

Updated as of May 13, 2021

Tutorial ASM.01: STEM-in-SEM—From Basic Transmission Imaging to Rigorous Quantitative Analysis
Session Chairs: Jason Holm and Gopal Rao
Saturday Morning, April 17, 2021
ASM

9:00 AM *

STEM-in-SEM—From Basic Transmission Imaging to Rigorous Quantitative Analysis Jason Holm;
National Institute of Standards and Technology, United States

Scanning electron microscopes and solid-state transmission electron detectors are widely available and generally easy to use, making the collection of imaging techniques referred to as Scanning Transmission Electron Microscopy in a Scanning Electron Microscope (STEM-in- SEM) more accessible today than ever before. These techniques are well suited to a host of transmission imaging applications including nanoparticle metrology, imaging beam-sensitive materials, grain texture studies, and defect analyses, for example. In this tutorial, we will describe how to obtain both qualitative and quantitative information from different transmission detectors including secondary electron conversion devices, different solid-state detectors, and a recently-developed programmable STEM (p-STEM) detector.

The first part of the presentation will briefly describe some of the pros and cons of low energy STEM-in-SEM imaging (i.e., with primary electron energies <30 keV). Different transmission imaging modes that can be accessed in a conventional SEM, and the types of information that can be gleaned from those modes will also be described. The importance of acceptance angle control will be emphasized. To that end, and because most commercially available STEM-in- SEM detectors enable only a few acceptance angle options, a straightforward and economical mask/aperture system [5] that can be adapted to most transmission detectors will be described. We briefly demonstrate how this approach can be used with a rudimentary solid-state STEM detector to obtain different imaging modes, and to quantify electron scattering distributions (i.e., diffraction patterns, Fig. 1b) for material systems amenable to this type of signal collection.

The second part of the presentation will emphasize an on-axis, pixelated detector for programmable scanning transmission electron microscopy (p-STEM). The apparatus includes a digital micromirror device (DMD) that enables imaging and diffraction in a single detector by directing different parts of the signal to different sensors. A CMOS digital camera is used to image the diffraction pattern, and a photomultiplier tube (PMT) synchronized with the microscope scanning system is used to generate a real space image by integrating (pixel-by-pixel) a portion of the diffraction pattern defined by the user. In effect, the DMD replaces the objective aperture in a transmission electron microscope (TEM) or an annular detector in a scanning transmission electron microscope (STEM). However, the DMD has the distinct advantage that arbitrary user-definable patterns (i.e., virtual apertures) can be programmed to it in real time, meaning that conventional imaging modes can be used to obtain quantifiable contrast and that non-conventional imaging modes can easily be explored. Detector operation is demonstrated by showing qualitative and quantitative information obtained from diverse samples including conventionally thinned (electropolished) stainless steel, oriented Au and Si films, and 2-dimensional materials. We will also show how the detector can be used to obtain information about the microscope including beam convergence angle and electron column alignment.

The third part of the presentation will present alternative and emerging imaging methods. For example, we will demonstrate how ptychography can be implemented in an SEM, how thermal diffuse scattering can be used as a local temperature probe, and different ways to ascertain sample strain.

Tutorial ASM.02: The Fundamentals of Nanoprobe Analysis
Session Chairs: Randal Mulder and Gopal Rao
Saturday Afternoon, April 17, 2021
ASM

5:00 PM *

The Fundamentals of Nanoprobe Analysis Randal Mulder; Silicon Labs., United States

As semiconductor technologies continue to decrease in size and the number of metallization layers increase, traditional methods for localizing the failure mechanism in failing semiconductor circuits such as micro-probing or light emission are severely limited if not impossible to perform. In response to this situation, nano-probe technologies have been developed to overcome this obstacle. In this tutorial, both AFM based and in-situ beam tool based (FIB/SEM) nano-probe technologies will be reviewed. Techniques for the characterization and identification of common semiconductor defects will be presented. Case studies for several types of defects will also be presented.

SYMPOSIUM BI01

Incorporating Sustainability into Materials Science Education, Training and Public Outreach
April 14 - April 18, 2021

Symposium Organizers

Ivana Aguiar, Universidad de la Republica
Yvonne Kavanagh, Institute of Technology Carlow
William Olson, ASM International
Daniel Steinberg, Princeton University

Symposium Support

Gold
National Science Foundation

* Invited Paper

Tutorial BI01: Industry's Current Approaches to Sustainable Practices and Strategic Planning for a Sustainable Future

Session Chairs: Tia Benson Tolle, Carolyn Duran, Yvonne Kavanagh, Daniel Steinberg and Jeffrey Whitford
Saturday Morning, April 17, 2021
BI01

9:00 AM *

Intel's Strategy for Corporate Responsibility—Responsible, Inclusive, Sustainable, Enabling Carolyn Duran; Intel Corporation, United States

Intel Corporation is a recognized leader in corporate responsibility and has a long history in taking action to advance progress in environmental sustainability, supply chain responsibility, diversity and inclusion, and social

impact. In this session we will demonstrate how Intel continues to raise the bar for ourselves in our own operations and supply chain, and the impact this has with our customers and society. This will include a deeper discussion on Intel's key actions in climate and energy, zero waste, and the circular economy. Additionally, we will share strategies around technology industry initiatives to accelerate change and adoption of best practices in responsible minerals, sustainable manufacturing and sustainable chemistry.

10:30 AM BREAK

10:45 AM *

Millipore Sigma and Data Driven Sustainability Planning Jeffrey Whitford; Merck KGaA, Germany

The instructor will discuss the need for quantification and how this is implemented in Merck with the DOZN quantitative analysis tool. He will address the question 'How do you embed quantitative analysis in the academic arena as a key lever for change?' and discuss the following topics:

Making data availability to the masses to encourage informed decision making

Creating and implementing sustainable design principles to drive change

Connecting the dots back to customers to understand the impact and opportunities for change.

12:15 PM BREAK

12:30 PM *

Sustainable Materials and Manufacturing in the Aerospace Industry Tia Benson Tolle and Kelsea Ballantyne; The Boeing Company, United States

Boeing recognizes climate change is a fundamental global challenge, and as we enable people to move freely across the planet we recognize the need to reduce the impact of flying. We are reducing carbon emissions and using resources efficiently through innovative solutions across our product life cycle, in our factories and at work sites. Additive manufacturing, also known as 3D printing, is changing the way we design and build products with fewer raw materials, creating less waste and improving fuel efficiency in our products. Innovative materials and processes are improving product efficiency in several ways. This session will discuss technical challenges and opportunities for sustainability in the aerospace materials and manufacturing industry.

SESSION BI01.01: Innovative Approaches I
Session Chairs: Ivana Aguiar and Daniel Steinberg
Sunday Morning, April 18, 2021
BI01

8:25 AM *BI01.01.02

Incorporating Uncertainty in Materials Industrial Ecology Elsa Olivetti; Massachusetts Institute of Technology, United States

The answer to most questions in environmental assessment for materials choice particularly around materials recovery is, "it depends". This presentation will focus on sustainability in curriculum within the materials science community and how we enable students to embrace the complexity of sustainability assessment while feeling entirely dissatisfied with the analytical methods used by practitioners. Examples will be drawn from impacts of materials choice on all aspects of the life cycle considering the context in which the material operates and on strategies for addressing and/or mitigating the impact of materials based on industrial ecology principles including dematerialization, substitution, and waste mining. This presentation will focus attention on how one might incorporate variation and uncertainty methodology in course work to account for the context in which the

material operates to understand the appropriateness of a particular mitigation strategy.

8:50 AM *BI01.01.03

Assessing the Contribution of Higher Education Programmes to the UN Sustainable Development Goals (SDGs) Vasiliki Kioupi and Nick Voulvoulis; Imperial College London, United Kingdom

Universities are engines of societal transformation and can nurture future citizens and navigate them towards sustainability through their educational programmes. In this talk, we will present an assessment framework we developed as part of our research at Imperial College London that Higher Education institutions can use to evaluate the contribution of their educational programmes to sustainability by reviewing the alignment of their intended learning outcomes (LOs) to the Sustainable Development Goals (SDGs) and the attainment of those LOs by students. The tool is based on a systemic grouping of the SDGs into eight sustainability attributes, namely, Safe Operating Space, Just Operating Space, Resilient Sustainable Behaviours, Alternative Economic Models, Health and Wellbeing, Collaboration, Diversity and Inclusion, and Transparency and Governance. Application of this tool in forty (40) environment and sustainability related Master's programmes highlighted gaps and areas for further consideration. In addition, we will present results on the application of the tool in a University case study to highlight how it can inform data driven decision-making around interventions to improve the integration of SDGs into curricula and the uptake of sustainability competences by students.

SESSION BI01.02: Online Teaching and Computational Resources

Session Chairs: Ivana Aguiar and Daniel Steinberg

Sunday Morning, April 18, 2021

BI01

10:30 AM *BI01.02.01

Materials Science for Sustainability—From Research Lab to Student Engagement Eva Hemmer;
University of Ottawa, Canada

Today's world faces global challenges, such as Societal Health, Environmental and Energy Concerns, that urgently have to be addressed for a sustainable development. While none of these concerns is easy to solve, material scientists are designing the building blocks that are key to sustainable energy and health strategies. Advanced optical materials act as novel optical bioprobes for reliable and early diagnosis of diseases or therapies. Novel optoelectronic/magnetic nanomaterials will increase device efficacy and endow them with yet unseen multifunctionality (photocatalysts, solar, storage devices). Herein, the remarkable optomagnetic properties of the rare-earths (RE) make RE-based materials ideal for biomedical and energy applications. Yet, challenges remain; low emission intensity and efficiency of small nanoparticles (NPs), and reliable and fast synthesis routes. As materials chemists, we are tackling these challenges with new designs of next-generation RE-NPs, accompanied by chemically controlled synthesis, application-oriented surface chemistry, and understanding of structure-property relationships.

While these research activities contribute to sustainability awareness of the small group of students working in our lab, the covid-19 pandemic has triggered a new format of teaching that has the potential to reach larger groups of students, raising their awareness of sustainability. This is the need to transform in-person classes into online courses. While this comes with new challenges, new opportunities arise: Seminar-style lectures for senior undergraduate and graduate students with experts from the fields of energy, environment, chemistry, physics and engineering were found to become popular at the University of Ottawa for students and educators alike. Will this new format of teaching find its permanent place in science curricula?

And how can we reach out further? The MRS Student Engagement Sub-Committee of the Academic Affairs Committee supports student-led activities at MRS events, including networking, science communication, and professional as well as personal development.^[1] This presentation will briefly introduce activities and

opportunities to interested students and senior mentors.

[1] D. Stadler, E. Hemmer, B. Anasori, Z. D. Hood, S. Mathur. Career progression through professional engagement: The impact of MRS student-led activities. *MRS Bulletin* 2020, 45 (4), 306.

10:55 AM *BI01.02.02

Teaching Sustainable Development to Engineering and Materials Students Tatiana Vakhitova, Marc Fry and Mauricio Dwek; Ansys Granta, United Kingdom

The Ansys Granta EduPack has supported undergraduate sustainability related teaching since 2007 with the introduction of an Eco Audit Tool – a teaching focused streamlined Life Cycle Assessment (LCA) Tool. The tool enables the energy and CO₂ emissions from each phase of a products life to be visualized, and the costs associated with each stage to be estimated. Based on positive educator and student feedback, in 2013 a new sustainability database was created that contains materials and process data with eco properties, socio-economic data on nations of the world, as well as legislation and regulations related to materials.

Further development added data on critical materials and materials risks.

This was followed in 2019 by the creation of a prototype Social Impact Audit Tool, which follows closely UNEP/SETAC guidelines on social life cycle assessment of products.

These existing and new developments aid teaching of courses on sustainable product design, sustainable engineering and many others, providing simple frameworks, tools and data to help students analyze complex sustainability systems and have informed discussion.

11:20 AM BI01.02.03

Materials Science Training Programs for Students and Masters with a Specialization in Electronics and Nanoelectronics Sergey M. Karabanov¹, Irina M. Kuvakova² and Yuriy Merkulov¹; ¹Ryazan State Radio Engineering University, Russian Federation; ²Social Sciences Institute, Russian Federation

Each stage of the social development creates its own set of intellectual, innovative directions in education. Currently, these areas are: artificial intelligence with the use of digital education (DE); A/B split testing in SEO-DE; video marketing in DE.

The development of materials science largely determines the development of the production of new materials for all areas of human life: medicine, building industry, transport, etc.

Materials science in the education system, especially in the field of electronics and nanoelectronics, ranks high. This is due to both the development of directions in instrument manufacture in the field of electronics and nanoelectronics (MEMS, NEMS, ultracapacitors, etc.), and invention and development of new materials (e.g, graphene). Creation of new methods and equipment for obtaining materials and testing their characteristics is also of great importance.

The paper considers the development of methods and programs for teaching materials science in the field of electronics and nanoelectronics using modern teaching methods (artificial intelligence, split-testing). The acquisition of the information during teaching depends on the initial level of preparation of the trained personnel. Therefore, educational programs correspond to different levels of preparation of the trained personnel: bachelors, masters, students of upgrade training courses. The role of online education, particularly, in teaching materials science is considered.

11:35 AM BI01.02.04

Incorporating Sustainability in Material Science Education—Adapting Computer Aid Programs in Teaching Materials Sustainability Burcu Ozden; The Pennsylvania State University, United States

In the century just ended, engineering recorded its grandest accomplishments. Despite these advances, the human being is face to poses challenges in the upcoming centuries. As the population grows and its needs and desires expand, the problem of sustaining civilization's continuing advancement, while still improving the quality of life, looms more immediate. The world needs engineers who will seek ways to put knowledge into

practice to come over the problem of sustainability. It is of great importance to incorporate concepts of sustainability into material science classes. In this work, I focus on the use of the sustainability component of SolidWorks, a Computer-Aided Design (CAD) tool, in teaching materials sustainability in online classes. The case study presents the virtual model of the product, the software capabilities, and the settings that have to be done for sustainability analysis and the results shown by the software.

11:50 AM BI01.02.05

Practices of Developing Undergraduate Curriculum on Green Engineering—Materials and Environment to Promote Active Learning Kaka Ma; Colorado State University, United States

As sustainability in product development and the relevant environmental impact raised increasing global attentions, it is critical to educate and train future workforce with the principles of green engineering and how to incorporate the principles in a broad context of science and engineering fields. This presentation will focus on development of undergraduate curriculum to incorporate sustainability into materials science education and the relevant pedagogy, including the online course - distanced learning session. I will share the experience of developing an undergraduate course on green engineering – materials and environment as a technical elective for engineering students and the feedback from the students. I will talk about three important aspects: link sustainability to the early design process, address the need of green engineering in the market, and integration of eco audit in CES Edupack in students' projects. Particularly, including some topic options on unrealistic materials in the project, e.g., the “uru metal” for Thor’s hammer from Marvel comics, turned out to be an effective pedagogy to motivate the students to look into the sustainability of material selection and processing, as well as to engage active learning.

SESSION BI01.03: Outreach Activities
Session Chairs: William Olson and Daniel Steinberg
Sunday Afternoon, April 18, 2021
BI01

1:00 PM *BI01.03.01

Learning Through Making—Integrating Makerspaces and United Nations Sustainable Development Goals in Science Learning Sara Rodriguez Martinez; ETH Zürich, Switzerland

Science thrives through the making of discoveries, building experiments, developing theories, solving problems. We are driven by all of these actions, but are we always taught that way? The theory of learning through making is not new; constructionism, or the education theory which focuses on how the making of artifacts supports the learner’s understanding of science, has been around for decades. Unfortunately, there’s little support on how to successfully turn theory into practice. In this talk, we will explore how to integrate learning through making in science learning, applicable to both formal and informal learning situations. We will look into finding support in community-led initiatives such as makerspaces and how to interact with such organizations to make our programs better. Makerspaces or Tinkerlabs are now ubiquitous all around the world, as their project-based nature fosters creativity, confidence and other necessary 21st Century Skills. Finally, we will draw from the United Nations Sustainable Development Goals for topics, projects and demo development, and how to turn them into a common ground for all of your science communication efforts.

1:25 PM BI01.03.02

The Big Compost Experiment—Using Citizen Science to Engage with the Public About Biodegradable Plastics Danielle Purkiss, Ayse Allison, Fabiana Lorencatto, Susan Michie and Mark A. Miodownik; University College London, United Kingdom

In 2018 the UK Plastics Pact set a target to make all plastic packaging 100% recyclable, reusable, or compostable, and to eliminate all unnecessary single-use packaging by 2025 [1]. Including compostable plastics in the target was important for two reasons: firstly, there are some items such as food packaging, wipes, tea bags, coffee pods, sachets, that being small and highly food contaminated are not suited to recycling or reuse; secondly, food waste is of major environmental importance and compostable liners play an important role in the route out of the home (government target for all UK households by 2023). But there is a fundamental problem. The biodegradable sector is currently the “wild west” of plastic packaging not just in the UK but also internationally. These materials are largely unregulated, the environmental claims around them exaggerated and the identification of them problematic. Nevertheless, these materials are starting to displace recyclable plastics such as PET due to their popularity with the public and brands. The displacement of reusable or recycling products is not the only problem, contamination of other waste streams is another: compostable plastics are currently incompatible with most Anaerobic Digestive, Industrial Composting systems and recycling systems [2]. Plastics Europe estimate the global market for biodegradable plastics is set to grow to 1.3 million tonnes in by 2023 [3] but it could be much greater if small item formats such as compostable snack packets and chocolate wrappers are produced to meet the Plastic Pact target.

The Big Compost Experiment (launched November 2019) [4] uses a citizen science approach to gather qualitative data on UK citizens’ opinion and behaviour towards biodegradable plastics and food waste strategies, and quantitative data about the performance of these items under UK home composting conditions. We engaged with more than 8000 citizens and report data from more than 300 home compost experiments from all over the UK [4]. This paper uses an interdisciplinary approach to data collection and analysis, and the evaluation of quantitative statistical and qualitative behavioural experiment data, and fits within a broader context of circular economy research and participatory citizen science.

Our citizen science research shows that 84% of UK households taking part reported that they are more likely to choose products that are marked as “biodegradable” or “compostable” but they are confused about what they are and how to dispose of them. We report on the fate of the biodegradable plastics tested, the majority of which did not fully biodegrade within a home composting environment [4]. We reflect on the role of citizen science in engaging with the public about behaviour change and the materials science of packaging.

1. UK Plastic Pact, www.wrap.org.uk/content/the-uk-plastics-pact (last accessed 28th Oct 2020)
2. Biodegradable plastics: An assessment of their role in the plastic waste crisis., www.plasticwastehub.org.uk(last accessed 28th Oct 2020)
3. Bioplastics Market Report (2018) www.european-bioplastics.org/wp-content/uploads/2016/02/Report_Bioplastics-Market-Data_2018.pdf (last accessed 28th Oct 2020)
4. Big Compost Experiment, <https://www.bigcompostexperiment.org.uk> (last accessed 28th Oct 2020)

1:40 PM DISCUSSION TIME

1:55 PM BI01.03.04

Raising Awareness About Materials Sustainability—Life Cycle Analysis as an Example Ivana Aguiar, Isabel Galain, Romina Keuchkerian, Maia Mombru and Maria Perez Barthaburu; Universidad de la República, Uruguay

When a consumer is faced with the decision of using a product made of a material or another, there are some preconceived ideas and an excess of information. Should I use a plastic or a paper bag? What factors should I consider? We designed and developed an activity for the general public in the University Chapter Udelar framework, which was carried out in different instances like the Heritage Day or the International Day of Women and Girl in Science in Uruguay. The objective was to help the consumers to make these decisions, providing information about life cycle analysis of different products, and explaining its concept and that of sustainability. Considering the COVID-19 pandemic, we had to design an appropriate demonstration which could involve an interaction with the participants, while at the same time complying with the sanitary measures.

We used three typical examples: a paper cup or ceramic mug, a paper or plastic bag, and disposable or cotton diapers. We presented the physical objects and asked the participants to compare the same object but made of different materials, in terms of five of the most common elements taken into account in a Life Cycle Analysis: energy use, water use, water contamination, CO₂ emissions, and solid waste. They have to choose which product was more or less intensive in terms of each category, and use the opportunity to speak with them about the relativity of geographic location and the efficiency improvement in productive processes. For this, we created a magnetic board with the items, which could be sanitized, and allowed participants to interact with the game. This involvement meant that participants would appropriate knowledge in a more organic way. In general, the public showed surprise with the results and claimed that this activity will change their actions in the future. Besides, they showed concern about deciding with the proper information, and demonstrated to us the necessity of disseminating this kind of data, to raise awareness about sustainability in our country and in our region.

2:10 PM BI01.03.05

Impact and Public Outreach of Socially Responsible Strategic Management of a Public Research Institution in the Effective Fight Against SARS-CoV-2 and COVID-19 Ivo Svejksky; Institute of Physics of the Czech Academy of Sciences, Czechia

In 2020, the whole world started to struggle with the SARS-CoV-2 pandemic and the coronavirus disease (COVID-19). As part of socially responsible research, the Institute of Physics of the Czech Academy of Sciences, as a public research institution in the Czech Republic, got involved in activities leading to the mitigation of the consequences of SARS-CoV-2 spread.

The main aim of this article is to propose a model of socially responsible management of a public research institution targeted at maximum positive impact for society, improvement of the image of an institution and wide public outreach in the time of the COVID-19 pandemic. Partial aims include the identification of key problems caused by COVID-19 to the inhabitants of the Czech Republic; the description of socially responsible strategic management of the FZU applied for the fight against COVID-19, the specification of the institute corporate culture and communication, the selection, description and evaluation of the most important FZU research projects with the accent on material physics and with a potential to contribute to the mitigation of the negative impact of the coronavirus on society, a set of recommendations for the application of the model to practice and its use in future crises.

For the research, both primary and secondary sources of data and the methods of induction and deduction have been used. The proposed model is based on real FZU strategic management and the functionality of the model has been verified in practical use.

It has been proven by the real use in the crisis time of the pandemic that the proposed model of socially responsible strategic management of a public research institution has brought positive results leading to the decrease in the danger of SARS-CoV-2 and COVID-19 in the Czech Republic. It is assumed that the model will be applicable and effective also when dealing with future crises. The broader issue of socially responsible strategic management of a public research institution in relation to crises has been growing in importance and will be researched further.

SESSION BI01.04: Technical Aspects

Session Chairs: William Olson and Daniel Steinberg

Sunday Afternoon, April 18, 2021

BI01

4:00 PM *BI01.04.01

Creating Sustainable Systems—From Stakeholder Decision-Making to Materials and Supply Chains

Carol Handwerker and Congying Wang; Purdue University, United States

When faculty, students, and even many practicing materials scientists think about sustainability, they frequently focus only on the materials and processes that they believe will lead to a sustainable product, very much a “build it and they will come” approach. University curricula in sustainable materials often mirror this view. In contrast, the NSF-funded Purdue-Tuskegee Integrative Graduate Education and Research Traineeship (IGERT) program “Global Traineeship in Sustainable Electronics” was based on the principle that people, their motivations for making certain decisions, and their ability to form trusted partnerships are central to the creation of sustainable materials, processes, and systems. To that end, the cornerstone of the IGERT program’s highly integrated curriculum, international fieldwork experience, and individual research topic mix was Elinor Ostrom’s General Framework for Analyzing the Sustainability of Social-Ecological Systems (Science, 2009) for which Ostrom was awarded the 2009 Nobel Prize in Economics. Faculty and three graduate student cohorts from Purdue and Tuskegee in multiple engineering disciplines, anthropology, management, toxicology, chemistry, physics, and mathematics collaborated over 7 years to build the program. In this talk I will present the key program elements and how they have been integrated to prepare students to participate in, and even become leaders in multi-stakeholder sustainable social-ecological systems.

4:25 PM BI01.04.02

En Route toward Sustainable Organic Electronics Clara Santato; Polytechnique Montréal, Canada

Consumer electronics has broadened access to education and information and contributed to improve our quality of life. Unfortunately, the pervasive expansion of electronics is generating an unsustainable growth of waste electrical and electronic equipment (WEEE) that contains toxic substances imposing great pressure on the environment and causing major health concerns (1). The electronics industry requires a paradigm shift: moving away from the planned obsolete strategy that has produced copious amounts of WEEE to an environmentally-responsible circular

approach, placing sustainability alongside performance at the heart of next-gen electronics design and manufacturing. To create this paradigm shift, the Collaborative Research and Training Experience in Sustainable Electronics and Eco-Design (CREATE SEED) initiative (2) trains a new generation of highly qualified personnel with a value-added experience in terms of an interdisciplinary approach, bringing together: chemistry, chemical engineering, engineering

physics, (eco)toxicology, electronic circuit design, hardware engineering, systems analysis, social sciences of the media, environmental economics, sustainable value chains and business models; professional skills in teamwork, communication, management, decision making and leadership. Within the context of CREATE SEED, to alleviate the environmental footprint of electronics and to extend their capabilities in emerging areas focusing on low human- and eco-toxicity, we design

& develop devices based on biodegradable organic electronic materials (3).

We will discuss the case of study of the pigment eumelanin, a bio-sourced candidate for environmentally benign (sustainable) organic electronics. The biodegradation of eumelanin extracted from cuttlefish ink was studied both at 25 °C (mesophilic conditions) and 58 °C (thermophilic conditions) following ASTM D5338 (4) and comparatively evaluated with the biodegradation of two synthetic organic electronic materials, namely copper (II) phthalocyanine (Cu-Pc) and poly(p-phenylsulfide) (PPS). Eumelanin biodegradation reached 4.1% (25 °C)

and 37% (58 °C) in 98 days, and residual material was without phytotoxic effects, while the two synthetic materials, conversely, were not biodegradable. The strikingly different results between bio-sourced and synthetic materials suggest that recurring to organic bio-sourced materials is a viable option to eco-design biodegradable organic electronic materials and devices. 1) Forti V., Baldé C.P., Kuehr R., Bel G. The Global E-waste Monitor 2020: Quantities, flows and the circular economy potential. United Nations University (UNU)/United Nations Institute for Training and Research (UNITAR) – co-hosted SCYCLE Programme, International Telecommunication Union (ITU) & International Solid Waste Association (ISWA), Bonn/Geneva/Rotterdam. 2) <https://www.polymtl.ca/create-seed/en>, an initiative funded by the Natural Sciences and Engineering Research

Council of Canada (NSERC). Clara Santato is the Principal Investigator. 3) Zvezdin A., Di Mauro E., Rho D.,

Santato C., Khalil M., MRS Energy and Sustainability, En route toward sustainable organic electronics, Vol. 7, 2020, E16. 4) Standard Test Method for Determining Aerobic Biodegradation of Plastic Materials Under Controlled Composting Conditions, Incorporating Thermophilic Temperatures.
<https://www.astm.org/Standards/D5338.htm>

4:40 PM BI01.04.03

3D Printing—Research, Training and Outreach in the Sustainability Ecosystem Rigoberto C. Advincula^{1,2,3}; ¹The University of Tennessee, Knoxville, United States; ²Oak Ridge National Laboratory, United States; ³Case Western Reserve University, United States

There is a high interest in using additive manufacturing or 3D printing to demonstrate sustainability, ecosystems in recycling, and biobased materials research. 3D printing to create devices from polymer and composite materials has appended the design functionality for new materials, including uses in biomedical devices, enabling rapid development. It is an important and emerging industrial production method. While 3D printed polymers can be further classified into thermoplastics, thermosets, and elastomers based on their thermo-mechanical properties, there are many desirable physical and chemical properties that can be combined with design. While important for materials research – it is important to integrate this into teaching curricula in materials science and broadcast in the public arena. This talk will demonstrate for the past 8 years: 1) integration in materials research, 2) teaching curricula development, 3) participation in the broad discussion of sustainable materials for affecting the circular economy. We will emphasize high impact factor peer-reviewed research, online and teaching curricula in 3D printing incorporating the circular economy, and participation in conferences to emphasize sustainability and high-performance materials research in 3D printing. The author has demonstrated these activities and paradigms in multi-institutions, multi-collaborations, and internationally.

SESSION BI01.05: How to Engage Materials Scientists and Students to Sustainability?

Session Chairs: Ivana Aguiar and William Olson

Sunday Afternoon, April 18, 2021

BI01

6:30 PM *BI01.05.01

Research and Publishing for the Sustainable Development Goals Ed Gerstner; Springer Nature, United Kingdom

The UN Sustainable Development Goals represent the most urgent, and difficult, challenges facing humanity. Many, such as SDG-13 on Climate Action, represent an existential threat. Meeting these challenges requires the involvement of physicists, chemists, earth scientists, biologists, mathematicians, computer scientists, engineers, clinicians, economists, entrepreneurs, social scientists and policymakers. But although they all share the same goal, and are try to solve the same sets of problems, they rarely attend the same conferences, read the same journals or even speak the same language. In this talk, I'll explore some of the philosophical, cultural and systematic barriers that researchers face, and what governments, funders, research institutions and, in particular, publishers need to do to help them make the world a better place.

6:55 PM *BI01.05.02

Incorporating Sustainability into Materials Science Education—Interest, Requirements and Opportunities Jeremy A. Theil^{1,2}, Ivana Aguiar³, Sudheer Bandla⁴, Ashley White⁵ and Yvonne Kavanagh⁶; ¹Xperi, United States; ²Mountain View Energy, United States; ³Universidad de República, Uruguay; ⁴Niagara Bottling, United States; ⁵Lawrence Berkeley National Laboratory, United States; ⁶Institute of Technology Carlow, Ireland

Throughout the Materials Science community (students, employers, faculty) there is interest in incorporating aspects of Sustainability into the educational experience. In order to quantify that interest as well as the needs of the community, interviews and a survey that recorded direct responses from more than 4% of the MRS membership were made. This survey confirmed the strong interest in implementing sustainability teachings from all peer groups, as evidenced by the high response rate. The major barriers to implementation in different regions, as well as the requirements of new educational resources will be discussed, along with guidance of effective educational experiences and resources encountered. Finally, methods to disseminate these materials to the community at large will be presented.

7:20 PM BI01.05.03

Engaging and Promoting Sustainability within Professional Societies Isabel Gessner¹, David Graf² and Sanjay Mathur²; ¹Massachusetts General Hospital, United States; ²University of Cologne, Germany

Sustainability encompasses almost all fields of our daily life and has become of increasing importance in the area of material science. While materials for sustainable future-leading technologies are developed, the sustainable production of these materials is likewise important. Professional societies such as the Materials Research Society (MRS) offer a versatile and interactive platform for those interested in engaging more in this topic. The aim of this presentation is to give an insight about MRS Focus on Sustainability Subcommittee, its task force activities and MRS Chapter activities that in many cases go beyond the sustainable development in the field of material science but also include inspirations for everyday life changes. Engagement in societies such as the MRS thereby provides a platform that allows to interact with a broad community of material scientists coming from both academia and industry, and therefore offers optimal conditions to find necessary facilitators and multipliers (refers to the UN Sustainable Development Goal no 17 'Partnerships for the Goals').

7:35 PM BI01.05.04

Materials Chemistry Incorporated into Building Science Identity Mary Sajini Devadas and Ellen Hondrogiannis; Towson University, United States

Science/STEM identity" is the sense of who students are, what they believe they are capable of, and what they want to accomplish with respect to science by interacting with others in the field. This requires intervention to help the "socializers" (i.e., STEM faculty and UGs) better understand the value and purpose of science literacy themselves so as to encourage students to appreciate science, be aware of possible career options in science, and enjoy learning and doing science. The project involves building "*science identity*" via the active involvement of Towson University's (TU) undergraduate student researchers (UG) in 1) engagement in research with the high school (HS) recruits through the apprenticeship model, 2) outreach activities in local high schools. The findings of this work will be presented.

7:50 PM *BI01.01.01

Sustainability as a Lens for Traditional Material Science Curriculums Gabrielle Gaustad; Alfred University, United States

The theoretical and methodological foundations of the sciences and engineering are essential to the removal of barriers to achieving sustainable systems. The teachings of these concepts still lie in traditional academic disciplines such as engineering, science, and mathematics. This structure can often manifest significant barriers to progress in tackling challenging sustainability issues due to an absence of a multi-faceted, interdisciplinary, systems approach. Material science has a particularly relevant set of foundational courses that lend themselves to interesting sustainability integration. Material selection approaches and software have begun to incorporate both economic and environmental "properties" in the decision analysis, highlighting the tradeoffs made in real applications(Ashby, Shercliff et al. 2013). Thermodynamics and kinetics principles can be illustrated in interesting energy conversion examples for next-generation renewable energy storage and production technologies. Other important contributions exist in fundamentals of mining, processing, alloying, phase equilibria, material flow analysis, etc. A variety of recent research is available with additional innovative

suggestions (Gipson and Prins 2015, Gunister, Ozturk et al. 2015, Mainali, Petrolito et al. 2015). Integration of sustainability issues into material science curriculum promotes nexus thinking. In many engineering curriculums it can be challenging to promote interdisciplinary thinking when the curricular approach is inherently siloed. This can often lead to a reductionist spiral where “solutions” produce unintended consequences or additional problems. Integration of sustainability into traditional disciplinary curriculums also promotes T-shaped or Pi-shaped student competencies. Broad, transversal skills are being emphasized more by employers; it is imperative that today’s student leave with not just a disciplinary degree but communication, organization, analysis, and critical thinking skillsets (Faris, Kolker et al. 2011, Connor, Sosa et al. 2017). These approaches also help to improve the translation of theory to practice, another key gap cited by employers. Students often struggle to take academic learning and use it directly for on the job skillsets; ABET has emphasized this need in its accreditation processes (Glasgow and Emmons 2007, Passow 2012). Specific examples will be illustrated for a diverse set of courses and curriculum. Results show such an approach can contribute to improved recruitment and retention number and preliminary results appear to also enhance student learning outcomes measured via traditional assessment methods.

SESSION BI01.06: Sustainability Education into Action I
Session Chairs: Ivana Aguiar and William Olson
Sunday Afternoon, April 18, 2021
BI01

9:00 PM *BI01.06.01

Sustainable Science—Let’s Green Our Labs! Rachael Relph; My Green Lab, United States

Recent years have seen the emergence of a green lab movement. Championed by a coalition of scientists, facility managers, engineers, designers, sustainability directors and non-profits, the movement seeks to institutionalize sustainability in laboratories through the adoption of green lab programs. These programs address laboratory sustainability holistically by encouraging scientists to reduce energy, water, waste and hazardous chemical use in the lab.

My Green Lab, a non-profit organization, is at the forefront of the green labs movement. My Green Lab runs several programs around the world for scientists in support of reducing the environmental impact of scientific research, including a Green Lab Certification Program, which uses a global standard for laboratory sustainability, and the ACT Label, which is the industry’s first eco-nutrition label for laboratory products.

This presentation will focus on how My Green Lab effectively engages scientists through the Green Lab Certification Program and will look at some examples of ways that materials scientists can incorporate sustainability into their daily work. We will also look at how manufacturers are using the ACT Label to design more sustainable products and how scientists can use it to make more informed purchasing decisions for their lab.

9:25 PM BI01.06.02

Intersecting Materials Science with Sustainability Education—A Single-Use Plastics Module for Undergraduate Curricula Ty Christoff-Tempesta and Noelle E. Selin; Massachusetts Institute of Technology, United States

Foundational principles of materials science and their application to related fields offer a critical toolkit for contextualizing and addressing pressing sustainability challenges. To this end, we developed an adaptable two-class module focused on the single-use plastics crisis for incorporation into undergraduate curricula. Designed for the gateway introduction to sustainability class at the Massachusetts Institute of Technology, “People and

the Planet: Environmental Governance and Science,” the module grapples with the proliferation of single-use plastics and their extensive environmental contamination. Students are introduced to a range of materials science principles in the module, including structure-property relationships, environmental interactions of materials, and life cycle analyses. Further, students are afforded the opportunity to consider the single-use plastics crisis through a variety of lenses, including as materials scientists, economists, policymakers, industrial stakeholders, chemists, and more. The module utilizes the Human-Technical-Environmental (HTE) framework and matrix-based approach to analyze the single-use plastics crisis through a pre-module background lecture and briefing paper, an in-class life cycle analysis (LCA) presentation and activity based on the UN Sustainable Development Goals, an in-class negotiation activity, pre- and post-class reflection questions, and readings for each class. The resources for this module are made readily accessible so that educators can incorporate any or all of its parts into their courses.

9:40 PM BI01.06.03

The Joint Undertaking for an African Materials Institute (JUAMI) Life Cycle Assessment Project Brian Iezzi¹, Timothy Tibesigwa², Edwin Richard³, David Maleko⁴, Tae Lim¹, Muhammad A. Hashmi¹, Jason Hawes¹, Carlos Biauou⁵, Kwasi Amofa⁵ and Steve Skerlos¹; ¹University of Michigan–Ann Arbor, United States; ²Makerere University, Uganda; ³Nelson Mandela African Institute of Science and Technology, Tanzania, United Republic of; ⁴Sokoine University of Agriculture, Tanzania, United Republic of; ⁵University of California, Berkeley, United States

Social, environmental, and economic life cycle assessments (LCA) have become critical decision-making tools in academia, industry, and government the world over. Materials LCA education has similarly become more common and best practices for teaching methodologies are in continuous development. This project is focused on a peer to peer mentorship model for LCA education in which PhD students in East Africa and the United States work together to develop and execute a comprehensive LCA to assess the sustainability of a local product or system. Specifically, the three pilot projects thus far have focused on biodiesel production in Uganda, the dairy industry in Tanzania, and the municipal solid waste system of Arusha, Tanzania. The model relies on vetted learning modules, developed at the Center for Socially-Engaged Design (CSED) at the University of Michigan, that step the students through the process of goal and scope identification, inventory creation, and impact assessment. This is coupled with close mentorship and support from students who have previously conducted LCAs, live and virtual day-long LCA workshops, and access to an open, high computing power server with best in class LCA software as well as critical databases such as EcoInvent and the Social Hotspot Database. This combined approach of peer to peer mentorship, curated educational materials and support, and access to critical computational infrastructure has proven to be successful in the implementation of the above-mentioned projects, with several currently under review for publication. We believe this model of a community-learning based approach to LCA education can be applied in other areas of the world to help train the next generation of global sustainability practitioners and educators. This project is supported by the National Science Foundation Joint Undertaking for an African Materials Institute (JUAMI) as well as the United Nations Environment Program (UNEP) Life Cycle Initiative.

9:55 PM BI01.06.04

Teaching High School Materials Science Through Research Kaci L. Kuntz; Rowland Hall, United States

At this pivotal moment, we are facing climate change, movements to increase diversity and equity in science, and a world-wide pandemic. Educators, researchers, and industry leaders are in the unique position to contribute to valuable and necessary changes. Materials scientists are well-suited to address these changes, particularly through sustainability research. With a strong correlation between mentorship in research, especially by teachers, and success of students in their life-long career in STEM (*Nature* 447, 791–797 (2007), *J. of Coll. Stud. Dev.* 49(4), 285-300 (2008)), we have developed an innovative curriculum to build mentor-mentee relationships in a high school classroom as students perform original materials science research with motivation to advance sustainable technologies for battery applications.

This course curriculum has three major pillars: **motivation, community, and skill development**. First, students are **motivated** by the broader impacts their research can have on the scientific community. With climate change and the need for improved energy technologies, we are inspiring and challenging the students to work on contributing to this research area. Moreover, to foster and model the culture of sustainability in research, students are first *computationally* investigating structure-property relationships and after identifying compounds with desired properties (e.g. charge/discharge rates, energy storage capacity, nontoxic, renewable, etc), they *experimentally* test the identified materials. On the experimental side, we are employing sustainable lab techniques, such as glove recycling and strategic experimental design to employ reusable equipment. Secondly, a research curriculum in a high school setting allows for **community**, collaboration, inclusivity, and diversity to be intentionally implemented into each class. Success and ideas from each student can be celebrated as a group; collaborations between students, mentor, and other scientists in industry and academic institutions can be fostered, and literature can be intentionally selected to highlight research content, diversity of researchers already in the field, and best sustainable research practices for the lab and industry settings. The aspects of allowing students to have mentors and to be exposed to other scientists with similar scientific identities can increase retention in STEM fields and future careers (*J. of Coll. Stud. Dev.* 49(4), 285-300 (2008)). Thirdly, this course allows students to readily apply their knowledge of math, physics, chemistry, biology, statistics, and engineering knowledge to real science (which is shown to improve retention in STEM (*Int. J. of STEM Edu.* 5(48) (2018))). They are gaining hands on experience and **developing the skills to**

- Perform literature reviews
- Design, engineer, and execute experiments
- Evaluate and interpret data and results
- Form conclusions
- Present findings, both verbally, orally, in writing, and in visual depictions.

The ability to consistently have a group of students gathered and working collaboratively on original materials science research allows for the mentoring and molding of future STEM leaders with a solid skill set foundation, sense of community and self-identity in science, and a motivation to pursue sustainable technologies with broader impacts for the scientific community and the world in this pivotal time.

In this work, we will discuss both the curriculum aspects of the course design and observed results from intentionally providing students with hands-on experience in materials science research in a classroom setting as we foster the growth of the future materials scientists.

SESSION BI01.07: On-demand
Wednesday Morning, April 14, 2021
BI01

8:00 AM *BI01.07.01

Teaching Materials for Mitigating Climate Change [Kevin S. Jones](#); University of Florida, United States

Teaching sustainability is a significant challenge given its broad reaching aspects. In a sustainable world our CO₂ levels are stable. Currently this is obviously not the case as the CO₂ level has exceeded 420ppm for the first time in human history. In an effort to teach students about the sources of CO₂ and ways to mitigate this challenge a new class entitled Materials for Mitigating Climate Change has been developed. The goal of this class is to explore the sources of CO₂ and how innovations in materials science are being used to address these challenges. The Environmental Protection Agency has divided up the sources of CO₂ into 5 categories including electricity, transportation, industry, commercial/residential and agriculture. The relative contributions of each of these sources to the 17GT of excess CO₂ produced each year is reviewed. Then each category is broken down by topic and the historical and recent impact of materials innovations on the CO₂ emission process are discussed. It is difficult to use these categories exactly given overlap in the areas. For example,

industrial source of CO₂ also involves transportation and buildings etc. In addition to it being difficult to place an exact figure on the relative contributions of each sector to the total CO₂ emissions, it is also difficult to place an exact figure on the potential impact of these innovations. Despite these instructional challenges, it is apparent materials innovations are going to play a critical role if we are to address the rising CO₂ levels. This talk will review the topics discussed in the class. It was found that asking the students to discover recent innovations external to the class proved to be an excellent method of engaging non-majors in this topic. While such stories can be captivating the challenge is placing numbers on the relative impact of these discoveries remains. This talk will conclude with asking the audience to contribute their ideas on aspects of this challenge that may have been overlooked.

8:20 AM BI01.07.03

Sustainable Polymer Degradation Using Concentrated Solar Energy Miriam Sanchez Pozos; Universidad Autónoma del Estado de México, Mexico

The widespread use of plastic has made plastic waste and its accumulation in the environment a matter of great concern because its natural degradation is very slow. However, there is a wide variety of synthetic polymers that subjected to photo-oxidative reactions produced by UV radiation from sunlight, degrade significantly. And if the wavelength of the UV radiation is adequate according to the type of plastic, for example 300 nm for polyethylene (Ibnelwaleed A, 2007), it is possible to maximize its degradation. Therefore, using solar concentration favoring the appropriate wavelength of UV radiation will allow to accelerate the photodegradation process of these wastes and will favor their rapid incorporation into the environment in a friendly way.

In the Faculty of Engineering of the Autonomous University of the State of Mexico in the Mechanical Engineering Degree program in the Materials Science subject, as well as in the Engineering Science Postgraduate course, (Materials and environmental sustainability), one of the issues addressed is the degradation of polymeric materials. The degradation of polymers is carried out under different schemes such as:

- 1- Natural weathering method, (CA)
- 2- QUV Accelerated weathering (Q-Lab), (CI)
- 3- Accelerated weathering using a solar concentrator, (CS)

With this practice, students learn that a wide variety of synthetic polymers absorb ultraviolet (UV) solar radiation. The Photo-oxidative degradation is the process of decomposition of the material by the action of light, which is considered one of the main sources of damage exerted on polymeric substrates under environmental conditions. Most synthetic polymers are susceptible to degradation initiated by UV visible light.

The methods to carry out the photodegradation practices are the natural weathering method; Outdoor exposure is performed on specimens mounted on test racks, oriented under standard conditions to expose the material to the full radiation spectrum as well as the temperature and humidity at that location. Another technique used is accelerated aging in accelerated weathering chambers that use UV radiation from the brand (Q-LAB). Finally a solar concentration system is used to super-accelerate the polymeric materials degradation . The materials degraded by the three techniques (CA, CI and CS), are analyzed to observe the formation of cracks, the embrittlement of the materials, the disintegration in powder, and the color changes. Finally, the degraded polymers are characterized by means of FTIR, and mechanical testing in order to determine the aging of the material as a function of time and the intensity of the radiation absorbed by them.

In the Faculty of Engineering of the UAEM, they are consolidated the experience about the development of solar concentration devices, with the knowledge and experience on plastics engineering, to develop postgraduate students' projects and laboratory practices of undergraduate, students about the use of solar energy in polymers degradation.

For the accelerated degradation practices, a solar concentrating system (patent MX/a/2015/000346) was designed and built. This solar concentrator was conceived to degrade plastic waste much faster than is done with UV radiation chambers (which only are used at the laboratory level). Therefore, this degradation technology can be considered as ecological, since it can be used with a very low environmental impact because it does not require more energy than from the Sun. This accelerated degradation system is mainly focused on treating plastic waste that is no longer susceptible to being reused or recycled.

With the use of the solar concentration system, students learn the scope of the use of solar energy, to replace the use of conventional equipment that consume too much electrical energy.

In the same way, students understand the effects of UV radiation on the degradation of polymers, and therefore the limited use they must make of them.

8:30 AM BI01.07.05

Late News: Plastics in View of Sustainability—An International Initiative Towards Education and Training of Young Scientists Natalia Tarazona¹, Rainhard Machatschek^{1,2}, Jinneth L. Castro Mayorga³, Felipe Salcedo Galán⁴ and Andreas Lendlein^{1,2}; ¹Helmholtz-Zentrum Geesthacht, Germany; ²University of Potsdam, Germany; ³Corporación Colombiana de Investigación Agropecuaria, Colombia; ⁴Universidad de los Andes, Colombia

In the race between technological progress and education, transformative changes are necessary to prepare a future workforce on sustainable thinking and practice, to act on authentic challenges (eg. ecosystem conservation and global economy) while making responsible use of natural resources. Such development of educational approaches could benefit from a strategic international collaboration, including scientific projects, joint programs and capacity building.

Here, we introduce the Transnational Network for Research and Innovation in Microbial Biodiversity, Enzymes Technology and Polymer Science –MENZYPOL, a team effort to integrate inclusive and equitable quality education into research collaboration projects. The project is jointly funded by the Colombian Administrative Department of Science, Technology and Innovation (Minciencias) and the German ministry of education and research (BMBF).

MENZYPOL aims to create a lasting partnership between Helmholtz Zentrum Geesthacht (HZG) in Germany, Universidad de los Andes (UniAndes) in Colombia and key partners from the Colombian agricultural sector (Agrosavia). The pilot project established in the network concentrates on the exploration of the Colombian biodiversity for the discovery and development of biocatalysts in polymer science. The main focus is to isolate microorganisms with the ability to produce advanced polyesters, and to obtain enzymes that can degrade polyesters from natural and synthetic origin.

Ideally, the DNA and protein sequences of the isolated microorganisms and enzymes, together with their specific activities, will be added to databases to support the identification of other species using predictive analytics. This integrated approach brings together researchers from two different continents aside from requiring a broad range of expertise, from molecular biology all through polymer science and bioinformatics. The participating students and early career researchers not only gain access to sophisticated research infrastructures or the microbial biodiversity of a megadiverse country, but also to scientific approaches that are far out of the scope of traditional scientific education. This is enabled by giving young scientists the opportunity to learn and to be mentored by experienced researchers. The ongoing COVID-19 pandemic presents a challenge by excluding short-term visits, and extended research stays, which can naturally only be offered to very few. Therefore, the lessons learned in the past months in virtualization of science education and exchange will be used to move activities to the digital world, thereby boosting outreach and accessibility.

8:40 AM *BI01.07.06

Low-cost and Recycled Electronics for Sustainable Education, Discovery and International Innovation Stoyan K. Smoukov; Queen Mary University of London, United Kingdom

Low cost and reusable technology is both a sustainable and scalable approach to education. We show examples of low-cost electronics which have resulted in an International Innovation Competition in Africa. Students are able to push the boundaries of what is possible and create new instruments, rather than only reproduce exercises pre-made for them. www.tinyurl.com/2020Africa

A new direction that grew out of a Trash-to-Treasure workshop - shows the power of up-cycling old electronics for education. Taking apart consumer electronics has long been a staple in materials education. It is a missed opportunity, however, to note how many times such devices fail for a simple reason, and much of them are still functional, capable of re-use in many other contexts, sometimes for even higher value.

The latter is illustrated with the case of dead hard-drives up-cycled to low-cost centrifuges, which have high specs. These can be used to carry out a number of biological tests. Understanding not only the materials but also the interdisciplinary principles of how such components integrate into a whole, dynamic system allow holistic teaching incorporating materials, electronics, 3D printing, sensing and more.

9:00 AM *BI01.07.07

Individual-Centric Approaches to Accessibility in Materials Science Education [Theresa Davey](#)¹ and [Rebecca Davenport](#)²; ¹Tohoku University, Japan; ²Max-Born Institute, Germany

A significant part of tackling sustainability in education is promoting access to quality education for all communities. Promoting diversity in university admissions is a vast challenge, involving addressing unconscious biases and perceptions of competence, but it doesn't solve the whole problem. Even if a diverse group of people are accepted to study materials science at university, that doesn't guarantee equal access to education. Time-pressured academics whose institutions undervalue teaching have an understandable overreliance on outdated teaching methods, which can have the unfortunate consequence of magnifying existing inequalities. This talk will present an discipline-based individual-centric approach to higher education teaching that will provide guidelines for working with students to create an inclusive learning environment.

The aim of this approach is to create an environment that promotes student empathy, self-awareness, and confidence in self-advocacy, while balancing competing needs and working within the limitations of a university environment such as large classrooms and non-ideal teaching spaces. The rapid shift to online learning has also revealed potential positive and negative aspects of out-of-classroom teaching, but has also put a significant strain on the mental health of both students and teachers, and exaggerated accessibility issues. Approaches that promote accessibility in the classroom do not always translate directly to online learning environments, but the key idea of individual-focussed education provides a framework for developing best practices for meeting a diversity of student needs and delivering positive student outcomes.

9:20 AM *BI01.07.08

The Repercussions of Gender Bias and Inequalities in Science Knowledge Making [Elizabeth Pollitzer](#); [Portia](#), United Kingdom

Gender equality, diversity, and inclusion have been identified as essential pre-requisites for excellence in science and scholarship, as well as for the socio-economic development of societies. Nevertheless, inequalities and gender gaps persist, e.g. underrepresentation of women and certain social groups in leadership positions. At the same time, previously overlooked issues emerge as critically important, e.g. the widespread occurrence of sexual harassment in academia. New issues also arise, for instance the gaps in knowledge revealed by the COVID pandemic, and the consequences of the pandemic for higher education and for academic and research careers. Another urgent issue is the lack of progress on gender equality in the UN Agenda 2030 and the need for better, more contextualised and gender-bias free approaches to SDGs implementation. Using the latest understanding of gender and diversity issues in science endeavours, complemented by examples pertinent to materials engineering, this presentation will focus on advancing gender equality, diversity and inclusion in the mechanisms of science knowledge making and application to achieve greater societal relevance and trust in science institutions and knowledge.

9:40 AM BI01.07.09

Writing-to-Learn in Introductory Materials Science and Engineering Hongling Lu, Leah Marks, Timothy Chambers, Solaire Finkenstaedt-Quinn, Ginger Shultz, Anne Gere and Rachel Goldman; University of Michigan–Ann Arbor, United States

M-Write is a campus-wide project which aims to transform teaching and learning in gateway courses through enhanced student engagement and transformative learning. In Materials Science and Engineering (MSE), we are implementing Writing to Learn (WTL) assignments and peer review in courses spanning from introductory undergraduate to advanced graduate levels. The WTL assignments enable students to apply content knowledge to “real-world” situations via writing, which promotes deeper thinking and compels students to explain concepts in their own words. The subsequent peer review and revision processes provide additional learning opportunities as the students give and receive feedback on content and critically self-assess their own work. In this project, we are quantifying the influence of WTL assignments on student understanding of key concepts in introductory MSE courses. The project involves evaluation of the effectiveness of the WTL assignments and their impact on student learning. Both quantitative and qualitative research methodologies are utilized, including pre/post assessment surveys and interviews, as well as analysis of writing products. In this presentation, we will discuss our use of WTL in Introductory MSE. For example, we have used WTL to assist student learning of polymer properties, with a prompt that focuses on polymer recycling and its impact on mechanical properties. Our research suggests that the polymer recycling WTL assignment was effective in promoting understanding of stress-strain behavior of polymers, but that further support is needed to help students connect polymer microscopic properties to macroscopic behavior [1]. The effectiveness of WTL assignments associated with other key concepts including the atomic packing in crystals, ductile vs. brittle failure, interpretation of phase diagrams, and corrosion as it relates to the Flint water crisis will also be discussed.

[1] S.A. Finkenstaedt-Quinn, A.S. Halim, T.G. Chambers, A. Moon, R.S. Goldman, A.R. Gere, and G.V. Shultz, J. Chem. Educ.94, 1610 (2017).

SYMPOSIUM CT01

In Situ/Operando Characterization of Solid–Liquid Interfaces for Sustainable Energy, Water and Environment
April 14 - April 23, 2021

Symposium Organizers

Ethan Crumlin, Lawrence Berkeley National Laboratory
Xiaofeng Feng, University of Central Florida
Feifei Shi, The Pennsylvania State University
Yingjie Zhang, University of Illinois at Urbana-Champaign

Symposium Support

Bronze
Bruker

* Invited Paper

SESSION CT01.01: Scanning Probe Characterization I
Session Chairs: Xiaofeng Feng and Yingjie Zhang
Thursday Morning, April 22, 2021
CT01

8:00 AM CT01.01.02

Visualizing ion adsorption and Crystal Growth at Charged Interfaces with Near-Atomic Resolution

Benjamin A. Legg^{1,2} and James J. De Yoreo^{1,2}; ¹Pacific Northwest National Laboratory, United States;
²University of Washington, United States

Solid-water interfaces can drive complex chemical phenomena, where processes such as ion adsorption become tightly coupled to phenomena such as surface charging and crystal growth. In-situ atomic force microscopy (AFM) provides a powerful tool to visualize these phenomena. Here we apply in-situ AFM to directly image individual aluminum ions at a mica-water interface and show how the mica-water interface drives changes in aluminum speciation (favoring the formation of hydrolyzed aluminum species). We subsequently investigate the assembly of these ions into dynamically fluctuating clusters, and the coalescence of these clusters to form 2D epitaxial aluminum hydroxide films with a persistent network of gaps. The cluster populations prior to film-growth reveal an energy landscape that deviates significantly from classical theories of heterogeneous nucleation, but these deviations can be explained when we consider the electrostatic energy associated with forming charged clusters at the solid-water interface. Monte Carlo simulations indicate that these charging effects can remove the classical barriers to crystal nucleation and enable a barrierless process of crystal growth by cluster coalescence.

8:15 AM *CT01.01.03

The Duality of Interfacial Water on Crystalline Surfaces—Hydration vs Expulsion and Replacement

Ricardo Garcia; CSIC, Spain

Interfacial liquid layers play a central role in a variety of phenomena ranging from friction to molecular recognition. Liquids near a solid surface form an interfacial layer where the molecular structure is different from that of the bulk. Yet the molecular-scale understanding of the interactions of liquid water with solid interfaces is unsatisfactory for the lack of high-spatial resolution methods. The presentation is divided in three sections. The first section is an introduction to the relevance of solid-liquid interfaces. The second section, presents the features and capabilities of 3D-AFM [1-2] to image with atomic resolution the **three-dimensional** interfacial structure of surfaces immersed in aqueous solutions. The third section reports the structure of interfacial water layers on different surfaces from graphene to a few layer MoS₂; from hexagonal boron nitride to pentacene. Those interfaces are characterized by the existence of a 2 nm thick region above the solid surface where the liquid density oscillates (Fig. 1) [3-4]. The distances between adjacent layers for graphene, few-layer MoS₂, h-BN and pentacene are ~0.50 nm. This value is larger than the one predicted and measured for water density oscillations (~0.30 nm). The experiments indicate that on extended hydrophobic surfaces water molecules are expelled from the vicinity of the surface and replaced by several molecular-size hydrophobic layers.

References

- [1] D. Martin-Jimenez, E. Chacon, P. Tarazona, R. Garcia, Nat. Commun. **7**, 12164 (2016).
- [2] T. Fukuma and R. Garcia, ACS Nano **12** 11785 (2018).
- [3] M.R. Uhlig, D. Martin-Jimenez and R. Garcia, Nat. Commun. **10** 2606 (2019).
- [4] M.R. Uhlig et al. (submitted)

8:40 AM CT01.01.04

Three-Dimensional Molecular Mapping of Ionic Liquids at Electrified Interfaces Shan Zhou, Kaustubh Panse, Mohammad H. Motevaselian, Narayana R. Aluru and Yingjie Zhang; University of Illinois at Urbana-

Champaign, United States

Electric double layers (EDLs) are key to electrochemical energy conversion and storage applications such as capacitive charging and redox reactions. However, most of the existing spectroscopy and atomistic imaging methods, such as X-ray spectroscopy and electron microscopy, can only probe the binding states and/or the planar distribution of strongly adsorbed species at the electrode interface, therefore the molecular scale structure of EDLs still remains elusive. Based on our recent success on high-speed 3D force mapping [1], here we report a novel technique, electrochemical three-dimensional atomic force microscopy (EC-3D-AFM), and use it to directly image the molecular scale EDL structure of an ionic liquid under different electrode potential. Our technique overcomes the limitations of existing 3D-AFM methods in measuring highly viscous liquids. From the 3D-AFM images, we observe rich 3D molecular distribution profiles and potential-dependent reconfigurations. In combination with molecular dynamics simulations, we are able to gain a molecular level understanding of the capacitive charging effects. We expect this mechanistic understanding to have profound impacts on the rational design of electrode-electrolyte interfaces for supercapacitors and batteries.

[1] Panse, K.*; Zhou, S.* and Zhang, Y. 3D Mapping of the Structural Transitions in Wrinkled 2D Membranes: Implications for Reconfigurable Electronics, Memristors, and Bio-Electronic Interfaces. *ACS Applied Nano Materials* **2019**, 2, 5779-5786.

8:55 AM CT01.01.05

Probing Electric Double Layers on MoS₂ Using *In situ* Atomic Force Microscopy Kaustubh Panse, Shan Zhou, Haiyi Wu, Narayana R. Aluru and Yingjie Zhang; University of Illinois at Urbana-Champaign, United States

There is an invigorated interest in using operando characterization techniques to analyze the electrode-electrolyte interface in various electrochemical materials systems. Various processes like ion adsorption, intercalation and electric double layer (EDL) charging on the electrode surfaces are responsible for the electrochemical performance, but the precise mechanisms remain unclear. Here we present in-situ electrochemical atomic force microscopy measurements to characterize the EDL structure on MoS₂ surfaces. We have specific interest in using MoS₂ as the electrodes due to their promising applications in batteries and supercapacitors.

We obtain atomic-scale 3D images of the electrode-electrolyte interfaces using a force mapping technique. In the current work, we vary the electrode potential and observe a change of the double layer structure. The observed fine molecular features near the electrode surface are unprecedented and reveal the charge storage mechanism of MoS₂ electrodes.

Reference:

Panse, K. S., Zhou, S., & Zhang, Y. (2019). 3D Mapping of the Structural Transitions in Wrinkled 2D Membranes: Implications for Reconfigurable Electronics, Memristors, and Bioelectronic Interfaces. *ACS Applied Nano Materials*, 2(9), 5779-5786.

9:10 AM *CT01.01.06

The Structure of Ionic Liquid Electric Double Layers and Their Functionality Investigated by Atomic Force Microscopy Nina Balke and Wan-Yu Tsai; Oak Ridge National Laboratory, United States

The structure and dynamics of the solid/liquid interface are of fundamental interest for various energy related technologies including energy storage, catalysis, lubrication, and many more. Of particular interest are room temperature ionic liquids (IL) which hold the promise of increasing the electrochemical stability windows for electrochemical capacitors and electrostatic gating of functional oxides. In both cases, the structure of the IL electric double layer (EDL) in three dimensions is the key to understand the device performance. Theories describing the EDL have been proposed showing a layering of cations and anion at solid interfaces. However, a full 3D description is lacking and experimental approaches to measure and understand the EDL's interfacial

structures, dynamics and reactivity are scarce. Due to the characteristic sizes of EDLs, this requires characterization techniques capable of resolving nm length scales. Atomic Force Microscopy (AFM) can investigate such length scales in 3D and has been shown to be suitable to image solid-liquid interfaces.

Here, we demonstrate the use of in-situ AFM techniques to understand processes at the solid/liquid interface and introduce statistical and theory coupled approaches. We will showcase the capabilities for two different systems. First, we will image the EDL of an ionic liquid at a graphite interface and report the direct observation of the structure and properties of topological defects. We will show the existence of structural domains parallel to the solid-liquid interface towards a full picture of the double layer structure and investigate their change with applied bias and shine light on their origin. Then we will apply the technique to IL gated oxide devices where the gating process is explained in terms of the interfacial IL structure. We will show that the transition between both ON and OFF states of the IL-gated amorphous indium gallium zinc oxide transistor is caused by a densification and preferential orientation of counter-ions at the oxide channel surface. This process occurs in three distinct steps, corresponding to regions of different electrical conductivity. In this case, the EDL thickness associated with the flat arrangement of cations at the surface results in extremely high charge density leading to high drain currents.

The work was supported by the Fluid Interface Reactions, Structures and Transport (FIRST), an Energy Frontier Research Center funded by the U.S. Department of Energy, Office of Science, Office of Basic Energy Sciences. Measurements were performed at the Center for Nanophase Materials Sciences (CNMS), which is sponsored at Oak Ridge National Laboratory by the Scientific User Facilities Division, Office of Basic Energy Sciences.

SESSION CT01.02: Atomistic Simulations
Session Chairs: Yuanyue Liu and Yingjie Zhang
Thursday Morning, April 22, 2021
CT01

10:30 AM *CT01.02.00

Determining Surface and Interfacial Structures—The Convergence of Computation, Experiments and Machine Learning Maria Chan; Argonne National Laboratory, United States

Determining atomistic structure at surfaces and interfaces is challenging because metastable surfaces/interfaces are likely accessible under realistic conditions, rendering energy-only searches insufficient, and experimental data often give incomplete information. Therefore, neither theory nor experimental data alone is sufficient to determine these structures. In this talk, we will discuss how we use machine learning to combine experimental and theory-based data to determine surface and interface structures.

10:55 AM *CT01.02.01

Interfacial Structure and Electrochemistry of Lithium and Zinc Batteries from Molecular Modeling Oleg Borodin, Travis Pollard and Jenel Vatamanu; U.S. Army Research Laboratory, United States

A molecular scale insight into ion transport and decomposition is important for understanding deficiencies of the currently used aqueous and non-aqueous electrolytes. In this presentation I will summarize progress made towards improving molecular scale understanding of the structure and electrochemistry for a wide range of aqueous and non-aqueous electrolytes. Double layer properties are obtained from classical MD simulations, while modeling of non-aqueous electrolytes will focus on the competitive solvent and salt reduction at the passivated electrochemical interfaces using Born Oppenheimer Molecular Dynamics (BOMD) simulations using DFT functionals. These BOMD simulations included critical factors needed to realistically represent

electrolyte reactivity at electrodes such as explicit description of the substrate – electrolyte interactions; accurate representation of electrolyte structure, ion pairing and aggregation near an electrode; and collection of sufficient statistics from multiple unique simulations that were initiated with differing initial configurations. For example, 20 BOMD simulations starting from different initial conditions using 2.0M LiPF₆ in THF tetrahydrofuran/2-methyl tetrahydrofuran showed no solvent decomposition nor HF formation while only LiF formation was observed as a result of LiPF₆ salt decomposition.¹ The most frequently observed reduction events included a PF₆⁻ coordinated to Li⁺ cations from the electrolyte and LiF surface that lead to anion defluorination and formation of 3LiF and PF₃ gas. The solvent separated LiPF₆ and did not actively participate in reduction. When surface defects in LiF were present near a high population of PF₆⁻ the anions there was a preference for the LiPF₆ reduction and repair the SEI without ether solvent decomposition. Interestingly, a number of fast diffusion events for F⁻ from the electrolyte | LiF interface to the LiF-lithium metal interface was observed that would be expected to occur during Li stripping indicating that F⁻ re-arrangement in the thin LiF passivation films should be also considered.¹ Electrolyte reduction at the passivated interfaces from these simulations will be contrasted with other solvents ranging from ethers with mixed salts or carbonates and results from the representative quantum chemistry (QC) calculations performed on the small model electrolyte clusters to estimate oxidation and reduction.

[1] J. Chen, Q. Li, T.P. Pollard, X. Fan, O. Borodin, C. Wang, *Materials Today*, 39 (2020) 118-126.

11:20 AM CT01.02.02

First-Principles Modeling of the Kinetics of Electrochemistry at Solid-Water Interface Xunhua Zhao and Yuanyue Liu; The University of Texas at Austin, United States

Kinetic information, such as the activation energy and transition state, is critical to understanding the reaction. However, the kinetic information of electrochemistry at solid-water interface is challenging to obtain from conventional models of density functional theory (DFT), as they often neglect the presence and/or the dynamics of the surface charge [1] and the solvent configuration, which are further coupled. Here we present a new model that accounts for these effects, by combining hybrid solvation, constant-electron-potential, and slow-growth sampling techniques together. We then apply this model to elucidate the active site structure and the mechanism of electrochemical carbon dioxide reduction catalyzed by single-nickel-atom embedded in graphene, which shows high performance in experiments while is not well understood [2].

[1] D. Kim, J. Shi, Y. Liu, *J. Am. Chem. Soc.* 2018, DOI: 10.1021/jacs.8b03002

[2] X. Zhao, Y. Liu, *J. Am. Chem. Soc.* 2020, DOI: 10.1021/jacs.9b13872

11:35 AM CT01.02.03

Computational Study of Ion Binding Mechanisms to Alkali Activated Materials Using Molecular Simulation Ahmed Abdelkawy¹, Mostafa Yousef¹ and Claire White²; ¹The American University in Cairo, Egypt; ²Princeton University, United States

Alkali activated cement (AAC) has proposed as a green alternative to ordinary Portland cement (OPC) due to reduced greenhouse gases emissions compared with the production of OPC powder. Here, we aim at computationally assessing the ability of the AAC binder phase to hinder the diffusivity of corrosive ions and hence protect the reinforcing steel in an AAC-based concrete. We have adopted the tobermorite 14Å crystal structure as a model system for the binder phase because it has Ca/Si ratio similar to sodium-containing calcium-alumino-silicate-hydrate (C-(N)-A-S-H gel that forms during alkali activation of blast furnace slag or class C fly ash. We have also incorporated sodium into the tobermorite structure since the hydration phases tend to be produced using sodium-based activators. To describe the interactions between ions we employed a force field that has been widely used to describe inorganic oxides and relies on representing the polarizability of the oxide ion using a core and a shell connected by a harmonic spring. We believe that this polarizability is needed to accurately describe the tobermorite/water interface. Water molecules have been described by a 3-point flexible model. We validated the transferability of the force field by computing several structural and mechanical properties for tobermorite and compared these with experiments and/or other force fields such as CLAYFF.

In this talk, we will present a detailed analysis of the structure, dynamics, and energetics of Na and Cl ions in bulk water and at the interface between water and tobermorite. We will also examine the effect of introducing and increasing the percentage of sodium as a dopant in tobermorite, with a focus on how this affects the behavior of interfacial ions. In our analysis, we rely on computing a set of time and space correlation functions to explain the mechanisms by which AAC can stop the ingress of corrosive ions such as chloride ions. Our work provides a key step in assessing the durability of reinforced concrete structures produced by AACs.

11:50 AM CT01.02.04

Multi-Stage Bubble Nucleation in Nanoscale Cavities Anirban Chandra, Shekhar Garde and Pawel Koblinski; Rensselaer Polytechnic Institute, United States

Vapor bubble nucleation plays an important role in a variety of evaporation/condensation based thermal transport processes such as evaporative cooling, boiling, etc. In most practical situations nucleation processes are heterogeneous. While homogeneous nucleation has been studied extensively using theory and simulations, heterogeneous nucleation mechanisms are still being actively researched as it is less amenable to standard theoretical/numerical techniques. In this study, we use molecular dynamics simulations to investigate homogeneous and heterogeneous (flat surfaces and cavities) bubble nucleation in water under negative pressures. The maximum negative pressure sustained by the system is used to determine the propensity of bubble nucleation. Our results indicate that trends in calculated nucleation pressures deviate from classical heterogeneous nucleation theory predictions due to the nanoscopic nature of the nucleated bubbles. Furthermore, we show that nanoscale cavities aid the nucleation process when weak interaction exists between the fluid and solid materials. In this weak interaction regime, we show that nucleation is a multistage process and also demonstrate the existence of an optimal groove geometry for heterogeneous nucleation.

12:05 PM CT01.02.05

Materials for Heterogeneous Catalysis—The Interface is *Still* the Device Giulia Galli and Wennie Wang; The University of Chicago, United States

We present the results of first principles calculations aimed at characterizing the electronic structure and charge transfers at heterogeneous interfaces between photo-absorbers, catalysts and water. We discuss the importance of considering realistic structural models at the atomistic level in order to predict the efficiency of solar energy conversion processes, and to tightly integrate theory, computation and experiment.

12:20 PM DISCUSSION TIME

SESSION CT01.03: Scanning Probe Characterization II
Session Chairs: Xiaofeng Feng and Yingjie Zhang
Thursday Afternoon, April 22, 2021
CT01

1:00 PM CT01.03.01

***In Situ* Study of the Lubrication Mechanism of Phosphonium Phosphate Ionic Liquid in Nanoscale Single-Asperity Sliding Contacts** Filippo Mangolini¹, Zixuan Li¹, Oscar Morales-Collazo¹, Jerzy Sadowski², Hugo Celio¹, Andrei Dolocan¹ and Joan F. Brennecke¹; ¹The University of Texas at Austin, United States; ²Brookhaven National Laboratory, United States

Ionic liquids (ILs) have gained considerable attention in the last two decades owing to their unique and tunable physico-chemical properties (*e.g.*, low vapor pressure, high thermal stability), which have made them potentially useful for a range of applications, including batteries, fuel cells, catalysis. Ionic liquids are

particularly attractive in lubrication, since their properties make them suitable for components working under extreme conditions, such as those found in engines, spacecraft, and micro-electromechanical systems. When ILs are used as lubricants, the interface between the IL and the surfaces of the components in relative motion plays a pivotal role in controlling the friction and wear response. Despite the scientific weight of published studies on the tribology of ILs, remarkably little is still known about the underpinning lubrication mechanism of ILs. The development of a fundamental understanding of the mechanism by which ILs reduce friction and/or wear requires shedding light on the processes occurring at nanoscale asperities within macroscale contacts. This constitute a significant challenge since observing and understanding the nanoscale mechanisms at play is inhibited by the hidden nature of the buried interface and the challenge of performing observations at the nanometer scale.

Here, we used atomic force microscopy (AFM) to visualize and quantify the processes occurring at sliding interfaces *in situ*, in single-asperity nanocontacts¹. The AFM experiments, in which a diamond tip was slid on steel in phosphonium phosphate IL (PP-IL) at high contact pressure (>5 GPa), indicated a significant friction reduction only after the removal of the native surface oxide from steel. Even though the AFM experiments allowed for the identification of changes in topography and friction *in situ* while sliding in PP-IL, they could not provide any information about the composition and structure of the regions scanned by AFM. The analysis of these regions is a challenging surface science problem owing to their limited lateral dimensions and the small thickness of the surface material modified by the mechanical action of AFM tips. To address this challenge and elucidate the origin of the friction reduction observed during AFM experiments, laterally-resolved *ex situ* analyses of the surface chemistry of steel were performed by synchrotron-based X-ray photoemission electron microscopy (X-PEEM), low energy electron microscopy (LEEM), and time-of-flight secondary ion mass spectrometry (ToF-SIMS). The analytical results indicated that the mechanically-induced exposure of metallic iron during AFM tests carried out in PP-IL leads to an increase in surface coverage of adsorbed phosphate anions together with a change in surface potential. These surface modifications are proposed to be caused by a change in surface roughness and adsorption configuration of phosphate anions on metallic iron compared to their configuration on iron oxide, which lead to the formation of a densely packed, lubricious boundary layer only on metallic iron.

The findings of this work² not only shed new light on the lubrication mechanism of ILs in general, but also provide guidance for engineering ILs with the aim of tuning their lubricating properties by controlling their interfacial structures with metal and metal oxides. These outcomes can enhance sustainable development through the reduction of the economic (*e.g.*, reduced fuel expenditure) and environmental (*e.g.*, less pollution) impact of tribology, while being a key factor in the attempt of achieving the challenging environmental objective of reducing greenhouse gas emissions.

References

1. Gosvami, N.N.; Bares, J.A.; Mangolini, F.; Konicek, A.R.; Yablon, D.G.; Carpick, R.W. *Science* **2015**, *348*, 102-106.
2. Li, Z.; Dolocan, A.; Morales-Collazo, O.; Sadowski, J.T.; Celio, H.; Chrostowski, R.; Brennecke, J.F.; Mangolini F. *Advanced Materials Interfaces* **2020**, *17*, 2000426

1:15 PM *CT01.03.02

Recent Advances in Nanoelectrochemical Imaging of Heterogeneous Surfaces Michael Mirkin, Koushik Barman, Tianyu Bo, Rui Jia, Sujoy Sarkar and Xiang Wang; The City University of New York, Queens College, United States

Scanning electrochemical microscopy (SECM) is a powerful tool for nanoscale imaging of heterogeneous surfaces. Emergent applications of this technique in studies of interfacial properties of materials and electrocatalysts require near-atomic scale spatial resolution and the capacity for measuring currents produced by inner-sphere electrochemical processes that typically deactivate nanoelectrode surface. In this paper we present some new approaches to high-resolution electrochemical imaging of surface reactivity and active site characterization. One of them is based on mediated electron transfer at nanoelectrodes that can be used as SECM tips for reactivity mapping and localized kinetic measurements of inner-sphere electrochemical

processes, such as hydrogen evolution reaction and oxygen reduction to hydrogen peroxide. Tunneling mode SECM experiments at flat samples are aimed at establishing the relationship between the electrochemical tunneling signal and local surface properties and developing single entity voltammetry for characterization of individual catalytic nanoflakes. Finally, we discuss SECM experiments in which a TEM finder grid is used as a substrate to enable multi-technique imaging of the same nanoscale portion of the catalytic surface and elucidate the nature of the active sites by correlating the electrochemical reactivity maps with atomic scale structural and bonding information obtained by TEM techniques.

1:40 PM CT01.03.03

A Comparison of Solid Electrolyte Interphase Evolution on Highly Oriented Pyrolytic and Disordered Graphite Negative Electrodes in Lithium-Ion Batteries Haoyu Zhu¹, Pete Barnes¹, Paul Davis¹, I. Francis Cheng², Eric Dufek³ and Hui (Clair) Xiong¹; ¹Boise State University, United States; ²University of Idaho, United States; ³Idaho National Laboratory, United States

In the early stage of lithium ion batteries (LIBs) cycling, the reaction of negative electrode with electrolyte will result in the formation of a thin film on the electrode surface.[1] This film is referred to solid electrolyte interphase (SEI), the stability of which is essential for practical LIBs. The most used negative electrode material in LIBs is graphite, due to its stability and low working potential.[2] Previous studies indicated that in graphite, the basal to edge plane ratio, particle size, pore size, degree of crystallinity and surface chemical composition affected the formation of SEI and its stability [2-5]. The defects in graphite is also a very important factor for SEI formation but has been rarely studied. Here, we investigated the SEI formation on an almost perfect graphite-HOPG (Highly Oriented Pyrolytic Graphite) and a synthetic defective carbon film - GUITAR (pseudo-Graphite from University Idaho Thermolyzed Asphalt Reaction) through operando electrochemical atomic force microscopy (EC-AFM). It was found that the defects on GUITAR promoted the electrolyte decomposition and SEI formation at a higher potential. Furthermore, the SEI particles evenly formed and densely packed on the GUITAR surface with a particle size of $172 \text{ nm} \pm 83 \text{ nm}$ and a thickness of about 50 nm. The SEI thickness on this defective electrode surface is very similar to that on HOPG (about 40-50 nm). It is also noteworthy that on HOPG, the formed SEI only partially covered the electrode surface, along with the graphite layer delamination from the step edge and bulging on the basal plane. This study showed direct evidence of how structural defects affect SEI nucleation and growth upon cycling.

1. Agubra, V.A. and J.W. Fergus, *The formation and stability of the solid electrolyte interface on the graphite anode*. Journal of Power Sources, 2014. **268**: p. 153-162.
2. An, S.J., et al., *The state of understanding of the lithium-ion-battery graphite solid electrolyte interphase (SEI) and its relationship to formation cycling*. Carbon, 2016. **105**: p. 52-76.
3. Tsubouchi, S., et al., *Spectroscopic Characterization of Surface Films Formed on Edge Plane Graphite in Ethylene Carbonate-Based Electrolytes Containing Film-Forming Additives*. Journal of The Electrochemical Society, 2012. **159**(11): p. A1786-A1790.
4. Joho, F., et al., *Relation between surface properties, pore structure and first-cycle charge loss of graphite as negative electrode in lithium-ion batteries*. Journal of Power Sources, 2001. **97-98**: p. 78-82.
5. Li, M., et al., *Cycle and rate performance of chemically modified super-aligned carbon nanotube electrodes for lithium ion batteries*. Carbon, 2014. **69**: p. 444-451.

1:55 PM *CT01.03.04

Mapping Alkali-Ion Fluxes at Battery Interfaces: Applications to Understand the Formation of the Solid-Electrolyte Interphase Zachary Gossage, Yunxiong Zeng and Joaquin Rodriguez-Lopez; University of Illinois at Urbana-Champaign, United States

The solid-electrolyte interphase (SEI) is a complex structure that forms on battery anodes as a result of decomposition reactions of solvent and electrolyte prompted by the high electrode polarizations. Understanding the SEI formation and its resulting properties is key to fabricating batteries more effectively, safely, and ensuring their sustained performance. In particular, in-situ analysis of the first stages of SEI formation would

allow us to better understand the ultimate fates of electron transfer and ion transport processes on these important structures. In this study, we explored the first stages of formation of the SEI using versatile redox and ionic probes based on scanning electrochemical microscopy (SECM). Specifically, we were interested in exploring how these new probes could be used to compare the behavior of Li⁺ based SEI's to those formed by Na⁺ and K⁺, which are of great interest for emerging batteries.

For ionic measurements, the principle is based on SECM probes that integrate mercury micro disk-well electrodes on which alkaline ions can be detected by means of fast-scan anodic stripping voltammetry. We unambiguously demonstrated the capability of these probes to detect alkali-ion fluxes at an electrode undergoing SEI formation and subsequent ion intercalation. Surprisingly, reversible Li⁺ fluxes were observed on SEI's formed at the edge plane of highly oriented pyrolytic graphite (HOPG), which we ascribe to the presence of reversible redox species on the SEI.[1] Further using a combination of redox imaging using sub-micron sized SECM probes and these new ion-sensitive probes, we elucidated key differences in the reactive evolution of the SEI for the Li⁺, Na⁺ and K⁺ systems. We will describe various correlations observed between the observed fluxes, electron transfer rates, and the presence of organic and inorganic structures observed at the corresponding SEIs. SECM mapping revealed aspects of surface reactivity that are lost during averaging in other electrochemical techniques, and allows a correlation of all reactive species, including ions and electrons, in complex interfacial structures.

[1] Gossage, Z.T.; Hui, J.; Zeng, Y.; Flores-Zuleta, H.; Rodríguez-López, J. Probing the reversibility and kinetics of Li⁺ during SEI formation and (de)intercalation on edge plane graphite using ion-sensitive scanning electrochemical microscopy. *Chem. Sci.* **2019**, 10, 10749-10754.

2:20 PM *CT01.03.05

Liquid Phase Peak Force Infrared Microscopy for Label-Free Chemical Imaging at Liquid/Solid Interface Xiaoji Xu; Lehigh University, United States

Abbe's diffraction limit prevents traditional optical spectroscopy to directly access the nanoscale structures and phenomena. One way to bypass the optical diffraction limit is through the detection of photothermal expansion from light absorption with atomic force microscopy (AFM). The combination of AFM and infrared excitation provides the ability to perform chemical-sensitive imaging and vibrational spectroscopy nanoscale spatial resolution. The peak force infrared (PFIR) microscopy is one of the emerging AFM-based infrared microscopies with spatial resolutions at sub 10 nm. In this presentation, we will describe the recent development of the PFIR microscopy into the liquid phase to address the needs for *in situ* characterization of materials at the liquid/solid interface. We equip the liquid-phase peak force infrared (LiPFIR) microscope with the capability of controlling fluid compositions during the measurement so as to initiate physical transformation and chemical reactions. LiPFIR microscopy is capable of tracking the polymer surface reorganization in fluids and detect the product of click chemical reaction in the aqueous phase. We also measure the hyperbolic phonon polaritons of hexagonal boron nitride submerged in water to reveal its dispersion relations in the fluid phase. As a biological application of the LiPFIR microscopy, the budding site of yeast cell wall particles is imaged in water. The super-resolution, label-free, non-destructive chemical imaging and spectroscopy capabilities of LiPFIR will facilitate investigations of chemical compositions and transformations at the liquid/solid interface.

2:45 PM DISCUSSION TIME

SESSION CT01.04: Electron Microscopy
Session Chairs: Feifei Shi and Yingjie Zhang
Thursday Afternoon, April 22, 2021
CT01

4:00 PM *CT01.04.01

Understanding Electrochemical Interfaces in Batteries via Liquid-Cell/Cryo TEM Reza Shahbazian-Yassar; University of Illinois at Chicago, United States

Electrochemical interfaces play a key role in governing the behavior of lithium batteries. However, access to these interfaces is limited due to the presence of liquid and the need for sealing the battery cells in high vacuum electron microscopes. Advanced in liquid-cell and cryo-holders now enables microscopists to investigate the local chemical and structural changes in battery interfaces. This presentation encompasses the efforts of PI in understanding the role of solid-liquid interfaces in controlling the electrochemical reactions kinetics and thermodynamics in lithium batteries. The first part of this presentation provides an overview on the challenges of

high-energy density rechargeable lithium-oxygen (Li-O₂) batteries due to their potential to surpass conventional lithium ion battery. This system is troubled by sluggish kinetics during the oxygen reduction reaction (ORR) and the oxygen evolution reaction (OER). We investigated the discharge/charge behavior in Li-O₂ batteries using *in situ* liquid-cell transmission electron microscopy (TEM). During ORR, Li₂O₂ particles formation is controlled by Li⁺ diffusion in the electrolyte and Li₂O₂ particles nucleate at the carbon electrode-electrolyte interface. Li₂O₂ nucleation and growth were also observed within the electrolyte where there was no direct contact with the carbon electrode. These Li₂O₂ particles exhibit growth following O₂⁻ diffusion-limited kinetics, which indicate the existence of non-Faradaic disproportionation reaction of intermediate LiO₂ into Li₂O₂. Our in-situ liquid TEM work depicts the ORR/OER fundamentals in Li-O₂ battery system under factors controlling the discharge and charge process. We expect findings here to guide both the electrode design and the electrolyte screening aiming for enhancement of the ORR and OER kinetics in Li-O₂ battery cells. We also show that the use of cryo-TEM can uncover electrochemical interfaces in polymer lithium cells. In particular, we were successful in understanding the composition and structure of SEI as a function of polymer electrolyte and lithium salts.

4:25 PM CT01.04.02

Operando Electroanalytical Liquid Cell Microscopy for Energy Applications Khim Karki¹, Rui Filipe Serra Maia², Eric A. Stach², Daan Hein Alsem¹ and Norman Salmon¹; ¹Hummingbird Scientific, United States; ²University of Pennsylvania, United States

Liquid electroanalytical measurements performed inside the transmission electron microscope (TEM) and X-ray microscope (XRM) are becoming more common and are used to study a wide range of electrochemical reaction-systems at the nanoscale [1-4]. The capability to apply stimuli such as electrical, heating and electrochemical measurements has already started to provide new insights on the dynamics and structural changes during nanoparticles synthesis [1,4], lithium charge and discharge [2], crystal growth [3], and metal corrosion [1]. However, the inability to acquire practical quantitative information in TEM/XRM, mimicking bulk behavior, has prevented researchers from interpreting data accurately and reliably. First, the hardware components are not optimized to perform in the reduced scale environment of the TEM/XRM [5]. Second, the chips configurations such as sizes and aspect ratios of different electrodes suitable for various electroanalytical measurements are poorly designed. Here, we present a newly developed electrochemical *operando* platform to obtain real-world bulk electrochemical analysis during liquid-phase TEM/XRM microscopy.

The *operando* liquid cell platform typically consists of two microfabricated chips sandwiched with electron transparent SiN_x membranes for encapsulating liquid and viewing in the microscope. We integrated newly developed bulk-sized electrochemical counter (CE), and reference electrodes (RE) with optimized electrochemistry chips equipped with a specialized working electrode (WE) surfaces with customizable chemical compositions, such as platinum, gold, carbon, and industrially used amorphous oxide films. This new configuration allows true quantitative measurements of electrochemical processes with details resembling the complete cycle of traditional bench-top bulk electrochemistry. To illustrate this capability, we present cyclic

voltammetry (CV) studies of two model electrochemical systems: electrodeposition and stripping of 0.1M CuSO₄ and redox cycling of 20 mM K₃Fe(CN)₆/20 mM K₄Fe(CN)₆ in 0.1M KCl solutions. In the former case, the copper deposition and stripping occur at the working electrode at distinct redox peaks in liquid cells. The use of an actual RE such as Ag/AgCl in the newly developed cell avoids using a pseudo-reference electrode (e.g., chip-patterned metal electrode), which is commonly used in traditional liquid cell microscopy. The bulk RE presents an opportunity to replicate data reminiscent of bulk-scale electrochemistry, particularly concerning the drift in the thermodynamic potential that severely affects electrochemical studies using pseudo-reference electrodes [6]. In the latter case, the current-potential (I-V) relationship in the in-situ cell shows similar Tafel slopes at the same potentials to the large electrode setup tests validating the high electrochemical fidelity of the in-situ cell [7]. The electrochemical data from the new liquid electrochemistry cell can be used to correlate the TEM/XRM structural and chemical analysis with the actual bulk behavior of these electrochemical reactions in a true *operando* condition. The work presented here highlights that with a suitable hardware system, the bulk behavior of the electrochemical processes can be observed and measured quantitatively [8].

References

- [1] F.M. Ross in "Liquid Cell Electron Microscopy," Cambridge University Press (2016).
- [2] J. Lim *et al.*, Science 353 (2016), p. 566.
- [3] Nielsen *et al.*, Science, 2014, 345 (6201), 1158-1162
- [4] Chee *et al.*, Micros. Microanal., 2014, 20 (2), 462-468
- [5] E. Fahrenkrug *et al.*, Journal of Electrochemical Society 164 (2017), p. H358.
- [6] D. Grujicic and B. Pesic, Electrochimica Acta 47 (2002), p. 2901.
- [7] N. Frenzel, J. Hartley, and G. Frisch, Phys. Chem. Chem. Phys., 19 (2017), p. 28841.
- [8] KK, DHA, and NS acknowledge funding from the Department of Energy, Office of Basic Energy Sciences, SBIR Grant # DE-SC0009573.

4:30 PM *CT01.04.03

***In Situ* Study of Electrode-Electrolyte Interfaces Using Liquid Cell Electron Microscopy** Haimei Zheng^{1,2};
¹Lawrence Berkeley National Laboratory, United States; ²University of California, Berkeley, United States

Liquid cell electron microscopy has attracted a lot of interest and significant progress has been made nowadays. In this talk, I will present the recent work in my group on the study of electrode-electrolyte interfaces with electrochemical liquid cell development. It is known that the formation of high quality solid-electrolyte interphase (SEI) is important to limiting lithium dendrite growth. However, how SEI may be modified during lithium deposition is hard to resolve due to challenges in *in-situ* investigation of the SEI with fine details. With electrochemical liquid cell TEM, we were able to directly observe that lithium dendrite growth was suppressed when a poly(diallyldimethylammonium chloride) (PDDA) cationic polymer film was applied on the electrode. Chemical mapping of the deposits provided remarkable details of SEI on individual nanogranules. It showed that lithium fluorides are uniformly distributed within the inner SEI layer, arising from the instantaneous reaction of the deposited lithium with PF₆⁻ ions accumulated by the cationic polymer film, thus the dendritic growth of lithium was prohibited. The ability to directly measure SEI chemistry at the nanoscale down to the individual grains *in-situ* and unveil its correlation with lithium deposition behavior opens future opportunities to explore unsolved mechanisms in batteries.

4:55 PM *CT01.04.04

***In Situ* and Cryogenic Electron Microscopy for Energy Materials** Yi Cui^{1,2}; ¹Stanford University, United States; ²SLAC National Accelerator Laboratory, United States

Developing new energy materials for batteries, solar cells, catalysts and gas storage requires understanding their structural evolution across multiple length and time scale. Over the past 15 years, the Cui group has been developing a set of electron microscopy tools to realize this purpose including in-situ electrochemical cell, in-situ gas reaction, in-situ mechanical indentation and cryogenic electron microscopy (cryo-EM). In this presentation, he will discuss how these advanced electron microscopy techniques impact energy materials. 1)

New generation of battery materials are accompanied by large volume and structure change and instability of interphase. He has developed in-situ electrochemical cells and in-situ mechanical deformation as powerful techniques for establishing the relationship of structural change with electrochemical performance, which provides fundamental guidelines for materials design. Cui has demonstrated the most important case on Si anodes: from fundamental understanding, materials design to realizing commercial success of high energy density batteries. 2) Many energy materials are highly sensitive to environment. Studying their reaction in-situ by environmental electron microscopy could provide insights on reaction mechanisms. Li metal reaction with gases as an important case will be presented. 3) Many energy materials are not stable under electron beam. Advanced cryo-EM recently developed in structure biology could be utilized and further developed for materials science. Cui pioneered the cryo-EM towards battery materials and obtained the first atomic resolution images of Li metal and solid electrolyte interphase. With cryo-EM he has answered many important fundamental questions which puzzled the battery field for a long time. He also demonstrated the power of cryo-EM to study a wide range of energy materials including metal-organic frameworks, perovskite and electrocatalysts.

5:20 PM *CT01.04.05

Understanding the Lithium-Electrolyte Interface in Liquid-Electrolyte and Solid-State Batteries Matthew T. McDowell; Georgia Institute of Technology, United States

Understanding how lithium metal behaves in liquid vs. solid electrolytes is key for developing stable, high-energy density lithium-metal batteries. This talk will discuss my group's efforts in understanding the interface of Li metal when in contact with liquid and solid electrolytes. I will first discuss our work in understanding how the lithium/electrolyte interface evolves in liquid-electrolyte batteries at low temperatures. Lithium metal is an attractive anode material for low-temperature batteries since it overcomes sluggish diffusion of Li^+ in graphite. However, most electrolytes exhibit extremely low Coulombic efficiency (CE) for lithium metal cycling at low temperatures. We have developed an ether-based electrolyte system with carbonate additives that substantially improves the CE of lithium metal cycling down to -60°C . Lithium metal deposited at low temperatures in this and other electrolytes shows a clear reduction in grain size with decreasing temperature, which is correlated with lower CE. Cryo-TEM and X-ray photoelectron spectroscopy investigation of the solid-electrolyte interphase (SEI) shows that this tailored electrolyte allows for greater inorganic content in the SEI at low temperatures, which enables a compact and conducting passivation layer. Next, I will present my group's work using *in situ* methods to understand the evolution of lithium interfaces in solid-state batteries. For NASICON-structured $\text{Li}_{1+x}\text{Al}_x\text{Ge}_{2-x}(\text{PO}_4)_3$ (LAGP), electrochemical experiments combined with multi-modal *in situ* investigation of interfacial reactions reveal how the formation of the interphase is linked to electrochemical degradation. *In situ* transmission electron microscopy (TEM) shows that the reaction of LAGP with lithium is similar to a conversion reaction, in which lithium insertion causes amorphization and volume expansion of $\sim 130\%$. *In situ* X-ray tomography experiments of operating LAGP-based cells reveal that the growth of the interphase causes fracture of the SSE, and quantification of the crack network shows that the extent of fracture with time is directly correlated to impedance increases within the cell. Based on this knowledge, we have found that interphase growth trajectories can be modulated through the deposition of interfacial protection layers, which can extend cycling stability of symmetric cells by almost two orders of magnitude. Finally, *operando* synchrotron X-ray tomography experiments have been developed and used to directly probe lithium/SSE interface dynamics using other SSEs. Together, the insights gained through these studies highlight the similarities and differences between lithium interfaces in liquid- and solid-electrolyte batteries, and building on this knowledge will be key for development of improved lithium metal batteries.

5:45 PM DISCUSSION TIME

SESSION CT01.05: Optical/Vibrational Spectroscopy
Session Chairs: Feifei Shi and Yingjie Zhang

8:15 PM *CT01.05.01

Using Vibrational Spectroscopy to Understand and Control Electrochemistry for Electrolyzers and Batteries Andrew Gewirth; University of Illinois at Urbana-Champaign, United States

This talk addresses the use of vibrational spectroscopy to evaluate the reactivity associated with CO₂ reduction electrolyzers and solid state batteries. In the first area, electrodeposition of CuAg, CuSn, or CuZn alloy films yields high surface area catalysts for the active and selective electroreduction of CO₂ to multi-carbon hydrocarbons and oxygenates. Alloy films containing Ag exhibit the best CO₂ electroreduction performance, with the Faradaic efficiency for C₂H₄ and C₂H₅OH production reaching nearly 60 and 25%, respectively, at a cathode potential of just -0.7 V vs. RHE and a total current density of ~300 mA/cm². Alloy films containing Sn exhibit greater efficiency for CO production relative to either Cu along or CuAg at low overpotentials. *In-situ* Raman and electroanalysis studies suggest the origin of the high selectivity towards C₂ products to be a combined effect of the enhanced stabilization of the Cu₂O overlayer and the optimal availability of the CO intermediate due to the Ag or Sn incorporated in the alloy. Sn-containing films exhibit less Cu₂O relative to either the Ag-containing or neat Cu films, likely due to the increased oxophilicity of the admixed Sn. CuZn films exhibit enhanced production of oxygenated products, particularly ethanol. Additionally, modification of the Cu electrode with certain polymers yields substantially enhanced reactivity, due in part to control of the Cu₂O layer.

Relevant to batteries, we discuss solid electrolytes (SEs) which have become a practical option for lithium ion and lithium metal batteries due to their improved safety over commercially available ionic liquids. The most promising of the SEs are the thiophosphates whose excellent ionic conductivities at room temperature approach those of commercially-utilized electrolytes. Spectroscopic and structural studies on these materials lead to new formulations exhibiting advantageous properties.

8:40 PM *CT01.05.02

Probing Electrode/Electrolyte Interface Using Plasmon Based Raman Spectroscopy—Recent Progress Guang Yang, Ilia Ivanov and Jagjit Nanda; Oak Ridge National Laboratory, United States

Plasmonic based Raman spectroscopic methods such as Surface and Tip- Enhanced Raman Spectroscopy (SERS and TERS) are extremely sensitive techniques with high interfacial selectivity.¹⁻³ However, applying these methods to obtain insights on the underlying interfacial phenomena at the electrode-electrolyte interphase in a functioning battery is challenging. In this regard, we have undertaken a systematic approach by first studying solvation properties of lithium-ion battery electrolytes using gold nanoparticle monolayer as a gap-mode SERS substrate. Specifically, we have chosen Lithium hexafluorophosphate (LiPF₆) salt in carbonate solvents -Ethylene Carbonate (EC) and dimethyl- carbonate (DMC). SERS studies shows the solvation shell surrounding Li-cation is different in at the bulk of the electrolyte than at the interface (close to the gold electrode). We have compared SERS results with normal Raman and FT-IR spectroscopy that captures the ensemble average. *In-situ* time resolved SERS studies showed dynamic changes in the Li-cation coordination close to the interface. Our findings here provide a unique high surface sensitive platform for studying the electrolytes molecules both qualitatively and quantitatively at interface. This work will create further interest in other areas where solid/liquid interface is essential, such as water desalination, heterogeneous catalysis, electrophoresis, corrosion, mass transport across bio membranes,

Acknowledgement

This work was supported by the US Department of Energy's Office of Energy Efficiency and Renewable Energy through the Vehicle Technology Office

Direct Operando Observation of Double Layer Charging and Early Solid Electrolyte Interphase Formation in

Li-Ion Battery Electrolytes, N. Mozhzhukhina et.al. **J. Phys. Chem. Lett.** 2020, 11, 4119–4123
Probing Electrolyte Solvents at Solid/Liquid Interface Using Gap-Mode Surface-Enhanced Raman Spectroscopy, G. Yang, J. Nanda et al. **J. Electrochem. Soc.** 166 (2) A1-A10 2019
Solvation Structure of Lithium-ion Battery Electrolytes using Gap Mode Surface Enhanced Spectroscopy, G. Yang, I. L. Ivanov, R. E. Ruther, R.L. Sacchi, V. Subjakova, D. L. Hallinan and J. Nanda, **ACS Nano.** 12, 10159–10170 (2018)

9:05 PM CT01.05.03

***In Situ* Raman Spectroscopy of Sulfate Phases in Early-Stage OPC Hydration** Hee Jeong Kim, Hyunchoe Loh and Admir Masic; Massachusetts Institute of Technology, United States

Carbon dioxide (CO₂) emissions during cement manufacturing are increasing daily, and the cement industry accounts for 7% of global CO₂ emissions (WBSCD, 2018). Research on cement hydration mechanism is the key for both understanding the physicochemical properties of the cement matrix and designing sustainable and durable construction materials. However, often it is difficult to characterize the initial hydration reactions of cement clinker (tricalcium silicate, dicalcium silicate, tricalcium aluminate, and tetra-calcium aluminate) that take place at the same time. Furthermore, it is difficult to identify the exact phase transformations during the cement hydration processes. Most physicochemical characterization methods applied to cement (BET, MIP, XRD, etc.) are performed on solid-state samples that have been prepared with hydration stoppage, dehydration, or pulverization, which could significantly affect the conditions. Also, the low crystallinity of the major hydrates such as calcium silicate hydrates (C-S-H) poses significant characterization challenges when traditional methods such as XRD are used. In this study, we used in-situ and operando confocal Raman spectroscopy to understand the early stage hydration kinetics of Ordinary Portland cement. In particular, 4% of the CaCO₃ powder was added to the mix to accelerate the hydration; we monitored the ettringite formation, which is closely related to the cement paste setting and its rheological properties. We spatially resolved and mapped the sulfate phase transformation with a high spatial (1-micron) resolution and an excellent signal-to-noise ratio.

WBSCD. (2018). Technology roadmap low-carbon transition in the cement industry. *World Business Council for Sustainable Development and International Energy Agency*.

9:20 PM BREAK

9:50 PM CT01.05.05

***In Situ* PM-IRRAS at the Air/Liquid/Solid Interface—Probing the Effects of Cations on Iron Surface Oxidation** Kathryn A. Perrine; Michigan Technological University, United States

Several techniques have been developed to measure *in situ* surface reactions at the gas/solid and liquid/solid interfaces from vacuum to ambient pressure environments. Probing chemical reactions in liquid environments become more complex with the addition of electrolytes, gases, and resulting interface transformations. Surface vibrational spectroscopy measures the effect of adsorbed surface species at the liquid/solid interface that can determine intermediate steps in environmental and electrochemical processes, that involve surface catalytic reactions. Our group has developed a new vibrational technique that simultaneously measures the air/liquid/solid interface using *in situ* polarized modulated infrared reflection absorption spectroscopy (PM-IRRAS). This technique was validated using a well-known system of alkanethiol adsorption on gold at the air/ethanol/gold interface in non-aqueous solutions and applying a model of a three-phase system. We present our investigation of the *in situ* iron interfacial oxidation from the influence of cations on the formation of inorganic scale, from corrosion. Iron interfaces are ubiquitous in soil, dust, and used as earth-abundant heterogeneous catalysts that undergo spontaneous redox reactions in the presence of oxygen and water, two key reactions in the corrosion mechanism. Chloride ions in electrolytes are found to catalyze the reaction in complex aqueous environments leading to different oxidation rates and results in different mineral

scale growth. In this study, different alkali and alkaline chloride electrolyte solutions were studied on the surface of iron to measure the influence of cations on surface corrosion. The electrolytic solutions are shown to either increase or decrease the rate of oxidation, producing different mineral scale from the reaction with air. These findings are corroborated with X-ray photoelectron spectroscopy and *in situ* liquid atomic force microscopy measurements, connecting oxidation states and surface morphology with surface vibrational signatures. These studies demonstrate how *in situ* PM-IRRAS reveals surface redox mechanisms that impact complex chemistry in the water and mineral cycles, electrochemical catalysis, and material degradation.

10:05 PM CT01.05.06

Operando Local pH Imaging in CO₂ Reduction Gas Diffusion Electrodes Using Confocal Microscopy

Alex J. Welch, Aidan Q. Fenwick, Ian Sullivan, Chengxiang Xiang and Harry A. Atwater; California Institute of Technology, United States

Here we report a new operando experimental technique to determine the local pH at various depths within an operating CO₂ reduction gas diffusion electrode (GDE). There is currently a lack of experimental data and understanding of the reaction conditions at the catalyst surface in CO₂ reduction GDEs - the thickness of the water layer and the local pH near the catalyst. Being able to observe these conditions *in situ* during GDE operation is important for understanding how the pH and local water quantity effect the selectivity and activity of the device. Measuring these quantities is typically difficult because of the opaque nature of materials used in GDEs and the short relevant length scales. We use a two-color fluorescent pH sensitive dye, DHPDS, with a pK_a of 7.33 and 8.53. The dye is dissolved in the electrolyte and excited by a 458 nm and 488 nm laser consecutively in a confocal microscope. The emission is collected from the two separate excitations and the ratio of the intensity is linearly proportional to the pH. The confocal allows us to excite the dye at specific planes in z, allowing us to see the pH at up to a 40um depth within the porous GDE. As a control we measured what the pH is at the surface of the electrode with no applied potential, and found that the local pH was greater than 9 while the bulk electrolyte (100mM KHCO₃ CO₂ saturated) had a pH of 6.8, when a potential -0.5V vs RHE is applied. This increase is due to the fact that protons are consumed during the CO₂ reduction reaction. The next step in the experiments is to characterize the pH at a range of potentials with operando microscopy observation of local reaction conditions in the pores of the electrode and to determine the uniformity of catalytic activity in the lateral direction, within the catalyst layer plane. We will also report results of experiments with several heterogeneous CO₂ reduction catalysts including Ag, Cu and their alloys, supported on different types of GDE materials with various hydrophobicity and structure. We anticipate that this technique will yield insights that inform future GDE design to optimize wetting and that knowledge about local pH will enhance our knowledge of catalytic mechanisms and control of catalytic selectivity and energy efficiency.

10:20 PM CT01.05.07

Fluorophores “Turned-on” by Corrosion Reactions Can Be Detected at the Single-Molecule Level Anuj

Saini; Case Western Reserve University, United States

Corrosion is an interfacial process that has a profound impact on society. While the mechanism of iron corrosion has been known for centuries, we haven't been able to visualize corrosion at the molecular scale due to the spatial and temporal limits of current microscopies and the long time scale of corrosion to develop larger microscale features. We demonstrate that fluorogenic molecules that “turn-on” upon redox reactions can sense the corrosion of iron at the single molecule scale. We first observe the cathodic reduction of non-fluorescent resazurin to fluorescent resorufin in the presence of iron in bulk solution. We show that the fluorescence signal is directly related to the amount of electrons that are available due to corrosion progression and can be used to quantify the catalyzed increase in the rate of corrosion by NaCl. By using modern fluorescence microscopy instrumentation we detect real-time, single-molecule “turn-on” of resazurin by corrosion, overcoming the previous limitations of microscopic fluorescence corrosion detection. Analysis of the total number of individual resorufin molecules shows heterogeneities during the progression of corrosion that are not observed in ensemble measurements.

SESSION CT01.06: Semiconductor–Liquid Interface
Session Chairs: Ethan Crumlin and Yingjie Zhang
Friday Afternoon, April 23, 2021
CT01

12:00 PM CT01.06.02

Probing the Liquid/Surface Interactions on Functionalized Graphene James Carpenter, Hyunchul Kim, Arend van der Zande and Nenad Miljkovic; University of Illinois at Urbana-Champaign, United States

The novel properties of 2D materials, such as graphene, are proposed to enable exciting applications in diverse areas such as sensing, electronics, and mechanics. However, the thinness of 2D materials and their sensitivity to environmental conditions present challenges when examining the fundamental liquid/solid interactions. For instance, it has been shown that the wettability, surface friction, and electrical conductivity of graphene on silicon dioxide can be tuned by adding bond terminations like hydrogen and fluorine to the graphene lattice. However, graphene's wettability, which is typically characterized using contact angle measurements, has also been shown to vary with its supported substrate—a phenomenon known as wetting transparency. This wetting transparency can further be complicated by the adsorption of volatile organic compounds (VOCs) that lower the surface energy of the substrate, raising the contact angle. Thus, to fully leverage the exciting properties of 2D materials for novel applications, we must develop a more rigorous understanding of the interactions between the 2D material, its supporting substrate, and its surroundings.

In this work, we used microgoniometry to examine the wettability of supported bare graphene and its functionalized forms, including fluorinated, hydrogenated, and hydro-fluorinated graphene. The diameter (50 – 100 microns) of the droplets produced using our microgoniometry apparatus eliminates the effects of gravity on the contact angle measurements, leading to high-fidelity results. The graphene samples were functionalized with hydrogen and/or fluorine bond terminations by indirect exposure to hydrogen plasma and xenon difluoride (XeF₂). We examined a range of substrates, including silicon dioxide, sapphire, gold, copper, and Parylene C. A combination of UV/Ozone exposure and plasma cleaning ensured that the graphene and substrates were cleaned properly to minimize the effects of residues from the graphene transfer process and volatile organic compounds. The effect of the cleaning and quality of the graphene was verified using XPS, ToF-SIMS, and Raman spectroscopy. We also systematically examined the effect of VOCs by exposing the samples to ambient conditions for specific amounts of time. The results indicate that the wetting transparency of graphene depends on the specific bond termination, underlying substrate, and exposure to VOCs. Our results offer guidance to those seeking to use graphene in novel applications where the liquid/solid interaction is of paramount importance, such as liquid phase sensors, actuators, and surface modifiers.

12:15 PM *CT01.06.03

(Photo)electrocatalysis at Work—Understanding Chemical Transformations Francesca Maria Toma; Lawrence Berkeley National Laboratory, United States

Artificial photosynthesis is a promising route for efficient conversion of solar energy to chemical fuels. To positively affect the *status quo*, polycrystalline, yet defective and heterogeneous, semiconductor materials are excellent candidates for targeting high efficiency, as well as low production cost, and long lifetimes of the device. However, a typical conundrum in this field is related to the fact that efficient materials are not durable, whereas durable materials show poor efficiency. In this context, characterization of materials transformation and charge transport mechanism is critical to enable design and development of new functional systems. We have established a suite of characterization techniques, including *in situ/operando* characterizations to provide insights into the materials chemical transformation in artificial photosynthesis. For instance, we use conductive

and electrochemical atomic force microscopy (AFM) to elucidate functional variations and structural changes at the nanoscale, and we utilize scanning transmission X-ray microscopy (STXM) to provide insights into the electronic structure and chemical composition of functional photoelectrochemical materials. Better understanding of the material behavior during operating conditions can lead to ultimate optimization of fuel cell efficiency.

12:40 PM *CT01.06.04

Nanoscale Probes of Carrier-Selective Catalyst/Semiconductor Contacts in Water-Splitting Photoelectrodes Shannon Boettcher; University of Oregon, United States

Heterogeneous electrochemical processes, including photoelectrochemical water splitting to evolve hydrogen using electrocatalyst-coated semiconductors, are driven by the accumulation of charge carriers and thus the interfacial electrochemical potential gradients that promote charge transfer. Conventional electrochemical techniques measure/control potentials at the conductive substrate or semiconductor ohmic contact, but are unable to isolate processes and electrochemical potentials at the surface during operation. I will present our recent work demonstrating that the nanoelectrode tip of an atomic-force-microscope cantilever can effectively sense the surface electrochemical potential of electrocatalysts coating semiconductor photoelectrodes during operation. This technique allowed us to unambiguously show that metal (oxy)hydroxide layers act as both hole collectors and oxygen-evolution catalysts on metal-oxide photoanodes such as Fe_2O_3 and BiVO_4 . We also discovered the critical role that heterogeneous interfacial barrier heights, and a related nanoscale pinch-off effect, play in building carrier-selective interfaces in semiconductor photoelectrodes for generating fuel from sunlight.

SESSION CT01.07: Electrocatalysis
Session Chairs: Ethan Crumlin and Feifei Shi
Friday Afternoon, April 23, 2021
CT01

2:15 PM *CT01.07.01

From Making Disinfectants and Rocket Fuels to Powering Heavy-Duty Vehicles—Single Atom Catalysts for Small Molecule Activation Huolin Xin; University of California, Irvine, United States

The ammonia you use to clean and disinfect your kitchen floor starts off as nitrogen, a gas that makes up almost 80 percent of Earth's atmosphere. But the conversion requires the breaking of a strong chemical bond in a high-heat, high-pressure industrial process known as the Haber-Bosch process. In nature, however, bacteria convert nitrogen gas to ammonia with a nitrogenase enzyme, whose active center is molybdenum, an abundant, nonprecious metal. By mimicking this biological nitrogen fixable process, my group has recently developed a series of new catalysts that can produce ammonia, rocket fuels, and power heavy-duty vehicles in a more sustainable way. The key is anchoring single metal atoms in a nitrogen/oxygen/carbon-coordinated environment to form a so-called single-atom catalyst (SAC). Unlike the Haber-Bosch process, which consumes massive amounts of energy and emits significant quantities of carbon dioxide to the atmosphere, these cheap, single-atom catalysts can be incorporated into modular and compact electrolyzing cells to produce commodities (ammonia, methane, and formate), as well as high-value-added chemicals like pharmaceuticals, with renewable solar or wind power. This emerging technology will not only make the traditional chemical production process greener but can also pave the way for a decentralized chemical industry.

2:40 PM CT01.07.02

Ultrahigh Oxygen Evolution Reaction Activity Achieved Using Ir Single Atoms on Amorphous CoOx Nanosheets Maoyu Wang and Zhenxing Feng; Oregon State University, United States

In the past decades, the renewable energy storage and energy conversion systems, such as fuel cells, water electrolysis, and metal-air batteries, have attract great attention. Oxygen evolution reaction (OER) is a key half reaction of water splitting to produce clean fuels. However, the sluggish kinetics of OER has significantly limited the performance and commercialization of such energy conversion devices. Up to now, the most efficient OER catalysts are still noble metal and metal oxides of Ruthenium (Ru) and Iridium (Ir), which are not cost-effective catalysts and unstable under high potentials. Recently, single atom catalysts have been used to improve the surface-to-volume ratio to increase OER catalytic activity. In our work, Ir single-atom catalysts supported by CoO_x amorphous nanosheets (ANSs) for OER. Experimental results show that Ir single-atoms are anchored by abundant surface-absorbed O in CoO_x ANSs. The Ir single-atom catalysts possess ultrahigh mass activity that is 160-fold of commercial IrO_2 . The OER of IrCoO_x ANSs reached a record-low onset overpotential of less than 30 mV. The *in-situ* X-ray absorption spectroscopy reveals that the Ir-O-Co pairs directly boosted the OER efficiency and enhanced the Ir stability.

2:55 PM CT01.07.03

Synthesis of FeCo-N-OLC Catalyst for Oxygen Reduction Reaction Brenda L. Vargas Pérez, Osvaldo E. E. González Sánchez, Yannelly A. Serrano Rosario, Kattia M. Gonzalez Aponte, Fabiola N. Sánchez Fonseca and Lisandro Cunci; Universidad Ana G Méndez, Puerto Rico

The world's main source of energy is fossil fuels, but fossil fuels are finite resources and can also irreparably harm the environment. According to the United States Energy Information Administration, the burning of fossil fuels was responsible for 76 percent of the US greenhouse gas emissions. Fossil fuels not only pollute the environment, but also affect human health. My research focuses on making a catalyst that is economical, efficient and above all friendly to the environment. The oxygen reduction reaction (ORR) is an important reaction for energy conversion systems, such as fuel cells. The fuel cells generate electricity directly by electrochemically reducing oxygen and oxidizing fuel in water as the only by-product. Onion-like carbon (OLC) are used as a catalytic support for fuel cell applications due to their high conductivity and high surface-to-volume ratio. The combination of carbon compounds with conductive polymers results in new materials and devices with possible practical applications. In recent decades, several studies have been conducted on nitrogen doped structures in carbon materials for the ORR. In my research we use nanodiamonds (NDs) to dope them with the polymerization of the aniline monomer. Then, through a pyrolysis process, we convert the ND/PANI particles into N-OLC. These particles are then polymerized using the aniline and pyrrole monomers to dope the OLCs with nitrogen. These particles are characterized using the following techniques, Raman, Fourier-transform infrared spectroscopy (FTIR), Scanning Electron Microscopy (SEM), Energy-dispersive X-ray spectroscopy (EDS) and X-ray Diffraction (XRD). Then the synthesis is carried out with the non-precious metals. The non-precious metals that we use are iron and cobalt. ORR experiments were performed with the FeCo-N-OLC particles. In future work we will characterize these samples using synchrotron techniques.

3:10 PM *CT01.07.04

***In Situ* Characterization of Electrocatalysts for the Oxygen Evolution and the CO_2 Reduction** Alexis Bell; University of California, Berkeley, United States

The electrochemical reduction of CO_2 using electrical energy derived from renewable sources (wind and solar) offers a potentially attractive means for producing carbon-based chemicals and fuels, particularly if the CO_2 can be recovered from the atmosphere. Accomplishment of this goal requires two types of catalysts – an anode catalyst that facilitates the oxidation of water to O_2 and either H^+ or OH^- , depending on the pH of the electrolyte, and a cathode catalyst that facilitates the reduction of CO_2 to hydrocarbons and oxygenated products. Extensive research has found that IrO_2 is the best catalyst for the oxygen evolution reaction (OER) in acidic electrolytes and FeNiOOH is the best catalyst for this reaction in basic electrolytes. On the other hand, Cu is the only metal that promotes the electrochemical reduction of CO_2 to hydrocarbons and oxygenates with high faradaic efficiency. This talk will focus on experimental techniques that have been used to characterize IrO_2 , FeNiOOH , and Cu under working conditions, i.e., *in situ*. The technique that will be discussed include

infrared spectroscopy, X-ray absorption spectroscopy, ambient-pressure X-ray photoelectron spectroscopy, and X-ray diffraction. We will see that use of these in situ techniques enables acquisition of critical information about the composition and structure of the working catalyst and, in some cases, the nature of adsorbed species on its surface under working conditions.

3:35 PM DISCUSSION TIME

SESSION CT01.08: Batteries
Session Chairs: Feifei Shi and Yingjie Zhang
Friday Afternoon, April 23, 2021
CT01

5:15 PM *CT01.08.01

Resolving the Controversy over the Elusive Components in Solid Electrolyte Interphase on Li Metal Anode Enyuan Hu¹, Zulipiya Shadike¹, Hongkyung Lee², Xia Cao², Jie Xiao² and Xiao-Qing Yang¹;

¹Brookhaven National Laboratory, United States; ²Pacific Northwest National Laboratory, United States

Lithium metal anode has great advantages such as extremely high theoretical specific capacity (3860 mA h g⁻¹), low density (0.59 g cm⁻³) and the lowest negative electrochemical potential (-3.040 V vs. the standard hydrogen electrode) and is considered as the ideal anode for rechargeable lithium batteries. Major challenges it faces include lithium dendrite formation and incompatibility with state-of-the-art electrolyte. Solid-electrolyte-interphase (SEI) plays a key role in determining the reversibility of lithium metal anode and engineering of SEI holds great promises for addressing the previously mentioned challenges. Understanding the properties of SEI is of great importance and has been the focus of many research. In this talk, three questions related to this topic will be discussed based on the results obtained from synchrotron-based scattering experiments. 1. Is LiH really an SEI component? 2. How come an ionic insulator like LiF can be considered as a good SEI component? 3. Is it possible to quantify crystalline/amorphous components in SEI? Strengths and limitations of currently available techniques for studying SEI will also be discussed.

5:40 PM DISCUSSION TIME

5:55 PM CT01.08.03

Electrochemical Generation of Liquid and Solid Sulfur on Two-Dimensional Layered Materials with Distinct Areal Capacity Ankun Yang^{1,2}, Guangmin Zhou¹ and Yi Cui¹; ¹Stanford University, United States;

²Oakland University, United States

Lithium-sulfur (Li-S) batteries are attractive candidates for energy storage in electric vehicles and grid-scale storage due to their high energy density and low-cost potential. Sulfur, the charge product in Li-S batteries, was believed to be solid, while we recently discovered that sulfur can stay in a super-cooled state as liquid sulfur. However, how the sulfur state (liquid or solid) affects Li-S battery performance is not clear. Here we demonstrate that liquid and solid sulfur provide very different areal capacities through in situ study of electrochemical sulfur generation. We report distinct growth behaviors of sulfur on two-dimensional (2D) layered materials: on the basal plane, only liquid sulfur accumulates; at the edge sites, liquid sulfur accumulates if the thickness of the 2D materials is small, while solid sulfur nucleates if the thickness is large. Based on our understanding of the edge-induced sulfur crystallization, we control the sulfur state (liquid or solid) and demonstrate much larger areal capacities from liquid sulfur compared to solid sulfur in the same charge time period. This work correlates the sulfur states with their electrochemical performance and provides insights on electrode designs for Li-S batteries and the application of 2D materials in Li-S batteries.

6:10 PM *CT01.08.04

Quantifying Capacity Losses Due to Solid-Electrolyte Interface Formation Michael F. Toney; University of Colorado Boulder, United States

Understanding the origins of failure and limited cycle life in lithium-ion batteries (LIBs) requires quantitative linking capacity-fading mechanisms to electrochemical and chemical processes. This is challenging in real systems where capacity is lost during each cycle to both active material loss and solid electrolyte interphase (SEI) evolution. In this talk, I will describe the model system-based approach that we have adopted that combines precision electrochemical measurements of the Coulombic efficiency (CE) and x-ray measurements of the SEI layer and active materials loss. By contrasting these independent quantities, we obtain insight into the SEI growth and evolution. I will discuss how we have used X-ray reflectivity (XRR) to obtain nanoscale insight into solid electrolyte interfaces (SEI) on model anode surfaces that implicate electrochemically formed LiF as playing a major functional role in the SEI. I will also describe how XRR tracks the thickness of a-Si thin films and when this is compared to the CE, we can quantify SEI growth over several cycles. The methodology we are adopting allows to quantitatively track the desirable and undesirable electrochemical processes.

SESSION CT01.09: X-Ray Characterization
Session Chairs: Ethan Crumlin and Feifei Shi
Friday Afternoon, April 23, 2021
CT01

8:15 PM CT01.09.01

Late News: *In Situ* X-Ray Scattering Studies of Organic Electrochemical Transistors Lauren Asselt¹, Nicholas D'Antona¹, Lucas Flagg¹, Tommaso Nicolini², Natalie Stingelin-Stutzmann³, Jonathan W. Onorato⁴, Christine Luscombe⁴, Chad R. Snyder¹ and Lee Richter¹; ¹National Institute of Standards and Technology, United States; ²Université de Bordeaux, France; ³Georgia Institute of Technology, United States; ⁴University of Washington, United States

Organic electrochemical transistors (OECTs) are a novel device architecture, emerging as a potential platform for biosensors and neuromorphic computing. In an OECT, volumetric doping (gating) of the active semiconductor is achieved through ingress of electrolyte ions, under potential control. This opens unique transduction modalities, due to the mixed (ionic and electronic) modes of conduction. This also challenges established paradigms for the operation of traditional, organic field-effect transistors as operation involves the dynamic swelling of the active layer by both solvent and ion. Thus, quantitative understanding of operation (and process-structure-function relationships) requires in-situ measurements of the films under potential control and in contact with electrolyte. Poly(3- (methoxyethoxyethoxymethyl)thiophene) (P3MEEMT) has emerged as an interesting, prototypical OECT material, differing from the classic OFET material, regioregular poly(3-hexyl)thiophene (P3HT), by the replacement of the non-polar alkyl side chains with oligoethylene glycol (OEG).[1] The OEG side chains facilitate ingress of aqueous electrolytes and introduce rich thermal processing behavior. Combining DSC with in-situ thermal GIWAXS we develop a detailed understanding of the thermal processing of P3MEEMT films. Annealing at (115 to 125)° C, above a crystal to liquid crystal transition, results in distinct semicrystalline morphology with predominantly face-on, pi-stacked domains with coherence length, l_c , along the lamella (100) direction up to 30 nm. Annealing above the liquid crystal melt results in a nearly isotropic crystal orientation distribution, characterized by significantly shorter l_c . The water vapor swelling of the thermally processed films is studied by both in-situ ellipsometry (total film swelling) and GIWAXS (crystalline domain swelling). The volumetric swelling varies with processing and at all times significantly exceeds the swelling of crystalline material, indicating the majority of the water is in the amorphous regions. Volumetric swelling does not exhibit simple Flory-Rehner behavior with a constant χ . Using a novel 'rolling drop' electrode, we are able to characterize the electrochemical doping of the films, as a function of both initial

thermal processing and of final water content, from contact with liquid water to equilibration with room relative humidity. The crystalline material exhibits changes similar to those observed for vapor phase doping of P3HT[2]: a small expansion of the (100) lamella separation and a contraction of the π - π separation. The (100) expansion and π - π collapse occur at potentials consistent with the transistor threshold, at doping densities of order $4 \times 10^{20} \text{ cm}^{-3}$.

[1] L.Q. Flagg, et al. *J Am Chem Soc* 2019, doi: 10.1021/jacs.8b12640

[2] E.M. Thomas, et al. *Adv Func Mat* 2018, doi: 10.1002/adfm.201803687

8:30 PM *CT01.09.02

Nanoscale Electrochemical Redox Processes in Liquid Electrolytes—Interplay Between Composition and Kinetics William C. Chueh; Stanford University, United States

Electrochemistry involves the redox of solids and molecules. In many solids, like electrodes for batteries and electrocatalysis, bulk redox processes occur due to the (de)insertion of ions like lithium and proton. These processes are usually heterogeneous and is controlled by local reaction and/or diffusion kinetics. In this talk, I will present characterization methods to measure nanoscale redox processes and correlate local composition to kinetics using LiFePO_4 and Co(OH)_2 as model redox-active solids.

8:55 PM *CT01.09.03

Interfacial Reactions in Electrochemical Energy Devices—*Operando* Studies Using Synchrotron X-Ray Scattering and Spectroscopy Zhenxing Feng; Oregon State University, United States

For electrochemical systems such as batteries and fuel cells, the liquid/solid interfaces are critical parts where many important reactions take place. It is critical to understand the interfacial changes for the better design of efficient energy systems. In the past years we have used various *operando* synchrotron-based X-ray techniques to study the atomic and electronic structure, chemistry and compositions of numerous electrochemical interfaces fuel cells, electrolyzers, lithium- and magnesium-batteries. In my talk, I will mainly focus on two examples. One is our efforts on using *operando* X-ray absorption spectroscopy (XAS) to study catalyst restructuring in many electrochemical reactions such as oxygen evolution reaction for water splitting and electrochemical CO_2 reduction. The second example will be focus on our recent works on aqueous sodium-ion batteries using the combination of *operando* X-ray diffraction and XAS.

9:20 PM CT01.09.04

Investigating Amphiphilic Polymer Surface Chemistry in Conditions from Vacuum to Hydration with Ambient Pressure XPS Mikayla Barry¹, Pinar Aydogan Gokturk², Rachel Segalman¹ and Ethan J. Crumlin²; ¹University of California, Santa Barbara, United States; ²Lawrence Berkeley National Laboratory, United States

Marine antifouling coatings represent an environmentally benign solution to the adhesion of marine organisms that markedly reduces fuel efficiency on ships. The success of these coatings is determined by molecular-scale interactions that take place between the polymer surface, water, and marine organisms. Because polymer surfaces restructure in response to the surrounding environment, *in situ* characterization is crucial for providing an accurate understanding of the surface chemistry in ambient conditions. To evaluate the surface chemistry of membrane-relevant polymers and their interactions with interfacial water (i.e. water sorption), we present synchrotron Ambient Pressure XPS (APXPS) studies performed on polymer surfaces in contact with water vapor. Amphiphilic side chains incorporated into these polymers showed surface-directing capabilities in conditions ranging from vacuum to the liquid interface present at 20 Torr water vapor, with side chains contributing more to the surface signal than predicted from the theoretical bulk composition. Depth probing in conditions up to 800 mTorr also indicates that these side chains are saturated at the top surface. Furthermore, substantial water sorption at 20 Torr water vapor suggests a surface with a less well-defined water-polymer interface that may aid the coating's performance as an antifouling material. These findings may be useful in designing and characterizing coatings that leverage favorable interactions with water for marine antifouling applications.

9:35 PM CT01.09.05

Probing the Role of Polymer Side-Chain Chemistry and Sorbed Counterion on Water Sorption—An *In Situ* APXPS Study Pinar Aydogan Gokturk¹, Mikayla Barry², Rachel Segalman^{2,3} and Ethan J. Crumlin^{1,1};

¹Lawrence Berkeley National Laboratory, United States; ²University of California, Santa Barbara, United States; ³University of California Santa Barbara, United States

Water interactions with polymer surfaces play an important role in nearly all aspects of life including cellular functions, electrochemistry and water purification. Yet the precise understanding and quantification of such interactions at a molecular level is still incomplete due to difficulty of operating many surface specific techniques under *in situ* conditions. To fill this gap, we use ambient pressure Tender X-ray Photoelectron Spectroscopy (APXPS [1-4]). Tender-APXPS combines the chemical specificity, high surface sensitivity and quantitative analysis of the surface composition of traditional XPS and allow studies at pressures up to 20 Torr. In this study, interaction of water vapor with model styrenic polymer thin film surfaces were investigated *in situ* from UHV up to 100% relative humidity (RH) with APXPS to understand the effect of functional groups, interaction types and counter ions. Our results suggest that the interaction of water with polymer surfaces is mediated by polar and charged functional groups. Additionally, we show that water sorption on polyelectrolytes is highly dependent on the counterion and the fraction of dissociated ionic groups.[5] This talk will also discuss the counterion specific potential developments on the polyelectrolyte/solution interface using the facile advantage of XPS to carry information on local potentials. We believe that these findings will provide direct insight into the critical role of side-chain and counterion chemistry in polymer-water interactions while also demonstrating the potential of APXPS with elemental and potential sensitivity to give valuable information to guide the design and control of future membrane-relevant materials for water and energy applications.

References:

- [1]. Axnanda, S.; Crumlin, E. J.; Mao, B. H.; Rani, S.; Chang, R.; Karlsson, P. G.; Edwards, M. O. M.; Lundqvist, M.; Moberg, R.; Ross, P.; Hussain, Z.; Liu, Z., Using "Tender" X-ray Ambient Pressure X-Ray Photoelectron Spectroscopy as A Direct Probe of Solid-Liquid Interface. *Scientific Reports* 2015, 5.
- [2]. Favaro, M.; Jeong, B.; Ross, P. N.; Yano, J.; Hussain, Z.; Liu, Z.; Crumlin, E. J., Unravelling the electrochemical double layer by direct probing of the solid/liquid interface. *Nature Communications* 2016, 7.
- [3]. Favaro, M.; Valero-Vidal, C.; Eichhorn, J.; Toma, F. M.; Ross, P. N.; Yano, J.; Liu, Z.; Crumlin, E. J., Elucidating the alkaline oxygen evolution reaction mechanism on platinum. *Journal of Materials Chemistry A* 2017, 5 (23), 11634-11643.
- [4]. Lichterman, M. F.; Hu, S.; Richter, M. H.; Crumlin, E. J.; Axnanda, S.; Favaro, M.; Drisdell, W.; Hussain, Z.; Mayer, T.; Brunschwig, B. S.; Lewis, N. S.; Liu, Z.; Lewerenz, H. J., Direct observation of the energetics at a semiconductor/liquid junction by operando X-ray photoelectron spectroscopy. *Energy & Environmental Science* 2015, 8 (8), 2409-2416.
- [5] Aydogan Gokturk, P.; Barry, M.; Segalman, R.; Crumlin, E. J., Directly Probing Polymer Thin Film Chemistry and Counterion Influence on Water Sorption. *ACS Applied Polymer Materials* 2020, ASAP.

9:50 PM *CT01.09.06

***In Situ* XPS study on Lithiation/Delithiation of a Silicon Electrode for All-Solid-State Lithium-Ion**

Batteries Takuya Masuda^{1,2}; ¹National Institute for Materials Science, Japan; ²Hokkaido University, Japan

Silicon is a promising candidate for an anode material of next-generation lithium batteries because of its high abundance, negative redox potential (0.35 V vs Li⁺/Li), and potentially high capacity density (4200 mAh g⁻¹). However, the details of the lithiation/delithiation reactions of the Si electrode in all-solid-state batteries have remained unclear. Transferring such air-sensitive samples from the battery testing environment to the measurement apparatus may significantly change the structure and chemical state of samples due to undesired side reactions. Furthermore, post-processing ex situ approaches using multiple samples may result in misinterpretation due to the variation of samples. Thus, in situ reaction analysis is essential to clarify the mechanism of lithiation/delithiation processes.

X-ray photoelectron spectroscopy (XPS) enables to determine the elemental composition, oxidation states, and electronic structure of sample surfaces in a vacuum chamber. The reaction process can be tracked in a stepwise manner without any influence of variation and inhomogeneity of samples if XPS can be applied to a certain position of the same battery sample under bias application conditions. Such in situ XPS allows us to assign each spectral feature properly to reaction products and to correlate the effect of reaction products on the reversibility of charge/discharge reactions.

Here, we have developed an in situ XPS apparatus equipped with a bias application system and applied it to the electrochemical lithiation/delithiation reactions of an amorphous Si electrode sputter-deposited on a $\text{Li}_6.6\text{La}_3\text{Zr}_{1.6}\text{Ta}_{0.4}\text{O}_{12}$ (LLZT). Upon the first lithiation, a broad Li peak appears at the Si surface, and peaks corresponding to bulk Si and Si suboxide significantly shift to lower binding energy, showing the formation of lithium-silicide and lithium-silicates due to the lithiation of Si and native oxide. Quantitative analysis of electrochemical response and photoelectron spectra determines the composition of lithium-silicide to be $\text{Li}_{3.44}\text{Si}$. Peak fitting of the broad Li peak shows the formation of Li_2O and Li_2CO_3 due to side reactions. After the delithiation, the peak corresponding to $\text{Li}_{3.44}\text{Si}$ phase shifts to higher binding energy to form $\text{Li}_{0.15}\text{Si}$ phase, while lithium-silicates, Li_2O , and Li_2CO_3 remains as irreversible species. Thus, electrochemical reactions accompanied with lithiation/delithiation processes are successfully observed.

Reference

R. Endo, T. Ohnishi, K. Takada, and T. Masuda, "In Situ Observation of Lithiation and Delithiation Reactions of a Silicon Thin Film Electrode for All-Solid-State Lithium-Ion Batteries by X-ray Photoelectron Spectroscopy", *J. Phys. Chem. Lett.* 2020, 11, 6649–6654.

10:15 PM DISCUSSION TIME

SESSION CT01.10: On-demand
Wednesday Morning, April 14, 2021
CT01

8:00 AM CT01.10.01

Platinum Nanocatalyst Degradation During the Oxygen Evolution Reaction Analyzed Through *In Situ* Liquid-Phase Transmission Electron Microscopy Rui Filipe Serra Maia¹, Yijin Kang² and Eric A. Stach¹;

¹University of Pennsylvania, United States; ²Northwestern University, United States

Photochemical water splitting is very promising because it converts solar energy into chemical energy in the form of molecular hydrogen (H_2), the most energy-rich chemical compound per unit of mass¹. However, this process is severely affected by catalyst degradation at the anode, where the strong oxidizing environment necessary for the oxygen evolution reaction (OER) causes fast platinum degradation, which is the most active catalyst for this reaction². Currently there are no efficient ways to prevent the catalyst degradation, which results in prohibitive industrial costs and prevents the widespread use of this technology to obtain H_2 and compete with fossil fuels³. This happens because it is very difficult to analyze how the chemistry and structure of platinum change at the atomic-scale when subjected to OER electrochemical potential in real-world conditions⁴.

We performed *in situ* liquid-phase Transmission Electron Microscopy (TEM) analysis to obtain a time-resolved analysis of platinum nanocatalysts subjected to OER electrochemical stress. The results show that surface Pt_xO_y play a key role in the mobility and dissolution of platinum nanocatalysts during the oxygen evolution reaction. Catalyst degradation involves grain aggregation and growth, followed by Pt_xO_y driven platinum dissolution. The electrochemical stress and degradation effects can be minimized by reducing grain boundary density and through application of intermittent electrochemical stress, which can be achieved by applying a pulsed potential as opposed to a continuous fixed potential. These insights allow correlating the catalyst degradation kinetics to the reaction conditions and catalyst properties, enabling rational optimization of variables such as crystallite size, grain boundary density and the electrochemical protocol for reverting the catalyst degradation and

enabling industrially sustainable hydrogen generation from water splitting.

References

1. Chu, S. & Majumdar, A. Opportunities and challenges for a sustainable energy future. *Nature* **488**, 294–303 (2012).
2. Seger, B. *et al.* Hydrogen Production Using a Molybdenum Sulfide Catalyst on a Titanium-Protected n+p-Silicon Photocathode. *Angew. Chemie* **124**, 9262–9265 (2012).
3. Habisreutinger, S. N. *et al.* Carbon nanotube/polymer composites as a highly stable hole collection layer in perovskite solar cells. *Nano Lett.* **14**, 5561–5568 (2014).
4. Klein, K., de Jonge, N. & Anderson, I. Energy-Loss Characteristics for EFTEM Imaging with a Liquid Flow Cell. *Microsc. Microanal.* **17**, 780–781 (2011).

SYMPOSIUM CT02

In Situ TEM Characterization of Dynamic Processes During Materials Synthesis and Processing
April 14 - April 18, 2021

Symposium Organizers

Madeline Dukes, Protochips, Inc.
Dongsheng Li, Pacific Northwest National Laboratory
Robert Sinclair, Stanford University
Daliang Zhang, Chongqing University

* Invited Paper

SESSION CT02.01: Structural Evolution and Structure-Property Correlation
Session Chairs: Madeline Dukes and Leopoldo Molina-Luna
Sunday Morning, April 18, 2021
CT02

8:00 AM *CT02.01.01

Insights on Structure-Property Correlations in Hafnia-Based RRAM Devices by *In Situ* TEM Leopoldo Molina-Luna, Robert Eilhardt, Alexander Zintler, Déspina Nasiou, Oscar Recalde, Stefan Petzold and Lambert Alff; TU Darmstadt, Germany

Hafnia based resistive random-access memory (RRAM) devices are promising candidates as next generation non-volatile memories and are appealing because of the compatibility with back-end-of-line processes in the current semiconductor fabrication process. Thus, improving device reliability is crucial for their use in future memory applications. Understanding the influence of the microstructure and the atomistic processes involved will help enhance device performance. As shown in recent work (1), grain boundary engineering the hafnia layer in TiN/HfO₂/Pt RRAM can yield forming free devices with threading grain boundaries that act as preferential pathways for conductive filament formation (2). The techniques that will be presented provide examples of how to correlate the local structure to the device properties. In situ experiments that involve heating as well as biasing have been carried out on devices mounted on MEMS-based chips by FIB in situ lift-out

techniques (3) and are key towards providing a component specific understanding of the physical/chemical mechanisms involved. Furthermore, we have performed a temperature-dependent study to directly monitor the microstructure evolution of the hafnia layer directly inside the microscope, thus giving a unique insight into the growth mechanism and formation of grain boundaries. The transformation from an amorphous/nanocrystalline to a polycrystalline state lowered forming voltages and device-to-device variability of the memory devices and served as a basis for a direct structure-property correlation. To further analyse the complex texture transfer mechanisms involved, phase-determination 4D-STEM experiments were carried out to locally correlate HfO₂ grain orientations with the underlying TiN electrode. A Machine Learning approach was implemented for analysing the generated 4D-STEM data sets (4).

References:

1. S. Petzold *et al.*, *Advanced Electronic Materials*. **5**, 1900484 (2019).
2. M. Lanza *et al.*, *Appl. Phys. Lett.* **100**, 123508 (2012).
3. A. Zintler *et al.*, *Ultramicroscopy*. **181**, 144–149 (2017).
4. A. Zintler *et al.*, *Microsc Microanal*, **1–3** (2020).

8:25 AM CT02.01.02

Late News: Atomic-Scale Friction Between Single-Asperity Contacts Under *In Situ* Transmission Electron Microscopy Xiang Wang and Scott X. Mao; University of Pittsburgh, United States

To date, visualizing the friction process between nanocontacts at an atomic scale is rarely accomplished. Here, through designing the nanocontact and performing controlled motion between asperities under high-resolution transmission electron microscopy (HRTEM), the real-time atomic-friction process is captured. Moreover, the interface dynamics and friction mechanism are illustrated by combining in-situ TEM observation with molecular dynamics simulation. For the first time under in-situ TEM, the atomic-friction between single-asperity nanocontacts is revealed to display a discrete stick-slip behavior and an asynchronous process for the accumulation and dissipation of the strain energy together with the nonuniform motion of interface atoms. This work provides a study approach to realize in-situ atomic-friction research and attains a fundamental understanding of friction phenomena at the atomic-scale.

8:40 AM CT02.01.03

***In Situ* X-Ray Fluorescence Microprobe (XFM) and Electron Energy-Loss Spectroscopy (EELS) to Determine Valence-State Configuration of CoPt Nanoparticles During Chemical Reaction** Alexandre Foucher¹, Nicholas Marcella², Ryan V. Tappero³, Anatoly Frenkel² and Eric A. Stach¹; ¹University of Pennsylvania, United States; ²Stony Brook University, The State University of New York, United States; ³Brookhaven National Laboratory, United States

The synthesis of bimetallic CoPt nanoparticles aims to optimize the use of expensive platinum for critical chemical reactions such as the oxygen reduction reaction (ORR). The crystallographic configuration of the intermetallic solution is directly related to its catalytic performance. For instance, the valence state influences the platinum oxygen bond strength, so it is necessary to know and control the crystal's electronic configuration at the atomic level to enhance catalytic properties. Hence, it is crucial to have a precise knowledge of the electronic configuration of Co and Pt and the atomic level to guide the future design of more efficient and active nanostructures.

To that end, we studied carbon-supported CoPt nanoparticles under reaction conditions with *in situ* XFM and *in situ* EELS. The sample was enclosed in an X-ray and electron-transparent closed-cell reactor, capable of providing both elevated temperatures and exposure to O₂ and H₂. The 1 μm XFM beam is a bulk approach that provides spectroscopic information over a large set of nanoparticles. In contrast, the EELS was performed in scanning transmission electron microscopy (STEM) mode with a probe size lower than 1 Å, allowing us to characterize the sample at the atomic level. This combination of approaches allows us to determine the chemical properties of individual particles and the overall system.

Results showed the progressive change of the oxidation state of cobalt upon reduction or oxidation. The valence state of cobalt could be determined, and we observe that it is spatially heterogeneous. Particle migration and coalescence was observed for a temperature above 400 °C and we determined the temperature where the reduction of cobalt is triggered. We also identified localized segregation of elements within the bimetallic structure, providing crucial information about the nanocatalysts' degradation mechanisms. This combined *in situ* approach can be applied to a large range of nanostructures and opens new opportunities to understand catalysts under reaction conditions.

8:55 AM CT02.01.04

Late News: Mapping the Element Distribution of Changing Materials: EDS for *In Situ* STEM and SEM
Meiken Falke and Igor Nemeth; Bruker, Germany

We discuss challenges and possibilities using energy dispersive X-ray analysis (EDS) in *in-situ/operando* experiments. EDS in TEM/STEM, SEM and T-SEM (electron transparent specimen in SEM) is a powerful and fast technique and well suitable for analyzing the whereabouts of particular species, be that static or during processes in liquids or gases, the application of force, changing temperature and involving specimen beam interaction. The time scale for useful EDS results lies in the range of minutes to seconds, depending mainly on spatial resolution (a 2D map or a spectrum of just one atom [1]) and characteristic X-ray yield. The latter again has various dependencies, which include probe current, radiation damage, collection angle, fluorescence yield and detector efficiency.

The dedicated sample holders and reaction cell designs, which are used for *in situ* experiments, often present a challenge for EDS analysis. It is important to understand how the holder design influences the spectroscopic efficiency and quantitative result. We discuss effects, such as spurious signals e.g. from holder materials, absorption e.g. in reaction cell windows, the influence of heat radiation on EDS spectra [2], specimen drift etc. Approaches and tools available so far to keep such effects under control and correct for respective analysis errors are shown. One simple step to take for example, is optimizing the geometry of the holder and EDS detector position. Adjusting the materials of holders and reaction cell windows to increase EDS efficiency and avoid parasitic signals would be a more complex task.

Furthermore, a stream of data from a changing specimen needs specific analysis strategies. Suitable data acquisition and processing tools, not only for EDS, but including complementary techniques, such as diffraction-based analysis options in SEM, are being developed.

[1] R. M. Stroud et al. *Appl. Phys. Lett.* **108** (2016) 163101

[2] T. T. van Omme et al., *Ultramicroscopy* **129** (2018) 14

9:00 AM *CT02.01.05

Liquid-Phase Electron Microscopy for Soft Matter Science and Biology Niels de Jonge^{1,2}; ¹INM – Leibniz Institute for New Materials, Germany; ²Saarland University, Germany

Innovations in liquid-phase electron microscopy (LP-EM) are discussed that have enabled experiments at the optimized conditions needed to examine soft matter [1]. Soft matter is referred to as a state of condensed matter that undergoes dynamic changes already at low energy, comparable to kT. Examples are polymers, weakly bound self-assembled structures, and biological systems. The main difficulty in such experiments is the occurrence of electron beam radiation effects, and the resulting complex experimental design and data interpretation that is inevitably influenced by those effects. By at least partially resolving the involved experimental difficulties, LP-EM is now capable of providing nanometer spatial resolution and sub-second temporal resolution for quantitative microscopy of soft matter in materials science and biology. This presentation will provide an overview of the different LP-EM systems available including graphene liquid cells, explain how the resolution does not depend much on the electron optical system but rather on the type of material, the available electron dose, and the sample thickness [2, 3]. Strategies for designing experiments are described as well including the usage of quantum dots [4]. An exciting new discovery is the ability to mitigate radiation damage so that the experiments can be carried out at much higher doses than what was previously expected [5]. Two examples will be given of the application of LP-EM, one in cancer research involving the

epidermal growth factor receptor in breast cancer [6], and one in the observation of quasi-crystals self-assembled in liquid from gold nanoparticles [7]. Finally, a perspective of directly imaging dynamic soft matter processes is given including a discussion on sparse imaging and artificial intelligence.

References

- [1] H. Wu, H. Friedrich, J.P. Patterson, N. Sommerdijk, N. de Jonge, *Adv. Mater.* 32, 2001582 (2020).
- [2] N. de Jonge, *Ultramicroscopy* 187, 113-125 (2018).
- [3] N. de Jonge, L. Houben, R.E. Dunin-Borkowski, F.M. Ross, *Nat. Rev. Mater.* 4, 61 (2019).
- [4] D.B. Peckys, C. Quint, N. Jonge, *Nano Lett.* 20, 7948 (2020).
- [5] S. Keskin, N. de Jonge, *Nano Lett.* 18, 7435 (2018).
- [6] D.B. Peckys, U. Korf, S. Wiemann, N. de Jonge, *Mol. Biol. Cell* 28, 3193 (2017).
- [7] E. Cepeda-Perez, D. Doblas, T. Kraus, N. de Jonge, *Sci. Adv.* 6, 1404 (2020).

9:25 AM CT02.01.06

Late News: Visualizing Oxidation Mechanisms in Few-Layered Black Phosphorus via In Situ Transmission Electron Microscopy Piran Ravichandran Kidambi; Vanderbilt University, United States

Layered two-dimensional (2D) black phosphorus (BP) exhibits novel semiconducting properties including a tunable bandgap and high electron mobility. However, the poor stability of BP in ambient environment severely limits potential for application in future electronic and optoelectronic devices. While passivation or encapsulation of BP using inert materials/polymers has emerged as a plausible solution, a detailed fundamental understanding of BP's reaction with oxygen is imperative to rationally advance its use in applications. Here, we use in situ environmental transmission electron microscopy to elucidate atomistic structural changes in mechanically exfoliated few-layered BP during exposure to varying partial pressures of oxygen. An amorphous oxide layer is seen on the actively etching BP edges, and the thickness of this layer increases with increasing oxygen partial pressure, indicating that oxidation proceeds via initial formation of amorphous P_xO_y species which sublime to result in the etching of the BP crystal. We observe that while fewlayered BP is stable under the 80 kV electron beam (e-beam) in vacuum, the lattice oxidizes and degrades at room temperature in the presence of oxygen only in the region under the e-beam. The oxidative etch rate also increases with increasing e-beam dosage, suggesting the presence of an energy barrier for the oxidation reaction. Preferential oxidative etching along the $[0\ 0\ 1]$ and $[0\ 0\ \bar{1}]$ crystallographic directions is observed, in good agreement with density functional theory calculations showing favorable thermodynamic stability of the oxidized BP $(0\ 0\ 1)$ planes compared to the $(1\ 0\ 0)$ planes. We expect the atomistic insights and fundamental understanding obtained here to aid in the development of novel approaches to integrate BP in future applications.

References:

Naclerio et al. *ACS Appl. Mater. Interfaces* 2020, 12, 13, 15844-15854, DOI:10.1021/acsami.9b21116

9:40 AM CT02.01.07

Late News: Dynamic Observation of Shear-Induced Reversible Low Angle Grain Boundary Formation in Gold Using *In Situ* TEM Shuang Li¹, Nanjun Chen¹, Bharat Gwalani¹, Mathew Olszta¹, Lei Li¹, Ayoub Soulami¹, Peter V. Sushko¹, Aashish Rohatgi¹, Yulan Li¹, Cynthia A. Powell¹, Suveen Mathaudhu^{1,2}, Arun Devaraj¹, Shenyang Hu¹ and Chongmin Wang¹; ¹Pacific Northwest National Laboratory, United States; ²University of California Riverside, United States

Processing pure metals by employing severe shear deformation can result in introduction of defects and thereby microstructural refinement. However, the atomic scale mechanisms of defect evolution and microstructural refinement during extreme shear deformation of pure metals is still at its infancy. Here, we report our observations of dynamic shear-induced low-angle grain boundary(GB) formation processes in nanocrystalline Au via *in-situ* shear deformation inside a high-resolution transmission electron microscopy. It is found that nanotwins nucleate from free surfaces and propagate inwards. This is accompanied by dislocations glide as well. The alignment of the gliding dislocations leads to the formation of low-angle GB. The collaborative

migration of nanotwins and dislocations result in the material being able to accommodate large plastic strain during shear deformation and fully recover under reversed loading with negligible damage accumulation. This nanotwin-mediated dislocation slip mechanism offers new insights for understanding low-angle GB formation during shear deformation of face centered cubic metals.

9:55 AM CT02.01.08

***In Situ* Transmission Electron Microscopy Temperature Measurement and Characterization of High-Temperature Behavior of Nanostructures** Daan Hein Alsem¹, Pawan Kumar^{2,2}, James Horwath², Deep M. Jariwala² and Eric A. Stach^{1,2}; ¹Hummingbird Scientific, United States; ²University of Pennsylvania, United States

Using controlled heat to control the structure of materials during processing is the most common *in-situ* transmission electron microscope (TEM) technique, as temperature causes atomic diffusion and thus allows structural re-ordering. Combining this with the high-resolution imaging and spectroscopy ability of the TEM, these experiments can provide detailed insights into what mechanism governs the relation between materials processing and structure.

Thin-film technology and its application to substrates for *in-situ* TEM has allowed heating systems with very localized heating of the specimen in TEM heating holders, enabling more stable imaging during *in-situ* TEM heating experiments. More recently, direct temperature measurements on these thin-film heating systems have made temperature measurements at the sample become closer to becoming a reality. Although double-tilt TEM heating holders have been available, they suffer from some of the same limitations as standard double-tilt TEM holders do, often to a greater extent because of the added electrical connections to operate the on-chip heater and sensor. Specifically, backlash in the tilting mechanism and lack of repeatability of the tilt makes it difficult to get the sample in exactly the right orientation and to know the exact angle of rotation. This work will use an optimized single and double-tilt *in-situ* TEM thin-film heating platform that minimizes mechanical artifacts in the tilting mechanism and provides very stable image performance when heated to temperatures up to 1000°C, where it can be run for more than 150 hours. Outside of standard temperature characterization of these thin-film heating TEM systems using different high resolution optical thermal imaging techniques, we will also report on experiments using melting standards to confirm the on-chip temperature sensor's accurate temperature response. We can identify very local and discrete melting events of samples with known melting points and correlate this to the sensor response, where local melting happens at very discrete moments (typically within a few frames). Surface diffusion occurs in matters of seconds following that. This results in *in-situ* TEM heating specimen holders that allow high-temperature imaging combined with double-tilt sample position control and accurate temperature indication.

This work will present how we used these new *in-situ* TEM sample heating systems to characterize two nanomaterial systems. Starting with gold nanorods to characterize particle motion and stability under the beam and then the phase transformation and (rapid) shape change at the melting point. We will present the rapid frame-to-frame phase transformation process of gold nanorods as we ramp the sample temperature to 1000°C and show that we can use the system to track phenomena in nanostructures over the full temperature range of the TEM heating system with good image stability.

We also show experimental data on few-layer 2D MoS₂ samples that were transferred onto the open viewing area of the heating chip. Depending on the heating rate, heating the MoS₂ sample *in-situ* resulted in either ordered crystalline hexagonal islands (<20 nm) that consist of a mixture of 2H and 3R phases or yielded a mix of nanocrystalline and amorphous regions [1]. Energy-dispersive X-ray spectroscopy (EDS) confirmed the chemical content of each segregated area.

These results illustrate this newly developed *in-situ* TEM double-tilt heating platform's optimized overall mechanical stability and temperature performance.

Reference:

[1] Pawan Kumar *et al.*, npj 2D Materials and Applications 4,16 (2020).

SESSION CT02.02: Phase Transformation and Structure-Property Correlation

Session Chairs: Biao Jin and Leopoldo Molina-Luna

Sunday Morning, April 18, 2021

CT02

10:30 AM *CT02.02.01

Gas Phase *In Situ* TEM Facilitates Improved Understanding of Nanoscale Processes Rainer Straubinger;
Protochips EMEA GmbH, Germany

In situ (scanning) transmission electron microscopy [(S)TEM] in a gas atmosphere has proven to be an outstanding technique for investigating dynamic processes in material structures under high resolution conditions. New innovations in-situ gas handling systems and in-situ software have enabled researchers to recreate complex environmental conditions inside the TEM by precisely controlling temperature, gas pressure, flow, and the introduction of gas and vapor mixtures to the sample during the course of the experiment. These advances have made it possible to investigate dynamic catalytic processes, such as the degradation catalytic material, one example being the strong metal support interaction (SMSI). These studies showed in real-time that an amorphous reduced titania layer is formed at low temperatures, and that the crystallization of the layer into either mono- or bilayer structures is dictated by the reaction environment and in accordance with the theory. Investigation these processes under high resolution conditions further allowed the correlation between the formation of the SMSI and a dramatic reshaping of the metallic surface facets.

Another field where in situ research can help to overcome the current limitations is in the field of semiconductor research. Compound semiconductors are promising candidates for optoelectronic applications on Si. Ga(N,As,P) for example could be capable of overcoming the efficiency limitations of gallium indium arsenide phosphide ((Ga,In)(As,P)) based structures. Unfortunately, the realization of good quality epitaxial layers of highly metastable materials is indeed very challenging. A successful approach to improve the layer quality and therefore increase the optical output of these structures is post-growth annealing. A robust mechanistic understanding cluster formation, desorption processes, and material distribution within the Ga(N,As,P) and Ga(P,Bi) layer due to thermal treatment is desirable, but replicating these experiments under in-situ TEM conditions is complicated due to the handling requirements of the necessary precursor gases. To overcome the issues handling toxic and pyrophoric group III and group V precursor gases, it was necessary to develop an in situ system which fulfills all of the technical- and safety-requirements of a modern MOVPE machine, the results of which will improve our understanding of the factors necessary to optimize the efficiency of semiconductor materials.

1. Zhang, S. et al. Dynamical Observation and Detailed Description of Catalysts under Strong Metal–Support Interaction. *Nano Lett.* 16, 4528–4534 (2016).

2. Straubinger, R., Beyer, A., Ochs, T., Stolz, W. & Volz, K. In Situ Thermal Annealing Transmission Electron Microscopy (TEM) Investigation of III/V Semiconductor Heterostructures Using a Setup for Safe Usage of Toxic and Pyrophoric Gases. *Microsc. Microanal.* 23, 751–757 (2017).

3. Straubinger, R. et al. Thermally Introduced Bismuth Clustering in Ga(P,Bi) Layers under Group V Stabilised Conditions Investigated by Atomic Resolution In Situ (S)TEM. *Scientific Reports* 8, 1–7 (2018).

10:55 AM CT02.02.02

Atomic Gradient Transitional Structures Induce High Photocatalytic Efficiency Dongsheng Li; Pacific

Polymorphs widely exist in nature and synthetic systems and are well known to determine material properties. Understanding phase transformation mechanisms among polymorphs enables the design of structures and tuning of phases to tailor material properties. However, current understanding is limited due to the lack of direct observations of the structural evolution at the atomic scale. Here, integrating (semi) *in situ* transmission electron microscopy and density functional theory, we report atomic structural evolutions of phase transformation from anatase (A) to rutile (R), brookite (B), R-phase, and TiO. Understanding the atomic structural evolution sheds light on interpreting and controlling TiO₂ polymorphs and interface structures for various applications. Here, we reveal the transitional atomic gradient structures, that form during phase transformation processes, alter electronic structures in 3D across the bulk of the crystals and thus substantially increase the active volume to separate electrons and holes and the resulting photoactivity. These new insights suggest that interphase matter based on gradient structures can be designed to induce new functions not achievable using abrupt interfaces. These findings enable a new materials design paradigm that can potentially be harnessed for a broad range of applications.

We also reveal the anisotropic nature of the electron-beam effect: dependence of crystallographic orientation with respect to electron-beam irradiation direction. The revealed electron-beam effects in our work provide guidance for *in situ* transmission electron microscopy studies.

11:10 AM BREAK

11:35 AM *CT02.02.05

***In Situ* Observations of Strain Induced Effects on Structure and Properties** Eva M. Olsson; Chalmers University of Technology, Sweden

Strain offers the possibility to tune the structure and properties of materials. The dimensionality of the material structures determines to what degree they can be strained prior to fracture. While bulk semiconductors fracture at 0.5-1.5 % strain and corresponding nanowires fracture at about 3-5 %, 2D structures can withstand up to 10% strain before fracture. This presentation will illustrate how *in situ* electron microscopy can reveal site specific information about the correlation between strain and catalytic activity, electrical, optical and thermal properties. We also show how strain can be introduced in nanostructures during their growth in solution and thereby tune the properties.

We have used high spatial resolution and precision using scanning transmission electron microscopy (STEM) to image the influence of atomic site-specific strain on catalytic activity of supported nanoparticles [1]. The data includes high precision information about the position of individual atoms as well as atom columns with varying number of atoms. We have also used *in situ* STEM to correlate nanoscale strain to electrical transport properties in III-V semiconducting nanowires [2]. The study shows an inhomogeneous strain distribution within nanowires where a uniaxial strain is applied. We have mapped the energy band gap and bulk plasmon as a function of tensile and compressive strain [3] in III-V nanowires. The work illustrates the potential of using combined *in situ* electrical and mechanical experiments where we have developed methods for *in situ* experiments and illumination with light for both scanning electron microscopes [4] and TEMs. We have performed *in situ* measurements of the resistance and thermal handling capabilities of wrinkled reduced graphene oxide [5].

[1] T. Nilsson Pingel, M. Jørgensen, A.B. Yankovich, H. Grönbeck and E. Olsson, “Influence of atomic site specific strain on catalytic activity of supported nanoparticles”, *Nature Communications* 9, 2722 (2018).

[2] L. Zeng, C. Gammer, B. Ozdol, T. Nordqvist, J. Nygård, P. Krogstrup, A.M. Minor, W. Jäger and E. Olsson, “Correlation between electrical transport and nanoscale strain in InAs/In_{0.6}Ga_{0.4}As core-shell nanowires”, *Nano Lett.* 18, 4949 (2018).

[3] L. Zeng, T. Kanne, J. Nygård, P. Krogstrup, W. Jäger and E. Olsson, “The effect of bending deformation on

charge transport and electron effective mass of p-doped GaAs nanowires”, Phys. Status Solidi RRL 13, 1900134 (2019).

[4] J. Holmér, L. Zeng, T. Kanne, P. Krogstrup, J. Nygård, L. De Knoop and E. Olsson, “An STM-SEM setup for characterizing photon and electron induced effects in single photovoltaic nanowires”, Nano Energy 53, 175 (2018).

[5] H.M. Nilsson, L. de Knoop, J. Cuming and E. Olsson, “Localized resistance measurements of wrinkled reduced graphene oxide using in situ transmission electron microscopy”, Carbon 113, 340 (2017).

12:00 PM CT02.02.06

***In Situ* Transmission Electron Microscopy and Multivariate Analysis of Phase Segregations in Cesium-Lead-Halide Perovskite Nanoparticles** Hannah Funk¹, Alberto Eljarrat², Oleksandra Shargaieva¹, Eva Unger¹, Christoph T Koch² and Daniel Abou-Ras¹; ¹Helmholtz-Zentrum Berlin, Germany; ²Humboldt-Universität zu Berlin, Guernsey

With power conversion efficiencies surpassing 25% in 2019, hybrid organic-inorganic lead-halide perovskites solar cells attract ever more interest in the photovoltaics community. Photo-induced phase separation has been reported for a range of mixed-halide perovskites, which limits the available band-gap energies for photovoltaic applications. An enhanced understanding of the phase separation mechanism is essential to rationalize limitations and design stable perovskite semiconductors. During electron microscope experiments, the electron beam may cause, in the same way as photons when using a laser beam for irradiation, phase transformations in halide perovskites. In the present work, we report about the in-situ monitoring of electron-beam-induced phase segregation in CsPb(Br,I)₃ crystallites by means of high-resolution imaging in a transmission electron microscope. The acquired time series were evaluated with multivariate analysis to classify the structural change over time. An algorithm “scans” the TEM image creating a diffractogram for each patch. The diffractogram patterns of all patches of the whole time series are collected into a two-dimensional image stack, which was then classified using principal component and the independent component analysis blind source separation. By this approach, it was possible to directly monitor and provide an atomistic picture of the in-grain phase segregation. The authors will provide insight into the various aspects of this in-situ approach for the study of nanoparticles.

SESSION CT02.03: Electrochemistry
Session Chairs: Dongsheng Li and Robert Sinclair
Sunday Afternoon, April 18, 2021
CT02

1:00 PM *CT02.03.01

Understanding the Role of Grain Boundaries in Solid Electrolytes for Batteries via *In Situ* Electron Microscopy Miaofang Chi; Oak Ridge National Laboratory, United States

Solid-state batteries are considered to be one of the most promising battery configurations for future energy storage with desirable properties including safety, capacity, and longevity. However, recent studies found that interfaces and grain boundaries in solid state batteries, regardless of the type of solid electrolyte, are the primary feature limiting their commercialization. One major advantage of solid-state batteries over conventional liquid electrolyte-based batteries was expected to be reduced dendrite growth, however, dendritic growth was recently observed and was revealed to be associated to grain boundaries. Interfacial resistances between electrolyte and electrodes are higher than projected and the majority of solid electrolytes are predicted to be unstable to lithium metal. Mitigating these issues can't be achieved without a fundamental understanding of the atomic and electronic structures of these interfaces and, more importantly, how they evolve upon electrochemical cycling. Here, we highlight several recent *in situ* microscopy studies that unveil the interface stability of model solid

electrolytes, e.g. LiPON and (Li₇La₃Zr₂O₁₂)LLZO, with lithium metal and compare their responses to different electrochemical cycling conditions. The role of grain boundaries in dendrite nucleation and propagation within LLZO is investigated by combining monochromated EELS with *in situ* microscopy imaging. The root cause of dendrite network formation in polycrystalline solid electrolytes will be discussed. We further provide a perspective as to how these issues, i.e. resistivity and dendrite growth at grain boundaries, could possibly be mitigated by controlling critical steps during synthesis.

Acknowledgement

Research sponsored by Oak Ridge National Laboratory's Center for Nanophase Materials Sciences (CNMS), which is a U.S. Department of Energy Office of Science User Facility.

1:25 PM CT02.03.02

Revealing Reaction Dynamics of Battery Electrolyte-Electrode Interfaces via *In Situ* Electrochemical TEM Alex W. Robertson¹, Shengda Pu¹, Chen Gong¹, Xiangwen Gao¹, Ziyang Ning¹, Sixie Yang¹, John-Joseph Marie¹, Boyang Liu¹, Robert House¹, Gareth O. Hartley¹, Jun Luo² and Peter Bruce¹; ¹University of Oxford, United Kingdom; ²Tianjin University of Technology, China

The critical area for understanding and progressing battery technology is the interface between the electrode and the electrolyte. The electrochemistry occurring at this interface, including the formation and evolution of an intermediate solid-electrolyte interphase (SEI) layer, is notoriously complex. Applying in-situ characterisation techniques to illuminate these dynamics will help with the diagnosis of the specific interfacial processes, and thus facilitate the design of better electrolytes. In this talk I will discuss some of our recent work using in-situ liquid-cell TEM to probe the evolving electrode interface in real time.[1]

Multivalent electrolytes, using chemistries based on Ca or Mg ions, are promising candidates for next-generation batteries. Recent breakthroughs are beginning to overcome the longstanding problem of devising effective multivalent electrolytes, yet a major challenge remains in designing electrolytes that yield a stable SEI that does not inhibit cycling. We performed extensive in-situ TEM characterisation of one of the more promising new electrolytes, a calcium borohydride salt in tetrahydrofuran (THF),[2] capturing the real-time nucleation, growth, and dissolution of calcium under various current density conditions. In-situ TEM imaging demonstrates the existence of a critical current density, beyond which adverse dendritic calcium plating morphologies dominate, and yielding detached isolated calcium deposits on stripping.[3]

Several other next-generation batteries are based on Li ion chemistries, and to attain peak performance desire a lithium metal anode. Yet ensuring that they remain stable over many cycles has proven challenging. One of the most effective avenues to combat this has been tailoring the SEI by adjusting the electrolyte composition with additives. These fluoride-rich interphases significantly improve cycling efficiency, yet diagnosing how they alter the structural dynamics of Li electroplating and stripping is difficult without in-situ imaging. I will discuss how using in-situ TEM can provide unique insights into the distinct morphological changes that occur to Li plated from electrolytes tailored to form a fluoride-rich interphase. Our observations reveal that the fluoride-rich SEI favours the formation of a densely interwoven Li deposit, as opposed to the more dendritic structures formed from standard electrolyte. This denser structure proved more amenable to uniform dissolution, leaving behind fewer isolated dead Li fragments, and thus yielding superior efficiency.

[1] Pu, S.; Gong, C.; Robertson, A. W. Liquid Cell Transmission Electron Microscopy and its Applications. Royal Society Open Science, 2020, 7, 191204.

[2] Wang, D.; Gao, X.; Chen, Y.; Jin, L.; Kuss, C.; Bruce, P. G. Plating and Stripping Calcium in Organic Electrolyte. Nature Materials, 2018, 17, 16-20.

[3] Pu, S.; Gong, C.; Gao, X.; Ning, Z.; Yang, S.; Marie, J. J.; Liu, B.; House, R. A.; Hartley, G. O.; Luo, J.; Bruce, P. G.; Robertson, A. W. Current-Density-Dependent Electroplating in Ca Electrolytes; From Globules to Dendrites. ACS Energy Letters, 2020, 5, 2283-2290.

1:40 PM BREAK

2:00 PM *CT02.03.04

Heaters and Electrode Materials for Expanding the Capabilities of Liquid Cell Electrochemistry Frances M. Ross¹, Shu Fen Tan¹, Kate Reidy¹, Serin Lee¹, Julian Klein¹, Nicholas Schneider², Haeyeon Lee¹, Ainsley Pinkowitz¹ and Jeung Hun Park³; ¹Massachusetts Institute of Technology, United States; ²Renata Global, United States; ³Princeton University, United States

Liquid cell transmission electron microscopy provides exciting opportunities for imaging processes in liquid with good spatial and temporal resolution. The quality and quantification of liquid cell data continue to improve, driven by advances in liquid cell equipment, control of local conditions, and theoretical understanding of electron beam effects. Liquid cell studies that combine imaging with electrochemical measurements have proved particularly useful in studies of energy materials, corrosion processes and crystal growth. The ability to control the temperature is important in extending the capabilities of liquid cell electrochemistry in probing these materials reactions. The electrode material is also important as it determines the reliability and consistency of the electrochemical measurements and can also affect the image resolution. Here, we explore the opportunities for liquid cell electrochemistry that arise from the use of heating as well as new electrode materials, specifically graphene and other two-dimensional (2D) materials. Heating is implemented by patterning electrodes over microfabricated liquid cell chips that already include a Pt resistance heater. 2D electrodes are implemented by transfer onto liquid cells that already include electrical contacts. We will describe the performance of combined heating and biasing chips and evaluate several 2D materials for their properties as electrodes in liquid cell electrochemistry, in comparison with conventional electrode choices such as Pt, Au or carbon. The minimal electron scattering from the 2D layer is especially helpful for preserving image resolution in electrochemical experiments carried out in plan view, where the imaging takes place through the electrode. Of the 2D materials we have tested we will focus on graphene as it appears to be particularly promising. We discuss its mechanical and electrochemical properties within the liquid cell, as well as the negligible voltage drop expected even in large area electrodes tens of micrometers across. We also discuss its stability under electron beam irradiation, even at the higher accelerating voltages often used in liquid cell electron microscopy. To demonstrate the capabilities of heating and graphene electrodes we deposit various metals from acidified electrolytes. Heating changes the kinetics, increasing the deposition rate at regions of elevated temperature. For graphene electrodes, the improved resolution allows us to explore nucleation and growth processes and demonstrate an unexpected coarsening process that occurs during deposition. We finally consider some future opportunities that will be enabled by the use of new chip designs in liquid cell electrochemistry. Particularly exciting are the possibilities of incorporating heating with novel electrode designs, and the performance of 2D materials that show favorable scavenging properties. The use of stacked 2D materials, as well as 2D layers patterned to control nucleation sites, will expand the opportunities further. We anticipate that both temperature control and incorporation of 2D materials into liquid cell design will open up new opportunities for investigating a wide range of problems relevant to energy storage and electrocatalysis as well as fundamentals of electrochemical reactions.

2:25 PM CT02.03.06

Vaporization and Diffusion of Pt/Pd from Pt/Pd/Al₂O₃ Under Redox Conditions Andrew C. Meng¹, Ke-Bin Low², Alexandre Foucher¹, Yuejin Li², Ivan Petrovic² and Eric A. Stach¹; ¹University of Pennsylvania, United States; ²BASF Corporation, United States

Al₂O₃-supported Pt/Pd bimetallic catalysts were studied using *in-situ* atmospheric pressure and *ex-situ* transmission electron microscopy. Significant metal vaporization was observed at temperatures above 600°C, both in pure oxygen and in air. This behavior implies that material transport through the vapor during typical catalyst aging processes for oxidation can play a more significant role in catalyst structural evolution than previously thought. Concomitantly, Pd diffusion away from metallic nanoparticles on the surface of Al₂O₃ can also contribute to the disappearance of metal particles. Electron micrographs from *in-situ* oxidation experiments were mined for data, including particle number, size, and aspect ratio using machine learning image segmentation. Under oxidizing conditions, we observe not only a decrease in the number of metal particles and

an increase in average size but also a decrease in the surface area to volume ratio. Some of the metal that had dissolved into the support can be regenerated and reappear back on the catalyst support surface under reducing conditions. Real-time observation of particles during separate oxidation and reduction processes provides nanometer-scale structural details of supported Pt/Pd particles at intermediate states not observable through typical *ex-situ* experiments. These observations represent a first step towards understanding how rapid cycling between oxidative and reductive catalytic operating conditions affects catalyst structure.

SESSION CT02.04: Crystal Growth and Particle Assembly Processes
Session Chairs: Qian Chen and Miaofang Chi
Sunday Afternoon, April 18, 2021
CT02

6:30 PM *CT02.04.01

Direct Imaging of Nanoparticle Superlattice Crystallization and Protein Fluctuation at the Nanoscale
Qian Chen; University of Illinois at Urbana-Champaign, United States

I will discuss my group's recent progress on capturing and understanding the intermediates and fluctuation dynamics at the nanometer resolution using liquid-phase TEM. The specific systems concern the nucleation and growth pathways of nanosized colloids into superlattices and moving membrane proteins in their native lipid and liquid environment. We find that prenucleation precursors and a layer-by-layer growth mode exist universally in diverse nanoparticle shapes. Single particle tracking, machine learning and simulations combined unravel the energetic and kinetic characteristics generic to the unexplored nanoscale, enabling advanced crystal engineering. For membrane proteins, we find that they exhibit real-time "fingering" fluctuations, which we attribute to dynamic rearrangement of lipid molecules wrapping the proteins. The conformational coordinates of protein transformation obtained from the real-space movies are used as inputs in our molecular dynamics simulations, to verify the driving force underpinning the function-relevant fluctuation dynamics. This platform invites an emergent theme of structural biophysics as we foresee.

6:55 PM CT02.04.02

Self-Assembled Nanoparticle Superlattices with Size-Dependent Reconfiguration Chang Qian¹, Binbin Luo¹, Ethan Stanifer², Xiaoming Mao² and Qian Chen^{1,1}; ¹University of Illinois at Urbana-Champaign, United States; ²University of Michigan–Ann Arbor, United States

We use liquid-phase transmission electron microscopy (TEM) to study the self-assembly of charged gold nanocubes, which showed a unique reconfigurable superlattice. The lattice can adopt two different states with same energy but different orientations, and our analysis showed the size-dependence of this reconfiguration process. Combining interaction modeling with simulation, we revealed the entropic nature of reconfiguration which dampens reconfiguration as the crystal size increases. We expect this tunable reconfiguration behavior to shed light on the design of responsive mechanical metamaterial.

7:10 PM CT02.04.03

Aqueous Dynamic Molecular and Particular Assembly of Amphiphilic Block Copolymer Visualized by *In Situ* LP-TEM Junho Hwang, Jun Hwa Hwang and Eunji Lee; Gwangju Institute of Science and Technology, Korea (the Republic of)

The self-assembly structure of a general amphiphilic block copolymer is carried out by direct dissolution into a selective solvent or through the gradual exchange from common solvents to selective solvent for one block. In this process, the self-assembled structure was either dynamically equilibrated in a solvent to have the lowest free energy or kinetically trapped to exhibit a uniform morphology. In the case of kinetically trapped

assemblies, morphological reconstruction and dynamic deformation occurred, implying the possible Brownian motion-based particle growth by collision and fusion. The self-assembly accompanying the dynamic nanoscale process of these organic molecules has not been directly observed, and basic mechanisms such as fusion, fragmentation, and growth are still subject to much research. The block copolymer self-assembly used in this study is a crew-cut micelle, not a star-shape micelle, and it can be confirmed that the volume fraction due to the ratio of the block length is controlled and the self-assembly structure transitions. Here, using the amphiphilic block copolymer, the self-assembly behavior of nanoparticles in real-time according to the molecular weight of the block in an aqueous solution was to be observed using a transmission electron microscope(TEM) and the dynamic behavior of the nanostructure was quantitatively analyzed by multiple object tracking analysis. This study provides a useful strategy for observing mechanisms of amphiphilic block copolymer self-assembly and the growth behavior of organic molecules based on Brownian motion.

7:15 PM BREAK

7:20 PM *CT02.04.04

Capture the Moment of Nucleation from a Solution Using a Transmission Electron Microscope Yuki Kimura; Hokkaido University, Japan

Our goal is to clarify what happens immediately before and after a nucleation event and how the nucleation pathway is determined. In the last decade, in situ observations of the crystallization processes in a solution have been performed for several materials and non-classical nucleation pathways have been reported based on a liquid-cell transmission electron microscope (TEM). Examples include oriented attachment growth of nanocrystals [1], and two-step nucleation of calcium carbonate (CaCO₃) and lysozyme protein crystals from amorphous/dense liquid particles [2, 3]. The unidirectional formation and growth of particles triggered by electron irradiation has also been observed. However, it is still difficult to directly observe crystals that follows the classical nucleation: grow beyond a certain large critical nucleus after fluctuations due to the competition between attachment and detachment of growth units. The difficulty is originating from their nanometric scale, rapidity, stochastic nature, and less ability to control the solution environment. We may be able to observe a crystallization process in lower magnification condition.

Then, unfortunately, crystalline nuclei cannot be observed separately as well as a conventional optical microscope.

To overcome the difficulties of direct observation, we have tried several approaches based on machine learning. One is a real-time prediction/detection at the moments of nucleation and the other one is enhancing the contrast of live images under very weak electron intensity. Both have been achieved based on machine learning.

Real-time prediction allows us to notify a nucleus before growth and, therefore, enable to observe and magnify it from a very beginning of nucleation. Enhances the contrast of TEM images allow us to magnify the nucleus at a constant electron intensity. This does not eliminate the effect of the beam completely, but it does minimize the change of a solution condition at higher magnification conditions. These have been evaluated by several nucleation and growth experiments. In the presentation, I will introduce more about our recent challenges and recent result of the early stages of crystallization.

[1] D. Li et al., Science 336 (2012) 1014.

[2] M. H. Nielsen et al., Science 345 (2014) 1158.

[3] T. Yamazaki et al. PNAS 114 (2017) 2154.

7:45 PM CT02.04.05

Self-Similar Mesocrystals Form via Interface-Driven Nucleation and Assembly Guomin Zhu^{1,2}, Maria Sushko², John Loring², Benjamin A. Legg², Miao Song², Jennifer Solits², Kevin Rosso² and James J. De Yoreo^{1,2}; ¹University of Washington, United States; ²Pacific Northwest National Laboratory, United States

Crystallization by particle attachment (CPA), which is a common mechanism of colloidal crystallization resulting in hierarchical morphologies, has been both exploited to create nanomaterials with unique, emergent

properties and implicated in the development of complex mineral textures. Oriented attachment (OA), a form of CPA in which crystalline primary particles align and attach along specific crystallographic directions, produces structures — typically referred to as mesocrystals — that diffract like single crystals, even though the constituent particle domains are still discernable. While the existence of mesocrystals has been well documented in a wide range of crystal systems and individual particle attachment events have been directly visualized, the mechanism by which these seemingly random events lead to well-defined, self-similar morphologies remains a mystery, as does the role of organic ligands, which are ubiquitous in nanoparticle systems. Combining *in situ* liquid phase TEM at 80°C with “freeze-and-look” TEM using indexed grids, we tracked formation of hematite (Hm) mesocrystals in the presence of oxalate and interpreted the results using classical density functional theory. The results show that formation of isolated Hm particles rarely occurs. However, once formed, interfacial gradients created by hematite-bound oxalate drive new hematite particles to repeatedly nucleate about 2 nm away from the new interface and then immediately undergo OA. We suspect our discovery reveals a widespread phenomenon with significant implications both for synthesis of materials and for understanding mineralization in natural environments. In addition, our discovery on the phenomenon close to solid interface highlights the complexity of material/solution interface, which lays the grounds for future research on the chemical and structural nature of the material/solution interface.

8:00 PM CT02.04.06

Crystallization Kinetics of Phase Change Materials Using Complementary *In Situ* Microscopic

Techniques Victoria Bird¹, Khalid Hattar², David LaVan³, Izak McGieson¹, Joseph McKeown⁴, Bryan W. Reed⁵, Feng Yi³ and Melissa K. Santala¹; ¹Oregon State University, United States; ²Sandia National Laboratories, United States; ³National Institute for Standards and Technology, United States; ⁴Lawrence Livermore National Laboratory, United States; ⁵Integrated Dynamic Electron Solutions, Inc., United States

Phase change materials (PCMs) are semi-conducting alloys with distinct optical and electrical properties in the amorphous and crystalline phases that make them useful for memory applications. In memory devices, amorphous bits are crystallized in nanoseconds by either laser or Joule heating, but the amorphous phase must also be stable against crystallization for long-term data retention. Crystal growth rates relevant to memory devices span orders of magnitude and fundamental questions regarding PCM crystallization mechanisms remain open, partly due to the difficulty in measuring crystallization kinetics in certain temperature regimes.

Ag-In-doped Sb-Te (AIST) alloys are an important class of PCMs that have been widely studied. Experiments using time-resolved reflectivity [1] and ultra-fast differential scanning calorimetry [2] have broadened the temperature range for which the crystallization kinetics of AIST have been characterized, but these indirect methods of measuring crystal growth have not yet resolved the kinetic behavior just above the glass transition temperature, T_g , which is of especial interest in the characterization of glass-forming materials. Direct methods of measuring crystal growth using microscopic methods which could more completely characterize crystallization behavior have emerged in recent years.

In this presentation, the application of multiple imaging techniques used to directly quantify crystal growth rates in PCMs over a broad range of temperatures will be described, with a focus on recent experiments on an AIST alloy with a nominal composition of $\text{Ag}_3\text{In}_4\text{Sb}_{74}\text{Te}_{17}$. The measurable growth rates from the different techniques span from $\sim 10^{-9}$ to >10 m/s and the *in-situ* imaging techniques applied include optical microscopy, conventional transmission electron microscopy (TEM), and dynamic TEM, a photo-emission TEM technique with nanosecond-scale time resolution [3]. It will be shown that crystal growth just above T_g could be imaged during *in situ* TEM through the use of sub-framing and a high-frame-rate direct electron detection camera [4]. The use of complementary *in situ* experimental techniques allow the crystal growth rates to be mapped over a large temperature range and can give insights into the crystallization kinetics of PCMs. Challenges associated with integrating results from different microscopic techniques, the issues with the determination of temperature during *in situ* TEM experiments, and the incorporation of nanocalorimetry with simultaneous TEM imaging [5,6] during crystallization will be discussed.

References

- [1] M. Salinga *et al.* *Nat Comms* **4** (2013) 1.
- [2] J. Orava *et al.* *Adv Funct Mater* **25** (2015) 4851.
- [3] V.L. Bird *et al.* *Microsc Microanal*, **24(S1)** (2018) 1868.
- [4] B.W. Reed *et al.* *Microsc Microanal* **23(S1)** (2017), 84.
- [5] M.D. Grapes *et al.* *Rev Sci Instrum* **85** (2014) 084902
- [6] M.D. Grapes *et al.* *Thermochimica Acta* 658 (2017) 72.

SESSION CT02.05: Materials Processing
Session Chairs: Madeline Dukes and Biao Jin
Sunday Afternoon, April 18, 2021
CT02

9:00 PM *CT02.05.01

***In Situ* and *Operando* Atomic Level Observation of Fluxional Behavior at Surface Sites In Ceria-Based Catalytic Systems** Joshua Vincent, Ramon Manzorro and Peter A. Crozier; Arizona State University, United States

The oxygen exchange and storage capacity of CeO₂ make it a common component in oxidation and reduction catalysts, with a wide range of applications such as automotive three-way catalysts, reforming, and fuel cells. These catalytic systems are typically based on a highly dispersed metal phase supported on CeO₂ nanoparticles, either pure or doped. In many cases, the fundamental catalytic mechanism usually involves reactant activation on the metallic component and oxygen transfer at or near the three-phase boundary that exists between the metal, oxide and gas phases. In the so-called Mars-van Krevelen type process, the reducible oxide support plays a key role by serving as a buffer to store and release oxygen to the reactant intermediates on the surface. The oxygen exchange process involves creation and annihilation of oxygen vacancies on the surface. Modelling with density functional theory suggests that the oxygen vacancy formation energy varies considerably depending on the characteristics of the surface site. To investigate the potential impact of surface heterogeneity during oxygen exchange, we have developed an *in situ* electron microscopy approach that allows us to directly observe the dynamic creation and annihilation of oxygen vacancies on CeO₂ surfaces and structural changes in Pt nanoparticles. We have employed this technique to explore the variation of lattice oxygen exchange with surface structural features such as nanofacets, step sites, adatom location and strain. In metal/oxide systems, the metal-support interface may be destabilized by these oxygen exchange events, giving rise to a surface that is constantly restructuring or fluxional behavior during catalysis. This presentation will discuss TEM based effort to determine in the oxygen exchange rate at different locations on CeO₂ nanoparticle surfaces and also at the metal/oxide interface of Pt/CeO₂ catalysts observed under *operando* conditions.

We gratefully acknowledge support of NSF grant NSF DMR (1840841, 1308085), CBET-1604971 and OAC-1940263.

9:25 PM CT02.05.02

Time Resolved Reflectometry With Pulsed Laser Melting of Implant Amorphized Si_{1-x}Ge_x Thin Films Jesse A. Johnson¹, Chris Hatem², Bruce Adams², Xuebin Li², David Brown^{3,1} and Kevin S. Jones¹; ¹University of Florida, United States; ²Applied Materials, Inc., United States; ³Air Force Research Laboratory, United States

Nanosecond pulsed laser melting using a frequency doubled Nd:YAG laser ($\lambda = 532$ nm) was performed on implant amorphized Si and Si_{1-x}Ge_x thin films. Undoped pseudomorphic Si_{1-x}Ge_x thin films were grown to a thickness of 40 nm on (100) Si wafers and Ge⁺ implants produced ~20 nm amorphous layers. The dynamic evolution of the single pulse laser melt process was probed in detail by using *in situ* time resolved reflectometry

(TRR) covering the sub-melt, partial and full amorphous melt, to full epi-layer melt regimes. TRR spectra were correlated as a function of energy density and Ge concentration with corresponding post-irradiation cross sectional TEM micrographs. It was shown that the resolution of the amorphous to crystalline conversion based on reflectivity differences allowed for the distinction between solid phase and liquid phase epitaxy regimes. Additionally, detection of the melt phase increased in sensitivity with increasing Ge concentration. Recovering the damage of implanted $\text{Si}_{1-x}\text{Ge}_x$ is a crucial step in CMOS manufacturing, and the metastable microstructures produced by pulsed laser melting of $\text{Si}_{1-x}\text{Ge}_x$ may be of interest for source/drain contact and channel strain engineering applications.

9:40 PM BREAK

9:45 PM CT02.05.03

Shining New Light on Perovskite Precursor Inks with Cryo-Electron Microscopy Nikita Dutta, Nakita Noel and Craig Arnold; Princeton University, United States

Lead halide perovskites have attracted great interest in recent years as promising materials for optoelectronics. Their ability to be solution processed is central to this interest, as it is a low-cost, scalable method with considerable flexibility. It has previously been observed that perovskite precursor inks are colloidal in nature, and that ink chemistry affects both the colloid distribution and the morphology of the deposited film. Yet, the mechanisms through which these effects arise are still poorly understood due in large part to the experimental difficulty of characterizing nanoscale colloids in solution. Here we demonstrate how cryo-electron microscopy can be used to overcome this challenge, presenting results from an interdisciplinary suite of methods that includes electron diffraction of vitrified inks and near-atomic resolution single particle averaging. Our results reveal for the first time that colloids in prototypical inks consist of a crystalline precursor phase, distinct from any of the starting materials. This shines light into the black box of perovskite solution processing and will ultimately enable better control of film morphology and optoelectronic properties.

10:00 PM CT02.05.04

Liquid-Liquid Phase Separation of CaCO_3 Revealed by *In Situ* Transmission Electron Microscopy Biao Jin¹, Harley Pyles², Ying Chen¹, Benjamin A. Legg¹, David Baker² and James J. De Yoreo^{1,2}; ¹Pacific Northwest National Laboratory, United States; ²University of Washington, United States

The nucleation of solids plays an important role in crystallization applications. Various intermediates have been proposed, including a dense liquid phase formed via liquid-liquid phase separation, but little is known about the occurrence of liquid-liquid phase separations at the nanoscale and the evolution of the dense liquid phase into a solid phase. Herein, taking CaCO_3 as a model system, our *in situ* liquid cell transmission electron microscopy directly shows that the dense liquid phase first appears from highly supersaturated solution in the presence of proteins as a stabilizer, which has also been demonstrated by *in situ* liquid NMR and ATR-FTIR results. By analyzing the behavior of coalescing droplets, it is found that the dense liquid phase may be a high viscosity fluid. In addition, when highly charged proteins are added, a network of the dense liquid phase forms, reminiscent of spinodal patterns in polymer melts near the interior of a spinodal. Subsequent dehydration of liquid droplets drives the formation of less hydrated amorphous calcium carbonate. This direct observation of dense liquid phase formation dynamics helps provide an in-depth understanding of the liquid-liquid phase separation mediated nucleation model.

10:15 PM CT02.05.05

Photoluminescence Mapping and Time-Domain Thermo-Photoluminescence for Rapid Imaging and Measurement of Thermal Conductivity of Boron Arsenide Shuai Yue^{1,2}, Geethal Amila Gamage², Mohammadjavad Mohebinia², David Mayerich², Vishal Talari², Yu Deng², Fei Tian², Shenyu Dai^{3,2}, Haoran Sun², Viktor G. Hadjiev², Wei Zhang⁴, Guoying Feng³, Jonathan Hu⁴, Dong Liu², Zhiming Wang¹, Zhifeng Ren² and Jiming Bao^{2,2}; ¹University of Electronic Science and Technology of China, China; ²University of Houston, United States; ³Sichuan University, China; ⁴Baylor University, United States

Cubic boron arsenide (BAs) is attracting greater attention owing to the recent experimental demonstration of ultrahigh thermal conductivity κ higher than 1000 W/m•K. However, its bandgap has not been settled and a simple yet effective method to probe its crystal quality is missing. Furthermore, traditional κ measurement methods are destructive and time-consuming, thus they cannot meet the urgent demand for fast screening of high κ materials. After we experimentally established 1.82 eV as the indirect bandgap of BAs and observed room-temperature band-edge photoluminescence, we developed two new optical techniques that can provide rapid and non-destructive characterization of κ with little sample preparation: photoluminescence mapping (PL-mapping) and time-domain thermo-photoluminescence (TDTP). PL-mapping provides a nearly real-time image of crystal quality and κ over mm-sized crystal surfaces; while TDTP allows us to pick up any spot on the sample surface and measure its κ using nanosecond laser pulses. These new techniques reveal that the apparent single crystals are not only nonuniform in κ but also are made of domains of very distinct κ . Because PL-mapping and TDTP are based on the band-edge PL and its dependence on temperature, they can be applied to other semiconductors, thus paving the way for rapid identification and development of high- κ semiconducting materials.

SESSION CT02.06: On-demand
Wednesday Morning, April 14, 2021
CT02

8:00 AM CT02.06.01

Structural and Chemical Analysis of Electrochemical AgAu De-Alloying at the Atomic Scale Through *In Situ* Transmission Electron Microscopy Rui Filipe Serra Maia and Eric A. Stach; University of Pennsylvania, United States

Nanoporous gold obtained through gold-silver dealloying exhibits unparalleled performance in catalysis, sensing, and battery electrodes¹⁻³. For example, combining metal oxides with nanoporous gold enables highly reversible cathodic reactions with significantly lower overpotentials than state-of-the-art electrodes for lithium-ion batteries⁴. The functionality and performance of nanoporous gold varies strongly with the synthesis conditions¹. However, the relationship between synthesis conditions and the final product's structural and morphological properties is still poorly understood. This is because it is difficult to obtain a time-resolved analysis of the dealloying process in real-world conditions^{5,6}.

We performed *in situ* liquid-phase Scanning/Transmission Electron Microscopy (S/TEM) to obtain a time-resolved analysis of the structure and chemistry of AuAg at the atomic scale during electrochemical dealloying at variable electrochemical and hydrodynamic conditions. The results indicate that pore formation occurs through a priming step of phase separation, where silver and gold form intertwined but separated domains and dealloying then proceeds through silver dissolution. The dealloying process is surface limited, and for that reason, thinner areas de-alloy faster than thicker ones. These results suggest that the previously observed inverse correlation between electrochemical overpotential and pore sizes is caused by an initiation of the second step before phase separation is complete when the separated domains are not fully developed. These insights allow direct correlations between processing parameters and the final properties, enabling rational optimization of properties such as crystallite size, grain boundary density and edge/terrace ratio for various technologic applications.

References

1. Seker, E., Reed, M. L. & Begley, M. R. Nanoporous gold: fabrication, characterization, and applications. *Materials (Basel)*. **2**, 2188–2215 (2009).
2. Wittstock, A., Biener, J. & Bäumer, M. Nanoporous gold: a new material for catalytic and sensor

applications. *Phys. Chem. Chem. Phys.* **12**, 12919–12930 (2010).

3. Kim, S. H. Nanoporous gold: Preparation and applications to catalysis and sensors. *Curr. Appl. Phys.* **18**, 810–818 (2018).

4. Chen, L. Y. *et al.* Nanoporous metal/oxide hybrid materials for rechargeable lithium–oxygen batteries. *J. Mater. Chem. A* **3**, 3620–3626 (2015).

5. de Jonge, N. Theory of the spatial resolution of (scanning) transmission electron microscopy in liquid water or ice layers. *Ultramicroscopy* **187**, 113–125 (2018).

6. Jungjohann, K., Evans, J., Aguiar, J., Arslan, I. & Browning, N. Atomic-Scale Imaging and Spectroscopy for In Situ Liquid Scanning Transmission Electron Microscopy. *Microsc. Microanal.* **18**, 621–627 (2012).

SYMPOSIUM CT03

Imaging Materials with X-Rays—Recent Advances with Synchrotron and Laboratory Sources
April 14 - April 20, 2021

Symposium Organizers

Arief Budiman, BINUS University
Margaret Murnane, University of Colorado Boulder
Olivier Thomas, Aix Marseille Universite
Ehrenfried Zschech, Fraunhofer IKTS

* Invited Paper

SESSION CT03.01: Coherent Diffraction Imaging
Session Chairs: Olivier Thomas and Ehrenfried Zschech
Monday Morning, April 19, 2021
CT03

8:00 AM INTRODUCTORY COMMENTS

8:05 AM *CT03.01.01

***In Situ* Coherent X-Ray Diffraction Imaging During the Catalytic Process** Hyunjung Kim; Sogang University, Korea (the Republic of)

Understanding structural changes in the atomic scale during the catalytic reaction process is crucial for revealing underlying mechanisms. However, it remains challenging to characterize the strain and defect evolution for a single nanocrystal catalyst in situ. Bragg coherent diffraction imaging (BCDI) is a powerful tool for investigating structural changes inside the nanoparticle in-situ in a non-destructive way. In my talk, I show how the atomic level of interaction of reactants affects the nanoparticles as strain-induced and the defect dynamics during the catalytic process by exploiting the merits of BCDI.

This work was supported by the National Research Foundation of Korea (NRF-2015R1A5A1009962 and NRF-2019R1A6B2A02100883) and Samsung Electronics..

8:30 AM *CT03.01.02

***In Situ* Structural Evolution of Model Catalysts Imaged by Bragg Coherent X-Ray Diffraction** Marie-

Ingrid Richard^{1,2}, Maxime Dupraz^{1,2}, Ni Li^{1,2}, Jerome Carnis^{3,2,4}, L. Wu^{2,3}, Stephane Labat³, Steven Leake², L. Gao⁵, J.P. Hofmann⁵, S. Fernández^{2,3}, M. Sprung⁴, A. Resta⁶, Tobias Schulli², E.J.M. Hensen⁵ and Olivier Thomas³; ¹Univ. Grenoble Alpes, CEA Grenoble, IRIG/MEM/NRS, France; ²The European Synchrotron, France; ³Aix Marseille Université, CNRS, Université de Toulon, France; ⁴PETRA III, Deutsches Elektronen-Synchrotron (DESY), Germany; ⁵Technische Universiteit Eindhoven, Netherlands; ⁶Synchrotron SOLEIL, France

Characterising the structural properties (strain gradients, chemical composition, crystal orientation and defects) inside nanostructures is a grand challenge in materials science. Bragg coherent diffraction imaging (Bragg CDI) can be utilised to address this challenge for crystalline nanostructures. A resolution of the structural properties of less than 10 nm is achieved up-to-date [1,2]. The capabilities of the Bragg CDI technique will be demonstrated on single nanoparticles for enhanced catalysis.

As an example, the Bragg CDI technique [3,4] allows understanding the interplay between shape, size, strain, faceting [5], composition and defects at the nanoscale. We will demonstrate that Bragg CDI on a single particle model catalyst makes it possible to map its local strain/defect field and directly image strain build-up close to the facets. We will also show results obtained during *in situ* [6,7] and *operando* Bragg CDI measurements: it was possible to track a single particle in gas or liquid phase environments to monitor its facet changes and to measure its strain/defect response to reaction.

This technique opens pathways to determine and control the internal structure of nanoparticles to tune and optimise them during catalytic and other chemical reactions. This technique should benefit from a unique opportunity: the ESRF EBS Upgrade. This should revolutionise imaging by making it possible to map evolving physico-chemical processes in a slow-motion movie.

- [1] S. Labat, M.-I. Richard, M. Dupraz, M. Gailhanou, G. Beutier, M. Verdier, F. Mastropietro, T. W. Cornelius, T. U. Schüllli, J. Eymery, and O. Thomas, *Inversion Domain Boundaries in GaN Wires Revealed by Coherent Bragg Imaging*, ACS Nano **9**, 9210 (2015).
- [2] N. Li, S. Labat, S. J. Leake, M. Dupraz, J. Carnis, T. W. Cornelius, G. Beutier, M. Verdier, V. Favre-Nicolin, T. U. Schüllli, O. Thomas, J. Eymery, and M.-I. Richard, *Mapping Inversion Domain Boundaries along Single GaN Wires with Bragg Coherent X-Ray Imaging*, ACS Nano **14**, 10305 (2020).
- [3] J. Carnis, L. Gao, S. Labat, Y. Y. Kim, J. P. Hofmann, S. J. Leake, T. U. Schüllli, E. J. M. Hensen, O. Thomas, and M.-I. Richard, *Towards a Quantitative Determination of Strain in Bragg Coherent X-Ray Diffraction Imaging: Artefacts and Sign Convention in Reconstructions*, Sci Rep **9**, 1 (2019).
- [4] N. Li, M. Dupraz, L. Wu, S. J. Leake, A. Resta, J. Carnis, S. Labat, E. Almog, E. Rabkin, V. Favre-Nicolin, F.-E. Picca, F. Berenguer, R. van de Poll, J. P. Hofmann, A. Vlad, O. Thomas, Y. Garreau, A. Coati, and M.-I. Richard, *Continuous Scanning for Bragg Coherent X-Ray Imaging*, Sci Rep **10**, 12760 (2020).
- [5] M.-I. Richard, S. Fernández, J. Eymery, J. P. Hofmann, L. Gao, J. Carnis, S. Labat, V. Favre-Nicolin, E. J. M. Hensen, O. Thomas, T. U. Schüllli, and S. J. Leake, *Crystallographic Orientation of Facets and Planar Defects in Functional Nanostructures Elucidated by Nano-Focused Coherent Diffractive X-Ray Imaging*, Nanoscale **10**, 4833 (2018).
- [6] M.-I. Richard, S. Fernández, J. P. Hofmann, L. Gao, G. A. Chahine, S. J. Leake, H. Djazouli, Y. De Bortoli, L. Petit, P. Boesecke, S. Labat, E. J. M. Hensen, O. Thomas, and T. Schüllli, *Reactor for Nano-Focused x-Ray Diffraction and Imaging under Catalytic in Situ Conditions*, Review of Scientific Instruments **88**, 093902 (2017).
- [7] S. Fernández, L. Gao, J. P. Hofmann, J. Carnis, S. Labat, G. A. Chahine, A. J. F. van Hoof, M. W. G. M. (Tiny) Verhoeven, T. U. Schüllli, E. J. M. Hensen, O. Thomas, and M.-I. Richard, *In Situ Structural Evolution of Single Particle Model Catalysts under Ambient Pressure Reaction Conditions*, Nanoscale **11**, 331 (2019).

8:55 AM CT03.01.03

Late News: Three-Dimensional Coherent X-Ray Imaging of Ferroelastic Domains in CsPbBr₃ Perovskite

Nanoparticles Dmitry Dzhigaev¹, Zhaojun Zhang¹, Lucas Marcal¹, Simone Sala², Alexander Björling², Anders Mikkelsen¹ and Jesper Wallentin¹; ¹Lund University, Sweden; ²MAX IV, Sweden

Halide perovskites attract significant interest due to their remarkable performance in solar cells. However, the gap in understanding of the relationship between their nanoscale structure and properties limits their application towards novel devices. Here we present a direct 3D imaging of twinned ferroelastic domains in single 500-nm CsPbBr₃ particles using Bragg Coherent X-ray Diffractive Imaging (BCDI) at sub-60 nm resolution. A preferential double-domain structure is revealed in several identical particles, with one (110)-oriented and one (002)-oriented domain and a similar domain volume ratio of 1:2.5. The domains exhibit a difference in lattice tilt of 0.59 degrees, in excellent agreement with calculations based on the lattice mismatch. The results in this work provide important insights both for the fundamental understanding of these materials and for the performance improvement of perovskite-based devices.

9:10 AM *CT03.01.04

Development of *In Situ* Broadband Laue Microdiffraction for Determination Crystallographic Orientation at the 34-ID-C Bragg Coherent Diffraction Imaging Instrument of the APS Ross Harder; Argonne National Laboratory, United States

Measurement of Bragg coherent diffraction imaging (BCDI) data relies on finding a Bragg diffraction signal from a single nanoscale crystal object. Often the object of interest can have unknown orientation in the sample or be one of many crystallites in a polycrystalline sample. In addition, even when a single Bragg reflection is found, the full crystallographic orientation remains unknown, and thus finding other Bragg reflections from the identical crystal becomes time-consuming or impossible.

In this talk, the commissioning of a movable double-bounce Si (111) monochromator at the 34-ID-C end station of the Advanced Photon Source will be described. The resulting capability aims at delivering multi-reflection BCDI as a standard tool in a single beamline instrument. The upgraded instrument enables, through rapid switching from monochromatic to broadband (pink) beam, the use of Laue diffraction to determine crystal orientation. With a proper orientation matrix determined for the lattice of a specific crystal, one can measure coherent diffraction patterns near multiple Bragg reflections, thus providing enough information to image the full strain tensor in 3D at the nanoscale. The design, concept of operation, the developed procedures for indexing Laue patterns, as well as automated measurement of Bragg coherent diffraction data from multiple reflections of the same nanocrystal will be presented. In addition, recent advances in identifying single grains of interest in a polycrystalline sample will be described.

9:35 AM *CT03.01.05

X-Ray Linear Dichroic Ptychography Jianwei (John) Miao¹, Yuan Hung Lo¹, Jihan Zhou¹, Arjun Rana¹, Drew Morrill², Christian Gentry², Bjoern Enders³, Young-Sang Yu³, Chang-Yu Sun⁴, David Shapiro³, Roger Falcone³, Henry Kapteyn², Margaret Murnane² and Pupa Gilbert⁴; ¹University of California, Los Angeles, United States; ²University of Colorado Boulder, United States; ³Lawrence Berkeley National Laboratory, United States; ⁴University of Wisconsin–Madison, United States

Ptychography, a powerful scanning coherent diffractive imaging technique, has attracted significant attention for its general applicability. Here we experimentally demonstrate x-ray linear dichroic ptychography for the first time and map the *c*-axis orientations of the aragonite (CaCO₃) crystal. Linear dichroic phase imaging at the oxygen K-edge energy shows strong polarization-dependent contrast and reveals the presence of both narrow (<35°) and wide (>35°) *c*-axis angular spread in the coral samples. These x-ray ptychography results are corroborated by 4D scanning transmission electron microscopy (STEM) on the same samples. Evidence of co-oriented but disconnected corallite sub-domains indicates jagged crystal boundaries consistent with formation by amorphous nanoparticle attachment. We expect that the combination of x-ray linear dichroic ptychography and 4D STEM could be an important multimodal tool to study nano-crystallites, interfaces, nucleation and mineral growth of optically anisotropic materials at multiple length scales.

SESSION CT03.02: Spectroscopy
Session Chairs: Arief Budiman, Margaret Murnane and Olivier Thomas
Monday Morning, April 19, 2021
CT03

10:30 AM *CT03.02.01

Correlative Multi-Modal 3D Imaging of Topologically Non-Trivial Magnetic Textures Emma M. Cating¹, Arjun Rana², Chen-Ting Liao¹, Yuan Hung Lo², Charles Bevis¹, Peter Johnsen¹, Sinead Ryan¹, Robert Karl¹, Xingyuan Lu², Christian Gentry¹, Michael Tanksalvala¹, Yuka Esashi¹, Bin Wang¹, John Badding³, Jianwei (John) Miao², Henry Kapteyn¹ and Margaret Murnane¹; ¹University of Colorado Boulder, United States; ²University of California, Los Angeles, United States; ³The Pennsylvania State University, United States

Understanding the structure and dynamics of spin textures in magnetic materials on the scale of the magnetic exchange interaction is both a question of fundamental physics and at the forefront of developing quantum technologies. Topologically stabilized magnetic textures such as skyrmions and the direct light-induced manipulation of spins hold promise for spintronics, low-energy data transport, and memory. However, because of their small size and low contrast, intricate nanoscale magnetic textures have proven difficult to image directly in 3D without prior knowledge of the sample.

Correlative multi-modal spectro-microscopy using complementary nanoscale imaging techniques and extreme ultraviolet and x-ray spectroscopies at both tabletop and facility scale provides access to a more complete range of elemental, chemical, electronic, magnetic, and structural and dynamic properties of complex samples. Resonant x-ray magnetic circular dichroism (XMCD) provides element-specific magnetic sensitivity; ptychography yields diffraction-limited images with phase contrast, ideal for low-contrast materials; time-resolved extreme UV (EUV) spectroscopies can capture new light-induced spin excitations; and x-ray reflectometry can image buried layers with sub-nm depth resolution. By combining these techniques, we are able to uncover new materials function and comprehensively characterize complex nanostructured, layered, and heterogeneous samples.

10:55 AM *CT03.02.02

Hyperspectral Imaging with Quick-XAS: Combining Micrometric Spatial- and Second Time-Resolutions with X-Ray Absorption Spectroscopy Camille La Fontaine, Olga Roudenko, Stéphanie Belin, Laurent Barthe and Valérie Briois; SOLEIL Synchrotron, France

X-ray Absorption Spectroscopy (XAS) is among the techniques widely employed to characterize materials providing atomic selective information on the materials structure and chemical speciation. Since the advent of 3rd generation synchrotron radiation facilities, a high photon flux is achieved at XAS beamlines which permits fast measurements and thus time-resolved monitoring of evolutionary processes. A wide range of materials science topics has taken advantage of this breakthrough (e.g. catalysis, energy storage, materials synthesis) through *in situ* and *operando* approaches. In order to access to a deeper and more accurate temporal description of the processes, multivariate data analysis is now commonly employed and provides spectra of the pure chemical species together with their concentration profiles.

Nevertheless, time-resolved XAS data are generally collected as macroscopic information related to the fraction of sample exposed to X-rays. At specialized beamlines, spatial resolution can be achieved using micro- or nano-focused beam while scanning the sample but with increased collection times. Alternatively, full-field sample illumination collected by a 2D detector can provide both spatial and time resolutions. Recent developments have been conducted at the ROCK beamline of SOLEIL synchrotron to allow time-resolved hyperspectral full-field X-ray imaging with XAS information.

ROCK is a XAS beamline tailored for *in situ* and *operando* investigations in the 4 to 40 keV energy range using Quick-EXAFS monochromators to achieve sub-second time resolution for macroscopic measurements. Hyperspectral full-field X-ray imaging experiments are operated at the beamline in transmission by collecting the visible light emitted from a thin scintillator imaging the sample absorption by a pixelated detector (ORCA Flash 4.0 V3 CMOS camera, Hamamatsu). Depending on the objective mounted on the camera, the pixel size and field of view (FoV) range from 0.65 μm to 1.625 μm and 1.3 mm to 3.3 mm, respectively, with a resolution of ca. 5 μm . Images at different energies of the XAS spectrum (typically ~ 600 images) are collected with an exposure time of 5 ms during the Quick-EXAFS monochromator energy scan yielding to one complete hyperspectral dataset every 10 s. XAS spectra can then be reconstructed on individual or binned pixels to improve the signal-to-noise (S/N) ratio when necessary. A specificity of ROCK is its versatile beam size from 0.4 to ~ 4 mm while keeping constant the flux delivered by the optics. Thus the beam size on the sample can be optimized considering the nature and size of the sample, the FoV and the S/N ratio of reconstructed spectra. Selected examples of studies using the methodology implemented at ROCK beamline will be presented in the field of pressure-induced spin transition, regeneration of heterogeneous catalysis, and cycling of Li-ion batteries. These examples illustrate the great potential of time-resolved XAS hyperspectral imaging and the gain obtained in comparison with macroscopic information for identifying potential dynamic heterogeneous behavior of materials.

Acknowledgment: The ROCK beamline construction and operation (2011-2019) were supported by a public grant overseen by the French National Research Agency (ANR) as part of the "Investissements d'Avenir" program (ref: ANR-10-EQPX-45).

11:20 AM CT03.02.03

Nanoscale Crystal Strain and Oxidation State Mapping of Primary $\text{LiNi}_{0.33}\text{Mn}_{0.33}\text{Co}_{0.33}\text{O}_2$ Particles

William Judge¹, Jordi Cabana¹, Martin Holt², Zhonghou Cai² and Brian May¹; ¹University of Illinois at Chicago, United States; ²Argonne National Laboratory, United States

Global concerns over the consistent consumption of finite fossil fuel stores have called for a transition to renewable energy sources. A significant stepping stone in completing this movement relies on the safety and reliability of energy storage technologies. Revolutionizing the industry John Goodenough, Stan Wittingham, and Akira Yoshinos were all critical of the development in current Lithium-Ion battery energy storage. However, their efforts are not without need of improvements. Sub-optimal reliability is caused by prevalent capacity fade at moderate working potentials. For global adoption in heavy uses cases (EV, power grid storage, etc.) this must be remedied. Degradation of the cathode material is narrowed down to three main categories; structural/chemical strain, electrolyte decomposition, and increase of surface-electrolyte interfaces. Narrowing these options, my focus is on cathode material strain characterization, both structural and chemical, at the nano-scale through the use of multiple techniques.

Well characterized, relevant $\text{LiNi}_{0.33}\text{Mn}_{0.33}\text{Co}_{0.33}\text{O}_2$ (LiNMC) material was chosen as an agent for nano-characterization. Ptychographic analysis methods with a resolution of 5 nm has been implemented in mapping transition metal oxidation states of a single particle for various states of charge. Further, lattice strain analysis has been carried out through the application of Scanning X-Ray Diffraction Microscopy. With a resolution of 30 nm, spatially resolving crystallographic spacing's for Pristine, Charged (to 4.75V), Discharged (to 2.7V) material was achieved. It was determined most point defect upon cycling effect primarily the chi regime of the diffraction patterns. Heterogeneities in both regards have given insight into degradation pathways for the LiNMC material.

11:35 AM DISCUSSION TIME

12:00 PM CT03.02.05

Micro X-Ray Fluorescence Microscopy as a Tool to Study Moisture-Dependent Inorganic Ion Diffusion in Individual Wood Cell Wall Layers Joseph Jakes; USDA Forest Service, Forest Products Laboratory,

The diffusion of chemicals and inorganic ions through wood cell walls is a critical process in nearly all woody biomass applications, including biorefineries, wood-based building materials, green electronics, and even as bioinspiration for new smart materials. Despite the near ubiquitous importance of intra-cell wall diffusion, the poorly understood diffusion mechanisms and rates are hindering progress. In this work, a new experimental methodology utilizing synchrotron-based X-ray fluorescence microscopy (XFM) was developed to study inorganic ion diffusion at submicron length scales in individual wood cell wall layers. Using a custom-built in situ relative humidity (RH) chamber, it was discovered that deposited K, Cu, Zn, and Cl ions only diffuse when the humidity is above 60% RH. Additionally, time-lapse XFM imaging was used to measure the time-dependent concentration profiles of implanted K, Cu, and Cl ions diffusing through cell wall layers. Time-lapse XFM imaging was performed at 70, 75, or 80% RH. Diffusion constants were calculated from the time-dependent concentration profiles using an analytical model developed based on Fick's second law for diffusion. Results revealed that diffusion rates increased with RH, the larger Cu ion diffused slower than the K ion, and the Cl ion diffusion constant was the same as the counter cation, indicating ions diffused together to maintain charge neutrality. The results also improve the understanding of the diffusion mechanisms. It is now understood that diffusion occurs via interconnecting pathways of rubbery amorphous polysaccharides, which contrasts the nearly century-old assumption of intra-cell wall transport occurring through interconnecting water pathways. With these new insights, researchers can now utilize polymer science approaches to engineer the molecular architecture of lignocellulosic biomass to optimize properties for specific end uses.

12:15 PM CT03.02.06

Non-Destructive Characterization of 3D Nanostructures via EUV Coherent Diffractive Imaging

Reflectometry—High-Resolution, Chemically Specific, Interface-Sensitive Maps [Michael Tanksalvala](#)¹, Christina Porter¹, Yuka Esashi¹, Nicholas W. Jenkins¹, Zhe Zhang¹, Naoto Horiguchi², Sadegh Yazdi¹, Jihan Zhou³, Michael Gerrity¹, Jianwei (John) Miao³, David Ren⁴, Laura Waller⁴, Henry Kapteyn^{1,5} and Margaret Murnane¹; ¹University of Colorado Boulder, United States; ²imec, Belgium; ³University of California, Los Angeles, United States; ⁴University of California, Berkeley, United States; ⁵KMLabs Inc., United States

The development and integration of next-generation nano and quantum devices is approaching a significant metrology hurdle. This is because nanoscale functional properties are no longer well-described by macroscopic models and can become almost entirely geometry- or interface-dominated. Moreover, the transport across interfaces (i.e. charge, spin and heat transport) impact various device properties, such as the switching energy of magnetic memory or the coherence time of quantum devices. This transport is difficult to measure and its in-situ measurement in working devices will be critical to further understanding and optimizing their synthesis and integration. Thus, there is a great need for non-destructive, non-contact imaging techniques applicable to general samples.

There exist many techniques for nano-characterization; however, most are destructive to the sample or insensitive to depth or composition. Milling techniques like secondary-ion mass spectroscopy (SIMS) and auger electron spectroscopy (AES) can determine the chemical composition through the sample's depth, but have a spatial resolution limited by the spot size of the milling beam, and destroy the sample in order to measure it. On the other hand, techniques based on transmission electron microscope (TEM) — such as energy-dispersive x-ray spectroscopy (EDS) or high-angle annular dark-field imaging (HAADF) — can measure composition or structure with atomic resolution, but require the sample to be extremely thin, and often require complex and destructive sample preparation (e.g. FIB-excitation). Non-destructive techniques like atomic-force microscopy (AFM) and scanning-electron microscopy (SEM) can do high-resolution imaging, but lack quantitative depth- or chemical-sensitivity.

Photon-based techniques such as x-ray reflectivity (XRR) and x-ray diffraction (XRD) perform non-destructive measurements that are sensitive to composition, layer thicknesses, and interface quality by measuring the reflectivity as a function of incidence angle (aka reflectometry). However, since XRR and XRD use hard x-rays, they must operate within 1deg of grazing-incidence to get sufficient reflectivity, and the resulting on-sample focus size limits their resolution to $>1\mu\text{m}$.

Extreme ultraviolet light (EUV, wavelength ~10-100nm) has many unique advantages for sample characterization. Many absorption edges lie in this region of the spectrum, providing excellent composition-sensitivity. Unlike x-rays, EUV absorption depths are 10nm-1 μ m, enhancing the depth-sensitivity of reflectometry. This work combines EUV reflectometry with ptychographic coherent diffractive imaging (CDI) to demonstrate a unique non-destructive microscopy whose resolution approaches the diffraction limit. Furthermore, the quantitative phase information also given by ptychography, which traditional XRR cannot measure, is extremely sensitive to the sample's composition and structure.

We use this technique to investigate a sample fabricated by imec. The sample consists of Si₃N₄ structures on an As-doped Si substrate (5x10²⁰ atoms/cm³). We investigated our technique's sensitivity to composition, layer thickness, interface quality and dopant level and found, for several, it approached or exceeded other techniques, while remaining non-destructive and high-resolution.

This work demonstrates a general nanoimaging technique that promises to fill a current gap in sample metrology. Our technique combines the unique advantages of coherent EUV light with the composition- and interface sensitivity of XRR and XRD and the resolution-enhancement and quantitative phase information of ptychography. This technique enables non-destructive, large-area, quantitative, 3D imaging of nanostructures and their chemical makeup, layer thicknesses, interface quality and dopant levels, without special sample preparation.

This work was financially supported by NSF STROBE STC (DMR-1548924); DARPA STTR (W31P4Q-17-C-0104); DARPA PULSE (W31P4Q-13-1-0015).

12:20 PM CT03.02.07

On-Line Microfluidics XRF and FTIR Spectroscopy for Fast Exploration of Liquid/Liquid Extraction Thermodynamics Ange Maurice¹, Varun Rai¹, Asmae El-maangar², Johannes Theisen², Thomas Zemb² and Jean-Christophe Gabriel^{1,3}; ¹Nanyang Technological University, Singapore; ²ICSM, University Montpellier, France; ³Université Paris-Saclay, France

Liquid-Liquid extraction can be a complex chemical **purification** process involving many thermodynamic and kinetic parameters. For instance, the **recycling** industry has an incoming waste stream with high variability. Thus, they need to constantly adjust their processes to match the variation in chemical composition. There is a need for fast process development tools to study liquid-liquid extraction. In this regard, downscaling an extraction system in microfluidics can be more accurate, faster and safer due to fluids being more stable and controlled.

We report on newly developed microfluidic devices integrated with Fourier Transform Infrared Spectroscopy (FTIR) and X-ray fluorescence (XRF) [1, 2]. These tools are primarily aimed at studying **liquid/liquid extraction** processes. First, using FTIR characterization of the vapor pressure, we study the **chemical activity** of the solvents [3]. Second, we perform, for the first time, **on-line XRF** quantification of metals to monitor liquid-liquid extraction in **microfluidics**[4]. The measurement is automated and performed for both aqueous and organic phase. This approach allowed us to quickly study the variation of free energies of transfer for the extraction and reverse-extraction of three rare-earth elements at different temperatures. Overall, thanks to a fully automated approach, we show that thermodynamics and kinetics of extraction can be obtained in **less than 12 hours** with a resulting liquid waste of **less than 20mL**.

1. Maurice, A., J. Theisen, and J.-C.P. Gabriel, *Microfluidic lab-on-chip advances for liquid-liquid extraction process studies*. Current Opinion in Colloid & Interface Science, 2020. **46**: p. 20-35.

2. Theisen, J., et al., *Effects of porous media on extraction kinetics: Is the membrane really a limiting factor?* Journal of Membrane Science, 2019. **586**: p. 318-325.

3. Kokoric, V., et al., *Determining the Partial Pressure of Volatile Components via Substrate-Integrated Hollow Waveguide Infrared Spectroscopy with Integrated Microfluidics*. Analytical chemistry, 2018. **90**(7): p. 4445-4451.

4. Unpublished results

SESSION CT03.03: NanoXRD
Session Chairs: Olivier Thomas and Ehrenfried Zschech
Monday Afternoon, April 19, 2021
CT03

1:00 PM *CT03.03.01

Nanoscale Materials Characterization Capabilities at NSLS-II Yong S. Chu, Mingyuan Ge, Hanfei Yan, Huang Xiaojing, Xianghui Xiao, Ajith Pattammattel and Lee Wah-Keat; Brookhaven National Laboratory, United States

The NSLS-II has outstanding nanoscale x-ray imaging capabilities in the hard x-ray regime, enabling a broad range of scientific research. The transmission x-ray microscopy (TXM) method, offered at the Full-field X-ray Imaging (FXI) Beamline, has the world-leading morphological and spectroscopic imaging capabilities with spatial resolutions from 20-50 nm. This full-field imaging capability with unprecedented imaging throughput finds excellent application in visualizing 3D chemical transformation in complex materials under in-situ controls [1-2].

With the focus size down to 12 nm, the Hard X-ray Nanoprobe (HXN) offers simultaneous multimodal imaging capabilities, which are ideal for visualizing material heterogeneity or defects with outstanding detection sensitivities. Some of the recent scientific applications include fluorescence tomography [3], high-sensitivity oxidation-state imaging [4], and strain imaging [5]. Significant efforts are directed toward achieving sub-10 nm 3D imaging using ptychography and performing more comprehensive material analysis by utilizing both full-field and scanning imaging modalities. The presentation will describe the latest technical capabilities and their applications for solving scientific problems.

References

- [1] Zhengrui Xu et. al., "Charge distribution guided by grain crystallographic orientations in polycrystalline battery materials," *Nat. Commun.* **11** (1), ID(83) (2020). 10.1038/s41467-019-13884-x
- [2] Cheng-Hung Lin et. al., "Systems-level investigation of aqueous batteries for understanding the benefit of water-in-salt electrolyte by synchrotron nanoimaging." *Sci. Adv.* **6** (10), eaay7129 (2020). 10.1126/sciadv.aay7129
- [3] Tiffany W. Victor et. al., "Lanthanide-Binding Tags for 3D X-ray Imaging of Proteins in Cells at Nanoscale Resolution," *J. Am. Chem. Soc.* **142** (5), 2145-2149 (2020). 10.1021/jacs.9b11571
- [4] Ajith Pattammattel et. al., "High-sensitivity nanoscale chemical imaging with hard x-ray nano-XANES". *Sci. Adv.*, **6**(37), eabb3615 (2020). 10.1126/sciadv.abb3615
- [5] Yue Cao et. al., "Complete Strain Mapping of Nanosheets of Tantalum Disulfide," *ACS Appl. Mater. Interfaces* **12** (38), 43173-43179 (2020). <https://dx.doi.org/10.1021/acsami.0c06517>

1:25 PM CT03.03.02

X-Ray Nano-Diffraction of Extremely Bent Single Nanowires Ullrich Pietsch¹, Arman Davtyan¹, Dominik Kriegner², Vaclav Holy³, Ryan Lewis⁴ and Julian Müller¹; ¹University of Siegen, Germany; ²Technical University of Dresden, Germany; ³Charles University, Czechia; ⁴McMaster University, Canada

Core-shell nanowires (NWs) with asymmetric shells allow for strain engineering of NW properties because of the bending resulting from the lattice mismatch between core and shell material. For this study GaAs core NWs were grown by molecular beam epitaxy (MBE) onto an Si(111) substrate and $\text{In}_x\text{Al}_{(1-x)}\text{As}$ shells were preferentially grown onto one side of the core only, for example onto the

(100) plane. Besides electron microscopy the bending of NWs has been observed by X-ray diffraction analysis using a micro- and nanofocused beam. Respective measurements have been performed at beamlines ID1 of ESRF and P23 of PETRA III, respectively. A new scheme of data recording has been developed in order to determine bending radii and strains of NWs with different nominal bending radius. For data analysis a kinematical diffraction theory for highly bent crystals was developed and applied. The homogeneity of the bending and strain was studied along the growth axis of the NWs, and it was found that the lower parts, i.e. close to the substrate/wire interface, are bent less than the parts further up. Extreme bending radii down to about 3 micron did result in strain variation of about 5% in the NW core.

1:40 PM CT03.03.03

Nano X-Ray Diffraction Imaging of Strain-Engineered LaSrFeO₃ Across the Metal-Insulator Transition

Travis D. Frazer, Dina Sheyfer, Tao Zhou, Zhonghou Cai, Jianguo Wen, Yuzi Liu, Deshun Hong, Changjiang Liu, Anand Bhattacharya and Yue Cao; Argonne National Laboratory, United States

Strongly correlated materials exhibit interesting emergent behavior, such as high temperature superconductivity, colossal magnetoresistance and metal-insulator transitions (MIT) [1-3]. For perovskites, these exotic functional properties can be tuned via strain engineering [4,5] due to the strong coupling between the charge, spin, and lattice degrees of freedom. It is still not fully understood how these degrees of freedom interrelate to produce exotic states, and part of the complexity comes from spatial inhomogeneities on the nanometer scale [1]. Moreover, real material systems contain defects that can greatly influence their behavior, such as phase transitions being pinned to and nucleated at point defects. It is thus critical to characterize the electronic and structural evolutions of correlated materials at the nanoscale, through their relevant phase transitions. As part of this effort, we use nano x-ray diffraction (nano-XRD) to image strain and structural changes in La_{1/3}Sr_{2/3}FeO₃ (LSFO) across its MIT. LSFO has a concurrent metal-insulator phase transition involving the spin and charge orders, along with a structural component, according to past work [6]. We synthesize LSFO films on SrTiO₃ (001) and (111) substrates, where both samples exhibit a MIT, but with onset temperatures that differ by 20 K. Whether these LSFO films are identical to the bulk LSFO, the nature of the MIT, and the role of the lattice strain are not fully understood. Utilizing the 30 nm spatial resolution and 10⁻⁵ strain sensitivity of nano-XRD, we image the evolution of strain with temperature for LSFO on the (111) substrate. We find that LSFO on STO (111) has a smooth structural response through the MIT, in contrast with the relatively sharp onset of the charge order. This differs from the sample on the (001) substrate, where the exact same charge order parameter cannot be found. Moreover, using nano-XRD, we see evidence of structural heterogeneity and domain formation in the (111) sample that becomes more pronounced 50K below the MIT, without a corresponding change in the charge order. Our results on the strain and lattice changes across the MIT will directly inform first principles calculations of correlated behavior in LSFO on STO. Clarifying the complicated energy balance between the lattice and electronic degrees of freedom in strain-engineered LSFO will have further implications for other MIT materials being investigated for next-generation memory devices. Time permitting, I will also discuss how simple machine learning techniques can enhance nano-XRD data analysis, independently extracting information on the film's local surface normal tilt and lattice plane spacing, in a single measurement.

The sample processing, experimental design, data collection, and development of new analysis methods were supported by the US Department of Energy, Office of Science, Basic Energy Sciences, Materials Science and Engineering Division. Work at the 26-ID-C and 33-ID-D beamlines of the Advanced Photon Source was supported by the US Department of Energy, Office of Science, Basic Energy Sciences, under Contract No. DE-AC02-06CH11357.

- [1] Dagotto, E. Complexity in Strongly Correlated Electronic Systems. *Science* **309**, 257–262 (2005).
- [2] Millis, A. J. Lattice effects in magnetoresistive manganese perovskites. *Nature* **392**, 147–150 (1998).
- [3] Imada, M., Fujimori, A. & Tokura, Y. Metal-insulator transitions. *Rev. Mod. Phys.* **70**, 1039–1263 (1998).
- [4] Wang, J. et al. Epitaxial BiFeO₃ Multiferroic Thin Film Heterostructures. *Science* **299**, 1719–1722 (2003).
- [5] May, S. J. et al. Quantifying octahedral rotations in strained perovskite oxide films. *Phys. Rev. B* **82**, 014110 (2010).

[6] Zhu, Y. et al. Unconventional slowing down of electronic recovery in photoexcited charge-ordered $\text{La}_{1/3}\text{Sr}_{2/3}\text{FeO}_3$. *Nat. Commun.* **9**, 1799 (2018).

1:55 PM *CT03.03.04

Nano-Imaging of Functional Nanomaterials by Spatially Resolved X-Ray Diffraction Tobias Schulli¹, Steven Leake¹, Marie-Ingrid Richard^{1,2}, Tao Zhou^{1,3} and Edoardo Zatterin¹; ¹ESRF, France; ²CEA Grenoble, France; ³Argonne National Laboratory, United States

Unprecedented tools to image crystalline structure distributions in materials have been made possible by recent advances in X-ray sources, X-ray optics and X-ray methods. Nanobeams combined with diffraction have made it possible to image parameters that were traditionally only addressed as ensemble averages. This enables the study of highly heterogeneous materials such as microelectronic devices and opens a new field of material science on the mesoscale. Furthermore, coherent nanobeams offer the opportunity to image nanomaterials in three dimensions with a resolution far smaller than the focused beam size. This has opened up new fields in X-ray diffraction in general and has become one of the main drivers for the enhancement of existing, and the construction of new, large scale scientific infrastructure projects around the world.

As one example, the ID01 beamline has been built to combine Bragg diffraction with imaging techniques to produce a strain and mosaicity microscope for materials in their native or operando state. A scanning probe with nano-focused beams, objective lens-based full-field microscopy and coherent diffraction imaging provide a suite of tools which deliver micrometre to few nanometre spatial resolution combined with the unrivalled strain resolution supplied by X-ray diffraction.

With worldwide efforts in the upgrading or new conception of synchrotron sources, improvements of several orders of magnitude in the throughput of these methods are expected in the next years. Our first results show the relevance of such new tools in complex experimental environments as encountered in nanotechnology and chemistry.

Although many basic principles and processes in what is in a wider sense called nanotechnology are known and exploited since more than a century, their development and improvement is still very much based on a trial and error approach. In the sector of energy materials such as batteries or electrochemical systems for energy conversion, the physiochemical complexity has prevented over decades a clear-cut understanding of processes and reactions at the nanoscale, essentially due to the absence of suited characterization tools. Looking at the example of batteries, and the worldwide implication of research groups on only a few prominent material systems, it becomes clear that rarely any progress in a technology depended so much on characterization and understanding of the complete reaction system. On the other hand, many common characterization techniques cannot assess such electrochemical systems under reaction but rather their constituents once isolated or extracted from the reactive system. Lab and synchrotron based powder X-ray diffraction has been a tool of choice for investigating nanomaterials in complex systems and under reaction. But only very recent developments permit to overcome the absence of spatial resolution of this method. We have developed several diffraction based microscopes that have proven their usefulness in microelectronic samples where high strain resolution needs to be combined with large fields of view and sub micrometer resolution. For typical nanostructures as present in catalytic reactions or batteries, coherent X-ray diffraction imaging tools will allow to zoom into single nanocrystallites with the potential of 3D nanometric imaging. While most published examples of the recent past aimed at high spatial resolution in static samples, current efforts are aiming at the operando assessment at a time resolution of relevance in chemical engineering, while preserving a 3D spatial resolution well below 10 nm. These tools that are today mainly limited to a small expert community are prone to quickly develop into one of the most powerful operando assessment methods; We will present the current state of the art of X-ray diffraction based microscopy with examples for imaging of individual nanostructures.

<!--!endif]---->

2:20 PM CT03.03.05

Local Structure and Switching of Ferroelectric/Ferroelastic Superdomains Probed by Scanning X-Ray NanoDiffraction Edoardo Zatterin¹, Marios Hadjimichael², Steven Leake¹ and Pavlo Zubko³; ¹European Synchrotron Radiation Facility, France; ²University of Geneva, Switzerland; ³University College London,

United Kingdom

Due to novel functionalities recently discovered at domain walls, thin-film ferroelectrics with dense ferroelastic domain structures represent promising candidates for a new generation of nanoelectronic devices [1]. Ferroelastic domain structures form to minimize epitaxial strain in the film, which can be tailored by selecting an appropriate combination of thin film and substrate material [2]. Certain combinations give rise to peculiar hierarchical organizations, whereby ferroelastic domains arrange in distinct “superdomain” bundles [3,4]. Recent studies have demonstrated that interconversion between superdomain states can be induced by the application of an external electric field [5] or stress [6], making these systems attractive for potential applications in reconfigurable electronics.

Little is still known about the superdomain arrangement locally, as well as the exact nature of its response to applied fields in device-like conditions. Studies to date have been confined to surface-limited Piezoresponse Force Microscopy (PFM) imaging or large area X-ray diffraction.

Here we attempt to fill this gap by employing synchrotron Scanning X-ray NanoDiffraction (SXND) [7]. An X-ray beam focused down to 50nm is swept across a ferroelectric thin film displaying a superdomain arrangement, giving local and spatially resolved access to its crystallography – with beam-size resolution. We use PbTiO₃ (PTO) // KTaO₃ (KTO) thin films as a prototype system for this study due to the rich mixture of both in-plane and out-of-plane domain bundles (the so-called “ a_1a_2/c ” structure) that PTO exhibits as a result of the moderate epitaxial tensile strain exerted by the KTO substrate.

The superdomain structure revealed by SXND displays a peculiar distribution of PTO tilt and tetragonality gradients [8], especially evident at the boundaries between a_1a_2 and ac bundles. We subsequently track changes in this spatial distribution of tilts as a function of in-plane electric field applied via interdigitated electrodes, observing 90 degree domain wall rotations to accommodate 180 degree switching of the in-plane polarization component as the applied field polarity is inverted. PFM data collected on the same regions corroborates our interpretation, and suggests that the peculiar nature of the superdomain boundaries plays a major role in the switching mechanism.

References

- [1] Sharma, P., et al. *Materials* 12, 2927 (2019)
- [2] Damodaran A. R., et al. *J Phys Condens Matter*, 28(26), p. 263001. (2016)
- [3] Langenberg, E. et al. *ACS Applied Materials & Interfaces*. 1944-8244 (2020).
- [4] Damodaran A. R. et al. *Advanced Materials*, 29, p. 1702069, (2017)
- [5] Matzen, S. et al. *Nature communications* 5, 4415 (2014).
- [6] Lu, X. et al. *Nature Communications* 10, 3951 (2019).
- [7] Schüllli, T. U., et al. *Current Opinion in Solid State and Materials Science*, 22(5), 188–201. (2018)
- [8] Catalan G., et al. *Nature Materials*, 10(12), 963–967. (2011)

2:35 PM CT03.03.06

Recent Commissioning of the Nanoprobe Endstation at the Submicron Resolution X-Ray Spectroscopy (SRX) Beamline at the NSLS-II Andrew Kiss, Evgeny Nazaretski, David S. Coburn, Jun Ma, Huijuan Xu, Mourad Idir, Lei Huang, Weihe Xu, Huang Xiaojing, Yang Yang, Randy Smith and Yong S. Chu; Brookhaven National Laboratory, United States

The Submicron Resolution X-ray (SRX) Spectroscopy beamline at the National Synchrotron Light Source II (NSLS-II) is a hard X-ray scanning-probe imaging and spectroscopy beamline. A focused X-ray beam is rastered over the sample to collect X-ray fluorescence (XRF) maps and spatially-resolved X-ray absorption spectroscopy (XAS) measurements from the sample. These techniques support a wide range of scientific fields including environmental and biological sciences, earth sciences, and material and energy sciences. Recently, a

new nano-endstation was commissioned to provide users with an increased spatial resolution and higher photon flux onto the sample. This nano-endstation is the result of a multiyear program coordinated by an in-house team of scientists and engineers to replace the existing micro-endstation at SRX by filling a gap in imaging spatial resolution at the NSLS-II and providing users with additional imaging capabilities.

The nano-endstation at the SRX was built downstream of the existing micro-endstation and utilizes all new equipment. A pair of fixed-curvature Kirkpatrick-Baez (KB) mirrors focus the incident beam onto the sample. These mirrors are installed in a vacuum chamber designed to provide high stability with a newly designed alignment mechanism and interferometer feedback. The KB mirrors were manufactured with tight tolerances to provide a sub-250 nm focus and have demonstrated a 225 nm focus from a knife-edge scan on a test pattern. The sample is mounted on a new piezo stage stack which uses coarse and fine stages to raster the sample through the focused beam. Additionally, a rotation stage is mounted to allow for tomographic measurements. The rotation stage with slip-ring connectors can be run with continuous rotation for advanced scan strategies. This is also important for operando measurements where an electrical connection is necessary, *e.g.* electrochemical cycling. An interferometer system is installed to monitor the sample position and correct for any potential run out. These enhancements and added capabilities at SRX enable our user community to collect the high-quality elemental maps and spectroscopy for their experiments, as well as collecting more information on their samples by extending from 2D images to 3D volumes.

SESSION CT03.04: Time Resolved
Session Chairs: Arief Budiman, Margaret Murnane and Olivier Thomas
Monday Afternoon, April 19, 2021
CT03

4:00 PM *CT03.04.01

Probing Thermal Transport in Nanostructured Materials with Coherent Extreme Ultraviolet Beams

Joshua Knobloch^{1,2,3}, Jorge Nicolas Hernandez Charpak^{1,2,3}, Brendan McBennett^{1,2,3}, Travis D. Frazer^{1,2,3}, Begoña Abad Mayor^{1,2,3}, Hossein Honarvar^{1,2,3}, Albert Beardo Ricol⁴, Luc Sendra Molin⁴, Javier Bafaluy⁴, Weilun Chao⁵, Weinan Chen⁶, H. Yang Cheng⁶, Alex Grede⁶, Pratibha Mahale⁶, Disha Talreja⁶, Yihuang Xiong⁶, Tom Mallouk⁶, Noel Giebink⁶, Venkatraman Gopalan⁶, Ismaila Dabo⁶, Vincent Crespi⁶, John Badding^{6,6}, Mahmoud I. Hussein^{3,3}, Juan Camacho⁴, F. Xavier Alvarez⁴, Henry Kapteyn^{1,2,3} and Margaret Murnane^{1,2,3}; ¹STROBE, United States; ²JILA, United States; ³University of Colorado Boulder, United States; ⁴UAB, Spain; ⁵Lawrence Berkeley National Laboratory, United States; ⁶The Pennsylvania State University, United States

Nanostructured materials can exhibit exotic properties and behaviors that enrich the landscape of bulk materials, due to the increased influence of dopants, surfaces, geometry, and interfaces. Moreover, at the nanometer length scale, conventional macroscopic models of materials fail to accurately describe their physical behavior. In addition, traditional metrology tools struggle to precisely measure their functional properties. Specifically, heat transport in dielectric and semiconductor materials—which is dominated by phonons—is traditionally considered to follow Fourier’s law of diffusion. However, when the relevant length scales of the system approach the scale of the phonon mean free paths, past experiments observed [1] and theories predicted [2] a breakdown of Fourier’s law. To date, experimentally probing thermal transport at the nanoscale for general geometries is an outstanding challenge, precluding the development of comprehensive models of heat flow in complex systems. These challenges are a current roadblock for nano- and quantum technologies, including the development of advanced nanoelectronics and efficient thermoelectric devices.

Fortunately, tabletop sources of ultrafast, coherent extreme ultraviolet (EUV) pulses, produced via high harmonic generation, have nanometer wavelengths and femtosecond pulse durations which are well-matched to the intrinsic length- and timescales of energy transport at the nanoscale [3]. Here, we demonstrate that a

dynamic scatterometry technique—based on these coherent EUV beams—is a versatile route for uncovering non-diffusive thermal transport behavior in nanostructured systems, from nanostructures on single crystal silicon to complex metalattices.

Using this new metrology capability, we map non-diffusive thermal transport away from 1D- and 2D-confined nanoscale heat sources on bulk substrates. This allows us to validate the counter-intuitive behavior that heat source periodicity (reduced spacing) can increase thermal dissipation efficiency [4,5]. We probe the full thermal transport landscape by studying varying heat source geometries on a variety of materials with drastically different phonon properties: silicon, silica, and diamond. Moreover, these EUV scatterometry results made it possible to develop and benchmark advanced mesoscopic and microscopic models to form a more general picture of phonon transport. We demonstrate that the kinetic-collective model, a mesoscopic model using a hydrodynamic-like transport equation, predicts the full thermomechanical response observed in the experiment—including non-diffusive transport behavior—over a wide range of length- and timescales. We also perform microscopic atomistic calculations to model experimentally relevant geometries and uncover the fundamental physics responsible for the observed counter-intuitive behavior.

Furthermore, we advance this EUV-based technique to probe transport in nanoengineered metalattices [6]. Metalattices are a powerful bottom-up approach to tuning the propagation of high frequency phonons—highly ordered nanoscale opal templates allow for precise control over structure, into which different materials can be infiltrated. Specifically, we explore the interplay between heat source geometry and the nanoscale structure of the metalattices. We observe that metalattices are capable of significantly reducing the thermal conductivity below the prediction of continuum models and support these findings with atomistic calculations. In conclusion, we highlight extensions of this scatterometry technique to novel modalities based on coherent EUV beams to probe behavior in general devices [7].

[1] Siemens et al. *Nat. Mater.* **9**, 26 (2010)

[2] Chen J. *Heat Transfer* **118**, 539 (1996)

[3] Rundquist et al. *Science* **280**, 1412 (1998)

[4] Hoogeboom-Pot et al. *Proc. Natl. Acad. Sci.* **112**, 4846 (2015)

[5] Frazer et al. *Phys. Rev. Appl.* **11**, 024042 (2019)

[6] Abad et al. *Nano Lett.* **20**, 3306 (2020)

[7] Karl Jr. et al. *Sci. Adv.* **4**, eaau4295 (2018)

4:25 PM CT03.04.02

Evaluating the Effects of Cyclic Stresses on the Microstructure of Ferrite—A Microsecond Time Resolved X-Ray Diffraction Based Technique Doriana Vinci¹, Vincent Jacquemain¹, Christophe Cheuleu¹, Olivier Castelnau¹, Vincent Michel¹, Véronique Favier¹, Cristian Mocuta² and Nicolas Ranc¹; ¹Laboratoire PIMM, Arts et Métiers Institute of Technology, CNRS, France; ²Synchrotron SOLEIL, France

Many mechanical systems are submitted to deformations repeated for a very large number of cycles during their service (e.g. several billion cycles, in what is called the gigacycle fatigue domain or very high cycle fatigue – VHCF - domain) and can break under stress lower than their ultimate tensile stress. This phenomenon, called fatigue of materials, can be encountered in many industrial sectors. Fatigue design is thus crucial in engineering and it requires the accurate characterization of material behavior under cyclic loadings to ensure the safety and reliability of structures throughout their life. The characterization of the fatigue behavior of materials has been largely investigated with fatigue tests requiring long testing time in standard laboratory. To overcome this inconvenient new approaches based on ultrasonic fatigue machines have been developed during the last decades. In particular, the present research focuses on a new method for the fast determination of fatigue behavior by interpreting diffraction patterns with a temporal resolution of $\sim 1 \mu\text{s}$ during an ultrasonic fatigue test at loading frequency of about 20kHz.

The present study points the estimation of the XRD peak broadening evolution during sample deformation due to ultrasonic fatigue cyclic loadings. This is a crucial parameter as it is strictly related to the microstructure of a material in term of mean elastic strain distribution and its fluctuation, intragranular strain heterogeneity and dislocation density.

A fully perlitic steel specimen was loaded using a 20kHz ultrasonic fatigue machine mounted on the six-circle diffractometer available at the DiffAbs beamline on the SOLEIL synchrotron facility in France. Since we are interested to investigate the VHCF domain, the amplitudes of the cyclic stresses ranges from 78 to 262 MPa. The diffraction patterns were acquired with a 2D hybrid pixel X-ray detector (XPAD3.2) with a temporal resolution of 1 μ s.

From the XRD patterns, peaks position and their respective broadening can be estimated. In particular, the evolution of diffraction peak broadening of ferrite (110) and (220) reflections is calculated by fitting the experimental data with an asymmetric Pearson-7 function. The results highlight an increase of the peak broadening with the amplitude of applied stresses. The micromechanical interpretation of these experimental data, based on a homogenization scheme capturing the strain heterogeneity inside the material, will be presented.

4:40 PM *CT03.04.03

Time-Resolved Synchrotron X-Ray Diffraction Studies of the Piezoelectric Response in Ferroelectric Thin Films Thomas W. Cornelius¹, Cristian Mocuta², Matthias Rössle³, Stephanie Escoubas⁴, Eudes B. Araujo⁵ and Olivier Thomas⁴; ¹CNRS, France; ²Synchrotron SOLEIL, France; ³Helmholtz-Zentrum Berlin für Materialien und Energie, Germany; ⁴Aix-Marseille Université, France; ⁵University of São Paulo State–UNESP, Brazil

Piezotransducers, based on piezoelectric materials, that convert electrical into mechanical energy (and vice-versa) are widely used in several communication, sensing and energy harvesting applications. Piezoelectric materials are thus used in various devices, including resonators, actuators and sensors, recently as thin films to facilitate their integration into microelectronic devices and for miniaturization purposes (at lowest energy consumption). Among piezoelectric materials it is well established that the piezoelectric coupling coefficients are very large in crystalline materials which are also ferroelectric, i.e. which exhibit a remanent electrical polarization, switchable by applying an external electric field.

Besides the intrinsic piezoelectric effect, extrinsic mechanisms related to the presence of domains contribute to the piezoelectric effect in ferroelectrics. The domains are regions in which the orientations of the polarization vector and the spontaneous strain tensor are uniform. They are separated by domain walls, within which polarization and strain change direction upon passing to an adjacent domain having different orientations of the polarization vector and spontaneous strain. When external fields are applied to the ferroelectric, the domain walls move to minimize the energy of the unfavourably oriented domains, thus contributing to the field-induced changes in polarization and strain. The intrinsic and extrinsic mechanisms are interdependent and, consequently, the total macroscopic response of a piezoelectric ceramic emerges from complex interactions of intrinsic and extrinsic mechanisms.

To investigate the physical properties of ferroelectric thin films various techniques, e.g. piezoelectric force microscopy (PFM), interferometry etc. are typically used. We use *in situ* synchrotron X-ray diffraction combined with the application of an electric field during measurements, which provides useful and precise information beyond the usual applications for structural studies [1-5]. It grants strain resolutions of the piezoelectrically-induced strain of better than 10⁻⁴. In addition, *time-resolved* X-ray diffraction gives access to the structural dynamics during electrical loading [6]. We present the electric field-dependence of structural dynamics in lead zirconate titanate (PZT) and lanthanum-modified lead zirconate titanate (PLZT) thin films with various La concentrations using *in-situ* and *time-resolved* X-ray diffraction with temporal resolutions down to few tens of nanoseconds. The build-in electric field effects on butterfly curves asymmetry in PZT films and the La-doping effects on the coexistence of nanodomains and coarse domains evolution in PLZT films is shown and discussed.

[1] J. Young *et al.*, Phys. Rev. Lett. 107, 055501 (2011)

[2] S. Gorfman *et al.*, Sci. Rep. 6, 20829 (2016)

[3] A. Davydok, T.W. Cornelius, C. Mocuta, E.C. Lima, E.B. Araújo, O. Thomas, Thin Solid Films 603, 29 – 33 (2016)

[4] T.W. Cornelius, C. Mocuta, S. Escoubas, A. Merabet, M. Texier, E.C. Lima, E.B. Araujo, A.L. Kholkin, O.

Thomas, J. Appl. Phys. 122, 164104 (2017)

[5] T.W Cornelius, C. Mocuta, S. Escoubas, L.R.M. Lima, E.B. Araújo, A.L. Kholkin, O. Thomas, Materials 13, 3338 (2020)

[6] C. Kwamen, M. Rössle, W. Leitenberger, M. Alexe, M. Bargheer, Appl. Phys. Lett. 114, 162907 (2019)

5:05 PM CT03.04.04

Transient Lattice Response upon Photoexcitation in CuInSe₂ Nanocrystals with Organic or Inorganic Surface Passivation Samantha Harvey; Northwestern University, United States

CuInSe₂ nanocrystals offer promise for optoelectronics including thin-film photovoltaics and printed electronics. Additive manufacturing methods such as photonic curing controllably sinter particles into quasi-continuous films and offer improved device performance. To gain understanding of nanocrystal response under such processing conditions, we investigate impacts of photoexcitation on colloidal nanocrystal lattices via time-resolved X-ray diffraction. We probe three sizes of particles and two capping ligands (oleylamine and inorganic S²⁻) to evaluate resultant crystal lattice temperature, phase stability, and thermal dissipation. Elevated fluences produce heating and loss of crystallinity, the onset of which exhibits particle size dependence. We find size-dependent recrystallization and cooling lifetimes ranging from 90 to 200 ps with additional slower cooling on the nanosecond time scale. Sulfide-capped nanocrystals show faster recrystallization and cooling compared to oleylamine-capped nanocrystals. Using these lifetimes, we find interfacial thermal conductivities from 3 to 28 MW/(m² K), demonstrating that ligand identity strongly influences thermal dissipation.

5:20 PM CT03.04.06

Advanced Material Characterization Using Quantitative Full-Field X-Ray Nano-Imaging Mingyuan Ge, Jiayong Zhang, Xianghui Xiao and Lee Wah-Keat; Brookhaven National Laboratory, United States

Transmission X-ray microscopy (TXM) is a full-field imaging technique. By taking advantage of using a synchrotron light source, TXM provides unique capabilities in fast 2D/3D imaging with nano-scale resolution. At the Full-field X-ray Imaging (FXI) Beamline at NSLS-II, we can routine perform 3D x-ray imaging with 1k x 1k x 1k voxels at a sub-50 nm resolution in less than one minute¹. While morphology characterization is the primary mode of the TXM application for vast samples, quantitative analysis in terms of material composition and oxidation states can be achieved through a TXM XANES method, where the imaging data are collected at multiple x-ray energies across one or more elemental absorption edges allowing spatially-resolved XANES analysis². The high-imaging rate at the FXI Beamline makes it possible to perform three-dimensional TXM XANES imaging under in-situ sample environment. In the presentation, we will report our recent instrument and data analysis development with few examples to describe the quantitative analysis using the data analysis tools we developed in-house³.

References:

1 Ge, M. Y. *et al.* One-minute nano-tomography using hard X-ray full-field transmission microscope. *Appl Phys Lett* **113** (2018).

2 Wang, J. J., Chen-Wiegart, Y. C. K. & Wang, J. In operando tracking phase transformation evolution of lithium iron phosphate with hard X-ray microscopy. *Nat Commun* **5** (2014).

3 Ge, M. Y. & Lee, W. K. PyXAS - an open-source package for 2D X-ray near-edge spectroscopy analysis. *J Synchrotron Radiat* **27**, 567-575 (2020).

8:00 AM *CT03.05.01

Insight into Biological Structures Using 3D Imaging Techniques Izabela B. Zglobicka¹, Jürgen Gluch², Qiong Li², Zhongquan Liao², Stephan Werner³, Peter Guttman³, Tomasz Plocinski⁴, Andrzej Witkowski⁵, Ehrenfried Zschech² and Krzysztof J. Kurzydłowski¹; ¹Bialystok University of Technology, Poland; ²Fraunhofer Institute for Ceramic Technologies and Systems (IKTS), Germany; ³Helmholtz-Zentrum Berlin (HZB), Germany; ⁴Warsaw University of Technology, Poland; ⁵University of Szczecin, Poland

Nature is not only a constant source of inspiration and knowledge for modern engineering but also most of all the source of materials with unique complex structures and properties. The structure optimized by millennial evolution can be used as a base for the preparation of advanced engineering materials. An essential requirement for this is the full understanding of the laws endowing the nature-built materials with superb properties. To this end, high resolution imaging techniques are essential for understanding the hierarchical structures formed in self-assembly processes.

Examples of inspirational organisms are diatoms. The particularly extensively studied diatom characteristic is their intricate cell wall structure, called frustule, mainly made of silicon dioxide (opal). These silica shells exhibit large variation in morphology as well as hierarchical architecture (from nano- to micro-metres).

In recent years, scientists have bridged the gap between biology and material science of diatoms by developing techniques for imaging diatom frustule cross-sections, using scanning electron microscopy (SEM) [1,2]. It enables imaging the fine details of the structure. However, an intrinsic limitation of this technique is the need of cross-sectioning of the studied species, e.g. applying Focus Ion Beam (FIB) milling. Recently, a new insight into the structure of diatoms has been provided by non-destructive visualization of interior structures using nano X-ray computed tomography (nano-XCT) [1,3-4].

The advantage of nano-XCT is demonstrated based on high-resolution 3D data sets describing the structure of diatoms non-destructively. These data sets are of particular importance and were complemented by high resolution three-dimensional structure information using soft X-ray nano-tomography (available at Helmholtz Zentrum Berlin HZB) combined with high-resolution transmission electron microscopy.

The associated imaging and composition analysis results from SEM/FIB, nano-XCT and TEM allow to describe the microstructure of frustules on multiple length scale. Those datasets are used to describe complex structure of diatoms frustules and to derive models in aim of fabrication of a self-similar, bio-inspired structure by applying 3D Selective Laser Melting (SLM) [3] as well as simulation to determinate mechanical properties of such shells [4].

Bibliography

- [1] Zglobicka I., Li Q., Gluch J., Plocinska M., Noga T., Dobosz R., Szoszkiewicz R., Witkowski A., Zschech E., Kurzydłowski K.J. (2017): Visualization of the internal structure of *Didymosphenia geminata* frustules using nano X-ray tomography. Scientific Reports, 7:9086. doi: 10.1038/s41598-017-08960-5.
- [2] Witkowski A., Plocinski T., Grzonka J., Zglobicka I., Bak M., Dabek P., Gomes A.I., Kurzydłowski K.J. (2019): Application of Focused Ion Beam Technique in Taxonomy-Oriented Research on Ultrastructure of Diatoms in J. Seckbach and R. Gordon (Eds.) Diatoms: Fundamentals and Applications, (113–126) © 2019 Scrivener Publishing LLC
- [3] Zglobicka I., Chmielewska A., Topal E., Kutukova K., Gluch J., Krüger P., Kilroy C., Swieszkowski W., Kurzydłowski K.J., Zschech E. (2019): 3D Diatom–Designed and Selective Laser Melting (SLM) Manufactured Metallic Structures. Scientific Reports, 9:19777. DOI: 10.1038/s41598-019-56434-7
- [4] Topal E., Rajendran H., Zglobicka I., Gluch J., Liao Z., Clausner A., Kurzydłowski K.J., Zschech E. (2020): Numerical and Experimental Study of the Mechanical Response of Diatom Frustules. Nanomaterials, 10, 959. doi:10.3390/nano10050959

8:25 AM CT03.05.02

Operando Tomography of Lead-Based Batteries for Improved Design of Energy Storage Systems Mark Wolfman, Alan Kastengren, Tiffany Kinnibrugh and Tim Fister; Argonne National Laboratory, United States

Lead-based rechargeable batteries are promising candidates for stationary grid storage due to their low cost, high stability, and fast discharge capabilities compared to other electrochemical energy storage chemistries. However, current lead-based batteries are unable to fully utilize the theoretical storage capacity, and are limited in their charging rates. Changes in particle size and porosity impact ion and electron transport dynamics between the electrolyte, active material, and current collector grid, ultimately affecting charge acceptance and cyclability. During cycling, large volume changes are encountered that strongly influence electrode morphology and hence battery performance. An improved understanding of this relationship is necessary in order to design more efficient batteries capable of meeting future energy storage needs. The strong attenuation of lead presents several challenges for conventional X-ray imaging. This work presents new techniques and tools developed to overcome these challenges including experimental design, instrumentation, and data analysis; then uses these tools to track the evolution of electrode morphology during initial formation and subsequent cycling of lead-acid batteries.

8:40 AM *CT03.05.03

Mechanical Set-Ups in Laboratory X-Ray Microscopy to Study *In Situ* Crack Propagation at Patterned Structures Kristina Kutukova, Jürgen Gluch, André Clausner and Ehrenfried Zschech; Fraunhofer Institute for Ceramic Technologies and Systems, Germany

The combination of high-resolution X-ray imaging with in-situ mechanical testing, particularly the application of specially designed test setups in a transmission X-ray microscope, allows the study of the fracture behaviour in heterogeneous materials, composites and micropatterned devices. A miniaturised micro double-cantilever beam test (micro-DCB) setup is integrated into a laboratory transmission X-ray microscope (TXM) to guide microcracks to the mechanically weakest region of a material, which is determined by the materials-dependent fracture toughness, the size and the shape of defects as well as the local stress, and to achieve stable crack propagation in a controlled way [1]. In-situ mechanical studies in a nano X-ray computed tomography (nano-XCT) system allow a 3D visualization of the micro-crack evolution in materials or in microchips with a spatial resolution of about 100 nm. During the micro-DCB experiment, the load is applied perpendicular to the optical axis of the X-ray microscope while images are collected. A force sensor allows to determine the mechanical load at certain stages of crack propagation. The local energy release rate can be determined quantitatively. The in-situ micro-DCB technique offers several benefits over existing methods and is applicable across a range of disciplines, including materials science (e.g. composites), microelectronics (e.g. interconnect stacks), and life sciences (e.g. tissue, bones).

High-resolution 3D image sequences based on nano-XCT are used to visualize crack opening and propagation in fully integrated multilevel on-chip interconnect structures of integrated circuits. The nondestructive study of the propagation of sub-micron cracks during the in-situ micro-DCB test allows to image cohesive failures in organosilicate glass (so-called low-k materials) or adhesive failure, i.e. delamination along Cu/dielectrics interfaces. Weakest layers and interfaces in the interconnect stack can be identified [2]. The quantitative determination of the energy release rate allows to judge the robustness of Cu/low-k interconnect stacks against process-induced thermomechanical stress and the effectiveness of so-called guard-ring structures. These data provide important input for the guard-ring design and for the selection of materials, particularly the insulating dielectrics. Eventually, the risk of failure of the patterned metal/dielectrics structures can be reduced.

[1] K. Kutukova, S. Niese, J. Gelb, R. Dauskardt, E. Zschech, "A Novel Micro-Double Cantilever Beam (micro-DCB) Test in an X-ray Microscope to Study Crack Propagation in Materials and Structures", *Mater. Today Comm.* 16, 293–299 (2018)

[2] K. Kutukova, S. Niese, C. Sander, Y. Standke, J. Gluch, M. Gall, E. Zschech, "A Laboratory X-ray Microscopy Study of Cracks in on-chip Interconnect Stacks of Integrated Circuits", *Appl. Phys. Lett.* 113, 091901 (2018)

9:05 AM BREAK

9:20 AM CT03.05.04

High Throughput Grain Mapping Using Advanced Acquisition Schemes with Laboratory Diffraction Contrast Tomography (LabDCT) Jun Sun¹, Florian Bachmann¹, Jette Oddershede¹, Hrishikesh Bale², Will Harris³ and Erik Lauridsen¹; ¹Xnovo Technology Aps, Denmark; ²Carl Zeiss X-ray Microscopy, United States; ³Carl Zeiss Microscopy, United States

Characterizing the polycrystalline grain microstructure of metals, alloys, ceramics or minerals in three dimensions nondestructively is paramount to better understanding the material properties. Often, such samples demand a larger representative volume/quantity to be statistically relevant or possess characteristic geometry (e.g. high aspect ratio rolling geometry) that is essential to interpret grain structure anisotropy.

Recent advances of Laboratory Diffraction Contrast Tomography (LabDCT) allow to record and reconstruct larger representative volumes seamlessly. We will present and discuss different approaches of data acquisition strategies attacking acquisition problems inherent to a given sample. Combining the 3D grain microstructure, i.e. grain morphology and crystallographic orientation, with traditional absorption contrast tomography gives unprecedented insights on the laboratory scale. Time resolved studies of the response of the material under investigation to external stimuli in- or ex-situ can be conducted.

9:35 AM CT03.05.05

Late News: Transparent X-Ray Beam Monitoring and Imaging with PIN diamonds Anna M. Zaniewski^{1,2}, Jesse Brown^{2,1}, Manpuneet Benipal² and Robert J. Nemanich^{1,2}; ¹Arizona State University, United States; ²Advent Diamond, United States

Advanced x-ray beam facilities support a wide range of scientific and technological development of materials. To maximize the value of these experiments, the x-ray beam itself needs to be well understood, with fine control over its position. As x-ray sources become more advanced, they will benefit from better beam monitoring and measurements. Most of the monitoring methods currently in use can only position the beam or measure beam flux before or after experiments; any drift in the beam position or intensity fluctuations that occur during the experiment would go unnoticed. Therefore, there is a need for real-time, direct beam monitoring which can be integrated with beam controls to quickly set up and control beam parameters, and image the beam. Recent advances demonstrate that thin diamond detectors are a viable technology for minimally invasive imaging of x-ray beams. The choice of diamond brings a number of advantages due to diamond's remarkable physical properties, such as large bandgap, semi-transparency to x-rays, extreme thermal properties, and fast electron and hole mobilities. In this work, we will describe our advances in producing a pixelated, thin, transparent x-ray beam monitor based on doped diamond, with a p-type/intrinsic/n-type (PIN) design, and preliminary results of testing the detector and readout system at the National Synchrotron Light Source II at Brookhaven National Lab.

9:50 AM CT03.05.06

Holistic Materials Analysis Through Scale-Bridging 3D X-Ray Microscopy Robin T. White, Tobias Volkenandt, Stephen T. Kelly and Will Harris; Carl Zeiss Research Microscopy Solutions, United States

X-ray Computed Tomography has proven to be a crucial method to properly characterize and understand a huge variety of materials applications. Due to the non-destructive 3D imaging capabilities, this imaging methodology provides unique insight into material properties with comparatively minimal sample processing. One limitation however has been resolution capabilities. Previously, X-ray tomography imaging has utilized the principle of geometric magnification to obtain resolution. This has several limitations, the main impact being the realistic resolution achievable. Recently, the application of using a photon-converting scintillator and objective lenses has enabled much higher resolution imaging. A unique ability of this system architecture is to enable non-destructive, multi-length scale visualization; with an imaging field of view range from tens of millimeters down to tens of micrometers, and resolution capabilities reaching 500 nm in instruments such as the ZEISS Xradia Versa. Alternatively, another X-ray imaging method is to use X-ray lenses such as Fresnel Zone Plates that can

achieve resolutions down to 50 nm and less, utilizing a quasi-monochromatic lab-based X-ray source in instruments such as the ZEISS Xradia Ultra. This system also employs an inline phase ring that enables Zernike phase contrast imaging which can greatly improve imaging contrast.

Due to the restrictions of lab-based equipment, each imaging solution requires its own imaging system. Often, this results in non-correlative imaging workflows – where a similar but different sample or region is imaged in each system to the maximum system resolution capabilities. This poses a number of inherent limitations in obtaining the full understanding of the sample in question: What does the sample look like as a whole and how representative is this region to another? Are there microscale properties that correlate to macroscale features? Additionally, knowing the exact resolution limit required to properly characterize a sample is an important question that can be difficult to answer without observing enhanced resolution of the exact same feature. Combining systems that can achieve different resolutions in a correlative workflow of the same sample also allows for advanced analysis, such as applying properties obtained from high resolution imaging to a large volume obtained from lower resolution imaging. For example, intra- and inter-particle porosity that is not resolved could inherently change simulation results without proper characterization.

We present here results combining two X-ray tomography systems, the Zeiss Xradia Versa and Zeiss Xradia Ultra instruments, into a correlative, multi-length scale analysis workflow through the use of specifically designed hardware and software tools. We demonstrate several applications using this combined approach to enable non-destructive, massively multiscale 3D imaging. Specific examples include combined quantitative studies in nuclear graphite material to facilitate a multiscale porosity and microstructural analysis, battery anode particles with combined machine learning upscaling as well as polymer electrolyte fuel cell device layers.

9:55 AM CT03.05.07

Structural Analysis of Dot-Core GaN Substrates Using X-Ray Topography Michael E. Liao, Yekan Wang, Kenny Huynh and Mark S. Goorsky; University of California, Los Angeles, United States

A refined systematic method for imaging and analyzing the structural characteristics of dot-core GaN substrates using X-ray topography is presented. Currently, fundamental understanding of the defect nature of dot-core GaN substrates and the impact on device performance is still in its infancy. Work by Raghothamachar et al.,¹ have previously used X-ray topography to catalogue various dislocations in dot-core GaN substrates. However, only rocked images were generated in that study, which are integrated images recorded by exposing a single film along different angular positions along an X-ray diffraction rocking curve. Our method involves generating single exposure images instead – images exposed at various points along the rocking curve with each image recorded on separate pieces of film. Rocked images were also generated for comparison. The measurements were performed at the 1-BM beamline of the Advanced Photon Source, Argonne National Laboratory using an X-ray energy of 8.05000 ± 0.00015 keV and a (111) Si beam expander to measure the (11 $\bar{2}$ 4) GaN reflection in the glancing incidence geometry. Unlike the rocked images, the single exposure images unequivocally preserve all the structural information pertaining to lattice tilt and distortion – both the magnitude of tilts and the spatial locations of tilt boundaries for example. The importance of preserving this structural information is that it enables us to describe quantitatively the distortion of the defects present. In fact, the single exposure images allow us to calculate the lattice curvature on two different scales: (1) globally across the entire dot-core GaN substrate (~tens of mm) and (2) locally across each highly distorted core (~500 μ m). One of the dot-core substrates measured had a radius of curvature of ~15 m across the entire substrate, while locally across individual cores the radius was on the order of ~0.2 m to ~0.4 m. This information is lost in rocked image measurements because the integration of images along different parts of the rocking curve loses angular information. Furthermore, the single exposure image method has the freedom of generating a ‘rocked image’ by superimposing each of these single exposure images together. Measured rocked images cannot be accurately deconvoluted into its image components. We demonstrate that a contour tilt map can be generated when superimposing many of these images together – an impossible task to accomplish from a measured rocked image. Lastly, many instances were found where dislocations that appeared in the single exposure image measurements were not present in the rocked image measurements. This is due to spatial overlapping of diffraction areas from recording images from different parts along the rocking curve on the same film when measuring rocked images.

References

1. B. Raghathamachar, et al., *J. Crys. Growth*, **544**, 125709 (2020).

The authors would like to acknowledge supported through the ARPA-E PNDIODES program under contract DE-AR0001116 at UCLA. This research used resources of the Advanced Photon Source, a U.S. Department of Energy (DOE) Office of Science User Facility operated for the DOE Office of Science by Argonne National Laboratory under contract no. DE-AC02-06CH11357. The synchrotron X-ray topography measurements were carried out at 1-BM Beamline of the Advanced Photon Source, Argonne National Laboratory.

SESSION CT03.06: AI/Modeling
Session Chairs: Olivier Thomas and Ehrenfried Zschech
Tuesday Morning, April 20, 2021
CT03

11:45 AM *CT03.06.01

AI-Enabled Phase Retrieval for Transmission and Bragg Ptychography Tao Zhou, Mathew Cherukara and Martin Holt; Argonne National Laboratory, United States

In this work, we demonstrate how machine learning and its related optimization tools can be used to replace conventional phase retrieval methods in X-ray transmission and Bragg ptychography. X-ray transmission ptychography has become a well-established technique for high resolution imaging and phase retrieval. We present PtychoNN, a novel approach to solve the ptychography problem based on deep convolutional neural networks. Once trained, PtychoNN is capable of generating high quality reconstructions up to hundreds of times faster compared to conventional iterative methods, essential for implementing real time phase retrieval. Moreover, by surpassing the numerical constraints of iterative methods, the sampling condition can also be significantly relaxed. The counterpart of transmission ptychography in diffraction condition is known as Bragg ptychography. The technique itself is less mature, as limited by the more complex diffraction geometry and data quality. Here we describe the forward propagation in Bragg ptychography using the Takagi-Taupin Equations (TTE). We show that, when combined with Automatic Differentiation (AD), TTE can be used as a general formalism for 3D phase retrieval, applicable to both Bragg ptychography and Bragg Coherent Diffraction Imaging. Compared to conventional Fourier Transform based methods, our approach accounts for additionally refraction, absorption, interference, dynamical effects, and is applicable to any kind of weakly strained material system. [1] M. J. Cherukara, T. Zhou, Y. Nashed, P. Enfedaque, A. Hexemer, R. J. Harder, M. V. Holt, *Appl. Phys. Lett.* 2020, 117, 044103. [2] T. Zhou, M.J. Cherukara, S.O. Hruszkewycz, M. Allain, N. Hua, O. Shpyrko, Y. Takamura and M.V. Holt, in submission.

12:10 PM CT03.06.02

Artificial Intelligence for Efficient Analytical Processing of X-Ray Diffraction Data Alex Ulyanenkov¹ and Alexander Mikhalychev²; ¹Atomicus LLC, United States; ²Atomicus OOO, Belarus

Artificial intelligence methods attract significant interest nowadays due to the general tendency of automating analysis procedures. Computer-based techniques are not only much faster and less demanding for expert knowledge of operators than manual techniques, but also provide reliability and reproducibility of the analysis results due to much lesser vulnerability to accidental errors. In this contribution, we focus on those two aspects of X-ray diffraction experiments: namely, we demonstrate how artificial intelligence can help in choosing the optimal measurement configuration and in data interpretation (both in powder and high-resolution X-ray diffraction). The approaches, discussed in our contribution are based on combining fundamental physical ideas with the two efficient mathematical tools: Bayes' theorem and Fisher information, which are quite often

overlooked by physicists.

Fisher information [1] quantifies the sensitivity of the measured data to the parameters of interest and, therefore, gives us a hint on choosing the most suitable way of data acquisition. Cramer-Rao bound [2] connects Fisher information to the reliability of the obtained results and the possible correlations between the model features. We demonstrate that fully automatic analysis of Fisher information is suitable for choosing the most informative reflections and measurement geometries when panning high-resolution X-ray diffraction (HRXRD) measurements. The decision is made adaptively, by rating all possible sets of scans and reciprocal-space maps, as well as diffractometer configurations, on the base of the amount of their information on the investigated sample. Also, analysis of the Fisher information structure (namely, detection of a banded diagonal shape of the inverse Fisher matrix) helps to reconstruct the sample parameters in a more efficient way: a problem with locally correlated parameters can be solved by iterative consideration of only a subset of parameters to be reconstructed at each step [3,4]. We apply this technique to the problem of automatic decomposition of an X-ray spectrum, consisting of a large number of strongly overlapping peaks, into contributions of individual peaks.

Bayes' theorem describes the update of our knowledge about the investigated sample by the obtained measurement results. It represents an efficient tool for quantitative ranking of models in the pattern recognition problems [3,5]. We apply a Bayesian approach to quantitative analysis of X-ray powder diffraction data (identification of phases from a measured X-ray spectrum), to peak indexing in HRXRD spectra (finding the correspondence between each measured peak with an expected Bragg peak, a layer thickness oscillation fringe or a superlattice fringe), and to the problem of decomposing strongly overlapping peaks (for power XRD data). The initial information about the investigated sample or dataset is encoded in prior probabilities for the models. The expected experimental inaccuracies caused by statistical and systematic noise are characterized by the likelihood function. Finally, models of the spectrum decomposition (peak identification, etc.) are ranked according to the estimated posterior probability. The approach is quite universal and can be easily adjusted to a particular physical problem: for example, additional systematic errors can be efficiently detected and corrected by introducing them into the analyzed model during powder phase identification. For all the mentioned tasks, the designed algorithms succeeded in automated solving of the problems.

1. Ly, A., et al, *Journal of Mathematical Psychology*, 2017, 80, 40–55.
2. Cramer, H., “Mathematical Methods of Statistics”, Princeton, Princeton University Press, 1946.
3. Mikhalychev, A., et al, *Ultramicroscopy*, 2020, 215, 113014.
4. Mikhalychev, A., et al, *Communications Physics*, 2019, 2, 134.
5. Mikhalychev, A. and Ulyanenko, A. *J. Appl. Cryst.* 2017, 50, 776-786.

12:25 PM CT03.06.03

Machine Learning Aided Image Reconstruction in X-Ray Tomography Jiayong Zhang, Thomas Flynn and Mingyuan Ge; Brookhaven National Laboratory, United States

Computer tomography has found broad application in material science and medical imaging, providing a versatile approach to visualize the internal structure of a 3D volume. For decades, there is extensive research on the improvement of reconstruction quality and fidelity to deal with the many challenges imposed by experimental data collection, such as noise and missing wedge. In this work, we introduce a neural network based method to tackle the missing wedge problem. Distinguished from existing machine learning architecture, we propose a new two-step model implemented through generative adversarial networks (GAN) and autoencoder to inpaint the miss-wedge sinogram. The results have demonstrated the state-of-the-art performance. More importantly, the proposed architecture is robust to insufficient training data, which provides uniqueness in distilling and expanding the knowledge learned from limited training data to un-seen categories as semi-supervised learning. We will also discuss the difference between our method and others' work, especially in the sense of how we can consistently improve the model performance in practical scientific applications when ground truth is not available. The ability to reconstruct images in X-ray tomography with high accuracy and fidelity would gain us more reliable insights into objects' intrinsic structure and deepen the

understanding of specific scientific problems. This work is supported by the LDRD program at the FXI facility at NSLS-II, Brookhaven National Laboratory (BNL).

12:40 PM *CT03.06.04

Performance Evaluation of Crystallographic Analysis Methodologies in Diffractive Characterization of Nanocrystalline Powders Hande Öztürk¹ and I C. Noyan²; ¹Ozyegin University, Turkey; ²Columbia University, United States

The potentials of facilitating nanocrystals in novel materials design and of enhancing existing materials in the form of advanced nanocomposites are attracting increasing attention to nanomaterials research. Due to the strong correlation between physical and chemical properties of nanocrystals and their sizes as well as atomic configurations, their production requires utmost control and precision. Hence developing accurate, reliable and robust characterization methods targeting nanocrystals is becoming an even more critical component of today's materials design and manufacturing activities. X-ray powder diffraction, being the gold standard of high-resolution materials characterization is the number one method employed in the analysis of nanocrystalline powders as well, although the fundamental principle behind the analysis of powder x-ray diffraction data is the assumption of infinitely-periodic stacking of atoms within individual grains, not strictly satisfied by nanocrystals due to their tiny sizes. That raises the question of whether we can use standard crystallographic analysis methods to solve for the average internal structure of nanocrystalline powders from their diffraction data.

In this talk I will address this question using computational modelling of powder diffraction from monodispersed nanocrystalline powders with grain sizes of 40 nm and below. To do that, I will first introduce our computational framework and present ideal diffraction data generated based on first-principle diffraction equations. This computed data will be treated as 'ideal experimental data' and then will be used to establish direct link between the diffracting nanocrystalline powder and its diffraction signature. Standard crystallographic analysis methodologies will be used to extract average structural characteristics of the nanocrystalline powder and they will be validated against the true structural parameters of the nanopowder by direct analysis of the atomic coordinates. Our conclusions are important in understanding the limits of applicability and validity of standard crystallographic analysis tools in x-ray diffraction data of nanocrystalline powders under ideal conditions, where the diffraction data is free from uncertainties and the diffracting sample is known down to the individual atomic positions. Moreover, our results will draw attention to the necessity of computational studies to investigate the diffraction phenomenon of x-rays from nanocrystalline powders and will motivate discussions on developing better data analysis algorithms compatible with the internal structure of nanocrystalline powders.

1:05 PM DISCUSSION TIME

1:20 PM CT03.06.06

Morphology-Informed Correlation Across Multimodal Microscopy Data Rishi Kumar, Xueying L. Quinn and David Fenning; University of California, San Diego, United States

Synchrotron-based study of material behavior often involves the use of multiple modes of characterization, whether in a synchronous correlative microscopy approach or via sequential measurement. While synchronous multimodal characterization is a growing area, these studies most commonly consist of various measurements on different instruments at different times, each with their own quirks resulting from practical constraints like sample orientation and tool resolution. The difficulty in strictly correlating data generated across measurements can be quite high, especially so for samples with asymmetric and non-extended morphology such as individual micro- or nanoparticles and rough or porous films as can be found in solar cells and battery electrodes. To address this challenge, we present a morphology-informed ray-tracing approach to simulate probe-sample interactions in raster scanning instruments, allowing for proper spatial correlation of the data acquired across synchrotron-based and benchtop setups.

First, we generate a three-dimensional model of our sample from a map of local thickness. We then perform ray-tracing of the X-ray beam with our sample, accounting for the X-ray-sample interaction and the orientation of the beam, sample, and involved detectors. As a demonstrative example, we analyze sequential nanoprobe X-ray diffraction and X-ray fluorescence maps of a state-of-the-art halide perovskite optoelectronic material. The ray-tracing yields a spatially-variant point-spread function weighting the contribution of all beam-intersected regions of the sample to the values recorded at the detectors at each point on the map, enabling deconvolution of the sample morphology from measured data and fair spatial correlation of data across measurements. Precise assessment of the sampled volume in correlative measurements will be increasingly necessary as experimental complexity increases at diffraction-limited storage rings.

1:35 PM CT03.06.07

Influence of Layer Charge on Hydration Properties of Synthetic Octahedrally Charged Na-Saturated Trioctahedral Smectites Doriana Vinci¹, Baptiste Dazas², Eric Ferrage², Martine Lanson³, Valérie Magnin³, Nathaniel Findling³ and Bruno Lanson³; ¹Laboratoire PIMM, Arts et Métiers Institute of Technology, CNRS, France; ²CNRS, IC2MP, Univ. Poitiers, France; ³Univ. Grenoble Alpes, Univ. Savoie Mont Blanc, CNRS, IRD, IFSTTAR, ISTERre, France

Smectite hydration impacts dynamical properties of interlayer cations and thus the transfer and fate of H₂O, contaminants, and nutrients in surficial environments where these ubiquitous clay minerals are often one of the main mineral components. The influence of key crystal-chemical parameters on hydration, organization of interlayer species, and related properties has been described for tetrahedrally substituted trioctahedral smectites (saponites). Despite the ubiquitous character of octahedrally substituted smectites, that make most of the world bentonite deposits, the influence of charge location on smectite hydration properties has not largely investigated. In this work a set of octahedrally substituted trioctahedral smectites (hectorites) with a common structural formula Na_xMg_{6-x}Li_xSi_{18.0}O₂₀(OH)₄ and a layer charge (x) varying from 0.8 to 1.6 was synthesized hydrothermally from stoichiometric gels. The distribution of charge-compensating Na⁺ cations and of associated H₂O molecules was determined experimentally from the modeling of X-ray diffraction data obtained along water vapor desorption isotherms. Distributions of charge-compensating cations and of associated H₂O molecules were also computed from GCMC simulations as a function of layer charge. Interlayer H₂O contents are similar in all Na-saturated smectite samples, independent of the location and amount of their layer charge. In contrast to synthetic saponite, for which stability of most hydrated layers was increased by increasing layer charge, the stability of synthetic hectorite hydrates is only slightly affected by layer charge. Consistently, the layer-to-layer distance of Na-saturated hectorite 2W (and 1W) layers is independent of layer charge. The contrasting hydration behavior of synthetic Na-saturated saponite and hectorite is likely due to different electrostatic attraction between the 2:1 layer and interlayer cation. Combined with previous results on saponites, the present data and sample set provides key constraints to assess the validity of force fields simulating clay-water interactions for an unmatched variety of smectite with contrasting locations and amounts of layer charge deficits.

SESSION CT03.07: Lab Sources

Session Chairs: Arief Budiman, Margaret Murnane, Olivier Thomas and Ehrenfried Zschech

Tuesday Afternoon, April 20, 2021

CT03

2:15 PM *CT03.07.01

Recent Innovations in Laboratory X-Ray Microscopes Wenbing Yun, Sylvia Lewis, David Vine, Benjamin Stripe, Sheraz Gul, Katie Matusik, Jeff Gelb, SH Lau and Janos Kirz; Sigray, Inc., United States

Innovations in laboratory x-ray source and x-ray imaging methodology are critical to realize intrinsic

advantages of x-ray microscopy for a wide range of applications. X-ray imaging using absorption, phase, and scattering/darkfield contrasts (tri-contrast) have been shown to provide unique and complementary structural information critical to many imaging applications, often missing in absorption contrast imaging alone. For example, scatter contrast has been shown to be superior to absorption contrast for imaging fine cracks. Phase contrast is far superior for imaging low Z (soft) materials than absorption contrast.

Significant improvement in tri-contrast x-ray imaging with laboratory x-ray sources is desirable, including options for operating over a wide energy range to image objects of various sizes and compositions, and to achieve high spatial resolution to visualize fine features.

Significant progress has been made in recent years in developing laboratory x-ray sources and methodologies to advance tri-contrast x-ray imaging. Sigray has developed a novel x-ray source using matrix array anode source technology (MAAST™) with an anode comprised of arrays of metal (e.g. Cu, W) microstructures as x-ray emitters embedded in a diamond substrate with excellent thermal conductivity. Under electron bombardment, the localized metal microstructures are effectively cooled due to the large thermal gradients relative to the diamond substrate.

The common approach to tri-contrast x-ray imaging involves the Talbot-Lau interferometer, which consists of three gratings. The first of these, the source grating, is used to provide the required coherence, but it has a number of drawbacks, including inefficient use of source x-rays as it absorbs more than 50%, narrow angular collimation with high aspect ratio grating structures for high energy x-rays and the consequent limit in imaging field of view. Additionally, for high energy x-rays, the fabrication of the source grating is extremely challenging. The MAAST x-ray source removes the need for the source grating entirely. It overcomes the drawbacks and offers many advantages.

Using these and other innovations, Sigray has developed x-ray microscopes with excellent capabilities. The design of the microscopes and their imaging performance will be reported and discussed.

2:40 PM CT03.07.02

Development of a New High-Energy X-Ray Diffraction NDT for High-Pressure Turbine Blades Alexiane Barbeau¹, Baptiste Joste² and Henry Proudhon²; ¹SAFRAN Tech, France; ²Mines Paristech, PSL University, Centre des Matériaux, CNRS UMR 7633, France

In the aerospace industry, single crystal nickel-based high-pressure turbine blades are the most critical part of the engine. The thermo-mechanical resistance of the blade is mostly due to the monocrystalline arrangement to increase the creep strength and to the design of internal cooling circuits with complex geometry to reduce the blade temperature.

To ensure the single crystal arrangement is maintained throughout the part after the foundry process, a non-destructive test (NDT) has been developed. Indeed, the presence of another grain into the part can critically impede the performance of the blade, which may cause irreversible damage to the engine motor.

The proposed solution is to develop a new industrial NDT system using high energy Laue transmission diffraction, which represents a technological breakthrough in the current industrial environment. A compact laboratory high energy Laue diffraction system has been designed, which uses a high-energy X-ray source, a motorized support sample setup and a high efficiency X-ray detector. A compact X-ray slit system is used to control the footprint of the beam on the sample and the motorized stage is used to scan the sample in front of the beam. Typical high energy X-ray sources are powerful enough to go through several millimeters of nickel-based alloy allowing to scan entire parts such as small turbine blades. Our experiments showed that to detect diffraction spots from the illuminated volume, the use of hybrid photon counting detector is desirable to increase the system performances (both faster data collection and detection of weak intensity reflection beams).

A forward simulation model of the Laue diffraction physics under the kinematic approximation has also been

developed and allows simulating any diffraction pattern according to the crystal structure. The forward model also takes into account the sample geometry, which can be as complex as a turbine blade with double walls and internal cavities. An in-house indexing algorithm based on the forward model, which takes into account the specificity of a laboratory system, allows to retrieve the crystal orientation from the experimental diffraction images and to detect new orientations in the pattern.

Experimental results show that Laue transmission diffraction method makes it possible to carry out an orientation mapping for an extended monocrystalline volume. Laue diffraction pattern analyses is able to reveal the potential presence of an undesirable grain in the volume.

2:55 PM CT03.07.03

Late News: Experimental Geometry Optimization of X-Ray Propagation-Based Phase Contrast Imaging
Hanna Dierks and Jesper Wallentin; Lunds universitet, Sweden

X-ray microscopy and tomography using propagation-based phase contrast (PB-PC) are powerful techniques to study low absorption samples on the micrometer scale. The main benefit of the technique is an increased contrast given by edge enhancement, that is, by near-field interference fringes around sharp edges. In setups with a divergent source, a trade-off between the distance dependent flux and the source coherence must be made. We present a systematical experimental and theoretical investigation of this trade-off, based on experiments with two different laboratory setups with high-resolution detectors: a custom-built system with a Cu microfocus source and a commercial system (Zeiss Xradia) with a W source.

The fringe contrast, contrast-to-noise ratio and fringe separation for a low-absorption test sample were measured for 130 different combinations of magnification and overall distances. We find that these figures-of-merit are sensitive to the magnification and that a theoretical optimum can be found that is independent of the overall source-detector distance. In general, we show that the theoretical models show excellent agreement with the measurements, if the X-ray source spectrum and the energy dependence of the detector sensitivity are considered. These results can be used when designing and optimizing the geometry of an imaging system, especially concerning the used magnification.

3:10 PM CT03.07.04

High-Resolution X-Ray Source with Advanced E-Beam Technology Emil Espes¹ and Anasuya Adibhatla²;
¹Excillum AB, Sweden; ²Excillum Inc, United States

Driven by needs from scientific research, healthcare and industrial manufacturing, X-ray microscopy has been successfully transferred from synchrotrons to the laboratory and the spatial resolution has been pushed to sub-micrometer. One way to further improve the resolution is to use an X-ray source with a very small focal spot. At Excillum, based on advanced electron beam and target technologies, a state-of-art nanofocus x-ray tube has been developed which enables an isotropic, resolution of 150 nm line-spacing.

Typical nanofocus X-ray tubes are normally limited in X-ray flux, which leads to long acquisition times when performing nano-CT outside of the synchrotrons. The newly developed nanofocus X-ray tube at Excillum, NanoTube N2, has a greatly improved brightness compared to its predecessor, achieving a minimum of 3x higher power loading while still maintaining the same sharp focus. The high brightness of Nanotube N2 brings the possibility of reduced scan times, helping to mitigate any motion blur from samples or imaging system to further improve the spatial resolution.

The advanced electron optics of the nanofocus X-ray tube has internal calibration and validation of the electron focus size, translating to the X-ray spot size. This gives the user a confirmation in what the maximum achievable resolution is for each scan, as well as a continuous feedback on the performance of the tube.

Until now the NanoTube has been integrated into different Nano-CT systems for applications of materials science [1], biomedical [2] and has recently been integrated in to commercially available NanoCT-systems [3].

This presentation will cover the technology enabling the new tube, as well as a few user examples of how the high resolution, high power density tube has helped researchers discover previously unseen features in their samples.

[1] C. Fella *et al.*, *Microscopy and Microanalysis*, 24(S2), 234-235 (2018)

[2] S. Ferstl *et al.*, *IEEE Transactions on Medical Imaging*, 1-1 (2019)

[3] <https://www.procon-x-ray.com/ct-alpha-nanotube/>

3:25 PM CT03.07.05

Late News: A Compact Light Source Providing High-Flux, Quasi-Monochromatic, Tunable X-Rays in the Laboratory Benjamin Hornberger and Jack Kasahara; Lyncean Technologies, Inc., United States

There is a large performance gap between conventional, electron-impact X-ray sources and synchrotron radiation sources. An Inverse Compton Scattering (ICS) X-ray source [1,2] can bridge this gap by providing a narrow-band, high-flux and tunable X-ray source that fits into a laboratory at a cost of a few percent of a large synchrotron facility. It works by colliding a high-power laser beam with a relativistic electron beam, in which case the energy of the backscattered photons is in the X-ray regime. So far, the only ICS source in regular user operation is the Munich Compact Light Source (MuCLS) [3], a combination of Lyncean Technologies' commercially available Compact Light Source (CLS) [4] and a beamline with two endstations built by researchers at the Technical University of Munich [5]. The application focus of the MuCLS is biomedical imaging of centimeter-sized samples in the 15-35 keV energy range, well-matched to the beam properties of the Lyncean CLS with ~4 mrad divergence and spectral bandwidth of 3-5%.

Here we present a concept for an ICS X-ray source that is about two orders of magnitude brighter than the existing CLS design. Depending on configuration, it covers an X-ray energy range of about 30-90 keV, or 60-180 keV, well-suited to many applications in materials science. It will provide X-ray flux of up to 4×10^{12} photons/s within a beam divergence of 4 mrad and a bandwidth of around 10%. This is well-suited for high resolution, micro-CT imaging of millimeter-sized samples at micron resolution, with a flux density similar to some high-energy synchrotron beamlines. The beam properties of the new design are also compatible with focused beam applications such as high-energy diffraction, since using a lower divergence part of the beam with lower bandwidth allows the use of several types of X-ray optics commonly used at synchrotron beamlines.

In this presentation, we will discuss the novel concepts applied to the design of this X-ray source as well as the resulting beam properties. We will discuss several application examples in the areas of imaging and diffraction where this system can approach or meet the performance of synchrotron beamlines. This will allow transferring many research and industrial applications from the synchrotron, where capacity is limited, and enable longitudinal studies that aren't compatible with the synchrotron access model, to a local lab.

[1] R. Hajima, "Status and Perspectives of Compton Sources," *Physcs Proc* 84, 35-39 (2016).

[2] M. Jacquet, "Potential of compact Compton sources in the medical field," *Phys Medica* 32, 1790-1794 (2016).

[3] E. Ettl, M. Dierolf, K. Achterhold *et al.*, "The Munich Compact Light Source: initial performance measures," *J Synchrotron Radiat* 23, 1137-42 (2016)

[4] B. Hornberger, J. Kasahara, M. Gifford *et al.*, "A compact light source providing high-flux, quasi-monochromatic, tunable X-rays in the laboratory," *Advances in Laboratory-based X-Ray Sources, Optics, and Applications VII*, A. Murokh and D. Spiga, Eds., 2, SPIE, San Diego, United States (2019).

[5] B. Günther, R. Gradl, C. Jud *et al.*, "The versatile X-ray beamline of the Munich Compact Light Source: design, instrumentation and applications," *J Synchrotron Radiat* 27, 1395-1414 (2020).

3:40 PM CT03.07.06

High Throughput Imaging Using Liquid MetalJet X-Ray Source Anasuya Adibhatla; Excillum Inc, United States

A conventional X-ray tube generates X-rays when highly energetic electrons are stopped in a solid metal anode. The fundamental limit for the X-ray power generated from a given spot size is when the electron beam power is so high that it locally melts the anode. The liquid-metal-jet anode (MetalJet) technology solves this thermal limit by replacing the traditional anode by a thin high-speed jet of liquid metal. Melting the anode is therefore no longer a problem as it is already molten, and significantly (about 10x) higher e-beam power densities can therefore be used making the MetalJet the brightest microfocus x-ray tube. The liquid-metal-jet technology results in stable and operational X-ray tubes running in over 100 labs around the world.

The applications include X-ray diffraction and scattering, several publications have also shown very impressive imaging results using liquid-metal-jet anode technology, especially in 2-D or 3-D phase-contrast imaging and X-ray microscopy. MetalJet sources also show their applicability in industrial imaging applications.

Phase-contrast imaging achieves a significant improvement on the contrast and resolution of soft-tissue with hard X-rays, however, the imaging quality, has been compromised by the low flux and brilliance using traditional microfocus tubes or adding optical elements. Therefore, the high brilliance liquid-metal-jet technology enables the development of laboratory-scale phase-contrast imaging systems. The high stability of the source meets the requirements of an ideal phase-contrast imaging technique. Several application examples will be given during the conference, illustrating the capability of MetalJet in commercial or in-house built X-ray microscopy system. The $K\alpha$ line of gallium, the main component of the liquid alloy is above absorption edge of copper making MetalJet beneficial for imaging copper structures with high contrast.

Excillum has recently introduced next generation MetalJet E1 increasing the brightness further by powering a 30 μm spot with 700W. The resulting flux is 70 times more than a conventional sealed tube microfocus tube in the energy range of 24-29 keV and 10 times more in the full spectrum. The applications where E1 dominates the performance are phase contrast imaging, high-pressure single crystal diffraction, small angle x-ray scattering, high speed x-ray imaging to name a few. The dual port capability provides flexibility to users in setting up experiments.

SESSION CT03.08: On-demand
Wednesday Morning, April 14, 2021
CT03

8:00 AM CT03.04.05

Late News: *In Situ* Analysis of Microstructural Evolution of Metallic Alloys Under High Speed Rotational Shear Deformation by Synchrotron XRD Arun Devaraj¹, Tingkun Liu¹, Mathew Olszta¹, Changyong Park², Bharat Gwalani¹, Stanislav Sinogeikin³, Suveen Mathaudhu¹ and Cynthia A. Powell¹; ¹Pacific Northwest National Laboratory, United States; ²Argonne National Laboratory, United States; ³DAC tools, United States

In order to develop shear-based solid phase processing methods, we aim to better understand the fundamental atomic scale mechanisms of mass and energy transfer in materials under shear deformation. To achieve this aim, we developed a first of its kind synchrotron-based in situ high-energy x-ray diffraction capability using a high-speed rotational diamond anvil cell (HSRDAC). HSRDAC provided time resolved synchrotron-based XRD results on lattice strain evolution and change in spatial variation of shear deformation induced alloying in Cu-Ni alloys. These in situ results were correlated with detailed microstructural characterization before and after shear deformation using transmission electron microscopy and atom probe tomography. This HSRDAC capability can provide new insights into the unique role of shear deformation in formation of metastable states, as well as in modifying the phase transformation pathways in a wide variety of alloy systems.

SYMPOSIUM CT04

Predictive Synthesis and Decisive Characterization of Emerging Quantum Materials
April 21 - April 21, 2021

Symposium Organizers

Panchapakesan Ganesh, Oak Ridge National Laboratory
Mingda Li, Massachusetts Institute of Technology
Kate Ross, Colorado State University
Hua Zhou, Argonne National Laboratory

* Invited Paper

SESSION CT04.01: Leaping Perovskite Quantum Materials
Session Chairs: Bethany Matthews and Hua Zhou
Wednesday Morning, April 21, 2021
CT04

8:00 AM *CT04.01.01

How the Polarization Quantum Can Cause Happiness or Distress at Perovskite Ferroelectric Surfaces, and Why It Matters for Energy Applications Nicola Spaldin; ETH Zurich, Switzerland

Using the example of multiferroic bismuth ferrite, we demonstrate how the interaction between the spontaneous ferroelectric polarization and the half-quantum-containing polarization lattice have a profound influence on the surface properties. With the help of density functional calculations, we identify energetically favorable happy (100) surface geometries, which are combinations of surface termination and polarization direction that lead to uncharged, stable surfaces. Switching the polarization causes these (100) surfaces considerable electrostatic distress, which must be compensated by the introduction of charged point defects or adsorbates such as water. We predict that the relative happiness or distress of the oppositely polarized surfaces should lead to an effective water splitting cycle on the bismuth ferrite (100) surface through polarization switching. We close by showing that there is an analogy between surface charge arising from ferroelectric polarization, and surface magnetization arising from magnetoelectric multipolization.

This work is in collaboration with Chiara Gattinoni and Ipek Efe

8:25 AM *CT04.01.02

Revealing Quantum Behavior by Point Defect Control in Complex Oxides Jung-Woo Lee¹, Tula R. Paudel², Anthony L. Edgeton¹, Neil Campbell³, Brenton A. Noesges⁴, Jonathon L. Schad¹, Katelyn Wada⁵, Jonathan Moreno-Rairez^{5,6}, Nicholas Parker⁵, Yulin Gan⁷, Hyungwoo Lee¹, Dennis V. Christensen⁷, Kitae Eom¹, Jong-Hoon Kang¹, Yunzhong Chen⁷, Thomas Tybell⁸, Nini Pryds⁷, Dmitri A. Tenne⁵, Leonard J. Brillson⁴, Mark S. Rzchowski³, Evgeny Y. Tsybal² and Chang-Beom Eom¹; ¹University of Wisconsin-Madison, United States; ²University of Nebraska-Lincoln, United States; ³University of Wisconsin-Madison, United States; ⁴The Ohio State University, United States; ⁵Boise State University, United States; ⁶Riverstone International School, United States; ⁷Technical University of Denmark, Denmark; ⁸Norwegian University of

Science and Technology, Norway

Point defects have played a major role in tuning the properties of materials over the last few decades. Controlling individual point defects in quantum heterostructures based on complex oxides presents new challenges, arising mostly from non-stoichiometry inherent to oxides. Here, we demonstrate the ability to tune point defects in LaAlO₃/SrTiO₃ (LAO/STO) oxide-based quantum heterostructures, using a newly-developed metal-organic pulsed laser deposition (MOPLD) growth technique with Ti flux provided by titanium tetraisopropoxide (TTIP). X-ray diffraction and Raman spectroscopy show that this approach opens a wide process window in which stoichiometry of STO can be controlled without structural changes. Depth-resolved cathodoluminescence spectroscopy reveals that STO films grown at higher TTIP flux have larger ratios of antisite Ti/Sr vacancies with lower concentration of oxygen vacancies. This leads to higher two-dimensional electron gas low-temperature mobilities at the LAO/STO interface and clear Shubnikov–de Haas oscillations. This result provides an essential part of the development of the next-generation complex oxide thin films and their heterostructures to investigate novel quantum phenomena.

This work was supported by the US Department of Energy (DOE), Office of Science, Office of Basic Energy Sciences, under Award DE-FG02-06ER46327.

8:50 AM BREAK

8:55 AM *CT04.01.03

Deciphering Electronic Correlations—An Atomic Perspective Yue Cao; Argonne National Laboratory, United States

Electronic correlation is arguably the most profound notion in condensed matter physics and often arises due to the strong interactions between the lattice and the electron charge, spin and orbital. Disentangling these degrees of freedom is thus critical to our understanding and manipulation of materials' properties but remains challenging due to the intricate interplay between these players. The difficulty fundamentally originates from the complicated energy landscape formed from often competing order parameters with almost degenerate energies. Here we demonstrate how a handful of experimental methods – electron diffraction, transport and X-ray pair distribution function – conspire to depict the role of atomic lattice vs. the electrons in the formation of electronic correlations.

In the Mott insulator Sr₂IrO₄ which structurally and electronically resembling the canonical high T_c superconductor cuprates, we recently observed a nematic order in the nonmagnetic normal state of the parent compound persisting below the Neel temperature and into the doped samples. The newly discovered nematic order has a correlation only a few nanometers and couples strongly to the lattice through the iridium 5d orbitals. We suspect the nematic order comes from competing ordering instabilities through the 'hidden' Fermi surface. Our observation challenges the accepted notions of nematicity in quantum materials and suggests that electronic nematicity can exist even in a correlated insulator and may cast new light on the understanding of non-conventional superconductivity.

9:20 AM CT04.01.04

Late News: Synthesis of Sr₂Ir_xRu_{1-x}O₄ via High-Pressure Floating Zone Technique Zachary Porter and Stephen D. Wilson; University of California, Santa Barbara, United States

In the past decade, researchers have uncovered a rich electronic phase diagram between the Mott insulating antiferromagnet Sr₂IrO₄ and the superconductor Sr₂RuO₄. However, sample size has constrained available measurements, and sample quality may be obscuring emergent magnetic phases. Here we describe the synthesis of single crystalline Sr₂Ir_xRu_{1-x}O₄ (0 < x ≤ 0.6) via a floating zone melting technique. We find that the use of a high pressure gas environment (~100 atm mixed O₂ and Ar) greatly decreases the evaporation of the IrO₂ reactant. The resultant gram-sized samples are more uniform in chemical composition and demonstrate unique

magnetotransport properties compared to previous work on flux-grown samples.

9:35 AM CT04.01.05

Late News: Post Electrocatalytic Cycling Examination of Defect Creation at Interfaces in LaFeO₃-SrTiO₃ Thin Films Bethany Matthews¹, Kayla Yano¹, Sandra Taylor¹, Michel Sassi¹, Rajendra Paudel², Andricus Burton², Byron Farnum², Ryan Comes² and Steven R. Spurgeon¹; ¹Pacific Northwest National Laboratory, United States; ²Auburn University, United States

Precise control of defects is paramount for control and manipulation of quantum phenomena. Defect formation at complex oxide interfaces can be caused by extreme environments. The inability to predict and control defect creation and evolution in environments, such as those encountered during catalytic cycling, predicates the ability to control and manipulate quantum properties and behavior and to access unique phenomena. To gain such control, it is important to understand the structural and chemical signatures associated with different defect types. LaFeO₃ (LFO) is a novel perovskite system with strongly defect-regulated catalytic properties, which makes it a rich system to explore defect manipulation. This work focuses on characterizing cation and oxygen defect populations developed near interfaces in single-crystal LFO grown on (001)-oriented SrTiO₃ substrates before and after electrocatalytic cycling. Scanning transmission electron microscopy (STEM) analyses are conducted using multiple modes of high-angle annular dark field, bright field, and annular bright field imaging to visualize the material microstructure. To complement imaging, local chemical and composition mapping is performed using electron energy loss spectroscopy (STEM-EELS). Our STEM-EELS measurements focus primarily on the O K edge, which is highly sensitive to local bonding and oxygen coordination environment. We discuss observed changes and their potential impact on the performance of this material.

9:50 AM CT04.01.06

Proximate Double Magnetic Transitions in BeCr₂O₄ Hector C. Mandujano¹, C. M. Naveen Kumar², Narayan Poudel³, Krzysztof Gofryk³, Thomas W. Heitmann⁴ and Harikrishnan S. Nair¹; ¹The University of Texas at El Paso, United States; ²Technische Universität Wien, Austria; ³Idaho National Laboratory, United States; ⁴University of Missouri–Columbia, United States

The coexistence of two order parameters is a particular occurrence in bulk single-phase materials. Such materials possessing (anti)ferromagnetism, ferroelectricity, and ferroelasticity are known as multiferroics. BeCr₂O₄ belonging to *Pbnm* and *Pcmn* space group is one of the earliest reported multiferroic compounds. In this work, we revisit this mostly unexplored material with a focus on multiple magnetic transitions at low temperatures. In this compound, Cr (III) occupies octahedral 4*a* site and Be (II) occupies the tetrahedral 4*c* site. This adopts a close packing structure with a 90° and 138° Cr – O – Cr bonds allowing for interesting magnetic superexchange interactions. In the present work, BeCr₂O₄ powder has been prepared using solid-state reaction method and verified the phase purity and crystal structure using laboratory and synchrotron X-ray diffraction. The Rietveld refinement of the powder X-ray data was carried out using *Pbnm* orthorhombic space group yielding lattice parameters, $a = 4.556 \text{ \AA}$, $b = 9.791 \text{ \AA}$, $c = 5.664 \text{ \AA}$. The magnetic susceptibility as a function of temperature revealed two close-by anomalies at $T_{N1} \sim 26.5 \text{ K}$ and $T_{N2} \sim 25.2 \text{ K}$, along with a third transition around 7.5 K, which are also observed in specific heat. Using the Curie-Weiss fit in the paramagnetic region, an effective magnetic moment is estimated to be 2.4 μ_B/Cr and the Curie-Weiss temperature is estimated to be -38 K indicating antiferromagnetic interactions. The reported antiferromagnetic structure is a noncollinear cycloidal spiral with a propagation vector along the *c*-axis with a large periodicity of 65 \AA , and abnormally low Cr moment, 1.55 μ_B . We will present microscopic details of multiple magnetic orders which are previously unreported, using magnetometry, specific heat, synchrotron X-ray diffraction, and neutron diffraction data.

11:45 AM *CT04.02.01

Insights into the Collective Electronic Losses at Surfaces with Momentum Resolution Francois C. Bocquet; Forschungszentrum Jülich GmbH, Germany

Investigating the dispersion of phonons and collective charge modes with high surface sensitivity is best achieved with high-resolution electron energy loss spectroscopy (HREELS) [1]. However, a systematic dispersion measurement over the whole Brillouin zone can take weeks with standard instruments, which measure the electron intensity sequentially, i.e., at one specific loss energy and one scattering angle at a time. Therefore, we have modified a high-resolution electron source to meet the requirements of commercial hemispherical electron analyzers with $E(k)$ imaging capabilities [2]. This allows the parallel detection of electrons in a broad range of momenta without sample movement. In this contribution I will show application examples of this new development for phonon, plasmon and exciton dispersion on 2D materials, quantum materials and organic single crystals.

[1] H. Ibach and D. L. Mills, *Electron energy loss spectroscopy and surface vibrations*, Academic Press, 1982.

[2] H. Ibach, F. C. Bocquet, J. Sforzini, S. Soubatch, and F. S. Tautz, *Electron energy loss spectroscopy with parallel readout of energy and momentum*, *Rev. Sci. Instrum.* **88**, 033903 (2017).

12:10 PM *CT04.02.02

New Capabilities of Inelastic Neutron Scattering for Studying Anharmonic Phonons Brent Fultz¹, Yang Shen¹ and Michael Manley²; ¹California Institute of Technology, United States; ²Oak Ridge National Laboratory, United States

The performance of the neutron source and instruments at the Spallation Neutron Source have now reached most of their full potential. The improvements in efficiency for inelastic neutron scattering are factors of hundreds beyond what was available a decade ago. With new experimental techniques, the momentum transfer Q can be aligned along all directions in a crystal, measuring energy spectra of phonons or magnons at all points in the Brillouin zone. Thermodynamic quantities that are sums over all phonons in a crystal can now be assessed phonon-by-phonon, and as functions of temperature.

Inelastic neutron scattering was used to measure all individual phonons in a single crystal of NaBr at temperatures of 10, 300 and 700 K. Even at 300 K the phonons, especially the optical phonons, showed large shifts in energy, with large broadenings from anharmonicity. Thermal expansion can be calculated by minimizing the free energy with respect to volume, V . In simple cases the free energy depends only on elastic energy and phonon entropy. Calculations were first performed with the quasiharmonic approximation (QHA), in which the phonon frequencies depend only on V , and on T only insofar as it alters V by thermal expansion. This QHA was an unqualified failure for predicting the temperature dependence of phonon energies, even 300 K. Ab initio computations of free energy that included anharmonicity from phonon-phonon interactions (and quasiharmonicity) successfully predicted both the temperature dependence of phonons and the large thermal expansion of NaBr. The anharmonicity was shown to arise from the cubic anharmonicity of nearest-neighbor Na-Br bonds. Anharmonicity is not a small correction to the QHA predictions of thermal expansion and thermal phonon shifts, but dominates the behavior.

A quantum Langevin model, similar to models developed for optomechanics, was used to predict intermodulation phonon sidebands (IPS). Ab initio calculations of anharmonic phonons in rocksalt NaBr showed sideband features qualitatively as "many-body effects." Inelastic neutron scattering measurements on a

crystal of NaBr revealed diffuse intensity at high phonon energy from the upper sideband. Its partner, the lower sideband, proves to be an "intrinsic localized mode." The spectral weight in the IPS pair is broadened and redistributed by interaction with the thermal bath, treated in the Langevin model as random noise.

These new studies on NaBr were made possible by new experimental capabilities for inelastic neutron scattering. The study of thermal expansion required the temperature dependence of all phonons in the first Brillouin zone. The observation of IPS required low backgrounds and high intensities. Both these studies are now practical with inelastic neutron scattering.

- D.S. Kim, et al., "Nuclear quantum effect with pure anharmonicity and the anomalous thermal expansion of silicon," P.N.A.S. 115, 1992 (2018).

- Y. Shen, et al., "The Anharmonic Origin of the Large Thermal Expansion of NaBr," Phys. Rev. Lett. 125, 085504 (2020). DOI: 10.1103/PhysRevLett.125.085504.

12:35 PM *CT04.02.03

Real-Time Observation of Dynamic Modulations Over a Ferro-Rotational Charge Density Wave Liuyan Zhao; University of Michigan, United States

Dynamic control over phases of matter with electromagnetic (EM) radiation receives increasing popularity in recent years because of both its ultrafast time scale and its access to thermodynamically unapproachable phenomena. Till now, the realization of dynamic manipulation of unconventional orders, such as a high-rank multipolar order, awaits to be explored largely because the coupling between multipolar orders and EM fields is nonlinear and nontrivial. In this talk, using the commensurate charge density wave (CCDW) in 1T-TaS₂ as the archetype, we demonstrate the dynamic control over the ferro-rotational order, the antisymmetric components of the second-rank electric quadrupolar order. We first show the ferro-rotational nature of CCDW in 1T-TaS₂, broken mirrors but preserved inversion, by performing temperature-dependent rotation anisotropy-second harmonic generation (RA-SHG). We then present the dynamic modulation of this ferro-rotational CCDW order, using time-resolved-RA-SHG (tr-RA-SHG) that adopts the optical-pump, RA-SHG-probe scheme. We show that this ultrafast modulation manifests itself as the breathing and the rotation of RA-SHG patterns at three different frequencies in the neighborhood of the previously reported CCDW amplitude mode frequency, with the mode of the highest (lowest) frequency primarily in the breathing (rotation) channel and the middle one in both channels. We further reveal a sudden shift of these three frequencies and a dramatic increase in the breathing and rotation magnitudes across a critical pump fluence of ~ 0.5 mJ/cm², by performing fluence dependent tr-RA-SHG.

1:00 PM *CT04.02.04

Probing Transient Lattice Dynamics of Photo-Excited Quantum Materials with Mega-Electron-Volt Ultrafast Electron Diffraction Xiaozhe Shen, Duan Luo, Fuhao Ji, Alexander Reid, Stephen Weathersby, Jie Yang and Xijie Wang; SLAC National Accelerator Laboratory, United States

Quantum materials under excitation from ultrafast laser pulses have shown exotic properties, such as ultrafast topological phase transition [1] and formation of transient charge density wave [2]. A complete understanding of such dynamical phenomena requires multimodal characterization techniques to reveal the dynamics associated with spin, charge, orbital and lattice degrees of freedom under nonequilibrium states. Ultrafast electron diffraction (UED) is an emerging tool to respond to this requirement by its capability of resolving transient lattice dynamics. SLAC National Accelerator Laboratory has built a UED with mega-electron-volt (MeV) electron beams to push the instrumental resolution to atomic spatial and temporal scales [3,4]. In this talk, the instrumental performance of SLAC MeV UED as well as the configuration of the experimental platform will be briefly reviewed. Selected experimental results on topological materials, charge density wave materials as well as heterostructures from two-dimensional materials will be highlighted. Research and development efforts to further expand the capabilities of SLAC MeV UED will be discussed.

References:

- [1] E. J. Sie, *et al.*, *Nature* **565**, 61 (2019)
[2] A. Kogar, *et al.*, *Nat. Phys.* **16**, 159 (2019)
[3] S. P. Weathersby, *et al.*, *Rev. Sci. Instrum.* **86**, 73702 (2015)
[4] X. Shen, *et al.*, *Ultramicroscopy* **184**(Pt A), 172 (2017)

1:25 PM CT04.02.06

Surface Characterization of Self-Catalyzed MBE Grown Be-Doped GaAs Nanowires and Te-Doped GaAsSb Nanowires for Infrared Photodetector Application. Priyanka Ramaswamy¹, Rabin Pokharel¹, Mehul Parakh¹, Shisir Devakota¹, Fred Stevie², Jia Li¹ and Shanthi Iyer¹; ¹North Carolina Agricultural and Technical University, United States; ²North Carolina State University, United States

Over the last decade, III-V semiconductor nanowires (NWs) have significantly attracted researchers due to one-dimensional architecture, quantum confinement effects, and a higher tolerance for stress-strain mismatch that allow greater freedom in engineering combinations of material systems in a variety of NW architectures to meet the demands of next-generation optoelectronic devices. Dopant incorporation in a well-controlled manner is essential to produce abrupt interfaces, to engineer work functions, and to realize advanced devices in NW configuration successfully. Unfortunately, the knowledge obtained from the thin film studies on dopant incorporation and carrier concentration cannot be directly translated to NWs due to the dopant's influence on the growth kinetics and growth mechanisms. Hall effect, field-effect, and capacitance-voltage are the commonly used measurement techniques in thin films for the determination of carrier concentration that require highly sophisticated lithography steps. For the assessment of dopants in NWs, several characterization methods have evolved. However, the sample preparation of off-axis electron holography is complex and requires additional information about the NW and homogeneity. Secondary ion mass spectrometry and atom probe tomography require a standard of known dopant concentration and are destructive. Hence, conductive-atomic force microscopy (C-AFM), scanning Kelvin probe microscopy (SKPM), X-ray photoelectron spectroscopy (XPS), and ultraviolet photoelectron spectroscopy (UPS), provide a set of excellent characterization methods for doping assessment, as they do not involve any complex contact fabrications.

In this work, we evaluate the incorporation of Beryllium (Be) dopants in GaAs NWs and Tellurium (Te) dopants in GaAsSb NWs grown using self-catalyzed molecular beam epitaxy (MBE) with variation in Be cell temperatures (T_{Be}) from 750 °C - 950 °C and Te cell temperatures (T_{GaTe}) from 500 °C - 570 °C, respectively. The extensive research interest in GaAs and GaAsSb NWs stems from its narrow bandgap region covering the important optical telecommunication wavelengths of 1.3 μm and 1.55 μm .

The topographical and I-V measurements using C-AFM of the vertical single NW exhibited a significant enhancement in current with photoresponse of 4 nA and 5 nA at -1 V for GaAs doped with T_{Be} at 950 °C and GaAsSb doped with T_{GaTe} at 550 °C. A statistical increase in the carrier concentration of Be-doped GaAs at T_{Be} of 750 °C, 850 °C, and 950 °C is found to be $9 \times 10^{15} \text{ cm}^{-3}$, $7 \times 10^{17} \text{ cm}^{-3}$, and $5 \times 10^{18} \text{ cm}^{-3}$, respectively from COMSOL Multiphysics fitting. An estimated carrier concentration of $7.1 \times 10^{17} \text{ cm}^{-3}$, $3.0 \times 10^{19} \text{ cm}^{-3}$, and $3.0 \times 10^{18} \text{ cm}^{-3}$ are determined for the Te-doped GaAsSb NWs at T_{GaTe} of 500 °C, 550 °C, and 570 °C, respectively. The elemental composition, work function, and carrier concentration of Be-doped GaAs and Te-doped GaAsSb NWs are further determined using XPS/UPS. With increasing T_{Be} for GaAs NWs, a shift in Fermi level (FL) towards the valence band provided evidence towards higher Be incorporation with T_{Be} -950 °C having work function and carrier concentration of 5.6 eV and $6.0 \times 10^{18} \text{ cm}^{-3}$. In Te-doped GaAsSb NWs, the FL is shifted towards the conduction band. The work function and the carrier concentration of Te-doped GaAsSb NWs at T_{GaTe} of 550 °C are found to be 3.6 eV and $2.8 \times 10^{19} \text{ cm}^{-3}$, respectively. The values of electron density from UPS concur very well with the values determined from C-AFM. The change in surface potential observed in doped NWs in SKPM also provided strong evidence of Be and Te incorporation. Hence, these surface analytical tools are found to be powerful characterization techniques for direct measurement of the dopant levels in NWs, which are critical for bandgap engineering design of optoelectronic devices.

Acknowledgment

This material is based upon research supported by the Air Force Office of Scientific Research (AFOSR) under grant number W911NF1910002.

SESSION CT04.03: Exploring Magnetic Topological and Quantum Phenomena
Session Chairs: Panchapakesan Ganesh and Mingda Li
Wednesday Afternoon, April 21, 2021
CT04

2:15 PM *CT04.03.01

Magnetic Topological Quantum Chemistry Bogdan A Bernevig; Princeton University, United States

Over the last 100 years, the group-theoretic characterization of crystalline solids has provided the foundational language for diverse problems in physics and chemistry. There exist two classes of crystalline solids: nonmagnetic crystals left invariant by space groups (SGs), and solids with commensurate magnetic order that respect the symmetries of magnetic space groups (MSGs). Whereas many of the properties of the SGs, such as their momentum-space corepresentations (coreps) and elementary band coreps (EBRs) were tabulated with relative ease, progress on deriving the analogous properties of the MSGs has largely stalled for the past 70 years due to the complicated symmetries of magnetic crystals. In this work, we complete the 100-year-old problem of crystalline group theory by deriving the small coreps, momentum stars, compatibility relations, and magnetic EBRs (MEBRs) of the single (spinless) and double (spinful) MSGs. We have implemented freely-accessible tools on the Bilbao Crystallographic Server for accessing the coreps of the MSGs, whose wide-ranging applications include neutron diffraction investigations of magnetic structure, the interplay of lattice regularization and (symmetry-enhanced) fermion doubling, and magnetic topological phases, such as axion insulators and spin liquids. Using the MEBRs, we extend the earlier theory of Topological Quantum Chemistry to the MSGs to form a complete, real-space theory of band topology in magnetic and nonmagnetic crystalline solids - Magnetic Topological Quantum Chemistry (MTQC). We then use this theory to perform a high through-put search of topological materials search, uncovering hundreds of topological magnetic materials.

2:40 PM *CT04.03.02

Realizing Gapped Topological Surface States in Magnetic Topological Insulators $\text{MnBi}_{2-x}\text{Sb}_x\text{Te}_4$ An-Ping Li; Oak Ridge National Laboratory, United States

Gapped surface states are a prerequisite for realizing several desired topological states like the quantum anomalous Hall effect showing dissipationless chiral edge states, the topological axion states displaying quantized magnetoelectric effects, and Majorana fermions obeying non-Abelian statistics. Recent research interest has turned extensively toward MnBi_2Te_4 , an intrinsic magnetic topological insulator, which is predicted to possess a large exchange gap in the surface states, potentially to exhibit exotic effects at room temperature. However, spectroscopic measurements with angle-resolved photoemission spectroscopy (ARPES) have shown contradictory results on the key feature needed for novel topological behavior: a magnetically induced gap between electronic energy bands. Some groups have observed the surface gap, while the others found no gap at Dirac point. The controversy can be ascribed to the large bulk carrier density of MnBi_2Te_4 coming from its highly electron-doped nature, whose fluctuation can significantly broaden the dispersion in ARPES data and overwhelm the fine structures around the Dirac point. It is thus imperative to engineer the materials to reduce the bulk carriers and to probe the surface electronic structures using local spectroscopy like scanning tunneling microscopy/spectroscopy (STM/STS).

Here we realize gapped surface states by tuning the bulk carrier density with Sb-substitution in $\text{MnBi}_{2-x}\text{Sb}_x\text{Te}_4$ (MBST) and characterizing the local band structure with quasiparticle interference (QPI) STM. Minimizing bulk carrier density results in the bulk-insulating MBST and allows us to access the surface states. A surface band gap of 50 meV has been revealed around the Dirac point inside the bulk band gap. *In situ* transport spectroscopy using our unique multiprobe STM has confirmed the surface nature of the carriers at the Fermi level through the exhibition of 100 % surface-dominant conductance. Moreover, the surface band gap is found

to be topologically protected and robust against magnetic field up to 9 T. Theoretical calculations based on density functional theory (DFT) have corroborated very well the experimental results, which reveal a topological axion insulator behavior of the MBST, consistent with recent observation of QAH effect. This research was performed at the Center for Nanophase Materials Sciences which is a DOE Office of Science User Facility.

3:05 PM BREAK

3:10 PM *CT04.03.03

MnBi₂Te₄.nBi₂Te₃—The Ideal Marriage of Magnetism and Topology Ni Ni; University of California, Los Angeles, United States

Magnetic topological material provides a great platform for discovering new topological states, such as the axion insulators, the Chern insulators, and the 3D quantum anomalous Hall (QAH) insulators. Recently, MnBi₂Te₄ was discovered to be the first material realization of a van der Waals intrinsic antiferromagnetic topological insulator (TI) where the QAH effect was observed at a record high temperature in its two-dimensional limit. Since the interplay of the magnetism and band topology determines their topological natures, understanding and manipulating the magnetism inside magnetic TIs will be crucial. In this talk, I will present our discovery of two new magnetic topological materials MnBi₂Te₄.nBi₂Te₃ (n=1 and 3) which consist of alternating [MnBi₂Te₄] and n[Bi₂Te₃] layers [1, 2]. I will show that by reducing the interlayer magnetic coupling with the increasing number of spacer [Bi₂Te₃] layers, MnBi₂Te₄.nBi₂Te₃ can be tuned from Z2 antiferromagnetic TIs (n=0,1,2) to ferromagnetic axion insulators. Furthermore, I will show that a continuous fine control of the magnetism in MnBi₄Te₇ can be made by Sb doping where an AFM to FM switching emerges due to the formation of the Mn/Sb antisite disorders [3]. Our study provides a rare tunable material platform to investigate various emergent phenomena arising from the marriage of magnetism and band topology.

[1] C. W. Hu, et.al, Nature Communications, 11, 97 (2020)

[2] C. W. Hu, et.al, Science Advances, 6, eaba4275 (2020)

[3] C. W. Hu, et.al, ArXiv: 2008.09097 (2020)

3:35 PM CT04.03.04

Late News: Comprehensive Database of Intrinsic Spin Hall Effect from High-Throughput Calculations Yan Sun¹, Yang Zhang¹, Qiunan Xu¹, Klaus Koepf², Roman Rezaev², Oleg Janson², Jakub Zelezny³, Tomas Jungwirth³, Jeroen van den Brink³ and Claudia Felser¹; ¹Max Planck Institute for Chemical Physics, Germany; ²Leibniz Institute for Solid State and Materials Research, Germany; ³Institute of Physics, Czech Academy of Sciences, Czechia

The spin Hall effect (SHE) has its special position in the field of spintronics, which allows transforming a charge current into a spin current and vice versa without the use of magnetic materials or magnetic fields. To gain new insight into the physics of the SHE and to identify materials with a substantial spin Hall conductivity (SHC), with the developed automatic high-symmetric atomic Wannier function projection, we performed high precision, high-throughput ab initio electronic structure calculations of the intrinsic SHC for over 20,000 non-magnetic crystals. The calculations reveal a strong and unexpected relation of the magnitude of the SHC with the crystalline symmetry, which we show exists because large SHC is typically associated with mirror symmetry protected nodal lines in the band structure. From the newly developed database, we identify new promising materials. This includes materials with a SHC comparable or even larger than that the up to now record Pt as well as materials with different types of spin currents. Furthermore, we find that the existence and magnitude of unusual symmetry spin currents that do not have perpendicular directions of spin current flow, spin polarization, and the electrical field can be in many materials tuned by the orientation of the electrical field with respect to the crystal [1]. This could be helpful for designing new types of spin-orbitronics devices.

[1] arXiv:1909.09605

3:50 PM CT04.03.05

Late News: New Chemical Strategy to Design Magnetic Skyrmion Host Materials Ebube E. Oyeka¹, Michal J. Winiarski², Artur Blachowski³, Keith M. Taddei⁴, Allen Scheie⁴ and Thao T. Tran¹; ¹Clemson University, United States; ²Gdansk University of Technology, ul., Poland; ³Pedagogical University of Cracow, ul., Poland; ⁴Oak Ridge National Laboratory, United States

Magnetic skyrmions, which are 3-dimensional topological excitations with a nano-sized particle character, have come to the forefront as potential applications in spintronic devices. These vortex-like spin nanostructures are stabilized by Dzyaloshinskii-Moriya asymmetric exchange interaction facilitated by strong spin-orbit coupling and broken inversion symmetry crystal lattice. However, designing new skyrmion-host materials presents a significant challenge. To address this, we propose a chemical strategy for inducing skyrmions in new classes of materials based on combinations of magnetic spin, asymmetric building units with stereo-active lone-pair electrons, and polar lattice symmetry. To demonstrate the viability of the proposed judicious design principles, we successfully synthesized Fe(IO₃)₃ with a non-centrosymmetric polar *P6₃* space group, by using low-temperature reactions and characterized the crystal structure using powder synchrotron X-ray diffraction and single-crystal X-ray diffraction. The magnetic structure and magnetic spin evolution of this material were investigated by performing neutron diffraction, ⁵⁷Fe Mössbauer spectroscopy, magnetization, and heat capacity measurements. Density functional theory calculations were also performed to gain better insights into chemical bonding and exchange interaction of Fe(IO₃)₃. Our results demonstrate a connection between topological magnetism and stereo-active lone-pair electrons in compounds having extended polar lattice, expanding avenues to create new skyrmion materials. The results and knowledge gained from this study will be discussed.

SESSION CT04.04: Probing Topological Quantum Systems and Theoretical Advances in Predicting Quantum Materials

Session Chairs: Panchapakesan Ganesh and Brenda Rubenstein
Wednesday Afternoon, April 21, 2021
CT04

5:15 PM *CT04.04.01

Topological Semimetals with Unique Optical Properties Joel Moore^{1,2}; ¹University of California, Berkeley, United States; ²Lawrence Berkeley National Laboratory, United States

This talk starts by reviewing known examples of how topological materials generate new kinds of electrodynamic couplings and effects. We then turn to how topological Weyl and Dirac semimetals can show unique electromagnetic responses, moving from linear optics to nonlinear optics, and the search for specific materials realizing these possibilities. We develop theories for why nonlinear optics is very strong in some Weyl semimetals such as TaAs, and how in others with structural chirality, there is the possibility of a quantized chiral photocurrent. This nonlinear effect has a natural quantum e^3/h^2 and appears in chiral Weyl semimetals over a finite range of frequencies. We discuss interaction and disorder corrections to nonlinear responses in closing, along with a related correction to the anomalous Hall coefficient at finite wavevector.

5:40 PM *CT04.04.02

Tuning the Chern Number in Quantum Anomalous Hall Insulators Cui-Zu Chang; The Pennsylvania State University, United States

A quantum anomalous Hall (QAH) state is a two-dimensional topological insulating state that has a quantized Hall resistance of $h/(Ce^2)$ and vanishing longitudinal resistance under zero magnetic field (where h is the Planck constant, e is the elementary charge and the Chern number C is an integer). The QAH effect has been realized in magnetic topological insulators and magic-angle twisted bilayer graphene. However, the QAH effect at zero

magnetic field has so far been realized only for $C = 1$. In this talk, I will briefly talk about the route to the QAH effect in magnetically doped TI films/heterostructures. I will focus on our recent progress on the realization of the QAH effect with tunable Chern number (up to $C = 5$) in multilayer structures consisting of alternating magnetic and undoped topological insulator layers. Moreover, the Chern number of a given multilayer can be tuned by varying either the magnetic doping concentration in the magnetic topological insulator layers or the thickness of the interior magnetic topological insulator layer. In the last part of my talk, I will discuss the potential applications of the QAH insulators with tunable high Chern number and what we can do along this direction in the future.

We acknowledge the support from the DOE grant (DE-SC0019064), the ARO grant (W911NF1810198), the NSF-CAREER award (DMR-1847811), and the Gordon and Betty Moore Foundation's EPiQS Initiative (Grant GBMF9063 to C.Z.C.).

6:05 PM BREAK

6:10 PM *CT04.04.03

Predicting Linear-, Nonlinear- and Hydrodynamic Phenomena in Quantum Materials Prineha Narang;
Harvard University, United States

Discoveries in quantum materials, which are characterized by the strongly quantum-mechanical nature of electrons and atoms, have revealed exotic properties that arise from strong correlations. We anticipate that quantum materials to be discovered and developed in the next years will transform the areas of quantum information processing including communication, storage, computing. To realize this promise, first principles theoretical and computational frameworks for quantum materials are essential. In this context, I will present our recent work in *ab initio* approaches to the microscopic dynamics, decoherence and optically-excited collective phenomena in quantum matter at finite temperature to quantitatively link predictions with 3D atomic-scale imaging, quantum spectroscopy, and macroscopic behavior. Capturing these dynamics poses unique theoretical and computational challenges. The simultaneous contribution of processes that occur on many time and length-scales have remained elusive for state-of-the-art calculations and model Hamiltonian approaches alike, necessitating the development of new methods in computational physics. I will show our predictions of linear-, nonlinear-, and hydrodynamics in Weyl semimetals, accounting for microscopic electron-electron and electron-phonon scattering processes. I will discuss the anomalous landscape for electron hydrodynamics in systems beyond graphene, highlighting that previously-thought exotic fluid phenomena can exist in both two-dimensional and anisotropic three-dimensional materials with or without breaking time-reversal symmetry. Our work identifies phonon-mediated electron-electron interactions as critical in a microscopic understanding of hydrodynamics. Non-diffusive electron flow, and in particular electron hydrodynamics, has far-reaching implications in quantum materials science, as I will show in this talk. Finally, I will discuss our recent work in driving quantum materials out-of-equilibrium to control the coupled degrees-of-freedom, and present an outlook on similarly controlling newly-synthesized topological systems.

6:35 PM *CT04.04.04

Correlation in 2D Materials—Magnetism, Proximity Effects and Reactivity Through the Lens of Quantum Monte Carlo Brenda Rubenstein, Daniel Staros, Gopal Iyer, Ravindra Nanguneri and Leonard Sprague; Brown University, United States

2D materials are an exciting new class of materials that hold great promise for a wide range of engineering applications because of their exceptional tunability. Indeed, these materials' band gaps, magnetic and topological properties, and conductivity can be dramatically altered just by stretching or stacking them. Despite their promise, however, our modern understanding of 2D materials is partially obscured by the fact that most have only been computationally modeled using Density Functional Theory (DFT), a theory that cannot readily describe electron correlation and is known to yield widely varying results for such central quantities as band gaps and molecular binding energies depending upon the exchange-correlation functional employed.

In this talk, I will describe my group's recent efforts to model an array of 2D materials using fully correlated quantum Monte Carlo (QMC) techniques and the unanticipated physics these efforts have revealed. First, I will discuss for which materials our simulations reveal the largest discrepancies between DFT and QMC. I will then illustrate the importance of using correlated methods in the modeling of proximity-induced magnetism and spin-orbit coupling in multilayer materials. Lastly, if time permits, I will detail how correlation influences carbon dioxide reduction on post-transition metal chalcogenides. Altogether, this work paints a more complete picture of the electronic structure and properties of this increasingly important class of materials.

SESSION CT04.05: Precise Manipulation, Modulation and Stabilization of Versatile Quantum States

Session Chairs: Jung-Woo Lee and Xiaozhe Shen

Wednesday Afternoon, April 21, 2021

CT04

8:15 PM CT04.05.01

Phase Selection of Nickel Sulfides via Precise Oxidation State Control in Molten Hydroxides—A High-Temperature Aqueous Analogue Xiuquan Zhou¹, David Mandia¹, Duck-Young Chung¹ and Mercuri G. Kanatzidis^{1,2}; ¹Argonne National Laboratory, United States; ²Northwestern University, United States

High-temperature solutions are promising for discovery of novel materials with interesting properties relevant to superconductivity, magnetism, energy conversion, etc. Despite highly effective for exploratory synthesis, they are much less predictable and offer little to no control of the oxidation state compared to aqueous solutions. Here, we demonstrate that molten hydroxides not only offers crystal growth but also exhibit similar acid-base chemistry like water. Although never before they have been used for the synthesis of a chalcogenide, we found it was surprisingly powerful. By precise oxidation state control in hydroxide mediums, not only we were able to grow single crystals of all known ternary K-Ni-S, we have successfully isolated several new phases. Among them, we have identified a new low-valence nickel-rich sulfide, KNi₄S₂ and discovered polytypism in the kinetically stabilized K₂Ni₃S₄. By controlling the polytypism in K₂Ni₃S₄, we could obtain a dilute Kagome lattice, which could be a new spin liquid materials. In addition, using KNi₄S₂ as a template, we obtained a new layered binary Ni₂S by deintercalating K and a LiOH-intercalated Ni₂S by exchanging K with LiOH. This new Van der Waals building block of Ni₂S proves to be a new host layer for intercalation chemistry. The rich acid-base chemistry in molten hydroxides can lead to rational discovery of new materials.

This new compound KNi₄S₂ share great structural similarities to the tetragonal KNi₂S₂. However, unlike KNi₂S₂, it consists of doubly stacked Ni square sheets between two sulfur square sheets instead of edge-sharing NiS₄ tetrahedra. Thus, each Ni forms both Ni-S ionic bonding and Ni-Ni metallic bonding. In addition to its exotic crystal structure, this low-valence Ni compound also shares great similarities with nickelate superconductors. Recently, new excitement emerges following the report of superconductivity (T_c up to 15 K) in a heterostructure of NiO₂ infinite-layer on perovskite.¹ One of the most extraordinary features of this nickelate superconductor is its oxidation state, +1.0-1.2, which is nearly isoelectronic with the hole-doped high- T_c cuprate superconductors.² However, unlike the parent phase of the cuprate superconductors (antiferromagnetic), no long-range magnetic ordering has yet observed in the nickelate system. Thus, it is of great importance to elucidate the underlying magnetic ordering or lack thereof in the low-valence nickelate system. Here, our new K₂Ni₃S₄ compound not only shares similar Ni-square net with both the nickelate and Fe-based superconductors, but also offers a rare opportunity to study the long-range magnetic ordering in low-valence Ni compounds.

To fully understand their electronic properties, we carried out density functional theory (DFT) calculations. Very interestingly, after deintercalation the binary Ni₂S does not show a simple change in electron-filling. Instead, close to its Fermi level, an electron pocket and almost a hole pocket appear at the G and M points,

respectively, whereas there was only an electron pocket at the G point for the parent KNi_4S_2 . This feature highly resemble the Fe-based superconductors especially the 122-type KFe_2Se_2 and the LiOH-intercalated FeSe. Although Ni_2S is not superconducting, but the magnetism is suppressed after the deintercalation. In addition, the Fermi surface nesting at the M point is not complete as there is no hole pocket for Ni_2S . However, if we can future oxidize Ni to between Ni +1-1.5, then a electron and hole pocket pair could be created and lead to superconductivity. This will link Fe-based superconductors to the new nickelate superconductors.

1. Li, D.; Lee, K.; Wang, B. Y.; Osada, M.; Crossley, S.; Lee, H. R.; Cui, Y.; Hikita, Y.; Hwang, H. Y. *Nature* **2019**, *572*, 624–627.
2. Bednorz, J. G.; Muller, K. A. *Zeitschrift fur Physik B Condensed Matter* **1986**, *64*, 189–193.

8:30 PM CT04.05.02

Uncovering the Mechanism of Single-Atom E-Beam Manipulation of Pnictogen Dopants in Silicon

Bethany M. Hudak^{1,2}, Alexander Markevich³, Jiaming Song⁴, Toma Susi³ and Andrew Lupini²; ¹U.S. Naval Research Laboratory, United States; ²Oak Ridge National Laboratory, United States; ³University of Vienna, Austria; ⁴Northwest University, China

Single-atom quantum devices, in which the spin state of an atom is used to encode a qubit, are promising architectures for quantum computers. In solid-state Si devices, this requires the precise positioning of subsurface qubit dopant atoms. The current state-of-the-art for single-atom positioning relies on scanning probe techniques such as atomic force microscopy (AFM) and scanning tunneling microscopy (STM). However, these techniques are limited to surfaces and often involve overgrowth layers to encapsulate the dopants, which could lead to the atoms diffusing from their intended positions. Recently, scanning transmission electron microscopy (STEM) has been demonstrated as a tool to directly position single atoms in graphene as well as in silicon by taking advantage of an Ångstrom-size probe that can be manually controlled. The ability to directly locate and position a single dopant atom in a 3D material opens up new avenues of device manufacturing, but the mechanism needs to be well-understood before the technique can be optimized and widely implemented. Here, we study the controlled positioning of subsurface pnictogen dopants in a thin silicon crystal. Using density functional theory molecular dynamics (DFT/MD) simulations, we uncover the atomistic mechanism through which the dopant atoms can be directed, unveiling a novel, damage-free atom exchange process. We study the Si group V dopants Bi, Sb, As, and P, revealing that the atom-exchange mechanism is limited to the large Bi and Sb dopants. New STEM experiments further demonstrate the ability to move the Sb dopants several lattice positions by dragging the electron probe across the sample, confirming that it is possible to manipulate Sb in the same manner that Bi could be directed.

8:45 PM CT04.05.03

Hydrogen Thermal Treatment Effects on Conductance Quantization in Pt/NiO/Pt Resistive Switching Cells Yusuke Nishi; National Institute of Technology, Maizuru College, Japan

Resistive random access memory (ReRAM) is the emerging nonvolatile memories, which has a metal-oxide-metal structure. A resistive switching (RS) phenomenon offers useful applications for not only nonvolatile memories but machine learning for neural network. The RS phenomenon in a transition metal oxide-based ReRAM cell is usually explained as nonvolatile transitions in the cell resistance between high- and low-resistance states by formation and dissolution of localized conductive filaments in the oxide thin film, which is created by the first voltage application, called forming. I reported that conductance quantization in nickel-oxide (NiO)-based ReRAM cells sandwiched by platinum (Pt) electrodes was observed during forming [1,2]. When the scale of the weakest spot in the filament reaches an atomic size, conductance quantization can be expected to appear. Therefore, the RS cell includes a conductive filament with a quantum point contact (QPC) upon the voltage sweep [1]. However, variation of voltage to reach the quantized conductance was large, because the amount controllability of oxygen vacancies was possibly inadequate. In this study, I investigate hydrogen thermal treatment effects on how the amount or distribution of the oxygen vacancies are controlled.

A 60-nm-thick Pt bottom electrode was deposited by sputtering on a silicon-dioxide/p-silicon substrate. Next, a polycrystalline 80-nm-thick NiO with a columnar structure layer was deposited by radio-frequency reactive sputtering under oxygen gas flow rate precisely regulated. Pt top electrodes were subsequently deposited on the NiO layer. Several Pt/NiO/Pt ReRAM cells showed the first abrupt current jump by an initial voltage sweep to the cell, which made the cell conductance equivalent to the quantized conductance ($=2e^2/h$). Moreover, the continued voltage sweep brought about conductance quantization in the cells, indicating the formation of a conductive filament with a QPC. However, variation of the voltage to start the current jump was large and only several cells showed conductance quantization.

I attempted various thermal treatment of the RS cells in reduced or oxidized gas ambience. Thermal treatment above 300°C during more than 20 min resulted in poor RS endurance, indicating deterioration of ReRAM cells by a strong heat effect. Meanwhile, argon and oxygen thermal treatment below 200°C led to a subtle change of initial cell resistance (less than 5%) and few effects on the voltage variation and how many cells showed clear conductance quantization. Therefore, thermal treatment below 200°C was conducted in hydrogen gas, which possesses a high reducing reaction, to prevent the cells from heat deterioration effect.

Although hydrogen thermal treatment between 150°C and 200°C resulted in the delamination of Pt top electrodes during even less than 10 min, initial resistance of cells fabricated with a higher oxygen gas flow rate during NiO deposition decreased to moderate values and RS endurance in the treated cells was almost improved by the hydrogen treatment below 150°C. In high-angle annular dark field scanning transmission electron microscopy analyses of the NiO layers after the hydrogen thermal treatment, brightness of bright spots observed at grain-boundary triple-points in the NiO layers was similar with each other. Energy dispersive X-ray spectroscopy revealed that the average composition ratio of O to Ni along the thickness direction at triple-points was comparatively constant and smaller than the value within grains. These results indicate that conductive filaments with a QPC are formed along Ni- or oxygen-vacancy-rich grain-boundary triple-points, and that reducing reaction by hydrogen thermal treatment below 150°C leads to restriction of voltage variation and improvement of appearance probability of conductance quantization.

[1] Y. Nishi et al., *J. Mater. Res.* **32**, 2631 (2017).

[2] Y. Nishi et al., *J. Appl. Phys.* **124**, 152134 (2018).

9:00 PM CT04.05.04

Stabilization of J-Aggregate Thin Films for Exciton-Polariton Microcavities Dane W. deQuilettes;
Massachusetts Institute of Technology, United States

Exciton-polaritons are a hybrid state of light and matter and are a quantum playground for exploring Bose-Einstein condensation, superfluidity, quantum vortices, and quantum entanglement. Although room-temperature polariton condensation has now been observed in carbon nanotubes, organic molecules, and in lower dimensional metal halide perovskites, these coherent quantum states are difficult to control and study due to rapid photodegradation. Here, we show orders-of-magnitude improvements in the photostabilization of the lower polariton branch emission from J-aggregated cyanine dyes through use of amine-based light stabilizers and hygroscopic crystal matrices. These results will likely enable condensation in a wide range of materials where these quantum effects were previously inaccessible.

SYMPOSIUM CT05

Artificial Intelligence and Automation for Materials Design
April 17 - April 20, 2021

Symposium Organizers

Amanda Barnard, Australian National University
Bronwyn Fox, Swinburne University of Technology
Manyalibo Matthews, Lawrence Livermore National Laboratory
Krishna Rajan, University at Buffalo, The State University of New York

Symposium Support

Silver
Army Research Office

* Invited Paper

Tutorial CT05: Computational Materials Discovery using the Automatic FLOW (AFLOW) Software
Session Chairs: Marco Esters, David Hicks, Manyalibo Matthews, Corey Oses and Cormac Toher
Saturday Morning, April 17, 2021
CT05

10:00 AM *

Introduction + AFLOW Installation Help Marco Esters; Duke University, United States

abstract

10:45 AM *

Materials Database Access—AFLOW.org and AFLUX Marco Esters; Duke University, United States

Computational materials databases play an important role in the design and synthesis of new compounds with desired physical properties. With more than three million entries, the AFLOW.org repository is the largest of its kind. This session will start with an introduction to AFLOW and its installation. It will conclude with a demonstration on how to use AFLUX, a search language developed for AFLOW, to query results from our database programatically. Python will be used to show how the data can be retrieved and returned in JSON format.

12:15 PM BREAK

12:30 PM *

Structural Analysis and Generation of Materials—AFLOW-SYM, AFLOW Prototype Encyclopedia, and AFLOW-XtalFinder David Hicks; Duke University, United States

Classification of crystallographic structures is necessary for understanding and tuning the properties of materials. Coupling structural analysis tools with automatic methods for modeling compounds accelerates materials design. This part will introduce the symmetry and structure generation engines inside AFLOW. Participants will learn the AFLOW prototyping system, how to create structure files in various ab initio code formats, how to calculate the symmetries of a material, and how to compare structures. Python interfaces and web interfaces to these tools will be provided as well.

2:00 PM BREAK

3:00 PM *

Thermodynamics—AFLOW-CHULL and CCE Cormac Toher; Duke University, United States

One of the most important aspects of computational materials discovery is the prediction of synthesizability. The AFLOW Convex HULL (AFLOW-CHULL) application provides the tools to assess the stability and synthesizability of materials. Attendants will be taught how to use AFLOW-CHULL through both the command line and our web application. This part will also demonstrate how to correct the formation enthalpies of polar compounds (e.g. oxides), which are often inaccurate in standard density functional theory calculations, using the Coordination Corrected Enthalpies (CCE) method.

4:30 PM BREAK

4:45 PM *

Disorder—AFLOW-POCC Corey Oses; Duke University, United States

Disordered materials such as high-entropy alloys have attracted considerable interest due to their enhanced physical properties such as high hardness. Modeling these materials, however, poses a considerable computational challenge. This section will cover AFLOW's Partial OCCupation (AFLOW-POCC) algorithm which has been successfully employed to predict six new high-entropy carbides. Participants will be introduced to the algorithm and learn how to use AFLOW to generate the structures to determine the properties of disordered materials.

6:15 PM Q&A

SESSION CT05.01: Machine Learning I
Session Chairs: Thomas Hammerschmidt and Krishna Rajan
Sunday Morning, April 18, 2021
CT05

8:00 AM *CT05.01.01

Network Theory Meets Materials Science Christopher Wolverton; Northwestern University, United States

One of the holy grails of materials science, unlocking structure-property relationships, has largely been pursued via bottom-up investigations of how the arrangement of atoms and interatomic bonding in a material determine its macroscopic behavior. Here we consider a complementary approach, a top-down study of the organizational structure of networks of materials, based on the interaction between materials themselves. We demonstrate the utility of applying network theory to materials science in two applications: First, we unravel the complete “phase stability network of all inorganic materials” as a densely-connected complex network of 21,000 thermodynamically stable compounds (nodes) interlinked by 41 million tie-lines (edges) defining their two-phase equilibria, as computed by high-throughput density functional theory. Using the connectivity of nodes in this phase stability network, we derive a rational, data-driven metric for material reactivity, the “nobility index”, and quantitatively identify the noblest materials in nature. Second, we apply network theory to the problem of synthesizability of inorganic materials, a grand challenge for accelerating their discovery using computations. We use machine-learning of our network to predict the likelihood that hypothetical, computer generated materials will be amenable to successful experimental synthesis. ** *In collaboration with V. Hegde, M. Aykol, S. Kirklin, L. Hung, S. Suram, P. Herring, and J. Hummelshoj*

References:

- Hegde, V. I., Aykol, M., Kirklin, S., & Wolverton, C. (2020). The phase stability network of all inorganic

materials. *Science Advances*, 6(9), eaay5606.

- Aykol, M., Hegde, V. I., Hung, L., Suram, S., Herring, P., Wolverton, C., & Hummelshøj, J. S. (2019). Network analysis of synthesizable materials discovery. *Nature communications*, 10(1), 1-7.

8:25 AM CT05.01.02

Late News: Optimizing Complex Geometries with Feed Forward Control and Machine Learning Clara Druzgalski, Gabe Guss, Ava Ashby, Simon Lapointe, Aiden Martin, Maria Strantza, Zachary Reese and Manyalibo J. Matthews; Lawrence Livermore National Laboratory, United States

Laser powder bed fusion (LPBF) enables the fabrication of complex metal parts for many industries. However, quality control of LPBF remains a challenge due to defects that negatively impact repeatability and reliability. Complex parts contain many features that are defect-prone such as overhangs, thin walls, and channels. Process parameters must be optimized to satisfy engineering requirements and reduce the likelihood of part failure. This work describes computational methods to identify defect-prone features and apply optimized parameters using feed forward control and machine learning models. This targeted approach adapts the laser parameters to improve dimensional accuracy and reduce porosity.

8:40 AM *CT05.01.03

Natural Language Processing for Materials Design—What Can We Extract From the Research Literature? Anubhav Jain; Lawrence Berkeley National Laboratory, United States

Traditionally, researchers have been able to leverage the tremendous wealth of information in the research literature only by reading and reviewing articles one at a time. This talk focuses on how advancements in natural language processing will make it possible to leverage the collective knowledge embedded in decades of previous research studies (often only represented in unstructured text documents) in novel ways. In this talk, I will provide a brief overview of natural language processing techniques and how they can be trained on the materials domain. Next, I will provide several examples of how such techniques are being leveraged to accelerate materials research. This includes the use of these algorithms to generate structured databases of materials properties (on which machine learning algorithms can be trained), to improve the ability to query and extract information from the body of research work, and even to make predictions of materials for functional applications. Finally, I will provide an outlook on the future of these techniques might be integrated into several different models of materials research and development.

9:05 AM CT05.01.04

Natural Language Processing for Insensitivity Classification of Energetic Materials Gaurav Kumar, Allen Garcia, Connor O'Ryan and Peter Chung; University of Maryland, United States

The vast and ever-increasing number of published text on energetic materials, written in natural language, opens doors for the application of Natural Language Processing (NLP) tools to extract information that can be used for characterization, design, and discovery of materials. In this work, we present how NLP can be used to extract information from open literature about energetics and their physical/chemical properties such as h₅₀ impact sensitivity. We combine text from ~20000 journal articles and US patents to form our corpus. Two types of classifiers are developed (1) A binary classifier which categorizes the energetics into two groups i.e. sensitive or insensitive, and (2) A multinomial classifier which computes the likelihood of energetics' sensitivity as a function of distance within an embedding vector space to five common energetics whose insensitivities are well known. The binary classifier is evaluated by comparing the classifier result with a reference list of the energetics. The evaluation of the multinomial classifier is based on Kolmogorov-Smirnov test, Jensen-Shannon, Hellinger, and Wasserstein distances between statistical distributions developed from NLP and those generated using actual h₅₀ data. The preliminary results indicate an accuracy of ~80% and an f-score of 0.86 for the binary classifier whereas the multinomial classifier consistently scores above a P-value of 0.90. This indicates that word embeddings can effectively capture the semantics of domain-specific language and that NLP, originally developed for natural language interpretation, can be extended to the study of materials, for instance, to

semantically learn how to characterize material properties and capture relationships between chemicals, their properties, and applications.

9:20 AM *CT05.01.05

Active Materials Exploration and Characterization with Bayesian Optimization Patrick Rinke; Aalto University, Finland

Data generation in materials science is often limited by the time it takes to perform experiments or simulations. To facilitate the exploration and characterization of complex materials, we have developed the Bayesian Optimization Structure Search (BOSS) code. BOSS is an active learning technique that strategically samples the parameter space of material-science tasks be it experimental or computational. BOSS proposes new data acquisition points for maximum knowledge gain, balancing exploitation with exploration. I will demonstrate BOSS' smart and efficient data strategy for two examples: 1) sustainable biomaterials and 2) hybrid organic-inorganic electronic materials. For 1), we extract lignin from wood samples with hydrothermal treatment. Lignin is further processed by chemical modification into sustainable composite materials (e.g. carbon fibers, thermoplastics and three-dimensional printed objects). Lignin extraction and processing is coupled to BOSS to visualize process-structure-property correlations and to efficiently optimize extraction and modification conditions. For 2), we couple BOSS to density-functional theory (DFT) calculations to study the adsorption of a camphor molecule on the Cu(111) surface. We identify 8 unique stable adsorbates. By matching the stable structures to atomic force microscopy (AFM) images, we conclude that the experiments feature 3 different structures of chemisorbed camphor molecules.

SESSION CT05.02: Automation and High Throughput I
Session Chairs: Nicholas Kotov and Prahalada Rao
Sunday Morning, April 18, 2021
CT05

10:30 AM *CT05.02.01

Materials Informatics and Manufacturing Scalability and Sustainability Elsa Olivetti; Massachusetts Institute of Technology, United States

Data has become a fundamental ingredient for accelerating and optimizing materials design and synthesis. Advances in applying natural language processing (NLP) to material science text has greatly increased the size and acquisition speed of materials science data from the published literature. This presentation will describe work to extract information from peer reviewed academic literature across a range of materials with particular focus on developing strategies for manufacturing scalability and sustainability challenges. Examples will be drawn from use of alternative feedstocks in cement as well as solid state electrolyte development.

10:55 AM *CT05.02.02

Automated Multimodal Manufacturing Optimization Brian Giera, Adam Jaycox, Kyle DeVlugt, Joseph Nicolino, Brian Au and Sam Ludwig; Lawrence Livermore National Laboratory, United States

The characterization and fabrication of manufactured parts is often a serial process, where different post-processing steps and quality measurements are obtained in a non-co-located and nonautomated fashion. The traditional process for taking components from the design stage to a final, qualified component is an extremely personnel intensive series of steps that are typically treated as siloed activities. Thus, the development cycle (e.g. part specification, fabrication, and qualification) is subject to bottlenecks, making part repeatability difficult and costly to achieve, quantify, and optimize. This is true for established manufacturing processes and especially true for emerging advanced manufacturing technologies. To address this, we adopt an "object-

oriented” or modular methodology at all stages of manufacturing, fabrication, inspection, and so on. For instance, on such inspection modality is an automated metrology system that can perform a variety of inspection routines on arbitrary objects. Another module is a comprehensive NoSQL database that can log all data acquired at each step for every part fabricated by our system. We also create digital twins of each inspection and fabrication module that evolve over time as insights are extracted from the growing database. Although we exercise these capabilities using a suite of fused deposition model printers, the object-oriented approach is agnostic to any given manufacturing approach or inspection system. During this talk, we walk through key capabilities demonstrated with these modules and the implications towards automation of process design.

11:20 AM *CT05.02.03

Autonomous End-to-End Systems for Materials Discovery Muratahan Aykol and Joseph Montoya; Toyota Research Institute, United States

Autonomous research platforms driven by artificial intelligence have the potential to enable rapid identification of improved material components for technological devices, such as batteries or fuel cells, at significantly reduced research costs. In this talk, we will present our recent progress on the development of an end-to-end autonomous platform that helps materials scientists efficiently find or expand the space of optimal candidate materials with minimal intervention. This platform provides a software framework for (i) designing and testing of goal-oriented research agents that can flexibly combine machine learning with physical and chemical constructs as well as heuristics to guide the experiments, and (ii) seamless deployment of the designed agents in actual closed-loop experimental settings. In particular, we will present a recent implementation of this framework for on-demand, cost-effective discovery of stable inorganic materials by automated, intelligent control of crystal structure selection and density functional theory simulations. This platform is running uninterrupted on cloud computing resources, and have found thousands of previously unreported ground state or nearly stable inorganic compounds in binary and ternary metal oxide, sulfide, phosphide and metal-alloy chemistries, notably augmenting the layout of the phase diagrams in many of these systems.

11:45 AM CT05.02.04

Robotics-Enabled Exploration of Multicomponent Lead Halide Perovskites via Machine Learning Kate Higgins¹, Sai M. Valleti², Maxim Ziatdinov³, Sergei Kalinin^{2,3} and Mahshid Ahmadi¹; ¹Joint Institute for Advanced Materials, United States; ²University of Tennessee, United States; ³Oak Ridge National Laboratory, United States

Metal halide perovskites (MHPs) have attracted considerable attention due to the combination of outstanding optoelectronic properties and low fabrication cost, making them uniquely attractive for various optoelectronic and sensing applications. Despite extensive effort, the synthesis of these materials preponderantly entails modifying a single compositional or synthesis variable and observing the structure and functionalities changes. Combined with lengthy processing and optimization times, this approach has largely been inefficient in its ability to explore vast design spaces. Here, we establish a workflow for the rapid synthesis and characterization of MHPs via combinatorial synthesis combined with rapid throughput photoluminescent measurements. We adopt an approach based on multivariate statistical analysis to gain insight into the variability of the photoluminescent properties across the compositional series. We map the compositional-dependent property (photoluminescence) and use the Gaussian Processing framework to determine associated uncertainties. From these uncertainties, we are then able to identify possible areas of interest and characterize them further. Overall, through the utilization of automated synthesis, we demonstrate how this workflow utilizes data-driven machine learning models for the accelerated discovery of large compositional spaces in MHPs with optimized properties for multifunctional optoelectronics.

1:00 PM *CT05.03.01

Machine Learning for the Modeling of Complex Energy Materials Nongnuch Artrith; Columbia University, United States

The properties of materials for energy applications, such as heterogeneous catalysts and battery materials, often depend on complicated chemical compositions and complex structural features including defects and disorder. This complexity makes the direct modeling with first principles methods challenging. Machine-learning (ML) potentials trained on first principles reference data enable linear-scaling atomistic simulations with an accuracy that is close to the reference method at a fraction of the computational cost. ML models can also be trained to predict the outcome of simulations (or experiments), bypassing explicit atomistic modeling altogether.

Here, I will give an overview of recent methodological advancements of ML potentials based on artificial neural networks (ANNs) [1-5] and applications of the method to challenging materials classes including metal and oxide nanoparticles and amorphous phases. Further, I will show an example of integrating large computational and small experimental data sets for the ML-guided discovery of catalyst materials [6].

References

1. J. Behler and M. Parrinello, *Phys. Rev. Lett.* **98** 146401 (2007).
2. N. Artrith, T. Morawietz, and J. Behler, *Phys. Rev. B* **83**, 153101 (2011).
3. N. Artrith and A. Urban, *Comput. Mater. Sci.* **114**, 135-150 (2016).
4. N. Artrith, A. Urban, and G. Ceder, *Phys. Rev. B* **96**, 014112 (2017).
5. A. Cooper, J. Kästner, A. Urban, and N. Artrith, *npj Comput. Mater.* **6**, 54 (2020).
6. N. Artrith, Z. Lin, and J. G. Chen, *ACS Catal.* **10**, 9438–9444 (2020).

1:25 PM CT05.03.02

Automated *In Silico* Screening of Nanoporous Materials for Enhanced CO₂ Capture Rodrigo F. Neumann¹, Fausto Martelli¹, Binqun Luan¹, Tonia Elengikal¹, Anshul Gupta¹, Guojing Cong¹, Mathias Steiner¹, Thomas Peters², Flor Siperstein³ and Breannan O Conchuir¹; ¹IBM Research, Brazil; ²University of Connecticut, United States; ³University of Manchester, United Kingdom

One of the strategies for carbon capture and storage is to leverage the adsorption properties of nanoporous materials. The carbon emissions of point sources, such as power plants, can be significantly reduced by applying these materials to the post-combustion capture of flue gas. Zeolites [1], Metal-Organic Frameworks [2], Zeolitic Imidazolate Frameworks [3] and Porous Polymer Networks [4] are examples of promising nanoporous materials which can efficiently trap flue gas molecules in their pores with diameters of a few (tens of) Angstroms.

Carbon dioxide, as a small gas molecule with 3.3 Angstroms of kinetic diameter, represents roughly 10% of the composition of flue gas coming out of coal-fired power station exhausts. In order to be a good carbon capture material, the nanoporous structure must not only adsorb flue gas components but *preferentially* adsorb CO₂ as opposed to more abundant flue gas components, such as N₂. Therefore, both the absolute adsorbate loading and the relative CO₂/N₂ selectivity are important performance figures-of-merit to be considered.

Millions of possible crystalline nanoporous materials [5] have been identified for carbon capture, extending far beyond our capability to quantify *in silico* the adsorption performance of each individual nanoporous structure by brute force calculations. Experimentally fabricating and measuring the adsorption properties of each framework is also unrealistic, due to the time and cost constraints, leading to the requirement for a pre-screening step to improve the resource allocation. In this talk, we present our work on optimising the

classification mechanisms for characterizing nanoporous structures, enabling efficient high-throughput screening of materials for carbon capture.

Our automated material screening tool leverages cloud resources to spawn multiple computational experiments in parallel to rapidly explore the vast space of relevant nanoporous materials. A full computational experiment comprises, of not only the realisation of Grand Canonical Monte Carlo (GCMC) adsorption simulations, but also a full geometrical and topological characterisation of the material in terms of its crystalline structure as represented by a point cloud of atomic positions. These can be combined with machine learning to accelerate the estimation of adsorption properties based solely on the atomistic structure of materials.

[1] Siriwardane, R. V., Ming-Shing S., and Edward P. F. Adsorption of CO₂, N₂, and O₂ on Natural Zeolites. *Energy & Fuels* **17**, 571-576 (2003). <https://doi.org/10.1021/ef0201351>

[2] Saha, D., et al. Adsorption of CO₂, CH₄, N₂O, and N₂ on MOF-5, MOF-177, and Zeolite 5A. *Environmental Science & Technology* **44**, 1820-1826 (2010). <https://doi.org/10.1021/es9032309>

[3] Hayashi, H., Côté, A., Furukawa, H. et al. Zeolite A imidazolate frameworks. *Nature Mater* **6**, 501–506 (2007). <https://doi.org/10.1038/nmat1927>

[4] Lu, W., et al. Porous polymer networks: synthesis, porosity, and applications in gas storage/separation. *Chemistry of Materials* **22**, 5964-5972 (2010). <https://doi.org/10.1021/cm1021068>

[5] Boyd, P., Lee, Y. & Smit, B. Computational development of the nanoporous materials genome. *Nat Rev Mater* **2**, 17037 (2017). <https://doi.org/10.1038/natrevmats.2017.37>

1:40 PM CT05.03.03

Late News: Machine Learning with Persistent Homology and Chemical Word Embeddings Improves Predictive Accuracy and Interpretability in Metal-Organic Frameworks Aditi Krishnapriyan^{1,2}, Joseph Montoya³, Maciej Haranczyk⁴, Jens Hummelshøj³ and Dmitriy Morozov¹; ¹Lawrence Berkeley National Laboratory, United States; ²University of California, Berkeley, United States; ³Toyota Research Institute, United States; ⁴IMDEA Materials Institute, Spain

Machine learning has emerged as a powerful approach in materials discovery. Its major challenge is selecting features that create interpretable representations of materials, useful across multiple prediction tasks. We introduce an end-to-end machine learning model that automatically generates descriptors that capture a complex representation of a material's structure and chemistry. This approach builds on computational topology techniques (namely, persistent homology) and word embeddings from natural language processing. It automatically encapsulates geometric and chemical information directly from the material system. We demonstrate our approach on multiple nanoporous metal-organic framework datasets by predicting methane and carbon dioxide adsorption across different conditions. Our results show considerable improvement in both accuracy and transferability across targets compared to models constructed from the commonly-used, manually-curated features, consistently achieving an average 25–30% decrease in root-mean-squared-deviation and an average increase of 40–50% in R² scores. A key advantage of our approach is interpretability: Our model identifies the pores that correlate best to adsorption at different pressures, which contributes to understanding atomic-level structure-property relationships for materials design.

1:55 PM *CT05.03.04

Defect Detection and Uncertainty Quantification in Property Prediction with Machine Learning Dane Morgan¹, Mingren Shen¹, Ryan Jacobs¹, Glenn Palmer¹ and Kevin Field²; ¹University of Wisconsin–Madison, United States; ²University of Michigan–Ann Arbor, United States

In this talk I will discuss two areas of applications of machine learning to materials science and engineering.

First, I will share recent results on extracting defects automatically from electron microscopy images. Electron microscopy is widely used to explore defects in crystal structures, but human tracking of defects can be time-consuming, error prone, and unreliable, and is not scalable to large numbers of images or real-time analysis. In this work I discuss application of machine learning approaches to find the location and geometry of different defect clusters in irradiated steels. We show that performance comparable to human analysis can be achieved with relatively small training data sets. We explore multiple deep learning methods that provide various features, e.g., fast processing for video and pixel level categorization to simplify defect dimension determination.

Second, I will share some studies we have been doing to assess accuracy of materials property prediction from machine learning models. Machine learning provides a powerful tool to predict materials properties, but relatively little attention has been paid to the critical issue of assessing the domain of the machine learning model and the accuracy of the predictions within that domain. In this talk I explore the effectiveness of some model error estimation methods, including ensemble and Bayesian methods, and consider how these might be used to obtain accurate error estimates within with the domain of the model. We apply the results on a realistic problem of modeling dilute impurity diffusion coefficients in a host, demonstrating that the model can predict accurate values for new systems but that the domain and errors are essential to consider for effective use of the model.

2:20 PM CT05.03.05

Machine Learning the Quantum-Chemical Properties of Metal–Organic Frameworks for Accelerated Materials Discovery with a New Electronic Structure Database Andrew S. Rosen¹, Shaelyn M. Iyer¹, Debmalaya Ray², Zhenpeng Yao³, Alan Aspuru-Guzik^{4,4}, Laura Gagliardi^{5,5}, Justin M. Notestein¹ and Randall Snurr¹; ¹Northwestern University, United States; ²University of Minnesota Twin Cities, United States; ³Harvard University, United States; ⁴University of Toronto, Canada; ⁵The University of Chicago, United States

Metal–organic frameworks (MOFs) are a widely investigated class of crystalline solids with tunable structures that make it possible to impart specific chemical functionality tailored for a given application. However, the enormous number of possible MOFs that can be synthesized makes it difficult to determine which materials would be the most promising candidates, especially for applications governed by electronic structure properties that are often computationally demanding to simulate and time-consuming to probe experimentally. Here, we have developed the first publicly available quantum-chemical database for MOFs (the “QMOF database”), which consists of properties derived from density functional theory (DFT) for over 14,000 experimentally synthesized MOFs. Throughout this study, we demonstrate how this new database can be used to identify MOFs with targeted electronic structure properties. As a proof-of-concept, we use the QMOF database to evaluate the performance of several machine learning models for the prediction of DFT-computed band gaps and find that crystal graph convolutional neural networks are capable of achieving superior predictive performance, making it possible to circumvent computationally expensive calculations. We also show how unsupervised learning methods can aid the discovery of otherwise subtle structure–property relationships using the computational findings in this work. We conclude by highlighting several MOFs with low band gaps, a challenging task given the electronically insulating nature of most MOF structures. The data and predictive models generated in this work, as well as the database of MOF structures, should be highly useful to other researchers interested in the predictive design and discovery of MOFs for the many applications dictated by quantum-chemical phenomena.

SESSION CT05.04: Material Informatics I
Session Chairs: Mathieu Bauchy and Wujie Wang
Sunday Afternoon, April 18, 2021
CT05

4:00 PM *CT05.04.01

Understanding and Visualizing Hyperspectral ToF-SIMS Data Sets Using Machine Learning Wil

Gardner^{1,2,3}, David Winkler^{2,4,5}, Davide Ballabio⁶, Benjamin Muir³ and Paul Pigram¹; ¹La Trobe University, Australia; ²La Trobe Institute for Molecular Science, La Trobe University, Australia; ³CSIRO Manufacturing, Australia; ⁴Monash Institute of Pharmaceutical Sciences, Monash University, Australia; ⁵School of Pharmacy, University of Nottingham, United Kingdom; ⁶Milano Chemometrics and QSAR Research Group, Department of Earth and Environmental Sciences, University of Milano-Bicocca, Italy

The application of multivariate analysis to mass spectral data sets has been thoroughly investigated in recent decades. Contemporary studies, however, frequently involve large scale and complex data collections comprising libraries of spectra or hyperspectral mass spectrometry imaging (MSI) or depth profiling. The understanding and visualizing the complex relationships between peaks, pixels and voxels embodied in these data remains a major challenge. It is now recognized that most mass spectral data contain non-linear relationships, which has led to increased application of machine learning approaches to provide unique insights into the underlying surface chemistry.

We have exemplified the use of the self-organizing map (SOM), a type of artificial neural network, for analyzing time-of-flight secondary ion mass spectrometry (ToF-SIMS) data derived from spectral libraries, hyperspectral images and depth profiles. Recently, we developed a novel methodology, SOM-RPM, which incorporates the algorithm relational perspective mapping (RPM) to improve visualization of the SOM for 2D ToF-SIMS images. We have also used SOM-RPM to characterize and interpret 3D ToF-SIMS depth profile data, voxel-by-voxel. An organic IrganoxTM multilayer standard sample was depth profiled using ToF-SIMS and SOM-RPM was used to create 3D similarity maps of the depth-profiled sample, in which the mass spectral similarity of individual voxels is modelled with color similarity. We used this similarity map to segment the data into spatial features, demonstrating that the unsupervised method meaningfully differentiated between Irganox-3114 and Irganox-1010 nanometer-thin multilayer films. The method also identified unique clusters at the surface associated with environmental exposure and sample degradation. Key fragment ions characteristic of each cluster were identified, tying clusters to their underlying chemistries. SOM-RPM has the demonstrable ability to reduce vast data sets to simple 3D visualizations that can be used for clustering data and visualizing the complex relationships within.

4:25 PM CT05.04.02

Charting the Low-Loss Region in Electron Energy Loss Spectroscopy with Machine Learning Laurien Roest¹, Sabrya E. van Heijst¹, Jaco ter Hoeve², Louis Maduro¹, Isabel Postmes^{1,2}, Juan Rojo² and Sonia Conesa-Boj¹; ¹Kavli Institute of Nanoscience Delft, Netherlands; ²VU Amsterdam & Nikhef, Netherlands

Electron energy-loss spectroscopy (EELS) within the transmission electron microscope (TEM) provides a wide range of valuable information on the structural, chemical, and electronic properties of nanoscale materials. A particularly important region of EEL spectra is the low-loss region, whose analysis makes possible charting the local electronic properties of nanomaterials from the characterisation of bulk and surface plasmons, excitons, and phonons to the determination of their bandgap and band structure. A major challenge for EELS data interpretation in this low-loss region is the presence of the zero-loss-peak (ZLP) associated to elastic scatterings. The presence of this ZLP often overwhelms the contribution from the inelastic scatterings between the TEM beam electrons with the sample such that relevant signals of low-loss phenomena risk becoming drowned in the ZLP tail. An accurate removal of the ZLP contribution is thus crucial in order to accurately map and identify key physical information from the low-loss region in EEL spectra. Several approaches to ZLP subtraction have been put forward in the literature. These methods are however affected by significant limitations: they based on specific, *ad-hoc* model assumptions about the ZLP, in particular concerning its parametric functional dependence on the electron energy loss ΔE , and they lack an estimate of the associated uncertainties.

Here we bypass these limitations by developing a model-independent strategy to realise a multidimensional determination of the ZLP with a faithful uncertainty estimate. Our approach is based on machine learning (ML)

techniques originally developed in high-energy physics to study the quark and gluon substructure of protons in particle collisions. It is based on the Monte Carlo replica method to construct a probability distribution in the space of experimental data and artificial neural networks as unbiased interpolators to parametrise the ZLP. The end result is a faithful sampling of the probability distribution in the ZLP space which can be used to subtract its contribution to EEL spectra while propagating the associated uncertainties. One can also extrapolate the predictions from this ZLP parametrisation to other TEM operating conditions beyond those included in the training dataset.

By means of this approach, we construct a ML model of ZLP spectra acquired in vacuum, which is able to accommodate an arbitrary number of input variables corresponding to different operation settings of the TEM. We demonstrate how this model successfully describes the input spectra and we assess its extrapolation capabilities for other microscope operation conditions. Further, we construct a one-dimensional model of the ZLP as a function of the energy loss ΔE from spectra acquired on two different specimens of tungsten disulfide (WS_2) nanoflowers characterised by a 2H/3R mixed polytypism. The resulting subtracted spectra are used to determine the value and nature of the WS_2 bandgap in these nanostructures as well as to map the properties of the associated exciton peaks appearing in the ultra-low loss region.

We also present results of further applications of our ML-subtracted EEL spectra to characterise the local electronic properties of TMD-based nanostructures. First, by means of the evaluation of the complex dielectric function via the Kramers-Kronig relations. Second, by implementing the automation of data analysis in spectral TEM images, where each pixel contains an individual EEL spectrum. By using ML regression and classification methods, one can identify relevant features of the spectra (peaks, edges, shoulders) with minimal human intervention and then determine how these features vary as we move along different regions of the nanostructure.

The framework presented in this work has been implemented and made available in an open source Python package, dubbed EELSfitter, and available from GitHub.

4:40 PM CT05.04.03

Discovery of Interpretable X-Ray Absorption Spectroscopy Signatures via Random Forest Machine Learning Models Steven B. Torrisi^{1,2}, Matthew Carbone³, Brian Rohr², Joseph Montoya², Yang Ha⁴, Junko Yano⁴, Santosh Suram² and Linda Hung²; ¹Harvard University, United States; ²Toyota Research Institute, United States; ³Columbia University, United States; ⁴Lawrence Berkeley National Laboratory, United States

X-ray absorption spectroscopy (XAS) produces a wealth of information about the local structure of materials, but interpretation of spectra often relies on easily accessible trends and prior assumptions about the structure. Recently, researchers have demonstrated that machine learning models can automate this process to predict the coordinating environments of absorbing atoms from their XAS spectra. However, machine learning models are often difficult to interpret, making it challenging to determine when they are valid and whether they are consistent with physical theories. In this work, we present three main advances to the data-driven analysis of XAS spectra: we demonstrate the efficacy of random forests in solving two new property determination tasks (predicting Bader charge and mean nearest neighbor distance), we address how choices in data representation affect model interpretability and accuracy, and we show that multiscale featurization can elucidate the regions and trends in spectra that encode various local properties. This multiscale featurization transforms the spectrum into a vector of polynomial-fit features, and is contrasted with the commonly-used “pointwise” featurization that directly uses the entire spectrum as input. We find that across thousands of transition metal oxide spectra, the relative importance of features describing the curvature of the spectrum can be localized to individual energy ranges, and we can separate the importance of constant, linear, quadratic, and cubic trends, as well as the white line energy. This work has the potential to assist rigorous theoretical interpretations, expedite experimental data collection, and automate analysis of XAS spectra, thus accelerating the discovery of new functional materials.

[1] S.B. Torrisi, M.R. Carbone, B.A. Rohr, J.H. Montoya, Y. Ha, J. Yano, S.K. Suram, L. Hung; *npj Computational Materials* **volume 6**, Article number: 109 (2020) <https://rdcu.be/b9n2Y>

4:55 PM CT05.04.04

Late News: Machine Learning Force Fields for Understanding the Thermodynamics of Li-Ion Cathodes
Joshua Gabriel, Juan C. Garcia, Noah Paulson, John J. Low, Marius Stan and Hakim Iddir; Argonne National Laboratory, United States

Machine Learning Force Fields (MLFF) have emerged as a tool to accelerate the atomic scale modeling of materials while preserving accuracy of density functional theory calculations. A workflow for developing such an MLFF, which leverages state of the art deep learning high performance computing architectures available at the national laboratories, is presented and discussed. The MLFF is used to study the thermodynamics and structural changes of lithium nickel oxide (LNO) battery cathode material during room temperature operation. The results emphasize the complexity of phase stability in this system and demonstrate the predictive power of the MLFF method.

5:00 PM CT05.04.05

Improvement of Adhesion Between NiTi Alloy and Diamond-Like Carbon Film by Bayesian Optimization Masafumi Toyonaga¹, Terumitsu Hasebe^{1,2}, Shunto Maegawa², Tomohiro Matsumoto^{1,2}, Atsushi Hotta¹ and Tetsuya Suzuki¹; ¹Keio University, Japan; ²Tokai University Hachioji Hospital, Japan

Surface coating is one of the most interesting methods for improving the mechanical, physical, chemical and biocompatible properties of materials and devices. Fluorine-incorporated diamond-like carbon (F-DLC) has received much attention as a coating material because of outstanding blood compatible properties which suppress fatal failure of the medical devices. However, it is well known that F-DLC thin films exhibit poor adhesion on metallic alloys and delamination or cracks are easy to occur after coating. In order to improve adhesion of F-DLC on metallic alloys, many scientific methods have been reported. Although some of these studies focused on introducing silicon-containing interlayers such as silicon-incorporated DLC (Si-DLC) between metallic alloys and F-DLC thin films to improve the adhesion properties, the film formation conditions of the interlayer that most improves the adhesion are not clear, and the method has not been established for optimizing the film formation conditions. Thus, we considered optimizing the structure of the interlayer using “Bayesian optimization”, which is known as one of machine learning. In this study, we optimize the structure of Si-DLC interlayer by Bayesian optimization to apply F-DLC to low blood compatible nickel-titanium (NiTi) alloy, which has been attracting attention as a material for medical devices due to superelasticity and shape memory.

The purpose of this study is evaluating the effectiveness of Bayesian optimization for determining optimal structures of interlayers between metallic substrates and F-DLC, and developing high blood compatible NiTi alloy by improving adhesion properties of F-DLC.

Si-DLC and F-DLC were prepared on NiTi substrates using radio frequency plasma enhanced chemical vapor deposition (RF-PECVD) equipment. The adhesion properties between NiTi substrates and DLC thin films were evaluated by the scratch test, and the structures of Si-DLC interlayer were updated successively by Bayesian optimization on the obtained data. Total of 30 Si-DLC interlayers were produced, and the highest adhesion could be improved to about 53 mN, while the lowest adhesion was about 22 mN. The one with the highest adhesion and the one with the lowest adhesion were deposited on the NiTi stents, and after performing the crimp test and the fatigue test, the surface was observed by Scanning Electron Microscope (SEM). As a result, no delamination was observed in the interlayer derived by Bayesian optimization, whereas delamination occurred in the sample in which structure was not optimized.

Therefore, this study shows that adhesion properties between metallic material and DLC thin film can be improved by Bayesian optimization. In addition, in the future, by applying machine learning in various researches in the field of materials, it is expected to develop materials with unprecedented excellent properties.

5:05 PM CT05.04.06

High-Throughput Electrochemical Screening of Deep Eutectic Solvent for Use in Redox Flow Batteries

Maria Politi and Jaime Rodriguez; University of Washington, United States

Deep eutectic solvents (DESs) are a class of materials with varied applications including catalysis and synthesis, extraction processes, drug solubilization and battery electrolytes. Their appeal stems from their broad electrochemical stability window, high electrical conductivity, low vapor-pressure, and low-flammability. These solvents present a depression in the melting point at specific molar ratios of organic components that can result in a liquid solution at moderate temperatures. A breadth of candidates with varying concentrations can be used to form DESs, leading to a vast design space. High throughput experiments and data-driven design strategies are key to accelerate the optimization of materials based on their physicochemical and electrochemical properties as well as engineering criteria (e.g. cost, safety, toxicity) for candidate DESs. The implementation of high-throughput tools allows for a rapid evaluation and screening based on metrics such as the melting point, potential stability window and ionic conductivity. Several high-throughput protocols have been designed for identifying the design space of molecules under investigation, their formulation and material characterization. Using data science principles, the molecules composing our basis set were identified using scoring based on metrics such as cost, melting point, toxicity and molecular weight. The formulation of deep eutectic solvents is automated through the use of a pipetting robot, combinatorial techniques and well-plates. Next, the melting point of the proposed mixtures is detected using an IR camera and hot-plate set-up. To screen for their electrochemical properties, 96-well plates with screen printed electrodes in combination with measurement techniques such as Cyclic Voltammetry (CV) and Electrochemical Impedance Spectroscopy (EIS) are implemented. Finally, to adapt high-throughput principles to the analysis of the data collection obtained through the aforementioned protocols, machine learning is leveraged for the data classification and data modeling. Furthermore, open-source Python-based packages have been developed and made available on GitHub. The combination of high-throughput experimentation and data analysis can greatly accelerate the design and screening candidate DES systems. This overall workflow could be easily adapted to other design spaces and applications.

5:10 PM CT05.04.07

Late News: A Materials-Informatics Based Study of Solid Electrolytes and Protective Coatings for Li Batteries Shreyas Honrao^{1,2}, Xin Yang³, Balachandran Radhakrishnan^{1,3}, Shigemasa Kuwata³, Hideyuki Komatsu⁴, Atsushi Ohma⁴ and John Lawson¹; ¹NASA Ames Research Center, United States; ²KBRR Wyle, United States; ³Nissan North America, United States; ⁴Nissan Motor Company, Japan

All-solid-state batteries with Li metal anode can address the safety issues surrounding traditional Li-ion batteries as well as the demand for higher energy densities. However, the development of solid electrolytes and protective coatings simultaneously possessing high ionic conductivity and wide electrochemical stability has proven to be a challenge. Here, we present a data-driven approach to explore the Li compound space for promising solid electrolytes and coatings. This is accomplished through the generation of a large database of battery-related materials properties of Li compounds by computing Li⁺ migration barriers using bond-valence-based pair potentials, and stability windows using density functional theory energies. Using this database, we implement machine learning models that can accurately predict migration barriers and electrochemical stability windows for any new Li compound. Through feature engineering, we ensure that our models are both accurate and interpretable. We perform feature importance analysis on our models to highlight materials properties that can be tuned for future design of coatings/electrolytes. Our database and informatics approach provide a valuable tool for the rapid discovery of new solid-state battery chemistries.

5:25 PM CT05.04.08

Late News: Prediction of Bulk and Grain Boundary Ionic Conductivities for Solid-State Li-Ion Conductors by Machine Learning Yen-Ju Wu¹, Takhiro Tanaka¹, Tomoyuki Komori², Mikiya Fujii², Hiroshi Mizuno², Satoshi Itoh¹, Tadanobu Takada¹, Erina Fujita¹ and Yibin Xu¹; ¹National Institute for Materials Science, Japan; ²Panasonic Corporation, Japan

A machine learning approach for identifying the important descriptors of the ionic conductivities of lithium solid electrolytes is proposed. This approach discriminates the factors of both bulk and grain boundary conductivities, which have been rarely reported. The effects of the interrelated structural, material, chemical and experimental properties on the bulk and grain boundary conductivities are investigated. The data are trained using the bulk and grain boundary conductivities of Li solid conductors at room temperature. Both the bulk conductivity and the grain boundary conductance of single grains were derived from 96 samples in three structural classes: perovskite, garnet, and NASICON. The important descriptors are elucidated by their feature importance and predictive performances, as determined by a nonlinear XGBoost algorithm: (i) the experimental descriptors of sintering conditions are significant for both bulk and grain boundary, (ii) the intrinsic bulk conductivity also changes with grain size, (iii) the local environment affects the grain boundary conductance that the lower coordinate number of Li shows higher grain boundary conductance. These findings can clarify ways of improving bulk conductivities and overcoming the limiting factors of grain boundary conductivities for solid-state Li-ion conductors.

SESSION CT05.05: Machine Learning II

Session Chairs: Clara Druzgalski, Rodrigo Neumann and Krishna Rajan

Sunday Afternoon, April 18, 2021

CT05

6:30 PM *CT05.05.01

End-to-End Differentiability and Tensor Processing Unit Computing to Accelerate Materials' Inverse Design Han Liu, Yuhan Liu and Mathieu Bauchy; University of California, Los Angeles, United States

Numerical simulations have revolutionized material design. However, although simulations excel at mapping an input material to its output property, their direct application to inverse design (i.e., mapping an input property to an optimal output material) has traditionally been limited by their high computing cost and lack of differentiability—so that simulations are often replaced by surrogate machine learning models in inverse design problems. Here, taking the example of the inverse design of a porous matrix featuring targeted sorption isotherm, we introduce a computational inverse design framework that addresses these challenges. We reformulate a lattice density functional theory of sorption in terms of a convolutional neural network with fixed hard-coded weights that leverages automated end-to-end differentiation. Thanks to its differentiability, the simulation is used to directly train a deep generative model, which outputs an optimal porous matrix based on an arbitrary input sorption isotherm curve. Importantly, this pipeline leverages for the first time the power of tensor processing units (TPU)—an emerging family of dedicated chips, which, although they are specialized in deep learning, are flexible enough for intensive scientific simulations. This approach holds promise to accelerate inverse materials design.

6:55 PM DISCUSSION TIME

7:10 PM CT05.05.03

Graphical Model Parameters for Formation of 3D Nanomolecular Complexes Minjeong Cha^{1,1}, Emine S. Turali-Emre^{1,1}, Xiongye Xiao², Paul Bogdan² and Nicholas A. Kotov^{1,1,1}; ¹University of Michigan, United States; ²University of Southern California, United States

The design of new functional materials for drug or anti-viral medicines is essential in the biomaterials and pharmaceutical field. However, due to the lack of generalized descriptors for the pairwise interactions of nano molecules, the automatic design and prediction of nanomaterials' function in the biosystem remain one of the most challenging problems. Here, to understand the comprehensive parameters for the formation of nano-biomolecular complexes, the protein complex information is investigated. The abundant protein topology data

from nature allow us to access the key structural aspects for detecting the interaction levels of molecule pairs. The newly introduced features originated from the graph network model would provide a universal description of local properties of any nanostructures and also play crucial roles in predicting the interaction level in protein pairs, defined by the distances. The feature correlation dynamics based on the distance classes validate the significant contribution of graph network features in the interaction prediction algorithms. As the proof-of-concept applications of nanomolecular complexes' interacting sites prediction, the SARS-Cov-2 nucleocapsid protein dimer and experimentally proven protein and nanoparticle pairs are analyzed. The rapid and straightforward prediction of interaction sites in pairwise molecular complexes will enhance our understanding of multi-dimensional structural model parameters for the design rules.

7:25 PM CT05.05.04

Graph Theory for Design of Complex Biomimetic Nanostructures Nicholas A. Kotov; University of Michigan, United States

The main hurdle on the pathway finding relationships between organization and properties of many biological materials is that the frameworks do not exhibit crystalline or any other long-range order that underpins many, if not all, structure-property correlations used for metals, ceramics, polymers, and other materials. Understanding of their organizational patterns and therefore, their mechanical, transport, electrical, and other properties will be essential for their engineering and requires a new approach to quantification of their structures.

This talk will address this problem and pave the way to comprehensive and quantitative description of structural patterns observed in different biomaterials using the graph theory (GT) extensively used in sociology and informatics for evaluation of complex network architectures.

The nanostructures represented by self-assembled chiral nanoparticles [1], biomimetic composites [2], and protein complexes [3] will be represented using GT representations based on discretization of nanostructures into nodes being connected with a network of edges. The resulting graphs can be utilized for enumeration of hierarchical architecture materials, information content (complexity), and *structure-property correlations*. Predictions of properties based on GT representations and machine learning algorithms will be presented.

References

[1] W. Jiang, Z.-B. Qu, P. Kumar, D. Vecchio, Y. Wang, Y. Ma, J. H. Bahng, K. Bernardino, W. R. Gomes, F. M. Colombari, A. Lozada-Blanco, M. Veksler, E. Marino, A. Simon, C. Murray, S. Ricardo Muniz, A. F. de Moura, N. A. Kotov, Emergence of Complexity in Hierarchically Organized Chiral Particles, *Science*, **2020**, 368, 6491, 642-648.

[2] Wang, M.; Vecchio, D.; Wang, C.; Emre, A.; Xiao, X.; Jiang, Z.; Bogdan, P.; Huang, Y.; Kotov, N. A. Biomimetic Structural Batteries for Robotics. *Sci. Robot.* **2020**, 5 (45), eaba1912.
<https://doi.org/10.1126/scirobotics.aba1912>.

[3] M. Baranwal, A. Magner, J. Saldinger, E. S. Turali-Emre, S. Kozarekar, P. Elvati, J. S. VanEpps, N. A. Kotov, A. Violi, A. O. Hero, Struct2Graph: A graph attention network for structure based predictions of protein-protein interactions, **2020**, *BioRxiv*, <https://doi.org/10.1101/2020.09.17.301200>.

7:40 PM CT05.05.05

Symmetry Incorporated Graph Convolutional Neural Networks for Solid-State Materials Weiyi Gong¹, Hexin Bai¹, Peng Chu¹, Haibin Ling² and Qimin Yan¹; ¹Temple University, United States; ²Stony Brook University, The State University of New York, United States

Recently, graph convolutional neural network (GCN) has been applied in crystal structures with a crystal graph representation to achieve an accurate prediction of material properties. However, graph convolutions used in previous work are mostly performed in real space based on the geometric information of crystal structures. The lack of space group symmetry information in real and reciprocal space limits the prediction accuracy of electron structure related properties. In this talk, we will demonstrate the development of a graph convolutional neural network with global and local symmetries in both real and reciprocal spaces incorporated. The newly proposed

model gives accurate predictions, compared to the state-of-the-art atom-based graph neural network models, and inspiring physical insights in the correlation between orbital symmetries and electronic structure properties of solid-state crystalline systems.

SESSION CT05.06: Materials Informatics II
Session Chairs: Stefano Curtarolo and Nuwan Dewapriya
Monday Morning, April 19, 2021
CT05

8:00 AM *CT05.06.01

Artificial Intelligence Towards Materials Maps Claudia Draxl^{1,2} and Matthias Scheffler^{2,1}; ¹Humboldt-Universität zu Berlin, Germany; ²Fritz Haber Institute of the Max Planck Society, Germany

High-throughput studies provide much information but will never cover the vast chemical and structural space of materials. Thus, Artificial Intelligence (AI) must enhance our research of tomorrow – starting today. To predict novel candidate materials for a given application, possibly even in regions of the materials space that no one would think of, our goal is to build a general “map of materials properties”. A FAIR (findable and AI ready; a further-reaching interpretation of the original acronym) data infrastructure will be an important step for achieving this goal [1]. The NOMAD Laboratory [2] is a community effort and a living example for such infrastructure in computational materials science, comprising the NOMAD Repository (raw data) and its Archive (normalized, i.e. code-independent data), the NOMAD Encyclopedia, and the NOMAD Analytics Toolkit. A final breakthrough is, however, only possible if the combined insight from synthesis, experiment [3], theory, and simulations are brought together. I’ll review where we are on this road that requires an immense but rewarding effort of the wide community.

[1] C. Draxl and M. Scheffler, *Big-Data-Driven Materials Science and its FAIR Data Infrastructure*, Invited Perspective in Handbook Andreoni W., Yip S. (eds) Handbook of Materials Modeling. Springer, Cham (2019).

[2] C. Draxl and M. Scheffler, *NOMAD: The FAIR Concept for Big-Data-Driven Materials Science*, MRS Bulletin 43, 676 (2018).

[3] A. Trunschke et al., *Towards Experimental Handbooks in Catalysis*, Topics in Catalysis, 1-17 (2020).

8:25 AM CT05.06.02

The Search for New Materials Joe Pitfield and Steven P. Hepplestone; University of Exeter, United Kingdom

Atomic scale structure prediction is a significant area of focus, yielding results such as the Materials Project [3] and tools such as AIRSS [1] and CALPYSO [2]. However, such approaches are focused on the isolated bulk whereas grain boundaries, interfaces and other phenomena dominate device development. Here, we demonstrate using MgO and graphite, how interface physics can lead to unique material formation, contrasting how this differs from the bulk, and what the resultant new properties are. To do this, we have developed A-RAFFLE, our structure at interfaces prediction tool, built upon the ARTEMIS interface prediction software [4]. Here, we demonstrate the base capability of RAFFLE as a structure prediction tool, highlighting its strengths and limitations compared to other approaches, and then discuss how RAFFLE has been implemented to predict structures at the interface between different materials.

References

[1] Chris J. Pickard and R. J. Needs. “High-Pressure Phases of Silane”. In: Phys. Rev. Lett. 97 (4 July 2006), p. 045504. doi:10.1103/PhysRevLett.97.045504. url:https://link.aps.org/doi/10.1103/PhysRevLett.97.045504.

[2] Yanchao Wang et al. “Crystal structure prediction via particle-swarm optimization”. In: Phys. Rev. B 82 (9 Sept. 2010), p. 094116. doi:10.1103/PhysRevB.82.094116. url:https://link.aps.org/doi/10.1103/PhysRevB.82.094116.

- [3] Anubhav Jain et al. “The Materials Project: A materials genome approach to accelerating materials innovation”. In: *APL Materials* 1.1 (2013), p. 011002. issn: 2166532X. doi:10.1063/1.4812323. url: <http://link.aip.org/link/AMPADS/v1/i1/p011002/s1%5C&Agg=doi>.
- [4] Ned Thaddeus Taylor et al. “ARTEMIS: Ab initio restructuring tool enabling the modelling of interface structures”. In: *Computer Physics Communications* 257 (2020), p. 107515. issn: 0010-4655. doi: <https://doi.org/10.1016/j.cpc.2020.107515>. url: <http://www.sciencedirect.com/science/article/pii/S0010465520302423>

8:40 AM BREAK

8:55 AM *CT05.06.04

Digital Infrastructures for Materials Research and Discovery Nicola Marzari; École Polytechnique Fédérale de Lausanne, Switzerland

We present our vision, implementation, and technology stack for a digital infrastructure for materials discovery. The three cornerstones are given by open-source quantum simulation codes tuned to the needs of pre- and exascale machines (Quantum ESPRESSO, SIRIUS); an operating system for high-throughput simulation with full reproducibility and data provenance (AiiDA), and a dissemination platform for raw and curated data, simulation services, and data analytics (Materials Cloud). An example will be given targeted at the discovery of novel two dimensional materials. Work done in collaborations with Giovanni Pizzi, and the AiiDA and Materials Cloud teams.

9:20 AM CT05.06.05

Automated Microstructural Feature Extraction for Accelerated Materials Discovery Baskar Ganapathysubramanian¹, Daniel Wheeler², Olga Wodo³ and Jaroslaw Zola³; ¹Iowa State University of Science and Technology, United States; ²National Institute of Standards and Technology, United States; ³University at Buffalo, The State University of New York, United States

Data-driven based approaches facilitate a systematic way to develop mappings between microstructure and microstructure-sensitive properties. Incorporating data-driven approaches with physically meaningful descriptors enables the elucidation of the underlying physical mechanisms linking structure with property (explainable or interpretable AI). One critical aspect of such an approach is the ability to represent materials and their structure in machine-friendly formats. In this talk, we present our framework to compute a library of generic descriptors for micrographs. We combine two approaches: statistical descriptors (e.g., n-point correlations) with morphological and topological descriptors (e.g., graph-based descriptors). Using this integrated approach, we will benchmark a few problems in the arena of discovering and mining microstructure-property maps. We explain how this work lays the foundation for machine learning of microstructure-property relationships and enables information fusion between multiple scales.

9:35 AM CT05.06.06

MPDD: Material-Property-Descriptor Database Adam M. Krajewski, ShunLi Shang, Yi Wang and Zi-Kui Liu; The Pennsylvania State University, United States

Fundamentally, each ML study predicts some property and comprises three elements: a database, a descriptor, and an ML algorithm. These are combined in two steps. First, the data representation is calculated using the descriptor. Then the model is iteratively evaluated on this representation or adjusted to improve it. Both processes are nearly instantaneous compared to ab-initio based methods; however, with extensive databases or materials modeled with large super-cells (e.g., glasses), times can grow into days or years. We present a tool that can speed up total process orders of magnitude by removing the most time-intensive step, i.e., the descriptor calculation.

To accomplish that, we move from traditional sharing of only the material-properties data to sharing of the

descriptors-properties data corresponding to the material as well, employing a NoSQL MongoDB database. This change not only enables orders-of-magnitude faster and effortless machine learning of materials but also serves as a tool for an automated and robust embodiment of prior knowledge about them in a graph-like fashion. Furthermore, since the descriptors are often reused for related properties, our database provides a tremendous speed-up in the design space exploration.

SESSION CT05.07: Data-Driven Chemistry I

Session Chair: Casey Brock

Monday Morning, April 19, 2021

CT05

10:30 AM CT05.07.01

Inverse Design of Self-Reporting Redox-Active Materials Using Quantum Chemistry Guided Active Learning Garvit Agarwal, Hieu A. Doan, Lily Robertson, Lu Zhang and Rajeev Surendran Assary; Argonne National Laboratory, United States

Redox flow batteries (RFBs) are a promising technology for stationary energy storage applications due to their flexible design, easy scalability and low cost. In RFBs, energy is carried in flowable redox-active materials (anolyte and catholyte redoxmers) which are stored externally and pumped to the cell during operation. Further improvement in energy density of RFBs requires design of redox-active materials with optimal properties i.e. wider redox potential window, higher solubility, and stability. Additionally, designing redoxmers with fluorescence enabled self-reporting functionality allows monitoring crossover of the redox-active material and state-of-health of the RFBs. Here we employ high-throughput density functional theory (DFT) calculations to generate database of reduction potentials, solvation free energies and absorption wavelengths of 1400 anolyte materials. Using simulated data, we develop accurate machine learning (ML) models to predict properties from simplified molecular input line-entry system (SMILES) representation of the molecular materials. The trained ML models are then used as surrogate models to drive the inverse material design loop using multi-objective Bayesian optimization to identify materials with optimum range of multiple properties. We demonstrate the improved efficiency of our active learning strategy as compared to the brute-force random search approach for discovering promising redox-active materials with desirable properties from a vast chemical search space of 2 million molecules.

10:45 AM CT05.07.02

Accelerated Prediction of Atomically Precise Cluster Structures Using On-the-Fly Active Learning Yunzhe Wang, Shanping Liu, Sam Norwood, Peter Lile and Tim Mueller; Johns Hopkins University, United States

The chemical and structural properties of nanoclusters are of great interest in numerous applications -- light emitting devices, catalysis, and biomedical imaging to name a few. A systematic study of structure-property relationship necessitates the knowledge of atomically precise structures of stable clusters over a variety of sizes. However, experimental characterization of the structures of these non-crystalline materials can be challenging. Computationally searching for stable structures is a feasible solution, but can be computationally expensive, as it is a global optimization problem. In this work, we present a procedure that can accelerate prediction of low-energy nanocluster structures by combining a genetic algorithm and an interatomic potential model actively learned on-the-fly. A pool-based genetic algorithm is implemented to efficiently sample the configuration space, and moment tensor potentials are used to rapidly relax and evaluate the energies of predicted clusters. The resulting procedure significantly accelerates the process of identifying low-energy cluster structures and is demonstrated on both bare and ligated clusters. The predicted lowest-energy nanoclusters are compared with the lowest energy structures reported in literature to validate this methodology. This workflow provides a feasible

way to systematically predict low-energy structures for nanoclusters at a large scale, which can greatly facilitate the discovery and design of novel nanomaterials for a wide range of applications.

11:00 AM CT05.07.03

Screening and Understanding Li Adsorption on Two-Dimensional Metallic Materials by Learning Physics Sheng Gong¹, Shuo Wang², Taishan Zhu¹ and Jeffrey C. Grossman¹; ¹Massachusetts Institute of Technology, United States; ²University of Maryland, United States

Two-dimensional (2D) materials have been applied on addressing challenges in Li-ion batteries (LIBs). However, it is hard to screen Li interaction with 2D materials by conventional first-principle calculations or purely data-driven machine learning. In this work, in order to screen Li interaction with 2D metallic materials, we build a high-throughput screening scheme that incorporate the process of learning physics into the screening circle. First, we use density functional theory (DFT) and graph convolutional networks (GCN) to calculate the minimum Li adsorption energies on a small set of 2D metals, then we propose a three-step adsorption mechanism based on previous understandings of charge-transfer and ionization-coupling to explain the found linear relation between minimum Li adsorption energy and work function of 2D metals. We propose that, during adsorption, a Li atom first ionizes to be a Li^+ and an electron with the energy cost equal to the ionization potential of Li, then the electron transfers to the 2D metal and release the energy equal to the work function, and finally the Li^+ couples with the negatively charged 2D metal with the energy change of coupling energy. We use chemisorption theory to support the proposed charge transfer direction, and we apply the linear dependence on explaining previous observation of enhanced Li adsorption by doping and functionalization and infeasibility of second-layer Li adsorption. For coupling, we find that the previously proposed image-charge coupling provides reasonable trend but fails for 0-height adsorption, and we use random forest model to predict and understand the coupling process, and find that variances of elemental properties of component elements and packing density are the most correlated features related to coupling. Finally, we apply our models on discovering potential high-voltage materials and find that some fluorides and chromium oxides have minimum Li adsorption energies lower than -7eV , which breaks the record, and we show that our physics-driven models have strong ability of extrapolation and higher accuracy and transferability than purely data-driven models. We hope this work can not only deepen human understanding of Li binding nature and promote the application of 2D materials on Li-ion batteries, but also inspire researchers to use physics to simplify learning problems by decoupling the target property into simpler properties in high-throughput screening for problems that are hard for conventional DFT calculations and purely data-driven machine learning.

11:15 AM CT05.07.04

Multi-Fidelity Information Fusion DFT Study of Doped-Graphene Single Atom Catalysts Hud Wahab, Gaurav Raj, Patrick Johnson, Lars Kotthoff and Dilpuneet S. Aidhy; University of Wyoming, United States

Cost versus accuracy trade-offs are common in materials science and engineering, where a particular property of interest can be measured/computed at different levels of accuracy or fidelity. Intuitively, the higher the accuracy the most resource and time intensive, while the low-cost quicker alternatives tend to be noisy. In such situations, machine-learning-based multi-information source fusion (MISF) approaches can be employed to fuse information accessible from varying sources of fidelity and make predictions at higher levels of accuracy. In this study, we perform a comparative study on traditionally employed single-fidelity (SF) and MISF strategies, such as multi-fidelity co-kriging (CK), to compare their relative prediction accuracies and efficiencies for accelerated property predictions and high throughput chemical space explorations. We perform our analysis using DFT-computed Gibbs free energy data set of H adsorption for doped graphene for single atom catalyst applications. We discuss how Sure Independence Screening and Sparsifying Operator (SISSO) methods can be used to select relevant descriptors. Finally, we elucidate whether MISF based learning schemes outperform the traditional SF machine learning methods, and discuss if this can be generalized for cases involving large chemical space explorations.

SESSION CT05.08: Applications II
Session Chairs: Patrick Parkinson and Andrew Rosen
Monday Afternoon, April 19, 2021
CT05

1:00 PM *CT05.08.01

Investigating the Shapes of Bottlebrush Polymers Using Machine Learning Sanket Deshmukh; Virginia Tech, United States

Bottlebrush polymers (BBPs) of thermosensitive polymers have potential applications in the field of biomedicine. They are a type of graft polymers in which thermosensitive polymer side-chains are grafted onto a polymer backbone. Above their lower critical solution temperature (LCST), the thermosensitive polymers can exhibit a coil-to-globule conformational transition. In this talk, we will discuss the effect of grafting density on the conformation of poly(N-isopropylacrylamide) (PNIPAM; LCST= ~305 K) side-chains in the BBPs with worm-like, cone-like, and cake-like shapes. We have performed coarse-grained (CG) molecular dynamics (MD) simulations of these BBPs at 290 K (below LCST) and 320 K (above LCST) in the presence of explicit CG water for 500 ns of these BBPs. The effect of temperature on the structure and shape of these BBPs were quantified by analyzing the simulation trajectories using convolutional neural network (CNN) based machine learning approach.

1:25 PM *CT05.08.02

Searching Order within Disorder with AI-Automation Stefano Curtarolo; Duke University, United States

Critical understanding of large amount of data leads to new spectral descriptors for discovering entropic ceramics (e.g. metastability, synthesizability), their phase transitions (e.g. mixing, melting) and their remarkable properties (hardness, elasticity) [Nat. Rev. Mater. **5**, 295 (2020)]. Research sponsored by DOD.

1:50 PM CT05.08.03

A Phase Mapping Algorithm to Accelerate High Throughput Experiments Ming-Chiang Chang¹, Sebastian Ament¹, Maximillian Amsler^{1,2}, Duncan R. Sutherland¹, Carla P. Gomes¹, R. Bruce van Dover¹ and Michael O. Thompson¹; ¹Cornell University, United States; ²University of Bern, Switzerland

Developing high-throughput methods, leveraging both experimental automation and computer agent based autonomous exploration, is crucial to accelerate materials discovery. Advances continue to be necessary in advanced synthesis techniques and equally in improved materials characterization tools. In work with lateral gradient Laser Spike Annealing (lgLSA), we have demonstrated the power of spatially resolved spectroscopic and diffraction methods for rapidly assessing both composition and processing impacts on material properties. However, lgLSA dramatically increases the amount of such spectral data produced during experiments with even a single library, data which must be processed rapidly and efficiently to prevent bottle necks during the decision making in autonomous high-throughput workflows. X-ray diffraction (XRD) data is particularly difficult to manage because of the complicated behavior of spectra with changing composition, texture, and grain size distribution with processing conditions. Peak shifting, peak broadening, and modification of scattering intensities are but a few of the challenges to existing phase identification algorithms.

We introduce a general algorithm to efficiently identify constituent phases in XRD data from a library of ICSD patterns. This phase mapping algorithm was developed to be particularly appropriate for lgLSA (autonomous) explorations, exploiting the unique characteristics of the dense, temperature-dependent, diffraction data across a single laser scan experiment. While recent work has proposed deep-learning-based models for this problem, our algorithm is inspired by compressed sensing and is particularly inexpensive to run due to the physically-induced sparsity of the phases. Further, our algorithm incorporates peak-shifting due to alloying, something which even a recent deep-learning-based approach cannot handle. We demonstrate the capabilities of this algorithm using data from the Bi-Ti-O material system, resolving complex XRD patterns into constituents based on known

phases from crystal structure databases. The algorithm has proven to be robust for phase identification even in the presence of doping, alloying, strain, and atomic disorder. Results from a variety of other systems demonstrate the general applicability of the algorithm. Finally, the ability to rapidly identify constituent phases in spectral data is especially valuable in an active learning context, where the phase identification can feed into experimental design. We will discuss how the algorithm is incorporated in an autonomous materials discovery workflow using in-situ experimental decisions and efficient synchrotron-based analysis. The algorithm has potential to be incorporated into many different high-throughput workflows, and can be equally used to provide physical knowledge to train machine learning models for accelerated materials discovery.

2:05 PM CT05.08.04

High Dimensional Model Representation - Gaussian Process Regression—A Powerful Tool to Learn Multivariate Functions from Sparse Data Mohamed A. Boussaidi¹, Owen Ren^{1,2}, Dmitry Voytsekhovskiy² and Sergei Manzhos¹; ¹INRS, Canada; ²Purefacts Inc, Canada

Machine learning approaches including neural networks (NN) and Gaussian process regression (GPR) are finding widespread use to recover functional dependencies from multidimensional data. As powerful as these approaches are, they may fail when data density is low, which is always the case in highly-dimensional cases. Some methods like GPR also cannot easily work with large datasets. Using modified high dimensional model representation (HDMR) to represent a multivariate function with machine-learned lower-dimensional terms allows recovering functions from very sparse data, down to ~2 data per dimension. Sub-dimensional component functions are easier to fit and to use. Specifically here we present a HDMR-GPR combination where the use of GPR to represent component functions allows nonparametric (unbiased) representation and the possibility to work only with functions of desired dimensionality, obviating the need to build an expansion over orders of coupling. All component functions are determined from a single set of samples. We test the method by fitting potential energy surfaces of polyatomic molecules as well as by computing vibrational spectra.

2:20 PM CT05.08.05

Comprehensive Comparison of Modern Sequential Design Approaches for Material Optimization—Application to Metal-Organic Frameworks Giovanni Trezza, Luca Bergamasco, Matteo Fasano and Eliodoro Chiavazzo; Politecnico di Torino, Italy

In a number of scientific contexts, the evaluation and optimization of an objective black-box function through the sequential performance of (physical and/or numerical) experiments can be prohibitively costly, especially when navigating in a high-dimensional domain. Modern sequential design algorithms based on machine learning are emerging as interesting options to address this issue, allowing to effectively explore particularly high-dimensional parameter spaces, with a minimal number of evaluations. In this framework, scientists can rationally choose the next experimental (or computational) setup to be analyzed while searching for the optimal candidate, without the need of relying on the luck of random guessing.

These general techniques find important applications in the broad area of material science (where the number of material descriptors or features can be impressively high), and hold promise to accelerate materials discovery and research. Here, we apply this approach to a database of 1000 Metal-Organic Frameworks (MOFs), which are innovative compounds employable in the energy field (e.g. thermal energy storage, carbon dioxide capture [1]). In particular, the aim is to find the best candidate in terms of a property of interest (e.g. water, carbon dioxide or other sorbate solubility) in the fewest number of trials navigating within a 58-dimensional feature space of properly selected material descriptors. In this work, we provide a comprehensive comparison of several state-of-the-art methodologies. This is accomplished both for the regression models over the initial set of 60 materials supposed to be known (random forest regression [2], Kriging [3], Gaussian process regression [4]) and for the strategies allowing to choose the next MOF to test (based on exploitation of high-performing candidates, exploration of poorly explored regions or entropic search [5]).

We observe that the convergence with these "smart" trajectories occurs before the average random guessing and, in many cases, in few dozens of evaluations. Differences among several strategies are shown and discussed.

References:

- [1] Boyd, P.G., Chidambaram, A., García-Díez, E. *et al.* *Nature* **576**, 253–256 (2019).
- [2] J. Ling, M. Hutchinson, E. Antono, S. Paradiso, and B. Meredig, *Integrating Materials and Manufacturing Innovation* **6**, 207 (2017).
- [3] S. N. Lophaven, H. B. Nielsen, J. Sondergaard, and A. Dace, Technical University of Denmark, Kongens Lyngby, Technical Report No. IMMTR-2002 12 (2002).
- [4] E. Brochu, V. M. Cora, and N. De Freitas, *arXiv preprint arXiv:1012.2599* (2010).
- [5] Wang, Zi, and Stefanie Jegelka, *arXiv preprint arXiv:1703.01968* (2017).

2:35 PM CT05.08.06

Machine Learning Tools to Accelerate Scalable Perovskite PV Manufacturing Nicholas Rolston¹, Zhe Liu², Austin Flick¹, Thomas W. Colburn¹, Zekun Ren², Justin Chen¹, Tonio Buonassisi² and Reinhold Dauskardt¹; ¹Stanford University, United States; ²Massachusetts Institute of Technology, United States

One of the key requirements for commercializing perovskite PV is to develop a scalable fabrication process to produce high-efficiency PV devices. We have identified that process optimization is the most time-consuming step during the development of scalable deposition technology for perovskite devices. Because the process optimization involves a large number of process variables (*e.g.*, typically 10 – 20 variables or more), it is difficult for human intuition to solve efficiently, for example, with the trial-and-error approach or the conventional design of experiment method (*e.g.*, one variable at a time). The state of the art for applying machine learning tools in process optimization is still at a preliminary stage. In this work, we address the challenges of ML-assisted optimization of scalable perovskite PV processing by developing the interpretable framework of sequential learning and establishing an adaptable ML model using transfer learning. The open-air rapid spray plasma process (RSPP) for depositing and curing of perovskite films is a unique platform to test and deploy the proposed ML-guided framework because RSPP is able to conduct optimization experiments at high throughput with easy access to adjusting a wide range of process variables.

In this work, we develop a novel Bayesian-optimization-based model that utilizes the visual inspection of film quality as a probabilistic constraint and conducts a local optimization of the trusted regions after the global optimization. Using the developed model, we adopt the sequential learning framework (also known as active learning), which utilizes a small dataset to initiate an ML regression model and iteratively suggests and collects new data points to achieve the optimization task. Specially, six process conditions are identified as the key parameters to systematically optimize (namely, substrate temperature, process speed, spray flow rate, plasma height, plasma gas flow, and plasma duty cycle) in RSPP perovskite devices. With less than 200 experimental conditions (which is a tiny fraction of 40k experimental conditions in a grid search), we achieve: (i) faster process optimization and (ii) a better understanding of the heuristic relationship between PV performance and process variables using an interpretable and transferable machine learning framework. Finally, with the help of this ML framework, we are able to produce the highest perovskite PV efficiencies ever reported in ambient.

SESSION CT05.09: Materials Informatics III
Session Chairs: Muratahan Aykol and Bin Ouyang
Monday Afternoon, April 19, 2021
CT05

4:00 PM *CT05.09.01

Towards Small-Data-Driven Materials Science Luca M. Ghiringhelli; Fritz Haber Institute of the Max Planck Society, Germany

The number of possible materials is practically infinite, while only few hundred thousands of (inorganic) materials are known to exist and for few of them even basic properties are systematically known. In order to speed up the identification and design of new and novel optimal materials for a desired property or process, strategies for quick and well-guided exploration of the materials space are highly needed. A desirable strategy would be to start from a large body of experimental or theoretical data, and by means of artificial-intelligence (AI) methods, to identify yet unseen patterns or structures in the data, and consequentially predictive (data-driven) models. This leads to the identification of maps (or charts) of materials where different regions correspond to materials with different properties. The main challenge on building such maps is to find the appropriate descriptive parameters (called descriptors) that define these regions of interest.

Here, I present novel methods for the AI-aided identification of descriptors and materials maps, based on symbolic regression, compressed sensing [1], and multi-task learning [2]. The methods are tailored to yield predictive models (also) with "small-data", and are shown applied to important materials-science challenges such as the prediction of stability of perovskite materials, of novel topological insulators, and more.

I focus on the (verified) predictive power of the learned maps, which goes beyond the mere interpolation of more "traditional" AI approaches, and analyze current and future challenges.

[1] R. Ouyang, S. Curtarolo, E. Ahmetcik, M. Scheffler, and L. M. Ghiringhelli. "SISSO: A compressed-sensing method for identifying the best low-dimensional descriptor in an immensity of offered candidates." *Physical Review Materials* 2, (2018): 083802.

[2] R. Ouyang, E. Ahmetcik, Ch. Carbogno, M. Scheffler, and L. M. Ghiringhelli. "Simultaneous learning of several materials properties from incomplete databases with multi-task SISSO." *Journal of Physics: Materials* 2, (2019): 024002.

4:25 PM CT05.09.02

Data-Driven Quantum Dot Synthesis Development in Flow Milad Abolhasani; North Carolina State University, United States

Inorganic lead halide perovskite (LHP) quantum dots (QDs) have recently emerged as a promising class of semiconducting materials for next-generation, solution-processed optoelectronic devices.¹ The unique properties of LHP QDs are mainly attributed to their high photoluminescence quantum yield (PLQY), high defect tolerance, facile bandgap tunability, and narrow emission linewidth.

Despite the substantial improvements in synthesis development of LHP QDs over the past five years, the conventional trial and error-based synthesis and formulation optimization methods have hindered their rapid adoption by energy technologies. Existing material development strategies very often fail to overcome the demands of colloidal QDs' vast synthesis and processing universe, resulting in time- and cost-intensive QD development efforts.

Recent advances in modular robotic material manufacturing and artificial intelligence (AI)-guided decision-making strategies, including deep neural networks (DNNs) and reinforcement learning (RL), provide an exciting opportunity to reshape the synthesis development and formulation discovery of precision-tailored QDs through the autonomous operation of a robotic QD synthesizer.²

In this work, we have developed the second generation of our *Artificial Chemist* technology;³ a modular microfluidic platform⁴ for data-driven, multi-step synthesis, optimization, and end-to-end manufacturing of colloidal LHP QDs. The AI-driven, multi-step chemical synthesis technique incorporates the modeling and uncertainty quantification of experimental responses and uses such models to strategically explore multivariate reaction space in a sequential, closed-loop, adaptive manner. This data-driven approach effectively couples the task of developing and training a surrogate model with the multi-objective optimization problem, which in practice results in accelerated chemical synthesis process development. The autonomous robotic QD synthesizer uses advanced DNNs and multi-stage decision-making policies trained on experimentally measured QD properties (generated *in house*) in tandem with state-of-the-art RL algorithms to strategically and intelligently explore QD design space, and thereby accelerate the synthesis optimization of LHP QDs for energy and chemical technologies. The reconfigurable *Artificial Chemist* technology utilizes a multimodal *in-situ* material diagnostic probe (absorption/photoluminescence (PL) spectroscopy) in conjunction with a real-time, ensemble DNN adaptive algorithm to enable simultaneous optimization of PLQY and size distribution of LHP QDs for

any desired emission color. The developed autonomous robotic experimentation technology with its modular flow reactors and QD processing modules can be readily adapted for data-driven development of other solution-processed nanomaterials.

References

1. Akkerman, Q. A., et al., *Nat. Mater.* **2018**, *17* (5), 394-405.
2. Abdel-Latif, K., et al., *Matter* **2020**, *3* (4), 1053-1086.
3. Epps, R. W., et al., **2020**, *32* (30), 2001626.
4. (a) Abdel-Latif, K., et al., *Advanced Functional Materials* **2019**, *29* (23), 1900712; (b) Epps, R. W., et al., *Lab Chip* **2017**, *17* (23), 4040-4047.

4:40 PM CT05.09.03

Machine Learning Prediction of Creep Rupture Behavior for Metal Alloys Reihaneh Jamshidi; University of Hartford, United States

The design of alloys and composites with high creep resistance is of great interest, especially in high-temperature applications. Here we show that machine learning algorithms can predict creep behavior of steel alloys, more specifically creep-rupture lifetime and rupture stress, as a function of the alloy composition and processing methods. The machine learning approach was applied on a data set of 2000 alloys, and the predicted creep-rupture lifetime and rupture stress were in good agreement with most of the experimentally measured values. The results were mutually confirmed by two algorithms.

4:45 PM CT05.09.04

Development of an Artificial Intelligence (AI) Based Image Processing Tool to Detect Microstructural Variations in AM Ti-6Al-4V Rohan Casukhela¹, Sriram Vijayan¹, Meiyue Shao¹, Matthew Jacobsen² and Joerg R. Jinschek¹; ¹The Ohio State University, United States; ²Air Force Research Laboratory, United States

Recent research progress has already indicated the promising potential of metal additive manufacturing (AM), e.g. when producing Ti-6Al-4V (Ti64) parts for aerospace applications. The AM process is inherently non-equilibrium in nature, caused by rapid thermal cycling and consequent steep thermal gradients, producing parts with complex, anisotropic, and metastable microstructures [1]. As a result, there is a limited understanding of the physical metallurgy of AM, which restricts the qualification of AM parts for use in critical applications. Therefore, in order to rapidly qualify AM Ti64 parts with targeted properties, AM processes must be optimized based on a fundamental understanding of the *AM Ti64 processing – microstructure – property (PMP)* space. This gap in understanding can be reduced by developing statistical models assisting mapping the PMP space. These models must be sufficiently flexible to be applicable on a vast variety of datasets obtained from processing, characterization, and testing methods across multiple length scales. However, the low volume of microstructural data obtained from characterization techniques across multiple length scales is often identified as a significant barrier when developing statistical models with low uncertainty.

In the case of AM Ti64, scanning electron microscopy (SEM) based techniques provide valuable information about the variation in α/β microstructure throughout the AM build. High-contrast SEM images require long(er) dwell times, which limits the volume of images acquired in a reasonable amount of time [1]. Here, we also acquired large-area SEM images using low dwell times and utilized a deep-learning network to improve image quality by denoising these low-resolution images. The accuracy of the extracted microstructural data was compared with findings based on high-quality SEM images [1]. Artificial intelligence (AI)-based image processing tools that were used to extract microstructural information from these denoised images can serve as an input to the regression-based PMP model for AM Ti64. The uncertainty associated with model predictions will be presented. Finally, significance of the model will be discussed and alternative designs for subsequent experimental iterations to refine the model will be proposed.

[1] Shao M., Vijayan S., Nandwana P., Jinschek J.R. The effect of beam scan strategies on microstructural variations in Ti-6Al-4V fabricated by electron beam powder bed fusion, *Materials and Design* 196, 109165 (2020)

4:50 PM *CT05.09.05

Coupling Machine Learning and Physics-Based Simulations to Accelerate Materials Design Bryce Meredig; Citrine Informatics, United States

Machine learning (ML) and physics-based simulations are highly complementary tools in computational materials design. ML models are flexible and computationally cheap, but they require sufficient training data and their accuracy suffers under extrapolation; physics-based simulations embed deep domain knowledge and often have broad applicability, but are computationally expensive. In this talk, we discuss using ML as a "glue" layer for multiscale simulations; automating physics-based simulations with the goal of enabling ML-driven sequential learning; and using uncertainty quantification in ML and simulations to improve both approaches to materials modeling.

5:15 PM CT05.09.06

Predicting Fracture Stress of Defective Graphene Samples Using Artificial Neural Networks Nuwan Dewapriya^{1,2}, Nimal Rajapakse^{1,3}, Priyan Dias⁴ and Ronald Miller²; ¹Simon Fraser University, Canada; ²Carleton University, Canada; ³Sri Lanka Institute of Information Technology, Sri Lanka; ⁴University of Moratuwa, Sri Lanka

The computational cost associated with atomistic modeling is often a bottleneck in the design and characterization of nanomaterials. For example, first-principles methods such as density functional theory can only be used to model a few hundred atoms at a time due to the extremely high computational cost associated with them, and therefore such methods cannot be used to study atomistic processes such as crack propagation. On the other hand, computationally efficient continuum mechanical approaches (e.g., finite element method) are not directly applicable to the nanomechanical problems because such methods do not generally consider surface energy effects and the discrete nature of atomic structures, which are quite significant when the characteristic dimension of a system is a few nanometers. Molecular dynamics (MD) simulations strike a balance between the computational cost and accuracy for nanomaterial modeling. Alternatively, machine learning techniques (e.g., neural networks) provide an opportunity to extract underlying features of data obtained from MD simulations while offering novel insights into the mechanics of nanoscale structures.

In this work, we employed both shallow and deep neural networks to predict the fracture stress of graphene samples containing various numbers and distributions of vacancy defects. Data required to model the neural networks was obtained from MD simulations. First, we developed shallow neural networks to predict the fracture stress of defective graphene samples at various temperatures and vacancy concentrations. Sensitivity analysis was performed to explore the features learned by the neural networks, and their behavior under extrapolation was also investigated. Subsequently, we developed deep convolutional neural networks to predict the fracture stress of graphene samples containing random distributions of vacancy defects. Results reveal that the neural networks have a strong ability to predict the fracture stress of defective graphene under various processing conditions. This work demonstrates some opportunities and challenges in modeling of neural networks using data obtained from MD simulations to solve complex nanomechanical problems.

Acknowledgement: This work was supported by the Natural Sciences and Engineering Research Council of Canada.

5:30 PM CT05.09.07

Explaining Neural Network Predictions of Material Strength Terrell N. Mundhenk¹, Ian A. Palmer², Brian Gallagher¹, Barry Chen¹, Gerald Friedland³ and Yong Han¹; ¹Lawrence Livermore National Laboratory, United States; ²Massachusetts Institute of Technology, United States; ³University of California, Berkeley, United States

We recently developed a deep learning method that can determine the critical peak stress of a material by looking at scanning electron microscope (SEM) images of the material's crystals. However, it has been somewhat unclear what kind of image features the network is keying off of when it makes its prediction. It is common in computer vision to employ an explainable AI saliency map to tell one what parts of an image are important to the network's decision. One can usually deduce the important features by looking at these salient locations. However, SEM images of crystals are more abstract to the human observer than natural image photographs. As a result, it is not easy to tell what features are important at the locations which are most salient. To solve this, we developed a method that helps us map features from important locations in SEM images to non-abstract textures. We do this as follows. We obtain the most salient locations from the network trained on SEM images using a method called FastCAM. We selected it because it has been empirically shown to produce saliency maps that correspond well to what is actually important in the image. We also run texture images from the Describable Texture Dataset (DTD) through the SEM image trained neural network. For both SEM and DTD images, we extract a feature vector from the most salient location in the activation tensors. This gives us a feature vector which has better definition than if we averaged across layers, which is the most common method. We then find the nearest neighbors between SEM feature vectors and DTD feature vectors. This tells us which textures are most like the salient locations in our SEM images. By correlating over the full set of SEM and DTD feature vectors we then have clear texture trends we can relate to critical peak stress. For instance, a low peak stress correlates strongly with textures described as stratified, braided or bumpy. High peak stress correlates with textures such as flecked, dotted or grid like. We had prior hypothesized that flecked and dotted like textures were associated with a higher peak stress. However, the other textures revealed yet unknown processes that might affect material strength. We will discuss the pro's and con's of using DTD to describe the textures of materials as it relates to critical peak stress. For instance, some textures in the set should probably be split into subcategories and in general can be ambiguous.

SESSION CT05.10: Deep Learning and Computer Vision
Session Chairs: Paul Pigram and Olga Wodo
Monday Afternoon, April 19, 2021
CT05

8:10 PM CT05.10.02

Using Deep Learning to Find High Performance Phase-Change Switchable Metasurface Reflectors

Jonathan Thompson^{1,2} and Matthew Mills²; ¹Azimuth Corporation, United States; ²Air Force Research Laboratory, United States

Metasurfaces of 1D gratings and 2D pillars arrays of the phase-change material $\text{Ge}_2\text{Sb}_2\text{Te}_5$ (GST) are investigated as an active switchable reflector. The large index contrast between the amorphous and crystalline phase-states, in conjunction with the highly tunable metasurface geometry, allows us to selectively engineer an agile device that shows both high reflectance and transmittance for $2\ \mu\text{m}$ wavelengths when switched between states. While the many degrees of freedom metasurfaces introduce are beneficial for spectral tuning, the large parameters spaces are also problematic insofar they are often impossible to exhaustively search when using traditional simulation methods like rigorous coupled wave analysis (RCWA). Nevertheless, we are able to completely search these large parameter spaces with millions of designs by employing artificial neural networks that have been trained using only a fraction of the total number of possible designs. These spectra predicting networks (SPN) achieve an accuracy of 98% and a simulation speed up of $10^5\times$ compared to the RCWA simulations that they were trained on. The exhaustive search using SPNs allows us to find optimal designs, where we discover several GST metasurface designs with $\sim 95\%$ reflectance and $\sim 80\%$ transmittance between phase-states.

8:25 PM CT05.10.03

Late News: Automatic Characterization of Single-Walled Carbon Nanotube Film Morphologies Using Computer Vision Phillip Williams, Nicole Rice and Benoit Lessard; University of Ottawa, Canada

When establishing the relationships between processing conditions, film morphologies and performance of Single-Walled Carbon Nanotube (SWNT) based devices, the device characteristics are easily measured and quantified, and the processing conditions are known and tightly controlled. On the other hand, the film morphology is often known either at a qualitative level, or through manual analysis which is both slow and error prone, as well as an inefficient use of a researcher's time. This gap presents a significant challenge to the construction of next-generation devices, since the current approaches focus on establishing processing condition to device performance relationships without being able to control for the actual morphologies of the SWNT devices which incidentally can vary significantly even at fixed processing conditions.

The use of Artificial Intelligence (AI) and Computer Vision (CV) can augment the current approaches used for analyzing devices by providing detailed metrics on the film morphologies using a software only approach, meaning that fast, accurate and reproducible analysis can be done at much larger scales and levels of detail than previously feasible. The analysis pipeline uses Atomic Force Microscopy (AFM) height data to calculate metrics that are currently collected manually – such as linear density – as well as providing entirely new information not available from any machine or manual technique, such as the positions, orientations, and lengths of each individual carbon nanotube in a device.

There are two main steps to the data analysis procedure. First, a file containing the height of the film at various positions is ingested and segmented into a bitmap which represents the presence or absence of a nanotube at a given position in the film. The second step is application of various algorithms to the segmentation bitmap to extract relevant metrics. The segmentation process consists of several steps which are designed to identify if a given point in a film belongs to a nanotube or not. This is accomplished by using adaptive thresholding techniques such as Otsu's method or Yen thresholding, as well as more traditional techniques such as edge detection, image filters and data preprocessing. The final output of this segmentation process is a matrix of true and false values, indicating if a given pixel belongs to a nanotube (true) or if belongs to the substrate that the nanotube was deposited on (false). Once the segmentation is complete, two solvers are applied to the data. The first is an algorithm that iterates through each row and column of the segmentation bitmap and detects how many nanotubes intersect with that row or column. This allows us to compute the linear density of the film at every point in the device, providing an obvious advantage over the current practice of graduate students hand-counting the intersections at a few positions in the AFM image. The other solver is a Genetic Algorithm (GA) based solver which attempts to find a set of nanotube parameters – orientations, positions and sizes – which would produce the same film morphology observed. Once the parameters of each individual nanotube is extracted, secondary processing can extract metrics such as the distribution of sizes and orientations of the nanotubes, to give a clear set of quantifiable observations describing the film morphology. Using our analysis methodology, we can automate characterization traditionally done manually, as well as produce entirely novel insights into the film morphology of SWNT devices in a matter of minutes or hours without the need for specialized equipment or multi-million dollar hardware.

8:40 PM CT05.10.04

Image Deconvolution and Resolution Enhancement in Scanning Probe Microscopy Using Deep Learning Lalith Krishna Samanth Bonagiri, Harry Feldman and Yingjie Zhang; University of Illinois at Urbana-Champaign, United States

Machine learning has been proved to substantially improve the existing imaging and characterization techniques in the field of material science. Currently, researchers in this area are using deep learning for classification and segmentation of the images/data for pattern recognition and thus enabling the automation of imaging techniques, particularly scanning probe microscopy (SPM). However, none of these well-developed deep learning techniques focussed on removing the tip convolution effect in SPM which would truly help in enhancing the spatial resolution of the resulting images. Tip convolution in SPM is a well-known phenomenon. To model this process mathematically, set theory and mathematical morphological operators such as dilation

and erosion have been used previously by many researchers. However, it is quite cumbersome to select the size of the structuring element and the morphological operation to obtain the tip shape and an accurate ground truth image. Apart from that, there are no existing learning-based algorithms, which are primarily required because the tip evolves with time and so does the artifact. Here in, we report a deep learning framework to remove the tip effect through a feature pyramid based neural network. We use nanoparticles of various shapes as model systems to perform AFM experiments and deconvolute tip-shape effects and are able to successfully reconstruct the actual nanoparticle shape using the neural network. This work can be generalized to all scanning probe microscopy techniques and can enable image deconvolution in real-time during experimental measurements.

8:55 PM BREAK

9:10 PM CT05.10.05

Rapid and Flexible Classification of Scanning Transmission Electron Microscopy Data Using Few Shot Learning Sarah M. Akers, Elizabeth J. Kautz, Bethany Matthews, Le Wang, Yingge Du and Steven R. Spurgeon; Pacific Northwest National Laboratory, United States

Control of property-defining materials defects for quantum computing and energy storage depends on the ability to precisely probe structure and chemistry at the highest spatial and temporal resolutions. Modern scanning transmission electron microscopy (STEM) is well-suited to this task, having yielded rich insights into defect populations in many systems. However, the dilute nature and complexity of materials defects, coupled with their varied representations in STEM data, makes reliable, accurate, high-throughput statistical defect analysis a significant challenge. Possible analysis approaches include low-level pixel processing, or even the application of machine learning methods for classification and image segmentation. However, the latter requires large sets of labeled training data that are difficult to obtain for many practical materials science studies. Here, we describe the use of an emerging few shot learning capability for rapid and flexible STEM data classification. This approach requires minimal information at the start of the analysis and uses a generally pre-trained encoder network to make inferences on experimental data. Our results show drastic improvements in data annotation costs, reproducibility, and scalability in comparison to neural network training from scratch. We demonstrate how few shot techniques can quickly extract feature maps and global statistics from a variety of STEM data, enabling a new quantitative understanding of defect populations.

9:25 PM CT05.10.06

Machine Learning to Reveal Nanoparticle Dynamics from Liquid-Phase TEM Videos Lehan Yao, Zihao Ou, Binbin Luo, Cong Xu and Qian Chen; University of Illinois at Urbana-Champaign, United States

Transmission electron microscopy (TEM) has been applied to nanomaterials characterization for decades, and with the recent development of liquid-phase TEM, the nanoscale dynamics including nanoparticle diffusion and superlattice crystallization can also be revealed. However, the quantitative parameter extraction directly from image/video data is still prone to challenges such as high noise and inhomogeneous background. Conventional manual measurement produces better accuracy but suffers from extremely low efficiency, while computer algorithm-assisted segmentation is fast but is tricky in terms of parameterization. Here, we integrate the computer-based fast analysis together with the smart vision of human beings by applying machine learning algorithms. The talk will be focused on automated image analysis of conventional TEM and nanoscale dynamics study from liquid-phase TEM, both enabled by machine learning. In our customized workflow, we develop methods to simulate TEM images, serving as the training dataset for the U-Net neural network. We then apply the trained neural network to liquid-phase TEM videos of different colloidal nanoparticle systems, revealing a diversity of properties including their diffusion and interaction, reaction kinetics, and assembly dynamics. We expect our framework to push the potency of TEM to its full quantitative level in a high-throughput and statistically significant fashion.

9:30 PM CT05.10.07

Deep Learning for Super-Resolved Atomistic Predictions from Atom Probe Tomography Aditi Sonal, Jith

Sarker, Baishakhi Mazumder and Kristofer Reyes; University at Buffalo, The State University of New York, United States

Atomistically resolved techniques such as Atom Probe Tomography (APT) and Molecular Dynamics simulations provide rich, complex and high-dimensional data. Often, however, such information is coarse-grained for ease of human-based analysis. Such coarse-graining results in loss of information present in the raw data. In this talk, we propose an alternative methodology using deep residual convolutional neural networks. We show how using such models, we can identify spatially-local, atomistically-resolved characterization of material structure. As an example, we apply the technique to identifying crystal phase in $\text{Al}_x\text{Ga}_{1-x}\text{O}_3$ material characterized by APT. We demonstrate a procedure for obtaining super-resolved identification of crystal structure to attenuate classification results in the face of noisy and incomplete data typical of APT. We also demonstrate how the use of synthetic atomistic simulations of crystal structure can assist in this atomistically-resolved structural characterization task, allowing the use of such DL-based techniques in situations where the presence of specific structures is ambiguous.

9:45 PM CT05.10.08

Late News: Advances in Image Driven Machine Learning for Microstructure Recognition and Characterization Arun Baskaran¹, Elizabeth J. Kautz², Wufei Ma¹, Aritra Chowdhury³, Bulent Yener¹ and Daniel Lewis¹; ¹Rensselaer Polytechnic Institute, United States; ²Pacific Northwest National Laboratory, United States; ³GE Global Research, United States

Machine learning (ML) or artificial intelligence (AI)-enabled materials design and discovery has recently emerged as a new paradigm in material science. An important sub-field within this broad area is image-driven machine learning (IDML), which has supplemented material characterization techniques beyond what was possible with conventional stereography and image analysis methods. Microstructure characterization is important for material design as it enables the development of processing-structure-property relationships that are critical to several research areas such as alloy design, assessment of corrosion resistance, failure analysis, etc. In this presentation, the state of the art of IDML for materials characterization is discussed using a set of functional modules, defined such that each module performs a specific role in the IDML workflow. Such an overview permits answering granular questions about the field such as the impact of IDML at different spatial length scales, the diversity of machine learning models adopted in the field, etc. One of the emerging techniques to have been adopted in the field is generative models for constructing synthetic and novel microstructures, and towards data augmentation. The results from applying a progressive growing generative adversarial network (pg-GAN) to generate a dataset of synthetic microstructures of a binary U-Mo alloy is detailed. The quality of the synthetic microstructures is evaluated by comparing these images and the real images in Fourier space, and investigating the presence of correlated background noise. Finally, the work in progress in using a transfer learning strategy on GANs to generate microstructures is reported, and the effect of this strategy on the microstructure quality, convergence time, and the size of the training dataset is discussed.

10:00 PM CT05.10.09

Leveraging Uncertainty from Deep Learning for Trustworthy Materials Discovery Workflows Jize Zhang, Bhavya Kailkhura and Yong Han; Lawrence Livermore National Laboratory, United States

We are witnessing a significantly growth of works that integrate deep learning to material application workflows. In such context, the uncertainty (or confidence) associated with the prediction from deep neural net would be of utmost importance, because it can be further leveraged to aid decision makings in cost-effective material discovery and synthesis process. Here, we investigate into answering several common challenging questions material scientists might encounter in such material application workflows, by leveraging the deep neural network's predictive uncertainty information. We first show that the uncertainty information enables the user to determine the necessary amount of training data for the deep neural net to achieve the desired accuracy level. Next, we present a framework that guides the deep learning model to avoid making predictions on confusing samples based on the uncertainty information. Finally, we show that the uncertainty is also helpful in

detecting out-of-distribution data. Specifically, we find out that an uncertainty-based out-of-distribution (OOD) detection scheme is already accurate to identify a wide range of real-world shifts in data, e.g., changes in the image acquisition conditions or changes in the synthesis conditions. We demonstrate the effectiveness of the proposed approach on a real-world example, where we classify molecular crystals produced under various synthesis/processing conditions from their microstructure information (scanning electron microscope images) using deep neural networks.

SESSION CT05.11: Applications III
Session Chairs: Manyalibo Matthews and Dane Morgan
Tuesday Morning, April 20, 2021
CT05

8:00 AM *CT05.11.01

Machine Learning Aided Discovery of Patterns in Crystal Chemistry Krishna Rajan; University at Buffalo, The State University of New York, United States

In this presentation we provide an overview of how we can transform the “genomics” paradigm in materials discovery to a “connectomics” approach to materials design. We provide examples of our new approach of mapping diverse information and discovering connections between structure and functionality in materials chemistry, by harnessing machine learning methods that utilize both the statistical and topological aspects of data. This can help to aid targeted materials discovery based on discovering the best pathways for future discoveries. We show how this “connectomics” approach can uncover hidden patterns associated with structure-property relationships in complex crystal chemistries.

8:25 AM CT05.11.02

Discovering Relationships Between OSDAs and Zeolites Through Data Mining and Generative Neural Networks Zachary Jensen¹, Soonhyoung Kwon², Daniel Schwable-Koda¹, Rafael Gomez-Bombarelli¹, Yuriy Roman-Leshkov², Manuel Moliner³ and Elsa Olivetti¹; ¹Massachusetts Institute of Technology, United States; ²Masdar Institute of Science and Technology, United States; ³Universitat Politècnica de València, Spain

Zeolites are crystalline, microporous materials extensively used in various industrial applications including catalysis, water decontamination, and NO_x abatement. Many of these zeolites are synthesized using an organic structure directing agent to guide towards that specific zeolite structure. Several strategies exist for finding suitable OSDAs for different zeolites including domain-specific heuristics, molecular dynamics simulations, and transition state mimicking. However, predicting new OSDAs for both existing and novel zeolite structures remains inexact and very challenging. To advance the goal of understanding interactions between OSDAs and zeolites, we take a data-driven approach that has been largely missing from the current state of research. We use natural language processing and text mining techniques to extract an exhaustive data set of known pairs of OSDAs and zeolites from the scientific literature. Next, we mine this data to elaborate on trends between the three-dimensional structure of the OSDA and the zeolite. Specifically, we examine several small-cage zeolites such as CHA, LTA, and AEI which exhibit strong correlations with OSDAs and have significant industrial applications. Finally, we develop a generative neural network trained on the literature data to suggest OSDA molecules for specific zeolites. We then use this model to examine several interesting zeolite systems including CHA and SFW to suggest potential replacement OSDAs.

8:40 AM CT05.11.03

Graph-Based Deep Learning for Designing Stable Interfaces for Solid-State Batteries Shubham Pandey¹, Vladan Stevanovic^{1,2}, Peter C. St. John² and Prashun Gorai^{1,2}; ¹Colorado School of Mines, United States; ²National Renewable Energy Laboratory, United States

Solid-electrolytes (SEs) offer numerous advantages over their liquid-state counterparts in solid-state batteries including, increased safety, wider operating temperatures, and higher energy densities. However, commonly used SEs and electrodes are thermodynamically unstable at the solid-solid interfaces. Decomposition phases forming at the interfaces may be ionically resistive or electronically conducting, which is undesired for battery design. There is a pressing need to search for new SEs and cathodes that will form stable metal anode-electrolyte and electrolyte-cathode interfaces. Thermodynamic stability of solid interfaces can be assessed through a convex hull construction based on the formation enthalpies of competing phases, which can be calculated from DFT total energies. To allow fast prediction of stability, in this work, we built crystal graph convolutional neural networks (CGCNNs) as a surrogate for predicting DFT total energies. Current implementations of CGCNN models for predicting total energy/formation enthalpy of inorganic materials are inaccurate for high-energy hypothetical structures. A model that is accurate for total energy predictions of not only ground-state (GS) but also high-energy hypothetical structures is desired when considering new materials for designing stable solid interfaces. To this end, we trained CGCNN models on DFT total energies from NREL Materials Database that contains GS or near-GS structures and a unique dataset containing ~10,000 hypothetical structures, including high-energy structures. The trained models achieve mean absolute errors of ~40 meV/atom for both GS and high-energy structures. These models will enable materials discovery efforts for designing stable interfaces in solid-state batteries as well as for other functional applications.

8:55 AM CT05.11.04

Machine Learning Stability Rules for Complex Ionic Compounds and Its Application in the Discovery of New NASICON Materials Bin Ouyang¹, Jingyang Wang¹, Tanjin He¹, Christopher J. Bartel¹, Haoyan Huo¹, Yan Wang², Valentina Lacivita², Haegyeom Kim³ and Gerbrand Ceder³; ¹University of California, Berkeley, United States; ²Samsung Research America, United States; ³Lawrence Berkeley National Laboratory, United States

Nowadays, various tools are readily available to perform high-throughput computational discovery of new materials. The next grand challenge is to bridge the gap between computational prediction and experimental accessibility. To fulfill this goal, elemental compatibility is the first thing to be understood. In the field of ionic solids established stability rules such as the Goldschmidt tolerance factor and the Pauling's rules work reasonably well in ionic solids that have relatively simple compositions and bond topologies, such as perovskites. However, when it comes to complex ionic compounds, the combinatorial space becomes very large and a handy stability model is mostly absent. To establish stability rules for complex ionic solids with the aid of machine learning tools, we take the NASICON type materials as a prototype system. The complexity of NASICONs is a challenge for ML as these compounds have four types of cation sites and are able to have both cation and polyanion mixing. In this work, we developed and applied a suite of high-throughput computation, physical interpretation, and machine learning tools to reveal the stability rules of NASICONs across all compositional and elemental space. We have decoupled the stability origin of NASICON materials into bond compatibility and site miscibility as well as present a two-dimensional "tolerance factor" that can be used to estimate the synthetic accessibility of NASICON materials with only basic elemental information. With the established stability principle, we have successfully synthesized more than ten new NASICONs in unexplored chemical spaces. We hope our work can provide insights in bridging the state-of-the-art machine-learning techniques and data-mining tools to accelerate the discovery of complex ionic compounds.

9:10 AM *CT05.11.05

Combining Machine Learning and Multiscale Modeling for Accelerated Battery Manufacturing Optimization Alejandro A. Franco^{1,2,3}; ¹Université de Picardie Jules Verne, France; ²Réseau du Stockage Electrochimique de l'Energie (RS2E), France; ³Institut Universitaire de France, France

Lithium ion batteries (LIBs) are playing a crucial role in the ongoing energy transition, in particular through the renewed emergence of electric vehicles. However, the increasing climate change requires us to develop innovative approaches to accelerate the optimization of LIBs. In this lecture i will present an innovative hybrid

computational approach, combining machine learning (ML) and multi-scale modeling (MSM), allowing to predict the impact of manufacturing parameters on lithium ion battery (LIB) electrode properties. Manufacturing parameters include electrode slurry composition and solid to liquid ratio, coating speed, slurry drying temperature, calendaring pressure, temperature and rolls speed. Resulting electrode properties include mesostructure information (spatial organization of active and inactive material particles, particles percolation, tortuosity factors, porosity, etc.) and electrochemical performance indicators (overpotentials and specific capacities upon galvanostatic discharge and charge). The ML techniques are used for predictive classification and regression, based on in house experimental databases, and for the acceleration of the parameterization of the physical-based models within the MSM workflow. The overall approach is developed in the context of the ARTISTIC project [1] and allows performing both direct and inverse design of the optimal manufacturing conditions maximizing given electrode descriptors such as energy and power density. Concrete demonstration examples will be provided on the basis of LIB electrodes made of graphite and Nickel-Manganese-Cobalt active materials, illustrating the strong capabilities of the approach to accelerate the optimization of LIB manufacturing processes.

References

- [1] ERC Consolidator Project ARTISTIC (Advanced and Reusable Theory for the In Silico-optimization of composite electrode fabrication processes for rechargeable battery Technologies with Innovative Chemistries) (<https://www.u-picardie.fr/erc-artistic/>).
- [2] Ngandjong, A.C., Rucci, A., Maiza M., Shukla, G., Vazquez-Arenas J., Franco, A.A., *J. Phys. Chem. Lett.*, **8** (23) (2017) 5966.
- [3] Lombardo, T., Hooek, J. B., Primo, E., Ngandjong, A. C., Duquesnoy, M., & Franco, A. A. (2020). Accelerated Optimization Methods for Force Field Parametrization in Battery Electrode Manufacturing Modeling. *Batteries & Supercaps*. <https://doi.org/10.1002/batt.202000049>
- [4] Rucci, A., Ngandjong, A. C., Primo, E. N., Maiza, M., & Franco, A. A. (2019). Tracking variabilities in the simulation of Lithium Ion Battery electrode fabrication and its impact on electrochemical performance. *Electrochimica Acta*, *312*, 168-178.
- [5] Chouchane, M., Rucci, A., Lombardo, T., Ngandjong, A. C., & Franco, A. A. (2019). Lithium ion battery electrodes predicted from manufacturing simulations: Assessing the impact of the carbon-binder spatial location on the electrochemical performance. *Journal of Power Sources*, *444*, 227285.
- [6] Shodiev, A., Primo, E. N., Chouchane, M., Lombardo, T., Ngandjong, A. C., Rucci, A., & Franco, A. A. (2020). 4D-resolved physical model for Electrochemical Impedance Spectroscopy of Li (Ni_{1-x-y}Mn_xCo_y)O₂-based cathodes in symmetric cells: Consequences in tortuosity calculations. *Journal of Power Sources*, 227871.
- [7] Cunha, R. P., Lombardo, T., Primo, E. N., & Franco, A. A. (2020). Artificial Intelligence Investigation of NMC Cathode Manufacturing Parameters Interdependencies. *Batteries & Supercaps*, *3*(1), 60-67.
- [8] Duquesnoy, M., Lombardo, T., M., Chouchane, Primo, E. & Franco, A. A. (2020). Data-driven assessment of electrode calendaring process by combining experimental results, in silico mesostructures generation and machine learning. *Journal of Power Sources*, in press (2020).

9:35 AM CT05.11.06

Calibration of Thermal Spray Microstructure Simulations to Experimental Data Using Bayesian Optimization David Montes de Oca Zapiain, Theron M. Rodgers, Dan S. Bolintineanu, Carianne Martinez, Aaron Olson and Nathan W. Moore; Sandia National Laboratories, United States

Thermal spray deposition is able to generate thick coatings of metals, ceramics and composites materials. This process is inherently stochastic and thus yields coatings that exhibit hierarchically complex internal structures that affect the overall properties of the coating. While, rules-based simulations are able to model the coating process; their accuracy and efficacy are governed by the set of pre-defined rules which are calibrated to specific material and processing conditions to accurately model particle spreading upon deposition. Nevertheless, not all parameters are able to be calibrated to experimental results. We present a protocol that automatically and efficiently determines the parameters that yield the synthetic microstructure with the closest statistics to the experimentally observed coating. This protocol starts by robustly quantifying the microstructure using 2-point

statistics and then representing the statistical quantification in a low-dimensional space using Principal Component Analysis. Subsequently, our protocol leverages a combination of Gaussian Processes Regression and Bayesian Optimization to determine the parameters that yield the minimum distance between synthetic microstructure and the experimental coating in this low-dimensional space in an accurate and computationally-efficient manner.

This work was supported by the Laboratory Directed Research and Development program at Sandia National Laboratories. Sandia National Laboratories is a multi-mission laboratory managed and operated by National Technology and Engineering Solutions of Sandia, LLC., a wholly owned subsidiary of Honeywell International, Inc., for the U.S. Department of Energy National Nuclear Security Administration under contract DE-NA0003525. The views expressed in the article do not necessarily represent the views of the U.S. Department of Energy or the United States Government. Sand no. SAND2020-11942 A

SESSION CT05.12: Data-Driven Chemistry II
Session Chairs: Alejandro Franco and Shubham Pandey
Tuesday Morning, April 20, 2021
CT05

11:45 AM *CT05.12.01

Machine-Learning the Structural Stability of Intermetallic Phases with Domain Knowledge of the Interatomic Bond Thomas Hammerschmidt; Ruhr University Bochum, Germany

The performance of machine-learning depends critically on the quality of the descriptors. In the case of learning atomic-scale properties, like formation energies obtained from density-functional theory (DFT) calculations, the descriptors are typically based on measures of the atomistic geometry and the distribution of chemical elements. Here, we construct descriptors that additionally include domain knowledge of the interatomic bond from a hierarchy of coarse-grained electronic-structure methods. In particular, we use tight-binding (TB) and analytic bond-order potentials (BOPs) that are derived from a second-order expansion of DFT. We demonstrate that a recursive solution of the TB problem and the closely related moments of the electronic density-of-states at the BOP level establish a smooth relation between the local atomic environment and the formation energy. This first level of domain knowledge of the interatomic bond shows high predictive power in machine-learning applications already with simple, qualitative TB/BOP models. We demonstrate this for the prediction of the formation energy and the band gaps of transparent conductors. As second level of domain knowledge we include the bond chemistry in terms of bond-specific TB Hamiltonians that are obtained from downfolding the DFT eigenspectrum of molecular dimers. As third level of domain knowledge we include the role of the valence electrons by determining approximate non-selfconsistent bond energies with BOP using bond-specific TB Hamiltonians. We demonstrate the application of these descriptors of the second and third level to the prediction of the formation energy of intermetallic phases and discuss their high relative importance as compared to other descriptors.

12:10 PM CT05.12.02

Late News: Machine Learning Potentials for Copper Alloys Angel Diaz Carral¹, Xiang Xu², Azade Yazdan Yar¹, Siegfried Schmauder² and Maria Fyta¹; ¹Institute for Computational Physics, University of Stuttgart, Germany; ²Institut für Materialprüfung, Werkstoffkunde und Festigkeitslehre (IMWF), Germany

Copper based alloys, due to their high electrical conductivity and high strength, are of great importance for electric and electronic applications such as connectors or lead frames. We investigate Cu-Ni-Si-Cr alloys with a different type and concentration of impurities through computational means. Our simulations provide us with structural data and energetics, which are further training Machine Learning (ML) algorithms to build ML

potentials. These will in turn be used in larger scale simulations to design alloys with desired properties. We first provide a methodological approach based on the comparison of different ML descriptors in order to better understand and model the Cu alloys. We discuss the impact of this approach in providing a framework for an optimum design of multicomponent materials, such as alloys.

12:25 PM CT05.12.03

Late News: Investigating Representations of Local Atomic Environments with Topology Optimization

Arindam Debnath and Wesley Reinhart; The Pennsylvania State University, United States

Advances in machine learning (ML) continue to accelerate materials discovery, but key challenges remain in knowledge representation for local atomic environments. State-of-the-art predictive performance can be obtained with many different types of features ranging from hand-crafted and human-interpretable features in the case of models like decision trees to learned features only meaningful to a computer in the case of approaches based on deep neural networks. Hand-crafted features informed by fundamental physics and human intuition often require less training to achieve robust performance, while purely learned features may provide less bias and greater predictive power since the model is free to identify the most salient descriptions of the data. In fact, many models fall in between these two extremes; a prevalent example are the rotation-invariant features which have been utilized to learn force fields for use in classical Molecular Dynamics (MD) simulations from ab initio calculations. While model development for these applications typically focuses on predictive performance, we are interested in the information that can be gleaned from the low-dimensional latent spaces which are learned as a by-product of these ML workflows.

We have recently developed a new representation of local atomic environments which is highly effective when combined with unsupervised manifold learning to embed the local environments of particles observed in classical MD simulations into a low-dimensional latent space. Our unsupervised scheme provides comparable performance to recent supervised methods while requiring only a fraction of the training data. However, this comes at a cost – our representation cannot be directly inverted to sample real-space structures from the latent space. Here we introduce a topology optimization scheme to generate ensembles of local atomic environments from the low-dimensional latent space. Representative samples of our rotation- and permutation-invariant features are drawn from the latent space in regions of interest such as metastable transition states. Then backpropagation is applied to optimize the real-space positions of atoms in the local environment to match the target features. This is similar in spirit to reverse Monte Carlo, except faster convergence can be achieved using gradient descent.

While less efficient for the inverse problem than deterministic, deep-neural-network-based approaches, our sampling scheme incidentally allows us to study the efficacy of different representations of local atomic environment. We investigate different choices of rotation- and permutation-invariant features by attempting to invert the environments observed in colloidal crystallization, ice nucleation, and binary mesophases back to real-space configurations. The results provide valuable information regarding advantages and limitations for different types of features, which should help select better features for predictive models in the future.

12:40 PM CT05.12.04

Late News: Machine Learning Prediction of the Hubbard U for Materials Containing Transition Metals

Casey N. Brock, Anand Chandrasekaran, Yuling An, Shaun Kwak and Mathew Halls; Schrödinger, Inc., United States

Standard approximations to the exchange-correlation functional for density functional theory (DFT) calculations tend to over-delocalize d and f electrons, causing critical systematic errors in predictions of material properties. A standard approach to correcting these errors is applying a Hubbard potential via an additional parameter, U. Often, the value of U is chosen empirically to reproduce measured values of the band gap or other properties. Alternatively, the Hubbard U value can be calculated explicitly using linear response or perturbation theory approaches, but these calculations are tedious and computationally expensive. In this work,

we outline a machine learning (ML) framework for predicting Hubbard U values for inorganic solids containing a single transition metal element. For this purpose, we generate a training set of over 200 periodic structures and the corresponding U values for the constituent transition metal sites based on density functional perturbation theory calculations. We then utilize descriptors for inorganic periodic systems to build ML models to predict Hubbard U values for novel structures outside the training set. The most important set of descriptors for predicting the Hubbard U potential for the examined materials systems are highlighted, with an analysis of outstanding trends and variations of its value across the d-block elements. Finally, we investigate the sensitivity of critical materials properties such as the formation energy and band-gap, to variations in the Hubbard U correction.

12:55 PM CT05.12.05

Automated Training of Many-Body Machine Learned Force Fields Jonathan Vandermause and Boris Kozinsky; Harvard University, United States

Machine learned (ML) force fields have emerged as a powerful tool for performing large-scale molecular dynamics simulations at near-DFT accuracy, but training many-body force fields that are interpretable, efficient, and uncertainty-aware remains an important open challenge. In this talk, we present Bayesian force fields that unite three popular frameworks—the Atomic Cluster Expansion (ACE), Gaussian Approximation Potentials (GAP), and Spectral Neighbor Analysis Potentials (SNAP)—opening the door to scalable, uncertainty-aware molecular dynamics simulations of complex materials. We first show how a multi-species generalization of the N-body ACE descriptor can be used to define a tunable many-body kernel similar to the Smooth Overlap of Atomic Positions kernel used in GAP models. We use this kernel to construct sparse Gaussian process (GP) force fields, and show that uncertainties derived from the predictive posterior distribution of the GP correlate with true model error on independent test sets.

The reliability of these uncertainties is the key feature of our approach that enables FLARE—Fast Learning of Atomistic Rare Events—an adaptive method for training force fields on the fly during molecular dynamics. This automated learning procedure takes an arbitrary structure as input and begins with a call to DFT, which is used to train an initial GP model on the forces acting on an arbitrarily chosen subset of atoms in the structure. The GP then proposes an MD step by predicting the forces on all atoms, at which point a decision is made about whether to accept the predictions of the GP or to perform a DFT calculation. The decision is based on the epistemic uncertainty of each GP force component prediction, which estimates the error of the prediction due to dissimilarity between the atom's environment and the local environments stored in the training set of the GP. In particular, if any uncertainty exceeds a chosen multiple of the current noise uncertainty of the model, a call to DFT is made and the training set is augmented with the forces acting on the highest uncertainty local environments, the precise number of which can be tuned to increase training efficiency. All hyperparameters are optimized whenever a local environment and its force components are added to the training set, allowing the error threshold to adapt to novel environments encountered during the simulation. We show that the final trained GP can be mapped onto an equivalent and much faster linear model resembling SNAP and qSNAP models, which we implement in the molecular dynamics program LAMMPS to scale our ML-driven simulations to tens of thousands of atoms over nanosecond timescales.

Our automated procedure for training fast Bayesian force fields allows a wide range of material compositions to be explored in a closed-loop fashion with minimal human supervision. As a demonstration, we apply our method to the shape memory alloy nitinol, and show that we accurately capture the martensite/austenite phase transition that occurs in this material at ambient pressure. We discuss how model uncertainties can be used to systematically expand the training set, enabling exploration of the effects of dopants, defects, and nonequiatomic compositions on the martensitic transition temperature.

SESSION CT05.13: Automation and High Throughput II
Session Chairs: Brian Giera and Kate Higgins
Tuesday Afternoon, April 20, 2021
CT05

2:15 PM *CT05.13.01

Heterogeneous Sensing and Scientific Machine Learning for Quality Assurance in Laser Powder Bed Fusion Aniruddha Gaikwad¹, Brian Giera², Gabe Guss², Jean-Baptiste Forien², Manyalibo Matthews² and Prahalada Rao¹; ¹University of Nebraska–Lincoln, United States; ²Lawrence Livermore National Laboratory, United States

Laser Powder Bed Fusion (LPBF) is the predominant metal Additive Manufacturing (AM) technique that benefits from a significant body of academic study and industrial investment. Despite LPBF's widespread use, there still exists a need for process monitoring to ensure reliable part production and reduce post-build quality assessments. Towards this end, we develop and evaluate machine learning-based predictive models using height map derived quality metrics for single tracks and the accompanying pyrometer and high-speed video camera data collected under a wide range of laser power and laser velocity settings. We extract physically intuitive low-level features representative of the molten pool dynamics from these sensing modalities and explore how these vary with the linear energy density. We find our Sequential Decision Analysis Neural Network (SeDANN) model – a scientific machine learning model that incorporates physical process insights – outperforms other purely data-driven black-box models in both accuracy and speed. The general approach to data curation and adaptable nature of SeDANN's scientifically informed architecture should benefit LPBF systems with an evolving suite of sensing modalities and post-build quality measurements.

2:40 PM CT05.13.02

High-Throughput Correlative Microscopy and Spectroscopy for Nano-Laser Development Ruqaiya Al-Abri, Hoyeon Choi and Patrick Parkinson; The University of Manchester, United Kingdom

Single-element monolithic lasers which can be heteroepitaxially grown or heterogeneously integrated onto a silicon platform have been long sought for photonic integrated circuitry, and as nanoscale light sources for research.

A promising solution for integrated coherent light is using semiconductor nanowires produced with III-V¹ or other emerging materials². These structures allow easy hetero-integration onto silicon³, and they act as both waveguide and gain material, however to date, silicon-integrated, room-temperature and continuous lasing has proven elusive. One key reason for this has been the challenge of repeatable characterisation – a small variation in the geometry or material properties (such as doping) of each nanowire can have an amplified effect on lasing due to the inherent non-linearity of this process, masking systematic properties of this system. In other words, ensemble measurements are meaningless, while single nanowire measurements are insufficient in the presence of heterogeneity.

High-throughput imaging and spectroscopy can be used to provide geometrical, material and functional measurements of large numbers of single nanowire lasers. By studying 100 to 100,000 nanowire lasers from each growth, we correlate performance metrics such as threshold or lasing wavelength with controllable characteristics such as wire length, diameter, doping or transfer process. Using this methodology we have demonstrated material optimization for high quantum efficiency via doping⁴, cavity analysis using time-resolved interferometry^{5,6}, and statistical improvements in fabrication⁷ processes. Each study has enabled record low optically pumped thresholds for III-V nanolasers towards room-temperature continuous lasing, and by integrating pick-and-place techniques⁸, we have demonstrated a combined high-throughput analysis and fabrication platform.

Our methodology – big-data for nano-optoelectronics – makes use of a high-speed data acquisition platform to generate large amounts of single-element data. We correlate electron microscopy, optical microscopy, spectroscopy and functional measurements on each wire through a self-registration process⁹ and stream this data

to a commodity database. This data can be analysed through a MATLAB or Python package, maximising the potential for data reuse. We demonstrate this approach for two applications: optimization of single perovskite nanowire laser, and for an intra-material study of end-facet reflectivity. This methodology is widely transferable to other material systems where single-element correlative study is essential to separate underlying physical processes from high levels of inter-object heterogeneity.

- (1) Eaton. *Nat. Rev. Mater.* **2016**, *1* (6), 16028.
- (2) Zhu. *Nat. Mater.* **2015**, *14* (6), 636–642.
- (3) Koblmüller. *Semicond. Sci. Technol.* **2017**, *32* (5), 053001.
- (4) Alanis. *Nano Lett.* **2018**, *19* (1), 362–368.
- (5) Zhang. *ACS Nano* **2019**, *13* (5), 5931–5938.
- (6) Skalsky. *Light Sci. Appl.* **2020**, *9* (1), 43.
- (7) Alanis. *Nanoscale Adv.* **2019**, *1* (11), 4393–4397.
- (8) Jevtics. *Nano Lett.* **2020**, *20* (3), 1862–1868.
- (9) Parkinson. *Nano Futur.* **2018**, *2* (3), 035004.

2:55 PM CT05.13.03

Implementation of Benchtop NMR as an Online, High-Throughput Sensor in Automated Synthesis Systems Anh Le-McClain; Magritek Inc., United States

The recent development of the high-performance benchtop Nuclear Magnetic Resonance (NMR) spectrometers equipped with high-resolution permanent magnets and flow cells enables a new way to do on-line/in-line monitoring of chemical reactions. Monitoring reactions with NMR provides not only the structural information about different chemical species generated during chemical reactions, but also their quantitative measurements (without the need of a calibration curve) to obtain the reaction's kinetics. Benchtop NMR with reaction monitoring capability can be conveniently incorporated as an online, high-throughput sensor in automated synthesis systems working with artificial intelligence (AI). This presentation will highlight the implementation of benchtop NMR in monitoring chemical reactions, as well as serving as a sensor for an organic synthesis robot using a convolutional neural network.

3:10 PM CT05.13.04

High-Throughput and Data-Driven Strategies for the Design of Deep Eutectic Solvent Electrolytes Jaime Rodriguez, Maria Politi and Lilo D. Pozzo; University of Washington, United States

Within the framework of green chemistry, Deep Eutectic Solvents (DES) have been identified as promising candidates for use in many applications, including battery electrolytes. DES are characterized by two or three materials that associate with each other through hydrogen bond interactions, resulting in a eutectic mixture whose freezing point is below that of the individual materials. This design space is overwhelmingly large and poses a challenge for screening a vast and diverse set of materials. Here we present a strategic approach consisting of high throughput experimentation (HTE) coupled with data science driven analysis to identify exceptional DES candidates based on key physiochemical and electrochemical properties. Much of our HTE adopts methods that are already used frequently in the biotech and pharmaceutical industries, most notably performing parallel syntheses and analyses in 96-well-plate formats. DES samples are first synthesized using an open-sourced automated liquid handling robot. DES melting points are then determined by monitoring the melting process with an infrared camera and identifying the temperature at which the thermal conductivity of the samples changes abruptly. The solubility of battery redox-species is determined via UV-VIS well-spectrophotometers. Finally, the electrochemical stability window and cycling properties of DES electrolytes are measured in high-throughput by using screen-printed electrodes on 96-well plates adapted for use with a standard potentiostat. The ability to rapidly and efficiently collect data also creates a need for the development and use of automated processes for data analysis, which have been developed in an open-sourced format by our group. This approach to HTE also allows for the incorporation of data science techniques, such as feature extraction and machine learning, that further aid in probing a design space that is ultimately too large for

experimental methods alone.

3:25 PM CT05.13.05

Machine Learning Modeling of Photodiode Signal for Selection of Laser Parameters in Laser Powder Bed Fusion Additive Manufacturing Simon Lapointe, Clara Druzgalski, Gabe Guss and Manyalibo Matthews; Lawrence Livermore National Laboratory, United States

Parts produced through metal additive manufacturing suffer from irregular quality, often exhibiting dimensional inaccuracies and defects such as cracks, pores, underfill, spatter, and balling. The development of approaches to control and optimize the additive manufacturing process are essential to improve part quality. Process parameters such as the laser power, velocity, beam size, and scan path should be optimized throughout the manufacturing process. However, incorporating the combined effects of material, geometry, and complex underlying physics into the optimization strategy can be particularly challenging. In this work, a data-driven approach for the selection of laser process parameters is proposed. Stainless steel parts of different shapes and sizes are printed with varying laser power and velocity strategies while collecting photodiode signal data. Using machine learning, a forward model is built to predict the track-wise photodiode signal along the scan path using laser parameters and geometry features as inputs. This model helps understand and quantify how the photodiode signal is influenced by the laser process parameters (laser power and velocity) and the part geometry (dimensions, overhangs, corners, etc.). Additionally, an inverse model is built to predict the laser parameters corresponding to a given track-wise photodiode signal and geometry features. The inverse model allows the selection of laser parameters to maintain a desired photodiode signal. The performance of the inverse model is assessed by deploying it on a test part which geometry differs from the parts used for training.

3:40 PM DISCUSSION TIME

3:55 PM CT05.13.07

Late News: High-Throughput Reaction Screening for Accelerated Materials Research Thomas Mustard; Schrodinger, United States

All specialty chemicals and advanced materials are produced from lower value feedstock or precursors by specialized chemical reactions. Empirical reaction tuning is a laborious and expensive process. In contrast, reliable and efficient first-principles workflows can be employed in a high-throughput fashion to survey chemical design space and inform experimental development. Systematic evaluation of steric and electronic contributions provides an unprecedented fundamental understanding of factors controlling a target reaction. With these structure-property relationships, one can re-design a reaction or catalyst to achieve desired activity. Paired with automated high throughput screening the rate of discovery and understanding is accelerated.

- Reaction/Catalysts activity and selectivity predictions from simulations
- High-Throughput automated methods for in silico reaction screening
- Examples in areas of hydroformylation, epoxy-amine thermosets

SESSION CT05.14: Data-Driven Chemistry III

Session Chairs: Sukriti Manna and Yen-Ju Wu

Tuesday Afternoon, April 20, 2021

CT05

9:25 PM CT05.14.02

Unique Challenges on NNP Development and Ways to Overcome Them Wonseok Jeong, Sungwoo Kang, Changho Hong, Jeong Min Choi and Seungwu Han; Seoul National University, Korea (the Republic of)

Recently, machine-learning (ML) approaches to developing interatomic potentials are attracting considerable attention because it is poised to overcome the major shortcoming inherent to the classical potential and density functional theory (DFT), i.e., difficulty in potential development and huge computational cost, respectively. In particular, the high-dimensional neural network potential (NNP) suggested by Behler and Parrinello is attracting wide interests with applications demonstrated over various materials. However, as ML potentials have a fundamental difference from traditional physics-based force fields, they have unique challenges to overcome for reliable accuracy. In this presentation, we share some of the challenges and our experiences in overcoming them with detailed examples.

First, we discuss the challenge of modeling defective systems. We found that to model defective systems with high accuracy, the sampling bias must be treated with care. Next, we show that when modeling dynamic systems with a large number of chemical reactions, the uncertainty estimation in atomic-resolution is necessary. The efficient uncertainty estimation in atomic-resolution can be obtained through a replica NNP ensemble. Furthermore, we will show that NNPs can be used as highly accurate surrogate models in exploring large space of crystal structures. This enables finding the stable crystal structure for complicated multicomponent systems. Finally, we discuss some of the future challenges in NNP development, and possible solutions to the challenges.

9:40 PM CT05.14.03

Late News: Analysis on the Strengthening Mechanism of Aluminum Alloys with Bayesian Learning for Neural Networks Shimpei Takemoto¹, Kenji Nagata², Takeshi Kaneshita¹, Yoshishige Okuno¹, Junya Inoue³ and Manabu Enoki³; ¹Showa Denko K.K., Japan; ²National Institute for Materials Science, Japan; ³The University of Tokyo, Japan

We discuss the strengthening mechanism of 2000 series aluminum alloy using neural networks. To understand the process-structure-property relationship in aluminum alloys, we have constructed a linear neural network with a single hidden layer whose input, hidden, and output layer nodes correspond to process parameters, structure features, and mechanical properties, respectively. We have applied the replica-exchange Monte Carlo method, an extended Markov chain Monte Carlo (MCMC) method, for the Bayesian inference of the optimal neural network architecture. When predicting ultimate tensile strength and tensile yield strength simultaneously, the Bayesian inference suggests that the neural network with two hidden layer nodes is optimal. This approach enables us to identify dominant combinations of additive elements and heat treatments for strengthening aluminum alloys. We have also conducted thermodynamic calculations of the equilibrium phase fraction using the Thermo-Calc software for each of the hidden layer nodes to discuss the strengthening mechanism of aluminum alloys.

9:55 PM CT05.14.04

Accurate Band-Gap Database for Semiconducting Inorganic Materials—Implementation of Hybrid Functional Sangtae Kim¹, Miso Lee¹, Changho Hong¹, Youngchae Yoon¹, Hyungmin An¹, Dongheon Lee¹, Wonseok Jeong¹, Dongsun Yoo¹, Youngho Kang², Yong Youn¹ and Seungwu Han¹; ¹Seoul National University, Korea (the Republic of); ²Incheon National University, Korea (the Republic of)

Among the various physical properties of materials, one of the fundamental characteristics of materials is band gap (E_g). The E_g of material provides a detailed description of the material's optoelectronic, optical, thermoelectric, and electronic properties, and is a good indicator in distinguishing materials (conductors, semiconductors, and insulators). In particular, semiconductors are used in various fields because of the unique characteristics of materials. For instance, in photovoltaic devices, materials with a direct E_g of ~ 1.3 eV, corresponding to the Shockley-Queisser limit, are favored as photo-absorbers that maximize the solar-cell efficiency. In power electronics, semiconductors with $E_g \geq 3$ eV are employed to sustain high electric fields. Currently, there are several inorganic material databases providing band gaps based on the Generalized Gradient Approximation (GGA) functional, including Materials Project, the Automatic Flow of Materials Discovery Library (AFLOWLIB), the Open Quantum Materials Database (OQMD), and the Joint Automated Repository for Various Integrated Simulations (JARVIS) (the JARVIS provides E_g based on meta-GGA, which significantly improves the accuracy). In spite of the importance of the band gap, however, calculated band gaps

are underestimated due to the limitation of the conventional density functional theory (DFT) scheme. As a related issue, many small-gap semiconductors such as Ge, InAs, PdO, Zn₃As₂, and Ag₂O, are misclassified as metals, which can affect selection of narrow-gap semiconductors in IR sensors, for instance. (In JARVIS, some of these errors are resolved by meta-GGA). In addition, the material containing un-filled d-bands shows an incorrect band gap because magnetics involved in spin configuration affect band splitting. For instance, the antiferromagnetic NiO has an experimental E_g of 4.3 eV, but the computational E_g ranges over 2.2-2.6 eV in the ferromagnetic ordering and GGA functional while the correct antiferromagnetic ordering produces 4.5 eV within the hybrid functional.

In this study, we construct an accurate bandgap database using Automated *Ab initio* Modeling of Materials Property Package (AMP²), which is a fully automated package for DFT calculations. The AMP² has an exclusive algorithm to correct the band gap more accurately: Density of state (DOS) Indicator and ‘One-shot’ hybrid calculation. In order to consider the magnetic properties of spin ordering, the Ising model was also introduced to improve the accuracy of the E_g . The Ising model simply describes the magnetic exchange energy from the spin pair and exchange parameters. We newly devised a method to calculate the exchange parameter through the fitting method and optimize that. The database consists of 10,481 materials that encompass most inorganic solids with E_g ranging between 0 and 5 eV. To verify our database, we compared it with the experimental band gap dataset and magnetic structure database (MAGNDATA). Through 116 benchmark materials for band gap, the root-mean-square error (RMSE) with respect to experimental data is 0.36 eV, significantly smaller than 0.75-1.05 eV in the existing databases. The resulting data are available online at SNUMAT.

10:00 PM CT05.14.05

Developing Machine-Learning Potentials from Disordered Structures for Crystal Structure Prediction

Changho Hong¹, Jeong Min Choi¹, Wonseok Jeong¹, Sungwoo Kang¹, Suyeon Ju¹, Kyeongpung Lee¹, Jisu Jung¹, Yong Youn² and Seungwu Han¹; ¹Seoul National University, Korea (the Republic of); ²National Institute for Materials Science, Japan

Crystal structure prediction (CSP) is a problem of finding a structure with global-minimum free energy. It can be broken down into two problems: a searching algorithm in configuration space of structures and a method of evaluating free energy. Various heuristic algorithms such as genetic algorithms have been developed for efficient search. First-principles calculation based on density functional theory (DFT) has been chosen as its non-empirical nature allows accurate evaluation of energies. The DFT-based CSP has been successful in identifying inorganic crystals under extreme conditions and organic crystals. One interesting field to apply CSP is structure prediction of ternary or higher (simply multinary hereafter) inorganic crystals at ambient conditions. CSP can accelerate the low throughput of experimental synthesis. Considering major technological breakthroughs in display and battery industries have been achieved from new materials such as InGaZnO₄ and Li₁₀GeP₂S₁₂, more rapid discovery of novel materials is very important. However, multinary materials have a momentous increase of atomic arrangements where permutation of different species becomes an important factor. This demands much more efficient methods of evaluating free energy than DFT. Recently, machine-learning potentials such as neural network potential (NNP) draw much attention for its accuracy of DFT and yet much faster speed. But absence of information on structures imposes a big hurdle to constructing training sets. To deal with this impediment, we propose a way to build NNP as a robust surrogate model of DFT for predicting the most stable structure of multinary compounds at ambient conditions. The central approach is to train an MLP over disordered structures such as liquid and amorphous phases. The molecular dynamics (MD) simulation of liquid phase can start from a random distribution and reach equilibrium quickly at high temperature. Then, the liquid phase is quenched to an amorphous phase. This makes it possible to forge training sets without any knowledge of unknown crystals except for the chemical composition. The short-range order in disordered phases resemble that of crystalline phases and local fluctuations during MD can also sample diverse local environments. To demonstrate accuracy of NNP, we compare NNP and DFT energies for Ba₂AgSi₃, Mg₂SiO₄, LiAlCl₄, and InTe₂O₅F over experimental phases as well as low-energy crystal structures that are generated theoretically. For every material, we find strong correlations between DFT and NNP energies, ensuring that the NNPs can identify the most stable structures and properly rank low-energy crystalline

structures. We also find that the evolutionary search combined with NNPs can evaluate low-energy metastable phases more efficiently than one with DFT. With this proposed way to training reliable machine-learning potentials for the crystal structure prediction, this research offers efficient method to search uncharted multinary phases.

10:05 PM CT05.14.06

Efficient Sampling for Training Set of Machine Learning Potentials Using Metadynamics Dongsun Yoo, Jisu Jung, Wonseok Jeong and Seungwu Han; Seoul National University, Korea (the Republic of)

Machine learning potentials (MLPs) are attracting enormous interests as a promising computational tool, which provides the accuracy of quantum mechanical calculations with the speed of classical interatomic potential. MLPs have extended their application to the complex system, including phase-change materials, nanoclusters, and catalysts. We have to make the training set cover diverse configurations, which can appear during the simulation, to get reliable simulation because MLPs can guarantee certainty only within the training set. The training set is made from a specific target static structure or DFT-based molecular dynamics (MD) simulations typically. However, such a manual sampling requires expertise in the target system and iterative trial-and-error data augmentation with enormous computation time.

Therefore, we suggest a metadynamics that uses the local environment of an atom, which is the input vector of MLPs, as collective variables. These collective variables keep the system from revisiting the symmetrically identical structure. We can sample a wide range of configurations autonomously where just high-temperature MD cannot visit. We demonstrate the metadynamics with a Pt surface with hydrogen, followed by an application on the GeTe system.

SYMPOSIUM CT06

From Quantum Mechanics to Materials Engineering—Recent Progress on the Development and Novel Applications of Ab Initio Methods in Materials Science
April 22 - April 23, 2021

Symposium Organizers

Amartya Banerjee, University of California, Los Angeles

Felipe Jornada, Stanford University

Lin Lin, University of California, Berkeley

Sivan Refaely-Abramson, Weizmann Institute of Science

Symposium Support

Silver

IOP Publishing

* Invited Paper

SESSION CT06.01: First-Principles Methods for Ground- and Excited-State Phenomena

Session Chairs: Amartya Banerjee and Sivan Refaely-Abramson

Thursday Morning, April 22, 2021

CT06

8:00 AM *CT06.01.01

Koopmans Spectral Functionals: Charged Excitations from Functional Theories Nicola Marzari; École Polytechnique Fédérale de Lausanne, Switzerland

I will discuss the theory and practice of Koopmans spectral functionals, aiming to reproduce total energies and spectra of molecules and materials with functional formulations. A comparison many-body perturbation theory is provided for ionization potentials and electron affinities of molecules and band structures of solids, showing an agreement with experiments comparable to the current state-of-the-art, and at a fraction of the computational costs. I will illustrate also the implementation in open-source periodic-boundary condition codes. Work done in collaboration with Nicola Colonna, Riccardo de Gennario, Edward Linscott, Linh Nguyen, and Andrea Ferretti.

8:24 AM *CT06.01.02

The Connector Theory Approach—Principles and Development of Functionals Ayoub Aouina¹, Marco Vanzini², Matteo Gatti^{3,1} and Lucia Reining^{3,1}; ¹Institut Polytechnique de Paris, France; ²EPFL, Switzerland; ³CNRS, France

One important approach for the description of quantum many-body systems is to design functionals: observables or effective potentials are expressed in terms of relatively simple quantities, such as the density or a one-body Green's function, instead of calculating expectation values with many-body wavefunctions. However, although efficient approximations for such functionals exist for some important observables, such as the total energy, they still lack precision for many applications, and other observables cannot be accessed in a satisfactory way. For example, Density Functional Theory (DFT) and Time-Dependent (TD) DFT still face major difficulties to describe strongly correlated systems, or excitonic effects in optical spectra. For other observables, even less is known about how to build good density functionals.

One way of designing approximations is to use results of model systems. In this talk we will show how model results can be used in an in principle exact way, called "Connector Theory", in order to describe observables and systems of interest. Within this approach, a quantity of interest is calculated for a model system as function of a parameter once and forever, and the results are stored. Under certain conditions, the result for an appropriate choice of parameter can then be used to replace a value of interest in a given real system. This choice of parameter is called "connector".

We will discuss the principles and general properties of such an approach. Of course, in practice, the connector has to be approximated. We will show that formulating the problem in this way is a convenient starting point for approximations, and a strategy to build systematic approximations will be presented. Some discussion and results can be found in [1,2].

[1] M. Vanzini, A. Aouina, M. Panholzer, M. Gatti, and L. Reining, *arXiv:1903.07930v3*

[2] M Panholzer, M Gatti, L Reining; *Phys. Rev. Lett.* 120, 166402 (2018).

8:48 AM *CT06.01.03

High-Throughput Computation of Raman- and Second Harmonics Optical Spectra for Automated Characterization of 2D Materials Kristian S. Thygesen; Technical University of Denmark, Denmark

Raman spectroscopy is frequently used to identify composition, structure and layer thickness of 2D materials. Here, we describe an efficient first-principles workflow for calculating resonant first-order Raman spectra of solids within third-order perturbation theory employing a localized atomic orbital basis set. The method is used to obtain the Raman spectra of around 1000 different monolayers selected from the Computational 2D Materials Database (C2DB)[1]. On basis of this database, we propose an automatic procedure for identifying a material based on an input experimental Raman spectrum and demonstrate it for the cases of MoS₂ (H-phase) and WTe₂ (T''-phase)[2]. Employing a similar computational methodology, we calculated nonlinear optical (NLO) spectra of about 400 non-centrosymmetric semiconducting monolayers. NLO phenomena such as harmonic generation, Kerr, and Pockels effects are of great technological importance for lasers, frequency converters, modulators, switches, etc. Recently, 2D materials have drawn significant attention due to their strong and unique NLO

properties. Sorting the non-resonant nonlinearities of the monolayers with respect to bandgap E_{gap} reveals an upper limit proportional to E_{gap}^{-4} , which is neatly explained by a generic two-band model. We identify multiple promising candidates with giant nonlinearities and band gaps ranging from 0.4 to 5 eV, some of which approach the theoretical upper limit and greatly outperform known materials[3].

The comprehensive libraries of ab initio Raman and NLO spectra are freely available via the C2DB website(<https://cmrdb.fysik.dtu.dk/c2db/>).

References:

[1] The Computational 2D Materials Database: High-Throughput Modeling and Discovery of Atomically Thin Crystals, S. Hastrup et al., 2D Materials 5, 042002 (2018)

[2] A library of ab initio Raman spectra for automated identification of 2D materials, A. Taghizadeh et al, Nature Comm. 11, 3011 (2020)

[3] Two-dimensional Materials with Giant Optical Nonlinearities Near the Theoretical Upper Limit, A. Taghizadeh et al, arXiv:2010.11596

9:12 AM *CT06.01.04

Partial Order-Disorder Transition in Thermoelectric Clathrates Revealed by a Novel Approach for Temperature-Dependent Properties of Alloys Claudia Draxl¹, Maria Troppenz¹, Santiago Rigamonti¹ and Jorge O. Sofo²; ¹Humboldt-Universität zu Berlin, Germany; ²The Pennsylvania State University, United States

Intermetallic clathrate compounds have a huge compositional and configurational space that allows for tailoring their properties towards a high thermoelectric efficiency. Semiconducting behavior is often difficult to achieve due to the intricate interplay between electronic structure, temperature, and disorder. For instance, in the complex clathrate compound $\text{Ba}_8\text{Al}_x\text{Si}_{46-x}$, the configuration of the Al atoms in the crystal framework drastically affects the electronic behavior [1]. This is most strikingly the case at the technologically relevant composition $x = 16$, whose ordered ground state is semiconducting, while disordered structures at higher energies are metallic. We have developed a multi-scale approach, based on statistical thermodynamics combined with the cluster-expansion method [2] and *ab initio* calculations which allows us to calculate the temperature-dependent effective band structure of alloys without relying on effective medium approximations [3]. With its help, we discover a semiconductor-to-metal transition that is accompanied by an order-disorder phase transition at 582 K.

[1] M. Troppenz, S. Rigamonti, and C. Draxl, Chem. Mater. 29, 2414 (2017).

[2] S. Rigamonti, et al., CELL: python package for cluster expansions with a focus on complex alloys. URL: <https://sol.physik.huberlin.de/cell>

[3] M. Troppenz, S. Rigamonti, J. Sofo, and C. Draxl, <https://arxiv.org/abs/2009.11137>

9:36 AM *CT06.01.05

Quantum Simulations of Heterogeneous Materials on Classical and Near-Term Quantum Computers Giulia Galli; The University of Chicago, United States

In this talk I will present strategies to predict and design materials for next generation technologies by combining theories based on quantum mechanics, and algorithms and codes running on high performance classical computers, and, in some cases, on near-term quantum computers. I will specifically focus on predicting and designing materials to build radically novel sensors and computers, so as to move in earnest into the quantum information age.

10:30 AM *CT06.02.01

Electronic and Optical Excitations from Screened Range-Separated Hybrid Density Functional Theory
Leeor Kronik; Weizmann Institute of Science, Israel

The concept of optimal tuning (OT) of range-separated hybrid (RSH) functionals has become an important tool for overcoming the fundamental gap problem and the charge transfer excitation problem in molecular systems. Here, this concept is extended to the solid state by introducing dielectric screening and orbital localization into the functional form. This approach, couched rigorously within the generalized Kohn-Sham formalism of density functional theory, can produce quantitatively the same one and two quasi-particle excitation picture given by many-body perturbation theory (MBPT), without any empiricism. Specifically, for covalent/ionic semiconductors and insulators, accurate band structures and optical absorption spectra, which agree well with those obtained from MBPT, are obtained. For molecular solids, the approach predicts the correct gap renormalization - even from single molecule calculations if a polarizable continuum model is used in an electrostatically consistent manner – and also predicts absorption spectra well.

10:55 AM CT06.02.02

Room Temperature Superfluorescence from a Single Nanocuboid John P. Philbin¹, Joseph Kelly², Lintao Peng³, Igor Coropceanu⁴, Dmitri V. Talapin^{4,3}, Eran Rabani^{5,6,7}, Xuedan Ma³ and Prineha Narang¹; ¹Harvard University, United States; ²Stanford University, United States; ³Argonne National Laboratory, United States; ⁴The University of Chicago, United States; ⁵Lawrence Berkeley National Laboratory, United States; ⁶Tel Aviv University, Israel; ⁷University of California, Berkeley, United States

Single-photon superradiance arises when a collection of identical emitters are spatially separated by distances much less than the wavelength of the light they emit and results in the formation of a superradiant state that spontaneously emits light with a rate that scales linearly with the number of emitters. This collective phenomena has only been demonstrated in a few nanomaterial systems, none of which have used quasi-2D nanoplatelets as the emitter. In this work, we rationally design a single colloidal nanomaterial that hosts multiple (nearly) identical emitters. Specifically, by combining molecular dynamics, atomistic electronic structure calculations, and model Hamiltonians methods, we show that quasi-2D nanoplatelets oriented along each face of a “nanocuboid” can serve as the (nearly) identical emitters required to observe both superradiant and subradiant phenomena. Utilizing layer by layer growth techniques to synthesize a nanocuboid, we demonstrate single-photon superfluorescence via single-particle time-resolved photoluminescence measurements at room temperature. The realization of superradiant and subradiant states in these single nanocuboids opens the door to ultrafast single-photon emitters and may provide an avenue to entangled multi-photon states via superradiant cascades.

This work is partially supported by the Army Research Office MURI (Ab-Initio Solid-State Quantum Materials) under Grant No. W911NF-18-1-0431. JP is a Ziff Fellow at the Harvard University Center for the Environment.

11:10 AM CT06.02.03

Symmetry Adapted Real Space Density Functional Theory for Helical Nanostructures—Application to Torsional Deformations in Group-IV Nanotubes Hsuan M. Yu and Amartya S. Banerjee; University of California, Los Angeles, United States

The mathematical framework for classifying nanostructures shows that a vast class of such materials can be described as being *helical*, i.e., their spatial atomic arrangement possesses helical symmetries. Helical nanostructures include important technological materials such as nanotubes, nanowires, nanoribbons and nanosprings; miscellaneous chiral structures encountered in chemistry; and examples from biology, including tail sheaths of viruses and many common proteins. Helical nanostructures have received much attention recently due to their unusual and interesting material properties, including e.g., their strong association with

ferromagnetism, ferroelectricity and superconductivity, unique transport characteristics, and the existence of strong coupling between their mechanical and optical/transport properties.

Given the relative abundance of helical nanostructures and their scientific and technological importance, there is a pressing need to have reliable and efficient computational tools for studying such structures. In this work, we will describe the formulation and implementation of a first principles simulation tool for helical nanostructures based on a symmetry adapted real space formulation of Kohn-Sham Density Functional Theory. Specifically, the computational method employs a finite difference discretization of the governing equations in so called *helical coordinates*, and handles symmetries arising from common helical groups by using an appropriate version of the Bloch theorem for such systems. This combination of features of the method allows one to simulate for example, the behavior of nanotubes of arbitrary chirality *ab initio*.

We utilize the newly developed computational tool to carry out a first principles study of various nanotubes. In particular, we will describe the behavior of group IV nanotubes under twisting deformations as revealed by our simulations. We will describe interpretation of some of the mechanical properties of these tubes, computed *ab initio*, from the perspective of elasticity theory. We will also highlight the interplay between mechanical strains and electronic states in these materials and comment on the effects of structural relaxation.

11:25 AM *CT06.02.04

Stochastic Many-Body Methods for Quasiparticle Excitations in Nanoscale Systems Vojtech Vlcek;
University of California, Santa Barbara, United States

I will present recent developments in predicting electronic excitations using the combination of stochastic computational techniques and many-body theory. The methodology relies on operators' decomposition via random vectors and recasting expectation values as statistical estimators. In practice, the implementation of diagrammatic methods employs real-time and real-space sampling.[1] This formalism leads to substantial computational savings and reduced scaling with the number of electrons; it enables first-principles predictions of quasiparticle energies in systems with thousands of atoms. In detail, I will describe our recent work on simulating nanoscale condensed systems within the linear scaling stochastic GW approximation.[2,3,4] Further, I will show that statistical sampling of interactions is an efficient route to go beyond GW: I will detail our work on the stochastic GW approach, which combines non-local vertex corrections in the screened Coulomb interaction and self-energy.[5] I will demonstrate that the vertex corrections affect unoccupied states, improve the quasiparticle energies, and capture multi-quasiparticle excitations otherwise missing in GW.[5,6] Despite the increased complexity of the self-energy, the stochastic GW scales linearly with the system size.

[1] V Vlcek, W Li, R Baer, E Rabani, D Neuhauser, Physical Review B 98 (7), 075107 (2018)

[2] J Brooks, G Weng, S Taylor, V Vlcek, Journal of Physics: Condensed Matter 32 (23), 234001 (2020)

[3] G Weng, V Vlcek The Journal of Physical Chemistry Letters 11 (17), 7177-7183 (2020)

[4] M Romanova, V Vlcek The Journal of Chemical Physics 153 (13), 134103 (2020)

[5] V Vlcek, Journal of Chemical Theory and Computation 15 (11), 6254-6266 (2019)

[6] C Mejuto-Zaera, et al., arXiv preprint arXiv:2009.0240122020

11:50 AM CT06.02.05

Improving Stochastic Green's Function Methods for Localized States in Low-Dimensional Heterostructures Mariya Romanova and Vojtech Vlcek; University of California, Santa Barbara, United States

First, we will present a new embedding approach [1] in the stochastic GW technique [2-4] that enables efficient treatment of the impurity states with high accuracy and minimal effort. The method is based on a partitioning of the Green's function and screened Coulomb potential into the deterministic subspace (usually containing localized states) and the stochastic subspace (the rest of the Hilbert space). The enhanced stochastic-deterministic sampling minimizes statistical errors in energies of localized quasiparticles.

Further, we will present a new technique for the stochastic decomposition of the many-body interactions into

additive subspace contributions. We partition the Hilbert space and compute the polarization self-energy via sampling selected charge density fluctuations in real space and time. The decomposition accounts for quasiparticle scattering by correlations from a particular subspace. We identify couplings among different areas (spatial or energetic), e.g., screening contributions in quantum interfaces.

We exemplify our approaches on N-vacancy defects in pristine monolayer and an hBN - graphene bilayer (> 2,000 electrons). We demonstrate the new hybrid stochastic-deterministic approach reduces statistical errors and leads to more than an order of magnitude savings in computational time. The computed subspace self-energy unveils how interfacial couplings affect electronic correlations and identifies contributions to excited-state lifetimes. While the embedding is necessary for the proper treatment of impurity states, the decomposition yields new physical insight into quantum phenomena in heterogeneous systems.

1. M. Romanova, V. Vlcek, J. Chem. Phys. 153, 134103, 2020
2. D. Neuhauser et al., Phys. Rev. Lett. 2014, 113, 076402
3. V. Vlček et al., Phys. Rev. B 2018 , 98 , 075107
4. V. Vlček et al., J. Chem. Theory Comput. 2017 , 13 , 4997–5003.

This work was supported by the NSF MRSEC Program through Grant No. DMR-1720256 and by the UCSB NSF Quantum Foundry Q-AMASE-i, Award No. DMR-1906325.

12:05 PM CT06.02.06

Late News: Electronic Structure of Mixed-Dimensional Metallophthalocyanine-MoS₂ Heterojunctions from Screened Range-Separated Hybrid Functionals Qunfei Zhou^{1,2}, Zhenfei Liu³, Tobin Marks¹ and Pierre Darancet²; ¹Northwestern University, United States; ²Argonne National Laboratory, United States; ³Wayne State University, United States

Mixed-dimensional heterojunctions (MDHJ) comprised of 0D molecules deposited on 2D materials are actively being explored for opto-electronic applications. As a result of the extreme heterogeneity in the density of states and dielectric screening of these systems, properties of MDHJs are impacted by numerous distinct and competing energy scales, including local and non-local electronic correlations, interfacial dipole and orbital hybridization, which complicates theoretical description of MDHJs accurately. Here we analyze the electronic structure of 0D-2D (metallophthalocyanines-MoS₂) heterojunctions using multi-objective optimization of range-separated hybrid functionals that incorporates screened exact exchange for asymptotically-correct Coulomb potential. We obtain electronic structures consistent with experimental photoemission results in both energy level alignment and electronic band gaps, representing a significant advance compare to standard DFT methods. We elucidate MoS₂ valence resonance with the transition-metal phthalocyanine non-frontier *3d* orbitals and how they contribute to emergent interfacial properties. This resonance is also highly dependent on the transition metal identity, enabling controlled tunability of the 0D/2D MDHJs. Based on our calculations, we derive parameter-free, model self-energy corrections to semi-local density functional theory for mixed-dimensional heterojunctions at different dielectric environment in an efficient way. In a broader context, these results illustrate how theory can impact the design and realization of precisely tailored mixed dimensional heterojunctions for specific opto-electronic functions.

12:20 PM DISCUSSION TIME

SESSION CT06.03: Ab Initio Techniques for Large-Scale Calculations and Multi-Scale Physics II

Session Chairs: Amartya Banerjee, Felipe Jornada, Lin Lin and Sivan Refaely-Abramson

Thursday Afternoon, April 22, 2021

CT06

1:00 PM *CT06.03.01

Subspace Embedding and Downfolding Techniques for the Bethe Salpeter Equation Diana Qiu; Yale University, United States

Ab initio many-body perturbation theory methods, like GW and GW plus Bethe Salpeter Equation (GW-BSE), are well-established and highly-accurate techniques for calculating the quasiparticle and optical properties of moderate-sized systems. There remain, however, a number of challenges when it comes to scaling up these techniques to address systems with a large number of heterogeneous atoms, various forms of aperiodicity, and large energy scales well-outside the optical regime. In this talk, I will discuss our newly developed subspace embedding and downfolding techniques for GW-BSE calculations on low-dimensional and amorphous systems that exemplify these challenges. In particular, we apply GW-BSE to study optical properties of heterostructures of quasi two dimensional (quasi-2D) materials, as well as the effect of electron-hole interactions on core-level spectra of quasi-2D materials and amorphous water, including dynamic effects due to scattering to the electron-hole continuum. The calculations are made possible through a combination of physically motivated approximations and algorithms, including non-uniform spatial sampling, low-rank approximations, and subspace embedding and matrix downfolding techniques. We find that electron-hole interactions play an essential role in the scattering of core-level excitations with excitations from the valence band.

1:25 PM CT06.03.02

Enabling Linear Scaling Exact Exchange for Heterogeneous Systems Hsin-Yu Ko¹, Zachary M. Sparrow¹, Marcos F. Calegari Andrade², Owen L. Crane¹, Brian G. Ernst¹, Peace Kotamnives¹, Yan Yang¹, Yang Yang¹, Eric G. Fuemmeler¹ and Robert DiStasio¹; ¹Cornell University, United States; ²Princeton University, United States

Hybrid functionals reduce the self-interaction error in semi-local density functional theory (DFT) and provide a semi-quantitative description of the electronic structure in systems throughout chemistry, physics, and materials science. However, the high computational cost associated with evaluating the exact exchange (EXX) interaction limits hybrid DFT from treating large-scale condensed-phase systems. To address this challenge, we have developed a linear-scaling real-space approach that exploits the sparsity in the EXX interaction using local orbitals (MLWFs). The resulting massively parallel algorithm (*exx*) provides an accurate evaluation of all EXX quantities and enables hybrid DFT based *ab initio* molecular dynamics (AIMD) of large-scale finite-gap systems with a wall time cost comparable to semi-local DFT [1]. Since *exx* was optimized to treat *homogeneous* systems, its performance degrades when treating highly anisotropic *heterogeneous* systems with multiple phases and/or components. In this work, we discuss three major theoretical and algorithmic advances that enable efficient and accurate hybrid DFT based AIMD of large-scale heterogeneous systems, and showcase the extended *exx* module when treating a complex solid-liquid interface.

[1] J Chem Theory Comput 16, 3757 (2020).

1:40 PM CT06.03.03

Molecular to Mesoscopic Design of Novel Plasmonic Materials—Combining First-Principles Approach with Electromagnetic Modelling Alireza Shabani¹, Mehdi Khazaei Nezhad², Neda Rahmani¹, Yogendra K. Mishra¹, Biplob Sanyal³ and Jost Adam¹; ¹University of Southern Denmark, Denmark; ²Ferdowsi University of Mashhad, Iran (the Islamic Republic of); ³Uppsala University, Sweden

To date, due to the rapid progress in science and technology, the efforts for reaching new plasmonic materials are extensively growing. Although the most often used noble metals, such as Au and Ag, demonstrate a strong optical response in plasmonics and metamaterials, some of their inherent features make them less suitable for real-world applications. In this work, we aim to seek new alternative plasmonic materials by proposing a novel and reliable method via manipulating the characteristic response of candidate compounds such as Al/Ga doped Zinc Oxide (A/GZO), ZrN, TiN and Silicon allotropes. This method merges two powerful computational

approaches, namely, density functional theory (DFT) and electromagnetic (EM) simulations by the finite-element method (FEM) and more rigorous methods (e.g. TMM, RCWA). We first perform a series of DFT calculations, including the structural relaxation of plasmonic material candidates, to find the crystal structure with minimum energy, for different exchange-correlation functionals such as GGA, LDA. In a second step, we analyse the simulated material's electronic and optical properties to illustrate potential metallic behaviour, from the viewpoint of material science, via electronic density of states (DOS), band structure and optical dispersion functions (real and imaginary parts). To evaluate the found material's performance in a semi-real plasmonic system, we subsequently extract the optical dispersion parameters, such as refractive index data as well as Drude-Lorentz parameters of complex dielectric permittivity from our calculated DFT. We finally feed the generated optical dispersion data into an EM-solver for optical simulations of any desired optical system and investigate its efficiency for suitability in plasmonic applications. Our method comprises the possibility for verification with experimental data on each level. From there on, we can optimize digitally the molecular structure, paving the way to predict the proposed compounds' plasmonic functionality, overcoming the persistent hurdles introduced by pure experimental works.

1:55 PM *CT06.03.04

Embedded Cluster Density Approximation for Performing High-Level Density Functional Theory Calculations in Large Systems Chen Huang; Florida State University, United States

We have developed the embedded cluster density approximation (ECDA) for scaling up high-level Kohn-Sham density functional theory (KS-DFT) calculations in large systems. ECDA is a local correlation method formulated in the framework of KS-DFT. In ECDA, a cluster is defined for each atom based on the density embedding theory. The cluster's exchange-correlation (XC) energy density is then calculated using advanced, orbital-based XC functionals. The system's XC energy is obtained by patching clusters' XC energy densities in an atom-by-atom manner. We have derived an efficient way to calculate the system's XC potential, making ECDA fully self-consistent and suitable for studying charge reorganization in heterogeneous materials. ECDA is a variational method, and analytical forces have also been derived. Numerical examples show that ECDA can be applied to various systems that have different bond types, which makes ECDA a nearly black-box method.

2:20 PM CT06.03.05

Uncovering Electron Scattering in Goniopolar Materials from First Principles Yaxian Wang and Prineha Narang; Harvard University, United States

Electron scattering on a non-trivial Fermi surface topology plays an important role in electron transport, thus giving rise to exotic phenomena such as violation of Wiedemann Franz law, hydrodynamic electron flow, unusual phonon decay etc. Recent experimental discoveries in axis-dependent conduction polarity, or goniopolarity, have observed that the charge carriers can conduct like either electrons or holes depending on the crystallographic direction they travel along in layered compounds such as NaSn₂As₂ and PdCoO₂, the latter of which also features hydrodynamic electron flow. In this talk, we present an ab initio study of electron scattering in such systems. Taking NaSn₂As₂ as an example, we study different microscopic scattering mechanisms from ab initio and present the electron-phonon scattering time distribution on its Fermi surface in momentum space, the anisotropy of which is proposed to be the origin of the axis-dependent conduction polarity. Further, we obtain the overall anisotropic lifetime tensors in real space at different electron chemical potentials and temperatures and discuss how they contribute to the macroscopic thermopower. While we find that the contribution of the in-plane and cross plane lifetimes exhibits a similar trend, the concave portion of the Fermi surface alters the electron motion significantly in the presence of a magnetic field, thus flipping the conduction polarity as measured via the Hall effect. Our calculations and analysis of NaSn₂As₂ also suggests the strong possibility of hydrodynamic electron flow in the system. These results together have implications for electron lifetimes in a broad class of new quantum materials and provide key, general insights into electron scattering on open Fermi surfaces.

2:35 PM CT06.03.06

Electron Hydrodynamics—Microscopic Origins and Effects of Macroscale Geometries George Varnavides¹, Adam S. Jermyn², Yaxian Wang³, Uri Vool³, Assaf Hamo³, Amir Yacoby³, Polina Anikeeva¹ and Prineha Narang³; ¹Massachusetts Institute of Technology, United States; ²Flatiron Institute, United States; ³Harvard University, United States

Electrons in condensed matter can flow collectively when their momentum is on-average conserved during microscopic scattering processes. This 'hydrodynamic' regime has been observed in graphene,¹⁻² and more recently in bulk materials such as WTe2 at moderately low temperatures and micrometer lengthscales.³⁻⁴ This enables direct observation of strong electron interactions otherwise challenging to measure. Competition between the ballistic, at low temperatures and nanometer lengthscales, and diffusive regimes, at high temperatures and millimeter lengthscales, suggests this phenomenon can only be observed in a narrow temperature/lengthscale window.

In this work, we compute temperature-resolved microscopic scattering rates for a broad range of materials, from first principles. We then utilize these, together with crystal symmetry constraints, to compute an effective viscosity tensor - which we use as a diagnostic tool for hydrodynamic material candidates.

Despite momentum conservation inside the material, electron scattering at the boundary lead to the unique spatial signatures, such as Poiseuille flow, observed in experiments.¹⁻⁴ We investigate the effect of nanoscale geometries on these viscous electron fluids by using two independent methods: i) Macroscopic solution of the electronic Navier Stokes equation using the ab-initio viscosity tensors computed above,⁵ ii) Microscopic solution of the spatially-resolved Boltzmann transport equation using the ab-initio scattering matrix.⁶

This work paves the path in experimentally-observable signatures of hydrodynamic electron flow based on first principles diagnostics.

¹ Sulpizio, J. A. et al. Nature 576, 75–79 (2019).

² Ku, M. et al. Nature 583 (2020)

³ de Jong, M. and Molenkamp, L., PRB 51 (1995)

⁴ Vool, U., Hamo, A., Varnavides, G., Yaxian, W. et al arXiv:2009.04477 (2020)

⁵ Varnavides, G., Jermyn, A.S., Anikeeva, P. et al. Nat Commun 11, 4710 (2020)

⁶ Varnavides G., Jermyn A.S., Anikeeva P. et al. Phys. Rev. B 100 115402 (2019)

SESSION CT06.04: Applications of Large-Scale First-Principles Calculations
Session Chairs: Amartya Banerjee, Felipe Jornada, Lin Lin and Sivan Refaely-Abramson
Friday Morning, April 23, 2021
CT06

8:00 AM CT06.04.01

Late News: Modeling Polaron Hopping in Ternary Spinel Oxides Maytal Caspary Toroker; Technion-Israel Institute of Technology, Israel

The small-polaron hopping model has been used for several decades for modeling electronic charge transport in oxides. Despite its significance, the model was developed for binary oxides, and its accuracy has not been rigorously tested for higher-order oxides. To investigate this issue, we chose the $Mn_xFe_{3-x}O_4$ spinel system, which has exciting electrochemical and catalytic properties, and mixed cation oxidation states that enable us to examine the mechanisms of small-polaron transport. Using a combination of experimental results and DFT+*U* calculations, we find that the charge transport occurs only between like-cations (Fe/Fe or Mn/Mn). And due to asymmetric hopping barriers and formation energies, we find that the polaron is energetically preferred to the

polaron, resulting in an asymmetric contribution of the Mn/Mn pathways.

Reference:

A. Bhargava, R. Eppstein, J. Sun, M. A. Smeaton, H. Paik, L. F. Kourkoutis, D. G. Scholm, M. Caspary Toroker*, R. D. Robinson*, “Breakdown of the small-polaron hopping model in higher-order spinels”, *Adv. Mat.*, 2004490 (2020).

8:15 AM CT06.04.02

Late News: Role of Surface Ligands and Disorder on Bandgap Tunability in Silicon Nanoparticles

Katerina Dohnalova Newell¹, Prokop Hapala² and Corentin Morice¹; ¹University of Amsterdam, Netherlands; ²Institute of Physics, Czechia

Silicon nanoparticles (Si-NPs) represent one of many types of nanomaterials, where the origin of emission is difficult to assess due to a complex interplay between the core and surface chemistry, especially due to silicon's strictly covalent chemistry. Band-gap tunability in ideal fully crystalline hydrogen capped Si-NPs is predicted to span from infrared to ultraviolet spectral range, but this is rarely observed in practice.

In this work, we simulate "fuzzy band structure", radiative rates and HOMO-LUMO energy (band-gap size) tunability of ~2nm Si-NPs. In particular we assess the role of surface, such as (i) covalently bonded atoms/molecules, (ii) strain and (iii) disorder. Simulations are done on the density functional theory level and compared with experimental results by a state-of-the-art single-dot correlative microscopy tool. By this method, the size of the individual NPs is measured by an atomic force microscopy (AFM) and the optical band-gap is evaluated from a single-dot photoluminescence measured on the very same NPs. We propose that (a) covalently bonded species alter the overall energy levels and transition rates, (b) strain reduces the radiative rates and (c) disorder reduces the bandgap tunability range. Our observations might explain the often observed puzzlingly fast radiative rates in organically capped Si-NPs and weak size tunability in most experimentally realized Si-NP systems.

8:30 AM CT06.04.03

Late News: Synthesis and Characterization of Up-Converting Gd₂O₃:Er³⁺, Yb³⁺, Mg²⁺ Nanoparticles

Aleksandra Wosztal^{1,1}, Krzysztof Fronc², Bożena Sikora², Tomasz Wojciechowski², Roman Minikayev², Wojciech Paszkowicz², Kamil Sobczak¹, Przemysław Kowalik², Katarzyna Lysiak¹, Danek Elbaum², Jacek Szczytko¹ and Izabela Kaminska²; ¹University of Warsaw, Poland; ²Institute of Physics, Polish Academy of Sciences, Poland

Nowadays there are many attempts in the world of science to harness quantum mechanics. One of the widely explored fields with the potential of practical usage is the anti-Stokes emission phenomena. Obtained during the research gadolinium oxide nanoparticles doped with selected metals were used to investigate energy transfer between erbium (Er³⁺) and ytterbium (Yb³⁺) ions and enhance the efficiency of anti-Stokes emission by doping structures with magnesium ions (Mg²⁺).

The examined materials were synthesized by a homogeneous precipitation method for 2 hours at a temperature of 85°C. The crystal structure arrangement was obtained by calcining at a temperature of 990°C for 3 hours. The nanoparticles were characterized with several methods. Size and form were analyzed by scanning electron microscopy (SEM) and transmission electron microscopy (TEM). The crystal structure was determined by X-ray diffraction (XRD). The atomic composition of the nanoparticles was characterized by energy-dispersive X-ray spectroscopy (EDS). Optical properties were analyzed by using photoluminescence measurements. Finally, nanoparticles were incubated with mouse mammary carcinoma (4T1) cells for 24h to examine their suitability for use in biology as luminescent markers.

As a result, nanoparticles show luminescence in the visible region - emission maxima occur at a wavelength of 565 nm (⁴S_{3/2} → ⁴I_{15/2}, ²H_{11/2} → ⁴I_{15/2}) and 663 nm (⁴F_{9/2} → ⁴I_{15/2}) during excitation with a semiconductor laser

with a wavelength of 980 nm (continuous wave). An increase in the effectiveness of the anti-Stokes emission process was observed - an 8-fold increase in red luminescence efficiency was obtained for nanoparticles doped with 2.5% Mg^{2+} compared with non-doped nanoparticles (Gd_2O_3 : 1% Er^{3+} , 18% Yb^{3+}). The measurements were carried out at a laser power density of $12 \text{ W} \times \text{cm}^{-2}$. The nanoparticles were dissolved in a dimethyl sulfoxide solution. The nanoparticles' diameter was 380 nm, 282 nm, and 260 nm (before calcining). The diameters of the obtained nanoparticles - are $302 \pm 37 \text{ nm}$ and $278 \pm 36 \text{ nm}$ (after a calcining) respectively.

8:45 AM CT06.04.04

Late News: Mechanistic Insights into the Reactivity of the Pd Catalyst for Hydrodechlorination of Trichloroethylene Chaitra Shenoy¹, Shelaka Gupta², Kirti Verma¹, Tuhin S. Khan³ and M. A. Haider¹; ¹Indian Institute of Technology Delhi, India; ²Indian Institute of Technology Hyderabad, India; ³CSIR - Indian Institute of Petroleum, India

Periodic, density functional theory calculations were employed to understand the hydrodechlorination of trichloroethylene (TCE) over different facets of a palladium catalyst. In order to accomplish this, the Pd surface was modelled as terrace sites (Pd(111)) and undercoordinated sites (Pd (211), Pd (100) and Pd (110)). The most stable binding configuration of TCE on the Pd surface was found to be through the di- σ mode of binding, wherein each carbon atom of the TCE molecule sits on top of the Pd atom. Comparing TCE adsorption over Pd facets, TCE shows the highest binding energy of -178 kJ/mol over Pd (110). TCE, upon adsorption on Pd, immediately undergoes dechlorination followed by subsequent hydrogenation of the hydrocarbon intermediates as the activation energies for C-Cl bond dissociation steps were quite low in comparison to the hydrogenation steps. As a result, the catalyst tends to undergo poisoning due to the chlorine atoms accumulated on the surface. Chlorine binds to the Pd facets as follows: Pd (110) > Pd (211) > Pd (100) > Pd (111), indicating rapid poisoning of the undercoordinated sites in comparison to the terrace site. This also suggests deactivation of smaller sized Pd nanoparticles. The strongly adsorbed Cl atoms react with hydrogen to form HCl.

9:00 AM CT06.04.05

Late News: Chemically Graded Metal/Ceramic Interface—A High Throughput DFT Study Prince Gollapalli and Satyesh K. Yadav; Indian Institute of Technology Madras, India

Interface between metal and ceramic is assumed to be atomically sharp as mixing of anions or cations (that is part of metal and ceramic) is not expected to be thermodynamically favorable. Contrary to this belief, we establish that in Ti/TiN system, it is thermodynamically favorable for N in TiN to cross over by forming N vacancy, to Ti forming interstitial solid solution. First-principles calculated value of N vacancy formation energy in TiN is 2.17 eV and N interstitial formation in Ti is -3.84 eV. Sum of the two values, which we call as driving force indicate that mixing of anions across the Ti/TiN interface is favorable.

To explore other combinations of metal/ceramic systems that could plausibly result in chemically graded interface by mixing of anions across the interface, we calculate C, N and O vacancy formation energy in range of carbides, nitrides and oxides respectively and interstitial formation energy in metals like, Ti, Zr, Hf, V, Nb, Ta, Al, Mg, Cr, and Fe. This covers range of technologically important metal/ceramic interfaces. We find that transition metals group elements, IV B and V B are more likely to form a chemically graded interface with nitrides and carbides. However, Al_2O_3 and MgO , show a large positive vacancy formation energy, are likely to form sharp interface with any metal, which explains the reason for using them as substrates for film growth. Formation of chemically graded interface results in gradual variation of structural parameter (like lattice parameter) and properties (elastic constants) across the interface. Such chemically graded interface could lead to better properties of the heterostructure involving metal/ceramic interfaces.

9:15 AM CT06.04.06

Late News: DFT Simulations to Understand Electrocatalytic Properties of Double Perovskite $\text{NdBa}_{1-x}\text{Sr}_x\text{Co}_2\text{O}_5+\text{d}$ ($x=0, 0.25, 0.50$) Jyotsana Kala, Uzma Anjum, Brajesh K. Mani and M. A. Haider; Indian Institute of Technology Delhi, India

$\text{LnBaCo}_2\text{O}_{5+d}$ type of layered double perovskite materials have received much attention as solid oxide fuel cell cathode materials owing to their high oxygen ion concentration, high electronic conductivity and catalytic activity towards oxygen reduction. In the present work, Nd-based double perovskites $\text{NdBa}_{1-x}\text{Sr}_x\text{Co}_2\text{O}_{5+d}$ (NBSCO, $x = 0, 0.25$ and 0.50) have been studied computationally.

Plane wave Density functional Theory based calculations using VASP were performed in order to examine the electrocatalytic properties of $\text{NdBa}_{1-x}\text{Sr}_x\text{Co}_2\text{O}_{5+d}$ double perovskite material. In view of the application of NBSCO material for SOFC cathodes, the bulk oxygen vacancy formation energies (E_{ov}) have been calculated computationally for oxygen vacancies created in all possible planes (BaSr/O, Nd/O and Co/O) and surface energies (γ) of the structure with different surface terminations (BaSr/Co, Nd/Co, Co/BaSr and Co/Nd) along (001) direction. Nd/O plane observed to have lowest oxygen vacancy formation energy among all the three possible planes in (001) direction of bulk NBSCO. This shows Nd/O plane to have high oxygen vacancy concentration. For $x=0, 0.25$ and 0.50 , BaSr/O plane have highest oxygen vacancy formation energy showing a difficulty in oxygen vacancy creation in BaSr/O plane as compared to other planes. This suggested less oxygen anion diffusivity in BaSr/O plane. However, on doping one fourth and half of the Ba with Sr resulted in an improved bulk oxygen vacancy characteristic of BaSr/O plane. Different energetics of different terminal surfaces shows importance of surface terminations. The results of first principles calculations for surface energies were analyzed and compared for different terminal surfaces. For NBSCO material, low surface energies have been observed for Ba/Co termination. Due to lower surface energies, Ba ions have tendencies to segregate towards surface. This is in accordance with the DFT simulations and molecular dynamics simulations of other Ba containing $\text{LnBaCo}_2\text{O}_{5+d}$ layered perovskites [1-5]. Doping the material with Sr have also shown similar trend in surface energies of BaSr/Co terminal surface.

References:

1. Anjum, U., Vashishtha, S., Sinha, N., & Haider, M. A. (2015). Role of oxygen anion diffusion in improved electrochemical performance of layered perovskite $\text{LnBa}_{1-y}\text{Sr}_y\text{Co}_{2-x}\text{Fe}_x\text{O}_{5+\delta}$ ($\text{Ln}=\text{Pr, Nd, Gd}$) electrodes. *Solid State Ionics*, 280, 24-29.
2. Anjum, U., Vashishtha, S., Agarwal, M., Tiwari, P., Sinha, N., Agrawal, A., & Haider, M. A. (2016). Oxygen anion diffusion in double perovskite $\text{GdBaCo}_2\text{O}_{5+\delta}$ and $\text{LnBa}_{0.5}\text{Sr}_{0.5}\text{Co}_{2-x}\text{Fe}_x\text{O}_{5+\delta}$ ($\text{Ln} = \text{Gd, Pr, Nd}$) electrodes. *International Journal of Hydrogen Energy*, 41(18), 7631-7640
3. Anjum, U., Khan, T. S., Agarwal, M., & Haider, M. A. (2019). Identifying the Origin of the Limiting Process in a Double Perovskite $\text{PrBa}_{0.5}\text{Sr}_{0.5}\text{Co}_{1.5}\text{Fe}_{0.5}\text{O}_{5+\delta}$ Thin-Film Electrode for Solid Oxide Fuel Cells. *ACS Applied Materials & Interfaces*, 11(28), 25243-25253
4. Anjum, U., Agarwal, M., Khan, T. S., & Haider, M. A. (2019). Mechanistic Elucidation of Surface Cation Segregation in Double Perovskite $\text{PrBaCo}_2\text{O}_{5+\delta}$ Material using MD and DFT Simulations for Solid Oxide Fuel Cells. *Ionics*, 26(3), 1307–1314
5. Anjum, U., Agarwal, M., Khan, T. S., Prateek, P., Gupta, R. K., & Haider, M. A. (2019). Controlling surface cation segregation in a nanostructured double perovskite $\text{GdBaCo}_2\text{O}_{5+\delta}$ electrode for solid oxide fuel cells. *Nanoscale*, 11(44), 21404-21418.

9:30 AM CT06.04.07

Late News: Construction of an EAM Type Interatomic Potential Model Describable of Metallic Polytype Energetics [Shinya Ogane](#)¹, Riku Sato¹, Taku Miyakawa², Yuta Tanaka², Kazumasa Tsutsui² and Koji Moriguchi^{1,2}; ¹Tohoku University, Japan; ²Nippon Steel Corporation, Japan

Many crystalline compounds are composed of one or more structural units. When these units can be “stacked” in different ways to form stable or metastable phases, the resulting phases are known as polytypes. Among these polytypes, the crystalline systems composed of close-packed (CP) layers have especially attracted attention on their fundamental and technological properties. While these polytypes are often experimentally observed in

wide-bandgap semiconductors, SiC systems are particularly known to show several hundred polytypes [1]. The long period stacking ordered (LPSO) Mg alloys with light weight, high specific strength, and high heat resistance are also recently drawing attention as a metallic system with similar polytypism to that in SiC [2, 3]. For both systems, the physical mechanism behind polytype selection is not yet fully understood.

Predicting polytype phase stability for a material has still been a long-standing issue in condensed matter physics and/or materials science. This stems from the fact that the atomistic interactions on polytype energetics might be surprisingly quite complex and delicate despite the simplicity of their geometrical structure. In this situation, some theoretical studies have recently been reported. Polytypism for the finite range Lennard-Jonesium based on the classical atomistic simulations has shown that its ground state structures can include not only fcc (3C) and hcp (2H) but a wide range of more complex stacking sequences depending on the interatomic interaction distance [4]. In addition, the enthalpy of any CP structure for a given element is recently found to be characterized as a linear expansion like a convergent series which describe the stacking configuration [5]. In the previous work, we have also presented a consideration of total energetics for the CP polytypes based on the geometrical analysis for the correlation between interlayer interactions and interatomic ones in CP polytypes [6]. These theoretical results suggest that short-range interactions are not enough to describe the CP polytype energetics and provide significant insights for creating interatomic models successfully showing the polytypes other than 3C and 2H structures as a ground state, those have never yet been implemented as far as the authors know.

Since the ground state for pure lanthanum (La) is the CP stacking structure with four layers along the c-axis in the unit cell, i.e. the double hexagonal CP structure (DHCP), the pure La can be an important reference system for studying the polytype formation. It is, therefore, possible to investigate the essential factors determining the polytype selection rule through the dynamical analyses for La. In the present work, we report on the process of constructing an interatomic potential with good descriptiveness on the La polytype energetics, that can be used for molecular dynamics (MD) simulations.

The Embedded Atom Method (EAM) type functions reported by Mishin et al. [7] are adopted for constructing the potential model in this study. Since our previous theoretical studies have shown that the long-range nature of interatomic interactions is an important factor in determining the ground state of polytype energetics [3, 6], the cutoff radius has been carefully selected considering the computational speed in MD simulations. Other basic properties and transferability of the EAM type potential constructed will be discussed in the presentation.

[1] K. Moriguchi, et al., J. Mater. Res. 28, 7 (2013).

[2] E. Abe et al., Phil. Mag. Lett, 91, 690 (2011).

[3] K. Moriguchi et al., 2020 Virtual MRS Spring/Fall Meeting & Exhibit, F.SF07.06.03 (2020) and submitted in MRS Advances.

[4] L. B. Pártay et al., Phys. Chem. Chem. Phys., 19, 19369 (2017).

[5] C. H. Loach and G. J. Ackland, Phys. Rev. Lett. 119, 205701 (2017).

[6] S. Ogane et al., 2020 Virtual MRS Spring/Fall Meeting & Exhibit, F.SF07.06.01 (2020) and submitted in MRS Advances.

[7] Y. Mishin et al., Phys. Rev. B 59, 3393(1999).

9:35 AM CT06.04.08

Late News: A Comparative Study on Convergent Series Lattice Models for Close-Packed Polytype Energetics Riku Sato¹, Shinya Ogane¹, Taku Miyakawa², Kazumasa Tsutsui², Yuta Tanaka² and Koji Moriguchi^{1,2}; ¹Tohoku University, Japan; ²Nippon Steel Corporation, Japan

Polytypism is a special case of polymorphism when the two polymorphs differ only in the stacking of identical two-dimensional sheets or layers. The polytypes are characterized by a stacking sequence with a given repeat unit along the hexagonal c-axis direction and are theoretically possible to have endless permutations of the sequences. Among these polytypes, the crystalline systems composed of close-packed (CP) layers have especially attracted attention on their fundamental and technological properties for many years.

Predicting polytype phase stability for a material has still been a long-standing issue in condensed matter physics and/or materials science. This situation stems from the fact that the atomistic interactions on CP

polytype energetics might be surprisingly quite complex and delicate despite the simplicity of their geometrical structure. We have proposed a computational method coupled with three theoretical tools (PGA: polytype generation algorithm; FPC-DFT: first-principles calculations based on the density functional theory; and ANNNI: axial next-nearest-neighbor Ising model), which can make us possible to efficiently investigate the structural energetics for diverse nonequivalent polytypes [1]. The equilibrium theories based on the ANNNI model that is well known in the field of statistical mechanics have played an efficient role in the study of the origins of polytypism [2, 3].

We have constructed an ANNNI model including interactions up to the third-nearest neighbor layer with four-spin term to investigate the static energetics of a wide variety of CP polytypes for 17 kinds of metallic elements in our recent work [4]. Using this ANNNI model, we can discuss phase stability of polytypes based on inter-layer interactions for the metallic systems [4]. We have also presented a theoretical consideration of total energetics for the close-packed (CP) polytypes based on the interlayer partial energy model where the total energy constructed from the two-body interatomic interactions is projected onto the interlayer interactions in CP polytype structures [5]. Our theoretical study suggests that the descriptiveness on polytype energetics changes according to the atomic interaction distance and the effective interatomic distance that controls the ground state for the polytype energetics can be inferred from the distribution of polytype structural energetics [5].

Loach and Ackland have recently proposed another convergent series lattice model on the polytype energetics where the stacking order description is different from that in the ANNNI model [6]. They emphasize that the model proposed is more useful than the classical ANNNI model since it converges more rapidly. While these theoretical results suggest that the convergent series lattice model such as the ANNNI and/or Loach's model is a powerful tool to describe the polytype energetics, the accuracy, the convergency and the physical meaning for each model have not been completely clarified and not been mutually compared with each other.

In the present work, a comparative study on convergent series lattice models for close-packed polytype energetics are carried out using both ANNNI and Loach's models. Using these models extracted from the first-principles calculations within the generalized gradient approximation (GGA), we will discuss the inter-layer interactions, the polytype phase diagrams, and the physical relation between the ANNNI and Loach's models.

[1] K. Moriguchi, et al., *J. Mater. Res.* 28 7-16 (2013).

[2] E. Rodriguez-Horta et al., *Acta Cryst.* A73, 377 (2017).

[3] J. J. A. Shaw and V. Heine, *J. Phys.: Condens. Matter* 2, 4351 (1990).

[4] K. Moriguchi et al., 2020 Virtual MRS Spring/Fall Meeting & Exhibit, F.SF07.06.03 (2020) and submitted in *MRS Advances*.

[5] S. Ogane et al., 2020 Virtual MRS Spring/Fall Meeting & Exhibit, F.SF07.06.01 (2020) and submitted in *MRS Advances*.

[6] C. H. Loach and G. J. Ackland, *Phys. Rev. Lett.* 119, 205701 (2017).

9:40 AM CT06.04.09

Late News: Evolution of Catalytic Active Sites in Methane Dehydroaromatization Reaction. Iqra Ahangar, Sonit Balyan, M. A. Haider and Kamal K. Pant; Indian Institute of Technology Delhi, India

With the discovery of new sources of natural gas, hydrocarbon products obtained from natural gas are providing a greater avenue to reduce dependence on coal and petroleum-based products. In this regard, direct conversion of methane to aromatics in non-oxidative environment is explored as an energy efficient route, as it eliminates the production of syngas and also eradicates the separation of CO_x from the product. For methane dehydroaromatization (MDA) reaction, Mo/HZSM-5 is widely used as the catalyst, yielding high selectivity for aromatics. Though, the catalyst is rapidly deactivated by coke formation in the form of polyaromatics hydrocarbon. And this remains an issue to be resolved. One thought to improve catalyst stability is arising from a detailed understanding of the catalytically active site which is dictating the protocols of catalyst synthesis, choice of the metal precursor, carburizing environment. Here in this work, utilizing density functional theory (DFT) calculations, we are discussing the implication of the oxycarbide species of molybdenum versus the carbide species in activating methane and formation of ethylene/acetylene intermediates. Overall, the results are highlighting the fundamental mechanistic insights on the active sight, which may provide a clue for rational

catalyst design.

9:45 AM DISCUSSION TIME

SESSION CT06.05: First-Principles Approaches for Large-Scale and Correlated Materials I
Session Chairs: Amartya Banerjee, Felipe Jornada, Lin Lin and Sivan Refaely-Abramson
Friday Morning, April 23, 2021
CT06

11:45 AM *CT06.05.01

Large-Scale Real-Space Electronic Structure Calculations Sambit Das¹, Bikash Kanungo¹, Phani Motamarri² and Vikram Gavini¹; ¹University of Michigan–Ann Arbor, United States; ²Indian Institute of Science, India

Electronic structure calculations, especially those using density functional theory (DFT), have been very useful in understanding and predicting a wide range of materials properties. Despite the success of DFT, and the tremendous progress in theory and numerical methods over the decades, the following challenges remain. Firstly, the state-of-the-art implementations of DFT suffer from cell-size and geometry limitations, with the widely used codes in solid state physics being limited to periodic geometries and typical simulation domains containing a few thousand electrons. This limits the complexity of materials systems that are accessible to DFT calculations. Secondly, most electronic structure calculations rely on the pseudopotential approximation, treating only the valence electrons. Recent studies have elucidated many scenarios where the pseudopotential approximation and the widely used pseudopotentials are unsatisfactory. Lastly, there are many materials systems (such as strongly-correlated systems) where the widely used model exchange-correlation functionals are inaccurate. Addressing these challenges will enable large-scale all-electron quantum-accuracy DFT calculations, and can significantly advance our predictive modeling capabilities of complex materials systems.

This talk will discuss our recent advances towards addressing the aforementioned challenges. In particular, the development of computational methods and numerical algorithms for large-scale real-space DFT calculations using adaptive finite-element discretization will be presented, which form the basis for the recently released DFT-FE open-source code. The computational efficiency, scalability and capability of DFT-FE will be presented, and contrasted with other widely used codes. In an effort to overcome the limitation of the pseudopotential approximation, recent progress in developing accurate, efficient, and scalable all-electron DFT calculations will be presented. Further, ongoing efforts, and related thoughts, on developing a framework for a data-driven approach to improve the exchange-correlation description in DFT will be discussed.

12:10 PM CT06.05.02

Quantum for Quantum—*Ab initio* Calculations in Chemical and Materials Sciences Using Near-Term Quantum Computation Stefan A. Bringuier and Pejman Jouzdani; General Atomics, United States

The use of *Ab initio* methods to address problems in chemical and material sciences (CMS) which are solved using classical computation is a mature and robust field. With the nascent field of quantum computing (QC) anticipated to grow and make advancements in the upcoming decades, now is a suitable time to investigate quantum algorithms and methodologies that positively augment or advance *Ab initio* calculations. We present a brief overview of leading quantum algorithms for noisy intermediate-scale quantum devices that target CMS problems, which include the successful variational quantum eigensolver (VQE). We discuss our two recent QC approaches for calculation of both ground and excited states. The first of these methods utilizes a subspace projection of a problem Hamiltonian in conjunction with the VQE algorithm to obtain the excited states accurately. The second method utilizes a quantum device to prepare and measure an effective Hamiltonian in

the computational basis of a qubit register. In this capacity, the quantum device acts as a coprocessor that can efficiently prepare the Hamiltonian for post-processing on a classical computer. The methods discussed are numerically demonstrated for small molecular systems (e.g., H₂, LiH), but in general, are suitable for larger chemical or material systems with appropriate quantum hardware resources. While mainstream QC may still be far away, we are at an opportunistic intersection for the materials community to think about how to address CMS problems using computing devices governed by quantum theory.

Acknowledgment: This material is based upon work supported by General Atomics internal R&D funding.

12:25 PM CT06.05.03

Quantum Algorithms for Predicting Strongly Correlated Matter Kade Head-Marsden and Prineha Narang; Harvard University, United States

Computationally tractable treatment of correlated quantum matter is a challenging problem relevant to chemistry, physics, and material science. It has been predicted that quantum computers have the potential to reduce the computational scaling from exponential to polynomial, however, environmental noise experienced by these devices has stymied the practical realization of this speed-up. With recent progress in quantum hardware, quantum devices are closer than ever to being capable of computationally investigating static and dynamic properties of strongly correlated systems. Here, I will discuss recently developed quantum algorithms to consider strongly correlated quantum systems. In particular I will focus on the dynamics of fermionic open quantum systems and static properties of condensed matter systems.

12:40 PM *CT06.05.04

Towards an Accurate and Efficient Order- N Framework for Real-Space Condensed-Phase Hybrid Density Functional Theory Robert DiStasio; Cornell University, United States

By including a fraction of exact exchange (EXX), hybrid functionals reduce the self-interaction error in semi-local density functional theory (DFT), and thereby furnish a more accurate and reliable description of the electronic structure in systems throughout chemistry, physics, and materials science. However, the high computational cost associated with hybrid DFT limits its applicability when treating large-scale and complex condensed-phase systems. To overcome this limitation, we have devised a highly accurate and linear-scaling (order- N) approach based on a local (MLWF) representation of the occupied space that exploits sparsity when evaluating the EXX interaction in real space [1]. In this work, we present a detailed description of the theoretical and algorithmic advances that are needed to perform hybrid DFT based *ab initio* molecular dynamics (AIMD) simulations of large-scale finite-gap condensed-phase systems using this approach. This is followed by a critical assessment of the accuracy and parallel performance of the *exx* algorithm when performing AIMD simulations of liquid water and several ice phases in the canonical (NVT) and isobaric-isothermal (NpT) ensembles. With access to high-performance computing (HPC) resources, we demonstrate that *exx* enables hybrid DFT based AIMD simulations of systems containing 500-1000 atoms with a wall time cost comparable to semi-local DFT. In the strong-scaling limit, this cost is split evenly between computation, communication, and processor idling; as such, we also discuss a three-pronged strategy that directly attacks each of these contributions and reduces the overall wall time cost by approximately an order of magnitude for large-scale heterogeneous systems. With these developments, this work takes us one step closer to routinely performing AIMD simulations of large-scale condensed-phase systems for sufficiently long timescales at the hybrid DFT level.

[1] J Chem Theory Comput 16, 3757 (2020).

1:05 PM CT06.05.05

Modeling Metal-Insulator Transition of VO₂ with GGA with Small Hubbard Parameters Daniel Koch, Kumar Prabhakaran, Mohamed Chaker and Sergei Manzhos; INRS, Canada

Studying the metal-insulator transition (MIT) of VO₂ from first-principles generally requires the use of computationally expensive hybrid density functionals, while the less resource-intensive functionals of the generalized gradient approximation (GGA) -type commonly fail to correctly describe the relative thermodynamic stabilities, crystal-, or electronic structures of the semiconducting and metallic monoclinic and rutile phases of VO₂. Unfortunately, investigating e.g. the effect of low-concentration doping on the VO₂ transition temperature requires simulation cell dimensions for which hybrid density functionals quickly become unfeasible. We present an overview of the underlying difficulties connected to the use of GGA functionals on the VO₂ MIT in commonly employed quantum chemistry codes and demonstrate that a computational setup using localized basis functions, pseudopotentials and a GGA functional with a small Hubbard correction helps achieving simultaneous description of qualitative band structure features, crystal geometries, and the MIT temperature of VO₂ correctly.

1:20 PM DISCUSSION TIME

SESSION CT06.06: First-Principles Approaches for Large-Scale and Correlated Materials II
Session Chairs: Amartya Banerjee, Felipe Jornada, Lin Lin and Sivan Refaely-Abramson
Friday Afternoon, April 23, 2021
CT06

2:15 PM *CT06.06.01

Towards First-Principles Quantum Monte Carlo for Quantum Materials Paul Kent; Oak Ridge National Laboratory, United States

We review recent advances towards first-principles quantum monte carlo (QMC) on general materials, including those where spin-orbital phenomena, strong electron correlation, and van der Waals interactions are significant. QMC methods provide very high accuracy and are in principle generally applicable. However fundamental improvements are required to study quantum materials as well as general materials incorporating elements from across the periodic table. Additionally, QMC methods generally make use of trial wavefunctions from other approximate theories to control the Fermion sign problem, introducing a systematic bias to the calculations. For simple bulk materials these trial wavefunctions can now be converged and the systematic error reduced[1,2]. This can accelerate methodological improvements by enabling cross validation and studies of the efficiencies of different QMC methods such as real space diffusion QMC and auxiliary field QMC. In terms of applications, these advances open the possibility to determining the total uncertainty in predicted properties of both quantum and general materials.

The methods described have been implemented in the open source QMCPACK code[3,4], <https://qmcpack.org>.

[1] F. Malone et al. "Systematic comparison and cross-validation of fixed-node diffusion Monte Carlo and phaseless auxiliary-field quantum Monte Carlo in solids", *Phys. Rev. B* 102, 161104(R) (2020).

<https://doi.org/10.1103/PhysRevB.102.161104>

[2] A. Benali et al. "Towards a Systematic Improvement of the Fixed-Node Approximation in Diffusion Monte Carlo for Solids", Accepted in *J. Chem. Phys.* (2020). <https://arxiv.org/abs/2007.11673>

[3] P. Kent et al. "QMCPACK: Advances in the development, efficiency, and application of auxiliary field and real-space variational and diffusion quantum Monte Carlo", *J. Chem. Phys.* 152 174105 (2020).

<https://doi.org/10.1063/5.0004860>

[4] J. Kim et al. "QMCPACK: an open source ab initio quantum Monte Carlo package for the electronic structure of atoms, molecules and solids" *J. Phys.: Condens. Matter* 30 195901 (2018).

<https://doi.org/10.1088/1361-648X/aab9c3>

2:40 PM CT06.06.02

Late News: Towards a Topological Quantum Chemistry Description of Correlated Systems—The Case of the Hubbard Diamond Chain Mikel Iraola^{1,2}, Niclas Heinsdorf³, Apoorv Tiwari^{4,5}, Dominik Lessnich³, Thomas Mertz³, Francesco Ferrari³, Mark Fischer⁴, Stephen Winter^{3,6}, Titus Neupert⁴, Frank Pollmann⁷, Roser Valentí³ and Maia García Vergniory^{2,8}; ¹University of the Basque Country, Spain; ²Donostia International Physics Center, Spain; ³Goethe University, Germany; ⁴University of Zurich, Switzerland; ⁵Paul Scherrer Institute, Switzerland; ⁶Wake Forest University, United States; ⁷Technical University of Munich, Germany; ⁸IKERBASQUE, Spain

The recently introduced topological quantum chemistry (TQC) framework has provided a description of universal topological properties of all possible band insulators in all space groups based on crystalline unitary symmetries and time reversal. While this formalism filled the gap between the mathematical classification and the practical diagnosis of topological materials, an obvious limitation is that it only applies to weakly interacting systems-which can be described within band theory. It is an open question to which extent this formalism can be generalized to correlated systems that can exhibit symmetry protected topological phases which are not adiabatically connected to any band insulator. In this work we address the many facets of this question by considering the specific example of a Hubbard diamond chain. This model features a Mott insulator, a trivial insulating phase and an obstructed atomic limit phase. Here we discuss the nature of the Mott insulator and determine the phase diagram and topology of the interacting model with infinite density matrix renormalization group calculations, variational Monte Carlo simulations and with many-body topological invariants. We then proceed by considering a generalization of the TQC formalism to Green's functions combined with the concept of topological Hamiltonian to identify the topological nature of the phases, using cluster perturbation theory to calculate the Green's functions. The results are benchmarked with the above determined phase diagram and we discuss the applicability and limitations of the approach and its possible extensions.

2:55 PM CT06.06.03

WITHDRAWN-NO REG (CT06.06.03) Identifying Design Principles for Solid State QM/MM Embedded Cluster Modelling Harry Jenkins and Andrew Logsdail; Cardiff University, United Kingdom

The current most popular computational method in modelling surface reactions is periodic planewave density functional theory (DFT)¹. Periodic DFT is both expansive in its functionality, and easy to use. However, there are still some major limitations. For instance, the preferred basis representation of planewaves is inefficient for high-level hybrid-DFT approaches; large models are needed for isolated catalytic chemistry, with many tens or hundreds of atoms included but redundant in calculations, as all atoms need to be treated quantum mechanically, even if they are far from the “active site”. In addition, periodic surface models cannot be used to model charged defects due to technical incompatibilities when trying to include any compensating background charge.

As an alternative, hybrid quantum- and molecular-mechanical (QM/MM) modelling can be coupled with an embedded cluster approach, which combines the high accuracy of QM modelling, with the high efficiency of MM modelling (MM), all in an aperiodic model that reproduces the bulk environment². However, the uptake of QM/MM in the solid-state community is limited by the bespoke nature of the model configuration, which typically requires empirical tuning to achieve accuracy comparable to the periodic DFT approaches.

In this work, we present our progress in outlining systematic design principles for QM/MM models, based initially on work using MgO. This has been pursued using the ChemShell³ software package, with FHI-aims⁴ used to perform DFT calculations, using both popular GGA approaches, compared to periodic DFT, and high-level exchange-correlation functionals (PBE0).

The focus of the work is understanding how cluster design principles, such as partitioning of the QM-region, determining coordinates of the unrelaxed cluster, and fixing different regions of the cluster during relaxation, affect the accuracy of measurable results. Our overall aim is to deliver an automated approach to cluster construction, with objective justification for each step involved.

¹ Becke, J. Chem. Phys. 140, 18A301 (2014)

² Groenhof, *Methods in Molecular Biology*, Ch.3 (2013)

³ Sherwood *et al.*, *J. Mol. Struct. (Theochem.)* 632, 1 (2003)

⁴ Blum *et al.*, *Computer Physics Communications* 180, 2175-2196 (2009)

3:10 PM *CT06.06.04

Coupled Cluster Methods and Other Techniques for Simulations of Materials Garnet Chan; California Institute of Technology, United States

Coupled cluster theory is usually viewed as a molecular theory, but I will describe its extension to treat spectra in materials, finite-temperature and non-equilibrium effects, and electron-phonon coupling.

3:35 PM CT06.06.05

Self-Interaction Corrected Functional Calculations as Alternative to Semi-Empirical DFT+U and Hybrid Functional Calculations Hannes Jonsson; University of Iceland, Iceland

While Kohn-Sham density functional theory (DFT) using GGA, meta-GGA functional approximations has been remarkably successful in a variety of applications, there are several important cases where it fails. Increasingly, this is being remedied by semi-empirical DFT+U or hybrid functional calculations where parameters are adjusted in one way or another to obtain acceptable results. A variational and self-consistent implementation of the Perdew-Zunger self-interaction correction (PZ-SIC) using complex optimal orbitals has instead been developed and applied to several such systems and found to give good results. Calculations of electronic holes in oxide crystals, transition metal clusters, Rydberg excited states and localized charge state that are absent in GGA and meta-GGA level calculations will be presented. The computational effort of the PZ-SIC calculations scales with system size in the same way as DFT/GGA calculations but the prefactor is large since an effective potential needs to be evaluated for each orbital (calculations that could, however, be carried out in parallel) and optimal orbitals need to be found in terms of the Kohn-Sham orbitals at each iteration. PZ-SIC is an example of an extended functional form where the energy depends explicitly on the orbital densities, not just the total electron density and thereby goes beyond Kohn-Sham DFT. While significant improvements are obtained with PZ-SIC, the orbital density dependent functional form could be exploited more generally to develop a self-interaction free functional rather than as a correction to Kohn-Sham functionals, thereby providing an optimal mean field theory for materials calculations.

3:50 PM DISCUSSION TIME

SESSION CT06.07: Beyond Equilibrium: First-Principles Spin and Structural Dynamics in Materials

Session Chairs: Amartya Banerjee, Amartya Banerjee, Felipe Jornada and Lin Lin

Friday Afternoon, April 23, 2021

CT06

5:15 PM *CT06.07.01

Spin-Forbidden Processes and Molecular Magnetism—New Theoretical Tools for Quantitative Modeling and Insight Anna I. Krylov; University of Southern California, United States

This lecture will describe theoretical aspects of spin-related phenomena in the context of novel molecular materials. Examples include spin-forbidden processes, which play an important role in photovoltaics, and molecular magnetism, which is of interest for quantum information science. Recent methodological developments within equation-of-motion coupled cluster theory will be discussed and illustrated by examples relevant to the design of novel materials.

5:40 PM CT06.07.02

Understanding phase stability and diffusion kinetics in structurally unstable but dynamically stabilized phases from first principles Sara Kadkhodaei; University of Illinois at Chicago, United States

The phase diagram of numerous materials of technological importance features high-symmetry high temperature phases that exhibit phonon instabilities. Leading examples include shape-memory alloys, as well as ferroelectric, refractory, and structural materials. In this talk I will introduce a new thermodynamic model for free energy calculation in these phases from first principles [1]. This model efficiently explores the system's ab-initio energy surface by partitioning it into piecewise polynomials around local minima, which is combined with a continuous yet constrained sampling in the vicinity of these local minima. I present the application of this model to the bcc phase of titanium as well as the austenite and martensite phases in NiTi and PtTi shape memory alloys, in which we illustrate that constant anharmonicity-driven hopping between local low-symmetry distortions stabilizes the system to maintain a high-symmetry time-averaged structure [2]. In addition, I will try to shed light on diffusion kinetics in dynamically stabilized phases based on a first-principles approach within the transition state theory [4]. Finally, I introduce the implementation of the model as an open-access and fully automated software toolkit called the Piecewise Polynomial Potential Partitioning (P4), which can be integrated into the Alloy Theoretic Automated Toolkit (ATAT)[3].

References

- [1] S. Kadkhodaei, Q.-J. Hong, and A. van de Walle, "Free energy calculation of mechanically unstable but dynamically stabilized bcc titanium," *Phys. Rev. B*, vol. 95, no. 6, p. 064101, Feb. 2017.
- [2] S. Kadkhodaei and A. van de Walle, "First-principles calculations of thermal properties of the mechanically unstable phases of the PtTi and NiTi shape memory alloys," *Acta Mater.*, vol. 147, pp. 296–303, Apr. 2018.
- [3] S. Kadkhodaei and A. van de Walle, "Software tools for thermodynamic calculation of mechanically unstable phases from first-principles data," *Comput. Phys. Commun.*, vol. 246, p. 106712, Jan. 2020.
- [4] S. Kadkhodaei and A. Davariashiyani, "Phonon-assisted diffusion in bcc phase of titanium and zirconium from first principles" *Phys. Rev. Materials* 4, 043802, April 2020

5:55 PM *CT06.07.03

Spin Dynamics and Exciton Recombination in Quantum Materials from First-Principles Yuan Ping; University of California, Santa Cruz, United States

Designing new quantum materials with long-lived electron spin states is in urgent need of a general theoretical formalism and computational technique to reliably predict spin lifetimes. We present a new, universal first-principles methodology based on density matrix (DM) dynamics for open quantum systems to calculate the spin-phonon relaxation time of solids with arbitrary spin mixing and crystal symmetry. In particular, this method describes contributions of the Elliott-Yafet (EY) and D'yakonov-Perel' (DP) mechanisms to spin relaxation, corresponding to systems with and without inversion symmetry, on an equal footing[1]. Our ab initio predictions are in excellent agreement with experimental spin lifetime for a broad range of materials, such as Si, Fe, MoS₂, graphene and its interfaces as well as GaAs.

We then implemented real-time DM dynamics for ultrafast Kerr rotation and studied spin dynamics under external electric and magnetic field. Through the complete theoretical descriptions of pump, probe and scattering processes including electron-phonon, electron-impurity and electron-electron scattering, our method can directly simulate the nonequilibrium ultrafast pump-probe measurements for coupled spin and electron dynamics and is applicable to any temperatures and doping levels. We use this method to simulate spin dynamics of GaAs and obtain excellent agreement with experiments. It is found that the relative contributions of different scattering mechanisms and phonon modes vary considerably between spin and carrier relaxation processes. Importantly, we point out that at low temperatures the electron-electron scattering becomes very important and causes the strong reduction of spin relaxation time under in-plane magnetic fields.

In addition, we will also introduce our recent work on radiative and nonradiative exciton recombination in two-

dimensional systems from many-body perturbation theory and its applications on designing point defects as single photon emitter and spin qubits in hexagonal BN[2-6]. Our work underscores the predictive power of first-principles techniques for key physical properties to quantum information science.

References:

- [1] J. Xu, A. Habib, S. Kumar, F. Wu, R. Sundararaman, and Y. Ping, *Nature Communications*, **11**, 2780, (2020)
- [2] F. Wu, T. Smart, J. Xu, Y. Ping, *Physical Review B*, **100**, 081407(R) (2019)
- [3] F. Wu, D. Rocca and Y. Ping, *Journal of Materials Chemistry C*, **7**, 12891, (2019)
- [4] F. Wu, A. Galatas, R. Sundararaman, D. Rocca, and Y. Ping, *Physical Review Materials*, **1**, 071001(R), (2017).
- [5] T. Smart, F. Wu, M. Govoni and Y. Ping, *Physical Review Materials*, **2**, 124002, (2018).
- [6] T. Smart, K. Li, J. Xu, Y. Ping, under review, arXiv:2009.02830, (2020)

6:20 PM CT06.07.04

Late News: Calculation of the Magnetostatic Dipole-Dipole Correction to Periodic Spin-Density Functional Theory Using an Auxiliary Magnetic Charge Density Lorien A. MacEnulty^{1,2} and David D. O'Regan¹; ¹Trinity College Dublin, Ireland; ²Drake University, United States

The dipole-dipole contribution to the total energy and potential due to unpaired electron spin is the magnetostatic analogue to the Hartree electrostatic term. It contributes at order $1/c^2$ in the Breit-Pauli Hamiltonian and is therefore neglected in both non-relativistic spin-density functional theory (DFT) and non-collinear DFT calculations including spin-orbit. The term is technologically important, however, since it induces the shape anisotropy effect critical in the design of nanoscale magnetic devices; in and of itself, the term perhaps warrants investigation as an intriguing physical phenomenon.

In this work, we develop a practical algorithm for non-self-consistent but non-perturbative calculations of the spin dipole-dipole correction to the total energy in periodic and molecular systems [1]. To this end, we make use of an auxiliary—and, ultimately, physically fictitious—magnetic charge density, determined via the magnetization intrinsic to the collinear (or non-collinear) spin-density associated with ground-state systems with vanishing free current density. The affiliated magnetic scalar potential is defined by means of a magnetic Poisson equation, and from this the magnetic field is calculated. Immersing the magnetization back into this magnetic field generates the non-self-consistent energy correction.

We developed a versatile module, compatible with the capacities of Mathematica, for calculating this energy for spin-densities in generalized periodic unit cells, to be used as a post-processing tool with any standard DFT code. Using this, we compared the strength of the magnetostatic energy to the electrostatic energy for a number of test systems, finding a ratio consistently on the order of the square of the fine structure constant, as is coherent with the term's position in the relativistic expansion. Our approach may highlight the magnetic charge density's aptitude both as an auxiliary for computing the properties of magnetic quantum systems and, more generally, for inclusion in the development of exchange-correlation functionals in relativistic DFT.

[1] L. MacEnulty and D. D. O'Regan, *Journal of Undergraduate Reports in Physics* **30**, 100005 (2020), DOI: 10.1063/10.0002045.

This research was funded by Science Foundation Ireland (SFI) through the Advanced Materials and Bioengineering Research Centre (AMBER, Grant No. 12/RC/2278).

6:25 PM CT06.07.05

Investigation of the Octahedral Center site Effect in the Antiperovskite Mn_3NiN Evelyn J. Triana and Andres C. Garcia Castro; Universidad Industrial de Santander, Colombia

The antiperovskite family Mn_3AN ($A = Zn, Cu, Ni, \dots$) exhibits negative thermal expansion, piezomagnetism, and non-collinear antiferromagnetism (AFM) due to the presence of magnetic frustration on the magnetic structure of the manganese atoms in the (111) planes [1]. Previous research on this material has been mostly focused on experimental findings, and it has dedicated primarily on understanding the magneto-structural properties of these antiperovskites. Interestingly, we found few theoretical studies devoted to elucidate the influence of the central anionic site in the Mn_3NiN antiperovskite. Therefore, our study focuses on theoretically investigating, through first-principles density functional theory (DFT) calculations, the effect of the nitrogen's site on the structural and electronic properties of the antiperovskites Mn_3NiN . Therefore, our main analysis consists of observing changes in the electronic structure by analyzing the band structure, density of states, and the oxidation state of the atoms in the presence and absence of nitrogen considering the allowed four noncollinear antiferromagnetic orderings. Our results show a tangible modification of the electronic structure close to the Fermi energy as well as structural changes, associated to the lattice parameter, due to the incorporation of nitrogen.

[1] Y. Wang, H. Zhang, J. Zhu, X. Lü, S. Li, R. Zou, and Y. Zhao, "Antiperovskites with exceptional functionalities," *Advanced Materials*, vol. 32, no. 1905007, p. 7, 2019.

6:30 PM CT06.07.06

Theoretical Investigation of the Spin-Phonon Coupling in the Antiperovskite Mn_3NiN Leonardo Florez Gomez and Andres C. Garcia Castro; Universidad Industrial de Santander, Colombia

The manganese-based antiperovskite nitrides family is formed by magnetic materials that exhibit non-collinear antiferromagnetism in the presence of magnetic frustration. Different reports have confirmed the existence of a strong coupling between the magnetic structure and the crystalline structure in the members of this family, for example in Mn_3NiN . As such, this coupling has been confirmed by piezomagnetism [1], magnetovolume effects [2], and negative thermal expansion [3] studies.

So far, theoretical studies focused on clarifying this coupling and phenomenon in antiperovskites are rare in the literature. This possibly because phonon calculations, including non-collinear magnetism formalism are a challenging task in these type systems. In this research, we theoretically studied the spin-phonon coupling in Mn_3NiN through first-principle DFT calculations. We aimed to understand the relation between the behavior of the phonons and the magnetic orderings of the material, taking into consideration correlation effects. To achieve this, we computed and analyzed the phonon frequencies, eigenvectors, and phonon dispersion curves for each of the two magnetic orderings that have been experimentally confirmed in the material [4]. From these results the phonon modes involved in the coupling were determined. Our results theoretically demonstrate the dependence of phonons on magnetic ordering and correlation effects in Mn_3NiN . With this study, we expect to contribute to future research in the field of antiperovskites that display a coupling between structure and magnetism.

[1] D. Boldrin, A. P. Mihai, B. Zou, J. Zemen, R. Thompson, E. Ware, B. V. Neamtu, L. Ghivelder, B. Esser, D. W. McComb, et al., "Giant piezomagnetism in Mn_3NiN ," *ACS applied materials & interfaces*, vol. 10, no. 22, p. 18863, 2018.

[2] K. Takenaka, M. Ichigo, T. Hamada, A. Ozawa, T. Shibayama, T. Inagaki, and K. Asano, "Magnetovolume effects in manganese nitrides with antiperovskite structure," *Science and technology of advanced materials*, vol. 15, no. 1, p. 1, 2014.

[3] M. Wu, C. Wang, Y. Sun, L. Chu, J. Yan, D. Chen, Q. Huang, and J. W. Lynn, "Magnetic structure and lattice contraction in Mn_3NiN ," *Journal of Applied Physics*, vol. 114, no. 12, p. 123902, 2013.

[4] D. Fruchart and E. F. Bertaut, "Magnetic studies of the metallic perovskite-type compounds of manganese," *Journal of the physical society of Japan*, vol. 44, no. 3, p. 781, 1978.

SYMPOSIUM CT07

Excited-State Properties of Materials—Theory and Computation
April 20 - April 20, 2021

Symposium Organizers

Ting Cao, University of Washington
Vladimir Falko, The University of Manchester
Diana Qiu, Yale University
Wang Yao, The University of Hong Kong

* Invited Paper

SESSION CT07.01: Excited-State I
Session Chairs: Ting Cao and Diana Qiu
Tuesday Morning, April 20, 2021
CT07

8:00 AM *CT07.01.01

Opto-Mechanics Driven Fast Martensitic Transition in Two-Dimensional Materials Ju Li; Massachusetts Institute of Technology, United States

Inspired by optical tweezers, we show that laser pulse with selected frequency can drive an ultrafast diffusionless martensitic phase transition of two-dimensional ferroelastic materials such as SnO and SnSe monolayers, where the unit-cell strain is tweezed as a generalized coordinate that affects the anisotropic dielectric function and electromagnetic energy density. At laser power of 10^{10} W/cm², the transition potential energy barrier vanishes between two 90°-orientation variants of ferroelastic SnO and SnSe monolayer, respectively, so displacive domain switching can occur within picoseconds. The estimated adiabatic thermal limit of energy input in such optomechanical martensitic transition (OMT) is at least 2 orders of magnitude lower than that in Ge-Sb-Te alloy. [Nano Lett. (2018) 7794]

8:25 AM CT07.01.02

***Ab Initio* Signatures of Phonon-Mediated Hydrodynamic Transport in Semimetals** Yaxian Wang¹, George Varnavides^{1,2} and Prineha Narang¹; ¹Harvard University, United States; ²Massachusetts Institute of Technology, United States

Hydrodynamic electron flow in condensed matters has been one of the most active research areas recently. While progress from both theory and experimental techniques are made, open questions regarding the underlying mechanisms still remain. We utilize *ab initio* techniques to treat the electron scattering events explicitly, and show in combination with Boltzmann transport equation a more applicable metric of hydrodynamic transport taking into account temperature, channel width, and impurity length, which can be directly verified by various experimental techniques. By investigating different electron scattering mean free

paths in PdCoO₂, ZrSiS, and TaAs₂, we show that that phonon mediated electron-electron interaction could lead to much shorter momentum conserving mean free path (l_{mc}) than momentum relaxing l_{mr} , facilitating hydrodynamic behavior in systems where the direct Coulomb interaction is largely screened.

We further discuss the momentum relaxing lifetimes on their Fermi surfaces, and show that at low temperatures, hole pockets feature much longer lifetimes than electron pockets, providing a window for momentum conserving scattering events to dominate. Importantly, our findings on TaAs₂ suggest that linear Dirac-Weyl bands as well as the bands that contribute to phonon-mediated diagrams are critical in search of promising candidates for hydrodynamic flow. Other key ingredients include high mobility carriers, low density of states compensated systems, and large electron-phonon matrix elements. The plethora of low symmetry crystals whose Fermi surfaces are composed of d orbitals from the transition metal and p orbitals from the metalloids provides a much larger pool for further study. This work provides *ab initio* signatures of material-specifics to explore hydrodynamic electron flow in a much larger family of condensed matter systems, and thus offers insights into study of electron interactions through transport phenomena.

8:40 AM *CT07.01.03

Excitons and Quantum Light-Matter Interactions in Layered van der Waals Structures Kristian S. Thygesen; Technical University of Denmark, Denmark

Two-dimensional (2D) materials like the transition metal dichalcogenides (TMDs) and their van der Waals bonded layered structures present interesting opportunities for studying and controlling light-matter interactions and for developing e.g. room temperature excitonic devices. Engineering of the dielectric environment represents a powerful strategy to control the excited states in 2D materials without compromising their structural integrity. We show that the quasiparticle band gap of a 2D semiconductor can be tuned by hundreds of meV by varying the concentration of free carriers in a nearby graphene sheet via electrostatic doping[1]. The recent development of high- κ 2D materials present new opportunities for dielectric engineering. We demonstrate that the exciton Rydberg series of a supported TMD monolayer changes qualitatively when the dielectric screening within the 2D semiconductor becomes dominated by the substrate. In this regime, the distance dependence of the screening is reversed and the effective screening increases with exciton radius, which is opposite to the conventional 2D screening regime. Consequently, higher excitonic states become underbound rather than overbound as compared to the Hydrogenic Rydberg series[2].

Bilayer TMDs present further opportunities for creating novel excitonic states and manipulating their properties. Indeed, interlayer excitons with electrons and holes located in different layers can be realized in structures with Type-II band alignment. I will present a joint theory-experiment collaboration demonstrating electrical control of interlayer excitons in bilayer MoS₂ up to room temperature. The large out-of-plane dipole of the interlayer excitons makes them highly sensitive to the perpendicular electric field and leads to giant Stark shifts of up to 60 meV. The work verifies an earlier theoretical prediction about the mixed intra-interlayer nature of the excitons in TMD homobilayers [3].

Finally, I will present some recent results on *ab-initio* calculations of spontaneous emission rates in van der Waals heterostructures. Specifically, it is shown that highly confined graphene plasmons can lead to extremely high Purcell factors for intersubband transitions in few-layer TMDs sandwiched between graphene and a perfect metal. Among other things, we demonstrate the importance of using *ab-initio* electronic wave functions (as compared to simpler model wave functions) for obtaining realistic rates.

References:

- [1] Electrically Controlled Dielectric Band Gap Engineering in a Two-Dimensional Semiconductor, A. C. Riis-Jensen et al., Phys. Rev. B 101, 121110(R) (2020)
- [2] Anomalous Non-Hydrogenic Exciton Series in 2D Materials on High- κ Dielectric Substrates, A. C. Riis-Jensen et al. arXiv:2009.12317
- [3] Interlayer Excitons with Large Optical Amplitudes in Layered van der Waals Materials, T. Deilmann and K. S. Thygesen, Nano Lett. 18, 2984 (2018)

9:05 AM *CT07.01.04

Frist-Principles Theory of Nonlinear Responses in Two-Dimensional Materials and Topological Materials

Xiaofeng Qian; Texas A&M University, United States

Materials with strong nonlinear responses play important roles in advanced optoelectronics and photonics. Large nonlinear responses such as second harmonic generation recently observed in 2D and topological materials spurred tremendous interest, offering great opportunities for developing ultrathin nonlinear optical devices free of phase-matching bottleneck. Here, we report our recent effort on first-principles theory and simulation of nonlinear responses in low-dimensional materials. First, we will present our study of second harmonic generation, shift photocurrent, and circular photocurrent in semiconducting 2D materials and reveal their microscopic origins in terms of interband and intraband contributions. We show that it is possible to realize ferroicity-driven nonlinear photocurrent switching by taking advantage of the inherent coupling between nonlinear susceptibility and underlying symmetry, ferroic order, and light polarization. Second, we will present on theoretical prediction and experimental demonstration of ferroelectric nonlinear anomalous Hall effect in time-reversal invariant few-layer WTe₂ and show that Berry curvature dipole and shift dipole can serve as new order parameters for noncentrosymmetric systems, paving the theoretical foundation for nonlinear quantum electronics such as Berry curvature memory. Finally, we will introduce our recent work on nonlinear photocurrent in PT-symmetry magnetic topological quantum materials. We predict that magnetic shift photocurrent can be magnetically switched between two antiferromagnetic states with time-reversed spin orderings in bilayer antiferromagnetic MnBi₂Te₄. External electric field can break PT-symmetry and enable normal shift photocurrent that are electrically switchable and tunable down to a few THz regime, suggesting bilayer antiferromagnetic MnBi₂Te₄ as a tunable platform with rich THz and magneto-optoelectronic applications. Nonlinear optical and photocurrent responses thus provide a powerful alternative for deciphering electronic structures and interactions, particularly fruitful for probing and understanding 2D materials, topological materials, and other quantum materials.

9:30 AM CT07.01.05

Crystal Phases of Charged Interlayer Excitons in van der Waals Heterostructures Igor Bondarev¹, Oleg Berman², Roman Kezerashvili² and Yurii Lozovik³; ¹North Carolina Central University, United States; ²New York City College of Technology, United States; ³Institute of Spectroscopy, RAS, Russian Federation

We study the properties of charged interlayer excitons (CIE) in highly excited vdW heterostructures [1] — a compound fermion system with the permanent dipole moment that was observed recently in Transition-Metal-Dichalcogenide bilayers [2]. We predict the existence of new strongly correlated collective CIE states, the long-range ordered phases of the excited bilayer heterostructure — the crystal phase and the Wigner crystal phase. We evaluate the critical temperatures and density for the formation of such many-particle cooperative compound fermion states. We demonstrate that they can be selectively realized with bilayers of properly chosen electron-hole effective mass ratio by just varying their interlayer separation distance. Compound fermion systems featuring permanent electric dipole moments are of both fundamental and practical importance due to their inherently unique many-body correlation effects between electric-dipole and spin degrees of freedom. The spin in such systems could potentially be used for quantum information processing and its correlation with the dipole moment provides an opportunity for spin manipulation through optical means. Fundamental cooperative crystallization phenomena we predict will greatly increase the potential capabilities of such systems to open up new avenues for experimental exploration and novel device technologies with van der Waals heterostructures.

Funding Acknowledgements:

DOE-DE-SC0007117 (I.V.B.), ARO-W911NF1810433 (O.L.B., R.Y.K.), RFBR-20-02-00410 (Y.E.L.)

[1] I.V. Bondarev, O.L. Berman, R.Ya. Kezerashvili, and Yu.E. Lozovik, Crystal Phases of Charged Interlayer Excitons in van der Waals Heterostructures, arxiv:2002.09988

[2] L.A.Jauregui, A.Y.Joe, K.Pistunova, D.S.Wild, A.A.High, Y.Zhou, G.Scuri, K.De Greve, A.Sushko, C.-

H.Yu, T.Taniguchi, K.Watanabe, D.J.Needleman, M.D.Lukin, H.Park, and P.Kim, Electrical Control of Interlayer Exciton Dynamics in Atomically Thin Heterostructures, Science 366, 870 (2019)

9:45 AM CT07.01.06

Charting the Rich Phenomenology of Novel Two-Dimensional Materials Nicola Marzari; École Polytechnique Fédérale de Lausanne, Switzerland

I will explore the properties and performance of novel two-dimensional materials that can be exfoliated from experimentally-known inorganic compounds. I will discuss the cases of novel topological insulators, superconductors, and high-mobility semiconductors. Work done in collaboration with Davide Campi, Davide Grassano, Antimo Marrazzo, Thibault Sohler, Marco Gibertini, and Giovanni Pizzi.

SESSION CT07.02: Excited-State II
Session Chairs: Ting Cao and Diana Qiu
Tuesday Morning, April 20, 2021
CT07

11:45 AM *CT07.02.01

Computational Spectroscopy from First Principles Giulia Galli; University of Chicago, United States

We discuss first principles, computational methods and strategies to predict light-activated processes in materials for sustainability (e.g. to understand and design photo-electrochemical cells) and for quantum information science (e.g. color centers in semiconductors). In particular we present methods to study materials at finite temperature, by coupling first principles molecular dynamics and many body perturbation theory.

12:10 PM CT07.02.02

Interpretations of Ground-State Symmetry Breaking and Strong Correlation in Time-Dependent Density Functional Theory John P. Perdew¹, Adrienn Ruzsinszky¹, Jianwei Sun², Niraj Nepal¹ and Aaron Kaplan¹; ¹Temple University, United States; ²Tulane University, United States

Strong correlations within a symmetry-unbroken ground-state wavefunction can show up in approximate density functional theory as symmetry-broken spin-densities or total densities. They can arise from soft modes of fluctuations (sometimes collective excitations) such as spin-density or charge density waves at non-zero wavevector. Familiar examples are the unobservable but revealing symmetry breaking in stretched H₂ and the observable symmetry breaking in antiferromagnetic solids. The example discussed here is the static charge-density wave/Wigner crystal phase of a low density ($\rho \approx 0.09$) jellium. Time-dependent density functional theory is used to show quantitatively that the static charge density wave is a soft plasmon. More precisely, the frequency of a related density fluctuation drops to zero, as found from the frequency moments of the spectral function. Our calculation is based on a recent constraint-based wavevector- and frequency-dependent jellium exchange-correlation kernel.¹ (Work supported by NSF DMR and DOE BES.)

¹ A. Ruzsinszky, N.K. Nepal, J.M. Pitarke, and J.P. Perdew, Physical Review B **101**, 245135 (2020).

12:25 PM *CT07.02.03

Electronic Excitations—Describing Couplings in Space and Time Lucia Reining^{1,2}; ¹Centre National de la Recherche Scientifique, France; ²Institut Polytechnique de Paris, France

Green's functions are efficient tools to study many-body systems. Because the one-body Green's function is non-local in space and time, it gives more direct access to phenomena which reflect coupling of different

regions of space and to memory effects in time, than approaches based on density functionals. Examples for such couplings are the occurrence of single and multiple plasmons, excitons, or satellite structure in excitation spectra. Still, existing approximations in the framework of many-body perturbation theory are often not sufficient to capture all these phenomena.

In this talk we will discuss extensions of Green's functions approaches beyond the previous state-of-the-art. This will include the description of coherent inelastic x-ray scattering [1], coupling of electron-hole excitations [2], and the description of charge dynamics. We will conclude by discussing promising routes for the future.

[1] Igor Reshetnyak, Matteo Gatti, Francesco Sottile, and Lucia Reining, Phys. Rev. Research **1**, 032010(R) (2019)

[2] Pierluigi Cudazzo and Lucia Reining, Phys. Rev. Research **2**, 012032(R) (2020)

12:50 PM *CT07.02.04

Transport in Gapped Bilayer Graphene Nanostructures Angelika Knothe and Vladimir Falko; National Graphene Institute, The University of Manchester, United Kingdom

Quantum nanostructures, e.g., quantum wires and quantum dots, are needed for applications in quantum information processing devices, such as transistors or qubits. In gapped bilayer graphene (BLG), one can confine charge carriers purely electrostatically, inducing smooth confinement potentials and thereby limiting edge-induced perturbances, while allowing gate-defined control of the confined structure. I will report on a series of works on electrostatically confined nanostructure in gapped BLG. We demonstrated, e.g., how some of BLG's unusual properties, i.e., its states' Berry curvature-induced orbital magnetic moment and the mini valleys and band inversions of its non-parabolic low-energy dispersion, translate into a BLG quantum wire's transport properties and a quantum dot's single- and two-electron states. We investigated both theoretically, and in collaboration with experiments, how to tune these features of BLG nanostructures externally to make them useful in future quantum technology applications.

1:15 PM *CT07.02.05

Ionic Gate Spectroscopy of 2D Semiconductors Alberto Morpurgo; University of Geneva, Switzerland

Owing to their very large geometrical capacitance, ionic liquid gated devices allow unique experiments to be performed. Possibly the best known example is the possibility to induce superconductivity at the surface of different insulators. Ionic liquid gated devices, however, have more to offer. In this talk I will show how ionic liquid gated transistors based on many different 2D semiconductors and van der Waals interfaces can be used to perform precise, quantitative spectroscopic measurements of the energy of band edges. These measurements allow the straightforward determination of the size of the band gap of many semiconducting 2D materials in mono, bi and multilayer form. They also allow the determination of the band alignment of two different materials used to form a van der Waals interface, a quantity that is normally difficult to measure reliably by means of other techniques. If time allows, I may also present very recent development on double gated devices, i.e. in devices in which a 2D semiconductor is coupled to two independent ionic gates on opposite sides.

SESSION CT07.03: Excited-State III
Session Chairs: Ting Cao and Diana Qiu
Tuesday Afternoon, April 20, 2021
CT07

2:15 PM *CT07.03.01

***Ab Initio* Many-Electron Green's Function Approach to Excited States in Materials—Correlated**

Multiparticle Excitations and Time-Dependent Phenomena Steven G. Louie^{1,2}; ¹University of California, Berkeley, United States; ²Lawrence Berkeley National Laboratory, United States

Many fascinating phenomena in nature owe their emergence from the interactions of large number of particles. In this talk, I will discuss some recent progress in understanding and computing excited-state phenomena in materials, especially those that are relevant to energy conversion, transport and storage. Many-electron interactions are dominant in many of these phenomena/properties. Several illustrative examples will be presented, including: strongly bounded correlated multiparticle excitations, such as trions and biexcitons, in quasi 1D and 2D semiconductors; universal slow yet tunable plasmons as well as giant excitonic enhancement of shift currents in 2D materials; and remarkable many-electron features in optical-field-driven, time- and angle-resolved photoemission spectroscopy (ARPES). *Ab initio* studies of these novel phenomena are made possible because of newly developed first-principles methods based on an interacting many-particle Green's function approach.

This work was supported by the U. S. Department of Energy and the National Science Foundation. I would like to acknowledge collaborations with members of the Louie group.

2:40 PM CT07.03.02

Exciton Dynamics in Pentacene Crystal from GW-BSE Galit Cohen¹, Dana Novichkova¹, Diana Qiu² and Sivan Refaely-Abramson¹; ¹Weizmann Institute of Science, Israel; ²Yale University, United States

Exciton dynamics underlie materials optoelectronic functionality, and it is of great interest to understand how material structure and composition influences the involved transport properties. In this work we study the connection between exciton dispersion and dynamics from a new approach, based on many-body perturbation theory within the GW-BSE approximation. By accounting for the exciton bandstructure, we relate its time-evolution and radiative recombination processes to the underlying material structure. We demonstrate this approach on the pentacene molecular crystal, a well-studied system with nontrivial excitonic processes and unique structural features. We explore exciton dispersion and relate it to the directionality of the light polarization due to crystal packing and to anisotropy in the exciton propagation. We further discuss band to band transitions that dominate the radiative lifetime and thermalization effects. Our results provide an insight into exciton transport properties as they are affected by the structural features of the pentacene crystal.

2:55 PM *CT07.03.03

Theoretical Spectroscopy from the UV to the Hard X-Ray Region—Example of Ga₂O₃ Claudia Draxl¹, Christian Vorwerk¹, Dmitri Nabok¹ and Francesco Sottile²; ¹Humboldt-Universität zu Berlin, Germany; ²LSI, Ecole Polytechnique, CNRS, CEA, Institut Polytechnique de Paris, France

Many-body perturbation theory (MBPT) is the state-of-the-art approach to determine neutral excitations in solids and has been applied with considerable success to determine optical, UV, and x-ray absorption spectra. However, theoretical studies so far have focused on a specific energy region, studying either core or valence excitations. In this talk, we present an all-electron MBPT approach that overcomes these limitations [1]. We show how it can be used to calculate absorption and inelastic scattering spectra, from the optical to the x-ray region. While these spectroscopic techniques probe either the valence or core excitations, the interplay of the two can be revealed by resonant inelastic x-ray scattering (RIXS). We present a novel many-body approach to determine RIXS spectra in solids [2], which makes use of the valence and core excitations determined within our all-electron approach. We demonstrate with the example of the wide-gap oxide Ga₂O₃ [3] how the excitation pathways determine the spectral shape of the emission, and demonstrate the nontrivial role of electron-hole correlation in the RIXS spectra. We also discuss how RIXS can be employed to determine the nature of bound valence excitons in this material.

[1] C. Vorwerk, B. Aurich, C. Cocchi, and C. Draxl, *Electronic Structure*, **1**, 037001 (2019).

[2] C. Vorwerk, F. Sottile, and C. Draxl, *Phys. Rev. Research* **2**, 042003(R) (2020).

[3] C. Vorwerk, D. Nabok, and C. Draxl, in preparation.

3:20 PM CT07.03.04

Late News: Quasiparticle Excitations and Band Structures in Organized Donor-Acceptor Copolymers
Guorong Weng and Vojtech Vlcek; University of California, Santa Barbara, United States

I will present our recent study of the quasiparticle excitations and band structures in organized donor-acceptor copolymers. We employ many-body perturbation theory, which accounts for the polarization effects among polymers, to calculate the quasiparticle energies in bulk polymers. Our computed results are in excellent agreements with the photoemission spectra data. We discover two types of states supporting band transport in bulk copolymers: the conjugated bands and impurity states. The non-local exchange interactions are found to enhance the band transport of hole along the polymer axis, but hinder the transport across the chain. The polarization interactions are found to stabilize charge carriers and hinder band transport. Further, we discover that depending on the molecular arrangement, bulk copolymers sustain electron and hole transport in two orthogonal directions; the holes are most efficiently transported along the polymer and the pi-pi stacking directions, while the electrons are transport along the edge-to-edge stacking direction.

3:35 PM *CT07.03.05

Progress in First-Principles Calculations of Electron-Phonon Couplings Feliciano Giustino; The University of Texas at Austin, United States

First-principles calculations of electron-phonon interactions are becoming an increasingly popular tool for the study of functional materials at finite temperature. As a result, several new techniques have been developed during the past decade to address a broad array of properties and phenomena, ranging from superconductivity to light-matter interactions [1]. Within this context, I will describe some recent developments in calculations of phonon-limited carrier transport and polaron physics. I will outline the Boltzmann transport formalism [2] and its application to the calculation of transport coefficients, and I will illustrate this technique by discussing carrier mobilities in wide-gap semiconductors [3], hybrid organic-inorganic halide perovskites [4] and two-dimensional materials [5]. Then I will describe our work phonon-mediated electron localization, and the formation of polarons in bulk and low-dimensional materials [6,7].

[1] F. Giustino, Rev. Mod. Phys. 89, 015003 (2017).

[2] S. Ponc , W. Li, S. Reichardt, and F. Giustino, Rep. Prog. Phys. 83, 036501 (2020).

[3] S. Ponc , D. Jena, and F. Giustino, Phys. Rev. Lett. 123, 096602 (2019).

[4] S. Ponc , M. Schlipf, F. Giustino, ACS En. Lett. 4, 456 (2019).

[5] W. Li, S. Ponc , F. Giustino, Nano Lett. 19, 1774 (2019).

[6] W. H. Sio, C. Verdi, S. Ponc , and F. Giustino, Phys. Rev. Lett. 122, 246403 (2019).

[7] W. H. Sio, C. Verdi, S. Ponc , and F. Giustino, Phys. Rev. B 99, 235139 (2019).

SESSION CT07.04: Excited-State IV
Session Chairs: Ting Cao and Diana Qiu
Tuesday Afternoon, April 20, 2021
CT07

5:15 PM *CT07.04.01

Understanding the Nature and Fate of Excitons in Complex Light-Absorbing Materials from First Principles Jeffrey B. Neaton^{1,2,3}; ¹University of California, Berkeley, United States; ²Lawrence Berkeley National Laboratory, United States; ³Kavli Energy NanoScience Institute, United States

The ability to synthesize and probe new classes of light-absorbing with tunable structure and composition – such as 2d transition-metal dichalcogenides, organic semiconductors, and halide perovskites – has driven the need for new intuition linking atomic- and molecular-scale morphology to their photophysics, and in particular the nature and fate of excitons. Here, I will discuss the use of ab initio density functional theory and many-body perturbation theory for computing photoactive excited states in complex light-absorbing materials including electron-phonon and exciton-phonon interactions. For transition metal dichalcogenides, we explore how exciton-phonon interactions renormalize defect levels and lead to decoherence channels for excitations associated with deep in-gap states; for organic acene crystals, we develop and use an approach to compute hopping diffusion rates for self-trapped excitons; and, finally, for halide perovskites, we discuss generalization of the BSE framework to include phonon screening via introduction of an exciton-phonon kernel, and demonstrate a significant renormalization of exciton binding energies. We also develop a general Wannier-Mott model for excitons including phonon screening, clarifying its importance in polar semiconductors. In each of the three examples presented, I will emphasize implications for experiments and new principles for the design of these systems materials. This work supported by the Department of Energy and the Department of Defense; computational resources provided by NERSC.

5:40 PM CT07.04.02

Tunable Edge States of Nanoribbons by Density Functional Theory and GW Approximations Adrienn Ruzsinszky, Hong Tang, Bimal Neupane and Niraj K. Nepal; Temple University, United States

Two dimensional materials (2D) are of interest due to their remarkable physical and chemical properties. Bending is the computationally efficient route to tune fundamental/optical gaps for device functionality [1]. Under mechanical bending, some transition metal dichalcogenide (TMD) monolayer nanoribbons undergo highly nonuniform local strain within the curved layers, much larger than uniaxial strain, making band edge states more tunable in these 2D materials. This helps to remove the strong Fermi-level pinning in the flat states, making the materials usable in contact-engineering. Many-body GW approximations can provide accurate band structures for solid materials. We use GW calculations along with recent meta-GGA density functionals to check the tunability of the band edges of MoS₂ nanoribbon with various widths. We are particularly focusing on non-empirical meta-GGAs developed for band-gap prediction [2], as computationally cheaper alternatives to hybrid functionals and GW approximations.

Work is supported by DOE-BES DE-SC0021263.

[1] L. Yu, A. Ruzsinszky, J.P. Perdew, Nano Lett. **16**, 2444 (2016)

[2] T. Aschebrock and S. Kümmel, Phys. Rev. Research, **1**, 033082 (2019)

5:55 PM *CT07.04.03

Moiré Twistronics in Transition-Metal Dichalcogenide Heterostructures David A. Ruiz-Tijerina; Universidad Nacional Autónoma de México, Mexico

Heterostructures formed by vertically stacked layers of transition-metal dichalcogenides (TMDs) exhibit a long-range atomic registry modulation known as a moiré pattern, caused by the slight incommensurability and/or twist angle between the layers. Carriers and excitons in the heterostructure perceive the moiré pattern as a superlattice potential capable of fundamentally altering their energy and optical spectra through miniband formation [1] and localization by confinement [2].

In this talk I shall discuss such effects, paying especial attention to heterobilayers formed by TMDs whose electron or hole band edges are nearly degenerate. This condition promotes resonant interlayer hybridization of both carriers and excitons, leading to the formation of hybridized exciton (hX) states, i.e., coherent superpositions of intra- and interlayer excitons that simultaneously possess a large oscillator strength and electric dipole moment [3]. At small twist angles, umklapp scattering by the moiré superlattice results in hX minibands, recently observed in MoSe₂/WS₂ structures [4]. The optical response of these moiré hX minibands is thus highly tunable by electrical means and twist angle control, providing an engineering pathway for the material's optoelectronic response. Finally, I will argue that hybridized excitons are ubiquitous in

heterostructures of TMDs and their alloys, and discuss their importance for new twistrionic materials for optoelectronics.

[1] D.A. Ruiz-Tijerina and V.I. Fal'ko. Phys. Rev. B 99, 125424 (2019)

[2] D.A. Ruiz-Tijerina, I. Soltero and F. Mireles. arXiv:2007.03754 [cond-mat.mes-hall]

[3] L.P. McDonnell, J.J.S. Vinier, D.A. Ruiz-Tijerina et al. arXiv:2010.02112 [cond-mat.mes-hall]

[4] E.M. Alexeev, D.A. Ruiz-Tijerina, M. Danovich et al. Nature 567, 81–86 (2019)

6:20 PM CT07.04.04

Determining the Linear Optical Properties of Transition Metal Doped Zinc Selenide from a First-Principles Approach Nicholas Pike^{1,2} and Ruth Pachter¹; ¹Air Force Research Laboratory, United States; ²UES, Inc., United States

Wide bandgap group II-VI chalcogenides have been used in multiple optical applications. For example, doping ZnSe by first-row transition metal atoms leads to localized states within the bandgap and thus changes to the structural, electronic, and optical properties of the ZnSe host. Here we explore the properties of ZnSe for a series of transition metal dopants using first-principle calculations. We discuss the level of theory applied for calculation of the electronic structures, using a metaGGA exchange-correlation functional with a Hubbard U correction. Our calculated absorption spectra in the infrared and visible spectral ranges demonstrate agreement with experimental measurements. The electronic structures correctly predict the spectroscopic fingerprints, and using Tanabo-Sugano diagrams, the crystal field energy in these materials.

6:35 PM CT07.04.05

Computational Analysis of Critical Points in Temperature Dependent and Time Resolved Ellipsometry Spectra of Ge Using Digital Filtering Carola Emminger¹, Stefan Zollner¹, Nuwanjula S. Samarasingha¹, Farzin Abadizaman¹, Jose Menendez², Shirly Espinoza³, Steffen Richter⁴, Mateusz Rebarz³, Oliver Herrfurth⁵, Martin Zahradnik³, Rudiger Schmidt-Grund⁶ and Jakob Andreasson³; ¹New Mexico State University, United States; ²Arizona State University, United States; ³ELI Beamlines, Czechia; ⁴Linköping University, Sweden; ⁵Universität Leipzig, Germany; ⁶TU Ilmenau, Germany

Critical points (CPs) are structures in the dielectric function (DF) which are related to interband transitions and depend on temperature and doping. We analyze CPs in the DF of bulk Ge measured with static and time-resolved spectroscopic ellipsometry using a linear filter technique based on Gaussian kernels recently introduced by Le, Kim, Kim, and Aspnes [1], which combines interpolation, noise reduction, scale change, and differentiation.

Utilizing this linear filter method, we calculate the second derivatives of the complex DF with respect to energy of experimental data taken in the spectral range of the direct band gap E_0 at various temperatures from 10 K to 718 K. The choice of the filter width is crucial to eliminate noise while preserving information at the same time and is defined according to the onset of white noise in the Fourier coefficients determined from a discrete Fourier transform of the data [1].

Applying a Levenberg-Marquardt algorithm, the second derivatives are fitted simultaneously with the imaginary part of the DF to a lineshape based on the Elliott-Tanguy theory [2] considering excitonic effects present at the direct band gap. The Elliott-Tanguy lineshape depends on the excitonic binding energy, the effective masses of the valence and conduction bands, the dipole matrix element, the threshold energy, and a broadening parameter. Effective masses of the conduction band and the heavy (hh) and light hole (lh) valence bands at cryogenic temperatures, as well as the matrix element are taken from literature. For the data set at 10 K, fitting only the band gap energy and the broadening parameters of the hh- and lh-bands provides reasonable fitting results for both the imaginary part and the second derivatives of the DF. For data above 10 K, the temperature dependence of the effective masses and the matrix element are considered. A red shift of the direct

band gap energy with increasing temperature is found as well as an increase in broadening which can be fitted using a Bose-Einstein statistical factor taking into account electron-phonon interactions.

The same analysis method is applied to the E_1 and $E_1+\Delta_1$ CPs of Ge dependent on photo-excited charge carrier density and temperature obtained from femtosecond pump-probe ellipsometry measurements [3]. Using a two-dimensional CP lineshape, the amplitude, excitonic phase angle, threshold energy, and broadening parameters are determined as functions of delay time. We find a distinctive change of the various parameters and a relaxation which starts at about 4 ps after the pump pulse. The decrease of the E_1 and $E_1+\Delta_1$ energies suggests a laser heating of about 20 K to 40 K, respectively. In the analysis of these data, we are especially interested in changes to the E_1 and $E_1+\Delta_1$ band gaps due to many-body effects (such as band gap renormalization and band filling), broadenings (due to screening of the electron-phonon interactions), spin-orbit coupling strengths, and excitonic phase angles as a function of the delay time between the pump and probe pulses.

[1] V. L. Le, T. J. Kim, Y. D. Kim, and D. E. Aspnes, *J. Vac. Sci. & Technol. B* **37**, 052903 (2019)

[2] C. Tanguy, *Phys. Rev. B* **60**, 10660 (1999)

[3] S. Espinoza, S. Richter, M. Rebarz, O. Herrfurth, R. Schmidt-Grund, J. Andreasson, and S. Zollner, *Appl. Phys. Lett.* **115**, 052105 (2019)

6:50 PM CT07.04.06

Tight-Binding DFT Investigation of Structural, Vibrational and Transport Properties of Graphene-Single-Walled Carbon Nanotube Hybrid Junctions Juhi Srivastava and Anshu Gaur; Indian Institute of Technology Kanpur, India

Single-walled carbon nanotubes (SWNT) and single-layer graphene (SLG) both are allotropes of sp^2 hybridized carbon with unusual and unique properties owing to their 1D and 2D nature, respectively. In recent years, there has been a push to use hybrids of carbon nanotube and graphene for various applications which take benefit of their unique properties while overcoming the limitations of individual components. A constitutive understanding of the interactions between SWNT and SLG will allow modification and tailoring of the properties of hybrid nanostructures as desired for various applications. This work focuses on the computational study of various interactions between SWNT and SLG in their hybrid nanostructures. In some of the recent experimental works, charge transfer between the constituents (SWNT and SLG), owing to their small work-function difference, is considered to be responsible for changes in their electronic and vibrational properties in the hybrid system. However, other forms of interaction between atoms of SWNT and SLG, such as van der Waal's (vdW) forces which may lead to localized structural deformations, may also have pronounced effect on measured properties. The interactions between carbon atoms of SWNT and SLG at close proximity may also result in electronic structure of the system that is unique to the hybrid nanostructure and different from either component (SWNT and SLG). These changes affect the overall performance of the devices based on SWNT-SLG hybrids with respect to the pristine constituents. We present the effect of various factors arising due to the interactions between atoms of SWNT and SLG, i.e. the van der Waal's (vdW) forces, structural deformation and the charge transfer, on the structural, vibrational, electronic, and transport properties of hybrid nanostructures, investigated computationally within the framework of tight-binding density functional theory (TB-DFT). These factors are already known to affect the vibrational properties on SWNT and SLG individually and are also seen to affect the Raman active phonon frequencies of SWNT and SLG within the hybrid system. In this work, we have explored the role of individual factors and interplay between them to estimate their relative contribution to the total changes observed in phonon frequencies in the hybrid systems. From our calculations, it is apparent that the structural deformations and the vdW forces acting on the atoms are the main factors to affect the vibrational properties of components within the hybrid, with structural deformation being the leading factor. We also observe that the charge transfer between SWNT and SLG is not enough at the equilibrium separation of ~ 3 Å to cause any significant changes in the Raman active phonon mode frequencies. With decreasing separation between SWNT and SLG, the charge transfer increases, however, the resulting vdW forces increase much more rapidly and hence would remain the prime factor to cause changes in vibrational properties. These interactions also affect the electronic structure and electronic transport (calculated within the non-equilibrium Green function (NEGF) formalism) in the hybrid nanostructures. The electronic structure of

hybrid nanostructures with various separations between SWNT and SLG and its effect on overall transport behavior is investigated to gain better understanding. We believe that our study would be helpful in comprehending experimentally observed behavior in hybrid nanostructures and may lead to the design of new hybrid systems with desirable properties.

SESSION CT07.05: Excited-State V
Session Chairs: Ting Cao and Diana Qiu
Tuesday Afternoon, April 20, 2021
CT07

9:00 PM *CT07.05.01

Exploiting Quantum Plasmonics for Enhanced Functionalities of Low-Dimensional Heterostructures

Zhenyu Zhang; University of Science and Technology of China, China

In systems of reduced dimensionality containing metals as constituent building blocks, the pertinent conduction electrons are quantum mechanically confined, and their collective excited states of motion are termed plasmons. Recent research has witnessed intensive efforts on exploiting the rich quantum nature of plasmonic excitations in a wide variety of processes, including photon entanglement, solar energy harvesting, electron dephasing, and catalysis, to name just a few. In this talk, we will briefly review situations where the quantum nature of plasmons is bound to play a vital role. Then we will use a few recent representative systems to demonstrate how quantum plasmonics can be exploited to enhance the performance of low-dimensional heterostructures for optimal functionalities. Our first example is the enhanced energy transfer between plasmons and excitons in the strongly coupled regime known as the plexcitons. Here, we reveal the various spectroscopic signatures of the coupling strength and its tunability in systems of molecular species adsorbed on noble metal nanoparticles. The next example is the demonstration and understanding of drastically enhanced phase coherence of the electron transport in graphene proximity coupled with a plasmonic system. Pushing further on the scope, we show in the third example how plasmons can join force with phonons in enhancing the superconducting transition temperatures of interfacial superconductors and beyond.

9:25 PM *CT07.05.02

Landau Levels and Energy Level Alignment for 2D Valleytronics and Spintronics Su Ying Quek; National University of Singapore, Singapore

Two-dimensional materials are promising candidates for next generation quantum devices. Rational bottom-up design of these functional materials rests on the ability to predict from first principles physical properties that are fundamental to the proposed functionalities. In this talk, we first present a first principles approach to predicting the Landau levels in monolayer H-phase transition metal dichalcogenides, which are 2D valleytronic materials. We obtain Landau levels that are symmetric in the K and K' valleys, shifted by a valley Zeeman term.[1] By using Hamiltonians with increasing levels of sophistication, we evaluate the effects of many-body interactions on the single-band orbital magnetic moments at the valleys. The resulting Landau levels are valley- and spin-polarized, and are in good agreement with recent experiments.[2] We next address the problem of energy level alignment in mixed-dimensional heterostructures, using state-of-the-art approaches to many-body perturbation theory in the GW approximation. Our GW approach (XAF-GW) [3] can be applied to large interface systems in the presence of non-covalent interfacial hybridization. We show that cobalt phthalocyanine (CoPc) molecules assembled on a 2D vanadium diselenide substrate are promising candidates for spintronics and quantum information applications. The spin on CoPc is not quenched, and spin-dependent tunneling barriers exist due to many-body interactions in the interface-hybridized states.[4] These same many-body interactions result in a shoulder in the unoccupied spectra which is also observed in experiment.

- [1] Physical Review Research, 2, 033256 (2020)
[2] Nature Nanotechnology, 12, 144 (2017)
[3] Journal of Chemical Theory and Computation, 15, 3824 (2019)
[4] Journal of Physical Chemistry Letters, 11, 9358 (2020)

9:50 PM CT07.05.03

Substrate Screening Effect on Quasiparticle Energies and Optical Properties of Two-Dimensional Interfaces with Lattice Mismatch Chunhao Guo¹, Junqing Xu¹, Dario Rocca² and Yuan Ping¹; ¹University of California, Santa Cruz, United States; ²University of Lorraine, France

Two-dimensional (2D) materials and their interfaces have recently emerged as promising platforms for exotic physical phenomena and outstanding applications. Previous methods of including substrate screening for quasiparticle energies can be only applicable to interfaces of two systems' lattice constants with certain integer proportion, which often requires a few percentage of strain. To solve this problem, we developed an efficient and accurate reciprocal-space interpolation technique for dielectric matrices that made quasiparticle energy calculations possible for arbitrarily mismatched interfaces free of strain [1]. We applied this method to obtain quasiparticle corrections at GW approximation for arbitrary mismatched 2D interfaces, by interfacing hexagonal boron nitride (hBN) with SnS₂ and phosphorene at their natural lattice constants.

We then employed this method to study the effect of substrates on optical properties of 2D materials, by solving the Bethe-Salpeter equation. We obtained a perfect agreement with experimental non-rigid 1s and 2s excitonic shifts with increasing layer thickness of WS₂, where the 1s peak is nearly unchanged with the number of layers, in a sharp contrast to 2s excitonic peak. Similarly, the 1s peak position of hBN was less sensitive than 2s excitonic peak when varying its substrate materials. We explained this observation in terms of the scaling relation of 1s and 2s exciton binding energy with a 2D hydrogen Wannier exciton model, and the linear scaling between exciton binding energy and quasiparticle band gap due to the environmental screening. At the end, we predicted a longer radiative lifetime of hBN with substrate screening than the one of free-standing hBN. [1] C. Guo et al, arXiv:2007.07982

*This work is supported by the National Science Foundation, under grant number 1760260.

10:05 PM CT07.05.04

Intersystem Crossing and Exciton-Defect Coupling of Spin Defects in Hexagonal Boron Nitride Tyler J. Smart^{1,2}, Kejun Li¹, Junqing Xu¹ and Yuan Ping¹; ¹University of California, Santa Cruz, United States; ²Lawrence Livermore National Laboratory, United States

Despite the recognition of two-dimensional (2D) systems as emerging and scalable hostmaterials of single photon emitters or spin qubits, uncontrolled and undetermined chemical nature of these quantum defects has been a roadblock to further development. Leveraging the design of extrinsic defects can circumvent these persistent issues and provide an ultimate solution. Here we established a complete theoretical framework to accurately and systematically design new quantum defects in wide-bandgap 2D systems. In particular, many-body interactions such as defect-exciton couplings are vital for describing excited state properties of defects in ultrathin 2D systems. Meanwhile, nonradiative processes such as phonon-assisted decay and intersystem crossing rates require careful evaluation, which compete together with radiative processes. From a thorough screening of defects based on first-principles calculations, we identified the Ti-vacancy complex as a promising defect in hexagonal boron nitride for spin qubits, with a triplet groundstate, large zero-field splitting, and a prominent intersystem crossing rate highly desirable for spin-state initialization and qubit operation.

- [1] T. J. Smart, K. Li, J. Xu, and Y. Ping, arXiv:2009.02830 (2020).

Funding Acknowledgement: NSF DMR-1760260, DMR-1956015, DMR-1747426. TJS acknowledges funding provided by LLNL Graduate Research Scholar Program. Part of this work was performed under the

auspices of the U.S. Department of Energy by Lawrence Livermore National Laboratory under Contract DE-AC52-07NA27344.

10:20 PM CT07.05.05

Single Crystal Growth and Transport Properties Studies of Non-Symmorphic Material CuBi_2O_4 Tekiyah Robinson, Kory Wells, Jonathan Valenzuela, Doyle Temple, Leroy Salary and Sunil Karna; Norfolk State University, United States

Topological materials having 8-fold electronic degeneracy protection by nonsymmorphic symmetries of a crystal exhibit double Dirac fermions which have been predicted in CuBi_2O_4 . Here, we have grown CuBi_2O_4 single crystal using floating zone crystal growth technique. Polycrystalline X-ray diffraction shows that CuBi_2O_4 crystallizes in the space group $P4/ncc$ which consists of planar $[\text{CuO}_4]^{6-}$ units with Bi^{3+} ions occupying the spaces between units. The magnetization and specific heat indicate a transition to the antiferromagnetic order at $T_N = 43$ K, in agreement with earlier literature reports. In this poster, the detailed magnetoresistance measurements in different crystal orientations will be also presented.

10:25 PM CT07.05.06

The Electronic States of MoS_2 -ITO—Experiment and Theory Manuel A. Ramos¹, Oscar Alberto López Galán¹, John Nogan², Torben Boll^{3,4} and Martin Heilmaier³; ¹Universidad Autónoma de Ciudad Juárez, Mexico; ²Sandia National Laboratories, United States; ³Karlsruhe Institute of Technology—Institute for Applied Materials, Germany; ⁴Karlsruhe Institute of Technology, Germany

The electronic states for indium-tin-oxide/molybdenum disulfide ($\text{In}_2\text{Sn}_2\text{O}_7/\text{MoS}_2$) crystal interface have been calculated by means of density functional theory using CASTEP code with ultrasoft pseudopotentials and revised Perdew-Burke-Ernzerhof (RPBE) functional in General Gradient Approximation (GGA). All molecular models were built using experimental information from atom probe tomography measurements on ITO- MoS_2 thin films as previously reported [1,2]. The experimental APT data indicates no segregation between species; however, some oxygen-molybdenum chemical bonding was detected corresponding to vertical $\langle 101 \rangle$ -direction growth of 2H- MoS_2 crystallites onto ITO during RF-sputtering deposits. The density of states indicate a semi-metallic character which are in agreement with Ohmic behavior of resistivity values of $\rho \sim 24\text{-}27$ (Ω/m) as measured by four-point probe in ITO/ MoS_2 thin film samples, as well bending of electronic semiconducting bands of MoS_2 when its on contact with ITO.

References

- [1] Manuel Ramos *et al.*, "Mechanical properties of RF-sputtering MoS_2 thin films", IOP: Surf. Topogr.: Metrol. Prop. 5 (2017) 025003.
[2] Manuel Ramos *et al.*, "Study of indium tin oxide MoS_2 interface by atom probe tomography", MRS Communications, doi:10.1557/mrc.2019.150

SYMPOSIUM CT08

Mechanochemical Coupling in Chemical Treatment and Materials Degradation—Modeling and Experimentation

April 21 - April 21, 2021

Symposium Organizers

Sheng Guo, Chalmers University of Technology

* Invited Paper

SESSION CT08.01: Chemical Treatments
Session Chairs: Sheng Guo and Jingli Luo
Wednesday Morning, April 21, 2021
CT08

8:00 AM *CT08.01.01

Diffusion and Chemical Stress—Induced Stress Effects in Ion Exchanged Inorganic Silicate Glass
Guglielmo Macrelli; Isoclima SpA, Italy

Diffusion of atoms, ions and molecules in solid materials may result in local mechanical stress. A review is presented of literature studies in semiconductor materials, high temperature oxidation and electrochemical charging and discharging of electrodes in lithium ion batteries. The main focus is inorganic silicate glasses submitted to alkali ion-exchange below glass transition temperature. Interdiffusion driven ion-exchange in glass results in stress effects that are used in technological applications for glass articles strengthening. These processes are extensively and widely used in screen covers for consumer electronics and structural windows for architectural and transportation applications. Optical effects are also discussed as a consequence of ion interdiffusion and its relationship with residual stress. Underpinning physics of ion exchange in glass is reviewed in respect to both stress build-up and relaxation considering, that ion exchange is a irreversible mass transfer process performed on a non-equilibrium state of matter which spontaneously relaxes towards a metastable supercooled liquid state.

8:25 AM CT08.01.02

Chemo-Mechanically Coupled Feedback Interactions and the Challenges to Building Robust Predictive Models Nithya Subramanian¹, Chiara Bisagni¹ and Laura Nielsen Lammers^{2,3}; ¹Delft University of Technology, Netherlands; ²Lawrence Berkeley National Laboratory, United States; ³University of California, Berkeley, United States

Novel materials enable solutions to the global challenges that we face today pertaining to energy and the environment. The realization of materials technology that allows for reliable lightweight structures, improved energy storage, improved efficiency of waste/nutrient recovery, etc. critically hinges on our understanding of strongly coupled material behavior under a wide range of conditions. Some natural as well as engineered material systems exhibit an interplay between their chemistry and mechanical response as the microstructures of these materials dynamically evolve as a response to their chemical composition/reaction kinetics. In some cases, even when our understanding of said coupled behavior is advanced, there are limitations to how we can account for them in computational models owing to a need for multiscale transfer of information. Building predictive mechanics models that can accurately capture the origins of material behavior by explicitly incorporating the chemical structure of constituents and reaction kinetics can be computationally prohibitive. This brings up the need for effective upscaling strategies in multiscale, multiphysical models that can preserve traceability across scales.

Here, we explore strategies for upscaling the mechanochemistry captured through all-atom classical and reactive molecular dynamics simulations in a few example materials such as polymer adhesives, engineered nanocomposites, and clay-rich porous media that are used in aerospace, electrochemical, and geological applications.

The polymer curing reaction in a multicomponent aerospace-grade epoxy is modelled based on a cut-off distance-based approach that determines bond formation. The resulting degree of conversion of the polymer and its glass transition temperature are confirmed with experimental data. We also studied the chemical and physical interactions in nanocomposites where carbonaceous nanoparticles are dispersed in a thermoset polymer. The interfacial adhesion (arising from chemical functionalization and non-bonded forces) between the nanoparticles and surrounding polymer is also quantified as a function of the degree of conversion of the polymer and the chemical composition (% wt. of nanoparticle in the nanocomposite). From a large combination of these simulations, we determined the effect of the nanostructure and chemistry of the polymers and nanocomposites on their elastic properties, crack initiation from bond breakage and chain sliding, traction-separation behavior at crack openings and fracture toughness. In the case of clay minerals whose chemical-mechanical coupling has tremendous implications for their role as geological barriers for the subsurface disposal of nuclear waste, we modelled the water and ion diffusion, clay swelling states and ion exchange selectivities for a range of pore fluid chemical compositions and concentrations. The swelling pressure, and therefore, the stress states of clay tactoids (containing multiple layers of clay minerals) was determined as a function of the local chemical composition.

In all the above-mentioned studies, the molecular models provide valuable insight into the dependence of stress states and interfacial load transfer on the chemical composition and the energetics of reactions. We then use a stochastic representative volume element (RVE) approach to march up the length scale while accounting for uncertainties characterized at the molecular scale. With the stochastic RVEs, we can predict the ‘bulk’ stress response and associated damage propagation under a given loading condition. The choice of parameters (and their probability distributions to make a stochastic prediction) to be included in the RVE model depends on the material system and its related performance parameter of interest. For example, in clay minerals, our interest is to predict the swelling and collapse of mineral layers (the swelling pressure & stress state) as a function of water activity and ambient conditions whereas the interest in polymer adhesives is to predict crack nucleation and propagation. Holistic computational models that can provide top-down/bottom-up traceability of chemical-mechanical coupling can be a valuable tool in our arsenal to advance and accelerate the design and certification of these material systems in critical applications.

8:40 AM *CT08.01.03

On the Role of Stress in Microstructure Evolution During Thermo-Chemical Surface Engineering Marcel A. Somers and Thomas L. Christiansen; Technical University of Denmark, Denmark

Thermochemical surface engineering of metals is characterized by a deliberate and targeted modification of the (sub)surface region of metals, with the aim to improve materials performance with respect to fatigue, wear, corrosion and combinations thereof. Generally, thermochemical surface engineering is understood in terms of thermodynamics and diffusion kinetics to describe the evolution of the microstructure under the influence of the chemical modification at elevated temperature. Associated with the change in composition in the surface-adjacent region strains and stresses are introduced. These strains/stresses affect the thermodynamics and the kinetics of the ingress of chemical species and, consequently, the microstructural evolution. This contribution illustrates several of the effects of composition-induced stresses/strains during thermochemical surface engineering with interstitials in metals through examples from activities in the authors’ research group. The presentation includes experimental as well as modelling aspects. The following examples are covered.

1. The dissolution of N and/or C into stainless steels and high entropy alloys (HEAs) at temperatures below 725 K for N and below 825 K for C is associated with the development of a supersaturated solid solution of interstitials in the fcc phase. This supersaturation is “kinetically stabilized” by sluggish decomposition, because of slow diffusion of substitutionally dissolved components. The lattice expansion caused by dissolution of N or C is accommodated elastically for low interstitial contents, leading to strengthening. As solid solution strengthening scales with the cube root of composition squared and biaxial compressive stresses caused by lattice expansion scale linearly with composition, plastic accommodation will occur above a threshold composition. Also, with an increase in N content long range ordering (LRO) of N atoms is encountered. The combination of elasto-plastic accommodation of lattice expansion and LRO leads to anisotropic growth of the developing case.

2. Hcp titanium can dissolve high contents of oxygen and is applied for surface hardening of Ti and its alloys. The thermo-chemical treatment of Ti in CO above the hcp-bcc transition temperature leads in principle to the uptake of both O and C. Since C has a very low solubility as compared to O, hence, primarily O is dissolved, thereby stabilizing a case of hcp-Ti atop bcc-Ti. The conversion of bcc to hcp is associated with the introduction of tensile stresses in the hcp case, leading to crack development in the hard and brittle part of the case close to the surface. Upon cracking, CO ingress leads to the development of a mixed interstitial compound Ti(C,O) along the crack surface, thereby converting this part into an extremely wear resistant Ti-surface, with a hardness of up to 3,000 HV.

3. Oxidizing of ZrCuAl-based bulk metallic glass (BMG) below the glass transition temperature is a potential thermo-chemical surface engineering treatment of BMGs. Within the BMG an internal oxidation zone (IOZ), consisting of nano-crystalline ZrO₂, develops. The volume expansion caused by zirconia formation leads to compressive residual stresses in the IOZ. The theoretical stresses are 30 times higher than the experimentally determined stress levels, indicating that stress relaxation has occurred. This is accomplished by shear band formation in the BMG adjacent to the IOZ, which later affects the ZrO₂ development of the advancing oxidation front. In addition, the compressive stresses induce outward diffusion of “noble” elements, as for example Ag (if present) and Cu. Surprisingly, segregation of these noble elements at free surfaces, as the outer surface, but also crack surfaces, leads to crystalline metallic regions, which can be considered as self-healing in the case of crack formation. Depending on the oxygen partial pressure, Cu can oxidize upon arrival at the surface.

9:05 AM CT08.01.04

Magnetic Force Microscopy Based Investigation of Molecule Impact on Magnetic Tunnel Junction Based Molecular Devices Pawan Tyagi; University of the District of Columbia, United States

This paper discussed the experimental magnetic force microscopy (MFM) studies on MTJMSDs. We showed that molecules are much more than simple spin channels between two magnetic electrodes. MFM produced vivid evidence showing that a paramagnetic molecule covalently bonded to the two ferromagnetic electrodes catalyzed a large-scale ordering on ferromagnetic electrodes and impacted several hundred-micron areas near molecular junctions. Transport studies showed that paramagnetic molecule induced long-range impact on ferromagnetic electrodes resulted in several orders of current suppression at room temperature. Future studies with various forms of magnetic tunnel junctions and molecules are in order. The present work provides the details about the efficacy of cost-effective, and mass producible liftoff based molecular device fabrication.

SESSION CT08.02: Materials Degradation I

Session Chairs: Sheng Guo and Jingli Luo

Wednesday Morning, April 21, 2021

CT08

11:45 AM *CT08.02.01

Novel Insights into Corrosion Processes by Advanced X-Ray Methods Christiane Stephan-Scherb^{1,2};

¹Federal Institute for Materials Research and Testing, Germany; ²Freie Universität Berlin, Germany

A variety of materials of technological interest change their properties through contact with reactive media. Solid-gas reactions lead to a variety of reaction products on the surfaces and internal interfaces. The observation of nucleation and growth processes in the environment where they occur (in situ) from a chemical-structural perspective is especially challenging for aggressive atmospheres. The talk presents innovative approaches to study corrosion mechanisms using advanced X-ray methods. Using energy dispersive X-ray diffraction and X-ray absorption spectroscopy in different tailor made environmental reaction chambers, valuable insights into high temperature oxidation and sulfidation processes were gained. Fe-based alloys were exposed to hot and

reactive atmospheres containing gases like SO₂, H₂O and O₂ at 650°C. During the gas exposure the tailor made reaction chambers were connected to a high energy diffraction end station at the synchrotron. The crystallization and growth of oxide and sulfide reaction products at the alloy surfaces were monitored by collecting full diffraction pattern every minute. Careful examination of shape and intensity of phase-specific reflections enabled to a detailed view on growth kinetics. These studies showed, oxides are the first phases occurring immediately after experimental start. As soon as reactive gas media enter the chamber, the conditions change and different reaction products, such as sulfides start to grow. A comparison of different gas environments applied, illustrated the differences in the type of reaction products. The in situ observation of high temperature material degradation by corrosion made it possible to study the contribution of phases, which are not stable at room temperature. For instance, wuestite (Fe_{1-x}O), was frequently observed at high temperatures in humid gases on Fe with 2 wt.% and 9 wt.% chromium, but not at room temperature. The strength of the occurrence of this phase additionally explains why, despite a higher Cr content, ferritic alloys with 9 wt.% Cr in a challenging atmosphere prevent the intrinsic formation of protective layers. The in situ observations were supplemented by careful considerations of thermodynamic boundary conditions and detailed post characterization by classical metallographic analysis. Additionally, the structure and chemistry of the dominant oxide layers were evaluated using X-ray absorption near edge structure spectroscopy. The talk will give an overview about chances and challenges for studying high temperature corrosion phenomena by advanced X-ray methods.

12:10 PM CT08.02.02

Modeling of Mass Transfer and Alpha Case Formation in Investment Casting of Titanium Alloys Sharon Uwanyuze, Stefan Schaffoener, Sanjubala Sahoo and Pamir Alpay; University of Connecticut, United States

Titanium alloys have excellent corrosion resistance, high-temperature strength, low density, and biocompatibility. Therefore, they are increasingly used for aerospace, chemical, and biomedical applications. Moreover, investment casting is a well-established process for manufacturing near-net-shape intricate parts for such applications. However, mass transfer arising from metal-mold reactions is still a major problem that drastically impairs the surface and properties of the castings. This work investigates the interfacial reactions and mass transfer problems that lead to alpha case formation. Improvements based on modeling and experimental validation are discussed, highlighting ceramic oxide refractories namely—zirconia, yttria, calcia, alumina, and novel perovskites particularly calcium zirconate and barium zirconate. It was found that while mold material selection is vital, alloy composition should also be carefully considered in mitigating metal-mold reactions and mass transfer.

12:25 PM *CT08.02.03

Degradation of Zirconium Alloys in Nuclear Reactors Studied by Atom Probe Tomography Mattias Thuvander, Johan Eriksson and Hans-Olof Andrén; Chalmers University of Technology, Sweden

The uranium dioxide nuclear fuel of light water reactors is contained in 4 m long tubes with a diameter of about 10 mm and a wall thickness of about 0.7 mm, called cladding tubes. The cladding tubes are made of zirconium alloys, the main reason being the very low cross section of Zr for thermal neutrons. The cladding tubes are subjected to several degradation mechanisms, including water-side corrosion, hydrogen pick-up and irradiation damage, affecting the mechanical integrity, which restricts the usage of the fuel. There are several different Zr alloys that are used for cladding tubes. We have studied Zircaloy-2, which is commonly used in boiling water reactors. It has a composition of Zr-1.5%Sn-0.15%Fe-0.1%Cr-0.05%Ni, and it is known that Fe, Cr and Ni play important roles for the performance of the alloy. These elements have a low solubility and precipitates of Zr₂(Fe,Ni) and Zr(Fe,Cr)₂ form. In order to study both the corrosion behavior and the neutron damage, atom probe tomography (APT) is a very useful technique, combining a sub-nm resolution in 3D with a high elemental sensitivity. By analyzing the oxide and the metal/oxide interface of samples corroded in autoclave it was shown that Fe and Ni were segregated at grain boundaries in the metal and that these segregations were inherited by the inwards growing oxide. Modeling provided support for that Fe present at oxide grain boundaries should reduce hydrogen pick-up, whereas the opposite should be true for Ni. We have also analyzed Zircaloy-2 after

in-reactor exposure, for three and nine years, respectively. The neutron irradiation leads to a gradual dissolution of the precipitates as well as formation of dislocation loops. It was found that the dissolved Fe, Cr and Ni segregates to the loops. This is very interesting, although it is not clear how this segregation affects the growth and stability of the loops, or the corrosion and hydrogen pick-up behavior.

12:50 PM CT08.02.04

Influence of Pack Cementation Time and Annealing on Microstructure of Cu Nanofoams Processed by Dealloying Hung T. Pham¹, Péter Jenei¹, Csilla Kádár^{1,2,3}, GiGap Han⁴, Heeman Choe⁴ and Jenő Gubicza¹; ¹Eötvös Loránd University, Hungary; ²Budapest University of Technology and Economics, Hungary; ³MTA–BME Lendület Composite Metal Foams Research Group, Hungary; ⁴Kookmin University, Korea (the Republic of)

Cu nanofoams processed by dealloying were studied as a promising applicant for anode material in lithium-ion batteries. Pack cementation were applied to produce the precursor materials for different times (3, 6, 12 and 15 h). The microstructure of the specimens was studied after the dealloying process. Samples produced with 6 h pack cementation time were also annealed to investigate the influence of heat treatment on the microstructure of Cu nanofoams. The foam structure was examined by scanning electron microscopy (SEM). The phase composition of the materials was determined using X-ray diffraction (XRD). Furthermore, X-ray line profile analysis (XLPA) was utilized for quantitative characterization of the diffraction domain size, the dislocation density and the twin fault probability.

SESSION CT08.03: Chemical Treatments and In Situ Experiments I
Session Chairs: Haihui Ruan and Daniel Schreiber
Wednesday Afternoon, April 21, 2021
CT08

2:15 PM *CT08.03.01

Characterization of Early Stages of Radiation Damage in Metals and Alloys with Positron Annihilation Spectroscopy Filip Tuomisto; University of Helsinki, Finland

The early stages of radiation damage in metals and alloys are governed by phenomena on the atomic scale. The most elementary are the creation of individual vacancies and interstitials (Frenkel pairs) and their motion that leads to either their annihilation or evolution towards larger defect clusters. The detailed mechanisms of the evolution of the radiation damage strongly depend on the defect-matrix-solute-impurity interactions. Experimental identification of the radiation-induced defects and the characterization of their properties is crucial for developing a detailed understanding and physics-based predictive models for radiation damage. Positron annihilation spectroscopy is a set of methods selectively sensitive to vacancy-type (open volume) defects [1]. It can be used to identify the sizes of the defects from mono-vacancies to clusters of tens of missing atoms, with concentration sensitivity in the range 10 ppb - 100 ppm. The chemical identity of the atoms immediately surrounding the vacancy-type defects can also be identified to a certain extent. Experiments can be performed with near-surface depth resolution up to a few microns, as well as in the bulk of the material, in a temperature range 10 - 1000 K, allowing for various in situ irradiation experiments.

I will review some of the recent positron annihilation experiments dealing with early-stage radiation damage in tungsten and high-entropy alloys (HEAs). The results obtained in tungsten include the direct determination of mono-vacancy and interstitial migration barriers [2] that employ irradiation experiments at cryogenic temperatures for freezing in the radiation-induced defects, and hydrogen-vacancy-cluster interactions at elevated temperatures [3]. In HEAs, the experiments reveal atomic-scale segregation already at the early stages (below 1dpa) of radiation damage [4] and non-trivial effects of C interstitials in the HEA matrix on hydrogen irradiation induced damage [5]. Finally, I will discuss preliminary results obtained in C and N interstitial

containing HEAs that show intriguing mono-vacancy migration barrier behavior most likely related to the unusual effects of these interstitials on the distribution of local lattice distortions.

[1] F. Tuomisto and I. Makkonen, Rev. Mod. Phys. 85, 1583 (2013).

[2] J. Heikinheimo et al., APL Mater. 7, 021103 (2019).

[3] M. Zibrov et al., J. Nuclear Mater. 531, 152017 (2020).

[4] F. Tuomisto et al., Acta Mater. 196, 44 (2020).

[5] E. Lu et al., J. Appl. Phys. 127, 025103 (2020).

2:40 PM *CT08.03.02

In Situ TEM Observation of Mechanochemical Coupling Induced Materials Degradation Chongmin Wang and Daniel Schreiber; Pacific Northwest National Laboratory, United States

Active functioning of materials will often trigger, or be accompanied by, one or more deleterious processes, such as oxidation, corrosion, fatigue, and thermal or mechanical effect, which in turn will couple with the active process to collectively affect the materials behavior and functionality. In a typical example, electrochemically driven functioning of a rechargeable battery inevitably induces thermal and mechanical effects that couple with the electrochemical process and collectively govern the performance of the battery. A direct visualization of such a coupling effect appears to be a fundamental challenge. In this presentation, we will discuss the utility of in-situ TEM to directly probe the mechanochemical coupling effect, intending to unravel mechanical effect on ionic transport, oxidation induce stress generation, mechanical effect on lithium dendrite growth, and electrochemical induced crystal deformation. We demonstrate that the intricate coupling of electrochemical, thermal, and mechanical effects will surpass the superposition of individual effects.

3:05 PM CT08.03.03

Late News: Electrolyte Conditions in Li-Ion Batteries in Presence of a Thermal Gradient Joaquin Guillamon¹, Corey Love², Rachel Carter², Xue Yang¹ and Amit Verma¹; ¹Texas A&M University - Kingsville, United States; ²U.S. Naval Research Laboratory, United States

Safety is an important concern in Li-ion battery operation and storage. As both energy stored per unit volume and higher current densities have increased in these batteries, energy dissipation in the form of heat has become one of the main issues for proper battery operation. As temperature increases, secondary chemical reactions may be initiated. These reactions release more heat and undesired products, triggering an auto-catalytic feedback process to occur, which is commonly classified into thermal-runaway mechanisms. This can potentially lead to a complete degradation of the battery, and possible explosion or combustion of the battery components.

Several researchers have worked on developing models to predict thermal behavior under conditions with potential thermal runaway outcomes on Li-ion batteries. The first studies proposed a model that emulates the solid electrolyte interface (SEI) decomposition and regeneration reactions on a standard 18650 cylindrical cell. Later works extended these models and included the reactions of cathode decomposition and electrolyte decomposition with potential combustion. Although macroscopic level energy balance helps to predict potential thermal behavior in a battery of multiple layers, the study of all the different transport mechanisms that happen inside a single layer battery is essential for a better understanding of the process taking place when temperature begins to rise. With the aim of improving heat dissipation inside a battery, the electrolyte is a key component to consider as it can potentially handle heat flux easier through convection within the solution.

This work investigates spatially dependent electrolyte conditions in the presence of a thermal gradient to produce an electrolyte-centric thermal runaway model. Non-current conditions are considered for this specific case study, emulating oven-test experiments, or storage conditions. The objective of the study is to model transport mechanisms that can potentially lead to thermal degradation of the battery. Li-ions, momentum, and thermal flux are the main components of the analysis. Numerical simulation techniques are used for this purpose. Findings show that non-uniform temperature distribution triggers free convection mechanisms within the electrolyte solution. According to our results, electrolyte stratification should be appreciated at the microscopic level. A thorough comprehension of the transport processes taking place inside the battery should

contribute to mitigate damage induced due to thermal abuse conditions.

3:20 PM CT08.03.04

Late News: Coupled Effects of Stress and Hydrogen on Stress Corrosion Cracking of Fe-Based Alloys
Arun Devaraj, Sten Lambeets, Mathew Olszta, Tingkun Liu, Joshua Silverstein and Daniel Perea; Pacific Northwest National Laboratory, United States

When Fe alloys are subjected simultaneously to an applied tensile stress and a corrosive, high-temperature aqueous medium, interplay of hydrogen and oxygen interactions with the alloy microstructure are thought to lead to intergranular stress corrosion cracking (SCC). Using transmission electron microscopy and in situ atom probe tomography we develop atomic scale understanding of this mechanochemical coupling during SCC of model Fe-18Cr-10Ni alloy. Specifically, the structure and composition of oxide layers and elemental partitioning as well as hydrogen segregation at the oxide-metal interface was revealed as a function of prior deformation. These new insights are expected to provide the scientific basis for tailoring the microstructure of metallic alloys used in nuclear and automotive applications to control the impact of coupled extreme environments of corrosion, stress, and temperature.

SESSION CT08.04: Materials Degradation II
Session Chairs: Jingli Luo and Haihui Ruan
Wednesday Afternoon, April 21, 2021
CT08

5:15 PM *CT08.04.01

Fundamental Insight into Crack Retardation Behavior Through Advanced Characterization Elaine West;
Naval Nuclear Laboratory, United States

Stress corrosion and corrosion fatigue cracking of structural materials used in the commercial nuclear power industry must be well understood to ensure the integrity of the reactor plant. While the cracking behaviors are generally recognized to show an Arrhenius temperature dependence, departure from this behavior has been observed at high temperatures. Mechanistic understanding of this behavior would support the development of improved predictive models for crack growth. Advanced characterization of crack tips and corrosion films have provided important insights into these behaviors. Chemical and mechanical signatures of crack retardation behavior will be discussed in the context of potential retardation mechanisms.

5:40 PM CT08.04.02

***Ab Initio* Study of Mechanochemical Coupling at Materials Interfaces** Zhuohan Li and Izabela Szułfarska;
University of Wisconsin–Madison, United States

Mechanical forces and chemical reactions at materials interfaces are often coupled to each other. This coupling is relevant to fields such as rock friction, micro/nano devices, wafer bonding. In particular, in sliding contacts, compressive and shear stress can activate interfacial chemical bonding reactions, resulting in higher friction and adhesion, higher wear rate, and higher tribofilm and tribo-polymerization production rate. The mechanochemical coupling has been generally described by phenomenological theories, including the Eyring model. In these theories, the activation energy for a chemical reaction is increased or decreased by the mechanical work done on the system, where σ is the stress acting on the system, and V^* is the activation volume. The physical meaning of activation volume has been under debate for decades, but the magnitude of the activation volume is often considered to be comparable to the dimension of the local deformation of chemical bonds participating in the reaction. However, recent experimental results showed that the range of activation volumes can be quite large even for the same material system. For example, for tribochemical wear of silicon

tips, where the wear is due to the chemical bond formation and breaking at the interface, the range of activation volumes can be as large as $\sim 6.7\text{-}115 \text{ \AA}^3$. With such a large range, the physical picture of the activation volume corresponding approximately to the dimension of the local volume involved directly in stretching or compressing of the chemical bonds might be oversimplified.

In order to understand the physico-chemical coupling at interfaces, we performed *ab initio* calculations of stress-induced reactions silica/silica interfaces. Our results show that the mechanochemical response arises not only from the interface region, where the chemical reaction occurs, but there is also a significant (and in some cases dominant) contribution from the deformation of the bulk solid. The relative contributions from each region depend on the stiffness of these regions, and the softer region dominates the response to the mechanical work done on the system. We also demonstrate that the contribution from the bulk region can be large even for stiff materials. This is because the near surface-region of the solid can be significantly softer than the bulk solid. The larger stresses experienced by the near-surface regions of two materials in contact can also lead to a larger mechanochemical response from the near-surface region. Our study provides new insights into the physical origins of the mechanochemical coupling at interfaces and the meaning of the activation volume.

5:55 PM CT08.04.03

Late News: Interplay Between Defect Transport and Cation Spin Frustration in Corundum-Structured Oxides [Amitava Banerjee](#), Aaron A. Kohnert, Edward E. Holby and Blas Uberuaga; Los Alamos National Laboratory, United States

Despite the fundamental importance of mass transport, there is still a lack of knowledge regarding the mechanisms in many materials. In particular, how the magnetic spin structure interacts with migrating defects is unclear. Here, using density functional theory to examine cation interstitial transport in corundum-structure oxides, Al_2O_3 , Cr_2O_3 , and Fe_2O_3 . These oxides have their own technological importance in various applications, such as diagnostic windows in nuclear energy systems, protective surface coatings, catalyst supports, magnetic storage, etc. In this study, we reveal an interplay between the migration of the interstitial and the magnetic structure of the oxide. The magnetic spin configuration impacts the migration energy of the migrating defect but, critically, the defect modifies the spin configuration. Thus, the two aspects change in concert to modify one other. This has profound implications for mass transport in magnetic materials.

6:10 PM CT08.04.04

Investigations on the Corrosion Resistance Enhancement of Electroless Ni-P Coating by Incorporating Corrosion Inhibitor-Loaded Nanocapsules Jiankuan Li, Chong Sun and [Jingli Luo](#); University of Alberta, Canada

The ever-increasing energy demand has driven the search for new oil and gas resources in harsh environments. However, corrosion problems of carbon steels in oil and gas production under harsh operational conditions and during the product transportation considerably impede the productivity and cause safety concerns. Majority of these corrosion problems are related to CO_2 corrosion. In the journey of seeking solutions, a high-phosphorus electroless Ni-P coating has gained growing attentions as an advantageous candidate to carbon steels due to its good balance between the outstanding anti-corrosion performance and reasonable cost.

When Ni and P atoms are co-deposited under the catalytic effect of adsorbed hydrogen atoms in the coating deposition process, H_2 gas bubbles are easily produced and left in the coating to form “micropores” that favor the penetration of aggressive medium and lead to coating degradation. To effectively mitigate electrolyte penetration and coating degradation, we designed a smart Ni-P coating incorporated with nanocapsules that enable the release of the pH-responsive corrosion inhibitor when corrosive medium reaches the micropores. In this work, the microstructure and chemical compositions of as-fabricated Ni-P coating and nanocapsule-incorporated Ni-P coating were analyzed by SEM, EDS, XPS and AFM, and the corrosion behaviors of the two coatings in the CO_2 -saturated NaCl solution were then evaluated by potentiodynamic polarization measurements and EIS. The results show that BTA-loaded nanocapsules are successfully incorporated into Ni-P coating without altering the microstructure and deposition rate, and the presence of nanocapsules significantly reduces the coating porosity by filling in the micropores. As a result, the corrosion resistance of the smart

coating notably increases due to the release of BTA originated from the local acidification of the micropores, as compared to the as-deposited coating. A good anti-corrosion stability is further confirmed by few noticeable corrosion pits and no evidence of lateral coating disbondment at the coating/substrate interface after immersion tests. This study offers new insights into developing smart electroless Ni-P coatings by incorporating nanoscale functionalized additives.

SESSION CT08.05: Chemical Treatments and In Situ Experiments II/Materials Degradation III
Session Chairs: Haihui Ruan and Daniel Schreiber
Wednesday Afternoon, April 21, 2021
CT08

8:15 PM *CT08.05.01

Special Water as New Constitution for Soft Materials Zhenhui Qi and Mehmood Elahi; Northwestern Polytechnical University, China

The inspiration derives from the concept of structural water in nature that water molecules are bound inside hydrophobic pockets and help to stabilize protein structures. However, water has rarely been found a similar role in material science. By using this water-activated glue, the resulting supramolecular polymeric materials exhibits strong adhesion to surfaces, and can be reused many times without losing its performance. Considering the unique feature of water, this discovery triggered the transition of negative role of water, and we started the water-centered the soft material design.

8:40 PM CT08.05.02

Modifying Surface Free Energy via Water Adsorption for Nano-Bonding™ Piezo-Electrics LiTaO₃ and LiNbO₃ with Si and SiO₂ at Room Temperature Mohammed Sahal, Abbie Ellison, Shefali Prakash, Srivatsan Swaminathan, Riley Rane, Brian Baker, Lauren Puglisi, Robert Culbertson and Nicole Herbots; Arizona State University, United States

The formation of hetero-structures between, either piezo-electric LiTaO₃ or LiNbO₃ with Si-based materials exhibits three major issues: the mismatch of crystal structure, of their lattice constants and of their coefficient of thermal expansion (CTE). In particular, the thermal expansion of LiTaO₃ or LiNbO₃ crystals is much larger. It differs from Si and SiO₂ by an order of magnitude.

The present work uses Nano-Bonding™ [1] to directly bond LiTaO₃ and LiNbO₃ to Si and SiO₂. This is done via Surface Energy Engineering (SEE). In synergy, SEE modifies the surface hydro-affinity and the surface energy to far-from-equilibrium states. These are more likely to react in air at room temperature. H₂O vapor is used to catalyze bonding of LiTaO₃ and LiNbO₃ to Si and SiO₂.

Hydro-affinity and surface energies are mapped across 4-6" wafers via Three Liquid Contact Angle Analysis (3LCAA). Mapping is done in air in a Class 100 Laminar Flood hood. Hydro-affinity is mapped via the water contact angle. Surface Energy is computed using van Oss-Chaudhury-Good theory [2], via the mapping of contact angles of two polar liquids (water and glycerin), and non-polar α -bromo-naphthalene. The measured surface energies are found to be close for the (110) orientation for both LiTaO₃ and LiNbO₃. They are 41 ± 2 mJ/m² for LiTaO₃ and 39 ± 2.5 mJ/m² for LiNbO₃ respectively.

The $\Delta G_{\text{Piezo-Si-H}_2\text{O}}$ of interaction computed from measured surface energies by applying van Oss- Chaudhury-Good theory [2] for 'as received' LiTaO₃, with 'after SEE' Si and SiO₂ were -0.1 mJ/m² and -16.8 mJ/m² and for 'as received' LiNbO₃, with 'after SEE' Si and SiO₂ were -13.4 mJ/m² and -28 mJ/m².

Thus $\Delta G_{\text{Piezo-Si-H}_2\text{O}}$ values are < 0 , to bond 'as received' hydrophobic LiTaO_3 and LiNbO_3 with 'after SEE' hydrophilic Si and SiO_2 in the presence of atmospheric moisture. Experimentally, SEE based on these computations is found to be successful in activating Nano-Bonding™ (at room temperature in 25 % HR) of LiTaO_3 to Si, and LiNbO_3 to SiO_2 .

[1] Nano-Bonding™, Herbots, et al. U.S. Pat. # 9,018,077 (2015), 9,589,801(2017), pend. (2020)

[2] Van Oss, et.al, (1988). "Interfacial Lifshitz-van der Waals and polar interactions in macroscopic systems". Chemical reviews, 88(6), 927-941

8:55 PM CT08.05.03

Computational Insights into Dopant Enhanced Li Vacancy Distribution and Energetic Changes in Ga Doped LLZO Changlong Li¹, Lindsay Roy², Nancy Birkner¹, Kyle Brinkman¹ and Lindsay Shuller-Nickles¹; ¹Clemson University, United States; ²Savannah River National Laboratory, United States

Ga-doped $\text{Li}_7\text{La}_3\text{Zr}_2\text{O}_{12}$ (LLZO) has been experimentally fabricated with high lithium ionic conductivity and is a promising candidate for the electrolyte in all-solid-state Li-ion batteries. However, the thermodynamic properties of Ga-doped LLZO remain underreported. In this study, Coulomb energy analysis for large disordered crystal with supercell program and density functional theory (DFT) calculations provide insights into the compositional and structural stability of $\text{Li}_{56-3x}\text{Ga}_x\text{La}_3\text{Zr}_2\text{O}_{12}$, where $x = 0, 1, 2, 4, 6, 8$. The lattice parameters decrease with increased Ga concentration because of the smaller ionic radii of the dopant and the formation of Li vacancies. Relationships between local coordination environment of Ga dopants and Li vacancies were considered, leading to an understanding of the configurational preferences in Ga-doped LLZO and the potential for correlated configurational dependencies of Li mobility. The enthalpy of formation as calculated based on the binary oxide reactants, for Ga-doped LLZO increases from -1540.72 kJ/mol for undoped tetragonal $\text{Li}_{56}\text{La}_{24}\text{Zr}_{16}\text{O}_{96}$ to -1411.70 kJ/mol for $\text{Li}_{32}\text{Ga}_8\text{La}_{24}\text{Zr}_{16}\text{O}_{96}$. The trend in enthalpy of formation with respect to the Ga concentration is in agreement with recently reported experimental calorimetry measurements, which are reported for the nominal formula unit $\text{Li}_{7-3x}\text{Ga}_x\text{La}_3\text{Zr}_2\text{O}_{12}$ (where $x = 0, 0.25, 0.5, 0.75$, and 1). Detailed energetic analysis associated with a stepwise increase in [Ga] were performed to understand the changes in thermodynamic stability with increased Ga content. The relation between Li-ion conductivity and the stability of the Ga-doped LLZO emphasizes that a balance must be achieved between the increase in Ga concentration, which drives the formation of Li vacancies necessary for Li migration.

9:10 PM BREAK

9:25 PM *CT08.05.05

Modeling of Microstructure Evolution of Metallic Materials Under the Influence of Diffusion, Chemical Reaction, Passivation, Sensitization, Electrical and Mechanical Loading San-Qiang Shi; The Hong Kong Polytechnic University, China

A computational framework based on multi-phase-field method was developed to study the complex microstructure evolution of metallic materials under the influence of chemical reaction, bulk and surface diffusion, surface passivation, sensitization, applied electrical and/or mechanical loading in aqueous or gas environment. The proposed framework makes use of the Allen-Cahn equation for phase variables, Cahn-Hilliard equation for conserved variables, Nernst-Planck equation and Poisson's equation for electrochemical condition, together with mechanical equilibrium equations. When chemical reactions were involved, the reaction rate was expressed as a function of the chemical (or electrochemical) potentials of reactants and products based on a detailed balance of reactions. The framework was applied to study pitting corrosion of steels with or without the formation of insoluble corrosion products, stress corrosion cracking, corrosion of metal matrix composite under mechanical loading, high temperature metal oxide formation under the influence of high PB ratio, intergranular corrosion of sensitized aluminum alloys, nano-porous structure evolution during chemical dealloying of binary alloys. The characteristics of the model predictions agree well qualitatively, in many cases also quantitatively, with the experimental observations. This work was supported by grants from the

9:50 PM CT08.05.06

Late News: Theoretical and Experimental Evaluation of Elastic Moduli of Fluoroethylene Carbonate and Vinylene Carbonate Polymers in Solid Electrolyte Interface of Silicon Anode Yuki Kamikawa¹, Koji Amezawa¹ and Kenjiro Terada²; ¹Institute of Multidisciplinary Research for Advanced Materials, Tohoku University, Japan; ²International Research Institute of Disaster Science, Tohoku University, Japan

Precisely evaluating the mechanical properties of polymeric components in a solid–electrolyte interphase (SEI) is crucial for ensuring its mechanical stability on silicon anodes, which significantly expand during lithiation. However, the complex inorganic/organic nanocomposite structure of SEIs hinders the ability to directly measure the elastic moduli of its constituent polymer components. To address this issue, in our prior DFT study, we proposed a theoretical methodology to determine these elastic moduli. First-principles calculations were performed to evaluate the energy barrier for a 1,2-radical shift in different carbons in the corresponding polymers. Using the identified crosslinking sites, the elastic moduli of the crosslinked fluoroethylene carbonate (FEC) and vinylene carbonate (VC) polymers were evaluated, which could not be directly measured on the formed SEI. Our calculations provided evidence of the elastic behavior of polymeric species in the SEI formed by the electrochemical reduction of FEC and VC on the surfaces of silicon anodes. Moreover, these findings suggested a new avenue for attaining mechanically stable SEIs on silicon anodes through the chemo-mechanical design of an inorganic/organic nanocomposite structure based on those mechanical properties. Then, cyclic nanoindentation tests and numerical methods were used to quantify the elasto- and viscoelasticity of SEIs as well as the effects of the stress field in the silicon anode material below the SEI, thus enabling the precise evaluation of the elastic modulus of the SEI. Instrumented nanoindentation was used to quantitatively measure the indentation force response on the heterogeneous surface of composite electrodes. The measured results showed that the mechanical properties of the SEI as determined by the Hertz model resulted in a significantly overestimated elastic modulus. The stress field in underlying Si significantly affected the results, especially for a thinner SEI thickness, and could cause the false appearance of a mechanically bilayered structure of the SEI with a hard, inorganic inner layer and a soft, outer polymeric layer. The elastic modulus of the SEI formed in the FEC electrolyte agreed with first-principles results and supported the recent solid-state NMR results demonstrating the existence of polymeric species in the interfacial region of the FEC-SEI and the silicon anode. In addition, the results corroborated recent transmission electron microscopy–electron energy loss spectroscopy and density functional theory results revealing that the FEC-SEI exhibits a nano-composite structure with inorganic particles distributed in crosslinked poly(FEC).

10:05 PM CT08.05.07

Screening Corrosion-Resistant Binary Magnesium Alloys Through High-Throughput Computations Yaowei Wang, Tian Xie and Hong Zhu; Shanghai Jiao Tong University, China

Magnesium (Mg) alloys have shown great potential as both structural and biomedical materials due to their high strength-to-weight ratio and good biocompatibility. However, poor corrosion resistance limits their further application, while alloying is believed to be one of the most effective strategies to develop corrosion-resistant Mg alloys. Traditional new magnesium alloy development is mainly based on the experiments, which is time-consuming and low-efficient. Recently, high-throughput computational method has become a useful tool to screen promising materials for various applications. In this work, we first collected 27919 (including repeated) Mg intermetallics structures from online databases, from which 332 stable candidates were selected. Then, the equilibrium potential based on Nernst equation were calculated and 50 Mg intermetallics with smallest equilibrium potential difference from that of Mg matrix and hence the lowest thermodynamic driving force of galvanic corrosion were reserved. Additionally, the adsorption energy of hydrogen adatom on the intermetallic surfaces were obtained for the further prediction of exchange current density based on the volcano curve. From the idea of small cathodic exchange current density and thermodynamic driving force of galvanic corrosion, several intermetallics were selected to be the promising phases for corrosion-resistant binary alloys. Our work not only predicts some new corrosion-resistant strengthening phases, but also provides a high-throughput

screening strategy for corrosion-resistant alloy design, which can also be extended to screen ternary intermetallics or other alloy systems.

10:20 PM CT08.05.08

Phase-Field Modelling of Chemo-Mechanical Coupling in High Temperature Oxidation and Aqueous Corrosion of Metals Chen Lin¹ and Haihui Ruan²; ¹Sun Yat-sen University, China; ²The Hong Kong Polytechnic University, Hong Kong

In this talk, a phase-field model (PFM) is introduced to study high temperature oxidation and aqueous corrosion of metals in a mechanico-chemical coupled field. The reaction rate is expressed as a function of the electrochemical potentials of reactants and products and conforms to the generalized Butler-Volmer relationship. The Gibbs free energy is expressed as a sum of chemical potential, interfacial energy, electrostatic potential energy, and mechanical strain energy of the system. And the variation of phase order parameter is governed by the Allen-Cahn type equation, which is derived from the equivalence of reaction rate and phase transformation rate. This governing equation captures the influences of reaction kinetics, elemental concentration, electric potential, and mechanical deformation. Coupled with the generalized Nernst-Planck equation, the Poisson equation, and the mechanical equilibrium equation, the complete set of phase-field equations are implemented. The proposed PFM is applied to study the corrosion mechanisms for the two typical scenarios: (i) the oxide scale roughening induced by high-temperature oxidation, and (ii) the localized corrosion in the wet environment. The numerical results of the first case unravel the roughening mechanism of oxide scale in an inward growth process, which is consistent with experimental results. In addition, it is shown that the initial metal surface morphology also significantly influences the resulted scale roughness, which renders a way to mitigate roughening-induced stress concentration and cracking in some applications. For localized corrosion, we study a complex corrosion process that involves mechano-electrochemical coupling, anodic dissolution, insoluble depositions (IDs) formation, and resulted Galvanic-pitting corrosion. Based on a quantitative investigation into the effects of Cl⁻ concentration, pH value, mechanical loading, and electric field, we reveal the autocatalytic process of pitting assisted by increasingly aggressive chemical environment and concentrated stress and study how the external electric field can arrest assisted corrosion and prolong service lifetime.

10:35 PM CT08.05.09

Completing the Picture of Oxidation on Copper Yun-Jae Lee¹, Ly T. Trinh², Taehun Lee^{1,3}, Krisztián Palotás⁴, Seyoung Jung⁵, Jungdae Kim² and Aloysius Soon¹; ¹Yonsei University, Korea (the Republic of); ²University of Ulsan, Korea (the Republic of); ³Princeton University, United States; ⁴Institute for Solid State Physics and Optics, Hungary; ⁵Pusan National University, Korea (the Republic of)

The oxidation of copper surfaces has been studied extensively in literature — from simple oxygen chemisorption structures to the formation of complex surface oxides and thin oxide films. Having an accurate atomistic model for this metal/oxide interface plays a pivotal role in determining interfacial processes in many copper-based technologies, ranging from electronic circuitry wirings to chemical catalysis in carbon dioxide reduction. The "29" and "44" complex surface oxides represent two of the most classical embryonic oxides on Cu(111). Although many attempts have been made to offer a detailed atomistic model of these surface oxides, their atomic structures remain elusive and ambiguous. In this work, we address this open question via state-of-the-art *ab initio* scanning tunneling microscopy (STM) and spectroscopy (STS) simulations that go beyond the simplistic Tersoff-Hamann's approach where the (functionalized) metal tips are explicitly included, and are corroborated by precise single crystal growth methods (with ultra-low surface roughness) and high-resolution STM/STS experiments. In particular, we reexamine the "29" structure and elucidate a complete atomistic model for the larger "44" surface oxide, thus completing the picture of early oxidation on copper.

Symposium Organizers

Derya Baran, King Abdullah University of Science and Technology
Xiaodan Gu, University of Southern Mississippi
Lynn Loo, Princeton University
Christine Luscombe, University of Washington

* Invited Paper

SESSION EL01.01: Organic Photovoltaics I
Session Chairs: Lynn Loo and Christine Luscombe
Sunday Morning, April 18, 2021
EL01

8:00 AM EL01.01.01

Late News: Organic Photovoltaic Cell—A Promising Indoor Light Harvester for Self-Sustainable Electronics Harrison Ka Hin Lee¹, Zhe Li¹, Jiaying Wu², Jeremy H. Barbe¹, Sagar Jain¹, Sebastian Wood³, Emily Speller¹, Fernando Castro³, James Durrant^{2,1} and Wing Chung Tsoi¹; ¹Swansea University, United Kingdom; ²Imperial College London, United Kingdom; ³National Physical Laboratory, United Kingdom

Organic photovoltaic devices have attracted significant interest for outdoor energy harvesting, as they have unusual properties including easy tunability of optical and electrical properties, and can be fabricated by low-cost, mass production methods. However, the potential for organic photovoltaic devices for indoor application (i.e. harvesting indoor light for self-sustainable electronics, e.g. power sensors) is much less explored. While there were a few initial studies on this topic, the power conversion efficiency of organic photovoltaic devices under indoor lighting (fluorescence lamp or white LEDs) is still low at that time. In 2016, our team revised the potential of organic photovoltaic devices for indoor applications by using the more state-of-the-art materials (at that time), which demonstrated good efficiency under indoor lighting. By exploring the design rules for indoor light harvesting, in 2018, we demonstrated a record high power conversion efficiency at that time (28% under 1000 lux fluorescent lamp: significantly better than silicon). These two crucial findings have then been leading to very active and significant amount of research on organic photovoltaic devices for indoor applications in the research community. In this talk, I will present the findings (and the design rules), and we believe that organic photovoltaic devices for indoor applications have much more promising potential to be commercialized (compared to outdoor applications), and can have significant impact on powering the "Internet of Things" for smart home, office, supermarket, buildings, etc.

8:15 AM EL01.01.02

Late News: Charge Separation in Blends of New C60 Fullerenes Derivatives and P3HT—In Search of Acceptors for Efficient Organic Photovoltaics Maciej Krajewski, Piotr Piotrowski, Wojciech Mech, Krzysztof P. Korona, Jacek Wojtkiewicz, Marek Pilch, Andrzej Kaim, Aneta Drabinska and Maria Kaminska; University of Warsaw, Poland

Organic solar cells (OSCs) have attracted a lot of attention in the last decade. The main advantage of OSCs is low-cost fabrication process and greater versatility than inorganic cells due to their flexibility and lightweight. The active layer of OSC comprises a blend of donor and acceptor material. The most frequently used donors are conductive polymers, such as P3HT and PTB7. The most widely used acceptor is C60 fullerene derivative:

phenyl-C61-butyric acid methyl ester, PC61BM.

To operate properly, the OSC structure must allow for the separation of photogenerated hole-electron pairs. The final efficiency (PCE) is strongly correlated with the effectivity of the charge separation process[1] occurring in the active layer, so the understanding of the charge transfer mechanism is necessary for further development of the OSCs. The main aim of this research was to determine the structural characteristics of fullerene derivatives important for improving the performance of OSCs.

In our study four newly synthesized fullerene C60 derivatives with different aromatic substituents and their blends with P3HT were selected to study the charge transport processes in the active layer. Two of them were functionalized with either one or two thiophene residues. Likewise the two others were functionalized with either one or two pyrene residues. To study these processes, light-induced Electron Spin Resonance (LESR) along with photoluminescence (PL) and time-resolved photoluminescence (TRPL) techniques were applied. During illumination PC61BM:P3HT blend exhibits exceptionally intense charge separation that is evident in the LESR spectrum as prominent two lines[2]. The intensities of these two lines provide information on the number of photoexcited and separated electrons and holes in the steady-state, which is one of the decisive factors influencing later the PCE of solar cells. The LESR signal of the all studied materials also showed two characteristic lines indicating charge transfer within the blend. Interestingly, blends with the molecules having only one aromatic substituent showed much stronger LESR signal, making them more predestinated for photovoltaic applications. Molecules with two aromatic substituents showed much more modest signal. PL and TRPL techniques were applied to trace the photo-carriers behavior inside the active layer. Radiative recombination and charge separation are two competing processes that lead to light emission and photocurrent generation, respectively. The observation of PL decay provides information on charge separation effectivity. Studies showed that the most effective PL decay is observed in blends of P3HT and fullerene derivatives with one aromatic substituent. On the other hand, blends of symmetric fullerene derivatives with P3HT did not exhibit significant PL attenuation. Therefore, it can be concluded that the separation of electrons and holes is ineffective in them.

The final step was to fabricate OSCs with an active layer made of blends of these new fullerene derivatives with P3HT, and their characterization. The results obtained with LESR and PL/TRPL techniques showed very high consistency with $J-V$ characteristics of OSCs. Best performing were the cells with fullerene derivatives, for which blends with P3HT exhibited two prominent LESR lines and fast PL decay. However, even the best PCE values obtained for cells with new fullerene derivatives were lower than PC61BM:P3HT reference cell (0.17% vs. 2.23%). This may be caused by lower solubility of these new materials and less optimized fabrication process. Still, the correlation of carrier separation efficiency, observed in the LESR and PL/TRPL measurements, with the PCE obtained from $J-V$ characteristics of the respective OSCs was clearly visible.

Acknowledgments: Research was co-funded by project TECHMATSTRATEG1/347431/14/NCBR/2018 (NCBiR).

[1] F. Laquai, *Macromol. Rapid Comm.*, 36, 1001–1025, 2015

[2] C. Deibe, *Adv. Mater.*, 22, 37, 4097–4111, 2010

8:30 AM EL01.01.03

Late News: Ultrafast Energy Transfer Triggers Ionization Energy Offset Dependence of Quantum Efficiency in Low-Bandgap NFA Solar Cells Julien F. Gorenflot¹, Safakath Karuthedath¹, Yuliar Firdaus¹, Catherine S. De Castro¹, George Harrison¹, Anastasia Markina², Neha Chaturvedi¹, Jafar Khan¹, Ahmed H. Balawi¹, Top A. Dela Peña¹, Wenlan Liu², Ru-Ze Liang¹, Anirudh Sharma¹, Sri Harish Kumar Paleti¹, Weimin Zhang¹, Yuanbao Lin¹, Erkki Alarousu¹, Dalaver Anjum¹, Pierre Beaujuge¹, Stefaan De Wolf¹, Iain McCulloch^{1,3}, Thomas Anthopoulos¹, Derya Baran¹, Denis Andrienko² and Frédéric Laquai¹; ¹King Abdullah University of Science and Technology, Saudi Arabia; ²Max Planck Institute for Polymer Research, Germany; ³University of Oxford, United Kingdom

In bulk heterojunction (BHJ) solar cells, the heterojunction interface between electron donor and acceptor drives the exciton-to-charge conversion, yet it also adds to energy and carrier losses. In principle, in low-bandgap non-fullerene acceptor (NFA) BHJs both electron affinity (EA) and ionization energy (IE) offsets should equally control the internal quantum efficiency (IQE). Allegedly, exciton-to-charge conversion is

efficient even for close-to-zero offsets. Here, we rebut both notions and demonstrate that counterintuitively, the charge transfer from the exciton rather than the further charge separation is the limiting step controlled by the IE offset and secondly, that sizeable IE offsets are required to reach high exciton-to charge conversion efficiency. We find that efficient Förster Resonant Energy Transfer to the low bandgap acceptor precedes the charge transfer, which thus always occurs via hole transfer from the acceptor, hence the unimportance of the EA offset. We discuss the reasons for the threshold IE offset in terms of interface energetics and find that two physical parameters are sufficient to describe the evolution of the IQE with IE offset on a very large range of material systems. Our model also explain other experimental observations such as barrierless charge separation and the difficulty of observing CT states emission and absorption in NFA based systems.

Intrinsic efficiency limits in low-bandgap non-fullerene acceptor organic solar cells. *Nat. Mater.* (2020). <https://doi.org/10.1038/s41563-020-00835-x>

8:45 AM EL01.01.04

Diluted Organic Semiconductor-Insulator Ternary Photovoltaics Chuanfei Wang¹, Xianjie Liu¹, Yiqun Xiao², Jonas Bergqvist³, Xinhui Lu², Feng Gao³ and Mats Fahlman¹; ¹Linköping University, Sweden; ²The Chinese University of Hong Kong, China; ³IFM, Linköping University, Sweden

The diluted organic semiconductor-insulator binary blend strategy recently has been used both in organic field electric transistors (OFETs) and polymer light emitting diodes (PLEDs) to improve (opt)electronic performance, processability, mechanical and environmental stability. The advantages shown in diluted OFETs and PLEDs potentially could be exploited in organic photovoltaics (OPVs) and thus the application of the diluted strategy in OPVs deserves attention. However, OPVs using the diluted semiconductor strategy have not yet been reported, possibly because introducing high concentration insulators ($\geq 10\%$) as filler in the bulk heterojunction binary donor-acceptor blend offers additional challenges as compared to the OFET and PLED applications. For example, exciton dissociation occurring at the bulk donor/acceptor interfaces will be suppressed if thick insulator regions form inside the donor/acceptor junctions. Similarly, transport and collection of free charge carriers following exciton dissociation can be hindered by either encapsulation of a donor/acceptor domain inside an insulator shell, or by insulator material segregation to either or both electrodes forming dense interface layers. Either inefficient exciton dissociation into free charges or decreased charge transport and collection is sufficient to significantly degrade the photovoltaic properties and thus prevent application of the diluted semiconductor strategy.

Here we successfully prepared solution-processed diluted OPVs by blending the state-of-the-art donor and acceptor polymers with commonly used insulators (Sol. RRL 2020, 4, 2000261). We show that “ideal” donor/acceptor bulk interfaces and interpenetrating donor/acceptor penetrating network can be maintained in the resulting ternary blends, yielding improved OPV performance such as: an order of magnitude improved hole mobility, reduced radiative and nonradiative recombination, as well as enhanced environmental and thermal stability. In addition, when the diluted organic solar cells are upscaled in area, the cell performance is 5 times less reduced compared to the pristine undiluted organic solar cells – a crucial advantage for commercial application. Finally, thicker ternary blend films can be deposited yielding the same degree of semi-transparency in the optical spectrum as the binary donor-acceptor blends, vastly improving printability of semi-transparent OPVs. Our findings imply that interpenetrating donor-acceptor network can be maintained in diluted ternary blend and the diluted strategy can be used to construct improved ternary devices involving internal penetrating donor-acceptor heterojunctions such as OPVs and organic photo detectors.

9:00 AM EL01.01.06

Counterintuitive Efficiency Trends in Dilute-Donor TAPC:C₆₀ Organic Solar Cell Blends Explained by Probing Ultrafast Charge Dynamics. Gareth J. Moore¹, Martina Causa¹, Josue Martinez Hardigree², Safakath Karuthedath³, Ivan Ramirez², Anna Jungbluth², Frédéric Laquai³, Moritz Riede² and Natalie Banerji¹; ¹University of Bern, Switzerland; ²University of Oxford, United Kingdom; ³King Abdullah University of Science and Technology, Saudi Arabia

Understanding the interplay between film morphology, photophysics, and its relation to device performance in bulk heterojunction organic photovoltaics remains challenging. Using the well-defined morphology of vapor-deposited TAPC:C₆₀ blends, from the surprisingly more efficient dilute-donor (5% TAPC) to the less efficient intermixed systems (50% TAPC), we see the morphological effects on charge generation and recombination on an ultra-fast time scale. With the use of ultrafast transient spectroscopy we are able to follow each step of the charge generation process and give an explanation for the counterintuitive efficiency trends in these organic solar cells.

First, we show that both Frenkel and Charge Transfer excitons generate photocurrent over the entire fullerene absorption range, giving advantage to the dilute-donor blend with more C₆₀.
Second, we show a novel technique for selectively monitoring interfacial and bulk C₆₀ clusters via their electro-absorption, demonstrating an energetic gradient that assists free charge generation.
Third, we identify a fast (<1 ns) recombination channel, where free electrons recombine with trapped holes on isolated TAPC molecules which should harm the performance of dilute solar cells. We, however, give evidence that this recombination is mitigated when electrons are rapidly extracted in efficient devices, reminding us that more than just the active layer needs to be considered when designing efficient organic solar cells. [1]

[1] J. Phys. Chem. Lett. 2020, 11, 14, 5610–5617

9:15 AM EL01.01.07

Improved Mechanical Properties of Polar Polythiophene Through Copolymerization or Blending with Urethanes Sepideh Zokaei¹, Renee Kroon¹, Mariavittoria Craighero¹, Johannes Gladisch², Claudia Cea³, Bryan Paulsen⁴, Lucas M. Kneissl¹, Wonil Sohn⁴, Dion Khodagholy³, Anna I. Hofmann¹, Anja Lund¹, Gustav Persson¹, Arne Stamm⁵, Per-Olof Syrén⁵, Eva M. Olsson¹, Jonathan Rivnay⁴, Eleni Stavrinidou² and Christian Muller¹; ¹Chalmers University of Technology, Sweden; ²Linköping University, Sweden; ³Columbia University, United States; ⁴Northwestern University, United States; ⁵KTH Royal Institute of Technology, Sweden

Polar polythiophenes with oligoethylene glycol side chains are an emerging class of materials that attract considerable attention for energy harvesting and storage as well as bioelectronics. The polar side chains enhance the compatibility with molecular dopants and improve the electrical conductivity and thermal stability of the doped material. However, polar polythiophenes are exceedingly soft at room temperature due to a sub-zero glass transition temperature. To enhance the versatility of these polymers, strategies are needed that permit to modulate their mechanical stiffness. In this contribution, we report our efforts to copolymerize a polar polythiophene with urethane blocks. Further, we describe wet spinning of its blend with polyurethane into fibers. The resulting materials feature elasticity and stretchability, yet higher stiffness. In addition, the copolymer and blend continue to display a high degree of electrochemical activity and electrical conductivity when chemically doped.

9:18 AM EL01.01.08

Smart Properties of PEDOT:PSS Carsten Dingler, Matthias Wieland, Henry Müller and Sabine Ludwigs; Institute of Polymer Chemistry, Germany

Polymer electronics has developed into an independent field of research as conducting polymers combine high, metal-like conductivity with the generally desired properties of commodity polymers. The additional responsiveness of conjugated polymers to various stimuli such as heat, electric voltage, or humidity has now also promoted efforts to fabricate sensors and actuators for wearable devices and electronic skin (e-skin). In this work, functional properties and the stimuli-responsiveness of smart materials such as particularly poly(3,4-ethylenedioxythiophene):poly(styrene sulfonate) (PEDOT:PSS) were studied. PEDOT:PSS has become one of the most promising candidate for applications in polymer electronics for, e.g., its remarkably high conductivity, the exceptional stability in air, and green processability from a dispersion in water.^[1] In addition, the electronic

conductivity of PEDOT combined with the polyelectrolytic PSS provide this polymer blend with a multi-responsivity.

The redox activity of PEDOT, for example, imparts electrochromism to PEDOT:PSS. This implies that the color can be switched through an electrochemical trigger,^[2] which is commonly used in electrochromic window or display applications. PEDOT:PSS exhibits not only a dark blue but also an almost colorless, transparent state when applied as a thin film. In one approach of this work, this could be exploited to make responsive photonic fibers.^[3] The hygroscopic nature of PSS also provides PEDOT:PSS with a dependence of various properties on the relative humidity (r.H.). This implies, for example, that electronic and ionic conductivity could be tuned and strongly depended on the water uptake of the films.^[4] Furthermore, swelling with water by absorbing humidity from the environment was used to fabricate humidity-triggered bilayer actuators.^[5] It could be demonstrated that for the tailor-made design of such actuators precise knowledge of the mechanical properties of the components as well as the corresponding dependence on r.H. is of utmost importance.^[5]

[1] A. Elschner, *PEDOT: Principles and Applications of an Intrinsically Conductive Polymer*, CRC Press, Boca Raton, FL, **2011**.

[2] M. Wieland, C. Malacrida, Q. Yu, C. Schlewitz, L. Scapinello, A. Penoni, S. Ludwigs, Conductance and spectroscopic mapping of EDOT polymer films upon electrochemical doping. *Flex. Print. Electron.* **2020**, *5*, 14016.

[3] C. Dingler, J. D. Sandt, M. Kolle, S. Ludwigs, Structurally Amplified Optical Contrast in a PEDOT:PSS-based Electrochromic Fiber Indicator, *in preparation*.

[4] M. Wieland, C. Dingler, R. Merkle, J. Maier, S. Ludwigs, Humidity-Controlled Water Uptake and Conductivities in Ion and Electron Mixed Conducting Polythiophene Films. *ACS Appl. Mater. Interfaces* **2020**, *12*, 6742–6751.

[5] C. Dingler, H. Müller, E. Ghobadi, M. Wieland, D. Fauser, H. Steeb, S. Ludwigs, Humidity Dependent Rheological Behavior and Curvature Prediction of PEDOT:PSS/PDMS Bilayer Actuators, *in preparation*.

9:21 AM EL01.01.09

The Effect of the Dielectric Environment on Electron Transfer Reactions at the Interfaces of Molecular Sensitized Semiconductors in Electrolytes Davide Moia^{1,2}, Masato Abe¹, Pawel Wagner³, Nagatoshi Koumura⁴, Jenny Nelson², Piers Barnes² and Shogo Mori¹; ¹Shinshu University, Japan; ²Imperial College London, United Kingdom; ³University of Wollongong, Australia; ⁴Interdisciplinary Research Center for Catalytic Chemistry, National Institute of Advanced Industrial Science and Technology, Japan

Electron transfer reactions at the interfaces of molecular sensitized semiconductors in electrolytes represent the basic steps in the working mechanism of several electrochemical and photo electrochemical systems for energy conversion and storage. For example, in dye sensitized solar cells, the design of interfaces that favor the desirable flow of photo-generated electronic charges towards the device contacts and that limit the rate of undesirable processes associated to energy loss is key to optimize device performance. [1] The identification of effective device design rules requires knowledge on the main factors influencing the kinetics of electron transfer. One such factor is the dielectric environment where charge transfer reactions occur. Electron transfer theories predict pronounced dependence of the rates of charge transfer between free molecules in solution on the polarity of the environment, where more polar solvents are expected to result in lower transfer rates. An appropriate description of this relation for electron transfer reactions involving molecules sensitizing semiconductors in electrolytes must account for the restricted geometry of these systems and is currently missing.

In this contribution, we present rates of electron transfer reactions involving photo-oxidized thiophene–carbazole-based molecules on oxide semiconductors in inert or redox-active electrolytes measured using transient absorption spectroscopy. [2] We explore the extent to which the dielectric properties of the surrounding medium can explain the rates of three different charge transfer processes occurring in these systems. We consider the hole hopping between molecules anchored to the semiconducting oxide surface, [3] the electron transfer from the oxide to the photo-oxidized molecule (electron-hole recombination) and the hole

transfer from the sensitizing molecules and a redox couple dissolved in the electrolyte solution (regeneration). Strikingly, we observe no clear correlation between the activation energy of hole hopping between molecules on oxide surfaces or the recombination rate between photogenerated electrons in the oxide and holes on the adsorbed molecules and the dielectric properties of the surrounding solvent. On the other hand, we show that fast electron transfer from cobalt complexes to photo-oxidized molecules is observed when using solvents with low polarity. Further to these findings, we show that the activation energy of hole hopping tends to increase with time following initial photogeneration of the holes, which emphasizes the role of energetic disorder in the molecular monolayer on charge transport. Moreover, we show that the recombination rate in different solvents scales with the hole hopping rate, consistent with our previous study. [4] Based on our findings, we highlight the importance of electronic coupling between the redox-active components and their solvation, besides the reorganization energy and the driving force, in the determination of electron transfer rates at molecular sensitized interfaces in electrolytes. Our study points to new strategies that allow to control electron transfer rates at interfaces of organic and hybrid photoelectrochemical systems and optoelectronic devices.

[1] A. Hagfeldt and M. Grätzel, *Chem. Rev.* **95**, 49 (1995).

[2] D. Moia, *et al. J. Phys. Chem. C* **124**, 6979 (2020).

[3] D. Moia *et al. Chem. Sci.* **5**, 281 (2014).

[4] D. Moia *et al. J. Am. Chem. Soc.* **138**, 13197 (2016).

9:24 AM EL01.01.10

Late News: Re-Assessment of Published Figures of Merit for Transparent Conducting Electrodes Aman Anand, Md Moidul Islam, Rico Meitzner, Ulrich S. Schubert and Harald Hoppe; Friedrich Schiller University Jena, Germany

Transparent conducting electrodes (TCEs) are one of the essential components of solar cells and other optoelectronic devices such as touch screens, electrochromic windows, flat panel displays, etc. Proper selection of specific TCEs is important to achieve efficient optoelectronic devices. A figure of merit (FOM) is an often-used quantity to rate the performance of TCEs. In this work, we have re-assessed the existing figures of merit and compare them with a new proposal from our side by applying them to specific material systems. It is demonstrated that the newly proposed FOM provides decisive information for the application specific development of material systems employed for TCEs.

9:27 AM EL01.01.11

The Role of ITIC and Its Derivatives on the Operational Stability of Organic Solar Cells Sri Harish Kumar Paleti¹, Sandra Hultmark², Leif Ericsson³, Ellen Moons³, Christian Muller² and Derya Baran¹; ¹King Abdullah University of Science and Technology, Saudi Arabia; ²Chalmers University of Technology, Sweden; ³Karlstadt University, Sweden

Despite advances in the power-conversion efficiencies of NFA-based organic solar cells, limited operational lifetime presents a stumbling block for their commercialization. Operational lifetime is assessed by the endurance of organic solar cell performance under constant thermal and light stress. Here, we study the operational stability of the organic solar cells based on the ITIC and its derivatives. We show that a fine-grained ternary blend including ITIC-4F and ITIC-4Cl mixture enhances the thermal stability. The halogenated ITIC derivatives readily co-crystallize and forms a fine-grained ternary blend with nanometer-sized domains. This results in a stable performance at 130 °C for at least 205 hours. We further show that the long-range order of the NFA crystals can only partly enhance the photo-stability of the organic solar cells. And, structural stability of the non-fullerene acceptor is also necessary to improve the photo-stability of the organic solar cells. These observations are confirmed using Nuclear Magnetic Resonance spectroscopy, High Resolution- Mass Spectroscopy, AFM-IR, and GIWAXS. Our results indicate that the ternary approach enables the use of high-temperature processing protocols and emphasizes the need for a more informed structural design of NFAs and unveils routes to minimize impurities, during synthesis, which affect the photostability of the NFA and thereby solar cells.

9:30 AM EL01.01.12

Influence of Side Chains on the N-Type Organic Electrochemical Transistor Performance David Ohayon¹, Achilleas Savva¹, Weiyuan Du¹, Bryan D. Paulsen², Jonathan Rivnay², Iain McCulloch¹ and Sahika Inal¹; ¹King Abdullah University of Science and Technology, Saudi Arabia; ²Northwestern University, United States

Organic bioelectronics has experienced tremendous growth over the past two decades thanks to the expansion of the library of organic electronic materials available. Electron conducting (n-type) polymers are particularly suitable to translate biological events that involve the generation of electrons. However, n-type polymers that are stable when addressed electrically in aqueous media are relatively scarce, and the performance of existing ones lags behind their hole conducting (p-type) counterparts. Here, we report a new family of donor-acceptor type polymers based on naphthalene-1,4,5,8-tetracarboxylic-diimide-bithiophene (NDI-T2) backbone where the NDI unit always bears an ethylene glycol (EG) side chain. We study how small variations in the side chains tethered to the acceptor as well as the donor unit affect the performance of the polymer films in the state-of-the-art bioelectronic device, the organic electrochemical transistor (OECT). First, we show that substitution of the T2 core with an electron withdrawing group (i.e., methoxy) or an EG side chain leads to ambipolar charge transport properties and causes significant changes in film microstructure revealed by ex situ X-ray scattering studies, which overall impairs the n-type OECT performance. We thus find that the best n-type OECT performer is the polymer that has no substitution on the T2 unit. Next, we evaluate the distance of the oxygen from the NDI unit as a design parameter by varying the length of the carbon spacer placed between the EG unit and the backbone. We find that the distance of the EG from the backbone affects the film order and crystallinity, and thus, the electron mobility. As such, we develop the best performing NDI-T2 based n-type OECT material to date. Our work provides new guidelines for the side chain architecture of n-type polymers for OECTs and insight on the structure-performance relationships for mixed ionic-electronic conductors, crucial for devices where the film operates at the aqueous electrolyte interface.

9:33 AM EL01.01.13

Late News: Optoelectronics of Disordered Solid-State Morphologies—Advances in Atomic-Scale Simulations Towards Design of High-Performance OLEDs Hadi Abroshan, Paul Winget, Casey N. Brock, Shaun Kwak and Mathew Halls; Schrödinger, Inc., United States

Organic-light emitting diodes (OLEDs) are becoming increasingly complex, consisting of multiple components with hybrid architectures. Hence, there is a growing demand for a computational approach to accurately describe sub-nanoscale phenomena, while being robust and scalable to unveil the origin of emergent layer and device-scale properties. To date, the majority of computational OLED designs rely on estimating materials properties in the gas phase. However, OLED materials are applied as thin solid films where intermolecular interactions have a significant impact on overall device performance. In this work, we present a multi-tiered computational workflow to efficiently study the optoelectronic properties of OLED materials in realistic disordered thin films. A range of robust and validated methods are combined to reveal impacts of the amorphous solid-state morphologies on the static and dynamic optoelectronic properties. The hierarchical approach of this work provides a thorough mechanistic understanding of materials performance for systematic design and development of future smart OLEDs as well as emerging electronic devices.

9:36 AM Q&A FOR ALL POSTERS

SESSION EL01.02: Organic Photovoltaics II
Session Chairs: Derya Baran and Xiaodan Gu
Sunday Morning, April 18, 2021
EL01

10:30 AM *EL01.02.01

Causal Structure-Property Relationships in Organic Photovoltaics by Integrating Resonant X-Rays and Device Dynamics Brian A. Collins; Washington State University, United States

With efficiencies >20% on the horizon, non-toxic and massively scalable organic solar cells are approaching economic viability. In order for the technology to approach limiting performance, it is necessary to establish a more definitive and detailed model on how molecular ordering drives device dynamics. Although many structure-property correlations can be found in the literature, it is critical to establish causal relationships to move the field forward. I will describe our advanced nanostructure characterization simultaneous to comprehensive device dynamics that are directly connected to performance. This allows us to analyze correlated trends in structure and dynamics to determine cause and effect more definitively. Our novel combination of synchrotron X-ray techniques allows us to derive a complete set of morphological parameters that includes details of donor-acceptor interfaces. We also have developed a photophysical measurement strategy using time-delayed collection field to quantify each fundamental stage in the charge generation process. By probing morphology on the devices themselves, our studies reveal unprecedented clarity on the effect of molecular mixing, crystallinity, and device interfaces on charge generation and extraction at operating conditions. The outcome is an increasingly resolved model of ideal device morphology. Such a model will enable new device processing strategies and help advise molecular design in pursuit of performance limits and commercialization of this exciting technology.

10:55 AM EL01.02.02

Late News: Development of Polymers for Scalable Organic Photovoltaics Alyssa Chinen-Mendez, Hualong Pan and Reed Eisenhart; Phillips 66, United States

ShieldPower™ polymers were developed at Phillips 66 for use in the photoactive layer of scalable organic photovoltaics. This talk will highlight their development from lab to pilot scale evaluation, focusing on the key parameters that enable ShieldPower™ polymers to reach high power conversion efficiencies using scalable coating techniques. The polymers combine high conductivity, as determined by time-resolved microwave conductivity experiments, and good solubility to enable photoactive layers with films >200 nm in thickness to be coated from non-halogenated solvents via slot-die coating in ambient air in a pilot fabrication line resulting modules that reach 5.3% power conversion efficiency. Further tuning the polymers' absorption properties and structures allows for blends with a stable non-fullerene electron acceptor to achieve power conversion efficiencies that remain constant over 250+ hours of illumination.

11:10 AM EL01.02.03

Late News: Understanding the Role of the Solubility of Axially Substituted SiPcs on Their Performance as Ternary Additives in Organic Photovoltaics Mário C. Vebber, Jaclyn Brusso and Benoit Lessard; University of Ottawa, Canada

Organic photovoltaics (OPVs) had their performance greatly improved in the past decade, thanks to careful molecular design and process optimization, even approaching the efficiency of single-junction inorganic devices. However, such state-of-the-art OPVs rely heavily on complex polymers and compounds, whose synthesis is not scalable and unlikely to make it to market. Thus, the enhancement of low-cost OPV active layers, such as P3HT:PC₆₁BM, is a relevant and often overlooked topic OPV research. A common way to improve P3HT:PC₆₁BM blends is to increase its relatively narrow light absorption range by adding a ternary additive that is sensitive to complementary wavelengths. Silicon phthalocyanines (SiPc) have been shown to be efficient ternary additives due to their strong light absorptivity, high electron mobility, chemical versatility and scalability of manufacture. The addition of a small amount of soluble, axially substituted SiPc (OR-SiPc) have been reported to increase the current of P3HT:PC₆₁BM devices by 25% and the overall efficiency by as much as 50%. One of the main challenges faced when engineering new or improving existent active layers is the lack of

robust design rules and property-performance relationships, leaving researchers and engineers to rely on time-consuming try-and-error approaches. In this context, we have synthesized 8 different OR-SiPc and evaluated how their properties impact their efficiency as additives in OPVs. The novel OR-SiPcs were synthesized by reacting different alkyl chlorosilanes of different lengths with Cl-SiPc. Characterization of the compounds has shown that all 8 OR-SiPcs possess similar surface energies and virtually identical optical and electronic properties, such as band gap (E_{bg}), ionization energy (IE), and energy levels. Alternatively, due to the different alkyl chain lengths in the axial positions, their solubility can change greatly. We were able to demonstrate that when OR-SiPc is added to P3HT:PC₆₁BM, device efficiency follows a nearly parabolic trend with respect to the additive solubility. The best performance was achieved by the additive whose solubility value was the closest to that of the donor polymer, P3HT. Based on these results and previously reported properties of the system, we have surmised that matching the solubility of the OR-SiPc and P3HT is beneficial because it favours the migration of the additive to the donor:acceptor interface, where its efficiency is maximized. OR-SiPc with solubilities below 20 mg ml⁻¹, for instance, tended to precipitate out of solution and form a separate crystalline phase, rather than migrating to the interface, making it less efficient at mediating the charge transfer between P3HT and PC₆₁BM. More research is needed to verify if a similar effect is observed in different systems and additives, nonetheless, this is an important step towards more robust design-rules for OPVs.

11:25 AM EL01.02.04

Color-Neutral, Semitransparent Organic Photovoltaics for Power Window Applications Yongxi Li¹, Hafiz K. Sheriff², Xia Guo³, Zhengxing Peng⁴, Harald Ade⁴, Maojie Zhang³ and Stephen Forrest¹; ¹University of Michigan, United States; ²University of Michigan–Ann Arbor, United States; ³Soochow University, China; ⁴North Carolina State University, United States

Semitransparent organic photovoltaic cells (ST-OPVs) are emerging as a solution for solar energy harvesting on building facades, rooftops and windows. However, the trade-off between power conversion efficiency (*PCE*) and the average photopic transmission (*APT*) in color-neutral devices limits their utility as attractive, power-generating windows. We demonstrate a semi-transparent OPV that achieves a high power conversion efficiency of 10.8% and visible transparency of ~50% using a simple non-fullerene acceptor (NFA) with strong near-infrared (NIR) absorption and simplified synthetic step. Contrary to expectations, stronger NIR absorption and closer molecular packing are obtained by employing an additive in these partially, instead of fully fused rigid NFAs. By combining NIR-absorbing material sets with an optical outcoupling structure that reduces trapping of visible radiation within the cell, that increases the NIR reflectivity, we overcome the trade-offs between efficiency, transparency, and device appearance. These results significantly surpass other semi-transparent solar cell technologies based on organic and other thin film materials systems, showing a promising future for ST-OPVs as power generating windows and other solar energy harvesting applications^[1].

[1] Yongxi Li, Xia Guo, Zhengxing Peng, Boning Qu, Hongping Yan, Harade Ade, Maojie Zhang* and Stephen R. Forrest*; Color-Neutral, Semitransparent Organic Photovoltaics. *PNAS*, 2020, 117, 21147-21154.

11:40 AM EL01.02.05

Late News: Linking Solution Phthalocyanine-Cannabinoid Interactions to Analyte Induced Changes for Organic Thin-Film Transistor Sensing Zachary Comeau, Benoit Lessard and Adam Shuhendler; University of Ottawa, Canada

Phthalocyanine (Pc) based organic thin-film transistors (OTFTs) have been demonstrated as a powerful platform for rapid low-cost sensors of atmospheric parameters, volatile gasses, and small organic molecules including cannabinoids. However, traditional characterization and testing of new materials or analytes requires highly specialized equipment and expertise. Alternatively, solution-based screening can limit manufacturing burden, allowing for a broad range of assays, and is employed here with the goal of expediting sensor development. Spectroelectrochemistry is used to probe molecular interactions between cannabinoids (Δ^9 -tetrahydrocannabinol (THC) or cannabidiol (CBD)) with and without a cannabinoid sensitive chromophore (Fast Blue BB) against a variety of phthalocyanines (Pcs). Spectroelectrochemical changes to the Q-band region

of the Pc spectra in the presence of analytes can be related to modified ratios of Pc-Pc orientations in solution. 2D-NMR is used to further elucidate unique Pc-Pc and Pc-analyte interactions, providing additional insight on atomic level interactions. Through altered Pc-Pc orientations, analytes can induce physical alterations to Pc thin-film morphology and structure, consequently, modifying electrical performance beyond charge trapping effects. Additionally, the effects of Pc peripheral and axial substitutions on analyte interactions and their relationship with film structure and performance is examined. Substitutions allow for an additional level of Pc tunability and are demonstrated to specifically further enhance OTFT sensing responses by up to 96%. Thus, with spectroelectrochemical solution-based screening, a range of potential materials for OTFT small organic molecules sensing applications can be rapidly assayed and OTFT responses can be predicted.

11:55 AM DISCUSSION TIME

12:10 PM EL01.02.07

Time-Resolved Optical Spectroscopy of Organic Mixed Conductors Priscila Cavassin, Olivier Bardagot, Julien Réhault and Natalie Banerji; University of Bern, Switzerland

Polymers that exhibit both electronic and ionic conductivity have garnered attention for their numerous applications in bioelectronics, neuromorphic systems and batteries. [1] In the field of bioelectronics, the organic electrochemical transistor (OECT) takes advantage of this property to interface with biological systems and convert ionic and electronic signals. [2] Despite recent advances in its fabrication and materials choice, there is a lack of understanding on central roles that are important for the optimal operation of the OECT, like the ionic transport and the morphological impact in its performance. [1] To this end, we have characterised the electrochemical doping and dedoping of poly(3-hexylthiophene) (P3HT) thin films using in-situ time-resolved Vis-NIR spectroscopy. We are able to follow the evolution of the doping with great time resolution, and by decomposing the spectra we can identify the different species involved in the process. Furthermore, we developed a kinetic model to describe the interconversion between the species. Additionally, by changing the degree of crystallinity of the P3HT films, we are able to identify can morphology affect ionic transport in the film.

[1] Chung, J.; Khot, A.; Savoie, B. M.; Boudouris, B. W., ACS Macro Lett. 2020, 9, 646–655.

[2] Rivnay, J.; Inal, S.; Salleo, A.; Owens, R. M.; Berggren, M.; Malliaras, G. G., Nat. Rev. Mater. 2018, 3, 17086.

12:13 PM EL01.02.08

Charge Transport on the Picosecond Time Scale in Non-Fullerene Acceptors Kaila M. Yallum and Natalie Banerji; Universität Bern, Switzerland

As the field of Organic Photovoltaics (OPVs) evolves, the need for fundamental understanding of the utilized materials grows along with it. Historically, OPVs feature fullerene-based electron acceptors, yielding efficiencies around 10-12%. Recently, efficiencies of over 17% have been achieved thanks to the use of non-fullerene acceptors (NFAs).

In order for the overall performance of OPVs to show such improvement, the processes involved in photocurrent generation must be optimized as well. Charge transport is one of the critical processes that requires further investigation in these systems. While single-carrier devices are commonly used in order to deduce the mobility of charge carriers in the steady state, Electromodulated Differential Absorption (EDA) spectroscopy is the principal technique employed in this project. This powerful technique can be used to qualify charge mobility on the picosecond time scale following photo-excitation, by recording the changes in electroabsorption (EA) over time with 100 femtosecond resolution. Carrying out these measurements in differing electric fields, drift and diffusion mechanisms of charge transport can be distinguished.

The highest performing OPVs of recent years, those achieving 17% photoconversion efficiencies, have featured

BTP-4F as the acceptor material. For this reason, the ITIC and BTP NFA families have been chosen for this project in order to qualify how charge transport changes with different molecular packing and core structures. In addition to investigating the sterics of these systems, the electronics will also be investigated by using a series of substitutions of the IC end group featured in both NFA families. Because the focus of this project is on the NFA domains of the OPV devices, the samples used for this project were neat NFA devices.

When studying these two NFA families under EDA conditions, it becomes quite clear that charge transport is largely influenced by the cores of these molecules. Further investigation is underway to understand how the morphology of the NFA regions will affect charge transport.

12:16 PM EL01.02.09

Late News: Molecular Design Optimization of Fused Electron-Deficient Semiconducting Polymers for N-Type Organic Thermoelectrics and Electrochemical Transistors [Maryam Alsufyani](#)¹, Rawad K. Hallani², Xingxing Chen², Suhao Wang³, Marc-Antoine Stoeckel³, Reem Rashid⁴, Xudong Ji⁴, Kai Xu³, Bryan Paulsen⁴, Helen Bristow¹, Hu Chen², Mingfei Xiao⁵, Henning Sirringhaus⁵, Jonathan Rivnay⁴, Simone Fabiano³ and Iain McCulloch^{1,2}; ¹University of Oxford, United Kingdom; ²King Abdullah University of Science and Technology, Saudi Arabia; ³Linköping University, Sweden; ⁴Northwestern University, United States; ⁵University of Cambridge, United Kingdom

N-type semiconducting polymers have been recently utilized in thermoelectric devices, however they have typically exhibited low electrical conductivities, in contrast to p-type semiconductors. This is due in particular to the n-type semiconductor's low doping efficiency, and poor charge carrier mobility. Strategies to enhance the thermoelectric performance of n-type materials include optimizing the electron affinity (EA) with respect to the dopant to improve the doping process, increasing the charge carrier mobility through enhanced molecular packing and introducing polar side chains to improve the miscibility with dopant. Here, we report the design, synthesis and characterization of three fused electron-deficient copolymers P1-P3, incorporating electron withdrawing lactone unit along the backbone. The polymers were synthesized using metal-free aldol condensation conditions to explore the effect of acene size and side chains, on the electrical conductivity. Acene size optimization of P1 and P2 has been investigated, their performance provided a great insight into designing P3, which incorporated polar side chains. The polymers have exhibited the largest electron affinity of -4.68 eV and when n-doped with N-DMBI, electrical conductivities of up to 1 S cm^{-1} , Seebeck coefficients of -220 mV K^{-1} and maximum Power factors of $5 \text{ mW m}^{-1} \text{ K}^{-2}$ were observed. Moreover, the polar nature of P3 has intrigued us to explore its performance in aqueous electrolytes of Organic electrochemical transistors (OECTs). OECT results indicated high transconductance of 0.35 S cm^{-1} and $[\mu\text{C}^*]$ of $0.92 \text{ F cm}^{-1} \text{ V}^{-1} \text{ s}^{-1}$, exceeding the state of the art materials. These results suggest a promising high-performance building block for both n-type organic thermoelectrics and OECTs, and also highlight that high electrical conductivities can be realized in conjugated polymers with careful molecular engineering.

12:19 PM Q&A FOR ALL POSTERS

SESSION EL01.03: Virtual Social Time
Session Chairs: Xiaodan Gu and Christine Luscombe
Sunday Afternoon, April 18, 2021
EL01

1:00 PM WE WILL BE HOSTING A VIRTUAL SOCIAL TO PROVIDE AN OPPORTUNITY FOR SYMPOSIUM PARTICIPANTS TO NETWORK. PLEASE BRING YOUR FAVORITE BEVERAGE ALONG WITH YOUR KIDS, PETS, OR ANYTHING ELSE THAT YOU'D LIKE TO SHARE WITH OUR COMMUNITY!

SESSION EL01.04: Organic Photovoltaics III
Session Chairs: Xiaodan Gu and Tianran Liu
Sunday Afternoon, April 18, 2021
EL01

6:55 PM EL01.04.02

Late News: Correlating Morphology with Mechanical Properties in High-Efficiency Ternary Organic Solar Cells Zhongxiang Peng¹, Yanhou Geng^{1,2} and Long Ye^{1,3}; ¹Tianjin University, China; ²International Campus of Tianjin University, China; ³North Carolina State University, United States

Organic photovoltaics (OPVs) based on nonfullerene small molecule acceptors have been the subject of renewable energy research in the past five years. Ternary photovoltaic blends comprising a polymer donor, a nonfullerene small molecule acceptor, and a fullerene acceptor have proved to be most efficient active layers for OPV devices. However, the morphological parameters and their relations with mechanical properties and photovoltaic performance of this type of highly efficient polymer:nonfullerene:fullerene OPVs are still unknown to date.

To address this question, we characterized the thin-film microstructure and mechanical behavior of the best-performing ternary OPV active layer (PM6:N3:PC₇₁BM). Specifically, we alter the relative weight ratio of acceptors and systematically examined the composition dependence of photovoltaic performance, surface/bulk morphology, and mechanical parameters of the ternary blend films. It is shown that the addition of 20 wt% PC₇₁BM to the acceptor component results in the highest power conversion efficiency (PCE) and crack-onset strain (COS) (Figure 1a). Most notably, we discover that it is possible to predict the elastic modulus of the ternary blend films by an extended Halpin-Tsai model (Figure 1b). This work provides simple guidelines for predicting the mechanical properties of many electronic devices based on ternary blends.

7:10 PM EL01.04.03

Late News: Thermodynamic Properties and Molecular Stacking Explain Performance of Four P3HT:Nonfullerene Organic Solar Cells Mengyuan Gao¹, Yanhou Geng^{1,2} and Long Ye^{1,3}; ¹Tianjin University, China; ²International Campus of Tianjin University, China; ³Department of Physics, Organic and Carbon Electronics Laboratories (ORaCEL), United States

The film morphology of polymer solar cells (PSCs) plays a significant role in the photovoltaic process that cannot be ignored, which associates with light-harvesting, exciton dissociation, and charge transport. In addition, the morphological stability of the PSCs is largely dependent on the amorphous-amorphous molecular interactions of the components, which can be described by the Flory-Huggins interaction parameter χ_{aa} . However, in the semi-crystalline blend systems, more complex thermodynamic interactions as reflected by crystal-amorphous interaction parameter (χ_{ca}), amorphous-crystal interaction parameter (χ_{ac}), and crystal-crystal interaction parameter (χ_{cc}), which are complementary to χ_{aa} . Here, we apply the Thermodynamic self-consistency theory coupled with Flory-Huggins theory to determine the various interaction parameters and establish the relationships between interaction parameter, morphology, and device performance of binary P3HT:nonfullerene blends, based on four nonfullerene small molecule acceptors (ITIC, Y6, O-IDTBR, ZY-4Cl). Moreover, the parameters related to molecular stacking are probed by grazing incidence X-ray diffraction and correlated partially with device performance. Chiefly, this study highlights the importance of both thermodynamic properties and molecular stacking to provide guidance for understanding morphology and device performance.

7:25 PM EL01.04.04

Endothermic Charge Separation in Efficient Non-Fullerene Organic Solar Cells Philip Chow; The

Organic solar cells based on non-fullerene acceptors can show high charge generation yields despite near-zero donor-acceptor energy offsets to drive charge separation and overcome the mutual Coulomb attraction between electron and hole, but the underlying mechanism remains unclear. In this talk I will present experimental results showing that free charges in these systems are generated by thermally activated dissociation of interfacial charge-transfer states. This process occurs over hundreds of picoseconds at room temperature, three orders of magnitude slower than comparable fullerene-based systems. Upon free electron-hole encounters at later times, both charge-transfer states and local emissive excitons are regenerated, thus setting up an equilibrium between local excitons, charge-transfer states and free charges. Our results suggest that the formation of long-lived and disorder-free charge-transfer states in these systems enables them to operate closely to quasi-thermodynamic conditions with no requirement for energy offsets to drive interfacial charge separation and achieve suppressed non-radiative recombination.

7:40 PM EL01.04.06

Quantitative Evaluation of Thermoelectric Characteristics of Small-Molecule Organic Semiconductors Based on Electronic Structure Calculations Masahiro Ohno, Koji Shimizu and Satoshi Watanabe; The University of Tokyo, Japan

Organic thermoelectric materials have attracted much attention as promising candidates for low-cost, near-room-temperature and flexible power generators which are desirable power supplies for flexible electronics. However, molecular design strategies to realize efficient thermoelectric conversion are not well established because little is known regarding microscopic origin of their thermopower. Many of recent studies employ conventional polymer semiconductors such as poly(3,4-ethylenedioxythiophene) (PEDOT) and poly(3-hexylthiophene-2,5-diyl) (P3HT) and focus on optimizing doping conditions and/or developing novel nanostructures. Aiming to break this situation, we propose a calculation method for quantitative evaluation of thermoelectric properties of organic semiconductors (OSCs) which facilitates preliminary screening of candidate materials and the exploration of novel organic thermoelectrics. We focus on small-molecule semiconductors in this study since their highly crystalline nature is advantageous for efficient thermoelectric conversion[1].

One of the present author (Ohno) and his collaborators have shown that the Seebeck coefficient (which is the most important indicator of the conversion efficiency and is defined as induced thermoelectric voltage per unit temperature difference) of crystalline OSCs can be calculated from the effective density of states (DOS) measured experimentally using the Mott formula[1]. Then the crucial point of our calculation method is the evaluation of the effective DOS of bulk small-molecule OSCs with taking account of the thermally induced structural fluctuation (which is non-negligible even at room temperature) originating from the fact that small-molecule OSCs usually form molecular solids bound by weak van der Waals force. To take account of this fluctuation, we propose to conduct classical molecular dynamics (MD) simulations followed by electronic structure calculation based on density functional theory (DFT).

To demonstrate the validity of the proposed method, we calculated the effective DOS and Seebeck coefficients of pentacene and rubrene whose thermoelectric properties are experimentally tested enough. In our MD simulations, we adopted the general AMBER force field, which describes intra- and inter-molecular interactions including van der Waals force and has been confirmed to be applicable to bulk OSC crystals. MD calculations were performed to simulate equilibrium states at the pressure of 1 atm at 300K, and 100 crystal structures were sampled every 5 ps (5000 steps) from the trajectories. For each sampled structure, DFT calculations were conducted using projector augmented wave method and Perdew-Wang 1991 (PW91) functional.

Although each of the DOS had sharp peaks owing to disorder-induced carrier localization, the effective DOS of bulk crystal were well approximated as an average of adequate number of DOS. Its exponentially decaying shape near the band edge was in good agreement with experimental results. The value of Seebeck coefficients estimated from the decay rates of the effective DOS were 0.26 mV/K for pentacene and 0.17 mV/K for rubrene. These values agree quantitatively with experimental results[2], so we expect that the proposed method is applicable to materials exploration. In the presentation, relationships between structures and thermoelectric

properties will also be discussed in depth.

[1] S. Watanabe and M. Ohno et al., *Phys. Rev. B* 100, 241201(R) (2019). [2] K. P. Pernstich et al., *Nat. Mater.* 7, 321 (2008).

7:55 PM EL01.04.07

Late News: Synthesis and Characterisation of Phosphonated PEDOT for Energy-Efficient, Bioelectronic Devices Jonathan A. Hopkins¹, Kristina Fidanovski¹, Lorenzo Travaglini¹, Pawel Wagner², Klaudia K. Wagner², Antonio Lauto³, David L. Officer² and Damia Mawad¹; ¹UNSW Sydney, Australia; ²University of Wollongong, Australia; ³Western Sydney University, Australia

Organic electrochemical transistors (OECTs) developed for integration in bioelectronic devices utilise a conjugated polymer (CP) as the active material in the channel. The utility of OECTs has been demonstrated in various bioapplications including monitoring and stimulating biological cells.^{1,2} In these applications, we want OECTs to be energy-efficient, requiring low threshold voltages to activate, and operating in accumulation mode such that they only use energy when switched “on”. Unfortunately, many existing CPs for aqueous OECTs lead to depletion mode operation, which requires a constant potential to keep the device “off” and so is more energy intensive. These materials also require crosslinking or post-treatment to prevent their dissolution in water,³ and their biocompatibility with certain cell lines may be limited by their high acidity.⁴

To overcome these limitations, we have synthesised a new CP, poly(ethylenedioxythiophene) bearing isopropyl-protected phosphonate groups (PEDOT-Phos), and performed its characterisation to elucidate its structure-property relationships. PEDOT-Phos is solution-processible from organic solvents, producing films which are readily proton doped with non-oxidising acids and undergo reversible electrochemistry in aqueous electrolytes. PEDOT-Phos can also be used in energy-efficient, aqueous OECTs with accumulation mode operation and low threshold voltages. These devices have the added advantages of high volumetric capacitances, good transconductances, and no requirement for additives or post-treatments. With these encouraging properties, PEDOT-Phos has great potential for emerging bioelectronic devices which combine good performance with improved energy efficiency.

References:

- (1) Hopkins, J.; Travaglini, L.; Lauto, A.; Cramer, T.; Fraboni, B.; Seidel, J.; Mawad, D. Photoactive Organic Substrates for Cell Stimulation: Progress and Perspectives. *Adv. Mater. Technol.* **2019**, 1800744, 1800744. <https://doi.org/10.1002/admt.201800744>.
- (2) Fidanovski, K.; Mawad, D. Conjugated Polymers in Bioelectronics: Addressing the Interface Challenge. *Adv. Healthc. Mater.* **2019**, 8 (10), 1–9. <https://doi.org/10.1002/adhm.201900053>.
- (3) Stavrinidou, E.; Leleux, P.; Rajaona, H.; Khodagholy, D.; Rivnay, J.; Lindau, M.; Saur, S.; Malliaras, G. G. Direct Measurement of Ion Mobility in a Conducting Polymer. *Adv. Mater.* **2013**, 25 (32), 4488–4493. <https://doi.org/10.1002/adma.201301240>.
- (4) Mantione, D.; del Agua, I.; Sanchez-Sanchez, A.; Mecerreyes, D. Poly(3,4-Ethylenedioxythiophene) (PEDOT) Derivatives: Innovative Conductive Polymers for Bioelectronics. *Polymers (Basel)*. **2017**, 9 (12), 354. <https://doi.org/10.3390/polym9080354>.

SESSION EL01.05: Organic Semiconductor Characterization I
Session Chairs: Fei Huang and Xiaoming Zhao
Sunday Afternoon, April 18, 2021
EL01

9:00 PM EL01.05.01

Late News: Resonant Tender X-Ray Diffraction for Disclosing the Molecular Packing of Paracrystalline Conjugated Polymer Films Chris McNeill¹, Guillaume Freychet², Eliot Gann³, Lars Thomsen⁴ and Xuechen Jiao¹; ¹Monash University, Australia; ²Brookhaven National Laboratory, United States; ³National Institute of Standards and Technology, United States; ⁴ANSTO, Australia

The performance of optoelectronic devices based on conjugated polymers is critically dependent upon molecular packing; however, the paracrystalline nature of these materials limits the amount of information that can be extracted from conventional X-ray diffraction. Resonant diffraction (also known as anomalous diffraction) occurs when the X-ray energy used coincides with an X-ray absorption edge in one of the constituent elements in the sample. The rapid changes in diffraction intensity that occur as the X-ray energy is varied across an absorption edge provide additional information that is lost in a conventional nonresonant experiment. Taking advantage of the fact that many conjugated polymers contain sulfur as heteroatoms, this work reveals pronounced resonant diffraction effects at the sulfur K-edge with a particular focus on the well-studied electron transporting polymer poly([N,N'-bis(2-octyldodecyl)-naphthalene-1,4,5,8-bis(dicarboximide)-2,6-diyl]-*alt*-5,5'-(2,2'-bithiophene)), P(NDI2OD-T2). The observed behavior is found to be consistent with the theory of resonant diffraction, and by simulating the energy-dependent peak intensity based on proposed crystal structures for P(NDI2OD-T2), we find that resonant diffraction can discriminate between different crystalline packing structures. The utilization of resonant diffraction opens up a new way to unlock important microstructural information about conjugated polymers for which only a handful of diffraction peaks are typically available.

9:15 PM DISCUSSION TIME

9:30 PM EL01.05.03

Thickness-Driven Polymorphism of Dinaphthothienothiophene (DNNT) Revealed by High-Resolution X-Ray Diffraction Nobutaka Shioya, Takafumi Shimoaka and Takeshi Hasegawa; Kyoto University, Japan

Among many promising organic semiconducting materials, dinaphthothienothiophene (DNNT) shows outstanding device performances in terms of charge transport and air stability, which exceeds those of the conventional prototypical material of pentacene. Although many reports demonstrate the excellent device performances of DNNT, a comprehensive understanding of thin film growth is lacking. In fact, the thin-film structure has long been believed to be identical to the single-crystal structure. In other words, polymorphs of DNNT have never been observed so far.

In the present study, the thickness-dependent structural evolution is revealed by means of high-resolution X-ray diffraction. This technique apparently reveals the existence of the “thin-film” phase [1], which has long been missed by the conventional analytical limit. This is also supported by infrared spectroscopy. The present study strongly suggests that a thickness-dependent structural change is a common phenomenon for rod-like organic molecules including DNNT. This study is believed to provide an in-depth understanding of thin film growth of common organic semiconductors.

[1] Shioya, N. et al., Appl. Phys. Express 2020, 13, 095505.

9:45 PM EL01.05.04

Late News: Collective Effects on Molecular Orientation in Growth of Organic Thin Films Sae Nagai, Yuta Inaba, Toshio Nishi, Hajime Kobayashi and Shigetaka Tomiya; Sony Corporation, Japan

Control of the molecular orientation in organic semiconductor (OSC) films is essential to improve the performance of organic electronic devices. However, specific parameters for controlling molecular orientation have not yet been fully understood. In this study, we focus on the impact of growth temperature on molecular orientation in OSC films. We used pentacene on SiO₂ as a model system and applied p-polarized multiple-angle incidence resolution spectrometry (pMAIRS) for investigating the variation of molecular orientation. The molecular orientation of films varied with growth temperature from lying (molecules orient parallel to the

substrate) to standing (molecules orient perpendicular to the substrate) orientation. This change suggests that the formation of a standing orientation is thermally activated compared with the lying state. The nucleation of standing-oriented islands occurs by molecular self-assembly at sufficiently high temperatures. Conversely, molecules deposit in a lying state at low temperatures owing to hinderance of the kinetic barrier to reorientation from lying to standing states. We defined a collective orientation barrier (COB) as an energy barrier for the reorientation processes throughout the growth. We estimated the COB from an Arrhenius plot of the probability to form a standing orientation, derived from the dichroic ratio measured by pMAIRS. We found that the COB in the growth of pentacene on the SiO₂ system was approximately 0.02 eV. The COB is a key parameter for determining the molecular orientation and can be utilized for the control of molecular orientation of OSC films to improve the performance of organic electronic devices.

SESSION EL01.06: New Organic Semiconductor Devices and Thermoelectrics I

Session Chairs: Enrique Gomez and Xiaodan Gu

Monday Morning, April 19, 2021

EL01

8:00 AM *EL01.06.01

How to Control the Thermoelectric Properties of Organometallic Coordination Polymers? Bob C. Schroeder; University College London, United Kingdom

Developing highly conducting and air-stable n-type semiconductors have proven to be extremely challenging, despite intensive research efforts and a need for better-performing materials. Not only would highly conducting interlayers facilitate charge extraction, respectively injection, when used in organic solar cells or light-emitting diodes, but also accelerate the development of emerging plastic electronic technologies like organic thermoelectrics. Thermoelectric generators convert heat into usable electricity, due to the Seebeck effect. Constructing an efficient thermoelectric generator based on organic semiconductors, however, has proven difficult, primarily due to a significant shortage of suitable materials. While organic p-type semiconductors are abundant and relatively easy to dope, there is a shortage of suitable n-type materials and appropriate dopants. One approach that has proven popular in recent years is extrinsic doping of conjugated polymers. By mixing molecular dopants into a polymer matrix, it is possible to enhance the overall conductivity of the semiconductor to a certain degree, before morphological instabilities take over and cause microscopic phase separation of the dopant and polymer matrix, significantly limiting the doping efficiency.

In this paper, we will present a new approach to intrinsic organic conductors, namely organometallic coordination polymers. We will discuss how the choice of ligand and coordinating metal cation affect the electrical properties of the material and demonstrate how both the ligand and metal cation can be exploited to control the electrical characteristics. We will discuss how material purification affects the overall performance and elucidate the charge transport mechanism in this material class. Contrary to extrinsically doped semiconducting polymers, the organometallic coordination polymers exhibit excellent ambient and morphological stability and could pave the way to a new class of robust organic conductors for plastic electronic applications.

8:25 AM EL01.06.02

Late News: N-Type Organic Thermoelectrics: Demonstration of $ZT > 0.3$ Jian Liu¹, Bas van der Zee¹, Riccardo Alessandri^{1,1}, Selim Sami^{1,1}, Jingjin Dong¹, Mohamad I. Nugraha², Alex J. Barker³, Sylvia Rousseva^{1,1}, Li Qiu^{1,1,4}, Xinkai Qiu^{1,1}, Nathalie Klasen^{1,1}, Ryan C. Chiechi^{1,1}, Derya Baran², Mario Caironi³, Thomas Anthopoulos², Giuseppe Portale¹, Remco W. Havenith^{1,1,5}, Siewert J. Marrink^{1,1}, Jan C. Hummelen^{1,1} and Lambert Jan Anton Koster¹; ¹University of Groningen, Netherlands; ²King Abdullah University of Science and Technology, Saudi Arabia; ³Istituto Italiano di Tecnologia, Italy; ⁴Yunnan University, China; ⁵Ghent

The ‘phonon-glass electron-crystal’ concept has triggered most of the progress that has been achieved in inorganic thermoelectrics in the past two decades. Organic thermoelectric materials, unlike their inorganic counterparts, exhibit molecular diversity, flexible mechanical properties and easy fabrication, and are mostly ‘phonon glasses’. However, the thermoelectric performances of these organic materials are largely limited by low molecular order and they are therefore far from being ‘electron crystals’.

Here, we report a molecularly n-doped fullerene derivative with meticulous design of the side chain that approaches an organic ‘PGEC’ thermoelectric material [1]. This thermoelectric material exhibits an excellent electrical conductivity of >10 S/cm and an ultralow thermal conductivity of <0.1 W/mK, leading to the best figure of merit $ZT = 0.34$ (at 120 °C) among all reported single-host n-type organic thermoelectric materials. The key factor to achieving the record performance is to use ‘arm-shaped’ double-triethylene-glycol-type side chains, which not only offer excellent doping efficiency ($\sim 60\%$) but also induce a disorder-to-order transition upon thermal annealing. This study illustrates the vast potential of organic semiconductors as thermoelectric materials.

[1] J. Liu, B. van der Zee, R. Alessandri, S. Sami, J. Dong, M.I. Nugraha, A.J. Barker, S. Rousseva, L. Qiu, X. Qiu, N. Klasen, R.C. Chiechi, D. Baran, M. Caironi, G. Portale, R.W. A. Havenith, S.J. Marrink, J.C. Hummelen, and L.J.A. Koster, *Nature Comm.* **11**, 5694 (2020).

8:40 AM EL01.06.03

Late News: Design Considerations for Conformable Hybrid X-Ray Detectors—Influence of Organic Semiconductor Molecular Weight Maheshani Prabodhi Alwis Nanayakkara¹, Mateus Masteghin¹, Laura Basirico², Ilaria Fratelli², Andrea Ciavatti², Beatrice Fraboni², Imalka Jayawardena¹ and S. Ravi P. Silva¹; ¹University of Surrey, United Kingdom; ²Università di Bologna, Italy

The use of X-ray radiation detectors has gradually increased over the past couple of decades in a wide variety of applications ranging from medical diagnostics, industrial inspection, scientific research, to cultural heritage preservation. However, the object of investigation in most situations is of complex shape and geometry, while the detectors available to study them are rigid and flat. Such incompatibility between the object and detector results in numerous issues including vignetting and distortion of images. As a result, there is a growing requirement for conformable or curved detectors. Organic-inorganic hybrid (OIH) semiconductors are one of the most rapidly advancing class of novel materials for X-ray detection, that can be effortlessly printed on flexible substrates by using low-temperature wet deposition techniques. Furthermore, the use of OIH semiconductors as a soft matrix is expected to enable the fabrication of conformable detectors. Among them, the OIH detector concept that involves X-ray stopping bismuth oxide (Bi_2O_3) nanoparticles (NPs) incorporated into an organic bulk heterojunction (BHJ) consisting of p-type polymer Poly(3-hexylthiophene-2,5-diyl) (P3HT) and the n-type [6,6]-Phenyl C71 butyric acid methyl ester (PC₇₀BM) is highly versatile due to its exceptional characteristics such as high broadband sensitivity, ultra-low dark currents, and fast response times^[1,2]. However, P3HT is generally regarded as a polymer that can crystallise depending on its molecular weight, and thereby influence the mechanical characteristics of the detector such as bendability, which is vital for conformable detectors. However, there has been very little work reported so far in this regard, especially for thick devices typically required for X-ray detection. In this study, we emphasize the importance of tuning the molecular weight of the P3HT polymer on achieving a perfect balance between the detector performance and bendability characteristics. Through fabricating conformable hybrid detectors with P3HT molecular weights in the range of 25-60 kDa, we demonstrate that there is a strong correlation between the detector performance, bendability characteristics, and crystallinity of the film. In particular, we observe the suitability of higher P3HT molecular weights for achieving detectors with a higher level of mechanical flexibility under repeated bending cycles. These observations are explained based on the internal microstructure of these films which results in higher mechanical cohesion within the film. This study highlights the importance of understanding and optimizing fundamental material properties towards designing highly conformable detectors, a fact that has not been reported in depth so far.

References

- [1] M. P. A. Nanayakkara, L. Matjačić, S. Wood, F. Richheimer, F. A. Castro, S. Jenatsch, S. Züfle, R. Kilbride, A. J. Parnell, M. G. Masteghin, H. M. Thirimanne, A. Nisbet, K. D. G. I. Jayawardena, S. R. P. Silva, *Adv. Funct. Mater.* **2020**, 2008482.
- [2] H. M. Thirimanne, K. D. G. I. Jayawardena, A. J. Parnell, R. M. I. Bandara, A. Karalasingam, S. Pani, J. E. Huerdler, D. G. Lidzey, S. F. Tedde, A. Nisbet, C. A. Mills, & S. R. P. Silva, *Nat. Commun.* **2018**, 9, 2926.

8:55 AM EL01.06.04

Diverse Anharmonic Structural Dynamics in Organic Semiconductors—Beyond the Quasi-Harmonic Approximation Maor Asher¹, Remi Jouclas², Nitzan Kahn¹, Guillaume Schweicher², Roman Korobko¹, Yves H. Geerts² and Omer Yaffe¹; ¹Weizmann Institute of Science, Israel; ²Université libre de Bruxelles, Belgium

The low-frequency lattice dynamics of small-molecule organic semiconductors have a significant impact on their transport properties. Many current studies do not take into account the possible strong anharmonic behavior of the lattice dynamics in these materials. In my presentation, I will show that similar molecules can have significantly different degrees and expressions of anharmonic lattice dynamics. I will do that by presenting the lattice dynamics of BTBT, ditBu-BTBT, diC8-BTBT, diPh-BTBT, and DNTT single crystals measured by polarization-orientation (PO) Raman combined with temperature-dependent Raman in the low-frequency range. I will show an expression of strongly anharmonic lattice dynamics in BTBT indicated by the change of the PO Raman dependence of the lattice vibrations as the temperature is increased. This anharmonic expression is almost completely suppressed in the other crystals. I will also show other expressions of anharmonicity in the form of an order-to-disorder phase transition in ditBu-BTBT and a polymorphic phase transition in diC8-BTBT. I will discuss the physical origin of these anharmonic expressions, addressing their large-amplitude motion and their anharmonic potential energy surface. I will argue that these expressions of anharmonicity are not captured within the quasi-harmonic framework. I will also talk about the effect of these anharmonic expressions on the nonlocal electron-phonon interactions, and their decoupled nature.

9:10 AM EL01.06.05

Predictive Modelling of Structure Formation in Semiconductor Films Produced by Meniscus-Guided Coating Jasper Michels¹, Ke Zhang¹, Philipp Wucher², Pierre Beaujuge², Wojciech Pisula¹ and Tomasz Marszalek¹; ¹Max Planck Institute for Polymer Research, Germany; ²King Abdullah University of Science and Technology, Saudi Arabia

Meniscus-guided coating methods, such as zone casting, dip coating and solution shearing, are scalable laboratory models for large-area solution coating of functional materials for thin-film electronics. Unfortunately, the general lack of understanding of how the coating parameters affect the dry-film morphology upholds trial-and-error experimentation and delays lab-to-fab translation. In this contribution we present a modelling study focusing on the prediction of dry-film morphologies produced by meniscus-guided coating of a crystallizing small molecular solute. Our model reveals how the interplay between coating velocity and evaporation rate determines the crystalline domain size, shape anisotropy and regularity. If coating is fast, evaporation drives the system quickly past supersaturation, giving isotropic domain structures. If coating is slow, depletion due to crystallization stretches domains in the coating direction. The predicted morphologies have been experimentally confirmed by zone-casting experiments of the organic semiconductor 4-tolyl-bithiophenyl-diketopyrrolopyrrole. Although here we considered a molecular solute, our model can be applied broadly to polymers and organic-inorganic hybrids such as perovskites.

9:25 AM *EL01.06.06

Controlled Crystallization and Electrochemical Doping Strategies of Films Based on the Two Work-Horses P3HT & P(NDI2OD-T2) Sabine Ludwigs; University of Stuttgart, Germany

Both, poly(3-hexylthiophene) (P3HT) and poly{[N,N'-bis(2-octyldodecyl)-1,4,5,8-naphthalenediimide-2,6-diy]-alt-5,5'-(2,2'-bithiophene) (P(NDI2OD-T2))}, can be regarded as the work-horses of the organic

electronics community.

Based on our earlier crystallization studies on P3HT¹ my talk will give an overview about our recent findings on structure-function relationships of (P(NDI2OD-T2))². The involvement of liquid-crystalline phases, in particular nematic-like preordering in highly concentrated solutions is demonstrated. Solvent vapor annealing is shown to lead to large area alignment in spherulite-like superstructures with semi-crystalline structures. Particularly nice is the applicability of blade-coating to achieve highly anisotropic fiber-containing films where both the bulk and the surface morphology can be determined.³ These findings show completely different growth behavior than previously developed for P3HT.¹

Using such well-defined morphologies we can access detailed structural insights into chemical and electrochemical doping mechanisms.^{4,5} An alternative way of inducing charge carriers in the bulk polymer film is *ex-situ* electrochemical doping.⁶ Here the charge carriers are generated inside a three-electrode setup in electrolyte by applying a static electrochemical doping potential. Our experiments show that the generated charged species are stable in the solid state enabling 4-line probe conductivity and absorption measurements. An advantage of our electrochemical doping technique is the ability to fine-tune the charge carrier density inside the polymer film and hence control the resulting conductivity. Conductivities as high as 220 S/cm over large electrochemical potential windows can be reached for P3HT films. Maximum conductivities in P(NDI2OD-T2) films are limited to 10⁻³ to 10⁻² S/cm which is ascribed to a mixed valence conductivity mechanism in such conjugated redox polymer films.⁴

- 1) E.J.W. Crossland, K. Tremel, F. Fischer, K. Rahimi, G. Reiter, U. Steiner, S. Ludwigs, **Adv. Mater.** 2012, 24, 839.
- 2) Y. M. Gross, and S. Ludwigs, **Synthetic Metals** 2019, 253, 73.
- 3) D. Trefz, Y. M. Gross, C. Dingler, R. Tkachov, A. Hamidi-Sakr, A. Kiriya, C. R. McNeill, M. Brinkmann, S. Ludwigs, **Macromolecules** 2019, 52, 43.
- 4) Y. M. Gross, D. Trefz, C. Dingler, D. Bauer, V. Vijayakumar, V. Untilova, L. Biniek, M. Brinkmann, S. Ludwigs, **Chem. Mater.** 2019, 31, 3542.
- 5) K. Bruchlos, D. Trefz, A. Hamidi-Sakr, M. Brinkmann, J. Heinze, A. Ruff, S. Ludwigs, **Electrochim. Acta** 2018, 269, 299.
- 6) D. Neusser, C. Malacrida, M. Kern, Y. Gross, J. van Slageren, S. Ludwigs, **Chem. Mater.** 2020, 32, 6003.

SESSION EL01.07: Doping of Organic Semiconductors

Session Chairs: Xiaodan Gu and Sabine Ludwigs

Monday Morning, April 19, 2021

EL01

10:30 AM *EL01.07.01

Pushing the Limits of Electron Microscopy of Conjugated Polymers Enrique D. Gomez; The Pennsylvania State University, United States

Imaging of polymers by transmission electron microscopy (TEM) or scanning transmission electron microscopy (STEM) remains a challenge due to the low contrast between domains and sensitivity to the electron beam. Recent advances in instrumentation for electron microscopy have aimed to push the resolution limit, leading to remarkable instruments capable of imaging at 0.5 Å. But, when imaging soft materials, the resolution is often limited by the amount of dose the material can handle rather than the instrumental resolution. Despite the strong constraints placed by radiation sensitivity, recent developments in electron microscopes have the potential to advance polymer electron microscopy. For example, we have used monochromatated sources for spectroscopy and imaging based on differences in the valence electronic structure of conjugated polymers, electron tomography to map nanoscale inhomogeneity in polymer density, and direct electron detectors to minimize the required dose for imaging and thereby image lattice planes in crystalline polymers. Key to these efforts is

characterization of the mechanism for radiation damage in the TEM, which suggests new strategies to minimize damage, and thereby push the resolution limit down to 3.6 Å (for example, for PffBT4T-20D). Altogether, the field of polymer electron microscopy is poised to make significant advances in the near future.

10:55 AM EL01.07.02

Late News: Computation of Meisenheimer Complexes Formed to Act as Dopants for Semiconducting Polymers Leading to High Power Factors for N-Type All-Organic Thermoelectrics Connor Ganley, Jinfeng Han, Tushita Mukhopadhyaya, Howard E. Katz and Paulette Clancy; Johns Hopkins University, United States

Organic semiconducting materials have already been commercialized for applications such as organic light-emitting diodes (OLEDs), organic field effect transistors (OFETs), and photovoltaic devices. Recent work in the Howard Katz group at Johns Hopkins University has produced two novel organic doped *n*-type polymer semiconducting thermoelectric materials, PNDIC1TVT and PBDOPVTT, with σ values of 0.2 S cm⁻¹ and 0.75 S cm⁻¹, respectively, and power factors (PF) of 67 μ W m⁻¹ K⁻² and 58.1 μ W m⁻¹ K⁻², respectively. A doped form of PNDIC1TVT appears to have the highest power factor value yet reported for a solution-processed conjugated organic-doped *n*-type polymer thermoelectric material. However, the molecular origin of this enhancement is uncertain, motivating a computational investigation of this system.

We used density functional theory to probe the nature, structure, and properties of an adduct forming between fluoride anion, an established but electrochemically unlikely *n*-dopant, and a model electron-accepting naphthalenetetracarboxylic diimide (NTCDI) subunit as a representative *n*-type conjugated polymer segment, to investigate the hypothesis that an adduct may act as an intermediate in the fluoride doping mechanism of the semiconducting polymer. Our contribution uses the ORCA code with Ahlrichs' def2-TZVP basis set with a B97-D3 functional, based on our previous investigations and recommendations by Grimme (*Phys. Chem. Chem. Phys.*, 2011). We confirmed adduct formation between the two species and identified three positionally unique sites at which a fluoride dopant was capable of *datively* bonding to the NTCDI, most strongly and somewhat surprisingly at the carbonyl carbons. Subsequent simulations explored the impact of positive counterions, cesium and tetramethylammonium. Our results confirmed the lack of experimental observations of cesium-containing adducts, which we predict would not form from a binding energy standpoint. We also found that the adducts had an ionization potential that was nearly 1 eV *less* than the dopants themselves, indicating a greater likelihood that the adduct was the source of doping rather than the pure fluoride salts. These results suggest that a fluoride ion-based Meisenheimer adduct could be a particularly effective fluoride intermediate to act as a dopant for *n*-type polymers and might be used for high-performance *n*-type organic thermoelectrics. We also conducted an analogous study on adduct structures using electron-donating thiophene oligomer segments and scandium triflate and tris(pentafluorophenyl)borane Lewis acids, which could also serve as *p*-dopants. Our results showed that the doped adduct electron affinities were at most 0.5 eV more negative than the pure Lewis acids, meaning that considering dielectric and entropic effects, they could serve as polymer *p*-dopants. This study strongly supports the hypothesis that adduct formation is a plausible mechanism for conjugated polymer doping by dopants that do not appear to have sufficient electrochemical driving force on their own, and suggests that adduct dopants could also contribute to useful density of states profiles for polymer thermoelectrics.

11:10 AM EL01.07.03

Late News: Reversible Charging of Redox-Active Conjugated Polymers Beyond the Polaronic State in Aqueous Electrolytes Alexander Giovannitti¹, Anna Szumska², Iuliana Petruta Maria² and Jenny Nelson²; ¹Stanford University, United States; ²Imperial College London, United Kingdom

Conjugated polymers are an interesting class of materials for electrochemical devices since their electrochemical properties can be tuned by chemical design strategies to enable redox activity in various electrolytes. For example, redox activity in aqueous electrolytes can be achieved by attaching polar side chains to the polymer backbone, which enables ionic transport and allows volumetric charging of polymer electrodes.^[1] While this approach has been beneficial for achieving low apparent redox potentials in aqueous solution, little is known about the relationship between water uptake during the electrochemical charging

process of conjugated polymers and their redox-potentials and stabilities, particularly for electron-transporting conjugated polymers. We find that excessive water uptake during the electrochemical charging of polymer electrodes is harming the reversibility of electrochemical processes and results in mechanical instabilities of the polymer electrodes, requiring control of the swelling through side-chain engineering. We show that small changes of the side chain composition can significantly increase the redox-stability of the materials in aqueous electrolytes, improving the capacity of the polymer by more than one order of magnitude. We further study the charging process by employing density functional theory calculations to explain shifts of the electrochemical redox-potentials of water-swollen polymer films. Our results show that water uptake is beneficial for achieving low redox-potentials. Additionally, we investigate the affinity of the charged polymer to undergo unwanted side reactions with the electrolyte and find a high retention of the charged, reduced, conjugated polymers in pH neutral aqueous electrolytes, but only in the absence of molecular oxygen. Our work shows the importance of chemical design strategies for achieving high redox-stabilities for conjugated polymers in aqueous electrolytes. [1] A. Giovannitti, I. P. Maria, D. Hanifi, M. J. Donahue, D. Bryant, K. J. Barth, B. E. Makdah, A. Savva, D. Moia, M. Zetek, P. R. F. Barnes, O. G. Reid, S. Inal, G. Rumbles, G. G. Malliaras, J. Nelson, J. Rivnay, I. McCulloch, *Chem. Mater.* **2018**, *30*, 2945.

11:25 AM DISCUSSION TIME

11:40 AM EL01.07.05

Late News: Quantifying Charge Carrier Localization in Chemically Doped Semiconducting Polymers

Riley C. Hanus, Shawn Gregory, Samuel Graham and Shannon Yee; Georgia Institute of Technology, United States

The use of semiconducting polymers continues to grow despite the lack of a robust theory for how chemical doping, polaron formation, and spatial inhomogeneity localize charge carriers in these materials. Charge transport in semiconducting polymers ranges from localized (hopping-like) to delocalized (metal-like), and no quantitative model exists to fully capture this spectrum of transport behavior and its dependency on charge carrier density. In this study, we develop and validate a charge transport model that quantifies charge carrier localization and can effectively capture the localized to delocalized transition. With the archetypal P3HT-FeCl₃ polymer-dopant system, we measure the temperature dependent electrical conductivity, Seebeck coefficient, quantify the extent of oxidation using XPS, and show that the transport function prefactor and the localization activation energy are functions of the charge carrier concentration ratio (i.e., the ratio of oxidized thiophene rings to total thiophene rings). From these observations, we develop a semi-localized transport (SLoT) model, which captures both localized and delocalized transport effects with broad application in describing the electro-thermal transport of many chemically doped polymers. By applying the SLoT model to published data on semiconducting polymers and carbon nanotube systems we demonstrate its broad applicability and utility. We are able to determine system dependent parameters such as (i) the maximum localization energy of the system in the low doping limit, (ii) how this localization energy changes with doping (iii) the amount of dopant required to achieve metal-like conductivity, and (iv) the hypothetical conductivity a system could have in the absence of localization effects. Ultimately, for the first time, this proposed SLoT model captures both localized and delocalized transport, and thereby improves our ability to predict and tailor electronic properties of doped-semiconducting polymers.

11:55 AM EL01.07.06

Structural Transformations in Conjugated Polymers Upon Electrochemical Doping from Aqueous Electrolytes Connor G. Bischak and David Ginger; University of Washington, United States

Electrochemically-driven ion insertion into conjugated polymers causes molecular structural changes that impact how ionic and electronic charge carriers move through the polymer matrix. Couplings between structural changes, ion motion, and electronic transport affect the performance of devices that rely on the mixed ionic electron conductivity of conjugated polymers, such as electrochemical capacitors, bioelectronics, and neuromorphic computing. Typically, the crystal structures of conjugated polymers change continuously upon

ion insertion. Yet, using *in situ* X-ray scattering, we find that conjugated polymers can undergo reversible first order structural phase transitions upon electrochemically-driven ion insertion. We also use nanoscale infrared imaging to characterize phase separation between ion-rich and ion-poor regions of the polymer during electrochemical doping. We find that structural phase transitions have important implications for the charging mechanism of conjugated polymers for electrochemical capacitors.

12:10 PM EL01.07.07

Designing Dopants to Produce Highly Mobile Carriers in Chemically Doped Conjugated Polymers Taylor Aubry, KJ Winchell, Jonathan Axtell, Alexander Spokoyny, Benjamin Schwartz and Sarah Tolbert; University of California, Los Angeles, United States

Doping conjugated polymers is an effective way to tune their electronic properties for thin-film electronics applications. Chemical doping of semiconducting polymers involves the introduction of a strong electron acceptor or donor molecules that can undergo charge transfer with the polymer. The charge transfer reaction creates electrical carriers on the polymer chain (usually positive polarons a.k.a. holes) while the dopant molecules remain in the film and serves as a counterion. Unfortunately, strong electrostatic attraction between counter-anions and most dopants will localize the polarons and reduce their mobility. Here, we employ a new strategy, utilizing substituted icosahedral dodecaborane (DDB) clusters as molecular dopants for conjugated polymers. DDBs provide a unique system in which the redox potential of the dopant can be rationally tuned via modification of the substituents without significant change to the size or shape of the dopant molecule. These clusters thus allow us to disentangle the effects of energetic offset on the production of free and trapped carriers in DDB-doped poly-3-hexylthiophene (P3HT) films. We find that the propensity for charge transfer is directly proportional to the energetic offset between P3HT and the DDB dopant. More importantly, by designing DDB clusters to have a high redox potential and good steric protection of the core-localized electron density, highly delocalized polarons with mobilities equivalent to films doped with no anions present are obtained. P3HT films doped with these boron clusters have conductivities and polaron mobilities roughly an order of magnitude higher than films doped with conventional small-molecule dopants such as 2,3,5,6-tetrafluoro-7,7,8,8-tetracyanoquinodimethane (F₄TCNQ) at the same doping level. The spectral shape of the IR-region absorption for our DDB-doped polymer film closely matches the calculated theoretical spectrum for the anion at infinite distance from the polaron. At the same time, grazing incidence diffraction indicates that, despite their large size, DDB clusters can intercalate within the polymer crystallites to create highly crystalline dope polymer films. We therefore conclude that these DDB clusters are able to effectively spatially separate polarons and counterion, and that this separation is a critically important aspect for producing high carrier mobilities in doped conjugated polymers.

SESSION EL01.08: New Organic Semiconductor Devices and Thermoelectrics II

Session Chairs: Christine Luscombe and Sarah Tolbert

Monday Afternoon, April 19, 2021

EL01

1:00 PM *EL01.08.01

Morphology Control to Realize Multi-Functionalities in Skin-Inspired Electronic Materials Zhenan Bao; Stanford University, United States

Skin-inspired electronic materials need to combine excellent electronic properties with additional requirements, such as stretchability, biodegradability and self-healability. In order to satisfy all the requirements, controlling multi-scale morphology through material design and processing is crucial. In this talk, I will present examples of such material systems.

1:25 PM *EL01.08.02

Plasmonics for Bright and Long-Lived Light Emitting Devices Michael Fusella, Renata Saramak, Rezlind Bushati, Vinod Menon, Michael S. Weaver, Nicholas J. Thompson and Julia J. Brown; Universal Display Corporation, United States

In this seminar, we introduce a new light emitting device combining the benefits of organic semiconductors, such as defect tolerance and chemical diversity, with the enhanced optical properties of plasmonic systems. Excitons formed in the organic layers of our novel LED architecture are intentionally coupled to the surface plasmon mode of a nearby metal electrode for decay rate enhancement and subsequently converted to photons in free space via a nanoparticle-based out-coupling scheme. Our architecture achieves a two-fold increase in operational stability at a given brightness compared to a conventional OLED while simultaneously outcoupling 8% of photons from the device. Our innovative approach augments materials design allowing for parallel development of increases in efficiency and stability and is applicable to all commercial applications of OLEDs, which include lighting panels, televisions, and mobile displays.

1:50 PM EL01.08.03

Late News: Pseudo-Self-Aligned Organic Field-Effect Transistors Jörn Vahland, Karl Leo and Hans Kleemann; TU Dresden - Institut für angewandte Physik, Germany

The gap in performance between organic and inorganic transistors is getting closer due to continuous improvements in charge carrier mobility and device designs. With record cutoff frequencies exceeding 150 MHz, organic transistors become increasingly attractive for high-frequency applications on flexible substrates, e.g., wireless communication.

However, a severe disadvantage of the state-of-the-art organic thin-film transistor (OTFT) technology is the lack of a self-aligned transistor architecture as routinely employed in silicon-based technology. In consequence, organic thin-film transistors suffer from large overlap capacitances reducing the frequency of device operation and causing large device-to-device variation due to the required alignment step. Hence, the development of a self-aligned organic transistor architecture based on a scalable and reliable process bears great potential for the improvement of printed and flexible circuits.

Here we propose a pseudo-self-aligned OTFT in a coplanar top-gate configuration in order to reduce parasitic capacitances originating from the source-gate and drain-gate overlap. Furthermore, these devices are fabricated by conventional photolithography and etching processes and do not require unreliable processes such as lift-off. The self-alignment is achieved by employing a spacing layer between the source and drain and the gate electrode. This spacer reduces the specific capacitance in this overlap region by about a factor of 10 from around 15 nF/cm^2 to 0.13 nF/cm^2 . While maintaining the overlap length L_{ov} , required for alignment during lithography, this reduces the total gate capacitance. A total device capacitance reduction from $1.34\text{ fF}/\mu\text{m}$ to $0.4578\text{ fF}/\mu\text{m}$ (normalized by channel width) for a channel length and overlap of $L=L_{ov}=3\mu\text{m}$ can be estimated.

2:05 PM EL01.08.04

Late News: Amplification of External Quantum Efficiency by Photomultiplication in Organic Photodetectors Jonas Kublitski¹, Axel Fischer¹, Shen Xing¹, Johannes Benduhn¹, Lucasz Baisinger¹, Donato Spoltore¹, Koen Vandewal² and Karl Leo¹; ¹Technische Universität Dresden, Germany; ²Hasselt University, Belgium

Photodetectors (PDs) find their applicability in several technological fields. In medical applications low signals need to be amplified, requiring external circuits, which increases the final price. In addition to low cost, flexibility and lightweight devices provided by organic materials, photomultiplication has been achieved in organic PDs, leading to remarkable external quantum efficiencies (EQEs). Drawbacks of such systems are the high dark currents (J_D), lack of spectral selectivity and high operation voltages, due to large injection barriers in reverse direction. By controlling the acceptor amount and with the aid of appropriated blocking layers, we force electrons to accumulate in the acceptor phase of ZnPc:C₆₀ blends, close to the cathode interface. Due to the increased field caused by the accumulated photocharges in this region a band bending arises, effectively

increasing the injection rate across the barrier. Under reverse bias, holes are able to tunnel through it, allowing for high hole injection. Because they can easily cross the device through the ZnPc phase, while electrons cannot easily reach the contact, an EQE of 200% is achieved in the visible range, under -5V. Simultaneously, under dark conditions, the band bending is absent and the J_D follows that of common photodiodes with values of 10^{-4} mA.cm⁻². Switching injection only by illumination leads to an on/off ratio of 10^5 . Controlling the trapping character of the acceptor phase allowed us to achieve photomultiplication in vacuum processed devices, leading to EQE higher than 100%. This results open the possibility to explore high responsivity controlled by the applied bias in the visible range for future applications in organic PDs.

2:20 PM EL01.08.05

Controlling Polymer-Dopant Interactions Through Molecular Design Christian Nielsen; Queen Mary University of London, United Kingdom

Polythiophenes are among the most studied organic semiconductors and they have found widespread use as the active material in organic field-effect transistors, bioelectronic sensors and as the electron donor component in organic photovoltaic devices. Here, we investigate how subtle structural modifications of archetypical polythiophenes such as poly(3-hexylthiophene) affect the optical, structural and electrical properties of the resulting polymer thin films. We furthermore discuss the implications of these structural modification for binary systems incorporating molecular dopants and outline molecular design strategies for controlling doping efficiency and electrical conductivity.

2:35 PM EL01.08.06

Late News: A Reassessment of the Characterization and Performance of Low-Noise Large-Area Organic Photodiodes Canek Fuentes, Wen-Fang Chou, Victor A. Rodriguez-Toro, Youngrak Park, Yi-Chien Chang, Oliver Moreno, Felipe A. Larrain and Bernard Kippelen; Georgia Institute of Technology, United States

Silicon photodiodes (SiPDs) are the foundation of light-detection technology but emerging applications such as wearable biometric monitoring, biomedical imaging, distributed ionizing-radiation detection, and others, require photodetectors with mechanical properties and form factors that are beyond those physically possible with SiPDs. Novel organic and hybrid semiconductors processed from solution at low temperatures have the potential to overcome current limitations of traditional SiPDs and to enable next-generation photodetector technology. Although the performance of photodiodes (PDs) based on these novel semiconductors has been reported to be similar or better than that of low-noise SiPDs, the claimed performance is in question because the approximations used to estimate relevant metrics are often not verified (1,2).

Questions in the characterization of PDs arise because the noise equivalent power (*NEP*) is seldom measured directly. Instead, it is extrapolated from responsivity values commonly measured with a low measurement bandwidth and at a high optical power that is much larger than the *NEP*. In addition, the electronic noise is not measured directly either. In this work, we present a reassessment of the characterization of PDs including direct measurements of the responsivity as a function of optical power, electronic noise, and a detailed derivation of the parameters that are relevant for the accurate estimation of a photodetector's performance. Insights derived from a detailed characterization, enable optimization of organic photodiodes (OPDs) based on polymeric bulk heterojunctions achieving a level of performance that within the visible spectral range, rivals that of low-noise SiPDs in all metrics, except response time. A comparison between small-area SiPDs and OPDs yields comparable median electronic noise currents of 37 fA, yielding comparable median noise equivalent power (*NEP*) values at 525 nm of ca. 200 fW and median specific detectivity (*D**) values of 2.1×10^{12} cm Hz^{1/2}/W at a low measurement bandwidth of 1.5 Hz. Champion OPDs show a *D** value as high as 8×10^{12} cm Hz^{1/2}/W. Detailed measurements of the electronic noise yields a reassessment of the physical origin of the different electronic noise contributions in OPDs, potential paths for optimization, and suggest that these OPDs could reach an extrapolated white-noise limited *NEP*_{ex,wn} of 2 fW and a *D**_{ex,wn} of $1.6 \times B^{1/2} \times 10^{14}$ cm Hz^{1/2}/W. This remarkable performance arises from the selection of photoactive layer materials and by the optimization of a device-geometry that does not make use charge-blocking layers. The superior design possibilities of OPDs in terms of area, form factor, weight, and custom shapes are also

demonstrated by fabricating on glass devices with an area of 0.9 cm^2 that achieve a D^* of $2 \times 10^{12} \text{ cm Hz}^{1/2}/\text{W}$ and flexible OPDs with an area of 1 cm^2 that yield a D^* of $1.1 \times 10^{12} \text{ cm Hz}^{1/2}/\text{W}$, both of which are comparable to small area OPDs on glass. Advantages of OPDs are further illustrated and quantified in a biometric monitoring application that uses ring-shaped, large-area, flexible OPDs, while maintaining low-noise SiPD-level performance.

[1] C. Fuentes-Hernandez, et al., *Science*, 370, 698 (2020).

[2] Y. Fang, et al., *Nature Photonics*, 13,1 (2019).

SESSION EL01.09: Organic Electronics
Session Chairs: Michael Fusella and Christine Luscombe
Monday Afternoon, April 19, 2021
EL01

4:00 PM EL01.09.01

Development of Benzodithiophene-Based Copolymers with Conjugated Indolin-2-One Side Chains as Wide Band Gap Donor Polymers for Efficient Non-fullerene Organic Solar Cells with a Large Open Circuit Voltage Marwa Abdellah, Wuqi Li and Yuning Li; University of Waterloo, Canada

We report the synthesis and development of benzodithiophene-based copolymers with conjugated indolin-2-one side chains (PTIBDT), and its fluorine derivative (PTIFBDT) with a donor backbone and acceptor side chains (Type II D-A polymer) as wide band gap donor polymers for efficient non-fullerene organic solar cells with a large open circuit voltage up to (1 eV) opposed to the conventional D-A polymers having both donor and acceptor units on backbone (Type I D-A polymers) with limited open circuit voltage values. PTIBDT and the fluorinated derivative PTIFBDT having a backbone consisting of benzodithiophene donor units and side chains containing indolin-2-one acceptor units were synthesized in a simple inexpensive route with a low-lying HOMO energy level of -5.59, -5.60 eV and a wide band gap of 1.91, 1.89 eV, respectively. In addition, both PTIBDT and PTIFBDT showed typical p-type semiconductor performance with ITIC were used as donor and acceptor to form a blend active layer, the best OSC device showed a short circuit current density (J_{sc}) of 15.60 and 13.70 mA cm^{-2} , an open voltage (V_{oc}) of 0.97 and 1.00 V, and a fill factor of 0.60 and 0.59, resulting in a power conversion efficiency (PCE) of up to 8.00 and 7.70 %, respectively.

4:03 PM EL01.09.02

Separating the Active Region from the Edges—Bulk Quantum Efficiency in Organic Photovoltaics Kan Ding¹, Xiaoheng Huang¹, Yongxi Li¹ and Stephen Forrest^{1,1,2}; ¹University of Michigan, United States; ²University of Michigan—Ann Arbor, United States

We introduce a convenient method for analyzing bulk heterojunction (BHJ) organic photovoltaics (OPVs) by calculating its “bulk quantum efficiency” (BQE), a quantity related to the recombination losses only within the BHJ, from device J - V characteristics. By testing the method against experimental results for both vacuum- and solution-processed OPVs with various BHJ, buffer layers and interface layers compositions, we show that direct measurement of BQE isolates the properties of the BHJ from device edges (i.e., buffer layers, interfaces and electrodes). The BQE analysis is then applied to study different degradation mechanisms in OPVs with various active layer materials and device structures. In solution-processed OPVs with non-fullerene acceptors (NFAs), we show that the primary mechanism for degradation is externally induced by the ZnO buffer layer. By inserting a self-assembled monolayer at the BHJ/ZnO interface, the degradation is significantly suppressed and the solution-processed NFA BHJs are stabilized. We also introduce an equation to quantitatively describe the degradation of BQE.

4:06 PM EL01.09.03

Late News: Probing the Role of Lateral Charge Transport in Organic Solar Cell Active Layers Pravini S. Fernando, Jeremy Mehta, Detlef M. Smilgies and Jeffrey M. Mativetsky; Binghamton University, United States

Solution processed organic bulk heterojunction (BHJ) solar cells offer a promising route towards lightweight, cost-effective, and flexible photovoltaics. Although the BHJ's nanoscale interpenetrating donor-acceptor network results in efficient charge photogeneration, it also creates complex three-dimensional pathways for collecting charge. Despite the three-dimensional nature of the charge transport, the importance of lateral pathways is generally ignored. In this work, we examine the extent of lateral current spreading during out-of-plane charge transport across BHJ active layers for insight into the impact of lateral pathways on charge collection. We first introduce a procedure, using conductive atomic force microscopy, to quantify lateral current spreading during out-of-plane charge transport. This method was used to study the dependence of lateral spreading on molecular orientation (face-on versus edge-on), molecule type (small molecule versus polymer), and film type (single component versus BHJ). Generally, charge transport is favored along the pi-pi stacking direction; hence, a face-on (edge-on) orientation normally favors vertical (lateral) charge transport. We observed in P3HT:PCBM active layers that lateral hole spreading was proportional to the edge-on to face-on population ratio of the P3HT, as determined by grazing-incidence X-ray diffraction. Interestingly, BHJ films with the greatest content of face-on P3HT did not have the highest out-of-plane current. Instead, an intermediate edge-on to face-on ratio exhibited a 20% higher out-of-plane current. We expect that the edge-on P3HT stacking plays an essential role in allowing holes to circumvent acceptor domains in which hole transport is excluded, enabling three-dimensional charge percolation. Predominantly edge-on P3HT, however, led to excessive lateral spreading and inefficient out-of-plane charge transport. We also observed that the polymer donor P3HT led to more lateral current spreading than the small molecule donor *p*-DTS(FBTTh₂)₂, owing to charge transport along the polymer backbone of P3HT. Less lateral current spreading was observed in BHJs compared to pure films, due to a disruption of lateral hole transport by the acceptor domains. These experiments provide insight into the effects of film morphology on charge percolation in BHJs, which will help promote efficient charge collection in organic solar cells.

4:09 PM POSTER Q&A

4:17 PM EL01.09.04

Morphological Origins of Non-Langevin Recombination to Realize Thick Yet Efficient Polymer-Fullerene Solar Cells Obaid Alqahtani^{1,2}, Seyed Hosseini³, Ardalan Armin⁴, Safa Shoaee³, Vicotr Murcia¹, Thomas Ferron¹, Terry McAfee¹, Kevin Vixie¹, Brian A. Collins¹ and Fei Huang⁵; ¹Washington State University, United States; ²Prince Sattam bin Abdulaziz University, Saudi Arabia; ³University of Potsdam,, Germany; ⁴Swansea University, United Kingdom; ⁵South China University of Technology, China

Scaling-up and commercialization of organic solar cells (OSC) using high throughput deposition techniques requires thicknesses >500 nm for reproducibility. Yet most OSC materials rapidly lose efficiency as thickness increases due to the recombination prior to extraction of charges. A novel electron-donating polymer NT812 exhibits efficient, micron thick solar cells when paired with a fullerene acceptor due to highly suppressed bimolecular recombination relative to diffusion-limited Langevin rate. In this system, bimolecular recombination depends on the blend ratio and solvent additives, pointing towards the role of nano-morphology. We investigate the morphological origins of the bimolecular recombination in blends of NT812. By combining results from a suite of X-ray techniques, we are able to quantify not only the crystallinity, domain size and purity but also the sharpness of the donor-acceptor interfaces, which are found to sharpen when introducing a plasticizing solvent additive. We find that all the investigated devices possess pure domains of polymer fibrils and fullerene aggregates regardless of the recombination reduction factor. This indicates that pure phases are insufficient for non-Langevin recombination. However, large well-ordered conduits free of molecular mixing and in particular, sharp interfaces help to maintain opposite charges away from one another and keep percolation pathways clear for enhanced charge transfer (CT) state dissociation rate. This structure-morphology relationship will be key to the successful commercialization of printed OSCs at scale.

4:20 PM EL01.09.05

Role of the Blend Ratio in Polymer:Fullerene Phototransistors Cinthya K. Trujillo Herrera, John G. Labram and Min Ji Hong; Oregon State University, United States

Because of their ability to combine detection and processing into a single element, phototransistors have the potential to be a disruptive optical detection technology. The complexity of commercial applications (as defined by number of vertical processing steps) can be reduced significantly when using phototransistors compared to photodiodes, for example. In addition, phototransistors have a gate-voltage-tunable responsivity (something for which there exists no analog in 2-terminal devices), with high gain from small changes in incident optical power density.

Organic phototransistors (OPTs) in particular offer the opportunity to develop devices with well-defined, tailored, optical response spectra. One of the most significant drawbacks to OPTs however is the complexity of the relationship between photocurrent and incident optical power density. In addition to the choice of two applied voltages (drain and gate), optically induced shifts in threshold voltage often lead to behavior that is difficult to predict and quantify.

In this work we have varied the composition of polymer:fullerene bulk heterojunction (BHJ) OPTs, in order to identify the respective role played by direct charge generation and optically induced shifts in threshold voltage. The current-voltage behavior of blends of poly(3-hexylthiophene-2,5-diyl) (P3HT) and phenyl-C₆₁-butyric acid methyl ester (PCBM) were studied under illumination at various intensities. It is demonstrated that even one percent (by weight) of P3HT in PCBM produces an appreciable response while remaining highly optically transparent to the excitation wavelength, making these organic phototransistors highly attractive for optically transparent detectors.

4:23 PM POSTER Q&A

4:35 PM EL01.09.07

Late News: Engineering Solution Processable N-Type Silicon and Tin Phthalocyanines for Organic Thin-Film Transistors Rosemary R. Cranston, Mário C. Vebber and Benoit Lessard; University of Ottawa, Canada

P-type organic semiconductors typically demonstrate higher mobilities and better chemical and environmental stability compared to n-type materials which are often air sensitive and insoluble. The development of soluble, stable, high performing n-type materials is critical for the fabrication of organic electronic devices for many of the novel applications organic semiconductors allow for. Due to their high degree of intermolecular stacking, crystallinity, chemical and mechanical versatility, and compatibility with solution processed fabrication technique, axially-substituted metal phthalocyanines (MPcs) are promising materials for applications in organic thin-film transistors (OTFTs). MPcs contain multiple functional sites, including the core, periphery and axial positions, allowing to chemically tune molecules to improve device performance. MPcs with tetravalent metal centers, such as silicon and tin phthalocyanines (SiPcs and SnPcs), are among the highest performing materials in this family, however remain relatively unexplored compared to commonly used divalent metal MPcs. Seven varying lengths of branched chain alkyl silane groups were incorporated into SiPc or SnPc at the axial positions to create fourteen solution processable n-type organic semiconductors, ten of which are novel materials never before used in OTFTs. Atomic force microscopy (AFM) images of the films show that variations in alkyl chain length and metal center result in drastic changes in film morphology and corresponding OTFT performance. OTFTs fabricated with the SnPc derivatives exhibited average mobilities in the range of $0.02 - 0.70 \times 10^{-2} \text{ cm}^2 \text{ V}^{-1} \text{ s}^{-1}$, with four of the seven compounds outperforming their SiPc counterparts whose mobilities ranged from $0.01 - 2.8 \times 10^{-2} \text{ cm}^2 \text{ V}^{-1} \text{ s}^{-1}$. The relationship between two key fabrication parameters, thermal annealing and spin time, on thin-film microstructure and OTFT performance was investigated through the electrical characterization of the highest performing material, bis(tri-*n*-butylsilyl oxide) SiPc, and related to grazing-incidence wide-angle x-ray scattering (GIWAXS) and x-ray diffraction (XRD) data. Thermal annealing

increased film crystallinity and altered the orientation of the SiPc molecule relative to the substrate, whereas spin time solely effected film crystallinity, thus exhibiting how these fabrication parameters can be used to change different aspects of the thin-film microstructure and modify device performance. The results of this work show the effectiveness of axial substitution as a strategy to control crystal packing and charge transport properties of SiPcs and SnPcs, and the potential of these materials as solution processable low cost n-type semiconductors.

4:50 PM EL01.09.08

Operando Scattering Reveals the Structural Origins of Regio-Chemistry Driven Improvements in Mixed Conducting Polymers Bryan D. Paulsen¹, Rawad K. Hallani², Christopher J. Takacs³, Micaela Matta⁴, Ruiheng Wu¹, Joseph Strzalka⁵, Qingteng Zhang⁵, Wonil Sohn¹, Alexander Giovannitti³, Anthony J. Petty II¹, Iain McCulloch⁶ and Jonathan Rivnay^{1,1}; ¹Northwestern University, United States; ²King Abdullah University of Science and Technology, Saudi Arabia; ³Stanford University, United States; ⁴University of Liverpool, United Kingdom; ⁵Argonne National Laboratory, United States; ⁶University of Oxford, United Kingdom

Conjugated polymers with oligoethylene glycol side chains are excellent mixed ionic-electronic conductors, and through volumetric capacitive coupling can efficiently interconvert ionic and electronic currents. These phenomena have been exploited for electrochromic, charge storage, biological sensor, neuromorphic, and organic electrochemical transistor (OECT) applications, amongst others. The polythiophene pg2T-TT, poly(2-(3,3'-bis(2-(2-(2-methoxy ethoxy)ethoxy)ethoxy)-[2,2'-bithiophen]-5-yl)thieno[3,2-b]thiophene), with its high capacitance (C^*), high hole mobility (μ), and high transconductance in OECTs (ionic-to-electronic transduction gain), has become a benchmark material for this emerging class of mixed conductors. Surprisingly, simply switching the side chain position on the bithiophene repeat unit from 3,3' to the 4,4' positions (producing pgBTTT) results in a marked improvement in mixed conducting properties. The product of pgBTTT's electronic mobility and volumetric capacitance ($\mu \times C^*$), which is the source of OECT transconductance, is double that of pg2T-TT, and represents a record high intrinsic figure of merit for enhancement mode OECT channel materials ($\mu \times C^* = 563 \pm 33 \text{ F cm}^{-1} \text{ V}^{-1} \text{ s}^{-1}$).

The source of this improvement is not immediately obvious. Traditional characterization methods typically carried out on dry polymer films do not reflect the operating conditions of these polymers in OECTs or other devices that exploit their mixed conducting properties, where they are swollen by a contacting electrolyte. Therefore, in situ and operando techniques are required. While X-ray scattering has become ubiquitous for structure determination, in situ or operando scattering of films emersed in aqueous electrolyte is severely limited by electrolyte scattering and absorption. This is especially critical for conjugated polymers which are weak scatterers and most often employed in (sub-micron) thin films. To overcome these challenges, we employ a new frit-based electrochemical cell that allows electrolyte contact of the thin film from below and incident X-rays to impinge from above, separating the electrolyte and x-ray path to provide unparalleled resolution of polymer microstructure in aqueous operando conditions. Leveraging this cell we compare the grazing incidence wide angle scattering (GIWAXS) patterns of dry, hydrated, electrolyte exposed, and electrochemical potential cycling pg2T-TT and pgBTTT, monitoring both molecular d-spacing and molecular packing coherence lengths. These operando measurements deviate markedly from equivalent ex situ measurements, highlighting the limited utility of ex situ experiments in elucidating the structure of electrolyte swollen polymer mixed conductors.

While pg2T-TT and pgBTTT show similar lamellar d-spacing expansions ($\sim 0.7 \text{ \AA}$) with hydration, upon electrolyte exposure further expansion of pg2T-TT lamellae (9.4 \AA) is over four times that of pgBTTT (2.1 \AA). This represents a fundamentally different degree of polymer electrolyte interaction that depends solely on the side chain regio-chemistry and gives rise to the difference in mixed conducting properties. Electrochemically doping pg2T-TT and pgBTTT produces similar pi-stack d-spacing contractions and relative lamellar expansions. UV-Vis and Raman spectroelectrochemistry was carried out to verify the similar degree of charging and nature of dopant induced charge carriers in pg2T-TT and pgBTTT.

These results highlight the sensitivity of mixed conducting properties to side chain architecture and the crucial

necessity of operando measurements to establish synthetic design rules for polymer mixed conductors. Further, the frit-based operando cell provides a new powerful tool to probe the previously inaccessible structure of solvent and electrolyte swollen polymer thin films with controlled electrochemical potential. This characterization capability is key for advancing the field of polymeric mixed conductors and likely other fields as well.

5:05 PM EL01.09.09

Stable Organic Electronic Devices Achieved Through the Characterization of Charge Carrier Traps in Organic Semiconductors Hamna Haneef¹, Qianxiang Ai², Karl Thorley², Hu Chen³, Iain McCulloch^{3,4}, Chad Risko², John Anthony² and Oana Jurchescu¹; ¹Wake Forest University, United States; ²University of Kentucky, United States; ³King Abdullah University of Science and Technology, Saudi Arabia; ⁴University of Oxford, United Kingdom

Given their low-cost processing, light weight, chemical versatility, and compatibility with flexible and biological systems, organic semiconductors (OSCs) are gradually becoming an integral part of our lives as active components of various optoelectronic devices. These systems undergo considerable electronic and structural transformations during device fabrication and operation which can profoundly impact their performance and stability. Characterization techniques that can elucidate the mechanisms of the time-dependent transformations occurring in these materials and devices are necessary to guide the processing and design of high performance and stable organic devices. For example, in organic field-effect transistors (OFETs), the basic building block of applications such as displays, radio frequency identification tags, and conformable sensors, identifying the sources and mechanisms leading to operational instabilities are crucial in eliminating their impact to ultimately achieve the much-needed stability to make these devices components in real-life applications. In this presentation, we describe an efficient characterization technique that serves as a quick and reliable diagnostic tool to identify with high accuracy the environmental and operational degradation pathways occurring in OFETs during device operation. Charge carrier trapping in electronic states generated in the bandgap of the OSC during operation has been identified as the main culprit for device instabilities. Therefore, by monitoring the energetic distribution and time evolution of trap states during OFET operation, and with guidance from density functional theory (DFT) calculations, we gained access to the sources of device degradation, clarified the nature of the traps generated during operation, and the parameter space that gives rise to these traps. This information guided the development of efficient design rules for device processing and delivered robust OFETs with unparalleled operational stability in both staggered and coplanar configurations regardless of the active material (small molecule and polymeric OSCs), as confirmed by the constant mobility and exceptionally low threshold voltage shift of $\Delta V_{th} = 0.1$ eV achieved under aggressive bias stress conditions for 500 min in ambient air.

SESSION EL01.10: Poster Session I: Organic Electronics I

Session Chairs: Xiaodan Gu and Yu Xia

Monday Afternoon, April 19, 2021

7:45 PM - 9:40 PM

EL01

7:45 PM OPENING COMMENTS

EL01.10.02

Heavy-Duty Flexible and Transparent Organic Solar Cells Wallace C. Choy^{1,2} and Jinwook Kim¹; ¹The University of Hong Kong, Hong Kong; ²Guangdong-Hong Kong-Macao Joint Laboratory for Photonic-Thermal-Electrical Energy Materials and Devices, China

While it is highly desirable to simultaneously achieve the features of good electrical/optical properties, low

surface roughness, robust mechanical flexibility under continuous operation bias for practical flexible electrodes, we demonstrate an outperformed a new class of Ag nano-network composite based transparent flexible electrode by a new one-step multifunctional chemical treatment. The robust electrical stability loaded with simultaneously continuous operation bias and mechanical bending is confirmed on the treated composite electrode. The organic solar cells based on our newly developed flexible composite electrode offer impressive performances as compared to the untreated device [1].

In details, we demonstrate a flexible transparent electrode showing the figure-of-merit value over 1000 (5.4 ohm/sq sheet resistance and >94% diffused transmission at 550 nm wavelength) via the new synthesis approach, simultaneously achieving selective welding at nanowires cross junctions to form Ag nano-network, removing PVP surfactants from Ag nanowires and PSS from PEDOT:PSS. In addition, with our proposed chemical treatment, the composite electrode can be completely detached from the supporting rigid substrate with no remained residues on the substrate, exhibiting extremely smooth topography (<1 nm root-mean-square roughness and <3 nm peak-to-valley roughness). Remarkably, we demonstrate robust electrical stability under simultaneously continuous operation bias and mechanical bending for the treated electrode for the first time. The OSC device with our proposed chemical treatment has achieved the best PCE of 15.41%, which is the best performance among ITO free flexible OSCs so far.

[1] J. Kim, D. Ouyang, H. Lu, F. Ye, Y. Guo, N. Zhao, W.C.H. Choy, *Adv. Energy Mater.*, DOI:10.1002/aenm.201903919.

7:51 PM Q&A

EL01.10.05

High Performance Indoor Photovoltaic Cells Using Main Chain Conjugated Copolymer Having Donor-Acceptor Heterojunctions Na Yeon Kwon, Su Hong Park, Hungu Kang, Young Un Kim, Hyo Jae Yoon, Min Ju Cho and Dong Hoon Choi; Korea University, Korea (the Republic of)

In general, the active layer of a high-performance polymer solar cell (PSC) has been fabricated by mixing a polymer donor and a low molecular acceptor. On the other hand, for future flexible photovoltaics, many studies are being conducted on *all*-PSCs that contain blend film of donor polymer and acceptor polymer to produce an active layer. However, despite the recent high power conversion efficiency(PCE) achievements of *all*-PSCs, the miscibility control and morphology reproducibility between the donor and acceptor polymers of the photoactive layer using two polymers remain a concern. This problem directly affects the stability of the device efficiency. Therefore, in order to overcome these shortcomings, studies have been conducted on polymers that can have heterojunctions in the internal structure of a main chain conjugated copolymer synthesized by covalent bonding between a donor and an acceptor unit.

And indoor photovoltaic (IPV) cells receive increasing attention because of their promising applications as power sources for devices of the Internet of Things ecosystem. The essential requirement for active materials of IPVs is that their absorption spectrum should overlap with the emission spectrum of light-emitting diodes (LEDs) that are often used as indoor lamps. Since IPVs require high harvesting efficiencies mainly in the visible range, the corresponding active material must be designed and applied differently from the molecular structure of the active material used in outdoor PVs. For this reason, photoactive materials for IPVs must display a narrow absorption spectrum in the visible wavelength range and a medium bandgap.

In this study, we successfully synthesized a crystalline main chain conjugated copolymer, P(BDBT-*co*-NDI2T), having BDBT donor-NDI2T acceptor heterojunctions in film states. Interestingly, the polymer exhibited a strong absorption band from 500 to 650 nm, which is overlapped well with the emission spectrum of white LED used as an indoor light source. IPV produced by using the P(BDBT-*co*-NDI2T) synthesized in this study as an active layer, showed a high power conversion efficiency of 12.70% (@500 lux) with a short circuit current density of 49.89 mA cm⁻². The PCE of the P(BDBT-*co*-NDI2T) film-based IPV was twice as high as that of the blend film-based IPV and showed excellent operational stability. This result was thought to be due to a smoother surface/internal morphology of the P(BDBT-*co*-NDI2T) films. Additionally, kelvin probe force

microscope(KPFM) data also indicated a relatively uniform distribution of the surface charge in the P(BDBT-*co*-NDI2T). These results may explain why P(BDBT-*co*-NDI2T)-based devices exhibit higher efficiency and very high operational stability compare to the blend film-based device. This study is the first time that the P(BDBT-*co*-NDI2T) has been applied to IPV, which suggests the potential for their widespread use in the development of indoor organic PVs in the future.

EL01.10.06

Tunable Light-Harvesting Property of Conjugated Terpolymers for Realizing High-Performing Indoor Photovoltaics Su Hong Park, Na Yeon Kwon, Young Un Kim, Diem H. Chau, Chai Won Kim, Seoung Uk Cho, Dong Won Lee, Min Ju Cho and Dong Hoon Choi; Korea University, Korea (the Republic of)

In addition to sunlight, we can see buildings (hospitals, shops, airports, offices, factories) illuminated for 24 hours, and artificial lighting is beginning to be recognized as a source of energy that needs to be harvested. Indoor light sources such as white light-emitting diodes (LEDs) can provide enough energy to operate most small wireless and low power consumption indoor electronics. Therefore, if organic photovoltaics (OPV), which are very sensitive to indoor light, are developed, they can be an ideal power source for indoor Internet of Things (IoT) wireless sensor networks due to their lightweight and mechanical flexibility. Thus, OPV has great potential to harvest energy that cannot be realized with powerful silicon-based inorganic photovoltaic cells. However, high-performance OPVs are typically fabricated using highly toxic solvents such as chlorinated aromatic solvents. These solvents can cause serious concerns about the side effects of human health in terms of germ cell mutagenicity, skin corrosion, and serious eye damage. From this point of view, the OPV material must be processed with a solvent that is harmless to the human body, and it must be designed to absorb indoor lighting to achieve high power conversion efficiency.

In this study, we introduced the fluorine-substituted benzotriazole (BTA) as a third monomeric unit into the benzo[1,2-*b*:4,5-*b'*]dithiophene (BDT-Cl)-benzo[1,2-*c*:4,5-*c'*]dithiophene-4,8-dione (BDD) alternating polymer, PM7 to increase electron-accepting property. PM7 is a famous donor polymer that shows very high performance in OPV cells. However, PM7 is only soluble in halogenated solvents such as CF, CB, and 1,2-dichlorobenzene but not soluble in a non-halogenated solvent such as toluene due to the highly rigid π -conjugated polymer with a strong aggregation effect. By introducing the BTA moiety into the PM7 as a relatively ductile unit, the terpolymer PM7-J52 (50) is successfully synthesized and it is well soluble in non-halogenated solvents, enabling environmentally friendly processing. When terpolymer was used as a donor polymer for indoor photovoltaics and processed using a non-halogenated solvent, PCE was measured as high as 11.34% in outdoor PV(AM1.5G) and 17.41% (500 lux) in indoor PV, respectively. Besides, the absorption spectrum of the blend film can be adjusted by changing the third monomer composition, which can improve the performance of PV devices using outdoor and indoor light sources. Our research has proposed a new ternary copolymer structure that can be used for fabricating outdoor or indoor PVs. In addition, the use of terpolymer has the advantage of being able to use non-halogenated solvents when fabricating PV devices.

8:13 PM Q&A

EL01.10.09

Introducing Oxide-Metal-Oxide Electrode with Heat Dissipating Thin Substrate to Geometrically Stretchable Organic Light-Emitting Diodes with Stable Color Coordinate Dong hyun Choi, Jun Su Yang, Dong Hyun Kim, Changmin Lee, Hyung Ju Chae, Geon Woo Jeong, Tae Wook Kim, Subrata Sarker and Seung Yoon Ryu; Korea University, Korea (the Republic of)

We implemented the geometrically stretchable organic light-emitting diodes (OLEDs) by breaking the stereotype that it is impossible to implement stretchable devices with a fragile oxide-type electrode under intense 2-dimensional random area strains with molybdenum trioxide (MoO₃)/gold (Au)/MoO₃ (MAM). The devices were fabricated on the pre-strained NOA63/3M elastomer and encapsulated with NOA63 for the waterproof sandwiched structure. The transmittance of the electrode was high enough to replace the semi-transparent silver (Ag) electrode, while the resistance was still lower than that. The work function of the

electrode could also be tuned through the MoO₃ dipole layer for excellent charge injection. Also, it was shown that the color coordinate did not change according to the angle. By comparing the glass- and the thick NOA63 film-based devices, it was found that the triplet-triplet annihilation was reduced through the heat sink mechanism that facilitated achieving a high exciton density. Also, significantly enhanced out-coupling was achieved by inserting silicon dioxide nanoparticles into NOA63. Consequently, the high current efficiency of ~82.5 cd/A and external quantum efficiency of ~22.6% were achieved by the horizontal emitter with a minimum efficiency roll-off.

EL01.10.10

Rational Design of Boron-Oxygen Bridged Acceptor Based Copolymer Host Materials for High Performance Solution-Processed Thermally Activated Delayed Fluorescent OLEDs Jinhyo Hwang, Chai Won Kim, Dong Won Lee, Seung Uk Cho, Min Ju Cho and Dong Hoon Choi; Korea University, Korea (the Republic of)

Organic polymers those exhibit features pertinent to functioning as host materials for thermally activated delayed fluorescence (TADF) emitters have considerable potential in solution-processable organic light-emitting diodes (OLEDs), allowing simple, low-cost, and large-area applications. In particular, polymer hosts have superior characteristics, including facile functionality to introduce various electron donor and acceptor entities, ability to uniformly disperse and contain small molecular dopants, and ability to produce more smooth and homogeneous films, compared to those of their small-molecule counterparts. This research describes the design and development of three new styrene-based copolymers (ABP91, ABP73, and ABP55) bearing diphenylacridine (DPAc) as the electron donor and 2,12-di-*tert*-butyl-7-phenyl-5,9-dioxa-13b-boranaphtho[3,2,1-de]anthracene (TDBA) as the electron acceptor.

In particular, the three polymers were synthesized via variations in the ratio of donor (DPAc) and acceptor (TDBA) monomers. A homopolymer (DHP) containing only DPAC units was also synthesized for comparison. Non-conjugated styrene backbone was employed as a linker between the donor and acceptors to restrict the conjugation length and thus accomplish a high E_T . Subsequently, the resulting copolymers featured E_{TS} values in the range of 2.73–2.75 eV.

We fabricated OLEDs via solution processing, employing a familiar t4CzIPN as TADF emitter using the following configuration: ITO/PEDOT:PSS (40 nm)/PVK (10 nm)/Host:t4CzIPN (20 nm, x wt %)/TPBi (40 nm)/LiF (0.8 nm)/Al (100 nm). The devices based on ABP91:t4CzIPN, ABP73:t4CzIPN, and ABP55:t4CzIPN achieve EQE/CE/PEs as high as 21.8%/71.4 cd A⁻¹/ 44.9 lm W⁻¹ (with CIE color coordinates of (0.29, 0.60)), 22.2%/70.1 cd A⁻¹/48.9 lm W⁻¹ (with CIE color coordinates of (0.27, 0.57)), and 19.7%/61.7 cd A⁻¹/43.1 lm W⁻¹ (with CIE color coordinates of (0.27, 0.56)), respectively. In contrast, the DHP-based devices were limited to only 14.5%/47.3 cd A⁻¹/27.4 lm W⁻¹ (with CIE color coordinates of (0.30, 0.59)) because of charge imbalance, attributed to its unipolar nature. Among the three hosts, ABP73 delivered the best performance, which is attributed to the high k_{RISC} , high PLQY, well-balanced charge-carrier transport ability, and homogeneous film formation with a small value of RMS roughness.

These results suggest that the development of copolymers, which consist of donor and acceptor entities in the side chain or pendent groups, is more suitable for highly efficient solution processing of TADF OLEDs. To our knowledge, this is, to date, the best performance that has ever been reported for polymer host materials in the area of TADF OLEDs. We strongly believe that this work will make a significant contribution through the introduction of a variety of copolymers that function as hosts for the development of proficient solution-processable TADF OLEDs.

EL01.10.11

Late News: Tetrabranched Photocrosslinker Enables Micrometer-Scale Patterning of Light-Emitting Super Yellow for High-Resolution OLEDs Wooik Jang, Hyewon Park, Jeehye Yang, Seunghan Kim, Hyunwoo Jo and Moon Sung Kang; Sogang University, Korea (the Republic of)

Development of a simple and effective patterning method applicable to solution-processible organic luminophores over a large area is critical for cost-effective production of organic light-emitting-diode (OLED)

displays. Here, we demonstrate high-resolution patterning of light-emitting polymer active layers using a highly efficient photocrosslinker (4Bx). The photocrosslinker is structured in a tetrabranched geometry, wherein a photocrosslinkable azide moiety is present at each of the four corners of the molecule, and each of these moieties can form a chemical bond with light-emitting polymer semiconductors under UV irradiation. Due to the high crosslinking efficiency of 4Bx, the use of an unprecedentedly small amount of 4Bx (0.1 wt%) allows fully crosslinking light-emitting Super Yellow polymer without degrading their photoluminescence and electroluminescence characteristics. Furthermore, precisely-defined photocrosslinked patterns of Super Yellow with feature sizes of 5 μm are formed by using p-xylene as the developing solvent that was carefully selected according to Hansen solubility parameter analysis.

EL01.10.12

A Comparison of Measurements of Organic Light-Emitting Diode with the Spectroradiometer and the Integrating Sphere Measurements Dong Hyun Kim, Changmin Lee, Hyung Ju Chae, Geon Woo Jeong, Dong hyun Choi, Tae Wook Kim, Subrata Sarker and Seung Yoon Ryu; Korea University, Korea (the Republic of)

There are two main ways to measure the performance of organic light-emitting diodes (OLEDs). One way is using a spectroradiometer (CS-2000) through the viewing angle and the other is the most widely used technique that involves an integrating sphere. In this study, we present a comparison of measuring the performance of OLEDs using the spectroradiometer and the integrating sphere. To improve the measurement accuracy of spectroradiometers, the viewing angles were set between -70° and $+70^\circ$ to avoid the out of focusing area. As the external quantum efficiency (EQE) estimated using the spectroradiometer was not coincident with that obtained using the integrating sphere method, we applied a mean estimation protocol to convert the EQE values obtained from the spectroradiometer by integrating the EQE values extracted from different viewing angles. The results were summarized for four different kinds of angular emission patterns. The data obtained from the conversion of EQE and electroluminescence (EL) of OLEDs measured with a spectroradiometer from all different angular emission patterns were similar to that measured with the integrating sphere with a small deviation. This study and the mean estimation protocol should help in understanding the accuracy of OLED measurements at a laboratory scale. As such, it is possible to reduce the recurring costs and the required time for these two measurement techniques by bypassing the integral sphere measurement

8:41 PM Q&A

EL01.10.13

Ultrasensitive, Selective and Fast Recovered Chemoreceptors Based on Interpenetrating Polymer Semiconductor Nano-Networks Hyukmin Kweon, Pureunsan Go, Han Wool Park, Chaeyoung Lee, Sang Jun Park, Joonseok Lee, Seon-Jin Choi and Do Hwan Kim; Hanyang University, Korea (the Republic of)

As air pollution has become an urgent issue worldwide, effective chemodetection and *in situ* monitoring of hazardous gases have been desired for public health. In this regard, high-performance of chemosensor have been demonstrated continuously based on conventional semiconducting materials, such as oxide semiconductors, 2-dimensional materials, and organic semiconductors (OSCs). Although oxide semiconductors based chemosensor possess high sensitivity and selectivity due to their high mobility and versatile surface functionalization, high temperature operation is a prerequisite for desired high sensitive chemodetection. On the other hand, OSCs can obtain high sensitive chemodetection at room temperature because of effective contact with target chemicals. However, OSCs cannot serve functionalization sites for selectivity, and exhibits poor recovery property by penetration of chemicals into an OSCs film. Therefore, in order to secure high sensitivity, selectivity, and ideal recovery property simultaneously, novel material design and scientific breakthrough in the field of chemosensors are strongly required.

Herein, we demonstrate an ultrasensitive, selective, and fast recovered NO_2 chemodetection based on interpenetrating polymer semiconductor nano-networks functionalized with amine based artificial chemoreceptors (NH_2 -IPSNs), in which polymer semiconductor chains are interpenetrated into a ladder-like organosilica network. The IPSNs serves unreacted silanol (Si-OH) groups acting as functional points on its

surface; by carefully manipulating the Si-OH groups, the NH₂-IPSNs film can be designed by simple solution process without a degradation of electrical performance. This surface engineering has been considered to be available in oxide semiconductor materials, however, through a novel approach of the IPSNs, it also could be allowable in OSCs. Consequently, the NH₂-IPSNs based chemosensor exhibited ultrahigh sensitivity (990% ppm⁻¹ at NO₂ 5 ppm) and superior selectivity in room temperature operation, even the sensing performance persisted in ambient environment. This is because the surface anchored NH₂ groups can build strong dipole moment interaction with NO₂ molecules. Furthermore, the surface NH₂ groups can suppress penetration of NO₂ molecules into the NH₂-IPSNs film effectively, so that fully recovery capability with fast recovery rate (240 s) was achieved. As a result, the NH₂-IPSNs based chemosensor can develop ultrasensitivity, selectivity, and ideal recovery property at room temperature simultaneously, which is attributed to our conceptual novelty to reconcile the characteristics of oxide and organic semiconductors. We believe that our rational design of new concept of semiconductor material represents a big step towards next-generation chemical monitoring system for various industry and public health.

EL01.10.14

Late News: Ionically Connected Floating Electrodes for Long-Distance (> 1 mm) Coplanar-Gating Graphene Transistors Hyunwoo Jo and Moon Sung Kang; Sogang University, Korea (the Republic of)

Exploiting the long-range polarizability of an electrolyte based on ion migration, electric double-layer transistors (EDLTs) can be constructed in an unconventional configuration;¹ here, the gate electrode is placed coplanarly with the device channel. For example, the current density of a transistor channel can be modulated using a gate electrode that is not located directly on top/below the channel but placed apart from the channel as long as the electrode is bridged with the channel through the electrolyte— which we refer to as the remote gating. In this paper, we demonstrate the influence of the distance factors of the electrolyte layer on the operation of EDLTs with a coplanar gate. As the promptness of the electric double-layer formation depends on the distance between the channel and the gate, the dynamic characteristics of a remote-gated transistor degrade with long distance. To suppress this degradation, we suggest using multiple coplanar floating gates bridged through ionic dielectric layers. Unlike remotely gated EDLTs that utilizes a single extended electrolyte layer, the devices with multiple segmented electrolyte layers operate effectively even when they are gated from a distance longer than 1 mm. The new device architecture provided here shows new opportunities to exploit graphene transistors.

Reference

1. Kim, B. J.; Lee, S. -K.; Kang, M. S.; Ahn, J. -H.; Cho, J. H. *ACS Nano* **2012**, 6, (10), 8646-8651.

EL01.10.15

Late News: Synthesis and Characterization of an Open-Shell Conjugated Polymer Containing a Quinoid Building Block with Diradical Yunseul Kim, Dongseong Yang, Yeon-Ju Kim and Dong-Yu Kim; Gwangju Institute of Science and Technology, Korea (the Republic of)

Quinoid platforms have attracted much attention because of their unique optical, electrical and magnetic properties, and can be applied to various organic electronics, such as organic field-effect transistors (OFETs), organic photovoltaics and organic spintronics. They exhibit low band-gap and redox amphotericism arising from stable quinoid-aromatic resonance structure and high structural planarity due to double bond formation between each ring. This quinoid structure often result in high and n-type charge carrier mobilities in OFETs. We also demonstrated high performance OFETs using quinoidal polymers recently. Interestingly, the quinoidal structure stabilizes the open-shell form with diradical upon recovery of aromaticity. The open-shell diradicaloids via introduction of quinoid building blocks into polymer require the experimental and theoretical analysis to comprehensively describe their unique optical and magnetic properties.

In this research, we will present our recent results on the investigation of structure-property relationship of an open-shell conjugated polymer embedded with stable diradicals. We designed and synthesized an azaisatin-terminated quinoid building block, azaquinoidal-bithiophene (azaQuBT), which has pyridine replacing benzene in the end of terminal isatin unit. This can lead to better coplanar conformation of polymer backbone due to

suppressing the rotation between quinoid-comonomer counterpart. Therefore, diradical occurred by open-shell form of azaQuBT could be well-delocalized into the polymer backbone, leading to stable ground-state diradical characters. An open-shell conjugated polymers, PazaQuBT-T, was successfully synthesized by Stille-polymerization. We characterized material properties by UV-Vis-NIR absorption, Raman spectroscopy and electron spin resonance (ESR) and discussed.

9:00 PM Q&A

EL01.10.17

Artificially Intelligent Tactile Ferroelectric Neuromorphic Skin Kyuho Lee, Chanho Park, Hyeokjung Lee, Seung Won Lee and Cheolmin Park; Yonsei University, Korea (the Republic of)

Lightweight and flexible tactile learning machines can simultaneously detect, synaptically memorize, and subsequently learn from external stimuli acquired from the skin. This type of technology holds great interest due to its potential applications in emerging wearable and human-interactive neuromorphic electronics. In this study, an integrated intelligent tactile learning electronic skin (e-skin) based on arrays of ferroelectric field-effect transistor memories with dome-shape tactile top-gates, which can simultaneously sense and learn from a variety of tactile information, is introduced. To test this device, tactile pressure is applied to a dome-shaped top-gate that measures ferroelectric remnant polarization in a gate insulator. This results in analog conductance modulation that is dependent upon both the number and magnitude of input pressure-spikes, thus mimicking diverse tactile and essential synaptic functions. Specifically, our device exhibits excellent cycling stability between long-term potentiation and depression over the course of 10,000 continuous input pulses. Additionally, it has a low variability of only 3.18 %, resulting in high-performance and robust tactile perception learning. Our 4×4 device array is also able to recognize different handwritten patterns using 2-dimensional spatial learning and recognition, and this is successfully demonstrated with a high degree accuracy of 99.66 %, even after considering 10 % noise.

EL01.10.18

Electropolymerized One-Dimensional Growth Coordination Polymer for Hybrid Electrochromic Aqueous Zinc Battery Wei Church Poh, Xuefei Gong and Pooi See Lee; Nanyang Technological University, Singapore

Conjugated polymers are attractive for rechargeable batteries owing to their reversible electrochemical redox reactions and/or intercalation abilities. However, conventional conjugated polymers are generally consisting of only organic backbones which tend to form highly reactive redox species during an electrochemical process or under light excitation, leading to undesirable side reactions. These side reactions such as irreversible oxidation occurred on the polymer backbones and its physical properties will be permanently altered, leading to degradation. This problem can be alleviated by incorporating redox-active transition metals into the conjugation system, helping to stabilize the generated redox species via coordination, or having itself undergoing a stable redox process.

Over the years, there has been an increasing interest focusing on nanostructured conjugated polymers as green and renewable electrodes for energy conversion and storage devices. Realizing an optically modulated energy storage device could unlock new applications including but not limited to variable optical attenuator, optical switches, displays, and smart windows for energy-efficient buildings. Herein, a rationally designed nanostructured coordination polymer has been prepared with the aim of realizing electrical modulated light transmission with stable electrochemical cathodic reactions. By utilizing the coordination conjugated polymer as the cathode and a zinc anode, an integrated hybrid electrochromic zinc battery device can be demonstrated with promising endurance.

From the electrochemical and optical analysis, the $\Delta E_{(\text{HOMO-LUMO})}$ of the polymer was found to be *ca.* 1.5 eV, suggesting that the polymer is behaving like an organic semiconductor with decent conductivity even with interrupted conjugation system due to metal inclusion. Based on the classical Johnson–Mehl–Avrami–Kolmogorov (JMAK) interpretation, the coordination polymer has undergone a one-dimensional growth process

which can be attributed to the judicious design of the monomeric transition metal complexes. During the designing of materials, the interplay between metal and ligands has been carefully considered from both thermodynamic and kinetic aspects in order to attain coordination systems with stable and robust redox process that is critical for both electrochromism and energy storage. Unlike the intercalation-deintercalation mechanism exhibited by metal oxides, the movement of ions flux in and out of the polymer could occur rapidly during the electrochemical reaction, offering a fast charge transfer process that is not possible in inorganic materials. The polymer-bound electrode has been configured into a hybrid device which is able to operate in an aqueous Zn electrolyte, achieving high color contrast of *ca.* 60 %, fast response time of <1s, and good stability for over 1000 consecutive charging-discharging cycles.

9:19 PM Q&A

SESSION EL01.11: Organic Ionic Conductors I
Session Chairs: Derya Baran and Alan Kaplan
Tuesday Morning, April 20, 2021
EL01

8:00 AM EL01.11.01

Late News: In Situ and In Operando Scattering Studies on Organic Solar Cells Based on Organic Semiconductors Peter Muller-Buschbaum; Technische Universität München, Germany

Based on novel organic semiconductors, organic solar cells are an interesting alternative to conventional silicon based solar cells as they feature new possibilities. Using wet chemical processing, they can be manufactured with large-scale production methods such as roll-to-roll printing. Consequently, the production of organic solar cells has the potential to become very cheap and easy. With in-situ grazing incidence small- and wide-angle X-ray scattering (GISAXS and GIWAXS) studies, we gain information on the kinetics of morphology formation of electrodes, blocking layers and active layers of the solar cells during processing.

In terms of large-scale usability, one of the major challenges for organic solar cells is to overcome their relatively short lifetime, as compared to their inorganic counterparts. To gain a deeper understanding of organic solar cell degradation with respect to changes in the active layer nano-morphology, we present in-situ studies on model donor-acceptor organic semiconductor based solar cells during the first hours of operation. The in-operando studies reveal information on both, its evolving current-voltage characteristics and the active layer nano-morphology. For that purpose, GISAXS / GIWAXS measurements and current-voltage (IV) tracking of the operating solar cell are performed simultaneously to gain fundamental understanding. Starting from an optimized morphology of the active layers in terms of highest efficiencies for organic solar cells, depending on the donor-acceptor organic semiconductor system, a mixing or demixing process are identified to cause changes of the morphology. The altered morphology is less optimal for charge transport through the active layer due to poor percolation in a too fine morphology or poor splitting of excitons in a too coarse morphology.

8:15 AM EL01.11.02

Late News: Phase Segregation Driven Ultra-Low Dark Currents in Organic-Inorganic Hybrid X-Ray Detectors Maheshani Prabodhi Alwis Nanayakkara¹, Lidija Matjacic², Andrew Nisbet³, Imalka Jayawardena¹ and S. Ravi P. Silva¹; ¹University of Surrey, United Kingdom; ²National Physical Laboratory, United Kingdom; ³University College London, United Kingdom

Organic-inorganic hybrid semiconductors have been identified as an emerging class of novel materials for direct conversion X-ray detection^[1,2]. Their success is attributed to a number of characteristics such as sensitivity over a broad energy range including high sensitivity for hard X-rays, low voltage operation, and conformability to complex shapes. However, previous generations of such detectors displayed dark currents that are $\times 1000$ -

10,000 higher than the industry standard of 10 pA mm^{-2} , therefore hindering their potential for commercialization. Herein, we introduce a new route to achieve ultra-low dark currents that are below 10 pA mm^{-2} even at electric fields as high as $\sim 4 \text{ V } \mu\text{m}^{-1}$ in hybrid detectors fabricated by incorporating high atomic number bismuth oxide nanoparticles into an organic bulk heterojunction consisting of p-type Poly(3-hexylthiophene-2,5-diyl) (P3HT) and n-type [6,6]-Phenyl C71 butyric acid methyl ester (PC₇₀BM). Such ultra-low dark currents are achieved through the enrichment of the hole selective p-type polymer near the anode contact, induced via vertical phase segregation within the hybrid film. The resulting hybrid detectors display broadband response with a record high sensitivity of $\sim 1.5 \text{ mC Gy}^{-1} \text{ cm}^{-2}$ and less than 6% variation in angular dependence response when tested under 6 MV X-rays from a clinical linear accelerator. Therefore, we anticipate that the above characteristics in combination with excellent dose and dose rate linearity, reproducibility, and long-term stability would stimulate further interest towards implementing such detectors for applications in dosimetry for medical and industrial applications.

References

- [1] M. P. A. Nanayakkara, L. Matjačić, S. Wood, F. Richheimer, F. A. Castro, S. Jenatsch, S. Züfle, R. Kilbride, A. J. Parnell, M. G. Masteghin, H. M. Thirimanne, A. Nisbet, K. D. G. I. Jayawardena, S. R. P. Silva, *Adv. Funct. Mater.* **2020**, 2008482.
- [2] H. M. Thirimanne, K. D. G. I. Jayawardena, A. J. Parnell, R. M. I. Bandara, A. Karalasingam, S. Pani, J. E. Huerdler, D. G. Lidzey, S. F. Tedde, A. Nisbet, C. A. Mills, & S. R. P. Silva, *Nat. Commun.* **2018**, 9, 2926.

8:30 AM EL01.11.03

Enhancing Long-Term Device Stability Using Thin-Film Blends of Small Molecule Semiconductors and Insulating Polymers to Trap Surface-induced Polymorphs Tommaso Salzillo^{1,2}, Antonio Campos¹, Adara Babuji¹, Raul Santiago³, Stefan Bromley^{3,4}, Carmen Ocal¹, Esther Barrena¹, Remi Jouclas⁵, Christian Ruzie⁵, Guillaume Schweicher⁵, Yves H. Geerts^{5,6} and Marta Mas-Torrent¹; ¹Institut de Ciència de Materials de Barcelona (ICMAB-CSIC), Spain; ²Weizmann Institute of Science, Israel; ³Universitat de Barcelona, Spain; ⁴Institució Catalana de Recerca i Estudis Avançats (ICREA), Spain; ⁵Faculté des Sciences Université libre de Bruxelles, Belgium; ⁶Université Libre de Bruxelles, Belgium

The 2,7-dioctyloxy[1]benzothieno[3,2-b]benzothiophene (C₈O-BTBT-OC₈) molecule, one of the most promising organic semiconductors, presents two different crystalline phases: a co-facial structure (bulk phase) and a herringbone structure also defined as surface-induced phase (SIP phase).¹ From solution deposition on Si/SiO₂ always the SIP phase has been detected so far and previous works have reported that with aging at ambient conditions or by solvent vapor annealing it transforms to the thermodynamically stable bulk structure.² The Bulk C₈O-BTBT-OC₈ phase crystallizes in a triclinic P-1 system with two molecules per unit cell presenting a displaced cofacial stacking, while the SIP phase has a monoclinic P2₁/c structure with a herringbone packing.^{1,3}

In this work we report the stabilization of the SIP phase by blending the C₈O-BTBT-OC₈ with an insulating polymer and preparing the thin film transistors (TFTs) by the bar-assisted meniscus shearing (BAMS) technique. All the TFTs based on C₈O-BTBT-OC₈ with polystyrene (PS) of low molecular weight (i.e., 3K) and high molecular weight (i.e., 100K) present the SIP structure and display good electrical properties with a field-effect mobility close to $1 \text{ cm}^2/\text{V s}$, a threshold voltage around 0 V and an on/off current ratio of 10^7 - 10^8 . However, after 3 months in ambient conditions the C₈O-BTBT-OC₈:PS100K film retain the same morphology, while the film based on the lower molecular weight PS presents the formation of different crystal domains on top of the pristine layer. The structural inhomogeneity of the C₈O-BTBT-OC₈:PS3K was investigated by micrometric spatially resolved Lattice phonon Raman spectroscopy.⁴

In order to compare the hole transport tendencies in the Bulk and SIP polymorphs of C₈O-BTBT-OC₈, we analyzed all independent pairwise HOMO-HOMO (Highest occupied molecular orbital) intermolecular electronic couplings (J_{HOMO}) in the two crystal structures using density functional theory (DFT) based calculations. Bulk phase show a highly anisotropic one dimensional (1D) electronic structure with only a single dominant J_{HOMO} value of 42 meV in a direction parallel to the *a*-axis of the crystal with all other J_{HOMO} values being $\leq 6 \text{ meV}$. In contrast, the SIP polymorphic phase has two main independent intermolecular couplings with

moderate J_{HOMO} values of 12-13 meV, which span over three different directions in the ab plane of the material, indicative of a more 2D electronic isotropy. Thus, although a larger electronic coupling is found in the Bulk phase, the electronic dimensionality in the SIP phase is enhanced.

Using the polymer blend we demonstrate the possibility to stabilize, during the time period studied of one year and a half, of the metastable SIP phase which present a 2D electronic isotropy compared with the 1D π -stacking arrangement of the bulk structure and thus to be preferred for thin film devices fabrication.⁵

[1] N. Bedoya-Martínez, B. Schrode, A. O. F. Jones, T. Salzillo, C. Ruzié, N. Demitri, Y. H. Geerts, E. Venuti, R. G. Della Valle, E. Zojer and R. Resel, *J. Phys. Chem. Lett.*, 2017, **8**, 3690–3695.

[2] B. Schrode, A. O. F. Jones, R. Resel, N. Bedoya, R. Schennach, Y. H. Geerts, C. Ruzié, M. Sferrazza, A. Brillante, T. Salzillo and E. Venuti, *ChemPhysChem*, 2018, **19**, 993–1000.

[3] C. Ruzié, J. Karpinska, A. Laurent, L. Sanguinet, S. Hunter, T. D. Anthopoulos, V. Lemaure, J. Cornil, A. R. Kennedy, O. Fenwick, P. Samorì, G. Schweicher, B. Chattopadhyay and Y. H. Geerts, *J. Mater. Chem. C*, 2016, **4**, 4863–4879.

[4] T. Salzillo, R. G. Della Valle, E. Venuti, A. Brillante, T. Siegrist, M. Masino, F. Mezzadri and A. Girlando, *J. Phys. Chem. C*, 2016, **120**, 1831–1840.

[5] T. Salzillo, A. Campos, A. Babuji, R. Santiago, S. T. Bromley, C. Ocal, E. Barrena, R. Jouclas, C. Ruzie, G. Schweicher, Y. H. Geerts and M. Mas-Torrent, *Adv. Funct. Mater.*, 2020, **2006115**, 1–9.

8:45 AM *EL01.11.04

Monitoring Ionic-to-Electronic Conduction in Bioelectronic Devices Sahika Inal; King Abdullah University of Science and Technology, Saudi Arabia

Organic mixed conductors and electrochemical phenomena at solid-liquid interface have garnered significant attention for applications in bioelectronics, electrochromics, energy storage/generation, neuromorphic computing, and thermoelectrics. These devices operate in electrolytes that render ions mobile in the film, making the coupling between electronic and ionic charges crucial. A prime example of such devices is the organic electrochemical transistor (OECT), a transducer used commonly to monitor bioelectronic signals. In this work, I will introduce the class of materials that have been used in OECT channels. Using *in operando* techniques, we find that the ions enter the semiconducting polymer channel hydrated and the excess swelling of the material has a significant effect on device characteristics, which can be traced back to changes in the overall structural order.^{1,2} We show that the infiltration of the hydrated dopant ions into the polymer film irreversibly changes the polymer structure and negatively impacts the OECT mobility, as well as the efficiency, reversibility, and speed of charge generation. We conclude that minimizing swelling of the polymer films during doping is a key parameter to design fast and highly efficient ion-to-electron transduction devices. Our work highlights the importance of characterizing the properties of these films *in-situ* (in their electrolyte swollen state) for drawing conclusions related to materials properties/device performance, which has a tremendous impact on the performance of biosensors. Lastly, I will show an n-type conjugated polymer that, against all the current design rules, shows high device performance, and introduce a new direction for the design of mixed conductors.

¹ Savva, A et al *Chem. Mater.* **2019** 31 (3), 927-937

² Savva, A et al *Adv. Funct. Mater.* **2020** 30 (11), 1907657

9:10 AM *EL01.11.05

Controlled and Reversible Volume Change in Conjugated Polymers via Electrochemical Addressing—An Experimental and Theoretical Study Johannes Gladisch¹, Sarbani Ghosh¹, Maximilian Moser², Iain McCulloch³, Magnus Berggren¹, Igor Zozoulenko¹ and Eleni Stavrinidou¹; ¹Linköping University, Sweden; ²University of Oxford, United Kingdom; ³King Abdullah University of Science and Technology, Saudi Arabia

Controlled volume change of soft materials is of interest for a wide range of applications, from actuators, microfluidics and drug delivery. Conjugated polymers can transform electrical energy into volume change when included in electrochemical devices via the exchange of ions and solvent. Recently we demonstrated a

glycolated polythiophene that reversibly expands by 300% upon addressing, relative to its previous contracted state, while the first irreversible actuation can achieve values of 10000%, outperforming any other conjugated polymers. Here I will present a study on a series of polythiophenes that differ in the length and/or in the distribution of the ethylene glycol side chains and how this impacts the volume change upon electrochemical addressing. In order to get insight on how the structure and morphology affect the volume change and reveal the mechanisms involved at the nanoscale we performed Molecular Dynamics. Finally, I will present how we can apply these materials for dynamic microfiltration.

SESSION EL01.12: Organic Ionic Conductors II
Session Chairs: Christine Luscombe and Eleni Stavrinidou
Tuesday Morning, April 20, 2021
EL01

11:45 AM EL01.12.01

Next-Generation Organic Mixed Ionic-Electronic Conductors—A Dynamic Study on Copolymers for Faster Electrochemical Devices Olivier Bardagot¹, Sanne Govaerts², Gonzague Rebetz¹, Priscila Cavassin¹, Frederic Schneider¹, Julien Réhault¹, Wouter Maes² and Natalie Banerji¹; ¹University of Bern, Switzerland; ²Hasselt University, Belgium

Improving the performance of organic mixed ionic-electronic conductors (OMIECs) favors not only the development of bioelectronic devices for healthcare and neuroscience applications, but also of optoelectronic and energy storage devices.[1] The performance of OMIECs can be explored using organic electrochemical transistors (OECTs). OMIECs bearing ionic side chains (called conjugated polyelectrolytes) present promising doping/dedoping cycling stability for applicative use.[2] Higher transconductance can be reached for copolymers bearing both alkyl and ionic side chains.[3] Nonetheless, the use of polar, glycolated, side chains remains to date the most effective strategy to concomitantly enhance the transconductance and response time of OECTs.[4] In this work, we compared P3HT-like polymers composed of: 100% alkyl, 100% ionic, 100% glycolated, and 50/50% ionic/glycolated side chains. Using *in operando* time-resolved UV-Vis-NIR absorption spectroscopy, with a time-resolution of a few milliseconds, and multivariate curve resolution (MCR) analysis, we elucidated the underlying processes driving the electrochemical doping kinetics of these OMIECs. Our findings suggest that introducing ionic side chains in glycolated polymers is an effective and easily transferable strategy to further enhance the response time of OECTs.

[1] B. D. Paulsen, K. Tybrandt, E. Stavrinidou, J. Rivnay, *Nature Materials* **2020**, 19, 13–26.

[2] E. Zeglio, M. M. Schmidt, M. Thelakkat, R. Gabrielsson, N. Solin, O. Inganäs, *Chem. Mater.* **2017**, 29, 4293–4300.

[3] P. Schmode, D. Ohayon, P. M. Reichstein, A. Savva, S. Inal, M. Thelakkat, *Chem. Mater.* **2019**, 31, 5286–5295.

[4] M. Moser, J. F. Ponder, A. Wadsworth, A. Giovannitti, I. McCulloch, *Advanced Functional Materials* **2019**, 29, 1807033.

12:00 PM EL01.12.02

Late News: Aqueous Formulation of Concentrated Semi-Conductive Fluid Using Polyelectrolyte Complexation My Linh Le¹, Dakota Rawlings¹, Scott Danielsen², Rachel Segalman¹ and Michael Chabinyc¹; ¹University of California, Santa Barbara, United States; ²Duke University, United States

There has been a growing interest in aqueous formulation of conjugated polymers to achieve more environmentally benign processing routes and to widen the utilization of these polymers in bioelectronics. The widely studied conducting polymer poly(3,4-ethylenedioxythiophene):polystyrene sulfonate (PEDOT:PSS) has

high electrical conductivity and aqueous processability, but suffers from ill-defined structure, poor synthetic tunability, and heavily post-processing dependent performance. Here, we demonstrate how coacervation of oppositely charged polymers can be used for formulating and processing conjugated polymers in aqueous media. By sampling a wide range of polymer concentrations and dielectric media, we obtained the mixing phase diagram of a PEDOT derivative substituted with alkoxysulfonate groups (PEDOT-S) with a polymeric ionic liquid (PIL). Using this phase diagram, we were able to find compositions that enabled the formation of a complex coacervate of these 2 polymers. This coacervate is a viscous fluid with extremely high polymer content (up to 60 wt%), and can be readily blade-coated to produce films of around 5 μm in thickness. Subsequent doping of the film with a strong acid increased the electrical conductivity of the coacervate to values that were higher than those of the neat PEDOT-S polymer. Optical spectroscopy showed that acid treatment led to a lower doping level in the coacervate than in neat PEDOT-S, suggesting a smaller charge carrier density and thus a higher carrier mobility within the coacervate. We postulate that in the coacervate, the conjugation length of PEDOT-S was enhanced due to the reduction in torsional disorder along the polymer chain upon the complexation. This work shows that polyelectrolyte complexation is a promising route to formulate conjugated polymers in aqueous media at high concentrations and that the resulting material is compatible with large-scale industrial processing protocols like blade coating. The complexation can also have beneficial impacts on charge transport through the improved control of the conformation of the conjugated polymer.

12:15 PM EL01.12.03

Late News: Characterizing Mixed Ionic-Electronic Conductors Using Grazing-Incidence Wide-Angle X-Ray Scattering (GIWAXS) with *In Situ* Potential Control Lucas Flagg¹, Maximilian Moser², Iain McCulloch^{3,2}, Dean DeLongchamp¹ and Lee Richter¹; ¹National Institute of Standards and Technology, United States; ²University of Oxford, United Kingdom; ³KAUST, Saudi Arabia

Organic mixed ionic-electronic conductors (OMIECs) are a class of materials that have recently drawn interest as materials for next generation biosensors, energy storage, neuromorphic computing and other organic electronic applications. This class of materials rely on counterions from an electrolyte solution to penetrate the volume of the organic layer in order to compensate injected electronic charges. Measuring the microstructure of these materials is uniquely challenging due to the essential role the electrolyte plays during operation of these types of devices. Traditional microstructure measurements are rarely performed in contact with liquid electrolytes, and therefore fail to fully characterize the most device relevant microstructure. Additionally, many of these materials are electrochemically unstable in the presence of air which limits the understanding we can gain from traditional *ex-situ* scattering techniques. These challenges motivate *in-situ* scattering experiments with both potential control and solvent present. Here we develop an *in-situ* grazing-incidence wide-angle x-ray scattering (GIWAXS) procedure based upon a “rolling drop” electrode, that allows us to interrogate the crystallite lattice while fully hydrated AND electrochemically doped. We explore a model series of polymers that display distinctly different swelling based upon the distribution of ethylene glycol in their side chains. Using this technique, we separate the active swelling of the polymer crystallites due to electrochemical oxidation/reduction from the passive swelling due simply to the hydration of the polymer lattice. Additionally, we use the identity of the dopant ion to change the hydrophobicity of the electrochemically doped polymer to further probe the role of hydration in this series of polymers.

12:30 PM EL01.12.04

Late News: Effect of Morphology, Composition and Mobile Anion on the Electronic Performance of Polyelectrolyte Block Copolymers Samantha Brixi, Alexander Peltekoff and Benoit Lessard; University of Ottawa, Canada

The growing demand for flexible, lightweight, and stretchable electronics has led to significant interest in printed electronics such as thin-film transistors (TFTs), which are used as foundational components in many emerging organic electronic devices such as displays and sensors. These applications require TFTs that can both operate at low voltages to minimize power utilization and be effectively produced by large scale printing methods to reduce cost.

Polyelectrolyte materials produce a large electrical double-layer capacitance (EDL) that is independent of layer thickness. This large EDL capacitance is exploited to produce TFTs that operate at low voltages. These materials are also compatible with large scale production methods that have less control over layer thickness. However, the resulting devices are typically slow-responding due to the slow ion migration during electrical double-layer formation. To improve this, the material's ionic conductivity must be improved. Ideally, an optimal polyelectrolyte gating material must insulate charge, have a high conductivity for fast switching speeds, and produce a large double-layer capacitance required for reduced operating voltages.

Our study investigates structure-property relationships between polymeric structural elements, such as morphology, polymer composition, anionic salt, and the materials' physical properties of interest: double-layer capacitance and conductivity. We synthesized a matrix of diblock copolymers consisting of insulating polystyrene first block followed by a second copolymer block consisting of an ionic liquid (IL) conductive monomer and soft PEGMA monomer. We varied the IL/PEGMA composition of the second block, the length of the second block, as well as the mobile anion associated with the ionic liquid monomer. Each material was tested in capacitors to determine the EDL capacitance and conductivity of each material to investigate structure-property relationships.

We found that microphase separation is critical for increased conductivity. Also, we found that increasing the PEGMA loading of the second block greatly improved conductivity. However, PEGMA loadings over 75% solubilized the first block eliminating the microphase separation and thus the nanochannel domains essential for conductivity. The double-layer capacitance can be changed by an order of magnitude depending on the anionic salt. We have identified structural design rules showing what chemical handle influences a specific material property.

Incorporating the dielectrics into top-gate top-contact TFTs with n-type semiconductor P(NDI2OD-T2), we found the devices could be operated at exceptional low voltages (< 1 V) while maintaining mobility values comparable to literature. We have also performed frequency-dependent measurements of the TFTs to compare the properties of the polyelectrolytes with different mobile anions, finding these results correlated well with observed TFT performance.

12:45 PM EL01.12.05

Quantitative Composition and *Operando* Structure Determination of Organic Mixed Ionic-Electronic Conductors Ruiheng Wu¹, Christopher J. Takacs², Maximilian Moser³, Bryan D. Paulsen¹, Joseph Strzalka⁴, Qingteng Zhang⁴, Iain McCulloch^{5,6} and Jonathan Rivnay^{1,1}; ¹Northwestern University, United States; ²SLAC National Accelerator Laboratory, United States; ³Imperial College London, United Kingdom; ⁴Argonne National Laboratory, United States; ⁵University of Oxford, United Kingdom; ⁶King Abdullah University of Science and Technology, Saudi Arabia

Organic mixed ionic-electronic conductors (OMIECs) are organic conjugated materials with the ability to uptake ions from aqueous electrolyte and transduce between ionic and electronic currents. The unique properties of OMIECs make them highly attractive in range of biological, energy and neuromorphic computing applications. For these materials operating in electrolyte emersed situations, the structure and composition is non constant during operation, and is difficult to characterize. This has become a major impediment to elucidation of structure property relationships that further the development of new materials. Here, we have filled these gaps of understanding that have been neglected in previous studies by quantifying the composition with ex situ X-ray fluorescence spectroscopy (XRF) and probing the device relevant structure with ex situ and operando grazing incident X-ray scattering. PEDOT:PSS and pg2T-TT were selected as model materials representing polyelectrolyte/conjugated polymer blends and homogeneous glycolated conjugated polymers, respectively. XRF studies of doped and dedoped PEDOT:PSS revealed the effect of Donnan exclusion due to the presence of PSS poly anions, preventing anion uptake and resulting in cation-only transport. Additionally, charge and mass balances revealed that the equilibrium between the polyanion and the proton contributed

significantly to the doping processes. XRF studies of doped and dedoped pg2T-TT quantified the dopant-anion concentration modulation, directly measured the minority role of cation transport, and revealed an unanticipated massive amount of charge trapping ($>10^{20}$ anions cm^{-3}) when exposed to electrolyte, that persists when reductively dedoped. The low conductivity of the reductively dedoped state confirmed the localized nature of the electronic charge counterbalancing the trapped anions. The pH dependence of dopant composition was investigated in both systems.

Ex situ grazing incident small-angle X-ray diffraction (GISAXS) confirmed the compositional homogeneity of both pg2T-TT and PEDOT:PSS polymer films. Operando grazing incident wide-angle X-ray diffraction (GIWAXS) of PEDOT:PSS, revealed the degree of polymer-electrolyte interaction resulting moderate lamellar expansions (1.6 Å) with electrolyte exposure, following a lamellar spacing relaxation upon ionic doping. Operando GIWAXS of pg2T-TT showed a moderate lamellar expansion (0.6 Å) with DI water exposure, but a much larger lamellar expansion (~ 10 Å) upon electrolyte exposure. The potential dependent π stack and lamellar d-spacing were quantified from the diffraction patterns. In contrast to PEDOT:PSS, the lamellar spacing of pg2T-TT was clearly increased during doping process.

Combining these multimodal results gives new insight into these systems. For instance, the XRF and GISAXS reveal that cations are evenly distributed in PEDOT:PSS contrary to common assumptions about the heterogeneous composition of PEDOT-rich and PSS-rich domains. Only when phase separation is driven by processing in strong acids, is an inhomogeneous distribution of cations observed. XRF and operando GIWAXS reveal the permanent structural modification that accompanies the high degree of charge trapping in pg2T-TT. As confirmed by GISAXS, this implies that anions must be present in both the amorphous and the crystalline regions of the polymer. These results represent the first quantitative compositional determination of OMIECs and the first operando scattering studies of weakly scattering homogenous OMIECs in aqueous conditions, and establish quantitative techniques necessary to produce meaningful structure-property relationships to drive the rational design of next-generation OMIECs.

1:00 PM EL01.12.06

Predicting Mechanical Properties from Molecular Parameters of Conjugated Polymers Abigail M. Fenton, Ralph H. Colby and Enrique D. Gomez; The Pennsylvania State University, United States

Conjugated polymers are used in many organic electronic devices such as organic photovoltaics, organic light emitting diodes, organic field effect transistors and bioelectronics. However, fundamental characteristics of these materials, such as mechanical properties and phase behavior, and their correlation with chemical structure, are not well understood. Nevertheless, controlling mechanical properties of conjugated polymers is crucial to enabling flexible and stretchable electronics. The plateau modulus G_N° , which is inversely related to the entanglement molecular weight M_e , can be used to predict the mechanical response of polymers for many orders of magnitude in frequency (along with the molecular weight distribution and relaxation time). The relationship between structural parameters (Kuhn length b and Kuhn monomer volume v_0) and mechanical stiffness (plateau modulus G_N°), initially proposed by Graessley and Edwards and experimentally investigated by Everaers, while well-studied for flexible and stiff polymers, has a large gap in experimental data between the flexible and stiff regimes. This gap prevents the validation of the crossover between flexible and stiff polymers and therefore, the prediction of mechanical properties from chain structure of any polymer in this region. Given the chain architecture, including a semiflexible backbone and side chains, conjugated polymers are an ideal class of material to study this cross-over region. Using small angle neutron scattering, oscillatory shear rheology, in-situ polarized optical rheology, along with the freely rotating chain model we have shown that twelve polymers with aromatic backbones, including conjugated polymers, populate a large part of this gap. We also have shown that a few of these polymers exhibit nematic ordering which explains a lower experimental G_N° than predicted using Everaers' plot, as nematic polymers have fewer entanglements than isotropic polymers. Nevertheless, when isotropic, these polymers follow the proposed relationship between b , v_0 , and G_N° .

1:15 PM EL01.12.07

High-Performance and Temperature-Resilient Redox Memories with Linear 20 ns Switching for Integrated Neuromorphic Computing Armantas Melianas¹, Tyler J. Quill¹, Garrett LeCroy¹, Yaakov Tuchman¹, Hilbert v. Loo^{2,1}, Scott Keene¹, Alexander Giovannitti¹, Hye Ryoung Lee¹, Iuliana Petruta Maria³, Iain McCulloch^{3,4} and Alberto Salleo¹; ¹Stanford University, United States; ²Technische Universiteit Eindhoven, Netherlands; ³Imperial College London, United Kingdom; ⁴King Abdullah University of Science and Technology, Saudi Arabia

Synaptic devices with linear resistance tuning are highly sought after for parallel programming of artificial neural network (ANN) weights in neuromorphic arrays. Conventional resistive memories however suffer from nonlinear and asymmetric conductance tuning and excessive write noise that are detrimental for accelerating learning in hardware ANNs. To address these challenges, we have recently introduced electrochemical random-access memories (ECRAMs), where resistive switching is controlled by ion insertion from the electrolyte into a semiconductor channel, enabling linear resistance tuning and parallel array programming [1]. However, state-of-the-art organic ECRAMs have not yet demonstrated stable and efficient operation at elevated 20-100 °C temperatures required for large scale integration with Si logic.

Here, we show that semiconducting polymers in combination with ion gels enable solid-state organic ECRAMs with stable and temperature-independent operation up to 110 °C. With a judicious choice of materials we demonstrate ECRAMs with linear conductance tuning (over 100x distinct states), fast switching (20 ns), rapid write-read cycles (<1 μs), low voltage (±1 V) and low energy (~100 fJ/write) operation, and excellent endurance (>10⁹ write-read operations at 90 °C). The use of novel polymers also improves the dynamic range to >2x. We use a series of photolithographically patterned devices and quantitative modelling to demonstrate that further scaling would lead to faster than 1 GHz switching. This shows that organic ECRAMs are temperature-resilient and meet the stringent device requirements for efficient neuromorphic computing. Demonstration of such high-performance solid-state ECRAMs [2] is a fundamental step towards their integration into synaptic arrays amenable to learning and inference.

[1] E. Fuller, S. T. Keene*, A. Melianas*, et al. *Science* 364 (6440), 570-574 (2019)

[2] A. Melianas, et al. *Science Advances* 6 (27), eabb2958 (2020)

SESSION EL01.13: Organic Semiconductor Characterization II

Session Chairs: Xiaodan Gu and Christine Luscombe

Tuesday Afternoon, April 20, 2021

EL01

2:15 PM *EL01.13.01

Assessment of Molecular Dynamics Force Fields for Conjugated Polymers Using Neutron and X-Ray Scattering Caitlyn M. Wolf and Lilo D. Pozzo; University of Washington, United States

Conjugated polymers can be ideal materials for the design of efficient photovoltaic devices, batteries, thermoelectric cells, light emitting diodes and many new technologies. Moreover, a large flexibility in organic synthesis methods enables the efficient application of molecular design principles to produce superior materials. Yet, the use of computational methodologies for conjugated polymers is still limited by a lack of properly validated simulation force fields that can be used to model structures and temporal fluctuations through molecular dynamics simulations. This presentation motivates the use of neutron and x-ray scattering techniques for the development of improved molecular simulation force fields and structural parameters specifically for poly-3-alkyl-thiophene, a model conjugated polymer. Quasi-elastic neutron scattering (QENS) experiments are used along with MD simulations to quantitatively compare proposed force fields to extensive sets of experimental data. X-ray and polarized neutron diffraction are also used to correlate experimental and model-

generated polymer structures. QENS validation of MD force fields presents a unique opportunity to increase the accuracy of highly uncertain parameters that are used in the simulation of conjugated polymers, including partial charges, Lennard-Jones and backbone torsion parameters. Many of these parameters are estimated from quantum mechanical calculations such as density functional theory but, unlike for force fields designed for small molecules, they are not often parameterized to experimental data. High variability is also observed in parameters for the small number of simulation force fields that have been proposed in the literature. A vision for the accelerated development of accurate force fields for these classes of materials is also proposed.

2:40 PM *EL01.13.02

What is the Assembly Pathway of Conjugated Polymers from Solution to the Solid State? Ying Diao; University of Illinois at Urbana-Champaign, United States

The hierarchical assembly of conjugated polymers has gained much attention due to its critical role in determining the optical/electrical/mechanical properties. The hierarchical morphology encompasses molecular scale intramolecular conformation (torsion angle, chain folds) and intermolecular ordering (π - π stacking), mesoscale domain size, orientation and connectivity, and macroscale alignment and (para)crystallinity. Such complex morphology in the solid state is fully determined by the polymer assembly pathway in the solution state, which in turn is sensitively modulated by molecular structure and processing conditions. However, molecular pictures of polymer assembly pathways remain elusive, due to the lack of detailed structural characterizations in the solution state and lack of understanding on how various factors impact the assembly pathways. In this talk, we discuss pre-aggregation and liquid-crystal mediated assembly pathways and their relationship. We develop SAXS models for in-depth analysis of the complex solution state structure of conjugated polymers complemented by imaging and spectroscopy. Further we discover a chiral, helical liquid crystal mediated assembly pathways from achiral conjugated polymers. We elucidate a hierarchical helical structure spanning the molecular scale to micron scale. We further trace the molecular origin of chiral liquid crystal assembly pathways. These studies change the way we perceive structure of conjugated polymers and may bring forth exciting new optoelectronic properties not imagined before.

3:05 PM EL01.13.03

Chiral Emergence in Multistep Hierarchical Assembly of Achiral Conjugated Polymers Kyung Sun Park and Ying Diao; University of Illinois at Urbana-Champaign, United States

Hierarchical structures are inherent to various soft material systems including biomolecules, mesogens and conjugated polymers. Structural chirality commonly results from the hierarchical organization of chiral building blocks, e.g., amyloids, M13 phage and chiral mesogen [1, 2]. Recently, it has been discovered that achiral mesogens/nanostructures can also form chiral, twisted structures due to symmetry breaking or topological defects [3-5]. This new finding can open a new degree of freedom for tuning electrical and optical properties and provide a fundamental understanding of complex supramolecular assembly and phase transition behaviors. In this work, we demonstrate chiral emergence from achiral donor-acceptor (D-A) conjugated polymers, a high-performance organic semiconductor. Our previous work demonstrated that the morphology of printed isoindigo-bithiophene-based conjugated polymer (PII-2T) films results in chiral, zigzag twinned domains despite the inherent molecular achirality [6]. We anticipate that the chirality is responsible for the multistep hierarchical assembly of achiral, torsional molecular structures. Still, several aspects regarding the nature of its multiscale organization and behavior remain a mystery. In conjugated polymers, the main intermolecular forces are π -interactions between the backbones and dispersion forces among the alkyl side chains. Such interaction often results in the presence of solution-phase aggregates and/or liquid crystalline phase. Given the importance of solvent in mediating these interactions, we also demonstrate how a solvent influences the development of mesophase and the relationship between pre-aggregation and mesophase formation. This study provides a clear map for the multiscale assembly pathway of conjugated polymers as we explore the possible hierarchical mesophase structures that can be used to enhance device performance

2. W. J. Chung *et al.*, *Nature* **478**, 364-368 (2011)
3. L. E. Hough *et al.*, *Science* **325**, 456-460 (2009)
4. M. R. Tuchband *et al.*, *P Natl Acad Sci USA* **116**, 10698-10704 (2019)
5. G. Singh *et al.*, *Science* **345**, 1149-1153 (2014)
6. K. S. Park *et al.*, *Sci Adv* **5**, eaaw7757 (2019)

3:20 PM EL01.13.04

Late News: Crystallization of Organic Thin Films and the Role of Thermal Properties and Molecular Structure Jordan Dull¹, Yucheng Wang¹, Holly Johnson¹, Komron J. Shayegan², Ellie Shapiro¹, Rodney Priestley¹, Yves H. Geerts³ and Barry P. Rand¹; ¹Princeton University, United States; ²California Institute of Technology, United States; ³Université libre de Bruxelles, Belgium

A group of organic small molecules, selected for small differences in molecular structure, are investigated for their ability to crystallize as a thin film. Each material is vapor deposited in a range of thicknesses between 20 - 80 nm and subsequently thermally annealed. The annealed films are categorized into three groups based on the crystal morphology as determined by polarized optical microscopy: platelet-forming, spherulite-forming, and those that resist crystallization. Differential scanning calorimetry is utilized to determine bulk thermal properties of these materials. We demonstrate that these thermal properties provide a reliable indicator of a material's crystallization motif. Platelet-forming materials tend to be characterized by high melting points (T_m) and a large crystallization driving force at the material's crystallization temperature (ΔG_c). The materials that resist crystallization as a thin film have small ΔG_c . These guidelines can help determine which organic molecules have a greater likelihood of growing into large-scale crystalline frameworks, a key step for improving charge carrier mobility and exciton diffusion length in organic semiconductors.

3:35 PM EL01.13.05

Late News: Using the High-Resolution *ac*-Hall Effect to Investigate the Effects of Grain Boundaries, Strain and Photoexcitation on the Charge Transport in Crystalline Organic Semiconductors. Vitaly Podzorov; Rutgers, The State University of New Jersey, United States

An exciting recent progress has been made in our understanding of fundamentals of charge carrier transport and photoconductivity of crystalline and polycrystalline organic semiconductors, largely achieved thanks to high-sensitivity *ac*-Hall effect measurements. This talk will cover one or more examples. For instance, we have elucidated the effect of grain boundaries on the Hall effect in high-performance, polycrystalline organic transistors, where it was found that capacitively charged grain boundaries may lead to an underestimated Hall mobility and an overestimated Hall carrier density [1]. In another example, the *intrinsic* mobility-strain relationship has been measured for the first time in organic semiconductors (here, in single crystalline rubrene). It became possible thanks to the *ac*-Hall effect and Raman measurements as a function of uniaxial mechanical strain applied to ultra-thin, flexible single-crystal rubrene OFETs. The study reveals a very strong, anisotropic and reversible modulation of the intrinsic (trap free) charge carrier mobility of these OFETs with strain, showing that an effective mobility of organic circuits can, in principle, be enhanced by up to ~ 80% with only 1% of compressive strain [2]. Finally, a photo-Hall effect has been measured in organic semiconductors for the first time [3]. These measurements have allowed us to directly access the mobility and density of charge carriers photogenerated at the surface and in the bulk of (ungated) organic crystals under *cw* photoexcitation. Our data reveal some unexpected properties of photoexcitation process, including the generation of mobile carriers of only one type (holes) and unconventional power exponents in photoconductivity. The data are also consistent with the mechanism of photoconductivity in rubrene based on an interaction of long-lived, mobile triplet excitons with surface electron traps, leading to a release of mobile holes [3].

References:

1. H. H. Choi, A. F. Paterson, M. A. Fusella, J. Panidi, O. Solomeshch, N. Tessler, M. Heeney, K. Cho, T. D. Anthopoulos, B. P. Rand and V. Podzorov, "Hall Effect in Polycrystalline Organic Semiconductors: The Effect of Grain Boundaries", *Adv. Funct. Mater.*, 1903617 (2019).
2. H. H. Choi, H. T. Yi, J. Tsurumi, J. J. Kim, A. L. Briseno, S. Watanabe, J. Takeya, K. Cho, V. Podzorov, "A

Large Anisotropic Enhancement of the Charge Carrier Mobility of Flexible Organic Transistors with Strain: A Hall Effect and Raman Study", *Adv. Science*, 1901824 (2019).

3. V. Bruevich, H. H. Choi, V. Podzorov, "The Photo-Hall Effect in High-Mobility Organic Semiconductors", *Adv. Funct. Mater.*, DOI:10.1002/adfm.202006178 (2020).

3:50 PM EL01.13.06

Late News: Application of Structure-Property Relationships of Silicon Phthalocyanines to Achieve Low Threshold Voltage N-Type Organic Thin-Film Transistors Benjamin King and Benoit Lessard; University of Ottawa, Canada

Metal and metalloid phthalocyanines (MPcs) are a large class of thermally stable organic semiconductor materials which can be manufactured with relatively inexpensive reagents and that have easily accessible synthetic routes. A wide variety of MPcs containing different metal cores have been incorporated into organic light-emitting diodes (OLEDs), organic solar cells (OPVs) and organic thin-film transistors (OTFTs), including copper (CuPc) and zinc (ZnPc), trivalent MPcs (one axial group) including aluminum (AlPc-Cl) and tetravalent MPcs (two axial groups) including silicon (SiPc-Cl₂) and tin (SnPc-Cl₂). To date, the greatest reported mobility for an MPc-based OTFT incorporates titanyl phthalocyanine (TiOPc) as the semiconductor, which exhibits a hole mobility (μ_h) on the order of $10 \text{ cm}^2\text{V}^{-1}\text{s}^{-1}$. Although MPcs are generally p-type, examples of n-type derivatives of these materials exist including SiPcs, SnPcs and peripherally-fluorinated F₁₆-CuPc.

SiPcs have recently shown promise as n-type or ambipolar organic semiconductors with various derivatives. The highest reported electron mobility (μ_e) of SiPcs is $\approx 0.5 \text{ cm}^2\text{V}^{-1}\text{s}^{-1}$ using pentafluoro-phenoxy silicon phthalocyanine (F₁₀-SiPc), indicating that high-performance SiPcs not only compare to but exceed other metal phthalocyanines (MPcs) in n-type OTFTs and can rival state-of-the-art organic semiconductors. Despite this excellent potential, only a few structure-property relationships have been established to determine the impact of the axial substituent on the electrical performance of SiPc-based OTFTs. For example, previous density functional theory (DFT) modelling data indicated that μ_e and other charge transport properties in fluorophenoxy SiPcs are dependant on the axis of transport and the number of substituted fluorine atoms on the axial pendant. Additionally, the choice of axial group affects SiPc packing in the single crystal, often changing the π - π stacking distance, herringbone angle, and degree of molecular overlap.

In this work, structure-property relationships for phenoxy-SiPcs were developed by fabricating bottom-gate top-contact OTFTs employing 11 derivatives. Characterization of thin-film properties in addition to electrical performance in devices was completed. Thin-film characterization techniques included x-ray diffraction (XRD), atomic force microscopy (AFM) Grazing-Incidence Wide-Angle X-ray Scattering (GIWAXS) and DFT modelling. One significant trend observed from electrical characterization was that increasing the electron-withdrawing character of axial pendant groups as characterized by their Hammett Parameter led to a reduction in threshold voltage, indicating that these substituents play a role beyond solid state packing and influencing morphology of thin-films. It was also determined that low molecular weight pendant groups contributed to a greater degree of crystalline order of SiPc materials in thin-films. These findings dictated the design of three additional novel SiPcs with phenoxy pendant group Hammett Parameters in the range of +0.66 to + 0.997. These materials exhibited threshold voltages as low as 4.8 V, exceeding the record low threshold voltage of 7.8 V reported for F₁₀-SiPc-based OTFTs fabricated in an identical architecture.

SESSION EL01.14: Poster Session II: Organic Electronics II

Session Chairs: Xiaodan Gu and Lilo Pozzo

Tuesday Afternoon, April 20, 2021

5:15 PM - 6:15 PM

EL01

EL01.14.01

Atom Probe Tomography of Molecular Organic Materials Matthew B. Jaskot, Andrew P. Proudian and Jeremy D. Zimmerman; Colorado School of Mines, United States

Many organic electronic devices, such as organic light-emitting diodes (OLEDs) and organic photovoltaics (OPVs), contain blends of molecules. The morphology, interface structure, impurities, and degradation pathways are all of great interest in improving device performance. Conventional analysis techniques, such as transmission electron microscopy, often provide critical but limited information in these materials. Atom probe tomography (APT) collects the mass-to-charge state of every ion detected with nanometer-scale resolution, providing previously inaccessible information that enables evaluation of nanometer-scale morphology, impurity analysis, and understanding degradation pathways in molecular organic electronic materials blends.

A wide variety of molecules can be analyzed with APT, ranging from fullerenes (e.g., C₆₀) to metalorganics (e.g., tris(2-phenylpyridine)iridium or Ir(ppy)₃) without indication of fragmentation. Sub-nanometer spatial resolution, sub-Dalton mass discrimination, and the ability to identify impurities or degradation products below 0.01 atomic% have been demonstrated [1,2]. We will introduce the APT technique, discuss techniques for creating APT samples, typical analysis conditions for organic small molecules, and highlight structure-property relationships in OLED and OPV devices enabled by APT analysis.

References:

- [1] A.P. Proudian, M.B. Jaskot, C. Lyiza, D. R. Diercks, B.P. Gorman, and J.D. Zimmerman, *Effect of Diels–Alder Reaction in C₆₀-Tetracene Photovoltaic Devices*, NanoLetters 16, 6086-6091 (2016)
- [2] A.P. Proudian, M.B. Jaskot, D.R. Diercks, B.P. Gorman, J.D. Zimmerman, *Atom Probe Tomography of Molecular Organic Materials: Sub-Dalton Nanometer-Scale Quantification*, Chemistry of Materials 31, 2241-2247 (2019).
- [3] The work was supported in part by grant DE-SC0018021 funded by the U.S. Department of Energy, Office of Science Early Career program.

EL01.14.02

Late News: Flexible Blade Coated Devices—Dual Functionality with Simultaneous Deposition Jasmine M. Jan, Juan Zhu, Jonathan Ting and Ana C. Arias; University of California, Berkeley, United States

Advances in printing techniques have given rise to low-cost, large-area, flexible electronics and systems. These printing methods have been used to fabricate organic electronics including light-emitting diodes (OLEDs), photodiodes (OPDs), solar cells (OSCs), and thin-film transistors (OTFTs) for various applications such as flexible displays, imagers, photovoltaics, smart tags, and logic circuits. However, in applications that require dual functionality, such as optoelectronic sensors with a combination of light sources and detectors, devices are fabricated separately in multiple processing steps. Additionally, the devices are often stacked together, reducing the mechanical flexibility of the overall system. To address these limitations, we utilize blade-coating in conjunction with surface-energy-patterning (SEP) to simultaneously deposit OLED and OPD films side-by-side on a single flexible substrate. This printing technique allows us to manufacture functionally distinct devices, while retaining the ability to individually optimize each device via ink parameters. The film thickness and device performance are compared and characterized for concentrations of 8, 10, and 12 mg/ml for OLEDs and 20, 35, and 50 mg/ml for OPDs. We chose the optimal ink concentration for the blade-coating process based on desired device performance – luminance for OLEDs and EQE for OPDs. The optimized OLEDs exhibit an average turn-on voltage of 3.4 V, and average luminance of 7000 cd/m² at 8 V. At 1000 cd/m², the current density, EQE and luminous efficacy of the OLEDs is 60.8 mA/cm², 1.35% and 9.5 lm/W with peak emission at 612 nm. OPDs exhibit EQEs of over 30% over the visible spectrum, and up to 45% in the near infrared region. The OPDs have a low dark current of 65.5 pA/cm², a cutoff frequency of 300 kHz, and LDR of over 120 dB.

EL01.14.03

Advanced Infrared Nanospectroscopy for Polymer Blend Characterization Nathaniel L. Prine¹, Zhiqiang Cao¹, Song Zhang¹, Tianyu Li², Kunlun Hong², Sarah Morgan¹ and Xiaodan Gu¹; ¹The University of Southern Mississippi, United States; ²Center for Nanophase Materials Sciences, United States

Characterizing the morphology of polymer blends is critical for improving the performance of next-generation sensors, photovoltaics, and pharmaceuticals. Unfortunately, blends containing materials that share similar chemical composition remain challenging to measure by traditional scanning probe microscopy due to poor topographical contrast. Coupling infrared spectroscopy with atomic-force microscopy, infrared nanospectroscopy (AFM-IR) overcomes this contrast barrier by distinguishing blended components by their unique infrared absorption response. While AFM-IR remains a robust technique for measuring surface morphology, the versatility of the technique has been largely unexplored. Herein, AFM-IR is used to determine blend composition using fundamental infrared spectroscopy theory for a series of immiscible and miscible blends. Second, nanoscale phase separation in isotope blends is explored using AFM-IR and confirmed by resonant soft X-ray scattering and small angle neutron scattering. These investigations highlight the widely unexplored potential of AFM-IR and its application for probing low-contrast, polymer blend morphology.

EL01.14.04

Engineering π -Stacking of an Anthracene Organic Semiconductor Through Cocrystallization Gonzalo Campillo-Alvarado and Ying Diao; University of Illinois at Urbana-Champaign, United States

Organic semiconductors (OSCs) are a rapidly emerging field in molecular electronics. Specifically, single-crystalline OSCs have received considerable attention due to the unique properties associated with long-range order, solution processing, absence of grain boundaries, and extremely low defect density [1] leading to a wide range of multi-functional materials (e.g., field-effect transistors, light-emitting diodes, photovoltaics). However, the lack of strategies to control and promote π -stacking in single crystals of OSCs has limited their diversification, property tunability, and application. While covalent modification of OSCs has arguably received the most attention [2], supramolecular modification of OSCs through weak, non-covalent interactions with additional molecules (i.e., cofomers) has been largely unexplored [3]. The resulting single-phase multicomponent solids (i.e., cocrystals) typically display enhanced or modulated properties compared to the parent OSC.

In this contribution, we introduce the use of halophenols as cofomers to promote π -stacking of a pyridyl-containing anthracene through hydrogen-bonding. Specifically, solution cocrystallization of the anthracene OSC results in single crystals with modulated π -stacking and is accompanied with significant changes in the photophysical properties. We envisage the supramolecular control of π -stacking in single crystals of OSCs with suitable cofomers could lead to a rapid diversification of multicomponent and multifunctional crystalline electronics with enhanced and tailored properties (e.g., flexible electronics).

References:

[1] Zhang, X., Dong, H., Hu, W., *Adv. Mater.* **2018**, *30*, 1801048.

[2] Anthony, J., *Angew. Chem. Int. Ed.*, **2008**, *47*, 452.

[3] Ray, K. K., Campillo-Alvarado, G., Morales-Rojas, H., Höpfl, H., MacGillivray, L. R., Tivanski, A. V., *Cryst. Growth Des.* **2020**, *20*, 3.

5:27 PM Q&A

EL01.14.05

Nanoscale Mapping of Morphology of Organic Thin Films Jongchan C. Kim; University of Michigan–Ann Arbor, United States

Understanding morphology is fundamental to revealing the structure-property relationships of solids.

Disordered materials are of particular interest since their morphology is rarely in the lowest energy, equilibrium state, and hence can be complex and metastable, or even unstable over time. Organic molecular solids are particularly important disordered materials since they are bonded by relatively weak van der Waals (vdW) forces. Here, we reveal the detailed nanoscale morphology within archetype organic electronic thin films using Fourier plane imaging microscopy (FIM). By depositing phosphorescent dye molecules at strategic positions within a host organic thin film, their luminescence provides high resolution, depth and area-dependent structural maps of the host. In this work, the FIM-plus-dye molecule combination is used to create 3D morphological maps of changes arising from thermal annealing in a stacked bilayer film comprising CBP (4,4'-Bis(N-carbazolyl)-1,1'-biphenyl) and TPBi (2,2',2''-1,3,5-Benzinetriyl)-tris(1-phenyl-1-H-benzimidazole), and at the interfaces. The volume resolution of the measurements is at the Ångstrom scale in the direction normal to the film plane that is limited only by the flatness of the predeposited film and the ability to accurately determine layer thickness during deposition, and has a resolution of approximately half the visible wavelength (~200 nm) within the plane. Our results provide a powerful tool for the high-resolution 3D morphological imaging of materials employed in a wide range of optoelectronic applications.

EL01.14.06

Conformally Vapor-Printed PEDOT on Fabrics for Foldable and Breathable Wearable Device

Application Michael Clevenger¹, Han Wook Song² and Sunghwan Lee¹; ¹Purdue University, United States; ²Korea Research Institute of Standard and Science, Korea (the Republic of)

Wearable electronics are a growing branch of technology that can have a large impact on various types of applications. The potential for the creation of new wearable devices from the most important medical applications to ones for novel enjoyment are extreme. In order to develop these wearable electronic devices, traditional inorganic conductive materials do not lend themselves to this type of application due to their mechanically brittle nature. Instead, polymeric materials with better mechanical flexibility are more advantageous to the development of wearable electronic components. Poly(3,4-ethylenedioxythiophene) (PEDOT) is one of the most promising conjugated polymers due to its high electrical conductivity as well as the environmental stability. PEDOT has been integrated in many electronic and optoelectronic devices such as organic thin film transistors (TFTs), solar cells and sensors. Due to these demonstrated performance together with mechanical flexibility, PEDOT has been garnering much attention more recently for potential use in wearable electronic applications.

For the development of wearable electronic devices with PEDOT, challenges remain particularly for clothing applications. Sustainable mechanical flexibility should be achieved over repeated folding and bending cycles as naturally occur in our daily use of clothing. Further, breathability, one of the principle functions of clothes should not be sacrificed after the coating of PEDOT.

In this presentation, in order to mitigate the challenges, oxidative chemical vapor deposition (oCVD) will be utilized, which uses mild thermal energy to generate a polymerization between a vaporized source material and an oxidizer in a vacuum chamber. We have investigated the electrical and structural stability of oCVD PEDOT and other thiophene-based polymers[1-3] and these polymers have been integrated in electrochromic devices[4]; TFTs[3, 5]; organic solar cells[6-8]; and chemical sensors[9-11]. In comparison to more conventional solution-based processes, oCVD lends itself to certain traits that are more beneficial when applied to the creation of wearable electronic devices and thin film deposition on fabric substrates. Films deposited from the use of oCVD better conform to the target fabric substrate. With the achieved excellent conformality, the fabric coated with oCVD PEDOT is still able to maintain its flexible properties as well as breathability, and can effectively be used in next generation devices on fabrics that work as clothing as well as electronics. In addition, no solvents are required for the oCVD deposition and therefore substrate distortion or damage is minimized.

What will be presented is a comparison of various properties of PEDOT thin films on both glass and fabric substrates as well as Si and glass substrates. Thin film deposition on Si and glass substrates is used as a control to compare the performance of oCVD PEDOT on fabrics. Specifically performance in regard to electrical,

mechanical, surface, and chemical properties will be discussed. To mimic daily use in clothing, mechanical bending tests of oCVD PEDOT were conducted and excellent performance stability was observed over 150 times bending cycles. General electrical properties include an analysis of conductivity, carrier density, and carrier mobility utilizing Hall Effect measurements system and four-point probe. AFM and SEM are used to determine and compare surface and cross-sectional microstructures. FTIR and UV-Vis spectroscopy are used to compare optical properties and chemical bonding information. Our findings on vapor-processed conjugated polymers on fabrics with high conductivity and mechanical flexibility is expected to significantly contribute to the realization of high performance and sustainable wearable clothing electronic devices that require enhanced uniformity, flexibility, and breathability.

EL01.14.08

Nanowire Morphologies Can Improve Ion Uptake Kinetics in Organic Electrochemical Transistors Rajiv Giridharagopal, Jiajie Guo, Jessica Kong and David Ginger; University of Washington, United States

Organic electrochemical transistor materials face a design tension between optimizing for ion mobility and for electronic mobility. These devices transduce ion uptake into electrical current, thereby requiring high ion mobility for efficient electrochemical doping and rapid turn-on kinetics, and high electronic mobility for maximum transconductance. Here we explore one method to improve operational kinetics in a high hole mobility conjugated polymer (poly[2,5-(2-octyldodecyl)-3,6-diketopyrrolopyrrole-alt-5,5-(2,5-di(thien-2-yl)thieno [3,2-b]thiophene)], DPP-DTT) by using a nanowire morphology. For equivalent thicknesses, the DPP-DTT nanowire films exhibit consistently faster spectroelectrochemical kinetics in KPF6 solution (~6-10X faster) compared to a standard DPP-DTT film. Nanowire devices also exhibit favorable shifts in the threshold voltage, making the nanowire architecture both faster and energetically easier to dope compared to neat films. We use nanoinfrared imaging via photoinduced force microscopy to show that these films exhibit ion diffusion throughout the film, suggesting there is a volumetric benefit to the nanowire architecture. We propose that, for higher-mobility materials that are often hydrophobic, casting the active layer in nanowire form may offer faster kinetics and possibly lower threshold voltage while maintaining desirable device performance, thereby providing one method to optimize ion mobility without sacrificing electronic mobility.

EL01.14.09

Simulation-Guided Design of Organic Devices for Cost-Effective and Scalable Electronics Matthew C. Waldrip¹, Hamna Haneef¹, Iain McCulloch^{2,3} and Oana Jurchescu¹; ¹Wake Forest University, United States; ²King Abdullah University of Science and Technology, Saudi Arabia; ³University of Oxford, United Kingdom

Interest in organic electronics is driven in large part by the applications they can address, yet a complete set of design rules is still absent for devices intending to fulfill those roles. Progress is assisted by general guidelines such as minimizing the Schottky barrier at injection interfaces or reducing defect states in the semiconductor layer, but improvements are achieved mainly through experimental trial-and-error, which is time, cost, and material intensive. Here we use physically-based numerical simulations to explore a vast parameter space with a high throughput in order to generate rules for material processing and device design, and optimize charge mobility and injection. For this purpose, the organic field-effect transistor (OFET) was selected as an experimental platform since current densities in OFETs ($\sim 10^4$ A cm⁻³) are much higher than in other organic devices, thereby allowing the exploration of charge injection and transport in the most extreme case. We have investigated the impact of the density of trap states and the injection barrier on the charge carrier mobility for both thick- and thin-dielectric devices, in a co-planar and staggered architecture. The simulations revealed that the performance of thin-dielectric devices (10 nm) is insensitive to large changes in the density of traps, while an injection barrier has a significant impact on mobility: only a 15% decrease in mobility was observed when raising the trap density by an order of magnitude in both architectures, but 60% and 95% decreases were observed when a 0.5 eV injection barrier was introduced in the staggered and co-planar devices, respectively. On the other hand, employing a thick dielectric (1000 nm) had the opposite trend: changes in the density of traps produced large reductions in mobility (by 60%), but the same 0.5 eV injection barrier decreases mobility by only 20% and 40% in the staggered and co-planar structures, respectively. Our results suggest that the

staggered structure and the thick dielectric are more tolerant to injection barriers. All these effects were also found to scale with the intrinsic mobility of the semiconductor. To test these predictions, we have fabricated and characterized a variety of OFETs and tuned the injection barrier via self-assembled monolayers (SAMs), oxide interlayers, and contact material selection, while the density of states was modified through altering film microstructure by processing. Notably, the experimental results agree well with the simulations, validating its use to predict and guide device design. With regards to the quality of the semiconductor and the contact/semiconductor interface, these results reevaluate the requirements necessary for optimizing OFETs. For example, given a good quality semiconductor with a low trap density, improving the injection barrier is not essential if a sufficiently thick dielectric is employed in the staggered architecture, allowing the selection of a more cost-effective and scalable contact material. Further parameter exploration combining both simulation and experiment will fine-tune the model and expand its predictive power.

5:47 PM Q&A

EL01.14.10

Dynamic Modulation of Charge Transport Properties Enabled by Cooperative Structural Transitions

Daniel Davies¹, Sangkyu Park¹, Prapti Kafle¹, Yuan Dafei², Hyunjoong Chung¹, Stefan Mannsfeld³, Danielle Gray¹, Ralph Weber⁴, Xiaozhang Zhu² and Ying Diao¹; ¹University of Illinois at Urbana-Champaign, United States; ²Institute of Chemistry, Chinese Academy of Sciences, China; ³Technische Universität Dresden, Germany; ⁴Bruker Corporation, United States

Cooperativity has long been used by living systems to circumvent energetic and entropic barriers to yield highly efficient molecular processes. Cooperative structure transition involves simultaneous, concerted displacement of molecules in a crystalline material, in stark contrast to the typical nucleation and growth mechanism occurring in a molecule-by-molecule fashion that often disrupt the material structural integrity. Cooperative transitions have acquired much attention in the research community for its low transition barrier, ultrafast kinetics, and structural reversibility. On the other hand, cooperative transition is rarely observed in molecular crystals and its molecular origin is not well understood. In 2-dimensional quinoidal terthiophene (2DQTT-o-B), a high-performance n-type semiconductor our research has shown prolific diversity in polymorphism and transition behavior resulting in 5 obtainable polymorphs showing large variations in electronic and optical behaviors. Along with the diversity of structure, both a cooperative and nucleation and growth transition has been reported simultaneously in the same system through 2 different thermally activated phase transitions. In situ microscopy, single crystal and grazing incidence X-ray diffraction, and Raman spectroscopy suggest a reorientation the alkyl side chains results in a cooperative transition behavior. While in stark contrast, we find the nucleation and growth mechanism occurs through a combination of side chain melting and increased core interactions resulting from a sudden increase in biradical nature of 2DQTT-o-B and is confirmed through in situ electron paramagnetic resonance. This is the first time, to our knowledge, that biradical interactions result in a structural change. Finally, we harness the cooperative phase transition behavior for a novel thermally actuated switching device. Through studying these fundamental mechanisms, we may establish design rules to rationally obtain polymorphic behavior for novel electronic applications.

EL01.14.12

High Anisotropic Self-Assembled Multilayered Films Used Simultaneously as Dielectric and Conducting Channel Material—A Novel Approach to Fabricate Solid-State Organic Field Effect Transistors

Gabriel Gaal^{1,2}, Maria L. Braunger¹, Varlei Rodrigues¹, Antonio Riul Jr.¹ and Henrique L. Gomes^{2,3}; ¹Universidade Estadual de Campinas, Brazil; ²Universidade do Algarve, Portugal; ³Universidade de Coimbra, Portugal

The next generation of organic-based electronic devices will require composite materials synergistically engineered to exploit novel and multi functionalities in a single device structure. Such multifunctional organic materials are attractive for various applications, including electronic skin, smart textiles, and self-healing batteries. Organic Field Effect Transistors (OFETs) have historically suffered from the lack of a single seamless material acting as both dielectric and channel. Typical OFET devices have defects and active electrical

impurities due to the quality of the dielectric/semiconductor interface critical for the device operation, which is the primary source of electrical instabilities and reliability issues. Such lack of quality control in the dielectric/semiconductor interface has until now, prevented, the commercialization of solid-state organic transistors. Here, we report a comprehensive investigation of process-friendly multilayered organic transistors without material discontinuities between dielectric and channel. The transistor design makes use of the high anisotropic electrical behavior of multilayered polyethylenimine/poly(acrylic acid) (PEI/PAA) composite thin films doped with reduced graphene oxide (rGO) and poly(3,4-ethylenedioxythiophene)-poly(styrenesulfonate) (PEDOT:PSS). The films were fabricated by self-assembled layer-by-layer (LbL) deposition technique, exploiting the spontaneous physical interactions that allow for the natural combination of various materials in a multilayered structure. Conductive layers formed by rGO nanosheets and the PEDOT:PSS nanofibers are dynamically ordered in a specific direction due to electrostatic interactions in the LbL film fabrication, creating highly anisotropic pathways. The in-plane film conductivity is 7 orders of magnitude higher than the conductivity normal to the multilayered planes. Temperature dependent measurements confirm the strong anisotropic electrical behavior. The charge transport mechanism is weakly thermal activated ($E_A = 33.4$ meV) along the aligned conductive phases while the charge transport normal to the plane is fitted with variable ranging hopping having an activation energy of 1.0 eV. The LbL films' high anisotropic electrical conduction is used to fabricate a novel field effect transistor where the same multilayered structure operates simultaneously as both dielectric and conductive channel. The transistor presents a low power consumption as it operates at the sub voltage regime. The dielectric part shows a high specific capacitance of $18 \mu\text{F}/\text{cm}^2$, and the semiconductor presents an n -type carrier transport having a field effect mobility of $4.0 \text{ cm}^2\text{V}^{-1}\text{s}^{-1}$. Moreover, the transistor threshold voltage (V_{th}) is zero, which shows that electrical active traps, which can charge upon the applied gate field and shield the external applied voltage are not active or do not exist. The entire applied gate field contributes to an increasing channel current, as expected in trap free devices. The results point to the development of a simple and efficient approach to fabricate solid-state OFETs relying on the high anisotropy of the LbL films, enhancing its potential for commercial applications.

6:06 PM Q&A

SYMPOSIUM EL02

Fundamentals of Halide Semiconductors for Optoelectronics
April 21 - April 23, 2021

Symposium Organizers

Xue Bai, Jilin University
Do Young Kim, Oklahoma State University
Jong Hyun Kim, Ajou University
William Yu, Louisiana State University Shreveport

Symposium Support

Bronze
Army Research Office

* Invited Paper

SESSION EL02.01: Low-Dimensional Halide Semiconductors I
Session Chairs: Xue Bai and Jong Hyun Kim

8:15 AM *EL02.01.01

Excitons and Phonons in 2D Perovskites Paulina Plochocka^{1,2}; ¹Laboratoire National des Champs Magnétiques Intenses, CNRS-UJF-UPS-INSA, France; ²Department of Experimental Physics, Faculty of Fundamental Problems of Technology, Poland

High environmental stability and surprisingly high efficiency of solar cells based on 2D perovskites have renewed interest in these materials. These natural quantum wells consist of planes of metal-halide octahedra, separated by organic spacers. Remarkably the organic spacers play crucial role in optoelectronic properties of these compounds. The characteristic for ionic crystal coupling of excitonic species to lattice vibration became particularly important in case of soft perovskite lattice. The nontrivial mutual dependencies between lattice dynamics, organic spacers and electronic excitation manifest in a complex absorption and emission spectrum which detailed origin is subject of ongoing controversy. First, I will discuss electronic properties of 2D perovskites with different thicknesses of the octahedral layers and two types of organic spacer. I will demonstrate that the energy spacing of excitonic features depends on organic spacer but very weakly depends on octahedral layer thickness. This indicates the vibrionic progression scenario which is confirmed by high magnetic fields studies up to 67T. Finally, I will show that in 2D perovskites, the distortion imposed by the organic spacers governs the effective mass of the carriers. As a result, and unlike in any other semiconductor, the effective mass in 2D perovskites can be easily tailored.

8:40 AM EL02.01.02

Late News: Vertically Aligned CsPbBr₃ Nanowire Arrays with Template-Induced Crystal Phase Transition and Stability Zhaojun Zhang, Klara Suchan, Jun Li, Crispin Hetherington, Alexander Kiligaris, Eva Unger, Ivan Scheblykin and Jesper Wallentin; Lund University, Sweden

All inorganic Metal halide perovskite (MHP) CsPbBr₃ nanowires (NWs) arrays have shown excellent performance in various optoelectronic applications such as laser, LED, and photodetection, *etc.* owing to its special properties have, such as one-dimensional photon/electron transport, enhanced light absorption, larger active surface area and higher charge injection efficiencies, *etc.*

The growth of CsPbBr₃ NWs and their various optoelectronic applications have been explored, e.g. for lasing, multicolor displays, control of emission anisotropy, and light guiding, as well as photodetection. However, most of these studies used unprotected in-plane NWs with horizontal alignment. A few studies have investigated vertically aligned MHP NW arrays, which have been proven to have high light extraction capability for LED devices and high resolution for pixel image sensors. So far, studies on vertically aligned CsPbBr₃ NWs arrays are limited.

Here, we report a low temperature solution growth of vertically aligned CsPbBr₃ NWs arrays with excellent stability, using anodized aluminum oxide (AAO) templates. AAO template is commonly used for nanocrystals synthesis, and it has also been used for MHP nanocrystals synthesis. However, the growth behavior and mechanism of micrometer length CsPbBr₃ NWs in AAO from a solution precursor have not been clearly investigated.

In this work, the growth behavior of CsPbBr₃ NWs in 5 μm thick AAO template from solution is clearly elucidated. Owing to the low concentration of precursor, the growth of micrometer length pure phase CsPbBr₃ NWs in AAO is different from the common way used for growing other MHP NWs such as MAPbI₃. The low solubility of its precursors makes it more challenging to fill the nanopores with CsPbBr₃, but it can be overcome by supplying sufficient solution as shown by our results. The NW diameter (10-250 nm) and the length (tens of nm to few μm) can be independently controlled. With decreasing diameter, the CsPbBr₃ NWs show a gradual photoluminescence blue-shift from 250 nm to 10 nm and crystal structure change from orthorhombic to cubic phase below 20 nm. This is the first observation of physical confinement induced phase transition for CsPbBr₃. The physical confinement of the CsPbBr₃ NWs in the AAO gives a remarkable stability to long term air storage.

Any significant degradation of these structures is not observed within 4 months, despite storing the sample in ambient air. Additionally, the CsPbBr₃-NWs/AAO composite shows good resistance to X-ray exposure, which makes it promising for applications in X-ray scintillation. The growth method proposed in this work should be viable for a wide range of MHP materials. The demonstrated stability makes the vertically aligned CsPbBr₃-NWs a promising foundation for a wide range of applications in many fields of optoelectronics.

8:55 AM EL02.01.03

Late News: Exciton Diffusion in Two-Dimensional Metal-Halide Perovskites Michael Seitz^{1,2,3}, Alvaro Magdaleno¹, Marc Meléndez¹, Nerea Alcázar-Cano¹, Tim Lubbers¹, Sanne W. Walraven¹, Sahar Pakdel⁴, Elsa Prada¹, Daniel N. Congreve^{2,3}, Rafael Delgado-Buscalioni¹ and Ferry Prins¹; ¹Universidad Autonoma de Madrid, Spain; ²Harvard University, United States; ³Stanford University, United States; ⁴Aarhus University, Denmark

There is an increasing interest in two-dimensional (2D) Ruddlesden-Popper perovskites for solar harvesting and light-emitting applications due to their superior chemical stability as compared to bulk perovskites.[1,2] Both, purely 2D and blends of 2D/3D phases have been successfully employed in solar cells with efficiencies of >18% and >21%, respectively.[3,4] As with earlier advances in the field of perovskites, these technological improvements are advancing at a pace that far exceeds our understanding of the physical mechanisms underlying their performance. Particularly, the reduced dimensionality in 2D perovskites results in excitonic excited states which dramatically modify the dynamics of charge collection. While the carrier dynamics in bulk systems is increasingly well understood, a detailed understanding of the spatial dynamics of the excitons in 2D perovskites is lacking.[5]

Here, we present direct measurements of exciton transport in single-crystalline layered perovskites. Using transient photoluminescence microscopy, we can follow the temporal evolution of a near-diffraction-limited exciton population with sub-nanosecond resolution revealing the spatial and temporal exciton dynamics. We observe two distinct temporal regimes: For early times excitons undergo unobstructed normal diffusion, while at later times exciton transport becomes subdiffusive as excitons get trapped. Interestingly, the diffusivity at early times depends sensitively on the choice of the organic spacer which can yield diffusion lengths that differ by up to an order of magnitude. We find a clear correlation between lattice stiffness and diffusivity, suggesting exciton–phonon interactions to be dominant in the spatial dynamics of the excitons in perovskites, consistent with the formation of exciton–polarons. Our findings provide a clear design strategy to optimize exciton transport in these systems.[6] In addition, we show that the complex exciton dynamics observed at later times can be leveraged to provide a detailed map of the trap-state landscape in 2D perovskites, in particular when used in combination with transient photoluminescence spectroscopy and a rigorous diffusion model that accounts for a distribution of radiative shallow trapping sites.[7]

1. Krishna, A., Gottis, S., Nazeeruddin, M. K. & Sauvage, F. Mixed Dimensional 2D/3D Hybrid Perovskite Absorbers: The Future of Perovskite Solar Cells? *Adv. Funct. Mater.* 29, 1806482 (2019).
2. Ortiz-Cervantes, C., Carmona-Monroy, P. & Solis-Ibarra, D. Two-Dimensional Halide Perovskites in Solar Cells: 2D or not 2D? *ChemSusChem* 12, 1560–1575 (2019).
3. Li, P. et al. Phase Pure 2D Perovskite for High-Performance 2D-3D Heterostructured Perovskite Solar Cells. *Adv. Mater.* 30, 1805323 (2018).
4. Yang, R. et al. Oriented Quasi-2D Perovskites for High Performance Optoelectronic Devices. *Adv. Mater.* 30, 1804771 (2018).
5. Straus, D. B. & Kagan, C. R. Electrons, Excitons, and Phonons in Two-Dimensional Hybrid Perovskites: Connecting Structural, Optical, and Electronic Properties. *J. Phys. Chem. Lett.* 9, 1434–1447 (2018).
6. Seitz, M. et al. Exciton diffusion in two-dimensional metal-halide perovskites. *Nat. Commun.* 11, 2035 (2020).
7. Seitz, M. et al. Mapping the Trap-State Landscape in 2D Metal-Halide Perovskites using

9:10 AM BREAK

9:15 AM EL02.01.04

Exciton-Phonon Coupling in 2D Perovskites—Role of Organic Spacer, Halide Cage Composition and Quantum Well Thickness Michal Baranowski¹ and Paulina Plochocka²; ¹Wroclaw University of Science and Technology, Poland; ²LNCMI, France

High environmental stability and surprisingly high efficiency of solar cells based on 2D perovskites have renewed interest in these materials. This natural quantum wells consists of planes of metal-halide octahedra, separated by organic spacers. Remarkable the organic spacers plays crucial role in optoelectronic properties of these compounds. Despite the bandedge states are composed from metal and halide orbitals the organic spacer imposes octahedral distortion and in this way controls band structure and carriers-phonon coupling. The characteristic for ionic crystal coupling of excitonic species to lattice vibration became particularly important in case of soft perovskite lattice. The nontrivial mutual dependencies between lattice dynamics, organic spacers and electronic excitation manifest in a complex absorption and emission spectrum which detailed origin is subject of ongoing controversy, because observed multiple sidebands are attributed to phonon replicas or distinct excitonic states.

Here we address this issue by systematic studies of 2D perovskites of different thickness of octahedral layer, different organic spacer, (namely phenethylammonium $C_6H_5C_2H_4NH_3$ (PEA) and long aliphatic chains (AC) $C_nH_{2n+1}NH_3$ (with $n=4,6,8,10,12$)) and halide cage composition. We found that energy spacing of excitonic feature depends on organic spacer but very weakly depends on octahedral layer thickness and metal ion. This support the vibronic progression scenario originating from coupling to organic spacer or halide cage motion. Our results show that in case of PEA spacer exciton couple dominantly to PEA vibration, while in case of AC excitons are coupled to octahedral layer vibration. We found that exciton-phonon coupling can be tuned by the quantum well thickness. The phonon related origin of complex spectral feature is additionally supported by high magnetic fields studies up to 67T. In all cases the equally spaced features exhibit identical shifts in magnetic field as can be expected for phonon replicas. The observed difference in exciton-phonon coupling can be consistently explained taking in to account mutual dependence between organic spacer, octahedral distortion and dielectric screening.

9:30 AM EL02.01.05

Strong Coupling Between Photon-Exciton Fano Resonances and Plasmonic Silver Nanoparticles in 2D Perovskites Franziska E. Muckel¹, Kathryn N. Guye², Shaun Gallagher², Yun Liu² and David Ginger²; ¹University Duisburg-Essen, Germany; ²University of Washington, United States

As easy-to-grow quantum wells with direct bandgaps, two dimensional Ruddleson-Popper perovskites carry great potential as excitonic components in strongly coupled polaritonic applications. Their combination of narrow excitonic features at room temperature and enhanced collective effects (i.e., coupling with multiple excitons) enable the observation of various regimes of light-matter interaction, including evidence of strong coupling with dielectric cavities or plasmonic nano-arrays.

Here we demonstrate that in $(C_4H_9NH_3)_2PbI_4$, butylammonium lead iodide (BAPI) thin films prepared via spin coating, the geometric morphology of the perovskite emitters needs to be considered to understand the excitonic spectrum and the light-matter interactions with localized cavities, in our case plasmonic silver nanoparticles. Specifically, we provide proof that a distinct exciton-photon Fano resonance in dark field scattering emerges from the coupling between the band edge exciton and the geometry-driven Rayleigh-like scattering background of the BAPI material itself, supported by finite-difference time-domain (FDTD) simulations and a classical coupled-oscillator model.

Through sequential spin coating, we combine the BAPI thin films with individual plasmonic silver nanocavities. Combining single particle dark field scattering spectroscopy and FDTD simulations, we demonstrate that the

BAPI Fano resonance exhibits strong coupling to the plasmon resonance of colloidal silver nanoparticle plasmonic cavities, although the total dark field scattering of the combined system is still dominated by the perovskite Fano resonance. We estimate a Rabi splitting of ~ 300 meV -- amongst the highest values ever reported for comparable material systems.

By adding a gold layer beneath the perovskite, we formed particle-on-mirror cavities, allowing us to access the out-of-plane excitonic component of the 2D perovskite. Due to the higher energy dissipation rate of the combined cavity, the combination of BAPI and particle-on-mirror cavity is found to exhibit intermediate coupling.

Our work not only highlights the potential of Ruddleson-Popper perovskites for polariton applications, but in addition provides new and unexpected insights into the principles governing the light matter-interaction of 2D halide perovskites.

SESSION EL02.02: Halide Perovskite LEDs I
Session Chairs: Do Young Kim and Zhibin Yu
Wednesday Morning, April 21, 2021
EL02

11:45 AM EL02.02.01

Late News: Critical Role of Additive-Induced Molecular Interaction on the Operational Stability of Perovskite Light-Emitting Diodes Chaoyang Kuang, Sai Bai and Feng Gao; Linköping University, Sweden

In spite of rapid improvements in efficiency and brightness of metal halide perovskite light-emitting diodes (PeLEDs), the poor operational stability remains a critical challenge hindering their practical applications. Herein, we demonstrate greatly improved operational stability of high-efficiency PeLEDs, enabled by incorporating dicarboxylic acids into precursor for the deposition of perovskite emissive layers. We reveal the critical role of carboxyl groups in enhancing the device stability through converting the active organic ingredients in perovskite emissive layers to stable amides, a process catalyzed by the alkaline zinc oxide substrate. The formed inert amides prohibit detrimental interfacial reactions between the perovskites and the charge injection layer underneath, greatly improving the thermal stability of the perovskite emissive layers and ensuring the long operational stability of the resulting PeLEDs. Through rationally optimizing the amidation reaction in the perovskite emissive layers, we achieve efficient PeLEDs with a peak external quantum efficiency of 18.6% and an outstandingly long half-life time of 682 h at 20 mA cm^{-2} , presenting an important breakthrough in PeLEDs.

12:00 PM *EL02.02.02

Organic-Inorganic Metal Halide Hybrids Beyond Perovskites—From Material Development to Device Integration Biwu Ma; Florida State University, United States

Organic-inorganic metal halide hybrids have attracted great research attention for their remarkable and useful optical and electronic properties with applications in a variety of areas, ranging from photovoltaic cells to light emitting devices, sensors, and detectors. In addition to the well-known 3D ABX_3 perovskite structure, organic-inorganic metal halide hybrids can have many other crystallographic structures, in which inorganic metal halide units, for instance, metal halide octahedrons, form 2D, 1D, and 0D structures surrounded by organic cations. These low dimensional materials exhibit unique and remarkable properties that are completely different from those of 3D ABX_3 perovskites. For instance, corrugated-2D and 1D organic metal halide hybrids exhibit broadband emissions from both direct and self-trapped excited states, and 0D organic metal halide hybrids exhibit broadband emissions from the reorganized excited states with high photoluminescence quantum efficiencies of up to 100 %. In this talk, I will present our recent efforts on the development and study of

organic-inorganic metal halide hybrids beyond perovskites. From 3D to 2D, 1D, and 0D structures at the molecular level, from mononuclear molecular metal halide species to multinuclear metal halide clusters, and from single-component homogeneous systems to multi-component heterogeneous systems, I will discuss how we can achieve synthetic control of this class of hybrid materials to realize desired properties with applications in various types of optoelectronics.

12:25 PM *EL02.02.03

Halide Perovskite-Polymer Composites for Fully Printed and Stretchable LEDs Zhibin Yu; FAMU-FSU College of Engineering, United States

Recently, astounding optoelectronic properties have been discovered in a group of halide perovskite materials. In this talk, our recent work of developing perovskite-polymer composites towards the realization of fully printed and stretchable light-emitting diodes (LEDs) will be presented. The perovskite-polymer composites possess all the remarkable optoelectronic characteristics of pristine perovskites. For instance, we have demonstrated their use for blue, green, and red LEDs. In addition, the device efficiencies are compatible to those of pristine perovskite LEDs. The perovskite-polymer composites have shown advantages in improving the processability and quality of the perovskite thin films; and enhancing the structural stability of the perovskites especially at humid fabrication and service environments. By embedding the perovskite crystals inside a polymer matrix, the perovskites can be less toxic and more environmentally benign compared to pristine perovskites; moreover, to enable new mechanical properties of perovskite LEDs.

12:50 PM EL02.02.04

All-Solution-Processed, Fully Inkjet-Printed Organometal Halide Perovskite Light-Emitting Diodes on Flexible Substrate Junyi Zhao¹, Li-Wei Lo^{1,1}, Haochuan Wan¹, Zhibin Yu^{2,2} and Chuan Wang^{1,1}; ¹Washington University in St. Louis, United States; ²Florida State University, United States

Organometal halide perovskite has already attracted extensive research attention owing to its great potential for ubiquitous optoelectronic applications. However, most hybrid perovskite-based optoelectronic devices are fabricated on rigid indium-tin-oxide (ITO) glass substrate inside the glove box with a vacuum-evaporated metal top electrode, which is a tedious and time-consuming process. In this work, we demonstrate an all-solution-processed perovskite light-emitting diodes (PeLEDs) fabricated entirely by inkjet printing in ambient conditions for high-resolution flexible display applications. The PeLEDs were constructed with an extremely simple 4-layer sandwich structure, consisting of a composite transparent bottom electrode of poly(3,4-ethylenedioxythiophene) polystyrene sulfonate (PEDOT:PSS) and poly(ethylene oxide) (PEO), a composite light-emissive layer of methylammonium lead tribromide ($\text{CH}_3\text{NH}_3\text{PbBr}_3$) and poly(ethylene oxide) (PEO), and a silver nanowire (AgNW) top electrode, all directly printed onto an ultrathin polydimethylsiloxane (PDMS) substrate. In addition, a printed polyethyleneimine (PEI) buffer layer inserted between the emissive layer and the top electrode was found to be effective in protecting the perovskite crystals from being attacked by the solvent in AgNW ink during the top electrode printing step. The device exhibits bright green emission with a turn-on voltage of 3.18 V, a maximum luminance intensity of $10\,227\text{ cd m}^{-2}$, and a peak current efficiency of 2.01 cd A^{-1} . By optimizing the ink formulation and printing recipe and taking full advantage of direct printing, we have also achieved scalable patterning of PeLEDs with resolution down to $250\text{ }\mu\text{m}$. The printed PeLEDs also exhibit good flexibility and can be conformably bent to a 3.5 mm radius convex curvature for over 100 bending cycles without degradation in performance. The combination of superior optical performance, simplified device structure, all-solution processability, and low-cost printing strategy is promising to pave way for emerging flexible display and wearable electronics applications.

2:15 PM *EL02.03.01

Organic-Inorganic Perovskites—Highly Diverse and Tunable Semiconductors David B. Mitzi; Duke University, United States

Hybrid perovskites offer an unprecedented degree of tunability through mixing and matching of diverse functionalities for inorganic and organic components [1]. The interfaces among organic cations and between the organic and inorganic components (mediated by hydrogen bonding and steric interactions) play an essential role in determining emergent properties within this semiconductor family. In this talk, we will examine how organic cation choice can profoundly impact spin, optical and thermodynamic properties, with a goal towards understanding how these characteristics can be rationally controlled. As an example, selection of appropriate chiral organic cations can lead to a transfer of chirality between the organic and inorganic components and an associated breaking of symmetry within the inorganic layer, which in turn provides a large Rashba-Dresselhaus splitting of the conduction band and associated control over spin texture [2]. Alternatively, organic cations with controlled HOMO and LUMO position can offer unique opportunities to fabricate self-assembling quantum well structures with distinct alignment of the energy levels [3]. Appropriate choice of the organic cation also leads to hybrids with melting temperature well below the decomposition point [4]. These examples of structure-property versatility yield new opportunities for fundamental science and prospective device applications.

References:

- [1] B. Saparov, D. B. Mitzi, *Chem. Rev.* 116, 4558 (2016).
- [2] M. K. Jana, R. Song, H. Liu, D. R. Khanal, S. M. Janke, R. Zhao, C. Liu, Z. V. Vardeny, V. Blum, D. B. Mitzi, *Nature Commun.* 11, 4699 (2020).
- [3] W. A. Dunlap-Shohl, E. T. Barraza, A. Barrette, S. Dovletgeldi, G. Findik, D. J. Dirkes, C. Liu, M. K. Jana, V. Blum, W. You, K. Gundogdu, A. D. Stiff-Roberts, D. B. Mitzi, *Mater. Horiz.* 6, 1707 (2019).
- [4] T. Li, W. A. Dunlap-Shohl, E. W. Reinheimer, P. Le Magueresc D. B. Mitzi, *Chem. Sci.* 10, 1168 (2019).

2:40 PM *EL02.03.02

Low-Dimensional Metal Halide Hybrid Perovskite Semiconductors for Light Emitting Devices Wanyi Nie; Los Alamos National Laboratory, United States

Metal halide perovskites are emerging class of semiconducting materials that make high performance photovoltaics. Recently, low dimensional perovskites, such as 2D perovskites and nanocrystals, show unique carrier transport and recombination processes. Low dimensional perovskites are thus demonstrated as ideal candidate for high efficiency light emitting diodes.

In my talk, I will discuss both 2D perovskites and perovskite nanocrystals and their applications in light emitting devices and radiation detectors. Firstly, the charge transport properties and surface properties will be discussed by scanning photocurrent microscopy measurement, where we found a long carrier diffusion length in 2D perovskite single crystals along in-plane direction. Secondly, we observed large degree of charge localization in the bromide 2D perovskite which yielded strong emission properties. Finally, I will introduce new perovskite nanocrystal structure that show stable and bright emission properties. Using low dimensional perovskite materials, we demonstrate bright light emitting diodes with external quantum efficiency of 10%~15% with stable operational lifetime.

3:05 PM *EL02.03.03

Structural and Electronic Impact of an Asymmetric Organic Ligand in Diammonium Lead Iodide Perovskites Antoine Kahn; Princeton University, United States

Reduced dimensionality forms of perovskites with alternating layers of organic ligands are a promising class of materials for achieving stable perovskite solar cells. Most work until now has focused on phases utilizing two ammonium terminated ligands per formula unit. However, phases utilizing a single diammonium ligand per formula unit are advantageous in that they can potentially have a thinner insulating organic layer between Pb-halide layers, yet the structural effects on their optoelectronic properties remain to be well understood. In this talk, we first rapidly summarize our recent work on the energetics of 2D Ruddlesden-Popper phase metal halide perovskites (MHP). We then turn to two Dion-Jacobson $n=1$ MHPs formed with butane 1,4- diammonium (BDA) and N,N-dimethylpropane diammonium (DMPD) spacers. Using ultraviolet and inverse photoelectron spectroscopies, BDAPbI₄ is shown to have a larger transport gap by 350 meV and a larger exciton binding energy by 140 meV than DMPDPbI₄. Through density functional theory calculations, the cause of this difference is traced to the out-of-plane tilting of the Pb-halide octahedra provoked by the asymmetric ligand in DMPDPbI₄. Parallel channels of nearly straight Pb-I-Pb bonds are formed in one direction, leading to enhanced electronic coupling and higher band dispersion in that direction. In BDAPbI₄, no such channels exist, resulting in greater electronic confinement and a larger band gap and exciton binding energy.

3:30 PM EL02.03.04

Long Periodic Ripple in a 2D Hybrid Halide Perovskite Structure Using Branched Organic Spacers Justin M. Hoffman¹, Christos Malliakas¹, Siraj Sidhik², Ido Hadar¹, Rebecca McClain¹, Aditya Mohite² and Mercouri G. Kanatzidis¹; ¹Northwestern University, United States; ²Rice University, United States

Two-dimensional (2D) halide perovskites have great promise in optoelectronic devices because of their stability and optical tunability, but the subtle effects on the inorganic layer when modifying the organic spacer remain unclear. Here, we introduce two homologous series of Ruddlesden-Popper (RP) structures using the branched isobutylammonium (IBA) and isoamylammonium (IAA) cations with the general formula (RA)₂(MA)_{n-1}Pb_nI_{3n+1} (RA = IBA, IAA; MA = methylammonium $n = 1-4$). [1] Surprisingly, the IAA $n = 2$ member results in the first modulated 2D perovskite structure with a ripple with a periodicity of 50.6 Å occurring in the inorganic slab diagonally to the [101] direction of the basic unit cell. This leads to an increase of Pb-I-Pb angles along the direction of the wave. Generally, both series show larger in-plane bond angles resulting from the additional bulkiness of the spacers compensating for the MA's small size. Larger bond angles have been shown to decrease the bandgap which is seen here with the bulkier IBA leading to both larger in-plane angles and lower bandgaps except for $n = 2$, in which the modulated structure has a lower bandgap because of its larger Pb-I-Pb angles. Photo-response was tested for the $n = 4$ compounds and confirmed, signaling their potential use in solar cell devices. We made films using an MAI additive which showed good crystallinity and preferred orientation according to grazing-incidence wide-angle scattering (GIWAXS). As exemplar, the two $n = 4$ samples were employed in devices with champion efficiencies of 8.22% and 7.32% for IBA and IAA, respectively.

References

[1] Hoffman, J. M.; Malliakas, C. D.; Sidhik, S.; Hadar, I.; McClain, R.; Mohite, A. D.; Kanatzidis, M. G. *Chem. Sci.*, **2020**, Advance Article.

3:45 PM EL02.03.05

Stability of 2D Hybrid Lead Halide Perovskites: Perspective from Bulk Crystals and Thin Films Eugenia S. Vasileiadou¹, Ido Hadar¹, Bin Wang², Ioannis Spanopoulos¹, Mikael Kepenekian³, Jacky Even⁴, Alexandra Navrotsky⁵ and Mercouri G. Kanatzidis¹; ¹Northwestern University, United States; ²University of California, Davis, United States; ³University of Rennes, France; ⁴INSA Rennes, France; ⁵Arizona State University, United States

Two-dimensional (2D) hybrid organic-inorganic halide perovskites are a promising class of environmentally stable semiconductors. Their inherent structural tunability and technological features provide a vast compositional space to engineer new materials for optoelectronic applications. Within this compositional space, several different homologous series and structure types of 2D perovskites have been developed for their successful fabrication in solar cells, light-emitting diodes and radiation detectors with attractive efficiencies.

Although 2D lead iodide perovskites exhibit superior stability over their 3D parent structures, a systematic understanding of their observed stability is missing. Herein, we actuate a comprehensive study on the relative stability of several distinct families of 2D halide perovskites in bulk crystal and film form. Thermochemical evaluation of the representative 2D structure types of Ruddlesden-Popper (RP) and Dion-Jacobson (DJ) perovskites was undertaken based on calorimetric measurements that reveal that the enthalpy of formation for the RP perovskites is negative while for the DJ perovskites is positive. Film stability tests demonstrate consistent observations with the thermochemical findings, where RP lead iodide perovskites are both thermodynamically and environmentally stable candidates for optoelectronic applications. Additionally, the methodical tailoring of the 2D perovskite structure's composition (organic and inorganic component), unveils trends in the comparison of 2D lead iodide and bromide perovskites, for the acquisition of halide perovskites with enhanced stability. Structural – crystallographic analysis of bulk, layered perovskites provides atomistic insight to control these materials' stability. Our work highlights the importance of the rational assessment of stability in 2D hybrid halide perovskites for the optimal synthetic design and engineering of environmentally robust perovskite materials for next-generation optoelectronic devices.

SESSION EL02.04: Halide Perovskite LEDs II
Session Chairs: Jong Hyun Kim and Sai Wing Tsang
Wednesday Afternoon, April 21, 2021
EL02

8:15 PM EL02.04.01

Late News: Highly Efficient Halide Perovskite Light-Emitting Diodes via Molecular Passivation Kang Wang, Aihui Liang and Letian Dou; Purdue University, United States

Metal halide perovskites are promising for applications in light-emitting diodes (LEDs), but still suffer from defects-mediated nonradiative losses, which represent a major efficiency-limiting factor in perovskite-based LEDs (PeLEDs). Here, we synthesized a series of new phenyl and thienyl-based molecular passivators with ammonium, formamidinium and imidazolium terminal groups, to examine the effects of different anchoring groups on defect passivation. After introducing the passivators, the as-prepared perovskite thin films display improved optoelectronic properties with low nonradiative recombination rate and high PLQY as well as reduced grain size and surface roughness. On this basis, we demonstrate highly efficient PeLEDs with an EQE of 15.6% using a novel imidazolium terminated passivator. Employing grazing incidence wide-angle X-ray scattering technique and single-crystal analysis, we further confirm that the in-situ formation of low-dimensional perovskite phase on the surface of 3D perovskite nanograins is responsible for the surface defects passivation, which lead to significantly enhanced device performances. This work not only provides us a deep insight into the interaction of organic molecules with perovskite lattice for defects passivation, but also guides the beginning of a new realm of molecular engineering for the development of high-performance perovskite-based optoelectronic devices.

8:30 PM *EL02.04.02

Comprehensive Defect Suppression of Halide Perovskite Nanoparticles for High-Efficiency Light-Emitting Diodes Young-Hoon Kim¹, Sungjin Kim¹, Arvin Kakekhani², Andrew Rappe² and Tae-Woo Lee¹; ¹Seoul National University, Korea (the Republic of); ²University of Pennsylvania, United States

Metal halide perovskite nanocrystals (PNCs) are regarded as promising light-emitters due to their high photoluminescence quantum efficiency and color purity. However, the electroluminescence efficiencies of perovskite light-emitting diodes (PeLEDs) based on PNCs are limited by lack of comprehensive materials design strategy both to suppress formation of defects causing non-radiative recombination and to enhance charge carrier confinement for more radiative recombination inside PNCs. In this work, we report a

reproducible method for producing PeLEDs based on PNCs that leads to unprecedentedly high current efficiency (CE) of $108 \text{ cd}\times\text{A}^{-1}$ (external quantum efficiency (EQE) of 23.4 %) in the PeLEDs and even higher CE of $205 \text{ cd}\times\text{A}^{-1}$ (EQE of 45.5 %) with a hemispherical lens. To accomplish this, we design a simple materials alloying strategy that generates smaller, monodisperse colloidal particles (improving charge carrier confinement) with fewer surface defects (suppressing non-radiative recombination). The governing concept is elegant only with one type of large organic cation dopant in colloidal PNCs. Doping of larger guanidinium (GA) into formamidinium (FA) lead bromide PNCs yields limited bulk solubility, above which extra GA segregates to the surface and stabilizes the under-coordinated sites. In bulk of PNCs, a small concentration of GA creates an entropy-stabilized phase. Increasing GA concentration requires higher surface/volume, leading to smaller PNCs for more carrier confinement inside PNCs. Additionally, the one dopant alloying strategy in PNCs was combined with a surface stabilizing a 1,3,5-tris(bromomethyl)-2,4,6-triethylbenzene overcoat which acts as a Br vacancy healing agent. Our world-leading efficiencies demonstrate that this design strategy provides a clear pathway to translate PNCs into PeLEDs for a new generation of high-efficiency display applications.

8:55 PM BREAK

9:35 PM *EL02.04.04

Achieving Bright and Stable Perovskite Light-Emitting Diodes via Surface Engineering Ni Zhao and Yuwei Guo; The Chinese University of Hong Kong, Hong Kong

In recent years metal halide perovskite based LEDs (PeLEDs) have attracted increasing research attention due to their solution processability and extraordinary electroluminescence performances. However, many PeLEDs exhibit significantly degraded radiance or shifted emission wavelength within hours of operation, thus limiting the practical applications of this technology. In this talk I will introduce our recent efforts in addressing the stability issues in high-efficiency PeLEDs. Firstly, the importance of eliminating iodide residues in the perovskite emissive layer will be discussed. Applying extensively excess ammonium halides in forming perovskites is a widely used approach to achieve high-performance PeLEDs. However, most of these PeLEDs suffer from severe external quantum efficiency (EQE) roll-off at high current densities, thereby restricting the realization of high-brightness PeLEDs and laser diodes. By combining voltage-dependent electrical stress measurements and *ex-situ* ion distribution analysis of the PeLEDs, we found that the electric-field driven diffusion of excess iodide ions, originated from the non-stoichiometric precursors, plays a dominant role in the EQE roll-off. Based on this discovery, we introduced a simple wash-off treatment with chloroform to remove the excess iodides from the perovskite surface and demonstrated that the treatment is highly effective in suppressing the roll-off behavior. Secondly, we further explored surface treatment of the FAPbI₃ perovskite films with phenylalkylammonium iodide molecules of varying alkyl chain lengths. Combining experimental characterization and theoretical modelling, we show that these molecules stabilize the perovskite through suppression of iodide ion migration. The stabilization effect is enhanced with increasing chain length due to the stronger binding of the molecules with the perovskite surface, as well as the increased steric hindrance to reconfiguration for accommodating ion migration. The passivation also reduces the surface defects, resulting in a high radiance and delayed EQE roll-off. Using the optimized passivation molecule, phenylpropylammonium iodide, we achieved a high radiance of $1282.8 \text{ W}/(\text{sr} \times \text{m}^2)$, a high critical current density (the current density corresponding to half of the EQE_{max}) of 2400 mAcm^{-2} and a record T₅₀ half-lifetime of 130 hrs under a high bias current density of $100 \text{ mA}/\text{cm}^2$.

10:00 PM *EL02.04.05

Dimensional, Interface and Optical Engineering for Efficient Blue and White Perovskite Light-Emitting Devices Hin-Lap Yip; South China University of Technology, China

Metal halide perovskite light-emitting diodes (PeLEDs) show great potentials to be the next-generation lighting technology, with external quantum efficiencies (EQEs) exceeding 20% for infrared, red and green LEDs. However, the efficiencies of blue and white devices severely lag behind. To improve the performance of blue

PeLEDs, we employed an integrated strategy combining dimensional engineering of perovskite film and recombination zone modulation in the LED device to obtain an EQE up to 5%.^[1] While further incorporating the strategy of interfacial engineering, highly efficient blue PeLEDs with EQEs over 10% have been successfully realized in our group, establishing an excellent platform for white-light emission. In our latest work, we demonstrated efficient white PeLEDs by optically coupling a blue PeLED with a red emitting perovskite nanocrystal layer in an advanced device structure, which allows to extract the trapped optical modes (waveguide and SPP modes) of blue photons in the device to the red perovskite layer via near-field effects. As a result, a white PeLEDs with EQE over 10% is achieved, which represents the state-of-the-art performance for white PeLEDs.

References:

[1] Z. Li[†], Z. Chen[†], H.-L. Yip* et al. *Nat. Commun.* 2019, 10, 1027; Z. Chen, H.-L. Yip* et al. *Adv. Mater.* 2017, 29, 1603157.

10:25 PM EL02.04.06

A Mechanistic Study on the Spectral Instability of Light-Emitting Diodes Based on Layered Mixed Halide Perovskites Yoonseo Nah¹, Omar Allam^{2,2}, Han Seul Kim³, In Soo Kim⁴, Seung Soon Jang² and Dong Ha Kim^{1,1}; ¹Ewha Womans University, Korea (the Republic of); ²Georgia Institute of Technology, United States; ³Korea Institute of Science and Technology Information, Korea (the Republic of); ⁴Korea Institute of Science and Technology, Korea (the Republic of)

Quasi-2D layered halide perovskites have been demonstrated as a promising class of materials for light-emitting applications. The interests in this class of materials derives from its attractive features including strong light absorption, narrow emission and unprecedented defect tolerance. Furthermore, halogen alloying offers an effective way for the finetuning of bandgap energy, hence a wide range of emission colors can be achieved by using mixed halide perovskites (MHPs). However, light-emitting diodes based on MHPs exhibit significant spectral shifts during the operation, which suggests that the fundamental understanding of the effects of mixed halide compositions should be preceded. Here, we report a novel mechanism of the spectral instability of layered mixed halide perovskites containing bromide and iodide. X-ray diffraction and absorption measurement indicate the uniform distribution of anions in the ambient environment. However, strong electric field which is applied during the device operation is found to drive the systematic migration of halides. The quantum mechanical density functional theory calculations reveal that slow equatorial-to-apical diffusion of bromide is responsible for the halide redistribution. In-depth analysis on the electroluminescence spectra also confirm that the spectral instability is responsible for the anion migration. Finally, we suggest that the dominant red electroluminescence from layered MHPs is attributed to the thermodynamically favored hole injection process. It is envisioned that our comprehensive study will provide new insights into the mechanism of spectral instability of multilayer electroluminescence devices based on MHPs.

SESSION EL02.05: Synthesis and Crystal/Defect Chemistry of Halide Semiconductors I

Session Chairs: Jong Hyun Kim and Ni Zhao

Thursday Morning, April 22, 2021

EL02

8:15 AM EL02.05.01

Late News: Synergistic Effect of A-Site Engineering and Surface Treatment in Tin Halide Perovskite Solar Cells Muhammad Akmal Kamarudin¹, Shahrir Razey Sahamir¹, Daisuke Hirotsu², Kohei Nishimura¹, Kenji Yoshino³, Takashi Minemoto⁴, Qing Shen¹ and Shuzi Hayase¹; ¹The University of Electro-Communications, Japan; ²Kyushu Institute of Technology, Japan; ³University of Miyazaki, Japan; ⁴Ritsumeikan University, Japan

Tin halide perovskite solar cells have attracted attention due to the less toxic nature of tin compared to lead compound. Currently, the efficiency of tin-based perovskite solar cells now reaching more than 13 % slowly catching up with that of lead-based perovskite solar cells showing the promise of tin-based perovskites. However, there are several issues with tin-based perovskites that need to be addressed in order for these materials to compete with lead-based perovskites. The susceptibility of Sn^{2+} to oxidize into Sn^{4+} upon exposure to air reduces the long-term device stability and this phenomenon also caused major surface recombination which will result in low open-circuit voltage. In addition, the energy levels in tin halide perovskites are shallow compared to that of lead-based perovskites which result in large energy mismatch when common charge transport carriers are used. In this work, we performed simultaneous A-site substitution and surface treatment on tin-halide perovskites to achieve efficiency of more than 10 % and device stability of more than 300 h. Upon partial A-site substitution, the energy barrier has been effectively reduced especially at the hole transport layer/perovskite interface leading to efficient hole carrier injection. While the surface passivation suppressed the formation of unreacted Sn species and hence surface recombination issue has been addressed successfully. Our hypotheses have been supported using Mott-Schottky and Electrochemical Impedance Spectroscopy measurements showing reduced intrinsic carrier density and enhanced carrier recombination resistance. Using X-ray Photoelectron Spectroscopy measurements, we confirmed the suppression of under-coordinated Sn species and oxidized Sn^{4+} .

8:30 AM EL02.05.02

Controlling Orientation of VLS-Grown Lead Iodide van der Waals Nanowires Leeku Huh and Naechul Shin; Inha University, Korea (the Republic of)

Lead iodide (PbI_2) with van der Waals (vdW) layered crystal structure is widely used as a precursor to prepare lead halide perovskites (LHPs) for diverse applications such as photovoltaics (PVs) or optoelectronics. Although the recent advances in the LHPs-based device applications are mainly based on the thin film-based technologies, fabrication of low-dimensional structures in precise manner would be beneficial for the enhancement of their physical properties. 1D nanowire is of particular interest since its structure intrinsically allows the increase in the light absorption, carrier lifetime, and mobilities, compared to its bulk counterpart. Furthermore, the ability to engineer the structure of 1D nanowires (e.g., phase, orientation, and heterojunction) promises advanced exploitation of the properties, as previously demonstrated for group VI or III-V semiconductor material system.

Here, we demonstrate that PbI_2 nanowires grown *via* vapor – liquid – solid (VLS) method, originally composed of vdW layers stacked along [0001] axis, can switch their orientation (i.e., kinking) by introducing PbBr_2 during the growth. Specifically, we can control two different types of kinking modes: (1) orientation with twin boundary (TB) formation, (2) orientation without TB, by differing the Br exposure time. Our systematic study controlling VLS growth parameters indicates that the incorporation of Br to the catalytic Pb seeds disturbs the triple-phase-line (TPL) and change interface energy, which determines the mode of kinking according to the Br concentration. Our kinked PbI_2 nanowires having different vdW stacking in a single domain exhibit interesting optical property such as localized photoluminescence and waveguide effect, suggesting their potential use in photonics or optoelectronics.

8:35 AM EL02.05.03

Late News: Formation Thermodynamics, Stability, and Decomposition Pathways of Perovskite Halides APbX_3 (A = methylammonium, Cs; X = Cl, Br, I) and Their Solid Solutions Dmitry S. Tsvetkov, Maxim Mazurin, Vladimir Sereda, Ivan Ivanov, Dmitry Malyshkin and Andrey Zuev; Ural Federal Univ, Russian Federation

Standard enthalpies of formation of APbX_3 (A = methylammonium, Cs; X = Cl, Br, I) perovskites and their solid solutions $\text{APb}(\text{X}_{1-z}\text{X}'_z)_3$ from halides and from elements at 298 K were measured using solution calorimetry. Standard entropies of CsPbX_3 (X = Cl, Br, I) at 298 K were determined using the results of EMF measurements of galvanic cells. Intrinsic and extrinsic stabilities of studied halides were analyzed and

compared with each other. The main difference between the stabilities of CsPbX_3 and $\text{CH}_3\text{NH}_3\text{PbX}_3$ halides was found to stem from the different chemical nature of cesium and methylammonium cations. Indeed, the enthalpies of formation of CsPbX_3 from binary constituent halides, $\Delta_f H_{\text{hal}}^\circ$, are only slightly more negative than those of $\text{CH}_3\text{NH}_3\text{PbX}_3$. Small values of $\Delta_f H_{\text{hal}}^\circ$ imply that the entropic contribution to the Gibbs free energy of formation of CsPbX_3 and $\text{CH}_3\text{NH}_3\text{PbX}_3$ is significant and, hence, of utmost importance for understanding the intrinsic stability of these compounds and their analogs. Regarding the extrinsic stability, the presence of gaseous O_2 , H_2O , and CO_2 was shown to be crucial for the stability of the iodide, CsPbI_3 , for which several decomposition reactions, exergonic at 298 K, were identified. At the same time, chloride, CsPbCl_3 , and bromide, CsPbBr_3 , are much less sensitive to these chemical agents. However, liquid water should degrade all the CsPbX_3 halides.

8:40 AM *EL02.05.04

Tin-Halide Perovskite Semiconductors—Defects Photophysics and Optimized Devices Architectures

Annamaria Petrozza; Center for Nano Science and Technology, Italy

Here, I will summarize our understanding of the nature of defects and their photo-chemistry in tin-halide perovskites thin films. We show that, in inert conditions, tin, p-doped, and lead (intrinsic) based perovskite thin film show comparable photoluminescence quantum yield, at comparable morphology. The thin film is also extremely stable under light soaking. On the other hand, photovoltaic devices, showing comparable device architecture show a dramatic reduction in power conversion efficiency for tin based devices. While so far, most of the community effort has been focused on the optimization of the perovskite thin film, very little work has been done on the design of the solar cell architecture. Here we will show new architectures for making tin based solar cells a competitive solution.

9:05 AM BREAK

9:10 AM EL02.05.06

Dependence of Phase Transitions on Halide Ratio in Inorganic $\text{CsPb}(\text{Br}_x\text{I}_{1-x})_3$ Perovskite Thin Films

Obtained from High-Throughput Experimentation Hampus Näsström^{1,1}, Pascal Becker^{1,1}, Jose Marquez Prieto¹, Oleksandra Shargaieva¹, Roland Mainz¹, Eva Unger^{1,2} and Thomas Unold¹; ¹Helmholtz-Zentrum Berlin für Materialien und Energie, Germany; ²Lund University, Sweden

Inorganic Cs-based lead halide perovskites have recently experienced a surge in interest, in part due to their enhanced stability compared with hybrid perovskites. The mixed $\text{CsPb}(\text{Br}_x\text{I}_{1-x})_3$ is especially interesting due to the tunable bandgap in the optimal range suitable for tandem solar cells as well as light emitting devices. However, in contrast to the pure CsPbI_3 and CsPbBr_3 , there has been very few investigations on the crystal phase dynamics of the halide mixture. In this work, we present the phase diagram of $\text{CsPb}(\text{Br}_x\text{I}_{1-x})_3$ ($0 \leq x \leq 1$, 300–585 K) obtained by high-throughput in situ GIWAXS measurements of a combinatorial thin film library¹. The thin film library is produced by combinatorial inkjet printing and measured at a high-flux liquid metal jet source. After synthesis, the films with lower Br/I ratio exhibit the non-photoactive delta-phase at room temperature, whereas the films with higher I/Br ratios are present in the metastable perovskite gamma phase. We find that during heating all compositions convert to the cubic perovskite phase at high temperature and that the presence of bromide in the films stabilizes the metastable perovskite phases upon cool down. In accordance with recent predictions from DFT-calculations, the phase transition temperatures are found to monotonically decrease with increasing bromide content.

¹Näsström et al., J. Mater. Chem. A, 2020, DOI: 10.1039/d0ta08067e

9:25 AM EL02.05.07

Late News: Glass Formation in Metal Halide Perovskites Akash Singh, Manoj K. Jana and David B. Mitzi; Duke University, United States

Crystalline metal halide perovskites (MHPs) have shown tremendous significance in the past decade, leading to momentous advancement in the interdisciplinary fields of materials, electronics and photonics. So far, these studies heavily focused on crystalline MHPs. Though crystallinity offers numerous advantages, the ability to induce glass formation in such semiconductors could provide unique opportunities to extend the associated structure-property relationships and broaden their application space. Despite significant efforts to amorphize MHPs under high pressure, an immediate reversal to a crystalline state upon pressure removal has so far impeded the study of the glassy MHP state and associated practical application, thus necessitating alternative routes. Further, the ability to melt-quench hybrid MHPs has largely been limited due to (i) degradation/loss of the organic component upon heating above 200°C and (ii) super-fast ordering kinetics of these melts. Herein, we demonstrate the first example of glass formation at ambient pressure and reversible switching between glassy and crystalline states in hybrid MHPs. Drawing inspiration from structure-property studies of chiral vs. racemic organic systems, we exploit bulky aromatic chiral organic cations to modify the bonding and packing characteristics and thereby enable an exceptionally low melting temperature ($T_m = 175^\circ\text{C}$) below the degradation point ($T_d \approx 205^\circ\text{C}$), as well as slow ordering kinetics in the exemplary 2D S-(-)-1-(1-naphthyl)ethylammonium lead bromide chiral MHP. These factors provide facile access to a stable glassy state of the said chiral MHP by melt-quenching both in thin-film and monolith configurations. Furthermore, the components of the melt can recrystallize (at $T_x \approx 100^\circ\text{C}$) upon heating above the glass-transition temperature ($T_g \approx 67^\circ\text{C}$), allowing reversible switching between the glassy and crystalline states with characteristic temperatures obeying the atypical sequence for MHPs, $T_g < T_x < T_m < T_d$. Formation of a semiconducting MHP glass, along with the demonstration of thermally-induced reversible switching between the glassy and crystalline states, each offering distinct semiconducting properties, unlocks a new research domain for MHPs with numerous prospective applications spanning the research fields of memory, computing, photonics, catalysis, batteries and meta-surfaces.

Reference: A. Singh et. al., Adv. Mater. 2021, 33(3), 2005868.

9:40 AM DISCUSSION TIME

SESSION EL02.06: Carrier Dynamics and Transportation Mechanisms I
Session Chairs: Jinsong Huang and Do Young Kim
Thursday Morning, April 22, 2021
EL02

10:30 AM *EL02.06.01

Understanding Function of Extrinsic Metal Ions in Perovskites Jinsong Huang; University of North Carolina at Chapel Hill, United States

Successful application of metal halide perovskites in different technologies stems from their demonstrated exceptional optoelectronic properties such as a long charge carrier diffusion length, tunable bandgap, low mid-bandgap trap density, high absorption coefficient, and efficient photoluminescence. However, one question still to be answered is whether these properties, particularly for those polycrystalline films used in most optoelectronic devices, are of intrinsic or extrinsic nature. For example, among all the intriguing optoelectronic properties of the polycrystalline thin perovskite films, the long carrier recombination lifetime is most attractive as it enables efficient perovskite solar cells. I will present some intriguing observation of how extrinsic metal ions affect the materials Morphology, optoelectronic properties and stability.

10:55 AM EL02.06.02

Nonradiative Energy Transfer and Long-Range Exciton Diffusion in Thickness-Controlled Halide Perovskite Nanoplatelets Andreas Singldinger, Michael Lichtenegger, Jan Drewniok, Moritz Gramlich, Carola

Despite showing great promise for optoelectronics, the commercialization of halide perovskite nanostructure-based devices is hampered by inefficient electrical excitation and strong exciton binding energies. To counteract these problems, an understanding of energy- and charge transfer processes in this material is crucial. Here, we study Förster resonance energy transfer (FRET) and charge carrier diffusion processes in quantum-confined two-dimensional CsPbBr₃-based nanoplatelets (NPLs). In thin films of NPLs with two predetermined thicknesses, we observe an enhanced acceptor photoluminescence (PL) emission and a decreased donor PL lifetime. This indicates a FRET-mediated process, benefitted by the structural parameters of the NPLs and with efficiencies of nearly $\eta_{\text{FRET}} = 70\%$.^[1] Additionally, films comprising NPLs of one thickness show signs of FRET-enabled long-range exciton diffusion with diffusion lengths of several hundred nanometers. Ultimately, a tailored energy funnel, in combination with a high diffusion length for perovskite NPLs could substantially improve the efficiency of blue-emitting nanostructure-based optoelectronic devices.

[1] A. Singldinger, M. Gramlich, C. Gruber, C. Lampe, A. S. Urban, ACS Energy Letters 5, 1380-1385 (2020)

11:10 AM EL02.06.03

Late News: Assessing Charge Carrier Extraction Rates in Halide Perovskite Heterojunctions Using Ultrafast THz and Optical Spectroscopies Edward Butler-Caddle¹, Imalka Jayawardena² and James Lloyd-Hughes¹; ¹University of Warwick, United Kingdom; ²University of Surrey, United Kingdom

Lead halide perovskites are one of the leading candidates as the light absorbing layer for new photovoltaic devices¹. As the fabrication of high quality perovskite layers has matured, the optimisation of the charge selective contacts has become increasingly important².

In a solar cell, the device asymmetry necessary to generate a photocurrent and photovoltage is provided by electron or hole selective transport layers (TLs) on either side of the light absorbing layer. At each interface, carrier selectivity may be provided by the relative band alignment, and can also be affected by any built-in fields at the interface. Built-in fields can also affect the interfacial recombination that competes with current extraction, so can have an important role in device performance. Together the two TLs may provide a built-in field throughout the perovskite layer which aids charge separation in the bulk.

Here we report time-resolved measurements of charge extraction into commonly used charge transport layers, by using the terahertz photo-conductivity, transient optical absorption and photoluminescence as non-contact spectroscopic probes. In order to isolate the carrier dynamics at a single interface, experiments were performed on bilayers consisting of the perovskite layer and a single transport layer. By investigating each transport layer in isolation, bulk fields were avoided and the behaviour of each interface was isolated independently. In this work we studied bilayers consisting of commonly used transport layers (Spiro-OMeTAD, PCBM and C60) deposited on top of a high-performance triple cation mixed halide perovskite³ layer (FA_{0.79}MA_{0.16}CS_{0.05})Pb(I_{0.83}Br_{0.17})₃. The ground-state bleach of the interband transitions (observed via transient absorption spectroscopy) probed the carrier density change, while the THz photoconductivity probed the product of the carrier density and mobility. By comparing the two techniques, the relative mobility of electrons and holes can also be observed, with holes found to have higher mobility. The optical techniques used here avoided the need for additional contacts, which may influence the data or confuse the interpretation of the results.

By tuning the optical excitation wavelength we created different initial carrier distributions in the perovskite. When using a short excitation wavelength to generate carriers close to the interface with the transport layer, rapid carrier extraction (within a picosecond) was observed, whereas when photogeneration was concentrated on the far side, negligible carrier extraction was observed over the first 3ns. Conversely, when using longer wavelengths to generate carriers more uniformly through the depth of the perovskite layer, very little extraction was observed over the first few nanoseconds. Therefore, concentrating carriers near the transport layer interface

gave extraction rates that were order of magnitudes faster than expected from diffusion alone.

We identify band bending near the interface as a potential route by which rapid charge extraction can occur. We explored the possible scenarios of drift-limited and diffusion-limited transport through a numerical solution to the drift-diffusion and Poisson equations. The importance of band bending (built-in fields) at the interface in perovskite heterojunctions was assessed.

1. Jena, A. K., Kulkarni, A. & Miyasaka, T. Halide Perovskite Photovoltaics: Background, Status, and Future Prospects. *Chem. Rev.* 119, 3036–3103 (2019).
2. Schulz, P., Cahen, D. & Kahn, A. Halide Perovskites: Is It All about the Interfaces? *Chemical Reviews* 119, 3349–3417 (2019).
3. Saliba, M. et al. Cesium-containing triple cation perovskite solar cells: Improved stability, reproducibility and high efficiency. *Energy Environ. Sci.* 9, 1989–1997 (2016).

11:25 AM BREAK

11:30 AM *EL02.06.04

Long-Range Hot Carrier Transport in Hybrid Perovskites Visualized by Ultrafast Microscopy Libai Huang; Purdue University, United States

The Shockley-Queisser limit for solar cell efficiency of ~ 33% can be overcome if hot carriers can be harvested before they thermalize. Recently, carrier cooling time up to 100 picoseconds was observed in hybrid organic-inorganic lead halide perovskites, but it is unclear whether these long-lived hot carriers can migrate long distance for efficient collection. We report direct visualization of hot carrier migration in $\text{CH}_3\text{NH}_3\text{PbI}_3$ thin films by ultrafast transient absorption microscopy, demonstrating three distinct transport regimes. Quasi-ballistic transport was observed to correlate with excess kinetic energy; resulting in up to 230 nanometers transport distance in 300 fs that could overcome grain boundaries. The nonequilibrium transport persisted over tens of picoseconds and ~ 600 nanometers before reaching the diffusive transport limit. These results suggest potential applications of hot carrier devices based on hybrid perovskites.

11:55 AM EL02.06.05

Light-dependent Impedance Spectra and Transient Photoconductivity in a Ruddlesden–Popper 2D Lead-Halide Perovskite Revealed by Electrical Scanned Probe Microscopy John A. Marohn¹, Ali Tirmzi¹, Ryan P. Dwyer² and Fangyuan Jiang³; ¹Cornell University, United States; ²University of Mount Union, United States; ³University of Washington, United States

We recently used electric force microscopy to discover persistent light-induced conductivity in a range of 3D lead-halide perovskite semiconductors. Here electric force microscopy was used to record the light-dependent impedance spectrum and time-resolved photoconductivity of a film of butylammonium lead iodide, BA_2PbI_4 , a 2D Ruddlesden–Popper perovskite semiconductor. The impedance spectrum of BA_2PbI_4 showed modest changes as the illumination intensity was varied up to 1400 mW/cm^2 , in contrast with the comparatively dramatic changes seen for 3D lead-halide perovskites under similar conditions. BA_2PbI_4 's light-induced conductivity had a rise time and decay time of 100 microseconds, 10^4 slower than expected from direct electron-hole recombination and yet 10^5 faster than the conductivity-recovery times recently observed in 3D lead-halide perovskites and attributed to the relaxation of photogenerated vacancies. What sample properties are probed by electric force microscope measurements remains an open question. A Lagrangian-mechanics treatment of the electric force microscope experiment was recently introduced by Dwyer, Harrell, and Marohn which enabled the calculation of steady-state electric force microscope signals in terms of a complex sample impedance. Here this impedance treatment of the tip-sample interaction is extended, through the introduction of a time-dependent transfer function, to include time-resolved electrical scanned probe measurements. It is shown that the signal in a phase-kick electric force microscope experiment, and therefore also the signal in a time-resolved electrostatic force microscope experiment, can be written explicitly in terms of the sample's time-

dependent resistance (*i.e.*, conductivity).

SESSION EL02.07: Synthesis and Crystal/Defect Chemistry of Halide Semiconductors II
Session Chairs: Biwu Ma and Zhibin Yu
Thursday Afternoon, April 22, 2021
EL02

1:00 PM *EL02.07.01

Perovskite Quantum Dots for Light Emission Edward Sargent and Yitong Dong; University of Toronto, Canada

I will discuss the synthesis and surface-management of perovskite quantum dots. I will address progress in managing ligand exchanges towards well-passivated inks that can then be processed directly into films. I will discuss the resultant photophysics and how the materials can be deployed in devices such as narrow-linewidth LEDs.

1:25 PM *EL02.07.02

***In Situ* Visualization of Ferroic-Ionic Interaction in Hybrid Organic Inorganic Perovskites** Olga S. Ovchinnikova; Oak Ridge National Laboratory, United States

Understanding the relationship between structure and functionality is particularly important for the future development of energy devices such as photovoltaics, batteries, catalysts, supercapacitors, optoelectronics, among a myriad of other important applications. In virtually all cases, it is the local inhomogeneities and defects that ultimately control macroscopic behavior and device performance by acting as nucleation centers for new phases, interactions, or failure sites. It is only by understanding the local mechanisms that we can hope to address these problems, and in doing so understand how to improve and enable the next generation of high conversion efficiency and long lifetime for optoelectronic materials. Hybrid organic-inorganic perovskites (HOIPs) such as methylammonium lead iodide ($\text{CH}_3\text{NH}_3\text{PbI}_3$) have attracted broad research interest due to their outstanding optoelectronic performance. However, fundamental understandings of the origin of high PCE and the anomalous current-voltage (I-V) hysteresis of HOIPs optoelectronic devices has proven elusive, even controversial. Although ferroelectricity has been suggested as the reason for this hysteric behavior, convincing evidence supporting this hypothesis is still incomplete. This is due in part to the strong ion motion in HOIPs that complicates the ferroic characterization. Here, using multi-modal functional and chemical imaging methods, we unveil the interaction between ferroic behavior and ion distribution in methylammonium lead iodide ($\text{CH}_3\text{NH}_3\text{PbI}_3$ or MAPbI_3). We demonstrate *in-situ* interaction of ions under the effect of local fields by introducing a new in-situ imaging mobility for time-of-flight secondary ion mass spectrometry (ToF-SIMS). By combining x-ray diffraction and ToF-SIMS we show that the ion redistribution is accompanied by a change in lattice strain, which is reversible. Additionally, Kelvin Probe Force Microscopy (KPFM) demonstrated a screening effect of the electric field and polarization in $\text{CH}_3\text{NH}_3\text{PbI}_3$ caused by ion migration. Overall, we demonstrate that local ion distribution can manipulate the formation of ferroelastic twin domain, providing a pathway to manipulate ferroelastic twin domains and hence optimize optoelectronic properties of HOIPs. This work offers an understanding of ferroic-ionic interplay in HOIPs, providing a pathway to develop novel devices based on HOIPs.

1:50 PM EL02.07.03

Tunable Broad Light Emission from 3D Bromide Perovskites Through Defect Engineering Ioannis Spanopoulos¹, Ido Hadar¹, Weijun Ke¹, Peijun Guo², Eve Mozur³, Emily Morgan³, Shuxin Wang³, G. N. Manjunatha Reddy⁴, Ram Seshadri³, Richard Schaller¹ and Mercouri G. Kanatzidis¹; ¹Northwestern University, United States; ²Argonne National Laboratory, United States; ³University of California, Santa Barbara, United

States; ⁴University of Lille, France

Hybrid halide perovskites have proven to be prominent candidates for many commercial applications, and despite their solution processable synthetic protocols, the resulting films and single crystals demonstrate a combination of optoelectronic properties which are not found to their fully inorganic semiconductor competitors. These features are attributed partly to their inherent defect tolerance.

In this work we take advantage of their defect tolerance to engineer a new family of 3D highly defective “hollow” bromide perovskites with general formula $(\text{FA})_{1-x}(\text{en})_x(\text{Pb})_{1-0.7x}(\text{Br})_{3-0.4x}$ (FA = formamidinium, en = ethylenediammonium, $x = 0-0.44$). The corresponding materials were characterized by a battery of techniques, including single crystal X-ray diffraction (XRD), high resolution powder X-ray diffraction (PXRD), and solid state nuclear magnetic resonance (NMR) measurements. Pair distribution function (PDF) analysis shed light on the local structural coherence, revealing a wide distribution of Pb-Pb distances in the crystal structure, validating further that the corresponding materials are lead deficient and that en inclusion has the same structural effect as in the case of the “hollow” iodide analogs.

By manipulating the number of defects, we finely tuned the optical properties of the pristine FAPbBr₃, by blue shifting the band gap from 2.20 eV to 2.60 eV for the 42% en sample. A most unexpected outcome was the fact that above 40% en incorporation the material exhibits strong broad light emission with 1% photoluminescence quantum yield (PLQY), that is maintained after exposure in air for more than a year. This is the first example of strong broad light emission from a 3D hybrid halide perovskite and is a clear demonstration that defect engineering can be utilized in our favour to add unusual, exotic optoelectronic properties to this versatile class of materials.

References

[1] Spanopoulos, I.; Hadar, I.; Ke, W.; Guo, P.; Mozur E. M.; Morgan E.; Wang S.; Reddy G. N. M.; Seshadri R.; Schaller, R. D.; Kanatzidis, M. G., *under submission*. 2020.

2:05 PM BREAK

2:10 PM EL02.07.04

Subgrain Structure and Ionic Segregation in Metal Halide Semiconductors Yongtao Liu^{1,2}, Patrick Trimby³, Liam Collins¹, Mahshid Ahmadi², Bin Hu², Sergei Kalinin¹, Roger Proksch⁴ and Olga S. Ovchinnikova¹; ¹Oak Ridge National Laboratory, United States; ²The University of Tennessee, Knoxville, United States; ³Oxford Instruments Nanoanalysis, United Kingdom; ⁴An Oxford Instruments Company, United States

Metal halide perovskites (MHPs) solar cells have shown great potential for optoelectronic applications. Although it has been well established how grain, grain boundary, and grain facet affect MHPs optoelectronic properties, less is known about subgrain structures. Recently, a sub-grain feature, twin domain, in MHPs has stimulated extensive discussion. Numerous calculation works have indicated that both domains and domain walls can significantly influence the optoelectronic properties of MHPs, while related experimental results are still missing. In this work, using electron backscatter diffraction (EBSD) and multiple advanced piezoresponse force microscopy (PFM) we studied the crystallographic and ferroic properties of twin domains in MHPs, respectively. Using EBSD, we identified the orientation relationship across the twin boundaries in CH₃NH₃PbI₃ and the directions parallel to the surface normal. Then, we performed multiple advanced PFM measurements to investigate whether the origin of PFM signals of these twin domains is ferroelectricity. We also investigated the behavior of twin domains and domain walls in polarization switching measurement and discovered nonferroelectric contributions to polarization switching measurement. Combining EBSD and PFM study, we found that the PFM signal in CH₃NH₃PbI₃ in the directions parallel to the surface normal (identified by EBSD) is not originated from piezoelectricity/ferroelectricity. These measurements were also carried out to study low-dimensional (2D) metal halide materials. A number of interesting phenomena have also been observed in 2D metal halide materials, including ferroic twinning, ion segregation, photoinduced strain, etc. This work offers a

picture describing the crystallographic orientation, twin domains, domain walls in MHPs, which is crucial for understanding the influence of subgrain structure on the optoelectronic properties of metal halide semiconductors.

2:25 PM EL02.07.05

Donor Doping of CsPbBr₃ John L. Lyons; U.S. Naval Research Laboratory, United States

The inorganic lead halide perovskite CsPbBr₃ exhibits many outstanding properties, in addition to possibly offering environmental stabilities better than their hybrid perovskite counterparts. The full utilization of these materials in optoelectronic applications would be aided by gaining the ability to control the electrical conductivity via impurity doping. One possible donor, bismuth, has been found to enhance solar cell efficiency, and an increase in the position of the Fermi level upon doping. Here I examine how bismuth incorporates into CsPbBr₃ using first-principles hybrid density functional theory. The stability of different configurations is considered as a function of chemical potential and Fermi level. Although bismuth prefers to substitute for lead under most conditions, it introduces a deep donor level ~500 meV from the conduction-band minimum, indicating it will not efficiently generate free carrier concentrations. Based on these results, doping strategies for CsPbBr₃ are reconsidered.

This work was supported by the Office of Naval Research through the Naval Research Laboratory's Basic Research Program

2:40 PM EL02.07.06

Late News: Surface Energy-Driven Preferential Grain Growth of Metal Halide Perovskites—Effects of Nanoimprint Lithography Beyond Direct Patterning Jiyoung Moon¹, Sunah Kwon¹, Masoud Alahbakhshi¹, Yeonghun Lee¹, Kyeongjae Cho¹, Anvar Zakhidov^{1,2}, Moon J. Kim¹ and Qing Gu¹; ¹University of Texas at Dallas, United States; ²ITMO University, Russian Federation

Hybrid organic–inorganic lead halide perovskites have attracted much attention in the field of optoelectronic devices because of their desirable properties such as high crystallinity, smooth morphology, and well-oriented grains. In addition, they can be easily implemented in many platforms using deposition techniques such as spin coating, methylamine gas vapor annealing, and vapor-assisted/gas-assisted solution processing.¹ However, direct patterning of perovskites is known to be challenging because they degrade when exposed to polar solvents and to UV and high electron energies that are used in photo- and e-beam lithography.² Recently, it was shown that thermal nanoimprint lithography (NIL) is an effective method not only to directly pattern but also to improve the morphology, crystallinity, and crystallographic orientations of annealed perovskite films.^{3,4} However, the underlining mechanisms behind the positive effects of NIL on perovskite material properties have not been understood. In this work, we study the kinetics of perovskite grain growth with surface energy calculations by first-principles density functional theory (DFT) and reveal that the surface energy-driven preferential grain growth during NIL, which involves multiplex processes of restricted grain growth in the surface-normal direction, abnormal grain growth, crystallographic reorientation, and grain boundary migration, is the enabler of the material quality enhancement. Moreover, we develop an optimized NIL process and prove its effectiveness by employing it in a perovskite light-emitting electrochemical cell (PeLEC) architecture, in which we observe a fourfold enhancement of maximum current efficiency and twofold enhancement of luminance compared to a PeLEC without NIL, reaching a maximum current efficiency of 0.07598 cd/A at 3.5 V and luminance of 1084 cd/m² at 4 V.

Reference

(1) Jung, M.; Ji, S. G.; Kim, G.; Seok, S. il. Perovskite Precursor Solution Chemistry: From Fundamentals to Photovoltaic Applications. *Chemical Society Reviews* **2019**, *48* (7), 2011–2038.

<https://doi.org/10.1039/c8cs00656c>.

(2) Melvin, A. A.; Stoichkov, V. D.; Kettle, J.; Mogilyansky, D.; Katz, E. A.; Visoly-Fisher, I. Lead Iodide as a Buffer Layer in UV-Induced Degradation of CH₃NH₃PbI₃films. *Solar Energy* **2018**, *159* (November 2017),

794–799. <https://doi.org/10.1016/j.solener.2017.11.054>.

(3) Li, Z.; Moon, J.; Gharajeh, A.; Haroldson, R.; Hawkins, R.; Hu, W.; Zakhidov, A.; Gu, Q. Room-temperature Continuous-Wave Operation of Organometal Halide Perovskite Lasers. *ACS Nano* **2018**, *12* (11), 10968–10976. <https://doi.org/10.1021/acsnano.8b04854>.

(4) Pourdavoud, N.; Haeger, T.; Mayer, A.; Cegielski, P. J.; Giesecke, A. L.; Heiderhoff, R.; Olthof, S.; Zaefferer, S.; Shutsko, I.; Henkel, A.; Becker-Koch, D.; Stein, M.; Cehovski, M.; Charfi, O.; Johannes, H. H.; Rogalla, D.; Lemme, M. C.; Koch, M.; Vaynzof, Y.; Meerholz, K.; Kowalsky, W.; Scheer, H. C.; Görrn, P.; Riedl, T. Room-Temperature Stimulated Emission and Lasing in Recrystallized Cesium Lead Bromide Perovskite Thin Films. *Advanced Materials* **2019**, *31* (39). <https://doi.org/10.1002/adma.201903717>.

2:55 PM EL02.07.07

Deep Levels in Cesium Lead Bromide from Native Defects and Hydrogen Michael W. Swift and John L. Lyons; U.S. Naval Research Laboratory, United States

Lead halide perovskites such as CsPbBr₃ have attracted widespread attention as optoelectronic materials, due in large part to their good performance despite high defect densities. This “defect tolerance” has often been explained by hypothesizing that there is negligible trap-assisted nonradiative recombination in these materials because none of the dominant defects give rise to deep levels in the gap. We refer to this as the “shallow defect hypothesis” (SDH). In this work, we reject the SDH for CsPbBr₃. Via a thorough first-principles inventory of native defects and hydrogen impurities, we show that a number of relevant defects do in fact have deep levels, most notably the bromine interstitial and hydrogen interstitial. This adds to a growing body of evidence against the SDH, suggesting that the observed defect tolerance may be due instead to relatively low recombination rates at deep levels. Guided by the theoretical identification of these defects, experiments can take steps to mitigate trap-assisted non-radiative recombination, further boosting the efficiency of lead halide perovskite optoelectronics.

* M.W.S. was supported by the Naval Research Laboratory Postdoctoral Fellowship through the American Society for Engineering Education. J.L.L. was supported by the ONR/NRL 6.1 Base Research Program.

SESSION EL02.08: Halide-Based Detectors
Session Chairs: Hyocheol Jung and Do Young Kim
Thursday Afternoon, April 22, 2021
EL02

4:00 PM EL02.08.01

Late News: Ultraflexible Perovskite X-Ray Detectors Interface Engineering Stepan Demchyshyn^{1,1}, Matteo Verdi², Laura Basirico^{2,3}, Andrea Ciavatti^{2,3}, Bekele Heilegnaw^{1,1,1}, Daniela Cavalcoli², Markus Scharber¹, Niyazi Serdar Sariciftci¹, Martin Kaltenbrunner^{1,1} and Beatrice Fraboni^{2,3}; ¹Johannes Kepler Universität Linz, Austria; ²Università di Bologna, Italy; ³National Institute for Nuclear Physics, Italy

The world around us consists of a myriad of objects with curved geometries and complex surfaces, yet the majority of sensors and detectors that we use to study them are rigid and planar. While state-of-the-art X- and gamma-ray detectors based on Si, a-Se, HgI₂ and CdZnTe have tremendously advanced the field of digital X-ray radiography, their mechanical stiffness, high thickness, and mass impose limits on their application and ultimate performance. Here we present first ultraflexible, lightweight, and highly conformable perovskite X-ray detectors, showing excellent performance that was achieved by means of thorough interfacial engineering study [1]. Our devices with an active area of 0.05 cm² show sensitivity of $9.3 \pm 0.5 \mu\text{C Gy}^{-1} \text{cm}^{-2}$ operated at 0 V (passive mode operation) with limit of detection down to $0.58 \pm 0.05 \mu\text{Gy s}^{-1}$ setting a current record for passive thin film perovskite detectors. Moreover, these ultraflexible detectors allow for isotropic operation, reliably

detecting X-rays impinging either on the back or the front side of the device. Ultraflexible, low-cost, and highly sensitive high energy radiation detectors are of great interest to the fields of medical diagnostics, dosimetry, industrial inspection, security, and defense. Low weight and high conformability of X-ray wearable dosimeters are appealing features for astronauts, nuclear power plants, and laboratory workers, as well as for imagers used in structural inspection and cultural heritage preservation.

[1] Demchyshyn S, Verdi M, Basiricò L, Ciavatti A, Hailegnaw B, Cavalcoli D, Scharber MC, Sariciftci NS, Kaltenbrunner M, Fraboni B. *Designing Ultraflexible Perovskite X-Ray Detectors through Interface Engineering*. *Advanced Science*. 2020 Dec;7(24):2002586.

4:15 PM EL02.08.02

Performance Losses in Perovskite Solar Cells Under Reverse Bias Due to Electrochemical Halide Reactions Jay Patel^{1,2}, Luca Bertoluzzi³, Kevin Bush³, Caleb Boyd^{3,1}, Ross Kerner¹, Brian O'Regan⁴ and Michael McGehee^{2,1}; ¹National Renewable Energy Laboratory, United States; ²University of Colorado Boulder, United States; ³Stanford University, United States; ⁴Sunlight Scientific, United States

Metal halide perovskite solar cells are now nearly as efficient as the best silicon solar cells but could cost less and be made with a less energy-intensive fabrication process. One of the most significant, but frequently overlooked challenges that must be addressed to allow commercialization of perovskite devices is their degradation under partial shading. When a solar cell is shaded in a module, the photogenerated current drops and a negative voltage (reverse bias) builds up as the other illuminated cells in series try to drive current through, leading to undesired efficiency losses.^(1, 2) Moreover, metal-halide perovskite-based photodetectors are showing real potential as x-ray detectors for medical imaging purposes. X-ray detectors are mainly operated in reverse bias for fast extraction of charge carriers.⁽³⁾ However there have been very few studies, investigating the behavior of devices under prolonged reverse bias. ^(2, 4, 5)

It is imperative to understand how these devices behave under reverse bias. Applying -1 V to -5 V (reverse bias) for a few seconds on perovskite devices with metal contacts induces irreversible device shunting and significant device degradation.⁽²⁾ Additionally, reports have shown some semi-transparent device architectures display substantial “s-kink” behavior in their $J-V$ scans after placed under extended reverse bias.⁽⁴⁾ However, the “s-kink” behavior is only one particular case of the reverse bias behavior. Many devices generally undergo short circuit, open circuit voltage and/or fill factor losses. Additionally, there have been observations of reverse bias induced halide phase segregation.^(2, 4) Consequently, while several processes may be occurring at reverse bias, the mechanisms provided do not entirely explain the severe efficiency losses (>50%) measured after reverse bias.

Here, we use an advanced drift-diffusion approach incorporating an electrochemical term to elucidate the short-circuit, open circuit and fill factor losses we experimentally measure after prolonged reverse bias. We show that holes can tunnel into the perovskite due to sharp band bending near the contacts, accumulate within the bulk of the perovskite absorber, and trigger the oxidation of halides. The density of the oxidized halide species is much higher in reverse bias as there are scarcely any electrons available to reduce the halogens. The resultant halogens act as bulk recombination centers. While the interstitial halogen density does decay when the cell is operated in forward bias, permanent degradation can occur if the iodine diffuses out of the perovskite layer. Our theory shows the significance of the mobile ions in controlling device performance and stability and suggests that reverse bias could be used to perform accelerated tests to quickly assess the robustness of perovskite devices to halide reactivity.

1. T. J. Silverman, M. G. Deceglie, X. Sun, R. L. Garris, M. A. Alam, C. Deline, S. Kurtz, Thermal and Electrical Effects of Partial Shade in Monolithic Thin-Film Photovoltaic Modules. *IEEE J. Photovoltaics*. **5**, 1742–1747 (2015).

2. A. R. Bowring, L. Bertoluzzi, B. C. O'Regan, M. D. McGehee, Reverse Bias Behavior of Halide Perovskite Solar Cells. *Adv. Energy Mater.* **8**, 1702365 (2018).

3. H. Wei, Y. Fang, P. Mulligan, W. Chuirazzi, H.-H. Fang, C. Wang, B. R. Ecker, Y. Gao, M. A. Loi, L. Cao, J. Huang, Sensitive X-ray detectors made of methylammonium lead tribromide perovskite single crystals. *Nat.*

Photonics. **10**, 333–339 (2016).

4. R. A. Z. Razera, D. A. Jacobs, F. Fu, P. Fiala, M. Dussouillez, F. Sahli, T. C. J. Yang, L. Ding, A. Walter, A. F. Feil, H. I. Boudinov, S. Nicolay, C. Ballif, Q. Jeangros, Instability of p–i–n perovskite solar cells under reverse bias. *J. Mater. Chem. A*, **8**, 242–250 (2020).

5. A. Rajagopal, S. T. Williams, C.-C. Chueh, A. K. Y. Jen, Abnormal Current–Voltage Hysteresis Induced by Reverse Bias in Organic–Inorganic Hybrid Perovskite Photovoltaics. *J. Phys. Chem. Lett.* **7**, 995–1003 (2016).

4:30 PM *EL02.08.03

Tunable Perovskite-Based Photodetectors in Optical Sensing Ruth Shinar; Iowa State University, United States

There is a continued and growing need for miniaturization of sensors to enable their integration into technologies, such as wearable electronics in medical testing and (bio)chemical analyses. Perovskite-based photodetectors (PPDs) are of special interest for integration with optical sensor components due to their thin structure and exceptional attributes of high responsivity and fast response. In this presentation we demonstrate the suitability and advantage of PPDs for optical analyte sensing by monitoring not only dose-dependent changes in the photoluminescence (PL) intensity of analyte-sensitive dyes, but also by measuring the PL decay times following an excitation pulse, which is a preferred monitoring approach. Two types of highly responsive PPD structures are described: (1) PPDs with wide band responsivity that are suitable for light detection over a broad spectral range, and (2) PPDs sensitive only over a tunable narrow spectral band, which makes them suitable for multi-analyte compact sensors arrays, with analytes that are detected in different spectral ranges. We show the functionality of such PPDs for monitoring gas-phase and dissolved oxygen (DO), as well as glucose. The effect of the PPDs attributes, e.g., size, response time, and responsivity spectrum on the sensors' components, mode of operation, and characteristics, including dynamic range, sensitivity, and limit of detection will be discussed. Advantages of such PPDs in comparison to Si photodiodes, thin film amorphous and nano-crystalline Si, as well as all-organic photodetectors will also be presented.

4:55 PM BREAK

5:00 PM EL02.08.04

Revealing Electrical Poling Induced Polarization Potential in Hybrid Perovskite Photodetectors Haiyang Zou, Zhiqun Lin and Zhong Lin Wang; Georgia Institute of Technology, United States

Despite recent rapid advances in metal halide perovskites for use in optoelectronics, the fundamental understanding of the electrical poling induced ion migration, accounting for many unusual attributes and thus performance in perovskite based devices, remain comparatively elusive. Herein, the electrical poling promoted polarization potential is reported for rendering hybrid organic inorganic perovskite photodetectors with high photocurrent and fast response time, displaying a tenfold enhancement in the photocurrent and a twofold decrease in the response time after an external electric field poling. First, a robust meniscus assisted solution printing strategy is employed to facilitate the oriented perovskite crystals over a large area. Subsequently, the electrical poling invokes the ion migration within perovskite crystals, thus inducing a polarization potential, as substantiated by the surface potential change assessed by Kelvin probe force microscopy. Such electrical poling induced polarization potential is responsible for the markedly enhanced photocurrent and largely shortened response time. This work presents new insights into the electrical poling triggered ion migration and, in turn, polarization potential as well as into the implication of the latter for optoelectronic devices with greater performance. As such, the utilization of ion migration produced polarization potential may represent an important endeavor toward a wide range of high performance perovskite based photodetectors, solar cells, transistors, scintillators, etc.

5:15 PM EL02.08.05

Perovskite-Based Sensing Scheme for Detecting Volatile Organic Compounds (VOCs) at Room Temperature Mohammad Shakhawat Hossain and Arash Takshi; University of South Florida, United States

Volatile Organic Compound (VOC) gases can contribute to the environmental pollution, leading to difficulty in breathing, nausea, eye irritation, and even damage of the central nervous system, specially in indoor environment. Sensing these gases plays a crucial role in environmental monitoring. This study aims to test the sensitivity and selectivity of methylammonium lead iodide (MAPbI₃) perovskites to various different VOC gases. Here, at first, microchannels were created on indium tin oxide (ITO) coated plastic substrates. The microchannels were filled with the perovskite precursor solution using the capillary motion force. After crystallization, the current-voltage (I-V) characteristic responses of the perovskite before and after the exposure to the gasses were studied, both under dark and light conditions. The variation of the photocurrent in response to ethanol, methanol, and acetone have been studied. While the sensor showed a negligible I-V changes in response to ethanol and acetone, the photocurrent was decreased by 25% when the device was exposed to methanol at 2.0 V voltage bias. The experimental results of detecting VOCs at room temperature are promising for the development of an array of low-cost and low-power perovskite-based gas sensors that can be integrated in lab-on-a-chip devices.

5:30 PM EL02.08.06

Late News: Multispectral Image Sensor Beyond Tristimulus Color Vision with Perovskites Md Wayesh Qarony^{1,2} and Mohammad I. Hossain²; ¹Lawrence Berkeley National Laboratory, United States; ²The Hong Kong Polytechnic University, Hong Kong

In this study, optical multispectral sensors based on perovskite semiconductors have been proposed, simulated, and characterized. The perovskite material system combined with the 3D vertical integration of the sensor channels allows for the realization of sensors with high sensitivities and a high spectral resolution. The sensors can be applied in several emerging areas, including biomedical imaging, surveillance, complex motion planning of autonomous robots or vehicles, artificial intelligence, and agricultural applications. The sensor elements can be vertically integrated on a readout electronic to realize sensor arrays and multispectral digital cameras. In this study, three- and six-channel vertically stacked perovskite sensors are optically designed, electromagnetically simulated, and colorimetric characterizations to evaluate the color science. The proposed sensors allow for the implementation of snapshot cameras with high sensitivity. The proposed sensor is compared to other sensor technologies in terms of sensitivity and selectivity.

5:45 PM DISCUSSION TIME

SESSION EL02.09: Carrier Dynamics and Transportation Mechanisms II

Session Chairs: Jong Hyun Kim and Sai Wing Tsang

Thursday Afternoon, April 22, 2021

EL02

8:15 PM *EL02.09.01

Influence of Charge Transport Layers on Capacitance Measured in Halide Perovskite Solar Cells Yanfa Yan; The University of Toledo, United States

To further improve the powder conversion efficiency of halide perovskite solar cells (PSCs), it is highly preferred to understand the electrical properties of the perovskite absorbers, since the PCE is determined by the electrical properties of PSCs, such as defect activation energy and density, carrier concentration, and dielectric constant. Capacitance-based techniques, such as thermal admittance spectroscopy (TAS) and capacitance-voltage (C-V), have been the choice of method for measuring electrical properties of semiconductor devices and have played important roles in the development of thin-film solar cell technologies. These techniques have been used to measure the electrical properties of PSCs such as defect activation energy and density, carrier

concentration, and dielectric constant, which provide key information for evaluating the device performance. We show that charge-transport layers can have significant influence on the measured capacitance, affecting the interpretation of the results. For example, the hole-transport layers (HTLs) can introduce high-frequency capacitance signature due to the response of charge carriers in HTLs. In literature, the so-called D1 signature was attributed to defects in perovskite defects. However, we found that the D1 signature is due to HTLs. For HTL-free PSCs, the D1 signature disappears and the high-frequency capacitance can be considered as the geometric capacitance for analyzing the dielectric constant of the perovskite layer.

8:40 PM EL02.09.02

Anisotropic Lattice Deformations Control Photocarrier Relaxation Dynamics in 2D Halide Perovskites

Hao Zhang^{1,1}, Wenbin Li^{1,1}, Joseph Essman¹, Claudio Quarti², Siraj Sidhik¹, Jin Hou¹, Isaac Metcalf¹, Jared Crochet³, Mercuri G. Kanatzidis⁴, Claudine Katan², Jacky Even⁵, Jean-Christophe Blancon¹ and Aditya Mohite¹; ¹Rice University, United States; ²Univ Rennes, France; ³Los Alamos National Laboratory, United States; ⁴Northwestern University, United States; ⁵Fonctions Optiques pour les Technologies de l'Information, France

Understanding hot-carrier cooling processes in hybrid (organic-inorganic) halide perovskites is crucial in photovoltaic applications. The dynamics of carrier-lattice interactions in perovskites strongly affect carrier lifetimes and diffusion lengths, which are key factors in device efficiency. Studies of 2D perovskite systems have revealed unique physics in terms of electron-lattice interactions, such as light-induced phonon coherences, phonon dynamical lattice disorder, and electron-phonon scattering through deformation potentials. Besides spectroscopic studies, we have performed direct structural probing of 2D perovskites using ultrafast electron diffraction (UED), and have shown multiple electron-phonon interactions during non-thermal carrier relaxation. Those electron-phonon scattering dynamics are dominated by structural deformation related to low-frequency phonon modes, induced by in-plane rotation of perovskite octahedra. Compared with the structural responses of 3D perovskites (MAPbI₃), our results on 2D crystals show distinct behavior in terms of both anisotropy and anharmonicity. These understandings could provide deeper insight in the dynamics of carrier-lattice interactions in 2D perovskites, and will bridge the knowledge gap of hot-carrier dynamics between 3D and 2D perovskite systems.

8:55 PM EL02.09.03

Direct Visualization of Large Polaron Formation in Hybrid Lead Halide Perovskites via Femtosecond Diffuse X-Ray Scattering

Burak Guzelturk¹, Thomas Winkler², Tim van de Goor², Matthew Smith³, Sean Bourelle², Sascha Feldmann², Mariano Trigo⁴, Samuel Teitelbaum⁴, Hans-Georg Steinrück⁴, Gilberto de la Pena⁴, Roberto Alonso Mori⁴, Diling Zhu⁴, Takahiro Sato⁴, Hemamala Karunadasa³, Michael Toney⁴, Felix Deschler² and Aaron Lindenberg^{3,4}; ¹Argonne National Laboratory, United States; ²University of Cambridge, United Kingdom; ³Stanford University, United States; ⁴SLAC National Accelerator Laboratory, United States

Lead halide perovskites uniquely offer long carrier diffusion lengths and high resilience against electronic defects, which are highly surprising for a solution-processed semiconductor. The microscopic mechanisms behind such favorable properties have not been fully understood to date. Main hypotheses revolved around dynamic structural responses and formation of large polarons in order to explain the slower carrier recombination and defect tolerances. Nevertheless, these dynamic structural aspects have not been monitored before mainly due to lack of available techniques that can track atomic-scale motions after photoexcitation. In this work, we perform optical pump / femtosecond diffuse x-ray scattering probe measurements using an x-ray electron free laser, the so-called LCLS at SLAC/Stanford [1]. The experiments clearly show that localized expansive strains build up following photoexcitation. It takes ~20 ps for the local distortions, on average, to reach about 5 nm in diameter. These lattice distortions then relax over the time window of the carrier recombination. Our finding undoubtedly demonstrates that the charge carriers in the perovskites strongly distort the atomic structure transiently while the distortion size extending over many unit cells, hence forming large polarons. In this experiment, we resolve the spatio-temporal evolution of the polarons for the first time enabled by phonon-momentum-resolved measurements in our experiment based on time-resolved diffuse x-ray

scattering.

[1] B. Guzelturk et al. Nature Materials (2020) DOI: 10.1038/s41563-020-00865-5

9:10 PM BREAK

9:15 PM EL02.09.04

Determination of Semiconductor Diffusion Coefficient by Optical Microscopy Measurements Dane W. deQuilettes¹, Roberto Brenes¹, Madeleine Laitz¹, Brandon Motes¹, Mikhail Glazov² and Vladimir Bulovic¹; ¹Massachusetts Institute of Technology, United States; ²Ioffe Institute, Russian Federation

Energy carrier transport and recombination in emerging semiconductors can be directly monitored with optical microscopy, leading to the measurement of the diffusion coefficient (D), a critical property for design of efficient optoelectronic devices. D is often determined by fitting a time-resolved expanding carrier profile after optical excitation using a Mean Squared Displacement (MSD) Model, where $D = [\sigma^2(t) - \sigma^2(0)]/2t$, with $\sigma^2(t)$ being the Gaussian variance as a function of time. Although this approach has gained widespread adoption, its utilization can significantly overestimate D due to the non-linear recombination processes that artificially broaden the carrier distribution profile. Here, we simulate diffusive processes in both excitonic and free carrier semiconductors and present revised MSD Models that take into account second-order (bimolecular) and third-order (Auger) processes to accurately recover D for various materials. For perovskite thin films, utilization of these models can reduce fitting error by orders of magnitude, especially for commonly deployed excitation conditions where carrier densities are $> 5 \times 10^{16} \text{ cm}^{-3}$. Contrary to what is generally accepted, we find that photon recycling does not have a significant impact on carrier profiles and that differences in grain size and boundary behavior, present in most polycrystalline films, can lead to distinct profiles that are not captured by MSD Models. Finally, we present clear strategies to investigate energy transport in disordered materials for more effective design and optimization of electronic and optoelectronic devices.

9:30 PM EL02.09.05

Modulating Charge Carrier Dynamics and Transfer Via Surface Modifications in Organometallic Halide Perovskite Quantum Dots William G. Delmas¹, Evan Vickers², Albert Dibenedetto¹, Calista Lum¹, Isaak Hernandez³, Jin Zhang² and Sayantani Ghosh¹; ¹University of California, Merced, United States; ²University of California, Santa Cruz, United States; ³Massachusetts Institute of Technology, United States

Controlled functionalization of colloidal quantum dot surfaces is key to the manipulation of their optoelectronic properties. Applying this principle to the study of organometallic halide perovskite quantum dots (PQD's), we investigate temperature-dependent optical and energy transfer properties of four PQD species, all functionalized with variations of benzoic ligands. These include benzoic acid (BA), phenylacetic acid (PAA), benzylamine (BZA), and isopropyl benzylamine (IPBZA). While the chemical structure of BZA/BA and IPBZA/PAA differ by just a few carbon atoms, this difference manifests as a significant variation in PQD properties. Charge transfer efficiency in PQD films comprising BA-ligated samples varies between 12- 95% as dot density is tuned from $10^2 - 10^5 \text{ dots}/\mu\text{m}^2$ but is consistently $\sim 92\%$ over that entire range for PAA-ligated PQDs. As temperature T decreases, initially, recombination is dominated by bound or trapped excitons, but for $T < 80 \text{ K}$, spectral broadening accompanied by free excitonic behavior is observed. Our results indicate enhanced charge delocalization at lower T , which reduces exciton confinement and recombination decay rates, underlining the importance of investigating PQD-ligand interactions at the fundamental level given the significant effect minute changes in ligand structures have on optoelectronic properties of quantum dots.

9:45 PM *EL02.09.06

On the Degradation and Self-Healing Mechanism in Perovskite Solar Cells Sai Wing Tsang; City University of Hong Kong, China

Ion dissociation in perovskite lattices has been recently identified to determine the intrinsic stability of

perovskite solar cells (PVSCs), the underlying degradation mechanism is still elusive. In this work, we demonstrate that by combining highly sensitive sub-bandgap external quantum efficiency (s-EQE) spectroscopy, impedance analysis as well as theoretical calculations, the evolution of defect states in PVSCs during the degradation can be monitored. It is found that the degradation of PVSCs can be divided into three steps: (1) dissociation of iodine ions (I^-) from perovskite lattices, (2) migration of I^- to interfaces, and (3) consumption of I^- by reacting with the metal electrode. Importantly, step (3) is found to be crucial as it will accelerate the first two steps and lead to continuous degradation. By replacing the metal with more chemically robust indium tin oxide (ITO) as the electrode, we find that the dissociated I^- under light soaking will only saturate at the perovskite/ITO interface without being consumed. Importantly, the dissociated I^- will subsequently restore to the iodine vacancies under dark condition to heal the perovskite and photovoltaic performance. Such shuttling of I^- without consumption in the ITO-contact PVSCs results in Harvest-Rest-Recovery (HRR) cycles in the natural day/night operation. We envision that the mechanism of the intrinsic perovskite material degradation reported in this work will lead to clearer research directions towards highly stable PVSCs.

10:10 PM DISCUSSION TIME

SESSION EL02.10: Non-Toxic Heavy-Metal-Free Halide Semiconductors

Session Chairs: Tae-Woo Lee and Bayrammurad Saparov

Friday Morning, April 23, 2021

EL02

8:00 AM EL02.10.01

Late News: Lead-Free Perovskite-Inspired Semiconductors for Indoor Photovoltaics Vincenzo Pecunia¹, Robert Hoyer², Yueheng Peng¹, Tahmida N. Huq³, Jianjun Mei¹, Luis Portilla¹, Robert Jagt³ and Judith L. MacManus-Driscoll³; ¹Soochow University, China; ²Imperial College London, United Kingdom; ³University of Cambridge, United Kingdom

Lead-free perovskite-inspired materials (PIMs) are receiving ever-growing attention in photovoltaics, optoelectronics, and beyond, due to their similarity to mainstream lead-based perovskites while being free of the toxicity concerns associated with the latter.^[1-3] Specifically, antimony- and bismuth-based PIMs have been identified as particularly promising. Nonetheless, the efficiencies of such PIMs in single-junction outdoor solar photovoltaics are yet to approach the levels of the lead-based counterparts. An important limiting factor lies in the bandgaps of these materials, which are in the region of 1.9 eV or greater, thereby preventing the optimal absorption of solar light for single-junction operation.

Going beyond the mainstream view of solely considering lead-free PIMs for outdoor solar photovoltaics, herein we show that these materials have considerable potential for indoor photovoltaics (IPV),^[4] a rapidly growing sector in energy harvesting for smart devices of the Internet of Things (IoT) ecosystem.^[5] With a focus on two representative lead-free PIMs with high photoconversion efficiencies, $Cs_3Sb_2Cl_xI_{9-x}$ ^[6] and BiOI,^[7] we show that their IPV efficiencies are up to ~5%, i.e., four times higher than under outdoor solar illumination and already within the performance range of mainstream commercial IPV based on hydrogenated amorphous silicon (a-Si:H).^[4] Further, based on power-dependent measurements and optical loss analyses, we provide insight into the current performance bottlenecks and identify strategies for future improvements toward the ultimate IPV efficiencies of these materials. Finally, by combining millimeter-scale $Cs_3Sb_2Cl_xI_{9-x}$ and BiOI IPV devices with ultralow-power printed electronics,^[8] we present the first-ever demonstration of printed thin-film-transistor electronics powered by IPV.^[4] By revealing the capability and potential of lead-free PIMs for indoor photovoltaics, our findings point to the opportunity provided by such environmentally-friendly semiconductors to sustainably power the growing IoT ecosystem.

References

- [1] R. Nie, R. R. Sumukam, S. H. Reddy, M. Banavoth, S. Il Seok, *Energy Environ. Sci.* **2020**, *13*, 2363.
- [2] V. Pecunia, L. G. Occhipinti, A. Chakraborty, Y. Pan, Y. Peng, *APL Mater.* **2020**, *8*, 100901.
- [3] Y.-T. Huang, S. R. Kavanagh, D. O. Scanlon, A. Walsh, R. L. Z. Hoyer, *Nanotechnology* **2021**, *32*, 132004.
- [4] Y. Peng, T. N. Huq, J. Mei, L. Portilla, R. A. Jagt, L. G. Occhipinti, J. L. MacManus-Driscoll, R. L. Z. Hoyer, V. Pecunia, *Adv. Energy Mater.* **2021**, *11*, 2002761.
- [5] Q. Hassan, Ed., *Internet of Things A to Z*, John Wiley & Sons, Inc., Hoboken, NJ, USA, **2018**.
- [6] Y. Peng, F. Li, Y. Wang, Y. Li, R. L. Z. Hoyer, L. Feng, K. Xia, V. Pecunia, *Appl. Mater. Today* **2020**, *19*, 100637.
- [7] R. L. Z. Hoyer, L. C. Lee, R. C. Kurchin, T. N. Huq, K. H. L. Zhang, M. Sponseller, L. Nienhaus, R. E. Brandt, J. Jean, J. A. Polizzotti, A. Kursumović, M. G. Bawendi, V. Bulović, V. Stevanović, T. Buonassisi, J. L. MacManus-Driscoll, *Adv. Mater.* **2017**, *29*, 1702176.
- [8] L. Portilla, J. Zhao, Y. Wang, L. Sun, F. Li, M. Robin, M. Wei, Z. Cui, L. G. Occhipinti, T. D. Anthopoulos, V. Pecunia, *ACS Nano* **2020**, *14*, 14036.

8:15 AM EL02.10.02

New Kid on the Block—An Emerging Quaternary Chalco-Halide for Stable High-Performance Solar Cells Seán R. Kavanagh^{1,2,2}, Aron Walsh² and David O. Scanlon¹; ¹University College London, United Kingdom; ²Imperial College London, United Kingdom

The exceptional optoelectronic performance of lead-halide perovskites (LHPs) has motivated enormous research efforts toward the discovery of ‘perovskite-inspired materials’ – compounds which aim to replicate the astonishing performance of LHPs while avoiding the infamous stability and toxicity pitfalls of these materials.^{1–3}

Recently, quaternary chalcogen halides of group IV / V elements have begun to attract attention, due to the presence of valence ns^2 lone pairs, a performance-defining feature of LHPs.⁴

Following the first experimental report of stable, solution-grown tin-antimony sulfoiodide ($\text{Sn}_2\text{SbS}_2\text{I}_3$) solar cells,⁵ with power conversion efficiencies above 4% (exceeding the first reported solar efficiency of methylammonium lead-iodide (MAPI)),⁶ we comprehensively characterize the structural and electronic properties of this emerging material. We find that the experimentally reported (non-ferroelectric) $Cmcm$ crystal structure is in fact an equipment artefact, representing an average over multiple (ferroelectric) $Cmc2_1$ configurations. The resemblance of this dynamic crystal structure and ferroelectric behavior to that of MAPI begs the question of its importance in high-performance defect-tolerant solar materials.

Moreover, using state-of-the-art *ab-initio* methods (hybrid Density Functional Theory including spin-orbit coupling effects), we rigorously assess the efficiency limits of this material on the basis of its electronic structure and predicted defect behavior.

Our work provides valuable insight regarding both the potential success of this emerging class of optoelectronic materials and structure-property relationships in perovskite-inspired materials, guiding design strategies and expanding the compositional space of candidate materials.

1 Y.-T. Huang, **S. R. Kavanagh**, D. O. Scanlon, A. Walsh and R. L. Z. Hoyer, *arXiv:2008.08959*.

2 **S. R. Kavanagh**, Z. Li et al, *J. Mater. Chem. A*, 2020, **8**, 21780–21788.

3 M. Buchanan, *Nature Physics*, 2020, **16**, 996–996.

4 R. Nie, R. R. Sumukam, S. H. Reddy, M. Banavoth and S. I. Seok, *Energy Environ. Sci.*, 2020, **13**, 2363–2385.

5 R. Nie, K. S. Lee, M. Hu, M. J. Paik and S. I. Seok, *Matter*, 2020, S2590238520304471.

6 A. Kojima, K. Teshima, Y. Shirai and T. Miyasaka, *Journal of the American Chemical Society*, 2009, **131**, 6050–6051.

8:30 AM *EL02.10.03

High-Efficiency Light Emission from Lead-Free Metal Halides Bayrammurad Saparov¹, Tielyr Creason¹ and Mao-hua Du²; ¹The University of Oklahoma, United States; ²Oak Ridge National Laboratory, United States

The emergence of lead halide perovskites for optical and electronic applications has been one of the most important discoveries of materials science and chemistry of the past two decades. To accelerate the industrial use of metal halide perovskites, there is a global search for alternative non-toxic, lead-free halides that demonstrate higher environmental stability and similarly outstanding optoelectronic properties while preserving the advantageous properties of lead halides. In this talk, our recent discoveries of brand-new families of lead-free high efficiency light-emitting materials will be summarized. These include all-inorganic copper(I) halides demonstrate low-dimensional non-perovskite structures, and consequently, very flat bands around the band gap, leading to very localized charges. Such charge localization and low-dimensional structures typically result in the presence of high stability self-trapped excitons at room temperature producing record high photoluminescence efficiencies approaching unity. On the other hand, families of low-dimensional hybrid organic-inorganic halides prepared in our show very diverse crystal structures and optical emission properties, including controllable emission from organic or inorganic components, or simultaneous emission from both. The talk will be concluded with a few examples of the potential practical applications of the luminescent metal halides mentioned in this talk.

8:55 AM BREAK

9:15 AM EL02.10.05

Late News: Emergence of Qualitatively Different Anharmonic Expressions in the Structural Dynamics of Halide Perovskites [Adi Cohen](#)¹, Thomas M. Brenner², Johan Klarbring³, Rituraj Sharma¹, Douglas H. Fabini⁴, Roman Korobko¹, Bettina Lotsch^{4,5}, Pabitra Nayak⁶, Olle Hellman³ and Omer Yaffe¹; ¹Weizmann Institute of Science, Israel; ²Weizmann institute of science, Israel; ³Linköping University, Sweden; ⁴Max Planck Institute for Solid State Research, Germany; ⁵Ludwig-Maximilians-Universität München, Germany; ⁶Tata Institute of Fundamental Research, India

Lead-based halide perovskite crystals have unique structural dynamics in that they exhibit, an-harmonic, liquid-like thermal fluctuations. This type of structural dynamics, that can not be treated within the classic framework of semiconductor physics, is intimately to the beneficial electronic properties of the lead based perovskites. In recent years, the double perovskite Cs₂AgBiBr₆, was studied as part of an effort to find a lead-free perovskite for optoelectronic applications. While the electronic properties of Cs₂AgBiBr₆ were extensively studied, little is known about its structural dynamics. We investigate the structural dynamics of Cs₂AgBiBr₆ and compare it to CsPbBr₃ which is its lead-based analog. By using temperature-dependent Raman measurements we found that both materials are strongly anharmonic. However, the expression of their anharmonic behaviour is markedly different. Cs₂AgBiBr₆ shows a soft-mode and a displacive phase transition similar to archetypical oxides perovskites. In contrary, CsPbBr₃ show an increase of a central Raman component, related to a large amplitude, relaxational motion. These differences are a result of different evolution with temperature of the tilting instability that exists in both crystals at low temperatures. This difference is important because it may explain why Cs₂AgBiBr₆ is not an effective material for optoelectronic applications compared to the lead-perovskites. In the course of our investigations, we also discovered a new phase of Cs₂AgBiBr₆ below 35 K.

9:30 AM EL02.10.06

A Direct Comparison of BiI₃, BiOI and Ag₃BiI₆ Layered Semiconductors for Optoelectronics [Andrea Crovetto](#), Alireza Hajjafarassar, Ole Hansen, Brian Seger, Ib Chorkendorff and Peter Vesborg; Technical University of Denmark, Denmark

The bismuth-based (oxy)iodides BiI₃, BiOI and Ag_xBiI_{x+3} share similar layered crystal structures, optimal band gaps for top absorbers in tandem solar cells, and moderate growth temperatures. Similarly to halide perovskite absorbers, they contain a heavy cation with a lone pair of electrons (Bi³⁺) which has been proposed as one of the features enabling defect tolerance in perovskites.

We have grown and characterized BiI₃, BiOI, and Ag₃BiI₆ absorbers and solar cells in a systematic manner by employing a consistent synthesis method ((oxy)iodization of metallic precursor) and a consistent analysis

routine [1]. In this way, the individual strengths and weaknesses of the three absorbers, as well as their common challenges, can be outlined.

The radiative efficiency of the three materials is within the same order of magnitude, indicating a similar degree of defect tolerance. Apart from that, each material has its own advantages and drawbacks, which will be outlined in this presentation.

Control of growth orientation should be a priority for all three materials in view of their anisotropic properties. P-type bulk doping and selection of alternative hole transport layers with deep valence bands would also be desirable to improve performance. At the device level, we report an improved open circuit voltage of BiI₃ solar cells with respect to the state of the art, and we report a proof-of-concept Ag₃BiI₆/silicon tandem cell.

Finally, we have observed at least one unusual, exciting property in each material: BiI₃ diodes have a very low dark ideality factor, on par with the highest-quality silicon solar cells. BiOI has a very convenient mix of moderate growth temperature and air stability. Ag₃BiI₆ is a mixed electronic-ionic conductor with fast ionic diffusion, which may find applications in neuromorphic, memory, or battery devices.

[1] Crovetto et al., Parallel Evaluation of the BiI₃, BiOI, and Ag₃BiI₆ Layered Photoabsorbers. *Chem. Mater.* **2020**, *32*, 3385–3395.

9:45 AM EL02.10.07

A₂MX₃ (A=Rb, K, NH₄; M=Cu, Ag; X= Cl, Br, I): High Stability, Nontoxic Group 11 Halides with Near-Unity Photoluminescence Quantum Yield Tielyr Creason¹, Hadiyah Fattal¹, Timothy M. McWhorter¹, Mao-hua Du² and Bayrammurad Saparov¹; ¹The University of Oklahoma, United States; ²Oak Ridge National Laboratory, United States

All-inorganic group 11 halides have recently gained interest in the optical materials community as viable, relatively non-toxic alternatives to luminescent lead halides. Bulk powder samples and single crystals of A₂MX₃ (A=Rb, K, NH₄; M= Cu, Ag; X= Cl, Br, I) were prepared using high temperature solid-state and solution techniques. The all-inorganic group 11 halides have been investigated through an in-depth optical characterization, including diffuse reflectance, photoluminescence, and radioluminescence. A₂CuX₃ are found to exhibit narrow blue photoluminescence peaks with record-high efficiencies as evidenced by the measured photoluminescent quantum yields up to unity (100 %). Conversely, A₂AgX₃ displays broad, white emission with tunability in color temperature. Through variation in the A⁺ cation site, the stability of the material can be dramatically increased, while retaining similar optical performance. For A₂CuX₃ the bright emission in this family has been attributed to self-trapped excitons localized on [CuX₃]²⁻ anionic substructure based on exhaustive photoluminescence studies supported by the density functional theory (DFT) calculations. Our combined experimental and computational study suggests strong potential of A₂MX₃ as phosphors for radiation detection and solid-state lighting applications.

SESSION EL02.11: Photophysics of Halide Semiconductors I

Session Chairs: Do Young Kim and Zhibin Yu

Friday Afternoon, April 23, 2021

EL02

12:10 PM EL02.11.02

Late News: Factors Influencing the Temperature-Dependent Amplified Spontaneous Emission (ASE) Threshold in Phase-Stable 3D Perovskite Films Isabel Allegro, Yang Li, Bryce S. Richards, Ulrich W. Paetzold, Uli Lemmer and Ian A. Howard; Karlsruhe Institute of Technology, Germany

Room-temperature continuous-wave (CW) lasing in quasi-two-dimensional perovskites was just recently demonstrated in thin films on a distributed feedback grating. However, CW lasing and amplified spontaneous emission (ASE) in three-dimensional (3D) perovskites was so far, only achieved at cryogenic temperatures. Factors limiting the 3D materials to sustain CW gain at higher temperatures include the temperature dependence of the charge carrier distribution in energy; the build-up of photo-induced non-radiative recombination channels; and the rates of bimolecular and Auger recombination. We investigate the latter in a phase-stable triple cation perovskite, by performing transient reflection measurements to determine the charge carrier dynamics from 80 K up to 290 K.

To accurately determine the Auger rate coefficient, we vary the initial carrier density reaching up to very high carrier concentrations where the Auger recombination plays a significant role. These carrier concentrations are above the ASE threshold for thin films prepared on conventional substrates, such as glass or sapphire. Therefore, we use a silicon substrate with a higher refractive index to completely suppress ASE in the film and its associated carrier depletion. Based on the power and temperature-dependent carrier dynamics measurements, we implemented a global fitting of the rate equation across the considered temperature range to extract the bimolecular and Auger recombination coefficients.

The results show that the bimolecular recombination rate decreases with increasing temperature (from $6.4 \times 10^{-10} \text{ cm}^{-3} \text{ s}^{-1}$ at 80 K to $1.1 \times 10^{-10} \text{ cm}^{-3} \text{ s}^{-1}$ at 290 K), as expected due to increased phonon scattering, whereas the Auger rate coefficient stays approximately constant across the entire temperature range (at approximately $3 \times 10^{-29} \text{ cm}^{-6} \text{ s}^{-1}$). Based on these results, we consider the carrier density at which the Auger recombination will dominate over the bimolecular recombination and discover that above 250 K, the ASE threshold density is lower than the carrier density at which the non-radiative Auger recombination dominates over the radiative bimolecular recombination. This means, that above 250 K, the ASE performance is limited by the Auger recombination and the threshold carrier density is in the roll-off region of the radiative emission efficiency due to Auger losses. At lower temperatures, the ASE threshold density is below the point at which Auger recombination starts dominating and the increase in ASE threshold is mainly determined by two factors: the rapid decrease in the bimolecular rate coefficient with temperature, and the energy dilution of the charge carriers. This energy dilution results in a reduced fraction of radiative emission in the ASE band, compared to the total photoluminescence spectrum. Both effects lead to a necessary increase in carrier density (and therefore pump rate) to maintain the same total emission rate in the ASE band. To increase the temperature at which CW ASE (and lasing) can be achieved in 3D perovskite films, strategies to increase the bimolecular recombination coefficient and keep a narrow emission bandwidth at higher temperatures should be investigated.

12:25 PM EL02.11.03

Late News: A New Photophysics for 2D and 3D Lead Halide Perovskites—Polaron Plasma in Equilibrium with Bright Excitons Michele Saba; Università di Cagliari, Italy

Rapid advances in perovskite photovoltaics have produced efficient solar cells, with stability and duration improving thanks to variations in materials composition, including the use of layered 2D perovskites. A major reason for the success of perovskite photovoltaics is the presence of free carriers as majority optical excitations in 3D materials at room temperature. On the other hand, the current understanding is that in 2D perovskites or at cryogenic temperatures insulating bound excitons form, which need to be split in solar cells and are not beneficial to photoconversion. Here we apply a tandem spectroscopy technique that combines ultrafast photoluminescence and differential transmission to demonstrate a plasma of unbound charge carriers in chemical equilibrium with a minority phase of light-emitting excitons, even in 2D perovskites and at cryogenic temperatures. We validate the technique with 3D perovskites and investigate 2D compounds based on both Pb and Sn as metal cation. The underlying photophysics is interpreted as formation of large polarons, charge carriers coupled to lattice deformations, in place of excitons. A conductive polaron plasma foresees novel mechanisms for LEDs and lasers, as well as a prominent role for 2D perovskites in photovoltaics.

12:40 PM BREAK

12:45 PM EL02.11.04

Late News: Large-Grain Double Cation Perovskites with 18 μ s Lifetime and High Luminescence Yield for Efficient Inverted Perovskite Solar Cells Emilio Gutierrez-Partida¹, Hannes Hempel², Sebastian Caicedo Davila², Meysam R. Raoufi¹, Carlos Peña-Camargo¹, Max Grischek^{2,1}, René Gunder², Pietro Caprioglio^{1,2}, Kai O. Brinkmann³, Hans Kobler², Steve Albrecht², Thomas Riedl³, Antonio Abate², Daniel Abou-Ras², Thomas Unold², Dieter Neher¹ and Martin Stollerfoht¹; ¹University of Potsdam, Germany; ²Helmholtz-Zentrum Berlin für Materialien und Energie, Germany; ³University of Wuppertal, Germany

Recent advancements in perovskite solar cell performance were achieved by stabilizing the α -phase of FAPbI₃ in *nip*-type architectures. However, these advancements could not be directly translated to *pin*-type devices. Here, we fabricated a high-quality double-cation perovskite (MA_{0.07}FA_{0.93}PbI₃) with low bandgap energy (1.54 eV) using a two-step approach on a standard polymer (PTAA).¹ The perovskite films exhibit large grains (1 μ m), high external photoluminescence quantum yields of 20% and outstanding Shockley-Read-Hall carrier lifetimes of 18.2 μ s without further passivation. The exceptional opto-electronic quality of the neat material was translated into efficient (up to 22.5%) *pin*-type cells with improved stability under illumination. The low-gap cells stand out by their high fill factor (83%) due to reduced charge transport losses and short-circuit currents 24 mAcm⁻². Using intensity dependent QFLS measurements, we quantify an implied efficiency of 28.4% in the neat material which can be realized by minimizing interfacial recombination and optical losses.

¹Gutierrez-Partida, et al. Large-grain double cation perovskites with 18 μ s lifetime and high luminescence yield for efficient inverted perovskite solar cells. *ASC Energy Letters*. **2021**, <https://dx.doi.org/10.1021/acsenenergylett.0c02642>

1:00 PM EL02.11.05

Novel Absorption Feature Due to Intrinsic Quantum Confinement in FAPbI₃ Adam D. Wright¹, George Volonakis^{1,2}, Juliane Borchert¹, Christopher Davies¹, Feliciano Giustino^{1,3,3}, Michael Johnston¹ and Laura Herz¹; ¹University of Oxford, United Kingdom; ²Institut des Sciences Chimiques de Rennes, France; ³The University of Texas at Austin, United States

Perovskite nanostructures have been engineered for LEDs, lasers and photodetectors^[1], their reduced dimensionality resulting in quantum confinement of charge carriers which yields dramatically different optoelectronic properties, including enhanced photoluminescence quantum yield^[2] and lower thresholds for amplified spontaneous emission^[3]. Although the creation of such perovskite nanostructures has clear advantages, it often relies on challenging top-down fabrication methods. It would therefore be highly advantageous if instead nanoscale domains were found to form intrinsically through self assembly in the perovskite.

In this study^[4], I report the discovery of intrinsically-occurring nanostructures in FAPbI₃, which exhibit quantum confinement effects manifested as an oscillatory absorption feature above the band gap. These features are present at room temperature but sharpen and become more apparent as the temperature is lowered towards 4 K. I demonstrate that the energetic spacings and temperature-dependence of the peaks vary in a manner consistent with quantum confinement intrinsically associated with the lattice of the material. I suggest the origin of this confinement to be nanodomains with an extent of approximately 10-20 nm. This interpretation is supported by correlating absorption spectra against *ab initio* calculations based on the bandstructure of FAPbI₃ in the presence of infinite barriers, and simulations for superlattices with moderate barrier heights. I further explore ferroelectricity/ferroelasticity and delta-phase twin boundaries as two possible causes of these domains. Altogether, such absorption peaks present a novel and intriguing quantum electronic phenomenon in a nominally bulk semiconductor, offering intrinsic nanoscale optoelectronic properties without necessitating cumbersome additional processing steps.

[1] Y. Fu, H. Zhu, J. Chen, M. P. Hautzinger, X.-Y. Zhu, S. Jin, *Nat. Rev. Mater.* **2019**, *4*, 169.

[2] L. Polavarapu, B. Nickel, J. Feldmann, A. S. Urban, *Adv. Energy Mater.* **2017**, 7, 1.

[3] M. Li, Q. Gao, P. Liu, Q. Liao, H. Zhang, J. Yao, *Adv. Funct. Mater.* **2018**, 28, 1707006.

[4] A. D. Wright, G. Volonakis, J. Borchert, C. L. Davies, F. Giustino, M. B. Johnston, L. M. Herz, *Nat. Mater.* **2020**. <https://doi.org/10.1038/s41563-020-0774-9>

1:15 PM EL02.11.06

Antisolvent Processing Dependent Photon Upconversion Performance in Perovskite-Sensitized Triplet-Triplet Annihilators Karunanantharajah Prashanthan^{1,2}, Boris Naydenov¹, Klaus Lips¹, Eva Unger^{1,3} and Rowan W. MacQueen¹; ¹Helmholtz-Zentrum Berlin für Materialien und Energie, Germany; ²University of Jaffna, Sri Lanka; ³Lund University, Sweden

Organolead halide perovskite thin films are an emerging class of triplet sensitizer for photon upconversion applications, with favourable semiconductor properties such as strong and broad optical absorption, large carrier diffusion lengths and pronounced spin-mixing. Our study aimed to identify connections between key properties of the perovskite film and the upconversion efficiency achieved in a standard bilayer upconverter structure. The perovskite film properties were deliberately altered by changing film processing conditions such as spin-coating speed, antisolvent type and antisolvent dripping time, while triplet-triplet annihilation photon upconverters were prepared in a bilayer structure consisting of thin film methyammonium lead iodide perovskite (MAPI) combined with a DBP-doped rubrene annihilator layer.

Photoexcitation of the perovskite film at 715 nm lead to delayed photoluminescence at 605 nm from the annihilator layer, with triplet formation in the rubrene layer sensitized by photogenerated charge carriers in the MAPI film. A stronger upconversion effect was observed for films which displayed brighter and more uniform perovskite photoluminescence. These attributes were highly sensitive to antisolvent dripping time, and were optimized at 20 seconds, measured relative to the start of the spinning process. Further, the choice of antisolvent also had a significant contribution in upconversion performance. Two different antisolvents, anisole and chlorobenzene, were utilized in the MAPI formation process. Films treated with anisole had on average a 10-fold increase in upconversion efficiency compared to the chlorobenzene-treated films.

Time-resolved photoluminescence measurements of the two MAPI variants revealed a stark difference in carrier lifetimes, which were 52 ns and 306 ns in the chlorobenzene and anisole-treated films, respectively. Owing to the near-identical appearance of the two films in a range of bulk-sensitive measurements, we proposed that the difference in carrier lifetime is due to a changing defect density at the MAPI/rubrene interface induced by the two antisolvent treatments. This may itself explain the pronounced difference in upconversion performance, since triplet exciton formation is driven by charge carrier interactions across the same interface, and presumably competes with defect-mediated electron-hole recombination.

1:30 PM EL02.11.07

Late News: Unconventional Scaling of Photoconductivity and Photoluminescence in Lead-Halide Perovskites and Novel Field-Effect Transistor Devices for Photoluminescence Control Vitaly Podzorov; Rutgers, The State University of New Jersey, United States

We have recently performed several fundamental magneto-transport (Hall effect), photoconductivity (PC) and photoluminescence (PL) studies of lead-halide perovskite single crystals, leading to a better understanding of the important charge transport and recombination properties of these materials [1,2,3]. Among these are the first reliable measurements of the dark- and photo-Hall effects in perovskites [1,2], revealing the intrinsic charge carrier mobilities and recombination parameters, as well as the first proposal of large polarons being an important type of carrier in these materials [4]. In this talk, I will focus more on the discovery of unconventional power exponents in photoexcitation flux dependence of PC and PL (including the “strange” power 3/2 in PL) in perovskite single crystals [3], and the demonstration of a novel type of an optoelectronic field-effect transistor device, where PL (rather than electric current) is modulated by a gate voltage [5].

References:

1. Y. Chen, H. T. Yi, X. Wu, R. Haroldson, Y. N. Gartstein, Y. I. Rodionov, K. S. Tikhonov, A. Zakhidov, X.-Y. Zhu, V. Podzorov, "Extended carrier lifetimes and diffusion lengths in hybrid perovskites revealed by steady-state Hall effect and photoconductivity measurements", *Nature Comm.* **7**, DOI: 10.1038/ncomms12253 (2016).
2. H. T. Yi, X. Wu, X.-Y. Zhu, V. Podzorov, "Intrinsic charge transport across phase transitions in hybrid organo-inorganic perovskites", *Adv. Mater.* **28**, 6509-6514, DOI: 10.1002/adma.201600011 (2016).
3. H. T. Yi, P. Irkhin, P. P. Joshi, Y. N. Gartstein, X. Zhu and V. Podzorov, "Experimental Demonstration of Correlated Flux Scaling in Photoconductivity and Photoluminescence of Lead-Halide Perovskites", *Phys. Rev. Applied* **10**, 054016, DOI: 10.1103/PhysRevApplied.10.054016 (2018).
4. X.-Y. Zhu and V. Podzorov, "Charge carriers in hybrid Organic-Inorganic Lead Halide perovskites might be protected as large polarons", *J. Phys. Chem. Lett.* **6** (23), 4758-4761 (2015).
5. H. T. Yi, S. Rangan, B. Tang, C. D. Frisbie, R. A. Bartynski, Y. N. Gartstein and V. Podzorov, "Electric-field effect on photoluminescence of lead-halide perovskites", *Materials Today*, DOI: 10.1016/j.mattod.2019.01.003 (2019).

SESSION EL02.12: Photophysics of Halide Semiconductors II

Session Chairs: Do Young Kim and Sai Wing Tsang

Friday Afternoon, April 23, 2021

EL02

5:15 PM *EL02.12.01

Formation of High-Temperature Giant Quantum States in Hybrid Perovskites Kenan Gundogdu and Franky So; North Carolina State University, United States

Optical excitation creates excitons in semiconductors. These quasiparticles most commonly exist in incoherent states. In extremely rare situations under critical conditions, these excitons might gain a collective electronic coherence through a process called spontaneous synchronization. This process is a symmetry breaking, i.e., second-order quantum phase transition, similar to Bose-Einstein condensation and superconductivity. When this happens, all oscillators form a giant dipole and radiate collectively, and act like a giant atom. This process was first proposed by Dicke and hence called Dicke superradiance. Since the electronic quantum phase is extremely fragile due to thermal phonon interactions, Dicke superradiance is only observable in a handful of solid state systems at cryogenic temperatures. In this presentation, we will present the results of our recent discovery of high-temperature Dicke superradiance in hybrid perovskites, and discuss the fundamental mechanism leading to such a macroscopic quantum phenomena in hybrid perovskites. Observation of superradiant phase transition in hybrid perovskites is important for developing emerging quantum applications using this versatile material family. Specifically, quantum sensing, communication, and computation applications require robust quantum oscillators. Observation of superfluorescence in hybrid perovskite can pave the way for such applications.

5:40 PM EL02.12.02

Distance Dependence of Förster Resonance Energy Transfer in 2D Perovskite Quantum Wells Shobhana Panuganti¹, Lucas V. Besteiro², Eugenia S. Vasileiadou¹, Alexander Govorov³, Stephen Gray⁴, Mercouri G. Kanatzidis¹ and Richard Schaller⁴; ¹Northwestern University, United States; ²Institut National de la Recherche Scientifique-Énergie, Matériaux et Télécommunications, Canada; ³Ohio University, United States; ⁴Argonne National Laboratory, United States

Two-dimensional (2D) materials are outstanding candidates for a variety of optoelectronic applications but are inhibited by low carrier mobilities and high exciton binding energies compared to their bulk counterparts. To that end, rapid Förster resonance energy transfer (FRET) presents an opportunity to quickly and purposefully direct energy through devices, which could improve the efficiency of existing applications and establish new

types of energy-funneling devices. The exciting observation of fast energy transfer that outcompetes other multiexcitonic effects, on the order of picoseconds, has been experimentally observed in 2D materials with requisite spectral overlap and electronic coupling between donor and acceptor, but high quality, clear data in such systems is sparse. Predictive models for FRET in 2D systems, particularly with respect to the distance between states, are underdeveloped.

In this work, we approach FRET in 2D perovskite quantum wells; these materials, in which layers of perovskite are electronically decoupled by organic spacer cations into 2D quantum wells of n octahedra in thickness, provide ideal systems for studying FRET given the precision with which various electronic and optical parameters may be synthetically adjusted. Though research into devices fabricated from such materials has skyrocketed, as they present ambiently stable and highly tunable alternatives to well-known hybrid organic inorganic perovskites, synthetic control for desired mixtures of n phases in thin-films that would enable a reliable energy transfer study are non-existent. Few studies exist that aim to discern energy transfer processes in these materials, and each suffers from a complete lack of control over sample composition, resulting in reported lifetimes of energy transfer that are orders of magnitude apart. In order to provide insights regarding FRET in this material class, we prepare thin-films with controlled mixtures of specific n phases of 2D perovskite quantum wells for the first time and use them to investigate binary arrangements of quantum well thicknesses to reveal fundamental behavior.

We examine rates of Förster resonance energy transfer in binary mixtures of 2D perovskites as a function of the distance between layers by incorporating alkylammonium cations of increasing chain length. Energy transfer is observed using transient absorption spectroscopy in each case. Evaluated rates in some instances outpace biexcitonic Auger recombination, and lifetimes become slower with increasing separation. We model these systems computationally, obtaining results in agreement with our empirically obtained lifetimes, and expand upon the model to survey effects of other influencing factors on energy transfer in 2D materials that may be, in principle, synthetically controlled. Our work begins building the necessary foundation for predictive models of FRET in 2D PQWs and further guides design principles for employing FRET in devices fabricated from 2D materials.

5:55 PM EL02.12.03

The Stark Effect as a Measure of Surface Passivation in Growing MAPbI₃ Perovskite Nanocrystals.

James C. Sadighian, Kelly Wilson, Michael Crawford and Cathy Wong; University of Oregon, United States

Organic-inorganic halide perovskite (OIHP) semiconductors are currently the focus of significant research interest due to their potential optoelectronic device applications. Quantum-confined nanocrystals (NCs) of these materials emit with high photoluminescence quantum yields and a narrow, tunable spectrum. These properties, coupled with the potential for low-cost, facile solution-based syntheses, make these NCs ideal for LEDs, lasers, and optical sensors. Due to their high surface area-to-volume ratio, the surface plays a critical role in determining the excited state dynamics, and thus optoelectronic properties, in these materials. In particular, the evolution of NC surface quality and the mechanisms by which surface states become bound by ligands during growth is still poorly understood. Under-coordinated surface atoms act as traps for charge carriers and can promote unwanted non-radiative recombination. The goal of this work is to understand how the NC surface becomes passivated during NC synthesis.

The fate of photogenerated species in NCs is typically studied using non-linear optical spectroscopies, such as transient absorption (TA), but these techniques have inherently long measurement timescales of up to several hours. OIHP NCs are traditionally formed through either a hot-injection or ligand-assisted reprecipitation synthesis. These reactions are typically complete within a few minutes, and nascent NCs are highly unstable and difficult to kinetically trap, precluding in situ investigation of dynamics with non-linear optical spectroscopies. This has limited our understanding of nucleation and growth processes in these systems. To overcome these limitations, we have developed a TA spectrometer that reduces the timescale required for measurement by spatially encoding the time delay in a tilted-pulse geometry. This allows collection of an entire broadband transient spectrum with a 60 ps time delay in just a few laser shots, and spectra with a good signal-to-noise ratio can be acquired within seconds. In this work we apply this novel instrumentation to a NC

synthesis whose reaction kinetics are limited by the solvation of precursors in a highly nonpolar solvent. Coupling this solvation-mediated synthesis to a rapid sampling technique has enabled the first-ever characterization of exciton dynamics in growing methylammonium lead triiodide NCs.

We observe the appearance of unique TA spectral features in newly formed NCs that slowly disappear over the remainder of the synthesis. Comparison to first and second order derivatives of the linear absorbance spectrum shows that photogenerated charge carriers become localized at surface trap states in nascent NCs, inducing a Stark effect that manifests in the TA measurements. The amplitude of the lineshape arising from this Stark effect declines as NC growth continues, suggesting that intermediate NCs possess unpassivated surface sites that can trap charge carriers and hamper optoelectronic performance. These sites are slowly passivated by capping ligands over the course of the synthesis. Our results contribute to a growing body of evidence suggesting that surface passivation occurs toward the end of NC growth in a final surface ligation stage of the reaction. This experimental technique provides researchers with a new tool to report on surface quality in growing NCs and has the potential to yield fundamental insights into the mechanism of nanocrystal nucleation and growth. A full understanding of these processes would allow for further synthetic control of NC properties by providing researchers the ability to tune reaction conditions *in situ* to target desired properties.

6:10 PM BREAK

6:15 PM EL02.12.04

Late News: The Role of Dopant Ions in Tuning the Optical Properties of Inorganic Lead Halide Perovskite Lijia Liu; University of Western Ontario, Canada

Inorganic lead halide perovskite (CsPbX_3 , X=Cl, Br, and/or I) have fascinating optical properties. By tuning the halide composition, the luminescence of CsPbX_3 can be tuned across the entire visible spectrum. The optical property of CsPbX_3 can also be modified upon the introduction of a new cation species, either a divalent or a trivalent metal ion. Depending on the type of cation, the synthesis strategy, and the nature of the perovskite host, how the introduced cations influence the optical property of the pristine perovskite could be entirely different. In this presentation, I am going to discuss three systems: (1) Mn-doped CsPbX_3 , in which the introduction of Mn results in dual-band emission, (2) Pr^{3+} -doped CsPbX_3 , in which heterovalent doping drastically enhance the perovskite bandgap emission, and (3) Eu^{2+} -doped CsPbBr_3 , in which Eu^{2+} induces a phase transformation of the perovskite host and producing a blue-emission band. The electronic structure of the doped perovskite and the luminescence mechanism is investigated using synchrotron-based X-ray absorption fine structure (XAFS) and X-ray excited optical luminescence (XEOL). These characterization techniques provide detailed structural information and energy transfer processes in these doped perovskites, and the information obtained is valuable for designing CsPbX_3 light-emitters with desired properties.

6:30 PM EL02.12.05

Light-Activated Contraction in Organic-Inorganic 2D Perovskites Enables High-Efficiency Photovoltaics Wenbin Li¹, Siraj Sidhik¹, Boubacar Traore², Reza Asadpour³, Hao Zhang¹, Jin Hou¹, Joseph Strzalka⁴, Esther Tsai⁵, Justin M. Hoffman⁶, Ioannis Spanopoulos⁶, Muhammad A. Alam³, Claudine Katan², Mercuri G. Kanatzidis⁶, Jacky Even², Jean-Christophe Blancon¹ and Aditya Mohite¹; ¹Rice University, United States; ²Institut National des Sciences Appliquées, France; ³Purdue University, United States; ⁴Argonne National Laboratory, United States; ⁵Brookhaven National Laboratory, United States; ⁶Northwestern University, United States

Understanding and tailoring the structure-induced physical behavior of materials under practical environments is critical for designing efficient and durable optoelectronic devices. Here, we report a new phenomenon - a sunlight-activated anisotropic lattice contraction in organic-inorganic 2D perovskites, which is reversible and strongly dependent of the specific structural phase and the organic interlayer cation bridging the perovskite octahedra. Modeling suggests that light-generated charge accumulation results in the build-up of a bulk compressive strain, which induces a continuous lattice contraction over minutes. In-situ structural

measurements on photovoltaic devices directly correlate the light-induced lattice contraction to an increase in the photovoltaic efficiency of Dion-Jacobson 2D perovskite solar cells from 13.8% to 16.4%. The increase in efficiency results from a combined increase in the open circuit voltage and fill factor, arising from the reduction of the potential barrier heights upon light-induced contraction

6:45 PM EL02.12.06

Multiplexed Nanocrystal Arrays of Halide Perovskites Jingshan S. Du, Donghoon Shin, Vinayak P. Dravid and Chad A. Mirkin; Northwestern University, United States

Halide perovskites have exceptional optoelectronic properties, making them attractive for photovoltaics, light-emitting technologies, and radiation detection. However, a poor understanding of the relationship between crystal dimensions, composition, and properties limits their use in integrated devices. In this presentation, we will discuss a multiplexed cantilever-free scanning probe method for synthesizing compositionally diverse halide perovskite nanocrystals spanning cm^2 areas. Single-particle photoluminescence studies reveal multiple independent emission modes due to defect-defined band edges with relative intensities that depend on crystal size for a fixed composition. Smaller particles, but ones with dimensions that exceed the quantum confinement regime, exhibit blue-shifted emission due to the reabsorption of higher-energy modes. The method reported herein is generalizable and has been used to synthesize six different halide perovskites, including a layered Ruddlesden-Popper phase. Importantly, it also enables the preparation of functional solar cells based upon a single nanocrystal. Additionally, the ability to pattern arrays of multi-color light-emitting nanocrystals opens avenues towards the development of sophisticated optoelectronic devices, including a wide variety of optical displays.

SYMPOSIUM EL03

Emerging Ionic Semiconductors—Research and Applications
April 22 - April 23, 2021

Symposium Organizers

Elif Ertekin, University of Illinois at Urbana-Champaign
Rafael Jaramillo, Massachusetts Institute of Technology
Yi-Yang Sun, Shanghai Institute of Ceramics, Chinese Academy of Sciences
Hao Zeng, SUNY-Buffalo

Symposium Support

Bronze
Army Research Office

* Invited Paper

SESSION EL03.01: Theory and Design of Ionic Semiconductors I
Session Chairs: Matthias Wuttig and Hao Zeng
Thursday Morning, April 22, 2021
EL03

10:30 AM *EL03.01.01

Chalcogenide Perovskites for Electronics and Optoelectronics Shengbai Zhang; Rensselaer Polytechnic Institute, United States

Most conventional semiconductors are covalent materials with four-fold coordination. The recent emergence of semiconducting perovskites, with six-fold coordination metal atoms in the skeleton framework and an exceptional success in photovoltaics, however, represent a different type of semiconductors distinctly different from any existing ones. For example, BaZrS₃ (a chalcogenide perovskite) has a direct band gap in the visible close to that of GaAs, but its ionicity, on average, is close to that of AlN. In other words, conventional semiconductors and perovskites represent two extremes in the ionicity spectrum. In this talk, I will discuss our recent theoretical efforts in advancing the knowledge on various forms of chalcogenide perovskites as a new class of semiconductors for electronic and optoelectronic applications [1-4]. Noticeably, a chalcogenide perovskite often exhibits a significantly higher density of states near the band gap than a conventional semiconductor due to the presence of transition-metal *d* states [1]. While the *d* bands are usually flatter than the (*s*, *p*) bands which is undesirable for carrier transport, their hybridizations exhibit noticeable anisotropy to resulting in favorable conduction channels with reasonably small effective masses. Also, indirect gap materials are often perceived as poor optoelectronic materials. However, due to these *d* bands, high optical absorption in indirect chalcogenide perovskites can take place at energies only a few tenths of an eV higher than the fundamental band gap [3], which could be beneficial for photovoltaic applications requiring both high absorption in the visible and long carrier lifetimes.

[1] Y. Y. Sun, et al., *Nano Lett.* **15**, 581 (2015).

[2] Y.-Y. Sun, et al., *Nanoscale* **8**, 6284 (2016).

[3] M. L. Agiorgousis, et al., *Adv. Theory Simul.* **2**, 1800173 (2019).

[4] H Zhang, et al, *Chin. Phys. Lett.* **37**, 097201 (2020).

10:55 AM *EL03.01.02

Electron Count and Ferroelectricity in Complex Oxides From First Principles Karin M. Rabe; Rutgers, The State University of New Jersey, United States

The electron count in complex oxide compounds can be controlled during growth via compositional substitution or formation of defects such as oxygen vacancies. Reversible control can be achieved through gating in heterostructures or through introduction of H or alkali metal interstitials. In this talk, I will present first-principles investigations of the effects of added charge on the crystal structure and bandstructure of illustrative systems, including BaTiO₃, ZnSnO₃, SmNiO₃, La_{1/3}Sr_{2/3}FeO₃ and perovskite titanate superlattices. In some systems, the added electrons or holes become free carriers, their mobility and concentration determining the resulting conductivity. When the system is ferroelectric, for example BaTiO₃ and ZnSnO₃, key questions include the effect of the free carrier concentration on the polar distortion, and the switchability of ferroelectrics with free carriers. Alternatively, the added charges can localize on transition metal ions and order, breaking translational and/or point symmetries. Combining the symmetry-breaking of the charge order with other symmetry-breaking factors, such as cation layering, epitaxial strain or the arrangement of the added interstitial ions, can produce charge-order-driven ferroelectricity. In these systems, coupling of charge order to the lattice is a key consideration in determining switchability between states of different polarization. Connections to experimental observations in the literature and to ongoing experiments will be discussed.

11:20 AM *EL03.01.03

Prediction of Novel Quinary Layered Oxychalcogenides Daniel W. Davies, Benjamin A. Williamson and David O. Scanlon; University College London, United Kingdom

N-type transparent conductors (TCs) are key materials in the modern optoelectronics industry. Despite years of research, the development of a high-performance p-type TC has lagged far behind that of its n-type counterparts, delaying the advent of “transparent electronics” based on transparent p-n junctions.[1] Here, we computationally investigate three layered oxychalcogenide structural motifs to try to predict new p-type TCs, namely the [Cu₂Ch₂][A₃B₂O₅] (325), [Cu₂Ch₂][A₄B₂O₆] (426) and [Cu₂Ch₂][A₂BO₂] (212) structural motifs.

Specifically, we have used a materials informatics approach (SMACT) to screen through the search space using low-cost heuristic tools.[2] This reduces the potential combinations from 1800 to a more computationally tractable 228, which then undergo DFT calculations to assess thermodynamic and dynamic stability. In this talk, I will present an update on how our search has predicted >50 novel semiconductors with potential applications ranging from TCs,[3] to photocatalysts,[4] solar absorbers and thermoelectrics.

[1] A. Walsh and J.-S. Park, The Holey Grail of Transparent Electronics, *Matter*, 3, 604 (2020)

[2] D. W. Davies, K. T. Butler, A. J. Jackson, A. Morris, J. M. Frost, J. M. Skelton and A. Walsh, Computational Screening of All Stoichiometric Inorganic Materials, *Chem*, 1 617 (2016)

[3] B.A.D. Williamson, G.J. Limburn, G.W. Watson, G. Hyett, and D.O. Scanlon. Computationally Driven Discovery of Layered Quinary Oxychalcogenides: Potential p-Type Transparent Conductors?, *Matter*, 3, 759 (2020)

[4] G. J. Limburn, M. J.P. Stephens, B. A. D. Williamson, A. Iborra-Torres, D. O. Scanlon and G. Hyett. Photocatalytic, structural and optical properties of mixed anion solid solutions $Ba_3Sc_{2-x}In_xO_5Cu_2S_2$ and $Ba_3In_2O_5Cu_2S_{2-y}Se_y$, *Journal of Materials Chemistry A*, 8, 19887 (2020).

11:45 AM *EL03.01.04

Data-Enabled Discovery of New Semiconductors for Energy Generation and Energy Storage Joseph W. Bennett; University of Maryland Baltimore County, United States

The interplay of first-principles density functional theory and experiments has led to the optimization of well-known families of oxides and chalcogenides whose members display a range of tunable band gaps, polarizations, and compositions. Here we combine crystallographic database mining and high-performance computing to discover and design new semiconductive functional materials that could be readily synthesized and potentially operate in different regimes of temperature, pressure, humidity, etc. Ultimately, we would like to examine a family of materials whose compositions span a wide set of cations and anions, specifically oxide and chalcogenides, to complement well-established materials like the ABX_3 perovskites and Ruddlesden-Popper phases. We focus on finding new examples of functional materials called ferroelectrics and antiferroelectrics since semiconductive ferroelectrics can find use as photovoltaics and antiferroelectrics are proposed to find use as materials capable of energy storage. Our work explores a candidate family of materials with a general formula of A_2BX_3 , where members have been assigned nonpolar, antipolar, and polar structure types. We use density functional theory to map out the potential energy landscape of this family by including both known and as-yet to be identified structure types. The results of our analysis show several known members to be either ferroelectric or antiferroelectric. We present a targeted set of oxide and chalcogenide semiconductors, and their compositionally tuned variants, that warrant further investigation as new functional materials.

12:10 PM EL03.01.05

Search for Inorganic Ternary Oxide-Nitrides Abhishek Sharan^{1,2} and Stephan Lany¹; ¹National Renewable Energy Laboratory, United States; ²Khalifa University, United Arab Emirates

Materials design from first principles enables exploration of uncharted chemical spaces. Broad computational searches have been reported for ternary mixed-cation oxides and nitrides. More recently, mixed-anion systems are gaining interest for computational discovery studies. Within this class, oxide-nitrides are particularly intriguing, because the two constituent systems exhibit remarkable commonalities (e.g., bond strength, elastic properties) and differences (e.g., formation enthalpies, electronic structure). A common limitation of computational discovery approaches is the reliance on prototype structures for total energy calculation which can miss the lowest energy structure. In addition, some known ternary oxide-nitrides form an ordered or disordered configuration derived from the crystal structure of a binary oxide, which may not be captured by prototypes selected from ternaries. We approach this challenge by letting two complementary structure sampling approaches compete. We use the Kinetically Limited Minimization (KLM) approach for high-throughput unconstrained crystal structure prediction in smaller cells up to 20 atoms, and, on the other hand, a configurational sampling on larger binary prototype structures. Using this approach, we searched 65 different

charge-balanced oxide-nitride stoichiometries, where 6 known systems were included as control sample. Within this set, we predict 8 new stable ternary oxynitrides, and an additional 5 new oxynitrides that are expected to be stable under activated Nitrogen conditions. The control sample was correctly recovered, providing confidence in the approach and clearing the path for future studies in a more extensive search space.

12:25 PM DISCUSSION TIME

SESSION EL03.02: Theory and Design of Ionic Semiconductors II
Session Chairs: Jayakanth Ravichandran and Shengbai Zhang
Thursday Afternoon, April 22, 2021
EL03

1:00 PM *EL03.02.01

Metavalent Bonding in Solids—Provocation or Promise? Matthias Wuttig^{1,2}; ¹RWTH Aachen University, Germany; ²FZ Jülich, Germany

Scientists and practitioners have long dreamt of designing materials with novel properties. Yet, a hundred years after quantum mechanics lay the foundations for a systematic description of the properties of solids, it is still not possible to predict the best material in applications such as photovoltaics, superconductivity or thermoelectric energy conversion. This is a sign of the complexity of the problem, which is often exacerbated by the need to optimize conflicting material properties. Hence, one can ponder if design routes for materials can be devised. In recent years, the focus of our work has been on designing advanced functional materials with attractive opto-electronic properties, including phase change materials, thermoelectrics, photonic switches and materials for photovoltaics. These materials are typically discussed as unconventional semiconductors, often but not always, with appreciable charge transfer. Phase Change Materials have provided a special challenge for materials optimization. They possess a remarkable property portfolio, which includes the ability to rapidly switch between the amorphous and crystalline state. Surprisingly, in PCMs both states differ significantly in their properties. This material combination makes them very attractive for applications in rewriteable optical and electronic data storage, as well as photonic switches. In this talk, the unconventional material properties will be attributed to a unique bonding mechanism (metavalent bonding). Further evidence for this bonding mechanism comes from a quantum-chemical map, which separates the known strong bonding mechanisms of metallic, ionic and covalent bonding. The map reveals that metavalent bonding is a new, fundamental bonding mechanism, which differs substantially from metallic, covalent and ionic bonding. This insight is subsequently employed to design phase change as well as thermoelectric materials. Yet, the discoveries presented here also force us to revisit the concept of chemical bonds and bring back a history of vivid scientific disputes about ‘the nature of the chemical bond’.

1:25 PM *EL03.02.02

Computational Screening of Light-Absorbing Materials for Tandem Devices Karsten W. Jacobsen; Technical University of Denmark, Denmark

In the talk I shall discuss recent efforts to computationally identify light-absorbing materials for use in solar cells and water splitting devices in particular with a tandem configuration. A range of materials are considered including sulfide perovskites, quaternary chalcogenides, and more broadly experimentally synthesized compounds, which have been structurally characterized. Key descriptors such as structure, stability, band gap, band structure, and defect states will be addressed. The possibilities of using machine learning to improve the efficiency of computational screening and structure determination will also be discussed.

1:50 PM EL03.02.03

K_{1-x}Na_xAsSe₂—New Low-Melting Noncentrosymmetric AAsQ₂ Semiconductors Abishek K. Iyer¹, Hye Ryung Byon², Jingyang He³, Shiqiang Hao¹, Benjamin Oxley¹, Christopher Wolverton¹, Venkatraman Gopalan³, Mercouri G. Kanatzidis¹ and Joon Jang²; ¹Northwestern University, United States; ²Songang University, Korea (the Republic of); ³The Pennsylvania State University, United States

Nonlinear optical (NLO) materials are used to convert the specific coherent wavelengths produced by lasers into wavelengths in other spectral regions such as UV-visible (0.2–2 μm) and infrared (IR) (3–20 μm), where lasers have poor efficiency. Metal chalcogenides with their smaller band gaps are appropriate for IR lasers, which are useful for visualization of tissue, environmental monitoring, and security applications. There are plenty of commercially available UV-visible NLO materials, but there only a few commercially available IR NLO materials. Even these materials suffer from problems such low laser damage threshold and two photon absorption, thus there is a need to search for new NLO materials in the IR-region. Alkali-metal chalcocarsenates (AAsQ₂) one such system that were discovered a decade ago which showed impressive NLO properties. AAsQ₂ (A = Li, Na and Q = S, Se) compounds are made up of 1-dimensional (1D) (1/∞) [AQ₂][−] chains which are connected by pyramidal AQ₃ units as observed in β-LiAsQ₂ (Cc) and γ-NaAsSe₂ (Pc) structures (Q = S and Se). γ-NaAsSe₂ have one of the highest second harmonic generation (SHG) intensities observed (~ 75 x AgGaSe₂) while, adding Na to the β-LiAsQ₂ structures resulted in increased SHG response as observed in γ-Li_{0.2}Na_{0.8}AsSe₂ (~ 65 x AgGaSe₂) and β-Li_{0.6}Na_{0.4}AsS₂ (~ 30 x AgGaSe₂). Structurally, the substitution of the smaller Li ions with larger Na ions weakens the interactions between adjacent (1D) (1/∞) [AQ₂][−] chains. A problem with γ-NaAsSe₂ (Pc) is a phase transition to the centrosymmetric δ-NaAsSe₂ (Pbca) upon melting, making it a challenge to grow large single crystals for NLO applications.

Here we have studied the effects of substituting γ-NaAsSe₂ (Pc) with the larger cation K to see if the interactions between the adjacent (1/∞) [AQ₂][−] chains are further weakened, thereby, its effect on their NLO properties. Additionally, K containing chalcocarsenates are usually low melting making them attractive for crystal growth which are essential for their application as NLO materials.

2:05 PM *EL03.02.04

Surface Structure, Defects and Reactivity of Perovskite Oxynitrides Ulrich Aschauer; University of Bern, Switzerland

The smaller band gap compared to pure oxides yields a superior light-absorption efficiency of perovskite oxynitride photocatalysts. While the bulk structure and properties of these materials have been extensively studied by computational methods, significantly less is known about their surfaces and consequently their photocatalytic reaction mechanisms. In this talk, I will present results of our density functional theory (DFT) calculations, highlighting anion-ordering phenomena at perovskite oxynitride surfaces, the effect of defects on their oxygen-evolution reaction (OER) activity as well as the potential of strain engineering these materials to become ferroelectric photocatalysts.

2:30 PM EL03.02.05

A Theoretical Exploration of Earth-Abundant Bismuth Oxyhalides for Thermoelectric Applications Maud Einhorn and David O. Scanlon; University College London, United Kingdom

Thermal energy is an unavoidable by product of myriad processes, spanning the industrial, domestic and transportation sectors, and presents an abundantly available and largely untapped source of clean energy. Thermoelectric devices, which are able to convert thermal energy into electricity, provide a route to significantly increase the overall energy efficiency of existing process across a range of sectors via waste-heat harvesting and yield a supply of clean energy.^[1] The effectiveness of a thermoelectric material is measured using the dimensionless figure of merit ZT , with the world record set at 2.6 for single-crystal SnSe along the through-plane direction.^[2] Realising reasonable conversion efficiencies generally requires high electrical conductivity and low thermal conductivity, with the maximum ZT of a material often limited by the strong correlation between these properties.

Despite efforts in the past few decades to identify promising novel thermoelectric materials, the champion thermoelectric materials tend to rely on non earth-abundant and toxic elements, such as bismuth telluride (Bi_2Te_3) and the lead chalcogenides. Oxides generally present properties valuable for thermoelectric applications, including low cost, thermal and chemical stability and environmental benignity, but broadly thermoelectric performance has been hindered by the inherent high lattice thermal conductivities.^[4] The performance of oxide thermoelectrics generally lagging behind the efficiencies achieved by chalcogenide-based materials, with poor carrier mobilities and high intrinsic thermal conductivities hampering progress.^[3]

In this study, we predict the maximum theoretical ZTs of a range of novel mixed-anion quaternary systems using state-of-the-art methods based on density functional theory. We have identified three materials with complex crystal structures, $\text{Bi}_2\text{YO}_4\text{Cl}$, $\text{Bi}_2\text{YO}_4\text{Br}$ and $\text{Bi}_2\text{YO}_4\text{I}$, which possess lower lattice thermal conductivities than usually seen in oxides, and excellent charge transport properties, calculated using methods superseding the traditionally used constant relaxation time approximation.⁵ We conclude that these materials have the potential to achieve ZTs greater than many existing oxide thermoelectric materials, and have the potential to perform as high-performance thermoelectric components. Additionally, the effects of nanostructuring these materials is discussed, to guide potential synthesis methods.

1. L. E. Bell, Cooling, heating, generating power, and recovering waste heat with thermoelectric systems. *Science* **321**, 1457–1461 (2008)
2. L-D, Zhao, S-H. Lo, Y. Zhang, H. Sun, G. Tan, C. Uher, C. Wolverton, V. P. Dravid and M. G. Kanatzidis, Ultralow thermal conductivity and high thermoelectric figure of merit in SnSe crystals. *Nature* **508**, 373-377 (2014)
3. G. Tan, L-D. Zhao, and M. G. Kanatzidis, Rationally designing high-performance bulk thermoelectric materials, *Chemical Reviews* **116**, 12123–12149 (2016)
4. J. He, Y. Liu and R. Funahashi, Oxide thermoelectrics: The challenges, progress and outlook, *J. Mater. Res.* **26**, 1762-1772 (2011)
5. Ganose, A. M.; Park, J.; Faghaninia, A.; Woods-Robinson, R.; Persson, K. A.; Jain, A. Efficient Calculation of Carrier Scattering Rates from First Principles. *arXiv:2008.09734 [cond-mat, physics:physics]* (2020)
6. Einhorn, M.; Williamson, B. A. D.; Scanlon, D. O. Computational prediction of the thermoelectric performance of LaZnOPn ($\text{Pn} = \text{P}, \text{As}$) *J. Mater. Chem. A*, **8**, 7914–7924 (2020)

2:45 PM DISCUSSION TIME

SESSION EL03.03: Progress in Ionic Semiconductor Thin Films

Session Chairs: Karsten Jacobsen and Rafael Jaramillo

Thursday Afternoon, April 22, 2021

EL03

4:00 PM *EL03.03.01

Thin Film Growth of Chalcogenide Perovskites by Pulsed Laser Deposition Jayakanth Ravichandran;
University of Southern California, United States

Chalcogenide Perovskites are a new class of semiconductors, which have tunable band gap in the visible to infrared part of the electromagnetic spectrum, large density of states with potentially high carrier mobility, and emergent photonic properties with anisotropy and non-linearity. In this talk, I will review the developments in thin film growth of perovskite chalcogenides and discuss some of the advances made in my research group on developing pulsed laser deposition as a growth method for chalcogenide perovskite thin films. We have successfully achieved textured growth of chalcogenide perovskite thin films on single crystalline oxide substrates. This advance presents new opportunities to probe the physical and chemical properties of this family

of novel electronic materials, their device implementations and applications, and also study the interfacial properties of oxides and chalcogenides. Specifically, I will outline the growth of model chalcogenide perovskite, BaZrS₃ and the quasi-1D hexagonal Perovskite-related sulfide, BaTiS₃ on compatible perovskite and other oxide single crystal substrates. Preliminary investigations on the physical properties accompanied by detailed structural and chemical characterizations and future outlook for the thin film growth of these materials will also be discussed.

4:25 PM EL03.03.02

Combinatorial Development of CaCuP Thin Films as P-Type Transparent Conductors Andrea Crovetto^{1,2}, Thomas Unold² and Andriy Zakutayev¹; ¹National Renewable Energy Laboratory, United States; ²Helmholtz-Zentrum Berlin für Materialien und Energie, Germany

Despite long-standing research efforts to develop p-type transparent conductive materials (TCMs), the current generation of optoelectronic devices still relies exclusively on n-type TCM contacts due to their much better trade-off between conductivity and transparency. An important issue in oxide-based p-type TCMs is the deep energy and localized nature of the 2p oxygen states in the valence band, which has negative consequences on both hole dopability and hole mobility in most oxides.

Recent computational work has identified the mixed ionic-covalent compound CaCuP as a promising material that could potentially outperform the existing p-type TCMs. On the one hand, the covalent bond between Cu and P produces a highly dispersive valence band, which favors high hole mobilities. On the other hand, the presence of an electropositive cation (Ca) implies that more ionic Ca-P bonds are also present in CaCuP. This plays an important role in widening the band gap (thus ensuring high optical transmission in the visible) and making CaCuP potentially suitable as a p-type TCM.

Using a unique combinatorial sputter chamber equipped with reactive PH₃ gas, we have grown CaCuP thin films for the first time. We have mapped the compositional and thermal phase space of CaCuP and evaluated its potential as a p-type TCM using high-throughput methods. Due to the high concentration of copper vacancies, the electrical conductivity of CaCuP under optimized growth conditions is almost on par with the conductivity of state-of-the-art n-type TCMs such as ITO and FTO, even in the absence of any extrinsic dopant. However, CaCuP films are only moderately transparent in the visible region due to unexpectedly high absorption strength above its indirect band gap. We will discuss possible solutions to this problem, together with the general prospects of CaCuP as a p-type TCM.

4:40 PM EL03.03.03

Realization of BaZrS₃ Chalcogenide Perovskite Thin Films for Optoelectronics Xiucheng Wei¹, Haolei Hui¹, Mengjiao Han², Junhao Lin², Yi-Yang Sun³, Shengbai Zhang⁴ and Hao Zeng¹; ¹University at Buffalo, The State University of New York, United States; ²Southern University of Science and Technology, China; ³Shanghai Institute of Ceramics, Chinese Academy of Sciences, China; ⁴Rensselaer Polytechnic Institute, United States

Recently published work reveals that the ionic chalcogenide perovskite BaZrS₃ possesses suitable properties for PV application, such as direct band gap of 1.7 to 1.8 eV, high stability against moisture and pressure, and strong light absorption. However, the lack of thin films hinders further exploration of this material's fundamental properties. Here we report the first work on BaZrS₃ films, by sulfurization of precursor films deposited by pulsed laser deposition and magnetron sputtering. The films are n-type semiconductors with carrier densities in the range of 10¹⁹ to 10²⁰ cm⁻³. The hall mobility ranges from 2.1 to 13.7 cm²/Vs depending on the sulfurization temperature. UV-Vis result shows an absorption coefficient of >10⁵ cm⁻¹ at a photon energy of >1.97eV. We further incorporate Ti to reduce the band gap of BaZrS₃ for better solar performance. Our thin film results pave the way to future device fabrication and validate BaZrS₃ as a viable candidate for optoelectronics.

4:55 PM EL03.03.04

Late News: Growth of BaZrS₃ Thin Films by Molecular Beam Epitaxy Ida Sadeghi, Kevin Ye and Rafael Jaramillo; Massachusetts Institute of Technology, United States

Chemical intuition, first-principles calculations, and recent experimental results suggest that chalcogenide perovskites are an outstanding class of semiconductors [1]. Chalcogenide perovskites feature the large dielectric response familiar in oxide perovskites, but also have band gap in the VIS-IR and strong light absorption. Preliminary results suggest that chalcogenide perovskites feature excellent excited-state charge transport properties familiar in halide perovskites, while also being thermally-stable and comprised of abundant and non-toxic elements. Nearly all experimental results on chalcogenide perovskites to-date were obtained on powder samples and microscopic single crystals [2-7]. Realizing the full potential of chalcogenide perovskites for optoelectronic applications will require the availability of high-quality, single-crystal thin films.

Here we report synthesis of BaZrS₃ thin films by molecular beam epitaxy (MBE) on oxide substrates. The film composition is confirmed by X-ray fluorescence and X-ray photoelectron spectroscopy. The phase is confirmed by X-ray diffraction and Raman spectroscopy. Photoluminescence spectroscopy showed peaks at 1.8 and 1.95 eV, suggestive of pristine and partially-oxidized material. We use spectroscopic ellipsometry to measure optical properties, confirming strong band-edge light absorption. As time allows we will present results of scanning transmission electron microscopy, impedance spectroscopy, the growth of BaZr(S,Se)₃ alloys with tunable band gap.

[1] R. Jaramillo, J. Ravichandran, APL Materials 7(10) (2019) 100902.

[2] S. Niu, D. Sarkar, K. Williams, Y. Zhou, Y. Li, E. Bianco, H. Huyan, S.B. Cronin, M.E. McConney, R. Haiges, R. Jaramillo, D.J. Singh, W.A. Tisdale, R. Kapadia, J. Ravichandran, Chemistry of Materials 30(15) (2018) 4882-4886.

[3] K. Hanzawa, S. Iimura, H. Hiramatsu, H. Hosono, Journal of the American Chemical Society 141(13) (2019) 5343-5349.

[4] S. Niu, J. Milam-Guerrero, Y. Zhou, K. Ye, B. Zhao, B.C. Melot, J. Ravichandran, Journal of Materials Research 33(24) (2018) 4135-4143.

[5] S. Niu, H. Huyan, Y. Liu, M. Yeung, K. Ye, L. Blankemeier, T. Orvis, D. Sarkar, D.J. Singh, R. Kapadia, J. Ravichandran, Advanced Materials 29(9) (2017) 1604733.

[6] Y. Nishigaki, T. Nagai, M. Nishiwaki, T. Aizawa, M. Kozawa, K. Hanzawa, Y. Kato, H. Sai, H. Hiramatsu, H. Hosono, H. Fujiwara, Solar RRL 4(5) (2020) 1900555.

[7] S. Filippone, B. Zhao, S. Niu, N.Z. Koocher, D. Silevitch, I. Fina, J.M. Rondinelli, J. Ravichandran, R. Jaramillo, Physical Review Materials 4(9) (2020) 091601.

5:10 PM EL03.03.05

SrHfS₃ Thin Films with Green Light Emission Haolei Hui¹, Xiucheng Wei¹, Zhonghai Yu², Yi-Yang Sun³, Sen Yang² and Hao Zeng¹; ¹University at Buffalo, The State University of New York, United States; ²Xi'an Jiaotong University, China; ³Rensselaer Polytechnic Institute, United States

SrHfS₃ belongs to the family of chalcogenide perovskite semiconductors with a bandgap of 2.43eV. Recently SrHfS₃ bulk crystals have been shown to exhibit strong green photoluminescence. It was also shown that it can be heavily doped to be both p- and n-type with strong emission, suggesting its bipolar doping capability and defect tolerance. It is thus a promising candidate to fill the green gap for solid state lighting applications. In this work, we show that SrHfS₃ thin films can be prepared by magnetron sputtering and CS₂ sulfurization. Raman spectrum matches closely with the theoretical calculations of a distorted perovskite structure. The film quality such as PL intensity and carrier concentration is highly dependent on sulfurization temperature.

5:25 PM EL03.03.06

Structure and Electronic Properties of Mixed-Bonded PbSe Epitaxial Thin Films on III-V Substrates Kunal Mukherjee^{1,2}, Brian Haidet², Eamonn Hughes², Leland Nordin³, Aaron Muhowski³, Kevin Vallejo⁴, Paul

Simmonds⁴ and Daniel Wasserman³; ¹Stanford University, United States; ²University of California, Santa Barbara, United States; ³The University of Texas at Austin, United States; ⁴Boise State University, United States

PbSe has emerged as a prototype for the study of unusual bonding in semiconductors. Recent work reveals the nature of bonding in PbSe and related IV-VI narrow band gap semiconductors as being distinct from covalent, ionic, and metallic.¹ We investigate the impact of such bonding on thin film growth, dislocation generation and dynamics, band-to-band carrier recombination, and field evaporation in epitaxial films grown directly on III-V substrates. These high quality engineered substrates serve as an excellent platform to probe and manipulate the properties of PbSe and its alloys.

We first demonstrate a route to prepare single crystal rocksalt PbSe films both on nearly lattice-matched and highly mismatched zincblende III-V substrates like InAs and GaAs using molecular beam epitaxy.² Our synthesis technique yields sharp heterointerfaces and we see clear structural distortions in the first few monolayers of PbSe mediating the significant bonding mismatch. These bare thin films strongly luminescence in the mid-infrared at room temperature even in the presence of threading dislocation densities exceeding $10^9/\text{cm}^2$, in sharp contrast to what may be expected from covalently bonded narrow bandgap III-V materials. We find minority carrier recombination lifetimes in our unintentionally doped PbSe films under low excitation in the 20–30 ns range and suggests a three carrier Auger process, although some very thin films deviate from this trend towards even longer lifetimes. Overall, these results are promising for the development of heterogeneously integrated mid-infrared light emitters.

Exploring this theme of unusual bonding further, the occurrence of elevated multi-atom evaporation events in atom probe tomography (APT) was recently hypothesized as a means to evaluate the nature of bonding in materials.³ We indeed see high rate of events with multiple atoms evaporating at once in voltage-pulsed APT of PbSe, supporting this suggestion, and finding even more such events localized around dislocation cores. However, in the same experiment we also see a high rate of multi-atom evaporation events in epitaxial layered-structure SnSe, which should be a mix of conventional covalent intra-layer and Van der Waals inter-layer bonding, showing exceptions are possible.

¹ M. Wuttig, V.L. Deringer, X. Gonze, C. Bichara, and J.-Y. Raty, *Advanced Materials* 30, 1803777 (2018).

² B.B. Haidet, E.T. Hughes, and K. Mukherjee, *Phys. Rev. Materials* 4, 033402 (2020).

³ M. Zhu, O. Cojocaru-Mirédin, A.M. Mio, J. Keutgen, M. Küpers, Y. Yu, J.-Y. Cho, R. Dronskowski, and M. Wuttig, *Advanced Materials* 30, 1706735 (2018).

SESSION EL03.04: Progress in Ionic Semiconductors/Theory and Design of Ionic Semiconductors III
Session Chairs: Chen Ming and Yi-Yang Sun
Thursday Afternoon, April 22, 2021
EL03

8:55 PM EL03.04.03

Characteristics of Silicon Nitride Thin Film with Plasma Treatment Chanwon Jung, Seokhwi Song, Suhyeon Park, Byunguk Kim, Youngjoon Kim, Eunjong Lee, Sunggwon Lee, Taehun Park and Hyeongtag Jeon; Hanyang University, Korea (the Republic of)

As the device's feature sizes continue to shrink, traditional floating gate NAND flash memory faces reliability issues such as cell-to-cell interference, reduced charge loss tolerance, and susceptibility to stress-induced leakage currents. 3D NAND flash memory was developed to overcome the above-mentioned problem. In 3D NAND flash memory, the charge storage material is silicon nitride (SiN_x), and the main trend for increasing

memory density is not scaling shrinking but stacking layers. Low-pressure chemical vapor deposition (LPCVD) is one of the most popular deposition methods to deposit SiN_x thin films on semiconductors due to its low hydrogen content and excellent step coverage and thermal stability. However, as more layers are stacked to increase memory density, the device's aspect ratio increases. The 1st generation 3D NAND flash memory has 24 layers and has an aspect ratio of 40:1. And currently, devices with more than 100 layers are required. As above, with the continuous aspect ratio increase, there is a demand deposition technology with accurate thickness control and high step coverage. Among various deposition methods to apply at high step coverage device, atomic layer deposition (ALD) is one of the best solutions to satisfy above-mentioned requirements. Due to self-limited ALD reaction, it enables to deposit thin film with high step coverage and good thickness control. Particularly, remote plasma ALD (RPALD) was utilized to enhance the reactivity between precursor and reactant gas for high film density with minimizing plasma damage. In RPALD, the plasma generation section is remotely outside of the reaction chamber and the radicals in plasma generation region enter into the reaction chamber for deposition.

In this study, we developed low-temperature SiN_x using bis(dimethylaminomethylsilyl)-trimethylsilyl amine (C₉H₂₉N₃Si₃, DTDN-2H₂) and N₂ reactant plasma as the precursor and reactant plasma. We studied the effect of plasma treatments that are 2 methods such as post plasma treatment and during deposition process plasma treatment. Various plasma processing processes were used in deposition processes to satisfy the defect density levels (5x10¹⁹/cm³). We investigated the effect of plasma treatment on the properties of SiN_x thin film. Auger electron spectroscopy (AES) was utilized to measure the stoichiometry. Samples treated by plasma treatment were stoichiometry thin film by 1:1.33 Si:N ratio. Because hydrogen content affects fault density, the hydrogen content of SiN_x film deposited was measured using secondary ion mass spectrophotometry (SIMS). X-ray photoelectron spectroscopy (XPS) was utilized for chemical binding state. N1s peak of H₂ plasma treatment SiN film had low-binding shift to 397.5eV from 397.7 eV (N-Si bond). The density of plasma-treated thin films was compared by X-ray reflectometry (XRR). In the case of thin film with plasma treatment, film density was higher than as deposition sample. And thin film with post H₂ plasma treatment was the highest density of 2.9g/cm³. In addition, studying defect properties of each thin film, we fabricated metal-Al₂O₃-silicon nitride-SiO₂-Si (MANOS) device. The trap density required by CTF device was satisfied by Ar plasma treatment during ALD process, post Ar plasma treatment, and post H₂ plasma treatment SiN thin film. Trap density of Post H₂ plasma treatment SiN films was increased to 7.65x10¹⁹/cm³

9:00 PM *EL03.04.04

Investigation on the Stability of Liquid-Like Thermoelectric Materials and Modules Pengfei Qiu;
Shanghai Institute of Ceramics, Chinese Academy of Sciences, China

Recently, the application of superionic conductors with liquid-like sublattice has been extended to the field of thermoelectrics. Extremely high thermoelectric figure of merit with the maximum $zT > 2.0$ have been observed and reported in a large family of novel Cu- and Ag-based liquid-like materials. However, despite the high performance, the stability and reliability of these liquid-like materials are key concerns for long-term service in the real applications. In this study, through systematically investigating the behavior of various liquid-like materials in an electric field or thermal gradient, we reveal the relations of atom migration, deposition, and material degradation. A general model is proposed to reveal the threshold for decomposition of liquid-like materials to prevent metal deposition upon atom migration. It is found that each liquid-like material has a threshold for metal deposition, named as the critical voltage. When the voltage stressed on the material is lower than the V_c , the mobile ions just form a steady concentration of gradient inside the material without any deposition. In this case, the liquid-like materials will demonstrate similar good stability with the traditional stable materials. With these understanding, a new strategy is proposed to design the stable and efficient TE modules based on liquid-like materials via geometry and interface optimization. By using this strategy, a TE module based on Cu₂Se with both good stability and high energy conversion efficiency up to 9.1% was successfully achieved.

9:25 PM EL03.04.06

Octahedron Rotation Evolution in 2D Perovskites and Its Impact on Optoelectronic Properties—The

Case of Ba–Zr–S Chalcogenides Chen Ming¹, Ke Yang^{2,3}, Hao Zeng⁴, Shengbai Zhang² and Yi-Yang Sun¹; ¹Shanghai Institute of Ceramics, Chinese Academy of Sciences, China; ²Rensselaer Polytechnic Institute, United States; ³Hunan University, China; ⁴University at Buffalo, The State University of New York, United States

Perovskite materials can have self-passivated surfaces without resorting to reconstructions or other passivating agents. This feature renders perovskite materials intrinsically suited for making two-dimensional (2D) materials. Previous studies often considered the structure of 2D perovskites to be directly terminated from the bulk. However, octahedron rotation (OR), being the distinctive structural feature of perovskite materials, appears to be an unexplored degree of freedom in 2D.

In this work, the OR patterns in 2D perovskites are systematically studied for the first time by employing an adapted Glazer's notation. Taking 2D Ba-Zr-S system as an example, we establish the relation between the OR pattern and slab thickness. It is found that as the thickness decreases, the OR pattern undergoes a transition by suppressing out-of-plane rotations. The OR in 2D chalcogenide perovskites could result in an anti-confinement effect, i.e., reducing the band gap to even below that of the bulk by countering the quantum confinement effect. In addition, we show that the Ba-Zr-S 2D perovskites exhibit reasonable electron mobility of $\sim 150 \text{ cm}^2 \text{ V}^{-1} \text{ s}^{-1}$ and large exciton binding energy of $\sim 0.9 \text{ eV}$. Our results suggest that the structure of OR is worth attention in future studies on 2D perovskites, and it provides a novel tuning knob for enhancing the properties of 2D materials, which is absent in existing 2D materials, such as graphene and transition metal dichalcogenides.

9:40 PM EL03.04.07

Chalcogenide Perovskite YScS₃ as a Potential p-Type Transparent Conducting Material Han Zhang¹, Chen Ming², Ke Yang^{3,4}, Hao Zeng⁵, Shengbai Zhang³ and Yi-Yang Sun²; ¹Shandong University, China; ²Shanghai Institute of Ceramics, Chinese Academy of Sciences, China; ³Rensselaer Polytechnic Institute, United States; ⁴Hunan University, China; ⁵University at Buffalo, The State University of New York, United States

Transparent conducting materials (TCMs) have been widely used in optoelectronic applications such as touchscreens, flat panel displays and thin film solar cells. These applications of TCMs are currently dominated by n-type doped oxides. High-performance p-type TCMs are still lacking due to their low hole mobility or p-type doping bottleneck, which impedes efficient device design and novel applications such as transparent electronics. Here, based on first-principles calculations, we propose chalcogenide perovskite YScS₃ as a promising p-type TCM. According to our calculations, its optical absorption onset is above 3 eV, which allows transparency to visible light. Its hole conductivity effective mass is $0.48 m_0$, which is among the smallest in p-type TCMs, suggesting enhanced hole mobility. It could be doped to p-type by group-II elements on cation sites, all of which yield shallow acceptors. Combining these properties, YScS₃ holds great promise to enhancing the performance of p-type TCMs toward their n-type counterparts.

9:55 PM EL03.04.08

Late News: Single-Site of Perovskite Unit Cell with d-d Transition in Electronic States Cong Wang; Beijing University of Technology, China

As one of low-cost and widely-utilized materials, perovskite type metal oxides have been extensively investigated and applied in environmental remediation and protection, energy conversion and storage, etc.^[1-7] Most of these diverse applications are results of a large diversity of the electronic states of metal oxides. Noticeably, however, many metal oxides present obstacles for applications in catalysis, mainly due to the lack of efficient active sites with desired electronic states. Continuous efforts and strategies have been devoted to create new structural units and functional activities of metal oxides. Single-site catalysis is one of most attractive solutions to explore new activities and enhance catalytic efficiencies.^[8-10] Here, we demonstrate the fabrication of single tungsten atom oxide (STAO), in which the metal oxide's active site unit reaches its minimum and a new electronic state is created. The catalytic mechanism in the STAO is determined by a new single-site physics mechanism, which is fundamentally distinct from the traditional size effect, and is also in

contrast to the standard condensed matter physics. The photogenerated electron transfer process is enabled by an electron in the spin-up channel excited from the highest occupied molecular orbital (HOMO) to the lowest unoccupied molecular orbital (LUMO)+1 state (both are largely tungsten atomic d-orbitals), which can only occur in STAO with W^{5+} . STAO results in a record-high and stable sunlight photocatalytic degradation rate of 0.24 s^{-1} , which exceeds the rates of available photocatalysts by approximately two orders of magnitude. The fabrication of STAO and its unique single-site photocatalytic mechanism lays a new ground for achieving novel physical and chemical properties using various single metallic atom oxides.

10:10 PM DISCUSSION TIME

SESSION EL03.05: Progress in Ionic Oxide and Nitride Semiconductors I
Session Chairs: Megan Butala and Ann Greenaway
Friday Morning, April 23, 2021
EL03

11:45 AM *EL03.05.01

Structure and Physical Properties of Complex Chalcogenides—Fundamental Research with an Eye Towards Applications George Nolas; University of South Florida, United States

Complex chalcogenides have demonstrated a variety of unique physical properties that are directly related to specific bonding schemes, and therefore continue to be investigated for different applications of interest. In addition, new chalcogenide compositions expand our library of materials and provide potential new avenues for discovery. Research that not only allows for a continuity of ongoing work into new and novel chalcogenide material systems but can also provide pathways for the design of materials or processing techniques with targeted properties for specific applications is paramount. The intellectual merit of these investigations is very closely tied to the particular bonding and structure types these materials possess. Developing a fundamental understanding of the underlying physical properties and their structure-property relationships is also of interest. I will present some of our recent progress on the structure-property relationships of specific materials, including layered materials, lanthanide metal polytellurides and new quaternary chalcogenides, provide insight into the search for new materials, and present results that demonstrate strong electron-phonon coupling and atypical transport of new chalcogenide materials.

12:10 PM EL03.05.02

Configurational Order-Disorder Transitions in $ZnGeN_2$ Jacob Cordell^{1,2}, Jie Pan², Adele Tamboli^{2,1}, Garritt J. Tucker¹ and Stephan Lany²; ¹Colorado School of Mines, United States; ²National Renewable Energy Laboratory, United States

The dependence of electronic structure on cation disorder in II-IV-V₂ materials with lattice parameters matched to their analogue III-V semiconductors makes these systems promising for tuning band gaps for use in energy-relevant devices such as LEDs and PV. Experimentally, however, properties do not always correlate with order as expected. In $ZnGeN_2$ specifically, the non-isovalent character of the disordered species (Zn^{2+} and Ge^{4+}) subjects the cation ordering to strong short-range order effects which influence band structure by decreasing the band gap relative to ordered $ZnGeN_2$. $ZnGeN_2$ exhibits pronounced discontinuities in enthalpy, entropy, and structural order parameters, which correspond to a first-order phase transition which is key to understanding the tunability of electronic properties. The steep nature of this transition suggests intermediate degrees of ordering are difficult or even impossible to obtain in single crystals or within crystalline grains. To model cation disorder, we use Monte Carlo (MC) simulations implementing a cluster expansion to approximate formation enthalpy. Representative configurations are relaxed in supercells containing 1,024 atoms using density functional theory calculations. From the Monte Carlo structures, we calculate the fractions of all possible

nitrogen coordination environments as a short-range order parameter and the Bragg-Williams and stretching parameters as long-range order parameters. We compare correlations between these order parameters as well as the mixing entropy and free energy of the system determined from thermodynamic integration to experimental literature on order in II-IV-V₂ materials.

12:25 PM EL03.05.03

Tuning the Electronic Properties of LaFeO₃ Thin-Films Photoelectrodes via Partial Cation Replacement

David J. Fermin¹, Xin Sun¹ and Devendra Tiwari²; ¹University of Bristol, United Kingdom; ²Northumbria University, United Kingdom

Fe₂O₃ thin-films have been extensively investigated as photoanodes, with a variety of different strategies being proposed to mitigate key performance limiting factors, namely short carrier lifetimes and surface recombination kinetics.¹ On the other hand, significantly less is known about the properties of perovskite ferrite absorbers, including LaFeO₃,²⁻⁴ YFeO₃,⁵ PrFeO₃,⁶ and BiFeO₃.⁷ These materials exhibit a wide range of intrinsic defects, which often lead to p-type conductivity. Our recent studies have shown that highly crystalline LaFeO₃ nanoparticles can promote hydrogen evolution under illumination at potential as positive as 1.47 V vs RHE,⁸ one of the highest photovoltages reported for a single p-type absorber layer. However, the performance of these perovskites is limited to quantum yields below 1%. In this contribution, we will examine the nature of the states involved in the loss of photogenerated carriers and the effect of partial substitution by alkaline-earth metal cations (AMC).

LaFeO₃ thin-film with a thickness of 95 nm were prepared by thermolysis (600 °C) of sol-gel precursors incorporating citric acid as chelating agent.⁹ The ratio of AMC (Mg²⁺, Ca²⁺, Ba²⁺ and Sr²⁺) to La³⁺ were adjusted in the range of 0 to 10% in the precursor solution, while keeping the Fe³⁺ concentration constant. XRD confirms the formation of single-phase cubic LaFeO₃ thin films across the whole composition range.

Interestingly, we observe subtle trends in lattice constant variations which are closely correlated to shifts in the binding energies of Fe 2p_{3/2} and O 1s measured by XPS. These trends are the result of the complex interplay between differences in ionic radii of the cations and changes in the oxidation state of Fe sites. Indeed, we establish a scaling factor between these two photoemission peaks, revealing a direct correlation between Fe oxidation state and Fe–O covalency. Electrochemical impedance spectroscopy (EIS) confirms the p-type characteristic of pristine LaFeO₃ thin-films, as well as the presence of sub-bandgap electronic state (A-states) close to the valence band edge. Partial AMC replacement leads to: (i) a decrease in the density of A-states, (ii) an increase in density of majority carriers (shallow acceptor states), and (iii) a shift of the valence band edge toward more positive potentials. In addition, AMC-substituted films exhibit deeper states centered at 0.6 eV above the valence band edge (B-states). These sub-band gap states have contrasting effects on the photoelectrochemical responses towards the oxygen reduction and the hydrogen evolution reactions. These trends are rationalized in terms of the position of the sub-bandgap states, majority carrier mobility, charge transfer and recombination kinetics.

References:

1. W. Yang, R.R. Prabhakar, J. Tan, S.D. Tilley and J. Moon, *Chem. Soc. Rev.*, **48**, 4979 (2019)
2. V. Celorrio, K. Bradley, O.J. Weber, S.R. Hall, and D.J. Fermin, *ChemElectroChem*, **1**, 1667 (2014)
3. G.P. Wheeler and K.S. Choi, *ACS Energy Lett.*, **2**, 2378 (2017).
4. G.P. Wheeler, V.U. Baltazar, T.J. Smart, A. Radmilovic, Y. Ping, and K.-S. Choi, *Chem. Mater.*, **31**, 5890 (2019)
5. M.I. Díez-García, V. Celorrio, L. Calvillo, D. Tiwari, R. Gómez, and D.J. Fermín, *Electrochim. Acta*, **246**, 365 (2017).
6. E. Freeman, S. Kumar, S.R. Thomas, H. Pickering, D.J. Fermín, S. Eslava, *ChemElectroChem*, **7**, 1365 (2020)
7. D. Tiwari, D.J. Fermín, T.K. Chaudhuri, A. Ray *J. Phys. Chem C*, **119**, 5872 (2015)
8. X. Sun, D. Tiwari and D. J. Fermín, *J. Electrochem. Soc.*, **166**, H764 (2019)
9. X. Sun, D. Tiwari and D. J. Fermín, *ACS Appl. Mater. Inter.*, **12**, 31486 (2020)

12:40 PM *EL03.05.04

Challenges and Opportunities in Ionic Chalcogenide Semiconductors Mercouri G. Kanatzidis^{1,1,2};

¹Northwestern University, United States; ²Argonne National Laboratory, United States

Metal chalcogenides define a large and important field of chemistry, and these materials continue to present appealing intellectual and scientific challenges. They are a large class with a broad set of chemical and physical properties involving diverse scientific phenomena and impact an astonishing variety of applications. The fields of science and technology impacted by chalcogenides continue to broaden. Some examples include nonlinear optics, thermoelectric energy conversion, radiation detectors, catalysis, topological insulators, science in two-dimensions, and unconventional superconductivity. Recently, the chemistry of these complex chalcogenides has witnessed the largest growth. We are in the middle of an impressive expansion in solid state chalcogenide chemistry with emphasis on materials with new compositions and structure types. In this regard, the development of novel synthetic methodologies is playing a major role in producing new materials, and this is a main objective in our program. We will highlight the general themes of synthesis science and structure-composition-property relationships with the following question being central: How does one develop the tools and concepts, both intellectual and experimental, to prepare new functional materials. There are several science drivers behind this research. Since crystal structure defines physical properties, of particular interest is learning to control structure dimensionality in complex systems. Another is learning how to incorporate two different metals in a single chalcogenide structure while avoiding phase separation. We will present relevant example in new materials with nonlinear optical properties and hard radiation and neutron detection capabilities and how they evolve as a function of composition and structure.

1:05 PM EL03.05.05

Late News: Structure and Bonding of AM₂Pn₂ (A=Ca, Mg, Yb; Pn=Bi, Sb) Compounds at High Pressure

Mario R. Calderon Cueva¹, Wanyue Peng¹, Clarke Samantha², Megan Rylko¹, Jingxuan Ding³, Allison Pease¹, Gill Levental¹, Benjamin Brugman¹, Susannah Dorfman¹ and Alexandra Zevalkin¹; ¹Michigan State University, United States; ²Lawrence Livermore National Laboratory, United States; ³Duke University, United States

Compounds in the structure type CaAl₂Si₂ have attracted great attention in recent years for their thermoelectric properties. In particular, MgMg₂Sb₂ and MgMg₂Bi₂ exhibit an impressive thermoelectric figure of merit zT due, in part, to their anomalously low thermal conductivity. In the present study, in situ high-pressure synchrotron X-ray diffraction was used to investigate the structure and bonding in binary and ternary AM₂X₂ compounds at pressures up to 50 GPa. Our results confirm prior predictions of isotropic in-plane and out-of-plane compressibility but reveal large disparities between the bond strength of the two distinct Mg sites. Using single-crystal diffraction, we show that the octahedral Mg–Sb bonds are significantly more compressible than the tetrahedral Mg–Sb bonds in MgMg₂Sb₂, which lends support to prior arguments that the weaker octahedral Mg bonds are responsible for the anomalous thermal properties of MgMg₂Sb₂ and MgMg₂Bi₂. Further, we report the discovery of a displacive and reversible phase transition ($C2/m$) in both MgMg₂Sb₂ and MgMg₂Bi₂ above 7.8 and 4.0 GPa, respectively. The transition to the high-pressure structure in these binary compounds involves a highly anisotropic volume collapse, in which the out-of-plane axis compresses significantly more than the in-plane axes. Further, we investigate the bond compressibility in ternary AM₂X₂ compounds using CaMg₂Sb₂ and YbMg₂Bi₂ to develop trends between bond compressibility and cation size and to study the stability of the CaAl₂Si₂ structure type.

1:10 PM DISCUSSION TIME

SESSION EL03.06: Progress in Ionic Oxide and Nitride Semiconductors II

Session Chairs: George Nolas and Kimberly See

2:15 PM *EL03.06.01

Structure-Property Relationships in Complex Early Transition Metal Oxides for High-Rate Energy Storage Megan M. Butala¹, Kit McColl², Kent J. Griffith³, Rebecca Dally⁴ and Igor Levin⁴; ¹University of Florida, United States; ²University College London, United Kingdom; ³Northwestern University, United States; ⁴National Institute of Standards and Technology, United States

As batteries are employed in larger numbers and for increasingly diverse applications, there is interest in electrode materials with improved safety, availability, and cost relative to commercial electrodes. Early transition metal oxides are one alternative material family showing promise, especially for high rate applications. However, we do not yet have a strong understanding of the role of composition, structure, and structural evolution with cycling for these materials, which tend to have large unit cells and complex structures.

To contribute to this fundamental understanding, we have studied the energy storage abilities and mechanism of complex niobate electrode materials KNb_3O_8 and NaNb_3O_8 . Using *ex situ* and *operando* X-ray diffraction, complemented by nuclear magnetic resonance spectroscopy and first principles calculations, we identify local and average structure changes and relate them to cycling performance and properties, including electronic conductivity over a charge induced metal-insulator transition. We also reflect on the role of these results in establishing a more general understanding of the structure-property relationships of other early transition metal oxides, for energy storage and beyond. This understanding is a necessary step toward the selection and design of electrode materials for the quickly-evolving energy landscape and our fundamental understanding of complex oxide semiconductors.

2:40 PM *EL03.06.02

Materials Chemistry of Ternary Nitride Semiconductors Andriy Zakutayev; National Renewable Energy Laboratory, United States

Nitride semiconductors is an interesting class of materials studied for diverse properties. Simple binary nitride semiconductors with wurtzite crystal structure such as GaN have been long used in many practical applications ranging from optoelectronic to telecommunication. The structurally related ZnGeN_2 or MgSnN_2 derived by cation mutation from the parent binary compounds have recently attracted attention for their disorder-tunable properties. However, these ternary nitride materials are mostly limited to II-IV-N₂ composition closely related to parent III-N compounds.

This invited presentation will focus on chemistry-inspired material design of unconventional ternary nitride semiconductors. First, chemical trends in crystal structure and thermodynamic stability of ternary nitrides containing Mg or Zn, and Zr, Nb, Mo transition metals will be presented. Second, the results will be shown for thin film synthesis and optoelectronic properties for some of these new ternary nitrides semiconductors beyond II-IV-N₂ family, such as Zn_2NbN_3 and Mg_3MoN_4 . Finally, kinetically controlled synthesis of metastable ternary nitrides will be discussed as one of the important next steps in the field.

3:05 PM EL03.06.03

Exploring the Nitride Perovskites Composition Space with Chemical Heuristics and First-Principles Calculations Daniel W. Davies¹, Aron Walsh² and David O. Scanlon¹; ¹University College London, United Kingdom; ²Imperial College London, United Kingdom

Oxide and halide perovskites of the form ABX_3 are a thoroughly studied class of material. They display a great breadth of interesting properties, which make them suitable for a variety of application areas from high-temperature superconductors to photovoltaic absorbers. More recently, the possibility of forming stable nitride perovskites have caught the interest of several research groups. While these are fairly illusive, which can be

understood in part due to the high oxidation states required on the A and B cations, the few that have been identified computationally and experimentally so far have shown interesting electronic properties.^{1,2}

In this study, we apply a computational screening workflow to further probe the composition space of nitride perovskite materials. By combining filters based on chemical heuristics from data-mined oxidation states³ we reduce the ABN₃ search space, where A and B are technologically relevant metals, from 3,906 to just 279 potentially feasible materials. We then carry out automated first-principles calculations to systematically investigate the stability of different octahedral tilting motifs in these materials. By mapping out the thermodynamic stabilities of the various tilts for each composition, we are able to provide the next level of resolution to the composition vs stability picture of this chemical space. Furthermore, we carry out phonon calculations on relevant subsections of the phase space to gain insight into dynamic stability and apply hybrid density functional theory (DFT) methods to determine accurate optoelectronic properties.

[1] R. Sarmiento-Pérez et al., *Prediction of Stable Nitride Perovskites*, *Chemistry of Materials*, **27** (2015)

[2] K. R. Tally et al., Synthesis of Ferroelectric LaWN₃ – The First Nitride Perovskite, arXiv preprint, **arXiv:2001.00633** (2020)

[3] D. W. Davies et al., *Materials Discovery by Chemical Analogy: Role of Oxidation States in Structure Prediction*, *Faraday Discussions*, **211** (2018)

3:20 PM *EL03.06.04

Mg-IV-N₂ Semiconductors—Polymorphism and Cation Disorder Ann L. Greenaway¹, Amanda Loutris¹, Rekha Schnepf^{1,2}, Karen Heinselman¹, Allison Mis^{1,2}, Rachel Woods-Robinson^{1,3}, Celeste Melamed^{1,2}, Jesse Adamczyk², M Brooks Tellekamp¹, Rachel Sherbondy^{1,2}, Dylan Bardgett¹, Sage Bauers¹, Andriy Zakutayev¹, Steven Christensen¹, Stephan Lany¹ and Adele Tamboli¹; ¹National Renewable Energy Laboratory, United States; ²Colorado School of Mines, United States; ³University of California, Berkeley, United States

As the search for new semiconductors expands, new paradigms for property control are emerging. Varying stoichiometry, polymorph, and alloying have, along with doping, enabled property control in binary semiconductors. Ternary and multinary compounds have additional degrees of freedom, such as lattice site disorder, which may enable unparalleled property control. In II-IV-N₂ compounds, which are analogs of the III-N semiconductors, cation site disorder can reduce the bandgap without substantially impacting lattice parameter,¹ but several members of this class are underexplored due to the historical difficulty in synthesizing nitrides. MgSnN₂ is a II-IV-N₂ with a predicted ~2.3 eV bandgap and wurtzite-derived ground state structure, making it of interest for optoelectronic properties and integration with existing III-N compounds. Here, we report on one of the first syntheses of MgSnN₂ and explore control of cation disorder and polymorphism in this material.

We first demonstrate combinatorial radio-frequency co-sputtering of MgSnN₂ across a range of cation compositions and up to 500 °C.² The predicted wurtzite-type polymorph forms across the explored temperature range, while a rocksalt-type polymorph not captured by previous predictions is found as a secondary phase at high Mg compositions below 200 °C. This phase is substantially metastable (>70 meV/atom) compared to the wurtzite-type ground state, and is predicted to be a wide bandgap, high dielectric constant material. Synchrotron x-ray diffraction confirms that both wurtzite- and rocksalt-type phases are cation-disordered, consistent with the reduced optical absorption onset of < 2 eV for the wurtzite-type phase *via* spectroscopic ellipsometry. We also demonstrate the heteroepitaxial growth of mixed wurtzite/rocksalt MgSnN₂ on GaN at 400 °C, where the close effective lattice match between GaN and the rocksalt-derived phase promotes its formation outside of the previously mapped temperature and cation composition range.

The existence of two accessible polymorphs of MgSnN₂, in addition to the possibility of cation ordering may enable additional control of materials properties. We exploit the ability to nucleate both polymorphs of MgSnN₂ on GaN in ongoing work investigating cation ordering in the rocksalt-derived MgSnN₂ using post-growth annealing, and further discuss related polymorph and cation order phenomena in the analogous compounds

MgSiN₂ and MgGeN₂. This work forms the basis for integrated materials control through both polymorph formation and lattice site disorder, bridging existing methods of manipulating semiconductor properties and emerging tools, while opening the door for a new set of semiconductors which can be integrated with well-established III-N compounds.

(1) Schnepf, R. R.; Cordell, J. J.; Tellekamp, M. B.; Melamed, C. L.; Greenaway, A. L.; Mis, A.; Brennecka, G. L.; Christensen, S.; Tucker, G. J.; Toberer, E. S.; Lany, S.; Tamboli, A. C. Utilizing Site Disorder in the Development of New Energy-Relevant Semiconductors. *ACS Energy Lett.* **2020**, 5 (6), 2027–2041.

(2) Greenaway, A. L.; Loutris, A. L.; Heinselman, K. N.; Melamed, C. L.; Schnepf, R. R.; Tellekamp, M. B.; Woods-Robinson, R.; Sherbondy, R.; Bardgett, D.; Bauers, S.; Zakutayev, A.; Christensen, S. T.; Lany, S.; Tamboli, A. C. Combinatorial Synthesis of Magnesium Tin Nitride Semiconductors. *J. Am. Chem. Soc.* **2020**, 142 (18), 8421–8430.

3:45 PM EL03.06.05

Controlled Synthesis and Electronic Structure Engineering of Metastable Ta₂N₃ via Oxygen

Incorporation Chang-Ming Jiang, Laura Wagner, Johanna Eichhorn and Ian Sharp; Technische Universität München, Germany

The binary Ta-N chemical system includes several compounds with notable prospects in microelectronics, solar energy harvesting, and catalysis. Among these, metallic TaN and semiconducting Ta₃N₅ have garnered significant interest, in part due to their synthetic accessibility. However, tantalum sesquinitride (Ta₂N₃) possesses an intermediate composition and largely unknown physical properties owing to its metastable nature. Herein, Ta₂N₃ is directly deposited by reactive magnetron sputtering and its optoelectronic properties are characterized. Combining these results with density functional theory provides insights into the critical role of oxygen in both synthesis and electronic structure. While the inclusion of oxygen in the process gas is critical to Ta₂N₃ formation, the resulting oxygen incorporation in structural vacancies drastically modifies the free electron concentration in the as-grown material, thus leading to a semiconducting character with a 1.9 eV bandgap. Reducing the oxygen impurity concentration *via* post-synthetic ammonia annealing increases the conductivity by seven orders of magnitude and yields the metallic characteristics of a degenerate semiconductor, consistent with theoretical predictions. Thus, this inverse oxygen doping approach – by which the carrier concentration is reduced by the oxygen impurity – offers a unique opportunity to tailor the optoelectronic properties of Ta₂N₃ for applications ranging from photochemical energy conversion to advanced photonics.

4:00 PM EL03.06.06

Cation Disorder in Zn-IV-N₂—Does Intrinsic Disorder Exist Besides Effects of Composition and Oxygen Content? Joachim Breternitz¹, Zhenyu Wang^{1,2} and Susan Schorr^{1,2}; ¹Helmholtz-Zentrum Berlin für Materialien und Energie, Germany; ²Freie Universität Berlin, Germany

Many of the materials considered for photovoltaic applications suffer from one or both of the barring arguments for truly sustainable materials: They contain elements that are either toxic (e.g. Pb, Cd) and/or scarce (e.g. Te, In, Ga). The use of more than 1000 ppm Pb in electrical devices is, for instance, banned in the European Union¹ and most other countries. Zinc-group IV-nitrides are being considered as promising candidates for photovoltaic absorber materials, containing uniquely elements of low toxicity and low resource criticality.² They can be formally related to binary III-V nitrides by replacing the trivalent cations of the latter with equimolar amounts of divalent and tetravalent ions. Further to band gap tuning by alloying group IV elements – in analogy to cation alloying in III-V's – it has been postulated based on DFT calculations that Zn-IV-N₂ compounds possess a second mechanism for bandgap tuning through cation disorder of the divalent and tetravalent species.³

The latter is unique to these ternary materials and marks the foundation of complex structure-property relationships in this class of materials, which need to be properly elucidated. Further, cation disorder is also

triggered by oxygen substituting nitrogen on the cation sites and the effects mimic each other in some way.⁴ The latter is particularly important, since a degree of oxygen presence is hardly avoidable in most nitride syntheses. Understanding the different effects on the structural features of these materials is key to their performance as photovoltaic materials.

Herein, we present a systematic study of $\text{Zn}_{1+x}\text{Ge}_{1-x}(\text{N}_{1-x}\text{O}_x)_2$ as model system for oxygen containing Zn-IV-N₂ materials. While the oxygen rich oxide nitrides appear as completely cation disordered and crystallise in the wurtzite type,⁴ oxygen poor compounds crystallise in the β -NaFeO₂-type that is also adopted by stoichiometric ZnGeN₂.⁵ Both crystal structures are closely related to each other with the latter being a subgroup of the wurtzite-type. The β -NaFeO₂-type, however, consists of two crystallographically independent cation positions that allow ordered cations, as well as a quantifiable degree of disorder. Since Zn²⁺ and Ge⁴⁺ are isoelectronic, they are virtually indistinguishable using X-ray diffraction and hence neutron diffraction is used for the reliable determination of disorder in this class of materials.

Combining chemical analyses and both, X-ray and neutron powder diffraction, we endeavour to disentangle the different phenomena leading to cation disorder and find evidence for oxygen-content related disorder as well as for cation disorder that does not relate to oxygen. However, the effects of oxygen and sample composition are largely predominant. Finally, we relate these structural findings with the optical bandgaps of the materials obtained through diffuse reflectance UV-VIS spectroscopy.

References

- 1 Restriction of the use of certain hazardous substances Directive (RoHS) 2011/65/EU.
- 2 P. Narang, S. Chen, N. C. Coronel, S. Gul, J. Yano, L.-W. Wang, N. S. Lewis, H. A. Atwater, *Adv. Mater.* **2014**, *26*, 1235-1241
- 3 D. Skachov, P. C. Quayle, K. K. Kash, W. R. L. Lamprocht, *Phys. Rev. B* **2016**, *94*, 205201.
- 4 J. Breternitz, Z. Y. Wang, A. Glibo, A. Franz, M. Tovar, S. Berendts, M. Lerch, S. Schorr, *Phys. Status Solidi A* **2019**, *216*, 1800885.
- 5 Z. Y. Wang, D. Fritsch, S. Berendts, M. Lerch, J. Breternitz, S. Schorr, *submitted*.

SESSION EL03.07: Progress in Ionic Semiconductor—Transport
Session Chairs: Elif Ertekin and Andriy Zakutayev
Friday Afternoon, April 23, 2021
EL03

5:15 PM *EL03.07.01

Origin of Unexpectedly Low Thermal Conductivity in Mg₃Sb₂ and Mg₃Bi₂ Thermoelectric Materials

Alexandra Zevalkink; Michigan State University, United States

In the past five years, Mg₃Sb₂ and Mg₃Bi₂ alloys have emerged as exceptional room-temperature thermoelectric materials, threatening to overthrow the decades-long reign of Bi₂Te₃. The success of these compounds is thanks in large part to their surprisingly low lattice thermal conductivity, which is rarely observed in simple, lightweight compounds. This talk will explore the chemical and thermodynamic origins of the anomalously low thermal conductivity in the Mg₃Pn₂ system (Pn = Sb, Bi). Temperature-dependent measurements of the elastic moduli and first principles phonon calculations were used to investigate the bond strength, rate of softening, and mode Grüneisen parameters. Compared with other isostructural compounds, we find that both Mg₃Sb₂ and Mg₃Bi₂ have anomalously soft shear moduli and large mode Grüneisen parameters. We attribute this behavior primarily to the small size of the Mg cations: Mg is undersized with respect to the 6-fold octahedral coordination environment, leading to weak anharmonic interlayer bonding and high rates of Umklapp phonon-phonon scattering. This is corroborated by the phonon spectra obtained from inelastic neutron scattering of

Mg₃Bi₂ and YbMg₂Bi₂ single crystals, which show significant softening of the acoustic phonons when Yb is replaced by the smaller Mg cation. In addition, we used *in-situ* high-pressure synchrotron X-ray diffraction to investigate the structure and bonding in Mg₃Sb₂ and Mg₃Bi₂ at pressures up to 50 GPa. By extracting the pressure-dependent volume change of the polyhedra using Mg₃Sb₂ single crystal diffraction data, we show that the octahedral Mg-Sb bonds are significantly more compressible than the tetrahedral Mg-Sb bonds, lending further support to our argument that the octahedrally-coordinated Mg is responsible for the anomalous thermal properties of the Mg₃Pn₂ system. Further, we report the discovery of a reversible high-pressure phase transition in Mg₃Sb₂ and Mg₃Bi₂ to a monoclinic structure at 7.8 GPa and 4.0 GPa, respectively.

5:40 PM EL03.07.02

The Effect of Multi-Band Transport on Thermal Conductivity Seen in Yb₁₄Mg_{1-x}Al_xSb₁₁ Max Wood^{1,2}, Chris Perez³, Francesco Ricci⁴, Geoffroy Hautier⁴, G. Snyder² and Susan Kauzlarich³; ¹NASA Jet Propulsion Laboratory, United States; ²Northwestern University, United States; ³University of California, Davis, United States; ⁴Université Catholique de Louvain, Belgium

The lattice thermal conductivity of a material above its Debye temperature should either decrease with increasing temperatures, as in a crystal, or remain independent of temperature, as in a glass. However, multiple literature reports of the Yb₁₄MgSb₁₁ crystal indicate its lattice thermal conductivity increases with increasing temperature well above its Debye temperature. Herein we study the thermal conductivity and electrical transport of the Yb₁₄Mg_{1-x}Al_xSb₁₁ solid solution and show this increase in lattice thermal conductivity can be attributed to an electronic effect arising from multi-band transport. We go on to show the effect multi-band transport has on thermal conductivity is pervasive in literature but is often misattributed to the thermal conductivity arising from phonon transport.

5:55 PM EL03.07.03

Conversion of Electrospun Layered Perovskite Nanofibers to Perovskite Oxynitrides for Visible Light Absorption Anja Hofmann and Roland Marschall; University of Bayreuth, Germany

The wide bandgap layered perovskites A₅M₄O₁₅ (A = Ba, Sr; M = Ta, Nb) are shown do be very active in photocatalytic water splitting under UV-light, resulting from the additional reaction sites in the crystal structure.[1] The activity can be improved either by the formation of heterojunctions such as Ba₅Ta₄O₁₅-Ba₃Ta₅O₁₅ or Ba₅Ta₄O₁₅-Ba₃Ta₅O₁₅-BaTa₂O₆. [2,3] Preparation of nanofibers can additionally solve the problem of the large mismatch between the small charge carrier diffusion length and the much larger light penetration depth, resulting in higher photocatalytic activity.[4,5] Visible light activity can be gained by the formation of heterojunctions such as Ba₅Ta₄O₁₅-AgVO₃[6] and Ba₅Ta₄O₁₅-C₃N₄[7] and via ammonolysis[8].

We are combining the positive effects of the nanofiber structure and the ammonolysis by preparing (111) layered perovskites nanofibers of Ba₅Ta₄O₁₅ and Ba₅Nb₄O₁₅ and converting them into perovskite oxynitrides. The samples were characterized with XRD and the conversion degree was determined. SEM characterization was performed, and Kr physisorption measurements were done to determine the BET surface area before and after ammonolysis. UV-Vis spectroscopy as well as hydrogen evolution measurements in water/methanol were performed.

In first experiments, conversion degrees of nearly 100% were obtained, yielding in a decrease of the band from 4.0 eV down to 2.0 eV for the niobium compound and from 4.6 eV down to 1.9 eV for the tantalum compound; giving visible light absorption abilities. The surface area is slightly increased. Morphology changes will be discussed in detail.

[1] H. Otsuka *et al.*, *Chem. Lett.* 2005, **34**, 822.

[2] R. Marschall, J. Soldat, and M. Wark, *Photochem. Photobiol. Sci.*, 2013, **12**, 671.

[3] J. Soldat, R. Marschall, and M. Wark, *Chem. Sci.*, 2014, **5**, 3746.

[4] N. C. Hildebrandt, J. Soldat, and R. Marschall, *Small* 2015, **17**, 2051.

[5] A. Bloesser and R. Marschall, *ACS Appl. Energy Mater.* 2018, **1**, 2520.

[6] K. Wang, X. Wu, G. Zhang, et al., ACS Sustain. Chem. Eng., 2018, **6**, 6682.

[7] E. Hua, G. Liu, G. Zhang, et al., Dalt. Trans., 2018, **47**, 4360.

[8] A. Mukherji, C. Sun, S. C. Smith, et al., J. Phys. Chem. C, 2011, **115**, 15674.

6:10 PM *EL03.07.04

Divalent Ion Conductors Kimberly A. See; California Institute of Technology, United States

Materials that conduct ions have long been studied for a variety of applications from solid state lighting to energy conversion technologies. Room temperature ionic conductivity is especially useful for energy storage applications and notable examples conduct monovalent Li^+ . Active materials in the cathode and anode must support facile ion diffusion and high electronic conductivity while solid-state electrolytes require high ionic conductivity but low electronic conductivity. Although Li-based systems work very well and have revolutionized energy storage, the desire to lower cost and increase availability motivates next-generation technologies based on new mobile ions including divalent Ca^{2+} , Mg^{2+} , and Zn^{2+} . We will discuss divalent ion conductivity in this context with a focus on Zn^{2+} conductivity in ZnPS_3 . ZnPS_3 supports Zn^{2+} conductivity with unexpectedly low activation energies (~ 350 meV) enabled by the flexible $[\text{P}_2\text{S}_6]^{4-}$ polyanion that distorts into the Van der Waals gap at the transition state.

6:35 PM EL03.07.05

Investigation of Thermoelectric Properties of $\text{Yb}_{14-x}\text{Na}_x\text{MgSb}_{11}$ Naomi Pieczulewski, Max Wood, Michael Toriyama, James Male and G. Snyder; Northwestern University, United States

The $\text{Yb}_{14}\text{MgSb}_{11}$ structural system is a record-breaking high temperature p-type material with applications in radioisotope thermoelectric generators. However, the single parabolic band model that has guided previous optimization efforts, pointing toward decreasing carrier concentration, do not take into consideration a second valence band that alters effective mass and electronic transport in the $\text{Yb}_{14}\text{MgSb}_{11}$ system. Here we conduct the first investigation to increase carrier concentration by Na doping $\text{Yb}_{14}\text{MgSb}_{11}$ based on an improved multiband model. To understand defect-controlled carrier concentration, we apply density functional theory (DFT) to investigate equilibrium phases, defect formation enthalpies and band diagrams. We found that the enthalpy of formation was more favorable for Na as an interstitial rather than a substitutional atom. Furthermore, experimental transport data on $\text{Yb}_{14-x}\text{Na}_x\text{MgSb}_{11}$ ($x=0, 0.05, 0.25, 1, 2, 3$) were prepared by ball milling and hot-pressing procedures. We show that Na increases Seebeck and resistivity leading to the conclusion that Na acts as a +1 electron donor interstitial atom decreasing carrier concentration.

6:50 PM EL03.07.06

Interplay Between Phononic and Electronic Properties in Determining Carrier Mobility in Heavily Donor-Doped CdO Thin-Films Zachary T. Piontkowski¹, Evan Runnerstrom^{2,3}, Angela Cleri⁴, Anthony McDonald¹, Jon Ihlefeld^{5,5}, Jon-Paul Maria⁴ and Thomas Beechem^{1,1}; ¹Sandia National Laboratories, United States; ²North Carolina State University, United States; ³U.S. Army Research Office—Materials Science Division, United States; ⁴The Pennsylvania State University, United States; ⁵University of Virginia, United States

Advances in CdO donor doping have realized carrier concentrations exceeding 10^{20} cm^{-3} while maintaining carrier mobilities of up to $500 \text{ cm}^2/\text{Vs}$ that together enable new mid-IR plasmonic applications. Despite this differentiating property combination, the underlying mechanisms dictating these properties remain incompletely understood. Unlike traditional semiconductors, mobility does not scale monotonically with carrier concentration in CdO as initial increases with dopant incorporation eventually level off and ultimately decrease. To explain these observations, we vibrationally resolve the lattice changes occurring upon doping and assess them in light with observed trends in mobility.

Raman spectroscopy, pre-resonant with the CdO band-gap, examined lattice strain, disorder, and exciton-impurity/phonon interactions occurring as a function of carrier concentration. Mobility is found to be inversely proportional to both the amount of strain and disorder that change with doping consistent with explanations for

dopant incorporation based on defect equilibria. Additionally, longitudinal optical phonon-plasmon coupled modes are identified and found to scatter by an impurity induced Fröhlich mechanism. Taken together, these coupling strengths also correlate linearly with the mobility, with decreased coupling associating with increased mobility. When viewed as a whole, the effects of strain, disorder and exciton-impurity/phonon interactions together dictate the carrier mobility, with phonon properties affecting the electronic properties and vice versa. These results have the potential to inspire new plasmonic materials which are engineered at the phonon level, revealing a new axis of device tunability.

Acknowledgements: Sandia National Laboratories is a multi-mission laboratory managed and operated by the National Technology & Engineering Solutions of Sandia, LLC, a wholly owned subsidiary of Honeywell International Inc., for the U.S. Department of Energy's National Nuclear Security Administration under contract No. DE-NA0003525.

7:05 PM DISCUSSION TIME

SESSION EL03.08: Progress in Ionic Oxide and Nitride Semiconductors III/Panel Discussion: Why New semiconductors?

Session Chairs: Yi-Yang Sun and Hao Zeng

Friday Afternoon, April 23, 2021

EL03

8:15 PM *EL03.08.01

Efficient Photocatalysts for Water Splitting to Produce Solar Hydrogen Kazunari Domen^{1,2}; ¹Shinshu University, Japan; ²The University of Tokyo, Japan

Sunlight-driven water splitting has received much attention as a means of large-scale renewable hydrogen production [1]. Both efficiency and scalability of water-splitting systems are essential factors for practical utilization of renewable solar hydrogen. Particulate photocatalyst systems do not involve any secure electric circuit and can be spread over wide areas by inexpensive processes potentially. Therefore, it is highly impactful to develop particulate photocatalysts and their reaction systems that efficiently split water.

The author's group has studied various semiconducting oxides, (oxy)nitrides, and (oxy)chalcogenides as photocatalysts for water splitting [2]. The water splitting activity of a SrTiO₃ photocatalyst can be boosted by two orders of magnitude by doping Al [3]. The apparent quantum yield of overall water splitting using a SrTiO₃ photocatalyst has been improved to 95% in the near UV region via refining the photocatalyst and cocatalyst preparation [4]. This quantum efficiency is the highest yet reported, and indicates that particulate photocatalysts can drive the uphill overall water splitting reaction as efficiently as the photon-to-chemical conversion process in photosynthesis.

The author's group has also been developing panel reactors in view of large-scale applications [3]. A prototype panel reactor containing Al-doped SrTiO₃ photocatalyst sheets splits water and releases product hydrogen and oxygen gas bubbles at a rate corresponding to a solar-to-hydrogen energy conversion efficiency (STH) of 10% under intense UV illumination. A 1-m²-sized photocatalyst panel reactor splits water under natural sunlight irradiation without a significant loss of the intrinsic activity of the photocatalyst sheets. A solar hydrogen production system with a greater size (100 m²) was recently built and its performance and system characteristics are under investigation. Panel reactors can accommodate various kinds of photocatalyst sheets and are expected to be built using light and inexpensive materials, thus being ideal for large-scale solar hydrogen production from water.

It is essential to develop photocatalysts active under visible light irradiation for practical solar energy harvesting. Ta₃N₅ and Y₂Ti₂O₅S₂ photocatalysts show activity in overall water splitting via one-step excitation under visible light irradiation [5,6]. Particulate photocatalyst sheets split water into hydrogen and oxygen via two-step excitation, referred to as Z-scheme, efficiently regardless of the size. In particular, a photocatalyst sheet consisting of La- and Rh-codoped SrTiO₃ and Mo-doped BiVO₄ split water into hydrogen and oxygen O₂ via two-step excitation, referred to as Z-scheme, and exhibit STH exceeding 1.0% [7,8]. Some other (oxy)chalcogenides and (oxy)nitrides with longer absorption edge wavelengths are also applicable to Z-schematic photocatalyst sheets.

In my talk, the latest progress in the development of photocatalytic materials and their reaction systems will be presented.

- [1] Hisatomi *et al. Nat. Catal.* **2019**, 2, 387.
- [2] Chen *et al. Nat. Rev. Mater.* **2017**, 2, 17050.
- [3] Goto *et al. Joule* **2018**, 2, 509.
- [4] Takata *et al. Nature* **2020**, 581, 411.
- [5] Wang *et al. Nat. Catal.* **2018**, 1, 756.
- [6] Wang *et al. Nat. Mater.* **2019**, 18, 827.
- [7] Wang *et al. Nat. Mater.* **2016**, 15, 611.
- [8] Wang *et al. J. Am. Chem. Soc.* **2017**, 139, 1675.

8:40 PM *EL03.08.02

Progress in Wide Gap Ionic Oxide Semiconductors Hideo Hosono^{1,2}; ¹Tokyo Institute of Technology, Japan; ²National Institute for Materials Science, Japan

The nature of conduction band minimum is totally different from that of valence band maximum. Thus, the materials design concept different from the conventional covalent type semiconductors are required for these materials. In this talk we review our progress in materials and device application:

Material Design and Example of Transparent Bipolar Semiconductors

Ambipolar wide gap oxide semiconductors were restricted to CuInO₂[1] and SnO₂[2]. We reported ambipolar materials ZrOS based on new design concept[3] and Cu₃N applying non-conventional doping approach[4].

Ultrawide gap amorphous oxide semiconductors and their TFTs

Ionic amorphous oxide semiconductors represented by IGZO is now widely used as the switching TFTs for high performance LCD and large-sized OLED TVs.[5] Here, ultra-wide gap(>3.5eV) amorphous oxide semiconductors[6] such as a-Ga₂O₃ [7] and their TFT characteristics are reported.

Crystal-amorphous nanocomposite semiconductors and their LED application

Nano-sized ZnO embedded in amorphous ZnO-SiO₂ has low work function by ~1eV than bulk ZnO keeping mobility of ~1 cm²/Vs and can form ohmic contacts with a wide range of electrode materials [8]. These features make it possible to boost the performance halide perovskite LEDs [9] and OLEDs[10].

- [1] Yanagi *et al. APL* 121, 15(2001), [2] Nomura *et al. Adv. Mat.* 23, 3431(2011), [3] Arai *et al. JACS* 139, 17175(2017), [4] Matsuzaki *et al. Adv. Mat.* 31, 1801968(2018), [5] Hosono, *Nat. Elect.* 1, 428(2018), [6] Kim *et al. a, NPG Asia Mater.* 9, e359 (2017), [7] Kim *et al. APL Mat.* 7, 022501(2019), [8] Nakamura *et al. Adv. Electr. Mat.* 4, 1700352 (2018), [9] Sim *et al. Appl. Phys. Rev.* 6, 031402(2019), [10] Hosono *et al. PNAS*, 114, 233(2017).

9:05 PM BREAK

9:20 PM *EL03.08.03

Panel Discussion: Why New Semiconductors? Hideo Hosono¹, George Nolas², Shengbai Zhang³ and Andriy Zakutayev⁴; ¹Tokyo Institute of Technology, Japan; ²University of South Florida, United States; ³Rensselaer Polytechnic University, United States; ⁴National Renewable Energy Laboratory, United States

Recent decades have seen exciting explosions of research into new and lesser-studied semiconductors, including such broad categories as complex halides, nitrides, and chalcogenides, and layered and two-dimensional materials. Even so, silicon has further consolidated its position as the leading material for computing, solar energy conversion, and even for some optoelectronics. In light of this friendly but often overmatched competition with silicon, we will ask four of the world's leading researchers what motivates them to continue work on new semiconductor materials.

Panelists will be Hideo Hosono, George Nolas, Shengbai Zhang and Andriy Zakutayev. Moderated by Rafael Jaramillo.

SYMPOSIUM EL04

Ultrawide Bandgap Materials, Devices and Systems
April 18 - April 20, 2021

Symposium Organizers

Masataka Higashiwaki, National Institute of Information & Comm Tech
Robert Kaplar, Sandia National Laboratories
Julien Pernot, University of Grenoble
Hongping Zhao, The Ohio State University

Symposium Support

Silver

Taiyo Nippon Sanso

* Invited Paper

SESSION EL04.01: AlGaN Materials and Devices
Session Chairs: Siddharth Rajan and Hongping Zhao
Sunday Morning, April 18, 2021
EL04

10:30 AM *EL04.01.01

AlN Nanowire pn Heterojunctions—A New Paradigm Towards UV-C LEDs Rémy Vermeersch^{1,2}, Alexandra-Madalina Siladie^{1,2}, Gwénolé Jacopin³, Ana Cros⁴, Nuria Garro⁴, Eric Robin^{1,5}, D. Calliste⁶, Pascal Pochet⁶, Fabrice Donatini³, Julien Pernot³ and Bruno Daudin^{1,2}; ¹Université Grenoble Alpes, France; ²CEA, IRIG-PHELIQS "Nanophysics and Semiconductors" Group, France; ³Institut Néel, Université Grenoble Alpes, CNRS, France; ⁴Universidad de Valencia, Spain; ⁵CEA, INAC-MEM, LEMMA, France; ⁶CEA, INAC-MEM, L-SIM, France

The desired realization of efficient solid state deep UV emission devices is currently limited by the difficulty to achieve efficient p-type doping of AlGa_N layers with high AlN molar fraction, due to the high ionization energy of single Mg impurity. However, if now using AlN nanowires (NWs), it will be shown that Mg/In codoping leads to an increased Mg solubility limit by more than one order of magnitude. Optimal electrical activation of acceptor impurities was achieved by electron irradiation [1]. Next, the formation of AlN NW p-n junction was

assessed by electron beam induced current (EBIC) experiments, putting in evidence the electrical field associated with the junction. Current-voltage characteristics in forward bias conditions have established that the current was varying as V^n , (with n larger than 6) before activation. By contrast, following acceptor activation, a space charge limited current regime was observed. Finally an AlGaIn active region consisting of either a short period AlN/GaN superlattice or of an AlGaIn section was inserted in the pn junction. The structural, electrical and electroluminescent properties of the resulting NW-based UVC LED will be discussed.

[1] A. M. Siladie et al, Nano Lett. 2019, 19, 8357–8364

10:55 AM EL04.01.02

Growth of (Al,Ga)N/GaN Heterostructures at Temperatures Below 600 °C by Metalorganic Vapor Phase Epitaxy Caroline E. Reilly, Nirupam Hatui, Shuji Nakamura, Steven P. DenBaars and Stacia Keller; University of California, Santa Barbara, United States

As the role of the nitrides in electronic applications expands, integrating group-III nitrides with other materials such as silicon based integrated circuits is an attractive route. Although bonding processes exist, the ability to grow III-N materials directly on already processed wafers would greatly widen the design space, an approach which is currently hampered by the high temperatures associated with nitride growth by metalorganic vapor phase epitaxy (MOVPE). For GaN and AlN, typical growth temperatures can exceed 1000 °C – too high to be compatible with many processed wafers or other sensitive substrates. High quality material growth, with low impurity incorporation and good morphology, is then desirable at low growth temperatures for integration with other materials. In this work, the MOVPE growth of (Al,Ga)N layers at temperatures below 600 °C was explored using a flow modulation epitaxy (FME) scheme. The latter was applied in order to compensate for the lower surface mobility of adsorbed species at these very low deposition temperatures.

All experiments were conducted via atmospheric pressure MOVPE on semi-insulating GaN-on-sapphire templates. Low temperature (LT) layers were grown using a FME scheme consisting of pulsing the group III precursor(s), trimethylaluminum (TMAI) and triethylgallium (TEGa), while continuously flowing ammonia. The LT layers were analyzed by Hall measurements, atomic force microscopy (AFM), X-ray diffraction (XRD), secondary ion mass spectrometry (SIMS), and X-ray photoelectron spectroscopy (XPS).

The FME growth scheme used in this study was previously optimized for GaN deposition with TEGa to allow for step flow growth at 550 °C. Upon the addition of TMAI, however, the surface no longer showed steps and instead a layer by layer growth mode was observed via AFM. The transition into a layer by layer growth mode with the addition of TMAI is consistent with the known lower surface mobility of Al adatoms. Despite losing the step flow growth mode, the RMS roughness of the AlGaIn layer was still sub-nanometer at 660 pm in comparison to 405 pm observed for the step-flow grown GaN, sufficiently smooth to be used for further studies. By using the same growth scheme exclusively with TMAI, layers with different thickness were grown varying the number of cycles between 94 and 563. The thinnest layer showed an RMS roughness of 470 pm and the thickest layer 535 pm. Layers with 282, 375, 469, and 563 cycles were additionally analyzed by XRD. The layer peak became sharper and shifted away from the substrate peak as the number of cycles was increased. This was the opposite trend of what may be expected if the shift in the XRD peak was solely due to increasing relaxation of the layer with increasing thickness. From SIMS and XPS data, it was confirmed that this shift was due to unintentional gallium incorporation, which was more pronounced in the thinner samples. Ga incorporation into AlN has been seen for higher temperature AlN growth on GaN following a similar trend to that seen herein.

Electrical characterization of the samples with varying thickness revealed that the two thinnest samples were too resistive to be measured. For all other samples, the sheet resistance decreased with increasing AlN thickness. The highest mobility measured was $400 \text{ cm}^2/(\text{V}\cdot\text{s})$ with a sheet charge of $1.65 \times 10^{13} \text{ cm}^{-2}$ for the sample with 469 cycles. Additionally, a sample with 8 nm LT GaN underneath a LT (Al,Ga)N layer exhibited a mobility of $230 \text{ cm}^2/(\text{V}\cdot\text{s})$ and a sheet charge of $1.60 \times 10^{13} \text{ cm}^{-2}$. More details on the effects of growth temperature, thickness, and composition on the characteristics of the (Al,Ga)N layers will be presented at the conference. This work is partially supported by the Solid State Lighting and Energy Electronics Center and Intel Corporation.

11:10 AM EL04.01.03

Influence of Chemical Potentials on Strain Development in Si-Doped Al_{0.7}Ga_{0.3}N Yan Guan¹, Shun Washiyam¹, Dolar Khachariya¹, Pegah Bagheri¹, Ji Hyun Kim¹, Pramod Reddy², Ramon Collazo¹ and Zlatko Sitar¹; ¹North Carolina State University, United States; ²Adroit Materials Inc., United States

AlGa_{0.3}N-based electronics and optoelectronics require Si doping for n-type conductivity. However, tensile stress is generated in AlGa_{0.3}N layers grown on foreign substrates with increasing Si concentration. High tensile stress could cause wafer bowing and cracking, which are detrimental to the device performance. Though several models have been proposed, the mechanism of the strain development by Si doping is still in debate. We have suggested that tensile stress is generated by dislocation climb. More vacancies and its complexes with Si are formed by the Fermi level shift brought by Si doping. Thus, the tensile stress is expected to be enhanced by lowering defect formation energy. This work reports the influence of chemical potentials on V_{III}-nSi complexes and the resulting strain development in Si-doped Al_{0.7}Ga_{0.3}N.

Si-doped Al_{0.7}Ga_{0.3}N layers were grown on unintentionally doped Al_{0.7}Ga_{0.3}N layers on top of c-plane AlN/sapphire substrates by MOCVD. Trimethylaluminum (TMA), triethylgallium (TEG), ammonia (NH₃), and SiH₄ were used as Al, Ga, N, and Si precursors, respectively. NH₃ flow rate was varied from 0.3 slm to 0.7 slm and 1.5 slm to control chemical potentials. SiH₄ flow rates were changed to control the Si concentration from 1E18 cm⁻³ to 1E19 cm⁻³. TMA and TEG flow rates were adjusted to control the growth rate and composition. Growth temperature and pressure were kept constant at 1100°C and 20 Torr, respectively. X-ray diffraction (XRD) was employed to determine the composition and strain development. Photoluminescence (PL) and Hall measurements were performed to characterize the influence of V_{III}-nSi complexes on electrical and optical properties.

First, the influence of growth rate on strain evolution was characterized. Growth rate was varied by metalorganic flow rates while SiH₄ flow rate, Al composition and NH₃ flow rate were kept constant at 30 sccm ([Si]~1e19 cm⁻³), 70% and 0.7 slm, respectively. Although strain increases linearly with thickness under the same growth condition (i.e., when growth time is varied), net strain was decreased from -0.19 % to -0.44 % (negative strain means compressive strain) as growth rate was increased from 600 nm/h to 900 nm/h for one hour growth. There are two possible reasons for the strain reduction by increasing growth rate: (1) as Si impurities are incorporated into the AlGa_{0.3}N layer in a mass transport limited process, [Si] is decreased at a higher growth rate; (2) metalorganic flow rate was increased to increase growth rate, and growth condition became more III-rich. Both lead to an increase in the formation energy of V_{III}-nSi complexes. Therefore, growth rate needs to be constant to characterize the role of chemical potentials in strain development.

When AlGa_{0.3}N layers were grown at a growth rate of 600±50 nm/h, an increase in strain towards a tensile state was clearly observed. Strain was increased from -0.41 % to -0.19 % and -0.04 % with increasing NH₃ flow rate. As the growth environment becomes more N-rich, the formation energy of V_{III}-related defects decreases, resulting in the increase in the V_{III}-related defect concentration. Under an equivalent growth rate, the Si concentration is constant for samples grown at different NH₃ flow rate. Thus, the observed high tensile strain at high NH₃ flow rate does not originate from the Si substitutional impurities by themselves, eg. formation of SiN_x or lattice expansion. Under N-rich conditions, more V_{III}-related defects are expected to be involved in surface mediated dislocation climb. The increase in the [V_{III}-nSi] was also confirmed from an increase in the V_{III}-nSi peak PL intensity and an abrupt decrease in the carrier concentration by self-compensation. In summary, we demonstrate that tensile stress induced by dislocation climb is governed by vacancy concentration rather than Si concentration, supporting and adding further details to the mechanisms previously discussed for the observation of strain in Si doped III-nitride layers.

11:25 AM EL04.01.04

Late News: Assessment of N-Type and P-Type Doping in (Al,Ga)N Heterostructures by Scanning Probe Microscopy Techniques Albert Minj¹, Ming Zhao¹, Benoit Bakeroot^{1,2}, Lennaert Wouters¹, Kristof Paredis¹, Thomas Hantschel¹ and Stefaan Decoutere¹; ¹imec, Belgium; ²Centre for Microsystems Technology (CMST), imec and Ghent University, Belgium

The current state of dopant assessment for the optimization of the wide band gap (Al,Ga)N-based

heterostructures for high-frequency and high-power applications relies heavily on quantitative chemical analysis techniques such as secondary-ion mass spectrometry. In such heterostructures, the determination of P-type carrier density of the cap layer, control of background concentration and assessment of polarization-induced confined carriers are necessary for the realization of optimal working devices. None of these can be completely inferred from the chemical analysis owing to several material and growth issues including the poor activation of Mg, the presence of O impurities and the amphoteric nature of carbon impurities. Here, as regions of interest in a typical epitaxial stack for GaN electronic devices consist of multiple triangular quantum wells with electron/hole confinement and doped layers, it demands electrical characterization at a nanoscale. In this context, the exploitation of the Schottky behaviour of nano-size metal-semiconductor junction formed between a metallic scanning probe microscopy (SPM) probe and (Al,Ga)N-nitride surface can be promising for carrier assessment by SPM techniques.

The two scanning probe microscopy techniques, scanning capacitance microscopy (SCM) and Conductive-atomic force microscopy (C-AFM), which are today routinely used for the characterization of Si- and Ge-based semiconductor structures with nanometer spatial resolution are investigated for their applicability on (Al,Ga)N heterostructures with energy band gap values larger than 3.4 eV. Our experiments make use of rectifying property of the electrical conduction at the nanoscale in both the modes. In this paper, it will be shown that by combining the two techniques, the nature of free carriers originating from extrinsic n-/p-type dopants and polarization-induced confined carriers, two-dimensional electron gas (2DEG) and hole gas (2DHG), can be revealed across (Al,Ga)N/Silicon heterostructures consisting of n-/p-doped GaN and AlGaN transition layers (TLs) [1]. Here, a simple phase shift of approximately 180° consistently observed between all n-type and p-type regions in SCM phase maps verifies the absolute and correct determination of the type of carriers in accordance with TCAD band simulation. We also found that by fabricating Ti/Al-based low resistance back contacts, the issues related to back-to-back Schottky configuration and surface charging were mitigated and it concurrently allowed C-AFM measurements at low DC biases. Our back-contact methodology also aided the SCM signal enhancement at low magnitudes of AC bias comparable to that used in conventional semiconductors like Si and Ge. A large SCM signal strength for AC bias ≤ 1 V was seen on both extrinsically (Si, Mg) doped regions and on the polarization induced 2D carrier gases near the interface, while no signal was recorded otherwise on undoped regions such as unintentionally doped GaN and AlGaN regions in the transition layers. Because of the rectifying property of the tip-sample junction for both n-type and p-type doped (Al,Ga)N regions, the type of the carriers can also be determined from the C-AFM measurements through selection of the polarity of the DC bias. Thanks to the small tip-sample contact area, the C-AFM technique eventually allowed resolving the 2DHG and 2DEG regions separated by an only 5 nm AlN layer. As the contact area can be further reduced with the use of sharper probe tips [2], this analysis can be extended to even narrower barriers. Our paper illustrates the high potential of the two techniques to study device heterostructures for high power and RF applications and multi-quantum well heterostructures as in optoelectronic devices.

References

- [1] A. Minj, M. Zhao, B. Bakeroot, and K. Paredis, Appl. Phys. Lett. 118, 032104 (2021)
- [2] T. Hantschel, M. Tsigkourakos, L. Zha, T. Nuytten, K. Paredis, B. Majeed, and W. Vandervorst, Microelectron. Eng. 159, 46 (2016)

11:40 AM EL04.01.05

Late News: Hanbury Brown and Twiss Correlations in a SEM—Imaging Carrier Lifetime at the Nanoscale in Ultra Wide Band Gap Materials Sylvain Finot¹, Vincent Grenier², Vitaly Zubialevich³, Catherine Bougerol¹, Pietro Pampili³, Joël Eymery⁴, Peter J. Parbrook³, Christophe Durand² and Gwénolé Jacopin¹; ¹University Grenoble Alpes, CNRS, Grenoble INP, Institut Néel, France; ²University Grenoble Alpes, CEA, IRIG, PHELIQS, NPSC, France; ³Tyndall National Institute, University College Cork, Ireland; ⁴University Grenoble Alpes, CEA, IRIG, MEM, NRS, France

In order to establish the relationship between luminous efficiency and material characteristics, it is essential to precisely measure the relative contribution of radiative and non-radiative recombinations. This is usually

obtained through the measurements of the luminescence decay time as a function of temperature. To do so, the commonly used technique is time-resolved photoluminescence spectroscopy [1]. However, this technique does not allow nanoscale resolution, which is the relevant scale for defect characterizations. In addition, when dealing with ultra-wide bandgap materials, it required expensive pulsed deep UV lasers.

To go beyond these limitations, fast electrons can be used as a highly localized excitation source for luminescence measurements. This technique is called cathodoluminescence (CL) spectroscopy. Recently, picosecond time-resolved CL technique has been developed to reach at the same time high spatial and high temporal resolutions [2,3]. However, it is difficult to obtain a high brightness pulsed electron gun, which leads to reduced spatial resolution, low CL intensity or photocathode aging issues.

In this work, to circumvent these limitations, we took advantage of the specific statistics of electron/hole pair generation by fast electrons. Indeed, in a secondary electron microscope, the interaction of the incident electron with the semiconductor generates almost instantaneously (< 1 ps) a bunch of electron/hole pairs (typically > 300). These electron/hole pairs can then radiatively recombine, according to their carrier lifetime. Hence, by studying the autocorrelation function of the CL intensity ($g_2(\tau)$), a strong bunching is expected at $\tau = 0$ ($g_2(\tau = 0) \gg 1$). More importantly, by fitting $g_2(\tau)$, we access the local carrier lifetime without the need for an expensive pulsed electron gun [4].

Thus, to measure the $g_2(\tau)$ of the CL signal, we built a Hanbury Brown and Twiss (HBT) interferometer to analyze the CL photon statistics. As an illustration, we applied this technique to the study of AlGaIn/GaN core-shell quantum wells on GaN microwires grown by metalorganic vapor phase epitaxy [5]. Due to the lattice mismatch between the GaN core and the AlGaIn shell, there is a formation of cracks. These cracks locally affect the material properties (strain, energy shift, CL intensity change...). Therefore, to quantify the impact of cracks on the luminous efficiency at the nanoscale, we recorded the carrier lifetime in this region. As expected, we observe a reduction of carrier lifetime near the crack, which indicates the creation of dangling bonds and point defects in the crack region. The CL results are then compared with transmission electron microscopy.

References

- [1] T. Langer *et al.*, Appl. Phys. Lett. **103**, 202106 (2013).
- [2] S. Chichibu *et al.*, Jpn. J. Appl. Phys. **59**, 020501 (2019).
- [3] W. Liu *et al.*, Appl. Phys. Lett. **109**, 042101 (2016).
- [4] S. Meuret *et al.*, ACS Photonics **3**, 1157 (2016).
- [5] S. Finot *et al.*, Appl. Phys. Lett. **117**, 221105 (2020).

11:55 AM *EL04.01.06

UV-VIS Photodetectors Using AlGaIn High Electron Mobility Transistors with GaN Nano-Dot Floating Gates Andrew Armstrong¹, Alexandra Brianna Klein¹, Andrew Allerman¹, Albert Baca¹, Mary Crawford¹, Jacob Podkaminer², Carlos Perez¹, Michael Siegal¹, Erica Douglas¹, Vincent Abate¹ and Francois Leonard¹;
¹Sandia National Laboratories, United States; ²Current Address: 3M Corporate Research Laboratory, United States

Visible-blind and solar-blind photodetectors were demonstrated using AlGaIn-channel high electron mobility transistors (HEMTs) with GaN nanodots as an optically-active floating gate. The effect of the photo-induced floating gate voltage was large enough to switch a HEMT from the off-state an on-state with illumination. Responsivity $> 10^8$ A/W was observed at room temperature with the HEMTs biased in the off-state in the dark for low dark current and low dc power dissipation. The absorption threshold was shown to be controlled by the AlN mole fraction of the HEMT channel layer, enabling the same device design to be tuned for either visible-blind or solar-blind detection. The influence of GaN nanodot position in the HEMT on the dynamic range of the photodetector was investigated. The responsivity and temporal response of the detectors as a function of optical intensity was investigated, and a gain-bandwidth product $> 10^9$ Hz was observed. The dependence of device performance on optical intensity was successfully modeled by treating the nanodots as a two-level system with

characteristic rates of carrier capture and recombination.

SESSION EL04.02: Nitrides Materials and Devices
Session Chairs: Bruno Daudin and Robert Kaplar
Sunday Afternoon, April 18, 2021
EL04

1:00 PM EL04.02.01

Late News: A Comprehensive Study of MOVPE Growth on 200 mm GaN-on-SOI for Monolithic Integrated GaN ICs Ming Zhao, Karen Geens, Xiangdong Li, Nooshin Amirifar and Stefaan Decoutere; imec, Belgium

With the mass production of discrete devices based on GaN-on-Si technology is just around the corner, the monolithic integrated GaN ICs (integrated circuits) has become a hot topic in recent years. This is largely attributed to its great potential in increasing the switching speed and efficiency, reducing the form factor and enabling a higher level of design flexibility, etc. We have proposed and experimentally validated the approach of using GaN-on-SOI combined with deep trench isolation as a technology platform to mainly eliminate the “back gating” effect which is associated with GaN-on-Si technology [1]. On the other hand, the MOVPE growth on SOI substrate, as a critical enabling technique, is far less studied compared to GaN-on-Si. In this work, we present a comprehensive study on multiple aspects of the MOVPE growth on 200 mm SOI substrates, including SOI substrate and buffer design. We further demonstrate the growth of HEMT device structures for voltage rating of 200 V, 650V and even beyond.

We found that the epitaxial growth on SOI substrates behaved very differently from the growth on regular Si substrate. The SOI wafer deformed much more strongly upon the lattice mismatch introduced stress. Further in-depth study pointed out that the phenomena is very likely associated with the strain partition effect. We have proven that the Si (111) device layer thickness is a tuning knob to alter the strain partition effect, which is in line with the strain partition theory. In addition, using Si (111) instead of Si (100) handling wafer can also to certain extent mitigate the strong wafer bowing of SOI substrate, which results from the higher stiffness of the Si (111) due to its higher biaxial modulus. Following our superlattice based GaN-on-Si buffer scheme but with dedicated modification, we have obtained a 200 mm GaN-on-SOI buffer platform with low wafer bow (<50 μm) and suitable for 200 V application. The vertical buffer breakdown voltage (voltage at which the leakage current reaches 1 $\mu\text{A}/\text{mm}^2$ at 25 $^\circ\text{C}$ and 10 $\mu\text{A}/\text{mm}^2$ at 150 $^\circ\text{C}$) is ~ 400 V at 25 $^\circ\text{C}$ and >300 V at 150 $^\circ\text{C}$. A high operating voltage of ~ 440 V is extrapolated (corresponding to a lifetime of 10 years at 175 $^\circ\text{C}$) based on time-dependent dielectric breakdown (TDDB) measurements. The buffer also shows a low buffer dispersion of < 10% at up to 150 $^\circ\text{C}$ using the “back-gating” method. This buffer platform has enabled the fabrication of E-mod p-GaN HEMT devices and the further demonstration of a functional 48V-to-1V buck converter with monolithic integrated half bridge and on chip drivers. However, it became extremely challenging to extend this buffer platform to a higher voltage, i.e. 650 V and beyond, by thickness scaling even using Si (111) handling wafer in the SOI substrate. It is very difficult to control the high in situ wafer deformation and to limit the post growth wafer bow <50 μm . We therefore proposed a novel buffer scheme by taking advantage unique properties of superlattice structure and the strain partition effect of SOI substrate. This buffer scheme consists of multiple superlattice blocks of different average Al% which allows to introduce alternatively the compressive and tensile stress along the buffer growth. Based on this buffer scheme we demonstrated a 4.8 μm buffer for 650 V application and a 6 μm buffer for a even higher voltage rating.

[1] X. Li et al., Proc IEEE Int. Electr. Dev. Meeting, San Francisco, CA, USA, 2019, pp. 4.4.1-4.4.4. and references therein.

1:15 PM EL04.02.02

Characterization of III-Nitride Epitaxial Layers by Scanning Spreading Resistance Microscopy Sizhen Wang, Jinho Kang, Bingjun Li and Jung Han; Yale University, United States

Scanning spreading resistance microscopy (SSRM) is an AFM-based technique, it detects the resistance of current spreading layer just below the tip-semiconductor contact region. This innovative nanoscale characterization techniques find its wide application in 2D carrier mapping in semiconductor material and device characterization because of its high resolution and ease of quantification. Although SSRM has been used to study GaN carrier concentration, AlGa_xN-GaN heterostructure, AlN-GaN quantum well, and related defects in III-nitride, there is still lack of research on dopant calibration and quantification on GaN materials. Here we presented a systematic research on GaN dopant calibration under variable tip stress condition using SSRM and apply this technology to characterize the detail structure of distributed Bragg reflector (DBR) of vertical cavity surface emitting laser (VCSEL).

First, n-GaN sample with staircase doping of Si, Ge was used to calibrate with variable tip force (range from 0.32 μN to 6.40 μN). Although the measured resistance $\log(R)$ decreased with increased tip force, the $\log(R)$ decreased monotonically as the dopant concentration (Si, Ge) increased, almost four order of magnitude doping range ($\sim 4 \times 10^{16} \text{cm}^{-3}$ for UID to $1 \times 10^{20} \text{cm}^{-3}$) can be distinguished for n-GaN thin film. And linear fitting curve was extracted to estimate the carrier concentration in heavy doping region. Then, the SSRM technology was used to reveal the fine DBR structure which consist of 25 pairs of Si-doped (43nm, $5 \times 10^{18} \text{cm}^{-3}$) and Ge-doped GaN (55nm, $9 \times 10^{19} \text{cm}^{-3}$), and the best contrast of 2D SSRM image of DBR structures was obtained with -0.1 V DC bias voltage and 2.56 μN tip force. Finally, the SSRM was applied to investigate the in-plane inhomogeneous incorporation of Ge dopants into GaN which was grown on Sapphire. 2D SSRM mapping results showed that as the Ge doping concentration was more than $3.0 \times 10^{19} \text{cm}^{-3}$, Ge incorporation become inhomogeneous. It was estimated that the light doping zones had only $8.90 \times 10^{18} / \text{cm}^3$ Ge dopant for sample with $6.0 \times 10^{19} / \text{cm}^3$ intentional Ge doping, while for sample with $1.4 \times 10^{20} / \text{cm}^3$ intentional Ge doping, the light doping zone was estimated only doped with $1.06 \times 10^{19} / \text{cm}^3$ Ge dopants. Using the ratio of nominal doping concentration to the minimum doping concentration as an indicator, its value changed from 6.69 to 13.23 as Ge doping of GaN epitaxial layer increased from $6.0 \times 10^{19} / \text{cm}^3$ to $1.4 \times 10^{20} / \text{cm}^3$. The inhomogeneous doping became worse with heavy Ge doping. And this issue might be related to anisotropic dopant incorporation efficiency at different facets which were exposed during GaN epitaxial growth.

1:30 PM EL04.02.03

Structural and Piezoelectric Properties of Sc_xAl_{1-x}N-GaN Heterostructures Grown by Molecular Beam Epitaxy Joseph Casamento, Celesta S. Chang, Yu-Tsun Shao, John Wright, David A. Muller, Huili (. Xing and Debdeep Jena; Cornell University, United States

Alloying with Scandium (Sc) into the III-nitride platform of InN, GaN, and AlN has gained tremendous interest in recent years, from fundamental research to transformative changes in technological applications. This is because isoelectronic alloying with Sc has been demonstrated to increase the piezoelectric response and induce ferroelectric behavior in Sc_xAl_{1-x}N alloys. ^[1,2] However, most studies of the fundamental properties Sc_xAl_{1-x}N have been focused on sputter deposited materials, where challenges such as sub-optimal crystallinity, microstructural instabilities, and chemical inhomogeneities have been encountered. Molecular beam epitaxy (MBE) aims to enable solutions to these issues via epitaxial deposition on single crystalline substrates in an ultra-high vacuum environment and thereby better elucidate the fundamental properties of Sc_xAl_{1-x}N.

In this work, ^[3] we report on the epitaxial growth studies of Sc_xAl_{1-x}N of various Sc compositions ($x = 0.18$ to 0.40) grown by MBE on n⁺ bulk GaN substrates and their corresponding structural and piezoelectric properties. Aluminum (Al) was supplied with a conventional Knudsen effusion cell and Sc was supplied via electron beam evaporation in a tungsten (W) crucible. Growth temperature was maintained at 600C, measured by a thermocouple. In-situ reflection high energy electron diffraction (RHEED) was used to assess the epitaxial nature of the films.

Phase purity and epitaxial relationship was further assessed using X-ray Diffraction (XRD). Films with a surface roughness of less than 1 nm were confirmed by atomic force microscopy (AFM). Out-of plane piezoelectric coefficients ($d_{33,eff}$) were analyzed with piezoresponse force microscopy (PFM) using a conductive AFM cantilever. High-angle annular dark field scanning transmission electron microscopy (HAADF-STEM) was utilized to study atomic level defects and to confirm the metal polar orientation of $Sc_xAl_{1-x}N$ grown on metal polar GaN.

Post-growth XRD measurements show a wurtzite 002 diffraction peak for the $Sc_xAl_{1-x}N$ layers at all Sc compositions studied ($x = 0.18$ to 0.40). XRD full-width-half maximum (FWHM) values ranged from 0.09 to 0.13 degrees (324-468 arcseconds) for $x = 0.18$ to $x = 0.33$, indicating superior crystalline quality. RHEED images suggested pure wurtzite phase $Sc_xAl_{1-x}N$ but decreasing crystallinity due to primary azimuthal streak broadening as Sc content increased. PFM results showed an increase in piezoelectric coefficient for $Sc_xAl_{1-x}N$ ($x=0.18$, 15 pm/V) relative to AlN (6 pm/V) and a decrease thereafter as Sc concentrations increased. Insight to this counterintuitive trend was given via HAADF-STEM, which showed the presence of zinc-blende inclusions bound by partial dislocations in the $Sc_xAl_{1-x}N$ ($x=0.40$) film. This contrasts with the RHEED images suggesting single-phase wurtzite crystals. The zinc-blende crystal structure is not thermodynamically stable and may arise from kinetic factors during the deposition process. The presence of zinc-blende inclusions likely hinders piezoelectric performance and is deleterious to potential ferroelectric behavior as zinc-blende point group prohibits ferroelectricity via symmetry arguments. This work gives insight into the fundamental behavior of epitaxial $Sc_xAl_{1-x}N$ and should provide guidance toward future optoelectronic applications based on these heterostructures. Future work will involve growth optimization and continued structural and electrical characterization to enhance piezoelectric performance and include ferroelectric behavior these epitaxial heterostructures.

[1] Akiyama, M et al. *Adv. Mater.* **21**, 593 (2009).

[2] Fichtner, S et al. *J. Appl. Phys.* **125**, 114103 (2019).

[3] Casamento, J et al. *Appl. Phys. Lett.* **117**, 112101 (2020).

1:45 PM EL04.02.04

Dielectric Properties, Electronic Transitions and Infrared Active Optical Phonon Modes of Molecular Beam Epitaxy $Sc_xAl_{1-x}N$ Determined by Spectroscopic Ellipsometry [Alyssa L. Mock](#)¹, Alan Jacobs², Eric Jin¹, Matthew Hardy² and Marko J. Tadjer²; ¹NRC Research Associateship Programs, United States; ²U.S. Naval Research Laboratory, United States

Significant interest has grown recently in alloying ultra-wide bandgap AlN with ScN in order to obtain unique and tunable properties. Such alloys could have impactful applications in high electron mobility transistor structures potentially enabling more efficient, compact, and powerful amplifiers critical to global communications infrastructure. Other possible applications include high frequency and broadband acoustoelectric filters and resonators. Further, the ferroelectric behavior of ScAlN with high scandium content has begun to garner notable attention of late with potential in sensor applications.

In our work, we employ spectroscopic ellipsometry to investigate (0001) wurtzite $Sc_xAl_{1-x}N$ ($0.00 \leq x \leq 0.20$) thin films grown by molecular beam epitaxy on c-plane sapphire substrates. We present the dielectric function obtained in the spectral region from 4-6.4 eV and report on the thicknesses and extracted critical point parameters from our best match model analysis. We find that the critical points associated with electronic transitions shift to lower energy as a function of increasing ScN alloy fraction. This is particularly interesting for tunability of band offsets between ScAlN and GaN in heterostructures, for example, critical for the development of next generation RF devices as the conduction band offset impacts the confinement and electron density in the two-dimensional electron gas that forms the channel of the device.

We also present the infrared dielectric functions and dielectric loss functions in the spectral region from 400-1200 cm^{-1} . From these we obtain infrared active phonon mode properties, which are fundamental material properties important for future device design. We find that all phonons shift to lower wavenumber as a function of scandium incorporation and we also see evidence of a decrease in crystal quality which is confirmed by x-ray diffraction measurements. Further, we report the high frequency and static dielectric constants as well as their

evolution with scandium content. We calculate the Born effective charge for each composition and find an increase with scandium content. Thus, we attribute the softening of the phonon modes with increasing scandium content to an increase in the effective metal ion mass and a corresponding increase of the dynamic effective charge. This work elucidates fundamental properties of MBE grown ScAlN thin films and contributes to improved understanding of Sc-based alloys currently under development for electronic and optoelectronic devices.

2:00 PM EL04.02.05

Growth of High Quality MOCVD Aluminum Nitride Using N₂ as Carrier Gas Samiul Hasan, Abdullah Mamun, Kamal Hussain, Dhruvinkumar Patel, Mikhail Gaevski, Iftikhar Ahmad and Asif Khan; University of South Carolina, United States

High quality, low dislocation density, AlN is required for high efficiency, high power, and long lifetime of the III-nitride based electronic and photonic devices. Several techniques have been reported to improve the quality of AlN, including substrate patterning, pulsed lateral overgrowth, high-temperature annealing, and modulation of temperature and precursors. All these growth processes have been done using ultra high purity H₂ as a carrier gas. The impact of carrier gases on the growth of AlN has rarely been studied. The rationale to study N₂ as a carrier gas for AlN growth in this research is to explore another carrier gas than H₂, which is safer and economical. Previously, the use of N₂ as a carrier gas resulted in inferior quality AlN layers. Here, we report the growth of high-quality AlN using N₂ as carrier gas on a basal plane sapphire substrate using metal-organic chemical vapor deposition (MOCVD). A series of samples with N₂ as carrier gas were grown with thickness varying from 1 μm to 4 μm by employing a two-step growth process. The process includes the formation of a thin buffer layer grown at 950° C with a high V/III ratio and a thick high-temperature growth at 1180° C with a low V/III ratio without introducing any intralayer. AlN samples were characterized using scanning electron microscopy (SEM), atomic force microscopy (AFM), high-resolution x-ray diffraction (HR-XRD), and Raman spectroscopy. SEM images show the formation of air pockets in the AlN layers, which acts as strain relief centers, reducing the dislocation densities. The XRD analysis of these samples shows the full width at half maxima of 289 arcsec of the omega scan for (10-12) plane and total dislocation density of 1.1x10⁹ cm⁻² for 4 μm sample, which are the best-reported values for AlN on a sapphire substrate using N₂ as the carrier gas. Raman study of a 4 μm AlN sample shows low compressive stress of 0.59 GPa. A systematic study of the evolution of the quality of AlN with thickness will be presented.

2:15 PM EL04.02.08

Late News: Polarization-Induced 2D Hole Gases in Undoped InGaN/AlN Heterostructures Grown on Single-Crystal AlN Substrates Jimmy J. Encomendero Risco¹, Zexuan Zhang¹, Reet Chaudhuri¹, Masato Toita², Debdeep Jena¹ and Huili Xing¹; ¹Cornell University, United States; ²Asahi Kasei Corporation, Japan

We report, for the first time, the epitaxial growth, structural characterization, and transport properties of polarization-induced 2D hole gases (2DHGs) homoepitaxially grown on high-quality single-crystal AlN substrates. By harnessing the polarization discontinuity at the InGaN/AlN heterointerface, a high density of free holes ($p > 5 \times 10^{13} \text{ cm}^{-2}$) is induced within AlN crystals without the need of acceptor impurities. This important feature, combined with the high structural quality of the homoepitaxial growth, results in the highest hole mobilities experimentally measured in bulk AlN substrates. The polarization origin of the 2D holes is experimentally confirmed by systematically increasing the Indium composition of the top InGaN layer, thereby inducing a higher density of free carriers at the InGaN/AlN heterojunction. Hole concentrations between $p = 5.2 \times 10^{13} \text{ cm}^{-2}$ and $p = 1.1 \times 10^{14} \text{ cm}^{-2}$ are measured at room temperature, as the indium composition is varied between 0% and 6%, showing a positive correlation with indium incorporation. X-ray diffraction reveals that over this composition range, the InGaN layers are coherently strained to the AlN lattice. Furthermore, the presence of strong interference fringes in the diffraction pattern and clear InGaN atomic steps indicates the presence of atomically smooth hetero-interfaces. Cryogenic Hall effect measurements show that hole concentrations are almost independent of temperature, ranging between $p = 2.5 \times 10^{13} \text{ cm}^{-2}$ and $p = 5.2 \times 10^{13} \text{ cm}^{-2}$ for indium compositions of 0% and 6%, respectively. These high hole densities, inaccessible by traditional

impurity doping at 77 K, attest to the electrostatic origin of the 2D holes. Our results constitute a pivotal step towards the manufacture of nitride-based p-type field effect transistors (FETs) that can take the advantage of the high thermal conductivity and high breakdown electric fields of single-crystal AlN substrates. As an added benefit, the simultaneous demonstration of complementary 2D electron gases (2DEGs) and 2DHGs in undoped heterostructures grown on single-crystal AlN substrates, enables an unmatched level of integration for high-power and high-frequency nitride-based electronics, raising hopes for all-nitride CMOS technology.

SESSION EL04.03: Other UWBG Semiconductors
Session Chairs: Robert Kaplar and Hongping Zhao
Sunday Afternoon, April 18, 2021
EL04

4:00 PM *EL04.03.01

Prospects of LiGaO₂ and NaGaO₂ as Ultrawide Band Gap Semiconductors Walter R. Lambrecht¹, Adisak Boonchun², Klichchukon Dabsamut², Dmitry Skachkov³, Santosh K. Radha¹ and Amol Ratnaparkhe¹; ¹Case Western Reserve University, United States; ²Kasetsart University, Thailand; ³University of Florida, United States

Inspired by the recent interest in β -Ga₂O₃ as ultra-wide-band-gap material, because of its combination of n-type dopability with a gap of about 4.9 eV, we propose two new even higher band gap materials and investigate their prospects for doping and transparent conducting applications in the ultraviolet range. We present a study of the phase stability, band structures, optical absorption and defect properties. LiGaO₂ is a material with a wurtzite derived orthorhombic structure with space group Pna2₁ at ambient conditions. It consists of an ordered arrangement of the Li and Ga cations on the wurtzite lattice and can be viewed as a I-III-VI₂ ternary derived from the binary II-VI compound ZnO. It has been considered in the past as ceramic material with piezo-electric properties and can be grown in bulk form by the Czochralsky method. Here we present quasiparticle self-consistent GW band structure calculations, showing that it has a direct gap of 5.6 eV (in agreement with experiment) when taking into account an estimated zero-point-motion correction of -0.2 eV. Furthermore, we find that transitions from the bottom of the conduction band to higher bands can only occur above 3.9 eV. The valence band maximum is split by crystal field splitting in three levels which leads to a polarization dependent absorption onset. The valence and conduction band effective mass tensors are determined. Defect calculations using the HSE hybrid functional show that the lowest energy of formation defect is the Ga_{Li} antisite, which is found to be a deep (negative U type) donor with a 2+/0 transition at 0.7 eV below the conduction band minimum. It is compensated by V_{Li}¹⁻ or Li_{Ga}²⁻ depending on chemical potential conditions. These defects pin the Fermi level deep in the gap leading to insulating behavior in intrinsic LiGaO₂. However, Si and Ge dopants are shallow donors and have low energy of formation. Thus n-type doping should be feasible. Sn leads to a somewhat deeper donor. Prospects for p-type doping are less promising: N_O is a deep trap with amphoteric character and Zn doping leads to self-compensation between Zn_{Ga} and Zn_{Li}. Ga vacancies are found to have high energy of formation but can be created by high-energy particle irradiation, while Li vacancies are expected to occur in as grown material. Their EPR signals have been reported and we find excellent agreement between our calculated g-tensors and hyperfine splitting with the experiment. Finally, to avoid potential problems with Li diffusion, we also study NaGaO₂ and find it to have a gap of 5.5 eV and to also be stable in the Pna2₁ structure. Both NaGaO₂ and LiGaO₂ can undergo a phase transition under pressure of about 8-14 GPa to an octahedrally coordinated phase. Among those phases, we find the R-3m phase to have lower energy than a rocksalt type phase. Even in this R-3m phase, the gap is above 5 eV but it becomes slightly indirect.

4:25 PM EL04.03.02

Electron and Hole Mobility of Rutile GeO₂ from First Principles—An Ultrawide-Band-Gap Semiconductor for Power Electronics Kyle Bushick, Kelsey Mengle, Sieun Chae and Emmanouil Kioupakis;

Rutile germanium dioxide (r-GeO₂) is an ultrawide-band-gap semiconductor with potential applications in high-power electronic devices or transparent conductors. In these devices, understanding the carrier dynamics is paramount to evaluate the possible performance of a new material. In this work we use first-principles calculations based on density functional and density functional perturbation theory to investigate carrier-phonon coupling in r-GeO₂ and predict its phonon-limited electron and hole mobilities as a function of temperature and crystallographic orientation. Our findings show that r-GeO₂ has relatively high carrier mobilities, and in particular high hole mobility compared to other UWBG materials. We find the room temperature mobilities are $\mu_{elec,\perp c} = 244 \text{ cm}^2 \text{ V}^{-1} \text{ s}^{-1}$, $\mu_{elec,\parallel c} = 377 \text{ cm}^2 \text{ V}^{-1} \text{ s}^{-1}$, $\mu_{hole,\perp c} = 27 \text{ cm}^2 \text{ V}^{-1} \text{ s}^{-1}$, and $\mu_{hole,\parallel c} = 29 \text{ cm}^2 \text{ V}^{-1} \text{ s}^{-1}$, with carrier scattering dominated by low-frequency polar-optical phonons. While the electron mobility compares readily with other UWBG materials such as β -Ga₂O₃, the hole mobility is notably high. This finding is complimented by other recent work that reports r-GeO₂ can be ambipolarly doped, enabling access to both n- and p-type devices. Paired with a wide band gap around 4.68 eV, the high carrier mobilities lead to a predicted Baliga figure of merit that surpasses an array of more established semiconductors, including Si, SiC, GaN, and β -Ga₂O₃. Through this work, we show that r-GeO₂ is a promising UWBG semiconductor with desirable properties for both n- and p-type high-power electronic devices.

4:40 PM EL04.03.03

Extremely Sharp Free Exciton Emission in Heteroepitaxial Cuprous Iodide Thin Films Grown by MBE Masao Nakamura¹, Sotato Inagaki², Yoshihiro Okamura², Makiko Ogino², Youtarou Takahashi^{2,1}, Licong Peng¹, Xiuzhen Yu¹, Yoshinori Tokura^{1,2} and Masashi Kawasaki^{2,1}; ¹RIKEN, Japan; ²The University of Tokyo, Japan

Triggered by the successful development of perovskite solar cells, halide semiconductors have gained extensive attention in the last few years. Cuprous iodide (CuI) is a representative wide-bandgap halide semiconductor with superior optical and electronic properties, such as direct bandgap and large exciton binding energy as well as high hole-mobility. In particular, the exciton binding energy and oscillator strength in CuI are comparable with or even surpassing those in well-known wide-bandgap semiconductors like GaN and ZnO. These prominent excitonic properties are of great advantage for future quantum optoelectronic applications, including ultraviolet lasers and quantum simulators utilizing the Bose-Einstein condensate of exciton-polariton. However, the studies towards such device applications have been of little progress in CuI due to the lack of high-quality thin films so far.

Recently, we have succeeded in a dramatic improvement in the quality of CuI thin films. Thin films were grown by the molecular beam epitaxy (MBE), which had been rarely employed for the fabrication of halide films but has a successful history in the growth of high-quality compound semiconductor films. As a substrate, we adopted InAs that is almost perfectly lattice-matched with CuI. The fabricated CuI film has a genuine single-crystalline structure with excellent lattice coherence and atomically-flat surface. The low-temperature photoluminescence spectra exhibit extremely-sharp luminescence peak assigned to the free-exciton emission, which has never been observed even in bulk single crystals. These results indicate that the optical quality of CuI film has reached to the level of much more extensively studied wide bandgap semiconductors.

The successful growth of the high-quality CuI film will facilitate the optoelectronic device applications of CuI. Moreover, the present result will open a new research direction to explore novel functionalities at the atomically-sharp heterointerface of halides.

4:55 PM EL04.03.04

Rutile GeO₂—An Ultra-Wide-Band-Gap Semiconductor for Power Electronics Sieun Chae¹, Kelsey Mengle¹, Kyle Bushick¹, Hanjong Paik², Nguyen Vu¹, John Heron¹ and Emmanouil Kioupakis¹; ¹University of Michigan, United States; ²Cornell University, United States

Ultra-wide-band-gap (UWBG) semiconductors have tantalizing advantages for power electronics as their wider band gaps enable higher breakdown voltages. A handful of materials such as AlN/AlGaN, β -Ga₂O₃, and

diamond have been developed for UWBG semiconducting devices, however, they are still facing numerous challenges, such as doping asymmetry and/or inefficient thermal conduction. In our work, we have identified rutile GeO₂ (r-GeO₂) to be a promising, yet unexplored UWBG (4.68 eV) semiconductor. Our first-principles calculations predict shallow ionization energies for donors such as Sb, As, and F, a phonon-limited electron mobility of 289 cm² V⁻¹s⁻¹, and a breakdown electric field of 7.0 MV cm⁻¹, which lead to a higher Baliga figure of merit than β-Ga₂O₃. r-GeO₂ also has superior thermal conductivity (51 W m⁻¹ K⁻¹ (experiment)) and p-type doping property (the calculated ionization energy for Al acceptors is 0.45 eV and the calculated phonon-limited hole mobility is 28 cm² V⁻¹s⁻¹). Though the thin-film synthesis of r-GeO₂ has remained challenging due to its highly metastable amorphous phase, we demonstrate the first synthesis of single crystalline epitaxial thin films of r-GeO₂ on a sapphire substrate using ozone-assisted molecular beam epitaxy. Also, Sb-doping of r-GeO₂ was achieved for r-GeO₂ single crystal nanorods. Our work motivates further exploration of r-GeO₂ as an alternative UWBG semiconductor that can overcome the limitations of the current state-of-the-art UWBG materials.

5:10 PM EL04.03.05

Late News: Thermal Imaging of Ultrawide Bandgap Devices Using MoS₂ Thermoreflectance

Enhancement Coatings Riley C. Hanus¹, Samuel Graham¹ and Asif Khan²; ¹Georgia Institute of Technology, United States; ²University of South Carolina, United States

Measuring the maximum operating temperature within the channel of ultrawide bandgap transistors is critically important, since thermal management often sets operational limits such as maximum power and lifetime. Thermoreflectance imaging is an optimal choice due to sub-micron spatial resolution, sub-microsecond transient characterization, and rapid data acquisition. Unfortunately, commercially available light sources are limited to energies less than ~3.9 eV and are therefore transparent to ultrawide bandgap materials. Here, we utilize an MoS₂ coating as a thermoreflectance enhancement coating which allows for the measurement of the surface temperature of (ultra)wide bandgap materials. This coating is a polycrystalline thin film with the c-axis preferentially aligned normal to the surface and is easily removable via sonication. The method is validated using electrical and thermal characterization of GaN and AlGaN devices. We demonstrate that this coating does not significantly influence the electrical and thermal behavior of the devices tested. A maximum temperature rise of 49 K at 0.59 W was measured within the channel of the AlGaN device, which is over double the maximum temperature rise obtained by measuring the thermoreflectance of the gate metal, demonstrating this method's value.

5:25 PM *EL04.03.06

Deep UV Optical Properties of High-Mg-Content Rocksalt-Structured MgZnO Takeyoshi Onuma¹, Kanta Kudo¹, Kyohei Ishii², Mizuki Ono¹, Yuichi Ota³, Kentaro Kaneko^{2,2,2}, Tomohiro Yamaguchi¹, Shizuo Fujita^{2,2} and Tohru Honda¹; ¹Kogakuin University, Japan; ²Kyoto University, Japan; ³Tokyo Metropolitan Industrial Technology Research Institute, Japan

Deep and vacuum UV light emitters have a variety of applications, such as in ozone cleaners, UV sterilization, medical care, and photolithography. Recently, the alternative use of 222-nm-DUV-light instead of conventionally-used 254-nm-DUV-light is proposed to sterilize human skin with suppressing DNA lesions based on the UV effects on the epidermis of hairless albino. [1] Indeed, action spectra for producing DNA lesions exhibit a peak at around 260 nm and subsequent increase in a wavelength range shorter than 220 nm and VUV region. [2] Enhancement of light absorption by a protein in the human epidermis in a shorter DUV and VUV regions enables selective inactivation of virus in an atmosphere. An effective wavelength range of 190 nm to 220 nm can be proposed by a tradeoff between the action spectra and the air absorption. However, most of commercially available DUV and VUV light sources are discharge-type lamps or lasers. Therefore, demands are increasing for developing solid-state DUV and VUV emitters since their cost, environmental impact, energy consumption are expected to be drastically reduced compared to the discharge-type light sources. AlGaN alloys are the most promising materials for DUV light emitters. [3,4] However, their shortest emission wavelength is limited to be around 210 nm for AlN. [5] In this study, we are focusing on high-Mg-content rocksalt-structured (RS) MgZnO alloys as alternative candidate materials for DUV and VUV emitters by virtue

of their wide variation of bandgap energy E_g from 4.5 eV for RS-ZnO to 7.8 eV for RS-MgO. Recently, successful growths of atomically-flat single crystalline RS-Mg_xZn_{1-x}O films on (001) MgO substrates by the mist chemical vapor deposition (mist CVD) method [6,7] and observation of DUV emission [6-8] were demonstrated. Further improvements in its crystalline quality [9] has resulted in the predominate observation of cathodoluminescence (CL) peak at around 199-217 nm for $x=0.92-0.95$. [9,10] Excitation-current-density dependent CL spectra were measured, and analyses based on a rate equation model confirmed that the DUV luminescence band is attributed to the near-band-edge emission. [10] Electronic structure calculations suggested predominate contribution of Γ - Γ direct transition for the RS-Mg_xZn_{1-x}O alloys with $x>0.5$. However, it is found that relatively broad tail-states expand toward deep UV spectral region. Consequently, CL peak energies show large Stokes-like shift of 0.7-0.8 eV. The E_g fluctuations and resultant exciton localization are possible origins of the large Stokes-like shift. Equivalent internal quantum efficiency is defined as spectrally integrated CL intensity at 300 K divided by that at 6 K. Relatively high values of 2-4% were obtained for the DUV NBE emission. The efficiencies were improved by employing the Mg_xZn_{1-x}O/MgO multi-layered structures. [11] This work was supported in part by Grants-in-Aid for Scientific Research Nos. 17H01263 and 20H00246 from MEXT, Japan.

[1] N. Yamano *et al.*, Photochem. Photobiol. **96**, 853 (2020). [2] T. Matsunaga *et al.*, Photochem. Photobiol. **54**, 403 (1991). [3] H. Hirayama, J. Appl. Phys. **97**, 091101 (2005). [4] M. Kneissl and J. Rass, III-Nitride Ultraviolet Emitters (Springer International Publishing, Cham, 2016). [5] Y. Taniyasu, M. Kasu, and T. Makimoto, Nature **441**, 325 (2006). [6] K. Kaneko *et al.*, Appl. Phys. Express **9**, 111102 (2016). [7] K. Kaneko *et al.*, J. Electron. Mater. **47**, 8 (2018). [8] T. Onuma *et al.*, Appl. Phys. Lett. **113**, 061903 (2018). [9] K. Ishii *et al.*, Appl. Phys. Express **12**, 052011 (2019). [10] M. Ono *et al.*, J. Appl. Phys. **125**, 225108 (2019). [11] K. Kudo *et al.*, in Compound Semiconductor Week 2019, Nara, May 20 (2019), MoE3-5.

SESSION EL04.04: Keynote Session: UWBG
Session Chairs: Masataka Higashiwaki and Hongping Zhao
Sunday Afternoon, April 18, 2021
EL04

6:30 PM *EL04.04.01

Materials and Device Engineering for AlGa_N and β -Ga₂O₃ UWBG Electronic Devices Nidhin K.

Kalarickal¹, Towhidur Razzak¹, Hao Xue¹, Zhanbo Xia¹, Chandan Joishi¹, Hongping Zhao^{1,1}, Asif Khan², Wu Lu¹ and Siddharth Rajan^{1,1}; ¹The Ohio State University, United States; ²University of South Carolina, United States

This presentation will review recent and ongoing work on ultra-wide band gap (UWBG) semiconductor electronic devices based on AlGa_N and β -Ga₂O₃. The high breakdown field strength of UWBG semiconductors such as AlGa_N and Gallium Oxide have opened exciting opportunities for achieving improved performance over well-established materials such as Si, GaN, and SiC. While these materials have several unique properties, they also share common challenges, such as relatively low mobility (compared to conventional Si and GaN), and the need for managing extreme electric fields

The first part of the presentation will discuss the development of AlGa_N-based transistors for RF and mm-wave applications. Device simulations show that despite the relatively low electron mobility, the high breakdown field in AlGa_N could enable performance enhancement for high frequency transistors. We will then discuss key recent developments in AlGa_N transistors that have enabled significant improvement in device performance. The use of electron affinity grading [1] and advanced epitaxial designs has enabled UWBG AlGa_N transistors with cutoff frequency over 40 GHz [2], and current density over 900 mA/mm. Introduction of high-permittivity materials in lateral device structures prevents premature gate breakdown, while improving field uniformity in transistor gate-drain regions [3]. We will discuss the application of this idea in BaTiO₃/AlGa_N lateral diodes,

where we achieved a breakdown field of 8.5 MV/cm [4] (breakdown voltage of 160 V), which represents the highest field achieved in a lateral device.

In the second part of the presentation, we will discuss recent work toward development of high-performance β -Ga₂O₃ lateral and vertical devices. We will discuss the growth of β -Ga₂O₃ and related alloys, and our investigation of fundamental electronic properties in these structures. The use of delta doping enables several key lateral electronic device structures. We will first give an outline of the relatively new mechanisms involved in Si delta doping using molecular beam epitaxy [5], and then discuss our work on growth of $(\text{Al,Ga})_2\text{O}_3/\beta\text{-Ga}_2\text{O}_3$ modulation-doped structures, including recent investigation into high sheet charge density modulation-doped structures [6]. We will then outline details of recent device demonstrations, including investigation of advanced passivation methods to reduce current collapse [7], scaled delta-doped transistors with cutoff frequency of 27 GHz [8], and modulation-doped field effect transistors state-of-art power switching figure of merit of 586 MW/cm².

The authors acknowledge funding from the Air Force Office of Scientific Research (AFOSR Grant No. FA9550-17-1-0227, Program Manager Dr. Kenneth Goretta) the DARPA DREaM program (No. ONR N00014-18-1-2033, Program Manager Dr. Young-Kai Chen, monitored by the Office of Naval Research, Program Manager Dr. Paul Maki), Air Force Office of Scientific Research under Award No. FA9550-18-1-0479 (GAME MURI, Program Manager Dr. Ali Sayir), NSF ECCS-1809682, and the Department of Energy / National Nuclear Security Administration under Award Number(s) DE-NA0003921.

- [1] Razzak, Towhidur, et al. *Applied Physics Letters* 115.4 (2019): 043502.
- [2] Xue, Hao, et al., *Applied Physics Express* 12.6 (2019): 066502.
- [3] Xia, Zhanbo, et al., *IEEE Transactions on Electron Devices* 66.2 (2019): 896-900
- [4] Razzak, Towhidur, et al., *Applied Physics Letters* 116.2 (2020): 023507
- [5] Kalarickal, Nidhin Kurian, et al., *Applied Physics Letters* 115.15 (2019): 152106
- [6] Kalarickal, Nidhin Kurian, et al., *Journal of Applied Physics* 127.21 (2020): 215706
- [7] Joishi, Chandan, et al., *IEEE Transactions on Electron Devices* (2020)
- [8] Xia, Zhanbo, et al., *IEEE Electron Device Letters* 40.7 (2019): 1052-1055.

6:54 PM *EL04.04.02

Current Status of Deep Level Defects in β -Ga₂O₃ Steven A. Ringel¹, Hemant Jagannath Ghadi¹, Joseph McGlone¹, Rachel Adams¹, Aaron R. Arehart¹, Zixuan Feng¹, A F M Anhar Uddin Bhuiyan¹, Yuxuan Zhang¹, Hongping Zhao¹, Zhanbo Xia¹, Nidhin K. Kalarickal¹, Siddharth Rajan¹, Alexander Senckowski² and Man Hoi Wong²; ¹The Ohio State University, United States; ²University of Massachusetts Amherst, United States

Beta phase gallium oxide (β -Ga₂O₃) is a strong contender as the basis for next generation high power and RF devices, and there has been significant progress and interest in developing this material system. Investigating the presence and properties of crystalline defects and their manifestation as bandgap states within the ~ 4.8 eV β -Ga₂O₃ bandgap has been paramount to improve material quality. With β -Ga₂O₃ rapidly advancing as a forward-looking semiconductor device technology, the exploration of deep level defect states has been extensive and is now broadening beyond initial baseline studies that continue to guide optimization of crystal growth and material quality. These directions include the characterization of the influence of high energy particle radiation, which represents envisioned applications of β -Ga₂O₃ devices used in harsh environments, direct investigations of deep level defect impacts on β -Ga₂O₃ transistor characteristics, and the characterization of intentional defect engineering such as using compensating deep acceptors for achieving semi-insulating layers that are needed in some device applications.

This presentation will first review the state of knowledge regarding deep level defect distributions in β -Ga₂O₃ based on the application of deep level optical spectroscopy (DLOS), deep level transient (thermal) spectroscopy (DLTS), and admittance spectroscopy to β -Ga₂O₃ materials and devices. This combination of techniques

enables quantitative characterization of defect states throughout the ultrawide β -Ga₂O₃ bandgap. A comparison of deep level distributions in energy and concentration will first be discussed based on materials grown using edge-defined film growth (EFG), metalorganic chemical vapor deposition (MOCVD), low pressure chemical vapor deposition (LPCVD), hydride vapor phase epitaxy (HVPE) and molecular beam epitaxy (MBE). Clear differences are observed depending on growth method, with the lowest total trap concentrations being found for MOCVD and HVPE materials. A deeper exploration of MOCVD materials reveal significant and inequivalent dependences of individual trap state concentrations on growth temperature, implying that the low total trap concentration in MOCVD material could be reduced further. Deep acceptor doping by Fe, Mg and N is also compared as a first step toward exploring the comparative efficacy of each impurity in enabling ideal semi-insulating behavior for β -Ga₂O₃, along with reviewing how Fe impacts the behavior of β -Ga₂O₃ transistors by virtue of its primary deep level position in the bandgap near $E_c - 0.8$ eV. Finally, the β -Ga₂O₃ response to proton irradiation will be discussed, detailing the dominant radiation-induced states that are formed and the subsequent radiation hardness.

7:18 PM *EL04.04.03

CVD Diamond P-I-N Structures for High Temperature Electronics, Radiation Detection and Electron Emission Robert J. Nemanich¹, Franz Koeck¹, Mohamadali Malakoutian², Harshad Surdi¹, Jason H. Holmes¹, Manpuneet Benipal³, Ricardo Alarcon¹, Srabanti Chowdhury⁴ and Stephen Goodnick¹; ¹Arizona State University, United States; ²University of California, Davis, United States; ³Advent Diamond Inc., United States; ⁴Stanford University, United States

Diamond is a semiconductor with extreme and unique properties, which enable applications for high temperature electronics, radiation detectors, and electron emitters for ultra-high voltage vacuum switches and traveling wave tube cathodes. The fundamental structure for each of these applications is the p-i-n diode prepared from epitaxial, doped diamond layers. The availability of high-quality diamond substrates and the development of plasma CVD of epitaxial doped and undoped diamond have enabled fabrication of diodes with high breakdown field. CVD growth of high purity intrinsic diamond has shown room temperature mobility of both electrons and holes > 5000 cm²/V-s. Boron and Phosphorus doped layers achieve p-type and n-type character, respectively. Highly doped layers $> 10^{19}$ cm⁻³ demonstrate low resistance through hopping conduction, which supports low resistance contacts. Epitaxial diamond PIN diodes show high current density injection mode transport described as space charge limited current. The unipolar hole current density through a Schottky diode intrinsic drift layer shows a V² dependence as described by the Mott-Gurney expression where the differential resistance decreases as the voltage increases. Similarly, the differential resistance of a p-i-n diode shows a decrease of on-resistance with V indicative of bipolar conductivity modulation. At higher forward bias, velocity saturation is expected to limit the current in both unipolar Schottky and bipolar p-i-n diodes. The injection limited current transport of the undoped intrinsic diamond layer can enhance the predicted Baliga's figure of merit for diamond relative to other wide bandgap semiconductors. Results on diamond p-i-n alpha particle detectors show essentially 100 % charge collection efficiency at an applied bias of < 20 V. Moreover, background from x-ray and gamma photons does not substantially impact the count rate. Similarly, efficient electron emission is observed from forward biased diamond p-i-n diodes. Here, improved n-type contact structures substantially enhances the emission. The tremendous progress in diamond applications is limited by materials challenges. As materials research progresses, new device concepts are being developed based on the outstanding, extreme and unique properties of diamond materials.

Acknowledgement: financial support by ARPA-E, DOE, NASA, NSF and ONR.

7:42 PM *EL04.04.04

Diamond Electronics for Quantum Sensing Mutsuko Hatano; Tokyo Institute of Technology, Japan

Diamond is an excellent host for spin-based qubits, and the spin in diamond has excellent properties. Nitrogen-vacancy (NV) center in diamond is one of the most promising candidates for quantum sensing. The energy levels of NV centers are sensitive to magnetic fields, electric fields, strain, and temperature, enabling scalable

applications from the atomic to the macroscopic range [1].

Core technologies on material, devices, quantum control technology, sensor systems, and applications for life science and energy electronics are introduced.

- Materials

Selectively-aligned NV ensemble formed by distinctive CVD-growth for scalable applications.

The heteroepitaxial growth of NV-contained diamond on Si substrate for large area and on-chip integration.

- Sensing devices using pn junctions.

- Multi-scale and multi-modal sensor systems for life-science and energy electronics applications [2-4].

This work was supported by MEXT QLEAP Grant Number JPMXS0118067395.

The author would like to thank Lab and Q-LEAP members for their contributions and helpful discussion.

[1] L. Doherty et al., Phys. Rep. 528, 1 (2013).

[2] A. Hoang et al., APL 118,044001 (2021)

[3] Y. Hatano et al., APL 118, 034001 (2021)

[4] Bang Yanget et al., Physical Review Applied 14, 044049 (2020).

8:06 PM *EL04.04.05

UV-C Laser Diode with Distributed Polarization Doped P-Cladding Layer Maki Kushimoto¹, Ziyi Zhang^{1,2}, Tadayoshi Sakai¹, Naoharu Sugiyama¹, Leo J. Showalter³, Yoshio Honda¹, Chiaki Sasaoka¹ and Hiroshi Amano¹; ¹Nagoya University, Japan; ²Asahi Kasei Corporation, Japan; ³Crystal IS, Inc., United States

UV laser diodes are candidates for health care applications such as water and air sterilization, medical sensing, and curing. Especially AlGaIn-based UV optical devices are compact, have a long lifetime, and is environmentally friendly compared with conventional UV light sources. Recently, UVC and UVB LDs [1,2] are realized a long time after the UVA LD is reported [3]. These were achieved by overcoming the several issues: low hole injection efficiency, high operation voltage, and optical loss caused by crystal defects. In particular, the the non-doped distributed polarization doping (DPD) [4] structure of the p-clad layer contributes to the lasing by improving the hole injection efficiency. The average Al composition of 85% and hole concentrations in the mid-17th power range can be expected to be obtained by this method. The p-clad layer with a non-doped DPD structure has other advantages. The high Al composition in the region close to the active layer acts as an EBL layer that suppresses the electron overflow. Mg doping is not performed in this layer, so that absorption of light emission in the p-cladding layer can be suppressed. This mean that non-doped DPD is well matched method with the UVC-LD structure for p-type conductivity control.

The device structure we have prototyped consists of n, p-AlGaIn cladding layer, guiding layer, single quantum well and p-contact layer. The p-type DPD cladding layer is constituted by continuously reducing the Al composition from AlN to AlGaIn with 70% Al composition. From the evaluation of the optical properties, it was found that the internal loss could be reduced to less than 10 /cm with the appropriate DPD layer thickness [5]. After electrode formation, the wafer cleavage and the deposition of HfO₂/SiO₂ distributed Bragg reflector were carried out. As a result, a pulsed LD operation of a 270 to 280 nm was observed at the room-temperature. Lasing was observed at a forward current density of 14 kA/cm².

We also demonstrated LDs by the combined of dry and wet etching method as LD mirror facet fabrication. This method generally known to fabricate LDs grown on heterogeneous substrates, and it is attractive for mass production and monolithic integration. Since DBR formation was a major issue in this method, we focused on ALD with good coverage. As a result, the lasing was achieved with this combined method as well as the conventional cleaved method.

Acknowledgments

The authors would like to acknowledge Mr. Kazuhiro Nagase, and Dr. Naohiro Kuze of Asahi Kasei Corporation for their invaluable discussion and considerable support. The authors would also like to acknowledge Dr. Nishii and working members of C-TEFs for their great contribution to development of laser diode process.

References

1. Z. Zhang, M. Kushimoto, T. Sakai, N. Sugiyama, L. J. Schowalter, C. Sasaoka, and H. Amano, Appl. Phys.

Express 12, 124003 (2019).

2. K. Sato, S. Yasue, K. Yamada, S. Tanaka, T. Omori, S. Ishizuka, S. Teramura, Y. Ogino, S. Iwayama, H. Miyake, et al., Appl. Phys. Express 13, 031004 (2020).

3. H. Yoshida, Y. Yamashita, M. Kuwabara, and H. Kan, Appl. Phys. Lett. 93, 241106 (2008).

4. D. Jena, S. Heikman, D. Green, D. Buttari, R. Coffie, H. Xing, S. Keller, S. DenBaars, J. S. Speck, and U. K. Mishra, et al., Appl. Phys. Lett. 81, 4395 (2002).

5. Z. Zhang, M. Kushimoto, T. Sakai, N. Sugiyama, L. J. Schowalter, C. Sasaoka, and H. Amano, JJAP 59 0904011 (2020).

SESSION EL04.05: GaN Power Electronics I
Session Chairs: Robert Kaplar and Hongping Zhao
Monday Morning, April 19, 2021
EL04

8:00 AM *EL04.05.01

Wide Bandgap Semiconductor Based Power Electronic Devices for Energy Efficiency Isik C. Kizilyalli¹ and Eric P. Carlson²; ¹U.S. Dept. of Energy, United States; ²Booz Allen Hamilton, United States

Abstract – Development of advanced power electronics with increased functionality, efficiency, reliability, and reduced form factor are required in an increasingly electrified world economy. Fast switching power semiconductor devices are key to increasing the efficiency and reducing the size of power electronic systems as a significant portion of the losses in the systems is dissipated in the power semiconductor devices. However, the prevailing power semiconductor devices, which are based on the semiconductor silicon, are fast approaching their operational limits due to the intrinsic Si material properties. Wide-bandgap (WBG) semiconductors, such as gallium nitride (GaN) and silicon carbide (SiC), with their superior electrical properties are enabling a new generation of power semiconductor devices that offer higher efficiency and higher power conversion densities in a wide range of applications. The U.S. Department of Energy's Advanced Research Project Agency - Energy (ARPA-E) has invested in WBG semiconductors to enable a new generation of power semiconductor devices that far exceed the performance of silicon-based devices. In 2017 ARPA-E launched the PN DIODES program to address a major barrier to fabricating GaN power electronic devices which is the lack of a viable selective area doping processes. At the launch of the program, the selective area doping processes commonly used for other semiconductor materials, such as ion implantation or solid state diffusion, had not produced satisfactory p-type regions or p-n junctions in GaN due to the thermodynamic decomposition of GaN at high temperatures which has limited the device fabrication processes. The selective area doping processes in GaN resulted in poor electrical performance not sufficient for power electronic applications. The goal of the PN DIODES program is to develop transformational advances and mechanistic understanding in the process of selective area doping in the group III-Nitride wide-bandgap semiconductor material systems in order to demonstrate arbitrarily placed, reliable, contactable, and generally useable p-n junction regions. The projects selected for funding as part of the PN DIODES program are developing innovative selective doping processes for GaN. These include cutting-edge high temperature annealing processes to activate implanted dopants and remove the damage caused by ion implantation while overcoming the thermodynamic limits of GaN decomposition, low temperature solid-state diffusion of dopants using pioneering mechanisms to increase the diffusion driving force, non-traditional selective area doping process using low damage patterned etching followed by GaN regrowth to form buried selectively doped regions, and nuclear transmutation techniques to convert host atoms to dopants *in-situ* through exposure to neutrons and/or high energy photons. The PN DIODES projects are using/developing advanced nanoscale characterization techniques to investigate the local optical, chemical, structural, and electrical properties of the selectively doped regions to gain a mechanistic understanding of the processes being developed. These include Photo and Cathodoluminescence, Raman Spectroscopy, Atom Probe Tomography, Secondary Electron Emission, X-ray Topography, Rutherford Backscattering Spectrometry/Channeling,

Electron Paramagnetic Resonance, Nuclear Magnetic Resonance, Scanning Spreading Resistance Microscopy, Scanning Capacitance Microscopy, Photoconductivity Spectroscopy, and Electron Holography. The progress and challenges of selective area doping processes being developed under the PN DIODES program is reviewed along with the mechanistic understanding being generated. Material and processing challenges, including reliability concerns, for GaN power devices are also described. A glimpse into the future trends in device development, system integration, and commercialization is offered.

8:25 AM EL04.05.02

Materials and Technology Issues of Vertical GaN Power FinFETs Ahmad Zubair, Joshua Perozek, John Niroula and Tomas Palacios; Massachusetts Institute of Technology, United States

By 2030, about 80% of all US electricity is expected to flow through power-electronic devices. To enable this vision, the next generation of power electronics will require much higher efficiency and smaller form-factor than today's silicon-based systems. III-Nitride semiconductors form an ideal material system for this thanks to the combination of excellent transport properties and the high critical electric field enabled by their wide bandgap.

Both lateral and vertical III-Nitride devices are being investigated. In this paper, we will study vertical GaN FinFETs, as the vertical fin channel offers excellent electrostatic and threshold voltage control, eliminating the need for epitaxial regrowth¹ or p-type doping² unlike other vertical power transistors. Vertical GaN FinFETs with 1200 V breakdown voltage (BV) and 5-A current rating have been demonstrated recently on free-standing GaN substrates³. Besides, the high current density of these devices, in combination with minimum parasitics, allow these devices to achieve beyond-state-of-the-art switching performance. This talk will discuss the recent progress of GaN vertical power FinFETs on native GaN substrates, highlighting the device and materials-level opportunities as well as some of the challenges to push the performance limits in these devices. In addition, the talk will review recent efforts on GaN vertical power FinFETs on non-GaN substrates⁴. In spite of their promising performance, the commercialization of vertical GaN FinFETs on native GaN substrates has been limited by the high cost (\$50-\$100/cm²) and small diameter (2-4 inch) of free-standing GaN substrates. The use of Si or engineered substrates with a matched thermal expansion coefficient could potentially reduce the substrate cost by 1000×, although key trade-offs between leakage currents and performance need to be carefully studied.

Acknowledgements - This research was supported by the ARPA-E SWITCHES and PN DIODES programs, monitored by Dr. Isik Kizilyalli.

[1] H. Nie *et al.*, IEEE EDL vol. 35, no. 9, p.939-941 (2014).

[2] T. Oka *et al.*, Appl Phys. Exp. vol. 7 no. 2, (2014).

[3] Y. Zhang *et al.*, IEDM Tech. Dig., p. 9.2.1, (2017).

[4] A. Zubair *et al.*, Device Research Conference (2020).

8:40 AM EL04.05.03

Laser-Assisted MOCVD GaN Epitaxy for Vertical Power Device Applications Yuxuan Zhang, Zhaoying Chen, Zixuan Feng and Hongping Zhao; The Ohio State University, United States

GaN and its alloys have been widely utilized in optoelectronics, photonics, and electronics. Due to its large band gap (3.4 eV), strong critical electric field (3.4 MV/cm) and high electron mobility (>1000 cm²/Vs), the Baliga's figure of merit (BFOM) of GaN is more than 500X and 3X higher than that of Si and SiC, exhibiting great potential for high power electronics. Vertical GaN PN diode with 5kV breakdown voltage has been demonstrated [1]. To further improve the device performance, thicker drift layer with lower controllable doping is desired. For MOCVD GaN growth, TMGa and NH₃ are typically used as Ga and N precursors. However, one of the challenges associated with current MOCVD technology is the low NH₃ cracking efficiency (<1%), due to its high chemical stability even under high temperature (1000 °C). Carbon is considered as the most common impurity which originates from TMGa precursor. It is most likely to be incorporated on nitrogen site to form a

deep acceptor (C_N) in n-type GaN [2], which compensates effective doping, thus increase on-resistance and leakage current in vertical GaN devices. Traditionally, C can be suppressed by increasing growth temperature (increase NH₃ cracking efficiency) and V/III ratio (increase NH₃ partial pressure) [3]. Recent study [4] indicated that NH₃ can be efficiently cracked by CO₂ laser in which the photon energy is coupled with N-H wagging mode. With laser-assisted MOCVD (LA-MOCVD), GaN growth window is expected to be expandable to lower temperature regime with faster growth rate and lower impurity incorporation.

In this work, we performed a systematic study on the growth of GaN via LA-MOCVD growth technique. A tunable CO₂ laser with wavelengths between 9.201 to 10.365 μm was utilized as external excitation source in a commercial MOCVD system. From our studies, NH₃ has a strong interaction with the CO₂ laser, while neither N₂ nor H₂ has much absorption of the laser beam. The MOCVD GaN growth condition is widely tuned, including the growth temperature, chamber pressure, NH₃ flow rate, and type of carrier gas, to understand the effect of CO₂ laser beam on the GaN growth. The preliminary results indicate that LA-MOCVD growth can suppress C incorporation in GaN. Meanwhile, the CO₂ laser can also lead to strong gas phase reaction between precursors, which in turn leads to the reduction of GaN growth rate. LA-MOCVD growth of GaN at lower temperature regime indicates the suppression of V-pits formation as compared to the conventional GaN growth without the laser. Smooth surface morphology of LA-MOCVD GaN was observed under optical microscope, AFM and SEM, with low RMS of 0.34 nm measured by AFM. Therefore, LA-MOCVD can become a novel growth technique to grow high quality GaN suitable for high power vertical devices.

In summary, for the first time, we performed CO₂ based LA-MOCVD GaN growth in a commercial MOCVD system. LA-MOCVD growth conditions are systematically mapped and comprehensive material characterization is performed. Results from this work indicate the great potential of using the novel LA-MOCVD growth method to achieve GaN epitaxy for vertical power devices with high breakdown voltages.

Acknowledgment: The authors acknowledge the funding support from Advanced Research Projects Agency-Energy (ARPA-E), U.S. Department of Energy (DE-AR0001036).

References:

- [1] H. Ohta, N. Asai, F. Horikiri, Y. Narita, T. Yoshida, and T. Mishima, Jpn. J. Appl. Phys. 58, SCCD03 (2019).
- [2] J. L. Lyons, A. Janotti, and C. G. Van de Walle, Phys. Rev. B 89, 035204 (2014).
- [3] D. D. Koleske, A. E. Wickenden, R. L. Henry, and M. E. Twigg, J. Cryst. Growth 242, 55 (2002).
- [4] H. Rabiee Golgir, Y. Gao, Y. S. Zhou, L. Fan, P. Thirugnanam, K. Keramatnejad, L. Jiang, J. F. Silvain, and Y. F. Lu, Cryst. Growth Des. 14, 4248 (2014).

8:55 AM EL04.05.04

GaN P-N Power Diodes with > 1.5 kV Breakdown Voltage Vishank Talesara, Zhaoying Chen, Yuxuan Zhang, Hongping Zhao and Wu Lu; The Ohio State University, United States

In this work, we report 1.5 kV GaN PN diodes on an HVPE substrate. The GaN layers were grown on a 2" HVPE GaN substrate using the Metal Oxide Chemical Vapor Deposition (MOCVD). The dislocation density of the substrate ranges between $2 \times 10^6 \text{ cm}^{-2}$ in the less dense regions to $1 \times 10^7 \text{ cm}^{-2}$ in regions that show the presence of dense dislocation clusters. The device structure consists of a 20 nm p+ GaN contact layer (Mg: $1 \times 10^{20} \text{ cm}^{-3}$), followed by a 500 nm p-GaN layer (Mg: $1 \times 10^{18} \text{ cm}^{-3}$), grown on an 8 μm n-GaN drift region (Si: $1.2 \times 10^{16} \text{ cm}^{-3}$) and 1.6 μm n+ GaN buffer layer (Si: $1.5 \times 10^{18} \text{ cm}^{-3}$) on a thick bulk HVPE GaN substrate. The hole concentrations in the p and p+ GaN layers are $1 \times 10^{17} \text{ cm}^{-3}$ and $5 \times 10^{17} \text{ cm}^{-3}$, respectively, measured by Hall measurements. CV measurements show that the drift layer has an electron concentration of $5.1 \times 10^{15} \sim 1.2 \times 10^{16} \text{ cm}^{-3}$. According to the analytical calculations, this device structure design has a theoretical punch-through breakdown voltage value of ~ 2.0 kV. For electrical field management, three layers of guard ring structures were designed and implemented by nitrogen ion implantation at the dose of $3.2 \times 10^{13} \text{ ions/cm}^{-2}$ at five ion energies which results in a depth of ~520 nm. Based on numerical simulations, the electrical field peaks at the edge of each guard ring and this device design should result in a breakdown voltage of 1670 V at a critical

field of 3.4 MV/cm. For device fabrication, Ti/Al-based metal scheme was used to form the contact to n-GaN as the back cathode. Pt/Ni/Au anodes were annealed at 350 °C for p-contacts with a specific contact resistivity of 0.6 mΩcm². The devices were then passivated by a 500 nm SiN layer after nitrogen ion implantation. The device size varies from 100 to 600 μm. The devices exhibit a breakdown voltage of 1530 V due to a clear avalanche process. The measured breakdown voltage has a remarkable agreement with numerical simulations. This suggests that the devices have an excellent breakdown efficiency > 75%. The reverse leakage current density is in the μA/cm² range till 500 V. The turn-on voltage is 4.9 V at 100 A/cm² and the device exhibited 1 kA/cm² current density at 6.0 V. The specific on-resistance for this device is 1.2 mΩ cm². This measured breakdown voltage and on-resistance lead to a figure of merit of 2.1 GW/cm². Considering the p-contact resistivity, this suggests that the n-drift layer has an electron mobility of 480 cm²/Vs. The devices have an ideal factor of 2.7 at 2.3 V, likely due to a resistive layer at the bulk GaN substrate and epitaxy interface. More statistical analysis of device performance will be presented at the conference. Overall, this work represents the state-of-the-art device performances of GaN power diodes.

This material is based upon work supported by the U.S. Department of Energy's Office of Energy Efficiency and Renewable Energy (EERE) under the Advanced Manufacturing Office, FY18/FY19 Lab Call.

9:10 AM DISCUSSION TIME

9:25 AM EL04.05.06

Low-Defect Etched-and-Regrown PN Diodes by *In Situ* Tertiarybutylchloride (TBCl) Etching Bingjun Li, Sizhen Wang and Jung Han; Yale University, United States

Gallium Nitride (GaN)-based devices are very attractive candidates for next-generation high-power applications, due to the intrinsic material properties. However, the lack of selective-area doping technique in GaN greatly limits the design flexibility and device performance. Due to the difficulty of post-ion-implantation annealing process in GaN material, selective-area etching (SAE), followed by selective area growth, is an alternative and promising approach to overcome this obstacle. Plasma-etching, as a well-developed technique to create smooth and high aspect-ratio trenches, induces serious optical and electronic defects and impurities on the treated surface. Therefore, we introduced a chlorine-based metal-organic (MO) precursor, tertiarybutylchloride (TBCl), into the MOCVD reactor to replace the role of plasma etching.

TBCl etching was also performed on 1.5μm unintentional-doped (UID) GaN templates grown on bulk GaN substrate to mitigate the effect of dislocation-mediated etching. Four samples are compared here. Sample A is a template. Sample B~D are templates etched by Cl-based plasma, TBCl and a combination of both, respectively. Photoluminescence (PL) showed strong near-band-edge emissions only from Sample A, C and D (Fig. 3(a)). And only Sample B had obvious Cl peak from x-ray photoelectron spectroscopy (XPS) (Fig. 3(b)). Both PL and XPS confirm that TBCl etching is able to remove the impurity (except Si and Al) and damage induced by plasma etching and does not introduce damage itself.

Besides, electrical properties were also evaluated. Four planar PN diodes were grown and fabricated. Device A is a continuous PN diode, while Device B~D were etched-and-regrown PN diodes. Three different etching were performed on 1.5μm UID drift layer grown on GaN substrate: plasma etching followed by AZ400K cleaning for Device B; plasma etching (ICP)+AZ400K cleaning+150nm TBCl etching for Device C; and 150nm TBCl etching for Device D. 300nm UID and 400nm p-GaN was regrown on the etched templates. Forward and reverse I-V characteristics were compared. No obvious difference is observed when they were forward biased. However, leakage behaviors are quite distinct. The TBCl-etched diode (Device D) shows the best leakage behavior among all three regrown devices, while ICP+TBCl-etched diode has the highest leakage current. From SIMS and CV measurement comparisons, Device C has the highest Si impurity concentration, which could explain the worst leakage behavior. On the other hand, a high concentration of deep traps was observed on ICP-etched diodes from CV measurement.

Acknowledgements

This work is supported by the Advanced Research Projects Agency-Energy (ARPA-E), U.S. Department of Energy, under Award Number DE-AR0000871 as part of the PNDIODES program managed by Dr. Isik Kizilyalli.

9:40 AM EL04.05.07

Scanning Capacitance Microscopy of GaN p-n Junction Through Planar and Selective Area Doping

Sizhen Wang, Bingjun Li and Jung Han; Yale University, United States

Scanning capacitance microscope (SCM) integrates a high-frequency capacitance sensor into the conductive atomic force microscope (C-AFM) to measure the change of capacitance of a well-known metal-oxide-semiconductor (MOS) or Schottky diode structure under an AC driving voltage. The dC/dV amplitude and phase of the output signal tells the doping type and carrier concentration, respectively. SCM has demonstrated the capability to delineate the p-n junction and form a 2-D dopant mapping on Si substrate accurately. In addition, doping characterization using SCM on GaN were also reported. Here, we demonstrated SCM characterization of a selective-area grown (SAG) lateral GaN p-n junction on bulk GaN substrate for the first time, which is a key building block of high-performance GaN-based high-power devices.

To quantify the doping concentration in a 2-D mapping, dC/dV amplitude and phase need to be calibrated with the known doping level at the beginning. Therefore, a sample consisting of multiple GaN layers with Si, Ge doping concentration ranging from unintentional doped GaN to $1 \times 10^{20}/\text{cm}^3$ were used for the calibration. And the dC/dV amplitude peak was selected as parameter for calibration, which can reduce noise impact and eliminate the contrast reverse issue. By applying different AC driving voltage, near four order of magnitude doping of GaN can be calibrated on bulk GaN. Similarly, p-GaN layers with Mg concentration range from 1×10^{19} to $8 \times 10^{19}/\text{cm}^3$ were also calibrated. Based on those calibration studies, we proposed an efficient operation procedure to characterize semiconductor samples with scanning capacitance microscopy and apply this procedure to investigate the continuously grown diodes, planar regrown diodes, and selective area regrown GaN diodes.

Several key results of applying SCM to characterize vertical GaN diode were summarized here: (1) to identify the p-n junction location, dC/dV phase is preferred to be used, because comparing to dC/dV amplitude, the dC/dV phase is much less susceptible to DC bias and AC driving signal. (2) SCM revealed that a thin n-type conducting layer existed at the regrown interface of planar regrown diode. This n-type layer, with increased conductivity comparing to UID-GaN, was related to ICP plasma damage. (3) For SAG regrown diodes, typical p-GaN layer was verified with SCM by applying proper DC bias condition, it was also found at the trench bottom (or regrowth interface), a typical n-type thin layer existed, which should not in ideal case. The possible n-type doping impurity might come from the out-gassing of the SiO_2 mask during the growth or other reactor parts made of quartz, which needs further investigation.

9:55 AM EL04.05.08

Late News: Surface Photovoltage Study of the Bulk Photovoltaic Effect in Carbon-Doped Gallium

Nitride Igal Levine¹, Ivan Gamov², Marin Rusu¹, Klaus Irmscher², Christoph Merschjann¹, Eberhard Richter³, Markus Weyers³ and Thomas Dittrich¹; ¹Helmholtz-Zentrum Berlin, Germany; ²Leibniz-Institut für Kristallzüchtung, Germany; ³Ferdinand-Braun-Institut GmbH, Leibniz-Institut für Höchstfrequenztechnik, Germany

Surface photovoltage (SPV) of carbon-doped gallium nitride single crystals (GaN:C) was investigated by Kelvin probe as a function of carbon doping.¹ GaN:C crystals are highly resistive due to compensating deep defect states. Depending on the carbon doping, SPV signals much larger than expected in relation to the band gap of GaN were detected setting on at photon energies of 2.5-2.6 eV due to excitation from defect states. Under constant illumination, the large SPV signals saturated at values above 20 V and even overshoot abruptly by up to several volts above the saturation value when switching off the light source. The sign of the large SPV signals changed from positive to negative when flipping the crystal from the Ga-polar to the N-polar surface. Therefore, the large SPV signals on GaN:C are not related to a conventional Demer photovoltage, which is

based on different mobilities for photogenerated electrons and holes, but rather to a bulk photovoltaic effect (BPVE) caused by a structure dependence of directed momentum transfer. It is proposed that (tri)carbon complexes are key for directed momentum transfer in GaN:C and the resulting observed BPVE.

(1) Levine, I.; Gamov, I.; Rusu, M.; Imscher, K.; Merschjann, C.; Richter, E.; Weyers, M.; Dittrich, T. "Bulk Photovoltaic Effect in Carbon-Doped Gallium Nitride Revealed by Anomalous Surface Photovoltage Spectroscopy". *Phys. Rev. B* **2020**, *101* (24).

SESSION EL04.06: GaN Power Electronics II
Session Chairs: Srabanti Chowdhury and Robert Kaplar
Monday Morning, April 19, 2021
EL04

10:30 AM *EL04.06.01

Design and Fabrication of Edge-Termination for Achieving Reliable GaN P-N Diodes for High Voltage Applications Srabanti Chowdhury¹, Andrew Allerman², Robert J. Kaplar², Andrew Armstrong², Jeramy Dickerson², Alan Jacobs³ and Karl Hobart³; ¹Stanford University, United States; ²Sandia National Laboratories, United States; ³U.S. Naval Research Laboratory, United States

Electrification drives us closer towards our goal of a sustainable energy system. Highly efficient and reliable ways of converting, delivering and conditioning power calls for innovations at every level, from system to materials. Silicon's role in the electrification has led to exploring wide- bandgap (WBG) materials. SiC led power electronics have revealed the large scope of improvement that one can expect to see out of WBGs due to an enhancement of the critical electric field. GaN, originally pushed for medium voltage (650V-900V) devices using the well-known HEMT configuration, has a lot more to offer in power electronics through its vertical configuration. Over the last decade a tremendous amount of progress has been made with the support from ARPA-E and ONR which resulted in the improvement of the epitaxial material, understanding of the underlying physics, optimization of design and processing of the devices, accurate failure analysis, and finally, laying the groundwork for mass production.

Under the current ARPA-E Open plus program our team is developing high voltage (towards 20 kV) GaN PN diodes for use as devices to protect the electric grid against electromagnetic pulses [1]. A common goal shared by both DOD and DOE is to have a foundry component in the US to successfully scale and produce vertical GaN devices for circuit implementation. Under the current program, we are bringing together all the research components starting from material development and wafer metrology to reliability and failure analysis. These are the essential components for successful manufacturing of GaN devices leading to its transfer to the foundry. Achieving a reliable p-n junction definitely is the first step towards high voltage (1.2kV and up) power devices. In this talk we will focus on various approaches of edge termination to realize a robust p-n junction. Bevel and junction termination extension (JTE) approaches are being pursued on p-n diodes to study their efficacies in field mitigation. Using the bevel termination technique for 1.2kV diodes, we are studying the reverse blocking strength of these diodes, by closely monitoring their avalanche capabilities. The foundry effort is utilizing as a primary path various combinations of nitrogen-implanted isolation structures, guard rings, and JTEs. The team, through a tight research collaboration, is working towards identification of the key challenges of edge- terminations and the best solution in GaN, to serve various voltage classes.

The authors gratefully acknowledge the support of ARPA-E's OPEN+ Kilovolt Devices Cohort managed by Dr. Isik Kizilyalli, and support of ONR managed by Mr. Lynn Petersen.

[1] R. Kaplar, et al. IEDM 2020

10:55 AM EL04.06.02

Variations in GaN Substrates and the Structural Evolution of Defects in Homoepitaxial GaN Layers
Yekan Wang¹, Michael E. Liao¹, Kenny Huynh¹, Andrew Allerman² and Mark S. Goorsky¹; ¹University of California, Los Angeles, United States; ²Sandia National Laboratories, United States

In this study, the structural defects in 40 mm homoepitaxial GaN grown on what is commonly referred to as dot-core GaN substrates were evaluated using synchrotron double crystal x-ray topography (XRT). 8.05 keV X-ray energy was used. The first crystal was an asymmetric Si (333) beam expander and the sample (2nd crystal) was oriented for diffraction of the (114) reflection. Films were obtained from single exposure at particular positions on the rocking curve and continuous exposure by rocking the sample (step size $\sim 0.008^\circ$) about the [100] axis through the Bragg condition.

For as-received dot core substrates, regions of high distortion around the cores are observed. These defective regions are not confined within the core regions. The effect of tilt and distortion distribute to further affect regions between the cores as well. Meanwhile, variations in the substrates are observed. The substrates curvature for three as-received dot core substrates from the same vendor is quite different, with a radius of curvature of 25m, 17m, and 7m respectively. The defect structure surrounding the cores in the three substrates is also different. The distortions around the cores in two of the three substrates have a few hundred μm white round (non-diffracting) regions around the cores while the other substrate shows irregular distorted regions. A few 'butterfly' shape patterns are present around some cores, which result from localized tilting of the lattice planes. Each side of the butterfly wing consists of contour lines representing regions of similar tilt. Rotating the sample every 60° and taking rocked images along different (1124) reflections, we found the 'butterfly' patterns follow the 60° rotation, suggesting that the lattice tilt around the cores occurs radially. The sample with 40 μm epilayer grown on a dot core substrate shows a change in the defect structure around the cores. Defective regions after epitaxial growth are more concentrated in the core areas. A hypothesis is that defects observed on the bare substrate propagate into the overlaying epilayer. However, during epitaxial growth, structural distortions are redirected towards the centers of cores. The surface shows haze and specular regions with variation in AFM roughness (1.3 nm vs 0.4 nm). More defective regions observed using XRT appears to be correlated with haze on the surface. Variation of distortions across the wafer can also be identified. There are circular spot features with bright contrast, corresponding to highly defective regions of tilt after the epitaxial growth. Between cores and over some cores, there is undistorted, low dislocation density ($\sim 10^5 \text{ cm}^{-2}$) material with uniform grey contrast, corresponding to higher quality GaN (hundreds of μm -size). Devices fabricated on such regions are expected to have better performance. In conclusion, the structural evolution of defects after the epitaxial growth is closely related to variations in the substrates. As a result, wafer screening and quality assessment using non-destructive techniques such as x-ray topography before and after the epitaxial growth are promised to help improve the overall quality of the homoepitaxial GaN structures.

The authors would like to acknowledge support through the ARPA-E PN DIODES program under contract DE-AR0001116 at UCLA. This research used resources of the Advanced Photon Source, a U.S. Department of Energy (DOE) Office of Science User Facility operated for the DOE Office of Science by Argonne National Laboratory under contract no. DE-AC02-06CH11357. The synchrotron X-ray topography measurements were carried out at 1-BM Beamline of the Advanced Photon Source, Argonne National Laboratory.

11:10 AM EL04.06.03

Application of Synchrotron X-Ray Topography to Characterization of Selective Area Doping Processes for the Development of Vertical GaN Power Devices
Yafei Liu, Hongyu Peng, Tuerxun Ailihumaer, Shanshan Hu, Balaji Raghothamachar and Michael Dudley; Stony Brook University, The State University of New York, United States

Selective area p-type doping of GaN is required for the development of vertical GaN devices that will help realize the potential of WBG semiconductor GaN in power electronics [1, 2]. Approaches being investigated include implantation followed by activation annealing by different methods, selected area etching and regrowth

of p-type regions [3], diffusion doping and neutron transmutation [4]. Using synchrotron X-ray topography [5] and complementary tools like HRXRD and Raman spectroscopy, the effect of substrate choice, implantation and annealing conditions have been evaluated on the structural quality and strain in the epilayers and regrown material. The choice of bulk GaN substrates plays an important role in the eventual extended defect configurations in the active layers. Ammonothermal-grown GaN substrate wafers show the best quality among all the wafers [6, 7]. These wafers, which are free of basal plane dislocations (BPDs), have low curvature and threading mixed dislocations (TMDs) dominant among the threading dislocations (TDs). Patterned HVPE GaN reveal a starkly heterogeneous distribution of dislocations with large areas containing low threading dislocation densities in between a grid of strain centers with higher threading dislocation densities and BPDs [8]. The strain level of HVPE GaN substrates is very high, and the dislocation density is around 10^5 - 10^6 cm⁻², which is much higher than 10^4 cm⁻² of ammonothermal samples and dislocation-free areas in the patterned HVPE samples. During epitaxial growth by CVD for implantation purposes, defects in substrates are shown to replicate into the epilayer and typically no new defects are observed to be introduced at the interface. On implantation, damaged layers are generated in the epilayer as revealed by satellite peaks in double axis rocking curves. The radiation fluence and energy determine the extent of damage. Depending on annealing conditions most of the damage is healed. However, the annealing temperatures greater than 1100 C can result in introduction of inhomogeneous strains and dislocation generation. While etching by TBCI is shown to be sensitive to certain types of threading dislocations, any thermal treatment is shown to introduce basal plane dislocations. Further investigations are underway to analyze the regrowth interface for the nucleation of new defects. Results will be discussed with implications for vertical device fabrication and expected impact on device performance.

References:

- [1] I.C. Kizilyalli, A.P. Edwards, H. Nie, D. Disney, D. Bour, IEEE Transactions on Electron Devices 60 (2013) 3067-3070.
- [2] I.C. Kizilyalli, A.P. Edwards, H. Nie, D. Bour, T. Prunty, D. Disney, IEEE Electron Device Letters 35 (2014) 247-249.
- [3] B. Li, S. Wang, M. Nami, J. Han, Journal of Crystal Growth 534 (2020) 125492.
- [4] R. Barber, Q. Nguyen, J. Brockman, J. Gahl, J. Kwon, Scientific Reports 10 (2020) 1-8.
- [5] B. Raghathamachar, M. Dudley, G. Dhanaraj, X-Ray Topography Techniques for Defect Characterization of Crystals, in: G. Dhanaraj, K. Byrappa, V. Prasad, M. Dudley (Eds.), Springer handbook of crystal growth, Springer Science & Business Media, 2010, p. 1425.
- [6] Y. Liu, S. Hu, H. Peng, T. Ailihumaer, B. Raghathamachar, M. Dudley, ECS Transactions 98 (2020) 21.
- [7] Y. Liu, B. Raghathamachar, H. Peng, T. Ailihumaer, M. Dudley, R. Collazo, J. Tweedie, Z. Sitar, F.S. Shahedipour-Sandvik, K.A. Jones, Journal of Crystal Growth 551 (2020) 125903.
- [8] B. Raghathamachar, Y. Liu, H. Peng, T. Ailihumaer, M. Dudley, F.S. Shahedipour-Sandvik, K.A. Jones, A. Armstrong, A.A. Allerman, J. Han, H. Fu, K. Fu, Y. Zhao, Journal of Crystal Growth 544 (2020) 125709.

11:25 AM EL04.06.04

Late News: Microstructure Impacts on Performance of GaN Power Switching Devices Brett Setera and Aris Christou; University of Maryland, United States

GaN power switching devices with thick epitaxial layers (3-15 microns) suffer from a high density of crystal defects, and specifically threading dislocations (TDs) in the epi-layer. Presence of dislocations leads to non-ideal performance and higher costs manifested in device voltage derating, limited die sizes, poor wafer yields, operating parameter instability, and limited device types. Microstructure analysis of defect type and location is crucial to correlating structure with device performance.

Experimental results with 10 μ m GaN epilayer grown on HVPE (hydride vapor phase epitaxy) + GaN indicate that threading dislocations can propagate through the epilayer to the contact, resulting in increased gate leakage current density. Cathodoluminescence (CL) imaging correlated with ECCI as well as AFM allow the conclusion to be reached that the main threading defects are the edge dislocations and dislocation loops which tend to be either tilted, exposing the edge dislocations, or parallel to the growth plane. Utilizing the three aforementioned non-destructive techniques allows measurement of as-grown defects before the device undergoes performance testing. Transmission x-ray topography analysis showed that the GaN is characterized by a nearly uniform

distribution of strain centers which are likely bundles of threading screw and edge dislocations. Strain free centers are then regions of relatively low dislocation densities. The threading dislocations are part of dislocation loops which are present in the GaN substrate and migrate through the interface. Cross-sectional TEM showed partial dislocation loops through the thickness of the GaN sample.

The two terminal GaN-on-GaN (HVPE) device was able to withstand 2.77 MV/cm before the contact to contact leakage current produced a gate – source short with an epilayer dislocation density of 10^6 cm^{-3} .

11:40 AM EL04.06.05

MOCVD GaN Epitaxy with Fast Growth Rates Yuxuan Zhang, Zhaoying Chen, Wenbo Li, Aaron R. Arehart, Steven A. Ringel and Hongping Zhao; The Ohio State University, United States

Gallium nitride (GaN) has been considered as a promising candidate for power electronic devices due to its wide bandgap (3.4 eV), high critical electric field (3 MV/cm), and high electron mobility ($>1000 \text{ cm}^2/\text{V s}$). As a key parameter to evaluate the performance of power devices, Baliga's figure of merit (BFOM) of GaN is more than 500X higher than silicon (Si) and 3X higher than silicon carbide (SiC) [1]. Vertical GaN PN diode with 5kV breakdown voltage has been demonstrated [2]. Although tremendous progress has been made in the past few years, challenges still exist to achieve vertical GaN power devices with $V_{BR}>10 \text{ kV}$, which requires the epitaxy of high quality GaN films with thick drift layer and low controllable doping with high mobility. Typical MOCVD GaN films with high mobilities were grown with growth rate of 2-3 $\mu\text{m/hr}$. Thus, it is important to develop and understand MOCVD GaN growth with fast growth rate, high crystalline quality, and controllable low carrier concentration.

In this work, the effect of increasing growth rate by increasing TMGa on the impurity incorporation, charge compensation, surface morphology and transport properties are systematically studied. Under optimized MOCVD GaN growth with a growth rate of 2 $\mu\text{m/hr}$, high quality GaN with stable low net charge density at $4 \times 10^{15} \text{ cm}^{-3}$ was demonstrated. [Si] and electron concentration ($N_d - N_a$) as a function of SiH_4 flow was studied. Stronger plummet of $N_d - N_a$ was observed with reduction of SiH_4 flow when $N_d - N_a$ is lower than $1 \times 10^{16} \text{ cm}^{-3}$, due to prominent compensation effect at low doping range. According to capacitance-voltage (CV) and secondary ion mass spectroscopy (SIMS) analysis, the [C] level was at $7 \times 10^{15} \text{ cm}^{-3}$ (SIMS detection limit). Low $N_d - N_a$ was achieved at $4 \times 10^{15} \text{ cm}^{-3}$ based on CV. Deep level transient spectroscopy / deep level optical spectroscopy (DLTS / DLOS) results show minimal electron trap concentration at $2.5 \times 10^{15} \text{ cm}^{-3}$, mainly from carbon related deep level defects. By increasing the TMGa flow rate, GaN with fast growth rate at 5.2 $\mu\text{m/hr}$ was achieved with stable $N_d - N_a$ at $1.5 \times 10^{16} \text{ cm}^{-3}$ and [C] at $2 \times 10^{16} \text{ cm}^{-3}$. Large area atomic force microscope (AFM) images on fast growth rate sample show smooth morphology with clear atomic strips and low surface roughness (RMS=0.647 nm). The Mn incorporation from the semi-insulating ammonothermal substrate into epilayer was observed. Controlled experiments show that Mn incorporation rate into epilayer is highly related to the growth rate, and Mn incorporation mechanism shares a similar behavior as Fe. SIMS showed that both Mn and Fe incorporation can be suppressed with faster growth rates. Room temperature Hall measurement showed that with electron concentration at around $1.5 \times 10^{16} \text{ cm}^{-3}$, electron mobility decreased from 852 cm^2/Vs to 604 cm^2/Vs as growth rate increasing from 2 $\mu\text{m/hr}$ to 5.2 $\mu\text{m/hr}$.

In summary, we studied the doping and compensation of n-type GaN as a function of growth rate. Low compensation level at 2 $\mu\text{m/hr}$ was confirmed by both DLTS/DLOS and CV. Increasing GaN growth rate led to the increase of carbon concentration while suppressing Mn and Fe incorporation. In order to achieve high quality thick GaN drift layer with controllable doping concentration at low- to mid- 10^{15} cm^{-3} range for high voltage vertical power devices, the key challenge is to reduce carbon incorporation in the GaN epilayer. The results from this work provide insights for GaN vertical power electronics.

Acknowledgment: The authors acknowledge the funding support from Advanced Research Projects Agency-Energy (ARPA-E), U.S. Department of Energy (DE-AR0001036), and U.S. Department of Energy's Office of Energy Efficiency and Renewable Energy (EERE) under the Advanced Manufacturing Office, FY18/FY19 Lab Call.

References:

[1] B. J. Baliga, Fundamentals of Power Semiconductor Devices (Springer Science & Business Media, 2010).

[2] H. Ohta, N. Asai, F. Horikiri, Y. Narita, T. Yoshida, and T. Mishima, *Jpn. J. Appl. Phys.* 58, SCCD03 (2019).

11:55 AM EL04.06.06

Influence of Surface Treatments on the Structure and Properties of GaN Layers Jiaheng He¹, Guanjie Cheng¹, Maggie Chen¹, Zhirong Zhang¹, Sam Frisone¹, Alexandra Zimmerman¹, Fabian Naab¹, Sizhen Wang², Bingjun Li², Jung Han² and Rachel Goldman¹; ¹University of Michigan–Ann Arbor, United States; ²Yale University, United States

Although silicon-based electronics are used to power light-emitting diodes and electric vehicles, their utility in high power applications is limited by slow switching and high on-state resistance. The most promising alternatives are vertical GaN devices, but these involve etching and selective-area re-growth which enhance the displacement of surface and near-surface Ga and N atoms. To understand processing-structure-property relationships relevant to vertical GaN devices, we are examining the influences of various surface treatments on the structure and properties of GaN layers. Utilizing ion beam analysis, we have examined the influence of ambient exposure and dry etching on the structure and properties of regrown p-i-n GaN structures. We show that dry etching improves the crystallinity of p-i interfaces, but also introduces interfacial H. In addition, we report on the influence of dry etching and metal-organic (MO) precursor treatment on the structure and properties of GaN substrates and epitaxial GaN layers. For these studies, we visualize the crystal symmetry and orientation using 2D planar ion channeling maps and angular yield profiles collected with a fully-automated 5-axis goniometer recently attached to the RC43 endstation of the 1.7 MeV Tandatron at the Michigan Ion Beam Laboratory. Our preliminary results suggest that the MO precursor reduces the density of displaced surface Ga atoms. To quantify the concentration and distribution of displaced atoms, we will compare 2D ion channeling maps with 2D Monte Carlo-Molecular Dynamics simulations using Flux 7.9.6. We will also present 2D maps of elastic recoil detection analysis spectra to evaluate the spatial distribution of H.

We gratefully acknowledge the support of ARPA-E through AWD0000191.

12:10 PM EL04.06.07

X-Ray Diffraction Studies of GaN p-i-n Structures for High Power Electronics Alexandra Zimmerman¹, Jiaheng He¹, Guanjie Cheng¹, Davide del Gaudio¹, Jordan Occena¹, Fabian Naab¹, Mohsen Nami², Bingjun Li², Jung Han² and Rachel Goldman¹; ¹University of Michigan–Ann Arbor, United States; ²Yale University, United States

Although silicon-based electronics are used to power light-emitting diodes and electric vehicles, their utility in high power applications is limited by a low breakdown voltage. The most promising alternative power devices consist of vertical GaN devices, which often require regrown active regions. Here, we report on x-ray diffraction studies of the crystallinity of the GaN p-i-n structures prepared with and without ex-situ ambient exposure and/or chemical etching. To quantify the mosaicity and threading dislocation (TD) densities at the p-i interfaces, we quantify and compare the full-width at half-maximum (FWHM) of both phi and omega x-ray diffraction scans. For the "in-situ" GaN structure, the screw-type TD densities are lowest, the edge-type TD densities are highest, and the interfacial near-band edge (NBE) and donor-acceptor pair (DAP) cathodoluminescence (CL) emissions are highest. Interestingly, elastic recoil detection analysis (ERDA) and Rutherford backscattering spectroscopy reveal minimal interfacial [H] but the highest fraction of displaced Ga atoms, suggesting efficient incorporation of Mg_{Ga}. On the other hand, for the ex-situ structures, minimal interfacial [H] is also observed, along with a high screw-type TD and low interfacial NBE and DAP CL emissions. Finally, for the etched/regrown structures, ERDA reveals the highest interfacial [H], along with moderate screw- and edge-type TD, moderate DAP CL, and significant yellow CL emission. The relationship between interfacial [H], displaced Ga, CL emission features, and screw- and edge-type TD densities will be discussed.

We gratefully acknowledge the support of ARPA-E through AWD0000191.

SESSION EL04.07: Ga₂O₃ I
Session Chairs: Sriram Krishnamoorthy and Hongping Zhao
Monday Afternoon, April 19, 2021
EL04

1:00 PM *EL04.07.01

Defects in b-Ga₂O₃—An Ultra High-Resolution Scanning/Transmission Electron Microscopy Imaging and Spectroscopy Nasim Alem and Adrian Chmielewski; The Pennsylvania State University, United States

Group III wide band gap (WBG) oxides are considered ideal materials systems for power electronics at extreme conditions. Due to their high band gap, this family of materials has a high breakdown voltage and high resistivity to electric field and temperature. Among WBG oxides, β -Ga₂O₃ is considered an ideal candidate for high power electronics due to its high band gap and its high breakdown electric field compared with GaN and 4H-SiC. Yet, defects currently limit the high performance of β -Ga₂O₃ crystal in high power electronic applications. While there have been a number of studies on the characterization of the defects in β -Ga₂O₃, little is known about the underlying atomic scale physics and chemistry of such defect complexes within the crystal, at the interfaces, and how they can affect the macroscale electronic properties. In addition, little is known about the stability and transition dynamics of the crystal under extreme conditions, i.e. thermal or electrical biasing, ultimately leading to its failure.

In this work we use advanced scanning/transmission electron microscopy imaging and electron energy loss spectroscopy to understand the atomic and chemical structure of b-Ga₂O₃ and epi thin film of b-Ga₂O₃/b-(Al_xGa_{1-x})₂O₃. We present the atomic and chemical structure of the defects, interfaces, and its structural transformation in the bulk b-Ga₂O₃ and epi thin film of b-Ga₂O₃/b-(Al_xGa_{1-x})₂O₃. In addition, nanoscale modulations in the electronic structure and the band gap in the epi thin films of b-Ga₂O₃/b-(Al_xGa_{1-x})₂O₃ is discussed. This presentation will further cover the nanoscale transition dynamics of b-Ga₂O₃ lattice under extreme environments such as high temperature and electric field. This fundamental study can bridge the gap between atomic scale structural modifications and macroscale materials functionality not only in b-Ga₂O₃ but also in the family of WBG oxides.

1:25 PM EL04.07.02

Mg Acceptor Doping in MOCVD (010) β -Ga₂O₃ Zixuan Feng, A F M Anhar Uddin Bhuiyan, Nidhin K. Kalarickal, Siddharth Rajan and Hongping Zhao; The Ohio State University, United States

Metalorganic chemical vapor deposition (MOCVD) of β -Ga₂O₃ thin films have been demonstrated with record-high room temperature and low-temperature mobilities that approach the theoretically predicted limit. [1,2] The extracted low acceptor concentration ($N_a < 10^{15} \text{ cm}^{-3}$) is extremely encouraging for its potential application in high power electronics. Among various impurities in MOCVD grown β -Ga₂O₃, Si represents the dominant one that contributes to the conductivity in the unintentionally doped (UID) films. It is commonly observed the Si spike at the growth interface between Ga₂O₃ substrate and the epitaxial layer. The existence of interface charges not only severely impacts charge transport characteristics [2], but also detrimentally affects device performance, such as causing buffer leakage current in lateral power devices. [3] In addition, controllable charge compensation serves as a key component in device designs, e.g., forming current blocking layer. Without effective p-type β -Ga₂O₃, an alternative route is to use semi-insulating layer to engineer the electric field in devices. Thus far, there are limited reports on the epitaxy of semi-insulating β -Ga₂O₃.

Among various acceptors in β -Ga₂O₃, Mg represents one of the most promising candidates with relatively shallow acceptor level and the lowest formation energy as compared to other cation-site acceptors from DFT calculation. [4] In this study, Mg in-situ doping in MOCVD β -Ga₂O₃ was conducted for the first time. Trimethylgallium (TEGa) and O₂ were used as Ga, O precursors and Ar as the carrier gas. Mg doping was introduced by using Cp₂Mg as precursor. Chamber pressure was set at 60 Torr in this study. The MOCVD growth temperature for β -Ga₂O₃ was expanded to the range from 650 °C to 900 °C. The growth was conducted

on commercial Fe-doped (010) β -Ga₂O₃ substrates. From secondary ion mass spectroscopy (SIMS), in-situ Mg doping concentration was tuned in the range of 10^{18} cm⁻³ to 10^{20} cm⁻³ by the variation of Cp₂Mg molar flow. H impurity concentration exhibits an obvious companion with Mg doping concentration, indicating possible Mg-H complex configurations in as-grown MOCVD Mg-doped β -Ga₂O₃.

In addition, we analyzed the SIMS diffusion characteristics of Mg acceptor under different growth temperature of 700 °C to 900 °C. Experimental results indicate Mg incorporation has a minimum dependence on the growth temperature. Instead, the Mg diffusion has a strong dependence on the growth temperature. The diffusion barrier energy of Mg in MOCVD β -Ga₂O₃ was estimated at ~0.9 eV based on numeric analysis of the SIMS profile. Capacitance-voltage (C-V) on lateral Schottky diode structures, with an Mg-doped buffer layer and a Si-doped channel layer, also verified the depletion of interface charge, demonstrating the effective charge compensation by in-situ Mg doping.

In summary, we demonstrated in-situ Mg acceptor doping in MOCVD growth of (010) β -Ga₂O₃ thin films. The growth conditions for Mg-doped MOCVD β -Ga₂O₃ were established with controllable doping between 10^{18} cm⁻³ to 10^{20} cm⁻³ and a wide growth temperature regime, ranging between 700 °C and 900 °C. The as-grown thin films were characterized to be electrically insulating despite the Mg-H chemical companion. Mg diffusion was observed strongly dependent on the growth temperature. With low growth temperature, Mg diffusion can be significantly suppressed while maintaining high crystalline quality. The demonstration of in-situ Mg-doping in MOCVD β -Ga₂O₃ can provide new routes for high-performance device design and device fabrication.

Acknowledgment: The authors acknowledge the funding support from the Air Force Office of Scientific Research No. FA9550-18-1-0479 (AFOSR, Dr. Ali Sayir).

References:

- [1] Z. Feng et al., Appl. Phys. Lett., 114, 250601 (2019).
- [2] Z. Feng et al., Phys. Status Solidi RRL 14, 2000145 (2020).
- [3] M. H. Wong et al., Jpn. J. Appl. Phys. 55, 1202B9 (2016).
- [4] J. L. Lyons, Semicond. Sci. Technol. 33, 05LT02 (2018).

1:40 PM EL04.07.03

Acceptors in Gallium Oxide Jani Jesenovc, Jacob Ritter, Christopher Pansegrau, John McCloy and Matthew D. McCluskey; Washington State University, United States

Monoclinic gallium oxide (β -Ga₂O₃) is an ultra-wide bandgap semiconductor with potential applications in power electronics. Semi-insulating substrates are required for most practical devices such as metal-oxide-semiconductor field effect transistors. This presentation will discuss recent experimental studies on Czochralski-grown β -Ga₂O₃ single crystals doped with Mg or Zn acceptors. These dopants result in semi-insulating material and are likely compensated by oxygen vacancies and shallow donors. Ir impurities originating from the crucible form deep donors that also compensate acceptors. The Ir⁴⁺ oxidation state gives rise to an absorption threshold in the visible/UV part of the spectrum and an IR absorption peak at 5150 cm⁻¹. Acceptors are passivated by hydrogen, an omnipresent contaminant, resulting in IR absorption peaks corresponding to O-H vibrational modes near 3300 cm⁻¹.

1:55 PM EL04.07.04

High-Mobility Low-Temperature Metalorganic Vapor Epitaxy Grown (010) β -Ga₂O₃ Homoepitaxial Films and Its Application to Realize Low Resistance Ohmic Contacts Arkka Bhattacharyya, Praneeth Ranga, Saurav Roy and Sriram Krishnamoorthy; The University of Utah, United States

Metalorganic vapor phase epitaxy (MOVPE) has emerged as the leading growth technique that allows for the growth of high-quality β -Ga₂O₃ epitaxial films with mobility values closer to the theoretical limit (~ 200 cm²/Vs). In the first part of this work, we report on the growth of high-mobility β -Ga₂O₃ homoepitaxial thin

films grown at a temperature **more than 200°C** less than the conventional growth temperature window for metalorganic vapor phase epitaxy [1]. Low-temperature β -Ga₂O₃ thin films **grown at 600°C** on Fe-doped (010) bulk substrates exhibit remarkable crystalline quality, which is evident from the measured room temperature **Hall mobility of 186 cm²/Vs** for the unintentionally doped films. N-type doping is achieved by using Si as a dopant, and a controllable doping in the range of 2×10^{16} – 2×10^{19} cm⁻³ is studied. Si incorporation and activation is studied by comparing the silicon concentration from secondary ion mass spectroscopy and the electron concentration from temperature-dependent Hall measurements. The films exhibit **high purity (low C and H concentrations)** with a very low concentration of **compensating acceptors ($\sim 2 \times 10^{15}$ cm⁻³)** even at this growth temperature. Additionally, an abrupt doping profile with a forward decay of **~ 5 nm/dec (10 times improvement compared to what is observed for thin films grown at 810°C)** is demonstrated by growing at a lower temperature due to suppression of Si dopant segregation [2].

In the second part of this work, we use this low-temperature growth regime to achieve degenerately n-type Si-doped ($>10^{20}$ cm⁻³) β -Ga₂O₃ layers to realize high-quality low resistance Ohmic contacts. We perform selective area regrowth of heavily-doped n⁺ β -Ga₂O₃ Ohmic contacts to lightly doped channel layers using a novel Ni/SiO₂ mask which is patterned by a combination of dry and wet etching technique. The Ohmic metal stack of Ti/Au/Ni (20nm/100nm/30nm) was selectively evaporated using photolithography patterning and lift off process. The doping in the n⁺ β -Ga₂O₃ layers was estimated to be $\sim 2 \times 10^{20}$ cm⁻³. TLM measurements on the n⁺ β -Ga₂O₃ layers show **R_{sh}, R_c and ρ_c** values to be **45 Ω /sq, 0.08 Ω .mm and 8.2×10^{-7} Ω .cm²** respectively. These results indicate that these MOVPE-grown n⁺ β -Ga₂O₃ layers were able to maintain good material quality even in this doping regime and is comparable to or better than that reported by other techniques such as MBE and PLD[3], [4]. **Fully MOVPE-grown FET** performance will be presented. The growth of high mobility films with an expanded growth window, MOVPE technique for Ga₂O₃ growths can now be considered more versatile. The ability to perform selective area regrowth of ohmic contacts expands the capability of the MOVPE technique in terms of device processing as well. This initial result of the low temperature growth and selective area regrowth using MOVPE shows the promise of this approach to realize high-quality channel layers as well as low resistance contacts for several lateral and vertical device topology.

ACKNOWLEDGEMENT: This work was supported by the Air Force Office of Scientific Research under Award No. FA9550-18-1-0507 (Program Manager: Dr. Ali Sayir). We also acknowledge the II–VI foundation Block Gift Program for financial support. This work was performed in part at the Utah Nanofab sponsored by the College of Engineering and the Office of the Vice President for Research.

REFERENCES:

- [1] A. Bhattacharyya *et al.* " Low-temperature homoepitaxy of (010) β -Ga₂O₃ by metalorganic vapor phase epitaxy: Expanding the growth window", Appl. Phys. Lett. **117**, 142102 (2020)
- [2] P. Ranga *et al.* "Delta-doped β -Ga₂O₃ films with narrow FWHM grown by metalorganic vapor-phase epitaxy," Appl. Phys. Lett. **117**, 172105 (2020)
- [3] K. D. Leedy *et al.*, Appl. Phys. Lett. **111**, 012103 (2017)
- [4] Z. Xia *et al.*, *IEEE Electron Device Letters*, vol. 39, no. 4, pp. 568-571, April 2018

2:10 PM EL04.07.05

MOCVD Epitaxy of β -(Al_xGa_{1-x})₂O₃ Films on (100) and (-201) β -Ga₂O₃ Substrates with Al Compositions up to 52% A F M Anhar Uddin Bhuiyan, Zixuan Feng, Jared M. Johnson, Hsien-Lien Huang, Jinwoo Hwang and Hongping Zhao; The Ohio State University, United States

β -Ga₂O₃ has gained a remarkable attention in high power electronic applications due to its higher bandgap energy (~ 4.85 eV), predicted high breakdown field strength (~ 8 MV/cm), and availability of high-quality native substrates with different orientations. β -(Al_xGa_{1-x})₂O₃ alloys, due to its bandgap tuning capability up to ~ 8.8 eV, can take advantage of its higher breakdown voltage in not only vertical power devices but also in high-performance lateral devices through device scaling. Recently, modulation doped field effect transistors have

been demonstrated with promising transport properties by forming 2-dimensional electron gas in β -AlGaO/GaO heterostructures with limited Al composition in β -AlGaO layer ($x < 20\%$). High quality β -AlGaO epitaxy with higher Al compositions is required to form heterostructures with large band offset and thus high 2D electron density. While theoretical studies have predicted that the solubility limit of Al_2O_3 in β - Ga_2O_3 is as high as $\sim 70\%$, very limited Al incorporation in (010) β - $(\text{Al}_x\text{Ga}_{1-x})_2\text{O}_3$ films has been observed experimentally ($x < 27\%$), as targeting for higher Al composition resulted in phase segregation [1].

In this work, for the first time, we have studied the growth of β - $(\text{Al}_x\text{Ga}_{1-x})_2\text{O}_3$ thin films on (100) and (-201) oriented β - Ga_2O_3 substrates via metalorganic chemical vapor deposition (MOCVD). Trimethylaluminum (TMAI), Triethylgallium (TEGa), and pure O_2 were used as Al, Ga and O precursors, respectively. Argon (Ar) was used as the carrier gas. By the systematic tuning of TEGa/TMAI molar flow ratio, pure β -phase $(\text{Al}_x\text{Ga}_{1-x})_2\text{O}_3$ films with Al compositions up to 52% were achieved on (100) β - Ga_2O_3 substrates [2]. X-ray diffraction (XRD) and X-ray spectroscopy (XPS) were used for determining the bandgaps and the Al compositions. Two-dimensional twin boundary defects in the β - $(\text{Al}_x\text{Ga}_{1-x})_2\text{O}_3$ films with different Al compositions were investigated by utilizing atomic resolution scanning transmission electron microscopy (STEM) imaging. Coherent growth of high quality (100) β -AlGaO/GaO superlattice (SL) structures with abrupt interfaces and uniform Al distribution were observed with Al compositions as high as 50%. Step flow growth with lower RMS roughness values (< 1.2 nm) were observed for higher Al composition samples. A mechanism was proposed for the step-flow growth of high-Al content films by considering Al adatoms as preferred nucleation sites for $(\text{Al}_x\text{Ga}_{1-x})_2\text{O}_3$ growths. The growth of β - $(\text{Al}_x\text{Ga}_{1-x})_2\text{O}_3$ films on (-201) oriented β - Ga_2O_3 substrates also revealed higher Al incorporation in pure β -phase ($x \leq 48\%$) without causing phase segregations [3]. The bandgap energies for (-201) β - $(\text{Al}_x\text{Ga}_{1-x})_2\text{O}_3$ films extracted from XPS spectra ranged between 5.20 ± 0.06 eV ($x = 21\%$) and 5.72 ± 0.08 eV ($x = 48\%$). The surface morphologies showed elongated features with granules along [010] direction, which were suppressed with the increasing Al content. The influence of the chamber pressure and temperature on Al incorporations and the surface morphologies were studied.

In summary, we have demonstrated MOCVD growth of (100) and (-201) β - $(\text{Al}_x\text{Ga}_{1-x})_2\text{O}_3$ films with high-Al compositions. Results from this work provide great promises for future device technologies based on this emerging ultrawide band gap semiconductor material system.

Acknowledgment: The authors acknowledge the funding support from the Air Force Office of Scientific Research No. FA9550-18-1-0479 (AFOSR, Dr. Ali Sayir) and the National Science Foundation (Grant No. 1810041, No. 2019753).

References:

- Bhuiyan et al., APL Mater. 8, 031104 (2020).
- Bhuiyan et al., Cryst. Growth Des. 20, 6722 (2020).
- Bhuiyan et al., Appl. Phys. Lett. 117, 142107 (2020).

2:25 PM EL04.07.06

Carrier Density in Ga₂O₃ Measured by Infrared Absorption Ernesto Gribaudo¹, Etienne Gheeraert¹ and Toshimitsu Ito²; ¹Université Grenoble Alpes, France; ²AIST, Japan

Gallium oxide Ga₂O₃ is a very promising material for the next generation wide bandgap semiconductor devices. Even if impressive electronic devices have already been fabricated, demonstrating the high potential of this new semiconductor, the knowledge about its electronic properties is still weak. The purpose of this work is to explore dopants and carriers by infrared absorption in gallium oxide. In regular semiconductor, such technique allows to identify at low temperature the ground level of dopants as shallow level centers, their excited states and photoionisation. At high temperature, when all the dopants are ionized, absorption by free carriers can be observed. All these information about the semiconductor electronic properties make infrared absorption a powerful technique.

In this work β - Ga_2O_3 crystals were grown by the floating-zone (FZ) method using no crucibles. By the zone-

refining that were executed by repeating the FZ procedure, very higher purity compared to that of regular growth method was obtained. Crystals were doped with Si with a concentration estimated from SIMS measurements from $2 \times 10^{17} \text{ cm}^{-3}$ to $1 \times 10^{19} \text{ cm}^{-3}$. Infrared was recorded in transmission from 5K to 300K. All the spectra exhibit a strong absorption continuum from 0.2 eV, with no measurable transmission below this value, and extending beyond 1.2 eV for high doping values. No absorption peak, that could have been assigned to a transition from the dopant ground level to an excited state was observed, whatever the temperature and the doping level.

The absorption intensity in the continuum, at 0.5 eV, is clearly correlated to the Si concentration. A linear relation is proposed, allowing the measure of the Si concentration in Ga_2O_3 in a non destructive way. This continuum is assigned to free electron infrared absorption.

The fact that no absorption peak is observed, even at 5K, and that the free absorption is observed whatever the temperature, suggest that silicon is ionized without any ionization energy. This could be attributed to an impurity band formed by very shallow silicon centers.

2:40 PM EL04.07.07

Late News: Ge Doping of Epitaxial β - Ga_2O_3 Films by MOCVD Fikadu Alema, George Seryogin, Alexei Osinsky and Andrei Osinsky; Agnitron Technology Incorporated, United States

We report on Ge doping of epitaxial Ga_2O_3 films by MOCVD using germane (GeH_4) balanced in nitrogen as a Ge source. The incorporation efficiency of Ge into Ga_2O_3 films grown using triethylgallium (TEGa) and trimethylgallium (TMGa) sources was studied by varying substrate temperature, GeH_4 flow rate, growth rate, and oxygen flow rates using SIMS. As expected, Ge incorporation increased with GeH_4 flow rate, but it incorporated well into films grown using TEGa than that grown using TMGa despite similar growth conditions. Hall Effect measurement and SIMS showed a strong dependence of Ge incorporation on the growth temperature. By decreasing the substrate temperature over a range of $\sim 200^\circ\text{C}$, the film's Ge concentration has increased by two orders of magnitude. The Hall Effect measurement also showed Ge doped films with RT electron mobilities ranging from ~ 40 to $\sim 150 \text{ cm}^2/\text{Vs}$ with the corresponding carrier concentration of $n = 3 \times 10^{19}$ to $n = 2 \times 10^{16} \text{ cm}^{-3}$ for Ge doped films. Temperature-dependent Hall Effect measurement will be discussed to investigate the donor activation energy and compensation concentration in representative TMGa and TEGa grown films. The results will be compared with similar films doped by Si. In this talk, the effect of Ge doping on the surface roughness and the incorporation of carbon and hydrogen impurities into the films will be discussed.

SESSION EL04.08: Ga_2O_3 II
Session Chair: Sriram Krishnamoorthy
Monday Afternoon, April 19, 2021
EL04

4:00 PM *EL04.08.01

Electro-Thermal Co-Design of a Gallium Oxide MODFET Sukwon Choi; The Pennsylvania State University, United States

To extend further the electrical performance envelope of wide bandgap (WBG) electronics based on gallium nitride (GaN) and silicon carbide (SiC), novel device structures based on ultra-wide bandgap (UWBG) semiconductors such as β -phase gallium oxide (Ga_2O_3) are being actively developed. While UWBG electronics target for higher power handling capabilities and smaller device footprints, the thermal conductivity of Ga_2O_3 is an order of magnitude lower than those for GaN and SiC. Therefore, device self-heating has become a major challenge to accomplish the successful transition from WBG electronics to the UWBG device technology. In this talk, the electro-thermal co-design process for a $(\text{Al}_x\text{Ga}_{1-x})_2\text{O}_3/\text{Ga}_2\text{O}_3$ modulation-doped field-effect

transistor (MODFET) will be demonstrated. First, the steady-state and transient thermal response of an operational MODFET is characterized using a recently developed 2D material-assisted Raman thermography technique. Second, a multi-physics device modeling scheme is used to reproduce the temperature-dependent electrical output characteristics as well as the self-heating behavior in response to the electrical inputs. Finally, this coupled electro-thermal model is used to design a device-level thermal management solution, taking advantage of a low thermal resistance composite substrate.

4:25 PM EL04.08.02

Thermal Annealing of α -Ga₂O₃ on the Millisecond Time Scale and the Observation of γ -Phase Inclusions

Katie R. Gann, Ming-Chiang Chang, Aine B. Connolly, Duncan R. Sutherland, Maximillian Amsler, R. Bruce van Dover and Michael O. Thompson; Cornell University, United States

β -Ga₂O₃ has shown significant promise as a wide bandgap, high-breakdown field semiconductor with extensive device applications. While the β -phase is the thermodynamically stable phase, there are a variety of polymorphs in the system, including the hexagonal α -phase with the widest bandgap, a defect spinel γ -phase, and an δ -phase with predicted piezoelectric properties. These alternate polymorphs, while metastable, readily form under various processing conditions. Laser spike annealing (LSA), with heating times from 150 μ s to 10 ms, has been shown to be effective in kinetically trapping metastable phases from a deposited amorphous phase. By varying the time and temperature, a processing-phase diagram for metastable phases can be rapidly developed using high throughput characterization methods.

The metastable phase formation sequence from amorphous Ga₂O₃, on a non-crystalline neutral substrate, was determined for annealing (dwell) times from 250 μ s to 10 ms (τ_{dwell}), and peak annealing temperatures (T_{peak}) between ambient and 1400 °C. Amorphous Ga₂O₃ films, 170 nm thick, were sputter deposited from a Ga₂O₃ target in an Ar(90%)/O₂(10%) ambient onto 100 mm oxidized (20 nm thermal SiO₂) Si wafers. Samples were annealed with 617 time/temperature conditions to fully characterize the time and temperature phase space using a CO₂ laser spike annealing system. The resulting thermally induced structural transformations were characterized with a variety of techniques, including optical imaging, reflectance spectroscopy, X-ray diffraction, and transmission electron microscopy. For temperatures below ~650 °C, no transformations were observed. Between 650 and 800-850 °C, and for all dwell times explored, the spinel γ -phase was observed in the quenched samples. At higher temperatures above 850-950 °C, the equilibrium β -phase was observed in the quenched samples. No other phases were observed under any processing conditions. TEM micrographs show that the γ -phase nucleated near the center of the deposited film homogeneously with minimal heterogeneous nucleation at either the SiO₂ interface or surface. We postulate that this phase is always the first to nucleate, with β -phase only nucleating heterogeneously off of the γ -phase at higher temperatures. This is supported by observations of extremely large grains of the β -phase at short annealing times, suggesting nucleation is limited with significant grain growth during the subsequent heating and cooling times of the thermal process. The low surface energy implied by the homogeneous nucleation also suggests a possible explanation for the widely observed γ -phase inclusions observed in MBE grown β - and α -phase films.

4:40 PM DISCUSSION TIME

4:55 PM EL04.08.04

Thermal Transport Across Metal/ β -Ga₂O₃ Interfaces Jingjing Shi¹, Chao Yuan¹, Shangkun Wang¹, Riley Hanus¹, Zhe Cheng^{1,2} and Samuel Graham^{1,1}; ¹Georgia Institute of Technology, United States; ²University of Illinois at Urbana-Champaign, United States

β -Ga₂O₃ is a very promising material to be applied in power and radio frequency devices because of its exceptional properties. However, the heat dissipation of its devices will be limited by its ultra-low thermal conductivity. Previous study showed that its device could achieve high power density with double-side cooling strategy and thin Ga₂O₃ layer. Therefore, the thermal transport across β -Ga₂O₃ interfaces becomes very important because the boundary resistance would be a main source of the total device resistance. In this work,

we study the thermal transport at β -Ga₂O₃/metal interfaces which play important roles in heat dissipation and as electrical contacts in β -Ga₂O₃ devices. A theoretical Landauer approach was used to model and elucidate the factors that impact the thermal transport at these interfaces. Experimental measurements using time-domain thermoreflectance (TDTR) provided data for the thermal boundary conductance (TBC) between β -Ga₂O₃ and a range of metals used to create both Schottky and ohmic contacts. From the modeling and experiments, the relation between metal cut-off frequency and the corresponding TBC is observed. Moreover, the effect of metal cut-off frequency on TBC is seen as the most significant factor followed by chemical reactions between the metal and the β -Ga₂O₃. Among all metal/Ga₂O₃ interfaces, for Schottky contacts, Ni/Ga₂O₃ interfaces show the highest TBC, while for ohmic contacts, Cr/Ga₂O₃ interfaces show the highest TBC. While there is a clear correlation between TBC and the phonon cutoff frequency of metal contacts, it is also important to control the chemical reactions at interfaces in order to maximize the TBC in this system.

5:10 PM EL04.08.05

Computational Fermi Level Engineering and Doping-Type Conversion of Ga₂O₃ via Three-Step Processing

Anuj Goyal¹, **Andriy Zakutayev**¹, **Vladan Stevanovic**² and **Stephan Lany**¹; ¹National Renewable Energy Laboratory, United States; ²Colorado School of Mines, United States

Ga₂O₃ is being actively explored for power electronics, deep-ultraviolet optoelectronics, and other applications due to its ultra-wide bandgap and low projected fabrication cost of large-size and high-quality crystals. N-type doping of Ga₂O₃ can be achieved and tuned, but p-type doping faces fundamental obstacles due to deep character of acceptor levels and polaron transport of resulting holes. However, successful engineering of Ga₂O₃ based devices requires critical control of doping density, Fermi level position, and free carrier concentration, providing opportunities for predictive process simulation. We use first-principles defect theory and defect equilibrium calculations to simulate a 3-step growth-annealing-quench protocol for hydrogen assisted Mg doping in Ga₂O₃, taking into account the hydrogen-oxygen-water gas phase equilibrium. We predict type conversion to a net *p*-type regime following O-rich annealing after growth under reducing conditions in the presence of H₂. This process is similar to the Mg acceptor activation by H removal in GaN. We show that there is an optimal temperature that maximizes the net acceptor density during the equilibrium annealing step for a given Mg doping level. Quenching of non-equilibrium annealed samples then results in a Fermi level E_F below mid-gap down to about $E_V + 1.5$ eV, creating a significant number of uncompensated neutral Mg_{Ga}⁰ acceptors. The resulting free hole concentration in quenched samples is very low ($10^9 - 10^{12}$ cm⁻³) due to deep energy level of these Mg acceptors, but this type converted Ga₂O₃ material can create a significant built-in field in a *p-n* junction with an adjoining n-type material. Additionally, the electron concentration is greatly suppressed in such acceptor-doped Ga₂O₃, which could enable the use as a current blocking layer to fabricate normally-off (enhancement-mode) vertical Ga₂O₃ based metal-oxide-semiconductor field effect transistors (MOSFETs), and as a guard ring for edge termination in MOSFETs and Schottky barrier diodes (SBDs) with increased breakdown voltage.

5:25 PM *EL04.08.06

Thermal and Electrical Properties of Ga₂O₃ FETs and Diodes Martin Kuball; University of Bristol, United Kingdom

Ga₂O₃ offers exciting new opportunities for power electronics with its ultra-wideband gap; numerous materials related challenges such as its low thermal conductivity, deep level traps and also the challenge to achieve “good” p-doping remain, however, these need to be resolved to be able to exploit Ga₂O₃’s full potential. I will review our latest results in this field, amongst them device temperature measurements and cooling mitigation strategies, trap generation during device stress also nitrogen implantation induced trap states, superjunction designs.

SESSION EL04.09: Ga₂O₃ III
Session Chairs: Nasim Alem, Masataka Higashiwaki and Hongping Zhao
Monday Afternoon, April 19, 2021
EL04

8:00 PM EL04.09.01

Late News: Prospects for Donor-Doping AIGO Alloys Joel Varley¹, Darshana Wickramaratne² and John L. Lyons²; ¹Lawrence Livermore National Laboratory, United States; ²U.S. Naval Research Laboratory, United States

Gallium oxide has emerged as a promising ultrawide-bandgap semiconductor partly due to its ability to be *n*-type doped. Alloying Ga₂O₃ with Al₂O₃ can further widen its band gap, potentially enabling novel device designs. But this alloying quickly leads to an increase in the position of the conduction-band minimum, and it is not clear whether (Al_xGa_{1-x})₂O₃ (“AIGO”) alloys will also be *n*-type dopable. Here we systematically explore the properties of group-IV (C, Si, Ge, and Sn) and transition metal (Hf, Zr, and Ta) substitutional dopants in AIGO alloys using first-principles hybrid functional calculations. In Ga₂O₃, all of these dopants act as shallow donors, but in Al₂O₃ they are deep defects characterized by the formation of either *DX* centers or positive-U (+/0) levels. Combining our calculations of dopant charge-state transition levels with information of the AIGO alloy band structure, we estimate the critical Al composition at which each dopant transitions from being a shallow to a deep donor. We identify Si as being the most efficient dopant to achieve *n*-type conductivity in high Al-content AIGO alloys, acting as a shallow donor over the entire predicted stability range for AIGO solid solutions.

This work was partially performed under the auspices of the U.S. DOE by the Lawrence Livermore National Laboratory under Contract No. DE-AC52-07NA27344 and supported by the Critical Materials Institute, an Energy Innovation Hub funded by the U.S. DOE, Office of Energy Efficiency and Renewable Energy, Advanced Manufacturing Office. JLL and DW were supported by the Office of Naval Research through the Naval Research Laboratory’s Basic Research Program.

8:15 PM EL04.09.02

Control of Surface Morphologies of M-Plane α -Al₂O₃ Homoepitaxial Films Using Plasma-Assisted Molecular Beam Epitaxy Riena Jinno and Hironori Okumura; University of Tsukuba, Japan

Rhombohedral α -Al₂O₃ (sapphire) ($E_g=8.8$ eV) and its alloys with α -Ga₂O₃ ($E_g\sim 5.3$ - 5.6 eV) have attracted for high power electronic devices and optical devices with function in the deep ultra-violet region due to the large predicted critical electric field and wide bandgap energy [1]. Insulating α -Al₂O₃ substrates have been widely used for the thin film growth of different materials because of the large-area and low-cost α -Al₂O₃ bulks grown by melting methods. However, the reports on homoepitaxial growth of α -Al₂O₃ thin films are limited [2]. In this study, we investigated the surface morphologies of α -Al₂O₃ thin films, which were grown by plasma-assisted molecular beam epitaxy (PAMBE) under various growth conditions.

The aluminum-oxide thin films were grown on a m-plane α -Al₂O₃ substrate with a miscut angle of 2 ° toward [0001] by PAMBE. The radio frequent power and oxygen flow rate were fixed at 150 W and 1.0 sccm, respectively. The thermocouple substrate temperature (T_{sub}) and Al beam equivalent pressure (BEP) were changed in the ranges of 130-830 °C and 4.0×10^{-6} - 1.8×10^{-5} Pa, respectively. The surface morphology was observed by atomic force microscopy.

The amorphous AlO_x films were grown for $T_{sub}<330$ °C, while the single-crystal α -Al₂O₃ films were homoepitaxially grown for $T_{sub}>530$ °C as revealed by reflection high energy electron diffraction and x-ray diffraction. The growth rate of the α -Al₂O₃ films increased with increasing the Al BEP, and showed a larger slope at the Al BEP higher than 1.3×10^{-5} Pa. The growth rate was independent on the substrate temperature between 130 and 830 °C. The α -Al₂O₃ surfaces exhibited root mean square (RMS) roughness smaller than 0.6 nm for the Al BEP lower than 1.3×10^{-5} Pa, while the α -Al₂O₃ surfaces suddenly increased the RMS roughness

larger than 10 nm for the Al BEPs higher than 1.3×10^{-5} Pa. The boundary between the smooth and rough surface morphologies corresponded with the singular point where the slope of growth rate versus the Al BEP changed. We consider that the Al BEP lower than 1.3×10^{-5} Pa agrees with the O-rich condition and that the Al-rich condition probably contributes to the rough surface morphologies and/or nonstoichiometry of the α -Al₂O₃ epitaxial films. From these results, the O-rich growth condition with higher growth temperature than 530 °C is suitable for the homoepitaxial growth of α -Al₂O₃.

This work was supported by NEDO Feasibility Study Program Uncharted Territory Challenge 2050.

[1] S. Fujita, et. al., Jpn. J. Appl. Phys. **55**(2016) 1202A3.

[2] T. Maeda, et al., J. Cryst. Growth, **177**(1997) 95-101.

8:30 PM EL04.09.03

Killer Defects in β -Ga₂O₃ Schottky Barrier Diodes Observed by Ultrahigh Sensitive Emission Microscopy and Synchrotron X-Ray Topography Makoto Kasu¹, Sayleap Sdoeung¹, Kohei Sasaki², Katsumi Kawasaki³, Jun Hirabayashi³ and Akito Kuramata²; ¹Saga University, Japan; ²Novel Crystal Technology, Inc., Japan; ³TDK Corporation, Japan

β -Ga₂O₃ with a bandgap of 4.5–4.8 eV is expected to serve as a high-power semiconductor surpassing the capabilities of SiC and GaN. Recently, we demonstrated the production of > 20 A-class β -Ga₂O₃ Schottky barrier diodes (SBDs) with a low on-state resistance of 6 m Ω .cm². However, the reliability of SBD plays a crucial role in the commercialization of SBDs in power system circuits. It is especially important to identify killer defects that can cause an increase of reverse leakage current and/or a decrease in the breakdown voltage. The sample was halide vapor phase epitaxy (HVPE)-grown ~10- μ m-thick epitaxial layer on EFG-grown β -Ga₂O₃ (001) substrate. Pt/Ti/Au Schottky electrodes with diameters of 50–1000 μ m were formed on the surface, and Ti/Au ohmic contacts were formed on the back surface. First, we observed light emission patterns from SBDs in operation using ultrahigh sensitive emission microscopy. The emission microscopy equipment consists of an ultrahigh sensitive electron-multiplying CCD camera and a probe station enabling the observation of light emission patterns of an SBD in real time.

In the reverse bias conditions, we detected emission patterns from SBDs with a high leakage current. The patterns were observed by AFM and synchrotron X-ray topography, and their cross-sections were observed by STEM. The killer defects were found to be stacking faults and polycrystalline defects in the HVPE epitaxial layer. Their properties will be reported.

8:45 PM EL04.09.05

Growth and Characterization of MOVPE-Grown Low Sheet Resistance β -(Al_xGa_{1-x})₂O₃/ β -Ga₂O₃ Heterostructure Channels Praneeth Ranga¹, Arkka Bhattacharyya¹, Adrian Chmielewski², Rujun Sun¹, Saurav Roy¹, Mike Scarpulla¹, Nasim Alem² and Sriram Krishnamoorthy¹; ¹The University of Utah, United States; ²The Pennsylvania State University, United States

In this work, we study the growth and characterization of β -(Al_xGa_{1-x})₂O₃/ β -Ga₂O₃ heterostructure channels with record low sheet resistance. In the past few years, β -Ga₂O₃ has emerged as a promising material for next-generation power electronics applications. The high bandgap of β -Ga₂O₃ leads to a very high predicted breakdown field of 6 – 8 MV/cm, larger than that of GaN and SiC. However, room temperature mobility of low-doped β -Ga₂O₃ is still limited to 200 cm²/V.s due to severe polar optical phonon scattering. Ab-initio calculations show that mobility of modulation-doped β -(Al_xGa_{1-x})₂O₃/ β -Ga₂O₃ channels could exceed that of uniformly-doped β -Ga₂O₃ layers at charge densities nearing 5×10^{12} cm⁻² [1]. This is attributed to enhanced screening of LO phonons modes at high 2DEG sheet charge densities. Currently, the sheet charge density of single β -(Al_xGa_{1-x})₂O₃/ β -Ga₂O₃ heterostructure is limited to $\sim 5 \times 10^{12}$ cm⁻² [2], which is in turn limited by the Al composition of the MBE-grown β -(Al_xGa_{1-x})₂O₃. To achieve such high sheet charge densities, a high Al content β -(Al_xGa_{1-x})₂O₃ barrier along with a sharp delta sheet is necessary. Recently, high-quality β -Ga₂O₃ films with mobilities close to 200 cm²/V.s have been realized MOVPE. Growth of (100) β -(Al_xGa_{1-x})₂O₃ layers up to 52% has been realized using the MOVPE technique [3]. In addition, n-type doping and delta doping were also achieved [4,5]. However, the FWHM of the Si delta sheet was found to be larger than that of MBE-grown β -

Ga₂O₃. By optimizing the growth conditions MOVPE-grown β -(Al_xGa_{1-x})₂O₃/ β -Ga₂O₃ heterostructures with high charge and mobility can be potentially attained.

Growth of delta-doped (010) β -Ga₂O₃ films is performed by Agnitron Agilis MOVPE reactor with TEGa, O₂ and silane (SiH₄) as precursors and argon as a carrier gas. Delta doping of β -Ga₂O₃ is achieved by interrupting the growth of β -Ga₂O₃ and supplying silane to the reactor. Multiple samples are grown under varying growth temperatures to characterize the spread of silicon donors β -Ga₂O₃. CV measurements are used to characterize the sheet charge density and FWHM of the silicon delta sheet. SIMS characterization revealed that surface segregation is the key mechanism, which leads to large FWHM Si delta sheets. By reducing the growth temperature to 600 C, CV measured FWHM of 3.2 nm is achieved, which is close to the FWHM of an ideal delta sheet. Similar growth conditions are utilized to realize a sharp delta sheet in β -(Al_xGa_{1-x})₂O₃/ β -Ga₂O₃ heterostructure. Two delta-doped β -(Al_xGa_{1-x})₂O₃/ β -Ga₂O₃ heterostructure are grown with different β -(Al_xGa_{1-x})₂O₃ spacer thicknesses (2- 4 nm) under identical growth conditions. MOVPE based low-temperature n⁺ regrowth process is utilized to achieve ohmic contacts to the channel. Hall measurements showed a sheet charge density of 6.4 x 10¹² to 1 x 10¹³ cm⁻² and mobility of 125 – 111 cm²/V.s. FET devices fabricated using heterostructure channels show a peak current of 22 mA/mm and transconductance of 7 mS/mm. Sheet resistance of 5.3 k Ω /square is realized at room temperature, which is the lowest value for a single heterostructure in current literature. CV and TLM characterization revealed similar charge density and sheet resistance values, confirming the properties of the heterostructure channel. These results show that high-quality β -(Al_xGa_{1-x})₂O₃/ β -Ga₂O₃ heterostructures with mobility exceeding 100 cm²/Vs can be realized using MOVPE technique. References: [1] Kumar.A et.al *Journal of Applied Physics* 128.10 (2020): 105703. [2] Kalarickal N.K et.al *Journal of Applied Physics* 127.21 (2020): 215706. [3] Bhuiyan AFM et.al *Crystal Growth & Design* 20, 6722-6730 (2020). [4] Ranga.P et al. *Applied Physics Express* 13.4 (2020): 045501. [5] Ranga.P et al. *Applied Physics Express* 12.11 (2019): 111004. Acknowledgments: This material is based upon work supported by the Air Force Office of Scientific Research under Award No. FA9550-18-1-0507 and monitored by Dr. Ali Sayir.

9:00 PM BREAK

9:15 PM EL04.09.06

Structural Analysis of Ion Implanted and Exfoliated (010) and (-201) β -Ga₂O₃ Michael E. Liao¹, Yekan Wang¹, Kenny Huynh¹, Fengwen Mu², Tiangui You³, Wenhui Xu³, Zhe Cheng⁴, Jingjing Shi⁴, Tadatomu Suga⁵, Xin Ou³, Samuel Graham^{4,4} and Mark S. Goorsky¹; ¹University of California, Los Angeles, United States; ²Institute of Microelectronics of Chinese Academy of Science, China; ³Shanghai Institute of Microsystem and Information Technology, Chinese Academy of Sciences, China; ⁴Georgia Institute of Technology, United States; ⁵Meisei University, Japan

The evolution of defects in both He⁺ and H⁺ ion implanted β -Ga₂O₃ for exfoliation was assessed using triple-axis x-ray diffraction and transmission electron microscopy. First, (010) and (201) substrates were He⁺ ion implanted simultaneously at -20 °C with an ion energy of 160 keV and a dose of 5 × 10¹⁶ cm⁻². Strain profiles for both implanted orientations were obtained from modeling the symmetric X-ray diffraction curves with dynamical simulations and the differences are attributed to the structural anisotropy of β -Ga₂O₃. After annealing at 200 °C to initiate He blister nucleation followed by 500 °C for up to 96 hours to induce He blister growth, the crack formation at the ion projected range beneath the surfaces also differed between the (010) and (201) implanted substrates. The annealed (010) substrates showed large continuous cracks at the projected range relatively parallel to the substrate surface. These cracks correspond to blistering directly above at the surface – a clear sign of exfoliation. In contrast, while the (201) annealed substrate showed disjointed cracks at the projected range, which would also be compatible with exfoliation, did not exhibit surface blistering. Furthermore, the cracks in this substrate were tilted at a series of angles ranging from 0° to 54° from the surface towards the (201) planes. Eighty percent of the cracks observed were tilted 54° – which is parallel to the (100) plane, a primary cleavage plane in β -Ga₂O₃. Note that the (100) is 90° from (010) and angled cracks were not observed in a previous effort¹ nor in this work. This directional dependence of the crack formation in the (201) substrate is a consequence of the anisotropic properties of the monoclinic structure, suggesting the (100)

cleavage plane plays an important role in crack propagation for exfoliation. After annealing at 500 °C for 96 hours, the strain was removed from the (010) substrates while the ($\bar{2}01$) substrates still exhibited residual strain. In a second set of samples that used H⁺ implantation at 35 keV, residual strain was also observed in annealed and exfoliated ($\bar{2}01$) β -Ga₂O₃ layers. These H⁺ implanted ($\bar{2}01$) substrates were exfoliated and bonded to (0001) 4H-SiC substrates. Exfoliation due to blister growth of the implanted ions with annealing typically corresponds to the removal of the implant-induced strain. However, as was the case for the He⁺ implant, diffraction measurements showed the presence of strain in the ($\bar{2}01$) β -Ga₂O₃ layers even after exfoliation that was only removed after further annealing. The analysis of the evolution of this strain is important because strain plays a significant role in important characteristics such as electrical and thermal transport. Subsequent annealing at 800 °C for 30 mins (with a ramp up rate of 5 °C/min), resulted in relieving this residual strain. Corresponding thermal measurements showed that the thermal conductivity of these β -Ga₂O₃ improved after annealing and removing the residual strain.

References:

1. M.E. Liao, et al., ECS J. of Solid State Sci. and Technol., 8(11), P673 (2019).

The authors M.E.L., Y.W., K.H., Z.C., J.S., S.G., and M.S.G. would like to acknowledge the support from the Office of Naval Research through a MURI program, grant No. N00014-18-1-2429.

9:30 PM EL04.09.07

Mg Acceptor Level in Ga₂O₃ as Studied by Photo-Induced Electron Paramagnetic Resonance Suman Bhandari and Mary E. Zvanut; The University of Alabama at Birmingham, United States

Gallium oxide is a wide band-gap (4.6-4.9 eV) semiconductor that has potential for power electronics. Doping Ga₂O₃ with Mg makes it semi-insulating material, which can be an integral part of power devices. For such applications, knowledge of the Mg-related defect level is essential. Theory predicts a Mg acceptor level (Mg⁻⁰) ~1.2 eV above valence band maximum (VBM) whereas thermal measurements using electron paramagnetic resonance (EPR) place the level ~0.65 eV above VBM [1, 2]. To address the disagreement between the reported defect levels, we investigate optical absorption of neutral Mg acceptors (Mg⁰) using photo-induced EPR. In this approach, we consider relaxation of the defect during optical excitation and determine the defect level and associated relaxation energy. Previously, using a similar technique, we have determined the Fe^{2+/3+} level and associated relaxation energy in Ga₂O₃ [3]. In this work, by examining two different Mg-doped Ga₂O₃ samples, which were grown by the Czochralski method at two different institutions, we show that the presence of other defects could affect the experimental results and possibly lead to misinterpretation. The crystals are irradiated with energies between 0.6 and 4.7 eV after Mg⁰ is generated with an LED (4.4±0.2 eV), and the effect on the amount of Mg⁰ is investigated at 130 K. The steady state EPR results show that, for one set of samples, the amount of Mg⁰ starts to decrease near 1.7 eV whereas for the other set of samples, the decrease begins at approximately 1 eV. The decrease in the amount of Mg⁰ indicates that Mg⁰ becomes Mg⁻ by either of the two processes: when electrons are excited 1) from valence band to Mg⁰ or 2) from other defects to conduction band and subsequently captured by Mg⁰. For samples with photo-threshold near 1.7 eV, no new defects appear nor do other existing defects change when the decrease of Mg⁰ is initiated. Therefore, we disregard the second process for these samples. Furthermore, a preliminary analysis of the optical cross section spectrum obtained from photo-EPR yields values for the defect level and relaxation energy that agree reasonably well with the predicted defect level for Mg⁻⁰ when a relaxation energy of ~1 eV is considered. On the other hand, for the set of samples with the 1 eV photo-threshold, an unknown defect 'X' increases when Mg⁰ starts decreasing, suggesting that the defect 'X' could be responsible for the decrease of Mg⁰. We suggest that the 1 eV threshold could represent a defect level for 'X', which lies approximately 1 eV below conduction band minimum. In the talk, we will show the analysis of the optical cross section spectrum for both sets of samples and discuss ambiguities caused by the presence of other defects. In addition, we will present a detailed analysis of the optical cross section spectrum to supplement our preliminary results suggesting that the ~1.7 eV photo-threshold likely represents the Mg⁻⁰ level accompanied by a large relaxation energy.

Acknowledgement:

NSF Grant: DMR-1904325 supports the work at UAB. We would like to acknowledge Jacob Leach, Kyma Inc. and Kevin Stevens, NG Synoptics, and Matthew D. McCluskey, Washington State University for the Mg-doped Ga₂O₃ samples.

Reference:

1. J. L. Lyons, *Semicond. Sci. Technol.* 33 (2018) 05LT02 (5pp)
2. Lenyk et al., *Appl. Phys. Lett.* 116, 142101 (2020)
3. Bhandari et al., *J. Appl. Phys.* 126, 165703 (2019)

9:45 PM DISCUSSION TIME

10:00 PM EL04.09.09

Recessed Gate Enhancement-Mode Ultrawide Bandgap Al_xGa_{1-x}N Channel MOSHFET with Drain Current 0.48 A/mm and Threshold Voltage +3.6 V Shahab Mollah, Kamal Hussain, Abdullah Mamun, Mikhail Gaevski, Grigory Simin, MVS Chandrashekhar and Asif Khan; University of South Carolina, United States

For ultra-wide bandgap (UWBG) devices to truly exploit their potential for power electronics applications, it is essential to develop enhancement mode (normally-off) devices. In the past, normally off devices have been made using p-gate, fluorine treatment and recessed gate techniques. Recently, enhancement mode devices were reported by Douglas *et al* using p-AlGa_N gate [1] and by Klein *et al* using fluorine treatment [2]. In the past, we have shown that the performance of normally-on UWBG AlGa_N HFETs can be significantly improved using insulating gate MOSHFET design with Al₂O₃[3] and ZrO₂ gate dielectrics [4]. Here we use stack of these two dielectric materials to make high-current recessed gate enhancement mode UWBG Al_{0.60}Ga_{0.40}N/Al_{0.40}Ga_{0.60}N MOSHFETs.

The epitaxial layers for the devices were grown by low pressure metal organic chemical vapor deposition on AlN (3 μm)/sapphire template on which a graded composition back-barrier Al_xGa_{1-x}N layer (x from 1 to 0.4) was grown. The back-barrier design enables a reduction in leakage currents by screening the substrate-epilayer growth interface. It also leads to a tighter confinement of the 2-DEG which improves the ON-OFF ratios, drain-currents, and the sub-threshold swing factor. It was followed by the Al_{0.40}Ga_{0.60}N channel layer of 185 nm thickness. On top of this a 170 Å thick n- Al_{0.60}Ga_{0.40}N barrier layer was grown which was followed by a 200 Å highly doped composition graded Al_xGa_{1-x}N layer with x-value changing from 0.60 to 0.3 towards the surface to facilitate the ohmic contact. The n-doping of this layer compensates the positive charges resulting from the reverse composition grading. The 2DEG sheet resistance was ~1900 Ω/square. Annealed source-drain ohmic contact metallization (Zr/Al/Mo/Au) yielded contact resistance of 1.7 Ω-mm. Gate recess etching through the top barrier, resulted in the positive shift of the threshold voltage by ≈ 12 V compared to devices without gate-recess (D-mode). Then a 25 nm thick ZrO₂-Al₂O₃ insulator stack was deposited in the recess region using Atomic Layer Deposition (ALD) to suppress leakage gate current and to enable positive gate bias operation. Gate electrode was made using Ni/Au metallization. The device exhibited a threshold-voltage (V_{TH}) of +3.6 V and drain source saturation current (I_{DS}) as high as 480 mA/mm at a gate voltage V_{GS} = +12 V. The peak extrinsic transconductance in the Al₂O₃-ZrO₂-MOSHFET is G_M ≈ 70 mS/mm.

To determine the factors leading to the high drain current we extracted the gate voltage dependencies of electron sheet density N_S and electron mobility μ. The extracted sheet carrier density is N_S ≈ 1.6 × 10¹³ cm⁻². μ is as high as 1600 cm²/(V.s) at low gate voltage near threshold V_G=2V and decreases down to 200 cm²/(V.s) at V_G +12V. The on-state field effect mobility is comparable to our depletion mode devices [3]. The E-mode MOSHFET shows a hysteresis of 0.5 V between forward and reverse sweep of gate voltage, higher than that of D-mode MOSHFET (0.2 V) indicating higher trap charges at semiconductor/oxide interface or bulk. For our E-mode MOSHFET, we estimated a sub-threshold slope (SS) value of 128 mV/decade and an ON/OFF ratio of more than 1.5x10⁸, while the SS value for D-mode device is ~100 mV/decade. This slight increase of SS is

consistent with the increased hysteresis in the transfer curve. The gate leakage currents at $V_G = -20V$ was 30 pA indicates the high quality of the oxide layer. Our studies suggest that UWBG AlGaIn MOSHFETs are very promising candidates for next generation power electronic devices.

References:

- [1] E. A. Douglas et al., J. Vac. Sci and Technol. B, **37**, 021208(2019).
- [2] B. A. Klein et al., Appl Phys. Lett., **114**, 112104(2019).
- [3] S. Mollah et al., phys. status solidi (a) **217**, 7, 1900802 (2020).
- [4] S. Mollah et al., Semicond. Sci. Technol., **34**,125001(2019).

SESSION EL04.10: Diamond I
Session Chairs: Robert Nemanich and Julien Pernot
Tuesday Morning, April 20, 2021
EL04

8:00 AM *EL04.10.01

Growth of High-Purity Diamond Films and Doping for Quantum Device Applications Tokuyuki Teraji;
National Institute for Materials Science, Japan

Formation and control of electron spin in diamond is attracting much attention for next-generation quantum information and quantum sensing devices. With this fact in mind, we provide a guideline for the growth of homoepitaxial diamond films that possess higher crystalline quality, higher chemical purity, and a higher carbon isotopic ratio and nitrogen doping. A custom-built microwave plasma-assisted chemical vapor deposition system was constructed to achieve these requirements. To improve both the purity and crystalline quality of homoepitaxial diamond films, an advanced growth condition was applied: higher oxygen concentration in the growth ambient. Under this growth condition for high-quality diamond, a thick diamond film of $>30 \mu\text{m}$ was deposited reproducibly while maintaining high purity and a flat surface [1, 2]. Then, combining this advanced growth condition for non-doped diamond (100) and (111) film with a unique doping technique that provides parts-per-billion order doping, single-color centers of either nitrogen-vacancy or silicon-vacancy centers that show excellent properties were formed [3, 4]. These advanced growth techniques are expected to accelerate the research fields of quantum information and quantum sensing devices using diamond.

The author would like to thank Dr. K. Ichikawa, Dr. C. Shinei, Dr. T. Kageura, Dr. S. Koizumi, Dr. K. Watanabe, Dr. S. Onoda, for helpful discussion and supporting characterization.

- [1] T. Teraji, J. Appl. Phys. 118, 115304 (2015).
- [2] T. Teraji, T. Yamamoto, K. Watanabe, Y. Koide, J. Isoya, S. Onoda, T. Ohshima, L. J. Rogers, F. Jelezko, P. Neumann, J. Wrachtrup and S. Koizumi, Phys Status Solidi A 212, 2365 (2015).
- [3] L.J. Rogers, K.D. Jahnke, T. Teraji, L. Marseglia, C. Müller, B. Naydenov, H. Schauffert, C. Kranz, J. Isoya, L.P. McGuinness and F. Jelezko, Nature Communications, 5, 4739 (2014).
- [4] P. Siyushev, M. Nesladek, E. Bourgeois, M. Gulka, J. Hruby, T. Yamamoto, M. Trupke, T. Teraji, J. Isoya and F. Jelezko, Science 363, 728 (2019).

8:25 AM EL04.10.02

Removal of Mechanical Polishing-Induced Nanoscale Damage in Diamond by Chemical Mechanical Polishing (CMP) Koji Koyama^{1,2}, Naoki Fujita¹, Seong-Woo Kim¹ and Mamoru Yoshimoto²; ¹Adamant Namiki Precision Jewel Co., Ltd., Japan; ²Tokyo Institute of Technology, Japan

1. Introduction

Surface finishing is a fundamental process to obtain the maximum performance from a material. Chemical

Mechanical Polishing (CMP) following to mechanical polishing is widely used for semiconductor materials, such as Si, GaAs, SiC, and GaN. Diamond has traditionally been, however, mechanically polished with diamond abrasive because it is the hardest material and ultimately inert. It is thought that nanoscale subsurface damage induced by mechanical polishing with diamond abrasive must be removed by CMP. Although there are many reports on diamond CMP, a detailed mechanism of diamond CMP has not been clarified yet. We proposed a new diamond CMP technology with chromium oxide abrasive. In this study, the time-dependent effect of the CMP treatment with chromium oxide slurry on the diamond substrate was investigated in the development of ideal diamond substrate with atomically flat and damage-less surfaces.

2. Experimental

We prepared four pieces of mechanically polished heteroepitaxial diamond substrates (KENZAN Diamond®) with diamond abrasive in order to obtain atomically flat surface prior to CMP. We applied CMP with chromium oxide slurry to three of them. The chromium oxide slurry was composed of 20 wt% of Cr₂O₃ abrasive, 70 wt% of water, and 10wt% of dispersant. The diamond substrate without CMP was also prepared as a reference sample. The surface morphology during/after CMP were observed with AFM and white-light interference microscopy.

We applied re-growth on the diamond substrates to evaluate the subsurface damage removal by CMP. The diamond thin film was grown on the polished substrates under the same growth condition. Surface morphology after re-growth was observed by SEM.

3. Results

We measured the surface roughness with white-light interference microscopy from a macroscopic viewpoint. The surface roughness drastically changed during CMP. In the initial stage from 0 to 5 hours, scratches appeared, and the surface roughness became extensive. Additional CMP up to 100 hours eliminated the scratches to attain a low surface roughness again. This phenomenon is known as a surface morphology change because of the subsurface damage removal among other hard-to-polish materials, such as sapphire, SiC, and GaN.

We observed the surface morphology with AFM from a microscopic viewpoint. An atomic step structure was observed on the 75-hours CMP substrate. The average step height was 0.09 nm, which is in good agreement with the atomic step height (a quarter of lattice constant) of the diamond (001). It is thought that the atomic step structure appears when CMP completely removes the subsurface damage induced by mechanical polishing. We re-grown a diamond film on the polished diamond substrates in order to confirm the subsurface damage removal. The surface pits on the homoepitaxially grown film became less with increasing the CMP time. No pits were observed in the SEM image of the 100-hours CMP substrate. It is reasonable that the surface pits after homoepitaxial growth were reduced with increasing the CMP time because of the removal of the subsurface damage by CMP.

4. Summary

Surface morphology and surface roughness change after/during CMP with the chromium oxide slurry were observed to clarify the effect of CMP on the subsurface damage of the diamond substrate.

Drastic surface roughness change during CMP was observed with white-light interference microscopy.

Atomic steps were observed with AFM on the 75-hours CMP substrate.

We observed the pits reduction with increasing CMP time in the homoepitaxially grown film.

All these results indicate that the CMP removed the subsurface damage induced by the mechanical polishing.

The diamond CMP with the chromium oxide slurry has the same effect on the subsurface damage removal as other reported diamond CMP technologies. Besides, this is the first time to report on the atomic step structure.

We expect this result contributes to clarifying the mechanism of the diamond CMP.

8:40 AM DISCUSSION TIME

8:55 AM EL04.10.04

618-V 2.63-mΩ cm² NO₂ P-Type Doped Diamond MOSFETs on a High-Quality Heteroepitaxial Diamond Layer Makoto Kasu¹, Niloy Chandra Saha¹, Seong-Woo Kim², Yuki Kawamata², Koji Koyama² and Toshiyuki Oishi¹; ¹Saga University, Japan; ²Adamant Namiki Precision Jewel Co., Ltd., Japan

Diamond semiconductors, owing to a wide bandgap of 5.47 eV and superior properties compared to SiC and GaN, can be used to develop high-power devices. Previously, we had proposed and demonstrated an NO₂ adsorbed hydrogen-terminated diamond field-effect transistor. [1] In a subsequent study, we demonstrated a diamond metal–oxide–semiconductor field-effect transistor (MOSFET) exhibiting a high drain current of 1.3 A/mm. [2] Kitabayashi and Kawarada *et al.* reported a diamond MOSFET with a high off-state breakdown voltage of 2021 V. [3] Diamond MOSFETs exhibiting either high current or high voltage have been reported predominantly until now. However, for a high radio–frequency power operation, a device with a combination of both high current and high voltage is necessary.

In this study, we fabricated NO₂ p-type doped diamond MOSFETs showing high current, high voltage, and the highest output power on a (001) heteroepitaxial diamond layer called the Kenzan diamond®. The heteroepitaxial diamond layer was grown on an Ir buffer layer on a (11-20) sapphire substrate. For delamination of the diamond layer from the substrate, the microneedle technique was used.

The heteroepitaxial diamond showed the lowest threading dislocation density and full width at half maximum of the (004) X-ray diffraction rocking curve of $1.4 \times 10^7 \text{ cm}^{-2}$ and 113.4 arcsec, respectively. Further, the NO₂ p-type doping was performed to generate high-density hole carriers in the diamond layer. Additionally, an Al₂O₃ double layer, optimized to both the hole channel and gate breakdown, was deposited on the NO₂ adsorbed diamond layer. To minimize the source resistance, the gate contact was formed adjacent to the source contact. The diamond MOSFET with a gate length of 1.4 μm exhibited a high drain-current density of –776 mA/mm with a negligible gate leakage current (less than 0.1 μA/mm). MOSFETs with a gate-to-drain length of 4.8 μm showed a high off-state breakdown voltage of –618 V and a specific on-resistance of 2.63 mΩ cm². The experimental Baliga’s figure-of-merit for the available output power density and maximum output power density were 145 MW/cm² and 12.3 W/mm, respectively. These values represent the highest values observed in diamond-based devices so far.

[1] M. Kubovic and M. Kasu, *et al.*, *Appl. Phys. Exp.* 2, 086502 (2009).

[2] K. Hiramata and M. Kasu, *et al.*, *Jpn. J. Appl. Phys.* 51, 090112 (2012).

[3] Y. Kitabayashi and H. Kawarada, *et al.*, *IEEE Electron Device Letters* 38, 363 (2017).

9:10 AM *EL04.10.05

Radiation Hard Diamond Electronics for Harsh Environmental Applications Hitoshi Umezawa; National Institute of Advanced Industrial Science and Technology (AIST), Japan

The huge earthquake and tsunami of 2011 in Japan caused the Fukushima Daiichi Nuclear Power Plant to lose all electricity and suffered a severe accident. The meltdown and subsequent hydrogen explosion caused harsh environmental conditions in the reactor containment vessels and the reactor buildings, with high radiation, high temperatures, and high humidity at the same time, which severely damaged the environmental monitoring equipment installed. Melted fuel, so called debris, are still in the damaged reactors and safe decommissioning operations are required under controlled conditions.

In order to increase the safety of next generation reactors and decommissioning operations, it is necessary to realize electronic circuits with semiconductor devices that can withstand the harsh environmental conditions. Diamond devices are known to realize long-term reliability at high temperatures [1] and are expected to be used as semiconductor devices for electronic circuits that can withstand severe accidents due to their high radiation hardness >10MGy [2]. The author and his colleague have developed active and passive devices based on diamond [2,3]. They have also succeeded in detecting pseudo-signals of radiations by a preamplifier circuit using diamond FETs under elevated temperatures. For the integration of diamond detector systems into nuclear reactors requires the development low noise circuits and mass production technology for the devices.

The author would like to thank Dr. J. H. Kaneko, Dr. A. Chayahara, Dr. S. Ohmagari and Dr. H. Kawashima for their great supports on experiments and discussion. The research is partially supported on the projects by Collaborative Laboratories for Advanced Decommissioning Science (CLADS) and MEXT, Japan.

References [1] K. Ikeda, *et al.*, *Appl. Phys. Express* 2 (1), 011202 (2009). [2] H. Umezawa, *et al.*, *Proc. 29th ISPSD*, 379-382 (2017). [3] S. Suzuki, *et al.*, *Thin Solid Films* 680, 81-84 (2019).

11:45 AM EL04.11.01

A Highly Modular Implantation System for the Creation of High-Density NV Centres in Diamond

Lahcene Mehmel¹, Midrel Ngandeu¹, Alexandre Tallaire^{1,2}, Ovidiu Brinza¹, Audrey Valentin¹, Fabien Bénédic¹ and Jocelyn Achard¹; ¹LSPM-CNRS, France; ²IRCP- Chimie Paristech, France

The negatively charged nitrogen-vacancy centre (so-called NV⁻ centre) in diamond is one of the most promising systems for applications in quantum technologies because of the possibility to optically manipulate and read out the spin state of this defect, even at room temperature. These specific spin properties have paved the way to ultra-sensitive, high-performance and innovative quantum sensors (magnetometers, gyroscopes, spectrum analysers, etc.) which could open up perspectives in investigating properties that would remain inaccessible by conventional devices.

For the development of these applications, it is necessary to have diamond films of very high crystalline quality in which the density, environment, orientation and spatial localization of the introduced colour centres are perfectly controlled which is now possible thanks to microwave Plasma-Assisted Chemical Vapour Deposition (PACVD) [1]. Nevertheless, obtaining high densities of NV centres (> 500 ppb) remains particularly difficult due to the low conversion efficiency between substitutional nitrogen N_s and NV centres. In addition, the localization of these NV centres very close to the surface by in situ doping remains very challenging. For all of these reasons, the development of versatile implantation systems allowing both introducing nitrogen using N⁺ or creating vacancies with He⁺ ion bombardment is seen as a promising route towards this aim. In this paper, we present a single cavity ECR (electron cyclotron resonance) source module for producing relatively high energy ion (10-50 keV) beams using different gas sources. Using an electro-optic system, the beam size can be shaped and fitted to the surface to be implanted. We will show that the creation of high-density NV centres can be achieved near the surface using 2 approaches: (1) irradiating high purity CVD diamonds with N⁺ and (2) irradiating highly nitrogen doped CVD diamond layers with He⁺.

[1] J. Achard. V. Jacques. A. Tallaire. Chemical vapour deposition diamond single crystals with nitrogen-vacancy centres: a review of material synthesis and technology for quantum sensing applications. Journal of Physics D: Applied Physics. 53 (2020) 313001. <http://dx.doi.org/10.1088/1361-6463/ab81d1>

12:00 PM EL04.11.02

Late News: Germanium Color Centre Formation Studies in CVD Nanocrystalline Diamond Rani Mary

Joy^{1,2}, Paulius Pobedinskas^{1,2}, Celine Noel³, Daen Jannis^{4,4}, Nicolas Gauquelin^{4,4}, Johan Verbeeck^{4,4}, Laurent Houssiau³ and Ken Haenen^{1,2}; ¹UHasselt, Belgium; ²IMEC vzw, Belgium; ³University of Namur, Belgium; ⁴University of Antwerp, Belgium

Diamond-based structures with luminescent defects are prominent platforms for photonics, sensing, imaging, and various other applications¹. Typically, high sensitivity systems with nitrogen vacancy (NV) centres in single crystal diamond (SCD) are demonstrated. However, challenges in scalable SCD processing and inferior optical properties of NV centres fuel the investigation for alternative emitters in micro- and nanocrystalline diamond (NCD) that offer wafer scale fabrication. A potential alternative is the Group IV defects that include silicon and germanium color centres².

In this study, we report *in-situ* fabrication of germanium vacancy (GeV) centres in polycrystalline diamond. NCD layers are grown on Ge substrates via the microwave plasma enhanced chemical vapour deposition technique under 1% CH₄ in H₂, 3000 W and 45 Torr process conditions. The deposition temperature is maintained at (700 ± 10)°C due to the proximity to Ge's melting point (937°C). The solid source Ge doping occurs via the gas phase by plasma etching of the substrate, followed by Ge-vacancy complex formation in the

deposited diamond layer^{3,4}. We demonstrate that Ge substrate does not form carbide layer. It is evidenced from electron energy loss spectroscopy that carbide phases are absent, instead an amorphous carbon layer of 2 nm forms at the diamond/substrate interface. Therefore, we were able to fabricate ~ 9 μm thick self-separating freestanding GeV incorporated diamond films with dimensions up to 1 × 1 cm². Scanning electron microscope analysis reveal faceted morphology of the NCD films while diamond formation is verified by Raman measurements. Room temperature photoluminescence (PL) measurements reveal 602 nm peak associated with the GeV formation in diamond. We also present time-of-flight secondary ion mass spectroscopy (ToF-SIMS) results that confirm Ge incorporation in NCD and discuss the non-uniformities in Ge incorporation in the film with PL mapping supported by the high resolution ToF-SIMS elemental imaging technique.

References

1. Aharonovich, I., Greentree, A. D. & Prawer, S. Diamond photonics. *Nat. Photonics* **5**, 397–405 (2011).
2. Bradac, C., Gao, W., Forneris, J., Trusheim, M. E. & Aharonovich, I. Quantum nanophotonics with group IV defects in diamond. *Nat. Commun.* **10**, 1–13 (2019).
3. Iwasaki, T. *et al.* Germanium-Vacancy Single Color Centers in Diamond. *Sci. Rep.* **5**, 1–7 (2015).
4. Ralchenko, V. G. *et al.* Observation of the Ge-Vacancy Color Center in Microcrystalline Diamond Films. *Bull. Lebedev Phys. Inst.* **42**, 157–164 (2015).

12:15 PM EL04.11.03

Demonstration and Analysis of 100 kA/cm² Diamond Diodes Harshad Surdi, Franz Koeck, Mohammad Faizan Ahmad, Trevor Thornton, Robert J. Nemanich and Stephen Goodnick; Arizona State University, United States

Diamond as a semiconductor exhibits excellent thermal conductivity (20W/cmK)[1] and therefore is very suitable for high power electronics where self-heating is often the primary reason for failure. Owing to a high thermal conductivity, very high forward current densities can theoretically be rectified through diamond Schottky-pn or Schottky-pin diodes before self-heating limitations. Although a high forward current density at 60 kA/cm² was demonstrated by Makino *et al.* [2], practical diodes start self-heating and fall short of the theoretical limits. It therefore becomes important to understand what the practical limitations in diamond diodes are, especially the effects of traps and recombination centers that limit the forward current density.

In this research we demonstrate a practical diamond Schottky-*pin* diode with a 114 kA/cm² forward current density at 17 V forward bias and fit theoretical drift-diffusion simulations to the measured data. The simulations were done with bulk trap densities of mainly three different energy levels uniformly distributed in the *i* and *n* regions of the diode. The trap energy and capture cross-sections for all trap levels were considered from Bruzzi *et al.* [3] and Ščajev *et al.* [4]. A hopping mobility is calculated for both electrons and holes to account for nearest neighbor and variable range hopping. We also observe velocity saturation in the *i* and *n* diode regions where the electric field gets large due to depletion from the Schottky metal contact as well as the *p-i-n* junction. Therefore, an electric field dependence in the mobility model is also considered. The simulations fit very well with the measured data and provide insight into different regions in the IV characteristics. Different regions in the IV characteristics are analyzed in detail by individually turning on the trap levels, field dependence on mobility and surface recombination effects. An ideal case for a theoretically possible current density before self-heating is also made.

References:

- [1] Isberg, Jan, *et al.* "High carrier mobility in single-crystal plasma-deposited diamond." *Science* 297.5587 (2002): 1670-1672.
- [2] Makino, Toshiharu, *et al.* "Diamond Schottky-pn diode without trade-off relationship between on-resistance and blocking voltage." *Physica Status solidi (a)* 207(9) (2010): 2105-2109.
- [3] Bruzzi, Mara, *et al.* "Deep levels and trapping mechanisms in chemical vapor deposited diamond." *Journal of Applied Physics* 91(9) (2002): 5765-5774.
- [4] Ščajev, P., *et al.* "Features of free carrier and exciton recombination, diffusion, and photoluminescence in undoped and phosphorus-doped diamond layers." *Diamond and Related Materials* 57 (2015): 9-16.

12:30 PM EL04.11.04

Towards the Implementation of Diamond Power Devices in Power Converters and Measurements of Their Switching Losses Nicolas Rouger¹, Damien Risaletto¹, Pierre Lefranc², Pierre-Olivier Jeannin², Hugo Cagnol¹, Gaetan Perez², Sébastien Vinnac¹, Julien Pernot³, David Eon³ and Etienne Gheeraert³; ¹Université de Toulouse ; LAPLACE ; CNRS ; INPT ; UPS, France; ²Univ. Grenoble Alpes, CNRS, Grenoble INP, G2Elab, France; ³Univ. Grenoble Alpes, CNRS, Institut Néel, France

Ultra wide bandgap (UWBG) materials such as monocrystalline diamond exhibit the best figure of merits for power semiconductor devices: the ultra-wide bandgap of 5.5eV translates into the highest electric field above 10MV/cm, which offers a thinner drift region with an associated higher doping level than with other Wide Bandgap (WBG) materials for the same breakdown voltage. Consequently, power semiconductor devices based on UWBG and diamond in particular have theoretically the lowest specific on state resistance, which leads to smaller active area and lower conduction and switching losses. Many different diamond power device architectures have been previously introduced, but the implementation of those in actual power converters was only reported in a limited number of communications [1-3]. Although the measurement of on state resistance is straight forward, the measurement of switching losses is challenging with the existing and future High Voltage (>600V) diamond power devices. First, diamond devices need to be packaged in order to be integrated in, at least, one power commutation cell (one transistor and one diode, or two transistors, with the same breakdown voltage). This packaging should also be compatible with a high junction temperature operation (above 150°C) to fully demonstrate the performances of diamond devices based on bulk conduction. Second, the active area of diamond devices can be relatively small compared to other available power devices. Consequently, the maximum switching speed of diamond power devices can be extremely fast, and the intrinsic parasitic capacitors much smaller than 1pF. Third, the total current rating of diamond power devices can be rather small (μ A to mA), which makes it difficult to probe the fast large signal variation of low drain currents, also with high voltage swings. Finally, the required gate to source driving voltages of diamond power transistors can be different from their Silicon and WBG alternatives, with large gate to source voltage swing [5]. For all these reasons, a specific experimental approach must be developed to adapt the implementation of diamond power devices in power converters, and to be able to accurately extract the large signal switching behavior of those devices.

In this work, we present the specific experimental characterization boards we designed and fabricated to achieve the fastest switching of diamond Schottky Barrier Diodes, and a flexible converter to extract switching losses of WBG and UWBG power transistors. The classical Double Pulse method is compared to the opposition method, where switching losses can be accurately measured without having to probe drain or source currents with fast dynamics. The converter is validated for high voltage inputs above 600V, load currents above 20A, switching frequencies above 100kHz, and flexible gate driver boards to adapt to specific gate voltages. Preliminary results on power switching with diamond MESFETs are also presented and discussed.

The research leading to these results has been performed within the GreenDiamond project (<http://www.greendiamond-project.eu/>), received funding from the European Community's Horizon 2020 Program (H2020/2014-2020) under grant agreement n° 640947 and is partially funded by French ANR Research Agency under grant ANR-16-CE05-0023 #Diamond-HVDC.

[1] Aboulaye Traoré et al 2017 Jpn. J. Appl. Phys. 56 04CR14

[2] V.D. Blank et al, Power high-voltage and fast response Schottky barrier diamond diodes, Diamond and Related Materials, Volume 57, 2015, Pages 32-36,

[3] G. Perez et al., "Diamond Schottky barrier diodes for power electronics applications," 2018 IEEE Energy Conversion Congress and Exposition (ECCE), Portland, OR, 2018, pp. 1956-1963

[4] C. Masante, J. Pernot, J. Letellier, D. Eon and N. Rouger, "175V, > 5.4 MV/cm, 50mOhm.cm² at 250°C Diamond MOSFET and its reverse conduction," 2019 IEEE ISPSD, Shanghai, China, 2019, pp. 151-154

12:45 PM EL04.11.05

Normally-OFF Diamond Reverse Blocking MESFET Jesus Canas^{1,2}, Alexander Pakpour-Tabrizi³, Etienne Gheeraert¹, Marina Gutierrez² and Richard Jackman³; ¹Univ. Grenoble Alpes, CNRS, Grenoble INP*, Institut Néel, France; ²Universidad de Cádiz, Spain; ³University College London, United Kingdom

Diamond transistors are promising for high temperature, high power and high frequency applications in harsh environments as a result of this material extraordinary properties, such as high electron and hole mobility ($4500 \text{ cm}^2\text{V}^{-1}\text{s}^{-1}$ and $3800 \text{ cm}^2\text{V}^{-1}\text{s}^{-1}$), low dielectric constant (5.7), high breakdown field (10 MV/cm), high thermal conductivity (10 W/cm K) or high radiation hardness. However, no shallow dopants are found and p-type doping is acquired using boron (0.37 eV) and n-type using phosphorous (0.6 eV). Because of its specificities, it is often more convenient to find original ideas for diamond transistors rather than using the classical designs. A normally-off inversion Diamond MOSFET was demonstrated in 2016. Nonetheless, fabricating a power inversion MOSFET requires a control of diamond growth and etching that has not been yet reached. Instead, most of Diamond transistors are normally-on MOSFETs, based on the 2D hole gas emerging due to transfer doping in H-terminated surface. But also, new transistors concepts like the diamond deep depletion MOSFET have shown promising results based on bulk boron doped diamond conduction.

In this work, we demonstrate a normally-off high breakdown voltage p-diamond reverse blocking MESFET. The source is fabricated using selective p+ diamond growth and Ti/Pt/Au Ohmic contacts, while the gate and drain Schottky contacts are made of Molybdenum on O-terminated Diamond. The major challenge in the fabrication of a normally off-MESFET is to target the correct layer thickness and doping concentration, in order to have a closed channel that can be opened applying a BIAS to the Schottky gate. Despite, the progress made in diamond growth allow us for the first time to design and fabricate such a device. The Drain and Gate Schottky contacts have been characterized showing a high ideality factor of 2.1 at room temperature, tentatively explained by an interface oxidized layer. The density of states of the interface is estimated as $\sim 10^{13} \text{ cm}^{-2}$ by the conductance method. The devices are normally off displaying undetectable gate leakage current. An on-state current level of 10^{-4} mA is reached in the ON-state at room temperature and 10^{-2} mA at 450 K. A breakdown voltage of $<1 \text{ kV}$ was measured for the device.

1:00 PM EL04.11.06

Hybrid Power Module with Diamond and SiC Power Devices—Modeling, Performances and Challenges

Nicolas Rouger¹, Anne Castelan^{1,2}, Idriss Nachete¹, Nazareno Donato³, Florin Udrea³ and Julien Pernot⁴; ¹Université de Toulouse ; LAPLACE ; CNRS ; INPT ; UPS, France; ²ICAM, France; ³University of Cambridge, United Kingdom; ⁴Univ. Grenoble Alpes, CNRS, Institut Néel, France

Ultra wide bandgap (UWBG) materials such as monocrystalline Diamond are foreseen as the next-generation power semiconductor devices [1], whereas wide bandgap (WBG) materials such as SiC and GaN are already pushing towards more efficient and more integrated power converters [2,3]. Diamond has outstanding physical properties such as the highest thermal conductivity ($20 \text{ W.cm}^{-1}\text{K}^{-1}$ at room temperature), a large critical electric field (10 MV.cm^{-1}), a wide doping range and a high carrier mobility in both P and N type doping types. Diamond devices are also maturing, with many improvements and breakthroughs in the recent years: Deep Depletion and inversion MOSFETs [4,5], 2DHG FETs with high current and high breakdown voltage capabilities [6], JFETs, high voltage and high temperature MESFETs, Schottky, PiN and Schottky PiN diodes [1]. Nonetheless, diamond devices based on bulk diamond conduction (e.g. MOSFETs, JFETs, MESFETs, Schottky diodes) suffer from the incomplete ionization of Boron dopants at typical operating junction temperatures (e.g. 300K-400K), which increases consequently the ON state resistance of such unipolar devices. Moreover, the active area of diamond can be limited by defect density and substrate size, which limits the high-current capability of diamond power devices in a short term.

How could one introduce as soon as possible diamond power devices in power modules to take benefits of their outstanding performances, while mitigating their weaknesses?

In this work, we propose to combine boron-doped diamond power transistors based on bulk conduction in a

hybrid association with WBG power devices such as SiC MOSFETs. Other hybrid associations between Si and SiC power devices have been previously proposed such as in [7], but UWBG such as diamond was never considered. A small area diamond power transistor is associated in parallel with a SiC MOSFET which is smaller than a SiC-only solution, and both SiC and diamond devices having the same breakdown voltage (1.7kV in this work). This hybrid association offer an attractive combination of the Positive and Negative Temperature Coefficients for the ON state resistance of SiC and Diamond power devices. This hybrid association is modeled, discussed and benchmarked with SiC-only (analytic and real datasheet) and Diamond-only solutions, considering representative specifications at the power converter level. Preliminary studies show a reduction of SiC active area by two. Particularly, the optimal sizing and the current sharing between the paralleled power devices are investigated as a function of operating conditions and junction temperatures. The thermal management solutions and electro-thermal coupling are also discussed based on analytical and numerical models.

- [1] N Donato *et al* 2019 *J. Phys. D: Appl. Phys.* **53** 093001
- [2] D. Johannesson *et al.*, "Assessment of 10 kV, 100 A Silicon Carbide mosfet Power Modules," in *IEEE Transactions on Power Electronics*, vol. 33, no. 6, pp. 5215-5225, June 2018.
- [3] Y. Zhang and T. Palacios, "(Ultra)Wide-Bandgap Vertical Power FinFETs," in *IEEE Transactions on Electron Devices*, vol. 67, no. 10, pp. 3960-3971, Oct. 2020.
- [4] T. Pham *et al.*, "Deep-Depletion Mode Boron-Doped Monocrystalline Diamond Metal Oxide Semiconductor Field Effect Transistor," in *IEEE Electron Device Letters*, vol. 38, no. 11, pp. 1571-1574, Nov. 2017.
- [5] Matsumoto, T. *et al.* Inversion channel diamond metal-oxide-semiconductor field-effect transistor with normally off characteristics. *Sci Rep* **6**, 31585 (2016).
- [6] M. Iwataki *et al.*, "Over 12000 A/cm² and 3.2 mΩ cm² Miniaturized Vertical-Type Two-Dimensional Hole Gas Diamond MOSFET," in *IEEE Electron Device Letters*, vol. 41, no. 1, pp. 111-114, Jan. 2020.
- [7] A. Deshpande and F. Luo, "Practical Design Considerations for a Si IGBT + SiC MOSFET Hybrid Switch: Parasitic Interconnect Influences, Cost, and Current Ratio Optimization," in *IEEE Transactions on Power Electronics*, vol. 34, no. 1, pp. 724-737, Jan. 2019.

SESSION EL04.12: Diamond III
Session Chairs: Jocelyn Achard and Nicolas Rouger
Tuesday Afternoon, April 20, 2021
EL04

2:15 PM *EL04.12.01

Boron Incorporation in Monocrystalline CVD Diamond Films for Schottky Barrier Diodes Ken Haenen^{1,2};
¹Hasselt University, Belgium; ²imec vzw, Belgium

Monocrystalline diamond is known as a material that possesses an extraordinarily combination of extreme properties. While this is an ideal starting point to become the next-gen electronic device material, several hurdles remain to be taken. The use of microwave plasma enhanced chemical vapour deposition (MW PE CVD) in combination with a wide parameter space enables the production of films with a wide window of doping concentrations and thicknesses that range from a few hundreds of nanometers to over a millimeter thick. Nonetheless, many times the device performance of electronic applications based on such layers remains far below the theoretical predictions. This is partly due to a lack in fundamental understanding in the relation between (varying) substrate quality, process conditions, dopant incorporation, and final crystalline properties. The latter will not only influence the actual dopant mobility and lifetime, but also the level of leakage currents in device structures based on such films.

Here, a detailed study on the methane concentration dependence of the plasma gas phase on the surface

morphology and boron incorporation in monocrystalline CVD diamond layers is presented. Both heavily doped p^+ films, with boron concentrations above the Mott transition ($\sim 3 \times 10^{20} / \text{cm}^3$), as well as lightly doped p^- films with acceptor concentrations down to $1 \times 10^{14} / \text{cm}^3$ will be discussed. A combined use of several characterisation techniques to assess the electronic, optical, and structural properties, including Hall measurements, Raman and absorption spectroscopy, AFM, and TEM, will shed light on the beforementioned relation between process conditions and subsequent film quality. The combination of said p^+/p^- layers in pseudo-vertical Schottky barrier diodes leads to devices that show a very low leakage current, down to 10^{-12} A, with forward current levels up to $\sim 10^3$ A/cm².

Finally, the experimental findings on impurity incorporation are corroborated by first principles calculations that give insight in the relation between methane concentration and preferential boron incorporation sites, also providing a route to understanding impurity incorporation in diamond on a general level, potentially of great importance for color center formation [1].

[1] R. Rouzbahani, S.S. Nicley, D.E.P. Vanpoucke, F. Lloret, P. Pobedinskas, D. Araujo, K. Haenen, "Impact of methane concentration on surface morphology and boron incorporation of heavily boron-doped single crystal diamond layers", *Carbon* **172** (2021), 463-473.

2:40 PM EL04.12.02

Interface Properties of ZrO₂/p-type O-Terminated (001) Diamond MOSCAP Beatriz Soto¹, Jesus Canas^{2,1}, M. Pilar Villar¹, Daniel Araujo¹ and Julien Pernot²; ¹University of Cádiz, Spain; ²Université Grenoble Alpes, France

Diamond has been exhaustively studied during the last few decades as semiconductor since it is theoretically the best candidate to meet the power electronics trade-off. However, the fabrication of devices based on diamond presents a set of challenges, for example the diamond available bulk size and surface termination quality and the fact of not having a native oxide among others, such problems prevent devices high performance and reliability. The present study is focused on the electrical and microstructural characterization of zirconium dioxide to be employed in diamond-based electronic devices for field effect transistor applications. Most of diamond Metal Oxide Semiconductor Capacitors (MOSCAPs) in literature were fabricated using Al₂O₃ or SiO₂ due to properties such as the wide band gap and their alignment with the diamond band setting. Based on those gate dielectrics, it has been recently demonstrated the first inversion channel normally-off Metal Oxide Semiconductor Field Effect Transistor (MOSFET) and a Deep Depletion MOSFET (D3MOSFET) showing great perspectives for the future of power electronics. However, in case of 2D hole gas channel, low channel mobility due to high density of interface states is still an issue so more effective passivation techniques are required to reduce losses of the performance. In this context, zirconia appears as a good candidate for the gate dielectric because of its high dielectric constant (with a minimum crystalline average value of about 19.7), high band gap (around 6eV) and its chemical and thermal stability favouring the oxide-diamond interface quality. In this work, the devices under test are MOSCAPs and Metal Oxide Metal capacitors fabricated on a p-type oxygen-terminated (001) diamond layer using an insulating layer of ZrO₂ grown by Atomic layer deposition (ALD). I-V, C-V and C-f measurements with temperature ranging between room temperature to 125 °C have been performed in order to extract information such as the doping concentration of the p- diamond layer, the MOSCAP flat band voltage, the oxide charge density or the interface state density. On the other hand, microstructural characterization through different techniques have been performed to determine the crystallinity degree and oxide thickness through High resolution electron microscopy (HREM) and the relate Fast Fourier transform (FFT) or X-ray diffraction (XRD), the oxide band gap has been analysed by Electron energy loss spectroscopy (EELS) and the stoichiometry analysis of the oxide has been based on Energy-dispersive X-ray spectroscopy (EDX). Finally, helped by finite element calculation of MOSCAP band diagram, the correlation between the electrical response and the microstructural nature of the device will be established and discussed.

2:55 PM EL04.12.03

Science and Technology of Integrated Super-High Dielectric Constant AlO_x/TiO_y Nanolaminates /

Diamond for MOS Capacitors and MOSFETs Orlando Auciello^{1,2}, Jiangwei Liu³, Elida I. de Obaldia^{4,1}, Bo Da³ and Yasuo Koide³; ¹The University of Texas at Dallas, United States; ²Original Biomedical Implants, LLC, United States; ³National Institute for Materials Science, Japan; ⁴Universidad Tecnológica de Panamá, Panama

A super-high dielectric constant AlO_x/TiO_y nanolaminate film is grown on hydrogenated crystalline diamond (H-diamond) to enable superior diamond-based metal-oxide-semiconductor (MOS) capacitors and metal-Oxide-Silicon-Field-Effect-Transistors (MOSFETs). In order to minimize or suppress leakage current, a nanometer thick AlO_x film is inserted at the AlO_x/TiO_y nanolaminate / H-diamond interface. The maximum values for the capacitance density and dielectric constant related to the summation of individual AlO_x and nanolaminate are 1.06 μF/cm² and 68.7, respectively. Capacitance density and dielectric constant for the AlO_x/TiO_y nanolaminate are as high as 5.22 μF/cm² and 308, respectively. Electrical properties of four H-diamond MOSFETs with gate lengths increasing from 2.4 μm to 10.1 μm were investigated. All of them showed p-type behavior and distinct pinch-off characteristics with drain current maxima of -47.4, -43.3, -26.6, and -24.6 mA/mm, respectively. On/off ratios and threshold voltages for the MOSFETs are higher than 10⁴ and lower than 0.55 ± 0.10 V, respectively. The low threshold voltages indicate that the AlO_x/TiO_y nanolaminate gate based MOSFETs can switch between ON and OFF stages at very low gate voltages. Effective mobilities of the H-diamond channel layers for all the MOSFETs raised firstly and dropped subsequently with increasing voltages, which can be explained by the effect of mobility limiting factors.

3:10 PM EL04.12.04

Time of Flight Measurement Using Electron Beam Induced Current on a Diamond Single Crystal

Alexandre Portier^{1,2}, Julien Pernot², Marie-Laure Gallin-Martel¹, Fabrice Donatini² and Denis Dauvergne¹;
¹Laboratoire de Physique Subatomique et Cosmologie (LPSC), France; ²Institut Néel, France

1. Introduction

Many techniques have already been used to characterize carriers' properties in diamond detectors by doing Time of Flight (ToF) measurements. The most common is to use alpha particles, which deposit their energy near the diamond surface [1, 2]. But some other techniques like using biphotonic absorptions [3] and neutrons [4] have already been carried out. Some experiments based on a pulsed laser [5] have found very high mobility at room temperature for electrons and holes. This high mobility is very interesting for fast timing and high rate detection applications. Time of flight using Electron Beam Induced Current (ToF-EBIC) is a new way to determine and study the carrier mobilities.

2. Time of Flight using Electron Beam Induced Current

The experiments were conducted through the following procedure: a CVD single crystal diamond is put in a scanning electron microscope chamber under vacuum, and biased by means of an external voltage source. A pulsed electron beam is focused on a small area of the diamond. The diamond works as a solid ionization chamber: electrons will lose their energy by creating electron-hole pairs in a small volume located close to the entrance surface. Because of the electric field, the carriers would drift to the negative electrode (holes) and to the positive electrode (electrons). The signal is extracted from the electrodes, amplified by a fast preamplifier (CIVIDEC C2-HV [6]) and the waveforms are digitized by an oscilloscope. Depending of the beam energy, the electrons are stopped in the first 1 to 5 μm from the diamond surface, which is quite small compared to the diamond bulk thickness (around 500 μm). Thus, one type of carrier is instantly collected (~10-100 ps) while the other one will drift a few nanoseconds to reach the opposite electrode. Then, it is possible to study separately the drift of electrons and holes so as to evaluate their mobilities for various bias voltages. In this work, thanks to this ToF-EBIC technique, diamond surface mapping for different depths (up to 5 μm) will be reported, charge carrier life time will be evaluated and carrier mobilities will be studied at different temperatures.

This work is supported by IDEX Université Grenoble Alpes and by DIAMTECH IN2P3.

[1] M. Pomorski, et al., *phys. stat. sol. (a)*, 203: 3152-3160 (2006). <https://doi:10.1002/pssa.200671127>

[2] H. Pernegger et al., *Journal of Applied Physics* 97, 073704 (2005). <https://doi.org/10.1063/1.1863417>

[3] C. Dorfer et al., *Appl. Phys. Lett.* 114, 203504 (2019). <https://doi.org/10.1063/1.5090850>

[4] C. Weiss, et al. Eur. Phys. J. A 52, 269 (2016). <https://doi.org/10.1140/epja/i2016-16269-8>

[5] J. Isberg, et al., Science 297, 1670 (2002). <https://doi.org/10.1126/science.1074374>

[6] CIVIDEC <https://cividec.at/>

SESSION EL04.13 Poster Session

Session Chairs: Masataka Higashiwaki and Hongping Zhao

Tuesday Afternoon, April 20, 2021

5:15 PM - 7:15 PM

EL04

EL04.13.01

Computational Prediction of P-Type Doping in Metastable AlScO₃ Perovskite with 8 eV Bandgap Cheng-Wei Lee^{1,2}, Prashun Gorai^{1,2}, Andriy Zakutayev² and Vladan Stevanovic^{1,2}; ¹Colorado School of Mines, United States; ²National Renewable Energy Laboratory, United States

This work centers on AlScO₃, one of the 14 candidate oxides identified in our recent computational survey of semiconductors for power electronics [1]. The survey utilized intrinsic materials properties entering Baliga figure of merit (BFOM) to gauge performance. AlScO₃ is a distorted ABO₃ perovskite (metastable high-pressure phase) typically investigated for phase transformation under high-temperature and -pressure conditions. However, its electronic properties and doping tendencies are rarely explored. Our first-principle calculations predict an indirect electronic band gap around 8.0 eV (HSE06+G₀W₀), which is much larger than those of typical ultrawide bandgap semiconductors. Such wide bandgap makes it a promising candidate semiconductor for high-temperature or/and high-voltage applications. A functional device requires the underlying semiconductor to be dopable and we addressed this issue by performing first-principle defect calculations. Specifically, we adopted the well-established supercell approach to perform defect calculations and the total energies are calculated using the standard HSE06 hybrid functional with the bandgap corrected by the many-body perturbation theory (G₀W₀). Our calculations of native defects point to the cation and oxygen vacancies as the dominant point defects. The exothermic nature of the cation vacancies for Fermi energies close to the conduction band minimum at both cation- and oxygen-rich conditions suggest n-type insulating behavior. On the other hand, at the oxygen-rich conditions, the anion vacancies allow p-type doping. We further investigated the formation energies of potential extrinsic p-type dopants, like Mg and Zn, and found them to be deep acceptors implying moderate p-type doping. Lastly, we examined the hole self-localization and found stable small hole polarons with ionization energies of the order of 0.1 eV. Ionization energy of this magnitude implies activated transport that should be largely overcome at moderate to high-temperature. Our computational results also call for further investigations into the electronic properties and the search for shallower acceptor dopants of this promising p-type ultrawide bandgap oxide.

[1] P. Gorai et al. *Energy Environ. Sci.*, 2019,12, 3338-3347

EL04.13.02

Design and Optimization of β -(Al_xGa_{1-x})₂O₃/Ga₂O₃ Delta-Doped High Electron Mobility Transistors Dawei Wang and Houqiang Fu; Iowa State University of Science and Technology, United States

Beta-Gallium oxide (β -Ga₂O₃) has garnered tremendous research interests for high power, high voltage, and high frequency applications due to its ultra-wide bandgap (~4.8 eV), high critical breakdown field of 8 MV/cm, and large Baliga's figure of merit. (Al_xGa_{1-x})₂O₃/Ga₂O₃ delta-doped high electron mobility transistors (HEMTs) have been experimentally demonstrated with high quality electron channel and good electron mobility. Delta-doping regulates the electrical characteristics of (Al_xGa_{1-x})₂O₃/Ga₂O₃ HEMTs since it is responsible for the formation of two-dimensional electron gas (2DEG) in the channel. With epitaxial growth techniques such as

MOCVD and MBE, delta-doping position and concentration can be precisely controlled. However, the effects of delta doping on device performance of $(\text{Al}_x\text{Ga}_{1-x})_2\text{O}_3/\text{Ga}_2\text{O}_3$ HEMTs are not comprehensively investigated.

In this work, we explore the design and optimization of $(\text{Al}_x\text{Ga}_{1-x})_2\text{O}_3/\text{Ga}_2\text{O}_3$ delta-doped HEMTs via TCAD SILVACO simulation, which can serve as critical guidance for experimental realizations. To date, there are very few reports on the simulation of $(\text{Al}_x\text{Ga}_{1-x})_2\text{O}_3/\text{Ga}_2\text{O}_3$ HEMTs, partly due to the immature status of Ga_2O_3 research and the lack of accurate material properties. In the simulations, we first calibrated our model with experimental electrical characteristics of $(\text{Al}_x\text{Ga}_{1-x})_2\text{O}_3/\text{Ga}_2\text{O}_3$ HEMTs such as their transfer and transconductance curves. Then a comprehensive series of design and optimization of delta doping in the HEMTs was conducted, including delta-doping concentration, delta-doping position, delta-doping width, and multiple delta-doping channels.

The simulated HEMT structure consisted of Ga_2O_3 substrate, 130 nm unintentionally doped (UID) Ga_2O_3 layer, and 27 nm $(\text{Al}_x\text{Ga}_{1-x})_2\text{O}_3$ layer, and two n^+ - Ga_2O_3 contact regions for the source and drain. The delta-doping region was modeled by a thin n - Ga_2O_3 slab with a donor concentration of $1 \times 10^{18} \text{ cm}^{-3}$, which is positioned inside the $(\text{Al}_x\text{Ga}_{1-x})_2\text{O}_3$ layer at 4 nm distance from the $\text{Ga}_2\text{O}_3/(\text{Al}_x\text{Ga}_{1-x})_2\text{O}_3$ interface. With increasing delta-doping concentration, the device transconductance and drain current increased significantly. When the delta-doping concentration was over $1 \times 10^{19} \text{ cm}^{-3}$, the device exhibited large leakage from the delta-doping region because the conduction band at the delta doping position was lower than that of the channel. The position of delta doping also played a critical role. It was found that the closer the delta doping to the interface, the larger the device transconductance and drain current. The largest breakdown voltage was obtained when the delta doping was 2 nm from the channel. We also simulated the effect of delta doping diffusion across the interface, which is a great concern during growth. The current collapse was observed due to the diffused impurities into the Ga_2O_3 layer, which decreased the large built-in electric field generated by the interface barrier. In addition, multiple delta-doping channels can also significantly impact device threshold voltage and breakdown voltages.

In short summary, these results provide critical references for the future development of high performance Ga_2O_3 high power and high frequency electronics.

EL04.13.03

Stability and Electronic Properties of Ga_2O_3 : Fe Alloys Studied Using Density Functional Theory

Calculations Luisa Scolfaro¹, Md Dalim Mia¹, Ahad Talukder¹, Brian Samuels¹, Pablo D. Borges², Wilhelmus J. Geerts¹ and Ravi Droopad¹; ¹Texas State University, United States; ²Universidade Federal de Vicosa, Brazil

Gallium oxide (Ga_2O_3) and its alloys are attracting great attention due to their potential in technological applications such as gas sensors, transparent conductive oxides for solar cells, UV detectors, magnetic sensors and devices, and high-power electronic devices. Doping Ga_2O_3 and/or alloying with foreign divalent elements, such as Mg^{2+} , Be^{2+} , Zn^{2+} , and Fe^{2+} are common ways to achieve high insulating materials needed in these applications. Although there have been few studies on the effects of iron in Ga_2O_3 , no systematic investigation about the stability and electronic properties of $(\text{Ga}_{1-x}\text{Fe}_x)_2\text{O}_3$ have been reported so far.

In this work, we present the results of Fe doping in Ga_2O_3 using density functional theory-based calculations performed for different Fe concentrations (and). The role played by oxygen vacancies is also investigated. The effects of strain in the pristine oxide reveals that the band gap decreases with increasing lattice constant. This behavior is also observed in the Fe-doped systems with increasing . The theoretical results are compared with recent experimental measurements using XRD measurements and obtained in $(\text{Ga}_{1-x}\text{Fe}_x)_2\text{O}_3$ samples grown with various Fe contents and in different growth conditions, allowing to get insight into the stability of the structure.

This work was supported in part by NSF through an DMR-MRI Grant under Award 1726970 and in part by DOD through a HBCU/MI grant (W911NF2010298).

EL04.13.04

A Computational Search for UWBG Semiconductors for High-Power and High-Temperature Electronics

Emily McDonald^{1,2}, Prashun Gorai^{1,2}, Andriy Zakutayev^{2,1} and Vladan Stevanovic^{1,2}; ¹Colorado School of Mines, United States; ²National Renewable Energy Laboratory, United States

As we move toward a more renewable, variable, and distributed electricity grid, we will need to find power electronic (PE) semiconductors that can withstand high power and high voltage applications. Ultra-wide band gap (UWBG) materials are promising candidates as they tend to exhibit large breakdown fields which increases the operating voltage limit for a given device size. However, currently explored UWBG materials either lack the thermal properties needed to dissipate heat at high power (Ga_2O_3), are difficult to synthesize as quality single crystals at scale (diamond, c-BN), or are difficult to dope to desired carrier concentrations (AlGaN). Using density function theory (DFT) calculations, we conduct a high-throughput computational search to identify promising UWBG semiconductors beyond those currently used or studied for n-type power electronic devices. We consider >1,500 total oxides, nitrides, sulfides, carbides, silicides, and borides. First principles generalized gradient approximation (GGA) calculations and semi-empirical models are used to evaluate the carrier mobility and critical breakdown field which are inputs to the well-known Baliga figure of merit. We use this metric along with the lattice thermal conductivity identify top potential candidates with performance better than the current market materials for high power (SiC-4H and GaN). The electronic structures of a sub-set of the most-promising oxide candidates are further assessed using low-throughput, higher-accuracy HSE06 hybrid calculations. Our results find more than 28 promising candidates that have higher lattice thermal conductivity than Ga_2O_3 and higher n-type Baliga figure of merit than SiC-4H and GaN which are the current materials used in high-power PE applications today. Of these candidates, 65% are oxides and 35% are nitrides, with chemistries covering binaries to quaternaries. We also conduct a qualitative assessment of n-type dopability of the top candidates by evaluating the governing material properties, considering acceptor defects as the limiting factor. Given the large number of oxides in the top candidates, these UWBG materials are promising for use in high-temperature electronic devices as well as high-power PE applications. This work provides guidance for selecting candidates with confidence for further experimental investigation. Portions of this work have been published by Gorai *et al.* in: *Energy Environ. Sci.*, 2019, **12**, 3338.

EL04.13.05

A Study of Structural and Electronic Properties of Rippled 2D and 2D/Diamond Heterostructures Pegah S. Mirabedini¹, Alex Greaney¹ and Mahesh Neupane^{1,2}; ¹University of California, Riverside, United States; ²U.S. Army Research Laboratory, United States

An external lattice perturbation may lead to localized height variations (ripples) in two-dimensional (2D) materials during the growth process, and as a result, affect their functionality. Here, we conduct a systematic first principle study of the effect of rippling on the structural and electronic properties of 2D layers (hBN, graphene) and the resulting 2D/Diamond heterostructures. We find the most favorable alignment of the layer on the hydrogen-terminated diamond (H-diamond (100)) substrate using a combined sampling and a machine learning approach. Rippling of sheets can arise from templating on a variety of substrates. The rippled structures we studied on H-diamond were found to have a stronger vdW interaction between the constituent layer and the substrate. A higher degree of charge transfer was observed in the heterostructures composed of a rippled hBN (graphene) layer, as compared to their planar counterparts. The transferred charges are confined within the vdW-gap between the 2D layer and H-diamond (100) surface. The higher thermodynamic stability, improved charge transfer, and additional tunability of the electronic properties in the rippled 2D/Diamond heterostructures make them better choices for application in diamond-based field effect transistors.

EL04.13.06

The Facile Exfoliation of $\beta\text{-Ga}_2\text{O}_3$ Layers and Prediction of a New Phase Sajib K. Barman and Muhammad N. Huda; The University of Texas at Arlington, United States

The transparent wide bandgap semiconductor, $\beta\text{-Ga}_2\text{O}_3$ has gained considerable attention due to its suitability to a wide range of applications. For example, its wide bandgap and small electron effective mass are suitable for power electronic devices. Interestingly, even though this is not a van der Waals material, it can be peeled along

(100) surface by a scotch tape method like in graphene. The resulting ultra-thin layers are used for high power device fabrications. The theoretical calculation has shown that out of the two possible (100) surface terminations, (100)B surface is the most stable one, which is also experimentally observed from scanning tunneling microscope study (STM). One of the interesting properties of this material is that thin layers preserve the pristine bulk-like electronic properties, making it even more promising for applications in power devices. It is then of paramount importance to understand why the exfoliation occurs facily even though the interlayer interaction in β -Ga₂O₃ is not van der Waals. This presentation will show the exfoliation phenomenon from the first principle thermodynamic total energy calculations and the mechanisms behind the easy exfoliation along (100)B surface. Lastly, we will show a theoretical prediction of a new phase of Ga₂O₃ obtained from the stacking of the exfoliated layers of β -Ga₂O₃. From the stability calculations, this phase is comparable to β -Ga₂O₃, as well as dynamically stable. From the hybrid density functional calculations, the new phase's bandgap is a little higher than the β -phase. The electronic and thermal properties of this new phase will be briefly presented and compared with β -Ga₂O₃. The methodology used and developed for this study can be utilized in general to understand bond breaking and forming in other wide bandgap materials as well. This understanding will give us better control to fabricate thin-film 2D devices, in general.

EL04.13.07

Anisotropic Thermal Boundary Conductance Across Metal/ β -Ga₂O₃ Interfaces Jingjing Shi¹, Yee Rui Koh², Akhil Mauze³, Chao Yuan¹, Shangkun Wang¹, Brian Foley^{1,4}, Takeki Itoh³, Yuewei Zhang³, James S. Speck³, Patrick Hopkins^{2,2,2} and Samuel Graham^{1,1}; ¹Georgia Institute of Technology, United States; ²University of Virginia, United States; ³University of California, Santa Barbara, United States; ⁴The Pennsylvania State University, United States

β -Ga₂O₃ is very promising to be applied in power electronic devices because of its superior properties, like the ultra-wide bandgap, high breakdown electric field, and the relatively low-cost growth of its single crystal. However, heat dissipation issue would limit the performance and reliability of β -Ga₂O₃ devices considering its extremely low thermal conductivity. A top-side cooling or double-side cooling strategy would be necessary to efficiently dissipate heat from the active region of β -Ga₂O₃ devices. As a result, thermal transport at the metal/ β -Ga₂O₃ contacts is very important for device thermal management, and a thorough understanding of the thermal boundary conductance (TBC) at metal/ β -Ga₂O₃ interfaces is needed. Anisotropy effects have been observed in the thermal conductivity of β -Ga₂O₃ but haven't been studied for TBC at β -Ga₂O₃ interfaces. In this work, we perform both experiments and theoretical simulations to study how the material orientation will affect the TBC at metal/ β -Ga₂O₃ interfaces at different temperatures. The Al/ β -Ga₂O₃ interface is studied as our model system because of the isotropic property of Al, which will not introduce other anisotropic mechanism into interfacial thermal transport. Both E-beam evaporated and molecular-beam epitaxy (MBE) grown Al/ β -Ga₂O₃ interfaces are studied to minimize the influence of other factors (like growth method related defects at interfaces) on TBC. We apply the time-domain thermoreflectance (TDTR) method to measure the TBC at Al/ β -Ga₂O₃ interfaces with different β -Ga₂O₃ substrate orientations (-201), (010), and (001), and the TBCs show strong anisotropy effect. In our theoretical calculation, to capture the anisotropy effect, a full first Brillouin zone k-space Landauer formula is applied. With the phonon information from ab initio calculations of the full first Brillouin in reciprocal lattice, there is no isotropic assumption and the influence of orientation can be captured and analyzed. Our modeling results are consistent with our experimental measurements that the TBC at (010) β -Ga₂O₃/Al interface is the highest, while the TBC at (-201) β -Ga₂O₃/Al interface is the lowest, and the difference is more than 50%. Our work shows that the anisotropy in β -Ga₂O₃ not only affects its thermal conductivity but its TBC as well. To capture the anisotropy effect, a modal approach with phonon information of the full first Brillouin zone is needed to accurately predict the TBC at β -Ga₂O₃ interfaces. The anisotropic TBC effect should be considered for the future thermal design of β -Ga₂O₃ devices.

EL04.13.08

The Structure and Properties of Amorphous Ga₂O₃ Julia E. Medvedeva; Missouri University of Science and Technology, United States

Gallium oxide has attracted a tremendous attention in recent years as a promising wide-bandgap semiconductor for power electronics and deep-UV optoelectronics. The optical properties of monoclinic β -Ga₂O₃ have been actively investigated both theoretically and experimentally, and a large range of the reported band gap values (from 4.3 eV to 5.1 eV) have been explained based on anisotropic onset of the optical absorption that originates from the crystallographic differences of the monoclinic gallium oxide phase.

Amorphous metal oxides have several advantages over their crystalline counterparts: the lack of lattice periodicity with defined crystal orientations, no grain boundaries, and an increased number of degrees of freedom for metal-Oxygen (MO) polyhedra packing in the disordered material lead to a uniform low-strain crack-resistant morphology, smooth surfaces over large areas, and in the case of ionic oxide semiconductors, a high carrier mobility. The effect of disorder on the optical properties of oxides is two-fold: on one hand, the fundamental band gap is determined by the nearest-neighbor interactions, i.e., the metal-oxygen bond strength, that is usually preserved upon amorphization; and on the other, disorder and structural defects may cause electron localization near the band edges, and these so-called tail states may contribute to the near-edge absorption.

In this work, computationally-intensive ab-initio molecular-dynamics liquid-quench simulations are combined with accurate electronic structure calculations using a hybrid functional in order to determine the structure and properties of amorphous Ga₂O₃ as a function of its density. Specifically, we calculate the coordination of individual Ga and O atoms in a large statistical ensemble of ten independent MD realizations at five different densities and predict changes in the coordination distribution as the density decreases to an optimal value for the amorphous oxide. In contrast to monoclinic β -Ga₂O₃ where half of the Ga atoms are octahedrally-coordinated with oxygen atoms and the other half is tetrahedrally coordinated, the number of the 6-fold GaO polyhedra is completely suppressed in amorphous oxide. These changes do not affect the electronic states in the conduction band which remains delocalized upon amorphization of stoichiometric Ga₂O₃. However, presence of 5-coordinated Ga and the resulting Ga coordination morphology determine the strong localization of the non-bonding O-*p*-states at the top of the valence band that contributes to the near-edge optical absorption. The calculated band gap of stoichiometric amorphous Ga₂O₃ is similar to the one in the crystalline phase, yet, the optical properties are isotropic in the disordered material. The effects of oxygen stoichiometry on the structure and properties of amorphous Ga₂O_{3-x} are also discussed.

EL04.13.09

Late News: Theoretical Investigation of Sn Deposition on Bare and Oxygenated Diamond (100) Surface Using Density Functional Theory (DFT) Sami Ullah and Neil Fox; University of Bristol, United Kingdom

Engineering a functionalised diamond surface that is stable and reproducible is of technological importance to future diamond electronic devices such as Schottky junctions and electron-emitting electrodes for field emission, thermionic energy converters, secondary electron multipliers.

One of the most interesting properties of diamond is the negative electron affinity (NEA) which means that the vacuum level lies below the conduction band, which makes diamond an efficient source of electrons. The NEA can appear when the surface carbon atoms are negatively charged which has been achieved by terminating the diamond surface suitably. Maier et al. [1] found EAs of 0.5 eV, -1.3 eV and 1.7 eV for the bare, H- and O-terminated (100) surfaces, respectively. A monolayer or sub-monolayer coverage of some of the electropositive group I and II metals and first-row transition metals (TMs) on the bare and oxygenated diamond surface have been found to be a suitable candidate for diamond surface termination. Transition metals like Cu, Ti, Ni and Co metals have been found theoretically to impart NEA to the diamond surface however their ability to do so depends upon their capacity to form a carbide on the diamond surface in which only Ti and V have been able to show higher NEA value than others. Most of these metals, however, do not form a stable monovalent bond with carbon which was solved by using an oxygen terminated diamond surface instead of a bare diamond surface. The key here is to induce stronger bonding between the metal layer and the underlying diamond surface and hence a large surface dipole. Recently Al was found to impart NEA of -1.47 eV at a layer thickness of 1 ML bare and -1.36 eV at 0.25 ML to the oxygenated surfaces of the diamond (100) [2].

Sn as termination on the bare and oxygenated surface of diamond has so far not been investigated although Sn is less electronegative than carbon and oxygen. Sn is also expected to form the carbide bonds and oxide on the surface of the diamond well. There has been a study on the same group elements (Si and Ge) termination of the diamond where they have been shown to bond well with the surface of diamond[3][4]. We wanted to study Sn as a potential NEA imparting termination on the bare and oxygenated surface of the diamond (100). DFT calculations were performed using CASTEP to model the system which contained 0.25 ML (Quarter Mono Layer), 0.5 ML (Half Monolayer) and 1 ML (Full Monolayer) Sn in different configurations on the bare and oxygenated surface of the diamond. It was found that Sn gives NEA on most of the absorption sites, largest being (-1.91 eV with an adsorption energy of -5.94 eV) in case of 0.5 ML (HML) Sn terminated oxygenated diamond surface. Sn on the bare surface gave NEA in all the configurations with lesser adsorption energies than the oxygenated diamond surface which again shows the important role of oxygen to improve the bonding between a metal atom and diamond surface and hence the properties.

References

- [1] L. Maier, F. and Ristein, J. and Ley, “Electron affinity of plasma-hydrogenated and chemically oxidized diamond (100) surfaces,” *Phys. Rev. B*, vol. 64, no. 16, p. 165411, 2001.
- [2] M. C. James, A. Croot, P. W. May, and N. L. Allan, “Negative electron affinity from aluminium on the diamond (1 0 0) surface: A theoretical study,” *J. Phys. Condens. Matter*, vol. 30, no. 23, p. 235002, May 2018, doi: 10.1088/1361-648X/aac041.
- [3] M. J. Sear *et al.*, “Germanium terminated (100) diamond,” *J. Phys. Condens. Matter*, vol. 29, no. 14, p. 145002, Apr. 2017, doi: 10.1088/1361-648X/aa57c4.
- [4] A. Schenk *et al.*, “Formation of a silicon terminated (100) diamond surface,” *Appl. Phys. Lett.*, vol. 106, no. 19, 2015, doi: 10.1063/1.4921181.

EL04.13.10

Late News: Mesa Edge Terminated Wide Bandgap β -Ga₂O₃/GaN Heterojunction Based Vertical p-n Diode Dinusha Herath Mudiyanse and Houqiang Fu; Iowa State University, United States

β -Ga₂O₃ is a wide bandgap (WBG) semiconductor material which has been extensively studied for power, optical and RF electronics due to its large bandgap of 4.7 - 4.9 eV and high breakdown field of \sim 8MV/cm. Most of the demonstrated β -Ga₂O₃ devices are unipolar like high electron mobility transistors (HEMTs) and Schottky barrier diodes, due to the lack of p-type Ga₂O₃. To overcome this constraint, other p-type materials, such as GaN and NiO, have been studied to produce Ga₂O₃ based p-n heterojunctions. GaN is also a WBG semiconductor which attracted especial interest in power devices and has a clear crystallographic relationship to β -Ga₂O₃ for epitaxial growth. Metalorganic chemical vapor deposition (MOCVD) is an industrial standard tool which can produce both β -Ga₂O₃ and GaN. The growth of high-quality GaN on Ga₂O₃ by MOCVD has been recently reported. β -Ga₂O₃/GaN p-n heterojunction by mechanically exfoliation has also showed decent rectifying behaviors. However, due to the absence of effective edge termination the breakdown capability of the β -Ga₂O₃ based p-n heterojunctions is still in an early stage. Here we report the design and simulation of mesa edge terminated vertical β -Ga₂O₃/GaN heterojunction based p-n diode using SILVACO TCAD simulator. The heterojunction was first calibrated with conduction and valance band offsets and the device with electrical properties of the materials. The device structure consisted of n⁺-Ga₂O₃ n-contact layer, 5 μ m unintentionally doped (UID) β -Ga₂O₃ drift layer and 500 nm p-GaN layer. The ideal breakdown voltage (BV) of the heterojunction was 1.37 kV, while the BV of the reference device without any mesa edge termination fall drastically to 300 V due to the electric field crowding at the device edge. Therefore, it is crucial to design and optimize the mesa edge termination of the β -Ga₂O₃/GaN p-n heterojunction to improve the BV.

In this work, namely three mesa edge termination structures: beveled mesa, step mesa, and deeply-etched mesa were investigated. The key parameter in determining the device BV for beveled mesa is the mesa angle θ , which was varied from 15° to 90° and obtained the highest BV of 1224 V for $\theta = 15^\circ$. For the edge termination with step mesa the width (W), depth (D), and the number of steps define the mesa structure. It was found that the device BV increased with increasing number of steps. The combination of (W , D) values of (0.5,0.5) and (0.5,1.0) and (1.0,1,0) was investigated, where all the values are in μ m. The highest value of BV was obtained for $W = 0.5 \mu$ m, $D = 1.0 \mu$ m and the number of steps = 5. It was found that smaller W and larger D gave better

BV. To clearly understand the edge termination effect, electric field distribution of devices at -300 V with different edge termination mechanism were studied. Without any effective edge termination, the peak electric field at the junction edge was ~ 4.2 MV/cm. Introducing the mesa edge termination the electric field crowding was alleviated, and the peak electric fields at the edges were reduced to 1.8 MV/cm and 2.4 MV/cm for the beveled and step mesa edge terminations, respectively. Deeply-etched mesa structure was also investigated for mesa depths of 0.5, 1.0, 2.0, to 3.0 μm which showed a more relaxed uniform electric field at the junction edge. The peak electric fields were decreased from 2.1, 1.8, 1.5 to 1.2 MV/cm, when the depth changes from 0.5 to 3.0 μm .

In brief, this work summarizes an extensive design and optimization of mesa edge terminations for the wide bandgap vertical $\beta\text{-Ga}_2\text{O}_3/\text{GaN}$ p-n heterojunction diode structure. Beveled mesa, step mesa and deeply-etched mesa structures were exploited to gain knowledge on how the mesa edge terminations can mitigate the electric field crowding at the junction edge and increase the device BV. $\beta\text{-Ga}_2\text{O}_3$ based bipolar high voltage and high power devices can use this work as a guidance to improve their performance.

EL04.13.11

Late News: Nanoscale Investigation of Extended Defects in Wide Bandgap Semiconductors Joshua D. Caldwell¹, Benedikt Hauer², Claire E. Marvinney³, Martin Lewin², Nadeemullah Mahadik⁴, Jennifer Hite⁴, Nabil Bassim⁵, Alexander Giles⁴, Robert Stahlbush⁴ and Thomas Taubner²; ¹Vanderbilt University, United States; ²RWTH Aachen University, Germany; ³Oak Ridge National Laboratory, United States; ⁴U.S. Naval Research Laboratory, United States; ⁵McMaster University, Canada

The use of wide-bandgap semiconductor materials like SiC and GaN can dramatically improve the performance of electronic devices at high powers and temperatures. However, the propensity of extended defects in these materials does challenge their implementation in commercial electronic and optical applications. Spectroscopic and microscopic tools for identifying and characterizing these defects typically offer either spectroscopic or microscopic information exclusively and/or may be destructive. Here, we show how extended defects within 4H-SiC manifest in the nanoscale infrared phonon response probed by scattering-type scanning near-field optical microscopy (s-SNOM), a nondestructive method capable of simultaneously collecting topographic and spectroscopic information with frequency-independent nanoscale spatial resolution (≈ 20 nm).

We correlate the s-SNOM response of various defects in 4H-SiC with UV-photoluminescence, secondary electron and electron channeling contrast imaging, and transmission electron microscopy. We identify evidence of step-bunching, recombination-induced stacking faults, and threading screw dislocations, and also demonstrate the interaction of surface phonon polaritons with extended defects. Phonon-enhanced infrared nanospectroscopy and spatial mapping via s-SNOM thus offer significant insights into extended defects within emerging semiconductor materials and devices. It thus serves as an important diagnostic tool to help advance material growth efforts for electronic, photonic, phononic, and quantum optical applications.

[1] B. Hauer, C. E. Marvinney, et al. *Advanced Functional Materials* **30**, 1907357 (2020).

EL04.13.12

Late News: Diamond Diode Detectors for (Nearly) Any Particle or Radiation Species—From Neutrons to X-Rays Jesse Brown^{1,2}, Anna M. Zaniewski^{1,2}, Manpuneet Benipal², Jason H. Holmes¹, Ricardo Alarcon¹ and Robert J. Nemanich¹; ¹Arizona State University, United States; ²Advent Diamond, United States

Radiation and particle detectors are a widely used technology for scientific, defense, environmental, industry, and other applications. However, many radiation detectors currently available on the market are bulky and many use fragile components. There is a great interest, therefore, in the development of solid state particle detectors. In this work, we will describe how we have designed, built, and tested breadboard versions of diamond diode-based particle detectors for a range of particle and radiation species, including: alpha particles, beta particles, neutrons, x-rays, and protons. This new class of radiation detectors are compact, rugged, low power, cost effective, easy to use, and reliable. Furthermore, for some species these detectors are capable of

energy measurements/spectroscopy for particle species/isotope identification, and real time dosimetry. We will describe our progress in bringing these detectors to the commercial market.

SYMPOSIUM EL05

Advanced Functional, Linear/Nonlinear and Quantum Materials for Metasurfaces, Metamaterials and Nanophotonics
April 17 - April 20, 2021

Symposium Organizers

Artur Davoyan, University of California, Los Angeles
Ho Wai (Howard) Lee, University of California, Irvine
Junghyun Park, Samsung Advanced Institute of Technology
Pin Chieh Wu, National Cheng Kung University

* Invited Paper

Tutorial EL05: Optical Metasurfaces—Materials, Design and Advanced Device Applications
Session Chairs: Jonathan Fan, Patrice Genevet, Ho Wai (Howard) Lee, Arka Majumdar and Junghyun Park
Saturday Morning, April 17, 2021
EL05

10:00 AM *

Metasurfaces—Then and Now Patrice Genevet; Université Côte d’Azur, CNRS, France

A class of planar and wavelength-thick optical components exhibiting exceptional optical properties have emerged in recent years. These artificial interfaces, known as metasurfaces, can manipulate the wavefront of light in almost any desired manner, leveraging on the scattering properties of the subwavelength nanostructures. To further develop this technology towards dynamic tuning, broadband applications and industrial production, new materials and new fabrication methods have been proposed.

In this tutorial, I will discuss basic design and fabrication methods of metasurfaces and summarize various applications for beam steering, polarization control and monolithic integration of metasurfaces in opto-electronic systems. As an alternative of conventional bulky, the development of this technology is expected to create a positive disruption in modern optical technologies, in particular in the fields of imaging, holography, 3D dynamic image rendering, AR/VR and LiDAR systems.

11:30 AM BREAK

11:45 AM *

Optimization and Machine Learning for Metasurface Design Jonathan A. Fan; Stanford University, United States

Inverse design, in which the design process is performed through iterative optimization, has the potential to push metasurface performance to the physical limits of composite materials engineering. In this tutorial, we will

discuss a range of state-of-the-art numerical optimization methods for metasurface design. We will introduce the objective-first and adjoint variables methods, which are gradient-based optimization concepts that can produce high performance freeform geometries. We will also provide an overview of machine learning techniques as applied to electromagnetics problems and show how generative neural networks can be harnessed as an effective global optimizer for photonic devices.

1:15 PM BREAK

1:30 PM *

Metastructures for Advanced Optical Applications Arka Majumdar; University of Washington, Seattle, United States

Dielectric metasurfaces are sub-wavelength diffractive optics, which can shape the phase, amplitude and polarization of the incident optical wavefront with high spatial resolution. While theoretically conceived decades ago, the availability of sophisticated nanofabrication techniques and computational techniques have recently rejuvenated this research field. In this tutorial, I will present the current state of the design and fabrication techniques of different metasurfaces. Going beyond single metasurface, I will present results with composite metasurfaces as well as tunable metasurfaces. Finally, I will show how computational post processing techniques coupled with metasurfaces can help create ultra-low-power and low-latency sensors.

SESSION EL05.01: Metasurfaces and Metamaterials
Session Chairs: Ho Wai (Howard) Lee and Pin Chieh Wu
Sunday Morning, April 18, 2021
EL05

8:00 AM *EL05.01.01

Metasurfaces for Orbital Angular Momentum Holography, Fibre Optical Trapping and Energy Harvesting Stefan A. Maier; Ludwig-Maximilians-Universität München, Germany

Metasurfaces allow the manipulation of the amplitude, phase, and polarization of light on an ultrathin platform, and have started to be explored also in the context of digitizing optical holograms. To increase the bandwidth of a metasurface hologram, essential for high-capacity holographic memory devices, different properties of light including polarisation, wavelength, and incident angles have been exploited for holographic multiplexing; however, the bandwidth of a metasurface hologram has remained too low for any practical use.

We present the design of a complex-amplitude metasurface hologram for ultrahigh-dimensional OAM-multiplexing holography in momentum space. To realise a complex-amplitude Fourier hologram, we have introduced an OAM diffuser array with a random phase function, capable of scaling down the amplitude variation in a typical Fourier image as well as eliminating the coherence of holographic image channels. We will demonstrate first realizations of holograms based on this concept.

8:40 AM EL05.01.02

Late News: Tunable Epsilon-Near-Zero Doped Zinc Oxide Thin Films Magdalena Nistor; National Institute for Laser, Plasma and Radiation Physics, Romania

Transparent conducting oxides (TCOs) continue to play an important role in optoelectronic applications due to the unique combination of optical transparency and electrical conductivity but recently TCOs have become an emerging class of nanophotonic materials with tailorable optical properties by synthesis, post-processing and optically generated free carriers [1].

Here we report on the Nd doped ZnO thin films with tunable epsilon-near-zero wavelength in the near-infrared region obtained by controlling the doping and the growth parameters. Epitaxial wurtzite Nd doped ZnO thin films with a wide range of optical and electrical properties were grown by pulsed electron beam deposition (PED) on c-cut single crystal substrates at relatively low substrate temperatures and gas pressures. PED is a well-established ablation method to grow thin films and has common features with the pulsed laser deposition [2, 3]. Rutherford backscattering spectrometry, X-ray diffraction and pole figure measurements were performed to determine the precise texture and in-plane epitaxial relationships between film and substrate in correlation with the electrical resistivity, mobility, carrier concentration and optical properties of the films. The physical basis of the metallic conductivity at room temperature of ZnO thin films leading to the observed optical tunability will be discussed, in particular the ability to precisely control the oxygen deficiency in these films together with the role of the Nd doping in both the carrier concentration and the structural disorder. This work demonstrates that degenerately ZnO thin films are promising epsilon-near-zero materials for nonlinear optical applications and nanophotonics. [1] S.Saha et al, Materials Today (2020), in press; [2] M. Nistor et al., RSC Adv. 6, 41465 (2016); [3] M. Nistor et al. Mater. Sci. Semicond. Process. 88, 45 (2018).

8:55 AM EL05.01.03

Molecular Platform for Frequency Upconversion at the Single-Photon Level Philippe Roelli¹, Diego Martin-Cano², Tobias J. Kippenberg¹ and Christophe Galland¹; ¹EPFL, Switzerland; ²Max Planck Institute for the Science of Light, Germany

As applications in fields like security or medicine require sensitive schemes in order to detect IR photons, an interesting strategy consists in converting weak IR signals into the optical domain where detectors with single photon sensitivity are readily available. We introduce here a novel platform for ultra-sensitive conversion and detection of far and mid-infrared signals, which is inspired by our previous work where we describe the interaction between molecular vibrations and plasmonic antenna using the model of cavity optomechanics. Our study quantified the nonlinear coupling rate and revealed that it could be as high as tens of THz. We also predicted signatures of optomechanical amplification that should be observable in state-of-the-art systems. Novel plasmonic platforms could thus enable the realization of protocols inspired by cavity quantum optomechanics.

The protocol that we suggest here benefits from the intrinsic ability of specific molecular vibrations to interact both with optical and IR fields as routinely observed in Raman and resonant absorption spectroscopy. To insure an optimal overlap between the two beams and the molecular system, doubly resonant nano-antennas confine the fields into similar mode volumes and increase therefore the efficiency of the conversion process.

In this conversion scheme, an incoming IR field drives resonantly a vibrational mode and modifies its excited state population, which is mapped onto the scattered anti-Stokes Raman signal produced during the interaction between the same vibrational mode and an optical pump beam. When the optical beam is red-detuned from the plasmonic resonance the interaction Hamiltonian reduces to a state swapping Hamiltonian, enabling an efficient optomechanical conversion process. Consequently, the modified vibrational population gives rise to an additional emission of coherent optical photons on the anti-Stokes sideband that can be detected with existing single photon counting techniques.

Our study demonstrates that the noise equivalent power (NEP) can be as low as few $\text{pW}\times\text{Hz}^{-1/2}$, improving on the state of the art for devices operating at room temperature. In addition to its low noise figure the sub-wavelength dimensions of the proposed converter promises the development of multi-spectral systems designed for IR source recognition and novel technological platforms harnessing the coherent nature of the conversion process.

9:10 AM EL05.01.04

Exciton-Resonance Tuning of an Atomically-Thin Lens Jorik Van de Groep^{1,2}, Jung-Hwan Song², Umberto Celano³, Qitong Li², Pieter Kik⁴ and Mark L. Brongersma²; ¹University of Amsterdam, Netherlands; ²Stanford

University, United States; ³imec, Belgium; ⁴CREOL, United States

Since the development of diffractive optical elements in the 1970s research has focused on replacing bulky optical elements such as lenses and grating by thin counterparts. Over the last decade, nanophotonic metasurfaces rapidly advanced the development of flat optical elements based on the realization that resonant optical antenna elements enable local phase control. Present applications of metasurface flat optical elements include lenses, polarization control, and beam steering.

Next-generation applications of flat optics such as light detection and ranging (LIDAR), dynamic holography, and computational imaging require dynamic control over optical functionalities, e.g. the focal position or efficiency of optical elements. However, most nanophotonic structures are static after design and fabrication. Current approaches for dynamic control like electrical gating exhibit limited tunability due to the finite electrorefraction and electroabsorption effects in metals and semiconductors.

Here, we demonstrate actively-tunable and atomically-thin optical lenses by carving them directly out of monolayer transition-metal dichalcogenides (TMDs) like WS₂ with a strong excitonic resonance in the visible spectral range. This turns the 2D material into the antenna or metamaterial and incorporation of active materials into larger antenna structures will no longer be needed. Due to their sub-nm thickness, these materials are highly tunable through external control. We fabricate 1 mm diameter lenses with a 2 mm focal length by patterning large-area monolayer WS₂ on sapphire using nanolithography and reactive-ion etching. Using an electrochemical cell, we electrostatically control the carrier density in the monolayer WS₂ and thereby gain active control over the excitonic light scattering amplitude. Using confocal scanning microscopy, we characterize the focal shape and analyze the focal efficiency.

We demonstrate dynamic electrical tuning of the focusing efficiency with a 33% modulation depth through manipulating of the excitonic material resonance properties as opposed to tuning of antenna resonances. The highly tunable nature of these exciton resonances opens an entirely new approach for the design of dynamic flat optics and metasurfaces with applications in free-space beam tapping, wavefront manipulation, and augmented/virtual reality.

9:25 AM EL05.01.05

"Perfect" Gradient Metasurfaces are Not the Most Efficient Hsiang-Chu Wang, Karim Achouri and Olivier J. Martin; Ecole Polytechnique Fédérale de Lausanne, Switzerland

Metasurfaces rely on the resonances of nanostructures with dimensions in the nanometer range for devices working in the visible regime. The corresponding fabrication technology requires E-beam exposure and can be quite challenging. It is prone to defects associated with the many subtle process steps during fabrication, resulting in missing, distorted, or displaced nanostructures within the metasurface. In this work, we analyze the robustness of gradient metasurfaces to a variety of such defects using both simulations and experiments on purposely miss-fabricated samples. Surprisingly, we observe that a "perfect" structure, without any defect, is not that which exhibits the best performance in terms of efficiency and angular response. We demonstrate that specific, well-controlled, defects can actually significantly enhance the performance of such a metasurface and explain this behavior using the resonance and near-field properties of the corresponding nanostructures. This work sheds very new light on the design strategies for metasurfaces and significantly alleviates some constraints on their fabrication accuracy.

9:40 AM EL05.01.06

Late News: Material and Geometry Optimization of Nonlinear Coupler Based on Hybrid Plasmonic Waveguides Aleksandr Ramaniuk and Marek Trippenbach; University of Warsaw, Poland

Hybrid plasmonic waveguides are often considered as an alternative to traditional plasmonic systems in integrated photonics, as they exhibit significantly smaller losses while maintaining small structure size [1].

Nonlinear optics is another field of application for hybrid plasmonic waveguides [2]. Multiple groups have considered using both plasmonic and hybrid plasmonic waveguides to create nonlinear couplers [3,4,5]. Most of these configurations use silicon and silicon oxide in order to remain compatible with silicon-on-insulator technological framework [4]. Other proposals used highly nonlinear organic materials, such as DDMEBT or paratoluene sulphonate [5] to achieve stronger self-modulation response.

In this work we propose hybrid plasmonic waveguides based on high-index dielectrics, such as silicon, germanium, germanium telluride and germanium antimony telluride. High refractive index allows us to introduce materials with higher nonlinear response, although low refractive index contrast leads to increase of modal area. Additionally, high-index materials provide efficient coupling to dielectric waveguides with good mode confinement. We also propose fabrication method for "two-ridges-one-slab" nonlinear coupler, based on common deposition and lithography technology. We use coupled mode theory based on Generalized Nonlinear Schrodinger Equation [6] to evaluate coupler performance. While nonlinear figure-of-merit remains relatively low ($F=\gamma*L_{prop} \sim 0.2 W^{-1}$) due to two-photon absorption, we report significantly smaller coupling distances (down to several micrometers), which allows to minimize the coupler. Our simulations show that influence of both conductor nonlinear response and nonlinear coupling processes is negligible in hybrid plasmonic waveguides.

- [1] Han, Z. H. and S. I. Bozhevolnyi (2013). "Radiation guiding with surface plasmon polaritons." Reports on Progress in Physics 76(1).
- [2] Li, G. Y., et al. (2016). "Figure of merit for Kerr nonlinear plasmonic waveguides." Laser & Photonics Reviews 10(4): 639-646.
- [3] Salgueiro, J. R. and Y. S. Kivshar (2010). "Nonlinear plasmonic directional couplers." Applied Physics Letters 97(8).
- [4] Dai, D. X. and S. L. He (2009). "A silicon-based hybrid plasmonic waveguide with a metal cap for a nano-scale light confinement." Optics Express 17(19): 16646-16653.
- [5] Pitolakis, A. and E. E. Kriezis (2013). "Highly nonlinear hybrid silicon-plasmonic waveguides: analysis and optimization." Journal of the Optical Society of America B-Optical Physics 30(7): 1954-1965.
- [6] Poletti, F. and P. Horak (2008). "Description of ultrashort pulse propagation in multimode optical fibers." Journal of the Optical Society of America B-Optical Physics 25(10): 1645-1654.

SESSION EL05.02: Metamaterials and Quantum Photonics I
Session Chairs: Ho Wai (Howard) Lee and Pin Chieh Wu
Sunday Morning, April 18, 2021
EL05

10:30 AM *EL05.02.01

Structuring Light with 4D Metamaterials Nader Engheta; University of Pennsylvania, United States

In this talk, I will present some of our most recent results in one of our ongoing research projects in my group, namely, how to manipulate and tailor light using four-dimensional (4D) metamaterials, i.e., structures with judiciously chosen spatial and/or spatiotemporal inhomogeneities, in order to provide exciting functionalities. Several topics, including metamaterial computing machines, "time-vs-space scattering", temporal anisotropy, spatiotemporal control of diffusion, and temporal cladding will be presented. Connection of these concepts with the photonic networks such as the Mach-Zehnder interferometers will also be given, and possible merging of these platforms will be mentioned. Potential applications of these results will also be discussed.

11:10 AM EL05.02.02

Optical Phonon Frequency Combs Dominik M. Juraschek¹, Adarsh V. Ganesan² and Prineha Narang¹;
¹Harvard University, United States; ²National Institute of Standards and Technology, United States

The generation of optical frequency combs has fundamentally advanced optical metrology and high precision measurements. Recently, frequency combs of acoustic phonons have been demonstrated in nonlinearly driven micromechanical resonators [1]. We take the theory underlying this comb generation to the atomic scale and investigate the possibility of optical phonon frequency combs [2]. Ultrashort laser pulses can be used to coherently excite infrared-active phonons, leading to atomic vibrations with large amplitudes. Nonlinear couplings between different phonons then arise from anharmonicities in the interatomic potential of the crystal lattice, which can be used for comb generation. A particularly challenging factor plays hereby the short lifetime of optical phonons, often on the order of several picoseconds. Using a combination of first-principles calculations and phenomenological modeling, we determine the atomistic parameters of materials that are required for a clear discrete spacing of frequency lines in the comb spectrum of the optical phonons. We propose a set of promising material candidates for displaying optical phonon frequency combs that would set a milestone in nonlinear phononic control of material properties.

[1] A. Ganesan, C. Do, and A. Seshia, Phys. Rev. Lett. 118, 033903 (2017)

[2] D. M. Jurashek, A. Ganesan, and P. Narang, in preparation

This work is supported by the Swiss National Science Foundation (SNSF) under Project No. 184259, the DARPA DSO under the Driven Nonequilibrium Quantum Systems (DRINQS) program, Grant No. D18AC00014, and by the Department of Energy ‘Photonics at Thermodynamic Limits’ Energy Frontier Research Center under Grant No. DE-SC0019140. This research used resources of the National Energy Research Scientific Computing Center (NERSC) under Contract No. DE-AC02-05CH11231.

11:25 AM EL05.02.04

Designer Tamm Plasmon Thermal Emitters Using Gradient Descent Regression Optimization Mingze He¹, [Joshua R. Nolen](#)¹, Josh Nordlander², Angela Cleri², Jon-Paul Maria² and Joshua D. Caldwell¹; ¹Vanderbilt University, United States; ²The Pennsylvania State University, United States

The mid-infrared (MIR) spectral range is often referred to as the molecular fingerprint region due to the multitude of molecular vibrational signatures it contains. As such, research focused on developing MIR optical sources of sufficiently narrow bandwidth, minimal power demands and small form factors are of great interest for potential spectroscopic and sensing applications such as bio- and chemical sensing, as well as the detection of harmful gases. One approach for such applications that has garnered significant attention recently has been frequency-selective thermal emitters. Here, by judiciously selecting and/or structuring semiconductor materials, the thermal photonic density of states can be tailored such that frequency-dependent far-field impedance matching, and therefore absorptivity, is achieved. Reciprocally, through Kirchhoff’s law, this results in an emissivity of equivalent direction and magnitude. Here we report on a powerful approach towards realizing narrowband thermal emitters with a high degree of frequency selectivity, without sacrificing narrow emission linewidths that is typically an issue with plasmonic-based emitters, through the inverse design of aperiodic Tamm plasmon (TP) devices.

Tps are optical interface states that form between a distributed Bragg reflector (DBR) and a metal or between two dissimilar DBRs. These excitations exhibit a parabolic dispersion that falls within the photonic bandgap of the DBR and the air light cone and are therefore accessible from free space without the need for expensive and time-consuming lithographic and etching fabrication steps. Here, we employ a gradient descent regression (GDR) algorithm to design TP-supporting films in the metal-DBR geometry and grow films that reproduce the predicted spectral features of our designs with great success. We utilize n-CdO deposited through high-power impulse magnetron sputtering as our metal layer. This highly-promising transparent conducting oxide (TCO) has been demonstrated to exhibit broad spectral tunability of the plasma frequency, while maintaining exceptionally low optical losses. This is due to CdO possessing both a low effective mass (ranging from 0.12 – 0.26 in epitaxially-grown films with carrier densities ranging from 10^{19} - 10^{20} cm⁻³) as well as electron mobilities extending upwards to 500 cm²/V-s. As TP modes correspond with the impedance-matched condition of the

DBR and the metal film, having such control over the impedance of both the DBR (through changes to individual layer thicknesses and dielectric index), and the CdO layer (through changes to the carrier density and layer thickness), grants significant flexibility to our design.

Inverse design has been used to design TP-supporting films in the past, however, these efforts have relied on computationally-expensive techniques, such as genetic algorithms, Bayesian optimization or deep learning, often requiring several hours or days to reach a final solution for a single-peak emission spectrum. In contrast, our GDR approach is capable of arriving at a solution on the timescale of seconds or minutes, all while running on a consumer-grade CPU. As we demonstrate, this opens the door to realizing thermal emitters with varying levels of spectral complexity. For example, realizing arbitrarily positioned single- and multi-peak thermal emission spectra, which can accurately match to the IR absorption spectra of greenhouse gases such as CO₂ and N₂O. We are also able to achieve quality-factors that far-exceed conventional plasmonic devices ($Q > 300$ for designed films), and control the full TP-dispersion and therefore spatial coherence of the thermal emission, all while maintaining a simple, planar structure. Therefore, the design principles used here outline a highly-tunable and potentially scalable platform for realizing applications such as filter-less non-dispersive infrared gas sensing and free-space communications.

11:40 AM *EL05.02.05

Engineering Light Emission for Frequency-Conversion Imaging and Quantum Technologies Mikhail Kats; University of Wisconsin-Madison, United States

This talk will discuss two recent developments related to engineering light emission. First, I will demonstrate a passive down-conversion imaging system that converts broadband ultraviolet light to narrow-band green light using perovskite nanocrystals, while preserving the directionality of rays, and thus enabling direct down-conversion imaging. The system preserves high transparency in the visible, enabling superimposed visible and ultraviolet imaging.

Then, I will discuss our design of a nanoscale light extractor (NLE) that enables efficient outcoupling and beaming of broadband light emitted by nitrogen-vacancy centers in diamond. The NLE consists of a patterned silicon layer on diamond and requires no etching of the diamond surface. Our design process is based on adjoint optimization using broadband time-domain simulations and yields structures that are inherently robust to positioning and fabrication errors.

SESSION EL05.03: Metamaterials and Quantum Photonics II

Session Chairs: Harry Atwater and Ho Wai (Howard) Lee

Sunday Afternoon, April 18, 2021

EL05

1:00 PM *EL05.03.01

Artificial-Intelligence Assisted Photonics Zhaxylyk Kudyshev, Alexander Kildishev, Vladimir Shalaev and Alexandra Boltasseva; Purdue University, United States

Discovering novel, unconventional optical designs in combination with advanced machine-learning assisted data analysis techniques can uniquely enable new phenomena and breakthrough advances in many areas including on-chip circuitry, imaging, sensing, energy, and quantum information technology. *Topology optimization*, which has previously revolutionized aerospace and mechanical engineering by providing non-intuitive solutions to highly constrained material distribution problems, has recently emerged as a powerful architect for *advanced photonic design*[1]. Compared to other *inverse-design* approaches that require extreme computation power to undertake a *comprehensive search* within a large *parameter space*, topology optimization

can expand the design space while improving the computational efficiency. This talk will highlight our most recent findings on 1) merging topology optimization with *artificial-intelligence-assisted algorithms* and 2) integrating *machine-learning based analysis* with *photonic design* and *quantum optical measurements*. Particularly, we will discuss our studies on implementing deep-learning assisted topology optimization for advanced metasurface design development[2-4]. Specifically, we will cover different generative network-based optimization strategies, covering local and global optimization frameworks. We will summarize our research on merging topology optimization technique with quantum device design for achieving ultrafast single-photon source that offers efficient on-chip integration. Finally, we will also describe our recent works on implementing a novel convolutional neural network-based technique for real-time material defect metrology at the quantum level that outperforms all existing approaches in terms of speed and fidelity. This new method rapidly extracts the values of the single-photon autocorrelation function at zero delays from sparse data and ensures one order speed up on solving “bad”/“good” emitter classification problems in comparison with conventional techniques[5]. Along with emitter classification, we will cover the ML-based regression schemes, which open up a way for the realization of rapid antibunching-induced super-resolution imaging applications.

References:

- [1] Sean Molesky, Zin Lin, Alexander Y. Piggott, Weiliang Jin, Jelena Vučković, Alejandro W. Rodriguez. Nature Photonics volume 12, pages 659–670 (2018)
- [2] Wei Ma, Zhaocheng Liu, Zhaxylyk A. Kudyshev, Alexandra Boltasseva, Wenshan Cai & Yongmin Liu, Deep learning for the design of photonic structures, Nature Photonics (2020) DOI: <https://doi.org/10.1038/s41566-020-0685-y>
- [3] Zhaxylyk A. Kudyshev, Alexander V. Kildishev, Vladimir M. Shalaev, and Alexandra Boltasseva, Machine-learning-assisted metasurface design for high-efficiency thermal emitter optimization, Applied Physics Reviews 7, 021407 (2020); <https://doi.org/10.1063/1.5134792>
- [4] Zhaxylyk A. Kudyshev, Alexander V. Kildishev, Vladimir M. Shalaev, and Alexandra Boltasseva, Machine learning-assisted global optimization of photonic devices, Nanophotonics (2020), DOI: 10.1515/nanoph-2020-0376
- [5] Zhaxylyk A. Kudyshev, Simeon I. Bogdanov, Theodor Isacsson, Alexander V. Kildishev, Alexandra Boltasseva, Vladimir M. Shalaev, Rapid Classification of Quantum Sources Enabled by Machine Learning, Advanced Quantum Technologies, Vol. 3, 10, 2020 DOI: <https://doi.org/10.1002/qute.202000067>

1:40 PM EL05.03.02

High Refractive Index Nanopillar Metasurface for Control of Coherent Light States Vahid Karimi and Viktoriia Babicheva; The University of New Mexico, United States

Metasurfaces of high-refractive-index materials, such as silicon, III-V compounds, and similar material groups, enable manipulation of light on a subwavelength scale and support well-defined Mie resonances. These ultra-thin optical nanostructures of high-refractive-index materials can be used at the subwavelength scale for amplitude and phase modulation. Hence, the metasurface supporting Mie resonances has a high potential in effective control of coherent light states. The integration of light-emitting devices, such as VCSELs and VeCSELs, and high-refractive-index metasurfaces is proven to be an efficient method for addressing light-emitting beam-shaping problems.

The monolithic integration approach is a new direction and offers many opportunities in designing beam-shaping VCSELs. The III-V compound nanopillar meta-atoms can be used in polarization-insensitive metasurface at the back-side surface of a bare VCSEL [1]. In this design, each nanopillar functions as an independent resonator with a low-quality factor. The large refractive index of the metasurface elements enables the large transmitted amplitude. Instead of modifying the laser cavity, the integrated III-V compound metasurface acts as a passive element that forms the laser beam profile on the emission surface.

We aim at designing metasurface with the desired phase modulation, and we study properties of III-V compound nanopillars of various dimensions. We study periodic nanopillar arrays on either high-index or low-index substrate with an intermediate layer in the visible and near-infrared frequencies [2]. Arrays of various

periodicity, with different heights and radii of nanopillars, as well as thicknesses of the intermediate layer are analyzed. Numerical simulations of III-V compound metasurfaces are carried out for arrays of different arrangements for reflection, transmission, and absorption spectral profiles.

The metasurface supports Mie type and other nanostructure resonances, and with an increase of intermediate layer thickness, the spectral positions of the nanostructure resonances move towards longer wavelengths. We report on the metasurface scattering characteristics to modulate the arbitrary beam shapes employing a phase-matching technique in the least-squares sense. We show the possibility of engineering the VCSEL's output beam shape by introducing nanopillars of specific arrangement and adding the intermediate high-index layer.

[1] Yi-Yang Xie, et al. Nat. Nanotechnol 15, 125 (2020).

[2] V. Karimi, V. E. Babicheva, Proc. SPIE 11460, Metamaterials, Metadevices, and Metasystems 2020, 114601F (2020).

1:55 PM *EL05.03.05

Engineering New Solid State Quantum Defects for Quantum Networks Nathalie P. de Leon; Princeton University, United States

Engineering coherent systems is a central goal of quantum science and quantum information processing. Point defects in diamond known as color centers are a promising physical platform. As atom-like systems, they can exhibit excellent spin coherence and can be manipulated with light. As solid-state defects, they can be produced at high densities and incorporated into scalable devices. Diamond is a uniquely excellent host: it has a large band gap, can be synthesized with sub-ppb impurity concentrations, and can be isotopically purified to eliminate magnetic noise from nuclear spins. Currently-known color centers either exhibit long spin coherence times or efficient, coherent optical transitions, but not both. We have developed new methods to control the diamond Fermi level in order to stabilize a new color center, the neutral charge state of the silicon vacancy (SiV) center. This center exhibits both the excellent optical properties of the negatively charged SiV center and the long spin coherence times of the NV center, making it a promising candidate for applications as a single atom quantum memory for long distance quantum communication. We have recently discovered bound exciton transitions associated with SiV⁰, which enable efficient optical spin polarization and optically detected magnetic resonance. Finally, I will describe our efforts to integrate SiV⁰ centers in nanophotonic devices, specifically in heterogeneously integrated III-V/diamond nanophotonic platforms designed to enhance the atom-photon interaction and achieve quantum frequency conversion to the telecom band.

SESSION EL05.04: Active Metasurfaces

Session Chairs: Ho Wai (Howard) Lee and Junghyun Park

Sunday Afternoon, April 18, 2021

EL05

4:00 PM *EL05.04.01

Active Metasurfaces: Reconfigurable Wavefront Control and Spatiotemporal Modulation Harry A. Atwater; California Institute of Technology, United States

A grand challenge for nanophotonics is the realization of comprehensively tunable metasurface nanoantenna arrays enabling dynamic, active control of the key constitutive properties of light – amplitude, phase, wavevector and polarization. Achieving this will open new photonics applications in phased-array optical beam steering, visible light modulation for communication and thermal radiation management. I will discuss the status and outlook for electronically tunable and reconfigurable plasmonic, excitonic and dielectric metasurfaces whose elements are arbitrarily reprogrammable, enabling a wide array of functions, including

steering, focusing, and frequency multiplexing of scattered radiation.

4:40 PM EL05.04.02

Late News: Tunable Cavity-Controlled Field Enhancement in Self-Assembled Plasmonic Metasurfaces

Timothy J. Palinski¹, Amogha Tadimety², Gary W. Hunter¹ and John X. Zhang²; ¹NASA Glenn Research Center, United States; ²Dartmouth College, United States

Locally enhanced electric fields in nanoplasmonic systems play an important role in a range of sensing and detection applications, including surface enhanced spectroscopies, fluorescence measurements, and refractive index-based biosensing. As these technologies move increasingly towards point-of-care applications, it is critical that sensor substrates maintain high-performance while being low profile, inexpensive, and easily fabricated. Here, we demonstrate tunable field enhancement in a self-assembled plasmonic metasurface via coupling to a stimuli-responsive photonic cavity. Our structure consists of a near-percolation plasmonic gold film on a polymer spacer above a gold mirror, creating a Fabry–Perot nanocavity. Simulations of the as-fabricated nanostructures reveal that the strongest field enhancement occurs when the cavity mode overlaps with the plasmonic top film, resulting in nearly perfect light absorption/trapping by the system. Compared to the nanoislands alone, the cavity-coupled system yields a ~4x increase in field enhancement. The random size and distribution of the plasmonic nanoislands contribute to its strong, broadband absorption >95% and corresponding field enhancement over 400-nm bandwidths. By varying the cavity thickness, the cavity mode overlap and resulting absorption-based field enhancement can be tuned to a spectral range of interest. Using a vapor-responsive polymer spacer, we demonstrate real-time, reversible tuning of these absorption bands across >100-nm ranges in wavelength in the presence of organic solvents. This structure was readily fabricated using standard wafer-scale thin-film deposition processes. The plasmonic top film can also be formed using other bottom-up techniques, including dispersion or printing of colloidal nanoparticles and seed-mediated particle growth, extending the range of potential applications and further simplifying the fabrication process. This platform forms the basis for a simple, dynamically tunable substrate which may be applied in a variety of sensing contexts, with potential application to other absorption-based processes such as energy harvesting and photodetection.

4:55 PM EL05.04.03

Late News: High Quality Factor Metasurfaces for Dynamic, Electro-Optically Controlled Wavefront

Shaping Sahil Dagli¹, Elissa Klopfer¹, David Barton², Mark Lawrence³ and Jennifer Dionne¹; ¹Stanford University, United States; ²Harvard University, United States; ³Washington University in St. Louis, United States

Wavefront shaping and control is essential for advancements in optical technologies including LiDAR, AR/VR, and LiFi systems. Metasurfaces offer a promising route for these technologies, as they allow for precise control of the amplitude, phase, and polarization of light in a sub-wavelength-thick footprint. However, most current metasurface designs are static, relying on fixed geometric patterning and lacking tunability once fabricated. Here, we design high quality factor (high-Q) metasurfaces that enable electro-optically tunable beam-steering through dynamic phase and amplitude control of the constituent nanoantennas. Our metasurface consists of a uniform array of subwavelength nanobars of Silicon, each 500 nm wide and 220 nm tall, atop 100 nm thick lithium niobate. By introducing subtle geometric perturbations into each constituent nanobar, we excite guided mode resonances with normally-incident light. Using full-field simulations, we show how these guided mode resonances excite strongly enhanced fields localized in the lithium niobate, with mode quality factors exceeding 20,000. Applying a voltage across individual nanoantennas shifts the spectral position of the high-Q resonance, modifying the antenna phase and amplitude. In reflection, we achieve a full 2 pi phase variation with applied bias, with a reflectance efficiency above 93%. Using these results, we computationally design a fully-reconfigurable, solid-state beam steerer: without bias light is directly reflected from the metasurface, whereas an applied biases of +9.2 V, 0 V, and -9.2 V across three constituent antennas diffracts the light to 30 degrees with 65% efficiency. Biases of 13 V, 2 V, -2 V, and -13 V across four constituent antennas diffracts the reflected light to 22 degrees. Near-continuous beam-steering can be achieved by modifying the bias across each antenna.

We also show how this platform can enable dynamic modulation of other optical transfer functions, including beam-splitting and lensing. Our high-Q electro-optic metasurfaces provide a foundation for light-weight, fully reconfigurable, solid-state classical and quantum information processing spanning LiDAR, LiFi, AR/VR, and quantum communications.

5:10 PM EL05.04.04

Beamforming Tradeoffs in Quasi-Static and Time-Modulated Optical Phased Arrays Raana Sabri, Mohammad Mahdi Salary and Hossein Mosallaei; Northeastern University, United States

Realization of dynamic beam steering for free-space data communication and light detection and ranging (LiDAR) technology, demands a class of high-performance devices with capability of generating fast-scanning and low-divergence beams. Optical phased arrays (OPAs), consisting of several typically identical optical nanoantennas, hold a great promise for achieving real-time beam steering, by imparting local, space-variant phase gradients on the incident light. Integration of dynamically tunable electro-optical materials into the constituent building blocks of OPAs facilitates active control over the intrinsic properties of subwavelength antenna elements with high speed and offers post-fabrication modifications to their optical response. The phase tuning mechanism of the active OPAs has thus far relied on the modulation of the resonant modes between the over-coupled and under-coupled regimes by applying external DC bias voltages to nanoantennas. This leads to high variations of amplitude during phase modulation and restricts the maximum achievable phase span into a narrowband critical coupling regime. Moreover, the phase modulations in such so-called quasi-static OPAs is typically less than 2π . Introducing time into OPAs, as an additional dimensionality, offers a way out to surmount these obstacles through generation of sideband signals and translating the spatial diversity of scattering into the spectral diversity. In this work, a comparative study on active beam steering performance of quasi-static and time-modulated reflective OPAs operating at near-infrared (NIR) spectral regime is presented. Plasmonic strip nanoantenna in a metal-insulator-metal (MIM) configuration integrated with indium-tin-oxide (ITO) is considered as the building block of the active OPA. First, the beamforming performance of the quasi-static OPA is analytically studied to highlight its main shortcomings including narrow bandwidth, limited angle-of-view, and large sidelobe level (SLL) as results of strong resonant dispersion of phase, limited dynamic phase span, and dramatic variations in amplitude. Moreover, a multiobjective evolutionary optimization is adopted to identify the non-intuitive beamforming tradeoffs between SLL and gain in the quasi-static OPA due to covarying amplitude and phase responses. Then, beam steering performance of a time-modulated OPA under the application of radio frequency biasing signals is investigated. Modulation waveform is optimized to achieve beam steering with uniform amplitude via non-resonant and dispersionless phase shift induced by modulation phase delay at the first order sideband. This dispersionless phase elevates time-modulated OPAs beyond their quasi-static counterparts in that it increases the functionality bandwidth, expands the angle-of-view, and minimizes the power coupled into undesired sidelobes by providing access to the full phase span (2π) with uniform amplitude. In addition, Taylor one-parameter distribution is employed to implement amplitude tapering for engineering of the beamforming tradeoffs between SLL and gain.

5:25 PM *EL05.04.05

On-Demand Beam Shaping Using a Reconfigurable Metasurface Hanwei Wang, Hsuan-Kai Huang, Yun-Sheng Chen and Yang Zhao; University of Illinois at Urbana-Champaign, United States

In magnetic resonance imaging (MRI), the signal-to-noise ratio (SNR) is the main figure of merit that assesses the imaging quality. Existing studies mainly focus on improving the magnetic field intensities of the constant homogenous field from the main coil or the oscillating field from the radio frequency (RF) coil. In addition to these options, SNR also depends on the coupling between the imaging subject and the RF coil during the signal reception, which has been largely ignored. Here we provide a different route towards enhancing the SNR of MRI by improving this coupling during the signal reception. We elucidate a theoretical design of an ultrathin metasurface with micrometer thickness and high flexibility. This metasurface is reconfigurable; it can selectively boost the SNR at a desired imaging region with any arbitrary shapes. Our design has shown that this metasurface can enhance SNR by up to 28 times in the

region of interest. At the same time, the metasurface is designed to minimally disturb the excitation fields by less than 1.6%, thus maintaining the uniformity of the excitation, which is important to achieve a high-quality MR image without artifacts.

SESSION EL05.05: Active and Quantum Metasurfaces
Session Chairs: Junghyun Park and Pin Chieh Wu
Sunday Afternoon, April 18, 2021
EL05

6:30 PM *EL05.05.01

Manipulating Photonic Quantum States by a Metasurface Xiang Zhang, Quanwei Li, Wei Bao, Zhaoyu Nie, Yang Xia, Yahui Xue, Yuan Wang and Sui Yang; University of California, Berkeley, United States

The two-dimensional designer metasurfaces have been established as a new class of versatile and powerful optical solution for controlling the classical light in various degrees of freedom such as phase, amplitudes, polarization and angular momentum. Expanding the control capability of metasurface from classical light to quantum state of single photons is an emerging direction that can lead to a new regime of light-matter interaction and applications for quantum technology. In this talk, we will present our proposal and experimental demonstration of manipulating photonic quantum states. The demonstrated control over the effective quantum interaction between single photons that is impossible by traditional optics has been enabled by an unprecedented design of metasurface. Our work greatly empowers the operations and functionalities of optical quantum technologies.

7:10 PM EL05.05.02

Extreme Color Tuning of Dynamic Metasurface via Electrochemical Intercalation of Lithium in TiO₂ Janna Eaves-Rathert¹, Elena Kovalik^{1,1}, Chibuzor Ugwu¹, Cary Pint^{2,1} and Jason Valentine¹; ¹Vanderbilt University, United States; ²Iowa State University of Science and Technology, United States

Faced with the ability to arbitrarily engineer the interaction of electromagnetic energy with a medium, the optics community is enchanted by the innumerable, though fixed, configurations of passive metamaterials. Looking forward, infusing such structures with dynamic tunability may help realize both practical applications and novel functionality. While many phase change materials are capable of wild property modulations induced by heat, electrochemical intercalation presents opportunities for complete rearrangement of atomic structure and composition in a reversible manner, resulting in potentially dramatic permittivity changes. In the age of the lithium ion battery, rapid materials innovation and research has uncovered numerous compounds which accommodate lithium, though the resulting changes in optical properties lack clarity. We explore the properties of titanium dioxide (TiO₂), which is both a high-index dielectric material with negligible absorption in the visible spectrum, making it popular for all-dielectric metasurfaces, as well as an established lithium anode material known for minimal volume expansion (<1%) and good cyclability. Upon lithiation to Li_{0.5}TiO₂, DFT calculations predict significant changes in dielectric constants in the visible and near-IR regions of the electromagnetic spectrum. These calculations are verified by air-free ellipsometry measurements on TiO₂ thin films deposited via atomic layer deposition and electrochemically lithiated, thereby reducing the refractive index by $\Delta n = 0.5$ at ~ 650 nm. When incorporated into metal-insulator-metal type metasurfaces, the resulting devices demonstrate sweeping spectral shifts across the visible regime with applied voltages < 2 V. Through unraveling the optical properties of this abundant, non-toxic battery material, our findings open the door to low-power, multistable, active metasurfaces for color modulation and tunable filters.

7:25 PM EL05.05.03

Strain-Tunable Resonators Based on an Integration of Bragg Reflectors and Metasurfaces Sravva

Nuguri¹, Benjamin Cerjan², Vince Einck¹, Mark Griep³, Naomi Halas² and James Watkins¹; ¹University of Massachusetts Amherst, United States; ²Rice University, United States; ³U.S. Army Research Office, United States

Bragg reflectors from layer by layer (LBL) assembly of Slide Ring elastomer and Zirconia Nanoparticles have been shown to offer desirable elasticity and strain tun-able optical properties. With a high loading of zirconia nanoparticles of nearly 80 wt% in the photonic crystal results in a refractive index contrast of 0.18 between the filled and unfilled layers of 6 periods. Further, we study an integration of Au meta-surfaces by utilising soft-imprinting lithography of 400 nm spaced rectangular pillars and other modulated nanofeatures on the Bragg Reflectors and harness the enhanced tuning ability. The nanoimprinting ink is composed of a bi-layer polymer resist, among which only the top layer renders lower viscosity that fills the stamp via capillary pressure. The resulting patterns are metallised with 50 nm of Au using e-beam evaporating technique and followed by transferring the metal features on the Bragg reflectors. By stretching the resulting photonic crystal over 40% strain we demonstrate the mechano-chromic sensing abilities in a span of wavelengths.

7:40 PM EL05.05.04

Self-Assembled BaTiO₃-Au_xAg_{1-x} Low-Loss Hybrid Plasmonic Metamaterials with Ordered “nano-Domino-Like” Microstructure Di Zhang¹, Shikhar Misra¹, Jie Jian¹, Ping Lu², Leigang Li¹, Ashley Wissel¹, Xinghang Zhang¹ and Haiyan Wang¹; ¹Purdue University, United States; ²Sandia National Laboratories, United States

Metallic plasmonic hybrid nanostructures have attracted enormous research interests due to the combined physical properties coming from different material components and the broad range of applications in nanophotonic and electronic devices. However, the high loss and narrow range of property tunability of the metallic hybrid materials has limited their practical applications. Here, a metallic alloy-based self-assembled plasmonic hybrid nanostructure, BaTiO₃-Au_xAg_{1-x} vertically aligned nanocomposite, has been integrated by a templated growth method for low-loss plasmonic systems. Comprehensive microstructural characterizations including (HR)STEM, EDS and 3D electron tomography demonstrate the formation of an ordered “nano-domino-like” morphology with the Au_{0.4}Ag_{0.6} nanopillars as the round cores, and the BTO as the squared shells. By comparing with the BTO-Au hybrid thin film, the BTO-Au_{0.4}Ag_{0.6} alloyed film exhibits much broader plasmon resonance, hyperbolic dispersion, low-loss, and thermally robust features in UV-Vis-NIR wavelength region. This study provides a feasible platform for complex alloyed plasmonic hybrid material design with low-loss and highly tunable optical properties towards all optical integrated devices.

SESSION EL05.06: Functional Metasurfaces and Plasmonic
Session Chairs: Junghyun Park and Pin Chieh Wu
Sunday Afternoon, April 18, 2021
EL05

9:00 PM *EL05.06.01

Multifunctional Metasurface and Its Applications ByoungHo Lee, Chusoo Choi, Jangwoon Sung and Gun-Yeal Lee; Seoul National University, Korea (the Republic of)

Metasurfaces are planar optics composed of artificially fabricated subwavelength meta-atoms with unique optical scattering characteristics. Thanks to their outstanding abilities to modulate electromagnetic waves, metasurfaces have been enthusiastically researched. The research on metasurfaces especially focuses on wavefront modulation and many approaches have been proposed to implement novel optical devices with versatile functionality. It has been demonstrated that metasurfaces can implement high-quality holographic light reconstruction with both amplitude and phase information at sub-wavelength scale spatial resolution, which is

expected to be applied to next-generation imaging technologies such as three-dimensional holographic imaging and optical data storage. In addition, metasurface lenses, called meta-lenses, have powerful features such as flatness, high numerical aperture, and versatility that cannot be found in conventional optical lenses. Based on these meta-optics, recent advances in metasurfaces have led to the development of various optical systems, and several studies have begun to be reported in recent years. In this talk, we will introduce our representative works that achieve significant progress of optical systems through utilizing elaborately designed multifunctional metasurfaces. The first part will introduce the passive and active type metasurfaces exhibiting enlarged light modulation capabilities with their practical applications. The passive type metasurface is designed to exhibit different scattering characteristics for two orthogonal polarizations of incidence light with their full-space controllability. Through exploiting multifunctionality, the polarizing beam-splitter and full-space holographic image generation are demonstrated. And, the active type metasurface is engineered to exhibit enlarged switching levels through exploiting optical-thermal analysis. To utilize the expanded switching level at best, the metasurface is designed to generate high-contrast holographic images according to the state change of metasurface. Thanks to the thermo-optical complexity of our active metasurface, the visual cryptosystem is demonstrated, providing an extremely high-security level. In the second part, we will introduce the novel concept of metalens, called see-through metalens for augmented reality (AR) device application. The see-through meta-lens effectively combines the real and virtual images in a compact manner thanks to the flatness and high-numerical-aperture of the proposed metalens. The proposed geometric-phase metalens can distinguish the two lights – light from outside object and one from an image projector based on polarization orthogonality. Especially, our study is highlighted for dramatically improving the field-of-view compared to previous AR imaging devices. Lastly, our perspective on the possibilities and challenges of metasurface hologram, metasurface multifunctional diffraction devices and metalens will be discussed.

9:40 PM DISCUSSION TIME

9:55 PM EL05.06.03

Dynamic Meta-Holograms with Designer Liquid Crystals for Interactive Displays and Unconventional Photonic Sensors Inki Kim, Won-Sik Kim, Young-Ki Kim and Junsuk Rho; Pohang University of Science and Technology, Korea (the Republic of)

Computer-generated holography (CGH) involves iterative numerical algorithms to obtain the phase and/or amplitude profiles needed to physically realize holograms. Metasurfaces consist of arrays of subwavelength nanoresonators that can control the wavefront of light in a desired way. They recently proved themselves to be an effective platform for CGH by surpassing the quality of traditional holograms in terms of image resolution and field-of-view. Those metasurface holograms showed prospects not only in imaging and display but also in security applications [1]. In particular, applying metaholograms to anticounterfeiting applications requires not only the technology of encoding multiple pieces of information, but also the manufacturability of highly efficient devices. To meet these complex needs, we have implemented high-efficiency metaholograms based on hydrogenated amorphous silicon (a-Si:H), which realize pragmatic images holograms working under unpolarized light (*e.g.* sunlight or flashlight of cellphone) and spin/direction-multiplexed metaholograms [2-4]. However, ‘real-time’ active operations of those flat optical devices have remained unresolved yet.

In this abstract, I will discuss our efforts in realizing dynamic metaholograms by leveraging specifically-designed (‘designer’) liquid crystals that can respond to target external stimuli. First, I will present high-efficiency interactive holographic displays, which can switch holographic images according to external stimuli like voltage, heat and touch sensing [5]. For examples, the voltage-responsive metahologram is able to switch the holographic images within few milliseconds promising for real-time video holographic displays demanding 60 ~ 120 frames/s. Also, the heat or touch-responsive metaholograms can monitor external temperature and impact by visualizing different hologram images according to the pre-programmed external stimuli standart. Such demonstrated systems may permit a diverse range of smart sensing and display applications such as smart hologram labels monitoring temperature/pressure/touch changes and interactive holographic displays recognizing haptic motions. Secondly, I will propose a compact gas sensor platform to autonomously sense the existence of a toxic volatile gas and provide an immediate visual holographic alarm [6]. By combining the

advantage of the rapid responses to gases realized by liquid crystals with the compactness of holographic metasurfaces, we develop ultra-compact gas sensors without the requirement of additional complex instruments or machinery to report the visual information of gas detection. It is expected that such a holographic metasurface gas sensor platform will provide a path to ubiquitous, compact, and smart unconventional photonic sensing applications that quickly alert users about harmful gases or biochemical leaks.

- [1] I. Kim *et al.*, *ACS Photonics* 5, 3876-3895 (2018)
- [2] I. Kim* *et al.*, *ACS Nano* 11, 9382-9389 (2017)
- [3] I. Kim* *et al.*, *Laser and Photonics Reviews* 13, 1900065 (2019)
- [4] I. Kim* *et al.*, *Nanoscale Horizons* 5, 57-64 (2020)
- [5] I. Kim *et al.*, *Advanced Materials* (2020) (in press)
- [6] I. Kim *et al.*, *Science Advances* (2020) (in review)

10:10 PM EL05.06.04

Collective Excitations and Optical Response of Ultrathin Carbon Nanotube Arrays Igor Bondarev and Chandra Adhikari; North Carolina Central University, United States

We develop a theory for collective near-field interactions and associated ElectroMagnetic (EM) response of planar, closely packed, periodically aligned Single-Wall Carbon Nanotube (SWCN) arrays embedded in finite-thickness ultrathin dielectric layers. The features that make this system interesting are the periodic CN alignment and the spatially periodic anisotropy associated with it. Additionally, the vertical confinement in dense ultrathin planar systems of finite thickness leads to the effective dimensionality reduction from 3D to 2D while still retaining the thickness as a parameter to represent the vertical size. This is the transdimensional regime [1] — neither 3D nor 2D but something in-between — turning into 2D as the thickness tends to zero, challenging to study what the 3D-to-2D continuous transition has to offer for new material functionalities [2-4]. The spatial anisotropy, periodic in-plane transverse inhomogeneity and vertical quantum confinement make the ultrathin array near-fields strong and anisotropically nonlocal, adding both extra challenges in developing the problem theoretically [3] and extra flexibility in designing CN films with desired EM properties experimentally [5]. Here, we derive the SWCN array EM response tensor in terms of the individual SWCN conductivity, plasma frequency and the volume fraction of CNs in the dielectric film. In the CN alignment direction the real part of the EM response has a sufficiently wide negative refraction band, indicating that the CN film behaves as a hyperbolic metamaterial [4]. Inhomogeneous and thermal broadening of the exciton and plasmon resonances lead to their overlap, making the exciton-plasmon hybridization possible. Being very stable and highly sensitive to the vertical size/CN-density/diameter/chirality variations, the ultrathin periodically aligned SWCN arrays and films show great potential to serve as a new flexible multifunctional nanomaterial platform for single-molecule detection and manipulation, including the near-field control of photoluminescence rate/directionality, chemical reactivity, and Casimir-Polder interactions [6,7].

Funding Acknowledgement: NSF DMR-1830874 (I.V.B.)

- [1] A.Boltasseva and V.M.Shalaev, Transdimensional Photonics, *ACS Photon.* 6, 1 (2019)
- [2] I.V.Bondarev, H.Mousavi, and V.M.Shalaev, Transdimensional Epsilon-near-zero Modes in Planar Plasmonic Nanostructures, *Phys. Rev. Research* 2, 013070 (2020); *MRS Commun.* 8, 1092 (2018)
- [3] I.V.Bondarev, Finite-Thickness Effects in Plasmonic Films with Periodic Cylindrical Anisotropy [Invited], *Opt. Mater. Express* 9, 285 (2019)
- [4] C.M.Adhikari and I.V.Bondarev, Optical Response of Ultrathin Periodically Aligned Single-Wall Carbon Nanotube Films, *MRS Advances*, DOI: 10.1557/adv.2020.234; see also arXiv:2010.00139
- [5] J.A.Roberts, S.-J.Yu, P.-H.Ho, S.Schoeche, A.L.Falk, and J.A.Fan, Tunable Hyperbolic Metamaterials Based on Self-Assembled Carbon Nanotubes, *Nano Lett.* 19, 3131 (2019)
- [6] I.V.Bondarev and Ph.Lambin, Near-field electrodynamics of atomically doped carbon nanotubes, In: *Trends in Nanotubes Research* (Nova Publishers, NY 2006). Ch.6, pp.139-183
- [7] J.Galego, F.J.Garcia-Vidal, and J.Feist, Suppressing photochemical reactions with quantized light fields,

10:25 PM *EL05.06.05

Linear and Nonlinear Plasmonic Properties of Metallic Particle-on-Film Nanocavities Dangyuan Lei; City University of Hong Kong, Hong Kong

Plasmonic nanocavities, consisting of metallic nanoparticles closely separated from a thin metal film by nanometric dielectric gaps, support hybridized plasmon modes with extremely small mode volumes and strongly enhanced local fields. They constitute a versatile nanophotonic platform for exploring many exotic light-matter interaction phenomena at the nanoscale, such as plasmon-enhanced nonlinear optics and quantum plasmonics.

This talk will review our recent studies on the linear and nonlinear plasmonic properties of metallic particle-on-film nanocavities (PoFNs), including plasmon resonance hybridization and decomposition [1-3], plasmon-enhanced polarized photoluminescence [4], and light-induced symmetry breaking for enhancing second-harmonic generation (SHG) [5]. I will present a new polarization-resolved spectral decomposition and color decoding approach for understanding the rich scattering radiation properties of two types of gold PoFNs. Our results reveal an unusual plasmon resonance in a gold nanosphere dimer-on-film nanocavity (absent in a nanosphere monomer counterpart), having strong radiation yet a large quality factor, which turns out to arise from the metal substrate-mediated dipole-quadrupole hybridization. Following this, I will show this strong yet narrow hybrid resonance gives rise to highly polarized photoluminescence emission from gold, with a 200-fold intensity enhancement and 5-fold linewidth reduction compared to a dimer of similar size on silica.

Finally, I will discuss a new mechanism for SHG enhancement in such plasmonic PoFNs, that is, the light-induced electromagnetic asymmetry. Our results show that such symmetry breaking efficiently suppresses the cancelling of locally generated SH fields and is further amplified in the SHG-induced plasmonic excitation through preferential coupling to the bright, bonding dipolar resonance mode of the nanocavity, leading to a record high far-field SHG efficiency of up to $3.56 \times 10^{-7} \text{ W}^{-1}$ in plasmonic nanostructures.

This work was supported in part by the Research Grants Council of Hong Kong (grant number: 15303417) and the National Natural Science Foundation of China (grant number: 62022001).

References:

- G.-C. Li, Y.-L. Zhang, and D. Y. Lei, "Hybrid plasmonic gap modes in metal film-coupled dimers and their physical origins revealed by polarization-resolved dark-field spectroscopy", *Nanoscale* **2016**, 8, 7199-7126.
- Q. Zhang, G.-C. Li, T. W. Lo and D. Y. Lei, "Polarization-resolved optical response of plasmonic particle-on-film nanocavities", *Journal of Optics*, **2018**, 20, 024010.
- G.-C. Li, Q. Zhang, S. A. Maier, D. Y. Lei, "Plasmonic particle-on-film nanocavities: A versatile platform for plasmon-enhanced spectroscopy and photochemistry", *Nanophotonics* **2018**, 7, 1865-1889.
- G.-C. Li, Y.-L. Zhang, J. Jiang, Y. Luo, D. Y. Lei, "Metal substrate mediated plasmon hybridization in a nanoparticle dimer for photoluminescence linewidth shrinking and intensity enhancement", *ACS Nano* **2017**, 11, 3067-3080.
- G.-C. Li, M. Qiu, W. Jin, A. Zayats, D. Y. Lei, "Light-induced electromagnetic asymmetry for enhancing second-harmonic generation from an untrathin plasmonic nanocavity", manuscript under review (**2021**).

SESSION EL05.07: Functional Metasurfaces and Nanophotonics

Session Chairs: Junghyun Park and Pin Chieh Wu

Monday Morning, April 19, 2021

EL05

8:00 AM *EL05.07.01

Vectorial Holography and Polarization-Maintaining Metasurfaces Qinghua Song¹, Arthur Baroni², Samira Khadir¹, Stéphane Vézian¹, Benjamin Damilano¹, Philippe de Mierry¹, Sébastien Chenot¹, Virginie Brandli¹, Patrick Ferrand² and Patrice Genevet²; ¹Université Côte d'Azur, CNRS, CRHEA, France; ²Aix Marseille Univ, CNRS, Centrale Marseille, Institut Fresnel, France

In this presentation, we will review our recent results on the realization of vectorial holograms. We will also introduce a specific computational imaging technique, dubbed Ptychography, to reconstruct the Jones matrix map of the metasurfaces at microscopic resolution, including all amplitude, phase and polarization effects. We also report on the realization of broadband polarization maintaining metasurfaces.

In this contribution, we will present **a general method that enables wavefront shaping with arbitrary output polarization** by encoding both phase and polarization information into pixelated metasurfaces[1]. We apply this concept to convert an input plane wave with linear polarization to a holographic image with arbitrary spatial output polarization. Our approach relies on pixelated metasurfaces, in which each pixel acts as a deflector able to encode both the polarization and the holographic phase information, resulting in a holographic image in a specific angle with arbitrary polarization.

Vectorial ptychography technique is introduced for mapping the Jones matrix to monitor the reconstructed metasurface output field and to compute the full polarization properties of the vectorial far field patterns, confirming that pixelated interfaces can deflect vectorial images to desired directions for accurate targeting and wavefront shaping.

Exploring further this concept of polarization addressing metasurface, we propose a general method for polarization-maintaining and angular nondispersive wavefront shaping with, essentially, unlimited bandwidth[2]. Our results show that we can eliminate the chromatic dispersion of material by properly designing the geometry of the meta-structures, resulting in perfect nondispersive optical properties. As a proof of concept we realize white-light broadband image projection, in which we control both the polarization and the projection angle over an unlimited spectral range.

Our work solves the problem of polarization mode dispersion and demonstrates that classical Pantcharatnam broadband metasurfaces, such as those published recently by several groups and that address broadband angular dispersion relying exclusively on the nanostructure dispersive properties, are unable to control the polarization over broadband frequency range. To really prove the performance of our approach, we have adopted a metasurface doublet configuration to address both angular and polarization dispersion, thus demonstrating the first broadband polarization-maintaining and dispersive-less metasurface.

Our experimental results prove that metasurfaces, designed and realized using precise nanofabrication methods could efficiently tailor the wavefront and control the polarization in the entire visible range, promising various applications in polarization imaging, augmented/virtual reality displays, full color display and broadband-polarimetry.

References

[1] *Ptychography retrieval of fully polarized holograms from geometric-phase metasurfaces*, Q Song, A Baroni, R Sawant, P Ni, V Brandli, S Chenot, S Vézian, B. Damilano, P. de Mierry, S. Khadir, P. Ferrand and P. Genevet, **Nature communications** 11 (1), 1-8 (2020)

[2] *Bandwidth Unlimited Polarization-Maintaining Metasurfaces*, Q. Song, S. Khadir, S. Vézian, B. Damilano, P. de Mierry, S. Chenot, V. Brandli and P. Genevet, **Science Advances**, in press (2020)

8:40 AM EL05.07.02

The Plasmonic Phase-Change Material In₃SbTe₂ as a Programmable Nanophotonics Material Platform for the Infrared Andreas F. Hessler¹, Sophia Wahl¹, Till Leuteritz², Antonios Anotonopoulos¹, Christina Stergianou¹, Carl-Friedrich Schön¹, Lukas Naumann², Niklas Eicker¹, Martin Lewin¹, Tobias Maß¹, Matthias Wuttig¹, Stefan Linden² and Thomas Taubner¹; ¹RWTH Aachen University, Germany; ²University of Bonn, Germany

The high dielectric optical contrast between the amorphous and crystalline structural phases of non-volatile phase-change materials (PCMs) provides a promising route towards tuneable nanophotonic devices [1-3]. Here [4], we employ the next-generation PCM In_3SbTe_2 (IST) whose optical properties change from dielectric to metallic upon crystallization in the whole infrared spectral range. This distinguishes IST as a switchable infrared plasmonic PCM and enables a new programmable nanophotonics material platform. We show how resonant metallic nanostructures can be directly written, modified and erased on and below the meta-atom level in an IST thin film by a pulsed switching laser, facilitating direct laser writing lithography without need for cumbersome multi-step nanofabrication. With this new technology, we demonstrate large resonance shifts of nanoantennas of more than 4 μm , a tuneable mid-infrared absorber with nearly 90% absorptance as well as screening and nanoscale “soldering” of metallic nanoantennas. Our novel concepts will empower new and improved designs of programmable nanophotonic devices for telecommunications, (bio)sensing and infrared optics, e.g. programmable infrared detectors, emitters and reconfigurable holograms.

[1] M. Wuttig, H. Bhaskaran and T. Taubner. Phase-change materials for non-volatile photonic applications. *Nature Photonics* 11, 465-476 (2017)

[2] A.-K. U. Michel, A. Heßler, S. Meyer et al.. Advanced optical programming of individual meta-atoms beyond the effective medium approach. *Advanced Materials* 31, 1901933 (2019)

[3] A. Leitis, A. Heßler, S. Wahl et al.. All-dielectric programmable Huygens’ metasurfaces. *Advanced Functional Materials* 30, 1910259 (2020)

[4] A. Heßler, S. Wahl, T. Leuteritz et al.. In_3SbTe_2 as a programmable nanophotonics material platform for the infrared. in submission (2020)

8:55 AM EL05.07.03

Exciton-Enhanced Light Scattering in Atomically-Thin Metasurfaces Ludovica Guarneri¹, Qitong Li², Jung-Hwan Song², Mark L. Brongersma² and Jorik Van de Groep¹; ¹University of Amsterdam, Netherlands; ²Stanford University, United States

Nanophotonic metasurfaces employ dense arrays of optically-resonant nanostructures to manipulate the properties of light in nm-thick optical coatings. By harnessing plasmonic or Mie resonances in metallic or dielectric nanoparticles, the phase and amplitude of the scattered light can be controlled at the nanoscale. Based on rapid advances in metasurface design, metasurfaces are now widely applied in flat optical elements for beam steering, lensing, and holography. However, novel applications in dynamic holography and augmented reality require metasurfaces and metadevices with actively-tunable functionality. So far, the use of plasmonic and Mie-resonances in dynamic metasurfaces is limited as their optical resonances are difficult to tune dynamically.

Monolayer transition metal dichalcogenides like WS_2 exhibit strong exciton resonances in the visible spectral range that dominate their optical response. The excitonic light-matter interaction in these 2D quantum materials is inherently very strong and highly tunable, which can be leveraged to realize mutable flat optical elements. To unleash the full potential exciton-enhanced light scattering in atomically-thin metasurface elements, it is essential to first achieve detailed understanding of the role of the exciton’s quantum mechanical properties in passive nanophotonic wavefront shaping.

Here, we employ atomically-thin metasurface lenses carved out of a monolayer of WS_2 to directly study the influence of exciton decay and dephasing on the metasurface functionality and spectral line shape. We fabricate 500 μm diameter zone plate lenses using electron-beam lithography and reactive-ion etching. At resonance, excitonic light scattering strongly enhances the focal intensity. We systematically characterize the focal shape and focusing efficiency as a function of wavelength using confocal microscopy. To study the influence of exciton-phonon scattering and dephasing on the optical functionality of the lens, we then characterize the efficiency spectrum as a function of temperature.

At ambient conditions, the spectrum shows a strong asymmetric line shape revealing that the scattered light fields are directly governed by the monolayer susceptibility. This enables an almost background-free measurement of the optical properties of the monolayer, and thereby the excitonic light-matter interaction.

Careful analysis of the line shape shows that the relative contribution from resonant excitonic light scattering is comparable to the non-resonant monolayer scattering. For decreasing temperatures on the other hand, the exciton's non-radiative decay and dephasing are suppressed and the exciton becomes fully radiative. As a result, the asymmetric line shape not only narrows and increases in amplitude, but also transitions into a symmetric line shape. This directly shows the increasing prevalence of the exciton resonance in the focusing efficiency. By comparing the results to numerical simulations and an analytical model, we show that the efficiency of the metasurface lens directly scales with the excitonic oscillator strength.

The results give direct insight in the role of exciton dynamics in optical wavefront shaping using atomically-thin metasurfaces. A full understanding of the role of exciton resonances in metasurfaces paves the way for dynamic components, combining tunable effects in quantum materials with classical metasurface optics.

9:10 AM EL05.07.04

Photovoltage Management with Surface Arrays of Subwavelength Silicon Formations Ashish Prajapati, Ankit Chauhan and Gil Shalev; Ben Gurion University of the Negev, Israel

Surface arrangements of subwavelength formations are extensively discussed in the context of photocurrent enhancement for photovoltaic (PV) applications. Recently, the potential contribution of such arrangements toward photovoltage augmentation is suggested. This study numerically demonstrates the potential for photovoltage management based on arrays composed of inverted silicon cones, referred to as light funnel (LF) arrays. The transition from an optimized nanopillar (NP) array into an LF array is examined. It is shown that a decrease in NP bottom diameter (D_b) is accompanied by an increase in open-circuit voltage (V_{oc}). The highest photovoltage enhancement is recorded for the smallest considered D_b $\frac{1}{4}$ 50 nm with a V_{oc} increase of 75 mV and reflects a 22% V_{oc} enhancement compared with the NP V_{oc} . It is shown that this V_{oc} increase is due to 250% increase in the excitation level, and that the spatially resolved excitation level of the array-nested LFs is more than two orders of magnitude higher than the highest spatially resolved excitation level in the array-nested NPs. Finally, it is shown that the suggested photovoltage management entails almost a factor of 2 increase in the nominal power conversion efficiency upon the transition from an NP PV cell into LF PV cell.

9:25 AM EL05.07.05

A Re-Configurable Infrared Metasurface Utilizing Acoustoelectric-Induced Charge Aggregation in Graphene Amun Jarzembski¹, Michael Goldflam¹, Thomas Beechem^{1,2} and Aleem Siddiqui¹; ¹Sandia National Laboratories, United States; ²Center for Integrated Nanotechnologies, United States

Acoustoelectric charge patterning of graphene is leveraged to create dynamically tunable infrared filters having expanded capability by not only modulating the properties of the plasmonic medium but the metasurface itself. While active spectral tuning within a graphene-based platform is well established, plasmon excitation has overwhelmingly been facilitated through a patterned metasurface whose properties derive from the physical shape of the material(s) involved thereby fixing its response at fabrication. The metasurface does not provide any tunability in itself but only excites the tunable plasmon. Here, in contrast, acoustoelectric induced charge aggregation of graphene permits a means to arbitrarily pattern charge distributions that can be modified in real time thus changing both the plasmonic dispersion and where on this dispersion the plasmon is excited.

To show the viability of a reconfigurable graphene metasurface controlled by a surface acoustic wave (SAW), a combined numerical and experimental methodology was employed. The interaction between the acoustic wave and graphene is obtained by solving for the coupling between the displacement field of the SAW and mobile charges at the graphene interface. In doing so, the periodic profile of the SAW-driven fields creates charge stripes in the graphene via the acoustoelectric effect, which in turn spatially modulates the two-dimensional material's optical properties. Numerically solving for the full-field spectral optical response under normal mid-infrared illumination at various acoustoelectric powers reveals a dynamic resonance behavior that tunes in both energy and depth. In particular, the plasmonic response can be switched on or off by simply enabling/disabling the SAW. Through careful consideration of both the optical and acoustoelectric design spaces, a single system

with compelling spectroscopic performance is obtained. Experimentally, charge stripes in graphene resting on top of a periodically poled substrate are observed via Raman imaging that confirms the achievable aggregation as well as the ability to spatially pattern graphene's optical properties. Subsequently, the effect is extended to acoustoelectric devices leveraging the SAW to induce charge aggregation in graphene. Future directions are highlighted, where the interdisciplinary acoustoelectric-optoelectronic interaction can further customize the graphene plasmon coupling mechanism and hence the device's optical response.

Acknowledgements: Sandia National Laboratories is a multi-mission laboratory managed and operated by the National Technology & Engineering Solutions of Sandia, LLC, a wholly owned subsidiary of Honeywell International Inc., for the U.S. Department of Energy's National Nuclear Security Administration under contract No. DE-NA0003525. We thank Zachary Piontkowski for technical review of this abstract.

SESSION EL05.08: Low Dimensional Photonics
Session Chairs: Ho Wai (Howard) Lee and Junghyun Park
Monday Morning, April 19, 2021
EL05

10:30 AM *EL05.08.01

Strainoptronics—A New Degree of Freedom for 2D Material Device Engineering Volker Sorger; George Washington University, United States

2D materials have a number of intriguing value propositions that could be harnessed for compact, tunable, high-performance optoelectronic devices when heterogeneously integrated in photonic circuits. Here I review our latest work including; (1) tunable TMD-based microring resonator with engineered critical-coupling condition, (2) a broadband graphene plasmon-slot detector ($R=0.7A/W$), (3) a bandgap-shifted strain-engineered absorption-enhanced MoTe₂ photodetector at 1.55 μ m ($R=0.5A/W$, low-dark-current $<10nA@-1V$), (4) a record-high responsivity ($R=1.4A/W$) slot-plasmon exciton-modulated MoTe₂ detector, all enabled by our recently developed method of cross-contamination-free yet deterministic dry transfer 2D material 'printer' mimicking a 3D printer for enabling rapid prototyping. These devices are based on heterogeneous integration of 2D materials into Silicon and SiN photonics, with the latter used for on-exciton modulation or exciton absorption.

11:10 AM EL05.08.02

Late News: Configurable Phonon Polaritons in Twisted α -MoO₃ Mingyuan Chen; Auburn University, United States

Van der Waals materials stacked with a relative twist angle are attracting tremendous interest in physics and have been intensively investigated to tune the electronic, magnetic, and optical properties of materials (known as "twistronics"). However, previous discoveries are based on the formation of peculiar moiré superlattices at small and specific twist angles. Here we report configurable nanoscale light-matter waves—phonon polaritons—by twisting stacked α -phase molybdenum trioxide (α -MoO₃) slabs over a broad range of twist angles from 0° to 90°. Our combined experimental and theoretical results reveal a variety of polariton wavefront geometries and topological transitions as a function of the twist angle, extending twistronics and moiré physics to nanophotonics and polaritonics. The origin of the polariton twisting configuration is attributed to the electromagnetic interaction of highly anisotropic hyperbolic polaritons in stacked α -MoO₃ slabs.

11:25 AM EL05.08.03

Late News: Hyperbolic Phonon Polaritons in Suspended α -MoO₃ Jiali Shen¹, Zhiren Zheng², Thao Dinh², Shuai Shao¹, Mingyuan Chen¹, Xiaojie Jiang¹, Nima Shamsaei¹, Qiong Ma³, Pablo Jarillo-Herrero² and

Siyuan Dai¹; ¹Auburn University, United States; ²Massachusetts Institute of Technology, United States; ³Boston College, United States

Polaritons are half-light-half-matter electromagnetic waves confined in materials. These nanoscale light-matter waves offer the access to optical properties and energy at the subwavelength scale. In this work, we studied the effect of environmental permittivity on polaritons in a prototype van der Waals materials of α -MoO₃. Different than majority polariton waves that spread towards all directions, polaritons in α -MoO₃ are highly anisotropic in the basal plane. Our nano-infrared imaging augmented with electromagnetics simulations reveal distinct effects of the sample suspension on the polariton parameters including wavelength, damping and dispersion, at various infrared frequencies. Our results are expected to offer guidance on engineering nano-polaritons propagation properties for desired nanophotonic functionalities.

11:40 AM EL05.08.04

Guided Mid-IR and Near-IR Light within a Hybrid Hyperbolic-Material/Silicon Waveguide

Heterostructure Mingze He¹, Sami Halimi¹, Thomas Folland^{2,1}, Sai S. Sunku^{3,3}, Song Liu⁴, James H. Edgar⁴, Dmitri Basov³, Sharon M. Weiss¹ and Joshua D. Caldwell^{1,1}; ¹Vanderbilt University, United States; ²The University of Iowa, United States; ³Columbia University, United States; ⁴Kansas State University, United States

Mingze He¹, Sami I. Halimi², Thomas G. Folland^{1,6}, Sai S. Sunku^{3,5}, Song Liu⁴, James H. Edgar⁴, Dmitri N. Basov³, Sharon M. Weiss², Joshua D. Caldwell^{1,2}

1, Department of Mechanical Engineering, Vanderbilt University, Nashville, TN 37212, USA. 2, Department of Electrical Engineering and Computer Science, Vanderbilt University, Nashville, TN 37212, USA. 3, Department of Physics, Columbia University, New York NY 10027, USA. 4, Tim Taylor Department of Chemical Engineering, Kansas State University, Manhattan, KS 66506, USA. 5, Department of Applied Physics and Applied Mathematics, Columbia University, New York NY 10027, USA. 6, Department of Physics and Astronomy, The University of Iowa, Iowa City, Iowa, 52242, USA

Silicon waveguides are the most indispensable building block in on-chip photonics. With demand for continuous increases in operational bandwidth, there is a desire to expand the operating frequency regime, as multiplexing of near- and mid-infrared (mid-IR) signals could provide unique applications for both signal processing and chemical sensing. However, this is challenging with integrated silicon photonics, since accommodating longer wavelength modes requires expanding the size of the silicon waveguide, which in turn would cause severe modal dispersion in the near-IR. Thus, an architecture that maintains the silicon waveguide's performance in the near-IR, while still providing confinement and propagation of mid-IR light would be highly beneficial.

Hyperbolic phonon polaritons (HPhPs) can compress long-wavelength free-space light to deeply sub-diffractive volumes and overcome the length-scale mismatch with structures designed for operation in the near-IR. Such HPhPs are supported within highly anisotropic media where the permittivity along orthogonal axes are opposite in sign, with hyperbolicity being demonstrated in an expanding list of natural materials, such as hexagonal boron nitride (hBN). Guiding of HPhPs in hBN has been studied previously using patterned strips and by introducing in-plane polaritonic refraction of HPhPs. However, previous research suffers from either unavoidable material damage of hBN or detrimental substrate absorption in the near-IR, which precludes the waveguide application at dual frequency domains. Thus, an architecture for frequency multiplexing of mid-IR and near-IR is yet to be demonstrated.

Here we address this challenge by realizing guided mid-IR and near-IR light within a hybrid hyperbolic-material/silicon waveguide heterostructure. By exploiting substrate-induced changes in polariton wavelength and thus in-plane polaritonic refraction, we demonstrate that the HPhPs supported by hBN can be confined laterally and guided by the underlying silicon waveguide structure, without the need for fabrication of the hyperbolic medium. Furthermore, we experimentally demonstrate that the hBN slab results in a negligible influence on waveguiding of near-IR light in the underlying Si waveguide. Thus, the prototype hybrid waveguide can operate in both the near- and mid-IR simultaneously. Such integration offers a generalizable approach for multiplexing dramatically different free-space wavelength light within a compact and on-chip footprint, offering a new toolset for nanophotonic design that maintains the low-loss properties of naturally

hyperbolic materials.

11:55 AM *EL05.08.05

Leveraging Optical Non-Locality and Block Co-Polymer Lithography to Create High Frequency Plasmonic Resonances in Graphene Victor Brar; University of Wisconsin--Madison, United States

I will discuss recent experiments aimed at creating plasmonic resonances in graphene in the short-wavelength infrared (SWIR). The plasmonic dispersion of graphene dictates that reaching such short wavelengths requires fabricating increasingly smaller nanostructures in the graphene surface, with lengthscales $< 10\text{nm}$. While conventional electron beam lithography has been shown to be effective at creating structures as small as 15nm , measurements of those systems revealed only mid-IR resonances, with wavelengths as short as $3.5\mu\text{m}$. We push to smaller lengthscales by introducing a new, bottom-up block co-polymer lithography method, which can easily pattern cm-scale sheets of graphene into 12nm nanoribbon arrays. Subsequent infrared absorption measurements from these samples reveals that they exhibit resonant behavior at frequencies much higher than predicted, reaching free-space wavelengths as short as $2.2\mu\text{m}$, well into the SWIR. We show that this behavior is due to strong non-local effects in the graphene, which effectively blue shifts the graphene plasmons at short wavelengths. This allows optoelectronic devices based on graphene plasmons to operate over a larger range than commonly assumed, possibly reaching the near infrared or visible. Another significant implication of this finding is that light-matter interactions driven by graphene plasmons are smaller than what is expected from first order calculations; for some spontaneous emission processes, these weaker interactions will create Purcell enhancements that are orders of magnitude smaller than expected. Finally, I will discuss recent attempts at integrating graphene nanoribbons derived using block co-polymer lithography with metal and dielectric metasurfaces, with an aim of creating an enhanced optoelectronic response.

SESSION EL05.09: Advanced Metasurfaces and Meta-Devices

Session Chairs: Ho Wai (Howard) Lee and Jeremy Munday

Monday Afternoon, April 19, 2021

EL05

1:00 PM *EL05.09.01

Topology Optimization of Artificial Photonic Materials with Deep Generative Networks Jonathan A. Fan; Stanford University, United States

Inverse design algorithms enable metasurfaces and other nanophotonic devices to achieve new functionalities and high efficiencies. Inverse algorithms based on global topology optimization networks (GLOnets), in which global optimization is framed as the training of a generative neural network, are a promising approach towards globally searching a non-convex design landscape. However, the relationship between the GLOnets algorithm and network architecture is not clear and the selection of a proper architecture is required to ensure GLOnets stability. We will discuss the role of network architecture in the GLOnets algorithm and show that, counterintuitively, relatively shallow networks are sufficient to performing stable global optimization. With select problems based on benchmark mathematical functions and diffractive nanophotonic systems, we discuss GLOnets in the context of problem-dependent architectures. We will also discuss viable and effective pathways towards conditional GLOnets, in which ensembles of related devices are co-designed.

1:40 PM EL05.09.02

Experimental Demonstration of Inverse-Designed Active Metasurface Arrays Prachi Thureja¹, Ghazaleh Kafaie Shirmanesh¹, Meir Grajower¹, Ruzan Sokhoyan¹, Katherine Fountaine² and Harry A. Atwater¹;

¹California Institute of Technology, United States; ²Northrop Grumman Corporation, United States

We experimentally demonstrate an array-level inverse design approach that accounts for the nonideal optical response to optimize the spatial array phase and amplitude profile of active metasurfaces for desired target functions [1]. Optical phase control in planar metasurfaces has recently been the subject of intensive worldwide research. While significant prior effort has addressed phase control in passive metasurfaces, active metasurfaces comprising of arrays of programmable nanoantennas have garnered widespread interest owing to their power for versatile wavefront shaping in real-time [2,3]. Notably, modulation of active metasurfaces generally relies on permittivity tuning near optical resonances in nanostructured antennas. This gives rise to an inherently nonideal optical response that creates strong interdependence between the scattered light phase and amplitude, and limits the accessible phase modulation range. As a consequence, conventional forward design of active metasurface phase profiles for beam steering results in significant losses of power coupling into undesired sidelobes, motivating our inverse design method, which enhances the performance of active metasurfaces with nonideal antenna components.

In contrast to passive metasurface design via shape optimization of individual antennas, active metasurfaces can be ‘designed’ by reconfiguration of independently gated, geometrically identical nanoantennas. This enables an array-level optimization of phase and amplitude for arbitrary user-defined metasurface functions, such as high-directivity dynamic beam steering. By performing optimization, we investigated the impact of phase and amplitude modulation on the beam steering performance of an active metasurface array of 100 non-interacting subwavelength antennas. We then examined the optical response of a nonideal plasmonic, electro-optically tunable metasurface using indium tin oxide as an active layer. The reflected light measurements indicate a limited phase modulation range of $\sim 220^\circ$ as well as covarying, non-unity amplitude at an operating wavelength of $\lambda = 1548$ nm. We find that nonintuitive array phase and amplitude profiles generate high performance despite a nonideal antenna optical response. Using inverse design, we demonstrate a reduction in the sidelobe radiation, thus increasing beam directivity compared to forward designs. We further used the array-level inverse design algorithm to experimentally validate high-directivity continuous beam scanning with a broad field-of-view of nearly 50° as well as simultaneous steering of beams in multiple different directions. Finally, we consider the impact of metasurface inter-antenna coupling on the beam steering performance. These findings highlight the power of array-level inverse design as a general approach for active metasurfaces, including all-dielectric metasurfaces. Inverse design thus has the potential to ultimately usher in a modern era of hierarchical co-design of nanophotonic materials, devices, and systems to realize highly efficient optical elements for complete space-time control of the scattered light wavefront.

[1] Thureja et al. ACS Nano (2020).

[2] Kafaie Shirmanesh et al. ACS Nano (2020).

[3] Shaltout et al. Science (2019).

1:55 PM EL05.09.03

Single-Crystal Noble Metal Films and Nanostructures from Solution—A Low-Loss, High-Yield, Green Strategy for Plasmonic Metasurfaces Gary W. Leach, Sasan V-Grayli, Finlay MacNab, Xin Zhang, Saeid Kamal and Dmitry Star; Simon Fraser University, Canada

The confinement of electromagnetic waves to nanometer-scale metal structures amplifies local fields that can be harnessed for application in information processing, energy harvesting, sensing and catalysis. Metal nanostructures offer the opportunity to manipulate the phases and amplitudes of electromagnetic waves to enable flat optics, subwavelength resolution imaging and patterning. However, the controlled fabrication of high-definition single-crystal subwavelength metal nanostructures has remained a significant hurdle due to the tendency for polycrystalline metal growth using conventional physical vapor deposition methods, and the challenges associated with placing solution-grown nanocrystals in desired orientations and locations on a surface to manufacture functional devices. Here, we introduce a scalable and green, wet chemical approach to monocrystalline noble metal thin films and nanostructures. The method enables the fabrication of ultrasubsmooth, epitaxial, single-crystal films of controllable thickness that are ideal for the subtractive manufacture of

nanostructure through ion beam milling, and additive crystalline nanostructure *via* lithographic patterning for large area, single-crystal metamaterials and high aspect ratio nanowires. Our single-crystal nanostructures demonstrate improved feature quality, pattern transfer yield, reduced optical and resistive losses, and tailored local fields to yield greater optical response and improved stability compared to polycrystalline structures, supporting greater local field enhancements and enabling practical advances at the nanoscale.

2:10 PM EL05.09.04

Topological Space-Time Photonic Transition Enabled by Time-Modulated Metasurfaces Hooman Barati Sedeh and Hossein Mosallaei; Northeastern University, United States

Light-matter interaction has been the heart of electromagnetic and optics for many years and thus an immense effort has been put into introducing different platforms and materials that can effectively control the flow of light in the desired fashion. Spatiotemporally modulated systems have gained the attention of the scientific community in recent years due to their extended dimensionality and enabling several exotic space-time phenomena. In particular, it has been established that the temporal frequency conversion of an optical mode in such systems is accompanied by a correlated change in its spatial frequency [1]. This phenomenon, which is known as space-time photonic transition, not only enables numerous exotic functionalities such as generating an effective magnetic field to control the flow of photons but also is the underlying mechanism for constructing optical isolators in space-time varying platforms [2]. Recently, it has been demonstrated that time-modulated metasurfaces (TMMs), which are planar structures whose subwavelength unit cells are tuned periodically in time via an external stimulus, can also enable nonreciprocal wavefront engineering and extend the degree of light manipulation through space-time photonic transitions. In addition to the nonreciprocal responses, TMMs have been shown to enable a wide range of other novel physical phenomena including wavefront engineering and signal camouflaging [3,4].

In this work, we introduce a new type of space-time photonic transition of light, dubbed as topological space-time photonic transition, which occurs upon the scattering of light from an angular-momentum-biased metasurface and gives rise to the generation of a twisted light beam that carries an orbital angular momentum (OAM) with proportional topological charge and shift in the temporal frequency. An angular-momentum-biased metasurface renders a virtually rotating TMM which yields a superposition of OAM-carrying beams at distinct frequencies, whose topological charges can be controlled via varying the applied phase delay modulation. The competency of topological space-time photonic transitions in the active tuning of OAM states with high mode-purity is analyzed, which yields minimal cross-talk between OAM channels in a mode-multiplexed communication system. Moreover, the role of the spatiotemporal modulation profile of the metasurface on the spatial and spectral diversity of OAM states is explored in detail. It is also demonstrated that the established concept can pave the way for hybridized mode-division and wavelength-division multiple access through the generation of distinct OAM states at different frequency harmonics. The nonreciprocity and broken time-reversal symmetry in topological space-time photonic transitions across the temporal frequency domain and Hilbert space of OAM states is also investigated giving rise to distinct twisted light channels in up- and down-links. To realize a time-modulated metasurface with angular-momentum biasing, a reflective dielectric metasurface is considered consisting of silicon nanodisk heterostructures integrated with indium-tin-oxide and gate dielectrics placed on a back mirror forming a dual-gated field-effect modulator. The metasurface is azimuthally divided into several sections where the nanodisk heterostructures are interconnected via biasing lines. This configuration enables addressing each section independently via a radio-frequency biasing signal and with a different modulation phase delay, thus enabling the flexible implementation of different spatiotemporal modulation profiles.

References

- [1] Winn, Joshua N., et al. *Physical Review B* 59.3 (1999): 1551.
- [2] Fang, Kejie, et al. *Nature photonics* 6.11 (2012): 782-787.
- [3] Salary, Mohammad Mahdi, et al. *New Journal of Physics* 20.12 (2018): 123023.
- [4] Liu, Mingkai, et al. *Physical Review Applied* 12.5 (2019): 054052.

2:25 PM *EL05.09.05

Bio-inspired Disordered Metaphotonic Devices for Medical Applications Radwanul H. Siddique¹, Daniel Assumpcao^{1,2} and Hyuck Choo²; ¹Samsung Semiconductor, Inc., United States; ²Samsung Advanced Institute of Technology, Korea (the Democratic People's Republic of)

Over the last decades, photonic metamaterials with tailored -i.e. with deliberately introduced- structural disorder have attracted considerable interest in various optical applications due to their extended spectral and angular range of effectiveness¹. However, millions of years of evolution in the biological world has developed a plethora of micro- and nanoscopic photonic structures with the deliberately introduced disorder in their respective geometries and compositions². In this talk, I will discuss how the development of metaphotonic devices harnessing bioinspired attributes can provide novel yet highly practical solutions for the global health sector. I will present our studies on biophotonic nanostructures found in butterfly wings that show unique optical properties with the tailored structural disorder, and their successful replication in laboratories using self-assembly based scalable nanofabrication techniques^{3,4,5}. We utilize this approach to pattern Si₃N₄-based metasurfaces onto a Fabry-Perot-resonator-based intraocular pressure (IOP) sensor for glaucoma management⁴. The metasurface integration onto the IOP sensor led to a 2.5-fold improvement in readout angle allowing easy handheld monitoring and in a one-month in vivo study conducted in rabbits, showed a 3-fold reduction in IOP error and a 12-fold reduction in tissue encapsulation and inflammation, compared to an IOP sensor without nanostructures. We will further discuss our second-generation metaphotonic IOP sensor that is made of only flexible nanostructured foil with a 3D hybrid periodic and amorphous photonic crystal using a newly developed colloidal lithography⁵. I will conclude the talk showing our recent progress in developing an ultra-compact optical spectrometer for smartphones using bioinspired tricks with high angular tolerance, resolution, and throughput, suitable for the realization of high-performance point-of-care biosensing⁶.

References

1. D.S. Wiersma, *Nature Photonics* **7(3)**, 2013.
2. V. E. Johansen, O.D. Onelli, L. M. Steiner, S. Vignolini. Photonics in nature: from order to disorder, *In Functional surfaces in biology III*, Springer, 2017.
3. R.H. Siddique*, Y.J. Donie*, G. Gomard, S. Yalamanchili, T. Merdzhanova, U. Lemmer, H. Hölscher, *Science Advances* **3(10)**, 2017.
4. V. Narasimhan*, R.H. Siddique*, J.O. Lee, S. Kumar, B. Ndjamen, J. Du, N. Hong, D. Sretavan, H. Choo, *Nature Nanotechnology* **13(6)**, 2018.
5. R. H. Siddique, L. Liedtke, H. Park, S. Y. Lee, H. Raniwala, D. Y. Park, D. H. Lim, H. Choo, *IEDM* 2020.
6. R.H. Siddique*, D. Assumpcao*, H. Choo, in preparation, 2021.

SESSION EL05.10: Novel Materials for Thermal and Nonlinear Emission Control

Session Chairs: Ho Wai (Howard) Lee and Pin Chieh Wu

Monday Afternoon, April 19, 2021

EL05

4:00 PM *EL05.10.01

Recent Advances and Applications of Epsilon-Near-Zero Materials—From Photodetectors and Hydrogen Sensors to Casimir Forces Jeremy N. Munday; University of California, Davis, United States

Materials whose dielectric functions approach zero have many unique properties ranging from enhanced non-linear behavior to suppression of quantum electromagnetic fluctuations. Beyond these interesting physical phenomena, epsilon-near-zero (ENZ) concepts can be applied to devices to exploit these effects. In this talk, I will discuss our recent work on the development of devices that take advantage of these effects to create super-absorbing optical films for novel photodetectors and hydrogen sensors, as well as quantum effects that can be

exploited using ENZ materials. Two examples of the later are the suppression of spontaneous emission and modifications to the Casimir force, a force that is purely quantum in nature and is related to the electromagnetic boundary conditions placed on vacuum fluctuations. We will conclude with an outlook for this emerging area of research.

4:40 PM EL05.10.02

Engineering the Spectral and Spatial Dispersion of Thermal Emission via Polariton-Phonon Strong Coupling Guanyu Lu¹, Christopher R. Gubbin², Joshua R. Nolen¹, Thomas G. Folland^{1,3}, Marko J. Tadjer⁴, Simone D. Liberato² and Joshua D. Caldwell¹; ¹Vanderbilt University, United States; ²University of Southampton, United Kingdom; ³The University of Iowa, United States; ⁴U.S. Naval Research Laboratory, United States

Phonon polaritons are quasiparticles comprising a photon and a coherently oscillating charge on a polar lattice, which are supported in the form of propagating (SPhP) and localized surface phonon polaritons (LSPHP). The promising properties of LSPHP modes are exceptionally high predicted Purcell enhancements and narrow resonance linewidths, with the potential for near-unity absorption (emissivity). However, one drawback is that as a highly localized mode, they offer no significant degree of spatial coherence (directionality) for thermal emission applications. Alternatively, high spatial coherence can be achieved using propagating SPhPs launched by grating elements. However, the non-localized nature of such propagating modes yields thermal emission into frequency-specific angles across the entire Reststrahlen band where such modes can be supported. The introduction of strong coupling between different polaritonic modes, therefore, provides us an opportunity to combine the virtues of the narrowband LSPHP resonances with the high spatial coherence associated with propagating SPhPs into a novel, mixed character polariton. Further, it has been proposed that strong coupling between LSPHPs with zone-folded longitudinal optic phonons (ZFLO) could provide a mechanism to use the longitudinal fields of an electrical bias to stimulate the transverse fields of SPhPs through Ohmic loss. Thus, we propose that through inducing strong coupling between LSPHPs, propagating SPhPs, and ZFLO phonons, that realization of a narrow-band, spatially coherent emitter amenable to electrically driven emission could be possible. Additionally, through coupling to such a ZFLO mode, the extremely narrow linewidths could be employed via strong coupling to further reduce the linewidths of the SPhP modes.

In this work, we report on three-oscillator strong coupling within a SPhP platform using nanopillar arrays fabricated into a 4H-SiC substrate. Here, we experimentally manipulate the dispersion relation of coupled SPhP modes by strongly coupling LSPHPs, propagating SPhPs, with the ZFLO. In the strong coupling regime, the formation of such hybrid modes with mixed character is expected. Furthermore, the strength of the interactions between such optical modes can be precisely controlled through the hybridization of three oscillators. We further report on the influence of such strong coupling upon thermal emission within the long-wave-IR (LWIR), demonstrating significant narrowing of the spectral and spatial dispersion of the individual modes within this strongly coupled regime. In our three-oscillator strong coupling platform, we simultaneously demonstrate a five-fold reduction in the angular spread of the thermally emitted light and a three-fold enhancement of the quality factor over that of the uncoupled LSPHP mode at the anti-crossing point where the splitting occurs. Furthermore, the high Q-factors (over 200) achieved are realized using traditional photolithography, enabling such devices to be produced at large-scale and reasonable costs. Our results demonstrate that by leveraging three-oscillator strong coupling that the spectral and spatial dispersion of thermal emission can be engineered for a variety of LWIR applications extending from spectroscopy, sensing, to free-space communications.

4:55 PM EL05.10.03

Experimental Observation of the Violation of Kirchhoff's Thermal Radiation Law Using a Guided Mode Resonator Coupled to Magneto-Optical InAs Komron J. Shayegan¹, Bo Zhao², Yonghwi Kim¹, Shanhui Fan² and Harry A. Atwater¹; ¹California Institute of Technology, United States; ²Stanford University, United States

For all thermal absorbers and emitters in equilibrium, the amount of radiation absorbed from a blackbody at a specific wavelength and incident angle is re-emitted reciprocally from the absorber back to the blackbody. This phenomenon has been formalized as Kirchhoff's law of thermal radiation (KLTR) and relies on the

absorber/emitter obeying time-reversal symmetry.

We report the first experimental observation of a reciprocity breaking of this reciprocal behavior in the mid-infrared wavelengths, using a magneto-optical device heterostructure. The device consists of a low-loss, Si guided mode resonant (GMR) grating waveguide structure made of Si on a top of degenerately-doped degenerately doped InAs wafer, which in an applied magnetic field, acts serving as our magneto-optical material. The degenerately-doped degenerately doped InAs, behaves responds optically as a Drude metal conductor with non-zero off-diagonal permittivity values when an applied magnetic field is applied. We design the Si GMR grating to critically couple to light at wavelengths (~ 17 microns) in the epsilon-near-zero regime of the InAs wafer, where the magneto-optical effect response is largest. Using this structure, we are able to break time-reversal symmetry by changing the direction of an in-plane magnetic field (~ 0.5 T) applied along the length of the grating. We are able to by measuring the polarization- and angle-dependent reflectivity and absorption, we obtained dispersion relations for the non-reciprocal, time-asymmetric InAs reflectivity and compared our results to theoretical predictions.¹ We do not observe a breaking of reciprocity for *s*-polarized infrared light but do see reciprocity a breaking of reciprocity for *p*-polarized light. This is, in agreement with the direction in which we apply our predicted field polarization required to break time-reversal symmetry. This work shows the constitutes the first experimental observation of reciprocity ability to break ring, and was performed using thermal radiation reciprocity in under room ambient conditions, and using modest magnetic fields attainable with permanent magnets.

[1] B. Zhao et al., *Optics Letters* **44**, 4203 (2019).

5:10 PM EL05.10.04

Noble-Transition Alloy Excels at Hot-Carrier Generation in the Near Infrared Kevin M. McPeak and Sara Stofela; Louisiana State University, United States

Above-equilibrium “hot” carrier generation in metals is a promising route to convert photons into electrical charge for efficient near-infrared optoelectronics. However, metals that offer both hot-carrier generation in the near-infrared and sufficient carrier lifetimes remain elusive. Alloys can offer emergent properties and new design strategies compared to pure metals. We will show that a noble-transition alloy, $\text{Au}_x\text{Pd}_{1-x}$, outperforms its constituent metals concerning generation and lifetime of hot carriers when excited in the near-infrared. At optical fiber wavelengths (e.g., 1550 nm), $\text{Au}_{50}\text{Pd}_{50}$ provides a 20-fold increase in the number of ~ 0.8 eV hot holes, compared to Au, and a 3-fold increase in the carrier lifetime, compared to Pd. The discovery that noble-transition alloys can excel at hot-carrier generation reveals a new material platform for near-infrared optoelectronic devices.

5:25 PM EL05.10.05

Photonic Crystal Waveguides as Thermal Concentrators for Catalytic Carbon Monoxide Reduction Haley Bauser, Xueqian Li, Magel Su and Harry A. Atwater; California Institute of Technology, United States

While photonic crystal waveguides have an extensive history in nanophotonics, we introduce a photonic crystal concept - as an infrared photon (thermal) concentrator, designed for solar-driven thermal heterogeneous catalysis for carbon monoxide reduction. A key goal in reducing global CO_2 emissions is the development of a net-zero carbon synthesis route for renewable generation of chemical fuels to replace conventional fossil fuels. Solar driven processes under mild conditions present a sustainable alternative to large-scale industrial processes that typically operate under high temperatures (>200 °C) and elevated pressures (>10 atm). However, thermal radiation losses typically prevent a catalyst photothermally heated by unconcentrated sunlight from reaching the minimum operating temperatures for heterogeneous catalysis of carbon monoxide which is generated by photoelectrochemical CO_2 reduction, to fuel and chemical products by the Fischer-Tropsch reaction pathway under direct 1 sun (1000 W m^{-2}) illumination. While higher temperatures can be reached through the use of geometry solar concentrators, these systems are difficult to scale up due to their complexity and reliance on solar tracking systems to optimize concentration.

Instead, building upon the concept of photonic crystals as medium for light trapping in photovoltaics, the emission of a catalyst coupled to an infrared photonic crystal can be trapped to infrared photons generate by

solar heating of a visible photoabsorber, thereby concentrating the solar-generated heat. A 3.5 micron thick lightly doped germanium is chosen as the photonic crystal waveguide material due to its high index, solar absorption coefficient stability in the visible range, and nearly lossless infrared characteristic. While two-dimensional photonic crystal designs can involve rod or hole arrays, the benefits of a hole array in this application are twofold: (1) stable trapping across a wide range of wavelengths, and (2) the ability to flow a reactive gaseous easily through the structure. We have designed a holey germanium photonic crystal with thermal infrared photon trapping efficiency above 90% for wavelengths from 8-15 microns. This prototype indicates promise for a first photonic crystal thermal concentrator to address scaling challenges and temperature requirements for solar thermochemical reactions under ambient sunlight.

SESSION EL05.11: Metasurfaces and Plasmonics/2D Material-Based Tunable Metasurface

Session Chairs: Junghyun Park and Pin Chieh Wu

Monday Afternoon, April 19, 2021

EL05

8:40 PM *EL05.11.03

Diatomic Metasurface for Multifarious Polarization Optics Zilan Deng and Xiangping Li; Jinan University, China

Metasurface based flat optics, an ultrathin layer of structured nano-antennas imparting local and space-variant abrupt phase changes, promises great potentials in shaping light's wavefronts in desirable manners. However, most of the reported metasurfaces are restrained by their design strategies and can only allow one or two physical parameters such as phase, polarization or amplitude to be controlled at the same time. Geometric metasurface provides dispersionless phases depending on the in-plane orientation angles of the meta-atoms. However, the polarization state of the incident light is restricted to circular polarization only. The combination of geometric phase with propagation phase was proposed to relieve the constraint and realize full control of the phase and polarization. However, this is achieved at the cost of increased thickness of the antennas to wavelength scale and concomitant massive computations for complicated meta-atom designs with intricate geometries at variant locations, meanwhile, the propagation phase is intrinsically dispersive, which restricts its ability to working at a specific wavelength. Here, we demonstrate a new dimerized metasurface design that can allow simultaneous control of the four basic parameters in one go as well as underpin variety of multi-functional optical elements. The proposed dimerized metasurface is consisting of two identical meta-atoms with exquisitely controlled in-cell displacements and orientations. Consequently, multi-functional holography that the amplitude, phase, polarization and color components of the diffracted beam can be completely controlled has been demonstrated. The proposed diatomic metasurfaces may extensively promote applications based on flat optics

9:10 PM BREAK

9:20 PM *EL05.11.04

Meta-Lens for Imaging, Sensing and Quantum Technology Mu Ku Chen¹, Lin Li^{1,2,3}, Zexuan Liu^{2,2,4}, Xifeng Ren^{5,5}, Shuming Wang^{2,2,4}, Vin-Cent Su⁶, Cheng Hung Chu^{7,8}, Hsin Yu Kuo^{8,7}, Ren Jie Lin^{7,8}, Biheng Liu^{5,5}, Wenbo Zang^{2,4}, Pin Chieh Wu⁹, Guangcan Guo^{5,5}, Lijian Zhang^{2,2,4}, Zhenlin Wang^{2,4}, Shining Zhu^{2,2,4} and Din-Ping Tsai^{1,8,7}; ¹The Hong Kong Polytechnic University, Hong Kong; ²Nanjing University, China; ³East China Normal University, China; ⁴Collaborative Innovation Center of Advanced Microstructures, China; ⁵University of Science and Technology of China, China; ⁶National United University, Taiwan; ⁷Academia Sinica, Taiwan; ⁸National Taiwan University, Taiwan; ⁹National Cheng Kung University, Taiwan

Meta-lens can achieve diffraction-limited focusing with nanoantenna array in a compact size. Many flat optical

devices have been demonstrated using meta-lens lately. For applications of full-color imaging and detections, the correction of chromatic aberration is a key issue. We introduced the integrated-resonant unit to incorporate with the geometric phase method to realize achromatic meta-lens. Broadband meta-lenses working over the near-infrared in reflection and entire visible spectrum in transmission are achieved. The full-color imaging is demonstrated by using GaN-based achromatic meta-lens. The high-dimensional light field imaging system was implemented by the nature-inspired 60×60 achromatic meta-lens array. The depth and velocity sensing of the imaging objects are achieved. A high-dimensional quantum entanglement light source is demonstrated by using a meta-lens array which composed of 10 by 10 meta-lenses. The meta-lens array can make multi-focusing spots into the nonlinear crystal simultaneously, and generate the multi entangled photon pairs. The entangled photon pairs are generated due to the spontaneous parametric down-conversion (SPDC) effect in the nonlinear crystal. We demonstrated the high-dimensional entanglement and 2-, 3- and 4-dimensional two-photon path-entanglement with different phases coded by the metalenses. It is a great progress for the quantum light source and quantum applications such as quantum computing, quantum cryptography, and quantum communication. We have developed optical meta-devices for beam deflection and reflection, polarization control and analysis, holography, second-harmonic generation, laser, tunability, imaging, absorption, color display, focusing of light, multiplex color routing, light-field sensing, and high-dimensional optical quantum source. The great advantages of meta-lens and meta-devices are their new properties, lighter weight, small size, high efficiency, better performance, broadband operation, lower energy consumption, and CMOS compatibility for mass production.

10:00 PM EL05.11.05

Spin Hall Effect of Light Using Structured Optical Materials Minkyung Kim, Dasol Lee and Junsuk Rho; Pohang University of Science and Technology, Korea (the Republic of)

Spin Hall effect of light (SHEL) refers to a spin-dependent and transverse splitting of light at an optical interface. This phenomenon can be readily found in various interfaces, but has been often left out of consideration because the splitting is much smaller than the wavelength. Thus, increasing the amount of the shift by using artificially structured materials has attracted scientific interests recently. We demonstrate that vertical hyperbolic metamaterial, or nanotrench structure consisting of metal and dielectrics, can be served as a platform to enhance the SHEL [1]. Under the same conditions of material combinations and total thickness, the enhancement, which is incident angle-dependent, can be higher than 800-fold when the incident angle is 5° , and 5000-fold when the incident angle is 1° . The gigantic SHEL in a vertical hyperbolic metamaterial will enable helicity-dependent control of optical devices including filters, sensors, switches, and beam splitters. This tendency of diverging shift as the incident angle decreases is not a unique characteristic of the vertical hyperbolic metamaterial, but is a universal feature that appears in many systems to increase SHEL. In other words, previous proposals to enhance the SHEL is limited to a small incident angle, on the order of milliradians. Diffraction can be used to improve SHEL at a large incident angle [2]. We present the enhancement of SHEL in a dielectric grating on a metal film by maximizing the difference between the transmission coefficients of two linear polarizations. The metal film impedes light transmission except the p-polarized first-order diffracted mode that is coupled to surface plasmon polaritons. These polarization-dependent transmission coefficients lead to a large SHEL at a large incident angle. Lastly, an approach to achieve a large SHEL with near-unity efficiency is proposed. Despite the remarkable enhancement of SHEL, the efficiency of the effect has been rarely discussed. The enhancement of SHEL in most of the previous proposals and demonstrations has been underpinned by small Fresnel coefficients, which in turn yield extremely low efficiency. In this last part, we present an approach using anisotropic impedance mismatching to attain a large SHEL with near-unity efficiency in the microwave spectrum [3]. A wire medium that has a near-unity transmission for one polarization and low transmission for the other is used to achieve high efficiency. The spin-dependent splitting is experimentally confirmed by measuring transmission coefficients and the spatial profile of Stokes parameters. The large SHEL with near-unity efficiency will enable highly efficient devices with spin-selective functionalities.

References

[1] M. Kim *et al.* *ACS Photonics* 6, 2530-2536, 2019

[2] M. Kim *et al.* *APL Photonics* 5, 066106, 2020

[3] M. Kim *et al.* *Laser & Photonics Reviews* (accepted)

10:15 PM EL05.11.06

Deep UV Surface-Enhanced Resonance Raman Spectroscopy for Ultrasensitive Label-Free DNA Detection and 2D Materials Using an Aluminum Film Abhishek Dubey¹, Ragini Mishra¹, Chang-wei Cheng¹, Wei-Lin Du¹, Ta-Jen Yen¹ and Shangjr Gwo^{1,2}; ¹National Tsing Hua University, Taiwan; ²Academia Sinica, Taiwan

Surface-enhanced Raman spectroscopy has been well investigated in the visible to the IR regime. In the visible to IR spectrum, several plasmonic materials have been given promised results like gold (Au) and silver (Ag). To explore the plasmonic properties in the Ultraviolet (UV) regime, aluminum (Al) has enormous potential to operate in the deep UV to the visible spectrum, so we present deep UV surface-enhanced resonance Raman Spectroscopy (SERRS) driven ultraviolet (UV) plasmonics through aluminum nanoholes. Therefore, the generation of deep UV range localized surface Plasmon resonance (LSPR) for electric field enhancement, the epitaxial aluminum film is grown by PA-MBE (plasma-assisted Molecular beam epitaxy) on sapphire substrate and CMOS compatible techniques are used to fabricate Al nanoholes. To assess, the deep UV SERRS nature of epitaxial Al film, we used the basis of nucleic acid and 2D materials as a benchmarked analyte. An ultra-thin layer (~ 1 nm) of Adenine, Thymine, Cytosine, and Guanine is sublimated on Al nanoholes and recorded the highest Raman intensity enhancement ($\sim 10^6$) with comparison to the non-plasmonic substrate. Here, we report the ultrasensitive detection limit of adenine and enhanced visualization of second-order Raman mode of MoS₂ using 266 nm wavelength Raman. This work thus enables, the sensitive detection of DNA and 2D materials.

10:30 PM DISCUSSION TIME

10:45 PM EL05.11.08

Electron Dynamics in Plasmons Hue T. Do^{1,1}, Wen Jun Ding², Zackaria Mahfoud², Lin Wu² and Michel Bosman^{1,2}; ¹National University of Singapore, Singapore; ²Agency for Science, Technology and Research, Singapore

The Particle-in-Cell (PIC) simulation is a widely used numerical method in plasma physics. We show that it can also be used to robustly describe plasmon resonances, similar to the conventional FDTD method, but with a unique emphasis on the motion of the electrons by tracking the individual conduction electrons in the time domain [1]. Our statistical studies of electron motions provide insight into the femtosecond time-scale dynamics of electrons in plasmons, including the plasmon dephasing, the contributions from different plasmon damping channels, and the electron kinetics during damping. An analysis of the time-resolved velocity distribution of the conduction electrons shows that only a small offset in this distribution constitutes the plasmon oscillation in each cycle. We describe the non-radiative damping through both electron-electron and electron-surface scatterings, where the latter is automatically and inherently included in the electron motions. Electron-surface scattering in PIC can be interpreted as a self-consistent interaction between the electrons and the enhanced local field at the surface. The presented framework will be particularly useful in future studies of plasmons in bimetallic nanostructures.

[1] Ding *et al.*, “*Particle Simulation of Plasmons*”, *Nanophotonics* 2020, 9(10), 3303–3313

[2] Do *et al.*, “*Electron Dynamics in Plasmons*”, (manuscript under review)

8:00 AM *EL05.12.01

Refractory Plasmonic Perfect Absorbers and Color Filters Using Transition Metal Nitride Metasurface

Yu-Jung Lu^{1,2}; ¹Academia Sinica, Taiwan; ²National Taiwan University, Taiwan

Broadband perfect absorbers in the visible have attracted a great deal of attention in many fields, especially for solar thermophotovoltaic (STPV) and energy harvesting systems. However, realizing light absorbers with high absorptivity, thermal stability and broad bandwidth remain a great challenge. In this work, we theoretically and experimentally demonstrate that a single-layer titanium nitride (TiN) metasurface absorber with a total thickness of 160 nm that exhibits broadband perfect absorption with an average absorption of more than 92% for a broad wavelength range from 400 nm to 750 nm in the visible. Unlike reported metamaterial absorbers based on the metal-insulator-metal (MIM) structure, we use a single-layer TiN metasurface, which simplifies the nanofabrication process and also maintains high absorption. The broadband perfect absorption of a single-layer TiN metasurface absorber is contributed by the combination of the intrinsic absorption of TiN and the broadband localized surface plasmon resonance (LSPR) of the lossy TiN nanodisk arrays. These results enable a new approach to realizing hot-carrier devices and solar-thermal energy conversion devices. In addition, we use the same concept of metasurface structure to design and fabricate the refractory color filters. We will also discuss the outlook for refractory metasurface in applications of the hot-carrier photodetection, photocatalysis, radiative cooling, and solar thermophotovoltaics.

8:30 AM EL05.12.02

Determination of the Absolute Chirality of Single Plasmonic Nanostructures in Solution Johannes Sachs^{1,2},

Jan-Philipp Günther^{1,2} and Peer Fischer^{1,2}; ¹Max Planck Institute for Intelligent Systems, Germany; ²University of Stuttgart, Germany

Chiral plasmonic structures, which exist in two distinct non-superimposable mirror-image forms, are interesting for (bio)chemical sensing. Almost all biomolecules are chiral, and are of only one handedness. Typically their handedness is detected via differential interactions with circularly polarized light. These interactions are weak, because the molecular dimensions are much smaller than the wavelength of light. Larger plasmonic nanostructures can boost the chiral signal and hence possibly yield high sensitivity and selectivity as well as permit detection in ultra-low volumes. Chiral metasurfaces exploit this and their interaction with chiral molecules, including proteins, has been studied. However, a difficulty in all experiments on metasurfaces to date is that – depending on their orientation – even achiral structures were reported to give chiral signals. This is because the experimental geometry (light in, object, light out) may become handed. It is then not trivial to distinguish the true (inherent real chirality) of a nanostructure from effects that arise due to the geometry of the setup.

We have succeeded in devising a new scheme to measure the true chirality of a single nanostructure that is free from artefacts and that reports a new observable [1]. The polarization-sensitive light scattered off a single nanoparticle can be measured while it is freely suspended in solution. For this, we have engineered a complex-shaped metal nanoparticle with defined handedness [2]. A novel spectrometer is introduced that can measure for the first time an artefact-free circular dichroism spectrum of a (reorienting) single nanoparticle. We thereby show that only the average spectrum taken over isotropic orientations of a single particle gives the same information as the corresponding ensemble spectra measured with the traditional instruments. This is in accordance with the ergodic principle, which is demonstrated for the first time in the context of chiroptical spectroscopy. Finally, we show that by growing hybrid nanostructures that contain a magnetic moment, we can re-orient single chiral metamaterials by means of an external field and obtain their spectral response as a function of their orientation.

[1] Sachs, J., Günther, J., Mark, A.G. *et al.* Chiroptical spectroscopy of a freely diffusing single nanoparticle. *Nat Commun* **11**, 4513 (2020). <https://doi.org/10.1038/s41467-020-18166-5>

[2] Mark, A., Gibbs, J., Lee, T. *et al.* Hybrid nanocolloids with programmed three-dimensional shape and

8:45 AM EL05.12.03

Late News: Influence of Plasmonic Surface Lattice Resonances Energy Transfer Between Two BODIPY Dyes Robert Collison¹, Vinod Menon², Joel Yuen Zhou³, Juan Perez-Sanchez³, Matthew Du³, Jacob Trevino⁴ and Stephen O'Brien²; ¹The Graduate Center of the City University of New York, United States; ²The City College of New York, United States; ³University of California, San Diego, United States; ⁴New York University, United States

To study the effect of surface lattice resonances (SLRs) on energy transfer, SLR-supporting square lattices of vertically layered Al-Al₂O₃-Al nanocylinders were fabricated onto a glass substrate. The substrate and lattices were coated with a film containing 800 mM (20 wt %) of the donor dye (P580) and 8 mM (0.16 wt %) of the acceptor (P650) dispersed in poly(methyl methacrylate) and the film's fluorescence spectra on the bare substrate and on the lattices were studied. In the absence of any SLR-supporting lattice, the fluorescence of the donor dye was less than that of the acceptor, with a donor-to-acceptor peak fluorescence ratio of 0.45, indicating that energy was readily transferred from donor to acceptor. In contrast, on a lattice that supports an SLR at 551 nm at $k_{\parallel} = 0$, coinciding with the donor dye emission peak at 550 nm, the fluorescence of the donor dye exceeded that of the acceptor, giving a donor-to-acceptor peak fluorescence ratio of 5.4. Additionally, the film exhibited a greater absolute donor fluorescence and a lesser absolute acceptor fluorescence on this lattice than on those that supported SLRs at other wavelengths. These results suggest that the SLR that coincides at $k_{\parallel} = 0$ with the donor dye's emission peak enhances the radiative decay of the donor at the expense of energy transfer to the acceptor. Notably, the SLRs that coincided with the donor emission peak at larger values of k_{\parallel} (at angles of emission of *ca.* 20° or 50°) did not have this effect.

9:00 AM EL05.12.04

Full-Field Imaging of Electromagnetic Fields via the Polarization Dependence of Photoemission Microscopy (DUV-PEEM) Thomas Beechem¹, Sean Smith¹, R. Guild Copeland¹, Fangze Liu² and Taisuke Ohta¹; ¹Sandia National Laboratories, United States; ²Los Alamos National Laboratory, United States

Through development of an electron-based imaging technique, the electromagnetic field profiles emanating from the edges of an atomically thin MoS₂ flake buried between Al₂O₃ and SiO₂ were characterized using photoemission electron microscopy excited by deep-ultraviolet light (DUV-PEEM). The photoemission yield is proportional to the square of the electric field for the single-photon process excited by the UV-light, thereby providing a pathway to the imaging of nanophotonic phenomena using emitted electrons. Because electrons are the sensing entity, the resulting images exhibit resolutions below the photon wavelength. To validate this concept, the dependence of photoemission yield on the wavelength and polarization of the exciting light was first measured and then compared to simulations of the optical response and the electric field quantified with classical optical theory. Close correlation between experiment and theory indicates that photoemission probes the optical interaction of the UV-light with the material stack directly. Utility is then demonstrated by employing the polarization dependence of photoemission to observe fringes indicative of the electromagnetic field profiles resulting from the interaction of the exciting UV-light with the MoS₂. Taken together, this “electron-based ellipsometric imaging” offers an analytical approach through which to visualize the electromagnetic field distributions central to many nanophotonic phenomena while simultaneously mapping optical property variation at sub-wavelength scales.

Acknowledgements: This work was performed under the Laboratory Directed Research and Development (LDRD) program at Sandia National Laboratories and undertaken, in part, at the Center for Integrated Nanotechnologies, an Office of Science User Facility operated for the U.S. Department of Energy (DOE) Office of Science. Sandia National Laboratories is a multimission laboratory managed and operated by National Technology & Engineering Solutions of Sandia, LLC, a wholly owned subsidiary of Honeywell International, Inc., for the U.S. DOE's National Nuclear Security Administration under contract DE-NA-0003525. The views expressed in the article do not necessarily represent the views of the U.S. DOE or the United States

Government.

9:15 AM EL05.12.05

Vectorial Holographic Color Prints for Double-Encrypted Optical Security Platform Inki Kim, Jaehyuck Jang, Gyeongtae Kim and Junsuk Rho; Pohang University of Science and Technology, Korea (the Republic of)

We propose bi-functional metasurface which contains structurally colored print and vectorial holograms with eight polarization channels towards advanced encryption applications. The encoded structural color prints can be observed under white light and the fully polarized holograms can be reconstructed using coherent laser source with combination of output polarizer/retarder. To encode multiple hologram images having different polarization states, a pixelated metasurface is adopted thereby digitalizing sets of phase distribution retrieved from the images into single metasurface. Such superpixel consists of four phase-gradient metaatom groups: meta-atom group rotated either clockwise or counterclockwise. Depending on the combination of clockwise and counterclockwise rotating meta-atom group, the polarization states of the reconstructed images are determined. The metaatom contains specifically designed geometric and propagation phase, and reflection spectrum at each spatial location. As a proof-of-concept, we devise electrically tunable optical security platform using our multifunction metasurface incorporated with liquid crystal. The optical security platform is double encrypted: Color printing image that can be decrypted by camera scanning provides first key and corresponding information will be used to fully unlock the double-encrypted information via projected vectorial hologram images. Such an electrically tunable optical security platform will provide a new route towards internet-of-things sensors for security and anticounterfeiting applications.

9:20 AM EL05.12.06

Gap-Plasmon-Mediated Luminescence Enhancement of Upconversion Nanoparticle-Sensitized Perovskite Quantum Dots in Metal-Insulator-Metal Configuration Minju Kim, Youngji Kim, Kiheung Kim, Jerome K. Hyun and Dong Ha Kim; Ewha Womans University, Korea (the Republic of)

All inorganic CsPbX₃ perovskite quantum dots (PeQDs) have received much attention due to their excellent properties such as large absorption coefficients, tunable bandgap, and narrow band emission. However, due to their low upconversion efficiency under near-infrared light excitation, potential applications have been limited. Recently, upconversion nanoparticle (UCNP) sensitized PeQD has been reported as a solution, but the low quantum yield of UCNPs and low photoluminescence (PL) intensity of PeQDs film have still remained challenges. In this study, enormous luminescence enhancement of PeQDs was achieved under near-infrared (NIR) excitation through sensitization by UCNPs and plasmonic coupling. To overcome the low luminescent quantum yield of UCNPs, gap plasmonic mode was integrated into the UCNP-perovskite film via metal-insulator-metal (MIM) configuration consisting of gold nanorods (AuNRs) and Ag thin film. The AuNRs-UCNPs/PeQDs-Ag film (MUPM) configuration is reported, for the first time, using UCNPs and PeQDs as an insulator layer, which provides high interfacial stability of perovskites-metallic nanostructures. Despite a thin active layer, a dominant green emission of PeQDs is observed under NIR excitation with high energy transfer efficiency by using similarly sized UCNPs and PeQDs. Furthermore, by capping AuNRs with the amphiphilic diblock copolymer, PL quenching and morphology deformation were suppressed. Therefore, an overall 29-fold upconversion enhancement was achieved for the green emission in the MUPM configuration owing to the strong localized electric field and the coupling of longitudinal localized surface plasmon resonance band of AuNRs with excitation of UCNPs. The present study provides a novel route to prepare highly efficient and effective emissive devices based on MIM configurations using an insulator layer composed of UCNPs and PeQDs, which can be expanded to serve a generalized platform in a broad range of applications.

12:15 PM *EL05.13.02

Instrument-on-a-Chip for *In Situ* Planetary Research Mahmooda Sultana; NASA Goddard Space Flight Center, United States

In situ measurements of trace gases in planetary environments are crucial for the understanding of atmospheric, geological, and possible biological processes. Currently, most planetary missions rely on large, heavy, high power instrumentation such as mass spectrometers for *in situ* chemical analysis. The size, weight and power (SWAP) of these payloads make the overall missions costly and challenging. In addition, some of the key species required for the origin of life as we know it, such as methane, ammonia, and water, are difficult to distinguish using mass spectrometry alone due to mass interference issues. To enable lower cost science missions, we have developed a highly miniaturized and compact multifunctional environmental sensor platform based on additive manufacturing techniques of low dimensional materials. The unique electrical and physical properties of nanomaterials coupled with the high surface area-to-volume ratio make them outstanding candidates as extremely sensitive gas detecting elements. In addition, our functionalized sensors are able to distinguish between key species of interest to astrobiology. The ability to print the sensor systems, heaters, interconnects and wireless antenna directly on the same substrate eliminates the need to integrate individually fabricated components. This makes the packaging significantly more robust and reduces the footprint of the overall instrument. In this talk, I will present the development and status of a unique instrument-on-a-chip for *in situ* planetary research, and potential upcoming mission opportunities.

12:45 PM EL05.13.03

Chiral Kirigami Metamaterials Wonjin Choi, Gong Cheng, Sang Hyun Lee, Theodore B. Norris and Nicholas A. Kotov; University of Michigan–Ann Arbor, United States

Kirigami, the art of paper cutting, presents a powerful tool to create complex and reconfigurable three-dimensional (3D) geometries from simple 2D cut patterns, which can be scaled across many orders of magnitude to yield macro- to nanoscale structures. The ability to achieve out-of-plane buckling, designed 3D shape, the robustness of the patterns under cyclic reconfiguration and the compatibility to conventional fabrication processes of kirigami structures together promise untapped possibilities for the efficient modulation of optical beams. Here we show that kirigami optics affords real-time modulation of THz beams with polarization rotation and ellipticity angles as large as 80° and 40° over thousands of cycles, respectively. The unusually large amplitudes of polarization rotation and ellipticity angles exceeding all known THz modulators were enabled by double-scale patterns composed of microscale metallic stripes together with submillimeter-scale kirigami cuts. We measured terahertz circular dichroism (TCD) spectra of several representative biological samples using chiral kirigami metamaterials and found distinctive TCD peaks. Kirigami metamaterials will also play an indispensable role for other applications, such as biomedical imaging, biosensors, line-of-sight telecommunication, information encryption and space exploration.

12:50 PM EL05.13.04

Computational Design of Buckypaper/Epoxy Shape Memory Polymer Nanocomposites Yelena Sliozberg¹, Martin Kröger², Todd Henry¹, Siddhant Datta³, Bradley Lawrence¹, Asha Hall¹ and Aditi Chattopadhyay³; ¹U.S. Army Research Laboratory, United States; ²ETH Zürich, Switzerland; ³Arizona State University, United States

The objective of this work is to understand the underlying molecular mechanisms of structural and mechanical properties of shape memory polymer (SMP) nanocomposites used for reconfigurable structures. In this work, we have performed coarse-grained molecular dynamics simulations and entanglement analysis of buckypaper (BP)/epoxy nanocomposites with a focus on their mechanical and shape memory performances, specifically on prediction of the Young's modulus of the material as a function of carbon nanotube (CNT) loading. We found

that the Young's modulus linearly increases with CNT volume fraction below 0.16 (40 wt%) followed by a sharp growth of the modulus at higher loading where the onset of entanglements of nanotubes was determined. Additionally, we found a significantly greater increase of the modulus at $T > T_g$ compared with the values below the glass transition temperature for all considered systems. The simulation suggests that incorporation of BP restricts relaxation of network strands of the polymer matrix and leads to resistance in the recovery process of composites. Computational results are compared with our experimental data on temperature controlled mechanical testing in tension of BP/epoxy nanocomposites.

12:55 PM EL05.13.05

A Quantum Leap in Nanophotonic Sensing: Ultrasensitive Fano Sensors Enabling SARS-CoV-2 Viral Load Detection Beyond the RT-PCR Techniques Xiangchao Zhu, Mustafa Mutlu, Reefat Inum, Ray Jara, Ahsan A. Habib and Ahmet A. Yanik; University of California, United States

A number of recent viral outbreaks, including the recent COVID-19 pandemic, have caused significant public health and economic concerns. Rapid and reliable point of care (POC) diagnostic technologies would provide a necessary first step for the proper treatment and management of these diseases [1]. State-of-the-art in vitro diagnostics (IVD) technologies including enzyme-linked immunosorbent assays (ELISA), and quantitative polymerase chain reaction (qPCR) are labor intensive, require cumbersome sample preparation, sophisticated equipment, and skilled operators. Here, using a novel nanophotonic approach, we present an ultrasensitive optofluidic diagnostic platform allowing detection of viral antigens with simple instrumentation at a concentration level five orders of magnitude lower than the most sensitive ELISA tests, and orders of magnitude more sensitive than the most advanced IVD technologies. In our tests with human serum samples, we experimentally demonstrated quantitative detection of viral antigens at attomolar sensitivities corresponding to 5-10 virus particles per 100 microliters. At this sensitivity level, our novel nanophotonic platform provided a compelling alternative to RNA-based quantitative-PCR tests for viral load detection.

[1] Cormac Sheridan, "Coronavirus and the race to distribute reliable diagnostics", *LNature Biotechnology* 38, 382-384 (2020)

1:00 PM EL05.13.06

Rapid Ge Diffusion Along Si/SiO₂ Interfaces During High Temperature Oxidation Chappel Sharrock¹, Benjamin Hicks¹, Emily Turner¹, Mark Law¹, George Wang² and Kevin S. Jones¹; ¹University of Florida, United States; ²Sandia National Laboratories, United States

In order to continue improving the performance of transistors beyond the 5nm node, there is interest in optimizing the use of Si and Ge in unique geometries [1]. A novel diffusion mechanism of Ge along an oxidizing Si/SiO₂ interface was reported, which resulted in the formation of strained Si nanowires [2]. Taking advantage of this diffusion mechanism has the potential of forming nanowires, nano-dots, and arbitrary shapes based on lithographic patterning; however, there is no understanding of the diffusion mechanism that results in the formation of these structures. To investigate this mechanism, alternating 20nm thick layers of Si and Si_{0.7}Ge_{0.3} were grown in a superlattice and patterned into fins via electron beam lithography. The final pattern contained multi-layered Si/SiGe fins with widths varying from 70 to 280nm with a single 100nm layer of Si at the base in which to observe the diffusion of Ge down the fin's sidewall during high temperature oxidation.

This lateral diffusion was observed over a range of times and temperatures between 800 and 950°C. Cross-sectional TEM samples were prepared after each anneal and the rate of diffusion was measured through analysis of HAADF-STEM images. The diffusion constant for Ge's lateral movement down the Si sidewall was measured to be approximately $1 \times 10^{-14} \text{cm}^2/\text{s}$ during 900°C oxidation. This is several orders of magnitude larger than Ge's interdiffusion with Si, which helps to explain why the nanowires and quantum dots are formed within these materials [3], [4]. The correlation between the thickness of the thermally grown oxide, the width of the SiGe layer forming on the side of the fin, and the length of the Ge diffusing down the side of Si sidewall has also been studied, providing additional insight into the diffusion mechanism. This analysis has been carried out

at multiple temperatures between 800 and 950°C, and the activation energy for Ge's lateral diffusion will be presented. These experimental results will be accompanied by a model using the Florida object-oriented process and device simulator (FLOOX), which has been using to assist in the extraction of diffusivities. Preliminary results using the process simulator's model will be compared to the experimentally observed evolution of the nanostructures.

Sandia National Laboratories is managed and operated by NTESS under DOE NNSA contract DE-NA0003525.

[1] T. David *et al.*, "New strategies for producing defect free SiGe strained nanolayers," *Sci. Rep.*, vol. 8, no. 1, pp. 1–10, Feb. 2018, doi: 10.1038/s41598-018-21299-9.

[2] W. M. Brewer, Y. Xin, C. Hatem, D. Diercks, V. Q. Truong, and K. S. Jones, "Lateral Ge Diffusion During Oxidation of Si/SiGe Fins," *Nano Lett.*, vol. 17, no. 4, pp. 2159–2164, Apr. 2017, doi: 10.1021/acs.nanolett.6b04407.

[3] R. Kube *et al.*, "Composition dependence of Si and Ge diffusion in relaxed Si_{1-x}Ge_x alloys," *J. Appl. Phys.*, vol. 107, no. 7, p. 073520, Apr. 2010, doi: 10.1063/1.3380853.

[4] Y. Dong, Y. Lin, S. Li, S. McCoy, and G. Xia, "A unified interdiffusivity model and model verification for tensile and relaxed SiGe interdiffusion over the full germanium content range," *J. Appl. Phys.*, vol. 111, no. 4, p. 044909, Feb. 2012, doi: 10.1063/1.3687923.

1:05 PM EL05.13.07

Late News: A Numerical Study of Near-Field Thermophotonic Devices Including Local Emission and Absorption Distributions Julien Legendre and Pierre-Olivier Chapuis; Univ Lyon, CNRS, INSA Lyon, Université Claude-Bernard Lyon 1, CETHIL UMR5008, France

Thermophotonics (TPX) is a technology close to thermophotovoltaics (TPV), where a heated light-emitted diode (LED) is used as the active emitter of the system [1]. With the development of LEDs and the increase of their achievable quantum efficiency, TPX has come out as an attractive concept for both energy harvesting and refrigeration [2]. The many studies on near-field (NF) thermal radiation and their application into efficient NF TPV devices [3] highlight the possibility to extend the concept to near-field thermophotonics [4], where enhanced energy conversion is due to both the electric control and wave tunneling.

This contribution explores the theoretical capabilities of NF-TPX systems. Ideal cases are compared with more realistic structures, involving materials such as Si, GaAs and GaN. Based on the local absorption and emission distributions [5], the results include detailed IV characteristics of the LED and PV cell sides around the maximum power point, and highlight in particular the advantages in comparison to far-field TPX and NF TPV. A particular attention is drawn to the search of optimal surface properties for the LED and the PV cell, which could potentially be approached by using metasurfaces. The impact of the temperature difference between these two elements, their quantum efficiency and the thickness of the different components are amongst the studied parameters.

[1] N. P. Harder and M. A. Green, *Semicond. Sci. Technol.* 18, S270, 2003. [2] T. Sadi *et al.*, *Nat. Phot.* 14, 205, 2020. [3] C. Lucchesi *et al.*, arxiv: 1912.09394, 2019. [4] B. Zhao *et al.*, *Nano Lett.* 18, 5224, 2018. [5] M. Francoeur *et al.*, *J. Quant. Spectr. Rad. Transf.* 110, 2002, 2009.

We acknowledge the funding of EU H2020 FET Proactive (EIC) programme through project TPX-Power (GA 951976).

1:10 PM *EL05.13.08

Meta-Optical Computational Imaging Systems for Large Aperture, Aberration-Free Imaging Arka Majumdar; University of Washington, United States

By exploiting computational backend, coupled with a designer meta-optics we demonstrate high-quality aberration free imaging using a single meta-optic in the visible wavelength range. The aperture is currently 0.5-1mm, but can be extended further. Several inverse design tools and end-to-end optimization are used to achieve such performance.

1:40 PM EL05.03.04

Tunable and Enhanced Absorption of Extended Short-Wave Infrared GeSn Nanopillar Arrays Anis Attiaoui, Etienne Bouthillier, Gerard Daligou, Aashish Kumar, Simone Assali and Oussama Moutanabbir; Polytechnique Montréal, Canada

Engineering light absorption in GeSn structures is crucial to enhance their basic device performance for a variety of applications such as MIR photodetectors and solar cells. Surface texturing to reduce the reflectivity is a key strategy to tune the optical properties. Since Group IV semiconductors typically have large refractive indices compared to air (between 3.4 and 4.2), planar opto-electronic devices are plagued by this refractive index mismatch. A promising method to circumvent this limitation is the use of semiconductor nanowires arranged in arrays covering an area of macroscopic dimensions. Top-down etched GeSn nanowire (NW) arrays were microfabricated with varying geometrical configuration. Visible and near IR spectroscopic ellipsometry measurement was undertaken in the spectral range from 900 nm to 2500 nm to evaluate the complex optical constant (n and k) for a 10% GeSn material. Detailed finite difference time domain (FDTD) simulations were combined with experimental analyses to systematically investigate light-GeSn nanowire interactions to tailor and optimize the NW array geometrical parameters and the corresponding optical response. The diameter-dependent leaky mode resonance peaks are theoretically predicted and experimentally confirmed with a tunable wavelength from 1.5 to 2.2 μm . A three-fold enhancement in the absorption with respect to GeSn thin film at 2.1 μm was achieved using nanowires with a diameter of 325 nm. The coupling between the HE_{11} and HE_{12} resonant modes manifests at NW diameters above 325 nm, while at smaller NW diameters and longer wavelengths the HE_{11} mode is guided into the underlying Ge layer. Additionally, the presence of tapering in NWs further extends the absorption range while minimizing reflection. The ability to manipulate light-matter interactions at the nanometer scale with GeSn is opening up new opportunities for spectral tunability in the extended short-wave infrared range.

SESSION EL05.14: Low Dimensional Photonics
Session Chairs: Ho Wai (Howard) Lee and Junghyun Park
Tuesday Afternoon, April 20, 2021
EL05

2:15 PM *EL05.14.01

Flat Optics for Dynamic Wavefront Manipulation Mark L. Brongersma; Stanford University, United States

Since the development of diffractive optical elements in the 1970s, major research efforts have focused on replacing bulky optical components by thinner, planar counterparts. The more recent advent of metasurfaces, i.e. nanostructured optical coatings, has further accelerated the development of flat optics through the realization that resonant optical antenna elements can be utilized to facilitate local control over the light scattering amplitude and phase. At the same time, researchers have aimed to identify ways to dynamically tune the properties of resonant optical antennas. The two developments are now leading to the development of dynamic flat optics.

In this presentation, I will highlight recent efforts in our group to realize electrically-tunable metasurfaces employing nanomechanics, electrochemistry, microfluidics, phase change materials, and atomically-thin semiconductors. Such elements can find application in systems for optical beam steering and wavefront manipulation as well as dynamic holography. I will illustrate how the proposed optical elements can be fabricated by scalable fabrication technologies, opening the door to many commercial applications.

2:55 PM EL05.14.02

Late News: Spectroelectrochemical Measurement and Modulation of Exction-Polaritons Wonmi Ahn¹ and

Blake S. Simpkins²; ¹Excet, Inc., United States; ²U.S. Naval Research Laboratory, United States

Quantum emitters strongly coupled to optical cavity modes create new hybrid states called polaritons, resulting in a vacuum Rabi splitting (Ω). Strikingly, the magnitude of this splitting correlates with modified emission properties and chemical reaction rates. However, active control of this coupling strength is difficult due to the fixed properties of the coupled oscillators (both, the quantum emitter and optical resonator). Here, we demonstrate active tuning of excitonic strong coupling in a system where organic dyes strongly couple to propagating surface plasmon polaritons (SPPs). After electropolymerization of a methylene blue (MB) film on a SPP-supporting Au surface, we demonstrated active control of coupling strength through reversible redox cycling of the MB film. Excitonic strong coupling was effectively cycled on and off with electrode potential either continuously tuned (*transient*) or held at a fixed value (*static*) and were quantitatively correlated with simultaneously measured electrochemical charge. Switching between reduced and oxidized forms of the dye resulted in Ω values tuned from ~ 0 to ~ 280 meV, *i.e.*, $\sim 14\%$ of the transition energy. The ability to control coupling strengths in a given emitter-cavity coupled system is a key capability for utilizing polaritonic states for cavity-mediated chemical reactions or optical devices.

3:10 PM EL05.14.03

Observation of Exciton-Polariton Emission in 2D Hybrid Perovskites with Intrinsic Cavity Induced Coupling Surendra B. Anantharaman¹, Jason Lynch¹, Baokun Song¹, Jin Hou^{2,2}, Huiqin Zhang¹, Kiyoung Jo¹, Pawan Kumar¹, Jean-Christophe Blancon², Aditya Mohite^{2,2} and Deep M. Jariwala¹; ¹University of Pennsylvania, United States; ²Rice University, United States

Hybrid states such as polaritons emerging from light-matter interaction are mostly observed in excitonic materials integrated in an external optical cavity. Two-dimensional (2D) hybrid organic/inorganic perovskites namely Ruddlesden-Popper (RP) perovskite have shown strong exciton confinement and oscillator strengths (12 ($n=1$) and 6 ($n=2$)).¹ Further, their optical constants suggest that the loss tangents in RP phase perovskites are among the highest for known excitonic semiconductor materials. These extraordinary optical properties can be exploited to create both the gain and cavity media in the semiconductor for strong light-matter interaction. Here, we show that intrinsic cavity mode formation in 2D perovskite flakes of intermediate thickness (~ 200 nm) on Au substrate leads to polariton state formation with Rabi splitting ~ 135 meV. In contrast, the thin flakes (15 nm) remain purely excitonic in nature. We confirm exciton-polariton formation from reflectance spectroscopy and associated emission spectroscopy at room temperature. Using transfer-matrix calculations, the experimentally observed exciton-polariton states can be modelled with two-coupled oscillators that corroborate well with the reflectance spectra. Further, temperature dependent photoluminescence and reflectance spectra shows the Rabi splitting and hybrid emission from exciton-polariton states present at room temperature, remains unperturbed down to 80 K. Tunable polariton formation from 520 nm to 610 nm by varying the perovskite composition will be presented. Rabi splitting increases with increase in oscillator strength of the perovskite as n is varied from 4 to 1. We believe that our work will open new avenues for exploring polariton in optoelectronic devices and photochemistry.

Keywords: Ruddlesden-Popper perovskites, Hybrid states, Polaritons, Rabi splitting, Intrinsic cavity mode

References:

1. Song, B. *et al.* Determination of Dielectric Functions and Exciton Oscillator Strength of Two-Dimensional Hybrid Perovskites. (2020) doi:<https://arxiv.org/abs/2009.14812>.

3:25 PM EL05.14.04

Ultrabroadband Nanophotonic 2D Material-Based Architecture for Reflection and Thermal Emission Control in Laser-Driven Lightsails John B. Brewer¹, Pawan Kumar², Matthew F. Campbell², Mohsen Azadi², George A. Popov², Igor Bargatin², Deep M. Jariwala² and Aaswath Raman¹; ¹University of California, Los Angeles, United States; ²University of Pennsylvania, United States

We present a holistic nanophotonic 2D material-based design strategy for ultrathin laser-driven lightsails that provides both high weight-constrained reflectance over a defined bandwidth and enhanced thermal emittance. Our investigation explores the use of hexagonal boron nitride (h-BN) and molybdenum disulfide (MoS₂) arranged in an inverse-designed layered photonic crystal architecture. Both the optical and thermal properties of the design are shown to be viable, emphasizing the holistic merit of its functionality. Relative to other designs, our concept exhibits impressive spectral emissivity values and accelerations for its mass, as well as the potential for excellent mechanical compliance. We compare its performance against other designs and show reasonable benchmarks of emissivity necessary to produce given steady state temperatures.

The Breakthrough Starshot Initiative aims to send a nanocraft to Earth's nearest habitable exoplanet, Proxima Centauri B, within 20 years of launch. To do so, the craft will use a reflective light sail accelerated by a ~100 GW phased array of lasers to speeds of $0.2c$ ¹. This requires a sail that is highly reflective over a Doppler-broadened wavelength range starting from the laser wavelength, is highly emissive in the mid-wave and long-wave infrared to effectively dissipate heat during acceleration, is mechanically robust enough to not degrade under the large forces acting on it, is correctly shaped to provide beam riding stability, and has a mass totaling ~1 g with a similarly-sized payload. Previous work has demonstrated designs using conventional dielectric materials such as Si₃N₄², Si, and SiO₂^{3,4}. Given the stringent weight and mechanical requirements of the sail, 2D materials may be ideally suited to serve as key lightsail components; however, to date they have not been extensively explored for this application. In addition, while several studies have considered optical factors in order to minimize acceleration distances, few have co-optimized thermal properties in order to present a holistic assessment of the overall suitability of a sail design.

Here we present an optimized 2D material-based nanophotonic sail design that is optically suitable and able to effectively dissipate heat as thermal radiation to maintain reasonable in-flight temperatures. This sail consists of a 1.264-gram multi-layer photonic crystal slab composed of h-BN and MoS₂ layers and is shown, through full-field electromagnetic simulations, of being capable of accelerating an equivalent mass payload to $0.2c$ within 14 gigameters. The materials utilized have refractive indices ranging from ~2.13 for h-BN to 3.98-3.87 for MoS₂ over the doppler broadened range. We show the sail's fabricability using currently available patterning and etching techniques, provide benchmark material emissivity values necessary to maintain a given steady-state sail temperature, and demonstrate how payload weight influences the optimal sail design. Additionally, we discuss thermal considerations such as vacuum evaporation of features and how maximum temperature limits of materials should be set to ensure sail viability. Finally, we discuss the need for high resolution measurements of 2 dimensional optical, thermal, mechanical, and coupled material constants to continue to improve simulation accuracy and true viability of future sail designs.

1) Atwater *Nat. Mater.* 17(2018)861

2) Jin, W. *ACS Photonics* 7(2020)9

3) Salary *Laser Photonics Rev.* 14(2020)1900311

4) Ilic *Nano Lett.* 18(2018)5583

3:40 PM *EL05.14.05

Tunable Light-Matter Interactions in Excitonic Semiconductors Deep M. Jariwala; University of Pennsylvania, United States

The isolation of stable atomically thin two-dimensional (2D) materials on arbitrary substrates has led to a revolution in solid state physics and semiconductor device research over the past decade. A variety of other 2D materials (including semiconductors) with varying properties have been isolated raising the prospects for devices assembled by van der Waals forces.¹ Particularly, these van der Waals bonded semiconductors exhibit strong excitonic resonances and large optical dielectric constants as compared to bulk 3D semiconductors. . First, I will focus on the subject of strong light-matter coupling in excitonic 2D semiconductors, namely chalcogenides of Mo and W. Visible spectrum band-gaps with strong excitonic absorption makes transition metal dichalcogenides (TMDCs) of molybdenum and tungsten as attractive candidates for investigating light matter interaction and applications as absorbing media in opto-electronics.^{2, 3} We will present our recent work

on the fundamental physics of light trapping in multi-layer TMDCs when coupled to plasmonic substrates. We systematically demonstrate via calculations and matching experiments that the presence of strong excitonic resonances in multilayers (< 20 nm thickness) combined with surface plasmon excitations of the nearby metals can achieve strongly coupled modes with apparent avoided crossings in reflectance spectra.⁴

Next, we will show the extension of these results to multilayers and superlattices of excitonic chalcogenides with alternating layers of boron nitride and aluminum oxide. These hybrid multilayers offer a unique opportunity to confine light in < 3 nm thick direct band gap absorbers over cm² scale areas. We will discuss the physics of strong light-matter coupling and applications of these multilayers. Finally, we will also present our recent and on-going works on tunable light-matter interactions in hybrid organic-inorganic perovskites⁵ where we observe exciton-polariton hybrid state emission at room temperatures in an external cavity-less geometry. Finally, I will also present our recent work on giant gate-tunability of optical constants in the telecom band in thin-films of high purity, semiconducting, carbon nanotubes.⁶ Our results highlight the vast opportunities available to tailor light-matter interactions in quantum confined materials in simple and practical designs enabling study of novel photonic phenomena and presenting avenues for practical technologies.

References:

1. Jariwala, D.; Sangwan, V. K.; Lauhon, L. J.; Marks, T. J.; Hersam, M. C. *ACS Nano* **2014**, 8, (2), 1102–1120.
2. Jariwala, D.; Davoyan, A. R.; Wong, J.; Atwater, H. A. *ACS Photonics* **2017**, 4, 2692-2970.
3. Brar, V. W.; Sherrott, M. C.; Jariwala, D. *Chemical Society Reviews* **2018**, 47, (17), 6824-6844.
4. Zhang, H.; Abhiraman, B.; Zhang, Q.; Miao, J.; Jo, K.; Roccasecca, S.; Knight, M. W.; Davoyan, A. R.; Jariwala, D. *Nature Communications* **2020**, 11, (1), 3552.
5. Song, B.; Hou, J.; Wang, H.; Sidhik, S.; Miao, J.; Gu, H.; Zhang, H.; Liu, S.; Fakhraai, Z.; Even, J.; Blancon, J.-C.; Mohite, A. D.; Jariwala, D. *arXiv preprint arXiv:2009.14812* **2020**.
6. Song, B.; Liu, F.; Wang, H.; Miao, J.; Chen, Y.; Kumar, P.; Zhang, H.; Liu, X.; Gu, H.; Stach, E. A.; Liang, X.; Liu, S.; Fakhraai, Z.; Jariwala, D. *ACS Photonics* **2020**, 7, (10), 2896-2905.

SESSION EL05.15: Active Metasurfaces and Nanophotonics I
Session Chairs: Ho Wai (Howard) Lee and Junghyun Park
Tuesday Afternoon, April 20, 2021
EL05

5:15 PM *EL05.15.01

High-Q Phase Gradient Metasurfaces for Compact Sensors and Modulators Jennifer Dionne, Jack Hu, Fareeha Safir, Mark Lawrence, David Barton and Jefferson Dixon; Stanford University, United States

High quality factor (“high Q”) cavities have revolutionized information processing, communications, sensing, and nonlinear optics by increasing photon storage times and significantly enhancing light-matter interactions. However, when the size of dielectric cavities is reduced to the nanoscale, resonant modes start to resemble point sources, scattering an incident wave in many different directions. While this scattering has been leveraged to create remarkable metasurfaces that precisely control the phase, amplitude, and polarization of light in an ultrathin footprint, metasurfaces generally exhibit high radiative loss rates and thus low Q-factors. Here, we present a general strategy for crafting high quality factor resonances in a phase gradient metasurface, and apply these results to achieve 1) multiplexed nucleic acid detection and 2) efficient electro-optic modulation. To create a high-Q metasurface, we introduce subtle structural perturbations to individual resonators to weakly couple free-space light into otherwise bound modes. We experimentally demonstrate control over the quality factor and resonant wavelengths in this scheme, achieving record phase-gradient metasurface Q’s greater than 2500. We highlight this scheme’s general applicability by designing and fabricating high-Q metasurfaces that act as beamsteerers to different angles, beam splitters, and lenses. Next, we show how high-Q metasurfaces can enable multiplexed nucleic acid detection. Our high-Q metasurfaces are functionalized with single-stranded DNA to target specific RNA gene sequences, then illuminated with a laser diode; the scattered intensity provides a

quantitative measure of the bound nucleic acid concentration. As a proof-of-concept, we focus on SARS-CoV-2 genetic sequences, including recent viral variants; through “multi-color” printing of the probe nucleic acid, we show multiplexed detection of viral variants within 15 minutes. Finally, we show how high-Q metasurfaces can be integrated with electro-optic materials for low-power metasurface modulation. Here, an array of uniform lithium niobate-on-Si antennas is individually addressed with an electrical bias, leading to a full 2π phase variation. We show how near-continuous beam-steering can be achieved by modifying the bias across each antenna, en-route to fully reconfigurable, solid-state information processing spanning LiDAR, LiFi, AR/VR, and quantum communications.

5:55 PM EL05.15.02

Self-Assembled Multi-Phase Metamaterials for Enhanced Magneto-Optical Anisotropy Xuejing Wang^{1,2}, Jie Jian¹, Haohan Wang³, Yash Pachaury¹, Ping Lu⁴, Xiaoshan Xu³, Anter A. El-Azab¹, Xinghang Zhang¹ and Haiyan Wang^{1,1}; ¹Purdue University, United States; ²Los Alamos National Laboratory, United States; ³University of Nebraska-Lincoln, United States; ⁴Sandia National Laboratories, United States

Magneto-optical coupling incorporates photon-induced change of magnetic polarization that can be adopted in ultrafast switching, optical isolators, mode convertors, and optical data storage components for advanced optical integrated circuits. However, integrating plasmonic, magnetic and dielectric properties in one single material system is challenging since one natural material can hardly possess multiple functionalities. We use a bottom-up self-assembling synthesis method to integrate multifunctional phases as a nanopillar-in-matrix thin film nanostructure that realizes epitaxial quality, sharp atomic interface and large throughput. Using titanium nitride (TiN) as a durable plasmonic matrix, a metal-free metamaterial platform with embedded nickel oxide (NiO) vertical nanorods that function as tunable ferromagnetic nanodomains has been demonstrated. Such a dissimilar ceramic-ceramic combination enables a strong hyperbolic dispersion in the visible and near infrared frequencies. More interestingly, when Au is introduced in TiN-NiO, a hybrid core-shell nanopillar array is formed where the two-monolayer Au shell serves to release the strain energy at the TiN/NiO interface. We demonstrate that a significantly enhanced long-range ordering of core-shell nanopillars can be achieved by using a template bottom-up growth process, which enables stronger Kerr anisotropy that is promising for building tunable and modulated all-optical nanodevices.

6:10 PM EL05.15.03

Semiconductor and Metal Metalattice Nanostructures—3D, Ordered and Extended Plasmonic Platforms for the NIR-VIS-UV Regime Parivash Moradifar¹, Lei Kang¹, Pratibha Mahale², Yunzhi Liu¹, Nabila Nova¹, Andrew Glaid¹, John Badding¹, Tom Mallouk², Douglas Werner¹ and Nasim Alem¹; ¹The Pennsylvania State University, United States; ²University of Pennsylvania, United States

Plasmonics is an emerging field in the intersection between nanotechnology, photonics and electronics. Surface plasmons are coupled collective excitations of conduction electrons and an applied electromagnetic field. Plasmons hereby enable enhancement, confinement and manipulation of light at the nanoscale level. Noble metal-based nanostructures are the most widely studied plasmonic materials since they exhibit strong electromagnetic field enhancement in the visible spectral range. However, strong dissipation originating from interband electronic transitions and losses in noble metals, makes it imperative to investigate alternative building blocks with lower losses and more diverse properties. Metamaterials are new emerging building blocks in electronics and photonics. They are proposed as versatile and tunable platforms supporting various surface plasmon modes exhibiting exotic plasmonic phenomena.

This study will focus on the plasmonic behavior of novel 3D hybrid metamaterials using monochromated electron energy loss spectroscopy (Mono-EELS) in conjunction with scanning/transmission electron microscopy (S/TEM) and X-ray energy dispersive spectroscopy (XEDS) to identify and spatially resolve various surface plasmon resonances (SPRs) over a wide spectral range of NIR-Vis-UV. Metalattices as a subgroup of metamaterials, are nanostructured 3D ordered hybrid materials on the range of sub 100 nm (sub wave-length scale). The metalattice nanostructures are high pressure confined CVD (HPcVD) synthesized

nanostructures, comprised of a SiO₂ close-packed template infiltrated by either Ag or Si-Ge, forming periodic and long-range interconnected structures. A void-free infiltration of these 3D ordered frameworks can provide a versatile and tunable platform as integrated plasmonic interconnects for large optical confinement and long propagation distance applications. By spatially and spectrally resolving the plasmonic response, localized and delocalized effects are studied, and the implications of confinement, interconnectivity, substrate effect, presence of cavity arrays as potential tools for modulating and tuning SPRs are explored. This work also utilizes theoretical calculations to further support the experimental measurements.

Plasmonic metalattice as a periodic and long-range interconnected structure is a novel route to make highly tunable and cost-efficient plasmonic materials with enhanced photonic properties providing a significant control over ultra-local modification of surface plasmon resonances. This understanding is a crucial key for a more efficient electromagnetic energy storage, enhanced biological, chemical sensing and next generation of transparent and flexible optoelectronic/plasmonic devices.

6:25 PM EL05.15.04

Porous Ceramics as a Near-Ideal Radiative Cooling Design Jyotirmoy Mandal; University of California, Los Angeles, United States

Passive radiative cooling (PRC) of terrestrial objects is achieved by radiative heat loss into space through the long wavelength infrared (LWIR) atmospheric transmission window. Due to its passive nature and net cooling effect, it is a sustainable way to cool human environments. A major goal of radiative cooling research is to create designs with near-ideal spectral properties – i.e. selective emittance in the LWIR ($\lambda \sim 8\text{-}13 \mu\text{m}$), and perfect reflectance elsewhere in the solar-thermal wavelengths ($\lambda \sim 0.2\text{-}40 \mu\text{m}$). However, most PRC designs are non-ideal with regard to selectivity [1-2], or else need multiple materials and complex architectures [3]. This presentation proposes a bilayer porous ceramics as selectively LWIR emissive radiative coolers with near-ideal optical performance. The selective emittance arises from the Christiansen effect, while the high reflectance elsewhere arises from the porous structure (for $\lambda < 8 \mu\text{m}$) and Restrahlen reflection (for $\lambda > 13 \mu\text{m}$). It theoretically shows how this can lead to near-ideal spectral properties, and demonstrate real examples that can achieve this behaviour. Along with their robustness and resistance to weathering, this makes porous ceramics near-ideal materials for radiative cooling.

[1] J. Mandal et. al., Science 362, 315 (2018)

[2] Y. Zhai et. al. Science 355, 1062–1066 (2017)

[3] A. Raman et. al., Nature 515, 541 (2014)

Jyotirmoy Mandal is supported by Schmidt Science Fellows, in partnership with the Rhodes Trust.

6:40 PM *EL05.15.05

Advancing Functional Materials for Robust and Dynamic Nanophotonics Nathaniel Kinsey, Dhruv Fomra, Kai Ding, Md. Ariful Hoque Sojib, Samprity Saha, Ray Secondo, Adam Ball, Vitaliy Avrutin and Umit Ozgur; Virginia Commonwealth University, United States

Materials drive innovation across science and technology, and photonic applications are no exception. In the last decade, a wide range of new and emerging materials have been realized to improve nonlinear interactions, support single-photon emission, and explore new realms of light-matter interaction. Among them, two classes of materials have had a particular impact in the area of nanophotonics, transition metal nitrides and transparent conducting oxides. The former has provided a robust and CMOS-compatible metallic alternative to traditional elemental metals while the latter has unlocked a new field of dynamic tunability and enhanced nonlinearities through epsilon-near-zero properties. In this talk, we will highlight our work to extend the development of two key materials, TiN and Al:ZnO, using new realms of scalable, low-temperature, CMOS-compatible plasma-enhanced atomic layer deposition. In addition, we will discuss some recent applications of these materials to realize robust plasmonic security devices, and enhanced dynamic applications for nonlinear optics and

integrated photonics.

SESSION EL05.16: Active Metasurfaces and Nanophotonics II
Session Chairs: Ho Wai (Howard) Lee and Junghyun Park
Tuesday Afternoon, April 20, 2021
EL05

9:00 PM *EL05.16.01

Dielectric Metasurfaces for Flat Optics—Wavefront Engineering and Future Applications Junsuk Rho;
Pohang University of Science and Technology, Korea (the Republic of)

Miniaturization is a main stream in modern technology, but reduction of conventional optical components accompanies performance degradation that limits the minimum feature size of optical devices. Metasurfaces that consist of ultrathin subwavelength antenna arrays can be a promising solution because metasurfaces provide an effective way of wavefront engineering without constraints on the device size. Electromagnetic responses of individual building blocks are determined by its geometric configurations, and many kinds of antennas have been explored to clarify the capability of metasurfaces; thereby, it has been verified that dielectric antennas can control amplitude, phase, and even both of them simultaneously.

The capability of wavefront engineering allows to realize versatile future applications such as holograms, lenses and color filters. Fundamental limitations of conventional holograms such as twin image and narrow viewing angle can be removed by metaholograms due to their sub-wavelength pixel size. Propagation phase of isotropic building blocks enables polarization-insensitive operation while geometric phase of anisotropic building blocks allows broadband operation of multifunctional metaholograms (*i.e.* image hologram, multiplexed metaholograms). Furthermore, both propagation phase and geometric phase can be considered in design of meta-atom, which enables a multicolor metahologram and complex-amplitude hologram. The recent advanced understanding of building blocks brings about an increase of the number of hologram encoded in the metasurface based on dispersion engineering and orbital-angular-momentum multiplexing. The metaholograms can also be extended to random point-cloud generation for application toward 3D object detection. The same design method described above can be applied to polarization independent broadband beam splitting and ultrathin light-focusing devices, *i.e.* metalenses.

Metasurfaces can engineer transmission/reflection spectrum in visible regime, *i.e.* sub-wavelength color printing. The building block to modulate scattering response is high-index dielectric Mie-scatterer which resonantly radiate light with fundamental modes when its size become comparable to wavelength of incident light. The metasurface, composed of arrays of Mie-scatters, transmit/reflect lights with the resonance modes, thus rendering structural colors which are changed according to the geometry of the scatterers. The metasurface which consists of asymmetric unit structure switch its colors depending on the polarization state of incident light, thus enabling application for optical cryptography. Adoption of phase change materials and stimuli-responsive materials enables active color filters.

Comprehensive metasurfaces that control both phase and amplitude have been realized by adjusting unit structures. The hologram resolution can be drastically improved by controlling complex amplitude using X-shaped antennas, and both functions of holography and color printing can be integrated in a single metasurface.

Recently, much metasurface research has aimed to embed nanoparticle-based hierarchy in building blocks to enhance the chirality²¹ and refractive index^{16,22,23}. Furthermore, actively tunable meta-holographic displays with designer liquid crystal modulators will enable interactive holographic displays and unconventional photonic sensor applications^{24,25}. In the future, metasurface research will be further expanded to a practical region by

exploiting diverse light properties (*e.g.* orbital angular momentum) to realize real-time 3D holographic video displays or advanced optical security labels⁶.

9:30 PM EL05.16.02

Complex Refractive Index Modulation of Hydrogenated Amorphous Silicon for Efficient Metasurfaces at the Visible Frequencies Younghwan Yang, Gwanho Yoon and Junsuk Rho; Pohang University of Science and Technology, Korea (the Republic of)

Hydrogenated amorphous silicon has emerged as materials for dielectric metasurfaces, which are promising optical platforms since it has compatibility with mature complementary metal-oxide-semiconductor processes. However, the bandgap of hydrogenated amorphous silicon filters electromagnetic waves at the visible frequencies, preventing it from being optical devices at the visible. Here, we investigate structural disorders of silicon and hydrogenation in order to suppress the bandgap of it to produce visibly transparent hydrogenated amorphous silicon. The structural configuration of silicon-hydrogen bindings is varied by the chemical deposition equilibrium of plasma-enhanced chemical vapor deposition chambers. The chamber atmospheres are changed by manipulating substrate temperatures, chamber pressures, radio frequency power, and input gas ratio. Chemical deposition equilibrium affects the bonding configurations and we reveal that substrate temperature and chamber pressure affect bonding configuration, providing wide coverages of complex refractive index at the visible frequencies. The refractive index of hydrogenated amorphous silicon can be changed from 3.0 to 4.1; the extinction coefficient can be as low as 0.09 at the wavelength of 450 nm. We also reveal the bonding configuration to interpret the relationship between bandgap and composition of hydrogenated amorphous silicon. The X-ray diffraction and Raman were conducted to uncover the crystallinity and stretching vibration, respectively. Micro-crystallinity induces a low extinction coefficient at the visible, and the polyhydride bonding contributes to high transparency. This low-loss hydrogenated amorphous silicon achieves the lowest values of the extinction coefficient are 0.082, 0.017, and 0.009 at the wavelengths of 450, 532, and 635 nm, respectively. Low-loss hydrogenated amorphous silicon is confirmed with beam steering metasurfaces, which deviate the incident light with precisely designed angles. Demonstrated low-loss metasurfaces achieve modulation efficiencies of 64.7% at 450 nm, 90.9% at 532 nm, and 96.6% at 635 nm, which are compatible with conventional low-loss dielectrics such as titanium dioxide and gallium nitride. The metasurfaces steer incident light with 9.9, 12.7, and 11.3 degrees operating at 450, 532, and 635 nm, respectively, which highly coincide with 10.8, 12.8, and 11.4 degrees at each wavelength. Considering its low optical losses and a large coverage of the complex refractive index, our low-loss hydrogenated amorphous silicon will be the dominant platform material at the visible frequencies.

9:45 PM EL05.16.03

Sub-Ambient Daytime Radiative Cooling by Silica-Coated Porous Anodic Aluminum Oxide Dasol Lee, Minkyung Kim and Junsuk Rho; Pohang University of Science and Technology (POSTECH), Korea (the Republic of)

Passive radiative cooling is a concept where an object on the Earth can radiate heat into outer space through the atmospheric window (AW) in the mid-infrared spectrum (8-13 μm). As the objects radiate, they cool down. For effective energy-free radiative cooling, the object must have low absorption of energy from the atmosphere, high emission through the AW, and minimal heat exchange with its surroundings. Passive cooling of an object under direct sunlight in the daytime can be achieved by radiating more energy away than what is absorbed. For this process, absorption of the strong solar radiation is undesirable, so it must be minimized by achieving high reflectivity in the ultraviolet (UV) and near-infrared (NIR) regime (0.3-2.5 μm), while simultaneously maximizing the emission of energy through the AW.

In this work, we propose an approach for passive radiative cooling that uses silica-coated porous anodic aluminum oxide (AAO), which shows near perfect spectral emissivity in the AW. Nanoporous structures have the benefits of simple and low-cost fabrication, and compatibility with engineering to achieve selective emissivity in the AW. However, conventional AAO has a large extinction coefficient over 10 μm and by itself, does not produce the required near perfect spectral emissivity band over the entire AW. To compensate for this,

thin layers of silicon dioxide (SiO₂) are coated on the porous AAO to achieve near perfect emissivity over the AW. The experimentally fabricated SiO₂-coated AAO membrane shows an average cooling flux of 65.6 W/m² during the daytime, and a maximum cooling of 6.1 °C below ambient temperature under direct sunlight.

Reference: *Nano Energy* **79**, 105426 (2021)

10:00 PM *EL05.16.04

Enhanced Photochemical Reactions Under Modal Strong Coupling Conditions Hiroaki Misawa^{1,2};

¹Hokkaido University, Japan; ²National Chiao Tung University, Taiwan

Metallic nanoparticles such as gold (Au) and silver (Ag) shows light absorption and scattering at the arbitrary wavelength of visible and near-infrared regions based on localized surface plasmon resonances (LSPRs). LSPRs which are collective oscillations of conductive electrons give rise to the enhancement of near-field and are expected as a light harvesting optical antenna for light energy conversion devices due to their spectrum tunability. We have successfully developed the plasmon-induced artificial photosynthesis systems such as water splitting and ammonia synthesis systems as well as solid-state plasmonic solar cells based on the principle of plasmon-induced charge separation between gold nanoparticles (Au-NPs) and the semiconductor photoelectrode.[1]-[7] Previously, the plasmon-induced charge separation has received considerable attention as a novel strategy for solar energy conversion.[8],[9] However, for the monolayer of Au-NPs on the semiconductor the insufficient absorption limited its solar energy conversion efficiency.

Recently, we reported Au-NPs/TiO₂/Au-film photoanode with a modal strong coupling between Fabry-Pérot nanocavity (FPnanocavity) mode and LSPR of Au-NPscan enhance water splitting reaction.[10] In particular, it should be noted that in addition to the absorption increment, the internal quantum efficiency (IQE) is enhanced under strong coupling conditions.

Additionally, we investigated the efficiency of hot-electron transfer under modal strong coupling conditions by monitoring the photocurrent generated at a plasmonic photoanode. We explored the effect of the modal strong coupling on the incident photon-to-current conversion efficiency (IPCE) and IQE in the presence of triethanolamine (TEOA) as a sacrificial electron donor to accelerate the surface reaction enough.[11] The absorption spectrum showed distinct dual bands, which corresponded to the strong-coupling-induced splitting of energy levels into upper and lower branches. The IPCE was dramatically enhanced as the TEOA concentration increased, and finally, the IPCE reached a maximum of ca. 4%. Additionally, both hybrid modes formed by the modal strong coupling contributed to the hot-electron transfers and photocurrent generation in the presence of TEOA because the IPCE action spectra can be separated into two peaks. Furthermore, the integrated IQE, which was obtained for wavelengths from 500 to 800 nm, was enhanced by approximately 5 times upon the addition of 1 vol% of TEOA and reached 3%.

References

1. Y. Nishijima, K. Ueno, H. Misawa et al. *J. Phys. Chem. Lett.* **1**, 2031 (2010).
2. Y. Zhong, K. Ueno, Y. Mori, X. Shi, T. Oshikiri, K. Murakoshi, H. Inoue, H. Misawa, *Angew. Chem. Int. Ed.*, **53**, 10350 (2014).
3. T. Oshikiri, K. Ueno, H. Misawa, *Angew. Chem. Int. Ed.*, **53**, 9802 (2014).
4. T. Oshikiri, K. Ueno, H. Misawa, *Angew. Chem. Int. Ed.*, **55**, 3942 (2016).
5. K. Nakamura, T. Oshikiri, K. Ueno, H. Misawa et al. *J. Phys. Chem. Lett.*, **7**, 1004 (2016).
6. C. V. Hoang, K. Hayashi, K. Ueno, H. Misawa et al. *Nat. Commun.*, **8**, 771 (2017).
7. T. Oshikiri, K. Ueno, H. Misawa, *Green Chem.*, **21**, 443 (2019).
8. K. Ueno, T. Oshikiri, H. Misawa, *ChemPhysChem*, **17**, 199 (2016).
9. K. Ueno, T. Oshikiri, Q. Sun, X. Shi, H. Misawa, *Chem. Rev.*, **118**, 2955 (2018).
10. X. Shi, K. Ueno, T. Oshikiri, Q. Sun, K. Sasaki, H. Misawa, *Nat Nanotechnol.*, **13**, 953 (2018).
11. Y. Cao, T. Oshikiri, X. Shi, K. Ueno, J. Li, H. Misawa, *ChemNanoMat*, **5**, 1008 (2019).

10:30 PM *EL05.16.05

Metasurfaces for Vortex Generation, Multiplexing and Laser Cheng-Wei Qiu; National University of Singapore, Singapore

Interfacial engineering via the artificially constructed structures of ultrathin thickness compared to the wavelength has enabled a plethora of advanced manipulations of light-matter interactions. I will report some of the most recent developments in my group as well as in the field of the interfacial engineering of manipulation of light-matter interactions, via the artificially nanostructured metasurfaces. Amongst various applications of metasurfaces, I will focus on how to design vortex metasurfaces¹ to generate and multiplex orbital angular momentums (OAMs), with other degrees of freedom of light such as polarization and frequency. Furthermore, we will show some more recent and exciting results about high-purity orbital angular momentum lasing by synergize the metasurfaces and cavities. It may provide an alternative paradigm toward an extremely compact and multifunctional nanodevices resorting to the OAM states of the light. The multiplexing and hybridization of OAM states with other properties of light open up new opportunities for the advanced flat-profile optics.

SYMPOSIUM EL06

Molecular and Colloidal Plasmonics—Synthesis and Applications
April 22 - April 23, 2021

Symposium Organizers

Viktoriia Babicheva, University of New Mexico
Yogendra Mishra, University of Southern Denmark
Svetlana Neretina, University of Notre Dame
Can Xue, Nanyang Technological University

* Invited Paper

SESSION EL06.01: Plasmonics I
Session Chairs: Yogendra Mishra and Svetlana Neretina
Thursday Morning, April 22, 2021
EL06

8:00 AM EL06.01.01

Late News: Plasmonic LASiS Metal Nanoparticles for Food Packaging Applications Margherita IZZI^{1,2}, Maria C. Sportelli¹, Antonio Ancona¹, Annalisa Volpe¹, Caterina Gaudioso¹, Amalia Conte³, Valentina Lacivita³, Matteo A. Del Nobile³, Rosaria Anna Picca^{1,2} and Nicola Cioffi^{1,2}; ¹University of Bari Aldo Moro, Italy; ²CSGI (Center for Colloid and Surface Science), Italy; ³University of Foggia, Italy

The application of metal and metal oxides in the form of nanostructures, to enhance physicochemical properties of materials has increasingly attracted the interest of materials scientists in different fields. Among other features, these nanomaterials show a broad antimicrobial activity and can be advantageous to design bioactive coatings and/or surfaces, with controlled metal ion release, exerting significant biological action and associated low toxicity for humans. In recent years, we have developed and deeply characterized many different nanoantimicrobial systems [1-3] as a powerful alternative route to fight bacterial resistance towards conventional antibiotics and disinfecting agents. In this study, bioactive Cu- and Ag- nanoparticles were

produced as ultra-stable [4] nanocolloids by means of laser ablation synthesis in solution (LASiS) for hypothetical food packaging application. We exploited the key features of LASiS, which is a green and versatile route to obtain nanoparticles without any toxic reductant or stabilizer. The resulting nanocolloids were used as additives for the controlled modification of different biodegradable polymeric matrices. Antibacterial ion release kinetics from modified surfaces was monitored, showing a tuneable and long-term release of bioactive species over time. The risk of entire nanoparticle release was ruled out by electron microscopy investigations of the contact solutions. Finally, the coatings' surface chemical composition (assessed by photoelectron and vibrational spectroscopies) was correlated with the ion release and bioactivity properties. They were examined in different cases of study, in order to evaluate their employment in active food packaging and bacteriostatic coatings for the car industry.

MCS acknowledges the project "Extension of the shelf-life of agri-food products through nanoantimicrobial and antibiofilm packaging with low environmental impact", Research for Innovation – European Social Fund network, n° 435A866B.

[1] M. C. Sportelli et al., *Scientific Reports*, 7 (2017), 11870.

[2] M.C. Sportelli et al., *Trends in Analytical Chemistry*, 84 (2016), 131-138.

[3] M.C. Sportelli et al., *Nanomaterials*, 7 (2016), 6.

[4] M. C. Sportelli et al., *Colloids and Surfaces A*, 559 (2018), 148–158.

8:15 AM EL06.01.02

Exploring the Chemical Reactivity of Gallium Liquid Metal Nanoparticles in Galvanic Replacement Laia Castilla i Amorós, Dragos Stoian, James R. Pankhurst, Seyedeh Behnaz Varandili and Raffaella Buonsanti; École Polytechnique Fédérale de Lausanne, Switzerland

Liquid metals are an interesting class of materials with fascinating properties deriving from their simultaneous metallic and liquid nature.¹ Besides their use as self-healing contacts in stretchable electronics, shrinking the size of the particles down to the nanoscale adds an extra dimension of complexity which generates new physicochemical properties and opens up new applications. Liquid metal micron- and nano-sized particles are being explored for biomedical applications, chemical sensors, imaging, and batteries. Nevertheless, the knowledge of their chemistry is still very limited compared to other classes of materials. Ga-based nanoparticles (NPs) are the most studied systems so far. Interestingly, Ga NPs have been demonstrated to possess plasmonic properties that are influenced by their size-dependent solid-liquid transition.^{2,3} Along with Ga, Cu is another non-noble metal presenting attracting catalytic and plasmonic behavior.⁴ Yet, the combination of these two metals at the nanoscale has not previously been reported.

In this work, we explore the reactivity of colloidal liquid Ga nanoparticles (NPs) toward a copper molecular precursor to synthesize bimetallic Cu-Ga NPs.⁵ Anisotropic mushroom-shaped Cu-Ga nanodimers, where the two segregated domains of the constituent metals share an interface, form as the reaction product. We combine transmission electron microscopy techniques, ICP elemental analysis, cyclic voltammetry and X-Ray absorption spectroscopy to investigate the formation mechanism of these anisotropic bimetallic nanostructures. We demonstrate that a galvanic replacement reaction (GRR) between the Ga seeds and a copper-amine complex takes place. GRRs are spontaneous electrochemical processes wherein one metallic domain (the sacrificial template) is oxidized by the cations of another metal that possesses a more positive reduction potential, usually resulting in alloyed hollowed structures in crystalline noble-metal systems. We, therefore, attribute the unusual final morphology of the bimetallic NPs to both the presence of the native oxide shell around the Ga NPs and their liquid nature, and we explain the reaction mechanism involving these phenomena. The same reaction scheme was then extended to the synthesis of Ag-Ga and Cu-In NPs, and their final morphologies further supported the above-stated hypothesis.

Based on this understanding, we also demonstrate that sequential GRRs to include more metal domains are possible and trimers including Ag-Cu-Ga were also obtained.

Overall, this first study on colloidal liquid metal NPs as sacrificial templates in GRRs showcases the very intriguing and peculiar reactivity of this class of materials at the nanoscale which has certainly been

underexplored to date. Furthermore, it opens the way toward achieving much more sophisticated and complex structures of Ga-based nanomaterials, which possess promising properties for top-scientific challenges including CO₂ electroreduction, sensing, plasmonics, and self-healing electronics.

1. Daeneke, T. *et al. Chem. Soc. Rev.* **2018**, *47*, 4073–4111.
2. Yarema, M. *et al. J. Am. Chem. Soc.* **2014**, *136*, 12422–12430.
3. Knight, M. W. *et al. ACS Nano* **2015**, *9*, 2049–2060.
4. Chan, G. H. *et al. Nano Lett.* **2007**, *7*, 1947-1952
5. Castilla-Amorós, L. *et al. J. Am. Chem. Soc.* **2020**, Accepted (10.1021/jacs.0c09458)

8:30 AM *EL06.01.03

Metal Chalcohalide Nanocrystals and Their Heterostructures with Halide Perovskite Nanocrystals

Liberato Manna; Istituto Italiano di Tecnologia, Italy

Halide perovskite semiconductors can merge the highly efficient operational principles of conventional inorganic semiconductors with the low temperature solution processability of emerging organic and hybrid materials, offering a promising route towards cheaply generating electricity as well as light. Following a surge of interest in this class of materials, research on the corresponding halide perovskite nanocrystals (NCs) as well has gathered momentum in the last years.¹ Another class of materials that has been recently investigated by us is that of metal chalcohalides. These materials offer a broad solid-state chemistry and they been investigated for applications in solar energy conversion, thermoelectrics, hard radiation detection, and superconductivity. Among them, lead chalcohalides have been rarely studied in the past. We have recently reported the synthesis of a series of lead chalcohalides, by means of colloidal approaches, delivering phases and compositions that had not been previously identified in the bulk.² These materials present indirect band gaps, they emit in the NIR region of the spectrum at cryogenic temperatures and have unique crystal structures. We will also show our recent results on the synthesis and advanced characterization of heterostructured nanocrystals in which one domain is a lead chalcohalide and the other domain is a cesium lead halide perovskite.³ The two domains are separated by a flat, atomically defined, epitaxial interface. In these materials, the photogenerated carriers are separated at their interface, and as such they might be promising in applications ranging from catalysis to photovoltaics.

References

1. Q. Akkerman *et al.* “Genesis, challenges and opportunities for colloidal lead halide perovskite nanocrystals”, *Nat. Mater.* 2018, *17*, 394–405.
2. S. Toso *et al.* “Nanocrystals of Lead Chalcohalides: A Series of Kinetically Trapped Metastable Nanostructures”, *J. Am. Chem. Soc.* 2020, *142*, 22, 10198.
3. S. Toso *et al.* “Halide Perovskite-Lead Chalcohalide Nanocrystal Heterostructures”, under review.

8:55 AM EL06.01.04

Late News: Study of the Surface Plasmon Resonances in Silicon Nanowires with Diameters Less Than 100 nm Giovanni Borgh^{1,2}, Corrado Bongiorno², Antonino La Magna², Giovanni Mannino², Salvatore Patané¹, Jost Adam³ and Rosaria A. Puglisi²; ¹Università degli Studi di Messina, Italy; ²Consiglio Nazionale delle Ricerche, Italy; ³University of Southern Denmark, Denmark

Silicon nanowires (Si-NWs) represent useful building blocks for nanoelectronic devices in many fields such as photovoltaics, photocatalysis, sensing or photodetectors. This is because they show interesting optical properties, including plasmon resonance (PR), the collective oscillation of free electrons, induced by an electromagnetic field at the proper frequency. PR is a versatile phenomenon because it is tunable depending on the intended application by modulating the nanosystem geometry, the medium covering or surrounding it and its shape. It allows, for example, to use Si-NWs to collect and amplify, by several orders of magnitude, radiant energy by generating a locally amplified electric field, a beneficial mechanism in many applications. Till now, however, there are no direct observations neither deep understanding in the literature on PR in Si-NWs. In this talk, the surface plasmon resonances triggered in isolated Si-NWs with diameters below than 100 nm are

visualized at high spatial resolution. We characterize the systems through transmission electron microscopy (TEM) coupled to electron energy loss spectroscopy (EELS) with a subnanometer electron probe. The plasmon behavior of the SiNWs is then modeled through theoretical calculations, and the results are in good agreement with the experimental data. The electrical field spatial distribution generated by the PR is mapped and rationalized. As an extension of our study, we show experimental and modeling data on SiNWs coated with different materials and structures, and we compare the plasmonic behavior to the one of pristine SiNWs.

9:10 AM EL06.01.05

Late News: Regular Self-Assembled Plasmonic Nanoparticle Superlattices—Characterization, Modelling and Applications Mathias Charconnet^{1,2}, Matiyas T. Korsaa³, Søren Petersen³, Luis M. Liz-Marzán^{2,4,5}, Jost Adam³ and Andreas Seifert^{1,4}; ¹CIC nanoGUNE BRTA, Spain; ²CIC biomaGUNE, Basque Research and Technology Alliance (BRTA), Spain; ³University of Southern Denmark, Denmark; ⁴IKERBASQUE, Basque Foundation for Science, Spain; ⁵Centro de Investigación en Red de Bioingeniería, Biomateriales y Nanomedicina(CIBER-BBN), Spain

Noble metal nanoparticles (NPs) are known for their ability to confine visible and near-infrared light at the nanoscale through plasmonic resonances. The plasmonic resonance frequency can be tuned by changing the nanostructure shape, material, or adjacent environment. To extend the features of plasmonic resonances, NPs can be arranged into periodic structures, also called superlattices. Such lattice structures potentially foster inter-particle and inter-cluster interactions through photonic coupling, giving rise to so-called lattice plasmons, which have interesting properties, the potential for high Q factors, strong near-field enhancement, and the potential to be tuned by period, incident angle and polarization. Moreover, the inner structure of a unit cell (cluster) of such periodic arrangement and its homogeneity has a strong influence on the plasmonic response.

Here, we present a self-assembly process that allows us to assemble a controlled number of nanospheres, nanorods or nano triangles into superlattices on large-scale. Capillary forces drive the NP self-assembly, via a nanostructured mold that confines the NPs in periodically arranged wells, yielding NP clusters in a superlattice. The chemical composition of the NP dispersion controls the formation of homogeneous NP superlattices. We studied the impact of homogeneity concerning extinction properties, near-field enhancement and irregularities of superlattices. Further, we demonstrate the generalization of our process regarding different shapes of NPs. The fabrication of superlattices with a defined number of NPs in each cluster allows us to compare their extinction properties, moreover, to study the formation of hybrid plasmonic modes originating from the individual clusters and the lattice.

We support our experimental studies by numerical modelling, thereby calculating the superlattice-induced extinction. To minimize the gap between electromagnetic simulations and experimental characterization, we combine statistical image analysis (based on SEM images of self-assembled clusters), finite-element modelling, and material and structure optimization. To identify the superlattice plasmonic shift for a varying lattice parameter, we analyze the cluster's near-field electromagnetic response, for weighed superpositions of statistically relevant particle arrangements identified by image analysis. Based on statistical analysis, we introduce and superimpose various geometric irregularities in our model, for matching the fabricated superlattice extinction curve, alongside optimization of particle radius, potential shell thickness and refractive index, and particle materials. By Mie theory and colloidal particle measurements, we calibrate our material model and incorporate the results regarding the gap between self-assembled NPs. We demonstrate polarization effects and extinction spectra with respect to variations of aforementioned parameters. As a special case, we additionally show how sensitive the system responds when irregularities are introduced.

Our results, corroborated by electromagnetic simulations and complemented by surface-enhanced Raman scattering (SERS) measurements, provide insight into the near-field enhancement of nanospheres, nanorods and nanotriangles, arranged in sub-wavelength superlattices of macroscopic dimensions, and give rise to new ideas for plasmon-coupled sensing.

9:25 AM *EL06.01.06

Designing Au Nanocrystal Assemblies for Optical Metamaterials Cherie R. Kagan; University of Pennsylvania, United States

We report the use of colloidal Au NCs as building blocks in the design of optical metamaterials. Chemical exchange of the long ligands used in NC synthesis with more compact ligand chemistries brings neighboring NCs into proximity and increases interparticle coupling.^{1,2} This ligand-controlled coupling allows us to tune through a dielectric-to-metal phase transition seen by a 10^{10} range in DC conductivity and a dielectric permittivity ranging from everywhere positive to everywhere negative across the whole range of optical frequencies.¹ For example, by partially exchanging the NC assemblies, we create strong, ultrathin film optical absorbers with a 6x increase in extinction in the infrared compared to that of bulk Au thin films.² For more complete ligand exchange and with thermal annealing, we realize strong optical scatterers useful in the design of optical metamaterials.³ Ligand exchange and annealing of NC films also triggers a large volume shrinkage. By juxtaposing plasmonic NCs and bulk materials, we exploit their different chemical and mechanical properties to transform lithographically-defined two-dimensional structures, upon ligand exchange, into three-dimensional structures.⁴ We use the three-dimensional structures to demonstrate large-area metamaterials with chiroptical responses of ~40% transmission difference between left-hand and right-hand circularly polarized light and that are suitable broadband circular polarizers.⁵

- (1) Fafarman, A. T.; Hong, S.-H.; Caglayan, H.; Ye, X.; Diroll, B. T.; Paik, T.; Engheta, N.; Murray, C. B.; Kagan, C. R. Chemically Tailored Dielectric-to-Metal Transition for the Design of Metamaterials from Nanoimprinted Colloidal Nanocrystals. *Nano Lett.* **2013**, *13* (2), 350–357. <https://doi.org/10.1021/nl303161d>.
- (2) Chen, W.; Guo, J.; Zhao, Q.; Gopalan, P.; Fafarman, A. T.; Keller, A.; Zhang, M.; Wu, Y.; Murray, C. B.; Kagan, C. R. Designing Strong Optical Absorbers *via* Continuous Tuning of Interparticle Interaction in Colloidal Gold Nanocrystal Assemblies. *ACS Nano* **2019**, acsnano.9b02818. <https://doi.org/10.1021/acsnano.9b02818>.
- (3) Chen, W.; Tymchenko, M.; Gopalan, P.; Ye, X.; Wu, Y.; Zhang, M.; Murray, C. B. C. B.; Alu, A.; Kagan, C. R. C. R. Large-Area Nanoimprinted Colloidal Au Nanocrystal-Based Nanoantennas for Ultrathin Polarizing Plasmonic Metasurfaces. *Nano Lett.* **2015**, *15* (8), 5254–5260. <https://doi.org/10.1021/acs.nanolett.5b02647>.
- (4) Zhang, M.; Guo, J.; Yu, Y.; Wu, Y.; Yun, H.; Jishkariani, D.; Chen, W.; Greybush, N. J.; Kübel, C.; Stein, A.; Murray, C. B.; Kagan, C. R.; Kubel, C.; Stein, A.; Murray, C. B.; Kagan, C. R. 3D Nanofabrication via Chemo-Mechanical Transformation of Nanocrystal/Bulk Heterostructures. *Adv. Mat.* **2018**, *30* (22), 1800233. <https://doi.org/10.1002/adma.201800233>.
- (5) Guo, J.; Kim, J.-Y.; Zhang, M.; Wang, H.; Stein, A.; Murray, C. B.; Kotov, N. A.; Kagan, C. R. Chemo- and Thermomechanically Configurable 3D Optical Metamaterials Constructed from Colloidal Nanocrystal Assemblies. *ACS Nano* **2019**, acsnano.9b08452. <https://doi.org/10.1021/acsnano.9b08452>.

9:50 AM DISCUSSION TIME

SESSION EL06.02: Plasmonics II
Session Chairs: Viktoriia Babicheva and Svetlana Neretina
Thursday Morning, April 22, 2021
EL06

10:30 AM *EL06.02.01

Plasmonic Gold Nanorods: Tuning Absolute Dimensions and Properties Catherine J. Murphy; University of Illinois at Urbana-Champaign, United States

Gold nanorods, first made in the mid-late 1990's by several groups, are the quintessential examples of shape-controlled properties at the nanoscale: the aspect ratio of the rods governs the positions of their transverse and longitudinal plasmon bands. The “standard” synthesis, a seed-mediated growth approach in aqueous solution, yields gold nanorods with diameters of 10-15 nm and tunable lengths from 20-80 nm. These standard gold nanorods exhibit corresponding extinction spectra that show a transverse plasmon band at ~520 nm and

longitudinal plasmon bands at ~600-850 nm. Recently our laboratory has expanded its capability to create “mini,” “maxi” and “mega” rods, where the range of aspect ratios are similar, and in some cases beyond, the standard rods. The fundamental absorption and scattering of light by this library of nanomaterials have been measured; and while the general expectation that larger particles scatter more light, and smaller particles absorb more light, is generally held, the details offer some surprises. The smallest nanorods enable surface chemical characterization by NMR; and recent STEM/EELS experiments show that the density of ligands at the ends and sides of the nanorods depends on ligand type and absolute rod dimension.

10:55 AM *EL06.02.02

It's Getting Hot in Here—Design of Thermally Stable Plasmonic Nanocrystals [Sara E. Skrabalak](#); Indiana University Bloomington, United States

Gold and silver nanostructures are common for applications in plasmonics. However, additional metals can be added to bring new function and enhanced properties. Here, the synthesis of branched gold-palladium nanostructures by seed-mediated co-reduction will be discussed. These nanocrystals have localized surface plasmon resonances (LSPRs) that can be tuned throughout the visible and near-infrared through control of particle size, composition, and finer features such as tip sharpness. Significantly, the LSPRs of the branched gold-palladium nanostructures display higher sensitivity to changes in refractive index compared to all-gold analogues. This feature opens up the potential of such materials in LSPR sensor applications. The branched gold-palladium nanostructures also display high structural stability in photothermal applications. Electromagnetic simulations reveal that the Pd content, and specifically its distribution, has a significant impact on optical properties and is an essential criterion for efficient heating. This insight provides new synthetic targets and highlights the importance of developing synthetic methods where the distribution of different metals in multimetallic structures can be precisely controlled.

11:20 AM EL06.02.03

Late News: Plasmonic Nanostructures for Photothermal Conversion [Yadong Yin](#); University of California, Riverside, United States

The plasmonic photothermal effect involves nonradiative conversion of light to heat by plasmonic nanostructures. It has attracted significant attention due to the widespread potential applications in developing energy conversion devices, therapeutic agents, and sensors and actuators. Here we report our recent progress on the design and preparation of plasmonic nanostructures for photothermal conversion. We first introduce the general principle of plasmonic photothermal conversion and then discuss the strategies for improving efficiency, which has been the focus of this field. We then discuss a number of typical application types, such as solar energy harvesting, steam generation, photothermal actuation, and color printing, to elucidate how to tailor the nanomaterials to meet the requirements of these specific applications. In addition to the photothermal effect, other unique physical and chemical properties can be coupled to further explore the application scenarios of plasmonic photothermal materials.

11:35 AM *EL06.02.04

In Situ Tracking Chemical Species at the Catalytically Active Surfaces of Silver Nanocrystals by Spectroscopy Fingerprinting [Dong Qin](#); Georgia Institute of Technology, United States

We report a mechanistic study of the Ag-catalyzed redox reaction between surface-bound nitroaromatic and isocyanide molecules for the production of an aromatic azo compound and isocyanate. We elucidate the mechanistic details by tracking the vibrational bands of all chemical species involved in the reaction through *in situ* surface-enhanced Raman spectroscopy (SERS). In a typical study, we functionalized the surface of Ag nanocubes with 1,4-phenylene diisocyanide (1,4-PDI) and demonstrated their adsorption by analyzing the Ag-bound N-C stretching band ($\nu_{\text{NC(Ag)}}$). When 4-nitrothiophenol (4-NTP) molecules were introduced onto the Ag surface covered with 1,4-PDI, we observed the decrease of the $\nu_{\text{NC(Ag)}}$ band and the appearance of the -NCO stretching band (ν_{NCO}) of isocyanate. Concurrently, we detected the formation of *trans*-4,4'-

dimercaptoazobenzene (*trans*-DMAB) at the expense of 4-NTP by characterizing the vibrational bands of these two species. Because the binding of isocyanide to Ag contributed to the formation of an electron-rich surface through σ donation, the redox reaction could occur when the oxygen atoms of the electron deficient nitro-groups of 4-NTP were extracted by the electron-rich Ag surface and subsequently used to oxidize the isocyanide to isocyanate. The coverage densities of both 1,4-PDI and 4-NTP on the Ag surface had a strong impact on the production of *trans*-DMAB. The redox reaction still took place when 1,4-PDI was replaced with 4,4'-biphenyldiisocyanide, confirming the pivotal role played by the isocyanide group.

SESSION EL06.03: Plasmonics III
Session Chairs: Yogendra Mishra and Svetlana Neretina
Thursday Afternoon, April 22, 2021
EL06

1:00 PM *EL06.03.01

A New Twist on Nanoparticle Assembly—Chiral Plasmonic Nanoparticle Superstructures from Molecular Peptide Precursors Nathaniel Rosi; University of Pittsburgh, United States

Replacing one atom or linkage in an organic molecule or polymer can dramatically affect its structure and properties. Chemists have long leveraged the power of synthesis to adjust and fine tune the properties of molecules and materials. Nanoparticles are a class of fundamental structural and functional building blocks for the construction of new materials. The properties of these materials depend on the size, shape, and composition of the constituent nanoparticles as well as their precise organization within the material. In order to fine tune the properties of the material, we must be able to carefully adjust the organization of its component nanoparticles. We are interested in using the power of synthetic chemistry to program and carefully adjust the structure and properties of hierarchical nanoparticle-based materials. This talk deals with peptide-based methods for controlling the synthesis and assembly of nanoparticles into well-defined chiral helical architectures. It will be demonstrated that the atomic make-up of the peptide constructs can be carefully adjusted and that these subtle yet purposeful modifications lead to significant structural changes to the chiral nanoparticle superstructure assembly and properties.

1:25 PM *EL06.03.02

Plasmon-Mediated Synthesis of Bimetallic Plasmonic-Catalytic Hybrid Nanomaterials Michelle L. Personick; Wesleyan University, United States

Bimetallic nanomaterials composed of a less reactive core metal with a dilute surface coverage of a second, catalytically active metal can exhibit improved catalytic performance resulting from a fine balance of activity and selectivity. Similarly, hybrid nanoparticles with a plasmonic core can be excited by visible light to influence the reactivity or selectivity at atoms or satellites of a more catalytically active metal localized at their surface. In both cases, the differing catalytic reactivity of the two component materials in the solid state is also reflected in differences in the reactivity of their metal salt precursors during nanomaterials synthesis. Our research group has developed a set of versatile synthetic tools for differentially controlling the rates of reduction of metal precursors to facilitate the growth of nanostructures with desired morphologies and surface compositions. Recently, we demonstrated that visible light excitation of a silver core nanostructure can be used to drive the plasmon-assisted reduction of platinum ions—a material that is not plasmonic in the visible region. This plasmon-mediated synthesis relies on the oxidation of a weak reducing agent, sodium citrate, by plasmonic hot holes to generate thermalized electrons that reduce platinum ions at the surface of the silver nanoparticle core. The approach overcomes key challenges in bimetallic nanomaterials synthesis, including accelerating the kinetically slow reduction of one metal precursor while also preventing competing galvanic exchange processes. Tuning of reduction kinetics controls the localization and amount of platinum deposited on the silver cores and

enables the selective generation of silver-platinum core-shell and core-satellite architectures, the latter of which are not accessible using standard thermal synthesis approaches.

1:50 PM *EL06.03.03

Solid State and Materials Chemistry (SSMC) in the Context of NSF's Division of Materials Research

Birgit Schwenzer; National Science Foundation, United States

An overview of the Solid State and Materials Chemistry (SSMC) program will be discussed in the context of the 2019 workshop "Frontiers in hybrid and interfacial materials chemistry research" (workshop report by B. S. Guiton et al., MRS Bulletin, 45(11), 951-964. doi:10.1557/mrs.2020.271). The workshop participants identified interdisciplinary challenges and opportunities as well as current areas of progress in subdisciplines including hybrid synthesis, functional surfaces, and functional interfaces. The scope of the workshop included several research topics beyond the scope of the SSMC program. To address this, the presentation will also briefly describe the other Topical Materials Research Programs (TMRPs) in DMR in addition to showcasing highlight outcomes of some recent research projects supported by SSMC.

2:15 PM *EL06.03.04

Light-Mediated, Directed Placement of DNA Ligands on Gold Nanoparticles Teri W. Odom; Northwestern University, United States

Nanoparticle assemblies show interesting optical properties and show distinct advances in sensing and therapeutics. Short, thiolated DNA strands are common linkers in gold nanoparticle (NP) assemblies; however, the precise placement of different DNA sequences on single NPs is challenging, which limits possible architectures. Moreover, because of the similar physical and chemical properties of different DNA sequences, the uniform gold NP core material makes regiospecific functionalization challenging. This talk will describe a gold NP platform and functionalization process that allows for the spatially-controlled placement of multiple DNA sequences on single NPs. We will discuss how gold nanostars fully conjugated with one DNA sequence can selectively release the DNA from the tips under excitation of fs-pulses at the plasmon wavelength of the branch. Then, we will show how these now bare Au regions can be functionalized with a different thiolated DNA sequence to result in constructs with different DNA strands at specific structural NP features. This selective functionalization can be further exploited to create unique nanoparticle assemblies by hybridization to other DNA-functionalized gold colloids.

2:40 PM EL06.03.05

The Essential Role of Reduction Potential in the Seed-Mediated Synthesis of Gold Bipyramids Dong He^{1,2},

Xing Zhang¹, Bhanu Sharma¹, Thomas Egan¹ and Gang Chen¹; ¹University of Central Florida, United States;

²Jilin University, China

Colloidal synthesis of nanoparticles is a complex process, which is subject to both thermodynamic and kinetic restrictions. Understanding and controlling these thermodynamic and kinetic factors are critical for the reproducible and reliable synthesis of nanoparticles. A common thermodynamic factor is the reduction potential of the reactants, whose role in nano-synthesis is not yet well understood. Here we took the gold bipyramids (GBPs) synthesis as an example to explore the quantitative relationship between reduction potential and synthetic products. For the convenience of comparison, phenol derivatives with similar structure (4-R-phenol) but different standard reduction potential were chosen as reductants, where R is chlorine, hydrogen, methyl, and methyl oxide, respectively. When they were used to reduce gold precursor, their actual reduction potential can be regulated easily through the pH value of the growth solution to study the effect of reduction potential on the products. For each phenol derivative we tested, it was found that there is an appropriate pH range, in which GBPs of high quality were synthesized and their longitudinal LSPR peak red-shifted with the increase of the initial pH value. This pH range is related to the substituent on phenol, those with electron-withdrawing groups are higher while those with electron-donating groups are lower. Although these phenol derivatives work in different pH ranges, the plots of the longitudinal LSPR peak of their resultant products versus the pH are quite

similar. When pH was substituted by the corresponding reduction potential calculated from the Nernst equation, these plots coincide together, meaning that the influence of reduction potential on the formation of GBPs is independent of the specific phenol derivatives (reductants), so the reduction potential is a fundamental factor in the synthesis of GBPs. This role of reduction potential is expected to be general in the synthesis of other types of nanoparticles, which is important not only for understanding the mechanism of nano-synthesis but for improving the reproducibility and reliability of nano-synthesis.

2:55 PM EL06.03.06

Highly Efficient Plasmonic Membrane Activation of Peroxide for Alcohol Oxidation Hao Tang, Guozheng Shao and Bruce Hinds; University of Washington, United States

Many industrial oxidation processes based on peroxide, have a difficulty of over oxidation in homogeneous solution principally due to faster oxidation rates of already oxidized species and high statistical probability of secondary oxidation near the completion of reaction. Ideal for stepwise oxidation is to limit the residence time of target molecule in a reaction zone to allow for single (or quantized) reaction events. This can be achieved in a membrane geometry where catalyst along a pore length and set flow velocity can precisely control residence time for oxidation. It is also known that Au nanoparticles can catalytically activate peroxide under light irradiation due to the formation of concentrated surface plasmon electromagnetic fields and thus hypothesized to be present in nanoporous planes. A plasmonic membrane was synthesized by evaporation of 25nm thick Au films onto pore entrances of anodized aluminum oxide membranes (AAO) with pore diameters of 20-200nm. This allowed solutions of peroxide and sec-phenethyl alcohol to flow through membrane and interact with Au surface plasmon upon exit of the membrane. Under light illumination of 10-100 mW/cm², quantum efficiencies (photon/peroxide radical) above 100% were seen (as high as around 250%), indicating a combination of both field induced activation of peroxide as well as a hot electron injection mechanism. By flowing sec-phenethyl alcohol and peroxide through the optimized Au@AAO system, the controlled single oxidation product of acetophenone was observed demonstrating the promise of the plasmonic flow membrane reactor design.

SESSION EL06.04: Plasmonics IV

Session Chairs: Viktoriia Babicheva and Svetlana Neretina

Thursday Afternoon, April 22, 2021

EL06

4:00 PM *EL06.04.01

Plasmonics for Hot-Electrons and Energy Applications Alexandra Boltasseva; Purdue University, United States

Hot carriers refer to energetic electrons/holes with energy distributions deviated from equilibrium Fermi-Dirac distributions. In metallic nanostructures, hot carriers can be generated from the decay of surface plasmons (SPs), which holds great promise for plasmon-enhanced photocatalysis, solar-energy harvesting devices, etc. One key knowledge needed for developing these applications is the hot-carrier energy distributions (HCEDs). Recently, an effective way to determine HCED experimentally utilizing a scanning tunneling microscope (STM)¹ was reported. With carefully chosen molecules that possess appropriate transmission characteristics between the plasmonic gold film and the gold tip of a STM, single-molecule junctions are created for current-voltage measurements at various voltage bias. The difference in the measured currents for the cases with and without plasmonic excitation reflects the so-called hot-carrier current which enables the direct quantification of HCED.

The knowledge of HCED is of fundamental and practical importance. Hot electrons/holes generated in metallic nanostructures can be transferred/injected to adjacent semiconductors with appropriate band structures for plasmon-enhanced photocatalytic or photovoltaic processes. Gold- and silver-semiconductor heterostructures

are most commonly studied for such applications based on hot electron transfer. In the last few years, titanium nitride (TiN) has been studied as an alternative plasmonic material with optical properties comparable to gold. Its chemical inertness plasmon resonance in the bio-transparent window (750 nm- 900 nm) makes it promising for biophotonic applications. We synthesized TiN@TiO₂ core-shell nanoparticles (NPs) and demonstrate that with the illumination of a 700 nm laser, such NPs efficiently convert free oxygen into singlet oxygen molecules (1O₂) which are key molecules used to kill cancer cells in photodynamic therapy (PDT).² We also show that hot electrons injected from TiN to TiO₂ play a major role in this photocatalytic process and provide an analytical model for evaluating the hot electron injection efficiency. Our study confirms the promise of TiN in hot electron-mediated applications especially in areas of biomedical and therapeutic interest.

Yet another direction that will be covered is a machine learning assisted topology optimization of thermal emitters for far-field thermophotovoltaic (TPV) applications. We have developed a unique optimization framework that allows to significantly speed-up meta-structure design optimization, and allows to significantly increase thermal emission reshaping efficiency of TiN based thermal emitters.³ Specifically, we have demonstrated that ML assisted optimization framework ensures more than 4900-time speed up of thermal emitters design development in comparison with conventionally used topology optimization. The developed thermal emitter design ensures more than 97% thermal emission efficiency.

1. H. Reddy, K. Wang, Z. Kudyshev, L. Zhu, S. Yan, A. Vezzoli, S. J. Higgins, V. Gavini, A. Boltasseva, P. Reddy, V. M. Shalaev, E. Meyhofer, *Science* 369, 6502 (2020).
2. X. Xu, A. Dutta, J. Khurgin, A. Wei, V. M. Shalaev, A. Boltasseva, *Laser Photonics Rev.* 14, 5 (2020).
3. Z. A. Kudyshev, A. V. Kildishev, V. M. Shalaev, A. Boltasseva. *Appl. Phys. Rev.* 7, 2 (2020).

4:25 PM *EL06.04.02

Plasmon-Induced Resonance Energy Transfer for Photoconversion, Sensing and Therapy Nianqiang Wu;
University of Massachusetts Amherst, United States

This talk will discuss the plasmon-induced resonance energy transfer process as the mechanism of energy transfer from plasmonic metals to semiconductors. It will show the effort to develop solar energy conversion devices, biosensors, and therapeutic agents based on this mechanism. This talk will demonstrate some application examples across several relevant fields.

4:50 PM *EL06.04.03

Optical Interaction in Metal and Hybrid Metal-Semiconductor Nanoparticle Assemblies Jing Zhao;
University of Connecticut, United States

Metal nanoparticles exhibit unique size and composition dependent optical properties, known as localized surface plasmon resonance (LSPR). When they assemble into small clusters, the optical coupling between the nanoparticles lead to new plasmonic properties. Specifically, when Ag or Au nanoparticles assemble into dimers and trimers, they exhibit polarization dependent optical spectra due to short range coupling. When they formed randomly arrays, the long-range coupling could result in changes in the LSPR band width and peak position. In addition, when semiconductor quantum dots (QDs) were placed closed to the metal nanoparticle assemblies, the plasmonic feature is altered due to the coupling between the exciton in the QDs and the plasmons. The fluorescence of the QDs changes as well due to this interaction. Under specific conditions, we observed peak splitting in both the dark-field scattering and fluorescence spectra of Au-QD-Au hybrid nanostructures.

5:15 PM *EL06.04.04

Prospect of Silicon Nanoparticles and Au-ZnO Nanowires in Energy and Health Sectors Ateet Dutt;
Universidad Nacional Autónoma de México, Mexico

A significant investigation has been done on understanding and implementing the well-known effect of surface plasmon resonance (SPR) in nanomaterials, and it has opened extensive research possibilities. Our lab has grown different nanomaterials such as Si nanoparticles and hybrid Au-ZnO nanowires to explore their

opportunity in solar cells, water splitting, and chemical/biosensing applications. The aim is to control these nanostructures' size and shape and study their influence on different properties. I will present the embedding of Si nanoparticles in various matrices such as SiO_x, SiN_x, SiO_xCy, and their unique properties for downshifting applications in the third generation of solar cells. Further, I will report the growth of hybrid Au-ZnO nanowires and the associated opportunities in hydrogen production and chemical/biosensing applications.

5:40 PM EL06.04.05

Ultra Efficient Hot Electron Generation with Aluminum Plasmonics: A Radiative Engineering Approach Enabling Photoinactivation of Multi-Drug Resistant Bacteria with Ambient Light Xiangchao Zhu¹, Mingran Liu¹, Michael Trebino², Jin H. Park², Fitnat A. Yildiz² and Ahmet A. Yanik¹; ¹University of California, United States; ²University of California, United States

Widespread misuse and overuse of antimicrobial drugs had led to emergence of multidrug-resistant (MDR) bacteria, placing tremendous pressure and even posing threat on health care worldwide. According to the recently released data by Infectious Diseases Society of America (IDSA), MDR infections are becoming the third leading cause of deaths (~160,000 deaths annually) in the United States. If left unchecked, MDR bacteria caused diseases could kill more people than cancer. Therefore, it is of crucial importance to develop effective antimicrobial approaches to combat bacterial infections, rather than merely relying on identification and development of new classes of antibiotics or antimicrobial agents. Recently, light-activated disinfection (LAD) has emerged as an efficient and efficacious way to eradicate biofilm-mediated microbial infections, advancing conventional concepts and bolstering current prevention efforts of bacterial disinfection. LAD approaches have shown excellent ability to instantaneously photo-inactivate a wide range of microbes and can work synergistically with medical antimicrobial agents. Ultraviolet (UV) germicidal irradiation is among one of most reliable and well-studied LAD-based antimicrobial technologies. It provides rapid and effective inactivation of drug-resistant microorganisms by destroying their nucleic acids and disrupting their DNA, rendering them incapable of reproducing and infecting. However, prolonged UV exposure can pose significant health risks to humans, causing skin cancer and eye damage, thus can only be applied at discrete moments in time (i.e. episodically). Especially for implementing the tool for continuous environmental cleaning activities within the clinical environment, this disinfection method is not suitable for prevention and control of healthcare-associated infections (HAI), which are a significant burden globally with millions of patients affected annually.

Violet-blue 405-nm light is emerging as a safe and cost-effective alternative to UV-based LAD technologies for continuous environmental decontamination since it can be used automatically without any downtime or side effects. Using sophisticated configured light emitting diode (LED) ballistic photons that are non-harmful to humans, this bactericidal visible light possesses outstanding antimicrobial properties against a wide range of bacterial and fungal pathogens. Nevertheless, its photo-inactivation efficiency is still several orders of magnitude lower than that of UV light. Here, we introduce a plasmonic approach enabling rapid (minutes) and extremely efficient (> 99.995%) inactivation of MDR *Vibrio Cholerae* biofilms with 405-nm light. We demonstrate nearly three orders of magnitude improvement in photo-inactivation efficiencies using 405-nm light activated radiatively coupled aluminum plasmonic nanoantenna arrays. We achieve highly effective light-induced local hyperthermia and toxic reactive oxidative species to irreversibly disrupt MDR biofilms. Our technique opens the door to light-activated smart antimicrobial coatings for continuous decontamination in occupied areas, thereby can help infection control practices by preventing mature biofilm development using low-intensity incoherent light.

5:55 PM DISCUSSION TIME

8:15 PM *EL06.05.01

Peptide Induced Chirality in Single Gold Nanoparticle Ki Tae Nam; Seoul National University, Korea (the Republic of)

Chiral structure controlled at nanoscale provides a new route to achieve intriguing optical properties such as polarization control and negative refractive index. However, asymmetric structure control with nanometer precision is difficult to accomplish due to limited resolution and complex processes of conventional methods. In this regard, utilizing chirality transfer occurring at organic-inorganic materials offers viable route to overcome these limitations. Previously we developed a unique synthesis strategy that characteristic of molecule is transferred to gold nanoparticle morphology. Based on the system, here, we demonstrated novel chiral gold nanostructures exploiting chirality transfer between peptide and high-Miller-index gold surfaces.

Enantioselective adsorption of peptides results in unequal development of nanoparticle surface and this asymmetric evolution leads to highly twisted chiral element in single nanoparticle making unprecedented 432 helicoid morphology. The synthesized helicoid nanoparticle showed strong optical activity (dissymmetry factor of 0.2 at 622 nm) which was substantiated by distinct transmittance color change of helicoid solution under polarized light. Modulation of peptide recognition and crystal growth enabled diverse morphological evolution and the structural alterations provided tailored optical response, such as optical activity, handedness, and resonance wavelength. We believe that our peptide directed synthesis strategy offers a truly new paradigm in chiral metamaterial fabrication and will be beneficial in the rational design of chiral nanostructures for use in novel applications.

8:40 PM *EL06.05.02

Plasmonic Nano-Molecules and Nano-Polymers Zhihong Nie; Fudan University, China

Plasmonic nanoparticles (e.g., gold, silver particles) show unique optical properties, such as localized surface plasmon resonance. Organization of plasmonic nanoparticles into discrete nanostructures with precise control allows for fine-tuning their interparticle plasmon coupling and collective properties. The assemblies of plasmonic nanoparticles have shown diverse applications in photonics, sensing, catalysis, and energy harvesting. In this talk, I will present our efforts to the fabrication of discrete plasmonic nanostructures with molecular-like and polymer-like configurations through directional bonding of nanoparticles and the exploitation of the plasmonic properties of the hierarchically assembled nanoparticles.

9:05 PM EL06.05.03

Hygroscopy-Induced Nanoparticle Reshuffling in the Ionic-Gold-Residue-Stabilized Gold Suprananoparticles Sungmoon Choi and Junhua Yu; Seoul National University, Korea (the Republic of)

Stabilization of nanoparticles is usually achieved by either charging the nanoparticle surface (electrostatic stabilization) or capping the nanoparticle surface with ligands (steric stabilization). Because organic capping ligands can also be used to tune the size, morphology, and chemical reactivity of nanoparticles during the nanoparticle formation process, attention has largely focused on how organic molecules influence the growth of nanoparticles.¹⁻² However, the roles of ionic precursors and the influence of their presence in the reaction mixture on their properties have been mostly overlooked. Gold nanoparticles are excellent species for investigating the impact of the ion residue in the reaction solution on the synthesis and properties of gold nanoparticles owing to their good stability and characteristic photophysical properties.³ We used polyethyleneimine (PEI) as the reducing and stabilizing agent for gold nanoparticles and tuned the ratio between PEI and Au(III) to adjust the abundance of gold ions in the nanoparticles. We found that a low level of the elemental gold and the stabilization of gold nanoparticle by an excess of gold ions contributed to the production of ultra-small nearly neutral gold nanoparticles.⁴ The cross-linking between gold

ions/PEI/nanoparticles further led to the assembly of these small gold nanoparticles into suprananoparticles that were stable in water. The hygroscopic Au(III) residues in the suprananoparticles absorbed moisture to form a micro-water pool and subsequently the nanoparticles in the new aqueous solution reshuffled to form larger nanoparticles, resulting in significant changes in their optical properties. This phenomenon was used to formulate a material for a fast, sensitive and straightforward detection of water content in organic solvents. Our results indicate that ionic precursors may play an important role in the formation and stabilization of nanoparticles. Moreover, the ionic residues, regardless of whether they are a part of the nanostructure or impurities, may introduce further characteristics and significantly change the properties of the nanostructure.

References.

1. Personick, M. L., et al., *J. Am. Chem. Soc.* **2013**, *135*, 18238.
2. Rycenga, M., et al., *Chem. Rev.* **2011**, *111*, 3669.
3. Daniel, M. C., et al., *Chem. Rev.* **2004**, *104*, 293.
4. Choi, S., et al., *Nanoscale Advances* **2019**, *1*, 1331.

9:20 PM EL06.05.04

Designing Janus Microspheres with Photonic and Plasmonic Faces for Active Color Pixels Jong Bin Kim¹, Su Yeon Lee², Nam Gi Min¹, Seung Yeol Lee¹ and Shin-Hyun Kim¹; ¹Korea Advanced Institute of Science and Technology, Korea (the Republic of); ²Korea Research Institute of Chemical Technology, Korea (the Republic of)

Nature and humans are inextricably linked to colors, and they adopt nanostructures—not a dye or chemical pigment—to generate nonfading colors that have unique optical properties. The nanostructures are dominantly embodied in two optical phenomena: photonic crystals and plasmonics. Photonic crystals give rise to the selective reflection of certain wavelengths as the periodic nanostructures create photonic bandgap inside the structures. Plasmonic colors happen at the metal surface of which morphology is defined in nanoscale; surface plasmon polariton (SPP) and localized surface plasmon resonance (LSPR) are largely known for the origins of plasmonic resonance. The two colors that have structural origins have great potentials when they are realized in a granular format. The structurally-colored granules serve as aesthetic pigments, microsensors that monitors microenvironment, optical barcodes, and nanoscale blocks constructing macroscopic structures. The granular combination of photonic and plasmonic colors are expected to couple two unique advantages into a single template.

Here, we utilize emulsion drops to create a plasmonically resonant surface on a microsphere with a photonic bandgap inside. The dual-mode Janus microspheres that exhibit plasmonic and photonic colors on the opposite side as a consequence of directional metal deposition. We microfluidically fabricate single emulsions with highly saturated colloids inside and on the interface at the same time, where the 3D crystallized colloids inside the emulsions develop a photonic bandgap, and the 2D crystallized colloids at the surface lead to the plasmonic color. We found the optimal range of suitable nanoparticle diameter for plasmonic colors from aluminum, from gold, and photonic colors to be 300-400, 200-300, and 180-250 nm in this system, respectively. It indicates that there is a limit to independently control the two colors so we adopt double emulsions of which the core and shell have crystallized nanoparticles with different diameters.

For the fabrication of Janus photonic/plasmonic microspheres, we disperse silica nanoparticles in an acrylate polymer, where silica nanoparticles are spontaneously crystallized by repulsive interactions from disjoining pressure. Silica nanoparticles are anchored at the emulsion interface and slowly exposed to the water phase as the emulsions are incubated in water. Also, the distance between nanoparticles becomes shortened with time because the polymer is slowly dissolved into water. The colloidal aging determines the surface nanostructure of the microparticles afterward, which determines plasmonic colors whereas the crystallization inside determines the photonic colors. Silica particles are removed and metal is deposited unidirectionally, which results in a continuous film with periodic pores on the top and metal bowls inside the pores. SPP occurs at the former and LSPR occurs at the latter, two of which are coupled to make plasmonic resonance by the incoming light. When the resonance occurs in the visible range, the surface generates plasmonic colors and longer incubation time blue-shifts the resonant wavelength so that the colors change from blue to purple to red. An incubation time of

emulsions thus changes the nanostructure and it is first to sophisticatedly control plasmonic colors in a granular format including all the rainbow colors. The colors are also adjusted by the metal type, metal thickness, and the relative location on the microspheres with respect to the metal-deposited apex. Finally, the anisotropic location of metal renders the microspheres react to an electric field so that the group of them makes a reflective display. The Janus microspheres are great candidates for microsensors with photonic barcodes, aesthetic colorants for secondary macrostructures, and active pixels for a reflective display.

9:25 PM EL06.05.05

SERS-active Microgels Produced by Simultaneous Photocross-Linking and Photoreduction for Direct Raman Analysis of Pristine Samples Jiwon Yoon¹, Dong Jae Kim¹, Dong-Ho Kim², Sung-Gyu Park² and Shin-Hyun Kim¹; ¹Korea Advanced Institute of Science and Technology, Korea (the Republic of); ²Korea Institute of Materials Science, Korea (the Republic of)

Raman spectroscopy is one of the riveting methods for molecular sensing as it provides noninvasive and label-free molecular identification. However, the intensity of Raman scattering is remarkably low, which makes it challenging to detect the infinitesimal amount of molecules. Metal nanostructures or nanoparticles can localize electromagnetic field on their surface for specific wavelengths of incident light through surface plasmon resonance, which can enhance Raman signal extraordinarily for the molecules near the surface; the phenomenon is referred to as surface-enhanced Raman scattering (SERS). SERS is a key to overcoming the weakness of Raman spectroscopy for molecular detection. However, metals are prone to contamination by adhesives such as protein, resulting in a reduction in Raman signal. Therefore, the pretreatment of samples is unavoidable for Raman analysis because many analytes are complex mixtures of small molecules, proteins, and/or cells. To prevent contamination, hydrogel networks have been employed as a protection layer. The hydrogels allow the infusion of smaller molecules than the mesh size while excluding larger molecules. Therefore, the hydrogel layer with a proper mesh size obviates the need for a time consuming and costly pretreatment, allowing the on-site analysis. One of the simple and practical structures as pretreatment-free SERS-based molecular sensors is metal nanoparticles encapsulated in hydrogel microparticles or microgels. For high Raman intensity and signal reproducibility, metal nanoparticles are required to be homogeneously embedded in the hydrogel matrix at a high concentration without local aggregates. However, it is very challenging to produce such a structure through post-encapsulation of metal nanoparticles due to the low dispersion stability of metal nanoparticles at a high concentration.

Here, we design SERS-active microgels containing a high density of gold nanoparticles through simultaneous photoreduction of gold precursor and photocross-linking of hydrogel precursor. To produce the microgels, the mixture of gold precursor, polyethylene glycol diacrylate (PEGDA), photoinitiator, sodium citrate, and distilled water is emulsified into monodisperse water-in-oil (W/O) emulsion droplets using a microfluidic device. The droplets are irradiated by ultraviolet (UV) for 2 min and incubated at 50°C for 2 days. During the UV irradiation, the photoinitiator is decomposed to form radicals, which cause photoreduction of gold precursors to form gold nanoparticles and photocross-linking of PEGDA to form a hydrogel network. During the thermal treatment, the unreacted gold precursor is reduced in the presence of sodium citrate, forming new gold nanoparticles or promoting the growth of preformed gold nanoparticles. The size and number density of gold nanoparticles formed in the hydrogel matrix strongly depend on the concentration of sodium citrate. The concentration of sodium citrate is optimized according to the intensity of Raman signals of the rhodamine 6G molecule. The microgels made using optimized sodium citrate concentration exhibit high Raman intensity as well as high signal uniformity, indicating high dispersion stability of gold nanoparticles at a high concentration. With the SERS-active microgels, we can detect pyocyanin dissolved in saliva without any sample pretreatment; the pyocyanin is one of the biomarkers for sepsis which is caused by infection of *Pseudomonas aeruginosa*. The limit of detection (LOD) is found to be 100 nM, which is two orders of magnitude lower than the typical concentration in clinical saliva samples of sepsis patients. It is noteworthy that the SERS-active microgels can detect the small molecules in the presence of large adhesives and cells in saliva. We believe that our microgels can be used as a general sensing platform for the on-site detection of small toxic molecules and biomarkers in various samples, including foods, drugs, biological fluids, and many others.

SESSION EL06.06: Spectroscopy
Session Chairs: Viktoriia Babicheva and Svetlana Neretina
Friday Morning, April 23, 2021
EL06

8:00 AM *EL06.06.01

Two-Dimensional Infrared Spectroscopy of Molecules on Metal Nanostructures Lev Chuntonov;
Technion–Israel Institute of Technology, Israel

Conformation and dynamics of small molecules, peptides, and proteins on the surface of metal nanostructures strongly affect the properties and applicability of these materials. However, despite the urgent need in understanding of molecule-surface and surface-induced intermolecular interactions, because of a great complexity of the associated phenomena and limitations of the available analytical methods, in many cases these details still remain elusive. Infrared spectroscopy, and especially its nonlinear two-dimensional variant conducted with sequences of femtosecond laser pulses, 2DIR, is a powerful method to elucidate molecular structure. Recently, the application of 2DIR spectroscopy was extended to studies of molecules on nanostructures. I will present results of our 2DIR experiments with molecules on two different classes of nanostructures: sub-wavelength colloidal silver nanoparticles with sizes of few to few tens of nanometers and half-wavelength gold infrared antennas of micrometer size.

Frequently, molecular organization within the nanoparticle capping layer has highly disordered character. Surprisingly, our 2DIR studies of a small tripeptide glutathione on silver nanoparticles revealed that under favorable conditions the interaction with silver surface leads to formation of highly-ordered intermolecular aggregates, with structure that apparently resembles tightly-stacked β -sheet-like layers wrapping the nanoparticle. This finding may have important implications in situations where ordered structure of the capping layer can impart unique chemical properties to the nanoparticles or can serve as a basis for design of multilayer macromolecular architectures.

In order to boost the sensitivity in 2DIR studies of surface molecules, we use resonant plasmonic infrared nano-antennas. The optical properties of these antennas can be controlled by the design of their size and shape to optimally suit the needs of the advanced nonlinear experiments. Signal enhancements factors of up to 10^5 have been observed, whereas molecular quantum dynamics probed by 2DIR spectroscopy have not been affected by the interaction with plasmonic antennas. Among the direct consequences of signal amplification are dispersive line shapes of the vibrational transitions, competition between the near-field coupling and the radiation damping enhancement mechanisms, and lack of the selectivity of molecular excitation to the laser light polarization, imposed by the surface boundary conditions. Interestingly, we observed that molecules subjected to the enhanced near-field of the plasmonic antennas are excited within the highly non-perturbative excitation regime, even though weak laser pulses are used for the excitation. This result can pave a way towards magnetic resonance-style spectroscopic experiments in the infrared.

8:25 AM *EL06.06.02

Novel Plasmonic Materials, Structures and Applications—A Computational Perspective Jost Adam;
University of Southern Denmark, Denmark

Working with plasmonic materials involves many scientific steps, including, aside from the laboratory-level experiments, the numerical creation, their comparison, and the device fabrication. Besides these challenging steps, the design of new plasmonic materials with unique physical and chemical characteristics, and outstanding optical properties, which are traditional realms of gold and silver, merits an important place. Optimizing the material properties to improve their functionality and performance in plasmonic applications is a subsequent challenge to be tackled, also through iterative feedback from the experiments.

This presentation will demonstrate an overview of recent advances in the computational design of potential future plasmonic materials, such as translational metals, transparent conducting oxides, or plasmonically active semiconductor allotropes, and their application in plasmonic structures, concepts, and devices. The extraction of complex dispersion characteristics from density functional theory (DFT) calculations allows the integration into subsequent electromagnetic modeling steps. This talk will illustrate the panorama of applying the so-developed materials into plasmonic particle investigations, ranging from isolated particles of various shapes and materials to self-assembled regular structures, exhibiting collective plasmonic crystal responses. The applications range from plasmonic sensing, metamaterials, and self-assembled particle clusters for surface-enhanced Raman scattering and catalysis.

The Computational Materials Group at SDU investigates computational pathways, from the first-principles calculation-based molecular design to the three-dimensional multi-physical modeling of plasmonic nanostructures and plasmonically enabled devices for sensing, lighting, and catalysis applications. Our group recently developed the "Photonic Materials Cloud," a cloud-based platform to support streamline the experimental, numerical, research, and education-based work on plasmonic materials. It allows for creating and comparing various material data via various methods and applying them to standard photonic applications, such as nanoparticle scattering and layered thin-film responses. The export of publication-ready graphics and column-based data facilitates its easy integration into a photonic materials science research line.

8:50 AM *EL06.06.03

Strong and Weak Vibrational Coupling in Metal Nanostructures Studied by Ultrafast Microscopy Greg Hartland¹ and Kuai Yu²; ¹University of Notre Dame, United States; ²Shenzhen University, China

The rapid heating induced by ultrafast excitation of metal nanostructures coherently excites the breathing vibrational modes of the structure. Detailed information about these modes can be obtained by studying single nanoparticles with transient absorption microscopy. However, in single particle experiments the breathing modes are usually heavily damped by radiation losses into the substrate. Recently we discovered that using low density substrates drastically reduces radiation losses and creates very high vibrational quality factors for gold nanoplates. This allows several new phenomena to be explored, including strong vibrational coupling between stacked nanoplates, and new vibrational modes that correspond to motion of the nanoplates relative to the substrate and, for the stacked nanoplates, relative to each other. The results from these experiments will be described in this talk, along with studies of mass loading effects for the nanoplates. In the mass loading experiments a localized change in vibrational frequency is observed when a particle is adsorbed onto the surface of a nanoplate. This is an unusual result, as the breathing modes of the nanoplates are normal modes that are spread out over the entire plate. This implies that the adsorbed mass hybridizes the normal modes. Insight into this effect is obtained from finite element simulations that model the vibrational modes of the coupled system.

9:15 AM EL06.06.04

Late News: Versatile Nanomasks for Fabrication of Plasmonic Resonators Aleksandra Szymanska, Mihai Suster and Piotr Wrobel; Faculty of Physics, University of Warsaw, Poland

Over the years, tremendous advances have been made in the design and fabrication of nano-size objects in a variety of geometries. Nanosphere Lithography is a large-area nanostructurization technique introduced in the early 80s which utilizes dielectric nanospheres for the preparation of nanoapertures or nanoparticles formed in the gaps between the nanospheres. The process is cost-effective and easily scalable, therefore it is often chosen in favor of expensive and time-consuming electron lithography or low-resolution photolithography.

In this report, we describe a simple method of preparing versatile plasmonic nanomasks based on electrostatic-driven assembly of silica nanoparticles (SNPs) of diameters ranging from 60 to 300 nm. This technique makes it possible to produce homogenous masks of uniform apertures on bare or PMMA-coated glass substrates covering an area of a few cm². Fabricating different nanomasks starting from single holes, through dimers or

trimers, up to long, nanowire-like apertures is possible due to a high degree of control of the sizes and concentrations of the SNPs, as well as of the temperature during the process. In combination with physical vapor deposition of metals, such as silver or gold, the masks can be used further as platforms for obtaining many different plasmonic nanostructures like discs, cones, dimers, or even more sophisticated shapes by simply changing the evaporation angle. Such plasmonic resonators are very suitable for SERS, photovoltaic and biosensing applications because of their high tunability stemming from a number of degrees of freedom within the described method of fabrication.

9:30 AM EL06.06.05

Coupling and Rabi Splitting of Plasmonic Modes in Nanopillar Array Dominic Bosomtwi, Marek Osinski and Viktoriia Babicheva; The University of New Mexico, United States

High light field enhancement and its nanoscale confinement in plasmonic nanostructures facilitate stronger light-matter interaction, including spontaneous emission rate, nonlinear response, light absorption, and so on. Plasmonic metasurfaces are two-dimensional nanoantennas arrays enabling subwavelength field localization. Because of the nanoscale light confinement, the metasurfaces provide an exceptional ability to manipulate light accompanied by unique spectral features, including high quality factor resonances.

We design the plasmonic metasurface that consists of multi-segment silver-silicon nanopillars, and we analyze the multiple mode excitations in this nanopillar array. The effect is similar to the excitations of multiple plasmonic modes at the complex interfaces of multilayer metal and dielectric structure. We numerically study the spectral response of a single and paired nanopillars in the unit cell of the periodic array [1]. Because of the hybrid silver-silicon multilayer design, we can realize Fano resonances and Rabi splitting in the metasurface's spectral response.

The study's emphasis has been placed on the analysis of bright and dark modes excited in the nanopillar array. Mode interplay and coupling give rise to asymmetric spectral profiles in often referred to as Fano resonances. Strong coupling between plasmonic states causes the energy levels to repel by splitting, and because of the mode coupling facilitated by the lattice, we observe their Rabi splitting.

The effects of multiple mode excitations and their Rabi splitting facilitated by the lattice can also be observed in another spectral range providing all parameters of the structure are scaled proportionally. However, it also imposes requirements on material properties in the spectral range of interest. In this case, a common condition for the observation of plasmonic resonances needs to be satisfied, and in particular, the real part of permittivity of the metal-like material should be comparable in magnitude to the semiconductor permittivity.

Support from the Navy HBCU-MI program under the grant N00014-18-1-2739 and the Office of Naval Research under the grant N00014-19-1-2117 is gratefully acknowledged.

[1] D. Bosomtwi, M. Osinski, and V. E. Babicheva, "Mode Coupling and Rabi Splitting in Transdimensional Photonic Lattices," *2020 IEEE 20th International Conference on Nanotechnology (IEEE-NANO)*, pp. 107-110 (2020).

9:45 AM EL06.06.06

Deep Learning Analysis of Vibrational Spectra of Bacterial Lysate for Rapid Antimicrobial Susceptibility Testing Regina Ragan; University of California, Irvine, United States

Even in the 21st century, bacterial infections are still treated empirically. Antibiotics are prescribed preemptively, because a proper diagnosis relies on culture growth which takes a day or more and can delay patient treatment, increasing morbidity. Yet the unnecessary administration of powerful, broad-spectrum antibiotics leads to the proliferation of antibiotic resistance. A bioinspired sensing platform, composed of 2-dimensional physically activated chemically (2PAC) assembled surface enhanced Raman scattering (SERS) sensors coupled with machine learning (ML) algorithms, has been developed for rapid phenotypic antibiotic

susceptibility tests (AST). This platform provides new diagnostic tools for antibiotic stewardship, complementing existing genomic tests that only provide feedback on known antimicrobial resistance mechanisms. Just as one can smell the difference between coffee and chocolate amongst multiple odors, SERS+ML rapidly measures and classifies spectral features of bacterial metabolite signatures in response to antibiotics, which are correlated with antibiotic lethality mechanisms. As individual odor receptors are incapable of identifying odorant molecules, so are individual SERS spectra unable to differentiate in a complex background.

SERS + ML is an exciting nascent area where some recent work using vector machines and artificial neural networks has greatly improved concentration predictions from SERS data. However, this is a longstanding challenge to produce large, high quality and reproducible data sets are needed for any ML analysis with SERS. Since the nanogap distance between gold nanospheres determines performance in SERS devices, small variations on the order of angstroms lead to large signal variations. 2PAC is low-cost, scalable, and reproducible chemical assembly method able to control of sub-nm nanogaps and is capable of reproducibly probing individual molecules over mm^2 areas. An implemented CNN regression model trained on SERS data of Rhodamine 800 resulted in limits of detection (LOD) and quantification (LOQ) of 10 fM ($\sim 10^{-5}$ ng/mL) with prediction accuracy (r^2 value) of 0.96 over a dynamic range of 6 orders of magnitude.

In order to reduce the time required for phenotypic AST, we present a metabolomics approach rather than direct measurement of cell growth or viability to detect phenotypic susceptibility or resistance to antibiotics. Yet there is an important price to pay to reduce AST time in this way: metabolomics approaches introduce an enormous parameter space. Consider that the *E. coli* metabolome contains over 2600 different metabolites. Nevertheless, SERS + ML allows for a fingerprinting approach to handle the complex data. Analysis of SERS data using a generative model, the variational autoencoder (VAE), is able to identify spectral features associated with molecular fingerprints in the cell lysate data associated with antibiotic efficacy. The high interpretability of the VAE generated SERS spectra allows us to identify useful vibrational information which guides additional targeted data collection to improve classification accuracy. Culture-free and easily acquired datasets of bacterial metabolites in aqueous solution can be leveraged to improve predictive models of complex metabolite response of bacterial communities and is one of the most significant advantages of using a generative model. Greater than 99% accuracy is achieved with unsupervised Bayesian Gaussian Mixture analysis when using data informed transfer learning with only a few training examples. Our results show differentiation of bacterial populations of ESKAPE pathogens based on antibiotic susceptibility in 10 min when using SERS + ML. This enormously reduces the amount of time needed to validate phenotypic AST with conventional growth assays and outlines a promising approach towards practical SERS AST.

SESSION EL06.07: Plasmonic Applications
Session Chairs: Viktoriia Babicheva and Yogendra Mishra
Friday Morning, April 23, 2021
EL06

11:45 AM EL06.07.01

Colloidal Nanoparticle Clusters for Efficient Conversion of Light to Chemical Energy Seunghoon Lee;
Ludwig-Maximilians-Universität München, Germany

The assembly of plasmonic metal nanostructures can efficiently merge the reactivity and energy harvesting abilities with enhanced plasmonic performance for visible light photocatalysis. Here we explore the influence of the presence of electromagnetic hotspots in the ability of plasmonic colloidal structures to induce efficient energy transfer for plasmonic catalysis. We report a novel synthetic strategy for the fabrication of colloidally assembled nanoparticles (NPs) in aqueous solution through fine controlled galvanic replacement between Ag nanoprisms and Au precursors.¹⁻⁵ Colloidally assembled nanostructures, e.g. Au particle-in-a frame and bimetallic assembled Au@M (M=Pd, Pt) nanostructures with catalytically active metals, exhibited superior

performance over their constituent nanostructure counterparts in plasmonic sensing, surface-enhanced Raman scattering (SERS), and plasmonic catalysis.¹⁻⁴ Recently, we successfully synthesize colloidal Au and Au@M (M=Pt, Pd) NP trimers with remarkable structural stability in various solutions.¹ These model systems allow us to study the synergy effect of hot spots and bimetallic composition in plasmonic catalysis. Our computational and experimental results highlight the synergy effect of geometry and composition of plasmonic catalysts in plasmon-driven chemical reactions. The plasmonic properties of NP trimers show that core-shell bimetallic NPs with hot spots can induce efficient light-to-chemical energy conversion as an increment of non-radiative plasmon decay to the catalyst surface. We monitored the plasmon-mediated reduction of 4-nitrobenzenethiol (4-NBT) using SERS for studying hot electron-induced chemical conversion. Core-shell bimetallic NP trimers show distinguishable photo-induced reduction of 4-NBT compared to their monomer or monometallic counterparts due to their efficient energy transfer. We expect that the present study can provide a new direction for the development of efficient photocatalysts.

References

1. **S. Lee**, H. Hwang, W. Lee, D. Scherbarchov, Y. Wy, J. Grand, B. Auguie, D. H. Wi, E. Cortés,* S. W. Han,* "Core-shell bimetallic nanoparticle trimers for efficient light to chemical energy conversion" (Just accepted in ACS Energy Letters).
2. **S. Lee**, J. Kim, H. Yang, E. Cortés, S. Kang, S. W. Han,* "Particle-in-a-Frame nanostructures with interior nanogaps" (Angew. Chem. Int. Ed. 2019, 58(44), 15890-15894).
3. Y. Wy, **S. Lee**, D. H. Wi, S. W. Han,* "Colloidal clusters of bimetallic core-shell nanoparticles for enhanced sensing of hydrogen in aqueous solution" (Part. Part. Syst. Charact. 2018, 35(5), 1700380).
4. **S. Lee**, Y. Wy, Y. W. Lee, K. Ham, S. W. Han,* "Core-shell nanoparticle clusters enable synergistic integration of plasmonic and catalytic functions in a single platform" (Small, 2017, 13(43), 1701633).
5. **S. Lee**, J. W. Hong, S.-U. Lee, Y. W. Lee, S. W. Han,* "The controlled synthesis of plasmonic nanoparticle clusters for efficient surface-enhanced Raman scattering platforms" (Chem. Commun. 2015, 51(42), 8793-8796).

12:00 PM *EL06.07.02

Macroscopically-Expanded 3D Nanostructures for High Brightness Illumination Applications Fabian Schuett¹, Maximilian Zapf², Lena M. Saure¹, Jürgen Carstensen¹, Carsten Ronning² and Rainer Adelung¹; ¹Kiel University, Germany; ²Institute for Solid State Physics, Germany

Laser diodes (LDs) are regarded as the next generation of ultra-efficient light sources, being able to produce more photons at high power densities than conventional light-emitting diodes.^[1] Even though most state-of-the-art technologies are based on a blue LD pumping a white-light-emitting phosphor, an all-laser wavelength mixing approach, e.g. a combination of three (RGB) or even four (RGBY) laser wavelengths would outperform the efficiency of any other known white-light source.^[2] However, in illumination applications, laser-based lighting systems still suffer from their monochromatic, low-divergent, and coherent nature, which demands a new generation of extremely efficient and versatile optical diffusers based on disordered nanostructured materials.^[2] In the here presented study, we demonstrate a macroscopically expanded, three-dimensional (3D) laser light diffuser based on a highly porous (>99.99%) nanoarchitecture, composed of interconnected hollow hexagonal boron nitride (h-BN) microtubes, with a wall thickness below 25 nm. The 3D hollow h-BN microtubular framework structure is synthesized by a novel template approach, which is based on a highly porous ceramic network consisting of tetrapodal-shaped microparticles.^[3] The synthesis results in a disordered and non-absorbing photonic network with thinly spread Rayleigh-type scattering centers, based on a combination of feature sizes greater than, equal to, and well below the magnitude of the impinging wavelength.^[4] With densities close to that of air, these aero-materials basically resemble an artificial solid fog, but with a defined hierarchical internal structure. This enables an isotropic 3D light distribution from energetic, highly directional, as well as coherent laser light, with speckle contrasts well below the human sensitivity limit. In combination with the excellent heat management of the 3D h-BN exceptionally high laser damage thresholds can be reached, enabling the usage of these aero-materials for high brightness illumination applications. Functionalization of these structures with photoactive materials will additionally open new fundamental

research prospects in the field of disordered photonics, including 3D plasmonic systems, random lasing, up/down conversion, and other non-linear optical effects.

References:

- [1] Laser & Photonics Reviews 7, **2013**, 963–993
- [2] Optics Express 19, **2011**, A982-90
- [3] Nature Communications 8, **2017**, 1215
- [4] Nature Communications 11, **2020**, 1437

*Corresponding Author: fas@tf.uni-kiel.de

12:25 PM *EL06.07.03

Plasmonic Nanoparticles with Unique Structures for Biosensing Xiaohu Xia; University of Central Florida, United States

Nanoparticles of gold and silver have been widely used in biosensing due to their fascinating plasmonic properties. Most of previously reported gold and silver nanoparticles are solid particles. Our recent studies showed that gold-silver alloyed nanoparticles with hollow interiors possess unique plasmonic properties that make them particularly suitable for biosensing applications. In the first part of this talk, I will introduce our new strategy to craft hollow gold-silver nanoparticles with unique physical and chemical parameters. Rational design and chemical synthesis of the nanostructures will be specified. In the second part, I will discuss the application of these hollow plasmonic nanostructures in biosensing. Examples of in vitro diagnostics of disease biomarkers will be highlighted.

12:50 PM *EL06.07.04

Photochemistry on Quantum-Sized Metal Nanoparticles Yugang Sun; Temple University, United States

The incompatibility of solar energy and the light absorption band of a chemical bond prevents the use of light to activate the chemical bond for interesting chemical reactions directly. This presentation will focus on a strategy that enables the efficient coupling of photon energy into chemical bonds to selectively promote the desired chemical reactions. The strategy relies on the excitation of hot electrons in quantum-sized metal nanoparticles (QSMNPs, with size in the range of 2 ~10 nm) upon photo-illumination and the following efficient injection of the hot electrons into specific chemical bonds. The redistribution of hot electrons in the chemical bonds dissipates the kinetic energy of hot electrons to the chemical bonds, activating the chemical bonds to promote the target chemical reactions. These sequential processes occur in a confined space, representing a series of quantum transitions, i) optical-to-electronic transition in quantum-sized metal nanoparticles (i.e., hot electron generation), ii) electronic-to-electrical transition at the nanoparticle/adsorbate interface (i.e., hot electron injection), and iii) electrical-to-electronic transition in adsorbate molecules (i.e., chemical bond activation). Selective oxidation of alcohols to aldehydes rather than ketones/acids, a class of important chemical reactions for many industrial processes (e.g., esterification), will be used as an example to highlight the use of QSMNPs for photo-driven selective chemical transformation on platinum group metal (PMG) nanoparticle catalysts, which do not exhibit strong optical absorption.

1:15 PM EL06.07.05

All-Gas Phase Plasma Synthesis of Plasmonic Zirconium Nitride for Advanced Photochemistry Applications Chris Rudnicki, Alejandro Alvarez, Stephen Exarhos, Carla Berroscope Rodriguez and Lorenzo Mangolini; University of California, Riverside, United States

Plasmonic nanomaterials interact strongly with light, and as a consequence there are of great interest in a broad variety of fields, such as photocatalysis, photochemistry, biophotonics, sensing, and wave-guiding. We present a novel technique for the synthesis of plasmonic zirconium nitride (ZrN) nanoparticles using a scalable non-thermal plasma process.¹ Cost, production concerns and most importantly thermal and chemical stability

motivate the search for alternative plasmonic materials to gold and silver², like Group IV transition metal-nitrides³ such as TiN⁴ and the relatively unexplored ZrN. Our ZrN nanoparticles display a plasmonic peak around 620 nm and from XRD and TEM we infer the crystallinity of the particles to be a cubic rock salt structure and a tunable size distribution below 10 nm. An attractive application of these plasmonic particles is the reduction of metals like platinum and chromium (VI) species in water which are extremely toxic.⁵ Here we have provided evidence of plasmon-driven photocatalytic activity within visible wavelengths to reduce platinum ions in solution.⁶ An aqueous solution of ZrN, methanol, and chloroplatinic acid (H₂PtCl₆) was illuminated using a monochromator to spectrally select wavelengths in the visible regime. Energy dispersive X-ray spectroscopy (EDS) was then used to determine the ratio of reduced platinum to zirconium at a given wavelength. A similar method was used to reduce Chromium (VI), a carcinogen commonly found in water, except we use the diphenyl carbazide method to determine the amount of Chromium (VI) in solution before and after exposing it to light. We then spectrally select visible wavelengths to compare the quantum yields of Chromium (VI) reduction between our synthesized ZrN and commonly used TiO₂ nanoparticles. We are able to achieve a quantum yield of up to 1.50% reducing Chromium (VI) to Chromium (III) using visible wavelengths, providing convincing evidence of photocatalytic response in this class of alternative plasmonic materials.

[1] Stephen Exarhos, Alejandro Alvarez-Barragan, Ece Aytan, Alexander A. Balandin, and Lorenzo Mangolini, Plasmonic Core–Shell Zirconium Nitride– Silicon Oxynitride Nanoparticles, *ACS Energy Letters*, 3 (10), 2349–2356, 2018.

[2] Naik, G. V., Shalaev, V. M., & Boltasseva, A. Alternative plasmonic materials: Beyond gold and silver. *Advanced Materials*, 25(24), 3264–3294, 2013.

[3] Guler, U., Shalaev, V. M., & Boltasseva, A. Nanoparticle plasmonics : going practical with transition metal nitrides. *Biochemical Pharmacology*, 18(4), 227–237, 2015.

[4] A. Alvarez Barragan, N. V. Ilawe, L. Zhong, B. M. Wong, and L. Mangolini, “A Non-Thermal Plasma Route to Plasmonic TiN Nanoparticles,” *J. Phys. Chem. C*, 121(4), 2316–2322, 2017.

[5] M. Valari, A. Antoniadis, D. Mantzavinos, and I. Poulios, “Photocatalytic reduction of Cr(VI) over titania suspensions,” *Catal. Today*, vol. 252, pp. 190–194, 2015.

[6] Barragan, A. A., Hanukovich, S., Bozhilov, K., Yamijala, S. S. R. K. C., Wong, B. M., Christopher, P., & Mangolini, L. Photochemistry of Plasmonic Titanium Nitride Nanocrystals. *Journal of Physical Chemistry C*, 123(35), 21796–21804, 2019.

1:30 PM DISCUSSION TIME

SYMPOSIUM EL07

Bioelectronics—Fundamentals and Applications
April 14 - April 22, 2021

Symposium Organizers

Tzahi Cohen-Karni, Carnegie Mellon University
Guosong Hong, Stanford University
Sahika Inal, King Abdullah University of Science and Technology
Jonathan Rivnay, Northwestern University

* Invited Paper

SESSION EL07.01: Neurotechnology I
Session Chairs: Tzahi Cohen-Karni, Sahika Inal and Jonathan Rivnay
Wednesday Morning, April 21, 2021
EL07

8:00 AM *EL07.03.03

A Look at Nonlinear Optic Polymers in Bioelectronics and Beyond Kaitlyn E. Crawford; University of Central Florida, United States

Bioelectronics, the integration of biology with electronics, encompasses sub-topics such as bioimaging, and transduction or actuation of biochemical or physiochemical signals using wearable or implantable devices. One component that these sub-topics have in common is the generation of large amounts of data, which feeds into Big Data. With Big Data comes emerging areas of AI-ML, data mining, deep learning, and neural networks. While bioelectronic topics and complementary disciplines are receiving significant attention, there is at least one other topic to consider: How to handle the transmission and storage of such large volumes of data? Copper wire is the traditional material to transmit information, but the theoretical speed and volume limits, at which electrons can travel through copper wire, are near capacity and cannot accommodate the projected global data demands. Compelling solutions using fiber optic cables are on the horizon as, compared to copper, they can handle 6000x the bandwidth, are of lower cost, lighter weight, and maintain lower temperatures. A bottleneck, however, for replacing copper with fiber optics cables, on the scale necessary to sustain our data transmission and storage needs, is the limited availability of nonlinear optic (NLO) materials that are necessary for optical modulation – which operate similar to the “on-off” modulation in electronics for coding information using 0s and 1s. Beyond optical modulators, NLOs also find broad application in areas such as: imaging, (bio)sensors, and terahertz spectroscopy. NLO materials are either inorganic such as lithium niobate, or organic such as electro optic polymers, wherein an asymmetric chromophore is combined with a glassy, amorphous polymer. *This talk will cover the development and characterization of a new family of easy to synthesize, stable, asymmetric chromophores, and their subsequent use in electro optic polymers for in demand, NLO modulator and sensing applications.*

8:25 AM EL07.01.02

Multi-Dimensional Fuzzy Graphene Bioelectronic Actuators Raghav Garg, Daniel San Roman, Yingqiao Wang and Tzahi Cohen-Karni; Carnegie Mellon University, United States

The ability to manipulate the electrophysiology of electrically active cells and tissues has enabled a deeper understanding of healthy and diseased states. This has primarily been achieved via bioelectronic actuators that interface engineered materials with biological entities. Graphene has gained recent interest as a building-block for bioelectronic actuators due to its advantageous electrochemical properties and biocompatibility. However, functional graphene bioelectronics exhibit a two-dimensional (2D) topology. This leads to inherent performance limitations due to the limited exposed surface-area and poor interactions with interfaced cells and tissues. Ideal geometry of graphene-based actuators needs to leverage the material’s high surface-area-to-volume ratio to facilitate maximum interaction with the electrode.

Here we report a breakthrough three-dimensional (3D) topology of graphene: 3D fuzzy graphene (3DFG), for actuation of electrically active cells and tissues. Using a bottom-up approach, we synthesize an interconnected network of free-standing graphene flakes. The 3D topology leads to enhanced surface-area compared to planar surfaces allowing 3DFG microelectrodes to exhibit lower electrode impedance than planar microelectrodes. 3DFG also exhibits greater cathodic charge storage capacity (CSC_C) and charge injection capacity (CIC). We further combine one-dimensional (1D) Si nanowires (NWs) with 3DFG to fabricate a truly 3D topology of graphene: NW-template 3D fuzzy graphene (NT-3DFG). The increased surface-area of NT-3DFG enhances the exhibited CSC_C and CIC. This enables miniaturization of graphene-based microelectrodes to ultra-microelectrodes for functional bioelectronics. Our results demonstrate the importance of extending the topology

of nanomaterials to 3D to push the physical and functional limits of conventional bioelectronics.

8:40 AM *EL07.01.03

Implantable Bioelectronics George Malliaras; University of Cambridge, United Kingdom

One of the most important scientific and technological frontiers of our time is the interfacing of electronics with the human brain. This endeavour promises to help understand how the brain works and deliver new tools for diagnosis and treatment of pathologies including epilepsy, Parkinson's disease, and brain cancer. Current solutions, however, are limited by the materials that are brought in contact with the tissue and transduce signals across the biotic/abiotic interface. Using novel organic materials coupled with thin substrates we make implants that are biocompatible and show exceptional performance in multimodal recordings and stimulation of the brain. I will outline examples of devices that simultaneously monitor the electrical and metabolic activity of the brain, and devices that locally deliver drugs with excellent spatiotemporal control. I will further discuss how the interface with soft robotics can enable devices that change shape and thereby decrease the invasiveness of neurosurgery.

9:05 AM EL07.01.04

Biological Modulation from Micro-Supercapacitor-Like Mesoporous Carbon Membranes Aleksander Prominski^{1,1,2} and Bozhi Tian^{1,1,2}; ¹The University of Chicago, United States; ²University of Chicago, United States

Electrical stimulation devices find numerous therapeutic applications, such as in the treatment of heart defects, epilepsy, and Parkinson's diseases. It is critical to search for new materials and methods to make these treatments safe and affordable to everyone in need. Design of bioelectronic devices requires materials with mechanical and electrochemical compliance to the cells and tissues to minimize their invasiveness. Recently, carbon nanostructures have been studied as bioelectronics components due to their excellent electrical and mechanical properties and the past success in energy research. Nevertheless, there is still a strong need to advance synthetic methods for the fabrication of cost-effective and safe carbon-based bioelectronics.

In this presentation, I will first discuss the synthesis of hierarchical meso- and macroporous carbon membranes using micelle-assisted self-assembly, as well as the fabrication of binder-free carbon-based microelectrode arrays using SU-8 as flexible support. The material design allows us to optimize its mechanical compliance and to leverage its biocompatible electrochemical properties for efficient biological stimulations. Inspired by micro-supercapacitors used in energy research, we explored the application of a comb-like interdigitated electrode design for *in vitro* stimulation and training of cells. For example, we applied the confined electric field to cardiomyocyte monolayer and achieved efficient overdrive pacing and subthreshold levels of training *in vitro*. We also explored the stimulation of retina and heart *ex vivo* and stimulation of a sciatic nerve *in vivo*, demonstrating efficient coupling between the carbon nanostructures and excitable tissues. Our results illustrate a promise of applying porous carbon materials for biological modulation and how traditional energy research tools can be adapted to design bioelectronic systems.

9:20 AM *EL07.01.05

Multiscale Bioelectronics from Liquid-Phase Processing of Nanoscale Carbides Flavia Vitale; University of Pennsylvania, United States

Bioelectronic technologies are enabling paradigm-shifting approaches to diagnosing and treating a number of disorders of the central and peripheral nervous systems. While tremendous progress has been made in the last decade, current bioelectronic interfaces are still dramatically inadequate to address the mechanical, chemical, and electrical properties of nervous structures. Nanostructured carbon materials are uniquely positioned to address these challenges, as they combine remarkable electronic and electrochemical properties, with intrinsically high mass-specific surface area and mechanical flexibility. Furthermore, they can be easily integrated within scalable solution-based processing, thus allowing easy modulation of their electronic,

mechanical, and optical properties.

In this talk, I will discuss how nanoscale soft conductors can be engineered into high-resolution, minimally invasive bioelectronic interfaces designed to seamlessly map and control the activity of excitable circuits at multiple scales. Specifically, I will introduce novel bioelectronic interfaces based on 2D transition metal carbides (a.k.a. MXenes) for recording and stimulation. I will discuss the fundamental electronic and electrochemical behavior of MXenes as well as present scalable liquid-phase processes to translate the remarkable molecular properties into high-resolution interfaces with customizable scale and coverage. Finally, I will present examples of applications in multiscale mapping and microstimulation of bioelectrical circuits *in vivo* in different models.

SESSION EL07.02: Poster Session I

Session Chairs: Tzahi Cohen-Karni, Guosong Hong, Sahika Inal and Jonathan Rivnay

Wednesday Morning, April 21, 2021

11:45 AM - 1:45 PM

EL07

EL07.02.01

Late News: Graphene Based Nanopore Sequencing—An Assessment on the Current State of Next Gen Sequencing Samuel Escobar, [Kiara Gonzalez-Gonzalez](#), Marcel Grau, Solimar Collazo Hernandez, Ernesto Espada, Brad Weiner and Gerardo Morell; University of Puerto Rico at Río Piedras, Puerto Rico

Using solid-state nanopores to sequence DNA is a promising third generation sequencing method. Graphene is used because it can provide a suitable membrane for sequencing applications. Sequencing DNA with graphene nanopores is a topic of interest for many researchers, but how does it work? As the DNA molecule passes through the nanopore, the nanopore will eventually be blocked by the negatively charged DNA molecule. Each nucleotide has presented a distinct current blockage signal as it interacts with the nanopore via the formation of temporary Van der Waals interactions. Therefore, the differentiation of each base is possible since we can observe different sources reporting distinct ionic currents for each nucleotide. It is by this principle that the DNA is sequenced. Here, we present how Graphene Nanopores could be ideal for DNA Sequencing by taking into consideration many factors that may help overcome the challenges that have been found within this method. These factors include: the functionalization - whether it is hydrogen functionalization, hydroxyl functionalization, or nitrogen functionalization - of the graphene, the number of graphene layers needed, the type of nanopore used, type of DNA, among others. All these variables have to be taken into consideration in order to obtain single-base resolution with all the advantages that graphene-nanopore sequencing has to offer.

EL07.02.02

Bioresorbable Primary Battery Built on Core-Double-Shell Zinc Microparticle Networks [Yutao Dong](#), Jun Li and Xudong Wang; University of Wisconsin–Madison, United States

Bioresorbable electronics, which decomposed in the physiological environment after a designed period of stable function and corresponding byproducts are resorbed and vanish, have gained increasing interests in state-of-the-art biomedical implants for pre-diagnosis, monitoring and treatment of diseases, drug delivery which only requires the function for a certain period of time. [1,2] Compared to other transient power supplies, such as piezoelectric nanogenerators, supercapacitors, bioresorbable batteries are promising power source with higher energy density and continuous output which typically are composed of bioresorbable material that degrade into non-toxic contents in physiological environment during and/or after discharge. State-of-the-art bioresorbable batteries are built upon Mg or Zn metal-based galvanic cells due to their good biosafety and electrochemical activity. Due to extreme high chemical activity of Mg, current Mg-based bioresorbable batteries all exhibited fluctuating voltage output and rapid output drops without a controllable lifetime, which cannot meet the

requirements of an implantable power supply. Additionally, the fast degradation rate could induce localized releasing of concentrated hydroxyl ions, leading to inflammation or other harmful effects. [3] Compared to Mg, Zn metal has moderate degradation rate which can circumvent undesirable local pH increase and minimize gaseous hydrogen evolution. [4] Furthermore, in all bioresorbable metal-based galvanic cell systems, although both anode and cathode are needed, it is the metal anode that dictates overarching electrochemical reaction and most battery characteristics. Nevertheless, almost all current models were built on bulky foils or plates, where their degradation occurred naturally on the metal surface. Therefore, there was no control over the degradation rate, direction and sequence, and thus all showed a poor controllability on the battery output and lifetime, which further limits their practical applications.

In this work, we report a bioresorbable zinc primary battery anode filament built on Zn micro-particles (MPs) coated with chitosan and Al₂O₃ nano-films. This battery filament exhibited a well-controlled dissolution direction and rate due to the mesoscale MP assembly, and the protective coatings. When discharged in 0.9% NaCl saline, single Zn MP filament with a 0.17 x 2 mm² cross-section exhibited a stable voltage output of 0.55 V at a current of 0.01 mA, where the current and voltage output could be simply designed by integration of the battery filaments in parallel or in series, respectively. The operational time could be directly adjusted by the length of filament. A stable 200-hour discharging time was achieved by a 15 mm Zn MP filament. By increasing the filament cross-sectional area, higher current output can be achieved at the same discharging voltage, raising the output power. The final discharging byproducts, mostly ZnO/Zn(OH)₂, could slowly dissolve in biofluids, making this composite filament completely degradable. This complete bioresorbable primary battery showed a full level of control of output and lifetime, providing a promising solution to *in vivo* powering transient bioelectronics.

EL07.02.03

Single-molecule Electrical Detection and Characterization of Biomolecules for New Bioelectronics

Applications in Biophysics and Biomedicine Juan M. Artes Vivancos, Keshani G. Pattiya Arachchillage and Subrata Chandra; University of Massachusetts Lowell, United States

The fundamental understanding of diverse processes in biology requires bridging the gaps between studies at different levels; organisms, tissues, cells, biomolecular complexes, and, ultimately, individual biomolecules. Biophysical characterization studies require new integrated experimental and computational approaches leading to a complete quantitative picture. Single-molecule biophysics has experienced a boom in the last decades. Not only the developments in optical microscopy¹ have allowed researchers to study biological details of fundamental processes with a high resolution, but nanoscience tools such as Scanning Probe Microscopies,² have led to biophysical studies at the single-molecule level. Notably, Scanning Tunneling Microscopy (STM)² has enabled researchers to perform single-molecule bioelectronic studies, including nucleic acids³⁻⁶.

Herein, we introduce examples of the new biomaterials science projects in our lab, where we are integrating these methods for the study of different biological systems. In particular, we recently demonstrated the first single-molecule electrical detection of a biologically-relevant nucleic acid^{6,7}. We are now applying these methods to:

The study of the biomolecular interactions in the RNA Induced Silencing Complex at the individual complex level and,

The single-molecule electrical detection of circulating tumor nucleic acids for the study of cancer biomarkers and the early diagnostics through liquid biopsy.

These methods and results could be applied to numerous biological problems, paving the way to a new body of knowledge in biophysics and materials science. On the applied research front, enabling single-molecule electrical detection in biomedical research and diagnostics constitutes a step forward in biosensors; this novel method is potentially simpler, faster, and cheaper than the established methods such as optical detection or PCR-based methods. These measurements are the first single-molecule electrical investigation of sequences from human origin.

References

1. WE Moerner and M Orrit. *Science*, 283(5408):1670–1676, 1999.
2. G Binnig, H Rohrer, C Gerber, and E Weibel. *Physical review letters*, 49(1):57, 1982.
3. JM Artes, Y Li, J Qi, MP Anantram, and J Hihath. *Nature communications*, 6:8870, 2015.
4. JM Artes, J Hihath, and I Diez-Perez. Biomolecular electronics. In *Molecular Electronics: An Experimental and Theoretical Approach*, 281–323. Pan Stanford, 2015.
5. Y Li, JM Artes, and J Hihath. *Small*, 12(4):432–437, 2016.
6. Y Li, JM Artes, B Demir, S Gokce, HM Mohammad, M Alangari, MP Anantram, E Oren, and J Hihath. *Nature Nanotechnology*, 13(12):1167, 2018.
7. J Veselinovic, M Alangari, Y Li, Z Matharu, J M Artés, E Seker, and J Hihath. *Electrochimica Acta*, 2019.

EL07.02.04

Understanding Different Biomolecular Interactions by Single-Molecule Electrical Methods Subrata Chandra, Keshani G. Pattiya Arachchillage and Juan M. Artes Vivancos; University of Massachusetts Lowell, United States

Biomolecular interactions are fundamental for any cellular function in organisms.[1] Understanding the interface between electronic materials and biological interactions with single molecule resolution can create a bridge between the knowledge gaps at different levels in organisms, tissues, cells, and, ultimately in individual molecules. This knowledge could also have a broader impact in elucidating the molecular basis of many diseases. [2] There is an urgent need for new concepts that appropriately describe the behaviour of biological interactions at the single-molecule level using bioelectronics. Determining the biophysical aspects of these interactions is also essential to understand the fundamental biology at interfaces which can tune the functionality and biocompatibility of next-generation bioelectronic devices.

Biomolecular electronics methods based on scanning probe microscopies can act as a promising alternative tool for measuring these interactions electrically.[3] We use single-molecule electrical methods to study electrical signals at these bioelectronic interfaces using the Scanning tunneling microscope-assisted break junction method (STM-BJ).[4] This technique has enabled the measurement of charge transport properties of biomolecules by reproducible conductance histograms related to the biomolecular structure and conformations.[5] STM-BJ measurements have recently shown the detection of RNA:DNA hybrids from E-coli by measuring their electrical conductance properties at the single-molecule level. [6] We aim at having a complete understanding of the interactions between different components of the RNA Induced Silencing Complex (RISC) applying these methods. RISC is a multiprotein complex that uses the siRNA or miRNA as a template to recognize complementary mRNA and plays a pivotal role in regulatory mechanisms. [7] This electrical approach also gives us a good opportunity to understand the signal transduction in RNA induced gene regulatory process.

The first step in our investigation is demonstrating the single molecule electrical detection of dsRNA. Next, we will measure the conductance of a protein (Argonaute) – dsRNA complex. This can give us a better understanding of the formation of the multiprotein complex and allowing the study of the thermodynamics and kinetics of regulation of gene expression at the individual complex level. The future work for this research will be exploring the specificity of these interactions, kinetics of those adducts and measure the thermodynamic quantities of those physical interactions. Lastly, we could use these fundamental results for designing next-generation smart biomaterials and biosensors that may address improved biological performances and advanced health monitoring in the future.

References:

1. Discher, Dennis, et al. "Biomechanics: cell research and applications for the next decade." *Annals of biomedical engineering* 37.5 (2009): 847.

2. Ryan, Daniel P., and Jacqueline M. Matthews. "Protein–protein interactions in human disease." *Current opinion in structural biology* 15.4 (2005): 441-446.
3. Artés, Juan Manuel, et al., (2016). Biomolecular Electronics in *Molecular Electronics: An Experimental and Theoretical Approach*. Bâldea, I. (Ed.). CRC Press.
4. Xu, Bingqian, and Nongjian J. Tao. "Measurement of single-molecule resistance by repeated formation of molecular junctions." *science* 301.5637 (2003): 1221-1223.
5. Artés, Juan Manuel, et al. "Conformational gating of DNA conductance." *Nature communications* 6.1 (2015): 1-8.
6. Li, Yuanhui, et al. "Detection and identification of genetic material via single-molecule conductance." *Nature nanotechnology* 13.12 (2018): 1167-1173.
7. Zhang, Yokota, Werner. Dubitzky, et al., RNA-induced Silencing Complex (RISC), in *Encyclopedia of Systems Biology*, Editors. 2013, Springer New York: New York, NY. p. 1876-1876.

EL07.02.05

Inkjet-Printed Stretchable PEDOT:PSS-Based Electrodes and Interconnects for Wearable Health Monitoring Devices Li-Wei Lo, Haochuan Wan, Junyi Zhao and Chuan Wang; Washington University in St. Louis, United States

Stretchable conductor is one of the key components in soft electronics that allows seamless integration of electronic devices and sensors on elastic substrates. Its unique advantages of mechanical flexibility and stretchability has enabled a variety of wearable or bioelectronic devices that can comfortably adapt to curved skin surface for long-term health monitoring applications. Here, we report a PEDOT:PSS-based stretchable material that can be patterned using a simple inkjet printing process while exhibiting low sheet resistance and accommodating mechanical deformations. We have systematically studied the effect various types of polar solvent additives on the electrical performance of the ink. The polar solvent induces the phase separation of the PEDOT and PSS grains and changes the conformation of PEDOT chain which leads to a more conductive film due to the charge hopping along the percolated PEDOT network. The optimal ink formulation is achieved by adding 5wt% of ethylene glycol into pristine PEDOT:PSS aqueous solution which results in a sheet resistance of as low as 58 Ω /sq. Elasticity can also be achieved by blending the above solution with soft polymer poly(ethylene oxide) (PEO). Thin-films of PEDOT:PSS-PEO polymer blends patterned by inkjet printing exhibits low sheet resistance of 84 Ω /sq and can resist up to 50% of tensile strain with minimal changes in electrical performance. With its low sheet resistance and high mechanical stability under deformations, we have further demonstrated the use of the polymer blend as stretchable interconnects on thin PDMS substrate for photoplethysmography (PPG) sensor for heart rate and cardiac output monitoring and stretchable dry electrodes for electrocardiography (ECG) recording applications.

EL07.02.06

Late News: Characterization by Electric Impedance Sensing of Normal Cell and Cancer Cell Attachment and the Effects of Ginseng Alejandra Martinez¹, Steffi Kong² and Maddy Behravan³; ¹University of Glasgow, United Kingdom; ²St George's University, Grenada; ³Converse College, United States

This research introduces an application of an electric impedance sensing technique to investigate cell attachment of normal epithelial cells (HaCAT) and cancerous cells (A431) before and after addition of Ginseng. In this study, an impedance sensing system is used to measure and characterize real-time changes in electric impedance (resistance and capacitance) with respect to an alternating current (AC) applied to HaCAT and A431 cell colonies. The impedance data is related to the properties of cell spreading, attachment, and delamination. The effect of Ginseng at various dosages on these cellular properties was inferred from impedance data. The

initial impedance data show that resistance is greater for A431 cells than HaCAT cells and that capacitance for A431 cells is less than the capacitance for HaCAT cells. Further, the data shows the resistance for HaCAT cells and for A431 cells increases with time, and the capacitance for both decreases with time. The impedance data analysis shows that Ginseng does not alter the impedance of HaCAT cellular matrix significantly over a long period. Ginseng results in partial detachment and reattachment of A431 cell-to-cell bonds, thus reordering the cellular matrix. This effect is not seen in HaCAT cell colonies.

EL07.02.07

Late News: Flexible Intra-Cardiovascular Monitoring Sensor and Electrode Device Ulises G. Vidaurri Romero; University of Texas Rio Grande Valley, United States

In recent years, triboelectric nanogenerators (TENGs) have been the center of attention for research due to its wide range of applications as microsystem components, energy harvesting devices, and health monitoring sensors. The flexibility and ability to produce energy of the TENGs are perfect attributes for a health monitoring sensor as well as an alternative to the conventional medical devices. This research focuses on an Intra-Cardiovascular Monitoring Sensor and Electrode Device (ICMSSED) that is biocompatible, cost-effective, and has high response to size ratio than other devices in its category. The framework can be implemented to achieve sensory applications as well as an electrical impulse supplier to the heart like a defibrillator in case of any cardiovascular failure. The fabrication of the device shows the combination of flexible Nitinol, with Poly-Dimethyl Siloxane (PDMS) and Poly-Vinylidene Fluoride (PVDF) polymers. Flexible nitinol wires are dip coated with these functional polymers and intertwined to achieve the framework. Nitinol wires are bi-laterally connected with the polymer coated nitinol sheets, which upon constant contact and separation within the cardiovascular system is capable to yield electrical output. Thus, as synthesized device can provide real-time data of vascular vibrations, vascular pressure, heartbeats per minute, Cardiac arrest, and defibrillation of the heart and vascular system. With its high output-to-size ratio, this Nitinol triboelectric nanogenerator is a promising step to a new chapter in medical advancements and devices.

Keywords

Cardio vascular system, Pacemaker, Nanogenerator, Triboelectric, Defibrillator, Health monitoring, Nitinol, Electrode, PDMS, PVDF

EL07.02.08

A Microfluidic Ion Sensor Array Harika Dechiraju, Chunxiao Wu, John A. Selberg, Brian Nguyen, Pattawong Pansodtee, Manping Jia, Mircea Teodorescu and Marco Rolandi; University of California, Santa Cruz, United States

A balanced concentration of ions is essential for biological processes to occur. For example, $[H^+]$ gradients power adenosine triphosphate synthesis, dynamic changes in $[K^+]$ and $[Na^+]$ create action potentials in neuronal communication, and $[Cl^-]$ contributes to maintaining appropriate cell membrane voltage. Sensing ionic concentration is thus important for monitoring and regulating many biological processes. This work demonstrates an ion-selective micro-electrode array that simultaneously and independently senses $[K^+]$, $[Na^+]$, and $[Cl^-]$ in electrolyte solutions. To obtain ion specificity, the required ion-selective membranes are patterned using microfluidics. As a proof of concept, the change in ionic concentration is monitored during cell proliferation in a cell culture medium. This microelectrode array can easily be integrated in lab-on-a chip approaches to physiology and biological research and applications.

EL07.02.09

Late News: Biodegradable Piezoelectric Ultrasonic Transducer for Brain Drug Delivery Thinh T. Le and Thanh Nguyen; University of Connecticut, United States

The blood-brain barrier (BBB), comprised of monolayers of endothelial cells, which prevents most therapeutics from accessing the brain tissue, is the major hurdle for treating brain diseases. The ultrasound has been shown

to be the most effective tool to disrupt the BBB. However, an external focused ultrasound system is complicated and tedious since it required MRI monitoring and a bulky transducer system, while the current implanted ultrasound transducers rely on non-degradable, toxic materials. Poly-L-lactic acid (PLLA), a biocompatible and biodegradable polymer, has been reported to exhibit piezoelectricity when appropriately processed. This research presents an air-backed unfocused biodegradable piezoelectric ultrasonic transducer made from piezoelectric electrospun nanofibers PLLA that can be implanted on the skulls to temporarily and locally disrupt the BBB for delivering drugs into the brain. The device will safely self-degrade, causing no harm to the body and avoiding invasive brain surgery for removal. We have also shown that the dextran model (3 kDa) can be delivered to the parenchyma of the mice brain by utilizing the ultrasound generated by this device. The improvements of this device can impact various medical fields such as sonodynamic therapy, sonothrombolysis, or ultrasound imaging.

EL07.02.12

Programmable Soft Liquid-Metal Electronics by Micromechanical Valving Xiangchao Zhu¹, Daniel Freitas², Yixiang Li¹, Sierra J. Catelani¹, Ismail Araci² and Ahmet A. Yanik¹; ¹University of California, United States; ²Santa Clara University, United States

The Internet of Things (IoT) is envisioned as a global infrastructure interlinking the physical and cyber worlds through “smart” objects continuously interacting with each other. It is predicted that IoT will connect more than 50 billions of “things” to each other by 2020, and have an economic impact surpassing 36 trillion of dollars by the year 2025. This will require tremendously large numbers of next-generation radio-frequency (RF) devices that can adapt to specific tasks, collect a wide variety of physical information, and exchange data wirelessly through communication networks. Reconfigurability in RF electronics is conventionally achieved by implementation of dynamically controllable components including semiconductor diodes and micro-electromechanical systems. However, these systems have certain limitations: nonlinearities and losses in p-i-n diodes and varactors cause degradation of the RF spectrum and yield low quality-factor responses, while MEMS switches demanding high strength fields suffer from self-actuation. Use of liquid-metals, offering high Q-factor response of a conductor in a versatile reconfigurable form, is an attractive alternative to these conventional approaches that use solid metals. Liquid-metal based reconfigurable methods, however, require large length scale (mm – cm) repositioning of liquid-metals in order to reshape them into a new electrical configuration, rendering long switching times.

Here, we introduce a scalable and electrically reconfigurable electro-microfluidic platform merging injection-based liquid-metal electrodes and micromechanical pneumatic microvalves. Without loss of generality, we demonstrate a PRogrammable INterdigitated Transducer (PRINT), an electro-acoustic RF transducer consisting of a sophisticated arrangement of two interlocking flexible comb-like electrodes conjugated with large arrays of individually addressable micromechanical valves. PRINT possesses precise and dynamically reconfigurable resonance tuning capability and high Q-factor (~ 334) resonance characteristics, both of which are challenging to achieve simultaneously. By directly compressing and modulating the electrical contacts between different liquid-metal microfluidic channel regions via microvalve actuation, we create electrically isolated regions with ultrasmall volumes (75 – 300 picolitres) and realize fast tuning of on-demand electrode configurations in a dynamic, reversible, and reliable way. Our electro-fluidic approach is distinctively different from the conventional methods that rely on emptying and refilling by pressure-driven flow or reshaping of the bulk material through electrowetting, electrocapillarity or electrochemical reactions. Our device architecture and reconfiguration scheme, employing microfluidic large-scale integration (mLSI) techniques, is generic and scalable to thousands of microvalves and hundreds of addressable chambers that are integrated in a single microfluidic chip. Complex reconfigurable device architectures for a number of different applications in the fields of RF electronics and electromagnetics could be created using on-chip multiplexers.

EL07.02.13

Late News: A Novel Green Bilayer Dielectric for High Performance Organic Thin-Film Transistors Mathieu Tousignant, Nicole Rice, Jukka Niskanen, Chloé Richard and Benoit Lessard; University of Ottawa,

Smart packaging is an emerging multi billion-dollar industry that relies on integrated flexible and inexpensive sensors to provide critical information such as temperature, pH, and time to aid with quality assurance. However, for these sensors to be incorporated into a wide variety of packaging they need to be flexible, biodegradable, and low cost.¹

These issues can be addressed using organic electronics, where carbon-based materials are used as the active layer within electronic devices. For example, organic thin film transistors (OTFTs) are commonly used in sensing applications. One of the active layers within an OTFT is the dielectric. The dielectric facilitates charge accumulation at the interface between the dielectric and the organic semiconductor when a source-gate voltage is applied. Ideally, we want a dielectric material with a high dielectric constant (high-k) and low leakage current. Unfortunately, most polymer dielectrics that meet these requirements are not environmentally friendly. However, poly(vinyl alcohol) (PVA) meets these requirements. It is a biodegradable, water soluble, high-k dielectric polymer. While, it does have some drawbacks such as poor film forming, sensitivity to moisture and large leakage currents; we found that the addition of low weight percentages of cellulose nanocrystals improved the film forming capabilities by increasing the viscosity of the solutions.² Building upon these findings, a thin layer of polycaprolactone (PCL) was deposited on top of our PVA dielectric to reduce the moisture sensitivity and leakage currents of PVA. PCL is a hydrophobic, low-K, biodegradable polymer with good insulating properties. The PCL layer was functionalized with toluene diisocyanate (TDI), which can be thermally cross-linked to the hydroxyl groups of PVA at the TDI-PCL/PVA interface. Bilayer crosslinking increased the thin film stability and facilitated orthogonal processing of the semiconducting layer. The fabricated PVA/PCL metal-insulator-metal capacitors were found to be highly stable, even after being exposed to 95% relative humidity, unlike pure PVA based devices. Finally, the TDI-PCL dielectric was used in the fabrication of single walled carbon nanotube top gate bottom contact OTFTs. When compared against native PVA, the TDI-PCL/PVA dielectric showed similar mobilities of $\sim 1 \text{ cm}^2/\text{Vs}$, a reduced average hysteresis of 0.2 V compared to 2.85 V for PVA, a negative threshold voltage shift and greater on/off ratios with a lower device variation. When compared against silicon dioxide the TDI-PCL/PVA dielectric had a six-fold decrease in operating voltage for both the output and transfer curves. These results demonstrate a novel method for using green dielectrics in high performing OTFTs while mitigating challenges associated with thin film processing and moisture sensitivity.

¹ Chen, S. *et al. J. Food Sci.* 85, 517–525 (2020)

² Tousignant, M. N. *et al. Langmuir* 36, (2020)

EL07.02.14

Late News: On Processing Sputtered Iridium Oxide Films (SIROF) for Neural Interfaces Tiffany W. Huang¹, Jens Duru², Zhijie C. Chen¹, Ludwig Galambos¹, Theodore I. Kamins¹ and Daniel Palanker¹; ¹Stanford University, United States; ²ETH Zürich, Switzerland

Porous sputtered iridium oxide films (SIROF) are relied upon for a variety of applications, including pH sensors and neural stimulation and recording electrodes. For neural applications, their ability to store and inject a high amount of charge is particularly important. This capability depends on the state of the material itself and access to its porous microstructure, which can be affected by a number of processes during fabrication. Of notable interest is the effect of heat treatment. Several processing steps require the use of heat, such as high temperature lithography (i.e., the SU-8 prebake typically performed at 150-250°C) or annealing of etch-related defects (i.e., a forming-gas anneal performed at 425°C). The currently available studies in this area are limited and relegated to effects of short anneals done by differential thermal analysis or temperature during deposition of SIROF. Additionally, the usage of aluminum as a sacrificial layer for electrical contacts would necessitate aluminum etchants used on SIROF, and the effect of such etchants has not been evaluated in the literature. Finally, ensuring that photoresist deposition on top of SIROF has no adverse effect and can be easily removed would give full confidence to depositing resist on SIROF for its protection during the device fabrication and release.

Here, we report on SIROF charge storage capacity (CSC) as a function of temperature and demonstrate only minimal effect of heating up to 300°C. We also show that two common etchants for aluminum, MF-26A (2.3%

tetramethylammonium hydroxide (TMAH)) and Aluminum Etch 80:3:15 NP (60-80% phosphoric acid, 5-15% acetic acid, and 1-5% nitric acid), significantly decreased SIROF capacitance and should thus be avoided in its processing. Additionally, we show that resist (20 μm spray-coated of a mixture of 7.5% SPR 220-7, 68% MEK, and 24.5% PGMEA) significantly decreases the SIROF capacitance, likely due to contamination of its pores, and thus affects performance in neural stimulation applications. We demonstrate that its capacitance can be restored by cleaning with N-methyl-pyrrolidone based solution Remover 1165 (5 min soak at 80°C followed by a 2 hr soak in NaClO). These results provide information about proper processing of SIROF for preservation of its charge injection capabilities for neural interfacing devices.

EL07.02.15

Bioelectronic Control of Chloride Ions and Concentration with Ag/AgCl Contacts Manping Jia, Harika Dechiraju, John A. Selberg and Marco Rolandi; University of California, Santa Cruz, United States

Translation between ionic currents and measurable electronic signals is essential for the integration of natural systems and artificial bioelectronic devices. Chloride ions (Cl^-) play a pivotal role in bioelectricity, and they are involved in several brain pathologies, including epilepsy and disorders of the autistic spectra, as well as cancer and birth defects. As such, controlling $[\text{Cl}^-]$ in solution can actively influence biochemical processes and can be used in bioelectronic therapies. Here, we demonstrate a bioelectronic device that uses Ag/AgCl contacts to control $[\text{Cl}^-]$ in solution by electronic means. We do so by exploiting the potential dependence of the reversible reaction, $\text{Ag} + \text{Cl}^- \leftrightarrow \text{AgCl} + \text{e}^-$, at the contact/solution interface, which is at the basis of the well-known Ag/AgCl reference electrode. In short, a negative potential on the Ag/AgCl contact transfers Cl^- from the contact to the solution with increasing $[\text{Cl}^-]$ and vice versa. With this strategy, we demonstrate precise spatiotemporal control of $[\text{Cl}^-]$ in solution that can be used to affect physiological processes that are dependent on $[\text{Cl}^-]$. As proof-of-concept, we use $[\text{Cl}^-]$ control to influence the membrane voltage on human pluripotent stem cells.

SESSION EL07.03: Neurotechnology II

Session Chairs: Tzahi Cohen-Karni, Guosong Hong, Sahika Inal and Jonathan Rivnay

Wednesday Afternoon, April 21, 2021

EL07

2:15 PM *EL07.03.01

Ultraflexible Electrodes for Brain Disorders Lan Luan; Rice University, United States

Brain functions and dysfunctions involve complex interactions between neural, vascular and other cellular activities in a dynamic and spatially resolved manner. This vast complexity demands the ability to simultaneously detect multifaceted brain activities at sufficient spatiotemporal resolutions and to longitudinally track their evolution over a long period of time. In this talk, I will discuss our efforts to meet these needs. These efforts include: 1) the development of ultra-flexible intracortical electrodes (the NanoElectronic Threads -- NETs) to prolong the recording longevity of spiking activities; 2) massively scaling up the recording channel number, density and coverage over brain regions; 3) integrating functional optical imaging techniques with long-lasting electrical recordings to resolve and track hemodynamic and neural activities longitudinally in ischemic brains, and 4) further extension of the spatiotemporal coverage by the co-implantation of NETs into deeper brain structures and a near-cortex-wide cranial window. These neurotechnology advances enables new opportunities for detecting, understanding, and potentially treating a broad spectrum of neurological and neurodegenerative disorders.

2:40 PM EL07.03.02

Late News: New Frontiers for Wireless, Battery-Free and Fully Implantable Neuromodulation Tools—

Transcranial Optogenetic Stimulation and Multimodal Operation in Freely Flying Animals Philipp Gutruf; University of Arizona, United States

Wireless, battery-free and fully implantable tools for the interrogation of the central and peripheral nervous system have quantitatively expanded the capabilities to study mechanistic and circuit level behavior in freely moving subjects. The light weight and small footprint of such devices enables full subdermal implantation that results in the capability to perform studies with minimal impact on subject behavior and yields broad application in a range of experimental paradigms.

Yet, current limitations in wireless power delivery require invasive modes of stimulus delivery that penetrate the skull and disrupt the blood brain barrier, causing tissue displacement, neuronal damage, and scarring. Power delivery constraints also sharply curtail arena volume, limiting operation to mostly rodent subjects in well controlled arena sizes. Here, we implement digitally managed, highly miniaturized, capacitive power storage to wireless and subdermal implants. This approach enables power delivery to optoelectronic components to enable two classes of new applications: transcranial optogenetic activation up to 5 mm deep into the brain without the need to penetrate the blood brain barrier and substantially increased arena volumes for rodents with a quadrupling of experimental arenas for wireless optogenetics to over 1 m² in size. By combining this technique with deep neural net enabled behavior guided primary antenna design we report multimodal optogenetic stimulation and physiological recording in freely flying songbirds for the first time and demonstrate optogenetic manipulation of song renditions, highlighting the capability to expand neuromodulation to a variety of animal model species.

2:55 PM *EL07.01.01

Wireless, Closed-Loop Photostimulation of the Nervous System Enabled by Miniaturized and Compliant Optoelectronic Implants Frederic Michoud¹, Claudia Kathe¹, Corey Seehus², Philipp Schoenle³, Qiuting Huang³, Clifford Woolf², Gregoire Courtine¹ and Stephanie P. Lacour¹; ¹EPFL, Switzerland; ²Harvard Medical School, United States; ³ETHZ, Switzerland

In the past decade, multiple approaches for optical stimulation of neurons have been proposed, mainly focused on the brain. Optogenetic activation of axons in the spinal cord or the peripheral nerves has specific challenges related to their anatomy, softness, opacity and demanding mechanics. We propose a wireless and implantable neurotechnology that offers safe and long-term photostimulation of any targeted neurons and pathways in untethered and unrestricted mice. The implantable system consists of (1) a conformable array of high efficiency micro-scale light emitting diodes, (2) elastic thin-film interconnects that dampen effects of local motion and join the LEDs via (3) a subcutaneous cable and (4) an ultraminiaturized, battery powered, head-mounted, wireless recording and stimulation platform. The platform is operated via a handheld tablet that displays a real-time preview of the acquired physiological signals, the timing of the photostimulation, and a feedback on the accurate delivery of the configured current.

The talk will review the design and manufacturing of the implantable system, highlighting critical steps to engineer compliant optoelectronic interfaces, safe and spatially-selective photostimulation in freely behaving animals. The versatility and robustness of the system will be demonstrated in the context of pain fibers modulation in the peripheral nerves and closed-loop control of spinal cord wherein the onset of a burst of muscle activity instantly triggers photostimulation.

3:20 PM *EL07.03.03

Magnetic Materials for Miniature Wireless Bioelectronics Jacob Robinson; Rice University, United States

Electrical stimulation of neural circuits is a key tool for studying brain function and developing new therapies for neurological disorders. Traditionally, these electrical stimulators include an implanted pattern generator (IPG) that includes a battery and a tether connecting the device to the stimulating leads. These components are one of the most common failure points of the system and comprise the vast majority of the implant volume. To create miniature neural implants without lead wires or large IPGs recent work has turned to wireless data and power delivery to miniaturize neural stimulators. The challenge for these devices, however, is the fact that the

body absorbs electromagnetic radiation often used to power miniature devices making it difficult to deliver sufficient power within operational safety limits. Here, we describe how magnetoelectric (ME) materials offer an efficient method to power millimeter-sized neural implants, achieving power levels of several mW well within the safety limits for human operation.

3:45 PM *EL07.03.04

Modulating Neurophysiology with Multifunctional Fibers Polina Anikeeva; Massachusetts Institute of Technology, United States

Integration of multiple disparate materials within flexible fibers has permitted simultaneous probing and modulation of multiple neurophysiological processes in behaving subjects. In this talk, I will highlight the recent materials and fabrication advances that extend applications of multimaterial fibers to long-term studies of brain dynamics, delivery and probing of neurochemicals, and modulation of neural circuits connecting the brain and the peripheral nervous system. For instance, I will show applications of hydrogels as a means of tuning the modulus of the fibers as well as a tool for drug delivery. Convergence drawing will be introduced as a means to expand the array of materials compatible with fiber fabrication. Finally, I will discuss the introduction of solid-state devices into fibers, and demonstrate their applications for wireless control of behavior and physiology.

SESSION EL07.04: Materials for Bioelectronics

Session Chairs: Tzahi Cohen-Karni, Sahika Inal and Jonathan Rivnay

Wednesday Afternoon, April 21, 2021

EL07

5:15 PM *EL07.04.01

Bioelectronic Modulation with Soft-Hard Composites Aleksander Prominski and Bozhi Tian; The University of Chicago, United States

Biointerface devices can probe fundamental biological dynamics and improve the lives of human beings. However, the direct application of traditional rigid electronics onto soft tissues or cells can cause signal transduction and biocompatibility issues, due to mechanical mismatch at the biointerfaces. One common mitigation strategy is the use of nanostructures or soft-hard composites to form more biocompatible interfaces with target cells or tissues. My group integrates nanoscience and soft matter physics with biophysics to study several semiconductor- or conductor-based biointerfaces. In this talk, I will first pinpoint domains where semiconductor properties can be leveraged for biointerface studies. Next, I will present a few recent studies from our lab and highlight key bioelectrical mechanisms underlying the non-genetic optical or electrochemical modulation interfaces. The non-genetic and soft-hard composite-based methods have the potential to overcome the limitations of current metal electrode-based devices such as bulk and cell membrane disruption, and are not dependent on genetic modifications. Finally, I will discuss new tissue-like materials and other biological targets that could catalyze future advances.

5:40 PM EL07.04.02

Exceptionally Tough and Self-Healing Polymer Blend for Electronic Skin Sung Hwa Hong; University of Toronto, Canada

Electronic skin is an emerging platform with multifunctionalities such as pressure, strain, temperature and humidity sensors while being soft, self-healable, flexible and stretchable. Such multifunctional materials are suitable for soft robotics, wearable devices and prosthetics. However, low toughness and manufacturability hinders the translation of the technology into practical applications.

Toughness is influenced by chemical structure of polymers and crosslinker. For instance, thermoplastic

polyurethane (TPU) is a commercially available polymer that has suitable mechanical properties for smart skin applications. However, most of TPUs have high elastic modulus and does not exhibit self-healability. There have been some attempts to endow self-healability, but the rate of healing typically took more than weeks for recovery. Recently, a TPU was labelled with covalently crosslinkable disulfide group and tuned with varying hard segments. This TPU with loosely packed hard segment facilitated the healing by thiol-disulfide exchange reaction. However, its Young's modulus above 5 MPa limits the application for smart skin. Herein, we report TPU blended with a synthesized self-healing polymer for highly tough and self-healable material. The self-healing polymer with a low Young's modulus is synthesized by using industrially friendly free radical polymerization involving methacrylic acid that enables crosslinking through metal-ligand interaction. This type of bond can be broken and re-formed easily, thus promotes self-healing. Subsequently, this polymer was blended with PU and electrospinning process was used to induce the film formation. Dynamic mechanical analyzer results revealed that the resulting film exhibits a toughness of 70 MJ/m³ and heals from macro-damages within 5 hrs. The film was further coated with polypyrrole endowing electrical conductivity. The material has been examined as a piezoresistive sensor and supercapacitor as to show its versatility for electronic skin application.

5:55 PM *EL07.04.03

Green Bioelectronic Interfaces Made from Protein Nanowires Jun Yao; University of Massachusetts Amherst, United States

Biosystems are made from biomaterials (e.g., protein), whereas conventional electronic systems or interfaces are made from non-biological materials. This leads to some inherent gap in terms of material compatibility in interfacing electronics with biosystems. We explore the possibility of making active electronic devices from protein nanowires harvested from microbe *Geobacter sulfurreducens* for 'green' bioelectronic systems/interfaces. We show how we can utilize the unique properties in the protein nanowires to realize energy devices, sensors, and computing devices, the three key basic elements for integrated electronic interfaces/systems. Specifically, we show 1) energy devices made from the protein nanowires can continuously harvest electric energy from ambient humidity to provide sustainable energy solution to microsystems; 2) neuromorphic devices (e.g., memristors) made from protein nanowires can achieve biological-amplitude functions for ultralow-power computation; and 3) protein nanowires can serve as the active sensing element in constructing electronic biosensors. The perspective of integrated systems/interfaces based on these elements will also be discussed.

6:20 PM EL07.04.04

Late News: Energetic Control of Redox-Active Polymers Towards Safe Organic Bioelectronic Materials Alexander Giovannitti; Stanford University, United States

In my presentation, I will explain the common electrochemical side reactions between redox-active conjugated polymers and aqueous electrolytes in ambient conditions. We find that electron-rich polymers such as PEDOT:PSS or pg2T-TT^[1] can undergo electron transfer reactions with molecular oxygen (oxygen reduction reaction), forming hydrogen peroxide (H₂O₂) as a side product. H₂O₂ itself is an oxidant that can cause harm to biological environments and devices and can also impact the device performance such as increasing the OFF currents of organic electrochemical transistors (OECTs). The origin for the side reaction is an electron transfer from the electron-rich conjugated polymers to molecular oxygen dissolved in the electrolyte where the ionization potential (IP) of the redox-active polymer determines if the reaction occurs spontaneously. By designing and synthesizing redox-active polymers with large ionization potentials (IP > 4.9 eV)^[2], we show that the side reaction can be avoided during the operation of electrochemical devices in ambient conditions. When tested in the OECT, the materials achieve low OFF currents (nAs), high ON/OFF ratios of >10⁵, and excellent redox-stability during continuous operation. This study elucidates the interaction of redox-active conjugated polymers and molecular oxygen which has previously been overlooked with potentially critical issues for operating electrochemical devices in oxygen-containing aqueous electrolytes (biological environments).

[1] A. Giovannitti, D.-T. Sbircea, S. Inal, C. B. Nielsen, E. Bandiello, D. A. Hanifi, M. Sessolo, G. G.

Malliaras, I. McCulloch, J. Rivnay, *Proc. Natl. Acad. Sci.* **2016**, *113*, 12017.

[2] A. Giovannitti, R. B. Rashid, Q. Thiburce, B. D. Paulsen, C. Cendra, K. Thorley, D. Moia, J. T. Mefford, D. Hanifi, D. Weiyuan, M. Moser, A. Salleo, J. Nelson, I. McCulloch, J. Rivnay, *Adv. Mater.* **2020**, *32*, 1908047.

6:35 PM *EL07.04.05

Controlling the Properties of Organic Mixed Ionic-Electronic Conductors Using Living Radical Polymerization Laure V. Kayser; University of Delaware, United States

Organic mixed ionic-electronic conductors (OMIECs) are materials capable of bridging the gap between biological entities ('soft' and ionically conductive) and electronic devices ('hard' and electronically conductive). They have therefore been used extensively in biosensors, organic electrochemical devices (OECTs), and wearable and implantable electronics. Among these OMIECs, the polyelectrolyte complex poly(3,4-ethylene dioxythiophene):poly(styrene sulfonate) (PEDOT:PSS) is the most commonly used for bioelectronic interfaces owing to its high conductivity, water and air stability, biocompatibility, and commercial availability. While the latter makes it easy to adopt and incorporate in devices, it limits our ability to modify the structure of PEDOT:PSS to achieve specific properties and performance. A possible solution to tune the properties of PEDOT:PSS is to use additives (plasticizers, polymers, crosslinkers, surfactant...). While effective at achieving the desired performance, additives often lead to other, sometimes undesirable, effects; making it difficult to predict and/or rationalize structure-property relationships. To address this issue, the Kayser laboratory specializes in modifying the PSS component to understand and *intrinsically* tailor the mixed ionic-electronic conduction, degradability, mechanical properties, and dynamic behavior of PEDOT:PSS derivatives. We use living radical polymerization techniques (e.g., reversible addition-fragmentation chain transfer polymerization, RAFT) to synthesize PSS with a control over the molecular weight and dispersity. For example, we found that we can precisely increase the conductivity of PEDOT:PSS, compared to its commercial form, without using external additives by synthesizing PSS with low molecular weight and dispersity ($M_n = 48$ kDa, $PDI = 1.2$). We are currently studying how these changes in the structure of PSS affect the transconductance of PEDOT:PSS in OECT devices. Another important factor for the integration of PEDOT:PSS in bioelectronics, besides conductivity, is its mechanical properties and compliance. In its commercial form, PEDOT:PSS is relatively 'hard' (Young's modulus \sim MPa) and poorly stretchable ($< 5\%$) which limits its use in wearable and implantable devices.¹ We have developed a method to obtain intrinsically stretchable samples by preparing block copolymers of PSS with poly(ethylene glycol methyl ether acrylate) (PEGMEA).² We are now exploring a similar copolymer strategy to obtain conductive materials with dynamic mechanical properties (i.e., stimuli-responsive PEDOT:PSS). A combination of published data and preliminary results will be presented that highlight our ability to control the intrinsic properties of PEDOT:PSS for applications in bioelectronics and human-machine interfaces.

¹ Kayser and Lipomi *Adv. Mater.* **2019**, *31*, 1806133.

² Kayser et al. *Chem. Mater.* **2018**, *30*, 4459.

SESSION EL07.05: Poster Session II

Session Chairs: Tzahi Cohen-Karni, Sahika Inal and Jonathan Rivnay

Thursday Morning, April 22, 2021

8:00 AM - 10:00 AM

EL07

8:00 AM INTRODUCTORY COMMENTS

EL07.05.02

EMIm-OTf Ionogel Coated Fibres—Characterisation and Development, Aiming at Ionic Smart Textiles

Claude Huniade¹, Shayan Mehraeen², Edwin Jager², Tariq Bashir¹ and Nils-Krister Persson¹; ¹The Swedish School of Textiles - University of Borås, Sweden; ²Linköping University, Sweden

Ions are prevalent within bioelectronics, as they are the main charge carriers in living systems. In contrast to electronic systems, ionic ones are closer to what can be found in our body; in muscles, neurons and nerves.

Textiles are a much used biomedical material, both in vivo and in vitro due to its membrane character, high efficient area, softness, biocompatibility and biodegradability. Modifying the physicochemical properties of the core or the surface of textile has been reported a countless amount of times, but still, its use in a bioelectrical context is limited.

Fibres are the building blocks of textiles and what make textiles an architected class of material. Then ionically conductive fibres are of great interest.

Here, we show the preparation of iono-conductive textile fibres through the (semi-)continuous dip-coating of ionogel on the cellulose-based viscose.

Ionogels are composed of salts in liquid state and a 3-dimensional solid network, in our case an ionic liquid (IL), 1-Ethyl-3-methylimidazolium trifluoromethanesulfonate, commonly named EMIm OTf or EMIm Triflate, and a thiol acrylate network, allowing the mobility of the ions within or in/out of the gel. This specific combination is a first effort towards the development of ionic textile fibres and ionic smart textiles, as a variety of ILs with different cations and anions exists, potentially allowing a large amount of different combinations.

We investigate how the coating of this ionogel affects the mechanical properties as well as the conductivity in AC or DC arrangement and their relation to temperature and humidity. Also, the thermal stability and sensitivity of degradation of the fibre system is studied.

Moreover, we introduce different textile structures, and potential applications directed to bioelectronics.

EL07.05.03

Proton-Activated Synaptic Plasticity of Synaptic Transistors Based on Peptide Min-Kyu Song¹, Seok Daniel Namgung², Daehwan Choi¹, Hyeohn Kim², Hongmin Seo², Misong Ju², Yoon Ho Lee², Taehoon Sung¹, Yoon-Sik Lee², Ki Tae Nam² and Jang-Yeon Kwon¹; ¹Yonsei University, Korea (the Republic of); ²Seoul National University, Korea (the Republic of)

With the recent advances on artificial intelligence, the need for advanced computing processors has been enormously growing to eliminate von Neumann bottleneck in conventional computing processors. To overcome this barrier, novel devices inspired by human brain have been newly proposed. Human brain processes neural signals with 10^{11} neurons and 10^{14} synapses which are connected in parallel while it consumes only 20 W which is extremely low compared to the super computers including IBM's Pohoiki Springs which consumes up to 500 W to emulate elementary brain tasks. To mimic the energy efficiency of biology, researchers in the area of nanoelectronics have proposed various neuromorphic devices. Among them, synaptic transistors have been regarded as the essential component for spiking neural network that emulates synaptic plasticity that pre-synaptic spikes induce timing-dependent post-synaptic responses.

In this work, we demonstrate the novel synaptic transistors that can be turned on and off by controlling humidity. Tyrosine-rich peptide was utilized for proton control layer (PCL) that proton conducting property is exponentially regulated by controlling humidity. IGZO and Au were used as a semiconducting layer and electrode, respectively. Electrical characteristics were measured as a function of relative humidity (RH). Long range gating effect was observed only in highly humid condition while no gating effect was observed in ambient condition. Capacitance-voltage (C-V) characteristics and impedance analysis indicate that the threshold effect of the electrostatic coupling is due to electric double layer (EDL) of protons in the peptide film. On the basis of this phenomenon, we demonstrate the synaptic functions of the device at high humidity including

paired pulse facilitation (PPF), spike-number dependent plasticity (SNDP) and transition from short-term plasticity (STP) to long-term plasticity (LTP). This result demonstrates not only the expansion of the controllability of synaptic function that proton is another control, but also the emulation of proton activation in acid sensing ion channel in biological synapse.

EL07.05.04

Late News: Current-Driven Organic Electrochemical Transistor for the Assessment of Biological Barriers Katharina Lieberth¹, Maximilian Brückner¹, Fabrizio Torricelli², Volker Mailänder^{1,3}, Paschalis Gkoupidenis¹ and Paul Blom¹; ¹Max-Planck-Institute, Germany; ²University of Brescia, Italy; ³University Hospital JGU Mainz, Germany

To use the organic electrochemical transistor (OECT) as a biosensor is of great importance, as it is a state-of-the-art technique in the field of drug delivery.^[1] Allowing ion-to-electron conversion and having a high amplification of gating due to volumetric capacitance, enables the OECT to operate with aqueous electrolytes at low voltages.^[2] When using the OECT as an inverter in a current-driven configuration, a constant current is applied at the channel by an external power supply. It was found that the OECT offers an enhanced sensitivity compared to standard transfer characteristics of an OECT.^[3] The impact of measurement scan rate on the inverter characteristics was also studied. Even small changes in the ionic current can be detected, which is required to study tight junction modulation.^[4] Tight junction barriers of epithelial cell layers impede the transcellular pathway of nutrients and drugs from organs into the blood.^[5,6] Hence, monitoring the effect of external stimuli such as poly-L-lysine (PLL) on tight junction modulations is crucial for drug delivery.^[7] As a well-established model for oral drug delivery, the epithelial colon carcinoma (Caco-2) cell line,^[8] found in the small intestine, was used to evaluate reversible modulation of tight junctions over time, under the effect PLL. Investigating PLL-concentration and TJ-modulation time dependence resumed that the exposure to a medium concentration of PLL initiates reversible modulation, whereas a too high concentration induces an irreversible barrier disruption. To support electrical measurements occluding-staining has been performed using immunofluorescence imaging. The results demonstrate the suitability of OECTs to *in-situ* monitor temporal barrier modulation and recovery, which can offer valuable information for drug delivery applications.^[9]

[1] N. Y. Shim, D. A. Bernards, D. J. Macaya, J. A. DeFranco, M. Nikolou, R. M. Owens, G. G. Malliaras, *Sensors* **2009**, 9896.

[2] J. Rivnay, P. Leleux, M. Sessolo, D. Khodagholy, T. Hervé, M. Flocchi, G. G. Malliaras, *Adv. Mater.* **2013**, 25, 7010.

[3] M. Ghittorelli, L. Lingstedt, P. Romele, N. I. Crăciun, Z.M. Kovács-Vajna, P.W.M. Blom, F. Torricelli, *Nat. Commun.* **2018**, 1441;

[4] L. V. Lingstedt, M. Ghittorelli, M. Brückner, J. Reinholz, N. I. Crăciun, F. Torricelli, V. Mailänder, P. Gkoupidenis, P. W. M. Blom, *Adv. Healthcare Mater.* **2019**, 8, e1900128.

[5] M. Ramuz, A. Hama, M. Huerta, J. Rivnay, P. Leleux, R. M. Owens, *Adv. Mater.* **2014**, 7083.

[6] L. H. Jimison, S. A. Tria, D. Khodagholy, Gurfinkel M., E. Lanzarini, A. Hama, G. G. Malliaras, R. M. Owens, *Adv. Mater.* **2012**, 5919.

[7] G.T.A. McEwan, M. A. Jepson, B. H. Hirst, N. L. Simmons, *Biochem. et Biophys. Acta* **1993**, 1148, 51.

[8] M. S. Balda, K. Matter, *Seminars in cell & developmental biology* **2000**, 11, 281.

[9] K. Lieberth, M. Brückner, F. Torricelli, V. Mailänder, P. Gkoupidenis, P.W.M. Blom, *Adv. Mater. Tech.* **2021** (accepted)

EL07.05.07

Late News: Study of Bio-Modified Gold Electrode for Forefront Point-of-Care Sensors Lucia Sarcina¹, Eleonora Macchia² and Luisa Torsi^{1,2,1}; ¹Università degli Studi di Bari Aldo Moro, Italy; ²Åbo Akademi University, Finland

In the last decade, there has been a growing demand for rapid, cost-effective point-of-care (POC) platforms for

early detection of clinically relevant biomarkers.^[1] This need gave rise to the implementation of novel bioelectronic systems, capable of interfacing biological samples with smart electronic devices. Thus, the robustness of transistor technology has been applied to the functional sensing of clinically relevant species, through the Electrolyte-gated Organic Field Effect Transistors (EGOFET) technology.^[2] Here a huge transducing surface is settled on the gate electrode by conjugating specific bio-elements, for the recognition of relevant analytes, such as protein, DNA strands or enzyme substrates.^[3] The subsequent interaction between the sensing pairs cause a variation on the electrode work-function, which is traduced in a sensor output modification, even at low analyte concentrations. This technology has been already employed for the label-free detection at the physical limit of different antigens such as the HIV-p24 protein.^[4] The sensor selectivity could be guaranteed by the proper functionalization of the sensing electrode. Thus, gold surfaces bio-modification has been deeply studied to investigate best configurations for the anchoring of specific antibodies, for the recognition of the target proteins, by means of a real-time Surface Plasmon Reference (SPR) assay. Through the well-known method of self-assembly of alkylthiols on gold, densely packed layer of 10^{11} - 10^{12} antibodies/cm² are covalently bound to the electrode and subsequently exposed to HIV-1 p24. Moreover, for testing the selectivity of the functionalized surface, the SPR response to a non-binding analyte, namely human C-reactive protein, was further investigated. In this perspective, the same method has been applied to the study of more complex systems as the detection of relevant bacteria. Both the SPR platform and EGOFET apparatus have been characterized, to assess functionalization procedures and electronic sensing evidences, competitive with current POC assays.

Reference

- [1] C. Dincer, R. Bruch, A. Kling, P. S. Dittrich, G. A. Urban, *Trends Biotechnol.* **2017**, *35*, 728.
[2] E. Macchia, R. A. Picca, K. Manoli, C. Di Franco, D. Blasi, L. Sarcina, N. Ditaranto, N. Cioffi, R. Österbacka, G. Scamarcio, F. Torricelli, L. Torsi, *Mater. Horizons* **2020**, *7*, 999.
[3] L. Sarcina, L. Torsi, R. A. Picca, K. Manoli, E. Macchia, *Sensors (Switzerland)* **2020**, *20*, 1.
[4] E. Macchia, L. Sarcina, R. A. Picca, K. Manoli, C. Di Franco, G. Scamarcio, L. Torsi, *Anal. Bioanal. Chem.* **2020**, *412*, 811.

EL07.05.08

Late News: Floating Gate Organic Electrochemical Transistors [Erica Zeglio](#)¹, Shirin Khaliliazar¹, Mahiar Hamedi¹ and Anna Herland^{1,2}; ¹KTH Royal Institute of Technology, Sweden; ²Karolinska Institutet, Sweden

Organic electrochemical transistors (OECTs) are electronic devices having conjugated polymers in conducting or semiconducting form as core components. In a typical OECT configuration, the channel is made by a drain and source metal contacts connected by a conjugated polymer film, which is then separated from a gate electrode by an electrolyte.^[1] The mixed electronic/ionic conductivity of conjugated polymers allows for low operating voltages, high amplification, and adaptability to various form factors, making OECTs appealing devices for bioelectronics, including biosensors and electrophysiological sensors.^[2]

For such sensing applications, it would be beneficial to explore configurations where the channel is physically separated from the target fluid containing the analyte or biological system of interest. Floating gates were introduced in electrolyte-gated transistors to provide such physical separation between the amplification and sensing compartments (though maintaining electronic connection).^[3] This configuration offers two main advantages: 1) the conjugated polymer and electrolyte can be chosen only based on device performance to maximize amplification, and 2) the sensing area can be built to optimize sensing in contact with biological fluids, such as electrolyte composition and electrode functionalization strategy (e.g. using simple thiol functionalization chemistry).^[4]

Here, we present an OECT with a floating gate configuration. We explore the effect of floating gate parameters (e.g. geometry and composition) on OECT operating and sensing performance. Our data suggest that the floating gate geometry is a promising strategy to maximize amplification while minimizing the volume of electrolyte required at the sensing area – something important for biological applications where the volume of the analyte is limited (e.g. DNA sensing).

- [1] E. Zeglio, O. Inganäs, *Adv. Mater.* **2018**, *30*, 1.
[2] L. Bai, C. G. Elósegui, W. Li, P. Yu, J. Fei, L. Mao, *Front. Chem.* **2019**, *7*, 313.
[3] S. P. White, K. D. Dorfman, C. D. Frisbie, *J. Phys. Chem. C* **2016**, *120*, 108.
[4] S. P. White, K. D. Dorfman, C. D. Frisbie, *Anal. Chem.* **2015**, *87*, 1861.

EL07.05.09

In-Operando Kinetic of PEDOT:PSS Electrochemical Doping Gonzague Rebetz, Olivier Bardagot, Julien Réhault and Natalie Banerji; University of Bern, Switzerland

Organic Electrochemical Transistors (OECTs) are sensitive sensors used in increasingly challenging biologic applications such as wearable textiles with integrated biosensors and *in vivo* recording of brain activity.^{1,2} They can be described as an ionic circuit embedded with an electronic circuit. The former arises from ions penetrating the organic channel upon gate bias, while the latter arises from source-drain electron flow across the organic channel.³ Even if our knowledge on OECT behavior and their performance has increased drastically during the last years, a complete picture of these two circuits and how they interact is still missing. Here, we innovatively combine two spectroscopic techniques to study the ionic and electronic transport processes in OECTs:

- 1) Time-resolved *in-operando* UV-vis-NIR absorption spectroscopy unravels the kinetics of the ionic circuit. This measurement monitors the ion penetration into the organic channel and the subsequent electrochemical doping processes with millisecond temporal resolution. Thanks to our multivariate curve resolution analysis,⁴ we extracted the neutral, polaron and bipolaron dynamics, providing insights to the limiting steps of the dedoping/redoping processes.
- 2) *In-operando* THz steady-state absorption spectroscopy investigates the electronic circuit. This measurement probes the nature and the nanoscale conductivity of the charges inside the organic channel.⁵ Connected to the doping level, the nanoscale conductivity grants further understanding about the nature of the interaction between the ionic and electronic circuit.

Results on PEDOT:PSS, the current state-of-the-art material in OECT applications, will be presented.

1. Gualandi I., Marzocchi M., Achilli A. *et al.* Textile Organic Electrochemical Transistors as a Platform for Wearable Biosensors. *Sci Rep* **6**, 33637 (2016).
2. Khodagholy D., Doublet T., Quilichini P. *et al.* In vivo recording of brain activity using organic transistors. *Nat Commun* **4**, 1575 (2013).
3. Rivnay J., Inal S., Salleo A. *et al.* Organic electrochemical transistors. *Nat Rev Mater* **3**, 17086, (2018)
4. De Juan A., Jaumot J., Tauler R. Multivariate Curve Resolution (MCR). Solving the mixture analysis problem. *Anal. Methodes* **6**, 4964-4976 (2014)
5. Unuma T., Yamada N., Nakamura A. *et al.* Direct observation of carrier delocalization in highly conducting polyaniline. *Appl Phys Lett* **103**, 053303 (2013)

EL07.05.10

Late News: Biocompatible and Biodegradable Solid-State Electrolyte for Organic Transistors Young Jin Jo and Tae-il Kim; Sungkyunkwan University, Korea (the Republic of)

Organic electronics are essential components of bio-integrated due to their flexibility and stretchability. There are various issues related to mechanical properties similar to those of skin, tissues and organs, reliability of electrical characteristics under deformations, biocompatibility, biodegradability and low-voltage operation. electrolyte-gated transistors (EGTs) are candidates for decrease of operating voltage using electrolyte as dielectrics in organic transistors. Electrolytes reduce the voltage of organic transistors by high capacitance from the electrical double layers. However most of electrolytes are liquid state that requires harsh passivation layer for stable working in the biological environment. Also, synthetic ion gel based on ionic liquid and polymers has

not been proved as being biocompatible and biodegradable. Here, we suggest a novel concept of solid-state electrolytes based on biocompatible levan polysaccharide for organic transistor. We also used choline based biocompatible and biodegradable ionic liquid by coupling acidic components found in nature. The electrolyte is flexible and highly transparent, also can be served as both dielectric and substrate for organic transistors. Therefore, we fabricated organic transistor on free-standing electrolyte films directly and we also utilized the electrolyte based organic transistors for measuring bio-signals on the skin or heart due to their flexibility, biocompatibility and biodegradability.

EL07.05.11

Late News: Catalytic Properties of Electropolymerized Poly(3,4-ethylenedioxythiophene) Films in Biological Media Prem D. Nayak, David Ohayon, Shofarul Wustoni and Sahika Inal; KAUST, Saudi Arabia

Various electrocatalytic and photocatalytic devices, promising for use as power supplies of bioelectronic devices, rely on oxygen reduction reaction (ORR). Poly(3,4-ethylenedioxythiophene), PEDOT, is an efficient ORR catalyst with hydrogen peroxide (H₂O₂) being the major product. Although H₂O₂ is an excellent green fuel for batteries and fuel cells, and an industrial oxidant, it is toxic for living systems when PEDOT films are used in bioelectronic devices. In this work, we investigated the ORR behavior and H₂O₂ production of a series of electropolymerized PEDOT films. By varying the counterion (monomeric vs. polymeric), including a hydroxyl terminated EDOT monomer in the polymer architecture, or adding a conductivity enhancer in the reaction mixture, we aimed to understand the synthetic parameters that govern the ORR properties. We found that the pristine doping level of the polymer – influenced by counterion type and the presence of the conductivity enhancer – controls the ORR pathway in PEDOT films. High levels of intrinsic doping leads to films with H₂O₂ as the ORR product. Using this information, we synthesized a new PEDOT derivative for which H₂O is the major ORR product. This systematic work will aid designing conducting polymers and choosing operational parameters that (i) maximize film performance in catalytic applications, and (ii) minimize the production of harmful chemicals in bioelectronic devices.

EL07.05.12

Late News: A Microfluidic and Nanoporous Membrane Integrated Organic Electrochemical Transistor for amyloid- β detection Anil Koklu¹, Shofarul Wustoni¹, Valentina Musteata¹, David Ohayon¹, Maximilian Moser², Iain McCulloch^{2,1}, Suzana Nunes¹ and Sahika Inal¹; ¹King Abdullah University Science and Technology, Saudi Arabia; ²University of Oxford, United Kingdom

Alzheimer's disease (AD) is a neurodegenerative disorder associated with a severe loss in thinking, learning, and memory functions of the brain. A common pathological indicator found in AD-affected brains is the aggregates of a protein named amyloid- β (A β). In this work, we developed an organic electrochemical transistor (OECT) integrated with a microfluidic platform and a nanoporous membrane for the label-free detection of A β aggregates in human serum. The nanoporous membrane is functionalized with Congo red (CR) showing a strong affinity for A β aggregates. The detection relies on the modulation of the electric field between the gate and the channel as the aggregates are captured by the membrane. Integration of the OECT with the microfluidics enables minute amounts of fluids to be processed and reduces the sample incubation time. Novel *p-type* and *n-type* semiconductors used at the OECT channel improve the sensitivity, decrease the detection limit, and lower the power requirements, ranking these sensors' performance beyond the state-of-the-art A β sensors. The high transconductance of the OECT, the precise porosity of the membrane, and the compactness endowed by the microfluidic enables protein detection as low as fM concentrations and over eight orders of magnitude wide concentration range in only 1 μ L of human serum.

10:30 AM *EL07.06.01

***In Vitro* Biomimetic Electronic Platforms** Francesca Santoro; Istituto Italiano di Tecnologia, Italy

The interface between biological cells and non-biological materials has profound influences on cellular activities, chronic tissue responses, and ultimately the success of medical implants and bioelectronic devices. The optimal coupling between cells, i.e. neurons, and materials is mainly based on surface interaction, electrical communication and sensing.

In the last years, many efforts have been devoted to the engineering of materials to recapitulate both the environment (i.e. dimensionality, curvature, dynamicity) and the functionalities (i.e. long and short term plasticity) of the neuronal tissue to ensure a better integration of the bioelectronic platform and cells.

On the one hand, here we explore how the transition from planar to pseudo-3D nanopatterned inorganic and organic materials have introduced a new strategy of integrating bioelectronic platforms with biological cells under static and dynamic conditions. Although a spontaneous penetration does not occur, adhesion processes are such that a very intimate contact can be achieved. On the other hand, we investigate how organic semiconductors can be exploited for recapitulating electrical neuronal functions such as long term and short term potentiation. In this way, both the topology and the material functionalities can be exploited for achieving in vitro biohybrid platforms for neuronal network interfacing.

10:55 AM EL07.06.02

About the Amplification Factors in Organic Bioelectronic Sensors Luisa Torsi and Eleonora Macchia; Università degli Studi di Bari Aldo Moro, Italy

Several three-terminal organic bioelectronic structures have been proposed so far to address the needs for a variety of biosensing applications. The most popular ones utilized organic field-effect transistors operated in an electrolyte, to detect both proteins and genomic analytes. They are endowed with selectivity by immobilizing a layer of bio-recognition elements. These features along with the foreseen low-cost for their production, make them very appealing for point-of-care biomedical applications. However, organic bioelectronic transistors do not always exhibit a performance level beyond state-of-the-art electrochemical sensors, which have been dominating the field for decades. This review offers a perspective view based on a systematic comparison between the potentiometric and amperometric electrochemical sensors and their organic bioelectronic transistor counterparts. The key-relevant aspects of the sensing mechanisms are reviewed for both, and when the mathematical analytical expression is actually available, the amplification factors are reported as the ratio between the response of a rationally designed transistor (or amplifying circuit) and that of a homologous electrochemical sensor. The functional dependence of the bioelectronic sensor responses on the concentration of the species to be detected enabling their correct analytical quantification, is also addressed.

11:10 AM EL07.06.03

Unraveling Enzyme/Conjugated Polymer Interactions for High Performance Metabolite Sensors David Ohayon and Sahika Inal; King Abdullah University of Science and Technology, Saudi Arabia

The tight regulation of metabolite metabolism in the body is crucial for balanced physiological function and any irregularities in metabolite uptake or consumption underlie various diseases. In our previous work, we demonstrated the development of a third-generation metabolite sensor, i.e., a microscale electrochemical device comprising an n-type conjugated polymer at the channel and as the gate electrode coating, which detects lactate or glucose without the need of an electron mediator.¹⁻² Here, we adopt a more fundamental approach to understand how the molecular structure of the n-type polymer enables the adsorption of the enzyme glucose oxidase on its surface. We investigate the interactions of the enzyme with six different n-type polymers which have the same backbone but different side chains. We find that depending on the polymer surface properties,

governed by the nature of the side-chains, the enzyme changes its conformation and footprint, which in turn determines the sensor sensitivity. Our work provides new guidelines for the structure-performance relationships of electronic materials with enzymes, crucial for the development of enzymatic metabolite biosensors and biofuel cells.

1. Ohayon, D.; Nikiforidis, G.; Savva, A.; Giugni, A.; Wustoni, S.; Palanisamy, T.; Chen, X.; Maria, I. P.; Di Fabrizio, E.; Costa, P. M. F. J.; McCulloch, I.; Inal, S., Biofuel powered glucose detection in bodily fluids with an n-type conjugated polymer. *Nature Materials* **2019**.

2. Pappa, A. M.; Ohayon, D.; Giovannitti, A.; Maria, I. P.; Savva, A.; Uguz, I.; Rivnay, J.; McCulloch, I.; Owens, R. M.; Inal, S., Direct metabolite detection with an n-type accumulation mode organic electrochemical transistor. *Sci. Adv.* **2018**, 4 (6).

11:25 AM EL07.06.04

Conjugated Molecularly Imprinted Polymers for Biological Sensing Christina J. Kousseff¹, Shofarul Wustoni², Fani E. Taifakou¹, Sahika Inal² and Christian Nielsen¹; ¹Queen Mary University of London, United Kingdom; ²King Abdullah University of Science and Technology, Saudi Arabia

The structure-based tuneability of the electronic and optical properties of conjugated polymers have enabled their application across a range of fields, including energy harvesting, photovoltaics, and medical imaging. However, in the context of biological sensing, the use of conjugated polymers has thus far incorporated little specificity in terms of covalent modification.

Developing robust, highly selective, biologically compatible sensing platforms is of critical importance because the measurement of analyte concentrations in biological samples is crucial for the management or detection of many diseases. For example, fluctuations above or below the optimal range of sodium ion concentration in many bodily fluids can impact blood pressure, nerve and muscle function, while glucose concentration in the blood must be monitored constantly in diabetes. Currently, commercial glucose sensors and many proposed alternatives rely on enzymes, which are expensive and subject to temperature and pH sensitivity, instability, and leaching over time. Meanwhile, other devices are based on complex composite designs featuring separate components to impart conductivity, analyte binding, or selective response. Synthetic strategy with conjugated polymers, especially using the technique of molecular imprinting, enables the efficient combination of analyte specificity, biological interfacing and electroactive or optical functionality into a single multipurpose material. In addition, these entirely organic systems offer affordability, stability, biocompatibility, and simple design and fabrication.

However, due to the well-known difficulties associated with the covalent modification of one of the most effective polymers for this application, poly(3,4-ethylenedioxythiophene) (PEDOT), one of the main challenges in this area thus far has been the attainment of specificity at a molecular level. I will present my work on the concept, design and synthesis of novel molecularly imprinted, electroactive polymers for biological sensing. This includes the creation of a sodium-chelating electrochromic polymer, and a cross-linked glucose-binding electroactive material, both based on covalently modified PEDOT. I will discuss the selectivity and sensing behaviour of these materials in response to the respective analytes, their properties when incorporated into transistor devices, and how this highly adaptable approach can be applied to create a range of materials for many applications across the field of biological sensing.

11:40 AM EL07.06.05

Ultra High Density Optical Nanoelectrode Arrays: Multi Million-Plex Electrophysiological Measurements with Subcellular Resolution Ahsan A. Habib¹, Xiangchao Zhu¹, Uryan Can², Maverick McLanahan¹, Pinar Zorlutuna² and Ahmet A. Yanik¹; ¹University of California, United States; ²University of Notre Dame, United States

Since the first measurement of the nerve impulse by Hermann von Helmholtz in 1849, understanding how a

network of neurons works has been one of the biggest scientific, engineering, and medical challenges [1]. The challenge remains unsolved in the realm of electrical technology, which has limited spatial resolution mainly due to the need for on-chip signal conditioning elements and tighter upper limits for the low noise transfer of spiking cell information by a multiplexed wire [2]. Here, we turn optics since light offers unprecedented spatiotemporal resolution and information-carrying capabilities [3]. Achieving electrophysiological recordings through optical means, on the other hand, largely depends on our ability to recruit reliable electro-optic translators converting electrophysiological signals into photons. After decades of research, state-of-the-art translators cannot provide the high signal-to-noise ratio requirements because of the low photon counts (e.g., voltage sensitive dyes) or low electric-field sensitivities (e.g., quantum dots). We recently invented a novel electro-optic probe by merging nanoionics, plasmonics, and electrochromism that we term "electro-plasmonic field probe" for the transduction of electrophysiological signals into high photon count optical signals [4]. Using the electro-plasmonic nanoprobe, we demonstrated a large scattering intensity change of ~7 % for low field values of 8×10^{-2} mV/nm consistent with the extracellular electric field. Our field probe compares favorably with the quantum dots that provide a ~11% change in photoluminescence signals for an applied field of 10 mV/nm. This field sensitivity is nearly two orders of magnitude lower than that of the electro-plasmonic nanoprobe. Moreover, our electrochromically loaded plasmonic nanoelectrodes have 10-100 million times larger cross sections than those of the widely-adopted genetically incorporated fluorescence molecules and therefore provide an extremely large signal-to-shot-noise ratio (~60-200) with a single loaded nanoelectrode compared to a low signal-to-shot-noise ratio (< 10) that millions of genetically incorporated fluorescence molecules could achieve. In our experiments, we realize extracellular label-free optical detection of electrophysiological activity with high signal-to-noise ratios at three orders of magnitude low light intensity conditions compared to genetically incorporated fluorescence molecules and demonstrate sub-millisecond temporal response time measurements (< 0.2 ms). Our novel approach presents a quantum technological leap for label-free optical imaging of electric-field dynamics with high spatiotemporal resolution.

References

- [1] Alivisatos AP, et al. The Brain Activity Map. *Science* **339**, 1284 (2013).
- [2] Tsai D, Sawyer D, Bradd A, Yuste R, Shepard KL. A very large-scale microelectrode array for cellular-resolution electrophysiology. *Nature Communications* **8**, 1802 (2017).
- [3] Scanziani M, Hausser M. Electrophysiology in the age of light. *Nature* **461**, 930 (2009).
- [4] Habib A, Zhu X, Can UI, McLanahan ML, Zorlutuna P, Yanik AA. Electro-plasmonic nanoantenna: A nonfluorescent optical probe for ultrasensitive label-free detection of electrophysiological signals. *Science Advances* **5**, eaav9786 (2019).

11:55 AM *EL07.06.06

Micro-Invasive Interfaces for Interstitial Fluid Sampling in the Brain and Beyond Ritu Raman
Massachusetts Institute of Technology, United States

Introduction: Biochemical dysregulation underlies many pathologies. Diagnosis and treatment of biochemical dysregulation involves monitoring biomarkers in bodily fluids. While methods for sampling bodily fluids such as blood are well-established, there is a need for robust micro-invasive methods for sampling the interstitial fluid (ISF) between cells, especially in delicate tissues such as the brain. The current state-of-the-art in neural ISF sampling, microdialysis, enables the collection of small, highly concentrated neurochemicals from ISF via diffusion across a semipermeable membrane. Large probe sizes (> 150 μm) limit spatial resolution, which leads to tissue scarring and limits chronic recording. Membranes also limit measuring neuropeptides and proteins, which are prone to nonspecific absorption and are present at very low concentrations in ISF, and preclude measuring dense core extracellular vesicles (EVs), which play critical roles in cell-cell signaling. There is thus a critical need for a micro-invasive interface that is membrane-free and enables sampling small ISF volumes from the brain. Such a platform can be readily adapted to other tissues *in vivo*, and also enables precise spatial and longitudinal tracking of biomarkers in tissue engineered constructs. We anticipate this tool will enable a deeper understanding of the onset, mechanism, and progression of diverse pathologies.

Methods: We have designed and built a micro-invasive membrane-free platform that enables direct sampling of

ISF from tissues *in vivo* and engineered tissues *in vitro*. The platform is composed of flexible hollow borosilicate probes (80 μm outer diameter, 50 μm inner diameter) coupled to a custom-made nanofluidic peristaltic pump (nanopump). Peristaltic flow within the nanopump is driven by the sequential contraction of nickel titanium alloy wires around flexible tubing (1 mm outer diameter, 100 μm inner diameter). The contraction of the wires is controlled via electrical currents that heat the material and trigger a phase transition. This simple two-component design enables bidirectional flow within a single lumen with nanoliter precision (3 nL stroke volume) and negligible dead volume (< 30 nL), capabilities not demonstrated by other low-flow pumps. Sampled fluid is analyzed via liquid chromatography-tandem mass spectrometry (LC-MS/MS) with processing protocols optimized for proteomics.

Results & Discussion: We have shown that our micro-invasive probes can be inserted into tissues *in vivo* and engineered tissues *in vitro* with minimal scarring. In fact, when the probes are chronically implanted in rodent brains, they demonstrate negligible gliosis and retain fluidic functionality for a year post-implantation. Performing nanopump-driven *in vivo* ISF sampling from the substantia nigra in three rats revealed this method was robust and repeatable. Of the 136 peptides identified, 77 overlapped with another biological replicate, while 28 were detected in all replicates. These included several biomarkers of interest such as brain acid soluble protein-1, myelin basic protein, gamma enolase, transthyretin, and kinesin-like protein 15. Ongoing studies will enable chronic tracking of covariant neuropeptides and EVs in physiological and pathological states. We have also shown that deploying this ISF sampling platform *in vitro* in engineered tissues of the central and peripheral nervous system enables spatially focused tracking of biomarkers in a high-throughput manner.

Conclusions: We have developed a novel tool for investigating the biochemical basis of diverse pathologies, with proof-of-concept demonstrations in one of the most challenging *in vivo* environments, the brain, as well as in diverse engineered tissues *in vitro*. Our ISF sampling platform has the potential to generate new fundamental knowledge and enable more accurate diagnosis and treatment of disorders caused by biochemical dysregulation.

12:20 PM DISCUSSION TIME

SESSION EL07.07: Flexible Bioelectronics

Session Chairs: Tzahi Cohen-Karni, Guosong Hong, Sahika Inal and Jonathan Rivnay

Thursday Afternoon, April 22, 2021

EL07

1:00 PM EL07.07.01

Evaluation of Partially Cracked Organic/Inorganic Multilayer Barrier Coatings for Compliant

Bioelectronic Interfaces Kyungjin Kim¹, Matthias Van Gompel², Kangling Wu¹, Florian Bourgeois², Yves Leterrier¹ and Stephanie P. Lacour¹; ¹École Polytechnique Fédérale de Lausanne, Switzerland; ²Comelec SA, Switzerland

A critical challenge to overcome to deploy miniaturized and compliant implantable bioelectronic interfaces *in vivo* is the design, synthesis, and validation of barrier coatings that combine hermeticity, biocompatibility, and microfabrication in agreement with physiological and therapeutic timescales.

Thin-film barriers prepared with vacuum deposition methods, e.g. atomic layer and chemical vapor deposition (ALD and CVD), are a promising strategy for conformal and hermetic coatings. Although ALD offers ultrathin metal oxides at low deposition temperature and low WVTR ($< 10^{-4}$ g.m⁻².d⁻¹), the presence of pinholes and defects hinder further improvement. Thus, to be suitable for *in vivo* conditions, organic-inorganic multilayers are investigated to offer a low water vapor transmission rate (WVTR $< 10^{-6}$ g.m⁻².d⁻¹) by separating such defects in the inorganic layers with the organic layer. Parylene C is an excellent candidate among engineered polymer films because of its low permeability and useful combination of dielectric properties and conformability. Besides, a wide range of medical implants already uses Parylene coatings. We, therefore, focused on a process enabling growth of the alternating stack of Parylene C and ALD Al₂O₃ / TiO₂ multilayers within a single

deposition chamber. Then, we assessed the chemical transport properties of these barrier films in parallel with their mechanical reliability and structural durability during flexural deformation.

The multilayer stack was deposited in a novel hybrid deposition equipment from Comelec SA, allowing for alternating deposition of Parylene then Al₂O₃ / TiO₂ films within a single batch process chamber and at low process temperature. Pristine samples were first characterized by a thin-film corrosion test, leakage current monitoring across interdigitated electrodes, and lifetime tests of coated optoelectronic devices under accelerated aging conditions. Then, we studied and observed channel cracks formed within the organic/inorganic multilayer structure using an in-situ optical microscopy tensile test and scanning electron microscopy with combined modeling. We calculated the fracture energies of the multilayers and applied these parameters to predict their failure mode. A cross-sectional area of a multilayer film strained to crack onset strain was ion-polished, and imaging confirmed the proposed channel crack configuration. Finally, we assessed the lifetime of structures coated with cracked multilayers, which surprisingly displayed an extended lifetime equivalent to 3 years. In summary, we have developed a multimodal characterization protocol to assess thin-film hermetic coating. Organic-inorganic multilayers are proposed as a potential solution for thin-film hermetic coating for in-vivo applications.

1:15 PM *EL07.07.02

Interfacing Skin-Inspired Electronics with Biological Systems Zhenan Bao; Stanford University, United States

Skin is the body's largest organ, and is responsible for the transduction of a vast amount of information. This conformable, stretchable, self-healable and biodegradable material simultaneously collects signals from external stimuli that translate into information such as pressure, pain, and temperature. The development of electronic materials, inspired by the complexity of this organ is a tremendous, unrealized materials challenge. However, the advent of organic-based electronic materials may offer a potential solution to this longstanding problem. Over the past decade, we have developed materials design concepts to add skin-like functions to organic electronic materials without compromising their electronic properties. These new materials and new devices enabled arrange of new applications in medical devices, robotics and wearable electronics. In this talk, I will discuss several projects related to engineering conductive materials and developing fabrication methods to allow electronics with effective electrical interfaces with biological systems, through tuning their electrical as well as mechanical properties. The end result is a soft electrical interface that has both low interfacial impedance as well as match mechanical properties with biological tissue. Several new concepts, such as "morphing electronics" and "genetically targeted chemical assembly - GTCA" will be presented.

1:40 PM EL07.07.03

Multifunctional Artificial Artery from Direct 3D Printing with Built-in Ferroelectricity and Tissue-Matching Modulus for Real-Time Sensing and Occlusion Monitoring Jun Li and Xudong Wang; University of Wisconsin-Madison, United States

Treating vascular grafts failure often requires complex surgery procedures and associates with a high mortality rate. Real-time monitoring vascular system could enable quick and reliable identification of complications and initiate safer treatments in the early stage. In this work, electric field-assisted 3D printing technology was developed to fabricate *in situ*-poled ferroelectric artificial arteries that offered battery-free real-time blood pressure sensing and occlusion monitoring capability. The complex functional artery architecture was made possible by the development of a printable ferroelectric bio-composite which could be quickly polarized during printing and reshaped into devised objects. Synergistic effect from the ferroelectric potassium sodium niobate (KNN) particles and the ferroelectric polyvinylidene fluoride (PVDF) polymer matrix yielded a superb piezoelectric performance (bulk-scale $d_{33} > 12$ pC N⁻¹, confirmed by piezometer) on a par with that of commercial ferroelectric polymers. The sinusoidal architecture brought the mechanical modulus down to the same level of human blood vessels. The desired piezoelectric and mechanical properties of the 3D-printed artificial artery provided an excellent sensitivity to pressure change (0.306 mV/mmHg, $R^2 > 0.99$) within the range of human blood pressure (11.25 to 225.00 mmHg). The high pressure sensitivity and the ability to detect

subtle vessel motion pattern change enabled early detection of partial occlusion (e.g., thrombosis), allowing for preventing grafts failure. This work demonstrated a promising strategy of incorporating multi-functionality to artificial biological systems for smart healthcare systems.

2:10 PM *EL07.07.05

Laser-Engraved Graphene-Based Wearable and mHealth Biosensors Wei Gao; California Institute of Technology, United States

Wearable sensors have the potential to provide rapid, non-invasive, and in-home health monitoring by real-time analyzing biomarkers in human sweat and saliva. However, most current biosensors suffer from low sensing accuracy for low-level analyte detection in biofluids and are difficult to fabricate on a large scale. In this talk, I will review our latest advances in developing fully-integrated laser-engraved graphene-based biosensors which can selectively and accurately measure a wide spectrum of sweat and saliva biomarkers including metabolites, nutrients, hormones, and proteins. The clinical value of these telemedicine platforms is evaluated through multiple human studies involving both healthy and patient populations toward metabolic monitoring and stress assessment. I will also introduce our recent work on a multiplexed wireless platform for the rapid COVID-19 test which could provide information on infection status, severity, and immunity. We envision that these telemedicine devices could open the door to a wide range of personalized healthcare applications.

2:35 PM *EL07.07.06

High-Sensitivity and Wide-Range Capacitive Pressure Sensors Enabled by the Hybrid Responses of a Porous Nanocomposite Nanshu Lu; The University of Texas at Austin, United States

Soft pressure sensors with high sensitivity over a wide pressure range are required for various applications such as electronic skins for human-mimetic robotics and electronic tattoos for pulse pressure measurement. In the last decade, most research aiming at increasing the sensitivity of capacitive pressure sensors focused on developing dielectric materials with added air gaps and/or higher dielectric constants. After extensive research, sensitivity has been significantly improved at low pressure range, e.g. 1 kPa, but drops drastically as the pressure increases. To overcome this challenge, we present a novel soft capacitive pressure sensor employing an electrically conductive porous nanocomposite with both piezoresistive and piezocapacitive responses. The porous nanocomposite is made out of functionalized carbon nanotubes and Ecoflex and can be inexpensively fabricated without MEMS technology. The nanocomposite is 600- μm thick, 85% porous, and open cell with tubular ligaments. An ultrathin dielectric layer was added between the conductive foam and the electrode to ensure the whole device is still capacitive. The sensor has a modulus of 2 kPa and an initial impedance of 47 M Ω with a phase angle of -86° . This capacitive sensor exhibits a sensitivity of 1.95 kPa $^{-1}$ within 0-1 kPa, 1.06 kPa $^{-1}$ within 1-5 kPa, 0.88 kPa $^{-1}$ within 5-10 kPa, 0.52 kPa $^{-1}$ within 10-30 kPa, and 0.35 kPa $^{-1}$ within 30-50 kPa of pressure ranges. The hybrid response is fully understood through a simplified circuit model, which has been validated by the experimental measurements. We have successfully applied this sensor to measure very subtle mechanophysiology on human body, including the pulse pressure of the jugular vein and the temporal artery.

SESSION EL07.08: Biosensors and In Vitro Platforms

Session Chairs: Tzahi Cohen-Karni, Guosong Hong, Sahika Inal and Jonathan Rivnay

Thursday Afternoon, April 22, 2021

EL07

4:00 PM EL07.08.01

Late News: Intrinsically Stretchable, Self-Adhesive, Conductive and Biocompatible PDA-PAM Hydrogel Electrode Enabled in Long-Term Continuous Electrophysiological Monitoring with Minimizing Motion Artifacts and Skin Irritation Fengjie He, Sijia Li, Yingtao Jiang and Shengjie Zhai; University of Nevada, Las

Since cardiovascular diseases (CVDs) are the number one cause of death in the US, long-term continuous electrocardiogram (ECG/EKG) monitoring has evolved to the forefront as a golden standard of ambulatory cardiac monitoring for precise CVDs diagnosis. However, the current commercial gel-type silver/silver chloride (Ag/AgCl) electrodes used in continuous ECG monitoring systems inevitably induce motion artifacts (noise signal) and occasionally cause signal loss. It is ascribed to the irregular impedance changes in the conductive layer between electrodes and skin resulting from the weak stretchability and decreased adhesiveness of the electrodes under intense human motion. On the other hand, some clinical cases reported that the commercial electrodes could cause severe skin irritations and allergies after long-term direct skin contact. Therefore, a self-adhesive, stretchable, and biocompatible hydrogel is highly desirable.

Polydopamine-polyacrylamide (PDA-PAM) hydrogel as a highly self-adhesive and stretchable biomaterial has been attracting tremendous attention. In particular, our previous experiments exhibited that PDA-PAM hydrogel has intrinsic electroconductive capacity due to a large amount of water (more than 70%) and abundant molecules and ions in the hydrogel. Thus, the PDA-PAM hydrogel is a perfect candidate to be integrated into ECG electrodes for continuous health monitoring. In this study, we successfully fabricated the PDA-PAM hydrogel-based ECG electrodes that can be readily connected to conventional ECG devices. As a proof of concept, three male and two female human subjects (age between 25-30 years) were employed to evaluate the proposed ECG electrodes' long-term continuous monitoring performance in this study. The ECG experimental acquisition successfully indicated that the proposed PDA-PAM-based ECG electrodes could simultaneously record continuous ambulatory ECG signals and minimize the motion artifacts under intense exercises, including running, stair climbing, butterfly sleeve, chest expansion. Besides, a 3-hour continuous wearing of the PDA hydrogel-based ECG electrodes test also showed that the ECG signal's quality did not degrade over time, and skin irritation such as itching or redness was not observed among all five human subjects. Notably, the signal-to-noise ratio (SNR) results of PDA-PAM-based ECG electrodes for different exercises demonstrated significant improvement compared to the commercial electrodes results (up to 59% improvement obtained from the running exercise). This significant improvement was attributed to the remarkable tissue adhesiveness and stretchability of the PDA-PAM hydrogel, which enabled the contact areas between electrode and skin to maintain consistent upon skin deformation during exercise and in turn minimized the motion artifacts in the collected signals. In summary, the developed PDA-PAM-based ECG electrodes were successfully employed in the continuous ECG monitoring with high SNR, low motion artifacts, and minimal skin irritation. Undoubtedly, the proposed PDA-PAM hydrogel will serve as a promising hypoallergenic conductive biomaterial for bioelectronics to record long-term continuous high-quality electrophysiological signals.

4:15 PM EL07.08.02

Sapphire-Supported Nanopores for Low-Noise DNA Sensing Pengkun Xia, Jiawei Zuo, Shinhyuk Choi, Xiahui Chen, Jing Bai and Chao Wang; Arizona State University, United States

Low-noise biomolecule sensing has proven to be a crucial method in biology, diagnostics, prognosis, etc. Solid-state nanopores have attracted considerable interest as a potentially high-speed, portable and low-cost solution for detecting a variety of biomolecules, such as proteins, RNA and DNA, as well as studying molecular interactions.

The high capacitive noise from conventionally used conductive silicon (Si) substrates, however, has seriously limited both their sensing accuracy and recording speed. To minimize the stray capacitance of the Si chip, conventional techniques introduce a thick insulating material at the nanopore vicinity. However, these fabrication schemes require complex, and manual processing techniques, such as selective membrane thinning, silicone/photoresist printing, glass bonding, *etc*, and thus are expensive, slow, and difficult to reproduce. Another approach is to replace conductive silicon with an insulating material, such as glass. The amorphous nature of glass substrates, however, prevents the formation of uniform membranes, and involves complex fabrication schemes, such as multiple lithography steps, as well as deposition and etching processes on individual chips. Accordingly, the broad availability of such glass-supported nanopore chips are very limited, primarily due to their low fabrication yield, poor reproducibility, and low throughput.

A new approach is proposed here for forming thin nanopore membranes on crystalline and insulating sapphire wafers as a means to eliminate stray capacitance from substrate conductance for low-noise biosensing. The method involves creating sapphire-supported (SaS) nanopore membranes by wet and anisotropic etching of 2-inch sapphire wafers in concentrated sulfuric and phosphoric acids, a process similar to bulk alkaline etching of Si, that has been widely used in MEMS and biosensing applications. Uniquely, we design a triangular membrane by leveraging the three-fold symmetry of the hexagonal c-plane sapphire lattice and developed a controllable process to produce nanopore membranes over a 2-inch wafer with average size as small as 10.6 μm with 6.8 μm deviation, which corresponds to picofarad level chip capacitance even considering nanometer-thin membranes in high-signal-to-noise-ratio (SNR) DNA detection. For validation, a SaS nanopore chip with a 100 times larger membrane area than conventional a silicon-supported (SiS) nanopore was tested, which showed 130 times smaller chip capacitance (10 pF) and 2.6 times smaller root-mean-square (RMS) noise current (18-21 pA over 100 kHz bandwidth, with 50 to 150 mV bias) when compared to a SiS nanopore (1.3 nF, and 46-51 pA RMS noise). Tested with 1k bp double-stranded DNA, the SaS nanopore enabled sensing at microsecond speed with a signal-to-noise ratio of 21, compared to 11 from a SiS nanopore.

By analyzing the device capacitance, noise current, and power density spectra of the SaS nanopore and comparing to the best reported SiS and glass-supported nanopores, we found our nanopore chips comparable to the best available low-noise sensors. In this work, the nanopore SNR in DNA sensing is mainly limited by the relatively large nanopore size (~ 7 nm) and relatively thick membranes (~ 30 nm). Further optimization in creating smaller nanopores (3-4 nm) and reducing membrane thickness, for example by integration with ultrathin 2D materials, is expected to greatly increase the sensitivity and boost the SNR. The SaS nanopore platform will find use in interrogating a variety of other biomolecules, and their molecular interactions at improved speed and accuracy. Beyond nanopores, our batch-processing compatible and potentially cost-effective manufacturing of the SaS membrane architecture, together with the high optical transparency of sapphire, may serve to establish a new fabrication and design strategy in bulk micromachining of sapphire wafers to broaden the applications in MEMS designs and optoelectronic devices.

4:30 PM EL07.08.03

Late News: Biomembrane Based Organic Electronic Devices for Probing Constituent Specific Changes in Supported Lipid Bilayers Samavi Farnush Bint E Naser, Han-Yuan Liu, Hui Su and Susan Daniel; Cornell University, United States

Supported lipid bilayers (SLBs) are extensively used to mimic and study membrane properties. However, they are generally formed on rigid, non-conducting supports which prevent label free sensing. Combining the insulating properties of biomembranes with bio-compatible conducting polymers (CPs) can enable the electrical detection of membrane disruptions and pathogen interaction. This type of sensing application broadens the use of organic electronic devices into biomedical engineering, biosensing applications, and fundamental membrane biophysics studies. To this end, we demonstrate the formation of lipid bilayers supported on a transparent, conducting polymer surface to investigate changes in membrane properties through constituent specific biomolecular interaction using both optical and electrochemical techniques. Specifically, we have studied methyl- β -cyclodextrin (M β CD) induced cholesterol transfer to and from SLBs and the binding of cholera toxin B subunit (CTB) to lipid bilayers containing GM1 receptor. For our investigation, we used PEDOT:PSS as the CP support because of its high conductivity, optical transparency, easy processing, and excellent biocompatibility. SLBs were formed on this conducting polymer via solvent assisted method since this method bypasses vesicle preparation, does not require vesicle affinity to CP surface, and is applicable to a wide range of lipid mixtures and compositions for which vesicle fusion is difficult. We confirmed the presence of the specific constituents, i.e., cholesterol and GM1 receptors in the lipid bilayers visually using fluorescence microscopy. Next, we explored the sensing capabilities of the developed platform through EIS measurements performed on PEDOT:PSS/ITO electrodes on glass substrates. We report on the successful detection and quantification of the changes in membrane properties, such as, diffusivity and resistance, resulting from cholesterol addition/deletion and receptor specific toxin binding activity using the CP supported SLBs. Our results demonstrate the tremendous potential of these platforms in biosensing application, such as, studying the therapeutic effects of β CD derivatives, drug-screening and examining drug delivery efficiency to prevent receptor specific toxin

interaction with the cell membrane.

4:45 PM *EL07.08.04

Shepherding Tissue Growth and Healing Using Bioelectric Interfaces Daniel J. Cohen; Princeton University, United States

Living cells have a remarkable capacity known as ‘electrotaxis’ where they can sense DC electric fields and orient their migration or growth along field lines. Such fields are surprisingly common *in vivo* and can be critical during embryonic development, wound healing, infection response, and tissue assembly. Essentially, ion gradients give rise to electrochemical DC fields ($\sim 1\text{V/cm}$) where the field direction orients cellular motion and the strength determines migration speed. The importance of such fields *in vivo* raises the question of whether we can develop bioelectric interfaces to mimic or manipulate these fields in order to literally program and ‘herd’ cellular growth and motion to heal injuries faster, grow bespoke tissues, or manipulate diseased tissue. This is an exciting opportunity, but many key challenges remain to be elucidated, especially at the material level. Firstly, new materials are required for the stimulation interface to reduce electrochemical damage and improve the resolution and subtlety of electrical control. I will discuss and highlight some of these challenges using the SCHEEPDOG platform—a multi-axis, microfluidic electrobioreactor developed in my laboratory—to emphasize both the extraordinary control electrotaxis affords and critical material limitations holding back more advanced interfaces. A second key challenge area is to relate bioelectric inputs to living material outputs as a tissue reconfigures itself in response to bioelectric stimuli. Here, I will introduce new work underlining the difficulties and limitations of using bioelectric cues to impose an external behavior on a living tissue material when the target behavior clashes with the natural behavior of the tissue. Overall, this talk will provide an attempt to provide a comprehensive introduction to electrotaxis spanning the basic biointerface biology of how DC fields are transduced by living cells, the design and constraints on DC bioelectric interfaces, and key challenges and opportunities in the field for the broader materials community.

5:10 PM EL07.08.05

Late News: Reliable, Low-Cost, Fully Integrated Hydration Sensors for Monitoring and Diagnosis of Inflammatory Skin Diseases in Any Environment Surabhi Madhvapathy¹, Heling Wang¹, Jessy Kong¹, Michael Zhang^{1,2}, Jongyoon Lee¹, Junbin Park¹, Hokyung Jang¹, Zhaoqian Xie^{1,3}, Jingyue Cao¹, Raudel Avila¹, Chen Wei¹, Vincent D'Angelo¹, Jason Zhu¹, Ha Uk Chung¹, Sarah Coughlin¹, Manish Patel^{1,4}, Joshua Winograd¹, Jaeman Lim¹, Anthony Banks¹, Shuai Xu¹, Yonggang Huang¹ and John A. Rogers¹; ¹Northwestern University, United States; ²Vanderbilt University, United States; ³Dalian University of Technology, China; ⁴University of Illinois at Chicago, United States

Present-day dermatological diagnostic tools are expensive, time-consuming, require substantial operational expertise, and typically probe only the superficial layers of skin ($\sim 15\ \mu\text{m}$). We introduce a soft, battery-free, noninvasive, reusable skin hydration sensor (SHS) adherable to most of the body surface. The platform measures volumetric water content (up to $\sim 1\ \text{mm}$ in depth) and wirelessly transmits data to any near-field communication-compatible smartphone. The SHS is readily manufacturable, comprises unique powering and encapsulation strategies, and achieves high measurement precision ($\pm 5\%$ volumetric water content) and resolution ($\pm 0.015^\circ\text{C}$ skin surface temperature). Validation on $n = 16$ healthy/normal human participants reveals an average skin water content of $\sim 63\%$ across multiple body locations. Pilot studies on patients with atopic dermatitis (AD), psoriasis, urticaria, xerosis cutis, and rosacea highlight the diagnostic capability of the SHS ($P_{\text{AD}} = 0.0034$) and its ability to study impact of topical treatments on skin diseases.

5:25 PM EL07.08.06

Late News: An Aerosol-Jet-Printed Graphene Biosensing Platform for Rapid Electrochemical Detection of Proteins and Small Molecules Sonal Rangnekar¹, Kshama Parate², Cicero Cardoso-Pola², Deyny Mendivelso-Perez^{2,3}, Dapeng Jing², Shaowei Ding², Ethan Secor¹, Emily Smith², Jesse Hostetter², Carmen Gomes², Jonathan Claussen² and Mark C. Hersam¹; ¹Northwestern University, United States; ²Iowa State University, United States; ³U.S. Department of Energy, United States

Inexpensive and rapid diagnostic biosensing is needed more than ever and may be achieved through the development of disposable electrochemical sensors. Graphene films are an ideal material for electrochemical biosensing due to their high electrical conductivity, large surface area, and biocompatibility. However, graphene films fabricated through chemical vapor deposition are too expensive for single-use applications, and low-cost manufacturing alternatives, such as screen and inkjet printing of graphene inks, do not provide sufficient control over electrode geometry to achieve favorable electrochemical sensor performance. In this work, aerosol jet printing (AJP) is leveraged to pattern solution-processed graphene inks into high resolution interdigitated electrodes (IDE) on a flexible polyimide substrate. After thermally curing in air, the IDEs are heated in CO₂ to create additional oxygen moieties on the graphene surface that are then reacted with EDC-NHS chemistry. The resultant graphene biosensing platform can be functionalized with arbitrary antibodies and blocking agents to create a highly sensitive and specific biosensor. This platform has been demonstrated for electrochemical detection of cytokines interleukin-10 (IL-10) and interferon-gamma (IFN- γ) to monitor immune system function (i.e., diagnosis of paratuberculosis in cattle) and for detection of histamine in food safety applications (i.e., determining fish spoilage). The limits of detection for each analyte (IL-10: 46 pg/mL; IFN- γ : 25 pg/mL; histamine: 31 μ g/mL) and sensing ranges (IL-10: 0.1-2 ng/mL; IFN- γ : 0.1-5 ng/mL; histamine: 6-200 μ g/mL) are appropriate for the respective applications. Furthermore, the biosensors are mechanically robust enough to withstand hundreds of bending cycles at high curvatures ($R = 3$ -11 mm) with minimal change in electrical and electrochemical signals. Overall, the low cost of manufacturing and short testing time (\sim 30 min to soak and sense) motivate the expansion of this printed graphene biosensor platform into other sensing applications, including wearable health monitoring and human health diagnostics.

5:40 PM EL07.08.07

Late News: Electrostatic Modulation of Signaling at the Cell Membrane—Waveform- and Time-Dependent Electric Control of ERK Dynamics Quan Qing; Arizona State University, United States

The dynamics of extracellular-signal-regulated kinase (ERK) signaling regulates a wide variety of stimulated cellular processes and plays an important role in cell survival, motility, differentiation and proliferation. Here we show that a new range of alternative current electric field (AC EF) in the tens of KHz could non-invasively activate EGFR-Ras-ERK signaling pathway with precise timing and single-cell resolution, where electroporation or Faradaic processes have been deliberately avoided by using high-k dielectric passivated microelectrodes. We have shown that the ERK activities can be synchronized with the response time independent of the distance from the electrodes, suggesting that the inter-cellular communication and diffusion-limited processes are not involved. Series of blocker tests pinpointed that the ERK activation were triggered by EF induced EGF-independent phosphorylation of EGFR without changes in pH, Ca²⁺ concentration or reactive oxygen species. Interestingly, we also discovered that the cell response was sensitive to the waveform and timing of the EF, and that inhibition of ERK could also be controlled with different dynamic characteristics, strongly suggesting the electrostatic nature of the coupling between AC EF and the membrane protein. Our work suggests a new exciting possibility that the dynamic signaling initiated by membrane proteins can be non-invasively and locally modulated by specifically tuned EF.

5:55 PM DISCUSSION TIME

SESSION EL07.09: On-demand
Wednesday Morning, April 14, 2021
EL07

8:00 AM EL07.09.02

Adaptive Self-Recoverable Electronic Epineurium Donghee Son; Sungkyunkwan University, Korea (the

Republic of)

Soft neuroprosthetics capable of bi-directionally monitoring sensory signals and delivering feedback motor information have pursued the perfect replacement for damaged nerves. Although such valuable efforts have been made to the long-term stability of the peripheral neural interfaces, nerve compression and tissue-induced device fatigue issues still remain challenging due to the lack of optimal materials that simultaneously meet tissue-device modulus matching, biocompatibility, and electrical/mechanical self-recovery. Here, we report a tissue-adaptive self-recoverable electronic epineurium that can prevent its electrical degradation induced by repetitive, non-uniform, and severe structural deformation occurred at a rat's sciatic nerve as well as undesired nerve compression. Such performances originate from its unique mechanical properties: i) spontaneous rearrangement of a ligand-decorated Au nanoshell-coated Ag flakes dispersed in a tough self-healing polymer matrix and ii) dynamic stress relaxation of the electronic epineurium enabling its mechanical adaptation to nerve modulus. Through these properties, we successfully demonstrate stable bidirectional neural recording and stimulation *in vivo* even under the harsh mechanical deformation.

8:10 AM EL07.09.03

A Protein-Based Free-Standing and Proton Conducting Transparent Polymer as a Sustainable Material for Large Scale Sensing Applications Nadav Amdursky; Technion–Israel Institute of Technology, Israel

In a world of depleted resources, and with our current acceptance that the materials we make can have a severe impact on the world, we now understand that we need to reconsider our strategy of making new materials. Accordingly, two materials-related approaches have been formulated. The first approach focusing on the environmental impact of the materials, also known as environmental chemistry, while the second approach is making/synthesizing new materials using green chemistry principals, also known as sustainable chemistry. The use of carbon-based polymers is a good example for the endeavor of making environmentally friendly materials, though not all polymers are environmentally friendly and many of them are not being synthesized in a green chemistry approach. In here, we are focusing on polymers exhibiting efficient ion transport capabilities, and specifically, proton conduction. Inspired by the natural role of mediating protons, we use proteins as the sole starting material for the formation of the polymer. Unlike synthetic polymers, protein-based polymers have inherent biocompatibility and biodegradability properties that promote their use in biomedical applications, either on the skin or *in vivo*. However, to date, protein-based proton conducting polymers cannot be translated to real applications due to two main reasons. The first being the low reported conductivity values compared to common synthetic proton conducting polymers, whereas the measured conductivity (at ambient conditions) across protein-based polymers are usually $<1 \text{ mS}\cdot\text{cm}^{-1}$, while the one of common polymers is $>5 \text{ mS}\cdot\text{cm}^{-1}$. The second most important challenge to overcome is the material formation protocol, whereas most of the conductive protein-based polymers have used genetically expressed proteins, which is not a viable solution as it is costly and time-consuming, even upon upscaling, and accordingly, cannot result in having highly affordable proteins in bulk quantities needed for the formation of materials in large scale. Here, we introduce a new sustainable approach of making proton conducting polymers using affordable and naturally available bovine serum albumin (BSA) proteins, which is in part due to being a 'waste product' of the extensive bovine industry. Hence, our choice of protein is both sustainable in terms that we are recycling waste products, in oppose of synthesizing or expressing something new, as well as highly economical with a commercial price tag of less than $2 \text{ USD}\cdot\text{gr}^{-1}$ of the protein starting material. An added novelty of our new approach here is in its simplicity, which is a one-pot process involving merely dissolving the protein at the right solvent mixture, polymerization and casting it. We show that by using our new methodology, we can form free-standing (self-supporting), insoluble transparent films with high measured proton conductivity at ambient conditions of $\sim 5 \text{ mS}\cdot\text{cm}^{-1}$, and highly attractive mechanical properties of the polymer, capable of stretching ~ 5 times its length. We show that an added value of using proteins as the building blocks is the breadth of functional groups, which are the amino acids residues, allowing performing a variety of post synthetic modifications, and in here we use them to increase the proton conductivity across the polymer. Taking into consideration the polymer stretchability, water containing, biocompatibility and biodegradability nature, we foresee its direct translation in various biomedical applications. Here, we show an immediate application route for our new polymer by its use as a solid-state ion

conducting polymer in electrical sensing of physiological signals, replacing the current cumbersome use of a conductive gel.

8:20 AM EL07.09.04

Flexible Graphene-Based Wireless mHealth System for Non-Invasive Stress Monitoring Jiaobing Tu, Rebeca Torrente-Rodriguez, Yiran Yang, Jihong Min and Wei Gao; California Institute of Technology, United States

Prompt and accurate detection of stress is essential to human performance analysis, stress-related disorder diagnosis, and mental health monitoring. Current approaches such as questionnaires are very subjective. To avoid stress-inducing blood sampling and to realize continuous, non-invasive, and real-time stress analysis at the molecular levels, we investigate the dynamics of a stress hormone, cortisol, in human sweat using an integrated wireless sensing device based on laser-enabled flexible graphene sensors that are mass producible at low cost. Highly sensitive, selective, and efficient cortisol sensing is enabled by a flexible sensor array that exploits the exceptional performance of laser-induced graphene for electrochemical sensing. We report a strong correlation between sweat and circulating cortisol and demonstrate the prompt determination of sweat cortisol variation in response to acute stress stimuli. Moreover, we demonstrate, for the first time, the diurnal cycle and stress-response profile of sweat cortisol, revealing the potential of dynamic stress monitoring enabled by this mHealth sensing system.

8:30 AM EL07.09.07

Control of the Debye Length at the Electrolyte-Oxide Interface of bioFETs with Tunable Surface Electric Fields Ie Mei Bhattacharyya¹ and Gil Shalev^{1,2}; ¹Ben Gurion University of the Negev, Israel; ²The Ilse-Katz Institute for Nanoscale Science & Technology, Ben Gurion University of the Negev, Israel

Biosensors based on field-effect devices (bioFETs) have gained immense research over the past few decades because of their numerous advantages over existing technologies. Yet, their commercialization remains very limited. The biggest challenge for bioFET realization is the extremely short Debye screening length at high ionic strengths. This problem becomes significantly more severe at the solution-oxide interface due to high ion concentration induced by the charged oxide surface groups which cripples any attempt to use field-effect mechanism to detect the presence of the target analytes. In this work, we propose an electrostatic approach to remove the excess concentration of counterions at the double layer (DL), thereby forcing the DL ion concentration to match the bulk concentration [1]. This consequently forces bulk screening length at the DL, thus 'exposing' target biomolecules to the underlying FET. In order to achieve this, local tunable surface electric fields are introduced to the DL using surface passivated-metal electrodes. The effect of these electric fields on the DL ion distribution are examined numerically and analytically. Also, the feasibility of the proposed approach is demonstrated numerically for a fully-depleted silicon-on-insulator based bioFET. We show how a significant twofold increase in the threshold voltage shift is achieved due to the presence of target molecules upon the removal of the surface excess ion population.

Reference

[1] I. M. Bhattacharyya, G. Shalev, Electrostatically-governed Debye screening length at the solution-solid interface for biosensing applications, *ACS Sensors*, 2020, 5, 1, 154-161.
<https://doi.org/10.1021/acssensors.9b01939>

8:40 AM EL07.09.08

Detecting Cancer Biomarkers Electrically Using Single-Molecule Techniques—Understanding Electrical Fingerprints at the Nucleic Acid Bioelectronic Interface Keshani G. Pattiya Arachchillage, Subrata Chandra and Juan M. Artes Vivancos; University of Massachusetts Lowell, United States

Cancer kills more than 8 million people per year and it is one of the most frequent causes of death globally.¹ Cancer biomarkers are promising for detecting cancers early.² There are various methods to analyze biomarkers

and liquid biopsy is one of them.³ Blood samples, or other body fluids, can contain circulating free tumor nucleic acids (ctNA) that can be used as cancer biomarkers.³ Detecting ctNA in the blood is challenging, because of the low ctNA concentration and the low frequency of mutations compared to wild-type sequences.³ Nanotechnology bioelectronics methods can help to address this challenge. In particular, the Scanning Tunneling Microscopic (STM)-assisted break junctions method (STM-BJ)⁴ has recently allowed the first demonstration of detection and identification of RNA from E.Coli via single-molecule conductance.⁵ This is an ideal method for liquid biopsy bioelectronics since it could detect cancer biomarkers such as ctNAs in liquid biopsy samples non invasively and quantify them with high sensitivity and specificity.³

In this work, we characterize ctNAs using the STMBJ to measure and compare the bioelectronics fingerprints of these ctNAs. The main hypothesis of the study is that the sequences of ctNAs can be used to detect cancers, by finding their unique electronic fingerprints. We focus the study on KRAS, BRAF, and Nras as effective cancer biomarkers, based on the recent literature.^{6,7} We have obtained some preliminary data for RNA sequences for a few candidate biomarkers and we expect to understand the bioelectronics interface between genetic material(ctNA) and nanostructured electrodes. Our results pave the way for the early detection of bioelectronics fingerprints from biomarkers, such as ctDNA and ctRNA,³ through liquid biopsy using nanotechnology. These methods may allow beginning treatments early, potentially saving many lives from cancer patients in the future.

References

1. Campbell PJ, Getz G, Korbel JO, et al. Pan-cancer analysis of whole genomes. *Nature*. 2020;578(7793):82-93. doi:10.1038/s41586-020-1969-6
2. Henry NL, Hayes DF. Cancer biomarkers. *Mol Oncol*. 2012;6(2):140-146. doi:10.1016/j.molonc.2012.01.010
3. Das J, Kelley SO. High-Performance Nucleic Acid Sensors for Liquid Biopsy Applications. *Angew Chemie - Int Ed*. 2019. doi:10.1002/anie.201905005
4. Xu B, Tao NJ. Measurement of single-molecule resistance by repeated formation of molecular junctions. *Science (80-)*. 2003;301(5637):1221-1223. doi:10.1126/science.1087481
5. Li Y, Artés JM, Demir B, et al. Detection and identification of genetic material via single-molecule conductance. *Nat Nanotechnol*. 2018;13(12):1167-1173. doi:10.1038/s41565-018-0285-x
6. Rheinbay E, Nielsen MM, Abascal F, et al. Analyses of non-coding somatic drivers in 2,658 cancer whole genomes. *Nature*. 2020;578(7793):102-111. doi:10.1038/s41586-020-1965-x
7. Detection of BRAF mutation in thyroid papillary carcinomas by mutant allele-specific PCR amplification (MASA) in: *European Journal of Endocrinology* Volume 154 Issue 2 (2006). <https://eje.bioscientifica.com/view/journals/eje/154/2/1540341.xml>. Accessed June 8, 2020.

8:50 AM EL07.09.09

Polydopamine as a Soft Material for Integration of Metabolically Active Photosynthetic Bacteria in Bioelectronics Danilo Vona¹, Gabriella Buscemi^{1,2}, Roberta Ragni¹, Francesco Milano², Gianluca M. Farinola¹ and Massimo Trotta²; ¹Università degli Studi di Bari Aldo Moro, Italy; ²Consiglio Nazionale delle Ricerche, Italy

Photosynthetic microorganisms and their subparts represent a very promising tool for the integration of biological photo transducers in bioelectronics and bioelectronic devices. [1,2] Light absorbed by these organisms can be converted into several energy forms exploitable for many external processes. Collect, extract, and transfer electrons from the photosynthetic microorganisms to electrodes represent one of the main issues in *Extracellular Electron Transfer* (EET). Unfortunately, EET often reduce microorganism's viability or leave bacteria in quiescent states inhibiting their reproduction. We present here a procedure for improving the communication between the bacterial cells and the electrode that does not jeopardize the activity and the viability of the bacteria. Cells from the purple non-sulphur bacterium *Rhodobacter sphaeroides* grown under photosynthetic conditions were used as model to test the ability of polydopamine to function as coating material that does not produce detrimental effect nor to the morphology of the cell, nor its basic metabolism, similarly to what previously reported in polygallic acid [3].

Acknowledgements: Funded by the FET-Open project HyPhOE (Grant agreement ID: 800926)

1. Reggente M, Politi S, Antonucci A, Tamburri E, Boghossian AA (2020) Design of Optimized PEDOT-Based Electrodes for Enhancing Performance of Living Photovoltaics Based on Phototrophic Bacteria. *Advanced Materials Technologies* 5 (3):Artn 1900931. doi:10.1002/Admt.201900931
2. Milano F, Punzi A, Ragni R, Trotta M, Farinola GM (2019) Photonics and Optoelectronics with Bacteria: Making Materials from Photosynthetic Microorganisms. *Adv Funct Mater* 29 (21):1805521. doi:10.1002/adfm.201805521
3. Vona D, Buscemi G, Ragni R, Cantore M, Cicco SR, Farinola GM, Trotta M (2020) Synthesis of (poly)gallic acid in a bacterial growth medium. *Mrs Advances* 5 (18-19):957-963. doi:10.1557/adv.2019.466

9:00 AM EL07.09.10

Integration of Bacterial Photoenzymes onto Electrodes—Towards Photosynthesis-Driven Optoelectronics

Gianluca M. Farinola¹, Gabriella Buscemi¹, Marco Lo Presti¹, Roberta Ragni¹, Rossella Labarile¹, Francesco Milano², Danilo Vona¹ and Massimo Trotta³; ¹Università degli Studi di Bari Aldo Moro, Italy; ²CNR-ISPA, Italy; ³CNR-IPCF, Italy

Photosynthetic microorganisms and their molecular components represent attractive tools for harvesting and conversion of solar light in integrated bioelectronic transducers [1].

We have recently investigated several approaches for addressing the Reaction Center (RC) photoenzyme, extracted from the purple non sulfur photosynthetic bacterium *Rhodobacter sphaeroides*, in optoelectronic devices for conversion of solar energy into photocurrent [2]. The RC has been covalently anchored on molecular organic semiconductors with reactive linkers, and the resulting active layer has been used in photodetector configuration [3]. A supramolecular approach based on specific interaction with another protein (Cytochrome C) has been used to create an oriented layer of RC on the gate electrode of an organic transistor device, resulting in the first example of light-driven Electrolyte Gated Organic Field Effect Transistor (LEGOFET) based on a photoenzyme [4]. More recently, we have used polydopamine (PDA) for attaching RC directly onto ITO electrodes, by simple polymerization of dopamine in aqueous media [5]. However, this convenient approach suffers from the low transparency of PDA, which limits the light absorption of the embedded RC. To overcome this issue, PDA has been tailored into a more transparent copolymer by using a degradative functionalization with ethylenediamine. After the encapsulation of RC into polydopamine, the diamine additive modifies the polymer structure, conferring modulable fluorescence properties to the RC-PDA nanoparticles, reducing their size and increasing the general transparency of the polymer. This leads to an enhancement of the light response of RC, with augmented production of charge separated states.

[1] F. Milano, A. Punzi, R. Ragni, M. Trotta, G. M. Farinola, *Adv. Funct. Mater.*, 29, 1805521, (2019).

[2] A. Operamolla, R. Ragni, F. Milano, R. R. Tangorra, A. Antonucci, A. Agostiano, M. Trotta, G. M. Farinola, *J. Mater. Chem. C.*, 3, 6471, (2015).

[3] E. D. Glowacki, R. R. Tangorra, H. Coskun, D. Farka, A. Operamolla, Y. Kanbur, F. Milano, L. Giotta, G. M. Farinola, N. S. Sariciftci, *J. Mater. Chem. C.*, 3, 6554-6564, (2015).

[4] M. Di Lauro, S. la Gatta, C. A. Bortolotti, V. Beni, V. Parkula, S. Drakopoulou, M. Giordani, M. Berto, F. Milano, T. Cramer, M. Murgia, A. Agostiano, G. M. Farinola, M. Trotta, F. Biscarini, *Adv. Electron. Mater.*, 6, 1900888, (2020).

[5] M. Lo Presti, M. M. Giangregorio, R. Ragni, L. Giotta, M. R. Guascito, R. Comparelli, E. Fanizza, R. R. Tangorra, A. Agostiano, M. Losurdo, G. M. Farinola, F. Milano, M. Trotta *Adv. Electron. Mater.*, 6, 2000140, (2020).

9:10 AM EL07.09.12

Self-Healable, Recyclable and Reconfigurable Wearable Electronics Jianliang Xiao; University of Colorado Boulder, United States

Stretchable/flexible electronics has attracted tremendous attention in the past 2-3 decades due to the

combination of its superior mechanical attributes and electrical performance. It can be applied in places that are not accessible by traditional rigid printed circuit boards (PCBs), such as seamless integration with soft tissues and organs of human body for healthcare, bio-inspired curvilinear imagers and artificial skins that mimic the mechanical and electrical properties of natural skin. Among all the exciting applications, wearable electronics represents one of the most important, as it is the most accessible to people, and can be integrated onto the surface of human body to provide many useful functions, including physical activity tracking, health monitoring, drug delivery, human-computer interface, and virtual/augmented reality. More recently, various chemistry and mechanisms have been explored to enable self-healability and degradability in wearable electronics.

All these developments could lead to an exciting bright future of applying technological advancements to improve the wellbeing of people and the society. However, on the other hand, mass production and application of electronics generate a large amount of electronic waste. By 2021, the total electric waste is estimated to reach 52.2 million tons, and the majority of the waste cannot be appropriately recycled. The consequence is that a large amount of heavy metals and other hazardous substances have been entering the eco-system, causing serious environmental problems and human health issues. To resolve this issue, we here report a fully recyclable multifunctional wearable electronic system, which can simultaneously provide excellent mechanical stretchability, self-healability and reconfigurability. Such wearable electronics is achieved by heterogeneous integration of rigid (chip components), soft (dynamic covalent thermoset polyimine) and liquid (eutectic liquid metal) materials through advanced mechanical design and low-cost fabrication method. In such wearable electronic system, off-the-shelf chip components provide high-performance sensing and monitoring of the human body, including physical motion tracking, temperature monitoring, and sensing of acoustic and electrocardiogram (ECG) signals. They are interconnected by intrinsically stretchable and robust liquid metal circuitry, and encapsulated by dynamic covalent thermoset polyimine matrix. Bond exchange reactions in the polyimine network, together with the flowability of liquid metal, enable the wearable electronics to self-heal from damage and to be reconfigured into distinct configurations for different application scenarios. Furthermore, through transimination reactions, the polyimine matrix can be depolymerized into oligomers/monomers that are soluble in methanol and are separated from the chip components and liquid metal. All recycled materials and components can be reused to fabricate new materials and devices.

9:20 AM EL07.09.13

Wireless Power Transfer System for Smart Contact Lenses Taiki Takamatsu, Hu Lunjie, Xiao Te, Qi Zhang and Takeo Miyake; Waseda University, Japan

Electronic contact lenses have been attracted much attention as health monitoring biosensors, wearable displays, and electrically-stimulated eye accommodation devices. Recent examples of their use are glucose sensing, lactate sensing, intraocular pressure measuring, light-emitting diode (LED) displays, and corneal electroretinogram recordings. As electrical lenses make continuous contact with the eyeball surface, their power source and all components must be flexible and safe. Constructing power sources on contact lenses is especially challenging, because the power device must be mounted on the restricted area of the lens without obstructing the vision. Here, we have developed wireless power transfer (WPT) system for smart contact lenses. The WPT system is based on two types of inductance(L)-capacitance(C) resonant circuits at the resonant frequency of 13.56 MHz [1]. Recently, we have developed a hybrid power generation device comprising a wireless power transfer system and a bioabsorbable metal–air primary battery, which provides a multifunctional direct current (DC) and/or alternating current (AC) output [2].

[1] *Advanced Materials Technologies*, 4, 1800671, 2019.

[2] *Advanced Functional Materials*, 30, 1906225, 2020.

9:30 AM EL07.09.14

Late News: Design of Novel Conjugated Polymers for Organic Electrochemical Transistor Biosensors
Maximilian Moser¹, Sahika Inal² and Iain McCulloch^{1,2}; ¹University of Oxford, United Kingdom; ²King Abdullah University of Science and Technology, Saudi Arabia

Organic electrochemical transistors (OECTs) are bioelectronic devices that have gained significant attention recently, as they have shown excellent performances as biomolecule sensors, implantable brain signal recorders, neuromorphic computing elements and many other biomedical applications.¹ Currently, the aqueous dispersion, poly(3,4-ethylenedioxythiophene):poly(styrenesulfonate) (PEDOT:PSS), has established itself as the OECT benchmark material, predominantly due to its commercial availability. PEDOT:PSS-based OECTs however display several disadvantages; namely i) their moderate OECT performances (quantified by the material-only dependent figure of merit μC^*), ii) their depletion-mode of operation, iii) their inability to conduct electrons and iv) PEDOT:PSS' highly complex structure preventing the formulation of structure-property relationships for future material design.² Based on these limitations, this work focuses on synthesizing novel, cheap and solution processable glycol-ether (GE) functionalized conjugated polymers to advance OECT and hence biosensor performance, while concomitantly also establishing design-rules for the development of future OECT materials.

Several molecular design strategies are investigated. These range from tailoring the GE side chain length, to varying the nature of the aromatic building blocks and modifying the chemical composition of the solubilizing chains.³⁻⁵ Ultimately, we show how judicious optimization of the molecular structures, involving polymer energy level, polymer morphology and polymer electroactive swelling modulation, allows us to achieve unprecedented performance and stability benchmarks with μC^* values of $522 \text{ F V}^{-1} \text{ cm}^{-1} \text{ s}^{-1}$ (*c.f.* typically $\sim 40 \text{ F V}^{-1} \text{ cm}^{-1} \text{ s}^{-1}$ for the PEDOT:PSS benchmark)⁶ and devices retaining 98% of their initial current over 2 h of continuous electrochemical cycling.⁴ We then proceed to show how the combined performance and stability advances of our newly developed materials can be exploited in the fabrication of higher performing biosensors, including better sensitivity and lower power consumptions.

References:

1. J. Rivnay, S. Inal, A. Salleo, R. M. Owens, M. Berggren and G. G. Malliaras, *Nat. Rev. Mater.*, **2018**, *3*, 17086.
2. M. Moser, J. F. Ponder, A. Wadsworth, A. Giovannitti and I. McCulloch, *Adv. Funct. Mater.*, **2019**, *29*, 1807033.
3. M. Moser, L. R. Savagian, A. Savva, M. Matta, J. F. Ponder, T. C. Hidalgo, D. Ohayon, R. Hallani, M. Rejsjalali, A. Troisi, A. Wadsworth, J. R. Reynolds, S. Inal and I. McCulloch, *Chem. Mater.*, **2020**, *32*, 6618.
4. M. Moser, T. C. Hidalgo, J. Surgailis, J. Gladisch, S. Ghosh, R. Sheelamantula, Q. Thiburce, A. Giovannitti, A. Salleo, N. Gasparini, A. Wadsworth, I. Zozoulenko, M. Berggren, E. Stavrinidou, S. Inal and I. McCulloch, *Adv. Mater.*, **2020**, *32*, 2002748.
5. M. Moser, A. Savva, K. Thorley, B. D. Paulsen, T. C. Hidalgo, D. Ohayon, H. Chen, A. Giovannitti, A. Marks, N. Gasparini, A. Wadsworth, J. Rivnay, S. Inal and I. McCulloch, *Angew. Chem. Int. Ed.*, **2020**, DOI: 10.1002/anie.202014078.
6. S. Inal, G. G. Malliaras and J. Rivnay, *Nat. Commun.*, **2017**, *8*, 1767.

9:40 AM EL07.09.15

Late News: Flexible Complementary Logic Circuit Featuring Two Identical Organic Electrochemical Transistors Lorenzo Travaglini¹, Adam Micolich¹, Claudio Cazorla¹, Erica Zeglio², Antonio Lauto³ and Damia Mawad¹; ¹University of New South Wales, Australia; ²KTH Royal Institute of Technology, Sweden; ³Western Sydney University, Australia

Conjugated polymers are commonly used as the electroactive channel in organic electrochemical transistors (OECTs).¹ Combination of *p*-type and *n*-type materials allow the realization of complementary logic circuits that would drastically impact on the sophistication of organic electronic devices. Improved functionalities can be achieved by building complementary circuits featuring two or more OECTs. To date, this aim is strictly related to the development of organic materials with respectively reliable hole and electron transport.² Coupling these two types of materials in circuits is challenging because of the requirement to have matching charge transport properties. While *p*-type OECTs are widely available, *n*-type OECTs are less common mainly due to poor performances and stability of the active material in aqueous electrolyte.³ In this study, we build a complementary logic circuit using a pair of OECTs featuring only polyaniline (PANI)

as the channel material in both transistors.⁴ PANI is chosen due to its unique behavior exhibiting a peak in current versus gate voltage when used as an active channel in an OECT. The voltage-transfer characteristic demonstrates the ability to switch from 0 to the supply voltage ($V_{DD} = \pm 0.2$ V) within a potential window suitable for physiological media, obtaining excellent performances with gain up to 7. We investigate concurrently the electrochemical and optical properties as the OECT was in operation to better understand the transfer characteristics of PANI. We further demonstrate the engineering of the complementary circuit into a flexible bioelectronic that operates in aqueous electrolyte.⁴ Our approach of using one material simplifies the synthesis and processing design and eliminates the need of sourcing a material with matching performance.

1. Rivnay, J., Inal, S., Salleo, A., Owens, R. M., *et al. Nat. Rev.* 3, 17086 (2018).
2. Sun, H., Vagin M., Wang, S., Crispin, X., *et al. Adv. Mater.* 30, 1–7 (2018).
3. Giovannitti, A., Nielsen, C., Sbircea, DT. *et al. Nat. Commun* 7, 13066 (2016)
4. Travaglini, L., Micolich, A., Cazorla, C., Zeglio, E., *et. al. Adv.Funct. Mater.* 2007205 (2020)

9:50 AM EL07.09.16

Late News: Solid-State Organic Electrochemical Transistors (OECTs) with Biomaterials for Electronic and Neuromorphic Applications Tung Nguyen-Dang, Kelsey Harrison, Alana Dixon, Alexander Lill, Erin Lewis, Shantonu Biswas, Yon Visell and Thuc-Quyen Nguyen; University of California, Santa Barbara, United States

Organic Electrochemical Transistors (OECTs) have emerged as a promising technology for the development of future bioelectronic and wearable devices. Indeed, a wide range of applications of low-operating voltage and low-power consumption OECTs in electronics are demonstrated, including flexible integrated circuits, wearable biosensors and in implantable brain recording devices. High-performance OECTs require high ionic conductivity and consequently, the majority of current work focus on the device physics and the applications of devices with liquid electrolytes. Nevertheless, liquid components in the transistors could severely impede their long-term stability and complicate their miniaturization. Tremendous attention has therefore been drawn to the development of solid-state materials for solid-state OECTs, among which biomaterial electrolytes are attractive candidates, thanks in part to their biocompatibility and environmental friendliness. Thus far, however, biomaterial-based OECTs have not been systematically studied. There still remains uncertainty surrounding the nature of the doping/dedoping process in the working principle of biomaterial-based OECTs, and as a result, there is a lack of strategies to enhance the performance of these transistors for applications. Here, we present a systematic study of biomaterial-based solid-state OECTs in which biogels consisting of gelatin and glycerol, two food-grade materials, are chosen as the model solid electrolyte. Such gels are fundamentally attractive for bioelectronics and wearable applications due to their superior and tunable electrical and mechanical properties. Their highly processability allows for the fabrication of all-solid-state organic transistors in conventional top-gate-bottom contact configuration and in novel printing-oriented floating-gate coplanar-contact configuration. By analysing the temperature dependence of the biogel OECTs and that of the gel electrolytes, we reveal the role of protonic doping/dedoping in the operation of these transistors. We then establish a relation between morphology and protonic-conductivity of the gels, allowing for the fabrication of gel-based OECTs with high performance. To illustrate this unique flexibility in tuning biogel OECT performance, we demonstrate solid-state organic transistors with high ON/OFF ratio and transconductance, possible ms-switching speed, and six-month stability in ambient air. Understanding ion-conduction in biogel OECTs also leads to better control of their state-retention property, enabling their employment as artificial synapses with various synaptic functions, such as frequency-based short-term and long-term plasticity. With advances in stretchable wearable electronic devices and in solid-state neuromorphic devices, we believe that naturally occurring gels, and gelatin-glycerol gels in particular, will play an essential role in the next generation of sustainable, bio-compatible electronics. As such, our study herein paves the way for the development of biomaterial-based electronics by providing guiding principles for future works that employ biomaterials in OECTs.

10:00 AM EL07.09.17

Late News: Tuning Strain Sensor Performance via Programmed Thin-Film Crack Evolution Juan Zhu,

Stretchable mechanosensors with specific mechanosensitivity and stretchability are ideal for a wide range of applications, from large deformation monitoring to subtle vibration detection. Currently, it is still a great challenge to fabricate stretchable mechanosensors with highly tunable stretchability and sensitivity with facile fabrication techniques. In this work, multifunctional sensors made from a metal film supported on an elastomer in conjunction with a novel programable cracking technology are reported. The cracking mechanism of the metal film can be effectively regulated by the surface chemistry of the elastomer, which results in finely controlled crack morphologies, allowing for strain sensors with well-defined sensitivity and stretchability. Benefitting from this strategy, our sensors demonstrate distinctive characteristics including unprecedented tunability, high sensitivity (Gauge Factor (GF) > 10000), broad stretchability (up to 100%), fast frequency response (5.2 Hz), and good cyclic stability (over 1000 cycles). Based on their superior performance, the sensors can be used for monitoring both subtle and drastic deformations in real-time. The fabrication process presented here, with one material system and a single approach, demonstrates a facile and efficient method for fabrication and regulation of strain sensors, making it an attractive approach for potential applications in wearable sensors, electronic skin and health monitoring platforms.

10:10 AM EL07.09.18

Late News: Stable and Conductive PEDOT:PSS:MXene Composites for Bioelectronics Shofarul Wustoni and Sahika Inal; King Abdullah University of Science and Technology, Saudi Arabia

Poly(3,4-ethylenedioxythiophene) (PEDOT) doped with poly(styrene sulfonate) (PSS) is the most commonly used conducting polymer in organic bioelectronics. However, electrochemical capacitances exceeding the current state-of-the-art are required for enhanced transduction and stimulation of biological signals. The long-term stability of conducting polymer films during device operation and storage in aqueous environments remains a challenge for routine applications. In this work, we electrochemically synthesize a PEDOT composite comprising the water dispersible two-dimensional conducting material Ti_3C_2 MXene. We find that incorporating MXene as a co-dopant along with PSS leads to PEDOT:PSS:MXene films with remarkably high volumetric capacitance and stability, outperforming single dopant-comprising PEDOT films, *i.e.*, PEDOT:PSS and PEDOT:MXene electropolymerized under the same conditions on identical surfaces. Furthermore, we demonstrate the use of a PEDOT:PSS:MXene electrode as an electrochemical sensor for sensitive detection of dopamine (DA). The sensor exhibited an enhanced electrocatalytic activity toward DA in a linear range from 1 μ M to 100 μ M validated in mixtures containing common interferents such as ascorbic acid and uric acid.¹ PEDOT:PSS:MXene composite is easily formed on conductive substrates with various geometries and can serve as a high performance conducting interface for chronic biochemical sensing or stimulation applications.

¹ S. Wustoni, A. Saleh, J.K. El-Demellawi, A. Koklu, A. Hama, V. Druet, N. Wehbe, Y. Zhang, S. Inal, MXene improves the stability and electrochemical performance of electropolymerized PEDOT films, *APL Materials* 8(12) (2020) 121105.

10:20 AM EL07.09.19

Late News: Amplification with Microfluidics Integrated N-Type Organic Electrochemical Transistor Sensor Anil Koklu, David Ohayon, Shofarul Wustoni, Adel Hama, Xingxing Chen, Iain McCulloch and Sahika Inal; King Abdullah University Science and Technology, Saudi Arabia

The organic electrochemical transistor (OECT) can translate biochemical binding events into an electrical signal with particularly high amplification. We herein present a compact and self-sufficient glucose sensor based on an *n-type* OECT.¹ The *n-type* polymer cast at the channel and on the gate electrode has specific interactions with the enzyme glucose oxidase, allowing for direct detection of glucose rather than hydrogen peroxide. The OECT was integrated with a microfluidic system, enabling higher channel current and transconductance, which, in turn, resulted in higher detection sensitivity, lower detection limit and an enhanced signal to noise ratio (SNR) compared to its microfluidic-free counterpart. Owing to the low noise endowed by the microfluidics, the low

magnitude gate current changes (\sim pA) upon enzymatic reaction could be resolved, revealing that while the relative changes in gate and drain currents are similar, the drain current output has a higher SNR. Our microfluidic-integrated design provides new insights into the mechanisms allowing for high sensor sensitivities, while the combination of redox enzymes and *n-type* polymers presents a new avenue for the development of portable and autonomous lab-on-a-chip technologies.

1. Koklu, A., Ohayon, D., Wustoni, S., Hama, A., Chen, X., McCulloch, I., & Inal, S. (2020). Microfluidics integrated n-type organic electrochemical transistor for metabolite sensing. *Sensors and Actuators B: Chemical*, 329, 129251.

SYMPOSIUM EL08

Next-Generation Interconnects—Materials, Processes and Integration
April 23 - April 23, 2021

Symposium Organizers

Silvia Armini, IMEC
Vincent Jousseume, CEA-LETI
Eiichi Kondoh, University of Yamanashi
Andrew Simon, IBM T.J. Watson Research Center

Symposium Support

Bronze
MilliporeSigma

* Invited Paper

SESSION EL08.01: Metallization and Reliability I
Session Chairs: Silvia Armini and Andrew Simon
Friday Afternoon, April 23, 2021
EL08

2:15 PM INTRODUCTORY COMMENTS

2:20 PM *EL08.01.01

The Search for the Most Conductive Interconnect Metal <10 nm Daniel Gall; Rensselaer Polytechnic Institute, United States

The effective resistivity of conventional Cu interconnect lines increases by more than two orders of magnitude as their width decreases from 30 to 6 nm. Alternative metals have the potential to mitigate the resulting resistivity bottleneck by (a) facilitating specular interface scattering with an insulating lattice-matched liner, (b) increasing the grain size or the grain boundary transmission through Fermi surface matching, and (c) choosing a metal with a low product of the bulk resistivity times the bulk electron mean free path. Electron transport measurements on epitaxial metal layers in combination with first-principles simulations are used to quantify the resistivity scaling for a series of metals including Cu, W, Ru, Mo, Co, Rh, and Ir, and to provide insight into the interface structure and chemistry requirements that lead to specular electron scattering and therefore a low resistivity for narrow interconnect lines.

2:45 PM EL08.01.02

Direct Printing of Metallic Interconnects at Micro/Mesoscale Using Localized Electrodeposition Md Emran Hossain Bhuiyan and Majid Minary; The University of Texas at Dallas, United States

Device integration in modern electronics has become complicated with increasing complexity in new generation of devices. Photolithography based conventional techniques are widely used for patterning materials for various electronics applications. These conventional techniques require multiple steps and high vacuum processing, which increase the fabrication cost. Direct printing of metallic interconnects in room temperature without mask and post processing step (high temperature thermal annealing) to achieve the electrical properties close to bulk can significantly reduce the manufacturing cost. Along with low manufacturing cost, superior quality of the printed metal is also highly demanding to be fit in the electronics applications.

Here, an additive printing process based on localized electrodeposition (LED) is demonstrated to print pure metallic interconnects at micro- and meso-scale on rigid and flexible substrates. LED is a 3D electrochemical nano-, micro-, meso- scale printing technology that allows the direct printing of high density, high aspect ratio, and good quality 3D metals and alloys structures at room environment. In the LED process, a nozzle containing the electrolyte of the metal or alloy of interest functions as the printing tool bit. A combination of SEM, XRD, FIB, AFM, nanoindentation, DSC, and electrical characterizations was used to characterize the structure and the properties of the printed interconnections. Microscopy and spectroscopy showed that the printed metal is solid with no porosity, smooth, and with low impurities. Electrical resistivity close to the bulk (~ 2 -time) was obtained without any thermal annealing. Mechanical characterization confirmed the mechanical strength close to the bulk with good adhesion strength of the printed interconnects to the silicon wafer. Thermal analysis further confirmed the melting point of the printed interconnects is close to the bulk. Promising electrical, thermal, and mechanical properties and good adhesion strength make this process attractive candidate for next-generation integrated circuit (IC) applications. Using this process, Cu or Ni micropillar bumps can be directly printed for flip chip interconnections and microscale interconnections for device integration. Such a process can also be used to fabricate functional devices.

3:00 PM EL08.01.03

Advances in Lateral Copper Electroplated Metallic Tracks—Production and Applications by Using Hydrogen Evolution Assisted Electroplating Sabrina Rosa and Arash Takshi; University of South Florida, United States

Recently we have demonstrated that hydrogen evolution assisted (HEA) electroplating can be used for rapid lateral growth of copper across a gap between two copper traces on a printed circuit board (PCB). In this work, the HEA approach has been applied for growing copper traces on three different fabrics of 1000 Denier Coated Cordura Nylon, Laminated Polyester Ripstop, and 100% Virgin Vinyl. To provide the conductive path for the electroplating, first, the desired pattern was applied as a template on the fabric using a conductive ink including multiwalled carbon nanotubes (MWNTs). The template was then metalized by lateral coating with copper. The fastest copper growth rate was achieved in 1000 Denier Coated Cordura Nylon sample (370.96 $\mu\text{m/s}$), while 100% Virgin Vinyl sample showed the slowest growth rate of 99.57 $\mu\text{m/s}$. Further study of the morphologies using the scanning electron microscopy technique showed that the material and the texture of the fabric directly affect the morphology of the electroplated copper. The results are very promising for developing a new method of fabricating wearable electronics by direct printing copper on different fabrics.

3:15 PM EL08.01.04

Two-Step Approach for Conformal Chemical Vapor-Phase Deposition of Ultra-Thin Conductive Silver Films Sabrina M. Wack, Petru Lunca Popa, Noureddine Adjeroud, Christèle Vergne and Renaud Leturcq; Luxembourg Institute of Science & Technology, Luxembourg

In the fabrication of microelectronic devices, which include DRAM capacitors, transistors, and back-end-of line

(BEOL) interconnects, copper (Cu) films are widely studied. However, in this field, silver (Ag) is of particular interest due to its low electrical resistivity and low residual stress compared to Cu. Moreover, a downscaling to less than 100 nm is possible without a considerable increase in resistivity. [1] All these arguments impose Ag as a potential replacement of Cu for contacts and interconnects. Besides microelectronics field, the outstanding optical properties of silver make it a good choice for several applications including optical coatings for plasmonics, windows or lenses, mirrors or sensors, while its chemical reactivity is used in antibacterial surfaces. More and more of these applications require a conformal growth of ultra-thin silver layers, which represents a challenge for most deposition methods. [2]

The deposition of highly uniform and conformal conductive ultra-thin films is also of great interest in the microelectronics industry where the miniaturization of semiconductor devices introduces complex three-dimensional structures with high aspect ratio. [3,4] Consequently, one of the main challenges is to be able to uniformly fill the metallic films into these structures. Conductive ultra-thin silver films are commonly deposited by line-of-sight methods (mainly sputtering) that do not allow conformal deposition on 3D structures with complex morphology such as in microelectronic devices, and have strong uniformity limitations for non-flat substrates such as curved glass. On the other hand, non-line-of-sight methods, such as chemical vapor deposition or atomic layer deposition, usually produce non-electrically-conductive films for low thickness, due to island growth mode. [4,5]

Our new approach relies on an original two-step plasma-enhanced chemical vapor-phase deposition [2], allowing us to reach the electrical performances of silver films obtained by physical approaches without the need of additional wetting layer. Indeed, we synthesized highly conductive and uniform Ag films with a critical thickness lower than 15 nm and a sheet resistance of 1.6 Ω /sq. for 40 nm thin film, corresponding to a resistivity of 6.4 $\mu\Omega$.cm. The high reflectance (up to 94%) and low absorbance (3%) in the infrared region further demonstrate the optical quality of the films, despite a still large rms roughness of 8.9 nm and justify the relevance of the product for high-performance IRR coatings. Moreover, we successfully demonstrate the high conformality of the deposited film on complex lateral high aspect ratio structures (up to 100), with better coverage than the one reported up to now for atomic layer deposition of silver.

This new processing approach opens a very promising route for the use of ultra-thin silver films for electronic and optoelectronic applications, and could be extended to other metals deposited from metal-organic precursors, in particular copper and gold, for which the deposition using chemical vapor based methods is a very active field.

[1] Amusan *et al.*, *J. Vac. Sci. Technol. A* **2016**, *34*, 01A126.

[2] Wack *et al.*, *ACS Appl. Mater. Interfaces* **2020**, *12*, 36329.

[3] Cremers *et al.*, *Appl. Phys. Rev.* **2019**, *6*, 021302.

[4] Hagen *et al.*, *Appl. Phys. Rev.* **2019**, *6*, 041309.

[5] Wack *et al.*, *J. Phys. Chem. C* **2019**, *123*, 27196.

3:30 PM *EL08.01.05

New Frontiers in Metrology for Advanced Interconnect Technologies Kavita Shah; Nova Measuring Instruments, United States

The recent years have proven to be a prime time for materials scientists, process and integration engineers working on interconnect technologies. Even a cursory look at the interconnect roadmap for the next 5 – 10 years will reinforce the observation that a sizeable portion of the periodic table is at play! The semiconductor industry continues to address several daunting challenges at an aggressive dimensional scale by introducing new materials and novel processes to meet modern processor requirements. These changes are not limited to just critical dimension interconnects. We also see rapid evolution for far-back-end technologies. Across the board, the challenge is developing new materials and techniques while meeting more stringent requirements for reliability, variability, and process control. However, identifying the sources of variability and resolving these

issues is becoming more difficult as the complexity evolves. New metrology techniques are needed to address these challenges; however, the mindset for process control back-end-of-line process control lags behind the materials' engineering advances. Fabs either live with older technologies or, in many cases, run the processes blind. The introduction of new integration schemes such as Selective Deposition further extends the need for novel metrology capabilities. We will explore the advent of new metrology techniques with better sensitivity and higher resolution to solve challenges for advanced interconnects in my talk. We will also discuss the unique implementation of materials and dimensional metrology techniques across a few different application types and highlight future development needs in metrology, algorithms, and machine learning techniques to advance the interconnect technology roadmap.

3:55 PM EL08.01.06

High Mobility Monolithic InAs Integration on Amorphous Substrates at Low Temperature Jun Tao, Debarghya Sarkar, Ragib Ahsan and Rehan Kapadia; University of Southern California, United States

Heterogeneous and scalable back-end-of-line (BEOL) compatible integration of high-quality crystalline III-V semiconductor materials and devices are fundamentally limited by two factors: (i) the lack of a crystalline growth surface and (ii) the $<400^{\circ}\text{C}$ thermal budget. Here, we demonstrate high electron mobility single-crystal InAs templated mesas can be monolithically integrated on amorphous substrates at a growth temperature of 300°C by low temperature templated liquid phase (LT-TLP) method. Importantly, a room temperature mobility of $5880\text{ cm}^2/\text{V}\cdot\text{s}$ and peak mobility of $6750\text{ cm}^2/\text{V}\cdot\text{s}$ at 50 K are measured, the highest mobility reported for any thin-film semiconductor material system directly grown on a non-epitaxial substrate. Detailed modeling of the scattering mechanisms in the grown material indicates that mobility is limited by surface roughness scattering, not the intrinsic material quality. The projected room temperature mobility can reach $10,000\text{ cm}^2/\text{V}\cdot\text{s}$ when reducing the RMS surface roughness of InAs from 1.8 to 1 nm, and result in $\sim 20,000\text{ cm}^2/\text{V}\cdot\text{s}$ at 0.5 nm RMS surface roughness, essentially identical with unencapsulated InAs thin films hetero-epitaxially grown by MOCVD or MBE. These results pave the way for the growth of high-mobility materials directly onto the back end of silicon CMOS wafers, and other non-epitaxial substrates such as glass, and polymers for flexible electronics.

4:10 PM DISCUSSION TIME

SESSION EL08.02: Manufacturing/Dielectric
Session Chairs: Vincent Jousseume and Andrew Simon
Friday Afternoon, April 23, 2021
EL08

5:15 PM *EL08.02.01

Low Temperature Direct Bonding Mechanisms Vincent Larrey; Univ. Grenoble Alpes, CEA, LETI, France

Low temperature direct bonding became a mass production technology used for various applications in the microelectronics and microsystems industries. From the first optical system elaboration in the sixties to emerging and promising 3D applications, processes continue to grow in maturity thanks to a progressive understanding of the direct bonding mechanisms. Nevertheless, many research areas still deserve further investigations.

We will first review the general requirements and the most common characterizations needed to track important parameters influencing the quality and reliability of bonded structures. Bonding strength energy measurement, acoustic microscopy, X Ray Reflectivity and Fourier Transform Infrared Spectroscopy, to name a few, are most useful help to fully understand the role of various process parameters.

Silicon and thermal silicon dioxide have been widely studied for the last thirty years as their assembly without

any added layers is required for SOI fabrication. These stable and reproducible materials are very interesting to describe the chemical and mechanical mechanisms at play in confined bonding interfaces. We will put some emphasis on the key role water has during and after bonding. Adsorbed water on the surfaces is indeed trapped at the bonding interface. A post bonding annealing is usually performed to strengthen the structures. It is then quite obvious that water management plays a key role. Hydrophilicity, asperities hydrolyzation, silanol to siloxane bonds conversion and water stress corrosion are fundamental notions to depict and understand the behavior of bonded structures. We will also describe the common surface preparation techniques used to improve the bonding strength and quality.

However, many microelectronics and microsystems applications require other material at the bonding interface. Previous considerations remains exact, however. New behaviors, models and mechanisms will benefit from such a background. Simply replacing thermal oxide with deposited oxide is not so easy, for instance. We will then have to deal with silanol groups in the oxide layer, as they will have an impact on water management. Other researches focus on alternative dielectrics and we will describe the specificity of alumina, silicon nitride and porous ultra low k materials.

We will then present some of the specificities of metallic direct bonding, with a focus on copper-to-copper direct bonding mechanisms. This technology can indeed address the growing 3D market, as it yields electrical contacts between microelectronic devices. To achieve such stacking, perfect hybrid surfaces (Silicon oxide and Copper) have to be prepared, aligned and contacted. We will discuss the surface topologies requirements and the latest bonding alignment improvements yielding stacks with connection pitches as low as 1 μ m.

Finally, we will discuss the main advantages and drawback of direct bonding compared to other bonding solutions, in order to propose a guideline to choose the best assembly technic.

5:40 PM EL08.02.02

Atomic Precision Advanced Manufacturing (APAM) of Ultra-Doped Nanostructures for Advanced

CMOS Devices and Interconnects David A. Scrymgeour, Esther Frederick, Connor Halsey, DeAnna Campbell, Evan Anderson, Scott Schmucker, Andrew Leenheer, Xujiao Gao, Jeffrey Ivie, Tzu-Ming Lu, Lisa Tracy and Shashank Misra; Sandia National Laboratories, United States

Atomic precision advanced manufacturing (APAM) is a promising platform for creating quantum structures and advanced silicon based electrical devices at the absolute limit of doping in silicon – at activated concentrations higher than achievable by ion implantation. In this process, a hydrogen-terminated Si(100) surface is patterned by selectively removing the bound hydrogen with an scanning tunneling microscope tip in chosen areas, leaving behind a depassivated (bare silicon) pattern. Subsequent exposure to phosphine molecules leads to dissociative chemisorption of phosphine molecules in the depassivated regions only, then the entire pattern is then protected with an epitaxial silicon cap. This creates a 2D delta layer of highly conductive phosphorous in silicon that can carry 2 mA/ μ m of current. This ultra-doping of Si provides unprecedented electronic behavior, virtually unrecognizable to traditional Si devices, and enables its future use in advanced silicon devices and interconnects.

Our recent work focuses on exploring various aspects of integrating APAM directly into CMOS architectures, as well as the consequences of APAM on potential Beyond Moore silicon devices. Our first focus involves overcoming traditional cryogenic temperature limitations of APAM devices, and we have recently demonstrated the use of APAM phosphorus nanostructures at room temperature, overcoming previous limitations. Our second goal is to assess the compatibility of APAM delta layers with operational CMOS conditions. We recently performed accelerated aging studies at high temperatures and drive currents and will discuss the robustness and failure mechanisms of the APAM materials. Lastly, we are exploring the chemical selectivity of hydrogen and silicon depassivated surfaces to achieve patterned atomic precision deposition (APD) and etch (APE).

This work was supported by the Laboratory Directed Research and Development Program at Sandia National Laboratories and was performed, in part, at the Center for Integrated Nanotechnologies, a U.S. DOE, Office of Basic Energy Sciences user facility. Sandia National Labs is a multimission laboratory managed and operated by National Technology and Engineering Solutions of Sandia, LLC. The views expressed in the article do not

necessarily represent the views of the DOE or the U.S. Government.

5:55 PM *EL08.02.03

Cryogenic Etching Applied to Next Generation Interconnects Remi Dussart, Thomas Tillocher and Philippe Lefaucheu; Université d'Orleans - CNRS, France

Cryogenic etching process was introduced more than 30 years ago by a Japanese team [1]. The idea was to cool the substrate to a very low temperature (-100°C) in order to freeze the chemical reactions on vertical sidewalls while maintaining them with silicon at the structure bottom submitted to the ion bombardment. A plasma of SF_6 was used to perform these experiments. However, it was shown later that oxygen was playing an important role by forming a SiO_xF_y passivation layer at the sidewalls [2]. Oxygen contamination was probably coming from SiO_2 sputtering in the reactor. SF_6/O_2 plasmas in interaction with a cooled silicon wafer can be used to form high aspect ratio structures. However, until recently, Bosch process [3] was usually preferred by companies to etch high aspect ratio silicon microstructures, for its better robustness and because it is a room temperature process, which does not require any liquid nitrogen to cool the substrate. Etching at low temperature of the substrate may have many advantages: reactions of interest mainly occur on cooled surfaces, higher etch rate can be obtained, it can be used for nanometric patterns and surface diffusion can be minimized ... [4] Moreover, new chillers are now available to cool down the wafer to very low temperatures without using liquid nitrogen. These assets make cryoetching generate more and more interest in the semiconductor industry.

In particular, cryogenic etching offers new opportunities for next generation interconnects. It can be used to anisotropically etch porous low-k materials. It is well known that ultra low-k material, which is used for the first levels of interconnection in CMOS technology, can be strongly damaged by plasma etching processes. Porous SiOCH is a typical low-k material used in microelectronics. Methyl depletion due to radical diffusion and reactions through the pores are some of the observed unwanted effects. Ion bombardment and VUV exposure can also damage the low-K material, leading to an increase of the k value [5]. In order to reduce Plasma Induced Damage, a technique based on the cryogenic process was introduced in 2013 [6]. It consists in cooling the substrate to a low temperature in order to reduce species diffusion and create a passivation layer on the sidewalls and on the pore surface. Several processes have been successfully tested involving $\text{C}_4\text{F}_8/\text{SF}_6$ plasma chemistry at -120°C . [7, 8]. The idea was to fill in the porous material by condensation of C_4F_8 before etching, and prevent plasma damage of the low-k material. Anisotropic etched profiles were obtained with an enhanced selectivity in $\text{SF}_6/\text{C}_4\text{F}_8$ plasma process at low temperature. The effect of the low temperature was clearly observed on the equivalent damage layer (EDL), which was evaluated by ex situ Fourier transform infrared (FTIR) spectroscopy and in situ ellipsometry. An anneal step at 350°C was also used to completely desorb the remaining CF_x species from the pores. An equivalent process at higher temperature was proposed using organic molecules having a higher boiling point (HBPO – Higher Boiling Point Organic).

[1] S. Tachi, K. Tsujimoto and S. Okudaira Appl. Phys. Lett. 52 616 (1988)

[2] J. W. Bartha et al. Microelectron. Eng., 27 453 (1995)

[3] F. Laermer and A. Schilp US Patent 5498312 (assigned to Bosch GmbH) (1996)

[4] R. Dussart et al., J. Phys. D: Appl. Phys. 47 123001 (2014)

[5] M. R. Baklanov et al. J. Appl. Phys., 133 041101 (2013)

[6] L. Zhang et al., J. of Solid State Sc. and Technol., 2(6), N131 (2013)

[7] F. Leroy et al., J. Phys. D: Appl. Phys. 48 435202 (2015)

[8] L. Zhang et al., J. Phys. D: Appl. Phys. 49 175203 (2016)

6:20 PM EL08.02.04

Late News: Effect of Non-Corrosive Gas Mixture on Etching of Nanometer-Scale Patterned Cu Thin Film Using Pulsed Modulated RF Source Plasma Ji Soo Lee, Eun Taek Lim, Sungyong Park, Yun Seong Park, Sung Hoo Cho and Chee Won Chung; Inha university, Korea (the Republic of)

As the critical dimensions of semiconductor devices are reduced for high performance, fast speed, and low operating power, copper has been used as the interconnect metals because it has low resistance and less electromigration. For the realization of copper interconnect into the devices, the etching of copper thin films are

necessary. However, the conventional dry etching of copper is difficult because conventional etching gases such as Cl_2 , HCl , HBr are formed nonvolatile by-products on the copper films. Currently, the damascene process is used for copper patterning. However, as the critical dimensions are further reduced down to 10s nm scale, the damascene process shows its limitation. Therefore, new etch process containing new gases needs to be developed.

In this study, the copper thin films were etched using non-corrosive gas mixture in pulse-modulated RF plasma. We investigated the effect of pulse-modulated RF plasma etching on etching characteristic compared to using the conventional continuous wave (CW) plasma etching. This modulated plasma can provide the specific plasma conditions modified by special matching system that can change on-off duty ratio of 13.56 MHz RF power and frequency on the specific duty ratio. In this research, the etching characteristics of copper thin film masked with nanometer-scale patterns were investigated in non-corrosive gases using pulse-modulated inductively coupled plasma reactive ion etching (ICP RIE). The effects of on-off duty ratio and frequency of pulsed plasma on the etch characteristics of copper were examined. Then, the etch profiles of copper thin films were observed by scanning electron microscopy and the etch mechanism was investigated using optical emission spectroscopy and X-ray photoelectron spectroscopy.

Acknowledgments

This research was supported by the MOTIE(Ministry of Trade, Industry & Energy (10080450) and KSRC(Korea Semiconductor Research Consortium) support program for the development of the future semiconductor device.

6:25 PM EL08.02.05

Late News: Inductively Coupled Plasma Reactive Ion Etching of Nanometer-Scale Patterned Copper Thin Films Using Organic Materials Sungyong Park, Eun Taek Lim, Ji Soo Lee, Yun Seong Park and Chee Won Chung; Inha University, Korea (the Republic of)

Copper interconnect, which has low resistivity, high electromigration resistance, and good mechanical properties, has replaced aluminum interconnect as the semiconductor devices are scaled down. However, copper interconnect could not be patterned by the conventional plasma etching technics because copper has very low reactivity and its etch byproducts are nonvolatile. Thus, copper patterning has been accomplished using 'damascene' process. However, as the critical dimensions of the devices decreased to nm scale, the resistivity of copper interconnect increased than that of the bulk resistivity. It occurs due to the surface scattering and grain boundary scattering of the copper as its dimensions are shrunk. Therefore, conventional dry etching method which can directly utilize low resistivity of the copper films should be developed.

Previously, dry etching of copper films using various halogen gases such as Cl_2 , SiCl_4 , HCl , and CCl_4 was performed, and the results were unsatisfactory due to the copper halide byproducts which were remained on the copper surface. On the other hand, organic chelator materials such as hexafluoroacetylacetone was used to the dry etching of the copper. Recently, inductively coupled plasma reactive ion etching using several organic materials were performed and good etching profile in the mm-scale copper line pattern was achieved. In this study, nanometer-scale patterned copper thin films have been etched using organic chelate materials with additives in inductively coupled plasma reactive ion etching. The influences of etch parameter such as gas concentration, ICP source power, bias voltage to the substrate, and process pressure have been investigated. The etch rate, etch selectivity, and etch profile of the copper film were examined by surface profilometer and field emission scanning electron microscopy. Then, the etch mechanisms were investigated using X-ray photoelectron spectroscopy and optical emission spectroscopy.

Acknowledgments This work was supported by Korea Institute for Advancement of Technology (KIAT) grant funded by the Korea Government (MOTIE) (0008458, PBL Oriented Semiconductor Equipment Engineer Recruits (POSEER), 2020 The Competency Development Program for Industry Specialist)

6:30 PM EL08.02.06

Low Dielectric Constant SiCOH Films by Plasma Enhanced Chemical Vapor Deposition of tetrakis(trimethylsilyloxy)silane and cyclohexane Precursors William Wirth, Jacob Comeaux and Seonhee

Jang; University of Louisiana at Lafayette, United States

In semiconductor industry, SiCOH films with low dielectric constant ($k \leq 4.0$) have been widely used as inter-metal dielectric (IMD) materials in the interconnects of semiconductor chips, to reduce a resistance-capacitance delay. In this study, the SiCOH films were deposited on silicon substrates using the plasma enhanced chemical vapor deposition of tetrakis(trimethylsilyloxy)silane (TTMSS) and cyclohexane (CHex) precursors. The chemical structure and materials performances of the SiCOH films strongly depended on deposition temperatures and flow rate ratios of TTMSS/CHex. Deposition temperatures varied in the range between room temperature and 400 °C. The flow rate ratios of TTMSS/CHex were determined by the control of argon carrier gas which transports each vaporized precursor from the bubblers to a process chamber. Physicochemical structures including porosity, density, and chemical composition of the SiCOH films affected their mechanical and electrical properties. The chemical bonds and compositions of the SiCOH films were investigated using Fourier transform infrared spectroscopy and X-ray photoelectron spectroscopy. The chemical bonds related with hydrocarbon and Si-O were the main characteristics of the SiCOH films. The mechanical properties including hardness and elastic modulus were measured by using a nanoindentation. The k values and leakage current density were determined by capacitance-voltage (C-V) and current-voltage (I-V) curves. The competition among hydrocarbon and Si-O bonds depending on deposition conditions affected the k values and mechanical strengths of the films. The enhanced mechanical and electrical performance with the optimized deposition conditions suggested the possibility of applying SiCOH films as IMD materials.

6:45 PM EL08.02.07

Design of Mechanically Reliable and Fracture Resistant Low-K Dielectric Hybrid Glasses for Next Generation Interconnects Karsu I. Kilic and Reinhold Dauskardt; Stanford University, United States

Despite their unusual properties, the reliable integration of low-k dielectric hybrid organosilicate glasses into interconnects for microelectronic device technologies is challenging due to their poor elastic and fracture properties. It is therefore crucial to explore the structure-property relationships of these materials to be able to design mechanically stiff and fracture resistant low-k dielectric hybrids for their successful integration into next generation interconnects. With our computational modeling, which is based on molecular dynamics simulations, we can generate highly accurate models of low-k dielectric hybrid organosilicate glasses with a wide range of structural characteristics and explore the effects of these structural characteristics on the resulting elastic and fracture properties. Our model low-k dielectric hybrid glasses have a range of different mean network connectivity, condensation degree and porosity; and they are derived from precursor molecules with a variety of geometrical features in terms of precursor chain length, molecular planarity and symmetry. Using molecular dynamics simulations, we can predict the structural stiffness of the model glass networks we generate and relate aforementioned structural features to the resulting elastic properties. As for the fracture properties, we have developed an algorithm named *Min-Cut Cohesive Fracture Model* which is based on a novel graph-theory approach to predict the fracture bond density and fracture morphology of our model hybrid glasses. In this approach, the glass network is treated as a graph where nodes and edges in the graph become atoms and bonds respectively. The algorithm operates on this mathematical framework and predicts the fracture path of the glass network to be the minimum cut that separates the graph, allowing us to explore fracture bond density and fracture patterns of several different low-k dielectric hybrid glass networks. Similar to elastic properties, we observe significant variations in the fracture path properties of low-k dielectric hybrid glass networks depending on their structural features. Remarkably, our results demonstrate that the hyperconnected low-k dielectric hybrid glass networks that are derived from cyclic and planar precursor molecules simultaneously enhance elastic and fracture properties. Specifically, the use of hyperconnected and cyclic planar precursors lead to *ultrastiff networks* which are stiffer than fully dense silica, and up to three times stiffer networks in comparison to traditional examples of low-k dielectric glasses such as the ethane-bridged oxycarbosilane (Et-OCS) glasses, while maintaining low density and low dielectric coefficient. Likewise, such networks also tend to exhibit more planar fracture paths (less fracture path meandering) with higher fracture bond density thereby significantly improving the fracture energy. This is a very important step towards the design of mechanically reliable and fracture resistant hybrid organosilicate low-k dielectric glasses for their successful integration to next generation

interconnects in microelectronic applications.

7:00 PM DISCUSSION TIME

SESSION EL08.03: Metallization and Reliability II
Session Chairs: Eiichi Kondoh and Andrew Simon
Friday Afternoon, April 23, 2021
EL08

8:15 PM *EL08.03.01

Low Temperature Deposition of Extremely Thin Barrier for Metallization Technology Mayumi Takeyama; Kitami Institute of Technology, Japan

In Si-LSI metallization technology and 3D-LSI, it is very difficult to obtain materials around metallization at low temperature and in a structurally- and thermally-stable state, because stability and temperature are generally inversely proportional. We have succeeded in forming at low temperatures insulating barriers and diffusion barriers. In particular, the sputtering method using radical reaction can form a thin film with excellent thermal stability without heating. I will explain the characteristics of the barrier film obtained by these technologies and an example of research on low-temperature deposition of barriers using the latest technology.

8:40 PM BREAK

8:55 PM EL08.03.03

Late News: Electrical Breakdown and Morphology Dependent Charge Transport Properties in Single TiO₂ Nanotubes Sourav K. Kajli, Debdutta Ray and Somnath C. Roy; Indian Institute of Technology Madras, India

Understanding the electrical conduction properties of a single nanostructure is essential for an insight into the fundamental charge transport through the 1D materials and also for exploring the collective behavior of an array of such nanostructures. TiO₂ nanostructures, such as electrochemically grown nanotubes, have been widely studied in recent times for several applications. The electrolyte plays a vital role in deciding the morphology, which, in turn, govern charge transport behavior. Here we present a comparative study of the charge transport through a single TiO₂ nanotube grown by electrochemical anodization using Ethylene Glycol and Dimethyl Sulphoxide electrolytes. The individual nanotubes are assembled into nanodevices using photolithography without relying on complex and sophisticated processes like electron beam lithography or focused ion beam deposition. The electric field dependent charge transport properties show Schottky emission at lower field regime and Poole-Frenkel emission in the higher region. The temperature-dependent electrical conduction (110K - 410K) is mediated by two thermal activation processes, attributed to shallow impurities in the low-temperature range ($T < 230$ K) and to the donors at deep intermediate levels at higher temperatures ($T > 230$ K). The activation energies for EG based nanotubes are found to be higher than that of DMSO nanotubes owing to the doubled wall morphology of the formed tubes. Also, the study of the electrical breakdown phenomena of these nanotubes reveals three distinct categories of collapse. 'Model A' type breakdown is characterized by a stepwise rise of current up to the breakdown point and fall to zero following a non-uniform step by step decrement, which is driven by crack formation near the electrode interface and its propagation. 'Model B' shows a transient rise and fall in current, leading to breakdown due to electromigration. Whereas 'Model C' type breakdown observed in a bundle of nanotubes shows a mixed trend of 'Model A' and 'Model B.' The data and analysis provide insight into the current limit through an individual nanotube or bundle of nanotubes and will be useful for designing prototype nanodevices from titania nanostructures.

9:10 PM *EL08.03.04

Amorphous Si-Rich W Silicide as a New Barrier and Contact Material for Advanced CMOS Naoya Okada, Noriyuki Uchida, Shinichi Ogawa and Toshihiko Kanayama; National Institute of Advanced Industrial Science and Technology, Japan

The electrical resistance in the back-end-of-line (BEOL) and middle-of-line (MOL) is becoming a critical factor more and more with recent shrinkage of Si CMOS. For interconnects, a thinner barrier film is required to keep the conductance in a narrower structure. Many researchers have already addressed this problem using various materials against Cu diffusion; yet, a new barrier material is strongly required. For the source/drain in transistors, Co is now a promising electrode; however, Co has a very high diffusivity in Si and a low reaction temperature easy to form silicide with Si; additionally, the Co/Si direct junction has a high contact resistance arising from a high electron Schottky barrier height (SBH) of $\sim 0.6\text{--}0.7$ eV for *n*-Si, owing to the Fermi-level pinning effect at the Si interface. The Co/Si junction therefore needs a diffusion barrier layer capable of the low SBH for Si. A promising solution is to use an atomically designed and engineered ultrathin barrier film. In this work, we demonstrate a novel barrier material with excellent barrier properties against Cu and Co diffusions and the low SBH for the Co/Si junction: the WSi_n ($n \leq 12$) composed of W-atom-encapsulated Si_n cage clusters.[1] The WSi_n film was prepared by the newly developed Cluster-Preforming Deposition (CPD) method.[2] In a hot-wall thermal deposition system, hydrogenated W-atom-encapsulated WSi_nH_x clusters with well-controlled n values ($n \leq 12$) are preformed by reaction of WF_6 and SiH_4 in the gas phase. The WSi_nH_x clusters are then deposited onto a substrate, where they are thermally dehydrogenated and coalesce to the WSi_n film with less hydrogen content. The formed films have an amorphous structure similar to the hydrogenated amorphous Si, but they are extremely stable against annealing up to 1100°C . We also confirmed that the WSi_n film exhibits an excellent step coverage over a high-aspect-ratio hole array with 40-nm diameter and 2- μm depth. [1]

The barrier properties of the WSi_n film against Cu diffusion were investigated using the two test structures with Cu electrodes: MOS capacitors with a 20-nm thermal oxide and $\text{p}^+\text{-n}$ diodes (junction depth of 100 nm) with and without the WSi_n insertion ($n = 12$, thickness = 5 nm). The WSi_n film exhibited excellent diffusion barrier properties for Cu contact; from the TDDDB lifetime of the Cu MOS capacitors, the diffusion barrier height was estimated to be 1.33 eV under 5 MV/cm stress and the Cu on Si diodes were stable against annealing up to 600°C . [3]

The contact properties for *n*-Si were investigated using the Co/Si Schottky diode with the WSi_n insertion ($n = 8$, thickness = 5 nm). Insertion of the WSi_n film reduced the electron SBH to 0.43 eV at Co/*n*-Si junctions. This is because the film is a semi-metal with a low work function close to the conduction band edge of Si. [4] These junctions have an excellent stability against annealing up to 700°C , leading to no appreciable interdiffusion. We directly observed that the WSi_n film prevented the Co diffusion by cross-sectional TEM and EDX. [5] These excellent diffusion barrier properties are because in the WSi_n film, all the Si atoms are strongly bonded to the W atoms forming W-atom-encapsulated clusters, suppressing the diffusion of Co and Cu atoms.

In conclusion, the WSi_n film exhibited excellent diffusion barrier properties for Cu and Co: a high barrier stability against annealing up to $600\text{--}700^\circ\text{C}$. Consequently, this film is a promising barrier and contact material in advanced CMOS.

[1] IEDM, 22.5, (2017). [2] J. Chem. Phys., 144, 084703 (2016). [3] IITC (2018). [4] APEX 13, 061005 (2020). [5] IITC (2019).

9:35 PM EL08.03.05

Late News: Reliability Failure in Microelectronic Interconnects by Electric Current Induced Chemical Reaction Sumit Kumar, Randhir Kumar, Praveen Kumar and Rudra Pratap; Indian Institute of Science Bangalore, India

The electric current-induced chemical reaction in Cr thin film by a micro/ nano-probe has been recently reported with detail characterization. Although the phenomenon has been employed for micro-nano fabrication

and the technique is called electroplating, this acts as a reliability failure of interconnection lines in the structure, where Cr is used as an adhesion layer, or main interconnects in microelectronic circuits. Here, for the first time, we present an investigation on the role of electric current density for such failure using a specifically designed sample. A 100 μm width, and 100 nm thin Cr film was deposited perpendicular to the Pt film of similar dimensions. The anode probe (20 μm diameter) was placed onto the Pt film whereas cathode probe onto the Cr film. The chemical reaction for an applied voltage initiated at the edge of the Pt film and not at the cathode probe. The analysis based on the COMSOL multiphysics simulation shows that the chemical reaction evolves at the high current density locations. The localized chemical reaction causes to damage the interconnection line. The study also builds a fundamental understanding of the mechanism of evolution of micro-nano patterning by electroplating.

9:40 PM DISCUSSION TIME

9:50 PM *EL08.03.02

Electroless Ni Plating—A Viable Approach for Fine-Pitch, Large Aspect-Ratio Vertical Interconnection Fabrication for 3D-LSI Integration and Packaging Mariappan Murugesan, Takafumi Fukushima and Mitsumasa Koyanagi; Tohoku University, Japan

The low-cost, high-throughput electro-less (EL) plating method has several potential advantages over the commonly used atomic layer deposition or physical vapor deposition processes to uniformly deposit barrier and seed metal layers inside the high aspect-ratio (AR) through-Si-via (TSV) interconnections for their immense applications in both the 2.5 D and 3D (three-dimensional) heterogeneous integration. By using an all-wet approach for TSV metallization, we have been able to fill the 8~10 mm-width Cu-TSVs with AR > 10 in Si-interposer for packaging applications. Also, the successful solid-filling of the sub-micron sized TSVs with AR close to 20 by EL plating of Ni enables one to achieve the vertical interconnections on 300 mm LSI wafer for the 3D-IC integration. Micro-structural and resistivity data on both sub- μm as well as 10 μm -width conventional Cu-TSVs with AR 12 to 17 revealed that the conformal Ni layer formed by EL-Ni plating is a very good seed layer for Cu electroplating. It is also evident from the morphological and the elemental analysis data that the EL-Ni plating forms nearly-uniformly thick metal layer all along the TSV sidewall and TSV bottom, which is otherwise difficult to realize by the even sophisticated PVD tool. Therefore, the EL plating method is proved to be a highly promising method for the conformal formation of barrier/seed layers inside the high AR TSVs for future 3D integration and packaging applications.

SYMPOSIUM EL09

Ferroelectricity and Negative Capacitance—Fundamentals, Applications and Controversies
April 14 - April 20, 2021

Symposium Organizers
Ru Huang, Peking University
Asif Khan, Georgia Institute of Technology
Changhwan Shin, Sungkyunkwan University
Pavlo Zubko, University College London

* Invited Paper

Tutorial EL09: Ferroelectricity in Advanced Microelectronics
Session Chairs: Sven Beyer, Jorge Iniguez, Asif Khan, Paul McIntyre, Kai Ni and Pavlo Zubko
Saturday Morning, April 17, 2021
EL09

10:00 AM *

Atomic Layer Deposition of Ferroelectrics Based on HfPO₂—Polycrystallinity, Polar Domains and Interfaces Paul McIntyre; Stanford University, United States

This tutorial will start with a general introduction to the atomic layer deposition (ALD) technique for industrial applications, the use of super-cycle ALD for fluorite structure oxides such as hafnium oxide and their nanolaminate and alloyed variants, and ferroelectricity therein. Afterwards, the main focus will be on microscopic aspects of such nanoscale, polycrystalline ferroelectrics for memory applications. Memory write and read operations require local reorientation and sensing of polar crystallographic domains, respectively. We will discuss the impact of such structural aspects on the miniaturization of the memory devices, physical principles relevant to polar domains, and methods for characterizing nanoscale domain structure in order to obtain a local picture for interpreting electrical data measured from ferroelectric memories. Lastly, we will elucidate the role of the interface layer structure, polarization charge screening, interface states and fixed charges on the performance and reliability of ferroelectric field-effect transistor based memories.

11:15 AM BREAK

11:30 AM *

Ferroelectric Field-Effect Transistors for 28nm Node and Beyond Sven Beyer; GlobalFoundries, Germany

With the discovery of ferroelectricity in HfO₂ based thin films 2011 and the co-integration of ferroelectric field effect transistors (FeFET) into standard high-k metal gate (HKMG) CMOS platforms 2016/17 by GLOBALFOUNDRIES, the FeFET has emerged from a theoretical dream to an applicable reality. Maturing in the beginning as a low-cost, low power eFLASH replacement, the FeFET yet is much more than a classical stiff eNVM cell. With its great HKMG CMOS compatibility, its flexibility and its unique switching properties, it is rather to be seen as a new versatile device that promises to open up new worlds. Especially the neuromorphic design community has shifted focus towards this novel device with game-changing potential. In this talk we will discuss the actual status of GLOBALFOUNDRIES FeFET technology, look into the operation and use of this device and sketch a potential roadmap.

12:45 PM BREAK

1:00 PM *

Ferroelectric Negative Capacitance Jorge Iniguez; Luxembourg Institute of Science and Technology, Luxembourg

We will discuss the effect known as “negative capacitance”, whereby some ferroelectric materials display an anomalous dielectric response (a negative permittivity) when subject to suitable electric boundary conditions. We will describe our current theoretical understanding, from both phenomenological and atomistic perspectives, drawing a clear distinction between equilibrium and transient negative-capacitance responses. We will also review the experimental evidence for both flavors of negative capacitance, and briefly present its expected technological applications (most notably in field-effect transistors, because of the concomitant “voltage amplification”). Finally, we will give our view of the current challenges and opportunities in the field.

2:15 PM BREAK

2:30 PM *

Numerical Models for Ferroelectric Memory Devices Kai Ni; Rochester Institute of Technology, United States

Ferroelectric memories based on the doped HfO₂ ferroelectric, including capacitor based 1T1C FeRAM and transistor based 1T FeFET, have received significant interests recently. The excellent scalability and CMOS compatibility of ferroelectric HfO₂ has allowed its integration into 2x technology node. Such scaling reveals novel physical phenomena not observed before in perovskite ferroelectric devices, such as degraded device variation with scaling, switching stochasticity, switching probability accumulation. In order to understand such phenomena and exploit them for novel energy efficient computation, accurate device models would be indispensable. In this lecture, we will present ferroelectric memory models developed so far, covering computationally efficient compact models, Monte Carlo models, and computationally intensive phase field models. By comparing with experimental data, the application range of each model will be identified and the potential for scaling/miniaturization of ferroelectric devices will be discussed.

SESSION EL09.01: Negative Capacitance
Session Chairs: Asif Khan and Pavlo Zubko
Sunday Morning, April 18, 2021
EL09

11:00 AM *EL09.01.01

Negative Capacitance Sayeeef Salahuddin; University of California, Berkeley, United States

Thermodynamics dictate that charge in an ordered system can be switched with lower energy than the Boltzmann limit known for non-interacting systems. Thinking about how to exploit it for computing led to the identification of negative capacitance in materials that show (anti)ferro-electric order [1]. In this presentation, we shall discuss this connection. Stabilization of negative capacitance needs careful consideration of electrostatic boundary condition. Especially, accounting for screening by metal electrodes is very important. In this regard, intuitive theoretical reasoning and simple schematics have often led to much confusion. We shall discuss our views on how to design experimental systems that are conducive to achieving the appropriate boundary conditions. While a single domain theory was used to elucidate the effect for simplicity, negative capacitance is not limited to single domains, as it has been pointed out early [2], and later by many authors [3,4].

Going back to the thermodynamic origin of switching more charge with less energy, the increase in capacitance has remained to be the simplest macroscopic test of the negative capacitance effect. However, modern imaging techniques allow probing the internal electric fields in a polar system with atomistic resolution. These experiments have revealed local energy maxima stabilized in the material, providing a direct imaging of stabilized negative capacitance [5]. These experiments confirm the prediction of local nature of the negative capacitance. In addition, they confirm the fact that negative capacitance originates in the regions of suppressed polarization.

One of the implications of Negative Capacitance is the possibility of subthermal ($<kT/q$) subthreshold swing in a MOSFET[6]. However, observation of subthermal swing has often been accompanied with Hysteresis or such swing has only been seen at very low currents. These led to questions such as: (i) Is subthermal subthreshold behavior intimately connected to Hysteresis? (ii) Does not observing this behavior mean that negative capacitance effect is fundamentally incorrect? In fact, in our view, most questions, confusions and so-called controversies can be traced back to these two questions. We will discuss these scenarios- specifically, the fact that these scenarios can be predicted from Landau's energy expressions together with appropriate boundary

conditions, as it has been discussed by many authors in literature. Therefore, observation of subthermal subthreshold swing is really a function of the properties of the channel material and the (anti)ferroelectric oxide and not observing it does not constitute a fundamental question on the negative capacitance effect itself. In fact, I will discuss other non-classical subthreshold behavior that ensues from negative capacitance, even if a subthermal subthreshold swing is not present. Such non-classical behavior is clearly observed in experiments.

Negative capacitance could find applications in different areas such as supercapacitors for energy storage, batteries, as enhanced capacitor for Dynamic Random Access Memory (DRAM) scaling, for back end capacitors in microchips, in addition to reducing supply voltage in transistors. I shall discuss some of our recent results in this regard. Specifically, I shall discuss experimental data that show how the original thermodynamic motivation of switching more charge with less energy can now be achieved [7,8] in the most advanced transistors, which could lead to supply voltage reduction and/or enhanced scaling capability beyond the roadmap.

[1] Salahuddin and Datta, Nanoletters, 8,2,2008

[2] Cano and Jimenez, APL, 97,13,2010

[3] Zubko et al, Nature 534 (7608), 524-528

[4] Lukyanchuk et al, Comm. Physics, 2,22, 2019

[5] Yadav et al Nature, 565, 7740, 468-471, 2019

[6] Salvatore et al, IEDM, 2008

[7] Cheema et al, Nature, 580 (7804), 478-482

[8] DW Kwon et al, IEEE EDL, 40,6,2019

11:25 AM *EL09.01.02

Enabling New Functionalities and Energy Efficiency with Negative Capacitance in 2D Devices Adrian Ionescu; Ecole Polytechnique Fédérale de Lausanne, Switzerland

In this talk we will present novel progress in the device functionality and energy efficiency when applying gate stacks with negative capacitance (NC) features to 2D devices. We will explore NC as technology booster for 2D/2D tunneling FETs based on WSe₂/SnSe₂ vdW heterojunctions, from low to high temperatures, including the energy losses per switching operation, together with the analysis of the advantages and challenges of using NC in doped high-k dielectrics like Si:HfO₂. We will report both DC and pulsed experiments trying to have further insights in recent controversies concerning the negative capacitance regime and the dynamics of nucleation processes in ferroelectrics.

11:50 AM *EL09.01.03

Static Reversible Negative Capacitance in Ferroelectric Nanodot with Domains and Topological Excitations Igor Lukyanchuk¹, Yurii Tikhonov¹, Anais Sene¹, Anna Razumnaya² and Valerii Vinokur³; ¹University of Picardie, France; ²Southern Federal University, Russian Federation; ³Argonne National Laboratory, United States

The idea of ferroelectric-based devices with negative capacitance (NC) in low-power nanoscale electronics triggered explosive activity in the field. This revived the thoughts of engineers of the early 1930-s on the possibility of negative circuit constants and the 40-years old fundamental question raised by Rolf Landauer, whether the capacitance can be negative, that is if the increase in the charge of the capacitor can decrease its voltage. Having stated that ferroelectrics can harbor the NC during the transient processes of switching, Landauer indicated that the very existence of the static NC as a part of steady-state is challenged by instability against spontaneous domain formation. For today, most of the research addressed transient NC, leaving the basic question of the existence of the steady-state NC unresolved. Here we demonstrate* that the ferroelectric nanodot capacitor hosts a stable two-domain state realizing the static reversible NC device.

* I. Luk'yanchuk, Y. Tikhonov, A. Sené, A. Razumnaya & V. M. Vinokur, Harnessing ferroelectric domains

SESSION EL09.02: Domains and Negative Capacitance
Session Chairs: Marty Gregg and Asif Khan
Sunday Afternoon, April 18, 2021
EL09

1:00 PM *EL09.02.01

Local Negative Permittivity and Topological-Phase Transition in Polar Skyrmions Ramamoorthy Ramesh;
University of California, Berkeley, United States

Topological solitons such as magnetic skyrmions have drawn attention as stable quasi-particle-like objects. The recent discovery of polar vortices and skyrmions in ferroelectric-oxide superlattices has opened up new vistas to explore topology, emergent phenomena, and approaches for manipulating such features with electric fields. Using macroscopic dielectric measurements, coupled with direct scanning convergent-beam electron diffraction (SCBED) imaging at the atomic scale, theoretical phase-field simulations, and second-principles calculations, we demonstrate that polar skyrmions in $(\text{PbTiO}_3)_n/(\text{SrTiO}_3)_n$ superlattices are distinguished by a sheath of negative permittivity at the periphery of each skyrmion. This enhances the effective dielectric permittivity compared to individual SrTiO_3 and PbTiO_3 layers. Moreover, the response of these topologically protected structures to electric field and temperature show a reversible phase transition from the skyrmion state to a trivial uniform ferroelectric state, accompanied by large tunability of the dielectric permittivity. Pulsed-switching measurements show a time-dependent evolution and recovery of the skyrmion state (and macroscopic dielectric response). The interrelationship between topological and dielectric properties presents an opportunity to simultaneously manipulate both of them by a single, and easily controlled, stimulus, the applied electric field.

1:25 PM EL09.02.02

Metal-Ferroelectric Supercrystals with Periodically Curved Metallic Layers Marios Hadjimichael¹, Yaqi Li^{2,3}, Edoardo Zatterin^{2,3,4}, Gilbert Chahine⁵, Michele Conroy⁶, Kalani Moore⁶, Eoghan O'Connell⁶, Petr Ondrejko⁷, Pavel Marton⁷, Jiri Hlinka⁷, Ursel Bangert⁶, Steven Leake⁴ and Pavlo Zubko^{2,3}; ¹University of Geneva, Switzerland; ²University College London, United Kingdom; ³London Centre for Nanotechnology, United Kingdom; ⁴European Synchrotron Radiation Facility, France; ⁵Université Grenoble Alpes, France; ⁶University of Limerick, Ireland; ⁷Institute of Physics of the Czech Academy of Sciences, Czechia

Domains in ferroelectric materials have been at the forefront of recent scientific research, mostly due to the fascinating properties of their boundaries, domain walls. As well as enhancing the macroscopic properties of ferroelectrics, domain walls exhibit symmetry and properties different from the bulk material, offering novel functionality. One scalable method to control domain wall configurations in ferroelectrics is epitaxial strain. Epitaxial strain and the interplay between electrostatic and mechanical energy allow for the formation of novel domain structures, such as regular arrays of flux closure domains or chiral vortex centres.

Here, we show that a stable supercrystal phase comprising a 3D ordering of nanoscale domains with tailored periodicities can be engineered in $\text{PbTiO}_3/\text{SrRuO}_3$ ferroelectric-metal superlattices under tensile strain. A combination of x-ray diffraction, piezoresponse force microscopy, transmission electron microscopy and phase-field simulations reveals a complex hierarchical superstructure, which consists of alternate vertical and horizontal flux closure patterns, and forms in order to minimize the elastic and electrostatic energy. Large local deformations of the ferroelectric lattice are accommodated by periodic lattice modulations of the SrRuO_3 layers, presenting a paradigm for engineering correlated materials with tailored modulated structural and electronic properties.

1:40 PM *EL09.02.03

Optimizing Steady-State Negative Capacitance Jorge Iniguez^{1,2}; ¹Luxembourg Institute of Science and Technology, Luxembourg; ²University of Luxembourg, Luxembourg

My group is interested in the behavior of ferroelectric materials that, in particular circumstances, display a persistent voltage drop that opposes the overall applied DC bias; that is, they behave as a static negative capacitance [1]. More precisely, we investigate PbTiO₃/SrTiO₃ ferroelectric/dielectric superlattices as a convenient model system [2,3], using second-principles simulation methods [2,4] to monitor their behavior as a function of the available control knobs: temperature, applied electric field, epitaxial strain and layer thickness. This allows us to better understand the factors affecting the negative-capacitance response of the PbTiO₃ layers, and thus identify strategies to optimize it. In this talk I will review our most recent results, focusing on the possible persistence of negative capacitance down to very low temperatures and the evolution of the differential capacitance as a function of applied electric field.

Work done in collaboration with M. Graf and H. Aramberri, postdocs at the Luxembourg Institute of Science and Technology. Funded by the Luxembourg National Research Fund through Grant INTER/RCUK/18/12601980.

[1] J. Iniguez et al., "Ferroelectric negative capacitance", Nature Reviews Materials 4, 243 (2019).

[2] P. Zubko et al., "Negative capacitance in multidomain ferroelectric superlattices", Nature 534, 524 (2016).

[3] S. Das et al., "Local negative permittivity and topological phase transition in polar skyrmions", Nature Materials (2020), <https://doi.org/10.1038/s41563-020-00818-y>

[4] J.C. Wojdel et al., "First-principles model potentials for lattice-dynamical studies: general methodology and example of application to ferroic perovskite oxides", J. Phys. Condens. Matt. 25, 305401 (2013).

2:05 PM EL09.02.04

Electric Field Control of Chiral Domains in PbTiO₃/SrTiO₃ Multilayers Piush Behera¹, Molly May², Margaret McCarter¹, Sujit Das¹, Archana Raja³, Markus Raschke² and Ramamoorthy Ramesh^{1,1}; ¹University of California, Berkeley, United States; ²University of Colorado Boulder, United States; ³Lawrence Berkeley National Laboratory, United States

Chirality, when an object cannot be superimposed on its mirror image, has been seen across a multitude of fields in materials science. From biological molecules to magnetic spin textures, chirality has played a key role in determining the functional properties of such systems. However, it is only recently that the chiral objects have appeared in ferroelectric materials systems. In PbTiO₃/SrTiO₃ (PTO/STO) thin film multilayers, boundary conditions set by epitaxial strain from the substrate and paraelectric layers of STO results the continuous rotation of electric dipoles in the PTO layer in the form of polar vortices.¹ Similar to magnetic vortices, the sense of rotation of the dipoles and the orientation of the axial polarization of the vortices can be used to classify them as left-handed or right-handed.² Although chirality and topology has been observed in a number of ferroic systems, the manipulation of the sense of chirality with electric fields has remained elusive. Using second harmonic generation circular dichroism (SHG-CD), we show that these vortices organize together to form chiral domains over length scales of 100s of nanometers. Each chiral domain consists of a multitude of vortex tubes of the same handedness, separated by a mobile chiral boundary. Using in-situ SHG-CD, we map chiral polar vortex domains as a function of in-plane electric field. We show that these domains can be elongated along the field direction, when the electric field is applied along parallel to the vortex tube. Moreover, by applying an electric field along the direction of rotation, we deterministically switched the chirality of the film by translation of the chiral boundary. Ab-initio and phase field simulations were used to show that the chiral switching arises from a reversal in the buckling of these vortices. In addition, piezoforce microscopy studies were performed to relate how the chirality arises from polarization of domains. This work illustrates the

first evidence of chiral switching in any materials system using an applied electric field, and highlights the use of lab-based mesoscopic probes of nanoscale chiral objects.

References

- [1] Yadav, A. K., C. T. Nelson, S. L. Hsu, Z. Hong, J. D. Clarkson, C. M. Schlepütz, A. R. Damodaran, et al. "Observation of Polar Vortices in Oxide Superlattices." *Nature* 530, no. 7589 (February 2016): 198–201.
- [2] Shafer, Padraic, Pablo García-Fernández, Pablo Aguado-Puente, Anoop R. Damodaran, Ajay K. Yadav, Christopher T. Nelson, Shang-Lin Hsu, et al. "Emergent Chirality in the Electric Polarization Texture of Titanate Superlattices." *Proceedings of the National Academy of Sciences* 115, no. 5 (January 30, 2018): 915–20.

2:20 PM *EL09.02.05

Effective Ferroelectric Permittivity in Metal-Ferroelectric-Insulator-Semiconductor (MFIS) Heterostructures—The Implications of Hard and Soft Domain Walls Atanu Kumar Saha and Sumeet Gupta; Purdue University, United States

The negative capacitance effect in ferroelectric (FE) based devices has not only attracted a significant research interest due to the possibility of achieving steep switching in transistors [S. Salahuddin et al., *Nano Lett.* 8, 2008], but has also intrigued a broader research community aimed at understanding the fundamental origin of such intriguing properties. In a microscopic sense, the ferroelectricity originates from the non-centrosymmetric crystal structure where the spontaneous displacement of atoms (and the corresponding electron gas and ion core) leads to a non-zero spontaneous polarization (P), which yields the minimum energy bi-stable states of the FE. However, in a heterogeneous system (*e.g.* FE-DE-semiconductor or MFIS stack), the value of P is determined by the minimum energy of the whole system rather than the energy of the FE itself. In such systems, the P -induced bound charge in the FE-DE interface induces a depolarization electric field in the FE layer. Such a depolarization effect tends to reduce the P magnitude of the FE layer causing an increase in its free energy. However, in this scenario, the fundamental electrostatics suggests the formation of multi-domain (MD) states that suppresses the depolarization effect without any significant increase in its free energy [A. Kopal et al., *Ferroelectrics* 223, 1999]. Moreover, the suppression of depolarization and free energy occurs in the cost of gradient energy (which is elastic in nature) due to the P gradient near the domain wall (DW). Therefore, the formation of the MD state appears as an interplay among different energy components for obtaining the minimum energy configuration [A. K. Saha et al., *Sci. Rep.* 10, 2020].

To investigate the MD state formation and its effect on the effective permittivity of FE, we have developed a phase-field simulation framework for Metal-Ferroelectric-Insulator-Metal (MFIS) heterostructure by self-consistently solving the Ginzburg-Landau equation, Poisson's equation, and semiconductor charge equations [A. K. Saha et al., *Sci. Rep.* 10, 2020]. According to our analysis, the applied voltage-driven P switching in the MD state is strongly dependent on the features of its DW. This further depends on the elastic, electrostatic, and physical properties of the FE layer and the dielectric/semiconductor layers that it interacts with. We show that, in the case of low elastic coupling (low gradient energy coefficient), the types of DWs are hard and the domain density depends on material parameters and physical dimensions of the heterostructure. In the hard DW regime, P -switching is hysteretic and can take place as a combination of domain nucleation and DW motion. During such a P -switching, the effective permittivity of FE becomes negative. However, even without P -switching (with voltages $<$ coercive voltage), the effective permittivity of the FE layer can increase (but remain positive) due to the electrostatic interactions among domains. This effect is more dominant when the domain density is large. As the domain becomes denser, the effective permittivity keeps increasing within the limit of hard-DW. On the other hand, for a sufficiently high elastic coupling (high gradient energy coefficient), the DW can become soft and the corresponding soft domain-wall displacement leads to non-hysteretic characteristics. In such a scenario, the effective permittivity of the FE layer becomes negative in a non-hysteretic fashion.

SESSION EL09.03: Dynamics of Negative Capacitance
Session Chairs: Asif Khan and Peide Ye
Sunday Afternoon, April 18, 2021
EL09

6:30 PM *EL09.03.01

Negative Capacitance in HfO₂ Based Ferroelectric Materials Michael Hoffmann^{1,2}, Stefan Slesazek¹ and Thomas Mikolajick^{1,3}; ¹NaMLab gGmbH, Germany; ²University of California, Berkeley, United States; ³Technische Universität Dresden, Germany

The feasibility of ferroelectric negative capacitance devices for ultra-low power electronics hinges on the availability of materials which are scalable and compatible with established semiconductor manufacturing technologies. Ferroelectrics of fluorite-structure based on the binary oxides HfO₂ and ZrO₂ fulfill both of these criteria. Recently, negative capacitance was observed in HfO₂ based ferroelectrics using pulsed electrical measurements. However, relatively large applied voltages have been necessary to observe negative capacitance in this material system so far. To move towards applications in negative capacitance devices, much lower operating voltages are needed. Furthermore, the microscopic domain dynamics underlying the negative capacitance effect in HfO₂ based ferroelectrics is still not understood, which hampers physical modeling and device design. Here, we discuss the available experimental data and outline pathways to move towards improving our understanding of negative capacitance in HfO₂ based ferroelectrics and prospective applications.

6:55 PM EL09.03.02

Differential Charge Boost in Hysteretic Ferroelectric-Dielectric Heterostructure Capacitors at the Steady State Nujhat Tasneem¹, Prasanna Venkatesan Ravindran¹, Zheng Wang¹, Jorge Gomez², Jae Hur¹, Shimeng Yu¹, Suman Datta¹ and Asif Khan¹; ¹Georgia Institute of Technology, United States; ²University of Notre Dame, United States

The ferroelectric (FE)-dielectric (DE) heterostructure is one of the commonly used model systems to probe negative capacitance effects.^{1,2} In such a system, the change in charge due to a change in source voltage can be larger than the change in charge when the same change in source voltage is experienced only by the constituent DE capacitor. Such a differential charge boost, when achieved without a hysteresis, can lower the power supply voltage and the energy dissipation in a negative capacitance field-effect transistor (NCFET). However, there is an ongoing debate on whether the charge boost in such a heterostructure is a transient phenomenon or a steady state one.

According to a transient model³ of ferroelectric negative capacitance, the charge boost in an FE-DE capacitor is a consequence of (1) the mismatch between the time scales for polarization switching and the screen charge dynamics in the FE, and (2) a charge imbalance between the FE and the DE. The change in the DE charge, ΔQ in such a scenario is expected to be larger than $C_{DE}\Delta V$ resulting in the so-called charge boost. The fundamental aspect of the transient model is that as the screening charges balance out the polarization charges, the boost in both V_{FE} and Q diminishes to values that are expected from a series combination of two positive capacitors, thereby leading to charge boost only in transience. Hence, ΔQ will be larger than $C_{DE}\Delta V$ only for a short amount of time. Whereas, if the charge boost was in fact a steady state response, then the charge boost stemming from it will prevail for the entire duration of the voltage pulse. Hence, the key test for transient and steady state model of negative capacitance is as follows: for a given change in voltage ΔV , is the charge supplied by the voltage source to a FE-DE capacitor ΔQ larger than $C_{DE}\Delta V$ only for a short duration of time (transient state) or an extended period of time (steady state)?

To answer this question, we present an experiment that tests the nature of the charge boost: steady-state or transient. To that end, we study a ferroelectric-dielectric (FE-DE) heterostructure with FE Hf_{0.5}Zr_{0.5}O₂ (10nm) and DE HfO₂ (5nm). We adopt a modified form of the well-known, positive up negative down (PUND)

technique where 'long' voltage pulses are applied on the FE-DE capacitor to measure its polarization vs voltage (P-V) characteristics. We find that the device under test (DUT) exhibits a differential charge boost of steady-state nature i.e., the charge boost remains intact after the initial transient effects subside and all the voltages in the system reach constant values and steady states. A SPICE-based model of the system that accounts for the multi-domain polarization switching dynamics in the FE-DE stack was also used to verify our experimental results.

In summary, the results obtained from the modified PUND measurement technique on an FE-DE structure reveals that the charge boost in a hysteretic FE-DE structure is prevalent for the entire pulse duration and hence a steady state response. The experimental results match with the predictions based on a multi-domain ferroelectric model eliciting the importance of domain dynamics in obtaining the ideal stabilized negative capacitance. Investigating NCFETs and NC Capacitors using this method will provide more insights into the charge dynamics of the systems which can be used to advance the designs and study the physics of these devices.

References:

1. S. Salahuddin and S. Datta, Nano letters 8, 405 (2008).
2. M. Hoffmann, F. P. Fengler, M. Herzig, T. Mittmann, B. Max, U. Schroeder, R. Negrea, P. Lucian, S. Slesazeck, and T. Miko-lajick, Nature 565, 464 (2019).
3. K. Ng, S. J. Hillenius, and A. Gruverman, Solid State Commu-nications 265, 12 (2017).

Prasanna Venkatesan Ravindran and Nujhat Tasneem both contributed equally to this project and will be co-presenting at the 2021 MRS Virtual Spring Meeting.

7:10 PM *EL09.03.03

Can NCFET Work as Steep-Slope Device for Ultralow-Power Logic Applications? Qianqian Huang, Mengxuan Yang, Chang Su, Huimin Wang and Ru Huang; Institute of Microelectronics, Peking University, China

Power dissipation is one of the most critical issues for nanoelectronic circuits. For low-voltage and low-power logic applications, novel steep-slope device concepts, which can break the fundamental limitation of subthreshold swing (SS) in MOSFETs (60mV/dec at room temperature), have attracted lots of attention. By utilizing the voltage amplification effect induced by the negative capacitance (NC) in the gate stack, the ferroelectric FET (FeFET) also has the capability of sub-60 SS, which is considered as NCFET. However, the NC effect in ferroelectric film has aroused great scientific controversy due to its unclear physical picture and lacking of direct experimental evidence.

Here we experimentally observed the NC effect in HfO₂-based ferroelectric film and systematically studied its fundamental physics from the perspective of material features including both relaxation polarization and transient polarization. Different from the stabilized NC, the observed NC effect of HfO₂-based FE material in this work is not a steady but a dynamic behavior, which is very sensitive with sweeping voltage and can be existed only under an extremely stringent operating frequency range. Moreover, even under this required frequency range, it is found that the SS of NCFET will inherently degrade with the increased gate voltage, which is not preferred for low-voltage logic operation.

Besides, it is found that the hysteresis theoretically exists, and there is an intrinsic optimization conflict between SS and hysteresis, which is a big challenge for logic applications. In addition, the hysteresis shows a strongly non-monotonic dependence on voltage sweeping rate, coupled with sweeping range, and can be even larger than the hysteresis of standalone FE capacitor for high-frequency applications. The possibility of NCFET as a steep-slope device for high-speed and low-voltage logic operation needs to be carefully re-assessed.

7:35 PM *EL09.03.04

Enhancement and Origin of Intrinsic Transient Negative Capacitance During Ferroelectric Switching Bin Xu^{1,2}, Sergey Prosandeev^{2,3}, Charles Paillard^{4,2} and Laurent Bellaiche²; ¹Soochow University, China;

²University of Arkansas–Fayetteville, United States; ³Southern Federal University, Russian Federation;

⁴Université Paris-Saclay, France

The reversal of polarization in a ferroelectric material involves overcoming an energy barrier and has been previously proposed and found to yield transient negative capacitance (NC) in the intermediate states of the switching process [1-3]. Homogeneous switching was assumed to interpret the experimental results of NC; however, inhomogeneous switching is a more abundant mechanism than homogeneous switching, but its possible effect on NC is basically unknown. Here, we use first-principles-based effective Hamiltonian techniques to investigate the occurrence of NC during these two types of switching processes in the super-tetragonal phase of BiFeO₃, which can be realized by changing the magnitude of the electric field. We find NC in both cases, but with the magnitude of the inverse of the capacitance being drastically larger in the inhomogeneous (nucleation limited) switching, as compared to the homogeneous switching. We further analyze the origin of the different NC effects, and point to the different energetic trajectories between these two representative switching mechanisms [4]. In addition, we derive analytical formulas and show that the capacitance can be negative under perfect screening conditions and for very different materials and switching mechanisms [5].

References:

- [1] A. I. Khan, K. Chatterjee, B. Wang, S. Drapcho, L. You, C. Serrao, S. R. Bakaul, R. Ramesh, and S. Salahuddin, *Nat. Mater.* 14, 182 (2015).
- [2] M. Hoffmann, M. Pešić, K. Chatterjee, A. I. Khan, S. Salahuddin, S. Slesazeck, U. Schroeder, and T. Mikolajick, *Adv. Funct. Mater.* 26, 8643 (2016).
- [3] A. K. Saha, S. Datta, and S. K. Gupta, *Journal of Applied Physics* 123, 105102 (2018).
- [4] Bin Xu, Sergey Prosandeev, Charles Paillard, and L. Bellaiche, *Phys. Rev. B* 101, 180101(R) (2020).
- [5] Sergey Prosandeev, Charles Paillard, B. Xu, and L. Bellaiche, *Phys. Rev. B* 101, 024111 (2020)

Acknowledgements:

B.X. and L.B. thank the DARPA Grant No. HR0011-15-2-0038 (MATRIX program). B.X. also acknowledges financial support from National Natural Science Foundation of China under Grant No. 12074277, the startup fund from Soochow University and the support from Priority Academic Program Development (PAPD) of Jiangsu Higher Education Institutions. S.P. thanks ONR Grant No. N00014-17-1-2818 and the support from Grant RMES No. 3.1649.2017/4.6, and also appreciates the financial support from Grant No. BAZ0110/20-3-08IF of Ministry of Science and Higher Education of the Russian Federation (State assignment in the field of scientific activity, Southern Federal University, 2020). C.P. acknowledges the support of ARO Grant No. W911NF16-1-0227. We are also thankful for the computational support from Arkansas High Performance Computer Center at the University of Arkansas.

SESSION EL09.04: Ferroelectric Materials
Session Chairs: Kisung Chae and Changhwan Shin
Sunday Afternoon, April 18, 2021
EL09

9:00 PM *EL09.04.01

Stability and Room Temperature Deposition of Ferroelectric Phase in Y-Doped (Hf, Zr)O₂ Films Hiroshi Funakubo¹, Takanori Mimura¹, Reijiro Shimura¹, Yoshiko Nakamura¹ and Takao Shimizu^{1,2}; ¹Tokyo Institute of Technology, Japan; ²National Institute for Materials Science, Japan

A discovery of ferroelectricity in doped HfO₂ films opens the door of the device application using very thin ferroelectric films because stable ferroelectricity is maintained below 10 nm even in polycrystalline films. We

demonstrate the fundamental understanding of HfO₂-based ferroelectric films using epitaxial films[1-8]. In addition, we demonstrate 1 mm-thick ferroelectric films that are useful for the piezoelectric applications[9-10]. Various devices including ferroelectric memories, ferroelectric tunnel junction, and piezoelectric transistors have been investigated. For these device applications, low temperature deposition of ferroelectric films is highly required to reduce the reaction between the film and the underlying layers.

In this study, we demonstrate the room temperature deposition of Y-doped (Hf, Zr)O₂ films by sputtering method[7]. Room temperature-deposited films showed almost similar ferroelectricity with the post heat-treated one above 800 °C. In addition, wide variety of composition show the ferroelectricity even for the films deposited at room temperature. In my presentation, we discuss the determination factors for the room temperature deposition.

- [1] Shimizu *et al.*, Appl. Phys. Lett., 107, 032910- 1 - 5 (2015);
- [2] Shimizu *et al.*, Sci. Rep., 6, 32931-1-8 (2016)
- [3] Shiraishi *et al.*, Appl. Phys. Lett., 108, 262904-1-5 (2016)
- [4] Mimura *et al.*, Jpn. J. Appl. Phys., 59, SGGB04-1-6 (2020).
- [5] Shimizu *et al.* Appl. Phys. Lett., 113, 212901-1-5 (2018)
- [6] Mimura *et al.*, Jpn J. Appl. Phys., 58, SB3B09-1-5 (2019).
- [7] Mimura *et al.*, Appl. Phys. Lett. 113, 102901-1-4 (2018).
- [8] Mimura *et al.*, Appl. Phys. Lett., 109, 052903-1-4 (2016)
- [9] Mimura *et al.*, Appl. Phys. Lett., 115, 032901 (2019).
- [10] Shimura *et al.*, J. Ceram. Soc. Jpn., 128, 539-543 (2020).
- [11] Mimura *et al.*, Appl. Phys. Lett., 116, 062901-1-5 (2020).

9:25 PM DISCUSSION TIME

9:40 PM EL09.04.04

Late News: Domain Patterns and Super-Elasticity of Freestanding BiFeO₃ Membranes via Phase-Field Simulations Ren-Ci Peng¹, Xiaoxing Cheng², Bin Peng¹, Ziyao Zhou¹, Long-Qing Chen² and Ming Liu¹; ¹Xi'an Jiaotong University, China; ²The Pennsylvania State University, United States

Super-elasticity of functional ferroelectric oxides offers promises for integrating ferroelectric films into flexible electronics. However, super-elastic deformation is a complex phenomenon related to possibly multiple concurrent mechanisms. Fundamentally understanding how multiple mechanisms contribute to the super-elasticity of ferroelectric oxides is crucial to realizing their potential flexible electronic applications. Here, we employ phase-field simulations to model the dynamics of ferroelectric domain patterns of freestanding BiFeO₃ membranes to understand the origin of their super-elasticity under substantial bending deformation (5% strain). It is demonstrated that both a reversible Rhombohedral-Tetragonal (R-T) phase transition and a nearly reversible domain evolution of BiFeO₃ membranes contribute to accommodating the large deformation and thus their super-elasticity. The dynamics of domain evolution also reveal the formation of an exotic ferroelectric vortex and polarization rotation before the phase transition. We constructed a diagram of phases and domain patterns as a function of the membrane thickness and bending angle, which allows one to readily predict the emergence of T phase and ferroelectric vortex in bent BFO membranes. These results not only provide fundamental understanding of mesoscale super-elastic mechanisms but also reveal exotic domain states of ferroelectric membranes.

9:55 PM EL09.04.06

Exploring Mixed-Cation Niobates for High-Performance Dielectric Nanocapacitors Seunghyun V. Oh, Woohyun Hwang and Aloysius Soon; Yonsei University, Korea (the Republic of)

With the increasingly high demand for high-performance dielectric nanocapacitors in electronics and energy storage devices, huge research efforts have been placed in developing high-performance multilayer ceramic capacitors (MLCCs) with a particular focus on advanced functional nanomaterials design and development. In

particular, the search for lead-free, low-loss ferroelectric oxides are considered as one of the most promising material candidates for this technology. In this study, using first-principles density-functional (perturbation) theory calculations, we investigate the influence of A-site alloying in potassium niobate, (K,A)NbO₃ on its optoelectronic, polarization, and dielectric properties, where A = Li, Na, Rb, and Cs. Using the special quasi-random structure model, we consider various alloy compositions of (K,A)NbO₃ and examine their mixing thermodynamics before moving on to characterizing their polar properties, establishing specific structure-property design rules for high-performance dielectric oxides. Together with complementary experimental findings, our work underscores the importance of how cation-exchange in these lead-free ferroelectrics on neoteric MLCC materials.

SESSION EL09.05: Domains and Ferroelectric Membranes

Session Chairs: Asif Khan and James LeBeau

Monday Morning, April 19, 2021

EL09

8:15 AM *EL09.05.01

Negative Capacitance in Copper-Chlorine Boracite Joseph Guy¹, Charlotte Cochard², Roger Whatmore³, Amit Kumar¹, Ray McQuaid¹ and Marty Gregg¹; ¹Queen's University Belfast, United Kingdom; ²University of Dundee, United Kingdom; ³Imperial College London, United Kingdom

During switching, the microstructure of a ferroelectric normally changes to best align internal dipoles with externally applied electric fields. Dipolar regions (domains), that are favourably oriented, grow at the expense of those in unfavourable orientations and this is manifested in a predictable field-induced motion of the walls that separate one domain from the next. In copper-chlorine boracite, however, we have discovered that head-to-head charged 90° domain walls move in the opposite direction to that expected: the polarisation that is anti-aligned with the applied electric field increases as a result of the field-induced wall movement. Polarisation-field (P-E) hysteresis loops, associated with the movement of these walls, hence show negative gradients throughout the entire P-E cycle. Negative capacitance is therefore implied. We have measured switching currents, generated by the relative motion between domain walls and sensing electrodes, by employing charge gradient microscopy. Such measurements reveal that the signs of the switching currents are opposite to those expected conventionally. Moreover, the switching current behaviour can be analysed to allow the negative capacitance component to be extracted and probed as a function of frequency.

8:40 AM EL09.05.02

Electro-Mechanical Control of Ferroelectric Domains in PbZr_{0.20}Ti_{0.80}O₃ Sergio Gonzalez Casa^{1,2}, Xiaofei Bai¹, David Albertini¹, Nicolas Baboux¹, Bertrand Vilquin¹, Pedro Rojo-Romeo¹, Solene Brottet¹, Matthieu Bugnet², Ingrid Cañero Infante¹ and Brice Gautier¹; ¹Institut des Nanotechnologies de Lyon, France; ²MATEIS, France

The control of ferroelectric domains and domain walls is the basis of a promising approach to imagine novel electronic devices. While the control of ferroelectric domains by the application of an electric field has been extensively studied, the application of a mechanical load and its consequences over the ferroelectric properties have been seldomly explored. Mechanical switching of ferroelectric domains by the application of a local stress has already been observed [1], however a complete explanation of the phenomena involved in the process may depend on the properties of the material studied. In order to propose a complete description of the mechanisms at play during switching, flexoelectricity has to be taken into account [1] in addition to piezoelectricity, which is a common property of all ferroelectrics, and along with ferroelasticity [2] and electrochemistry [3].

In this contribution, we apply a mechanical stress by pressing the surface with the tip of an atomic force

microscope. We show that mechanical switching in sol-gel grown ferroelectric $\text{PbZr}_x\text{Ti}_{1-x}\text{O}_3$ ($x=0.2$) thin films is possible under different conditions of mechanical stress up to large thicknesses (200 nm). We vary the experimental conditions that allow effective mechanical switching of layers of different thicknesses, and combine electrical and mechanical switching to modify the threshold force needed to switch the polarization. The results are supported by the cross-sectional observation of the films by scanning transmission electron microscopy (STEM), which brings information about the nanoscale structure and chemistry of the films.

Our results suggest two ways of controlling the threshold force. Firstly, the prior application of an electric field would modify the value needed to switch domains mechanically. This effect is probably due to charge trapping that decreases the magnitude of the electric field created by the applied stress. Secondly, the mechanical switching is affected by the presence of nanometer-scale cavities within the sample, either aligned in specific regions of the film or randomly distributed as evidenced by STEM images, which modify the boundary conditions of the domains created by mechanical stress and their stability. The combination of both external electrical field and cavities tends to show that it is actually possible to tune the force threshold to suit the desired purpose. We will discuss these results with the aim to provide a larger understanding of means to exploit the mechanical switching in integrated ferroelectric devices. [4]

[1] H. Lu, et al., *Science*, 335(6077):59–61, (2012).

[2] D. Edwards et al, *Adv. Mater. Interfaces*, 3, 1500470 (2016)

[3] Y. Cao, et al., *Physical Review B* 96, (2017)

[4] S. Gonzalez-Casal et al. In preparation.

8:55 AM EL09.05.03

Free-Standing Ferroelectric Oxide Superlattices Yaqi Li¹, Edoardo Zatterin^{1,2}, Alexander Björling³, Michele Conroy⁴, Kalani Moore⁴, Adam Clancy¹, Sungmyung Kang¹, Marios Hadjimichael¹, Dirk Groenendijk⁵, Edouard Lesne⁵, Anastasiia Pylypets⁶, Fedir Borodavka⁶, Andrea Caviglia⁵, Jiri Hlinka⁶, Ursel Bangert⁴, Steven Leake² and Pavlo Zubko¹; ¹University College London, United Kingdom; ²European Synchrotron Radiation Facility, France; ³Lund University, Sweden; ⁴University of Limerick, Ireland; ⁵Delft University of Technology, Netherlands; ⁶The Czech Academy of Sciences, Czechia

Ferroelectric oxide thin films and superlattices have attracted broad interest on account of their novel physical and functional properties. The strong coupling between strain and polarization in these materials allows mechanical and electrical boundary conditions to be utilized to induce novel polar phases, unusual polarization textures and surprising behaviour, as exemplified by the negative capacitance phenomenon. In such heterostructures, an epitaxial strain is usually induced through a lattice-parameter mismatch between the epitaxial layers and a monocrystalline substrate. This substrate-imposed strain is an invaluable tool, which plays a crucial role in determining the domain structures and the resulting properties; however, it also presents significant limitations to accessing a wealth of yet unexplored phase transitions in complex oxide heterostructures and hinders their applications in flexible electronics and integration in semiconductor electronic circuits.

With the development of new methods for releasing thin films from the underlying substrate, free-standing complex oxide heterostructures become excellent candidates to explore and harness the full potential of strain engineering. In this work, ferroelectric-dielectric superlattices with ordered nanoscale domains were released from the substrate, allowing the thin-film oxide components to share the strain elastically with each other. The free-standing superlattices were studied with a combination of laboratory and synchrotron x-ray diffraction, piezoresponse force microscopy, transmission electron microscopy and Raman spectroscopy. Our measurements show that the spatial distributions of strain are introduced, which lead to the three-dimensional deformation of films. The released superlattices adopt a new, complex polarisation structure with an unexpected

local anisotropy, which is correlated with the local film curvature.

9:10 AM EL09.05.04

Giant Piezo-Driven Magnetoelectric Coupling in (011) PMN-PT Membrane Heterostructures Shane Lindemann¹, Julian Irwin¹, Gi-Yeop Kim², Kitae Eom¹, Bo Wang³, Jianjun Wang³, Jiamian Hu¹, Long-Qing Chen³, Si-Young Choi², Chang-Beom Eom¹ and Mark S. Rzchowski¹; ¹University of Wisconsin–Madison, United States; ²Pohang University of Science and Technology, Korea (the Republic of); ³The Pennsylvania State University, United States

Relaxor ferroelectrics, such as $(1-x)\text{Pb}(\text{Mg}_{1/3}\text{Nb}_{2/3})\text{O}_3$ - $(x)\text{PbTiO}_3$ (PMN-xPT), exhibit giant piezoelectricity which arises from the presence of multiple symmetries near a Morphotropic Phase Boundary (MPB). The MPB in PMN-xPT lies around $x = 35\%$ and separates a Rhombohedral (R) phase, with spontaneous polarization along the $\langle 111 \rangle$ crystallographic directions, from a Tetragonal (T) phase whose polarization lies along $\langle 100 \rangle$. For compositions near the MPB, the presence of bridging Monoclinic (M) and Orthorhombic (O) phases help to facilitate large lattice distortions as the spontaneous polarization rotates between the competing symmetries in order to align with the applied field.

Bulk studies using (011) oriented PMN-PT single crystals have been used to demonstrate non-volatile 71/109 degree switching between in-plane and out-of-plane R polarization directions. Such switching can result in distinct strain states and forms the basis of low-power, ultrafast, memory storage devices when coupled with a ferromagnetic (FM) material [1,2]. Achieving low power, however, necessitates the use of thin films of PMN-PT. Additionally, the films must be removed from their substrates in order to prevent substrate clamping that eliminates their giant piezoelectricity. Here we demonstrate growth of epitaxial (011) PMN-PT thin films, followed by removal of the substrate via etching of a sacrificial layer. By coupling with a FM Nickel overlayer, we achieve manipulation of in-plane magnetic anisotropy under 3V applied bias across the PMN-PT film, which is much lower than the $>100\text{V}$ needed using bulk PMN-PT. However, we do not see evidence of the 71/109 degree switching as observed in the bulk studies. Instead we find that the piezo-driven coupling is dominated by polarization rotation from the nominally $\langle 111 \rangle$ oriented R state towards the [011] O state along the applied field direction. Our findings have significant implications on the design of strain-mediated devices based on relaxor-ferroelectrics such as PMN-PT.

[1] Wu, T.; Bur, A.; Zhao, P.; Mohanchandra, K. P.; Wong, K.; Wang, K. L.; Lynch, C. S.; Carman, G. P. *Appl. Phys. Lett.* 2011, 98 (1), 012504

[2] Hu, J.-M.; Li, Z.; Chen, L.-Q.; Nan, C.-W. *Nat. Commun.* 2011, 2, 553

9:25 AM *EL09.05.05

Complex Polarisation Texture and Emergent Functionalities at Twin Domain Crossings in Ferroelectric Thin Films Patrycja Paruch; University of Geneva, Switzerland

Ferroelectric materials can host a wider range of novel functional properties as well as unusual structural features, potentially useful for nanoelectronics applications. At domain walls or in regions with high strain gradients, in particular, the complex interaction between polarisation, electrostatics, and strain can lead to localised chiral polarisation textures, electrical conductivity, and charge or chemical segregation. One promising highly strained structure is the intersection between ferroelastic twins.

In $\text{Pb}(\text{Zr}_{0.2}\text{Ti}_{0.8})\text{O}_3$ thin films, investigating such twin domain intersections with a combination of scanning probe microscopy and nonlinear optical microscopy, we find a characteristic localised piezoelectric and response and evidence of a more complex rotational or closure structure in second harmonic generation polarimetry analysis. The heart of the twin domain crossing presents an extremely high susceptibility to local application of electric bias or pressure, dominating the polarisation switching dynamics in this region. We also observe distinct mechanical properties and enhanced electrical conduction at the intersection.

SESSION EL09.06: Switching and Negative Capacitance
Session Chairs: Beatriz Noheda and Pavlo Zubko
Monday Morning, April 19, 2021
EL09

10:30 AM *EL09.06.01

Domain Switching and Imprint in Ferroelectric HfO₂ Capacitors Alexei L. Gruverman; University of Nebraska, United States

Application of HfO₂-based films to ferroelectric memory and logic devices has generated considerable interest as they allow overcoming significant problems associated with poor compatibility of perovskite ferroelectrics with CMOS processing. However, detailed studies of such application-relevant properties as imprint and polarization switching dynamics with respect to the electrode material and processing condition are still sparse. Here, we use a combination of Piezoresponse Force Microscopy (PFM) and pulse switching techniques to analyze the time- and field-dependent evolution of the domain structure in HfO₂-based thin film capacitors. Switching spectroscopy-PFM (SS-PFM) maps revealed the electrode-dependent spatial variations in the local potential landscape, which strongly affect the domain switching kinetics. It is shown that stronger oxidation reduces the internal imprint bias while also leading to an increase in the remanent polarization. Development of “fluid imprint” determined by the sample switching pre-history is reported. A particularly slow polarization reversal in the absence of an external field - termed as inertial switching - due to the interface entrapment of the charge injected during pulse application is shown to have a strong impact on polarization retention.

10:55 AM DISCUSSION TIME

11:10 AM EL09.06.03

Transient Negative Capacitance Behaviour in Constant Series R-C FETs Ashwani Kumar, Xiaoyao Song and Maria M. De Souza; The University of Sheffield, United Kingdom

Current research effort in transient negative capacitance phenomena is focussed on attempts to separate out the components arising from change in polarisation (dP/dt) in a Ferroelectric material from circuit components such as those expressed by the Miller model [1][2]. The phenomenon of transient negative capacitance, despite having completely disparate origins in the case of multi-domain as opposed to single-domain ferroelectric, remains closely interlinked with negative capacitance as governed by the Landau-Khalatnikov (LK) equation [3]. The single-domain regime, which is governed by the LK equation, can be expressed by a series R-C circuit in parallel with an oxide capacitor C_{ox} , where C is non-linear and can attain negative values for a certain range of polarisation. In contrast, the multi-domain approximation is modelled by the Kolmogorov-Avrami-Ishibashi (KAI) model, which utilises a time-dependent polarisation [4] or the Miller model [5], which akin to the LK framework, can be equivalently described as a series R-C circuit. However, C in the Miller model remains strictly greater than 0. In different variations of such models at least one of the elements between R and C is always considered non-linear (with respect to polarisation) [6] to help explain the steep switching behaviour. Here we establish that the phenomenon of transient negative capacitance can be considered to be more general than reported earlier. We demonstrate the conditions for sub-60 mV/dec switching in an RC-FET, even if the R and C were constant. The voltage dropped across an equivalent series RC circuit can be represented as $V_{ox} = R(dQ_{ch}/dt) + (Q_{ch}/C)$, where V_{ox} and Q_{ch} are the voltage across gate dielectric and sheet charge density in the channel, respectively. This leads us to the necessary condition for achieving a body factor $m < 1$ along both forward and backward sweeps. However, when combined with the semiconductor charge $(dQ_{ch})/(d\Psi_s) = (q/(k_B T))Q_{ch}$, where Ψ_s is the surface potential, it is seen that sub-60 mV/dec switching is possible only if $Q_{ch} > 0$ (i.e. when the transistor is ON) during the backward sweep. We believe this insight contributes further understanding to the causes of hysteresis in commonly used SPICE models of FE-FETs.

References: [1] J. Gomez et al., “Hysteresis-free negative capacitance in the multi-domain scenario for logic applications,” Tech. Dig. - Int. Electron Devices Meet. IEDM, vol. 2019-Decem, no. i, pp. 138–141, 2019. [2] J.

Gomez et al., “Significance of Multi and Few Domain Ferroelectric Switching Dynamics for Steep-Slope Non-Hysteretic Ferroelectric Field Effect Transistor,” in 2019 Device Research Conference (DRC), 2019, vol. 2019-June, no. 574, pp. 247–248. [3] L. D. Landau and I. M. Khalatnikov, “On the anomalous absorption of sound near a second order phase transition point,” in Dokl. Akad. Nauk SSSR, vol. 96, 1954, pp. 469–472. [4] Y. J. Kim et al., “Voltage Drop in a Ferroelectric Single Layer Capacitor by Retarded Domain Nucleation,” Nano Lett., vol. 17, no. 12, pp. 7796–7802, 2017. [5] M. N. K. Alam, P. Roussel, M. Heyns, and J. Van Houdt, “Positive non-linear capacitance: the origin of the steep subthreshold-slope in ferroelectric FETs,” Sci. Rep., vol. 9, no. 1, pp. 1–9, 2019. [6] M. A. Alam, M. Si, and P. D. Ye, “A critical review of recent progress on negative capacitance field-effect transistors,” Appl. Phys. Lett., vol. 114, no. 9, 2019.

11:25 AM *EL09.06.04

Dynamics Studies of Ferroelectric Switching on Hafnium Zirconium Oxide Peide P. Ye; Purdue University, United States

In this work, we present the first experimental determination of nucleation time and domain wall (DW) velocity by studying switching dynamics of ferroelectric (FE) hafnium zirconium oxide (HZO) according to the nucleation limited switching (NLS) model in ferroelectricity. Experimental data and simulation results were used to quantitatively study the switching dynamics. The switch speed can be degraded in high aspect ratio devices due to the longer DW propagation time or with dielectric interfacial layer due to the required additional tunneling and trapping time by the leakage current assist switch mechanism. The work is in collaborations with Xiao Lyu, Mengwei Si from Purdue University, Pragya R. Shrestha, Kin P. Cheung from NIST, Panni Wang, Shimeng Yu from GaTech.

11:50 AM EL09.06.05

Late News: Interplay of Negative Quantum Capacitance and Negative Ferroelectric Capacitance for Low-Power Transistor Operations Karpur Shukla, Meng-Ju Yu and Jimmy Xu; Brown University, United States

Since the initial proposal [1] of using ferroelectric negative capacitance to realize voltage transform for low-power transistors, substantial theoretical and experimental progress has been made in determining their fundamental properties and realizing negative capacitance transistors with improved device characteristics. Nevertheless, substantial gaps remain between observed performance and model expectations.

Most pressingly, model analyses [2,3] seem to imply substantial limits on the ability of ferroelectric negative capacitance to improve the subthreshold swing of well-designed transistors. Due to the small subthreshold gate capacitances of well-designed transistors, these models suggest that negative capacitance enhanced lowering of the subthreshold swing is only achievable with rather thick ferroelectric layers, at scales impractical for large-scale integration.

A central conclusion of these models is that the design space of negative capacitance FETs is constrained largely by the quantum capacitance of the channel, and thus that lowering the quantum capacitance of the channel allows for an expanded design space. In doing so, these models make the implicit assumption that the quantum capacitance of the channel remains positive. However, lowering the quantum capacitance exposes the channel to the prospect of negative *quantum* capacitance [4], itself a phenomenon of interest in enhancing low-power electronic device operation. Negative quantum capacitance can arise [5] in channels with strong electron correlation effects at a low electron density in a number of materials, including silicon.

Here, we discuss the effects of negative quantum capacitance in FET channels on the operations of ferroelectric negative capacitance FETs. In particular, we find that for small negative quantum capacitance values, the subthreshold swing begins exhibiting hysteresis. While hysteresis could be desirable in some neuromorphic applications, it puts a lower limit on the density of charge carriers in the channel for conventional low-power electronics. However, we further find that for larger magnitudes of the negative quantum capacitance, hysteresis

again disappears from the subthreshold swing. This adds a new region of design space to the fundamental model of ferroelectric negative capacitance FETs. We discuss the specific regime at which large negative quantum capacitance can provide steep-slope subthreshold switching, and examine the implications for ferroelectric negative capacitance FET design.

- [1] S. Salahuddin and S. Datta, *Nano Lett.* **8**, 405 (2008)
- [2] M. Kobayashi and T. Hiramoto, *AIP Adv.* **6**, 025113 (2016)
- [3] W. Cao and K. Banerjee, *Nat. Comm.* **11**, 196 (2020)
- [4] T. Kopp and J. Mannhart, *J. Appl. Phys.* **106**, 064504 (2009)
- [5] P. Tsipas *et al.*, *Adv. Elec. Mat.* **2**, 1500297 (2016)

SESSION EL09.07: Poster Session
Session Chairs: Michael Hoffmann and Asif Khan
Monday Afternoon, April 19, 2021
1:00 PM - 3:00 PM
EL09

EL09.07.01

Switchable Photovoltaic Properties in PZT Epitaxial Thin Films Komalika Rani, Stéphane Gable, Thomas Maroutian, Philippe Lecoeur and Sylvia Matzen; Université Paris-Saclay, France

Epitaxial ferroelectric thin films are currently investigated for their potential in photovoltaic (PV) applications [1], mainly because of their large open circuit voltage and switchable photovoltaic effect. Indeed, in a ferroelectric film, the sign of the photovoltaic current can be controlled by the direction of the ferroelectric polarization, allowing in theory to achieve a 100% switchability of the photocurrent with the polarization, which is of great interest for potential applications, as photoferroelectric memories. However, switchability is not always achievable in integrated ferroelectric films between electrodes, because of extrinsic parameters, such as the nature of the electrode-ferroelectric interface (Schottky barrier) [2] or the amount of non-mobile charged defects. In addition, switchable photocurrent can also be affected by the migration of charged defects, such as oxygen vacancies, under applied electric field [3]. So, disentangling the impact of defects, electrodes, and polarization on the PV properties is not an easy task.

In this work, a careful study of the switchability of the PV properties of epitaxial lead zirconate titanate (PZT) thin films has been conducted in order to investigate the role played by the ferroelectric polarization. 100 nm thick PZT films were grown using pulsed laser deposition (PLD) and integrated in capacitor geometry between SrRuO₃ bottom and Pt top electrodes and the photoinduced current in the PZT devices were studied under UV illumination (above the PZT band gap), in different polarization states. A voltage pulse protocol was used to pole the device under increasing electric fields to reach different electrical states while measuring their polarization value. These results revealed the critical role of the depolarizing field as the driving force for the photocurrent and allowed us to extract to screening efficiency of electrodes. In addition, the contribution from electrode-ferroelectric interface was evidenced for particular photon energy, especially with ITO top electrodes.

- [1] C. Paillard, X. Bai, I. C. Infante, M. Guennou, G. Geneste, M. Alexe, J. Kreisel, and B. Dkhil, *Photovoltaics with Ferroelectrics: Current Status and Beyond*, *Adv. Mater.* 2016, 28, 5153–5168
- [2] L. Pintilie, C. Dragoi, I. Pintilie, *Interface controlled photovoltaic effect in epitaxial Pb(Zr,Ti)O₃ films with tetragonal structure*, *J. Appl. Phys.* 2011, 110, 044105.
- [3] Y. Guo, B. Guo, W. Dong, H. Li, H. Liu, *Evidence for oxygen vacancy or ferroelectric polarization induced switchable diode and photovoltaic effects in BiFeO₃ based thin films*, *Nanotechnology* 2013, 24, 275201.

EL09.07.04

Origin of the Ferroelectric Response in the Sr(Nb,Ta)O₂N Oxynitrides Juan S. Gelves Badillo¹, Aldo Romero^{2,3} and Andres C. Garcia Castro¹; ¹Universidad Industrial de Santander, Colombia; ²West Virginia University, United States; ³Benemérita Universidad Autónoma de Puebla, Mexico

Heteroanionic materials have recently positioned in the center of multiple investigations. The latter is motivated by the physical, optical, and chemical properties that can emerge when properly combining different, but compatible anions, within the same compound. Oxynitride perovskite compounds have shown to offer a wide range of different tunable properties depending on the O/N rate, for instance, the absorption of light in the visible regime makes them ideal candidates for photocatalysis applications where polar compounds offer a notable advantage [1].

In this study, we theoretically explored the origin of the polar and ferroelectric responses experimentally observed in perovskite oxynitrides SrNbO₂N and SrTaO₂N [2,3]. With this aim, first-principles calculations of the structural and vibrational properties were performed. We show that such ferroelectric behavior is extremely sensitive to the anionic ordering in both Sr(Nb,Ta)O₂N systems, where *cis*- and *trans*- orderings are identified as the most probable orderings in the crystals. Furthermore, We found that both *cis*- and *trans*- type can hold ferroelectricity, although the mechanisms in how such a stable phase emerges in each ordering are quite different. Additionally, we show that spontaneous polarization characterizing such ferroelectric phases can be considerably enhanced by applying in-plane epitaxial strain, achieved by using strontium titanate as substrate.

[1] Fuertes, A. (2015). “Metal oxynitrides as emerging materials with photocatalytic and electronic properties”. *Materials Horizons*, 2(5), 453-461.

[2] Kim, Y. I., Woodward, P. M., Baba-Kishi, K. Z., & Tai, C. W. (2004). “Characterization of the structural, optical, and dielectric properties of oxynitride perovskites AMO₂N (A= Ba, Sr, Ca; M= Ta, Nb)”. *Chemistry of materials*, 16(7), 1267-1276.

[3] Kikkawa, S., Sun, S., Masubuchi, Y., Nagamine, Y., & Shibahara, T. (2016). “Ferroelectric response induced in *cis*-type anion ordered SrTaO₂N oxynitride perovskite”. *Chemistry of Materials*, 28(5), 1312-1317.

EL09.07.05

Theoretical Investigation of the Electronic Properties of Ruddlesden-Popper Oxynitrides Sr₂AO_{4-x}N_x(A=Nb, Ta)(x=0.5, 1) Juan A. Pinto Castro and Andres C. Garcia Castro; Universidad Industrial de Santander, Colombia

In condensed matter, Ruddlesden-Popper (RP), considered as an intergrowth of n-layers ABX₃ perovskites with an AX layer with structure: (AO)(ABO₃) have attracted a lot of attention due to their potential applications. As such, perovskites-like materials are notably at the vanguard of technological developments thanks to their versatility offered by the partial substitution of anionic sites as in the case of oxygen replacement by nitrogen sites (i.e. oxynitrides). These substitutions possible due to the similarities in electronegativity, polarizability, ionic radius, and coordination states and bringing modifications of their physical properties such as electrical, optical, catalytic, and magnetic responses [1]. Therefore, the study and research on new RP oxynitrides phases constitute an area of huge interest.

Here we present significance outcomes due to partial substitution of nitrogen for oxygen in structures Sr₂AO_{4-x}N_x(A=Nb, Ta)(x=0.5, 1), that show symmetry inequivalent structures that I have analyzed, These structures are more stable thermodynamically compared with oxides and nitrides structures, and the most stable is a *trans*-type configuration structure. The direct bandgap is reduced to benefit the performance of photocatalysis. Likewise, by researching the relationship of vibrational behaviour of *trans*-type configuration, it becomes evident that these RP-phases hold a ferroelectric response.

First-principles calculation reveals that strontium oxynitrides RP-phases are strongly correlated materials due to underestimation in the bandgap. So we have used, instead DFT, DFT+U for consistent results.

[1] Inorg. Chem. 2004, 43, 25, 8010–8017

EL09.07.06

Dielectric Anomalies and Magnetodielectric Effect in Layered Perovskite-Type $\text{Pr}_2\text{Ti}_2\text{O}_7$ Single Crystal
Moein Adnani¹, Liangzi Deng¹, Melissa Gooch¹, Huiyuan Man², Alireza Ghasemi², Collin Broholm^{2,2}, Seyed Mojtaba Koohpayeh^{2,2} and Ching-Wu Chu^{1,3}; ¹University of Houston, United States; ²Johns Hopkins University, United States; ³Lawrence Berkeley National Laboratory, United States

The ternary oxides of the compound family with the general formula $\text{A}_2\text{B}_2\text{O}_7$, where A is a trivalent cation and B is a transition metal, have been widely studied because of their interesting physical properties and their technological applications. Among the relatively less explored members of this family are the rare-earth titanates ($\text{RE}_2\text{Ti}_2\text{O}_7$), which have a monoclinic layered perovskite-type structure and have been of interest for their ferroelectric, piezoelectric, non-linear optical, and photocatalytic properties and their high Curie temperature. Here we present our low-temperature dielectric study of high structural quality, stoichiometric single-crystal $\text{Pr}_2\text{Ti}_2\text{O}_7$. This compound has a monoclinic polar crystal structure ($P2_1$) that consists of four layers of corner-sharing TiO_6 octahedra separated by two layers of Pr cations. We will review the crystal structure and some of the magnetic and ferroelectric properties of the compound. We will then discuss our dielectric and magnetodielectric results, in particular the field-dependent anomalies in the dielectric constant and the mutual coupling between dielectric properties and magnetization in this compound.

The work in Houston is supported by US Air Force Office of Scientific Research Grants FA9550-15-1-0236 and FA9550-20-1-0068, the T. L. L. Temple Foundation, the John J. and Rebecca Moores Endowment, and the State of Texas through the Texas Center for Superconductivity at the University of Houston.

The work in Johns Hopkins University is supported as part of the Institute for Quantum Matter, an Energy Frontier Research Center funded by the U.S. Department of Energy, Office of Science, Basic Energy Sciences under Award No. DE-SC0019331.

EL09.07.07

Late News: Ferroelectric Properties and Magnetic-Induced Behavior of Magnetoelectric Multiferroic BiFeO_3
Xiang Li, Yongjian Tang, Hyunjea Lee, Joseph Casamento, Antonio B. Mei, Phillip Dang, Zexuan Zhang, Ludi Miao, Debdeep Jena, Darrell G. Schlom, Daniel C. Ralph and Huili Xing; Cornell University, United States

Magnetoelectric multiferroic materials have received increasing attention by the research community since they simultaneously possess magnetization and ferroelectricity and the two order parameters are coupled by magnetoelectric effects. BiFeO_3 (BFO), one of the few room-temperature magnetoelectric multiferroic materials, is of special interest. For instance, BFO can be potentially used in the magnetoelectric spin-orbit (MESO) device¹, spin-orbit torque field-effect transistor (SOTFET)², etc. However, to date, most studies on BFO have been focused on the electric field induced switching instead of magnetic field driven behavior. Despite difficulties in directly switching ferroelectricity in BFO by an external magnetic field, the exchange interaction between BFO and an adjacent ferromagnetic (FM) material³ might enable a new way for switching by applying a magnetic stimulus via spin-orbit torque if the materials parameters fall in the right window, as proposed in the modeling work of SOTFET². In this work, a SrRuO_3 (SRO)/BFO/SRO heterostructure is used to study the ferroelectric properties and magnetic-induced behavior of BFO.

The SRO/BFO/SRO (20/100/20nm) heterostructure was grown epitaxially by molecular-beam epitaxy (MBE) on (110) DyScO_3 substrates using similar growth conditions in [4]. No ion irradiation was done post growth. Ti/Pt (5/50nm) was blanket deposited by sputtering, and subsequently patterned into top metal contacts of capacitors by photolithography and ion milling. Large area Ti/Pt top contacts are effectively shorted to the bottom SRO layer thus serving as the opposite electrode of the capacitors.

First, we discovered that these MBE BFO layers are highly insulating, unlike the ones reported in [4], where post-growth MeV-ion irradiation had to be applied to curb the leakage through polarization domains. The low

leakage in these MBE BFO films directly enabled us to study its ferroelectric properties by the positive-up-negative-down (PUND) measurement at both RT and 5 K, a common method to obtain polarization-electric field (P-E) loops by measuring the displacement and switching currents. Conductive AFM was also carried out: very low current level (~ 10 pA up to 10 V) was measured across the sample and no leakage pattern was observed. The PUND data revealed a saturation polarization (P_s) of 60-80 $\mu\text{C}/\text{cm}^2$ and a coercive field of 0.6-1 MV/cm, but no clear dependence on temperature.

Next, we applied out-of-plane (oop) or in-plane (ip) magnetic fields up to 6 T, respectively, during the PUND measurements, at both RT and 5 K to investigate if an external magnetic field can influence the measured P-E loop in BFO. At RT, the SRO layers serve as simple metal electrodes; while at 5 K, we expect the SRO layers will be polarized by the external magnetic fields since SRO has a ferromagnetic Curie temperature of ~ 150 K. In this BFO/FM heterostructure, no noticeable shift in the P-E loop is observed at 5 K under the magnetic field condition used in this study. At RT, a systematic shift in the P-E loops was observed; however, after carefully correlating the shift with the order of measurements, we believe the shift arose primarily from the ferroelectric imprint effect not the magnetic field. Overall, these observations are consistent with our modeling predictions². Due to the relatively large thickness (100 nm) and P_s (~ 70 $\mu\text{C}/\text{cm}^2$), the switching energy barrier in BFO is too high. If the coupling strength between the two order parameters remains the same or increases, it is more likely to observe magnetic-induced behavior in thin La-doped BFO with reduced P_s .

[1] Manipatruni, et al, Nature 565, 35(2019). [2] Li, et al, APL 116, 242405(2020). [3] Heron, et al, Nature 516, 370(2014). [4] Mei, et al, APL Mater. 7, 071101(2019).

* This work was supported in part by the SRC nCORE task 2758.001 and NSF E2CDA program (ECCS 1740286). This work was performed in part at the CNF, an NNCI member supported by NSF Grant NNCI-2025233.

EL09.07.08

Magnetocaloric Study of $\text{Mg}_{0.5}\text{Zn}_{0.125}\text{A}_{0.375}\text{Fe}_2\text{O}_4$ (A = Co, Cu, and Ni) Ferrites Dipesh Neupane¹, Jeotikanta Mohapatra², Surendra Dhungana¹ and Sanjay R. Mishra¹; ¹The University of Memphis, United States; ²The University of Texas at Arlington, United States

Magnetic refrigeration (MR) is a crucial subject as a future cooling technology based on magnetocaloric effect (MCE) that replaces the conventional vapor compression technique for energy saving, high efficiency, minimal environmental impact, and reliability. MR of magnetic materials is based on the change in entropy when the materials are subjected to the field. Therefore for more efficient, materials should have large entropy changes. Spinel ferrites are one of the essential magnetocaloric materials that consist of transition metal ions (MFe_2O_4 , M = Mn, Zn, Co, Ni, Cu, and Mg). Among different spinel ferrites, the Mg-Zn spinel ferrite is considered necessary due to its remarkable magnetic and electrical properties. The MCE in ferrite is observed ~ 1.36 at 350K. The current effort is to broaden the MCE operating temperature. In view of the above, in this study, a comparative study of magnetocaloric effect (MCE) in $\text{Mg}_{0.5}\text{Zn}_{0.125}\text{A}_{0.375}\text{Fe}_2\text{O}_4$, A = Co, Cu, and Ni is reported. The samples were prepared via auto-combustion method and heat-treated in the air at 1100°C for 12 h. The phase identification of the powders performed using x-ray diffraction shows that all the samples exhibit a high-purity cubic spinel structure. The lattice parameter is affected due to different ionic radii of substituted elements. With Co and Ni substitution, a gradual shift in the peaks to the left as compared to Cu is observed that showed a decrease in lattice parameters from 8.510 Å to 8.356 Å due to smaller ionic radii of Co^{2+} ion (0.65 Å), Ni^{2+} ion (0.69 Å) than Cu^{2+} ion (0.73 Å). Morphology and size of the $\text{Mg}_{0.5}\text{Zn}_{0.125}\text{A}_{0.375}\text{Fe}_2\text{O}_4$, A = Co, Cu, and Ni particles were investigated by scanning electron microscopy (SEM). SEM shows the particle diameter was $\sim 40 - 170$ nm, indicating that the nanoparticles were polycrystalline. Magnetic measurements were performed using a Quantum Design Superconducting Quantum Interference Device (SQUID) magnetometer. The magnetization as a function of the temperature for all sample, under an applied magnetic field of 100Oe, were measured to see the phase transition. When the temperature decreased, the samples exhibited a paramagnetic (PM) - ferromagnetic (FM) transition at the Curie temperature (T_C). The transition temperatures increased from 550 K to 600 K for Cu to Co. Ni substituted sample showed transition temperature in between Cu and Co. Saturation magnetization for $\text{Mg}_{0.5}\text{Zn}_{0.125}\text{A}_{0.375}\text{Fe}_2\text{O}_4$, A= Cu, Ni, and Co reached 23 emu/g, 27emu/g, and 33 emu/g at 10K. Large magnetic properties for Co is due to the superexchange interaction and magnetic coupling.

To evaluate the MCE of the samples, the isothermal magnetization curves were collected at different fixed temperatures ranging from 300 to 700 K. The temperature measurements are at intervals $T=10\text{K}$. The magnetic entropy change ΔS_M has been calculated from the M–H curves using the Maxwell relation. The maximum entropy change $|\Delta S_M^{\text{Max}}|$ as a function of temperature increases from $1.25 \text{ J.Kg}^{-1}\text{K}^{-1}$ to $3.16 \text{ J.Kg}^{-1}\text{K}^{-1}$ under an applied magnetic field of 5T Cu to Co substitution. The peak position of ΔS_M vs. T curve was independent with applied fields for the same material, whereas the peak shifted towards lower temperature as for Cu sample and higher temperature for Co sample compare to Ni sample. This magnetocaloric behavior is mainly due to superexchange interaction between Fe – Fe ions and particle size. These values are relatively high and comparable to other ferrite systems. Arrot plots showed the positive slope of the curve for all samples indicating a second-order phase transition. Cooling efficiency can be calculated from the peak position of ΔS_M called relative cooling power (RCP). The RCP was found to be 51 to 126 J/Kg for Cu, 62 to 135 J/kg for Ni, and 76 to 165 J/kg for Co sample calculated from 0.5T to 5T, respectively. Significantly higher ΔS_M^{Max} and curie temperature make our compounds promising materials for magnetic refrigeration technology for higher temperatures.

EL09.07.09

Late News: Ferroelectricity and Enhance Energy Storage Density in 0.70Pb(Zr0.52Ti0.48)O3-0.30Pb(Fe0.5Nb0.5)O3 Nanoscale Ferroelectric Thin Film Prepared by Pulsed Laser Deposition Technique Karuna K. Mishra, Ivan Castillo and Ram Katiyar; University of Puerto Rico, United States

Highly (001) oriented 0.70Pb(Zr_{0.52}Ti_{0.48})O₃-0.30Pb(Fe_{0.5}Nb_{0.5})O₃(0.70PZT-0.30PFN) magnetic ferroelectric thin films were deposited on La_{0.67}Sr_{0.33}MnO₃ (LSMO) buffer layer coated on (LaAlO₃)_{0.3}(Sr₂AlTaO₆)_{0.7} (001) substrates by following two subsequent laser ablation processes in oxygen atmosphere employing pulse laser deposition technique. The 0.70PZT-0.30PFN films were found to grow in tetragonal phase with orientation along (001) plane as inferred from x-ray diffractometry analysis. The temperature dependent dielectric measurements (80-750 K) were performed on metal-ferroelectric-metal heterostructure capacitors in the frequencies range of 10^2 – 10^6 Hz was observed to be diffused over a wide range of temperature 400–700 K and exhibits high dielectric constant ~ 2200 at room temperature. The well saturated slim loop of thin films capacitors suggesting nano-scale ferroelectric behaviors (relaxor type) of 0.70PZT-0.30PFN thin films in line with diffuse dielectric response results. An excellent high energy storage density (U_{re}) $\sim 51 \text{ J/cm}^3$ with efficiency $\sim 62 \%$ was estimated at applied voltage 1.5 MV/cm. High DC breakdown strength, larger dielectric constant and high restored energy density values of our 0.70PZT-0.30PFN ferroelectric thin films indicate its usage in high energy storage applications. These results will be presented in details at the meeting.

EL09.07.10

Realizing New Multiferroic Double Perovskites for Photovoltaic Applications—First-Principles Approach Neda Rahmani^{1,2}, Mohammad E. Ghazi², Morteza Izadifard², Alireza Shabani¹, Biplab Sanyal³ and Jost Adam¹; ¹University of Southern Denmark, Denmark; ²Shahrood University of Technology, Iran (the Islamic Republic of); ³Uppsala University, Sweden

Clean and renewable solar energy is regarded as one of the most reliable and abundant sources to tackle the prevalent energy crisis. The photovoltaic effect, directly converting sunlight into electricity, is an important way to harvest solar energy, and many efforts have been devoted to the development of photovoltaic technology. Toward the next-generation photovoltaics, multiferroic materials (MFs), with the coexistence of ferroelectricity and magnetism in the same phase, show promise as candidates for harvesting energy, especially from sunlight. The spontaneous polarisation of such type of non-centrosymmetric materials is the origin of charge carrier separation. On the other hand, magnetic ordering induces a small bandgap, typically due to electronic states of the magnetic atom in the Fermi energy region. One method to find these rare materials is to employ double perovskites (DPs) with general formula $A_2BB'X_6$, in which one of the sublattices is magnetic, and the other one is ferroelectric. This study intends to develop and apply theoretical tools to predict and improve the photovoltaic properties in new double perovskites with multiferroic properties. In that light, the structural, magnetic, electronic, and photovoltaic properties of new MF-DPs $A_2\text{MnBO}_6$ (A=Sn, Bi and B=V, Ta, Ti) using ab initio

simulations based on DFT method are systematically investigated. The electronic band structure and density of states demonstrate the semiconducting behaviour of these double perovskites with the values of band gaps falling within the desired range for optimal photovoltaic performance. Structural calculations, including distortion parameters and bond angles, indicate that these DPs undergo a significant octahedral tilting and distortion which may result in a considerable value of electric polarization and hence, may be suggested as potential multiferroic materials. In the MnO_6 octahedra, Jahn-Teller effect, which is related to the Mn^{3+} electron configuration, distorts the Mn-O bonds. Whereas, in $\text{Ta}(\text{Ti})\text{O}_6$ octahedra, the Second Order Jahn-Teller effect originating from d^0 electron configuration of $\text{Ta}^{5+}(\text{Ti}^{4+})$ is responsible for the off-centering displacement of Ta(Ti) atoms and the distortion of $\text{Ta}(\text{Ti})\text{O}_6$ octahedra. Optical properties, including absorption coefficient (α) calculations, show that the value of α in the visible region is in the order of 10^5 cm^{-1} , comparable to the absorption coefficient of some well-known photovoltaic materials. These results draw an intense theoretical research interest to explore the photovoltaic properties of new multiferroic double perovskites to characterize them as potential solar materials.

EL09.07.11

PVD TiN Development to Improve Ferroelectric Properties of HZO Films in MFM Capacitors David Lehninger, Konstantin Merstens, Lukas Gerlich, Maximilian Lederer, Tarek Ali and Konrad Seidel; Fraunhofer Institute for Photonic Microsystems (IPMS), Germany

The discovery of ferroelectricity in doped hafnium oxide thin films revived the interest in ferroelectric (FE) memory concepts [1]. Compared to other dopants, zirconium doped hafnium oxide (HZO) crystallizes at low temperatures (e.g. $T_{\text{cryst.}} < 400^\circ\text{C}$), which makes this material ideal for the implementation of ferroelectric functionalities into the Back-End-of-Line (BEoL) [2]. For this approach, metal-ferroelectric-metal (MFM) capacitors are very interesting. Integrated in the BEoL, they can be connected either to the drain- or gate-contact of a standard logic located in the Front-End-of-Line (FEoL) to realize ferroelectric random access memories (FeRAMs) or ferroelectric field effect transistors (FeFETs), respectively. It is beneficial to deposit the top electrode of the MFM stack by physical vapor deposition (PVD) processes like sputtering. It is fast, can be done at room temperature, and is a low-cost and reproducible process.

Here, we present the impact of the top TiN electrode, deposited by reactive magnetron sputtering using a metallic titanium (Ti) target and nitrogen / argon plasma, on the ferroelectric properties of HZO films embedded in MFM capacitors. By using different nitrogen (N_2)- and argon (Ar) flows, TiN film with various compositions (measured by X-ray-photoelectron spectroscopy) and thicknesses (measured by ellipsometry) have been realized. The crystallinity and different phases have been determined by X-ray diffraction (GI-XRD). The influence of the mentioned parameters on the ferroelectric properties of the HZO film are discussed by taking additional effects like film stress into account. Furthermore, the low temperature PVD TiN is compared with high temperature chemical vapor deposited (CVD) TiN.

[1] T. S. Böscke et al., Appl. Phys. Lett. 2011, 99, 102903.

[2] D. Lehninger et al., pss(a) 2020, 217, 1900840

EL09.07.12

Cross-Domain Optimization of Ferroelectric Parameters for Negative Capacitance Transistors Sai Surya Kiran Pentapati¹, Rakesh Perumal², Sourabh Khandelwal³, Michael Hoffmann⁴, Sung Kyu Lim¹ and Asif Khan¹; ¹Georgia Institute of Technology, United States; ²NVIDIA, United States; ³University of South Florida, United States; ⁴NaMLab gGmbH, Germany

Field Effect Transistors with a ferroelectric gate stack provide a negative capacitance (NC) effect and show a sub 60mV/decade sub-threshold slope (SS) [1–3]. This improves the cell delay and total power (using supply voltage scaling) without traditional Moore's law scaling. [4–5] study the impact of the ferroelectric properties (coercive field E_c and polarization P_0) at transistor, gate, and full-chip level. Using a wide range of non-hysteresis $E_c(1, 4)\text{MV/cm}$, $P_0(10, 40)\mu\text{C/cm}^2$ values, we introduce the idea of optimality of ferroelectrics (those within 5% of the lowest achievable power at given voltage while meeting target delay). An open-source 15nm

FinFET with 0.8V supply voltage is used for target delay baselines and to generate the NCFET libraries.

Transistor Level analysis at $V_{DD}=0.4V$ shows sub-threshold slope(SS) and I_{on} improves as the (E_c, P_0) is closer to hysteresis boundary (this is the curve beyond which NCFETs have hysteretic behavior). NC effect increases as we move closer to the boundary, and higher I_{on} and SS do not coincide as a strong NC effect also has a smaller range of operation in terms of V_{gs} . So, a steep SS caused by large NC effect saturates quickly, while a slightly smaller slope remains active for a longer range of V_{gs} achieving higher I_{on} . Gate level analysis inverter provides of power and delay metric evolution.

Gate Level: The voltage amplification effect [1] of NCFET decreases the V_{th} and devices go to saturation at a smaller $|V_{gs}|$. This increases the saturation mode of operation to a wider range of V_{gs} and the voltage transfer curves become smoother. So, short-circuit current is higher at large SS, and gate capacitance ($\propto I_{on}$) is higher when I_{on} is large. At low V_{DD} , the NC effect does not saturate for V_{gs} within the operation range $(0, V_{DD})$ and the effects at hysteresis boundary vary due to this. NC saturation also causes the delay to increase with V_{DD} in extreme cases counter-intuitive to the traditional delay- V_{DD} curves. The optimality region also changes with V_{DD} as a higher NC effect is required to meet target delay when V_{DD} is decreased for NCFETs. At iso-delay, we achieve 92% reduction in total power using a $V_{DD}=0.2V$ and a high NC effect ferroelectric. The same NCFET creates 87% reduction (best observed) in full chip power analysis as well.

Not all benefits at gate level translate to a full-chip level. Using various types of cells in full chip optimization, the NCFETs that lie out of the optimal range in gate-level analysis can be within the wider optimal range of full-chip. While a subset of the optimal range in full-chip can be estimated using inverter level analysis, different cells behave differently with NC effect, and a full chip design with a large number of cells and good variation in types of cells gives a detailed optimal NCFET ranges for a given supply voltage and technology.

[1] S. Salahuddin and S. Datta. Use of Negative Capacitance to Provide Voltage Amplification for Low Power Nanoscale Devices, 2008 Nano Lett., doi: 10.1021/nl071804g

[2] K. Li et al., "Negative-Capacitance FinFET Inverter, Ring Oscillator, SRAM Cell, and Ft," 2018 IEEE International Electron Devices Meeting (IEDM), doi: 10.1109/IEDM.2018.8614521

[3] Z. Krivokapic et al., "14nm Ferroelectric FinFET technology with steep subthreshold slope for ultra low power applications," 2017 IEEE International Electron Devices Meeting (IEDM), doi: 10.1109/IEDM.2017.8268393

[4] S. Pentapati et al., "Cross-Domain Optimization of Ferroelectric Parameters for Negative Capacitance Transistors—Part I: Constant Supply Voltage," in IEEE Transactions on Electron Devices, Jan. 2020, doi: 10.1109/TED.2019.2955018.

[5] S. Pentapati et al., "Optimal Ferroelectric Parameters for Negative Capacitance Field-Effect Transistors Based on Full-Chip Implementations—Part II: Scaling of the Supply Voltage," in IEEE Transactions on Electron Devices, Jan. 2020, doi: 10.1109/TED.2019.2955010.

EL09.07.13

Impact of FeFET Drain Current Variation in Processing-in-Memory Architectures Nathan E. Miller, Zheng Wang, Saurabh Dash, Asif Khan and Saibal Mukhopadhyay; Georgia Institute of Technology, United States

We analyze the impact of drain current (I_{DS}) variation in 28 nm high-K metal-gate Ferroelectric FET devices on FeFET-based processing-in-memory (PIM) deep neural network accelerators. Non-Normal variation in I_{DS} is observed due to repeated read operation on two devices with different channel dimensions at various read frequencies. Device-circuit co-analysis using the measured current distribution shows a 1 to 3 percent accuracy degradation of an FeFET-based PIM platform when classifying the Fashion-MNIST dataset with the LeNET-5 DNN model. This accuracy drop can be fully recovered with variation-aware training methods, showing that FeFET current variation is not prohibitive to the design of DNN accelerators.

SESSION EL09.09: Ferroelectric Devices I
Session Chairs: Asif Khan and Nujhat Tasneem
Monday Afternoon, April 19, 2021
EL09

9:00 PM *EL09.09.01

Ferroelectric-HfO₂ FeFET for 3D High-Density Memory Application Masaharu Kobayashi; The University of Tokyo, Japan

In the research field of memory devices, ferroelectric memory has been attracting much attentions because of the newly discovered ferroelectric HfO₂ (FE-HfO₂) material which is fully CMOS compatible [1]. Ferroelectric memory device can inherently operate at high-speed and low-power. One-transistor memory, ferroelectric FET (FeFET), has a small footprint and non-destructive read-out [2], which is promising for high-density storage memory application. Recently, 3D stacked FeFET has been proposed and demonstrated[3], which can possibly compete with NAND flash memory in terms of memory capacity and power consumption.

There are, however, several challenges to realize such 3D stacked FeFET using conventional poly-Si channel. Poly-Si channel has low mobility and forms a low-k interfacial layer which causes voltage loss and reliability degradation by charge trapping. In this work, we propose to use amorphous oxide semiconductor (AOS), IGZO [4,5], as an alternative channel material. IGZO channel provides high mobility as a deposited channel and prevent low-k interfacial layer formation. IGZO has been already in production for flat panel display, and high reliability has been already proved.

We fabricated FE-HfO₂ capacitor by capping with IGZO layer. IGZO layer works as preferable capping for HfZrO₂ and induces ferroelectric orthorhombic phase. Electrical characterization shows sharp hysteresis and large spontaneous polarization charge, which can be explained by process-induced strain by IGZO capping. FE-HfO₂ capacitor with IGZO capping also shows wake-up free endurance characteristics, which can be due to the engineered itnerface between the FE-HfO₂ and IGZO layer avoiding interface defect such as oxygen vaccancy [6]. Then we fabricated FeFET with IGZO channel, in which we introduced back gate. Back gate can help to fix the IGZO body potential so that the elecric field is effectively applied to the FE-HfO₂ layer for erase operation. The field-effect mobility is as high as 10cm²/Vs, which is the same as Hall mobility and the mobility of transistor with SiO₂ gate insulator. There is no mobility degradation with FE-HfO₂. DC I-V sweep and pulse write operation both show >0.5V memory window with almost ideal subthreshold swing. This subthrsold characteristics is attributed to the low interface trap (<10¹¹1cm²) and bulk defect, and junctionless operation. These results are promising for high-density and low power storage memory application.

[1] J. Muller et al., *Nano Lett.* 12, pp. 4318–4323 (2012), [2] J. Muller et al., *IEDM Tech. Dig.*, pp. 280-283 (2013), [3] K. Florent et al., *IEDM Tech. Dig.*, pp. 43-46 (2018), [4] K. Nomura et al., *Nature*, 432, 25, pp. 488-492 (2002), [5] F. Mo et al., *VLSI Tech. Symp.*, pp. 42-43 (2019), [6] F. Mo et al., *Appl. Phys. Expr.*, 13, 074005 (2020).

9:25 PM EL09.09.02

Ultrathin HfO₂-Based Ferroelectric Tunnel Junctions on Silicon Nirmaan Shanker¹, Suraj Cheema¹, Cheng-Hsiang Hsu¹, Adhiraj Datar¹, Jongho Bae¹, Daewoong Kwon¹ and Sayeef Salahuddin^{1,2}; ¹University of California, Berkeley, United States; ²Lawrence Berkeley National Laboratory, United States

Ferroelectric materials offer significant promise for nonvolatile memories and low-power logic transistors [1] due to stable polarization states which can be reversed under an applied electric field. With the recent discovery of ferroelectricity in HfO₂ [2], fluorite-structure binary oxides have attracted considerable interest as they are compatible advanced semiconductor processes, unlike prototypical perovskite-structure ferroelectrics. Accordingly, ultrathin HfO₂-based ferroelectrics have received significant attention in charge-based

ferroelectric random-access memory (FeRAM), ferroelectric field-effect transistors (FeFETs), and even negative capacitance FETs [3]. Meanwhile, resistive-switching materials have emerged as promising candidates for novel beyond-CMOS computing paradigms [1]. In this context, ferroelectric tunnel junctions (FTJs) present a promising energy-efficient resistive switching memory as FTJs exploit the polarization-dependent tunneling barriers across thin ferroelectric barriers. However, a critical requirement for FTJs is to achieve a sufficiently high tunneling current while still exhibiting a large ON/OFF ratio (tunneling electroresistance), which requires robust ferroelectricity as the tunneling barrier is reduced to the ultrathin limit, presenting a materials challenge preventing realistic FTJ-based memories.

In this work, we demonstrate FTJs with ultrathin Zr-doped HfO₂ (Zr: HfO₂) ferroelectric barriers down to a thickness corresponding to two unit cells, grown by atomic layer deposition on silicon [4,5]. These tunnel junctions exhibit large polarization-driven electroresistance (19000 %), the largest value reported for HfO₂-based FTJs. In addition, due to the ultrathin ferroelectric barrier, these junctions provide large tunneling current ($> 1 \text{ A cm}^{-2}$) at low read voltage, orders of magnitude larger than reported thicker HfO₂-based FTJs. Furthermore, the data retention ($> 10^4 \text{ s}$) and endurance characteristics ($> 10^3$ cycles) in these ultrathin HfO₂-based FTJs are comparable to those obtained with much thicker HfO₂-based ferroelectric layers. Scanning probe microscopy techniques – piezoresponse force microscopy (PFM) and conductive atomic force microscopy (C-AFM) – help establish polarization-driven switching is indeed responsible for the observed resistive switching. Thus, the ultrathin ferroelectric barriers not only allow robust memory operation, but also enable simultaneous occurrence of large electroresistance and large current, critical for practical applications.

[1] S Salahuddin, K Ni & S Datta. “The era of hyper-scaling in electronics.” *Nat. Electron.* **1**, 442–450 (2018).

[2] TS Böske *et al.* Ferroelectricity in hafnium oxide thin films. *Appl. Phys. Lett.* **99**, 102903 (2011)

[3] D Kwon, S Cheema, N Shanker [...] S Salahuddin. “Negative Capacitance FET with 1.8-nm-Thick Zr-Doped HfO₂ Oxide.” *IEEE Electron Device Lett.* **40**, 993–996 (2019).

[4] S. Cheema*, N. Shanker* [...] S. Salahuddin. “One nanometer HfO₂-based ferroelectric tunnel junctions on Si.” *arXiv* 2007.06182 (2020).

[5] S Cheema, D Kwon, N Shanker [...] S Salahuddin. “Enhanced ferroelectricity in ultrathin films grown directly on silicon.” *Nature* **580**, 478–482 (2020).

9:40 PM BREAK

10:20 PM EL09.09.04

Performance Comparison of Negative Capacitance in Si Nanowire and Nanosheet Field Effect Transistors Md. Azizul Hasan, Fahimul I. Sakib and Mainul Hossain; University of Dhaka, Bangladesh

The superior electrostatic control and high scalability of nanowire (NW) and nanosheet (NS) gate-all-around field-effect-transistors (FETs) make them promising alternatives to FinFETs in advanced technology nodes. Negative capacitance (NC) effect, originating from a ferroelectric (FE) material in the gate stack, can provide an elegant solution for the much-needed voltage scaling in these aggressively scaled devices. In this work, a comparative analysis on the performance of NC-NWFETs and NC-NSFETs is presented through fully calibrated, three-dimensional TCAD simulations. For the same layout footprint (LF), both single channel NC-NSFETs and those, with vertically stacked NSs, have been considered. Single channel NC-NSFET exhibits 9% lower subthreshold swing (SS) and 35% higher ON-current (I_{ON}) than NC-NWFET of comparable device dimensions. In contrast to NC-NWFET, capacitance matching between the FE and the underlying metal-oxide-semiconductor (MOS) capacitance is achieved with a thinner FE layer in NC-NSFET. This is particularly significant, since a thinner FE layer enables further scaling of these NC devices. In addition, NC-NSFET, with vertically stacked NSs, can achieve $4\times$ higher I_{ON} and $\sim 50\%$ lower SS than NC-NWFET, owing to higher effective width and better capacitance matching. A high I_{ON}/I_{OFF} ratio of 10^6 , with low operating voltage ($V_{DD} = 0.2\text{V}$), is obtained for the NC-NSFET. The significantly higher I_{ON} in NC-NSFET also results in faster switching, with significantly lower power consumption, at $V_{DD} < 0.3 \text{ V}$. The performance of stacked NC-NSFETs can be optimized by tuning the width and thickness of the NSs. Negative differential resistance (NDR)

is found to be more pronounced in NC-NSFET, enabling these devices to attain a stronger drain-induced-barrier-rising (DIBR) and steeper SS for gate lengths (L_G) as small as 10 nm. The results presented here pave the way for performance optimization of NC-NWFETs and NC-NSFETs, in ultra-scaled and high-density logic applications, for 10 nm and beyond technology node.

10:35 PM EL09.09.05

Low Voltage Operating Ferroelectric Memory Transistor with MoTe₂ Channel and P(VDF-TrFE)

Yongjae Cho, Ji Hoon Park and Seongil Im; Yonsei University, Korea (the Republic of)

MoTe₂ channel-based P(VDF-TrFE) ferroelectric nonvolatile memory is fabricated, which operates at minimum switching pulse voltage and minimum drain voltage. For the minimum switching voltage of 8 V, bottom-gate architecture is employed and its advantages are investigated. By using bottom-gate structure, we could avoid a dead layer formed at the interface between thermally-deposited Al and P(VDF-TrFE) at top-gate architecture. A dead layer in top-gated ferroelectric memory transistors increases the coercive voltage so as the switching pulse voltage. And, for the minimum drain voltage, a novel method of H₂O₂ treatment is developed. By oxidizing the source/drain area of MoTe₂ surface by H₂O₂ solution, Ohmic contact between Pt and MoTe₂ is achieved even without thermal annealing which would have a destructive effect on the crystal quality of P(VDF-TrFE). To demonstrate the benefit of our memory transistor in aspect of power saving, it is integrated into an OLED operating circuit.

SESSION EL09.10: Hafnia-Based Ferroelectrics and Devices

Session Chairs: Asif Khan and Pavlo Zubko

Tuesday Morning, April 20, 2021

EL09

8:15 AM *EL09.10.01

Impact of Interfaces and Dopants on Ferroelectric Properties of Epitaxial HfO₂ Films Tingfeng Song, Saúl

Estandía, Jike Lyu, Jaume Gàzquez, Ignasi Fina and Florencio Sanchez; Instituto de Ciencia de Materiales de Barcelona (ICMAB-CSIC), Spain

Ferroelectric HfO₂ is a promising material for new memory devices, but the microstructure of the films needs to be better controlled and some properties, mainly endurance, need to be improved. Research on ferroelectric HfO₂ has been focused mainly on polycrystalline films. In contrast, epitaxial films, of great interest to understand properties and prototyping devices, are scarcely investigated. The recently achieved stabilization of the orthorhombic ferroelectric phase in epitaxial Hf_{0.5}Zr_{0.5}O₂ films on perovskite La_{0.7}Sr_{0.3}MnO₃ electrodes has allowed to, among other results, control the crystalline polymorphs through substrate selection, achieve high polarization, endurance and retention in sub-5 nm films, and fabricate epitaxial ferroelectric tunnel junctions. Studies on epitaxial films are still in a nascent state, and little is known about the effects of dopants and interfaces, whose critical influence has been demonstrated in polycrystalline films. We will show the relevance to the stabilized phases and ferroelectric properties (polarization, endurance and retention) in epitaxial HfO₂-based capacitors of i) substrates and electrodes, and ii) chemical composition of the HfO₂-based films.

8:40 AM EL09.10.02

Impact of the Interface Layer on the Wake-Up Behaviour of Hafnium Oxide Maximilian Lederer,

Konstantin Merstens, Alireza Kia, Jennifer Emara, Ricardo Olivo, Yannick Raffel, David Lehninger, Tarek Ali, Kati Kühnel, Konrad Seidel and Thomas Kämpfe; Fraunhofer Institute for Photonic Microsystems, Germany

Ferroelectric field effect transistors based on hafnium oxide have become a viable option as embedded non-volatile memory solution due to its high coercive field as well as its compatibility to complementary metal-

oxide-semiconductor (CMOS) processes [1]. In comparison to ferroelectric capacitors, these devices comprise an additional interface layer, which impacts the electrical field distribution in the gate stack and yields a depolarization field counteracting the polarization of the ferroelectric, affecting properties like endurance and retention [2,3]. In consequence, this is expected to affect the wake-up behaviour of the hafnium oxide layer. Additionally, this layer is already present during the crystallization of the ferroelectric at high temperature. As diffusion processes cannot be excluded at these temperatures, influences on the crystallization behaviour are expected.

Here, we present the impact of different annealing temperatures on the layer stack. Diffusion processes inside the layer stack during the crystallization anneal were investigated using time-of-flight secondary ion mass spectroscopy (ToF-SIMS). For high annealing temperatures, changes in the chemical composition of the interface layer were observed. Furthermore, electrical characterization of the ferroelectric properties revealed a strong impact of the annealing temperature, which resulted in an increased presence of the wake-up effect for lower annealing temperatures. Additional transmission Kikuchi diffraction (TKD) analysis revealed strong differences in the microstructure and crystallographic texture, which are most likely responsible for the observed behaviour.

[1] Müller, J. et al.; ECS J. Solid State Sci. Technol. 4, N30-N35 (2015).

[2] Müller, J. et al.; NVMTS, (2016).

[3] Gong, N. and Ma, T.-P.; IEEE Electron Device Lett. 37, 1123 (2016).

8:55 AM EL09.10.03

Influence of Antiferroelectric-Like Behavior on Tuning Properties of Ferroelectric HZO-Based

Varactors Sukhrob Abdulazhanov, Maximilian Lederer, David Lehninger, Tarek Ali, Jennifer Emara, Ricardo Olivo and Thomas Kämpfe; Fraunhofer Institute for Photonic Microsystems, Germany

With the progress in wireless networks, including the upcoming 5G and Internet of Things, there is a high concern in exploring of materials for passive or active RF devices. The main criteria are good CMOS-compatibility, low tuning voltage, low chip size and low power consumption. Ferroelectric materials, like barium strontium titanate (BST) [1] have been widely used as tunable capacitors - varactors. However they lack CMOS compatibility and require relatively high tuning voltages. Hafnium zirconium oxide (HZO) is a fully CMOS-compatible material [2], with a good back-end-of-line integration possibility due to its low thermal budget [3]. It is a good candidate for varactor applications [4], with a high miniaturization possibility [5],[6]. Here, we investigate the capacitance-voltage (CV) characteristics of $\text{Hf}_x\text{Zr}_{1-x}\text{O}_2$ MFM thin film capacitors with various Zr doping, thicknesses and annealing temperatures. The impact of field cycling during the wake-up on the tunability was analyzed and an optimized bias region for the maximum tunability was determined. Additionally, the effect of antiferroelectric-like (AFE) behavior on tuning was investigated. The superposition of ferroelectric and AFE regime shows an interesting behavior, where less bias for tuning is needed, but tunability is reduced. A usefulness of such a behavior for varactor application was also examined. We have also investigated the ferroelectric and antiferroelectric-like properties at elevated temperatures. It was shown that with increase of temperature tunability deteriorates. Temperature measurements also comply with recent studies of ferroelastic nature of AFE behavior [7].

[1] N. K. Pervez et al., Appl. Phys. Lett. 85, 19, 4451, (2004).

[2] T. S. Böske et al., Appl. Phys. Lett. 99, 10, 102903, (2011).

[3] D. Lehninger et al., pss(a), 217(8), 1900840, (2020)

[4] M. Dragoman et al., Appl. Phys. Lett. 110, 10, 103104, (2017).

[5] S. Abdulazhanov et al., IEEE MTT-S IMWS-AMP., p.46 (2019).

[6] S. Abdulazhanov et al., IEEE MTT-S IMWS-AMP., p.175 (2019).

[7] M.Lederer et.al., Appl. Phys. Lett. 115, 22, 222902, (2019)

9:10 AM EL09.10.04

Rethinking Reliability of Ferroelectric Transistors for Memory and Logic Applications Nicolo Zagni¹,

Kamal Karda², Francesco Maria Puglisi¹, Paolo Pavan¹ and Muhammad A. Alam²; ¹Università degli Studi di

Introduction Despite the remarkable development in ferroelectric FETs, endurance and reliability of these devices still represent serious concerns in both memory and logic applications. In this work, we present recent results discussing the reliability of HfO₂-based FeFETs [1] employed as either non-volatile memory elements or as steep-switching NCFET logic transistors. For FeFET, we analyze the role of interface and bulk trap generation on memory window closure leading to limited endurance. For NCFET, we discuss the beneficial role of negative capacitance (NC) effect in reducing the persistent reliability issue of negative bias temperature instability (NBTI). We utilize a common theoretical framework based on the Landau Theory to describe ferroelectric energy landscape that allows capturing: *i*) the hysteretic I-V characteristics of FeFETs when employed for memory applications; and *ii*) the NC effect when aiming at steep-slope (hysteresis-free) switching for logic transistors [2].

Endurance Limits of FeFETs Endurance is the total number of repeated program/erase cycles after which the states of a memory become indistinguishable. One of the main factors limiting the endurance of FeFETs is the generation of traps at the interfacial layer inserted in the gate stack between the ferroelectric and semiconductor body. In [3], we developed an experimentally validated analytical model to describe the effects of aging on the memory window (MW). This model captures the degradation of programmed/erased states depending on the amount of generated traps that in turn is related to the amplitude and duration of the writing pulses. As such, the analytical model could serve either as an add-on to traditional techniques or as a stand-alone method to characterize generated defect densities under a variety of stress conditions. For instance, it is possible to estimate the net generated traps from the MW expression derived in [3], thus allowing to correlate MW measurements with generated traps. The estimation drawn from the simple analytical model can be helpful to develop next-generation FeFETs with improved endurance.

NBTI Suppression In NC-FETs The primary mechanism for NBTI-induced degradation in MOSFETs is the increase in interface trap density with stress time. The NBTI degradation can be fully compensated by adding a ferroelectric (FE) layer of proper thickness for stabilized NC operation. This enables steep-slope, hysteresis-free operation needed for switching. NBTI reduction comes from the extra capacitance given by the parasitic source/drain overlap regions that cause the capacitance matching (between the negative capacitance and the intrinsic MOSFET gate capacitance) to improve over stress time. Since achieving an optimum FE layer thickness needed for obtaining NBTI-free operation can be challenging, we performed simulations for various thicknesses to find that even for relatively thin FE (e.g., 7 nm) NBTI degradation is reduced [4]. In other words, even if the FE thickness needs to be determined exclusively by process integration and capacitance matching constraints, it would still lead to NBTI reduction.

Conclusions Reliability aspects in ferroelectric FETs for both memory and logic applications were investigated by means of either analytical models or self-consistent numerical simulations based on the framework based on Landau Theory. The modeling approach presented in this work allows gaining useful insights into how to improve reliability of ferroelectric FETs and accelerate the path towards widespread commercialization.

Acknowledgments Authors thank prof. L. Selmi (Univ. of Modena and Reggio Emilia) for useful discussion. This research has received partial funding from the European Commission's Horizon 2020 BeFerroSynaptic project, grant agreement n°871737 via the IU-NET consortium.

References [1] J. Muller et al., IEDM, 2013. [2] M. A. Alam et al., APL, 114, 2019. [3] N. Zagni et al., APL, 117, 2020. [4] K. Karda et al., TED, 67, 2020.

9:25 AM EL09.10.05

CMOS Backend Compatible Ferroelectric Tunnel Junction Memory Device Keerthana S. Nair^{1,2}, Marco Holzer^{1,2}, Sourish Banerjee¹, Catherine Dubourdieu^{1,2} and Veeresh Deshpande¹; ¹Helmholtz-Zentrum Berlin für Materialien und Energie, Germany; ²Freie Universität Berlin, Germany

Ferroelectric tunnel junction (FTJ) memories have gained prominence among emerging non-volatile memories due to low power consumption, high switching speed, and potential for neuromorphic applications [1]. Recent development of doped hafnium oxide ferroelectric layer enables integration of FTJ memory devices with CMOS technology. In FTJ devices, the tunneling current is directly dependent on the remnant polarization of

the ferroelectric layer. While the tunneling current is higher across a thin ferroelectric layer (around 1-4 nm), it is challenging to have a high remnant polarization in these layers and simultaneously achieve a high tunneling electro resistance (TER) ratio. FTJs with a composite stack of Metal-Ferroelectric-Dielectric-Metal, allow the use of a thick ferroelectric layer (~10 nm) while obtaining high TER, as demonstrated recently [2, 3]. However, the crystallization of the ferroelectric layer is carried out at high temperatures (500-600°C) which are incompatible with the CMOS back-end-of-line. In this work, we demonstrate a highly CMOS backend compatible FTJ stack with a 400°C crystallized Hf_{0.5}Zr_{0.5}O₂ (HZO) ferroelectric layer and TiN-Al₂O₃-HZO-W stack. Such a stack with a TiN bottom metal and a W top metal allow seamless integration with the CMOS back-end-of-line, particularly at contact level and has not yet been explored. The FTJ devices show on-current and TER that are comparable to the state-of-the-art. The devices also show multi-level resistance behavior necessary for neuromorphic applications. We will also discuss a detailed investigation of the switching transients, voltage, and device resistance dependence on switching cycles. As the composite stack is similar to those used in the study of negative capacitance, the polarization switching behavior of the device is of importance to a broader community. Furthermore, we will also discuss device characteristic dependence on dielectric thickness and identify parameters to improve the TER, on-state current and retention.

- [1] M. Benjamin et al., “Ferroelectric Tunnel junction based on ferroelectric – dielectric Hf_{0.5}Zr_{0.5}O₂/Al₂O₃ capacitor stacks,” *European Solid-State Device Research Conference (ESSDERC)*, pp. 142-145, 2018.
- [2] M. Benjamin et al., “Direct correlation ferroelectric properties and memories characteristics in ferroelectric tunnel junctions,” *IEEE Journal of Electron Device Society (J-EDS)*, vol. 7, pp. 1175-1181, 2019.
- [3] R. Hojooon et al., “Ferroelectric tunnel junctions based on aluminium oxide/zirconium-doped hafnium oxide for neuromorphic computing,” *Scientific Reports*, vol. 9, pp. 1-8, 2019.

SESSION EL09.11: Structure and Functional Characterization of Ferroelectric Thin Films and Polar Textures
Session Chairs: Patrycja Paruch and Pavlo Zubko
Tuesday Morning, April 20, 2021
EL09

11:45 AM *EL09.11.01

Hafnia-Based Ferroelectric Devices—A Singular Type of Switching P. Nukala^{1,2}, D. Carbone³, M. Ahmadi¹, Y. Wei^{1,4}, Sylvia Matzen⁵ and Beatriz Noheda^{1,1}; ¹University of Groningen, Netherlands; ²Indian Institute of Science, India; ³Lund University, Sweden; ⁴École Polytechnique Fédérale de Lausanne, EPFL, Switzerland; ⁵University Paris-Saclay, CNRS, France

Hafnia-based films are changing the way we think of ferroelectric switching. Ferroelectricity in these materials arises from metastable phases that are easier stabilized at the smallest dimensions. In addition they present low leakage as well as CMOS compatibility [1], making them ideal candidates for memory and logic devices. In addition, their switching takes place, quite uniquely, without involving domain wall motion, which allows experimental access to negative capacitance states[2]. Multiferroic tunnel junctions (MTJs) fabricated with (La,Sr)MnO₃ electrodes and ferroelectric Hf_{0.5}Zr_{0.5}O₂ barriers show both tunneling magnetoresistance (TMR) and tunneling electroresistance effect (TER), displaying four resistance states by magnetic and electric field switching[3]. Moreover, under electric field cycling, the TER effect can reach values as large as 10⁶%. Experiments indicated that polarization switching alone cannot be responsible for those changes[4]. In this talk we will show direct evidence, by means of *operando* transmission electron microscopy[5], as well as synchrotron x-ray diffraction experiments with *in-situ* application of electric fields[6], of the mechanisms that come into play during electric field switching in hafnia-based devices, as well as their relative importance determining the properties of these devices.

- [1] U. Schroeder, C. S. Hwang, and H. Funakubo, Ferroelectricity in doped hafnium oxide: materials, properties

and devices, Woodhead Publishing, 2019

[2] M. Hoffmann, F.P.G. Fengler, M. Herzig, T. Mittmann, B. Max, U. Schroeder, R. Negrea, P. Lucian, S. Slesazeck & T. Mikolajick, *Nature* 565, 464 (2019).

[3] Y. Wei, S. Matzen, T. Maroutian, G. Agnus, M. Salverda, P. Nukala, Q. Chen, J. Ye, P. Lecoeur, and B. Noheda, “Magnetic tunnel junctions based on ferroelectric $\text{Hf}_{0.5}\text{Zr}_{0.5}\text{O}_2$ tunnel barriers,” *Physical Review Applied* 12, 031001 (2019)

[4] Y. Wei, S. Matzen, C. P. Quinteros, T. Maroutian, G. Agnus, P. Lecoeur, B. Noheda “Magneto-ionic control of spin polarization in magnetic tunnel junctions”, *npj Quantum Materials* 4, 62 (2019).

[5] P. Nukala, M. Ahmadi, Y. Wei, S. de Graaf, S. Matzen, H. W. Zandbergen, B. Kooi, B. Noheda, “Operando observation of reversible oxygen migration and phase transitions in ferroelectric devices”, arXiv:2010.10849 (submitted)

[6] P. Nukala, G. Carbone, E. Stylianidis, R. Hamming Green, M. Salverda, Y. Wei, A. Burema, T. Banerjee, A. Bjorling, D. Mannix, S. Matzen, B. Noheda, (in preparation)

12:10 PM EL09.11.02

***In Situ* Transmission Electron Microscopy of Field-Induced Polarization Switching in Antiferroelectric Zirconia** Sarah Lombardo¹, Christopher Nelson², Kisung Chae^{3,3,4}, Sebastian E. Reyes-Lillo⁵, Mengkun Tian¹, Nujhat Tasneem¹, Zheng Wang¹, Michael Hoffmann⁶, Kyeongjae Cho⁴, Andrew Kummel³, Josh Kacher¹ and Asif Khan^{1,1}; ¹Georgia Institute of Technology, United States; ²Oak Ridge National Laboratory, United States; ³University of California, San Diego, United States; ⁴The University of Texas at Dallas, United States; ⁵Universidad Andres Bello, Chile; ⁶NaMLab/TU Dresden, Germany

Ferroelectric and antiferroelectric oxides have gained attraction in recent years for use as gate oxides in field effect transistors (FETs), along with potential applications toward random access memories and high-density energy storage, owing to their hysteretic charge-voltage characteristics and negative capacitance phenomena. Exploiting this negative capacitance can lead to lower operating voltages, and therefore, operation of transistors beyond their current limits. The origin of negative capacitance is thought to stem from the energy barrier of first order field-induced phase transitions. In the case of antiferroelectric materials, interesting non-linearities in their polarization-voltage characteristics (i.e. double hysteresis loops) are observed and attributed to an electric field-induced first-order, structural phase transition between a non-polar, parent phase and a polar active phase. However, direct observation and identification of such phase transitions and their relation to ferroelectric/antiferroelectric properties has yet to be unanimously determined, leaving significant gaps in our fundamental understanding of the microstructure-property relationship of such materials. Since polarization correlates with microstructure, the application of an electric field alters the microscopic features, enabling electrical properties suitable for non-volatile memory, analog synapses, and artificial neurons, but also poses significant challenges to performance such as variability, reliability, and endurance.

The first step in identifying the crystallographic pathways involved in polarization switching of antiferroelectric ZrO_2 -based thin films is the direct imaging of the polarization switching at the atomic scale with applied bias via *in situ* transmission electron microscopy (TEM). *In-situ* TEM characterization can provide simultaneous biasing and imaging of atomic structure in real time. Field-induced phase transitions and microstructural evolution of antiferroelectric zirconia are investigated via high resolution, in-situ TEM biasing, coupled with DFT-calculated atomic models, to identify the origin of antiferroelectricity in these materials. Such characterization techniques highlight the ability of advanced electron microscopy to provide insight into structure-property relations of fluorite-type binary FE/AFE oxides, thereby improving our fundamental understanding of the microscopic mechanisms behind device performance for the advancement of logic and memory technologies.

12:25 PM EL09.11.03

Late News: Atomic Scale Crystal Field Mapping of Polar Vortices in Oxide Superlattices Sandhya Susarla^{1,2}, Pablo García-Fernández³, Colin Ophus¹, Pablo Aguado-Puente⁴, Sujit Das², Peter Ercius¹, Lane W. Martin², Ramamoorthy Ramesh^{2,1,2} and Javier Junquera³; ¹Lawrence Berkeley National Laboratory, United States; ²University of California, Berkeley, United States; ³Universidad de Cantabria, Spain; ⁴Queen's

Polar vortices in oxide superlattices exhibit complex polarization topologies. In this presentation, I will talk about using a combination of energy loss near-edge structure analysis, crystal field multiplet theory, and first-principles calculations to probe the electronic structure within such polar vortices in $[(\text{PbTiO}_3)_{16}/(\text{SrTiO}_3)_{16}]$ superlattices, at the atomic scale. The peaks in Ti -edge EEL spectra shift systematically depending on the position of the Ti^{4+} cations within the vortices i.e., the direction and magnitude of the local dipole. First-principles computation of the local projected density of states on the Ti orbitals, together with the simulated crystal field multiplet spectra derived from first-principles are in good agreement with the experiments. This combined experimental and theoretical approach can serve as a fundamental basis to study macroscopic properties such as chirality and circular dichroism.

12:40 PM EL09.11.04

Atomic-Scale Design of Negative Capacitance in Ultrathin $\text{HfO}_2\text{-ZrO}_2$ Ferroic Heterostructures on Silicon Suraj Cheema¹, Nirmaan Shanker¹, Cheng-Hsiang Hsu¹, Yu-Hung Liao¹, Shang-Lin Hsu^{2,2}, Steven K. Volkman¹, Vladimir Stoica³, Zhan Zhang⁴, John Freeland⁴, Padraic Shafer², Jim Ciston², Mohamed Mohamed⁵, Chenming Hu¹ and Sayeef Salahuddin^{1,2}; ¹University of California, Berkeley, United States; ²Lawrence Berkeley National Laboratory, United States; ³The Pennsylvania State University, United States; ⁴Argonne National Laboratory, United States; ⁵Lincoln Laboratory, Massachusetts Institute of Technology, United States

Negative capacitance [1] has emerged as a promising solution to overcome fundamental energy-efficiency limits in conventional electronics, in which internal ferroelectric order within the gate stack of a field-effect transistor can enable low-power operation [2,3]. Thus far, negative capacitance has been primarily demonstrated in thick perovskite- and fluorite-structure ferroelectric thin films, but integration into advanced semiconductor technology nodes will require stabilization at the ultrathin regime. Here, we present evidence of negative capacitance in atomic-scale $\text{HfO}_2\text{-ZrO}_2$ heterostructures [4] down to two-nanometers thickness, leveraging our recent work examining the 2D limits of fluorite-structure ferroelectricity on silicon [5-7]. $\text{HfO}_2\text{-ZrO}_2\text{-HfO}_2$ trilayers on Si-SiO₂ demonstrate sub-7 Å effective oxide thickness (EOT) without having to scavenge the SiO₂ interlayer, in stark contrast to conventional high- κ metal gate (HKMG) technology. Accordingly, in comparison to industrial HKMG benchmarks, these SiO₂-buffered ferroic heterostructures boast the lowest reported leakage for such aggressively-scaled EOT gate oxides, possible via negative capacitance.

In contrast to previous reports of negative capacitance in thicker ferroelectric HfO_2 -based films [8], the microscopic origin of negative capacitance in these ultrathin $\text{HfO}_2\text{-ZrO}_2$ multilayers arises from mixed ferroelectric-antiferroelectric order. Remarkably, this fluorite-structure family fosters the stabilization and competition of such ferroic order at the atomic-scale regime [5-7]. We first demonstrate ultrathin ferroic order – a crucial requirement for negative capacitance – down to one-nanometer in doped- HfO_2 films [5,6] and five-angstroms in conventionally-antiferroelectric ZrO_2 films [7]. To establish polarization switching in these ultrathin films, hysteretic characterization – via scanning probe, electrical tunnel junction and dielectric measurements – in various device geometries (in-plane, out-of-plane) diagnose competing antiferroelectric-ferroelectric order. In conjunction, electron microscopy and synchrotron X-ray characterization monitor structural signatures of the competing ferroic phases. These results indicate not only the absence of a ferroelectric critical thickness, but also ultrathin-enhanced polar distortion in fluorite-structure thin films [5,7], critical breakthroughs towards exploiting ferroic-based phenomena at ultra-scaled dimensions. Finally, pulsed electrical measurements and Landau phenomenology help explain the underlying origins of negative capacitance in this mixed-ferroic system. Therefore, this work not only broadens the ferroic origins of negative capacitance beyond ferroelectricity, but also allows one to design negative capacitance in atomic-scale $\text{HfO}_2\text{-ZrO}_2$ heterostructures on silicon [4], paving the way towards realistic ferroelectric-based computing.

[1] S Salahuddin & S Datta. “Use of Negative Capacitance to Provide Voltage Amplification for Low Power Nanoscale Devices. *Nano Lett.* **8**, 405–410 (2008).

[2] D Kwon*, S Cheema* [...] S Salahuddin. “Negative Capacitance FET with 1.8-nm-Thick Zr-Doped HfO_2

Oxide.” *IEEE Electron Device Lett.* **40**, 993–996 (2019).

[3] D Kwon*, S Cheema* [...] S Salahuddin. “Near Threshold Capacitance Matching in a Negative Capacitance FET with 1 nm Effective Oxide Thickness Gate Stack.” *IEEE Electron Device Lett.* **41**, 179–182 (2020).

[4] S Cheema [...] S Salahuddin. “Negative capacitance in atomic-scale HfO₂-ZrO₂ ferroic heterostructures for advanced transistors.” *[in preparation]*

[5] S Cheema*, D Kwon* [...] S Salahuddin. “Enhanced ferroelectricity in ultrathin films grown directly on silicon.” *Nature* **580**, 478–482 (2020).

[6] S Cheema [...] S Salahuddin. “One nanometer HfO₂-based ferroelectric tunnel junctions on silicon.” *arXiv* 2007.06182.

[7] S Cheema [...] S Salahuddin. “Emergence of sub-nanometer mixed antiferroelectric-ferroelectric order on silicon.” *[in preparation]*

[8] M Hoffmann *et al.* *Nature* **565**, 464–467 (2019).

12:55 PM EL09.11.05

Ferroelectric HZO Capacitor with W/TiN Bottom Electrode with No Wakeup Harshil Kashyap¹, Mahmut S. Kavrik¹, Chenghsuan Kuoo¹, Ajay Yadav² and Andrew Kummel¹; ¹University of California, San Diego, United States; ²Applied Materials, Inc., United States

Ferroelectric HfO₂ is being investigated for neuromorphic computing and back-end memory due to its scalability and compatibility with the current CMOS processing. However, for low power operation, low switching voltage (sub +/-1V) is desired. To achieve this, thinner FE HZO films are required along with no interfacial oxide/dead layers. In this study, Ni(top)/HZO/W/TiN MIM capacitors grown at high temperature were explored to achieve low voltage operation. Sputtered W/TiN bottom electrodes were deposited on a Si wafer. Samples were annealed in-situ prior to deposition in UHV at 350°C for 30 min in homebuilt ALD tool. HZO was deposited using TDMAH, TDMAZ and H₂O ALD precursors at 350°C substrate temperature. 50 nm Ni top electrodes were deposited using thermal evaporation. Oxide thickness was measured using ellipsometry on a Si witness sample. Samples were annealed at 450°C in N₂ for 2min. Electrical characterization was performed using a Keithley 4200A-SCS characterization system.

A sample with 200 cycles HZO (12 nm) was fabricated and characterized. Cross sectional TEM measurements revealed an oxidized W film which is reduced at the W/HZO interface; this was confirmed by EDS (not shown). This results in abrupt W/HZO interface and low voltage switching because there is no interfacial dielectric layer which inducing a voltage drop as observed in other electrode materials such as TiN and Si. The sample shows steep switching and high 2Pr of 41 μC/cm² at +/-5V. To reduce the operating voltage, the device was scaled. 100 cycles of HZO were deposited; ellipsometry was used to confirm the thickness as 6 nm. Endurance test was performed at 1MHz +/-1.8V (~3 MV/cm) to study the device performance over time.

The device showed a 2Pr = 39 μC/cm² at +/-1.8V (3MV/cm) and a maximum 2Pr = 62 μC/cm² at +/- 3.1V along with sharp switching I-V. The voltage scaling with thickness, as shown by the comparison of two devices is consistent with the absence of interfacial oxides. The endurance performed is superior to typical TiN/HZO/TiN structures and is sufficient for many applications. Furthermore, the devices do not show any wake-up which is beneficial since this complicates operation in a practical circuit. The absence of wake-up is consistent with the absence of oxygen vacancies at the W/HZO interface because the HZO ALD was performed on oxidized W film which was reduced to W metal during high-temperature ALD; confirmed by EDS (not shown). It is well known that oxygen vacancies at the electrodes result in the pinning of FE grains which reduces Pr. By operating with subloops with less than full Pr, +/-1V operation can be achieved and this will further increase the endurance.

1:10 PM *EL09.11.06

Directly Connecting Local Chemistry and Structure to Relaxor Properties Using Scanning Transmission Electron Microscopy James M. LeBeau; Massachusetts Institute of Technology, United States

Relaxor ferroelectrics are characterized by diffuse dielectric and piezoelectric properties, which distinguishes them from traditional ferroelectrics. To formulate models of local polar behavior, the structural and chemical complexity in relaxor systems have largely been probed with diffuse scattering using X-rays, neutrons, and electrons. These techniques, however, provide a measure of the average global and local structure across a relatively large volume of the material. Consequently, the origin of relaxor properties continues to be debated although these materials have been studied extensively. In this talk, I will discuss how aberration corrected scanning transmission electron microscopy (STEM) can be used to directly separate nanoscale structural and chemical inhomogeneities in relaxors. Here, we apply these techniques to $\text{Pb}(\text{Mg}_{1/3}\text{Nb}_{2/3})\text{O}_3\text{-PbTiO}_3$ (PMN-PT). Through simultaneous acquisition of images that are sensitive to chemistry (angle annular dark-field STEM) and light elements (integrated differential phase contrast STEM), we directly connect nanoscale chemical order regions, distorted oxygen octahedra, and local polarization. We find that the degree of chemical order smoothly varies within ordered domains and approaches a minimum at anti-phase boundaries, as well as regions of correlated oxygen octahedral tilting are found to be anti-correlated with regions of maximal chemical order. Comparing with the projected polarization, we observe that the regions of greatest variation in polarization correspond to the regions of maximum chemical order and maximum octahedral distortion. Based on these results, we show that both structural and chemical inhomogeneities act as a barrier for polarization rotation and thus frustrate long range polar order.

SESSION EL09.12: Ferroelectric Devices II

Session Chairs: Michael Hoffmann, Asif Khan and Andrew Kummel

Tuesday Afternoon, April 20, 2021

EL09

2:15 PM *EL09.12.01

Status and Outlook for Ferroelectric Hf-Based Films and Devices Robert Clark; TEL Technology Center, America, LLC, United States

The recent discovery that with certain dopants hafnium oxide can be crystallized in a form that exhibits ferroelectricity has opened up a range of device possibilities(1). We chose to work within the Hf/Zr system for our initial studies. The advantages of the Hf/Zr doping system include the similarity in precursors which can enable several running modes for the ALD process including a co-pulsing scenario, as well a cycle ratio scenario for controlling the Zr doping. In addition, the relative range of doping for which a strong remnant polarization is observed is much broader for the Hf/Zr system than for other dopants such as Al, Si, etc. which means this system should be more tolerant of small variations in composition, temperature and thickness than the other doping schemes. These factors along with a relatively low thermal budget suggest the CMOS-friendly Hf/Zr system could provide the basis for a number of ferroelectric memory devices. Other potential uses for these films include the possibility to create multi-domain ferroelectric FETs that can be used within a neuromorphic device to mimic synapse behavior. This talk will review and update our work to date on these films and their potential uses. References: 1. T. S. Böescke, J. Müller, D. Bräuhäus, U. Schröder and U. Böttger, in *Technical Digest of the International Electron Devices Meeting*, p. 24.5.1 (2011).

2:40 PM EL09.12.02

Scaling FeFET Towards 7nm Node—A TCAD Perspective Gihun Choe, Jae Hur and Shimeng Yu; Georgia Institute of Technology, United States

Ferroelectric materials have been explored for device structures such as ferroelectric random-access memory, ferroelectric tunnel junction, and ferroelectric field-effect transistors (FeFETs) [1]-[3]. Among the device structures, the FeFETs have been considered as one of the most versatile devices to implement the non-volatile memory and in-memory compute. It has low write energy as it is electric field driven, non-destructive read-out

mechanism and relatively fast program/erase speed [3]. The discovery of ferroelectric material based on doped HfO₂ has made FeFETs more attractive. Hafnia based ferroelectric material has good compatibility with the complementary metal-oxide-semiconductor (CMOS) fabrication process. Even more, its ferroelectric properties could be controlled depending on the dopant materials and doping concentration, which enables fine-tuning of FeFETs' performance.

Industrial development of FeFETs stays at 28nm/22nm today [4] [5], primarily because high voltage (~3V) is required to program the polarization states in the conventional ferroelectric gate MFIS stack (metal/doped HfO₂/interfacial layer/silicon). The unmatched charge between the Fe-cap and MOS-cap creates enhanced electric field in the interfacial layer, resulting in trap generation, reliability degradation and exacerbated variability.

Making FeFETs compatible with 7nm FinFET-like structure, if successful, could enable the emerged memory-logic circuit designs that take the advantages of high-performance 7nm logic transistors. Scaling down the ferroelectric layer thickness while maintaining ferroelectric properties is especially critical. In a recent research [6], 1~2 nanometers of the hafnia-zirconia-based ferroelectric layer were demonstrated. GlobalFoundries prototyped high-k/metal-gate bulk FeFETs at 28 nm [4] and fully-depleted SOI (FDSOI) FeFETs at 22 nm using silicon doped HfO₂ based material [5].

In this work, we simulated FeFETs from 22 nm node of FDSOI to 7 nm node of ferroelectric FinFET (Fe-FinFET) using a Sentaurus TCAD to assess its scalability. Simulation parameters including ferroelectric properties were fitted with experimental results of a 22nm FDSOI FeFET for accurate expectation and future suggestion. Quasi-static I-V characteristics of the FeFET were modeled using the multi-domain Preisach model built in TCAD and domain phase variations were considered. Eventually, the design guideline for 7 nm technology node of Fe-FinFET was suggested with an aim to optimize the write voltage below 1.5V. The memory window of Fe-FinFET could be enhanced using innovative gate stack design and/or employing higher-k materials for an interlayer oxide.

Reference

- [1] J. Okuno *et al.*, "SoC compatible 1T1C FeRAM memory array based on ferroelectric Hf_{0.5}Zr_{0.5}O₂," *IEEE Symposium on VLSI technology and Circuits*, virtual, June 2020.
- [2] M. Kobayashi, Y. Tagawa, F. Mo, T. Saraya, and T. Hiramoto, "Ferroelectric HfO₂ Tunnel Junction Memory With High TER and Multi-Level Operation Featuring Metal Replacement Process," *IEEE J. Electron Devices Soc.*, vol. 7, pp. 134–139, 2019.
- [3] E. Yurchuk *et al.*, "Impact of Scaling on the Performance of HfO₂ -Based Ferroelectric Field Effect Transistors," *IEEE Trans. Electron Devices*, vol. 61, no. 11, pp. 3699–3706, Nov. 2014.
- [4] M. Trentzsch *et al.*, "A 28nm HKMG super low power embedded NVM technology based on ferroelectric FETs," *IEEE International Electron Devices Meeting (IEDM)*, San Francisco, CA, USA, Dec. 2016, p. 11.5.1-11.5.4.
- [5] S. Dunkel *et al.*, "A FeFET based super-low-power ultra-fast embedded NVM technology for 22nm FDSOI and beyond," *IEEE International Electron Devices Meeting (IEDM)*, San Francisco, CA, USA, Dec. 2017, p. 19.7.1-19.7.4.
- [6] S. S. Cheema *et al.*, "Enhanced ferroelectricity in ultrathin films grown directly on silicon," *Nature*, vol. 580, no. 7804, pp. 478–482, Apr. 2020.

2:55 PM EL09.12.03

DFT Modeling of Scaling Limits in FEFETs [Kisung Chae](#)^{1,2}, Andrew Kummel¹ and Kyeongjae Cho²;

¹University of California, San Diego, United States; ²The University of Texas at Dallas, United States

Atomic stack models in ferroelectric (FE) hafnium-zirconium oxide (HZO) based on density functional theory have been developed to elucidate the atomic and electronic structure level origin of fatigue behavior, i.e., deteriorating memory window with field cycling. Stack models to mimic metal-FE-metal (MFM) capacitor and metal-FE-semiconductor FE field effect transistor (FEFET) were developed. There were three key findings. (1) For a metal in direct contact with the FE layer, the field inside the FE is eliminated and local potential profile inside the FE is unchanged upon polarization switching. Conversely, the field inside the FE is not completely eliminated by a relatively less polarizable semiconductor electrode, and there is an asymmetric potential profile

due to polarization switching. (2) When a DE interlayer is placed at the interfaces in MFM and FEFET stacks, a significant internal field is induced in both cases. Strength of the field is dependent on the thickness of the FE layer, decreasing for thicker FE layers, and for ultrathin films (<4 nm) can exceed the breakdown voltage, consistent with difficulty in synthesizing FE HZO films thinner than 5 nm. (3) Since the field within the FE layer is reversed each time the polarization switches, this will promote charge-compensating defect generation. With a significant accumulation of defect density, most likely O vacancies, the FE phase of HZO would become thermodynamically unstable, and transition to a non-polar phase losing the spontaneous polarization. This would explain the fatigue behavior of the FE devices. The suggested mechanism would be more significant for a FEFET due to the lower polarizability of semiconductor vs metal electrodes and the spontaneous formation of insulating oxide DE interlayers, for example silicon oxide on silicon, which is consistent with unsatisfactory endurance for FEFET devices compared to MFM capacitors. The atomic models have developed a fundamental understanding to enable experimental optimization strategies for desired device performance.

3:10 PM EL09.12.04

Multidomain Ferroelectric Switching Dynamics Studied with a Physics-Based Circuit Compatible Model for Phase-Field Simulations Chia-Sheng Hsu¹, Sou-Chi Chang², Dmitri Nikonov², Ian Young² and Azad Naeemi¹; ¹Georgia Institute of Technology, United States; ²Intel Corporation, United States

The multidomain nature of ferroelectric (FE) polarization switching dynamics has recently attracted a great deal of research attention due to the discovery of the doped hafnium oxides as an FE material compatible with transistor fabrication processes. To study Zr-doped hafnium oxides (HZO), we develop a physics-based circuit compatible model for phase-field simulations, where the 3-dimensional time-dependent Ginzburg–Landau (TDGL) equation and Poisson’s equation are self-consistently solved with the SPICE simulator. Systematically calibrated based on the experimental measurements of metal–ferroelectric–metal (MFM) capacitors, the model well captures transient negative capacitance (NC) in pulse switching dynamics, with domain interaction and viscosity being the key factors. The influence of pulse amplitudes on voltage transient behaviors is found to be attributed to the fact that the FE free energy profile strongly depends on how the domains interact. In addition, we extract the domain viscosity dynamics during polarization switching according to the experimental measurements. For the first time, a physics-based circuit-compatible SPICE model for multidomain phase-field simulations is established to reveal the impact of microscopic domain interaction on the NC effect. The findings of this article may have important implications for the charge boost induced by the stabilization of NC in an FE/dielectric (DE) stack at a specific operating voltage or frequency.

3:25 PM EL09.12.05

MIT Virtual Source Ferroelectric FET (MVSFE) Model—Application to Scaled- L_g FeFET Analog Synapses Ahmad Zubair, Ujwal Radhakrishna, Mark Theng, Dimitri Antoniadis and Tomas Palacios; Massachusetts Institute of Technology, United States

Conventional multi-purpose hardware based on von-Neumann architecture does not satisfy the energy efficiency requirements of large-scale implementations of deep neural networks (DNN). Hardware accelerators that reduce data movement are therefore key to improve the power efficiency of many big data applications based on deep learning, such as image classification and speech recognition. Emerging non-volatile memory devices such as resistive random-access memory, phase change memory, floating gate memory and ferroelectric field effect transistors (FEFETs) are potential candidates for these DNN accelerators due to their synaptic functionality *i.e.* analog conductance modulation.

FeFET analog synapses are 3-terminal devices that have been proposed to improve the classification accuracy and yield low latency in non-volatile memory-based DNN accelerators. This is due to their high conductance ratio, operation capability with sub-100 ns pulse [1] and seamless integration with CMOS process flow. This work presents a simulation framework to evaluate novel ferroelectric and anti-ferroelectric devices, such as doped HfO₂ ferroelectric-transistors, and their impact in system-level neuromorphic applications. The study uses a new, comprehensive, physics-based compact Verilog-A model, the MIT Virtual Source Ferroelectric FET (MVSFE) model that describes transistors with ferroelectric (FE)-oxides in their gate-stack. We expanded

physics-based MIT Virtual Source model benchmarked against scaled 45nm [2] MOSFET to capture the physics of ferroelectric oxide using VDST-P [3,4] model calibrated against experimental FE HZO characteristics. The model captures underlying FET incorporating ballistic transport and charges for advanced technology node FeFETs (with or without internal gate). Our model extends the scope of [1] to the highly scaled L_g required for energy efficient system-level implementation of DNN [5] We also use the framework to show that engineering the device with multiple t_{FE}/V_T elements along width direction engineering is effective to improve system-level performance metrics (i.e. linearity and classification accuracy) of DNN built using analog synapses. The results provides insight on improved device design, and its system-level performance impact in a multilayer perceptron neural network.

[1] M. C. Jerry, P -Y.; Zhang, J.; Sharma, P.; Ni, K.; Yu,S.; Datta, S., "Ferroelectric FET Analog Synapse for Acceleration of Deep Neural Network Training," 2017.

[2] C. Auth, A. Cappellani, J. S. Chun, A. Dalis, A. Davis, T. Ghani, *et al.*, "45nm high-k plus metal gate strain-enhanced transistors," *2008 Symposium on Vlsi Technology*, pp. 99-+, 2008.

[3] B. Jiang, P. Zurcher, R. E. Jones, S. J. Gillespie, and J. C. Lee, "Computationally efficient ferroelectric capacitor model for circuit simulation," *1997 Symposium on Vlsi Technology*, pp. 141-142, 1997.

[4] J. Chow, A. Sheikholeslami, J. S. Cross, and S. Masui, "A voltage-dependent switching-time (VDST) model of ferroelectric capacitors for low-voltage FeRAM circuits," *2004 Symposium on Vlsi Circuits, Digest of Technical Papers*, pp. 448-449, 2004

[5] T. Gokmen and Y. Vlasov, "Acceleration of Deep Neural Network Training with Resistive Cross-Point Devices: Design Considerations," *Front Neurosci*, vol. 10, p. 333, 2016.

3:40 PM EL09.12.06

First-Principles Theory and Insights of Two-Dimensional Ferroelectric Semiconductors and Semimetals

Xiaofeng Qian; Texas A&M University, United States

Nanoscale ferroelectric materials hold great promises in miniaturized device applications such as ferroelectric capacitor, transducers, actuators, sensors, photovoltaics, etc. Here we present first-principles theoretical predictions and understandings of three materials classes of two-dimensional ferroelectrics, including (a) semiconducting 2D group IV monochalcogenides [1], (b) semiconducting 2D multiferroic semiconductors in monolayer transition metal phosphorus chalcogenides (TMPCs) with coexisting ferroelectricity and ferromagnetism [2], and (c) semimetallic few-layer WTe_2 [3,4]. We show that monolayer group IV monochalcogenides hold highly anisotropic and large ferroelectric polarization with visible-spectrum excitonic gap and sizable exciton binding energy and strain-tunable ferroelectric transition barrier. We will further discuss our study and understanding of domain wall, phase transition and domain switching in 2D ferroelectric group IV monochalcogenide using first-principles based machine-learning force field developed in our group. In contrast to group IV monochalcogenides, monolayer TMPCs hold coexisting ferroelectricity and ferromagnetism where Cu atoms spontaneously move away from the center atomic plane and result in out-of-plane electric dipole moment, suggesting the possibility of controlling electric polarization by external vertical electric field. Finally, we will present our study of ferroelectric polarization in semimetallic few-layer WTe_2 where small interlayer sliding induces ferroelectric transition with small kinetic barrier, enabling facile ferroelectric switching upon electric gating and ferroelectric nonlinear anomalous Hall effect demonstrated in experiment very recently [4].

References: [1] 2D Materials 4, 015042 (2017). [2] Applied Physics Letters 113, 043102 (2018). [3] npj Computational Materials 5, 119 (2019). [4] Nature Physics 16, 1028-1034 (2020).

9:00 PM *EL09.14.01**Polycrystalline Ferroelectric HfZrO₂-Based Negative Capacitance FETs with Polarization Phases and Domains** Min-Hung Lee; National Taiwan Normal University, Taiwan

The integrating ferroelectric gate stack into FETs with negative capacitance (NC) effect [1][2] for subthreshold swing (SS) improvement has attracted lots of attention due to hafnium (Hf)-based oxide with ferroelectricity. The prospect of ferroelectric Hf-based oxide by ALD (Atomic Layer Deposition) has been wide and intensive studied due to lots of applications. The HfO₂ with suitable dopants and annealing for ferroelectric (FE) transition would be studied, and demonstrated NC effect for steep-slope FET (SS-FET) and memory applications [3][4].

Pursuing steep-SS with accompanying hysteresis is a challenge for NC-FET development, as well as the issue of asymmetric SS of bi-directional sweep [5][6]. Furthermore, the reduced NC onset voltage is another issue to boost steep SS at low operation bias [7]. The antiferroelectric (AFE) Hf_{1-x}Zr_xO₂ with adopting as gate would overcome partial issues and make comparison with ferroelectric Hf_{1-x}Zr_xO₂ [8][9]. Note that the FE and AFE characteristics of HfZrO₂-based is achieved by Zr incorporation content by ALD supercycle.

Device dimension scaling down, such as FinFET and GAA, to comparable with domain size of polycrystalline ferroelectric HfZrO₂ (HZO) is evaluated for SS and drain-induced barrier lowering (DIBL) [10][11]. The multi-domain modeling of polarization randomly located in HZO and the probability with Gaussian distribution HZO are confirmed by measurement data within limitation polarization, and presented NC effect for voltage amplification with opposite direction of E-field in FE and IL. The experimental data of FinFET and planar FET are used to validate the simulation results and the direction effect of domain quantity.

The compatible CMOS process and scaling film thickness are the advantages to integrate into semiconductor industry by comparison with perovskite material. The high scalability and CMOS-compatibility of ferroelectric Hf-based oxide is a key technology enabler for energy-efficient computing to serve for smart power management in IoT applications.

Acknowledgment

The authors are grateful for the funding support from the National Science Council (MOST 109-2213-E-003-003 and 109-2622-8-002-003), process supported by Taiwan Semiconductor Research Institute (TSRI), Nano Facility Center (NFC), and computing support was provided by the National Center for High-Performance Computing (NCHC), Taiwan.

References:

[1] S. Salahuddin et al, *NanoLetters*, 8, 405, 2008. [2] S. Salahuddin et al, in *IEDM*, 2008, 693. [3] M. H. Lee et al, in *IEDM*, 2015, 616. [4] K.-S. Li et al, in *IEDM*, 2015, 620. [5] W. Chung et al, in *IEDM*, 2017, 365. [6] M. H. Lee et al, in *IEDM*, 2017, 565. [7] M. H. Lee et al, in *IEDM*, 2016, 306. [8] X. Lyu et al, in *VLSI Symp.*, 2019, T44. [9] M. H. Lee et al, in *IEDM*, 2019, 447. [10] M. H. Lee et al, in *IEDM*, 2018, 735. [11] K.-T. Chen et al, *SST*, 35, 125011, 2020.

9:25 PM EL09.14.02**Late News: Low Temperature (350 °C) Annealing for Ferroelectric Hf_{0.5}Zr_{0.5}O₂ Thin Films**

Zhouchangwan Yu, Balreen Saini, Fei Huang, Wilman Tsai and Paul McIntyre; Stanford University, United States

HfO₂-based ferroelectric thin films are promising for memory and neuromorphic applications. Compared to conventional perovskite-structure ferroelectric materials, HfO₂-based ferroelectrics have excellent CMOS compatibility, and they are better able to meet back-end-of-line (BEOL) thermal budget requirements. In this work, we demonstrate that high polarization ($P_r > 20 \mu\text{C}/\text{cm}^2$) Hf_{0.5}Zr_{0.5}O₂ (HZO) thin films are achieved by a

rapid thermal anneal (RTA) at a very low temperature (350°C). Orthorhombic phase formation of HZO is studied as a function of RTA time.

In the ferroelectric HZO capacitor structure, 10 nm HZO is sandwiched between 10 nm top and bottom TiN electrodes. The HZO film is deposited by a plasma-enhanced atomic layer deposition (PE-ALD) process at 250°C. The bottom and top TiN are deposited by reactive sputtering of Ti in N₂ atmosphere. After top TiN deposition, the capacitors are annealed by RTA at 350°C in N₂ atmosphere from 30 to 600 seconds. Finally, Pt contacts are deposited on the TiN top electrodes to facilitate for electrical measurements. Capacitor areas are defined by etching Pt/TiN stack in SC1 solution.

All HZO capacitors display polarization switching after annealing at 350°C, even after only 30 s anneal. The remnant polarization (P_r) increases as the RTA time increases from 30 s to 120 s, and the P_r saturates for longer RTA times ($P_r > 20 \mu\text{C}/\text{cm}^2$). For all devices, there is no evidence of an anti-ferroelectric hysteresis loop observed even in the as-processed (pristine) state, and no significant polarization “wake-up” effect is observed during voltage cycling. Grazing incidence X-ray diffraction (GI-XRD) is performed to analyze the phase evolution of the HZO thin film in this low temperature anneal process. The observed O(111) peak is consistent with formation of the orthorhombic phase. HZO films annealed for longer RTA time display higher O-phase peak intensities. Also, weak peaks indexed as the monoclinic phase begin to appear as the RTA time increases. Synchrotron XRD are performed for quantitative analysis on the phase evolution structure as a function of RTA time.

The ALD temperature used in deposition of the HZO film is a key factor enabling a low RTA thermal budget. HZO deposited at 200°C required a higher temperature for formation of films exhibiting a programmable polarization (> 500°C). Also, significant wake-up behavior is observed during voltage cycling, suggesting that the tetragonal phase and orthorhombic phase co-exist in the pristine state for films deposited at this lower ALD temperature, later transforming to the orthorhombic phase during cycling. Possible structural origins of this ALD temperature-induced change in phase formation sequence will be discussed.

9:40 PM EL09.14.03

High-Performance and High-Endurance Hafnia-Based Ferroelectric Field Effect Transistor with 3-Dimensional Structural Approach Taeho Kim, Junghyeon Hwang, Giuk Kim, Minhyun Jung and Sanghun Jeon; Korea Advanced Institute of Science and Technology, Korea (the Republic of)

Since the discovery of fluorite-structure oxides with ferroelectricity, especially doped-HfO₂, the ferroelectric field effect transistor (HfO₂-FeFET) has attracted huge attention as an emerging memory device. One of the serious challenges of the HfO₂-FeFETs is their limited endurance, which has been attributed to the degradation of the interface layer before the polarization fatigue of the HfO₂-ferroelectric layer. The main mechanisms of the interface layer degradation of FeFETs represented by metal-ferroelectric-insulator-semiconductor (MFIS) are charge injection/trapping and interfacial defect generation, which is mainly induced by high electric field through the interfacial dielectric layer. In this work, we propose strategies to minimize the interfacial electric field by approaching from two viewpoints of ferroelectric material properties and device structure. In this study, we present a structural approach and ferroelectric characteristics of a device that can have a larger dielectric capacitance compared to ferroelectric capacitance to improve the memory window and reliability characteristics. When it comes to 1T-1C type FeRAM, material and process are designed to have a high spontaneous polarization (P_s) value. However, for large memory window and reliable 1T type FeFET, it requires a certain value of spontaneous polarization value. We found that MFMS (metal-ferroelectric-metal-insulator-semiconductor) FeFET with a three-dimensional channel structure is very effective to improve the memory window and reduce the electric field through the interfacial layer. In particular, the latter contributes greatly to improving reliability characteristics.

9:55 PM EL09.14.04

Architecture Dependent Ferroelectric Material Considerations in Planar and Nanowire Transistors

Negative capacitance field effect transistors (NCFET) have the potential to lower the subthreshold swing below 60 mV/decade at room temperature. This can be achieved through an internal amplification for which the magnitude of ferroelectric capacitance (C_{FE}) must be lower than the oxide capacitance (C_{OX}) i.e. $|C_{FE}| < C_{OX}$ [1]. Since the transistor architecture has evolved from traditional planar to nanowire, the geometrical considerations for C_{FE} and C_{OX} have become relevant in the choice of ferroelectric material [2]–[3]. Our analytical investigation for a long channel metal–ferroelectric–insulator–semiconductor (MFIS) NCFET has shown that the circular cross-section of the nanowire yields more negative ferroelectric capacitance along with a higher oxide capacitance than that exhibited by the planar device. Also, $|C_{FE}|$ increases significantly as compared to C_{OX} in a cylindrical geometry as compared to planar NCFET, which translates into the requirement of a thicker ferroelectric layer (T_{FE}) to sustain the internal amplification and the associated sub-60 mV/decade current transition. In order to mitigate the above condition of using a relative thicker T_{FE} , a ferroelectric material with a higher coercive field or lower remnant polarization is more suited for nanowire architecture. For an interfacial oxide layer of 1 nm, a double gate NCFET with Al-HfO₂ [2], Y-HfO₂ [4], Gd-HfO₂ [5] and HZO [4] requires a minimum T_{FE} of 5 nm, 8 nm, 12 nm, and 21 nm, respectively, to sustain internal amplification. However, for a cylindrical nanowire NCFET, the minimum T_{FE} values increase to 7 nm, 11 nm, 23 nm, and 69 nm, respectively. This difference between the minimum values of T_{FE} is least (~2 nm) for Al-HfO₂ (exhibits a high coercive field) and highest (48 nm) for HZO based NCFET. This difference between the minimum ferroelectric thickness of a planar double gate and a nanowire NCFET is governed by the coercive field and remnant polarization of the ferroelectric material. Since nanowire architecture can effectively suppress short channel effects, the maximum possible nanowire diameter should be selected so as to further limit the minimum T_{FE} for sustaining the internal amplification. For a thinner interfacial oxide layer thickness, the minimum T_{FE} for cylindrical NCFET can also become comparable to that required for a planar NCFET. The above mentioned inferences indicate the suitability of a ferroelectric material with a higher coercive field (or lower remnant polarization) along with thinner interfacial oxide or larger nanowire diameter for nanowire transistor architecture.

References

- [1] S. Salahuddin *et al.*, *Nano Lett.*, 8 (2007), 405–410.
- [2] A. D. Gaidhane *et al.*, *IEEE Trans. Electron Devices*, 65 (2018), 2024–2032.
- [3] D. Jimenez *et al.*, *IEEE Trans. Electron Devices*, 57 (2010), 2405–2409.
- [4] S. Semwal *et al.*, *IEEE Trans. Electron Devices*, 67 (2018), 3868 - 3875.
- [5] M. Hoffmann *et al.*, *Adv. Funct. Mater.* 26 (2016), 8643–8649.

10:10 PM EL09.14.05

Analysis of Ferroelectric Negative Capacitance—Hybrid MEMS Actuator Using Energy Landscape
Raghuram Tattamangalam Raman, Arvind Ajoy and Revathy Padmanabhan; Indian Institute of Technology Palakkad, India

Electrostatic MEMS (Micro Electro Mechanical System) actuators are widely used in various applications like RF (Radio Frequency) MEMS, Digital Micromirror Devices etc. These devices inherently consume low-power. However, they demand high operating voltages. A novel method proposed to mitigate this large voltage requirement, is to connect a ferroelectric capacitor, exhibiting negative capacitance, in series with the MEMS actuator thereby forming a hybrid MEMS actuator¹. This technique is adapted from the emerging and recently reported use of ferroelectric negative capacitance in realizing steep slope (Subthreshold Swing $SS < 60$ mV/decade) low-voltage transistors. The response of the electrostatic MEMS actuator depends heavily on the applied input (static and dynamic inputs). Hence, it is necessary to develop a physics-based unified framework that facilitates an easy analysis of the hybrid MEMS actuator for different inputs.

We propose an energy-based framework to systematically analyze the statics and dynamics of the hybrid MEMS actuator. The proposed method uses graphical energy-displacement and phase portrait plots to

investigate static pull-in, dynamic pull-in and pull-out phenomena of the hybrid MEMS actuator. The ferroelectric capacitor is governed by the Landau-Khalatnikov equation, which relates the voltage across the ferroelectric to its charge. The MEMS actuator, however, is governed by the nonlinear force-balance differential equation, expressed in terms of the electrode displacement. Therefore, we employ a coordinate transformation from the charge to the displacement, to obtain the Hamiltonian of the hybrid MEMS actuator in terms of its displacement. A mapping function, based on the MEMS capacitor charge-voltage relationship, is used for this transformation².

Using this framework, we show that the static pull-in, dynamic pull-in and pull-out voltages of the hybrid actuator are significantly reduced due to the ferroelectric negative capacitance, as compared to the standalone MEMS actuator. The results obtained are in agreement with the numerical SPICE (Simulation Program with Integrated Circuit Emphasis) simulations of the hybrid MEMS actuator³. The framework is unified because the same Hamiltonian is used for examining the static pull-in, dynamic pull-in, and pull-out phenomena. Since the proposed framework uses only graphical plots for the analysis, it eliminates solving intricate nonlinear differential equations that govern the dynamics of the hybrid actuator. Therefore, this serves as a quick analysis tool to predict the pull-in and pull-out voltages of the hybrid MEMS actuator. The proposed energy-based framework also has the capacity to include the adhesion between the contacting surfaces. We model the adhesion using Van der Waals force and illustrate the reduction in the pull-out voltage in the hybrid MEMS actuator due to the presence of adhesion. The proposed framework could be further enhanced to include other phenomena such as fringing field capacitance. It could also be used for different MEMS structures by suitably modifying the mapping function, used for the coordinate transformation.

[1] M Masuduzzaman and M A Alam, Nano Lett., vol. 14, no.6, 2014.

[2] R. Tattamangalam Raman, A Ajoy and R Padmanabhan, IEEE Trans. Electron Devices, vol. 67, no. 10, Oct. 2020.

[3] R. Tattamangalam Raman and A Ajoy, IEEE Trans. Electron Devices, vol. 67, no. 11, Nov. 2020.

SESSION EL09.15: On-demand
Wednesday Morning, April 14, 2021
EL09

8:00 AM EL09.15.01

Physical Investigation and Modeling of the Dynamic Hysteresis in Ferroelectric-based Negative Capacitance FET Chang Su¹, Kaifeng Wang¹, Liang Chen¹, Zhongxin Liang¹, Mengxuan Yang¹, Qianqian Huang^{1,2} and Ru Huang^{1,2}; ¹Institute of Microelectronics, Peking University, China; ²National Key Laboratory of Science and Technology on Micro/Nano Fabrication, China

While power consumption density significantly increases with scaling down of MOSFETs, novel low power devices have triggered lots of interest, among which ferroelectric-based negative capacitance (NC) FET is regarded as a promising candidate due to its capability of sub60 subthreshold swing (SS) and high on current. Up to now, although domain nucleation and growth theory is reasonable to explain experimental phenomena observed such as steep SS in NCFET and V-drop in R-FE circuit, the physical mechanism of hysteresis in FeFET lacks a thorough analysis, making it difficult to unambiguously determine the contribution of domain switching to hysteresis. Besides, the specific model aimed at hysteresis is missing, while the conventional method relies on extraction from pre-existing transfer curve, which is too time-consuming to approximate and systematically offer the explicit guideline with high efficiency. In this work, an accurate efficient quantitative model of hysteresis in multi-domain FeFET is proposed, based on modeling of FE polarization switching dynamics mediated by domain nucleation and growth, including history effect, minor loop operation, voltage and time dependence. The proposed model can accurately capture the dynamic mechanism of hysteresis without

time-consuming iteration process, unveiling its non-monotonic dependence on voltage sweeping rate, coupled with sweeping range, which is also briefly discussed in physics. Moreover, the FE material-related parameters impact on hysteresis in FeFET is investigated by model and physically analyzed to draw a comprehensive conclusion. Furthermore, we re-evaluated the prerequisite of NC origin and requirement of hysteresis-free, showing that there exists a fundamental challenge of FeFET for high-speed and low-voltage operation as a logic device.

8:10 AM EL09.15.02

The Impact of Body Biasing on Externally-Connected Al:HfO₂-Based Ferroelectric Field Effect

Transistor Yejoo Choi, Seungjun Moon, Jaemin Shin and Changhwan Shin; Sungkyunkwan University, Korea (the Republic of)

Since the physical dimension of integrated circuit device (especially, memory device) has been aggressively scaled down over the past a few decades, it has been faced with a few critical/technical issues such as ever-increasing power dissipation and even incommensurate integration density because of the physical scaling limit [1]. As one of the promising solutions, ferroelectric field effect transistor (FeFET) has been emerged as a candidate for future nonvolatile memory (NVM) device because of its scalability and compatibility to CMOS (complementary metal oxide semiconductor) technology. In real, among various ferroelectric materials, HfO₂-based ferroelectric material doped with various dopants such as Zr, Al, and Si are being adopted in FeFET. Al-doped HfO₂ (HAO) shows its stable ferroelectricity in thermal process (e.g., 500 °C ~ 900 °C). Moreover, by modulating various conditions of fabrication process, the ferroelectricity of HAO can be optimized. This indicates that HAO can be widely used for future FeFETs.

In this work, the performance of HAO-based ferroelectric capacitor is presented with various fabrication conditions since the ferroelectricity of ferroelectric material requires appropriate conditions for crystallization. To explore many fabrication options for HAO-based ferroelectric capacitor, following conditions are taken into account and modulated: 1) the doping concentration of HAO (i.e., the cycle ratio of ALD deposition); 2) oxygen exposure time in ALD deposition process; 3) ALD substrate temperature; 4) annealing temperature. Then, the HAO capacitor is externally connected to the gate stack of the baseline MOSFET to electrically form a FeFET. Note that 500nm-long-channel MOSFET (metal oxide semiconductor field effect transistor) is fabricated to explicitly analyze the effect of the body biasing as well as to avoid short channel effects [2]. The modulation of memory window (MW) by body biasing in FeFETs with HAO-ferroelectric capacitor are experimentally investigated.

[1] Wang, P., Wang, Z., Shim, W., Hur, J., Datta, S., Khan, A. I., & Yu, S. (2020). Drain–erase scheme in ferroelectric field-effect transistor—Part I: Device characterization. *IEEE Transactions on Electron Devices*, 67(3), 955-961.

[2] Kim, H. W., & Kwon, D. (2020). Impact of body-biasing for negative capacitance field-effect transistor. *Journal of Physics Communications*, 4(9), 095019.

Acknowledgements

This work was supported by the National Research Foundation of Korea (NRF) through a grant funded by the Korea government (MSIP; No. 2020R1A2C1009063, 2020M3F3A2A01081672, 2020M3F3A2A01082326, and 2020M3F3A2A02082473).

SYMPOSIUM EN01

Symposium Organizers
Philipp Stadler, Johannes Kepler University Linz
Patchanita Thamyongkit, Chulalongkorn University
Shihe Yang, Peking University
Tsukasa Yoshida,

* Invited Paper

SESSION EN01.01: Advanced Electrocatalytic CO₂ Reduction
Session Chairs: Philipp Stadler and Patchanita Thamyongkit
Thursday Morning, April 22, 2021
EN01

8:00 AM *EN01.01.01

Developing Electrocatalysis Systems for CO₂ Reduction Edward Sargent; University of Toronto, Canada

I will update on progress in energy utilization and carbon balance in electrochemical reduction of CO₂ to ethanol and ethylene. I will discuss key advances in both system design and catalyst design, synthesis, and realization.

8:25 AM EN01.01.02

Optimizing the CO₂-to-CO Electrochemical Conversion From 2D Silver Nanoprisms via Superstructure Assembly Kun Qi, Yang Zhang, Ji Li and Damien Voiry; University of Montpellier, France

Electro-reduction of CO₂ in a highly selective and efficient manner is a crucial step toward the utilization of CO₂ but still requires the development of novel fabrication strategies for improving the activity and selectivity of the catalytic materials. The catalytic properties are largely dictated by the electronic structure because the performance of catalysts follows the Sabatier principle, which predicts that interactions between reactants (and intermediates) and the catalyst surface must be ideally balanced¹. Owing to their reduced dimensionality, two-dimensional (2D) materials have emerged as interesting platforms for studying electrocatalysis².

In this context, nanostructured Ag catalysts have been found to be effective candidates for CO₂ to CO conversion³. However, the ambiguous determination of the CO₂ reduction active sites and the maximization of the density of exposed active sites has greatly limited the use of Ag towards the realization of practical electrocatalytic devices. Herein, we report a superstructure design strategy prepared by the self-assembly of two-dimensional Ag nanoprisms for maximizing the exposure of active edge ribs⁴. The self-assembled Ag nanoprisms allow exposing > 95% of the edge sites which translates into high selectivity and activity towards the production of CO from CO₂. Our first principle calculations combined with electrocatalytic measurements point out the reduced binding energy of COOH* intermediate on the low-coordinated Ag surface atoms at the corner and edges ribs of the nanoprisms. Electrochemical measurements on individual nanoprisms and the corresponding superstructures allowed us to identify the edge ribs as the active sites with an onset potential for the CO₂RR reaction of 190 mV and a turnover frequency of $5.2 \times 10^{-3} \pm 2.8 \times 10^{-3} \text{ s}^{-1}$ at an overpotential of 0 mV. When tested in an H-cell, the Ag superstructure demonstrates a selectivity over 90% for 100 hours together with a current retention of $\approx 94\%$ at -600 mV vs. RHE.

References:

Sabatier, P. *La Catalyse en Chimie Organique*. (Paris & Liège Ch. Béranger Editeur, 1920).
Voiry, D.; Shin, H. S.; Loh, K. P.; Chhowalla, M. *Nature Reviews Chemistry* 2018, 2, 0105.

Liu, S. et al. *Chem. Soc.* 2017, 139, 6

Qi, K. et al. *In Preparation*, 2020

8:40 AM EN01.01.03

Electrocatalytic CO₂ Reduction on Green Synthesized Copper Nanoarchitectures to C₂ and C₂₊ Value-Added Products Supported Over Gas Diffusion Layers Venkata Siva Rama Krishna Tandava¹, Sebastian Murcia¹ and Joan Ramon Morante^{1,2}; ¹Catalonia Institute for Energy Research (IREC), Spain; ²Universitat de Barcelona, Spain

Circular economy of CO₂ is nowadays a hot issue for our society. Nevertheless, its successful implementation still requires a lot of new knowledge of reliable systems. Electrochemical CO₂ reduction (ECO₂R) is one of several promising strategies to mitigate CO₂ emissions. Developing novel advanced functional nanostructured catalyst materials and systems for electro conversion of CO₂ to alternative fuels or value-added products in order to meet the global energy needs and so as a means to curb the increasing amounts of CO₂ in the atmosphere is of utmost importance. To date, Copper (Cu) and Copper-based materials are the only heterogeneous catalyst systems that have shown a propensity to produce valuable hydrocarbons and alcohols such as ethylene and ethanol.

Copper nanoparticles were synthesized by a simple wet chemical reduction method at mild temperatures using *L*-Ascorbic acid, a widely used green reducing agent, and different additives for the morphological control. X-Ray Diffraction studies revealed the presence of Cu₂O particles with varied crystallographic orientation, which can be selective towards ethylene and C₂₊ products, while SEM analysis showed the formation of specific morphologies such as cubes, cuboctahedrons, and truncated octahedron morphologies. The as-synthesized nanoparticles were directly drop cast on 3D porous substrates (e.g., carbon Toray and copper foam). The electrodes were evaluated in conventional H-type and flow filter-press cells with Gas Diffusion electrodes under neutral and alkaline electrolyte conditions. A clear correlation between working voltage, structural electrocatalyst properties, pH, and product distribution was observed, with higher selectivity towards ethylene generally obtained at intermediate potentials. Other aspects such as hindering the Hydrogen Evolution Reaction and evaluating the role of halide species were also considered. The results and both selectivity favoring and limitation factors were discussed and potential solutions were addressed here.

This work is supported by **European Union's Horizon 2020 DOC-FAM** program under the **Marie Skłodowska-Curie Actions** Grant Agreement No **754397**.

8:55 AM *EN01.01.04

Novel Materials for Oxygen and Carbon Monoxide Electrocatalysis Maria Escudero-Escribano; University of Copenhagen, Denmark

The design and development of active, stable, and selective electrocatalysts for renewable energy conversion reactions is key for the transition towards a decarbonised future. This talk will present some recent strategies aiming to understand and engineer the interfacial structure and properties for oxygen and carbon monoxide/carbon dioxide electrocatalysis.

The first part will be focused on the development of self-supported high surface area nanostructured catalysts for the oxygen reduction and evolution reactions (ORR and OER, respectively). In the second part, I will present our recent work on Cu-based well-defined electrodes in contact with different electrolytes aiming to understand the structure sensitivity for CO₂ and CO reduction. We show how model studies are essential to understand the structure-property relationships and design efficient electrocatalysts for sustainable energy conversion.

9:20 AM EN01.01.06

Late News: Au Decorated Cu(OH)₂ Nanoneedle Catalysts for Electrochemical CO₂ Reduction Kim R. Gustavsen, Erik A. Johannessen and Kaiying Wang; University of South-Eastern Norway, Norway

The industrialization of the planet has created an increasing demand for energy which unfortunately has been linked to rising levels of carbon dioxide (CO₂) in the atmosphere. Thus, incentives to utilize alternative methods of energy generation is becoming more and more important. While renewable energy technologies are developing rapidly, they still suffer from intermittency. They will therefore be dependent on the development of new energy storage technologies if the transition to a renewable energy economy should be successful.

Electrochemical CO₂ reduction is a promising candidate for energy storage since it can generate valuable chemicals and fuels (such as hydrocarbons) while at the same time close the carbon cycle. The only metal catalyst capable of efficient hydrocarbon production is copper, despite being unselective and known to generate a wide range of products simultaneously. This greatly reduces the efficiency of the desired product, and much effort has been aimed at tuning the selectivity of copper-based catalysts. However, a highly selective Cu based catalyst that is functional over a prolonged period without suffering deactivation is yet to be found.

Copper hydroxide has shown great promise for CO₂ reduction reaction (CO₂RR), and have a greater affinity towards C₂ products such as ethylene at the cost of methane formation [1]. Similar to oxide-derived Cu (OD-Cu), the oxidation state of the surface is believed to play an important role in the enhanced selectivity towards ethylene. However, the existence of sub-surface oxide during reaction conditions is a controversial topic, and factors like increased surface roughness is also suggested as being responsible. Nevertheless, while favorable C-C coupling energetics are observed for Cu(OH)₂ based catalyst compared to polycrystalline Cu, the Faradaic efficiency (FE) for ethylene is still relatively low (38.1%) [2].

In this work we attempt to further enhance the C₂ selectivity of Cu(OH)₂ nanoneedles by depositing a thin Au coating. The Au sites will generate CO, which can be transferred to adjacent Cu sites by either readsorption or surface diffusion to undergo further reduction. The Cu(OH)₂ nanoneedles were synthesized by anodizing Cu foils in 3M KOH at a constant current density (~3.2 mA/cm²) for 10 minutes. Subsequently, the Cu(OH)₂ nanoneedles were decorated with Au using DC magnetron sputtering. The catalyst performance was evaluated in an H-cell and the gaseous products were quantified by gas chromatography in an on-line configuration .

References

1. Iijima, G., et al., *Role of a Hydroxide Layer on Cu Electrodes in Electrochemical CO₂ Reduction*. *ACS Catalysis*, 2019. **9**(7): p. 6305-6319.
2. Lee, S.Y., et al., *Mixed Copper States in Anodized Cu Electrocatalyst for Stable and Selective Ethylene Production from CO₂ Reduction*. *Journal of the American Chemical Society*, 2018. **140**(28): p. 8681-8689.

9:25 AM DISCUSSION TIME

SESSION EN01.02: Novel Concepts in Sustainable Electrocatalysis—Carbon and Metal-Free Electrocatalysts
Session Chairs: Maria Escudero-Escribano and Philipp Stadler
Thursday Morning, April 22, 2021
EN01

10:30 AM *EN01.02.01

From Organic Electronics Towards Bio-Organic Systems for CO₂ Recycling Niyazi Serdar Sariciftci;
Johannes Kepler Universität Linz, Austria

Organic photovoltaic cells are maturing from the academic research into the industrial development, entering the markets. Pure organic nanostructures and organic/inorganic hybrid nanostructures are comparatively studied

for such devices. This talk gives an overview of materials' aspect and devices.

In order to account for a sustainable future, the application of biodegradable and biocompatible systems for organic optoelectronics are needed. The use of cheap electronic devices in a large scale will introduce a "consumable electronics" into the market of "consumer electronics". Therefore environmentally friendly materials are important to use. This is a next great challenge to material science in organic electronics. New developments of bio-inspired and/or bio-origin, bio-compatible materials from our institute will be reported. Such materials can also be used to interface the biological and biomedical research with the organic electronics field.

Last but not least the conversion of CO₂ to methane (or other synthetic fuels) using solar energy is an important step to make an efficient, large scale energy storage. At the same time this will make a cyclic and sustainable CO₂ economy. We report organic as well as bio-organic catalysts which can be used in photo-electro-catalytic conversion devices. Such bio-catalysts can be enzymes as well as living bacteria immobilized on electrodes. Selectivity of such bio-catalysts is very high and combined with the room temperature operation of such bio-electro-catalytic systems makes them industrially highly attractive.

10:55 AM *EN01.02.02

Chiral molecules and the Electron's Spin—New approach to Spin Controlled Chemistry Ron Naaman;
Weizmann Institute of Science, Israel

Spin based properties, applications, and devices are commonly related to magnetic effects and to para or ferro magnetic materials. However, we found that chiral organic molecules act as spin filters for photoelectrons transmission, in electron transfer, in electron transport. The effect, termed Chiral Induced Spin Selectivity (CISS), [[1],[2]] lead to the discovery that when chiral molecules are charge polarized, there is a transient spin polarization [[3]]. At each electrical pole, the (partially) unpaired electron is spin polarized with opposite polarization at the positive and negative poles. Which spin is associate with which pole depends on the handedness of the molecule. This finding sheds new light on enantio-specific interactions and it allows to construct novel methods for enantio-separation. [[4],[5]] It also opens new ways to induce spin polarization in semiconductors and to obtain temperature activated ferromagnetism in chiral metallo-organic crystals [[6]].

[[1]] R. Naaman, Y. Paltiel, David Waldeck, *Nature Reviews Chemistry* 3, 250 (2019).

[[2]] R. Naaman, D. H. Waldeck *Ann. Rev. Phys. Chem.* 66, 263 (2015).

[[3]] A. Kumar, E. Capua, M. K. Kesharwani, J. M. L. Martin, E. Sitbon, D. H. Waldeck, R. Naaman, *PNAS*, **114**, 2474–2478 (2017).

[[4]] K. Banerjee-Ghosh, O. Ben Dor, F. Tassinari, E. Capua, S. Yochelis, A. Capua, S.-H. Yang, S. S. P. Parkin, S. Sarkar, L. Kronik, L. T. Baczewski, R. Naaman, Y. Paltiel, *Science* **360**, 1331 (2018).

[[5]] F. Tassinari, J. Steidel, S. Paltiel, C. Fontanesi, M. Lahav, Y. Paltiel, R. Naaman, *Chemical Science*, **10**, 5246–5250 (2019).

[[6]] A. K. Mondal et al. *ACS Nano* (2020) in press. DOI: 10.1021/acsnano.0c07569.

11:20 AM EN01.02.03

Late News: Electrochemical- Thermally-Activated Chemical (E-TAC) Water Splitting Hen Dotan^{1,2}, Avigail Landman^{2,1}, Gideon Grader^{2,1} and Avner Rothschild^{2,1}; ¹H2Pro, Israel; ²Technion--Israel Institute of Technology, Israel

Electrolytic hydrogen production faces technological challenges to improve efficiency, economic value and

rapid scale up. In conventional water electrolysis, the water oxidation and reduction reactions are coupled in both time and space, as they occur concurrently at an anode and a cathode in the same cell. This introduces challenges such as product separation, and sets strict constraints on material selection and process conditions. Another major challenge is to improve efficiency, which is limited by the large (> 400 mV) overpotential loss of the four-electron oxygen evolution reaction (OER).

The Electrochemical – Thermally-Activated Chemical (E-TAC) water splitting cycle decouples these reactions by dividing the process into two stages; an electrochemical (E) stage that reduces water at the cathode and charges (oxidizes) a nickel hydroxide ($\text{Ni}(\text{OH})_2$) anode to nickel oxyhydroxide (NiOOH), followed by a chemical (TAC) stage that reduces the charged anode (NiOOH) spontaneously (without applied bias) back to its initial state ($\text{Ni}(\text{OH})_2$) by oxidizing water. This chemical reaction is accelerated at elevated temperatures (60 - 100°C), providing a handle to control the evolution of oxygen in the cell so as to avoid mixing with hydrogen. The E-TAC cycle enables overall alkaline water splitting at an average cell voltage of ~ 1.5 V in a membraneless cell architecture that offers potential for cost reduction by eliminating membranes and sealing components, and supports high-pressure hydrogen production. High electrolytic efficiency of $98.7\%_{\text{HHV}}$ is achieved by dividing the four-electron OER into four one-electron reactions wherein four Ni(II) sites are charged (oxidized) to Ni(III). The operational challenges that arise from swinging between the E and TAC stages and the material challenges that arise from the finite capacity of the nickel (oxy)hydroxide anode will be discussed in the talk.

11:35 AM EN01.02.04

Catalyst Optimization for Electroreduction of Nitrates to Ammonia Marcelo E. Chavez, Sebastian Murcia and Joan Ramon Morante; Catalonia Institute for Energy Research, Spain

A combination of the increased awareness about nitrogen-oxyanions contamination in waters and the value of certain nitrogen-based products as key commodities, potential fuel or chemical precursors, have opened a novel approach line within the circular economy, framed in the development of both: novel materials and optimal processes for nitrate electroreduction to ammonia as main reaction product. The vast literature in the field of water denitrification points to the most promising materials for nitrate electroreduction. Pure transition and noble metals, in combination with organic and inorganic substrates have been tested in this process with different outcomes, among which the most remarkable are the catalytic activities of copper, gold, silver and iron. However, most of the materials that showed excellent properties for one step of the complete reduction of nitrate, did not show good results in terms of faradaic efficiencies towards most of the nitrogen-based valuable products. In this work, ammonia is presented as main product given its essential role in modern agriculture and as a potential energy carrier. In this context, in a sustainable process, not only the catalytic activity defines the ideal material, but its combination with the faradaic efficiency and stability of the electrocatalyst. Having copper as the most active material for nitrate electroreduction, it is important to combine it with a substrate that provides stability, resistance to operative conditions, and selectivity to ammonia. The reasons stated above have conducted the research to define materials for nitrate electroreduction as copper nanoparticles supported by carbon-based and titanium structures. Copper nanoparticles obtained by electroless reduction and deposited on 3D carbon and metallic substrates, combined with the optimal electrochemical conditions of working potential, nitrate concentration and ammonia recovery system are presented in this work to open a potential alternative route to the traditional high energy consuming Haber-Bosch process for ammonia production.

11:50 AM EN01.02.05

Late News: Selective Hydrogen Catalysis via Carbon Nanotube Encapsulation and Oxide Layer Deposition Samuel S. Hardisty, Kobby Saadi and David Zitoun; Bar-Ilan University, Israel

Catalysts undergo poisoning and degradation during their utilization in many different fields. Common examples are the CO poisoning of Pt, or the degradation of Pt/C catalysts during start-stop procedures, both occurring in polymer electrolyte fuel cells (PEMFCs). Another energy technology that features prominent catalyst degradation is the hydrogen bromine redox flow battery (H_2 - Br_2 RFB). H_2 - Br_2 RFBs are a cheap and efficient solution to large scale energy storage. The main hinderance of the technology is the poisoning of the hydrogen evolution reaction/hydrogen oxidation reaction (HER/HOR) catalyst by bromine species which have

crossed over the proton exchange membrane. Without a revolution in membrane development, this crossover appears unpreventable. Therefore, we sought to protect the catalyst locally. Two possible solutions were found to impart catalyst active site selectivity: Pt encapsulation in single walled carbon nanotubes (SWCNTs) and metal oxide deposition on catalysts via atomic layer deposition (ALD).

Platinum nanoparticles were synthesized within the internal cavities of small diameter SWCNTs, through a simple impregnation and drying procedure. High resolution transmission electron microscopy (HRTEM), atomic force microscopy (AFM) and scanning tunneling electron microscopy (STEM) were used to characterize the particles and demonstrate that they were confined within the SWCNTs. The typical hydrogen under potential deposition peaks were observed on a cyclic voltammogram of the sample, whereas the oxide region was heavily suppressed compared to Pt/C. Some diffusion limitation was observed during the HOR, indicating that the electrolyte diffusion pathway is through the SWCNTs, but the same mass transport limited current was attained. The oxygen reduction reaction (ORR) mass transport limited current was much lower than expected for Pt (2 mA cm^{-2}), indicating a transport selectivity for hydrogen over oxygen. The stability of these platinum nanoparticles in the presence of bromide/tribromide solution was vastly increased compared to the standard 50% Pt/C catalyst, shown by x-ray photoelectron spectroscopy (XPS) and electrochemistry. It is proposed that this effect is caused by steric and electrostatic repulsion of the large tribromide ion by the SWCNT cavity (internal diameter of 2 nm). The encapsulated platinum also features a vastly higher mass activity when cycled in a cell, indicating better Pt utilization due to the small particle size. This opens a new route for imparting selective access to active sites of a catalyst, hence increasing the stability of the catalyst, a potential solution to many problems faced by technologies that rely on catalysts.

Another possible solution to prevent catalyst poisoning is through a protective oxide coating on its surface. ALD was chosen due to its highly controllable, conformal deposition, but also as it can be applied to a wide range of commercial catalysts, making it highly applicable for real world applications. Different thicknesses of vanadium oxide were deposited on a commercial 50% Pt/C catalyst. XPS and HRTEM confirmed the ALD process had deposited vanadium oxide species on the catalyst. The HOR was unaffected by this deposition, indicating diffusion of hydrogen could occur through the oxide layer. Stability of the material in the presence of bromide/tribromide solution was superior to the uncoated commercial catalyst, showing the oxide coating successfully protected the catalyst. Again, whilst it has been demonstrated for bromine poisoning of Pt, this approach should be applicable to many poisoning problems facing other catalysts/applications.

12:05 PM EN01.02.06

Late News: The Relationship Between Energy Levels of Polymeric Organic Semiconductors and Their Reactivity Towards the Oxygen Reduction Reaction Alexander Giovannitti, Tyler Mefford, William C. Chueh and Alberto Salleo; Stanford University, United States

We present the development of electron-transporting polymeric organic semiconductors as a new class of metal-free electrocatalysts for the oxygen reduction reaction in aqueous electrolytes. The polymeric organic semiconductors are based on conjugated polymers with large electron affinities (equivalent to materials with low lying lowest unoccupied molecular orbital (LUMO)), where polar side chains are attached to the backbone to process materials from solution and to improve the ionic charge transport properties.^[1] This design concept results in fast charging polymer electrodes where volumetric charging of thick electrodes ($> 1 \mu\text{m}$) is achieved due to the balanced ionic and electronic charge transport properties of the polymer. The outstanding mixed ionic/electronic transport properties also enable the utilization of single-phase electrodes where no additives or binders are needed for the electrode to function in aqueous electrolytes.

We will further explain the working principle of the polymeric electrocatalyst, for which the polymeric organic semiconductor is first activated by an electrochemical doping reaction (reduction, n-type doping) that increases the reactivity of the material towards molecular oxygen. By employing in-situ spectroelectrochemical measurements and rotating ring disk electrode (RRDE) measurements, we find that the polymer achieves its highest performance when charged to the polaronic, singly charged, state. The polymers predominantly yield hydrogen peroxide through the 2-electron reduction of oxygen. The selectivity towards peroxide and water (4-electron product) is influenced by electrolyte pH. We hypothesize that chemically tuning the polymer's energy levels and side chains will pave the way for the successful development of low-cost, metal-free, and solution-

processable electrocatalysts for energy conversion technologies.

[1] A. Giovannitti, C. B. Nielsen, D.-T. Sbircea, S. Inal, M. Donahue, M. R. Niazi, D. A. Hanifi, A. Amassian, G. G. Malliaras, J. Rivnay, I. McCulloch, *Nat. Commun.* **2016**, 7, 13066.

[2] D. Moia, A. Giovannitti, A. A. Szumska, I. P. Maria, E. Rezasoltani, M. Sachs, M. Schnurr, P. R. F. Barnes, I. McCulloch, J. Nelson, *Energy Environ. Sci.* **2019**, 12, 1349.

12:20 PM EN01.02.07

Conducting Biopolymers as Metal-Free Electrocatalysts Philipp Stadler^{1,1}, Halime Coskun¹, Abdalaziz Aljabour¹, He Sun^{1,1} and Tsukasa Yoshida²; ¹Johannes Kepler Universität Linz, Austria; ²Yamagata University, Japan

The most active and efficient catalysts for the electrochemical hydrogen evolution reaction rely on noble metals, a fact that increases the cost of producing hydrogen and thereby limits the widespread adoption of this fuel. Here we present metal-free polydopamine and polyguanine as selective organic hydrogen electrocatalysts¹⁻³. The conducting functional polymers incorporate selective hydrogen-affine hydrogen bonds that possess a similar hydrogen binding energies and work function as e.g. platinum or palladium. We report the synthesis of hydrogen-selective electrocatalytic polyguanine and polydopamine and demonstrate the enhancement of the rate-determining step in the proton reduction. We further present mechanistic spectral IR-operando studies on the catalytic hydrogen bonded motifs and showcase the surface tunability between hydrogen evolution and hydrogen electrosorption including steps towards scaling the material for continuous electrolysis for several 100 hours/cycles without notable degradation.

(1) Coskun, H.; Aljabour, A.; Schoefberger, W.; Hinterreiter, A.; Stifter, D.; Sariciftci, N. S.; Stadler, P. Cofunction of Protons as Dopant and Reactant Activate the Electrocatalytic Hydrogen Evolution in Emeraldine-Polyguanine. *Adv. Mater. Interfaces* 2020, 7 (2), 1901364 DOI: 10.1002/admi.201901364.

(2) Coskun, H.; Aljabour, A.; Luna, P.; Sun, H.; Nishiumi, N.; Yoshida, T.; Koller, G.; Ramsey, M. G.; Greunz, T.; Stifter, D.; Strobel, M.; Hild, S.; Hassel, A. W.; Sariciftci, N. S.; Sargent, E. H.; Stadler, P. Metal-Free Hydrogen-Bonded Polymers Mimic Noble Metal Electrocatalysts. *Adv. Mater.* 2020, 32 (25), 1902177 DOI: 10.1002/adma.201902177.

(3) Coskun, H.; Aljabour, A.; Greunz, T.; Kehrer, M.; Stifter, D.; Stadler, P. Electrochemical Hydrogen Storage in Amine-Activated Polydopamine. *Adv. Sustain. Syst.* 2020 DOI: 10.1002/adsu.202000176.

12:25 PM EN01.02.08

Synthesizing a Novel Janus Carbon Nano-Onions Modified as a Catalyst Support for Oxygen Reduction Reaction Angelica Del Valle-Perez, Armando J. Nieves-Carrasquillo and Lisandro Cunci; Universidad Ana G. Mendez, Puerto Rico

Carbon materials have been awakening scientific interest for research because it allows chemical functionalization for multiple applications in the sciences, especially in energy applications. Carbon Nano-onions (CNO) are spherical structures composed of multilayers of fullerenes, these layers are connected in a way that shows the shape of an onion. Its development begins with the use of nano-diamonds, a carbon material of strong structure which it forms in a very violent environment. The nano-diamonds are taken to a furnace at a temperature of 1650°C to finally obtain the CNO. Janus particles are receiving increasing attention because of their dual properties, where each side can be functionalized to have distinctive characteristics. The modifications on the surface of these nanoparticles can provide different chemical and physical properties. The interesting properties of Janus nanoparticles are that they have different sizes and shapes which have now been able to be studied in more detail. The purpose of this project is to use asymmetrically modified CNO as a support for metal nanoparticles to avoid agglomeration and, thus, increase their surface area and efficiency. Janus nanoparticles will be designed by a Wax-paraffin Pickering Emulsion process using CNO on its surface. The deposition of Platinum (Pt) was carried out by a chemical process using sodium borohydride. The removal process of the paraffin involves the dispersion of the wax-paraffin/CNO-Pt particles in Chloroform, repeating the process by six times and rinse with isopropanol to finally obtain the amphiphilic nanoparticle. The differences on the surface of the particles before and after removing the paraffin were observed by Scanning

Electron Microscopy (SEM). The Energy-Dispersive Spectroscopy was used to validate the elemental information of the particles and assure the deposition of 20% of Pt on the surface of the particles. Transmission Electron Microscopy (TEM) provided us with information on the dispersion of Pt on the surface of CNO. Through X-ray diffraction (XRD) and Raman Spectroscopy, we were able to confirm the paraffin removal and presence of Pt in these particles. Cyclic Voltammetry was used to characterize the proposed catalyst and comparison with the commercial catalyst Pt/Vulcan. The Pt-CNO/CNO catalyst was tested for its performance for the Oxygen Reduction Reaction (ORR) using the Rotating Ring Disk Electrode (RRDE). Polarization curves of ORR were obtained with RRDE rotations at 0,100,400,900,1600 and 2500rpm in a O₂-saturated 0.1M KOH solution.

SESSION EN01.03: Advanced Electrocatalysis—Deeper Insights and Mechanistics I
Session Chairs: Ron Naaman and Philipp Stadler
Thursday Afternoon, April 22, 2021
EN01

1:00 PM *EN01.03.01

Mechanistic Studies of the Electrochemical CO₂ Reduction on Single Site, Metallic and Hybrid Electrocatalysts Peter Strasser; Technische Universität Berlin, Germany

In this talk, I will highlight some recent advances in our understanding of the catalytic reaction mechanism of the direct electrochemical reduction of CO₂ and of related mixed feeds into value-added fuels and chemicals on smooth polycrystalline metallic surfaces, on non-metallic, single metal-site electrocatalysts, and on metallic/non-metallic tandem catalyst schemes. Methods used include in situ X-ray analytical techniques and time-resolved Differential Electrochemical Mass Spectrometry (DEMS) conducted in novel capillary flow cells. The DEMS flow cells enable milli-second resolved analysis of reaction products under stationary and transient conditions, providing access to accurate onset potentials of a wide variety of reaction products.

1:25 PM EN01.03.02

Combinatorial Investigation of Metal Based Compounds as Electrolyzers for Oxygen Evolution Reaction Hannah N. Barad¹, Gerardo Salinas², Eran Oren¹, Mariana Alarcon-Correa¹, Florian Peter¹, Alexander Kuhn² and Peer Fischer¹; ¹Max Planck Institute for Intelligent Systems, Germany; ²Universite de Bordeaux, France

Combinatorial materials science (CMS) is a highly promising method for fast discovery of new functional materials, such as low T_c superconductors, shape-memory alloys, and photoabsorbers. CMS has been used to form thin films with composition and thickness gradients, consequently, synthesizing, on a single substrate, a range of samples with systematically varying properties, which is the first step in finding new materials and device structures. Apart from the composition or thickness, film morphology and nanostructuring can be especially important for an assortment of applications ranging from catalysis and photovoltaics to magnetic materials, as morphology governs the chemical reactivity, determines the surface area, and is important for charge mobility and recombination processes. However, heretofore CMS research did not encompass film morphology as a study parameter.

Here we describe how we vary nano-scale morphology and material composition at the same time using an adapted shadow growth method based on glancing angle deposition (GLAD), which eliminates the commonly used wet chemical steps for nanostructure synthesis. In a one-step well-controlled growth we quickly obtain a large number of nano-columnar structures, including nanorods, nanohelices, and nano-zigzags, with varying material compositions. Adapting GLAD and introducing it into CMS, with accompanying high-throughput characterization, constitutes an integrated approach for discovering new materials and structures for a multitude of applications in many scientific fields.

We use this method to fabricate a multi-component nanocomposite electrolyzer and study its compositional and

structural variations. The system is a multinary elemental metal-based library, where each material has an impact on the resulting nanostructure as well as the chemical composition and state. After investigating the physical and chemical properties of the library, it is then examined as an electrocatalyst for oxygen evolution reaction (OER). The OER activity shows a dependence on the nanostructuring of the library as well as on the chemical and compositional variation. By using CMS and high-throughput analysis, we are able to gain insights that the standard experimental techniques would not be able to achieve, thus indicating the importance and impact CMS has in the field of electrolyzers for the future.

1:40 PM EN01.03.03

Hydrazine Oxidation Electrocatalysis on Multi-Doped Carbons—Who Does What? David Eisenberg; Technion–Israel Institute of Technology, Israel

Electrocatalysis of hydrazine oxidation, a promising non-carbon fuel, is both a practical goal, and a scientific paradox. Hydrazine is a famous reductant in chemical synthesis, yet the onset potential for its electro-oxidation reaction is highly dependent on the catalytic surface. Some excellent catalysts have been developed in recent years towards direct hydrazine fuel cells. Most of these catalysts, however, are either prohibitively expensive (e.g. Pt-based ones), or easily deactivated (e.g Ni-based ones).

We have recently discovered a family of multi-doped carbons with record-breaking electrocatalytic activity towards hydrazine oxidation in alkaline pH.^{1,2} They contain many components, all of which postulated to be possible candidates for hydrazine oxidation active sites: from Mo-doped Fe₃C nanoparticles, to the N-doped, graphitic, hierarchically porous carbon. They provide the first example of hydrazine oxidation on carbides. Moreover, they are stable, efficient, and easy to make on a large scale.

In our quest to understand the source of activity in these fascinating materials, we launched a systematic study into each of the component, and into their combination. On the way, we discovered how Mo-doping is actually unnecessary, and how Zn and Cu direct the nanostructure by different mechanisms.² Furthermore, we demonstrated that the carbon matrix itself is highly active toward the reaction.³ At this point, we raised even larger questions: are the carbide nanoparticles even participate in the reaction? What does it really take for a carbon material to electro-oxidize hydrazine? To answer these questions, we combined electrochemical measurements, broad scope material characterization, and mechanistic quantum-mechanical calculations.⁴

In this talk I will present unpublished and recently published results, clearing the field of hydrazine oxidation on doped carbons, and explaining the individual catalytic, cooperative and structural roles of each component. While much remains to be understood about the activity and selectivity of these elusively simple material, and their excellent performance makes this challenge both technologically and scientifically appealing.

(1) Ojha, K.; Farber, E. M.; Burshtein, T. Y.; Eisenberg, D. *Angew. Chem. Int. Ed.* **2018**, *57*, 17168.(2) Burshtein, T. Y.; Farber, E. M.; Ojha, K.; Eisenberg, D. *J. Mater. Chem. A* **2019**, *7*, 23854.(3) Farber, E. M.; Ojha, K.; Burshtein, T.; Eisenberg, D., *J. Electrochem. Soc.* **2020**, *157*, 064517.(4) Burshtein, T.; Tamakuwala, K.; Sananis, M.; Ioffe, K.; Hirsch, S.; Farber, E. M.; Grinberg, I.; Eisenberg, D., *under preparation*.

1:55 PM EN01.03.04

Enhancing Hydrogen Evolution Reaction Assisted by Metal-Free Hot Electron Driven Electrode Hyun Uk Chae, Ragib Ahsan, Jun Tao and Rehan Kapadia; University of Southern California, United States

To pull through the emerging energy crisis, cost-effective, stable, and highly active electrocatalysts are required. Hydrogen evolution reaction (HER) is one of the electrochemical processes which allows direct conversion of electrical energy to chemical energy. However, the efficiency of this conversion process is limited by the overpotential required to reach a high enough current density. Up to date, transition metals such as platinum having the narrow d-orbital have been treated as a good electrocatalyst. They enable the activation energy to be reduced by lowering the energy of the transition state via strong interaction between the adsorbed hydrogen

atoms and the energy states of the catalyst. However, the high cost as well as low abundance in the Earth has been limiting their widespread use in commercial electrocatalysis. Herein, we show that the turn on voltage of the electrochemical reaction can be adjusted in a semiconductor-insulator-plasma etched graphene (SIEG) device. O₂ plasma etched graphene was introduced as a top electrode to increase the number of electrochemical active sites. This breaks the limitation of the catalytic property of pristine graphene limited by its large hydrogen adsorption energy and lack of electrochemically active sites. The Oxide-semiconductor layer plays a role to tune the hot electron population by biasing the graphene-semiconductor junction. The shift of the onset potential of HER can be achieved up to ~0.8V while reaching a current density of 90 mA/cm² at an overpotential of -0.5V vs RHE. Importantly, this occurs without the assist of any noble metal catalyst and uses only abundant elements such as silicon, aluminum, and carbon. This potentially introduces a new pathway in which electrocatalysts could be engineered through control over the number of active sites and electron distribution.

2:10 PM EN01.03.05

Lattice Oxygen Evolution Reaction and Its Role in Electrochemical Stability of Iridium Oxides Vitaly Alexandrov; University of Nebraska–Lincoln, United States

Electrocatalytic water splitting has received a great deal of attention as an attractive way of storing energy in the form of pure hydrogen. RuO₂ and IrO₂ catalysts are archetypical materials used for the anodic oxygen evolution reaction (OER) in acidic media, but even for the most stable oxides the long-term stability represents a critical issue. Theoretical analysis based on the use of Pourbaix diagrams have emerged as a powerful tool to identify acid-stable materials for electrocatalysis. Despite the great utility of these diagrams, they do not capture the whole complexity of reaction conditions that may affect materials stability such as highly oxidizing non-equilibrium conditions of the OER. For example, it has been recently demonstrated by both simulations and experiments for a number of complex oxides including rutile IrO₂ that stability of a catalyst can suffer from the active participation of lattice oxygen in the OER. In this work we employ density functional theory (DFT) calculations to investigate the thermodynamics of the OER through both the conventional and the lattice oxygen evolution reaction mechanisms across a series of iridium-oxide based catalysts. We show that lattice oxygen participation should be attainable for a number of iridium-oxide phases that are predicted to be thermodynamically stable based on the Pourbaix diagrams. These results suggest that lattice oxygen evolution reaction should be taken into account when analyzing electrode stability under electrochemical conditions. The obtained theoretical results will be discussed in the context of available experimental data.

2:25 PM EN01.03.06

Mechanistic and Experimental Insights Towards Laser-Ablated Holey Nanocarbons in Single-Atom Catalysis (SAC) via Fundamental Dangling Bond Concepts Kishwar Khan¹, Zhengtang Luo¹ and Khalil Amine²; ¹The Hong Kong University of Science and Technology, Hong Kong; ²Argonne National Laboratory, United States

Single-atom catalyst (SAC) is a key player in catalysis these days owning a tiny amount of metal atoms could increase its intrinsic activity towards efficient catalyst in numerous reactions. However, it is the remaining challenge and questionable to control its stability, benchmark performance, superior energy consumption during the complex synthesis process, and above the average temperature that encourages single metal atoms to become agglomerate. Herein we report a new approach based on laser ablation techniques to make laser irradiated doped holey graphene support (LGO), and subsequently make it hetero-doped laser irradiated macroporous graphene (NLG). Used the fundamental dangling bonds concept of nanocarbons to trap the metal atoms from Iron and Cobalt foams. We applied the optimized process conditions so that M⁰ could transfer electrons to NLG via dangling oxygen groups to become M^{σ+}. These dangling surface bonds of oxygen synchronizes with M^{σ+} to make metal-oxide (M-O) bonds. Dry the material at ambient conditions to make stronger dangling bonds between M-O, and then sonicate it afterwards to take away metal atoms from bulk counterparts to metal single atoms (MSA) anchored on the NLG via dangling bonds associated with oxygen groups. This new synthesis approach for making SAC is easy, economical, and sustainable as the metal foam is

working here like photocopying machine, and we can use the same foam for a long time as a metal precursor. Furthermore, we demonstrated this idea on the synthesis of two catalysts, namely Co-SAC@NLG towards hydrogen evolution reaction (HER) and Fe-SAC@NLG for oxygen reduction reaction (ORR) electrocatalysts. The morphology was experimentally verified by different tools, including aberration-corrected scanning transmission electron microscopy (AC-STEM). At the same time, bonding states, and surrounding environment of MSA are dually confirmed by X-ray absorption near edge structure (XANES) and extended X-ray absorption fine structure (EXAFS). For mechanism understanding, first-principle calculation density functional theory (DFT) was applied to justify its working mechanism in detail based on thermodynamics using grand canonical potential kinetics (GCP-K) quantum mechanics to obtain for various overpotentials to get minimum free energy using Legendre transformation (LT) to relate applied voltage and net charge of the structure. Apart from the demonstration of a new synthesis approach, the detailed experimental insights, and understanding the theoretical mechanism from this study will expand the existing knowledge in the field of heterogeneous single-atom catalyst towards different reactions.

2:40 PM EN01.03.07

Control of Oxygen Vacancies to Tune the Electronic Structure and OER Activity of Orthorhombic SrIrO₃ Matthew Sweers, D. Bruce Buchholz and Linsey Seitz; Northwestern University, United States

Human-induced climate change, driven by rising levels of carbon dioxide in the atmosphere, is one of the greatest challenges humanity has ever faced. Electrolysis holds the potential to be a valuable option for carbon-free energy storage especially when coupled with renewable electricity sources. Hydrogen produced by electrolysis can be used to generate electricity in a fuel cell or as a feedstock for vital chemicals. Current electrolysis technology lacks the necessary efficiency to be economically viable at an industrial scale due to the lack of adequate catalysts for the Oxygen Evolution Reaction (OER), the more complex of the necessary half-reactions, in acidic environments.

The best catalysts for the OER in acid are iridium- and ruthenium-based. By pushing these compounds to higher performance, we can identify which material properties are responsible for high OER activity. From recent literature on cobalt-based OER catalysts in alkaline conditions, increased covalency of the metal-oxygen bond results in involvement of lattice oxygen in the reaction and decreased formation energies for intermediate oxygen species, both resulting in higher activity. We examine whether similar effects of metal-oxygen bond covalency occur in the analogous system of iridium-based catalysts in acidic environments, recognizing that Ir and Co are both group 9 transition metals. We build upon this test by tuning the O 2p band through manipulation of the anion sub-lattice of the exceptionally active perovskite catalyst, orthorhombic SrIrO₃ (SIO). Precise control and variation of the concentration of oxygen vacancies allows us to perturb the electronic structure, compare the results with a concurrent DFT study, and measure the resulting changes in catalytic activity of SIO. This study first requires a reliable deposition method, which has been achieved by investigating factors that control the growth, crystallinity, and composition of the films.

We developed a consistent method for depositing atomically smooth thin films of SIO via pulsed laser deposition. The films have been extensively characterized using x-ray diffraction, spectroscopy methods, and multiple forms of microscopy, revealing several trends that highlight key deposition parameters. For example, the x-ray photoelectron spectroscopy of the Ir4f peaks signifies an unexpected but critical dependence of the film's iridium content on the position of the substrate within the vapor plume during deposition. This phenomenon is likely due to the relative masses of the vaporized species. This revelation, along with other trends, led to the consistent deposition protocol that provided a platform to vary oxygen content in SIO films. Deliberate formation of oxygen vacancies typically includes doping with foreign cations, which may result in unintended changes to electronic structure and catalytic activity, overshadowing the effect of the oxygen vacancies. Thus, we investigate alternative routes to control oxygen content without introduction of foreign species: 1) varying the oxygen partial pressure during deposition, and 2) annealing films in mixtures of O₂ and N₂ post-deposition. Characterizing the oxygen-deficient films, such as with x-ray absorption spectroscopy, in conjunction with electrochemical OER testing allows us to investigate the electronic structure changes and their effects on catalytic activity. For example, a clear relationship has been identified correlating decreased oxygen content with increased Ir4f binding energy, making plain the influence of anion stoichiometry on electronic

structure. Exploring these relationships enhances our understanding of the drivers of OER catalytic activity and helps in the development of better catalysts. Improvement of OER technology will enable electrolysis to become a financially viable option for energy storage and sustainable chemical production, aiding in our fight against climate change.

2:55 PM EN01.03.08

Electrochemical Analysis of Au and Cu Surface Alloys During Hydrogen and CO₂ Reactions In Aqueous Media Emily M. Marquez, Kim Hong Kue, Diana Godoy and Hadi Tavassol; California State University, Long Beach, United States

We report on electrochemical analysis and stress measurements of hydrogen and CO₂ reactions on Au and Cu surfaces in aqueous solutions with different pHs. Hydrogen and CO₂ reactions are important for the production of chemical fuels using water electrolysis and reduction of CO₂ to CO or small hydrocarbons. However, room temperature electrocatalysis of H₂ production and CO₂ reduction on earth-abundant surfaces remain challenging. Hydrogen reactions ($2\text{H}^+ + 2\text{e}^- \leftrightarrow \text{H}_2$) are efficient on Pt and Pd surfaces but are not as feasible on many earth-abundant transition metal surfaces particularly at higher pHs. CO₂ reduction is slow on even most active surfaces and requires transfer of multiple electrons and protons ($\text{CO}_2 + 2\text{H}^+ + 2\text{e}^- \rightarrow \text{CO} + \text{H}_2\text{O}$). Interestingly, surfaces with high activity toward CO₂ (e.g. Au and Cu) are not active toward hydrogen reactions. Here, we explore the reaction mechanism and early stages of catalysts activation during hydrogen and CO₂ reactions on these surfaces using electrochemical analysis and *in-situ* stress measurements. Well-defined Au and Cu surfaces are prepared using evaporation and atomic layer electrochemical deposition. Electrochemical analysis shows changes in surface reactivity toward HER and CO₂ reduction as the surface composition and structure is altered. Our stress analysis shows that hydrogen activation on surfaces causes a compressive stress, that can be used as a signature for activity toward hydrogen reactions. Interestingly, *in-situ* stress measurements of Au surfaces do not show proton activation even at low pHs. However, our analysis reveals stress responses corresponding to CO₂ interaction with Au surface at low pHs. The CO₂ stress responses are evident at *ca.* 0.2-0 V vs. RHE. The stress response is different from what is observed for hydrogen activation on surfaces. We will particularly discuss how these signature features of hydrogen and CO₂ reactions changes as a function of solution pH. We also use rate dependence of stress response to identify surface charge effects of primary activation steps. Our studies show that at higher pHs water is involved in the hydrogen reactions even on Pt surfaces. We will discuss how CO₂ activation changes surface charge dynamics during activation steps. These studies will provide insight into activity and selectivity descriptors for hydrogen production and CO₂ reduction reactions in aqueous media.

SESSION EN01.04: Advanced Electrocatalysis—Deeper Insights and Mechanistics II

Session Chairs: Ulf-Peter Apfel and Philipp Stadler

Thursday Afternoon, April 22, 2021

EN01

4:25 PM EN01.04.02

Metal-Organic Framework based Cobalt Oxide and Cobalt Sulfide as Efficient Electrocatalysts and High-Performance Supercapacitors Jonghyun Choi, Tenzin Ingsel, Khamis Siam and Ram Gupta; Pittsburg State University, United States

The increasing global population and advancement in energy-dependent devices have caused increased energy use in consumer and industrial appliances, electronic devices, and automobiles, creating an urgent need for clean and renewable energy sources. Electrochemical water-splitting is one of the greenest ways to generate clean and high-performance fuel. Water-splitting produces hydrogen and oxygen gases. The generated hydrogen gas can be used as fuel, whereas evolved oxygen gas can be used in metal-air batteries or released in the

atmosphere as a clean gas. The electrocatalytic properties of most of the materials for water splitting depend upon several factors such as morphology, phase purity, defects, etc. Additionally, electrochemical energy storage devices garner considerable research interest because of their high storage energy and long lifecycle; supercapacitor's global market reached \$2 billion in 2015. This project has synthesized metal-organic framework (MOF) derived cobalt oxide and cobalt sulfide using a facile method. 2-methyl imidazole and cobalt nitrate hexahydrate were used for the synthesis of MOF-derived cobalt oxide and MOF-derived cobalt sulfide electrodes. The electrode with MOF-derived cobalt oxide went through a solvothermal process while the electrode with MOF-derived cobalt sulfide was sulfurized hydrothermally. The structural and electrochemical properties of these electrodes were studied in detail. The MOF-derived cobalt oxide and sulfide's electrocatalytic activities were studied in 1M KOH solution for oxygen evolution reaction and 3M KOH solution for capacitive behaviors and storage capabilities. MOF-derived cobalt oxide showed an overpotential of ~ 375 mV to achieve a current density of 10 mA/cm^2 . A significant improvement in electrocatalytic properties was observed with the electrode that went through sulfurization. MOF-derived cobalt sulfide displayed an overpotential of ~ 278 mV at 10 mA/cm^2 . The specific capacitance obtained by the cobalt sulfide-based electrode (MOF-derived) was $\sim 2537 \text{ F/g}$ at 1 A/g while the cobalt oxide-based electrode (MOF-derived) was $\sim 484 \text{ F/g}$ at 1 A/g . Our results suggest that a facile method of sulfurization of the MOF-derived compound is a way to achieve high electrocatalytic activities for oxygen evolution reaction in the water-splitting process and increased capacitive capabilities.

4:30 PM EN01.04.03

How Strain Modifies the Electrochemical CO₂ Reduction Pathway on Cu Taewoo Kim, Rishi Kumar, Jeffrey A. Brock, Eric E. Fullerton and David Fenning; University of California, San Diego, United States

Copper is an attractive electrocatalyst for CO₂ conversion to valuable carbonaceous products. However, the poor selectivity remains as a challenge to achieve high energetic efficiency. In this work, using model Cu (001) surfaces, we clarify how tensile strain influences CO₂ reduction reaction pathway, shifting products selectivity away from single-carbon to value-added, multi-carbon products.

We establish varying built-in tensile strain on epitaxially grown Cu (001) surfaces on single-crystal Si substrate by changing film thickness. With decreasing film thickness, we observe increasing in-plane tensile strain at the surface that shifts the Cu *d*-band center toward the Fermi level, in good agreement with *d*-band theory. In CO₂ electrolysis at moderate overpotential, we find a suppression of single-carbon products with this upshifting *d*-band center. The change in selectivity indicates a change in adsorption energy for reaction intermediates and perhaps the promotion of hydrogenation of *CO-to-*CHO, one of the key descriptors for CO₂ conversion to multi-carbon products. These findings provide direct experimental evidence that strain can tune the CO₂ conversion reaction pathway to produce energy dense products, providing new opportunities to design efficient and selective catalysts even without changing catalyst composition.

4:45 PM DISCUSSION TIME

5:00 PM EN01.04.05

Late News: Direct Electrosynthesis of Pure Aqueous H₂O₂ Solutions up to 20% by Weight Using a Solid Electrolyte Yang Xia and Haotian Wang; Rice University, United States

Hydrogen peroxide (H₂O₂) is a crucial chemical with a wide range of applications in civil and industrial fields. It is currently produced from the industrial energy- and waste-intensive anthraquinone process. Its centralized feature also makes it rely heavily on the storage and transportation of H₂O₂, which is unstable and hazardous. Electrocatalytic oxygen reduction reaction (ORR) to H₂O₂ provides an alternative to realize green and delocalized production, with the only inputs from renewable electricity, water and air. However, this route still faces two challenges: 1) lack of catalysts which selectively drive the $2e^-$ ORR towards H₂O₂ (instead of H₂O); 2) generated H₂O₂ are typically in mix with solutes in traditional electrolyzers, which necessitates complicated separation processes to recover pure H₂O₂ solutions for applications.

To make the electrochemical route more reliable in the future scaling-up, we reported a direct and continuous production of pure H₂O₂ solutions for the first time, through rational design of both catalyst and reactor. Here, we report a direct electrosynthesis strategy that delivers separate hydrogen (H₂) and oxygen (O₂) streams to an anode and cathode separated by a porous solid electrolyte, wherein the electrochemically generated H⁺ and HO₂⁻ recombine to form pure aqueous H₂O₂ solutions. By optimizing a functionalized carbon black catalyst, we achieved over 90% selectivity for pure H₂O₂ at current densities up to 200 mA cm⁻², which represents a H₂O₂ productivity of 3.4 millimoles per square centimeter per hour (3660 moles per kilogram of catalyst per hour). A wide range of pure H₂O₂ concentrations up to 20 wt.% could be obtained by tuning the water flow through the solid electrolyte, and the catalyst retained activity and selectivity for 100 hours. The as-generated H₂O₂ solutions were also demonstrated to reduce the Total Organic Carbon (TOC) level of local rainwater to that of drinking water.

5:15 PM EN01.04.06

Size-Composition Catalytic Activity Maps for Alloy Nanoparticles Liang Cao and Tim Mueller; Johns Hopkins University, United States

We present the use of *ab-initio* calculations to calculate the coverage-dependent catalytic activity of alloy nanoparticles with realistic sizes (5 nm-10 nm) by explicitly predicting atomic-scale structures and adsorbate binding energies. We demonstrate our approach using Pt-Ni nanoparticles as catalysts for the oxygen reduction reaction (ORR). We achieve our results by constructing a quaternary Pt-Ni-OH-Vacancy cluster expansion model to explicitly predict OH adsorption energies on nanoparticles of varying shape, size, and atomic structure. The OH coverage-dependent ORR activity is calculated through a kinetic Monte Carlo (KMC) simulation. This model enables us to accurately investigate the catalytic activity of various surface sites with different coordination numbers and local atomic environments. Using this model, we evaluate how different parameters affect the ORR activity of Pt-Ni nanoparticles, including size (2 nm-10 nm), Pt composition (60%-100%), and shape. Through the use of KMC-enabled kinetic simulations of structural evolution we evaluate how the activities of the particles change due to Ni dissolution. Our approach identifies OH coverage at the atomic scale and provides theoretical insights into how to tune the structures of alloy nanoparticles to optimize catalytic activity.

5:30 PM EN01.04.07

Late News: Structural Dynamics of Nanoalloy Catalysts for Fuel Cells by In Situ Total X-Ray Scattering Valeri Petkov; Central Michigan University, United States

Many catalysts for energy related applications, in particular metallic nanoalloys, readily undergo atomic-level changes during electrochemical reactions. The origin, dynamics and implications of the changes for the performance of the catalysts inside operating devices though are not well understood. This is largely because they are studied on model nanocatalysts under controlled laboratory conditions. We will present results from combined x-ray spectroscopy and total scattering studies on the dynamic behavior of Pt/Pd-3d transition metal nanoalloys inside an operating proton exchange membrane fuel cell [1]. The results indicate that the catalysts change profoundly under the erosive conditions inside the cell, including leaching of transition metal species and continuous re-alloying leading to the emergence of structure states with an improved activity and stability.

I. V. Petkov et al. *Nanoscale* 11 (2019) 5512.

5:45 PM EN01.04.08

Characterization of CeO_x-Decorated Pd/C Catalysts Synthesized By Controlled Surface Reactions for Hydrogen Oxidation in Anion Exchange Membrane Fuel Cells Richard Andres Ortiz Godoy^{1,1,2}, Jasna Jankovic^{1,1,2} and Mariah Batool¹; ¹University of Connecticut, United States; ²Center for Clean Energy Engineering, United States

The sluggish kinetics of hydrogen oxidation reaction (HOR) at the anode in alkaline electrolytes are one of the

biggest hurdles in the development of next generation non-Pt catalyst for anion Exchange Membrane Fuel Cells (AEMFCs) having an efficient HOR catalyst¹⁻³. Lately, Pd has been extensively used because of the need of developing HOR electrocatalysts based on more abundant and cheaper elements than Pt. Additionally, in order to increase the HOR kinetics of Pd, previous studies focused their efforts on the development of Pd-CeO₂ composites because CeO₂ is an oxygen-deficient compound that allows for a fast OH⁻ saturation. Lately, Pd has been extensively used because of the need of developing HOR electrocatalysts based on more abundant and cheaper elements than Pt. Additionally, to increase the HOR kinetics of Pd, previous studies focused their efforts on the development of Pd-CeO₂ composites because CeO₂ is an oxygen-deficient compound that allows for a fast OH⁻ saturation. Controlled Surface Reactions (CSR) process has been used to selectively deposit different atomic ratios (0, 0.24, 0.38 and 0.59 at. ratio ICP-AES Measured bulk Ce/Pd) between CeO_x onto carbon supported Pd catalysts nanoparticles with the main goal of improving the efficiency of HOR catalysts expecting a homogenous distribution of CeO_x nano-islands preferentially attached to Pd nanoparticles (NPs) in order to achieve highly active CeO_x-Pd/C catalysts for HOR⁴. In recent years, when it comes to study the relationship between morphology and structure of nanoparticles that constitute the fuel cells catalyst and the correlation to their electrocatalytic activity, Transmission Electron Microscopy (TEM) has become the state-of-the-art characterization technique. Here I present a comprehensive characterization approach for the synthesized highly active catalyst, and correlate obtained structural/compositional parameters to the performance. The characterization of the catalysts was carried out via Inductively Coupled Plasma-Atomic Emission Spectroscopy (ICP-AES), High-Resolution Transmission Electron Microscopy (HR-TEM), Scanning Transmission Electron Microscopy (STEM) - Energy Dispersive Spectroscopy (EDS), Electron Energy Loss Spectroscopy (EELS), and X-ray Photoelectron Spectroscopy (XPS) to confirm the bulk composition, phases present, morphology, elemental mapping, local oxidation state and surface chemical states, respectively. The HRTEM images indicated that Pd NPs were uniformly distributed on the carbon support with only some minor agglomeration. Additionally, the achieved high interfacial contact between CeO_x and Pd acquired on single NPs was, for the first time, segmented and calculated using High-resolution STEM-EDS maps and Image J processing program by measuring the overlap intensities between Pd and Ce NPs; the results clearly showed that CeO_x NPs were in intimate contact with Pd and their interfacial contact area increased with the addition of CeO_x, reached a maximum at a ratio 0.38 CeO_x -Pd/C, then decreased due to the formation of large CeO_x islands upon the further addition of CeO_x. The attained interfacial contact area also seems to be much higher than other previously reported Pd-CeO₂ catalysts synthesized by other methods⁴⁻⁷.

REFERENCES: 1.Davydova, et al. ACS Catal 2018. 8, 6665–6690; 2.Dekel, Curr. Opin. Electrochem 2018. 12, 182–188; 3.Dekel, J. Power Sources 2018. 375, 158–169; 4.Singh, et al. Adv. Funct. Mater 2020. 30, 1–11; 5.Miller, et al. Angew. Chemie 2016. Int. 55, 6004–6007; 6.Hamish et al. Nano Energy 2017, 293–305; 7.Yu, et al. Nano Energy 2019. 57, 820–826.

5:50 PM EN01.04.09

Late News: Oxygen Reduction Reaction Activity of Nanocolumnar Pt Thin Film Electrocatalyst Deposited on Carbon Support by High Pressure Sputtering Assem Basurrah^{1,2}, Busra Ergul¹, Zhiwei Yang³, Ranjitha Hariharalakshmanan¹ and Tansel Karabacak¹; ¹University of Arkansas at Little Rock, United States; ²University of Jeddah, Saudi Arabia; ³Raytheon Technologies Research Center, United States

Proton-exchange membrane fuel cell (PEMFC) is one of the most important sources of clean energy especially for automotive applications, which currently utilizes platinum nanoparticles dispersed on carbon (Pt/C) as a catalyst. However, the catalyst activity and durability need to be improved and the cost of the fuel cell need to be reduced for successful commercialization. Extensive research has been done to improve the catalyst activity and durability, reduce the amount of platinum used and reduce its manufacturing cost. Continuous thin film layer approach is a promising candidate for non-conventional catalysts to address these challenges. For this purpose, nanocolumnar Pt thin film (Pt-TF) layers supported on carbon was fabricated by high pressure sputtering (HIPS) and investigated as oxygen reduction reaction electrocatalysts for PEMFCs. HIPS is a simple physical vapor deposition method that is scalable and easily applicable to industrial sputter deposition systems, in which atoms come to the substrate surface with oblique angles and form columnar structures. Different Pt-TF/C weight ratios ranging from 5% to 20% and Pt: Ni (1:3) TF/C were studied. Weight loading was controlled

by changing the sputter deposition time. X-ray diffraction analysis revealed the existence of Pt and formation of the Pt: Ni alloy on carbon support. Electrochemical characterization of the carbon-supported Pt-TF samples was conducted by cyclic voltammetry and rotating disk electrode measurements in an aqueous perchloric acid electrolyte. The electrochemically active surface area, mass activity and specific activity of the Pt-TF/C samples were found to be increasing as the Pt-TF/C ratio was increased.

5:55 PM EN01.04.10

Late News: Catalytic Performance of Porous Yb₂O₃ Sesquioxide Alina Aftab, Richard Blair, Katerina Chagoya and Nina Orlovskaya; University of Central Florida, United States

Ytterbium Oxide (Yb₂O₃) is a rare earth oxide that has been used in various applications, including sensor and laser technology, sintering aid and doping of different ceramics, and catalytic applications. Although Yb₂O₃ has been considered a potential catalyst for reactions such as vapor phase catalytic dehydration, to the best of our knowledge, there is no reported research for the use of Yb₂O₃ in the hydrogenation of syngas in Fisher-Tropsch chemical reactions. In order to add to the current state of knowledge, the possibility of using porous Yb₂O₃ as a catalyst for converting syngas (CO+H₂) into liquid hydrocarbons using the Fischer-Tropsch process was explored. 99.99% pure Yb₂O₃ ceramic powder was pressureless sintered at 900 °C for four hours in the air to create cylinders with an average porosity of 45%. The crystal structure and lattice parameters of Yb₂O₃ were then measured using neutron diffraction and Yb₂O₃ was confirmed to be cubic (*Ia-3*) with $c=10.43731$ Å lattice parameter. The spectral vibrational signature of Yb₂O₃ attained by micro-Raman spectroscopy corresponded fully to the one published in the literature. Two plug flow catalytic experiments, at temperatures of 250 °C and 500 °C, were performed for the catalytic studies. It was found that Yb₂O₃ is catalytically active and can be used to convert syngas into useful hydrocarbons. Production of methane, ethene, and ethane was detected in the catalytic experiment at 500 °C, but propane, propene, butane, and methanol were also detected in the experiment at 250 °C. It was concluded that more data points are required to be collected to determine if the products' mass distribution followed Flory-Schulz's distribution. Raman spectroscopy and neutron diffraction were also performed on samples used in the catalytic experiment. The crystal structure did not change during the catalytic experiment and the lattice parameter was $c=10.43582$ Å. A slight shift in the Raman active peaks was detected in the Raman spectra and an extra peak had to be added to obtain the curve fitting.

SESSION EN01.05: Advanced Electrocatalysis—Novel Routes for Energy Cycles

Session Chairs: Yongye Liang and Tsukasa Yoshida

Thursday Afternoon, April 22, 2021

EN01

8:15 PM *EN01.05.01

Redox Catalytic Energy Conversion Through an Electrochemical-Chemical Cycle Qing Wang; National University of Singapore, Singapore

Conventionally, the operation of electrochemical energy conversion and storage devices is inherently dictated and constrained by the redox reactions at electrode-electrolyte interface. The redox-mediated process, a chemical reaction between an electrolyte-borne redox species electrochemically generated on electrode and a material (either soluble or insoluble in electrolyte) off the electrode, provides additional flexibility in circumventing the constraints intrinsically confronted by the conventional electrochemical devices. One example is the redox-mediated hydrogen and oxygen evolution reactions (HER & OER) for spatially decoupled water electrolysis. The concurrent electrochemical-chemical cycle enables continuous reactions between an electrolyte-borne redox mediator and a HER/OER catalyst loaded in a fixed-bed reactor spatially separated from the cell, which is believed to be advantageous to enhanced safety, operation flexibility and H₂ purity. Another example is redox-mediated nitrogen reduction reaction (NRR) for ammonia synthesis. Judiciously selected

redox species serve both as electron and proton carriers circulating between the cell and N₂-filled catalyst bed and present considerably promoted NRR reaction yield. In this talk, I will report our latest progress in the above areas. In addition, I will briefly introduce some other studies on redox-mediated reactions, such as redox targeting-based battery for low-grade waste heat harnessing based on a thermal-electrochemical cycle.

References:

1. F. Zhang, S. Huang, X. Wang, C. Jia, Y. Du, and Q. Wang, Redox-Targeted Catalysis for Vanadium Redox-Flow Batteries. *Nano Energy*, **52**, 292-299 (2018).
- Y. G. Zhu, F. W. Goh, R. Yan, S. Wu, S. Adams, and Q. Wang, Synergistic Oxygen Reduction of Dual Redox Catalysts Boosting the Power of Lithium-air Battery. *Phys. Chem. Chem. Phys.*, **20** (44), 27930-27936 (2018).
- R. Yan and Q. Wang, Redox-Targeting-Based Flow Batteries for Large-Scale Energy Storage. *Adv. Mater.*, **30**, 1802406 (2018).
- Y. Chen, M. Zhou, Y. Xia, X. Wang, Y. Liu, Y. Yao, H. Zhang, Y. Li, S. Lu, W. Qin, X. Wu, and Q. Wang, A Stable and High Capacity Redox Targeting-based Electrolyte for Aqueous Flow Batteries. *Joule*, **3** (9), 2255-2267 (2019).
- M. Zhou, Y. Chen, M. Salla, H. Zhang, X. Wang, S. R. Mothe, Q. Wang, Single-Molecule Redox-Targeting Reactions for a pH-Neutral Aqueous Organic Redox Flow Battery. *Angew. Chem. Int. Ed.*, **59** (34), 14286-14291(2020).

8:40 PM DISCUSSION TIME

9:00 PM EN01.05.04

Size-Dependent Activity for N₂ Electroreduction on Metal Nanocatalysts Xiaofeng Feng; University of Central Florida, United States

Electrochemical reduction of N₂ to NH₃ has recently received considerable attention, because it may enable sustainable, distributed production of NH₃ when powered by solar- or wind-generated electricity. However, typical catalysts show a low activity and selectivity for N₂ reduction reaction (NRR) due to the barrier for N₂ activation and the competing hydrogen evolution reaction (HER). A rational design of NRR catalysts relies on our understandings of structure-activity relationships and active sites for the NRR, and such study requires model catalysts with well-defined structures. Here we present a study of size-dependent activity for the NRR on Ru nanoparticle catalysts. We first tried colloidal synthesis method with polyvinylpyrrolidone (PVP) as a surfactant to control the size of Ru nanoparticles, while the derived Ru catalysts showed negligible activity for NRR, which was attributed to residual surfactant molecules that blocked catalyst surfaces. Therefore, we used atomic layer deposition (ALD) method to prepare Ru nanoparticles with controlled sizes and clean surfaces. We also quantified the electrochemical active surface areas of Ru samples and measured surface-area-normalized activity for the NRR. Consequently, the effect of Ru nanoparticle size on the NRR activity and Faradaic efficiency was revealed, which can provide insights into the active sites for the NRR and guidance on the design of NRR catalysts via surface site engineering.

9:15 PM EN01.05.06

Late News: An Experimentally Verified LC-MS Protocol Towards an Economical, Reliable and Quantitative Isotopic Analysis in Photo(Electro)Catalytic Nitrogen Reduction Reactions Sandra E. Saji; The Australian National University, Australia

To substitute the energy-intensive Haber-Bosch process for the synthesis of ammonia, some labile techniques, such as photocatalysis, electrocatalysis, photoelectrocatalysis, and photothermocatalysis, have emerged and attracted intense research interest. However, the contamination of the reaction system is one of the major concerns on how to reliably and accurately evaluate the performance of these catalysts, which is why various control studies are involved. Isotopic labelling studies are one of the most reliable control strategies in nitrogen fixation experiments, to ensure the fact that N₂ is exclusively the source of the generated ammonia. As a convenient, sensitive and accurate technique distinguished with a quantitative atomic mass resolution, liquid

chromatography-mass spectrometry (LC-MS) has been extensively employed for the detection of ammonia in aqueous electrolyte systems. However, the previously reported protocols for $^{15}\text{N}_2$ isotopic analysis using LC-MS either involved hazardous procedures which could potentially damage the instrument, or lacked in their experimental verification using real samples. In this work, we present a safe, reproducible and economical protocol for the detection of ammonia using LC-MS, exhibiting an exponentially steep progressive detectivity of ^{15}N abundance, which was well verified with a series of experimental results for nitrogen reduction reactions. This is expected to provide a prudent, cost-effective and sustainable gateway into isotopic analysis.

9:30 PM EN01.05.07

Late News: Understanding the Interaction of Solvents and Biogenic Impurities with Heterogeneous Catalysts Haseena K V and M. A. Haider; Indian Institute of Technology Delhi, India

The integration of chemo and biocatalysis for the sustainable production of high-value chemicals and fuels from bio-renewable resources like lignocellulosic biomass has attained notable attention in the past decade. The catalytic reactions for transforming platform chemicals obtained from fermentation are often carried out in the liquid phase. Catalyst deactivation caused by the biogenic impurities such as amino acids and proteins arriving from the fermentation media is a key challenge in this line. To understand the role of solvents and biogenic impurities, the hydrogenation reaction of fermentation-derived 6-acyl- α -pyrone (6PP) was explored. Reactions using pure 6PP was carried out in solvents with different dielectric constants. Cyclohexane was found to be the best solvent providing >99% 6PP conversion and 79% DDL yield in 10 min using (10%) Pd/C. Further, the same reaction was carried out at different temperatures and almost complete conversion was obtained at 433 K. With an increase in temperature 6PP conversions increased along with DDL yield. However, reactions using fermentation-derived 6PP showed reduced conversion and product yield. Experiments revealed that even trace quantities of biogenic impurities such as amino acids and proteins from the fermentation media interact with the catalyst and cause significant deactivation of the catalyst. DFT simulations using the Vienna ab initio simulation package (VASP) was employed to unravel the interaction of amino acids on the catalyst surface. Amino acid Methionine (Met), bound through sulfur atom in its most stable adsorption mode with a binding energy=-186 kJ/mol, and it underwent C-S bond cleavage to form SCH_3 species with an activation barrier $E_a = 136$ kJ/mol. This species was found to be stable on the surface. A plausible mechanism for the dissociation of Met on Pd (111) surface is proposed capturing the energetics of the dissociation steps. Much stronger adsorption and relatively lower dissociation barriers were found in the case of Cys on the same surface. Interestingly the observed experimental trend in deactivation also aligns well with simulation results. A combined experimental and computational approach is used to develop deeper insights into the interaction of solvents and biogenic impurities in heterogeneous catalysis.

9:45 PM EN01.05.08

Late News: Metal/organic Hybrid Electrocatalyst for CO₂ Reduction by Reductive Conversion of CuSCN / Neutral Red Hybrid Thin Film Yuki Tsuda¹, Tensho Nakamura¹, Philipp Stadler² and Tsukasa Yoshida¹; ¹Yamagata University, Japan; ²Johannes Kepler Universität Linz, Austria

Reducing atmospheric carbon dioxide (CO_2) is one of the most important challenges for sustainable society. Electrocatalysis for CO_2 reduction reaction (CO_2RR) to energy-rich chemicals has been intensively studied. The catalyst needs to be developed out of earth-abundant elements and should be efficient, fast and selective for useful product.

Recently, Coskun et al. have reported high catalytic activity of metal-free polydopamine towards CO_2RR [1]. Aside from its conductivity, its hydrogen-bonding nature is supposed to be important for stabilization of reaction intermediates. Among traditional electrocatalytic metals, copper (Cu) is outstanding to yield useful hydrocarbons, although its product selectivity is limited. If we can now combine both of them, namely, by introducing hydrogen-bonding organic molecules into Cu, selective production of hydrocarbon such as methane may be achieved by forming concerted catalytic sites.

In this study, the above-mentioned hybrid catalyst has been aimed by employing electrochemical self-assembly (ESA) of CuSCN / neutral red (NR) hybrid thin films. Minor addition of NR, one of phenazine dyes bearing

many amino groups in its structure, to the bath for cathodic electrodeposition of CuSCN resulted in ESA of red-colored and nanostructured CuSCN/NR hybrid thin films, which is then electrochemically transformed into Cu/NR hybrid by electrolysis at -1.0 V vs. Ag/AgCl in an aqueous 0.1 mol dm⁻³ KCl under N₂. Formation of metallic Cu and remainder of NR have been confirmed by XRD and FT-IR, respectively.

Thus prepared thin film electrodes were tested for CO₂RR in an aqueous 0.1 mol dm⁻³ KCl (pH 6.8) While nanostructured Cu made by reductive conversion of NR-free CuSCN showed a reasonable activity to achieve -1.3 mA cm⁻² at -1.2 V (vs. Ag/AgCl) under CO₂, about 3 times enhanced from that under N₂, the Cu/NR hybrid showed a unique feature to reduce potential (for -0.75 mA cm⁻²) from the initial -1.01 to -0.73 V upon 10 times repetition of voltammetric potential scanning, indicating its activation for CO₂RR. It is possible that NR molecules re-organize to form catalytic sites during the electrolysis.

At this stage, we haven't identified the products and their selectivity. These preliminary results, however, already indicate successful strategy to obtain hybrid electrocatalyst to combine Cu and hydrogen-bonding organic molecules to enhance the activity for CO₂RR.

[1] Halime Coskun et al., *Science Advances*, Vol. 3, no. 8, e1700686 (2017).

9:50 PM EN01.05.09

Atomic Probing of Defects Engineered Nanocarbon Support Concurrence with Bimetallic Atoms Towards Electrocatalysis and Zn-Air Batteries Kishwar Khan¹, Zhengtang Luo¹ and Khalil Amine²; ¹The Hong Kong University of Science and Technology, Hong Kong; ²Argonne National Laboratory, United States

The mechanistic understanding of defects engineering in nanocarbons, and its hybrid with single metal atoms towards electrocatalysis are vital to study in-depth, and still its remains very challenging. Herein, we advocate the fundamental understanding of the nature of active sites in ample edge defects nitrogen-doped graphene (DG) fascinated with specific coordination of carbon atoms rings. The concept of defect mechanism revealed that the topological defect (*e.g.* multiple edge pentagon, pentagon—octagon—pentagon or pentagon—heptagon—pentagon rings) appeared correspondingly in the combination of carbon atoms that avoided random dislocations and disclinations that brought active sites during reactions. We anchored Ni and Fe isolated single metals on DG support towards enhanced O₂ response. X-ray absorption spectroscopy evidences the embedding nature of NiFe metal atoms within the DG surface. The precise structural characterizations using high-resolution transmission electron microscopy/high-angle annular dark-field (HAADF) images in scanning transmission electron microscopy (STEM) techniques to probe the atomic level understanding of such defects, its different coordination of atoms. Density functional theory (DFT) further trust these specific grouping of carbon atoms and frilling of NiFe single atoms on the tip-enhanced local electric field of the carbon support that active upsurge sites and promotes the kinetics for ORR and OER. This study offers new prospects and underscores the importance of identifying topological defects in nanocarbons with the addition of single metal atoms towards the active species for multiple reaction catalysts.

SESSION EN01.06: Advanced Electrocatalysis—Deeper Insights and Mechanistics III

Session Chair: Philipp Stadler

Friday Morning, April 23, 2021

EN01

8:00 AM *EN01.06.01

Hybridization of Molecular and Metallic/Semiconductor Materials for CO₂ Catalytic Reduction Marc Robert; Université de Paris, France

Reduction of carbon dioxide has as main objective the production of useful organic compounds and fuels - renewable fuels - in which solar energy would be stored. Molecular catalysts can be employed to reach this

goal. They may in particular provide excellent selectivity thanks to easy tuning of the electronic properties at the metal and of the ligand second and third coordination sphere. Hybridization of these catalysts with conductive or semi-conductive materials may lead to enhance stability and new catalytic properties. This approach bridges between homogeneous and heterogeneous, and it raises new fundamental questions that may further lead to breakthrough in CO₂ reduction chemistry.

Our recent results in this area will be discussed. [1-5]

1. M. Wang, L. Chen, T-C. Lau, M. Robert, *Angew. Chem. Int. Ed.* **2018**, *57*, 7769-7773.
2. S. Ren, D. Joulie, D. Salvatore, K. Torbensen, M. Wang, M. Robert, C. Berlinguette, *Science* **2019**, *365*, 367-369.
3. E. Boutin, M. Wang, J. C. Lin, M. Mesnage, D. Mendoza, B. Lassalle-Kaiser, C. Hahn, T. F. Jaramillo, M. Robert, *Angew. Chem. Int. Ed.* **2019**, *58*, 16172-16176.
4. B. Ma, G. Chen, C. Fave, L. Chen, R. Kuriki, K. Maeda, O. Ishitani, T-C. Lau, J. Bonin, M. Robert, *J. Am. Chem. Soc.* **2020**, *142*, 6188-6195
5. P. B. Pati, E. Boutin, R. Wang, S. Diring, S. Jobic, N. Barreau, F. Odobel, M. Robert, *Nat. Commun.* **2020**, *11*:3499.

8:25 AM *EN01.06.02

Operando Insight into the CO₂ Electrocatalytic Reduction Reaction Beatriz Roldan Cuenya; Fritz Haber Institute of the Max Planck Society, Germany

The efficient electrochemical conversion of CO₂ (CO₂RR) to valuable fuels and feedstocks is a highly sought process towards the minimization of the carbon footprint. However, higher selectivity towards C₂₊ products must be achieved before a broad industrial use can be envisioned. Better efficiency can be attained by tuning the morphology (size, shape, dispersion), oxidation state, composition of the catalysts, NP/support interactions, and by a rational selection of the electrolyte. In addition, understanding the changes that a catalyst may experience on its surface during a reaction is crucial in order to establish structure/composition-reactivity correlations. Here, mechanistic insight into CO₂RR will be provided by using as target materials size- and shape-controlled mono and bimetallic NPs including Cu, Cu₂O, Zn, Cu-Zn, Cu-Ag NPs with spherical, cubic and triangular-base prism shapes, and Cu₂O cubes decorated with monodispersed Ag nanoparticles on the surface.

A synergistic combination of spectro-electrochemical methods, *in situ* microscopy (EC-AFM, L-TEM), *operando* X-ray absorption spectroscopy (XAS), *operando* high-energy X-ray diffraction (HE-XRD), *operando* Raman spectroscopy and *quasi in situ* X-ray photoelectron spectroscopy (XPS) were used to gain insight into the morphological, structural, and chemical transformations undergone by the NPs during CO₂RR. I will illustrate that the as-prepared state of the mono and bimetallic NPs is drastically different from the structure and surface composition of the working catalyst. Thus, our study gives a comprehensive insight into C₂₊-forming state of Cu-based catalysts and sheds light into the selectivity-determining catalyst properties for CO₂RR.

8:50 AM DISCUSSION TIME

9:05 AM EN01.06.04

Design and Mechanistic Understanding of Earth-Abundant Metal Chalcogenide Electrocatalysts for Selective Electrosynthesis of Hydrogen Peroxide Hongyuan Sheng, Aurora N. Janes, J. R. Schmidt and Song Jin; University of Wisconsin-Madison, United States

Hydrogen peroxide (H₂O₂) is a versatile and green oxidant with a variety of distributed applications such as environmental remediation, disinfection, and household sanitation, but its centralized chemical production via the anthraquinone process poses significant cost, energy, and safety concerns. Decentralized electrosynthesis using renewable electricity to selectively reduce O₂ to H₂O₂ via the two-electron oxygen reduction reaction (2e⁻ ORR) could better satisfy end-user demands on-site, yet robust, earth-abundant catalysts that are active and selective in acidic (or neutral) solutions are lacking. Here we present our recent joint efforts combining theory and experiments to establish rational design rules for selective and stable acidic 2e⁻ ORR electrocatalysts based

on earth-abundant metal chalcogenide compounds. We first showed that pyrite-type cobalt disulfide (CoS_2) selectively catalyzes the acidic $2e^-$ ORR at low overpotentials due to the spatial separation of active metal sites by anions, which kinetically suppresses the scission of O-O bond in OOH^* adsorbate and the undesired $4e^-$ ORR. We further established both pyrite- and marcasite-type cobalt diselenide (CoSe_2) polymorphs as more stable and leaching-resistant acidic $2e^-$ ORR catalysts because of the much weaker binding of O^* adsorbate to Se sites. This stability allows for the bulk accumulation of practically useful 547 ppm H_2O_2 and the effective electro-Fenton degradation of organic pollutant for on-site environmental remediation. Building on the new mechanistic understanding, our ongoing developments and future perspectives of earth-abundant metal compound-based $2e^-$ ORR electrocatalysts will also be discussed.

9:20 AM EN01.06.05

Late News: Highly Active Co–Fe–P Nanoparticles Decorating Carbon Fibers Electrodes for the Oxygen Evolution Reaction María Isabel Díez García, Guillem Montaña Mora, Andreu Cabot Codina and Joan Ramon Morante; Institut de la Recerca de la Energia de Catalunya, Spain

Electrocatalytic decomposition of water is a promising route for hydrogen production, which nowadays is one of the best candidates as energy vector for a future carbon-free economy. The involved catalysts must have high electrocatalytic activity (and high selectivity) for lowering the applied voltage to the cell and long-term stability for the durability of the device. Apart from that, the materials should be composed by Earth-abundant elements and be environmentally friendly. Besides, the synthetic route should be cheap and scalable for industrial production. For the oxygen evolution reaction (OER), the Ir/Ru oxides show excellent electrocatalytic performance for water oxidation in alkaline media, however, the scarcity of these metals and their high cost are detrimental for practical applications. Fueled by a growing interest in new materials that could be advantageous against precious metal-based catalysts, metal phosphides have attracted particular attention. Most of them exhibit good catalytic properties toward hydrogen evolution reaction (HER) and OER and a high conductivity compared with the corresponding metal oxides/hydroxides. In this work, we investigate CoFeP nanoparticles supported on two different 3D electrodes, nickel foam and carbon felt substrates. Electrodes using nickel foam display higher current densities due to a lowered Tafel slope and higher conductivity of the substrate. For CoFeP deposited on nickel foam, overpotentials lower than 300 mV are achieved for 10 mA/cm^2 . The influence of the Co/Fe ratio, particle size, morphology and structure of CoFeP nanoparticles deposited on the electrode supporting materials have been investigated and compared with the monometallic phosphides emphasizing the role of the use of bimetallic based systems combined with the advantageous expected role of the phosphides.

9:35 AM EN01.06.06

Ultrathin Bismuth Oxyiodide Nanosheets for Photocatalytic Ammonia Generation from Nitrogen and Water Under Visible to Near-Infrared Light Mohammadjavad Mohebinia¹, Chunzheng Wu², Guang Yang¹, Shenyu Dai³, Alireza Hakimian¹, Tian Tong¹, Hadi Ghasemi¹, Zhiming Wang², Dezhi Wang¹, Zhifeng Ren¹ and Jiming Bao^{1,1,1}; ¹University of Houston, United States; ²Institute of Fundamental and Frontier Sciences, University of Electronic Science and Technology of China, China; ³Sichuan University, China

Artificial photosynthesis of ammonia using atmospheric nitrogen and water is a sustainable but challenging alternative to the Haber-Bosch process. Bismuth oxyiodide (BiOI) is a promising candidate due to its superior light absorption capability (bandgap of around 1.8 eV) and abundant surface oxygen vacancies. However, its improper band edge positions made it inactive for overall water-splitting and N_2 fixation. In this work, ultrathin BiOI nanosheets were synthesized through a simple surfactant (PVP) assisted hydrothermal route. The nanosheets split pure water into H_2 and O_2 and converted nitrogen and water into ammonia under visible or near-infrared light. PVP capping not only reduced the thickness of BiOI sheets but also upshifted its band edge positions due to the surface electric dipole induced by polyvinyl pyrrolidone molecules on the BiOI surface, thus enabling the water oxidation and nitrogen reduction half-reactions simultaneously.

11:45 AM *EN01.07.01

Power-to-X Technologies—Bioinspired Catalyst and Device Design Mathias Smialkowski¹, Kai Junge Puring¹, Kevinjeorjios Pellumbi^{2,1}, Lucas Hoof², Daniel Siegmund² and Ulf-Peter Apfel^{1,2}; ¹Ruhr University Bochum, Germany; ²Fraunhofer UMSICHT, Germany

The efficient reduction of protons and CO₂ under mild conditions is a current challenge for modern society. Nature utilizes enzymatic machineries that comprise iron- and nickel- containing active sites to perform these transformations.^[1] Recently, we reported on the formidable HER activity of bulk Fe_{4.5}Ni_{4.5}S₈ electrodes revealing similar structural and functional properties of the enzymes.^[2,3] We herein set out to explore the influence of the Fe : Ni ratio on the performance of the electrocatalyst.^[4] Using linear sweep voltammetry, we show that the increase in the Fe or Ni content, respectively, lowers the activity of the bulk electrocatalyst towards HER. Additionally, with increasing Se content in Fe_{4.5}Ni_{4.5}S_{8-x}Se_x, the HER performance is significantly lowered.^[5,6] Thus, specific Fe-Ni interactions seem to be the key for materials reactivity. In addition, we show that a temperature increase leads to a significant decrease of the overpotential. Furthermore, due to the resemblance of such sulfides with CO₂ converting enzymes, we likewise investigated Fe_{4.5}Ni_{4.5}S₈ electrodes to perform CO₂ reduction.^[7] In non-aqueous conditions as well as in supercritical CO₂, this material is indeed a potential catalyst affording CO or formic acid, respectively, as main product with high Faradaic yields.

Notably, the reactivity of the pentlandite materials can be further tuned by the reactor environment as well as the electrodes shape which was found to be equally important as the catalyst.

References.

- [1] Möller, F. ; Piontek, S. ; Miller, R. G. ; Apfel U.-P. ; *Chem. Eur. J.* **2018**, *24*, 1471-1493.
- [2] Konkena, B.; junge Puring, K.; Khavryuchenko, O.; Sinev, I. ; Piontek, S.; Muhler, M.; Schuhmann, W.; Apfel, U.-P. ; *Nature Commun.* **2016**, *7*:12269, DOI: 10.1038/ncomms12269.
- [3] Zegkinoglou, I.; Zendegani, A.; Sinev, I.; Kunze, S.; Mistry, H.; Zhao, J.; Hu, M. Y.; Alp, E. E.; Piontek, S.; Smialkowski, M.; Apfel, U.-P.; Hickel, T.; Neugebauer, J.; Roldan Cuenya, B.; *J. Am. Chem. Soc.* **2017**, *139*, 14360-14363.
- [4] Piontek, S.; Andronescu, C.; Zaichenko, A.; Konkena, B.; junge Puring, K.; Marler, B.; Antoni, H.; Sinev, I.; Muhler, M.; Mollenhauer, D.; Roldan Cuenya, B.; Schuhmann, W.; Apfel, U.-P.; *ACS Catalysis* **2018**, *8*, 987-966.
- [5] Smialkowski, M.; Siegmund, D.; Pellumbi, K.; Hensgen, L.; Antoni, H.; Muhler, M.; Apfel, U.-P.; *Chem. Comm.* **2019**, *55*, 8792-8795.
- [6] Pellumbi, K.; Smialkowski, M.; Siegmund, D.; Apfel, U.-P. ; *Chem. Eur. J.* **2020**, *26*, 9938 –9944.
- [7] Piontek, S.; junge Puring, K.; Siegmund, D.; Smialkowski, M.; Sinev, I.; Roldan Cuenya, B.; Apfel, U.-P.; *Chem. Sci.* **2019**, *10*, 1075–1081.

12:10 PM EN01.07.02

FeP/C 3D Cathodes as Highly Efficient Electrodes for Hydrogen Production María Isabel Díez García, Sebastian Murcia and Joan Ramon Morante; Catalonia Institute for Energy Research (IREC), Spain

The deployment of carbon-free energy technologies that could compete with the price of fossil fuels is expected to be a key factor for sustaining the future energy requirements of the world population. In this regard, H₂ is a promising energy vector that could be produced using solar energy, and one of the approaches consists on coupling an electrolyzer to a photovoltaic cell. Among electrode materials used as cathodes, iron phosphide has

engaged interest in the last years. Apart from the fact that it is composed of two elements highly abundant in the Earth crust, the new synthetic routes are making its synthesis simpler and cheaper. In this work, a 3D electrode composed by FeP directly deposited on carbon fibers is fabricated by a simple impregnation method and subsequent heat treatment. The intermediate iron species are converted to FeP by in situ PH_3 generation at 300-400 °C, leading to a highly porous electrode with a high surface area. Electrodes are optimized by exploring different synthetic conditions, such as heat treatment temperatures or catalyst loading. The intermediate Fe species are found to influence the final FeP/C configuration. Optimized FeP/C electrodes exhibit high activity towards hydrogen evolution reaction (HER) in both acidic and alkaline electrolytes displaying low overpotentials and excellent stability. Additionally, the doping with some particular metals is also studied, unveiling the role of the dopant in the HER activity. A further demonstration of performance in a flow cell is presented, confirming the feasibility of our electrodes as cathodes for HER in continuous operation.

12:25 PM EN01.07.03

Late News: Topological Engineering of Pt-Group-Metal-Based Chiral Crystals Toward High Efficiency Hydrogen Evolution Catalysts Qun Yang and Claudia Felser; Max Planck Institute for Chemical Physics of Solids, Germany

It has been demonstrated that topological nontrivial surface states can favor heterogeneous catalysis processes such as the hydrogen evolution reaction (HER), but a further decrease in mass loading and an increase in activity are still highly challenging. The observation of massless chiral fermions associated with large topological charge and long Fermi arc (FA) surface states inspires the investigation of their relationship with the charge transfer and adsorption process in the HER. In this study, it is found that the HER efficiency of Pt-group metals can be boosted significantly by introducing topological order. A giant nontrivial topological energy window and a long topological surface FA are expected at the surface when forming chiral crystals in the space group of $P2_13$ (#198). This makes the nontrivial topological features resistant to a large change in the applied overpotential. As HER catalysts, PtAl and PtGa chiral crystals show turnover frequencies as high as 5.6 and 17.1 s^{-1} and an overpotential as low as 14 and 13.3 mV at a current density of 10 mA cm^{-2} . These crystals outperform those of commercial Pt and nanostructured catalysts. This work opens a new avenue for the development of high-efficiency catalysts with the strategy of topological engineering of excellent transitional catalytic materials.

12:40 PM EN01.07.04

Mesoporous NiFe_2O_4 with Tuneable Pore Morphology for Electrocatalytic Water Oxidation Christopher Simon¹, Jana Timm¹, David Tetzlaff^{2,3}, Jonas Jungmann¹, Ulf-Peter Apfel^{2,3} and Roland Marschall¹; ¹University of Bayreuth, Germany; ²Ruhr-University Bochum, Germany; ³Fraunhofer Institute for Environmental, Safety, and Energy Technology UMSICHT, Germany

Electrocatalytic water splitting using renewable energies to form green hydrogen and oxygen has attracted a widespread interest to replace fossil fuels as major energy carrier. Currently, the oxygen evolution half reaction (OER) is regarded to be the major bottle-neck of water splitting due to its hampered kinetics involving a multi-step proton and electron transfer. Noble metal electrocatalysts, such as RuO_2 and IrO_2 are widely used for OER, however, their prohibitive scarcity and cost limit their potential widespread use in electrolyzers.

Among multiple transition metal oxides, ferrites with the general formula $\text{M(II)Fe}_2\text{O}_4$ ($\text{M} = \text{Ca, Zn, Mg, Ni, Co, Mn}$ etc.) have gained considerable attention due to their compositions made up from earth-abundant elements and widespread application fields including electrocatalysis.[1-4] Especially nickel ferrite has been considered as efficient OER electrocatalyst, with outstanding high stability in alkaline media, excellent redox properties, and ferromagnetism facilitating the catalyst separation from solution. [5]

We will report on the successful synthesis of mesoporous NiFe_2O_4 materials with narrow pore size distribution for the oxygen evolution reaction. The materials are prepared by a soft-templating strategy using citric acid and the optional addition of the commercially available block copolymer Pluronic® P-123, followed by calcination. The mesopore evolution during thermal treatment is examined systematically giving insights into the formation process of mesoporous NiFe_2O_4 . The formation of intermediate carbonate species induced by the use of citric

acid in the synthesis plays a key role in the formation mechanism of the templated mesoporous structure. Furthermore, citric acid is also crucial to obtain phase-pure NiFe₂O₄.

Detailed nitrogen physisorption analysis including desorption scanning experiments will be presented to reveal the exceptional accessibility of the mesopores generating surface areas of up to 200 m²/g. The ability of the NiFe₂O₄ powders to perform electrocatalytic oxygen evolution reaction under alkaline conditions was investigated, highlighting the advantages of mesopore insertion. The performance was ascribed to be dependent of the electrochemical surface area, which increased with the relative surface area of the prepared materials. In general, the highly accessible mesoporous and amorphous structure with large surface areas seem to be key parameters for OER, whereas high crystallinity turns out to be not beneficial.

References

- [1] X. F. Lu, L. F. Gu, J. W. Wang, J. X. Wu, P. Q. Liao, G. R. Li, *Adv. Mater.* **2017**, *29*, 1604437.
- [2] G. Liu, K. Wang, X. Gao, D. He, J. Li, *Electrochim. Acta* **2016**, *211*, 871–878.
- [3] Q. Qin, L. Chen, T. Wei, Y. Wang, X. Liu, *Catal. Sci. Technol.* **2019**, *9*, 1595–1601.
- [4] M. Li, Y. Xiong, X. Liu, X. Bo, Y. Zhang, C. Han, L. Guo, *Nanoscale* **2015**, *7*, 8920–8930.
- [5] Z. Wu, Z. Zou, J. Huang, F. Gao, *ACS Appl. Mater. Interfaces* **2018**, *10*, 26283

12:55 PM EN01.07.06

Late News: Synthesis, Properties and Electrocatalytic Activity of Phosphorus-Rich 3D Metal Phosphides
Edward G. Gillan; University of Iowa, United States

Transition-metal phosphides (MP_x) have received significant scrutiny as water splitting electrocatalysts, particularly those with nanostructured morphologies that facilitate the electrocatalytic hydrogen evolution reaction (HER). The most synthetically accessible structures are those from the metal-rich side of metal-phosphorus phase diagrams (e.g., FeP, CoP, Ni₂P, or Cu₃P). Our group has developed a solvent-free chemical exchange synthesis for metal phosphides that can directly produce both crystalline metal-rich and less-studied phosphorus-rich metal phosphides at moderate temperatures near 500 °C. This reaction relies on the direct insertion/exchange reaction between metal halides and elemental phosphorus to form PCl₃ and the MP_x products. In some cases, addition of a tin flux facilitates redox processes and MP_x growth along with SnCl₂ byproduct formation. Single metal phosphides from the 3d metal group can be targeted through changes in synthetic conditions to form metal-rich and phosphorus-rich crystalline materials such as FeP versus FeP₂, CoP versus CoP₃, and Ni₂P versus NiP₂ or NiP₃. The synthesis and characterization of different compositions in the Fe/Co/Ni phosphide families will be described.

Several of the MP₂/MP₃ phases show hydrogen evolution reaction (HER) activity analogous to that observed for their metal-rich counterparts despite lower metal content. Even for 3d metal catalysts, a decrease in metal content without large corresponding loss in surface catalytic activity is desirable for sustainable catalytic solutions. The P-rich structures appear to resist (electro)chemical degradation in acidic environments during electrocatalytic HER experiments over extended 18-hour periods. In contrast to the metal-rich phosphides with extensive metal-metal bonding, MP₂/MP₃ structures contain polyphosphide anions that may better encapsulate metal centers and can enable electrocatalytically useful polyphosphide anion redox activity. Comparisons of local structure and properties and their possible impact on surface reactions in electrocatalytic HER will be described.

1:10 PM EN01.07.07

Late News: Topological Materials as Electrochemical Catalysts Guowei Li and Claudia Felser; Max Planck Institute for Chemical Physics of Solids, Germany

Exotic electronic states are realized in various topological phases, from topological insulators to recently reported Weyl/Dirac semimetals, nodal line semimetals, and magnetic semimetals. They strongly influence the surface electronic structures of the investigated materials and could serve as a good platform to gain insight into the catalytic mechanism of surface reactions. Topological Semimetals such as PtSn₄ and Co₃Sn₂S₂ adopt quasi-

two-dimensional structures and could expose the crystal surfaces constructing by transition metal atoms. Topological non-trivial surface states are observed at the crystal surfaces, which are located near the Fermi level. These topological surface states can act as both electron acceptors or donators for small adsorbed molecules, consequently tailoring the adsorption energy and Gibbs free energy in the electrochemical catalytic reactions.

1:25 PM DISCUSSION TIME

SESSION EN01.08: Transition Metal-Organic and -Dichalcogenide Materials for Electrocatalysis
Session Chairs: Philipp Stadler and Tsukasa Yoshida
Friday Afternoon, April 23, 2021
EN01

5:15 PM EN01.08.02

Enhanced Water Splitting Performance of MoS₂ and PdSe₂ Using Heterostructuring Edward A. Baker, Joe Pitfield and Steven P. Hepplestone; University of Exeter, United Kingdom

Two dimensional materials, such as the transition metal dichalcogenides (TMDCs) are a good candidate for water splitting catalysts [1,2], as they often have larger band gaps than their bulk counterparts. However, this had to be balanced by the thin layers having a small absorption cross section and difficulties in mounting on a suitable substrate. PdSe₂ is being suggested as a potential water splitting candidate [3]. However its bulk band gap is too small for water splitting [4]. We propose to use this structure as a surface coating to a second TMDC with a larger band gap such as MoS₂ and use this as an example of how such heterostructures could function.

Using density functional theory, implemented in the Vienna Ab-initio Simulation Package, we have investigated the surfaces of TMDC monolayers MoS₂ and PdSe₂, and a Hetero-bilayer of the two, for their potential application as photocatalytic water splitters. The different functional groups involved in the Hydrogen and Oxygen evolution reactions have been added to the monolayers and the hetero-bilayer to determine their energetics. In addition to this, we have looked at how stable these materials are, to both adsorptions and substitutions, in both air and water environments.

References:

- [1] Qing Tang and De En Jiang. ACS Catalysis, 6(8):4953–4961, Aug 2016.
- [2] B. Amin, et al . Phys. Rev. B, 92:075439, Aug 2015.
- [3] C. Long, et al . ACS Appl. Energy Mater., 2, 1, 513-520, 2019.
- [4] G. Zhang, et al . Appl. Phys. Lett., 114, 253102, June 2019.

5:30 PM *EN01.08.03

Molecular Engineering of Metal Phthalocyanine Electrocatalysts for the Carbon Dioxide Reduction Reaction Yongye Liang, Zhan Jiang and Huan Li; Southern University of Science and Technology, China

Molecular electrocatalysts are attractive due to their well-defined structures and easy regulation of chemical properties. However, in heterogeneous systems, molecular electrocatalysts are usually inferior to noble metal based materials in terms of activity and stability, and the molecular engineering of electrocatalytic performance remains a grand challenge. Herein, we present our recent work on the development of molecularly dispersive electrocatalysts (MDEs) and their molecular engineering regulation strategies for the carbon dioxide reduction reaction. These MDEs were constructed by anchoring metal phthalocyanine molecules on side walls of carbon nanotubes, which could effectively overcome the issues of poor electrical conductivity and molecular aggregations. The electrocatalytic performance could be further improved by tuning metal centers and

substitution groups on phthalocyanine. The designed nickel phthalocyanine MDE system exhibited high selectivity and good stability for the conversion to carbon monoxide at high current densities in gas-diffusion electrodes, setting new records of noble-metal-free and molecule-based electrocatalysts. The cobalt phthalocyanine MDE system could catalyze the six-electron reduction of carbon dioxide to methanol with high selectivity and good stability, which had not been achieved by molecular electrocatalysts. The MDEs with well-defined active centers also facilitated understanding the underlying mechanism on structural factors affecting electrocatalytic performance with the help of in-situ/operando characterizations and theoretical calculations. These studies pave a new path for the development of high-performance electrocatalysts.

5:55 PM EN01.08.04

Unzipping 2D Transition Metal Dichalcogenides for Hydrogen Evolution Reaction Catalysis Suchithra Padmajan Sasikala; KAIST, Korea (the Republic of)

Discovery of 2D atomic structures, including graphene, transition metallic dichalcogenides (TMDs), *h*-boron nitride, phosphorene, and mxene, has unveiled new possibilities in materials science. Unzipping of the basal plane is a general issue to uniquely control the material signatures of the 2D materials, as evidenced by the effective transformation of intrinsically metallic graphene into semiconductors, while unzipped into few-nanometer-wide graphene nanoribbons. Nonetheless, reliable unzipping has been reported for graphene and phosphorene thus far. Single elemental nature of those materials allows straightforward understanding of chemical reaction and property modulation involved with such geometric transformations. Here we present spontaneous linear ordered unzipping of bi-elemental 2D MX₂ transition metal chalcogenides as a general route to synthesize 1D nanoribbon structures. Strained metallic phases (1T') of MX₂ are found to undergo highly specific longitudinal unzipping owing to the self-linearized oxygenation at chalcogenides. Stable dispersions of 1T' MoS₂ nanoribbons with widths of 10-120 nm and lengths up to ~4 μm are produced in water. Edge abundant 1T' MoS₂ nanoribbons reveal the hidden potential of idealized electrocatalysis for hydrogen evolution in a competitive level with precious Pt catalyst.

6:10 PM EN01.08.05

Designing Polymorphic Nanoporous Iridium Oxides for Oxygen Evolution Catalysis SangSeob Lee, Giyeok Lee and Aloysius Soon; Yonsei University, Korea (the Republic of)

Oxygen evolution reaction (OER) is the key anodic catalytic reaction for many important clean energy processes. To date, the search for an active, selective, and stable electrocatalysts has not ceased and a detailed atomic-level design of the OER catalyst remains an outstanding (if not, compelling) problem. Only recently, a computational high-throughput study of iridium oxides (for both IrO₂ and IrO₃) has highlighted the role of polymorphism and stoichiometry to precisely engineer iridium oxides for efficient and stable OER catalysis. However, it seems surprising that nanoporous (i.e. crystal structures containing nanopores and nanochannels) iridium oxides – which have been proposed in various experiments – were not examined in that study. In this work, we have further extended the previous computational report to include many metastable nanoporous iridium oxide polymorphs – inspired both from experiments and also analogous crystal structures from manganese oxides. Using van der Waals corrected density-functional theory calculations, we investigate the thermodynamic stability, intercalation properties, and electronic structure of these nanoporous iridium oxides. We focus on understanding how the charge, size, and concentration of the intercalation ions (e.g. K⁺, Ca²⁺, etc.) may be taken advantage of for engineering the desired OER descriptor – the ratio of Ir³⁺/Ir⁴⁺ in these intercalated polymorphs, for the neoteric OER electrocatalysts.

6:15 PM DISCUSSION TIME

6:30 PM EN01.08.07

High-Throughput Data-Mining of Transition Metal Carbides and Nitrides for Promising Conductive Low-Cost Heterogeneous Catalyst Supports Giyeok Lee¹, Taehun Lee^{1,2} and Aloysius Soon¹; ¹Yonsei University, Korea (the Republic of); ²Princeton University, United States

Transition metal carbides and nitrides are suggested as promising candidates for conductive low-cost heterogeneous catalyst supports given their superior structural durability and electronic structure to effectively promote charge transfer across the catalyst interface. To architecture the most optimal carbide and/or nitride for conductive supports, we consider a range of group VI and V metal carbides and nitrides (in their rock-salt bulk phase) and perform high-throughput first-principles density-functional theory (DFT) calculations using the Vienna *Ab initio* Simulation Package (VASP) within our automated high-throughput in-house python code via the Atomic Simulation Environment (ASE). Namely, from the low Miller-index surfaces of these carbides and nitrides, we calculate and analyze their surface thermodynamic stability, surface work function modulations, and electronic structure analysis to examine the magnitude/origin of charge transfer across the catalyst interface. Furthermore, we introduce point defects at the pristine surfaces of these carbides and nitrides to inspect the variations in surface work functions and electronic structure to anticipate a wider range of tunability of their support properties in heterogeneous catalysis. Through these high-throughput DFT calculations, we have successfully screened out the most promising candidates and propose an *ab initio* design rule to engineer the next-generation hybrid heterogeneous catalysts.

6:35 PM EN01.08.08

Single Ni Atom Decorated Networked Carbon for pH-Universal Oxygen Electroreduction for Fuel Cell Application Alekha Tyagi¹, Kamal K. Kar^{1,1} and Hiroyuki Yokoi²; ¹Indian Institute of Technology Kanpur, India; ²Kumamoto University, Japan

In the present era of depleting conventional energy resources, it is urgent to inspect and develop substitutional fuel resources and suitable energy storage and conversion systems for their exploration. Further, in light of the increasing pollution concerns, it is desirable that the alternative systems are suitable for environment-friendly energy conversion. Polymer electrolyte membrane fuel cell (PEMFC) and the metal-air batteries are the prospective devices, which need dedicated research efforts to overcome the shortcomings and reach commercialization. The major performance limiting factor is the sluggish reaction kinetics of the oxygen reduction reaction (ORR) at the cathode. Noble metal nanoparticles supported on carbon are employed as cathode catalyst to enhance the reaction rate. But, these catalysts are not economical and suffer from poisoning and fuel-crossover issues. Suitable cost-effective, highly active and durable catalyst system are very much needed to enhance the rate of the ORR.

Here, we are presenting an atomic Ni decorated N, S doped hierarchical porous networked carbon synthesized by employing an optimized inert pyrolysis followed acid-treatment strategy. Nickel nitrate and guanidine thiocyanate are chosen as precursors for metallic entity and doped porous support, respectively. The catalyst possesses a novel morphology with atomically dispersed Ni atoms and nickel sulfide entities on networked N, S-doped carbon backbone.

The sample synthesized at 750 °C, which is further treated with 1 M HCl (Ni-GT-750-A) exhibit superior pH-universal ORR performance with an onset potential ($V_{\text{Onset}} = 0.91 \text{ V}$ (0.1 M KOH) and 0.89 V (0.1 M HClO₄) versus reversible hydrogen electrode (RHE). The excellent current stability (95.0 and 60 %) and resistance to methanol poisoning (90.6 and 80.3 %) are observed through chronoamperometric studies as comparison to the state-of-the-art catalyst (Pt/C) (65.0, 27, -33.0 and 16.5 %) in alkaline and acidic media, respectively. This electrochemical performance marks the suitability of the proposed catalyst in wide range of electrolytic media.

The observed ORR performance of the prepared electrocatalyst is attributed to the localized single-metal atom type ORR active sites over carbon matrix, which decreases the potential barriers for intermittent reactions due to enhanced atom utilization efficiency, which in turn increases the ORR kinetics. These atomic species are visualized using high-angle annular dark field- scanning transmission electron microscopy (HAADF-STEM). The hierarchical porous morphology as confirmed through N₂ adsorption-desorption isotherms and pore size distribution in addition to the defects in the carbon support owing to the present heteroatoms as can be visualized by Raman studies also contributed in the overall ORR performance in a synergistic manner. The

explored physicochemical traits and ORR activity of Ni-GT-750-A paves the way for exploration of its catalytic activity for other electrochemical reactions and as electrode material for energy storage devices.

This work is published as:

A. Tyagi, K K. Kar, H. Yokoi, J. Colloid and Interface Sci., 571 (2020) 285-296

<https://doi.org/10.1016/j.jcis.2020.03.043>

SYMPOSIUM EN02

Sustainable Routes to Fuels and Commodity Chemicals Production via Electrochemical Methods

April 21 - April 23, 2021

Symposium Organizers

Fatwa Abdi, Helmholtz-Zentrum Berlin

Simelys Hernandez, Politecnico di Torino

Yun Hao Ng, City University of Hong Kong

Francesca Maria Toma, Lawrence Berkeley National Laboratory

Symposium Support

Silver

Helmholtz-Zentrum Berlin

* Invited Paper

SESSION EN02.01: Lightning Presentations: (Photo)electrochemical CO₂ Reduction

Session Chairs: Fatwa Abdi and Francesca Maria Toma

Wednesday Morning, April 21, 2021

EN02

11:45 AM *EN02.01.01

Metal and Semiconductor Photocatalysts for Selective Carbon Dioxide Reduction Harry A. Atwater;

California Institute of Technology, United States

Recent work has shown intriguing possibilities for non-equilibrium carrier generation in metal nanostructures at semiconductor interfaces to modify the rates and pathways for photochemical reactions at the nanoscale, suggesting that light can play a new role as an agent of photocatalytic selectivity – beyond its traditional role of charge carrier generation. Key open questions in this field include: i) how hot are the hot carriers? ii) how hot carriers are transported and whether they modify interfacial reactions? iii) ultimately, how efficiently can these processes generate chemical products from sunlight? We show that hot carrier photocatalytic reactions at the Au/p-GaN and Cu/NiO nanoparticle interfaces alter the Faradaic efficiency for carbon dioxide reduction relative to dark electrocatalysis. Notably, at both of these interfaces, charge carrier separation occurs via photoexcited hot hole injection into the p-type wide bandgap semiconductor, localizing electrons in the metal catalyst nanoparticles. An exciting new result is the observation of self-sustaining, unassisted photocatalytic gas phase carbon dioxide reduction in metal/p-GaN structures, where the CO₂ reduction reaction is balanced by water oxidation on gallium nitride. In this work, we have address carrier generation, transport and interface dynamics with first-principles theory, and experimental observation of carrier dynamics via hot-carrier

photocurrent spectroscopy, ultrafast transient absorption spectroscopy, and photoelectrochemical measurements.

Another key future photocatalyst challenge for solar fuels from carbon dioxide reduction is design of earth-abundant tandem photocatalysts with both appropriate bandgaps and sufficiently high photovoltages to efficiently drive carbon dioxide reduction reactions at solar photocurrent densities, with validated durability and long lifetime. We survey options for photocatalysts comprised of metal oxide, metal nitride and tandem heterostructure components.

12:10 PM EN02.01.02

Calculations of the Electrochemical Reduction of CO₂ and the Competing Hydrogen Formation Hannes Jonsson; University of Iceland, Iceland

Results of theoretical calculations of electrochemical CO₂ reduction to formate, hydrocarbons and alcohols will be presented. The mechanism for the formation of various products is established and the rate evaluated and compared with experimental measurements. The rate of the main side reaction, the hydrogen evolution reaction, is also estimated. The calculations are based on a detailed atomistic model of the electric double layer (metal slab and water layer) and density functional theory calculations to evaluate not only the free energy of intermediates as a function of applied voltage but also the activation energy for each elementary step, both Heyrovsky and Tafel reactions [1]. Comparison is also made with calculations using an implicit solvation model [2]. A range of close packed metal surfaces are compared, including Cu, Ag, Au, Ni, Fe, Rh, Ir and Pt. The results are in remarkably good agreement with the available measurements. A two parameter descriptor is established that can help identify improved catalysts for this important reaction. The elucidation of the reaction mechanism of CO₂ electroreduction to hydrocarbons and alcohols as well as the competing hydrogen evolution reaction is an important step towards the design of a selective and energy efficient catalyst for small scale, decentralized fuel production using renewable energy sources and CO₂ as reactant.

[1] J. Hussain, H. Jónsson and E. Skúlason, ACS Catalysis 8, 5240 (2018).

[2] M. Van den Bossche, E. Skúlason, C. Rose-Petruck and H. Jónsson, J. Phys. Chem. C 123, 4116 (2019).

12:15 PM EN02.01.03

Electrocatalytic CO₂ Reduction on CuZnAl-Based Oxide Catalysts—Tuning of the H₂/CO Ratio Hilmar Guzmán^{1,2}, Daniela Roldán¹, Adriano Sacco², Micaela Castellino¹, Marco Fontana², Nunzio Russo¹ and Simelys Hernandez^{1,2}; ¹Politecnico di Torino, Italy; ²Istituto Italiano di Tecnologia, Italy

Electrochemical Reduction of CO₂ (ER-CO₂) is a very attractive alternative to tackle Global Warming.[1] Cu-based materials have shown increased yields of hydrocarbon and oxygenate products, while its selectivity towards CO is low.[2] Inspired by the thermocatalytic process, a traditional co-precipitation method was employed to synthesize CuZnAl-based oxide catalysts with a mesoporous structure. This CuZnAl catalyst was tested for the first time for the ER-CO₂ under ambient conditions. The Physico-chemical properties of the catalysts were studied by several characterization techniques (e.g., XRD, XPS, BET, SEM, TEM) and electrochemical impedance spectroscopy at different applied-potentials to understand the role of the modification of the catalyst components during operation in the final selectivity and activity. Results revealed that adding amphoteric metal oxides like ZnO and Al₂O₃ to the CuO-based catalyst contributed to promote CO formation over H₂. XPS measurements on the fresh samples revealed that the ternary CuZnAl catalyst presented a lower percentage (5%) of Cu⁰ + Cu¹⁺ mixture on the surface than the other catalysts, being mainly constituted by Cu⁺². This material reached a Faradaic efficiency towards syngas of almost 95% at -0.89 V vs. RHE. Nevertheless, the highest production rate of syngas was obtained at the most negative applied potential (~ 17 μmol h⁻¹ cm⁻² at -1.14 V vs. RHE). A tunable H₂/CO ratio was achieved by applying different potentials, reaching lower values by increasing applied negative potential (CO current density increased). In fact, a syngas with a H₂/CO ratio of ~2 was obtained at -0.89 V vs. RHE, which is a suitable raw material for further methanol synthesis. The enhanced performance for syngas production of the developed CuZnAl catalyst is

demonstrated to be attributed to its surface properties (i.e., alkalinity and the oxidation state on the surface, its lowest diffusional mass transfer resistance, its highest total pore volume, and the lowest Cu crystals size among the prepared catalysts).

Acknowledgments

This work has received funding from the European Union's Horizon 2020 Research and Innovation Action program under the Project SunCoChem (Grant Agreement No 862192).

Reference

- [1] H. Guzmán, M.A. Farkhondehfal, K. Rodolfo Tolod, N. Russo, S. Hernández, Photo/electrocatalytic hydrogen exploitation for CO₂ reduction toward solar fuels production, in: Sol. Hydrog. Prod. Process. Syst. Technol., Elsevier Inc., 2019: p. 560. <https://doi.org/10.1016/C2017-0-02289-9>.
- [2] J.J. Velasco-Vélez, T. Jones, D. Gao, E. Carbonio, R. Arrigo, C.J. Hsu, Y.C. Huang, C.L. Dong, J.M. Chen, J.F. Lee, P. Strasser, B. Roldan Cuenya, R. Schlögl, A. Knop-Gericke, C.H. Chuang, The Role of the Copper Oxidation State in the Electrocatalytic Reduction of CO₂ into Valuable Hydrocarbons, ACS Sustain. Chem. Eng. 7 (2019) 1485–1492. <https://doi.org/10.1021/acssuschemeng.8b05106>.

12:20 PM EN02.01.04

Late News: Immobilization of a Molecular Re Complex on MOF Derived Hierarchical Porous Carbon for CO₂ Electroreduction in Water/Ionic Liquid Electrolyte Domenico Grammatico^{1,2}, Huan Ngoc Tran³, Yun Li³, Silvia Pugliese^{3,2}, Laurent Billon¹, Bao-Lian Su² and Marc Fontecave³; ¹University of Pau and Pays del'Adour, France; ²University of Namur, Belgium; ³Collège de France, France

The development of molecular catalysts for CO₂ electroreduction within electrolyzers requests their immobilization on the electrodes. Several methods have been explored for the heterogenization of homogeneous complexes, we here report a novel approach using a hierarchical porous carbon material, derived from a Metal Organic Framework, as a support for the well-known molecular catalyst [Re(bpy)(CO)₃Cl] (bpy = 2,2'-bipyridine). This cathodic hybrid material, named Re@HPC, has been tested for CO₂ electroreduction using a mixture of an ionic liquid (1-Ethyl-3-methylimidazolium tetrafluoroborate, EMIM) and water as the electrolyte. The present study reveals that thanks also to the hierarchical porosity and structure of the porous carbon, the Re@HPC is a remarkable catalyst, enjoying excellent activity (high current densities and high turnover numbers) and good stability. Interestingly, it catalyzes the conversion of CO₂ into a mixture of carbon monoxide and formic acid, with a selectivity that depends on the applied potential. These results emphasize the advantages of integrating molecular catalysts onto such porous carbon materials for developing novel, stable and efficient, catalysts for CO₂ reduction.

12:25 PM EN02.01.05

Dynamic Surface Structure of Cu Thin-Film Electrode Under CO₂ Reduction Conditions from *In Situ* X-Ray Characterization SooHong Lee¹, John C. Lin^{2,3}, Apurva Mehta³, Ryan C. Davis³, Thomas Jaramillo^{2,3}, Christopher Hahn³ and Walter Drisdell¹; ¹Lawrence Berkeley National Laboratory, United States; ²Stanford University, United States; ³SLAC National Accelerator Laboratory, United States

Identifying the chemical state of the catalytic surface at the electrode-electrolyte interface is of significant interest, but the *in situ* characterization of the active surface during the CO₂ reduction reaction (CO₂RR) remains challenging due to the formation of bubbles from gaseous products and mass transport limitations. These hurdles limit state-of-art *in-situ/operando* techniques from characterizing catalyst surfaces under the reaction conditions. In particular, there is great interest in whether Cu oxide species exist at the surface or near-surface of Cu-based CO₂RR catalysts under these conditions, and if such species play a role in the catalytic pathway to multi-carbon products.

Here, we conducted *in-situ* characterization of the atomic and electronic structure of the near-surface of a Cu thin-film using synchrotron X-ray methods under the high current CO₂RR conditions relevant for device operation. The structural evolution of the near-surface region of polycrystalline Cu electrodes under *in situ*

conditions was investigated through a combination of grazing incidence X-ray absorption spectroscopy (GIXAS) and X-ray diffraction (GIXRD). The *in situ* GIXAS shows that the surface oxide is fully reduced to metallic Cu before the onset potential for CO₂RR, and the catalyst surface retains the metallic state across the potentials relevant to the CO₂RR. In addition, *in-situ* GIXRD results showed that potential-dependent surface reconstruction from polycrystalline Cu to a Cu(100)-like surface was observed only in the presence of CO₂ reactants. Previously believed to be a sole potential-induced effect, our findings suggest that surface reconstruction is increased by the CO₂RR chemistry and that this reconstruction occurs across the macroscopic (mm-scale) surface. These findings show that the surface of Cu electrocatalysts is dynamic during the CO₂RR, and underscore the need for *in-situ* studies to accurately understand the catalyst surface state during catalysis.

12:30 PM ORAL Q&A

12:45 PM EN02.01.06

Carbon Dioxide Capture and Electrochemical Conversion with Ionic Liquids [Alessia Fortunati](#)¹, María José Rubio¹, Boyan Iliev², Nunzio Russo¹ and Simelys Hernandez¹; ¹Politecnico di Torino, Italy; ²Iolitec Ionic Liquids technologies GMBH, Germany

The exponential increase in the concentration of greenhouse gasses in the atmosphere is considered one of the most important reason for climate change. Carbon Dioxide is the most significant anthropogenic gas that contributes in global warming.

CO₂ capture and storage (CCS) has been proposed as one of the most important invention to mitigate CO₂ emissions. Moreover, conversion of carbon dioxide into energy-rich chemicals is a viable approach to reducing the global carbon footprint. The most common techniques to remove CO₂ from gas streams are the chemical and physical adsorption by liquid solvents. Traditionally, aqueous amine solutions have been used as chemical solvents because of their high selectivity, high reactivity and low price. Unfortunately, they present also many disadvantages associated with the high energy demand required for the solvent regeneration, corrosion issues and loss of solvent because of their high volatility. Hence, in the need to find more efficient solvents for CO₂ capture and conversion, Ionic Liquids (ILs) have been highlighted as very good alternatives to common amine solution. (1)

Within this field lies this research, which in turn is part of a much broader European project called SunCoChem. For this project we are testing the stability and performance of various ionic liquids, provided by Iolitec Ionic Liquids technologies GMBH, and in particular their ability to capture and electrochemically convert a pure CO₂ stream to CO with high efficiencies.

The ionic liquids were tested in a two-compartment H-type electrochemical cell. In the anodic chamber a nickel mesh electrode was immersed in a solution of potassium hydroxide and in the cathodic one a silver foil cathode was employed in a solution of CH₃CN and ionic liquid. An organic solvent was used to favor the dissolution of the ionic liquid and the homogenization of the solution. The Ionic Liquids (ILs) tested so far have a cationic part based on imidazole, which is expected to stabilize and lower the activation energy for the reduction of CO₂, namely [BMIM][BF₄], [BMIM][CH₃CO₂], [BMIM][CF₃CO₂] and [BMIM][CF₃SO₃]. This trend was confirmed by a shift to more positive potentials of the onset (~ 0.5V) for the CO₂ reduction reaction in the presence of these Ionic Liquid.

During the CP studies, some ILs evidenced a decrease in the applied potential indicating the increase of the electrolyte conductivity on difference to the behavior of the most commonly used [BMIM][BF₄] IL in the same organic solvent.

Our results evidence relevant current density values, a good stability during chronopotentiometry (CP) tests and a high selectivity towards the target product: CO, which however change depending on the used IL.

ACKNOWLEDGMENT

This work has received funding from the European Union's Horizon 2020 Research and Innovation Action programme under the Project SunCoChem (Grant Agreement No 862192).

References:

(1) Shokat Sarmad et al, Carbon Dioxide Capture with Ionic Liquids and Deep Eutectic Solvents: A New Generation of Sorbents, 2016, <https://doi.org/10.1002/cssc.201600987>

12:47 PM EN02.01.07

Influence of Sonication on Co-Precipitation Synthesis of Copper Oxide Catalyst for CO₂ Electroreduction

Daniela Roldán¹, Hilmar Guzmán^{1,2}, Nunzio Russo¹ and Simelys Hernandez^{1,2}; ¹Politecnico di Torino, Italy; ²Center for Sustainable Future Technologies, Italy

The need to reduce greenhouse gas emissions and increase our energy supply makes the electrochemical reduction of CO₂ (CO₂R) a very attractive alternative to produce non-fossil-based fuels or chemicals. Copper-based catalysts is one of the catalyst that most efficiently promote the formation of species with one or more carbon-carbon bonds from the electrochemical reduction of CO₂ [1]. Because the catalyst preparation method has an influence on the physicochemical properties and on the electrocatalytic performance[2], in this work, it was decided to evaluate the effect of the ultrasound application (US) on the shape and size of the particles obtained, its electrocatalytic activity and its selectivity to products of interest. For this purpose, sonication was carried out at different percentage amplitudes of ultrasonic power (23, 30 and 37%) during the aging time of the synthesis. Physical characterization was carried out by using different techniques including X-ray diffraction, BET and field-emission scanning electron microscopy (FESEM). Electrochemical tests for CO₂ reduction were done under ambient conditions. Regarding the physical characteristics, we found that pore size distribution is narrower by increasing the US amplitude. On the other hand, there is no significant difference in morphology and dimension of particles. However, the surface area increased with the use of ultrasound, this is attributed to a better dispersion created by acoustic cavitation. Ultrasound has also an effect on Copper-based catalysts performance; in this case, the selectivity towards H₂ and C₁ products (CO and formate) was enhanced. In addition, an increase in productivity of CO₂R products was obtained with respect to the synthesized catalysts that were not assisted by ultrasound (> 3-fold). These results motivate us to further explore in what other ways acoustic cavitation phenomenon can influence the physical characteristics of the catalysts and, in turns, their performance for the electrochemical reduction of CO₂.

Acknowledgement

This work has been performed with the financial support of Eni SpA and the R&D Program Energy Transition (Cattura e Utilizzo CO₂).

References

- [1] Hilmar Guzmán; M.Amin Farkhondehfar; Kristine-Rodulfo Tolod; Simelys Hernández; Nunzio Russo, Chapter 11: Photo/electrocatalytic hydrogen exploitation for CO₂ reduction toward solar fuels production. In Solar Hydrogen Production, Francesco Calise, M. D. D. A., Massimo Santarelli, Andrea Lanzini, Domenico Ferrero, Ed. Elsevier Inc.: 2019; pp 365-418.
- [2] Dasireddy, V. D. & Likozar, B., 2019. The role of copper oxidation state in Cu/ZnO/Al₂O₃ catalysts in CO₂ hydrogenation and methanol productivity. Renewable Energy, Volumen 140, pp. 452-460.

12:49 PM POSTER Q&A

12:59 PM *EN02.01.08

Copper-Based Systems for CO₂ Reduction—From an Electrochemical to a Photoelectrochemical Approach Jonathan Albo; University of Cantabria, Spain

To reverse the impact of increasing CO₂ emissions would need not only curbing the reliance on fossil fuels but also developing effective strategies to capture and utilize CO₂. There are also increasing attempts to consider CO₂ as a resource and a business opportunity rather than a waste with a cost of disposal. Among the several available strategies, the electrochemical reduction of CO₂ to produce value-added chemicals becomes a feasible mechanism of storing intermittent renewable energy that is entering the stage of gradual implementation [1]. When electrochemical reduction integrates a light source to provide energy for redox reactions, we have a

photoelectrochemical device, which have attracted an intense attention in recent years [2]. In principle, such integration enables higher energy efficiency by reducing the requirements of external energy and by reducing losses in transporting electricity to the electrolysis cell. Ideally, these systems may be completely operated under the sun without the need of an external bias between cathode and anode compartments, which may additionally reduce system capital costs [3].

Since CO₂ is a thermodynamically stable molecule, its multistep reduction confronts many fundamental technical hurdles. The kinetics for CO₂ reduction are also, in general, more sluggish than the thermodynamically favorable two-electron H₂ evolution reaction, which competes with CO₂ reduction. The electro-and-photoelectro-chemical processes are thus highly dependent on the development of efficient materials capable of selectively reducing CO₂ at low overpotentials. Of the myriad cathode materials that have been used, copper and copper oxides are regarded unique with both intermediate hydrogen overpotentials and CO adsorption [4] allowing further reduction of CO₂ to fuels and commodity chemicals such as methanol [5] or ethylene [6] at moderate reaction rates.

With this communication, the author presents the research activities in the electro-and-photoelectro-chemical conversion of CO₂ to alcohols and hydrocarbons at copper-based systems in the DePRO research group of the University of Cantabria, to provide new insights and guidance to the field. A filter-press dual-chamber cell is used for the continuous conversion of CO₂ under different phases involved (i.e. gas or liquid-phase), electrode/cell designs (e.g. GDE, MEA or photoanode/photocathode) and key operating conditions. Many of these factors are often intertwined, which complicates advances in the field, but with continued research efforts these sustainable technologies for CO₂ conversion might become technically and economically feasible in the near future.

ACKNOWLEDGEMENT

The author gratefully acknowledge the financial support from the Spanish Ministry of Science and Innovation (MICINN) through the project PID2019-104050RA-I00 as well as Ramón y Cajal programme (RYC-2015-17080).

References

- [1] Chauvy, R., Meunier, N., G. De Weireld, T. Selecting emerging CO₂ utilization products for short- to mid-term deployment. *Appl. Energ.* 236, 2019, 662–680.
- [2] Vignesh, V., Bartlett, J., Pillai, S. C. Photoelectrochemical conversion of carbon dioxide (CO₂) into fuels and value-added products. *ACS Energy Lett.* 5, 2, 2020, 486–519
- [3] Castro, S., Albo, J., Irabien, A. Photoelectrochemical reactors for CO₂ utilization. *ACS Sustain. Chem. Eng.* 6, 12, 2018, 15877-15894.
- [4] Garza, A. J., Bell, A. T., Head-Gordon, M. Mechanism of CO₂ reduction at copper surfaces: Pathways to C₂ products. *ACS Catal.* 8, 2, 2018, 1490–1499.
- [5] Albo, J., Alvarez-Guerra, M., Castaño, P., Irabien, A. Towards the electrochemical conversion of carbon dioxide into methanol. *Green Chem.* 17, 2015, 2304-2324.
- [6] Ma, W., Xie, S., Liu, T., Fan, Q., Ye, J., Sun, F., Jiang, Z., Zhang, Q., Cheng, J., Wang, Y. Electrocatalytic reduction of CO₂ to ethylene and ethanol through hydrogen-assisted C–C coupling over fluorine-modified copper. *Nat. Catal.* 3, 2020, 478–487.

SESSION EN02.02: Lightning Presentations: (Photo)electrochemical Engineering of Reactions and Devices I
Session Chairs: Fatwa Abdi and Simelys Hernandez
Wednesday Afternoon, April 21, 2021
EN02

2:15 PM *EN02.02.01

Optimizing Organic Electrosynthesis Through Electrochemical Engineering Approaches and Bayesian

The chemical industry propelled human progress by using energy from fossil fuels and, in the process, inadvertently contributed to anthropogenic climate change. This industry outputs >70,000 products (1.2 billion tons in total), impacts more than 25% of the US GDP, and is responsible for ~5% of the US primary energy consumption (4.5 Quads). Thermochemical processes in this industry account for >93% of this energy consumption (>87% in the form of fossil-fuel-derived heat). Decarbonization of this industry would represent a giant step towards mitigating global warming. This urgent transition must integrate renewable energy sources with chemical manufacturing, ultimately resulting in the electrification of this industry *via* large-scale implementation of electrochemical manufacturing. Currently, however, two major challenges prevent the deployment of electrosynthesis reactors at scale: their low selectivity and their low production rates. This presentation will discuss reaction engineering opportunities to enhance the performance of organic electrosynthesis reactors. Specifically, I will present our work on understanding and improving the electrohydrodimerization process for the production of adiponitrile (ADN), a precursor to Nylon 6,6. Although this model reaction is the largest and most successful organic electrosynthesis implemented in industry, it faces many challenges owing to its limited energy conversion and selectivity. Through a combination of experimental electroanalytical characterization and Bayesian machine learning, we elucidate guidelines for the optimal operation of ADN electrosynthetic reactors. Our results provide insights into mass transport limitations that affect the selectivity of organic electrosynthesis processes and on how to dynamically control electrode processes to mitigate them.

2:40 PM *EN02.02.02

Mass Transport Considerations for High Performance CO₂ Electrolysers Wilson Smith^{1,2}; ¹National Renewable Energy Laboratory, United States; ²University of Colorado Boulder, United States

Electrocatalytic CO₂ reduction has the dual-promise of neutralizing carbon emissions in the near future, while providing a long-term pathway to create energy-dense chemicals and fuels from atmospheric and waste CO₂. The field has advanced immensely in recent years, taking significant strides towards commercial realization. Gas diffusion electrodes (GDEs), composed of solid electrocatalysts on porous supports positioned near the interface of a conducting electrolyte and CO₂ gas, have been able to demonstrate the substantial current densities needed for future commercialization. These higher reaction rates have often been ascribed to the presence of a three-phase interface, where solid, liquid, and gas provide electrons, water, and CO₂, respectively. Conversely, mechanistic work on electrochemical reactions implicate a fully two-phase reaction interface, where gas molecules reach the electrocatalyst's surface by dissolution and diffusion through the electrolyte. Here, we first outline the macro, micro and atomistic phenomena occurring within a gas-diffusion electrode to provide a focused introduction to the architecture of the often-discussed three-phase region for CO₂ electrolysis. In addition, we use a 2-D model to examine the concentration gradients in the gas and electrolyte flow channels across a GDE, which provides longitudinal information along the length of a flow cell. In doing so, we quantify the extent of concentration overpotentials and ohmic drops throughout the catalyst layer across a range of applied potentials and flow rates. Various process parameters were modified to explore the effects on the CO₂ mass transfer-limited current density, conversion, and outlet concentrations of CO₂, CO and H₂. Our model suggests that ohmic losses largely determine the current density distributions at low conversion rates where small gradients in concentration exist. However, as the concentration profiles become less uniform (e.g. high conversion rates), the non-electrochemical consumption of CO₂ starts to overtake electrochemical conversion, and leads to non-uniform performance across the electrode. In addition, while higher flow rates allow the ability to substantially increase current density, this comes at the expense of ohmic drops and losses in selectivity, which become more prominent at high conversion rates. The ability to understand the interplay between process conditions and local environment will be necessary to further develop the science and technology of electrochemical CO₂ reduction.

3:05 PM BREAK

3:10 PM EN02.02.04

Nanoporous Au and Cu Gas Diffusion Electrodes for Selective, High Current Density Carbon Dioxide Reduction Aidan Q. Fenwick^{1,2}, Alex J. Welch^{1,2}, Ian Sullivan² and Harry A. Atwater^{1,2}; ¹California Institute of Technology, United States; ²Joint Center for Artificial Photosynthesis, United States

Nanoporous (NP) transition metals offer a high surface area and edge-rich catalytic environment capable of selective electrolysis of carbon dioxide (CO₂) when utilized as a catalyst in a gas diffusion electrode (GDE). While the copper and gold have been extensively explored as catalysts for the carbon dioxide reduction reaction (CO₂RR) in both aqueous and vapor fed electrolyzes, a fully nanostructured catalytic environment remains unexplored. Here, we report the development and electrochemical performance of NP gold and copper GDEs deposited on a carbon or polytetrafluoroethylene (PTFE) microporous layer (MPL). NP GDEs are synthesized by vapor deposition of an alloy onto the MPL followed by a chemical or electrochemical dealloying process that yields a continuous porous electrode with nanoscale dimensions forming a NP catalyst layer. The average ligament and pore sized can be tuned by varying the temperature, solvent and length of the dealloying process. We observe that carbon paper-based, NP GDEs are prone electrolyte flooding due to the hydrophilicity of the bare metal surface. The contact angle of the NP GDE can be tailored from 40° to 150° via a 2 step application of 1) Nafion ionomer and 2) Nafion:carbon black mixture applied to the NP GDE. This system is capable of electrochemical generation of carbon monoxide with a partial current density of 650 mA/cm² in a 250mM KHCO₃ electrolyte that can be maintained for over 48 hours of continuous electrolysis. We will also report results of experiments of NP Cu/Au on PTFE and the effects of ligament thickness, pore size, catalyst structure and hydrophobicity on CO₂RR. These studies demonstrate that nanoporous catalyst environments can play an important role in governing the product selectivity and achievable current density of CO₂RR in a GDE.

3:15 PM EN02.02.05

Stabilization of Local pH Gradient and Separation of Product Gases by Buoyancy-Driven Fluid Dynamics in Solar-Driven Water Splitting Keisuke Obata and Fatwa F. Abdi; Helmholtz-Zentrum Berlin, Germany

In order to achieve a sustainable society driven by the abundant solar energy, the intermittency of sunlight needs to be overcome. One attractive solution is to store solar energy in the form of chemical fuels, e.g., the generation of hydrogen and oxygen in solar-driven water splitting. To this end, tremendous efforts have been devoted to developing efficient semiconductors and electrocatalysts, which resulted in a significant improvement of the reported solar-to-fuel efficiency in the last couple of decades. As the next stage, designing device architectures that are scalable and efficient is paramount in order to fully translate the developed materials towards practical applications. Indeed, it has been shown that major performance losses can be obtained from ineffective design,^{1,2} especially when scaling-up devices to larger area. A key component of the device operation is the fluid dynamics, as it plays an important role to determine the mass-transport phenomena in the device and the resultant energy efficiency. In this study, we highlight the buoyancy effects driven by (photo)electrochemical reactions and evaluate their influences on the ion distribution in the electrolyte solutions and product separation.

In the first part, pH changes during water splitting in a stagnant electrochemical cell with near-neutral electrolyte are monitored in-situ by a pH-sensitive fluorescence sensor foil placed between the anode and cathode. Electrolyte close to the anode and cathode gets more acidic and more alkaline, respectively, in unbuffered and buffered neutral-pH conditions. A closer look at the pH distribution within the cell further reveals that natural convection is generated by the electrochemical reactions under non-stirred conditions. Specifically, at low current densities (≤ 2 mA/cm²), the acidic and alkaline regions move to the top and bottom of the cell, respectively. Based on this observation, we develop a model that considers natural convection driven by buoyancy forces due to local changes in the density of the electrolyte, which reveals that buoyancy-driven convection significantly helps to stabilize local pH gradients. Our extended simulations further predict the great contribution of buoyancy-driven convection towards the production of value-added aqueous chemicals even at high current density range.

Buoyancy-driven fluid dynamics is also considered in terms of product separation in a solar-driven water splitting device. We consider a membrane-less flow cell as an attractive technique to separate gaseous products through the electrolyte flow without having any membrane-associated complexity and losses. We introduce Euler-Euler multiphase fluid dynamics simulations, which calculate the volume fraction of liquid and gas phases, to investigate the crossover in the presence of gas bubbles. We specifically consider realistic implementation of solar-driven water splitting device by taking into account the tilt orientation of the device. Our simulations reveal that gas bubbles, often ignored in previous studies,^{2,3} contribute more to the crossover rather than dissolved gases. We also extensively evaluate various important parameters that affect the overall product crossover, e.g., the device tilt angle, bubble diameter, bubble formation efficiency, etc. For example, smaller gas bubbles are found to suppress the crossover due to the stronger momentum exchange between the liquid and gas phases. This suggests the potential benefit of using surfactants, which are known to decrease the bubble diameter, for efficient product separation in membrane-less devices. Overall, our study highlights the critical importance in understanding and controlling the bubble formation under operating conditions to design efficient membrane-less water splitting devices.

1. Ahmet, *et al.*, *Sustainable Energy Fuels*, 2019, **3**, 2366.
2. Abdi, *et al.*, *Sustainable Energy Fuels*, 2020, **4**, 2734.
3. Holmes-Gentle, *et al.*, *Sustainable Energy Fuels*, 2017, **1**, 1184.

3:20 PM ORAL Q&A

3:40 PM EN02.02.07

Strategies for improving GDE Performance by a Uniform Dispersion of Catalyst Nanoparticles and an Optimal Nafion Content Federica Zammillo¹, Hilmar Guzmán^{1,2}, Nunzio Russo¹ and Simelys Hernandez^{1,2}; ¹Politecnico di Torino, Italy; ²Istituto Italiano di Tecnologia, Italy

In the context of the strategies needed to mitigate CO₂ emissions and combat climate change, the electrochemical CO₂ reduction represents a promising alternative. Among the different reactors, GDE-based ones are widely studied systems: here, the limitations shown by configurations with CO₂ dissolved in electrolyte solutions can be overcome by feeding CO₂ directly in gaseous form. In this work, the manufacturing process of the Cu-based gas diffusion electrode, namely the catalytic ink deposition on a porous carbon paper support, was carried out both by airbrushing (manual) and by spray-coating (automated) techniques. The characterization of the electrodes was performed by using X-Ray Diffraction, X-Ray Photoelectron Spectroscopy and Field Emission Scanning Electron Microscopy techniques. To assess electrodes behavior, cyclic and linear sweep voltammetry techniques were conducted. When comparing the achieved current densities at the highest applied potential, the electrode obtained with the spray coater displayed a better electrocatalytic activity (~10 mA/cm² higher at about -2.5 V vs Ag/AgCl), with respect to that fabricated with the airbrush. A thorough study of the GDEs performance was accomplished, testing the so obtained electrodes and thereby evaluating the effect of a variation of Nafion content in the productivity and selectivity results toward the desired products. A promising outcome was achieved when boron (B) has been incorporated in the Cu-catalyst material: indeed, in this case, the hand-made GDE revealed a FE of about 6% toward alcohols (mostly ethanol). The catalyst layer dispersion is a critical aspect of electrochemical CO₂ reduction and, confirming previous studies on the different deposition methods, a more uniform distribution of the catalyst particles enabled the spray coated GDEs to outperform the hand-made ones. Furthermore, the variation of Nafion content on the GDE structure had a relevant effect on the electrode performance, allowing to considerably reduce the side-production of hydrogen and increasing at the same time the CO generation. Finally, the role of local pH was taken into account: a preliminary model highlighted that a higher pH on the electrode surface may promote the hydration of CO₂ to carbonate and bicarbonate species, thus lowering CO₂ concentration at the triple-phase-boundary and hindering liquid products formation.

Acknowledgement

This work has received funding from the European Union's Horizon 2020 Research and Innovation Action

programme under the Project SunCoChem (Grant Agreement No 862192) and from the Piedmont Region under the Saturno project (<https://saturnobioeconomia.it/>).

3:42 PM EN02.02.08

Late News: Nitrogen Vacancy Enhanced Ni₃N/Ni Catalysts for Si Photocathodes with High Activity and Stability Doudou Zhang; The Australian National University, Australia

Magnetron sputtering is a scalable and eco-friendly approach of developing high-performance non-noble electro(co)catalysts with strong adhesion for durability. Herein, a 3D triangular pyramid nickel nitride with tunable nitrogen vacancies was created through magnetron sputtering, which is different from conventional nitridation process with high temperature and hazardous resource. Continuous sputtering the Ni₃N/Ni catalysts with poor-crystalline and good wettability delivered 99 mV overpotential at 10 mA cm⁻², a Tafel slope of 28 mV dec⁻¹ and durability 75 hours, which is approximate to Pt sputtering on FTO and exceeds the other reported catalysts on the planar substrates in alkaline media. Based on the theoretical calculations, it is further verified that the presence of nitrogen vacancies effectively enhances the adsorption of water molecules and ameliorates the adsorption-desorption behavior of intermediately adsorbed hydrogen, which leads to an advanced HER activity of Ni₃N/Ni. Then, the Ni₃N/Ni grown on c-Si photocathode showed the current density of 37.3 mA cm⁻² at 0 V RHE with 0.6 V onset potential, and applied bias photon-to-current efficiency (ABPE) 8.9% toward PEC-HER with stability in strong media 50 hours including the power on-off and continuous reaction. DFT calculations verified the surface structure with N-vacancies surface and high HER activity of the Ni₃N/Ni catalyst under working conditions. The demonstration has showed the potential for practical, large-scale manufacturing of the nitrides cocatalysts for composite photoelectrodes.

3:44 PM POSTER Q&A

3:50 PM *EN02.02.09

Electrolyte Effects on the Electrochemical Reduction of CO₂ Chong-Yong Lee, Jinshuo Zou and Gordon Wallace; University of Wollongong, Australia

Electrochemical reduction of CO₂ offers an eco-friendly recycling strategy in producing economically valuable fuels and chemical feedstocks. This process is readily tuned by employing suitable electrocatalysts, electrolytes, and electrochemical cell configurations to achieve preferred products. The nature of the anions and cations used in the electrolyte, could either having neutral, promoting or detrimental effect on the CO₂ electroreduction; underlying the complexity of such electrocatalytic reaction. This talk will present two recent studies on how the electrolytes could significantly influence the CO₂ electroreduction performance. The dramatic influence of electrolyte alkalinity in widening the potential window for CO₂ electroreduction in a flow-cell system utilized SnS catalyst will be discussed. Alkaline electrolyte was found suppressing the H₂ evolution across all potentials particularly at the less negative potentials, as well as suppress CO evolution at more negative potentials. This in turn widens the potential window for formate conversion. Mechanistic aspects of the role of alkalinity in widening the electrochemical potential window will be elucidated. In another study, seawater was employed as an electrolyte for CO₂ electroreduction. Under the applied cathodic potential and in the presence of CO₂, calcium ions in the seawater resulting in detrimental effect of calcium carbonate deposition onto the catalyst surface. We proposed a strategy in preventing calcite deposition onto the catalyst, hence enabling seawater to be used as a viable electrolyte for CO₂ electroreduction.

SESSION EN02.03: Lightning Presentations: Ab Initio/DFT Calculations and In Situ/Operando Characterization

Session Chairs: Yun Hao Ng and Francesca Maria Toma

Thursday Morning, April 22, 2021

EN02

10:30 AM *EN02.03.01

Selectivity Tuning of CO₂ Electroreduction Catalysts Under Dynamic Reaction Conditions Beatriz Roldan Cuenya; Fritz Haber Institute of the Max Planck Society, Germany

The utilization of fossil fuels as the main energy source gives rise to serious environmental issues, including global warming caused by the continuously increasing level of atmospheric CO₂. The electrochemical conversion of CO₂ (CO₂RR) to chemicals and fuels driven by electricity derived from renewable energy has been recognized as a promising strategy towards sustainable energy.

In my talk I will provide examples of the dynamic transformations undergone by well-defined CO₂RR catalysts (e.g. Cu single crystals, Cu nanocubes) under reaction conditions and their influence on the catalyst selectivity. In particular, I will discuss how important morphological motives and chemical sites can be created and regenerated in potentiodynamic (pulsed) electrochemistry experiments. Additionally, the determining role of the electrolyte in the surface restructuring, reaction activity and selectivity will be illustrated.

In situ and *operando* characterization methods (e.g. EC-AFM, Liquid-TEM, LEEM/XPEEM, XAS, XPS, XRD) will be used to gain in depth understanding on the structure- and electrolyte-sensitivity of real CO₂RR catalysts under working conditions. Our results are expected to open up new routes for the reutilization of CO₂ through its direct selective conversion into higher value products such as ethylene and ethanol.

10:55 AM EN02.03.02

Influence of Fe-Dopant Clustering on the Activity and Selectivity of MoS₂ Towards Nitrogen Reduction Reaction Akash Jain¹, Maya Bar-Sadan^{2,2} and Ashwin Ramasubramaniam¹; ¹University of Massachusetts Amherst, United States; ²Ben-Gurion University of the Negev, Israel

The Haber-Bosch process is widely used in the fertilizer industry for ammonia (NH₃) production, but it depends heavily on fossil fuels and involves very high temperatures and pressures. The electrochemical nitrogen reduction reaction (NRR) when combined with renewable sources of energy potentially offers a sustainable and fossil-fuels-free route for NH₃ production at moderate temperatures and pressures. However, for scalable NRR, a highly active, selective, and low-cost electrocatalyst is still needed, which motivates the search and rational design of NRR electrocatalysts. Recently, molybdenum disulfide (MoS₂), a layered transition metal dichalcogenide, has attracted significant interest as an NRR electrocatalyst, because of its highly catalytically active edges and defect sites on the basal plane. Yet, MoS₂ shows overall poor NRR activity and selectivity because of the high thermodynamic energy barriers, sluggish reaction kinetics, and relatively unfavorable thermodynamics than the competing hydrogen evolution reaction (HER). Here, we show that substitutional doping of MoS₂ monolayer with iron (Fe) dopants can improve significantly its NRR activity and selectivity. Using density functional theory (DFT) calculations, we study the influence of isolated Fe-dopant and clusters of Fe-dopants on the stability and local structure of MoS₂ basal plane and edges. Also, we study the thermodynamics of three competing reactions: NRR, HER, and electrochemical desulfurization reaction on the basal plane, and edges of undoped and Fe-doped MoS₂ monolayers. Key finding from our study is that Fe-doping promotes the formation of S-vacancy (V_S) sites on MoS₂ and clustering of Fe-dopants in the basal plane results in the spontaneous (thermodynamically favorable) formation of Fe-dopants and S-vacancy defect (Fe-V_S) complex. The Fe-V_S complex renders Fe and Mo atoms available for NRR reaction intermediates and substantially suppresses HER, increasing the NRR selectivity of MoS₂. Overall, our DFT calculations highlight the role of Fe-dopants in improving the NRR activity and selectivity of MoS₂ and rationalize the observations of recent experiments on Fe-doped MoS₂ nanoflowers that display significantly improved NRR faradaic efficiency and yield compared to undoped MoS₂ nanoflowers.

11:00 AM EN02.03.03

Electronic Structure Based Intuitive Design Principle of Single-Atom Catalysts for Efficient Electrolytic Nitrogen Reduction Ritesh Kumar and Abhishek K. Singh; Indian Institute of Science, India

As an alternative to the cost-and energy-intensive Haber-Bosch process, the implementation of electrolytic ammonia synthesis from the dinitrogen molecule has been a long-sought goal. State-of-the-art electrocatalysts for nitrogen reduction reaction (NRR) face not only activity but also selectivity problems with the competitive hydrogen evolution reaction (HER). Recently, single-atom catalysts (SACs) have emerged as promising for various reactions as they combine the best of homogeneous and heterogeneous catalysts. The reason for their high activity compared to their bulk and nanoparticle counterparts are yet to be completely understood. Inspired by the structure of the nitrogenase FeMo cofactor, we studied 13 transition metals anchored on MoS₂ monolayer at Mo-top positions, as possible electrolytic NRR catalysts using first-principles methods. Employing the implicit solvation model, we calculated free energy barriers for proton abstraction by N₂ molecule in end-on configuration and adsorption free energy of hydrogen on all SACs. Based on these two parameters, Fe, Co, and Ru were found to be the most active and highly selective electrolytic NRR catalysts. Compared with other mechanisms, the limiting potentials (and hence activity) for enzymatic mechanisms were found to be higher on these three SACs, with Ru SAC having a very low overpotential of 0.38V versus Standard Hydrogen Electrode (SHE). Bader charge transferred from transition metal to N₂ molecule and group number of transition metals correlate strongly with the NRR activity and hence emerge as two key descriptors for catalytic activity. These intuitive principles for rational designing of promising alternatives to the currently used bulk Ru(0001) catalyst could accelerate the search for highly efficient and selective SACs for electrolytic NRR.

11:05 AM EN02.03.04

Mechanistically Understanding of PEC Self-Improving Si/GaN Photocathode Using Suite of Advanced Characterization Techniques and First-Principle Calculation Guosong Zeng¹, Tuan Anh Pham², Srinivas Vanka³, Guiji Liu¹, Zetian Mi³, Tadashi Ogitsu² and Francesca Maria Toma¹; ¹Lawrence Berkeley National Laboratory, United States; ²Lawrence Livermore National Laboratory, United States; ³University of Michigan–Ann Arbor, United States

To advance the application of solar water splitting for renewable energy, tremendous works have been put on the development of state-of-the-art protective coatings for long-term stability and high efficiency, whereas more effort needs to be focused on the fundamental study of materials' stability/degradation mechanisms. In this work, we report Si/GaN photocathodes for sustained hydrogen production via a self-improving mechanism. By employing state-of-the-art characterization techniques, we show the presence of an oxynitride-like layer, which behaves similarly to electrocatalyst for better mediating charge transfer. DFT simulation shows that replacing the nitrogen atoms by oxygen to form oxynitride can not only passivate the surface for further stability, but also provide more active sites for HER. This work also sets a prototype for fundamental understanding of stability mechanism of protective layers in PEC water splitting application, and the gained knowledge provides feedback for development of further improved design of durable and efficient photoelectrode.

11:10 AM EN02.03.06

Late News: Operando Spectroelectrochemical Observation of Surface States and Active Sites in Chalcopyrite Photocathodes for Solar Water Reduction Yongpeng Liu, Néstor Guijarro and Kevin Sivula; Swiss Federal Institute of Technology Lausanne (EPFL), Switzerland

Photoelectrochemical (PEC) water splitting is emerging as a technology that could potentially sustain a low-carbon hydrogen-based economy. Among the different photoactive materials suitable for operation in a PEC device, Cu(In,Ga)S₂ (CIGS) is drawing increasing attention as a photocathode owing to its outstanding optoelectronic properties and tunable band gap. However, serious bottlenecks for the implementation of this material arise from the costly fabrication of PV-grade thin-films using non-scalable vacuum techniques, and the need for overlayers/catalysts to extract charges and perform the hydrogen evolution reaction.

Recently, we reported an all-solution-processed CIGS photocathode that demonstrates a significant and stable photocurrent response towards water reduction, even in the absence of overlayers or co-catalysts. Although the photocurrent onset potential is substantially negative with respect to the flat-band potential, the bare CIGS photocathode offers an intriguing system for gaining fundamental insights. Motivated by its intrinsic catalytic

properties and unsatisfactory photovoltage, we combined three complementary operando spectroelectrochemical techniques including photoelectrochemical impedance spectroscopy (PEIS), intensity-modulated photocurrent spectroscopy (IMPS) and operando Raman spectroscopy with density-functional theory (DFT) calculations to understand the fate of photogenerated charge carriers. Through PEIS, photoluminescence spectroscopy and DFT calculations, we resolved atom-specific surface trapping states that restrict the photovoltage of CIGS. In addition, we performed the first operando Raman study on CIGS photocathodes where we identified the catalytically active sites. Computational methods further confirm these sites requiring the least free energy to adsorb protons for hydrogen evolution reaction. Overall, these fundamental findings suggest the composition of an improved surface for defect passivation and active sites exposure, which paves the way for rational design of this material for PEC water reduction.

11:15 AM EN02.03.10

Late News: Electronic Excitations of α -Fe₂O₃ Thin Films Measured by Resonant Inelastic X-Ray Scattering at the Fe L_{III}-Edge—Momentum, Temperature and Dopant Dependence David S. Ellis¹, Ru-Pan Wang^{2,3}, Deniz Wong⁴, Jason K. Cooper⁵, Christian Schulz⁴, Yi-De Chuang⁵, Yifat Piekner¹, Daniel Grave^{1,6}, Markus Schleuning⁷, Dennis Friedrich⁷, Frank M. de Groot⁸, Roel Van de Krol⁷ and Avner Rothschild¹; ¹Technion–Israel Institute of Technology, Israel; ²University of Hamburg, Germany; ³Deutsches Elektronen-Synchrotron DESY, Germany; ⁴Helmholtz-Zentrum Berlin für Materialien und Energie, Germany; ⁵Lawrence Berkeley National Laboratory, United States; ⁶Ben-Gurion University of the Negev, Israel; ⁷Helmholtz-Zentrum Berlin für Materialien und Energie GmbH, Germany; ⁸Debye Institute, Utrecht University, Netherlands

Hematite (α -Fe₂O₃) is a promising candidate for a photoanode material for photo-electrochemical hydrogen production, meeting several key criteria. A photoanode's performance depends on optical absorption and electronic transport, which are manifestations of its electronic structure. In spite of hematite's Earth abundance and deceptively simple chemical formula, the electronic and magnetic interactions arising from its Fe *d*⁵ orbitals and neighboring oxygens, and longer range interactions, is surprisingly intricate. Here we interrogate hematite's electronic structure with Resonant Inelastic X-Ray Scattering (RIXS). After a brief introduction to the technique, we present our Fe L_{III}-edge RIXS spectra of heteroepitaxial hematite thin films, both undoped and variously doped, measured for several momentum transfers (**q**), at both low temperature (T=14K) and room temperature. Although there could be some weakly dispersive excitations present in the spectra, a possible sign of charge transfer excitations, we conclude that the bulk of the observed L_{III}-edge RIXS intensity in the visible range originates from ligand-field d-d excitations, which is corroborated with the help of spin-multiplet simulations. The temperature dependence, which showed some highly temperature-sensitive features, identically for undoped, 1% Sn-doped, and 1% Zn-doped samples, is discussed.

11:20 AM ORAL Q&A

11:40 AM EN02.03.07

Late News: Electronic Structure Modulation of Manganese Incorporated Ni₂P Leading to Enhanced Activity for Water Splitting Lakshay Dheer; Jawaharlal Nehru Centre For Advanced Scientific Research, India

The cornerstone of the emerging hydrogen economy is hydrogen production by water electrolysis with concomitant oxygen generation. Incorporating a third element in metal phosphides can tune the crystalline and electronic structure, hence improving the electrocatalytic properties. In this work using first-principles theoretical calculations, Mn-substituted Ni₂P has been explored as an excellent catalyst for water splitting. The catalytic activity of Ni₂P improves drastically on Mn-substitution for hydrogen evolution reaction as we obtain a close to optimum ΔG_H (-0.14 eV) and the work function of Ni_{1.5}Mn_{0.5}P which falls just below the hydrogen reduction potential. The oxygen evolution activity of Ni₂P is also explored upon Mn-substitution. We find a 32% reduction in the overpotential (η) towards OER for Ni_{1.5}Mn_{0.5}P. The effect of surface oxygen (metal-

oxides) species on the catalytic performance of Ni_{1.5}Mn_{0.5}P is further studied and the η further reduces thus improving the OER activity of the catalyst. We show that substitution of a second metal species in metal phosphides alters the electronic structure and induces synergistic interactions in the system leading to an enhanced catalytic activity towards water splitting.

11:42 AM POSTER Q&A

11:54 AM *EN02.03.09

Understanding Charge Transport in Transition Metal Oxides with Novel First-Principles Computational Methods Marco Bernardi; California Institute of Technology, United States

Advances in first-principles calculations enable accurate predictions of charge carrier mobility and scattering mechanisms in semiconductors. However, many transition metal oxides of technological interest remain an open problem as they exhibit soft phonon modes due to structural phase transitions, strong electron-phonon (e-ph) interactions leading to polaron effects, and electron correlation due to open *d* shell, or combinations of these features.

This talk will present a range of new ab initio approaches for treating e-ph interactions and charge transport in oxides. We will first present methods to address soft phonon modes and large-polaron effects, and demonstrate their application to SrTiO₃ perovskite as a paradigmatic case. A recent study of a wide range of oxides with room temperature mobilities ranging from low to high will then be presented, highlighting materials design rules for high mobility. The second part of the talk will focus on recent progress, including studies of e-ph interactions in the frameworks of DFT+U and dynamical mean field theory, and their application to understanding the transport properties of various transition metal oxides. If time permits, we will briefly discuss a new approach to predict the formation of self-localized (small) polarons in oxides with inexpensive e-ph calculations.

SESSION EN02.04: Lightning Presentations: (Photo)electrochemical Engineering of Reactions and Devices II

Session Chairs: Fatwa Abdi and Simelys Hernandez

Thursday Afternoon, April 22, 2021

EN02

1:00 PM *EN02.04.01

Modeling, Design and Optimization of Robust Photoelectrodes Sophia Haussener; EPFL, Switzerland

Photoelectrochemical (PEC) approaches for the processing of solar fuels and materials are interesting, provided they can be efficiently, stably, scalably, and sustainably implemented.

There is still significant process required on the development of earth abundant and efficient but also stable and robust materials. The rapid identification of novel and promising photoelectrode materials or components is needed in order to provide a faster turnover of potential novel candidate materials (and different synthesis processes). Identifying and quantifying the key parameters limiting the efficiency and the stability of the photoelectrodes is fundamental to providing material and mesostructural design guidelines. This quantification is experimentally not accessible given by the multi-physical nature of the processes taking place in the photoelectrodes. Computational modeling can provide the necessary insights but requires the detailed knowledge of material parameters that are often unknown for new photoelectrode materials and requires to account for the complex mesostructure of the photoelectrode.

First, I will discuss versatile and validated computational models that allow for the material characterization, material parameters optimization, and mesostructural optimization of photoelectrodes. I will distinguish between involved multi-dimensional and multi-scale models and rapid screening models based on analytical

correlations. I will then show how models can be extended to incorporate degradation (specifically photocorrosion) processes in order to understand and increase stability. I will show how important the local reaction environment is for the stability of a component, and how heterogeneity in the operating variables (current density, species concentration, temperature, etc.) affect degradation. I will end with providing general guidelines on materials and component integration into efficient and stable photoelectrodes and full devices, while also discussing the robustness of material and device efficiency and stability when exposed to varying, non-design-point operating conditions (such as will be expected in on-sun operation).

1:25 PM *EN02.04.02

Recent Progress on Oxide-Based Tandem Devices for Solar Water Splitting Roel Van de Krol^{1,2};

¹Helmholtz-Zentrum Berlin für Materialien und Energie GmbH, Germany; ²Technische Universität Berlin, Germany

Practical photoelectrochemical devices for solar water splitting should generate photovoltages in excess of 1.7 V to reach viable efficiencies. Currently, the only practical way to achieve this is to combine two or more absorbers in a tandem configuration. With silicon being a nearly ideal candidate as a bottom absorber, the main challenge is to find a suitable top absorber material that combines good chemical stability with a bandgap of around 1.9 eV. I will discuss recent progress on $\text{Cu}_5\text{V}_2\text{O}_{10}$, $\text{b-Cu}_2\text{V}_2\text{O}_7$, $\alpha\text{-SnWO}_4$, and CuBi_2O_4 , all of which have a bandgap that is close to the ideal value. We have synthesized all these materials with pulsed laser deposition in an attempt to obtain films of high electronic quality. Although all these materials show relatively modest photocurrents, some show surprisingly high photovoltages and reasonable stability under certain conditions. The opportunities for these materials and challenges that have to be addressed will be critically discussed. In the second part, I will show several examples of tandem water splitting devices. One is an all-oxide device based on $\text{p-CuBi}_2\text{O}_4$ and W:BiVO_4 , the second is based on a top absorber of nanostructured $\text{WO}_3/\text{BiVO}_4$ with a flat silicon wafer as a bottom absorber. I will finish with some considerations on the scale-up of these devices and show some recent results on the importance of natural convection near electrode surfaces.

1:50 PM EN02.04.03

High Throughput Evaluation of Multi-Element, Multi-Functional Coatings for Improved Photoanodes

and Photocathodes Joel Haber¹, Zemin Zhang², Guiji Liu², Aniketa Shinde¹, Lan Zhou¹, Dan Guevarra¹, Ryan Jones¹, Kevin Kan¹, John Gregoire¹, Francesca Maria Toma² and Jason K. Cooper²; ¹California Institute of Technology, United States; ²Lawrence Berkeley National Laboratory, United States

The development of efficient, stable photoanodes and photocathodes remains a primary materials challenge in the establishment of a scalable technology for artificial photosynthesis. The typical photoelectrode architecture consists of a semiconductor light absorber coated with a metal oxide that serves a combination of functions, including corrosion protection, electrocatalysis, light trapping, carrier transport, and elimination of deleterious surface recombination sites. We describe high throughput investigations of the variation in performance and photo-response of integrated photoanode and photocathode libraries. The photoanode assembly libraries consist of uniform BiVO_4 light absorbers coated with films varying in composition and loading and evaluated at pH 9 and 13. The photocathode assembly libraries, for example, consist of uniform CuBi_2O_4 light absorbers coated with film libraries varying in composition and loading. Photoelectrode assemblies based on promising coating compositions and loadings were characterized in detail.

1:55 PM EN02.04.05

Late News: Semi-Monolithic Tandem Solar Cell Architecture for Photoelectrochemical Water Splitting

Kai C. Outlaw-Spruell, Joshua Crunk, Wilman Septina and Nicolas Gaillard; Hawaii Natural Energy Institute, United States

Tandem devices are necessary architectures for unassisted photoelectrochemical water splitting because of their ability to maximize the power conversion efficiency and provide a high photo-voltage necessary to drive the

reaction. The traditional tandem integration process involves a monolithic tandem stack where the wide bandgap top cell is grown onto the narrow bandgap bottom cell, which places limitations on material selection and fabrication processes due to restrictions such as deposition techniques and temperature. To overcome this challenge and provide flexibility in material selection and manufacturing processes, a semi-monolithic tandem device architecture is investigated.

The semi-monolithic tandem device architecture is a novel approach of tandem cell manufacturing aimed at providing cost-effective, scalable photoelectrochemical water splitting technology. This technique employs a lift off and transfer method to combine two independently processed cells into one cell architecture using a transparent conductive adhesive (TCA) to create a multi-junction photovoltaic stack. This allows combination of materials which a standard deposition technique would not allow due to bottom cell degradation during deposition.

In this communication, we report of our latest results to integrate wide bandgap chalcopyrite absorbers into semi-monolithic tandem devices for PEC water splitting. Being an essential steppingstone in the semi-monolithic tandem manufacturing process, characterization of the relative conversion efficiency of a single junction solar cell before and after the lift off process was investigated. The cell was exfoliated using a soda lime glass substrate and a TCA that exhibited ~90% transmittance from 300-2000 nm as well as an out-of-plane series resistance on the order of $10^{-1} \Omega\text{-cm}^2$ (comparable to that of molybdenum in Cu(In,Ga)Se₂ solar cells). Using a 1.8 eV CuGa₂Se₅ cell integrated with CdS, ZnO and ITO, our results showed that approximately 100% of the baseline efficiency, short-circuit photocurrent density and open-circuit voltage was preserved after exfoliation. Then, the wide bandgap device was integrated with a 1.1eV narrow bandgap silicon solar cell using our lift-off/transfer technique to create a semi-monolithic tandem device. An open circuit voltage (Voc) of 1.2V was obtained, corresponding to over 83% of the sum of the sub-cells Voc. These promising results confirm the viability of the semi-monolithic approach to create efficient tandem devices for PEC water splitting.

2:00 PM EN02.04.06

Multifunctional CoMoO₄ for Supercapacitors, Oxygen Evolution and Methanol Oxidation Tenzin Ingsel, Felipe de Souza, Ram Gupta and Khamis Siam; Pittsburg State University, United States

The depletion of nonrenewable fossil fuels and its adverse impact on the environment has intensified the search for alternative, sustainable, and clean energy sources for the last several decades. Concurrently, the researchers have focused on designing and developing innovative materials to convert and efficiently store energy. Oxides and sulfides of transition metals have become the state-of-the-art material for energy conversion and storage, mainly attributed to their rich faradic reaction in electrode-electrolyte interface. These materials' potential applications have been extensively studied for electrode material in batteries, supercapacitors, electrocatalyst for water splitting, and fuel cell applications. In this project, metal molybdate CoMoO₄ was prepared via two different methods, binder-free/in situ and dip coating. The two different CoMoO₄ electrodes' specific capacitance was calculated at different current densities and scan rates. Sharp differences between the two electrodes were observed regarding how much specific capacitance they can deliver based on various current densities and scan rates. The in-situ electrode displayed a specific capacitance of 2853 F/g, whereas the dip-coated achieved 357 F/g, both recorded at 1 mV/s. When the OER performances of CoMoO₄ in situ and dip-coated electrodes were compared, in situ CoMoO₄ required a lower overpotential of 324 mV whereas, dip-coated electrodes exhibited 381 mV, both at 10 mA/cm². In situ CoMoO₄ showcased faster kinetics with a more downward Tafel slope of 70 mV/dec compared to dip-coated electrode with 90mV/dec. With the introduction of 0.5 M methanol in the 1M KOH electrolyte, an improved current density signal was observed in both the electrodes. A current density signal of 200 mA/cm² (@20 mV/s) and 25 mA/cm² (@20 mV/s) with and without 0.5 M methanol were observed in dip-coated CoMoO₄. With 0.5 M methanol in electrolyte, an improved current density signal of 135 mA/cm² was obtained in the binder-free electrode from an initial current density signal of 30 mA/cm² (@20 mV/s). Such findings indicate the facile construction of molybdate-based electrocatalysts for methanol oxidation.

2:02 PM Q&A

2:25 PM *EN02.04.07

The Optical Properties and Electronic Structure of CuBi₂O₄ and the Spatiotemporal Dynamics of Photoexcited Plasmonic Gold Nanospheres for Applications in Light Driven Chemistry Jason K.

Cooper^{1,2,3}; ¹Joint Center for Artificial Photosynthesis, United States; ²Lawrence Berkeley National Laboratory, United States; ³Liquid Sunlight Alliance, United States

The economies of the future and the sustainability of the planet's ecosystems will rely on green energy technologies such as through the capture of sunlight to drive chemical transformations. In particular, light-harvesting photoelectrodes dictate the generation of photovoltage and photocurrent so understanding the underlying physics governing performance and stability limitations are critical to advance related technologies. Specifically, CuBi₂O₄ is a natively p-type semiconductor with 1.5 – 1.8 eV optical bandgap; as a photocathode it has been demonstrated to have a photocurrent onset potential greater than 1 V_{RHE} yet remains limited to about 1.5 mA cm⁻². In this investigation we characterize the electronic structure (valence and conduction band orbital composition) of the material using a suite of advances spectroscopic techniques in conjunction with DFT modeling. These results suggest the limited electron polaron diffusion length of 45 nm is related to charge localization at Cu 3d states in the conduction band. Photoelectrodes made of plasmonic nanostructures are interesting for energy conversion applications due their dual function acting both as catalytic centers and light absorbers thus localizing the light energy directly at the catalytic site. Hollow-gold nanospheres (HGNs), thin shells of gold which can be readily dispersed in water, have a plasmon resonance absorption which can be tuned from 520 nm to the near infrared based on the shell diameter and thickness making them excellent structures to harvest a large portion of the terrestrial solar flux. After the plasmon is excited, the energy is rapidly converted to heat the particle. In this study, through a combination of transient absorption (TA) spectroscopy and full scale molecular dynamics (MD) on 30 nm particles surrounded by water, the spatiotemporal temperature and pressure profiles reveal that photoexcitation of the HGN creates a high temperature and high-pressure environment particularly suited for thermal catalysis. These studies taken together identify an unique opportunity for coupled reaction micro-environments to take advantage of photoelectrochemical and photothermal reaction mechanisms.

SESSION EN02.05: Lightning Presentations: (Photo)electrocatalysis—Novel Materials and Understanding I
Session Chairs: Yun Hao Ng and Francesca Maria Toma
Thursday Afternoon, April 22, 2021
EN02

8:15 PM *EN02.05.01

Application of Photocorrosive Metal Sulfide Photocatalysts to Artificial Photosynthetic Reactions Akihiko Iwase; Meiji University, Japan

Artificial photosynthesis including water splitting and CO₂ fixation using photocatalysts is an attractive research field toward realizing sustainable society. The metal sulfides with narrow band gaps are a promising material group as a photocatalyst for hydrogen evolution under visible light irradiation. Although the metal sulfide is a favorable material for visible light absorption, the metal sulfide itself is oxidized by photogenerated holes (photocorrosion). We have successfully utilize metal sulfide photocatalysts in Z-schematic water splitting and CO₂ reduction upon using a reduced graphene oxide as a solid-state electron mediator.¹⁻³ In the present study, we will present the successfully developed and improved Z-scheme systems using the metal sulfides prepared by a flux method with various alkaline chloride salts.

A single phase of metal sulfides was successfully prepared by a solid-state reaction and a flux method with various flux alkaline chloride salts. The particle size and aggregation degree depended on the preparation temperature in the flux method. Highly crystalline large particles were obtained at high temperature. The

particle size was smaller than that of a solid-state reaction. All samples showed photocatalytic activity for sacrificial H₂ evolution under visible light irradiation. The metal sulfides prepared by the flux method showed the higher activity for sacrificial H₂ evolution than that prepared by a conventional solid-state reaction. The metal sulfide prepared by the flux method also functioned as a H₂-evolving photocatalyst in the Z-scheme systems with a reduced graphene oxide as an electron mediator. The solar water splitting activity was higher than that using the metal sulfide prepared by a solid-state reaction.⁴⁾ The Z-scheme system was also active for CO₂ reduction under visible light irradiation.

Thus, we successfully developed and improved Z-scheme systems for water splitting and CO₂ reduction using photocorrosive metal sulfide photocatalysts under visible light irradiation.

1) K. Iwashina, A. Iwase, Y. H. Ng, R. Amal, A. Kudo, *J. Am. Chem. Soc.* **2015**, *137*, 604.

2) A. Iwase, S. Yoshino, T. Takayama, Y. H. Ng, R. Amal, A. Kudo, *J. Am. Chem. Soc.* **2016**, *138*, 10260.

3) T. Takayama, K. Sato, T. Fujimura, Y. Kojima, A. Iwase, A. Kudo, *Faraday Discuss.* **2017**, *198*, 397.

4) S. Yoshino, A. Iwase, Y. H. Ng, R. Amal, A. Kudo, *ACS Appli. Energy Mater.* **2020**, *3*, 5684.

8:40 PM *EN02.05.02

Electrolyte Engineering for Water Splitting Tatsuya Shinagawa; The University of Tokyo, Japan

Converting the water molecule that sits at the bottom of the free energy landscape into hydrogen can serve as a core-technology in the future sustainable society, if driven by renewable energy sources. Photocatalytic and photoelectrochemical water splitting falls in this category of technologies, which proceeds, upon the irradiation of light, via a complex photophysical and electrocatalytic process involving photon absorption, exciton separation, carrier diffusion, carrier transport, surface reaction, and mass-transport.^[1,2] Achieving solar hydrogen production at a high efficiency thus requires these steps to function efficiently and simultaneously despite of their differing time scales, however, the complex reaction network hinders its quantitative understanding and thus rational designing. Notably, by decoupling the steps, the photophysical and electrocatalytic events during water splitting can be independently addressed, which would shed light on the system and pave a way for its development.^[1,2]

This contribution describes the electrocatalytic water splitting at near-neutral pH levels, whose milder condition than the extreme pH counterparts is compatible with photocatalytic and photoelectrochemical systems, with a particular focus placed on the electrolyte.^[3-7] Electrocatalytic water splitting at the near-neutral pH levels experiences a reactant-switching.^[3] The hydrogen evolution reaction (HER) proceeds as the reduction of proton at smaller reaction rates, which switches to that of the water molecule at higher reaction rates due to the diffusional constraints of the proton. Likewise, the oxygen evolution reaction (OER) proceeds as the oxidation of the hydroxide ion and the water molecule at lower and higher reaction rates, respectively. Adding the buffering species, e.g., phosphate, into the solution mitigates such local pH alteration by in-situ providing the proton and hydroxide ions, although beyond this simple buffering action, the added buffering species plays a variety of decisive roles.^[3-6] For instance, the molality of the buffering species needs to be sufficiently high to attain improved buffering capacity for maintaining the local pH levels, which however is counterbalanced by the enlarged viscosity at high molalities, resulting in a slowed mass-transport flux of the buffering species.^[3,4] Also, the identity of ions, either kosmotropic or chaotropic, has similarly large influences on the electrolysis. Particularly, at molalities higher than 0.1 mol kg⁻¹, the mean activity coefficient of the added ions is no longer unity, and the association of the ions need to be taken into account that is determined by the identity and combination of the ions.^[3,5] All in all, looking at the electrolysis from the viewpoint of electrolyte quantitatively elucidates the bottleneck of the water splitting at the near-neutral pH levels and provides the guideline to improve its performance, highlighting the significance of *electrolyte engineering*.^[3] The aspect of electrolyte engineering detailed herein can be extended to the regulation of the gas cross-over during water splitting and quantitative understanding of mass-transport during photocatalytic water splitting.

References:

[1] K. Takanabe, *ACS Catal.* **2017**, *7*, 8006-8022.

[2] T. Shinagawa, Z. Cao, L. Cavallo, K. Takanabe, *J. Energy Chem.* **2017**, *26*, 259-269.

[3] T. Shinagawa, K. Takanabe, *ChemSusChem* **2017**, *10*, 1318-1336.

- [4] T. Shinagawa, K. Takanabe, *J. Phys. Chem. C* **2015**, *119*, 20453-20458.
[5] T. Shinagawa, K. Takanabe, *J. Phys. Chem. C* **2016**, *120*, 1785-1794.
[6] T. Shinagawa, K. Obata, K. Takanabe, *ChemCatChem* **2019**, *11*, 5961-5968.
[7] T. Naito, T. Shinagawa, T. Nishimoto, K. Takanabe *ChemSusChem*, accepted. DOI: 10.1002/cssc.202001886

9:05 PM BREAK

9:20 PM EN02.05.03

Rational Design of Photoelectrocatalytic Materials for CO₂ Reduction [Guiji Liu](#); Lawrence Berkeley National Laboratory, United States

Due to the rapid depletion of fossil fuels and related environmental issues, developing technologies for producing renewable, clean fuels for our future is of great importance. Artificial photosynthesis via CO₂ reduction offers an attractive and cost-effective route to achieve this goal. However, the uncontrollable chemical transformations of existing photoelectrocatalytic materials under operating conditions greatly limit their applications for artificial photosynthesis technologies. Understanding their chemical transformations is a prerequisite to achieve sustainable energy conversion and storage into chemical bonds. Herein, we unravel the transformation mechanisms of photoelectrodes by systematic chemical and photoelectrochemical analysis and consequently provide an efficient protection scheme for light driven CO₂ reduction, using cuprous oxide as a model system.

9:25 PM EN02.05.05

Hierarchical Bimetallic Phosphide of Ni₂P-Cu₂P on Ni-Foam-Graphene-CNTs Substrate—Efficient and Super-Stable Electrocatalyst for Overall Water Splitting [Sk Riyajuddin](#)¹, Mansi Pahuja¹, Sushil Kumar¹, Takahiro Maruyama² and Dr Kaushik Ghosh¹; ¹Institute of Nano Science and Technology, India; ²Meijo University, Japan

The depletion of fossil fuels and the increase in environmental pollution have quest the scientific society to develop renewable and environment-friendly resources that can fulfill the needs of energy demands. Amidst all the existing clean energy resources, hydrogen energy is the most economical and has already captured a prime place in recent technological developments. Having high energy density, hydrogen can stand as an alternative to traditional fossil fuels. Water splitting via the electrochemical process to generate hydrogen for a fuel cell is an economic and green approach to resolve the looming energy and environmental crisis. It involves two half-cell redox reactions i.e. cathodic hydrogen evolution reaction-HER ($2\text{H}^+ + 2\text{e}^- \rightarrow \text{H}_2$) and anodic oxygen evolution reaction-OER ($4\text{OH}^- \rightarrow \text{O}_2 + 2\text{H}_2\text{O}$) but due to their sluggish kinetics, its desires to develop highly active electrocatalysts to accelerate the electron transfer process. So far, the precious noble metals like Pt (for HER) and RuO₂/IrO₂ (for OER) have been proven to be the best electroactive catalyst but their extortionate cost and dearth restrain the industrial-grade applications. Besides that, these noble metals (Pt, RuO₂, IrO₂) are incompetent to make their position in the same electrolyte for continuous overall water splitting. Developing cheap, stable, scalable, and efficient electrocatalyst is in need to explore the suitable cost-effective replacement of noble metal-based electrocatalyst for future scale-up industrial viability. Herein, we report a rationally design seamless super-hydrophilic homogeneous bimetallic phosphide of Ni₂P-Cu₂P on Ni-foam-Graphene-CNTs heterostructure using facile electrochemical metallization followed by phosphorization without the intervention of metal oxides or hydroxides. The bimetallic phosphide shows extraordinary water electrolysis activity in terms of ultra-low overpotential (HER-12 mV@10 mA/cm², 124 mV@100 mA/cm² in acid medium and OER-140 mV@20 mA/cm², 190 mV@50 mA/cm² in basic medium) and high turn-over frequency (1s⁻¹@100 mV for HER and 1s⁻¹@310 mV for OER). The excellent stability at least for 10 days at a high current density of 500 mA/cm² without much deviation, infers the practical utilization of the novel catalyst towards green fuel production. The low Tafel slope (41 mV/dec for both HER and OER), low charge transfer resistance (18 ohm-HER), large electrochemical active surface area (959 cm²-HER, 630 cm²-OER), and large active site density (4.26x10⁻⁴ mol/cm²-HER, 2.12x10⁻⁴ mol/cm²-OER) indicating super electrocatalytic properties. The versatility

of the catalyst has been observed when it shows remarkable performance in overall water splitting with a very low cell voltage of 1.45 V @10 mA/cm² in 1M KOH solution and long-term stability up to 40 hours with minimum loss (3%) of current density. The theoretical density functional study reveals that H-binding energy distribution among P-sites of CuP₂ and Ni₂P and d-band sifting among metal atoms in the heterostructure (Ni₂P-CuP₂) favour the HER and OER activity, respectively. Besides, the catalyst demonstrates an alternate transformation of solar energy to green H₂ production using a standard silicon solar cell. This research unveils a new avenue to design and synthesize highly stable electrocatalyst against an attractive paradigm of commercial water electrolysis for renewable electrochemical energy conversion.

9:30 PM ORAL Q&A

9:42 PM EN02.05.07

Late News: Electrochemical Methane Conversion with CuO/CeO₂ Catalysts Jaehyun Lee, Jiwoo Yang and Jun Hyuk Moon; Sogang University, Korea (the Republic of)

The oxidation of methane, driven by electrochemical potential, is desirable as a strategy to overcome the low selectivity in thermochemical catalytic reactions, but improving productivity remains a challenge. We demonstrate the electrochemical conversion of methane to methanol in a CuO/CeO₂ oxide catalyst. We confirm the highest methane oxidation activity at Cu:Ce=6:4. we achieve the highest production rate of 752.9 μmol/g_{cat}/hr (6 hr reaction) at ambient pressure; Among the oxygenates, a CH₃OH selectivity of 79% is obtained. In a high pressure reaction at 10 bar, productivity of 1,832.2 μmol/g_{cat}/hr and 21,986.6 μmol/g_{cat} is achieved. We confirm the formation of methanol by oxidation of methane by active oxygen on the catalyst, and also present a side reaction pathway by further oxidation of methanol.

9:44 PM POSTER Q&A

9:50 PM *EN02.05.08

Molecular-Semiconductor Hybrid Systems for Photocatalytic and Electrochemical CO₂ Reduction Takeshi Morikawa; Toyota Central R&D Labs., Inc., Japan

For the development of systems to convert CO₂ into useful energy-rich chemicals under sunlight or electrical energy, the use of metal-complex catalysts is one of attractive approaches because CO₂ selectivity and reaction rates can be controlled by ligand modification [1]. The combination with semiconductor photosensitizers is also one of promising approaches to promote the reaction under photoirradiation. To realize a CO₂ reduction system which utilizes water molecule as an electron donor in the CO₂ reduction reaction (CO₂RR), we previously proposed the a hybrid molecular-catalyst/semiconductor system for the visible-light driven CO₂RR, and demonstrated systems of particulate photocatalyst and photoelectrode utilizing Ru-bipyridine complex polymer catalysts linked with semiconductors of N-doped Ta₂O₅[2], GaP:Zn[3], InP:Zn[4], (CuGa)_{0.8}Zn_{0.4}S₂[5], (AgIn)_{0.22}Zn_{1.56}S₂[4], ZnS:Ni[4], etc. The photoelectrode system demonstrated a monolithic tablet-formed device, and it generated formate with a solar-to-chemical conversion efficiency (E_{solar}) of 4.6 % in an aqueous solution [4]. DFT calculation and related experiments clarified that the very low onset potential (-0.18 V vs RHE) for CO₂ reduction at the Ru-bipyridine complex is dependent on combination of carbon support and K⁺ in solution, which enabled the demonstration of the monolithic device [6].

One recent topic is a visible-light-driven Z-schematic CO₂ reduction using H₂O as an electron donor in aqueous particulate suspension which can be operated in a simple mixture of [Ru(4,4'-diphosphonate-2,2'-bipyridine)(CO)₂Cl₂] ([Ru(dpby)]) modified (CuGa)_{1-x}Zn_{2x}S₂ (CGZS) hybrid photocatalyst as a CO₂ reduction, BiVO₄ photocatalyst as a water oxidation and Co-complex as an electron mediator [7]. The CO₂ reduction activity was significantly dependent on the composition of CGZS, and utilization of [Ru(dpby)]/CGZS at x=0.7 ($E_g = 2.36$ eV) showed the highest Z-schematic CO₂ reduction activity for CO and HCOO⁻ production accompanying O₂ generation under visible-light irradiation. The very high CO₂ reduction selectivity exceeding 90 % under visible light irradiation as the aqueous particulate suspension suggests that particulate Z-schematic reaction is also applicable to the highly selective and efficient photocatalysis for solar fuel generation by CO₂

fixation.

As for the electrochemical system, our recent approach is the use of earth-abundant elements. As well as lowering system costs, reduction in CO₂ emissions from raw materials mining to final catalyst synthesis further confirms the feasibility of this earth-abundant systems. A silicon photovoltaic cell (Si-PV) was connected to a [Mn-bpy] cathode for CO₂RR [5] and an β -FeOOH anode combined with Ni hydroxide for OER [8, 9]. The system operated in a one-compartment reactor filled with pH 6.9 aqueous solution saturated with CO₂ [10], and exhibited E_{solar} of over 10 % in production of mixture of CO and H₂ as syngas.

- References

- [1] K. Kamada, S. Saito et al., *J. Am. Chem. Soc.* **2020**, 142, 10261–10266.
- [2] S. Sato, T. Morikawa, et al, *Angew. Chem. Int. Ed.* **2010**, 49, 5101-5105.
- [3] S. Sato, T. Arai, T. Morikawa, et al., *J. Am. Chem. Soc.*, **2011**, 133, 15240-15243.
- [4] T. M. Suzuki, A. Kudo, T. Morikawa, *Applied Catalysis B: Environmental* **2018**, 224, 572–578.
- [5] T. Arai, S. Sato, T. Morikawa, *Energy Environ. Sci.*, **2015**, 8, 1998-2002.
- [6] S. Sato, et al., *ACS Catal.* **2018**, 8, 4452–4458.
- [7] T. M. Suzuki, A. Kudo, T. Morikawa, et al., *Chem. Commun.*, **2018**, 54, 10199-10202
- [8] T. M. Suzuki, et al., *Sustainable Energy Fuels*, **2017**, 1,636-643.
- [9] T. M. Suzuki, T. Morikawa, et al., *Bull. Chem. Soc. Jpn*, **2018**, 91, 778–786.
- [10] T. Arai, et al., *Chem. Commun.*, **2019**, 55,237-240.

SESSION EN02.06: Lightning Presentations: (Photo)electrochemical Engineering of Reactions and Devices III
Session Chairs: Fatwa Abdi and Yun Hao Ng
Friday Morning, April 23, 2021
EN02

8:25 AM EN02.06.02

α -SnWO₄ Photoelectrodes Prepared by Pulsed Laser Deposition—An Overview of the Recent Progress

Patrick Schnell, Moritz Kolbach, J. Mark C. M. Dela Cruz, Markus Schleuning, Keisuke Obata, Rowshanak Irani, Ibbi Y. Ahmet, David E. Starr, Roel Van de Krol and Fatwa F. Abdi; Helmholtz-Zentrum Berlin für Materialien und Energie, Germany

Direct photoelectrochemical hydrogen production is a promising route towards a clean and sustainable energy supply. To obtain high solar-to-hydrogen (STH) efficiencies, a suitable semiconducting material with a band gap of 1.7 to 1.9 eV is needed as the top absorber in tandem solar water splitting devices [1]. An interesting candidate is α -SnWO₄, a ternary metal oxide with an ideal band gap of 1.9 eV and a flatband potential of ~ 0 V vs. RHE. Several deposition methods have been used for the deposition α -SnWO₄ thin films. The highest reported photocurrent so far of 0.75 mA/cm² has been achieved by pulsed laser deposited (PLD) α -SnWO₄ films covered with an NiO_x overlayer [2].

In this study, we provide an overview of our current understanding of α -SnWO₄ films prepared by pulsed laser deposition. First, although the deposition of NiO_x is crucial to obtain the above-mentioned record photocurrent, it limits the photovoltage as observed from the cyclic voltammetry and open circuit potential analysis (OCP). This suggests that the interface between α -SnWO₄ and NiO_x is not ideal, and understanding this interface is important to improve the performance further. We therefore present a thorough α -SnWO₄/NiO_x interface investigation by means of synchrotron-based hard X-ray photoelectron spectroscopy (HAXPES). These data are complemented with OCP analysis and Monte-Carlo-based photoemission spectra simulation. Our study reveals that the deposition of NiO_x with PLD introduces a strong upwards band bending (~ 400 meV) at the interface, which is favorable for charge separation. However, significant oxidation of Sn²⁺ to Sn⁴⁺ can be simultaneously observed at the interface with increasing NiO_x layer thickness. Our photoemission spectra simulation indicates that this can be attributed to the formation of SnO₂ at the interface. Control experiments show that such a layer

can indeed be responsible for the reduction of photovoltage; its formation has to therefore be avoided to overcome the photovoltage limitation of α -SnWO₄. In the second part of this study, a systematic investigation of the photoelectrochemical stability of α -SnWO₄ is performed in electrolytes with a broad pH range (2 – 13) at various applied potentials. Inductively coupled plasma optical emission spectroscopy (ICP-OES) is combined with X-ray photoelectron spectroscopy, X-ray diffraction and electron microscopy to reveal the mechanisms behind the stability or degradation at respective pH and applied potential. Finally, we show the operation conditions in which a self-limiting passivation layer is formed on α -SnWO₄. While this layer blocks further charge transfer, such a self-limiting process relaxes the requirement for the protective overlayer, i.e., it allows for the presence of a limited number of pinholes. Overall, this overview suggests that despite the previously reported challenges, α -SnWO₄ is a promising material for photoelectrochemical water splitting. Further performance improvements can be achieved by optimizing the interfacial properties between α -SnWO₄ and the overlayer as well as taking advantage of the beneficial self-passivation mechanism.

[1] Seitz et al., *ChemSusChem* 7 (2014) 1372 – 1385

[2] Kölbach et al. *Chem Mater.* 30 (2018) 8322-8331

8:30 AM EN02.06.03

Late News: Rational Design of Photoelectrochemical Perovskite-BiVO₄ Tandem Devices for Selective Syngas Production Virgil Andrei, Geani M. Ucoski, Motiar Rahaman, Chanon Pornrungrroj, Esther Edwardes Moore, Bertrand Reuillard, Qian Wang, Demetra S. Achilleos, Robert A. Jagt, Chawit Uswachoke, Hannah J. Joyce, Robert Hoye, Judith L. MacManus-Driscoll, Richard H. Friend and Erwin Reisner; University of Cambridge, United Kingdom

Metal halide perovskites have recently emerged as promising alternatives to commonly employed light absorbers for solar fuel synthesis.^[1,2] These semiconductors enabled photoelectrochemical (PEC) perovskite-BiVO₄ tandem devices which can perform unassisted water splitting,^[3,4,6] as well as the more challenging CO₂ reduction to syngas.^[5,7] While the bare perovskite light absorber is rapidly degraded by moisture, recent developments in the device structure have led to substantial advances in the device stability, from seconds to days.

In this contribution, we give an overview of the latest progress from the field of perovskite PEC devices, introducing design principles to improve their performance and reliability. For this purpose, we will discuss the role of charge selective layers in increasing the device photocurrent and photovoltage, by fine-tuning the band alignment and enabling efficient charge separation. A further beneficial effect of hydrophobicity is revealed by comparing devices with different hole transport layers (HTLs). A threefold increase in the lifetime of perovskite photocathodes is obtained by replacing a hydrophilic PEDOT:PSS HTL with an inorganic NiO_x HTL.^[3] A further leap in stability up to 96 h can be demonstrated by introducing a hydrophobic PTAA HTL, which acts as an additional barrier to lateral moisture infiltration while further increasing the onset potential for H₂ evolution to approximately 1.0 V vs. RHE.^[6]

On the manufacturing side, we will provide new insights into how appropriate encapsulation techniques can extend the device lifetime to a few days under operation in aqueous media.^[3,5] Many prototypes rely on low melting alloys as encapsulants, however the demand on rare elements can be detrimental for the overall cost and scalability of the tandems, whereas metals can suffer from chemical corrosion. To avoid these drawbacks, we introduce graphite epoxy paste as a conductive, hydrophobic encapsulant.^[6,8] This abundant, metal-free composite can reduce the device cost^[6] while enabling a more facile integration of perovskite devices with inorganic,^[6,7] molecular^[5] and bio-catalysts.^[4] The combined advantages of these approaches are demonstrated in a perovskite-BiVO₄ tandem configuration, leading to selective unassisted CO₂ reduction to syngas.^[7]

[1] Chen, J.; Dong, C.; Idriss, H.; Mohammed, O. F.; Bakr, O. M. Metal Halide Perovskites for Solar-to-Chemical Fuel Conversion. *Adv. Energy Mater.* 2019, 1902433.

- [2] Samu, G. F.; Janáky, C. Photocorrosion at Irradiated Perovskite/Electrolyte Interfaces. *J. Am. Chem. Soc.* 2020, 142 (52), 21595.
- [3] Andrei, V.; Hoyer, Robert L. Z.; Crespo-Quesada, M.; Bajada, M.; Ahmad, S.; de Volder, M.; Friend, R.; Reisner, E. Scalable Triple Cation Mixed Halide Perovskite–BiVO₄ Tandems for Bias-Free Water Splitting. *Adv. Energy Mater.* 2018, 8, 1801403.
- [4] Edwardes Moore, E.; Andrei, V.; Zacarias, S.; Pereira, I. A. C.; Reisner, E. Integration of a Hydrogenase in a Lead Halide Perovskite Photoelectrode for Tandem Solar Water Splitting. *ACS Energy Lett.* 2020, 5, 232.
- [5] Andrei, V.; Reuillard, B.; Reisner, E. Bias-free solar syngas production by integrating a molecular cobalt catalyst with perovskite–BiVO₄ tandems. *Nat. Mater.* 2020, 19, 189.
- [6] Pornrunroj, C.; Andrei, V.; Rahaman, M.; Uswachoke, C.; Joyce, H. J.; Wright, D. S.; Reisner, E. Bifunctional Perovskite-BiVO₄ Tandem Devices for Uninterrupted Solar and Electrocatalytic Water Splitting Cycles. *Adv. Funct. Mater.*, 2008182.
- [7] Rahaman, M.; Andrei, V.; Pornrunroj, C.; Wright, D.; Baumberg, J. J.; Reisner, E. Selective CO production from aqueous CO₂ using a Cu₉₆In₄ catalyst and its integration into a bias-free solar perovskite–BiVO₄ tandem device. *Energy Environ. Sci.* 2020, 13 (10), 3536.
- [8] Andrei, V.; Bethke, K.; Rademann, K. Adjusting the thermoelectric properties of copper(i) oxide-graphite-polymer pastes and the applications of such flexible composites. *Phys. Chem. Chem. Phys.* 2016, 18 (16), 10700.

8:35 AM EN02.06.04

Manufacturable Processes for Si-Based Metal-Insulator-Semiconductor Photoanodes for Solar-Driven Water Oxidation Soonil Lee¹, Li Ji² and Edward Yu¹; ¹The University of Texas at Austin, United States; ²Fudan University, China

Si-based photoelectrodes have attracted substantial interest due to their potential for cost-effective conversion of water into clean fuel using solar energy. However, Si-based photoanodes for the oxygen evolution reaction (OER) are still challenging due to the requirements of large overpotential and low stability in alkaline solutions. To achieve high efficiency and long-term stability, metal-insulator-semiconductor (MIS) structures have been widely explored. In Si-based MIS photoanodes, the insulator needs to prevent Si corrosion in alkaline solutions and also transport carriers efficiently. In this work, we demonstrate a series of highly manufacturable processes for fabricating Ni/SiO₂/Si MIS photoanodes with SiO₂ insulating layers up to 90nm thick and localized, non-lithographically fabricated Ni catalyst contacts. The resulting photoanode structures show high efficiency and long-term stability in alkaline solutions. Specifically, a Ni/SiO₂/n-Si photoanode yielded onset potential and photocurrent density of ~1.0 V versus RHE and ~25 mA/cm², respectively, while a Ni/SiO₂/p⁺n-Si photoanode yielded an onset potential of 0.7 V versus RHE and saturation current density of 32 mA/cm², all in 1 M KOH alkaline solutions. Moreover, in stability testing in 1 M KOH aqueous solution, a constant photocurrent density of ~15.5 mA/cm² was maintained at 1.3 V versus RHE for 48 hours. This approach yields an enhancement in OER performance of Si-based MIS photoanodes with highly manufacturable fabrication processes that are amenable to large-scale commercial fabrication.

8:40 AM EN02.06.05

Chances and Challenges of Thermally Coupled Solar Water Splitting Moritz Kolbach¹, Kira Rehfeld² and Matthias M. May³; ¹Helmholtz-Zentrum Berlin für Materialien und Energie, Germany; ²Ruprecht-Karls-Universität Heidelberg, Germany; ³Universität Ulm, Germany

Hydrogen is a versatile energy carrier. When produced by water splitting using renewable energy sources, it is a greenhouse gas-free alternative to fossil fuels. The industrialization process of this technology is currently dominated by electrolyzers powered by electricity from wind turbines or photovoltaic solar cells. This approach is, for now, the most advanced and feasible. However, there are indications that the long-term goal to produce Hydrogen on a TW-scale only by wind power could face physical limitations,^[1] not present for the solar route, which we will discuss.

Furthermore, it is debated in the community whether more integrated device designs for solar water splitting

can optimize hydrogen production due to lower balance of system costs and a smarter thermal management.^[2,3,4] Such a more integrated device—with the photoabsorber immersed in the electrolyte or not—offers the opportunity to thermally couple the absorber and the electrolyte. In this way, heat losses in the photoabsorber can be turned into an efficiency boost for the device via simultaneously cooling the absorber, enhancing the catalytic performance of the water splitting reactions, and decreasing the ohmic losses.^[5] However, the complex influence of different weather and climate conditions on the efficiency of such a thermally coupled device is poorly understood. Here, we introduce an open-source Python-based model that combines solar cell physics, electrochemistry, thermal fluxes, and climate data as part of the “YaSoFo” environment.^[6] This model allows us to find suitable device configurations and quantify the efficiency-benefits for multi-junction photoelectrochemical devices. In addition, we scrutinize our predictions under idealized laboratory conditions. Our modelling and experimental results give important insights into the chances and challenges for thermally coupled water splitting.

[1] A. Kleidon, L. Miller, F. Gans, Physical Limits of Solar Energy Conversion in the Earth System. In: Tüysüz H., Chan C. (eds) Solar Energy for Fuels, Top. Curr. Chem. **2015**, 371, Springer, Cham

[2] T. J. Jacobsson, Energy Environ. Sci. **2018**, 11, 1977-1979

[3] R. van de Krol, B. Parkinson, MRS Energy Sustain. **2017**, 4(e13), 1-11

[4] M. Reuß, J. Reul, T. Grube, M. Langemann, S. Calnan, M. Robinius, R. Schlattmann, U. Rau, D. Stolten, Sustain. Energy Fuels **2019**, 3, 801-813

[5] S. Tembhurne, F. Nandjou, S. Haussener, Nat. Energy **2019**, 4, 399-407

[6] M. M. May, D. Lackner, J. Ohlmann, F. Dimroth, R. van de Krol, T. Hannappel, K. Schwarzburg, Sustain. Energy Fuels **2017**, 1, 492-503

8:45 AM CONTRIBUTED Q&A

9:00 AM EN02.06.06

Electrocatalytic CO₂ Reduction to C₂₊ Products on B-Doped CuO Catalysts Hilmar Guzmán^{1,2}, Daniela Roldán¹, Nunzio Russo¹ and Simelys Hernandez^{1,2}; ¹Politecnico di Torino, Italy; ²Istituto Italiano di Tecnologia, Italy

Since the industrial revolution, anthropogenic activities have impacted the planet's carbon cycle by the emissions of large amounts of greenhouse gases (GHGs), shifting the equilibrium of human history. The electrocatalytic CO₂ reduction (EC CO₂R) is an interesting technology because, driven by renewable energy sources, can be used to store both renewable electricity and CO₂ in added-value products such as liquid fuels (ethanol and other high-octane alcohols (>C₂)).^[1] To date, researchers have focused on observing the effects of surface modification (e.g., nano-structuring and surface tailoring) on catalyst selectivity and activity to produce C₂₊ products. Nonetheless, it still remains an ongoing challenge due to high C-C coupling barriers. Among these studies, incorporation of the light element boron (B) into the Cu catalyst has been reported to induce the formation and stabilization of Cu⁺¹/Cu interfaces and reduce the barrier of the *CO dimerization, promoting a high activity for EC CO₂R towards C₂ products.^[2] We have developed a B-doped Cu oxide catalyst by the ultrasound-assisted co-precipitation method and B₂O₃ impregnation, which were tested for this technology. The catalyst materials have been fully characterized by different Physico-chemical methods like X-ray diffraction, BET, porosimetry, field-emission scanning electron microscopy (FESEM), among others, before and after the catalytic tests. The results revealed that for producing C₂₊ alcohols, the catalyst must overcome the 1^o RDS of *CO formation, and then this *CO can be converted by dimerization to superior products. Thus, Faradaic efficiency towards alcohols (> 95% selectivity to ethanol) increases, and B-doping reduces H₂ production up to an optimum B amount. Therefore, under the optimum synthesis condition, a partial current density of about 3 mA cm⁻² for alcohols was reached. The physical and chemical properties of the nanostructures synthesized materials define concerted efforts that can be manipulated to tune the performance of the electrochemical reaction. These interesting results could help find a suitable electrocatalyst to establish this technology at the industrial level.

Acknowledgments

This work has been performed with the financial support of Eni SpA and the R&D Program Energy Transition (Cattura e Utilizzo CO₂).

References

- [1] H. Guzmán, M.A. Farkhondehfar, K. Rodulfo Tolod, N. Russo, S. Hernández, Photo/electrocatalytic hydrogen exploitation for CO₂ reduction toward solar fuels production, in: Sol. Hydrog. Prod. Process. Syst. Technol., Elsevier Inc., 2019: p. 560. <https://doi.org/10.1016/C2017-0-02289-9>.
- [2] C. Chen, X. Sun, L. Lu, D. Yang, J. Ma, Q. Zhu, Q. Qian, B. Han, Efficient electroreduction of CO₂ to C₂ products over B-doped oxide-derived copper, Green Chem. 20 (2018) 4579–4583. <https://doi.org/10.1039/c8gc02389a>.

9:02 AM EN02.06.08

Facile and Scalable Synthesis of Cu₂O-SnO₂ Catalyst for the Photoelectrochemical CO₂ Conversion

Maddalena Zoli^{1,2}, Daniela Roldán¹, Hilmar Guzmán^{1,2}, Simelys Hernandez^{1,2}, Angelica Chiodoni², Katarzyna Bejtka² and Nunzio Russo¹; ¹Politecnico di Torino, Italy; ²Istituto Italiano di Tecnologia, Italy

The conversion of the atmospheric CO₂ to value-added compounds is more and more attractive to the scientific community, since natural sink cannot keep up with the constant anthropogenic emission and amplification processes. Recently, CO₂ concentration in the atmosphere exceeds 410 ppm, and its growth has remained constant since the 50s^[1]. Renewable and green approaches to CO₂ recovery are aimed to minimize the worrying impact of its emission to the environment, and to drive the transition to a new circular economy approach in chemistry and energy production. Within the depicted scenario, electrochemical and photoelectrochemical CO₂ reduction are being widely investigated as promising methods to transform CO₂, under mild reaction conditions, into useful chemicals or fuels. For instance, alcohols, CO and HCOOH that can be exploited as renewable energy sources or as key intermediates for the chemical industry.

Among the non-precious metal oxides, Cu₂O is a cheap, abundant and intrinsically p-type semiconductor. Due to its narrow band gap (~ 2 eV) and the suitable positioning of conduction and valence bands, Cu₂O is an ideal photocatalyst for CO₂RR. Simultaneously, SnO₂ is an n-type direct band-gap semiconductor with noticeable electron mobility together with an intrinsic stability. It openly transpires the dual role of Cu₂O, as photoabsorber and forming a p-n junction with tin oxide.

In this work, the synthesis of photoactive copper-tin-oxide-based catalyst was optimized by a co-precipitation method^[2], employing Cu(NO₃)₂·3H₂O and SnCl₄·5H₂O into a stirred and heated reactor. A solution of Na₂CO₃ was added as a precipitant agent, while NaBH₄ as the reducing one^[3], in order to promote the Cu₂O formation. The work-up protocol, based on copious MilliQ water washings, was implemented and finally optimized. The characterization step included Field Emission Scanning Electron Microscopy (FESEM), Energy Dispersive X-ray Analysis (EDX) X-rays Diffraction Analysis (XRD), UV-Visible Spectroscopy analysis, among others, and allowed the morphological assessment, the porosity value estimation and the crystalline phase evaluation. With the latter, it has been found a correspondence to the cubic crystalline phase (cuprite) of Cu₂O and consequently confirmation that the reduction process has been successfully carried out.

The so obtained catalyst was then deposited it onto a GDL (Gas Diffusion Layer) and FTO-based substrates by spray coating of an ink containing: the catalysts, Vulcan carbon (to increase the electrode conductivity), Nafion as binder and Isopropanol as carrier. The photo-electrochemical activity for the CO₂ reduction reaction was tested in the dark and under sunlight simulated conditions by means of Linear Sweep Voltammetry (LSV) and Chrono-Potentiometry (CP) analyses. Relevant current density (*j*) values of up to 40 mA/cm² were observed, and from the products analysis during the CP a high Faradaic Efficiency to CO was obtained. The influence of the ink composition was accurately investigated in terms of interaction among all the components and with respect to the employed substrate, taking into account sun-light activity and stability of the prepared electrodes towards their future utilization in a device for the sun-driven CO₂ conversion to high-added value products.

ACKNOWLEDGMENT

This work has received funding from the European Union's Horizon 2020 Research and Innovation Action

programme under the Project SunCoChem (Grant Agreement No 862192).

[¹] X. Lan, B. D. Hall, G. Dutton, J. Mühle, and J. W. Elkins. (2020). Atmospheric composition [in State of the Climate in 2018, Chapter 2: Global Climate].

[²] Schuth F., et al., Journal of Catalysis, (2008), 258

[³] *Angew. Chem. Int. Ed.* 10.1002/anie.201808964

9:04 AM POSTER Q&A

9:14 AM *EN02.06.09

Extraction of Mobile Charge Carrier Photogeneration Yield Spectrum in Metal Oxide Photoelectrodes

Daniel Grave¹, David S. Ellis², Yifat Piekner², Moritz Kolbach³, Hen Dotan², Asaf Kay², Patrick Schnell³, Roel Van de Krol³, Fatwa F. Abdi³, Dennis Friedrich³ and Avner Rothschild²; ¹Ben Gurion University, Israel; ²Technion–Israel Institute of Technology, Israel; ³Helmholtz-Zentrum Berlin für Materialien und Energie, Germany

In conventional solar cell materials, above-bandgap photon absorption generates free electrons and holes, which travel freely through the material and contribute to the photocurrent. In metal oxides, however, light can excite electrons and holes into a variety of different electronic states, some of which are, or can eventually become mobile charge carriers, while others do not contribute to photocurrent. For example, the visible absorption spectrum of hematite (α -Fe₂O₃), one of the leading photoanode candidates for solar water splitting, is thought to be composed of both ligand-to-metal charge transfer (LMCT) bands which are responsible for the photocurrent and more localized *d-d* bands which do not generate free charge. As a result, much of the optical absorption is wasted. Since both the LMCT and *d-d* bands span the visible spectrum, the photogeneration yield, defined as the probability of an absorbed photon to generate mobile charge carriers, depends strongly on wavelength. Here, we introduce a new method to empirically extract the mobile charge carrier photogeneration yield spectrum of semiconductor photoabsorbers using optical and external quantum efficiency measurements of ultrathin films. We apply this method to hematite photoanodes in photoelectrochemical cells under *operando* conditions and show agreement between the extracted photogeneration yield spectrum and the photoconductance spectrum measured by time-resolved microwave conductivity. We demonstrate that mobile charge carrier generation fundamentally limits the conversion efficiency of hematite photoanodes, and provides an upper limit to the achievable photocurrent that is lower than that predicted by its bandgap. We then extend the analysis more generally to other photoelectrode materials and demonstrate its value towards understanding optical absorption mechanisms and charge carrier generation in complex materials.

9:39 AM DISCUSSION TIME

SESSION EN02.07: Lightning Presentations: (Photo)electrocatalysis—Novel Materials and Understanding II

Session Chairs: Simelys Hernandez and Francesca Maria Toma

Friday Morning, April 23, 2021

EN02

11:45 AM *EN02.07.01

Semi-Permeable Oxide Coatings for Selective (Photo)electrocatalysis Daniel Esposito; Columbia University, United States

Conventional electrocatalysts used in fuel cells, electrolyzers, and photoelectrochemical systems are typically comprised of metallic nanoparticles that lower energy barriers for electrochemical reactions at the electrocatalyst/electrolyte interface. Typically, these nanoparticles are partially or fully exposed to a liquid phase that contains the reactants and products of interest. In contrast, this presentation describes an emerging

class of (photo)electrocatalysts for which the active electrocatalyst sites are completely encapsulated by ultrathin layers of permeable oxides that can exhibit membrane-like properties. These so-called membrane coated electrocatalysts (MCECs)^[1] offer many potential advantages over conventional electrocatalysts, including the ability to simultaneously mitigate degradation,^[2] alter reaction selectivity,^[3] and improve reaction kinetics at the buried interface between the overlayer and active catalyst.^[4] This talk will focus on describing recent case studies of silicon oxide (SiO_x) and titanium oxide (TiO_x)-encapsulated Pt electrocatalysts that demonstrate the ability of nanoscopic overlayers to greatly modulate reaction selectivity, even in cases where the thermodynamics and/or kinetics of the undesired reaction are highly favored compared to the desired reaction. By systematically changing the properties of well-defined oxide overlayers, this work uncovers design principles that can be used to tune reaction selectivity for a wide range of electrochemical reactions of interest for the sustainable production and use of fuels and commodity chemicals.

References

- [1] D.V. Esposito, “Membrane Coated Electrocatalysts—an Alternative Approach to Achieving Stable and Tunable Electrocatalysis“, *ACS Catalysis*, vol. 8, pp 457–465, 2018..
- [2]. N. Y. Labrador, et al., “Enhanced Performance of Si MIS Photocathodes Containing Oxide-Coated Nanoparticle Electrocatalysts”, *Nano Letters*, vol. 16, 6452-6459, 2016.
- [3] N. Y. Labrador, et al., “Hydrogen Evolution at the Buried Interface between Pt Thin Films and Silicon Oxide Nanomembranes”. *ACS Catalysis*, vol. 8, pp 1767–1778, 2018.
- [4] J.E. Robinson, et al., “Silicon Oxide-Encapsulated Platinum Thin Films as Highly Active Electrocatalysts for Carbon Monoxide and Methanol Oxidation”. *ACS Catalysis*, vol. 8, pp 11423–11434, 2018.

12:10 PM EN02.07.03

Novel Approach to Extract Reaction and Recombination Rates of the Photoelectrode Peter Cendula¹, Prangya P. Sahoo², Gabriel Cibira¹ and Pavel Simon¹; ¹University of Zilina, Slovakia; ²Slovak Academy of Sciences, Slovakia

Semiconductor/electrolyte interfaces attract intense interest to convert solar energy to chemical fuels. Although many analytical models describing the photocurrent-voltage response of these devices exist, they have difficulty to reproduce full numerical simulations under small anodic bias.

We recently derived an analytic model of a weakly absorbing n-type semiconductor/electrolyte interface with a slow rate of water oxidation reaction, fast recombination rate and under small voltage bias [1]. Excellent overlap of our model was demonstrated with full numerical simulations. Our model enabled us to simplify calculation of the impedance of the semiconductor/electrolyte interface derived in the work of Bertoluzzi et al[2]. The comparison of analytic and measured impedance allows to extract the reaction rate for redox reaction from the dark impedance and the direct bulk recombination constant of the semiconductor from the impedance under illumination.

This work provides easy-to-use recipe for the quantitative comparison of the recombination and reaction properties of the various semiconductor photoelectrodes by impedance spectroscopy.

References

- [1] Cendula et al., 10.1021/acs.jpcc.9b07244
- [2] Bertoluzzi et al., 10.1039/C5TA03210E

Acknowledgement

We acknowledge support of Operational Program Integrated Infrastructure 2014 - 2020 of the project: Innovative Solutions for Propulsion, Power and Safety Components of Transport Vehicles, code ITMS 313011V334, co-financed by the European Regional Development Fund.

12:15 PM EN02.07.04

Heterostructures of Cadmium Chalcogenide Quantum Dots and MoS₂ Nanoplatelets Prepared by Linker-Assisted Assembly—Influence of Ligand Properties on Excited-State Charge Transfer and Photocatalysis Arianna Rothfuss, Nuwanthi Suwandarathne and David Watson; University at Buffalo, The State University of New York, United States

Heterostructures of semiconductors can achieve photoinduced charge separation for a wide variety of applications in photocatalysis, including photoelectrochemical (PEC) water splitting. Heterostructures comprised of quantum dots (QDs) and MoS₂ nanoplatelets have demonstrated potential as architectures for PEC water splitting and hydrogen generation.¹ Linker-assisted assembly (LAA) is a promising synthetic method for these heterostructures. In LAA, colloidal QDs are pre-synthesized, affording substantial control over size and energetics, and then interfaced with the nanoplatelets. Moreover, charge-transfer properties of the heterostructures can be tuned with properties of the bridging ligand.

This presentation will focus on the effects of varying the length of molecular linkers between QDs and MoS₂ on the dynamics of charge transfer and the efficiency of redox photocatalysis. Mercaptoalkanoic acid ligands, ranging from 3 to 16 carbon atoms, as well as cysteine were used to attach the QDs to MoS₂. We hypothesized that tuning the alkyl chain length of the ligand would modulate the rate of electron transfer, due to the variable spatial separation between the components. LAA-derived QD/MoS₂ heterostructures were initially synthesized with cysteine as the linker and exhibited rapid electron transfer from the QDs to MoS₂ due to the type-II energetics. These heterostructures also produced oxidative photocurrent and demonstrated photoelectrochemical and photocatalytic hydrogen generation. The LAA-derived QD/MoS₂ heterostructures with mercaptoalkanoic acid linkers also exhibited dynamic quenching, relative to free QDs, in time-resolved emission experiments, which provided evidence for excited-state charge transfer.

Measured electron-transfer rate constants for the heterostructures were tunable over three orders of magnitude by varying the alkyl chain length. LAA-derived heterostructures oxidized lactic acid to pyruvic acid, and oxidative photocurrents varied by approximately 4-fold with the length of the bridging ligand. These results highlight the extent to which the properties of bridging ligands affect excited-state charge transfer and photocatalysis within QD-MoS₂ heterostructures, and, more generally, provide insight into the design of materials architectures for PEC water splitting.

1. Cho, J.; Suwandaratne, N. S.; Razek, S.; Choi, Y.-H.; Piper, L. F. J.; Watson, D. F.; Banerjee, S., Elucidating the Mechanistic Origins of Photocatalytic Hydrogen Evolution Mediated by MoS₂/CdS Quantum-Dot Heterostructures. *ACS Applied Materials & Interfaces* **2020**, *12* (39), 43728-43740.

12:20 PM EN02.07.05

Probing the Photoelectrochemical Properties of Fe₂TiO₅ Using Epitaxial Thin-Film Photoanodes Motoki Osada^{1,2,2}, Kazunori Nishio^{1,2,3}, Kyuho Lee^{1,2}, Harold Hwang^{1,2} and Yasuyuki Hikita¹; ¹SLAC National Accelerator Laboratory, United States; ²Stanford University, United States; ³Tokyo Institute of Technology, Japan

Recently, Fe₂TiO₅ has emerged as a promising photoanode material for water photo-oxidation due to its suitable bandgap of 2.1 eV, high chemical stability, and scalability consisting of earth-abundant elements [1]. It has been reported that photoelectrochemical (PEC) performance is enhanced in heterostructure forms such as Fe₂TiO₅/α-Fe₂O₃ or Fe₂TiO₅/TiO₂ [2,3]. However, these investigations have been limited in polycrystalline nanostructures that hinders the elucidation of the intrinsic PEC properties of Fe₂TiO₅.

Building on our successful fabrication of single-phase Fe₂TiO₅ epitaxial thin films using pulsed laser deposition [4], here we report the comprehensive characterization of the intrinsic PEC properties of Fe₂TiO₅ using the most well-defined surface and bulk structures available. We demonstrate that Fe₂TiO₅ exhibits highly efficient charge transfer efficiency of 20% at the Fe₂TiO₅-electrolyte interface at 1.23 V vs. RHE, while it is only 1% for α-Fe₂O₃. This excellent surface property is further corroborated by forming heterostructures with α-Fe₂O₃ epitaxial thin films, in which the photocurrent enhances by an order of magnitude and the onset potential improves by ~300 mV compared to a pure α-Fe₂O₃ photoanode. Details of the epitaxial photoanode fabrication, photocurrent-voltage curves, transient photocurrent analysis, and impedance spectroscopy will be discussed in the presentation.

[1] D. S. Ginley, and M. A. Butler, *J. Appl. Phys.* **48**, 2019 (1977).

[2] Q. Liu *et al.*, *Nat. Commun.* **5**, 1 (2014).

[3] P. S. Bassi *et al.*, *Nano Energy* **22**, 310 (2016).

[4] M. Osada *et al.*, *APL Mater.* **6**, 056101 (2018).

*Supported by DOE BES MSD (DE-AC02-76SF00515) and the LDRD program at SLAC National Accelerator Laboratory.

12:25 PM CONTRIBUTED Q&A

12:40 PM EN02.07.07

Late News: Effect of Varying Magnetic Field on the Alignment of Tandem Semiconductor Microparticles for Unassisted Water-Splitting [Saumya Gulati](#) and Josh Spurgeon; University of Louisville, United States

There has been a vast improvement in photovoltaic (PV) technology in the last couple of decades; however, solar PV technology has a lot of drawbacks, including that it is intermittent, broadly dispersed, and non-transportable. Hence, cost-effective solar energy storage is critical for widespread implementation of solar energy as the primary energy source. My project focuses on the development of tandem semiconductor microparticles which when placed in water under 1 Sun condition could spontaneously split water into hydrogen and oxygen with solar-to-hydrogen efficiency of >10%.

In the present work, we have acquired customized microwire array structures made on silicon (Si) wafer by deep reactive ion etching method and formed a diode on these particles via a doping process. We have also been able to produce a TiO₂ tandem junction for additional photovoltage. Nickel, which serves multiple purposes in the design, has been deposited on Si via an electroless photo-deposition process. It acts as a hydrogen evolution catalyst while protecting the Si from oxidation. Secondly, owing to its ferromagnetic property, an electromagnet can orient these particles to achieve current-matching, in the series-connected Si and TiO₂. This is hypothesized to achieve higher efficiency.

For proof-of-concept, the magnetic alignment analysis has been done on Ni coated Si microwire particles. Future work aims at replicating similar analyses for tandem microwire particles and testing its effect on the eventual solar-to-hydrogen efficiency.

12:42 PM POSTER Q&A

12:56 PM *EN02.07.10

Recent Developments in Understanding Ternary Oxide Photoelectrodes Using BiVO₄ as a Model System Dongho Lee, Ann Lindberg and [Kyoung-Shin Choi](#); University of Wisconsin–Madison, United States

Oxide-based photoelectrodes recently have been at the forefront of research for photoelectrochemical water splitting. While most oxide-based photoanodes suffer from severe electron-hole recombination, BiVO₄ photoanodes are known to achieve exceptionally high electron-hole separation efficiencies. However, an understanding of what features of BiVO₄ lead to this desired property is currently lacking. In this study, we sought to elucidate these features by investigating PbCrO₄, which has electronic and structural similarities to BiVO₄. For this goal, we prepared PbCrO₄ as a high-quality photoanode and compared its photoelectrochemical properties and stability with those of BiVO₄. In this presentation, we will discuss the photoelectrochemical similarities and differences between PbCrO₄ and BiVO₄ in detail, which can provide useful guidelines to develop high-performance oxide-based photoanodes. Another topic to be discussed in this presentation is the effects of surface termination/composition of a ternary photoelectrode on the interfacial energetics. For ternary oxide photoelectrodes, there exist numerous ways to terminate the surface even for the same facet and their surface composition can be different from their bulk composition. However, the effects of surface termination/composition on a ternary oxide photoelectrode have not been systematically studied. In this presentation, we will compare BiVO₄ photoelectrodes with V-rich and Bi-rich surfaces and demonstrate that the surface composition has a considerable effect on the surface energetics and photocurrent generation of BiVO₄ even for the same facet. We will also discuss the atomic origin of the impact that the surface of photoelectrodes has on their surface energetics and photoelectrochemical properties.

SYMPOSIUM EN03

Intercalation Energy Storage Materials and Systems for Beyond Li-Ion Batteries
April 14 - April 23, 2021

Symposium Organizers

Xin Li, Harvard University
Anton Van der Ven, University of California, Santa Barbara
Hui (Clair) Xiong, Boise State University
Naoaki Yabuuchi, Yokohama National University

Symposium Support

Platinum

BICI USA Co., Ltd

Gold

Science | AAAS

Bronze

Rigaku

* Invited Paper

SESSION EN03.01: Zn and Mg Ion Batteries
Session Chairs: Hui (Clair) Xiong and Naoaki Yabuuchi
Wednesday Morning, April 21, 2021
EN03

8:00 AM *EN03.01.01

With High-Performance Two-Electron, Dendrite-Suppressing Zinc Anodes in Hand, Time for Battery Cathodes to Catch Up Debra R. Rolison¹, Samuel Kimmel^{2,1}, Christopher Rhodes², Christopher N. Chervin¹, Brandon J. Hopkins³, Nathaniel L. Skeele¹, Jeffrey W. Long¹ and Joseph F. Parker¹; ¹U.S. Naval Research Laboratory, United States; ²Texas State University, United States; ³NRL-NRC Postdoctoral Associate, United States

Although lithium-ion batteries are today's go-to high-energy battery technology, the inherent safety issues of Li-ion remain a persistent challenge, especially when Li-ion battery packs are required, as in electrified vehicles and distributed microgrids. The monolithic three-dimensional (3D) zinc "sponge" developed at the U.S. Naval Research Laboratory (NRL) solves long-standing performance limitations for zinc anodes and paves the way for next generation Ni-Zn batteries competitive with the specific energy of Li-ion systems plus adding improved safety inherent to aqueous, nonflammable electrolytes. However, the current performance of β -Ni(OH)₂ composite electrodes does not provide sufficient performance or energy density to match that of Zn sponge anodes and represents a critical bottleneck to Ni-Zn batteries with high energy density. We are investigating Ni-based cathodes redesigned as architectures to wire the electrode volume in 3D while building on Texas State's microwave synthesis of multi-substituted α -Ni(OH)₂ to increase the capacity, minimize the parasitic oxygen evolution reaction, and provide stable multi-electron cycling of the active material.

8:25 AM *EN03.01.02

Covalent Organic Framework Cathodes for Zinc-Ion and Metal-Sulfur Batteries Aninda J. Bhattacharyya, Ruth Gomes and Akshatha Venkatesh; Indian Institute of Science, India

This presentation discusses the application of covalent organic frameworks (COFs) as cathodes in battery chemistries beyond the Li-ion viz. non-aqueous liquid electrolyte-based Li/Na-S and aqueous Zn-ion batteries.

We have designed covalent organic framework nanosheets over end-opened multi-walled carbon nanotubes (CNT-CON) and explored their role as sulfur host in metal sulfur batteries. The carbon nanotubes provide the conductivity and confine the elemental sulfur, whereas the covalent organic nanosheets layer acts as a porous (chemical) trap to prevent polysulfide dissolution electrolyte. Numerous experimental methods investigated the crystallinity, porosity, and framework composition of the cathode material. The molecularly designed covalent organic framework viz. the CNT-CON/S when employed as the cathode in Li-S and Na-S battery exhibited a significant improvement in electrochemical performance (specific capacity and cycling efficiency) as compared to CNT/S and COF/S cathode. All these studies convincingly show that COFs grafted on to conducting carbon structures can serve as alternative (organic) electrodes for high-performance metal-sulfur battery systems (Ruth Gomes et al. *ACS Sustainable Chem. Eng.* 2020).

The second part of the lecture will discuss a redox-active two-dimensional COF and its graphene oxide composite (COF-GOPH) as a cathode in an aqueous rechargeable Zn-ion battery (ZiB). Zinc metal anode and varying concentrations of Zn^{2+} -ion and Li^+ -ion electrolytes were used in the cell with COF-GOPH cathode. The best battery performance was obtained when the composition of the Zn and Li-based electrolytes are 1:1. Combination and X-ray photoelectron spectroscopy and conductivity measurements reveal that optimum concentration of Li^+ ions in the mixed-ion electrolyte was beneficial for better facilitation of Zn^{+2} diffusion into the electrode, providing superior electrochemical performance. The COF-Zn aqueous mixed-ion system offers a better alternative to conventional aqueous organic batteries with a single type of ions. It ensures excellent electrochemical performance in cycling stability reversibility and capacity retention (Akshatha Venkatesh et al. *submitted*, 2021).

The above examples of employing COF in battery chemistries beyond the Li-ion further broadens the potential of COFs. The work clearly demonstrates that COFs can be used in the development of new and efficient battery systems that are safe, cost-effective, eco-friendly, and, most importantly, providing a sustainable future.

8:50 AM EN03.01.03

WITHDRAWN-NO REG (EN03.01.03) Biosourced Sepia Melanin as Universal Organic Cathode for Post-Li-Ion (Zn^{2+} , Al^{3+}) Aqueous Rechargeable Batteries Abdelaziz M. Gouda and Clara Santato; Polytechnique Montréal, Canada

The increasing demand for energy especially from renewable and intermittent resources (e.g. sun and wind) along with the colossal demand for portable electronics and the growing popularity of electric vehicles, push the community to be more dependent on energy storage technologies, especially Lithium-ion battery (LIB)). Concurrent with this booming LIB technology, an emerging topic of research has been dedicated to curtailing the environmental concerns, the Li mining geopolitical issues, as well as providing other cost effective and environmental benign alternatives. Rechargeable zinc and aluminum aqueous batteries hold promise owing to the affordability, high capacity and safety [1, 2]. Eumelanin is the most common form of the pigment melanin in the human body, with diverse functions including photoprotection, antioxidant behavior, metal chelation, and free radical scavenging [3]. Sepia Melanin is a natural eumelanin extracted from the ink sac of cuttlefish. The poor solubility of melanin in most of organic solvent combined with the density of metal-binding catechol groups that reversibly bind mono and multivalent metal ions, constitutes the foundation and stability for its use in energy storage systems [4, 5]. In this work, we report on the use of sepia melanin with reduced graphene oxide (as conductive binder) grafted on carbon paper as a highly stable, biosourced, environmentally benign and biocompatible cathode for Zn^{+2} and Al^{+3} aqueous rechargeable batteries. This stable, environmentally benign and bio compatible cathode will enable applications from biomedical devices to grid storage.

- [1] Kundu D, Oberholzer P, Glaros C, Bouzid A, Tervoort E, Pasquarello A and Niederberger M 2018 Organic cathode for aqueous Zn-ion batteries: taming a unique phase evolution toward stable electrochemical cycling *Chem. Mater.* **30** 3874-81
- [2] Elia G A, Marquardt K, Hoeppe K, Fantini S, Lin R, Knipping E, Peters W, Drillet J F, Passerini S and Hahn R 2016 An overview and future perspectives of aluminum batteries *Adv. Mater.* **28** 7564-79
- [3] Di Mauro E, Xu R, Soliveri G and Santato C 2017 Natural melanin pigments and their interfaces with metal ions and oxides: Emerging concepts and technologies *MRS Communications* **7** 141-51
- [4] Jo K Y, Wei W, Sang Eun C, F. W J and J. B C 2014 Catechol Mediated Reversible Binding of Multivalent Cations in Eumelanin Half Cells *Adv. Mater.* **26** 6572-9
- [5] Kim Y J, Wu W, Chun S E, Whitacre J F and Bettinger C J 2013 Biologically derived melanin electrodes in aqueous sodium ion energy storage devices *Proceedings of the National Academy of Sciences* **110** 20912-7

9:05 AM DISCUSSION TIME

9:20 AM EN03.01.05

Analysis of MoS₂ Coatings on Zn-Anode for High Efficiency Zn-Ion Rechargeable Battery Gerardo Gamboa, Sanket Bhojate and Wonbong Choi; University of North Texas, United States

Zn-ion battery is an increasingly attractive alternative energy storage system compared to traditional Li-ion batteries due to their low cost, high theoretical capacity, and increased safety. However, dendrite formation limits the stability of the Zn metal anode and restricts the practical use of Zn-ion batteries. In our early work, MoS₂ via electrodeposition has been proven to be an effective barrier to Zn dendrite growth, however, the growth of such MoS₂ thin films has not been well studied. For this study, a series of tests on the deposition of MoS₂ on Zn of different grain size proved that Zn grain boundaries are favorable sites for the start of MoS₂ growth. The Zn coated anodes were then tested for their efficiency in symmetrical cell testing. The MoS₂ layer, as thin at 50 nm, increased the anodic diffusion of Zn ions and improved overall battery performance. The structure-property relations of MoS₂ coatings on Zn has been studied systematically. The Zn ion conductivity of the MoS₂ coated anode with the variation of the coating thickness and morphology of MoS₂ also has been studied. This study further reinforces the possibility of creating practical Zn-ion batteries as next generation energy storage systems.

9:35 AM EN03.01.06

Investigating Magnesium Ion Insertion in WS₂ Cathodes and Mg-CNT Composite Anodes Mayukh Nandy, Todd Houghton, Srivatsan Swaminathan, Arjun Modi and Hongbin Yu; Arizona State University, United States

Today, Lithium ion batteries are often the primary means of providing electrical power to a diverse ecosystem of devices, from mobile phones to electric vehicles. However, while capacity, cost, and reliability of Li-ion chemistries have steadily improved over the past two decades, limitations of the technology have become increasingly apparent. Indeed, despite considerable investment in LIBs, it is not clear the technology will reach optimal energy density and per-cell cost targets, laid out in industry and government-sponsored roadmaps, by the year 2030 at its current rate of progress. Furthermore, cost fluctuations in the price of raw materials used to fabricate LIBs and environmental impacts caused by both production and disposal have yet to be fully addressed.

Given the present and anticipated limitations of LIBs, investigations into alternative divalent metal-ion battery chemistries which utilize magnesium or zinc have continued to gain traction within the scientific and engineering community. Mg-ion cells offer a theoretical volumetric capacity which exceeds that of lithium while utilizing an element more abundant in the earth's crust. Mg anodes are also dendrite free, allowing greater practical capacities than what is currently achievable with intercalation-type anodes used for LIBs. However,

Mg-ion battery cells consisting of sulfur-containing chalcogenide cathodes and Mg metal anodes must utilize unconventional and often volatile electrolyte solutions to inhibit anode surface passivation.

Here, the electrochemical behavior of WS₂ cathodes and Mg-CNT composite anodes in contact with a conventional EC/PC polymer-gel (PVDF-HPF) electrolyte is investigated within the context of Mg-ion insertion. Indeed, the atomic structure and interlayer spacing of WS₂ is similar to other Mg-insertion cathodes such as TiS₂ and MoS₂, while Mg-CNT composite anodes have demonstrated compatibility with perchlorate-containing electrolytes. Analysis of WS₂ cathodes via cyclic voltammetry shows a reversible redox reaction involving Mg species at the cathode/electrolyte interface, indicating a possible intercalation mechanism. Additional cathode and anode surface data is provided by XPS, Powder XRD, and Raman Spectroscopy. Cell fabrication details and analysis of reacted cathodes and anodes in the context of Mg-ion intercalation will be discussed.

SESSION EN03.02: Solid State Batteries
Session Chairs: Xin Li and Anton Van der Ven
Wednesday Morning, April 21, 2021
EN03

11:45 AM *EN03.02.01

Solid Electrolyte-Modified 4V Layered Cathodes for High-Voltage and Solid-State Lithium Batteries

Yuan Yang; Columbia University, United States

The development of next-generation energy storage demands electrode materials with higher capacity. One potential solution is to charge layered oxides, such as LiCoO₂ and Li(Ni_xCo_yMn_z)O₂ (NCM) cathodes, to a higher electrode potential so that more Li⁺ ions can be removed. However, this is often impeded by performance degradation arising from following phenomena: 1) phase transition in the bulk electrode, 2) surface reconstructions, and 3) electrolyte oxidation. In this talk I will present our recent studies on using ceramic electrolyte-based coatings to alleviate these issues. With a thin layer of Li_{1.5}Al_{0.5}Ge_{1.5}(PO₄)₃ (LAGP) coating, phase transition and surface reconstruction of LiCoO₂ are suppressed. Consequently, LAGP protected LiCoO₂ shows a discharge capacity of 196 mAh g⁻¹ at 0.1 C when charged to 4.5 V vs. Li⁺/Li. The capacity retention is 88% over 400 cycles. The LAGP coating also suppresses electrolyte oxidation when layered oxides are combined with polyethylene oxide (PEO)-based solid polymer electrolytes. While PEO is easily oxidized above 4 V vs. Li⁺/Li when it is in contact with bare LiCoO₂ and NCM523, it is stable up to 4.3-4.4 V vs. Li⁺/Li with a LAGP coating. When charged to 4.3 V, capacity retention of 89.7% over 200 cycles, and 93.8% over 100 cycles are achieved in LAGP-LiCoO₂/PEO/Li cells and NCM523/PEO/Li cells, respectively. The corresponding average coulombic efficiencies are ~99.8%. These studies show that solid electrolyte coating is an effective approach to enhance interfacial stability of 4V layered oxide cathodes with various electrolytes at high electrode potentials.

12:10 PM EN03.02.02

Zeolite-Templated Carbon—A Model Framework Solid for Beyond Lithium-Ion Battery Cathodes

Romain J. Dubey^{1,2}, Erin E. Taylor³, Kostiantyn Kravchyk^{1,2}, Maksym Kovalenko^{1,2} and Nicholas Stadie³; ¹ETH Zürich, Switzerland; ²Empa, Swiss Federal Laboratories for Materials Science & Technology, Switzerland; ³Montana State University, United States

Beyond lithium-ion battery (LIB) chemistries demand new electrode materials exhibiting unique features to accommodate the larger and/or multivalent active ions. Zeolite-templated carbon (ZTC) is an ordered microporous carbon scaffold that is molecularly thin, electrically conductive, and connected in three dimensions. Its narrow pore size distribution is centered at 1.2 nm, permitting the controlled introduction and

ultrafast conduction of a wide range of molecular guests. We report methodological studies of the serviceability of ZTC as a stable cathode material across wide voltage ranges for both bulky, polyatomic anions (as in dual-ion electrochemistries) and divalent cations (as in magnesium-ion electrochemistries) in high energy density and high power density electrochemical cells. Charge storage proceeds by a purely capacitive mechanism at the cathode, mated with the faradaic mechanism of metal plating and stripping at the anode. Solid-state NMR spectroscopy sheds insight into the roles of the ion and solvent in charge/discharge cycling within the microporous framework of ZTC, with intuitive trends revealed based on ion size, solvent size, and solvent viscosity.

12:25 PM EN03.02.03

Comparison of Hong versus von-Alpen Type Nasicon Membranes for Use in a Rechargeable Seawater Battery Jeffrey B. Wolfenstine¹, Wooseok Go², Jeff Sakamoto³ and Youngsik Kim²; ¹Solid Ionic Consulting, United States; ²Ulsan National Institute of Science and Technology (UNIST), Korea (the Republic of); ³University of Michigan–Ann Arbor, United States

The rechargeable seawater battery (SWB) is one of the potential candidates as a large-scale energy storage system due to its low cost and eco-friendliness compared to Li-ion batteries. However, the current seawater battery using a Hong Nasicon ($\text{Na}_3\text{Zr}_2\text{Si}_2\text{PO}_{12}$) [H-NASICON] Na-conducting membrane suffers from high ohmic polarization as a result of its low ionic conductivity. One way to reduce to this polarization is to use a Na-conducting membrane with higher ionic conductivity than H-NASICON. In this regard von-Alpen type NASICON ($\text{Na}_{3.1}\text{Zr}_{1.55}\text{Si}_{2.3}\text{P}_{0.7}\text{O}_{11}$) [VA-NASICON] was investigated as a possible replacement membrane for use in a SWB. The electrical, mechanical, chemical stability and SWB cell testing of VA-NASICON and H-NASICON were evaluated and compared. It was observed that VA-NASICON exhibited both a higher bulk and grain boundary conductivity leading to a total ionic conductivity of 3 times higher than that for H-NASICON. The results will be explained in terms of the difference in structure and microstructure between the two materials. The difference in the mechanical properties; hardness, fracture toughness and fracture stress between the two materials will be explained based on their microstructural differences. The ionic conductivity, structure and microstructure of VA-NASICON were unchanged after testing in seawater, suggesting it is chemically stable in seawater. Testing of VA-NASICON in SWB coin cells revealed it exhibited about 1.5 x the power compared to H-Nasicon. This value is in close agreement the lower ohmic resistance of VA-NASICON compared to H-NASICON. The results of this study suggest that of the two materials evaluated, VA-NASICON is the better choice for a Na-ion conducting electrolyte in a SWB than the current H-NASICON.

12:40 PM DISCUSSION TIME

12:55 PM EN03.02.05

Tuning Ionic Conductivity in Argyrodite Solid Electrolytes with Pseudohalides Annalise E. Maughan; National Renewable Energy Laboratory, United States

All-solid-state batteries hold the potential to transform electrochemical energy storage technologies. Replacing the flammable liquid electrolyte with a solid-state ion conductor can improve battery safety and may further increase battery energy density when paired with lithium metal anodes. However, widespread implementation of all-solid-state batteries is hindered in part by the fact that candidate solid-state electrolytes typically exhibit ionic conductivities that are several orders of magnitude lower than liquid electrolytes, which typically results in slow charge/discharge rates. While there are a multitude of candidate electrolyte materials for all-solid-state batteries, rapid advancements in this field necessitate a fundamental understanding of the relationships between composition and ionic conductivity. These design principles may then be leveraged to identify and target new materials with ionic conductivities that are competitive with existing liquid electrolyte technologies. One such family of materials is the argyrodites of the general formula $\text{Li}_6\text{PS}_5\text{X}$ (X = halide or pseudohalide), as they can achieve ionic conductivities that are nearly competitive with liquid electrolytes. Because the X-site can be occupied by either halides or larger pseudohalides, these materials provide an exciting system to understand the underlying relationships between structure, composition, and ion conduction in candidate solid electrolytes. In

this work, I have prepared new argyrodite materials with pseudohalides at the X-site and have determined the structure-property relationships that contribute to low activation barriers and high ionic conductivities in these materials. This work highlights an exciting approach to tuning ionic conductivity in new electrolyte materials for potential applications in all-solid-state batteries.

1:10 PM EN03.02.06

Anharmonic Phonons, Superionic Diffusion and Ultralow Thermal Conductivity in Argyrodite Cu_7PSe_6
Mayanak K. Gupta¹, Jingxuan Ding¹, Dipanshu Bansal¹, Douglas Abernathy², Georg Ehlers², Naresh Osti², Wolfgang Zeier³ and Olivier Delaire^{1,1,1}; ¹Duke University, United States; ²Oak Ridge National Laboratory, United States; ³Justus-Liebig-University, Germany

We present a combined experimental and theoretical investigation of atomic dynamics in the superionic compound Cu_7PSe_6 , rationalizing the atomistic diffusion mechanism and the impact of host lattice dynamics. Inelastic neutron scattering (INS) and quasi-elastic neutron scattering (QENS) were performed as a function of temperature and were complemented with ab-initio molecular dynamics extended to long time scales with the use of machine-learned potentials (MLMD). INS data reveal characteristic changes at the onset of superionic behavior, providing insights into the role of the host lattice dynamics, while QENS probes the superionic Cu diffusion via the jump length, residence time, and diffusion constant. The MLMD simulations reveal that the long-range Cu diffusion is limited by an inter-cluster hopping step, which is strongly coupled to the host phonon dynamics. Further, MLMD simulations enable us to capture the ultralow lattice thermal conductivity within the Green-Kubo framework. These results supersede the traditional quasiharmonic phonon picture to capture the strong anharmonicity in this superionic system.

This research was supported by the U.S. DOE.

1:25 PM EN03.02.07

Late News: Recycling $\text{Li}_7\text{La}_3\text{Zr}_2\text{O}_{12}$ (LLZO) and $\text{Li}_{1.5}\text{Al}_{0.5}\text{Ge}_{1.5}(\text{PO}_4)_3$ (LAGP) -Based Electrolyte Composites Using the Cold Sintering Process Yi-Chen Lan and Enrique D. Gomez; The Pennsylvania State University, United States

The anticipated commercialization of all-solid-state lithium batteries highlights the urgent need to develop recycling strategies for solid-state electrolytes. Garnet type, $\text{Li}_7\text{La}_3\text{Zr}_2\text{O}_{12}$ (LLZO), and NASICON-type, $\text{Li}_{1.5}\text{Al}_{0.5}\text{Ge}_{1.5}(\text{PO}_4)_3$ (LAGP) electrolytes are particularly promising because of their high conductivity and good chemical stability against lithium metal and air, respectively. Here, we use cold sintering process to recycle degraded electrolytes with poor structural integrity. The low temperature allows co-sintering of composites, which still remains challenging for conventional sintering. Two model systems, LLZO with polypropylene carbonate (PPC) and lithium perchlorate (LiClO_4), and LAGP with bis(trifluoromethanesulfonyl)imide (LiTFSI) salts, are studied. LLZO-PPC- LiClO_4 shows a reprocessibility for eight times with ionic conductivities in excess of 10^{-4} Scm^{-1} at room temperature and relative densities of 76~80%, which are comparable with the values of pristine sample. LAGP-LiTFSI reprocessed composites exhibit high relative densities of around 90% and ionic conductivities above 10^{-5} Scm^{-1} at room temperature. Thus, we demonstrate the use of cold sintering to recycle ceramic-salt and ceramic-salt-polymer integrated electrolytes.

SESSION EN03.03: Electrochemical Evolution in Li, Na, K Batteries
Session Chairs: Hui (Clair) Xiong and Naoaki Yabuuchi
Wednesday Afternoon, April 21, 2021
EN03

5:15 PM *EN03.03.01

Multi-Electron Intercalation Cathodes M. Stanley Whittingham; Binghamton University, The State University of New York, United States

The Olivine lithium iron phosphate cathode provides a very stable and high rate cathode for lithium and lithium-ion intercalation batteries. However, its energy density is much lower than that of the NMC layered oxides. This can be helped by switching to lithium manganese phosphate, which has an 0.5 V higher cell potential. To achieve energy densities approaching those of the layered oxides, it will be necessary to achieve a two-electron reaction per redox center. In principle, the anode can be lithium, sodium, magnesium or calcium. Vanadium is one of few suitable transition metal centers where a two-electron can be achieved, as vanadium can readily undergo between the +5 and +3 oxidation states, and in some cases to the +2 state. The earliest two-electron cathode was vanadium diselenide, VSe₂, [1] with relatively low cell potentials as the reaction uses the +4 to +2 oxidation states. VS₂ would be expected to have more attractive potentials. Vanadium phosphates are found to readily and reversibly intercalate both two lithium or two sodium ions [2,3], with the former having cell potentials around 4 and 2.5 volts. The challenges facing these systems will be discussed [4].

[1] M. S. Whittingham, Mater. Res. Bull., 13, 959-965 (1978)

[2] M. S. Whittingham et al., Accounts of Chemical Research 51, 258-264 (2018). DOI: 10.1021/acs.accounts.7b00527

[3] C. Siu et al., Chem. Commun., 54, 7802-7805 (2018). DOI: 10.1039/c8cc02386g

[4] N. A. Chernova et al, Advanced Energy Materials, in press. DOI: 10.1002/aenm.202002638.

5:40 PM *EN03.03.02

The Effect of Crystal Structure on the Activity of Cu in Na-Ion Cathode Materials Enyuan Hu¹, Qinchao Wang¹, Yiman Zhang², Jue Liu² and Xiao-Qing Yang¹; ¹Brookhaven National Laboratory, United States; ²Oak Ridge National Laboratory, United States

Sodium-ion batteries are important for energy storage because sodium is much more abundant than lithium which is the fundamental element for lithium-ion batteries. From chemical point of view, sodium-ion cathodes open up opportunities for utilizing novel electrochemistries that are not possible in lithium-ion cathodes. For example, Fe³⁺/Fe⁴⁺ and Cu²⁺/Cu³⁺ redox cannot be utilized in lithium-ion cathode because of structural disorder or/and exceedingly high voltage that is incompatible with currently available electrolyte. In sodium-ion cathodes, structural ordering enabled by the large size of sodium ion, the diversity of structures, and the relatively low voltage make it possible to utilize the Fe³⁺/Fe⁴⁺ and Cu²⁺/Cu³⁺ redox couples. This talk will focus on the latter one. Two kinds of materials with the same stoichiometry (Na_{2/3}Cu_{1/3}Mn_{2/3}O₂) but different structures (P2 and P3) are synthesized and characterized to understand the structure-property relationship in these materials. Synchrotron and neutron scattering as well as DFT calculations are used to understand the bulk structural changes during electrochemical cycling. Synchrotron-based hard and soft x-ray spectroscopies are used to understand the chemistries both in the bulk and at the surface in these two materials. The effect of crystal structure on the activity of Cu will be explained and the possibility of O activity will also be discussed.

6:05 PM EN03.03.03

Hierarchical Intercalant Orderings in Layered Oxides for Na- and K-Ion Battery Electrodes Jonas Kaufman and Anton Van der Ven; University of California, Santa Barbara, United States

Layered transition-metal oxides have been successfully employed as electrode materials for Li-ion batteries, however, intercalating Na or K instead often introduces effects that can diminish reversibility and rate capability. Within these materials, Na and K tend to stabilize additional host crystal structures accessed via topotactic phase transitions and display a stronger preference for ordering within the intercalation layers to minimize electrostatic energy. In some cases, rather than discrete orderings appearing at some particular intercalant concentrations, the stable orderings within a concentration range form a continuum, or a "Devil's staircase," of hierarchical orderings based on some underlying motifs. Using a first-principles statistical mechanical approach, we have identified several such sets of orderings in common layered oxides intercalated

with Na or K, within the O3/P3/O1 structure family. An important set of orderings appears in the P3 structure at intermediate concentrations, in which variants of one particular ordering are separated by periodically spaced antiphase boundaries. The overall density of boundaries in this case determines the average composition. Another notable set of orderings is predicted for K intercalation at high concentrations, where alternating regions of octahedrally and prismatically coordinated K exist in the same intercalation layer. This mixed coordination leads to significant distortions of the host structure. We discuss these sets of orderings in the context of phase stability predictions for several systems and compare our results to experimentally observed voltage profiles and structural evolution during cycling. We also explore ramifications for ion diffusion and electrode performance.

6:20 PM EN03.03.04

Origins of Irreversibility in Layered $\text{NaNi}_x\text{Fe}_y\text{Mn}_z\text{O}_2$ Cathode Materials for Sodium Ion Batteries Eric Gabriel¹, Changjian Deng¹, Paige Skinner¹, Sungsik Lee², Pete Barnes¹, Chunrong Ma¹, Jihyeon Gim², Miu Lun Lau¹, Eungje Lee² and Hui (Clair) Xiong¹; ¹Boise State University, United States; ²Argonne National Laboratory, United States

Layered $\text{NaNi}_x\text{Fe}_y\text{Mn}_z\text{O}_2$ cathode (NFM) is of great interest in sodium ion batteries due to its high theoretical capacity and utilization of abundant, environmentally-friendly elements. However, the evolution of the local bonding of the transition metals (TMs) beyond the first charge/discharge cycle is not well understood. In this work, we investigate the reversibility of TM ions in layered NFMs with varying Fe contents and potential windows after multiple cycles. Utilizing *ex situ* synchrotron X-ray absorption near edge spectroscopy (XANES) and extended X-ray absorption fine structure (EXAFS) of pre-cycled samples the valence and bonding evolution of the TMs are elucidated. Our results indicate that Fe redox ($\text{Fe}^{3+}/\text{Fe}^{4+}$) is active in the first several cycles in these $\text{NaNi}_x\text{Fe}_y\text{Mn}_z\text{O}_2$ samples, but on the 5th cycle Fe no longer participates in charge compensation. Manganese was found to be inactive for all cycles. The Ni redox couple contributes most of the charge compensation for NFMs beyond the 1st cycle. Ni redox is quite reversible in the cathodes with less Fe contents. However, the Ni redox couple shows significant irreversibility with high Fe content of 0.8, suggesting an interaction between Ni and Fe bonds. The electrochemical reversibility of the NFM cathode becomes increasingly enhanced with the decrease of either Fe content or with lower upper charge cutoff potential.

6:35 PM DISCUSSION TIME

6:50 PM *EN03.03.06

Open-Framework Polyanionic Compounds as Potassium Insertion Host Shinichi Komaba¹, Tomooki Hosaka¹, Shahul Hameed^{1,2}, Mirai Ohara¹, Tetsuya Takahashi¹, Kei Kubota^{1,2} and Ryoichi Tatara^{1,2}; ¹Tokyo University of Science, Japan; ²Kyoto University, Japan

We reported the high working voltage of K-ion battery (KIB) comparable to Li-ion and higher than Na-ion batteries based on the fact that the standard potential of potassium is lower than those of lithium and sodium in nonaqueous electrolyte [1,2]. In 2015, our group reported a graphite negative electrode delivering $>250 \text{ mAh g}^{-1}$ with excellent reversibility [1]. Furthermore, a Prussian blue analogue (PBA) of $\text{K}_2\text{Mn}[\text{Fe}(\text{CN})_6]$ demonstrated highly reversible potassium insertion/extraction and 4 V operation, realizing a 4 V-class $\text{K}_2\text{Mn}[\text{Fe}(\text{CN})_6]/\text{graphite}$ full cell [3]. The previous studies revealed that a three-dimensional open framework structure of PBAs is suitable for insertion/extraction of large K^+ ion. In addition to the PBAs, polyanionic compound and metal organic phosphate open framework (MOPOF) materials are potential positive electrode materials for KIBs due to their open framework structure and inductive effect. In this talk, our recent studies on potassium insertion into various polyanionic compounds and MOPOFs, such as orthorhombic KFeSO_4F (o- KFeSO_4F), KFePO_4F , $\text{K}_6(\text{VO}_2)(\text{V}_2\text{O}_3)_2(\text{PO}_4)_4(\text{P}_2\text{O}_7)$ (K6V6P6), and $\text{K}_2[(\text{VOHPO}_4)_2(\text{C}_2\text{O}_4)]$ [4,5], will be presented to give a perspective of potassium insertion material design.

We have reported a reversible potassium extraction and insertion into o- KFeSO_4F , which has KTiOPO_4 -type structure providing large channels for K^+ ion diffusion. In this study, potassium insertion mechanism of $\text{KFe}(\text{III})\text{PO}_4\text{F}$ having the same crystal structure was examined and compared with that of o- $\text{KFe}(\text{II})\text{SO}_4\text{F}$.

KFe(III)PO₄F exhibited reversible potassium insertion and extraction based on the Fe³⁺/Fe²⁺ redox couple. In addition to the KTiOPO₄-type structure materials, other open-framework materials of K₆V₆P₆ and K₂[(VOHPO₄)₂(C₂O₄)] were investigated. K₆V₆P₆ delivered a reversible capacity of ca. 60 mAh g⁻¹ with a plateau at 4.0 V. K₂[(VOHPO₄)₂(C₂O₄)] exhibited a large discharge capacity of >100 mAh g⁻¹ and excellent rate capability due to the facile migration of K⁺ ions in the framework. From these results, we will present our future insight into electrochemical potassium insertion chemistry for battery applications.

References

- [1] S. Komaba *et al.*, *Electrochem. Commun.*, **60**, 172 (2015).
- [2] T. Hosaka, S. Komaba *et al.*, *Chem. Rev.*, **120**, 6358 (2020).
- [3] X. Bie, K. Kubota, S. Komaba *et al.*, *J. Mater. Chem. A*, **5**, 4325 (2017).
- [4] T. Hosaka, T. Shimamura, S. Komaba *et al.*, *Chem. Rec.*, **19**, 735 (2019).
- [5] A. S. Hameed, S. Komaba *et al.*, *Adv. Energy Mater.*, 1902528 (2019).

SESSION EN03.04: Battery Anode
Session Chairs: Hui (Clair) Xiong and Naoaki Yabuuchi
Wednesday Afternoon, April 21, 2021
EN03

8:15 PM *EN03.04.01

The Ultimate Intercalation Limit in Disordered Rock Salt Electrodes Shyue Ping Ong, Haodong Liu, Zhuoying Zhu, Ping Liu and Xingyu Guo; University of California, San Diego, United States

Rechargeable lithium-ion batteries with high energy density that can be safely charged and discharged at high rates are desired for electrified transportation and other applications. In this talk, I will report the discovery of a disordered rocksalt (DRS) Li₃V₂O₅ anode with near-optimal intercalation potentials for safe, fast-charging batteries. In particular, we will demonstrate that the outstanding electrochemical performance of these DRS electrodes can be attributed to a hitherto undiscovered redistributive lithium intercalation reaction with low energy barriers. Beyond the immediate practical applications, the discovery of this novel high-rate intercalation reaction opens a completely new space for the search of metal oxide electrodes for fast-charging, long-life lithium-ion batteries. Further, I will discuss a statistical analysis of the ultimate limits of intercalation into DRS type materials.

8:40 PM *EN03.04.02

Computational Study on the Intercalation Energy Storage Mechanism of Transition-Metal-Carbide MXene by Quantum-Classical Hybrid Simulation Yasunobu Ando^{1,2}; ¹AIST, Japan; ²Kyoto University, Japan

Two-dimensional transition-metal carbide MXenes has been known as a promising material of high-performance electrode for energy storage applications with both non-aqueous and aqueous electrolytes because it has electronic conductivity, ion capability in interlayer nanospace, and the redox activity of Ti. Especially, as an electrode of electrochemical capacitors, MXenes have a unique dependence of capacitance on intercalated cation species and a distinctive behavior that is both capacitive and pseudocapacitive depending on the electrolyte. To better understand electrochemical mechanism of these behaviors, we performed a microscopic theoretical analysis of the electric-double layer (EDL) in the interlayer nanospace of the MXene electrode by combining first-principles calculations based on density functional theory (DFT) and classical implicit solvation theory named three dimensional reference-site interaction model (3D-RISM) method [1]. By using the quantum-classical hybrid simulation, solvation effect at the interlayer nanospace of MXene electrode was taken into consideration appropriately with low computational cost comparable with conventional DFT simulation.

For the unique dependence of capacitance on intercalated cation species, our simulation results showed that the capacitance of EDL capacitors can be enhanced by a factor of 1.8, when the water molecules are strongly confined into the two-dimensional nanoslits of titanium carbide MXene electrode. This is because that dipolar polarization of strongly confined water overscreens an external electric field applied on the EDL and enhances capacitance with a characteristically negative dielectric constant of a water molecule [2, 3].

Another investigated feature is the distinctive behavior that is both capacitive and pseudocapacitive depending on the electrolyte. As a result of their electronic states simulated via the quantum-classical hybrid simulation, it was found that the hydration shell of intercalated ions prevents orbital coupling between MXene and the intercalated ions, which leads to the formation of an EDL and capacitive behavior. However, once the cations are partially dehydrated and adsorbed onto the MXene surface directly, because of orbital coupling of the cation states with the MXene states, particularly for surface-termination groups, charge transfer occurs and results in a pseudocapacitive behavior [4].

9:05 PM EN03.04.03

Correlating Crystallinity of Nb₂O₅ Fibers with Electrochemical Performance as Sodium-Ion Battery Electrode Carla G. Real¹, Davi Marcelo Soares², Gurpreet Singh² and Hudson Zanin¹; ¹University of Campinas - UNICAMP, Brazil; ²Kansas State University, United States

Research on niobium pentoxide (Nb₂O₅)-based electrodes for electrochemical energy storage devices is gaining traction because of its ability to store charge at high rates despite its wide bandgap and low electronic conductivity—a phenomenon not observed in other widely studied transition metal oxides electrode materials. Crystalline form of Nb₂O₅— orthorhombic and pseudohexagonal phases— also presents superior electrochemical stability and rapid ion transport of alkali-metal ions throughout the a–b plane. This work investigated the effect of different crystalline structures of Nb₂O₅ in micro/nano fiber geometry as working electrode in sodium half-cells. The micro/nano fiber geometry promoted Na-ion de/intercalation reactions combined with capacitive reactions. Results show that these materials present excellent cycling stability and specific capacity within 0 to 2.25 V potential window. Orthorhombic Nb₂O₅ outperform amorphous Nb₂O₅ and many other traditional high capacity metal oxide-based electrodes such as birnessite such as MnO₂ and RuO₂.

9:20 PM BREAK

9:35 PM *EN03.04.04

The Architectures for the Si and Li-Metal Anode Based Batteries with High Performances In Kim^{1,2}, Cary Hayner¹ and Xin Li²; ¹NanoGraf Corporation, United States; ²Harvard University, United States

Currently, pure electric vehicles (EV) are produced from many car makers. And it is becoming more popular with the public. However, an additional increase of driving range with long life and high safety is necessary to make EV popularized completely. Also, aviation service such as air-taxi will be commercialized soon. Therefore, the application of new materials such as Si and Li-metal anode is essential to increase energy density dramatically at this moment. And proper electrode engineering has brought Si-based anode materials closer to commercialization from consumer applications. However, Si technology has not yet been significantly commercialized due to a number of shortcomings. In particular, cycle life and irreversible capacity losses due to side reactions continue to be issues that plague their widespread use. Thus, the addition of only thimbleful silicon is possible right now for practical batteries, and it is difficult for the dramatic increase of energy density of batteries.

In this presentation, we can check the current status of approaches for commercialization of Si anode based batteries. Also, newly developed advanced architecture with offering higher battery capacity and faster rate performance, all while being produced via a low-cost solution chemistry-based manufacturing process will be introduced. This scalable manufacturing procedures of silicon-based anode can lead to significantly improved performance of next-generation batteries, which have high energy density, long-term cycling stability, and fast

charging ability.

In the case of Li-metal, the electrode structure is going to be porous rapidly and the growth of Li dendrite is going to be generated rapidly. And those lead short cycle life performance, low safety and poor reliability. Thus, Li-metal anode is not possible to be applied to EV, and it is tested for the application of drones that have low requirement for life and safety.

In this presentation, we are going to introduce hybrid Li-metal battery, having high energy density (-800 Wh/L, -360 Wh/kg), high safety and long cycle life performance, which is applicable to practical EV. We applied hybrid Li-metal anode technologies and additional support from safe materials to retard thermal runaway.

10:00 PM *EN03.04.05

Phase Evolution and Interfacial Strain in Electrode Materials for Energy Storage Dong Su; Institute of Physics, Chinese Academy of Sciences, China

Advanced (scanning) transmission electron microscopy ((S)TEM) techniques have been intensively applied to study the reaction kinetics of electrode materials for secondary ion batteries. With/Combining different TEM techniques, including in-situ TEM and diffraction, HAADF-STEM, and STEM-electron energy-loss spectroscopy, researchers are able to probe local structural and chemical information of electrode materials at atomic resolution. This talk will focus on using in-situ and analytical TEM to characterize the oxide electrode material for lithium ion batteries. After reviewing the recent advances of in-situ TEM investigations on both anode and cathode, we will discuss the dynamical study on the phase evolution, strain effect and passivation layer of conversion-type Fe₃O₄, aiming to understand how reaction pathways affect the batteries performances [1-3]. In addition, this talk will present our investigations on effects of defects on capacity fade of Ni-rich Li(Ni, Mn, Co)O₂ cathode [4].

References:

- [1] He K. et al., Visualizing non-equilibrium lithiation of spinel oxide via in situ transmission electron microscopy, *Nature Communications*, 7,11441 (2016)
- [2] Hwang S. et al., Strain coupling of conversion-type Fe₃O₄ thin film for lithium ion battery, *Angewandte Chemie*, 56,7813, (2017)
- [3] Li J. et al. Phase evolution of conversion-type electrode for lithium ion batteries, *Nature Communications*, 10,2224 (2019)
- [4] Li S. et al., *Angewandte Chemie International Edition*, (2020) <https://doi.org/10.1002/anie.202008144>

10:25 PM EN03.04.06

Enabling Low-Temperature Operation of Alkali Metal Anodes through Electrolyte Design Akila C. Thenuwara, Pralav P. Shetty and Matthew T. McDowell; Georgia Institute of Technology, United States

Low temperature (< -20 °C) operation of conventional Li-based secondary batteries is severely hindered by increased cell polarization, which can be attributed mainly to the low ionic conductivity of electrolytes and sluggish solid-state diffusion in graphite. Additionally, charging of graphite-based Li-ion batteries under low-temperature conditions can cause undesirable Li plating; thus, there is a substantial need for next-generation anodes that can operate over a wide temperature range. In this regard, the Li metal anode has previously shown some promise for ultra-low temperature operation; however, it generally exhibits limited cycling capability and low Coulombic efficiency. Here, we develop advanced electrolyte formulations (which consist of dual salts and/or dual solvents) and show that these formulations can substantially improve the Coulombic efficiency (CE) of both Li and Na metal anodes down to -60 °C.¹⁻² For example, we show that pure ether based electrolytes exhibit CE < 50 % for Li cycling at -40 °C, but using FEC additives increases CE to over 90 %. The origins for this improved performance are primarily due to beneficial alterations of the solid-electrolyte interphase (SEI) at low temperatures when these additives are used. We perform cryo-transmission electron microscopy (TEM) and X-ray photoelectron spectroscopy to link SEI chemistry and structure as a function of temperature to cycling performance. Furthermore, we investigate the solvation structure of Li⁺ and Na⁺ in the electrolyte and relate solvation structure to SEI formation. Our results provide important guidance for designing electrolytes and interfaces for efficient operation of high-energy batteries at low temperatures.

References

1. Thenuwara, A. C.; Shetty, P. P.; Kondekar, N.; Sandoval, S. E.; Cavallaro, K.; May, R.; Yang, C.-T.; Marbella, L. E.; Qi, Y.; McDowell, M. T., Efficient Low-Temperature Cycling of Lithium Metal Anodes by Tailoring the Solid-Electrolyte Interphase. *ACS Energy Letters* **2020**, *5* (7), 2411-2420.
2. Thenuwara, A. C.; Shetty, P. P.; McDowell, M. T., Distinct Nanoscale Interphases and Morphology of Lithium Metal Electrodes Operating at Low Temperatures. *Nano Letters* **2019**, *19* (12), 8664-8672.

SESSION EN03.05: Li and Na Ion Batteries
Session Chairs: Xin Li and Anton Van der Ven
Thursday Morning, April 22, 2021
EN03

10:30 AM *EN03.05.01

High Valent Redox for Li and Na-ion Electrodes William C. Chueh; Stanford University, United States

High-valent redox at the positive electrodes are required to achieve high-energy density in intercalation lithium and sodium-ion batteries. Yet, high-valent redox is usually accompanied by strong structural irreversibility and hysteresis. In this talk, I will present a unified understanding of high valent redox that integrates redox chemistry with point defect chemistry and coulombic interaction. I will draw examples from lithium-ion electrode chemistries based on 3d, 4d and 5d transition metals.

10:55 AM *EN03.05.02

Stacking-Fault Enhanced Lattice Oxygen Redox in Layered Cathode Materials Yan-Yan Hu^{1,2}; ¹Florida State University, United States; ²National High Magnetic Field Laboratory, United States

Many layered Li and Na cathode materials deliver additional capacity via lattice oxygen redox reactions. However, its origin is under debate. The irreversibility and hysteresis of lattice oxygen redox limit its practical applications. With combined magnetic resonance spectroscopy and computational studies, we have discovered that layered structures with stacking faults can afford additional removal of lithium accompanied by lattice oxygen redox. The insights gained in this work may inspire materials design which employs structural disorder for achieving high-capacity stable cathode materials.

11:20 AM *EN03.05.03

Anionic Redox Chemistry in Layered Chalcogenide Cathode Materials for Sodium Batteries Zulipiya Shadike¹, Tian Wang², Ding-Ren Shi², Enyuan Hu¹, Zheng-Wen Fu² and Xiao-Qing Yang¹; ¹Brookhaven National Laboratory, United States; ²Fudan University, China

The discovery of anionic redox chemistry in layered compounds was traced back to ligand-hole chemistry in chalcogenides, in which the redox of S_2^{2-} , Se_2^{2-} or Te_2^{2-} ions in layered structures might be involved. In recent years, investigation of oxygen redox chemistry in cathode materials has attracted a lot of attention based on the potential to increase the energy density of Li-ion batteries. The reversible oxygen redox reactions in layered cathode materials such as Li-rich NMC and $Li_{12}Ru_{0.5}Mn_{0.5}O_3$ are considered to be responsible for their extraordinary specific capacity. Similarly, the reversible sulfur redox reaction in layered chalcogenides is considered a promising approach to increase the specific capacities in sodium-ion batteries. However, only a limited number of studies on the nature of anionic redox chemistry in layered chalcogenides have been reported in the literature. Issues about whether the redox mechanism is based on reversible formation/decomposition of S-S dimers or formation of electron holes on S are still under debate. We have designed and synthesized a series of layered cathode materials such as $NaCrS_2$, Ti substituted $NaCrS_2$ and Se substituted $NaCrS_2$ for a systematic

investigation about the nature of anionic redox chemistry of sulfur, including the formation of localized electron holes, anionic dimers, and disulfide-like species during the charging process. The charge compensation mechanisms and structural evolution of these cathode materials have been investigated using synchrotron-based multi-model characterization techniques such as in situ/ex situ x-ray absorption spectroscopy, x-ray diffraction, x-ray pair distribution function analysis as well as spatially resolved x-ray fluorescence mapping combined with DFT calculation. These results provided valuable information for the development of high energy cathode materials based on the anionic redox reaction for sodium batteries.

Acknowledgment

The work at Brookhaven National Laboratory was supported by the Assistant Secretary for Energy Efficiency and Renewable Energy, Vehicle Technology Office of the U.S. Department of Energy through the Advanced Battery Materials Research (BMR) Program under contract DE-SC0012704. This research used resources at beamlines 7-BM (QAS), 8-BM (TES) of the National Synchrotron Light Source II, a U.S. Department of Energy (DOE) Office of Science User Facility operated for the DOE Office of Science by Brookhaven National Laboratory under Contract No. DE-SC0012704.

11:45 AM EN03.05.04

Mechanism of Non-Hysteretic Redox Exceeding Conventional Transition Metal Capacity in Na-Ion Cathode Materials Daniil A. Kitchaev, Julija Vinckeviciute and Anton Van der Ven; University of California, Santa Barbara, United States

Harnessing electrochemical activity exceeding the limit of conventional transition metal redox, observed in Li-excess and Na-excess cathodes, is one of the most promising routes towards dramatically increasing the energy density of battery materials. However, the majority of materials exhibiting such anomalous capacity suffer from substantial voltage hysteresis and structural degradation. Two prominent exceptions are $\text{Na}_2\text{Mn}_3\text{O}_7$ and Li_2IrO_3 , which are model systems for non-hysteretic redox beyond the transition metal limit. Nonetheless, the mechanism of their redox behavior and stability to structural transformation remains controversial, with significant inconsistencies between experimental observations and the "O-redox" theories proposed as explanations of their behavior. We derive the first redox mechanism to consistently explain all experimental observations in $\text{Na}_2\text{Mn}_3\text{O}_7$ and Li_2IrO_3 , based on the oxidation of a delocalized, π -bonded network of metal- d and oxygen- p orbitals. This mechanism, which we term π -redox, leads to a unique behavior wherein the oxidation potential, capacity and structural evolution is dictated by the long-range structure of the π -network rather than local bonding environments. We show that π -redox competes with oxidation-driven transition metal migration, which is dominant in layered Li-excess materials based on Li_2MnO_3 but may be suppressed in layered Na-ion cathodes. The π -redox mechanism establishes the first rigorous framework for engineering non-hysteretic redox beyond the limit of transition metal capacity, which is particularly promising in layered Na-ion materials.

12:00 PM EN03.05.05

Controlling Covalency and Anion Redox Potentials Through Anion Substitution in Li-Rich Chalcogenides Joshua J. Zak¹, Andrew J. Martinolich¹, David N. Agyeman-Budu², Seong Shik Kim¹, Nicholas H. Bashian³, Ahamed Irshad³, Sri Narayan³, Brent C. Melot³, Johanna Nelson Weker² and Kimberly A. See¹; ¹California Institute of Technology, United States; ²SLAC National Accelerator Laboratory, United States; ³University of Southern California, United States

Conventional positive electrode materials for Li-ion batteries utilize a Li^+ intercalation mechanism charge-balanced by redox on transition metals within an oxide host lattice. Moving forward, multielectron cathodes that exhibit contributions to the redox from structural anions are of interest for the potential to dramatically increase charge storage capacity. Oxidation of Li-rich oxides can achieve >1 electron oxidation per transition metal, but, due to the high-voltage redox, electrolyte degradation and other unwanted side reactions can convolute interpretation of the electrochemistry. Later group chalcogenides, however, operate within the potential window of the electrolyte preventing complications associated with electrolyte decomposition. Capacity beyond that

compensated by a one-electron oxidation on a transition metal is often attributed to anion oxidation enabled by covalent interactions with the metal. Here, we report anion redox in a solid solution, $\text{Li}_2\text{FeS}_{2-y}\text{Se}_y$, where the metal-anion covalency is tuned through systematic substitution of the anion to further understand the role of covalency on reversible anion redox. Multielectron redox is observed in all materials in the solid solution along with a systematic shift of the high-voltage plateau associated with anion oxidation. Spectroscopic studies indicate concomitant Fe and S/Se oxidation throughout charging contrary to the discrete Fe and S redox observed in Li_2FeS_2 . Perselenide bonds are found to form in Li_2FeSe_2 accompanied by the irreversible formation of a new, high-impedance phase, which leads to poor cyclability. Therefore, while tuning metal-chalcogenide covalency provides a handle to control anion redox, the structural changes incurred through anion-anion bonding can be deleterious to material performance. As such, developing holistic understanding of the electronic and structural response to anion redox is necessary to design next-generation multielectron energy storage materials.

SESSION EN03.06: Advanced Performance and Phenomena in Batteries
Session Chairs: Anton Van der Ven and Hui (Clair) Xiong
Thursday Afternoon, April 22, 2021
EN03

1:00 PM *EN03.06.01

Charge Transfer in Intercalation Cathode Materials—Towards Extreme Fast Charging Christopher S. Johnson; Argonne National Laboratory, United States

Due to their exceptional high energy density, lithium-ion batteries are of central importance in many modern electrical devices. A serious limitation, however, is the slow charging rate used to obtain the full capacity. Thus far, there have been no ways to increase the charging rate without losses in energy density and electrochemical performance. Here we show that the charging rate of a cathode can be dramatically increased via interaction with white light. We find that a direct exposure of light to an operating LiMn_2O_4 3-D intercalation cathode during charging leads to a remarkable lowering of the battery charging time by a factor of two or more. This enhancement is enabled by the induction of a microsecond long-lived charge separated state, consisting of Mn^{4+} (hole) plus electron. This results in more oxidized metal centers and ejected lithium ions are created under light and with voltage bias. We anticipate that this discovery could pave the way to the development of new fast recharging battery technologies.

1:25 PM *EN03.06.02

Insight on the Local Structure and Electronic Structure of Positive Electrode Materials for Na-Ion Batteries Using Solid State NMR Dany Carlier^{1,2}, Long Nguyen^{1,2,3}, Yohan Biecher¹, Paula Sanz Camacho^{1,2}, Jacob Olchowka^{1,2}, Marie Guignard¹, Christian Masquelier^{3,2}, Claude Delmas¹ and Laurence Croguennec^{1,2}; ¹Institut de Chimie de la Matière Condensée de Bordeaux, France; ²RS2E, France; ³Laboratoire de réactivité et de chimie des solides, France

For energy storage, nowadays, Li-ion and Na-ion batteries are major technologies for mobility applications and also for large-scale storage of energy and their integration in the grid. In the scope of finding new positive electrode materials with improved performances, the deep understanding of the link between their structure, electronic structure and electrochemical behavior is crucial. To that extent, Magic Angle Spinning Nuclear Magnetic Resonance (MAS-NMR) appeared to be a key tool, as for paramagnetic materials, it allows to probe both, the local structure and the local electronic structure thanks to the hyperfine interaction.

Using MAS-NMR we showed that several phosphate materials as $\text{Na}_3\text{V}_2(\text{PO}_4)_2\text{F}_3$, which is a promising materials for positive electrode application Na-ion batteries exhibit some O-defects leading to the formation of V^{4+} ions locally. These V^{4+} ions are forming a vanadyl-type bond with the defect O, and affect the

electrochemical cycling performances. ^{23}Na , ^{31}P MAS (and ^{19}F) NMR was also used to probe the local structure and electronic structure of the solid solution series $\text{Na}_3\text{V}_2(\text{PO}_4)_2\text{F}_{3-y}\text{O}_y$ and other $\text{Na}_3(\text{V},\text{M})_2(\text{PO}_4)_2\text{F}_{3-y}\text{O}_y$ materials with $\text{M} = \text{Fe}$ or Al . These studies combined with DFT calculations lead to a better understanding of the local arrangement and the local electronic structure.

Layered Na_xMO_2 oxides are also interesting for application in Na-ion batteries. Among them, $\text{P2-Na}_x\text{CoO}_2$ appears to be a model material with a very specific phase diagram and unusual physical properties. ^{23}Na MAS NMR was used to characterize the changes in the electronic structure during Na deintercalation. It was shown that the position of the signal is governed by an interplay between the Fermi contact interaction due to localized electrons and the Knight interaction due to the delocalized ones. Depending on the Na content, the evolution of the ^{23}Na shift provides then information about the local electronic structure in the material.

1:50 PM EN03.06.03

Na/K Ion Exchange Mechanism in Layered $\text{Na}_3\text{Ni}_2\text{SbO}_6$ Cathode—“Na Redistribution by K Insertion”
Haegyeom Kim¹, Deok-Hwang Kwon², Jaechul Kim³, Bin Ouyang², Hyunchul Kim¹, Juila Yang² and Gerbrand Ceder^{2,1}; ¹Lawrence Berkeley National Laboratory, United States; ²University of California, Berkeley, United States; ³Stevens Institute of Technology, United States

Recently, an ion exchange reaction that can stabilize potassium intercalation oxides was proposed as a new approach to develop cathode materials for K-ion batteries (KIBs).¹⁻⁴ Such ion exchange method indeed has frequently used for the development of novel Li-layered oxides to attain structural features of Na layered oxides.⁵⁻⁷ This ion exchange reaction has the potential to discover novel layered cathode materials by accessing the metastable states that cannot be achieved by conventional high-temperature calcination. However, the solid-state ion-exchange mechanism and the resulting phase evolution are not well understood.

In this work, we systematically investigate electrochemical Na^+/K^+ ion exchange in layered oxides using O3-type $\text{Na}_3\text{Ni}_2\text{SbO}_6$ as a model system.⁸ We found intriguing phase transitions according to the relative Na/K content upon K intercalation by *in-situ* XRD: (i) coexist of K-rich and Na-rich phases during charging and discharging and (ii) phase transformation of Na-rich phase upon K intercalation. Strong electrostatic repulsion between Na and K ions that have radically different bond lengths to coordinating oxygen ions can result in this complex phase evolution. We uncovered that upon Na^+/K^+ ion exchange Na ions remaining in the desodiated $\text{Na}_x\text{Ni}_2\text{SbO}_6$ phase are pushed away from the intercalating K ions, thereby separating Na-rich and K-rich phases in a particle. Interestingly, this phenomenon creates complex, three-phase equilibrium during the desodiation and potassiation processes in $\text{Na}_x\text{K}_y\text{Ni}_2\text{SbO}_6$: phase equilibrium between one K-rich and two Na-rich phases or two K-rich and one Na-rich phase is observed, as dictated by the Gibbs phase rule. Our computational study further demonstrated that this phase separation originates from the large lattice mismatch along the *c*-axis between the K-rich and Na-rich phases. Our observations and interpretations demonstrate that “ion-exchanged” systems may be more complex to interpret than the previously understood. Our analysis should be applicable to other ion-exchange systems where the exchanged ions are not well miscible in the host structure.

References

- [1] S. Baskar et al. *ECS Transactions* **2017**, 80, 357.
- [2] N. Naveen et al. *Chem. Mater.* **2018**, 30, 2049.
- [3] J. Y. Hwang et al. *Energy Environ. Sci.* **2018**, 11, 2821.
- [4] H. Zhang et al. *Chem. Commun.* **2019**, 55, 7910.
- [5] C. Delmas et al. *Mater. Res. Bull.* **1982**, 17, 117.
- [6] A. R. Armstrong et al. *Nature* **1996**, 381, 499.
- [7] F. Capitaine et al. *Solid State Ionc.* **1996**, 89, 197.
- [8] H. Kim et al. *Chem. Mater.* **2020**, 32, 4312.

2:05 PM EN03.06.04

Re-Examining the Electronic Structure of Layered NaMO_2 Electrodes Christopher Savory and David O. Scanlon; University College London, United Kingdom

Ab initio modelling is a useful tool in the study of battery electrodes, able to support experimental findings and predict new phases and behaviours, providing a suitable and accurate method is used. Regular Density Functional Theory (DFT) functionals such as the commonly used PBE, however, are impacted by the 'self-interaction error' which severely impacts the accuracy of calculations involving the highly-correlated 3d valence electrons in transition metals (TMs).¹

Historically, the study of battery cathodes using DFT has been improved through the addition of 'U' parameters, which correct for the self-interaction error,² however these parameters require tuning to experimental measurements on the specific system in question, while also need to be varied during intercalation (with changes in oxidation state) and can be highly sensitive to changes in transition metal composition. This makes them unideal for the description of complex cathode systems containing multiple transition metals and valencies, weakening them as a predictive tool for new systems.

Additionally, with the increased development behind the theory of anionic redox in cathodes, accurate assessment of the charge transfer transition, which standard DFT tends to underestimate, is crucial.³ Minimally-parameterised hybrid DFT functionals such as HSE06 are routinely used to accurately predict the band gaps of semiconductors, however previous studies have highlighted disagreement between hybrid DFT and band gaps recorded from XPS-BIS for TM cathode materials, as well as overestimation of predicted intercalation voltages.^{4,5}

In this study, we address this issue, using a combination of HSE06 and high-level quasiparticle self-consistent GW calculations (with the inclusion of additional terms to W from the Bethe-Salpeter equation) to explore the electronic structure of sodium intercalation cathodes such as NaCoO₂ and NaFeO₂, as well as comparisons to their lithium counterparts, at the highest feasible level of ab initio theoretical methods. We demonstrate how the inclusion of additional screening terms to the on-site Coulombic interaction leads to changes in the valence electronic structure of the cathodes not seen in cheaper methods. Secondly, we examine how the inclusion of corrections for the van der Waals forces, crucial to simulation of deintercalation behaviour, varies between hybrid and standard DFT. In doing so, we hope to set out a blueprint for guiding accurate future calculations of cathodes that rely less on parameterisation, and as such demonstrate reliable predictive power.

(1) Urban, A.; Seo, D.-H.; Ceder, G. *npj Comput. Mater.* **2016**, 2 (October 2015), 16002.

(2) Zhou, F.; Cococcioni, M.; Marianetti, C. A.; Morgan, D.; Ceder, G. *Phys. Rev. B - Condens. Matter Mater. Phys.* **2004**, 70 (23), 235121.

(3) Ben Yahia, M.; Vergnet, J.; Saubanère, M.; Doublet, M. L. *Nat. Mater.* **2019**, 18 (5), 496.

(4) Seo, D. H.; Urban, A.; Ceder, G. *Phys. Rev. B - Condens. Matter Mater. Phys.* **2015**, 92 (11), 115118.

(5) Aykol, M.; Kim, S.; Wolverton, C. *J. Phys. Chem. C* **2015**, 119 (33), 19053.

2:20 PM EN03.06.05

Exploration of A-Mn-O System with A=Li, Na, K for Cathode Material in Non Aqueous Batteries Valerie Pralong, Justine Jean, Erwan Chandler, Audric Neveu, Melanie Freire and Evan Adamczyk; CNRS CRISMAT, France

One of the major challenges of the 21st century is our ability to solve energy-related problems caused by ever-higher consumption, demography and standard of living. It is therefore imperative to anticipate this energy demand and this in a context of sustainable development. Storage technologies are highly dependent on the materials used and it is necessary to search for new materials with advanced properties that are also ecological and economical. Despite the high performance of lithium-based materials, its cost is driving scientists to develop alternative systems based on sodium and potassium, which are widely abundant in the earth's crust.

Manganese based oxide materials are promising cathodes for alkaline ion batteries due to their high energy density, low-cost and low-toxicity. Focusing on layered-type structures, one has to cite of course the A_xMnO₂ families showing interesting insertion properties in all the system based on lithium, sodium and even more recently potassium. Moreover, we notice that the system A-Mn-O are extremely rich in term of original structures. For example, we found a new lithium rich composition Li₄Mn₂O₅ with a disordered rock salt structure that was showing an exceptional capacity of about 300mAh/g. Interestingly, the material Na₄Mn₂O₅ has been reported with a layered type structure, different from the lithiated phase and we will discuss the

relationship between the structure and insertion properties. Also, we have reported the electrochemical properties of the phase $\text{Na}_2\text{Mn}_3\text{O}_7$ with a lamellar structure built of $[\text{Mn}_3\text{O}_7]^{2-\infty}$ anionic layers held by sodium ions; a reversible discharge capacity of 160 mAh/g at 2.1V vs Na^+/Na through a biphasic process is observed.

In recent years, we can see a growing interest of researchers for K-ion batteries (KIBs). Thus, many compounds have been studied belonging to families already studied for Li-ion and Na-ion batteries (LIBs and NIBs, respectively). So far, only lamellar phases K_xMnO_2 are reported. We will discuss on the possibility to explore and find other composition for this application.

In this presentation, we will discuss and compare the three system Li-Mn-O, Na-Mn-O and K-Mn-O in terms of structure and properties towards the insertion of alkaline ions.

2:35 PM EN03.06.06

Direct Electrochemically Grown Layered Na Transition Metal Oxides as High-Capacity High-Rate Cathodes for Na-Ion Battery Arghya Patra, Beniamin Zahiri, Patrick Kwon and Paul Braun; University of Illinois at Urbana-Champaign, United States

State-of-the-art synthesis for layered oxide cathodes for Na ion batteries involves prolonged high temperature ($>700^\circ\text{C}$) processing for long reaction times (~ 24 hours) under high oxygen pressure, followed by slurry casting after mixing with binders and additives. Here, we introduce, an intermediate temperature (350°C), dry molten sodium hydroxide mediated electrodeposition process to grow air and moisture sensitive layered sodium transition metal oxides, Na_xMO_2 ($\text{M}=\text{Co}, \text{Mn}, \text{Ni}, \text{Fe}$) as binder-and-additive-free cathode materials for Na ion battery. Despite being synthesized at the lowest reported synthesis temperature and reaction times, our electrodeposited oxide cathodes retain the key structural and electrochemical performance observed in the high temperature bulk synthesized analogues. We demonstrate that tens of microns thick, $>80\%$ dense Na_xCoO_2 and Na_xMnO_2 can be deposited at a growth rate of $\sim 5\text{-}20$ $\text{mg}/\text{cm}^2/\text{hr}$, with near theoretical gravimetric capacity, rate capability and chemical diffusion coefficient of Na^+ ions. The electrodeposited oxide cathodes can be accessed as both the thermodynamically stable O3 and metastable P2 polytypes. Growth texture, tortuosity and microstructure of the electroplated oxide cathodes are controlled by careful tuning of the deposition parameters and bath chemistry. Fast Na^+ ion conducting 110, 101 and 104 facets can be vertically oriented, enabling electrodeposited cathodes with ultrahigh loading ($30\text{-}40$ mg/cm^2), low tortuosity and reversible high areal capacity ($3\text{-}4$ mAh/cm^2) while operating at high current densities (~ 1 mA/cm^2).

SESSION EN03.07: Panel Discussion: Beyond Li Ion Battery

Session Chairs: Xin Li and Anton Van der Ven

Thursday Afternoon, April 22, 2021

EN03

8:15 PM *

Panel Discussion: Beyond Li Ion Battery M. Stanley Whittingham¹, Shinichi Komaba², Christopher S. Johnson³ and Debra R. Rolison⁴; ¹State University of New York at Binghamton, United States; ²Tokyo University of Science, Japan; ³Argonne National Laboratory, United States; ⁴U.S. Naval Research Laboratory, United States

Four distinguished panelists will share their vision with the audience on the topic of beyond Li-ion batteries through short presentations that are followed by a panel discussion. Next generation Li, Na, K and Zn ion batteries will be discussed in this 2 hour panel session with a particular focus on advanced cathode, anode and electrolyte concepts and designs. The audience will have the opportunity to directly interact with the panelists.

Schedule:

Introductory Remarks by Anton Van der Ven

Presentation by Stanley M. Whittingham—*Li Batteries for Energy Storage to Green the Environment - Is There Another Battery Alternative?*

Presentation by Shinichi Kimoba—*Sodium and Potassium Chemistry for Batteries*

Presentation by Christopher Johnson—*Calendar Life of Si Anodes in LIBs: Time is Ticking*

Presentation by Debra Rolison—*The Case for Zinc*

Panel Discussion

Closing Remarks by Anton Van der Ven

This session will be moderated by Anton Van der Ven and Xin Li

SESSION EN03.08: Poster Session

Session Chairs: Xin Li and Naoaki Yabuuchi

Friday Morning, April 23, 2021

8:00 AM - 10:00 AM

EN03

EN03.08.01

A Hierarchical Three-Dimensional Porous Graphene Film for Suppressing Polysulfide Shuttling in Lithium-Sulfur Batteries Eman Alhajji; King Abdullah University of Science and Technology, Saudi Arabia

The lithium-sulfur (Li-S) battery is a promising next-generation rechargeable battery with high energy density. Given the outstanding capacities of sulfur (1675 mAh g^{-1}) and lithium metal (3861 mAh g^{-1}), Li-S battery theoretically delivers an ultrahigh energy density of 2567 Wh kg^{-1} . However, this energy density cannot be realized due to several factors, particularly the shuttling of polysulfide intermediates between the cathode and anode, which causes serious degradation of capacity and cycling stability of a Li-S battery. In this work, a simple and scalable route was employed to construct freestanding laser-scribed graphene (LSG) interlayer with nano-sized carbon particles, which effectively suppresses the polysulfide shuttling in Li-S batteries. Thus, a high specific capacity (1160 mAh g^{-1}) with excellent cycling stability (80.4% capacity retention after 100 cycles) has been achieved due to the unique structure of hierarchical three-dimensional pores in the freestanding LSG.

EN03.08.02

The Effect of Microwave Heating Time on Electrochemical Energy Storage of Nickel Hydroxide Nanomaterials Nuha A. Alhebshi, Sumaih F. Alshareef and Faten E. Al-Hazmi; King Abdulaziz University, Saudi Arabia

The significant attention toward developing flexible electronic devices and smart textiles have been encouraging the utilization of various flexible current collectors as well as investigating their interface effects on the device performance. Using the traditional fabrication of supercapacitors and batteries onto textile fabrics and polymeric substrates requires additional processes of conductive-layer coatings and non-conductive binder additives. In this work, binder-free flexible electrodes of nickel hydroxide are directly deposited on conductive carbon cloth (CC) using a simple and short-time synthesis assisted by microwaves. The growth of nickel hydroxide nanoflakes is observed using x-ray diffraction and scanning electron microscopy after 10 min and 30 min of the microwave heating time at a fixed temperature. All our samples are tested as supercapacitor electrodes in potassium hydroxide aqueous electrolyte at room temperature. In specific, electrochemical impedance spectroscopy is used to study the electrode/electrolyte interface in terms of ions diffusion and charge transfer resistance. The redox Faradic mechanism of energy storage is confirmed by the cyclic voltammetry and

the galvanostatic charging-discharging techniques. Nickel hydroxide nanoflakes that are prepared in 30 min show a conformal coating on all substrate microfibers and a consequently larger electrochemical active area which results in higher capacitance than the electrodes prepared in 10 min. Such optimization in the design and fabrication of binder-free electrodes and current collectors could improve the flexibility of electronic devices and promote their implantation into functional textile applications.

EN03.08.03

Computational Modeling of Halogen Intercalation in Cathode Hosts for High Energy Density Dual Ion Batteries Naman Katyal and Graeme Henkelman; The University of Texas at Austin, United States

High voltage dual-ion batteries (DIBs) have been reported using a water-in-bisalt electrolyte, metal halides, and graphite electrodes but the full cell energy density is lower than commercialized batteries. Replacing graphite with heteroatom substituted graphite lamellar structures like BC_3 , $B_3C_{10}N_3$ can improve the performance of the dual ion battery. Heteroatom substituted graphite materials have been studied for metal ion intercalation in anodes and show similar electronic conductivity as graphite but remain unexplored for the halogen intercalation process. Halogen intercalation process in cathode host is of significant importance because it is directly related to the capacity and cycling of the battery. Halogen intercalation in graphite has been explored using diffraction and isothermal based studies but a rigorous thermodynamic and kinetic investigation is still missing. From a thermodynamic standpoint, only one study has reported the existence of chlorine intercalated graphite structure but a range of bromine intercalated graphite structures have been reported although there is no consensus about the staging process or the composition of bromine in graphite layers at every stage. Hence, a computation model to understand the halogen intercalation processes in graphite structures is needed to resolve the inconsistencies that can be used to study heteroatom substituted graphite structures. Through this model, our aim is to predict materials that can replace graphite as host structures in dual ion batteries to achieve high energy densities and longer cyclability.

In this paper, we aim to find answers to fundamental questions about the thermodynamics and kinetics of bromine and chlorine intercalated graphite structures: a.) Develop a convex energy hull diagram for bromine-intercalated structures and study the staging at every composition from the most stable structure, b.) Find, if any, thermodynamic stable chlorine-intercalated graphite structures, c.) Develop a convex energy hull diagram for bromine and chlorine co-intercalated structures and study the staging at every composition from the most stable structure, d.) Kinetic investigation of halogen diffusion in graphite using adaptive kinetic Monte Carlo techniques. All the calculations in this work have been performed using Density Functional Theory (DFT) methods in Vienna ab-initio Simulation Package (VASP). For all the structures modeled in this work, we will model structural properties using Raman Spectrum, Extended X-Ray Fine Spectrum, X-Ray Diffraction, and Pair distribution functions that are directly accessible via experiments as well. This will help us guide experiments towards an informed choice of cathode hosts for dual ion batteries using water in the salt electrolytes from our computational results.

EN03.08.04

Machine and Deep-Learning for Intercalation Compounds—Elucidating Structure-Property Relationships Kaci L. Kuntz, Yuchen Yang, Elena K. Barker, Daniel Carlebach, Mahit Dagar, Madeleine K. Eatchel, Tyler L. Gerstein and Anna K. Jiricko; University of Utah, United States

With the extensive research of intercalation in layered materials beginning in 1841, these compounds have since found use in battery, optoelectronics, and biomedical wearable devices (*Inorg. Chem. Front.* 2016, 3, 452; *Adv. Mater.* 2019, 1808213). With essentially limitless possibilities of intercalation compounds due to combinations of different host lattices and guest species (e.g. donor, acceptor, and neutral compounds), intercalation chemistry creates the unique opportunity to engineer and design future compounds for specific applications such as electrodes. However, this is only feasible if structure-property relationships of intercalated materials are extracted. Due to the large quantity of data on intercalation compounds, machine learning (ML) is an ideal approach (*J. Phys. Mater.* 2019, 2 032001). Previous ML studies of graphite intercalated compounds have often

been limited in scope to alkali metal guests (*J. Mater. Chem. A* 2019, 7, 19070-19080; *ACS Appl. Mater. Interfaces* 2019, 11(20), 18494–18503). Here, we employ ML and deep-learning (DL) to elucidate structure-property relationships in bulk graphite intercalation compounds with donor, acceptor, and neutral guests. Furthermore, we explore the application of these structure-property relationships to single and few-layered intercalation compounds where surface adsorption and intercalation of these ultra-thin materials can play significant roles in resulting properties of the intercalation compound as the 2D limit is approached.

EN03.08.05

Spin Structure and Magnetic Ordering of $\text{Li}_2\text{Ni}_2\text{TeO}_6$ Kory Wells, Tekiyah Robinson, Jonathan Valenzuela, Sunil Karna and Doyle Temple; Norfolk State University, United States

We studied tellurium containing oxide $\text{Li}_2\text{Ni}_2\text{TeO}_6$ using x-ray diffraction, magnetic measurements, and neutron powder diffraction. $\text{Li}_2\text{Ni}_2\text{TeO}_6$ crystallizes in the orthorhombic crystal structure having $Fddd$ space group. The magnetic susceptibility measurements performed at $H_a = 1$ kOe exhibits an upturn below ~ 80 K and maintains its constant value up to lower temperatures. The magnetic hysteresis is seen at lower temperatures below 80 K indicating the development of a ferromagnetic component that get disappears above 80 K revealing a ferromagnetic transition at ~ 80 K. Both ferromagnetic and antiferromagnetic peaks are revealed in neutron powder diffraction patterns below 80 K.

EN03.08.06

Transition Metal Monochalcogenides as Anodes for Metal-Ion Batteries Shakir Bin Mujib, Marren Ellis, Porter Herold and Gurpreet Singh; Kansas State University, United States

As the most promising energy storage system (ESS), rechargeable alkali metal-ion batteries have been attracting great attention. The selection of suitable electrode material is a fundamental step in the development of metal-ion batteries to achieve enhanced performance. In the present study, we have explored the feasibility of monolayers of phosphorene analogs, namely, group IV monochalcogenides. The monochalcogenide layers form structures belonging to the same orthorhombic crystal system and possess similar hinge-like structures like phosphorene. Just this unique hinge-like structure and the isolation of 2D forms will introduce strong anisotropic properties endowing them with fascinating properties, such as tunable bandgaps, high carrier mobility, and predominantly anisotropic and optical properties. We present two-dimensional (2D) sheets of germanium and tin sulfides and tellurides as promising high-capacity and stable materials for energy storage. GeS, GeTe, SnS, and SnTe with layered structures are prepared via a simple liquid-phase exfoliation approach. As-synthesized 2D nanosheets can effectively increase the electrolyte-electrode interface area and facilitate metal ion transport. As a result, GeS, GeTe, SnS, and SnTe nanosheets deliver a high areal capacity of 1.76 mAh cm^{-2} , 1.05 mAh cm^{-2} , 2.66 mAh cm^{-2} , 1.22 mAh cm^{-2} respectively as anodes in lithium-ion batteries (LIBs). Further analysis of these monochalcogenides in sodium-ion batteries (SIBs) and potassium-ion batteries (KIBs) suggest that layered monochalcogenides can be potential anodes in other metal-ion batteries.

EN03.08.07

Late News: Detailed Redox Mechanism and Self-Discharge Diagnostic of 4.9 V $\text{LiMn}_{1.5}\text{Ni}_{0.5}\text{O}_4$ Spinel Cathode Revealed by Raman Spectroscopy Ankush Bhatia, Jean Peirre Pereira-Ramos and Rita Baddour-Hadjean; Institut de Chimie et des Matériaux Paris-Est (ICMPE) UMR 7182 CNRS, France

Lithium-ion rechargeable batteries have been widely used as a power source for portable devices and are available for applications to electric vehicles, which demand high power, high energy, inexpensive and safe batteries[1]. Their continuous improvement is tightly bound to the understanding of lithium (de)intercalation phenomena in electrode materials. Here we address for the first time the use of Raman spectroscopy to understand the mechanisms involved in high voltage spinels $\text{LiNi}_x\text{Mn}_{2-x}\text{O}_4$ ($x = 0$; $x = 0.5$).

Although the “classical” lithium-containing spinel LiMn_2O_4 (LMO) has been extensively studied, certain points remain unclear. For instance, very little is known on the nature of the intermediate composition $\text{Li}_{0.5}\text{Mn}_2\text{O}_4$

postulated halfway during charge/discharge for which attempts to model a lithium/vacancy ordering have been made. On the other hand, compositions within the solid solution $\text{LiNi}_x\text{Mn}_{2-x}\text{O}_4$ ($0 < x \leq 0.5$) are of interest as they exhibit increasing voltage upon lithium extraction. The best compromise is found for $\text{LiNi}_{0.5}\text{Mn}_{1.5}\text{O}_4$ (LNMO): with a high specific capacity of 140 mAh g^{-1} available along a wide potential plateau at $\approx 4.7 \text{ V}$ vs Li^+/Li , LNMO is widely studied as a next-generation positive electrode material for Li-ion batteries. LNMO exists as two polymorphs, “disordered” ($Fd-3m$) where Mn/Ni occupy $16d$ sites randomly and “ordered” ($P4_332$) where Ni and Mn sit on ordered $4a$ and $12d$ sites. So far, the disordered form has outperformed the ordered form from an electrochemical point of view [2]. The delithiation/lithiation mechanism of disordered LNMO has been previously investigated using mainly X-ray and neutron diffraction and *in situ* synchrotron. Although these methods provide a picture of the phase evolution during cycling, we still lack information about the atomic level variations as lithium ions deintercalate/intercalate in the crystal structure of LNMO. Raman spectroscopy on the other hand is a very appropriate tool to enrich the knowledge of the structure of Li intercalation compounds at the scale of the chemical bond. A wealth of structural information including symmetry changes, local disorder, changes in bond lengths, emergence of secondary phases, etc... can be extracted from the Raman study of various Li intercalated host lattices, providing therefore a better insight into the mechanisms governing the electrode performances [3].

In this work, Raman spectroscopy (RS) is used to explore the short-range environment in LMO and LNMO. We provide here for the first time a complete assignment of the LMO and LNMO Raman fingerprint as well as a detailed qualitative and quantitative picture of structural and vibrational changes during the charge-discharge of these cathode materials. A careful RS investigation led on the LMO cathode during the first charge process provides the first detailed experimental evidence of an ordering scheme at the scale of the chemical bond of the intermediate composition $\text{Li}_{0.5}\text{Mn}_2\text{O}_4$. A combined approach using XRD and RS allows picturing changes in LNMO crystal structure and in the oxidation states of the nickel during stages of the charge-discharge process. Raman spectra collected between 3.5 and 4.9 V display rich and varying features. Appropriate analysis based upon Raman spectra fittings allow access to a quantitative estimation of the different Ni^{2+} , Ni^{3+} and Ni^{4+} redox species in the LNMO spinel oxide at different oxidation-reduction states. This makes RS a powerful probe to evaluate the state of charge of the cathode material. Finally, we demonstrate the great efficiency of RS as an efficient and simple diagnostic tool of the self-discharge phenomenon occurring in the LNMO electrode.

References

- [1] J. M. Tarascon, M. Armand, Nature 414 (2001) 359.
- [2] A. Manthiram, K. Chemelewski, E. S. Lee, Energy Environ. Sci. 7 (2014) 1339.
- [3] R. Baddour-Hadjean, J. P. Pereira-Ramos, Chem. Rev. (2010) 110, 1278.

EN03.08.09

Late News: High-Throughput Screen Printing of Supercapacitors Based on Vanadium Dioxide Amal Alamri¹, Mohammad Vaseem², Nuha A. Alhebshi^{1,1}, Bashaer Minyaw¹ and Atif Shamim²; ¹King Abdulaziz University, Saudi Arabia; ²King Abdullah University of Science and Technology, Saudi Arabia

Vanadium dioxide-based materials have promising structural, electrical, and chemical properties that promote it as an essential component in electronics, energy conversion, and storage devices such as supercapacitors. One of the main challenges that may limit the implementation of vanadium dioxides in large-area applications is the vacuum-based synthesis processes such as chemical vapor deposition. In addition, the high-cost and complication of the conventional fabrication of supercapacitor electrodes are considered as other challenges. In this research, our high-quality vanadium dioxide-based ink is synthesized using a solution process [1]. Then, the ink is monolithically printed on flexible substrates. The printing technique is straightforward, scalable, and cost-effective. The electrochemical impedance spectroscopy was used to measure the resistance of the printed supercapacitors, while the cyclic voltammetry was conducted to confirm the energy storage mechanism of our materials. The areal electrode capacitances are calculated from the galvanostatic charging-discharging experiment to be in the range of $650\text{-}200 \mu\text{F}/\text{cm}^2$ at areal currents of $10\text{-}80 \mu\text{A}/\text{cm}^2$. Interestingly, the effects of the material properties on the device performance are investigated and deeply correlated to explain the results.

Such innovative printed supercapacitors would attract attention as energy storage components that can be fully integrated into systems of flexible electronic devices, the Internet of Things, and smart textiles.

[1] Weiwei Li, Mohammad Vaseem, Shuai Yang, and Atif Shamim, Flexible and reconfigurable radio frequency electronics realized by high-throughput screen printing of vanadium dioxide switches. *Nature-Microsystems and Nanoengineering* 6, 77 (2020). <https://doi.org/10.1038/s41378-020-00194-2>.

SESSION EN03.09: On-demand
Wednesday Morning, April 14, 2021
EN03

8:00 AM EN03.09.01

Electrochemical Studies of TaS₂ as Electrode Material for Monovalent-Ion Batteries Davi Marcelo Soares and Gurpreet Singh; Kansas State University, United States

Electronic and automotive industries are strategic towards economic development owing to their substantial participation in the gross domestic product of several countries. Currently, these industries converge on the pursuit of higher energy density batteries for their products, for instance, wearable electronic devices and electric cars. Furthermore, beyond lithium-ion battery systems are also gaining traction given the uncertainty of lithium supply in the future. As a consequence, in order to develop high-performance monovalent-ion batteries further understanding of intercalation process of monovalent ions – such as Li⁺, Na⁺ and K⁺ – in layered materials is desirable, because this process is the stepping-stone towards novel battery technologies. Belonging to transition metal dichalcogenides (TMD) family, tantalum disulfide (TaS₂) is a layered polymorph with superconducting behavior that, unlike several TMD, presents metallic conductivity in its 2H phase. In addition, the interlayer spacing of TaS₂ – approximately 6% larger than TiS₂ – makes it a promising host material for intercalation of alkali metal ions with radii larger than Li⁺. Here we report 2H-TaS₂ as electrode material for lithium- (LIB), sodium- (SIB), and potassium-ion (PIB) batteries in a comprehensive electrochemical study to unveil aspects such as charge storage mechanism, ionic diffusion coefficient calculation, and impedance information obtained in the frequency domain analysis in half-cell configuration. Results indicate that first cycle charge specific capacity of LIB is 344 mAh g⁻¹. Moreover, long term cycling reveals reasonable stability with capacity decay of 0.23% per cycle within 40 cycles as PIB at 50 mA g⁻¹. To summarize, this work intends to shed light on the understanding of charge storage mechanism of 2H-TaS₂, and ultimately contribute towards the development of high-performance electrode materials for monovalent-ion batteries.

8:10 AM EN03.09.03

Effect of Sodium Dodecyl Benzene Sulfonate on Self-Discharge in Electric Double-Layer Capacitors Tareq Kareri^{1,2} and Arash Takshi^{1,1}; ¹University of South Florida, United States; ²Najran University, Saudi Arabia

One of the most important obstacles that make supercapacitors an inappropriate option to replace batteries at this time is self-discharge. Energy loss in supercapacitors is significant, especially when the charging time is short. Reducing the charge redistribution, by enlarging electrodes porosity is a possible solution to minimize the self-discharge. More focus has been given in this work to study the effect of sodium dodecyl benzene sulfonate (SDBS) on the spontaneous voltage drop in electric double-layer capacitors (EDLCs). Different concentrations of SDBS were added to change the porosity of PEDOT:PSS-based electrodes. The lowest voltage drop (ΔV) (-11.3%) was achieved in the PEDOT:PSS-based electrode with 2.0 wt% of SDBS. Also, the experimental results showed that increasing the concentration of SDBS more than 2.0 wt% leads to a reduction in the slope of the self-discharge curve and voltage drop directly. The samples with a high percentage of SDBS showed a sharp initial voltage drop due to high leakage current and high internal resistance. At the high scan rate of 200 mV/s,

the highest measured specific capacitance of 11.4 F/g was reached in the electrode with 2.0 wt% of SDBS. Results indicated that the porosity structure of the electrode has an important role in decreasing the self-discharge in EDLCs by reducing the spontaneous voltage drop.

8:20 AM EN03.09.04

Elucidating the Na, and K Intercalation and Diffusion in Carbon Anodes – Insights from Computational Modelling at the Atomic Scale Emilia Olsson and Qiong Cai; University of Surrey, United Kingdom

DFT simulations of Na, and K on different carbon motifs (defective graphene basal planes, planar graphitic layers, cylindrical pores, and combinations of these) found in hard carbon anode materials were conducted to investigate their effect on the metal intercalation. We show that both oxygen-, and nitrogen-containing defects are energetically favorable to form on these carbon motifs (in agreement with experimental characterization),³⁻⁵ both at the basal plane, in the graphitic stacks, and on strained edge sites. Assessing the effect of these defects on Na, and K interaction with the carbon structure, we found that these defects improve the initial sodiation and potassiation steps, but that the strong interaction between the metals and the defects can limit their diffusion, leading to irreversible capacity loss. To elucidate the effect of the same defects on divalent ion battery metals (Ca, Mg, and Zn) we expanded our study to also include these. Ca was shown to have the highest affinity towards these anode models, whereas neither Mg or Zn could not be shown to favorably adsorb. Intercalation in expanded graphitic pores showed that the narrow graphitic stacks with interlayer distance of $< 3.4 \text{ \AA}$ for Na, and $< 3.8 \text{ \AA}$ for K is inaccessible for intercalation. Graphitic stacks with interlayer distance $< 6 \text{ \AA}$ were found to be important for metal storage, whereas wider planar pores and cylindrical pores are beneficial for Na and K diffusion.² These simulations further showed that both these pore shapes and sizes are instrumental in the electrochemical performance of these anodes and need to be considered in computational modelling.

Acknowledgment

The financial support from EPSRC (Engineering and Physical Sciences Council) under the grant number EP/M027066/1, and EP/R021554/2, is acknowledged.

References

- ¹ A.C.S. Jensen, E. Olsson, H. Au, H. Alptekin, Z. Yang, S. Cottrell, K. Yokoyama, Q. Cai, M.-M. Titirici, and A.J. Drew, *J. Mater. Chem. A* **8**, 743 (2020).
- ² E. Olsson, J. Cottom, H. Au, Z. Guo, A.C.S. Jensen, H. Alptekin, A.J. Drew, M.-M. Titirici, and Q. Cai, *Adv. Funct. Mater.* **30**, 1908209 (2020).
- ³ H. Alptekin, H. Au, A.C. Jensen, E. Olsson, M. Goktas, T.F. Headen, P. Adelhelm, Q. Cai, A.J. Drew, M.-M. Titirici, and A.C. Jensen, *ACS Appl. Energy Mater.* acaem.0c01614 (2020).
- ⁴ H. Au, H. Alptekin, A.C.S. Jensen, E. Olsson, C.A. O'keefe, T. Smith, M. Crespo-Ribadeneyra, T.F. Headen, C.P. Grey, Q. Cai, A.J. Drew, and M.M.-M. Titirici, *Energy Environ. Sci.* (2020).
- ⁵ E. Olsson, G. Chai, M. Dove, and Q. Cai, *Nanoscale* **11**, 5274 (2019).

8:30 AM EN03.09.05

Outlook on K-Ion Batteries Mauro Pasta and Shobhan Dhir; University of Oxford, United Kingdom

Due to the rapid battery market expansion, and the limited and geographically concentrated lithium and cobalt resources, there is significant concern regarding the short-term supply and long-term sustainability of lithium-ion batteries (LIBs). Potassium-ion batteries (KIBs) are emerging as a promising complementary technology to LIBs due to the relative abundance of potassium. KIBs can also use graphite anodes providing a critical advantage over sodium-ion batteries (NIBs).

In my talk, I will provide a brief overview of the most promising cathodes [1], anodes [2] and electrolytes to date and a concise techno-economic model of KIBs. I will then discuss the critical research challenges that need to be addressed for KIBs to become a viable technology [3].

References

1. Fiore M, Wheeler S, Hurlbutt K, Capone I, Fawdon J, Ruffo R, et al. Paving the Way toward Highly Efficient, High-Energy Potassium-Ion Batteries with Ionic Liquid Electrolytes. *Chem Mater.*, 2020.
2. Capone I, Aspinall J. Electrochemo-Mechanical Properties of Red Phosphorus Anodes in Lithium, Sodium, and Potassium Ion Batteries. *Matter*, 2020.
3. Dhir S, Wheeler S, Capone I, Pasta M. Outlook on K-Ion Batteries. *Chem*, 2020.

8:40 AM EN03.09.06

Practical Li||NMC Batteries Enabled by Designs of Fluorinated Electrolyte Solvents Hansen Wang, Zhiao Yu, William Huang and Yi Cui; Stanford University, United States

Development of Li metal anodes is critical to the realization of next generation high specific energy batteries. Commercialization of Li metal anodes, however, is plagued by its poor cyclability. This is because Li metal inevitably reacts with electrolytes, forming mechanically vulnerable solid-electrolyte interphase (SEI). With the significant volume fluctuation during Li metal cycling, the SEI easily cracks, leading to dendritic growth and continuous capacity loss. Electrolyte engineering recently arises as one of the most promising approaches to address these issues. Novel electrolyte systems alter the Li-ion solvation structure, enabling much improved Li deposition homogeneity and Coulombic efficiency (CE). However, further studies are still in demand. First, recently developed electrolyte recipes are usually complicated or cost-inefficient (high concentration, multi-solvent, multi-salt, etc.). Second, understandings on the working mechanisms of these Li-compatible electrolytes are still controversial. **Here, we design and synthesize a family of fluorinated ether molecules that enables practical Li metal battery cycling performances with optimized electrolyte formulations and study their working mechanisms.**

Fluorinated 1,4-dimethoxybutane (FDMB), 1,5-dimethoxypentane (FDMP), 1,6-dimethoxyhexane (FDMH) and 1,8-dimethoxyoctane (FDMO) are designed and synthesized for the first time as solvents for Li metal battery electrolytes. When Li salts are dissolved, the O and F atoms on these molecules chelate onto Li-ions simultaneously, leading to a unique brownish electrolyte color and **high stability to metallic Li as well as high voltage cathodes.** With these molecules, we demonstrate two electrolyte formulations that enables practical Li metal battery cycling performances. In the first formulation, we combine FDMB with 1 M LiFSI salt. It achieves excellent CE (over 99.5%) with a single-salt-single-solvent electrolyte configuration. As a result, a Cu||NMC532 anode-free pouch cell (~250 mAh) runs for 100 cycles before 80% capacity retention under lean electrolyte condition. In the first formulation, we use FDMH as the main solvent. Due to its reduced Li salt solubility, small portion of dimethoxyethane (DME) is added to enable much reduced ionic and interfacial resistance, resulting in the 1 M LiFSI/6FDMH-DME electrolyte. It enables 250 cycles of 20 μ m Li||NMC811 cells before 85% capacity retention. Cu||NMC811 anode-free pouch cells also last for 120 cycles before reaching 75% of initial capacity. We show that the molecular design of solvent molecules could serve as one of the most promising strategies enabling practical Li metal batteries. Additionally, with an **advanced pouch cell pressure sensing platform**, we show that the cycling performances of these electrolytes are weakly affect by the operational pressure.

With characterization tools, we further demonstrate the working mechanism of these electrolytes. XPS shows an FSI anion-derived SEI chemistry with LiF nanoparticles accumulating with cycling on the deposited Li metal surface. This inorganic, anion-derived SEI chemistry is further confirmed by Cryo-STEM and AFM characterizations. With electrochemical experiments, we verify that **the formation of an anion-derived, LiF rich rSEI (residual SEI, SEI remaining on the electrode after Li stripping) framework is likely the key to homogeneous Li deposition and prolonged cycle life in these electrolytes**, as well as other previously reported Li-compatible electrolyte systems with LiFSI. These findings will serve as critical guides to the electrolyte designs of Li metal battery in the future.

8:50 AM EN03.09.07

First-Principles Predictions of New Lithium Iron Oxysulfides for Battery Applications Bonan Zhu and David O. Scanlon; University College London, United Kingdom

Historically, the identification of new Li-ion cathode materials has led to significant advances in the field, and currently, they underpin the overall performance and production costs of batteries. Accurate first-principles calculations, coupled with the database-based big-data approach, has led advances and predictions into new materials in the past¹. The scarcity of data among the underexplored chemical spaces, however, has limited the ability of such approaches for computationally predicting truly new materials. In this work, we apply *ab initio* random structure searching (AIRSS)^{2,3}, an unbiased massively parallel structure prediction method, to search for stable phases in the Li-Fe-O-S chemical space. Experimentally, an anti-perovskite phase Li₂FeSO₄ had been shown to be a promising low-cost earth-abundant cathode material with good rate capacity. Our search was able to re-discover this phase and its low-temperature distortions, along with a range of other previously unknown stable and metastable phases. Their potential for battery applications has been assessed. The use of crystal structure prediction helps us pursue fundamental structure-property relationships in cathodes, and thus will also help the field to explore and find new paradigms in the future.

References:

- (1) Hautier, G.; Fischer, C.; Ehlacher, V.; Jain, A.; Ceder, G. Data Mined Ionic Substitutions for the Discovery of New Compounds. *Inorg. Chem.* **2011**, *50* (2), 656–663. <https://doi.org/10.1021/ic102031h>.
- (2) Pickard, C. J.; Needs, R. J. Ab Initio Random Structure Searching. *Journal of physics. Condensed matter : an Institute of Physics journal* **2011**, *23* (5), 053201–053201. <https://doi.org/10.1088/0953-8984/23/5/053201>.
- (3) Pickard, C. J.; Needs, R. J. High-Pressure Phases of Silane. *Phys. Rev. Lett.* **2006**, *97* (4), 045504. <https://doi.org/10.1103/PhysRevLett.97.045504>.
- (4) Lai, K. T.; Antonyshyn, I.; Prots, Y.; Valldor, M. Anti-Perovskite Li-Battery Cathode Materials. *J. Am. Chem. Soc.* **2017**, *139* (28), 9645–9649. <https://doi.org/10.1021/jacs.7b04444>.

9:00 AM EN03.09.08

Theoretical Exploration on the Defect Chemistry of Sodium Titanates for High Power Sodium-Ion Anodes Yong-Seok Choi^{1,2,1}, Sara I. Costa^{3,2}, Nuria Tapia-Ruiz^{3,2} and David O. Scanlon^{1,2,1}; ¹University College London, United Kingdom; ²The Faraday Institution, United Kingdom; ³Lancaster University, United Kingdom

The low cost and abundance of sodium have driven growing interest in Na-ion batteries (NIBs) as a possible alternative to Li-ion batteries. Nevertheless, fundamental differences between Na and Li, such as ionic radius and reduction potential, make it challenging to develop suitable electrode materials for embedding Na ions. Among the various electrodes explored to date, sodium titanates (Na₂Ti_nO_{2n+1}) anodes arise as one of the most promising candidates due to its large abundance and nontoxicity^[1,2].

Early approaches on improving electrochemical performance of sodium titanates revealed that the adjustment of *n* value of Na₂Ti_nO_{2n+1} can change the arrangements of constituent TiO₆ octahedra and thus, affect the capacity and cycle life of the anodes^[3-5]. In general, sodium titanates with higher Na contents (e.g. Na₂Ti₃O₇) possess layered structures with high capacity, whereas those with lower Na contents (e.g. Na₂Ti₆O₁₃) have tunnel structures with long cycle life^[6]. Despite these efforts, titanate anodes without any materials modifications commonly suffer from poor rate performance, which mainly results from the intrinsic insulating nature of titanate anodes associated with large band gap of 3.7-3.9 eV^[3,7].

One of the most effective ways to improve the electrical conductivity is to narrow the band gap of materials. The defect chemistry of sodium titanates, however, has not been fully analyzed, and remains a bottleneck in the design of anodes for high power applications. In this study, using layered Na₂Ti₃O₇ and tunneled Na₂Ti₆O₁₃ as testbed materials, we analyze the intrinsic defects and their effects on electronic structures and fermi level position. Using hybrid Density Functional Theory calculations, we evaluate the dominant native defects, and provides guidelines for defect engineering for anodes with improved performance.

- (1) *Advanced Functional Materials* 26.21 (2016): 3703-3710.
- (2) *Nano Energy* 18 (2015): 20-27

- (3) *Advanced Energy Materials* 3.9 (2013): 1186-1194
- (4) *Small* 12.22 (2016): 2991-2997
- (5) *ACS applied materials & interfaces* 10.1 (2018): 437-447
- (6) *Physical Chemistry Chemical Physics* 14.7 (2012): 2333-2338
- (7) *ACS applied materials & interfaces* 10.44 (2018): 37974-37980

9:10 AM EN03.09.09

Transition-Metal Dichalcogenide Heterostructures for Use as Electrodes in Li-Ion Batteries Conor J. Price, Francis Davies, Edward A. Baker and Steven P. Hepplestone; University of Exeter, United Kingdom

In order to address the ever-increasing demand for better battery materials [1], we present a study exploring the potential of multi-layered heterostructures made from transition-metal dichalcogenides (TMDCs) in order to understand the benefits and drawbacks such layered materials could have as potential device electrodes.

Layered materials of atomically thin sheets have demonstrated promise as electrode materials due to their interlayer spacing allowing for easy lithium intercalation and diffusion. One family of such materials is the transition metal dichalcogenides (TMDCs) [2,3], which have already demonstrated promise in this application [4]. Further, recent advances in CVD [5] have allowed the development of novel materials formed from the heterostructuring of component TMDCs. These 'designed' materials allow for tailoring of material properties by utilising the new physics that arises from their combination. In particular, the opportunity to optimise transport, diffusion barriers and maintain the higher capacities that some structures offer, could provide a new generation of electrode materials.

We show how the properties of heterostructures and superlattice systems change compared to the constituents, highlighting the advantages and disadvantages of these materials, and estimate the maximum capacity of these structures. We do this using first principles density functional theory, explaining how the open-circuit voltage profiles and lithium diffusion barriers change for the composites, and the potential such structures have for future battery development.

REFERENCES

- [1] Saxena, S et al . *IEEE Industrial Electronics Magazine*, 2017.
- [2] Lin, L et al . *Energy Storage Materials*, 2019, 19.
- [3] Chhowalla, M. et al. *Nature Chemistry*, 2013, 5.
- [4] Zhang, L et al. *Nano Letters*, 2018, 18, 1466-1475.
- [5] Sherrell, P et al. *ACS Appl. Energy Mater.* 2019, 2, 8, 5877-5882.

9:20 AM EN03.09.10

Structure-Dependent Sodium-Ion Storage Mechanism of Cellulose Nanocrystal-Based Carbon Anodes for Highly Efficient and Stable Batteries Jung-Eun Lee, Su Jeong Yeom, Hyun-Wook Lee and Han Gi Chae; UNIST, Korea (the Republic of)

In the recent time, sodium-ion batteries (SIBs) has been attracted as a substitute of lithium-ion batteries (LIBs) due to the depletion of Li and the similar physicochemical properties of Na to Li. However, because of the larger ionic radius of Na^+ (102 pm) than Li^+ (78 pm), the hard carbon which shows wider interlayer spacing and porous structure compared to graphite has been actively investigated for use as anodes of SIBs. In the current study, spray-dried cellulose nanocrystals (CNCs) carbonized over a wide temperature range (i.e., 800–2500 °C) were prepared for carbon anodes of SIBs. The carbonized CNCs exhibited low surface area of 1.5 m²/g which is required to ensure minimal loss of Na ions for SEI layer formation. The structural variations in the CNC-based carbon anodes are correlated with the sodiation mechanism by investigating the galvanostatic voltage profiles, and it is found that Na ion adsorption takes place in the less-ordered carbonaceous structures followed by intercalation into the more ordered internal carbon structure with an average interlayer spacing of >0.37 nm. Among the various anodes examined, the CNCs carbonized at 1500 °C (C1500) deliver the highest reversible

specific capacity of 311 mA h g⁻¹ at a current density of 10 mA g⁻¹, and exhibit an outstanding rate capability (273 mA h g⁻¹ at 400 mA g⁻¹). In addition, they also possess an excellent specific capacity retention of 92.3% even after 400 cycles at 100 mA g⁻¹, along with an initial coulombic efficiency of 85%. Density functional theory (DFT) calculation exhibits that the energy barrier for Na ion intercalation of C1500 (0.20 eV) is almost a half that of the CNCs carbonized at 2500 °C (0.39 eV). We therefore believe that our results establish a foundation for the materials and their corresponding electrochemical properties, in addition to providing a novel route for the development of highly effective SIB systems.

9:30 AM EN03.09.16

Anchored Mediator Enabling Shuttle-Free Redox Mediation in Lithium-Oxygen Batteries Youngmin Ko and Kisuk Kang; Seoul National University, Korea (the Republic of)

Redox mediators (RMs) are considered an effective countermeasure to reduce the large polarization in lithium-oxygen batteries. Nevertheless, achieving sufficient enhancement of the cyclability is limited by the trade-offs of freely mobile RMs, which are beneficial for charge transport but also trigger the detrimental shuttling phenomenon. Here, we successfully decoupled the charge-carrying redox property of RMs and shuttling phenomenon by anchoring the RMs in polymer form, where physical RM migration was replaced by electron self-exchange along polymer chains. Using a model system of a polymer, PTMA (2,2,6,6-tetramethyl-1-piperidinyloxy-4-yl methacrylate), whose repeating unit contains the well-known RM tetramethylpiperidinyloxy (TEMPO), it is demonstrated that PTMA is capable of functioning as a stationary RM, preserving not only the redox activity of TEMPO, but also the charge-carry property enabled by electron exchange along polymer chain. Anchoring the RM in air electrode as polymer foam successfully prevents the shuttle phenomena. Consequently, the efficiency of RM-mediated Li₂O₂ decomposition remains remarkably stable without the consumption of oxidized RMs or degradation of the lithium anode, resulting in marked improvement of the performance of the lithium-oxygen cell.

9:40 AM EN03.09.17

Performance of Selenium-Graphene Composite as Potassium Ion Battery Cathode Vidushi Sharma and Dibakar Datta; New Jersey Institute of Technology, United States

Current advancements in energy technologies rely on combining the high-performance active electrodes with two-dimensional materials such as graphene for enhanced conductivity, mechanical stability and flexibility. Understanding the physical and electrochemical attributes of the formed interfaces can assist in device designing and performance. We utilize Density functional theory (DFT) to present an insightful analysis of selenium (Se) and graphene (Gr) composite cathode for potassium ion batteries. Se is replacing S as a favored cathode choice for being less reactive, free from shuttle effects, and possessing superior electrical conductivity. However, it falls short on electronic conductivity and abundance as per the industrial scale. Thus, Se based electrodes are consistently used with a carbon-based conductive additive to target long product life and weighted efficiency. To this end, the electrochemical performance of the Se-K cathode is determined by open-circuit voltage (OCV) plot and is compared with its counter-part Gr interfaced Se-K cathode. Significant variation in voltage plot and inter-atomic distances is seen due to the presence of Gr additive. To further the interface analysis, the interface strength of the Se/Gr 3D/2D interface has been quantified and correlated to the crystal structure, size, surface chemistry, and surface potential of the interfacing materials. The present analysis covers the chemical, physical and electrochemical contributions of Gr additive to the Se-K cathode for potassium ion battery which can assist the experimentalist and industries in fine-tuning the design of Se/Gr composite cathodes.

9:50 AM EN03.09.18

Deep Learning Inverse Design of Vascular Porous Structures for High Rate Performance Batteries Po-Chun Hsu; Duke University, United States

Vascular channel structures are ubiquitous in nature. Examples such as roots, blood vessels, and lung alveoli

show how vasculatures represent the optimal structures with a perfect balance between surface area and mass transport. For lithium-ion batteries, creating vascular porous channels in the electrodes can potentially enhance the transport and kinetics by ensuring the fresh supply of electrolyte that mitigates the electrode polarization and thereby achieve high power or fast charging without damaging the electrode. However, it is challenging to optimize for the vascular structure from the immense parameter hyperspace. Variables such as radii, angles, and branch numbers constitute millions of possible combinations. In addition, even if the vascular structure could be optimally designed, it is nontrivial to fabricate them at the scale of battery cells. In this talk, I will show our recent research progress that uses deep learning and finite element modeling to quickly predict the battery performance and also to inverse-design the parameters of the most efficient vascular electrode structure. Depending on the model complexity, we can arbitrarily choose the performance criteria among charge capacity, cycle life, maximum local temperature, and maximum local stress. The performance of the predicted vascular electrode is then validated by microfabrication. By connecting artificial intelligence and micromanufacturing, we envision this research will significantly broaden our design parameter hyperspace of high-rate energy storage devices and provide an effective general approach for solving multiscale and multiphysics problems in reactive flow systems.

10:00 AM EN03.09.20

Unforeseen Electrical Breakdown Properties of Metal-Aluminum Oxide-Metal Structures Herbert Kliem and Kapil Faliya; Saarland University, Germany

The electrical breakdown properties of metal-aluminum oxide-metal structures are investigated. The structures are prepared on silicon wafers in vacuum. A bottom electrode consisting of Cu (thickness 600nm) and Al (60nm) is prepared by thermal evaporation first. Then the aluminum oxide film (200nm) is deposited by electron beam evaporation from ceramic powder with a low oxygen support. Au, Cu or Pd (85nm) are evaporated on top using a shadow mask. The diameter of the top electrodes varies between .1mm and 1.9mm. The whole structure is prepared without breaking the vacuum.

Capacitance vs. frequency measurements of the device reveal a relaxational dielectric permittivity caused by fluctuating protons in the amorphous oxide [1]. Then a ramp voltage positive at the top electrode with speed 1V/s is applied. Before the sample finally has an electrical breakdown in fields of up to 4.5MV/cm single partial breakdown spots are visible at the top electrode. They appear in fields above 1MV/cm. At comparable voltages the density of the spots is three to four times higher at the Pd electrode than at the Cu and Au electrodes. A similar observation was published by P. Ball [2]. Pd electrodes can exhibit an electrochemical mechanical damage because of a high H flux and hydrogen evolution.

On the top the breakdown spots have a diameter of about 20 micrometer. Using an AFM it is found that the spots form caves or craters which are as deep as 1.5 micrometer. They penetrate the bottom electrode and reach down into the silicon substrate [3]. Considering the crater's volume and the specific heats of the different materials the energy necessary to form the craters by thermal energy can be calculated. This energy is compared to the electrostatic energy stored in the capacitance at the voltage where the spot appears. For the smallest capacitance of about 3pF with a diameter of .1mm and a spot voltage of 36V the electrostatic energy available from the structure is 50 times smaller than the energy necessary to melt the materials. If the materials are evaporated, the electrostatic energy is even 350 times smaller than the required evaporation energy [3].

It seems that the electrical breakdown with its hot plasma channel triggers another so far unknown process which delivers the energy necessary to form the craters. At the present moment one can only speculate about the physical nature of this effect. It remains an open question if this process is somehow related to the supposed cold fusion reported 31 years ago [4] and recently discussed again in [2].

[1] L. Kankate, C. Nies, W. Possart, H. Kliem, IEEE TDEI, vol. 25, 1508 (2018)

[2] P. Ball, MRS BULLETIN, vol. 44, 833 (2019)

[3] H. Kliem, K. Faliya, IEEE TDEI, vol. 27, 1080 {2020}

[4] M. Fleischmann, S.Pons, J. Electroanal. Chem. Interfacial Electrochem., vol. 261, 301 (1989)

10:10 AM EN03.09.22

Design Optimization of Low Cost, Highly Efficient Aqueous Zinc-Iodide Flow Battery Monalisa

Chakraborty¹, Sebastian Murcia¹, Joan Ramon Morante^{1,2} and Teresa Andreu Arbella^{1,2}; ¹Catalonia Institute for Energy Research, Spain; ²University of Barcelona, Spain

Redox flow batteries offer a reliable solution for future grid-scale energy storage due to its flexible design in decoupling energy and power independently. In comparison with mostly investigated and commercialized all vanadium redox flow batteries, aqueous zinc-iodide flow battery (ZIFB) is a highly promising contender due to its cost-effectiveness, environment friendliness, safety, and high energy density. Currently it is possible to achieve a ZIFB with high energy density based on aqueous ZnI₂ as electrolytes. However, there are still obstacles to overcome before utilizing its full potential. Therefore, various research is under investigation to improve the battery design by optimizing its components towards the development of high-performance batteries. For example, achieving reversible Zn deposition/dissolution is highly challenging in Zn-based batteries. Inhomogeneous growth of metallic Zn on the surface of the anode during charging, can lead the cell to improper discharge. Herein, we have carried out the performance comparisons of different carbon based anodes on the basis of their physical structure, hydrophilic properties and electrical conductivities. We have found that planar, graphitized and highly conductive anode can lead to efficient Zn deposition/dissolution, resulting the cell to achieve high energy efficiencies. On the other hand, electrolyte has a major contribution in scaling up the battery performance. Due to an imbalance of concentration of solutes between the anode and cathode compartments during electrochemical cycling, the differential osmotic pressure results in water migration through the ion-permeable membrane from the compartment with lower ionic strength to the compartment with higher ionic strength, which is usually overlooked by using a static positive compartment, limiting its capacity. The addition of extra solute to the electrolyte solution is a way out to resolve this issue and reach an ionically balanced situation between two compartments. In this work, we have carried out the experimental analysis of a lab-scale Zn-I flow battery as per our theoretical ionic strength calculations to reach an overall balanced system. From the theoretical calculation, it has been proven that by adding extra potassium iodide (KI) to an electrolyte of 1:1 ZnI₂: KI, the ionic balance between the compartments could be achieved. We have performed electrochemical impedance spectroscopic (EIS) as a tool to study the solution resistance and ionic conductivity of the half-cell compartments. Further full cell cycling following post-mortem analysis of the half-cell electrolytes ensured no water migration between compartments during cycling, also excellent cycling efficiencies have been achieved. Overall, the mechanisms of optimizing anode material and electrolyte design, show an promising path to enhance the performance Zn-I flow batteries, which enlighten a step forward to the research in the next-generation aqueous flow batteries.

The work was funded by MINECO/ERDEF through WINCOST (ENE2016-80788-C5-5-R) and CCU+Ox (PID2019-108136RB-C33) projects.

M. Chakraborty received PhD grant from the EU Horizon 2020 research and innovation programme (DOC FAM COFUND 2016) under the Marie Skłodowska–Curie grant agreement No 754397.

10:20 AM EN03.09.24

Enabling Highly Efficient High-Voltage Potassium-Ion Batteries with Ionic-Liquid Electrolytes Samuel J. Wheeler¹, Michele Fiore^{1,2}, Kevin Hurlbutt¹, Isaac Capone¹, Jack Fawdon¹, Riccardo Ruffo² and Mauro Pasta¹; ¹University of Oxford, United Kingdom; ²University of Milano-Bicocca, Italy

Potassium-ion batteries are a promising alternative to conventional lithium-ion batteries. They have the potential to be low cost and sustainable as they can contain only cheap and abundant elements. In potassium-ion batteries lithium is replaced with potassium, the copper current collector is replaced with aluminium, and high-performance cathodes do not require cobalt. They have the crucial advantage over sodium-ion batteries that graphite, the commercial lithium-ion anode, can reversibly intercalate potassium but not sodium.

Potassium manganese hexacyanoferrate (KMnHCF₆), a Prussian blue analogue, operates at a high voltage of around 4 V vs. K⁺/K and has a high theoretical specific capacity of 155 mA h g⁻¹. During a recent analysis of non-aqueous potassium-ion batteries we identified KMnHCF₆||graphite as one of the most promising potassium-ion battery chemistries [1]. However, numerous challenges remain such as preventing aluminium

current collector corrosion at high voltage and minimising parasitic reactions from water remaining in the KMnHCFe structure, both of which reduce the coulombic efficiency. Additionally, an electrolyte that performs well with both the KMnHCFe cathode and graphite anode must be developed.

In this work we make two key advancements to address the challenges presented by the KMnHCFe||graphite system [2]. Firstly, a systematic optimisation of the citrate-assisted synthesis of KMnHCFe was performed, using high-throughput synthesis and characterisation tools, to reduce the defect and water content whilst controlling for particle size. Secondly, an ionic-liquid based electrolyte, 1 M KFSI in Pyr_{1,3}FSI (potassium bis(fluorosulfonyl)imide in N-butyl-N-methylpyrrolidinium bis(fluorosulfonyl)imide)), was employed that forms stable passivating layers on both the cathode and anode, leading to highly efficient half-cell cycling. The electrochemical performance of KMnHCFe was observed to be highly dependent on particle size, the larger particles showing lower specific capacity but better cyclability. An optimised KMnHCFe material displayed a specific capacity of 119 mA h g⁻¹ and a stable coulombic efficiency of 99.3%, a significant improvement over the previous state of the art. In the same electrolyte graphite displays excellent electrochemical performance maintaining 99% of its specific capacity after 400 cycles and a stable coulombic efficiency of 99.94%.

References:

[1] Dhir, S.; Wheeler, S.; Capone, I.; Pasta, M. *Chem* **2020**, *6* (10), 2442–2460.

[2] Fiore, M.; Wheeler, S.; Hurlbutt, K.; Capone, I.; Fawdon, J.; Ruffo, R.; Pasta, M. *Chem. Mater.* **2020**, *32* (18), 7653–7661.

10:30 AM EN03.09.26

Understanding the Nuclear Quantum Effects on Proton Transfer in Ti₃C₂T₂ MXene with Co-Cation (Li⁺, Na⁺, K⁺) Intercalation Using ReaxFF Path-Integral Molecular Dynamics Karthik Ganeshan and Adri C. van Duin; The Pennsylvania State University, United States

Due to the fast intercalation kinetics and the potential for pseudocapacitance, layered materials are promising for supercapacitor energy storage and understanding the role of ion confinement and transport is critical in enhancing the required properties of high energy and power density. Two-dimensional metal carbides and nitrides of early transition metals (MXenes) are one such class of materials that enable fast surface redox reactions and combine properties of high conductivity with hydrophilicity [1]. High volumetric capacitance of 1500 F cm⁻³, has been achieved with the most widely used Ti₃C₂ MXene with aqueous H₂SO₄ electrolyte [2], indicating a dominant role of proton transport and surface protonation reactions contributing to the enhanced energy storage.

Nuclear quantum effects (NQEs), e.g. tunneling, on the structural and dynamical properties might be of significance due to the delocalization of light nuclei such as hydrogen but are often ignored in computational simulations. Here, we explore the NQEs on proton under confinement and under the influence of co-cation intercalation of Li⁺, Na⁺, and K⁺ using ReaxFF Path-Integral Molecular Dynamics (PIMD) simulations. Considering two cases of Ti₃C₂O₂ MXene with sparse intercalation of water and a single layer of water, we use grand-canonical monte carlo to reach equilibrium of intercalated protons for each system with/out co-cation intercalation, followed by thermostatted ring polymer MD method of PIMD to capture NQEs. The difference in the number of protons intercalated show a strong interplay between the protons, co-cation, water and the MXene surface. Benchmarking against equivalent classical MD simulations of bulk water, first we show that the NQEs enable a broadening of the O-H and O-O radial distribution functions (RDFs), indicative of bond stretching due to proton delocalization. Although capturing NQEs in simulations is vital in matching experimentally obtained properties of bulk water [3], we investigate its importance in proton transport mechanism in the MXene configurations considered using RDFs, hydrogen-bonding network and proton/water diffusion coefficients.

These insights into the NQEs may help understand the proton transfer mechanism more accurately and lead

towards a rigorous procedure for the associated simulations.

References

- [1] B. Anasori, *et al.*, Nat. Rev. Mater. 2, 16098 (2017)
- [2] M. R. Lukatskaya, *et al.*, Nat. Energy 2, 17105 (2017).
- [3] M. Ceriotti, *et al.*, Chem. Rev. 116, 7529 (2016).

10:40 AM EN03.09.27

Paramagnetic Molecule Induced More Than Five Orders of Current Suppression on Magnetic Tunnel Junctions at Room Temperature Pawan Tyagi, Christopher Riso and Edward Friebe; University of the District of Columbia, United States

Magnetic tunnel junction (MTJ) can serve as an excellent testbed for connecting molecule between two ferromagnetic electrodes. A paramagnetic molecule covalently bonded to two ferromagnetic electrodes with two thiol functional groups can produce intriguing transport and magnetic properties. We have chemically bonded paramagnetic molecules between two ferromagnetic electrodes of a MTJ along the exposed side edges. In this paper we discussed the observation of molecule induced dramatic changes in the magnetic and transport properties of the conventional magnetic tunnel junctions. Paramagnetic molecules were chemically bonded to ferromagnetic electrodes to bridge them across the insulating spacer along the exposed edges. Paramagnetic molecular channels along the tunnel junction edges decreased the overall current, through tunnel barrier and molecular channels, > 5 orders of magnitude below the leakage current of the bare tunnel junction at room temperature. These molecules caused significant changes in the spin density of states due to potential spin filtering effect. Also, paramagnetic molecules produced antiferromagnetic coupling between the affected magnetic electrodes. In this state spin transport in the magnetic tunnel junction based molecular devices plummeted by several orders. It is also noteworthy that our experimental studies provide a platform to connect a vast variety of ferromagnetic leads to the even broader array of high potential molecules such as single molecular magnets, porphyrin, and single ion molecules. The strength of exchange coupling between ferromagnetic electrodes and molecules can be tailored by utilizing different tethers and terminal functional groups. The MTJMSD can provide an advanced form of logic and memory devices, including a testbed for the molecule-based quantum computation devices. Future studies about the interaction between molecular magnets and ferromagnets and the interaction of thiol ended alkanes with ferromagnets will be of very valuable. This study indicates the potential of magnetic molecules as a means of transforming conventional magnetic tunnel junctions and producing unprecedented magnetic and transport properties.

10:50 AM EN03.09.28

Late News: High-Voltage K-Ion Battery Cathode Using a Spinel $\text{LiNi}_0.5\text{Mn}_1.5\text{O}_4$ Oxide Ankush Bhatia, Jean Peirre Pereira-Ramos and Rita Baddour-Hadjean; Institut de Chimie et des Matériaux Paris-Est (ICMPE) UMR 7182 CNRS, France

On the recent research front for the next generation secondary batteries beyond Li, potassium insertion into graphite in non-aqueous cells has brought new insights into the electrochemical K^+ intercalation behavior and introduced advantageous benefits from potassium. Since potassium resources are much abundant and the standard potential of K^+/K is 0.13 V below that of Li^+/Li , potassium-ion batteries can be regarded as an appealing alternative to LIBs to realize high voltage systems with low cost. The crucial issue is the development of cathode materials able to accommodate the large K-ion without displaying detrimental structural changes toward cycle life and rate capability performance. The 4.7 V $\text{LiMn}_{1.5}\text{Ni}_{0.5}\text{O}_4$ spinel is already a promising cathode for the next generation of high voltage LIBs, and its host structure, $\lambda\text{-Mn}_{0.75}\text{Ni}_{0.25}\text{O}_2$, could be of great interest for K-ion batteries. Here, we investigate for the first time the potassium insertion properties into electrochemically prepared $\lambda\text{-MnO}_2$ ($\lambda\text{-MO}$) and $\lambda\text{-Mn}_{0.75}\text{Ni}_{0.25}\text{O}_2$ ($\lambda\text{-MNO}$) spinels^{1,2}. We show the $\lambda\text{-MNO}$ material is capable of reacting with potassium ions along the first discharge in $\text{KPF}_6/\text{EC}/\text{PC}$ electrolyte to convert to a layered phase, $\text{K}_{0.5}\text{Mn}_{0.75}\text{Ni}_{0.25}\text{O}_2$ (KMNO). Then, a highly reversible potassium extraction/insertion is observed, corresponding to the exchange of $\approx 0.3 \text{ K}^+$ (90 mAh g^{-1}) during the first cycle at a C/20 rate at an

average potential of 3.3 V vs K⁺/K. Excellent cycling stability is observed from the 15th cycle with 70 mAh g⁻¹ still available after 60 cycles. Note also that 65% capacity is retained after 350 cycles at a C/5 rate. A comparative analysis between λ-MO and λ-MNO highlights the even greater performance of λ-MNO as high voltage cathode material for K⁺-ion batteries. Moreover, the origin of the attractive electrochemical performances of λ-MNO is investigated by XRD, Raman, and EDS experiments after discharge and charge cycles.

[1] A. Bhatia, J.P. Pereira-Ramos, N. Emery, B. Laik, Ron I. Smith, R. Baddour-Hadjean*. “An exploratory investigation of spinel LiMn_{1.5}Ni_{0.5}O₄ as cathode material for K-ion battery”, 2020, *ChemElectroChem*, **article** (DOI: doi.org/10.1002/celec.202000462)

[2] A. Bhatia, J.P. Pereira-Ramos, N. Emery, B. Laik, Ron I. Smith, R. Baddour-Hadjean*. “An exploratory investigation of spinel LiMn_{1.5}Ni_{0.5}O₄ as cathode material for K-ion battery”, 2020, *ChemElectroChem*, **front cover**(DOI: doi.org/10.1002/celec.202000890)

11:00 AM EN03.09.29

Late News: Modified H₂V₃O₈ as Cathode Material for Na-Ion Batteries Daniela Söllinger, Jürgen Schoiber and Simone Pokrant; Paris Lodron University of Salzburg, Austria

Today the implementation of renewable energy supply is an important task for society. In this context, efficient energy storage is a key element for the successful realization of the energy turnaround. One of the most promising electrochemical energy storage concepts relies on rechargeable batteries such as Li-ion batteries as a very prominent example. [1]

However, lithium is listed as critical raw material since the production of lithium is only controlled by a few countries (e.g. in South American countries). [2] Therefore, new alternatives for anode-materials have to be found, which offer a higher accessibility combined with a high standard electrode potential. One promising candidate is sodium since it is an abundant resource in the earth crust and offers easy access worldwide. [3][4]

In addition to identifying alternatives for lithium as anode material, suitable cathode materials, which are electrochemically active versus Na⁺-intercalation, have to be found. In this context, layered vanadium oxides like hydrated vanadium oxide (H₂V₃O₈ or V₃O₇·H₂O) offer a flexible platform for cathode materials based on metal ion insertion. [5] H₂V₃O₈ possesses mixed valence states of V⁴⁺ and V⁵⁺ and due to its open framework it allows for reversible intercalation of various ions like Li⁺, Na⁺ or Zn²⁺. By changing its morphology from particles to thin fibers, faster charging and higher charge densities are enabled.

In this contribution, we present structural and morphological properties of H₂V₃O₈ synthesized under hydrothermal conditions with additives (e.g. rGO) in addition to the electrochemical properties. We show that conductive additives lead to higher energy densities combined with higher cycling stabilities for Na-ion batteries. Further modifications such as presodiation of H₂V₃O₈ are explored to compensate the loss of Na⁺-ions due to the formation of the solid electrolyte interface (SEI) in the first cycles.

[1] Arianna Moretti et. al., *Adv. Energy Mater.* **2016**, 6, 1600868

[2] Ashby, Michael F., Butterworth-Heinemann, **2013**, 349-413

[3] Xiaoxiao Liu et. al., *Adv. Funct. Mater.* **2019**, 29, 1903795

[4] Iqra Moez et. al., *ACS Appl. Mater. Interfaces* **2019**, 11, 41394–41401

[5] Aura Tolosa et. al., *ACS Appl. Energy Mater.* **2018**, 1, 3790–3801

11:10 AM EN03.09.30

Late News: Crystal Structures and Local Environments of NASICON-Type Na₃FeV(PO₄)₃ and Na₄FeV(PO₄)₃ Positive Electrode Materials for Na-Ion Batteries Sunkyu Park^{1,2,3}, Jean-Noël Chotard^{1,4,5},

Dany Carlier^{2,4,5}, Iona Moog³, Mathieu Duttine², Antonella Iadecola⁴, François Fauth⁶, Christian Masquelier^{1,4,5} and Laurence Croguennec^{2,4,5}; ¹Laboratoire de Reactivite et de Chimie des Solides, France; ²Institut de Chimie de la Matière Condensée de Bordeaux, France; ³TIAMAT Energy, France; ⁴RS2E, Réseau Français sur le Stockage Electrochimique de l'Energie, France; ⁵ALISTORE-ERI European Research Institute, France; ⁶CELLS-ALBA Synchrotron, Spain

NASICON-type $\text{Na}_3\text{V}_2(\text{PO}_4)_3$ (NVP) is promising as positive electrode material for Na-ion batteries due to its robust crystal structure, providing long cycle life and great rate capability.^[1,2] However, it is able to exchange only two Na^+ ions per two Vanadium transition metals leading to a moderate specific capacity of 118 mAh/g. Therefore, it has been an important challenge in the research field to improve the specific capacity while keeping the solid framework of NASICON structure. Recently, several new NASICON-type materials such as $\text{Na}_{3+x}\text{Mg}_x\text{V}_{2-x}(\text{PO}_4)_3$,^[3] $\text{Na}_4\text{MnV}(\text{PO}_4)_3$,^[4-6] and $\text{Na}_4\text{MnCr}(\text{PO}_4)_3$,^[7] have been reported attempting to gain higher specific capacity and have better sustainability. Surprisingly, $\text{Na}_4\text{FeV}(\text{PO}_4)_3$ has not been reported yet in literature. We thus decided to study the Fe/V-mixed system demonstrating possible extraction of three Na^+ ions per two transition metals. Sol-gel and solid-state methods with various synthesis parameters were investigated to synthesize the target material, $\text{Na}_4\text{FeV}(\text{PO}_4)_3$. We obtained the NASICON-type phase with small amount of secondary phases (NaFePO_4 and Na_3PO_4). To obtain the pure phase, $\text{Na}_3\text{FeV}(\text{PO}_4)_3$ has been synthesized and electrochemically sodiated to form $\text{Na}_4\text{FeV}(\text{PO}_4)_3$. Herein, we present for the first time crystal structures of the NASICON materials, $\text{Na}_3\text{FeV}(\text{PO}_4)_3$ and $\text{Na}_4\text{FeV}(\text{PO}_4)_3$, using high resolution Synchrotron X-ray diffraction (SXRD) as well as the electrochemical performances. 2.64 Na^+ were extracted from the $\text{Na}_4\text{FeV}(\text{PO}_4)_3$ upon charge process, corresponding to a specific capacity of 146.3 mAh/g. We could clearly observe a superstructure in $\text{Na}_3\text{FeV}(\text{PO}_4)_3$ due to Na^+ ordering, which is different from the structure reported in the literature.^[6] Thermal analyses of $\text{Na}_3\text{FeV}(\text{PO}_4)_3$ were performed combining *in situ* temperature XRD and differential scanning calorimetry (DSC). An ordered/disordered phase transition is observed at 123°C with an increase symmetry from monoclinic (Space Group: $C2/c$) to rhombohedral (Space group: $R-3c$). The superstructure reflections from the ordered phase completely disappear at high temperature, which reversibly appear again as temperature goes down. The fully electrochemically sodiated $\text{Na}_4\text{FeV}(\text{PO}_4)_3$ crystallizes in a rhombohedral unit cell ($R-3c$) with all the sodium sites almost fully occupied. Since Vanadium and Iron share the same crystallographic site synchrotron X-ray absorption spectroscopy (XAS) at V and Fe K-edges and Mossbauer spectroscopy were performed. These technics allow to differentiate the local V, and Fe environments, respectively, and their oxidation states in both $\text{Na}_3\text{FeV}(\text{PO}_4)_3$ and $\text{Na}_4\text{FeV}(\text{PO}_4)_3$. Extended X-Ray Absorption Fine Structure (EXAFS) analysis shows that average bond distance of Fe – O increases from 1.99 Å in $\text{Na}_3\text{FeV}(\text{PO}_4)_3$ to 2.06 Å in $\text{Na}_4\text{FeV}(\text{PO}_4)_3$ while that of V – O remains unchanged as 2.02 Å suggesting the reduction of Fe^{3+} to Fe^{2+} without noticeable distortion of the MO_6 octahedra. The details of the local environments and oxidation states evolution and the electrochemical performances will be discussed.

References

- [1] J.-N. Chotard, G. Rouse, R. David, O. Mentré, M. Courty, and C. Masquelier, *Chem. Mater.*, **27**, 5982–5987 (2015).
- [2] K. Saravanan, C.W. Mason, A. Rudola, K.H. Wong, and P. Balaya, *Adv. Energy Mater.*, **3**, 444–450 (2013).
- [3] A. Inoishi, Y. Yoshioka, L. Zhao, A. Kitajou, and S. Okada, *ChemElectroChem*, **4**, 2755–2759 (2017).
- [4] F. Chen, V.M. Kovrugin, R. David, O. Mentré, F. Fauth, J.-N. Chotard, and C. Masquelier, *Small Methods*, **1800218**, 1800218 (2018).
- [5] M. V Zakharkin, O.A. Drozhzhin, I. V Tereshchenko, D. Chernyshov, A.M. Abakumov, E. V Antipov, and K.J. Stevenson, *ACS Appl. Energy Mater.*, **1**, 5842–5846 (2018).
- [6] W. Zhou, L. Xue, X. Lü, H. Gao, Y. Li, S. Xin, G. Fu, Z. Cui, Y. Zhu, and J.B. Goodenough, *Nano Lett.*, **16**, 7836–7841 (2016).
- [7] J. Wang, Y. Wang, D.H. Seo, T. Shi, S. Chen, Y. Tian, H. Kim, and G. Ceder, *Adv. Energy Mater.*, **1903968**, 1–10 (2020).

11:20 AM EN03.09.31

Late News: Restoring Relevance to Old Battery Chemistry via Direct Cathode Upcycling [Anthony](#)

Montoya and Jack Vaughey; Argonne National Laboratory, United States

In recent years, the increase in demand for lithium-ion batteries (LIBs) has brought attention to the supply of the raw materials used in production of the cathode. Using a direct recycling process to reclaim spent cathodes for second use not only recovers the component elements, but also aims to keep the existing structure in-tact and minimize steps and costs associated with reprocessing the material. Cobalt in particular is a high value material of concern and is a major component of the commonly used $\text{Li}(\text{Ni}_x\text{Mn}_y\text{Co}_z)\text{O}_2$ (NMC) class of cathodes. While NMC materials have gained marketplace acceptance, their exact composition has evolved. For instance five years ago NMC111 was commonly used, versus NMC622 or NMC811 are more common now. This change in composition over time presents a challenge to directly recycling cathode materials since those coming out of service are no longer in line with current compositions. The goal of this work is to upcycle an NMC111 powder to the more relevant Ni-rich NMC622 target composition. Reactions with different Ni-rich coatings were explored as a method of incorporating nickel into the structure through solid state methods. The challenges of obtaining identifying reaction conditions which avoid the formation of undesired oxides and lead to a more homogeneous material will be discussed. Structural and compositional analysis will be detailed.

11:30 AM EN03.09.32

Late News: Electrolyte-Dependent Phase Heterogeneity and Its Atomic Origin within Primary Cathode Nanoparticles Wenxiang Chen¹, Xun Zhan¹, Renliang Yuan¹, Heonjae Jeong², Cheng Zhang², Kim Ta², Hyosung An¹, Paul Braun¹, Ryan Stephens³, Andrew Gewirth², Hong Yang², Elif Ertekin², Jian-Min Zuo¹ and Qian Chen¹; ¹University of Illinois at Urbana Champaign, United States; ²University of Illinois at Urbana-Champaign, United States; ³Shell International Exploration and Production Inc, United States

We study the electrochemical and structural responses of primary cathode nanoparticles for magnesium ion insertion. By systematically varying the electrolyte, we observe a successful Mg^{2+} insertion and the consistent solid-solution phase transition in the nanoparticles. Further examination by scanning electron nanodiffraction (SEND) in scanning transmission electron microscope (STEM) revealed two distinctive strain and phase distribution patterns in the cathode nanoparticles at nanometer resolution regulated by the electrolyte. One is consist of a uniform, major phase domain distribution due to an elastic strain relaxation mechanism at the atomic level, whereas the other one is consist of a non-uniform, scattered phase domain distribution or “core-shell” structure with a plastic strain relaxation mechanism. The varied chemo-mechanical behaviors are associated with the coherency strain and charge screening effect occurred in the Mg^{2+} insertion revealed at the atomic level by STEM imaging and DFT calculations. Our work shows that electrochemical parameters such as the electrolyte have a direct influence on the cathode structural heterogeneity during Mg ion insertion, which rationally guide the design of battery materials with high stability and capacity.

11:40 AM EN03.09.33

Late News: MD Simulation Study of Sodium-Ion Transport In Na-Ion Battery Cathode Materials Deepak Seth, M. A. Haider, Manish Agarwal, Uzma Anjum, Shaharyar Wani and Tuhin S. Khan; Indian Institute of Technology Delhi, India

Classical molecular dynamics (MD) simulations are applied to study the transport of Na-ions in cathode materials for Na-ion batteries (SIB). Two different materials (in $\text{Na}_x\text{Ti}_2(\text{PO}_4)_3$) are studied to access and compare the level of Na-ion diffusion in electrode structure. Sodium constitute a potential alternative of Lithium in alkali metal batteries, since sources of Li are limited, and Na is readily available. titration, impedance measurements etc.) diffusivity estimates specifically from impedance curves are often measured away from the equilibrium and fitting parameters are prone to produce large errors. MD simulations using universal force field have provided a direct assessment of self-diffusion coefficient of Na-ions in the structure of $\text{Na}_x\text{V}_4\text{O}_{10}$ with varying concentrations of Na-ions ($0.33 < x < 1.33$), calculating a diffusion coefficient of $5.75 \times 10^{-8} \text{ cm}^2/\text{s}$ for $x=0.66$ at 300 K, which is in good agreement with experiments. Mean square displacement (MSD) and Na-ion density plots are further providing a mechanistic insight on the route of Na-ion transport.

As a next generation material, NASICON structured type ($\text{NaTi}_2(\text{PO}_4)_3$) SIB material, are investigated for Na-ion transport. Inter-atomic based partial charge potential model is applied, and concentration of Na-ion is varied (from $0.82 < x < 0.98$) in the supercell (total of 9000 atoms) of $\text{Na}_x\text{Ti}_2(\text{PO}_4)_3$ at 323 K. Na^+ transport of different sets of runs are calculated and MD trajectory are visualized. MSD of Na^+ as a function of time. Self-diffusion coefficient of Na^+ is calculated from the slope of MSD vs time plot for the three-dimensional transport, following Einstein's relation. Calculated diffusivities are in the range of $\sim 10^{-8}$ - 10^{-9} cm^2/s and corresponding ionic conductivity is estimated to be ($\sim 10^{-4}$ S/cm). These values are in agreement with experimentally measured values of Na-ions in the same structure.

References

Saroha, R., Khan, T.S., Chandra, M., Shukla, R., Panwar, A.K., Gupta, A., Haider, M.A., Basu, S. and Dhaka, R.S., 2019. Electrochemical properties of $\text{Na}_{0.66}\text{V}_4\text{O}_{10}$ nanostructures as cathode material in rechargeable batteries for energy storage applications. *ACS omega*, 4(6), pp.9878-9888.

Wani, M.S., Anjum, U., Khan, T.S., Dhaka, R.S. and Haider, M.A., 2020. Understanding Na-Ion Transport in $\text{Na}_x\text{V}_4\text{O}_{10}$ Electrode Material for Sodium-Ion Batteries. *Journal of Electronic Materials*, pp.1-6.

SYMPOSIUM EN04

Towards High Safety and High Energy Density—Solid-State Batteries
April 14 - April 22, 2021

Symposium Organizers

Liangbing Hu, University of Maryland

Yoon Seok Jung, Yonsei University

Wei Luo, Tongji University

Jennifer Rupp, Massachusetts Institute of Technology

* Invited Paper

SESSION EN04.01: Interface I

Session Chairs: Corsin Battaglia and Yoon Seok Jung

Wednesday Morning, April 21, 2021

EN04

8:00 AM *EN04.01.01

Challenges Facing Solid-State Batteries with Alkali Metal Anode—Voids and Dendrites Ziyang Ning¹, Dominic Spencer Jolly¹, Jitti Kasemchainan¹, Stefanie Zekoll¹, Gareth O. Hartley^{1,2}, T. J. Marrow¹ and Peter Bruce^{1,2,3}; ¹University of Oxford, United Kingdom; ²The Faraday Institution, United Kingdom; ³The Henry Royce Institute, United Kingdom

All-solid-state batteries could deliver a step change in energy density and improved safety through the use of an alkali metal anode and a ceramic electrolyte. However, dendrites form at the anode that penetrate the ceramic electrolyte is one of the greatest challenge facing solid-state batteries. While dendrite formation on charging

directly leads to short-circuit and cell failure, the formation of voids on discharging can also lead to interfacial contact loss and trigger dendrite initiation. To enable the use of an energy dense alkali metal anode, voids and dendrites both need to be fundamentally understood.

We have investigated the process of stripping as a function of current density and stack pressure in both Li/Li₆PS₅Cl/Li and Na/Na-β"-alumina/Na cells, revealing the dominant role of metal creep in preventing void accumulation and cell failure. By using a combination of 3-electrode cells, scanning electron microscopy and X-ray tomography, we show that there is a critical stripping current density, above which voids will not only form at the interface but increase in number and size on cycling, eventually leading to dendrite formation on charge. The combined effect of stack pressure and temperature have been studied to better understand and potentially eliminate void formation on stripping. We show that by applying high stack pressure, or moderate pressure at higher temperature, higher current densities can be achieved with stable cycling.

For a better mechanistic understanding of Li ingress into solid electrolytes, we've utilised *in-situ* phase-contrast tomography combined with spatially mapped X-ray diffraction to follow penetration of Li into ceramic electrolyte and the associated propagation of cracks. Based on our observation, the new understanding of how dendrites grow in solid-state batteries will be discussed.

8:25 AM *EN04.01.02

4 V All-Solid-State Battery Enabled by a Passivating Cathode/hydroborate Solid Electrolyte Interface

Ryo Asakura, David Reber, Léo Duchêne, Seyedhosein Payandeh, Arndt Remhof and Corsin Battaglia; Empa—Swiss Federal Laboratories for Materials Science and Technology, Switzerland

Designing solid electrolytes for all-solid-state-batteries that can withstand the extreme electrochemical conditions in contact with an alkali metal anode and a high-voltage cathode is challenging, especially when the battery is cycled beyond 4 V. Here we demonstrate that a hydroborate solid electrolyte Na₄(CB₁₁H₁₂)₂(B₁₂H₁₂), built from two types of cage-like anions with different oxidative stability, can effectively passivate the interface to a 4 V-class cathode and prevent impedance growth during cycling. We show that [B₁₂H₁₂]²⁻ anions decompose below 4.2 V vs Na⁺/Na to form a passivating interphase layer, while [CB₁₁H₁₂]⁻ anions remain intact, providing sufficient ionic conductivity across the layer. Our interface engineering strategy enables the first demonstration of a 4 V-class hydroborate-based all-solid-state battery combining a sodium metal anode and a cobalt-free Na₃(VOPO₄)₂F cathode without any artificial protective coating. When cycled to 4.15 V vs Na⁺/Na, the cells feature a discharge capacity of 104 mAh g⁻¹ at C/10 and 99 mAh g⁻¹ at C/5, and an excellent capacity and energy retention of 78% and 76%, respectively, after 800 cycles at C/5 at <0.2 MPa at room temperature. Increasing the pressure to 3.2 MPa enables a discharge capacity of 117 mAh g⁻¹ at C/10 with a mass loading of 8.0 mg cm⁻², corresponding to an areal capacity close to 1.0 mAh cm⁻². The cell holds the highest average discharge cell voltage of 3.8 V and specific energy per cathode active material weight among all-solid-state sodium batteries reported so far. Combined with their low gravimetric density <1.2 g/cm³, low toxicity, high thermal and chemical stability [2], stability vs lithium and sodium metal anodes [3], soft mechanical properties enabling cold pressing [4], compatibility with solution impregnation [5] and infiltration [6], and potential for low cost [7, 8], hydroborate electrolytes represent a promising option for a competitive future all-solid-state battery technology.

References:

- [1] R. Asakura, D. Reber, L. Duchêne, S. Payandeh, A. Remhof, H. Hagemann, C. Battaglia, *Energy Environ. Science*, DOI: 10.1039/d0ee01569e
- [2] R. Asakura, L. Duchêne, R.-S. Kühnel, A. Remhof, C. Battaglia, *ACS Appl. Energy Mater.* 2019, 2, 6924
- [3] L. Duchêne, R.-S. Kühnel, D. Rentsch, A. Remhof, H. Hagemann, C. Battaglia, *Chem. Comm.* 2017, 53, 4195
- [4] L. Duchêne, A. Remhof, H. Hagemann, C. Battaglia, *Energy Storage Mater.* 2020, 25, 782
- [5] L. Duchêne, R.-S. Kühnel, E. Stilp, E. Cuervo Reyes, A. Remhof, H. Hagemann, C. Battaglia, *Energy Environ. Science* 2017, 10, 2609

- [6] L. Duchêne, D. H. Kim, Y. B. Song, S. Jun, R. Moury, A. Remhof, H. Hagemann, Y. S. Jung, C. Battaglia, *Energy Storage Mater.*, 2020, 26, 543
- [7] A. Gigante, L. Duchêne, R. Moury, M. Pupier, A. Remhof, H. Hagemann, *ChemSusChem* 2019, 12, 4832
- [8] S. Payandeh, R. Asakura, P. Avramidou, D. Rentsch, Z. Lodziana, R. Cerny, A. Remhof, C. Battaglia, *Chem. Mater.* 2020, 32, 1101

8:50 AM EN04.01.03

A Li Metal Ink Towards Ultrathin Li Foils and Interface Compatible Solid-State Li Metal Batteries

Wangyan Wu and Wei Luo; Institute of New Energy for Vehicles, China

Li metal anode, after being in the doghouse for several decades, revived in recent years due to the merits of lowest potential (-3.04 V vs. SHE), low density and high specific capacity (3860 mAh/g) under the circumstance that the intercalation chemistry is reaching the ceiling of energy density. Nonetheless, it is not until the chronic diseases related with Li metal and organic electrolyte, such as dendrite growth, excessive N/P ratio, being knocked off can its commercialization be realized. Plagued by the incompatibility with organic electrolytes, one of the research directions branches out towards the combination of Li and inorganic solid-state electrolytes, where the poor interface brings a new challenge. Focusing on resolving the issue, here, a Li metal ink was prepared by introducing biomass-derived carbon particles into molten Li.^[1] Due to the significantly decreased surface tension, the ink is able to directly write on copper foils or other substrates that customized thickness and **ultrathin Li foils with a remarkably small thickness (<10 μm)** can be achieved. Moreover, when the ink directly writes on garnet-type LLZTO pellets, a desirable interface is obtained and therefore an extremely **low interfacial resistance of 6 Ω cm²** is delivered, in sharp contrast to 939 Ω cm² of pure Li and the garnet. Thanks to the distinguished interfacial compatibility, **a critical current density of 2.5 mA/cm²** and stable plating/stripping more than 800 h in symmetric cells are achieved. Full cells consisting of the ink, garnets and NCM523 also enable to deliver stable cycling performance. Due to the successful partnership with non-flammable solid-state electrolytes, the Li metal ink may have a chance to bring us very close to the use of solid-state lithium metal batteries with high safety and high energy density.

Reference

- [1] Wu W., et al. A writable lithium metal ink. *Sci. China Chem.*, 2020, 63, 1483-1489.

9:05 AM EN04.01.04

Revealing the Role of the Cathode-Electrolyte Interface on Solid-State Batteries Beniamin Zahiri¹, Arghya Patra¹, Chadd Kiggins², John B. Cook² and Paul Braun¹; ¹University of Illinois at Urbana-Champaign, United States; ²Xerion Advanced Battery Corporation, United States

Interfaces play crucial, but still poorly understood roles in the performance of secondary solid-state batteries (SSBs). Using crystallographically oriented and highly faceted thick cathodes, we directly assess the impact of cathode crystallography and morphology on long-term performance of SSBs. The controlled interface crystallography, area, and microstructure of these cathodes enables understanding interface instabilities unknown (hidden) in conventional thin film and composite solid-state electrodes. A generic and direct correlation between cell performance and interface stability is revealed for a variety of both lithium and sodium-based cathodes and solid electrolytes. Our findings highlight that minimizing interfacial area, rather than its expansion as is the case in conventional composite cathode, is key to both understanding the nature of interface instabilities and improving cell performance. Our findings also point to the use of dense and thick cathodes as a new path for increasing the energy density and stability of SSBs.

9:20 AM EN04.01.05

Computation-Guided Discovery of Materials for Stabilizing Interfaces in High-Energy Solid-State Lithium-Ion Batteries Adelaide M. Nolan, Yunsheng Liu and Yifei Mo; University of Maryland, United States

The continued improvement in operating time and lifetime of electric vehicles and portable electronic devices requires higher energy density lithium ion batteries. The energy density of lithium-ion batteries can be increased

by implementing high-voltage cathodes, but these cathodes are reactive and unstable during cycling with the electrolyte. To design coatings or solid electrolytes that can stabilize these cathodes, an understanding of how different chemistries interact with high-voltage cathodes is critically needed. We employ novel thermodynamic analyses based on a large-scale computation database to systematically evaluate the thermodynamic stability of a broad range of solid-state chemistries with common cathodes. By analyzing a large number of materials in high-throughput computation, we find a trade-off in that materials stable with lithiated cathodes are often unstable with delithiated cathodes, which limits the possible choice of materials stable throughout the cycling voltage. In addition to reaffirming previously demonstrated coating and solid electrolyte chemistries, our computation predicts several new chemistries, including lithium phosphates and lithium ternary fluorides, are promising solid-state chemistries stable with high-voltage cathodes. Additionally, we systematically study the chemical and electrochemical stability of coatings at the interface between promising solid electrolytes and high-capacity cathodes for all-solid-state lithium-ion batteries, which are a promising next-generation battery technology. Based on our new computation approach and our high-throughput materials analyses, we offer suggestions to improve the stability of the interface for application in all-solid-state batteries. Our computational study provides guiding principles for designing coating materials with long-term stability with high-voltage cathodes for lithium-ion batteries.

9:35 AM EN04.01.06

Characterization of Interface Evolution in Argyrodite Solid Electrolytes with Li Metal Anode for Practical, High Energy Density Solid-State Batteries [Sudarshan Narayanan](#)¹, Ulderico Ulissi² and Mauro Pasta¹; ¹University of Oxford, United Kingdom; ²Nissan Technical Centre Europe, United Kingdom

An all solid-state approach is fast becoming the most promising direction in realizing the goal of rechargeable Li-ion batteries with improved safety and performance for widespread use in portable electronics and electric vehicle applications. Such an approach employing solid electrolytes enables the use of Li metal as the anode, thereby extending access to much higher energy densities than previously envisioned in cells with liquid electrolytes. While a variety of material systems such as oxides, anti-perovskites, garnets, sulfides, and polymers, to name a few, have been extensively explored for their suitability as solid electrolytes (SE), most SEs are known to be unstable in contact with Li metal, leading to formation of decomposition products that can affect the performance of the electrochemical cell. Among these SE material systems, a class of sulfides called argyrodites ($\text{Li}_6\text{PS}_5\text{X}$, X = Cl, Br, I) have been identified as most promising candidates for practical solid-state Li-ion batteries owing not only to their relatively high ionic conductivities but also easy manufacturability and scalability^[1].

Our study probes the chemistry at the interface of Li metal and argyrodite SE surface and the evolution of decomposition products thus formed through X-ray photoelectron spectroscopy (XPS) under ex-situ and in-situ conditions. Previous studies by Janek and coworkers, Schlenker et al. and Wood et al.^[2-4] have reported interfacial characteristics in related cell materials, considering some of these aspects, but contrasting chemistries and a lack of consensus on electrode-electrolyte interphase products underscores the complexity of such a system. In my talk, I will discuss the effect of using different methods of depositing/plating Li metal on the SE surface while comparing and contrasting the interphasial products therein. I will also present a characterization of the evolution of the interface when subjected to electrochemical cycling under “in-operando” conditions, closely simulating a practical system. Additionally, investigations of the effect of surface roughness of the argyrodite SE as a means to understanding Li metal to SE contact will also be reported.

References:

- [1] Pasta, M., Armstrong, D., Brown, Z.L., Bu, J., Castell, M.R., Chen, P., Cocks, A., Corr, S.A., Cussen, E.J., Darnbrough, E., et al. “2020 roadmap on solid-state batteries”. *Journal of Physics: Energy* **2** (2020), p 032008
- [2] Wenzel, S., Sedlmaier, S.J., Dietrich, C., Zeier, W.G., and Janek, J., “Interfacial reactivity and interphase growth of argyrodite solid electrolytes at lithium metal electrodes”. *Solid State Ionics* **318** (2018) pp 102–111
- [3] Schlenker, R., Stepien, D., Koch, P., Hupfer, T., Indris, S., Roling, B., Miß, V., Fuchs, A., Wilhelmi, M., and Ehrenberg, H. Understanding the Lifetime of Battery Cells Based on Solid-State $\text{Li}_6\text{PS}_5\text{Cl}$ Electrolyte

Paired with Lithium Metal Electrode. ACS Applied Materials and Interfaces **12** (2020), pp 20012–20025
[4] Wood, K.N., Steirer, K.X., Hafner, S.E., Ban, C., Santhanagopalan, S., Lee, S.H., and Teeter, G. Operando X-ray photoelectron spectroscopy of solid electrolyte interphase formation and evolution in Li₂S-P₂S₅ solid-state electrolytes (2018) Nature Communications **9**, pp 1-10.

SESSION EN04.02: Interface II
Session Chairs: Liangbing Hu and Yifei Mo
Wednesday Morning, April 21, 2021
EN04

11:45 AM *EN04.02.01

Understanding Interfacial Atomistic Mechanisms of Lithium Metal Stripping and Plating in Solid-State Batteries Yifei Mo; University of Maryland, College Park, United States

The all-solid-state battery based on the Li metal anode is a promising next-generation energy storage system, but is currently limited by the low current density and short cycle life of the anode. Further research to improve the Li metal anode is impeded by the lack of understanding in its failure mechanisms at the lithium-solid interfaces, in particular the fundamental atomistic processes responsible for interface failure. Here, we perform the large-scale atomistic modeling study of lithium stripping and plating on solid-electrolyte interfaces by explicitly considering key fundamental atomistic processes and interface atomistic structures. Our simulations found the interface failure mechanisms and the effects of interface structures, lithium diffusion, adhesion energy, and applied pressure on such failure. By systematically varying the independent parameters of our simulations, we provide a guiding map of selecting solid-state lithium cells, in which indicates the required high interfacial adhesion energy and high applied pressure for inhibiting interface failure during cycling. Optimal solid interfaces and new research strategies are also predicted for the research and development of solid-state Li-metal batteries.

12:10 PM *EN04.02.02

Multi-Modal Operando Analysis of Lithium-Solid Electrolyte Interfaces Neil P. Dasgupta; University of Michigan, United States

Solid-state batteries have seen a dramatic increase in research in recent years because of their ability to address safety challenges associated with flammable liquid electrolytes, and the potential to enable Li metal anodes. However, the formation of solid-solid interfaces poses unique challenges compared to solid-liquid interfaces. This requires new methods to study the fundamental behavior of solid-solid interfaces, and understand their dynamic evolution during cycling¹.

In this talk, I will present a suite of multi-modal *in situ/operando* characterization approaches that we have used to study Li metal-solid electrolyte interfaces during cycling. First, to gain an improved understanding of the electrochemical stability, I will discuss *operando* X-ray photoelectron spectroscopy (XPS) analysis of lithium metal-solid electrolyte interfaces². This approach allows us to directly observe interphase formation and evolution as the electrochemical potential of the solid-electrolyte surface is biased to potentials below the thermodynamic potential for Li plating. A range of sulfide and oxide ceramic electrolytes were explored, since they exhibit a range of (in)stability levels during Li metal plating.

To compliment these spectroscopic measurements, a range of *in situ/operando* microscopy techniques will also be presented. First, *operando* optical microscopy results will be presented, which allow for direct observation of the nucleation and growth of Li filaments both into, and out of, solid electrolyte surfaces²⁻³. By time synchronizing the optical video analysis with the electrochemical signatures of plating and stripping, new

insights into the dynamic evolution of morphology and associated electrochemical analysis can be obtained. This micro-scale imaging will also be complimented by *in situ* analysis at the nanoscale. By integrating the observations across this multi-modal characterization approach, the implications for SSB performance and stability will be discussed, and critical needs for future research will be described.

1) K. B. Hatzell, X. C. Chen, C. L. Cobb, N. P. Dasgupta, M. B. Dixit, L. E. Marbella, M. T. McDowell, P. P. Mukherjee, A. Verma, V. Viswanathan, A. S. Westover, W. G. Zeier "Challenges in Lithium Metal Anodes for Solid State Batteries" *ACS Energy Lett.* **5**, 922 (2020).

2) A. L. Davis, R. Garcia-Mendez, K. N. Wood, E. Kazyak, K.-H. Chen, G. Teeter, J. Sakamoto, N. P. Dasgupta "Electro-Chemo-Mechanical Evolution of Sulfide Solid Electrolyte/Li Metal Interfaces: Operando Analysis and ALD Interlayer Effects" *J. Mater. Chem. A* **8**, 6291 (2020).

3) E. Kazyak, R. Garcia-Mendez, W. S LePage, A. Sharafi, A. L. Davis, A. J. Sanchez, K.-H. Chen, C. Haslam, J. Sakamoto, N. P. Dasgupta "Li Penetration in Ceramic Solid Electrolytes: Operando Microscopy Analysis of Morphology, Propagation, and Reversibility" *Matter* **2**, 1 (2020).

12:35 PM EN04.02.03

Fast Charge Transfer Across the LLZO Solid Electrolyte/LCO Cathode Interface—A Thin-Film Model System Jordi Sastre-Pellicer, Xubin Chen, Abdessalem Aribia, Ayodhya Tiwari and Yaroslav Romanyuk; Empa–Swiss Federal Laboratories for Materials Science and Technology, Switzerland

Thin film batteries can be valuable model systems to investigate interface charge dynamics and to serve as playgrounds for interface engineering, without the complexity of bulk systems. Here we investigate the charge transfer properties between the lithium garnet $\text{Li}_7\text{La}_3\text{Zr}_2\text{O}_{12}$ (LLZO) solid electrolyte and the LiCoO_2 cathode using a thin-film model system, with the aim of reducing the interface resistance and allowing high charge-discharge rates.

We developed a method for fabricating crystalline LLZO thin films using magnetron co-sputtering followed by an annealing step at 700°C (significantly below the standard processing temperatures). The resulting 500 nm-thick Ga-doped LLZO thin films show densities and ionic conductivities (2×10^{-4} S/cm) comparable to the values observed in bulk ceramic pellets.[1]

Based on this thin film fabrication process, we fabricated an all-thin-film model system to investigate the LLZO / LCO cathode interface. This architecture provides an easy access to the interface for characterization, allowing one to identify the degradation processes taking place at the interface under high-temperature co-sintering. Introducing an in situ-lithiated Nb_2O_5 diffusion barrier at the interface, it was possible to lower the LLZO / LCO charge transfer resistance to about $50 \Omega \text{ cm}^2$. The low interfacial resistance combined with the high conductance through the LLZO thin-film electrolyte allows charge transfer at high charge-discharge rates up to 40 C (0.9 mA/cm^2).[2]

[1] Sastre, Jordi, et al. "Lithium Garnet $\text{Li}_7\text{La}_3\text{Zr}_2\text{O}_{12}$ Electrolyte for All-Solid-State Batteries: Closing the Gap between Bulk and Thin Film Li-Ion Conductivities." *Advanced Materials Interfaces* (2020): 2000425.

[2] Sastre, Jordi, et al. "Fast Charge Transfer across the $\text{Li}_7\text{La}_3\text{Zr}_2\text{O}_{12}$ Solid Electrolyte/ LiCoO_2 Cathode Interface Enabled by an Interphase-Engineered All-Thin-Film Architecture." *ACS Applied Materials & Interfaces* 12.32 (2020): 36196-36207.

12:50 PM EN04.02.04

Aluminum Oxide Interlayer Enabling Facile Li-Ion Transfer Between LiCoO_2 and Garnet Electrolyte Yaoyu Ren, Angelique Jarry, Gary Rubloff and Eric Wachsman; University of Maryland, United States

$\text{Li}_7\text{La}_3\text{Zr}_2\text{O}_{12}$ (LLZO) garnet-type lithium-ion conductors are being investigated as a promising solid electrolyte for solid-state lithium batteries. To enable a functional all-solid-state configuration intensive investigations have focused on reducing the cathode/electrolyte interfacial resistance which contributes the most to cell performance loss [1]. Among the commercial cathode materials investigated so far, LiCoO_2 (LCO) is one of the most stable with garnet electrolytes as only a superficial reaction has been detected between the two materials.

However, even this minor reaction would block the Li-ion transport through the interface, resulting in deteriorated cell performance.

In this work, we demonstrate that a thin aluminum oxide layer (5 nm) can be an effective interlayer to impede the formation of harmful interphase and enable facile Li-ion transfer between LCO and LLZO garnet. Room-temperature-sputtered LCO thin films were employed to form an interface with the garnet electrolyte and annealed at various temperatures to reveal the effect of the extent of the interfacial reaction on the Li-ion transfer across the interface. The aluminum oxide layer was then introduced between LCO and the garnet electrolyte by sputtering a metallic aluminum layer which is then annealed together with the upper LCO layer in oxygen. Compared to the cells without an aluminum oxide interlayer, those with the interlayer exhibited much-improved performance, i.e., a stable discharge capacity of up to 110 mAh/(g LCO) at a C/10 rate and a rate capability up to the 3C rate. Atomic layer deposition was also employed to fabricate the aluminum oxide interlayer and a similarly improved cell performance was observed. The specific conditions for implementing the two methods for depositing the aluminum oxide layer and their effectiveness are compared to distinguish their capabilities in practical cell application.

[1] T. Liu, Y.Y. Ren, Y. Shen, S. X. Zhao, Y. H. Lin, C. W. Nan, *Journal of Power Sources*, 324 (2016) 349-357.

1:05 PM EN04.02.05

Towards Uniform Lithium Plating for Anode-Free Solid-State Batteries Using Amorphous Carbon Interlayers Moritz H. Futscher, Thomas Amelal, Jordi Sastre-Pellicer, Sebastian Siol and Yaroslav Romanyuk; Empa–Swiss Federal Laboratories for Materials Science and Technology, Switzerland

To keep pace with the ever-increasing demands for high energy density, low cost, and long cycle life of rechargeable batteries, advanced battery designs are needed. The greatest improvement over conventional batteries is expected to come from the use of metallic lithium as an anode. However, non-uniform electroplating of lithium metal results in the formation of dendrites, which greatly shortens battery life.

Researchers from Samsung have recently shown that introducing an amorphous interlayer of Ag-C composite leads to a long term stability without dendrite formation.[1] However, the reason why the interlayer shows this advantageous behaviour is not understood. We deposit amorphous carbon interlayers with different properties between anode and solid-state electrolyte by direct current and high power impulse magnetron sputtering. We show the influence of the microstructure and conductivity of the carbon interlayer on lithium plating through lithium phosphorus oxynitride and garnet-type solid electrolytes. Our results shed light on the key factors that enable homogeneous lithium plating and thus the use of lithium metal in solid-state batteries.

[1] Y.-G. Lee et al. High-energy long-cycling all-solid-state lithium metal batteries enabled by silver–carbon composite anodes. *Nat. Energy* **5**, 299–308 (2020)

1:20 PM EN04.02.06

Elucidating Interfacial Instability in All-Solid-State Lithium Batteries from First-Principles Simulations Liwen Wan, Aniruddha M. Dive, Marissa Wood, Kwangnam Kim, Tian Li and Brandon Wood; Lawrence Livermore National Laboratory, United States

All-solid-state batteries offer great promise for safer and higher-energy-density storage compared to conventional liquid-based Li-ion batteries. Yet they suffer greatly from high interfacial resistance caused by poor physical contact, structural and chemical heterogeneity and formation of undesired secondary phases that are detrimental to Li-ion transport. To overcome these challenges, atomic-scale visualization of the interfaces and a detailed understanding of how the structure and chemistry of the interface evolve during processing and operation, which ultimately dictates device performance is critical. In this talk, I will address how we combine high-temperature ab initio molecular dynamics simulations with machine-learning and global optimization algorithms to study the structural and chemical evolutions of solid-electrolyte/cathode interfaces in all solid-state lithium batteries. I will also demonstrate how we integrate first-principles based simulations with high-

resolution microscopy and spectroscopy to unravel the atomic details of these interfaces under different processing conditions and discuss the implications of structural and chemical inhomogeneity at the interfaces towards Li-ion transport. Examples will be discussed in this talk includes the garnet and perovskite solid-electrolytes interfacing with layered lithium cobalt oxide cathode.

This work was performed under the auspices of the U.S. Department of Energy by Lawrence Livermore National Laboratory under Contract DE-AC52-07NA27344.

1:35 PM EN04.02.07

Cryo-Electrical Microscopy Platform for Battery and Quantum Energy Applications Khim Karki, Daan Hein Alsem and Norman Salmon; Hummingbird Scientific, Afghanistan

The introduction of cryogenic cooling of specimens in the (scanning) transmission electron microscopy (S/TEM) has recently allowed in understanding various quantum interfaces and phase co-existence in strongly correlated systems [1]. Understanding those quantum properties at the fundamental level had been difficult due to limited characterization techniques with inadequate spatial and temporal resolution. Quantum materials must be studied at cryogenic temperatures because many of the relevant properties in these quantum materials only manifest themselves at these low temperatures. Cryogenic S/TEM has also led to the observation of critical structural information related to battery interfaces at atomic resolution, which are traditionally difficult to achieve because they are air-sensitive and are prone to electron beam damage in the S/TEM [2-5]. Thus, most materials require cryo-transfer and-cryo preservation of the sample using cryogenic coolant (liquid nitrogen), limiting the studying of the sample to post-mortem analysis. The cryo-electrical holder previously tested was limited in applying electrical stimulus to the sample at cryogenic temperature, and the primary focus was on imaging[5]. Here, we present the development cryo-electrical biasing S/TEM holder that simultaneously allows electrical stimulus and high-resolution imaging of a sample in-situ at various cryogenic temperatures.

The newly developed cryo-electrical holder will enable the understanding of critical interfaces in battery systems and surface-electronic behavior of quantum topological insulators such in two-dimensional (2D) materials, among others, for artifact-free evaluation of the studied devices in high-resolution imaging and spectroscopy modes. Here, we present an example of studying battery processes using a single nanowire system from room temperature down to liquid nitrogen temperature as close as around -170°C. Electrical biasing is performed in a nanowire sample that sits across the electrodes on the biasing chip. A constant current experiment at cold temperatures on the nanowire shows a voltage drop as the reaction proceeds with a growth of the dendrite layer plated on the nanowire's surface. The cryo-electrical TEM holder will be vital in enabling scientists to expand the knowledge of structure-property relationships in materials, specifically the relation between temperature and electronic properties, and will allow for the accelerated development of the next generation of electronic, quantum, and energy storage materials devices [6]

References

- [1] K. A. Moler, *Nat. Mater.* **2017**, *16*, 1049.
- [2] Y. Li, et al., *Science (80-.)*. **2017**, *358*, 506 LP.
- [3] X. Wang, et al., *Nano Lett.* **2017**, *17*, 7606.
- [4] M. J. Zachman, et al., *Nature* **2018**, *560*, 345.
- [5] K.A. Spoth, et al., *Microsc. Microanal (Suppl 2)* **2019**, 1660-1661
- [6] KK, DHA, and NS acknowledge funding from the Department of Energy, Office of Basic Energy Sciences, SBIR Grant # DE-SC0019627.

2:15 PM *EN04.03.01

Identifying the Structural and Compositional Features that Create High Li-Ion Mobility in Solid-State Compounds Gerbrand Ceder; Lawrence Berkeley National Laboratory, United States

High Li mobility is required in cathode materials as well as in solid-state electrolytes. While computationally driven searches have had considerable success in identifying new solid-state electrolytes in sulfides, considerably less high mobility oxide conductors have been discovered. In this presentation, I will show the four mechanisms that we have identified to produce high Li mobility in solids. These insights apply universally to solid ion conductors as well as to high-rate cathode materials. For each of the four mechanisms we have performed a high-throughput computational search through the relevant part of known compound space in order to develop new solids with the potential to have very high mobility. Our results indicate that there many oxides that are likely to have considerably higher Li-ion conductivity than LLZO. Time permitting, I will also show how the same principles apply to creating high rate cathode materials.

2:40 PM *EN04.03.02

Ultrafast High Temperature Sintering (UHS) Toward Solid-State Battery Manufacturing Chengwei Wang¹ and Liangbing Hu²; ¹HighT-Tech LLC, United States; ²University of Maryland, United States

Ceramic-based solid-state electrolytes (SSEs) are attractive materials for improving battery safety. To develop improved ceramic SSEs, computational predictions based on first principles methods can be a valuable tool in accelerating materials discovery. Experimental confirmation is essential after such predictions; however, materials screening rates are limited by the long processing time of conventional ceramic synthesis and sintering techniques, which are also prone to poor compositional control due to volatile element loss. These problems also cause great challenges for the manufacturing of solid state batteries.

To overcome these limitations in SSE synthesis and manufacturing, we develop an ultrafast high-temperature sintering (UHS) process for the fabrication of ceramic materials by radiative heating that features a record-high temperature of up to 3,000 °C and an ultrafast heating rate of up to 100,000 °C/minute (Science 368.6490 (2020): 521-526). The UHS method can directly sinter oxide precursors into solid, dense ceramics in seconds. Compared with previous furnace-based fabrication techniques, the UHS process is >100–1000-times faster (e.g., reducing the sintering time from hours to ~10 s). As a result, we are able to achieve excellent compositional control of ceramics containing volatile components (e.g., Li in solid-state electrolytes), as well as prevent uncontrolled grain growth for outstanding material performance. Additionally, the UHS process can also be applied to manufacture SSE membranes with high conductivities and provide excellent sintering at material interfaces with limited interdiffusion, which are essential for devices such as thin film batteries. Furthermore, this technique is compatible with 3D printing to produce novel ceramic structures and devices that are otherwise impossible to achieve by other rapid sintering methods. Finally, the UHS process is universal, allowing us to synthesize a wide range of new ceramic materials with novel composition and structure. This technique has the potential to transform and expand the discovery of ceramic compounds, with significant impacts for rapid materials screening and manufacturing of solid-state batteries.

We also extended the method for sintering printed thin film batteries (Science advances 6.47 (2020): eabc8641) and multielement metals (Advanced Science, Rapid Synthesis and Sintering of Metals from Powders, accepted), which will be discussed briefly as well.

3:05 PM BREAK

3:20 PM EN04.03.04

Dopant type (Al, Ga, Ta) on the Mechanical, Electrical and Electrochemical Behavior of Li₇La₃Zr₂O₁₂ Jeffrey B. Wolfenstine¹, GiGap Han², Heeman Choe² and Jeff Sakamoto³; ¹Solid Ionic Conducting, United

States; ²Kookmin University, Korea (the Republic of); ³University of Michigan–Ann Arbor, United States

Owing to its potential to improve battery performance compared to state-of-the-art Li-ion, there has recently been a resurgence in the development of Li metal anode technology. However, to date, efforts to cycle Li metal using liquid electrolytes with sufficient coulombic efficiency and safety have been largely insufficient to demonstrate commercial viability for electric vehicles. However, Li-ion conducting solid electrolytes are attracting considerable attention to overcome the issues associated with liquid electrolytes. One such solid electrolyte that meets many of these requirements is cubic Li-garnet of the nominal composition $\text{Li}_7\text{La}_3\text{Zr}_2\text{O}_{12}$ (LLZO). One of the major issues with cubic LLZO is increasing its critical current (charging current at which dendrites form). It was been shown that the critical current of LLZO is a function of its electrical and mechanical properties. It is the purpose of this talk to discuss the effect of three different aliovalent dopants (Al, Ta, Ga) on the electrical (total, grain, grain boundary conductivity), mechanical (hardness, fracture strength, fracture toughness) and critical current of hot-pressed near theoretical dense cubic $\text{Li}_7\text{La}_3\text{Zr}_2\text{O}_{12}$. These results will be correlated with the resulting microstructure. This information is required if LLZO is to be used as an electrolyte in solid-state batteries. In addition, implications of these results on the performance of all-solid-state batteries with a Li metal anode will be discussed.

3:35 PM EN04.03.05

Exploration of Li-P-S-O System for Discovery of New Solid Electrolyte Audric Neveu¹, Vincent Pele², Christian Jordy² and Valerie Pralong¹; ¹CNRS, France; ²SAFT, France

With the aim of making lithium batteries safer, the scientific community is looking in recent years to replace the liquid solvents used as electrolyte with a solid ionic conductor compound. Several families of materials have been developed, leading to major improvements in this technology (NASICON, perovskites, Garnets [1]). In addition, the thio-phosphate family is widely explored and several compounds have been discovered in the pseudo-binary $\text{Li}_2\text{S}-\text{P}_2\text{S}_5$ diagram such as Li_3PS_4 , $\text{Li}_7\text{P}_3\text{S}_{11}$ or Li_7PS_6 [2]. In 2011, R. Kanno and al. [3] had discovered a new phase: $\text{Li}_{10}\text{GeP}_2\text{S}_{12}$ showing ionic conduction of 12 mS/cm. Unfortunately, this structure is unstable with respect to lithium metal [4] and germanium remains a very expensive element. In order to improve the stability of this structure, a partial substitution of sulfur by oxygen has been successfully proposed [5]. Very recently, the germanium-free phase $\text{Li}_{9.6}\text{P}_3\text{S}_{12}$ has been obtained and exhibits better stability towards lithium despite a lower conductivity [6]. Recently we published about the effect of adding oxygen in this compound [7]. Here, we present the effect of added oxygen on the structure, on the ionic conductivity and during cycling in all solid-state battery.

[1] F. Zheng, M. Kotobuki, S. Song, M. O. Lai, and L. Lu, *Review on Solid Electrolytes for All-Solid-State Lithium-Ion Batteries*, Journal of Power Sources **389**, 198 (2018).

[2] Ö. U. Kudu, T. Famprikis, B. Fleutot, M.-D. Braida, T. Le Mercier, M. S. Islam, and C. Masquelier, *A Review of Structural Properties and Synthesis Methods of Solid Electrolyte Materials in the $\text{Li}_2\text{S} - \text{P}_2\text{S}_5$ Binary System*, Journal of Power Sources **407**, 31 (2018).

[3] N. Kamaya, K. Homma, Y. Yamakawa, M. Hirayama, R. Kanno, M. Yonemura, T. Kamiyama, Y. Kato, S. Hama, K. Kawamoto, and A. Mitsui, *A Lithium Superionic Conductor*, Nature Materials **10**, 682 (2011).

[4] S. Wenzel, S. Randau, T. Leichtweiß, D. A. Weber, J. Sann, W. G. Zeier, and J. Janek, *Direct Observation of the Interfacial Instability of the Fast Ionic Conductor $\text{Li}_{10}\text{GeP}_2\text{S}_{12}$ at the Lithium Metal Anode*, Chemistry of Materials **28**, 2400 (2016).

[5] Y. Sun, K. Suzuki, K. Hara, S. Hori, T. Yano, M. Hara, M. Hirayama, and R. Kanno, *Oxygen Substitution Effects in $\text{Li}_{10}\text{GeP}_2\text{S}_{12}$ Solid Electrolyte*, Journal of Power Sources **324**, 798 (2016).

[6] Y. Kato, S. Hori, T. Saito, K. Suzuki, M. Hirayama, A. Mitsui, M. Yonemura, H. Iba, and R. Kanno, *High-Power All-Solid-State Batteries Using Sulfide Superionic Conductors*, Nature Energy **1**, 16030 (2016).

[7] A. Neveu, V. Pelé, C. Jordy, and V. Pralong, *Exploration of Li-P-S-O Composition for Solid-State Electrolyte Materials Discovery*, Journal of Power Sources **467**, 228250 (2020).

3:50 PM EN04.03.06

Tunable Lithium-Ion Transport in Mixed-Halide Argyrodites Sawankumar v. Patel¹, Swastika Banerjee²,

Haoyu Liu¹, Pengbo Wang¹, Po-Hsiu Chien³, Jue Liu³, Xuyong Feng¹, Shyue Ping Ong² and Yan-Yan Hu¹; ¹Florida State University, United States; ²University of California, San Diego, United States; ³Oak Ridge National Laboratory, United States

Argyrodites, with fast Li⁺ ion conduction, are promising for applications in rechargeable solid-state batteries. Here, we investigate a new compositional space of argyrodite superionic conductors, Li_{6-x}PS_{5-x}XY_x [X and Y are halides], with a remarkably high ionic conductivity of 24 mS/cm at 25 °C. In addition, the extremely low Li-migration barrier of 0.155 eV makes it distinct and promising for low-temperature operation of SSBs. Average structure analysis via neutron Bragg diffraction reveals the retention of parent argyrodite structure with cubic space group (F-43m) with significant anion site disorder among the Cl⁻, Br⁻, and S²⁻ anions at Wyckoff 4a and 4d sites. Neutron pair distribution functions reveal the short-range order of anions in a monoclinic space group. Further characterization of the local structures by solid-state NMR confirms anion reordering. High-resolution ⁶Li NMR reveals lithium disorder induced by diversifying the anion sublattice. ⁷Li NMR relaxometry shows gradual increase in Li ion dynamics, eventually yielding a “melted” Li⁺ sublattice with a flattened energy landscape when increasing x. In addition, the diversity of anion species and Li-deficiency induce hyper coordination and coordination entropy for the Li-sublattice, resulting in higher jump rates of lithium ions. Electrochemical impedance spectroscopy unveils enhanced Li⁺-ion transport with increasing x. This study demonstrates that mixed-anion frameworks can help stabilize highly conductive structures in a compositional space otherwise unstable with lower anion diversity.

4:05 PM EN04.03.07

Late News: Investigation of Ionic Liquid Crystal Materials as Non-Solvating Lithium-Ion Conductors
Jiacheng Liu, Lingyu Yang, Hannah Collins, Emma Kerr and Jennifer Schaefer; University of Notre Dame, United States

Liquid crystals (LC) are known for forming hexagonal, smectic, and gyroid phase structures. These traits are favorable for LC electrolytes as they may contain ordered ion transport pathways that allow for higher ionic conductivity than isotropic materials. Furthermore, LC system is helpful for studying ion-transport mechanism in ion-aggregates which is a novel concept introduced by Winy and Frischknecht. Current research on LC electrolytes is mostly focused on ion-transport properties of organic ion pairs or metal-ions with solvation sites. Despite the promising potential, thus far there have been limited research performed on non-solvating LC electrolytes that lack polar matrices for ion-solvation; limited works of non-solvating LC have been done and focused on sulfonate/metal ion pairs with addition of solvent to promote charge dissociation. The ion transport property with non-solvating and higher charge delocalization anions have rarely been reported. Previously, we reported on the synthesis and characterization of side-chain, non-solvating single-ion LC polymer electrolytes with various anions and found that delocalization effect of the anion has a strong influence on the Li⁺ conductivity. It was shown using broadband dielectric spectroscopy analysis that the ion transport is correlated with dielectric relaxation. In this contribution, we report on the ion transport properties of an ionic liquid crystalline electrolyte with -TFSI anions for lithium-based batteries. This class of materials exhibits a wide smectic phase temperature window and a conductivity above 10E-5 at 60 °C. The influence of addition of high dielectric constant moiety on phase transition, ion conductivity, and transport mechanism will also be discussed.

SESSION EN04.04: Advanced Characterization
Session Chairs: Liangbing Hu and Hongli Zhu
Wednesday Afternoon, April 21, 2021
EN04

5:15 PM *EN04.04.01

Advanced NMR and MRI Studies of Ion Conduction and Dendrite Formation in Solid-State Batteries

Yan-Yan Hu^{1,2}; ¹Florida State University, United States; ²National High Magnetic Field Laboratory, United States

Solid-state rechargeable batteries, which afford new chemistry with enhanced energy density and safety, are promising energy storage media. Solid electrolytes with fast ion conduction, good compatibility with electrodes, and superior electrochemical stability are key to the success of solid-state batteries. The development of such solid electrolytes rely on our fundamental understanding of important processes, such ion conduction and dendrite formation, which requires advanced characterization tools that can non-invasively examine various aspects of these processes.

Nuclear magnetic resonance spectroscopy (NMR) and imaging (MRI) are known as powerful and versatile tools to study structure and ion dynamics, particularly suitable for investigating the aforementioned topics. In this discussion, we will present our work on: i) ion transport mechanisms and their dependence on structure and compositions in superionic conductors studied with NMR spectroscopy and relaxometry. The insights from this study have enabled the discoveries of new materials with unprecedented ionic conductivities with the lowest activation barriers for Li⁺ ion transport. ii) The origin of dendrite formation in solid-state batteries and its propagation process investigated with 3D *in situ* MRI combined with tracer-exchange. This unravels dendrite formation process in the solids, very different from liquid-electrolyte based systems.

5:40 PM *EN04.04.02

***In Operando* Study of All-Solid-State Lithium Batteries Coupling Thioantimonate Superionic Conductors with Metal Sulfide** Hongli Zhu; Northeastern University, United States

All-solid-state lithium batteries (ASLBs) employing solid-state electrolytes (SEs) are considered as promising next-generation energy storage systems with high safety due to the elimination of the flammable liquid electrolyte used in convention lithium ion batteries. Among various SE candidates, sulfide SEs are one of the most studied species because of their ultrahigh ionic conductivity. However, sulfide SEs suffer from poor compatibility with the conventional transition metal oxide cathode, which is a challenging issue for the further application in ASLBs. In this work, an ASLB pairing a novel thioantimonate conductor, Li_{6.6}Ge_{0.6}Sb_{0.4}S₅I, with high capacity sulfide cathode FeS₂ is characterized by operando techniques, and a superior performance is achieved. Generally, FeS₂ is highlighted with high specific capacity, earth abundance and environmentally benignity, but constrained by fast-decaying performance in batteries using liquid electrolyte. Herein, sulfide SEs can successfully address the severe mass loss caused by the aggregation of Fe⁰ nanoparticles and shuttle effect of polysulfides during cycling. Li_{6.6}Ge_{0.6}Sb_{0.4}S₅I exhibits high stability with FeS₂ in an optimized voltage range. The operando energy dispersive X-ray diffraction (EDXRD) was firstly used to in situ study the interface stability. As a result of excellent compatibility between FeS₂ and Li_{6.6}Ge_{0.6}Sb_{0.4}S₅I, outstanding capacity and cycling stability is achieved at the same time.

6:05 PM EN04.04.03

***Operando* Probing of Lithium Metal Interfaces in Solid-State Batteries Using Synchrotron X-Ray Tomography** John Lewis, Francisco Javier Quintero Cortes, Yuhgene Liu, Jared Tippens and Matthew T. McDowell; Georgia Institute of Technology, United States

Solid-state lithium metal batteries have garnered significant interest in recent years due to the potential for solid-state electrolytes (SSEs) to enable a lithium metal anode by suppressing dendrite growth and eliminating hazardous liquid electrolytes. However, the development of solid-state lithium metal batteries has been limited by numerous challenges that exist at the interface between lithium and SSEs, such as lithium metal penetration through the electrolyte, void formation at the interface, and electrochemical decomposition to form an interphase. Here, we characterize the interface between lithium metal and the sulfide SSE Li₁₀SnP₂S₁₂ using *operando* synchrotron X-ray tomography. Owing to the high ionic conductivity of Li₁₀SnP₂S₁₂ ($> 10^{-3}$ S cm⁻¹), we were able to electrochemically test symmetric Li/Li₁₀SnP₂S₁₂/Li cells at the relatively high current density of 1 mA cm⁻² while simultaneously collecting 3D images of the cell. Interphase growth and the formation of

interfacial voids were observed throughout the electrochemical experiments. Segmentation and detailed image analysis enabled quantitative analysis of these phases, which were coupled to electrochemical measurements to establish links between interphase growth and void formation to cell failure. We ultimately found that the loss of interfacial contact area caused by void formation at the lithium interface is primarily responsible for failure, with current constriction effects exacerbating the voltage polarization in the cell due to the formation of smaller contact spots with highly localized current flow. Our results highlight the power of *operando* X-ray imaging to probe buried interfaces in solid-state batteries during relevant electrochemical processes.

6:20 PM EN04.04.05

Three-Dimensional ^7Li MRI Investigation of Li Microstructure Formation in Solid Electrolytes Haoyu Liu¹, Po-Hsiu Chien¹, Ghoncheh Amouzandeh², Jens Rosenberg², Samuel C. Grant² and Yan-Yan Hu^{1,2};
¹Florida State University, United States; ²National High Magnetic Field Laboratory, United States

Li-ion batteries (LIBs) using solid-state electrolytes (SSEs), known as all-solid-state batteries (ASSBs), have gained much attention due to their improved safety as well as energy density compared with the current generation of LIBs. However, Li microstructure/dendrite growth still persists as the major issue that largely compromises stability and causes short circuits of batteries especially at high cycling rates, which hinders the success of ASSBs for practical applications. While much effort has been invested to understand where, when, and how Li microstructures grow in SSEs, direct evidence has yet to emerge to illustrate where the growth of Li dendrite initiates in SSEs, either from SSEs–Li interfaces or the bulk of SSEs and how it propagates. Herein, for the first time, we report 3D images of Li microstructures to reflect the variations of lithium density distribution in $\text{Li}_7\text{La}_3\text{Zr}_2\text{O}_{12}$ (LLZO) upon electrochemical polarization of a Li/LLZO/Li cell via non-invasive ^7Li Magnetic Resonance Imaging (MRI). By combining *ex situ* high-resolution 3D MRI of cycled LLZO pellets and *in situ* 2D MRI of the Li/LLZO/Li cell upon electrochemical cycling, the process of Li microstructure formation is revealed, which proves to be significantly different from the liquid-electrolyte-based LIBs. The techniques developed and demonstrated in this work will also benefit studies of other material systems.

6:35 PM EN04.04.06

Isolating and Analyzing the Behavior of Single Grain Boundaries in $\text{Li}_7\text{La}_3\text{Zr}_2\text{O}_{12}$ Solid-State Electrolyte Alexandra C. Moy¹, Grit Haeuschen², Martin Finsterbusch² and Jeff Sakamoto¹; ¹University of Michigan, United States; ²Forschungszentrum Jülich GmbH, Germany

The need for improved battery performance and safety has created the impetus to replace carbon-based anodes used in state-of-the-art batteries with lithium metal. However, it is generally known that lithium metal anodes cannot cycle with state-of-the-art liquid electrolytes due to dendrite formation. Owing to its stability and stiffness, the solid-state electrolyte, lithium lanthanum zirconium oxide (LLZO), is known to physically stabilize lithium during cycling. However, LLZO is typically polycrystalline and there is evidence that grain boundaries potentially serve to initiate lithium filament growth. Thus, there is a need to better understand the behavior and properties of the individual grain boundaries and how grain boundary networks may or may not affect lithium filament penetration in LLZO.

Single crystal and bi-crystal LLZO doped with aluminum were fabricated using rapid induction hot pressing. Grain size and crystallographic orientation were confirmed by x-ray diffraction and electron backscatter diffraction. The ability to grow grains larger than a millimeter enabled electrochemical characterization of single grains and grain boundaries based on orientation and position. Characterization techniques included electrochemical impedance spectroscopy and chronoamperometry. This work presents electrochemical characterization of single grain boundaries and single crystals, increasing the understanding of grain boundary and bulk effects on solid-state electrolyte performance. With this understanding, optimal design and fabrication of solid-state electrolytes can be determined to allow for the implementation of lithium metal anodes into advanced battery technology.

References

1. Krauskopf, T; Richter, FH; Zeier, WG; Janek, J. "Physicochemical Concepts of the Lithium Metal Anode in Solid-State Batteries." *Chemical Reviews* **2020** *120* (15), 7745-7794.
2. Sharafi, A.; Haslam, CG; Kerns, RD; Wolfenstein, J; Sakamoto, J. "Controlling and Correlating the Effect of Grain Size with the Mechanical and Electrochemical Properties of LLZO Solid-State Electrolyte." *Journal of Materials Chemistry A* **2017** *5* (40), 21491-21504.

6:50 PM EN04.04.07

Low Tortuosity Ice Templated Composite Solid-State Cathodes Stephen K. Heywood¹, Eongyu Yi², Stephen Sofie¹, Marca Doeff² and Guoying Chen²; ¹Montana State University, United States; ²Lawrence Berkeley National Laboratory, United States

The solid-state lithium garnet structured electrolyte $\text{Li}_{6.25}\text{Al}_{0.25}\text{La}_3\text{Zr}_2\text{O}_{12}$ (LLZO) has shown strong viability in the fabrication of solid-state lithium batteries given its stability with lithium metal anodes than can drive nearly double the specific energy density of conventional lithium ion batteries. However, the integration into low cost battery systems with high capacity for electric vehicles requires a means of minimizing lithium transport distance from the electrolyte into cathode of a bulk 3D electrolyte to overcome the increased ohmic resistance of solid-state lithium garnets. To reduce lithium transport length in bulk solid batteries, our approach is to utilize scalable and aqueous based freeze tape casting to create low tortuosity porous scaffolds of LLZO co-sintered with a dense LLZO film to form a bi-layer battery architecture that can be incorporated with high nickel NMC cathodes. LLZO bi-layer micro-structure development for Li ion transport and NMC incorporation as well as methods to ameliorate interfacial resistance in the solid-state composite cathode without added liquid/polymer electrolytes will be presented.

SESSION EN04.05: Solid-State Batteries I
Session Chairs: Kyung Yoon Chung and Wei Luo
Wednesday Afternoon, April 21, 2021
EN04

8:15 PM *EN04.05.01

Polymer-Based Hybrid Solid Electrolytes for Highly Safe Rechargeable Lithium Batteries Dong-Won Kim; Hanyang University, Korea (the Republic of)

Rechargeable lithium-ion batteries (LIBs) have become the main power sources for portable electronic devices, and their applications have rapidly expanded to electric vehicles and large-scale energy storage systems due to their high energy density and excellent cycle life. Although current commercialized LIBs employing liquid electrolytes exhibit superior cycle performance compared to other rechargeable battery systems, there are still concerns related to the use of liquid electrolytes, such as solvent leakage, high volatility and flammability, which make full utilization for large capacity applications very challenging due to the safety issues. As a strategy for enhancing battery safety, all-solid-state lithium battery assembled with a solid-state electrolyte has gained great attention. Among the various types of solid electrolytes, solid polymer electrolytes have attractive properties such as absence of leakage problem, non-flammability, easy processing for producing a thin film, low cost, design flexibility, cuttable shapes and good interfacial contacts with electrodes. However, solid polymer electrolytes exhibited low ionic conductivities at ambient temperature, and their mechanical properties were often poor and thin free-standing films could not be obtained without a thermal curing process. In our work, different types of polymer-based hybrid solid electrolytes with high ionic conductivity and good mechanical property are prepared and applied to rechargeable lithium- batteries. First, the solid polymer electrolytes supported by porous polymer membrane are prepared and their electrochemical properties are characterized. Second, the solid-state hybrid electrolytes composed of ion-conductive polymer and oxide-based inorganic conductive materials are investigated. Third, the hybrid solid electrolytes based on highly conductive $\text{Li}_6\text{PS}_5\text{Cl}$

was prepared in the form of thin film and their electrochemical characteristics are investigated. All types of the polymer-based solid-state electrolytes are applied to Li/LiNi_xCo_yMn_{1-x-y}O₂ cells, and their electrochemical performance will be reported.

8:40 PM *EN04.05.02

Understanding Stability Issues Related to Sulfide Based Solid Electrolytes and Composite Cathodes for All-Solid-State Lithium-Ion Batteries Jae-Ho Park^{1,2}, Jiwon Jeong^{1,2}, Da-Seul Han³, Eun-Seong Kim^{1,4}, Jun Tae Kim¹, Hun-Gi Jung^{1,4}, Kyung-Wan Nam³, Woo Young Yoon² and Kyung Yoon Chung^{1,4}; ¹Korea Institute of Science and Technology, Korea (the Republic of); ²Korea University, Korea (the Republic of); ³Dongguk University-Seoul, Korea (the Republic of); ⁴KIST School, Korea University of Science and Technology, Korea (the Republic of)

All-solid-state lithium-ion batteries (ASLBs) have been proposed due to the expectation that they can overcome two major problems on the present lithium-ion batteries based on organic liquid electrolyte : (1) thermal instability of the liquid electrolyte with flammable organic solvent, (2) limited energy density of battery. Sulfide based solid electrolytes are attracting attention, owing to their high formability and high ionic conductivity which enable favorable interfaces between solid electrolyte and active material particles. The well-connected interfaces can lead to increasing in lithium ion channels and energy density of active materials, however, it also causes a side reactions which form a resistive layer and decreases long cycling life of ASLBs. In this regard, many researchers focused on solving interface problems of ASLBs. To solve these problems, it is important to analyze the stability issues concerning sulfide solid electrolytes and their interfacial reactions accurately with various analysis techniques.

In this talk, we will present the results of comparative analysis on chemical and electrochemical stability with two sulfide-based solid electrolytes, Li₇P₃S₁₁ and Li₆P₅SCl which have been widely studied. We will also report the results of electrochemical characterization for composite cathodes by applying each of solid electrolytes. Furthermore, our recent research results of post-mortem analysis for composite cathodes using X-ray based analytical techniques will also be presented.

9:05 PM EN04.05.04

Late News: Rational Design of Solution-Processable Sulfide Solid Electrolytes for All-Solid-State Lithium-Ion Batteries Yong Bae Song¹, Hiram Kwak^{1,2} and Yoon Seok Jung¹; ¹Yonsei University, Korea (the Republic of); ²HYU, Korea (the Republic of)

Application of lithium-ion batteries (LIBs) has been expanded to large-scale energy storages, such as electric vehicles and energy storage systems. However, safety issues of conventional LIBs have emerged as the most critical concern in recent years. In this respect, all-solid-state batteries (ASBs) have been regarded as one of the most promising alternatives. Especially, ASBs employing sulfide solid electrolytes have shown outstanding performances compared with those fabricated with others such as oxides and polymer electrolytes. Specifically, Li argyrodites are unique due to their solution processability that offers the practical fabrication process of ASB electrodes and intimate ionic contacts between active materials and SEs. However, solution-processable Li argyrodites have been studied only for a composition of Li₆PS₅X (X = Cl, Br, I) with insufficiently high Li⁺ conductivities (~10⁻⁴ S cm⁻¹). Recently, notable progress on new-compositional Li argyrodites has been achieved.

In this presentation, compositional design of solution-processable Li argyrodites and microstructural analyses are presented. Also, promising electrochemical performances of ASBs prepared by an infiltration of solution-processable new Li argyrodites are shown.

References

- [1] *Adv. Energy Mater.* **2018**, *8*, 1800035.
- [2] *Adv. Mater.* **2016**, *28*, 1874–1883.

[3] *Nano Lett.* **2017**, *17*, 3013–3020.

[4] *Nano Lett.* **2020**, *20*(6), 4337–4345.

9:20 PM BREAK

9:35 PM EN04.05.05

Late News: Slurry-Fabricable Li⁺-Conductive Dry Polymer Electrolyte Binders with Sulfide Solid Electrolytes for Practical All-Solid-State Batteries Kyu Tae Kim, Dae Yang Oh, Seungwoo Jun, Yong Bae Song and Yoon Seok Jung; Yonsei University, Korea (the Republic of)

The solidification of electrolytes using inorganic materials has great potential of enhancing safety and energy density. While sulfide solid electrolytes (SEs) have been considered as a promising candidate due to their high conductivity and mechanical deformability, the chemical instability for organic polar solvents complicates the wet-slurry fabrication of sheet-type electrodes and SE films for all-solid-state Li batteries (ASLBs). Thus far, only a limited number of organic solvents has been investigated with lacking systematic approach. In addition, the disruption of interfacial Li⁺ conduction by binders has been regarded as the origin of the poor electrochemical performances. This could be relieved by hybridizing with liquid electrolytes but at the expense of the ASLBs' thermal stability.

In this presentation, we will show our recent development of dry polymer electrolyte (DPE) binders via a tactical approach considering reactivities between organic solvents and SEs. New liquid-free DPE-based Li⁺-conductive binders that could cope with practically adaptable processing solvents are thus tested. Significant improvements in utilizing electrode active materials and their outstanding thermal stability, enabled by slurry-fabricable DPE-based binders, are demonstrated.

9:50 PM EN04.05.06

Late News: Electron and Ion Transfer Across Interfaces of the NASICON-Type LATP Solid Electrolyte with Electrodes in All-Solid-State Batteries—A Density Functional Theory Study via an Explicit Interface Model Hong-Kang Tian¹, Randy Jalem^{1,2}, Bo Gao¹ and Yoshitaka Tateyama^{1,2}; ¹National Institute for Materials Science (NIMS), Japan; ²Kyoto University, Japan

NASICON-type oxide Li_{1+x}Al_xTi_{2-x}(PO₄)₃ (LATP) is expected to be a promising solid electrolyte (SE) for all-solid-state batteries (ASSBs) owing to its high ion conductivity and chemical stability. However, its interface properties with electrodes on the atomic scale remain unclear, but it is crucial for rational control of the ASSBs performance. Herein, we focused on the LATP SE with $x = 0.17$ and investigated the electron and ion transfer behaviors at the interfaces with the Li metal negative electrode and the LiCoO₂ (LCO) positive electrode via explicit interface models and density functional theory calculations. Ti reduction was found at the LATP/Li interface. For the LATP/LCO interface, the results indicated the Li-ion transfer from LCO to LATP upon contact until a certain electric double layer is formed under equilibrium, in which LCO is partially reduced. The calculation results agree well with experimental observations. Co–Ti exchange was also found to be favorable where the Li ion moves with Co³⁺ to LATP. We also explored the possible interfacial processes during annealing by simulating the oxygen removal effect and found that oxygen vacancy can be more easily formed in the LCO at the interface. It implies that partial Li ions move back to LCO for the local charge neutrality. The calculation results are well in line with the experiments. We also demonstrated higher Li chemical potential around the LATP/LCO interfaces, leading to the dynamical Li-ion depletion upon charging. The calculation results and the deduced mechanisms well explain the experimental results so far [1-2] and provide insights into the interfacial electron and ion transfer upon contact, during annealing, and charging [3].

References:

[1] Yamamoto, Y. and Muto, S. et al. *J. Am. Ceram. Soc.* **2020**, *103*, 1454–1462.

[2] Tsuchiya, B., Iriyama, Y., and Morita, K. et al. *Adv. Mater. Interfaces* **2019**, *6*, 1900100.

[3] Tian, H.-K. and Tateyama, Y. et al. *ACS Appl. Mater. Interfaces* **2020**, *12*, 54752–54762.

10:05 PM DISCUSSION TIME

10:20 PM EN04.05.08

Late News: Fe³⁺-Substituted Li₂ZrCl₆: New Halide Li⁺ Superionic Conductors for All-Solid-State Batteries Hiram Kwak^{1,2}, Da-Seul Han³, Juhyoun Park^{1,2}, Yoonjae Han^{1,2}, Kyung-Wan Nam³ and Yoon Seok Jung¹; ¹Yonsei University, Korea (the Republic of); ²Hanyang University, Korea (the Republic of); ³Dongguk University, Korea (the Republic of)

For the development of all-solid-state Li batteries with improved safety and energy density, solid electrolytes (SEs) showing a high Li⁺ conductivity ($\geq 10^{-3}$ S cm⁻¹) are the key. This is met by several types of inorganic compounds of sulfides, oxides, borohydrides, and halides. Among them, sulfide materials have been considered to be highly promising due to their mechanical deformability which enables scalable cold-pressing-based fabrication. However, uncoated conventional layered LiMO₂ (M = Ni, Co, Mn, Al) cathodes showed poor performances in combination with sulfide SEs, which is due to poor oxidation stability of sulfide SEs and (electro)chemical reactions between LiMO₂ and sulfide SEs. Since new halide SEs of Li₃YX₆ (X = Cl, Br) showing high Li⁺ conductivities (0.51 and 1.7 mS cm⁻¹ for Li₃YCl₆ and Li₃YBr₆, respectively) and excellent (electro)chemical oxidation stabilities as well as mechanical deformability were reported, much efforts have been focused on the developments of halide superionic conductors. Despite advances in developments of halide SEs, high Li⁺ conductivities of $\sim 10^{-3}$ S cm⁻¹ have only been achieved using scarce and expensive elements such as Y, Er, Sc, and In.

In this presentation, our recent results on the development of new cost-effective Li⁺ superionic conductor, Fe³⁺-substituted Li₂ZrCl₆, and their application to all-solid-state batteries will be presented.

10:35 PM EN04.05.10

Late News: Crystal Structure of Li_{3-x}Yb_{1-x}M_xCl₆ Modulated by Heat Treatment Temperature for All-Solid-State Batteries Juhyoun Park^{1,2}, Da-Seul Han³, Hiram Kwak^{1,2}, Yongjung Choi³, Kyung-Wan Nam³ and Yoon Seok Jung¹; ¹Yonsei University, Korea (the Republic of); ²Hanyang University, Korea (the Republic of); ³Dongguk University, Korea (the Republic of)

The application area of lithium ion batteries (LIB) has been expanded from mobile electronics to electric vehicles and energy storage systems. Safety issue of LIBs employing organic liquid electrolytes has mounted as a serious problem. In this regard, all-solid-state lithium batteries using inorganic solid electrolytes (SEs) are considered as one of the most promising candidates. While sulfide SEs have been extensively investigated for practical, ASLBs owing to their high ionic conductivities and mechanical sinterability, they suffer from poor electrochemical stability, especially when combined with conventional layered LiMO₂ cathodes. Recent reinvestigation of halide SEs derived via mechanochemical method (Li₃YCl₆) has demonstrated high ionic conductivities of $> 10^{-3}$ S cm⁻¹, which was contrasted by low conductivities of $10^{-4} \sim 10^{-6}$ S cm⁻¹ for samples prepared by conventional heat-treatment in the past. Importantly, halide SEs showed excellent (electro)chemical oxidation stabilities, which enables stable cycling of conventional LiMO₂ cathodes. Thus far, it has been considered that multiple factors such as bulk/local structures and contents of Li and central metals could affect ionic conductivities of halide SEs.

In this presentation, effects of crystal structures of Li₃YbCl₆ substituted with tetravalent metals on Li⁺ conductivities, which are modulated by heat-treatment temperature, are presented.

SESSION EN04.06: Solid State Electrolytes and Anodes

Session Chairs: Yoon Seok Jung and Mauro Pasta

Thursday Morning, April 22, 2021

EN04

8:00 AM *EN04.06.01

SOLBAT—The Faraday Institution’s Solid-State Li-Metal Anode Project Mauro Pasta; University of Oxford, United Kingdom

Li-ion batteries have revolutionized the portable electronics industry and empowered the electric vehicle (EV) revolution. Unfortunately, the traditional Li-ion chemistry is approaching its physicochemical limit. The demand for higher density (longer range), high power (fast charging) and safer EVs has recently revamped the interest in solid state batteries (SSB). Historically, research has focused on improving the ionic conductivity of solid electrolytes, yet ceramic solids now deliver sufficient ionic conductivity. The barriers lie within the interfaces between the electrolyte and the two electrodes, in the mechanical properties throughout the device, and in processing scalability.

In 2018 the Faraday Institution, the UK’s independent institute for electrochemical energy storage research, launched the SOLBAT (solid-state lithium metal anode battery) project aimed at understanding the fundamental science underpinning the problems of SSBs, recognising that the paucity of such understanding is the major barrier to progress.

In my talk I will present an overview of the fundamental challenges that are impeding the development of SSBs, the advances in science and technology necessary to understand the underlying science, and the multidisciplinary approach that the SOLBAT researchers are taking to face these challenges.

References

1. Pasta M, Armstrong D, Brown ZL, Bu J, Castell MR, Chen P, et al. 2020 roadmap on solid-state batteries. *J Phys Energy*. 2020;2(3):32008.

8:25 AM *EN04.06.02

Monolithic Solid-State Lithium-Ion Batteries with Sulfide Electrolytes Liangliang Li; Tsinghua University, China

Solid-state lithium (Li)-ion batteries are attracting a lot of interest due to good safety and high energy density. Sulfide solid electrolytes have many advantages such as high ionic conductivity and easy processability. Recently, monolithic solid-state Li-ion batteries that utilize sulfide electrolytes as both the active material and ionic conductor have been developed. With a monolithic structure, the active material loading and active sites for electrochemical reaction can be increased and the unwanted interfacial reaction between the cathode and the electrolyte is avoided. In this talk, we will discuss monolithic solid-state batteries with argyrodite $\text{Li}_6\text{PS}_5\text{Cl}$ and $\text{Li}_2\text{S-P}_2\text{S}_5$ glass-ceramic solid electrolytes. First, the synthetic methods of these sulfide electrolytes are introduced and the property optimization of the electrolytes is given. Second, monolithic all-solid-state batteries based on $\text{Li}_6\text{PS}_5\text{Cl}$ and $\text{Li}_2\text{S-P}_2\text{S}_5$ sulfide electrolytes are fabricated and tested. The monolithic batteries show long cycle life and high discharge capacity at room temperature. The electrochemical activity of these sulfides is systematically analyzed and the main factors that affect the long-term cycling performance of the monolithic batteries are discussed.

8:50 AM EN04.06.03

“Water-in-Salt” Polymer Electrolyte for Li-Ion Batteries Jiaxun Zhang, Chongyin Yang and Chunsheng Wang; University of Maryland, United States

Lithium ion batteries (LIBs) deliver a high energy density, a long cycle stability and a high energy efficiency. While the intrinsic safety problem of LIBs impedes the application of current LIBs in large scale energy storage. Aqueous rechargeable lithium ion batteries resolve several challenges of conventional LIBs. However, the electrochemical stability window of aqueous electrolytes is less than 2.0 V, beyond which H_2 or O_2 gas generated owing to the electrolysis of H_2O . Recently, the ground-breaking of “water-in-salt” electrolyte (WiSE) successfully expanded the ESW of water to 3.0 V. To enhance energy density of WiSE batteries, the cathodic limitation of 1.9 V needs to further reduced, and a high Coulombic efficiency (CE) of $> 99.9\%$ at a matched areal capacities of cathode/anode at a low charge/discharge rates is required for a long-term cycling. Here, by

incorporating WiSE with UV-curable methacrylic polymer, we designed a solid-state aqueous polymer electrolyte (SAPE), in which the abundant hydrophilic groups stabilized water molecules due to the sluggish water mobility in SAPE and formed a water-less thin passivation interphase between anode and electrolyte. Moreover, the anode was pre-coated with a strongly basic water-free solid polymer electrolyte to further promote the formation of passivation interphase. All of these contributed the formation of a more robust SEI to reduce the water reduction reactions on anode surface. An extended electrochemical stability window of 3.86 V is achieved at 12 mol kg⁻¹ aqueous polymer electrolyte enabled 3 V full cells with an unprecedented high initial CE of 90.5% and average CE of 99.97%. The SAPE exhibits intrinsic safety and tolerance of drastic mechanical abuse, the flexible full cell with super robustness can be widely used for low-cost and high-safety flexible electronic devices. The UV-cured polymerization process possesses the merit of facile and high efficiency, and the whole process have the potential to be practical used in a large scale. Also, the high-voltage bipolar cell is fabricated to demonstrate aqueous solid state battery. Overall, this newly developed reduced salt concentration WiSE not only reduces the cost of aqueous electrolyte, but also opens up another perspective on future directions and guidance for the design of aqueous electrolyte for high-energy-density Li-ion batteries in practical applications.

9:05 AM EN04.06.04

Transformations in Structured Alloy Anodes for Solid-State Batteries Sang Yun Han¹, Chanhee Lee^{1,2}, Yuhgene Liu¹, John Lewis¹ and Matthew T. McDowell^{1,1}; ¹Georgia Institute of Technology, United States; ²Ulsan National Institute of Science and Technology, Korea (the Republic of)

Alloy anode materials are promising for Li-ion batteries, as they have greater specific capacity than conventional graphite electrodes. Metals that form alloys with Li can electrochemically react to form Li-rich alloys at room temperature, such as Li₂₂Sn₅, Li₁₃In₃, and Li₁₅Si₄, with specific capacities of 990 mAh g⁻¹ for Sn and 1012 mAh g⁻¹ for In, as compared to 372 mAh g⁻¹ for graphite. However, the severe volume changes associated with charging and discharging alloy anodes remain a problem. In the case of all-solid-state batteries, these electrode volume changes can substantially exacerbate chemomechanical degradation because of the all-solid nature of the battery system and the propensity for fracture of the solid electrolyte. Here, we investigate electrochemical transformations in alloy materials in solid-state batteries and correlate these transformations to stress evolution within the solid-state stack. Metal foils with bicontinuous porosity are shown to exhibit improved capacity and cycling behavior in solid-state batteries made from sulfide-based electrolytes. In particular, porous indium showed much better specific capacity, capacity retention, and cycle life than dense indium foil with similar mass loading in solid-state batteries. The porous metal foils are synthesized by chemically dealloying Li-rich alloys in dry methanol and directly used them as the anode for the solid-state cells. This performance enhancement is likely due to the capability of the porous material to accommodate volume changes during charging/discharging while minimizing mechanical damage to the solid electrolyte. An integrated force sensor within the solid-state cells allows for real-time measurement of subtle changes of stack pressure within the cell, and the porous vs. dense films show different evolution of stack pressure. We have also investigated the impact of anode geometry (foil vs. particulate anode structure) on stress evolution and accumulated mechanical damage. Our results demonstrate the importance of controlling volume changes and stress evolution at the anode of solid-state batteries.

9:20 AM EN04.06.05

Enhancement of Ion Conduction via Anion Structural Disorder in Li_{6-x}PS_{5-x}Br_{1+x} Pengbo Wang¹, Haoyu Liu¹, Sawankumar v. Patel¹, Xuyong Feng¹, Po-Hsiu Chien¹, Yan Wang² and Yan-Yan Hu^{1,3}; ¹Florida State University, United States; ²Samsung Research America, United States; ³National High Magnetic Field Laboratory, United States

All-solid-state batteries (ASSBs) using fast-ion conductors as electrolytes are promising energy storage technology for enhanced energy density and safety. Among them, Li-argyrodites have attracted increasing attention because of their high ionic conductivity above 10 mS/cm and structural flexibility that can tolerate a variety of modifications in the anion sublattices. Here, we synthesized Li_{6-x}PS_{5-x}Br_{1+x} with different amount of

Br^- at Wyckoff 4d sites which are predominantly occupied by S^{2-} in the pristine structure. The highest ionic conductivity of 11 mS/cm at 25 °C is achieved with low activation energy of 0.18 eV for $\text{Li}_{15.3}\text{PS}_{4.3}\text{Br}_{1.7}$. The influence of $\text{Br}^-/\text{S}^{2-}$ mixing on ion conduction is systematically investigated with multinuclear solid-state NMR coupled with X-ray diffraction and impedance spectroscopy. Distinctive atomic arrangements (4S, 3S1Br, 2S2Br, 1S3Br, and 4Br) at 4d sites in the sublattices and a statistically random distribution of Br^- and S^{2-} at 4d sites are observed with ^{31}P NMR. The resulting local structures regulate the jump rates of their neighboring Li ions and Li redistribution. As a result, the increased Li^+ occupancy at Wyckoff 24g sites promotes fast ion conduction. Meanwhile, $^6\text{Li} \rightarrow ^7\text{Li}$ tracer-exchange NMR unveils that Li (24g) is more frequently visited than Li (48h). Experimental evidence combined with density functional theory calculations has revealed that the particular arrangement of 1S3Br at 4d sites maximizes overall Li^+ conduction. This insight applies to other argyrodites and will be useful to the design of new fast-ion conductors.

9:35 AM DISCUSSION TIME

SESSION EN04.07: Solid-State Batteries II
Session Chairs: Jordi Sastre-Pellicer and Wangyan Wu
Thursday Morning, April 22, 2021
EN04

10:30 AM *EN04.07.01

Tools for Automated Rapid Screening of Fast Ion Conducting Solids Stefan N. Adams; National University of Singapore, Singapore

Identifying new materials that combine high ionic conductivity with structural and electrochemical stability so far remains a slow trial and error search process. To rationally accelerate materials design and exploit the opportunities in the materials genome a dependable rapid screening of materials is required so that promising structures can be shortlisted for higher level computational as well as experimental characterization. Here we report on the progress of our softBV bond-valence site energy-based automated pathway analysis that provides rapid and simplified visualization of pathways, in order to bridge the gap between experimentalists and simulation specialists [1,2]. Thereby meaningful approximate predictions of ion transport pathways can be achieved from crystal structure models within seconds or minutes providing a speedup factor of 3 to 5 orders of magnitude compared to DFT-based NEB methods. Combined with a graphical user interface our software suite (that is available free for academic use from [2]) this aims to enable experimentalists to quickly identify candidate solid electrolyte materials. We also aim to integrate the pre-screening into an automated workflow for subsequent DFT characterization [3]. Results are benchmarked against both experimental and DFT NEB migration barriers. Besides the migration barriers the approach now also comprises an AI-based dopant predictor focusing on bond-valence-based crystal chemical descriptors to assist experimentalists in exploring favorable substitutional doping strategies.

We will also compare the predictability of absolute room temperature conductivities from static energy landscape analysis, bond-valence based empirical MD simulations and ab initio molecular dynamics (AIMD) simulations. While for small fast-ion conductor structures at sufficiently high temperatures AIMD appears to be the gold standard, the less reliable but computationally empirical approaches have an advantage in modelling complex disordered interfaces at low temperatures over longer periods. This eliminates the hazards involved in extrapolations down to room temperature properties for the frequent cases of order-disorder phase transitions at intermediate temperatures. As an example we will discuss lithium and sodium compounds containing multiple (poly)anions, in particular the combination of thiophosphate and halide anions or various MS_4 polyanions. Based on computational screening using our bond valence site approach and DFT studies several thiophosphate halides along the $\text{A}_3\text{PS}_4\text{-LiX}$ (Cl, Br, I; A = Li, Na) tie line [4] and the $\text{A}_x(\text{MS}_4)_y(\text{M}'\text{S}_4)_z$ phase space [5] have been explored and their properties discussed based on BVSE pathway models and molecular dynamics

simulations in combination with experimental (X-ray and neutron) diffraction, solid state NMR and electrochemical characterisation. The simplicity of the approach also facilitates the study of homogeneity ranges as exemplified for the solid solution systems $\text{Li}_{4-x}\text{PS}_4\text{I}_x$ ($0 < x < 0.67$) and $\text{Na}_{9+x}(\text{MS}_4)_{3-x}(\text{SnS}_4)_x$ or compound series such as LiTX_4 . Thereby we also explore under which circumstances the predictions based on static BV calculations have to be complemented by dynamic simulations to capture the role of polyanion librations in promoting ion transport.

References:

- [1] L.L. Wong, K.C. Phuah, R. Dai, H. Chen, W.S. Chew, S Adams; submitted.
- [2] <http://www.dmse.nus.edu.sg/asn/software.html>
- [3] B. He, S. Chi, A. Ye et al.; npj Scientific Data 7 (2020) 151;
L. Zhang, B. He; Q. Zhao et al.; Advanced Functional Materials 30 (2020) 2003087.
- [4] R. Prasada Rao, H. Chen, S. Adams; Chemistry of Materials 31 (2019) 8649-8662.
- [5] A. Sorkin, S. Adams, Materials Advances 1 (2020) 184-196.

10:55 AM EN04.07.02

Photonic Methods for Rapid Annealing of Cathode Films on Flexible and Temperature-Sensitive Substrates for Thin-Film Solid-State Batteries Jordi Sastre-Pellicer¹, Xubin Chen¹, Matthias Rumpel², Andreas Flegler², Patrik Hoffmann^{1,3} and Yaroslav Romanyuk¹; ¹Empa–Swiss Federal Laboratories for Materials Science and Technology, Switzerland; ²Fraunhofer Institute for Silicate Research ISC, Germany; ³École Polytechnique Fédérale de Lausanne, Switzerland

High temperature and prolonged thermal annealing for the crystallization of cathode films in thin-film solid-state batteries (TF-SSBs) restricts the choice of current collector and substrates and causes lithium loss in the cathode. This work explores photonic-based alternatives for cathode crystallization, specifically xenon flash-lamp annealing (FLA), ultra-violet excimer laser irradiation (UV-laser) and infrared laser (IR) annealing. The effect of these methods is systematically compared to that of thermal annealing in terms of processing time, crystal structure and electrochemical performance of two model thin-film cathodes LiMn_2O_4 (LMO) and LiCoO_2 (LCO).

FLA can crystallize LMO cathode films in less than 6 minutes compared to the reference thermal processing time of 60 minutes at 600 °C. The performance of the FLA-processed LMO cathodes (crystallinity, capacity, diffusion coefficient) is comparable to that of the thermal reference. LCO cathodes with thicknesses up to 5 μm could be crystallized by FLA.

To demonstrate the fast crystallization of thin-film cathodes on temperature-sensitive substrates, we applied FLA to LCO cathode films deposited on flexible aluminum foil. Flexible TF-SSBs composed of LCO as cathode, lithium phosphorus oxynitride (LiPON) as solid electrolyte and Li metal as anode were fabricated and exhibited an energy density and power density up to 800 $\mu\text{Wh cm}^{-2}$ and 7000 $\mu\text{W cm}^{-2}$, respectively. Such performance is comparable to state-of-the-art thermally-annealed TF-SSBs on rigid substrates.

11:10 AM EN04.07.03

Quantifying the Density and Mobility of Mobile Ions in Solid Electrolytes by Transient Current Measurements Moritz H. Futscher, Jordi Sastre-Pellicer and Yaroslav Romanyuk; Empa–Swiss Federal Laboratories for Materials Science and Technology, Switzerland

Solid electrolytes are a key component in enabling new technological advances for rechargeable batteries by mitigating many of the challenges associated with the use of liquid organic electrolytes. One of the key properties of solid electrolytes is their ability to transport ions between the anode and the cathode. This ion migration is usually characterized by measuring the ionic conductivity by means of impedance spectroscopic measurements. However, the ionic conductivity is proportional to both the density and the mobility of mobile ions. Only the mobility represents the actual velocity of the mobile ions.

Using lithium phosphorus oxynitride (LiPON), we show how measuring the temperature-dependent current transients can be used to independently quantify both the mobility and the density of mobile ions in solid electrolytes. By changing the mobile ion density in $\text{Li}_7\text{La}_3\text{Zr}_2\text{O}_{12}$ (LLZO) solid electrolyte by co-sputtering LLZO and Li_2O , we show how samples that seem to have the same ionic conductivity can still differ in ionic mobility. Finally, we employ this method to quantify the effects of Al and Ga doping on the ion migration in LLZO solid electrolytes. The proposed approach in quantification of mobile ions can be extended to other solid electrolytes for a better understanding of ion migration and the influence on battery performance.

11:25 AM EN04.07.05

Fast Li-Ion Solid Electrolytes for Solid-State Batteries Jan Allen; U.S. Army Research Laboratory, United States

Solid Li-ion conducting electrolytes are one pathway towards future, energy-dense, intrinsically-safe solid-state batteries. Thus, it is of interest to study novel fast Li-ion solid electrolyte materials. Here we report the synthesis and characterization of a new family of oxide solid electrolytes. We detail the compositions that were explored and give the results of the synthesis, densification and the structural, physical and electrochemical characterization and its interface with electrode materials. The properties of the new materials will be compared and contrasted to well-known solid Li electrolytes such as garnet and NASICON structured materials.

11:40 AM EN04.07.06

Conditioning Hybrid Organic-Inorganic Solid Electrolytes for Improved Cation Mobility Vazrik Keshishian and John Kieffer; University of Michigan–Ann Arbor, United States

Conventional lithium-ion batteries that use liquid electrolytes are not very desirable due to lack of chemical stability, safety issues and cost of production. Solid state electrolytes (SSEs) not only have the potential to correct these drawbacks, but improve performance characteristics such as energy density and power density can also be improved. To simultaneously achieve high ionic conductivity and mechanical stiffness, a composite materials design approach for creating the novel SSEs is indicated. Here we report on our development of hybrid organic-inorganic electrolytes, in which a silica backbone is formed by sol-gel synthesis routes to provide a mechanically rigid backbone. The fluid in this nano-porous structure is subsequently replaced with polymer solutions. The polymer is grafted onto the backbone through reactive groups, and thus anchored into structure to establish the ion conducting phase. This unique approach allows us to decouple the influence of mechanical properties on ionic transport properties of materials and achieve both high elastic stiffness and ionic conductivity. We discovered that the network structure of a gel-cast material can be further conditioned by influencing the structural evolution during drying. Changing sample aspect ratio various degrees of anisotropy and spatial gradients can be achieved in the network topology. This is revealed through nano-mechanical characterization of the materials, using Brillouin light scattering. Since there is a strong correlation between the adiabatic elastic modulus and the activation energy of ion hopping, this anisotropy also affects ionic conductivity. Here we elaborate on strategies to harness this structural conditioning to create better performing SSE (Acknowledgement: NSF-DMR 1610742.)

11:55 AM EN04.07.07

Late News: Controlling the Cation Ordering on a $\text{LiNi}_0.5\text{Mn}_1.5\text{O}_4$ Thin-Film Model System by Modifying the Cooling Rate During Annealing Andrea I. Pitillas Martinez^{1,2,3}, Christophe Detavernier³ and Philippe Vereecken^{1,2}; ¹imec, Belgium; ²KU Leuven, Belgium; ³Ghent University, Belgium

The introduction of cathode materials that have both intrinsically higher capacities as well as higher operating potentials can help to further move towards the usage of electric vehicles and renewable energies. In this regard, high energy density cathodes which are cobalt free are of high interest in the field of batteries, mainly due to their lower cost, as well as for environmental reasons. The high cost of cobalt [1], as well as the environmental conditions under which it is extracted are the main determining factors which rise major concerns in the continuing use of cobalt containing cathodes.

In this regard, cobalt free cathodes such as $\text{LiNi}_{0.5}\text{Mn}_{1.5}\text{O}_4$ (LNMO) are of high interest due to its high operating potential (4.7 V vs Li^+/Li) as well as its high specific capacity (147mAh/g). However, regardless of the intensive research done over the years, this material has not yet really made it into the market. One of the reasons being the contradictory results reported in literature trying to correlate the composition, material properties and electrochemical performance with the crystal structure as well as differentiating its bulk and interface properties when in contact with electrolytes [2].

For this reason, in this work, we would like to present the potential of using a thin film $\text{LiNi}_{0.5}\text{Mn}_{1.5}\text{O}_4$ model system to address this issue. So, it is possible to relate more accurately the composition, crystallinity and cation ordering of this material with its electrochemical performance.

Thin film LNMO has been previously reported as model system for study of cation ordering in LNMO. Yet only the effect of the pressure during RF sputter deposition was investigated so far, which, however, can affect both the cation ordering and the composition of the thin film [3],[4]. As such the correlation between the electrochemical performance with the cation ordering was challenging, as it is also dependent on composition. Herein, we present an approach to control the cation ordering of a thin film LNMO while maintaining the composition constant based on controlling the cooling rate during the annealing step after sputtering at the same deposition pressure.

References:

- [1] Materials Today, Volume 18, Issue 5, 2015, Pages 252-264
- [2] Journal of Power Sources 467 (2020) 228318
- [3] Chem. Mater. 2017, 29, 14, 6044-6057
- [4] Energy Storage Materials 15 (2018) 396-406

12:10 PM DISCUSSION TIME

SESSION EN04.08: Solid-State Batteries III
Session Chairs: Liangbing Hu and Bilge Yildiz
Thursday Afternoon, April 22, 2021
EN04

1:00 PM *EN04.08.01

Structure, Chemistry and Charge Transfer Resistance of the Interface Between Garnet Solid Electrolyte and Oxide Cathodes Bilge Yildiz; Massachusetts Institute of Technology, United States

All-solid-state batteries promise significant safety and energy density advantages over liquid-electrolyte batteries. The interface between the cathode and the solid electrolyte is an important contributor to charge transfer resistance. Strong bonding of solid oxide electrolytes and cathodes requires sintering at elevated temperatures. Knowledge of the temperature dependence of the composition and charge transfer properties of this interface is important for determining the ideal sintering conditions. To understand the interfacial decomposition processes and their onset temperatures, model cathode systems of LiCoO_2 (LCO) and $\text{LiNi}_{0.6}\text{Mn}_{0.2}\text{Co}_{0.2}\text{O}_2$ (NMC622) thin films deposited on cubic Al-doped $\text{Li}_7\text{La}_3\text{Zr}_2\text{O}_{12}$ (LLZO) pellets were studied as a function of temperature, gas composition and electrochemical conditions. The methods combine interface-sensitive techniques, including X-ray photoelectron spectroscopy (XPS), synchrotron X-ray absorption spectroscopy, hard X-ray photoemission (HAXPES), and synchrotron X-ray diffraction. In this talk, we will present the found precipitation products at the interface as a function of synthesis and electrochemical conditions, their role in altering the interface resistance to Li transfer, and compare the LCO and NMC related cathodes in terms of their instability onset conditions.

1:25 PM EN04.08.02

Lithium Insoluble Interlayer Aids Dendrite Suppression and Enhanced Current Densities in Lithium Solid-State Batteries Vikalp Raj, Varun Kankanallu, Bibhatsu Kuiri and Naga Phani Aetukuri; Indian Institute of Science, Bangalore, India

Lithium ion batteries (LIBs) have been in prevalence for over two decades. They find use in portable electronics, electric vehicles and also grid storage. The conventional Li-ion battery technology employs electrolytes that have flammable organic solvents as key constituents. In addition, these electrolytes are thermodynamically unstable at voltages beyond 4 V; stability at voltages beyond 4 V is essential for the development of high voltage and therefore, high energy density Li-ion batteries. Moreover, state-of-the-art lithium ion batteries use a graphitic anode, which has a low theoretical specific capacity of 372 mAh/g. Due to this low specific capacity, conventional LIBs are limited in scope with respect to their energy and power density. Lithium metal anodes with a theoretical specific capacity of 3860 mAh/g are ideal for the development of high energy density Li-ion batteries. However, Lithium metal when used with liquid electrolytes tends to form filament like structures called dendrites due to uneven deposition of Li metal leading to short battery lifetime and also possible battery fires.

Over the years, solutions to this challenge included the development of solid-state electrolytes that could mechanically suppress dendrite growth. Solid-state electrolytes are non-flammable, mechanically robust and (electro)chemically stable. Several solid (inorganic and organic materials) have been proposed as candidate materials. However, dendrite growth is experimentally observed in most of these solid electrolytes. For example, garnet based Li-ion conductor $\text{Li}_7\text{La}_3\text{Zr}_2\text{O}_{12}$ (LLZO) and its doped variants have been extensively studied as potential candidates for utility in solid-state batteries. Garnet solid-state electrolytes have several favourable properties that are desired for solid-state Li-ion battery applications. However, dendrite growth at current densities as low as $100 \mu\text{A}/\text{cm}^2$ has been observed. Improvements to the interface between lithium anode and the solid electrolyte via the use of metal interlayers and surface modification techniques, have been shown to mitigate dendrite growth at current densities exceeding $100 \mu\text{A}/\text{cm}^2$. When such interfacial improvements have been coupled with an external mechanical pressure of several hundred kilopascal, cells were shown to sustain higher current densities without any dendrite growth. Although such high stack pressures are impractical for batteries development.

In this work we have synthesized high ion conductivity pure cubic phase LLZTO and studied dendrite growth mechanism. We observe that voids at Li/LLZTO interface act as field concentrators and have prime role to play in nucleation of dendrites. We suggest that these voids might be inevitable owing to nature of this battery system and propose the use of electron conducting interlayers which have no solubility with lithium metal as way of suppressing voids and mitigating dendrite growth.

1:40 PM EN04.08.03

A Proposed General Solution for Li Dendrite Penetration into Solid Electrolytes Yue Qi¹, Chunmei Ban² and Stephen J. Harris³; ¹Brown University, United States; ²University of Colorado Boulder, United States; ³Lawrence Berkeley National Laboratory, United States

Solid electrolytes (SEs) face significant technical challenges, in large part because lithium/sodium dendrites readily penetrate through SEs, leading to short circuits, even though early-on the high mechanical strength of ceramic separators was expected to suppress lithium growth. The ability of such a soft material (Li or Na metal) to penetrate through a ceramic is surprising from the point of view of models widely used in the Li battery field. We introduce a concept, new to the battery field, for suppressing penetration of lithium dendrites through SEs by putting the SE surfaces into states of residual compressive stress. For a sufficiently high compressive stress, cracks have difficulty forming, and cracks that do form are forced to close, blocking dendrite penetration. This approach is widely used to solve commercially important stress corrosion cracking problems in metals and static fatigue problems in ceramics and glasses (e.g., Gorilla Glass). However, the technique will not be useful for SEs if the Li ion transport rate through a SE is substantially reduced when the SE is in compression.

Our molecular dynamics calculations for Li ion transport through a common SE demonstrate that the introduction of even very high residual compressive stresses (10 GPa) has only a modest effect on Li ion transport kinetics, suggesting that the approach is viable and capable of providing a new paradigm for developing highperformance and mechanically strong SEs.

1:55 PM EN04.08.04

Solid-State Li-Ion Battery Performance and Electrolyte Conductivity Modeling in Python Maya Horii¹, Rebecca Christianson², Heena Mutha² and Chris Bachman¹; ¹California State University, Los Angeles, United States; ²Draper Laboratory, United States

High Li-ion conductivity solid electrolytes can allow for higher energy density and safer solid-state Li-ion batteries. One promising solid electrolyte is $\text{Li}_7\text{La}_3\text{Zr}_2\text{O}_{12}$ (LLZO) as it has both a high conductivity and stability. However, processing of ceramic electrolytes that are thin, dense, and have limited grain boundaries is a challenge. Additionally, understanding the effect of these properties on battery performance is not well understood. To analyze the effect of LLZO grain structure, a resistor mesh model was created. By solving for voltage using successive over-relaxation of Kirchhoff's Law, we can calculate the conductivity and diffusion coefficient of a material with varying grain sizes, grain boundary thicknesses, and voids. This model was coupled with a continuum battery performance model, which uses the Nernst-Planck equation to track the concentration of Li throughout a battery with an LLZO electrolyte, a Li metal negative electrode, and a LiCoO_2 positive electrode. Then, using the concentration data, the overpotential from diffusion, charge transfer, and resistance were found using the Nernst equation, Butler-Volmer equation, and the integral of the electric field in the electrolyte, respectively. By adding the overpotentials to the equilibrium voltage based on state of charge, we obtained charge/discharge curves, energy, and power for the battery under varying conditions. Combining these models, we can determine the effect of grain structure on overall battery performance. This modeling method can be used to evaluate the suitability of solid-state electrolyte materials and manufacturing methods.

As expected, the model predicted increasing energy output as grain size increased and grain boundary thickness decreased, due to the low conductivity of LLZO grain boundary. Similarly, it was able to predict increasing energy at lower C-rates. It was found that below ratios of grain size to grain boundary thickness of 10000, the diffusion coefficient begins to appreciably decrease. The low electrolyte diffusion coefficient has the largest detrimental effect at high C-rates, where the electrolyte becomes the limiting factor and is unable to support the Li diffusion.

2:10 PM EN04.08.06

From Atomistic Understanding of Correlation and Transport to Solid Polymer Electrolyte Design Nicola Molinari¹, Jonathan Mailoa² and Boris Kozinsky^{1,2}; ¹Harvard University, United States; ²Bosch, United States

Electrolytes control battery recharge time and efficiency, anode/cathode stability, and ultimately safety, consequently electrolyte optimization is crucial for the design of modern energy storage devices. However, conductivity and general transport properties of the cation/anion pair(s) dissolved in the electrolyte often pose a technological limitation to the viability of the battery, and progress in fundamental insights into the origin of transport limitations are challenging yet extremely valuable. We adopt theoretical and molecular modeling techniques to shine light on transport properties and correlation effects in solid polymer electrolyte systems.

Poly(ethylene oxide) (PEO) -based solid polymer electrolytes have a long history of research due to the easy processability and good transport properties, yet new observations that challenge our conventional understanding are still reported, especially at high salt concentrations relevant for technological applications. Our study of such regimes for PEO-Li-bis(trifluoromethane)sulfonimide (TFSI) reveals the central role of the anion in coordinating and hindering Li ion movements. In particular, we observe significant competition between the anion and the polymer backbone to coordinate lithium atoms and surprising formation of asymmetric cation-anion clusters. The latter observation resonates well with recent experimental findings,

where negatively-charged Li-anion clusters were speculated to exist to justify the negative lithium transference number measured in this system. We then leverage the atomistic understanding developed for PEO to propose and study a new class of poly(anhydride)-based solid polymers electrolytes. Remarkably, we find that the electrolyte consisting of Li-TFSI dissolved in poly(cis-hept-4-enoicanhydride) has a 50% higher conductivity than PEO and a lithium transference number as high as 0.79. We then rationalize these results by investigating the complex anion-polymer chain competition in coordinating lithium.

2:25 PM EN04.08.07

Late News: LiBH₄-Oxide Composite as Solid-State Electrolyte for Solid-State Lithium-Ion Battery

Valerio Gulino^{1,2}, Matteo Brighi³, Peter Ngene¹, Radovan Černý³, Marcello Baricco² and Petra de Jongh¹;

¹Utrecht University, Netherlands; ²University of Turin, Italy; ³University of Geneva, Switzerland

Solid-state electrolytes (SSEs) are promising candidates for resolving the intrinsic limitations of the organic liquid electrolyte currently employed in Li-ion batteries. Nevertheless, an SSE must fulfil several requirements to be employed in an all-solid state battery (SSB), such a high ionic conductivity. Complex hydrides (*e.g.* LiBH₄) are suggested as solid-state electrolytes.¹ Among the different polymorphs of LiBH₄, only the hexagonal phase, which is stable at temperatures above 110°C, has a remarkable high ionic conductivity ($\sim 10^{-3}$ S cm⁻¹ at 120 °C). To practically access a room temperature (RT) SSB, a promising approach to enhance the Li-ion conductivity of LiBH₄ at RT is the development of new high conductive interface by mixing it with oxide nanoparticles (such as SiO₂, Al₂O₃ and MgO).²

In this work the Li-ion conductivity of LiBH₄ has been enhanced by means of MgO-mixing, optimizing the composition of LiBH₄-based composites in order to obtain a RT operating SSE. The optimum composition of the mixture results 53 v/v % of MgO, showing a Li-ion conductivity of $2.86 \cdot 10^{-4}$ S cm⁻¹ at 20 °C, four order or magnitude higher than pure LiBH₄ and comparable to the Li-ion conductivity of a liquid electrolyte. The improved Li-ion conductivity relies on the formation of a conductive interface that can be described by a core-shell model where the fraction of LiBH₄ (the core) is in direct contact with the oxide (the shell).

The formation of the composite does not affect the electrochemical stability window, which is similar to that of pure LiBH₄ (about 2.2 V vs. Li⁺/Li). The mixture has been incorporated as solid-electrolyte in a TiS₂/Li all-solid-state Lithium metal battery. A freshly prepared battery failed at RT only after 5 cycles. On the other hand, a stable solid electrolyte interphase can be obtained by a pre-conditioning cycling at 60 °C. Afterward, a capacity retention of about 80 % at the 30th cycle was obtained operating at RT. We illustrate that the addition of oxide nanoparticles to LiBH₄ offers a promising strategy to obtain novel SSE candidates for Li-based SSB.³

(1) Matsuo, M.; Orimo, S. Lithium Fast-Ionic Conduction in Complex Hydrides: Review and Prospects. *Adv. Energy Mater.* **2011**, *1* (2), 161–172. <https://doi.org/10.1002/aenm.201000012>.

(2) Gulino, V.; Barberis, L.; Ngene, P.; Baricco, M.; de Jongh, P. E. Enhancing Li-Ion Conductivity in LiBH₄-Based Solid Electrolytes by Adding Various Nanosized Oxides. *ACS Appl. Energy Mater.* **2020**, *3* (5), 4941–4948. <https://doi.org/10.1021/acsaem.9b02268>.

(3) Gulino, V.; Brighi, M.; Murgia, F.; Ngene, P.; de Jongh, P. E.; Černý, R.; Baricco, M. Room Temperature Solid-State Lithium-Ion Battery Using LiBH₄-MgO Composite Electrolyte. *ACS Appl. Energy Mater.* **2021**, *accepted*. <https://doi.org/10.1021/acsaem.0c02525>.

2:40 PM DISCUSSION TIME

SESSION EN04.09: Solid-State Batteries IV

Session Chairs: Jennifer Rupp and Yan Yao

Thursday Afternoon, April 22, 2021

EN04

4:00 PM *EN04.09.01

High-Energy All-Solid-State Organic–Lithium Batteries Yan Yao; University of Houston, United States

The race to safer and higher-energy batteries is prompting a transition from the liquid electrolyte-based lithium-ion batteries to all-solid-state lithium batteries. Recent studies have identified unique properties of organic battery electrode materials such as moderate redox potentials and mechanical softness which are uniquely beneficial for all-solid-state batteries based on ceramic electrolytes. Here we further explore the promise of organic materials and demonstrate a sulfide electrolyte-based organic-lithium battery with a specific energy of 828 Wh kg^{-1} , rivaling the state-of-the-art of all-solid-state batteries. Two innovation steps are responsible for the accomplishment. First, the combination of lithium anode and the high-capacity cathode material pyrene-4,5,9,10-tetraone ensures a high theoretical specific energy. Second, the microstructure of the organic cathode is optimized with the introduction of cryomilling, a technique common to processing soft materials but not familiar to electrode fabrication. The cathode material utilization increases to 99.5% as a result, up from the 55–89% previously reported for ceramic electrolytes-based solid-state organic batteries. The improvement highlights the special requirements of solid-state organic electrodes for microstructural engineering while preserving the chemical integrity of components.

4:25 PM EN04.09.02

Late News: Design of High-Voltage Stable Hybrid Electrolyte with an Ultrahigh Li Transference Number Chen Liao^{1,2} and Kewei Liu¹; ¹Argonne National Laboratory, United States; ²Joint Center of Energy Storage Research, United States

Considering the high energy consumption during processing, and the low compliance and adhesion of ceramic electrolytes, the integration of polymer into ceramic electrolytes provides a way to mitigate the interfacial issues. However, the severe ion concentration gradient, low ionic conductivity, and instability toward Li metal and high-voltage cathodes become the major concerns in applying hybrid electrolytes. In this work, we report a single-ion-conducting hybrid electrolyte with a new electrolyte-chemical stable polymer and LLZO. The composite electrolyte exhibited a high Li transference number of 0.94 and electrochemical stability up to 5.6 V vs Li/Li⁺. Promising averaged Coulombic efficiencies of 99.97% and 99.91% were achieved in cells with LiNi_{0.8}Co_{0.15}Al_{0.05}O₂ (NCA) and LiNi_{0.6}Mn_{0.2}Co_{0.2}O₂ (NMC622) cathodes for 400 and 200 cycles, respectively.

4:40 PM EN04.09.03

Late News: Structural Insights into Mechanisms of Fast Ion Conduction in Li-Argyrodite Po-Hsiu Chien and Jue Liu; Oak Ridge National Laboratory, United States

Promoting fast ion conduction in solid electrolytes is of technological importance to the development of all-solid-state rechargeable batteries. Among solid electrolytes, it has reported that Li-Argyrodite has the potential to achieve high Li-ion conductivity on par with conventional organic liquid electrolytes. The anion-site disorder has been proposed as the root cause of flattening the energy landscape for 3D Li⁺ migration. However, the structural origin in terms of ion migration pathways responsible for the high Li⁺ conductivity remains unclear. It, therefore, prompts us to investigate the Li-ion conduction in Li-Argyrodite (Li₆PS₅X, X = Cl, Br, and I) using variable-temperature neutron diffraction in combination with maximum entropy method (MEM) analysis, bond valence site energy (BVSE), and impedance spectroscopy. Several novel insights are obtained in this work: (1) Li⁺ is found suitable to occupy an interstitial site 16e, which then facilitates the 3D ion conduction by 48h–16e–48h jump with lower activation energy. This finding indicates that the 48h–48h jump alone is insufficient to describe the commonly accepted picture of long-range cage-to-cage ion conduction, (2) we find that the Li⁺ conductivity is, despite rare discussion, influenced by the Li⁺ distribution that can be altered by effective anion charge locating in the center of Li-cage, and (3) a rational approach, i.e., equal negative charge (ENC), is employed to improve the Li⁺ conductivity (from 6 mS/cm at r.t. in Li₆PS₅Cl) through manipulating the distribution of anion charge over 4c and 4a sites in Li_{5.7}PS_{4.7}ClBr_{0.3} (9 mS/cm at r.t.).

4:55 PM EN04.09.04

Late News: Chiral Salts for Solid-State Lithium Metal Batteries Lixin Qiao^{1,2}, Heng Zhang³ and Michel Armand¹; ¹Centre for Cooperative Research on Alternative Energies (CIC energiGUNE), Basque Research and Technology Alliance (BRTA), Spain; ²University of the Basque Country (UPV/EHU), Spain; ³Key Laboratory of Material Chemistry for Energy Conversion and Storage (Ministry of Education), School of Chemistry and Chemical Engineering, Huazhong University of Science and Technology, China

Solid-state lithium metal (Li^o) batteries (SSLMBs) are considered as the most promising alternatives to improve the energy density and safety of state-of-the-art liquid-based lithium-ion batteries.¹ Solid polymer electrolytes (SPEs) with excellent processability and flexibility have attracted great attention in the development of practical SSLMBs.

The chemistry of lithium salts plays a pivotal role in dictating the physicochemical and electrochemical performance of SPEs, thus influencing the cyclability of SSLMBs.² In addition to the most popular salt, lithium bis(trifluoromethanesulfonyl)imide anion (LiTFSI), several new salts have been proposed to improve further the ionic conductivity of SPEs, such as lithium (difluoromethanesulfonyl)(trifluoromethanesulfonyl)imide (LiDFTFSI),² lithium (trifluoromethanesulfonyl)(*N*-bis(methoxyethyl)sulfonyl)imide (LiEFA).³ The implementation of these salts in SPEs resulted in significant improvement of lithium-ion conductivities. However, to date, little attention has been paid to chiral salts and their possible impacts on the physicochemical and electrochemical properties of SPEs.

In this work, we report a new type of chiral salts built from commercially available camphorsulfonic acid and their use as electrolyte salts for poly(ethylene oxide) (PEO)-based SPEs. The fundamental properties of the neat salts and PEO-based electrolytes are comprehensively characterized, in terms of surface morphology, thermal stability, phase transition, ionic conductivity, and electrochemical stability... The role of chirality on the properties of the PEO-based electrolytes is intensively revealed via a combination of experimental and computational methods.⁴

References

- [1] X. Judez, G. G. Eshetu, C. Li, L. M. Rodriguez-Martinez, H. Zhang and M. Armand, *Joule*, **2** (2018), 2208–2224.
- [2] H. Zhang, U. Oteo, H. Zhu, X. Judez, M. Martinez-Ibañez, I. Aldalur, E. Sanchez-Diez, C. Li, J. Carrasco and M. Forsyth, *Angew. Chem. Int. Ed.*, **131** (2019), 7911–7916.
- [3] H. Zhang, F. Chen, O. Lakuntza, U. Oteo, L. Qiao, M. Martinez-Ibañez, H. Zhu, J. Carrasco, M. Forsyth and M. Armand, *Angew. Chem. Int. Ed.*, **131** (2019), 12198–12203.
- [4] Q. Lixin, S. Alexander, Z. Yan, M.-I. Maria, S.-D. Eduardo, L. Elias, T. Marcel, J. Patrik, Z. Heng and A. Michel, *J. Electrochem. Soc.* **167** (2020), 120541.

5:10 PM EN04.09.05

Late News: Structure and Ionic Mobility of Anti-Perovskite Compounds as Solid-State Electrolytes

Annie-Kim Landry^{1,2}, Gillian Goward³, Dany Carlier^{2,4}, Frédéric Le Cras¹ and Brigitte Pecquenard^{2,5,6};

¹Commissariat à l'Énergie Atomiques et aux Énergies Alternatives, France; ²Institut de Chimie de la Matière Condensée de Bordeaux, France; ³McMaster University, Canada; ⁴Université de Bordeaux, France; ⁵Centre National de la Recherche Scientifique, France; ⁶Bordeaux INP, France

The interest for solid-state electrolyte has increased over the last decade with the emergence of high-performance materials which avoid safety issues associated to inflammable solvents. Anti-perovskite compounds, which present an inverse perovskite-type structure where the anionic and cationic sites have been exchanged, are promising materials as solid electrolyte for all-solid-state batteries as they show a high ionic conductivity [1]. The stability of the cubic structure depends on the size of the ions and can result in a distorted system with a lower symmetry such as an orthorhombic or tetragonal structure.

This work investigates the Li_{3-x}H_xOCl compounds to understand the relationship between the structure and the

ionic mobility of the lithium ions in anti-perovskite compounds. For these compounds, the cubic structure leads to a greater ionic mobility due to the anisotropic migration pathway. Li_2OHCl shows a phase transition from orthorhombic to cubic structure around $37\text{ }^\circ\text{C}$ which leads to an increase of conductivity of one order of magnitude. To stabilize the cubic phase at room temperature, the Li/H ratio has been modified and the $\text{Li}_{2.1}\text{H}_{0.9}\text{OCl}$ has been synthesized. Li_2OHCl and $\text{Li}_{2.1}\text{H}_{0.9}\text{OCl}$ are characterized by variable temperature ^7Li and ^1H static and Magic-Angle Spinning Nuclear Magnetic Resonance (MAS-NMR) and by Pulsed-Field Gradient NMR (PFG-NMR). The two compounds are also studied by variable temperature synchrotron X-Ray Diffraction (XRD), Electrochemical Impedance Spectroscopy (EIS) and other characterization techniques. Other similar materials with an anti-perovskite structure where the halide has been partially or totally substituted by a superhalogen (BH_4^- , BF_4^- and AlH_4^-) have been investigated by density functional theory calculations and tend to show a higher ionic conductivity [2] as shown experimentally by Sun et al [3]. First syntheses were achieved with BH_4^- and characterized by XRD, EIS and NMR.

References:

[1] Y. Zhao and L. L. Daemen *J. Am. Chem. Soc.* **2012**, 134, 15042-15047.

[2] H. Fang *et al. J. Mater. Chem. A* **2017**, 5, 13373-13381.

[3] Y. Sun *et al. J. Am. Chem. Soc.* **2019**, 141, 5640-5644.

5:25 PM EN04.09.06

The Effect of Li and Na Mechanical Behavior on the Electrochemical Performance of Solid-State Batteries Jeffrey B. Wolfenstine¹, Michael Wang² and Jeff Sakamoto²; ¹Solid Ionic Consulting, United States; ²University of Michigan–Ann Arbor, United States

Recently, there has been renewed interest in the use of pure alkali metals (e.g., Li, Na) as anodes for rechargeable batteries. Using a pure alkali metal anode with a liquid electrolyte can lead to dendrite shorting and flammability issues. To overcome the issues associated with liquid electrolytes solid-state batteries consisting of Li-ion and Na-solid electrolytes combined with Li and Na anodes and solid cathodes are attracting considerable attention. In the case of a solid-state battery it is anticipated that the alkali metal anode will be under load to maintain contact between it and the solid-state electrolyte. For example, one of the major issues with these batteries is that at high discharging currents voids form near the electrolyte/metal interface which results in an increase in cell resistance which eventually leads to cell failure. One way to achieve high discharge currents is to increase stack (cell) pressure which increases the creep rate of the metal and consequently, prevents void formation and hence, avoiding cell death. Thus, it is important to determine the creep mechanism of metal anodes to be able to predict and understand the effect of stack pressure on creep rate and hence, cell life. In addition, to creep behavior of the anode other mechanical properties such as; yield stress and elastic constants must be determined in order to optimize the performance of solid-state batteries with Na or Li anodes. It is the purpose of this talk to present and compare the elastic properties, yield stress in tension/compression and the creep behavior in tension/compression for Na to Li and limited existing values in the literature and show how these properties effect the charging/discharging behavior and cycle life of solid-state batteries with Li and Na anodes. In addition, provide new insights in the design, modeling, and understanding of solid-state batteries utilizing alkali metal anodes

5:40 PM DISCUSSION TIME

SESSION EN04.10: Li and Na-Based Solid-State Batteries

Session Chairs: Yoon Seok Jung and Wangyan Wu

Thursday Afternoon, April 22, 2021

EN04

8:15 PM *EN04.10.01

Development of Cation-Substituted Na₃SbS₄ Solid Electrolytes Akitoshi Hayashi; Osaka Prefecture University, Japan

Na-ion conducting solid electrolytes are a key to develop all-solid-state sodium rechargeable batteries. Sulfide materials are suitable electrolytes because of their high conductivity and good deformability. In 2012, we reported cubic-Na₃PS₄ metastable phase, which was precipitated by crystallization of the mother glass, exhibited the conductivity of 10⁻⁴ S cm⁻¹ [1]. Na₃SbS₄ with a higher Na⁺ conductivities of 10⁻³ S cm⁻¹ is developed [2]. In this study, we have focused on cation-substituted Na₃SbS₄ electrolytes to increase their conductivity. The electrolytes were prepared via mechanochemistry, followed by heat-treatment to enhance their crystallinity. A part of Sb was replaced by W to form solid-solutions Na_{3-x}Sb_{1-x}W_xS₄ and increased their conductivity. The sulfide superionic conductor with the composition of Na_{2.88}Sb_{0.88}W_{0.12}S₄ exhibited a room temperature conductivity of 3.2 × 10⁻² S cm⁻¹ in a sintered body [3], which is higher than the best Li⁺ conductivity of 2.5 × 10⁻² S cm⁻¹ in LGPS-type Li_{9.54}Si_{1.74}P_{1.44}S_{11.7}Cl_{0.3} [4]. Partial substitution of Sb with W induced the Na vacancy doping and the tetragonal to cubic phase transition. A similar conductivity increase was also observed by a partial substitution of Mo. Conductivity enhancement in the W- and Mo-substituted Na₃SbS₄ was discussed by the first-principles calculations [5]. In addition, the Na_{2.88}Sb_{0.88}W_{0.12}S₄ electrolyte was successfully prepared from an aqueous solution [6] and its precursor solution is useful for close contact with active material particles. All-solid-state Na/S cells with the Na₃SbS₄ electrolyte showed an almost full reversible capacity of 1560 mAh per gram of S and good cyclability at 25°C [7].

Acknowledgements: This work was supported by Element Strategy Initiative of MEXT, Grant Number JPMXP0112101003 and JSPS KAKENHI Grant Number 18H01713 and 19H05816.

References

- [1] A. Hayashi *et al.*, *Nat. Commun.* 3 (2012) 856.
- [2] A. Banerjee *et al.*, *Angew. Chem. Int. Ed.* 55 (2016) 9634.
- [3] A. Hayashi *et al.*, *Nat. Commun.* 10 (2019) 5266.
- [4] Y. Kato *et al.*, *Nat. Energy*, 1 (2016) 16030.
- [5] R. Jalem *et al.*, *Chem. Mater.*, 32 (2020) 8373.
- [6] S. Yubuchi *et al.*, *J. Mater. Chem. A*, 8 (2020) 1947.
- [7] T. Ando *et al.*, *Electrochem. Commun.*, 116 (2020) 106741.

8:40 PM EN04.10.02

Production and Purification of Anhydrous Sodium Sulfide William Smith, Jerry Birnbaum and Colin A. Wolden; Colorado School of Mines, United States

Anhydrous sodium sulfide (Na₂S) is a key component in sodium-sulfur batteries as well as an important chemical reagent. However, anhydrous Na₂S is currently prohibitively expensive for applications outside of research labs (>\$10 g⁻¹) and purity is a concern. Herein, we compare the properties of three forms of anhydrous Na₂S: (i) commercially supplied, (ii) Na₂S produced through dehydration and purification of commercial hydrate flakes (Na₂S·xH₂O), and (iii) Na₂S formed by the reaction of hydrogen sulfide with dissolved sodium alkoxide and recovered through solvent evaporation. Crystallinity, purity, thermal stability, and morphology of the various forms of Na₂S were characterized by XRD, FTIR/Raman, TGA, and SEM respectively. Vacuum annealing of low-cost Na₂S hydrate at 150 °C produced anhydrous Na₂S. This dehydrated material retains impurity signatures attributed to polysulfide (Na₂S_x) and sulfite groups (S=O) that were also observed in commercially supplied Na₂S. These impurities could be removed by heating to 400 °C under flowing H₂, the kinetics of which are well-described by a shrinking core model. The solution-based approach resulted in the direct synthesis of crystalline Na₂S anhydride at low temperatures (100 °C) without need for further purification. Both approaches presented herein are inherently scalable with materials costs that are one to two orders of magnitude lower than the current price of anhydrous Na₂S.

8:55 PM BREAK

9:25 PM EN04.10.04

Late News: Surface-Dependent Stability of the Interface Between Li₇La₃Zr₂O₁₂ Solid Electrolyte and the Li Metal from First-Principles Calculations Bo Gao¹, Randy Jalem^{1,2,3} and Yoshitaka Tateyama^{1,2}; ¹National Institute for Materials Science, Japan; ²Kyoto University, Japan; ³Japan Science and Technology Agency (JST), Japan

The garnet-type Li₇La₃Zr₂O₁₂ (LLZO) solid electrolyte is of particular interest because of its high Li-ion conductivity, wide electrochemical window, and good chemical stability under atmospheric conditions, suitable for practical all-solid-state batteries (ASSBs). However, some stability issues, including the reduction of Zr [1] and the contact loss [2], at the LLZO/Li interface has been observed in a number of studies, leading to poor cycle stability and high interfacial resistance. Herein, we have revealed the origin of these instabilities by performing a comprehensive first-principles investigation with a high-throughput interface structure search scheme, based on the density functional theory framework. [3,4] Based on the constructed phase diagrams of low-index surfaces, we found that the coordinatively unsaturated (i.e. coordination number < 6) Zr sites exist widely on the low-energy LLZO surfaces. These undercoordinated Zr sites are reduced once the LLZO surface is in contact with the Li metal, leading to the chemical instability of the LLZO/Li interface. The employments of the approaches such as controlling the synthesis atmosphere are needed for preventing the reduction of LLZO against the Li metal. Besides, the calculated formation and adhesion energies of interfaces suggest that the Li wettability on the LLZO surface is dependent on the termination structure, which may result in the inhomogeneous Li depletion and contact loss. The present analysis with comprehensive first-principles calculations provides a novel perspective for the rational optimization of the interface between LLZO electrolyte and Li metal anode in the ASSB. [5]

References:

- [1] Y. Zhu, J. G. Connell, S. Tepavcevic, P. Zapol, R. Garcia-Mendez, N. J. Taylor, J. Sakamoto, B. J. Ingram, L. A. Curtiss, J. W. Freeland, D. D. Fong, and N. M. Markovic, *Adv. Energy Mater.* **9**, 1803440 (2019).
- [2] T. Krauskopf, H. Hartmann, W. G. Zeier, and J. Janek, *ACS Appl. Mater. Interfaces* **11**, 14463 (2019).
- [3] B. Gao, P. Gao, S. Lu, J. Lv, Y. Wang, and Y. Ma, *Sci. Bull.* **64**, 301 (2019).
- [4] B. Gao, R. Jalem, Y. Ma, and Y. Tateyama, *Chem. Mater.* **32**, 85 (2020).
- [5] B. Gao, R. Jalem, and Y. Tateyama, *ACS Appl. Mater. Interfaces* **12**, 16350 (2020).

9:40 PM EN04.10.05

Late News: Operando Differential Electrochemical Pressiometry for Probing Electrochemo-Mechanical Evolution in Li[Ni,Co,Mn]O₂/Graphite All-Solid-State Batteries Seunggoo Jun, Young Jin Nam, Hiram Kwak, Kyu Tae Kim, Dae Yang Oh and Yoon Seok Jung; Yonsei University, Korea (the Republic of)

Due to their potential of improved safety, energy density, and operating temperature ranges, all-solid-state batteries (ASBs) have been emerging as a promising power source for electric vehicles. Sulfide solid electrolytes (SEs), such as Li₁₀GeP₂S₁₂ (12 mS cm⁻¹) and Li_{5.5}PS_{4.5}Cl (12 mS cm⁻¹), are attractive candidates for practical ASBs because of their high ionic conductivities being comparable to those of conventional liquid electrolytes (~10 mS cm⁻¹) and mechanical sinterability. In ASBs that lacks soft components, electrochemo-mechanical evolutions originating from breathing volumetric strains of electrode active materials upon charge-discharge are imperative in the viewpoints of not only improving performances but also comprehensive understanding complex interfacial phenomena.

In this presentation, we report newly developed operando differential electrochemical pressiometry (DEP) for ASBs. The pressure change signals reflecting volume changes of electrode active materials feature phase transitions of electrode active materials in LiMO₂/Gr all-solid-state cells. Thus, it is demonstrated that DEP analysis enables offering nondestructive determination of state-of-charges of ASBs. Complementary analysis results via ex situ X-ray diffraction measurements is also presented.

9:55 PM DISCUSSION TIME

10:05 PM *EN04.10.08

Silver-Carbon Composite Anodes for All-Solid-State Lithium Metal Batteries Yong-Gun Lee and Dongmin Im; Samsung Advanced Institute of Technology (SAIT), Samsung Electronics, Korea (the Republic of)

An all-solid-state battery with a lithium metal anode is a strong candidate for surpassing conventional lithium-ion battery capabilities. However, undesirable Li dendrite growth and low Coulombic efficiency impede their practical application. We have found that a silver-carbon nanocomposite anode layer, when employed in combination with solid electrolyte, prohibits the dendrite formation and allows the homogeneous Li metal plating and stripping on the surface of current collector. The high Coulombic efficiency thus achieved also eliminates the need of excessive Li metal, further increasing the cell energy density and decreasing the production cost. The silver particles are dissolved in the Li metal during the charging process and appear to assist the homogeneous Li plating. On the other hand, the carbon layer keeps the solid electrolyte physically separated from Li metal, preventing the chemical degradation of solid electrolyte and the Li metal penetration through it. Consequently, the nanocomposite anode formed on a current collector can offer high energy density (>900 Wh/L) and long cycle life (>1,000 times) in the solid-state batteries (0.6 Ah prototype pouch cell).

SESSION EN04.11: On-demand
Wednesday Morning, April 14, 2021
EN04

8:00 AM EN04.11.01

Doped Pyrochlores as Versatile Reagents for Formation of Lithium Conducting Garnet Solid Electrolytes Jon M. Weller and Candace Chan; Arizona State University, United States

Lithium conducting garnets in the family of doped lithium lanthanum zirconates (nominally $\text{Li}_7\text{La}_3\text{Zr}_2\text{O}_{12}$, LLZO) are of great interest as oxide solid electrolytes for solid-state lithium-metal batteries. Despite the promising properties of LLZO in terms of electrochemical stability and ionic conductivity, processing of garnet solid electrolytes is still a challenge. Many synthetic approaches have been investigated to-date, including sol-gel, co-precipitation, spray pyrolysis, combustion, and molten salt synthesis, not to mention the standard solid-state reaction method. Most of the aforementioned methods can generate LLZO with the expected properties, but nearly all are either costly or not amenable to producing thin films of LLZO, which are necessary for practical solid-state batteries based on lithium conducting garnets. Interestingly, in nearly all of these approaches the lanthanum zirconate pyrochlore phase ($\text{La}_2\text{Zr}_2\text{O}_7$, LZO) is seen as an intermediate phase before conversion of precursors to LLZO, nearly irrespective of precursor type. In this work, nanocrystalline, off-stoichiometric, doped pyrochlores based on the LZO structure are synthesized as a quasi-single-source precursor for formation of LLZO, maintaining a 3:2 ratio of La:Zr instead of the conventional 1:1 ratio in stoichiometric pyrochlores, while also incorporating necessary dopants to stabilize the cubic phase of LLZO after densification. Using these novel, nanosized pyrochlore precursors, LLZO is formed by the simple addition of a Li_2O source. Conversion of doped LZO to LLZO in molten salts is demonstrated as a novel synthetic approach, requiring only low synthesis temperatures (as low as 400 °C). Additionally, doped pyrochlores may be directly converted to garnets in a single reactive sintering step, resulting in both high density (> 90% relative density) and ionic conductivity (> 0.5 mS cm^{-1}), presenting a streamlined approach to formation of garnet solid-electrolytes amenable to more facile processing methods than conventional ceramic sintering.

SYMPOSIUM EN05

Materials Challenges and Opportunities in Concentrated Solar Power Technologies
April 20 - April 20, 2021

Symposium Organizers

Andrea Ambrosini, Sandia National Laboratories
Adrianus Aria, Cranfield University
Ramon Escobar Galindo, Universidad de Sevilla
Christopher Muhich, Arizona State University

Symposium Support

Bronze
MilliporeSigma

* Invited Paper

SESSION EN05.01: Thermal Storage and Corrosion and Poster Session
Session Chairs: Adrianus Aria and Ramon Escobar Galindo
Tuesday Morning, April 20, 2021
EN05

8:00 AM *EN05.01.01

Challenges with High Temperature Thermophysical Property Measurements Shannon Yee; Georgia Institute of Technology, United States

Robust and accurate thermophysical properties, namely thermal diffusivity, thermal conductivity, and specific heat of high-temperature (>1000 K) containment materials (CMs) and heat transfer materials (HTMs) are lacking, (i) because few measurement techniques exist, and (ii) unbeknown measurement inaccuracies exist in many commercially available techniques that are not well documented in literature. This has resulted in surprisingly large spread in reported thermophysical properties at high temperatures of both CMs and HTMs, begging the question what are the true thermophysical properties of many CMs and HTMs. This presents a unique challenge for designing high-temperature thermal systems when there is such large uncertainty in physical properties of materials. It has been challenging to calculate (or model) the thermophysical properties due to the composite (or multi-component alloy) nature of these materials often resulting in microstructural phase transitions and spatially heterogeneous composites. At elevated temperatures chemical stability (both oxidation and corrosion) and radiation effects make accurate measurements exceedingly difficult. To address this challenge, numerous repeated measurements on multiple samples spanning both spatial (e.g., heterogeneity) and temporal (e.g., aging) variations and subsequent statistical analysis (e.g., 95% confidence-interval) are required to confirm or refute the often single-measurements reported on material specification sheets or literature. This invited talk will highlight some “problematic materials” whose properties have been misreported previously, commenting on “likely” sources of error. This talk will also highlight new measurement techniques that are trying to address some of these identified shortcomings. And finally, this talk will present “lessons learned” from a more robust statistical approach to reporting thermophysical properties.

8:25 AM EN05.01.02

Nickel-Aluminide Based Anticorrosion Coatings Prepared by Plasma Spray for Concentrating Solar Power Applications Sarah Yasir¹, Adrianus I. Aria¹, Elena Guillen² and Jose Endrino³; ¹Cranfield University, United Kingdom; ²PROFACTOR GmbH, Austria; ³Basque centre of materials, Spain

The use of solar energy for power generation provides an efficient sustainable energy solution. Among a

number of technologies developed for power generation using solar energy, concentrating solar power (CSP) is encouraging because of the capability of thermal energy storage that makes it possible for the generation beyond sunset and in times of cloud cover. Although the use of molten salts as heat transfer fluid and thermal storage in CSP has various advantages, they have a major disadvantage as they make the component systems highly susceptible to corrosion. Different approaches to prolong life by suppressing corrosion have been adapted including the use of high alloy steels and the use of high purity molten salts, coating is a promising option because coatings are believed to provide shield to suppress corrosion.

In this study, we investigate the use of protective coatings to enhance the corrosion resistance of the component systems against molten salts at an elevated temperature. Nickel aluminide coatings are deposited using plasma spray system, as they hold high-temperature mechanical strength and it has a remarkable oxidation resistance performance as substrate component. Moreover, nickel aluminide has low solubility in the molten nitrate salt. Ni₃Al coatings are much preferred to be used as corrosion resistant coatings as they possess strength at high temperature, oxidation protection and creep properties.

Corrosion behaviour of stainless steel 347 (SS347) and Ni₃Al coated SS347 was investigated in molten nitrate salt (60wt% NaNO₃ + 40wt% KNO₃) immersion at 565°C for 500 hours intervals up to 3000 hours. A growth of stratified oxide layers was observed on SS347 sample surface comprising of NaFeO₂, Fe₂O₃ and Fe₃O₄. The Ni₃Al coated SS347 samples were observed to undergo rapid oxidation within first 500 hours. The results presented in this study suggest that Ni₃Al coating suppresses the formation of oxide layers on the surface of stainless steel substrates and can be used to suppress corrosion in presence of molten nitrate salts. The fact, that Ni₃Al coated SS347 gives mass change of one order of magnitude lower than the bare SS347, it means that these coatings can be used to prolong the lifetime of bare SS347 in molten nitrate salt at 565°C, which is of relevance to thermal energy storage applications. In my presentation, I will show the corrosion test results and discuss the potential of nickel aluminide coatings to suppress hot corrosion by molten salts in an environment that simulates that of concentrating solar power plants.

8:40 AM EN05.01.03

Wear in Particle Based CSP Systems From Particle Abrasion and Attrition at High Temperature Nipun Goel¹, Tessa Mei-lin Fong¹, John Shingledecker², Andrew Russell¹, Michael W. Keller³, Siamack A. Shirazi³ and Todd Otanicar¹; ¹Boise State University, United States; ²Electric Power Research Institute, United States; ³The University of Tulsa, United States

High temperature particle-based receivers offer distinct advantages over conventional molten salt receivers due to their ability to achieve temperatures above 700 C, direct absorption of solar energy as they fall through a beam of concentrated sunlight, and the relative ease of storage (and retrieval using a secondary working fluid) in insulated storage tanks. The use of particles, however, also raises concerns with material degradation from the flow of hot or cold particles through discharge hoppers or along the inner receiver surfaces and other system components (e.g. tubes, valves etc.), depending on operating mode of the receiver. The flow of particles over surfaces may result in loss of material from abrasive wear, impact erosion from impingement under gravitational fall and particle attrition as particles fall and move on top of each other.

In the present study, the performance of candidate materials and particles were evaluated through a series of abrasion erosion and particle attrition experiments at room temperature as well as at 800 C. Candidate materials were subject to abrasive wear from particles at low particle to material velocities inside a resistance heated kiln, and analyzed for changes in mass and surface morphology using cross-sectional scanning electron microscopy (SEM) and energy dispersive x-ray spectroscopy (EDS) tests. The wear rate for different specimens was noted to be largely driven by the strength of chromia scales built on the specimens from exposure to high temperature. Particle attrition measurements explored the susceptibility of particles to breakdown from particle to particle interaction and the generation of fines from this process. At the low velocities expected in particle based Concentrated Solar Power (CSP) plants, the particles tested exhibited near negligible breakdown. However, changes in the particle hardness at 800 C resulted in a significantly higher particle breakdown to sizes <40 microns raising potential environmental concerns. In addition to particle breakdown, it was also noted that the sample had oxides from the stainless steel test setup mixed in with the particles. Similar oxides can be expected to turn up in the utility scale particle based CSP plants as well. The presence of oxide was also noted to affect

the solar absorptivity of the mixture compared to a clean initial specimen, potentially resulting in a change in the overall efficiency of the CSP plant.

8:55 AM EN05.01.04

Frequency-Domain Hot-Wire Measurements of Molten Nitrate Salt Thermal Conductivity Andrew Z. Zhao¹, Matthew Wingert^{1,2} and Javier Garay¹; ¹University of California, San Diego, United States; ²PsiQuantum, United States

The thermal conductivity of liquids has traditionally been determined by measuring either the steady-state temperature gradient or time-dependent temperature rise in a sample due to an applied heat flux. The transient hot-wire method has become the standard for measuring liquid thermal conductivity; in this method, direct current Joule heats a long, thin wire immersed in a liquid sample, and the measured temperature rise over a particular time interval is fit to a heat transfer model to extract the thermal conductivity of the liquid. However, in the high-temperature environments of molten salts, long metal wires are vulnerable to corrosion, and convection errors are magnified in larger volumes of molten salts. Here, we utilize a new frequency-domain, corrosion-resistant, short hot-wire technique (sensor and model) to measure the thermal conductivity of molten NaNO₃ (2.78% standard uncertainty), KNO₃ (2.38% standard uncertainty), and Solar Salt mixture (2.66% standard uncertainty). Operating in the frequency domain and utilizing a full 3D model allows the use of short sensor wires, reducing the total contact area to minimize corrosion, and the use of small sample volumes, mitigating convection errors. An alternating current at varying frequencies Joule heats a short platinum wire sensor (6.5 mm), which is protected by a 1.6 mm thick Al₂O₃ coating, submerged in molten salt. The frequency-dependent temperature response of the sensor surrounded by salt is measured and fit to a 3D thermal model to obtain the thermal conductivity of the molten salt. Together, the new sensor design and 3D model keep the probed molten salt volume below 1 μL. Our frequency-domain measurements show an ~11-15% higher thermal conductivity of molten nitrate salts than the current reference correlations made from steady-state and time-domain measurements.

9:10 AM *EN05.01.05

Robust High-Temperature Materials for Concentrated Solar Power Ken Sandhage¹, Yujie Wang¹, Priyatham Tumurugoti¹, Jorge Velasco-Ramirez¹, Alexander Strayer¹, Gregory Scofield¹, Adam Caldwell¹, Supattra Singnisai¹, Qingzi Zhu², Mehdi Pishahang², Michael Sangid¹, Asegun Henry², Kevin Trumble¹, Grigorios Itkos¹ and Mario Caccia¹; ¹Purdue University, United States; ²Massachusetts Institute of Technology, United States

The efficiency of concentrated solar power (CSP) plants for generating electricity may be appreciably increased by operating at higher temperatures. By increasing turbine inlet temperatures to $\geq 750^\circ\text{C}$ and by using high-pressure, supercritical carbon dioxide (sCO₂) power cycles, instead of conventional cycles at $\leq 550^\circ\text{C}$, the relative heat-to-electricity conversion efficiency may be increased by $>20\%$ (a key step towards direct competition with fossil fuel power plants and a large decrease in greenhouse gas emissions). However, inlet sCO₂ temperatures for CSP turbines are severely limited by current printed-circuit-type heat exchangers (PCHEXs) that are used to transfer heat to the sCO₂; that is, conventional metal alloys used in such PCHEXs exhibit a significant decrease in mechanical performance at $>600^\circ\text{C}$.

Here we present a robust composite of zirconium carbide (ZrC) and tungsten (W) for use in PCHEXs at $\geq 750^\circ\text{C}$. Co-continuous ZrC/W composites possess an attractive combination of properties for this application. ZrC and W are chemically compatible; that is, these solids exhibit limited mutual solid solubility, do not react to form other compounds, and exhibit a solidus temperature of 2800°C . Measurements of the thermal diffusivity and heat capacity of co-continuous ZrC/W composites have yielded an average thermal conductivity value of 66 W/m-K at 800°C , which is appreciably higher than values reported for advanced Ni-based alloys at this temperature (e.g., 22.1 W/m-K for IN740H). Polycrystalline ZrC and W exhibit similar modest values of thermal expansion from 25°C to 750°C , and have been found to be resistant to thermal cycling and extreme thermal shock (e.g., $>1000^\circ\text{C}/\text{sec}$). The interconnected carbide phase can provide ZrC/W composites with high-

temperature stiffness and creep resistance, whereas W exhibits high-temperature ductility for enhanced resistance to fracture relative to monolithic ZrC. Indeed, co-continuous ZrC/W composites have been found to possess average failure strengths at 800°C of 600 MPa (well above the maximum allowed stresses of Ni-based superalloys at this temperature at elevated pressures). Although not inherently resistant to high-temperature oxidation, ZrC/W composites have been endowed with such resistance via modest CO additions to sCO₂ (to generate a supercritical reducing fluid) and by placing a layer of Cu (a relatively noble metal) on the ZrC/W surface. Such Cu-bearing ZrC/W composites have exhibited negligible oxidation after 1000 h at 750°C in mixtures of sCO₂ with 50 ppm CO at 20 MPa.

The fabrication of PCHEXs comprised of dense co-continuous ZrC/W-based HEX plates with tailorable channel patterns will also be discussed. Porous WC preform plates with desired channel patterns may be generated by low-cost forming (e.g., casting, pressing) of WC/organic mixtures, followed by organic pyrolysis and light (initial stage) sintering. The resulting rigid, porous WC preform plates can then be converted into dense ZrC/W plates via reactive pressureless infiltration with a Zr-bearing liquid. The Zr in the liquid undergoes a displacement reaction with the WC in the preform to yield ZrC and W as solid reaction products. These products possess a combined volume that is larger than the volume of WC consumed, so that the prior pores in the preform become filled with these new solids with little change in external preform shape, surface features, and size (typically <1% dimension changes). Because the channels present in the easily-formed porous WC preforms are retained in the dense ZrC/W plates, prolonged chemical etching (required for current metal-based PCHEXs) is not needed to produce such channels, and unique channel morphologies (higher aspect ratios, non-circular cross-sections) can be generated for tailored fluid flow and heat transfer. Techno-economic analyses indicate that ZrC/W-based PCHEXs can strongly outperform Ni-superalloy PCHEXs at lower cost.

9:35 AM BREAK

9:40 AM EN05.01.06

Magnetically-Accelerated Solar-Thermal Energy Storage within High-Temperature Molten Salt Phase Change Materials Peng Tao, Chao Chang and Tao Deng; Shanghai Jiao Tong University, China

Thermal energy storage within high-temperature molten salts is critical to overcome solar illumination intermittency and ensure stable operation of concentrated solar-thermal systems. Current molten salt phase change materials, however, generally suffer from a low thermal conductivity, which seriously limits both the charging and discharging processes. It is challenging to effectively increase the thermal conductivity of high-temperature molten salts without affecting their heat storage capacity and other inherent thermophysical properties. In this work, we reported that magnetically moving mesh-structured solar absorbers within solar salts along the solar illumination path could significantly accelerate the solar-thermal energy storage rates. The mesh absorber continuously advances the melting solid/liquid interface thus achieves fast latent heat storage of solar-thermal energy within solar salts. Compared to conventional static charging processes, such magnetically-accelerated movable charging strategy increases the latent heat solar-thermal energy harvesting rate by 107% and maintains 100% heat storage capacity of solar salts. We also demonstrated that the movable charging supports large-area charging of solar salts with small-sized solar-thermal converters and continuous batch-to-batch solar-thermal storage. The movable charging system can be readily integrated with heat exchanging systems to serve as energy sources for water and space heating by using abundant clean solar-thermal energy. Alternatively, the high-temperature heat stored within melted solar salts can be direct converted to electricity through thermoelectric conversion, and the converted electricity can simultaneously light up multiple LEDs.

9:45 AM EN05.01.07

Doped ALPO-5 Zeolites as Promising O₂ Sorption Pump Materials—A Density Functional Theory Study Steven A. Wilson, Ellen Stechel, Ivan Ermanoski and Christopher Muhich; Arizona State University, United States

Many chemical processes depend on having an environment that is low in oxygen partial pressure ($PO_2 < 100$

Pa); sorption pumps are a promising route to establishing that environment by either oxygen pumping or oxygen separation from an inert gas. Near ambient sorption-based processes rely on either pressure or thermal swings, requiring no moving parts, no electricity, and neither very high nor very low temperatures. In this work, we use ab initio calculations to explore zeolites as a class of materials for sorption based oxygen pumping/separation. Our calculations indicate that while the neat ALPO-5 zeolite does not adsorb O₂, O₂ does adsorb on zeolites selectively doped with transition metals and metalloids and hence, can enable separation and pumping. ALPO-5 doped with Si, Ge, Sn, Pd, Pt, Ti, V, Cr, Mn, Zr, Mo, Hf, W, Ce, and Pr provides ad-sorption energies ranging from -0.19 to -3.92 eV, (-) indicates exothermic process. Additionally, we provide a comprehensive understanding of what controls the adsorption energy: 1) the dopant must be able to adopt an oxidation state that is more positive than the cation it replaces, and 2) the size of the pore into which the O₂ adsorbs to the wall. Lastly, we conduct a thermodynamic analysis of a thermal swing cycle to approximate the optimal O₂ binding energy for low energy O₂ pumping/separation. We find that the minimum energy cost likely occurs when the adsorption energy is in the range of 0.75 – 1.00 eV (72 – 97 kJ*mol⁻¹), which corresponds to Ge, V, Pt, or Ce doped ALPO-5.

9:50 AM EN05.01.09

Best Practices for Synthesizing Single Phase Thermochemical Materials in Multinary Systems Robert T. Bell¹, Dan Plattenberger¹, Sarah Shulda¹, Nicholas Strange^{1,2}, Karen Heinselman¹, James E. Park³, Andrea Ambrosini³, Michael F. Toney^{2,4}, Philip Parilla¹, Anthony H. McDaniel³, Eric Coker³ and David Ginley¹; ¹National Renewable Energy Laboratory, United States; ²SLAC National Accelerator Laboratory, United States; ³Sandia National Laboratories, United States; ⁴University of Colorado Boulder, United States

Materials for solar thermochemical production of hydrogen (STCH) and other fuels often relies on the use of highly thermally stable multinary oxides. Often these oxides possess three or more cations and represent an alloy or line compound within a complex multinary phase space. These complex phase spaces often possess one or more other refractory phases which, if formed during synthesis, remain as secondary phases through repeated sintering. These secondary phases are typically inactive thermochemically, create a convoluted signal in measurements which can complicate isolating the performance and behaviors of candidate materials. This work discusses a number of best practices and potential routes for synthesizing single phase multinary oxides for thermochemical applications. Common synthetic routes discussed include mixed carbonate and oxide sintering, unary oxide blends, and modified Pechini sol-gel processing. The formation of different secondary phases based on the synthesis route is demonstrated for example systems such as BaCe_{0.25}Mn_{0.75}O₃. Results of sintering model systems at different peak temperatures demonstrate the need for furnace temperature in excess of 1200°C in many systems. Additionally, the effect of isothermal reduction and re-oxidation cycling on removing secondary phases, especially containing softer cations such as Mn, is demonstrated. These reduction and oxidation cycling results partially explain the commonly observed drift in performance during the initial few cycles of STCH materials. This work provides an important roadmap to synthesizing single phase thermochemical materials.

SESSION EN05.02: Solar Thermochemical Water Splitting I & Solar Thermochemistry and Energy Storage

Session Chairs: Adrianus Aria and Ramon Escobar Galindo

Tuesday Morning, April 20, 2021

EN05

11:45 AM *EN05.02.01

Metal Oxide-Based Thermochemical Redox Processes for Producing Solar Fuels and Storing Ellen Stechel¹, Alberto de la Calle¹, Ivan Ermanoski² and James E. Miller²; ¹Arizona State University, School of Molecular Sciences, United States; ²Arizona State University, School of Sustainability, United States

High temperature endothermic reduction of metal oxides, which can liberate oxygen gas at achievable conditions, converts thermal energy to stored chemical energy. A subsequent re-oxidation step either recovers the stored energy as heat or utilizes it to drive other chemical reactions. If the re-oxidation step restores the material to its original state so that the two-steps can repeat indefinitely, the sequence of reactions constitutes a thermochemical cycle. Two related processes (reversibly re-oxidizing with oxygen or affecting bond breaking by re-oxidizing with CO₂ and/or water) are somewhat analogous; the fuel production option is significantly more constrained by thermodynamics and hence subject to greater challenges to efficiency and cost. Nonetheless, both chemistries have been of increasing interest due to their potential for high efficiency utilization of the sun and economic competitiveness for clean energy and most recently as a role in achieving negative emissions and closing the carbon cycle.

This presentation will discuss thermodynamic requirements and opportunities presented by the redox-active metal oxide thermochemistry and show recent progress towards developing the materials and cycles for thermochemical energy storage and CO₂/H₂O splitting.

12:10 PM EN05.02.02

Gaining Mechanistic Insight into the Relationship Between Electronic Structure and Reduction of Thermochemical Materials through Combined Empirical and Modeling Experimentation Sarah Shulda¹, Robert T. Bell¹, Dan Plattenberger¹, James E. Park², Anuj Goyal¹, Nicholas Strange¹, Karen Heinselman¹, Eric Coker², Josh Sugar², Andrea Ambrosini², Stephan Lany¹, Sami Sainio³, Michael F. Toney⁴, Philip Parilla¹, Anthony H. McDaniel² and David Ginley¹; ¹National Renewable Energy Laboratory, United States; ²Sandia National Laboratories, United States; ³SLAC National Accelerator Laboratory, United States; ⁴University of Colorado Boulder, United States

The layered perovskite BaCe_{0.25}Mn_{0.75}O₃ (BCM) is a proven solar thermochemical (STCH) water splitting material demonstrating higher hydrogen generation and improved redox kinetics relative to current state of the art materials. Recent results have revealed that BCM belongs to a larger family of STCH materials, BXM (X = Ce, Nb, Pr). Despite the three materials having identical structures, and differing only in 1/8 of their cation species, their water splitting performances are markedly different. Improved understanding of the mechanisms and material properties that determine performance of STCH materials is necessary for designing materials that better synergize with the operating temperatures of concentrated solar power (CSP). In this work, we present a comparative study of the electronic response of BXM materials to varying degrees of reduction, and use modeling to reveal the mechanisms driving these changes. Probing the oxygen with X-ray absorption spectroscopy (XAS) reveals substantial differences in the electronic structure between the BXM materials in both oxidized and reduced states. These results demonstrate that the oxygen K-edge is sensitive to even small concentrations of oxygen vacancies in large part due to the finding that the effect of vacancies on the electronic structure of the material extends far beyond second nearest neighbors. Comparisons of the oxygen K-edge measured by XAS and the complementary technique electron energy loss spectroscopy (EELS) confirm the veracity of the observed changes in electronic structure. Local density of states (LDOS) calculations carried out on oxidized and defected structures enable specific peaks in the XAS spectra to be correlated to hybridized molecular orbitals, providing valuable insights into the underlying electronic changes resulting in shifts in energy and intensity. These LDOS calculations correctly predict changes in XAS due to reduction. These results are a key component of elucidating structure-property relationships for this class of STCH materials.

12:25 PM EN05.02.03

A Renewable, Carbon-Neutral Route to Ammonia via Concentrating Solar Thermochemistry Andrea Ambrosini¹, Kevin Albrecht¹, H. E. Bush¹, Alberto de la Calle², Ivan Ermanoski², Tyler Farr³, Xiang Gao², Matthew W. Kury¹, Peter Loutzenhiser³, Nhu ". Nguyen³ and Ellen Stechel²; ¹Sandia National Laboratories, United States; ²Arizona State University, United States; ³Georgia Institute of Technology, United States

Ammonia (NH₃) is an energy-dense chemical and a vital component of fertilizer. In addition, it is a carbon-neutral liquid fuel and a potential candidate for thermochemical energy storage for high-temperature

concentrating solar power (CSP). NH_3 is currently synthesized via the Haber-Bosch process, which requires pressures of 15- 25 MPa and temperatures of 400-500 °C. Nitrogen (N_2) and hydrogen (H_2) are essential feedstocks for producing NH_3 : H_2 is generally derived by steam reforming of methane, and N_2 is sourced from air, after O_2 removal, via combustion of methane. Burning hydrocarbons produces the heat and mechanical energy required to drive the NH_3 reaction. All three processes (sourcing the energy, producing H_2 and N_2) produce CO_2 emissions. The development of a renewable pathway to NH_3 synthesis that utilizes concentrated solar irradiation for the process heat instead of hydrocarbon combustion and operates under relatively low pressure, will result in both a decrease (or elimination) in greenhouse gas emissions and avoid the cost, complexity, and safety issues inherent in high-pressure processes.

The aim of the Solar-Thermal Ammonia Production (STAP) project is to develop a solar thermochemical looping technology to produce and shuttle N_2 from air for the subsequent production of NH_3 in an advanced two-stage process. The endothermic thermal reduction of redox-active metal oxide particles is driven by concentrated solar irradiation; subsequent exposure to air re-oxidizes the particles, removing O_2 and producing relatively pure N_2 gas. The N_2 serves as a feedstock for a renewable NH_3 production process in an advanced two-step, low pressure, looping process. In the first step, H_2 reacts with metal nitride particles to produce NH_3 , resulting in a reduced (nitrogen deficient) metal nitride. In the second step, the nitride is regenerated utilizing the nitrogen produced in the air separation step. The net result is NH_3 produced from sunlight, air, and (green) H_2 , while the metal oxide and nitride particles are recycled.

The STAP project consists of four thrusts: (1) Systematic synthesis, characterization, and thermodynamic analysis of oxides for N_2 recovery from air; (2) materials investigation and development of nitrides for NH_3 production and re-nitridation; (3) process and reactor design, modeling, fabrication, and small-scale demonstration; and (4) full system and techno-economic analyses. The system concept will be summarized in this presentation, and the synthesis and characterization of the working materials will be discussed, including x-ray diffraction, thermogravimetric analysis, and reaction performance.

Sandia National Laboratories is a multimission laboratory managed and operated by National Technology & Engineering Solutions of Sandia, LLC, a wholly owned subsidiary of Honeywell International Inc., for the U.S. Department of Energy's National Nuclear Security Administration under contract DE-NA0003525.

12:40 PM EN05.02.04

Thermochemical Energy Storage Using Phosphatic Pebbles Sesha Srinivasan, Mc Ben Joe Charles, Haley Royce, Scott Wallen and Richard Matyi; Florida Polytechnic University, United States

Phosphatic Pebble or Dolomite, calcium magnesium carbonate ($\text{CaMg}(\text{CO}_3)_2$), is considered an undesirable mined resource for phosphoric acid production in Florida; as such, large quantities of the mineral are available. This study is aimed to characterize the phosphatic high concentration dolomite pebbles received from the Florida Industrial and Phosphate Research Institute (FIPR) and investigated their feasibility for thermochemical energy storage (TCES). The chemical composition of these dolomite minerals was studied using different techniques such as X-ray Fluorescence (XRF), Fourier-transform infrared spectroscopy (FTIR), and Scanning electron microscopy with energy-dispersive X-ray spectroscopy (SEM, EDS), which confirmed the phosphatic pebbles received from FIPR contained high percentages of dolomite. Thermogravimetric analysis (TGA) was used to calculate the activation energy for calcination and carbonation of the dolomite pebbles in Nitrogen (N_2) ambient and CO_2 ambient conditions respectively, and with temperatures up to 800°C. Values important for thermochemical energy storage such as heat capacity and enthalpy of reaction were also calculated using this TGA data. Changes in crystal structure after calcination, carbonation, and wet ball milling of the dolomite minerals were observed using X-ray diffraction (XRD). The effects of wet ball milling to reduce particle size were observed on the cyclic stability and carbonation of the dolomite pebbles. Particle size and surface area were measured using XRD and N_2 adsorption with the BET method. The structural characteristics of dolomite as explored via metrological techniques (QEMSCAN) thus demonstrating the presence of magnesium and calcium in combinations of carbonates, Calcium Oxide, Magnesium Oxides, and residual Carbon dioxide.

12:55 PM EN05.02.05

Materials for Concentrated Solar Energy-Driven Sulphur-Based Thermochemical Cycles Christos Agrafiotis¹, Vamshi Krishna Tanda¹, Dennis Thomey¹, Lamark de Oliveira¹, Lutz Mevißen², Hiroki Noguchi³, George Karagiannakis⁴, Martin Roeb¹ and Christian Sattler^{1,5}; ¹DLR - German Aerospace Center, Germany; ²RWE Generation SE, Germany; ³Japan Atomic Energy Agency, Japan; ⁴CERTH - Centre for Research & Technology, Hellas, Greece; ⁵TU Dresden, Germany

Thermochemical cycles of the sulphur family recycle sulphur as the central element that appears in different compounds at changing oxidation state. Such cycles like the Hybrid Sulphur (HyS) and the Sulphur-Iodine (SI) cycle were originally conceived to produce hydrogen via water-splitting, but can be modified to produce solid sulphur that can be combusted in air to produce high-temperature heat and hence can be used both as a renewable fuel as well as a seasonal solar energy storage means. The HyS, SI and solid sulphur-based thermochemical cycles share the common step of the decomposition reaction of sulphuric acid: first thermally to steam and SO₃ and subsequently the catalytic SO₃ dissociation (splitting) to SO₂ and oxygen. The latter is their highest-temperature (700-900°C), endothermic reaction step that can be aided by heat supplied by concentrated solar irradiation, either directly on porous ceramic volumetric receivers/sulphuric acid decomposition reactors or indirectly via solar-receiver-heated gaseous or solid particle streams operating as heat transfer fluids and transferring their enthalpy to the sulphuric acid decomposer downstream of the solar receiver. A common issue in all cycles has to do with the particular characteristics of sulphuric acid chemistry: highly corrosive environment combined with high temperatures. These peculiarities impose further necessities and research needs with respect to the structural materials and components to be employed, in addition to research on catalyst compositions and reactor designs. The work will present recent progress in this field in the context of designing, building and operating a novel, sulphuric acid decomposer/sulphur trioxide splitting reactor indirectly heated via hot moving particle streams. Aspects to be covered include materials solutions for the manifolds for the injection of the sulphuric acid solution, evaporator tubes, sealants, special ceramic adhesives to join anti-corrosive metallic-to-ceramic tubing e.g. (stainless steel to SiC) and materials and reactor solutions to compensate for thermal expansion/contraction. These results will be complemented with analogous results from long-term testing (up to 1,000 operation hours) of sulphur trioxide catalyst compositions shaped in the form of either catalytic particles or structured porous ceramic assemblies - and relevant post-operation characterization studies. The final technical solutions are articulated into an integrated sulphuric acid decomposer/sulphur trioxide splitting reactor from qualified materials and concepts, capable of concentrated solar irradiation-driven, long-term operation under the required demanding conditions.

1:10 PM EN05.02.06

Pure and Mixed Metal Oxides for High-Temperature Thermochemical Energy Storage via Reversible Redox Reactions Marco Gigantino, Daniel Notter and Aldo Steinfeld; ETH Zürich, Switzerland

Concentrated solar energy provides a clean source of process heat in excess of 600 °C and thus enables the decarbonization of several key energy-intensive industrial processes, such as mineral and metallurgical extraction, lime and cement manufacturing, biomass pyrolysis and gasification, as well as thermal production of power and fuels. These processes can be performed round-the-clock with solar process heat by making use of the endothermic-exothermic effect associated with the reduction-oxidation (redox) of metal oxides to store and release the high-temperature heat. This category of thermochemical energy storage (TCS) materials typically features high values of energy storage density and the advantage of employing ambient air as gaseous reagent. Of particular interest are the redox pairs BaO₂/BaO, Co₃O₄/CoO, CuO/Cu₂O, Fe₂O₃/Fe₃O₄ and Mn₂O₃/Mn₃O₄, which have their equilibrium temperature above 600 °C in atmospheric air. A common problem for these metal oxides when approaching their melting point is thermal sintering, which progressively reduces the gas-solid contact area and, hence, their redox rate and redox cyclic performance. In this work, we described the manufacturing of mm-size granules with tailored morphological properties that exhibit stable reaction kinetics and cyclic performance over multiple redox cycles. The material synthesis process involved the mixing of the reactive metal oxide with pore formers and sintering inhibitors - e.g., Al₃O₄, CaO, CeO₂, Fe₂O₃, MgO, Mn₃O₄,

SrO, Y₂O₃-stabilized ZrO₂ (YSZ) - which were added in different concentrations and combinations to form binary and ternary mixtures. The synthesized granules were tested by thermogravimetry over up to 100 consecutive redox cycles at conditions relevant for the intended TCS applications. Thermodynamic and kinetics analyses were carried out for each binary and ternary system. In terms of cyclic stability, the best performing materials were Fe₂O₃ in pure form, the binary mixture CuO-YSZ (65-35wt%), and the ternary mixtures Co₃O₄-YSZ-MgO (80-15-5wt%), CuO-Al₂O₃-YSZ (70-22.5-7.5wt%), and CuO-Al₂O₃-MgO (60-30-10wt%), yielding gravimetric heat storage capacities of 421, 559, 609, 565, 439 kJ for kg of oxidized mixture, respectively. In these materials, the additives served as inert supports. The binary mixtures Mn₂O₃-Al₂O₃, Mn₂O₃-Fe₂O₃, Mn₂O₃-MgO, where the additives participated in the redox reactions, exhibited stable cyclic performance as well.

1:25 PM DISCUSSION TIME/Q&A

SESSION EN05.03: Coatings & Town Hall—The Future of Concentrating Solar Power
Session Chairs: Andrea Ambrosini and Adrianus Aria
Tuesday Afternoon, April 20, 2021
EN05

2:15 PM *EN05.03.01

Solar-Selective Coatings for High-Temperature Solar Applications Based on a Selective Transmitter on Top of a Black Body Absorber Matthias Krause¹, Frank Lungwitz¹, A. Mendez^{1,2}, M. Hoppe¹, J. Sonnenberg¹, A. Garcia-Valenzuela¹, F. Munnik¹, J. Grenzer¹, R. Hübner¹ and Ramon Escobar Galindo³; ¹Helmholtz-Zentrum Dresden, Germany; ²Nano4Energy, Spain; ³Universidad de Sevilla, Spain

An alternative concept to achieve solar selectivity for solar thermal materials and applications consists in the use of spectrally selective transmitter coatings.[1] These are characterized by a high transmittance in the solar range and a high reflectance in the thermal range of the electromagnetic spectrum. Suitable materials for selective transmitters are dielectric/metal/dielectric multilayers and transparent conductive oxides (TCOs).[2] The concept has a series of advantages compared to multilayer- or cermet-based solar-selective coatings (SSCs) like the easiness of manufacturing, the possibility to use standard materials as transmitter (e.g., indium tin oxide (ITO)) and absorber (e.g. Pyromark or black chrome), and the adaptability to specific requirements with respect to receiver temperature and solar concentration factor.

After a conceptual introduction, the analysis of solar plant parameters, i.e., operation temperature and solar concentration, for which this concept provides a better solar efficiency than state-of-the-art bare black body absorber, will be given.[3] We will then review the recent developments in the field, which include an excellent high-temperature in-air stability of such type of solar coatings.[4] In the second part of the talk, we will report own results toward a new TCO on black body absorber coating. Vacuum and in-air stability of the TCO SnO₂:Ta at 800 °C and its structural properties before and after heat exposure are demonstrated. As potential absorber, the formation, structure, and optical properties of dense, PVD-grown CuCr₂O₄ thin films are studied. They are obtained in high purity from as-deposited samples by a simple in-air annealing step at 800 °C and absorb light in the whole solar range from 300 nm to 2500 nm.

[1] C.E. Kennedy, Review of Mid- to High-Temperature Solar Selective Absorber Materials, NREL Technical Reports, NREL - National Renewable Energy Laboratory, Golden, Colorado, USA, 2002.

[2] J.C.C. Fan, F.J. Bachner, Transparent heat mirrors for solar-energy applications, Applied Optics 15(4) (1976) 1012-1017.

[3] F. Lungwitz, R. Escobar-Galindo, D. Janke, E. Schumann, R. Wensch, S. Gemming, M. Krause, Transparent conductive tantalum doped tin oxide as selectively solar-transmitting coating for high temperature

solar thermal applications, *Solar Energy Materials and Solar Cells* 196 (2019) 84-93.

[4] H. Wang, I. Haechler, S. Kaur, J. Freedman, R. Prasher, Spectrally selective solar absorber stable up to 900 degrees C for 120 h under ambient conditions, *Solar Energy* 174 (2018) 305- 311.

2:40 PM EN05.03.02

Spectral Emissivity Measurements and Conversion Efficiency Estimation in Black Spinel and Nanoneedle-Based Coatings for Solar Tower Plants Telmo Echaniz¹, Iñigo González de Arrieta^{1,2}, Raquel Fuente¹, Lizzie Rubin^{3,3}, Renkun Chen^{3,3}, Josu Mirena Igartua¹, Manuel José Tello¹ and Gabriel Alejandro López¹; ¹University of the Basque Country, Spain; ²Université de Orléans, France; ³University of California, San Diego, United States

Infrared emissivity measurements at working temperatures are of great importance for solar absorber coatings in central tower plants, as they allow proper estimations of the conversion efficiencies of these materials, as well as heat transfer management. This is especially important in situations where the concentration flux of the plant is reduced (e.g., the start-up phase). To that end, the high-temperature directional spectral emissivities of new copper-alloyed spinel coatings with different structures have been researched for concentrated solar power applications.

Four new coatings based on black spinel nanoparticles [1], as well as two nanoneedle-based ones [2], were measured up to their desired temperature operation range (800 °C and 600 °C, respectively). The nanoparticle-based coatings feature improved thermal stability that allows them to withstand higher temperatures than the industry standard Pyromark® 2500. The emissivities of these coatings are highly dependent on the morphology of the nanoparticle agglomerates, even more than on sample composition. In particular, a porous $\text{Cu}_{0.5}\text{Cr}_{1.1}\text{Mn}_{1.4}\text{O}_4$ coating showed a promising combination of an enhanced solar absorptance and emissivity in the normal direction, and a reduced total hemispherical emissivity at all temperatures. Both effects can be linked to the porosity of the sample, by means of enhanced light trapping in the normal direction and increased semitransparency at high polar angles of emission. Thus, this coating shows signs of directional selectivity. Besides, using a porous coating would be more cost-effective, since less mass of the material would be required for the coating. When combined with absorptance measurements, these emissivity measurements allow estimating the real efficiencies of the coatings, which can even reach values around 0.93 [3].

CuCo_2O_4 nanoneedle-based coatings, on the other hand, possess an extremely high 99% solar absorptance, which is also coupled with very high hemispherical emissivity values, with values between 0.82 and 0.92 at working temperatures. It was observed that coating these nanostructures with aluminum-doped zinc oxide (AZO) is highly effective in increasing their emissivities at all angles and temperatures. Thus, outside of concentrated solar power applications, these thermally stable thin coatings can also find use as highly efficient black absorbers in the visible and IR ranges.

[1] E.B. Rubin, Y. Chen, R. Chen, Optical properties and thermal stability of Cu spinel oxide nanoparticle solar absorber coatings, *Sol. Energy Mater. Sol. Cells* 195 (2019) 81–88.

[2] E.B. Rubin, S. Shin, Y. Chen, R. Chen, High-temperature stable refractory nanoneedles with over 99% solar absorptance, *APL Mater.* 7 (2019) 031101.

[3] I. González de Arrieta, T. Echaniz, R. Fuente, E. Rubin, R. Chen, J.M. Igartua, M.J. Tello, G.A. López, Infrared emissivity of copper-alloyed spinel black coatings for concentrated solar power systems, *Sol. Energy Mater. Sol. Cells* 200 (2019) 109961.

2:55 PM EN05.03.03

Design, Spectral Properties and Thermal Stability of High-Temperature Solar-Selective Coatings Based on Cr(Al)N Multilayer Stacks Ramon Escobar Galindo¹, Teresa Cristina Rojas², Alvro Caro² and Juan Carlos Sanchez-Lopez²; ¹Escuela Politécnica Superior, Universidad de Sevilla, Spain; ²Instituto de Ciencia de Materiales de Sevilla (CSIC-Univ. Sevilla), Spain

Two multilayer solar selective absorber coatings [$\text{Al}/\text{CrN}_{0.95}/\text{Cr}_{0.96}\text{Al}_{0.04}\text{N}_{1.08}/\text{Cr}_{0.53}\text{Al}_{0.47}\text{N}_{1.12}/\text{Al}_2\text{O}_3$ (stack #1) and $\text{Cr}_{0.96}\text{Al}_{0.04}\text{N}_{0.89}/\text{Cr}_{0.62}\text{Al}_{0.38}\text{N}_{1.00}/\text{Cr}_{0.53}\text{Al}_{0.47}\text{N}_{1.12}/\text{Al}_2\text{O}_3$ (stack #2)] were deposited on 316L steel by

combining direct current (DC) and high power impulse magnetron sputtering (HiPIMS) technologies with the aim of increasing the working limit temperature. The composition and thickness of the constituent layers were optimized using CODE software to achieve a high solar absorptance (α) and low values of thermal emittance (ϵ) in the infrared region. The deposited multilayered stacks were heated for 2 hours in air at 600, 700 and 800 °C to study their thermal stability and optical performance. Compositional, structural and optical characterization of the stacks (as-prepared and after thermal treatment) was performed. Both stacks presented a good solar selectivity with $\alpha > 95\%$ and $\epsilon_{25^\circ\text{C}} < 15\%$, were stable up to 600 °C and fulfilled the performance criterion $\text{PC} < 5\%$ after 600 and 700 °C treatments. Despite the stacks suffered chemical transformations above 600 °C, partial oxidation (stack #1) and Cr_2N formation (stack #1 and #2), the optical properties were optimum up to 700 °C for stack #1 ($\alpha = 94\%$, $\epsilon_{25^\circ\text{C}} = 12\%$) and 600 °C for stack #2 ($\alpha = 93\%$, $\epsilon_{25^\circ\text{C}} = 13\%$). The solar-to-mechanical energy conversion efficiencies (η) of the as-deposited and annealed (600 and 700 °C) samples were up to 20 percentage points higher than the absorber paint commercially used (Pyromark). At 800 °C, they underwent a further structural transformation, provoked by the oxidation of the inner layers, and they consequently lost their solar selectivity.

3:10 PM EN05.03.04

Late News: Design of High-Temperature Solar Selective Coatings Based on Cr(Al)N: Microstructure and Optical Properties of CrN_y and $\text{Cr}_{1-x}\text{Al}_x\text{N}_y$ Films Teresa Cristina Rojas, Alvro Caro, G. Lozano and Juan Carlos Sanchez-Lopez; Instituto de Ciencia de Materiales de Sevilla, Spain

In this work we present the microstructural and optical characterization of CrN_y and $\text{Cr}_{1-x}\text{Al}_x\text{N}_y$ films to be used in multilayered solar selective coatings (SSC) for high temperature application. The films were prepared by direct current (DC) and high-power impulse magnetron sputtering (HiPIMS) technology. The deposition parameters: N_2 flux, HiPIMS frequency and the aluminum power target, were modified to get a wide variety of stoichiometries. The composition, morphology, phases and electronic structure of the films were characterized in depth. The optical behavior was determined by UV-Vis-NIR and FTIR spectroscopies, and the optical constants were obtained from the measured transmittance and reflectance spectra based on appropriate dielectric function models. Small changes in the layer composition influence the optical constants. Our results indicate that a metallic-like behavior was obtained for CrN_y layers with N vacancies ($y=0.67$ and $y=0.95$) while a semiconductor-like behavior was observed for $y=1.08$. The optical properties of $\text{Cr}_{1-x}\text{Al}_x\text{N}_y$ layers can also be tuned from metallic to semiconductor-like behavior depending on the chemical composition. In particular, we demonstrated that CrN_y films could be used as effective absorber layer in multilayer-based SSC, and namely, the $\text{CrN}_{0.67}$ film also as IR reflector/absorber layer. Indeed, the absorption coefficients of $\text{Cr}_{1-x}\text{Al}_x\text{N}_y$ films with optimized Al content and N-vacancies are comparable to those reported for state-of-the-art materials such as TiAlN or TiAlCrN . In addition, a $\text{Cr}_{0.96}\text{Al}_{0.04}\text{N}_{0.89}$ film was found to be a suitable IR reflector/absorber layer. The ensemble of results highlights the potential of these materials as efficient components in multilayer-based SSC for high temperature applications. Three different multilayered-SSC were designed by applying optical simulations, obtaining excellent optical selective properties ($a > 95\%$ and $e < 15\%$).

3:15 PM EN05.03.05

Late News: Opportunities of HiPIMS Technology for Designing Complex Multilayered Cr(Al)N Coatings for Solar Selective Applications Juan Carlos Sanchez-Lopez, Alvro Caro, Juan Martinez-Romero and Teresa Cristina Rojas; Instituto de Ciencia de Materiales de Sevilla, Spain

High power impulse magnetron sputtering (HiPIMS) technology has emerged as a recent promising physical vapor deposition technique for coating with improved properties. The application of short high power pulses to the magnetron sources enables higher plasma densities and ionization rates, leading to improved film density and functionality. In this paper we explore the possibilities of this technique to design multilayered systems based on Cr(Al)N with controlled chemical composition and microstructure for solar selective absorption. By changing the pulse length (20 to 100 ms) and frequencies (200 to 1000 Hz) differences in the film stoichiometry, crystallinity, lattice parameters and morphology can be obtained, influencing the properties of interest for the foreseen application. In particular, we will present how to tailor the optical properties and the

oxidation resistance thanks to the variation of pulse parameters in the single individual layers. The benefits obtained by combining the high power pulse delivered to the target with a negative voltage applied to the substrate (bias) will be shown. A full design based on a multilayered CrAlN systems capped with an antireflective Al₂O₃ layer is prepared on 316L steel with and without the application of bias. The results demonstrated that the bias helped to densify the structure, decreasing the intercolumnar spaces, although affected the targeted film stoichiometry. The thermal stability and oxidation resistance properties of both stacks will be compared and discussed to establish a relationship between synthesis conditions and practical performance at different temperatures (room temperature, 600, 700 and 800°C).

3:20 PM TOWN HALL DISCUSSION—THE FUTURE OF CONCENTRATING SOLAR POWE

SESSION EN05.04: Heat Exchange Materials and Alloys
Session Chairs: Andrea Ambrosini and Christopher Muhich
Tuesday Afternoon, April 20, 2021
EN05

5:40 PM EN05.04.01

Oxide Dispersion Particle Clustering Using Phase Field Modelling in Nickel-Based Superalloys Bryan T. Kinzer, Aditya Sundar and Rohini Bala Chandran; University of Michigan—Ann Arbor, United States

Nickel-based superalloys are promising materials for next generation heat-exchangers in concentrated solar power technologies, including the supercritical CO₂ Brayton cycle, due to their superior corrosion resistance at high-temperatures of 1000 °C. However, many of these alloys lack sufficient yield and creep rupture stress required in power plants as strengthening from gamma prime precipitates is no longer effective at these elevated temperatures. One of the most promising methods of increasing yield stress at high temperatures is through the introduction of oxide dispersion strengthening (ODS) particles. At these high temperatures grain boundary sliding is activated; the ODS particles pin the grain boundaries reducing sliding improving creep and yield stress. Using the existing Reppich particle pinning model, our results indicate that by simply mixing in 0.3 wt% of 40 nm diameter ODS (Y₂O₃) particles, the yield stress of a typical Ni alloy, Haynes 214, can more than double at 1000 °C showing the promise of the ODS approach. Increasing the amount of ODS particles can result in improved strengthening of the base alloy, but only up to a certain mass-fraction. As the weight percent of ODS powders is increased clusters of ODS particles form causing stress concentrations, which leads to alloy cracking and to changes in grain recrystallization. Traditionally, the maximum mass-fraction of ODS powders is determined through trial and error, based on observing its effects on cracking during solidification. This process is time consuming and offers limited insight about the fundamental mechanisms at play. In this work, we apply phase-field modelling to inform how the microstructural evolution is influenced by the mass-fraction and initial distribution of the ODS particles. The model will be applied to explore the effect of ODS particle clustering on grain growth, which can influence creep and strength. Processing parameters, such as cooling rate, will be linked to initial ODS particle distribution offering insight into the driving forces that lead to particle clustering. These findings will shed light onto the mechanisms that determine the effectiveness of oxide dispersion particle strengthening on improving mechanical properties for high temperature applications to help enable next generation concentrated solar power technologies.

5:55 PM EN05.04.02

Multiscale Porous High-Temperature Heat Exchanger Design Using Ceramic Co-Extrusion Xiangyu Li, Chad Wilson, Lenan Zhang, Bikram Bhatia, Lin Zhao and Evelyn Wang; Massachusetts Institute of Technology, United States

We propose a high performance, compact and durable ceramic heat exchanger design capable of operating over

1200 °C and 250 bar for aerospace and CSP applications. Our checkered pattern design leverages porosity at the centimeter-scale that serves as macrochannels for the flow of working fluids. Meanwhile, a micrometer-scale porous core is embedded into these channels to significantly improve heat transfer and structural strength. Compared to traditional porous media approach, this multiscale porous configuration with straight ducts enables high heat transfer and a low pressure drop penalty. Furthermore, these structures can be fabricated using a ceramic co-extrusion process capable of creating both the channels and porous internal structure in one step. Overall, the heat exchanger is able to operate with hot flows over 1200°C and supercritical CO₂ at 300°C and 250 bar, providing high volumetric power density and less than 1% pressure drop.

Due to the large difference in the feature size of the heat exchanger, it is computationally prohibitive to include all the detailed feature in one simulation. Therefore, a hierarchical model is proposed to optimize the design and predict the mechanical strength, pressure drop and thermal performance. An analytical thermal resistance model is also developed to optimize the thermal performance of the heat exchanger. Thermal performance is evaluated and optimized as volume power density, weight power density and effectiveness.

The proposed high-performance counterflow heat exchanger can enable efficient heat exchange at extreme conditions in a wide range of power generation application, due to its high thermal performance, low volume, light weight and scalable fabrication process.

6:10 PM EN05.04.03

Oxidation and Carburization Behavior of Iron- and Nickel-based Alloys in Supercritical CO₂

Environments Aditya Sundar, Bryan T. Kinzer and Rohini Bala Chandran; University of Michigan–Ann Arbor, United States

Advanced Iron (Fe) and Nickel (Ni) based alloys are potential candidates to serve as reactor components in high temperature, super-critical carbon dioxide (s-CO₂) heat exchangers. These high temperature (up to 1100°C) and high pressure (up to 20 atm s-CO₂) conditions pose the critical challenge of carburization induced corrosion, in addition to enhanced surface oxidation. In this work, we evaluate the relative performance of 3 such alloys: Fe-based Inconel MA 956, Ni-based Haynes 214 and Ni-based Amdry 386. Thermodynamic calculations and kinetic simulations are implemented using a CALPHAD (CALculation of PHase Diagrams) based approach to understand the propensity of oxide and carbide formation. Thermodynamic analysis supports reported experimental findings that that carbide precipitates (M₂₃C₆, M₇C₃ etc.) are stable at the interface between the surface oxide (Corundum, rutile, spinel etc.) and the underlying metallic alloy. We propose a diffusion-driven model that combines oxide growth rates and gas transport through the oxide, to estimate the carbon activity at this interface. The reduction of carbon dioxide (CO₂) to carbon monoxide (CO) results in the formation of elemental Carbon (C), enhancing the thermodynamic driving force for carburization. Under similar boundary conditions for the interfacial carbon activity, Ni-based alloys exhibit better carburization resistance as compared to Fe-based alloys. Further, we also implement isothermal and non-isothermal heat treatment simulations to study the microstructural changes resulting from exposure to high temperatures and pressures (upto 1100°C and 20 atm). Thermo-kinetic nucleation and growth models employed in this study will be used to inform experiments about the design of particular heat treatments that promote/arrest the growth of desired high strength precipitate phases. The results from our work will guide the selection and processing of structural materials used as high temperature components in the next generation of concentrated solar power technologies.

6:25 PM *EN05.04.04

Optically Transparent and Thermally Insulating Aerogel Solar Collectors Thomas Cooper, Bikram Bhatia, Lee A. Weinstein, Lin Zhao, Yi Huang, Elise Strobach, Kenneth McEnaney, Sungwoo Yang, Evelyn Wang and Gang Chen; Massachusetts Institute of Technology, United States

Aerogels can be made transparent in the solar spectrum but opaque in the infrared spectrum. Such optically transparent and thermally insulating aerogels can be used in solar collectors, replacing the need for selective surfaces and vacuum in solar thermal systems. This talk will summarize several aspects of aerogel solar

collectors. Theoretical modeling suggests that aerogel collectors can have attractive performance. Optimization of the synthesis process for silica aerogel has led to highly transparent aerogels across the entire solar spectrum. Several experimental implementations of the aerogel collectors will be discussed. One configuration is to combine solar thermal with solar PV in one optical path to increase dispatchability of PV, enabled by the transparent aerogel. In another configuration, transparent aerogel will be used in linear Fresnel concentrators to achieve high temperatures. Experimental results on the system performance will be discussed. The transparent aerogel also enables nonconcentrating system to achieve high temperatures for other thermal applications such as sterilization.

6:50 PM DISCUSSION TIME/Q&A

SESSION EN05.05: Solar Thermochemical Water Splitting II
Session Chairs: Andrea Ambrosini and Christopher Muhich
Tuesday Afternoon, April 20, 2021
EN05

9:00 PM *EN05.05.01

Pathways to Renewable Fuels Using Concentrated Sunlight [Anthony H. McDaniel](#); Sandia National Laboratories, United States

Population growth and continued industrialization of developing countries may double global energy consumption by 2035. If such energy demands are largely met by fossil fuels, the deleterious effects of anthropogenic carbon loading of the earth's ecosystems will greatly intensify. As such, developing technologies to create renewable and sustainable fuels from sunlight is widely seen as a global imperative.

While technologies for converting solar irradiance into hydrogen or hydrocarbons predicated on low-temperature pathways such as electrolysis and natural or artificial photosynthesis offer potential solutions, there is significant recent interest in utilizing high-temperature pathways powered by concentrated solar energy. Here we offer a perspective on a process that utilizes highly concentrated thermal energy from the sun to drive chemical reactions that split water into hydrogen or carbon dioxide into carbon monoxide, thereby creating simple fuels or precursors to more complex energy carriers like fungible liquids. Our implementation for converting sunlight to fuel is based upon a deceptively simple two-step redox cycle. In step one, a concentrated solar resource heats and reduces a non-stoichiometric oxide, spontaneously creating oxygen defects and depositing the solar energy directly into the reduced oxide, much like charging a battery. Once "charged," the reduced oxide is exposed to water or carbon dioxide in a second step under conditions that result in spontaneous gas splitting, yielding molecular hydrogen or carbon monoxide (i.e., solar fuel or solar syngas).

Effective and efficient redox-active materials are key to the commercial success of solar thermochemical water splitting technologies, and material discovery efforts at laboratories around the globe are currently underway. This talk will discuss the use of complex, multi-cation oxides to accomplish the redox cycle chemistry and describe our efforts to explore the fundamental underpinnings of important relationships between oxide composition, electronic structure, and functionality. Furthermore, we will review progress made by the HydroGEN Advanced Water Splitting Materials Consortium (h2awasm.org), which is a research community brought together and funded by the US DOE as an Energy Materials Network initiative in late 2017 and tasked with using high throughput computational material science approaches to discovering thermochemically active oxides. We will also review challenges and opportunities for discovering new redox cycle chemistries within the context of achieving high solar-to-fuel conversion efficiency in engineerable and appropriately designed solar reactors.

9:25 PM EN05.05.02

Designer Perovskites with Dual Reduction on A and B Sites—Lowering the Peak Temperature of Thermochemical Hydrogen Production Cycles Robert T. Bell¹, Sarah Shulda¹, Dan Plattenberger¹, Eric Coker², Josh Sugar², Sami Sainio³, Nicholas Strange^{1,3}, Karen Heinselman¹, Philip Parilla¹, Anthony H. McDaniel², Michael F. Toney^{4,3}, Sai Gautam Gopalakrishnan^{5,6}, Emily Carter^{5,7}, Ellen Stechel⁸ and David Ginley¹; ¹National Renewable Energy Laboratory, United States; ²Sandia National Laboratories, United States; ³SLAC National Accelerator Laboratory, United States; ⁴University of Colorado Boulder, United States; ⁵Princeton University, United States; ⁶Indian Institute of Science, India; ⁷University of California, Los Angeles, United States; ⁸Arizona State University, United States

Lowering the peak temperature required by solar thermochemical hydrogen (STCH) production cycles might be key to overcoming a range of technology readiness challenges. For oxide perovskite based STCH, the peak cycling temperature occurs during the oxide reduction step where reactive oxygen vacancies are generated, typically at temperatures >1300°C. Generally, oxygen vacancies are charge compensated by reduction of a single cation species on either the A or B site. However, recent modeling suggests a strategy for reducing the temperature would be to tune the enthalpy through doping while maximizing the entropy of reduction with dual reduction on both A and B site cations. We will report on experimentally validating these models and demonstrating dual cation reduction of Ce⁴⁺ to Ce³⁺ and Mn³⁺ to Mn²⁺ in (Ca,Ce)(Mn,Ti)O₃ perovskite. We designed techniques to measure samples with varying degrees of reduction in ex situ experiments through complementary use of in situ measurements. In situ techniques including TGA and XRD were used to quantify the reduction of ex situ samples, where reduced states are quenched into samples cooled under reducing environments. The oxidation state of cations in samples, both oxidized and reduced, were then determined through a combination of ex situ X-ray absorption spectroscopy (XAS) and X-ray photoelectron spectroscopy (XPS) measurements. We report the performance of this material during temperature and pO₂ cycling. These experiments both validate predicted routes to design STCH materials and demonstrate techniques to quantifiably quench reduction into samples for ex situ measurements.

9:40 PM EN05.05.03

Late News: Solar Thermochemical Hydrogen Production on Layered Perovskite BaX_{0.25}Mn_{0.75}O₃ (X = Ce, Nb, Pr) and BaTi_{0.5}Mn_{0.5}O₃ James E. Park, Eric Coker, Mark Rodriguez, Andrea Ambrosini and Anthony H. McDaniel; Sandia National Laboratories, United States

Solar thermochemical hydrogen production (STCH) is a two-step process that utilizes concentrated solar heat and metal oxide materials to produce hydrogen gas by splitting water molecules through oxide redox chemistry. Among the many different materials investigated, perovskite (ABO₃) materials, including Sr_xLa_{1-x}Mn_yAl_{1-y}O₃ (x, y = 0.4, 0.6)¹ and ATi_{0.5}Mn_{0.5}O₃ (A = Ca and Sr),^{2,3} have been reported that are competitive with CeO₂, the current benchmark material. Multiple combinations of perovskite-like materials are possible with diverse crystal structures due to partial cation substitution and vacancy formation on the metal and oxygen sites, which influence the electronic structure and consequent STCH performance. Recently, BaCe_{0.25}Mn_{0.75}O₃ (BCM), a layered perovskite, was shown to have faster water oxidation kinetics than Sr_xLa_{1-x}Mn_yAl_{1-y}O₃ (x, y = 0.4, 0.6) and better hydrogen production capability than ceria at a lower thermal reduction temperature (T_R=1350 °C).⁴ In the course of determining the chemical underpinnings of BCM's performance, three new water-splitting and isostructural materials, BaNb_{0.25}Mn_{0.75}O₃ (BNM), BaPr_{0.25}Mn_{0.75}O₃ (BPM), and BaTi_{0.5}Mn_{0.5}O₃ (BTM), were synthesized and characterized. Comparing the performance and structural changes of these materials *in operando* aids in the understanding of the relationship between hydrogen production capability and the different local environments of the metal-oxygen bonds resulting from the chemical modification. From this, a better fundamental understanding can be developed to aid in identifying new materials for solar thermochemical fuel production.

1. McDaniel, A. H.; Miller, E. C.; Arifin, D.; Ambrosini, A.; Coker, E. N.; O'Hayre, R.; Chueh, W. C.; Tong, J. *Energy Environ. Sci.* **2013**, *6*, 2424.

2. Qian, X.; He, J.; Mastronardo, E.; Baldassarri, B.; Yuan, W.; Wolverton, C.; Haile, S. M. *Matter* **2020**, *4*, 1.

3. Qian, X.; He, J.; Mastronardo, E.; Baldassarri, B.; Wolverton, C.; Haile, S. M. *Chem. Mater.* **2020**, *32*, 9335.
4. Barcellos, D. R.; Sanders, M. D.; Tong, J.; McDaniel, A. H.; O'Hayre, R. P. *Energy Environ. Sci.* **2018**, *11*, 3256.

Sandia National Laboratories is a multi-mission laboratory managed and operated by National Technology and Engineering Solutions of Sandia, LLC., a wholly owned subsidiary of Honeywell International, Inc., for the U.S. Department of Energy's National Nuclear Security Administration under contract DE-NA0003525. The views expressed in this article do not necessarily represent the views of the U.S. Department of Energy or the United States Government.

9:55 PM EN05.05.04

***Ab Initio* Study of Atomic and Electronic Structure of Promising $\text{BaX}_{0.25}\text{Mn}_{0.75}\text{O}_3$ (X=Nb, Ce, Pr) Oxides for Solar Thermochemical Hydrogen Production** Anuj Goyal and Stephan Lany; National Renewable Energy Laboratory, United States

The two-step metal oxide water-splitting cycle is one of the most viable approach for Solar Thermochemical Hydrogen (STCH) production. Challenges exist in finding suitable oxides that can satisfy thermodynamics of the STCH redox cycle under viable range of temperatures and partial pressures. Recently, BXM family members, *i.e.*, $\text{Ba}_4\text{NbMn}_3\text{O}_{12}$ (BNM), $\text{Ba}_4\text{CeMn}_3\text{O}_{12}$ (BCM), $\text{Ba}_4\text{PrMn}_3\text{O}_{12}$ (BPM) are discovered to exhibit promising STCH performance. However, the magnetic degrees of freedom of their experimental crystal structures is not characterized, and only hypothetical models exist for their electronic structure. We performed Monte-Carlo sampling for the magnetic spin arrangement of Mn atoms to provide explicit atomic structure models for their ground state 12R polytype and determined the most stable spin configuration for each member after structure relaxation using density functional theory (DFT) calculations. We also elucidate the most stable charge configuration ($\text{Mn}^{3+}/\text{Mn}^{4+}$ arrangement) for BNM among the existing hypothesis in literature. We investigate these strongly correlated oxides using different levels of theory (DFT+*U*, Hybrid-DFT) to develop better understanding of their electronic structure. These calculations allowed us to develop a model based on molecular orbital interactions that help explain the observed changes in their experimental x-ray spectroscopy measurements. Thereby, help link differences in electronic structure of BXM family members to their varying water-splitting behavior. These structure models will further facilitate future in-depth defect studies to model STCH redox cycle of these oxides.

10:10 PM EN05.05.05

Testing and Characterization of Liquid Metal Alloys for Hybrid Thermo-Electro-Chemical Water Splitting Cycles Laura Achola, Anthony H. McDaniel, Witman Matthew, Margaret Gordon and Andrea Ambrosini; Sandia National Laboratories, United States

Renewable and sustainable sources of energy are playing a much larger role in powering modern society driven by the need to limit global CO₂ emissions and mitigate the anthropogenic influences on climate change. Hydrogen, a clean energy source with a high gravimetric energy density (≈ 140 MJ kg⁻¹) and zero carbon emission, is a possible clean route to lowering emissions from transportation and as an alternate source of energy storage. Currently, the majority of hydrogen is produced from reforming of fossil fuels which is carbon intensive and non-renewable. Renewable production of hydrogen, such as electrolysis and solar thermochemical, are less developed and more expensive than hydrocarbon reforming. The primary challenge of renewable hydrogen production is reducing the cost of production technologies to make the resulting hydrogen cost competitive with conventional transportation fuels. We propose a novel route to hydrogen production via a hybrid thermochemical-electrochemical process utilizing liquid metal solutions (LMS) to effect a water splitting reaction. The process can be driven by heat and electricity from renewable concentrating solar power (CSP). In the first step, steam is thermochemically reduced by the LMS producing hydrogen and a metal oxide by product, while in the second step, an endothermic process, the metal oxide is electrochemically reduced back to metal, and oxygen is evolved. The LMS process has the potential to produce hydrogen via water splitting at temperatures much lower than current CSP-driven thermochemical processes ($\gg 1000$ °C) and at applied potentials lower than conventional high-temperature electrolysis. A number of possible binary LMS

compositions that reduce at reasonably low overpotentials have been identified using machine learning. Here we test several alloy candidates for their ability to produce hydrogen in a flow reactor set-up. The basic proof of concept will be elucidated. X-ray diffraction and scanning electron microscopy of the LMS before and after the reaction to analyze byproducts and changes in microstructure, grain sizes of tin oxide, coalescence will be presented.

10:25 PM EN05.05.06

Rutherford Backscattering Spectrometry (RBS) for Quantification of Oxygen and Vacancies in Solar Thermochemical Hydrogen Production Materials Karen Heinselman, Robert T. Bell, Dan Plattenberger, Sarah Shulda, Philip Parilla and David Ginley; National Renewable Energy Laboratory, United States

Many classes of materials for production of solar thermochemical hydrogen (STCH) and other fuels depend on reversible formation of oxygen vacancies which react with oxygen in steam or other gases. The change in oxygen vacancy stoichiometry during the gas reduction step ($\Delta\delta$) is directly proportional to the hydrogen produced each cycle. Despite being a key property of STCH materials, the oxygen stoichiometry is rarely quantitatively measured with sufficient accuracy to capture changes in vacancy concentration. In many cases, thermal gravimetric analysis (TGA) is used to observe mass loss during cycling, which is then attributed to oxygen loss. However, the dynamic nature of TGA measurements prevent its use to directly measure vacancy content of ex-situ and postmortem samples used in other measurements. In this work, we introduce the use of Rutherford Backscattering Spectrometry (RBS) to directly measure the oxygen and cation stoichiometry of multinary STCH oxide samples, both powders and thin films, at sufficient accuracies to determine the vacancy stoichiometry by comparing oxidized and reduced samples. The operating principles of RBS are described, and the capabilities of the technique are compared to complimentary elemental analysis techniques including X-ray fluorescence spectroscopy (XRF), energy-dispersive X-ray spectroscopy (EDX), X-ray photoelectron spectroscopy (XPS), and Inductively Coupled Plasma Mass Spectrometry (ICP-MS). The non-destructive depth profiling capabilities of RBS are demonstrated on representative STCH materials. Additionally, the sensitivity of RBS to light elements allows the determination of whether secondary phases are forming at surfaces, including the formation of carbonates which is a concern for STCH materials featuring alkaline rare earth elements. Together, this work demonstrates an underutilized technique for quantitative analysis of oxygen vacancy stoichiometry in STCH materials; a key material property to STCH performance which has been under-reported in the field.

10:40 PM EN05.05.07

First-Principles Screening of Ca-Ce-M-O (M = 3d transition metal) Oxide Perovskites for Solar Thermochemical Applications Sai Gautam Gopalakrishnan^{1,2}, Ellen Stechel³ and Emily Carter^{1,4}; ¹Princeton University, United States; ²Indian Institute of Science, India; ³Arizona State University, United States; ⁴University of California, Los Angeles, United States

Solar thermochemical (STC) processes have the potential to be an efficient way to generate renewable fuels or fuel precursors using concentrated sunlight. Specifically, an STC process can use redox-active, transition-metal oxide substrates to split water and CO₂, generating syngas, H₂ and CO. Importantly, STC processes benefit from oxide substrates that can *i*) withstand large temperature swings, *ii*) sustain high degrees of oxygen off-stoichiometry and *iii*) be resistant to adverse phase transformations. Currently, the state-of-the-art material used in STC applications is pure CeO₂; identifying materials that can operate at lower temperatures and achieve higher efficiency is an active area of research. Here, we explore the chemical space of Ca-Ce-M-O (M=3d transition metal) oxide perovskites, with Ca and/or Ce occupying the A site and M occupying the B site within an ABO₃ framework, as potential STC candidates, using density functional theory (DFT) based calculations. To account properly for electron exchange and correlation, we use the strongly constrained and appropriately normed functional, with an appropriately determined Hubbard *U* correction to reduce the inherently large self-interaction error DFT engenders when describing 3d (M) and 4f (Ce) electrons. While we consider only Ca and/or Ce on the A-site because of their similar size and the potential redox-activity of Ce, we evaluate all 3d transition metals except Zn on the B-site (Zn⁺³ is uncommon in solids). We evaluate the oxygen vacancy

formation energy (~enthalpy of reduction in an STC process), electronic properties, and thermodynamic stability of ternary Ca-M-O, Ce-M-O, and quaternary Ca-Ce-M-O perovskites, identify promising candidates, and extract metrics that govern the enthalpy and entropy of reduction that are key to improving STC efficiencies.

SYMPOSIUM EN06

Frontier Energy Sciences in Halide Perovskites
April 14 - April 20, 2021

Symposium Organizers

Michael Saliba, Stuttgart University
Elizabeth von Hauff, Vrije Universiteit Amsterdam
Yuanyuan Zhou, Hong Kong Baptist University
Kai Zhu, National Renewable Energy Laboratory

Symposium Support

Silver

Journal of Energy Chemistry

Bronze

Matter | Cell Press

* Invited Paper

SESSION EN06.01/EN07.01: Joint Session I: When Perovskite Meets Chalcogenide
Session Chairs: Michael Saliba and Byungha Shin
Sunday Morning, April 18, 2021
EN06

8:00 AM *EN06.01/EN07.01.01

Charge Carrier Dynamics and Non-Radiative Recombination in Chalcogenide and Halide Perovskite Photovoltaic Materials Thomas Unold; Helmholtz Zentrum Berlin für Materialien und Energie GmbH, Germany

Application of semiconductor thin film materials in photovoltaic devices requires optimized optoelectronic properties and thus understanding of the underlying physical mechanisms and limits governing carrier transport and recombination. Although material parameters such as doping density, recombination lifetimes and mobilities belong to the most basic properties eventually defining the solar cell operation, they can be quite elusive or ambiguous in their characterization. Here, chalcogenides (e.g. chalcopyrite and kesterite) and halide perovskites share some similarities, but also a number of differences. Considerable discussion prevails about the role of interface versus bulk recombination in devices, the values of carrier mobilities, doping levels and minority carrier lifetimes. Combining different characterization techniques such as time-resolved luminescence, photoluminescence quantum yield as well as pump-probe terahertz spectroscopy we attempt to draw a relatively consistent picture of material properties and device function, exposing current limits and paths to improvement.

8:25 AM *EN06.01/EN07.01.02

Towards Perovskite-CIGS Large Area Tandem Architectures Valerio Zardetto¹, Marcel Simor¹, Pieter Jan Bolt¹, Tom Aernouts², Gianluca Coletti¹, Mariadriana Creatore³, René A. Janssen³, Veronique Gevaerts¹, Sjoerd Veenstra¹, Hans Linden¹ and Ronn Andriessen¹; ¹TNO partner in Solliance, Netherlands; ²IMEC partner in Solliance, Thin Film PV, Belgium; ³Eindhoven University of Technology, Netherlands

The fabrication of cost-effective multi-junction (MJ) device architectures is presently considered the strategy to increase the Power Conversion Efficiency (PCE) of the solar cells in order to lower the levelized cost of energy (LCOE), decreasing therefore the price of an installed photovoltaic (PV) system. The outstanding advancement of metal halide perovskite absorber (PSC) technologies in the last years motivates the PV community to investigate tandem hybrid architectures, consisting of a perovskite based top cell with a commercial bottom PV device such as crystalline silicon (c-Si) or copper indium gallium selenide (CIGS). The combination with the latter, in particular, offers unique advantages: i) compatibility with lightweight flexible plastic or metal foils as substrates, in view of a roll to roll (R2R) manufacturing line, further reducing the manufacturing and the installation costs, as well as the environmental footprint of the KWh generated; ii) large scale integration of PV devices in, amongst others, buildings (BIPV) and vehicles (VIPV).

This contribution will provide an overview of the activities within the Solliance consortium on 4 terminal tandem and preliminary work on 2 terminal architectures, on rigid, as well as flexible substrates. In order to increase the overall PCE of the tandem hybrid configuration, the optimization of the sub-cells' performance with respect to their spectral responses is required. Several combinations of suitable complementary band gaps of the two absorbers are explored, as well as the optimization of the near infrared transparency of the top perovskite cell by tuning the free carrier absorption of the TCO adopted. Furthermore, in the case of the 2-terminal architecture, the development of an efficient interconnected layer among the two sub-cells is utmost crucial to provide the monolithic series interconnection and, at the same time, to minimize the parasitic absorption.

Optimized TCO, transport layers and anti-reflective properties lead to a near-infrared transmittance of about 90% (an average taken from the wavelength range of 700-800 nm to 1200 nm) on glass or plastic based top PSC optimizing therefore the response of the filtered CIGS. As a result, coupling a semitransparent glass-based PSC and a flexible CIGS we calculate a 4T tandem PCE of 25.2% on small area devices (<0.1 cm²). When using a flexible semi-transparent perovskite solar cell, a record-breaking power conversion efficiency of 23.0% is calculated. We also evaluated the PSC-CIGS combination on a larger area (> 80 cm²), currently adopting a non-optimized (in the NIR region) large area perovskite module. We calculated already a 1.9% absolute increase in the efficiency with respect to the single CIGS device, with a further improvement that can be achieved by improving the light management and fine tuning the perovskite band gap. Whereas the 4T architecture offers already a significant increment in performance with respect to the single junction devices, the development of the 2T tandem PSC-CIGS exhibits more challenges. As observed by the first results, the efficiency of the flexible 2T tandem PSC-CIGS, still lags behind the power conversion efficiency of the single CIGS. New upscalable perovskite formulations as well as the optimization of the recombination layer will also be addressed as crucial topics to boost the overall performance.

8:50 AM BREAK

9:05 AM *EN06.01/EN07.01.03

Chalcogenide Perovskite Thin Films for Energy Conversion—Prospects, Challenges and Routes Forward Corrado Comparotto, Kostiantyn Sopiha and Jonathan Scragg; Uppsala University, Sweden

Great progress in perovskite photovoltaics has been enabled by the excellent intrinsic material properties of lead-halide perovskites. These relatively newly-available materials are already opening paths to higher performance in mass-market PV technologies, including tandem PV modules. Nonetheless, reaching competitive levelized energy costs will hinge on achieving comparable robustness to existing silicon-based technology. This is a high and rising benchmark, which has not yet been approached by halide perovskite technologies. This makes it less likely that investors will support the upscaling and deployment of perovskite-

based solar technology.

Chalcogenide perovskites, in which halide anions are replaced by chalcogenides (O, S, Se) could offer a new path forward. Examples include BaZrS₃ and SrHfS₃, among several others. The solar cell-relevant properties of these materials are projected to be comparable to halide perovskites. More critically though, their chemistry provides them with excellent stability under conditions for which halide perovskites would rapidly degrade, e.g. in water, humid air or at high temperatures.

The major challenge with chalcogenide perovskites has been to synthesise them in thin film form with good quality. Therefore, despite impressive measurements from bulk materials, it has not been possible to validate their application in thin film solar cells. There are several reasons for the synthetic difficulties, connecting to intrinsic material properties as well as to the use of inappropriate synthesis methods. To date, we still have incomplete understanding of the growth processes of these materials.

In this presentation, we briefly summarise the potential of the chalcogenide perovskites based on prior literature. Then, our own progress toward thin films suitable for solar-cell integration will be presented. A number of sputter-based growth routes to BaZrS₃ have been investigated and evaluated using combinatorial approaches. Materials have been characterised using XRD, STEM-EDS, SEM/TEM imaging, XAFS, Photoluminescence mapping and Ion-beam techniques including RBS and ERDA, to construct a picture of the growth sequence and final compositional, microstructural and optoelectronic characteristics of the films. This is a means to establish the first “cookbook” for chalcogenide perovskite films suitable for solar cells, i.e. the optimal growth conditions for high quality material. Film formation will be discussed in the context of thermodynamic and kinetic aspects, applicable to any type of growth method. The aim of this talk is to promote and support research into these highly interesting materials in other labs, and stimulate collaboration on this exciting topic.

9:30 AM EN06.01/EN07.01.04

Effect of the HTM/TCO Interface on the Electrical Properties of Semi-Transparent Perovskite Solar Cells for Tandem Applications Emilie Raoult^{1,2,3}, Marion Provost², Romain Bodeux^{1,2}, Sébastien Jutteau^{1,2}, Marie Legrand^{1,2}, Samuel Rives^{1,2}, Armelle Yaiche^{1,2}, Damien Coutancier^{2,4}, Jean Rousset^{1,2} and Stéphane Collin^{2,3}; ¹Electricité De France (EDF), France; ²Institut Photovoltaïque d'Ile-de-France (IPVF), France; ³Centre for Nanoscience and Nanotechnology (C2N), France; ⁴CNRS, France

Spiro-OMeTAD, CuSCN and PTAA are attractive hole transport materials (HTM) in conventional n-i-p architectures for perovskite cells¹. In this work, we combine these three HTMs on semi-transparent (ST) solar cells with different sputtered electrodes made of In₂O₃-SnO₂ (ITO) or In₂O₃-ZnO (IZO) to study their impact on the optical and electrical properties of the cells.

First, thanks to an optical model based on the Transfer Matrix Method and careful material characterizations^{2,3}, a good agreement has been obtained between the transmission, reflection and absorption spectra of the complete structure of the ST cell with Spiro and ITO. This model allows to simulate the efficiency of a tandem cell with a silicon bottom cell, to identify optical losses and to optimize the thickness and properties of the each layer. It is shown that the Spiro and ITO layers have a non-negligible parasitic infrared absorption in the IR, resulting in a lower efficiency for the filtered silicon cell. The gain in efficiency enabled by the use of PTAA, CuSCN and IZO, which are almost transparent in the IR region, is assessed.

Second, triple cation perovskite solar cells with these three HTMs are synthesized and characterized in detail using scanning electron microscopy, ellipsometry spectroscopy, glow discharge emission optical spectroscopy, X-ray diffraction and transmission spectroscopy. Regarding the electrical properties, the Spiro is a layer known for its sensitivity, and the poor reproducibility obtained on ST cells is often associated with degradation due to energetic sputtering⁴. Investigations using CuSCN as HTM showed a slightly better reproducibility than Spiro but strong light soaking effects also appeared, and the resulting efficiencies are low. The replacement of the

Spiro by PTAA has improved the reproducibility of cells, while maintaining good performances. A 17.4% efficiency perovskite semi-transparent cell with PTAA was obtained and which is significantly above our previous results with Spiro (16.4%)⁵.

After electrode sputtering deposition, a characteristic S-shape appears in IV characteristics. By regularly following the cells over time while keeping them under vacuum atmosphere and in the dark, IV curves recovered until the S-shape disappeared completely. For example, a cell with Spiro and ITO have 8.7% efficiency and 43% Fill Factor (FF) the first day and reach 16.8% with FF=70% after 66 days. When the Spiro is replaced by PTAA, the S-shape is less pronounced and the recovery time markedly reduced to 15 days. These effects are not visible on cells with CuSCN.

Lee et al.⁶ obtained a similar S-shaped curve on perovskite cell with a Spiro/silver electrode, with a short recovery time of about one day. A local reaction between the dopant Li-SIF and the silver could cause the deoxygenation of the Spiro at the surface, which would create a temporary electrical barrier. It is interesting to note that this dopant is common to PTAA and Spiro but not to CuSCN. Preliminary results obtained by time resolved photoluminescence (TRPL) shows a decrease of the PL signal over time. Experiments are underway to determine if the cause of this decrease is due to improved extraction at the HTM/TCO barrier as suggested by Lee et al.⁶, or if it comes from a reduction in radiative recombination related to defect healing. We will discuss the reaction mechanisms for these three HTM.

[1] Z. Shariatnia, *Renew. Sustain. Energy Rev.*, 119, 109608, 2020

[2] E. Raoult *et al.*, *36th Eur. Photovolt. Sol. Energy Conf. Exhib. 757*, 2019

[3] E. Raoult *et al.*, *SPIE: Physics, Simulation, and Photonic Engineering of Photovoltaic Devices IX*, 2020

[4] H. Kanda *et al.*, *J. Phys. Chem. C*, 120, 50, 28441, 2016

[5] F. J. Ramos *et al.*, *Sci. Rep.*, 8, 1, 2018

[6] D. G. Lee *et al.*, *ACS Appl. Mater. Interfaces*, 11, 51, 48497, 2019

9:45 AM EN06.01/EN07.01.05

Late News: A Transparent Polymer Impregnated with Conductive Particles for Tandem Photovoltaic Devices Joshua Crunk, Kai C. Outlaw-Spruell and Nicolas Gaillard; Hawaii Natural Energy Institute, United States

Tandem photovoltaic (PV) devices offer great advantages over individual photovoltaic cells including the potential to reach power conversion efficiencies (PCEs) greater than that of the composing individual cells. The current record PCE for a PV tandem cell is over 29%, set by a perovskite/Si tandem. Perovskite solar cells (PSCs) are ideal for tandem devices because they have proven to be highly efficient and the bandgap can be tuned. However, PSCs are extremely sensitive to air and light. Another great candidate for tandem devices are chalcopyrite thin-film solar cells. Chalcopyrite cells also have tunable bandgaps and high efficiencies. The manufacturing process for chalcopyrite cells includes parameters that would degrade the performance of the bottom cell in a monolithic tandem device and the architecture of the cell prohibits a sufficient amount of energy below the bandgap from reaching the bottom cell. Thus, we present a strategy for fabricating a semi-monolithic chalcopyrite/perovskite tandem device by employing a transparent polymer impregnated with conductive particles (TPCP).

The TPCP was designed for electrically coupling solar cells into tandem devices. The TPCP can be employed in three ways: (i) fully-bonded, (ii) semi-bonded, and (iii) freestanding. When fully-bonded, the TPCP permanently bonds two surface allowing for passage of light and electrical current. TPCPs have been used to fabricate a CuGaSe₂/Si tandem device with an open circuit voltage of 1.04 V and PCE of 2.45%. Fully-bonded TPCPs were used to exfoliate the CuGaSe₂ cell at the MoSe₂ layer with an FTO-coated glass handle. The exfoliated CuGaSe₂ cell was then fully bonded with the TPCP to a Si bottom cell. The semi-bonded TPCP passes light and electrical current while also providing the protective features of a polymer over a surface. The semi-bonded TPCP has successfully been employed as an encapsulation technique for preserving PSCs. The TPCP encapsulation did not affect the performance of the PSC. An encapsulated PSC exposed to air and light

for 14 days did not show any visible signs of degradation. The freestanding TPCP enables the coupling of PV cells without permanently bonding the cells. Ultraviolet-visible spectroscopy measured over 90% transmittance across the visible spectrum. The resistance of the TPCP measured by linear sweep voltammetry yielded a series resistance to the order of $10^{-1} \Omega \cdot \text{cm}^2$.

Based on the successful fabrication of the CuGaSe₂/Si tandem device and encapsulation of the PSC, we will investigate the fabrication of a chalcopyrite/perovskite tandem device composing of a wide bandgap chalcopyrite top cell and a narrow bandgap PSC. Additionally, the application of the freestanding TPCP to fabricate a tunable tandem device with exchangeable cells will be attempted.

SESSION EN06.02: Ion Moves in Perovskite Semiconductors

Session Chairs: Ivan Mora-Sero and Elizabeth von Hauff

Sunday Morning, April 18, 2021

EN06

10:30 AM *EN06.02.01

Ion Transport and Redistribution in Bulk and at Interfaces of Halide Perovskites Joachim Maier; Max Planck Institute for Solid State Research, Germany

The first part of the presentation summarizes parts of our work on bulk ion conductivity in halide perovskites. It discusses contributions from halide ions and methylammonium cations, and their relevance for polarization phenomena and stability [1]. The finding that light enhances the ion conductivity in the iodides [2] but not in the bromides, offers a simple explanation for the light induced demixing [3]. How far this surprising light effect on ion conduction has the potential to lead to novel “opto-ionic” devices is discussed [4].

The second part of the presentation refers to interfaces. It is shown that mobility of ions and the significant fraction of ionic charge carriers also gives rise to ionic built-in potentials, a point that had not been addressed in the photovoltaic literature and might lead to a paradigm change in the understanding of photoactive interfaces [5].

[1] A. Senocrate and J. Maier, *J. Am. Chem. Soc.* 141 (2019) 8382

[2] G.Y. Kim et al., *Nat. Mater.* 17 (2018) 445

[3] G.Y. Kim et al., *Photo-effect on ion conduction in mixed cation and halide perovskites and implications for photo de-mixing*, *Angew. Chem.*, to be published

[4] A. Senocrate et al., *Helv. Chim. Acta* 103 (2020) e2000073

[5] G.Y. Kim et al., *Adv. Funct. Mater.* 30 (2020) 2002426

10:55 AM *EN06.02.02

In Situ Monitoring of Iodine Migration in Mixed Halide Perovskites Preethi S. Mathew, Jeffrey DuBose and Prashant Kamat; University of Notre Dame, United States

Trapping of holes at iodide sites in mixed halide perovskite, MHP (MAPbBr_{1.5}I_{1.5}) films cause iodide ions to migrate toward grain boundaries, thus inducing the formation of iodide rich phases and bromide rich phases. When mixed halide perovskite films are in contact with solution, the migration of iodine extends beyond phase segregation as it gets expelled into solution. The selective removal of iodine from MHP upon continued irradiation transforms the perovskite film into a bromide-rich perovskite film. Substituting A-site cation of MHP with cesium (Cs) slows down iodide expulsion due to increased thermodynamic stabilization of MHP lattices. Similar lattice stabilization has also been observed in Cl-alloyed perovskites. Furthermore, photoinduced iodide expulsion process in MHPs can be modulated through externally applied electrochemical bias. At anodic potentials, electron extraction at TiO₂/MHP interfaces becomes more efficient, leading to hole build-up within MHP films. This improved charge separation, in turn, favors iodine migration as evident from

the increased apparent rate constant of iodine expulsion ($k_{\text{expulsion}} = 0.0030 \text{ s}^{-1}$). Conversely, at cathodic bias (-0.3 V vs. Ag/AgCl potential) electron-hole recombination is facilitated within MHP films, slowing down iodine expulsion by an order of magnitude ($k_{\text{expulsion}} = 0.00018 \text{ s}^{-1}$). The tuning of the E_{Fermi} level through external bias modulates electron extraction at the TiO_2/MHP interface indirectly controls the build-up of holes, which ultimately induces iodine migration/expulsion. Suppressing iodine migration in perovskite solar cells is important for attaining greater stability since they operate under internal electrical bias.

11:20 AM DISCUSSION TIME

11:35 AM EN06.02.04

Modulation of Photo-Induced Iodide Expulsion in Mixed Halide Perovskites with Electrochemical Bias

Jeffrey DuBose^{1,2}, Preethi S. Mathew^{1,2} and Prashant Kamat^{1,2}; ¹Radiation Laboratory, United States;

²University of Notre Dame, United States

Mixed halide perovskites (MHPs) under photoirradiation phase segregate into iodide- and bromide-rich domains. When in contact with a solvent, the perovskite film expels iodine into solution. The trapping of holes at iodide sites dictates the overall iodide migration process. We have now succeeded in modulating the iodide expulsion process in MHPs through externally applied electrochemical bias. At anodic potentials, electron extraction at the electrode interface becomes more efficient, leading to build-up of holes within the MHP film. This in turn favors phase segregation and increases the rate iodine expulsion ($k_{\text{expulsion}} = 0.0030 \text{ s}^{-1}$ at 0.5 V vs. Ag/AgCl). Conversely, at cathodic bias we facilitate electron-hole recombination within the MHP film and slow down iodine expulsion ($k_{\text{expulsion}} = 0.00018 \text{ s}^{-1}$ at -0.3 V vs. Ag/AgCl). The tuning of E_{Fermi} through external bias modulates charge extraction at the perovskite electrode interface and indirectly controls the build-up of holes, which in turn induces iodine expulsion. Suppressing iodine migration in perovskite solar cell is important for attaining greater stability of perovskite solar cells since they operate under internal bias.

11:50 AM EN06.02.05

Late News: Towards Understanding the Origin of the Light-Induced Phase Segregation in the Mixed-Halide Perovskites

Lyubov Frolova¹, Sergey Luchkin², Ernst Kurmaev³, Sergey Aldoshin¹ and Pavel Troshin¹;

¹IPCP RAS, Russian Federation; ²Skolkovo Institute of Science and Technology, Russian Federation; ³Ural Federal University, Russian Federation

Tunability of optoelectronic properties of lead halide perovskites achieved through halide mixing can potentially enable their multiple applications e.g. in tandem solar cells and light-emitting diodes. However, mixed halide perovskites are unstable under illumination due to their segregation into Br-rich and I-rich phases, which negatively affects the performance characteristics and operational stability of devices. Research efforts over the past years provided a substantial understanding of the factors influencing light-induced halide phase segregation. While several mechanisms were proposed, none of them could account for all available experimental data; and hence the origin of the effect is still under active debate. Herein, we thoroughly investigated the photodegradation of CsPbI_2Br and $\text{Cs}_{1.2}\text{PbI}_2\text{Br}_{1.2}$ using a set of complementary techniques. *In-situ* atomic force microscopy provided a spectacular visualization of the real-time halide phase segregation dynamics demonstrating that iodoplumbate is selectively expelled from the mixed halide perovskite grains and nucleates as a separate I-rich phase at the grain boundaries. We propose a mechanism based on the reversible $\text{Pb}^{2+}/\text{Pb}^0$ and I/I_3^- redox (photo)chemistry, which explains our experimental findings and other previously reported results. Furthermore, it sheds new insights on the underlying mechanisms of multiple phenomena related to light- or electric field-induced degradation of various lead halide perovskites.

More details can be found in our recently accepted paper: L. A. Frolova et al., Reversible $\text{Pb}^{2+}/\text{Pb}^0$ and I/I_3^- redox chemistry drives the light-induced phase segregation in all-inorganic mixed halide perovskites. *Adv. Energy Mater.* 2021, DOI: 10.1002/aenm.202002934.

12:05 PM EN06.02.06

Late News: Quantized Halide Diffusion in 2D Perovskite Vertical Heterostructures

Akriti Akriti¹, Enzheng

Shi^{2,1}, Stephen B. Shiring¹, Brett M. Savoie¹ and Letian Dou¹; ¹Purdue University, United States; ²Westlake University, China

Solid state devices based on halide perovskites are now competing with other well-established semiconductors like silicon and gallium arsenide. However, the intrinsic instability of three-dimensional (3D) perovskites poses a great challenge in their widespread commercialization. The soft crystal lattice of hybrid halide perovskites facilitates anionic diffusion which impacts material stability, optoelectronic properties, and solid state device performance. Two-dimensional (2D) halide perovskites with bulky organic barriers have been used for improving the extrinsic stability as well as suppressing intrinsic anionic diffusion. With this strategy, devices with enhanced stability and reduced hysteresis have been achieved. Nevertheless, a fundamental understanding of the role of compositional tuning, especially the impact of organic cations, in inhibiting anionic diffusion across the perovskite-ligand interface is missing. Through this study, we demonstrate a quantitative investigation of the anionic inter-diffusion in flat 2D vertical heterojunctions between two arbitrarily determined phase-pure halide perovskite single crystals. Contrary to their 3D counterparts, anion diffusion across 2D halide perovskite vertical heterostructures does not follow the classical Fickian diffusion featuring continuous concentration profile evolution. Instead, the assembled vertical heterostructures show a “quantized” layer-by-layer diffusion behavior governed by a local free energy minimum and ion-blocking effects of the organic cations. We found that for a given organic cation, 2D perovskites ($n = 1$) are better inhibitors of halide diffusion compared to quasi 2D ($n > 1$) and 3D perovskites. Surprisingly, halide inter-diffusion coefficients for 2D perovskites capped with short aliphatic organic cations (*e.g.* butylammonium) are only 1~2 order of magnitudes smaller than that of 3D perovskites, suggesting the ineffectiveness of these cations in blocking the anionic migration. Furthermore, we found that bulkier and more rigid π -conjugated organic cations inhibit halide inter-diffusion much more effectively ($D < 10^{-20}$ m²/s) compared to aliphatic cations. These results offer significant insights into the mechanism of anionic diffusion in 2D perovskites and provide a new materials platform for heterostructure assembly and device integration.

SESSION EN06.03: Re-Inventing Perovskites for Versatile Applications

Session Chairs: Yen-Hung Lin and Li Na Quan

Sunday Afternoon, April 18, 2021

EN06

6:30 PM *EN06.03.01

Mercury Rising in Perovskites Tze Chien Sum; Nanyang Technological University, Singapore

Slow hot carrier cooling in halide perovskites holds the key to the development of perovskite hot carrier (HC) and multiple exciton generation (MEG) solar cells that could potentially overcome the Shockley-Queisser limit. In this talk, I will focus on the new photophysical insights from our recent works on the hot carrier phenomena in halide perovskites.

6:55 PM *EN06.03.02

Narrowband Near-infrared Perovskite/Polymer Hybrid Photodetectors Zhaojue Lan, Linfeng Cai and Furong Zhu; Hong Kong Baptist University, Hong Kong

Solution-processable halide perovskite semiconducting materials have unique optoelectronic properties for applications in perovskite solar cells and photodetectors (PDs). The discrete perovskite PDs have a broadband photoresponse, which is sensitive over the visible wavelength range, while the discrete polymer PDs exhibit a broadband photoresponsivity with extended absorption in the near-infrared (NIR) wavelength range, *e.g.*, from visible light to the NIR wavelength of >1100 nm. The visible-blind NIR photodetection with these broadband PDs requires the use of the filters or the specially designed photonic structures for attaining the photodetection

over a well-defined wavelength range. However, the use of the external filters adds additional cost and reduces the overall photosensitivity of the PDs.

Different narrowband photodetection approaches have been attempted, e.g., incorporating a microcavity structure and using charge collection narrowing (CCN) effect in the PDs. In the CCN-type PDs, a relatively thick photoactive layer, e.g., > 2500 nm thick photoactive layer, is adopted to reduce the collection efficiency of the charge carriers generated by the visible light absorbed near the upper region of a thick photoactive layer. The use of a thick active photoactive layer in a CCN-type PD faces some technical challenges: (1) The responsivity of the CCN-type PDs is limited as a large amount of the incident light is attenuated by the thick photoactive layer. (2) Perovskite PDs with a thick photoactive layer often associates with a slower response speed due to the decrease in its carrier transit time limited cut-off frequency. (3) The photodetection spectrum in the CCN-type PDs is limited by the absorption edge of the photoactive layer. This talk discusses a novel hybrid PD with a heterostructure perovskite/polymer photoactive layer for alleviating the challenges: (1) to achieve high hole transport efficiency by incorporating a thinner perovskite, (2) to realize narrowband NIR detection through buildup of the space charges at the perovskite/polymer interface, and (3) to improve the device design freedom by incorporating different combinations of perovskite charge transporting layer and the NIR absorbing layer in the perovskite/polymer structure. The hybrid PDs with a thinner photoactive layer results in an obvious increase in the responsivity and response speed. The hybrid PDs thus demonstrated have a narrowband NIR detection and a -3 dB cut-off frequency of 300 kHz, offering an exciting option for a plethora of applications in bio-imaging, environmental detection, and security monitoring.

7:20 PM EN06.03.03

A Perovskite Retinomorph Sensor John G. Labram and Cinthya K. Trujillo Herrera; Oregon State University, United States

Designed to outperform conventional computers when performing machine-learning tasks, neuromorphic computation is the principle whereby certain aspects of the human brain are replicated in hardware. While great progress has been made in this field in recent years, almost all input signals provided to neuromorphic processors are still designed for traditional (von Neumann) computer architectures. For example, in a CCD detector an array of pixels is sampled at fixed intervals in time.

In this work we have taken inspiration from the human retina and demonstrated an event-driven sensor which pre-processes optical signals by design. Using a metal halide perovskite thin film as one dielectric layer of a bilayer capacitor, we demonstrate a device which changes its capacitance under illumination. When in series with a resistor, and a constant bias is applied across this device, the voltage dropped across the resistor will spike temporarily as the capacitor (dis)changes, before returning to its equilibrium value. The result is a sensor which spikes in response to changes in illumination, but otherwise outputs zero voltage. A simple model was developed to parameterize and simulate these sensors.

It is hoped that this work represents the first step towards a paradigm shift for the design of sensing systems for neuromorphic computation, and artificial intelligence in general. When combined with similar spiking sensors that respond to other stimuli (e.g. sound, vibration, temperature, etc..), the academic and commercial communities should be able to realize complex sensing systems for a broad range of applications in artificial neural networks. Such a sensor is not only optimized for use with spiking neuromorphic processors but anticipated to have broad appeal from fields such as LIDAR (light detection and ranging), autonomous vehicles, facial recognition, navigation, and robotics.

7:35 PM DISCUSSION TIME

7:50 PM EN06.03.05

Enhanced Memory Properties in Tailored 2D/3D Halide Perovskite Heterointerface Resistive Switching Memory SangMyeong Lee, Won Bin Kim, Gill Sang Han and Hyun Suk Jung; Sungkyunkwan University,

Korea (the Republic of)

Halide perovskites (HPs) has been conceived as resistive switching (RS) memory devices; this is due to their low operation voltage, high on/off ratio, and tunable band gap. However, the HP-based RS memory devices have several challenges owing to the short endurance of 350 cycles, data retention of 4×10^3 s and stability of perovskite film.^{1,2} Herein, 2D/3D halide perovskite heterointerface was made by a low-temperature all-solution process. The 2D/3D halide perovskite RS memory devices exhibits excellent performance with an endurance of 2700 cycles, a high on/off ratio of 10^6 , and data retention of 10^4 s. The 2D halide perovskite layer could disturb the Ag ion migration into the 3D halide perovskite layer by calculated thermally-assisted ion-hopping activation energy and the results of the time-of-flight secondary ion mass spectroscopy. Moreover, the 2D halide perovskite layer controls the rupture of the Ag conductive filament. Therefore, the 2D halide perovskite layer enhances the RS memory properties by controlling both Ag migration and filament rupture. This study provides another strategy for improving memory properties of HPs based resistive switching memory devices.

Reference

1. E. Yoo, M. Lyu, J.-H. Yun, C. Kang, Y. Choi and L. Wang: Bifunctional resistive switching behavior in an organolead halide perovskite based $\text{Ag}/\text{CH}_3\text{NH}_3\text{PbI}_3-x\text{Cl}_x/\text{FTO}$ structure. *Journal of Materials Chemistry C* **4**, 7824 (2016).
2. J. Choi, S. Park, J. Lee, K. Hong, D.H. Kim, C.W. Moon, G.D. Park, J. Suh, J. Hwang, S.Y. Kim, H.S. Jung, N.G. Park, S. Han, K.T. Nam and H.W. Jang: Organolead Halide Perovskites for Low Operating Voltage Multilevel Resistive Switching. *Advanced Materials* **28**, 6562 (2016).

8:05 PM EN06.03.06

Lead Iodide Hybrids with Aromatic Diammonium Cations—From 2D Dion-Jacobson Perovskites to 3D Hybrid Structures. Xiaotong Li¹, Weijun Ke¹, Yihui He¹, Peijun Guo², Mikael Kepenekian³, Boubacar Traore³, Jacky Even³, Claudine Katan³, Constantinos Stoumpos¹, Richard Schaller² and Mercouri G. Kanatzidis¹; ¹Northwestern University, United States; ²Argonne National Laboratory, United States; ³University of Rennes, France

Aromatic diammonium cation, x-(aminomethyl)pyridinium (AMPY, x = 3 or 4) can form 2D Dion-Jacobson lead iodide perovskite, which adopt the general formula of $(x\text{AMPY})(\text{MA})_{n-1}\text{Pb}_n\text{I}_{3n+1}$ (MA = methylammonium, n = 1–4). By modifying the position of the $-\text{CH}_2\text{NH}_3^+$ group from 4AMPY to 3AMPY, the stacking of the inorganic layers changes from exactly eclipsed to slightly offset. The perovskite octahedra tilts are also different between the two series, with the 3AMPY series exhibiting smaller bandgaps than the 4AMPY series. Compared to the aliphatic cation of the same size (AMP = (aminomethyl)piperidinium), the aromatic spacers increase the rigidity of the cation, reduce the interlayer spacing and decrease the dielectric mismatch between inorganic layer and the organic spacer, showing the indirect but powerful influence of the organic cations on the structure and consequently on the optical properties of the perovskite materials. Preliminary solar cell devices based on the n = 4 perovskites as absorbers of both series exhibit promising performances. More interestingly, when using 1:4 ratio of AMPY:PbO as starting materials, totally different structures with 3D connection motif form instead. However, because of the steric requirement of the Goldschmidt tolerance factor rule, it is impossible for $(x\text{AMPY})\text{M}_2\text{I}_6$ to form proper perovskite structures. Instead, a combination of corner-sharing and edge-sharing connectivity is adopted in these compounds leading to the new 3D structures. Devices of $(3\text{AMPY})\text{Pb}_2\text{I}_6$ crystals exhibit clear photoresponse under ambient light without applied bias, reflecting a high carrier mobility (μ) and long carrier lifetime (τ) and great potential for photo and X-ray detection applications.

SESSION EN06.04: What Happens at Perovskite Semiconductor Interfaces

Session Chairs: Yuanyuan Zhou and Kai Zhu

Sunday Afternoon, April 18, 2021

EN06

9:00 PM *EN06.04.01

High Performance Perovskite Solar Cells via Two-Step Deposition Jingbi You; Chinese Academy of Sciences, China

The champion efficiency of perovskite solar cells is over than 25%, which is great potential for practical application. Most of the high performance perovskite solar cells are based on the one step deposition with solvent engineering. Two-step deposition is easily controlled, and could be good for deposition of uniform and large area devices, while the efficiency of the device using two-step method is lag behind the one step. Here, we rationally designed the two-step method, and pushed the perovskite solar cells performance close to 25%.

9:25 PM *EN06.04.02

Smart Interface Engineering to Achieve Perovskite Solar Cells with Low Energy Loss, High Operational Stability and the Capability to Capture Degraded Pb-Containing By-Products Alex Jen; City University of Hong Kong, Hong Kong

Minimizing energy loss is a key aspect to transcend the current limitations on the performance of perovskite photovoltaics (PVSC). Our recent study combined composition and interface engineering to dramatically improve the efficiency and long-term operational stability of the PVSC. Moreover, a very innovative approach has also been developed to combine both efficient charge extraction and the ability to trap decomposed Pb-containing perovskites into one material to address the most challenging environmental contamination issue for the commercialization of PVSCs.

This talk will be divided into two parts: (1) Progress of achieving the highest efficiency (23.4%) in inverted perovskite solar cells (PVSCs) through smart engineering of the interfaces; (2) Demonstration of the simultaneous achievement of high PCE (>22%), excellent operational stability (85°C at MPP for 1000h under 1 Sun illumination), and the ability to capture degraded Pb-containing by-products by employing 2D metal-organic frameworks (2D-MOF) as a charge extraction layer in PVSCs.

9:50 PM *EN06.04.03

Interfacial Engineering for High Voltage (>1.4V) Performance of Inorganic Perovskite Solar Cells Tsutomu Miyasaka^{1,2}; ¹Toin University of Yokohama, Japan; ²Waseda University, Japan

Molecular design for improving and modifying the quality of the interfacial structures involved in carrier transports is becoming the major challenge towards high performance and stable perovskite solar cells (PSCs). Various approaches of interfacial engineering have been attempted in the past decade by using modulator molecules and mixing 2D and 3D structures to perovskites, as overviewed by our group as a comprehensive review.¹ These efforts lead to enhance the stability of the organic—inorganic hybrid perovskite devices, which have currently achieved a record efficiency of 25.5%. However, organic cations in hybrid perovskites (methylammonium, etc.) and use of diffusible ionic dopants in hole transport materials (HTMs) are responsible for low stability of perovskites at high temperatures (>120°C). In this respect, use of all-inorganic perovskite materials and dopant-free HTMs will be a main direction of perovskite photovoltaics.² CsPbX₃ (X=Br, I) is the widely studied candidate of the all-inorganic materials although the stability of its photo-active black phase depends on the halide composition and CsPbI₃ lacks in high stability. We have conducted the device fabrication using CsPbI₂Br as the perovskite absorber. The CsPbI₂Br film was made into junction with a solution-processed film of dopant-free HTMs which are copolymer materials and thermally stable up to 300°C. The quality of interfacial structure at the CsPbI₂Br and HTM junction was improved by inserting an ultra-thin layer (<3 nm) of amorphous SnO_x. The all-inorganic and dopant-free PSCs thus fabricated yielded a power conversion efficiency exceeding 15%. Further we could enhance the open-circuit voltage (V_{oc}) of this PSC up to 1.42V as the highest V_{oc} ever achieved with a single perovskite cell.³ In preparation of all-inorganic perovskites, a big challenge should also be directed to development of lead-free perovskite materials for environmental safety in

practical applications.²

All-inorganic dopant-free PSCs are expected to have robust stability against high temperatures. Among extensive applications, use of thermally robust PSCs in space environments is promising because the device is exposed to temperatures in the range of -100 to $+100^{\circ}\text{C}$. Further, thin perovskite photovoltaic films demonstrate high stability and tolerance against exposure to high energy particle irradiations (proton and electron beams).^{4,5} In the near future, perovskite photovoltaics will undergo more research for space applications.

References:

1. A. K. Jena, A. Kulkarni, and T. Miyasaka, *Chem. Rev.* **2019**, 119, 3036–3103.
2. T. Miyasaka, A. Kulkarni, G. M. Kim, S. Oez and A. K. Jena, *Adv. Energy Mat.*, **2019**, 1902500.
3. Z. Guo, T. Miyasaka, et al. *J. Am. Chem. Soc.* **2020**, 142, 21, 9725–9734.
4. Y. Miyazawa, M. Ikegami, H.-W. Chen, T. Ohshima, M. Imaizumi, K. Hirose, and T. Miyasaka, *iScience* **2018**, 2, 148-155.
5. S. Kanaya, G. M. Kim, M. Ikegami, T. Miyasaka, K. Suzuki, Y. Miyazawa, H. Toyota, K. Osonoe, T. Yamamoto and K. Hirose, *J. Phys. Chem. Lett.*, **2019**, 10, 6990-6995.

10:15 PM EN06.04.04

Interface Passivation by Atomic Layer Deposition of Alumina in Inverted (p-i-n) Perovskite Solar Cells Tamanna Mariam, Ramez Hosseinian Ahangharnejhad, Zhaoning Song, Abdul Quader, Zahrah Almutawah, Suman Rijal, Kamala Khanal Subedi, Adam Phillips, Yanfa Yan, Randy J. Ellingson and Michael Heben; University of Toledo, Wright Center for Photovoltaics Innovation and Commercialization, United States

Over the past decade heavy investment in understanding perovskite solar cells have led to high power conversion efficiency (PCE) regular (n-i-p) structure devices fabricated from low cost, scalable methods. In recent years, interest in the inverted structure (p-i-n) perovskite solar cells due to suppressed hysteresis effects, lower temperature processing, flexibility, and, most importantly, applications in tandem structures. However, the device performance of inverted structure devices lags behind, likely due to added recombination at one or both of the perovskite/charge transport layer (CTL) interfaces. Here, we investigate passivation of both of these interfaces to reduce the interfacial recombination in the inverted planar perovskite solar cell. For this study we use fully solution processed Poly[bis(4-phenyl) (2,5,6-trimethylphenyl) amine (PTAA) hole transport layer (HTL) and (6,6)-phenyl C61 butyric acid methyl ester (PCBM)/Bathocuproine (BCP) electron transport layer (ETL). For the absorber perovskite material, we use a triple cation and mixed halide material with composition $\text{Cs}_{0.05}(\text{FA}_{0.83}\text{MA}_{0.17})_{0.95}\text{PbI}_{0.83}\text{Br}_{0.17}$ and 1.62 eV bandgap. For the passivation layer we use alumina (Al_2O_3) deposited via atomic layer deposition. We fabricated devices with and without alumina at the HTL/perovskite, perovskite/ETL and both CTL/perovskite interfaces. The unpassivated devices show V_{oc} of 1.08 V, fill factor (FF) of 72.1% and PCE of 15.4%. The V_{oc} does not change when the alumina is included at the HTL/perovskite interface, but the FF improves to 74.8%, leading to a PCE of 15.7%. When less than 1nm of alumina is added at only the perovskite/ETL interface, the V_{oc} does not change, but the FF and PCE increase to 75.8% and 16.2%, respectively; however, when the alumina thickness is 1-1.6 nm, the V_{oc} , FF and PCE increase to 1.10 V, 76.0% and 16.5%, respectively. When 1-1.6 nm of alumina is included at both CTL/perovskite interfaces, the performance increases further, with champion devices exhibiting PCEs of 18.3% with V_{oc} of 1.11 V and FF of 76.8%. In addition, the passivated devices show less hysteresis than unpassivated devices. These results demonstrate that the interface between the CTL and perovskite affects the devices performance, and that thin layers of inorganic materials can be used to reduce the interfacial recombination. In addition, incorporation of an inorganic layer at both perovskite interfaces may lead to an encapsulation-like effect and reduce degradation of the devices through several mechanisms, including limiting water ingress. The device performance is being monitored to investigate if this is the case. The results show a promising next step toward developing high PCE and stable inverted perovskite solar cells via interface passivation.

10:30 PM EN06.04.05

Fracture Behavior of Organic-Inorganic Halide Perovskite Thin Films for Solar Cells Zhenghong Dai,

Organic-inorganic halide perovskites (OIHPs) has emerged as the most promising light-absorber materials in the photovoltaic community due to their near-ideal bandgaps. However, the low formation energies of OIHPs render them unstable. While significant progress has been made in improving the stability of OIHPs, perovskite solar cells (PSCs) will also need to be mechanically reliable if they are to service satisfactorily for years. In this context, we study the fracture behavior of PSCs by measuring their cohesion energies (G_c) using double cantilever beam method and report a novel approach to strategically enhance the interfacial adhesion and performance of PSCs by interface modification. The reliability was greatly improved after interfacial toughening. This work points to a new route for designing mechanically robust PSCs with long-term durability.

10:45 PM EN06.04.06

Late News: Conversion of P-Type to N-Type Surface of Tin-Lead Perovskite Leading to Efficiency More Than 22% Gaurav Kapil^{1,2}, Takeru Bessho², Qing Shen¹, Hiroshi Segawa² and Shuzi Hayase¹; ¹The University of Electro-communications, Japan; ²The University of Tokyo, Research Center for Advanced Science and Technology, Japan

Introduction

Tin-lead (Sn-Pb) perovskite solar cells (PSCs) are now getting great attention due to the rapid increase in photoconversion efficiency (PCE) more than 20%, which brings them near to their Pb counterparts [1]. They possess the bandgap of 1.2-1.3 eV, which is according to Shockley-Queisser (SQ) limit can give higher PCE than Pb-PSCs where bandgap lies in between 1.45-1.55 eV. Also, according to SQ limit the Voc of 0.9-1 eV is possible for the solar absorbing materials with a bandgap of 1.2-1.3 eV [2]. In our previous work, we have reported a PCE of 20.4% using $\text{Cs}_{0.025}\text{FA}_{0.475}\text{MA}_{0.5}\text{Sn}_{0.5}\text{Pb}_{0.5}\text{I}_3$ (1.27 eV) perovskite as the absorber layer in PSCs with a Voc of 0.81 V [3]. In the work, we revealed that lattice strain relaxation is one of the important properties to look for cation mixing at A position of ABX_3 (where, A is monovalent cation, B is bivalent cation and X is halide anion) perovskite. Therefore, following the same strategy, in the present research, we added a small fraction of Br anion with I anion at X position that led to further decrease in lattice strain and reduction of Urbach energy that resulted into increase in Voc. In addition to this, we used Lewis base surface passivation that solved the two major problems of Sn-Pb perovskite, first is the reduction in formation of amount of Sn^{4+} and second is neutralization of positive surface of perovskite due to I anion vacancy. Further, it is shown that Lewis base post treatment of tin-lead perovskite led to the evolution of n-type surface that resulted in increased electron diffusion length and charge collection in the device.

Results and discussion

The perovskite used in the study is $\text{Cs}_{0.025}\text{FA}_{0.475}\text{MA}_{0.5}\text{Sn}_{0.5}\text{Pb}_{0.5}\text{I}_{3-x}\text{Br}_x$ (where $x=0, 0.025, 0.05, 0.1$). Four devices with different concentration of Br anion are prepared such as Br 0%, Br 2.5%, Br 5% and Br 10%. Device with Br 2.5% showed a best PCE of 21.10% with a FF of 0.81, Voc of 0.84V and Jsc of 31.22 mA/cm^2 . The change PCEs with Br concentration is well supported by UV, PL, SEM, XRD, XPS analysis of perovskite films. Finally, PSC with 22.64% (highest so far in Sn-Pb) after optimization will be reported.

References

- K. Xiao and H. Tan et al., *Nature Energy*, 2020, 5, 870-880.
- W. Shockley, H. J. Queisser, *J. Appl. Phys.* 1961, 32, 510.
- G. Kapil and S. Hayase et al., *ACS Energy Letters*, 2019, 4, 1991-1998.

SESSION EN06.05: Perovskite Semiconductor Goes Low-Dimensional

Session Chairs: Li Na Quan and Yuanyuan Zhou

Monday Morning, April 19, 2021

EN06

8:00 AM *EN06.05.01

Tetrazine-Incorporating Layered Halide Perovskites Featuring Type II Electronic Interface—A Small Cation with Several Optical and Electronic Resonances Emmanuelle Deleporte¹, Ferdinand Lédée^{1,1}, Pierre Audebert¹, Gaëlle Trippé-Allard¹, Laurent Galmiche¹, Damien Garrot¹, Jérôme Marrot¹, Jean-Sébastien Lauret¹, Claudine Katan², Jacky Even² and Claudio Quarti^{2,3}; ¹Université Paris-Saclay, France; ²Univ Rennes, France; ³University of Mons, Belgium

2D-layered perovskites form assembled natural quantum well structures, where the perovskite layer is separated by large organic cations. They have been known for decades, but they are attracting growing interest, for their strong photoluminescence properties, their chemical versatility and their low sensitivity to external degradation mechanisms due to UV light and moisture. In particular, the chemical versatility of the organic part is a decisive advantage compared to their 3D counterparts.

Energy matching and band alignment engineering between the organic/inorganic parts can either be done by tuning the halide composition, by modifying the number of haloplumbate layers or by adjusting the HOMO/LUMO gap and/or levels of the organic spacer, that is to say by incorporating optically active molecules in the perovskite structure. In this case, instead of playing a simple passive barrier role, the organic part can be used to engineer the optoelectronic properties to these materials. Depending on the optical matching, defined for hybrid perovskites as the spectral overlap between the perovskite and organic absorbers optical transitions, along with the type I/II of interface, charge and/or energy transfers can be induced between the inorganic and organic moieties

We have synthesised two novel layered perovskites containing optically active s-tetrazine (R-C₂N₄-R) as sole included organic spacer. Thanks to the various energy resonances between the inorganic and the organic component, both at the level of the single particle electronic states and at the level of many-body exciton states, this system represents the ideal test case to discuss in the detail charge and energy transfer processes at the type II interface. Furthermore, the incorporation of this novel chromophore as spacer is based on a new design concept, which exploits heterocycles with large fraction of nitrogen, rather than extending the size of carbon-based pi-core. We further performed extensive optical characterization supported by computational studies, in order to gain a complete picture of all potential charge and energy transfer processes ongoing in this complex perovskite-luminophore system. More specifically, both excited states as well as band alignment were studied to rationalize the complete quenching of the perovskites light-emission. We conclude that several decay channels may coexist between the s-tetrazine and the perovskite frame, and highlight the necessity of depicting these materials at the level of both excitonic and mono-electronic states.

Reference : F. Lédée et al, Materials Horizons 2021, <https://doi.org/10.1039/D0MH01904F>

8:25 AM *EN06.05.02

Superfluorescence in Assemblies of Cesium Lead Halide Quantum Dots Michael Becker¹, Gabriele Rainò^{2,3}, Franziska Krieg^{2,3}, Ihor Cherniukh^{2,3}, Yuliia Berezovska^{2,3}, Maryna Bodnarchuk^{2,3}, Rainer Mahrt¹, Maksym Kovalenko^{2,3} and Thilo Stoeferle¹; ¹IBM Research Europe - Zurich, Switzerland; ²ETH Zürich, Switzerland; ³Empa–Swiss Federal Laboratories for Materials Science and Technology, Switzerland

Fully inorganic cesium lead halide nanocrystals exhibit giant oscillator strength and long dephasing times at cryogenic temperature, making them ideally suited to explore settings that make use of their exceptionally strong intrinsic light-matter coupling. Through drying-mediated self-assembly of the colloidal perovskite nanocrystals, we can realize various superlattice geometries.

In these assemblies, we observe coherent, cooperative emission so-called superfluorescence. There the quantum dots spontaneously synchronize, thereby forming effectively a giant dipole, and emit an intense burst of light. We will discuss the characteristic signatures of excitation-dependent decay acceleration, superlinear burst intensity and Burnham-Ciao ringing within the different assemblies. Furthermore, we will compare the behavior in these assemblies to giant nanocrystals.

Our experiments demonstrate that in contrast to many other quantum dot systems, cesium lead halide nanocrystals can be made with sufficiently small energy spread to efficiently couple many of them and explore collective optical properties. Superlattices of these nanocrystals are a versatile tool that opens a new door to

investigate these effects.

8:50 AM *EN06.05.03

New 2D Iodide Perovskites for Stable Photovoltaics Mercouri G. Kanatzidis; Northwestern University, United States

The 2D halide perovskites layers can be formed by the introduction of bulky organic cations that tend to interdigitate between the perovskite sheets. It is a multi-member family of materials with variable thickness of the inorganic slabs presents natural quantum wells (QW) type structures with increased Coulombic shielding, lowering the exciton binding energy and increasing the effective charge carrier mobility. These materials are enabling higher solar cell stabilities and record-breaking efficiencies. It is important to understand the thermodynamic and chemical limitations of their structures and how they vary from one 2D member to the next. We employ a combination of synthetic chemistry, calorimetry and crystallography to obtain and identify the thickest known 2D halide perovskite compound characterized to date and we use thermodynamics analysis to assess the enthalpy of formation for these compounds. The current application of these low dimensional semiconductors in stable photovoltaics will be discussed.

9:15 AM *EN06.05.04

Mixed-Metal Perovskites and Expanded Perovskite Analogs Kurt Lindquist¹, Daiki Umeyama^{2,1}, Michael Boles¹, Adam Slavney¹, Stephanie Mack^{3,4}, Linn Leppert⁵, Jeffrey B. Neaton^{4,3} and Hemamala Karunadasa^{1,6}; ¹Stanford University, United States; ²National Institute for Materials Science, Japan; ³University of California, Berkeley, United States; ⁴Lawrence Berkeley National Laboratory, United States; ⁵University of Twente, Netherlands; ⁶SLAC National Accelerator Laboratory, United States

Halide perovskites provide a flexible platform for tuning optoelectronic properties through changes in composition, connectivity, and dimensionality. I will present our recent studies on further increasing the accessible electronic structures of this versatile family of materials by synthesizing mixed-metal perovskites and expanded analogs of halide perovskites. Through both stoichiometric and substoichiometric metal substitutions we can synthesize a variety of halide perovskites, including those with unprecedented lattices and unusual electronic structures. I will also discuss our recent efforts on expanding the cavities in typical 3D perovskites to incorporate more complex organic ions, including aromatic molecules with low-lying states that form the conduction band and organic radicals that add spins to the lattice.

SESSION EN06.06: Processing and Stabilizing Perovskites

Session Chairs: Yen-Hung Lin and Kai Zhu

Monday Morning, April 19, 2021

EN06

10:30 AM *EN06.06.01

Room Temperature Printing and *In Situ* Investigation of Perovskite Thin Films for Printable Solar Cells Gang Li; The Hong Kong Polytechnic University, Hong Kong

Hybrid organo-metal halide perovskite solar cells (PSCs) are promising candidates for next generation photovoltaic device primarily due to their high efficiency, printability and low cost. PSCs have exhibited externally verified power conversion efficiencies (PCE) exceeding 25% outclass from 3.8% in 2009, which have encouraged recent efforts on scalable coating technique in PSCs towards manufacturing. However, devices fabricated by scalable techniques are still lagged the state-of-the-art spin coated devices because the power conversion efficiency (PCE) is highly dependent on the morphology and crystallization kinetics under a controlled environment, and delicate solvent system engineering.

In this talk, we will present the recent works using in-situ technique to guide the development of high performance PSCs using blade coating technology.

(a). Via a laminar air-knife assisted room temperature meniscus coating approach to control the drying kinetics during the solidification process, we recently manufacturing friendly, antisolvent-free room-temperature coating of hysteresis-free PSCs with power conversion efficiency (PCE) of 20.26% for 0.06 cm² and 18.76% for 1 cm² devices. Moreover, this approach offers a solid model platform for in-situ UV-vis and microscope investigation of the perovskite film drying kinetics.

(b) One step further, based on the widest studied champion perovskite solution system DMF-DMSO, we report air-knife assisted fabrication of perovskite solar cell in AMBIENT condition at high relative humidity of 55±5%. In-depth in-situ time-resolved UV-vis spectrometry is carried out to investigate the impact of solvent removal and crystallization rate, which are proven to be a critical factor on influencing the crystallization kinetics and morphology due to moisture attack. The UV-vis spectrometry also enables accurate determination of wet precursor film thickness – a key parameter for fabrication. Anti-solvent free, high humidity ambient coating of hysteresis-free PSCs with PCE of 21.1% and 18.0% are demonstrated for 0.06 cm² and 1 cm² devices, respectively. These PSCs coated in high humidity ambient conditions also show comparable stability with those made in N₂ glovebox.

(c) The room temperature meniscus coating of high-quality perovskite films incorporated with a multifunctional sulfobetaine based zwitterionic surfactant. Systematic in-situ studies uncover the perovskite crystallization pathway and emphasize the surfactant's synergistic role in film construction, crystallization kinetics modulation, defect passivation, and moisture barrier protection. This strategy is applicable across perovskite compositions and device architectures with the enhanced power conversion efficiencies up to 22%. In addition, this approach significantly improves the stability of perovskite films and devices under different aging conditions.

REFERENCES

- [1] H Hu, Z Ren, PWK Fong, M Qin, D Liu, D Lei, X Lu, G Li*. Room Temperature Meniscus Coating of >20% Perovskite Solar Cells: A Film Formation Mechanism Investigation. *Advanced Functional Materials*, 1900092 (2019).
- [2] PWK Fong, Gang Li. Under review.
- [3] K. Liu et al. Zwitterionic Surfactant Assisted Room Temperature Coating of Efficient Perovskite Solar Cells. 2020. <https://doi.org/10.1016/j.joule.2020.09.011>

10:55 AM *EN06.06.02

Halide Perovskite Perovskite Stabilization by the use of Embedded Nanostructures and Outdoor Characterization Ivan Mora-Sero; Universitat Jaume I, Spain

The interaction of halide perovskite and colloidal semiconductor nanostructures (quantum dots or nanoplatelets) can produce interesting synergistic interactions. We show that the interaction of PbS quantum dots and nanoplatelets can produce the stabilization of FAPbI₃ and FACsPbI₃ perovskite black phase and also the increase of the efficiency, stability and reproducibility of the photovoltaic devices prepared with these halide perovskites. Incorporation of PbS QDs allows the dramatic decrease of the annealing temperature for the formation of black FAPbI₃ phase perovskite thin film, from the 170C required without QDs to 85C when QDs are present. In addition, stability of these systems including embedded nanostructures is extended not just for samples prepared in the glove box but fabricated in ambient conditions. These result points the interest of Perovskite-Quantum Dot Nanocomposites, for further development of advanced optoelectronic devices. In addition, a new methodology to analyze halide perovskite outdoor will be described. We will show that this methodology complement the analysis obtained with the figure of merit T₈₀, parameter that refers to the time at which the device reaches 80% of its initial rated power, providing further physical insight into the recombination mechanism dominating the performance, improving the understanding of the degradation processes and device characterization.

11:20 AM *EN06.06.03

Dynamical 2D/3D Interfaces a Boost to Perovskite Solar Cell Stability—Processes and Energetics Behind Giulia Grancini; Università degli Studi di Pavia, Italy

Engineering two-/three- dimensional (2D/3D) perovskite solar cells is nowadays a popular strategy for efficient and stable perovskite solar cells ¹⁻³.

However, the exact function of the 2D/3D interface in controlling the long-term device behavior and the interface physics therein are still obscure.

Here I will discuss the 2D functions which can simultaneously act as surface passivant, electron blocking layer, a sheath to physically protect the 3D underneath, but also impact on the ion movement and charge accumulation. We found a peculiar dynamical structural mutation happening at the 2D/3D interface: the small cations in the 3D cage move towards the 2D layer, which acts as an ion scavenger. If structurally stable, the 2D physically blocks the ion movement at the interface boosting the device stability. Otherwise, the 2D embeds them, dynamically self-transforming into a quasi-2D structure. ²

In concomitance, we discovered that the stable 2D perovskite can block ion movement, improving the interface stability on a slow time scale. ^{2,4}

The judicious choice of the 2D constituents is decisive to control the 2D/3D kinetics and improve the device lifetime, but also can impact on the interface energetics, which can vary and influence the interface processes and ultimately device open circuit voltage. This knowledge turns fundamental for device design, opening a new avenue for perovskite interface optimization.

References

- [1] J.-P. Correa-Baena et al., *Science* **358**, 739–744 (2017).
- [2] A. Sutanto et al. *J. Mater. Chem. A* **8**, 2343-2348 (2020).
- [3] V. Queloz et al. *J. Phys. Chem. Lett.* **10**, 19, 5713-5720 (2019).
- [4] A. Sutanto et al. *Nano Lett* **20**, 3992-3998 (2020)

Acknowledgements I acknowledge the “HY-NANO” project that has received funding from the European Research Council (ERC) Starting Grant 2018 under the European Union’s Horizon 2020 research and innovation programme (Grant agreement No. 802862).

11:45 AM EN06.06.04

Rapid Open-Air Fabrication of Perovskite Solar Modules Nicholas Rolston¹, William Scheideler², Austin Flick¹, Justin Chen¹, Hannah Elmaraghi¹, Andrew Sleugh¹, Oliver Zhao¹, Michael Woodhouse³ and Reinhold Dauskardt¹; ¹Stanford University, United States; ²Dartmouth College, United States; ³National Renewable Energy Laboratory, United States

We report on the scalable open-air fabrication of large-area perovskite solar modules comprising several key advances in the field including scalable large-area spray deposition, new scribing techniques for monolithic integration, advanced optoelectronic characterization using photoluminescence, and a demonstration of reproducibility and high-throughput manufacturability across multiple module batches and open-air process environments. The Rapid Spray Plasma Processing (RSPP) method enables crystallization of perovskite films in ambient with linear speeds of 12 m/min without a post-anneal. RSPP is a moisture-resistant process with better device performance, higher luminescent yield over the largest reported field of view in literature, and carrier lifetimes > 10X than spin coated perovskite to achieve the highest device performances for open-air perovskite deposition. Manufacturability and reproducibility of RSPP is shown using monolithic integration of series-connected modules with 17 subcells on active areas of 5.9 cm² with a rapid fiber laser scribing method. This low-cost, 1064 nm laser scribing process using a unique indirect ablation mechanism has not been demonstrated in literature and is fully compatible with all scribing processes for monolithic integration. A stable cell and module power output of 18.0% and 15.5%, respectively, was achieved with a subcell V_{oc} > 1.06 V that is reproducible and significantly outperforms spin-coated modules. A comprehensive and complete technoeconomic model for the full 9-step in-line perovskite manufacturing process starting with the glass substrate and ending with the junction box of the encapsulated module is used to calculate the module manufacturing cost, to estimate the balance of system costs and to determine a leveled cost of energy for a range of module efficiencies and lifetimes. The analysis provides novel insights and guidelines for necessary

tool speeds, efficiencies, and lifetimes to enable the viability of perovskite module manufacturing for utility-scale energy generation.

12:00 PM EN06.06.05

***In Situ* Grazing-Incidence Wide-Angle X-Ray Scattering Reveals Mechanisms for Phase Distribution and Disorientation in 2D Halide Perovskite Films** Justin M. Hoffman¹, Joseph Strzalka², Nathan C. Flanders¹, Ido Hadar¹, Shelby A. Cuthriell¹, Qingteng Zhang², Richard Schaller², William Dichtel¹, Lin X. Chen² and Mercuri G. Kanatzidis¹; ¹Northwestern University, United States; ²Argonne National Laboratory, United States

Two-dimensional (2D) hybrid halide perovskites with the formula $(A')_2(A)_{n-1}Pb_nI_{3n+1}$ have remarkable stability and promising efficiency in photovoltaic and optoelectronic devices, yet fundamental understanding of film formation, key to optimizing these devices, is lacking. In particular, understanding the processes that lead to the perpendicular orientation of the layers in relation to the substrate, essential for charge carrier extract, and the phase distribution, which has been shown to have a beneficial carrier cascade effect, is needed. Here, in-situ grazing-incidence wide-angle X-ray scattering (GIWAXS) is used to monitor film formation during spin-coating.[1] This elucidates the general film formation mechanism of 2D halide perovskites during one-step spin-coating. There are three stages of film formation: sol-gel, oriented 3D, and 2D. Three precursor phases form during the sol-gel stage and transform to perovskite, first giving a highly oriented 3D-like phase at the air/liquid interface followed by subsequent nucleations forming slightly less oriented 2D perovskite. Furthermore, heating before crystallization leads to fewer nucleations and faster removal of the precursors, improving orientation. This outlines the primary causes of phase distribution and perpendicular orientation in 2D perovskite films and paves the way for rationally designed film fabrication techniques.

References

[1] Hoffman, J. M.; Strzalka, J.; Flanders, N. C.; Hadar, I.; Cuthriell, S. A.; Zhang, Q.; Schaller, R. D.; Dichtel, W. R.; Chen, L. X.; Kanatzidis, M. G. *Adv. Mater.*, **2020**, *32*, 2002812.

12:15 PM EN06.06.06

Using Electrohydrodynamic Deposition as a Potentially Useful Method for In-Space Manufacture of Perovskite Solar Cells Samuel Erickson¹, William G. Delmas¹, Albert Dibenedetto¹, Lyndsey McMillon-Brown², Timothy Peshek² and Sayantani Ghosh¹; ¹University of California, Merced, United States; ²NASA Glenn Research Center, United States

The difficulty in fabricating lightweight, stable, and efficient photovoltaic devices is compounded when in done *in situ* during space missions. Popular deposition techniques like spin coating and drop casting require gravity, making them useless in orbit. To overcome this problem, we have developed a thin film preparation technique utilizing electrohydrodynamic deposition (EHD). This technique entails drawing bi-solvent perovskite precursor solution from a source needle to substrate via an applied electric field. The difference in vapor pressure between the solvents drives surface coverage and film formation in a phenomenon known as Marangoni flow. Thus, EHD is not only a versatile and scalable method, but uniquely suited to our goal of developing stable and high-efficiency thin film devices without assistance from a gravitational field.

In addition to the deposition technique, other factors, including the chemical composition of the absorbing layer, selection of charge transport layers, and thickness of each layer, are among the dozens of choices that must be made when making a photovoltaic device. To best direct our research, metrics such as power conversion efficiency (PCE), annealing temperature, and long-term stability were extracted from literature published during between 2012 and the present. These variables were then analyzed to find useful correlations and compositions among high-performing cells.

A key trend among devices is the moderate correlation between number of cations in a cell and its efficiency.

While this may not be surprising, we found that the efficiency of methylammonium/formamidinium (MA/FA) lead perovskite cells was comparable to, or better than, cesium/MA/FA (Cs/MA/FA) cells. Since Cs greatly complicates fabrication and is generally added for increased stability (unnecessary for cells in space), we choose to focus on MA, followed by MA/FA films. Another influential finding was that cells with high PCE used tin oxide as their electron transport layer (ETL), which will also be incorporated in our devices. Other key findings include interesting trends regarding the relative roles of open circuit voltage versus short circuit current, and the halide composition of the perovskite.

This talk will focus on the EHD process, the data analytics, and our results in thin film fabrication.

*This work was supported by NASA grant no. NNX15AQ01

SESSION EN06.07/EN07.10: Joint Session II: When Perovskite Meets Chalcogenide

Session Chairs: Byungha Shin and Yuanyuan Zhou

Monday Afternoon, April 19, 2021

EN06

7:45 PM *EN06.07/EN07.10.01

Compositional and Defect Engineering in Halide Perovskite and Multinary Chalcogenide Solar Absorber Materials David B. Mitzi; Duke University, United States

Chalcogenide CdTe and Cu(In,Ga)(S,Se)₂ (CIGS) and halide-perovskite-related (e.g. CH₃NH₃PbI₃) semiconductors represent the fastest growing commercial and the most vigorously studied thin-film photovoltaic (PV) technologies, respectively. Alternatives to these semiconductors are also being sought to mitigate toxicity and elemental abundance concerns, for improved compatibility with pervasive scaling of the technologies. Inherent to these pursuits, is the need to understand materials and device limitations, especially as they relate to defects. In this talk, we will consider additive engineering and doping in CH₃NH₃PbI₃-related semiconductors [1,2], as well as proposed defect-resistant Cu₂Ba(Sn,Ge)(S,Se)₄ materials [3,4], and employ a range of characterization techniques, including carrier-resolved photoHall, conventional Hall effect, terahertz spectroscopy and other time-resolved spectroscopies, to understand associated properties and performance-limiting or -enhancing mechanisms.

References:

- [1] O. Gunawan, S. R. Pae, D. M. Bishop, Y. Virgus, J. H. Noh, N. J. Jeon, Y. S. Lee, X. Shao, T. Todorov, D. B. Mitzi, B. Shin, *Nature* 575, 151 (2019).
- [2] J. Euvrard, O. Gunawan, D. B. Mitzi, *Adv. Energy Mater.* 9, 1902706 (2019).
- [3] D. Shin, B. Saporov, D. B. Mitzi, *Adv. Energy Mater.* 7, 1602366 (2017).
- [4] G. C. Wessler, T. Zhu, J.-P. Sun, A. Harrell, W. P. Huhn, V. Blum, D. B. Mitzi, *Chem. Mater.* 30, 6566 (2018).

8:10 PM *EN06.07/EN07.10.02

Searching Stable Perovskite Solar Cell Materials Using Materials Genome Techniques and High-Throughput Calculations Su-Huai Wei; Beijing Computational Science Research Center, China

The solar cells based on the emerging organic-inorganic hybrid halide perovskite is progressing rapidly in the last decade, but the commercialization of the perovskite solar cells still faces significant challenges. The major issues are the poor long-term stability and toxicity. In light of this, materials design and screening of novel stable perovskites is becoming an important research direction. In contrast to conventional *trial-and-error* processes, materials genome techniques and high-throughput calculations have played important roles in this area and accelerated materials discovery. In this talk, I will present a review that summarizes our recent progress in this field, mainly focusing on four classes of perovskites including AM²⁺X₃ halide single

perovskites, $AM^{4+}Y_3$ chalcogenide single perovskites, $A_2M^+M^{3+}X_6$ halide double perovskites, and $A_2M^{3+}M^{5+}Y_6$ chalcogenide double perovskites. The stability, electronic, optical, and defect properties of these materials in terms of their applications as solar cell absorbers are discussed.

8:35 PM *EN06.07/EN07.10.03

Carrier-Resolved Photo-Hall Effect in High Performance Perovskite Solar Absorbers Okie Gunawan¹, Seong Ryul Pae², Byungha Shin², Douglas M. Bishop¹ and David B. Mitzi³; ¹IBM T.J. Watson Research Center, United States; ²Korea Advanced Institute of Science and Technology, Korea (the Democratic People's Republic of); ³Duke University, United States

Majority and minority carrier properties such as type, density and mobility represent fundamental yet difficult to access parameters governing semiconductor device performance, most notably solar cells. Obtaining this information simultaneously under light illumination would unlock many critical parameters such as recombination lifetime, recombination coefficient, and diffusion length, however this goal has remained elusive. We demonstrate here a new carrier-resolved photo-Hall technique that rests on a new equation relating hole-electron mobility difference ($\Delta\mu$), Hall coefficient (H), and conductivity (σ), and a rotating parallel dipole line ac-field Hall system with Fourier/lock-in detection for clean Hall signal measurement (Nature 575, 151, 2019). We successfully apply this technique to a world-record-quality perovskite film and map the results against varying light intensities, demonstrating unprecedented simultaneous access to the above-mentioned parameters.

9:00 PM BREAK

9:15 PM *EN06.07/EN07.10.04

Advances and Challenges for Commercialization of Perovskite Solar Cells Yulia Galagan; National Taiwan University, Taiwan

The interest in perovskite photovoltaics has significantly increased over the last few years. High power conversion efficiencies (PCE) and low-cost manufacturing make perovskite PVs a very promising candidate for future applications. Despite the very advantageous features of perovskite materials, several issues still need to be solved before the commercialization of perovskite solar cells (PSCs). The main challenges of bringing perovskite technologies to the market are (i) scaling-up of the cells and modules dimension, (ii) usage of lead in the perovskite solar panels and (iii) stability of the PSC modules. These three challenging topics will be discussed in the presentation, and possible solutions to overcome these issues will be proposed. The implementation of the proposed measures will help to demonstrate the feasibility of high-volume production. It is an important milestone towards the industrial manufacturing of perovskite photovoltaics and their future commercialization.

9:40 PM EN06.07/EN07.10.05

Analysis for Efficiency Potential of II-VI Compound, Chalcopyrite and Kesterite Based Tandem Solar Cells Masafumi Yamaguchi¹, Hitoshi Tampo², Hajime Shibata², Nobuaki Kojima¹ and Yoshio Ohshita¹; ¹Toyota Tech. Inst., Japan; ²National Institute of Advanced Industrial Science and Technology, Japan

PV-powered vehicle application are very attractive for reducing CO₂ emission and creation of new market. Development of high-efficiency (> 30%) and low-cost solar cell modules is necessary [1]. The II-VI compound, chalcopyrite and kesterite based tandem solar cells are thought to be one of the most promising PV devices because of high-efficiency and low-cost potential. However, efficiencies of II-VI compound, chalcopyrite and kesterite based tandem solar cells (27.2% with III-V/CIGS 3-junction, 24.2% with perovskite/CIGS 2-junction, 16.8% with CdZnTe/Si 2-junction, 15.3% with CdTe/CISE 2-junction, 8.5% with CGSe/CIGSe 2-junction, 3.5% with CZTS/Si 2-junction tandem solar cells) are lower compared to 37.9% with III-V 3-junction and 35.9% with III-V/Si 3-junction tandem solar cells. Therefore, it is necessary to clarify and reduce several losses of tandem solar cells. This paper presents high efficiency potential of II-VI compound, chalcopyrite and kesterite based tandem solar cells analyzed by using our analytical procedure [2] and discusses about non-

radiative recombination losses in those tandem solar cells.

One of problems to attain the higher efficiency II-VI compound, chalcopyrite and kesterite based tandem solar cells is to reduce non-radiative recombination loss. The open-circuit voltage V_{oc} drop compared to bandgap energy ($E_g/q - V_{oc}$) is dependent upon non-radiative voltage loss ($V_{oc, nrad}$) that is expressed by external radiative efficiency (ERE). Open-circuit voltage is expressed by

where the second term shows non-radiative voltage loss, is radiative open-circuit voltage and 0.23V was used as $\Delta (= E_g/q -)$ in this study.

Correlation between V_{oc} values for II-VI compound, chalcopyrite and kesterite based tandem solar cells reported in the references and ERE values estimated by eq. (1) suggests that II-VI compound, chalcopyrite and kesterite based tandem solar cells have larger non-radiative loss and further improvements in efficiency are thought to be possible by improving external radiative efficiency (ERE). The ERE values estimated in this study are 0.00116% for 27.2% III-V/CIGS 3-junction, 0.024% for 24.2% perovskite/CIGS 2-junction, 0.00162% for 16.8% CdZnTe/Si 2-junction, $1.17 \times 10^{-5}\%$ for 15.3% CdTe/CISe 2-junction, $5.87 \times 10^{-8}\%$ for 8.5% CGSe/CIGSe 2-junction, and $8.05 \times 10^{-10}\%$ for 3.5% CZTS/Si 2-junction tandem solar cells compared to 2.2% for 37.9% III-V 3-junction and 1.62% for 35.9% III-V/Si 3-junction tandem solar cells. According to our analysis [3], the 2-junction and 3-junction tandem solar cells have potential efficiencies of more than 36% and 42%, respectively. Several non-radiative recombination losses such as bulk recombination, interface recombination and so forth in tandem solar cells are discussed in this paper. In addition, resistance loss of tandem solar cells including inter-connection is discussed in this study.

References

- [1] M. Yamaguchi et al., *Prog. Photovolt.* (2020) <https://doi.org/10.1002/pip.3343>.
- [2] M. Yamaguchi et al., *J. Mater. Res.* **32**, 3445 (2017).
- [3] M. Yamaguchi et al., *J. Phys. D. Appl. Phys.* **51**, 133002 (2018).

9:55 PM EN06.07/EN07.10.06

Late News: Bandgap Tuning for Pt-Based Mixed Halide-Chalcogenide Perovskites Kristen Tagaytayan¹, Rubaiya Murshed¹, Ivano Castelli², Benedikt Ursprung^{3,4}, Edward S. Barnard⁴ and Shubhra Bansal¹; ¹University of Nevada, Las Vegas, United States; ²Technical University of Denmark, Denmark; ³Columbia University, United States; ⁴Lawrence Berkeley National Laboratory, United States

Organic-inorganic hybrid halide perovskite solar cells (HPSCs) have attracted immense attention because of excellent optoelectronic properties and a record power conversion efficiency (PCE) that has surpassed 25.5% within a few years. HPSCs are competitive with conventional thin-film and c-Si photovoltaic technologies because of their high efficiency, tunable bandgap, high absorption coefficient, and easy and low-cost fabrication. However, despite the very high efficiency already attained by (FA,MA,Cs)Pb(I,Br)₃ single-junction solar cells, the toxicity of Pb and stability of these materials are challenges to commercialization of this technology. Many Pb-free technologies have been developed such as GeI₂ doped Sn based perovskites with promising PCE > 13%. However, a major challenge for Pb-free perovskites is poor power conversion efficiencies as divalent Sn²⁺ and Ge²⁺ tend to oxidize into 4+ oxidation state, generating excessive defects (Sn and Ge vacancies), and result in short carrier diffusion lengths.

Cs₂PtI₆ is a high absorption coefficient and optimal bandgap ($E_g = 1.4$ eV) material, which has shown promising power conversion efficiency of > 12%[1]. The material has shown high absorption coefficient, carrier lifetime > 2 μ s and stability to heat and light soaking stress. ITO/SnO₂/Cs₂PtI₆/PCBM/Carbon devices have also shown to be stable in air without encapsulation for 60 days[2]. Hamdan and Chandiran have demonstrated Cs₂PtI₆ photoanode to be stable under AM1.5G illumination and extreme pH for over 12 hours, making the material promising for photoelectrochemical devices[3]. Although Pt offers an ideal model system, the search for a low-cost, stable, and high performance Pb-free halide perovskite continues. Replacement of Pt with Ni for A₂BX₆ is expected to reduce the bandgap with the reduction in cation size[4]. Here, we explore the effect of Pt precursor, solvents, and Pt-Ni solid solution on optical bandgap, absorption coefficient, structure, and morphology of

Cs₂PtI₆ films.

Cs₂PtI₆ films processed with PtI₄ precursor in a solvent mixture of DMF:DMSO[5] results in crystalline films with an optical bandgap of ~ 1.4 eV. PtI₂ precursor processed with a solvent mixture of DMF:GBL also results in structure and optical bandgap albeit with higher film porosity and preferred crystallographic orientation. Both these processes result in low oxygen content in the films as confirmed by EDS and XPS. On the other hand, films processed with PtI₂ precursor in DMF:DMSO solvent mixture results in oxygen containing films with a bandgap measured as 2.2 eV using UV-Vis-NIR and photoluminescence spectroscopy. Intermixing of B cation with a 50 at% of Pt and 50 at% of Ni results in an optical bandgap of 1.48 eV with the crystal structure of Cs₂PtI₆. Detailed composition analysis shows oxygen is incorporated at anion site resulting in a mixed halide-chalcogenide phase with a tunable bandgap with oxygen concentration. Cs₂(Pt_xNi_{1-x})(I_yO_z)₆ offers an interesting material with tunable bandgap for optoelectronic and sensor applications.

[1] Schwartz, D.; et al. *Phys. Status Solidi Rapid Res. Lett.* **2020**, *14*, 2000182.

[2] Yang, S.; et al. *ACS Appl. Mater. Interfaces* **2020**, *12*, 40, 44700–44709.

[3] Hamdan, M.; Chandiran, A. K. *Angew. Chem., Int. Ed.* **2020**, *59* (37), 16033– 16038.

[4] Cai, Y.; et al. *Chem. Mater.* **2017**, *29*, 7740– 7749.

[5] Abbreviations: DMF = Dimethylformamide, DMSO = Dimethyl sulfoxide, GBL = γ -Butyrolactone, EDS = Energy-dispersive X-ray spectroscopy, XPS = X-ray photoelectron spectroscopy, UV-Vis-NIR = Ultraviolet-Visible-near-Infrared

SESSION EN06.08: Take a Closer Look at Perovskite Semiconductors
Session Chairs: Ivan Mora-Sero, Michael Saliba and Elizabeth von Hauff
Tuesday Morning, April 20, 2021
EN06

8:00 AM EN06.08.01

Superlattice Formation in the Perovskite Solar Cell and Enhancement of the Photovoltaic Performance
Satoshi Uchida¹, Naoyuki Shibayama², Ryota Jono³ and Hiroshi Segawa¹; ¹The University of Tokyo, Japan; ²RIKEN, Japan; ³Research Organization for Information Science and Technology, Japan

Recently organic–inorganic halide perovskite solar cell have great attention for its high performance together with easy production and wide variety of the process & flexibility of substrate materials. The power conversion efficiency has already reached over 25% in 2020 much beyond another solar cells such as CIGS or amorphous Si. The further performance still looks promising toward the Shockley–Queisser limit at around 30%. For that purpose, physical chemistry understanding based on the crystallography must be essential to design the good light harvesting, good charge separation and good charge transfer.

Recently we reported the scientific revelation that the crystal phase of thin film CH₃NH₃PbI₃ consists of the mixture of tetragonal phase and cubic phase. Moreover bold zebra pattern with d-spacing with 14.2Å (2 θ =6.22° for CuK α) was clearly observed by high resolution TEM with FIB processing that consists with tetragonal and cubic phase superlattice. To make more high performance, here the crystal phase control with liquid nitrogen quenching just after the hot plate heating was newly examined. The resulting cell performance was impressive, about 2% more than that without Liq. N₂ treatment. For such treatment the detail about the TEM observation will also be discussed.

8:15 AM *EN06.08.02

Guiding Automated Synthesis of Metal Halide Perovskites Towards Enhanced Stability Kate Higgins¹,

Maxim Ziatdinov², Sergei Kalinin² and Mahshid Ahmadi¹; ¹University of Tennessee, Knoxville, United States; ²Oak Ridge National Laboratory, United States

Metal halide perovskites (MHPs) have significant potential to revolutionize optoelectronics yielding the next generation of highly efficient, low cost devices including solar cells, light-emitting diodes, and photodetectors. However, a new materials engineering approach is required to realize the full potential of these compounds, since MHPs have a broad range of compositions and crystal structures that yield a multitude of diverse and yet unexplored property combinations. Currently, the primary concern at the forefront of scientific and application-driven research is the stability of these materials in the pure or device-integrated form.

An automated experimental workflow based on guided combinatorial synthesis and rapid throughput characterization has been developed to explore properties and stability of metal halide perovskite systems in ambient conditions [1]. We also develop a machine learning-based workflow to quantify the evolution of each system as a function of composition based on overall changes in photoluminescence spectra, as well as specific peak positions and intensities. We will discuss the stability dependence on composition and extremely non-uniform behavior within the composition space. The interpolative regression analysis of photoluminescent properties helps to distinguish mixtures that form *solid solutions* from those that *segregate* into multiple materials in ambient conditions. In addition, the analysis of bandgap energy provides key information about the optimal compositions for certain applications. This workflow is a necessary step to guide the material synthesis and to gain an insight into the intrinsic materials stability by studying the complex phase diagram of mixed perovskites. The workflow allows not only to explore large composition spaces, but also identify stability behavior. Furthermore, it is universal, simple and can be applied to other perovskite systems and solution-processable materials and can be implemented at low cost as compared to systems reported previously, a necessary condition of rapid adoption of these approaches. To further explore the materials level stability, we have studied several compositions of MHPs using time of flight secondary ion mass spectroscopy (ToF-SIMS) under operation condition in a laterally designed electrode configuration [2,3]. To interpret the multidimensional data obtained from such experiments, we develop a machine learning workflow combining the Hough transform and non-negative matrix factorization and non-negative tensor decomposition, to avoid this limitation and extract salient features of associated chemical changes and to separate the light- and voltage-dependent dynamics. Combining these *in-situ* characterizations and this machine learning workflow provides comprehensive information on the chemical nature of moving species, ion accumulation, and interfacial electrochemical reactions in metal halide perovskites devices, feeding back into automated discovery process.

References:

- [1] Higgins, K., Valletti, S. M., Ziatdinov, M., Kalinin, S. V., Ahmadi M. (2020) *ACS Energy Letters*, 5, 3426-3436
- [2] Higgins, K., Lorenz, M., Ziatdinov, M., Vasudevan, R. K., Ievlev, A. V., Lukosi, E. D., Ovchinnikova, O. S., Kalinin, S. V., Ahmadi, M. *Advanced Functional Materials* (2020) 30, 2001995.
- [3] Liu, Y., Borodinov, N., Lorenz, M., Ahmadi, M., Kalinin, S. V., Ievlev, A. V., Ovchinnikova, O. S. *Advanced Science* (2020) 7, 2001176.

8:40 AM *EN06.08.03

Watching and Understanding the Formation of Hybrid Metal Halide Perovskites Carolin M. Sutter-Fella; Lawrence Berkeley National Laboratory, United States

Material synthesis is a very important aspect in human kinds endeavor to discover and create new materials for energy applications. In order to make materials with desired functions we need to know how these functions relate to structure, synthetic variables, arrangement of atoms and molecules and how functions evolve during synthesis.

In this regard, the field of halide perovskites moved towards more and more complex compositions enabling improved device performance and stability. Most of the improvements however, are chemical intuition driven or achieved through empirical optimization of processing conditions. Establishing the relationships between synthesis condition and film properties will enable active control of synthesis parameters and increase

reproducibility. The formation of halide perovskites from colloidal precursors including the initial stages of formation and the physicochemical evolution of properties via polydisperse nanocrystal nucleation and solvent-complexation will be discussed. We identified for example how the precursor and antisolvent influence the crystallization pathway, how morphology can be templated, and how additives can aid room temperature processing. By correlating diffraction and photoluminescence (PL) measurements, it will be demonstrated how *in situ* PL can reveal subtle changes throughout all synthesis steps including the onset of film decomposition.

9:05 AM *EN06.08.04

How *In Situ* Experiments Can Help Us to Understand Multication Perovskite Formation, Stability and Composition Ana F. Nogueira; University of Campinas, Brazil

Multicomponent perovskite solar cells have reached the recent efficiency breakthrough of 25.5%, higher than silicon polycrystalline photovoltaics. Such fantastic result was only possible due to a precise control and engineering of the morphology, interfaces and the use of multiple cations in perovskite A-site, as Rb, Cs, MA (methylammonium) and FA (formamidinium). For tandem perovskite solar cells, a mixture of different anions, as Br and I is also desired to adjust the band gap. Such cocktail of different cations and anions influences the formation of intermediates, new phases, favours halide homogenization, etc; so that at the end, the efficiency of the device is closely related to not only the optical quality of the film (e.g. crystallinity), but morphology and composition.

In this presentation, we will summarize important results using *in situ* experiments to probe perovskite formation (2D and 3D), stability and composition. We employed time-resolved grazing incidence wide angle x-ray scattering (GIWAXS), small angle x-ray scattering (SAXS) and high-resolution XRD taken at the Brazilian Synchrotron National Laboratory and SSRL-Stanford.

In situ GIWAXS experiments allowed us to understand the influence of the solvents, time to initiate the crystallization, humidity in the preparation of perovskite films and to get important information about final composition and morphology [1]. It is well known that a 2D layer on the top of a 3D bulk perovskite improves stability and performance. *In situ* GIWAXS revealed us that during thermal annealing the 2D layer transforms itself into a disorder layer, improving hole transfer and stability [2]. This technique was also employed to identify the first intermediates formed during the degradation of different Cs and Br perovskite compositions under ambient conditions [3].

In situ SAXS is another powerful technique to follow the first stages of the 2D perovskite's formation. Our results suggest that the formation of the individual slabs in $\text{BA}_2[\text{FAPbI}_3]\text{PbI}_4$ is quite fast (within the first 10 s) and, then, these slabs self-assemble into bulk crystallites during the next 40 minutes [4].

Another topic of interest is the photoinduced phase segregation in FACs-based perovskite films. We investigated this phenomenon by photoluminescence (PL) studies and *in situ* high-resolution XRD (dark and under illumination). We found out that cubic-tetragonal transition is able to stabilize the samples with higher Br and Cs content, however this is not true for the films with 17% Br. Thus, other mechanisms must be operating and ruling phase segregation [5].

[1] R. Szostak, et. al, "Revealing the perovskite film formation using the gas quenching method by *in situ* GIWAXS: morphology, properties and device performance", *Advanced Functional Materials*, in press, 2020 (DOI: 10.1002/adfm.202007473)

[2] A. Sutanto, R. Szostak, et. al., "In Situ Analysis Reveals the Role of 2D Perovskite in Preventing Thermal-Induced Degradation in 2D/3D Perovskite Interfaces", *Nano Letters*, 20(5) 3992-3998 (2020)

[3] P. E. Marchezi, et. al., "Degradation mechanisms in mixed-cation and mixed-halide $\text{Cs}_x\text{FA}_{1-x}\text{Pb}(\text{Br}_y\text{I}_{1-y})_3$ perovskite films under ambient conditions" *J. Mater. Chem. A*, 9, 9302-9312 (2020)

[4] R. F. Moral, et. al. "Synthesis of Polycrystalline Ruddlesden-Popper Organic Lead Halides and Their Growth Dynamics", *Chemistry of Materials*, 31 (22) (2019), 9472-9479

[5] R.E Beal, A. F. Nogueira, et. al., "Structural Origins of Light-Induced Phase Segregation in Organic-Inorganic Halide Perovskite Photovoltaic Materials" *Matter*, v.2, Issue 1, (2020)

9:30 AM *EN06.08.05

A Machine Learning Approach to Deconvolute the Role of Stressors in Perovskites' Stability Marina S.

Leite; University of California, Davis, United States

A complete understanding of the influence of the individual and combined effects of extrinsic (humidity and oxygen) and intrinsic (light, bias, and temperature) stressors on halide perovskite materials is key for the ultimate development of stable optoelectronic devices. Here, we present a suite of optical and electrical complementary tools that provide a detailed description of the dynamic responses within these materials. We unfold the impact of distinct humidity levels on charge carrier radiative recombination in $\text{Cs}_x\text{FA}_{1-x}\text{Pb}(\text{I}_y\text{Br}_{1-y})_3$ perovskites through *in situ* PL, where we temporally and spectrally measure light emission within loops of critical relative humidity (rH) levels. Our results demonstrate that the Cs/Br ratio strongly affects the spectral stability of light emission hysteresis, as well as its extent. The photo-emission dynamics in metal halide perovskites with both I and Br is also interrogated by environmental PL, where we find that the presence of Br suppresses hysteresis. We realize a machine learning (ML) approach based on supervised learning combined with environmental PL measurements and determine the (ir)reversible changes that takes place in MAPbBr_3 and MAPbI_3 model systems, and in state-of-the-art multication compositions such as $\text{Cs}_{0.05}\text{FA}_{0.79}\text{MA}_{0.16}\text{Pb}(\text{I}_{0.83}\text{Br}_{0.17})_3$ and $(\text{Cs}_{0.07}\text{Rb}_{0.03}\text{FA}_{0.76}\text{MA}_{0.14}\text{Pb}(\text{I}_{0.85}\text{Br}_{0.15}))_3$. We further resolve transient processes such as ion motion by spatially resolving the local photovoltage and photocurrent at the nanoscale. Here, we quantify how the addition of Rb reduces the inactivity of the perovskites' grains. Combined, the macro- and nanoscale environmental measurements performed provide a comprehensive platform for tracking, in real-time, the relevant changes that can lead to degradation. Moreover, they represent a reliable diagnosis tool that can be expanded to any perovskite chemical composition.

9:55 AM PANEL DISCUSSION

SESSION EN06.09: Bring Perovskites to the Real World for a Smart Future

Session Chairs: Yen-Hung Lin and Kai Zhu

Tuesday Afternoon, April 20, 2021

EN06

9:00 PM *EN06.09.01

High Efficiency Perovskite/Silicon Solar Cells and Solar Hydrogen Systems Kylie Catchpole; Australian National University, Australia

Combining perovskites with well-established photovoltaic materials such as silicon is an attractive option for producing cheap, high efficiency and high voltage solar cells. Perovskite/silicon tandems have the potential for further progress in increasing the efficiency to 30% and beyond, and we discuss some of the key ways forward to achieving this goal. We demonstrate a 4-terminal tandem perovskite/silicon configuration in which the efficiency is as high as 27.7% through a passivation approach using 2D perovskites. We also demonstrate efficiency above 21% and fill factor of 83% for a 1cm^2 single junction perovskite cell using a nanotextured electrode transport layer. Perovskite/silicon tandems integrated with an appropriate catalyst are also a promising way to achieve high efficiency solar hydrogen generation. Using this approach we demonstrate a water-splitting system with a solar to hydrogen efficiency over 17%.

9:25 PM *EN06.09.02

Space within Perovskite/Silicon Tandem Solar Cells—Plenty of Opportunities for Perovskite Solar Cells Xiaodan Zhang; Nankai University, China

Perovskite/Silicon tandem solar cells (PSTSCs) have potentially remarkable energy conversion efficiency at a reasonable cost, which can significantly boost the future PV landscape. Recently, a newly certification efficiency of 29.15% had been reported, which further demonstrated the potential commercialization of this

devices. Despite these advances, stability and large area are the barriers which hinder the industrialization of the tandem devices. And, these issues are closely related to perovskite top cells. Therefore, eliminating the instability problem of perovskite materials and further increasing the efficiency of large scale perovskite devices which will promote the application of perovskite/Silicon tandem cells in the real world condition. In a word, there are many opportunities for perovskite devices to accelerate the development of PSTSCs.

9:50 PM *EN06.09.03

Perovskite Tandems Edward Sargent and Bin Chen; University of Toronto, Canada

I will discuss advances in perovskite tandems, both silicon:perovskite and perovskite:perovskite. I will discuss challenges in achieving the union of operating stability and high performance (especially high Voc) in both the small-bandgap and the large-bandgap cells making up the tandem stack.

10:15 PM EN06.09.04

Optical Design Guidelines for Perovskite/Perovskite Tandem Solar Cells in a Material Independent Approach Mehmet Koç, Zeynepnur Sahinel and Selcuk Yerci; Middle East Technical University, Turkey

Solar cells have presented significant improvements since their first introduction, and every day new developments are still being reported for different solar cell technologies.¹ Conversion efficiency improvements slow down as they become closer to their practical limits and it becomes a more challenging task for researchers to further boost the conversion efficiency. Researchers are continuously searching for alternative routes to surpass fundamental limits. One of the most promising routes is using tandem solar cell structures, which has a long proven success.²

Tandem solar cells enable better utilization of available illumination spectrum which leads to a higher conversion efficiency mainly by better spectral matching. However, some major design challenges are waiting to be addressed such as obtaining maximum absorption in absorbers of both subcells while having electrically advantageous design thicknesses in a material-independent way. Perovskite solar cells have attracted a lot of researchers since their introduction due to their excellent optoelectronic properties. The vast number of researches yields a very broad range of functional materials such as electron/hole transport layers, and transparent conductive electrodes (TCE); as well as various perovskites with different optical properties and bandgaps. Hence, optical design guidelines of perovskite solar cells should be carried out in a way to account for the optical properties of different materials. Therefore, previously we have documented optical design guidelines in a material independent approach for the perovskite solar cells in their standalone configurations.³ In this work, first, bandgaps of perovskite absorbers in both subcells are varied to find optimum pairs that yield the highest power output for both connection configurations, four- and two terminal. Subsequently, optimum optical design parameters for each layer in the tandem structure for a broad range of refractive index of conceptualized functional layers are computed. This expands the applicability of this approach to provide design guidelines for the already documented and future materials. Optimizations are carried out with the integration of machine learning algorithms due to the vastness of the parameter sets. Finally, optical loss mechanisms are quantized and alternative ways of addressing them are discussed.

1 Green MA, Dunlop ED, Hohl Ebinger J, Yoshita M, Kopidakis N, Hao X (2020) Solar cell efficiency tables (version 56). Progress in Photovoltaics: Research and Applications 28:629–638.

<https://doi.org/10.1002/pip.3303>

2 Graydon O (2009) Solar success for Sharp. Nature Photonics 3:684–684.

<https://doi.org/10.1038/nphoton.2009.224>.

3 Koç M, Soltanpoor W, Bektas G, Bolink HJ, Yerci S (2019) Guideline for Optical Optimization of Planar Perovskite Solar Cells. Advanced Optical Materials 7:1900944. <https://doi.org/10.1002/adom.201900944>

10:30 PM EN06.09.05

Real-Time Optical Monitoring for Rapid Diagnosis of the Thermal Stability of Device Architectures for Perovskite Solar Modules Thomas W. Colburn, Oliver Zhao, Justin Chen and Reinhold Dauskardt; Stanford

University, United States

When exposed to elevated temperatures, metal halide perovskites suffer from decomposition to PbI_2 , volatilization of the organic component from the crystal structure, and even metal diffusion of the top contact through the top carrier selective contact to the perovskite. Current methods to evaluate perovskite solar cell thermal stability involve fabrication of full cells and repeated testing over 1000+ hours, requiring considerable manual labor, equipment, and resources.

In our work, we employ a custom-built photo enclosure for high-resolution and real-time optical monitoring of large-area module test architectures during thermal aging for over 1000+ hours. The photo enclosure consists of an optical camera, adjustable light source, heated stage, and standardized color panel that act to normalize the RGB values of the illuminated samples between batches.^[1] We analyze the color of the perovskite layer and establish threshold color intensity values corresponding to critical color changes in the film signaling an appreciable quantity of PbI_2 formation. These color changes indicate the presence of thermal degradation without the need for confirmation through extensive characterization methods. We map the entire module surface for color changes to determine both local and regional degradation modes to identify trends in spatial non-uniformities of modules. From the optical degradation profile of the module, we subsequently apply localized characterization techniques to highlight different features or high-interest areas without analyzing the full sample area. Furthermore, we employ our optical monitoring system to a wide range of strategies designed to mitigate thermal degradation, including incorporation of perovskite additives, perovskite surface functionalization, and hybrid organic-inorganic transport layers. The ability to rapidly evaluate thermal stability without the need for complex characterization equipment and time and resources for fabrication and testing of full devices streamlines the design iteration process towards achieving fully stable perovskite solar modules.

[1] Sun, Shijing; Tiihonen, Armi; et al. (2020): A Physical Data Fusion Approach to Optimize Compositional Stability of Halide Perovskites. ChemRxiv. Preprint. <https://doi.org/10.26434/chemrxiv.12601997.v2>

10:45 PM EN06.09.06

Late News: Avoiding Upscaling Losses for Perovskite Photovoltaics—Advantages of Fully-Evaporated Layer Fabrication and All-Laser-Scribed Interconnections David B. Ritzer¹, Tobias Abzieher², Thomas Feeney², Felix Laufer², Agit Basibüyük¹, Stefan Bergfeld³, Bryce S. Richards^{1,2} and Ulrich W. Paetzold^{1,2}; ¹Institute of Microstructure Technology, Germany; ²Light Technology Institute, Germany; ³Bergfeld Lasertech, Germany

Perovskite-based semiconductors have considerable potential to become an important technology for the fabrication of efficient thin-film photovoltaics (PV). Owing to the ease of fabrication by various wet-chemical deposition techniques, outstanding optoelectronic properties as well as simple bandgap tunability, the international research community puts great effort into the technology's development, resulting in small-area perovskite solar cells exceeding 25% power conversion efficiency (PCE) within only a decade of research. However, perovskite-based PV still faces several challenges, such as low operational stability and the need for upscaling of the fabrication processes to application relevant device areas. In this context, literature reports a clear trend of significant PCE losses during upscaling of device area, as many established deposition processes become increasingly complex to control over larger areas.

In this work, we present for the first time the combination of an all-evaporated layer stack sequence with all-laser-scribed module interconnections as a promising method to close the gap between small-area record solar cells and large-area solar modules. By bringing together the ease of upscaling deposition area by vacuum-based techniques and the high-quality, high-throughput laser scribing method for fabrication of interconnections, a synergy employable as future industrial approach for high-quality module fabrication with excellent reproducibility and production yield is formed. First, an optimization of the laser scribing lines required for efficient serial interconnections is performed, eliminating reported problems such as incomplete ablation, redeposition of ablation debris and flake formation. Based on this, all-evaporated small area solar cells with an aperture area of 0.1 cm^2 are scaled up by a factor of up to 500 to a total aperture area of 51 cm^2 , with geometric

fill factors of up to 96% and most importantly without significant upscaling losses. An in-depth analysis of the fabricated devices utilizing current-density-voltage-characteristics, laser-beam-induced current mapping and photoluminescence measurements reveals excellent layer homogeneity and interconnection quality. The fabricated solar modules reach PCEs of up to 16.5% for aperture areas above 51 cm² (active area PCE of 17.5% with small-area solar cells achieving a PCE of 18.0%), being a world record for fully-evaporated perovskite solar modules. The difference between small- and large-area devices corresponds to an exceptionally low upscaling loss close to 0.5%_{abs} per magnitude of upscaled area, which significantly surpasses not only the upscaling efficiency of other solution-based upscaling methods of perovskite PV but also that of other thin-film technologies such as CIGS. Finally, the investigations are used to comprehensively assess the employed upscaling strategy, identifying further potential for improvement with the ultimate objective of approaching the industrial application of the perovskite PV technology.

SESSION EN06.10: On-demand
Wednesday Morning, April 14, 2021
EN06

8:00 AM EN06.10.01

Late News: Pressure-Assisted Fabrication of High-Quality Perovskite Crystals for Efficient and Stable Perovskite Solar Cells Junsheng Luo; University of Electronic Science and Technology of China, China

The grain boundaries of organic-inorganic halide perovskite films not only function as defect centers, but also behave as intrinsic ion migrating channels and extrinsic moisture-induced degradation initiators, which are detrimental to the efficiency and stability of perovskite solar cells (PSCs). Here, an effective methodology for fabrication of high-quality perovskite layers with reduced non-radiative recombination, suppressed ion migration and increased moisture stability is reported for the first time, referred as the pressure-assisted solution processing (PASP). Through PASP strategy, the nucleation and growth of perovskite crystals can be controlled, leading to the micron-sized grains and microsecond-range carrier lifetimes. The resultant PSC shows champion power conversion efficiency (PCE) as high as 20.74% and a stabilized efficiency exceeding 20%, with superior long-term stability, maintaining above 90% of initial PCE even aging 60 days or continuous 1-sun illumination for 200 h in ambient environment without encapsulation. We unambiguously believe that the control of perovskite crystal nucleation and growth with high quality will be an important direction to improve the efficiency of PSCs to the theoretical limit, as well as to stabilize perovskite-based materials and devices.

8:10 AM EN06.10.02

Late News: Enhanced Optoelectronic Performance of Perovskite Solar Cells Integrated with Front Metal-Oxide Nanoholes Mohammad I. Hossain^{1,2}, Md Shahiduzzaman³, Safayet Ahmed², Rashedul Huque¹, Md Wayesh Qarony^{2,4}, Ahmed Mortuza Saleque², Md Akhtaruzzaman⁵, Dietmar Knipp⁶, Yuen H. Tsang² and Juan Antonio Zapien¹; ¹City University of Hong Kong, Hong Kong; ²The Hong Kong Polytechnic University, Hong Kong; ³Kanazawa University, Japan; ⁴University of California, Davis, United States; ⁵National University of Malaysia, Malaysia; ⁶Stanford University, United States

Improvement of optoelectronic properties of perovskite solar cells (PSCs) can be realized by employing efficient front contact. This study aims to enhance the optical and electrical performances of PSCs by utilizing metal-oxide nanoholes at the front. Such front nanostructures significantly contribute to the broadband light-incoupling and light trapping in a solar cell, resulting in an improvement of quantum efficiency (QE) and short-circuit current density (J_{sc}), leading to further enhancement of energy conversion efficiency (ECE). Furthermore, the metal-oxide contact exhibits high lateral conductivity, high optical transparency, and a suitable work function, facilitating PSC's optoelectronic performance. As most high-performance PSCs explore only the device's electrical properties, the current study reveals a detailed understanding of PSC optics, electrical

characteristics, and their practical fabrication process for achieving high ECEs. The optics, optimization, and electrical effects of PSCs are investigated by advanced three-dimensional electromagnetic simulations with the combination of finite-difference time-domain (FDTD) and finite element method (FEM) techniques. The investigation implies that the nanophotonic-structured front contact allows enhancing the J_{sc} by 11~27% while improving the light incoupling by 10~12%, compared to that of planar configuration. Herein, the validation of numerical modeling was performed by fabricating PSC in a superstrate configuration that was optimized to reach an ECE of 17.5%, V_{oc} of 1.02 V, J_{sc} of 22.1 mA/cm², and FF of 80%. Detailed descriptions of the nanophotonic contact, device, and fabrication process are provided.

8:20 AM EN06.10.03

Impact of Annealing Temperature on Mixed A-Site Halide Perovskite Device Stability Laura E. Mundt¹, Fei Zhang², Axel Palmstrom², Kai Zhu², Joseph J. Berry² and Laura T. Schelhas²; ¹SLAC National Accelerator Laboratory, United States; ²National Renewable Energy Laboratory, United States

The term ‘perovskite’ denotes the crystal structures made of corner-sharing octahedra with ions placed in the octahedral interstitials with the ABX₃ formula. Particular attention has been targeted at compositions with the X-site occupied by a halide and the B-site by a metal, due to interesting functional properties, particularly those associate with photovoltaics (PV). A vast variety of elements and molecules have been incorporated into metal halide perovskite structures, the most prominent are methyl ammonium (MA⁺), and/or formamidinium (FA⁺) as A-site cations, Pb²⁺ and/or Sn²⁺ as the B-site metal, as well as I⁻ and Br⁻ on the X-site. The ability to maintain the perovskite structure, from a geometric point of view, is given by the Goldschmidt tolerance factor t_G . It takes into account the geometric constrains in the crystal lattice and is defined as the ratio of the octahedral interstitial and the A-site cation size. Compositions with non-ideal geometric conditions, such as FAPbI₃ and CsPbI₃, are prone to transition into unfavorable δ -phases. By utilizing a mixture of ions, the geometric conditions in the crystal structure can be finely tuned and thereby improve the inherent structural stability. As a consequence, the mixed perovskite composition of FA_{1-x}Cs_xPbI₃ with optimized tolerance factors features superior structural stability compared to the pure FA- or Cs-compositions.^[1] However, previous studies showed that PV devices, featuring mixed perovskite compositions with similar tolerance factors as absorber layers, do not necessarily exhibit similar stability in structure or device performance. This strongly suggests there are further mechanisms that play a significant role in the structural and device stability in perovskite solar cells (PSCs). In this study, we explore the structure-function relationship in state-of-the-art mixed A-site halide PSCs and reveal the impact of annealing conditions of the device stability.

Time-of-flight secondary ion mass spectroscopy (ToF-SIMS) measurements on neat FA_{0.83}Cs_{0.17}PbI₃ perovskite films that had been annealed at different temperatures revealed local variations in the perovskite composition for low annealing temperatures.^[2] Based on these findings we hypothesize that insufficient annealing leads to incomplete mixing. Local deviations from the mixed phase, either Cs-rich or FA-rich, can nucleate further phase segregation into the parent δ -phases. In sum, reaching thermal equilibrium during the film annealing is crucial for device stability.

We present a study that unambiguously correlates device performance with structural properties, revealing degradation mechanisms in FA_{0.83}Cs_{0.17}PbI₃ PSCs: Operando X-ray diffraction (XRD) allows us to probe the structure function relationship. By utilizing high-energy synchrotron X-rays, we are able to penetrate the perovskite absorber layer through the metal contact in a complete device held at max power. In order to accelerate degradation and to mimic realistic operational temperature conditions, the experiment is performed at elevated temperatures (50°C - 80°C). Using this technique, we compared devices annealed at 100°C and at 180°C. We clearly find superior performance and stability for the samples annealed at higher temperatures. Furthermore, we can identify δ -phases forming for insufficiently annealed samples, corroborating our hypothesis.

In conclusion, we present a study of state-of-the-art mixed A-site halide PSCs, directly correlate processing conditions to device stability and elucidate the underlying degradation mechanisms. Our findings help inform optimized processing protocols to lay the ground for efficient and long-term stable perovskite PV.

[1] Z. Li, M. Yang, J. S. Park, S. H. Wei, J. J. Berry, K. Zhu, *Chem. Mater.* **2016**, *28*, 284.

[2] L. T. Schelhas, Z. Li, J. A. Christians, A. Goyal, P. Kairys, S. P. Harvey, D. H. Kim, K. H. Stone, J. M. Luther, K. Zhu, V. Stevanovic, J. J. Berry, *Energy Environ. Sci.* **2019**, *12*, 1341.

8:30 AM EN06.10.04

Efficient Interlayer Exciton Transport in Two-Dimensional Metal-Halide Perovskites Alvaro Magdaleno, Michael Seitz, Michel Frising, Ana Herranz de la Cruz, Antonio I. Fernández-Domínguez and Ferry Prins; Universidad Autónoma de Madrid, Spain

Two-dimensional (2D) metal-halide perovskites have emerged as a more robust alternative to their three-dimensional counterparts. Due to quantum and dielectric confinement effects, excitons dominate the energy transport characteristics in thinnest members of the 2D perovskites family. Recently we have reported on the in-plane exciton diffusion using transient photoluminescence microscopy, where high diffusivities were found ($0.2 \text{ cm}^2/\text{s}$ for PEA_2PbI_4). Using the same technique, here, we will show that this material exhibits remarkably efficient out-of-plane exciton transport ($0.06 \text{ cm}^2/\text{s}$) as well. This out-of-plane diffusivity translates to a diffusion length of exceeds 100 nm, making it relevant to device design. Moreover, our result show that the individual energy transfer steps that underly the out-of-plane transport occur on a sub-ps timescale. Such ultrafast timescales are over two orders of magnitude faster than predictions using Förster theory. We will discuss the shortcomings of Förster theory for the case of excitons in the layered perovskites. Most importantly, our results show that the excitonic energy transport is considerably less anisotropic than charge-carrier transport for 2D perovskites.

[1] Seitz, M. et al, *Nat. Commun.* <https://doi.org/10.1038/s41467-020-15882-w>

[2] Magdaleno, A. J. et al, *ChemRxiv*. <https://doi.org/10.26434/chemrxiv.13073153.v1>

8:40 AM EN06.10.05

Changes in Dielectric Constant of Metal Halide Perovskites Studied via Frequency-Dependent Time-Resolved Microwave Conductivity Min Ji Hong and John G. Labram; Oregon State University, United States

Metal Halide Perovskites (MHPs) have drawn significant attention due to their outstanding optoelectronic properties, such as high absorption coefficient and long carrier lifetime. While MHPs offer industry and the academic community many exciting opportunities, consistent mechanistic understanding and consensus still lag behind more established systems. One notable property of this class of materials is their large dielectric constant, which has been observed to change significantly under illumination. [1] While the polarizability of this system has been invoked to explain many of its unusual properties, the behavior of the dielectric constant under illumination is still poorly understood.

In this study, we have used frequency dependent Time Resolved Microwave Conductivity (TRMC) to investigate how the dielectric constant changes under illumination as a function of time, in a range of MHPs. Both changes in photoconductance and change in dielectric constant are analyzed as a function of time, with nanosecond precision. We observe that photo-induced change in dielectric constant are roughly proportional to photo-induced carrier density but decay over different timescales, indicating that the presence of charge carriers alone is not the only factor in changes in polarizability.

[1] E. J. Juarez-Perez, R. S. Sanchez, L. Badia, G. Garcia-Belmonte, Y. S. Kang, I. Mora-Sero, and J. Bisquert, *Photoinduced Giant Dielectric Constant in Lead Halide Perovskite Solar Cells*, *J. Phys. Chem. Lett.* **5**, 2390 (2014).

8:50 AM EN06.10.06

3D-to-2D Transition of Anion Mobility in CsPbBr_3 Under Pressure Thijs Smolders, Matthew Wolf and Alison Walker; University of Bath, United Kingdom

Unlike typical inorganic semiconductors, lead–halide perovskites exhibit significant ionic conductivity, which is believed to affect their performance and stability. Here, we present a detailed theoretical study of the atomic scale effects of pressure on anion migration in the low temperature orthorhombic *Pnma* phase of CsPbBr₃, using nudged elastic band calculations based on density functional theory. We compute all symmetrically inequivalent activation barriers for anion migration to their closest neighbours, as a function of hydrostatic pressure in the range 0.0–2.0 GPa, which we then use as parameters in a kinetic model which allows us to connect the atomic scale calculations to the macroscopic anion mobility tensor as a function of applied pressure.

We find that the mobility is enhanced by pressure in the plane spanned by the [100] and [001] lattice directions, while along the [010] direction it is severely diminished, leading to an effective 3D-to-2D transition of the mobility at elevated pressures. This can be explained by the fact that a network of only a few symmetrically inequivalent paths dominates the mobility at elevated pressures. Our results demonstrate the significant influence of pressure on both the rate and direction of anion migration in CsPbBr₃, which we consider likely to hold for other lead–halide perovskites.

9:00 AM EN06.10.07

Nanotemplating Effects on the Thermodynamic Stability of Perovskite-Phase CsPbI₃ Arkita Chakrabarti and Aaron Fafarman; Drexel University, United States

Perovskite phase cesium lead iodide CsPbI₃ has emerged as a promising all-inorganic photovoltaic (PV) absorber material for its remarkable optoelectronic properties such as a suitable band gap, high absorptivity, high charge carrier lifetime and solution processability, all desired qualities for PV cells. However, under ambient conditions, CsPbI₃ transforms into a high density, non-functional, non-perovskite yellow phase. However, perovskite-phase CsPbI₃ can be stabilized in the form of quantum dots and thin films. Proceeding with the hypothesis that this is an effect of reduced dimensionality, we have sought a robust approach for enforcing controlled nanostructure. To do so, we synthesized CsPbI₃ in the pores of various inorganic scaffolds: prefabricated anodized aluminum oxide (AAO) membranes and TiO₂ nanoparticle scaffolds. Nano-structuring provides a truncated crystal lattice, which we hypothesize weakens the impact of the long-range, compressive electrostatic forces that act upon the CsPbI₃ unit cell. Under such reduced compression, we hypothesize that the lower density, black perovskite phase, is favored. Herein is described a study of phase transition thermodynamics of CsPbI₃ for perovskite synthesized in scaffolds with pore sizes ranging from few nanometers to mesoscopic dimensions. X-ray diffraction is employed to quantify the resulting expansion of the lattice. We found a 250 C drop in the phase transition temperature and enhanced thermal and moisture stability as a consequence of nano-templating in AAO with pore sizes lower than 80nm; crystals synthesized in larger pores and mesoscopic TiO₂ showed standard phase transition temperature of 330 C, consistent with bulk CsPbI₃. This approach could potentially stabilize the functional perovskite phase of CsPbI₃ at near ambient conditions.

9:10 AM EN06.10.08

Bridging the Defect Chemistry and Device Physics of Hybrid Perovskite Devices Davide Moia, Gee Yeong Kim, Ya-Ru Wang, Mina Jung, Alessandro Senocrate, Jaehyun Lee and Joachim Maier; Max Planck Institute for Solid State Research, Germany

Hybrid perovskites are the first photovoltaic material class presenting competitive solar cell performance and, at the same time, significant mixed ionic electronic conduction at room temperature. Several studies have pointed out that the long time scale electrical response of hybrid perovskite solar cells can be related to the migration of ionic defects in the material, specifically to electrode polarization, [1] stoichiometric polarization [2] and ionic-to-electronic current amplification. [3] Yet, quantitative information on the contribution of each of these processes as a function of device properties and working conditions is still missing to date. Given that long time scale behavior has direct consequences on the photo-conversion mechanism and long time scale degradation in these materials, it is desirable to develop comprehensive device models that successfully describe both electronic and ionic phenomena. Progress in the understanding of these aspects will enable improved device design and is a most urgent challenge in the field.

In this contribution, we address such question using a combined experimental and numerical approach. First, we evaluate the contribution of different ion-related processes on the electrical response of hybrid perovskite devices. We carry out electrochemical conductivity measurements while varying the iodine partial pressure during the measurement, the device contact materials and the electrode geometry. Our results show that the behavior of bulk and interfaces are different under dark equilibrium vs out of equilibrium conditions, with consequences on the interpretation of the long time scale response. The data also highlight the need to combine multiple techniques when quantifying charge carrier conductivities in hybrid perovskite devices under light or voltage bias.

Next, we develop and validate a model that encapsulates the ionic and electronic properties of perovskite based devices. Our approach combines knowledge on the analytical description of mixed conductors and of the electronic processes determining much of the electrical behavior in solar cells under operation. First, we map the functional dependence of the recombination currents in perovskite semiconductors as a function of recombination mechanism and working conditions. By coupling electronic generation and recombination to the drift diffusion equations of electronic and ionic charge carriers, we develop a model bearing analytical consistency with the expected semiconductor and mixed conductor physics of hybrid perovskites' bulk. We then consider different descriptions for the device interfaces, and highlight the importance of majority carriers' behavior at establishing charge carrier equilibrium and quasi-equilibrium at these boundaries. [4] Based on these considerations, we develop equivalent circuit models that simulate impedance spectra of hybrid perovskite devices. Our numerical results give supporting evidence for our interpretation of the experimental measurements on horizontal devices under dark or under illumination.

Finally, we critically assess the potential of our model and its applicability to the experimental characterization of solar cell devices. We demonstrate the generality of the model and present a number of approximated versions, which are relevant to hybrid perovskite, but also to other traditional photovoltaic materials. The proposed approach will aid the interpretation of electrical measurements on perovskite solar cells, with also implications on other mixed conducting devices.

[1] S. Ravishankar *et al.* *J. Phys. Chem. Lett.* **8**, 915 (2017).

[2] T. Y. Yang *et al.* *Angew. Chemie - Int. Ed.* **54**, 7905 (2015).

[3] D. Moia *et al.* *Energy Environ. Sci.* **12**, 1296 (2019).

[4] G. Y. Kim *et al.* *Adv. Funct. Mater.* **30**, 1 (2020).

9:20 AM EN06.10.09

Thermodynamics and Kinetics of Photo-Demixing and Dark-Remixing in Two-Dimensional Mixed Lead Halide Perovskites Ya-Ru Wang¹, Alessandro Senocrate¹, Gee Yeong Kim¹, Algirdas Dučinskas², Jovana V. Milić², Davide Moia¹, Michael Grätzel² and Joachim Maier¹; ¹Max Planck Institute for Solid State Research, Germany; ²EPFL, Switzerland

Mixed halide perovskites are promising materials for solar cells, light-emitting diodes and other optoelectronic devices due to their tunable bandgaps. However, under light, these systems show segregation into two phases with different halide compositions (photo-demixing). Interestingly, these two phases tend to remix back in the dark (dark-remixing)^[1]. This phase instability is undesirable when aiming for solar cells with stable output, while it opens opportunities towards new device architectures.^[2] The observed light-induced evolution of different phases involves significant ion transport. Therefore, an improved understanding of the underlying defect chemical mechanisms involved in photo-demixing (and dark remixing) can help both preventing and controlling this effect.

While several studies have characterized photo-demixing in 3D mixed halide perovskites, the role of decreasing dimensionality on this process has not yet been fully clarified. In the case of two-dimensional (2D) lead halide perovskites, increased resilience against intrinsic and extrinsic degradation routes has been attributed to the

suppression of ion migration in these materials with respect to the 3D counterparts.^[3-4] It is therefore interesting to probe how the photo-demixing relates to the structure and composition of these mixed halide perovskite systems.

Here, we demonstrate that also 2D mixed halide perovskites show reversible demixing under light. The kinetics of the process is slower for the 2D systems compared with their 3D counterpart. We investigate the evolution of optical and structural properties of 2D perovskite thin films under different light bias conditions, providing information on the thermodynamics and the kinetics of the photo-demixing and dark-remixing processes. These techniques, combined with in-situ conductivity measurements, also allow us to assess the influence of light intensity, thin-film composition, substrate, and encapsulation. Lastly, we propose a model that describes photo-demixing and dark-remixing in 2D mixed lead halide perovskites based on our previous analysis of the 3D systems.^[5] Our study contributes to defining the thermodynamic picture of 2D mixed halide perovskites, which will aid the compositional engineering of optoelectronic devices where photo-demixing is controlled.

[1] Hoke ET, Slotcavage DJ, Dohner ER, Bowring AR, Karunadasa HI, McGehee MD. Reversible photo-induced trap formation in mixed-halide hybrid perovskites for photovoltaics. *Chem Sci* 2015, 6(1): 613-617.

[2] Mao W, Hall CR, Bernardi S, Cheng YB, Widmer-Cooper A, Smith TA, et al. Light-induced reversal of ion segregation in mixed-halide perovskites. *Nat Mater* 2020.

[3] Cho J, DuBose JT, Le ANT, Kamat PV. Suppressed Halide Ion Migration in 2D Lead Halide Perovskites. *ACS Materials Letters* 2020.

[4] Grancini G, Nazeeruddin MK. Dimensional tailoring of hybrid perovskites for photovoltaics. *Nature Reviews Materials* 2019, 4(1): 4-22.

[5] Kim GY, Senocrate A, Wang Y-R, Moia D, Maier J. Photo-effect on ion transport in mixed cation and halide perovskites and implications for photo demixing. *Angewandte Chemie International Edition*, n/a(n/a).

9:30 AM EN06.10.11

Physical Passivation of Grain-Boundaries and Defects in Perovskite Solar Cells by PMMA Efrain Ochoa¹, Mario Ochoa², Roberto D. Ortuso¹, Parnian Ferdowsi¹, Romain Carron², Ayodhya Tiwari², Alke Petri-Fink¹, Ullrich Steiner¹ and Michael Saliba^{3,4}; ¹Adolphe Merkle Institute, Switzerland; ²Empa–Swiss Federal Laboratories for Materials Science and Technology, Switzerland; ³Institute for Photovoltaics (ipv), Germany; ⁴Forschungszentrum Jülich, Germany

The present study analyses the use of poly(methyl methacrylate) (PMMA) interlayers as passivation agents between the photoactive perovskite films and the carrier transport layers in Perovskite Solar Cells (PSCs). Our study finds that the deposited PMMA acts exclusively as a very good electrical isolator. By accumulation at perovskite grain boundaries and defects, it physically prevents charge carriers from reaching these locations, rather than chemically passivating electronic trap states that may arise from surface defects. Spin-coating a very low concentration PMMA solution onto perovskite layers increases the shunt resistance and the fill factor, without increasing the series resistance, giving rise to an improvement in cell efficiency.

The characterization of the degree of passivation provided has been assessed through spatially and time-resolved photoluminescence, while a detailed atomic force microscopy analysis, complemented with ellipsometric and electrical measurements, allows distinguishing the PMMA morphology once deposited onto the perovskite film and its effect on finished devices.

This mechanism should apply to any perovskite composition or device architecture. Since the perovskite remains in immediate contact with the surrounding carrier transport layers, this method can be used in combination with other surface passivation methods, which could be applied before or after the PMMA treatment.

9:40 AM EN06.10.12

Can Structuring Make Hybrid Perovskite's $A_xA'_{1-x}PbX_yX'_{1-y}$ Result in a More Effective Stand-Alone

Hybrid Solar PV Material? Edmund Chan, Ned Taylor and Steven P. Hepplestone; University of Exeter, United Kingdom

Hybrid perovskite solar cells (with chemical formula ABX_3) are of great interest due to the recently measured power conversion efficiency of greater than 25% (but theoretically, 33.7%). Perovskite structures are easily customisable, with a range of options for A, B and X. This enables us to both tune the electronic band gap and the stability by varying the composition. Two promising perovskites are the $CH_3NH_3PbI_3$ (MAPI) and $CH(NH_2)_2PbBr_3$ (FAPB) structures. By varying the ratio of FA and MA and doping with Br, we can potentially tune the band gap and effective masses (and hence electronic transport).

We present a theoretical investigation of the structural and electronic properties of $MA_xFA_{1-x}PI_yBr_{1-y}$, performed using first-principles density functional theory. Our results show that in a solid-state solution setting, decreasing fractions of y dominates the fall of cell volume which increases the band gap. We discuss why the formation energies at the most favourable ground-state hexagonal phase and the experimentally observed cubic phase vary in these compositions, including the effects of the rotation of the organic groups, affect the effective masses and, ultimately, the transport. We also explore the effects of clustering and intermixing on these structures and their stability.

In order to compromise for a more desirable bandgap for stand-alone PV and better structural stability, the hybrid perovskite constituents are then strategically layered, with n:1 ratio, into superlattice form. We explore the bulk properties and interfacial engineering to improve the material's electronic transport.

9:50 AM EN06.10.13

Voltage Bias Stress Effects in Metal Halide Perovskites Laura Flannery¹, Jonathan Ogle¹, Daniel Powell¹, Christopher Tassone² and Luisa Whittaker-Brooks¹; ¹The University of Utah, United States; ²Stanford Synchrotron Radiation Lightsource, United States

The solar-to-power power conversion efficiencies (PCEs) of metal halide perovskites (MHP) have been improved over the last decade using a wide variety of methods, such as composition manipulation, dopant introduction, and interfacial buffers. These methods, however, have taken little regard for the electronic and interfacial effects such alterations may cause within devices under voltage bias stress - a condition required for most device operation. Here, we investigate the effect of halide and cation substitution in MHP structures [mainly, $CH_3NH_3PbI_{2.87}Cl_{0.13}$ and $Cs_{0.1}(MA_{0.17}FA_{0.83})_{0.9}Pb(I_{0.83}Br_{0.17})_3$] to understand current behavior while under a range of voltage bias stress in both light and dark conditions. With the use of a second device structure, without transport layers, the same voltage bias stress effects unique to the different MHP structures are observed thus confirming that the difference in the current trends are due to intrinsic behavior of the perovskite structure, rather than interfacial recombination and interactions with the transport layers. We also determine how changes in morphology and crystallite orientation in $CH_3NH_3PbI_{2.87}Cl_{0.13}$ and $Cs_{0.1}(MA_{0.17}FA_{0.83})_{0.9}Pb(I_{0.83}Br_{0.17})_3$ thin film absorbers can influence ion migration and therefore alter charge transport and current stability in MHP photovoltaic devices.

10:00 AM EN06.10.14

Lead-Free $Cs_4CuSb_2Cl_{12}$ Layered Double Perovskite Nanocrystals Tong Cai, Wenwu Shi and Ou Chen; Brown University, United States

Concerns about the toxicity of lead-based perovskites have aroused great interest for the development of alternative lead-free perovskite-type materials. Recently, theoretical calculations predict that Pb^{2+} cations can be substituted by a combination of Cu^{2+} and Sb^{3+} cations to form a vacancy-ordered layered double perovskite structure with superior optoelectronic properties. However, accessibilities to this class of perovskite-type materials remain inadequate, hindering their practical implementations in various applications. Here, we report the first colloidal synthesis of $Cs_4CuSb_2Cl_{12}$ perovskite-type nanocrystals (NCs). The resulting NCs exhibit a layered double perovskite structure with ordered vacancies and a direct band gap of 1.79 eV. A

composition–structure–property relationship has been established by investigating a series of $\text{Cs}_4\text{Cu}_x\text{Ag}_{2-2x}\text{Sb}_2\text{Cl}_{12}$ perovskite-type NCs ($0 \leq x \leq 1$). The composition induced crystal structure transformation, and thus, the electronic band gap evolution has been explored by experimental observations and further confirmed by theoretical calculations. Taking advantage of both the unique electronic structure and solution processability, we demonstrate that the $\text{Cs}_4\text{CuSb}_2\text{Cl}_{12}$ NCs can be solution-processed as high-speed photodetectors with ultrafast photoresponse and narrow bandwidth. We anticipate that our study will prompt future research to design and fabricate novel and high-performance lead-free perovskite-type NCs for a range of applications.

10:10 AM EN06.10.15

Optical, Morphological and Electrical Characterization of Methyl Ammonium Lead Iodide Perovskite Films for Solar Cells Shambhavi R. Sakri, Liang-Chieh Ma, Bushra Alharbi and Anupama Kaul; University of North Texas, United States

There are varied approaches toward the synthesis of three-dimensional (3D) perovskites based on methyl-ammonium-lead-iodide ($\text{CH}_3\text{NH}_3\text{PbI}_3$) absorbers for solar cells which have now yielded power conversion efficiencies (PCEs) approaching $\sim 26\%$. In this work, we explored multiple synthesis routes to systematically optimize the films through a careful analysis of their optical, morphological and electrical characteristics. In the first technique, a stable Lewis base adduct solution of $\text{CH}_3\text{NH}_3\text{I}$ - PbI_2 -DMSO in dimethylformamide (DMF) is formulated, where an antisolvent of diethyl ether is gently cast on the adduct film during spin coating to reduce the rapid evaporation of DMF from the film surface. Through this careful control of the antisolvent, the growth kinetics lead to the evolution of the $\text{CH}_3\text{NH}_3\text{PbI}_3$ morphology from needle or rod-like toward the preferred platelet-like topology. Other commonly used anti-solvents such as toluene are limited in usage because they tend to wash off the dimethyl sulfoxide (DMSO) which contributes towards stability and reduction of pin-holes. In the second technique, $\text{CH}_3\text{NH}_3\text{I}$ and PbI_2 in a ratio of 1:3 by weight was stirred overnight at 60°C in gamma-butyrolactone. In this technique, grain growth of 3D perovskite crystal is primarily dependent on stirring time of the precursor solution and annealing temperature. The third technique involves a two-step approach where the PbI_2 (in DMF) and $\text{CH}_3\text{NH}_3\text{I}$ (in 2-propanol) precursors are deposited in succession on the substrate and annealed. Loading time, i.e. exposure of $\text{CH}_3\text{NH}_3\text{I}$ to PbI_2 before spinning is initiated, influences growth of the 3D perovskite on the mesoporous titanium dioxide, where the latter serves as the electron transport layer in the solar cell stack. The loading time was optimized to obtain a cuboid morphology with large size. We can confirm that our absorber is optically active with all the three techniques used, where a sharp photoluminescence peak of high intensity is obtained at the ideal location of ~ 774 nm. The onset of absorption in the UV-VIS spectra occurs at 826 nm and increases gradually up to 490 nm. The bandgap of our film calculated using the Tauc method was found to be consistent with our PL inferred bandgap at ~ 1.6 eV. From scanning electron microscopy (SEM) imaging, a uniform sized continuous granular platelet morphology of the absorber was evident for the optimized film, with a tightly controlled roughness as well. We calculate the average grain size, and a grain size of at least $1 \mu\text{m}$ in the homogeneous and smooth films is optimal for incorporation into the solar cell stack. The X-ray diffraction (XRD) analysis shows characteristic peaks for the tetragonal perovskite structure at room temperature. Current-voltage characteristics revealed that the absorber was electrically conductive in the dark and under illumination for our photo-responsive measurements, prior to its integration into the solar cell stack for the PCE characterization studies.

10:20 AM EN06.10.18

Interfacial Trap-Assisted Triplet Generation in Lead Halide Perovskite Sensitized Solid-State Upconversion Lili Wang; Massachusetts Institute of Technology, United States

Photon upconversion via triplet-triplet annihilation (TTA) has promise for overcoming the Shockley–Queisser efficiency limit for single-junction solar cells by allowing the utilization of sub-bandgap photons. Recently, bulk perovskites have been employed as sensitizers in solid-state upconversion devices to circumvent poor exciton diffusion observed in previous nanocrystal-sensitized devices. However, an in-depth understanding of the underlying photophysics of perovskite-sensitized triplet generation is still lacking due to the difficulty of

precisely controlling interfacial properties in fully solution-processed devices. In this study, interfacial properties of upconversion devices are adjusted by a mild surface solvent treatment, which specifically alters perovskite surface properties without perturbing the bulk, and thermal evaporation of the annihilator precludes further solvent contamination. Sequential charge transfer and interfacial trap-assisted triplet sensitization are demonstrated by comparing the upconversion performance, transient dynamics, and magnetic field dependence of the upconversion devices. Incomplete triplet conversion from transferred charges and consequent triplet-charge annihilation (TCA) are also confirmed as two limiting factors for upconversion performance. Our observations highlight the importance of controlling interfacial properties and provide guidance for further device design and optimization of upconversion devices using perovskites or other semiconductors as sensitizers.

10:30 AM EN06.10.19

Improved Crystallization of Triple Cation Perovskites Assisted by Mixed Antisolvents for High Performing Solar Cells Banashree Gogoi, Aditya S. Yerramilli, Terry Alford and William Petuskey; Arizona State University, United States

In the case of Perovskite solar cells, the active perovskite layer acts as a crucial component in influencing the solar cell's efficiency. Crack free perovskite films with enlarged grain size are essential for a highly efficient solar cell. Triple cation perovskite mainly relies on solvent-antisolvent engineering for achieving good crystal growth and enlarged grains. In recent years many kinds of research have been done involving antisolvents in Triple cation perovskites. The Antisolvent assisted crystallization (ASAC) method is considered one such way to obtain better film quality. However, the perovskite films prepared by this ASAC method still suffers from low coverage and rapid degradation. Thus, the choice of antisolvent or mixture of antisolvents can be crucial in effectively precipitating the perovskite and demonstrating high efficiency. To achieve an ideal choice of antisolvents, we have examined a mixture consisting of Ethyl acetate (EA) with Chlorobenzene (CB) and EA with Isopropyl alcohol (IPA) in different ratios for the fabrication of the perovskite layer. In this case, EA acts as a solvent that will assist in dissolving the excess perovskite precursor due to its polar nature; and, IPA and CB will enhance crystallization by reducing the solubility of the perovskite. The devices fabricated using these mixtures of antisolvents improved efficiency by more than 13% when compared to only 8% for those prepared using only EA, CB, and IPA individually. High quality, crack free perovskite layers with enhanced grain sizes were attained from using mixtures of CB and EA, which lead to improved photovoltaic properties.

10:40 AM EN06.10.20

Strain in Ruddlesden-Popper Films with Target- n Emission Rhys M. Kennard¹, Clayton J. Dahlman¹, Juil (Jay) Chung¹, Benjamin L. Cotts², Naveen R. Venkatesan¹, Ryan DeCrescent¹, Lingling Mao¹, Alberto Salleo², Jon A. Schuller¹, Ram Seshadri^{1,1} and Michael Chabinye¹; ¹University of California, Santa Barbara, United States; ²Stanford University, United States

Keywords: Strain engineering, structural formulation, light-matter interaction, 2D films, phase purity, photoluminescence emission.

Two-dimensional Ruddlesden-Popper (RP) hybrid perovskites have been instrumental to the unprecedented development in the areas of energy harvesting and light emission technologies, as well as to studying cutting-edge fundamental science. RP formulations exhibit the $(A')_2(A)_{n-1}B_nX_{3n+1}$ structure, where A' is the spacer cation between A -Pb-X sheets, the A cation residues between Pb-X octahedra and X is a halide. A major challenge surrounding RP hybrid perovskites with $n > 1$ has been poor phase control when casting the materials as films. Competing reaction pathways and stacking faults cause phase heterogeneity at the nanoscale, inducing charge carrier funneling to the lowest-bandgap phase, and poor optoelectronic control. This prohibits both fundamental film characterizations and use of RP formulations in photodetector and light-emitting devices.

Here, we experimentally identified A' and A -site cations for which large- n RP films retain the photoluminescence emission of the single crystal formulations. Notably, the emission did not contain undesired

n RP emission, nor the large 3D-like emission typical of other spin-cast RP films. We correlated changes in the proportions of different emissive features with strain and morphology, and further controlled emission using small amounts of additives. These results will help push RP-based perovskite fundamental characterization and energy-based technologies to the next level.

10:50 AM EN06.10.22

Effect of the Chemical Composition on Structural, Thermodynamical and Mechanical Properties of CsBX₃ (B = Pb, Sn; X = Cl, Br) All-Inorganic Perovskites Pablo Sánchez-Palencia Vallejo^{1,2}, Gregorio García Moreno^{1,2}, Perla Wahnón Benarroch^{1,2} and Pablo Palacios Clemente^{3,2}; ¹Universidad Politécnica de Madrid, E.T.S.I. Telecomunicación, Spain; ²Universidad Politécnica de Madrid, Instituto de Energía Solar, Spain; ³Universidad Politécnica de Madrid, E.T.S.I. Aeronáutica y del Espacio, Spain

Despite their vertiginous growth in power conversion efficiency (PCE) terms and their ultra-competitive cost, perovskite solar cells (PSC) carry stability as their main warhorse towards commercialization. Pursuing solutions to a key problem of instability in most commonly used MAPbI₃ caused by the rotation of the complex organic molecules located in the A position (chemical formulae ABX₃), all-inorganic perovskites like CsPbI₃ and relatives are attracting considerable attention, although in comparison they present only promising results yet, being necessary a profound study of their properties to overcome new problems. Set the focus on stability, a review of the main structural, thermodynamical and mechanical properties of all-inorganic halide perovskites with general formula CsPb_{1-b}Sn_b(I_{1-x}Br_x)₃ is flagged as crucial, with the goal of elucidate the connection of those properties with the stability and its dependence upon the composition of the compounds.

In this work, a DFT-based study has been performed, allowing to cover a wide range of chemical compositions and knowing in detail how the composition changes affect those different properties and consequently the stability. Firstly, stability has been assessed through a series of structural tolerance parameters, like the Goldschmidt factor, the Sun's parameter and the intrinsic hardness. Also, thermodynamical stability in terms of formation enthalpies considering different competitor phases and compounds have been evaluated according to standard procedures. Furthermore, several mechanical properties defining response to different kind of stresses, as an important characteristic for their integration in complex multilayer devices or flexible and wearable applications, having also a big impact on their absorptivity which relies on their crystallinity and stress state, have been obtained from the elastic constants following the stress-strain methodology. All those properties will define a complete set that properly describes the different facets of the intrinsic stability of these halide perovskites and their correlation, providing a guide of how to improve that weak point through composition engineering.

11:00 AM EN06.10.23

Exciton Fine Structure of Individual CsPbBr₃ Nanoplatelets in a Vector Magnetic Field Alexander Schmitz^{1,1}, Federico Montanarella², Maksym Kovalenko² and Gerd Bacher^{1,1}; ¹Universität Duisburg-Essen, Germany; ²ETH Zürich, Switzerland

Nanoplatelets (NPL) of all-inorganic perovskites are promising candidates for application in light-emitting devices due to their high exciton binding energy, their exceptionally high quantum efficiency, and their improved stability.¹ While quantum dots of this material class have been studied excessively in the weak or intermediate quantum confinement regime providing interesting information on their exciton fine structure^{2,3}, such signatures are expected to be strongly modified when introducing strong confinement conditions in a selected direction, as in nanoplatelets.

In this work, we examine the exciton fine structure of individual CsPbBr₃ nanoplatelets with a thickness of five monolayers at cryogenic temperatures by means of polarization-resolved micro-photoluminescence spectroscopy. We find photoluminescence signatures comprised of either two or three clearly resolvable emission lines with linewidths down to 300 μ eV and a fine structure splitting of \sim 1 meV. Such splitting has already been observed in quantum dots of the same material and was attributed to intrinsic Rashba effects in the orthorhombic structure.³ The two lowest energy emissions exhibit strong linear polarization of up to > 90 %

with orthogonal polarization directions, corresponding to the dominant lateral crystal axis. This correlation enables us to derive the relative orientation of the NPL under investigation relative to the observation direction and substrate orientation.

To further elucidate the exciton fine structure, we apply a rotating vector magnet field of up to 5 T to the individual NPLs. The observed emission lines split up into doublets with rising magnetic field, with an average splitting of $\sim 300 \mu\text{eV}$ at 5 T. This behavior clearly indicates that all three emission lines are spin-degenerate at zero field and it yields a small effective g-factor of < 1.1 for the strongly confined perovskites. A systematic study of a variety of individual NPLs in the vector magnetic field further yields insights into the anisotropy of the exciton fine structure.

References

¹ Bertolotti *et al.* (2019): ACS Nano 13 (12), S. 14294. DOI: 10.1021/acsnano.9b07626.

² Pffingsten *et al.* (2018): Nano Lett. 18 (7), S. 4440. DOI: 10.1021/acs.nanolett.8b01523.

³ Becker *et al.* (2018): Nature 553 (7687), S. 189. DOI: 10.1038/nature25147.

11:10 AM EN06.10.24

Enhanced Optical Absorption via Mixed-Valent Doping of Vacancy-Ordered $\text{A}_3\text{B}_2\text{X}_9$ Triple Perovskites

Seán R. Kavanagh^{1,2,2}, Aron Walsh², David O. Scanlon¹ and Robert Palgrave¹; ¹University College London, United Kingdom; ²Imperial College London, United Kingdom

Vacancy-ordered triple perovskites have recently come under the scientific spotlight as promising materials for high-performance next-generation optoelectronic technologies.¹⁻³ Their $\text{A}_3\text{B}_2\text{X}_9$ stoichiometry facilitates the replacement of the toxic Pb^{2+} cation with a benign isoelectronic B^{3+} cation (e.g. Bi^{3+} or Sb^{3+}) while preserving the perovskite crystal structure. Unfortunately, however, these materials tend to exhibit large bandgaps (> 2 eV), impeding their application in many photo-catalytic/voltaic devices.^{3,4}

In this work, we demonstrate a drastic shift of over 1 eV in the optical absorption onset of $\text{Cs}_3\text{Bi}_2\text{Br}_9$ (from 2.58 eV to 1.39 eV), upon doping with tin. The origin of this broadband absorption is identified through a combination of detailed theoretical and experimental characterization of this novel material. Sn atoms are found to disproportionate in the doped material, inducing a strong intervalence charge transfer (IVCT) transition, whilst preserving the structural integrity of the perovskite framework. Moreover, using hybrid Density Functional Theory, including spin-orbit coupling effects, alongside the Marcus-Hush theory of IVCT behavior, we comprehensively elucidate the origin of unusual concentration dependence of absorption in the doped perovskite.

Our work provides valuable insight regarding the effects of mixed-valency and structure-property relationships in perovskite-inspired materials, guiding design strategies and expanding the compositional space of candidate materials. Furthermore, we anticipate that this massive reduction in absorption onset could aid charge transport and/or photo-catalytic performance, opening the door to unexplored applications of this material class.

¹ Y.-T. Huang, **S.R. Kavanagh**, D.O. Scanlon, A. Walsh, and R.L.Z. Hoye, ArXiv:2008.08959 (2020).

² **S.R. Kavanagh**, Z. Li, M. Napari, R.G. Palgrave, M. Abdi-Jalebi, Z. Andaji-Garmaroudi, D.W. Davies, M. Laitinen, J. Julin, M.A. Isaacs, R.H. Friend, D.O. Scanlon, A. Walsh, and R.L.Z. Hoye, J. Mater. Chem. A **8**, 21780 (2020).

³ M. Buchanan, Nature Physics **16**, 996 (2020).

⁴ K.K. Bass, L. Estergreen, C.N. Savory, J. Buckeridge, D.O. Scanlon, P.I. Djurovich, S.E. Bradforth, M.E. Thompson, and B.C. Melot, Inorg. Chem. **56**, 42 (2017).

⁵ R. Nie, R.R. Sumukam, S.H. Reddy, M. Banavoth, and S.I. Seok, Energy Environ. Sci. **13**, 2363 (2020).

11:20 AM EN06.10.25

Temperature-Dependent Ferroelectric Measurement of Methylammonium Lead Iodide Allen Zhao^{1,2}, Zhaoning Song¹, Rasha Awni¹, Manoj Jamarkattel¹, Michael Heben¹ and Yanfa Yan¹; ¹The University of Toledo, United States; ²University of Michigan–Ann Arbor, United States

Organic-inorganic metal halide perovskites are a family of semiconductor materials with a number of unique and multifaceted optoelectronic properties, making it suitable for a wide range of applications. Despite the rapid progress of halide perovskite research in recent years, many challenges remain in understanding the fundamental properties of these materials. Among them, probing the ferroelectric response of halide perovskite-based devices has been shown to be challenging due to the soft lattice of halide perovskite and the large electronic and ionic contributions to conductivity. To date, there is limited research on ferroelectricity in metal halide perovskite thin films, and as a result, the existence and impact of these ferroelectric characteristics remain under debate. Here, we use a facile Sawyer-Tower measurement circuit with tunable stimulated frequencies to measure the ferroelectric hysteresis loop of perovskite capacitors and photodiodes at temperatures varying from 90 to 300 K. Utilizing this setup, we investigated variations in the polarization-electric field (P-E) hysteresis of different perovskite-based devices as a result of increasing and decreasing temperatures. We observed different temperature-dependent hysteresis behaviors in capacitors and photodiodes based on a prototype perovskite, methylammonium lead iodide ($\text{CH}_3\text{NH}_3\text{PbI}_3$). It was noted that the critical points of change in the P-E curves of these devices were observed at $\sim 150\text{K}$, which is attributed to the phase transition from the tetragonal to the orthorhombic crystal structure resulting from the temperature change. The Sawyer-Tower measurements, combined with thermal admittance spectroscopy measurements provide insights to understanding the material and device properties of halide perovskites.

This work is supported by National Science Foundation under contract number DMR-1807818.

11:30 AM EN06.10.26

Impact of Processing and Solution Engineering on the Film Formation of Lead-Free Halide Double Perovskite $\text{Cs}_2\text{AgBiBr}_6$ Maged A. Abdelsamie¹, Finn Babbe¹, Kevin Cruse², Gerbrand Ceder² and Carolin M. Sutter-Fella¹; ¹Lawrence Berkeley National Laboratory, United States; ²University of California, Berkeley, United States

Lead-Free halide double perovskites with enhanced stability have gained attention as a promising environmentally friendly alternative to lead halide perovskites. Amongst different halide double perovskites, $\text{Cs}_2\text{AgBiBr}_6$ has shown attractive optoelectronic properties and stability, making it a promising candidate for stable high-efficiency optoelectronic devices. Motivated by a text-mining effort that not only illustrates the prevalence of powder over thin-film synthesis but also the discrepancy between the number of compositions experimentally realized and studied as compared to the many predicted compositions we present here on the intricacies of thin-film synthesis of $\text{Cs}_2\text{AgBiBr}_6$. Understanding the role of processing strategies on film formation pathways is of crucial importance as crystallization strongly affects the film microstructure, stability, and functionality in optoelectronic devices. Herein, using time-resolved spectroscopy, we investigate the film formation of $\text{Cs}_2\text{AgBiBr}_6$ *in situ* during blade-coating, spin coating, and the subsequent post-deposition thermal annealing under different processing conditions including antisolvent- and additive (HBr)-assisted synthesis. We show how different processing routes affect the film formation and microstructure of $\text{Cs}_2\text{AgBiBr}_6$. For films prepared by spin-coating and thermal annealing, we show that dropping anti-solvents during spin coating induces immediate supersaturation and crystallization of the wet film, whereas the time point of dropping the antisolvent has implications on the film formation dynamics and the final microstructure. Furthermore, due to the limited solubility of precursor salts, the thickness of the films is constrained by the low concentration of the precursor solution. HBr additive increases the solubility of precursor salts allowing to obtain thicker and pinhole-free films. We also show how the addition of HBr induces colloid formation in solution and thus influences the crystallization pathway during thin-film processing. For films prepared by blade-coating, our findings reveal that using blade-coating not only affects the crystallization pathway but also promotes the formation of highly crystalline films with preferential orientation as compared to films prepared by spin-coating followed by thermal annealing. Our work highlights the importance of real-time investigations to provide a mechanistic understanding of film formation and therefore can inform synthetic parameter choice.

11:40 AM EN06.10.28

Late News: An Efficient and Hydrophobic Molecular Doping for High-Efficiency and Stable Perovskite Solar Cells Junsheng Luo; University of Electronic Science and Technology of China, China

Longevity has been a long-standing challenge for perovskite photovoltaics. In general, Li-TFSI/*t*-BP are the state-of-the-art bi-dopants for the hole-transporting layer (HTL) in perovskite solar cells (PSCs), although such dopants significantly diminish the stability of devices. Here, we reported a novel dopant of fluorinated iron(III) porphine (Fe(III)-PP) as a potential alternative to the Li-TFSI/*t*-BP. The optimized PSCs exhibit a champion power conversion efficiency (PCE) of 21.734%, which is the highest efficiency among the ever reported PSCs based on novel dopant in HTL and also outperforms the standard bi-dopants Li-TFSI/*t*-BP (21.065%). The high migration barrier together with the hydrophobic nature of the Fe(III)-PP, which in turn suppress intrinsic ion migration and alleviate extrinsic moisture-induced degradation, resulting in prominent improvement of long-term stability of PSCs up to 1200 h under air exposure without encapsulation.

11:50 AM EN06.10.29

Late News: Applying Small Perturbation Techniques on Perovskite Solar Cells—Combining Experiments with Drift Diffusion Modelling Antonio J. Riquelme¹, Lawrence Bennett², Francisco Gálvez¹, Nicola Courtier², Lidia Contreras-Bernal^{1,3}, Matthew Wolf⁴, Hernan Miguez³, Alison Walker⁴, Giles Richardson² and Juan Anta¹; ¹Universidad Pablo de Olavide, Spain; ²University of Southampton, United Kingdom; ³Centro de Investigación Superiores Científicas, Spain; ⁴University of Bath, United Kingdom

Metal Halide Perovskites (MHPs) are mixed electronic–ionic semiconductors with an extraordinary complex optoelectronic behaviour and a record efficiency surpassing 25%. Interpreting small perturbation response of perovskite solar cells (PSCs) is significantly more challenging than for most other photovoltaics. This is for a variety of reasons, of which the most significant are the mixed ionic-electronic conduction properties of metal halide perovskites and the difficulty in fabricating stable, and reproducible, devices. Experimental studies, conducted on a variety of PSCs, produce a variety of spectra shapes, with different physical interpretations. The impedance response has commonly been analyzed in terms of sophisticated equivalent circuits that can be hard to relate to the underlying physics and which complicates the extraction of efficiency-determining parameters. By a combination of experiment and drift-diffusion (DD) modelling of the ion and charge carrier transport and recombination within the cell, the main features of common impedance spectra are well reproduced by the DD simulation. Based on this comparison, we show that the high frequency response contains all the key information relating to the steady-state performance of a PSC, focusing on the charge collection efficiency of the device. We also analyze Intensity Modulated Photocurrent Spectroscopy (IMPS) data in MHPs based on the analysis of the internal quantum efficiency, connecting them to the charge collection obtained from Impedance, and the time signals featuring in the frequency spectra. We look at the change of each signal when optical excitation wavelength, photon flux, and temperature are varied for an archetypical methyl ammonium lead iodide solar cell. We compare the Perovskite IMPS results with relatively simpler dye-sensitized solar cells (DSC) with viscous and non-viscous electrolytes to help us to understand the origin of the three signals appearing in MHP cells and the measurement of the internal quantum efficiency.

12:00 PM EN06.10.30

Late News: On the Origin of Current Losses in Lead-Tin Perovskite Solar Cells and Beyond Jarla Thiesbrummel¹, Vincent M. Corre², Carlos Peña-Camargo², Fengjiu Yang³, Steve Albrecht³, Dieter Neher², Henry J. Snaith¹ and Martin Stollerfoht²; ¹University of Oxford, United Kingdom; ²University of Potsdam, Germany; ³Helmholtz-Zentrum Berlin, Germany

The power conversion efficiency of mixed metal lead-tin perovskite solar cells still lags behind those of their full-lead equivalents. One reason for this is that Sn²⁺ is easily oxidised to Sn⁴⁺, which leads to the formation of charge carrier trap states and to p-doping. Though several strategies have been developed to prevent or limit this oxidation, the degradation of the perovskite layers upon exposure to oxygen remains problematic. Moreover, the

exact influence of self-doping on the performance of lead-tin perovskites is poorly understood. On top of that, other factors that could strongly affect device performance, such as the influence of mobile ions, have barely been explored for this system. Here, we take a closer look at the origin of current losses in lead-tin perovskite solar cells and find that, beside optical losses, the cells also suffer from significant charge collection losses. Voltage dependent photoluminescence (PL) measurements at open-circuit (V_{oc}) demonstrate a significant reduction in PL upon a switch from open- to short-circuit, indicative of efficient charge extraction. However, then the PL rises again over the course of several seconds, before stabilising at about 6% of the PL value obtained at V_{oc} . The current decays on the same timescales as the extraction becomes less efficient due to band flattening, amounting to a loss of 1.4 mA cm^{-2} under 1 sun illumination. In the following, we show that the reduction in the charge extraction efficiency and band flattening is linked to the movement of mobile ions in the perovskite rather than electronic charge (doping) and we show that this effect is well reproduced by numerical simulations. Importantly, as far as we could assess in this research, doping in mixed lead-tin perovskites is not directly causing current losses as the doping density is insufficient to screen the built-in field. Finally, we generalise our findings to lead-based perovskites, where we also find that the timescales of the band flattening and current loss correspond to the timescales of mobile ions. Hence, the mechanisms appear to be generic for Pb and Pb/Sn based perovskites, which paves the way towards understanding a key loss mechanism in perovskite cells.

12:10 PM EN06.10.31

Late News: Nonlinear Band Gap Dependence of Mixed B-Site 2D Ruddlesden-Popper Perovskites

Cameron Underwood, David Carey and S. Ravi P. Silva; Advanced Technology Institute, University of Surrey, United Kingdom

Ruddlesden-Popper phase (RPP) perovskites have the general form $A_{1-n-1}A_2B_nX_{3n+1}$. The reduced dimensionality and structural characteristics of RPPs reportedly improve the stability of these crystals in comparison to their 3D perovskite counterparts¹. Two dimensional (2D) Ruddlesden-Popper perovskites (RPPs) of the form ABX_4 can be used as the tunable active layer in photovoltaics, as the passivating layer for 3D perovskite photovoltaics or as light emitting diodes.

Here we show a nonlinear band gap behaviour with Sn content in mixed phase 2D RPPs of the form $AB_{1-x}B_2xI_4$. GGA level density functional theory calculations (with and without spin-orbit coupling) are employed to study the effects of the short range ordering of B1 and B2 in $AB_{1-x}B_2xI_4$ compositions with $x = 0, 0.25, 0.5, 0.75$ and 1. The origins of the nonlinearity are shown to be due to the chemical behaviour of the relative energies of the B s states in the VBM composition, much like in 3D perovskites². This is also influenced by the relative X-B-X angles, where increased angles result in a higher overlap between X and B orbitals, resulting in a higher dispersion and a decreased band gap. The short range ordering of B site atoms is discussed, especially in the case of $x = 0.5$, where the short range ordering is most significant, the band gap energy is shown to be dependant on this. We have also highlighted the role of using SOC in calculations of 2D RPPs, discussing that SOC does not significantly affect the nonlinearity of the band gap, but strongly affects the linear term, and is also crucial for understanding other electronic properties of 2D RPPs, such as accurate effective masses. This research underlines the importance of supercell permutations as well as providing a good platform to study other 2D perovskites, such as other A sites, other mixed B sites, or mixed halide RPPs.

[1] - Spanopoulos, I.; Hadar, I.; Ke, W.; Tu, Q.; Chen, M.; Tsai, H.; He, Y.; Shekhawat, G.; Dravid, V. P.; Wasielewski, M. R., et al. Uniaxial Expansion of the 2D Ruddlesden-Popper Perovskite Family for Improved

Environmental Stability. Journal of the American Chemical Society 2019, 141, 5518–5534.

[2] - Goyal, A.; McKechnie, S.; Pashov, D.; Tumas, W.; Van Schilfgaarde, M.; Stevanovic, V. Origin of Pronounced Nonlinear Band Gap Behavior in Lead–Tin Hybrid Perovskite Alloys. Chem. Mater. 2018, 30, 3920–3928.

12:20 PM EN06.10.32

Late News: DFT Calculations of Neutral and Charged Tin-Halide Perovskites Cameron Underwood¹, Zhou Wang², Guosheng Shao², David Carey¹ and S. Ravi P. Silva¹; ¹Advanced Technology Institute, University of Surrey, United Kingdom; ²Zhengzhou University, China

3D bulk perovskites have shown amazing promise as photovoltaic devices, but are still curbed by various instabilities. Sn based perovskites in particular are extremely susceptible to oxidation in both air and moisture. We report on the evolution of the electronic structure with partial oxidation state of tin and iodine from ASnI_3 to a charged system of $[\text{ASnI}_3]^{2+}$, where A = CH_3NH_3 (MA), $\text{CH}(\text{NH}_2)_2$ (FA) or Cs. When a simulated charge cell is tested, most of the charge is reduced in the SnI_3 unit due to the valence band edge being dominated by Sn 5s and I 5p antibonding states, this charge reduction is accompanied by a reduction in unit cell volume in $[\text{ASnI}_3]^{2+}$ compared to ASnI_3 . Generalized gradient approximation (GGA) level density functional theory (DFT) band structure calculations with spin orbit coupling show semiconducting behaviour in ASnI_3 , with metallic behaviour in $[\text{ASnI}_3]^{2+}$. We also show a similar behaviour for APbI_3 and $[\text{APbI}_3]^{2+}$, where the Pb atoms lose less partial charge than Sn due to the higher relative energy of the Pb 6s states compared to Sn 5s states. Phonon band structure calculations show an increase in imaginary modes in the charged system, for both Sn and Pb based systems.

12:30 PM EN06.10.33

Late News: Multi-Functional Conjugated Ligand Engineering for Stable and Efficient Perovskite Solar Cells Ke Ma and Letian Dou; Purdue University, United States

With the advancement in understanding the device physics of perovskite solar cells, tremendous attention has been paid on the interface between perovskite layer and the charge transporting layer, where the significant efficiency loss and degradation occur. Surface passivation is an effective way to improve the efficiency and stability of perovskite solar cells. However, a key challenge faced by most of the passivation strategies is reducing the interface charge recombination while avoiding imposing energy barriers to charge extraction. This is usually achieved through fine control of the passivation process. In this talk, I will present a novel multi-functional semiconducting organic ammonium cationic interface modifier for post-treatment of the perovskite surface, to overcome this dilemma through molecular engineering. The conjugated organic ammonium halide salt can simultaneously facilitate charge extraction, improve energy level alignment, reduce interface recombination, and stabilize the perovskite lattice. The conjugated ligand treatment also exhibits a high degree of tolerance to the capping condition and capping layer thickness, owing to its semiconducting properties. Based on this strategy, a triple-cation mixed-halide medium-bandgap perovskite solar cell is delivered with an excellent power conversion efficiency of 22.06% (improved from 19.94%). More interesting, the ion migration and halide phase segregation in perovskite films are significantly suppressed due to the lattice anchoring effect of conjugated ligand, which lead to a long-term stability of over 1000 hours under continuous illumination. Our molecular engineering strategy provides a new practical method of interface engineering in perovskite solar cells towards improved efficiency and stability.

12:40 PM EN06.10.34

Late News: A Strategy for Constructing Dispiro-Based Dopant-Free Hole-Transporting Material—Spatial Configuration of Spiro-bifluorene Changes from Perpendicular to Parallel Arrangement Zhongquan Wan; University of Electronic Science and Technology of China, China

Due to the low intrinsic hole mobility caused by orthogonal conformation of two fluorene units in Spiro-

OMeTAD which is a classic hole-transporting material (HTM) in perovskite solar cells (PSCs), Spiro-OMeTAD based PSCs generally can only obtain high performances through a sophisticated doping process with dopants/additives which adds to the cost and complicity of device fabrication, but also adversely affects the stability of PSC device. Herein, a novel dispiro-based HTM, WH-1, is designed by cleverly replacing the central carbon atom of Spiro-OMeTAD with cyclohexane, and the spatial configuration of HTM is changed from vertical orthogonality of the two fluorene units to parallel arrangement, which is beneficial to the formation of homogeneous and compact HTM film on the surface of perovskite film, improvement of intermolecular electronic coupling and intrinsic hole mobility. WH-1 is obtained in a two-step facile synthesis with a high yield from commercially available materials. WH-1 is used in PSCs as dopant-free HTM, which is the first time that the dispiro-based molecule is applied as dopant-free HTM, and power conversion efficiency (PCE) of 19.57% is obtained, rivaling Li-TFSI/t-BP doped Spiro-OMeTAD in PCE (20.29%), and showing obvious superior long-term stability.

12:50 PM EN06.10.35

Late News: A Periodic Half-Cylinder Photonic Plate to Polarize and Recycle Light Using Perovskite Solar Cells Applicable to Liquid Crystal Displays Guillermo Martínez-Denegri¹, Catarina G. Ferreira¹, Johann Toudert¹, Mariia Kramarenko¹, Paul Fassl^{2,3}, Marco A. Ruiz-Preciado^{2,3}, Saba Gharibzadeh^{2,3}, Ulrich W. Paetzold^{2,3} and Jordi Martorell^{1,4}; ¹ICFO - Institute of Photonic Sciences, Spain; ²Light Technology Institute - Karlsruhe Institute of Technology, Germany; ³Institute of Microstructure Technology - Karlsruhe Institute of Technology, Germany; ⁴Universitat Politècnica de Catalunya, Spain

Liquid crystal displays (LCDs) are widely used to obtain high resolution full color images in many electronic devices. Unfortunately, such devices are far from being energetically efficient. In fact, in current portable electronics or large TV monitor screens based on LCDs, a considerable amount of light emitted by the light-emitting diodes does not reach the eye of the user but instead it is lost as heat somewhere in the device. Here, we propose a novel light guiding system which we name half-Cylinder Photonic Plate (h-CPP). The h-CPP is based on a periodic array of intercalated half-cylinders where light propagates chaotically and transversally to the cylinders, exiting the array from the top surface with a diffused light intensity pattern. By applying inverse electromagnetic design to modify the optical properties of such periodic array surface, we are able to induce a lossless polarization selectivity which can be made suitable for LCD applications. Furthermore, the design of the h-CPP allows to collect the non-transmitted light, unusable for the display and otherwise wasted, by two perovskite solar cells. Thereby, this light can be recycled back to electricity, considerably increasing the overall device efficiency. Based on such h-CPP, we will present a combination of numerical and experimental results demonstrating the polarization as well as light recycling capacities of our novel design.

1:00 PM EN06.10.36

Investigation of Heterogeneous Charge Trapping Dynamics at Nanoscale Defects in Triple Cation Mixed Halide Perovskite Thin Films Sofia Kosar¹, Andrew Winchester¹, Stuart Macpherson², Christopher E. Petoukhoff¹, Julien Madéo¹, Michael K. Man¹, Samuel Stranks² and Keshav M. Dani¹; ¹Okinawa Institute of Science and Technology, Japan; ²University of Cambridge, United Kingdom

Hybrid organic-inorganic perovskites (HOIPs) have been introduced as promising semiconductor materials for fabrication of photovoltaic (PV) devices about a decade ago [1]. Since then the photoconversion efficiencies of record HOIP PV devices have exceeded 25 % [2], which approaches efficiencies of traditional single crystal Si solar cells. Nevertheless, theoretical calculations predict that there is potential to boost the efficiency of HOIP PV devices even further, to more than 30 % [3]. However, to do so we need to first overcome limitations that prevent these materials from reaching their theoretical efficiencies.

One of the main performance-limiting factors for HOIP PVs has been attributed to the presence of non-radiative losses [4]. These non-radiative losses have been shown to be inhomogeneously distributed at the nanoscale, implying local carrier trapping. Therefore, understanding the nature of these non-radiative losses and their detrimental impact on PV device performance, requires use of techniques having high degrees of spatial and

temporal resolution. Recently, using a custom-designed time-resolved photoemission electron microscope (TR-PEEM), we have directly imaged nanoscale distribution of defects that induce non-radiative losses in HOIP thin films, identified their formation sites with respect to surface microstructure, and revealed their hole-trapping nature [5].

Here, we further elucidate the nature of nanoscale defects in triple cation mixed halide perovskite thin films that have been fabricated by solution-processing methods. We employ the TR-PEEM technique to explore the nanoscale electronic properties of these defects, including their spatial distribution, energy-level position within the band gap, and their charge trapping dynamics. We correlate these defects to non-radiative recombination sites, and to the surface morphology. We find the presence of multiple types of defects, the formation of which is related to the growth stoichiometry. We reveal that these nanoscale defects have inhomogeneities in their charge trapping dynamics. Our study provides insight into the relationship between composition of HOIP thin films and formation of nanoscale performance-limiting defects.

References: [1] Kojima *et al.*, *J. Am. Chem. Soc.*, 131, 17, 6050 – 6051 (2009); [2] Best Research-Cell Efficiency Chart, nrel.gov (2020); [3] Park and Segawa, *ACS Photonics* 5, 8, 2970 - 2977 (2018); [4] Stranks, *ACS Energy Lett.*, 2, 7, 1515 - 1525 (2017); [5] Doherty, Winchester *et al.*, *Nature*, 580, 360 - 366 (2020).

1:10 PM EN06.10.37

Photo-Effect on Ion Transport in Mixed Cation and Halide Perovskites and Implications for Photo Demixing Ya-Ru Wang, Gee Yeong Kim, Alessandro Senocrate, Davide Moia and Joachim Maier; Max Planck Institute for Solid State Research, Germany

Since the discovery of anomalous polarization phenomena in solar cells based on organic-inorganic hybrid perovskites, much attention has been devoted to the mixed ionic-electronic conducting properties of these materials.^[1, 2] Strikingly, investigation of mixed conduction in methylammonium lead iodide (MAPbI₃) under light showed – along with the expected increase in electronic conductivity – huge enhancement of ionic conductivity (photo-ionic effect).^[3] The photo-induced ion conductivity is assumed to be the consequence of hole localization that neutralizes iodide locally; the so-formed neutral iodine atoms can occupy interstitial sites where they are further stabilized by the polarizable environment in MAPbI₃.

As mixed-cation/anion perovskites show the greatest potential for achieving high-efficiency solar cells, understanding the role of cations and anions on this “photo-ionic effect” is of utmost importance. Here, we quantitatively deconvolute ionic and electronic transport properties in which the A-site cation or the anion is partially or fully substituted. Specifically, the electronic and ionic conductivities of MAPbBr₃, CsPbI₃, CsPbBr₃, as well as FAPbI₃-MAPbI₃ and MAPbBr₃-MAPbI₃ mixtures are investigated.^[4] As far as the photo-ionic effect is concerned, we find that A-site substitution was of only small influence compared with anion substitution. By substituting I by Br, a significant lowering of the photo-ionic effect was observed. This corroborates our hole trapping mechanism for the photo-induced ion transport owing to the fact that Br is less polarizable than the counterpart of I. Our electrical characterization performed on mixed halide perovskite MAPb(I_{1-x}Br_x)₃ thin films as a function of x confirms the previously reported phase instability under light of these materials in the intermediate composition range. On the basis of these observations, we draw a possible interpretation explaining the photo-demixing in mixed halide perovskites where the formation of neutral iodine interstitial defects stabilizes the coexistence of I-rich and Br-rich domains. This factor may represent an important contribution to the driving force for phase segregation and emphasizes the importance of the coupling between electronic and ionic defects in the phase behavior of halide perovskites.

[1] Yang TY, Gregori G, Pellet N, Gratzel M, Maier J. The Significance of Ion Conduction in a Hybrid Organic-Inorganic Lead-Iodide-Based Perovskite Photosensitizer. *Angew Chem Int Ed Engl* 2015, 54(27): 7905-7910.

[2] Senocrate A, Moudrakovski I, Kim GY, Yang TY, Gregori G, Gratzel M, et al. The Nature of Ion

Conduction in Methylammonium Lead Iodide: A Multimethod Approach. *Angew Chem Int Ed* 2017, 56(27): 7755-7759.

[3] Kim GY, Senocrate A, Yang T-Y, Gregori G, Grätzel M, Maier J. Large tunable photo effect on ion conduction in halide perovskites and implications for photodecomposition. *Nature materials* 2018, 17(5): 445-449.

[4] Kim GY, Senocrate A, Wang Y-R, Moia D, Maier J. Photo-effect on ion transport in mixed cation and halide perovskites and implications for photo demixing. *Angewandte Chemie International Edition*, n/a(n/a).

1:20 PM EN06.10.38

Untangling the Ionic Conductivity Tuning by Changing A-Site Cation and X-Site Anion in Hybrid Perovskites by Photoelectrochemical Impedance Spectroscopy Priya Srivastava, Ramesh Kumar and Monojit Bag; Indian Institute of Technology Roorkee, India

Mixed electronic-ionic conductors such as hybrid perovskite materials exhibit the complexity in conduction. A deeper understanding of both ionic conductivity and electronic conductivity is important. Herein, the role of A-site cation and X-site halide ion was investigated by employing Photoelectrochemical Impedance Spectroscopy technique on perovskite-electrolyte interface-based devices in controlling the charge and ionic conductivity of the perovskite material. It was observed that ionic conductivity of the perovskite material can be easily tuned either by changing the A-site cation (MA⁺/FA⁺) or by changing the X-site halide ion (I⁻/Br⁻). Significantly different (opposite) photo-induced ionic conductivity in different cation or different halide-based perovskites was noted. Therefore mixed-cation or mixed-halide perovskite can be utilized to reduce photo-induced ion conductivity of the material. Furthermore, very fine-tuning is also possible by modulating the externally applied voltage. The effect of ion accumulation and migration on the charge storage and transport property of the device is analyzed using vacancy hopping and jump relaxation model. Ionic conductivity spectra revealed Jonscher's law dependence at mid- and low- frequency regime with a constant plateau at high-frequencies. It was concluded that the interplay of ion migration and accumulation dictates the resulting conduction and storage property of the complete device structure. These perovskite/electrolyte-based devices, therefore, can be promising candidates for electrolyte gated perovskite field-effect transistors where switchable ion conductivity can be achieved either by external applied electric field or photo-excitation.

1:30 PM EN06.10.39

Late News: Spatial Chemical Heterogeneity Circumvents Power Losses from Local Electronic Disorder in High-Performance Halide Perovskite Solar Cells Kyle Frohna¹, Miguel Anaya^{1,1}, Stuart Macpherson¹, Jooyoung Sung¹, Tiarnan A. Doherty¹, Yu-Hsien Chiang¹, Andrew Winchester², Keshav M. Dani², Akshay Rao¹ and Samuel Stranks^{1,1}; ¹University of Cambridge, United Kingdom; ²Okinawa Institute of Science and Technology, Japan

Halide perovskites perform remarkably in optoelectronic devices^{1,2}. This class of materials exhibits a considerable defect tolerance, with long charge carrier lifetimes in spite of large concentrations of defects, which has been related to exotic phenomena such as polarons, Rashba effect and photon recycling^{3,4}. However, their performance is still not properly understood given they exhibit compositional and structural heterogeneity in addition to large concentrations of deep charge carrier traps in well localized spatial clusters^{5,6}. In this talk, we resolve this paradox revealing that compositional disorder of the perovskite can induce carrier funneling away from deep trap states, improving performance⁷.

We use a series of multimodal microscopy techniques based on synchrotron nanoprobe and optical spectroscopic techniques, including hyperspectral and transient absorption microscopy. We map the local chemical and structural heterogeneity of device relevant FA_{0.79}MA_{0.16}Cs_{0.05}Pb(I_{0.83}Br_{0.17})₃ (FA=formamidinium, MA=methylammonium) perovskite samples on the nanoscale using nano X-ray fluorescence and diffraction. We spatially correlate these measurements with local values of quasi-Fermi level

splitting and Urbach energy, which are important device metrics, as well as ultrafast carrier dynamics from transient absorption microscopy. We show that local quasi-Fermi level hotspots are caused by carriers funneling onto local regions with low electronic disorder. Importantly, this funneling mechanism collects charges over micrometers and thus sequesters carriers away from trap clusters associated with higher electronic disorder. The visualization of this nanoscale landscape provides an explanation for the purported defect tolerance in these materials and may open an avenue for a new class of intrinsically disordered but high performing materials.

1. Kim, Y.-H. et al. Comprehensive defect suppression in perovskite nanocrystals for high-efficiency light-emitting diodes. *Nat. Photonics*, doi:10.1038/s41566-020-00732-4 (2021).
2. Al-Ashouri, A. et al. Monolithic perovskite/silicon tandem solar cell with >29% efficiency by enhanced hole extraction. *Science* 370, 1300, doi:10.1126/science.abd4016 (2020).
3. Frohna, K. et al. Inversion Symmetry and Bulk Rashba Effect in Methylammonium Lead Iodide Perovskite Single Crystals. *Nat. Commun.* 9, 1829 (2018).
4. deQuilettes, D. W., Frohna K. et al. Charge-Carrier Recombination in Halide Perovskites. *Chemical Reviews*, doi:10.1021/acs.chemrev.9b00169 (2019).
5. Doherty, T. A. S. et al. Performance-limiting nanoscale trap clusters at grain junctions in halide perovskites. *Nature* 580, 360-366, doi:10.1038/s41586-020-2184-1 (2020).
6. Tennyson, E. M., Doherty, T. A. S. & Stranks, S. D. Heterogeneity at multiple length scales in halide perovskite semiconductors. *Nat. Rev. Mater.*, doi:10.1038/s41578-019-0125-0 (2019).
7. Frohna, K., Anaya, M. et al. Spatial Chemical Heterogeneity Circumvents Power Losses from Local Electronic Disorder in High-Performance Halide Perovskite Solar Cells. Submitted (2021).

1:40 PM EN06.10.40

Late News: Perovskite Solar Cells for Space Application Lennart Reb¹, Michael Böhmer¹, Benjamin Predeschly¹, Sebastian Grott¹, Goran I. Ivandekic¹, Renjun Guo¹, Christoph Dreißigacker², Roman Gernhäuser¹, Andreas Meyer² and Peter Muller-Buschbaum^{1,3}; ¹Technische Universität München, Germany; ²Deutsches Zentrum für Luft- und Raumfahrt, Germany; ³Heinz Meier-Leibniz Zentrum, Germany

Perovskite solar cells possess a revolutionary potential for space applications. The thin-film solar cells can be processed onto thin polymer foils that enable an exceptional specific power, i.e. obtainable electric power per mass, being superior to their inorganic counterparts. However, research towards space applications was mainly restricted to terrestrial conditions so far. We report the first demonstration of operation of perovskite solar cells in space conditions [1]. A stabilized payload orientation allowed us to obtain current-voltage characteristics under stable irradiance conditions in low Earth orbit altitudes. By tracking the evolution of short-circuit currents we can identify phases of direct solar irradiation and weak diffuse-light irradiation arising from the Earth's surface. During phases of strong solar irradiance, both perovskite solar cell types (planar and mesoscopic nip-type) exceeded power densities (power per area) of 14 mW cm⁻². Thus, the different solar cells reached their performance expectations exposed to space conditions. Also during a phase of being turned away from the sun, the solar cells still generated power, just collecting faint scattered light from the Earth. Interestingly, the power densities reached levels as anticipated for deep-space irradiance conditions. These results highlight both the suitability for near-Earth applications as well as the potential for deep space missions for perovskite cells.

[1] L. Reb et al., *Joule* 4,1880-1892 (2020), <https://doi.org/10.1016/j.joule.2020.07.004>.

1:50 PM EN06.10.41

Investigating the Role of Band Alignment of the Transparent Conductor and Electron Transport Layer Interface in Wide-Bandgap Perovskite Solar Cells Jared Friedl, Ramez Hosseinian Ahangharnejhad, Adam Phillips and Michael Heben; The University of Toledo, United States

Wide-bandgap mixed-halide perovskites such as CH₃NH₃Pb(I_xBr_{1-x}) are of great interest because of their favorable bandgaps for use as top subcells in multijunction photovoltaic devices. Recently, we have shown

through numerical simulation that the performance of single junction wide-bandgap perovskite devices strongly depends on the energetic alignment between the absorber and the charge transporting layers. Those results showed interesting behavior in the power conversion efficiency at high conduction band offset between the electron transport layer (ETL) and wide-bandgap absorber; namely, the open circuit voltage rapidly increased, but the fill factor decreased just as drastically. These results suggest the formation of a large potential barrier that impedes electron flow out of the absorber. Such a barrier was not evident at the ETL/absorber interface but may be the result of poor band alignment at the transparent conducting oxide (TCO)/ETL interface. Here, we investigate the impact of TCO band alignment with the ETL in wide-bandgap perovskite solar cells. We show that varying the conduction band position of the TCO can lead to reductions in both the recombination and fill factor loss. The reduction in recombination allows the device to maintain a high fill factor, near 90%, not previously observed for a wide range of conduction band offsets (CBOs) between the ETL and wide-bandgap absorber. Simultaneously, varying the conduction band position of the TCO preserves a high V_{OC} and results in a 1-2% increase in efficiency compared to our previous modeling with a standard TCO and optimized ETL/absorber CBO. These results indicate that as the bandgap of the perovskite absorber layer is increased, the choice of ETL and TCO will have a significant joint effect on performance.

2:00 PM EN06.10.42

Triple Halide Perovskite Composition Exploration Assisted by DFT and Data Science Methods Qingmu Deng¹, Zachary del Rosario¹ and Rebecca Belisle²; ¹Olin College of Engineering, United States; ²Wellesley College, United States

Lead halide perovskites are promising materials for tandem solar cell applications due to their easily tunable bandgap through cation and halide compositions. However, photo-induced halide segregation in iodide-bromide perovskite chemistries often results in iodine-rich and bromine rich domains and limits the efficiency of tandem solar cells. One approach to mitigate such segregations reported in the literature is the addition of chlorine to the cesium-formamidinium iodide-bromide perovskite compositions. However, the literature on the effects of varying degrees of chlorine incorporation in thin-film perovskite is limited. In this study, we present an experimental study of the iodine-bromine-chlorine composition space aided by density functional theory (DFT) calculations and data science methods. By loosening cesium-to-formamidinium ratio at the same time, we allow for more possible selections of triple halide compositions that could fall in the optimal range of Goldschmidt's tolerance factor and result in stable perovskite. Among these selections, we look for compositions whose band gaps are optimized for tandem applications and whose halide segregation effects are minimized. Since all possible hybrid-cation mixed halides samples at one percent increments are too numerous to fabricate, we perform a screening informed by DFT and data science methods to intelligently search the compositional space. Through iterative experimental and computational exploration, we identify triple halide perovskite compositions with optimized opto-electronic properties well suited for tandem applications. Our data science and DFT approach demonstrates an expedition to experimental work in material discovery and characterization, which could be adapted to optimizing perovskite chemistries for alternative optoelectronic applications.

2:03 PM EN06.10.43

MAPbBr₃ Single Crystal Stability with Co-Exposure of Oxygen and Light Ke Wang¹, Benjamin Ecker¹, Jinsong Huang² and Yongli Gao¹; ¹University of Rochester, United States; ²University of North Carolina at Chapel Hill, United States

The stability of methylammonium lead bromide (MAPbBr₃) single crystal was investigated when subjected to simultaneous oxygen exposure and light illumination of one solar intensity. The exposure process was monitored with X-ray photoelectron spectroscopy (XPS) with detailed control of the exposure time and pressure. It was found that with light the oxygen degradation process of the MAPbBr₃ was substantially accelerated. Quantitative analysis showed that Carbon, Bromine and Nitrogen lost 52%, 56% and 90% of their initial concentration respectively at 10¹² Langmuir of oxygen exposure. It further showed that ~11% of the perovskite's Pb degraded to metallic Pb at 10⁹ Langmuir, and then was oxidized with the increase of the oxygen pressure.

2:06 PM EN06.10.45

Unraveling the Role of Alkali Cations on Perovskite Phase Segregation of Multi-Cation and Mixed-Halide Perovskites Ming-Chun Tang^{1,2}, Siyuan Zhang^{1,3}, Nhan V. Nguyen¹ and Christina A. Hacker¹;

¹National Institute of Standards and Technology (NIST), United States; ²University of Maryland, United States;

³Theiss Research, United States

Control and prevention of perovskite phase segregation are crucial to realizing stable and tunable multi-cation and mixed-halide perovskite optoelectronic devices. Herein we report the comprehensive analysis of band structure, compositional heterogeneity, and phase segregation in the novel alkali cesium (Cs⁺) and potassium (K⁺)-doped 3D perovskites using a suite of powerful and highly complementary techniques [such as X-ray photoemission spectroscopy (XPS), depth profiling, ultraviolet photoelectron spectroscopy (UPS) and grazing incidence wide-angle X-ray scattering (GIWAXS)]. Perovskite phase segregation information has been extracted from the optical or electrical properties using techniques such as absorption and photoluminescence spectroscopy, external quantum efficiency (EQE), transient difference absorption spectroscopy, and photovoltaic performance. However, all of these techniques provide indirect compositional information and cannot reveal the spatial distribution. We found that the incorporation of metal cations raises the conduction band minimum (CBM), facilitating electron transfer to the electron transport layer. Notably, the depth profile by XPS and GIWAXS analysis show that the formation of iodide- and bromide-rich regions are strongly correlated to the alkali metal cation concentrations: low metallic concentration (5%) can prevent phase segregation where the halides and cations are distributed evenly across the films, while high metallic cation ratio (20%) leads to halide segregation where the concentration of iodide decreases accompanied with the increase of bromide and metal cation concentration as the sampling depth increases. These differences in electronic properties, element distribution, and film morphology were reflected in solar cell performance: >20 % of power conversion efficiency (PCE) was demonstrated with low Cs⁺ incorporated perovskite, while ≈16.7 % of PCE with high Cs⁺ concentration perovskite. Similar trends were also observed in the K⁺-doped perovskite system. We believe this work will advance the perovskite community by providing a direct and straightforward route to characterize the impacts of perovskite phase segregation.

2:09 PM EN06.10.46

Extraction of Perovskite Solar Cell Parameters Based on a Consistent Device Model Andreas Schiller^{1,2}, Martin T. Neukom^{1,2}, Simon Züfle¹, Evelyne Knapp², Christoph Kirsch², Balthasar Blülle¹, Sandra Jenatsch¹ and Beat Ruhstaller^{1,2}; ¹Fluxim AG, Switzerland; ²Zurich University of Applied Sciences, Switzerland

Parameter extraction based on numerical simulation is error-prone because model parameters are often correlated [1]. The accuracy of the extracted parameters can be improved by combining multiple steady-state and transient measurement techniques to reduce these correlations. This method has been successfully applied to organic solar cells [2].

Modelling perovskite solar cells, however, involves additional complexity. Characteristic features, such as IV curve hysteresis [3,4] and slow transient current rise [5,6] indicate the presence of mobile ionic charges in the perovskite layer. Simulation models including ionic charges could qualitatively reproduce these individual features [3-5]. However, the reliable determination of these ionic parameters additionally requires suitable characterization techniques.

To increase the trustability of the model, we systematically study the influence of individual model parameters on different experimental techniques. We therefore model multi-layer methylammonium lead iodide (MAPI) perovskite solar cells in a coupled opto-electrical simulation including mobile ionic charge carriers, charge trapping, Shockley-Read-Hall (SRH) recombination and doped transport layers. We find a single set of parameters to explain the combined results from various measurement techniques in DC, AC, and transient regime [6]. The applied techniques include IV curves with different scan rates, light intensity dependent open circuit voltage, impedance spectra, intensity-modulated photocurrent spectra (IMPS), transient photocurrents and transient voltage step responses. As expected, the various measurement techniques show different sensitivities to material and device parameters, which a model fit can benefit from.

Yet correlated parameters remain an issue. Namely it is difficult to distinguish between concentration and mobility of ionic charge carriers [6]. M.H. Futscher et al. [7] recently applied a measurement technique called transient ion drift to perovskite solar cells. This technique was originally developed for inorganic p-n junctions and allows to individually and quantitatively measure both concentration and mobility of slowly moving mobile charges [8]. It is unfortunately restricted to materials with low concentrations of mobile charges and comparably high doping [7-8]. Using our model we evaluate this characterization technique for devices beyond these restrictions. Specifically we investigate materials with high concentrations of mobile ions or absence of doping, as many perovskite materials meet one or both of these specifications. We further investigate the correlation between other parameters and the extracted ones.

Our consistent device simulation model allows for a better understanding of the governing physical effects and provides a powerful tool to study the influence of device parameters on the solar cell performance and efficiency. The variety of applied measurement techniques allows one to reduce the correlation between parameters. Furthermore, an in depth parameter study suggests possible paths towards an optimized device [6].

References

- [1] M.T. Neukom et al., *Sol. Energy* (2011), 85, 1250.
- [2] M.T. Neukom et al., *Organic Electronics* (2012), 13, 2910-2916.
- [3] S. van Reenen, M. Kemerink and H.J. Snaith, *J. Phys. Chem. Lett.* (2015), 6, 3808-3814.
- [4] P. Calado et al., *Nat. Commun.* (2016), 7, 13831.
- [5] S.E.J. O'Kane et al., *J. Mater. Chem. C* (2017), 5, 452-462.
- [6] M.T. Neukom et al., *ACS Appl. Mater. Interfaces* (2019), 11, 26, 23320-23328.
- [7] M.H. Futscher et al., *Mater. Horiz.* (2019), 6, 1497-1503.
- [8] T. Heiser and A. Mesli, *Appl. Phys. A: Solids Surf.* (1993), 57, 4, 325-328.

2:12 PM EN06.10.50

Probing the Mechanism of Anion Exchange and Dopant Migration in Cesium Lead Halide Perovskites
Kyle Kluherz^{1,2}, James J. De Yoreo^{2,1} and Daniel Gamelin¹; ¹University of Washington, United States; ²Pacific Northwest National Laboratory, United States

Colloidal CsPbX₃ (X = Cl, Br, I) perovskite nanocrystals have attracted a great deal of interest due to their bright, narrow emission, high photoluminescence quantum yields, tunable band gap, and defect tolerance. Various dopants have been successfully incorporated in their structure, including notably Mn²⁺ and Yb³⁺, allowing for novel emission properties such as broadband emission and quantum cutting. However, the structure and chemistry of dopants within the perovskite lattice are not well understood. A characteristic property of CsPbX₃ nanocrystals is their facile anion-exchange chemistry in the liquid or gas phase, which allows ready conversion between different halide structures, formation of mixed halide compositions, and access to materials that are difficult or impossible to synthesize directly. The mechanism(s) by which this anion exchange occurs are still poorly understood, as are its effects on dopant sites. Our work focuses on probing these reactions at the atomistic level to gain mechanistic insight into this important chemical transformation. We have employed X-ray total scattering measurements of the ensemble anion exchange reaction to observe structural changes during this process. These indicate a continuum shift in the structure during anion exchange, with expected expansions in the long-range order. A substantial change in the majority of atom pair positions and intensities was also observed in the Mn-doped system, while the Yb-doped system is nearly identical to the undoped structure, except for a small shift in the Pb-Cl peak. Furthermore, we are pursuing a combination of environmental TEM and HR-STEM with EDX mapping at multiple points ex-situ and in-situ in the gas phase in order to understand the mechanism of anion exchange in doped and undoped halide perovskite nanomaterials.

2:15 PM EN06.10.51

Does Mechanical Strain Drive Ion Migration in Mixed Halide Perovskites? Jacob Bolduc and Aaron Fafarman; Drexel University, United States

Metal halide perovskites possess fascinating material properties and significant technological promise. The

materials consist of a nominal formula of $APbX_3$, where A is a large cation (e.g. Cs, MA or FA), and X is a halide, however much attention has been devoted to the alloys composed from mixtures thereof, e.g. (MA/Cs/FA)Pb(Br/I)₃. Alloying at the X -site provides bandgap tunability while alloying at both sites can significantly enhance stability towards both phase change and moisture-catalyzed degradation. Recent studies have identified the phenomenon of light induced halide demixing, whereupon illumination drives the formation of pure-phase halide clusters. This entirely reversible process has been hypothesized to be due to strain induced by photoexcited polarons. The facile and reversible nature of ion mobility in this system makes it an ideal setting for studying the coupling between external perturbations and the spatial distribution of ions in mixed alloys. These experiments test whether mechanically induced strain is another such external perturbation capable of driving ion migration. To determine the extent of ion migration in mixed halide perovskites to mechanically-induced strain, polycrystalline thin films of MAPbBr₂ were placed under deliberate tensile strain and measured via steady-state photoluminescence for changes in the spatial distribution of halides at the point of strain as a function of time.

2:18 PM EN06.10.52

Late News: Organic and Inorganic A-Site Cation Induced Trends in the Electronic Structure of Lead Bromide Perovskites Gabriel J. Man; Uppsala University, Sweden

The presence of an organic or inorganic A-site cation has been associated with subtle differences in the electronic structures of lead bromide perovskite compounds. Through a bromine- and lead-selective core level spectroscopic study of three archetypal hybrid-organic and all-inorganic APbBr₃ compounds, including the first high-resolution hard X-ray absorption spectroscopy measurements on lead halide perovskite single crystals, we find the A-site cation has a substantial effect on the unoccupied states and a relatively smaller effect on the occupied states. We examine the conduction band states with Br K-edge X-ray absorption spectroscopy, finding Pb-Br states near the conduction band edge and higher-lying (A cation)-Br states. We find a linear correlation between relative Goldschmidt tolerance factors and relative conduction band widths. Through a combination of non-resonant X-ray emission spectroscopy and hard X-ray photoelectron spectroscopy, we find that the occupied states of the three compounds differ primarily at the valence band edge. We directly access lead-bromide bonding ionicity via X-ray emission spectroscopy and account for relative shifts in the energy levels with the chemical shift. Our findings have implications for interfacial energy level alignment in perovskite devices, the defect tolerance hypothesis, slow hot carrier cooling and other intriguing effects in this class of materials.

SYMPOSIUM EN07

Thin-Film Compound Semiconductor Photovoltaics
April 14 - April 20, 2021

Symposium Organizers

Charles Hages, University of Florida
Mike Scarpulla, University of Utah
Byungha Shin, Korea Advanced Institute of Science and Technology
Mirjam Theelen, TNO

Symposium Support

Bronze
Angstrom Engineering Inc.

* Invited Paper

Tutorial EN07: Young Scientist Tutorial on Characterization Techniques for Thin-Film Solar Cells
Session Chairs: Daniel Abou-Ras, Alexandra Bothwell, Mirjana Dimitrievska, Veronique Gevaerts and Arthur Onno
Saturday Morning, April 17, 2021
EN07

10:00 AM INTRODUCTION - DANIEL ABOU-RAS

10:05 AM *

J-V and IQE—Measurement Fundamentals and Introductory Device Modelling with Advanced Analysis for Photovoltaic Applications Alexandra Bothwell; Colorado State University, United States

Introduction to current density-voltage (J-V) and quantum efficiency (QE) measurements including essentials to measurement setup and data analysis. Expanded application of J-V and QE data to photovoltaic performance loss quantification: how the combination of meaningful measurements and fundamental photovoltaic concepts such as the Shockley-Queisser limit and non-ideal diode equation can be used to understand dominant loss mechanisms in solar cells. Basic outline of SCAPS 1-D modeling as a companion analysis tool to supplement interpretation of device operation.

11:35 AM BREAK

11:50 AM *

Tandem Devices and Advanced Measurements Veronique Gevaerts; Netherlands Organization for Applied Scientific Research, Netherlands

Introduction into tandem and multijunction devices: boosting solar cell efficiencies, tandems with Perovskites, and 2T vs 4T. Semitransparent electrodes and recombination layers for tandem fabrication. Challenges in analyzing electrical J-V measurements of so-called two terminal (2T) devices and how to properly measure EQE with bias illumination and voltage.

1:05 PM BREAK

1:20 PM *

Photoluminescence Characterization of Photovoltaic Materials and Devices—From Material Properties to Loss Analysis Arthur Onno; Arizona State University, United States

- Theoretical background on semiconductor photoluminescence
- Basic photoluminescence measurement setup
- Spectrally resolved photoluminescence: impact of absorptance spectrum, temperature, injection level, and defect states
- Time-resolved photoluminescence: measurement technique, competing emission dynamics within samples, potential and pitfalls
- Quantitative photoluminescence: accessing the quasi-Fermi-level splitting from a rapid nondestructive measurement

Photoluminescence playbook case study: combining spectrally resolved, quantitative, and time-resolved photoluminescence to understand to origin of voltage losses in cadmium selenium telluride solar cells.

2:35 PM BREAK

2:50 PM *

Raman Spectroscopy Characterization from Structure to Defect Engineering Mirjana Dimitrievska; École Polytechnique Fédérale de Lausanne, Switzerland

Introduction into Raman spectroscopy: regular, resonance, and polarization measurements. How to conduct proper Raman measurements, the most common mistakes. Application of Raman spectroscopy for structural and crystal quality assessments, as well as defect and secondary phase identification. Building Raman-based methodologies for defect identification and correlation with optoelectronic properties through combinatorial studies.

4:05 PM FINAL DISCUSSION AND FAREWELL

SESSION EN07.02: Advances in CdTe-Based Solar Cells I
Session Chairs: Alexandra Bothwell and Mike Scarpulla
Sunday Morning, April 18, 2021
EN07

10:30 AM *EN07.02.01

Thin Film Solar Cells Using n-CdTe Absorber Layers Ken Durose¹, Luke Thomas¹, K Cheetham^{1,2}, M Isaccs³, Theo Hobson¹, N Tarbuck¹, L Phillips¹ and Jon Major¹; ¹University of Liverpool, United Kingdom; ²STFC Daresbury Laboratory, United Kingdom; ³Research Complex at Harwell, United Kingdom

There are good reasons to abandon the usual p-type absorbers in CdTe-based solar cells in favour of n-type ones. Despite recent advances in CdTe PV (e.g. eliminating CdS, the use of CdSeTe and intentional p-type doping using CdTe:As), the basic design of ‘superstrate’ CdTe-based devices remains unchanged since the 1960s: light enters through the glass/transparent conducting electrode/window layer and generation takes place in a shallow homojunction in the CdTe-based absorber layer - which is otherwise p-type. These cells have limited V_{oc} . The use of n-type CdTe absorbers sidesteps two fundamental physical limitations of p-CdTe and replaces them with technological challenges: For p-type CdTe it is well known that formation of Ohmic contacts requires that a barrier be overcome (this being the value of the electron affinity plus a large fraction of the bandgap). Also, wide- and medium-gap semiconductors cannot stably be doped p-type at a high density due to self-compensation limitations imposed by native defects. Such factors limit the V_{oc} achievable from CdTe-based devices. For n-type CdTe, doping with indium can achieve close to 100% activation and allows higher stable doping densities to be achieved than with CdTe:As for example. Ohmic contacts to it may be formed without issue. Both the n-doping and Ohmic contacts are well-known for single crystal n-CdTe.

Hence the challenge for n-type devices, lies elsewhere, notably in the choice of partner layers and their electrodes, the selection of a device architecture and the control of n-doping in the context of thin film growth and processing. There are essentially four choices of device architecture: A) ‘substrate’ devices in which the light enters through the glass/TCO combination and then first encounters either a) n-CdTe or b) a p-type partner layer or B) ‘superstrate’ devices in which the light enters through a transparent electrode and then first encounters either a) n-CdTe or b) its p-type partner layer. To sum them up in other words: there is either an n- or a p-type window layer. We ruled out using p-type TCOs immediately - since they have low conductivity - and instead we considered other options. In a preliminary simulation study (using SCAPS) we identified a range of materials choices and architectures for n-CdTe devices that gave $V_{oc} \geq 1V$. This indicated that experimentation would be worthwhile.

For the CdTe:In doping we have been trialling post-growth introduction of indium into CSS-grown CdTe using

elemental indium (with and without pre- or post-treatment using MgCl_2), both aqueous and methanolic InCl_3 and also treatments with and without nitric/phosphoric etching. We will report conductivity measurements, transfer length measurements (contacts), SIMS and XPS results. There is some indication that diffusion can be blocked by surface oxides. As an alternative we are trialling intentionally pre-doped CdTe:In source material for use in close space sublimation film growth directly. At the time of writing device work is in progress using a variety of wafer (test structure) and thin film partner layers including organics. This part of the work is at an early stage and we will report on progress at the conference.

10:55 AM EN07.02.02

Reconciliation of Theory with Experiment for Defects in CdTe—The Case of the Cadmium Vacancy Seán R. Kavanagh^{1,2,2}, Aron Walsh² and David O. Scanlon¹; ¹University College London, United Kingdom; ²Imperial College London, United Kingdom

The ability to accurately model, understand and predict the behaviour of crystalline defects would constitute a significant step towards improving photovoltaic device efficiencies and semiconductor doping control, accelerating materials discovery and design. In this work, we apply state-of-the-art *ab initio* techniques - hybrid Density Functional Theory (DFT) including spin-orbit coupling - to accurately model the atomistic behaviour of the cadmium vacancy (V_{Cd}) in cadmium telluride (CdTe). In doing so, we resolve several longstanding discrepancies in the extensive literature on this subject.

CdTe is a champion thin-film absorber for which defects, through facilitation of non-radiative recombination, significantly impact photovoltaic (PV) performance, contributing to a reduction in efficiency from an ideal (Shockley-Queisser) value of 32% to a current record of 22.1%. Despite over 70 years of experimental and theoretical research, many of the relevant defects in CdTe are still not well understood, with the definitive identification of the atomistic origins of experimentally-observed defect levels remaining elusive.¹⁻³

In this work, through identification of a tellurium dimer ground-state structure for the neutral Cd vacancy, we obtain a single negative-U defect level for V_{Cd} at 0.35 eV above the VBM, finally reconciling theoretical predictions with experimental observations. Moreover, we reproduce the polaronic, optical and magnetic behaviour of V_{Cd}^{-1} in excellent agreement with previous Electron Paramagnetic Resonance (EPR) characterisation.⁴

The origins of previous discrepancies between theory and experiment, namely incomplete mapping of the defect potential energy surface (PES) and inherent qualitative errors in lower levels of electronic structure theory, are analysed in detail. Accordingly, this work helps to establish robust procedures for accurate and reliable modelling of defect processes in emerging materials, informing future investigations and enabling the acceleration of materials discovery and design procedures.

1 A. Lindström, S. Mirbt, B. Sanyal and M. Klintonberg, *J. Phys. D: Appl. Phys.*, 2015, **49**, 035101.

2 J.-H. Yang, W.-J. Yin, J.-S. Park, J. Ma and S.-H. Wei, *Semicond. Sci. Technol.*, 2016, **31**, 083002.

3 A. Shepidchenko, B. Sanyal, M. Klintonberg and S. Mirbt, *Scientific Reports*, 2015, **5**, 1–6.

4 P. Emanuelsson, P. Omling, B. K. Meyer, M. Wienecke and M. Schenk, *Phys. Rev. B*, 1993, **47**, 15578–15580.

11:10 AM EN07.02.04

In Situ Doping for CSS Growth of n-CdTe Hetero-Structures Theo Hobson, Luke Thomas, Laurie Philips, Jon Major and Ken Durose; University of Liverpool, United Kingdom

In this work we investigate the use of pre-doped n-type CdTe source material to fabricate PV devices via close-space sublimation (CSS). The more readily dopable n-type CdTe offers the potential advantages of easier Ohmic contacting and higher V_{oc} than are achieved with conventional p-type CdTe material. Metallic indium was incorporated into bulk CdTe source material (Sigma Aldrich 6N) in quartz capsules sealed

under vacuum and heated above the melting point of 1091°C for 3 days. In order to achieve doping in the range $10^{18} - 10^{16} \text{ cm}^{-3}$ successive dilution steps were required. The resulting material was qualified by chemical analysis using EDX (to determine homogeneity for the highly doped compositions) and by ICP-OES to determine the absolute indium concentrations in the bulk material more generally. XRD was used to confirm the phase purity.

Thin films of CdTe:In deposited using CSS onto NSG TEC-AB substrates (highly resistive SnO₂ on glass) were examined. Incorporation of the indium during the CSS deposition was investigated by quantitative SIMS of the films, and by scraping off the material for ICP-OES analysis. Growth on the resistive TEC-AB substrates also allowed for in-plane conductivity and contact resistance measurements using the transmission line method (TLM). C-V measurements were carried out on glass/Mo/CdTe:In/In structures and were used to give estimates of the carrier concentration. The carrier type was confirmed using the hot probe method.

In addition to the characterisation of the films, we also investigated the use of n-CdTe in test-structures and devices based on p-type semiconductor wafers. Simple evaluations of the band line-ups between n-CdTe and p-type wafers of Si, GaAs, and InP, using the Anderson model, indicated favourable junction properties. We therefore grew these structures by CSS transport of CdTe:In onto (001) oriented wafers. Initial deposition tests indicated that the films adhered well to their substrates and were crystalline in appearance. The junction properties and PV performances of these structures will be reported.

11:15 AM BREAK

11:25 AM EN07.02.05

Post-Growth Doping of N-Type CdTe for Thin-Film Devices Luke Thomas¹, M Isaccs², K Cheetham³, Theo Hobson¹, Jon Major¹ and Ken Durose¹; ¹Stephenson Institute for Renewable Energy, United Kingdom; ²HarwellXPS, United Kingdom; ³STFC, Daresbury Laboratory, United Kingdom

The motivation of this work is to deploy intentionally doped n-type CdTe in place of the more conventional p-type: this offers the possibility of high, stable doping in the absorber layer which has the potential to give high V_{oc} in photovoltaic devices. In this work we explore the use of post-growth doping of CSS-grown CdTe films, both to investigate the feasibility of doping and in preliminary devices.

Several approaches to post-growth doping with indium were trialled, including in-diffusion of evaporated indium metal, and the annealing of films that had been sprayed with InCl₃ in either aqueous or methanolic solutions. Annealing was conducted either in air or under flowing nitrogen.

The surface chemistry of the treated samples was investigated using XPS. The instrument used was a Kratos Axis Ultra-DLD photoelectron spectrometer with a monochromatic AlK α x-ray source. The elements/peaks screened for were Cd3d, Te3d, In3d, Cl2p and O1s. The In MNN Auger line was also measured since it exhibits larger chemical shifts than the In3d XPS line. A pass energy of 20 eV was used for the XPS lines and 80 eV for the Auger.

Chemical incorporation of the indium in the CdTe films was evaluated by quantitative SIMS. Implantation standards were created using single crystal THM-grown B surfaces of CdTe (Japan Energy) with xxx-In and yyy-Cl. SIMS measurements were done by Loughborough Surface Analysis using a Cameca IMS 7F-auto SIMS instrument using O²⁺ and Cs⁺ as the primary ion species at an energy of 10 keV. Profiles were obtained for Cd, Te, In, Cl, O and Sn. It was found that indium could be incorporated throughout an approx. 5 μm thick film at a density of $6 \times 10^{18} \text{ cm}^{-3}$. The conductivity of the films and contact resistances were measured using the transmission line method (TLM) and the hot probe method was used to verify the carrier type.

A variety of 'superstrate' device structures were considered, for example glass/FTO/n-CdTe/ZnTe/P3HT/Au and SCAPS simulations indicated that many were capable of achieving V_{ocs} of $> 1 \text{ V}$ in principle. Preliminary devices were fabricated on NSG TEC15 FTO/glass. ZnTe was evaporated from a powder source while the CSS-grown CdTe films were post-growth doped using the indium metal route. Device and diode characterisation

results will be presented.

11:30 AM DISCUSSION TIME

11:45 AM EN07.02.07

Combinatorial Development of MZO Emitters for Emerging CdTe Based Solar Cells Gavin Yeung¹, Carey Reich², Adam Danielson², Walajbad Sampath² and Colin A. Wolden¹; ¹Colorado School of Mines, United States; ²Colorado State University, United States

Due to the low material and manufacturing costs of polycrystalline CdTe-based solar cells, it is the leading thin-film photovoltaic technology. Magnesium zinc oxide ($\text{Mg}_x\text{Zn}_{1-x}\text{O}$) has proven to be a highly effective emitter layer due to its transparency and ability to tune the conduction band alignment with CdTe. State-of-the-art devices employ graded $\text{CdSe}_y\text{Te}_{1-y}$ (CST) layer at the interface, and emerging absorbers employ group V doping with significantly higher carrier concentrations. The goal of this work is to engineer MZO to adapt to the evolving nature of the absorber. Combinatorial libraries of MZO were fabricated by reactive sputtering and characterized by ellipsometry, XRD, UV-visible spectroscopy, 4-point probe, and Hall effect. After screening to identify promising compositions, uniform MZO films are used to optimize device performance. For standard CdTe the optimum Mg content was found to be $x \sim 0.15$, producing $>16\%$ devices. With CST based devices the optimum Mg content increased to $x \sim 0.25$, producing $>19\%$ devices. The as-deposited MZO is highly insulating, so Ga was added to increase carrier concentration. GMZO libraries are fabricated with band gaps spanning 700 mV and whose electrical resistivity may be systematically varied >6 orders of magnitude by controlling the rate of Ga deposition. We plan to report on the efficacy of these promising GMZO libraries to optimize band gap and carrier concentration for both CST and CST:GrV based devices.

</div></div>

12:00 PM DISCUSSION TIME

12:05 PM *EN07.02.09

What Limits the Voltage of CdSeTe Solar Cells—Material Quality, Surface Passivation or Contact Selectivity? Arthur Onno¹, Adam Danielson², Carey Reich², Siming Li³, William Weigand¹, Darius Kuciauskas³, Walajbad Sampath² and Zachary Holman¹; ¹Arizona State University, United States; ²Colorado State University, United States; ³National Renewable Energy Laboratory, United States

Polycrystalline cadmium telluride (CdTe) and cadmium selenide telluride (CdSeTe) photovoltaic devices suffer from a sizable voltage deficit when compared with competing technologies (*e.g.*, crystalline silicon, perovskite, III-V). Record-efficiency devices have not yet broken the 900-mV open-circuit voltage limit, even though, given the wide direct bandgap of CdSeTe absorbers (1.4–1.5 eV depending on the selenium content), a voltage above 1100 mV could be theoretically expected. Yet, a precise understanding of the origin of this voltage deficit and, more importantly, a clear pathway to overcome it are currently lacking.

The historically poor material quality of polycrystalline CdTe absorbers with, until recently, minority carrier lifetimes τ in the nanoseconds at best, has long been held responsible for these poor V_{oc} performances. To remedy this, extensive work has focused on increasing both the lifetime and the acceptor (*i.e.* activated dopant) concentration N_A , as the quasi-Fermi-level separation is a direct function of the $N_A \times \tau$ product. Double heterostructure CdSeTe samples, with both surface passivated with either magnesium zinc oxide (MZO) or Al_2O_3 , have reached lifetimes in the hundreds of nanoseconds, indicating that excellent material quality was achievable with CdSeTe absorbers and suggesting that poor *surface passivation*—*i.e.*, passivation of the absorber front and back interfaces, as opposed to passivation of defects at the grain boundaries—was an important contributor to the limited voltages measured on finished devices. Similarly, arsenic doping of the absorber has led to acceptor concentrations in excess of 10^{16} cm^{-3} .

Yet, these improvements in both lifetime and acceptor concentration have not translated into meaningful increases in V_{oc} . Two questions thus arise:

1) What limits the voltage of Cd(Se)Te devices?

2) How can we easily and systematically decouple the sources of voltage loss in finished devices? In this work, we answer these two questions by comparing the thermodynamic voltage limit $V_{oc,ideal}$ of finished solar cells with their quasi-Fermi-level splitting (QFLS)—also referred to as the *internal* or *implied* open-circuit voltage iV_{oc} (QFLS= $q \times iV_{oc}$ with q the elementary charge)—and their *external* or *terminal* voltage V_{oc} . We calculate $V_{oc,ideal}$ from the external quantum efficiency (EQE) of the device and access iV_{oc} through measurement of the device external radiative efficiency (ERE) using a calibrated photoluminescence tool, while V_{oc} is measured through standard J - V curve tracing. We show that As-doped cells with Al_2O_3 -passivated contacts can exhibit EREs in excess of 1%—surpassing the best crystalline silicon devices and on par with the best perovskite devices—but, concurrently, band tails limit their thermodynamic voltage limit. Nevertheless, our best device achieves an *internal* voltage $iV_{oc} > 980$ mV. This is close to 100 mV higher than the *external* open-circuit voltage (V_{oc}) of the record-efficiency polycrystalline CdSeTe solar cell. Thus, in these highly luminescent devices, the voltage is limited by the contact selectivity rather than by the material quality of the absorber. We then propose a novel passivated and selective back contact structure—based on an Al_2O_3 passivating layer followed by a p-type boron-doped hydrogenated amorphous silicon (a-Si:H) hole selective layer—with the goal of translating these high iV_{oc} values into high V_{oc} values and achieving $V_{oc} > 1$.

SESSION EN07.03: Advances in CdTe-Based Solar Cells II
Session Chairs: Eric Colegrove and Charles Hages
Sunday Afternoon, April 18, 2021
EN07

1:00 PM *EN07.03.01

On the Fundamental Aspects of Performance and Stability of CdTe Solar Cells Dmitry Krasikov; First Solar, United States

First Solar is the largest solar manufacturer in Western Hemisphere. While possessing CdTe cell and module efficiency records of 22.1% and 18.2%, respectively, we continue research to further push the boundaries of CdTe cell technology. In particular, we conduct fundamental studies of losses and instabilities within active layers of CdTe cells.

The current Cu-doped CdTe technology suffers from insufficient absorber doping caused by atomic interactions between Cu and Cl. Besides limiting the maximum doping achievable in practical fabrication process, defect reactions between Cu and Cl cause further reduction in absorber doping during field operation, which contributes to slow degradation of Cu-doped devices.

High and stable absorber doping of $1 \times 10^{16} \text{ cm}^{-2}$ and above could be achieved in chlorinated CdTe films by replacing Cu with arsenic acceptors. However, taking the full advantage of heavily-doped CdTe absorbers requires high quality front interface with small conduction band offset. Our atomic simulations predict strong conduction band offset at CdTe/ SnO_2 interface, which prevents achieving high V_{oc} values. Additional performance improvement of arsenic-doped cells could be achieved by further increase in doping activation, which is currently limited by formation of kinetically-stabilized deep donors that not only reduce the built-in potential, but may also limit the bulk lifetime.

Another important aspect of CdTe cell performance is reversible short-range metastabilities present both in Cu- and As-doped devices. Our kinetic device modeling suggests that observed metastable phenomena are caused by the defect reactions at the front interface.

1:25 PM EN07.03.02

Investigating Carrier Dynamics in CdTe Full Device Studied with Time-Resolved Terahertz and Photoluminescence Spectroscopies Mohammad Mehdi Taheri¹, Triet M. Truong¹, Shannon L. Fields², William N. Shafarman², Brian McCandless² and Jason Baxter¹; ¹Drexel University, United States; ²University of Delaware, United States

Understanding the nature of recombination and its dependence on defects and interfaces is essential for engineering materials and contacts for higher V_{oc} and power conversion efficiency in photovoltaic (PV) devices. Time-resolved photoluminescence (TRPL) has conventionally been used to evaluate recombination, but not all materials are strongly emissive or otherwise suitable. Pump – probe spectroscopy presents valuable complementary information, wherein an optical pump pulse photoexcites carriers within the absorber and the transient photoconductivity is probed with a terahertz (THz) pulse. Until now, experimental constraints have limited the use of THz probes to interrogate full device stacks, and measurements were instead made on exfoliated films or films grown on unconventional substrates. However, interfaces are critical to the behavior of photoexcited carriers in solar cells, and the substrates themselves often influence the film growth and bulk properties. Therefore, it is important to probe the behavior of PV absorbers as close as possible to their normal operating conditions.

Here we report on cross-cutting metrology tools based on time-resolved THz spectroscopy (TRTS) and TRPL that enable *in operando* characterization of carrier dynamics and recombination mechanisms in working PV devices. Through a combination of experiments and modeling, we can obtain key parameters including Shockley-Read-Hall (SRH) lifetime, minority carrier mobility and diffusion length, and interface recombination velocity using non-contact probes. By varying pulsed photoexcitation conditions, the contributions of interface and bulk recombination can be determined as a function of applied bias.

TRTS has been applied to thin film absorbers but has not been used for full devices because the conductive contacts absorb or reflect the THz radiation. Here we create wire-grid patterns using conventional laser scribing to increase the signal-to-noise ratio by at least 5-fold compared to unscribed samples. The TRTS signal corresponds to transient photoconductivity, while TRPL arises from radiative recombination. We can simulate both of these by numerical solution of the continuity equations and Poisson's equation. Best-fit values of the SRH lifetime and surface and interface recombination velocities are then determined by global fitting of multiple TRTS and TRPL data sets having different photoexcitation conditions.

We have developed and validated this approach using CdTe thin film PVs. For instance, we found a bulk lifetime of 1.6 ns, CdTe/CdS interface recombination velocity of less than 100 cm/s, and back surface recombination velocity of $\sim 2 \times 10^3$ cm/s for a CdTe device treated with CdCl₂. In contrast, as-deposited films without CdCl₂ treatment had bulk lifetime of only ~ 50 ps and higher interface and back-surface recombination velocities of $\sim 2 \times 10^4$ cm/s. We are now applying this approach to understand how dynamics change depending on processing conditions designed to enable high doping densities and on choice of buffer material.

By determining the locus and mechanisms of performance-limiting recombination, we can accelerate the development of thin film PVs with high higher V_{oc} and efficiency. While the method has been demonstrated here using CdTe, it is also applicable to perovskites, CIGS, CZTSSe, and other emerging technologies.

1:40 PM EN07.03.03

Towards Large-Grain Epitaxial CdTe Solar Cells Made by Close-Spaced Sublimation (CSS) or Vapor Transport Deposition (VTD) Mahisha Amarasinghe^{1,2}, David S. Albin², Matthew Reese², John Moseley², Helio R. Moutinho² and Wyatt Metzger²; ¹University of Illinois at Chicago, United States; ²National Renewable Energy Laboratory, United States

Polycrystalline CdTe thin films for solar energy applications are deposited by fast high throughput deposition techniques on glass coated with nanocrystalline transparent conducting oxides. While this approach makes polycrystalline CdTe solar panels a cost leader, the deposition has resulted in small grain sizes on the order of microns for decades.

Grain boundaries (GBs) are active recombination centers that reduce overall carrier lifetime and hence the device performance of CdTe solar cells [1,2]. Therefore, increasing grain size and reducing GB density, especially at the critical junction region, can improve carrier lifetime and solar cell performance [3-5].

The CdTe community relies on CdCl₂ treatments to facilitate grain growth and passivate GBs, increasing the aggregate lifetime from ps to tens of ns. This passivation combined with CdSeTe bandgap engineering has improved CdTe record efficiency to 22.1%. Material challenges are that CdTe grain growth during CdCl₂ anneals is driven by Ostwald ripening, which has historically been limited to the order of the film thickness (i.e. a few microns). Furthermore, CdCl₂ treatments do not completely passivate GBs [4]. For example, correlated GB recombination velocities have been measured to be as high as 10⁵–10⁶ cm/s [6]. Finally, Cl compensation may reduce activation ratios in Group-V doped CdTe devices resulting in microscopic potential fluctuations and lower V_{oc} [7].

Colossal grain growth (CGG) was recently reported in micron-thick Cd(Se,Te) thin films deposited on glass [8]. The resulting CdTe structures had extremely large ~ 1-mm lateral size grains that were much larger than anything previously reported and a layer structure relevant for CdTe solar cells.

In this work, we will illustrate that the resulting, near single-crystal thin films can be used as a growth template for epitaxy of subsequent CdTe layers by techniques appropriate for making devices. Starting device structures have been made using Corning 7059/75-nm Cd₂SnO₄/60-nm MgZnO substrates upon which a CdSe_{0.10}Te_{0.9} layer was evaporated for CGG. Because of its lower bulk resistivity, Cd₂SnO₄ films could be made thin enough for devices and smooth for CGG of the Cd(Se,Te) layer. After the Cd(Se,Te) was deposited, CdCl₂ treatments with temperatures ranging from 420 °C to 500 °C (with and without oxygen) were carried out before and after the CGG anneal, and subsequent CdTe was deposited epitaxially by using either close-spaced sublimation or vapor transport deposition. Lifetime, device performance, and cathodoluminescence results will be presented for both glass/Cd₂SnO₄/MgZnO/CGG-Cd(Se,Te)/CdTe and glass/Cd₂SnO₄/MgZnO/CGG-Cd(Se,Te) structures at the conference.

References:

1. Moseley, J. et al., *IEEE J. Photovolt.* 4, 1671–1679 (2014)
2. Moseley J. et al., *J. Appl. Phys*, 118, 025702 (2015)
3. Kanevce A. et al., *J. Appl. Phys*, 121, 214506 (2017)
4. Amarasinghe M. et al., *Adv. Energy Mater.* 2018, 8, 1702666
5. Amarasinghe M. et al., *IEEE J. Photovolt.* 8 (2), 600-603 (2018)
6. Moseley J. et al., *J. Appl. Phys*, 124, 113104 (2018)
7. Moseley J. et al., *Journal of Applied Physics*, 128, 103105 (2020).
8. Albin D. et al., *J. Phys Energy*

1:55 PM EN07.03.04

Direct Microscopy Imaging of Nonuniform Carrier Transport in Polycrystalline Cadmium Telluride Chuanxiao Xiao; National Renewable Energy Laboratory, United States

Inhomogeneous microscopic carrier transport is difficult to study but important in many condensed-matter applications. For example, the role of grain boundaries (GBs) in polycrystalline semiconductors has been controversial for 20 years. In cadmium telluride (CdTe) solar cells, electron-beam-induced current (EBIC) measurements consistently demonstrate enhanced current collection along GBs, which is argued as evidence for interpenetrating CdTe *p-n* current-collection networks critical to high efficiency. Conversely, cathodoluminescence (CL) measurements consistently indicate that GBs are deleterious low-lifetime regions. Here, we apply transport imaging (TI) in conjunction with spatially correlated EBIC, CL, and scanning Kelvin probe force microscopy measurements to understand carrier drift, diffusion, and recombination in polycrystalline CdTe. We simultaneously observe GB potential wells, reduced carrier lifetime at GBs, and seemingly contradictory enhanced GB current collection, then describe their coexistence with microscopic TI and physical arguments. The results provide visualization of inhomogeneous transport that is critical to understanding and engineering polycrystalline solar technology.

2:10 PM *EN07.03.05

N-Type CdTe Thin Films and Solar Cells Chris Ferekides, Vasilios Palekis, Wei Wang, Sheikh Tawsif Elahi and Md Zahangir Alom; University of South Florida, United States

Recent developments in cadmium telluride (CdTe)-based thin film technology has demonstrated record efficiencies for both CdTe cells (22.1 %) and modules (18.6 %). Even with this progress, record-efficiency CdTe solar cells have open-circuit voltage $VOC \sim 880$ mV, which is considerably lower than the theoretical limit of $VOC \sim 1.15$ V. Much of the focus on CdTe has been associated with increasing its net p-type doping concentration in order to increase the device VOC. High p-type doping in CdTe has been challenging, while various studies have shown $10^{16} - 10^{19}$ cm⁻³ n-type doping in crystalline CdTe using In grown by the Bridgman or molecular beam epitaxy (MBE) methods. Recent studies of In doped crystalline CdTe have shown lifetimes exceeding 2 μ s and solar cells fabricated with this material demonstrated VOC greater than 1 V. In this paper the effect of indium (In) doping on CdTe thin film solar cells will be discussed. CdTe thin films were deposited using the elemental vapor transport (EVT) technique under various Cd/Te gas phase ratios and In vapor concentrations. Solar cells of the superstrate configuration (glass/TCO/CdS/n-CdTe/p-ZnTe/BC) have been fabricated and characterized. There was a correlation between the concentration of In in the vapor phase and net n-type doping for CdTe devices fabricated near Cd/Te stoichiometric ratio. Increasing the amount of In vapors resulted in higher n-type doping in CdTe. From C-V measurements doping levels $>10^{16}$ cm⁻³ were achieved. Devices were also fabricated at various Cd/Te vapor ratios at a constant In vapor concentration. Films deposited under Cd-rich conditions exhibited higher lifetimes than those deposited under Te-rich conditions. On the other hand, films deposited at under Te-rich conditions exhibited higher n-type doping. To-date n-type CdTe solar cells yielded devices with $VOC = 730$ mV, $JSC = 20$ mA/cm², $FF = 62$ % and efficiency near 9 %. SCAPS and AMPS solar cell simulation tools were used to better understand and aid the development of n-type CdTe solar cells. Doping, carrier lifetimes, and interface states of the CdTe-absorber and ZnTe window layer are being investigated.

2:35 PM *EN07.03.06

Progress and Challenges in Doping Polycrystalline CdTe-Based Alloys with Arsenic Amit H. Munshi, Akash Shah, Ramesh Pandey, Pascal Jundt, Carey Reich, Adam Danielson and Walajbad Sampath; Colorado State University, United States

Improvement in polycrystalline CdTe photovoltaics efficiency is primarily limited by the deficit in open-circuit voltage. The deficit can be overcome by reducing the carrier recombination while improving carrier concentration in the film. Traditionally, CdTe-based devices have been doped with copper. However, increasing carrier concentration using copper while reducing recombination is fundamentally limited by various complexes copper may form. To overcome this issue, doping with group V elements has been of interest to the research community for decades and more recently it has been one of the primary focuses of the CdTe research community.

Using sublimation as the deposition method, our research has shown that arsenic can be effectively used to improve carrier concentration while simultaneously reducing recombination. Doping with arsenic is certainly not devoid of challenges as various defects such as the presence of dimers, tetramers, AX-centers, and arsenic clusters in the device pose challenges. However, using an advanced fabrication approach guided by state-of-the-art predictive computational simulation models, we have been able to overcome several of these limitations. Using the method that will be discussed, we have been able to demonstrate carrier lifetimes greater than 2 μ s, carrier concentration over 5×10^{15} cm⁻³, and surface recombination velocity less than 100 cm/s. Following fabrication of films with characteristics suitable for high performing devices, several other factors in the film fabrication process and device structure had to be refined to employ the advantages of doping CdTe-based devices with arsenic as shown by various numerical simulations.

In addition to improvement in device performance, using arsenic as the doping element for CdTe-based photovoltaics may have advantages in terms of longevity of the modules in the field as well. With optimized doping in CdTe with copper, large volumes of modules have been commercially manufactured and installed. However, arsenic doping in polycrystalline films is found to have superior metastability. This is one of the critical factors to be taken into consideration as the elimination of copper may improve projected life of CdTe-based photovoltaic panels from 25 years currently to over 50 years.

4:00 PM EN07.04.01

Optoelectronic and Material Properties of Solution-Processed Earth-Abundant $\text{Cu}_2\text{BaSn}(\text{S}, \text{Se})_4$ Films for Solar Cell Applications Betul Teymur¹, Sergiu Levcenko², Hannes Hempel², Eric Bergmann³, Jose Marquez Prieto², Thomas Unold², Ian Hill³ and David B. Mitzi^{1,1}; ¹Duke University, United States; ²Helmholtz-Zentrum Berlin für Materialien und Energie GmbH, Germany; ³Dalhousie University, Canada

$\text{Cu}_2\text{BaSn}(\text{S}, \text{Se})_4$ (CBTSSe) has been gaining attention as a prospective solar absorber, since it employs low-toxicity and abundant metals, while offering low-cost manufacturing options, controllable stoichiometry, high absorption coefficient ($>10^4 \text{ cm}^{-1}$) and bandgap (E_g) tunability (1.5-2.0 eV). Besides these suitable optoelectronic properties, CBTSSe does not suffer from anti-site disorder in contrast with $\text{Cu}_2\text{ZnSn}(\text{S}, \text{Se})_4$, as confirmed by Shin et al. with *vacuum-deposited* films [1]. The current study focuses on *solution-deposited* nominally stoichiometric CBTSSe films [2] with a bandgap of 1.59 eV and explores the fundamental film properties using several spectroscopic techniques. Temperature- and excitation-dependent photoluminescence studies reveal a dominant defect emission at ~ 1.5 eV and a second deep defect feature at 1.15 eV. Time-resolved terahertz spectroscopy measurements show few tens of picoseconds (~ 50 ps) surface and few nanoseconds (~ 3 ns) bulk lifetimes, as well as $\sim 140 \text{ cm}^2/\text{Vs}$ mobility, the latter of which is in the range of reported values for CZTSSe. The solution-processed CBTSSe films suffer from exacerbated surface recombination at the junction of CdS and CBTSSe, due to cliff-like band alignment with 0.63 eV conduction band offset (as measured by ultraviolet photoemission spectroscopy). Employing these films in an Al-Ni/ITO/ZnO/CdS/CBTSSe/Mo photovoltaic device structure, we report open-circuit voltage (V_{OC}), short-circuit current density, fill factor, and efficiency of 470 mV, $14.3 \text{ mA}/\text{cm}^2$, 43.6%, and 2.93%, a record performance level among solution-processed CBTSSe devices. Device performance in this study may be mainly limited by interfacial properties and inadequately selected device structure (e.g., poorly matched buffer layer), which both enhance recombination-associated losses in V_{OC} . The physical measurements provided for the nominally stoichiometric solution-processed CBTSSe absorber point to critical areas for future improvement of CBTSSe and related photovoltaic cells in the quest for higher efficiency devices based on earth-abundant metals.

Reference

[1] D. Shin, B. Saparov, T. Zhu, W. P. Huhn, V. Blum, D. B. Mitzi, $\text{BaCu}_2\text{Sn}(\text{S}, \text{Se})_4$: Earth-Abundant Chalcogenides for Thin-Film Photovoltaics, *Chem. Mater.*, 28 (2016), 4771-4780.

[2] B. Teymur, Y. Zhou, E. Ngaboyamahina, J. T. Glass, D. B. Mitzi, Solution-Processed Earth-Abundant $\text{Cu}_2\text{BaSn}(\text{S}, \text{Se})_4$ Solar Absorber Using a Low-Toxicity Solvent, *Chem. Mater.*, 30 (2018), 6116-6123.

4:15 PM EN07.04.02

Silver Doping of Enargite (Cu_3AsS_4) Absorbers Using Amine-Thiol Chemistry for the Fabrication of Solar Cells Apurva A. Pradhan, Scott A. McClary, Joe Andler and Rakesh Agrawal; Purdue University, United States

Enargite (Cu_3AsS_4) is an emerging candidate for photovoltaic applications with a direct band gap of 1.41 eV, consisting of earth abundant elements with differing ionic radii and consequently lower likelihood of cation disorder, ideal predicted and experimentally verified optoelectronic properties, and demonstrated use in working thin-film solar cells. Previous experimental work on this material from our group has demonstrated that enargite films have a Shockley-Read-Hall, or defect assisted, recombination lifetime on the timescale of nanoseconds, relatively shallow defect energies, and carrier concentrations on the order of 10^{15} cm^{-3} . However, carbonaceous

fine grain layers, secondary phases, pinholes in the film, and poor band alignment with n-type CdS may be part of the reason that power conversion efficiencies for enargite-based solar cells remained below 0.5%. While investigating suitable n-type junction partners is a subject of a parallel research effort, in this work, we present a novel solution-processed route to create enargite films using an amine-thiol based molecular precursor approach that eliminates carbonaceous fine grain layers, creates phase-pure films, and improves film morphology.

A mixture of amine and thiol has shown to be a very versatile solvent system for dissolving a variety of metal chalcogenides for the fabrication of thin films and nanoparticles. Arsenic sulfides and copper sulfides can undergo reactive dissolution in amine-thiol solvents to form complexes that can decompose at relatively low temperatures. These molecular precursor solutions can be combined into an ink that can be directly coated onto conductive substrates to create tennantite ($\text{Cu}_{12}\text{As}_4\text{S}_{13}$) films that transform and coarsen into micron-sized enargite grains with low surface roughness and no detectable secondary phases after heating in an arsenic-sulfide atmosphere at 425°C . Unfortunately, shunt resistances on devices made using this approach remained low and SEM has confirmed the presence of pin-holes in the film. To improve film morphology and increase shunt resistances, inspiration was taken from silver alloyed $\text{Cu}(\text{In,Ga})\text{Se}_2$ thin films.

Silver alloying in $\text{Cu}(\text{In,Ga})\text{Se}_2$ (CIGSe) solar cells has been an area of active research over the past decade. In CIGSe, Ag alloying has been shown to lower the valence band edge, increase the bandgap, increase grain size, and reduce structural defects, partially due to the lower melting temperature of these alloyed films. The amine-thiol solvent system allowed for facile incorporation of varying concentrations of silver sulfide into coating inks for the creation of silver doped enargite films. With silver incorporation, we observed significant improvements in film morphology that fused adjacent enargite grains in the film together and eliminated pinholes. Preliminary optoelectronic characterization on these films have revealed a shift to higher energy bandgaps with increasing silver content. Devices created with silver-doped enargite show increased shunt resistance and produced champion device efficiencies exceeding 0.6%. This is higher than past demonstrated efficiencies for this material and shows that silver alloying has the potential to improve film properties and device efficiencies. Further optimization of film growth conditions and silver content is expected to allow for further increases in device efficiencies.

4:30 PM EN07.04.03

Embedded Au and Ag Nanoparticles in Pulsed Laser Deposited Photovoltaic Thin Films Mehmet A. Sahiner, Jasmyne Emerson, Faith Akinlade, Matthew Herington and Venise Castillon; Seton Hall University, United States

We have used pulsed laser deposition to deposit nanoparticles (Ag, Au) to investigate the effects of these impurities on the photovoltaic properties of the CdS/CdTe based thin films. The main objective was to investigate how the inclusion of nanoparticles will affect light scattering in the at the interfaces and whether the different size and shape of nanoparticles will have a positive effect on the overall electrical performance of these thin film solar cells. In our previous studies, we have investigated the effects of the embedded Ag nanoparticles on the photoelectric conversion efficiency on CdS/CdTe based thin film solar cells as synthesized by Pulsed Laser Deposition (PLD). Silver was shown to enhance the photovoltaic performance by almost doubling the photovoltaic conversion efficiency of the conventional CdS/CdTe films [1]. A careful comparison of photovoltaic performance of Au/Si versus Ag embedded thin films of CdS/CdTe on indium tin oxide coated glass substrates have been performed. Our results on the Ag case revealed electrical performance of these cells have correlates with the particles density and the particle size on the CdS/CdTe interface. This study concentrates on the Au and Ag nanoparticle deposition on the CdS/CdTe interface with varying particle size and distributions. Structural and compositional characterization were performed using XRD, AFM, and SEM/EDX. Photovoltaic properties were measured using a LabView assisted Keithley Sourcemeter set-up. The comparison of Ag vs Au nanoparticles on the structure and photovoltaic conversion efficiency will be presented. Ag and Au nanoparticles have contrasting effects on the photovoltaic conversion efficiency in terms of their relative coverage at the interface, This will be discussed in the light of plasmonic resonances and effective light scattering for Ag and Au particles.

[1] Olivia Rodgers, Anthony Viscovich, Yunis Yilmaz, Mehmet Sahiner, “The Effect of Embedded Ag Nanoparticle on the Photovoltaic Conversion Efficiency in CdTe/CdS Thin Films”, American Physical Society Bulletin, X17.13 (2018).

This work is supported by NSF Award #:DMI-0420952

4:35 PM EN07.04.04

Synthesis and Characterization of Selenium-Alloyed Bournonite—A Prospective Semiconductor for Optoelectronic Applications Eric T. Chang, Gabrielle Koknat, Volker Blum and David B. Mitzi; Duke University, United States

In the search for solar absorber materials for thin-film photovoltaics (PV), the materials class of complex chalcogenides has maintained consistent interest. In the past two decades, the kesterite $\text{Cu}_2\text{ZnSn}(\text{S},\text{Se})_4$ (CZTSSe) has proven promising as an earth-abundant, nontoxic solar absorber. However, with an efficiency plateauing at 12.6%, a necessary search for novel earth-abundant and nontoxic chalcogenide PV candidates continues. Recently, bournonite (CuPbSbS_3) has been identified as a potential ferroelectric photovoltaic material with a bandgap (1.2-1.3 eV) appropriate for single junction photovoltaic devices (1-1.6 eV). Bournonite is an appealing candidate for a number of reasons, including its structural and electronic three dimensionality, absorption coefficients comparable to that of MAPbI_3 and GaAs, an optical dielectric constant similar to that of hybrid perovskites, high predicted defect tolerance, and the potential for Rashba/Dresselhaus splitting, a phenomenon that has been linked to slow electron hole recombination in lead-halide perovskites.¹ Additionally, as a naturally occurring mineral, bournonite is predicted to be stable, avoiding the instability challenges that face the highly popular perovskites. In the past year, progress in bournonite’s application for PV has accelerated with two studies reporting thin-film processing of bournonite.^{2,3} One such study also reported the first PV device to employ bournonite as the absorber layer (PCE of 2.23%).³ In an effort to explore band gap engineering of bournonite, we report the solid state bulk synthesis of selenium-alloyed bournonite ($\text{CuPbSb}(\text{S}_{1-x}\text{Se}_x)_3$) across the full range of selenium concentrations ($x = 0.0 - 1.0$). We characterize the crystal structure and band gap of the samples using x-ray diffraction and diffuse reflectance spectroscopy, reporting a band gap that approaches 1.1 eV near $x = 0.5$. We compare these results with computational band structure predictions.

1. Wallace, S. K.; Svane, K. L.; Huhn, W. P.; Zhu, T.; Mitzi, D. B.; Blum, V.; Walsh, A., Candidate photoferroic absorber materials for thin-film solar cells from naturally occurring minerals: enargite, stephanite, and bournonite. *Sustainable Energy & Fuels* **2017**, *1* (6), 1339-1350.
2. Koskela, K. M.; Melot, B. C.; Brutchey, R. L., Solution Deposition of a Bournonite CuPbSbS_3 Semiconductor Thin Film from the Dissolution of Bulk Materials with a Thiol-Amine Solvent Mixture. *Journal of the American Chemical Society* **2020**, *142* (13), 6173-6179.
3. Liu, Y.; Yang, B.; Zhang, M.; Xia, B.; Chen, C.; Liu, X.; Zhong, J.; Xiao, Z.; Tang, J., Bournonite CuPbSbS_3 : An electronically-3D, defect-tolerant, and solution-processable semiconductor for efficient solar cells. *Nano Energy* **2020**, *71*, 104574.

4:40 PM EN07.04.05

Fabrication of pn Homojunction of SnS and Its Photovoltaic Properties Issei Suzuki¹, Sakiko Kawanishi¹, Sage Bauers², Andriy Zakutayev², Hiroyuki Shibata¹, Hiroshi Yanagi³ and Takahisa Omata¹; ¹Tohoku University, Japan; ²National Renewable Energy Laboratory, United States; ³University of Yamanashi, Japan

Tin sulfide (SnS) is a promising light-absorbing material for next-generation solar cells due to its safe and abundant constituent elements and suitable optical properties. SnS homojunction structure is expected to overcome the limitation of conversion efficiency (η) of the conventional SnS solar cells based on the heterojunction between p-type SnS and n-type CdS or Zn(O,S) with η of 4-5% at maximum[1]. However, SnS homojunction has not been reported due to difficulties in realizing n-type SnS. In recent years, we have demonstrated the n-type conductive SnS single crystals with halogen (Cl or Br) doping[2], and growth of large single crystal in centimeter-scale[3]. In this study, a p-type SnS thin film was deposited on the large size n-type

crystal to form a pn homojunction, and its photovoltaic properties were evaluated.

Cl-doped large n-type SnS single crystals were prepared by the flux method using Sn as the main solvent. A p-type SnS thin film with a diameter of 1 mm and a thickness of 270 nm was deposited at 340° C on the (100) cleavage plane of the n-type single crystal by RF sputtering. The device structure was GaIn/n-type SnS single crystal/p-type SnS thin film/ZnO/ITO. Structural and electrical properties of the film and homojunction were evaluated. Photovoltaic properties were studied by I-V and C-V measurements.

The p-type SnS thin film deposited on the single crystal was <100>-oriented in the growth direction and was also gently oriented in the growth plane. In addition, there was no void at the n-type single crystal/p-type thin film interface, and the change in Cl concentration was very abrupt. The open circuit voltage (V_{OC}) was 360 mV, which is comparable to the highest value of the previously reported SnS homojunction cells (372 mV[1]). Since the built-in potential of the homojunction was 920 mV and much larger than the previous heterojunction (~700 mV), it should be possible to improve the V_{OC} further. The conversion efficiency was 1.4%, which is lower than the record η of heterojunction (4-5%), mainly due to its low closed circuit current density (J_{sc}) of 7.5 mA/cm². Once the device structure of the homojunction cell is optimized to efficiently collect the photogenerated carriers and achieve a comparable J_{sc} as the conventional heterojunction cells (~25 mAcm⁻²), conversion efficiency exceeding 4-5% would be realized with homojunction with improving the V_{oc} .

[1] P. Sinsermsuksakul et al., *Adv. Energy Mater.*, 4, 1 (2014).

[2] H. Yanagi et al., *Appl. Phys. Express*, 9, 051201 (2016); Y. Iguchi et al., *Inorg. Chem.*, 57, 6769 (2018).

[3] S. Kawanishi et al., *Cryst. Growth Des.* 20, 5931 (2020).

4:45 PM BREAK

5:00 PM EN07.04.06

Synthesis of Cu₂ZnSnS₄ Using Low-Temperature, Water-Based Binary Sulfide Nanoparticle Inks for Sustainable, Low Cost Photovoltaics Han Wang, Nathaniel J. Quitariano and George P. Demopoulos; McGill University, Canada

Kesterite Cu₂ZnSnS₄ (CZTS) is a promising semiconductor material for next-generation thin film photovoltaics since it has earth-abundant and nontoxic elements, a stable structure, and strong light absorption properties. Nanoparticle, solution-based methods have been demonstrated as a potential route for the deposition of CZTS thin films, but many of these methods incorporate organic solvents or additives which can leave a carbon residue that affects device performance. In addition, these organic solvents can create problems with scalability and sustainability. The presented work demonstrates the capability of an environmentally friendly, aqueous-based nanoparticle ink to create the CZTS absorber thin film. Metal chalcogenide complexes formed with ammonium sulfide and tin sulfide are used to stabilize a mixture of component binary sulfides in water without other additives, which are deposited as a compact absorber film with spin coating. It is shown that the concentration of the ammonium sulfide content greatly affects the ink stability, the thin film morphology, and optoelectronic properties of the absorber layer. Furthermore, the incorporation of the tin sulfide complex enables a low temperature transition from binary sulfide nanoparticles to the CZTS phase.

5:05 PM EN07.04.08

TiO₂-CuO Heterostructure for Cost-Effective and Better Optoelectronic Properties of Solar Cell Sajal Islam¹, Ariful Haque^{2,2}, M.F.N. Taufique³ and Kartik Ghosh¹; ¹Missouri State University, United States; ²North Carolina State University, United States; ³Pacific Northwest National Laboratory, United States

Oxide heterostructures have drawn great attention recently, because of its environment-friendly properties and potential applications in optoelectronic devices like LEDs and Solar Cells. In this work, we have performed a simulation study of the heterojunction solar cell with SCAPS (a Solar Cell Capacitance Simulator) using TiO₂ as an n-type layer and CuO as a p-type layer. The thickness and the dopant dependent simulation studies have shown that the solar cell operates at a maximum efficiency of 19.15% when the thickness of the TiO₂/CuO layers are chosen 1.4µm/1.2µm. We carried out an indium doped tin oxide (ITO) vs Fluorine doped tin oxide

(FTO) comparison study as well where FTO worked better as the anode in this structure. We chose gold as the cathode from the simulation study of a range of elements and observed that efficiency increases with better metal work function. Based on these simulation results we have fabricated the oxide-based heterojunction solar cell on FTO substrates using pulsed laser deposition (PLD) for the TiO₂ layer and spin coating for the CuO layer. We have conducted structural-property correlations of individual layers using x-ray diffraction (XRD), Raman analysis, photoluminescence spectroscopy (PL), scanning electron microscopy (SEM), energy-dispersive x-ray spectroscopy (EDX), and different electrical measurements e.g. hall measurements, and sheet resistance measurements. Using specific PLD parameters, we have successfully grown both the rutile phase and anatase phase of TiO₂ separately on several FTO substrates. The results and analysis from the characterizations confirm the successful growth of high-quality oxide thin film layers of TiO₂ on FTO and CuO on TiO₂. Finally, to make the cathode layer of gold, the sputtering technique is used. The solar cell characterization is performed by the I-V measurement using a standard solar simulator and UV-VIS. We have used Origin, Vesta, and MATLAB software for data analysis. The analysis of the solar cell characterization results will be presented at the conference. This facile and cost-effective process of fabrication of all oxide-based heterojunction solar cells will reduce the overall cost of solar cells and increase efficiency with a better optoelectronic performance.

5:10 PM EN07.04.09

Solar Cell Effect on Ferromagnetic Metal-Based Molecular Spintronics Devices Pawan Tyagi and Christopher Riso; University of the District of Columbia, United States

Can spin property of electron lead to a novel form of solar? This question is critical because almost all the solar cells created so far are based on electronic charge. This paper reports the solar cell phenomenon based on the spin property of electrons. The spin-based solar cell effect was observed on magnetic tunnel junction based molecular spintronics devices (MTJMSD). MTJMSDs were produced by covalently bonding organometallic molecular clusters (OMCs) between the top and bottom ferromagnetic electrodes along the exposed side edges of magnetic tunnel junctions with Co/NiFe/AlO_x/NiFe thin film configurations. The MTJMSD configuration showing the photovoltaic effect also exhibited OMC induced strong antiferromagnetic coupling[1] and room temperature current suppression by >five orders of magnitude[2]. Our MTJMSD was fabricated below 100-degree C temperature and employed earth-abundant transition metals like nickel and iron. This paper shows that MTJMSD's photovoltaic effect was susceptible to the magnetic field, temperature, and light intensity. MTJMSDs exhibited three different current states termed as high (μ A), medium (nA), and low (pA). In each state, light radiation produced the photovoltaic effect. OMC molecule appears to create robust exchange coupling between the two ferromagnetic electrodes of the magnetic tunnel junctions leading to significant changes in the electrical, magnetic, and optical properties of the ferromagnetic electrodes. OMC induced changes in the ferromagnetic electrodes also propagated outside the MTJ's perimeter. Magnetic studies, KPAFM, and Raman studies suggested that OMC transformed a ferromagnetic film into photoresponsive material and produced a built-in potential in the MTJMSD. MTJMSD's ability to absorb white light radiation and the ability to separate opposite spins in the three different current states lead to the net photovoltaic effect. MTJMSD's photovoltaic response responded to the magnetic field. This paper mainly reports the experimental observations. Further investigation about the deeper understanding of the spin-photovoltaic effect is needed. We were also not able to provide an exact estimate of the energy conversion efficiency. It was experimentally challenging to determine the exact area responding to light radiation. Future work may focus on simultaneous KPAFM, MFM, and I-V measurements under dark and light for further understanding and new insights.

5:15 PM EN07.04.10

Late News: Stability, Electronic and Optical Properties in Ternary Nitride Phases of MgSnN₂—A First Principles Study Bishal B. Dumre¹, Daniel Gall² and Sanjay Khare¹; ¹The University of Toledo, United States; ²Rensselaer Polytechnic Institute, United States

We studied the disordered-rocksalt, orthorhombic and disordered-wurtzite phases of the ternary nitride semiconductor MgSnN₂ from first principles methods using density functional theory (DFT). We find that MgSnN₂ is mechanically and dynamically stable in all three phases. However, COHP analysis suggests that the

disordered rocksalt structure has anti-bonding states below the Fermi level between -5 eV to -2 eV as compared to the bonding states in other two phases, indicative thermodynamic metastability. Computed lattice constant and electronic band gap values of 4.56 Å and 2.69 eV of MgSnN₂ in disordered rocksalt structure compare well with experimentally reported values of 4.48 Å and 2.3 eV respectively. Furthermore, band gaps were computed in MgSnN_{2-x}O_x, with x = 0.5, 1.0, 1.5, 2.0, to elucidate the role of possible oxygen impurity. Of the three phases, disordered-rocksalt structure shows the lowest charge carrier effective masses. Moreover, this phase has promising absorption coefficient and reflectivity to be used as the absorber layer of tandem solar cells in the higher energy region of the visible portion of the solar spectrum. The other two phases can be utilized as a window layer of solar cells owing to their larger band gap values of 4.36 eV and 4.86 eV respectively.

5:20 PM EN07.04.11

Late News: Photocurrent Transient Characteristics of Chemically Synthesized Lateral and Vertical PbS Photovoltaics for Application as High Performance Infrared Photodetectors Emmanuel K. Ampadu¹, Eunsoo Oh¹, Jungdong Kim¹, DeaKwan Noe¹, KeunSoo Kim² and DongYun Lee²; ¹Chungnam National University, Korea (the Republic of); ²Department of Physics and Graphene Research Institute-Texas Photonics Center International Research Center (GRI-TPC IRC), Korea (the Republic of)

Infrared (IR) photodetectors play a major role in numerous applications, including communications, environmental monitoring and security [1]. Various materials have been used for the purposes of infrared photo detection. Notable among them include Ge, InGaAs and InAs [2]. Research on lead based chalcogenide (PbTe, PbS, and PbSe) for infrared applications have been extensively explored by the scientific community due of the possibility to tune the bandgap in the infrared wavelength range even up to the Terahertz (THz) region [3]. Various photodetectors have been commercialized; photoconduction type which employ the use of an external bias and photovoltaic type detectors which operate with no external bias.

Owing to high transmission in the infrared region, high electrical conductivity, excellent atomic lattice structure and the broad applications for industrial purposes, great attention from the scientific community has been focused on graphene. Graphene is also a very good material for the purposes of transparent contacts in optoelectronic devices operating in the mid - to - far - infrared range, where other transparent oxides such as ITO are no longer desirable due to their free carrier absorption [4]. The increasing interest in the need for bendable, flexible and high performance optoelectronic devices makes graphene a good candidate and has therefore led to various functional materials/graphene hybridized materials [5-6]. Great efforts on the achievement of high-performance graphene-based photodetectors have been concentrated on the development of graphene (G) hybrid structure such as G-semiconductors, G-quantum dots (QD) and G-polymer. Studies have also been conducted to form epitaxial junctions by directly depositing various functional materials on large area CVD-graphene [7].

We fabricated vertical photovoltaic type G/PbS/Ti device by taking advantage of Ti/PbS Schottky junction and discussed the photocurrent transient characteristics. Lead sulfide (PbS), which has a bandgap of 0.42 eV at room temperature, was deposited directly on post-annealed large-area CVD (Chemical vapor deposition) graphene by CBD (Chemical bath deposition). Using a metal mask and an e-beam evaporator, we deposited Ti on glass/G/PbS. Temperature dependent photocurrent spectra of our G/PbS/Ti photovoltaic devices were measured by a Fourier transformed infrared (FTIR) set-up. Post-annealing was found to be an important activity for the adhesion of PbS films on G/glass. As the bandgap energy of PbS decreases with decreasing temperature, the cut-off wavelength increases to longer wavelength, as temperature decreases.

We also fabricated a lateral type device which was comprised of two (2) Ti electrodes separated by a gap of 7 nm and a PbS layer and discussed the laser power dependent photocurrent transient. Because we could obtain fast photo-response from the lateral type device, photocurrent spectrum at room temperature using a FTIR equipment was measured. The cut off wavelength of the detector was found to be ~3.2 μm at room temperature (300 K) which is typical for PbS devices. Our photovoltaic PbS devices can detect not only short - to - mid - infrared but also terahertz radiation at room temperature, which is highly applicable in many fields.

5:25 PM EN07.04.12

N-Type SnS Thin Films Applicable for Homo Junction Solar Cells Issei Suzuki¹, Sakiko Kawanishi¹, Sage

Bauers², Andriy Zakutayev², Hiroyuki Shibata¹, Minesok Kim³, Hiroshi Yanagi³ and Takahisa Omata¹;
¹Tohoku University, Japan; ²National Renewable Energy Laboratory, United States; ³University of Yamanashi, Japan

Since tin (II) sulfide (SnS) is a semiconductor composed of abundant and safe elements and possesses a bandgap (1.1-1.3 eV) suitable for solar cells, it is expected as a light absorber for the next-generation thin film solar cells. The acceptor-type defects, such as Sn antisite (Sn_S) and Sn vacancy (V_{Sn}), are easy to be formed in SnS due to their low formation enthalpy, SnS typically exhibits p-type conduction and it is difficult to convert it into n-type [1]. SnS solar cells, therefore, have adopted a heterojunction structure with p-type SnS and n-type semiconductors such as CdS, however, the conversion efficiency is still 4-5% at maximum [2]. Such low efficiencies are attributed to an unfavorable band offset and interface defects at the hetero interfaces.

Homojunction structure is expected to exhibit higher conversion efficiency and therefore many efforts have been made to realizing n-type SnS. In recent years, it has been reported that n-type SnS sintered compact and single crystals are obtained by halogen (Cl or Br) doping, which paved the way for SnS homojunction [4]. However, the n-type SnS thin films have not been reported so far and it remains as a barrier towards realizing homojunction devices. In this study, we succeeded in obtaining n-type Cl-doped SnS thin films by RF sputtering deposition under a use of RF atomic sulfur supplier (sulfur cracker).

Cl-doped SnS thin films were deposited by RF sputtering on a SiO₂ glass substrate heated at 220-340 °C. Atomic sulfur was supplied to the deposition field of the thin film at the same time from the sulfur cracker installed next to the sputtering cathode. The electrical conductivity, Hall coefficient, chemical compositions, and optical absorption spectra of the obtained thin films were studied.

All of the obtained SnS thin films were p-type conductive without using sulfur cracker and n-type conductive with sulfur cracker, which indicates that supply of the atomic sulfur to the deposition suppresses the formation of acceptor-type defects. Whereas the n-type films exhibited sharp absorption due to the direct band gap around 1.3 eV, p-type films additionally exhibited a broad absorption in the range of 0.9 to 1.2 eV. This broad absorption indicates that there are defect levels with a large density of states within the band gap, which supports the above speculation that the acceptor-type defects were suppressed by performing the deposition with the sulfur cracker.

[1]J. Vidal et al., *Appl. Phys. Lett.*, **2012**, 100, 032104.

[2]P. Sinsersuksakul et al., *Adv. Energy Mater.* **2014**, 4, 1400496.

[3]H. Yanagi et al., *Appl. Phys. Express*, **2016**, 9, 051201.

SESSION EN07.05: Characterization and Passivation I

Session Chairs: Xiaojing Hao and Byungha Shin

Sunday Afternoon, April 18, 2021

EN07

6:30 PM EN07.05.01

First Principles Prediction of Incoherent Interfaces for CdTe/SnO₂ Abhishek Sharan and Stephan Lany;
National Renewable Energy Laboratory, United States

The electronic structure properties of interfaces are of central importance to photovoltaics. Computational approaches can provide information complementary to experimental characterization. In particular, first principles methods can establish an unambiguous link between atomic structures features and their electronic consequences. This strength is also a challenge, because realistic atomic structure models must be available for such calculations. Only for highly idealized situations, such as the epitaxial interface between two reasonably lattice matched materials with the same crystal structure (coherent interface), can the atomic interface structure be trivially constructed. The situation becomes much more complicated when the interface must accommodate

incommensurate surface unit cells for the two materials. In this case, the interface becomes incoherent, i.e., exhibiting a reduced periodicity requiring a larger surface unit cell or even forming an essentially (2-dimensionally) amorphous non-periodic structure.

In this work, we adopted the kinetically limited minimization (KLM) approach, previously utilized for unconstrained crystal structure prediction, to sample atomic structures for SnO₂/CdTe interfaces without and with the presence of CdCl₂. The simulations treat SnO₂ as a substrate, and CdTe as a thin film, with a variable number of atomic layers. No initial assumptions are made about the CdTe atomic structure. Both the correct zinc-blende bulk structure and the known surface structures of the (110) and (001) back-surfaces are reproduced over the course of the sampling. The inclusion of CdCl₂ results in improved bonding and periodicity, and considerably lowers the total interface energy. While the full sampling of the compositional and configurational space remains challenging, this work provides a proof of concept for first principles atomic structure prediction for incoherent interfaces.

6:45 PM EN07.05.02

High Throughput, Single-Source Scribing Mechanism for Optimal Interconnections in Thin-Film Photovoltaic Modules Austin Flick and Reinhold Dauskardt; Stanford University, United States

The advancement of thin film photovoltaic devices requires the successful implementation of a series of high-performing, low-cost scribes for efficient module interconnections. These scribes, which serve to electrically isolate the front electrode (P1) and rear electrode (P3), and provide the electrical interconnection (P2) between adjacent cells, have been explored using a wide variety of scribing options, primarily laser-based mechanisms. Laser scribing offers the benefits of high tunability and alignment accuracy, allowing for the selective removal of specific layers while mitigating dead area losses. Different laser wavelengths and process parameters are often employed to achieve this selectivity; however, the demand for multiple unique laser systems for complete module fabrication results in high equipment costs and increased process complexity.

Our work demonstrates the successful implementation of a single-source scribing mechanism capable of performing the P1, P2, and P3 scribes, enabling further simplification and cost reduction over other laser scribing methods. This mechanism utilizes one of the most commercially available laser wavelengths (1064nm) without the need for expensive yet commonly employed ultrashort laser pulsed systems, relying exclusively on interactions between the laser and front electrode material and thus demonstrating broad applicability across a variety of materials and architectures. This unique scribing mechanism is compatible with extremely high throughputs on the order of several meters per second, an order of magnitude increase over the speeds of other laser scribing mechanisms. An improvement at this scale further enables reductions in cost of over 90% for the laser scribing steps in a MW-scale photovoltaic system.

6:50 PM *EN07.05.03

New Analysis Methods for Dopant Fluctuations in Thin-Film Solar Cells John Moseley; National Renewable Energy Laboratory, United States

Quantifying the performance impacts of band tails on CdTe, CIGSe, and CZTS thin-film solar cells remains a significant challenge to further development of these technologies. Band tails are prevalent in CdTe, CIGSe, and CZTS absorption, quantum efficiency, and luminescence data and are believed to reduce the open-circuit voltage (V_{oc}). However, quantifying band-tail related performance impacts is not straightforward. Tailing present in macroscopic optoelectronic data may arise from inhomogeneous impurity/matrix-element distributions, from structural defects such as dislocations and grain boundaries, or from intentional compositional grading [e.g., Cu(In_xGa_{1-x})Se₂]. Furthermore, inhomogeneities may span from nm to mm in scale. Thus, quantifying performance impacts includes the challenges of separating tailing due to inhomogeneities and structural defects from tailing due to compositional grading; determining the characteristic length scale of inhomogeneity; and reconciling macroscopic and microscopic data and models.

The thin-film solar cell community knows well that fluctuations in dopant densities produce electrostatic

potential fluctuations. However, the community still relies heavily on early theoretical work (from Shklovskii and Efros and others) to estimate potential fluctuation magnitudes. Commonly used expressions were only meant to provide first-order estimates and are potentially inadequate for describing fluctuations occurring in thin-film solar cell materials. In this talk, I will summarize our recent efforts to develop realistic estimates of fluctuation impacts on performance, using Cd(Se)Te solar cells as an example.

Optoelectronic data on Cd(Se)Te cells doped with arsenic show an increasing tail below the bandgap that is correlated with increasing arsenic incorporation level. These cells have As-dopant activation levels of only 1-5%, and an inverse relationship exists between dopant activation and incorporation, consistent with self-compensation mechanisms. Macroscopic photoluminescence and microscopic cathodoluminescence measurements were conducted at room and low temperature. The data indicate that, to a large extent, the tailing observed in macroscopic measurements, and the inhomogeneity that causes it, is present within individual μm -size grains.

Consistent with this picture, we consider that tails are created by randomly distributed As donor and acceptor (shallow) defects. The densities of donor and acceptor defects are based on incorporation (secondary-ion mass spectrometry) and carrier-density (capacitance-voltage) data. Donor and acceptor defects are randomly distributed in a cube and each is assigned a screened coulomb potential. Fluctuations in the potential can be clearly seen and we confirm that this numerical approach reproduces results from early semiclassical band-tail theory. Furthermore, we apply semiclassical theory to estimate V_{oc} losses in Cd(Se)Te solar cells.

Addressing the weaknesses of semiclassical theory, we develop self-consistent numerical methods to analyze random dopant fluctuations. We distribute donor and acceptor defects randomly within a 2D domain and solve Poisson's equation with density-gradient corrections to the electron and hole densities. The results show how compensation can enhance potential fluctuation amplitudes and induce large carrier-density fluctuations. Interestingly, we find that the effective band gap energy is not constant but has a distribution with a low energy tail. Finally, we use simple formulas to show how the effective bandgap tail can produce tails in absorption and luminescence spectra. These methods can potentially be used to form realistic models of fluctuation impacts on thin-film solar cell performance and facilitate progress.

7:15 PM BREAK

7:30 PM *EN07.05.04

Impact of Se Alloying on Metastable Defect Properties in Cd-Rich Group-V Doped CdTe Single Crystal
Akira Nagaoka¹, Kensuke Nishioka¹, Kenji Yoshino¹, Koji Kimura², Kouichi Hayashi², Darius Kuciauskas³ and Mike Scarpulla⁴; ¹University of Miyazaki, Japan; ²Nagoya Institute of Technology, Japan; ³National Renewable Energy Laboratory (NREL), United States; ⁴University of Utah, United States

Cadmium telluride (CdTe) photovoltaic (PV) modules are relatively easy to produce at a low cost, making them one of the most competitive commercially available PV technologies. Recently, the world-record PV cell has a power conversion efficiency of 22.1%, which is well below the theoretical limits. The improvement of efficiency without increasing the production costs will make PV generation more competitive with fossil fuels. The practical strategy for higher efficiency is improvements of open-circuit voltage (V_{oc}) and short-circuit current (J_{sc}).

Recently, it was discovered that group-V element doping (P, As, Sb, or Bi) and Cd-rich composition are key technologies for increasing V_{oc} , and these results were attributed to high p-type doping and long minority carrier lifetime. PV devices fabricated with P-doped CdTe single crystals as absorbing layer and with Cd-rich composition could result in hole concentration of $\sim 10^{17} \text{ cm}^{-3}$, minority carrier lifetime of several hundreds of nano second, and V_{oc} exceeding 1 V. However, it is difficult to obtain group-V doping higher than 10^{17} cm^{-3} because doping efficiency typically becomes lower with higher dopant incorporation (above $\sim 10^{16} \text{ cm}^{-3}$). The origin of this doping limit has not been established, but theoretical studies suggest that it may be caused by the formation of self-compensating AX center or defect complex. The AX center is formed due to a large lattice

relaxation of the substitutional dopant which results in conversion to a donor state. Recently, with in situ As-doping in polycrystalline thin film CdTe-based PV devices larger than 20% power conversion efficiency was achieved, but dopant activation remained low (2-4%).

On the other hand, CdTe alloying with Se (CdTeSe) has attracted strong interest for improving J_{sc} because lower bandgap leads to increased absorption in the long wavelength part of the spectrum. Bandgap tuning through alloying is widely used in PV. For example, high-efficiency $Cu(In_xGa_{1-x})Se_2$ (CIGS) absorbers employ bandgap grading by controlled variation of In/Ga composition.

We combine both approaches to develop more efficient CdTe solar cells: group V doping and alloying with Se. We have grown high-quality As-doped Cd-rich CdTeSe single crystals from metal Cd solvent near thermodynamic equilibrium using the traveling heater method (THM). In this presentation, we will report growth and characterization of group-V doped Cd-rich CdTeSe single crystals from THM. It is not clear how the formation of CdTeSe alloy affects the activation of group-V doping, defect compensation mechanism and PV performance, and we propose some possible answers to these questions.

7:55 PM EN07.05.06

Semi-Transparent and Ultra-Thin Silicon Solar Cells Fabricated by the Surface-Bulk Micromachining

Erfan Pourshaban, Aishwaryadev Banerjee, Chayanjit Ghosh, Adwait Deshpande, Hanseup Kim and Carlos Mastrangelo; The University of Utah, United States

Widespread research in the field of wearable electronics, has ignited interest in stand-alone and efficient power generators. Photovoltaic devices are promising candidates for such applications. Due to their high stability and biocompatibility, Si solar cells are an attractive choice. However, the absorption coefficient of Si is highest in the visible and NIR region of the EM spectrum. Thus, efficient Si cells are opaque, which makes them undesirable for a wide range of applications that require the on-board electronics to be transparent.

Additionally, the thickness of the conventional Si solar cells is $\sim 200\text{-}300\ \mu\text{m}$ which makes them rigid and unsuitable for applications that require the system components to be thin and flexible. Here, we present the design, fabrication, and performance evaluation of semi-transparent ($T \sim 30\%$ and 60%) and ultra-thin ($15\ \mu\text{m}$) Si solar cells fabricated by surface-bulk micromachining (SBM) process.

A $\langle 111 \rangle$ boron-doped Si wafer with an average bulk resistivity of $5\text{-}10\ \Omega\cdot\text{cm}$ was used as the substrate and base region. $400\ \text{nm}$ of SiO_2 was thermally grown which acts as the diffusion barrier for subsequent doping steps. Phosphorous doping was performed at $1000\ ^\circ\text{C}$ for 60 minutes to define the emitter region (sheet resistance = $8\ \Omega\cdot\text{sq}^{-1}$). Micro holes (with a diameter of $170\ \mu\text{m}$) were then lithographically patterned in a hexagonal arrangement to achieve different levels of transparency in the fabricated Si solar cell. Next, deep reactive ion etching (DRIE) was performed on these patterns to realize trenches of $15\ \mu\text{m}$ depth. This defines the final thickness of the solar cell. After this, $300\ \text{nm}$ of LPCVD low-stress Si nitride was deposited on the sidewalls of the trenches as an etch resistant layer. This was followed by patterning and a second DRIE (DRIE 2) to dig deeper trenches than those achieved previously. The final transparency and effective surface area of the Si solar cell is determined during this step. The diameter of DRIE 2 micro holes was designed to be $\sim 150\ \mu\text{m}$ with a filling ratio of 25% and 50% that corresponds to an inter-hole distance (s) of $138\ \mu\text{m}$ and $54\ \mu\text{m}$, respectively. This inter-hole spacing determines the required minimum depth of DRIE 2 trenches (h), which is crucial to release the ultra-thin device from the underlying substrate. Since (111) family planes have a negligible etch rate in KOH/TMAH, they act as an effective etch-stop layer. Therefore, to ensure that the etchant completely undercuts the device before reaching the etch-stop layer, the DRIE-2 depth (h) must be higher than $s \cdot \tan(19.47^\circ)$. The DRIE-2 trench depth for 25% and 50% filling ratio devices were designed to be $394\ \mu\text{m}$ and $154\ \mu\text{m}$, respectively. Finally, the samples were dipped into a 10 wt% tetramethylammonium hydroxide (TMAH) solution at $100\ ^\circ\text{C}$ for completely releasing the structures. The time taken to release devices with 25% filling ratio and 50% filling ratio was 10 hours and 4 hours, respectively. After fishing out the released devices from the TMAH solution and removing the remaining Si nitride by CF_4/O_2 RIE dry-etching, $20\ \text{nm}$ of SiO_2 was deposited as a passivation layer on the bottom of the solar cell and the sidewalls of DRIE trenches.

$15\ \mu\text{m}$ thick Si solar cells with a transparency of $\sim 30\%$ and $\sim 60\%$ were fabricated using the proposed method. Photocurrent-voltage measurements were conducted under indoor white light condition with an input power density of $13\ \text{mW}\cdot\text{cm}^{-2}$. I-V results demonstrate the open-circuit voltage of 300, 120 mV and the short circuit

current density of 34, 1.4 $\mu\text{A}\cdot\text{cm}^{-2}$ for the 30% and 60% transparent silicon solar cells, respectively.

8:00 PM *EN07.05.07

Controlling the Defects of Kesterite Solar Cells Xiaojing Hao; University of New South Wales, Australia

The Kesterite $\text{Cu}_2\text{ZnSn}(\text{S},\text{Se})_4$ (CZTSSe) semiconductor is a compelling emerging light-harvesting material for low-cost, environment-benign, and high-efficiency thin-film photovoltaics. The highest power conversion efficiency so far for kesterites are 11% and 12.6 % for pure sulfide kesterite and Se-containing kesterites, respectively. The current state-of-the-art kesterite devices suffer from the challenge of controlling defects (e.g. cation—disordering defects, defect clusters), which generally results in severe potential fluctuation, low minority carrier lifetime, and thereby unsatisfactory device performance. Identifying effective ways of controlling these defects is of vital importance for further efficiency breakthroughs. In our recent work, we demonstrated that some of these defects can be suppressed by either controlling the local chemical environment during the chalcogenisation synthesis of kesterite, or lithium post-deposition-treatment. By controlling the local chemical environment in time when the kesterite phase starts to form, we demonstrated an independently confirmed 12.5% efficiency for CZTSe solar cells with high V_{oc} of 491 mV, showing the promise of these defect control strategies.

SESSION EN07.06: Advances in CIGS Solar Cells I

Session Chairs: Alex Redinger and Mike Scarpulla

Monday Morning, April 19, 2021

EN07

8:00 AM *EN07.06.01

Ag-Alloying in $\text{Cu}(\text{In},\text{Ga})\text{Se}_2$ Marika Edoff, Jes Larsen, Jan Keller, Kostyantyn Sopiha, Tobias Törndahl and Lars Stolt; Uppsala University, Sweden

The chalcopyrite family has emerged as a material with many possibilities and has yielded high efficiencies above 23 % [1]. One of the additions to this family is alloying with silver to form $(\text{Ag},\text{Cu})(\text{In},\text{Ga})\text{Se}_2$ (ACIGS). Among the features of Ag alloying as compared to $\text{Cu}(\text{In},\text{Ga})\text{Se}_2$ (CIGS) without Ag, are a lower melting temperature, that leads to large grains also for relatively low deposition temperatures, but also lower voltage losses as compared to the Shockley Queisser limit [2], and a slight increase in bandgap, due to Ag, accompanied by lowering of both the conduction band minimum and of the valence band maximum energy [3]. These advantages open up interesting applications for ACIGS as e.g. top cells in tandem devices, either in combination with low bandgap CuInSe_2 (with or without Ag) or with Si as bottom cells. Due to its electronic band structure, ACIGS with high bandgap up to 1.5 eV yields high efficiencies with a conventional buffer layer like CdS, but also with ZnSnO and $\text{Zn}(\text{O},\text{S})$ [4]. In addition to high efficiency, also long-term performance is essential for all applications and there are some questions related to phase stability for the ACIGS material, that need to be investigated further, but where we have obtained new insights with the help of first principle calculations [5]. Among the studies made in our group during the last few years are ACIGS with Ag/(Ag+Cu) ratios varying from 10 to 100 % and with varying Ga/(Ga+In) from 0 to 100 %. We have also applied ACIGS to solar cells with submicron thick absorber layers, as well as investigated the impact of post deposition treatments to this type of materials. In the talk, a short review of the state-of-the art of ACIGS will be given together with some of our insights from this line of research.

[1] Nakamura et al, IEEE Journal of Photovoltaics, 2019, 9 (6), 1863-1867

[2] Edoff et al, IEEE Journal of Photovoltaics, 2017, 7 (6), 1789-1794

[3] Boyle et al, Journal of Applied Physics, 2014, 115 (22), 223504

[4] Keller et al, Progress in Photovoltaics, 2020, 28 (4), 237-250

[5] Sopiha et al, Journal of Materials Chemistry A, 2020, 8 (17), 8740-8751

8:25 AM EN07.06.02

The Effect of Damp Heat—Illumination Exposure on CIGS Solar Cells—A Combined XRD and

Electrical Characterization Study Mirjam Theelen¹, Ruud Hendrikx², Nicolas Barreau³, Henk Steijvers¹ and Amarante Bottger²; ¹TNO Solliance, Netherlands; ²Delft University of Technology, Netherlands; ³Institute des Matériaux Jean Rouxel (IMN)-UMR, France

In order to obtain long-term stable and low-cost photovoltaic modules, it is important to know possible degradation mechanisms. In order to identify long term behavior, unpackaged Cu(In,Ga)Se₂ solar cells were simultaneously exposed to damp heat and illumination (settings: 85°C/85% relative humidity and 1000 W/m² BAA illumination) [1]. In-situ monitoring of their electrical parameters demonstrated a rapid decrease of the efficiency, mainly driven by changes in the series and shunt resistances. Moreover, non-degraded and degraded solar cells were studied by in-depth XRD and SIMS to investigate the material changes leading to efficiency loss.

SIMS revealed the migration of sodium and potassium, likely leading to a severe decrease in the shunt resistance (from 500±100Ω to 20-30Ω within 200 hours) and voltage. It also displayed the ingress of hydroxide, especially in the ZnO:Al film. Extensive XRD measurements showed that molybdenum oxide was formed, which likely affected the Ohmic contact between Mo and CIGS. Moreover, an in-plane stress increase in the ZnO:Al film from -183±29 to -450±40 MPa was observed. This stress increase is most likely due to the incorporation of species like hydroxides and carbonates in the grain boundaries of the ZnO:Al film. These phenomena could lead to the observed increased series resistance in the solar cells [2].

[1] M. Theelen *et al.*, JoVE 140 (2018)

[2] M. Theelen *et al.*, Sol. Mat. Sol. Cells 157 (2016) 943–952

8:40 AM EN07.06.03

Late News: Investigation of the Aptness of Pulsed Laser Deposition for the Sequential Fabrication of

Cu(In,Ga)Se₂-Based Thin-Film Solar Cells Evripides Kyriakides, Panagiotis Ioannou, Christiana Nicolaou, Vasiliki Paraskeva, Maria Hadjipanayi, George E. Georghiou, Paris Papagiorgis, Grigorios Itskos and John Giapintzakis; University of Cyprus, Cyprus

Thin-film photovoltaic (PV) technologies, and Cu(In,Ga)Se₂ (CIGS) thin-film solar cells in particular, have been the subject of increasingly rigorous study of late. There are several motivating factors for the development of thin-film photovoltaics, such as the reduction in raw material usage, the decrease in solar cell weight, and the possibility of deposition on flexible substrates. Furthermore, CIGS-based thin-film solar cells hold several advantages compared to rival solar cell technologies. Specifically, they have the highest conversion efficiencies among chalcogenide thin-film PV technologies (23.35% for cells and 17.5% for modules), high radiation resistance, and outstanding stability.

The typical CIGS-based solar cell consists of a soda-lime glass (SLG) substrate, a Mo back contact, CIGS as the p-type absorber layer, CdS as the n-type buffer layer, and i-ZnO/ZnO:Al as the decoupling and transporting window layers, respectively. However, in the state-of-the-art CIGS-based solar cells, each of these layers is deposited with a different method; co-evaporation for the CIGS layer, chemical bath deposition for the CdS layer, and reactive sputtering for the i-ZnO/ZnO:Al bilayer.

This work reports on the utilization of pulsed laser deposition (PLD) as a single technique for the preparation of the aforementioned layers of a complete CIGS-based solar cell stack. Employing a single deposition technique greatly reduces manufacturing complexity. Furthermore, it potentially decreases processing time and associated fabrication costs through streamlined production lines.

The presented results discuss the challenges faced in the completion of this task. The properties of the PLD-grown thin films with respect to structure, composition and morphology are parametrically investigated through

X-ray diffraction (XRD), energy-dispersive X-ray spectroscopy (EDS), scanning electron microscopy (SEM) and atomic force microscopy (AFM). Hence, the influence of PLD process parameters on film growth is evaluated. TCAD simulations realized in Synopsys Sentaurus Device are utilized for the optimization of the function of the cell. Electrical and optical measurements carried out in a solar simulator are used to assess the photovoltaic behavior of the complete structure and, critically, the CdS/CIGS junction heterointerface. The solutions implemented, involving modifications to the typical PLD process, are discussed. Finally, the resulting improvement in conversion efficiency is demonstrated.

8:45 AM BREAK

9:30 AM *EN07.06.06

High Efficiency Solar Cells Based on Co-Evaporated $\text{CuIn}_{0.7}\text{Ga}_{0.3}\text{S}_2$ —Correlation Between Growth Process and Absorber Characteristics Nicolas Barreau; Université de Nantes, CNRS, Institut des Matériaux Jean Rouxel, IMN, France

$\text{CuIn}_{0.7}\text{Ga}_{0.3}\text{S}_2$ semi-conductor has a bandgap energy of 1.7 eV, which is well adapted to applications as top cell in tandem structures with c-silicon bottom cell. Recently, we have shown that solar cells with standard structure, namely Glass/Mo/ $\text{CuIn}_{0.7}\text{Ga}_{0.3}\text{S}_2$ /CdS/ZnO/AZO, can reach efficiencies above 14 %; the $\text{CuIn}_{0.7}\text{Ga}_{0.3}\text{S}_2$ layer being grown by co-evaporation following a 3-stage process. Determination of compositional depth profile of these absorbers revealed that the distribution of group III elements (*i.e.* In and Ga) is not homogeneous throughout the layers, as expected for films grown by means of sequential process. However, in contrast to V-shaped GGI evolution commonly observed in selenide absorbers, these sulfide films appear composed of two distinct layers, a first with GGI $\sim 0.7/0.8$ near the back contact and a second with GGI $\sim 0.2/0.3$ close to the surface; note that the abrupt interface between these layers is located at about half of total film thickness. A large part of the present contribution will focus on the origins for such bilayered compositional structure, which will be discussed accounting relative phase stability while copper content is increased during the second stage. In addition, although optimal bulk material quality could be achieved, device performance still appears limited by dominant interface recombination. To further explore that issue, the first results on epitaxial $\text{CuIn}_{0.7}\text{Ga}_{0.3}\text{S}_2$ layers will be presented.

SESSION EN07.07: Advances in CIGS Solar Cells II
Session Chairs: Nicolas Barreau and Mirjam Theelen
Monday Morning, April 19, 2021
EN07

10:30 AM *EN07.07.01

Development of Ultrathin $\text{Cu}(\text{In,Ga})\text{Se}_2$ Solar Cells Jessica de Wild¹, Thierry Kohl¹, Gizem Birant¹, Dilara G. Budu¹, Guy Brammertz¹, Marc Meuris¹, Jef Poortmans² and Bart Vermang¹; ¹IMOMECE, Belgium; ²imec, Belgium

Thin film solar cells have the possibility to be made flexible, semi-transparent and/or may be applied for tandem structures or building integrated. Having multiple usages, it is of interest to make these thin film solar cells as fast and cheap as possible. From the available thin films, $\text{Cu}(\text{In,Ga})\text{Se}_2$ (CIGS) has one of the best solar cell performance [1]. There are concerns about the usage of indium though when CIGS will be widely applied. Therefore, making the CIGS layer thinner and thereby reducing the amount of In, is an interesting option to explore. When the absorber material becomes thin, interfaces are generally limiting the performance and the path length to absorb all the incoming light may be too short to absorb the longer wavelengths. There are various approaches to tackle these problems. Passivation of the back contact by applying a dielectric is the main route investigated. Not only reduces it the interface recombination at the Mo/CIGS back contact but it also

increases the reflection. We will present here various approaches which are aimed to be industrial viable and easy to make to reduce the losses in ultrathin CIGS solar cells. This also holds for the absorber layers which are made by a single stage coevaporation process. In this case, the Ga gradient at the back is replaced by a passivation layer and no copper rich stage is applied. The effect of the simplified growth is mostly visible in the grain boundaries [2]. As passivation layer, AlO_x is often used. As this layer blocks the current flow, it has to be either sufficiently thin to allow tunneling or requires holes allowing for the current to flow to the Mo back contact. We will show that the latter approach can be applied for layers up to 6 nm without lithography steps by simply adding NaF before CIGS growth [3]. When applying a thin Ag layer under the AlO_x the cells also show optical improvement. This is likely due to formation of scattering particles, making the CIGS rougher and thereby increasing the optical path length. To improve the absorber layer itself alkali treatments are applied [4]. At the front, the CIGS/buffer interface may also need to be adapted. Application of a passivation layer at the front, either with holes or thin enough for tunneling, is investigated. Before applying a passivation layer on the CIGS surface, cleaning treatments need to be applied [5]. To analyze the effect of the various treatments a combinatorial approach based on bias dependent admittance spectroscopy and (time resolved (TR)) photoluminescence (PL) is developed. Generally, with (TR)-PL a quick analysis whether the treatments are improving the absorber/interface quality before finishing into a device is possible. Features like interference and blue shifts of the spectra may be observed as well and can be related to the emission profile and scale of the potential fluctuations in the absorber layer [6]. However, improvement due the various treatments observed in the (TR)-PL does not necessarily translates into better solar cell performance. This can indicate that the treatments are sensitive to the processing conditions of the window layers for instance and/or that barriers are formed. With bias-dependent admittance spectroscopy losses at interfaces and bulk can be found by introducing a so-called CVf loss map [7]. These maps visualize the losses in the solar cell, which makes it possible to distinguish defects in the bulk from the interface and barriers at front or back interfaces. The bottlenecks observed when developing ultrathin CIGS solar cells will be discussed and possible options to mitigate them are investigated.

- [1] M.A. Green, DOI: 10.1002/pip.3303
- [2] T. Kohl, DOI: 10.1021/acsaem.0c00610
- [3] G. Birant, DOI: 10.1016/j.solener.2020.07.038
- [4] J. de Wild, DOI: 10.1021/acsaem.9b01370
- [5] D. G. Buldu, DOI:10.1002/pssa.202000307
- [6] J. de Wild, DOI: 10.1063/5.0024840
- [7] G. Brammertz, DOI: 10.1109/JPHOTOV.2020.2992350

10:55 AM EN07.07.02

Sputtered Gallium Oxide Applied to the Front Side of Cu(In,Ga)Se₂ Thin-Film Solar Cells Wolfram Witte, Wolfram Hempel, Stefan Paetel, Richard Menner and Dimitrios Hariskos; Zentrum für Sonnenenergie- und Wasserstoff-Forschung Baden-Württemberg (ZSW), Germany

Oxide-based materials could be candidates for buffer, passivation, or high resistive (HR) layers in Cu(In,Ga)Se₂ (CIGS) thin-film solar cells. In recent years, oxide materials like (Zn,Mg)O, Al₂O₃, Zn_xTi_yO [1], (In,Ga)₂O₃ [2] and Sn_{1-x}Ga_xO_y [3] were under investigation. Most of them were deposited by atomic layer deposition. However, from an industrial point of view a very fast method, with deposition times <1 min for a complete layer, would be preferable for buffer, passivation, or HR layer growth.

In this study, we present our results with rf-magnetron sputtered Ga₂O₃ buffer layers as a substitute for our solution-grown CdS buffer in combination with i-ZnO as HR layer and ZnO:Al front contact. So far, best cells achieved efficiencies up to 14% without post-annealing compared to the CdS-buffered reference cells, which exhibit efficiencies up to 17%. As a result of the very high bandgap energy around 4.7 eV of Ga₂O₃, as determined on quartz glass by optical transmittance measurements, and reduced parasitic absorption even higher J_{sc} values could be achieved compared to the CdS-buffered reference cells. Nevertheless, the difference in efficiency is mainly due to reduced Voc and FF values of the CIGS cells with Ga₂O₃.

The solar cell performance of cells with Ga₂O₃ buffers strongly depends on the deposition conditions as well as

on the thickness of the sputtered Ga₂O₃ layers. We observed poor cell efficiencies for cells with Ga₂O₃ sputtered at room temperature and good values for films grown at elevated substrate temperatures (120 – 200 °C). This result is similar to the behavior we observed for CIGS cells with sputtered Zn(O,S) and In_xS_y buffers [4]. The Ga₂O₃ layers deposited in the relevant temperature range for solar cell applications are X-ray amorphous. When using CIGS absorber layers with a RbF post-deposition treatment, a wet chemical treatment of the CIGS surface before the Ga₂O₃ deposition has a significant positive impact to achieve decent efficiencies. Non-rinsed samples could exhibit poor efficiencies, mainly due to bad FF values. In addition, we could achieve a comparable good efficiency of 19.4% (with anti-reflective coating) with Ga₂O₃ applied as an HR layer instead of i-ZnO (19.7%) in combination with CdS as a buffer and ZnO:Al as front contact.

[1] J. Löckinger et al., ACS Appl. Mater. Interfaces **10** (2018) 43603

[2] T. Koida et al., IEEE J. Photovolt. **5** (2015) 956

[3] F. Larsson et al., J. Vac. Sci. Technol. A **37** (2019) 030906

[4] D. Hariskos et al., Appl. Sci. **10** (2020) 1052

11:10 AM EN07.07.03

Chemical and Electronic Structure of GaO_x/Cu(In,Ga)Se₂ Interfaces in Thin-Film Solar Cells with RbF Post-Deposition Treatment Dirk Hauschild^{1,1,2}, Elizaveta Pyatenko^{1,1}, Vladyslav Mikhnych¹, Ralph Steininger¹, Mary Blankenship², Dimitrios Hariskos³, Wolfram Witte³, Michael Powalla³, Clemens Heske^{1,1,2} and Lothar Weinhardt^{1,1,2}; ¹Karlsruhe Institute of Technology (KIT), Germany; ²University of Nevada, Las Vegas (UNLV), United States; ³Zentrum für Sonnenenergie- und Wasserstoff-Forschung Baden-Württemberg (ZSW), Germany

The introduction of post-deposition treatments (PDTs) has increased the Cu(In,Ga)Se₂-based (CIGSe) thin-film solar cell efficiencies to >23 % on a laboratory scale. Such high-efficiency devices are often processed with a solution-deposited CdS buffer layer. However, the CdS band gap leads to absorption losses in the buffer layer, reducing the solar-cell efficiency. Hence, there is a strong interest to replace CdS with an alternative wide(r) band gap material. In addition to merely increasing the buffer layer band gap, using such an alternative material would also lead to various changes at the buffer/absorber interface, including the electronic and chemical structure. A detailed knowledge of these changes is crucial for further device optimization.

In this contribution, we report on industrially relevant CIGSe absorbers with and without an NH₃-based rinsing step applied after the RbF PDT. Their interface with a wide band-gap GaO_x buffer layer is studied using x-ray photoelectron spectroscopy (XPS), hard XPS (HAXPES) at the synchrotron, and a combination of UV photoelectron spectroscopy (UPS) and inverse photoemission spectroscopy (IPES). The results paint a comprehensive picture of the GaO_x/CIGSe interface and will be discussed in view of the performance of the corresponding CIGSe solar cells.

11:25 AM BREAK

11:35 AM EN07.07.04

Late News: Atomic Layer Deposition of Zn_{1-x}Mg_xO as Transparent Conducting Films for Chalcopyrite Solar Cells Poorani Gnanasambandan^{1,2}, Mohit Sood², Noureddine Adjeroud¹, Renaud Leturcq¹ and Susanne Siebentritt²; ¹Luxembourg Institute of Science and Technology, Luxembourg; ²University of Luxembourg, Luxembourg

We investigate atomic layer deposited zinc magnesium oxide films with varying Mg content as transparent conducting films and as electron transport layers for chalcopyrite solar cells. Optimizing a ternary process by mixing two binary ALD process has its challenges [1]. We achieve high degree of control on composition by optimizing the growth conditions with varying deposition temperatures and supercycle parameters such as pulse ratios and bilayer period. We examine the effect of these films on the performance of high-bandgap solar cells

based on Cu(In,Ga)S₂ absorbers.

Previous studies on the impact of Zn_{1-x}Mg_xO:Al as transparent electrodes and Mg doped ZnO thin films for the window layer of CIGS Cu(In,Ga)(S,Se)₂ solar cells employed co-sputtering, electrodeposition and ALD respectively [2][3][4][5]. With the advantage of low temperature and highly conformal thin film growth, we study ALD grown Zn_{1-x}Mg_xO with x varying from 0.1 to 0.4 and elucidate the effect of doping on the band alignment, electrical and optical properties. With variation in Mg content we were able to achieve 11% efficient Cu(In,Ga)S₂ solar cell with an open-circuit voltage of 941 mV.

- [1]. Mackus, Adriaan JM, et al. "Synthesis of doped, ternary, and quaternary materials by atomic layer deposition: a review." *Chemistry of Materials* 31.4 (2018): 1142-1183.
- [2]. Kuwahata, Yoshihiro, and Takashi Minemoto. "Impact of Zn_{1-x}Mg_xO: Al transparent electrode for bufferless Cu (In, Ga) Se₂ solar cells." *Renewable energy* 65 (2014): 113-116.
- [3]. Wang, Mang, et al. "Electrodeposition of Mg doped ZnO thin film for the window layer of CIGS solar cell." *Applied Surface Science* 382 (2016): 217-224.
- [4]. Inoue, Yukari and Hala, Matej et al. "Optimization of buffer layer/i-layer band alignment" in 42nd IEEE Photovoltaic Specialist Conference (IEEE, New Orleans, 2015), pp. 1
- [5]. Hiroi H, Iwata Y, Adachi S, Sugimoto H, Yamada A. New World-Record Efficiency for Pure-Sulfide Cu(In,Ga)S₂; Thin-Film Solar Cell With Cd-Free Buffer Layer via KCN-Free Process. *IEEE J Photovolt.* 2016;6(3):760-763.

11:50 AM EN07.07.05

Solution Processed Bismuth Halide and Chalcohalide Thin-Film Solar Cells David J. Fermin¹ and Devendra Tiwari²; ¹University of Bristol, United Kingdom; ²Northumbria University, United Kingdom

Solution processing of inorganic thin-film solar cells is a key challenge in the growing area of system integrated photovoltaics. The ability of processing high quality materials at temperatures below 200 °C enables the fabrication of devices onto flexible composite materials. Semiconductor compounds with high degree of defect tolerance are an exciting class of materials particularly well-suited to these applications. Indeed, compounds based on Bi³⁺ can lead to attractive opto-electronic properties similar to those observed in Pb²⁺ hybrid perovskites, such as large spin-orbit coupling, dielectric constant and band dispersion.¹

In this contribution, we will discuss the structure and opto-electronic properties of phase-pure BiI₃ and BiSI obtained by solution based method. BiI₃ is prepared by spontaneous gas-phase iodination of Bi₂S₃ films at 200 °C,² while BiSI is generated by thermolysis of a precursor solution composed of Bi(NO₃)₂, thiourea and NH₄I.³ In addition to accurate structure refinement from XRD data of the thin-films, we find excellent correlation between experimental Raman spectra and Raman modes calculated by density functional perturbation theory. Interestingly, BiI₃ exhibits p-type conductivity (acceptor density of the order of 10¹⁵ cm⁻³) and a band gap of 1.7 eV, while BiSI is n-type with a donor density in the range of 10¹⁹ cm⁻³. Quasi-particle G₀W₀ calculations of both materials show that the conduction band is more dispersed than the valence band due to spin-orbit coupling promoted by Bi³⁺. Band edge energy values are estimated by electrochemical impedance spectroscopy, enabling the design of PV devices with appropriate band alignment. Devices with the structure Glass/FTO/TiO₂/BiI₃/F8/Au and Glass/FTO/SnO₂/BiI₃/F8/Au, where F8 is Poly(9,9-di-n-octylfluorenyl-2,7-diy), display open-circuit voltage above as high as 600 mV and record power conversion efficiency of 1.32% under AM 1.5G illumination. We will expand the discussion to other complex Bi chalcogenides,⁴ addressing the key limiting factor in the PV performance of these materials, i.e. their short carrier lifetimes.

References:

- 1- A.M. Ganose et al. *Chem. Commun.* 2017, **53**, 20
- 2- D. Tiwari and D.J. Fermin, *ACS Energy Lett.* 2018, **3**, 1882
- 3- D. Tiwari et al. *ACS Appl. Energy Mater.* 2019, **2**, 3878
- 4- D. Tiwari et al. *Chem. Mater.* 2020, **32**, 1235

12:05 PM *EN07.07.06

Development and Application of Transparent Back Contacts in CIGSe Solar Cells Roland Scheer¹, Thomas Schneider¹, Johanna Troendle¹, Bodo Fuhrmann¹, Frank Syrowatka¹, Heiko Kempa¹, Torsten Hoelscher¹, Marcel Placidi^{2,3} and Alejandro Perez-Rodriguez^{2,4}; ¹Martin-Luther-Universität-Halle-Wittenberg, Germany; ²IREC, Spain; ³Polytechnic University of Catalonia, Spain; ⁴Universitat de Barcelona, Spain

Replacing the established Molybdenum back contact in Cu(In,Ga)Se₂ solar cells by a transparent conducting layer would enable a variety of new applications: Bifacial solar modules, semitransparent building integration without back side mirroring, and ultrathin solar cells with scattering back reflector. In this work, we review the status of alternative back contacts for CIGSe solar cells and present own work using ITO. It is shown that for low temperature CIGSe deposition, the ITO back contact is on par with the Mo standard regarding PCE, and may even surpass Mo for ultrathin devices. Admittance measurements on ITO back contacts indicate the absence of a back contact barrier and thus the avoidance of the wellknown reach-through effect. Using bifacial illumination, the back contact recombination velocity is determined to around 10⁵ cm/s for the ITO/CIGSe interface formed at around 480°C by co-evaporation of CIGSe on sputtered ITO. Cells of 300 nm CIGSe thickness demonstrate quantum efficiency of 55% if illuminated from the back side. If the ITO layer is grown on top of a reflective back contact of 100 nm Aluminum, ultrathin devices can be constructed. Here, the Aluminum acts as the optical reflector and the ITO serves as a diffusion barrier and electronic back contact. This back contact can be further functionalized by light scattering elements. In experiment, a 300 nm structure element height below a 500 nm CIGS film gives the highest current density, which amounts to 88% of that of a 2.8 μm reference solar cell on Molybdenum.

SESSION EN07.08: Novel Absorber Materials II
Session Chairs: Alex Redinger and Mike Scarpulla
Monday Afternoon, April 19, 2021
EN07

1:00 PM *EN07.08.01

Bismuth Oxyiodide Solar Cells—Defect Tolerance, Device Engineering and Indoor Light Harvesting
Robert Hoyer; Imperial College London, United Kingdom

Lead-halide perovskites have emerged as a leading thin film solar absorber over the past decade. One of the key enabling properties is their tolerance to point defects, which enables them to achieve long charge-carrier lifetimes despite high defect densities when grown by low-temperature, simple fabrication methods. However, the toxicity of the water-soluble lead content may limit their widescale adoption. This talk examines bismuth-based semiconductors as a low-toxicity and stable alternative to lead-halide perovskites, with particular focus on bismuth oxyiodide (BiOI). We show that BiOI replicates the tolerance of lead-halide perovskites to point defects using experimental and computational methods [1,2]. An all-inorganic device structure is developed, and we achieve photovoltaic devices with external quantum efficiencies of up to 80% at 450 nm wavelength. Both the BiOI absorber and devices are stable in air. Although the 1.9 eV band gap is too wide for single-junction devices under 1-sun illumination, this band gap is ideal for indoor light harvesting. We demonstrate BiOI devices with comparable performance to hydrogenated amorphous silicon (the industry standard for indoor photovoltaics) under fluorescent and white LED lighting. We show that these devices, with lab-scale millimetre-squared areas, are sufficient to power carbon nanotube-based inverters [3]. Finally, we discuss the key limiting factors that need to be overcome to achieve further improvements in performance [1,3,4], as well as the potential of the broader family of bismuth-based perovskite-inspired materials for applications in solar energy and indoor light harvesting [3].

- [1] R. L. Z. Hoye, *et al. Adv. Mater.* **2017**, *29*,1702176
 [2] T. N. Huq, L. C. Lee, ..., R. L. Z. Hoye, *Adv. Funct. Mater.* **2020**, *30*, 1909983
 [3] Y. Peng, T. N. Huq, J. Mei, ..., R. L. Z. Hoye, V. Pecunia, *Adv. Energy Mater.* **2020**, Under Revision
 [4] R. A. Jagt, ..., R. L. Z. Hoye, *J. Mater. Chem. C* **2020**, *8*, 10791

1:25 PM EN07.08.02

Defect Identification and Full Lattice Dynamics of Zinc Phosphide, an Earth-Abundant Semiconductor for Photovoltaics Elias Z. Stutz¹, Diego A. Sandoval Salaiza¹, Alexander P. Litvinchuk², Mahdi Zamani¹, Simon Escobar Steinvall¹, Rajrupa Paul¹, Jean-Baptiste Leran¹, Anna Fontcuberta i Morral^{1,1} and Mirjana Dimitrievska¹; ¹École Polytechnique Fédérale de Lausanne, Switzerland; ²University of Houston, United States

Zinc phosphide (Zn₃P₂) is an earth-abundant semiconductor material capable of addressing the rising demand for low-cost and efficient optoelectronic devices. Its 1.5 eV direct bandgap, long minority carrier diffusion length (5-10 μm), and high absorption coefficient make it very promising for applications as an absorber in thin films solar cells. Furthermore, it has the added benefit of being a binary phase over more complex multinary materials.

Two crucial challenges need to be overcome to produce high-efficiency devices. First, poor crystal quality when grown on commercially available substrates due to high interface defect densities and high coefficient of thermal expansion. This challenge has been recently solved in our laboratory, as we have demonstrated different fabrication methods of high-quality reproducible thin films, with the possibility of facile transfer onto commercially available substrates.[1] [2] The second challenge is the control of bulk defects and doping, which is crucial for optoelectronic performance. Usually, uncontrolled growth results in p-doped material due to the formation of intrinsic acceptor defects.

To solve the challenge of defect control, we have investigated structural defects in the room-temperature-stable phase of zinc phosphide (α-Zn₃P₂, space group P4₂/nmc) using Raman spectroscopy. For that purpose, we have first fully characterized the lattice dynamics of zinc phosphide by combining density functional theory (DFT) calculation with polarized micro-Raman measurements on single-crystalline zinc phosphide. This is the first complete analysis of phonons in Zn₃P₂, essentially providing a reference for further characterization of this material. We identified 33 of the 39 expected Raman lines and have calculated the atomic displacement in all vibrational modes[3].

Then, using factorial and combinatorial studies of Zn₃P₂, along with the micro-Raman spectroscopy and previously mentioned results, has allowed us to probe different structural defects within Zn₃P₂. Systematic changes in the peak position, intensity, and widths in correlation with the presence of Zn and P interstitials and vacancies are presented and discussed. This work demonstrates the possibility of defect engineering in Zn₃P₂, which is of the foremost importance for the improvement of solar cell performance, as well as the potential of Raman scattering for point defect assessment in this system.

- [1] R. Paul *et al.*, “Van der Waals Epitaxy of Earth-Abundant Zn₃P₂ on Graphene for Photovoltaics,” *Cryst. Growth Des.*, vol. 20, no. 6, pp. 3816–3825, 2020.
 [2] S. Escobar Steinvall *et al.*, “Multiple morphologies and functionality of nanowires made from earth-abundant zinc phosphide,” *Nanoscale Horizons*, vol. 5, pp. 274–282, 2020.
 [3] E. Z. Stutz *et al.*, “Raman spectroscopy and lattice dynamics calculations of tetragonally-structured single crystal zinc phosphide (Zn₃P₂) nanowires,” *Nanotechnology* (accepted)

1:40 PM EN07.08.03

Novel Photovoltaic Materials—Multinary Adamantine Phases Derived from Ternary Chalcopyrites Yvonne Tomm¹ and Susan Schorr^{1,2}; ¹Helmholtz-Zentrum Berlin für Materialien und Energie, Germany; ²Freie Universität Berlin, Germany

Adamantine-type compounds, including kesterites, are currently the most promising material for a fully inorganic thin film photovoltaic technology that is free of critical raw materials and thus provides sustainable solutions.

Adamantines are compounds crystallizing in a structure, in which every atom is tetrahedrally bonded to four nearest neighbours [1]. To find new compounds for absorber layers as well as window materials for thin film solar cells, the $A^I B^{III} X^{VI}_2$ chalcopyrite compound family, belonging to the Adamantine compounds, can be extended by chemical substitution. Coming from the chalcopyrite-type structure (space group I-42d), one A^{+1} (occupying the structural site 4a) and one B^{+3} cation (occupying the structural site 4b) are replaced by one four-valent cation ($A^{+1} + B^{+3} \leftrightarrow C^{+4}$). This substitution will consequently lead to the formation of cation vacancies. In this way a quaternary “defect adamantine” [1] such as I-[-III-IV-VI]₄ is formed.

Here we report on the growth of $Cu[]BCX_4$ single crystals, with $B = Ga, In, C = Ge, Sn$ and $X = S, Se$ such as $CuGaGeS_4$, $CuInGeS_4$, and $CuGaSnS_4$, and the analysis of their structural as well as optoelectronic properties. The single crystals were grown by chemical vapor transport using iodine as transport agent. The evolved material and the grown crystals were characterized by X-ray fluorescence spectroscopy (XRF) for chemical composition as well as by X-ray diffraction (XRD) at 298K. The obtained powder patterns were analyzed by LeBail refinement to determine the lattice parameter. The chalcopyrite-like crystal structure was used as a structural model in the refinement.

The band gap energy of the material was revealed by solid-state UV/Vis reflectance spectroscopy. The obtained data were analyzed using the Kubelka–Munk pseudo-absorption function and the Tauc-plot method. The structure-property relations of $CuGaGeS_4$ and $CuGaSnS_4$ will be discussed in detail in the presentation.

We present first results on the growth and characterization of the novel compound semiconductor $CuGaGeS_4$ as well as $CuGaSnS_4$. These indicating a potential for future applications.

[References]

[1] B.R. Pamplin, Prog. Crystal Growth Charact. vol.3, pp. 179-192 (1981)

1:55 PM BREAK

2:05 PM EN07.08.04

Towards Defect-Free Thin Films of the Earth-Abundant Absorber Zinc Phosphide Through Nano-Patterning Simon Escobar Steinvall¹, Elias Z. Stutz¹, Rajrupa Paul¹, Mahdi Zamani¹, Nelson Y. Dzade², Valerio Piazza¹, Martin Friedl¹, Virginie de Mestral¹, Jean-Baptiste Leran¹, Reza R. Zamani³ and Anna Fontcuberta i Morral^{1,4}; ¹Laboratory of Semiconductor Materials, Institute of Materials, Ecole Polytechnique Fédérale de Lausanne, Switzerland; ²School of Chemistry, Cardiff University, United Kingdom; ³Interdisciplinary Centre for Electron Microscopy, Ecole Polytechnique Fédérale de Lausanne, Switzerland; ⁴Institute of Physics, Ecole Polytechnique Fédérale de Lausanne, Switzerland

Zinc phosphide (Zn_3P_2) is an earth-abundant semiconductor with optoelectronic properties suitable for photovoltaic applications, such as a direct bandgap (1.50 eV), long minority carrier diffusion lengths (up to 10 μm), and high absorption in the visible range.^{1,2} However, applications of the material has been limited due to challenges introduced by the lack of substrate with a matching lattice constant (for epitaxial growth) and thermal expansion coefficient, and the doping due to off-stoichiometry composition resulting in the formation of self-interstitials. Molecular beam epitaxy overcomes this by providing a low-temperature growth route with precise control over the composition, facilitating the fabrication of high-quality zinc phosphide.

A technique which can be used to further improve the material quality is selective area epitaxy (SAE).^{3,4} Using a nano-patterned oxide mask on indium phosphide substrates we demonstrate the selective growth in the holes, limiting the interface area to improve its quality.⁵ The SAE grown zinc phosphide first grows as nanopillars. By controlling the growth time and pitch they can be made to overgrow the oxide and coalesce, forming a thin film. The structural properties of the material and the epitaxial relationship were investigated through transmission electron microscopy, which also showed the influence of hole size on the composition of the zinc phosphide and the formation of rotational core-shell structures. Furthermore, using conductive atomic force microscopy (CAFM) and photoluminescence spectroscopy (PL) we evaluated the functional properties of the material. The CAFM measurements showed a diode-like behavior when the zinc phosphide is grown on an n-type substrate, whilst the PL showed clear bandgap emission at 1.53 eV, ideal for photovoltaic applications.

This approach has shown great potential in producing high-quality zinc phosphide, and upcoming studies will use it to transfer the growth to an earth-abundant substrate (silicon), and making prototype photovoltaic devices based on SAE grown zinc phosphide.

References

1. G. M. Kimball *et al.* *Appl. Phys. Lett.*, **95**, 112103 (2009).
2. M. Y. Swinkels *et al.* *Phys. Rev. Applied*, **14**, 024045 (2020).
3. M. Friedl *et al.* *Nano Lett.*, **18**, 2666–2671 (2018).
4. C. –Y. Chi *et al.* *Nano Lett.*, **13**, 2506–2515 (2013).
5. F. Glas *Phys. Rev. B*, **74**, 121302 (2006).

SESSION EN07.09: Advances in CIGS/CZTS Solar Cells
Session Chairs: Shubhra Bansal and Charles Hages
Monday Afternoon, April 19, 2021
EN07

4:00 PM *EN07.09.01

Metastability in CIGS Solar Cells with Na and RbF Alkali Treatments with Variation in Buffer Layers
Shubhra Bansal; University of Nevada, Las Vegas, United States

The effects of Na and RbF alkali treatment on the metastability behavior of Cu(In,Ga)Se₂ solar cells with two different buffers have been investigated with stress factors of heat, junction bias and illumination.

For CdS buffer, four device types with and without Na or RbF treatments have been subjected to heat- and light-soaking under open- and short-circuit (OC, SC) junction bias. Low-Na devices show a higher bandgap due to increased minimum Ga content, higher recombination current and lower open-circuit voltage (V_{OC}). Devices with RbF post-deposition treatment (PDT) show an improvement in net doping density $\sim 10^{16} \text{ cm}^{-3}$, V_{OC} and efficiency. Heat- and light-soaking under OC junction bias provokes an increase in net carrier concentration and V_{OC} irrespective of the alkali treatments. After SC stress, a decrease in V_{OC} and net carrier concentration are observed which can be stabilized by RbF-PDT. ToF-SIMS measurements reveal an increase in Na and O concentration in CIGS for baseline and reduced-Na devices, respectively, after OC stress. Oxygen concentration in CdS decreases after heat- and light-soaking for devices without RbF-PDT, whereas it remains unchanged for devices with RbF-PDT. The atomic concentration profiles in CIGS significantly stabilize as a function of stress with the addition of RbF-PDT.

Devices under open-circuit (OC) light soaking show an increase in V_{OC} with CdS buffer, however, V_{OC} decreases for ZnOS buffer devices. All devices show an increase in net carrier concentration after OC light soak irrespective of RbF-PDT or the buffer layers, even though ZnOS buffer devices show degradation. Under short-circuit (SC) light soak CdS buffer devices with RbF-PDT show stabilization of V_{OC} attributed to the increase in ionized acceptors in ordered vacancy compound (OVC) or buffer donor density. ZnOS buffer devices, on the other hand, show a decrease in V_{OC} under both OC and SC light soak irrespective of RbF treatment. A comprehensive discussion of effect of interface defects, conduction band offset and near interface doping density will be presented for ZnOS based CIGS solar cells.

4:25 PM EN07.09.02

Tailoring the Amine-Thiol Solvent System for the Deposition of High Quality Metal Selenide Films to Fabricate Cu(In,Ga)(S,Se)₂ Solar Cells Jonathan Turnley, Swapnil Deshmukh and Rakesh Agrawal; Purdue University, United States

The solution processing of thin-film solar cells is of great interest due to the potential of this method to decrease

costs and dramatically increase manufacturing throughput compared to the vacuum analogue. By utilizing hydrazine as a solvent, researchers have fabricated solution-processed Cu(In,Ga)(S,Se)₂ devices with efficiencies greater than 17%. However, hydrazine is highly toxic and explosive, potentially limiting its use in large-scale manufacturing. Several alternative solution processing methods are under investigation, though none have matched hydrazine in efficiency. Because of the difficulty in producing a soluble selenium species, these methods will often deposit a nanocrystalline sulfide precursor film. The precursor film is then converted to a large-grain selenide film by heating in a selenium atmosphere. During this conversion, grain growth is achieved as the nanocrystalline sulfide material dissolves in a liquid selenium front and then recrystallizes into micron-scale selenide grains. This process often results in a distinct “fine-grain” layer, particularly as film thickness increases, limiting researchers to absorber layer of 1-1.5 μm in thickness.

The amine-thiol solvent system has emerged as one of the most promising alternatives to hydrazine, producing Cu(In,Ga)(S,Se)₂ devices with efficiencies above 15%. With its ability to dissolve metals and metal chalcogenides, the amine-thiol solvent system is able to avoid potential anionic impurities that arise when using other metal salts. Additionally, because selenium and many metal selenides can be dissolved in amine-thiol, this system has the potential to tune the sulfur to selenium ratio of the precursor film, as is done in the hydrazine system. One challenge, however, is that the metal-thiolates produced in this dissolution can easily decompose into metal sulfides upon heating, often leading to significant sulfur content in the precursor film, along with some residual carbon.

In this research, we will discuss investigations into amine-thiol dissolutions of metal chalcogenide species through the use of ¹H-NMR, Raman, and ESI-MS. By developing a deeper understanding of the chemistry in this reactive dissolution, we can then make carefully controlled modification to the resulting metal complexes. We will present the various methods we have developed to alter the metal-chalcogenide bonding in the soluble precursor species, thereby changing the decomposition products and allowing for additional control over precursor film fabrication. We will also discuss the implications of the precursor film chalcogen composition on the further processing of the absorber layer, particularly as it relates to grain growth and will show how it can help reduce the carbon content in the film. To this end, we have utilized this new chemistry to produce the first ever 2 μm-thick, solution-processed absorber films with no fine-grain layer. Finally, we will discuss how these strategies can be implemented to further the ultimate goal of high efficiency, solution-processed solar cells. In conclusion, this research focuses on developing an understanding of the fundamental chemistry of the metal complexes created with the amine-thiol solvent system and connecting this knowledge with the practical application of solution-processed thin-film PV.

4:40 PM EN07.09.03

Chemical and Electronic Properties of CdS/Cu(In,Ga)Se₂ Interfaces with High Ga/(Ga+In) Ratio and Post-Deposition Treatment Mary Blankenship¹, Dirk Hauschild^{1,2,2}, Elizaveta Pyatenko^{2,2}, Wolfram Witte³, Dimitrios Hariskos³, Wanli Yang⁴, Nan Jiang^{1,4}, Monika Blum^{4,4}, Michael Powalla³, Lothar Weinhardt^{1,2,2} and Clemens Heske^{1,2,2}; ¹University of Nevada, Las Vegas (UNLV), United States; ²Karlsruhe Institute of Technology (KIT), Germany; ³Zentrum für Sonnenenergie- und Wasserstoff-Forschung Baden-Württemberg (ZSW), Germany; ⁴Lawrence Berkeley National Laboratory (LBNL), United States

The conversion efficiency of Cu(In,Ga)Se₂-based (CIGSe) thin-film solar cells has reached values above 23% on a laboratory scale. To further increase the solar cell performance, higher open-circuit voltages can be achieved by increasing the Ga/(Ga+In) (GGI) ratio to create a larger absorber band gap and/or by applying a post-deposition treatment (PDT) to the absorber surface. Consequently, it is crucial to understand how a high GGI *and* a PDT affects the chemical structure and band alignment at the buffer/absorber interface.

We have investigated in-line deposited and industrially relevant CIGSe absorbers with high bulk and surface GGI ratios. Two sample series, one with and one without RbF PDT, were prepared, and their interfaces with a chemical bath deposited CdS buffer layer were characterized with a combination of electron and soft x-ray spectroscopies. For this purpose, laboratory-based x-ray and UV photoelectron spectroscopy (XPS and UPS, respectively), inverse photoemission (IPES), and x-ray-excited Auger electron spectroscopy (XAES) were combined with synchrotron-based soft x-ray emission spectroscopy (XES). A detailed picture of the electronic

and chemical structure at and near the interface can be painted, which will be discussed in relation to the performance of the corresponding CIGSe solar cells.

4:55 PM BREAK

5:00 PM *EN07.09.04

Cell-Level Reliability Starring Cu(In,Ga)Se₂ Thin-Film Photovoltaics Lorelle M. Mansfield, Ingrid L. Repins, Stephen Glynn, Christopher P. Muzzillo, Bart Stevens, Peter Hacke, Kent Terwilliger, Steve Johnston, Steven P. Harvey, Matthew R. Young, Helio R. Moutinho, C.S. Jiang, Chuanxiao Xiao, Darius Kuciauskas and Timothy J. Silverman; National Renewable Energy Laboratory, United States

The reliability of photovoltaics is commonly studied at the module level. Many reliability problems do originate from module attributes, such as metal interconnections to cells, junction boxes, etc. However, significant work in reliability can also be done before an entire module is designed. In this talk I summarize how we investigated three reliability concerns in Cu(In,Ga)Se₂ (CIGS) photovoltaics at the cell level. The first is metastability, which in CIGS presents as an increase in V_{oc} over time during prolonged light exposure. Although increasing V_{oc} is not detrimental to module performance, it does complicate accurately measuring a module's performance and subsequent rating. The second is shading-induced hot spots where cells are irreversibly damaged by reverse voltage. This can happen in less than 1 second of partial shading, and the damage is often visible to the eye. Finally, we looked at potential-induced degradation (PID) or a decrease in performance caused by voltage differentials which drive ion diffusion. PID is a growing concern as the number of modules wired in series rises, hence increasing voltage differentials. Examining these perceived problems required developing robust measurement protocols including the fabrication of novel testing structures. These efforts ensured that we were incorporating the right metrics for investigating the phenomena and provided insights for improvement strategies.

NREL is in a unique position to test reliability at the cell level as we are making improvements to PV technology. If we look at reliability earlier in the research cycle, we have the potential to avoid commonly known module reliability problems before cell changes are implemented on a large scale. Cell-level reliability studies could thus lower the rates of module failures in the field and provide confidence to investors that new technologies will perform as advertised.

5:25 PM EN07.09.05

Late News: Enhanced Efficiency of Solution-Processed CuIn(S,Se)₂ Solar Cells by *In Situ* Incorporation of Al₂O₃ Wilman Septina¹, Christopher P. Muzzillo², Craig Perkins², Anne Curtis Giovanelli¹, Thomas West¹, Kenta Ohtaki¹, Hope Ishii¹, John Bradley¹, Kai Zhu² and Nicolas Gaillard¹; ¹University of Hawaii, United States; ²National Renewable Energy Laboratory, United States

In recent years, passivation of Cu(In,Ga)Se₂ (CIGSe) surface and/or interfaces with insulator materials has attained lots of attention to further increase efficiency. Such passivation is usually achieved with a thin layer of Al₂O₃ (<50 nm) deposited either before or after fabrication of CIGSe, most predominantly by atomic layer deposition method. The application of Al₂O₃ layer has been shown to reduce the number of electrically active defects at the semiconductor surface, which in turn lowers surface recombination velocities. This led to a decrease in interface recombination and resulted in improved efficiency. Passivation with Al₂O₃ has also been applied successfully to other thin film absorbers such as Cu₂ZnSn(S,Se)₄ and CdTe.

In this report, we present a novel approach to improve solution-processed CuIn(S,Se)₂ (CISSe) solar cell efficiency by in-situ incorporation of Al₂O₃. Specifically, AlNO₃ was added to inks containing CuCl, InCl₃, and thiourea dissolved in methanol. After spin coating of these solutions performed in air, samples were subjected to a selenization process. Our study showed that the Al formed amorphous nanosized-Al₂O₃ covering parts of the film top and bottom surfaces as well as within bulk and grain boundaries. Power conversion efficiency (PCE) as high as 11.6% was measured on cells using CISSe incorporated with Al₂O₃, a value higher than that measured on CISSe fabricated from Al-free ink (maximum PCE: 8.3%). This efficiency boost stemmed primarily from an increase in both in open-circuit voltages and fill factors. Defect passivation via this in-situ formed Al₂O₃ is

thought to play a major role in the improvement of the solar cell performance through defect passivation, while permitting Cd diffusion to take place at the absorber sub-surface. Details of the fabrication process, materials, and photovoltaic characterization will be discussed.

5:30 PM EN07.09.06

Silver Indium Diselenide—A High Mobility, Low-Defect Chalcopyrite Material with Potential for Thin-Film Photovoltaics David J. Rokke, Kyle G. Weideman, Anna Murray and Rakesh Agrawal; Purdue University, United States

An area of interest in the thin film photovoltaics community that has grown in recent years is the alloying of Cu(In,Ga)(S,Se)₂ (CIGS) with silver to create (Ag,Cu)(In,Ga)(S,Se)₂ (ACIGS). Alloying of silver in CIGS has resulted in favorable device characteristics such as increasing the bandgap to optimize devices for top cells in tandem architectures, reduced structural disorder (observed by lower Urbach energies) and lower open circuit voltage losses. However, we anticipate that the alloying of silver may only complicate the fabrication of CIGS devices by introducing a sixth element that must be controlled in the material. Indeed, a recent report¹ showed that high bandgap ACIGS devices have a low tolerance to off-stoichiometry, and another recent study² has suggested that the ACIGS system may be prone to phase segregation at certain temperatures and compositions. These observations foreshadow possible complications in the controlled scale-up of ACIGS devices.

In this work, we propose that some advantages of silver incorporation in chalcopyrite materials could be harnessed differently, by moving away from the complex stoichiometry of ACIGS to the far simpler AgInSe₂ (AIS). AIS has been studied only briefly in the literature, but initial findings suggest that the material is worth investigating further as a photovoltaic absorber material. By eliminating copper and gallium, the possibility for phase segregation is greatly reduced and the challenges presented by ACIGS are avoided. In addition, AIS has a direct bandgap in the ideal range for single-junction cells at 1.24eV, has been shown to have a carrier mobility much higher than CIGS, and has been predicted to have higher defect formation energy than CIGS.

To explore the potential of this material, we have fabricated thin films of AgInS₂ through the amine-thiol solution processing route by dissolving silver sulfide and metallic indium in a monoamine-dithiol solvent mixture, creating a solution of bis(1,2-ethanedithiolate) indium (III) and oligomeric Ag(I) thiolates. These solutions were cast on to molybdenum-coated glass substrates and annealed to form orthorhombic AgInS₂ films. These were then selenized in an elemental selenium atmosphere to create chalcopyrite thin films.

Our preliminary electronic characterization of AgIn(S,Se)₂ thin films suggest that the carrier concentration is roughly $1 \times 10^{13} \text{ cm}^{-3}$. In previous literature³ it has been shown that the carrier concentration can be controlled by changing the concentration of selenium in the annealing atmosphere. We find that carrier mobilities and photoluminescence characteristics are superior to similarly fabricated CIS thin films. From these initial results, we expect AIS to have superior electronic properties and defect characteristics when compared to CIS/CIGS films.

A side effect of the use of silver instead of copper is a change of the majority carriers from holes (p-type) to electrons (n-type). Taking full advantage of AIS will require a redesign in the optimal device architecture, as incorporation in to a heterojunction with CdS or Zn(O,S,OH) (as is done with CIGS) is no longer a viable approach. Our ongoing work is exploring possible junction partners for AIS to propose viable device architectures for further investigation.

In this work, we have developed a solution processing route for the synthesis of AgIn(S,Se)₂ thin films and demonstrated exciting electrical properties of this under-studied material. Along with our results, we point out the promise that this material holds for the thin film PV community.

(1) Keller, J.; Stolt, L.; Sopiha, K. V.; Larsen, J. K.; Riekehr, L.; Edoff, M. *Sol. RRL* **2020**, 2000508 (1), 2000508

(2) Sopiha, K. V.; Larsen, J. K.; Donzel-Gargand, O.; Khavari, F.; Keller, J.; Edoff, M.; Platzer-Björkman, C.; Persson, C.; Scragg, J. J. S. *J. Mater. Chem. A* **2020**, 8 (17), 8740

(3) Tell, B.; Shay, J. L.; Kasper, H. M. *J. Appl. Phys.* **1972**, 43 (5), 2469

5:35 PM *EN07.09.07

The High Efficiency CZTSSE Solar Cells on Flexible Metal Foils Jin-Kyu Kang^{1,2}, Dae-Ho Son¹, Seung-Hyun Kim¹, Se-Yun Kim^{1,2}, Dae-Kue Hwang¹, Shi-Joon Sung¹, Kee-Jeong Yang¹ and Dae-Hwan Kim¹; ¹Daegu Gyeongbuk Institute of Science and Technology (DGIST), Korea (the Republic of); ²Kyungnam University, Korea (the Republic of)

The development of flexible solar cells is necessary for achieving market competitiveness through the implementation of low cost solar cells and for applying customized business models, such as building integrated photovoltaics (BIPV) and mobile applications. In addition, low-cost flexible substrates can be used to lower manufacturing costs, which can contribute to the expansion of the renewable energy market by shortening the energy payback time. Solar cells with the CZTS-based ($\text{Cu}_2\text{ZnSnS}_4$, $\text{Cu}_2\text{ZnSnSe}_4$, $\text{Cu}_2\text{ZnSn}(\text{S},\text{Se})_4$) absorbers are advantageous for lowering the cost, but the development of high efficiency solar cells based on flexible substrates has been relatively unexplored. In this work, flexible CZTSSE solar cells applying the Mo and SUS foil substrate were developed. When we used the metal precursor, double CZTSSE layer, voids and ZnSSe secondary phase were observed. The ZnSSe layer formed during soft annealing plays important role as a layer that blocks the volatilization of Zn. Large void can cause the formation of unwanted secondary phase and non-uniform composition. Applying SnS precursor is a good strategy as a way to suppress void formation. To optimize the processes of the flexible CZTSSE thin film solar cells, Na doping, back contact modifying, blister formation suppression were studied. Applying NaF decreased the defect level and Voc deficit ($E_g - q\text{VOC}$). This improvement can be explained by the associated decrease in defects, which are considered the recombination centers in the CZTSSE absorber layer. The weak adhesion between CZTSSE and Mo layers and the high stress of CZTSSE layer can form blisters. The increase of adhesion between CZTSSE and Mo layers can prevent the formation of blister. The best power conversion efficiency of the prepared CZTSSE solar cell on flexible Mo foil is 11.59%, which is world top efficiency record on flexible substrate.

Acknowledge: This work was supported by the DGIST R&D Program of the Ministry of Science and ICT (19-BD-05) and the Korea Institute of Energy Technology Evaluation and Planning (KETEP) and the Ministry of Trade, Industry & Energy (MOTIE) of the Republic of Korea (No. 20173010012980).

SESSION EN07.11: Advances in CIGS Solar Cells III
Session Chairs: Daniel Abou-Ras and Mirjam Theelen
Tuesday Morning, April 20, 2021
EN07

8:00 AM *EN07.11.01

Grain Boundaries and Dislocations in $\text{Cu}(\text{In},\text{Ga})\text{Se}_2$ Solar Cells Daniel Abou-Ras; Helmholtz-Zentrum Berlin für Materialien und Energie, Germany

Owing to the polycrystalline nature of $\text{Cu}(\text{In},\text{Ga})\text{Se}_2$ (CIGS) thin films in high-efficiency solar cells, the impact of grain boundaries in these thin films on the photovoltaic performance has always been of concern. The present contribution will give an overview on the current understanding of this matter and show that even in high-efficiency devices, the enhanced nonradiative recombination at CIGS grain boundaries leads to a V_{oc} loss of 20-30 mV. In contrast, nonradiative recombination at dislocations does not seem to be enhanced with respect to the CIGS bulk. Differences between grain boundaries and dislocations will be discussed as well as the issue of potential passivation of grain boundaries by, e.g., alkali metals.

8:25 AM EN07.11.02

Urbach Energy of Alkali-Treated $\text{Cu}(\text{In},\text{Ga})\text{Se}_2$ Single Crystals Omar Ramirez and Susanne Siebentritt; University of Luxembourg, Luxembourg

Alkali post-deposition treatments in polycrystalline Cu(In,Ga)Se₂ absorbers have demonstrated to yield an increase in open-circuit voltage. The origin of such improvement has been attributed to reduced non-radiative recombination in the bulk, where the underlying mechanism has been proposed to be due to passivation of charged defects at grain boundaries as a result of the accumulation of heavy alkali elements conveying a reduction in band bending and tail states¹. However, the density of tail states is also impacted by disorder in the crystal itself, and in the case of Cu(In,Ga)Se₂, prompted by electrostatic potential and bandgap fluctuations. The Urbach energy describes the extension of the states into the band gap, and has recently been proposed as an indicator of the absorber's quality since a correlation between Urbach energy and open-circuit voltage deficit has been observed².

In this contribution, we study the influence of different alkali post-deposition treatments on the crystal itself. We measure the Urbach energy and the quasi-Fermi level splitting (qFLs) of NaF and KF-treated Cu(In,Ga)Se₂ single crystals grown by metalorganic vapor phase epitaxy. Our results show that the post-deposition treatments with NaF, and to a lesser extent KF, can effectively decrease the Urbach energy. In a similar way, an improvement in qFLs is obtained after the post-deposition treatments. The fact that alkali incorporation into the grains have an impact on the Urbach energy, suggests that the decrease in tail states observed in polycrystalline absorbers with heavy alkali post-deposition treatments is not exclusively grain boundary-related. Both effects: the reduction of tail states and the increased qFLs are explained by increased net-doping due to the alkalis. The effects on grain boundaries have to be complemented by the effects on the grain interiors, to understand the observed improvements and to devise ways for further efficiency improvements.

References

[1] S. Siebentritt et. al., *Advanced Energy Materials* **2020**, 10, 1903752.

[2] S. De Wolf, J. Holovsky, S.-J. Moon, P. Löper, B. Niesen, M. Ledinsky, F.-J. Haug, J.-H. Yum, C. Ballif, *The Journal of Physical Chemistry Letters* **2014**, 5, 1035.

8:40 AM EN07.11.03

Band Gap Energy Variations in Chalcogenide Compound Semiconductors: Influence of off-Stoichiometry Susan Schorr^{1,2} and Galina Gurieva¹; ¹Helmholtz-Zentrum Berlin für Materialien und Energie, Germany; ²Freie Universität Berlin, Germany

The photoactive band gap energy E_g of a solar cell device is determined by the band gap of the absorber layer material which has to be optimized to reach high conversion efficiencies.

One of the reasons for the success of Cu(In,Ga)Se₂ (CIGS) based thin film solar cells is the remarkable flexibility of its chalcopyrite crystal structure, accepting large stoichiometry deviations. The structural flexibility is a key for the quaternary kesterite-type compounds too. Cu₂ZnSn(S,Se)₄ (CZTSSe) based thin film solar cells reach the highest efficiency with a Cu-poor and Zn-rich composition of the absorber layer. Such deviations from the stoichiometric composition lead to the formation of intrinsic point defects (vacancies, anti-sites, and interstitials) in the compound, which significantly influence the electrical and optical properties of the material.

The existence of off-stoichiometric CZTS, CZTSe and CZTSSe has been shown in extended and systematic studies of powder series [1,2]. The off-stoichiometric composition of the kesterite-type phase corresponds to certain point defects. This correlation is the basis for defining off-stoichiometry types referred to as A–L [2,3]. For example, A-type off-stoichiometric kesterites, which are Cu-poor and Zn-rich, contain copper vacancies (V_{Cu}) and Zn_{Cu} anti-sites. The off-stoichiometry type model has been confirmed experimentally on the basis of neutron diffraction studies [2, 4].

We have determined the band gap energy of these series of off-stoichiometric kesterite-type compounds (powder) by diffuse reflectant spectroscopy. The optical band gap was extracted from Tauc plots obtained by plotting $(F(R) \cdot hv)^2$ versus the photon energy [5]. We can show, that in off-stoichiometric CZTS and CZTSe the band gap energy varies strongly in dependence on the off-stoichiometry (which can be expressed by the cation ratios) of the kesterite-type phase. For instance in A-B type CZTSe the band gap energy E_g increases from 0.88 eV to 1.0 eV in dependence on decreasing Cu/(Zn+Sn) and increasing Zn/Sn ratio (Cu/(Zn+Sn) decreases from 0.96 to 0.81 and Zn/Sn increases from 1.04 to 1.15).

Comparing such band gap energy variations in Cu-poor CZTS and CZTSe with those in off-stoichiometric Cu-

poor chalcopyrites (like CuInS₂, CuInSe₂ and CuGaS₂) then surprisingly one finds a different behavior. When looking at the same off-stoichiometry range the band gap energy variations in Cu-poor chalcopyrites are very small.

This can have serious consequences for kesterite-based solar cell device. The absorber layer shows generally an inhomogeneous chemical composition thus different off-stoichiometric kesterite phases, this means different off-stoichiometry types, occur coexisting. This may cause remarkable variations in band gap energy within the absorber layer.

- [1] L.E. Valle Rios, K. Neldner, G. Gurieva and S. Schorr, *J. Alloys Compd.* 657 (2016) 408.
- [2] G. Gurieva, L.E. Valle Rios, A. Franz, P. Whitfield and S. Schorr, *J. Appl. Phys.* 213 (2018) 161519.
- [3] A. Lafond, L. Coubrac, C. Guillot-Deuden, P. Deniard, S. Jobic, *Z. Anorg. Allg. Chem.* 638 (2012) 2571.
- [4] S. Schorr, G. Gurieva, M. Guc, M. Dimitievaska, A. Perez-Rodriguez, V. Izquierdo-Roca, C. Schnohr, J. Kim, W. Jo, J. M. Merino, *J. Phys.: Energy* 2 (2020) 012002.
- [5] Tauc, J., R. Grigorovici and A. Vancu, *Physica Status Solidi* 15 (1966) 627.

8:55 AM BREAK

9:10 AM EN07.11.04

Towards 1V Open-Circuit Voltage and Beyond—Reducing Bulk and Interface Losses in Wide Bandgap Chalcopyrite CuInGaS₂ Solar Cell Mohit Sood, Shukla Shukla, Damilola Adeleye, Michele Melchiorre and Susanne Siebentritt; University of Luxembourg, Luxembourg

Bandgap tunability of copper indium gallium disulfide Cu(In,Ga)S₂ from 1.55eV (CuInS₂) to 2.5eV (CuGaS₂) makes it an excellent top cell option for use in a tandem devices.[1] An open-circuit voltage (V_{OC}) of 973 mV and a power conversion efficiency of 15.5% Cu(In,Ga)S₂ demonstrates its promises for tandem solar cells in combination with silicon or Cu(In,Ga)Se₂. [2,3] However, even the best devices still suffer from a significant V_{OC} deficit (~600 mV) compared to its bandgap owing to non-radiative recombination in the device. Further advancements require a better comprehension of the recombination channels limiting the V_{OC} of the device, whether they lie in the bulk or at the interface.

We present investigation on a composition series of Cu(In,Ga)S₂ absorbers grown under different Cu concentration *i.e.* different [Cu]/[In+Ga] (CGI) ratio with bandgap (E_g) around ~1.6 eV, suitable for combination with record efficiency bottom cells. We have shown in the past that a variation in CGI of CuInS₂ drastically influences the recombination in the bulk. [4] Here we study higher band gap films with a band gap gradient. The opto-electrical properties are probed with photoluminescence measurements, and the electrical properties by current-voltage and capacitance measurements on solar cells fabricated with either CdS or Zn(O,S) buffer. The results of low temperature photoluminescence demonstrate suppression of deep defects as the CGI is decreased from 1.02 to 0.93, consequently leading to a maximum quasi-Fermi level splitting (qFLs) of 972 meV. Current-voltage measurements of devices prepared with CdS and Zn(O,S) buffer layer exhibit efficiencies close to 13 % with a V_{oc} deficit of 650 mV in Cu-poor (CGI<1) Cu(In,Ga)S₂ devices. Temperature dependent V_{OC} measurements show the presence of strong front interface recombinations in all devices, independent of buffer layer used, except one. The device prepared from absorber with CGI < 1 using Zn(O,S) buffer layer, temperature dependent V_{OC} measurements show V_{OC} extrapolation to the bandgap of the absorber at 0 Kelvin, demonstrating front interface passivation in the device. Recently front interface passivated Cu(In,Ga)S₂ device with high V_{OC} have been demonstrated, although with a lower bandgap.[5] Our study with higher bandgap allows differentiating between the influence of a defective surface layer and unfavorable band alignment. The findings demonstrate that high qFLs and V_{OC} is achieved only with an unetched, *i.e.* undamaged surface and suitable band alignment. In this case, V_{OC} is limited by bulk recombination. We investigate the deep defects responsible. Finally, capacitance-voltage measurements conclude rather low doping values in Cu poor Cu(In,Ga)S₂, an increase in which could lead to further improvement in qFLs and hence the V_{OC} of the device and take it to beyond 1 V.

- [1] B. Tell, J. Shay, and H. J. P. r. B. Kasper, *Electrical Properties, Optical Properties, and Band Structure of*

CuGaS₂ and CuInS₂, *Phys. Rev. B.*, vol. 4, no. 8, p. 2463, 1971.

[2] H. Hiroi, Y. Iwata, H. Sugimoto, and A. Yamada, Progress toward 1000 mV open circuit voltage on chalcopyrite solar cells, *IEEE J. Photovolt.*, vol. 6, no. 6, pp. 1630-1634, 2016.

[3] H. Hiroi, Y. Iwata, S. Adachi, H. Sugimoto, and A. Yamada, New World Record Efficiency for Pure-Sulfide Cu(In,Ga)S₂ Thin-Film Solar Cell With Cd-Free Buffer Layer via KCN-Free Process, *IEEE J. Photovolt.*, vol. 6, no. 3, pp. 760–763, 2016, doi: 10.1109/JPHOTOV.2016.2537540.

[4] A. Lomuscio *et al.*, Quasi-Fermi-Level Splitting of Cu-Poor and Cu-Rich CuInS₂ Absorber Layers, *Phys. Rev. Appl.*, vol. 11, no. 5, p. 054052, 2019.

[5] S. Kim, T. Nagai, H. Tampo, S. Ishizuka, and H. Shibata, Large open-circuit voltage boosting of pure sulfide chalcopyrite Cu (In, Ga) S₂ prepared using Cu-deficient metal precursors, *Prog. Photovolt.*, 2020.

9:25 AM *EN07.11.05

Sulfides and Selenides, Cu-Rich and Cu-Poor—What is Better for Solar Cells? Susanne Siebentritt and Thomas P. Weiss; University of Luxembourg, Luxembourg

Sulfide chalcopyrites have suitable band gaps to be used as top cells in tandem photovoltaic devices. Traditionally the sulfide solar cells were made from Cu-rich absorbers, i.e. absorbers grown under Cu-excess. The latest record device with an efficiency of 15.5% however, was made from Cu-poor material - which also results in the better solar cells in selenide chalcopyrite. Yet, in contrast to the selenides, the quasi-Fermi level splitting, i.e. the internal voltage of the absorber is higher in Cu-rich CuInS₂ than in Cu-poor CuInS₂. We will discuss the similarities and differences between sulfide and selenide material, in particular in terms of Cu dependent properties, as well as the defect spectra.

SESSION EN07.12: Characterization and Passivation II

Session Chairs: Nicolas Barreau and Charles Hages

Tuesday Morning, April 20, 2021

EN07

11:45 AM *EN07.12.01

On the Surface Properties of CIGSe Absorbers Alex Redinger; University of Luxembourg, Luxembourg

In this contribution, I will present an overview of the most important scanning probe microscopy results acquired on Cu(In,Ga)Se₂ (CIGSe) absorber surfaces over the last years. Then I will summarize some of our latest results acquired on polycrystalline and epitaxial CIGSe with different Cu-content. I will present a scanning tunneling microscopy (STM) study, where we analyzed the electronic effect of Cd²⁺ pre-electrolyte treatment [1]. I will show how Cd-ions effectively passivate defects and increase surface band bending. Then I will critically discuss the current status of Cu-rich CIGSe and present a detailed STM and Kelvin Probe Force Microscopy study, which we carried out on the rear-surface of the absorbers [2]. We do find strong evidence for a Cu_xSe precipitation at the back of Cu-rich absorbers. Finally, I compare measurements acquired on polycrystalline and epitaxial absorbers before and after K deposition and show how a short air exposure alters the work function distribution and the interpretation of grain boundary band bending.

[1] Boumenou, C. K. *et al.* Passivation of the CuInSe₂ surface via cadmium pre-electrolyte treatment. *Phys. Rev. Mater.* **4**, 045405 (2020).

[2] Boumenou, C. K. *et al.* Electronic and compositional properties of the rear-side of stoichiometric CuInSe₂ absorbers, *Prog Photovolt. Res. Appl.* 2020, *in press*.

12:10 PM EN07.12.02

Late News: Nanocrystalline Silicon Tunnel Junctions in High Efficiency Solar Cells—Characterization

and Deep Insight Apolline Puaud¹, Laurie-Lou Senaud², Delfina Muñoz¹ and Bertrand Paviet-Salomon²;
¹CEA-INES, France; ²PV-Center CSEM, Switzerland

With the increasing use of nanocrystalline silicon layers and tunnel junctions in high-efficiency tandem and single-junction solar cells, the understanding of the transport mechanisms in these layers becomes mandatory. Moreover, some solar cells can be composed of an NPN junction: (n)nc-Si:H/(p)nc-Si:H/n-type transparent conductive oxide (TCO) with complex intern mechanisms not explained in the state-of-the-art. In this work, two approaches of tunnel junction from CSEM [1] and CEA [2] are compared and deeply characterized in a cross experiment.

We performed dark I-V measurements under variable temperature on several heterojunction test-structures. We used different n-type TCOs and nanocrystalline silicon layers to decorrelate the mechanisms at the interface with the TCO and at the interface between n-type and p-type nanocrystalline silicon layers. Structures without front-side TCO and with Aluminum metallization are also used to help this decorrelation. Moreover, we calculated contact resistivity (ρ_c) of each possible stack and corresponding contact activation energies.

Each test-structure is composed of a (n)c-Si wafer, a known and Ohmic backside and a variable frontside. By measuring symmetrical structures (with equivalent backside and frontside) and using the expanded Cox and Strack Method presented by Wang Et al. [3], we extracted the backside resistances and corresponding contact resistivity. With the poor lateral conductivity of amorphous silicon layers compared to the c-Si(n) bulk, we assume that the current spreading only occurs in the bulk, so we calculate the backside resistance, R_{back} with the following equations: $R_{back}=(R_{tot} - R_{bulk})/2$ with $R_{bulk}=(\rho/d\pi).\arctan(4t/d)$ where d is the front-side circular electrode diameter, t the wafer thickness and R_{tot} the total resistance extracted from I-V curves. By plotting the contact resistivity on an Arrhenius plot, we obtained contact activation energies.

Same analysis were performed for the whole test-structures of the study by using the equation $R_{front}=R_{tot}-R_{bulk}-R_{back}$ to obtain frontside resistances. Structures without TCO on the frontside and Aluminum metallization on (n)nc-Si:H presents a good Ohmic behaviour, with contact resistivity under $250 \text{ m}\Omega.\text{cm}^2$ at ambient temperature, which confirms a good contact between n-type nanocrystalline silicon layer and Aluminum. Contrariwise, for structures with the stack (n)nc-Si:H/(p)nc-Si:H/Al, Ohmic contacts are only obtained at high temperatures with the two thinner tunnel junctions and contact resistivities are larger than $400 \text{ m}\Omega.\text{cm}^2$. For the thicker tunnel junction, Ohmic behaviors were observed at all temperatures in all test-structures, which results in very low contact resistivity (under $40 \text{ m}\Omega.\text{cm}^2$). Moreover, in this case, we observed a very low front-resistance variation from 200K to 290K and an increase of this resistance from 275K to 350K when the bulk resistance becomes dominant. The differences in thermal behavior could be explained by a huge contribution of transport via tunneling, which is a mechanism less temperature dependent than thermoionic emission. In fact, with the vertical nanocrystalline growth, thicker is a layer; the better is the vertical conduction that permits the current to flow through the junction. A complete analysis of transport mechanisms and the results with the different front-side TCOs will be presented in the full study.

[1] B. Paviet-Salomon *et al.*, *Sol. Energy*, vol. 175, pp. 60–67, Nov. 2018, doi: 10.1016/j.solener.2018.01.066.

[2] A. Puaud, A.-S. Ozanne, L.-L. Senaud, D. Munoz, and C. Roux, *IEEE J. Photovolt.*, pp. 1–7, 2020, doi: 10.1109/JPHOTOV.2020.3038600.

[3] W. Wang *et al.*, *IEEE J. Photovolt.*, vol. 9, no. 4, pp. 1113–1120, Jul. 2019, doi: 10.1109/JPHOTOV.2019.2917386.

12:25 PM EN07.12.03

Assessing the Defect Tolerance of Kesterite-Inspired Solar Absorbers Andrea Crovetto¹, Sunghyun Kim², Moritz Fischer¹, Nicolas Stenger¹, Aron Walsh², Ib Chorkendorff¹ and Peter Vesborg¹; ¹Technical University of Denmark, Denmark; ²Imperial College London, United Kingdom

Various thin-film I₂–II–IV–VI₄ photovoltaic absorbers derived from kesterite have been synthesized, characterized, and theoretically investigated in the past few years. The availability of this homogeneous

experimental/computational dataset is an opportunity to examine trends in the defect properties of kesterite-derived materials and identify criteria to (hopefully) find new defect-tolerant semiconductors in this vast chemical space.

First, we find that substitutions on the Zn site lead to a smooth decrease in band tailing as the ionic radius of the substituting cation increases. Unfortunately, this substitution strategy does not ensure the suppression of deeper defects and non-radiative recombination [1].

Then, we argue that Gaussian and Urbach band tails in kesterite-inspired semiconductors are two separate phenomena caused by two different antisite defect types. Deep Urbach tails are correlated with the calculated band gap narrowing caused by the $(2I_{II} + IV_{II})$ defect cluster. Shallow Gaussian tails are correlated with the energy difference between the kesterite and stannite polymorphs, which points to the role of $(II_I + I_{II})$ defect clusters involving Group IB and Group IIB atoms swapping across different cation planes. This finding can explain why in-plane cation disorder and band tailing are uncorrelated in kesterites.

Finally, we will discuss some PV-relevant properties of two relative newcomers to the $I_2-II-IV-VI_4$ family (Cu_2SrSnS_4 and Cu_2BaSnS_4) in a more detailed manner. The properties are: bulk defect landscape, band tailing, absolute band positions, and surface band bending [2].

[1] Crovetto et al., Assessing the defect tolerance of kesterite-inspired solar absorbers. *Energy Environ. Sci.*, 2020, **13**, 3489–3503.

[2] Crovetto et al., Experimental and first-principles spectroscopy of Cu_2SrSnS_4 and Cu_2BaSnS_4 photoabsorbers, *ACS Appl. Mater. Interfaces*, <https://doi.org/10.1021/acsami.0c14578>

12:30 PM EN07.12.05

Hole Transport Across Graphene Electrodeposited Cu_2O Interfaces Himanshu Singh; Indian Institute of Technology, India

Growing demand for energy sources that are cleaner and economical lead to intensive research on alternative materials for solar cells which does not require energy intensive fabrication procedures. Cuprous oxide (Cu_2O) is the among earliest semiconductor to be evaluated for photo-voltaics which is still being investigated for its earth abundant composition, cost effectiveness and bandgap. Cu_2O , a p-type semiconductor with a direct band gap of 2-2.2eV, is an attractive semiconductor material for photovoltaic conversion due to its high optical absorption coefficient in the visible range and can also be used as anode material in thin film lithium batteries. To maximize the photocurrent efficiency, it is coupled to charge transfer and transport pathways of Inorganic materials such as Vanadium pentoxide (V_2O_5), Molybdenum trioxide (MoO_3) and Nickel oxide (NiO). However, such realization requires cost intensive high vacuum plasma enhanced deposition processes and graphene is an ideal alternative to such hole transport layers.

Graphene is a transparent conductor which can be roll to roll processed in a cost effective fashion. These hole extraction layer requires a high work function to allow for the built-in electric field across the active layer and for holes to transport toward the anode. Graphene and it's derivatives, due to their ambipolar behaviour allowing work function tunability, are suitable candidates for hole transport layer (HTL). The most important character of such an implementation is the contact resistance between P- Cu_2O and the graphene film. Here we study the interface conductivity of graphene and Cu_2O films grown using electrochemical methods.

A compact, non-porous, stoichiometric Cu_2O was electrodeposited on graphene coated glass plates. The contact resistance of the Cu_2O thin film with commonly used metals such as Au, Pt, Ti was measured using a standard transfer length measurement technique. The contact resistance of graphene with the same set of metals were also measured. Finally, the crucial contact resistance of graphene- Cu_2O interfaces were measured for the first

time. We draw conclusions on the electrodeposited doping density, Schottky barrier between the Cu₂O thin films and the metals and finally the efficiency of graphene as an efficient hole injector.

12:35 PM BREAK

12:55 PM EN07.12.07

Atomistic Approach to the Doping of Compound Semiconductors Olivier C. Gagné; Carnegie Institution for Science, United States

Activation and tuning of the useful properties of semiconductors intended for photovoltaic, electronic and/or electrochemical applications hinges on their successful release of charge carriers, a process typically achieved in appreciable quantity via substitutional incorporation of foreign ions into the host crystal structure, i.e. extrinsic doping. As it stands, the rate-limiting step in designing efficient semiconductors is the identification of the most viable dopant ions to achieve n- and/or p-type conductivity – a process that is severely clouded by our incomplete understanding of chemical bonding behavior in solids. Today, doping studies rely exclusively on resource-intensive first-principles calculations, with little chemical guidance available to computationalists regarding where to focus their resources. Below, we argue that an atomistic understanding of the factors underlying ion substitutions in solids would provide such guidance, and would allow proactive calculations to be made for host/dopant combinations prior to their synthesis in lieu of expanding costly resources in low-return compositional spaces.

Three major factors underlie doping difficulties in semiconductors: [1] dopant insolubility, where defect formation energies are prohibitively high, [2] un-ionizability of dopant, where the charge carrier is not released to the system at operating temperature, and [3] compensated dopants, where formation of an opposite-charge native defect negates the effect of the intentional dopant. Factor [3] is terminal whereby formation of compensated defects is caused by the charge carrier itself, and not the identity of the dopant. However, difficulties associated with factors [1] and [2] may be circumvented via appropriate dopant selection, whose ease of substitution in the host crystal structure (in the form of defect formation energies) dictates dopant level depth in the band structure. Factors known to influence dopant level depth include similarities in atomic orbital energies, local atomic geometry (crystal-chemical behavior), and size of the substituting ions – all of which amenable to guidance via an adequate, systematized understanding of crystal-chemical behavior. Substantial discrepancy between the dopant and substituted ions for any of these parameters results in deep dopant levels, which are generally undesirable as they provide uncontrolled recombination channels.

Systematic investigation of crystal-chemical behavior begins with wide-scale analysis of chemical bonding in solids, in the form of bond-length dispersion analyses. Results from the largest bond-length dispersion analysis for inorganic solids were recently reported for cations bonded to O²⁻ and N³⁻,^[1] covering 177,446 reliable bond lengths hand-picked from 9210 crystal-structure refinements for oxides, and 6,770 bond lengths from 720 crystal-structure refinements for nitrides; equivalent analysis for cations bonded to S²⁻, Se²⁻ and Te²⁻ is underway. We use these data to systematically identify structural, electronic and/or bond-topological effects underlying anomalous bonding behavior across the periodic table. Considering that the chemical insight derived from these bonding data holds at the local scale, our analyses enable an atomistic understanding of dopant behavior at point defects which we use to investigate and model the fundamental principles underlying the coexistence of ions in crystallographic sites, taking us one step closer to a quantitative assessment of dopant viability in compound semiconductors – and an atomistic resolution to the doping bottleneck.

References:

[1] Gagné, O. C. & Hawthorne, F. C. (2016). *Acta Cryst.* B72, 602–625; Gagné, O. C. (2018). *Acta Cryst.* B74, 49–62; Gagné, O. C. & Hawthorne, F. C. (2018a). *Acta Cryst.* B74, 63–78; Gagné, O. C. & Hawthorne, F. C. (2018b). *Acta Cryst.* B74, 79–96; Gagné, O. C. & Hawthorne, F. C. (2020). *IUCrJ* 7, 581–629; Gagné, O. C. (2020). *ChemRxiv*. 11626974

1:00 PM EN07.12.08

An Investigation of Doping and Quasi-Homojunction Thin-Film Solar Cells Based on Sb₂Se₃ Donglou Ren, Michel Cathelinaud, Hongli Ma and Xianghua Zhang; Université de Rennes, France

The development of traditional commercial thin film solar cells based on copper indium gallium selenide (CIGS) and cadmium telluride (CdTe) in large-scale production is limited due to the scarcity of In, Ga and Te and the toxicity of Cd.

Earth-abundant and low-toxic antimony chalcogenides Sb₂X₃ (X = S, Se, S/Se) have received an increased attention from the photovoltaics community thanks to their excellent optoelectronic properties. After only 7 years of research, the record power conversion efficiency (PCE) of Sb₂Se₃ based solar cells has reached 10.5%¹. Consequently, they are more and more considered as a promising next generation absorber materials. Despite the huge progress, the efficiency is still far lower than the values reported for CIGS and CdTe, largely owing to the absorber's low carrier density and high defects concentration². Doping is an effective method to improve the properties of semiconductors, however, only few works have been reported in this field.

In this work, we investigated the effects of several dopants (Na, In, Cu, I, and Te) on the electric and electronic properties of Sb₂Se₃ prepared using melt-quenching method. Different techniques including X-ray diffractions and observation under high-resolution electronic microscopes have been used to observe that the elements of Na and In are not doped into Sb₂Se₃ lattice, leading to phase separation. Surprisingly, two novel heterojunctions Sb₂Se₃/NaSbSe₂ and Sb₂Se₃/β-In₂Se₃ were successfully in-situ synthesized and they exhibited interesting photocatalytic activity for methyl orange degradation, taken as an example, due to the effective separation and transport of photo-generated carriers.

Most importantly, the effective p-type doping (Cu) and n-type doping (I and Te) are obtained, remarkably enhancing the photoelectric properties of Sb₂Se₃. Quasi-homojunction thin film solar cells using doped Sb₂Se₃ with Cu and I, have been fabricated via radio frequency (RF) magnetron sputtering technology. Encouraging PCE of 2.41%, fill factor (FF) of 41%, J_{sc} of 20 mA/cm², and V_{oc} of 294 mV have been achieved. The preparation, characterization, and loss mechanisms of these solar cells will be presented and discussed. This is the first work on homojunction solar cells based on Sb₂Se₃.

References

¹ X. Wang, et al., Manipulating the Electrical Properties of Sb₂(S,Se)₃ Film for High-Efficiency Solar Cell, *Adv. Energy Mater.* 2020, 2002341.

² C. Chen, et al., Characterization of Basic Physical Properties of Sb₂Se₃ and its Relevance for Photovoltaics. *Front. Optoelectron.* 2017, 10, 18–30.

1:15 PM EN07.12.09

Late News: Origin of Low Conversion Efficiency of Cu₂ZnSnS₄ Kesterite Solar Absorber—The Actual Role of Cation Disorder Wei Chen¹, Diana Dahliah¹, Gian-Marco Rignanese¹ and Geoffroy Hautier^{1,2};

¹Université catholique de Louvain, Belgium; ²Dartmouth College, United States

As an emerging class of nontoxic and earth-abundant solar absorbers, kesterite Cu₂ZnSn(S,Se)₄ has been the focus of much attention from the photovoltaic community. However, despite years of optimization, the kesterite solar cells struggle to attain a power efficiency higher than 13%, far behind the other thin-film technologies such as CIGS and perovskites. The open-circuit voltage (V_{oc}) is in particular low given the material's band gap. The low efficiency and the low V_{oc} of kesterite solar cells are often attributed to the Cu-Zn cation disorder, although such an assignment is still a subject of debate. Here, the controversial role of cation disorder in the extraordinarily low V_{oc} of Cu₂ZnSnS₄ (CZTS) kesterite absorber is examined through a statistical treatment of disorder within the cluster-expansion method. It is demonstrated that the extensive Cu-Zn disorder alone cannot be responsible for the large Urbach tails observed in many CZTS solar cells. While the band gap is reduced as a result of the Gaussian tails formed near the valence-band edge due to Cu clustering, band-gap fluctuations contribute only marginally to the V_{oc} deficit, thereby excluding Cu-Zn disorder as the primary source of the low efficiency of CZTS devices. On the other hand, the extensive disorder stabilizes the formation of Sn_{Zn} antisite and complexes, which as nonradiative recombination and minority carrier trapping centers dominate the

V_{oc} loss in CZTS. Our analysis indicates that current CZTS devices might have already approached the maximum conversion efficiency given the limited growth conditions and the remnant cation disorder even after post-annealing. In view of the improved efficiency achieved with CZTS-derived kesterite absorbers, the methodology presented in this work offers an avenue to understanding and optimizing these emerging kesterite solar devices towards higher efficiency.

1:30 PM EN07.12.10

Cu/Zn Disorder vs Solar Cell Efficiency—The $\text{Cu}_2\text{ZnSn}(\text{S}_x\text{Se}_{1-x})_4$ Monograin Case Galina Gurieva¹, Alexandra Franz¹, Sergiu Levcenko¹, K. Muska², Kaia Ernits² and Susan Schorr^{1,3}; ¹Helmholtz-Zentrum Berlin für Materialien und Energie, Germany; ²crystalsol OÜ, Estonia; ³Freie Universität Berlin, Germany

In the last years quaternary chalcogenides have gained a lot of attention; especially the kesterite type semiconductor compounds $\text{Cu}_2\text{ZnSn}(\text{S},\text{Se})_4$ which consist mostly of earth abundant and non-toxic elements. These compounds are a promising low cost alternative absorber material for thin film solar cells due to its suitable criteria for photovoltaic applications: *p*-type semiconductor behavior, direct band-gap between 1.0-1.5 eV and absorption coefficient $>10^4 \text{ cm}^{-1}$ [1]. The record conversion efficiency of 12.6 % reported for a $\text{Cu}_2\text{ZnSn}(\text{S},\text{Se})_4$ based thin film solar cell was reached when the polycrystalline CZTSSe absorber layer exhibits an off-stoichiometric composition [2]. Deviations from stoichiometry cause intrinsic point defects (vacancies, anti-sites, interstitials), which determine the electronic properties of the semiconductor significantly [3]. It is agreed in literature that large band tailing observed in Cu-based kesterite-type semiconductors causes voltage losses limiting the efficiency of kesterite-based devices. The Cu/Zn disorder (Cu_{Zn} and Zn_{Cu} anti-sites in Cu-Zn planes at $z=1/4$ and $3/4$), which is always present in these compounds [4, 5], is discussed as a possible reason for band tailing. Conventional structural characterization is done with X-ray diffraction, but in case of isoelectronic cations, like Cu^+ and Zn^{2+} , they are difficult to distinguish. Nevertheless, the neutron scattering length of Cu and Zn is different, by neutron diffraction we can distinguish between Cu^+ and Zn^{2+} site occupation in the crystal structure [4, 5]. Kesterite-type based thin films solar cell technologies are mainly based on polycrystalline absorber layers, which makes it quite hard to correlate the crystallographic structure (determined via neutron diffraction) to the performance of these materials. A promising low cost alternative technology uses $\text{Cu}_2\text{ZnSn}(\text{S},\text{Se})_4$ (CZTSSe) monograins (single crystals of 50-100 μm size) which are fixed in a polymer matrix to form a flexible solar cell [6].

The experimental determination of the order parameter Q which is a quantitative measure of the degree of Cu/Zn disorder [7] requires a differentiation between the isoelectronic cations Cu^+ and Zn^{2+} . An in depth analysis of neutron diffraction data provides information on the cation distribution in the crystal structure allowing the determination of type and concentration of intrinsic point defects including a distinction between Cu and Zn [5]. On the other hand neutron diffraction requires large sample volumes, thus kesterite monograins offer the unique possibility to correlate structural disorder in kesterite-type absorbers with device performance parameters.

We will present a detailed structural investigation of CZTSSe monograins based on neutron powder diffraction experiments, the influence of the purity of the starting material as well as small changes in the chemical composition on the Cu/Zn disorder resulting in different power conversion efficiencies of the respective devices. A further investigation of the effect of the disordering procedure and the long low temperature – “ordering” annealing on the Cu/Zn disorder and optical properties of the CZTSSe monograins will be presented as well.

Reference:

- [1] S. Delbos, EPJ Photovoltaics 2012; 3: 35004.
- [2] W.Wang et al., Adv. Energy Materials, 2013.
- [3] M. Guc et. al., in preparation
- [4] S. Schorr, Solar Energy Materials & Solar Cells 2011; 95: 1482-1488
- [5] G. Gurieva et. al., J Appl Phys 2018; 123: 161519/1-12
- [6] www.crystalsol.com
- [7] Toebbens et al. Phys. Stat. Sol. B 253 (2016) 1890

SESSION EN07.13: On-demand
Wednesday Morning, April 14, 2021
EN07

8:00 AM EN07.13.01

Late News: Modulus Spectroscopic Estimation of Two Local Built-In Potentials in CZTSe: Ge Bi-Layers Solar Cells Sanghyun Lee¹ and Kent Price²; ¹Indiana State University, United States; ²Morehead State University, United States

Kesterite or CZTSSe ($\text{Cu}_2\text{ZnSnS}_x\text{Se}_{4-x}$) solar cells has been steadily emerging third-generation thin-film solar cells as cost-effective CZTSSe solar cells have shown <12.6 % efficiency. In particular, we reported that CZTSe Ge bi-layers devices have shown greatly improved performance with the enhanced grain and grain boundary properties. CZTSe: Ge bi-layers devices consist of several different functional parts such as carrier generation and carrier separation, associated with electric field in the depletion region. The current-voltage (I-V) measurements can provide the device performance of photovoltaic devices (DC characteristics), but the electrical property associated with each interface junction of CZTSe: Ge bi-layers devices cannot be readily accessed with DC characteristics. Conversely, AC characteristics (modulus spectroscopy) can provide each interface junction's properties in the frequency domain as a certain range of frequency separately reveals them. In this study, we fabricated and analyzed CZTSe: Ge bi-layers devices to accurately evaluate the electrical structure at hetero and back contact junctions by modulus spectroscopic characteristics. Moreover, we studied the dependence of light and voltage biases with respect to impedance and modulus behaviors of hetero and back contact junctions. We used an equivalent circuit model for CZTSe: Ge bi-layers devices that describes the junction modulus and impedance characteristics. This model is utilized to extract the most appropriate device parameters under various voltage bias conditions, which agrees with Sentaurus TCAD numerical simulation results.

Fabricated devices are analyzed with an equivalent circuit model, and LEVM/LEMW software resolved two different parallel circuit branch components. Modeling with LEVM/LEMW software accurately fits our model to modulus spectroscopy combined with impedance spectra in the given testing frequency domain. Using TCAD numerical simulations, we examine a variety of device models with a set of built-in potentials for appropriate parallel circuits with two capacitance and two resistance ($R^2=0.99$). Our study shows that heterojunction built-in potential is 801 meV, which is ~10 % smaller than a theoretical value, 894 meV. Conversely, the built-in potential of the back contact junction is 428 meV. The total built-in potential is 373 meV. All in all, modulus data combined with impedance spectra agree well with modeling and numerical simulation results.

SYMPOSIUM EN08

Progress in Understanding Charge Transfer at Electrochemical Interfaces in Batteries
April 22 - April 23, 2021

Symposium Organizers

Vijayakumar Murugesan, Pacific Northwest National Laboratory
Nav Nidhi Rajput, Tufts University

* Invited Paper

SESSION EN08.01: NMR Analysis of Heterogeneous Interfaces
Session Chairs: Karl Mueller and Vijayakumar Murugesan
Thursday Morning, April 22, 2021
EN08

10:30 AM *EN08.01.01

Unraveling the Chemistry and Transport of Multi-Valent Cations in the Bulk and at Interfaces Karl Mueller¹, Venkateshkumar Prabhakaran¹, Grant E. Johnson¹, Linda Wangoh¹, Yingge Du¹, Kee Sung Han¹, Jian Zhi Hu¹, Ying Chen¹, Rajeev Surendran Assary² and Vijayakumar Murugesan¹; ¹Pacific Northwest National Laboratory, United States; ²Argonne National Laboratory, United States

The design and achievement of superior battery systems (i.e., those that are more efficient, higher in energy density, safer, more environmentally friendly, etc.) requires knowledge of fundamental chemical and physical properties of the system and its components while under true operating conditions. Such advanced knowledge can be obtained through both modeling and experimental efforts. In the case of battery systems designed to replace the well-known lithium ion battery systems, new chemistries in particular are being explored, classified, and improved using state-of-the-art characterization and computational tools. New analytical tools have been developed for the study of these advanced battery systems in destructive, post-mortem modes as well as while the battery is under operating conditions. Further, certain aspects of the battery chemistry and operation can also be modeled and reproduced with varying degrees of fidelity through computational studies that cross scales from the atomic and molecular to the sizes of pores and beyond. The combination of these experimental techniques and computational tools will eventually lead to predictive understanding of battery components and their operation in the complete battery system. This presentation will focus on progress in merging both post-mortem and operando studies that use advanced spectroscopies and computational methods to understand components of complex battery systems. In this work, we focus on enabling the prediction and creation of bespoke interfaces and transformative interphases for energy storage through atomistic- and molecular-level understanding of the role of interface structure and composition on interphase properties, as well as the design and discovery of novel interface constructs for facile charge transport.

10:55 AM *EN08.01.02

Exploring Transition Metal-Complexes as Redox Mediators in Li-O₂ Battery Aninda J. Bhattacharyya and Subhankar Mandal; Indian Institute of Science, India

Identification of oxygen as a high energy density storage material marked a paradigm shift from solid-state intercalation chemistry form of energy storage such as Li-ion batteries. Nearly three decades ago, Abraham and co-workers demonstrated a rechargeable metal-oxygen (Li-O₂) battery. Li-O₂ batteries display a theoretical energy density of over 3505 Wh. Kg⁻¹, much higher than Li-ion batteries. However, Li-O₂ electrochemistry is non-trivial. The electrolyte, electrocatalysts, and solid-porous O₂-scaffold influences the multistep O₂ → Li_xO_y reaction. The reversibility of the transformation of O₂ → Li_xO_y is crucial for stable battery performance, and this is directly associated with the kinetics of oxygen evolution reaction (OER) and the formation of insoluble oxides (Li_xO_y) during oxygen reduction reaction (ORR). There has been intense research on the Li-O₂ battery system's different components over the last two decades. Our strategy here is to develop efficient soluble redox mediators/electrocatalysts that reside at porous O₂-electrode|electrolyte interface. This is in contrary to the conventional approach of immobilization of electrocatalyst(s) on the porous cathode (O₂)-scaffold. The

efficiency of the redox-mediator is finely determined by the redox reversibility of the transition metal site and oxygen binding capability of the complex. While this strategy may lead to efficient metal-oxygen batteries, it will also pose new and non-trivial challenges on interfacial charge transfer and transport. This presentation will discuss porphyrin (bare hemin and heme proteins, Rudra N. Samajdar et al. *J. Phys Chem. C* 2019) and phthalocyanines (Pc) (Subhankar Mandal et al. *submitted*, 2021) from groups 6-12, e.g., MnPc, FePc, CoPc, NiPc, CuPc, ZnPc, and MgPc (d^0 system, group 2) as the redox mediators in Li-O₂ batteries. Due to the redox mediator's residence at the electrode | electrolyte interface, the insulating Li-oxides do not form on the air-cathode scaffold and block the pores. In the context of the porphyrin, due to their superior ability to combine with O₂, the protein performs better than the bare heme. In the case of the Pcs, the electrochemical processes are observed to be highly dependent on the metal centre. The experimental findings in case of the Pcs are additionally supported by theoretical studies based on DFT.

11:20 AM EN08.01.03

Insights into the Functionality of an Alkylated Li_xSi_yO_z Interphase for High Energy Cathodes from High Sensitivity NMR Spectroscopy Shira Haber¹, Rosy Sharma^{2,3}, Arka Saha^{2,3}, Arava Zohar¹, Malachi Noked^{2,3} and Michal Leskes¹; ¹Weizmann Institute of Science, Israel; ²Bar-Ilan University, Israel; ³Bar-Ilan Institute of Nanotechnology and Advanced Materials, Israel

Deposition of thin protective films on the cathode surface is an efficient approach to overcome interfacial degradation processes and control ionic mobility across the interface. An essential requirement of a good coating layer is that in addition to surface passivation, it will enable unimpeded ion transport between the electrode and electrolyte. To date, the rational design of such protective layers is limited, mostly due to the lack of sensitive characterization tools that can provide atomic-molecular level insight into both the *structure* and *function* of thin amorphous layers.

Here I will present a new approach to examine thin interphases and gain atomic level insight into their composition, 3D structure and lithium ion transport properties by using **solid state nuclear magnetic resonance** (ssNMR) spectroscopy. The approach is based on (i) 10-10⁴ fold increase in ssNMR sensitivity provided by **Dynamic nuclear polarization** (DNP), a process in which the high electron spin polarization is transferred to surface nuclei in the sample, enabling the detection of otherwise invisible nanometer-thick layers, and (ii) tracking ⁶Li-⁷Li isotope exchange processes across the electrode-electrolyte interface.

I will describe the application of this approach to a novel surface treatment for high energy cathodes, lithium rich LiNi_xMn_yCo_zO₂ (NMC), which leads to substantial improvements in rate performance and capacity retention. Specifically, I will show how the combination of DNP and ssNMR provides a detailed chemical map of the surface composition and structure of this lithium-silicate protection layer. The permeability of the coating and the role of lithiated interphases was assessed by ^{6,7}Li exchange experiments on coated and uncoated NMC and further compared to Electrochemical Impedance Spectroscopy (EIS) results.

The combination of structural insight from high sensitivity ssNMR and lithium exchange brings us closer to understanding the functionality of electrode surface layers.

11:35 AM EN08.01.05

Solvation Structures, Molecular-Level Dynamics and Evolution of Electrolytes in Solution and at Interfaces Using Advanced NMR Techniques Jian Zhi Hu¹, Ying Chen¹, Kee Sung Han¹, Nathan Hahn², Kevin R. Zavadil², Kristin Persson³, Vijayakumar Murugesan¹ and Karl Mueller¹; ¹The Joint Center for Energy Storage Research (JCESR), Pacific Northwest National Laboratory, United States; ²Sandia National Laboratories, United States; ³Lawrence Berkeley National Laboratory, United States

Nuclear magnetic resonance (NMR), a quantitative and non-destructive atomic-isotope specific tool, is idea for studying a system without compromising control of both pressure and temperature. We will show how NMR and associated capabilities (1D and 2D solid/liquid state NMR spectroscopy, pulsed-field-gradient-NMR, and DFT computational modeling of NMR parameters) combined with molecular dynamics simulations can be utilized to study the solvation structures and the molecular-level dynamics of electrolytes in solution and at the solid-electrolyte interface. The following examples will be highlighted to demonstrate the power of our

combinations of approaches: (i) Mechanisms of desolvation associated with $\text{Mg}(\text{TFSI})_2 + \text{G}_2$ on surfaces of nano-sized MgO solids; (ii) Role of solvent rearrangement on Mg^{2+} solvation structures in dimethoxyethane solutions; and (iii) Origin of unusual acidity and Li^+ diffusivity in a series of water-in-salt electrolytes.

References

- Hu, J. Z.; Rajput, N. N.; Wan, C.; Shao, Y. Y.; Deng, X. C.; Jaegers, N. R.; Hu, M.; Chen, Y. W.; Shin, Y.; Monk, J.; Chen, Z.; Qin, Z. H.; Mueller, K. T.; Liu, J.; Persson, K. A., Mg-25 NMR and computational modeling studies of the solvation structures and molecular dynamics in magnesium based liquid electrolytes. *Nano Energy* 2018, 46, 436-446. <https://doi.org/10.1016/j.nanoen.2018.01.051>
- Hu, J.Z.; Jaegers N. R.; Y. Chen, Y.; Han, K.; Wang, H.; Murugesan, V.; and Mueller, K.T. Adsorption and thermal decomposition of electrolytes on nanometer magnesium oxide: An in situ ^{13}C MAS NMR study. *ACS Applied Materials & Interfaces* 2019, 11, 42:38689-38696. DOI:10.1021/acsami.9b11888
- Chen, Y.; Jaegers, N. R.; Wang, H.; Han, K.; Hu, J. Z.; Mueller, K. T.; and Murugesan, V. Role of Solvent Rearrangement on Mg^{2+} Solvation Structures in Dimethoxyethane Solutions Using Multimodal NMR Analysis. *J. Phys. Chem. Lett.* 2020, 11, 15, 6443–6449. <https://doi.org/10.1021/acs.jpcclett.0c01447>.
- Han, K.; Zhou Yu, Wang, H.; Redfern, P. C.; Ma, L.; Cheng, L.; Chen, Y.; Hu, J. Z.; Curtiss, L. A.; Xu, K.; Murugesan, V.; and Mueller, K. T. Origin of Unusual Acidity and Li^+ Diffusivity in a Series of Water-in-Salt Electrolytes. *J. Phys. Chem. B* 2020, 124, 5284–529. <https://pubs.acs.org/doi/10.1021/acs.jpccb.0c02483>

11:50 AM EN08.01.06

Multivalent Electrolytes: Controlling Interfacial Resiliency Through Selective Cation Coordination

Nathan Hahn^{1,2} and Kevin R. Zavadil^{1,2}; ¹Sandia National Laboratories, United States; ²Joint Center for Energy Storage Research, United States

While several multivalent battery working ions such as Mg^{2+} or Ca^{2+} present the theoretical promise of high pack-level energy density, numerous challenges stand in the way of their successful development to commercialization. One of the key challenges is maintaining electrolyte stability during the working ion (de)solvation and charge transfer events at the potential extremes of the anode and cathode electrified interfaces. Stability under these conditions is heavily influenced by the interactions of the strongly polarizing multivalent cation of interest with the supporting salt or solvent species. In this work, we evaluate the efficacy of using selective coordination strategies to tune interfacial stability at magnesium and calcium battery electrodes. A combination of electrochemical, solvation, and surface analyses will be presented to provide a holistic view of the extent to which targeted salt or solvent additives mitigate electrolyte decomposition. These findings help guide electrolyte design efforts aimed at achieving high voltage multivalent batteries.

12:05 PM DISCUSSION TIME

SESSION EN08.02: Ion Transport Across Interfaces

Session Chairs: Nav Nidhi Rajput and Kevin Zavadil

Thursday Afternoon, April 22, 2021

EN08

1:00 PM *EN08.02.01

Ion Clustering in Electrolytes—Implications on Electrochemical Stability and Transport Properties Boris Kozinsky^{1,2}; ¹Harvard University, United States; ²Bosch Research, United States

Electrochemical stability windows of electrolytes largely determine the limitations of operating regimes of lithium-ion batteries, but the degradation mechanisms are difficult to characterize and poorly understood. Using computational quantum chemistry to investigate the oxidative decomposition mechanisms that govern voltage

stability of multi-component organic electrolytes, we find that electrolyte decomposition is a process involving the solvent and the salt anion and requires explicit treatment of their coupling. We find that the ionization potential of the solvent-anion system is often lower than that of the isolated solvent or the anion. This mutual weakening effect is explained by the formation of the anion-solvent charge-transfer complex, which we study for 16 anion-solvent combinations relevant for Li-ion battery electrolytes. This understanding of the oxidation mechanism allows to formulate a simple predictive model that explains experimentally observed trends in the onset voltages of degradation of electrolytes near the cathode. This model opens opportunities for rapid rational design of stable electrolytes for high-energy batteries. [1]

Our charge complex model suggests an explanation of why ionic liquids are typically found to be more electrochemically stable at high voltage than conventional organic solvent-based electrolytes. At the same time, ion complexes in ionic liquids affect ionic transport due to correlation effects. Using molecular dynamics simulations of transport properties, we find that strong ionic interactions result in significant deviations from ideal solution behavior. By adopting rigorous concentrated multicomponent solution theory, we show that anomalously low and even negative Li transference numbers emerge in vast range of different ionic liquid chemistries, suggesting a universal behavior of this class of electrolytes. Finally, we propose chemical strategies for mitigating the detrimental effects of clustering and for increasing transference number and conductivity. [2-4]

[1] E. Fadel et al, “*Role of solvent-anion charge transfer in oxidative degradation of battery electrolytes*”, Nature Comm., 10, 3360 (2019)

[2] N. Molinari, J. P. Mailoa, B. Kozinsky, “*General Trend of Negative Li Effective Charge in Ionic Liquid Electrolytes*”, J. Phys. Chem. Lett. 10, 2313 (2019)

[3] N. Molinari, J. P. Mailoa, N. Craig, J. Christensen, B. Kozinsky, “*Transport Anomalies Emerging from Strong Correlation in Ionic Liquid Electrolytes*”, J. Power Sources, 428, 27 (2019)

[4] N. Molinari and B. Kozinsky, “*Chelation-Induced Reversal of Negative Cation Transference Number in Ionic Liquid Electrolytes*”, J. Phys. Chem. B 124, 13, 2676–2684 (2020).

1:25 PM EN08.02.02

ALD Niobium Oxide for Improved Rate Capability and Cycle Life of Cathode Films for Li-Ion Batteries

Abdessalem Aribia, Jordi Sastre-Pellicer, Xubin Chen, Gilshtein Evgeniia, Ayodhya Tiwari and Yaroslav Romanyuk; Empa–Swiss Federal Laboratories for Materials Science and Technology, Switzerland

Layered oxide cathode materials are widely used in modern Li-ion batteries. However, during device operation they suffer from surface degradation, transition metal oxide dissolution and destructive phase transitions at the cathode-electrolyte interface. One way to suppress the chemical instability and reactivity of the cathode with the electrolyte is to coat the cathode surface with inert oxides.

We investigate niobium oxide cathode coatings with an intention of improving performance at ultra-high C rates and long-term cyclability of Li-ion batteries. The effect of the coating was evaluated in a thin-film LiCoO₂ model system. The niobium oxide was deposited by atomic layer deposition (ALD), which enables a conformal coating over the cathode material. The niobium oxide film was lithiated by annealing it together with the cathode. The electrochemical properties could be significantly improved compared to uncoated samples by systematically investigating the battery performance as a function of coating thickness. Thereby, 47 % remaining initial capacity was observed at 100 C for 30 nm niobium oxide-coated cathode films. For the same coating thickness, the cells retained 80% of the initial capacity after 493 cycles at 10 C, more than doubling the cycle life of the uncoated cathode. Impedance investigation indicated a strong retardation of the interfacial resistance growth during cycling. Elemental analysis revealed a bulk and surface contribution of the niobium oxide coating. These results suggest that ALD as coating method can also have a strong impact for high rate discharging of bulk cathode powders.

1:40 PM *EN08.02.03

Mechanisms of Diffusive Charge Transport and Surface Adsorption in Redox-Active Polymer Solutions

Liliana Bello and Charles E. Sing; University of Illinois at Urbana-Champaign, United States

Redox-active polymers (RAPs) are a promising material for energy storage in flow batteries due their large size preventing detrimental redox material crossover and adjustable molecular chemistry and architecture for optimized performance. There has been a recent effort to understand the physics governing charge diffusion in RAPs, both in the bulk and near surfaces. We use simulations and theory to show how a variety of molecular charge transport mechanisms affect diffusive motion in RAP solutions. To simulate these RAP solutions, we employ a hybrid Brownian dynamics and kinetic Monte Carlo model that accounts for both the conformational degrees of freedom and charge hopping dynamics. This model uses a coarse-grained representation that can be altered to reflect a variety of physicochemical properties of RAPs, in particular using the molecular charge hopping kinetics as either a tunable variable or an input parameter. We perform these simulations for both isolated, single-chain and interacting, multi-chain systems to demonstrate the interplay between a variety of transport mechanisms (e.g. intra-polymer self-exchange, polymer segmental motion, inter-polymer collisions). We develop theoretical scaling arguments to describe the diffusive motion of charge via these mechanisms, showing excellent agreement with simulations. Our predictions suggest the existence of three charge transport regimes, which distinguish between inter- and intra-molecular processes and dilute and semi-dilute solutions. We extend our understanding of these solution dynamics to model of the kinetics of surface adsorption, providing a molecular connection between surface interactions and charge transport.

2:05 PM EN08.02.04

Cooperative Anion Effects for Reversible Plating/Stripping of Divalent Metals Justin Connell, Milena Zorko, Garvit Agarwal, Mengxi Yang, Chen Liao, Rajeev Surendran Assary, Dusan Strmcnik and Nenad Markovic; Argonne National Laboratory, United States

One of the biggest challenges facing the development of multivalent batteries is the fact that the majority of promising electrolytes demonstrated to date are incompatible with either metallic anodes or high voltage cathodes, both of which are required for multivalent systems to compete with existing Li-ion technologies. For example, many electrolytes shown to exhibit reversible plating/stripping of Mg metal rely on the presence of significant concentrations of Cl^- , precluding their use with oxide cathode materials due to parasitic reactions that take place at high voltage. In light of this limitation, it is imperative that a more complete understanding be developed of the specific role of Cl^- in promoting reversibility in multivalent systems in order to develop design rules for synthesizing new electrolytes that can avoid the use of Cl^- altogether. Through systematic rotating disk and ring-disk electrode (RDE and RRDE) investigations of metal plating/stripping in multivalent electrolytes utilizing the bis-(trifluoromethane sulfonyl) imide (TFSI⁻) anion with varying concentrations of Cl^- , a cooperative effect is observed between both anions that yields the overall more reversible behavior of mixed TFSI⁻/ Cl^- electrolytes relative to electrolytes containing only TFSI⁻. This effect is shown to be general across multiple multivalent systems (i.e., Mg, Zn and Cu), and mechanistic understanding of the role of Cl^- in improving reversibility of TFSI-based electrolytes is provided through the combination of R(R)DE experimental results with computational evaluation of the activity and stability of various TFSI⁻ and Cl^- -based solution complexes. The cooperative anion effect can be further generalized to other electrolyte systems, suggesting a set of general design principles for developing new multivalent electrolytes.

2:20 PM EN08.02.05

Realizing Reversible Magnesium Plating/Stripping by Interface Controls Hui Wang^{1,2}, Jaegwon Ryu^{1,2} and Yuyan Shao^{1,2}; ¹Pacific Northwest National Laboratory, United States; ²Joint Center for Energy Storage Research, United States

Rechargeable Mg batteries hold a great potential for a new low-cost, high energy density energy storage solution due to the high volumetric capacity (3,833 mAh cm⁻³) and natural abundance (2.33% in earth crust) of Mg. Despite its promising electrochemical metrics, the absence of proper electrolytes that enable reversible Mg plating-stripping and compatible pairing with cathode materials hindered the practical use of Mg metal anodes. More importantly, there is very limited fundamental understanding of the critical factors to drive the reversible

Mg anodes at the Mg/electrolyte interface. Here, we investigated the interfacial chemistry between Mg and modified Mg cationic clusters in Mg(TFSI)₂ with Mg(BH₄)₂ cosalt through operando electrochemical analyses to rationalize the improved reversibility of Mg plating-stripping. Meanwhile, the electrochemically evolved artificial film was developed to stabilize the fresh Mg deposits, which showed ultrafast charge transfer and low film resistance in the conventional electrolyte of Mg(TFSI)₂-MgCl₂.

2:35 PM DISCUSSION TIME

SESSION EN08.03: Interphases for Ion Intercalation
Session Chairs: Rajeev Surendran Assary and Kevin Zavadil
Thursday Afternoon, April 22, 2021
EN08

4:00 PM *EN08.03.01

Optimizing Bulk and Interfacial Kinetic Limitations in Nanostructured Battery Materials Sarah Tolbert;
University of California, Los Angeles, United States

In bulk battery materials, solid-state diffusion of ions frequently limits rate capabilities, and phase transitions or phase separation processes often limit stability. Many of these limitations can be overcome by moving to the nanoscale, as diffusion distances are shortened, and phase transitions or phase separation can either be suppressed, or occur on much shorter length-scales. Nanoporous materials, in particular, are very promising, as they offer reduced diffusion lengths without significantly reducing electrical conductivity, as often occurs in nanocrystal based materials. While the advantages of nanostructured electrode materials can be significant, they have the marked disadvantage of increased interfacial area that can lead to increased SEI formation and reduced coulomb efficiency. In this talk, we explore a number of systems where we seek to optimize the trade-off between bulk kinetic limitations and interfacial or charge transfer limitations, with a specific focus on how nanoscale architecture can be tuned to produce an ideal balance between these limitations. Systems that will be addressed include high rate nanoporous cathodes based on both conventional oxides, using LiNi_{0.80}Co_{0.15}Al_{0.05}O₂ (NCA) as a prime example, and on metal phosphates, using LiVPO₄F (LVPF) as an example. In both cases, nanoporous materials are produced by combining polymer templating with sol-gel methods. For both systems, in addition to optimizing nanoscale size, we find that the key to high rate behavior is incorporation of a conductive artificial SEI layer. In the oxide cathodes, in particular, conjugated polymers can be highly effective at increasing stability and rate capabilities, a process that should derive from a combination of enhanced electrical conductivity and reduced SEI formation. A variety of new conjugated polymer binders will be discussed. Finally, we will consider nanostructured alloy anodes produced by selective etching of metals. In these systems, dramatic structural changes upon lithiation require the use of nanophase materials to achieve stable cycling. Here, the interplay between nanoscale architecture, material composition, and surface layers will be explored using *operando* transmission X-ray microscopy (TXM), which allows us to directly image the evolution of the nanoscale pore structures during battery operation. Taken together these results demonstrate the rich design space that is available when nanoscale architecture and interfacial engineering are combined to optimize the performance of battery materials.

4:25 PM *EN08.03.02

Probing Local Ion Intercalation Processes Through Electro-Chemo-Mechanical Coupling Behaviors Nina Balke and Wan-Yu Tsai; Oak Ridge National Laboratory, United States

Electrode deformations during charging and discharge process are directly related to the power performance and cyclability of the energy storage devices. Understanding the electrode deformation and changes in mechanical responses during electrochemical events and their impact on devices' performance is crucial for achieving high

power and high energy storage devices. In-situ atomic force microscopy (AFM) is well suited to tackle this task as it allows tracking local sub-nanometer volume changes and other mechanical responses. With a spatial resolution of tens of nanometer, this approach is capable of mapping the electro-chemo-mechanical behavior under the conditions close to the device operation and access information about local redox mechanisms and investigate its heterogeneity.

In this work, the local electro-chemo-mechanical coupling behaviors of proton insertion into WO_3 electrodes is studied. The concept of mechanical cyclic voltammetry (mCV) curves is introduced, and the relationship between electrochemical current and strain are discussed in the context of simplified models. The results show that different mechanical responses are involved during ion insertion and extraction. The mechanical CV mapping highlighted the local heterogeneity and showed that the charging mechanisms varied across the electrode. These local variations could be further correlated to local morphology, crystal orientations or chemical compositions. Besides providing information of redox heterogeneity, the mCV methodology allows us to circumvent the common issues that are often encountered in the global electrochemical characterizations, for example cell resistance and unwanted parasitic reaction. We further demonstrate that the mCV approach is applicable to a variety of energy storage materials with increasing complexity of current-deformation relationships.

The work was supported by the Fluid Interface Reactions, Structures and Transport (FIRST), an Energy Frontier Research Center funded by the U.S. Department of Energy, Office of Science, Office of Basic Energy Sciences. Measurements were performed at the Center for Nanophase Materials Sciences (CNMS), which is sponsored at Oak Ridge National Laboratory by the Scientific User Facilities Division, Office of Basic Energy Sciences.

4:50 PM EN08.03.03

Advanced Electrode/Electrolyte Interphases for High Voltage Lithium Metal Batteries Xiaodi Ren, Xianhui Zhang, Ji-Guang Zhang and Wu Xu; Pacific Northwest National Laboratory, United States

Rechargeable batteries with high energy density are of significant importance to the energy storage market, especially for portable electronics and electric vehicles. Although the use of lithium (Li) metal anode and high capacity cathode at high operation voltage can achieve the high energy density of batteries, the development of Li metal batteries is greatly limited by the inferior performances because of the issues related to the Li metal anode (dendrite growth and low Coulombic efficiency) and the intercalation cathode under high voltages and challenging temperatures. The main reason is the electrode/electrolyte interphases on both Li metal anode and the high voltage cathode are not stable and effective enough to protect the two electrodes from the continuous side reactions with the electrolyte. In this presentation, we report to design and in situ generate highly stable electrode/electrolyte interphases on both Li anode and LiCoO_2 cathode with an advanced electrolyte, with which greatly improved cell performances of $\text{Li}||\text{LiCoO}_2$ batteries are achieved under a high charge voltage of 4.5 V and a wide temperature range from -30 to 55 °C. More details will be discussed at the presentation.

5:05 PM EN08.03.04

Designing Stable Electrode/Electrolyte Interphases for Lithium-Ion Batteries with Low-Flammability Electrolytes Hao Jia, Yaobin Xu, Xianhui Zhang, Sarah Burton, Mark Engelhard, Peiyuan Gao, Chongmin Wang and Wu Xu; Pacific Northwest National Laboratory, United States

As the energy density of lithium ion batteries (LIBs) increases, safety of the battery is raising intensive concern. Flammability of the electrolyte is a critical link of the overall safety property of LIBs. The conventional approach to reduce the flammability of liquid electrolytes is to introduce a certain amount of a miscible organic phosphate solvent as flame retardant (FR) additive or co-solvent into the LiPF_6 -organocarbonates electrolytes.[1] However, due to the intercalation of the phosphate molecules into the graphite electrode, the introduction of such FR usually induces incompatibility between the FR and the graphite electrode and deterioration in battery cycling performance. Moreover, as the FR is gradually consumed by the parasitic

reactions at the electrode/electrolyte interfaces, the flame retarding effectiveness of the FR decays.[2] In response to these challenges, the concept of localized high-concentration electrolyte (LHCE) with an organic phosphate solvent FR is utilized to adjust the electrode/electrolyte interphases on both graphite anode and high voltage cathode. By adopting the unique solvation structure of LHCE and the incorporation of a small amount of electrolyte additive, the electrode/electrolyte interphases can be designed and tuned. Consequently, the graphite||LiNi_{0.8}Mn_{0.1}Co_{0.1}O₂ cells using such phosphate-based LHCEs can achieve the capacity retention of 85.5% after 500 charge/discharge cycles, being significantly higher than that of conventional LiPF₆-organocarbonate electrolyte (75.8%). Meanwhile, ignition test shows that these LHCEs are much less flammable than the conventional LiPF₆-organocarbonate electrolytes. More details will be reported during the presentation.

References

- [1] X. Yao, S. Xie, C. Chen, Q. Wang, J. Sun, Y. Li, S. Lu, *Journal of power sources* 2005, 144, 170.
- [2] T. Dagger, C. Lürenbaum, F. M. Schappacher, M. Winter, *Journal of Power Sources* 2017, 342, 266.

5:20 PM EN08.03.05

Ion Clustering and Transport in MgCl₂-Based Electrolytes for Rechargeable Magnesium Batteries

Vallabh Vasudevan¹, Mingchao Wang¹, Nick Birbilis² and Nikhil Medhekar¹; ¹Monash University, Australia; ²The Australian National University, Australia

Non-aqueous Rechargeable Mg batteries (RMBs) represent a safer, cheaper and more powerful alternative to lithium ion battery technology.^{1,2} However, the high charge density of Mg²⁺ ions triggers the formation of ion impermeable deposits with solvents at electrode/electrolyte interfaces called Solid-Electrolyte Interfaces (SEIs). To overcome the stability and reversibility issues caused by SEIs, the electrolytes used must be stable against reductive reactions at the anode/electrolyte interface during charge/discharge cycles in RMBs.^{3,4} Magnesium halide salts are an exciting prospect as stable and high-performance electrolytes for RMBs. By nature of their complex equilibria, these salts exist in solution as a variety of electroactive species (EAS) in equilibrium with counter ions such as AlCl₄⁻. Here we investigated ion agglomeration and transport of several such EAS in MgCl₂ salts dissolved in ethereal solvents under both equilibrium and operating conditions using large scale atomistic simulations.⁵ We find that the solute morphology is strongly characterized by the presence of clusters and is governed by the solvation structures of EAS. Specifically, the isotropic solvation of Mg²⁺ results in slow formation of bulky cluster, compared with chain-like analogues observed in the Cl-containing EAS such as Mg₂Cl₃⁺, MgCl⁺ and Mg₂Cl₂²⁺. We further illustrate these clusters can reduce the diffusivity of charge-carrying species in the MgCl₂ based electrolyte by at least an order of magnitude. We highlight the role of the solvent in determining cluster morphology and ion mobility by controlling ion diffusion pathways and ion coverage. Our findings of the cluster formation, morphology and kinetics can provide useful insight into the electrochemical reactions at the anode/electrolyte interface in RMBs.

References

1. C. B. Bucur, T. Gregory, A. G. Oliver and J. Muldoon, *The Journal of Physical Chemistry Letters*, 2015, **6**, 3578-3591.
2. M. John, B. C. B. and G. Thomas, *Angewandte Chemie International Edition*, 2017, **56**, 12064-12084.
3. P. Baofei, H. Jinhua, H. Meinan, B. S. M., V. J. T., Z. Lu, B. A. K., Z. Zhengcheng and L. Chen, *ChemSusChem*, 2016, **9**, 595-599.
4. K. A. See, K. W. Chapman, L. Zhu, K. M. Wiaderek, O. J. Borkiewicz, C. J. Barile, P. J. Chupas and A. A. Gewirth, *Journal of the American Chemical Society*, 2016, **138**, 328-337.
5. V. Vasudevan, M. Wang, J. A. Yuwono, J. Jasieniak, N. Birbilis and N. V. Medhekar, *The Journal of Physical Chemistry Letters*, 2019, **10**, 7856-7862.

5:35 PM DISCUSSION TIME

8:15 PM *EN08.04.01

Single Molecule Charge Transport at Electrode Interfaces Charles M. Schroeder and Jialing Li; University of Illinois at Urbana-Champaign, United States

The development of new energy storage systems has attracted substantial attention in the scientific community. The overall performance of energy storage in batteries, including rates of charge/discharge and system reliability, largely depends on the resiliency of the electrode/electrolyte interface. Despite recent progress, major challenges lie developing new electrolytes and electrodes for redox-flow batteries to enhance charge transfer rates and to achieve extended operation lifetimes. In recent years, bulk-scale methods have been used to characterize and understand redox-active electrolyte behavior at interfaces, however, bulk measurements tend to 'average out' and obscure charge transport events at the molecular level. In this work, we use single molecule methods to directly characterize charge transport at the electrode interface. In particular, we use a custom electrochemical scanning tunneling microscope-break junction (ECSTM-BJ) instrument to understand interfacial charge transport and redoxmer degradation at the molecular level. ECSTM-BJ enables the direct measurement of molecular charge transport and conductance as a function of applied bias, external gate voltage, and the chemical identity of the redox-active species or supporting electrolytes. Materials with different chemical structures and charge transport channels are identified as different molecular subgroups, thereby revealing otherwise hidden molecular sub-populations that underlie bulk-scale behavior. Using this approach, we investigate two different redox-active systems: viologen-based molecules and mesolytic cleavage of redoxmers. Electrostatic gating is used to tune charge transport in viologen-based molecules by adjusting the potential drop across the double layer and the associated redox states in the electrochemical environment. In contrast to non-redox-active counterparts, our results show that the conductance of viologen-containing molecules is a strong function of the gate voltage as the viologen redox center is reduced. Moreover, the reduced state of the molecules weakens the interaction between the molecules and the electrode, which is indicated by changes in junction length. In a related study, we show that intermolecular charge transport is effectively regulated by the formation of a pH-responsive supramolecular host-guest complex. In this way, we present intriguing new avenues for intermolecular complexation for controlling the charge transport process. Finally, we discuss the direct molecular characterization of self-immolating redoxmers that degrade upon being damaged via mesolytic cleavage. Interestingly, our results show that strong electric fields near electrode interfaces induce mesolytic cleavage, followed by the dimerization of the reaction products, which is detected by single molecule conductance. Overall, our results highlight the use of single molecule techniques to characterize charge transport at the electrode/electrolyte interface.

8:40 PM EN08.04.02

Interfacial Solvation Dynamics of Multivalent Cations—Peculiarities and General Principles of Ion Solvation Engineering Artem Baskin^{1,2}, David Prendergast² and John Lawson¹; ¹NASA Ames Research Center, United States; ²Lawrence Berkeley National Laboratory, United States

The essential electrochemical processes at electrode interfaces are closely related to the changes of coordination environments and solvation structures of cations. The thermodynamics of these processes including reactivity and stability of interfaces are largely determined by the spatial speciation profile in the interfacial regions whereas kinetics of the charge transfer is governed by the stiffness of solvation spheres of cations and their coordination states. However, the atomistic details and thermodynamic characteristics of ion (de-)solvation process in the confined environment (e.g., near an electrode) remain largely unknown. Specifically, for multivalent cations that are prone to the formation of ion-pairs and neutral aggregates in low dielectric solvents and show a non-trivial concentration dependence of population of various ionic species these characteristics are

very difficult to probe both experimentally and computationally. The key questions we want to address are the following: 1) how different the population of ionic/neutral species at the interface is as compared to the bulk electrolyte at various electrode potentials; 2) in which form the active matter (metal cations) is delivered to the interface; 3) what is the dynamics of the cation solvation and coordination environment along the most thermodynamically favorable pathways of a cation that approaches the interface from a bulk electrolyte; and finally 4) what is the locus and a particular cation solvation/coordination state at which the charge transfer occurs.

Using a multiscale methodology based on classical and *ab initio* free energy sampling techniques we analyze a solution of MgTFSI₂ in THF next to graphene and show that the anion-coordinated species are the vehicle that delivers the Mg-cation to the interfaces at shorter distances and in lower coordination states. This allows us to formulate the key and general interfacial descriptors that can be used to control the balance between the chemical stability of an interface and the overpotential associated with the charge transfer kinetics. We identified the optimal free energy pathways and a generalized coordinate that describe the (de-)solvation dynamics of the Mg-cation. Finally, we show how the interfacial solvation dynamics can be manipulated using the ion solvation multiplicity.

[1] A. Baskin and D. Prendergast, *J. Phys. Chem. Lett.* **10**, 4920–4928 (2019)

[2] A. Baskin and D. Prendergast, *J. Phys. Chem. Lett.* **11**, XXX, 9336–9343 (2020)

8:55 PM *EN08.04.03

Atomic-Scale Insight into Charge Transfer Processes at Electrochemical Interfaces Donald Siegel;
University of Michigan–Ann Arbor, United States

Interfacial charge transfer processes strongly influence the performance of electrochemical energy storage devices in many different ways. For example, ion deposition from electrolytes onto electrodes influences the efficiency, morphology, and stability of anodes based on high-capacity metals. Electronic transfer between electrodes and solid electrolytes can impart undesirable electrical conductivity and precipitate harmful chemical reactions. Ion transport in solid electrolytes can be highly sensitive to internal interfaces such as grain or particle boundaries. This presentation will summarize recent computational studies of the atomic-scale phenomena that underlie charge transfer processes on electrode surfaces, between electrodes and electrolytes, and at internal interfaces in solid electrolytes. Multiple computational techniques, ranging from large scale classical MD to many-body perturbation theory, are used to tackle the different length scales spanned by these systems.

9:20 PM EN08.04.04

Interfacial Reactivity of Electrolytes in Multivalent Batteries—Insights from Density Functional Theory Calculations and XPS Experiments Garvit Agarwal¹, Swadipta Roy², Venkateshkumar Prabhakaran², Grant E. Johnson², Vijayakumar Murugesan² and Rajeev Surendran Assary¹; ¹Argonne National Laboratory, United States; ²Pacific Northwest National Laboratory, United States

Multivalent batteries, particularly Mg-metal batteries, are promising technology for next-generation energy storage applications due to their theoretically high volumetric energy density. One of the critical challenges in multivalent batteries is to create a stable and functional electrochemical interphase (solid electrolyte interphase) that facilitates reversible plating and stripping of charge carrying ions and impedes electronic transport to limit electrolyte degradation. This requires fundamental understanding of the reactivity of electrolyte (solvent and salt) species with Mg-metal anode. To address this, we employ in-operando X-ray photoelectron spectroscopy (XPS) experiments in combination with density functional theory (DFT) calculations to elucidate the decomposition mechanisms of two commonly used etheral solvents, diglyme (G2) and tetrahydrofuran (THF) on the Mg-metal anode surface. The solvent molecules are exposed to sputter cleaned Mg-metal surface and high-resolution XPS spectra are collected at different temperatures to analyze the reaction products. DFT calculations are performed to model the adsorption and to compute the reaction energy profiles to elucidate decomposition reaction pathways of G2 and THF on pristine Mg (0001) surface. The decomposition pathways are modeled as a series of C-O and C-H bond cleavage reactions. The climbing image nudged elastic band (CI-

NEB) calculations are carried out to compute the transition states and energy barriers for the various C-O and C-H bond cleavage reactions. Further, Bader charge analysis is performed to estimate the effect of charge transfer on the stability of intermediate species formed during the surface decomposition reactions. The computed reaction energy profiles indicate higher reactivity of diglyme molecule compared to a THF molecule at Mg (0001) surface, in agreement with experimental observations. Our approach enables a detailed atomic-level understanding of the reaction mechanisms and explain the nature of key reaction products of solvent decomposition on Mg-metal anode surface.

9:35 PM DISCUSSION TIME

SESSION EN08.05: Theoretical Analysis of Interfacial Reactivity
Session Chairs: Nav Nidhi Rajput and Rajeev Surendran Assary
Friday Morning, April 23, 2021
EN08

8:00 AM *EN08.05.01

Elucidating Cation Electrodeposition—The Roles of Electrolyte Composition and Surface Structure Perla Balbuena, Stefany Angarita-Gomez and Fernando A. Soto; Texas A&M University, United States

The use of lithium metal anodes is expected and desired in the new generation of high energy density batteries. However, the high reactivity of Li metal electrodes creates a series of issues that keep them away from practical applications. For example, electrolyte degradation reactions due to electron transfer from the surface induce the formation of a solid-electrolyte interphase (SEI) film, that starts at open circuit conditions. This multicomponent SEI film has different passivation properties and morphologies depending on the electrolyte. However, during battery charge, another phenomenon takes place simultaneously with SEI growth, and this is cation electrodeposition and metal nucleation or “plating”. As expected, at fixed current rate, phenomena such as cation diffusion and desolvation depend strongly on the type of electrolyte and the stage of formation of the SEI. Here we analyze cation electrodeposition from first principles simulations, including ab initio constrained molecular dynamics coupled to thermodynamic integration in the Blue Moon ensemble. We characterize the possible free energy pathways of the cation in various environments and the influence of the electrolyte composition and its decomposition, and the surface structure.

8:25 AM EN08.05.02

Effects of Functionalized Cathode and Electrolyte Composition on Structure and Dissolution of Polysulfide Species in Li-S Batteries Rasha Atwi and Nav Nidhi Rajput; Stony Brook University, The State University of New York, United States

A major breakthrough in battery materials is required to meet the ever-increasing proliferation of portable electronic devices, electric vehicles and their variants, as well as the need for incorporating renewable energy resources into the main energy supply [1]. In this context, lithium-sulfur (Li-S) batteries are promising candidates due to their very high energy density (2,600 Wh kg⁻¹) and specific capacity (1,675 mAh g⁻¹) and significantly lower weight and cost, compared to lithium-ion batteries (LIBs) [2]. Fully packaged, it is expected that future Li-S batteries can operate at close to 500 Wh kg⁻¹, which is more than twice the energy density of LIBs (200 Wh kg⁻¹) [3]. However, several issues including the dissolution of Li-Polysulfide (PS) species into the electrolyte have prevented this technology from being broadly commercialized [4]. In this talk, I will present our computational approach of attaching functional groups to the cathode surface to create thermodynamic barriers to the dissolution of PS in an electrolyte. Beginning with theoretical analysis of the structure and interactions of generic LiPS moieties and a large set of functional groups via high-throughput density functional theory (DFT) calculations, I show that it is possible to identify functional groups that anchor to the cathode and

exert high enough binding affinity to LiPS formed near electrode/electrolyte interface to prevent their loss to the solution. The selected candidates are used in detailed molecular dynamics (MD) studies to develop a fundamental understanding of the effect of various electrolyte variables (components, PS chain length, salt concentration) on structural and dynamical properties at the functionalized interface [5, 6]. In addition, I show how we are applying such a multi-scale modeling approach using our group's newly developed computational infrastructure that combines DFT calculations with MD simulations, resulting in a database of well-characterized materials to be used for building machine-learning models as well as for testing computationally identified structures in experiments. This work provides crucial information to mitigate the dissolution of PS species during cycling, which is the main reason for rapid capacity decay in Li-S batteries.

References

1. Larcher, D. and J.-M. Tarascon, *Towards greener and more sustainable batteries for electrical energy storage*. Nature chemistry, 2015. 7(1): p. 19.
2. Manthiram, A., X. Yu, and S. Wang, *Lithium battery chemistries enabled by solid-state electrolytes*. Nature Reviews Materials, 2017. 2(4): p. 1-16.
3. Fang, R., et al., *More reliable lithium-sulfur batteries: status, solutions and prospects*. Advanced materials, 2017. 29(48): p. 1606823.
4. Manthiram, A., Y. Fu, and Y.-S. Su, *Challenges and prospects of lithium-sulfur batteries*. Accounts of chemical research, 2013. 46(5): p. 1125-1134.
5. Rajput, N.N., et al., *Elucidating the solvation structure and dynamics of lithium polysulfides resulting from competitive salt and solvent interactions*. Chemistry of Materials, 2017. 29(8): p. 3375-3379.
6. Andersen, A., et al., *Structure and dynamics of polysulfide clusters in a nonaqueous solvent mixture of 1, 3-dioxolane and 1, 2-dimethoxyethane*. Chemistry of Materials, 2019. 31(7): p. 2308-2319.

8:40 AM DISCUSSION TIME

8:55 AM EN08.05.04

Understanding Ion Transport and Interfacial Stability in Fluorine Containing Lithium Argyrodite Electrolytes for Solid-State Lithium-Sulfur Batteries Varun Shreyas, William Arnold, Saransh Gupta, Jacek Jasinski, Gamini Sumanasekera, Hui Wang and Badri Narayanan; University of Louisville, United States

Rechargeable all solid-state lithium-sulfur batteries (ASLSBs) hold tremendous promise for use in electric vehicles due to their high theoretical capacity (~1675 Ah/kg; ~5-6 times higher than state-of-the-art Li-ion batteries), high promised energy density (400 Wh/kg) and cycle life, and low costs owing to natural abundance of sulfur. Lithium argyrodites (e.g., Li₇PS₆, and its halogen-doped derivatives) have emerged as a lucrative class of solid-state electrolytes (SSEs) for ASLSBs; owing to their high Li-ion conductivity (~10⁻³ S/cm), good elastic stiffness (~30 GPa), and low flammability. Despite their promise, ASLSBs (even using argyrodite SSEs) remain far from commercialization due to paucity of fundamental understanding of physical factors underlying key electrochemical phenomenon including ion-conduction, charge transport, structural evolution, and interfacial reactions (e.g., dendrite growth, electrolyte decomposition etc.). Specifically, such knowledge gap has thwarted development of high-performance SSEs that provide rare combination of superionic Li conduction and interfacial stability. Here, we integrate *ab initio* molecular dynamics (AIMD) simulations, density functional theory (DFT) calculations, liquid-phase synthesis and characterization methods to advance the understanding of lithium-ion conduction and interfacial reactions in fluorine (F) containing lithium argyrodites. The choice of F-containing argyrodites was motivated by recent reports indicating that F (or LiF) could suppress formation of deleterious dendrites at the Li-anode. Our AIMD simulations showed that lithium argyrodite doped with F alone, Li₆PS₅F possesses much lower Li-ion conductivity (~0.32 mS/cm) as compared to state-of-the-art Li₆PS₅Cl electrolytes (~0.9 mS/cm). Interestingly, we found that simultaneous doping of argyrodites with two dissimilar halogens (e.g., F and Cl) results in much higher Li⁺ ion conductivity as compared to the counterparts doped with one halogen. For instance, we found that the Li⁺ ion conductivity of Li₆PS₅F_{0.5}Cl_{0.5} electrolyte (2 mS/cm) is ~2.2 times higher than that of Li₆PS₅Cl (0.9 mS/cm) and ~6 times that of Li₆PS₅F (0.32 mS/cm); consistent with our experimental measurements. Careful analysis of our AIMD trajectories, and DFT calculations indicate that this enhanced Li-ion diffusion can be attributed to the unique

defect structure stabilized by F ions, and halogen-mediated hopping of Li ions across the SSE. More importantly, we found that such mixed halogen doping enhances stability of SSE against Li-anode, as evidenced by our galvanostatic Li stripping/plating experiments that show flat voltage profile and low polarization voltage for $\text{Li}_6\text{PS}_5\text{F}_{0.5}\text{Cl}_{0.5}$ even at current density of 0.2 mA/cm^2 ; in contrast, the cells with $\text{Li}_6\text{PS}_5\text{F}$ and $\text{Li}_6\text{PS}_5\text{Cl}$ electrolytes die at 0.05 mA/cm^2 and 0.1 mA/cm^2 respectively. AIMD simulations show that this enhanced interfacial stability in $\text{Li}_6\text{PS}_5\text{F}_{0.5}\text{Cl}_{0.5}$ SSE is enabled by formation of strong Li-F bonds at the anode/electrolyte interface, which reduce the dissociation of PS_4^{3-} tetrahedra. These results will be discussed in the context of developing novel solid-state electrolytes for high-performance all solid-state lithium-sulfur batteries.

9:10 AM EN08.05.05

Late News: DFT Sampling Study on Ion Transfer at Heterogeneous Solid-Solid Interfaces in Batteries

Yoshitaka Tateyama^{1,2}, Keitaro Sodeyama^{1,2} and Bo Gao¹; ¹National Institute for Materials Science, Japan; ²Kyoto University, Japan

Interfacial charge-transfer processes in batteries govern their performance and stability, where both electronics and ionics play crucial roles. However, the electronic and atomistic understanding of such interface processes is still difficult in the conventional computational as well as experimental approaches. From theoretical side, we have addressed this issue based on the first-principles density functional theory (DFT) calculations of the explicit solid-solid interfaces. Firstly, we explored techniques to obtain the energetically probable disordered solid-solid interfaces. If soft materials consist of the interface, one can use the DFT molecular dynamics (MD) sampling. We applied this procedure for the Li-intercalated graphite LiC_x anode / Li_2CO_3 inorganic solid electrolyte interphase (SEI) [1]. For the solid electrolyte (SE) - cathode interfaces in all-solid-state batteries (ASSBs), we developed, “Heterogeneous Interface (HI)-CALYPSO method”, allowing systematic sampling of heterogeneous solid-solid interface structures, based on the particle swarm optimization (PSO) [2].

With the obtained probable interfaces, we calculated the free/potential energy profiles of the Li-ion transfer across the interfaces. For the LiC_x anode / Li_2CO_3 SEI interface, we demonstrated that the Li-ion energy (a sort of electrochemical potential) in the anode is much higher than in the SEI [1]. The energy difference is attributed to the negative-charge environment surrounding the Li-ions. The obtained energy profiles correspond to the discharge process where Li-ions flow into the electrolyte side. To explain the charging process, we proposed that the energy profiles are modulated by the electric field by the excess electrons. These results also suggest a continuous energy profile model for Li-ion in the whole battery. We have also examined the energy profiles across the $\beta\text{-Li}_3\text{PS}_4$ (LPS) SE / LiCoO_2 (LCO) cathode interfaces in ASSB, which supports the current profile model. Though several hypotheses still exist, the present results will give a novel and useful insight into the Li-ion transport in batteries.

The work was partly supported by MEXT as “Program for Promoting Researches on the Supercomputer Fugaku” (Fugaku Battery & Fuel Cell Project) and JSPS KAKENHI “Interface IONICS” Grant Number JP19H05815.

References: [1] T. Baba, Y. Tateyama *et al.*, Phys. Chem. Chem. Phys. 22, 10764 (2020). [2] B. Gao, R. Jalem, Y. Ma, Y. Tateyama, Chem. Mater. 32, 85 (2020).

SESSION EN08.06: Metal Anode Interfacial Design
Session Chairs: Vijayakumar Murugesan and Kevin Zavadil
Friday Morning, April 23, 2021
EN08

11:45 AM *EN08.06.01

Controlling Interphase Generation and Interfacial Charge Transfer at Magnesium Anode–Electrolyte Interfaces Brett A. Helms¹, Sung-Ju Cho¹, Benjamin Cousineau², Jingbo Zhao¹, Emily Carino³, Julian Self¹, Kristin Persson^{1,2}, Rajeev Surendran Assary³, Garvit Agarwal³ and Kevin R. Zavadil⁴; ¹Lawrence Berkeley National Laboratory, United States; ²University of California, Berkeley, United States; ³Argonne National Laboratory, United States; ⁴Sandia National Laboratories, United States

The inherent reactivity of magnesium metal toward electrolytes promotes the formation of insulating surface films which inhibit ionic charge transfer at the anode-electrolyte interface of magnesium metal batteries. It remains a significant challenge to realize reversibility with high energy efficiency due to the exceedingly high overpotential to plate and strip the anode at high current densities. Here, we will discuss recent efforts in our group to control interphase generation at the magnesium anode-electrolyte interface with de novo designed materials. We find that tailoring the solvation environment of magnesium in the interphase is a critical factor and explains both successes and failures in rechargeable cells. We further find that both structure and dynamics play important roles, which we elucidate by comparing molecular dynamics simulations with Raman, IR, and X-ray spectroscopic studies as well as X-ray scattering. Together, these collective insights feed back into the design of artificial interphases, which have decidedly different design rules than those that are used in alkali metal batteries (i.e., Li-metal, Na-metal, or K-metal). We will also highlight how computational materials design and high-throughput screens becomes indispensable tools to quickly navigate important structure–transport relationships in artificial interphases for magnesium metal batteries.

12:10 PM EN08.06.02

Sodium Stripping and Plating from Na-β"-Alumina Ceramics beyond 1000 mA/cm² Daniel Landmann, Gustav Graeber, Meike Heinz and Corsin Battaglia; Empa–Swiss Federal Laboratories for Materials Science and Technology, Switzerland

Sodium-nickel chloride batteries are based on abundant, non-critical raw materials (namely rock salt, nickel, and alumina). These batteries have a proven track record for backup power applications, but also show great potential for large-scale stationary electricity storage. To enable increased deployment of this battery technology, charge and discharge rate capabilities need to be improved (>1C), and cell production cost needs to be reduced.

While lithium-ion battery cells are currently developed towards generation 3b, the current sodium-nickel chloride cell design stems from the early 1990s. In this study, we assess the rate limiting processes in state-of-the-art sodium-nickel chloride cells and propose measures to improve their performance. We deconvolute the battery's performance into anode and cathode processes in order to develop next-generation sodium-nickel chloride batteries with enhanced cell design and chemistry. By these measures, we target to improve nominal discharge current rates from currently C/3 to 1C (200 mA/cm²), and maximum pulse discharge rates from currently 1.5C to 3C (600 mA/cm²) [1].

On the anode side, we investigate plating and stripping of liquid sodium metal from a ceramic Na-β"-alumina electrolyte at 250 °C, applying a specially designed high-temperature electrochemical cell. Employment of a porous carbon electrode coating allows us to (1) prevent dewetting of plated liquid sodium from, and (2) to supply liquid sodium upon stripping to, the sodiophobic Na-β"-alumina surface. By this measure we are able to eliminate the mass transport limitations at the sodium/ Na-β"-alumina interface and demonstrate current densities above 1000 mA/cm² at cumulative plated capacity of 10 Ah/cm² without dendrite formation [2]. These values are two orders of magnitude higher than the corresponding values measured at room temperature [3] and exceed practical continuous current densities by a factor of 5.

On the cathode side, we characterize the chlorination and de-chlorination reaction of nickel by cyclic voltammetry, galvanostatic techniques, and electrochemical impedance spectroscopy. We deconvolute the cathode behavior into single processes by dedicated experiments. We identify the rate-limiting processes and link the overall electrochemical performance of the battery to the local degree of chlorination. By enhancing the general understanding of the working principles in sodium-nickel chloride cells, we strive to enhance cycle-life and increase charge and discharge rates for next-generation sodium-nickel chloride batteries.

- [1] M. V.F. Heinz, G. Graeber, D. Landmann, C. Battaglia, J. Power Sources 2020, 465, 228268
[2] D. Landmann, G. Graeber, M. V. F. Heinz, C. Battaglia, Materials Today Energy 2020, 18, 100515
[3] M.-C. Bay, M. Wang, R. Grissa, M. V. F. Heinz, J. Sakamoto, C. Battaglia, Adv. Energy Mater. 2019, 201902889

12:25 PM EN08.06.03

Kinetic- vs Diffusion-Driven Three-Dimensional Growth in Magnesium Metal Battery Anodes Janna Eaves-Rathert¹, Kathleen Moyer^{1,1}, Murtaza Zohair^{1,1} and Cary Pint^{1,1,2}; ¹Vanderbilt University, United States; ²Iowa State University of Science and Technology, United States

Until now, a key barrier toward realizing a high energy density Mg^{2+} battery has been the limited understanding of mechanisms governing multivalent metal electrodeposition. This, compounded with recent observations of Mg dendrites, highlights the need for better fundamental insight into multivalent systems. We present a comprehensive study of electrodeposition in practical coin cell configurations to evaluate the mechanisms of growth from common $Mg(TFSI)_2$ -based electrolytes. Our findings indicate a transition from charge transfer-limited to diffusion-limited electrodeposition processes that govern the morphological evolution of Mg deposits. We observe the signature of cell shorting under a wide range of current densities which we attribute to 3-D hemispherical growth of Mg deposits that form under mixed diffusion and kinetic control and are distinguished from traditional fractal dendrites. Our results highlight synergy with classical electrochemical theories for growth and lay groundwork for future approaches to achieve stable electroplated multivalent metal electrodes.

12:40 PM EN08.06.04

Dendrite Formation during Charging of Li-Metal Batteries: Transport Limitations within the SEI Control Dendrite Initiation Adam M. Maraschky and Rohan Akolkar; Case Western Reserve University, United States

High-energy density batteries are the critical component which could enable electric aircraft and more powerful portable devices. The Li metal anode offers the highest theoretical specific capacity among the available anode materials. The most significant barrier to the development of secondary Li-metal batteries is the dendritic electrodeposition of Li during the battery charging process. In this presentation, we will characterize the onset time of dendritic growth that occurs when charging Li-metal anodes. Using a combination of electrochemical techniques and optical microscopy, we observe that Li dendrites initiate at a time when the surface overpotential during galvanostatic electrodeposition reaches a maximum value. The dendrite onset time (τ_{onset}) is shown to increase with increasing temperature and decrease with increasing current density and initial solid electrolyte interphase (SEI) thickness. These observations form the basis of an analytical transport model wherein the Li^+ concentration available for Li plating decreases gradually within the SEI as the layer becomes thicker during electrodeposition. At $t = \tau_{\text{onset}}$, the mobile Li^+ concentration at the Li-SEI interface approaches zero. Due to this Li^+ concentration depletion, the roughness of the Li electrode amplifies, eventually producing dendrites. Once dendrites form, they rupture the SEI, lowering the surface resistance for Li plating. Model predictions of how τ_{onset} varies with current density, initial SEI thickness, and temperature are found to be in qualitative agreement with experimental observations. The analytical model explains mechanistically how transport limitations within the SEI control the onset time of dendrites during Li electrodeposition. Our results highlight the need for stable SEI materials that suppress or eliminate solid-state Li^+ concentration depletion, which is shown herein to be the key process controlling the formation of dendrites during Li-metal battery charging.

12:55 PM EN08.06.05

Superior Lithium Metal Anode Composed of Porous Carbon Electrodes Layered with Metal-Organic Framework Juran Noh, Wenmiao Chen, Yutao Huang, Peng Wu, Jian Tan, Hong-cai Zhou and Choongho Yu; Texas A&M University, United States

Lithium-based energy storage system has faced a critical limit of gravimetric/volumetric capacity in commercial

graphite anode (340 mAh g^{-1}). Lithium metal is a holy grail for the next generation anode with high specific capacity (3850 mAh g^{-1}), but still has big challenges caused by lithium dendrites and large volume changes particularly at high current density and capacity. Three-dimensional (3D) lithium host materials may compensate for the volume change with pores in the host material but limited lithium-ion diffusion through porous media has resulted in clogging at the pore inlet and thereby initiated lithium dendrite growth on the surface. While artificial solid-electrolyte interphase (SEI) coated lithium metal anode could avoid lithium dendrite growth on the surface but repeated large volume change may cause the detachment of the SEI layer. In this study, a two-dimensional metal-organic framework (MOF) has been attached to carboxylated CNTs via strong coordination bonding. We observed that MOF-layered 3D CNT scaffolds stored a large amount of lithium metal without dendrite growth and volume expansion until a high capacity of 24 mAh cm^{-2} at a high current density of 8 mA cm^{-2} . With the utilization of inner void space to store lithium, high volumetric capacity ($\sim 1000 \text{ mAh cm}^{-3}$) and gravimetric capacity ($\sim 1690 \text{ mAh g}^{-1}$) was achieved, which are much higher than those of commercial graphite anode (570 mAh cm^{-3} and $\sim 340 \text{ mAh g}^{-1}$). This study discloses a promising approach for a high-energy-density anode with lithium metal, which has been arduous in utilizing lithium metal for Li batteries in practice.

1:10 PM EN08.06.06

Late News: High-Performance Low-Temperature Molten Sodium Batteries Enabled by Improved Charge Transfer Across Interfaces Martha M. Gross, Stephen Percival, Rose Lee, Amanda Peretti, Mark Rodriguez, Erik Spoeerke and Leo Small; Sandia National Laboratories, United States

Managing electrochemical interfaces in molten sodium batteries is key to achieving high battery performance. Traditional molten sodium batteries operate a high temperature ($\sim 300 \text{ }^\circ\text{C}$) which facilitates charge transfer at the interfaces between molten sodium and solid electrolyte, solid electrolyte and catholyte, and catholyte and current collector. Dramatically lowering the operating temperature to near the melting temperature of sodium ($97.8 \text{ }^\circ\text{C}$) introduces substantial charge transfer resistances at these key interfaces. To enable high battery efficiency, longevity, and resiliency, the molten sodium battery must be re-engineered from the bottom up to improve charge transfer and lower interfacial resistances. Here, we describe a low-temperature molten sodium battery capable of high performance, long-term operation at the low temperature of $110 \text{ }^\circ\text{C}$. This is achieved by the modification of battery interfaces and materials design of the metal-halide sodium iodide molten salt catholyte. The use of engineered Sn-based coatings on the solid electrolyte surface at the interface with molten sodium to increase sodium wetting on NaSICON is shown to dramatically lower interfacial resistance, allowing battery operation at higher current densities. The activation of the cathode current collector to enhance charge transfer at the catholyte-current collector interface further reduces resistance at this interface, enabling high cyclability of the battery. Materials design of the metal-halide sodium iodide molten salt catholyte results in further improvements in interfacial resistance, resulting in a high-performance, low-temperature molten sodium battery of great promise for large-scale electrochemical energy storage. Sandia National Laboratories is a multimission laboratory managed and operated by National Technology & Engineering Solutions of Sandia, LLC, a wholly owned subsidiary of Honeywell International Inc., for the U.S. Department of Energy's National Nuclear Security Administration under contract DE-NA0003525.

1:15 PM EN08.06.07

Late News: Electrochemistry of the NaI-AlBr₃ Low Temperature Molten Salt System—Implications for Applied Battery Performance Stephen Percival, Rose Lee, Martha M. Gross, Amanda Peretti, Leo Small and Erik Spoeerke; Sandia National Laboratories, United States

Development of a new class of redox active, fully inorganic, low temperature (c.a. $100 \text{ }^\circ\text{C}$) molten salt electrolytes is necessary for the continued development of safe, low cost sodium battery technologies. The discussed, redox active, NaI-AlBr₃ system demonstrates many physical properties that are desirable for the use in a battery system. These properties have been investigated and experimentally evaluated with focus to energy storage considerations, including the conductivity and melting point of various compositions at different temperatures allowing the construction of a simple phase diagram. The electrochemical properties of the various

molten salt composition showed lower than expected iodide oxidation current density along with variable diffusion coefficients of reactant. Choice of electrode material was found to significantly affect the reaction kinetics, where carbon is found to hinder reaction rate as compared to tungsten, potentially dictating battery cell engineering and cost.

This work was supported by the U.S. Department of Energy's Office of Electricity through the Energy Storage Research Program, managed by Dr. Imre Gyuk. Sandia National Laboratories is a multi-mission laboratory managed and operated by National Technology and Engineering Solutions of Sandia, LLC, a wholly-owned subsidiary of Honeywell International, Inc., for the U.S. Department of Energy's National Nuclear Security Administration under contract DE-NA0003525. This paper describes objective technical results and analysis. Any subjective views or opinions that might be expressed in the paper do not necessarily represent the views of the U.S. Department of Energy or the United States Government.

1:20 PM DISCUSSION TIME

SESSION EN08.07: X-Ray Spectroscopy of Interfacial Process
Session Chairs: Vijayakumar Murugesan and Kevin Zavadil
Friday Afternoon, April 23, 2021
EN08

2:15 PM EN08.07.01

Lithium Interface Dynamics in Coated LiFePO₄ Nanoparticles Peter Benedek¹, Xueyan Zhao¹, Emanuel Billeter², Elisabetta Nocerino³, Ola Forslund³, Nami Matsubara³, Andreas Borgschulte², Fanni Juranyi⁴, Martin Månsson³ and Vanessa Wood¹; ¹ETH Zürich, Switzerland; ²Empa–Swiss Federal Laboratories for Materials Science and Technology, Switzerland; ³KTH Royal Institute of Technology, Sweden; ⁴Paul Scherrer Institute, Switzerland

During the last decade, the (dis)charge behaviour of LiFePO₄ (LFP) particles has been widely studied. While LFP typically charges in a phase separation reaction forming LiFePO₄ and FePO₄-rich domains, these domains vanish into a single Li_xFePO₄ solid solution at faster rates or smaller particle size.¹ Using phase-field modelling, an involvement of the interface has been proposed where autocatalytic reactions and resistances may affect the LFP charging dynamics and hence the rate-limiting steps.^{2,3} However, due to the lack of understanding of the LiFePO₄ interfaces, existing experiments do not suffice to validate this model.

Here, we rationalize the interface dependent delithiation mechanism in LFP particles by introducing coatings that affect ion dynamics and hence the resistances.⁴ With a combination of electronic structure calculations and *ab-initio* molecular dynamics modelling, we show that insulating oxide coatings such as ZnO hamper lithium ion interface diffusion, whereas carbon coatings lead to faster Li ion transport. We validate our models by synthesizing coated LiFePO₄ nanoparticles and measuring their electronic structure using ultraviolet absorption and x-ray photoemission spectroscopy. Measuring lithium ion interface diffusivity on the coated LFP nanoparticles via muon spin spectroscopy confirms our calculations.⁵ Finally, using operando x-ray diffraction, we can track interface dependent changes in the delithiation behaviour. Based on our findings, we offer a rational design strategy for interfaces in lithium ion batteries that homogenize the current density and reduce the strain throughout the battery materials providing longer battery lifetime at increased rate capabilities.

References

- [1] Y. Li, *Solid State Ionics* **323**, 142 (2018).
- [2] N. Nadkarni et al., *Phys. Rev. Mater.* **2**, 8, 85406 (2018).

- [3] M. Z. Bazant, *Faraday Discuss.* **199**, 423-463 (2017).
[4] P. Benedek et al., *In Preparation*.
[5] P. Benedek et al., *ACS Appl. Mater. Interfaces* **12**, 14, 16243 (2020).

2:30 PM EN08.07.02

Using Operando SQUID Magnetometry to Monitor Charge Transfer Processes in Li- and Na-Ion Battery Cathodes Stefan Topolovec¹, Gregor Klinser¹, Heinz Krenn² and Roland Würschum¹; ¹Graz University of Technology, Austria; ²University of Graz, Austria

Further development in the field of modern battery materials requires advanced characterization techniques that can yield insights into the atomic and chemical processes occurring during charging and discharging. Therefore, over the last years, a variety of in situ/operando methods were developed, probing the transfer of ions and electrons mainly at the electrode-electrolyte interface [1,2]. To achieve a complete picture of the processes in the electrodes, additional bulk sensitive methods, probing the whole volume of the material, would be beneficial. By developing an operando SQUID magnetometry technique, our group has established such a method, which enables a continuous monitoring of the oxidation states of the transition metal ions and therefore an identification of the redox active ions [3]. In this talk, first the electrochemical cell that enables operando measurements in a SQUID magnetometer will be presented and then an overview about recent results obtained with this new characterization technique will be given.

Measurements of the variation of the magnetic susceptibility of the technologically important class of NMC cathode materials have shown that different charge transfer processes occur for the two compositions $\text{LiNi}_{0.33}\text{Mn}_{0.33}\text{Co}_{0.33}\text{O}_2$ and $\text{LiNi}_{0.6}\text{Mn}_{0.6}\text{Co}_{0.2}\text{O}_2$. For $\text{Li}_x\text{Ni}_{0.33}\text{Mn}_{0.33}\text{Co}_{0.33}\text{O}_2$ first Ni acts as redox active ion and changes its oxidation state stepwise from Ni^{2+} to Ni^{3+} and then from Ni^{3+} to Ni^{4+} . Upon extracting more than 66% of Li, a simultaneous oxidation of Co^{3+} and O^{2-} ions was observed that is associated with irreversible capacity losses [4]. The charge compensation process for $\text{Li}_x\text{Ni}_{0.6}\text{Mn}_{0.6}\text{Co}_{0.2}\text{O}_2$ could also be divided into three steps. First a simultaneous oxidation of Ni^{2+} and Co^{2+} ($1 \geq x > 0.53$), followed by a sole Ni^{3+} oxidation ($0.53 > x > 0.21$), and finally by a contribution of Ni^{3+} and Co^{3+} or by Co^{3+} and O^{2-} ($x < 0.21$) [5].

The potential of the developed operando technique will also be demonstrated for post Li-ion batteries. Studies on $\text{NaV}_2(\text{PO}_4)_3$ cathodes revealed that vanadium is the only ion undergoing oxidation and reduction upon battery operation and that parasitic side reactions take place in the first charging cycle [6].

All in all, we could proof that operando magnetic susceptibility measurements can serve as a sensitive fingerprint for the charge compensation processes taking place in Li-ion and Na-ion battery cathodes. Therefore, this technique is highly suitably as complementary method for the characterization of the electron transfer reactions at electrode interfaces.

- [1] M. G. Boebinger et al., *ACS Energy Lett.* **5** (2020) 335
[2] D. Liu et al., *Adv. Mater.* **31** (2019) 1806620
[3] S. Topolovec et al., *J. Solid State Electrochem.* **20** (2016) 1491
[4] G. Klinser et al., *Appl. Phys. Lett.* **109** (2016) 213901
[5] G. Klinser et al., *J. Power Sources* **396** (2018) 791
[6] G. Klinser et al., *Phys. Chem. Chem. Phys.* **21** (2019) 20151

2:45 PM EN08.07.03

Atomic-scale Computational Study of the Solid Electrolyte Interphase in Na-Ion Batteries with a Nanoporous Hard Carbon Anode Emilia Olsson and Qiong Cai; University of Surrey, United Kingdom

The solid electrolyte interphase (SEI) is known to have a direct impact on sodium ion battery performance. The composition of the SEI has been shown to have a compositional dependence upon electrolyte, cycling time, anode material, and sodium salt. For hard carbon anodes with organic solvent and NaPF_6 there are a number of

common features. These involve the fluoridation of the hard carbon surface suggested to result from the salt dissociation, in addition the breakdown of the electrolyte molecules can result in carboxyl, carbonyl and carbonate motifs being observed, together with both inorganic and organic SEI constituents.^{1,2} This makes the atomic scale understanding of the anode electrolyte interphase, and its influence on both charge transfer and electrochemical performance challenging.

In this study, we combine atomic scale computational modelling with experimental characterisation of anode electrolyte interphases to investigate the structure, charge transfer, and electronic processes at the hard carbon anode electrolyte interphase in Na-ion batteries.^{3,4} Hard carbons are complex disordered carbon structures with randomly oriented graphene sheets, closed and open pore systems, and turbostratically stacked graphitic stacks. Adding to their complexity, these anode materials are also prone to defects and oxygen functionalities. This complex anode material structure leads to a plethora of different anode electrolyte interphase structures, which all can have different influence on the electrochemical performance.⁴⁻⁷ Here, we construct, based on experimental guidance, a number of different interphase models to capture the effect of anode surface termination, roughness, defects, functional groups, pore size, and combinations of these on the electrochemical performance and charge transfer across the electrolyte anode interphase. Through a combination of ab initio molecular dynamics, and density functional theory simulations, the electronic structure, ionic diffusion, and electrolyte dissociation products can be investigated. These simulations showed, using an organic solvent based electrolyte that the local structure of the anode surface directly influences the solvent molecule breakdown and interphase immobile solvent molecule layer. Introducing carbon vacancy defects, and oxygen functionalities, together with different pore systems were further shown to affect the organic solvent molecule breakdown and lead to irreversible capacity loss. Similarly, the sodium ion transfer from the electrolyte bulk to the anode (both through intercalation and surface adsorption) was probed at different interphases to explore the effect of morphology, the liquid phase composition, and electronic structure on charge transfer.

Acknowledgment

The financial support from EPSRC (Engineering and Physical Sciences Council) under the grant number EP/M027066/1, and EP/R021554/2, is acknowledged.

References

- ¹ G.G. Eshetu, T. Diemant, M. Hekmatfar, S. Grugeon, R.J. Behm, S. Laruelle, M. Armand, and S. Passerini, *Nano Energy* **55**, 327 (2019).
- ² C. Bommier and X. Ji, *Small* **14**, 1703576 (2018).
- ³ H. Au, H. Alptekin, A.C.S. Jensen, E. Olsson, C.A. O'keefe, T. Smith, M. Crespo-Ribadeneyra, T.F. Headen, C.P. Grey, Q. Cai, A.J. Drew, and M.M.-M. Titirici, *Energy Environ. Sci.* (2020).
- ⁴ H. Alptekin, H. Au, A.C. Jensen, E. Olsson, M. Goktas, T.F. Headen, P. Adelhelm, Q. Cai, A.J. Drew, M.-M. Titirici, and A.C. Jensen, *ACS Appl. Energy Mater.* acaem.0c01614 (2020).
- ⁵ E. Olsson, J. Cottom, H. Au, Z. Guo, A.C.S. Jensen, H. Alptekin, A.J. Drew, M.-M. Titirici, and Q. Cai, *Adv. Funct. Mater.* **30**, 1908209 (2020).
- ⁶ E. Olsson, G. Chai, M. Dove, and Q. Cai, *Nanoscale* **11**, 5274 (2019).
- ⁷ A.C.S. Jensen, E. Olsson, H. Au, H. Alptekin, Z. Yang, S. Cottrell, K. Yokoyama, Q. Cai, M.-M. Titirici, and A.J. Drew, *J. Mater. Chem. A* **8**, 743 (2020).

3:00 PM *EN08.07.04

Synchrotron Characterization of Chemo-Mechanical Transformations in All-Solid-State Batteries Kelsey B. Hatzell and Marm Dixit; Vanderbilt University, United States

Transportation accounts for 23% of energy-related carbon dioxide emissions and electrification is a pathway toward ameliorating these growing challenges. All solid state batteries could potentially address the safety and driving range requirements necessary for widespread adoption of electric vehicles. However, the power densities of all-solid state batteries are limited because of ineffective ion transport at solid|solid interfaces. New insight into the governing physics that occur at intrinsic and extrinsic interfaces are critical for developing engineering strategies for the next generation of energy dense batteries. However, buried solid|solid interfaces

are notoriously difficult to observe with traditional bench-top and lab-scale experiments. This talk will discuss opportunities for tracking phenomena and mechanisms in all solid state batteries *in-situ* using advanced synchrotron techniques. Synchrotron techniques that combine reciprocal and real space techniques are capable of tracking multi-scale structural phenomena from the nano- to meso-scale. This talk will discuss the role microstructure plays on transport and interfacial properties that govern adhesion. Quantification of salient descriptors of structure in solid state batteries is critical for understanding the mechanochemical nature of all solid state batteries.

3:25 PM EN08.07.05

Phase Controlled Synthesis and Properties of Mn₃O₄ Spinel Oxides Electrodes for Multivalent Batteries Using Molecular Beam Epitaxy Linda Wangoh, ZhenZhong Yang, Le Wang, Mark Bowden, Karl Mueller, Vijayakumar Murugesan and Yingge Du; Pacific Northwest National Laboratory, United States

Rechargeable multivalent batteries have attracted extensive research due to their low cost and higher energy density compared to Li-ion batteries. However, most cathode materials have several major challenges such as slow charge/discharge cycle and irreversible phase transitions that hinder their practical use as multivalent cathodes. Therefore, identifying and synthesizing the ideal electrode material is therefore essential in advancing multivalent battery technology. Furthermore, fundamental nature of the diffusion mechanism and its effects on the host structure is necessary to improve the performance of these systems.

Manganese-based spinel oxides are a particular class of promising materials for multivalent electrodes due to their increased energy density and higher specific capacity. However, their performance is highly dependent on their synthesis conditions and phase purity due to the existence of a multiple Manganese oxidation states (Mn²⁺, Mn³⁺, Mn⁴⁺). In this presentation, we highlight the use of epitaxial thin films, grown using Molecular Beam Epitaxy (MBE), a technique that provides precise control over interface structure and thickness, to study host structures for multivalent cathodes. We begin with epitaxial Fe₃O₄ thin film as a model system to highlight the utility of well-defined interfaces and smooth surfaces to perform fundamental studies in cation diffusion. In addition, we investigate the electronic and structural properties of Mn₃O₄ spinel epitaxial films. In particular, we highlight the phase selective growth of phase pure Mn₃O₄ is highly dependent on the growth parameters such as flux rate and oxygen partial pressure. Furthermore, to understand the evolution of Mn₃O₄, thermal annealing of the material is performed to promote cation diffusion and structural transitions. These changes are monitored using high-resolution *in-situ* and *ex-situ* characterization techniques such as x-ray photoelectron spectroscopy, x-ray absorption near edge structure and x-ray diffraction.

3:40 PM DISCUSSION TIME

SESSION EN08.08: Chemical Imaging of Interfaces

Session Chairs: Nav Nidhi Rajput and Kevin Zavadil

Friday Afternoon, April 23, 2021

EN08

5:15 PM *EN08.08.01

Identifying Intact Electrode Interfaces with Cryogenic Electron Microscopy Katherine L. Jungjohann¹, Daniel Long¹, Steven Randolph², Renae Gannon³, Luara Merrill⁴, Subrahmanyam Goriparti⁴ and Katharine Harrison⁴; ¹Center for Integrated Nanotechnologies, United States; ²Thermo Fisher Scientific, United States; ³University of Oregon, United States; ⁴Sandia National Laboratories, United States

Increasing the energy storage capacity of portable, rechargeable Li-ion batteries would find the most gains by implementing a Li-metal anode. Li-metal anodes at high-charging rates are needed for high power applications, such as for electric vehicles. However, Li-metal anodes experience significant capacity losses and limited

lifetimes as a result of the uncontrolled Li morphology during plating and stripping, especially at high-charge rate. The resultant morphology is commonly seen as high aspect ratio grains, which have a large surface area that can react with the electrolyte and form the solid electrolyte interphase (SEI) layer. The SEI layer is a determinant factor of the performance of the Li anode, as cyclic Li plating and stripping steps produce significant surface volume changes that present fresh surfaces for further SEI formation. This causes the SEI to continuously grow over the lifetime of the battery. This is a barrier for implementation of Li-metal anodes into commercial batteries, as the continuous formation of SEI consumes the Li inventory (resulting in capacity loss) and electrolyte (reducing pathways for Li-ion transport through the cell).

The visualization of the Li/SEI/electrolyte interfaces allows for understanding the co-dependence of the different stacked materials within a battery and the failure mechanisms that result from effects of stack pressure, electrolyte, separator, and cycling rate. Cryogenic electron microscopy techniques allow for the intact characterization of solid-liquid interfaces from atomic-scale resolution [1], up to complete cross-sectional visualization of frozen coin-cell batteries. We present analysis of SEI/Li metal interfaces using cryogenic focused ion beam (FIB) cross-sectional imaging in a scanning electron microscope, and the subsequent lamella preparation for cryo-scanning/transmission electron microscopy analysis [2]. Additionally, using a cryo stage on a laser plasma-FIB [3], we visualize a complete coin cell in cross section at representative areas of a millimeter in width. Both structural mapping methods are combined with elemental mapping using x-ray spectroscopy for identification of the electrode/electrolyte interfaces. We propose a mechanism for Li plating through a separator based on our analysis, as it is known that Li metal itself does not have the mechanical integrity to puncture the polymeric material unassisted [4,5].

References:

[1] Y Li et al., *Science* **358** (2017), p. 506.

[2] MJ Zachman et al., *Nature* **560** (2018), p. 345.

[3] MP Echlin et al., *Materials Characterization* **100** (2015), p. 1.

[4] CD Fincher et al., *Acta Materialia* **186** (2020), p. 215.

[5] This work was funded by Sandia National Laboratories' Laboratory Directed Research and Development program. It was performed, in part, at the Center for Integrated Nanotechnologies, an Office of Science User Facility operated for the U.S. Department of Energy (DOE) Office of Science. Sandia National Laboratories is a multi-mission laboratory managed and operated by National Technology and Engineering Solutions of Sandia, LLC., a wholly owned subsidiary of Honeywell International, Inc., for the U.S. Department of Energy's National Nuclear Security Administration under contract DE-NA-0003525.

5:40 PM EN08.08.02

The Effect of Anions in the Calcium Solvation Under Operando Conditions Probed by *In Situ* Soft X-Ray absorption spectroscopy Feipeng Yang¹, Xuefei Feng¹ and Jinghua Guo^{1,2}; ¹Lawrence Berkeley National Laboratory, United States; ²University of California, Santa Cruz, United States

While there is considerable interest in multivalent batteries, calcium has not attracted much attention compared to magnesium or aluminum until a recent work showing that calcium can be plated and stripped at room temperature with good capacities and stabilities. Additionally, because of the higher mobility of Ca^{2+} compared to that of Mg^{2+} as a result of the lower charge density of Ca^{2+} , the interest in calcium batteries has been growing rapidly. The problem now inhibiting the development of calcium batteries is the understanding of the solvation and charge transfer mechanism at the electrode/electrolyte interface and how different types of anions will affect the calcium solvation at this interface while under in-situ/operando electrochemical conditions. It has been reported that when $\text{Ca}(\text{BH}_4)_2$ is substituted by the more weakly coordinated calcium hexafluoroisopropoxyborate ($\text{Ca}(\text{BHFIP})_2$), ionic conductivity increases by an order of magnitude, which demonstrates the strong coordination of BH_4^- compared to Ca^{2+} in THF. To probe the calcium coordination chemistry difference at the electrode/electrolyte interface as a function of the type of anions, total electron yield (TEY) mode soft X-ray absorption spectroscopy (XAS) was employed under operando electrochemical conditions. It was observed that the $\text{Ca}(\text{BHFIP})_2$ in THF shows a small shoulder on the right side of the L_2 -edge and a pre-edge peak on the left side of the L_2 -edge peak. A less prominent pre-edge peak is also observed on the left side of the L_3 -edge peak. These signatures become more prominent when the potential is swept negatively

and are not reversible when the potential is swept positively in a cyclic voltammetry cycle. On the other hand, the $\text{Ca}(\text{BH}_4)_2$ in THF is more reversible, and no shoulder peak on the right side of the L_2 -edge peak was observed. The detailed solvation structure of the calcium still needs to be resolved with the DFT calculations but such TEY spectra indicate their differences in the calcium coordination chemistry at the electrode/electrolyte interface as a result of the anions and it will guide the future development of electrolytes for calcium batteries.

5:55 PM *EN08.08.03

Unveiling a New Facet in Magnesium Battery Electrochemistry Rana Mohtadi and Oscar Tutusaus; Toyota Research Institute of North America, United States

The pursuit of eco-friendly battery technologies that meet the industrial requirements for portable, stationary and automotive applications in terms of safety, cost, energy density, performance reliability and sustainability has propelled research efforts toward battery chemistries beyond Li-ion. Thus far, none of the battery chemistries that promise high energy densities such as those based on Li metal (Li-S, Li-air) and multivalent batteries such as Mg have demonstrated their potential owing to intrinsic material challenges. For example, Li-S and Li-air suffer from complex cathode conversion reactions and dendrite prone Li metal. On the other hand, issues in multivalent batteries like Mg stem from the high polarizability of Mg^{2+} that results in strong interaction with solvents and host solid state structures.^[1,2,3,4] This unfortunate phenomena has often resulted in sluggish diffusion kinetics and high overpotentials, which undermine the practicality of Mg batteries. Herein, we will discuss how fundamental studies we conducted inspired a potential path forward towards overcoming these challenges and allowed us to discover new possibilities towards enabling Mg rechargeable batteries.

References

- [1] Choi J. W. Aurbach D. Nature Reviews Materials 1, 2016, 16013, 1.
- [2] Mohtadi R., Orimo S., Nature Reviews Materials, 2016, 2,16091, 1311.
- [3] Mohtadi R., Mizuno F. Beilstein J. Nanotechnol. 2014, 5, 1291.
- [4] Kar M., Tutusaus O., MacFarlane D.R., Mohtadi R., Energy & Environmental Science, 2019, 12, 566.

6:20 PM EN08.08.04

Multimodal Characterization of Electrodeposited Calcium Metal and Its Native Interphases for Next-Generation Battery Applications Scott A. McClary, Daniel Long, Paul Kotula, Mark Rodriguez, Timothy Ruggles, Katherine L. Jungjohann and Kevin R. Zavadil; Sandia National Laboratories, United States

Rechargeable batteries based on divalent Ca anodes have attracted considerable research attention due to their high theoretical energy densities, reduction potentials approaching lithium's, high crustal abundance, and low propensity for dendrite formation [1,2]. The highly reductive nature of calcium means that a solid-electrolyte interphase (SEI) layer spontaneously forms to protect the growing deposit from parasitic reactions. Many SEI components formed from typical calcium electrolytes (e.g. CaF_2) are poor ionic conductors [3], leading to failure upon cycling [4], but a select few (e.g. borate species, CaH_2) support limited calcium transport, enabling more extensive cycling [3,5]. To date, the formation mechanisms and transport properties of interphases in Ca electrodeposits have been sparsely studied.

In this contribution, we present multimodal characterization of electrodeposited and cycled Ca metal from $\text{Ca}(\text{BH}_4)_2$ -THF and related electrolytes, with emphasis on the properties of native interphases. We identify primary and secondary phases in electrodeposits using techniques including XRD, SEM, and ToF-SIMS. We discuss the transport properties of key interphase components as determined through electrochemical methods. We then show results of characterization of thin calcium lamellae including TEM and STEM imaging, selected-area diffraction, and EDS and EELS mapping, revealing the chemical identity, nano-scale structure, and spatial distribution of interphases, while drawing connections to bulk microstructure when possible. We also discuss the use of cryogenic techniques to freeze the native electrolyte in place, allowing for insight into an evolving

calcium deposit under realistic battery operating conditions.

Our results are an important step towards the rational design and engineering of favorable protective interphases required for high efficiency plating and stripping of calcium metal anodes [6].

References:

[1] M. E. Arroyo-de Dompablo et al. *Chem. Rev.* **2020**, 120(14), 6331-6357.

[2] A. M. Melemed et al. *Batteries and Supercaps* **2020**, 3(7), 570-580.

[3] J. Forero-Saboya et al. *Energy Env. Sci.* **2020**, 13(10), 3423-3431.

[4] A. Shyamsunder et al. *ACS Energy Lett.* **2019**, 4(9), 2271-2276.

[5] D. Wang et al. *Nat. Mater.* **2018**, 17(1), 16-20.

[6] This work was performed, in part, at the Center for Integrated Nanotechnologies, an Office of Science User Facility operated for the U.S. Department of Energy (DOE) Office of Science. Sandia National Laboratories is a multimission laboratory managed and operated by National Technology & Engineering Solutions of Sandia, LLC, a wholly owned subsidiary of Honeywell International, Inc., for the U.S. DOE's National Nuclear Security Administration under contract DE-NA-0003525. The views expressed in the article do not necessarily represent the views of the U.S. DOE or the United States Government.

6:35 PM EN08.08.05

Late News: Scanning Electrochemical Cell Microscopy Based Nanoscale Electrochemistry Study Jiali Zhang and Byong Kim; Park Systems, Inc., United States

The objective in electrocatalysis and energy storage is to correlate electrochemical activity with nanostructured electrochemical interfaces (electrodes) [1]. However, it is challenging to quantify the heterogeneity of electrode structures or study the local structure-activity relationship for these interfaces using conventional macroscopic electrochemical techniques. Scanning electrochemical cell microscopy (SECCM) is a new nanoelectrochemical scanning probe technique designed to investigate the local electrochemical properties of electrode surfaces. In this study, the electrochemically reversible $[\text{Ru}(\text{NH}_3)_6]^{3+/2+}$ electron transfer process at a highly ordered pyrolytic graphite (HOPG) surface was recorded with SECCM technique using Park NX12 AFM system. A single barrel glass nanopipette with a Ag/AgCl quasi-reference counter electrode (QRCE) is utilized [2]. Using previous successful experience in commercializing pipette-based electrochemical microscopy [3], Park Systems's hardware and software enable localized nanoscopic cyclic voltammetry each time the meniscus contacts the surface. The redox process at the HOPG surface is detected with high reproducibility and robustness, with a current limit as minute as a few pA. Position dependence electrochemical current mapping is demonstrated. These results suggest that the effectiveness of Park Systems's commercial SECCM option for quantitative electroanalysis at the nanoscale. This capability could also facilitate the rational design of functional electromaterials with potential applications in energy storage (battery) studies and corrosion research.

[1] Guell, A. G., Ebejer, N., Snowden, M. E., Macpherson, J. V., & Unwin, P. R. (2012). Structural correlations in heterogeneous electron transfer at monolayer and multilayer graphene electrodes. *Journal of the American Chemical Society*, 134(17), 7258-7261.

[2] Gao, R., Edwards, M. A., Qiu, Y., Barman, K., & White, H. S. (2020). Visualization of Hydrogen Evolution at Individual Platinum Nanoparticles at a Buried Interface. *Journal of the American Chemical Society*, 142(19), 8890-8896.

[3] Shi, W., Goo, D., Jung, G., Pascual, G., Kim, B., & Lee, K. Simultaneous Topographical and Electrochemical Mapping using Scanning Ion Conductance Microscopy–Scanning Electrochemical Microscopy (SICM-SECM).

6:50 PM DISCUSSION TIME

8:15 PM *EN08.09.01

Accessible Electrode Surface Area and Its Impact on Redox Flow Battery Performance Fikile Brushett^{1,2};
¹Massachusetts Institute of Technology, United States; ²Joint Center for Energy Storage Research, United States

Carbon-fiber electrodes exhibit many desirable material properties including conductivity, porosity, and chemical stability, and, accordingly, are employed in a range of electrochemical technologies.¹ These electrodes are particularly important in redox flow battery (RFB) systems, as they support multiple critical functions including providing surface area for electrochemical reactions, distributing liquid electrolytes, and conducting electrons and heat. While commercial materials possess suitable permeability and conductivity, the performance of pristine substrates is limited and oxidative treatment prior to use is common practice.^{2,3} Partial oxidation of the electrode surface has been shown to introduce a range of oxygen functional groups, which improve hydrophilicity and, in some cases, catalyze redox reactions, as well as to increase surface area available for the electrochemical reactions.^{4,5} Both effects are posited to improve electrode performance but their relative importance and effectiveness remains unclear.⁶

Here, we critically assess the nature of the surface area generated by thermal pretreatment in air and its role on RFB electrode performance. Using Freudenberg H23 as a model substrate, we systematically vary pretreatment time and temperature to create different surface morphologies and develop structure-function relations. First, we use Brauner Emmanuel Teller gas adsorption (e.g., N₂, Kr, Ar/CO₂) and mercury porosimetry to estimate physical surface area and pore size distribution. In parallel, we use voltammetry and impedance spectroscopy to determine electrochemically active surface area with different electrolyte compositions. In general, we find that only a fraction of the physical surface area is accessible for electrochemical redox reactions due, in large part, to the nanoscopic dimensions of the added surface area. Second, we develop a simple mathematical model to assess the effectiveness of the available surface area of carbon fibers for Faradaic reactions. We find that, under typical RFB operating conditions, external mass transfer limitations govern performance, limiting the utilization of recessed areas generated during pretreatment. Ultimately, these results highlight the potential limits of performance improvement strategies based on increasing surface area of fibrous substrates and motivate new approaches for electrode development.

Acknowledgements

The authors acknowledge the financial support of the Joint Center for Energy Storage Research, an Energy Innovation Hub funded by the United States Department of Energy. The author also acknowledges the Center for Nanoscale Systems and the NSF's National Nanotechnology Infrastructure Network (NNIN) for the use of Nanoscale Analysis facility for electrode property characterization.

References

1. M. H. Chakrabarti et al., *Journal of Power Sources*, **253**, 150–166 (2014).
2. T. J. Rabbow, M. Trampert, P. Pokorny, P. Binder, and A. H. Whitehead, *Electrochimica Acta*, **173**, 17–23 (2015).
3. N. Pour et al., *The Journal of Physical Chemistry C*, **119**, 5311–5318 (2015).
4. B. Sun and M. Skyllas-Kazacos, *Electrochim. Acta*, **37**, 8 (1992).
5. T. J. Rabbow and A. H. Whitehead, *Carbon*, **111**, 782–788 (2017).
6. K. V. Greco, A. Forner-Cuenca, A. Mularczyk, J. Eller, and F. R. Brushett, *ACS Applied Materials & Interfaces*, **10**, 44430–44442 (2018).

8:40 PM EN08.09.02

Mechanisms Underlying the Electrochemical Oxidation of Nitroxide Radicals in Ethaline Deep Eutectic Solvent Nora A. Shaheen¹, Mahesh Ijjada¹, Miomir B. Vukmirovic² and Rohan Akolkar¹; ¹Case Western Reserve University, United States; ²Brookhaven National Laboratory, United States

Deep eutectic solvents (DESs) are emerging as promising electrolytes for electrochemical energy storage applications. Electroactive nitroxide-radical-containing organics can be dissolved in DESs to facilitate redox reactions; however, mechanistic insight of their charge transfer kinetics at the electrode surface is limited. Here, we investigate the mechanism underlying the electrochemical oxidation of 2,2,6,6-tetramethylpiperidine-1-oxyl (TEMPO) and 4-hydroxy-2,2,6,6-tetramethylpiperidine-1-oxyl (4-hydroxy-TEMPO). Using polarization measurements on a platinum rotating disk electrode (RDE) and micro-electrode, we show that the anodic charge transfer coefficient (α) for one-electron transfer oxidations of TEMPO and 4-hydroxy-TEMPO approaches 0.9 in DES as well as in aqueous electrolytes, i.e., a significant deviation from $\alpha \approx 0.5$ expected for symmetric redox behavior. To explain this observation, a two-step oxidation mechanism is proposed wherein the nitroxide-containing species undergo fast charge transfer at an electrode surface followed by slow rate-limiting desorption of the adsorbed oxidized species. Numerical simulations are reported to characterize how the proposed two-step mechanism manifests in transient electrochemical behavior of the 4-hydroxy-TEMPO oxidation reaction, and good agreement with experiments is noted. Further evidence, based on voltammetry coupled with gravimetry (e-QCM), will be presented in support of the surface adsorption-desorption phenomena. Ramifications of the mechanistic understanding gained to the design of future high-performance DES electrolytes for energy storage will be discussed.

8:55 PM *EN08.09.03

Reaction Rate Mapping at Electrodes for Redox Flow Batteries—Impacts of Adsorption and Electrode Structure Dipobrato Sarbapalli¹, Michael Counihan¹, Tylan Watkins², Kevin R. Zavadil² and Joaquin Rodriguez-Lopez¹; ¹University of Illinois at Urbana-Champaign, United States; ²Sandia National Laboratories, United States

Long-lasting, high performance redox flow batteries (RFBs) will require robust electrode interfaces capable of enabling thousands of cycles while sustaining high rates of charge transfer. In this context, understanding the mechanisms of charge transfer as affected by processes such as precipitation/adsorption, molecular or electrode degradation, and the distinct reactivity of heterogeneous surface features, seems of great relevance to develop electrodes that ensure sustained RFB performance. We posit that to achieve this understanding, a versatile approach that achieves a quantitative evaluation of electron transfer rates and relates them to these chemical processes and structural attributes is necessary.

In this presentation, we will discuss how we have combined the redox imaging capabilities of scanning electrochemical microscopy (SECM) with other in-situ and ex-situ characterization techniques such as atomic force microscopy (AFM) and secondary-ion mass spectrometry (SIMS), as well as with versatile multi-layer graphene (MLG) electrodes to elucidate reaction attributes of model redox-active dialkoxybenzene derivatives, 2,5-di-*tert*-butyl-1,4-bis(2-methoxyethoxy)benzene (C1) and 2,3-dimethyl-1,4-dialkoxybenzene (C7).[1] Specifically, during cycling of the redox mediators, we observed the formation of interfacial films with distinct redox and mechanical properties compared to those of cleaved graphitic surfaces, and exclusively during reduction of electrogenerated radical cations. These films modified the rate and distribution of the electron transfer rate constants causing a significant deviation from Butler-Volmer kinetics. However, their impact was also found to be highly dependent on the surface features investigated, which were conveniently probed using the spatially-resolved capabilities of SECM. Bolstered by our findings with C1 and C7, we have also investigated other molecules used as catholytes in RFBs as well as the impact of redox-active concentration on the observed rate constants. The diversity of effects observed through our electrochemical imaging methodology highlights the importance of understanding how heterogeneous reactivity might impact RFB performance.

[1] Watkins, T.; Sarbapalli, D.; Counihan, M.J.; Danis, A.S.; Zhang, J.; Zhang, L.; Zavadil, K.R.; Rodríguez-

López, J. A Combined SECM and Electrochemical AFM Approach to Probe Interfacial Processes Affecting Molecular Reactivity at Redox Flow Battery Electrodes. J. Mater. Chem. A. 2020, **8**, 15734-15745.

9:20 PM DISCUSSION TIME

9:35 PM EN08.09.05

Binding Energies and Electronic Coupling Calculations of Redox Flow Molecules at the Carbon Surface

Jason D. Howard and Larry Curtiss; Argonne National Laboratory, United States

For charge transfer to occur in a redox flow battery the molecules must come in proximity to the electrode surface and because of this the binding energy of the constituent molecules is a crucial aspect of the net charge transfer of the system. In this work the process of computing charged binding energies is discussed along with theoretical ambiguities. The methods of using either cluster or periodic models are compared. The results overall suggest that charged redox flow molecules can bind strongly to a carbon surface. Results also show that binding energies are strongly affected by an applied potential. For cases where spontaneous charge transfer occurs within standard density functional theory simulations, constrained density functional theory is used to get a more physical binding energy. Finally some results of the electronic coupling for diabatic states prepared with constrained density functional theory are presented in the context of Marcus theory.

SYMPOSIUM EN09

Advances in Conversion Electrodes for Reliable Electrochemical Energy Storage

April 14 - April 21, 2021

Symposium Organizers

Vitaly Alexandrov, University of Nebraska-Lincoln

Aaron Hollas, Pacific Northwest National Laboratory

Huilin Pan, Zhejiang University

Noah Schorr, Sandia National Laboratories

* Invited Paper

SESSION EN09.01: Metal Anodes and Conversion Cathodes I

Session Chairs: Vitaly Alexandrov and Noah Schorr

Wednesday Morning, April 21, 2021

EN09

8:00 AM *EN09.01.01

Understanding and Addressing the Fundamental Challenges in Rechargeable Lithium Metal Batteries

Xiao; Pacific Northwest National Laboratory, United States

To significantly boost the energy of the state-of-art lithium ion (Li-ion) batteries, one of the most effective approaches is to replace graphite anode with Li metal which is ultralight but energy concentrated. However, its thermodynamically instable nature in liquid electrolytes causes many well-known problems such as dendrite formation which plagues the implementation of the proposed technology. Although many approaches have been

proposed to rescue Li metal anodes, most of the work are performed in small-scale coin cells and tested in the conditions drastically different from the reality. A full knowledge of Li metal activities at the cell level is lacking but extremely critical for the success of developing next-generation rechargeable Li metal batteries. This talk will discuss the fundamental challenges of utilizing Li metal anode in at cell-level. A Li metal prototype pouch cell with 350 Wh/kg energy with more than 350 cycles will be demonstrated. The key fundamentals that enable the long-term cycling of Li metal anodes in pouch cells are discussed and the root causes of the poor cycling of realistic Li metal pouch cells have been revisited. A series of fundamentally new insights have been provided to inspire scientific innovations to tackle the real challenges of developing next-generation battery technologies.

8:25 AM DISCUSSION TIME

8:40 AM *EN09.01.04

The Effects of Applied Interfacial Compression on Lithium Metal Cycling Behavior Katharine Harrison, Subrahmanyam Goriparti, Daniel Long, Benjamin Warren, Luara Merrill, Zachary Casias, Brad L. Boyce, Brian Perdue and Katherine L. Jungjohann; Sandia National Laboratories, United States

Conversion cathode materials have traditionally been paired with lithium metal for use in non-aqueous primary batteries to enable high energy density. Due to the demand for high energy density rechargeable batteries, there is great interest in replacing conventional lithium insertion materials currently used in lithium-ion batteries with conversion cathodes and lithium metal anodes. Essentially, these batteries are similar to lithium primary batteries but with the added complication of recharge. Rechargeability is extremely challenging due to the need to chemically convert species with large volume expansion and multiple discharge products back to their original forms during charge. In conjunction, these already challenging battery systems also rely on repeatable and efficient electroplating and stripping of lithium metal. Despite decades of research, efficient and reliable lithium-metal anode cycling remains a major challenge in commercializing rechargeable batteries based on conversion chemistries.

Interfacial stack pressure in cells consisting of conversion cathodes and lithium-metal anodes is a critical parameter to tune and control. The large volume changes associated with cycling high capacity conversion cathodes and lithium-metal anodes will likely cause significant pressure changes in cells during cycling, unlike the small volume changes typically observed for intercalation electrodes. Furthermore, our previous studies suggest that the absence of interfacial compression greatly impacts lithium-metal anode morphology and Coulombic efficiency during cycling.¹ In an effort to understand these impacts more systematically, we fabricated lithium versus copper pouch cells and subjected them to varied applied interfacial compression.

We cycled pouch cells at high and low current densities in 4 M lithium bis(fluorosulfonyl)imide in 1,2-dimethoxyethane (4 M LiFSI in DME) for 50 cycles at a variety of pressures ranging from 0-10 MPa. This very promising electrolyte was used because it has been shown to enable lithium-metal anode cycling with high Coulombic efficiency, a dense morphology, and a compact solid electrolyte interphase.² We disassembled pouch cells after the first and 51st plating cycles to understand morphology of the lithium deposits using cryo focused ion beam and cryo electron microscopy techniques. We confirm through these experiments that interfacial compression plays an important role in lithium-metal anode plating and stripping behavior. Lithium morphology and Coulombic efficiency can be improved through tuning the applied interfacial compression.

Supported by the Laboratory Directed Research and Development program at Sandia National Laboratories, a multimission laboratory managed and operated by National Technology and Engineering Solutions of Sandia, LLC., a wholly owned subsidiary of Honeywell International, Inc., for the U.S. Department of Energy's National Nuclear Security Administration under contract DE-NA-0003525.

1. Harrison, Katharine L., Kevin R. Zavadil, Nathan T. Hahn, Xiangbo Meng, Jeffrey W. Elam, Andrew Leenheer, Ji-Guang Zhang, and Katherine L. Jungjohann. "Lithium self-discharge and its prevention: direct

visualization through in situ electrochemical scanning transmission electron microscopy." ACS nano 11, no. 11 (2017): 11194-11205.

2. Qian, Jiangfeng, Wesley A. Henderson, Wu Xu, Priyanka Bhattacharya, Mark Engelhard, Oleg Borodin, and Ji-Guang Zhang. "High rate and stable cycling of lithium metal anode." Nature communications 6, no. 1 (2015): 1-9.

9:05 AM DISCUSSION TIME

9:20 AM *EN09.01.06

Functional 2D Materials and Devices for High-Power Energy Storage Xinliang Feng; Technische Universität Dresden, Germany

High-power electrochemical energy storage devices are important components for various industrial applications, ranging from individual electronics to grid storage. The demand for power and energy supply is equally imperative in actual use and is keen to expand in the future. Thus, it is highly desirable to design new electrochemical batteries and supercapacitors to mitigate the trade-off between power density and energy density. On the other hand, as growing requirements for intelligent electronic devices and internet-of-things, extensive attentions have been attracted to functional (particularly, smart and stimuli-responsive) energy storage devices, which are rapidly responsive to the variations of devices or the external environment, *e.g.*, configuration, voltage, deformation, light, and temperature, etc. Meanwhile, the portable, implantable, and wearable electronics are advancing toward miniaturization as well as ultralight, and safe, long-term, and high-speed operation, thus stimulating the urgent pursuit for miniaturized energy storage devices.

In this lecture, we will present our recent efforts in developing functional graphene and 2D materials for high-power energy storage devices, especially for the flexible/micro-supercapacitors with smart functions.

Electrochromism, thermo-response, and photo-response can be integrated into such devices which provide the possible means to monitor the electrochemical process using external stimulus, thus opening up windows for realizing the power systems for intelligent electronic devices. Towards realizing high-power electrochemical batteries, we will discuss our recent progress in the development of dual-ion energy storage devices, which involve different charge storage chemistry in contrast to the conventional "rocking-chair" mechanism.

SESSION EN09.02: Metal Anodes and Conversion Cathodes II

Session Chairs: Aaron Hollas and Noah Schorr

Wednesday Morning, April 21, 2021

EN09

11:45 AM *EN09.02.01

Deeply Rechargeable Zinc Anodes for Ultra-Safe High-Energy Rechargeable Batteries Nian Liu; Georgia Institute of Technology, United States

Metallic zinc as a rechargeable anode material for aqueous batteries has gained tremendous attention with merits of intrinsic safety, low cost, and high theoretical volumetric capacity (5,854 mAh/cm³). Among zinc-based batteries, Zn-air batteries are promising with the highest theoretical volumetric energy density (4,931 Wh/L). Rechargeable zinc anode has recently achieved progress in neutral electrolytes, yet developed slowly in alkaline electrolytes, which are kinetically favorable for air cathodes. Passivation, dissolution, and hydrogen evolution are three main reasons for irreversibility of zinc anodes in alkaline electrolytes, which limits the rechargeability and usable energy density. In this talk, I will present our recent works on using nanoscale material design to overcome passivation, dissolution, and hydrogen evolution issues of zinc anode, towards a deeply rechargeable zinc-based battery. I will also introduce the battery-gas chromatography quantitative analysis, as well as in situ microscopy methodologies we have developed, to quantify gas evolution side

reaction, as well as visualize the reaction on electrodes during operation.

12:10 PM EN09.02.02

3D- Printed Zinc-Carbon Composite Anode for High Performance Zinc-Ion Battery Stephen Amoko, Sanket Bhoyate, Narendra Dahotre, Yijie Jiang and Wonbong Choi; University of North Texas, United States

Recently, aqueous Zinc ion batteries have caught research attention due to intrinsic safety, low cost, and high theoretical volumetric capacity. However, insufficient utilization of Zn ions from anode can result in an inferior battery performance and limit practical application. Using 3D printed structures, the active surface area of Zn anode can be increased efficiently utilizing the Zn ions from anodes for battery reactions. Here, we develop a 3D printable zinc-carbon composite anode using direct ink writing (DIW) method to obtain porous anode structure with an increased surface area for high performance Zn ion batteries. Porous anode structure exhibits an increased electrochemical performance as compared to commercial Zn plate anodes resulting in higher specific capacity. By varying filament distancing and path, we can 3D print the zinc anode with different active surface areas, area to volume ratio, and porosity. Carbon in the composite improved conductivity, and mechanical stability of 3D printed zinc anode. Our 3D printed composite anodes allows flexible designing of batteries surpassing conventional battery designs such as coin cells or pouch cells and can be used to design printed energy storage systems.

12:25 PM EN09.02.03

High Performance Printed AgO-Zn Rechargeable Battery for Flexible Electronics Lu Yin, Jonathan Scharf, Joseph Wang and Y. Shirley Meng; University of California, San Diego, United States

The rise of flexible electronics calls for cost-effective and scalable batteries with good mechanical and electrochemical performance. In this presentation, we report on our development of printable, polymer-based AgO-Zn batteries that feature flexibility, rechargeability, high areal capacity, and low impedance. Using elastomeric substrate and binders, the current collectors, electrodes, and separators can be easily screen-printed layer-by-layer and vacuum-sealed in a stacked configuration. The batteries are customizable in sizes and capacities, with the highest obtained areal capacity of 54 mAh/cm² for primary applications. Advanced micro-CT and EIS were used to characterize the battery, whose mechanical stability was tested with repeated twisting and bending. The batteries were used to power a flexible E-ink display system that requires a high-current drain and exhibited superior performance than commercial coin-cell batteries. The developed battery presents a practical solution for powering a wide range of electronics and holds major implications for the future development of practical and high-performance flexible batteries.

12:40 PM *EN09.02.04

Advances in Alkaline Conversion Batteries for Grid Storage Applications Timothy N. Lambert¹, Noah B. Schorr¹, David J. Arnot¹, Matthew Lim¹, Nelson S. Bell¹, Andrea M. Bruck², Jonathon N. Duay¹, Maria Kelly¹, Rachel Habing¹, Logan Ricketts¹, Julian Vigil¹, Joshua W. Gallaway², Igor Kolesnichenko¹, Stephen Budy¹, Elijah Ruiz¹, Gautam G. Yadav³, Meir Weiner³, Aditya Upreti³, Jinchao Huang³, Michael Nyce⁴, Damon Turney⁴, Sanjoy Banerjee^{4,3}, Birendra Magar⁵, Nirajan Paudel⁵, Igor Vasiliev⁵, Erik Spoerke¹ and Babu Chalamala¹; ¹Sandia National Laboratories, United States; ²Northeastern University, United States; ³Urban Electric Power, United States; ⁴The City University of New York, United States; ⁵New Mexico State University, United States

For energy storage to become ubiquitous in the grid, safe, reliable low-cost electrochemical storage technologies that can be manufactured at high volumes with low capital expenditures are needed. Rechargeable alkaline batteries based on the use of a Zinc conversion anode are well suited due to Zn's high capacity (820 mAh g⁻¹), elemental abundance and established materials supply chain resulting in low production costs. Alkaline-based cells are also inherently safe and do not have the temperature limitations of Li-ion or Pb-acid batteries, thereby removing the need for complicated thermal management control strategies, and providing for simpler systems with lower integration costs. To realize the highest energy density batteries Zn needs to be

coupled with a similarly low cost, abundant and high capacity conversion electrode. Historically Zn/MnO₂, Zn/CuO and Zn/S are primary battery chemistries; however, MnO₂ (616 mAh g⁻¹), CuO (674 mAh g⁻¹) or S (1675 mAh g⁻¹) conversion cathodes are enticing candidates and if a reversible battery can be proven.

This talk will cover recent endeavors to develop cost effective and reliable energy dense alkaline batteries for grid storage applications in a Department of Energy, Office of Electricity (OE) funded program, whose success depends on the ability to effectively pair Zn anodes with a high capacity conversion cathode. This presentation will include an introduction into the OE funded program and the recent developments of rechargeable Zn/MnO₂. Progress towards rechargeable Zn/Cu₂S and Zn/CuO batteries, which have now been demonstrated at commercially relevant areal capacities (~ 10-40 mAh cm⁻²) and energy densities (~ 100-250 Wh/L), and aspects of their battery chemistries and cycling properties will also be provided.

This work was supported by the U.S. Department of Energy, Office of Electricity, Energy Storage Program, Dr. Imre Gyuk, Program Manager, and the Laboratory Directed Research and Development program at Sandia National Laboratories. Sandia National Laboratories is a multi-program laboratory managed and operated by National Technology and Engineering Solutions of Sandia, LLC., a wholly owned subsidiary of Honeywell International, Inc., for the U.S. Department of Energy's National Nuclear Security Administration under contract DE-NA-0003525. The views expressed herein do not necessarily represent the views of the U.S. Department of Energy or the United States Government.

1:05 PM *EN09.02.05

Wiring Electrons and Ions Throughout Architected Zinc Anodes Enables Rechargeable Aqueous Zinc Batteries Debra R. Rolison, Brandon J. Hopkins, Ryan H. DeBlock, Christopher N. Chervin, Nathaniel L. Skeele, Megan B. Sassin, Jeffrey W. Long and Joseph F. Parker; U.S. Naval Research Laboratory, United States

The inherent safety issues of Li-ion batteries and the high-risk supply chain of necessary elements in their active materials provides ample reason to revisit safer aqueous-based batteries. In terms of the specific energy of the system (not the single cell) and the system cost per kW h⁻¹, zinc-based batteries can outshine Li-ion and are undergoing a 21st-century renaissance. We have demonstrated that a monolithic three-dimensional (3D) aperiodic form factor zinc “sponge” developed at the U.S. Naval Research Laboratory (NRL) suppresses formation of dendrites, even when cycling the cell versus nickel, silver, or air cathodes at high rate and to deep utilization of all the zinc in the cell. This performance breakthrough arises because the entire electrode volume is directly wired to the current collector through an inner core of always-present metallic zinc thereby improving uniformity of electroreaction. The co-designed feature of through-connected porosity in 3D plays an important role in ensuring within the confined volume that the ultimate end-product of discharge in alkaline electrolyte, zinc oxide, precipitates onto that internal electrified interface. The historic limitations of zinc anodes in alkaline electrolyte are now history paving the road to next-generation, safer electrochemical energy storage.

1:30 PM Q&A

SESSION EN09.03: Metal Anodes and Conversion Cathodes III

Session Chairs: Aaron Hollas and Noah Schorr

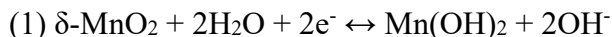
Wednesday Afternoon, April 21, 2021

EN09

2:15 PM *EN09.03.01

Mechanistic Role of Dopants in Conversion Reactions of Layered Birnessite MnO₂ Joshua W. Gallaway, Andrea M. Bruck, Matthew A. Kim, Tristan Owen, Erick Ruoff and Katelyn Ripley; Northeastern University, United States

Rechargeable alkaline Zn-MnO₂ batteries have become the subject of a large research effort because they provide a pathway to high energy density rechargeable batteries that are potentially low cost (<\$50/kWh) and have a non-flammable electrolyte. Since aqueous batteries are more limited in voltage than non-aqueous systems, achieving high reversible capacity is key to increasing energy density and lowering cost. A full two-electron reaction of MnO₂ from its layered birnessite form to the layered hydroxide pyrochroite results in a theoretical capacity of 617 mAh/g.



However, discharge of reaction (1) proceeds through a mixed mechanism: initially the layered structure is maintained and charge is compensated by insertion of ions; later the layered structure breaks down through dissolution and a new layered structure is formed. The charging reaction is similar in nature, but not necessarily a simple reversal of the same path. Furthermore, side reactions can permanently reduce the capacity, as material is instead converted to a stable and resistive spinel form Mn₃O₄ that results in electrode failure. Layered birnessite, which has the ideal structure $\delta\text{-MnO}_2$, can accommodate foreign cations in the interlayer as well as interlayer water. For example K-birnessite incorporates some K⁺ from the electrolyte as well as some neutral H₂O as $\delta\text{-(K}_x\text{)MnO}_2 \bullet w\text{H}_2\text{O}$. However, the K⁺ charge is compensated by some reduction of Mn^{IV} to Mn^{III}, and because K⁺ is not electrochemically active in the stability window of water, this results in a theoretical capacity much lower than 617 mAh/g. If the inserted cations are instead electrochemically active (as with some transition metals) they can themselves participate in the electrochemical reaction and provide capacity. It has long been known that doping $\delta\text{-MnO}_2$ with Bi³⁺ reduces or eliminates the detrimental side reactions resulting in Mn₃O₄, producing a rechargeable electrode. This doping is most effective in thin electrodes of low areal capacity. However, a dual-doping strategy involving both Bi³⁺ and Cu²⁺ extends the effect to high areal capacity electrodes that are thick, have high mass loading, or both. In such a case there are many electrochemically active species in the material, and the sequential electrochemistry of Mn(IV/III), Cu(II/I), Mn(III/II), Cu(I/0), and Bi(III/0) have all been observed on the surface of an MnO₂ particle using operando $\mu\text{-XANES}$ during electrode discharge.

Here we present findings concerning the mechanistic role of intercalated cations in the conversion reactions of doped $\delta\text{-MnO}_2$, with a particular focus on the part played by Bi³⁺. Bi-doped MnO₂ can be prepared in a number of ways, and is often treated in the literature as a single interchangeable material. However, there is evidence that different synthesis methods result in materials that differ in morphology, crystallinity, and in amount and site of Bi-doping. In this study we prepare a series of crystalline $\delta\text{-(K}_x\text{, Bi}_y\text{)MnO}_2 \bullet w\text{H}_2\text{O}$ materials in which y is systematically varied, and these model compounds allow the structural effect of Bi³⁺ to be observed. Operando characterization of these compounds during cycling reveal the dynamic effect of Bi dopants and their interaction with Mn during reaction (1). A multimodal study of synchrotron X-ray diffraction (XRD) and quick X-ray absorption (QAS) shows that during charging of Bi-doped MnO₂ there is an extended period of overlapping electrochemical activity of Bi(0/III) and Mn(II/III), and that this period corresponds to the disappearance of the discharge product, crystalline Mn(OH)₂, but no corresponding charge product is observed by diffraction. Operando Raman spectroscopy reveals that during this period the vibrational signature of $\delta\text{-MnO}_2$ is present, which indicates a disordered $\delta\text{-MnO}_2$ is the initial charge product. Without Bi³⁺ this disordered material is not observed.

2:40 PM DISCUSSION TIME

3:05 PM *EN09.03.03

Novel Materials and *Operando* Methods for Electrical Energy Storage Technologies Héctor D. Abruña;
Cornell University, United States

This presentation will deal with the development of novel materials and *operando* methods for the study and characterization of battery materials. The presentation will begin with a brief overview of the methods

employed. Particular emphasis will be placed on the use of X-ray diffraction (XRD), X-ray absorption spectroscopy (XAS) X-ray microscopy and tomography and confocal Raman under active potential control. The utility of these methods will be illustrated by selected examples including Li/S, Li/Se batteries and Li metal deposition and dendritic growth, as well as the use of organic based materials. The presentation will conclude with an assessment of future directions.

3:30 PM EN09.03.04

Reaction Heterogeneity in High-Energy Lithium–Sulfur Pouch Cells Lili Shi, Chaojiang Niu, Cassidy Anderson, Shuo Feng, Dianying Liu, Dongping Lu, Jie Xiao and Jun Liu; Pacific Northwest National Laboratory, United States

Lithium sulfur (Li–S) battery as one of the most promising next generation energy storage technologies has been extensively studied because of the high theoretical energy, low cost, and environmental friendliness of sulfur.¹ Significant progresses have been made on new materials and advanced characterization techniques for mechanism understandings.² However, further commercialization is currently hindered by the limited cell energy and cycle life of realistic batteries.³ To close the gap between the material-level discoveries to the practical cell-level demonstration, we designed and fabricated realistic Li–S pouch cells, compared the key parameters required for high energy batteries, investigated the reaction processes and their correlations to the cycle behaviors and failure mechanisms. It is found in addition to the electrolyte depletion, heterogeneous electrolyte diffusion and redistribution are dominant factors of the high energy cell decay at electrolyte extremely lean conditions.⁴ Utilization of spatially resolved characterization and theoretical simulation on the practical pouch cells provides a full spectrum view of the dynamic interactions of key cell components in Li–S batteries. New finding of the research will be presented and discussed at the meeting.

References

1. A. Manthiram, Y. Fu, S.-H. Chung, C. Zu and Y.-S. Su, *Chemical reviews*, 2014, **114**, 11751-11787.
2. X. Ji, K. T. Lee and L. F. Nazar, *Nature materials*, 2009, **8**, 500-506.
3. D. Lv, J. Zheng, Q. Li, X. Xie, S. Ferrara, Z. Nie, L. B. Mehdi, N. D. Browning, J. G. Zhang and G. L. Graff, *Advanced Energy Materials*, 2015, **5**, 1402290.
4. L. Shi, S.-M. Bak, Z. Shadike, C. Wang, C. Niu, P. Northrup, H. Lee, A. Y. Baranovskiy, C. S. Anderson and J. Qin, *Energy & Environmental Science*, 2020.

3:45 PM *EN09.03.05

Improving Cell Resistance and Cycle Life with Solvate/Thiophosphate Hybrid Electrolytes in Lithium Metal and Lithium Sulfur Batteries Andrew Gewirth; University of Illinois at Urbana-Champaign, United States

Solid electrolytes (SEs) have become a practical option for lithium ion and lithium metal batteries due to their improved safety over commercially available ionic liquids. The most promising of the SEs are the thiophosphates whose excellent ionic conductivities at room temperature are comparable to those of the commercially-utilized ionic liquids. Hybrid solid-liquid electrolytes exhibit higher ionic conductivities than their bare solid electrolyte counterparts due to decreased grain boundary resistance, enhanced interfacial contact with electrodes, and decreased degradation at the interface.

In this study, we evaluate a series of hybrid electrolytes made from a ‘solvate’ electrolyte in both Li-Li symmetric cells and in a full cell with a Li₂S cathode relative to their bare Li/SE/Li counterparts. Interestingly, hybrid electrolytes made by combining HFE-modified solvates and SE exhibit all the benefits of the interlayer modified SEs, without the necessity of pellet manufacture. The solvate-integrated cathode layer is additionally beneficial for achieving high active material utilization, maintaining intimate interfacial contact, and providing buffer space for volume contraction and expansion. The hybrid Li₂S cell exhibited superior cycling performance compared to the solid-state cells in terms of Li₂S loading, utilization, and cycling stability. Finally, we discuss the use of hybrid electrolytes to enable other cathode chemistries, particularly those involving conversion.

4:10 PM EN09.03.06

Enhanced Performance of Iron-Based Material for Aqueous Rechargeable Battery Fenghua Guo, SaeWon Kim, Xiaoqiang Shan, SathyaNarayanan Jagadeesan and Xiaowei Teng; University of New Hampshire, United States

Electrochemical energy storage has always been an essential part of the application of electricity, as electricity itself cannot be stored. Aqueous electrochemical energy storage is one of the most important and long-lasting research fields due to its cost-effective and environmentally benign nature. The utilization of transition metal oxides/hydroxides in rechargeable batteries has attracted increasing research interests over the years for their multiple valence states, making it possible to have one or more redox couples and the relatively high abundance of transition metal on earth. Among them, the iron as the fourth most abundant element on the earth crust saw its application in the energy storage as early as when Thomas Edison developed the famous Nickel-Iron Battery in 1901.

Our study was devoted to bringing further understanding of the electrochemical behavior of lepidocrocite (γ -FeOOH) in the alkaline system and its application as the anode in full cells. Unlike commonly used alkaline solution with high concentration, we focus on a mild environment (pH=12, 13). By bringing in additional anion group into the system, we observed enhanced capacity with a different redox behavior, which was attributed to the formation of the green rust phase by *in-situ* X-ray Diffraction measurements. Full cell data showed that the capacity retention was also improved significantly by enabling the anion intercalation. Our study opens a way to improve the performance of iron-based electrode materials in an alkaline system.

SESSION EN09.04: Metal Anodes and Conversion Cathodes IV

Session Chairs: Vitaly Alexandrov and Huilin Pan

Wednesday Afternoon, April 21, 2021

EN09

5:15 PM *EN09.04.01

Multiple Sulfur Reduction Pathways and Hidden Lithium Storage Mechanisms for Extra Discharge Capacity Revealed by First Principles Simulations Perla Balbuena and Saul Perez Beltran; Texas A&M University, United States

Lithium-Sulfur batteries are among the most promising for desired high energy density applications such as electric vehicles. The batteries are usually configured with a Li metal anode and a sulfur-carbon (S-C) cathode electrode, in addition to an electrolyte typically composed by an ether solvent, a salt, and some additives. However, the formation of soluble polysulfide species during discharge reactions, and their migration to the anode side create severe problems that result in drastic reduction of the battery capacity during cycling. One possible solution is to modify the structure and chemical composition of the S-C cathode, by creating chemical S-C bonds. One of the best materials that contain such S-C bonds results from special thermal treatments (under an excess of sulfur) of polyacrylonitrile (PAN), that results in a new material called SPAN. During discharge, this material does not generate long-chain polysulfides, thus avoiding one of the main problems of this type of batteries. However, the underlying microscopic mechanisms occurring in the cathode during lithiation are not yet fully understood. In this work, we use ab initio molecular dynamics simulations to model a cathode material that reproduces experimental data of SPAN's graphitization and conjugated ordering, sulfur-carbon covalent bonding, sulfur loading, and elemental composition, including nitrogen doping. Our study reveals atomistic details regarding voltage profiles including the roles of S, N, and C atoms during lithiation, and provides new insights into the origins of irreversible capacity loss between the first and second cycles.

5:40 PM EN09.04.02

Rational Design of Sulfur Cathode for High-Energy Lithium-Sulfur Batteries Shuo Feng^{1,2}, Lili Shi¹,

Cassidy Anderson¹, Yuehe Lin², Jie Xiao¹, Jun Liu¹ and Dongping Lu¹; ¹Pacific Northwest National Laboratory, United States; ²Washington State University, United States

A crucial prerequisite for a high energy lithium-sulfur (Li-S) battery is the integration of a high-loading sulfur cathode, a lean amount of electrolyte, and a limited Li anode 1-4. However, simultaneous application of these parameters often leads to the rapid deterioration of the cell performance. Fundamental mechanisms of the cell failure are still not very clear; materials that can fulfill both high energy density and long cycle life of the Li-S batteries are still facing significant challenges. Highly porous and nanosized carbon materials are widely explored as effective sulfur hosts to improve Li-S battery's performance. However, these nano materials tend to form extremely porous and thick sulfur cathodes which require a large amount of electrolyte for pore filling, and thus a very high electrolyte to sulfur ratio (E/S ratio > 10 $\mu\text{L}/\text{mgs}$) is usually used for cell test. To address those issues, rational designs for both materials and electrode structures are urgently needed to enable the operation of low porosity sulfur cathodes (<50%) under lean electrolyte condition (E/S ratio < 4 $\mu\text{L}/\text{mgs}$), conserving more proportion of electrolyte for cell cycling. In this research, sulfur/carbon composite with controllable secondary particle sizes were synthesized and used as example materials to understand the impacts of materials and electrodes on sulfur reactions at realistic conditions. It is found that the larger sulfur/carbon particles (> 90 μm) demonstrate significant superiorities over the smaller ones (< 20 μm) in terms of electrolyte permeability, sulfur utilization rate, electrochemical polarization, and shuttling effect. As a result, at an extremely low electrode porosity of 45%, the high loading sulfur cathode (>4 mg/cm^2) can deliver a high initial discharge capacity of 1001 mAh/g under lean electrolyte conditions (E/S ratio = 4 $\mu\text{L}/\text{mgs}$) with a much improved cycling stability. New findings of the research will be presented and discussed at the symposium.

References

1. Lv, D.; Zheng, J.; Li, Q.; Xie, X.; Ferrara, S.; Nie, Z.; Mehdi, L. B.; Browning, N. D.; Zhang, J.-G.; Graff, G. L.; Liu, J.; Xiao, J., High Energy Density Lithium-Sulfur Batteries: Challenges of Thick Sulfur Cathodes. *Advanced Energy Materials* **2015**, *5* (16).
2. Shi, L.; Bak, S.-M.; Shadike, Z.; Wang, C.; Niu, C.; Northrup, P.; Lee, H.; Baranovskiy, A. Y.; Anderson, C. S.; Qin, J.; Feng, S.; Ren, X.; Liu, D.; Yang, X.-Q.; Gao, F.; Lu, D.; Xiao, J.; Liu, J., Reaction heterogeneity in practical high-energy lithium-sulfur pouch cells. *Energy & Environmental Science* **2020**, *13* (10), 3620-3632.
3. Lu, D.; Li, Q.; Liu, J.; Zheng, J.; Wang, Y.; Ferrara, S.; Xiao, J.; Zhang, J. G.; Liu, J., Enabling High-Energy-Density Cathode for Lithium-Sulfur Batteries. *ACS Appl Mater Interfaces* **2018**, *10* (27), 23094-23102.
4. Liu, J.; Bao, Z.; Cui, Y.; Dufek, E. J.; Goodenough, J. B.; Khalifah, P.; Li, Q.; Liaw, B. Y.; Liu, P.; Manthiram, A.; Meng, Y. S.; Subramanian, V. R.; Toney, M. F.; Viswanathan, V. V.; Whittingham, M. S.; Xiao, J.; Xu, W.; Yang, J.; Yang, X.-Q.; Zhang, J.-G., Pathways for practical high-energy long-cycling lithium metal batteries. *Nature Energy* **2019**, *4* (3), 180-186.

5:55 PM *EN09.04.03

High Donor Electrolytes for Lithium-Sulfur Batteries with Lean Electrolyte Conditions Jang Wook Choi; Seoul National University, Korea (the Republic of)

Li-S batteries have experienced remarkable progress in the past decade, mainly in terms of cycle life. The shuttling process, the main capacity fading mechanism, was addressed by a variety of strategies targeting all of sulfur electrode, electrolyte, and separator. Nonetheless, the main progress was based on ether-based electrolytes that have a certain level of compatibility with Li metal counter electrode. To achieve more competitive energy density, electrolyte amount should be controlled to be low thus satisfying the necessity of lean electrolyte conditions. In this talk, I will introduce recent progress in identifying high donor electrolytes. High solubility of polysulfides contributes directly to boosting the volumetric energy density. I will also discuss how to secure the compatibility with Li metal anode so that high donor electrolytes can be adopted in commercially viable conditions.

6:20 PM *EN09.04.04

The Role of Superoxide Solvation and Crystal Growth in Enabling Rechargeable, High Capacity Metal

Oxygen Batteries Naga Phani B. Aetukuri; Indian Institute of Science, India

Batteries with energy density higher than that of state-of-the-art Li-ion batteries are considered critical for mass adoption of electric automobiles. Alkali metal-X batteries such as Li-O₂, Na-O₂, K-O₂ and Li-S batteries have been extensively researched over the past few years as high energy density alternatives to Li-ion batteries. Amongst these battery types, metal-oxygen batteries afford the highest energy density for a given alkali metal. Elementary steps that are common to all alkali metal-oxygen batteries are, i) the electrolyte crystal growth during discharge and ii) dissolution of alkali metal peroxides such as Li₂O₂ (in Li-O₂ batteries) or superoxides such as NaO₂ or KO₂ (in Na- or K-O₂ batteries, respectively). In general, at least one of these steps was found to be slow or inefficient in aprotic metal-oxygen batteries. However, the parameters that limit the rate of crystal growth and dissolution, and therefore the ultimate practical energy densities and rechargeability attainable in these batteries, are poorly understood. For example, Li₂O₂ and NaO₂, the discharge products in Li- and Na-O₂ batteries respectively, are both electronic insulators. Therefore, electrochemical deposition of Li₂O₂ and NaO₂ might lead to battery electrode passivation and to low practical specific energy. However, electrode-passivation limited capacities were observed in Li-O₂ batteries, but not in Na-O₂ cells. In this talk, we will present experimental results backed by theoretical calculations that suggest the capacity limitations in alkali metal-oxygen batteries can be overcome by suitable electrolyte design that enhances solution-mediated electrochemical deposition of Li₂O₂ and NaO₂. This mechanism leads to a higher specific energy than that limited by electrode passivation. Further, we will discuss the role of ion-pairing on the growth of crystals in metal-oxygen batteries and propose suitable additives to enhance crystal growth in metal-oxygen batteries. Finally, we will also discuss design rules for selecting electrolyte solvents that favor the solution deposition of discharge products while also being electrochemically stable.

6:45 PM EN09.04.05

Competition of Intercalation and Conversion Reactions for FeOF Cathode—A Combined Study with Atomic Simulations and Experiment Qisheng Wu¹, Haotian Wang², Gary Rubloff², Chuan-Fu Lin^{2,3} and Yue Qi¹; ¹Brown University, United States; ²University of Maryland, United States; ³The Catholic University of America, United States

The iron oxyfluoride (FeOF) cathode has been attracting great research interests since it inherits both the high output voltage of fluorides (FeF_x) and the good kinetics of oxides (FeO_x). The lithiation of the rutile FeOF starts with intercalation up to a certain concentration (Li_{0.6}FeOF) followed by conversion reaction to form new phases (e.g., rock salt LiFeO_x, LiF, and Fe metal). It is not surprising that the thermodynamically favorable conversion reaction does not happen in the very beginning due to kinetic barriers for solid-state phase transformation. The atomistic mechanism of the competition between the intercalation *vs.* conversion for FeOF is yet to be understood. In this work, a combined study with atomic simulations and experiments is performed to resolve this issue.

We propose by density functional theory (DFT) calculations a new intermediate rock salt structure, which has lower interface energy with the dominating converted phases (LiFeO₂ and FeO). Therefore, the intermediate rock salt structure will have a smaller barrier for conversion reactions. It is identified from the transition state calculations via NEB method that phase transition from the intercalated rutile structure to the intermediate rock salt structure is accompanied by a volume expansion. Therefore, compression stress imposed by a coating layer can prevent the transformation to the intermediate rock salt structure and delay the onset of the converting reaction. This explained the previous experimental observation that a thin solid electrolyte (LiPON) deposition on the FeOF cathode extended the Li insertion process to higher concentrations (Li_{1.0}FeOF). Since the intercalation process is more reversible than the conversion reaction, the LiPON coated FeOF cathode retained 89% of its capacity for more than 100 cycles. This suggests that mechanical constraints can be used to control the competition of intercalation and conversion reactions to design durable high capacity conversion-type cathode materials for Li-ion batteries.

7:00 PM EN09.04.06

Density Functional Theory and Experimental Investigation of Voltage Profile and Rechargeability in CF_x Batteries Kevin Leung¹, Noah B. Schorr¹, Matthew Mayer², Timothy N. Lambert¹, Y. Shirley Meng² and Katharine Harrison¹; ¹Sandia National Laboratories, United States; ²University of California at San Diego, United States

Graphite Fluoride (CF_x) exhibits one of the highest theoretical energy capacities among primary batteries, and has recently been reported to be rechargeable in Na/CF_x cells[1]. Although CF_x is widely used, key aspects of CF_x cell operations remain poorly understood. For example, the practical operational voltage is far below the theoretical (thermodynamic) average of 4.66 V for Li/CF_x [2] (Fig. 1a). The discharge rate is slow, and rechargeability for Li/CF_x, which can lead to high energy density secondary batteries, has yet to be demonstrated. A deeper understanding of the CF_x discharge mechanism, which is still disputed, will improve battery capabilities. In this presentation, we will report ab initio molecular dynamics (AIMD) simulations of CF_x defluorination by a Li-droplet on CF_x edges (i.e., under short-circuit conditions). We also perform static, zero temperature Density Functional Theory (DFT) calculations of equilibrium voltages motivated by insights obtained in these AIMD simulations. From these predictions, we propose a discharge mechanism with a voltage range which is in broad agreement with our Galvanostatic Intermittent Titration Technique (GITT) measurements. We also calculate defluorination energy barriers associated with C-F bond breaking and relate these predictions to kinetic values estimated from experiments. Finally, solvent effects and constant-voltage electrochemical (including “overpotential”) conditions will be considered in DFT calculations.

References

- [1] Y. Shao et al., “Synthesis and Reaction Mechanism of Novel Fluorinated Carbon Fiber as a High Voltage Cathode Material for Rechargeable Na Batteries.” *Chem. Mater.* 28, 1026 (2016).
[2] A.J. Valegra *et al.*, “Thermodynamic and Kinetic Data of Carbon Fluorine Compounds.” NTIS Report AD-776 990 (1972).

SESSION EN09.06: On-demand
Wednesday Morning, April 14, 2021
EN09

8:00 AM *EN09.05.04

Screening Interfaces of Energy Materials Using First-Principles Calculations Pieremanuele Canepa;
National University of Singapore, Singapore

In 2000, during his noble prize lecture Prof. Herbert Kroemer stated “The interface is the device”[1]; he was referring to the phenomenal success in design and application of semiconductor heterojunction devices in microelectronics. Arguably, Kroemer's statement has an ever-increasing relevance across a range of technologies far beyond transistors, where heterojunctions found their initial success. Researchers are increasingly finding that interfaces between materials represent a rich space for the exploration of exotic properties that are not present in bulk materials, such as two-dimensional electron gases (or liquids) and quantum topological states. It is clear that the importance of the interface can only grow with the evolution of modern technological applications. Simultaneously, progress in computational materials science in describing complex interfaces is critical for improving the understanding and performance of energy materials, including rechargeable batteries and catalysts [2].

In this talk, I will elucidate how first-principles calculations, based on density functional theory, can be applied to large pools of materials to rationalize their behaviors when forming functional interfaces [3–7]. Focus will be given to topical materials in rechargeable batteries, where controlling interfaces is paramount to curb degradation phenomena [3–7].

- [1] H. Kroemer, “Nobel Lecture: Quasielectric fields 1065 and band offsets: teaching electrons new tricks,”

Rev. Mod. Phys. 73, 783–793 (2001).

[2] K. T. Butler, G. Sai Gautam and P. Canepa, Designing Interfaces In Energy Materials Applications With First-Principles, npj Computational Materials (2019).

[3] P. Canepa, G. Sai Gautam, D. C. Hannah, R. Malik, M. Liu, K. G Gallagher, K. A Persson and G. Ceder, Chem. Rev., 117, 4287–4341(2017)

[4] P. Canepa et al, Particle Morphology and Lithium Segregation to Surfaces of the Li₇La₃Zr₂O₁₂ Solid Electrolyte, Chem. Mater., 30 (9) 3019–3027 (2018).

[5] T. Chen, G. Ceder, G. Sai Gautam and P. Canepa, Evaluation of Mg compounds as coating materials in Mg batteries, Front. Chem. (2019) 10.3389/fchem.2019.00024

[6] T. Chen, G. Sai Gautam and P. Canepa, Ionic transport in Potential Coating Materials, Chem. Mater., 31 (19) 8087-8099 (2019).

[7] Z. Deng, G. Sai Gautam, S. K. Kolli, J.-N. Chotard, A. K. Cheetham, C. Masquelier and P. Canepa, Phase Behavior in Rhombohedral NaSiCON Electrolytes and Electrodes, 32 (18) 7908-7920 (2020).

SYMPOSIUM EN10

Transformation, Reaction and Organization at Functional Interfaces for Sustainable Energy Systems and Environmental Managements
April 17 - April 18, 2021

Symposium Organizers

Zhenxing Feng, Oregon State University
Carmen Murphy, Johnson Matthey
Elizabeth Podlaha-Murphy, Clarkson University
Huolin Xin, University of California, Irvine

* Invited Paper

Tutorial EN10: Interfaces in Energy Storage and Water-Energy Nexus Systems
Session Chairs: Seth Darling, Zhenxing Feng and Kang Xu
Saturday Morning, April 17, 2021
EN10

9:00 AM *

Interfacing Electrolytes in Batteries Kang Xu; U.S. Army Research Laboratory, United States

This tutorial provides a colloquial introduction to the interface science in electrochemistry, and the central role played by interfaces and interphases in the advanced batteries. It will also cover the recent advances in the field of high energy battery chemistries and materials.

10:30 AM BREAK

10:45 AM *

Interfaces in Water-Energy Systems Seth Darling; Argonne National Laboratory, United States

Interfaces between materials and water or aqueous fluids are central to the performance of almost all water-energy systems. In this tutorial, Dr. Darling will first introduce global-scale challenges related to the water-energy nexus and then reveal how the properties of water/solid interfaces are interconnected with these challenges. He will present various strategies that are used by researchers to manipulate interfacial properties, ranging from mussel-inspired dopamine chemistry to atomic layer deposition and related techniques. He will provide examples of applications implementing such approaches, including anti-fouling surfaces, catalytically active materials, membranes with unusual transport properties, selective sorbents, and photothermal systems for solar steam generation.

SESSION EN10.01: Electrocatalysis in General
Session Chairs: Zhenxing Feng and Carmen Murphy
Sunday Morning, April 18, 2021
EN10

8:00 AM *EN10.01.01

Probing Buried Electrochemical and Catalytic Interfaces Under Working Conditions Robert Weatherup;
University of Oxford, United Kingdom

Revealing the chemical reactions that occur at catalytic and electrochemical interfaces under realistic conditions is critical to selecting and designing improved materials for chemical synthesis, energy storage, and corrosion prevention. Obtaining chemical information with nm-scale interface sensitivity is however a significant challenge given these interfaces are typically buried between a bulk support and dense reaction environment.^{1,2}

Here we introduce and apply several complementary methods based on soft X-ray spectroscopies and neutron reflectometry for studying electrochemical and catalyst interfaces under realistic liquid- and gas-phase environments. This includes *membrane-based* approaches which we have been involved in developing over recent years that enable *operando* x-ray photoelectron and absorption spectroscopy (XPS/XAS) of solid-liquid and solid-gas interfaces at atmospheric pressures and above.²⁻⁵ These rely on reaction cells sealed with X-ray/electron-transparent membranes such as thin (<100 nm) silicon nitride or graphene membranes that remain impermeable to gases and liquids.

We demonstrate how these approaches can track the chemical evolution of solid-gas interfaces such as copper surfaces during methanol oxidation,⁶ and supported nanoparticle catalysts in atmospheric pressure environments.⁴ We also show how total electron yield (TEY) mode XAS can monitor the evolution of solid-liquid interfaces under electrochemical control, including the oxidation/reduction of Ni electrodes in aqueous media, and solid-electrolyte interphase (SEI) formation on Li-ion battery anodes.⁵ This is complemented by neutron reflectometry which reveals the precise thickness of the layers formed on electrode surfaces with sub-nm depth resolution, even for light elements such as Li, C, O. We are thus able to follow the chemical and structural evolution of the solid-electrolyte interphase during its formation under realistic electrochemical conditions. We further introduce some promising new methods for accessing the chemistry of electrode-electrolyte interfaces in solid-state batteries,⁷ using Hard X-ray Photoelectron Spectroscopy.

We expect these methods to be valuable in understanding a wide range of interfacial reactions across the electrochemical and catalytic sciences, and will summarize outstanding challenges in this area that are still to be overcome.

References

1. Wu et al. *Phys. Chem. Chem. Phys.* **2015**, *17*, 30229.
2. Weatherup et al. *Top. Catal.* **2018**, *61*, 2085.

3. Velasco-Velez et al. *Angew. Chemie* **2015**, *54*, 14554.
4. Weatherup et al. *J. Phys. Chem. Lett.* **2016**, *7*, 1622.
5. Weatherup et al. *J. Phys. Chem. B* **2018**, *122*, 737.
6. Eren et al. *Phys. Chem. Chem. Phys.* **2020**, *22*, 18806
7. Brugge et al. *J. Mater. Chem. A* **2020**, *8*, 14265

8:25 AM *EN10.01.02

Intermetallic PtCo Catalysts with Enhanced Stability Jacob Spendelow¹, Chenyu Wang¹ and David Cullen²;

¹Los Alamos National Laboratory, United States; ²Oak Ridge National Laboratory, United States

Polymer electrolyte fuel cell performance is limited mainly by the cathode, where poor oxygen reduction reaction (ORR) kinetics and slow transport of O₂ to active sites lead to large overpotentials. State-of-the-art high surface area Pt alloy catalysts also suffer from poor durability due to loss of surface area (particle growth) and leaching of base metals. We have recently demonstrated that the use of intermetallic nanoparticle catalysts such as L1₀-PtCo can enable significant improvements in long-term performance due to improved stabilization of base metal in the ordered lattice. We have also demonstrated a strong role of the catalyst support in determining catalyst performance and durability, providing additional opportunities to control and tune catalyst properties through control of support morphology, porosity, and graphitization. New catalysts based on L1₀-CoPt combined with advanced support structures have shown excellent durability in fuel cell membrane electrode assemblies (MEAs), meeting DOE targets for accelerated stress tests (30K voltage cycles in MEA) with minimal performance degradation. Recent results and future directions for this catalyst research will be discussed.

8:50 AM EN10.01.03

Highly Dispersed RuOOH Nanoparticles on Silica Spheres—An Efficient Photothermal Catalyst for Selective Aerobic Oxidation of Benzyl Alcohol Qilin Wei and Yugang Sun; Temple University, United States

Photothermal catalysis represents a promising strategy to utilize the renewable energy source (e.g., solar energy) to drive chemical reactions more efficiently. Successful and efficient photothermal catalysis relies on the availability of ideal photothermal catalysts, which can provide both large areas of catalytically active surface and strong light absorption power simultaneously. Such duplex requirements of a photothermal catalyst exhibit opposing dependence on the size of the catalyst nanoparticles, i.e., smaller size is beneficial for achieving higher surface area and more active surface, whereas larger size favors the light absorption in the nanoparticles. In this article, we report the synthesis of ultrafine RuOOH nanoparticles with a size of 2–3 nm uniformly dispersed on the surfaces of silica (SiO_x) nanospheres of hundreds of nanometers in size to tackle this challenge of forming an ideal photothermal catalyst. The ultrasmall RuOOH nanoparticles exhibit a large surface area as well as the ability to activate adsorbed molecular oxygen. The SiO_x nanospheres exhibit strong surface light scattering resonances to enhance the light absorption power of the small RuOOH nanoparticles anchored on the SiO_x surface. Therefore, the RuOOH/SiO_x composite particles represent a new class of efficient photothermal catalysts with a photothermal energy conversion efficiency of 92.5% for selective aerobic oxidation of benzyl alcohol to benzaldehyde under ambient conditions.

9:05 AM DISCUSSION TIME

9:20 AM EN10.01.05

Aging and Recovery of Fe-Ni-Co Electrocatalysts for the Alkaline Oxygen Evolution Reaction (OER)

Elizabeth Podlaha-Murphy; Clarkson University, United States

Earth-abundant Fe-Ni-Co oxide are recognized electrocatalysts for the oxygen evolution reaction (OER) in water splitting. In the present work, Fe-Ni-Co alloy thin films are electrodeposited onto copper substrates and surface oxides generated by voltammetry in 1 M KOH. The electrocatalysts are aged until changes in the OER are observed at different applied current densities. Regenerated catalysts occur via a cathodic post-treatment.

Stability of the electrocatalysts are examined with voltammetry, chronopotentiometry and XANES analyses. Fresh, unaged samples show predominately Fe(III), Ni(II) and metallic Co states present in the oxide. Changes of the electron density distribution were observed upon aging of the electrocatalysts that could be reversed through the regeneration step. The Fe-Ni-Co thin films were fabricated by electrodeposition from a boric acid-containing electrolyte onto rotating cylinder electrodes. The OER activity of the electrodeposits in 1 M KOH was a function of deposit composition, as expected although alloys with a small amount of Co maintained a constant Tafel slope over a larger range than a comparable Fe-Ni electrocatalyst. Chronopotentiometric aging during an anodic current density of 10 mA/cm² for 30 hours, was followed by a cathodic post treatment current density, that fully recovered the OER activity, and the limits of the cathodic post treatment with more extreme aging conditions will be discussed.

SESSION EN10.02: Interfaces in Electrochemical Energy Storage
Session Chairs: Xiaofeng Feng and Yingjie Zhang
Sunday Morning, April 18, 2021
EN10

10:30 AM *EN10.02.01

Operando 3D Imaging of Electrodes and Electric Double Layers at the Atomic Scale Yingjie Zhang;
University of Illinois at Urbana-Champaign, United States

The interconversion between chemical energy and electricity relies critically on electrode-electrolyte interfaces, which consists of the electrode surface regions and the solvation layers, also called the electric double layers (EDLs). While the electrode structures have been extensively studied using in-situ characterization techniques, to date the structure of EDLs remains largely unexplored. This is not surprising, considering the weakly ordered, partially mobile, and vacuum-incompatible nature of the liquid molecules in the EDL. To address this challenge, we have developed a novel technique, electrochemical three-dimensional atomic force microscopy (EC-3D-AFM), to directly image both the electrode surface and EDLs under operando conditions. Utilizing ultrasensitive force detection techniques, we are able to achieve atomic and molecular resolution. I will discuss our recent findings on the potential-dependent EDLs of graphitic and other van der Waals electrodes using the EC-3D-AFM method. In addition, I will also discuss our efforts on operando spectroscopy of electrode-electrolyte interfaces, as well as joint experiment-theory approaches to understand the hidden mechanisms of interfacial electrochemical energy conversion processes.

10:55 AM EN10.02.02

Lithium-Ion Battery Separators—The Influence of Separator Structure on Battery Performance
Christina Sauter, Raphael Zahn and Vanessa Wood; ETH Zürich, Switzerland

Separators in Lithium Ion Batteries (LIBs) are electronically isolating membranes that prevent physical contact between the two electrodes while allowing ionic transport. Therefore, they are considered to be a crucial part in battery safety.¹ In commercially available LIBs, separators are predominately made from porous polyolefin films such as polypropylene (PP) or polyethylene (PE). They can be coated with thin layers of ceramics (e.g., Al₂O₃, MgO₂, ...), which improves their stability against shrinking under thermal stress and their resistance to electrochemical oxidation by high voltage positive electrodes.³

Traditionally, the effective transport coefficient (ratio between porosity and tortuosity) is used for the characterization of LIB separator performance. However, to fully capture all aspects of battery performance, additional structural parameters like pore space connectivity are necessary.^{4 5} Here, we show how the 3D structure of the separator pore space directly influences separator wetting and thereby battery performance. Our research group developed an approach to visualize and quantify LIB separators with focused ion beam scanning electron microscopy (FIB-SEM).² Using FIB-SEM we acquired the 3D tomographic data of

commercial coated and uncoated PE separators. Comparing the effective transport coefficients, pore connectivity and mechanical stability of the two different separators, we quantify the influence of the ceramic coating on structure and performance.

The 3D data sets also allow us to simulate the wetting of the separator membranes with liquid electrolyte. We see that during this so-called imbibition-process up to 30% gas is entrapped in the separator. Using partial wetting theory, we show that the specific 3D structure of the separator is responsible for this incomplete wetting. Comparing the wetting simulations to separator performance measurements, we demonstrate, that incomplete wetting can explain the discrepancy between theoretically predicted and experimentally measured transport coefficients. We also show that quasi-static wetting models overestimate the amount of residual gas in the membranes and that realistic wetting models have to consider both, the physico-chemical properties of the liquid electrolyte and the 3D structure of the separator pore space.⁶

1. Zhang, S. S. A review on the separators of liquid electrolyte Li-ion batteries. *J. Power Sources* **164**, 351–364 (2007).
2. Lagadec, M. F., Ebner, M., Zahn, R. & Wood, V. Communication—Technique for Visualization and Quantification of Lithium-Ion Battery Separator Microstructure. *J. Electrochem. Soc.* **163**, 992–994 (2016).
3. Lee, H., Yanilmaz, M., Toprakci, O., Fu, K. & Zhang, X. A review of recent developments in membrane separators for rechargeable lithium-ion batteries. *Energy Environ. Sci.* **7**, 3857–3886 (2014).
4. Lagadec, M. F., Zahn, R., Müller, S. & Wood, V. Topological and network analysis of lithium ion battery components: The importance of pore space connectivity for cell operation. *Energy Environ. Sci.* **11**, 3194–3200 (2018).
5. Lagadec, M. F., Zahn, R. & Wood, V. Characterization and performance evaluation of lithium-ion battery separators. *Nat. Energy* **4**, 16–25 (2018).
6. Sauter, C., Zahn, R. & Wood, V. Understanding Electrolyte Infilling of Lithium Ion Batteries. *J. Electrochem. Soc.* **167**, (2020).

11:10 AM EN10.02.03

Enhanced Voltage Generation Through Electrolyte Flow on Liquid Filled Surfaces Bei Fan, Prab Bandaru and Li Cheng; University of California, San Diego, United States

The generation of electrical voltage through the flow of an electrolyte over a charged surface may be used for energy transduction. Here, it is shown that enhanced electrical potential differences/streaming potential (V_s) may be obtained through the flow of salt water on *LFS* (liquid filled surfaces) infiltrated with lower dielectric constant liquid, such as oil, harnessing electrolyte slip and associated surface charge. A record large figure of merit, in terms of the voltage generated per unit applied pressure, of 0.043 mV/Pa, was obtained through the use of the *LFS*, greater by a factor of 1.4, when compared to air filled surfaces (*AFS*). These results lay the basis for innovative surface charge engineering methodology for the study of electrokinetic phenomena at the microscale with applications to new electrical power sources.

We will also discuss a methodology for substantially indicating the magnitude of the electrokinetic streaming potential (V_s) from ~ 0.02 V to ~ 1.6 V, based on experimental results. The underlying idea is to use textured *LFS*, filled with low viscosity oils, for electrolyte flow. The charge density at the electrolyte-oil interface as well as the enhanced slip is thought to be responsible for the enhancement of the V_s . The specific influence of the filling oil viscosity on the V_s was probed with respect to the viscosity. It was found, through experimental analysis as well as computational simulations, that the fluid slip length was inversely proportional to the filling oil viscosity, and influences the V_s . The obtained results provide new perspectives related to complex electrolyte flow conditions as may be relevant to chemical and biological separations.

11:25 AM EN10.02.04

New Long Life/ Safer Lithium Ion Battery with Low Cost/Li-Corrosion Resistant Ultrananocrystalline Diamond-Coated Components Elida I. de Obaldia^{1,2}, Orlando Auciello^{2,3} and Jesus J. Alcantar-Peña⁴;

¹Universidad Tecnológica de Panamá, Panama; ²The University of Texas at Dallas, United States; ³Original

Biomedical Implants, LLC, United States; ⁴Center for Engineering and Industrial Development, Mexico

Novel low cost/electrically conductive/corrosion resistant nitrogen-doped ultrananocrystalline diamond (N-UNCD) coating provides excellent chemically robust encapsulation of commercial natural graphite (NG)/copper (Cu) anodes and new textured Si-based anodes, currently under development for Li-ion batteries (LIB), providing a solution to the problem of LIBs' anode materials degradation due to chemical corrosion induced by Li ions. The N-UNCD encapsulating coating allows for good conductivity of both electrons and Li-ions while exhibiting outstanding chemical and electrochemical inertness to Li ions-induced corrosion, eliminating de Li-induced chemical corrosion of graphite powder in current commercial graphite/copper composite anodes, which result in degradation of the capacity energy after undesirable relatively short numbers of charge/discharge cycles of LIBs. In addition, the electrically conductive N-UNCD coating produce a substantial increase in the mechanical strength of the anode's graphite powder and will also produce the same results for structured Si anodes, resulting in the formation of robust Solid-Electrolyte Interface (SEI) films, which effectively eliminate unceasingly cracking of SEI, observed in graphite/copper anodes, which expose fresh graphite anode surface, thus, repairing of the SEI by electrochemical reduction of the electrolyte and the formation of additional SEI compounds, which increase the impedance for the lithium ion diffusion and causes the electrolyte to be prematurely depleted in anodes without the N-UNCD coating. In addition to the excellent protection to chemical attack of anodes, new preliminary R&D will be presented indicating that electrically conductive N-UNCD coatings can also be used to coat LIB's oxide cathodes to protect them from Li-induced corrosion, as well, and that insulating/corrosion resistant UNCD coating can be used to coat the inner walls of novel metallic aluminum LIB's cases and membranes to protect them from corrosion induced by the Li-based battery environment, and thus enabling to use aluminum as a LIB's case, thus to replace current more expensive partially corrosion resistant metals. The pathway to commercialization of the new UNCD coating technology for LIBs and other LI-based batteries, like thermal Li-sulfur batteries will be discussed.

11:40 AM DISCUSSION/Q&A/SOCIAL

SESSION EN10.03: Interfaces in Electrocatalysts 2 Characterizations

Session Chairs: Zhenxing Feng and Jacob Spendelow

Sunday Afternoon, April 18, 2021

EN10

1:00 PM *EN10.03.01

The Use of Synchrotron Techniques to Characterize Oxide-Supported Catalysts Richard L. Kurtz;

Louisiana State University, United States

Synchrotron-based characterization methods can provide valuable information on the nature of catalyst/adsorbate interactions and a number of soft X-ray based techniques will be reviewed in this presentation. We will focus our discussion on systems involving catalyst clusters supported on single-crystalline oxides, particularly TiO₂, ZnO, and Fe₂O₃. The examples that we will present include studies related to electrochemistry as well as environmental chemistry.

With synchrotron ultra-violet light one can provide information on occupied valence electronic structure and charge-transfer mechanisms occurring during reaction and adsorbate bonding using ultra-violet photoemission (UPS) and by tuning the photon energy it's possible to use excitation resonances to enhance sensitivity to defect states. Synchrotron-based X-ray photoelectron spectroscopy (XPS) is another valuable tool for probing surface reactions and cross-sections for core-level excitations can also be tuned with photon energy. Since XPS involves photoexcitation from a core level to a plane-wave final excited state far above E_F , the measured binding energies reflect potential shifts in the *occupied* core levels reflecting the chemistry of the atomic

bonding. Another valuable measurement is to probe the *empty* electronic states just above the Fermi level by monitoring the X-ray absorption near edge structure (XANES). This can provide further information on the changes induced by chemical bonding and the hybridization of empty electronic states and we will show that it provides valuable information that is complementary to the UPS/XPS probes of the occupied states. In the case of the L edges ($2p$ states), the dipole-allowed transition to empty $3d$ states are very sensitive to details of the changes in the empty-state electronic structure, crystal-field splitting, and other effects induced in the interfaces on chemical adsorption and reaction.

It is helpful to combine this data with models to better understand the local atomic and electronic states and density-functional theory (DFT) calculations allow one to model surface structures and compute electronic band structures, including empty states. A Bader analysis can provide information on charge-transfers that are involved, and methods have been developed to compute the XANES spectra directly, including spectra considering the presence of the ($2p$) core hole. We will contrast data with predictions to show how progress is being made in understanding the underlying chemistry involved. We will conclude with a summary of how synchrotron studies, combined with DFT calculations, will provide valuable information on the atomic and electronic origins of interface structures.

1:25 PM *EN10.03.02

Revealing Coupled Surface Transformation and Reorganization on Metal Oxide in Oxygen Evolution Reaction Hua Zhou; Argonne National Laboratory, United States

Electrocatalysts are materials designed to provide a facilitating environment for electrochemical conversion and synthesis of materials and fuels from atmospheric molecules, which is one of the most important challenges facing societal need of energy in 21st century. One of the major hurdles developing electrocatalysts is the lack of holistic information of the evolving surface structure of materials during electrochemical operation. This is particularly formidable for oxygen evolution reaction (OER), where the oxidizing environment is corrosive and can significantly rearrange the electrocatalyst surface structure. Therefore, identifying how the surface structure of materials evolves during the OER is essential to the development of more active and stable electrocatalysts and broadly to the prospect of materials and energy sustainability. Surface-sensitive X-ray probes from modern synchrotron sources including surface X-ray scattering and grazing incidence X-ray spectroscopy provide a very powerful suite of toolkits to decipher the surface subtlety and evolution. If utilizing these techniques in a well-coordinated approach, one can deliver thorough and deep fundamental insights of surface transformations (e.g. structural, chemical and electronic) during the electrocatalytic process.

In this talk, I will firstly render a brief survey of various surface sensitive X-ray techniques to specifically probe structural and chemical aspects of electrocatalytic materials, in particular the combined approach to differentiate the contribution from surface and bulk layers. In particular, I will introduce the high energy surface X-ray diffraction technique which facilitates fast capturing of structural evolution of less stable surface under electrocatalytic conditions. Following the survey, I would like to present a comprehensive study of the emergent surface transformation of SrIrO_3 , the most active OER electrocatalyst reported to date, especially the amorphous boundary layer that forms from the pristine crystalline structure on the surface with OER cycling. In virtue of multimodal X-ray probing, a step-by-step transformation mechanism of the amorphization process could be explicitly illuminated. Our X-ray results show that the amorphization is triggered by the lattice oxygen activation and the structural reorganization facilitating coupled cation and anion diffusions is key to the realization of the OER active structure in the final Sr_yIrO_x form which exhibits stronger disorder than conventional amorphous IrO_x , partially explaining its champion OER activity.

1:50 PM EN10.03.03

The Active Sites of *In Situ* Generated CoO_x Catalyst for Electrochemical Water Splitting Maoyu Wang and Zhenxing Feng; Oregon State University, United States

The high-efficiency and low-cost catalysts for oxygen evolution reaction (OER) are critical for electrochemical

water splitting to generate hydrogen as the clean fuel for sustainable energy conversion and storage. The development of those catalysts relies on discovering their active sites and understanding of their catalytical states so that rational design strategies can be applied. Transition metal sulfides are an emerging type of OER catalyst that exhibits superior activity even better than commercial standards such as RuO₂. However, they undergo structural and compositional change during the reaction, which adds difficulties in studying catalytic active sites. Here, we use cobalt sulfide, Co₉S₈, as a representative example. Utilizing multimodal operando characterizations including Raman spectroscopy, X-ray absorption spectroscopy, and X-ray reflectivity, we find that Co₉S₈ ultimately converts to oxide cluster (CoO_x) containing six oxygen coordinated Co as the basic unit which is the true catalytic center to promote high OER activity. The density functional theory (DFT) calculations verify the in-situ generated CoO_x consisting of di-μ-oxo Co-Co motifs in CoO₆ octahedral clusters as the actual active sites. Our results also provide insights to design other transition metal X-ides (X: C, P, N, S, etc.) as efficient electrocatalysts that experience a similar restructuring in OER.

2:05 PM EN10.03.04

Tuning Metal Nanoparticle Exsolution on Perovskite Surface with Strain-Modified Point Defect

Formation Jiayue Wang¹, Jing Yang¹, Alexander K. Opitz^{1,2} and Bilge Yildiz^{1,1}; ¹Massachusetts Institute of Technology, United States; ²Technische Universität Wien, Austria

A central theme in renewable energy technologies today is to design nanostructured catalysts at the solid/gas and solid/liquid interfaces towards desired reactions. A recent advance in materials for electrochemical energy and fuels conversion is to synthesize oxide supported metal nanoparticles in a process termed “exsolution”. Exsolution generates stable and catalytically active metal nanoparticles via phase precipitation out of a host oxide. Unlike traditional nanoparticle infiltration techniques, the nanoparticle catalysts from exsolution are anchored in the parent oxide. This anchored structure makes the exsolved nanoparticles more resistant against particle agglomeration as compared to the infiltrated ones. As a promising technique, exsolution has now been successfully implemented to produce stable supported nanoparticle catalysts in a wide range of applications, including H₂O and CO₂ splitting, three-way catalysts, solid oxide fuel cells, and ceramic membrane reactors.

The current exsolution studies typically report metal nanoparticles of 10s of nm size and separation of 10s-100s of nm. While the obtained improvement in reaction kinetics is already promising, there is *plenty of room at the bottom* to increase the density and dispersion of exsolved nanoparticles to achieve higher catalytic activities. In this work, we propose that point defect formation in the oxide lattice to be the fundamental knob to control exsolution and demonstrate this approach in epitaxial La_{0.6}Sr_{0.4}FeO₃ (LSF) thin films. By quantifying surface defect states with ambient pressure X-ray spectroscopy (APXPS), we identify the initial oxygen vacancy formation and the following Schottky defect formation as the primary defect reactions in exsolution. Then, by tuning the formation energy of these two defects in LSF with biaxial lattice strain, we examined their impacts on metallic iron (Fe⁰) exsolution. Lattice strain tunes the formation energy, and thus, the abundance of these defects, and alters the amount and size of the resulting exsolution particles. As a result, the LSF surface that has more of these point defects, also has the highest Fe⁰ concentration, the largest particle density, as well as the finest particle size. Finally, with the aid of density functional theory (DFT), and Monte Carlo (MC) calculations, we suggest surface oxygen vacancy clusters to be the nucleation sites for the exsolved particles. These observations highlight the critical role of surface point defects in controlling the size and density of the exsolved nanoparticles on the perovskite surfaces.

2:20 PM EN10.03.05

Probing the Initial Stages of Iron Surface Corrosion Using AP-XPS Chathura de Alwis¹, Mikhail Trought¹, Slavomir Nemsak², Ethan J. Crumlin² and Kathryn A. Perrine¹; ¹Michigan Technological University, United States; ²Advanced Light Source, Lawrence Berkeley National Laboratory, United States

Iron-based materials, prevalent in steel infrastructures as well as soils and minerals, participate in chemical reactions in the water cycle. Iron surfaces undergo corrosion, an electrochemical redox process, with oxidation of the iron anode and the cathodic reaction driven by O₂ and water. The surface corrosion occurs in ambient

conditions and in complex environments, where ions are known to catalyze the rate of oxidation. Metallic iron readily transforms in the presence of water and O₂ to form a complex mixture of iron oxides, hydroxides and oxyhydroxides, known as rust. Therefore, to understand the surface processes and changes in oxidation states, decreasing the reaction rate is required to measure factors on the surface oxidation mechanism.

Ambient pressure X-ray photoelectron spectroscopy (AP-XPS) was used to measure surface oxidation of iron. An iron substrate with and without NaCl, was exposed to varying partial pressures of O₂ and H₂O vapor. The O1s, C1s, Fe2p, Na2s, and Cl2p regions were analyzed in comparison to the pristine iron surface. The evolution of oxide species in the O1s and C1s regions were observed with increasing O₂ pressure, which we interpreted as an irreversible formation of carbonates and bicarbonates at the surface. The results were corroborated by the lab-based *ex situ* XPS following the air exposure. Combination of the experiments helped to understand the fundamental steps of oxidation and the role of O₂ for changing surface composition in the corrosion reaction. The ions from NaCl play a significant role in surface oxidation, during the initial stages of surface corrosion, impacting surface chemistry in energy processes, mineral cycling and material degradation.

2:25 PM EN10.03.06

Valence Band Spectra Reveals Phase Transformations of Fe₃O₄(001) During Ambient Pressure

Reduction and Oxidation [Mikhail Trought](#)¹, Slavomir Nemsak², Ethan J. Crumlin² and Kathryn A. Perrine¹;
¹Michigan Technological University, United States; ²Lawrence Berkeley National Laboratory, United States

Iron oxide surfaces play a significant role in catalytic reactions such as water splitting, the Haber process, and in mineral cycling in naturally-occurring environmental processes. These processes rely on the change of the oxidation state of the iron oxide surface by oxidation-reduction reactions. Many of these transformations occur in the high-pressure regime, which makes these reactions difficult to investigate at the atomic level due to extraneous factors affecting the surface at the equilibrium/reactive conditions. However, it is still important to identify the phase transformation of iron oxide materials *in situ* during these processes.

In this study, iron oxide surface transformations are investigated using ambient pressure - X-ray photoelectron spectroscopy (AP-XPS). The Fe₃O₄(001) surface was exposed to reducing and oxidizing conditions by dosing hydrogen and oxygen gases, respectively at various temperatures and pressures. AP-XPS was used to measure changes in the surface electronic structure and oxidation states of the Fe₃O₄(001) surface near ambient pressure conditions in the Fe 2p, O 1s, and valence band regions. The shape of the valence band spectra was used to track changes in the surface electronic structure during the reactions. These studies suggest that Fe₃O₄(001) reduces when annealed in ultra-high vacuum and exposed to H₂ and upon oxidation, Fe₂O₃ is produced. These experiments are compared with α -Fe₂O₃(0001) that reduces to Fe₃O₄ when annealed in ultra-high vacuum. This study gives an important insight to the *in situ* surface redox chemistry and phase transformations of iron oxide surfaces relevant for catalytic and environmental processes.

2:30 PM DISCUSSION/Q&A/SOCIAL

SESSION EN10.04: Interfaces in Electrocatalysts 3 Characterizations

Session Chairs: Zhenxing Feng and Elizabeth Podlaha-Murphy

Sunday Afternoon, April 18, 2021

EN10

4:00 PM *EN10.04.01

Tuning the Catalyst Microenvironment for CO₂ Gas-Diffusion Electrolysis [Xiaofeng Feng](#); University of Central Florida, United States

Electrochemical reduction of CO₂ provides a promising route for sustainable production of fuels and chemicals such as multi-carbon hydrocarbons and oxygenates. While most efforts are focused on developing catalytic

materials for CO₂ electroreduction, it is also critical to understand other factors beyond catalytic materials such as the local environment of the catalysts, which can mediate the transport and local concentration of reaction species and influence reaction pathways. Here we present our recent study of catalyst microenvironment for CO₂ electroreduction in flow cells with gas-diffusion electrodes (GDEs). For proof-of-concept, we use commercial Cu nanoparticles and homogeneously disperse polytetrafluoroethylene (PTFE) nanoparticles in the catalyst layer, which created a hydrophobic microenvironment of the Cu catalysts. The Cu/C/PTFE electrode showed a significant improvement in the activity, Faradaic efficiency, and C₂₊ product selectivity for CO₂ reduction compared to a regular Cu/C electrode without added PTFE. Moreover, the CO₂ reduction activity on the Cu/C/PTFE electrode increased with the CO₂ gas flow rate, suggesting a gas-phase transport of CO₂ inside the catalyst layer. The improved performance is attributed to the reduced diffusion layer thickness that accelerates CO₂ mass transport, increases the local concentration of CO₂ near the catalyst surface, and enhances CO₂ adsorption for the reaction. Compared to regular GDEs, the electrode with added PTFE creates a balanced gas/liquid microenvironment and solid-liquid-gas interfaces inside the catalyst layer, which can enhance the mass transport and kinetics of CO₂ electrolysis, providing a general approach to improve gas-involving electrocatalysis.

4:25 PM *EN10.04.02

Spatially Resolved Analysis of Degradation in Polymer Electrolyte Fuel Cells and Novel Electrode Designs for Improved Efficiency of Polymer Electrolyte Water Electrolysis Severin Vierrath and Matthias Breitwieser; Universität Freiburg, Germany

Fuel cells and electrolysis based on a polymer electrolyte membrane (PEM) are key technologies for a hydrogen society to produce green hydrogen, store large amounts of energy or electrify heavy-duty vehicles. However, durability and efficiency of the membrane electrode assembly is still a major focus of research. This talk gives two examples on investigating ageing phenomena in a fuel cell electrode. The first examines carbon corrosion in the electrode via Focused-Ion-Beam (FIB) tomography, showing that the major mechanism of this degradation phenomenon is loss of active catalyst^[1]. In the second investigation, the polymer degradation in the membrane is studied via Raman, showing that the polymer degradation is favored on the anode side^[2]. The second part of the talk deals with reducing the iridium catalyst loading in the anode of PEM water electrolysis. In the effort of reducing the catalyst, a major problem arises in the in-plane conductivity of the electrode, which leads to poor efficiencies^[3]. Two alternatives are presented, which counter this problem by increasing the electrical conductivity. Employing a nanofiber interlayer enabled an 80% reduction of catalyst material without compromising efficiency or durability^[4]. In the second more simplistic approach, blending the polymeric binder in the electrode with PEDOT:PSS, an electronically conductive polymer, yielded a similar effect^[5].

[1] Hegge, F., Sharman, J., Moroni, R., Thiele, S., Zengerle, R., Breitwieser, M., & Vierrath, S. (2019). Impact of Carbon Support Corrosion on Performance Losses in Polymer Electrolyte Membrane Fuel Cells. *Journal of The Electrochemical Society*, 166(13), F956.

[2] Böhm, T., Moroni, R., Breitwieser, M., Thiele, S., & Vierrath, S. (2019). Spatially resolved quantification of ionomer degradation in fuel cells by confocal Raman microscopy. *Journal of The Electrochemical Society*, 166(7), F3044.

[3] Bernt, M., Siebel, A., & Gasteiger, H. A. (2018). Analysis of voltage losses in PEM water electrolyzers with low platinum group metal loadings. *Journal of the Electrochemical Society*, 165(5), F305.

[4] Hegge, F., Lombeck, F., Cruz Ortiz, E., Bohn, L., von Holst, M., Kroschel, M., ... & Vierrath, S. (2020). Efficient and Stable Low Iridium Loaded Anodes for PEM Water Electrolysis Made Possible by Nanofiber Interlayers. *ACS Applied Energy Materials*.

[5] Ortiz, E. C., Hegge, F., Breitwieser, M., & Vierrath, S. (2020). Improving the performance of proton exchange membrane water electrolyzers with low Ir-loaded anodes by adding PEDOT: PSS as electrically conductive binder. *RSC Advances*, 10(62), 37923-37927.

4:50 PM EN10.04.03

Late News: Variable Temperature Raman Spectroscopic Analysis of the Formation of Harmful Defects in Photoanodes During Synthesis Rodney Smith; University of Waterloo, Canada

Semiconducting photoelectrodes may possess numerous types of structural defects, with each exerting influence over material properties and photoelectrochemical performance. We previously demonstrated that Raman spectroscopy can identify distortions within the crystal lattice of hematite electrodes that were synthesized by the annealing of lepidocrocite. The distortion inhibited photoelectrocatalysis and was tentatively attributed to protohematite, a form of hematite where hydroxyl ligands are trapped within the crystal lattice. Here, the mechanism of hematite formation while annealing lepidocrocite is probed through *in-situ* variable temperature Raman spectroscopy and conventional thermal analysis. Results show a branching pathway, where protohematite forms between 200 and 400 °C in a reaction environment-dependent fashion. Once formed, the protohematite is remarkably persistent and harmful to photoelectrocatalysis. These results demonstrate a powerful method to study solid state phase transitions and provide insight into the formation of a harmful defect in hematite photoanodes that was previously not considered.

5:05 PM EN10.04.04

Modulation of Surface Electronic States in Ferroelectrics for Enhanced Hydrogen Evolution Activity Pedram Abbasi, Tod A. Pascal and David Fenning; University of California, San Diego, United States

Traditionally, catalysts are limited by adsorbate-surface interactions that lead to a “volcano” behavior of activity as a function of binding energy, qualitatively described by the Sabatier principle. Thus one of the grand challenges in modern catalysis is the rational design of systems that can surpass this optimum. Ferroelectric perovskites are an interesting class of nanomaterials since they can present two distinct chemical surfaces depending on the polarization direction. This dual presentation potentially frees catalyst design from the constraints of a simple Sabatier framework, where on any single catalytic surface the adsorbates involved in the reaction must bind neither too weakly nor too strongly. Here we demonstrate a polarization-dependent electrochemical performance of ferroelectric BaTiO₃ (BTO) thin films for the hydrogen evolution reaction (HER).

A combination of detailed surface sensitive, core-level spectroscopy and first-principles computation are used to gain insight into the catalytic effects of a change in the polarization state of the BTO. The model BTO catalyst is grown by molecular beam epitaxy and exhibits an excellent ferroelectric response in Piezo-force microscopy (PFM) and polarization-filed (P-E) hysteresis measurements. We use electrochemical poling to control the polarization direction of the single-crystal thin film, enabling sensitive measurements of the catalytic surface in both up and down polarization states. Angle-resolved X-ray photoelectron spectroscopy and Ultra-violet Photoelectron spectroscopy reveal a lower work function and high valence band density of states at the surface of BTO when poled up.

These measurements are complemented by density functional theory (DFT) calculations, employed to gain insights into the localized density of states in BTO slabs, as well as the effect of polarization switching on the HER reaction barriers. Our calculations demonstrate that upward polarized samples have a higher density of electrons near the solid-electrolyte interface and predict a lower barrier for proton adsorption as the rate-limiting step for HER reaction. Experimentally, we observe a higher exchange current density on the upward polarized BTO, consistent with the first-principles result.

By leveraging model single-crystal thin film catalysts in experiments with well-defined polarization, we gain insights into the effects of ferroelectric polarization at the catalytic surface, paving the way for further development of ferroelectric-enhanced electrocatalysis.

5:20 PM DISCUSSION/Q&A/SOCIAL

6:30 PM *EN10.05.01

Transformation, Reaction and Organization at Functional Interfaces for Sustainable Energy Systems Using Microreactor-Assisted Nanomaterial Deposition Process Chih-Hung Chang; Oregon State University, United States

Microreactor-Assisted Nanomaterial Deposition (MAND) process combines the merits of microreaction technology and chemical synthesis of nanomaterials. This technique uses continuous flow microreactors for the synthesis, assembly, and deposition of nanomaterials. In synthesis, microreactor technology offers large surface-area-to-volume ratios within microchannel structures to accelerate heat and mass transport. This accelerated transport allows for rapid changes in reaction temperatures and concentrations, leading to more uniform heating and mixing in the deposition process. The possibility of synthesizing nanomaterials in the required volumes at the point-of-application eliminates the need to store and transport potentially hazardous materials while providing new opportunities for tailoring novel nanostructures. MAND processes control the heat transfer, mass transfer, and reaction kinetics using well-defined microstructures of the active unit reactor cell that can be replicated to produce higher chemical production volumes. This critical feature opens a promising avenue in developing scalable nanomanufacturing. Furthermore, the continuous flow microreactor opens up the opportunity to conveniently assemble unique nanostructures and nanostructured thin films. There are many innovative solution-based routes towards syntheses of nanomaterials. The majority of these syntheses, however, were carried out using small-batch reactors. Results-to-date demonstrates the possibility to control the reacting flux, including small intermediate-reaction molecules, nanoclusters, nanoparticles, and structured assembly of nanomaterials.

I will discuss recent progress in using continuous microreactors to control the chemical transformation, reaction, and organization of functional nanomaterials and the applications of these functional nanomaterials for sustainable energy systems (e.g., solar photovoltaics). There is a significant opportunity to improve all solar PVs to maximize annual energy yield and increase service lifetime by engineering the interface. First, a portion of the light is reflected when light encounters an abrupt change in the refractive index. Thus, it is essential to reduce reflection for improving efficiency. Besides, the accumulated mass (i.e., soils, dust, pollutants, and air particles) on a cover can significantly reduce the power output of a solar PV module ranges from 1% to as much as 70% in some areas without cleaning. One way to mitigate the soiling effect is to regularly clean the solar arrays, which increase the LCOE and requires water. We have investigated the use of MAND to control the interfaces on installed solar modules in the field to mitigate these issues.

6:55 PM EN10.05.02

Durable and Washable Paper-Based Electronics for Wearable Applications Su Yang, Xiaoming Tao, Su Liu and Xujiao Ding; Hong Kong Polytechnic University, China

Nowadays wearable electronics are playing a more and more important part in daily life. Therein, paper-based electronics stand out by virtue of various advantages like low-cost, lightweight, and high flexibility. Nevertheless, it is still challenging to achieve long-term use of paper-based electronics due to their poor electromechanical durability and washability. This work adopts a novel high-performance polyimide paper as substrate and compact parylene encapsulation as a protective and reinforced layer, simultaneously enhancing electromechanical durability and machine-washability for the first time. The result shows parylene-encapsulated PI paper-based electronics show greatly electromechanical performance, abrasion resistance, bending durability, and outstanding machine washability. Moreover, such paper-based electronics demonstrates outstanding stability over different harsh environments. With 1D circuit board assemblies design and fabrication, the resultant electronic yarns are easily integrated into fabrics for wide wearable applications. Such water-resistant

paper-based electronics show great feasibility for wearable applications other than dry disposable electronics.

7:10 PM EN10.05.03

Development of Polymer Nano-Composite Based Aerogels via Supercritical Drying Ying Mu, Xiaoli Li and Marilyn L. Minus; Northeastern University, United States

Since the development of aerogels in the 1930s, they have attracted much attention due to their unique porous structure and lightweight properties. Such structures are useful for many applications including thermal and sound insulation, energy storage, waste-water treatment, and flame retardant materials. To date, silica-based aerogels have dominated the industry and research interests, although, while limited, some polymeric-based materials exist. More recently, polymer-based aerogels have drawn much attention, but to date have primarily been processed via freeze drying methods. While this method is more tunable for polymer-based aerogels, the resultant morphology and properties are inferior to aerogels processed using supercritical drying (SCD). In this work, SCD process optimization and process-structure-property studies on polymer nano-composite based aerogels will be presented. The mechanisms of solvent exchange and diffusion during gel and aerogel processing will also be investigated and discussed. Boron nitride nanotubes (BNNTs) have been chosen as a filler candidate for these composite aerogels due to their lightweight, oxidative, structural, and radiation shielding properties. Current work has shown that the composite precursor gels exhibit enhanced mechanical and thermal performance. To this end, a fundamental study regarding these materials will be presented and include multi-scale characterization results and analyses.

7:25 PM EN10.05.04

Ultrasensitive Electrochemical Sensors Based on van der Waals Materials Fujia Zhao, Shan Zhou and Yingjie Zhang; University of Illinois at Urbana-Champaign, United States

Dissolved oxygen (DO) and hydrogen peroxide are important indicators of water quality. Hydrogen peroxide is also widely used in water and pollutant treatment as an excellent oxidizer. Thus, an aqueous oxygen and hydrogen sensor with high sensitivity, rapid response and good selectivity is in high demand. However, previously reported sensors, which are mainly based on enzymes, noble metals or metal oxides, have drawbacks of either high cost or weak response. Here, we introduce a novel electrochemical sensor based on van der Waals materials. Our sensors exhibit ultrahigh sensitivity and low detection limit for oxygen and hydrogen peroxide detection, outperforming typical noble metal-based electrochemical sensors. Through electrochemical kinetic analysis and simulations, we quantify the reaction kinetics and find that the high performance can be attributed to the facile charge transfer at the electrode-aqueous solution interface.

7:40 PM EN10.05.05

Conceptualization, Proof-of-Concept and Material Challenges of the Brayton Electrochemical Refrigeration Cycle Aravindh Rajan; Georgia Institute of Technology, United States

One path towards mitigating the global warming consequences of the rising global cooling demand is the search for alternative refrigeration technologies. We have identified one such technology that has electrochemical origins and remains to be experimentally demonstrated. The entropy of carefully chosen cathodic and anodic reactions may be utilized to induce refrigeration by employing them in either Brayton or Stirling type cycles. In this work, the concept of the Brayton Electrochemical Refrigeration (BECR) cycle will be first introduced. This will include an overview of the working of the system, the governing material properties and operating parameters, and predictions of its performance. Then, the development and results of the experimental proof-of-concept of the BECR cycle will be discussed. Finally, the material level challenges to a commercial product will be discussed. Arguments will be made as to why the commonly leveraged solvation entropy is not a promising pathway to commercialize the BECR cycle and thermally regenerative electrochemical systems in general. A less explored alternative mechanism of entropy change is proposed.

7:55 PM EN10.05.07

Realization of Entire Substrate Area Selective Emitters via Thin Film Interference Minsu Oh, Emily Carlson and Thomas Vandervelde; Tufts University, United States

Selective thermal emitters have attracted researchers due to their utility in applications such as gas sensing or thermophotovoltaic (TPV) energy harvesting. Depending on the application, the desired emission spectrum of an emitter can vary. For example, in TPV applications, a broadband emitter can increase the output power density of the diode at the cost of lower energy conversion efficiency due to excess energy in higher energy photons being lost to thermalization of the carriers. Meanwhile, a narrowband emitter can improve the conversion efficiency via reduced thermalization of the diode, resulting in lowered output power density. A narrowband selective emitter designed with its absorption energy spectrum placed just above the bandgap could also be paired with a TPV diode for cases where the diode heating needs to be minimized. For this reason, a balance between the output power density and conversion efficiency is needed for the optimal performance of a TPV system. As such, one of the approaches to optimizing a TPV system's performance is utilizing a selective emitter with multiple narrowbands and stacking of a number of TPV diodes whose bandgaps correspond to the different peak emission wavelengths of the emitter. Photonic crystals (PhCs)/metamaterials (MMs) have been used to create selective emitters with different peak emission wavelengths and bandwidths. However, most PhC/MM emitters are limited to a single band emission spectrum, and only a few MMs have been reported with a multiband emission spectrum. Moreover, PhC/MM emitters that work at shorter wavelengths such as the visible or near-/mid-infrared are based on nanometer scale feature sizes where it is challenging to write the pattern over a large area and fabrication imperfections can lead to lowered performances. The thermal stability of a nano-patterned emitter could also decrease at high temperatures. In this work, we report multiband selective emitters that are built with a planar, thin layer of a dielectric material deposited on top of a metallic layer. The multiple emission bands of these emitters directly result from the interference fringes in reflectance, as the transmittance of the structure is zero over the wavelength spectrum studied. The peak emission wavelengths of these emitters can be tuned by varying the thickness of the dielectric layer due to the dependence of reflectance on the film's thickness. Compared to PhC/MM emitters, the thin-film emitters reported here do not need nano/micro patterning, which makes the fabrication process longer and more complicated, and can be fabricated over the entire area of the substrate with ease. Therefore, we believe that our work can provide a path forward for optimizing thermal applications such as TPV energy harvesting via selective emitters with a large working area, fabrication ease, and multiple emission bands.

8:00 PM DISCUSSION/Q&A/SOCIAL

SESSION EN10.06: Interfaces in Electrocatalysts 1 Materials

Session Chairs: Zhenxing Feng and Hua Zhou

Sunday Afternoon, April 18, 2021

EN10

9:00 PM *EN10.06.01

Entropy-Maximized Materials for Electrocatalysis Applications Sheng Dai^{1,2}; ¹Oak Ridge National Laboratory, United States; ²The University of Tennessee, United States

Until recently the design and synthesis of heterogeneous catalysts have been dominated through enthalpic factors (e.g., charge-charge interactions, charge-transfer interactions). With emergence of high entropy materials (HEMs), another avenue to design and synthesize catalytic materials has opened up. The definition of HEMs is any material that consists of the solid solution of more than five components that allow great flexibility in tuning surface compositions and interfacial functionalities. Here we present the synthesis of high entropy electrocatalysts that potentially outperform the traditional catalysts in energy-related catalysis reactions. The synthesis strategies through entropy maximization will be discussed.

9:25 PM *EN10.06.02

Chemical Design of Colloidal Copper-Based Nanorod Electrocatalyst Xingchen Ye and Soojin Jeong; Indiana University Bloomington, United States

In this talk, I will discuss our recent progress on the development of heterometallic seed-mediated synthesis for monodisperse penta-twinned Cu nanorods using Au nanocrystals as seeds. The nanorod aspect ratio can be readily adjusted from 2.8 to 13.1 by varying the molar ratio between Au seeds and Cu precursor, resulting in narrow longitudinal plasmon resonances tunable from 762 to 2201 nm. The growth pathway features coevolving shape and composition whereby nanocrystals become progressively enriched with Cu concomitant with nanorod growth. The nanorods possess active surface sites for the high-rate electrochemical reduction of carbon dioxide into liquid fuels.

9:50 PM EN10.06.03

Transition Metal Sulfide-Based Electrocatalysts for Water Oxidation Reaction Brian Muhich and Zhenxing Feng; Oregon State University, United States

Water splitting reactions represent a promising future avenue for clean energy storage and fuels, and the development of inexpensive and commercially friendly electrocatalysts is essential for the widespread utilization of such processes. Oxygen evolution reaction (OER), also known as water oxidation reaction, is a key component of the overall water splitting reaction, and currently, the most effective catalysts for OER are RuO₂ and IrO₂. Due to the scarcity of noble metals like Ru and Ir, effective catalysts composed of more abundant transition metals are desired. Among these transition metal catalysts, (Ni, Co)S materials have shown significant promise as effective OER catalysts. In this project, we explore the enhanced OER activity through the use of (Ni, Co)S catalysts and also explore different means by which to optimize these catalysts through different NiCo compositions. Through the use of electrochemical tests, we have observed favorable reaction kinetics at higher concentrations of Co and lower overpotentials at higher concentrations of Ni, with good stability overall. We attribute these characteristics to the *in-situ* development of NiOOH active sites and the higher conductivity of Co. This work provides insights in the development of efficient and noble metal free OER electrocatalysts based on the optimization of transition metal compositions, and future physical characterization can advance our understanding of a catalyzed water splitting mechanism and the development of chemically stable electrocatalysts.

9:55 PM EN10.06.04

CeO₂-TiO₂ Nanoparticle—Nanorod Heterojunction for Efficient Photoelectrochemical Water Splitting Sutapa Dey and Somnath C. Roy; Indian Institute of Technology Madras, India

Limited fossil fuel reserves and green house emissions have driven intense research activities over the past few decades on the development of clean and renewable energy sources. Hydrogen is one such source with a high gravimetric energy density and the combustion of which does not generate carbon contained products. However, hydrogen needs to be generated from sources such as water or hydrocarbons, and such processes become viable only when input energy is supplied through renewable sources. Photoelectrochemical (PEC) water splitting is such a suitable pathway to generate hydrogen from water using solar energy. In this process, a semiconductor based material generates electron-hole pair by harvesting solar energy, which paves the way to produce hydrogen mediated by chemical reactions through decomposition of water. However, in spite of about 50 years since its discovery by Fujishima and Honda, PEC water splitting remains a challenging task because of a lack of suitable material. In general, metal oxide such as Titanium dioxide (TiO₂) acts as an excellent photocatalyst material¹, but suffers from limited light absorption window (in ultra violet region which is only 5% of full solar spectrum) and relatively higher recombination of the photogenerated charges. In this regard, CeO₂, a rare earth metal oxide with a more negative conduction band position and lower band gap is one of the most efficient companion of TiO₂ leading to suitable band alignment in a CeO₂-TiO₂ heterojunction². Moreover, CeO₂ shows visible light sensitivity and good electron transfer ability mediated by its variable Ce valences such

as Ce^{3+} and Ce^{4+} , high capacity for oxygen storage, capture and release and high thermal stability³. Here we demonstrate that by using TiO_2 nanorods functionalized with CeO_2 nanoparticles, photocurrent density enhances 3 times over that obtained from the bare TiO_2 nanorods. The TiO_2 nanorods are fabricated on FTO coated glass substrates by hydrothermal technique. The size and distribution of the CeO_2 nanoparticles grown over these nanorods can be precisely controlled by optimizing the deposition/growth parameters and at an optimum condition, an effective heterojunction forms enabling easy transfer of photogenerated charges. This is also confirmed by Electrochemical Impedance Spectroscopy (EIS), where lowest charge transfer resistance is observed for CeO_2 - TiO_2 heterojunction photoanodes. Further, Applied Bias Photo-to-current Efficiency (ABPE %) shows a 2.52 times enhancement for the heterojunctions compared to that of bare TiO_2 nanorods. In addition to expected effect of heterojunction in assisting charge separation, visible light absorption by CeO_2 (marked by a 50 nm red-shift in the absorption spectra) also helps in achieving better performance in the PEC operation. We conclude that such heterojunctions made with all oxide components (CeO_2 and TiO_2) may serve better for PEC applications by virtue of their chemical stability under aqueous media. The results of this work with extensive details will be presented.

References

1. Li, C. *et al. J. Am. Chem. Soc.* 137, 1520–1529 (2015). 2. Zhou, Q. *et al. Electrochim. Acta* 209, 379–388 (2016). 3. Montini, T., Melchionna, M., Monai, M. & Fornasiero, P *Chem. Rev.* 116, 5987–6041 (2016).

10:00 PM DISCUSSION/Q&A/SOCIAL

10:25 PM EN10.06.06

D-Band Contraction of Metal Nitride Nanosheets for Highly Efficient and Stable Electrochemical Oxidation of Ammonia Shi He, Yufeng Cheng, Mengdi Wang, Peter Novello, Siyuan Zhu and Jie Liu; Duke University, United States

Ammonia is a promising hydrogen carrier as it reduces the cost of long-range transportation of hydrogen. Ammonia electrolysis provides a convenient method to extract hydrogen from ammonia at end users. However, the conventional platinum carbon electrode suffers from fast degradation and electrode fouling at electrode-electrolyte interface during the ammonia electrochemical oxidation (AOR). Here, we report that nitriding electrochemical deposited nickel cobalt layered double hydroxide nanosheets can achieve high electrocatalytic activity for AOR in non-aqueous solution. The AOR onset overpotential of NiCo_2N nanosheets is 0.55 V which is about 0.25 V lower than that of the platinum carbon electrode. Ultraviolet-visible and Mass spectroscopy studies reveal NiCo_2N nanosheets can suppress the formation of metal amine complex and preferentially oxidize ammonia to N_2 with a faradic efficiency of over 90 percent. DFT calculation indicates that the downshift of the metal d-band center on NiCo_2N nanosheets surface accelerated the generation of NH_x^+ cations and desorption of final N_2^* , boosting ammonia electrochemical oxidation toward N_2 . Overall, this work introduces a practical strategy for synthesizing an active and stable electrocatalyst for AOR.

SYMPOSIUM NM01

Superconductors as Quantum Materials
April 18 - April 18, 2021

Symposium Organizers

Badih Assaf, University of Notre Dame
Liangzi Deng, University of Houston
Danfeng Li, City University of Hong Kong
Peng Wei, University of California, Riverside

Symposium Support
Bronze
Lake Shore Cryotronics
Oxford Instruments America, Inc.

* Invited Paper

SESSION NM01.01: Cuprates, Oxides, Heavy Fermions
Session Chairs: Danfeng Li and Ming Yi
Sunday Morning, April 18, 2021
NM01

8:00 AM *NM01.01.01

A p-type Transparent Conducting Oxide with 2D Superconductivity Akira Ohtomo and Takuto Soma; Tokyo Institute of Technology, Japan

We report on epitaxial synthesis, excellent p-type transparent conductivity, and two-dimensional superconductivity of the layered lithium niobate [1]. The superconducting films were prepared through the following three steps. Amorphous films of the stoichiometric LiNbO_2 were first deposited on (111) spinel substrates, and then heated to high temperatures for obtaining highly crystalline epitaxial films. A fraction of Li ions were removed from the films by immersing in an iodine solution so that the equivalent amount of hole carriers were introduced. The obtained films showed superconductivity below 4.2 K, and averaged transmittance to the visible light of 77% despite large number of hole carriers. Moreover, we found that the normal-state conductivity and the transmittance simultaneously increased with increasing hole carriers. This behaviour is unusual because higher conductivity usually leads to larger free-carrier absorption. We explained it in terms of strongly correlated electrons at the largely isolated Nb $4d_{z^2}$ band. The two-dimensional superconductivity in $\text{Li}_{1-x}\text{NbO}_2$ will be briefly discussed in terms of the observed BKT transition and the electronic phase diagram that was established by electrochemical doping experiments [2].

[1] T. Soma, K. Yoshimatsu, A. Ohtomo, *Sci. Adv.*, **6**, eabb8570 (2020).

[2] K. Yoshimatsu, M. Niwa, H. Mashiko, T. Oshima, A. Ohtomo, *Sci. Rep.*, **5**, 16325 (2015).

8:25 AM *NM01.01.02

High Temperature Superconductivity in Monolayer Cuprates Yuanbo Zhang; Fudan University, China

The two-dimensional CuO_2 plane plays a fundamental role in the physics of cuprates. Indeed, cuprates (and all other families of high temperature superconductors) adopt a layered atomic structure. In BSCCO, the weak van der Waals interaction between adjacent bismuth-oxygen layers makes the crystal easily cleavable, making atomically-thin BSCCO an ideal system for investigating high temperature superconductivity in the two-dimensional limit. By fabricating samples in an inert atmosphere, we are able to obtain half-unit-cell-thick single crystals (referred to as monolayer) of BSCCO samples and to probe the evolution of superconductivity as the dimensionality is reduced. We probe the electronic structure of monolayer $\text{Bi}_2\text{Sr}_2\text{CaCu}_2\text{O}_{8+\delta}$ (Bi2212) and $\text{Bi}_2\text{Sr}_2\text{CuO}_{6+\delta}$ (Bi2201) with electronic transport measurements, as well as scanning tunneling microscopy (STM) and scanning tunneling spectroscopy (STS) techniques.

8:50 AM *NM01.01.03

Local Moment Pairing in the Heavy-Fermion Superconductor CeCoIn_5 Laura Greene; Florida State University, United States

The heavy-fermion superconductor CeCoIn_5 has a pairing symmetry of $d_{x^2-y^2}$ but the pairing mechanism

remains unknown. Our planer tunneling spectroscopy measurements on single crystals into the three major crystallographic orientations as a function of temperature down to 20 mK and fields up to 18 T are reproducible, and our diagnostics show transport across the barrier is predominately single-step elastic tunneling. [1] At low temperatures, on the (100) and (001) faces, we find sharp coherence peaks with an estimated gap of 0.65 meV, and on the (110) face, a broad zero-bias peak. Previously published STM work reports observing pair potentials above $T_c = 2.3$ K [2]; we also find pre-formed pairs up to $T_p \sim 5$ K. Below T_p , with increasing applied field, the pairing gap evolves smoothly to a field-induced gap, that grows linearly up to 18 T, the highest field measured. At higher temperatures, no field-induced gap is observed, showing that pairing and the field-induced gap exist concomitantly. Kondo scattering plays a role in the pairing mechanism, and omposite pairing remains a possible explanation. [3]

[1] K. Shrestha, S. Zhang, L.H. Greene, J.D. Thompson, Y. Lai, R.E. Baumbach, K. Sasmal, M. B. Maple, and W.K. Park, "Spectroscopic Evidence for the Direct Involvement of Local Moments in the Pairing Process of the Heavy-Fermion Superconductor CeCoIn₅" Submitted.

[2] Ernst et al Phys. Stat, Sol B (2010); Fasano et al Physical B (2018).

[3] Flint and Coleman PRL (2010); Flint, Dzero, Coleman NatPhys (2008)

This work was supported by NSF/DMR-1704712 (FSU), NSF/DMR-1157490 (FSU) NSF/DMR-1644779 and the State of Florida (NHMFL), DOE, Office of BES, and Division of MSE (LANL), and NSF/DMR-1810310 (UCSD).

9:15 AM NM01.01.04

Cavity Probes and Control of Antiferromagnetic Fluctuations in a Mott Insulator Jonathan Curtis¹, Andrey Grankin², Nicholas Poniatowski¹, Prineha Narang¹, Victor Galitski² and Eugene Demler¹; ¹Harvard University, United States; ²University of Maryland, United States

Using THz electromagnetic cavities to probe and control correlated phases of matter has recently seen a surge in activity, in large part due to remarkable advances in experimental techniques. Some of the most interesting compounds from this point of view are the cuprate high-temperature superconductors and their Mott-insulating parent compounds, which often exhibit long-range antiferromagnetic order. In this work, we present a mechanism by which the electromagnetic field of such a THz cavity can be coherently coupled to the quantum fluctuations of this antiferromagnetic order in a simplified model of an undoped cuprate. In addition to the direct magnetic-dipole interaction between the electromagnetic field and the local moments, we also consider a more elaborate coupling which exploits spin-orbit effects to produce coupling between the antisymmetric spin-exchange interaction and the electric field. Within linear spin-wave theory, we show how these terms can lead to the formation of Neel magnon-polariton resonances, as well as allow for optical parametric driving of spin-waves in the insulating phase. We identify clear experimental signatures to look for and argue these are within experimental reach. Finally, we conclude by speculating on what happens once the system is hole-doped with charge carriers, in light of our outlined coupling scheme.

J.B.C. acknowledges support from the Harvard Quantum Initiative (HQI).

9:30 AM NM01.01.05

Ultra-High Critical Current Density at the Quantum Critical Point of YBa₂Cu₃O_{7-d} Superconducting Thin Films Teresa Puig¹, Alex Stangl¹, Anna Palau¹, Guy Deutscher² and Xavier Obradors¹; ¹Institut de Ciència de Materials de Barcelona-CSIC, Spain; ²Tel Aviv University, Israel

Doping is one of the most relevant paths to tune the functionality of cuprates, it determines carrier density and the overall physical properties of these impressive superconducting materials. We present an oxygen doping study of YBa₂Cu₃O_{7-d} (YBCO) thin films from underdoped to overdoped state, correlating the measured charge carrier density, n_H , the hole doping, p , and the critical current density, j_c . Our results show a continuous increase

of j_c with charge carrier density, reaching 90 MA/cm² at 5 K for p-doping at the Quantum Critical Point (QCP), linked to an increase of the superconducting condensation energy. The ultra-high j_c achieved corresponds to a third of the depairing current, i.e. a value 60% higher than ever reported in YBCO films. The overdoped regime is characterized by a sudden increase of n_H , associated to the reconstruction of the Fermi-surface at the QCP. Pulsed laser and chemical solution deposited films have been studied. Overdoping YBCO, therefore, opens a promising route to extend the current carrying capabilities of REBCO coated conductors for applications.

9:45 AM NM01.01.06

Late News: Electrochemically-Induced Insulator-Metal Transition in Ionic-Liquid-Gated NiS₂ Single Crystals Sajna Hameed, Bryan Voigt, William Moore, John Dewey, Bhaskar Das, Bing Luo, Nicholas Seaton, Chris Leighton and Martin Greven; University of Minnesota Twin Cities, United States

Motivated by the existence of superconductivity in pyrite CuS₂ [1], we explore the possibility of ionic-liquid-gating-induced superconductivity in the related antiferromagnetic Mott insulator pyrite NiS₂. A clear gating-induced insulator-metal transition is observed, with progressively decreasing low temperature sheet resistance with increasing positive gate bias. We deduce an electrochemical gating mechanism through formation of S vacancies, however, which is entirely non-volatile and irreversible. This is in striking contrast to the completely reversible, volatile electrolyte-gating-induced insulator-metal transition in pyrite FeS₂ [2]. We attribute the difference in behaviors to the much larger S diffusion coefficient in NiS₂ compared to FeS₂ [3,4], analogous to the situation in electrolyte-gated oxides [5].

[1] H. S. Jarrett et al, Phys. Rev. Lett., **21**, 617 (1968)

[2] J. Walter, B. Voigt, E. Day-Roberts, K. Heltemes, R. M. Fernandes, T. Birol, and C. Leighton, Sci. Adv. **6**, eabb7721 (2020)

[3] C. Clark and F. Friedemann, J. Mag. Mag. Mat. **400**, 56 (2016)

[4] E. B. Watson, D. J. Cherniak, and E. A. Frank, Geochim. Cosmochim. Acta, **73**, 4792 (2009)

[5] H. Wang, J. Walter, K. Ganguly, B. Yu, G. Yu, Z. Zhang, H. Zhou, H. Fu, M. Greven and C. Leighton, Phys. Rev. Mater. **3**, 075001 (2019)

Funding: This work was supported primarily by the National Science Foundation through the University of Minnesota MRSEC under Award Number DMR-2011401.

SESSION NM01.02: Superconductivity Under High Pressure and Fe-based Superconductors

Session Chairs: Liangzi Deng and Danfeng Li

Sunday Morning, April 18, 2021

NM01

10:30 AM *NM01.02.01

Higher T_cs Beyond That Predicted by the Universal T_c-Dopant Relation Paul C. W. Chu^{1,2}, Liangzi Deng¹, Yongping Zheng³, Zheng Wu¹, Shuyuan Huyan¹, Hung-Cheng Wu¹, Yifan Nie³ and Kyeongjae Cho³;

¹University of Houston, United States; ²Lawrence Berkeley National Laboratory, United States; ³The University of Texas at Dallas, United States

Achieving higher transition temperature (T_c) is a primary goal in superconductivity research. T_c and doping have been found to have a dome-like universal relation where the peak position is the maximum T_c (T_{c-max}), which is consistent with previous experimental results in the lower pressure range. By using our newly developed ultra-sensitive magnetization measurement technique under high pressure, we have discovered a universal resurgence of T_c passing the peak predicted by the general T_c-p (doping) or -P (pressure) relation for the BSCCO cuprate high temperature superconductors and have attributed the resurgence to a pressure-induced

electronic transition, which is supported qualitatively by our density functional theory calculations. This offers a new path to raise the T_c of the layered cuprate high temperature superconductors to a new height.

We have investigated the bulk superconducting state *via* dc magnetization measurements by deploying our newly developed HP-DAC/MPMS technique. We discovered a common resurgence of the T_c s of the monolayer $\text{Bi}_2\text{Sr}_2\text{CuO}_{6+\delta}$ (Bi2201) and the bilayer $\text{Bi}_2\text{Sr}_2\text{CaCu}_2\text{O}_{8+\delta}$ (Bi2212) to beyond the respective $T_{c\text{-max}}$ s predicted by the universal relation between T_c and p or P at higher pressures. The T_c of underdoped Bi2201 initially increases from 9.6 K at ambient to a peak at ~ 23 K at ~ 26 GPa and then drops as expected based on the universal T_c - P relation. However, at pressures above ~ 40 GPa, T_c rises rapidly without any sign of saturation up to ~ 30 K at ~ 51 GPa. Similarly, the T_c for the slightly overdoped Bi2212 increases after passing a broad valley at 20-36 GPa and reaches ~ 90 K without any sign of saturation at ~ 56 GPa. We have therefore attributed this T_c -resurgence to a possible pressure-induced electronic transition in the cuprate compounds due to a charge transfer between the Cu $3d_{x^2-y^2}$ and the O $2p$ bands projected from a hybrid bonding state, leading to an increase in the density of states at the Fermi level, in agreement with our density functional theory calculations. Similar T_c - P behavior has also been reported previously in the trilayer $\text{Bi}_2\text{Sr}_2\text{Ca}_2\text{Cu}_3\text{O}_{10+\delta}$ (Bi2223). These observations suggest that higher T_c s than those previously reported for the layered cuprate high temperature superconductors can be achieved by breaking away from the universal T_c - P relation through possible electronic transitions induced by the application of higher pressures.

The work at Houston is supported in part by US Air Force Office of Scientific Research Grants FA9550-15-1-0236 and FA9550-20-1-0068, the T. L. L. Temple Foundation, the John J. and Rebecca Moores Endowment, and the State of Texas through the Texas Center for Superconductivity at the University of Houston.

10:55 AM *NM01.02.02

Hot Superconducting Superhydrides Russell Hemley; University of Illinois at Chicago, United States

Realizing superconductivity in the vicinity of room temperature in hydrogen-rich materials under pressure is a topic of great current interest. Specifically, high-pressure experiments motivated by density-functional theory and conventional electron-phonon coupling models have uncovered new classes of hydrogen-rich metal hydrides, or superhydrides, with superconducting critical temperatures (T_c) in the vicinity of room-temperature at megabar pressures (i.e., >100 GPa). Original calculations for the rare-earth hydrides predicted that LaH10 and YH10 would form dense hydride clathrate structures exhibiting T_c 's of 257-326 K at pressures of 200-300 GPa.^{1,2} X-ray diffraction experiments on the La-H system confirmed the formation and stability of the LaH10 structure near the predicted pressures,³ and subsequent electrical conductivity and critical current measurements confirmed the very high-temperature superconductivity of the phase.^{4,5} Experiments that used ammonia borane (NH_3BH_3) as the hydrogen source indicated T_c 's beginning at 260 K, including conductivity onsets as high as 290 K that have been confirmed in more recent work.⁶ It was proposed that the high and variable T_c arises from incorporation of N and/or B in the structure from the ammonia borane starting material.^{5,6} Moreover, in experiments that confirmed the structure⁷ and high-temperature superconductivity^{5,6} of LaH10, Drozdov et al.⁸ reported a slightly lower maximum T_c of 250 K in experiments conducted without ammonia borane. Using methods developed previously and applied to H3S, B and N doping of the La-based superhydride increases the T_c of the material to room temperature. These techniques were also used to examine the doping of C on the superconductivity of H3S. As found for the La-based superconductor, low-level substitution of C for S can fine-tune the Fermi energy to match the peak in the electronic density-of-states peak, thereby maximizing the electron-phonon coupling and boosting the critical temperature from the original 203 K to 289 K at 260 GPa for 4% doping of C for S in H3S.⁹ The results provide an explanation for the recent experimental observation of room-temperature superconductivity in a highly compressed C-S-H mixture.¹⁰ The above findings open new avenues for creating 'hot' hydrogen-rich superconductors with T_c 's above room temperature.

* Work done in collaboration with M. Ahart, R. Kumar, M. Somayazulu, H. Liu, N. Salke, I. I. Naumov, R. Hoffmann, N. W. Ashcroft, Y. Meng, M. Baldini, Z. M. Geballe, S. W. Tozer, A. D. Grockowiak, E. Zurek, F. Zhang, Y. Ge, R. Dias, Y. Yao, and H. Wang. This research was supported by NSF (DMR-1933622) and DOE (DE-SC0020340 and DE-NA0003975).

- 1 H. Liu et al., Proc. Natl. Acad. Sci. 114, 6990 (2017).
- 2 F. Peng et al., Phys. Rev. Lett. 119, 107001 (2017).
- 3 Z. M. Geballe et al., Angew. Chem. Inter. Ed. 57, 688 (2018).
- 4 M. Somayazulu et al., Phys. Rev. Lett. 122, 027001 (2019).
- 5 R. J. Hemley, M. Ahart, H. Liu, & M. Somayazulu, Road to Room Temperature Superconductivity (Areces, Madrid, Spain, 2018) p. 199.
- 6 A. D. Grockowiak et al., arXiv: 2006.03004.
- 7 H. Liu et al., Phys. Rev. B. 98, 100102 (2018).
- 8 A. P. Drozdov et al., Nature 569, 528 (2019).
- 9 Y. Ge, F. Zhang, R. Dias, R. J. Hemley & Y. Yao, arXiv: 2011.12891.
- 10 E. Snider et al., Nature 586, 373 (2020).

11:20 AM *NM01.02.03

Topological States and Transport Properties in Iron Chalcogenide Superconductors Qiang Li^{1,2}; ¹Stony Brook University, The State University of New York, United States; ²Brookhaven National Laboratory, United States

Superconducting iron chalcogenides $\text{FeSe}_x\text{Te}_{1-x}$ (FST) have attracted a great deal of interest in both fundamental physics and potential applications. While very high upper critical fields make FST an excellent candidate for high-field magnets and energy applications, Majorana zero-modes identified in FST superconductors hold promise for topological quantum computing. In this talk, we discuss multiple topological states and possible broken time reversal symmetry in FST, and their impacts to charge transport, which we studied in both FST single crystals and thin films having a broad range of superconducting transition temperature driven by strain or gating.

11:45 AM *NM01.02.04

Low Temperature Emergence of an Orbital-Selective Mott Phase in $\text{FeTe}_{1-x}\text{Se}_x$ Ming Yi; Rice University, United States

Electronic correlation is of fundamental importance to high temperature superconductivity. Iron-based superconductors are believed to possess moderate correlation strength, which combined with their multi-orbital nature makes them a fascinating platform for the emergence of exotic phenomena. Previously, it has been reported that iron-chalcogenide superconductors exhibit strong orbital-dependent correlation effects and that by raising temperature they crossover into an orbital-selective Mott phase. Here, we report spectroscopic evidence of the reorganization of the Fermi surface from FeSe to FeTe as Se is substituted by Te. This evolution is observed to be accompanied by a redistribution of the orbital-dependent spectral weight near the Fermi level together with a divergent behavior of a band renormalization in the d_{xy} orbital. All of our observations are further supported by our theoretical calculations to be salient spectroscopic signatures of such a non-thermal evolution from a strongly correlated metallic phase towards an orbital-selective Mott phase in $\text{FeTe}_{1-x}\text{Se}_x$ as Se concentration is reduced.

12:10 PM NM01.02.05

Nematic Fluctuations in Iron-Based Superconductors $\text{BaFe}_2(\text{As}_{1-x}\text{P}_x)_2$ Zhaoyu Liu, Qianni Jiang, Yue Shi, Zaiyao Fei, Paul Malinowski, Josh Mutch and Jiun-Haw Chu; University of Washington, United States

Nematicity is a many-body quantum phase that breaks rotational symmetry while preserving translational symmetry. It has been discovered in the phase diagrams of both iron-based and cuprate high-temperature superconductors [1-3]. In the iron-based superconductors, the optimal doping of superconducting phase coincides with the putative nematic quantum critical point, suggesting the possibility of superconducting pairing enhanced by nematic quantum fluctuations [2,4]. However, a comprehensive study of the nematic fluctuations is still absent in the $\text{BaFe}_2(\text{As}_{1-x}\text{P}_x)_2$, which exhibits the cleanest signature of quantum criticality among all the iron-based superconductors. In this talk, I will present a detailed study of the nematic fluctuations of $\text{BaFe}_2(\text{As}_{1-x}\text{P}_x)_2$.

xP_x)² using the elastoresistivity measurement. I will also present the study of strain dependence of superconducting T_c , which shed light on the intricate relations between nematicity and superconductivity.

SESSION NM01.03: Superconductivity—Proximity Effects Including Topological
Session Chairs: Seul-Ki Bac and Peng Wei
Sunday Afternoon, April 18, 2021
NM01

1:00 PM *NM01.03.01

Phase-Dependent Dissipation in SNS Junctions—Topology and Non-Equilibrium Dynamics Meydi Ferrier; Universite of Paris-Saclay, France

An (SNS) junction with two superconductors coupled by a normal metal hosts Andreev bound states whose energy spectrum is phase-dependent and exhibits a minigap, resulting in a periodic supercurrent. However, phase-dependent dissipation also appears due to finite-time relaxation of Andreev bound states, providing an ultra-sensitive tool for the carrier dynamics.

In the weakly driven regime, we have measured dissipation in a phase-biased junction built around a bismuth nanowire, a second order topological insulator which was previously shown to host one-dimensional ballistic edge states. We have found absorption peaks at the Andreev level crossings in accordance with predictions of telltale signs of topological junctions [1,2].

I will also present our most recent results on SNS junctions strongly driven out of equilibrium by microwave field where novel physics emerges due to redistribution of quasiparticles, whose understanding is still incomplete. Strong driving power can significantly modify the distribution function from thermal equilibrium, activating additional transitions. We have measured the evolution of both the supercurrent and dissipation, extracted simultaneously from the ac magnetic susceptibility of a phase-biased graphene-superconductor ring driven out of equilibrium by microwave irradiation [3]. Increasing the frequency beyond the system relaxation rate has several measurable consequences: Firstly, the phase dependence of supercurrent is modified. In particular, the Fourier coefficients dependence on power deviates from the Bessel function expected in the adiabatic ac Josephson effect in qualitative agreement with time-dependent Usadel equations. Secondly and more interestingly, the dissipation with irradiation frequency higher than the minigap shows a distinct enhancement around $j = 0$ where the minigap is the largest and the dissipation is very weak in equilibrium. Using Kubo formalism, we explain this effect by the nonequilibrium distribution function with partial occupation above the minigap permitting transitions between levels on the same side of the minigap (intra-band). More generally, our results demonstrate that phase dependent dissipation measurement allows a much deeper understanding of the relaxation mechanisms than supercurrent in superconducting junctions.

[1] Murani et al, Phys. Rev. Lett. **122**, 076802 (2019)

[2] Fu and Kane, Phys. Rev. B **79**, 161408(R) (2009)

[2] Dou et al, arXiv:2011.07308

1:25 PM *NM01.03.02

2D Platforms for Majorana States and Phase Measurement of Topological Superconductivity Igor Zutic¹, Tong Zhou¹, Jong Han¹, Matthieu C. Dartiailh², William Mayer², Andrew Kent², Javad Shabani², Narayan Mohanta³ and Alex Matos-Abiague³; ¹University at Buffalo, The State University of New York, United States; ²New York University, United States; ³Wayne State University, United States

Topological transition transforms common superconductivity into an exotic phase of matter, which holds promise for fault-tolerant quantum computing [1]. A hallmark of this topological transition is the emergence of Majorana bound states (MBS), quasiparticles that nonlocally store a single electron. Their non-Abelian

exchange statistics allows for the implementation of quantum gates through braiding operations [1]. While most of the MBS proposals were focused on 1D systems [2], their geometry has inherent difficulties for technological implementation and realizing braiding. MBS detection typically relies on the measurement of zero-bias conductance peak [2,3] that could also arise in topologically-trivial systems. To overcome these challenges, we propose 2D platforms, which could support scalable MBS and their braiding. First we discuss how spin valves, common in spintronics, can be used through their fringing fields [4,5] to proximitize two-dimensional electron gas to implement MBS and their braiding [6,7]. Next we show our measurements of topological superconductivity in epitaxial Al/InAs Josephson junctions [8]. The closing and reopening of the superconducting gap with increasing magnetic field is simultaneously accompanied by the measurement of p-jump in the superconducting phase [8]. Remarkably, this topological transition can be controlled by gate voltage. We propose X-shaped topological junctions [9] in which the observed topological transition can be used to realize scalable MBS and their braiding.

[1] D. Aasen et al., Phys. Rev. X **6**, 031016 (2016).

[2] H. Zhang et al., Nature **556**, 74 (2018).

[3] K. Sengupta, I. Zutic et al., Phys. Rev. B **63**, 144531 (2001).

[4] T. Zhou et al., Phys. Rev. B **99**, 134505 (2019).

[5] N. Mohanta et al., Phys. Rev. Appl. **12**, 034048 (2019).

[6] G. Fatin et al., Phys. Rev. Lett. **117**, 077002 (2016).

[7] A. Matos-Abiague et al., Solid State Commun. **262**, 1 (2017)

[8] W. Mayer et al., arXiv:1906.01179, preprint.

[9] T. Zhou et al., Phys. Rev. Lett. **124**, 137001 (2020)

1:50 PM *NM01.03.03

Josephson Coupling Between Topological Superconducting Surfaces Guo-Xing Miao; University of Waterloo, Canada

The proximity effect from superconductors is . Inducing superconductivity on topological insulator surface states through proximity effect is an attractive approach to realize topological superconductivity, and provides great freedom in potential device engineering. Here we aim to look at the coupling between the opposite surfaces of a topological insulator thin film. Using high quality BiSbTe thin films as the tunnel barrier and MgB₂ to induce superconductivity, the top and bottom surfaces of the same topological insulator can readily couple between themselves. Other than Josephson coupling between bulk superconductors, one can also identify signatures from the coupling between surface zero-modes, while other modes are largely suppressed due to the opposite spin textures. Interestingly, the edges of the micro sized pillars offer another channel of conductance across the junction. When unfolded, the device is practically equivalent to an in-plane junction with a 1D channel between two topological superconductors and a periodic boundary condition. This circular 1D edge channel can potentially become a host for Majorana-like edge modes on vertical pillar structures.

2:15 PM *NM01.03.04

Controlling Vortex Matter in Superconductors with Nano-Textured Structures Wai-Kwong Kwok; Argonne National Laboratory, United States

Advances in nanofabrication has opened new venues for controlling vortex matter, which is responsible for the electro-magnetic response of all applied superconductors. For example, nano-hole and blind-hole structures with innovative patterns have emerged as a versatile platform for controlling and optimizing vortex pinning and dynamics in superconductors for enhanced critical current. Magnetic field pinning of vortices with nanoscale structures has also shown great potential for in-situ manipulation of vortex behaviour. Moreover, magnetic pinning is relatively temperature independent compared with core pinning. I will present recent highlights of our work on tailoring vortex dynamics with magnetic texturing. Namely, we use nano-magnetic patterned structures based on spin-ice rules to explore the effect of pinning, dynamic rectification and geometric frustration in a flux quanta system. In addition, we demonstrate that magnetic pinning can be used to 'pin' vortices in the liquid state in high temperature superconductors.

This work was supported by the U.S. Department of Energy, Office of Science, Materials Sciences and Engineering Division.

2:40 PM NM01.03.05

Late News: An Epitaxial GaN/NbN Heterostructure Exhibiting Concurrent Superconductivity and Quantum Hall Effect Phillip Dang¹, Guru Khalsa¹, Celesta S. Chang¹, D. Scott Katzer², Neeraj Nepal², Brian Downey², Virginia Wheeler², Alexey Suslov³, Andy Xie⁴, Edward Beam⁴, Yu Cao⁴, Cathy Lee⁴, David A. Muller¹, Huili Xing¹, David Meyer² and Debdeep Jena¹; ¹Cornell University, United States; ²U.S. Naval Research Laboratory, United States; ³National High Magnetic Field Laboratory, United States; ⁴Qorvo, Inc., United States

Superconductivity is a phenomenon that allows for lossless electrical transport and exceptional precision in voltage due to flux quantization, while the quantum Hall effect (QHE) is a paragon of topological protection in electronic states that allows for part-per-billion precision in resistance. Creating seamless heterostructures harboring these two unique electronic phases is highly desirable for the discovery new physics as well as the application of these electronic phases to topological quantum computing. Unfortunately, the quantum Hall state and the superconducting state are typically thought to be incompatible because the same magnetic field that creates the quantum Hall state destroys the superconducting state. In this work, we show that by using growth advances to develop a heterostructure of superconducting NbN and a GaN two-dimensional electron gas (2DEG), the two electronic phases can be seen concurrently in the same structure.

The epitaxial nitride structure begins with a 50 nm NbN layer, which is grown on a 3-inch diameter semi-insulating 6H-SiC wafer by plasma-assisted molecular beam epitaxy (PAMBE). We then use metal organic chemical vapor deposition (MOCVD) to grow a 20 nm AlN nucleation layer, a 1.5 μm GaN buffer layer, and an AlN spacer/AlGaIn barrier/GaN cap stack that defines the 2DEG. Gated Hall bar devices were fabricated by using 15 nm of Al₂O₃ as a gate insulator and Ti/Al/Ni/Au annealing for ohmic contacts to the 2DEG. Resistivity and Hall-effect measurements were taken on the gated Hall bars in magnetic fields up to 45 T and at temperatures as low as 350 mK. Over the range of gate voltages used, the 2DEG densities vary from less than $1.1 \times 10^{12}/\text{cm}^2$ to $6.7 \times 10^{12}/\text{cm}^2$, and the 2DEG mobilities vary from 1200 cm²/Vs to 8500 cm²/Vs at 390 mK. The GaN 2DEG was able to enter the integer QHE regime in magnetic fields as low as 15 T. We then made electrical contact to the buried NbN layer to extract the superconducting critical temperature and critical fields via resistance measurements. The T_c is 16.5 K with a sharp transition of $\Delta T = 0.16$ K in width, and the maximum out-of-plane H_c is 17.8 T. Therefore, superconductivity and the integer QHE are concurrent in this structure for $T < 1$ K and $15 \text{ T} < \mu H < 17.8 \text{ T}$. Analysis of these results shows that this window of temperatures and magnetic fields can be significantly expanded, suggesting that the nitride material system could potentially become an industrially viable platform for robust quantum devices based on topologically protected transport.

SESSION NM01.04: 1D Superconductivity and Nickelates

Session Chairs: Badih Assaf and Yi-Ting Hsu

Sunday Afternoon, April 18, 2021

NM01

4:00 PM *NM01.04.01

Neutron Scattering Studies in Quasi- One-Dimensional Superconducting Systems Clarina R. dela Cruz and Keith M. Taddei; Oak Ridge National Laboratory, United States

Quasi-one-dimensional A₂Cr₃As₃ (with A=K, Cs, Rb) is an intriguing new family of superconductors which exhibit many similar features to the cuprate and iron-based unconventional superconductor families. Yet in contrast to these systems, no charge or magnetic ordering has been observed which could provide the electronic

correlations presumed necessary for an unconventional superconducting pairing mechanism - an absence which defies predictions of first principles models. We report the results of neutron scattering experiments on polycrystalline $\text{K}_2\text{Cr}_3\text{As}_3$ ($T_c \sim 7\text{K}$) which probed the low temperature dynamics near T_c . Neutron diffraction data evidence a strong response of the nuclear lattice to the onset of superconductivity while inelastic scattering reveals short-range magnetic fluctuations. These observations suggest that $\text{K}_2\text{Cr}_3\text{As}_3$ is in close proximity to a magnetic instability and that the incipient magnetic order both couples strongly to the lattice and competes with superconductivity - in direct analogy with the iron-based superconductors. Further studies of charge doping of KCr_3As_3 via H intercalation revealed very interesting results. We show that the previously reported ethanol bath deintercalation of $\text{K}_2\text{Cr}_3\text{As}_3$ to KCr_3As_3 has a secondary effect whereby H from the bath enters the quasi-one-dimensional Cr_6As_6 chains. Furthermore, we find that - contrary to previous interpretations - the difference between non-superconducting as-grown KCr_3As_3 samples and superconducting hydrothermally annealed samples is not a change in crystallinity but due to charge doping with the latter treatment increasing the H concentration in the CrAs tubes effectively electron-doping the 133 compound. These results suggest a new stoichiometry $\text{KH}_x\text{Cr}_3\text{As}_3$, that superconductivity arises from a suppressed magnetic order via a tunable parameter and paves the way for the first charge-doped phase diagram in these materials.

4:25 PM *NM01.04.02

Superconductivity in Infinite Layer Nickelates Harold Hwang^{1,2}; ¹Stanford University, United States; ²SLAC National Accelerator Laboratory, United States

Ever since their discovery, superconductivity in cuprates has motivated the search for materials with analogous electronic or atomic structure. Here we present how soft chemistry approaches can be used to synthesize superconducting infinite layer nickelates from their perovskite precursor phase, using topotactic reactions [1,2]. We will present the synthesis and transport properties of the nickelate superconductors, and our current understanding of aspects of the electronic structure, including the unusual role of rare-earth hybridization [3,4]. A particular focus will be on the observation of a doping-dependent superconducting dome in $(\text{Nd,Sr})\text{NiO}_2$, similar to cuprates [5]. However, while cuprate superconductivity is bounded by an insulator for underdoping and a metal for overdoping, here we observe weakly insulating behavior on either side of the dome. Furthermore, the normal state Hall coefficient is always small and proximate to a continuous zero crossing in doping and in temperature, in contrast to the $\sim 1/x$ dependence observed for cuprates. This suggests the presence of both electron- and hole-like bands, consistent with band structure calculations.

[1] D. F. Li, K. Lee, B. Y. Wang, M. Osada, S. Crossley, H. R. Lee, Y. Cui, Y. Hikita, and H. Y. Hwang, *Nature* **572**, 624 (2019).

[2] K. Lee, B. H. Goodge, D. F. Li, M. Osada, B. Y. Wang, Y. Cui, L. F. Kourkoutis, and H. Y. Hwang, *APL Mater.* **8**, 041107 (2020).

[3] M. Hepting, D. Li, C. J. Jia, H. Lu, E. Paris, Y. Tseng, X. Feng, M. Osada, E. Been, Y. Hikita, Y.-D. Chuang, Z. Hussain, K. J. Zhou, A. Nag, M. Garcia-Fernandez, M. Rossi, H. Y. Huang, D. J. Huang, Z. X. Shen, T. Schmitt, H. Y. Hwang, B. Moritz, J. Zaanen, T. P. Devereaux, and W. S. Lee, *Nat. Mater.* **19**, 381 (2020).

[4] B. H. Goodge, D. F. Li, M. Osada, B. Y. Wang, K. Lee, G. A. Sawatzky, H. Y. Hwang, and L. F. Kourkoutis, *PNAS* **118**, e2007683118 (2021).

[5] D. F. Li, B. Y. Wang, K. Lee, S. P. Harvey, M. Osada, B. H. Goodge, L. F. Kourkoutis, and H. Y. Hwang, *Phys. Rev. Lett.* **125**, 027001 (2020).

4:50 PM NM01.04.03

Synthetic Route Towards Higher-Crystallinity Superconducting Infinite-Layer Nickelates Kyuhoo Lee^{1,2}, Danfeng Li^{1,2}, Motoki Osada^{1,2}, Bai Yang Wang^{1,2}, Berit H. Goodge^{3,4}, Lena Kourkoutis^{3,4} and Harold Hwang^{1,2}; ¹SLAC National Accelerator Laboratory, United States; ²Stanford University, United States; ³Cornell University, United States; ⁴Kavli Institute at Cornell for Nanoscale Science, United States

The recent discovery of superconductivity in the infinite-layer nickelates $\text{Re}_{1-x}\text{Sr}_x\text{NiO}_2$ ($\text{Re} = \text{Nd, Pr}$)^{1,2} has

sparked significant interest in the investigation of the intrinsic superconducting and normal-state properties of this new superconducting system. However, the non-trivial inclusions of defects and structural imperfections in this thermodynamically unstable material^{3,4} remain a major materials challenge. The main factors contributing to these imperfections include the unusually high formal nickel valence in the perovskite precursor phase due to the chemical doping of strontium, the unavoidable epitaxial mismatch with the substrate due to the large in-plane lattice change during the topotactic transition, and the decomposition and secondary-phase formation issues arising during the soft-chemistry reduction step.³⁻⁵ Upon careful optimization of the growth and reduction conditions, we have identified the key parameters for achieving higher crystallinity and established a reproducible method to stabilize high-quality Nd_{1-x}Sr_xNiO₂ (001) epitaxial thin films on SrTiO₃ (001) substrate by pulsed-laser deposition and CaH₂-assisted topochemical reduction. In particular, x-ray diffraction and scanning transmission electron microscopy measurements of the newly optimized samples reveal that the Ruddlesden-Popper-type faults prevalent in the previous generation of samples (Ref. 3) are now largely eliminated, indicating major improvements in the crystallinity of this material. The optimization process and the resultant evolution of the structural properties of the nickelate films will be discussed. In addition, the improvement in the crystallinity affects the transport properties and the superconducting dome^{5,6} of this material, the details of which will be discussed.

1 Li, D. *et al.* Superconductivity in an Infinite-Layer Nickelate. *Nature* **572**, 624 (2019).

2 Osada, M. *et al.* A Superconducting Praseodymium Nickelate with Infinite Layer Structure. *Nano Lett.* **20**, 5735 (2020).

3 Lee, K. *et al.* Aspects of the Synthesis of Thin Film Superconducting Infinite-Layer Nickelates. *APL Mater.* **8**, 041107 (2020).

4 Wang, B.-X. *et al.* Synthesis and Characterization of Bulk Nd_{1-x}Sr_xNiO₂ and Nd_{1-x}Sr_xNiO₃. *Phys. Rev. Mater.* **4**, 084409 (2020).

5 Zeng, S. *et al.* Phase Diagram and Superconducting Dome of Infinite-Layer Nd_{1-x}Sr_xNiO₂ Thin Films. *Phys. Rev. Lett.* **125**, 147003 (2020).

6 Li, D. *et al.* Superconducting Dome in Nd_{1-x}Sr_xNiO₂ Infinite Layer Films. *Phys. Rev. Lett.* **125**, 027001 (2020).

*Supported by DOE BES MSD (DE-AC02-76SF00515), the Moore Foundation (GBMF9072), and DOD AFOSR (FA 9550-16-1-0305).

5:04 PM NM01.04.04

Electronic Structure and Interface Effects in Superconducting Nickelate Thin Films Berit H. Goodge^{1,1}, Danfeng Li^{2,3}, Kyuho Lee^{2,3}, Motoki Osada^{2,3}, Bai Yang Wang^{2,3}, Harold Hwang^{2,3} and Lena Kourkoutis^{1,1}; ¹Cornell University, United States; ²SLAC National Accelerator Laboratory, United States; ³Stanford University, United States

The stabilization of superconducting infinite-layer nickelate thin films [1,2] presents a long-awaited platform for experimental comparison to the analogous cuprate superconductors and exploration of the underlying physical mechanisms. Unlike the bulk-synthesized cuprates, however, the thin film geometry of the superconducting nickelates has important implications for both the materials physics and the experimental methods used to probe it. Here, we harness atomic-scale scanning transmission electron microscopy (STEM) and localized electron energy loss spectroscopy (EELS) to explore both the lattice and electronic structure with high real-space resolution across a wide series of nickelate thin films. State-of-the-art electron spectroscopy reveals key electronic differences between the nickelate and cuprate superconductors [3]. Beyond the experimental considerations, the thin film geometry of the nickelate superconductors has also raised speculation about possible phenomena at the nickelate-substrate interface [4-6]. Harnessing the ability of cross-sectional measurements by atomic-resolution STEM and EELS, we discuss the details of both lattice and electronic structure in these materials across the substrate-film interface.

1. Li, D. *et al.* Superconductivity in an Infinite-Layer Nickelate. *Nature* **572**, 624 (2019).

2. Osada, M. *et al.* A Superconducting Praseodymium Nickelate with Infinite Layer Structure. *Nano Lett.* **20**, 5735 (2020).
3. Goodge, B. H. *et al.* Doping evolution of the Mott-Hubbard landscape in infinite-layer nickelates. arXiv:2005.02847 (2020).
4. He, R. *et al.* Polarity-induced electronic and atomic reconstruction at NdNiO₂/SrTiO₃ interfaces. *Physical Review B* **102**, 035118 (2020).
5. Geisler, B. and Pentcheva, R. Fundamental difference in the electronic reconstruction of infinite-layer versus perovskite neodymium nickelate films on SrTiO₃(001). *Physical Review B* **102**, 020502(R) (2020).
6. Bernardini, F. and Cano, R. Stability and electronic properties of LaNiO₂/SrTiO₃ heterostructures. *J. Phys. Mater.* **3** (2020) 03LT01.

*Supported by DOD AFOSR (FA 9550-16-1-0305), DOE BES MSD (DE-AC02-76SF00515), and the Moore Foundation (GBMF9072).

5:18 PM NM01.04.06

Penetration Depth Measurements of Infinite-Layer Nickelates Shannon Harvey, Bai Yang Wang, Danfeng Li, Motoki Osada, Kyuho Lee, Varun Harbola, Sam Crossley and Harold Hwang; Stanford University, United States

The discovery of superconductivity in infinite-layer nickelates [1] has the potential to help reveal the origins of high-temperature superconductivity. To do this, we must first develop an understanding of superconductivity in nickelates by measuring their fundamental properties. In this talk, I will present our measurements of the in-plane penetration depth of (Nd,Sr)NiO₂ thin films across the doping-dependent superconducting dome [2]. The penetration depth provides information about the superfluid density and pairing symmetry of the superconducting state, which will help to inform our understanding of the nature of superconductivity in these materials.

[1] Li, D. *et al.* Superconductivity in an infinite-layer nickelate. *Nature* **572**, 624–627 (2019).

[2] Li, D. *et al.* Superconducting Dome in Nd_{1-x}Sr_xNiO₂ Infinite Layer Films. *Phys. Rev. Lett.* **125**, 027001 (2020).

Supported by DOE BES MSD (DE-AC02-76SF00515) and the Moore Foundation (GBMF4415)

5:32 PM NM01.04.07

Isotropic Pauli-Limited Superconductivity in the Infinite-Layer Nickelate Nd_{0.775}Sr_{0.225}NiO₂ Bai Yang Wang^{1,2}, Danfeng Li^{1,2}, Berit H. Goodge³, Kyuho Lee^{1,2}, Motoki Osada^{1,2}, Shannon Harvey^{1,2}, Lena Kourkoutis³, Malcolm Beasley¹ and Harold Hwang^{1,2}; ¹Stanford University, United States; ²SLAC National Accelerator Laboratory, United States; ³Cornell University, United States

The recent observation of superconductivity in thin film infinite-layer nickelates [1] offers fresh terrain for investigating superconductivity in layered oxides. A wide range of perspectives [2-4], emphasizing single- or multi-orbital electronic structure, Kondo or Hund's coupling, and analogies to cuprates, have been theoretically proposed. Clearly, further experimental characterization of the superconducting state is needed to develop a foundational understanding of the nickelates. In this talk, I will discuss using magnetotransport measurements to probe the superconducting anisotropy in Nd_{0.775}Sr_{0.225}NiO₂. We find that the upper critical field is surprisingly isotropic at low temperatures, despite the layered crystal structure. We deduce that under magnetic field, superconductivity is strongly Pauli-limited, such that the paramagnetic effect dominates over orbital de-pairing. Underlying this isotropic response is both an enhanced electronic magnetic moment, the measurement of which can serve as a critical test of our interpretation and a substantial anisotropy in the superconducting coherence length, at least four times longer in-plane than out-of-plane. A prominent low-temperature upturn in the upper critical field indicates the likelihood of an unconventional ground state.

- [1] Li, D. et al. Superconductivity in an infinite-layer nickelate. *Nature* **572**, 624–627 (2019).
- [2] Lee, K.-W. & Pickett, W. E. Infinite-layer LaNiO₂: Ni¹⁺ is not Cu²⁺. *Phys. Rev. B* **70**, 165109 (2004).
- [3] Jiang, M., Berciu, M. & Sawatzky, G. A. Critical nature of the Ni spin state in doped NdNiO₂. *Phys. Rev. Lett.* **124**, 207004 (2020).
- [4] Botana, A. S. & Norman, M. R. Similarities and differences between LaNiO₂ and CaCuO₂ and implications for superconductivity. *Phys. Rev. X* **10**, 011024 (2020).

*Supported by the Moore Foundation (GBMF9072) and DOD AFOSR (FA 9550-16-1-0305).

SESSION NM01.05: Topological Superconductivity
Session Chairs: Badih Assaf and Peng Wei
Sunday Afternoon, April 18, 2021
NM01

6:30 PM *NM01.05.01

Superconductivity, Topological Edge States and Electron-Hole Pairing in a Single Monolayer Material, WTe₂ David H. Cobden; University of Washington, United States

In the semimetal WTe₂, low symmetry, band inversion, heavy carrier mass, near-perfect compensation, strong electron-phonon interactions and strong spin-orbit coupling all combine to provide a promising setting for correlated and topological phenomena. Undoped, a monolayer of WTe₂ behaves as a two-dimensional topological insulator with helical conducting edge states. Anisotropic magnetoresistance measurements of the edge conduction reveal the direction of the spin polarization, and surprisingly it is found to be independent of the edge termination. We infer that it is inherited from the bulk bands which are also spin polarized along a special axis, and show that this is consistent with theory. In addition, several lines of evidence indicate that the insulating behavior involves electron-hole pairing, with the possible formation of an excitonic insulator state near the compensated state. Meanwhile, at a surprisingly low level of electrostatic doping the insulating state converts into a metal which superconducts about 0.8 K. It is therefore quite likely that the superconductivity is tilted-Ising like and competes with excitonic ordering. Multi-terminal measurements also suggest that the topological edge states persist while being very weakly coupled to the bulk superconductivity.

6:54 PM *NM01.05.02

Majorana Corner Modes in Superconducting Topological Metals—A Case Study of Monolayer WTe₂ Yi-Ting Hsu; University of Notre Dame, United States

Monolayer WTe₂, an inversion-symmetric transition metal dichalcogenide, has recently been established as a quantum spin Hall insulator and found superconducting upon gating. It is therefore natural to wonder whether this discovered superconductivity is topological. In this talk, I will first show that gated monolayer WTe₂ is a promising candidate for a "higher-order" topological superconductor, which features Majorana zero modes localized at sample corners. Then I will present a general recipe for realizing superconductors hosting such Majorana corner modes without utilizing proximity effect. Finally, I will discuss systematic searches for new material candidates in databases guided by topological invariants that are applicable to ab initio band structures and can diagnose Majorana boundary types.

7:18 PM DISCUSSION

7:42 PM *NM01.05.04

Half-Quantum Flux in Topological Superconductors Yufan Li; Johns Hopkins University, United States

Spin-triplet superconductors (SCs) are highly desirable but rarely realized. On the other hand, there are surging interest in the spin-triplet p-wave pairing due to its close relevance to topological superconductivity and noise-resilient quantum computing. The superconducting gaps of triplet and singlet SCs with odd and even parity respectively can be exploited for unequivocal identification. We show that the magnetic flux quantization, one of the defining characteristics of a superconductor (SC), is a decisive phase-sensitive method to distinguish triplet-pairing SCs from the more common spin-singlet SCs. A superconducting ring with triplet pairing may demonstrate half-integer flux quantization $(n + \frac{1}{2}) \Phi_0$, where n is an integer, i.e., half flux quanta with half-integer quantum numbers of $1/2, 3/2, 5/2, \text{etc.}$ instead of the exclusive integer quantization $n\Phi_0$ observed in singlet SCs. We have observed half-quantum flux in mesoscopic rings of superconducting β -Bi₂Pd thin films [1]. The result provides conclusive evidence for spin-triplet p-wave pairing in β -Bi₂Pd as a leading candidate of intrinsic topological SCs. We have also observed half-quantum flux in noncentrosymmetric α -BiPd, where an admixture of singlet and triplet pairing is expected from the absence of parity symmetry [2]. Our findings establish a new paradigm for identifying spin-triplet pairing, and usher in new venues for studying topological superconductivity.

[1] Y. Li, X. Xu, M.-H. Lee, M.-W. Chu, C. L. Chien, Science 366, 238-241 (2019).

[2] X. Xu, Y. Li, C. L. Chien, Physical Review Letters 124, 167001 (2020).

8:06 PM *NM01.05.05

Superconductivity and Topological Phases in Two-Dimensional Materials Kam-Tuen Law; The Hong Kong University of Science and Technology, Hong Kong

In recent years, superconductivity and topological phases (such as quantum spin Hall and anomalous Hall phases) have been discovered in atomically thin two-dimensional materials such as in transition metal dichalcogenides (TMDs) and twisted bilayer graphene. These materials exhibit novel physical properties due to their crystal symmetries, band structures and interaction effects.

In this talk, I would like to discuss:

1. The properties of superconducting 2H-structure TMDs which we called Ising superconductors. In the case of gated 2H-structure MoS₂ for example, superconductivity can survive even in the presence of an in-plane magnetic field up to 60 Tesla. We showed that this is due to a special form of spin-orbit coupling (SOC) which we called Ising SOC. We will also discuss how Ising superconductors can be used to realize Majorana fermions which are important for topological quantum computation. [1-4]

3. The current-induced magnetization switching in twisted bilayer graphene. Recently, quantum anomalous Hall effect with spontaneous ferromagnetism was observed in twisted bilayer graphenes (TBG) near 3/4 filling by Goldhaber-Gordon's group at Stanford [6] and Young's group at UCSB [7]. Importantly, it was observed that an extremely small current can switch the direction of the magnetization. This offers the prospect of realizing low energy dissipation magnetic memories. However, the mechanism of the current-driven magnetization switching is poorly understood as the charge currents in graphene are generally believed to be non-magnetic. In this talk, the observed current-induced magnetization effect will be explained [8].

1. Science 350, 1353 (2015),

2. Nature Physics 12, 139-143 (2016),

3. Nature Materials 17, 504-508 (2018),

4. Physical Review Research 2, 013026 (2020),

5. A. Sharpe etc. Science 365, 605 (2019),

6. M. Serlin etc. Science 367, 895 (2020),

7. Nature Communications 11, 1650 (2020).

9:00 PM *NM01.06.01

Topological Superconductivity and Majorana Zero Mode in Iron-Based Superconductors Hong Ding;
Institute of Physics, Chinese Academy of Sciences, China

In this talk I will report our recent discoveries of topological superconductivity and Majorana zero mode in iron-based superconductors. We have observed a superconducting topological surface state of Fe(Te, Se) with $T_c \sim 14.5\text{K}$ by using low-temperature ARPES [1], and a pristine Majorana zero mode (MZM) inside a vortex core of this material by using low-temperature STM [2]. We have also observed a half-integer level shift of vortex bound states [3] and quantized Majorana conductance [4] in this material, which are hallmarks of MZMs. In addition, we have also found that most of Fe-based superconductors [5], including monolayer Fe(Te, Se)/STO [6], have similar topological electronic structures. One of them, $\text{CaKFe}_4\text{As}_4$, an Fe-As bilayer superconductor ($T_c \sim 35\text{K}$), is found to possess MZM and other bound states that can be well reproduced by a simple theoretical model [7]. Our observations offer a new, robust platform for realizing and manipulating MZMs, which can be used for quantum computing at a relatively high temperature.

References

- [1] Peng Zhang et al., Science 360, 182 (2018)
- [2] Dongfei Wang et al., Science 362, 334 (2018)
- [3] Lingyuan Kong et al., Nature Physics 15, 1181 (2019)
- [4] Shiyu Zhu et al., Science 367, 189 (2020)
- [5] Peng Zhang et al., Nature Physics 15, 41 (2019)
- [6] Xun Shi et al., Science Bulletin 62, 503 (2017)
- [7] Wenyao Liu et al., Nature Communications 11, 5688 (2020)

9:25 PM *NM01.06.02

Novel Physics Induced by Dimensional Reduction from 3D to 2D in Layered Materials Xianhui Chen;
University of Science and Technology of China, China

Two-dimensional (2D) materials have attracted plenty of interests due to the novel physical properties induced by the reduction of dimension compared to three-dimensional (3D) system, and the practical and potential application of revolutionary current technologies as well. It is of great significance to extensively investigate the fundamental physics of the related materials in the two-dimensional limit. The success of 2D materials is based on the development of suitable synthesis methods, mainly including exfoliation, chemical vapour deposition and various solution-phase methods. New and more efficient methods are under developing. Recently, we have successfully intercalated organic ion cetyltrimethyl ammonium (CTA^+) and tetrabutyl ammonium (TBA^+) into several layered crystals via electrochemical intercalation method, realizing two-dimensionalization of the related functional layers and observing some intriguing new physical phenomena. We intercalated CTA^+ and TBA^+ into the FeSe single crystal by the electrochemical method, achieving high superconducting transition temperature (T_c) to be 45 and 50 K for $(\text{CTA})_{0.3}\text{FeSe}$ and $(\text{TBA})_{0.3}\text{FeSe}$, respectively. By measuring Knight shift and nuclear spin-lattice relaxation rate, we unambiguously observed a pseudogap behavior below $T_p \sim 60$ K in these two kinds of layered FeSe-based high-temperature superconductors, and revealed that the pseudogap behavior is related to strong superconducting fluctuations due to the quasi-2D nature induced by the organic-ion intercalations. With intercalating the same organic ions into an intrinsic semiconductor SnSe_2 , superconductivity with T_c to ~ 6.4 (TBA^+) and 7.1 K (CTA^+) was achieved. We also synthesized an organic-ion intercalated transition-metal dichalcogenides $(\text{TBA})_{0.3}\text{VSe}_2$, where the metallic charge-density-wave (CDW) state with transition temperature (T_{CDW}) of 110 K in the pristine system was changed to an insulating CDW state

with T_{CDW} of 165 K by the intercalation. With TBA^+ -intercalation, the insulating ferromagnetic van der Waals material $Cr_2Ge_2Te_6$ with Curie temperature T_{curie} of 67 K was altered to a metallic ferromagnet with T_{curie} of 208 K, accompanied by the magnetic easy axis changing from $\langle 001 \rangle$ direction to the ab plane. Our work indicated that the 3D-to-2D crossover induced by intercalation of the large organic ion CTA^+ and TBA^+ between functional layers plays a key role in the dramatic changes of the physical properties in the several material systems, and demonstrated that the intercalation of organic ions with large size can serve as a convenient and efficient approach to explore and manipulate the versatile electronic and magnetic properties in the layered crystals.

References:

- [1] M. Z. Shi, N. Z. Wang, B. Lei, C. Shang, F. B. Meng, L. K. Ma, F. X. Zhang, D. Z. Kuang, and X. H. Chen, *Phys. Rev. Mater.* 2, 074801 (2018).
- [2] M. Z. Shi, N. Z. Wang, B. Lei, J. J. Ying, C. S. Zhu, Z. L. Sun, J. H. Cui, F. B. Meng, C. Shang, L. K. Ma and X. H. Chen, *New J. Phys.* 20, 123007 (2018).
- [3] B.L. Kang, M.Z. Shi, S.J. Li, H.H. Wang, Q. Zhang, D. Zhao, J. Li, D.W. Song, L.X. Zheng, L.P. Nie, T. Wu and X.H. Chen, *Phys. Rev. Lett.* 125, 097003(2020).
- [4] L. K. Ma, M. Z. Shi, B. L. Kang, K. L. Peng, F. B. Meng, C. S. Zhu, J. H. Cui, Z. L. Sun, D. H. Ma, H. H. Wang, B. Lei, T. Wu, X. H. Chen, *Phys. Rev. Mater.*, 4, 124803 (2020).
- [5] F. B. Meng, Z. Liu, L. X. Yang, M. Z. Shi, B. H. Ge, H. Zhang, J. J. Ying, Z. F. Wang, Z. Y. Wang, T. Wu and X. H. Chen, *Phys. Rev. B* 102, 165410 (2020).
- [6] N. Z. Wang, H. B. Tang, M. Z. Shi, H. Zhang, W. Z. Zhuo, D. Y. Liu, F. B. Meng, L. K. Ma, J. J. Ying, L. J. Zou, Z. Sun, X. H. Chen, *J. Am. Chem. Soc.* 141, 17166-17173 (2019).

9:50 PM NM01.06.03

Late News: Fermi-arc Criterion for Surface Majorana Modes in Superconducting Time-Reversal Symmetric Weyl-Semimetals Rauf O. Giwa and Pavan Hosur; University of Houston, United States

A Majorana-fermion is an exotic particle that is its own anti-particle and can occur in superconductors, where charge conjugation is realized as a particle-hole symmetry. In recent years, many clever realizations of Majorana-fermions in condensed-matter have been predicted. Many have been verified by exploiting the interplay between superconductivity and band topology in metals and insulators. On the other hand, Weyl-semimetals are three-dimensional materials in which the bulk band-gap closes at an even-number of discrete points (Weyl nodes) in the Brillouin zone. Weyl-summits are characterized by topologically protected surface states consisting of disjoint, open Fermi-arcs, projected from bulk Weyl-nodes to the surface.

Realizations of Majorana-fermions in semimetals remain less explored. We ask, "under what conditions do superconducting vortices in time-reversal symmetric Weyl-semimetals trap Majorana-fermions on the surface?" If each constant- k_z plane, where z is the vortex axis, contains equal numbers of Weyl nodes of each chirality, we predict a generically gapped vortex and derive a topological invariant ν in terms of the Fermi arc structure that signals the presence or absence of surface Majorana fermions. In contrast, if certain constant- k_z planes contain a net chirality of Weyl nodes, the vortex is gapless.

We analytically calculate the topological invariant ν within a perturbative scheme and provide numerical support with an orthorhombic lattice model. Using our criteria, we predict phase transitions between trivial, critical and topological vortices by simply tilting the vortex. Finally, we propose $Li(Fe_{0.91}Co_{0.09})As$ with broken inversion symmetry as a candidate for realizing our proposals.

10:05 PM *NM01.06.04

Phenomena and Physics in Pressurized Superconductors Revealed by Our Recent Studies Liling Sun¹, Jing Guo¹, Yazhou Zhou¹, Genda Gu², Cheng Huang¹, Qi Wu¹, Tao Xiang¹ and Robert J. Cava³; ¹Institute of Physics, Chinese Academy of Sciences, China; ²Brookhaven National Laboratory, United States; ³Princeton University, United States

It has been established that the superconductivity in a material is dictated by its degrees of freedom of electronic charge, orbital, spin and crystallographic structure, which can be manipulated by the control parameters such as pressure, magnetic field and chemical composition. Pressure is a ‘clean’ way to tune basic electronic and structural properties without changing the basic chemistry, and can help to search for new phenomena and understand the corresponding physics. In this talk, I will present some interesting phenomena obtained by our recent high-pressure studies, including crossover from two-dimensional to three-dimensional superconducting states in bismuth-based cuprate superconductor [1] and discovery of the *RSrVS* superconductors [2-5].

References:

- [1] J. Guo and L. Sun et al, Nature Physics 16,295(2020)
- [2] C Huang and L. Sun et al, PRM (R) 4, 071801(2020)
- [3] J. Guo and L. Sun et al, Adv. Mater. 31, 1807240 (2019)
- [4] L. Sun and J.R. Cava, PRM 3, 090301(2019)
- [5] J. Guo and L. Sun et al, PNAS 114, 13144 (2017)

10:30 PM *NM01.06.05

Clathrate Superhydrides Under High Pressure—A Class of Extraordinarily Hot Conventional Superconductors Yanming Ma; Jilin University, China

Room-temperature superconductivity has been a century long-held dream of mankind and a focus of intensive research. In an effort to search for room-temperature superconductors, we proposed in 2012 the first-ever clathrate superhydride CaH₆1 stabilized at an extreme pressure 150 GPa that shows a potential of high temperature superconductivity at T_c about 235 K. In 2017, we extended the superconducting clathrate structures into rare earth (RE, e.g., Sc, Y, La, Ce, Pr., etc) superhydrides at high pressure conditions that commonly have three clathrate structured stoichiometries of REH₆, REH₉, and REH₁₀, some of which exhibit extraordinarily high-temperature superconductivity². Subsequent experiments synthesized the as-predicted clathrate superhydrides YH₆, YH₉, and LaH₁₀ and measured T_c values at 224, 243, and 260 K, respectively, setting up new T_c records among known superconductors. These discoveries open up the door of achieving superconductors that could work at room temperature (300 K) in superhydrides under high pressures. In the talk, I will give an overview on the current status of research progress on superconductive superhydrides, and then discuss the design principle for achieving room temperature superconductor. Our prediction on a hot superconductor (T_c = ~400 K) in a clathrate Li₂MgH₁₆ superhydride found in a ternary Li-Mg-H system³, and other recent results on clathrate superhydrides together with future research direction along this line will be discussed.

References:

- ¹Wang, et al., PNAS 109, 6463 (2012)
- ²Peng, et al., PRL 119, 107001 (2017)
- ³Sun, et al., PRL 123, 097001 (2019)

SYMPOSIUM NM02

Superconducting Materials and Applications
April 14 - April 22, 2021

Symposium Organizers
Qiang Li, Brookhaven National Laboratory

Floriana Lombardi, Chalmers University of Technology
Paolo Mele, Shibaura Institute of Technology
Teresa Puig, CSIC

Symposium Support
Bronze
MilliporeSigma

* Invited Paper

SESSION NM02.01: Recent Development of REBCO Films and Coated Conductors
Session Chairs: Qiang Li and Xavier Obradors
Wednesday Morning, April 21, 2021
NM02

8:00 AM *NM02.01.01

New Opportunities for Nanostructured Coated Conductors: Solution Derived Ultrafast Transient Liquid Assisted Growth Xavier Obradors¹, Teresa Puig¹, Juri Banchewski¹, Silvia Rasi¹, Albert Queraltó¹, Kapil Gupta¹, Lavinia Saltarelli¹, Diana Garcia¹, Adrià Pacheco¹, Roxana Vlad¹, Laia Soler¹, Júlia Jareño¹, Ziliang Li¹, Roger Guzman¹, Natalia Chamorro¹, Bohores Villarejo¹, Cornelia Pop¹, Max Sieger¹, Susagna Ricart¹, Jordi Farjas², Pere Roura², Cristian Mocuta³, Ramon Yañez⁴ and Josep Ros⁴; ¹ICMAB - CSIC, Spain; ²University Girona, Spain; ³Soleil Synchrotron, France; ⁴Universitat Autònoma de Barcelona, Spain

Coated conductors of YBa₂Cu₃O₇ (CC-YBCO) have emerged as the most attractive opportunity to reach unique performances in an extended range of temperatures and magnetic fields making them attractive for power and magnet applications. Reducing the cost/performance ratio, however, continues to be a key objective. Chemical solution deposition (CSD) is a competitive cost-effective technique which has been used to obtain nanocomposite films and CCs. However, the typical growth rates (0.5-1 nm/s) of the fluorine-based CSD approach remain too low thus limiting its throughput.

We will show in this talk how CSD-based nanocomposite YBCO films can be obtained using metalorganic colloidal solutions including preformed BaMO₃ (M=Zr, Hf) nanoparticles. This approach can be easily combined with Inkjet printing and other scalable deposition techniques for thick film preparation.

Transient Liquid Assisted Growth (TLAG) is a novel growth approach [1] allowing to combine the already well established CSD methodologies with ultrahigh growth rates based on a non-equilibrium liquid-mediated approach (100-1000 nm/s). This novel approach uses fluorine-free metalorganic precursors and is also compatible with the colloidal solution approach to nanocomposite coated conductors. We will show that using properly TLAG requires to generate new knowledge about kinetic phase diagrams that we have reached using fast in-situ XRD analysis (100 nm/frame) under synchrotron radiation. Critical current densities up of 5 MA/cm² at 77K are already realized in thin films and the suitability of using IBA buffered metallic substrates will be also demonstrated. A modified nanostructure is demonstrated based on epitaxial BaMO₃ nanoparticles thus generating a new opportunity to deeply analyse the key influence of defect structure on vortex pinning of nanocomposite superconductors.

We acknowledge funding from EU-ERC_AdG-2014-669504 ULTRASUPERTAPE and EU-PoC-2020-IMPACT projects, and the Excellence Program Severo Ochoa SEV2015-0496

[1] L. Soler et al, Nature Communications, 11, 344 (2020)

8:25 AM *NM02.01.02

Strong Pinning at High Growth Rates in Rare Earth Barium Cuprate (REBCO) Superconductor Films

Grown with Liquid-Assisted Processing (LAP) During Pulsed Laser Deposition Judith L. MacManus-Driscoll¹, John Feighan¹, May Lai¹, Ahmed Kursumovi¹, Haiyan Wang², Di Zhang², Jae Hun Lee³ and Seung Hyun Moon³; ¹University of Cambridge, United Kingdom; ²Purdue University, United States; ³sunam, Korea (the Republic of)

We present a simple liquid assisted processing (LAP) method, to be used in-situ during pulsed laser deposition growth to give both rapid growth rates (>250 nm/min) and strong pinning. Achieving these two important features simultaneously has been a serious bottleneck to date. LAP enhances the kinetics of the film growth so that good crystalline perfection can be achieved at up to 60 x faster growth rates than normal, while also enabling artificial pinning centres to be self-assembled into fine nanocolumns. In addition, LAP allows for RE mixing (80% of Y with 20% of Yb, Sm, or Yb+Sm) to create effective point-like disorder within the REBCO lattice and which leads to strongly improved pinning at 30 K and below. Overall, LAP is a simple method which could be adopted by other in-situ physical or vapour deposition methods (i.e PLD, MOCVD, evaporation, etc) to significantly enhance both growth rate and performance.

8:50 AM *NM02.01.03

Advanced Second Generation Wire Development at AMSC Martin W. Rupich¹, Qiang Li², Vyacheslav Solovyov³ and Amit Goyal⁴; ¹AMSC, United States; ²Brookhaven National Laboratory, United States; ³Brookhaven Technology Group, United States; ⁴University of Buffalo, United States

AMSC is exploring the development of advanced wire architectures which can double the I_c of the standard Second Generation (2G) high temperature superconducting (HTS) wire and significantly enhance performance in the presence of magnetic fields. The Second Generation HTS wires are generally based on a composite architecture consisting of a thin YBCO superconducting layer deposited on one side of a thin, flexible metal substrate. This composite HTS/substrate structure is typically surrounded by an electroplated Cu layer or laminated between metal strips to provide mechanical and electrical stability. AMSC has been developing an alternative architecture consisting of 2 distinct HTS layers deposited on each side of a metal substrate. This double HTS layer composite is then surrounded by an electroplated Cu layer or laminated between two metal strips, resulting in a wire package nearly indistinguishable from the standard single HTS layer wire. The novel architecture results in a 2G wire with double the critical current of the standard single layer wire.

The enhanced pinning performance of the wire is achieved by the introduction of a uniform defect structure produced by a reel-to-reel irradiation of the HTS layers by ions such as Au⁵⁺. The ion irradiation produces an extremely uniform distribution of pinning defects that enhances I_c by a factor of up to 3 times. By controlling the irradiation process, the performance can be engineered for the temperatures and fields of the targeted applications.

In this presentation, we will review the performance of the novel 2G wire architecture and describe the structure and properties of the irradiation induced pinning landscapes.

This work is supported by EERE under contract DE-EE0007870.

9:15 AM NM02.01.04

Late News: Reel to Reel BZO-Doped REBCO Coated Conductors by Direct-Resistance Heating Technique in Advanced MOCVD Reactor Mahesh Paidpilli, Kalyan Boyina, Eduard Galstyan, Goran Majkic and Venkat Selvamamickam; University of Houston, United States

Advanced metal organic chemical vapor deposition (A-MOCVD) has been developed to grow long-length, thick film REBCO coated conductors in a single pass with superior in-field performance. Multiple long-length 5% Zr doped REBCO coated conductors with film thickness ranging from 1-4 μ m have been produced in A-MOCVD Reactor. The critical current density of these conductors has been examined by scanning hall probe microscopy. REBCO coated conductors with $\sim 4\mu$ m thickness exhibit magnetization critical current density (J_c) over 1.5 MA/cm² at 65 K, 1.5 T and 5.4 MA/cm² at 4.2 K, 13 T. The microstructure, out-of-plane and in-plane texture of REBCO coated conductors will also be presented.

9:30 AM NM02.01.05

Fast Screening of TLAG-CSD REBCO Superconductors Fabrication by High-Throughput

Experimentation [Albert Queraltó](#)¹, Juri Banchewski¹, Kapil Gupta¹, Adrià Pacheco¹, Lavinia Saltarelli¹, Diana Garcia¹, Cristian Mocuta², Susagna Ricart¹, Xavier Obradors¹ and Teresa Puig¹; ¹Institut de Ciència de Materials de Barcelona, Spain; ²European Synchrotron Radiation Facility, France

High-throughput screening of materials is a novel development strategy that is envisaged to accelerate discovery, development, and optimization of materials. Chemical solution deposition (CSD) techniques such as drop-on-demand inkjet printing (DoD IJP) are ideal to perform high-throughput studies through the fabrication of complex combinatorial samples with locally-uniform or graded compositions, and high spatial precision that enables parallel investigations on morphological, structural and functional properties.

The current work shows the implementation of such approach to expedite the optimization of REBCO superconducting films fabricated with the newly developed transient-liquid assisted growth chemical solution deposition (TLAG-CSD) method, which has been able to attain growth rates 100 times larger than with other fabrication methods. The preparation of combinatorial samples was done through mixing different rare earth cuprate precursor solutions with DoD IJP to explore the influence of rare-earth and liquid phase compositional changes on the epitaxial growth characteristics. The use of computational methods allowed the successful merging of precursor inks and high sample homogeneity, as confirmed by EDX and high-resolution XRD.

Epitaxial growth studies were then conducted for the fast identification of the best ranges of processing conditions and compositions. We use the advantages of this strategy to rapidly analyze different compositions in one single step by in-situ XRD synchrotron radiation experiments. Finally, we combined this knowledge with machine learning approaches to widen the understanding and rapid optimization of epitaxial growth of high-temperature REBCO superconducting films.

References:

- [1] Soler et al. Nat. Comm. 11, 344 (2020).
- [2] Rasi et al. J. Phys. Chem. C 124, 15574-15584 (2020).
- [3] Queraltó et al. submitted. <div id="gtx-trans" style="position: absolute; left: 5px; top: 334px;"> <div class="gtx-trans-icon"> </div> </div>

9:45 AM NM02.01.06

A Microstructural Perspective of the Ultrafast Transient Liquid Assisted Growth of High Current

Density YBCO Superconducting Films [Kapil Gupta](#)¹, Lavinia Saltarelli¹, Albert Queraltó¹, Laia Soler¹, Júlia Jareño¹, Juri Banchewski¹, Roger Guzman¹, Silvia Rasi¹, Adrià Pacheco¹, Diana Garcia¹, Susagna Ricart¹, Jordi Farjas², Pere Roura-Grabulosa², Xavier Obradors¹ and Teresa Puig¹; ¹Institut de Ciència de Materials de Barcelona (ICMAB-CSIC), Spain; ²University of Girona, Spain

The outstanding ability of $\text{YBa}_2\text{Cu}_3\text{O}_{7-x}$ (YBCO) films to carry high currents at high magnetic fields offers an unparalleled opportunity to be used in large scale superconducting power applications and high field magnets. In an essential need of high performance, high throughput, and low cost manufacturing, chemical solution deposition (CSD) has become a very competitive cost-effective and scalable methodology to produce epitaxial thin films, with enhanced performance at high magnetic fields by the incorporation of secondary phase nanoparticles (NPs) [1]. However, their growth rates are rather small (0.5-1 nm/s). In this regard, we have developed a novel growth approach, entitled, Transient Liquid Assisted Growth (TLAG) [2], which is able to combine CSD methodologies for fluorine-free metalorganic precursors with ultra-fast growth rates (100 nm/s) by facilitating a non-equilibrium liquid-mediated approach and several intermediate reactions. Critical current densities up of 5 MA/cm² at 77K are already realized in TLAG-CSD grown YBCO thin films. In order to further improve the thin film's crystal quality and superconducting properties, understanding of initial nano-phases in pyrolysis process and all the intermediate reactions during growth, as well as, fine tuning of growth parameters is essential. For this purpose, the microstructure of pyrolyzed YBCO thin films and the intermediate

phases of quenched thin films along with grown YBCO thin films, investigated via high resolution transmission electron microscopy (HRTEM), scanning transmission electron microscopy (STEM), electron energy loss spectroscopy (EELS) and energy dispersive X-ray spectroscopy (EDX), will be presented. Furthermore, the current-carrying capabilities of high temperature superconductors (HTS) are determined by its microstructure and it can be enhanced by the presence of well-controlled nano-defects inside the epitaxial superconducting matrix acting as vortex pinning centers. TLAG-CSD has demonstrated the growth of nanocomposites to increase flux pinning at high magnetic fields by incorporating pre-formed NPs to the metalorganic initial inks. Therefore, using aberration-corrected STEM combined with high angle annular dark field (HAADF) and EELS, we explore the detailed microstructure of grown TLAG-CSD YBCO films and nanocomposites, with a focus on new defects landscape at the atomic level, secondary phases, and strain effects. An additional advantage of TLAG-CSD is that preformed NPs can be incorporated to the metalorganic ink to prepare superconducting nanocomposites with enhanced vortex pinning, which will also be presented. Finally, the recent progress in TLAG-CSD, in terms of microstructure correlation with growth mechanisms and growth rate will be discussed.

SESSION NM02.02: Topology, Josephson Junction and Superconducting Electronics I
Session Chairs: Sergey Kubatkin and Floriana Lombardi
Wednesday Morning, April 21, 2021
NM02

11:45 AM *NM02.02.01

Revealing the Second-Order Topological Character of Bismuth-Based Josephson Junction Sophie Gueron and Helene Bouchiat; Université Paris Saclay et CNRS Laboratoire de Physique des Solides, France

In Second-Order Topological Insulators (SOTI), bulk and surfaces are insulating while the edges or hinges conduct current in a quasi-ideal (ballistic) way, being insensitive to disorder. Crystalline bismuth has been shown to belong to this class of materials [1,2,3]. Just like the case of Quantum Spin Hall edges of 2D Topological Insulators, current is expected to be carried without dissipation by counter-propagating ballistic helical states, with a spin orientation locked to the momentum. Such edge or hinge states open many possibilities, from dissipationless charge and spin transport to new avenues for quantum computing. We have investigated Crystalline Bi nanowires based Josephson junctions and found that they exhibit saw-tooth current phase relations robust in high magnetic field which is the signature one-dimensional ballistic edge states. We also demonstrate the topological nature of Andreev states in these junctions when coupled to a microwave resonator in a phase-biased configuration. We find absorption peaks at the Andreev level crossings, whose temperature and frequency dependencies point to protected topological crossings with an accuracy limited by the electronic temperature of our experiment.

References :

- [1] A. Murani *et al*, Nature Communications 8, 15941 (2017).
 - [2] Frank Schindler *et al*, Nature Physics 14, 918–924 (2018).
 - [3] A. Murani *et al*, Phys. Rev. Lett. 122, 076802 (2019).
- Helene Bouchiat's email is helene.bouchiat@u-psud.fr

12:10 PM *NM02.02.02

Josephson Junctions with Topological Interlayers Alexander Brinkman; University of Twente, Netherlands

In order to study Majorana and parafermionic quasiparticles a platform is needed that combines superconductivity and topology. A candidate platform is a Josephson junction with standard s-wave superconductors as leads and a topological interlayer in which electron spin is coupled to momentum direction.

We will show results for junctions based on topological materials with transport in 3D bulk Dirac semimetals, 2D topological surface states as well as 1D higher order topological hinge states, progressively trying to reduce the number of non-topological additional modes.

For the Dirac semimetal $\text{Bi}_{0.97}\text{Sb}_{0.03}$ we revealed that the required spin-momentum locking is present for the bulk carriers and that the degeneracy of the Dirac cone can be lifted in parallel electric and magnetic fields [1]. Indeed, Josephson junctions with this material reveal that part of the supercurrent is carried by bound states that are 4π -periodic, as evidenced from microwave irradiation experiments [2]. The g-factor of the interlayer turns out to be gigantic [3]. We will discuss in what sense these bound states can be considered topological despite their degeneracy in spin.

Going one dimension lower, the spin momentum locking of 2D topological surface states can be used. For the Dirac semimetal Cd_3As_2 we show that part of the supercurrent is carried by the Fermi arc surface states [4]. For the use of the surface states of topological insulators we developed technology that allows for in-situ fabricated interfaces and in-situ defined nanostructures [5]. The use of selective area growth is especially promising for the purpose of reducing the number of modes in the nanodevices by size quantization, in order to maximize the 4π signal.

In order to avoid any non-topological Andreev modes in the junctions at all, the 1D situation is preferred. For this purpose we focused on higher order topological 1D hinge states that might exist in Dirac semimetals. For Cd_3As_2 we showed that this is indeed the case by analyzing the supercurrent modulation by magnetic field and electric gating [6].

1. Monopole diffusion in Dirac semimetal $\text{Bi}_{0.97}\text{Sb}_{0.03}$, J. de Boer *et al.*, Phys. Rev. B **99**, 085124 (2019).
2. 4π periodic Andreev bound states in a Dirac semimetal, Chuan Li *et al.*, Nature Mater. **17**, 875 (2018).
3. Zeeman-effect-induced $0-\pi$ transitions in ballistic Dirac semimetal Josephson junctions, Chuan Li *et al.*, Phys. Rev. Lett. **123**, 026802 (2019).
4. Fermi-arc supercurrent oscillations in Dirac semimetal Josephson junctions, Cai-Zhen Li *et al.*, Nature Communications **11**, 1150 (2020).
5. Selective area growth and stencil lithography for in situ fabricated quantum devices, P. Schüffelgen *et al.*, Nature Nano. **14**, 825 (2019).
6. Reducing Electronic Transport Dimension to Topological Hinge States by Increasing Geometry Size of Dirac Semimetal Josephson Junctions, Cai-Zhen Li *et al.*, Phys. Rev. Lett. **124**, 156601 (2020).

12:35 PM NM02.02.03

Late News: Circuit-QED Probing of Majorana Bound States in TI Nano Josephson Junctions [Thilo Bauch](#)¹, Ananthu Pullukattuthara Surendran¹, Gunta Kunakova^{2,1}, Jana Andzane², Donats Erts² and Floriana Lombardi¹; ¹Chalmers University of Technology, Sweden; ²University of Latvia, Latvia

The interest in hybrid Topological Insulator (TI) Josephson junctions was boosted after the prediction by Fu and Kane of an unconventional chiral p-wave symmetry of the proximity induced order parameter into the topological surface states. The chiral induced p-wave is a prerequisite for the nucleation of localized Majorana states in a tri-junction geometry, which is instrumental for topological quantum computation. In a multimode hybrid TI Josephson junction with two terminal geometry, Majorana physics manifests as peculiar properties of a part of the Andreev bound states carrying the Josephson current: they give rise to an unconventional 4π periodic current phase relation (CPR) coexisting with a 2π periodic CPR of the conventional Andreev bound states. The relative weight between the 4π and 2π periodic Andreev bound states increases with the transparency

of the junction and, in general, by reducing the number of channels. A direct way to achieve a low number of transport channels is to use TIs with reduced dimensionality like very thin and narrow nanoribbons. Indeed, quite recently, various theoretical proposals have shown the advantage to using Josephson junctions with TI nanoribbons, with suppressed bulk conduction, to realize Majorana fermions.

To obtain information about the bound state spectrum we have implemented a circuit-QED readout scheme for our Al-Bi₂Se₃-Al hybrid junctions. Here we embedded a TI Josephson junction-based RF SQUID in a superconducting resonator. The dispersive microwave read out of the resonator/RF-SQUID setup allows us to extract information about the bound state spectrum of the TI junction. In fact, the low amplitude microwave readout ensures a relative low perturbation of the junction (in respect to the critical current) as compared to typical “Shapiro step” measurements, where the large microwave drive can cause undesirable population of higher lying bound states. Moreover, the dispersive readout enables us to characterize decoherence sources eventually affecting the performance of a TI junction based topological quantum bit. Finally, we present preliminary results of two-tone spectroscopy envisaged to extract the phase dispersion of single bound states directly.

12:50 PM NM02.02.04

Late News: Unconventional Current Phase Relation of Topological-Insulator Nanoribbon-

Superconductor Hybrid Junctions Ananthu Pullukattuthara Surendran¹, Gunta Kunakova^{1,2}, Jana Andzane², Donats Erts², Floriana Lombardi¹ and Thilo Bauch¹; ¹Chalmers University of Technology, Sweden; ²University of Latvia, Latvia

Hybrid material systems with a conventional superconductor in proximity to a semiconductor or an unconventional conductor have recently acquired a vast interest due to their potential to host exotic phenomena.^[1-3] Current studies on superconductor-topological insulator (TI)-superconductor junctions based on exfoliated film and nanoribbons have shown unconventional current phase relations (CPR) that could be associated with Majorana fermions, which may help realize topologically protected quantum computing.^[4-8] In a 3D TI based junction, the Majorana modes should appear in the surface modes as a doublet of gapless Andreev bound states whose energy varies 4π periodically with the phase across the junction alongside the normal 2π periodic Andreev bound states. But in most of the studies on these systems, there is an unavoidable contribution from the bulk, and experiments based on 3D-TI nanoribbons (TINRs) with a reduced number of transport modes are much needed. We make use of Al-Bi₂Se₃-Al junctions fabricated using TINRs grown by physical vapor deposition.^[9-11] To extract the current phase relation of our TI-junction, we utilize an asymmetric dc-SQUID measurement technique. The TI-junction to be studied is connected parallel to a reference junction on the same TINR with a higher critical current, typically 10-15 times more, thus forming a SQUID device. This asymmetry in critical current is achieved by varying the TI-junction width, keeping the distance between the electrodes constant. Now, considering a large ratio between the critical currents and a small SQUID loop inductance (i.e., screening parameter much less than one), the phase across the reference junction stays constant on the application of magnetic flux while the phase across the test junction is changing linearly with the applied magnetic flux. From the modulations of the SQUID critical current, we directly determine the CPR of the small TI-junction. We observe clear deviations from standard sinusoidal CPR of typical tunnel junctions in all our devices. This skewed CPR at low temperatures results from highly transparent modes in our TI junctions. For increasing temperature and one obtains the sinusoidal current phase relation consistent with the thermal population of the Andreev bound states.

Reference:

- [1] L. Fu et al., Phys. Rev. Lett. 100, 096407 (2008)
- [2] C. Nayak et al., Rev. Mod. Phys. 80, 1083–1159 (2008)
- [3] G. Y. Huang et al., Phys. Rev. B: Condens. Matter Mater. Phys. 95, 155420–6 (2017)
- [4] J. Wiedenmann et al., Nat. Comm, 7:10303 (2016)
- [5] C. W. J. Beenakker et al., Annu. Rev. Condens. Matter Phys. 4, 113–136 (2013)
- [6] L. P. Rokhinson et al., Nat. Phys. 8, 795–799 (2012)
- [7] K. L. Calvez et al., Commun. Phys. 2, 4 (2018)

- [8] P. Schüffelgen., Nat. Nanotechnol. 14, 825–831 (2019)
[9] G. Kunakova et al., Nanoscale 10, 19595–19602 (2018)
[10] G. Kunakova et al., Appl. Phys. Lett. 115, 172601 (2019)
[11] G. Kunakova et al., J. Appl. Phys. 128, 194304 (2020)

1:05 PM NM02.02.05

Late News: Giant Fractional Shapiro Steps in Anisotropic Josephson Junction Arrays Ritika Panghotra¹, Clécio C. de Souza Silva², Bart Raes¹, Ivo Cools¹, Wout Keijers¹, Jeroen E. Scheerder¹, Victor V. Moshchalkov¹ and Joris Van de Vondel¹; ¹Quantum Solid-State Physics, Department of Physics and Astronomy, KU Leuven, Belgium; ²Departamento de Física, Universidade Federal de Pernambuco, Brazil

The current phase relationship (CPR), describes the relation between the supercurrent, I_s , through a Josephson junction (JJ) and the gauge invariant phase difference across the junction, $\Delta\theta$. The exact relation, is determined by the details of the Andreev bound state spectrum that exists in the junction. For conventional SIS junctions, the CPR is sinusoidal, $I_s = I_c \sin(\Delta\theta)$, where I_c is the junction critical current. With the advances in materials sciences and the realization of novel link materials, exhibiting non-conventional CPRs, JJ with new functionalities arise having a tremendous potential for applications.

The harmonic content of the CPR in these novel weak link materials can be revealed by experiments relying on detecting the phase-locked response of a current driven Josephson junction when subjected to a high frequency radiation field of frequency, ν_{rf} [1]. In case the weak link is characterized by a conventional sinusoidal CPR, this resonant response manifests itself as constant voltage plateaus, so called Shapiro steps, in the VI-characteristics at voltages $V_n = n\Phi_0\nu_{rf}$, where n is an integer number and Φ_0 the flux quantum. However, for a weak link having a non-sinusoidal CPR, the response exhibits, in addition to the conventional integer Shapiro steps, steps at fractional values $V_{n/q} = (n/q)\Phi_0\nu_{rf}$, where the q^{th} ($q \neq n$) fractional step originates from the phase-locked response with the q^{th} harmonic of the CPR.

Despite the experimental accessibility of these techniques, the detailed interpretation of such experiments is complicated by the non-linear nature of the Josephson response. Moreover, the use of a single junction makes these experiments challenging mainly due to its low response. Josephson junction arrays (JJAs) containing many junctions provide the natural alternative to provide the necessary enhancement of the coherent response. Although JJAs hold a strong promise to study the CPR, the impact of the particular CPR on the high frequency response remains until now unexplored.

We investigate the potential of anisotropic JJAs to study the harmonic content of the CPR in a broad frequency range (down to 50 MHz). Introducing anisotropy results in a giant collective high frequency phase-locked response that reflects the properties of a single junction. We demonstrate experimentally the appearance of giant fractional Shapiro steps in anisotropic JJAs as unambiguous evidence of a skewed current phase relationship. This in contrast to prior observations of giant fractional Shapiro steps in JJAs as resulting from magnetic flux quantization in the two-dimensional array.

- [1] S. Shapiro, *Phys. Rev. Lett.* **11**, 80 (1963)
[2] R. Panghotra, B. Raes, Clécio C. de Souza Silva, I. Cools, W. Keijers, J.E. Scheerder, V.V. Moshchalkov, and J. Van de Vondel, *Communications Physics* **3**, 53 (2020)

2:15 PM *NM02.03.01

Making the High-Pressure-Induced High- T_c Phases Practical for Applications Paul C. W. Chu^{1,2}, Liangzi Deng¹, Trevor Bontke¹, Melissa Gooch¹, Shuyuan Huyan¹, Rabin Dahal¹ and Zheng Wu¹; ¹University of Houston, United States; ²Lawrence Berkeley National Laboratory, United States

Raising T_c and setting new T_c records by discovering new compounds, modifying known compounds, and/or developing novel mechanisms to meet new challenges in science and technology have lured many scientists and engineers to superconductivity ever since its discovery. Great progress has been made in the last three decades in both the stable compounds, such as cuprates and iron-pnictides and -chalcogenides, and the unstable compounds of hydrogen-rich molecular solids. Both have T_c s within practical ranges: air-conditioning for the former and cryogen-free ambient for the latter. While the temperature barrier has been brought down, the pressure becomes a formidable obstacle to practical applications. Should this obstacle be overcome by retaining these high pressure (HP)-induced high- T_c phases at ambient, their technological impact would be profound and limited only by the imagination. We have thus explored the possibility of retaining these HP phases at ambient *via* pressure-quenching following appropriate thermodynamic paths like those for diamond from graphite and black phosphorus from red phosphorus. Model material systems of Sb, Bi, FeSe, and Cu-doped FeSe have been chosen for the study. We have successfully retained at ambient many superconducting and non-superconducting phases induced under HP up to 64 GPa in these materials. The thermal stability of the pressure-quenched phases has also been resistively examined. The experimental details are briefly described below:

I. Non-superconducting Sb and Bi Single Crystals

1. Determined resistively the phase diagrams, R-P and T_c -P, of the superconductors investigated and compared them with existing ones when available.
2. Identified the HP-induced phases with their different T_c s to retain at ambient.
3. Pressure-quenched these HP-induced phases by rapid removal of the pressure at 77 K.
4. Cooled the pressure-quenched phases from 77 K down to 1.2 K to determine whether each superconducting phase has been quenched in. If so, warmed up the sample to room temperature and cooled it down again to 1.2 K. The superconducting transition will disappear if the superconducting phase is associated with pressure-quenching and if the thermal stability of this phase ceases to exist at 300 K.
5. By repeating such R-T measurements on cooling to 1.2 K after warming to various temperatures above 77 K, the thermal stability of each pressure-induced superconducting phase quenched at 77 K is determined.
6. An anomaly in the R-T curve is also detected in the temperature region when the superconducting transition disappears.
7. Indeed, some of the HP-induced superconducting phases have been successfully pressure-quenched at ambient at 77 K with different thermal stability ranges.

II. Superconducting FeSe Single Crystals

Following the same steps taken for Sb and Bi, we have shown that the HP-induced superconducting phases, as well as the non-superconducting phases, can be pressure-quenched at ambient with a thermal stability up to 300 K.

III. Non-superconducting Cu-Doped FeSe Single Crystals

Following the same protocol for the above compounds, we have unambiguously pressure-quenched in at ambient the HP-induced superconducting and non-superconducting phases.

We have thus demonstrated that the superconducting and non-superconducting phases in Sb, Bi, FeSe, and Cu-doped FeSe single crystals induced under HP up to 64 GPa can be pressure-quenched in at 77 K and ambient pressure with different thermal stabilities up to 300 K. The observations hold great promise for practical applications of the high-temperature superconducting cuprate HBCCO with a T_c of 164 K at ~ 31 GPa and of C-S-H with a T_c of 287 K at 267 GPa.

The work in Houston is supported by US Air Force Office of Scientific Research Grants FA9550-15-1-0236 and FA9550-20-1-0068, the T. L. L. Temple Foundation, the John J. and Rebecca Moores Endowment, and the State of Texas through the Texas Center for Superconductivity at the University of Houston.

2:40 PM *NM02.03.02

Significantly Enhanced Pinning Efficiency of 1D BaZrO₃ Artificial Pinning Centers with Coherent Interfaces with YBa₂Cu₃O_{7-x} Matrix Judy Z. Wu; University of Kansas, United States

One-dimensional c-axis aligned BaZrO₃ (BZO) nanorods are regarded as strong one-dimensional artificial pinning centers (1D-APCs) in YBa₂Cu₃O_{7-x} (YBCO) films. However, a microstructure analysis has revealed a highly defective, oxygen-deficient YBCO column of 2-3 nm in thickness around the BZO 1D-APCs due to the large lattice mismatch of ~7.7% between the BZO (3a=1.26 nm) and YBCO (c=1.17 nm). A hypothesis of reduced pinning potential height due to this defective YBCO column has been confirmed recently on much lower pinning efficiency of the BZO 1D-APCs as compared to BaHfO₃ (BHO) 1D-APCs that form a coherent interface with YBCO. Herein, we report a dynamic Ca/Cu replacement approach on tensile strained YBCO lattice immediately after the BZO 1D-APCs formation to induce c-axis elongation of the YBCO lattice near the BZO 1D-APC/YBCO interface to prevent the interfacial defect formation by reducing the BZO/YBCO lattice mismatch. An YBCO elongated c-axis up to 1.24 nm via Ca/Cu replacement and a defect-free, coherent BZO 1D-APC/YBCO interface are confirmed in transmission electron microscopy and elemental distribution analyses. Excitingly, up to five-fold enhancement of $J_c(H)$ at magnetic field $H=9.0$ T//c-axis and 65-77 K was obtained in the ML samples as compared to their BZO/YBCO single-layer counterpart's. This has led to a record high pinning force density F_p together with significantly enhanced H_{max} at which F_p reaches its maximum value $F_{p,max}$ for the BZO 1D-APCs at H//c-axis. At 65 K, $F_{p,max} \sim 157$ GN/m³ and $H_{max} \sim 8.0$ T in the 6 vol.% BZO/YBCO ML samples represent a significant enhancement over $F_{p,max} \sim 36.1$ GN/m³ and $H_{max} \sim 5.0$ T on the 6 vol.% BZO/YBCO SL counterparts. This result not only illustrates the critical importance of the BZO 1D-APC/YBCO interface in the pinning efficiency, but also provides a facile scheme to repair this interface for higher pinning efficiency of the BZO 1D-APCs.

Acknowledgements

This research was supported in part by NSF contracts Nos: NSF-DMR-1909292 and NSF-DMR-1508494, the AFRL Aerospace Systems Directorate, the Air Force Office of Scientific Research (AFOSR), and the U.S. National Science Foundation (DMR-1565822 and DMR-2016453) for TEM characterization.

3:05 PM NM02.03.03

Late News: Anisotropic Superconductivity in the Spin-Vortex Antiferromagnetic Superconductor CaK(Fe_{0.95}Ni_{0.05})₄As₄ Beilun Wu; Instituto Nicolás Cabrera and Condensed Matter Physics Center (IFIMAC), Universidad Autónoma de Madrid, Spain

CaKFe₄As₄ is a newly discovered iron pnictide superconductor which shows optimal critical temperature T_C of 38 K at the stoichiometric compound. Electron doping with Ni or Co atoms induces a decrease in T_C and the onset of a particular hedgehog antiferromagnetic order, without sign of structural instability or nematicity. The influence of this new form of magnetic order on the superconducting state has been till now poorly investigated. Here, we present quasiparticle interference study on CaK(Fe_{0.95}Ni_{0.05})₄As₄ using scanning tunneling microscope at dilution fridge temperature[1]. Unlike in the undoped system[2], we reveal in the Ni doped system a four-fold highly anisotropic superconducting state, in association with the hedgehog antiferromagnetic order present in this system.

[1] J.Llorens et als., arXiv:2009.11246 (2020)

[2] A.Fente et als., Phys. Rev. B 97, 134501 (2018)

3:20 PM NM02.03.04

Late News: Superconducting Properties of 1144-type Iron-Based Superconductors by Mechanochemically Assisted Synthesis Andrea Masi^{1,2}, Achille Angrisani Armenio², Andrea Augieri², Giuseppe Celentano², Chiarasole Fiamozzi Zignani², Aurelio La Barbera², Francesco Rizzo², Alessandro Rufoloni², Enrico Silva¹, Angelo Vannozzi² and Francesca Varsano²; ¹Università degli studi Roma Tre, Italy; ²ENEA, Italy

Iron-based superconductors (IBSC) represent a group of superconducting materials that attracted significant attention in recent years both for academic research and practical applications due to the exotic coupling of magnetism and superconductivity and to their large critical current densities at high magnetic fields. All iron-based superconductors are based on a common structural element, namely a layer composed by Fe atoms tetrahedrally coordinated by pnictogen (P,As) or chalcogen (S,Se,Te) atoms. Several elements and molecules can be intercalated among these planes, giving rise to the different families of the IBSCs. Among these, the so called “1144” compounds are obtained when alternate layers of alkaline and alkaline-earth metals are intercalated among Fe-As planes. These group of IBSCs is characterized by critical fields and critical currents among the highest for what concerns IBSCs single crystals, hence, being very attractive in perspective of high field applications.

In previous works, we have demonstrated the appeal of a mechanochemically assisted synthesis route as opposed to the common high temperature (e.g. $T \sim 900$ °C) process, allowing a finer control of the experimental variables. In particular, we exploit High Energy Ball Milling (HEBM), a low cost and easily scalable mechanochemical powder processing methodology, to ensure the intimate mixing of the elemental powders, and therefore a high degree of homogeneity and reactivity in the starting reactants. Coupling the HEBM with intermediate temperature (e.g. $T \sim 700$ °C) thermal treatments represents an effective strategy to drop the issues related to volatile compounds (e.g. As, K) and ensure at the same time the required homogeneity.

In this work we focus on the properties of Ca/K-1144 polycrystalline materials obtained by the mechanochemically assisted synthesis route. The materials have been characterized in their structure and morphology by means of X-ray diffraction and scanning electron microscopy techniques. Superconducting properties are evaluated by means of electrical resistance and magnetization measurement carried out in different magnetic field conditions up to 18 T. High field measurements allow to highlight granularity phenomena – often observed in these class of compounds – most likely due to weak links at grain or grain aggregates boundaries and to the random orientation of the crystallites that characterizes these bulk samples.

3:35 PM NM02.03.05

Late News: Investigating the Impact of Magnetism on Superconductivity in the Magnetic-Superconductor RbEuFe₄As₄ via Scanning Hall Probe Microscopy David Collomb¹, Simon Bending¹, Alexei Koshelev², Mathew Smylie^{2,3}, Liam Farrar¹, Jin Ke Bao², Duck-Young Chung², Mercuri G. Kanatzidis^{2,4}, Wai-Kwong Kwok² and Ulrich Welp²; ¹University of Bath, United Kingdom; ²Argonne National Laboratory, United States; ³Hofstra University, United States; ⁴Northwestern University, United States

The possible coexistence between magnetism and superconductivity has fascinated scientists ever since the latter's discovery over 100 years ago. New insights into the interaction between these two forms of order may lead to the realisation of exciting new applications including superconducting spintronics, skyrmionics and fluxonic devices for the next generation of computing hardware. RbEuFe₄As₄ is a recently-discovered spin-singlet iron-based superconductor with a superconducting transition temperature of $T_c = 37$ K and a magnetic transition temperature of $T_m = 15$ K, below which both superconductivity and magnetism are present. This large coexistence temperature window makes RbEuFe₄As₄ an ideal material in which to study the interactions between the two forms of order in detail. Magnetic force microscopy and optical conductivity measurements on RbEuFe₄As₄ have suggested a weak suppression of superconductivity in the vicinity of T_m [1], while angle-resolved photoemission spectroscopy measurements indicate a more complete isolation of the two sublattices [2]. Here we use quantitative scanning Hall probe magnetic imaging of superconducting vortices in RbEuFe₄As₄ to probe changes in key superconducting parameters near the magnetic ordering temperature. Model fits to the vortex profiles as a function of temperature reveal a significant increase in the penetration depth near T_m , followed by a gradual reduction at lower temperatures, revealing that the magnetic ordering

leads to a significant reduction in the superfluid density [3]. We corroborate these results with a recently-developed model describing the suppression of superconductivity by correlated magnetic fluctuations [4]. The qualitative agreement between our data and the model suggests that the coupling between the Eu moments and Cooper pairs is weak enough that superconductivity is never destroyed, yet still strong enough to substantially weaken superconductivity. Our results have important implications for understanding coexistence phenomena in other materials systems, which could pave the way to exploiting such materials in future hybrid applications.

[1] V. Stolyarov, A. Casano, M. Belyanchikov, A. Astrakhantseva, S.Y. Grebenchuk, D. Baranov, I. Golovchanskiy, I. Voloshenko, E. Zhukova, B. Gorshunov, A. V. Muratov, V. V. Dremov, L. Y. Vinnikov, D. Roditchev, Y. Liu, G.-H. Cao, M. Dressel, and E. Uykur. Unique interplay between superconducting and ferromagnetic orders in $\text{EuRbFe}_4\text{As}_4$, *Phys. Rev. B* **98**, 140506 (2018).

[2] T. Kim, K. Pervakov, D. Evtushinsky, S. Jung, G. Poelchen, K. Kummer, V. Vlasenko, V. Pudalov, D. Roditchev, V. Stolyarov, D. V. Vyaikh, V. Borisov, R. Valenti, A. Ernt, S. V. Ereemeev, and E. V. Chulkov. When superconductivity does not fear magnetism: Insight into electronic structure of $\text{RbEuFe}_4\text{As}_4$, arXiv preprint arXiv:2008.00736 (2020).

[3] D. Collomb, S. J. Bending, A. E. Koshelev, M. P. Smylie, L. Farrar, J-K. Bao, D. Y. Chung, M. G. Kanatzidis, W-K. Kwok, and U. Welp. Observing the suppression of superconductivity in $\text{RbEuFe}_4\text{As}_4$ by correlated magnetic fluctuations, arXiv preprint arXiv:2010.09901 (2020).

[4] A. E. Koshelev, Suppression of superconducting parameters by correlated quasi-two-dimensional magnetic fluctuations, *Phys. Rev. B* **102**, 054505 (2020).

3:50 PM NM02.03.06

Late News: Direct-Writing of Advanced 3D Nano-Superconductors Rosa Córdoba¹, D. Mailly², A. Ibarra³, Roman O. Rezaev⁴, E. Smirnova⁴, Oliver G. Schmidt⁴, Vladimir M. Fomin⁴, Uli Zeitler⁵, I. Guillamón⁶, Hermann Suderow⁶ and JM De Teresa⁷; ¹Molecular Science Institute (ICMol), Spain; ²Centre de Nanosciences et de Nanotechnologies, France; ³University of Zaragoza, INA, LMA, Spain; ⁴Institute for Integrative Nanosciences, Germany; ⁵High Field Magnet Laboratory (HFML-EFML), Radboud University, Netherlands; ⁶Universidad Autónoma de Madrid, Spain; ⁷Instituto de Nanociencia y Materiales de Aragón (INMA), Spain

Nowadays, superconductors are commonly utilized in several applications such as energy generators and storage due to their unique capability of transferring electricity without energy losses. In some applications, their nanoscale patterning enhances their performance and gives rise to new physical phenomena.

Innovative schemes have taken advantage of the third dimension (3D) for the development of advanced electronic components. The fabrication of complex 3D nano-architectures opens fascinating novel routes in the fields of material science, physics and nanotechnology. Thus, 3D nano-superconductors could be implemented in the next generation of energy efficient electronic devices. Nevertheless, their fabrication and characterization are still challenging and only a few works addressing the growth of real 3D nanosuperconductors have been reported so far¹⁻⁴.

In this contribution, we introduce a direct-write nanolithography method to fabricate at-will advanced 3D nano-superconductors. This specific technique called focused ion beam induced deposition (FIBID) is based on chemical vapour deposition process assisted by a charged particle beam focused to a few nanometers. Particularly, we have prepared 3D superconducting W-C hollow nanowires by decomposing tungsten hexacarbonyl molecules with a highly-focused He^+ ion beam, with outer diameters down to 32 nm and inner ones down to 6 nm⁵. In addition, by modifying the ion beam current, hollow nanowires with controllable inner and outer diameters have been achieved⁶. The growth of the vertical W-C nanowire occurs around the ion beam spot, mainly due to the interaction of secondary electrons with the adsorbed precursor molecules, whereas a cavity at the center of the nanowire is created due to the He^+ beam milling effect on the growing material. As shown by transmission electron microscopy, nanowires microstructure displays grains of large size fitting with face-centered cubic WC_{1-x} phase. In addition, we have grown nanohelices with at-will geometries, with dimensions down to 100 nm in diameter, and aspect ratio up to 65. These nanotubes and nanohelices become superconducting at 7 K and show large critical magnetic field and critical current density. Particularly, these nanohelices display superconductivity up to 15 T depending on the direction of the field with respect to the nanohelix axis. This suggest that their helical 3D geometry and their orientation in a magnetic field play a

significant role in the superconducting phase transition, which can be qualitatively explained using an approach for the properties of thin-film superconductors. Moreover, fingerprints of vortex and phase-slip patterns are experimentally identified and supported by numerical simulations based on the time-dependent Ginzburg-Landau equation ⁷.

The fabrication of such advanced 3D nanomaterials with outstanding properties makes this technique at the cutting edge of nanofabrication methods based on focused beams of charged particles.

References

- (1) Li, W. et al., *J. Nanosci. Nanotechnol.* **2010**, *10* (11), 7436–7438.
- (2) Romans, E. J. et al., *Appl. Phys. Lett.* **2010**, *97* (22), 222506.
- (3) Li, W. et al., *Nanotechnology* **2012**, *23* (10), 105301.
- (4) Porrati, F. et al., *ACS Nano* **2019**, acsnano.9b00059.
- (5) Córdoba, R. et al. *Nano Lett.* **2018**, *18* (2), 1379–1386.
- (6) Córdoba, R. et al., *Beilstein J. Nanotechnol.* **2020**, *11* (1), 1198–1206.
- (7) Córdoba, R. et al., *Nano Lett.* **2019**, *19* (12), 8597–8604.

Acknowledgement:

“This project has received funding from the EU-H2020 research and innovation programme under grant agreement No 654360 NFFA-Europe.”

4:05 PM NM02.03.07

Late News: Topological Transitions in Superconductor Nanomembranes Under a Strong Transport Current Roman O. Rezaev^{1,2}, E. Smirnova¹, Oliver G. Schmidt^{1,3,3} and Vladimir M. Fomin^{1,4}; ¹Leibniz IFW Dresden, Germany; ²Tomsk Polytechnic University, Russian Federation; ³TU Chemnitz, Germany; ⁴National Research Nuclear University MEPhI, Russian Federation

Topological defects such as vortices and phase slips in a superconductor system manifest spatial patterns and dynamics that are closely associated with the geometric design in curved micro- and nanostructures of superconductors [1]. This study is motivated by the recent progress in fabrication of complex 3D nanoarchitectures (e.g., open nanotubes and nanohelices) by using the advanced 3D roll-up self-organization and nanowriting techniques based on focused ion beams. To simulate the superconducting properties of complex nanoarchitectures, a numerical platform has been developed based on a set consisting of the time-dependent Ginzburg-Landau equation coupled with the Maxwell equations [2].

The topological transitions between vortex-chain and phase-slip transport regimes unveiled in curved superconductor nanostructures as a function of the applied magnetic field under a strong transport current [3] open up a possibility to efficiently tailor the superconducting properties of nanostructured materials by inducing a nontrivial topology of superconducting screening currents. We report on a topological transition between superconducting vortices and phase slips under a strong transport current in an open superconductor nanotube with a submicron-scale inhomogeneity of the normal-to-the-surface component of the applied magnetic field. When the magnetic field is orthogonal to the axis of the nanotube, which carries the transport current in the azimuthal direction, the phase-slip regime is characterized by the vortex/antivortex lifetime $\sim 10^{-14}$ s versus the vortex lifetime $\sim 10^{-11}$ s for vortex chains in the half-tubes, and the induced voltage shows a pulse as a function of the magnetic field. This non-monotonous behavior is attributed to the occurrence of a phase-slip area at such magnetic fields, when the quasi-stationary pattern of vortices changes from single to double chains in each half-turn, followed by reentrance of the superconducting state with a chain of moving vortices when the magnetic field further increases. A three-fold voltage peak occurs in an ultrathin open Nb tube of radius 400 nm at the magnetic field about 10 mT. The topological transition between the vortex-chain and phase-slip regimes determines the magnetic-field–voltage and current–voltage characteristics of curved SC nanomembranes to pursue high-performance applications in advanced electronics (e.g., as novel superconductor switching-based detectors) and quantum computing.

References

- [1] Fomin, V. M. *Self-rolled Micro- and Nanoarchitectures: Topological and Geometrical Effects*, De Gruyter, Berlin-Boston, **2021**, 148 p.
- [2] Smirnova, E. I.; Rezaev, R. O.; Fomin, V. M. *Low-Temperature Physics* **2020**, *46*, 325-330.
- [3] Rezaev, R. O.; Smirnova, E. I.; Schmidt, O. G.; Fomin, V. M. *Communications Physics* **2020**, *3*, 144, 1-8.

Acknowledgement

This work has been supported by DFG projects #FO 956/5-1, #FO 956/6-1, COST Action #CA16218 (NANOCOHYBRI), MEPhI Academic Excellence Project # 02.a03.21.000, RFBR and Tomsk Region under the project #19-41-700004.

SESSION NM02.04: MgB₂ Wires and Cryogenics
Session Chairs: Christopher Kovacs and Mary Ann Sebastian
Wednesday Afternoon, April 21, 2021
NM02

5:15 PM NM02.04.01

Late News: Significant Progress in MgB₂ Transport J_c and n Value with Vapor-Solid Reaction Route and C/Dy₂O₃ Additions Mike D. Sumption and Fang Wan; The Ohio State University, United States

In this work a vapor-solid reaction route was developed for MgB₂ conductors with a multifilamentary structure of subelements with a Mg infiltration-based subelement design. The individual subelements consisted of Mg rods surrounded by B powder, all encased in a Nb chemical barrier. This design, used previously for liquid infiltration routes, was used for a lower temperature vapor-solid reaction route, with significant improvements in layer J_c, conductor I_c, and conductor n-value. This result is explained in terms of a two process model, including percolation through the strand, and local reactive diffusion to form the MgB₂ phase. The model shows that much deeper infiltration and a more complete reaction is possible with a vapor-solid route. Whole conductor J_e values of 9 x 10⁴ A/cm² are obtained at 4 T, 4.2 K, (I_c = 500 A in our 0.83 mm OD, 18 filament conductor). Index values above 30 were obtained at 6 T. These conductors had co-additions of 2 mol% C and 2 wt% Dy₂O₃. A variety of C doping fractions and Dy₂O₃ additions are compared, and the best properties are found in samples with co-additions. It is seen that Dy₂O₃ suppresses T_c more slowly than C doping and thus is a useful co-additive at elevated temperatures. Co-additions are in every case superior to single additive designs, although the optimal amount of Dy₂O₃ additions depends on the intended temperature of use. This result is explained in terms of the relative fraction of inter- and intra-band scattering with C doping and Dy₂O₃ additions.

5:30 PM NM02.04.02

Late News: Cryogenic/Superconducting Considerations for Electric Aircraft Drivetrains Mary Ann Sebastian^{1,2}, Timothy Haugan², Mike D. Sumption³ and Bang-Hung Tsao¹; ¹University of Dayton Research Institute, United States; ²Air Force Research Laboratory, United States; ³The Ohio State University, United States

Transportation is a leading source of green-house gas emissions, with aircraft contributing to 10% of the CO₂ emissions at 900 million metric tons of CO₂/yr. Employing electric aircraft drivetrains would greatly diminish CO₂ emissions. However, implementation of all-electric, hybrid, and turboelectric propulsion systems does present many difficult challenges in regards to power capability, specific power, and specific energy. Superconducting power transmission and cryogenic machines have unique properties that can help overcome these challenges. Superconducting power transmission has no ohmic losses, lower transmission voltage, and utilizes smaller, lightweight conductors. Cryogenic machines utilizing superconducting wire possess very high

efficiency and supply a large current density. This presentation discusses cryogenic/superconducting considerations for electric aircraft drivetrains and provides an analysis of mass and heat loss scaling laws for various components of the electric drivetrain: such as metal conductors, busbars, current leads, metal/superconducting T-joints, HTS cables, and cryoflex tubing.

5:45 PM NM02.04.03

Late News: Current Sharing, Stability and Thermal Management in an Extremely Low AC Loss MgB₂ Conductor Christopher Kovacs¹, Timothy Haugan², Mike D. Sumption³, Mike Tomsic⁴ and Matt Rindfleisch⁴; ¹National Academies of Sciences, Engineering, and Medicine, United States; ²Air Force Research Laboratory, United States; ³The Ohio State University, United States; ⁴Hyper Tech Research Inc., United States

In the push to develop high power electric aircraft, superconducting technology promises to significantly reduce mass and volume of motors and generators. However, challenges related to AC Loss and thermal management are a significant factor in preventing the proliferation of aerospace superconducting technologies. Increasing the resistance of the metal matrix stabilization has only gone so far in reducing coupling currents for higher frequency applications. In this research, Multiphysics simulations were used to investigate using a very high thermal conductivity electrical insulator replacing the main slightly resistive metal matrix of an MgB₂ composite wire. The insulator separates the MgB₂ filaments entirely, only allowing transient current sharing to occur with the high purity (typically Niobium) diffusion barrier. The results of these simulations and a process to make this composite in a realistic manner using a molten salt impregnation process are then presented.

SESSION NM02.05: REBCO and Iron-Based Superconductors and Nanostructures

Session Chairs: Kazumasa Iida and Yutaka Yamada

Wednesday Afternoon, April 21, 2021

NM02

8:15 PM *NM02.05.01

Prediction of Flux Pinning Properties of APC-Doped REBCO Coated Conductor by TDGL Method Kaname Matsumoto; Kyushu Institute of Technology, Japan

Optimizing the critical current density J_c of REBa₂Cu₃O_{7-x} (REBCO, RE = rare earth) coated conductors at a given temperature T and magnetic field B is particularly important in applications such as high magnetic field coils. To that end, it is necessary to know more about how the introduced artificial pinning centers (APCs) immobilize the motion of quantized vortices. In order to solve this problem, we fabricated coated conductor samples in which BaMO₃ (BMO : M=Hf, Zr, Sn) APCs were introduced into REBCO thin films and investigated in detail the effect on J_c under 4.2 – 20 K and $B//c$, 0-25 T magnetic fields. The thin film preparation conditions were adjusted to change the size and density of the BMO nanorods, and to control the concentration of random pinning centers such as oxygen vacancies. Information on nanostructures including BMO-APCs was obtained from REBCO samples by TEM observation, and vortex pinning simulation was performed by large-scale time-dependent Ginzburg-Landau (TDGL) equations for high kappa limit, with nanostructure information as input parameters. Thereafter, the predicted J_c and the measured J_c were compared. According to the experimental results, the maximum value of the global pinning force $F_p (= J_c \times B)$ of the sample varied from 0.7 to 1.7 TN/m³ depending on the concentration of BMO. When the concentration of BMO was high, the F_p value reached a peak of 1.7 TN/m³ at 8-10 T and formed a plateau. The plateau continued to the high magnetic field region of 25 T, the upper limit of the present experiment. When the concentration of BMO was low, the maximum value of F_p decreased to about half and gradually increased toward the high magnetic field side. On the other hand, according to TDGL simulation, when the concentration of BMO was high, F_p reached about 1.7 TN/m³ in the vicinity of 8-10 T (strong pinning regime), and then the F_p value was saturated to form a similar plateau (collective pinning, plastic pinning regime). In addition, when

the BHO concentration was halved, J_c decreased to about half, and the experimental results were successfully reproduced almost accurately. Large-scale TDGL simulations were expected to have splendid J_c prediction power, but now it is clear that the experimental J_c values of REBCO coated conductors with APCs can be simulated almost accurately. Additional random pin effects such as oxygen vacancies can be also incorporated into the TDGL simulation. The optimal structure of APC that maximizes J_c can be predicted under given T and B conditions by these methods, which can help improve the performance of coated conductors with real complex microstructures.

8:40 PM *NM02.05.02

Development of High- T_c Superconducting DC Cable System and Related Basic Studies Noriko Chikumoto, Hirofumi Watanabe, Yury Ivanov, Hirohisa Takano and Satarou Yamaguchi; Chubu University, Japan

For the social implementation of superconducting cables, the key point is how long the liquid nitrogen used to cool the superconducting cables can be circulated maintaining a predetermined temperature. In order to obtain the properties required to get a future prospect for longer length cable system, we participate a national project called Ishikari project that include the construction of two dc power lines, "Line 1" with 500m-length (5kA, 100 MVA) and "Line 2" with 1000m-length (2.5 kA, 50 MVA) and the circulation and current test using the system. The project had been started from 2013 and successfully ended on 2016 [1,2]. From the analysis of various data we have got the prospect that we can circulate the LN2 for more than 20 km. [3]. However, there are issues to be considered for the realization of 10-20 km system, such as improvement of thermomechanical characteristics, simplification of cable connection, weight reduction, and further improvement of cooling efficiency. We will discuss about these technical issues and show some of the basic research concerning them.

[1] S. Yamaguchi, et al., *IEEE Trans. Appl. Supercond.*, **25**, # 5402504 (2015).

[2] N. Chikumoto, et al., *IEEE Trans. Appl. Supercond.*, **26**, # 5402104 (2016).

[3]H. Watanabe, et al., *IEEE Trans. Appl. Supercond.*, **27**, # 5400205 (2017).

9:05 PM *NM02.05.03

Development of High-Performance $Ba_{1-x}K_xFe_2As_2$ Tapes for High-Field Magnet Applications Yanwei Ma^{1,2}; ¹Institute of Electrical Engineering, Chinese Academy of Sciences, China; ²University of Chinese Academy of Science, China

Iron-based superconductors exhibit high upper critical fields and low electromagnetic anisotropy, making them particularly attractive for high-field applications. IEE-CAS continues to address iron-based wire development and fabricating methods to improve characteristics and performance of the wires and tapes. The highest J_c value has reached 0.15 MA/cm² at 4.2 K and 10 T with a combination of densification and texturing processes in mono-core silver sheathed $Ba_{1-x}K_xFe_2As_2$ (Ba-122) tapes. By employing high strength Cu/Ag and stainless steel/Ag as sheath materials, larger than 0.1 MA/cm² at 4.2 K in an external magnetic field of 10 T was recently achieved for Ba-122 tapes by the scalable flat-rolling process. Furthermore, transport J_c of 100 m long tapes was further enhanced, higher than 30000 A/cm² (4.2 K, 10 T). We will show a summary of the recently achieved properties and give an outlook on the next development steps on our program roadmap.

9:30 PM NM02.05.04

Late News: Evidence of Ambient Superconductivity in Engineered Au-Ag Nanostructures Anshu Pandey; Indian Institute of Science, India

We had recently proposed the existence of room temperature, ambient pressure superconductivity in Au-Ag nanostructures. This presentation will provide an overview of the structural, electronic, magnetic and optical properties of these materials. It is shown that below a certain critical temperature that is dependent on sample structure and composition, these materials show transitions to a diamagnetic, zero resistance state. We further show that along with emergence of unusual magnetic and electrical properties, these materials also exhibit unconventional optics. In particular, we observe the suppression of usual metallic plasmon resonances and the appearance of a broad dissipation less resonance. A theoretical framework for correlating and explaining some

of these material properties is described.

SESSION NM02.06: Superconductors Wires/Tapes and Applications
Session Chairs: Teresa Puig and Carmine Senatore
Thursday Morning, April 22, 2021
NM02

8:00 AM *NM02.06.01

Frontiers of Nb₃Sn and REBCO Conductor Technology for Future Applications in High Magnetic Fields

Carmine Senatore¹, Florin Buta¹, Gianmarco Bovone¹, Marco Bonura¹, Tommaso Bagni¹, Davide Matera¹, Amalia Ballarino², Simon Hopkins², Bernardo Bordini² and Lucio Rossi²; ¹University of Geneva, Switzerland; ²CERN, Switzerland

Low Temperature Superconductors (LTS) have today more widespread application than ever, with a large market pulled by Magnetic Resonance Imaging (MRI), Nuclear Magnetic Resonance (NMR) spectroscopy and large-scale science projects. In particular, Nb₃Sn is the prime candidate to develop accelerator magnets for the post-LHC collider, where unprecedented collision energies in the region of 100 TeV are envisaged. This goal has led to a baseline configuration requiring dipoles generating 16 T in a 100 km tunnel that translates into a requirement for critical current densities substantially beyond state-of-the-art for commercial Nb₃Sn wires and eventually close to the ultimate limit of the material. On the other hand, High Temperature Superconductors (HTS) were intended at the beginning as a vehicle for a new class of applications in the electric utility network. However, the game changing opportunity now coming from HTS and, in particular, from REBCO tapes results from the possibility to operate at high current densities in very high magnetic fields and at high cryogenic temperature. These properties raised the interest of both high-energy physics and fusion communities. High fields beyond the reach of LTS, in the range of 20 T, would enable a further increase of the collision energy in the next generation hadron colliders and are making possible the conception of compact fusion devices, which are crucial for the fusion's commercial realization. Moreover, the low sensitivity of the critical current to temperature, apart from the obvious simplification of the refrigeration system, would bring an improved stability of the magnet system, which is an essential requirement both in a particle collider and in a dynamic fusion environment. In this talk, I will address the current state and the directions in which the technology needs are driving the property evolution of Nb₃Sn and REBCO with a particular focus to the recent developments at UNIGE.

Research supported by the Swiss National Science Foundation (Grant No. 200021_184940), by the European Organization for Nuclear Research (CERN), Memorandum of Understanding for the FCC Study, Addendum FCC-GOV-CC-0112 (KE3646/ATS) and Addendum FCC-GOV-CC-0175 (KE 4663/ATS) and by the Accelerator Research and Innovation for European Science and Society (ARIES) project. ARIES has received funding from the European Union's Horizon 2020 Research and Innovation programme under Grant Agreement No 730871.

8:25 AM *NM02.06.02

Challenges in Designing Superconducting Magnets for the European DEMONstration Fusion Power Plant Valentina Corato; ENEA, Italy

Fusion power offers the prospect of an almost inexhaustible source of energy for future generations. The design and R&D of future fusion reactor concepts is expected to benefit largely from the experience gained in the design, construction and operation of ITER. However, harnessing fusion energy and deploying reliable magnetic confinement fusion power plants, requires to overcome the design challenges and to address the remaining readiness gaps.

Many realizations of the DEMONstration Fusion Power Plant (DEMO) are proposed in the world, featuring different concepts and approaches. In this framework Europe is starting the Conceptual Design Phase for building a superconducting tokamak and starting operations around the middle of the century. The aim is demonstrating the production of 500 MWs of net electricity, the feasibility of operation with a closed tritium fuel cycle, and maintenance systems capable of achieving adequate plant availability.

Superconducting magnets have the crucial role to produce high magnetic fields used for initiating, confining, shaping and controlling the fusion fuel in the form of plasma. The main challenges related to magnets regard the design layout (pancakes vs. layers), the superconducting materials (Low-Temperature vs. High-Temperature Superconductors) and technology (React&Wind vs. Wind&React manufacturing approach) and the possible use of radial plates.

An overview of the state-of-the-art and the main perspectives of the superconducting magnet technology considered for DEMO will be illustrated.

8:50 AM NM02.06.04

Late News: Angular Dependence of Pinning Unfolds the Difference Between YBCO and Fe(Se,Te) Films

Gaia Grimaldi¹, Antonio Leo^{2,1}, Angela Nigro^{2,1}, Masood Khan², Valeria Braccini¹, Carlo Ferdeghini¹, Francesco Rizzo³, Andrea Augieri³ and Marina Putti⁴; ¹CNR, Italy; ²University of Salerno, Italy; ³ENEA, Italy; ⁴University of Genova, Italy

The study of pinning landscape is crucial to implement any coated conductor technology based on superconducting materials. In particular, the race to obtain a more isotropic material among High Temperature Superconductors has been pursued by the introduction of effective pinning centers in HTS. The advance of Iron-Based Superconductors can be boosted not only by the fact that Fe-chalcogenides are some of the most isotropic superconductors but also overcoming some conventional beliefs. The Fe(Se,Te) thin films, indeed, are very weak anisotropic superconductors with low values of both the anisotropy factors γ_j and γ_H , in the critical currents and critical fields, respectively. Nevertheless, a common feature with HTS is their layering crystallographic structure. Therefore a puzzling issue arises from the angular dependence of pinning in Fe(Se,Te) compared with YBCO films. We measure the irreversibility field $H_{irr}(\theta)$ and the activation pinning energy $U_p(\theta)$ as a function of the angle between the c -axis of the films and the applied magnetic fields up to 16 T. $H_{irr}(\theta)$ experimental data reveal similarities and differences between YBCO and Fe(Se,Te) films. Owing to their common material layered structure they both show an anisotropic $2D$ behavior of the intrinsic pinning contribution, whereas the extrinsic pinning component unveils the $3D$ isotropic pinning of Fe(Se,Te) against the $2D$ pinning anisotropy of YBCO. A stronger endorsement comes from $U_p(\theta)$ data that show a steep peak around $\theta=0^\circ$ (H parallel to the ab -planes) for both YBCO and Fe(Se,Te) films, which is the fingerprint of their flux pinning ability into the layering structure. By continuously rotating θ towards 90° degrees, only YBCO shows a smooth spread peak around $\theta=90^\circ$ (H parallel to the c -axis), whereas no peak is observed for Fe(Se,Te). All these features promote Fe-chalcogenide superconducting material as the right candidate for coated conductor technology.

9:05 AM NM02.06.05

Late News: Improved Properties in Gd-Doped YBCO Film Grown by Chemical Solution Deposition

Valentina Pinto¹, Angelo Vannozzi¹, Achille Angrisani Armenio¹, Francesco Rizzo¹, Andrea Masi^{1,2}, Andrea Augieri¹, Antonino Santoni¹, Alessandro Rufoloni¹, Antonella Mancini¹, Laura Piperno^{1,2}, Valentina Galluzzi¹, Massimo Tomellini³, Silvia Orlanducci³ and Giuseppe Celentano¹; ¹ENEA, Italy; ²Roma Tre University, Italy; ³Tor Vergata University, Italy

The replacement of Y^{3+} in $YBa_2Cu_3O_{7-\delta}$ (YBCO) by rare earth elements (REs) such as Gd^{3+} to form alternative $REBCO$ compounds has been extensively studied and demonstrated to be very effective for the preparation of materials with enhanced superconducting properties. Chemical Solution Deposition (CSD) of GdBCO is widely adopted for the production of films, but film growth is more sensitive to process parameters with respect to YBCO synthesis. With the aim of overcoming this limitation and improving superconducting properties, mixed $Y_{1-x}Gd_xBa_2Cu_3O_{7-\delta}$ compounds have been successfully studied. To our knowledge, the introduction of Gd in the

form of Gd_2O_3 or GdBCO, added in excess with respect to YBCO, has been reported only by two papers (on bulk or film grown by sol-gel) and demonstrated to have a positive influence on superconducting properties. In this work, we propose a similar study applied to YBCO film deposited by CSD. The aim is to obtain the advantages related to the presence of Gd using the robust and reproducible process adopted for YBCO. In particular, when Gd is added in excess with respect to Y, it can form oxides as Gd_2O_3 or it can substitute Y to form GdBCO, whereas Y can form other oxides such as Y_2O_3 . In both cases, many different defects might originate and act as artificial pinning centers, contributing to the overall improvement of superconducting properties.

CSD of Gd-doped YBCO (YBCO-Gd) film was carried out following the metal organic decomposition approach and *in-situ* route. Three dopant concentrations, i.e. 5, 10 and 20mol%, were studied. Film morphology and crystalline structure were deeply investigated by scanning and transmission electron microscopy (SEM and TEM), X-ray diffraction and photoelectron spectroscopy (XRD and XPS). In general, a well *c*-axis oriented grain structure was observed through XRD. However, YBCO-Gd5% and 10% samples show, with respect to pure YBCO, improved film coalescence and an increase of stacking faults number, as recognized by TEM. XPS allowed verifying the Gd distribution in the film and which phase Gd formed. Superconducting properties, assessed through electrical and magnetic measurements, were evaluated at different temperatures, magnetic field directions and intensities. Higher zero-field critical current densities were measured in the temperature range from 10 K to 77 K with 5% and 10% Gd concentrations (i.e. 28, 27 and 13 MA/cm² respectively for YBCO-Gd5%, YBCO-Gd10% and YBCO at 10K). This improvement by a factor two remains up to 12T and from 10 K to 65 K.

Preliminary data on YBCO-Gd20% evidenced the need for further process optimization aimed at reducing the porosity and the *a*-axis content well evident in the studied films. Nevertheless, the in-field superconducting properties were better than pure YBCO and comparable to YBCO Gd5% and YBCO Gd10%, although a different pinning strength acting in YBCO Gd20% samples could be recognized.

The obtained results confirm the efficacy of Gd addition for the enhancement of transport properties and the existence in YBCO-Gd films of a pinning mechanism particularly significant at low temperatures and different with respect to pure YBCO. The possible origin of such outcomes will be proposed and discussed.

Acknowledgments

V.P. work has been carried out within the framework of the XXXIII Doctoral program in Chemical Sciences, Department of Chemical Science and Technologies, University of Rome Tor Vergata.

This work has been carried out within the framework of the EUROfusion Consortium and has received partial funding from the Euratom research and training programme 2014-2018 and 2019-2020 under grant agreement N°633053. The views and opinions expressed herein do not necessarily reflect those of the European Commission.

This project has received funding from the European Union's Horizon 2020 research and innovation programme under grant agreement N°823717 – ESTEEM3 (Nano-engineered YBCO Superconducting Tapes for High Field Applications, NESTApp).

9:20 AM NM02.06.06

Late News: Intrinsic Anisotropy and Pinning Anisotropy as Revealed by Surface Impedance

Measurements in $YBa_2Cu_3O_{7-d}$ and $FeSe_xTe_{1-x}$ Thin Films [Enrico Silva](#)¹, Jorge Alcalá², Andrea Alimenti¹, Andrea Augieri³, Elena Bartolomé⁴, Valeria Braccini⁵, Giuseppe Celentano³, Xavier Obradors², Anna Palau², Valentina Pinto³, Nicola Pompeo¹, Teresa Puig², Marina Putti⁶, Francesco Rizzo³ and Kostiantyn Torokhtii¹; ¹Università Roma TRE, Italy; ²Institut de Ciència de Materials de Barcelona, Spain; ³ENEA, Italy; ⁴Escola Universitaria Salesiana de Sarrià, Spain; ⁵CNR-SPIN, Italy; ⁶Università degli Studi di Genova, Italy

Anisotropy is fundamental in layered superconductors $YBa_2Cu_3O_{7-d}$ (YBCO) and Fe-based compound like $FeSe_xTe_{1-x}$ (FeSeTe). The sources of anisotropy are many. The unavoidable anisotropic electron effective mass (whence the anisotropic coherence length) gives rise to what we call here *intrinsic anisotropy* γ . The layered structure and extended defects like twin planes, grain boundaries, columnar or other linear defects such some artificial pinning centres (APC) introduce additional directional and a complex *pinning anisotropy*.

In magnetic-field dependent measurements all sources of anisotropy contribute to the overall response, with a difficult identification of the different contributions. Microwave measurements are able to disentangle the intrinsic from pinning anisotropy: high-frequency oscillating vortices experience the effect of vortex drag (the usual mechanism of flux-flow resistivity ρ_{ff} , which depends on the anisotropy through the effective vortex mass), pinning recall force (given by the pinning constant k_p), and flux-creep jumps (quantified by a normalized dimensionless parameter χ) [1]. By measuring the complex surface impedance $Z=R+iX$ as a function of the applied dc magnetic field H and the field orientation θ , possibly at different frequencies, all these contributions can be singled out, gaining separately access to the intrinsic and pinning anisotropy [2].

We perform measurements of $Z(H,\theta)$ with different dielectric resonator setups [3], operating at 16, 27 and 47 GHz, in dc fields up to 1.3 T at different field orientations. We investigate and compare the behaviour of YBCO thin films grown by Chemical Solution Deposition [4] and Pulsed Laser Deposition (PLD) [5], with and without APC in the shape of nanoparticles and nanorods, to the results obtained in pristine $\text{FeSe}_x\text{Te}_{1-x}$ thin films grown by PLD from $\text{FeSe}_{0.5}\text{Te}_{0.5}$ targets [6]. We extract the intrinsic anisotropy γ of the various samples, obtaining in YBCO consistent values $\gamma = 5.0 \pm 0.5$ [7] irrespectively of the kind of APC, and $\gamma \approx 2$ in FeSeTe . On the other hand, we obtain very different pinning anisotropies in all compounds. In YBCO, the pinning anisotropy is related in a complex fashion to the different directional APC, while in FeSeTe we do not measure in the angular dependence of the pinning constant significant departures from the effective mass effect.

This work has been carried out within the framework of the EUROfusion Consortium and has received funding from the Euratom programme 2014–2018 and 2019–2020 under Grant Agreement No. 633053. The views and opinions expressed herein do not necessarily reflect those of the European Commission. Work partially supported by Italian MIUR-PRIN project “Hibiscus”, Grant No. 201785KWLE. We acknowledge financial support from Spanish Ministry of Economy and Competitiveness through the Severo Ochoa Programme for Centres of Excellence in R&D (FUNFUTURE CEX2019-000917-S) and SUMATE project RTI2018-095853-B-C21, co-financed by the European Regional Development Fund.

References

- [1] M. Golosovsky, M. Tsindlekht, and D. Davidov, *Supercond. Sci. Technol.* **9**, 1 (1996) (review paper)
- [2] N. Pompeo and E. Silva, *IEEE Trans. Appl. Supercond.* **28**, 8201109 (2018)
- [3] A. Alimenti et al., *Meas. Sci Technol.* **30**, 065601 (2019)
- [4] A. Llordés et al, *Nat. Mater.* **11**, 329 (2012)
- [5] F. Rizzo et al, *APL Mater.* **4**, 061101 (2016); doi: 10.1063/1.4953436
- [6] N Pompeo et al., *Supercond. Sci. Technol.* **33**, 114006 (2020)
- [7] E. Bartolomé et al., *Phys. Rev. B* **100**, 054502 (2019); N. Pompeo et al., *Supercond. Sci. Technol.* **33**, 044017 (2020)

9:35 AM NM02.06.07

Late News: MgB₂—A Promising Material for Large Scale Applications of Superconductivity Jacques Noudem^{1,2}, Yiteng Xing^{1,2} and Pierre Bernstein^{1,2}; ¹Normandie University, France; ²ENSICAEN, France

While most applications of bulk superconductors are based nowadays on REBCO (RE: Rare earth) or BSCCO materials, the possibility to use liquid hydrogen as a fuel for airplanes and other applications on the one hand and the availability of powerful cryo-coolers on the other hand make light MgB₂ superconductors very attractive for large scale applications. The low density of this light material and its strong mechanical hardness are well suited to its possible use in electric aircrafts and windmill generators. Using the Spark Plasma Sintering technique, bulks can be manufactured in much less time than cuprates and the bulks can be given complex shapes. This is much more difficult with cuprates. These advantages make already MgB₂ a privileged material for the investigation of functional superconducting properties. As an example, we'll report the results of our studies on i) the effect of the thickness and the diameter of cylindrical superconductors on the levitation force and the condition for stability in superconducting magnetic levitation and ii) the role of the starting material on the critical current density of MgB₂ bulks and its dependence on the applied magnetic field.

10:30 AM *NM02.07.01

Understanding Sources of Decoherence In Superconducting Quantum Devices with High Quality Factor Superconducting Resonators Sebastian de Graaf¹, Tonia Lindstrom¹, Alexander Tzalenchuk¹, Lev Ioffe^{2,3}, Lara Faoro⁴, Andrey Danilov⁵ and [Sergey Kubatkin](#)⁵; ¹National Physical Laboratory, United Kingdom; ²University of Wisconsin–Madison, United States; ³Google Inc, United States; ⁴Sorbonne Université, France; ⁵Chalmers University of Technology, Sweden

Despite the promises of superconducting qubits, their performance is presently limited by short coherence times due to defects intrinsic to materials. As a result, future quantum computers would require massive error correction circuits, which seem to be very challenging to build. Another more promising path would be to improve this coherence time, which would relax the constraints on the quantum error correction circuits and would thus make a quantum computer more feasible. This task is considered one of the main challenges in the field, and we contribute to its solution by measurements on high quality factor superconducting resonators [1,2]. Our approach gave vital clues to the long-standing problem of noise and decoherence in superconducting devices: a technique for on-chip Electron Spin Resonance (ESR) allowed to identify the chemical species responsible for the flux noise in superconducting circuits [3]. Furthermore, the noise measurements in superconducting resonators point to the link between charge and flux noise in superconducting circuits [4]: a mild sample treatment has led to tenfold reduction of the density of the surface spins, responsible for the flux noise, as evidenced by ESR, and this treatment has also led to tenfold reduction of the low frequency noise in superconducting resonator, usually associated with charge noise.

Another major challenge comes from non-equilibrium quasiparticles (QPs) that result in qubit relaxation and dephasing. We reveal a previously unexplored decoherence mechanism in the form of a new type of Two-Level Systems (TLS) originating from trapped QPs, which can induce qubit relaxation. Using spectral, temporal, thermal and magnetic field mapping of TLS-induced fluctuations in frequency tunable resonators [2], we identify a highly coherent subset of the general TLS population with a low reconfiguration temperature around 300 mK, and a non-uniform density of states. These properties can be understood if the TLS are formed by QPs trapped in shallow subgap states formed by spatial fluctuations of the superconducting order parameter. This implies that even very rare QP bursts will impact coherence over exponentially long timescales. Summarizing this part, some spurious two-level systems observed in superconducting devices are attributed to long-lived quasiparticles trapped in gap inhomogeneities [5].

Finally, we study a single highly coherent environmental two-level system. We trace the in-time spectral diffusion of this individual TLS and demonstrate that it originates from the TLS coupling to a countable number of low energy incoherent fluctuators (TLF). From the analysis of these fluctuations, we can access relevant parameters of these otherwise elusive low energy TLFs including TLF-TLF interaction energies. Our approach opens up for deriving the macroscopic observables of glassy media from direct measurements of local TLF dynamics at microscopic level - a route towards substantiating commonly accepted models for a decohering environment.

In summary, the use of high-Q superconducting resonators contributes to the construction of full microscopic model for interacting TLS and will then present a solid foundation for building up an ensemble level description of a glassy TLF media. Such a development, in turn, will provide so much needed understanding of decoherence mechanisms at microscopic level and indicate approaches for mitigation of decoherence.

[1] Journ. of Appl. Phys. 112, 123905, (2012)

[2] Phys. Rev. Applied, 2020, in print

[3] Phys. Rev. Lett. 118, 057702, (2017)

[4] Nature Comms. 9, 1143, (2018)

[5] Sci. Adv. 2020, accepted

10:55 AM *NM02.07.02

Temperature Dependence of Quasiparticle Tunneling as a Probe of Transmon Quality Cihan Kurter; IBM T.J. Watson Research Center, United States

Non-equilibrium quasiparticles are possible sources for decoherence in superconducting qubits because their tunneling across the Josephson junction can lead to relaxation. In this talk, we will present the impact of intrinsic properties of our transmons on quasiparticle tunneling (QPT) and discuss how this affects the device quality and performance. We find that the QPT rate to be sensitive to the choice of materials and to the geometry of the capacitive pads shunting the Josephson junctions in transmons. In some of our devices, we observe an anomalous temperature dependence of the QPT rate below ~ 100 mK that deviates from a flat background associated with non-equilibrium quasiparticles. One hypothesis for this trend which will be discussed is that sites of high transparency in the Josephson junction give rise to such behavior.

11:20 AM NM02.07.03

Late News: Investigate Microwave Losses of Materials with Superconducting Resonators Chan U Lei¹, Suhas Ganjam¹, Lev Krayzman¹, Ignace Jarrige², Luigi Frunzio¹ and Robert Schoelkopf¹; ¹Yale University, United States; ²Brookhaven National Laboratory, United States

Improving the coherence of superconducting circuits is one of the biggest challenges in superconducting quantum computing. Superconducting quantum circuits are built from materials such as dielectrics and superconductors. The microwave dissipations from these materials limit the coherence of the circuits. Since the dissipated power of the constituent materials combines in parallel, the materials' quality of all the dominating loss channels needs to be improved simultaneously to enhance the coherence. Therefore, identifying and quantifying materials' microwave losses in superconducting circuits is crucial to developing quantum circuits with very high coherence. In this talk, we will present how to use superconducting resonators to characterize and measure microwave losses of materials in superconducting circuits.

11:35 AM NM02.07.04

Late News: Low Frequency AC Josephson Effect in Ultrasmall Josephson Junctions Hermann Suderow; Universidad Autónoma de Madrid, Spain

The Josephson effect is the consequence of coupling between two superconducting electrodes and consists of a Cooper pair current flowing between the two superconductors at zero bias voltage $V=0$ and coherent emission of photons with energy eV at a finite bias voltage $V>0$. Here we show that ultra small Josephson junctions embedded in a circuit with a feedback oscillate between zero and finite voltage states. We measure the resulting AC oscillations in Pb-Pb, Al-Al and Pb-NbSe₂ atomic size Josephson junctions with a millikelvin Scanning Tunneling Microscope (STM). We discuss prospects and applications of the newly found AC behavior.

11:50 AM NM02.07.05

Late News: Direct Ion Beam Writing of Josephson Junctions in Superconducting Nitrides Aki Ruhtinas and Ilari Maasilta; University of Jyväskylä, Finland

Direct writing of Josephson junctions using focused ion beam was recently demonstrated in YBCO [1] and MgB₂ thin films [2]. This method can simplify and extend the fabrication of Josephson junctions for superconducting devices. We use this approach for superconducting nitride thin films, and show how disorder-driven superconductor-insulator transition (SIT) can be used in Josephson junction fabrication using a helium ion beam. We use high quality superconducting thin films of NbN, TiN and NbTiN that we grow with an infrared pulsed laser deposition technique [3], and demonstrate that in all of the studied nitrides superconductivity can be suppressed by helium ion irradiation, with a higher helium ion fluence resulting in a lower critical temperature T_c . This controllable T_c suppression combined with the high spatial resolution of the

helium ion microscope enables us to successfully fabricate SNS-type Josephson junctions with highly tunable weak links. First results indicate that the most promising candidate among the three superconducting nitrides studied is NbTiN, because of its high T_c (~ 15 K), low resistivity and easily controllable SIT transition. In addition, we demonstrate that NbTiN thin films can be pushed to the insulating side of the SIT transition with a high enough helium ion fluence. Thus, we also managed to fabricate insulating barrier SIS Josephson junctions with NbTiN, in addition to SNS- type devices.

[1] S. Cybart et al., *Nature Nanotech.* 10, 598 (2015)

[2] L. Kasaei et al., *AIP Advances* 8, 075020 (2018)

[3] S. Chaudhuri, M. R. Nevala, T. Hakkarainen, T. Niemi and I. J. Maasilta, *IEEE Trans. Appl. Supercond.* 21, 143 (2011); A Torgovkin et al., *Supercond. Sci. Technol.* 31, 055017 (2018)

12:05 PM NM02.07.06

Superconducting rf-SQUIDs Based Metamaterials Operated in 3WM and 4WM Regimes for Travelling Microwaves Luca Fasolo^{1,2}, Angelo Greco^{1,2}, Alessio Rettaroli³, Luca Piersanti³, Giovanni Maccarrone³, Carlo Ligi³, Daniele Di Gioacchino³, Claudio Gatti³, Matteo Beretta³ and Emanuele Enrico^{1,2}; ¹Istituto Nazionale di Ricerca Metrologica, Italy; ²Piemonte Quantum Enabling Technologies Laboratory - PiQuET, Italy; ³Istituto Nazionale di Fisica Nucleare - Laboratori Nazionali di Frascati, Italy

At microwave frequencies, Josephson parametric amplifiers (JPA), based on a resonant architecture, have demonstrated quantum-limited noise and are currently used in emerging fields like axion search or solid state qubits read out. Despite significant advances allowing improved bandwidth and saturation power JPAs are however still insufficient for addressing the needs of the above-mentioned applications. Traveling Wave Parametric Amplifiers (TWPAs) represent a potential solution. At microwave frequencies, a TWPA is designed as a nonlinear metamaterial that exploits the signal response of reactive parts (typically inductance) in a superconducting circuit. A large pump tone modulates this inductance, coupling the pump (f_p) to a signal (f_s) and idler (f_i) tone via frequency mixing such that $2f_p = f_s + f_i$ (4-wave mixing, 4WM) or $f_p = f_s + f_i$ (3-wave mixing, 3WM).

Parametric amplifiers are currently the only known method to achieve quantum-limited sensitivity to microwave signals but achieving a large enough and sufficiently flat bandwidth over the entire needed band is still a challenging task. Worldwide, research efforts are under way to solve these problems, by developing several prototype functional amplifiers. TWJPA appear as the ultimate microwave amplifiers since they promise large gain, wide bandwidth, high saturation power and low noise approaching the quantum limit, making it robust, easily integrable into experimental setups, and cost-effective application in detectors read out and in quantum information sciences.

In recent times, the concept of a parametric amplifier with microwaves travelling along a transmission line with embedded Josephson junctions (TWJPA) was developed in several groups. These devices have already demonstrated quantum-limited noise and are used to readout superconducting qubit. TWJPA are classically designed for operating only in the 4WM regime. In this approach, the necessary phase matching of the travelling microwaves requires sophisticated dispersion engineering which still cannot ensure perfect phase matching in a sufficiently wide frequency range. This results in undesirable resonance dips and considerable ripple in the gain versus frequency dependence. Recently, a wide-band parametric amplifier operating in the regime of 3WM, has been proposed. The proposed design consists of a 3WM TWJPA based on microwave transmission line formed by a serial array of non-hysteretic rf-SQUIDs. This one-dimensional metamaterial possesses large quadratic nonlinearity and nominally zero (unwanted) cubic (Kerr-like) nonlinearity. Proof-of-principle measurements performed at a temperature $T = 4.2$ K on Nb/AlOx/Nb trilayer samples have demonstrated the validity of the concept of this practical TWJPA with great promise for quantum-limited performance. It is expected that TWJPA devices operating in the three-wave mixing mode will outperform state-of-the-art parametric amplifiers with respect to simultaneously achieving large gain and high bandwidth. In the present work several characterizations of TWJPAs based on Al standard Josephson junctions technology will be presented. The DC current tunability of such a rf-SQUIDs based metamaterial will be investigated by focusing on the 4WM and 3WM regimes. Single tone transmission spectroscopy and signal gain evaluation by means of the so-called pump-on-pump-off method will be discussed with particular attention to real devices

non-idealities that introduces a complex behaviour of the amplifier response.

12:20 PM NM02.07.07

Late News: Large Fluctuations of T_1 in Long-Lived Transmons Kungang Li, Sudeep Dutta, Rui Zhang, Zachary Steffen, Dylan Poppert, Shahriar Keshvari, Jeffery Bowser, Benjamin Palmer, Christopher Lobb and Frederick Wellstood; University of Maryland, United States

As the relaxation time T_1 of transmons has increased in recent years, apparently so has the size of the fluctuations in T_1 . To investigate the cause of these fluctuations we measured the T_1 of transmons made with an electrode layer of pure aluminum and a counter-electrode layer made with either pure Al or oxygen-doped granular Al. The superconducting energy gap of the counter-electrode depends on the layer's thickness and the grain size, which depends on the oxygen doping. At 20 mK an oxygen-doped device showed T_1 variations between about 80 μ s and a maximum of 300 μ s, while an un-doped device on the same chip showed uncorrelated T_1 variations between about 50 and 100 μ s. Measurements of the fluctuations versus temperature reveal that the standard deviation of T_1 is proportional to T_1 , even above 150 mK, where the transmon relaxation is dominated by thermally generated quasiparticles. We discuss why this behavior is not consistent with the two most commonly proposed mechanisms, fluctuations in two-level-system dielectric loss or fluctuations in the density of non-equilibrium quasiparticles and propose an alternative mechanism that is consistent with this behavior.

SESSION NM02.08: REBCO Films and Coated Conductors

Session Chairs: Fedor Gomory and Joffre Gutierrez

Thursday Afternoon, April 22, 2021

NM02

1:00 PM NM02.08.01

REBa₂Cu₃O_{7-x} Coated Conductors Integration in High-Energy Physics Applications Joffre Gutierrez¹, Artur Romanov¹, Patrick Krkotic^{2,3}, Guilherme Telles¹, Joan O'Callaghan³, Francis Perez², Montse Pont², Xavier Granados¹, Ilya Korolkov⁴, Sergio Calatroni⁵ and Teresa Puig¹; ¹Institut de Ciència de Materials de Barcelona, Spain; ²ALBA Synchrotron, Spain; ³Universitat Politècnica de Catalunya, Spain; ⁴Institut de Física d'Altes Energies, Spain; ⁵CERN, Switzerland

On the 19th of June 2020, the European Strategy Group announced the 2020 update of the European Strategy for Particle Physics, identifying the ambition to operate a proton-proton collider (FCC-hh) at the highest achievable energy as long term future priority. CERN's FCC-hh is the most ambitious scenario for a post LHC machine. It will operate as an 80-100 km acceleration ring where 16-18 T magnets will steer proton bunches producing center-of-mass collision energies of 100 TeV. In order to protect the superconducting magnets, the 35.4 W/m/beam synchrotron radiation emitted by the protons will be absorbed by a stainless steel tube, the so called beam-screen chamber, held at a temperature window of 40-60 K. Image currents will be induced into the steel walls of the beam-screen endangering the beam stability. To counteract this effect, the interior of a beam-screen chamber has to be coated with a highly conductive material. Our consortium explores the possibility to replace the conventional beam-screen coating Cu with REBa₂Cu₃O_{7-x} (RE = rare earth) Coated Conductors (CCs) in order to increase the beam stability margin.

In this contribution, we demonstrate why commercially available REBCO CCs are promising candidates for the FCC-hh beam screen coating. Critical current densities measured up to 9 T at 50 K, which is the operating reference temperature of the beam screen chamber, point towards a superconducting performance that can sustain the induced peak image currents of 25 A at FCC conditions. We present the surface resistance R_s of CCs and Cu colaminated on stainless steel at 8 GHz and in a wide range of cryogenic temperatures and magnetic fields. We find that CCs outperform Cu under operating conditions close to those to be found in the FCC-hh. In

addition, high frequency vortex parameters like the depinning frequency are extracted from the data by fits with the Gittleman-Rosenblum model. This allows a discussion on the limits of the mean-field model and the correlation between surface resistance and microstructure of different REBCO CCs. The next steps towards an aspect ratio study of Cu and CCs in order to minimize trapped fields in the beam screen chamber, their assembly in the beam screen and the expansion of measurement conditions to the more realistic 16 T and 1 GHz will be discussed.

1:15 PM NM02.08.02

Late News: Direct Visualization of Current-Stimulated Oxygen Migration in YBa₂Cu₃O_{7- δ} Thin Films

Alejandro Silhanek¹, Stefan Marinković¹, Alejandro Fernández-Rodríguez², Simon Collienne¹, Sylvain Blanco Alvarez¹, Sorin Melinte³, Boris Maiorov⁴, Gemma Rius⁵, Xavier Granados², Narcis Mestres² and Anna Palau²;
¹Université de Liège, Belgium; ²Institut de Ciencia de Materials de Barcelona, ICMAB-CSIC, Spain;
³Université Catholique de Louvain, Belgium; ⁴Los Alamos National Laboratory, United States; ⁵Institute of Microelectronics of Barcelona, Spain

The past years have witnessed major advancements in all-electrical doping control on cuprates. In the vast majority of cases, the tuning of charge carrier density has been achieved via electric field effect by means of either a ferroelectric polarization or using a dielectric or electrolyte gating. Unfortunately, these approaches are constrained to rather thin superconducting layers and require large electric fields in order to ensure sizable carrier modulations. In this work, we focus on the investigation of oxygen doping in an extended region through current-stimulated oxygen migration in YBa₂Cu₃O_{7- δ} superconducting bridges. The underlying methodology is rather simple and avoids sophisticated nanofabrication process steps and complex electronics. A patterned multiterminal transport bridge configuration allows us to electrically assess the directional counterflow of oxygen atoms and vacancies. Importantly, the emerging propagating front of current-dependent doping δ is probed in situ by optical microscopy and scanning electron microscopy. The resulting imaging techniques, together with photoinduced conductivity and Raman scattering investigations, reveal an inhomogeneous oxygen vacancy distribution with a controllable propagation speed permitting us to estimate the oxygen diffusivity. These findings provide direct evidence that the microscopic mechanism at play in electrical doping of cuprates involves diffusion of oxygen atoms with the applied current. The resulting fine control of the oxygen content would permit a systematic study of complex phase diagrams and the design of electrically addressable devices.

1:30 PM NM02.08.03

Late News: Analytical Modelling of the Functional Properties of Superconductors—A Useful Tool

Complementary to Numerical Simulation Pierre Bernstein, Yiteng Xing and Jacques Noudem; Normandy University, France

Most investigations on the functional properties of bulk superconductors, such as the trapped field and the levitation force, are done nowadays by numerical simulations combining the finite element method and the A, H or T- Ω formulations of the differential Maxwell equations. By comparison, analytical models require generally a regular distribution of the applied field and are practical with simple superconductor shapes with a high level of symmetry only. They have however the advantages to require much less computation time than numerical simulations and to show physical laws that are not always obvious in the results of the simulations. In this contribution we'll present analytical mean field models of superconducting magnetic levitation (SML) reproducing the levitation force on the one hand and the guidance force on the other hand. We'll show that these models give very useful information for the design of the applications of SML concerning: i) the localization of the shielding currents in the superconductors and ii) the condition for stability of axisymmetric levitating systems.

1:45 PM NM02.08.04

Late News: Reducing Cross-Field Demagnetization in Stacks of REBCO Tapes by Soldering

Enric Pardo¹, Mykola Solovyov¹, Anang Dadhich¹, Shuo Li², Marek Mosat¹ and Jan Souc¹; ¹Slovak Academy of Sciences, Slovakia; ²Northeastern University, China

The most powerful remnant-magnetic-field magnets are stacks of REBCO high-temperature superconducting tapes, which can trap up to 17.7 T. However, relatively low alternating magnetic fields perpendicular to the trapped magnetic field can demagnetize, or even fully demagnetize, the stacks [1]. This is a problem for many power devices, such as rotating machines with stacks of tapes in the rotor. Promising applications are aircraft propulsion motors for hybrid or electric airplanes [2], where ripple fields are of the order of 1 kHz or higher. At this frequency, a flight of only 1 hour corresponds to more than 3 million ripple-field cycles, which can fully demagnetize the stack, if the ripple field amplitude is high enough [1]. In this contribution, we present a solution to reduce cross-field demagnetization for many cycles, based on soldering the tapes. We base our study in both measurements and modeling. For modeling, we use the Minimum Electro-Magnetic Entropy Production (MEMEP) [3] to find the screening currents, taking into account the effect of soldering the tapes with a finite resistivity [4]. For the measurements, we magnetize the stack in liquid nitrogen with a superconducting magnet and later apply a transverse alternating field by means of a copper coil for frequencies of up to 500 Hz. Modeling shows that soldering the tapes with low enough resistance can drastically reduce the cross-field demagnetization. In order to achieve sufficiently small tape-to-tape resistance, we solder the tapes face-to-face in the experiments, confirming the findings from modeling. With this contribution, we show that soldered stacks with low resistance between tapes are very interesting for applications, and hence it is worth to dedicate efforts in this direction.

[1] A Dadhich, E Pardo. Modeling cross-field demagnetization of superconducting stacks and bulks for up to 100 tapes and 2 million cycles, *Scientific Reports* **10**, 19265 (2020)

[2] F Grilli et al. Superconducting motors for aircraft propulsion: the Advanced Superconducting Motor Experimental Demonstrator project. *Journal of Physics: Conference Series* **1590**, 012051 (2020)

[3] E Pardo and M Kapolka. 3D computation of non-linear eddy currents: Variational method and superconducting cubic bulk. *J. Comp. Phys.* **344**, 339-363 (2017)

[4] S Li, J Kováč, E Pardo. Coupling loss at the end connections of REBCO stacks: 2D modelling and measurement. *Supercond. Sci. and Technol.* **33**, 075014 (2020)

2:00 PM NM02.08.06

Late News: Controlling the Doping of YBCO Nanowire Through Electromigration Edoardo Trabaldo, Riccardo Arpaia, Eric Wahlberg, Floriana Lombardi and Thilo Bauch; Chalmers University of Technology, Sweden

The understanding of copper oxide superconductors, and in particular $\text{YBa}_2\text{Cu}_3\text{O}_{7-\delta}$, is inextricably tied to the complex electronic phases of those materials in their normal state. Here various nanoscale ordering phenomena occur as a function of doping and temperature and thus two key factors need to be addressed: 1) study the material at the nanoscale and thus the characteristic length scales of the phenomena under study, 2) precise control of the charge doping, which determines its properties.

Nanowires with different oxygen content are the ideal platform to study the electronic properties of YBCO as a function of doping. Alas, their fabrication is challenging, and each doping level requires a separate fabrication process. Moreover, the nanowire properties at different doping levels might vary due to different fabrication conditions. As an alternative solution, we use electromigration (EM) to control ex-situ the doping level of YBCO nanowires.

This process involves the displacement of the dopant oxygen atoms by applying a strong electric current. Pulsed EM can be used to gradually reduce the doping of a YBCO nanowire, while DC biased EM can be conversely used to restore the oxygen content of the same nanowire. These EM processes result in high-quality YBCO nanowires and can be used to fine tune their doping level. Indeed, with a single nanowire we were able to recover most of the YBCO phase diagram, with critical temperatures ranging from 90 K to 45 K.

The ex-situ control of the doping level in YBCO nanowires is a milestone towards an in-depth study of the phase diagram of cuprates. The EM bypasses the challenges of different fabrication techniques and opens the way for using the same nanowire to study the entire phase diagram. Moreover, this technique is interesting for the technological applications of YBCO weak links, where the tuning of the nanowire properties, such as

critical current and kinetic inductance, is required.

2:15 PM NM02.08.07

Late News: Development of Hot Spot in Coated Conductor Tape Due to Local Reduction of Critical Current Fedor Gomory and Jan Souc; Slovak Academy of Sciences, Slovakia

Coated conductor (CC) tapes with functional layer of high-temperature superconductor REBCO (RE = Y, Gd, Er,...) exhibit impressive capability of transporting large amounts of electricity when the critical current, I_c , could commonly reach 1000 A in a tape 12 mm wide when cooled down to 77 K. However, when checking this property along the tape length, it quite often reveals the existence of locations with suddenly reduced I_c value. It is then not obvious which value of current should be taken as the limitation for a steady DC transport. We expect that a current slightly surpassing the local critical value could be sustained, but at its further increase the temperature will rise quickly creating the “hot spot” with enormous local dissipation causing an irreparable damage.

We present the model allowing to investigate the evolution of temperature in the location with reduced critical current analytically. It was found, that at surpassing the local I_c this temperature could stabilize at an elevated value, provided the dissipation is balanced by the cooling capability of surrounding environment. However, for a given tape architecture and cooling conditions, there is always the value of transported current that triggers the development of a hot spot. Advantage of our approach is that it allows in rather simple way to predict the result of DC transport at currents larger than the local minimum of critical current. Experiments with the tapes optimized for use in a resistive fault current limiter confirmed the validity of our theoretical formulas.

SESSION NM02.09: Vortex Pinning and Critical Current

Session Chairs: Qiang Li and Mike Sumption

Thursday Afternoon, April 22, 2021

NM02

4:00 PM NM02.09.01

Late News: Strong Increases in Transport Current, Grain Refinement and Point Pining with Internal Oxidation of Ti, Zr, and Hf Solutes in APC Nb3Sn Superconductors Mike D. Sumption¹, Xingchen Xu², Jacob Rochester¹, Xuan Peng³, Gabriel Ortiz¹ and Jinwoo Hwang¹; ¹The Ohio State University, United States; ²Fermilab, United States; ³Hyper Tech Research, United States

Over the last few years, it has been shown that an internal oxidation process can be used to more than double the layer J_c of state-of-the-art Nb₃Sn conductors, with ternary level Bc₂ values and practical conductor layouts. Part of the reason for this large increase is that the grain size is reduced, and since conventional Nb₃Sn pins flux exclusively at the grain boundaries, this leads to large transport increases. This grain boundary refinement is caused by Zener pinning associated with oxide nanoparticles generated by the oxygen which has diffused in during the internal oxidation process. However, the oxide nanoparticles themselves pin flux directly. As the size of the nanoparticles decreases and their density increases, we can shift the character of the pinning from grain boundary to point pinning, as quantified by the shape of the pinning curve. In this work we compare various members of the group-IVB elements (Ti, Zr, Hf) as internal oxidants, showing that the size decreases while density increases as we move from Ti to Zr to Hf. We also confirm that internal oxidation is required to obtain the largest grain reductions and required for any level of peak shift. We use TEM to show the size and distribution of the precipitates, as well as map their distribution across the growth layer. We see that the TiO particles are typically 100 nm, while those of the ZrO are 5-10 nm, and those of the HfO are below 5 nm. We discuss the role of classic nucleation and growth in determining these factors. We find that the J_p curve shifts from 0.2 Birr for unoxidized Hf and control samples to 0.25 Birr for ZrO precipitates to 0.27 Birr for HfO. Further consideration of the underlying mechanisms should allow yet further improvements in conductor

performance. Our results, in particular the influence of the precipitates on peak shift, suggests that internal oxidation is presently the most promising route for high field performance increases in Nb₃Sn.

4:15 PM NM02.09.02

Late News: Optimizing Supercurrent Transmission in NiFe Ferromagnetic Josephson Junctions Using Ni "Dusting" Swapna Sindhu Mishra, Robert M. Klaes, Reza Loloee and Norman O. Birge; Michigan State University, United States

Josephson junctions with ferromagnetic layers where the ground-state phase difference can be reliably controlled are a potential candidate for applications in cryogenic memory devices, which can greatly reduce the ever-growing energy requirements for large-scale computing. Phase control has been successfully demonstrated with junctions containing a Ni fixed layer and a NiFe free layer [1,2]. However, there are still several improvements that can be made to increase the efficiency and reliability of these junctions. We present work on improving the transmission efficiency of single layer NiFe junctions by "dusting" the NiFe with thin layers of Ni on both sides. We also present a study of the 0- π transitions in these Ni "dusted" NiFe junctions.

This work is supported by Northrop Grumman Corporation.

[1] E. C. Gingrich, B. M. Niedzielski, J. A. Glick, Y. Wang, D. L. Miller, R. Loloee, W. P. Pratt, and N. O. Birge, Nat. Phys. 12, 564 (2016).

[2] I. Dayton, T. Sage, E. Gingrich, M. Loving, T. Ambrose, N. Siwak, S. Keebaugh, C. Kirby, D. Miller, A. Herr, Q. Herr, and O. Naaman, IEEE Magn. Lett. 9, 3301905 (2018).

4:30 PM NM02.09.03

Late News: Understanding the Role of Interfilament Bonding on the Critical Current Density of Bi-2212 Round Wires and Optimization of Wire Architecture Imam Hossain, Jianyi Jiang, Peter J. Lee, Temidayo Abiola Oloye, Fumitake Kametani, David Larbalestier and Eric Hellstrom; Florida State University, United States

Currently, the record J_c achieved in Bi-2212 short samples is around 9600 ampere per mm² at 5 T in 4.2 K. However, this performance has not yet been reproduced in long length coils and to date, the maximum J_c achieved in a coil is much lower compared to short samples. One possible reason for this lower J_c in coils is because the Bi-2212 wire in the coils has more interfilamentary bonding than in short Bi-2212 wires. This difference in amount of bonding can be explained by the amount of time the Bi-2212 spends in the melt state (t_{melt}) during the heat treatment. Short samples are heat treated in small overpressure (OP) furnaces and the heat treatment parameters can be controlled precisely. Large coils, which have large thermal masses, have to be heat treated in large OP furnaces where precise temperature control is not straight forward and small variations can cause significant changes in t_{melt} . We find that J_c depends on t_{melt} and this dependence is more prominent in wires with shorter distance between the Bi-2212 filaments compared to wires with larger filament separation. For a given t_{melt} , wires with smaller filament separation have more filament bonding than wires with larger filament separation. We believe the amount of filament bonding impacts the degree of Bi-2212 alignment, with longer t_{melt} resulting in less aligned Bi-2212 and therefore lower J_c . We are studying the underlying mechanism of how interfilament bonding impacts the electromagnetic properties of Bi-2212 wires. In our studies, we have found that interfilament bonding causes fluctuations in Bi-2212 filament cross-sections along the length of the wire, which possibly reduces the critical current. We have begun studying the kinetics of interfilament bond formation so we can quantitatively describe the amount of bonding that occurs in different wires as a function of time during the OP heat treatment. Our goal is to use this kinetic data to optimize the distance between Bi-2212 filaments to minimize the impact t_{melt} has on J_c , which should make it easier to OP heat treat coils in large OP furnaces, and will improve coil performance.

4:45 PM NM02.09.04

Late News: High Speed MgO Buffer Layer Deposition System for Commercial HTS Tape Production

James A. Greer¹, Larry Scipioni¹, Alexey Mankevich², Anton Markelov² and Alexander Molodyk²; ¹PVD Products, United States; ²S-Innovations, Russian Federation

The rapidly growing field of compact nuclear fusion technology is driving the need for HTS-equipped electromagnets. The amount of tape needed just to build a single demonstrator reactor outstrips – by an order of magnitude – the present worldwide capacity to produce tape. Thus, higher speed tape manufacturing is a critical need. One of the bottlenecks in the production of buffered tape is the epitaxial MgO layer deposited on amorphous oxide. In the Stanford process, ion beam assisted deposition (IBAD) produces the biaxially textured template for subsequent addition of epitaxial MgO (EPI) by electron beam evaporation on heated substrates. The IBAD growth rate is limited by the available ion beam flux, which must match the arriving flux of MgO molecules at the tape substrate.

PVD Products has developed and commercialized a dual-chamber system for high speed production of IBAD/EPI layers. The system can process 1 kilometer of 100 μm thick tape at a speed of 200 meters/hour. Longer lengths of thinner tape are possible due the high capacity electron beam sources. The system features extended length deposition zones with multiple tape passes and, most importantly, a unique IBAD geometry pairing one evaporator with two large rectangular RF ion sources. The EPI layer chamber is likewise equipped with dual evaporation sources to support growth of thick EPI MgO at high processing speed. Multi-pass deposition handles 12 mm wide tape, and the tool is also designed to handle a single lane of 10 cm wide tape, albeit at a lower tape speed of ~ 50 m/hour. Two dedicated, differentially pumped RHEED chambers provide real-time feedback on film quality of both the IBAD and EPI processes without exposing the RHEED system to evaporant or high gas pressure. The tool has demonstrated processing 1 km of tape in a continuous 5-hour run. Due to the robust design, initial testing has also been extended to web speed up to 350 m/hr while still producing good RHEED patterns from both chambers. We will give an overview of the technology and present results from initial characterization the films deposited on metal tapes, including post-processing of LMO and ReBCO to complete the HTS stack.

SESSION NM02.10: Superconducting Films and Coated Conductors Applications

Session Chairs: Noriko Chikumoto and Kaname Matsumoto

Thursday Afternoon, April 22, 2021

NM02

8:15 PM *NM02.10.01

Recent Progress of HTS R&D and Production at Shanghai Superconductor Technology Yutaka

Yamada^{1,2}, Yue Zhao^{2,3}, Jiamin Zhu^{2,3}, Guangyu Jiang², Chunsheng Cheng², Zhiyong Hong^{2,3} and Zhijian Jin³;

¹Chubu university, Japan; ²Shanghai Superconductor Technology Co., Ltd, China; ³Shanghai Jiao Tong University, China

Recent efforts to develop REBCO wire at Shanghai Superconductor Technology will be presented. Mainly two kinds of wire, GdBCO and EuBCO with/without pinning center are constantly produced at a high-speed deposition rate of 50nm/sec. Monthly production of the wire achieved in 2020 achieved about 50 to 100km/month. Not only mass-production but also R&D for high-field application are also being developed. For example, we achieved high critical current, I_c , and pinning force at 4K, 18T of 430 A/4 mm-width and 806.2 GN/m³, respectively. In addition to these main R&D, efforts to improve production system are being done for wire precise size control, Hastelloy substrate thickness, and so on.

8:40 PM *NM02.10.02

SuperOx Research and Development Strategy for Customization of Commercial REBCO Coated Conductors for Various Applications Sergey Lee; SuperOx Japan, Japan

During 10 years since its foundation SuperOx Japan has been successfully developing IBAD/PLD approach for manufacturing of 2G HTS wires and in collaboration with SuperOx and S-Innovations (Russia) delivered hundreds of kilometers of REBCO based coated conductors for R&D and commercial projects worldwide. SuperOx strategy based on customization of 2G HTS superconducting wires for application in particular temperature and field ranges. Based on the operating conditions in terms of magnetic field strength and temperature the company outlined five target areas for the development of new 2G HTS wires including:

- 1) Superconducting fault current limiters (SFCL, operating in self-field at 77K);
- 2) Rotating machines, particularly motors for aircrafts (1-3T and 65-70K);
- 3) Magnets for induction heaters, flywheels and MagLev (3-5T, 30-40K);
- 4) Coils for fusion reactors (12-20T, 20K);
- 5) Inserts for high-field NMR (>25T, 4.2K).

The R&D strategy for new line of SuperOx 2G HTS products relied on the combination of following approaches:

Variation of composition by chemical substitutions;
Optimizing the overall superconducting material stoichiometry;
Controlling of hole doping level (oxygen content);
Introduction of pinning centers including fabrication of multilayers;
Heavy ion irradiation of the HTS wires.

By the end of 2020 SuperOx companies reached production capacity of 300 km of 2G HTS wires per year and in 2021 we are planning to approach the level of 1000 km/year. In the course of production, it was revealed that new tapes demonstrate extremely attractive properties, for instance critical current (I_c) up to 1000A/12mm (s.f, 77K) record high engineering current (J_e) exceeding 1000A/mm² at 20K-20T and over 2000A/mm² at 4.2K and 20T was demonstrated.

In this work we carried out systematic analysis of large number of industrially produced tapes studied by XRD, SEM-EDX, TEM, micro Raman techniques and their connection with final I_c -B- θ characteristics. Several important features responsible for superior I_c -B characteristics were identified which was very helpful to stabilize the production of tapes with improved I_c -B characteristics and to increase the production yield.

9:05 PM *NM02.10.03

Strong Vortex Pinning in (Ba,K)Fe₂As₂ Epitaxial Thin Films by Grain Boundary Engineering Kazumasa Iida^{1,2}, Dongyi Qin³, Chiara Tarantini^{4,5}, Takafumi Hatano^{1,2}, Hikaru Saito^{6,2}, Yiming Ma⁶, Chao Wang⁶, Satoshi Hata^{6,6,2}, Michio Naito^{3,2} and Akiyasu Yamamoto^{3,2}; ¹Nagoya University, Japan; ²JST CREST, Japan; ³Tokyo University of Agriculture and Technology, Japan; ⁴National High Magnetic Field Laboratory, United States; ⁵Florida State University, United States; ⁶Kyushu University, Japan

Significant progress on the thin film growth of iron-based superconductors (FBS) has been achieved over the last decade. As a result, high quality, epitaxial thin films of the technological important FBS [e.g., Fe(Se,Te), doped $LnFeAsO$ (Ln : lanthanoid) and doped $AeFe_2As_2$ (Ae : alkali earth elements)] are realised on different kinds of single crystalline substrates and technical substrates except for (Ba,K)Fe₂As₂.

Recently, we have successfully fabricated (Ba,K)Fe₂As₂ epitaxial thin films on fluoride substrates[1], which gives a great opportunity to investigate electrical transport properties. Here, we report on a high critical current density J_c of 14.6 MA/cm² at self-field and 4 K, corresponding to the pinning efficiency $\eta=J_c/J_d$ of 8.8% (J_d : depairing current density). This value is much higher than the single crystal with artificial isotropic defects ($\eta=3.5\%$) [2]. The angular-dependent J_c always shows a large c -axis peak below 25 K, which is the opposite behaviour to the expected one from the upper critical field anisotropy. Microstructural analysis by transmission electron microscope revealed the presence of many grain boundaries located almost parallel to the crystallographic c -axis. These results suggest that low-angle grain boundaries work as strong correlated pinning centres.

This work was supported by JST CREST Grant Number JPMJCR18J4. A portion of work was performed at the National Magnetic Field Laboratory, which was supported by National Science Foundation Cooperative Agreement No. DMR-1644779, US Department of Energy Office of High Energy Physics under the grant

number DE-SC0018750, and the State of Florida. This work was also partly supported by Advanced Characterization Platform of the Nanotechnology Platform Japan sponsored by the Ministry of Education, Culture, Sports, Science and Technology (MEXT), Japan.

[1] D. Qin, K. Iida, T. Hatano, H. Saito, Y. Ma, C. Wang, S. Hata, M. Naito, A. Yamamoto, submitted.

[2] V. Mishev, M. Nakajima, H. Eisaki, M. Eisterer, *Sci. Rep.* **6**, 27783 (2016).

9:30 PM NM02.10.04

Late News: Critical Current Density in Ca and Ce Counter-Doped YBCO Jamil Tahir-Kheli and Carver Mead; California Institute of Technology, United States

A recent paper (<https://arxiv.org/abs/1702.05001>) suggests that the D-wave gap symmetry of cuprate YBCO may be changed to S-wave gap symmetry by simultaneous doping of an electron doping atom and a hole doping atom into the parent compound. An S-wave gap symmetry creates better Josephson junctions across grain boundaries in poly-crystalline YBCO and would lead to an increase of its critical current density, J_c . A low J_c in poly-crystalline cuprates has been a major technological roadblock to fabricating high- J_c cuprate wires. We synthesized $Y(1-x-y)Ca(x)Ce(y)Ba_2Cu_3O(7-d)$, where the Ca and Ce atoms substitute onto Y sites as hole and electron donors, respectively. We find that over a broad range of Ca and Ce dopings (x and y each varying from 0.0 to 0.32), the T_c of the cuprates is in the range of 72-77 K. This T_c stability to a large quantity of impurities is incompatible with a D-wave superconducting gap and suggests the appearance of S-wave gap symmetry. In order to study the J_c of our samples, we have designed a non-contact radiofrequency (RF) resonator that measures changes in the AC resistance and inductance in order to extract the J_c . In this talk, we will present our results for J_c as a function of temperature and Ca and Ce doping.

SESSION NM02.11: On-demand
Wednesday Morning, April 14, 2021
NM02

8:00 AM NM02.11.01

Late News: Critical Current Distributions of Bi-2212 Compared to Benchmark Nb-Ti Superconductors Shaon Barua^{1,2}, Daniel Davis², Yavuz Oz², Jianyi Jiang², Eric Hellstrom², Chiara Tarantini², Ulf Trociewitz² and David Larbalestier²; ¹Florida State University, United States; ²National High Magnetic Field Laboratory, United States

In composite superconductors, the local critical current can vary along the length due to variable vortex pinning interactions, as well as variations in filament connectivity due to filament shape variation and, especially in HTS conductors, variations in grain-to-grain connectivity. This critical current (J_c) distribution can be extracted from a d^2V/dI^2 treatment of the $V-I$ curves, as originally proposed by Baixeras and Fournet [1] and used by Warnes [2] to study filament-sausaging degradation of critical current density (J_c) in Nb-Ti. High J_c is now available in Bi-2212 round wires and there is intense interest in further optimization of these wires. Brown [3] recently studied wires with almost 6 times variation in J_c made over almost a decade and found that their normalized $J_c(H)$ characteristics were almost identical, from which we concluded that their vortex pinning was identical and that J_c was determined by their grossly varying connectivity. In Nb-Ti there is concern about filament connectivity only when filaments are overdrawn and they start to sausage, unlike Bi-2212 where cross-sectional non-uniformity is built into the filament shape due to the large shape anisotropy of Bi-2212 grains and many poor grain-to-grain connections further degrade filament connectivity. Attainable J_c values in Nb-Ti reach ~ 0.2 of the depairing current density (J_d), while reaching only $\sim 0.01 J_d$ in Bi-2212, suggesting significant room for raising J_c if better connectivity can be obtained (Bi-2212 does however have higher J_c than Nb-Ti now). Our measurements show that J_c in Bi-2212 depends significantly on both powder source and the heat treatment used

to densify and grain-align the 2212. We find that the standard deviation to mean ratio s/m of various Bi-2212 wires range from $\sim 0.1 - 0.2$, while our benchmark Nb-Ti conductor is about 0.05 at $\sim 0.5H_{irr}$. We find it interesting that (i) there are clear trends that J_c rises as s/m declines and (ii) that the s/m values are only about twice as high as our fully optimized Nb-Ti wire, which unlike Bi-2212 is isotropic and has one single value of H_{irr} . We conclude that this technique is valuable for comparison of various Bi-2212 conductors and for comparison to more traditional Nb-Ti and Nb₃Sn conductors.

References

- [1] J. Baixeras and G. Fournet, "Vortex displacement losses in a non-ideal type II superconductor," *Journal of Physics and Chemistry of Solids*, vol. 28, no. 8, pp. 1541–1547, Aug. 1967.
- [2] W. H. Warnes and D. C. Larbalestier, "Critical current distributions in superconducting composites," *Cryogenics*, vol. 26, no. 12, pp. 643–653, Dec. 1986.
- [3] M. D. Brown *et al.*, "Prediction of the $J_c(B)$ behavior of Bi-2212 wires at high field," *IEEE Transactions on Applied Superconductivity*, vol. 29, no. 5, pp. 1–4, Aug. 2019.

8:10 AM NM02.11.03

Late News: Probing Materials Losses with Planar Superconducting Resonators Corey Rae H. McRae^{1,2};
¹University of Colorado Boulder, United States; ²National Institute of Standards and Technology, United States

Materials losses from native oxides on superconducting metal surfaces, interfaces between materials, and bulk dielectrics are the dominant source of decoherence in superconducting quantum processors. Superconducting microwave resonators can act as a convenient qubit proxy for assessing loss performance and characterizing loss mechanisms such as two-level system loss, non-equilibrium quasiparticles, and magnetic flux vortices. This talk will provide an overview of accurate resonator loss measurement, summarizing techniques that have been evolving for over two decades, and will conclude with recommendations for future measurements in this field.

8:20 AM NM02.11.04

Late News: Effect of Varying the Cooling Rate (R_F) on Over Pressure Heat Treated (OPHT) Bi-2212 Round Wires Temidayo Abiola Oloye, Jianyi Jiang, Imam Hossain, Eric Hellstrom, David Larbalestier and Fumitake Kametani; Florida State University, United States

Advances in precursor powder and processing technology has increased the potential of Bi₂Sr₂CaCu₂O_x (Bi-2212) as a capable material for application in high field high temperature superconducting (HTS) magnets. The record high critical current densities ($J_c [4.2K, 30T] = 4670A/mm^2$) was achieved by improved precursor powder, in particular the recent Engi-Mat powder. Further understanding and optimization of the processing stage will provide another avenue for further increases in the J_c of Bi-2212 round wires (RW). The use of Over Pressure Heat Treatment (OPHT) has greatly simplified the processing of Bi-2212 RW with less time and resources spent in the processing stage. Notwithstanding these advantages of OPHT, the exact influence of the key OPHT parameters, most especially the rate of cooling (R_F) and the time in the melt (t_{melt}) on the micro- and nano- structure of fully heat treated Bi-2212 RW is still not fully understood. In this study, we systematically vary R_F and t_{melt} for 2 wire diameters (1mm and 1.2mm) and investigate how this affects the microstructure, grain texture, and overall J_c of the recent Bi-2212 RWs made with the new Engi-Mat powder. We found that the 1mm diameter wire showed minimal variation in J_c (about 5%) and microstructure, while at 1.2mm, the wires showed significant variation microstructure and J_c (about 20%). Overall, our results showed the possibility of achieving minimal variation in J_c with a wide OPHT processing window. This study is particularly important for scaling up Bi-2212 processing from short sample OPHT to large coil processing while maximizing the J_c of Bi-2212 RW. Further details will be given in the presentation.

8:30 AM NM02.11.05

Late News: Experimental and 3D Modelling Investigation of DC Magnetic Shielding by Machinable MgB₂ Bulks Michela Fracasso^{1,2}, Samuele Ferracin¹, Roberto Gerbaldo^{1,2}, Gianluca Ghigo^{1,2}, Francesco Laviano^{1,2}, Andrea Napolitano^{1,2}, Daniele Torsello^{1,2}, Mykola Solovyov³, Fedor Gomory³, Marco Truccato^{2,4},

Mihai A. Grigoroscuta⁵, Mihail Burdusel⁵, Aldica Gheorghe⁵, Petre Badica⁵ and Laura Gozzelino^{1,2},
¹Politecnico di Torino, Italy; ²Istituto Nazionale di Fisica Nucleare INFN, Italy; ³Slovak Academy of Science, Slovakia; ⁴University of Torino, Italy; ⁵National Institute of Materials Physics, Romania

Bulk superconductors (SC) have recently found a mighty application in magnetic shielding [1], with MgB₂ bulks as a very promising option [2]. For this purpose, a combination of modelling procedure and growth technique able to manufacture properly shaped products with high and homogeneous critical current density, can be a successful approach guiding the whole optimization process.

This work focuses on the shielding properties of tube- and cup-shaped MgB₂ bulks with small height/outer radius aspect ratio. Moreover, the effect of adding a ferromagnetic (FM) sheet around the superconductor is addressed. All the SC samples were produced by processing the starting commercial MgB₂ powders added with hexagonal BN into high-density bulks via spark plasma sintering, obtaining fully machinable samples [3]. Starting from the experimental analysis, a 3D modelling evaluation was then carried out.

In more details, first, the properties of both SC and hybrid SC/FM shields were measured in both axial- (AF) and transverse-field (TF) configurations using cryogenic Hall probes [4,5]. In a second step, the experimental results were reproduced by finite element calculations with COMSOL Multiphysics® [4], exploiting a 3D magnetic vector-potential (**A**) formulation [6]. The good agreement obtained by comparing the computed induction fields with those measured experimentally allowed us to validate this modelling approach for our application.

Finally, this numerical procedure was applied to explore new shield design with similar aspect ratio but optimized performance. In particular, the shielding efficiency of three different cup-shaped arrangements were compared both in AF and TF configurations, studying the effect of superimposing ferromagnetic vessels of different sizes around the superconductor.

Acknowledgements

Slovak team acknowledges the support of Grants APVV-15-0257 and APVV-16-0418.

[1] K. Hogan et al., Supercond. Sci. Technol. 31, 015001 (2018)

[2] D. Barna et al., IEEE Trans. Appl. Supercond., 29, 4101310 (2019)

[3] G. Aldica M. Burdusel, V. Cioca, P. Badica Patent No RO130252-A2, DPAN 2015-383635

[4] L. Gozzelino et al., Supercond. Sci. Technol., 32, 034004 (2019)

[5] L. Gozzelino et al., Supercond. Sci. Technol., 33, 044018 (2020)

[6] M. Solovyov and F. Gömöry, Supercond. Sci. Technol., 32, 115001 (2019)

8:40 AM NM02.11.06

Late News: Investigating the Use of 2G REBCO Coated Conductors in Magnetic Confinement Fusion Devices William Iliffe, Chris Grovenor and Susannah Speller; University of Oxford, United Kingdom

The toroidal field (TF) magnets of magnetic confinement fusion (MCF) power plants need to operate at high current density for extended periods to be cost effective. This requires these TF magnets to use superconducting current carriers. To aid in their design, this work aims to better understand how ReBCO coated conductors will perform when subjected to the exotic particle environment present in electricity producing MCF devices. This has been achieved using a combination of irradiation damage simulation and ion bombardment experiments.

Simulation based investigations have been used to determine the predominant changes to ReBCO during neutron irradiation in several settings (fusion and fission). Ion bombardment experiments included 2 irradiation campaigns performed with room temperature samples. These used 2MeV He⁺ and 3.1MeV O₂⁺ ions to mimic the effects of neutron irradiation. The results using each ion species, were compared with those of published neutron irradiation experiments. The 3rd ion bombardment campaign involved the in-situ irradiation and superconducting property measurement of ReBCO samples whilst at their operating temperature. This required a new, dedicated experiment to be designed and built, in collaboration with Surrey University's Ion Beam Centre.

A summary of the findings of the irradiation damage simulations, results from the 3 irradiation campaigns and a summary of the in-situ irradiation and testing experiment will be presented, along with proposed next steps.

8:43 AM NM02.11.07

Late News: Optimization of Milling Energy Density and Heat Treatment Temperature for Enhancing Intergrain Critical Current Density in K Doped Ba-122 Bulks Shah Alam Limon, Chongin Pak, Chiara Tarantini, Eric Hellstrom, David Larbalestier and Fumitake Kametani; Florida State University, United States

Iron based superconductors (FBS) are interesting materials that have high intragranular J_c of $\sim 6 \times 10^5 \text{ Acm}^{-2}$ as thin film single crystal at 4.2 K and 15 T, high irreversibility field of $> 90 \text{ T}$, T_c of $> 35 \text{ K}$, and very low critical field anisotropy. An increase of intergranular J_c is needed to make these materials suitable for high field magnet applications. Intergrain connectivity issues must be overcome for achieving high J_c . Extrinsic factors, such as impurity phases and grain boundary porosity, are the present cause of poor intergrain connectivity in FBS polycrystalline bulks and wires. Combining high-pressure heat treatment and clean synthesis protocol, we studied how the milling energy density and heat treatment (HT) temperature affect the superconducting properties of $\text{Ba}_{0.6}\text{K}_{0.4}\text{Fe}_2\text{As}_2$ (K-Ba-122). By changing RPM and milling time of planetary ball mill, we precisely evaluated milling energy density E_{BM} , ranging from 65 MJ/kg to 1 GJ/kg in different bulks. A novel two-stage heat treatment was used for each bulk. In 1st stage, different HT temperature and ambient pressure was applied in different bulks. We fixed the 2nd stage HT temperature and pressure consistent (600 °C and 193 MPa). We obtained after the 1st HT a T_c of $\sim 38 \text{ K}$, which is close to the highest T_c reported for optimally doped K-Ba-122 single crystals. However, in all cases, T_c drops by 3-4 K after the high pressure 2nd HT. Optimization of 1st stage HT for any E_{BM} was achieved at 750°C, where magnetization J_c after the complete two-stage HT was highest compared with other 1st HT temperatures. Maximum J_c of $1.1 \times 10^5 \text{ Acm}^{-2}$ at 1T is achieved by synthesizing bulk at 100 MJ/kg and 750 °C 1st HT, followed by the high-pressure 600 °C 2nd HT. In this specific case, T_c after 1st HT was 37.6 K and after 2nd HT 34.6 K. The milling energy of 100 MJ/kg at 1st milling appeared to contribute reducing the formation of current-blocking FeAs phase. In this presentation, we will discuss about the correlation between milling energy, heat treatment temperature, connectivity and improved superconducting properties in polycrystalline K doped Ba-122.

8:53 AM NM02.11.08

Late News: The Influence of the Pre-Magnetization Value on the Levitation Force of HTS Tape Stacks Aleksandr Starikovskii, Maxim Osipov, Irina Anishchenko and Igor Rudnev; National Research Nuclear University MEPhI, Russian Federation

This study presents new results on investigation of the levitation force between a permanent magnet and pre-magnetized GdBCO superconducting tape stacks containing from 20 to 100 tapes of 12 mm × 12 mm. The stacks were cooled with liquid nitrogen in the field of a superconducting magnet with a magnetic induction of 3 T and then they were placed in a cryostat of the levitation force measuring system. Stacks of 100 tapes were cooled in different applied fields with magnetic induction in the range of 0.1-1 T. The field captured by the tapes was measured with a Hall sensor 5 minutes after magnetization. Experimental data on levitation force value and the effect of lateral displacement on it for stacks of tapes with different thicknesses and trapped flux have been obtained. Levitation force decay during the lateral displacements above a permanent magnet was observed for different stacks. Based on the obtained results, it was concluded that pre-magnetized stacks show greater repulsive forces than non-magnetic ones, and the difference increases with the number of tapes in the stack. Capture of the magnetic flux not only provides a greater levitation force, but also leads to a greater attenuation of the levitation force at lateral displacements which increases with increasing magnetization. The captured flux depends on the external field as follows: it increases with an increase in the applied field up to 0.4 T, after which it reaches saturation. The observed physical processes were simulated, and obtained results are in good agreement with the experimental data.

This work was supported by a grant from the Russian Science Foundation (Project 17-19-01527).

8:56 AM NM02.11.09

Late News: Dissipation Caused by Phase Slip Center in NbTi Superconducting Bridge Khalil Harrabi, Abdelkarim Mekki and Hocine Bahlouli; KFUPM, Saudi Arabia

We report on the dissipation caused by step current pulse in NbTi superconducting filament on fused silica. The non-equilibrium state is induced by a current exceeding the critical current I_c . A voltage appears after a certain delay time t_d , and close to T_c the dissipation is governed by the phase slip center phenomena. It bears similarity to single photon detection using a superconducting nanowire biased with a current smaller than the critical current I_c . The film cooling time is deduced from fitting the data with the Time-Dependent Ginzburg-Landau (TDGL) theory due to M. Tinkham. We find that the film cooling time is longer close to T_c than at lower temperature and this is attributed to the number of phonon population that increased.

9:06 AM NM02.11.10

Late News: Simplified Colloidal Route for Preparation of Nanostructured Au-Ag Films with Superconductivity in the Ambient Navyashree Vasudeva, Pritha Mondal, Subham K. Saha, Rekha Mahadevu, Anand Sharma and Anshu Pandey; Indian Institute of Science, India

Au-Ag nanostructures have been posited as potential room temperature, ambient pressure superconductors in past studies. This presentation will summarize recent progress made towards the growth of films of these materials. Au-Ag nanostructures comprise discrete ~ 1 nm Ag nanocrystals embedded at specific loading densities into an Au matrix. This motif is nontrivial to produce through standard colloidal techniques that rely upon spherically or axially symmetric growth around a central nucleus. I will present methods developed by us that enable a simplified route for the preparation of these materials. The structural properties of Au-Ag materials produced through this method will be described. This presentation will further provide an overview of their unconventional optical and electrical properties. In particular, we will describe the suppression of plasmon resonances within these materials along with the emergence of a broad non-dissipative resonance over the visible. We will further describe the observation of zero resistance in films of these materials. In certain samples, these states with resistivity below 10^{-10} ohm-m are also observed at temperatures as large as 400 K. Other aspects including stability, and sensitivity of these materials towards air exposure, will be discussed.

9:16 AM NM02.11.11

Late News: Theoretical Insights into the Unconventional Electronic Structure and Optics of Engineered Au-Ag Nanostructures Pritha Mondal, Subham K. Saha, Awadhesh Narayan and Anshu Pandey; Indian Institute of Science, India

Recently it was shown that bimetallic nanostructured films composed of gold and silver exhibit certain unconventional electrical and optical properties which are not expected from any conventional metallic films. To account for these observations, we have developed a coarse grained theoretical model to explain the experimental findings. We adopt a jellium model for the gold silver material. A metal-insulator transition mediated by correlation enhancement is described. I will show that the system is associated with two temperature scales with a potential superconducting transition occurring below the electron localization temperature.

9:26 AM NM02.11.12

Late News: Unconventional Optical, Structural and Magnetic Properties of Au-Ag Nanostructures with Superconductivity in the Ambient Subham K. Saha¹, Rekha M¹, Pritha Mondal¹, Navyashree Vasudeva¹, Samartha Channagiri¹, Pavithra Bellare¹, Arpita Mukherjee², Nihit Saigal¹, Guru P. Rajasekar¹, Dev K. Thapa¹, Biswajit Bhattacharyya¹, Narayanan Ravishankar¹ and Anshu Pandey¹; ¹Indian Institute of Science, India; ²University of Gothenburg, Sweden

Recent studies on engineered Au-Ag nanostructure assemblies have attracted tremendous interest due to their unconventional electrical and magnetic properties. Briefly, these nanostructures have been shown to exhibit an

immeasurably low resistive state, typically with resistivity below 10^{-10} ohm-m and also a highly diamagnetic state at temperatures approaching and greater than the ambient. Along with these observations, they also exhibit an unusual optical response which is not anticipated from their constituent material. Generally, Au or Ag nanostructures show their definitive plasmon resonances under optical excitation. This corresponds to the collective oscillations of free electrons which leads to an excitation of dipolar modes. Contrary to conventional Au and Ag materials, Au-Ag nanostructures do not show any definitive plasmon resonance at a particular frequency but rather show a broad extinction over the entire UV-VIS optical window even extending up to NIR. We de-convolve the extinction into constituent scattering and absorption components. It is found that extinction entirely comprises of scattering with negligible absorption. Further, these nanostructures do not show any dissipative dynamics in pump-probe spectroscopy. We shed further insights into the unconventional properties of these materials through EELS and structure correlated single particle microscopy. Our findings indicate significant electronic reconfiguration in these nanostructures that gives rise to deviations from the usual dielectric response of Au and Ag.

SYMPOSIUM NM03

Topological and Quantum Phenomena in Intermetallic Compounds and Heterostructures
April 22 - April 23, 2021

Symposium Organizers

Elena Hassinger, Technische Universität München
Anderson Janotti, University of Delaware
Jason Kawasaki, University of Wisconsin
Lukas Muechler,

Symposium Support

Gold
National Science Foundation

* Invited Paper

SESSION NM03.01: Topology and Magnetism
Session Chairs: Ana Akrap and Elena Hassinger
Thursday Morning, April 22, 2021
NM03

8:00 AM *NM03.01.01

Manipulating of Magnetism and Band Structure in the Topological Semimetal EuCd_2As_2 Na Hyun Jo^{1,2,3}, Brinda Kuthanazhi^{1,2}, Yun Wu^{1,2}, Thais V. Trevisan^{1,2}, Erik Timmons^{1,2}, Tae-Hoon Kim¹, Lin Zhou¹, Lin-Lin Wang¹, Benjamin G. Ueland^{1,2}, Andriy Palasyuk^{1,2}, Dominic H. Ryan⁴, Robert J. McQueeney^{1,2}, Kyungchan Lee^{1,2}, Benjamin Schrunck^{1,2}, Anton A. Burkov⁵, Ruslan Prozorov^{1,2}, Peter P. Orth^{1,2}, Sergey Budko^{1,2}, Adam Kaminski^{1,2} and Paul C. Canfield^{1,2}; ¹Ames Laboratory, United States; ²Iowa State University, United States; ³Lawrence Berkeley National Laboratory (current affiliation), United States; ⁴McGill University, Canada; ⁵University of Waterloo, Canada

With the steady rise of topological materials, attention of the community is now shifting to magnetic

incarnations that host a largely unexplored territory from both a theoretical and experimental perspective. Magnetic topological materials allow for the formation of new structures (as the spin can introduce new periodicities) and are yet to be mapped out in generality and resultantly harbor a lot of potential for novel effects. Hence, having a stable material platform is of tremendous interest to underpin both theory and experimental progress in this direction. So far, several materials are reported as magnetic Weyl semimetal though a material with a single pair of Weyl points that readily offers tuning of its topological states is yet to be found. EuCd_2As_2 is a magnetic semimetal that has the potential of manifesting nontrivial electronic states, depending on its low temperature magnetic ordering. By discovering and taking advantage of the chemical tunability of EuCd_2As_2 , we report the successful growths of single crystals of EuCd_2As_2 with the ferromagnetic and antiferromagnetic ground state. In addition, we will discuss a detailed temperature-dependent Angle-resolved photoemission spectroscopy (ARPES) study on the ferromagnetic EuCd_2As_2 .

This work was supported by the Center for Advancement of Topological semimetals, an Energy Frontier Research Center funded by the U.S.DOE, Office of Basic Energy Sciences. Work at the Ames Laboratory was supported by the U.S. Department of Energy, Office of Science, Basic Energy Sciences, Materials Sciences and Engineering Division. The Ames Laboratory is operated for the U.S. DOE by Iowa State University under Contract No. DEAC0207CH11358.

8:25 AM *NM03.01.03

Exotic Quantum Magnets and Competing States—New Yb Kondo Systems Emilia Morosan; Rice University, United States

Novel physics discoveries heavily rely on the design and synthesis of new materials, which, in turn, depends a lot on the growth method. I will use the backdrop of my group's discoveries of several Kondo systems, to emphasize the importance of the interplay between chemistry, materials science and physics in unveiling new materials' properties. In particular, I will focus on YbT_3M_7 where the transition metal T is either Rh or Ir, and the metal M is Si or Ge. These are rhombohedral compounds, chemically and structurally very similar, with some similar physical properties and substantive differences. They all show evidence for strong electronic correlations and Kondo physics; one orders ferromagnetically (YbIr_3Ge_7) while the other two have antiferromagnetic ground states. Most remarkable, YbIr_3Si_7 shows long range antiferromagnetic order and non-Fermi liquid behavior even within the ordered state, while the electrical resistivity indicates bulk insulating behavior with ARPES and DFT calculations pointing to a conductive surface. We reconcile the observed Kondo physics, long range magnetic order and the insulating-to-metal crossover from bulk to surface with a proposal of Kondo exhaustion and evidence for a Yb valence transition from magnetic ($3+$ in the bulk) to non-magnetic ($2+$ on the surface).

8:50 AM NM03.01.04

Late News: Tunable Chiral Symmetry Breaking in Symmetric Weyl Materials Sahal Kaushik¹, Evan Philip² and Jennifer Cano¹; ¹Stony Brook University, United States; ²Brookhaven National Laboratory, United States

Asymmetric Weyl semimetals, which possess an inherently chiral structure, have different energies and dispersion relations for left- and right-handed fermions. They exhibit certain effects not found in symmetric Weyl semimetals, such as the quantized circular photogalvanic effect and the helical magnetic effect. In this work, we derive the conditions required for breaking chiral symmetry by applying an external field in symmetric Weyl semimetals. We explicitly demonstrate that in certain materials with the T_d point group, magnetic fields along low symmetry directions break the symmetry between left- and right-handed fermions; the symmetry breaking can be tuned by changing the direction and magnitude of the magnetic field. In some cases, we find an imbalance between the number of type I left- and right-handed Weyl cones (which is compensated by the number of type II cones of each chirality.)

9:05 AM NM03.01.05

Late News: A New Cubic Hall Viscosity in Three-Dimensional Topological Semimetals Iñigo Robredo^{1,2}, Pranav Rao³, Fernando de Juan^{1,4}, Aitor Bergara^{1,2}, Juan Luis Mañes², Alberto Cortijo⁵, Maia Vergniory^{1,4} and Barry Bradlyn³; ¹Donostia International Physics Center, Spain; ²University of the Basque Country, Spain; ³University of Illinois at Urbana-Champaign, United States; ⁴Basque Foundation for Science, Spain; ⁵Universidad Autónoma de Madrid, Spain

In this work, we study the non-dissipative viscoelastic response of three dimensional crystals. We show that for systems with tetrahedral symmetries, there exist new, intrinsically three-dimensional Hall viscosity coefficients that cannot be obtained via a reduction to a quasi-two-dimensional system. To study these coefficients, we specialize to a tight binding model for a chiral magnetic metal inspace group $P2_13$ (198), which features a threefold degenerate “spin-1” fermion at the Fermi level. Using the Kubo formula for viscosity, we compute the non-dissipative Hall viscosity for the spin-1 fermion in two ways. First we use an electron-phonon coupling ansatz to derive the “phonon” strain coupling and associated phonon Hall viscosity. Second we use a momentum continuity equation to derive the viscosity corresponding to the conserved momentum density. We conclude by discussing the implication of our results for hydrodynamic transport in three-dimensional magnetic metals, and discuss some candidate materials in which these effects may be observed.

SESSION NM03.02/NM04.07: Joint Session: Skyrmions
Session Chairs: Lukas Muechler, Johanna Nordlander and Leslie Schoop
Thursday Morning, April 22, 2021
NM03

10:30 AM *NM03.02/NM04.07.01

Atomic-Scale Studies and Design of Topological Spin Textures and Majorana States in Magnet-Superconductor Hybrid Systems Roland M. Wiesendanger; University of Hamburg, Germany

Since the discovery of the existence and manipulation possibilities of individual nanoscale skyrmions in ultrathin transition metal films on heavy-element substrates [1] by spin-polarized scanning tunneling microscopy (SP-STM) [2], the field of magnetic skyrmions [3,4] has gained significant interest due to their great potential for future magnetic memory and logic devices [5,6]. In particular, the small size, enhanced stability and unidirectional current-driven movement of chiral magnetic skyrmions make them interesting for novel types of magnetic device concepts. These unique properties of skyrmions are intimately linked to interfacial Dzyaloshinskii-Moriya (DM) interactions [7,8] which recently have been studied directly at the level of individual magnetic atoms on surfaces of heavy-element substrates [9]. Based on these fundamental investigations of the distance- and material dependencies of interfacial DM interactions, it has become possible to design non-collinear spin textures in low-dimensional systems based on the powerful combination of SP-STM and single-atom manipulation techniques [10,11]. Proximity-coupling of such well-defined low-dimensional non-collinear spin-states with elemental superconductors allows the design of yet another type of interesting topological states, i.e. Majorana zero modes, which offer great potential for topological quantum computation [11,12]. Besides the emergence of Majorana states in quasi-1D hybrid systems consisting of spin-spirals interacting with elemental superconductors, we will also discuss most recent progress towards the observation of Majorana states in quasi-2D skyrmion-superconductor hybrid systems [13].

References

- [1] N. Romming et al., *Science* **341**, 6146 (2013).
- [2] R. Wiesendanger, *Rev. Mod. Phys.* **81**, 1495 (2009).
- [3] A.N. Bogdanov and Ch. Panagopoulos, *Nature Reviews Physics* **2**, 492 (2020).

- [4] A.N. Bogdanov and Ch. Panagopoulos, *Physics Today* **73**(3), 44 (2020).
- [5] R. Wiesendanger, *Nature Reviews Materials* **1**, 16044 (2016).
- [6] A. Fert, N. Reyren, V. Cros, *Nature Reviews Materials* **2**, 17031 (2017).
- [7] M. Bode et al., *Nature* **447**, 190 (2007).
- [8] S. Heinze et al., *Nature Physics* **7**, 713 (2011).
- [9] A. A. Khajetoorians et al., *Nature Commun.* **7**, 10620 (2016).
- [10] M. Steinbrecher et al., *Nature Commun.* **9**, 2853 (2018).
- [11] H. Kim et al., *Science Advances* **4**, eaar5251 (2018).
- [12] A. Palacio-Morales et al., *Science Advances* **5**, eaav6600 (2019).
- [13] A. Kubetzka et al., *Phys. Rev. Mater.* **4**, 081401(R) (2020).

10:55 AM *NM03.02/NM04.07.02

Skyrmions and Chiral Spin Textures in Non-Centrosymmetric Magnetic Materials Roland Kawakami;
The Ohio State University, United States

Magnetic domain structures are fundamentally altered by the presence of the Dzyaloshinskii-Moriya interaction (DMI), which introduces a preference for the twisting of neighboring spins. This produces various chiral spin textures including topological skyrmion bubbles, helical phases, and chiral domain walls. Two important directions for the field are to (1) explore and visualize the complex magnetic phases down to the atomic scale and (2) develop small skyrmions at room temperature for potential high-density memory applications. For this, we are investigating skyrmions and chiral spin textures in thin films of FeGe, MnGe, and Fe-rich FeGe grown by molecular beam epitaxy. These materials have a B20 structure with broken inversion symmetry to generate a bulk-like DMI, which yields skyrmions that are often studied by the topological Hall effect or other macroscopic probes. In our work, we visualize the spin textures from the submicron-scale down to the atomic-scale using spin-polarized scanning tunneling microscopy, magnetic force microscopy, and Lorentz transmission electron microscopy. I will discuss our team's advances in atomic-layer engineering for FeGe to boost the Curie temperature above room temperature while shrinking the skyrmion size down to < 20 nm, the atomic-scale visualization of helical spin textures with topological defects in MnGe, and initial work toward skyrmions in epitaxial 2D magnets.

The work was done in collaboration with Tao Liu, Camelia Selcu, Jake Repicky, Jay Gupta, David McComb, Mohit Randeria, Prasanna Balachandran, Nuria Bagues Salguero, Binbin Wang, Po-Kuan Wu, Shuyu Cheng, Tim Hartnett, Denis Pelekhov, Perry Corbett, Brendan McCullian, Adam Ahmed, Chris Hammel.

11:20 AM *NM03.02/NM04.07.03

Skyrmions and Topology in Magnetic Materials Claudia Felser; Max Planck Institute Chemical Physics of Solids, Germany

Topology a mathematical concept became recently a hot topic in condensed matter physics and materials science, a complete classification of all non-magnetic inorganic materials are available [1,2]. Recently the focus have shifted to magnetic materials, first antiferromagnetic materials are classified, too [3]. In magnetic materials the Berry curvature in real and reciprocal space lead to new topological properties such as Skyrmions [4] and Antiskyrmions [5] and in magnetic Weyl semimetals to giant responses in antiferromagnetic [6] and ferromagnetic compounds [7]. Heusler compounds as tunable materials are interesting for both categories, they might even allow for the investigation the relation between Berry curvatures in real and reciprocal space. In materials hosting Antiskyrmions the Dzyaloshinskii Moriya-Exchange and the dipol-dipol interaction is important. The dipol-dipol interactions allows for interesting mesoscopic effects. New materials can be designed by changing the symmetry, magnetic moments (ferro, ferri, antiferro, compensated ferri) and magnetic crystalline anisotropy [8].

- [1] Bradlyn et al., *Nature* **547**, 298, (2017)
- [2] Vergniory, et al., *Nature* **566**, 480 (2019)

- [3] Xu, et al., Nature (2020) accepted, preprint arXiv:2003.00012
[4] Mühlbauer, et al. Science 323, 915 (2009)
[5] Nayak, et al., Nature 548, 561 (2017)
[6] Nayak, et al., Science Advances 2 e1501870 (2016)
[7] Liu, et al. Nature Physics 14, 1125 (2018)
[8] Manna, et al., Nature Reviews Materials 3, 244 (2018)

11:45 AM *NM03.02/NM04.07.04

Anti-Skyrmions and Skyrmions in Heusler Compounds Stuart Parkin; Max Planck Institute of Microstructure Physics, Germany

Heusler compounds are a large family of compounds which exhibit a wide range of properties. The inverse tetragonal Heusler compounds exhibit unidirectional magnetic anisotropy. Some of these compounds, in particular those containing heavy elements, exhibit non-collinear spin structures, that are derived from a Dzyaloshinskii-Moriya (DMI) vector exchange interaction. We show that such materials can exhibit a range of spin textures including both anti-skyrmions and elliptical Bloch skyrmions in the same compound, as well as helical spin textures that propagate along particular crystal directions. Another fascinating aspect of these structures is that the size of the anti-skyrmion and the wavelength of the helices can be varied from sub 100 nm to more than a micron by varying the thickness of the lamella in which the structures are observed. This is due to the important role of long-range magneto-dipole interactions that are more much important in these Heusler compounds than, for example, in the widely studied cubic B20 compounds in which skyrmions have been extensively explored. Chiral spin textures in ferro-, ferri- and anti-ferrimagnetic materials and thin film heterostructures are of fundamental interest with great potential for spintronic applications especially Racetrack Memory.

SESSION NM03.03: Layered Compounds + 2D Magnets
Session Chairs: Anderson Janotti and Jason Kawasaki
Thursday Afternoon, April 22, 2021
NM03

1:00 PM *NM03.03.01

Modulation Doping via the 2D Crystalline Acceptor RuCl₃ Kenneth Burch; Boston College, United States

Two-dimensional (2d) nano-electronics, plasmonics, and emergent phases require clean and local charge control, calling for layered, crystalline acceptors or donors. Here I will describe how the Relativistic Mott Insulating state of RuCl₃ provides a new opportunity to introduce modulation doping into 2D materials. Specifically, we demonstrate and optimize this charge transfer with extensive Raman, photovoltage, and electrical conductance measurements combined with ab initio calculations. Also, we find the doping is exceptionally local, can occur through hBN, works with various exfoliated, CVD, and MBE materials. Time permitting, I will discuss new opportunities this opens for nanoplasmonic, optoelectronics, and correlated phases.

1:25 PM *NM03.03.02

Exploring and Expanding the Compositional and Microstructural Space of Transition Metal-Based 3D and 2D Carbides and Nitrides Jan Paul Siebert¹, Niels Kubitzka², Minh Hai Tran², Andreas Reitz¹, Robert Brilmayer², Annette Andrieu-Brunsen² and Christina Birkel^{1,2}; ¹Arizona State University, United States; ²Technische Universität Darmstadt, Germany

Transition metal-based carbides that belong to the family of MAX phases are an intriguing class of materials –

particularly in terms of their mechanical properties – as they combine characteristics of metals and ceramics. More recently, some of their members have also been discussed in terms of their magnetic behavior, whereas most studies are conducted on thin film samples and the synthesis of bulk materials with later transition metals (e.g. Mn) is still a real challenge. Besides, MAX phases are used as precursors for a relatively new class of 2D materials, the so-called MXenes that are investigated in the context of a plethora of potential applications, for example in catalysis, battery and biomedical research.

Our group utilizes a diverse set of synthesis techniques to prepare new MAX phases as well as known ones with unique morphologies. In this talk, I will focus on the following two examples: (i) The synthesis of MAX phase Cr₂GaC by an initially wet chemical approach that allows a new type of processability of the soluble precursors. (ii) Design of a “smart” hybrid MXene with switchable conductivity and temperature as an external stimulus. We employ X-ray powder diffraction and electron microscopy techniques to study the structure and microstructure of the products, respectively. In the case of the wet chemical-based synthesis of Cr₂GaC, we conducted detailed thermal analysis and ex-situ Neutron diffraction to propose a formation mechanism of the MAX phase particles.

1:50 PM *NM03.03.03

Near-Fermi-Level Electronic States in Hexagonal ABC Intermetallic Compounds from First Principles

Karin M. Rabe; Rutgers, The State University of New Jersey, United States

Ternary ABC intermetallic compounds exhibit a rich variety of crystal structures and electronic properties. In this work, we study the structural energetics and band structures of real and hypothetical ABC intermetallic phases with structures obtained by stacking binary honeycomb layers with single layers of interstitial atoms in various ways, using first principles calculations to determine the structural parameters and the bands in each phase. We use this dataset to analyze and model the bands near the Fermi level to classify the systems considered and to extract a set of rules that allows us to predict and design hexagonal ABC intermetallic materials with targeted transport and optical properties, connecting to experimental measurements on known hexagonal ABC phases. In particular, we investigate the rich physics of polar metals in this family of materials, which offer the promise of functional properties switchable by appropriate applied fields and stresses.

2:15 PM NM03.03.04

Berry Curvature and Topological Nernst Effect in Biased Bilayer WSe₂ Vassilios Vargiamidis¹, Panagiotis Vasilopoulos² and Neophytos Neophytou¹; ¹University of Warwick, United Kingdom; ²Concordia University, Canada

We investigate the anomalous thermoelectric transport in bilayer WSe₂ with broken inversion symmetry, due to a gate electric field, regardless of time-reversal symmetry. We compare the cases in which the spin-orbit coupling (SOC) is absent or present. In the presence of SOC and of a valley-contrasting Berry curvature, anomalous spin and valley Nernst responses are generated. The Nernst signals exhibit peaks and dips, as the chemical potential is varied, that have the signs of the Berry curvatures of the bands and are proportional to their magnitudes. In the absence of SOC but with an electric field present, the Nernst responses are the same in the conduction and valence bands due to particle-hole symmetry. The anomalous valley Nernst coefficient is enhanced by increasing the electric field strength. When time-reversal symmetry is violated, e.g., upon using an insulating magnetic substrate, the total Nernst coefficient is finite and exhibits a dip-peak feature. We also analyze the orbital magnetization and the orbital magnetic moment. In the absence of a gate electric field the magnetization vanishes due to the spin degeneracy of the bands. In the presence of electric field, the magnetization and its two contributions, one due to the magnetic moment and one due to the Berry curvature, are calculated and interpreted in terms of opposite circulating currents of the bands in the two layers. The results are pertinent to other transition metal dichalcogenides and future caloritronic applications.

2:30 PM NM03.03.05

Late News: Structural Defects and Low Temperature Twisting of Kagomé Layers in Intermetallics

Mekhola Sinha¹, Hector K. Vivanco¹, Cheng Wan¹, Maxime Siegler¹, Veronica J. Stewart¹, Lucas A. Pressley¹,

Tanya Berry¹, Ziqian Wang¹, Isaac Johnson¹, Mingwei Chen^{1,2}, Thao T. Tran^{1,3}, W. Adam Phelan^{1,4} and Tyrel M. McQueen¹; ¹The Johns Hopkins University, United States; ²Tohoku University, Japan; ³Clemson University, United States; ⁴Los Alamos National Laboratory, United States

Kagomé intermetallics with 2D lattices have served as an ideal platform to study the exotic quantum phenomenon associated with flat bands and Dirac-type dispersions. It is essential to explore the electronic properties of these structures for the experimental realization of 2D kagomé lattice in bulk materials. We explore a specific family of kagomé intermetallics with the formula MT_6X_6 compound where $M = \text{Mg, Lu, Y}$; $T = \text{Co, Fe, Cr}$; and $X = \text{Ge}$. Single crystals of MgCo_6Ge_6 were grown by laser Bridgman technique. X-ray precession images and electron diffraction measurements collected at $T = 293(2)$ K show that the compound crystallizes in space group $P6/mmm$, with $a = 5.06094(15)$ Å, $c = 7.7271(2)$ Å. Residual electron maps provide evidence of columnar disorder along c axis while no defects were found in the electronic structures of flux-grown LuFe_6Ge_6 and YCr_6Ge_6 crystals. Further investigation of the crystal structure reveals spontaneous twisting of the Co kagomé layers in MgCo_6Ge_6 . We look into crystal orbital hamiltonian population analysis to understand the cooperative twisting between layers within the Co-kagomé network and the interlayer tetragonal bonding. Despite the appearance of static tilting, no evidence of a phase transition was found in magnetization, resistivity, or specific heat measurements, implying that the twisting exists at all temperatures, but is thermally fluctuating at room temperature. This behavior is further supported by looking into related materials to understand the pairwise twisting and bonding in layered structures.

Funding:

This work was supported by the David and Lucile Packard Foundation. HKV, VJS and TTT acknowledge support of the Institute for Quantum Matter, an Energy Frontier Research Center funded by the United States Department of Energy, Office of Science, Office of Basic Energy Sciences, under Award DE-SC0019331. MKS, LAP, TB, and WAP acknowledge support of the Platform for the Accelerated Realization, Analysis, and Discovery of Interface Materials (DMR-1539918), a National Science Foundation Materials Innovation Platform. ZW, IJ and MC acknowledge support of Whiting School of Engineering, the Johns Hopkins University, and the NSF (NSF DMR-1804320). CW acknowledges the support of Hopkins Extreme Materials Institute (HEMI). Access to the Bruker 1172 instrument was also possible via the Hopkins Extreme Materials Institute (HEMI).

2:45 PM NM03.03.06

Late News: Temperature and Composition Evolution of Charge Density Wave and Superconducting Orders in Ta-Based Dichalcogenides by Total X-Ray Scattering Valeri Petkov; Central Michigan University, United States

A characteristic feature of quantum materials is the presence of various lattice degrees of freedom manifesting themselves as local structural distortions leading to competing ground state phases of the electronic system and exotic behavior. More often than not, the distortions are not well expressed and/or perfectly periodic, making it difficult to identify and quantify them using traditional crystallographic techniques. We will demonstrate the advantages of total x-ray scattering and large-scale structure modeling in studying lattice instabilities in archetypal quantum materials such as Ta-based dichalcogenides. In particular, we will show that the low-temperature charge density wave state in trigonal prismatic 2H-TaSe₂ emerges via a gradual buildup of locally correlated clusters of Ta atoms, and not via a spontaneous emerging of Ta superstructure at the transition temperature [1]. We will also show the presence of a hierarchical relationship among the crystal lattice, charge density wave and superconducting orders in ternary Ta-Te-Se solid solutions, where different degrees of crystal lattice order-disorder appear to promote and maintain the different orders to a different extent. The relationship may well explain the observed irregular evolution of the superconducting transition temperature with the relative Te to Se ratio [2].

1. V. Petkov et al. *Phys. Rev. B* **101**, 121114(R) (2020).
2. V. Petkov et al. *Phys. Rev. B* **102**, 134119 (2020).

SESSION NM03.04: Topological Materials I
Session Chairs: Jason Kawasaki and Lukas Muechler
Thursday Afternoon, April 22, 2021
NM03

4:00 PM *NM03.04.02

Frontiers of Crystal Growth and Characterization of Topological and Quantum Intermetallics Tyrel M. McQueen; Johns Hopkins University, United States

Materials by design is the rational prediction and creation of functional materials with defined properties. Its goal is to meet current and future societal needs for better or more complex materials, from biocompatible materials in medicine to lightweight alloys for space applications and energy generation, storage, and transport. Unfortunately the chemistry underlying modern materials science and engineering has lagged other sub-fields in an extremely critical area: the ability to selectively make and break bonds in the solid state. This is due to limited synthetic methodology and method development. True materials by design cannot be achieved until reliable synthetic capabilities are developed that can actually produce the specified materials. In this talk, I will highlight the progress being made in such synthesis by design, with a particular focus on intermetallic quantum materials necessary to realize new electronic and magnetic states of matter including topological superconductivity and axion insulators. Efforts to build and maintain US leadership in the area of new materials discovery and synthesis – particularly via the JHU Institute for Quantum Matter and PARADIM, the Platform for Accelerated Realization, Analysis, and Discovery of Interface Materials (PARADIM), an NSF-MIP National User Facility, and opportunities for use of these capabilities by the community, will also be presented.

4:25 PM *NM03.04.03

Weyl Nodes and Magnetostructural Instability Samuel M. Teicher and Ram Seshadri; University of California, Santa Barbara, United States

The room temperature ferromagnetic phase of the cubic antiperovskite Mn_3ZnC is known from first-principles calculation to be a nodal line Weyl semimetal. Features in the electronic structure that are the hallmark of a nodal line Weyl state—a large density of linear band crossings near the Fermi level—can also be interpreted as signatures of a structural and/or magnetic instability. We examine this system carefully, and use it as a jumping off point to understand the possible implications of Weyl-like features in the electronic structures, and Peierls-like structural distortions and related structural and magnetic instabilities.

4:50 PM NM03.04.06

Exciting Features of Electronic Band Dispersion of IrGa & RhGa Compounds from First-Principles Joshua Steier^{1,2}, David Gordon³, JeanPierre Alvarez³, Kalani Hettiarachchilage¹ and Neel Haldolaarachchige³; ¹Seton Hall University, United States; ²Stony Brook University, The State University of New York, United States; ³Bergen Community College, United States

Dirac materials have recently been one of the most significant attractions of the scientific community. We present an ab initio study of electronics properties of IrGa and RhGa compounds, with the absence and presence of spin-orbit interaction using first-principles calculations. Linearly dispersed band crossings, which are characteristic of topological semimetals, were identified near Fermi energy. These include type I and II Dirac points and nodal lines. Additionally, the sensitivity of Dirac points to physical pressure was studied by applying compressive and tensile stress to the lattice axis. The unusual electronic structure of IrGa will be useful to search for novel Dirac Fermions and it is a good candidate for further research and experimental studies.

SESSION NM03.05: Novel Superconductivity and Magnetism I
Session Chairs: Valentin Taufour and Masaki Uchida
Thursday Afternoon, April 22, 2021
NM03

8:15 PM *NM03.05.01

Insulator-Metal Transition, Topological Superconductivity and Parity Violation in UTe₂ Youichi Yanase¹, Jun Ishizuka¹, Shuntaro Sumita² and Akito Daido¹; ¹Kyoto University, Japan; ²RIKEN, Japan

We theoretically study magnetism and superconductivity in UTe₂, which is a recently discovered strong candidate for an odd-parity spin-triplet superconductor. Theoretical studies for this compound faced difficulty because first-principles calculations predict an insulating electronic state, incompatible with superconducting instability. To overcome this problem, we take into account electron correlation effects by a GGA+U method and show the insulator-metal transition by Coulomb interaction. Using Fermi surfaces obtained as a function of U, we clarify the topological properties of possible superconducting states. Fermi surface formulas for the three-dimensional winding number and three two-dimensional Z₂ numbers indicate topological superconductivity at an intermediate U for all the odd-parity pairing symmetry in the Immm space group. Symmetry and topology of superconducting gap nodes are analyzed, and the gap structure of UTe₂ is predicted. Topologically protected low-energy excitations are highlighted, and experiments by bulk and surface probes are proposed to link Fermi surfaces and pairing symmetry. We show that a recent ARPES experiment is consistent with the topological superconductivity.

Next, we provide and analyze a periodic Anderson model for UTe₂. The 24-band tight-binding model reproduces the band structure obtained from a GGA+U calculation consistent with an ARPES experiment. The Coulomb interaction of *f*-electrons enhances Ising ferromagnetic fluctuation along the *a*-axis and stabilizes the spin-triplet superconductivity of either *B_{3u}* or *A_u* symmetry. When effects of pressure are taken into account in hopping integrals, the magnetic fluctuation changes to an antiferromagnetic one, and accordingly, the spin-singlet superconductivity of *A_g* symmetry is stabilized. Based on the results, we propose pressure-temperature and magnetic field-temperature phase diagrams revealing multiple superconducting phases. Interestingly, a mixed-parity superconducting state with spontaneous parity violation is predicted.

8:40 PM *NM03.05.02

Local Magnetic Measurements of Unconventional Superconductors Katja C. Nowack; Cornell University, United States

A fundamental property of a superconductor is its response to an applied magnetic field. In this talk, I will discuss how we use scanning superconducting quantum interferences device (SQUID) microscopy to study the local magnetic response in two different types of superconductors. First, I will discuss measurements on focus ion beam defined microstructures fabricated from single crystals of the heavy-fermion superconductor CeIrIn₅. By imaging the local diamagnetic response, we observe that the superconducting transition temperature, T_c, varies throughout the structure in a complex pattern. This pattern arises due to the interplay of a non-trivial strain field from the differential thermal contraction of the substrate and microstructure and the sensitivity of T_c in CeIrIn₅ to the strength and direction of strain. Devices with different geometry show that the spatial modulation of T_c can be tailored in agreement with predictions based on finite element simulations. These results offer a new approach to manipulate strain-sensitive electronic order on micrometer length scales in strongly correlated matter. Second, I will show how we use scanning SQUID to perform local magnetic measurements on few-layer van der Waals superconductors. We can directly probe the diamagnetic response as a function of temperature and other tuning parameters despite the extremely small sample volume. I will discuss

how we can extract the superfluid stiffness and other characteristics of the superconducting state from our measurements.

Imaging of CeIrIn₅ microstructures was primarily supported by the Department of Energy, Office of Basic Energy Sciences, Division of Materials Sciences and Engineering, under Award DE-SC0015947. Measurements of van der Waals superconductors were supported by the Cornell Center for Materials Research with funding from the NSF MRSEC program (DMR-1719875) and the NSF (DMR-2004864).

9:05 PM *NM03.05.03

Topological and High-Field Reentrant Superconductivity in UTe₂ Nicholas P. Butch^{1,2}; ¹NIST Center for Neutron Research, United States; ²University of Maryland, United States

Spin triplet superconductivity is found in UTe₂ below 1.6 K. Remarkably, it coexists with strong spin fluctuations, has an extremely high upper critical field of 35 T, and breaks time reversal symmetry. I will describe how superconductivity in UTe₂ differs from conventional superconductivity and I will present evidence that this phase is topologically nontrivial. I will also discuss how in UTe₂ large magnetic fields give rise to a new, reentrant, superconducting phase, between 40 T and 65 T, the highest values reported for any material.

9:30 PM NM03.05.04

Scanning SQUID Microscopy of the Quantum Anomalous Hall Effect George M. Ferguson¹, Run Xiao², David Low¹, Ling-Jie Zhou², Anthony Richardella², Cui-Zu Chang², Nitin Samarth² and Katja C. Nowack¹; ¹Cornell University, United States; ²The Pennsylvania State University, United States

We report magnetic imaging of Cr-doped (Bi,Sb)₂Te₃ heterostructures in the quantum anomalous hall regime. We used a scanning superconducting quantum interference device (SQUID) microscope with micrometer scale spatial resolution to image the magnetic fields above current biased devices. Using these images we reconstructed the current density, allowing us to visualize where current flows in the devices. We also used top and back gates to study how the magnetization is affected by electrostatic gating. By performing these measurements as a function of current bias, gate voltage and magnetization direction we construct a comprehensive picture of electronic transport in our devices.

9:45 PM NM03.05.06

Late News: Quantum Magnetism in EuPd₃S₄ Tanya Berry¹, Vincent Morano¹, Micheal Nickolas², Xin (Jason) Zhang¹, Qun Yang², Topias Foerster³, Zhijun Zhu⁴, Rafal Wawrzynczak², Tom Halloran¹, Walter Schnelle², Johannes Gooth², Jeffrey Lynn⁴, Claudia Felser², Collin Broholm¹ and Tyrel M. McQueen¹; ¹Johns Hopkins University, United States; ²Max Planck Institute for chemical Physics of Solids, Germany; ³HZDR – Helmholtz-Zentrum Dresden-Rossendorf, Germany; ⁴National Institute of Standards and Technology, United States

Double Dirac materials are a topological phase of matter that have an unprecedented eightfold electronic degeneracy. They display a host of exotic charge transport properties that are strongly impacted by magnetic fields. Quantum magnets are known to exhibit a variety of magnetic phases of matter with emergent quasiparticles. Here we report the discovery of quantum magnetism in the Dirac material EuPd₃S₄. The zero-field magnetic structure is found to be a 2-sublattice antiferromagnetic state with no magnetic coupling between sublattices at the mean-field level that results in an emergent degree of freedom corresponding to the relative orientation of the sublattice magnetizations. Application of a magnetic field drives domain ordering before collapsing to a fully ferromagnetic state. These magnetic states are found to dramatically impact the electronic structure of EuPd₃S₄, resulting in the destruction of the 8-fold degenerate state and formation of mostly likely Weyl states. Our findings open the door to the experimental and theoretical explanation of the interplay between novel magnetic states and topological phases of matter.

SESSION NM03.06: Novel Superconductivity and Magnetism II
Session Chairs: Nicholas Butch and Elena Hassinger
Friday Morning, April 23, 2021
NM03

8:00 AM *NM03.06.01

Even and Odd Parity Superconductivity in CeRh₂As₂ Javier F. Landaeta¹, Seunghyun Khim¹, Jacintha Landaeta¹, Nyantakyi Bannor¹, Manuel Brando¹, Philip Brydon², Daniel Hafner¹, Robert K uchler¹, Raul Cardoso¹, Ukrike Stockert¹, Andrew Mackenzie^{1,3}, Daniel Agterberg⁴, Christoph Geibel¹ and Elena Hassinger^{1,5}; ¹Max Planck Institute for Chemical Physics of Solids, Germany; ²University of Otago, New Zealand; ³University of St Andrews, United Kingdom; ⁴University of Wisconsin–Milwaukee, United States; ⁵Technical University Munich, Germany

Multiple new forms of unconventional superconductivity have been discovered over the past four decades. In most cases, the strong electronic correlations and the interplay between superconductivity and other phases (magnetic ones, among others) leads to understanding that the simple frame of electron-phonon superconductivity breaks down. Because this implies that complex phase diagrams with different superconducting states are expected, it is striking that many materials only show a single-component superconducting phase diagram. Here, we report the discovery of two-phase unconventional superconductivity in CeRh₂As₂ with a transition temperature of 0.26 K. Using thermodynamic and magnetic probes, we establish that the superconducting critical field is as high as 14 T for magnetic fields along the c-axis. Furthermore, a c-axis field drives a transition between two different superconducting states. In spite of the fact that CeRh₂As₂ is globally centrosymmetric, we show that local inversion-symmetry breaking at the Ce sites enables Rashba spin-orbit coupling to play a key role in the underlying physics. More detailed analysis identifies the transition from the low- to high-field states to be associated with one between states of even and odd parity.

8:25 AM NM03.06.02

Late News: Epitaxy, Exfoliation and Strain-Induced Magnetism in Rippled Heusler Membranes Dongxue Du¹, Sebastian Manzo¹, Vivek Saraswat¹, Konrad Genser², Karin M. Rabe², Paul M. Voyles¹, Michael Arnold¹ and Jason K. Kawasaki¹; ¹University of Wisconsin, United States; ²Rutgers, The State University of New Jersey, United States

Single-crystalline membranes of functional materials enable the tuning of properties via extreme strain states; however, conventional routes for producing membranes require the use of sacrificial layers and chemical etchants, which can both damage and limit the ability to make membranes ultrathin. Here we demonstrate the epitaxial growth of the cubic Heusler compound GdPtSb on graphene-terminated Al₂O₃ substrates. The weak Van der Waals interactions of graphene enable the mechanical exfoliation to yield free-standing GdPtSb membranes. Despite the presence of the graphene interlayer, the Heusler films have epitaxial registry to the underlying sapphire, as revealed by x-ray diffraction, reflection high energy electron diffraction, and transmission electron microscopy. Whereas unstrained GdPtSb is antiferromagnetic, we show that the large strains or strain gradients in rippled membranes induce a spontaneous magnetic moment at room temperature, with a saturation magnetization of 5.2 bohr magneton per Gd atom, approaching the ~ 7 bohr magneton limit expected for ferromagnetic ordering. Our membranes provide a novel platform for tuning the magnetic properties of intermetallic compounds via strain (piezomagnetism and magnetostriction) and strain gradients (flexomagnetism).

8:40 AM NM03.06.04

Carrier Conduction and Magnetic Interactions in a Nanostructured Epitaxial

Ferromagnet/Semiconductor Fe: FeVSb Estiaque Haidar Shourov, Chenyu Zhang, Paul M. Voyles and Jason K. Kawasaki; University of Wisconsin–Madison, United States

Magnetic semiconductors are attractive for memory devices and spintronic applications [1]. However, the practical utility of dilute magnetic semiconductors (DMS) such as Mn: GaAs, albeit having all key ingredients for these applications, are hindered due to low Curie temperature. On the other hand, narrow bandgap semiconductors often make excellent thermoelectric candidates. A conventional strategy for improving the thermoelectric figure of merit (ZT) is to decrease the phonon thermal conductivity via nano-structuring [2]. Recently, it has been suggested that magnon drag (spin wave) [3], spin fluctuations [4], and enhanced effective mass [5] are alternative strategies to enhance thermoelectric performance by enhancing the power factor. Here we demonstrate the controllable synthesis of a ferromagnet/semiconductor nanostructured system: Fe nanoparticles embedded epitaxially within a semiconducting FeVSb matrix. Transmission electron microscopy confirms that the nanoparticle formation is mediated by bulk segregation for all composition greater than 10% excess Fe in stoichiometric FeVSb. Our Fe: FeVSb thin films, grown by molecular beam epitaxy, display magnetic moment and anomalous Hall effect that scale with the volume fraction of Fe nanoparticles. The parent stoichiometric FeVSb is predicted to be diamagnetic, but our stoichiometric films also exhibits magnetic signatures in transport and magnetometry at 300K. This suggests that within the solubility limit of Fe, $\text{Fe}_{1+\delta}\text{VSb}$, where δ is the bound of solubility, is a potential dilute magnetic semiconductor with Curie temperature greater than room temperature. Additionally, the ferromagnetic nanoparticles can induce spin polarized charge carriers in the semiconducting matrix due to proximity effect, making this highly controllable and tunable system appealing for spintronics. Our angle-resolved photoemission spectroscopy (ARPES) measurements on the parent semiconductor FeVSb reveal an enhanced effective mass due to electronic correlations [6]. The combination of nanostructure precipitates, magnetic interaction, and electronic correlation in this highly tunable heterostructure presented here offers a promising route for new thermoelectric application for practical waste heat recovery.

References:

- [1] Y. Ohno, D. K. Young, B. Beschoten, F. Matsukura, H. Ohno and D. D. Awschalom, Nature (London) **402**, 790 (1999).
- [2] H. Scherrer and S. Scherrer, in Handbook of Thermoelectrics, edited by D. M. Rowe (CRC Press, New York, 1994), pp. 211– 237.
- [3] M. V. Costache, G. Bridoux, I. Neumann and S. O. Valenzuela, Magnon-drag thermopile, Nat. Mater. **11** (2012).
- [4] N. Tsujii, A. Nishide, J. Hayakawa, and T. Mori, Science advances **5**, eaat5935 (2019).
- [5] Y. Pei, X. Shi, A. LaLonde, H. Wang, L. Chen, and G. J. Snyder, Nature **473**, 66 (2011).
- [6] E. H. Shourov et al, arXiv preprint, arXiv:2009.11489 (2020).

8:55 AM NM03.06.05

Complex Magnetic Phases in Polar Tetragonal Intermetallic NdCoGe₃ Binod K. Rai^{1,2}, Ganesh Pokharel^{3,1}, Hasitha Suriya Arachchige^{3,1}, Seung-Hwan Do¹, Qiang Zhang¹, Masaaki Matsuda¹, Matthias Frontzek¹, Vasile O. Garlea¹, Andrew D. Christianson¹ and Andrew F. May¹; ¹Oak Ridge National Laboratory, United States; ²Savannah River National Laboratory, United States; ³The University of Tennessee, Knoxville, United States

Polar materials can host a variety of topologically significant magnetic phases, which often emerge from a modulated magnetic ground state. Relatively few noncentrosymmetric tetragonal materials have been shown to host topological spin textures and new candidate materials are necessary to expand the current theoretical models. This presentation will discuss the anisotropic magnetism in the polar, tetragonal material NdCoGe₃ via thermodynamic and neutron diffraction measurements. The H-T phase diagram shows several magnetic field-induced phases with an applied field in the plane. Neutron diffraction data reveal that NdCoGe₃ hosts complicated magnetic order derived from modulated magnetic moments, with the ground state characterized by the propagation vector $\mathbf{k} = (0.494, 0.0044, 0.385)$ at 1.8 K.

9:10 AM *NM03.06.06

Topology Enabled Unconventional Superconductivity in a Time-Reversal Symmetry-Breaking Bulk Superconductor Valentin Taufour, Jackson Badger, Yundi Quan, Matthew Staab, Antonio Rossi, Kasey Devlin, Peter Klavins, Susan Kauzlarich, Inna Vishik and Warren Pickett; University of California, Davis, United States

In recent years, much efforts have been made towards the discovery of topological superconductors. Topological superconductivity can be artificially engineered in hybrid structures combining topological materials with conventional superconductors, or it can exist intrinsically in certain unconventional superconductors. Odd-parity superconductors are candidates for intrinsic topological superconductivity because topologically non-trivial gap functions naturally show up in these materials. These superconductors can be discovered in the proximity of magnetic instabilities such as in the superconducting ferromagnets, or in structural families that lack inversion symmetry. In this presentation, I will present our experimental and computational results on a new superconductor that breaks-time reversal symmetry because of its intrinsic topological properties. The normal state band structure includes Dirac lines and a Dirac loop at the Fermi level resulting from non-symmorphic symmetry operations, as well as Dirac points robust against splitting from SOC. The topology of the Fermi surface provides a platform for inter-band pairing and time-reversal symmetry breaking superconductivity. Our results illustrate a new route to realize spin-triplet superconductivity in a centro-symmetric structure without the need for a nearby magnetic instability.

9:35 AM NM03.06.07

Pressure-induced suppression of axionic charge density wave and onset of superconductivity in the chiral Weyl semimetal Ta₂Se₈I Qingge Mu¹, Dennis M. Nenno², Yanpeng Qi³, Fengren Fan¹, Cuiying Pei³, Moaz ElGhazali¹, Johannes Gooth¹, Claudia Felser¹, Prineha Narang² and Sergey Medvedev¹; ¹Max Planck Institute for Chemical Physics of Solids, Germany; ²Harvard University, United States; ³ShanghaiTech University, China

The Weyl points with opposite chiralities can be coupled by charge density wave (CDW) resulting in axion quasiparticle in condensed matter physics^{1,2}. Recently, the Weyl semimetal Ta₂Se₈I was reported to exhibit axions in the collective mode of CDW, the sliding CDW which is detected with nonlinear *V-I* curves³. Here we investigate the electrical transport property and crystal structure under pressure. Upon applying pressure, the axionic CDW is suppressed, which is manifested by the decrease of transition temperature and corresponding single particle energy gap. A superconducting transition appears at the vicinity of the complete suppression of the CDW. The superconducting *T_c* is enhanced monotonically to 4.5 K with pressure up to 47 GPa. No main structural transition is detected from Raman spectra and synchrotron XRD patterns. However, partial amorphization is observed in which the stretching mode of Se-Se survives, and Ta₂Se₈I evolves into superconducting state at low temperature indicating that the TaSe₄ chains may play an important role in the pressure-induced superconductivity. Our investigations construct a complete phase diagram depicting the evolution of anionic CDW and superconductivity with respect to pressure, giving further understanding of correlated topological states.

1. Li R, Wang J, Qi X L, Zhang S C. Dynamical axion field in topological magnetic insulators. *Nature Physics* **6**, 284-288 (2010).
2. Wang Z, Zhang S C. Chiral anomaly, charge density waves, and axion strings from Weyl semimetals. *Physical Review B* **87**, (2013).
3. Gooth J, *et al.* Axionic charge-density wave in the Weyl semimetal (TaSe₄)₂I. *Nature*, (2019).

11:45 AM *NM03.07.01

Tunable Quantum Anomalous Hall Effect by the Exchange Coupling Between vdW Magnetic Layers Huixia Fu¹, Jiewen Xiao¹, Chaoxing Liu² and Binghai Yan¹; ¹Weizmann Institute of Science, Israel; ²The Pennsylvania State University, United States

The layered antiferromagnetic MnBi₂Te₄ films have been proposed to be an intrinsic quantum anomalous Hall (QAH) insulator with a large gap. It is crucial to open a magnetic gap of surface states. However, recent experiments have observed gapless surface states, indicating the absence of out-of-plane surface magnetism, and thus, the quantized Hall resistance can only be achieved at the magnetic field above 6 T. We propose to induce out-of-plane surface magnetism of MnBi₂Te₄ films via the magnetic proximity with magnetic insulator CrI₃. A strong exchange bias of ~40 meV originates from the long Cr-*e_g* orbital tails that hybridize strongly with Te *p* orbitals. By stabilizing surface magnetism, the QAH effect can be realized in the MnBi₂Te₄/CrI₃ heterostructure. Moreover, the high-Chern number QAH state can be achieved by controlling external electric gates. In addition, we have derived a simple electron-counting rule to predict the magnetic exchange coupling between general vdW layers for both homo- and hetero-vdW junctions.

12:10 PM *NM03.07.02

Chern Numbers and Nodal Points in Topological Semi Metals Maia Vergniory; Donostia International Physics Center, Spain

Nonmagnetic topological materials have dominated the landscape of topological physics for the past two decades. These breakthroughs in nonmagnetic materials have not yet been matched by similar advances in magnetic compounds. Using magnetic band theory and topological indices obtained from Magnetic Topological Quantum Chemistry (MTQC), I will present a systematic way of identifying magnetic topological materials. I will then, focus on high order magnetic semimetals, and provide a topological classification of different fermions in these phases. Finally I will present new experimental realizations in materials. In particular I will focus on the pyrite compound CoS₂, using complementary bulk- and surface-sensitive angle-resolved photoelectron spectroscopy and ab-initio calculations we discovered Weyl-cones at the Fermi-level and we directly observed the topological Fermi-arc surface states that link the Weyl-nodes, which will influence the performance of CoS₂ as a spin-injector by modifying its spin-polarization at interfaces.

12:35 PM *NM03.07.03

Seeing the Topological Ground States Through Infrared Spectroscopy Ana Akrap; University of Fribourg, Switzerland

Nowadays we know of many gapless electronic phases with conical bands, such as graphene, Dirac semimetals, and Weyl semimetals. Their low-energy excitations resemble truly relativistic particles.

To see those excitations, we have to capture the physics at a milli-electron-volt scale.

In our experiments, we access electronic structures at these low energies by combining Landau level spectroscopy, infrared spectroscopy, and effective Hamiltonian models.

1:00 PM NM03.07.04

Topological Engineering Through Nonlinear Phononics Dominik M. Juraschek¹, Nesta B. Joseph², Prineha Narang¹ and Awadhesh Narayan²; ¹Harvard University, United States; ²Indian Institute of Science, India

Topological properties in quantum materials promise applications in lossless electronics and quantum information processing. Recently, dynamical control of the topological phase of the Weyl semimetal WTe₂ has been demonstrated, in which a terahertz-field induced charge current leads to interlayer shear strain that

dynamically changes the Weyl nodes of the system [1]. Here, we theoretically describe an alternative route for topological phase control that is based on a nonlinear phonon coupling. The interlayer shear and breathing modes of layered topological materials couple to infrared-active phonon modes that can be resonantly excited with ultrashort terahertz pulses. The nonlinear coupling leads a transient distortion along the coordinate of the shear and breathing modes that in turn induce changes in the topological phase of the material. Using a combination of first-principles calculations and phenomenological modeling, we demonstrate that the Dirac and Weyl nodes in WTe_2 and ZrTe_5 can be modulated through this excitation. Our results suggest that nonlinear phononic rectification of the crystal lattice is a powerful tool for dynamical control of topology in layered quantum materials.

[1] E. J. Sie et al., Nature 565, 61 (2019)

[2] D. M. Juraschek, N. B. Joseph, P. Narang, and A. Narayan, in preparation

This work is supported by the Swiss National Science Foundation (SNSF) under Project No. 184259, the DARPA DSO under the Driven Nonequilibrium Quantum Systems (DRINQS) program, Grant No. D18AC00014, and by the Department of Energy ‘Photonics at Thermodynamic Limits’ Energy Frontier Research Center under Grant No. DE-SC0019140. This research used resources of the National Energy Research Scientific Computing Center (NERSC) under Contract No. DE-AC02-05CH11231.

SESSION NM03.08: Topological Materials III
Session Chairs: Anderson Janotti and Lukas Muechler
Friday Afternoon, April 23, 2021
NM03

2:15 PM NM03.08.01

Late News: Filling Anomaly for General 2D and 3D S_4 Symmetric Lattices Yuan Fang and Jennifer Cano; Stony Brook University, The State University of New York, United States

We derive symmetry indicator formulas for the filling anomaly on 2D square lattices with and without time reversal, inversion symmetry, or their product, in the presence of spin-orbit coupling. We go beyond previous work by considering lattices with atoms occupying multiple Wyckoff positions. We also provide an algorithm using the Smith normal form that systematizes the derivation.

The formulas determine the corner charge in 2D atomic or fragile topological insulators, as well as in 3D insulators and semimetals by studying their 2D slices. We apply our results to a 3D tight-binding model on a body-centered tetragonal lattice, whose projection into the 2D plane has two atoms in the unit cell. We apply these results to several antiperovskites as material examples.

2:30 PM *NM03.08.02

Topological Magnets in 2D and 3D M. Zahid Hasan; Princeton University, United States

Electrons organize in ways to give rise to distinct phases of matter such as insulators, metals, magnets or superconductors. In the last ten years or so, it has become increasingly clear that in addition to the symmetry-based classification of matter, topological consideration of wavefunctions plays a key role in determining distinct or new quantum phases of matter [see, for an introduction, Hasan & Kane, Reviews of Modern Physics 82, 3045 (2010)].

In this talk, I briefly introduce these new topological concepts in the context of their experimental realizations in magnetic materials. As examples, I present how tuning a topological insulator whose surface hosts an unpaired Dirac fermion can give rise to Weyl fermion (massless charged fermion) in nonmagnetic and magnetic semimetals with “fractional” Fermi surfaces, and in strongly correlated magnets such as the Heusler, Kagome

and related materials. These exotic topological matter harbor novel and unprecedented properties that may lead to the development of next generation quantum technologies including novel qubits.

2:55 PM *NM03.08.03

New Insights into Topological Semimetals Jennifer Cano^{1,2}; ¹Stony Brook University, The State University of New York, United States; ²Flatiron Institute, United States

The field of topological semimetals continues to reveal new insights. I will discuss recent developments starting with the classification of nodal fermions in both magnetic and non-magnetic space groups. I will then introduce higher order Fermi arcs as a bulk-edge correspondence for Dirac fermions, and discuss a refinement of the symmetry indicators that predict these hinge states. Finally, I will discuss some material predictions.

SESSION NM03.09: Topological Films

Session Chairs: Anderson Janotti and Jason Kawasaki

Friday Afternoon, April 23, 2021

NM03

5:15 PM *NM03.09.01

Topological States of Cadmium Arsenide Films Grown by Molecular Beam Epitaxy Susanne Stemmer; University of California, Santa Barbara, United States

Interfaces and heterostructures with topological semimetals offer new opportunities to control and manipulate their unique electronic states and a wealth of associated phenomena, for example, via electric field effect, strain, or symmetry breaking. In this presentation, we will discuss recent progress in heterostructures of a prototype three-dimensional Dirac semimetal, cadmium arsenide (Cd_3As_2), which are grown by molecular beam epitaxy. We show that high-mobility, epitaxial Cd_3As_2 films can be grown in different crystallographic orientations. We discuss the nature of the quantum Hall effect of thin Cd_3As_2 films grown in different orientations and using different measurement geometries that uniquely identify the quantum Hall effect from single Dirac fermions on the surfaces. We will discuss other remarkable phenomena in the quantum limit of (001) films. We will also discuss pathway towards realizing novel topological systems.

5:40 PM *NM03.09.02

Quantized Transport on Topological Semimetal Fermi Arcs Masaki Uchida; The University of Tokyo, Japan

Cd_3As_2 is an ideal system for investigating quantum transport in topological semimetals. In addition to its high electron mobility and long mean free path, its natural growth orientation is different from the rotational axis connecting the two Dirac nodes. This allows us to detect orbital motions in topological semimetal surfaces. We have successfully developed a growth technique realizing high mobility Cd_3As_2 films with excellent surface flatness, and first observed quantum Hall states induced by quantum confinement [1]. Related film techniques such as electric gating and chemical doping of Zn also enable systematic transport studies of the Dirac semimetal films, with controlling the bulk dimensionality [1, 2], Fermi energy [3, 4], and band topology [3, 4]. By carefully fabricating $(\text{Cd}_{1-x}\text{Zn}_x)_3\text{As}_2$ films with three-dimensional and uniform thickness, we have observed surface quantum oscillations and their evolution into quantized states in films [5, 6]. This is evidenced by distinct differences in oscillation frequency, field angle dependence, and temperature change from the bulk ones. Moreover, we have found intrinsic coupling between two spatially-separated surface states in Weyl orbits by measuring dual-gate devices [7]. Independent scans of top- and back-gate voltages reveal concomitant modulation of doubly-degenerate quantum Hall states, which is not possible in conventional surface orbits as in topological insulators. Our results evidencing the unique spatial distribution of Weyl orbits provide new

opportunities for controlling the novel quantized transport. In particular, fabrication of heterointerfaces for proximitizing the surface Fermi-arcs with ferromagnets [8] and superconductors will be promising, as well as another chemical doping of Sb for increasing band-inversion energy [9].

References

- [1] M. Uchida *et al.*, Nat. Commun. **8**, 2274 (2017).
- [2] Y. Nakazawa, M. Uchida *et al.*, Sci. Rep. **8**, 2244 (2018).
- [3] S. Nishihaya, M. Uchida *et al.*, Sci. Adv. **4**, eaar5668 (2018).
- [4] S. Nishihaya, M. Uchida *et al.*, Phys. Rev. B **97**, 245103 (2018).
- [5] S. Nishihaya, M. Uchida *et al.*, Nat. Commun. **10**, 2564 (2019).
- [6] Y. Nakazawa, M. Uchida *et al.*, APL Mater. **7**, 071109 (2019).
- [7] S. Nishihaya, M. Uchida *et al.*, submitted.
- [8] M. Uchida *et al.*, Phys. Rev. B **100**, 245148 (2019).
- [9] Y. Nakazawa, M. Uchida *et al.*, Phys. Rev. B **103**, 045109 (2021).

6:05 PM *NM03.09.03

Investigations of Topological and Quantum Phenomena in Heusler and Rare-Earth Monopnictide Epitaxial Thin Films Chris J. Palmstrom; University of California, Santa Barbara, United States

Controlling electronic properties via bandstructure engineering is at the heart of modern semiconductor devices. We have extended this concept to semimetals utilizing confined thin film geometries and hetero-epitaxial interfaces to engineer electronic structure in rare-earth monopnictide and half-Heusler semimetallic systems. In the case of the rare-earth monopnictide, LuSb, quantum confinement changes the carrier compensation and differentially affects the mobility of the electron and hole-like carriers resulting in a strong modification in its large, non-saturating magnetoresistance behavior. Bonding mismatch at the heteroepitaxial interface of the semi-metal (LuSb) and a semiconductor (GaSb) leads to the emergence of a novel, two-dimensional, interfacial hole gas and is accompanied by a charge transfer across the interface that provides additional avenues to modify the electronic structure and magnetotransport properties in the ultra-thin limit.

The prediction and observation of topological surface states in half-Heusler compounds raises exciting possibilities to realize exotic electronic states and novel devices by exploiting their multifunctional nature. However, their position with respect to the Fermi level and the high density of bulk carriers has made it difficult to detect them through transport measurements. Here, we introduce compensation doping in epitaxial PtLuSb thin films as an effective route to tune the chemical potential and simultaneously reduce the bulk carrier concentration by more than two orders of magnitude compared to the parent compound. Linear magnetoresistance is shown to appear as a precursor phase that transmutes into a quantum Hall phase arising from the topological surface states on further reduction of the coupling between the surface states and the bulk carriers. Our approach paves the way to both reveal and manipulate exotic properties of topological phases in Heusler compounds.

6:30 PM NM03.09.04

Magnetic Properties on Bulk MnBi₂Te₄ Samples Grown by MBE Seul-Ki Bac¹, Logan Riney¹, Jiashu Wang¹, Kerrie Koller^{2,1}, Xinyu Liu¹, Maksym Zhukovskiy¹, Tatyana Orlova¹, Malgorzata Dobrowolska¹, Jacek Furdyna¹ and Badih Assaf¹; ¹University of Notre Dame, United States; ²Saint Mary's College, United States

Intrinsic magnetic topological insulator MnBi₂Te₄ has been extensively studied due to the theoretical prediction that it will provide a platform for novel topological phases, such as the quantum anomalous Hall effects (QAHEs), the axion insulators (AIs), and the type-II magnetic Weyl semimetals depending on thickness. Recently, the QAHE and AI have been observed on MnBi₂Te₄ flakes with odd and even number of layers, respectively. However, further progress on this novel material is hindered by the difficulty in preparing its high-quality thin films with well-controlled composition and thickness. Here we report on the magnetic properties of MnBi₂Te₄ samples grown by molecular beam epitaxy (MBE) with various thicknesses. We observed two main

results: magnetic phase transitions and the linear dependence between the Hall conductance and the magnetization. Both transport and SQUID measurements clearly show magnetic phase transitions between a ferromagnetic to an antiferromagnetic state and vice versa, which brings the possibility of hosting those new topological phases on MBE grown samples. In addition, we verify that the origin of the anomalous Hall effect of MnBi₂Te₄ is intrinsic, from its linear dependence of magnetization. Our results enable the realization of quantum anomalous Hall effects in the large area MnBi₂Te₄ films with thickness precisely controlled by MBE.

6:45 PM NM03.09.05

Characterization of the Sr Impurity in Bi₂Se₃ Thin Films by Molecular Beam Epitaxy Logan Riney¹, Xinyu Liu¹, Christian Bunker¹, Dominic Battaglia¹, Seul-Ki Bac¹, Jiashu Wang¹, Yum Chang Park², Malgorzata Dobrowolska¹, Jacek Furdyna¹ and Badih Assaf¹; ¹University of Notre Dame, United States; ²National Nanofab Center, Korea (the Republic of)

The Bi-chalcogenides are the most prominent topological materials to be studied to date. Alloying transition and alkali metals into the Bi-chalcogenides has enabled the discovery of topological superconductor candidates Sr-, Nb, and Cu- doped Bi₂Se₃. In this work, we synthesize Sr_xBi₂Se₃ thin film by molecular beam epitaxy on GaAs(111) substrates. While we do not succeed in obtaining superconductivity, our results provide insight on the mechanism by which Sr is alloyed into Bi₂Se₃. First, X-ray diffraction measurements indicate an increasing c-axis lattice parameter suggesting the formation of some Sr interstitials. Second, the mobility extracted from transport measurements and phonon linewidths extracted from Raman spectroscopy indicate that Sr likely alloys into the structure. Third, an increasing n-doping is seen with increasing Sr content. And lastly, a reduction of the electron coherence length with increasing Sr suggests that inelastic charged impurity or electron-electron scattering is enhanced. It is thus clear that Sr leads donor type impurities and more n-doping in Bi₂Se₃ despite. The thermodynamics of the MBE codeposition process seem to be generally unfavorable to the formation of Sr interstitials, thus making the synthesis of superconducting films highly challenging.

7:00 PM NM03.09.06

Late News: Two-Dimensional Quantum Oscillations Observed in Magnetic Topological Semimetal EuSb₂ Films Mizuki Ohno¹, Masaki Uchida^{1,2,3}, Ryosuke Kurihara^{4,5}, Susumu Minami⁶, Yusuke Nakazawa¹, Shin Sato¹, Markus Kriener⁵, Motoaki Hirayama^{1,5}, Atsushi Miyake⁴, Yasujiro Taguchi⁵, Ryotaro Arita^{1,5}, Masashi Tokunaga^{4,5} and Masashi Kawasaki^{1,5}; ¹Dept. of Appl. Phys., the Univ. of Tokyo, Japan; ²PRESTO, Japan Science and Technology Agency (JST), Japan; ³Department of Physics, Tokyo Institute of Technology, Japan; ⁴ISSP, the Univ. of Tokyo, Japan; ⁵RIKEN CEMS, Japan; ⁶Dept. of Phys., the Univ. of Tokyo, Japan

Topological nodal-line semimetals (TNLSMs) have attracted burgeoning attention because unprecedented quantum transport and magnetoelectric response originating from the Zak phase have been theoretically expected. Moreover, recent computational exploration has accelerated efforts to find magnetic TNLSM materials for controlling these topological phenomena by magnetic fields. In general, however, time-reversal symmetry breaking by magnetic ordering destroys robustness of the nodal lines, and thus only few magnetic TNLSM materials have been reported so far. In addition, quantum oscillations have never been observed in these magnetic topological nodal-line semimetals. Namely, discovery of a new magnetic TNLSM and fabrication of its high-mobility films have been strongly desired.

In order to introduce magnetic moments into typical nonmagnetic TNLSM CaSb₂, we prepare isostructural EuSb₂ single-crystalline films by molecular beam epitaxy (MBE). Our first-principles calculations demonstrate that EuSb₂ hosts topological nodal lines protected by nonsymmorphic symmetry even under antiferromagnetic ordering of the Eu²⁺ spins. An X-ray diffraction rocking curve is very sharp, ensuring high crystallinity of the obtained film. Observed Shubnikov-de Haas oscillations with multiple frequency components exhibit small effective masses and two-dimensional field-angle dependence even in a 250 nm thick film, suggesting possible contributions of surface states.

Our demonstration of the new magnetic TNLSM and first observation of quantum magnetotransport in its films will stimulate further investigation and control of exotic transport phenomena proposed for magnetic topological semimetals.

SYMPOSIUM NM04

Magnetic Skyrmions and Topological Effects in Materials and Nanostructures
April 14 - April 21, 2021

Symposium Organizers

Vincent Cros, Centre National de la Recherche Scientifique
Max Hirschberger, The University of Tokyo
Johanna Nordlander, Harvard University
Leslie Schoop, Princeton University
Oleg Yazyev, Ecole Polytechnique Federale de Lausanne

Symposium Support

Gold

Swiss National Science Foundation

* Invited Paper

SESSION NM04.01: Magnetic Skyrmions and Topological Effects in Materials and Nanostructures I
Session Chairs: Vincent Cros and Max Hirschberger
Wednesday Morning, April 21, 2021
NM04

8:00 AM *NM04.01.01

Skymions in Magnetic Multilayers Hongying Jia, Markus Hoffmann, Gustav Bihlmayer and Stefan Bluegel; Forschungszentrum Jülich GmbH, Germany

Spin-orbit interaction in combination with structural inversion asymmetry on magnetic surfaces, interfaces, hetero- and nanostructures is a source for a variety of spin-dependent transport phenomena and novel magnetic textures, with the chiral magnetic skyrmions [1] being the best known. In this presentation, we discuss our efforts to optimize magnetic multilayers for skyrmions [2-7] in potential applications. We elaborate on the issues of skyrmion size [7], stability and lifetime [8], and detection [9, 10]. Furthermore, we discuss multilayers of monolayer-thick films and compare those to results of stacks of thicker films. Motivated to enable efficient material screening, we report on our efforts to replace the Dzyaloshinskii–Moriya interaction (DMI) with a descriptor (e.g. work function, electric dipole moment [11]) that is easier to evaluate or measure.

Our investigations make use of a multiscale approach based on (i) density-functional theory (DFT) (the FLAPW method as implemented in the FLEUR code [12] and the Korringa-Kohn-Rostoker (KKR) method as implemented in juKKR [13]) combined with (ii) the atomistic spin dynamics code SPIRIT [14,15] by which the lifetime of the skyrmions are determined combining the Geodesic Nudged Elastic Band method (GNEB) [16] or the Systematic Saddle Point Search method [8] with the Harmonic Transition State Theory (HTST) and (iii) micromagnetic reasoning.

We acknowledge funding by the DARPA TEE program (#HR0011831554) from DOI, from Deutsche Forschungsgemeinschaft (DFG) through SPP 2137 “Skyrmionics” (Project No. BL 444/16), the Collaborative

Research Centers SFB 1238 (Project C01) as well as computing time from JARA-HPC and Jülich Supercomputing Centre.

- [1] Stefan Heinze *et al.*, Nat. Phys. **7**, 713 (2011).
- [2] Ashis Kumar Nandy *et al.*, Phys. Rev. Lett. **116**, 177202 (2016).
- [3] Abdu Belabbes *et al.*, Phys. Rev. Lett. **117**, 247202 (2016).
- [4] Bertrand Dupé *et al.*, Nat. Commun. **7**, 11779 (2016).
- [5] Bernd Zimmermann *et al.*, Appl. Phys. Lett. **113**, 232403 (2018).
- [6] Hongying Jia *et al.*, Phys. Rev. B **98**, 144427 (2018).
- [7] Hongying Jia *et al.*, Phys. Rev. M **4**, 094407 (2020).
- [8] Gideon P. Müller *et al.*, Phys. Rev. Lett. **121**, 197202 (2018).
- [9] Dax M. Crum *et al.*, Nat. Commun. **6**, 8541 (2015).
- [10] Manuel dos Santos Dias *et al.*, Nat. Commun. **7**, 13613 (2016).
- [11] Hongying Jia *et al.*, Phys. Rev. M **4**, 024405 (2020).
- [12] For a program description, see www.flapw.de.
- [13] For a program description, see <https://jukkr.fz-juelich.de>
- [14] For a program description, see <https://spirit-code.github.io>
- [15] Gideon P. Müller *et al.*, Phys. Rev. B **99**, 224414 (2019).
- [16] Pavel F. Bessarab *et al.*, Sci. Rep. **8**, 3433 (2018).

8:25 AM *NM04.01.03

Stability and Ultrafast Topological Switching of Magnetic Skyrmions Felix Buettner; Helmholtz-Zentrum Berlin, Germany

Magnetic skyrmions are long-lived topological excitations in a small subset of magnetic materials, such as some heavy-metal / ferromagnet multilayers with strong interfacial spin-orbit interactions. These materials can host a high density of skyrmions without any topological counterparts, which defines these states as topological phases with a large net topological charge. A transition from a topological trivial state to a skyrmion state is hence considered a topological phase transitions. Such topological phase transitions, which involve the nucleation or annihilation of magnetic skyrmions, are in principle allowed due to the discrete nature of the lattice. However, they are still suppressed by the same strong energy barriers that also allow skyrmions to exist at room temperature [1]. Topological phase transitions are therefore expected to be of first order, with hysteresis and a transition dynamics characterized by slow and heterogeneous nucleation, as known, e.g., from freezing of water. In fact, we find that heterogeneous nucleation is the underlying principle of electrical skyrmion nucleation, which crucially relies on materials defects to break the translational symmetry [2].

Surprisingly, however, we find that picosecond homogeneous nucleation of an extended topological phase, comprising a dense array of nanometer-scale magnetic skyrmions, can be induced by a single femtosecond laser pulse.

In this talk, after giving an introduction to the stability [1] and the spin-orbit torque nucleation [2] of magnetic skyrmions, I will discuss the nucleation dynamics of this all-optical topological phase transition, which we were able to follow in real time during the early user operation of beamline SCS at the European XFEL [3]. Using time-resolved small angle x-ray scattering, we discovered that rapid, homogeneous nucleation of the skyrmion phase is mediated by a previously undisclosed transient fluctuation state. This state, which is characterized by high spatial frequency magnetic fluctuations, persists for approximately 100 ps after exciting our magnetic multilayer with a femtosecond, infrared laser pulse. The topological phase emerges from these fluctuations by nucleation and coalescence, a mechanism that goes well beyond existing theories of topological phase transitions such as the Kibble–Zurek mechanism and the Berezinskii–Kosterlitz–Thouless transition. The process is completed on a time scale of 300 ps. Using atomistic spin dynamics simulations, we confirm that the fluctuation state is key to the ultrafast increase of the global topological charge, enabled by an almost complete elimination of the topological energy barrier in this transient state of matter.

[1] F. Büttner, I. Lemesh, and G. S. D. Beach, Theory of isolated magnetic skyrmions: From fundamentals to room temperature applications. *Scientific Reports* 8, 4464 (2018).

[2] F. Büttner, I. Lemesh, M. Schneider, B. Pfau, C. M. Günther, P. Helsing, J. Geilhufe, L. Caretta, D. Engel, B. Krüger, J. Viehhaus, S. Eisebitt, and G. S. D. Beach, Field-free deterministic ultrafast creation of magnetic skyrmions by spin-orbit torques. *Nature Nanotechnology* 12, 1040 (2017).

[3] F. Büttner, B. Pfau, M. Böttcher, M. Schneider, G. Mercurio, C. M. Günther, P. Helsing, C. Klose, A. Wittmann, K. Gerlinger, L.-M. Kern, C. Strüber., C. von Korff Schmising, J. Fuchs, D. Engel, A. Churikova, S. Huang, D. Suzuki, I. Lemesh, M. Huang, L. Caretta, D. Weder, J. H. Gaida, M. Möller, T. R. Harvey, S. Zayko, K. Bagschik, R. Carley, L. Mercadier, J. Schlappa, A. Yaroslavtsev, L. Le Guyarder, N. Gerasimova, A. Scherz, C. Deiter, R. Gort, D. Hickin, J. Zhu, M. Turcato, D. Lomidze, F. Erdinger, A. Castoldi, S. Maffessanti, M. Porro, A. Samartsev, J. Sinova, C. Ropers, J. H. Mentink, B. Dupé, G. S. D. Beach, and S. Eisebitt, Observation of fluctuation-mediated picosecond nucleation of a topological phase. *Nature Materials* (2020).

8:50 AM *NM04.01.04

Kinetically Controlled Skyrmion Flow Christian Pfleiderer; Technische Universität München, Germany

The non-trivial topology of skyrmions in magnetic materials results in a massively enhanced coupling to spin currents and an emergent electrodynamic directly observable in the transport properties. We report an investigation of the conditions and characteristics of the unpinning and subsequent motion of skyrmions in the class of chiral magnets as inferred from the transverse and longitudinal susceptibility as well as kinetic neutron scattering.

9:15 AM *NM04.01.05

Stability of Néel-Type Skyrmion Lattice Against Oblique Magnetic Fields in GaV₄S₈ and GaV₄Se₈
Martino Poggio; Universität Basel, Switzerland

Magnetic skyrmions have mostly been studied in cubic chiral helimagnets, in which they are Bloch-type and their axes align along the applied magnetic field. In contrast, the orientation of Néel-type skyrmions is locked to the polar axis of the host material's underlying crystal structure. In the lacunar spinels GaV₄S₈ and GaV₄Se₈, the Néel-type skyrmion lattice phase exists for externally applied magnetic fields parallel to this axis and withstands oblique magnetic fields up to some critical angle. Here, we map out the stability of the skyrmion lattice phase in both crystals as a function of field angle and magnitude using dynamic cantilever magnetometry. The measured phase diagrams reproduce the major features predicted by a recent theoretical model, including a reentrant cycloidal phase in GaV₄Se₈. Nonetheless, we observe a greater robustness of the skyrmion phase to oblique fields, suggesting possible refinements to the model. Besides identifying transitions between the cycloidal, skyrmion lattice, and ferromagnetic states in the bulk, we measure additional anomalies in GaV₄Se₈ and assign them to magnetic states confined to polar structural domain walls.

SESSION NM04.02: Magnetic Skyrmions and Topological Effects in Materials and Nanostructures II

Session Chairs: Vincent Cros and Oleg Yazyev

Wednesday Morning, April 21, 2021

NM04

11:45 AM *NM04.02.01

Skyrmions for Unconventional Computing and Revealing Latent Information Karin Everschor-Sitte;
Johannes Gutenberg Universität Mainz, Germany

Novel computational paradigms in combination with proper hardware solutions are required to overcome the limitations of our state-of-the-art computer technology, in particular regarding energy consumption. Due to the inherent complex and non-linear nature, spintronics offers the possibility towards energy-efficient, non-volatile hardware solutions for various unconventional computing schemes.[1-3]

In this talk, I will address the potential of magnetic skyrmions for in particular two unconventional computing schemes – reservoir computing and stochastic computing. Reservoir computing is a computational scheme that allows drastically simplifying spatial-temporal recognition tasks. We have shown that random skyrmion fabrics provide a suitable physical implementation of the reservoir [4,5] and allow to classify patterns via their complex resistance responses either by tracing the signal over time or by a single spatially resolved measurement. [6] Stochastic computing is a computational paradigm that allows speeding up a calculation while trading for numerical precision. Information is encoded in terms of bit-streams as a probability. A key requirement and simultaneously a challenge is that the incoming bitstreams are uncorrelated. The Brownian motion of magnetic skyrmions allows creating a device that reshuffles the bit-streams. [7,8]

In any type of hardware-based computation, finally, some sort of readout of the system is needed. While often a significant effort is made in enhancing the resolution of an experimental technique to obtain further insight into the sample and its physical properties, advantageous data analysis has the potential to provide a deeper insight into a given data set. This is particularly relevant when the signal is close to the resolution limit, i.e. where the noise becomes at least of the same order as the signal. [9]

[1] J. Grollier, D. Querlioz, K. Y. Camsari, KES, S. Fukami, M. D. Stiles, Nature Electronics (2020)

[2] E. Vedmedenko, R. Kawakami, D. Sheka, ..., KES, et al., J. of Phys. D (2020)

[3] G. Finocchio, M. Di Ventra, K.Y. Camsari, KES, P. K. Amiri and Z. Zeng, arXiv:1907.07176

[4] D. Prychynenko, M. Sitte, et al, KES, Phys. Rev. Appl. 9, 014034 (2018)

[5] G. Bourianoff, D. Pinna, M. Sitte and KES, AIP Adv. 8, 055602 (2018)

[6] D. Pinna, G. Bourianoff and KES, arXiv:1811.12623

[7] D. Pinna, F. Abreu Araujo, J.-V. Kim, et al, Phys. Rev. Appl. 9, 064018 (2018)

[8] J. Zazvorka, F. Jakobs, D. Heinze, ..., KES, et al., Nat. Nanotech. 14, 658 (2019)

[9] I. Horenko, D. Rodrigues, T. O’Kane and KES, arXiv:1907.04601

12:09 PM *NM04.02.02

Local Spectroscopy on Magnon Modes in Skyrmion-Hosting Materials in the Microwave Frequency Regime Dirk Grundler; EPFL, Switzerland

After the discovery of the magnetic skyrmions in the A-phase of a chiral magnet [S. Mühlbauer et al., Science 323, 915 (2009)], the interest in non-collinear spin structures has substantially increased. Such nanoscale spin structures depend crucially on the material, temperature and energy contributions relevant to magnetically ordered states such as symmetric Heisenberg exchange, antisymmetric Dzyaloshinskii–Moriya exchange interactions, Zeeman energy, magnetocrystalline and shape anisotropy. The engineering of materials and energy terms is now decisive to harvest the promised functionalities of skyrmions e.g. as racetrack memory [A. Fert et al., Nat. Nano. 8, 152 (2013)], probabilistic computing approach [D. Pinna et al., Phys. Rev. Applied 9, 064018 (2018)] and microwave oscillator [S. Zhang et al., New J. Phys. 17, 023061 (2015)]. For all these possible applications a detailed understanding of spin dynamics in the technologically relevant GHz frequency regime [Y. Onose et al., Phys. Rev. Lett. 109, 037603 (2012), S.A. Montoya et al., Phys. Rev. B 95, 224405 (2017)] is of utmost importance. At the same time eigenresonances provide a fundamental insight into the relevant energy terms [T. Schwarze et al., Nat. Mater. 14, 478 (2015)].

In the talk we report on broadband spectroscopy performed on non-collinear spin structures supported by different materials systems such as the chiral bulk magnet Cu_2OSeO_3 and multilayers prepared from FeGd. The low magnetic damping in both systems allowed us to observe rich magnon spectra which depended characteristically on the different magnetic phases. Our experiments range from about 10 K to room temperature. Beyond broadband spin-wave spectroscopy we performed Brillouin light scattering with a focused laser beam (bulk Cu_2OSeO_3) and x-ray magnetic circular dichroism microscopy (FeGd multilayers grown on a

membrane). Specific cooling cycles and magnetic field histories applied to Cu_2OSeO_3 induced metastable phases which displayed eigenmode spectra not known from the earlier publications [Y. Onose et al., Phys. Rev. Lett. 109, 037603 (2012); T. Schwarze et al., Nat. Mater. 14, 478 (2015)]. We report our latest experimental results obtained on the dynamics of non-collinear spin structures in the bulk chiral magnet Cu_2OSeO_3 and FeGd multilayers.

The work was possible due to excellent cooperation with Ping Che, and M. Albrecht, A. Bauer, K. Baumgaertl, M. Bechtel, H. Berger, E. Catapano, M. Garst, J. Gräfe, M. Heigl, A. Kúkol'ová, A. Magrez, A. Mucchietto, C. Pfeleiderer, H.M. Rønnow, T. Schönenberger, G. Schütz, J.-R. Soh, I. Stasinopolous, M. Weigand, J. Waizner. The research is funded by SNSF via grant 171003 (sinergia project Nanoskymionics) and by DFG via transregio TRR80.

12:33 PM *NM04.02.03

Skyrmion and Tetartion Lattices in Twisted Bilayer Graphene Achim Rosch; University of Cologne, Germany

Recent experiments on twisted bilayer graphene show an anomalous quantum Hall (AQH) effect at filling of 3 electrons per moiré unit cell. The AQH effect arises in an insulating state with both valley- and ferromagnetic order. We argue [1], that weak doping of such a system leads to the formation of a novel topological spin texture, a 'double-tetartion lattice'. The building block of this lattice, the 'double-tetartion', is a spin configuration which covers 1/4 of the unit-sphere twice. In contrast to skyrmion lattices, the net magnetization of this magnetic texture vanishes. Only at large magnetic fields more conventional skyrmion lattices are recovered. But even for large fields the addition of a single charge to the ferromagnetic AQH state flips hundreds of spins. Our analysis is based on the investigation of an effective non-linear sigma model which includes the effects of long-ranged Coulomb interactions.

[1] Thomas Boemerich, Lukas Heinen, and Achim Rosch, Phys. Rev. B **102**, 100408(R) (2020).

12:57 PM *NM04.02.04

Exploring Magnetic Skyrmions in Co-Zn-Mn Compounds—From Far-From-Equilibrium States to Effects of Magnetic Frustration Jonathan White; Paul Scherrer Institute, Switzerland

First discovered in 2009 to form a lattice of whirlpool-like twists in MnSi, magnetic skyrmions have since been explored extensively in other bulk magnetic crystals, and in synthetic systems such as magnetic mono- and multilayers. Regardless of the host system, the topological winding of skyrmions is the common ingredient that leads to unique physical properties attracting significant interest. In particular, it is established that skyrmions when created display a robustness against perturbation and decay that is generally referred to as topological protection. This is a central concept underlying the stability of skyrmions and their suitability for use in applications, either within equilibrium phases or far-from-equilibrium states.

In this talk, we will review our recent experimental studies of Co-Zn-Mn compounds [1-6], a family of high-temperature chiral cubic magnets discovered recently to host Bloch-type chiral skyrmions over an extended temperature range, including room temperature [1]. Amongst the remarkable properties displayed by these materials, we will focus first on how skyrmions phases fall out of thermal equilibrium remarkably easily on supercooling to form robust metastable skyrmion states [2-3]. These metastable skyrmion states extend unprecedentedly across the majority of the phase diagram, and can even display a thermally-reversible structural transformation that surprisingly does not trigger a decay to the thermodynamic ground state.

Second, we focus in on the $\text{Co}_7\text{Zn}_7\text{Mn}_6$ composition, the phase diagram of which hosts two thermodynamically distinct equilibrium skyrmion phases [5]. One of these skyrmion phases is the so-called A-phase, stable just below the transition temperature and familiar to all chiral cubic magnets. The second skyrmion phase in this system is much more unusual, being stable at much lower temperatures, with this fact alone implicating multiple skyrmion stability mechanisms exist in this single system, and the existence of a new

skyrmion phase stability mechanism at low temperature. From extensive recent experiments [6], we will argue that the stability of the low temperature skyrmion phase is due to a cooperative interplay between chiral magnetism and the magnetic frustration that arises due to a hyper-kagome structural motif in the crystal structure.

Overall, our experiments on Co-Zn-Mn compounds showcase this system as a rich playground for exploring the connection between topological skyrmions, the physics of far-from-equilibrium topological states and magnetic frustration.

- [1] Y. Tokunaga *et al.*, Nature Communications **6**, 7638 (2015)
- [2] K. Karube, J.S. White *et al.*, Nature Materials **15**, 1237 (2016)
- [3] K. Karube, J.S. White *et al.*, Phys. Rev. Materials **1**, 074405 (2017)
- [4] K. Karube, J.S. White *et al.*, Science Advances **4**, eaar7043 (2018)
- [5] K. Karube, J.S. White *et al.*, Physical Review B **102**, 064408 (2020)
- [6] V. Ukleev *et al.*, submitted for publication.

1:21 PM *NM04.02.05

Ferromagnetic and Synthetic Antiferromagnetic Skyrmions in Magnetic Multilayers—3D Textures and Investigations of the Dzyaloshinskii-Moriya Interaction Nicolas Reyren¹, Yanis Sassi¹, Matthieu Grelier¹, Cyril Léveillé², Fernando Ajejas¹, Erick Burgos-Parra^{1,2}, Sachin Krishnia¹, Titiksha Srivastava^{1,3}, William Legrand¹, Davide Maccariello¹, Sophie Collin¹, Aymeric Vecchiola¹, Karim Bouzehouane¹, Nicolas Jaouen², Stefania Pizzini⁴, André Thiaville⁵, Vincent Cros¹ and Albert Fert¹; ¹Unité Mixte de Physique, CNRS, Thales, Paris-Saclay, France; ²Synchrotron Soleil, France; ³SPEC, CEA-Saclay, France; ⁴Institut Néel, France; ⁵Laboratoire de Physique des Solides, France

Magnetic skyrmions are localized magnetic textures in magnetic films, behaving as particles and topologically different from the uniform ferromagnetic state. In metallic magnetic multilayers (MML) with perpendicular magnetic anisotropy (PMA), non-collinear chiral spin textures are stabilized by interfacial Dzyaloshinskii-Moriya interaction (DMI), which favours a unique sense of magnetization rotation. Magnetic skyrmions in MML were identified to be extremely promising for applications, as well as of fundamental interest. [1] The magnetism community provided a great effort during the last years to control skyrmions properties, notably size, velocity, and stability in field and temperature.

We soon realized that the increase of repetitions of the multilayers serving the thermal stability of the magnetic textures has the *a priori* adverse effect of stabilizing hybrid magnetic textures that is a depth dependence of the chirality (of domain walls or skyrmions) due to the competitions between dipolar fields and DMI. [2] We will describe ferromagnetic skyrmion propagation in different type of structures and discuss the role of their three-dimensional (3D) magnetic textures with hybrid chirality.

The dipolar fields are also responsible for the increase in skyrmion diameter. Both the hybrid chirality and the size increase suggest that reducing the role of dipolar fields is desirable in view of applications. A solution is to use ferromagnetic layers coupled antiferromagnetically through Ruderman-Kittel-Kasuya-Yoshida (RKKY) interaction, namely synthetic antiferromagnetic (SAF) MML. Manipulating the SAF MML is of course difficult using external magnetic fields only, and a solution using a bias layer will be discussed. [3] Studying SAF systems with conventional magnetic force microscopy (MFM) and other techniques is challenging. We will present experimental investigations using MFM in vacuum [3], NV-center microscopy, electrical transport measurement [4] and x-ray scattering techniques [5] to investigate the magnetization textures, and, in particular, the skyrmions in SAF.

Understanding precisely our observations requires a detailed understanding of the DMI. Therefore, we investigate systematically the DMI using Brillouin light scattering, stripe domain period, and domain wall propagation in several types of multilayers to measure its dependence with thickness [6] and materials [6,7]. In

particular, we unravel a strong correlation between the work function and the DMI amplitude [7].

- [1] A. Fert, N. Reyren and V. Cros, *Nat. Rev. Materials* **2**, 17031 (2017)
- [2] W. Legrand *et al*, *Sci. Adv.* **4**, eaat0415 (2018)
- [3] W. Legrand *et al*, *Nat. Mater.* **19**, 34 (2020)
- [4] D. Maccariello *et al*, to appear in *Phys. Rev. Appl.*
- [5] C. Léveillé, E. Burgos-Parra *et al*, in preparation.
- [6] W. Legrand *et al*, in preparation.
- [7] F. Ajejas *et al*, in preparation.

French ANR grant TOPSKY (ANR-17-CE24-0025), DARPA TEE program grant (MIPR#HR0011831554), FLAG-ERA SOgraphMEM, and EU grant SKYTOP (H2020 FET Proactive 824123) are acknowledged for their financial support.

SESSION NM04.03: Magnetic Skyrmions and Topological Effects in Materials and Nanostructures III
Session Chairs: Vincent Cros and Dirk Grundler
Wednesday Afternoon, April 21, 2021
NM04

2:15 PM *NM04.03.01

Skyrmions, Hopfions and Related Topological Defects in Chiral Magnets and Liquid Crystals Avadh Saxena; Los Alamos National Laboratory, United States

Nontrivial topological defects such as two- and three-dimensional skyrmions, skyrmion tubes and hopfions have been observed in a variety of materials including chiral magnets, nematic liquid crystals and even in ferroelectrics as well as other materials (e.g. multiferroics) and physical contexts such as condensates. I will present a comparative study of these topological entities in terms of modeling them using the relevant variable, e.g. magnetization, polarization or the director field. I will also focus on their energetics, a variety of topological invariants that characterize them and how to study their properties for potential applications.

2:39 PM *NM04.03.02

Tailoring and Measuring Anisotropy in Skyrmion Hosts Istvan Kezsmarki; Universität Augsburg, Germany

The impact of magnetic anisotropy on the skyrmion lattice (SkL) state in non-centrosymmetric magnets has been overlooked for long, partly because a semi-quantitative description of the equilibrium SkL phase forming near the Curie temperature could often be achieved without invoking anisotropy effects. Recently, anisotropy has been reported to play a crucial role in the formation of low-temperature equilibrium SkLs in cubic helimagnets, the transformation between different metastable SkLs and the deformation of skyrmions in axially symmetric polar magnets. While these findings highlight the importance of magnetic anisotropy with regard to the stability, symmetry and shape of individual skyrmions and SkLs, systematic experimental studies quantifying the strength of anisotropy in skyrmion hosts are virtually non-existing. Here, we determine the type and the strength of magnetic anisotropy in various skyrmion-host families, using multi-frequency electron spin resonance spectroscopy, and report on strong variations of anisotropy driven by composition, temperature or even by magnetic field.

3:03 PM *NM04.03.05

Thermodynamic Phenomena of Skyrmions Wanjun Jiang; Tsinghua University, China

Skyrmions are particle-like topological spin textures stabilized by the Dzyaloshinskii-Moriya interaction, which

have recently stimulated great interests in spintronics community. The dynamics of which have been frequently studied via using magnetic fields and current-induced spin torques. On the other hand, a comprehensive understanding of thermal effects, including random thermal fluctuation and directional thermal currents, on the dynamics of skyrmions are not fully established yet.

In this talk, I will first discuss our recent experimental observation of the thermal fluctuation-induced random walk of a single isolated Néel-type magnetic skyrmion in an interfacially asymmetric Ta/CoFeB/TaO_x multilayer. In particular, an intriguing topology dependent Brownian gyromotion behavior of skyrmions has been identified. The onset of Brownian gyromotion of a single skyrmion induced by the thermal effects, including a nonlinear temperature-dependent diffusion coefficient and topology-dependent gyromotion are further formulated based on the stochastic Thiele equation.

Subsequently, I will discuss the thermal generation, manipulation and detection of nanoscale skyrmions, which were made in microstructured devices made of different multilayers – [Ta/CoFeB/MgO]₁₅, [Pt/CoFeB/MgO/Ta]₁₅ and [Pt/Co/Ta]₁₅ integrated with on-chip heaters, by using a full-field soft X-ray microscopy. In particular, the thermal generation of densely packed skyrmions at the device edge, together with the unidirectional diffusion of skyrmions from the hot region towards the cold region were experimentally observed. These thermally generated skyrmions can be further electrically detected by measuring the accompanied anomalous Nernst voltages. These results could open another exciting avenue for enabling skyrmionics, and promote interdisciplinary studies among spin caloritronics, magnonics and skyrmionics.

[1] W. Jiang, et al., Science, 349, 283 (2015).

[2] W. Jiang, et al., Nature Physics, 13, 162 (2017).

[3] W. Jiang, et al., Physics Reports, 704, 1-49 (2017).

[4] J. Zázvorka et al. Nature Nanotechnology **14**, 658-661 (2019).

[5] L. Zhao, et al., Phys. Rev. Letts. 125, 027206 (2020).

[6] Z. Wang, et al., Nature Electronics, 3, 672-679 (2020).

3:27 PM *NM04.03.04

Advanced Transmission Electron Microscopy of Magnetic Skyrmions at the Nanoscale Rafal Dunin-Borkowski, Andras Kovacs, Thibaud Denneulin and Fengshan Zheng; Forschungszentrum Jülich GmbH, Germany

Off-axis electron holography is a powerful technique, which can be used to record the phase shift of an electron wave that has passed through an electron-transparent specimen in a transmission electron microscope. According to the Aharonov-Bohm equation, the phase shift is sensitive to local variations in electromagnetic potential, which are in turn dependent on nanoscale properties of a specimen of interest, such as charge density or magnetization. The determination of such properties from a recorded phase image is an ill-posed problem that is difficult to tackle. We have developed a model-based iterative reconstruction technique, which can be used to retrieve the projected in-plane magnetization distribution from the magnetic contribution to a recorded phase image, or alternatively the three-dimensional magnetization distribution from a set of at least two tilt series of magnetic phase images. The technique is based on the optimized implementation of a forward model, which maps a given magnetization distribution onto one or more phase images. The forward model utilizes sparse matrix multiplications for efficient projections and Fourier-transform-based convolutions with pre-calculated convolution kernels based on analytical solutions for the magnetic phase images of simple geometrical objects. The ill-posed problem is tackled by replacing the original problem by a least squares minimization, which is augmented by regularization techniques to find a solution for the reconstructed magnetization distribution. Tikhonov regularization of first order is used to apply smoothness constraints to the magnetization, which is justified by the minimization of exchange energy. *A priori* information about the positions and sizes of magnetic objects in the field of view are utilized in the form of a three-dimensional mask, which reduces the number of unknowns to be retrieved. The model-based approach is flexible and can account for arbitrary linear phase ramps and phase offsets, as well as for untrustworthy (low confidence) regions in input images. We have applied it successfully to reconstruct in-plane (projected) magnetization distributions from

individual experimental magnetic phase images and three-dimensional magnetization distributions from tilt series of phase images. Diagnostic measures, which are based on optimal estimation theory, have been used to analyze the quality of the reconstruction results. The influence of the regularization strength has been assessed, in order to obtain the best solution in the presence of noise and other artefacts.

In order to visualize the magnetization distributions of Bloch-type magnetic skyrmions in three dimensions, we have used model-based iterative reconstruction to study patterned FeGe nanostructures that host individual skyrmions in the absence of applied magnetic fields, allowing tomographic tilt series of off-axis electron holograms to be recorded. We have also identified novel superstructures of skyrmion strings in thin films of chiral magnets that form characteristic patterns in phase images recorded using off-axis electron holography.

In order to visualize the magnetization distributions of Néel-type skyrmions that are stable at room temperature, we have studied perpendicularly-magnetized multilayers of heavy metals and ferromagnets sputtered on SiN membranes by tilting the sample with respect to the incident electron beam direction in the presence of applied magnetic fields and compared experimental phase images with simulated phase images derived from atomistic models. Furthermore, we have studied two-dimensional magnetic materials, which possess strong perpendicular magnetocrystalline anisotropy and show Néel-type skyrmion bubbles after field cooling.

3:51 PM *NM04.03.03

Curvilinear Magnetism—Geometrically Curved Ferro- and Antiferromagnets Denys Makarov;
Helmholtz-Zentrum Dresden-Rossendorf e.V., Germany

The main origin of the chiral symmetry breaking in magnetic materials is associated with the intrinsic Dzyaloshinskii-Moriya interaction (DMI). At present, tailoring of DMI is done rather conventionally by optimizing materials, either doping a bulk single crystal or adjusting interface properties of thin films and multilayers. A viable alternative to the conventional material screening approach can be the exploration of the interplay between geometry and topology. The research field in magnetism, which is dealing with the study of the impact of geometrical curvature on magnetic responses of curved 1D wires and 2D shells is known as curvilinear magnetism [1]. The perspective of the development of curvilinear magnetism is outlined in the 2017 and 2020 Magnetism Roadmaps [2,3]. In this presentation, we will discuss on the recent achievements in the field and address the following topics:

A fully 3D approach to treat curvilinear effects in ferromagnetic nanowires and thin shells of arbitrary shape is established by Gaididei et al. back in 2014 [4] and was recently extended by Sheka et al. [5] to properly account for effects of non-locality due to the presence of long-range magnetostatic interaction. Volkov et al. has proven that the exchange-driven chiral effects in curvilinear ferromagnets are experimental observables [6] and can be used to realize nanostructures with tunable magneto-chiral properties from standard magnetic materials.

In contrast to the intrinsic DMI, a concept of mesoscale Dzyaloshinskii-Moriya interaction was put forth, which is a result of the interplay between the intrinsic (spin-orbit-driven) and extrinsic (curvature-driven) DMI terms [7]. The mesoscale DMI governs the magneto-chiral properties of any curvilinear ferromagnetic nanosystem and depends both on the material and geometrical parameters. Its strength and orientation can be tailored by properly choosing the geometry, which allows stabilizing distinct magnetic chiral textures including skyrmion and skyrmionium states as well as skyrmion lattices [8-10]. Interestingly, skyrmion states can be formed in a material even without an intrinsic DMI [8,10].

Sheka et al. [5] discovered a novel non-local chiral symmetry breaking effect, which does not exist in planar magnets: it is essentially non-local and manifests itself even in static spin textures living in curvilinear magnetic nanoshells. To identify this new interaction, a generalized micromagnetic theory of curvilinear ferromagnets was constructed accounting for local and nonlocal effects. The curvature leads to the emergence of the new magnetostatic charge, the geometrical charge, determined by the local characteristics of the surface. This newcomer is responsible for the appearance of novel fundamental chiral symmetry breaking effect.

The field of curvilinear magnetism was recently extended towards curvilinear antiferromagnets. Pylypovskiy et al. [11] demonstrated that intrinsically achiral one-dimensional curvilinear antiferromagnet behaves as a chiral helimagnet with geometrically tunable DMI, orientation of the Neel vector and the helimagnetic phase

transition. This positions curvilinear antiferromagnets as a novel platform for the realization of geometrically tunable chiral antiferromagnets for antiferromagnetic spinorbitronics.

- [1] Streubel et al., J. Phys. D: Appl. Phys. 49, 363001 (2016).
- [2] Sander et al., J. Phys. D: Appl. Phys. 50, 363001 (2017).
- [3] Vedmedenko et al., J. Phys. D: Appl. Phys. 53, 453001 (2020).
- [4] Gaididei et al., PRL 112, 257203 (2014).
- [5] Sheka et al., Communications Physics 3, 128 (2020).
- [6] Volkov et al., PRL 123, 077201 (2019).
- [7] Volkov et al., Scientific Reports 8, 866 (2018).
- [8] Kravchuk et al., PRB 94, 144402 (2016).
- [9] Kravchuk et al., PRL 120, 067201 (2018).
- [10] Pylypovskiy et al., Phys. Rev. Appl. 10, 064057 (2018).
- [11] Pylypovskiy et al., Nano Letters (2020). doi:10.1021/acs.nanolett.0c03246.

SESSION NM04.04: Magnetic Skyrmions and Topological Effects in Materials and Nanostructures IV
Session Chairs: Johanna Nordlander and Oleg Yazyev
Wednesday Afternoon, April 21, 2021
NM04

5:15 PM *NM04.04.01

Imaging Skyrmions in Ferromagnets and Antiferromagnets with Scanning NV-Center Microscopy

Aurore Finco; Laboratoire Charles Coulomb, Université de Montpellier and CNRS, France

NV-center magnetometry emerges as a powerful technique to investigate complex magnetic textures at the nanoscale under ambient conditions. It makes use of the response to magnetic field of the single spin of an NV-center [1], which is a defect in the crystalline structure of diamond consisting of a nitrogen atom and a vacancy. We demonstrate here its imaging capabilities both on ferromagnetic skyrmions stabilized at zero external field and on antiferromagnetic domain walls and skyrmions in a synthetic antiferromagnet.

To observe non-collinear textures in ferromagnets, we operate the NV magnetometer in photoluminescence quenching mode, allowing the detection of stray field producing areas by measuring the spatial variations of the emitted NV center photoluminescence. In addition, the use of a diamond probe ensures that the experiment is carried out in the absence of external magnetic perturbation. To illustrate this, we show that skyrmions with a diameter about 60 nm [2] are stabilized by the exchange bias coming from the interface between the antiferromagnet IrMn and the ferromagnet NiFe in an optimized Pt/Co/NiFe/IrMn stack.

In addition to ferromagnets, antiferromagnets have recently attracted a great interest in spintronics owing to the robustness of their magnetic textures and their fast dynamics. However, since they exhibit no net magnetization, antiferromagnets are challenging to work with. Therefore, we introduce a new imaging mode of the scanning NV-center microscope which does not rely on the measurement of the static magnetic stray field but on the detection of magnetic noise originating from spin waves inside the non-collinear antiferromagnetic textures of interest. The presence of magnetic noise accelerates the NV spin relaxation. As a consequence, the emitted photoluminescence is reduced, allowing a simple detection of the noise sources [3].

We demonstrate this new technique on synthetic antiferromagnets [4] consisting of two ferromagnetic Co layers antiferromagnetically coupled through a Ru/Pt spacer. We first image domain walls and prove that we perform noise-based imaging by measuring a shorter NV spin relaxation time above an antiferromagnetic domain than above a domain wall. Calculations of the spin waves dispersion both in the antiferromagnetic domains and in

the domain walls as well as maps of simulated magnetic noise intensity enable us to conclude that the noise which we probe arises from spin waves channelled in the domain walls.

Going further, we tune the composition of the synthetic antiferromagnet stacks in order to stabilize spin spirals or antiferromagnetic skyrmions. In both cases, our relaxometry-based technique is able to image the non-collinear structures, demonstrating its efficiency and opening new avenues of exploration in the characterization of complex structures in magnetically-compensated materials.

This work was done in collaboration with Spintec in Grenoble, France, the Unité Mixte de Physique CNRS/Thalès in Palaiseau, France and the Center for Nanoscience and Nanotechnology (C2N) in Palaiseau, France. This project has received funding from the European Union's Horizon 2020 research and innovation programme under the Marie Skłodowska-Curie grant agreement No 846597 and from the DARPA TEE Program.

- [1] L. Rondin et al, Rep. Prog. Phys 77, 056503 (2014)
- [2] K. Gaurav Rana et al, Phys. Rev. Appl., 13, 044079 (2020)
- [3] A. Finco et al, arXiv:2006.13130 (2020)
- [4] W. Legrand et al, Nat. Mater., 19, 34 (2020)

5:40 PM *NM04.04.02

Skyrmion Dynamics in MnSi Tobias Weber¹, David Fobes², Johannes Waizner³, Paul Steffens¹, Greg Tucker⁴, Martin Boehm¹, Lukas Beddrich⁵, Chris Franz⁵, Henrik Gabold⁵, Rob Bewley⁴, David Voneshen⁴, Markos Skoulatos⁵, Robert Georgii⁵, Georg Ehlers⁶, Andreas Bauer⁵, Christian Pfleiderer⁵, Peter Boeni⁵, Marc Janoschek⁷ and Markus Garst⁸; ¹Institut Laue-Langevin, France; ²Los Alamos National Laboratory, United States; ³University of Cologne, Germany; ⁴ISIS Pulsed Neutron and Muon Source, United Kingdom; ⁵Technische Universität München, Germany; ⁶Oak Ridge National Laboratory, United States; ⁷Paul Scherrer Institute, Switzerland; ⁸Karlsruhe Institute of Technology, Germany

For temperatures in the range between ca. 28 and 29 K and for magnetic fields of about 0.16 – 0.21 T, the itinerant magnet MnSi features a vortex-like skyrmion order [1] of its electron spins. The study of the structure of magnetic skyrmions has generated much experimental and theoretical interest since its discovery over ten years ago. Here, we present the first comprehensive study of the dynamics of the skyrmion phase.

MnSi's non-centrosymmetric space group has profound consequences for dynamics in all ordered magnetic phases of MnSi. Namely, it introduces a Dzyaloshinskii-Moriya term which leads to magnon creation at energies that are different from those for magnon annihilation, with this phenomenon being restricted to reduced momentum transfers whose vector q has components perpendicular to the skyrmion plane. The dynamical magnetic structure factor $S(q, E, H)$, with $q = Q - G$ and lattice vector G , thus becomes asymmetric ("non-reciprocal") with respect to changing the sign of either q , the energy transfer E , or the magnetic field H , but is symmetric upon interchanging the signs of any two of these variables. Such an asymmetric behavior could so far also be observed for the field-polarized [2, 3], the paramagnetic [4] and the conical [5,6] phase of MnSi.

For our recently completed study [7] we fully mapped out the magnetic dynamics in the skyrmion phase of MnSi. To that end, we employed polarized triple-axis, time-of-flight and spin-echo experiments. Apart from an in-depth analysis of the non-reciprocal dynamics, we succeeded in observing a splitting of the magnon energies into closely-spaced Landau levels for momentum transfer vectors inside the skyrmion plane. Theoretically, we describe our results using a mean-field linear spin-wave model. A correction of the theory for instrumental resolution yields an excellent quantitative agreement between experiment and theory.

- [1] S. Mühlbauer, B. Binz, F. Jonietz, C. Pfleiderer, A. Rosch, A. Neubauer, R. Georgii, and P. Böni; Science 323 (5916), 915–919 (2009).
- [2] S. V. Grigoriev, A. S. Sukhanov, E. V. Altynbaev, S.-A. Siegfried, A. Heinemann, P. Kizhe, and S. V.

Maleyev; Phys. Rev. B 92, 220415 (2015).

[3] T. J. Sato, D. Okuyama, T. Hong, A. Kikkawa, Y. Taguchi, T. Arima, and Y. Tokura; Phys. Rev. B 94, 144420 (2016).

[4] B. Rössli, P. Böni, W. E. Fischer, and Y. Endoh; Phys. Rev. Lett. 88, 237204 (2002).

[5] T. Weber, J. Waizner, G. S. Tucker, R. Georgii, M. Kugler, A. Bauer, C. Pfleiderer, M. Garst, and P. Böni; Phys. Rev. B 97, 224403 (2018).

[6] T. Weber, J. Waizner, P. Steffens, A. Bauer, C. Pfleiderer, M. Garst, and P. Böni; Phys. Rev. B 100, 060404(R) (2019).

[7] T. Weber, D. M. Fobes, J. Waizner, P. Steffens, G. S. Tucker, M. Böhm, L. Beddrich, C. Franz, H. Gabold, R. Bewley, D. Voneshen, M. Skoulatos, R. Georgii, G. Ehlers, A. Bauer, C. Pfleiderer, P. Böni, M. Janoschek, and M. Garst; submitted (2020).

6:05 PM NM04.04.03

Magnetic Ordering and Magnetoresistance of Antiferromagnet CaFe_2O_4 Jonathan Valenzuela, Tekiyah Robinson, Kory Wells, Sunil Karna and Doyle Temple; Norfolk State University, United States

The oxide compounds containing iron are widely studied because of many interesting phenomena including charge disproportionation, spin polarization, and the magnetoresistive effect. CaFe_2O_4 crystallizes in the orthorhombic $Pbnm$ structure which consists of distorted FeO_6 distorted octahedra through edge- and corner-sharing with intercalated Ca atoms. We have recently grown a large single crystal of CaFe_2O_4 by the optical floating-zone method. The two transitions $T_1 \sim 240$ K and $T_2 \sim 200$ K are observed in our magnetic susceptibility measurements. Our neutron powder diffraction reveals two competing magnetic phases, Γ_6 and Γ_3 , at low temperatures which are distinguished by their c -axis stacking of ferromagnetic b -axis stripes. Γ_6 -type magnetic phase develops below 240 K that starts to reduce with the emergence of Γ_3 -type magnetic phase below 200 K. The detailed magnetoresistance measurements in different crystal orientations will also be discussed in the presentation.

6:20 PM *NM04.04.04

Emergent Topological Structures and Phase Transitions in Ferroelectric Superlattices Lane W. Martin^{1,2}; ¹University of California, Berkeley, United States; ²Lawrence Berkeley National Laboratory, United States

In superconductivity, colossal magnetoresistance, and multiferroism, emergent phenomena arise from the interplay of various degrees of freedom and competing phases that drive nanoscale complexity (*i.e.*, chemical, ionic, electronic, etc. variations) that can be readily controlled using external stimuli and can result in colossal changes in physical responses. Leveraging advances in *ab initio* design, atomically precise synthesis, and multi-modal characterization of materials researchers can now induce such competition in an on-demand fashion and probe the resulting order in ways never imagined before. While non-trivial topological magnetic textures such as skyrmions have generated particular interest due to their topological protection and their potential for use in memory applications, similar effects in ferroelectrics were not expected. Such topologically protected structures or concomitant topological-phase transitions in ferroelectric were thought to be unlikely because the primary order parameter is strongly coupled to the lattice distortion and thus continuous evolution of the order parameter would result in a large elastic-energy cost. But advances in materials heterostructuring, superlatticing, nanostructuring, *etc.* are now opening the door to previously unexpected effects – including the observation of novel structures reminiscent of topological structures in magnetic systems in such polar materials.

Here we will summarize and highlight recent advances in the study of ferroelectric/dielectric superlattices such as $(\text{PbTiO}_3)_n/(\text{SrTiO}_3)_n$, wherein unit-cell-level control enables one to place the Landau, electrical, elastic, and gradient energies into competition which drives the formation of topologically non-trivial structures including so-called polar vortices and skyrmions. We will introduce and explore a number of aspects of these systems, including: the fundamental nature of the features that can be produced and the mechanisms behind their formation, routes to tune the morphology of the emergent structures to produce both polar vortices and skyrmions with a skyrmion number of +1, observations of phase coexistence (mediated by a first-order phase

transition) between such emergent, non-trivial phases and trivial ferroelectric phases, the potential for the formation of a novel multi-order-parameter state which belongs to a class of gyrotropic electrotoroidal compounds, the realization of electric-field control of such mixed-phase systems which permits interconversion between the non-trivial emergent states and trivial ferroelectric phases concomitant with order of magnitude changes in piezoelectric and nonlinear optical responses, the potential for a non-classical, BKT-like topological phase transition in these materials, electric-field and light susceptibilities, the potential for exotic dielectric phenomena, and much more. All told, this work will provide a primer on this growing field, highlight similarities and differences with the magnetic community, and show how multi-modal approaches are rapidly rewriting our understanding of this class of materials.

6:45 PM NM04.04.05

Comprehensive Screening and Alloy Design of Inverse Heusler Antiskyrmion Hosts Daniil A. Kitchaev and Anton Van der Ven; University of California, Santa Barbara, United States

The scarcity of bulk materials capable of hosting (anti)skyrmions over a wide range of ambient temperatures remains one of the most substantial obstacles to moving from proof-of-concept experiments to practical skyrmion-based devices. We have recently demonstrated that achieving a wide temperature range for skyrmion stability requires moving from the cubic symmetry seen in conventional bulk skyrmion hosts, to uniaxial symmetries[1], alongside ensuring a high Curie temperature. Several high-temperature antiskyrmion host materials consistent with these criteria have been experimentally reported within the family of inverse Heusler alloys[2,3]. We report a comprehensive computational exploration of the inverse Heusler family of compounds in search of synthesizable compositions capable of hosting antiskyrmions and other helimagnetic phases over a wide range of temperatures near ambient conditions. We develop a universal model connecting the chemical, structural, and magnetic phase stability of these alloys, building from first-principles calculations of their structure, to finite temperature and mesoscale behavior. While very few ordered ternary inverse Heuslers may host antiskyrmions, we identify an abundance of disordered quaternary inverse Heusler alloys that are likely to support these magnetic phases, in addition to those previously reported. These results establish the first set of rational design criteria for engineering thermally-robust topological magnetism, and identify a number of promising chemical spaces for experimental exploration.

[1] Kitchaev, D. A., Schueller, E. C., Van der Ven, A. *Physical Review B*, 101(5), 054409. (2020)

[2] Nayak, A. K., Kumar, V., Ma, T., et al. *Nature*, 548(7669), 561-566. (2017)

[3] Jena, J., Stinshoff, R., Saha, R., et al. *Nano letters*, 20(1), 59-65. (2019)

SESSION NM04.05: Magnetic Skyrmions and Topological Effects in Materials and Nanostructures V

Session Chairs: Max Hirschberger, Johanna Nordlander and Leslie Schoop

Wednesday Afternoon, April 21, 2021

NM04

8:15 PM NM04.05.01

Distinct Topological Skyrmion Lattices in Tetragonal Heusler Compounds Jacob Gayles^{1,2}, Toni Helm^{3,1} and Claudia Felser²; ¹University of South Florida, United States; ²Max Planck Institute for Chemical Physics of Solids, Germany; ³Dresden High Magnetic Field Laboratory, Helmholtz Zentrum Dresden Rossendorf, Germany

Tetragonal Heusler compounds that lack inversion symmetry was shown to stabilize an antiskyrmion lattice, even above room temperature. Recently, multiple distinct Skyrmion states have been proposed to emerge in the Heusler ferromagnetic metal $Mn_{1.4}PtSn$. The compound displays a transition from A.S.K. to Bloch-type Skyrmions, as seen from Lorentz transmission electron microscope results, placing $Mn_{1.4}PtSn$ in a select category. This Heusler compound forms in a superstructure with the D_{2d} symmetry, which allows for an

anisotropic Dzyaloshinskii-Moriya interaction (D.M.I.) perpendicular to the tetragonal axis. We use density functional theory calculations of $Mn_{1.5}XY$ and Mn_2XY to extract the relevant exchange interactions that determine the rich phase diagrams in these materials. The exchange interactions are between the comparatively large moments on the Mn atoms $\sim 4 \mu_B$, which show magnetic states that are ferrimagnetic non-collinear up to the spin reorientation. The D.M.I. and anisotropy's primary source is the X ion, either Rh, Pd, Ir, or Pt, which also influences the exchange interactions. The Fermi level can be tuned by the Y ion, either In, Sn or Sb. The interplay of these microscopic exchange interactions leads to a rich phase diagram that can display distinct skyrmion phases in external fields.

The Topological Hall effect (THE), a direct measurement of the topological magnetic excitations in conductive compounds, has proven a subject in detecting Skyrmion lattice phases. We calculate the anomalous Hall effect and topological Hall effects in these regimes to capture the electronic structure's influence on the Berry curvature. Here we report new insights of the magnetotransport, which is compared to experimental findings in the magneto-optical Kerr effect, magnetic force microscopy studies, ferromagnetic resonance, specifically in the intriguing magnetic properties of $Mn_{1.4}PtSn$. We show how the contribution of Skyrmions can be detected in transport devices. Our results provide evidence for the existence of antiskyrmions and ferrimagnetic in-plane Skyrmions depending on a wide range of temperatures and the orientation of an external magnetic field. These findings lead to a unique possibility to stabilize distinct skyrmions and for detection by all-electrical means.

8:30 PM DISCUSSION

8:45 PM NM04.05.04

Topological Nature of Magnetic and Electronic Structures in Cubic B20 Nanostructures Nitish Mathur¹, Matthew J. Stolt¹, Fehmi Yasin², Xiuzhen Yu² and Song Jin¹; ¹University of Wisconsin Madison, United States; ²RIKEN, Japan

Nanostructured platform for materials with real space (magnetic skyrmion) and momentum space (Weyl fermions) topological features could enable efficient memory and quantum computing devices. We have developed “bottom-up” chemical vapor deposition (CVD) techniques to synthesize single-crystal nanostructures of non-centrosymmetric cubic B20 FeGe (magnetic skyrmion host) and CoSi (Weyl semimetal). Magnetic skyrmions are depicted as two-dimensional spin texture, in reality, they possess a three-dimensional structure of skyrmions that looks like elongated strings extending throughout the thickness of the sample. We report the creation and annihilation of skyrmion strings in FeGe nanostructures under in-plane magnetic field (H_{\parallel}) using magnetotransport and defocused Lorentz transmission electron microscopy (LTEM) detection techniques for the first time. Unusual asymmetric and hysteretic magnetoresistance (MR) features are observed during magnetic phase transitions within the skyrmion strings stability regime when H_{\parallel} is along the nanostructure's long edge, which increase the sensitivity of MR detection. On the other hand, CoSi are found to possess unconventional chiral fermions with higher Chern number and chirality dependent band dispersion. We synthesized novel merohedral twinned nanowires of Weyl semimetal that could possess a topological defect (exhibits spontaneous symmetry breaking) connecting/separating two enantiomeric atomic arrangements inside the crystal itself. We discuss here the notable synthesis results, experimental techniques, and challenges to explore the topological nature of magnetic and electronic structures in nanostructure morphology.

9:00 PM NM04.05.05

Real-Space Observation of Topological Skyrmions/Antiskyrmions and Their Controlled Transformation in Non-Centrosymmetric Magnets Licong Peng¹, Kosuke Karube¹, Rina Takagi¹, Wataru Koshibae¹, Kiyomi Shibata¹, Kiyomi Nakajima¹, Taka-hisa Arima^{1,2}, Naoto Nagaosa^{1,2}, Shinichiro Seki¹, Yoshinori Tokura^{1,2,2}, Yasujiro Taguchi¹ and Xiuzhen Yu¹; ¹RIKEN Center for Emergent Matter Science (CEMS), Japan; ²University of Tokyo, Japan

Topological skyrmions and antiskyrmions have attracted enormous attention due to their different emergent phenomena and potential applications to spintronics. In this talk, we will present the real-space observations of skyrmions/antiskyrmions and their transformation in two kinds of non-centrosymmetric magnets^[1,2] by Lorentz

transmission electron microscopy. We will show the stability and manipulation of the square-shape antiskyrmions in a square lattice and elliptically-deformed skyrmions with opposite helicities as determined by the interplay of magnetic dipole interaction and anisotropic Dzyaloshinskii–Moriya interaction. We then show that their topological nature, such as topological charge, helicity, and lattice form, is highly controllable by manipulating the in-plane and out-of-plane magnetic fields, temperature, and thickness, etc..

References:

[1] L. C. Peng, R. Takagi, W. Koshibae, K. Shibata, K. Nakajima, T. Arima, N. Nagaosa, S. Seki, X. Z. Yu and Y. Tokura. *Nat. Nanotech.* **15**, 181-186 (2020)

[2] K. Karube*, L. C. Peng*, J. Masell, X. Z. Yu, F. Kagawa, Y. Tokura & Y. Taguchi, submitted (2020) (*equally contributed)

9:15 PM *NM04.05.06

Emergent Electromagnetic Induction in Helical-Spin Magnets Yoshinori Tokura^{1,2}; ¹RIKEN, Japan; ²The University of Tokyo, Japan

We report on the inductor function as designed and realized via emergent electromagnetic field (EEMF) in metallic magnets with helical spin orders. An inductor is one of the most fundamental circuit elements for modern electronic device. The magnitude of such a conventional inductance is proportional to the volume of an inductor's coil, which is known as a hardly-solvable hindrance to miniaturization of inductors. Here, we demonstrate an inductance of quantum-mechanical origin, that is originating from the emergent electric field induced by current-driven dynamics of spin helices in a magnet. In microscale rectangular-shaped devices of a magnet with nanoscale spin helices, e.g. Gd₃Ru₄Al₁₂, we observed that the inductance is prominently enhanced in spin helically-modulated phases, showing a typical inductance value (L) as large as sub micro-henry for the device whose volume is $\sim 10^{-6}$ times smaller than the inductor available at present. The observed inductance is enhanced by the nonlinearity in current and shows non-monotonous frequency dependence, both of which result from the current-driven dynamics of the spin-helix structures. We discuss the possibility of the highly inductive helimagnets working beyond room temperature as a most distinct outcome of EEMF in quantum materials.

9:40 PM NM04.05.07

Late News: Magnetic Skyrmions in a Thermal Gradient-Experimental Observation and Critical Speed-Up Jan Masell¹, Xiuzhen Yu¹ and Naoto Nagaosa^{1,2}; ¹RIKEN CEMS, Japan; ²The University of Tokyo, Japan

When a magnetic insulator is subject to a temperature gradient, an effective magnon current flows from the hot to the cold side of the sample. It was theoretically proposed that this magnon current exerts a torque on the magnetization, similar to a spin-transfer torque in a bulk magnet, which can move magnetic skyrmions towards the source of heat [1,2,3].

I will present recent experimental observations which confirm the directed motion of skyrmions in the chiral magnetic insulator Cu₂OSeO₃ when a heat gradient is applied. The experimentally observed skyrmion velocity is in qualitative agreement with our theoretical predictions. Moreover, our theoretical analysis predicts an enhancement of the magnon current at the phase transition from a conical to a field-polarized background. The embedding phase is therefore expected to have a strong impact on the motion of skyrmions in a thermal gradient, including a critical speed-up at the aforementioned phase transition, which I will discuss in this presentation.

[1] L. Kong and J. Zang, *Phys. Rev. Lett.* **111**, 067203 (2013)

[2] A. A. Kovalev, *Phys. Rev. B* **89**, 241101(R) (2014)

[3] S.-Z. Lin, C. D. Batista, C. Reichhardt, and A. Saxena, *Phys. Rev. Lett.* **112**, 187203 (2014)

9:55 PM *NM04.05.08

Control, Drive and Manipulation of Various Topological Spin Textures Xiuzhen Yu; RIKEN, Japan

Exotic topological spin textures¹⁾ and their dynamics attract much attention to fundamental physics²⁾ and applications to novel electron-devices³⁾ owing to their topological nature and emergent electromagnetic properties. Here, I will present how to control, drive and manipulate nanometer-scale topological spin textures and their lattice forms, such as (anti) skyrmion, (anti) meron and their transformations between antiskyrmions and skyrmions, merons and skyrmions, and transformations of their lattice forms between square lattice (sq.-ML) and triangular lattice (hex-SkL), with finely tuning the external magnetic field in several magnets⁴⁻⁶⁾ with non-centrosymmetric crystalline structure. On the other hand, the minute (atomic-scale) skyrmions have been successfully manipulated in centrosymmetric magnets with Ruderman–Kittel–Kasuya–Yoshida (RKKY)-type electronic coupling⁷⁻⁸⁾. To manipulate and track individual skyrmions and its lattice form using a relatively low electric current, we make a microdevice composed a thin helimagnet of FeG with a small notch⁹⁾, which allowed the spin current to be localized in a specific area near the corner of the notch. Drift, Hall and torque motions of single 80-nm-size skyrmions and their clusters are tracked with directional current at low current density, a thousand times weaker than those used in that for drives of magnetic domain walls.

These works were done in collaborations with Profs. Yoshinori Tokura, Naoto Nagaosa, Masashi Kawasaki, Taka-hisa Arima, Yusuke Tokunaga, Shinichiro Seki and Masahiko Mochizuki and Drs. Tasujiro Taguchi, Fumitaka Kagawa, Max Hirschberger, Wataru Koshibae, Naoya Kanazawa, Kosuke Karube, Jan Masell, Licong Peng, Fehmi Yasin, Khanh Nguyen Daisuke Morikawa, Masao Nakamura, Kiyoun Shibata, and Rina Takagi.

References:

- ¹⁾ X. Z. Yu, J. Masell, et al., *Nano Lett.* 20, 7313 (2020)
- ²⁾ N. Nagaosa and Y. Tokura, *Nat. Nanotechnol.* 8, 899 (2013).
- ³⁾ W. Legrand, *Nat. Mater.* 19, 34 (2020).
- ⁴⁾ L.C. Peng, et al., *Nat. Nanotechnol.* 15, 181 (2020)
- ⁵⁾ F. Yasin, *Adv. Mater.* (2020) DOI: 10.1002/adma.202004206
- ⁶⁾ X. Z. Yu, et al., *Nature* 564, 95 (2018)
- ⁷⁾ M. Hirschberger, et al., *Nat. Commun.* 10, 5831 (2019)
- ⁸⁾ K. Nguyen, et al., *Nat. Nanotechnol.* 15, 444 (2020)
- ⁹⁾ X.Z. Yu, et al., *Sci. Adv.*, 6, eaaz9744 (2020)

10:20 PM NM04.05.09

Shubnikov de-Haas Oscillation and Quantum Hall Effect in Bulk CaCuSb Single Crystal—Evidence of 2D Charge diffusion Souvik Sasmal¹, Rajib Mondal², Arumugam Thamizahvel¹, Bahadur Singh¹ and Vikram Tripathi¹; ¹Tata Institute of Fundamental Research, India; ²UGC DAE Consortium For Scientific Research, India

As the charge carriers in 3D materials are not confined and free to move in all spatial dimensions, Quantum Hall Effect (QHE) in 3D is rare and it is relatively unexplored in experiments due to the limited choice of viable candidate materials. Here, we report on the observation of weak antilocalization (WAL) and QHE followed by Shubnikov de-Haas (SdH) oscillations with oscillation frequency 314 T and effective mass in bulk CaCuSb single crystal. It crystallizes in the hexagonal structure (P6₃/mmc). One of the unique features of this crystal structure is to possess two Cu-Sb layers in the unit cell that act as the conduction channels. Significant anisotropy in electrical transport measurements along crystallographic *a*- and *c*- direction suggests that magneto-transport effect is due to charge diffusion on Cu-Sb planes but not along *c*- axis. A cusp like behavior in the low field region of magnetoresistance reveals WAL in this compound, as observed in *ABC*- type hexagonal structure CaAgBi¹⁾. Magnetoconductance (MC) follows 2D scaling law as reflection of merging MC data as a function of normal component of magnetic field for different angles. Quantized Hall plateaus are observed in the $1/\rho_{xy}$ vs $1/B$ plot are attributed to the multiple 2D conduction channels in the system. The first-principles calculations show that CaCuSb is a semimetal with dominant hole carriers at the Fermi level. Our study shows that CaCuSb can provide a unique platform to study QHE in high magnetic fields.

Reference:

[1] Souvik Sasmal *et al.*, *J. Phys.: Condens. Matter* 32, 335701 (2020)

10:35 PM *NM04.05.10

Topological Quasiparticles—Magnetic Skyrmions Axel Hoffmann; University of Illinois at Urbana-Champaign, United States

Magnetic skyrmions are topologically distinct spin textures and can be stable with quasi-particle like behavior.¹ This makes them interesting for information technologies,² where data is envisioned to be encoded in topological charges, instead of electronic charges as in conventional semiconducting devices. Using magnetic multilayers we demonstrated that inhomogeneous charge currents allow the generation of skyrmions at room temperature in a process that is remarkably similar to the droplet formation in surface-tension driven fluid flows.³ Micromagnetic simulations reproduce key aspects of this transformation process and suggest a second mechanism at higher currents that does not rely on preexisting magnetic domain structures.⁴ Indeed, we demonstrated this second mechanism experimentally using non-magnetic point contacts.⁵ Using this approach, we demonstrated that the topological charge gives rise to a transverse motion on the skyrmions, i.e., the skyrmion Hall effect.⁶ Finally, I will provide an outlook on dynamic excitations of magnetic skyrmions.^{7,8}

This work was supported by the U.S. Department of Energy, Office of Science, Materials Sciences and Engineering Division and by NSF through I-MRSEC.

References:

1. W. Jiang, *et al.*, *Phys. Rep.* **2017**, 704, 1–49.
2. A. Hoffmann and S. D. Bader, *Phys. Rev. Appl.* **2015**, 4, 047001-1–047001-18
3. W. Jiang, *et al.*, *Science* **2015**, 349, 283–286.
4. O. Heinonen, *et al.*, *Phys. Rev. B* **2016**, 93, 094407-1–094407-6.
5. Z. Wang, *et al.*, *Phys. Rev. B* **2019**, 100, 184426-1–184426-9.
6. W. Jiang, *et al.*, *Nature Phys.* **2017**, 13, 162–169.
7. M. Lonsky and A. Hoffmann, *Phys. Rev. B* **2020**, 102, 104403-1–104403-11.
8. M. Lonsky and A. Hoffmann, *APL Mater.* **2020**, 8, 100903-1–100903-12.

SESSION NM04.06: On-demand
Wednesday Morning, April 14, 2021
NM04

8:00 AM NM04.06.02

Late News: Disordered Spin Textures and Emergent Magnetic Transport Properties in Tb₅Sb₃ Single Crystal Aki Kitaori¹, Naoya Kanazawa¹, Jonathan White², Victor Ukleev², Yoshichika Onuki³ and Yoshinori Tokura^{1,3}; ¹University of Tokyo, Japan; ²Paul Scherrer Institute, Switzerland; ³RIKEN, Japan

Non-collinear magnetic structure induces emergent magnetic field on conduction electrons, resulting in such as a geometrical Hall effect and so on [1]. Especially in helimagnets with short magnetic periods, the geometrical or topological Hall effect can dominate Hall resistivity profile [2]. Such systems have been attracting attention as a material platform where emergent magnetic fields can be utilized.

Some Mn₅Si₃-type rare-earth compounds, such as Dy₅Si₃ and Ho₅Sb₃, are known for famous material examples to exhibit helimagnetic orderings. Among them, Tb₅Sb₃ has been identified as a helimagnet that hosts various magnetic structures.

We have succeeded in growing single crystals of Tb₅Sb₃ and revealed the magnetic and electric transport properties. We found peculiar magnetic-field dependences of Hall resistivity showing peak structures, which

cannot be explained by anomalous Hall effect proportional to the magnetization and may indicate the emergent field contributions. We have also identified the possible formation of a disordered helimagnetic state by small-angle neutron scattering (SANS). In this poster, we will discuss the relation between the Hall resistivity profile and the disordered helical magnetic structure.

[1] S. Gao *et al.*, *Phys. Rev. B* 100, 241115(R) (2019)

[2] T. Kurumaji *et al.*, *Science* 365, 6456, 914-918 (2019)

8:10 AM NM04.06.03

Late News: Solution-Processed Yttrium Iron Garnet Thin Films as Novel Magnetostrictive Materials

Shreya K. Patel and Sarah Tolbert; University of California, Los Angeles, United States

Many spintronic devices require low damping materials that also exhibit high magnetostriction.^{1,2} However, the efficiency of such devices is limited by the high conductivity of metallic magnetostrictive materials, causing significant electrical losses from eddy currents and increased damping. Yttrium iron garnet ($\text{Y}_3\text{Fe}_5\text{O}_{12}$, or YIG) is a promising alternative to metallic magnetostrictive materials since it exhibits low Gilbert damping.^{3,4} Additionally, YIG exhibits acceptable magnetic properties for spintronic devices including a relatively low coercivity.^{4,5} Despite these advantages, YIG intrinsically exhibits near-zero magnetostriction. Theoretical and experimental data has shown that doping YIG with cerium (substituting for yttrium) can significantly increase magnetostriction due to increased spin-orbit coupling in bulk, single crystal materials.^{5,6} We utilize solution processing for facile stoichiometry control as well as integrability into a future device. The synthesis and characterization of these novel magnetostrictive YIG materials will be presented.

References: 1) *J. Phys. Condens. Matter.*, **2017**, 29, 1-22. 2) *Nat. Commun.*, **2017**, 8, 296. 3) *APL Mater.* **2014**, 2, 106. 4) *Solid State Phys.*, **2013**, 64, 157-191. 5) *J. Appl. Phys.*, **1967**, 38, 3737-3739. 6) *AIP Conf. Proc.*, **1972**, 5, 704-706.

SYMPOSIUM NM05

Functional Nanoparticle Materials—Synthesis, Property and Applications

April 14 - April 20, 2021

Symposium Organizers

Mei Cai, General Motors

Ou Chen, Brown University

Yu Han, King Abdullah University of Science and Technology

Han Htoon, Los Alamos National Laboratory

* Invited Paper

SESSION NM05.01: Functional Nanoparticle Materials—Synthesis, Property and Applications I

Session Chairs: Mei Cai and Ou Chen

Sunday Morning, April 18, 2021

NM05

8:00 AM NM05.01.03

Remarkable Dependency of the Chirality Transfer Efficiency on the Shape of Nanoscale Chiral Additives Ahlan Nemati, Sasan Shadpour and Torsten Hegmann; Kent State University, United States

Intelligent nanoscale tuning of chirality in liquid crystal media holds great potential for deciphering the level of homochirality and origin of chirality in the living systems. Notably, we have reported some of the highest ever-reported value of the helical twisting power in achiral N-LCs for chiral ligand-coated GNRs [1-2]. Moreover, we demonstrate how the amplification of chirality facilitated by GNRs decorated with chiral molecules can be used to clearly distinguish the chiral induction strength of a homologous series of binaphthyl derivatives, differing only in the length of a non-tethered aliphatic chain, in the induced chiral N*-LC phase [3-4]. Recent further research shows that we are now able to accurately control the helical pitch and the helical twisting power values in N-LC/nanoparticle composites. These composites include mixtures of N-LCs with diverse chiral ligand-coated nano shapes (spherical, rod, prism, disk, and star) and varying aspect ratios (2-10) of gold nano shapes. Finally, we additionally support our experimentally derived arguments of a more comprehensive understanding of the chirality transfer's dependency on shape by calculations of a suitable pseudoscalar chirality indicator [5].

References:

- [1] Nemati, A., Shadpour, S., Querciagrossa, L., Mori, T., Gao, M., Zannoni, C., Hegmann, T., *Nature Communication*, **9**, 1, 1-13 (2018).
- [2] Sharma, A., Mori, T., Lee, H.C., Worden, M., Bidwell, E., Hegmann, T., *ACS Nano*, **8**, 12, 11966-11976 (2014).
- [3] Nemati, A., Shadpour, S., Querciagrossa, L., Mori, T., Zannoni, C., Hegmann, T., *ACS Nano*, **13**, 9, 10312-10326 (2019)
- [4] Mori, T., Sharma, A., Hegmann, T., *ACS Nano*, **10**, 1, 1552-1564 (2016).
- [5] Nemati, A., Shadpour, S., Querciagrossa, L., Zannoni, C., Hegmann, T., Gonçalves, D., Cui, X., Ai, R., Wang, J., *ibid.*

8:15 AM NM05.01.04

Late News: Thermodynamically Stable Colloidal Solids—Interfacial Free Energy-Particle Size Distribution Correspondence Andrew Nelson and Lawrence Friedman; National Institute of Standards and Technology, United States

The thermodynamics of solid-solution interfaces is one of the most basic topics of interest in colloid science. The work of interface formation, called in varying contexts the surface or interfacial energy or tension, is the thermodynamic parameter that dictates the stability and evolution of suspensions, gels, emulsions, and many other systems. From the perspective of the synthetic chemistry of solid nanoparticles, the interfacial energy usually is taken to be responsible for a serious obstacle in the preparation and use of these highly dispersed materials: where the free energy of interfaces is positive, systems will inevitably coarsen to minimize this quantity. Establishing a system in which interfaces are actually stable, by the controlled reduction of the interfacial energy, offers a framework for preparing stable, reproducible, and controllable nanoparticle dispersions for both fundamental and engineering applications. Such dispersions of solids, in analogy to the much better-characterized case of microemulsions, have been prepared but not yet systematized. From the statistical thermodynamics of nanoparticle dispersions and using the tools of classical nucleation theory and liquid mixtures, we provide a simple analytical expression giving a one-to-one correspondence between the measurable size distribution of a colloidal suspension at equilibrium and the size-dependent interfacial free energy. The size distribution can be given only in terms of parameters that are relatively easy to control, estimate, or measure, such as the molecular solubility, densities, and cohesive energies. Consideration of older experimental data, in light of this framework, allows us in principle to characterize different modes through which different colloidal solutions are stabilized in equilibrium, such as through preferred curvature or electrostatic charging. Finally, we indicate the parameters that must be optimized in order to solve the problem of preparing monodisperse nanoparticles and discuss whether previous syntheses may have reached the narrowest achievable size distribution allowed at equilibrium.

8:30 AM NM05.01.05

Silver Ion Cluster Formation and Xe Sorption in Silver-Exchanged Zeolites—Insights Toward

Accelerated Materials Design Eric Hoar and Lindsay Roy; Savannah River National Laboratory, United States

The trace analysis of xenon is an indicator of nuclear activity and as such the collection of Xe isotopes from the environment is of great importance for environmental monitoring and treaty verification. Silver clusters have been shown to selectively sorb Xe better from the environment when integrated into an aluminosilicate zeolite framework system vs. other systems such as MOFs. Despite the large amount of research on these Ag-zeolites, resolving the role of silver (Ag) in the sorption mechanism remains a complex issue with several contradictory reports in the literature. Prior to the design of novel sorption materials, research must first address the fundamental questions of why Ag-zeolites outperform other porous adsorbents with respect to Xe uptake. To better understand the role of silver ion cluster formation in the sorption of Xe, this talk will focus on using density functional theory (DFT) methods to identify specific structure-property relationships in Ag-exchanged chabazites which contribute to increased sorption uptake. The results show that small, highly charged clusters form high-index facets within the large cavities of the zeolite, which could allow for rapid sorption of Xe onto their surface. Optimization of these features must be considered when designing high-performance, low-cost adsorbents for noble gases. Ultimately, these results will be used to develop strategies for exploring Xe sorption uptake using a machine learning sorption model amenable to straightforward validation by first-principles simulation and experimental data.

8:45 AM NM05.01.06

Material Interdiffusion During Low Temperature Sintering of Nanoporous Metals Natalya Kublik¹,

Stanislau Niauzorau¹, Sridhar Niverty², Nikhilesh Chawla² and Bruno Azeredo¹; ¹Arizona State University, United States; ²Purdue University, United States

In the past decade, nanoscale metals have found use in reactive metal inks due to its ability to fuse at lower temperatures and create electrically conductive traces. [1] This study examines a new class of nanoscale metals and their morphology evolution during sintering. Specifically, interdiffusion of atoms in nanostructured metals is investigated during low temperature (e.g. 44% of T_m of AuCu eutectic point) sintering of nanoporous Au thin films and Cu powders. Both powders and thin-films are synthesized by chemical dealloying yielding ligaments that are 46 and 64 nm, respectively, and the former is dispersed over the latter as an initial condition for sintering. Samples are transferred into the tube furnace while wet in dehydrated alcohol to prevent oxide formation [2] and are sintered in a reducing atmosphere (H₂/Ar mixture, 5% of H₂) at 400 °C. After sintering, cross-sections through the neck zone between powders and thin-film are obtained via focused ion beam milling and the concentration profiles across the welded interface are measured via energy dispersive X-ray spectroscopy with large diffusion penetration depths (0.8 μm) across the interface being detected. Before and after sintering SEM images not only show thermal coarsening of the ligaments in both materials, but also evidence of neck formation between ligaments bridged across their original interface. Our results will be presented in the context of existing literature for neck formation and welding between bulk and nanoscale metals. This study might shed a light on the interdiffusion of porous metals during low temperature sintering.

References:

[1] Lu, Y., Huang, J., Wang, C. *et al.* Cold welding of ultrathin gold nanowires. *Nature Nanotech* **5**, 218–224 (2010). <https://doi.org/10.1038/nnano.2010.4>

[2] S. Brett Walker and Jennifer A. Lewis. Reactive Silver Inks for Patterning High-Conductivity Features at Mild Temperatures. *Journal of the American Chemical Society* **2012** *134* (3), 1419-1421. DOI: 10.1021/ja209267c

9:00 AM NM05.01.07

Late News: Optimization of NanoCluster Beacons (NCB) Using an NGS Platform and Machine Learning

Yu-An Kuo, Oliver S. Zhao, Soonwoo Hong, Trung D. Nguyen, Yuan-I Chen, Chien-Yu Lin and Tim Yeh; The

University of Texas at Austin, United States

The key to future fluorescence sensing lies in the use of new methods for fluorescence modulation, beyond what is currently available. DNA-templated silver nanoclusters (DNA/AgNCs; for instance, Ag₈, Ag₁₀ and Ag₁₆) offer such an opportunity as their fluorescence emission color can be tuned by their DNA hosts or activated by nearby DNA strands termed the activators. The resulting complexes, called NanoCluster Beacons (NCB), have found applications in sensing nucleic acids, proteins, small molecules, enzyme activities and cancer cells. Whereas new applications of this unique molecular probe are emerging across a broad range of disciplines, it is unclear what sequence features of the activators ultimately control the fluorescence activation color and brightness of NCB. Further diversification and optimization of NCB will require a large ligand composition space (of the activator) to be scanned, beyond what robotic plates or test tube method can provide.

Here we introduce a high-throughput approach to study the fluorescence activation behavior of silver nanoclusters. By using a next-generation sequencing (NGS) chip (Illumina *MiSeq*), more than 10⁴ activators can be screened in a single experiment, which is nearly 100-fold higher than the throughput of current robotic plate method. The activation results reveal that the middle six nucleobases (of the 18nt-long activator) are the most critical in determining the activation intensity of silver nanoclusters, as randomizing these nucleotides leads to many dark NCBs. Interestingly, position 4-6 of the activator are found particularly important in stabilizing yellow NCB, while position 2-4 are hotspots for creating red NCB.

Taking advantage of our high-throughput chip screening platform, we have identified many pairs of NCB which only differ by a single nucleotide in their activator sequences but give drastically distinct activation outcomes (either by color difference or intensity difference). These extreme pairs are termed the polar opposite twins (POT). We have identified red and yellow POTs with intensity difference as high as 8-fold (T to C at position 4) and 29-fold (C to G at position 5), respectively. Moreover, based on the NGS selection results, a workflow to generate new activator designs using random sampling and support vector machine is established. We successfully obtained a new red-emissive NCB having intensity difference as high as 2.9-fold compared to selected red NCB standard.

9:15 AM NM05.01.08

Late News: Novel Tools for Nanoparticle Characterisation Niamh Mac Fhionnlaioich, Ye Yang and Stefan Guldin; University College London, United Kingdom

Advancing colloid science & engineering requires a detailed understanding of building blocks, their spatial arrangement and interaction with chemical and biological targets. In my group, we have developed a number of novel analytical approaches. I will introduce the measure of information entropy as a powerful statistical method to evaluate the dispersity of colloidal populations and optimise synthetic parameters [1]. We have recently established an alternative route to evaluate 2D colloidal ordering based on the so-called spatial distribution function [2]. In comparison to conventional approaches, such as the radial distribution function or the 2D fast Fourier transform, this method is particular powerful for assemblies displaying limited order. I will further elaborate on how a simple protocol, based on quartz crystal microbalance with dissipation monitoring (QCM-d), for the stepwise in situ quantification of AuNPs immobilisation and subsequent uptake and release of chemical and biological binding partners [3]. Crucially, the frequency shift patterns offered by QCM-d enabled us to model the binding kinetics and calculate binding parameters, such as the association and dissociation rate constants (k_{on} and k_{off}) and apparent binding constant K_a . In combination with a recently developed synthetic protocol for decoupled control of size and surface composition [4], this analytical toolbox provides a powerful platform for systematic studies on colloidal behaviour, ligand-shell mediated nanoparticle-stimuli interactions and rational optimisation of material design for environmental and biomedical applications.

References:

[1] Information entropy as a reliable measure of nanoparticle dispersity - N. MacFhionnlaioich, S. Guldin, *Chemistry of Materials*, vol. 32, pp. 3701 – 3706, 2020.

- [2] Application of the Spatial Distribution Function to colloidal ordering - N. MacFhionnlaioich, R. Qi, S. Guldin, *Langmuir*, vol. 35, pp. 16605 – 16611, 2019.
- [3] Probing nanoparticle-analyte interaction in real time via quartz crystal microbalance with dissipation monitoring - Y. Yang, G. Poss, N. Nianias, Y. Weng, R. Qi, H. Zheng, E. Kay, S. Guldin, *Nanoscale*, vol. 11, pp. 11107 – 11113, 2019.
- [4] A versatile AuNP synthetic platform for decoupled control of size and surface composition - Y. Yang, L.A. Serrano, S. Guldin, *Langmuir*, vol. 24, pp. 6820 – 6826, 2018.

SESSION NM05.02: Functional Nanoparticle Materials—Synthesis, Property and Applications II
 Session Chairs: Mei Cai and Ou Chen
 Sunday Morning, April 18, 2021
 NM05

10:30 AM *NM05.02.01

Nanoparticles for Ultrasensitive Biosensing Molly Stevens; Imperial College London, United Kingdom

This talk will provide an overview of our work in the design of functionalised polymer and inorganic nanoparticles for applications in ultrasensitive biosensing [1]. We engineer simple conceptually novel approaches to detect disease biomarkers, such as abnormally regulated enzymes, to extend the detection window for early disease diagnostics. We aim to design biosensing strategies that are simple, cost-effective and easy deploy to the point-of-care to democratise access to advanced diagnostic technology. We will discuss impactful sensing applications for infectious and non-communicable diseases for example innovative smartphone enabled tests for epidemic surveillance in the field [2] and injectable nanoparticle-based sensing probes for in vivo detection of cancer that produce a colorimetric response in urine in under 1 hour [3]. This talk will also provide an overview of our recent advances in Raman spectroscopy characterisation techniques for high-throughput tracking of surface functionalisation in single nanoparticles [4].

- [1] A. Creamer, C. S. Wood, P. D. Howes, A. Casey, S. Cong, A. V. Marsh, R. Godin, J. Panidi, C. H. Burgess, T. Wu, Z. Fei, I. Hamilton, M. A. McLachlan, M. M. Stevens, M. Heeney. “Quantitative post-polymerisation functionalisation of conjugated polymer backbones and its application in multi-functionalised semiconducting polymer nanoparticles.” *Nature Communications*. 2018. 9: 3237.
- [2] C. S. Wood, M. R. Thomas, J. Budd, T. P. Mashamba-Thompson, K. Herbst, D. Pillay, R. W. Peeling, A. M. Johnson, R. A. McKendry, M. M. Stevens. “Taking connected mobile-health diagnostics of infectious diseases to the field.” *Nature*. 2019. 566: 467-474.
- [3] C. N. Loynachan, A. P. Soleimany, J. S. Dudani, Y. Lin, A. Najer, A. Bekdemir, Q. Chen, S. N. Bhatia, M. M. Stevens. “Renal clearable catalytic gold nanoclusters for in vivo disease monitoring.” *Nature Nanotechnology*. 2019. 14: 883–890.
- [4] J. Penders, I. J. Pence, C. Horgan, M. Bergholt, C. Wood, A. Najer, U. Kauscher, A. Nagelkerke, M. M. Stevens. “Single particle automated Raman trapping analysis.” *Nature Communications*. 2018, 9: 4256.

10:55 AM NM05.02.02

Late News: Leveraging Critical Phenomenon in Multi-Scale Nanoparticle Networks to Make Large Area Field Effect Transistors for Sensing Applications Abhijeet Prasad^{1,2}, Michael Stoller² and Ravi F. Saraf^{1,2};

¹University of Nebraska–Lincoln, United States; ²Vajra Instruments Inc, United States

Phenomenon of Coulomb blockade (CB) due to single electron (local) charging in nanogranular metallic system has long been a scientific curiosity due to their exotic electronic properties. The attraction is an insulator-to-metal transition observed at cryogenic temperatures where the electron transport is affected by local charging of the nano-grains by just a single electron. We have observed functionally similar behavior in large nanoparticle array of a quasi-one dimensional (1D) nanoparticle necklace network (N³) of 10 nm Au particles from 4 K to

room temperature (RT). Here, we demonstrate a new class of field effect transistor (FET) operating at RT where the conductance of N^3 devices is modulated over two orders of magnitude by a gate electrode. The demonstrated gain is $\sim 500x$ higher, sensing area is $\sim 150x$ larger, and the current is 10^4x higher than previously published close-packed nanoparticle array FET's. Remarkably, the N^3 FET I-V behavior exhibits universality, where the conduction gap is invariant and the I-V behavior can be superimposed in a master curve at different gate voltages. To understand universality of I-V behavior the network topology is quantitatively mapped by leveraging the local-1D structure of N^3 . Simulations using topological maps indicate that conduction pathways morph with "fractal-like" growth of conducting channels as charging barriers are systematically overcome by gate bias. Due to self-similar conduction path morphing, we conclude that at RT electron transport in these disordered systems is primarily driven by critical phenomenon, akin to second order phase transformations. The high gain, large sensing area, and flexibility for functionalization of Au can allow N^3 devices to serve as a platform for a new class of high sensitivity sensors.

11:10 AM NM05.02.03

Late News: Colorful Applications of Fluorescent Silica Nanoparticles—Interactions Between Bio-Organic Molecules and Inorganic Surfaces Aashani D. Tillekaratne, Chamari Hettiarachchi, Sewwandi Kuruppu, Nirojan Lalichchandran, Kasun Ananda and Navindra Keerthisinghe; University of Colombo, Sri Lanka, Sri Lanka

Silica nanoparticles are known as versatile inorganic materials that provide an efficient platform to interact with biological molecules. These interactions are believed to have occurred on prebiotic Earth at the origin of life. Experimentally, the interaction between silica and biomolecules is granted feasible due to the ease of synthesis and the ease of their surface modification. Having rich surface chemistry due to the presence of silanol groups extending out of their surface and available for bonding, these nanoparticles can be conjugated with fluorescent dyes which can further be functionalized to be conjugated with biological and/or organic counterparts leading to a variety of colorful and interesting applications. In the present study, we have synthesized fluorescent silica nanoparticles by the reverse microemulsion method and using three different fluorescent dyes, fluorescein isothiocyanate (FITC), Rhodamine-B, and Tris(2,2'-bipyridyl)dichlororuthenium(II) hexahydrate (commonly known as Rubpy). In the synthesis, the microemulsion is prepared by mixing cyclohexane, n-hexanol, and Triton X-100 (or dioctyl sulfosuccinate sodium salt). To this microemulsion, the fluorescent dye which is conjugated with the linker, 3-aminopropyltriethoxysilane (APTES) is added followed by the silica precursor, tetraethylorthosilicate (TEOS). Hydrolysis and condensation are then initiated by adding ammonia. After stirring for 24 hours, the microemulsion is broken with acetone and the nanoparticles are recovered after centrifugation and washing. Scanning electron microscopy images showed spherical shaped particles with an average diameter of around 150 nm. These fluorescent silica nanoparticles showed excellent photostability and minimal dye leakage over a period of one hour which is a reasonably long duration for the proposed bioconjugation experiments. To facilitate the bioconjugation process, these dye-doped nanoparticles were functionalized, first with amine groups using APTES and then with carboxyl groups using succinic anhydride. Fourier Transform Infrared (FTIR) spectra confirmed the surface functionalization. These fluorescent silica nanoparticles were used to detect latent fingerprints on the surfaces of aluminum foil, stainless steel, glass, plastic, and wood using the powder dusting method and the suspension method. Powder dusting on aluminum foil produced the best results after exposing the surfaces to the nanoparticles for 30 minutes after the fingerprint was placed on the surface. On top of this, the most interesting application of these fluorescent silica nanoparticles was their use in the detection of *Escherichia coli*, which is considered the best biological indicator for coliform contamination in food and water. The anti-*E. coli* antibody was immobilized on the fluorescent nanoparticle surface by reacting the carboxyl functionalized nanoparticles with the protein at room temperature. Then the *E. coli* culture was mixed with the antibody-conjugated nanoparticles in phosphate-buffered saline (PBS). After incubation, a smear was made on a microscopic slide and observed under the fluorescence microscope. For the nanoparticles doped with all three dyes, FITC, Rhodamine-B, and Rubpy, fluorescence microscopic images were obtained with the resolution of observing up to a single bacterial cell. Staining of the moving live cells was also observed. These interesting results demonstrate the effectiveness of the fluorescent silica nanoparticles in the use of chemical and biological sensors. Their excellent photostability and the ability

to retain the dye for longer periods in the nanoparticle matrix compared to the free dye in solution are added advantages when these sensors are developed.

11:25 AM NM05.02.04

Late News: Fluorescence Enhancement and Functionalization of Nanodiamonds for Optically Trackable Drug Delivery Pietro Aprà^{1,2}, Mirko Sacco¹, Veronica Varzi¹, Valentina Boscaro¹, Margherita Gallicchio¹, Alessandro Barge¹ and Federico Picollo^{1,2}; ¹University of Torino, Italy; ²National Institute for Nuclear Physics, Italy

Currently, a strong interest has been focused on the employment of nanoparticles as promising tools in biomedical research, diagnostics and therapy. In this frame, Nanodiamonds (NDs) earned a solid reputation due to their interesting features, such as inertness, fluorescence, biocompatibility and the possibility of modifying their surface termination [1]. Aim of this work is the realization of diamond-based drug delivery systems which are optically trackable during *in-vitro* experiments, by exploiting the fluorescence properties deriving from the Nitrogen–Vacancy (NV) lattice defects [2], consisting in a substitutional nitrogen atom nearby to a vacancy defect. This system is optically active, with a wide excitation spectrum around 500 – 600 nm and emission at 600 – 800 nm, and provides a photostable label suitable for different types of bio–imaging and bio–sensing applications. By mean of ion–beam induced damaging, more defects can be introduced in the crystal lattice, thus creating new NV centers and enhancing the fluorescence of NDs [3]. To this scope, in the first part of the work the NDs were irradiated with a 2 MeV proton beam, exploring a wide range of fluences (between 10^{14} – 10^{17} protons cm^{-2}). Raman and Photoluminescence (PL) spectroscopy were employed as elective investigation techniques to quantify the ion–implanted NDs fluorescence. As a result, PL spectra showed that the creation of new NV centers by proton–irradiation led up to two orders of magnitude increase in fluorescence with respect to the unirradiated samples.

In the second part of the work, the NDs surface was chemically modified to allow a proper covalent–linking functionalization with cetuximab (NDs–Ctx), a monoclonal antibody specific for EGFRs, which are receptors typically overexpressed on colon–rectal cancer cells membrane. The successful surface grafting procedure was verified by means of Thermogravimetric Analysis. NDs–Ctx were then administrated to cultured DiFi rectal carcinoma cells and their internalization degree (compared to a control sample of unmodified NDs) was evaluated by confocal microscopy. From the analysis of the acquired images, a high uptake level was observed in the platelets of NDs–Ctx treated DiFi cells, while weak or no NDs fluorescence signal was assessable inside the cells in the case of unirradiated NDs administration.

In conclusion, post–synthesis treatments and proton–beam irradiation of NDs were effective in strongly enhancing their fluorescence yield. Moreover, cetuximab was successfully conjugated on NDs surface and the targeting and uptake–inducing properties of the system were observed on DiFi cell line. These results reinforce the suitability of NDs as promising nano–tools for both biolabeling and drug delivery applications, worthy of further investigations to combine these two potentials.

[1] Mochalin, V. N., Shenderova, O., Ho, D., Gogotsi, Y. (2012) The properties and applications of nanodiamonds. *Nat. Nanotechnol.*, 7:11–23

[2] Van der Laan, K., Hasani, M., Zheng, T., Schirhagl, R. (2018) Nanodiamonds for in vivo applications. *Small*, 14:1703838 (2018)

[3] Waldermann, F.C. et al. (2007) Creating diamond color centers for quantum optical applications. *Dia. Relat.Mat.*, 16:1887–1895

11:40 AM NM05.02.05

Luminescence Properties and Cell Uptake Analysis of Nanophosphors for Bio-Imaging Applications Dalia H. Chavez¹, Karla O. Juárez-Moreno^{2,3}, Gustavo Hirata⁴ and Rosella Reyes¹; ¹Centro de Enseñanza Técnica y Superior, Mexico; ²Centro De Nanociencias y Nanotecnología-UNAM, Mexico; ³CONACYT-CNyN-UNAM, Mexico; ⁴Centro de Nanociencias y Nanotecnología-UNAM, Mexico

Nanotechnology is providing new tools for cell imaging and diagnosis through the synthesis and tuning of

nanophosphors with special physicochemical properties. Yttrium oxide (Y₂O₃) host has gained broad research interest due to its excellent chemical stability, good thermal stability and low cost; this host can be used to synthesized luminescence upconversion nanoparticles (UCNPs) and downconversion nanoparticles (DCNPs) that can be used as biolabels for fluorescence imaging. The UCNPs absorb near infrared photons to upconvert them to emit in the visible spectra; also, the DCNPs absorb UV photons and emit in the visible spectra. In this study we analyzed biocompatible UCNPs and DCNPs co-doped with rare earth ions, they were functionalized with amino groups and folic acid ligands (FA) that bind to folate receptors (FR) overexpressed on certain types of cancer cells, the functionalized nanoparticles (FA-NPs) were internalized into the cancer cells studied via endocytosis by the conjugation FA-FR. We present a nanotoxicological study that includes cytotoxicity, genotoxicity, hemocompatibility and in vitro inflammatory studies. The study demonstrated that bare and functionalized NPs are no cytotoxic and no genotoxic at the tested concentrations (0.01 to 20 mg/ml) in three cell lines (breast, skin cancer and osteoblasts). Also they are hemocompatible and do not exert nitric oxide production in vitro by macrophages. The FA-NPs were clearly localized into the cell cytoplasm with bright red luminescence. We can conclude that these nanoparticles are biocompatible and can be further used for cancer cells bioimaging.

11:55 AM NM05.02.06

Late News: *In Vitro* Evaluation of the Antimicrobial Activity by the Nebulization Method of Hydrogen Peroxide and AgNPs Synthesized by the Green Route Juan Carlos Martinez¹, Hiram D. Gonzalez Martinez², José Alejandro López Venzor², Christian Gabriel Carranco Torres¹ and Raúl Carrera Cerritos¹; ¹Instituto Politécnico Nacional, Mexico; ²Nabicron S.A.P.I. de C.V., Mexico

Since 2019, institutions and governments around the world have faced the challenge of containing the progress of the COVID-19 pandemic caused by the Sars-CoV-2 coronavirus. According to the WHO, one of the main transmission routes for COVID-19 is contact with contaminated surfaces. For this reason, a thorough disinfection is essential to prevent contagion. In this sense, nanotechnology has attracted significant attention due to its cross-cutting properties in different disciplines. Silver nanoparticles (AgNPs) have been one of the most investigated nanomaterials and recently applied by various industries. In this work, the synergistic effect of the *in vitro* antimicrobial activity of hydrogen peroxide with biosynthesized AgNPs from a geranium plant extract was evaluated. AgNPs were characterized by HRTEM, UV-Vis spectroscopy as well as ICP-MS for their analytical determination where an average particle diameter less than 50 nm was obtained with a spherical morphology and a concentration of 1,474.6 mg / L. The air disinfection method (ADM) was used for the evaluation of the antimicrobial effect in vitro against *Escherichia coli* ATCC 25922. This test showed a 99.99% of bacterial growth reduction with a dose of 76.6 mg / L of AgNPs and 0.55% hydrogen peroxide, after eight minutes of nebulized exposure of the solution. These results provide valuable information on the way to explore new bionanotechnological antimicrobial agents to promote the safety, innocuousness and hygiene of products, spaces and surfaces.

12:00 PM NM05.02.07

Late News: *In Vitro* Microbiological Test of Silver Nanoparticles Extracted by Green Method on *Pseudomonas aeruginosa* Juan Carlos Martinez, Raúl Carrera Cerritos, Karla Paola Sánchez Guerrero and Rocío Alejandra Silva Contreras; Instituto Politécnico Nacional, Mexico

Recently, antibacterial solutions have been investigated in the medical area, since the excessive use of antibiotics has caused microorganisms to express greater resistance to this type of antibiotics. In this research work, the effect of Ag nanoparticles on *Pseudomonas aeruginosa* bacteria (ATCC27853) was verified as a function of time. Different concentrations of colloidal solution were prepared and exposed during the incubation time in order to identify the minimum inhibitory concentration (1:2, 1:4, 1:8 and 1:16). Nanoparticles synthesized by the green route were used using *Pelargonium spp* extract as a reducing agent. Average diameters of nanoparticles <50 nm was obtained, which were characterized with a JEOL JEM1010 transmission electron microscope. The inhibitory effect of nanoparticles in *Pseudomonas aeruginosa* was verified by counting colony forming units (CFU) for 0, 2 and 4 hours of bacterial incubation. The tests showed that the 1: 2 concentration

ratios exhibited a 100% inhibition since the initial interaction of the colloidal solution with the growing bacteria and during the four hours of monitoring. While in the 1: 4 ratio, 100% inhibition was observed up to 2 hours after the initial time of the nanoparticles-bacteria interaction. For the rest of the dilutions, there were gradual inhibitions as a function of time, however, they were not 100%. Finally, we conclude that the use of nanomaterials generated by green routes are an alternative for their application in biological systems that are currently a health problem in living beings. As a perspective of this work we suggest to perform cytotoxicity tests in cellular biological systems for biomedical applications.

12:05 PM NM05.02.08

Late News: Development of SERS-Active Gelatin Based Hydrogels for Label Free Detection of Bio-Analytes [Zahra Khan](#)^{1,2}; ¹A*STAR, Singapore; ²UCL, United Kingdom

— Hydrogels are a macromolecular network of hydrophilic copolymers with physical or chemical cross-linking structure with significant water uptake capabilities. They are a promising substrate for Surface-enhanced Raman Spectroscopy (SERS) as they are both flexible and biocompatible materials. Conventional SERS-active substrates suffer from limitations such as instability and inflexibility which restricts their use in broader applications. Gelatin based hydrogels have been synthesised in a facile and relatively quick method without the use of any toxic cross-linking agents. Composite gel material was formed by combining the gelatin with simple polymers to enhance the functional properties of the gel. Gold nanoparticles, prepared by a reproducible seed-mediated growth method, was combined into the bulk material during gel synthesis. After gel formation, the gel was submerged in the analyte solution overnight. SERS spectra was then collected from the gel using a standard Raman spectrometer. A wide range of analytes were successfully detected on these hydrogels showing potential for further optimization and use as SERS substrates for biomedical applications.

12:10 PM NM05.02.09

Heavy Metal Extraction from Water by the Filtration with Iron-Tannic Acid Complex [Sujoy Saha](#) and Hemali Rathnayake; University of North Carolina at Greensboro, United States

Water purification by the removal of heavy metals is one of the most challenging fields of scientific research. In natural waters, heavy metals are generally present in trace amounts but most of them have a wide range of hazardous and detrimental effects to the human body even at very low concentrations. Heavy metals especially lead, and cadmium can cause severe health effects including cancer, nervous system damage, organ damage, and in extreme cases, death. Thus, it is very important to extract heavy metal from industrial wastewater along with drinking water. In this research, we used the Iron-Tannic Acid complex for the filtration of water and could successfully extract Pb^{2+} , Cd^{2+} , and Ag^{+} cations from different water samples containing those heavy metal. The amount of heavy metal in the water was detected by Inductively Coupled Plasma - Optical Emission Spectrometry (ICP-OES). The presence of large numbers of carboxylic acid groups in the Iron-Tannic Acid complex is therefore responsible for the strong binding of the heavy metal cations. Among all of the heavy metal filtration materials, the Iron-Tannic Acid complex has the greatest potential in heavy-metal extraction processes for future applications.

Keywords: Heavy metal extraction, Metal-organic complex, water purification

12:25 PM NM05.02.10

Late News: Surface Charge-Dependent Toxicity of Hematite Nanoparticles [Svetlana Vihodceva](#)¹, Andris Šutka¹, Mariliis Sihtmae², Merilin Rosenberg^{2,3,4}, Maarja Otsus², Krišjanis Šmits⁵, Līga Bikše⁵, Kaja Kasemets² and Anne Kahru²; ¹Riga Technical University, Latvia; ²National Institute of Chemical Physics and Biophysics, Estonia; ³University of Tartu, Estonia; ⁴Tallinn University of Technology, Estonia; ⁵University of Latvia, Latvia

In the current study, the antibacterial activity and ecotoxicity of positively and negatively charged hematite (α - Fe_2O_3) nanoparticles were studied. α - Fe_2O_3 nanoparticles were obtained by simple green hydrothermal synthesis, while surface charge was controlled by a surface functionalization with citrate coating. The antibacterial activity was evaluated to Gram-negative bacterium *Escherichia coli* and Gram-positive bacterium

Staphylococcus aureus. Microbes were exposed to different concentrations of α -Fe₂O₃ nanoparticles in deionized water for 30 minutes and 24 h at room temperature and evaluated for the post-exposure colony forming ability. The positively charged α -Fe₂O₃ showed *E. coli* bactericidal activity already after 30 minutes. Extending the exposure to 24 h increased the antibacterial effect with minimal bactericidal concentration values between 100-1000 mg/L. Bactericidal activity against *S. aureus* was not observed. Negatively charged α -Fe₂O₃ did not exhibit any activity against both tested bacteria. Our results confirmed that deionized water could be a model medium for the antibacterial testing. Additionally, ecotoxicity studies with *Vibrio fischeri* showed no ecotoxicity of α -Fe₂O₃ - EC₅₀ > 1000 mg/L. No reactive oxygen species production in abiotic or biotic conditions in the dark was observed. Confocal laser microscopy images analysis by MicrobeJ confirmed that more positively charged nanoparticles were associated with generally negatively charged bacterial cells than negatively charged nanoparticles and this effect was larger for *E. coli* which is also in concordance with positive charged α -Fe₂O₃ nanoparticles being more toxic to *E. coli* than *S. aureus*.

Acknowledgments: This work has been supported by the European Regional Development Fund within the Activity 1.1.1.2 “Post-doctoral Research Aid” of the Specific Aid Objective 1.1.1 “To increase the research and innovative capacity of scientific institutions of Latvia and the ability to attract external financing, investing in human resources and infrastructure” of the Operational Programme “Growth and Employment” (No. 1.1.1.2/VIAA/2/18/331).

SESSION NM05.03: Functional Nanoparticle Materials—Synthesis, Property and Applications III
Session Chairs: Yu Han and Han Htoon
Sunday Afternoon, April 18, 2021
NM05

1:00 PM NM05.03.02

Late News: Elucidating Alloying Strategies for Ni-Based Bimetals Using Geo-Inspired Perovskite Oxides
Kandis L. Abdul-Aziz¹, Soham Shah¹, Mingjie Xu² and Xiaoqing Pan²; ¹University of California, Riverside, United States; ²University of California, Irvine, United States

In-situ exsolution of reducible transition metals from geo-inspired perovskite precursors allows for the synthesis of strongly-adhered nanoparticles that are thermally-stable and homogeneous in size and shape. The perovskite oxides are materials that can reversibly exsolve transition-metal cations as nanoparticles under fluctuating reducing and oxidizing reaction conditions. The exsolution process occurs when the cation dopant diffuses from the bulk of the perovskite and form nanoparticles on the surface under reducing conditions. Earlier work on perovskite oxide precursors has determined that bulk defects can modulate the ionic diffusion of dopant metal monomers. This presentation extends the notion of exploring the rich defect chemistry of geo-inspired perovskite oxides to control the formation and growth of regenerable Ni-Fe nanoparticles from Ni-doped LaFeO₃ perovskite oxide precursors [1]. The Ni-doped lanthanum ferrite perovskite precursors were prepared with varying ratios of the La and Fe in the parent perovskite of either 0.9:1, 1:0.9, and 1:1. The exsolved Ni-Fe nanoparticles exhibited notable ranges in composition, size, and dispersion. The systems were characterized using High-angle annular dark-field imaging scanning transmission electron microscopy (HAADF – STEM), X-ray diffraction (XRD) and in situ X-ray Absorption Spectroscopy (XAS). This presentation will discuss recent work to address the existing materials chemistry challenges for Ni-based bimetallic nanoparticles' controlled formation.

1. S. Shah, S. Sayono, J. Ynzunza, R. Pan, M. Xu, X. Pan, K.L. Gilliard-Abdulaziz, The effects of stoichiometry on the properties of exsolved Ni-Fe alloy nanoparticles for dry methane reforming, AIChE J. In press (2020). <https://doi.org/https://doi.org/10.1002/aic.17078>.

1:15 PM NM05.03.03

Cu_{2-x}S/PbS Core/Shell Nanocrystals with Improved Solubility and Chemical Stability Patrick Yee¹, Sarah Brittman², Nadeemullah Mahadik², Joseph Tischler², Rhonda Stroud², Alexander Efros², Peter Sercel³ and Janice Boercker²; ¹National Research Council, United States; ²U.S. Naval Research Laboratory, United States; ³California Institute of Technology, United States

Excitonic PbS nanoparticles have shown excellent photosensitivity in the IR region, but limited device efficiencies because short diffusion lengths restrict film thicknesses to less than the absorption length. They also have slow radiative recombination rates, which limit the performance of light-emitting diodes. To address these limitations, we work to couple PbS excitons with plasmons on the nanoscale in order to increase the radiative rates and absorption cross sections. For the plasmonic component, we use the doped plasmonic semiconductor, Cu_{2-x}S, which has a tunable plasmon resonance that can be designed to overlap with the excitonic absorption of PbS in the short-wave infrared regime.

We demonstrate a synthetic method to add a thin PbS shell layer, with a controlled thickness, to Cu_{2-x}S cores using Pb oleate and bis(trimethylsilyl)sulfide as the Pb and S precursors. Energy-dispersive X-ray maps and high angle annular dark field images collected with scanning transmission electron microscopy confirm the Cu_{2-x}S/PbS core/shell architecture. Absorbance spectroscopy shows a blueshift in the plasmon resonance of the Cu_{2-x}S/PbS core/shell nanoparticles relative to the parent Cu_{2-x}S nanoparticles. Using X-ray diffraction, we show that this blueshift is due to the oxidation of the Cu_{2-x}S cores (an increase in x) upon PbS shell deposition. The shell thickness is controlled by tuning the amount of Pb and S precursors. Transmission electron microscopy indicates progressive growth in the core/shell nanoparticle diameter with increasing Pb:Cu ratios and a monodisperse distribution of nanoparticles.

While no photoluminescence is observed from the PbS shell, these core/shell nanocrystals are highly promising for studying exciton-plasmon coupling in binary superlattices with PbS nanocrystals for three reasons: 1) the Pb shell increases the Cu_{2-x}S core solubility, aiding in assembly, 2) the PbS shell blueshifts and enhances the plasmon resonance of the Cu_{2-x}S core such that it overlaps better with the PbS exciton energy range, and 3) the PbS shell hinders the Cu_{2-x}S cores from chemically quenching the photoluminescence of neighboring PbS nanocrystals in solution. The ability to hinder quenching is dependent on the PbS shell thickness in the Cu_{2-x}S/PbS core/shell nanoparticles, with the thicker PbS shells better preserving the excitonic PbS photoluminescence. Thus, the Cu_{2-x}S/PbS core/shell nanoparticles provide an opportunity to controllably investigate plasmon-exciton coupling in a variety of binary superlattice symmetries and stoichiometries.

1:30 PM NM05.03.06

Late News: Ultralow-Platinum Pt@Ni@Pt Core-Bishell Nanorods Bifunctional Oxygen Evolution and Reduction Electrocatalyst in Alkaline Medium Melina Zysler, Victor Shokhen, Samuel S. Hardisty, Anya Muzikansky and David Zitoun; Bar Ilan University, Israel

Pt-Ni nanoparticles were vastly explored because of the synthetic tunability and the high electrochemical performance toward oxygen reduction reaction (ORR), the application and high-efficiency catalytic activity are commonly confined for acidic medium due to the Pt corrosion in alkaline medium. The alternative Ni-rich nanoparticles investigated as oxygen evolution reaction (OER) catalyst have shown insufficient efficiency in the acidic medium because of the known transition metal leaching process. The novelty in our work is the ability to produce an active bifunctional catalyst that accomplishes both ORR and OER in alkaline medium. Our advance was accomplished by a comprehensive investigation of the synthesis parameters and by a rational material design.

The ultralow-platinum Pt@Ni@Pt core-bishell nanorods achieve an unprecedented (for a Pt-based catalyst) overpotential of 0.29 V at 10 mA cm⁻² and current density of 162 mA μg⁻¹Pt at 1.6 V (vs. RHE) for the OER, while still maintaining a very decent value of 0.32 A mg⁻¹Pt at 0.85 V for the ORR. These values outperform the standard Pt catalyst for the ORR and the Ni catalyst for the OER, using less than 1%wt. Pt. This work advances the field of ultra-low platinum content, which in our point of view will be one of the critical issues that will allow the green energy technology to be implemented.

Also, this research revealed a unique methodology that allows morphology and size tunability of Pt@Ni core-

shell nanoparticles. The kinetic control of the core and the shell was achieved by combining two commonly used solvents as reducing agents while keeping the (111) plane electrochemically active. We highlight that the understanding of the relationships between the composition of a material and its structure and properties is a fundamental objective and a key challenge in nanoscience research.

1:35 PM NM05.03.07

Enhanced Combustion Performance of Functional Metal Nanoparticle Materials Sungwook Hong and Roxanne Esparza; California State University, Bakersfield, United States

Aluminum nanoparticles (ANPs) have been considered attractive additives for solid-fuel rockets due to a high energy density with an increased burning rate. Unfortunately, the use of the ANPs is limited by the following reasons: ANPs can be readily sintered and oxidized, prior to the combustion process, degrading the combustion performance. In order to resolve these problems, a surface coating of the ANPs by hydrocarbons has been proposed. While previous studies reported that the hydrocarbon coating is essential for the ANPs to be used as combustible materials, atomic-scale understanding of thermal behaviors of the hydrocarbon-coated ANPs has yet to be achieved. Here we perform reactive molecular dynamics (RMD) simulations to investigate effects of hydrocarbon coating on the combustion performance of the ANPs. Our RMD simulations reveal detailed reaction steps for the sintering process of the bare/hydrocarbon coated ANPs. As such, our RMD simulations provide a valuable input for experimental synthesis of functional metal nanoparticle materials for energy conversion applications.

S.H. and R.E. acknowledge the new tenure-track faculty start-up fund from School of Natural Science, Mathematics and Engineering at California State University, Bakersfield (CSUB).

References

- [1] Yetter, R. A.; Risha, G. A.; Son, S. F. Metal Particle Combustion and Nanotechnology. *Proc. Combust. Inst.* **2009**, 32, 1819–1838
- [2] Park, K.; Rai, A.; Zachariah, M. Characterizing the Coating and Size-Resolved Oxidative Stability of Carbon-Coated Aluminum Nanoparticles by Single-Particle Mass-Spectrometry. *J. Nanopart. Res.* **2006**, 8, 455–464.
- [3] Guo, L.; Song, W.; Hu, M.; Xie, C.; Chen, X. Preparation and Reactivity of Aluminum Nanopowders Coated by Hydroxyl-Terminated Polybutadiene (Htpb). *Appl. Surf. Sci.* **2008**, 254, 2413–2417.
- [4] Senftle, T. P.; Hong, S.; Islam, M. M.; Kylasa, S. B.; Zheng, Y.; Shin, Y. K.; Junkermeier, C.; Engel-Herbert, R.; Janik, M. J.; Aktulga, H. M. The ReaxFF Reactive Force-Field: Development, Applications and Future Directions. *npj Comput. Mater.* 2016, 2, 15011.

1:40 PM NM05.03.08

Late News: Citrus Limon as Reducing Agent for the Synthesis of Gold Nanoparticles by Multiwave Ultrasonic Technique Juan Carlos Martinez, Julio Cesar Ramos Dominguez, César Fernando López Sánchez and Raúl Carrera Cerritos; Instituto Politécnico Nacional, Mexico

Nanotechnology has studied applications in biomedical areas, for which several nanomaterials have been synthesized that present limitations such as toxicity and instability in organisms, so green methodologies have been developed that help reduce this problem. In this work we report the green synthesis of AuNPs using as a reducing agent lemon extract (Citrus limon), and the multiwave ultrasonic technique as an excitation element. As the precursor reagent, trihydrated chlorouric acid ($\text{HAuCl}_4 \cdot 3\text{H}_2\text{O}$, Sigma Aldrich SKU 520918) was used, and as a reducing agent the lemon juice extract. The reaction was carried out in an ultrasonic bath at a frequency of 40kHz, at 55 ° C for one hour (Branson 2800 series). The final solution obtained showed a purple coloration, and was characterized by UV-VIS spectrophotometry and transmission electron microscopy (JEOL JEM 1010). Peak absorbance peak at 530 nm was observed and particle diameters between 12 and 16 nm were obtained.

The reported results could be of interest to carry out fusion of nanometric inorganic materials by the ultrasonic technique, and by controlling the temperature and frequency, metal structures with different morphology and properties could be generated.

1:45 PM NM05.03.09

Late News: Nanoporous Ni Produced from the Reduction of NiO Nanoparticle Dispersions and Implications for Low-Cost Functional Applications Mark Atwater and Beck Boan; Liberty University, United States

Porous Ni has many potential applications, such as energy storage, fuel cells, and catalysis, which account for its rapid rise in publication frequency in recent years. Nanoporous Ni is less commonly reported, but it is expected to have enhanced properties due its higher surface area. Dealloying is the most developed method for creating nanoporous metals, with Ni precursors including Ni-Mn, Ni-Mn-Cu, or the classic Ni-Al alloys, first developed and patented by Murray Raney in 1927, and therefore referred to as “Raney” nickel. The general strategy of dealloying is well-developed and provides a valuable method for achieving nanoscale porosity. The commonality among dealloying methods is the preferential removal of a sacrificial phase. That phase must be carefully removed in its entirety, as any residue will alter the final properties. Here we present the removal of a second phase to create nanoscale porosity in a scheme broadly similar to dealloying; however, the sacrificial phase is an oxide, not another metal. This oxide reduction provides a single-metal strategy for nanoporosity (e.g., Ni+NiO), thereby eliminating any source of metallic contamination. Furthermore, the opportunity exists to intentionally alloy with greater accuracy by alloying before or during oxide reduction. For example, Ni and Cu can be alloyed during milling in metallic phase or, as a simple extension, CuO would be added with NiO so that the desired metallic composition is obtained after reduction. Any number of permutations to this approach can be employed for completely unique control of the final structure and composition. This technique is remarkably simple and scalable. The precursors are created through standard powder metal processes (milling, compaction, etc.), and the required temperatures are quite modest. Additionally, this provides an environmentally friendly alternative to chemical etching by acids, which are commonly employed in dealloying. The processing, properties, and applications will be reviewed.

2:00 PM NM05.03.10

Late News: Facile Synthesis of Ru-ZrP Catalysts with Nano-Anadem Structure and Its Application in Hydrogenation of Acetophenone Xiaoyu Li and Qiang Zhang; Washington State University, United States

As a reaction generally used in industrial processes, the catalytic hydrogenation of organic compounds containing carbonyl groups using nanomaterials is extensively studied. Herein, we describe the preparation of an unusual nanomaterial, ruthenium nano-anadem decorated zirconium phosphate nanoplatelets, which can be used to realize the selective hydrogenation reaction of ketone. We choose acetophenone (AP) for main study as it is the simplest ketone and can lead to important hydrogenation products, such as ethylcyclohexane (EC) for bio-oils and 1-cyclohexylethanol (CE) for many polymers production and biofuel purpose.

α -zirconium phosphate (α -ZrP) serving as a solid support has been widely studied. We obtained α -ZrP nanoplatelets with high yield and good quality by using a modified refluxing method. Through an ion-exchange and reduction reaction pathway, Ru nanoparticles can be loaded on ZrP nanoplatelets to yield Ru-ZrP nano-anadem structures. The obtained Ru-ZrP composites with different loading amount were characterized *via* powder X-ray diffraction (PXRD), nitrogen adsorption and de-adsorption, transmission electron microscopy (TEM), Scanning electron microscopy (SEM), and X-ray photoelectron Spectroscopy (XPS). We also explained the detailed growth mechanism. The successful synthesis of Ru-ZrP nanoplatelets were also supported by its excellent catalytic performance in the hydrogenation reaction of acetophenone. To obtain an optimized reaction condition, many factors such as reaction time, reaction temperature and pressure of hydrogen gas were investigated. Conversion and yield were determined by gas chromatography mass spectrometry (GCMS). Conversion rates of AP could be achieved 100% at room temperature. The resulting products include at least 93% yield rate of CE and EC as the rest. The stability and possible mechanism for Ru-ZrP catalyzed AP were discussed. It shows very good stability after 5 runs of recycle. The kinetics of this reaction were discussed as

well as some rare intermediates in details. The results suggest that there is a great potential for this novel Ru-ZrP nanostructures in catalytic applications.

SESSION NM05.04: Functional Nanoparticle Materials—Synthesis, Property and Applications IV
Session Chairs: Ou Chen and Han Htoon
Sunday Afternoon, April 18, 2021
NM05

4:00 PM *NM05.04.01

Synthesis and Machine Learning of Patchy Nanoparticles Qian Chen; University of Illinois at Urbana-Champaign, United States

I will discuss my group's two recent progresses on constructing a library of hybrid patchy nanoparticles. Synthetically, we applied the concept of "island formation" established for planar substrates, where ligands cluster as they adsorb, to preparing gold nanoparticles of diverse shapes with precisely sized polymer patches. These polymer patches adapt their configuration in response to external stimulus and modulate the self-assembly behaviors of the nanoparticles. Meanwhile, we applied machine learning based data-mining method to relate synthesis conditions with the patterns of the patchy nanoparticles, to allow for predictive synthesis and design. Such fundamental understanding of the synthesis, interaction and assembly of patchy nanoparticles can bear relevance to their increasing ramifications in addressing staggering national needs in environment, energy, and health.

4:25 PM NM05.04.02

Late News: Spatially Resolved Fourier Transform Impedance Spectroscopy—A Technique to Rapidly Characterize Composite Materials, Interfaces and Devices Mathew Kelley, Grigory Simin, Kamal Hussain, Asif Khan, Andrew Greytak and MVS Chandrashekar; University of South Carolina, United States

We demonstrate a technique to quickly build and spatially map the frequency response of optoelectronic devices. The transfer function of a linear system is the Fourier transform of its impulse response. Such an impulse response is obtained from transient photocurrent measurements of devices such as photodetectors and solar cells. We introduce and apply Fourier Transform Impedance Spectroscopy (FTIS) to a PbS colloidal quantum dot (QD)/SiC heterojunction photodiode and validate the results using intensity-modulated photocurrent spectroscopy. Cutoff frequencies in the devices were as high as ~10kHz, showing their utility in advanced thin film and flexible electronics. The practical frequencies for FTIS lie in the mHz-kHz range, ideal for composite materials such as QD films that are dominated by interfacial trap states. These can lead to characteristic lengths for charge collection ~20-500 μm dominated by transmission line effects, rather than intrinsic diffusion and drift length scales, enabling extraction of interfacial capacitances and series/parallel resistances.

4:40 PM NM05.04.03

Late News: Understanding Intermediates in Cluster Synthesis Using Mass Spectrometry Grant E. Johnson¹, Michael Hewitt², Marshall Ligare¹, Ulises Reveles³, Niranjana Govind¹ and Heriberto Hernandez²; ¹Pacific Northwest National Laboratory, United States; ²Grinnell College, United States; ³Advanced Career Education Center, United States

Rational synthesis of size- and composition-selected clusters with predetermined properties for applications in catalysis, energy conversion and storage, and chemical separations will be facilitated by a mechanistic understanding of cluster nucleation, growth, and etching in solution. We have characterized the formation of triphenylphosphine (PPh₃) ligated gold clusters in the Au₁₋₂₂ size range using online reaction monitoring

combined with high-mass-resolution electrospray ionization mass spectrometry. To improve the sensitivity and mass resolution of larger clusters for unambiguous identification, we increased the number of scan averages and reduced the width of mass collection windows, thereby mitigating mass and abundance bias resulting from small gold-ligand species present in high abundance. We have identified new clusters including $\text{Au}_5(\text{PPh}_3)_5^+$, $\text{Au}_{12}(\text{PPh}_3)_9\text{HCl}^{2+}$, $\text{Au}_{15}(\text{PPh}_3)_9\text{Cl}^{2+}$, $\text{Au}_{16}(\text{PPh}_3)_{10}\text{Cl}_2^{2+}$, $\text{Au}_{17}(\text{PPh}_3)_{11}^{3+}$, $\text{Au}_{18}(\text{PPh}_3)_{10}^{2+}$, $\text{Au}_{19}(\text{PPh}_3)_{10}\text{Cl}^{2+}$, $\text{Au}_{20}(\text{PPh}_3)_{12}\text{H}_3^{3+}$, $\text{Au}_{21}(\text{PPh}_3)_{10}\text{Cl}^{2+}$, and $\text{Au}_{22}(\text{PPh}_3)_{10}\text{Cl}_2^{2+}$, indicating that a full range of clusters between Au_{1-22} is present in solution. We present evidence that the Au_{12-14} size range is a transition point in cluster nucleation where smaller clusters exhibit a one-to-one gold-to-ligand ratio while larger clusters feature additional gold atoms without an equal number of accompanying ligands. Our results show that differently functionalized phosphines may be used to direct the size and abundance of gold clusters in solution. While for PPh_3 -ligated clusters the most abundant species are Au_{6-9} , for methyldiphenylphosphine (PPh_2Me) and dimethylphenylphosphine (PPhMe_2)-ligated clusters the most abundant species are Au_{10-11} and Au_{12-14} , respectively. We also present evidence that small hydrogen-containing intermediates ($\text{Au}_2(\text{PPh}_3)_2\text{H}^+$ and $\text{Au}_4(\text{PPh}_3)_4\text{H}^+$) are responsible for the growth of larger clusters. Degradation of these intermediates and growth of larger clusters are shown to be dependent on irradiation of the solution with light. Together, our findings advance the mechanistic understanding of the size-selective synthesis of clusters in the subnanometer size regime where “each atom counts” toward tuning the properties of clusters for eventual applications.

4:54 PM NM05.04.05

Dielectrophoretic Control of Particle Suspensions with Topographical Features Albanie Hendrickson-Stives and Christine Keating; The Pennsylvania State University, United States

Alternating current (AC) electric fields can be used for the reconfigurable, directed self-assembly of particles as a result of forces such as dielectrophoresis. Electrodes patterned via photolithography and 3D microprinting create a gradient in the AC electric field to control particle assemblies. Since these systems are spatially controllable and reconfigurable, they are of interest for realizing tunable metamaterials and optical responses. Here we focus on assemblies with topographical electrodes and particles with materials properties for desired interactions with electromagnetic radiation. Current work is focused on single and multicomponent assemblies with particles of varying composition (e.g. SiO_2 , TiO_2 , PMMA). Because of their different properties, each of the particle types has distinct assembly structures and orientations that can be obtained based on the electric field conditions. The various assembly structures can then have their own distinct interactions with light based on the particles present and their orientation.

4:59 PM NM05.04.07

Monte Carlo Simulations Reveal the Properties of Magnetic Tunnel Junction-Based Molecular Spintronic Devices Due to Exchange Coupling Between Paramagnetic Molecules and Two Ferromagnetic Electrodes Marzieh Savadkoobi, Bishnu R. Dahal, Andrew Grizzle, Christopher D'Angelo and Pawan Tyagi; University of the District of Columbia, United States

Magnetic Tunnel Junction (MTJ)-based Molecular Spintronic Devices (MTJMSDs) can lead to new forms of metamaterials and devices for the futuristic computers. MTJMSD is produced by chemically bonding a paramagnetic molecule between two ferromagnetic layers of a MTJ. Variation in coupling strength and nature of molecule-FM layer can produce an unprecedented testbed to observe novel phenomenon. Fundamental understanding of MTJ-based devices and their characteristics needs investigation of various factors such as molecular coupling strength and nature with the two FM electrodes. It is extremely challenging to study the impact of wide range of molecule-FM coupling strengths on MTJMSD via experiments. This paper focuses on Monte Carlo Simulations (MCS) to investigate the impact of molecular coupling with two FM electrodes. We utilized continuous MCS process and Metropolis algorithm¹ to study molecular coupling effect. Our model is a cross junction form MTJMSD where molecules are placed between two elongated FM electrodes representing FM-molecule-FM configuration. In this paper we focused on Heisenberg type exchange coupling. We studied various permutations when molecule formed ferromagnetic or antiferromagnetic coupling with the two FM electrodes. The MTJMSD device used in this study was defined with $H \times W \times L$ ($=11 \times 50 \times 50$) dimension where H

is the height, W is the width and L is the length of device. Molecular plane is along the H side of the device structure and located between equal number of atomic FM layers (5×5). We changed the Heisenberg exchange coupling strengths and nature between the paramagnetic molecule and left FM electrode (JmL) and right FM electrode (JmR). To achieve the equilibrium energy state, we conducted 200 million iterations and studied the spatial and temporal evolution of the FM electrodes and MTJMSD as a function of JmL and JmR. The magnitude and nature of JmL and JmR affected the MTJMSD's magnetization, heat capacity, and magnetic susceptibility. For positive JmL and JmR the MTJMSD attained the highest magnetization due to the molecule induced parallel configurations of the two FM electrodes. However, when JmL and JmR were opposite in nature, molecule induced antiparallel magnetizations on the two FM electrodes. With opposite JmL and JmR MTJMSD magnetic moment settled closed to zero. Our MCS study also showed that molecular coupling effect spreads over a long range with respect to the molecular junction sites. According to our MCS results, molecular coupling impacted the whole junction when the critical magnitude of JmL and JmR was ~20% of the Curie temperature of two FM electrodes. These MCS studies also explain the experimentally observed strong molecule induced exchange coupling. Our group observed long range effect of antiferromagnetic coupling between the FM electrodes of an MTJ via organometallic molecular clusters (OMCs)¹⁻³. Studying the effect of different thermal energies on MTJMSD's magnetization properties is the next milestone of this ongoing project and will be studied in parallel to experimental works.

This work is supported by National Science Foundation-CREST Award (Contract # HRD- 1914751), Department of Energy/ National Nuclear Security Agency (DE-FOA-0003945).

References:

1. P. Tyagi, C. Baker and C. D'Angelo, *Nanotechnology* 26, 305602 (2015).
2. P. Tyagi and E. Friebe, *J. Mag. Mag. Mat.* 453, 186-192 (2018).
3. P. Tyagi and C. Riso, *Organic Electronics* 75, 105421 (2019).

5:13 PM NM05.04.08

A Computational Approach to Fundamentally Understand Blending Thermodynamics Between Polymers and Single-Wall Carbon Nanotubes Yichen Deng, Ying Mu and Kenneth Benson; Northeastern University, United States

Motivated by the idea that 1D nanomaterials can be used as templates for polymer chain alignment and orientation, carbon nanotubes (CNTs), a typical 1D nanomaterial, have been widely used as nano-fillers for reinforcing the polymer matrix in order to improve mechanical/structural properties of composite materials. Dispersing CNTs in the polymeric matrix remains a major challenge to address in order to increase the efficiency of enhancement. Experimental work of our lab has shown that the use of a non-solvent induced phase separation process can lead to regions of complete CNT-polyacrylonitrile (PAN) interaction within the matrix. To systematically explore the mechanism behind this phenomenon, full atomistic simulation is used to study the energy profile within the CNT/PAN/DMF system. To connect the simulation with the experimental work, a coarse-grained model using dissipative particle dynamic (DPD) method has been built to scale-up the simulated system. In this study, small angle X-ray scattering and thermal gravimetric analysis (TGA) techniques are employed as a tool to validate the interaction parameter setting of our DPD model. This parameter will provide important information/feedback needed to estimate a 'chi' parameter for PAN-CNT interaction. More broadly this coarse-graining approach can also be applied to other 1D-polymer systems to determine whether selective interaction is possible.

SESSION NM05.05: Functional Nanoparticle Materials—Synthesis, Property and Applications V

Session Chairs: Mei Cai and Ou Chen

Sunday Afternoon, April 18, 2021

NM05

9:00 PM NM05.05.01

Nonthermal Plasma Synthesis of Nitrogen-Doped Titanium Dioxide Nanoparticles with Visible Light Photocatalytic Activity Qiaomiao Tu, Chad Beaudette and Uwe Kortshagen; University of Minnesota Twin Cities, United States

Titanium dioxide (TiO₂) has been extensively studied for water splitting,¹ dye-sensitized solar cells,² and photocatalysis³ due to its chemical stability and efficient photon-electron transfer. However, the wide bandgap (3.0-3.2 eV) and rapid recombination rate limit its utilization of visible solar radiation when used as a photocatalyst. Nitrogen doping has proven to be an effective way to alter the band structure and extend the photoactive region to visible light.⁴ Despite these advantages, a single-step synthesis route with wide tunability of nitrogen doping is still desirable.

Here, we demonstrate the synthesis of nitrogen-doped titanium dioxide nanoparticles with enhanced visible light absorption and photocatalytic activity via a one-step nonthermal plasma route. We investigated the plasma power influence on the particle growth and nitrogen incorporation under various reactor geometries, which allows for tuning of the substitutional and interstitial nitrogen doping level, bandgap and thus light absorption behaviors. By adjusting the locations of the electrode and the oxygen injection into the plasma, the particles transitioned from entirely interstitial nitrogen-doped to substitutional nitrogen-doped. The reactor design also allowed for phase tuning from amorphous, to crystalline anatase, rutile, and mixed anatase/rutile.

Photocatalytic performances of the as-synthesized nanoparticles were evaluated through the degradation efficiency of organic dyes methyl orange (MO) and methylene blue (MB) under natural sunlight irradiation. The low concentration of TiO₂ required in this work for degradation of both MO and MB dyes without external facilitation of metal ion doping or hydrogen peroxide addition indicates that the nitrogen-doped TiO₂ nanoparticles are efficient visible-light photocatalyst.

This work expands the scope of nonthermal plasmas for functional oxide nanocrystal fabrication, demonstrating its versatility in tuning material composition and structure. The discussion on the relationship between plasma conditions and nanoparticle properties provides fundamental insights into engineering nanoparticle growth and functionalization.

This work was supported by the National Science Foundation under MRSEC grants DMR-1420013 and DMR-201140.

References:

- [1] Tang, J.; Durrant, J. R.; Klug, D. R. Mechanism of Photocatalytic Water Splitting in TiO₂. Reaction of Water with Photoholes, Importance of Charge Carrier Dynamics, and Evidence for Four-Hole Chemistry. *J. Am. Chem. Soc.* **2008**, *130* (42), 13885–13891.
- [2] Hwang, Y.-K.; Park, S. S.; Lim, J.-H.; Won, Y. S.; Huh, S. Preparation of Anatase/Rutile Mixed-Phase Titania Nanoparticles for Dye-Sensitized Solar Cells. *J. Nanosci. Nanotechnol.* **2013**, *13* (3), 2255–2261.
- [3] Shah, M. W.; Zhu, Y.; Fan, X.; Zhao, J.; Li, Y. Facile Synthesis of Defective TiO_{2-x} Nanocrystals with High Surface Area and Tailoring Bandgap for Visible-Light Photocatalysis. *Sci. Rep.* **2015**, *5*, 15804.
- [4] Cong, Y.; Zhang, J.; Chen, F.; Anpo, M. Synthesis and Characterization of Nitrogen-Doped TiO₂ Nanophotocatalyst with High Visible Light Activity. *J. Phys. Chem. C* **2007**, *111* (19), 6976–6982.

9:15 PM NM05.05.03

Full Daytime Sub-Ambient Radiative Cooling in Commercial-Like Paints with High Figure of Merit Xiangyu Li^{1,2}, Joseph Peoples¹, Zhifeng Huang³, Zixuan Zhao¹, Jun Qiu⁴ and Xiulin Ruan¹; ¹Purdue University, United States; ²Massachusetts Institute of Technology, United States; ³Wuhan University, China; ⁴Harbin Institute of Technology, China

Radiative cooling is a passive cooling technology that acts by reflecting sunlight and emitting radiation in the sky window. Although highly desirable, full daytime sub-ambient radiative cooling in commercial-like single-layer particle-matrix paints has not been achieved. Here, we demonstrate full daytime sub-ambient radiative cooling in CaCO₃-acrylic paint by using large band gap CaCO₃ fillers, a high particle concentration of 60%, and

a broad size distribution. Our paint shows a high solar reflectance of 95.5% and a high normal emissivity of 0.94 in the sky window. Field tests show cooling power exceeding 37 W/m^2 and a surface temperature of $>1.7^\circ\text{C}$ below ambient at noon. A figure of merit RC is proposed to compare the cooling performance independent of weather conditions. The standard RC of our paint is 0.49, among the best radiative cooling performances, while offering the benefits of convenient paint form, low cost, and compatibility with commercial paint fabrication processes.

9:30 PM NM05.05.04

Ligand Identity Determines Carrier Dynamics in CuInSe₂ Nanocrystals Samantha Harvey; Northwestern University, United States

Semiconductor nanocrystals (NCs) continue to garner interest for their unique optoelectronic properties that are controllable through size, shape, and composition. CuInSe₂ NCs have been hailed as a less-toxic alternative to Cd and Pb based materials and exhibit bandgaps similar to Si making them ideal for photovoltaic application. Synthesis of these materials has allowed them to be prepared using a variety of ligands. Broadly it is well known that ligands play a key role in stabilizing these colloids and passivating surfaces, but they can also be crucial to intraband and interband relaxation as well as electronic and thermal conductivity. Very little research has focused on the effects of ligands on photophysics in CuInSe₂. Here we demonstrate through a variety of optical techniques the strong impact that ligands have on carrier dynamics in CuInSe₂ NCs.

9:45 PM NM05.05.05

Enhanced Infrared Photodiodes Based on PbS/PbCl_x Core/Shell Nanocrystals Adam Colbert¹, Diogenes Placencia¹, Erin Ratcliff², Janice Boercker¹, Paul Lee², Edward Aifer¹ and Joseph Tischler¹; ¹U.S. Naval Research Laboratory, United States; ²The University of Arizona, United States

The performance of short-wave infrared (SWIR) photodetectors based on colloidal lead sulfide (PbS) depends critically on advances in passivation strategies to address the more complex surface structure of large-diameter particles. Nanocrystals prepared using PbCl₂ precursors result in formation of a thin PbCl_x shell, providing improved air stability and photoluminescence quantum yields compared to those derived from other lead sources. We directly compare the performance of SWIR photodiodes fabricated with PbS/PbCl_x (core/shell) nanocrystals versus their PbS-only (core) counterparts. Despite their inherently similar bulk properties, the core/shell-based devices exhibit greater external quantum efficiencies and reduced dark current densities, while the core-based devices suffer from shunting and inefficient charge extraction. To elucidate the implications of the shell chemistry on device performance, we evaluate the thickness-dependent energy level offsets and interfacial chemistry of the nanocrystal films with the zinc oxide electron-transport layer. Our results suggest the disparate device performance between the two synthetic routes is associated with unfavorable interface dipole formation and a high prevalence of surface defect states in the core-only system, due to incomplete removal of the native organic ligands using conventional thin-film halide exchange. The PbCl_x shell offers a promising route to passivate the additional surface facets of large nanocrystals, that previously established ligand treatments fail to adequately address.

10:00 PM NM05.05.06

Resistance Variations for Different Pattern Designs of Printed Conductors Due to Non-Uniform Ink Drying Milad Ghalamboran and Gerd Grau; York University, Canada

Printed electronics is a promising low-cost and high-throughput technology for electronic device fabrication. Printed electronics can create flexible electronics on flexible, large-area, thin, and lightweight substrates such as plastic or paper. Wearable electronics, flexible displays, and sensor tags are promising applications of flexible-printed electronics. Conductive, dielectric, and semiconductor patterns can be printed by adding different nanoparticles to a solvent with specific agents to improve printability and prevent particle agglomeration. Printed materials require drying to evaporate the solvent and solidify the material. Electrical conductivity is one of the most important properties of printed metal nanoparticle conductors. Conductivity should be the same

irrespective of pattern design: size, location, or density of adjacent patterns. However, we demonstrate here that inconsistencies in the drying process for printed patterns with close proximity cause resistivity variations. We studied these resistivity variations experimentally in arrays of printed square electrodes. Silver nanoparticle ink is used to inkjet print 9, 25, and 49 square shape electrodes in 3x3, 5x5, and 7x7 arrays to study the resistivity variation between squares at different positions in the array. Electrical resistivity measurement shows higher resistivity for printed squares at the center of each array, while printed squares at the corners exhibit lower resistivity after drying on a hot plate. This variation depends not only on the location of each electrode in an array but also on the number of electrodes. This means, for the same drying temperature and duration, the array with a larger number of electrodes shows higher resistivity variation due to the higher evaporation rate of the corner electrodes than the center. As an example, the resistivity variation for 3x3 and 7x7 arrays is 40% and 69%, respectively. Compared to a single isolated electrode, the resistivity at the center of a 7x7 array is 81.7% higher. We studied this phenomenon also for printed squares with three times larger area (9 mm²), and the results show the same trend but with an overall larger resistivity. Different types of patterns, such as lines and square spirals, show the same trend when features are printed in close proximity, which is inevitable for a spiral. After drying, nanoparticles are sintered in a second post-treatment process to improve the electrical conductivity of the printed metal nanoparticle film. In the sintering process, metal nanoparticles melt and merge to form larger grains with fewer grain boundaries, so the modified morphology of the printed structure can improve the electrical conductivity. Conventionally, sintering is performed at an elevated temperature. Here, we find that sintering on a hotplate at 120 °C results in a reduction in the resistivity variation between different electrodes in a 7x7 array to 9.6%. Compared with conventional thermal sintering, intense pulsed light (IPL) sintering is preferable for high-throughput manufacturing. IPL, as a fast sintering method, applies short, high-intensity light pulses from a Xenon lamp to the printed patterns to improve their electrical conductivity while the substrate temperature stays low. Using IPL can also reduce the resistivity variations of the printed square patterns in an array. There are three parameters for controlling the total energy from the light pulses in IPL. Optimization is necessary to find an optimum number of pulses, on-time, and voltage to achieve the highest electrical conductivity of printed silver nanoparticle ink as well as the lowest resistivity variation. With optimum IPL parameters, the resistivity variation changed to 20% and 22% for 3x3 and 7x7 arrays, respectively. This understanding of printed metal conductor post-processing is important for circuit designers who need to consider resistivity variations and proximity effects in complex circuit patterns.

10:15 PM NM05.05.07

Defect Mediated Site-Specific Nucleation of Aligned Carbon Nanotubes Supriti Sen, Mula Raju and Chacko Jacob; Indian Institute of Technology Kharagpur, India

Oxygen vacancy defects in silicon dioxide substrates act as defect-mediated nucleating sites for metal nanoparticles. Site-specific nucleation of metal catalyst particle and the subsequent growth of nanostructures could thus be accomplished by modulating the number density of these oxygen vacancies on specific substrate sites. This study demonstrates surface passivation dictated site-selective growth of vertically aligned multiwall carbon nanotubes (MW-CNTs), on a SiO₂/ Si patterned substrate. Contrasting choice of growth site of MWCNTs is observed for substrates pre-treated in a reducing atmosphere versus that pre-treated in a mildly oxidizing atmosphere. The different substrate pre-treatments alter the number density of oxygen vacancies on the SiO₂ and Si terraces of the substrate which in turn alters the preferred nucleation site for the metal catalyst particle, resulting in the observed switching of site-selectivity. Scanning electron microscopy of the as-synthesized CNT architectures revealed a high degree of site-selectivity in the growth pattern. Hermans orientation factor revealed a reasonably high degree of alignment of the MWCNTs for both the growth patterns. Transmission electron microscopy and Raman spectroscopy have been employed to study the structure and quality of the synthesized tubes and the catalyst particles. Auger electron spectroscopy was used to study the chemical state of the substrate surfaces and the nucleated catalyst particles. The results demonstrate the significance of surface defects in the nucleation and the subsequent growth of nanostructure.

8:00 AM *NM05.06.01

Plasmon-Mediated Synthesis of Periodic Arrays of Gold Nanoplates Using Substrate-Immobilized Seeds Lined with Planar Defects Svetlana Neretina, Robert A. Hughes and Spencer D. Golze; University of Notre Dame, United States

The architectural diversity realized by plasmonic nanostructures is in large part due to seed-mediated colloidal growth modes that are seeded, not only by single-crystal seeds, but by seeds with a well-defined internal defect structure. Multi-twinned seeds have, for example, been used to generate colloids with icosahedral and decahedral structures while seeds with planar defects realize nanoplate geometries. Recently, we demonstrated a nanofabrication route that synergistically combines nanoimprint lithography, directed assembly, and liquid-phase epitaxy to obtain periodic arrays of complex noble metal nanostructures over a square centimeter area. This benchtop process leverages a synthetic strategy in which seed-mediated liquid-phase growth modes are carried out on substrate-immobilized seeds. While the strategy has led to the generation of substrate-based structures with considerable architectural diversity, it is fundamentally limited by the inability to fabricate seeds with the same internal defect structure as those routinely used in colloidal chemistry. Here, we demonstrate a large-area processing route for generating substrate-based Au seeds lined with stacking faults and use them to synthesize arrays of epitaxially aligned Au nanoplates using a plasmon-mediated growth mode. The work advances the possibility of bringing an exciting nanoplate chemistry to the substrate surface and, in doing so, provides the building blocks needed to enable on-chip plasmonic devices.

8:25 AM NM05.06.02

***In Vivo* Clustering of Gold Nanoparticles and Quantum Dots via Copper-Free Click Reaction for Real-Time Imaging and Tumor Sensing** Vu O. Pham-Nguyen, Ji Un Shin, Mao Wei, Ju Won Lee, Jae Keun Park, Miso Lee, Wan Ho Cho and Hyuk Sang Yoo; Kangwon National University, Korea (the Republic of)

Nowadays, fabrication of biosensors for cancer detection, monitoring of angiogenesis or cancer metastasis and cancer imaging holds vast potential. We herein proposed a biosensor based on clustering of matrix metalloproteinase (MMP)-responsive gold nanoparticles (AuNP) and quantum dots (QD) by azide-alkyne copper-free click reaction. Briefly, AuNP were surface-decorated with two types of poly(ethylene glycol) (PEG); 1) short chain of azide-terminated PEG, 2) long chain composed of double PEG chains with a connecting peptide (MMP CP) vulnerable for MMP digestion. We precisely controlled the immobilized PEG ratios so that the azide moieties can be exposed only when MMP externally digests the long chain of PEG. Deshielded AuNPs will be subsequently clicked to alkyne-functionalized QD. Due to the high concentration of MMP at tumor site, the fluorescence resonance energy transfer (FRET) between QD and AuNP during clusters formation is speculated that can be used for tumor sensing. To characterize the surface decoration of AuNP, UV-Vis spectrum and Raman spectroscopy of decorated AuNP were analyzed. A red shift in UV-Vis spectrum according to the size change of AuNP during decoration and 2 distinct peaks for PEG in Raman spectrum were clearly observed confirmed the successful decoration of carboxylate-PEG and mPEG-MMP CP on AuNP surface. The size changes of decorated AuNP was further confirmed by DLS and TEM, where a huge increase in hydrodynamic diameter of the AuNP was confirmed in the order of AuNP (~40nm), AuNP/PEG (~60nm) and AuNP/PEG/MMP CP (~90nm). In consistence with the DLS results, shell thickness of AuNP obtained by analyzing TEM images showed the same trend according to stepwise decoration of AuNP. Moreover, when AuNP/PEG-azide was labeled with alkyne fluorescence dye, a significant increase of the fluorescence intensity was recorded by spectrofluorophotometer and IVIS in comparison to AuNP-dye suspension confirmed the click-functionality of AuNP/PEG-azide. Thus, AuNP/PEG-azide was speculated that can be used for click reaction toward alkyne-QD. The enzyme responsive clustering process was investigated by incubating with

different concentration of MMP-2. There was a dramatic increase of AuNP diameter up to about 400nm and the FRET efficiency also increased up to ~58% after 2h of incubation confirmed the cluster formation of AuNP and QD. This results suggesting that AuNP and QD can be employed for tumor sensing due to the elevated MMP-2 concentration at tumor site. To stimulate *in vivo* clustering behaviors, AuNP and QD were incubated with the supernatants of cell cultured medium. The diameter of the clusters and FRET efficiency also increase after 2h of incubation. Furthermore, we monitored the fluorescence intensities of QD by IVIS when co-injected with AuNP to tumor bearing mice. Consequently, after 6h post injection, the fluorescence intensity of QD was clearly reduced confirmed the feasibility of our platform for real-time imaging and tumor sensor *in vivo*.

8:40 AM NM05.06.03

Sintering of Silver Nanoparticle Patterns Using Formic Acid Vapors Justin Courville, Muhibbur Rahman and Seonhee Jang; University of Louisiana at Lafayette, United States

The use of metal nanoparticles (NPs) for printed conductive patterns are gaining a lot of attention because of the low cost and shorter manufacturing time in the fabrication of flexible electronic devices. Flexible electronics include organic thin film transistor (OTFT), organic light-emitting diode (OLED), sensors, and wearable devices. Metallic NP inks mainly comprised of metal NPs such as gold (Au), silver (Ag), and copper (Cu) are commonly used for printing of conductive patterns on flexible substrates. After printing of NP inks, sintering process is required to achieve high conductance of the patterns. Metallic NP inks also contain the organic capping molecules and additives which are barrier to high conductance. Through sintering process, these organic compounds should be removed. Ag NPs are the most widely used in many applications due to their high electrical conductivity and chemical stability. In this study, the effect of sintering atmosphere on the conductivity of printed patterns is investigated. Sintering atmosphere is chosen among air, nitrogen (N₂), and N₂-bubbled through formic acid. The sintering temperature is maintained below 200°C to avoid the deformation and degradation of flexible substrate. The formic acid atmosphere shows a better removal of the organic compounds than air or N₂. At the beginning of thermal sintering, the organic capping molecules surrounding the NPs decompose and necking between the adjoining NPs occurs, followed by grain growth and densification. The electrical conductivity of Ag film is dependent on sintering conditions. It is observed that the resistances of Ag films decrease as the sintering temperatures increase when sintering atmosphere is chosen between air and N₂. Ag films sintered under N₂-bubbled through formic acid shows low resistances below 0.14 Ω even at temperatures below 100°C. In comparison, the resistances of Ag films sintered under air or N₂ drastically decreases from 1.59-2.57 and 0.20-0.22 Ω when the sintering temperatures increase from 80 to 140°C. The microstructure and chemical composition of the printed conductive patterns under different sintering conditions such as temperature, time, and type of atmospheres are analyzed. The grain growth, pore distribution, and level of organic residues determine the conductivity of the printed patterns. Formic acid vapors play an important role in decomposition of organic molecules, neck formation of NPs, and densification of the film, compared to the patterns sintered under air or N₂. The average hardness and elastic modulus of the films sintered under formic acid vapors and N₂ are higher than that sintered under air at sintering temperature of 140°C.

8:55 AM NM05.06.04

Late News: Label Free Detection of Small Molecules Using Surface-Enhanced Raman Spectroscopy (SERS) with Gold Nanoparticles Synthesised with Various Capping Agents Zahra Khan^{1,2}; ¹A*STAR, Singapore; ²UCL, United Kingdom

SERS has received increased attention in recent years focusing toward biological and medical applications due to its great sensitivity as well as molecular specificity. In the context of biological samples there are generally two methodologies for SERS based applications: label free detection and the use of SERS tags. Necessity of tagging can make the process slower and limits the use for real life. Label-free detection offers the advantage that it reports direct spectroscopic evidence associated with the target molecule rather than the label. Reproducible, highly monodisperse gold nanoparticles (Au NPs) were synthesised using a relatively facile seed mediated growth method. Different capping agents (TRIS, citrate and CTAB) were used during synthesis and characterization was performed. They were then mixed with different analyte solutions before drop-casting onto

a glass slide prior to Raman measurements to see which NPs displayed the highest SERS activity as well as their stability. A host of different analytes were tested, both non-biomolecules and biomolecules which were all successfully detected using this method at concentrations as low as 10^{-3} M with salicylic acid reaching a detection limit in the nanomolar range. SERS was also performed on samples with a mixture of analytes present whereby peaks from both target molecules were distinctly observed. This is a rapid and effective way of testing samples and offers potential applications in the biomedical field as a tool for diagnostic and treatment purposes.

9:10 AM NM05.06.06

Probing Charge Transport Kinetics in Plasmonic Environment with Cyclic Voltammetry Mohammad Shahabuddin, Ashleigh K. Wilson, Natalia Noginova, Md A. Rab and Joyce Fields; Norfolk State University, United States

Modification of physical and chemical phenomena is observed in vicinity of metamaterials may involve different mechanisms specific for nanostructured and plasmonic media. In order to better understand the factors responsible for modification of electrochemical reactions in plasmonic environment, we employ the cyclic voltammetry method and investigate how the vicinity to nanostructured metallic surfaces affects the electron-transfer process and charge transport kinetics. In addition, we explore effects of laser light illumination and discuss the results taking into account photoinduced electric potentials and plasmon-related heating.

9:15 AM NM05.06.07

Late News: Carbon Fibers for Energy Storage Devices—Electrochemical Double Layer Supercapacitors, Pseudocapacitors and Zn-Air Batteries Zahra Abedi, Desiree Leistenschneider, Weixing Chen and Douglas G Ivey; University of Alberta, Canada

Development of inexpensive energy storage devices is crucial due to the ever increasing demand for sustainable energy. The material used as the electrode material in energy storage devices is one of the most important factors affecting the device's performance, price and sustainability. Asphaltene, as a high carbon content by-product of the oil sands industry, can be used as the base material for the electrodes in electrochemical double layer supercapacitors (EDLC), pseudocapacitors and the air electrode in Zn-air batteries (ZAB). Asphaltene is the most polar fraction and heaviest part of oil sands bitumen. Approximately 20 wt% of bitumen produced from the oil sands consists of asphaltene.

Carbon fibers (CF) derived from asphaltene were chemically activated to prepare activated carbon fibers (ACF). ACF were used to prepare stable and high performance flexible EDLC and pseudocapacitor electrodes as well as air electrodes for ZAB.

ACF used as the active electrode material in EDLC showed a specific surface area (SSA) as high as $2290 \text{ m}^2 \text{ g}^{-1}$ and total porosity of $1.27 \text{ cm}^3 \text{ g}^{-1}$ that included $0.88 \text{ cm}^3 \text{ g}^{-1}$ of micropores (pore width $< 2 \text{ nm}$) and $0.29 \text{ cm}^3 \text{ g}^{-1}$ of mesopores ($2 \text{ nm} < \text{pore width} < 50 \text{ nm}$). The maximum specific capacitance (C_s) reached was 311 F g^{-1} at a specific current (I_s) of 0.04 A g^{-1} that dropped to 248 F g^{-1} at 1 A g^{-1} (in 6 M KOH); capacitance retention was 91% after 10,000 cycles. This material was later used in an EDLC device with an ionic liquid electrolyte (EMIMBF₄, 1-ethyl-3-methylimidazolium tetrafluoroborate); specific energy (E_s) and power (P_s) values of 35.7 Wh kg^{-1} at a P_s of 525.4 W kg^{-1} , respectively, were achieved. These were comparable to energy and power values delivered by some batteries.¹

Because of the high performance and high conductivity of ACF used in the EDLC devices, this material was chosen to be used in ACF/MnO₂ composite electrodes to aid the pseudocapacitive performance of MnO₂. Birnessite-type MnO₂ (δ -MnO₂) was prepared through a hydrothermal process; its microstructure was subsequently thermally modified to reduce its crystallinity by introducing defects. These defects acted as active sites to enhance electrolyte ion adsorption/desorption, which can increase C_s , E_s and P_s . The maximum C_s reached by the composite electrode was 395 F g^{-1} at a specific current of 0.04 A g^{-1} , with 282 F g^{-1} at 1 A g^{-1} . Capacitance retention was 74% after 5,000 cycles. The maximum P_s in 6 M KOH for the composite electrode was 2.57 kW kg^{-1} at E_s of 6 Wh kg^{-1} .

Asphaltene based carbon fibers were chosen to prepare homemade gas diffusion layers (GDL) for use in air electrodes in ZAB. Air electrodes were prepared with CF carbonized at three different temperatures, i.e., 500

°C, 800 °C and 1500 °C. The oxygen reduction reaction (ORR) and oxygen evolution reaction (OER) activity of the electrodes, as well as commercially purchased electrodes, were tested in 1 M KOH. All homemade electrodes showed much better OER activity than the purchased ones. ORR activity was similar for both commercial electrodes and homemade electrodes prepared with CF at 1500 °C (CF-1500). CF-1500 will be tested in full ZAB cells to determine their performance and cycling behavior and compared with purchased electrodes. Finally, electrodes, prepared with CF-1500 and electrocatalysts consisting of Mn-mixed metal oxides, will be tested in ZAB half cells and full cells.

9:30 AM NM05.06.08

Elucidating the Plasmonic Modes in Metal Nanojunctions with Nanoparticle Libraries Jingshan S. Du, Charles Cherqui, George Schatz, Vinayak P. Dravid and Chad A. Mirkin; Northwestern University, United States

Plasmonic resonances in metal nanostructures have enabled the creation of a new class of chemical sensors, photocatalysts, and therapeutics. In particular, coupling plasmonic metals to other functional nanostructures provides an effective way to generate multi-functional materials, tailored to respond to controlled light inputs in specific ways. Remarkably, these advances have occurred despite a lack of understanding of how energy transfer occurs between metallic domains and the geometric and dielectric effects on the plasmonic properties in hetero-nanostructures. Here, we present a nanoparticle library approach designed to explore the plasmonic modes of metal nanojunctions with various geometries, metal types, and composition ratios. Polymer nanoreactors generated by scanning probe lithography were used to prepare location-encoded particle libraries on electron-transparent substrates where the individual nanoparticles have precisely defined size and composition. Single-particle level far-field light scattering and near-field energy-loss maps were sequentially collected from the same nanojunctions, allowing for mode identification of the entire plasmonic spectrum and correlation between the near-and-far-field properties of the system. Notably, a dipole injection from a plasmonically active metal to a lossy metal is revealed in the nanojunctions, suggesting that field enhancement on the surface of the lossy metal is responsible for photocatalytic “energy transfer” in reactions on the lossy metal. We report on a new group of hetero-nanoprisms containing both active and lossy metals in a planar configuration. The unique plasmonic mode distribution uncovered by our methods yields a design paradigm for creating the next generation of low-cost (due to elemental composition), multi-functional nanomaterials.

SESSION NM05.07: Functional Nanoparticle Materials—Synthesis, Property and Applications VII
Session Chair: Ou Chen
Monday Morning, April 19, 2021
NM05

10:30 AM *NM05.07.01

Integrated Synthesis and Process Design Enabling Kinetic and Structural Control in Self-Assembled Polymer-Grafted Nanocrystal Superstructures Xingchen Ye; Indiana University Bloomington, United States

Polymer-inorganic nanocomposites based on polymer-grafted nanocrystals (PGNCs) are enabling technologically relevant applications owing to their unique physical and chemical properties. While diverse PGNC superstructures have been realized through evaporation-driven self-assembly, this approach presents multifaceted challenges in understanding and ultimately controlling the assembly kinetics and superstructure selection. In this presentation, I will first discuss our work on the rapid assembly of multicomponent superstructures from a homogeneous disordered PGNC mixture. We find that controlling the nature of assembly environment allows for exquisite control of the rate and extent of PGNC assembly. Characterization of kinetically arrested intermediates reveals a multistep crystallization pathway defying classical nucleation theory. Next, I will discuss examples on polymer-grafted anisotropic nanocrystals. It is found that the interplay between

nanocrystal shape and interaction softness give rise to tunable assembly phase behavior.

10:55 AM NM05.07.02

Shape-Driven, DNA-Mediated Engineering of Colloidal Superlattices Wenjie Zhou^{1,2}, Haixin Lin^{1,2}, Yuanwei Li^{1,2}, Zizhuo Liu¹, Ziyin Huang^{1,2}, Devleena Samanta^{1,2}, Koray Aydin¹ and Chad Mirkin^{1,1,2};
¹Northwestern University, United States; ²International Institute for Nanotechnology, United States

The emergence of order from disorder has fascinated, puzzled, and inspired generations of scientists. Colloidal assembly of nanoscale objects is of particular interest as a wide range of hierarchical structures can be obtained simply by changing the size, shape, and surface chemistry of the nanomaterials. Over the past decade, advances in colloidal nanocrystal (NC) synthesis have provided access to a library of well-defined nanoscale building blocks. The organization of isotropic NCs, i.e. uniformly functionalized nanoscale spheres or pseudo-spheres, has been extensively studied and design rules have been empirically set or theoretically explained. In contrast, very few design rules exist for anisotropic NCs, such as asymmetrically functionalized spheres, rods, plates, and polyhedral NCs, and the rules that do exist are often challenged by unusual cases. Therefore, our current understanding of the self-organization process of anisotropic NCs has yet to achieve the leap from “discovery by chance” to “synthesis by design”. In this presentation, we present synthetic methodologies towards the assembly of designer 2D and 3D NC superlattices using DNA-functionalized polyhedral NCs and a series of geometry-inspired strategies.

For 2D structures, we have developed a shallow template-assisted DNA-mediated assembly strategy to precisely arrange colloidal NCs onto surfaces with single-particle orientational control across millimeter areas. In addition to our precise control over the in-plane arrangement, the oligonucleotide bonds between the NCs and substrate can be reversibly expanded and contracted, enabling post-synthetic tunability. As an example, we have synthesized a tunable NC-based metasurface that rapidly responds to changing solution polarity and, therefore, is promising for the fabrication of reconfigurable 2D optical devices. To achieve 3D structures, we have developed a series of PEG-DNA ligands that enabled the assembly of polyhedral NCs into ordered and dense-packed superlattices, which is challenging due to the rigidity of pure DNA. Taking advantage of the highly customizable nature of oligonucleotides and geometry inspired designs, polyhedral NCs of different sizes and shapes were densely assembled/co-assembled. This resulted in the introduction of eleven new structures to the DNA-engineered colloidal crystal family, including the first colloidal quasicrystal engineered with DNA. Moreover, we have shown the ability to inversely design and experimentally produce ordered superlattices based on polyhedral complementarity. Importantly, these colloidal organization platforms may enable systematic exploration of structure-functional relationships, as well as on-demand design and fabrication of highly ordered nanoscale architectures which will be of interest to the metamaterial communities.

11:10 AM NM05.07.03

Assembly of Covalently-Linked Quantum Dot Heterostructures: Characterization of Excited-State Charge-Transfer Dynamics in Dispersed and Multilayered Systems Caitlin R. McGranahan, Guy Wolfe II and David Watson; University at Buffalo, The State University of New York, United States

Semiconductor quantum dots (QDs) are prime candidates as harvesters of light and donors of excited charge carriers for solar energy conversion. The unique properties of QDs can be exploited to generate desirable energetic offsets to promote interfacial charge transfer between QDs. Our group's recent efforts have established the validity of utilizing carbodiimide-mediated coupling chemistry to selectively tether two QDs through the formation of an amide bond between the terminal functional groups of capping ligands [1]. We previously reported on excited-state hole transfer in colloidal CdS/CdSe QD heterostructures, which exhibit quasi-type-I interfacial energetic offsets [1]. Type-I energetics rely on the excitation of one QD component, which results in unidirectional charge transfer and hindered charge separation.

This presentation reports on our efforts to improve and expand upon our previous work in two ways. First, we synthesized and characterized covalently tethered colloidal CdSe/CdTe QD heterostructures via formation of amide bonds. These heterostructures exhibit type-II energetics that promote interfacial charge separation,

irrespective of which constituent QD is initially excited, and afford enhanced control over the thermodynamic driving forces for charge transfer. Within these heterostructures, photogenerated electrons are transferred from CdTe to CdSe, and photogenerated holes are transferred from CdSe to CdTe, on timescales of 10^{-8} s. Second, we prepared ternary CdSe/CdTe heterostructures by immobilizing a covalently-linked bilayer of these QDs on a metal oxide substrate. When compared to colloidal heterostructures, thin films consisting of QDs adsorbed to a metal oxide substrate introduce the possibility of an additional stepwise excited-state charge transfer process. We hypothesized that a stepwise process such as this should facilitate extended spatial separation of charge carriers and longer charge-separated state lifetimes, such that energy is harvested more efficiently and desirable processes can more effectively compete with recombination. Dynamic quenching of emission was observed in heterostructure-modified thin films, consistent with excited-state charge transfer. Rate constants for photoinduced electron and hole transfer between QDs are on the order of 10^8 s⁻¹ and 10^7 s⁻¹, respectively. The bidirectional interfacial charge transfer within these type-II QD heterostructures, both in dispersion and within films, further reveals the potential of this system for use in light harvesting and solar energy conversion. This presentation will highlight these recent results as well as our ongoing time-resolved spectroscopic characterization of photoinduced charge transfer in CdSe/CdTe QD heterostructures.

[1] Sellers, D. G.; Button, A. A.; Nasca, J. N.; Wolfe, G. E.; Chauhan, S.; Watson, D. F., Excited-State Charge Transfer within Covalently Linked Quantum Dot Heterostructures. *The Journal of Physical Chemistry C* **2015**, *119* (49), 27737-27748.

11:25 AM NM05.07.05

Late News: Gas-Phase Nitrogen Doping of Monolithic TiO₂ Nanoparticle-Based Aerogels for Efficient Visible-Light-Driven Photocatalytic H₂ Production Junggou Kwon, Kyoungjun Choi, Murielle Schreck, Tian Liu, Elena Tervoort and Markus Niederberger; ETH Zürich, Switzerland

Hydrogen production using abundant solar energy and semiconductor photocatalysts holds significant potential as a clean and sustainable energy system. Macroscopically sized aerogel monoliths synthesized from preformed anatase nanoparticles are promising three-dimensional photocatalysts due to their immense surface area, high porosity, translucency, and the nanoscale characteristics of the semiconducting crystalline building blocks. Recent studies showed that such titania aerogels decorated with metals are effective for gas-phase photocatalytic CO₂ reduction and H₂ production [1, 2]. However, TiO₂ nanoparticle-based aerogels remain limited to UV-driven photocatalysis due to the intrinsic wide bandgap (3.2 eV). To increase conversion efficiency from solar energy to H₂ production, visible-light sensitization is necessary. Here, we present a facile method for the doping of the aerogel monoliths postsynthetically to make them visible-light active for H₂ production. A CVD gas-phase reaction and plasma utilization at low temperature provided efficient nitrogen incorporation into preformed TiO₂ aerogels without affecting their initial properties. The nitridation improves the optical absorption and charge separation efficiency through an appropriate balance between doping amount and coexistent defects. In comparison to the non-doped sample, the nitrogen-doped aerogels show a significant enhancement in visible-light-driven photocatalytic H₂ production (3.1 mmol h⁻¹ g⁻¹) with excellent stability over 5 days. Our approach of gas-phase nitridation of preformed aerogel monoliths offers a powerful tool to improve their properties as visible-light active photocatalysts.

[1] F. Rechberger, et. al., *Mater. Horiz.* **4**, 1115 (2017)

[2] A. L. Luna, et. al., *Appl. Catal. B.* **267**, 118660 (2020)

11:30 AM NM05.07.06

Alignment Frustration in Block Copolymer Films with Polymer Grafted Nanoparticles under Soft-Shear Cold Zone Annealing Saamil Samant¹, Shimelis Hailu², Maninderjeet Singh³, Nihar Pradhan⁴, Kevin Yager⁵, Alamgir Karim³ and Dharmaraj Raghavan²; ¹Intel Corporation, United States; ²Howard University, United States; ³University of Houston, United States; ⁴Jackson State University, United States; ⁵Brookhaven National Laboratory, United States

Block copolymers (BCPs) provides a platform to sequester nanoparticles in a specific polymeric domain of a BCP system and fabricate aligned nanostructures that can be of significant importance in design of electrostatic capacitors. To aid in the dispersion of nanoparticles in the BCP system, polymer grafted nanoparticles were synthesized using grafting to and grafting from methods. Here, we report the influence of loading of polymer grafted nanoparticles (homopolymer and BCP grafted) on the dispersion and assembly of nanoparticles within cylinder forming BCP (c-BCP) of PS-*b*-PMMA films under static and sharp dynamic thermal gradient soft shear. The application of static thermal field via oven annealing on BCP-g-NP filled as-cast c-BCP films induced a morphology transition from poorly ordered cylinders to mixed morphology, while under dynamic thermal field via cold-zone annealing with soft-shear (CZA-SS), a morphology transition from poorly ordered cylinders to long range ordered parallel morphology was observed. However, at high nanoparticle loading (~10%), there is frustration in the unidirectional alignment of the BCP matrix due to aggregation of functionalized nanoparticles. These findings will be compared and contrasted with homopolymer grafted nanoparticles loaded BCP to establish the significance of graft ligand chemistry in entropic contribution to the frustration in the unidirectional alignment of BCP matrix.

This work is supported by NSF DMR1901127.

11:35 AM NM05.07.07

Colloidal Crystal Engineering with Metal–Organic Framework Nanoparticles and DNA Shunzhi Wang^{1,2}, Sarah S. Park^{1,3}, Cassandra Buru¹, Omar Farha¹ and Chad Mirkin¹; ¹Northwestern University, United States; ²University of Washington, United States; ³Pohang University of Science and Technology, Korea (the Republic of)

Colloidal crystal engineering with nucleic acid-modified nanoparticles is a powerful way for preparing 3D superlattices, which may be useful in many areas, including catalysis, sensing, and photonics. To date, the building blocks studied have been primarily based upon metals, metal oxides, chalcogenide semiconductors, and proteins. Here, we show that metal–organic framework nanoparticles (MOF NPs) densely functionalized with oligonucleotides can be programmed to crystallize into a diverse set of superlattices with well-defined crystal symmetries and compositions. Electron microscopy and small-angle X-ray scattering characterization confirm the formation of single-component MOF superlattices, binary MOF–Au single crystals, and two-dimensional MOF nanorod assemblies. Importantly, DNA-modified porphyrinic MOF nanorods (PCN-222) were assembled into 2D superlattices and found to be catalytically active for the photooxidation of 2-chloroethyl ethyl sulfide (CEES, a chemical warfare simulant of mustard gas). Taken together, these new materials and methods provide access to colloidal crystals that incorporate particles with the well-established designer properties of MOFs and, therefore, increase the scope of possibilities for colloidal crystal engineering with DNA.

11:50 AM NM05.07.09

Room Temperature Thermoelectric Behavior of GO-TiO₂@PEDOT: PSS Hybrid Composite Shivani Shisodia^{1,2}, Djamila B. Hourlier², Dharmendra P. Singh³, Benoit Escorne⁴, Abdelhak Hadj Sahraoui¹ and Michael Depriester¹; ¹Université du Littoral Côte d'Opale, France; ²Centre National de la Recherche Scientifique, France; ³Université du Littoral Côte d'Opale, France; ⁴Pôle de Recherche "Environnement, Milieux Littoraux et Marins" (EMLM), France

The ability of thermoelectric (TE) materials to convert waste heat, produced from fossil fuels, into electricity is an interesting approach to harvest thermal energy. Till now, inorganic TE materials are best known for their high ZT values but they suffer from high toxicity, high cost, and hideous processing. On the other hand, the low TE efficiency of organic materials is lagging behind their inorganic counterparts. Therefore, we propose a hybrid material as an alternative to obtain a high dimensionless figure of merit.

We utilize the hybrid organic-inorganic approach by taking advantage of the low thermal conductivity of organic polymers, and large Seebeck coefficient of inorganic materials, which is essential for obtaining an improved TE efficiency. Nevertheless, accomplishing a high electrical conductivity whilst keeping a low

thermal conductivity is difficult; and optimization of both parameters is of utmost importance.

To surmount the aforementioned difficulties, we propose a p-type hybrid composite made of an organic polymer poly (3,4-ethylene dioxythiophene): polystyrene sulfonate (PEDOT: PSS) filled with inorganic graphene oxide-titanium dioxide (GO-TiO₂), as a cost-effective and scalable outcome for future TE applications. A facile two steps synthesis route has been opted to synthesize GO-TiO₂@PEDOT: PSS hybrid nanocomposite. The oxo (C=O) and hydroxyl groups (-O-H) of GO have been firstly attached to TiO₂ nanoparticles and then used as a template for the oxidative polymerization of EDOT.

As-synthesized hybrid nanocomposites were analyzed by XRD, SEM, FTIR, UV-Vis spectroscopy, and TG-DSC. The thermal conductivity of the materials was done by the photothermal radiometry (PTR) technique and obtained results were in good agreement with the theoretical predictions proposed in Nan's model. Seebeck coefficient measurements were done by a home-made setup based on two probe method.

The influence of filler on the thermoelectric properties of PEDOT: PSS has been studied. It was observed that the thermal conductivity of PEDOT: PSS has been decreased by half; whereas, the Seebeck coefficient was increased by 2.5 times with the addition of 5wt% GO-TiO₂ into the PEDOT: PSS polymer matrix. The obtained hybrid material can be utilized in various applications such as power generation, cooling, and refrigeration, printing applications, etc. up to 300°C as suggested by the thermogravimetric analysis results.

SESSION NM05.08: Functional Nanoparticle Materials—Synthesis, Property and Applications VIII
Session Chairs: Yu Han and Han Htoon
Monday Afternoon, April 19, 2021
NM05

1:00 PM NM05.08.01

Late News: PbSe Nanorod Degree of Organization Dictated by the Ligand Structure Tugba Hacıfendioğlu and Demet Asil; Middle East Technical University, Turkey

PbSe nanorods have been considered as one of the most promising nanoparticles for solar energy field owing to their high multiple exciton generation yield. As a design rule in solar cell applications, strongly coupled nanoparticles with low exciton binding energy are necessary. In this respect, successful integration of nanorods into solar cells, where an efficient exciton dissociation is demanded, requires fundamental understanding of nanorod ligand interactions. This study discloses the effect of ligand type on the nanorod ordering and on the photovoltaic performance. We found that the ligands which are flexible and have free rotation about the axis of the ligand molecules lead to ordered nanorods whereas completely disordered nanorods are obtained when rigid ligand molecules with torsional degrees of freedom are used for the ligand exchange process. We utilized high-resolution transmission electron microscopy imaging technique to study the effect of ligand structure on nanorod ordering. Steady state photoluminescence measurements were performed to investigate the effect of degree of order on the photo-physical properties. Finally, photovoltaic characteristics of the solar cells based on different ligands were investigated.

1:15 PM NM05.08.02

Late News: Scalable Synthesis of Nanoporous Atomically Thin Graphene Membranes for Dialysis and Molecular Separations via Facile Iso-Propanol-Assisted Hot Lamination Piran Ravichandran Kidambi; Vanderbilt University, United States

Scalable graphene synthesis and facile large-area membrane fabrication are imperative to advance nanoporous atomically thin membranes (NATMs) for molecular separations. Although chemical vapor deposition (CVD)

allows for roll-to-roll high-quality monolayer graphene synthesis, facile transfer with atomically clean interfaces to porous supports for large-area NATM fabrication remains extremely challenging. Sacrificial polymer scaffolds commonly used for graphene transfer typically leave polymer residues detrimental to membrane performance and transfers without polymer scaffolds suffer from low yield resulting in high non-selective leakage through NATMs. Here, we systematically study the factors influencing graphene NATM fabrication and report on a novel roll-to-roll manufacturing compatible isopropanol-assisted hot lamination (IHL) process that enables scalable, facile and clean transfer of CVD graphene on to polycarbonate track etched (PCTE) supports with coverage $\geq 99.2\%$, without compromising support integrity/porosity. We demonstrate fully functional centimeter-scale graphene NATMs that show ~ 2 - 3 orders of magnitude higher permeance and better selectivity than commercially available state-of-the-art polymeric dialysis membranes, specifically in the 0-1000 Da range. Our work highlights a scalable approach to fabricate graphene NATMs for practical applications and is fully compatible with roll-to-roll manufacturing processes.

Cheng et al. *Nanoscale*. 2021

Cheng et al. *Nano Lett.* 2020

Kidambi et al. *Adv. Mat.* 2018

Kidambi et al. *Adv. Mat.* 2018

Kidambi et al. *ACS App. Mat. Int.* 2018

Kidambi et al. *Adv. Mat.* 2017

Kidambi et al. *Adv. Mat.* 2017

Kidambi et al. *Nanoscale* 2017

1:30 PM NM05.08.03

Late News: Polymer-Ligated Monodisperse Metal Chalcogenide Nanoparticles with Markedly Improved Stabilities Shuang Liang and Zhiqun Lin; Georgia Institute of Technology, United States

Metal chalcogenide semiconducting nanoparticles (NPs) possess appealing optoelectronic properties that render a wide range of applications, including photovoltaics, photodetectors, and light-emitting diodes (LEDs). Yet, the instability of this class of low-bandgap NPs in ambient conditions remains a key challenge for their practical use. Herein, we demonstrate an unconventional strategy by employing star-like diblock copolymers as nanoreactors to in-situ craft monodisperse metal chalcogenide (e.g., PbSe) NPs with precisely tailorable size, surface chemistry, near-IR optical properties, and significantly improved stabilities in air. The surface of PbSe NPs is intimately and permanently ligated with polymer hairs (i.e., the outer blocks of star-like block copolymers), imparting the protection of PbSe NPs against oxidation and preventing them from aggregation. Intriguingly, alternating the composition and chain lengths of the outer blocks affords a remarkable control over the enhancement of stability of PbSe NPs in ambient conditions.

1:45 PM NM05.08.04

Photocatalytic Activity of Semiconductors Zn-Based Quantum Dots Josian Luciano-Velázquez¹, Carla I. Quiles-Vélez¹, Sebastián A. Cruz-Romero¹, Gabriel E. Torres-Mejías² and Sonia J. Bailón- Ruíz²; ¹University of Puerto Rico, Mayagüez, Puerto Rico; ²University of Puerto Rico, Ponce, Puerto Rico

Semiconductor quantum dots like zinc sulfide have interesting potential applications, consequent to their size-dependent optical properties. These nanostructures can be used on agriculture, environmental chemistry, and fluorescence microscopy, among others. The great rise in nanotechnology has sparked interest in the scientific community in nanomaterials for the use of photodegradation in aquatic bodies. Quantum Dots (QDs) like ZnS nanoparticles (NPs) can absorb electromagnetic radiation and generate photo-excited nanostructures which would be generating reactive oxygen species directly in aqueous phase. The presence of ROS in aquatic environments can be used to destroy organic contaminants by photocatalysis processes. Previous studies had evidenced that the presence of impurities (i.e. copper) into the crystalline structures of QDs can enhance their optical properties and consequently their catalytic capacity. Because of this, the present investigation was focused on generating water-stable ZnS nanoparticles with catalytic properties. This work had three objectives:

1) synthesis of pure and doped ZnS nanoparticles following a reflux method; 2) characterize nanostructures; and 3) study the photocatalytic properties of these nanostructures. A redshift was observed in the photoluminescence peak of pure ZnS nanoparticles when they were doped with heavy metals. Pure ZnS NPs and Cu-doped ZnS NPs evidenced luminescent peaks at 446 nm and, 541 nm, respectively. Nanoparticles (pure and doped) evidenced sizes less than 5 nm and morphologies mainly spherical. Photodegradation studies were evaluated in presence of organic dyes like methylene blue and different concentrations of pure and doped quantum dots (250 and 500 ppm). The destruction of organic dyes in the presence of photo-excited ZnS nanoparticles is envisioned as a fast and clean technology.

2:00 PM NM05.08.05

Sulfur-Infusion Hole Transport Layers for Improved Charge Collection in Colloidal Quantum Dot Solar Cells Arlene Chiu, Eric Rong, Christianna Bambini, Yida Lin, ChengChangfeng Lu and Susanna Thon; Johns Hopkins University, United States

Colloidal quantum dot (CQD) materials have many optoelectronic applications such as in photodetection, light emitting diodes and solar energy harvesting. However, CQD devices are limited in their efficiency in comparison to bulk semiconductor materials, particularly in the field of PbS CQD solar cells. We have identified the hole transport layer (HTL) as a critical component limiting the performance of these devices. Here, we introduce a new method of sulfur infusion via electron beam evaporation to the current ethanedithiol-passivated PbS CQD-based HTL (PbS-EDT), used in the highest-performing PbS CQD solar cell architectures, to increase the carrier mobilities and doping densities.

We used 1D optoelectronic simulations to identify specific factors associated with the HTL that limit the performance of PbS CQD solar cells, including low electron mobility, low doping density, and non-optimal energy band levels. Because the function of the HTL is to block electrons and transport holes, the discovery of low electron mobility in the HTL as a limiting factor in solar cell efficiency was an unexpected result. We hypothesized that this could indicate that significant photogeneration occurs in the HTL and that low electron mobility in this layer is therefore limiting the ability to extract those photogenerated charges. To further test this hypothesis, we increased the thickness of the PbS-PbX₂ (X = Br, I) CQD absorbing layer in simulations and found that there was a point at which an increase in electron mobility in the HTL no longer impacted the performance of the solar cell. This, along with optical simulations of the electric field distribution in the layered solar cell structure, confirmed our hypothesis.

Based on the results of the simulations, we aimed to develop a new HTL with high electron mobility and doping density. We performed stoichiometric control of the HTL by introduction of elemental sulfur to increase carrier mobilities and doping densities, testing effective sulfur thicknesses of 1-15 Å. To characterize our new HTL, we obtain doping densities using capacitance–voltage (Cap-V) measurements, carrier mobilities using space-charge-limited current (SCLC) measurements, and performed current density–voltage (J-V) measurements under simulated solar illumination to measure solar cell device performance parameters. We verified that our new HTL materials had increases in both doping density and electron mobility of an order of magnitude compared to the standard HTL materials, while the hole mobility remained relatively unchanged. We were also able to achieve a clear improvement in device performance of 1% absolute power conversion efficiency (PCE). The primary effects of our sulfur infusion method were an increase in electron mobility through reduction of the surface trap state density and an increase in p-type doping density by shifting the film stoichiometry. The improvement in these two properties correlated with an increase in the solar cell PCE through increases in the short circuit current and fill factor, as expected.

We demonstrated new HTL materials for CQD solar cells based on sulfur infusion of PbS-EDT CQDs that enable high electron mobility and doping density. Our new HTL increased device performance, from a maximum of 9.3% to 10.4% PCE. Elemental sulfur infusion is a facile and effective method to boost performance in PbS CQD solar cells and could provide a means for improved efficiencies in other PbS CQD-based optoelectronics.

2:15 PM NM05.08.07

Processability of a Thermally Stiffening Polymer Nanocomposite with Diffuse Interface Chen Gong¹, Donovan Weiblen¹, Deniz Rende¹, Pinar Akcora² and Rahmi Ozisik^{1,1}; ¹Rensselaer Polytechnic Institute, United States; ²Stevens Institute of Technology, United States

Thermally stiffening polymer nanocomposites were synthesized by chemically grafting or physically adsorbing a high-glass-transition-temperature polymer onto a nanofiller and then embedding this into a polymer matrix that has a glass transition temperature that is less than that of the grafted/adsorbed polymer. In the current study, we investigate the effect of extrusion at three different shear rates on the structure and properties of two different thermally stiffening polymer nanocomposites: poly(bisphenol A carbonate), PC or poly(2-vinyl pyridine), P2VP-adsorbed silica nanofillers embedded in a poly(ethylene oxide), PEO, matrix. Results were compared to bare silica containing PEO nanocomposites and neat PEO. Results indicate that extrusion at 80 °C led to some degree of agglomeration of the silica nanofillers and formation of structures at different length scales as characterized by small angle X-ray scattering (SAXS). Crystallinity of PEO was found to decrease upon extrusion in all nanocomposite samples but those PC and P2VP-adsorbed systems had higher crystallinity compared to bare-silica containing nanocomposites, and the crystallinity of P2VP-adsorbed system was the highest among all nanocomposite samples. This was attributed to the formation of nanofiller agglomerates and to the greater isolation of the matrix PEO chains from the silica nanoparticles due to the presence of adsorbed polymer layer; which were also supported with attenuated total reflectance–Fourier transform infrared spectroscopy (ATR-FTIR) results. Viscoelastic properties of the PC-adsorbed systems were found to recover their pre-extruded properties whereas all other nanocomposites showed large degree of decreases in their viscoelastic responses upon extrusion.

SESSION NM05.09: Functional Nanoparticle Materials—Synthesis, Property and Applications IX
Session Chairs: Ou Chen and Han Htoon
Monday Afternoon, April 19, 2021
NM05

4:00 PM *NM05.09.01

Probing Crystallization Pathways of Aluminum Hydroxide Nanoparticles Xin Zhang¹, Ying Chen¹, Suyun Wang¹, Mehran Amiri², May Nyman², Sebastian Mergelsberg¹, Carolyn Pearce¹, Lili Liu¹, Mowei Zhou¹, Duo Song¹, Eric Bylaska¹, Jian Zhi Hu¹, Nancy Washton¹, Karl Mueller¹, Zheming Wang¹, James J. De Yoreo¹, Sue Clark¹ and Kevin Rosso¹; ¹Pacific Northwest National Laboratory, United States; ²Oregon State University, United States

Aluminum is the third-most abundant element in Earth's crust. As a result, aluminum hydroxide polymorphs, such as gibbsite, bayerite and nordstrandite are abundant minerals in soils and dominate aluminum ores. Because of their various properties such phases have been deployed widely as adsorbents, fire retardants, coatings, catalysts, and luminescence powders, as well as comprising important precursors to various alumina products. Understanding the crystallization pathways of the aluminum hydroxide polymorphs is thus important to geochemistry, environmental science, energy storage, catalysis, biomedicine, industrial processing, and even nuclear waste treatment. Here we use *in situ* magic angle spinning nuclear magnetic resonance (MAS-NMR), scanning electron microscopy (SEM), scanning/transmission electron microscopy (S/TEM), atomic force microscopy (AFM), small angle X-ray scattering (SAXS), X-ray absorption spectroscopy (XAS), electrospray ionization (ESI)-mass spectrometry, high resolution powder X-ray diffraction (XRD), and X-ray pair distribution function (PDF) techniques to probe the nucleation and crystal growth mechanisms of various aluminum hydroxide nanoparticles in details. By focusing on understanding the role of aluminum coordination change dynamics from tetrahedral in solution to octahedral in solids and vice versa, and by quantifying

intermediate polyoxoaluminate cluster formation, some unifying principles governing these transformations emerge. Furthermore, various advanced techniques reveal the transformation and aggregation of aluminum-oxo clusters during the hydrothermal process, which indicate cluster assembly pathways to aluminum hydroxide nanoparticle nucleation and crystal growth. These findings are important for developing new methods to morphology and size-controlled synthesis of aluminum hydroxide nanoparticles, and may aid in the design of chemical processes for managing the aluminum inventory in nuclear waste.

4:25 PM NM05.09.02

Laser Photothermal Nano-Assembly of Palladium Nanoparticles and 3D Porous Graphene Pilgyu Kang^{1,1}, Byoung Gak Kim², Seung Min Lee¹, Minsu Kim², Farbod Moghaddam¹, Daniel Mitchell¹ and Heeyoung Jeong²; ¹George Mason University, United States; ²Korea Research Institute of Chemical Technology, Korea (the Republic of)

A facile, rapid, and scalable manufacturing method for nano-assembly of palladium nanoparticles (PdNPs) and graphene is desired for broad applications in energy storage and harvesting, sensing and detection, and catalysis. However, existing approaches to obtain the organic-inorganic hybrid nanostructures involve multi-step processes for synthesis of constituent elements. Graphene nanomaterials are synthesized by chemical vapor deposition and reduction of graphene oxides and metal nanoparticles are combined by electrodeposition, solution-based chemical processing, and thermal annealing. Laser-based method recently demonstrated rapid, cost-effective production of 3D porous graphene called laser-induced graphene (LIG) by pulsed laser irradiation of various polymers as a carbon/graphene precursor such as polyimide, and the laser method and LIG showed a promise to facile, scalable, rapid manufacturing of nanostructured graphene and functional devices for broad applications including sensing and detection, energy storage and harvesting and nanocatalysts. However, the laser photothermal generation of inorganic-organic nanostructured composite materials has not been explored. Here, we present a one-step, rapid, scalable laser photothermal nano-assembly method to synchronously generate Pd NPs and porous graphene by using polymer films that contains Pd and carbon precursors. We use the polymers of intrinsic microporosity (PIM-1) as a graphene precursor, which has high solubility in volatile solvent and miscibility with inorganic materials. The outstanding compatibility with inorganic materials and solubility in volatile organic solvents of PIM-1 allow for homogeneous films without phase separation, and formation of the films only by removing volatile solvents at ambient condition. A pulsed CO₂ laser irradiation on the homogeneous films of PIM-1 and Pd-ligands induces localized graphitization (carbon atoms in the polymer chains become sp² hybridized) yielding nano- to microscopic 3D porous graphene while the organic functional groups of Pd-ligands are vaporized and Pd atoms nucleate and crystallize in nanoparticles. Thus, our laser-induced photothermal local heating yields synchronous nano-assembly of highly dense and monodispersed PdNPs in porous nanostructured graphene. Based on low energy requirements of PdNPs to form palladium hydrides (PdH_x) and exceptional electrical properties of the porous graphene including high conductivity and electron mobility we used the laser nanomanufactured hybrid nanostructures for highly sensitivity hydrogen gas sensing with the limit of detection down to 1 ppm. We also demonstrated fast and reversible hydrogen gas detection in the range of 1-50 ppm H₂, which is attributed to chemical reversibility of the hybrid nanostructures. We showed mechanically flexible, wearable H₂ sensor with outstanding mechanical flexibility and reliability of the hybrid nanostructures under cyclic bending strain of 0.22% as well as cyclic twisting angles of ±90° up to 10,000 cycles. Furthermore based on our hybrid nanostructures we developed a wireless H₂ gas sensor platform enabling monitoring with a smartphone. Our approach combining the laser photothermal method and the versatile polymer of the PIM-1 has potential to manufacture hybrid nanostructured materials of various metal nanoparticles and porous graphene for broad fields in energy storage and harvesting, sensing and detection, and catalysis as well as diverse applications including electrochemical sensors, gas storage systems, and supercapacitors.

4:40 PM NM05.09.03

Late News: How 3D Printed Polymeric Scaffolds Optimize Geometry, Mechanical Stability and Photocatalytic Performance of Nanoparticle-Based Aerogels Murielle Schreck, Nicole Kleger and Markus Niederberger; ETH Zürich, Switzerland

Photocatalytic hydrogen production is one of the most important techniques, which have to be part of a sustainable energy system to ensure the survival of our polluted planet. The search for the most efficient photocatalyst for this technique includes not only finding the right material, but as importantly, finding the right structure. We suggest 3D, translucent, nanoparticle-based aerogel monoliths as promising candidates for the photocatalytic hydrogen production in the gas phase. To achieve the best photocatalytic performance, the right fit between the geometries of especially 3D photocatalysts and reactors measuring their performance is crucial. Here, we report how we take control of the geometry of the photocatalyst by introducing 3D printed polymeric scaffolds into the aerogels. Thanks to these scaffolds, we can investigate the gas flow through the aerogel, the UV light penetration into the aerogel and the optimal fit with our custom-made continuous gas flow reactor to maximize the hydrogen production rate. We manage to raise the hydrogen production rate from originally $433 \mu\text{mol g}^{-1} \text{h}^{-1}$ by a factor of almost 4 to $1578 \mu\text{mol g}^{-1} \text{h}^{-1}$ just by modifying the geometry of the aerogels. Additionally, the rigid scaffolds enhance the mechanical stability of the fragile aerogels, increasing the fabrication yield and, therefore, saving material, money and time. With the possibility to engineer these 3D printed polymeric scaffolds, we can match the geometry of any 3D, template-free, self-supporting photocatalyst to the geometry of reactors built for any photocatalytic gas phase reaction and maximize the photocatalytic performance.

4:55 PM NM05.09.04

Late News: Printable Dielectric Thin Films of Metal-Polymer Core-Shell Nanoparticles [Roman Buchheit](#)¹, Björn Kuttich¹, Lola González-García¹ and Tobias Kraus^{1,2}; ¹INM – Leibniz Institute for New Materials, Germany; ²Saarland University, Germany

Printable dielectrics are important materials for flexible and inkjet-structured electronics. Many of them are composites with a polymer and a nanoparticle component. Non-conductive nanoparticles, for example oxides with high dielectric constant, form dielectric composites that can be described by effective-medium theory and often contain a large volume fraction of particles [1]. Conductive metal nanoparticles at low concentrations form dielectric polymer composites with properties that are usually discussed using percolation theory [2]. The volume fraction of the metal has to be kept low in order to avoid short circuits.

Here, we present a dielectric material with a microstructure and properties that range in between the two cases introduced above. We electrically insulate conductive gold nanoparticles with a covalently bound polystyrene shell. These hybrid core-shell nanoparticles are then dispersed and deposited in thin dielectric films. The distribution of the gold in the polystyrene matrix is controlled by the structure of the covalently bound polymer shell and its interactions. We tune the amount of the organic phase in the final dielectric layer by different conditions during ligand exchange, which leads to different polymer ligand densities on the gold core. We will discuss the dielectric constants and the microstructure of dielectric layers prepared from ink of core-shell hybrid nanoparticles with 5 nm diameter gold cores and thiol-terminated polystyrene shells (PS) of different molecular weights ($M_n=5000$ Da or $M_n=11000$ Da) with different densities. Thermal Gravimetric Analysis (TGA) data of the dry films indicated gold volume content between 4.9 vol% and 21.1 vol% depending on the polymer shell density. Small-Angle X-ray Scattering (SAXS) and Transmission Electron Microscopy (TEM) revealed different microstructures of the dielectric films that ranged from crystalline bcc packings to fully disordered, but homogeneous packing as visible in TEM. Impedance measurements in the frequency range from 100 Hz up to 1 MHz indicated a dielectric constant of 3.5 for the highest grafting density of polystyrene at a dielectric loss of below 2% at 1 kHz, while the lowest grafting density of polystyrene led to a dielectric constant of up to 40 with a dielectric loss of below 5% at 1 kHz.

We believe that the covalent attachment of polymer ligands to metal cores is a promising approach to “molecular hybrid” films that can be deposited by wet processing without agglomeration. Our approach solves the problems of particle agglomeration in earlier nanocomposites of metal nanoparticles in polymers at high particle loading [3,4]. The strong attachment of the insulating polymer ligands prevents dielectric failure that otherwise besets nanocomposites at increased metal contents.

References:

- [1] Dang, Zhi-Min; Yuan, Jin-Kai; Zha, Jun-Wei; Zhou, Tao; Li, Sheng-Tao; Hu, Guo-Hua (2012): Fundamentals, processes and applications of high-permittivity polymer–matrix composites. In *Progress in Materials Science* 57 (4), pp. 660–723. DOI: 10.1016/j.pmatsci.2011.08.001.
- [2] Nan, C.-W.; Shen, Y.; Ma, Jing (2010): Physical Properties of Composites Near Percolation. In *Annu. Rev. Mater. Res.* 40 (1), pp. 131–151. DOI: 10.1146/annurev-matsci-070909-104529.
- [3] Toor, Anju; So, Hongyun; Pisano, Albert P. (2017): Dielectric properties of ligand-modified gold nanoparticle/SU-8 photopolymer based nanocomposites. In *Applied Surface Science* 414, pp. 373–379. DOI: 10.1016/j.apsusc.2017.04.096.
- [4] Toor, Anju; So, Hongyun; Pisano, Albert P. (2017): Improved Dielectric Properties of Polyvinylidene Fluoride Nanocomposite Embedded with Poly(vinylpyrrolidone)-Coated Gold Nanoparticles. In *ACS applied materials & interfaces* 9 (7), pp. 6369–6375. DOI: 10.1021/acsami.6b13900.

5:10 PM NM05.09.05

Light Activated Gas Sensing Application of Assembly of Sol-Gel Synthesized CuO Bundles Rutuja Bhusari, Jean-Sébastien Thomann and Renaud Leturcq; Luxembourg Institute of Science and Technology, Luxembourg

Chemiresistive gas sensors based on sol-gel synthesised colloidal materials with controlled size, shape and composition have demonstrated notable sensing properties [1]. In our earlier work we showed that ordered assemblies of ZnO nanorods produced in solution via wet chemical synthesis lead to formation of network like structures on electrodes, with sensing capabilities at room temperature [2]. Current passing through such a network between one electrode to another, is modulated based on the surface chemistry taking place between surrounding environment and material deposited [2].

In this work, we extend our previous work to assembly of CuO bundles forming a network between gold electrodes. Copper oxide (CuO) is a well-known p-type material used for variety of applications including chemiresistive gas sensors. CuO is known to have excellent optical and chemical properties which can be tuned for variety of applications. For example, Hou et al. have studied study the effect of morphology and surface structure of CuO nanostructures on the CO sensing properties [1]. In addition to this, CuO nanostructures have been found to be sensitive to a variety of reducing and oxidising gasses [2, 3, 4]. In this work, synthesis and characterisation of CuO bundles network is presented, followed by sensing response towards oxygen. The properties are tuned by annealing of the network, which acts on the junctions between the bundles. Moreover, we investigate the optical properties of such an assembly of structures to improve its electrical characteristics and enhance its gas sensing response using light activation.

- [1] Hou, L., Zhang, C., Li, L., Du, C., Li, X., Kang, X. F., & Chen, W. (2018). CO gas sensors based on p-type CuO nanotubes and CuO nanocubes: Morphology and surface structure effects on the sensing performance. *Talanta*, 188, 41-49.
- [2] Caicedo, N., Leturcq, R., Raskin, J. P., Flandre, D., & Lenoble, D. (2019). Detection mechanism in highly sensitive ZnO nanowires network gas sensors. *Sensors and Actuators B: Chemical*, 297, 126602.
- [3] Hoa, N. D., Van Quy, N., Jung, H., Kim, D., Kim, H., & Hong, S. K. (2010). Synthesis of porous CuO nanowires and its application to hydrogen detection. *Sensors and Actuators B: Chemical*, 146(1), 266-272.
- [4] Wang, C., Fu, X. Q., Xue, X. Y., Wang, Y. G., & Wang, T. H. (2007). Surface accumulation conduction controlled sensing characteristic of p-type CuO nanorods induced by oxygen adsorption. *Nanotechnology*, 18(14), 145506.

5:25 PM NM05.09.06

Resolving the Atomic Structure of Sequential Infiltration Synthesis Derived Indium Oxyhydroxide Clusters Alex Martinson, Xiang He and David Tiede; Argonne National Laboratory, United States

Sequential infiltration synthesis (SIS) is a route to the precision deposition of inorganic solids in analogy to atomic layer deposition (ALD), but occurs within (vs upon) a soft material template. We reveal a possible pathway for the sequential infiltration synthesis of InO_xH_y clusters in a PMMA host matrix and the inorganic films (after annealing) composed of sub-6 nm In_2O_3 nanocrystals. Interestingly, small InO_xH_y clusters with only

1 to 3 In atoms were found to form after a single SIS cycle. These small InO_xH_y clusters serve as sites for reaction in subsequent cycles and/or subsequent condensation with other small nuclei that first proceeds linearly and, later, more three-dimensionally. Although the structures of as-grown InO_xH_y clusters lack long-range crystallographic order, they exhibit local coordination environments similar to cubic In_2O_3 and $\text{In}(\text{OH})_3$. Crystallization of the InO_xH_y clusters is easily achieved by annealing the hybrid $\text{InO}_x\text{H}_y/\text{PMMA}$ thin films in air, which leads to the formation of denser, but still microporous, In_2O_3 thin films. The size and subtleties of the In_2O_3 structure depend on the number of SIS cycle used to deposit the inorganic phase before annealing. Lattice expansion, longer In-O bond lengths, and larger atomic displacement were observed in samples with greater SIS cycles. These methods and findings may provide fundamental insights into other SIS processes as well as map a route to the precision synthesis of discrete-atom-number clusters.

5:40 PM NM05.09.07

Investigation of Optical Properties of TiO_2 , WO_3 , and Y_2O_3 Nanoparticles Sergey Mamedov; HORIBA Scientific, United States

Metal oxide nanoparticles are attractive materials for many applications but have recently become an essential part of dye-sensitized solar cells and highly efficient catalysis materials. The material's efficiency depends on size, shape, and surface chemistry, which critically determine their properties and interaction.

Raman spectroscopy is a powerful method to investigate nanoparticles' vibrational properties, as the Raman band's peak and width are very sensitive to the local structure. Besides, phonons' behavior at the nanoparticles boundary strongly depends on the particle size and is a critical factor in creating a highly efficient material. It was shown that the Raman peak of TiO_2 at 142.9 cm^{-1} shifted to a high-frequency region with a decrease in the nanoparticles' size. However, Raman spectroscopy of nanopowders of WO_3 and Y_2O_3 were not investigated yet. Nanopowders of TiO_2 , WO_3 , and Y_2O_3 with the mean size ranged from 5 to 40 nm were investigated by Raman spectroscopy in the broad spectral range. The phonon confinement model was applied to calculate the Raman spectra of these materials. The correlation length of the phonons calculated from the spectra of nanoparticles shows a significant difference between large ($> 40 \text{ nm}$) and small ($< 10 \text{ nm}$) nanoparticles. Grain size can be extracted from the Raman spectra of nanomaterials by applying a model of confined phonons. Results showed a good correlation between grain sizes obtained from Raman spectra and XRD. Raman spectra are more sensitive to nanoparticles' structural motive compared to XRD. The Raman spectra may be different even if X-ray diffraction shows that the particle size is the same. It reflects the differences in the surface structure of nanoparticles.

SESSION NM05.10: Functional Nanoparticle Materials—Synthesis, Property and Applications X

Session Chairs: Mei Cai, Ou Chen and Han Htoon

Monday Afternoon, April 19, 2021

NM05

7:45 PM NM05.10.01

Late News: Direct White Light Emission (WLE) via Controlling the N Doping Centres in Carbon Dots (CDs) Barun K. Barman and Tadaaki Nagao; National Institute for Materials Science, Japan

Direct white light emission (WLE) from single-component emitters, free from rare-earth and toxic metals have been strongly required in industry, but it is still a grand challenge. Recently, fluorescent carbon dots (CDs) has emerged as a new class of metal-free luminescent materials that are composed mainly of C, O, H. Their fluorescence properties are tuned by the doping centre and surface functional groups leading to multiple emission in the entire visible spectra. The systematic investigation of the N-doping centres and surface functional groups has provided a vital understanding of the emission property. For example, the optimized synthetic strategy enabled us to dope graphitic N centres and lead to the broadband WLE extended in the entire

visible spectra (400 to 750 nm). The decrease or increase of the graphitic N centres into the CDs led to the green and orange emission, respectively. Because the graphitic N creates mid-gap states within the HOMO–LUMO gap of the pristine CDs, as a result, the light absorption is red-shifted which gives rise to the low energy fluorescence in the visible spectrum. These as synthesized CDs show direct and ideal WLE both in solution and in solid forms with CIE value of (0.33, 0.34) and high colour rendering index (CRI 92). These CDs can form transparent and efficient WLE film with long term stability, when they are mixed in the polymer matrix and excited via UV light. This study provides an important guiding principle for CDs syntheses for realizing spectrally tuned emission and direct WLE.

8:00 PM NM05.10.02

Late News: Ammonia Uptake of a Metal Organic Framework Adsorbent from Ultralow to Ambient Pressure Dae Won Kim¹, Dong Won Kang¹, Minjung Kang¹, Jung-Hoon Lee², Jong Hyeak Choe¹, Yun Seok Chae¹, Doo San Choi¹, Hongryeol Yun¹ and Chang Seop Hong¹; ¹Korea University, Korea (the Republic of); ²Korea Institute of Science and Technology, Korea (the Republic of)

Even though various porous adsorbents have been examined as NH₃ capture applications, these materials generally displayed insufficient NH₃ uptake, low affinity at the ppm level, and poor chemical stability against humid NH₃. Herein, we report the NH₃ capture properties of iso-reticular series metal-organic frameworks M₂(dobpdc) (M= Mg, Mn, Co, Ni, and Zn) that contain open metal sites. Among the series, the Mg analogue recorded highest ammonia uptake, outperforming any other existing benchmark materials with 23.9 mmol g⁻¹ at 1 bar and 8.25 mmol g⁻¹ at 570 ppm in ambient temperature. From the NH₃-temperature programmed desorption curves we could compare the strength of the interaction between NH₃ and Lewis acidic open metal sites and activation energy of desorption of NH₃, which was further supported with van der Waals-corrected density functional theory calculations. The structural stability of Mg₂(dobpdc) upon exposure to wet NH₃ was superior to that of the other M₂(dobpdc) and the frameworks tested, displaying intact structural integrity over 3 days. The NH₃ breakthrough experiments in humid conditions revealed that Mg₂(dobpdc) could selectively capture NH₃ in wet conditions without structural degradation or capacity loss for multiple cycles. The NH₃ adsorption mechanism of Mg₂(dobpdc) in dry and wet conditions was elucidated with in-situ FT-IR spectroscopy, showing that ammonium ion was accompanied in wet condition. To summarize, these results demonstrated that Mg₂(dobpdc) is a recyclable compound that selectively capture NH₃ with significant NH₃ affinity and capacity. We envision that Mg₂(dobpdc) is promising candidate for real-world NH₃-capture applications.

8:05 PM NM05.10.05

Late News: Fundamental Study of the Dispersion of Carbon Nano-Onions Armando J. Nieves-Carrasquillo, Angelica Del Valle-Perez and Lisandro Cunci; Universidad Ana G. Méndez, Puerto Rico

Multi-shell fullerenes, known as carbon nano-onions (CNOs) discovered by Ugarte in 1992, are structured by concentric shells of carbon atoms. Different methods for their synthesis have been developed and their properties have been widely studied. The chemical functionalization of CNOs has been investigated and several synthetic pathways were found to be applicable for the introduction of a variety of functional groups. CNOs exhibit poor solubility in both aqueous and organic solvents due to aggregation. This is promoted by strong intermolecular interactions such as van-der-Waals forces. To overcome this tendency to aggregate, functionalization of the surface of the carbon materials is the method of choice. The purpose of this project is to make the oxidized CNOs bear a relative centrifugal force at different time durations. Analyzing between two functionalizing methods, furnace and via synthesis. How well the material disperses, provides a fundamental concept for the synthesis efficiency. According to preliminary results, there is a tendency on which the concentrated CNOs (obtained via synthesis) difference in weight gets narrow, as duration of the centrifugal force increases. Because of their structure, high conductivities, and dispersion properties, CNOs acquired by synthesis are often used as conductive additives in electrochemical energy storage devices, such as battery and supercapacitor electrodes, where an increase in the rate performance (power) of the device is necessary. Chemically modified CNOs were probed in different fields of application and have revealed to be a promising nanomaterial that attracts a growing interest among researchers and opens new avenues for investigation. CNOs

can be implemented as a catalytic support. In addition, this material can be used as a metal-free catalyst that can increase its catalytic performance by doping with polymers providing nitrogen or phosphorus atoms to the surface. Both methods start using nano-diamonds; a carbon nanomaterial of strong structure which undergo a temperature of approximately 1650°C inside a furnace to obtain the CNOs structure. The CNOs oxidized through synthesis requires a constant temperature and stirring to attain oxygen based functional groups. The preliminary elemental detection of oxygen atoms was gathered by Energy-Dispersive Spectroscopy. To detect states in the CNO's molecular system, Raman Spectroscopy was utilized to confirm the carbon structure of CNOs by the identification of the peaks D and G characteristic of this carbon material. An in-depth characterization analysis was done using X-Ray Diffraction, providing detailed information about chemical composition, and crystalline structure. The morphology and microstructure of CNOs were studied using a Transmission Electron Microscope and Scanning Electron Microscopy.

8:10 PM NM05.10.06

Late News: The Rates of Unlayered Graphene Formation in a Supercooled Carbon Melt at Low Pressure

Philip Chrostoski, Chathuri Silva and Philip Fraundorf; University of Missouri, United States

Elemental carbon has important structural diversity, ranging from nanotubes through graphite to diamond. Previous studies of micron-size core-rim carbon spheres extracted from primitive meteorites; whose isotopic signatures indicate an origin in red-giant star nucleosynthesis [ApJLett **578** L152 (2002), Elements **10** 441 (2014)], suggest they formed around such stars via the solidification of condensed carbon-vapor droplets, followed by gas-to-solid carbon coating to form the graphite rims. Similar core-rim particles result from the slow cooling of carbon vapor in the lab [Hundley LPSC 2018 HAL-02238804]. Although experimental indications from particle slicing suggest that this core material may not have special strength, it's properties as a diffusion barrier may be quite interesting if one can synthesize material with graphene sheets as large (e.g. 600 atoms or 4 nm widths) and abundant (e.g. $6 \times 10^{19}/\text{cc}$) as we find in the presolar cores [M&M **26** 2838 (2020)]. Although we've not yet done any percolation theory modeling, the small size of pores in a single graphene sheet [Nature **579** 229 (2020)] suggest that this material may be able to stop diffusion of even small atoms like helium over astrophysical (not just geologic) time scales. Before working on oven design, we first want to model nucleation and growth as a function of time at temperature to see what laboratory conditions are likely to be required. This is also relevant, of course, for astrophysicists in understanding conditions of carbon condensation around the types of stars that created the carbon atoms of which we are made [COSPAR 2021]. Our preliminary results suggest that the presolar cores solidified over longer times (say tens of seconds) at lower temperatures (say 2400K) compared to the laboratory cores (say tenths of seconds) at higher temperatures (say 3050K). The analytical models so far follow the "few parameter" approach of Turnbull and Fischer [JChemPhys **17** 71 (1949)] for reaction (not diffusion) limited nucleation & growth. Using this model, with preliminary energy values extracted from atomistic data and/or experimental constraints in the lab-grown case, we generated an analytical growth model to compare with pre-solar and lab-grown data, which gave us the above-quoted preliminary numbers. We looked at our "liquid model" systems for set temperature molecular dynamics anneals at experimentally-estimated densities of 1.8 g/cc. Our system had a 42-atom graphene sheet with the rest of the liquid atoms randomly placed with a nearest neighbor $> 1.9 \text{ \AA}$. Looking at 2D growth, we see when at temperatures ranging from 1700 – 4200 K the growth rate increases as temperatures increase. Future work to refine these models will hopefully generate better-constrained energy values from our atomistic simulations, to use with such analytical models. Along with this, downward temperature ramps will be examined instead of fixed temperature anneals as rates of cooling are likely the key parameter in both laboratory and astrophysical settings. We will also be looking at models for supercooling thresholds with containerless liquid metals – [Nucleation in Condensed Matter (2010)] and the uses of dynamical atomistic models of both nucleation and growth [JPetrology **54** 913 (2013), *Handbook of Continuous Crystallization* (2020)].

8:15 PM NM05.10.07

Magnetoactive Multi-Walled Carbon Nanotube for 3D Motion Tracking Electroluminescence Display

Seung Won Lee, Chanho Park, Hyeokjung Lee, Kyuho Lee and Cheolmin Park; Yonsei University, Korea (the Republic of)

Development of human-interactive display enabling the simultaneous sensing, visualisation, and memorisation of a magnetic field remains a challenge. Here we report a skin-patchable magneto-interactive electroluminescent display, which is capable of sensing, visualising, and storing magnetic field information, thereby enabling 3D motion tracking. An alternating current (AC) EL display is developed with a magnetoactive conductive fluid of multi-walled carbon nanotubes (MWNTs), decorated with superparamagnetic iron oxide (Fe_3O_4) nanoparticles, in n-hexadecane on which an AC-field responsive emissive layer is placed with two parallel electrodes. By constructing mechanically flexible arrays of magneto-interactive displays, a skin-patchable and pixelated platform is realised. The magnetic field varying along the z-axis enables the 3D motion tracking (monitoring and memorisation) on 2D pixelated display. This 3D motion tracking display is successfully used as a non-destructive surgery-path guiding, wherein a pathway for a surgical robotic arm with a magnetic probe is visualised and recorded on a display patched on the abdominal skin of a rat, thereby helping the robotic arm to find an optimal pathway.

8:30 PM NM05.10.10

Efficient Radiative Cooling of Low-Cost BaSO_4 Nanoparticle-Paper Dual-Layer Thin Films Andrea L. Felicelli, Joseph Peoples, Jie Wang, George Chiu and Xiulin Ruan; Purdue University, United States

Radiative cooling allows for effective dissipation of heat into deep space, making it an environmentally clean as well as passive cooling technology. It has been shown to be effective at reducing energy consumption from the cooling requirements of many widespread systems including commercial and residential buildings and outdoor electronic equipment. The development of versatile and cost-effective materials with good radiative cooling performance is critical to furthering the range of applications of this technology as well as improving the potential for the technology within existing applications. The BaSO_4 nanoparticle-embedded coatings we have developed have consistently shown strong radiative cooling performance with a solar reflectance of greater than 95% and an emissivity of greater than 0.90 in the "sky window", which is the region of the atmosphere that is transparent (corresponding to 8-13 μm wavelengths). These performance parameters demonstrate these coatings to be a potentially promising material to continue to study for radiative cooling applications. Specifically, it is also highly desirable to reduce the coating thickness and preserve the high performance. Doing so promotes cost-effectiveness and maintains energy savings that the material can provide. The work presented demonstrates a thin and cost effective dual-layer BaSO_4 -paper structure with a high radiative cooling performance. We have coated BaSO_4 -nanoparticle-embedded layers with varying thickness on transparency films or commercial cotton-based paper, which allowed us to form a series of dual-layer thin films. Their spectral and total optical reflectance, transmittance and absorptance (or emissivity) are characterized across the ultraviolet, visible, near-infrared and mid-infrared wavelength range. The results allow for the decoupling of the effects of the developed BaSO_4 nanoparticle-embedded coatings from the effects of moderately-to-highly reflective substrates they may be applied over, demonstrating the effectiveness of the coatings themselves for radiative cooling applications versus other surfaces that appear visually similar. Furthermore, the transparency film substrates alone show high emissivity in the sky window but low reflectance in the solar spectrum, while the inexpensive and widely-available commercial cotton-based paper shows high emissivity in the sky window and moderately high reflectance in the solar spectrum. We have been able to demonstrate that by coating the paper with just a thin layer of our BaSO_4 -based nanocomposites, we can significantly increase its radiative cooling performance to be comparable with other state-of-the-art approaches. This is demonstrative that the developed BaSO_4 nanoparticle-paper dual-layer film could be a cost effective and high performance radiative cooling material at small thicknesses.

8:45 PM NM05.10.12

Brown TiO_2 Incorporated Novel 3D MXene as Efficient ORR/OER Electrocatalysts for Lithium-Air Batteries Nur Aqlili Riana Che Mohamad, Haeji Hong, Filipe Marques Mota and Dong Ha Kim; Ewha Womans University, Korea (the Republic of)

A key step to assure the practical application of Li-air batteries involves replacing O_2 with air due to their

expected high practical specific energy densities from 1000 to 2000 Wh kg⁻¹ which could even match with 1700 Wh kg⁻¹ of the gasoline energy system. The Lithium-air batteries involve the oxygen reduction reaction (ORR) during the discharge and the oxygen evolution reaction (OER) in the charging process thus structured ORR/OER electrocatalyst greatly governs the performance of the battery. The promising 2D materials like MXene gained much attention over recent years due to the displayed properties of both ceramics and metals, such as high electrical and thermal conductivity, certain softness, unusual damage tolerance, as well as excellent oxidation resistance, and withstand the volumetric expansion during lithiation. In order to maximize the benefits of MXene, the utilization of 3D MXene could further provide a larger surface area with high exposed specific active sites, high robustness, and 3D conductive network. In this study, we accessed the promise of incorporating the active and stable oxygen vacancies in Brown TiO₂ into the novel 3D network of MXene which is believed to accelerate the Li₂O₂ formation and decomposition by lowering the reaction energy barrier of the reversibly decomposing discharge products. Coupled electrochemical and spectroscopic analyses in the present study disclose the systematic discharge formation and decomposition through the controlled tailoring of active vacancy sites as well as manipulating the morphology of novel 3D MXene network.

8:50 PM NM05.10.15

Late News: Design and Engineering of Cu₂O-CuO Nanostructured Heterojunctions Subish John and Somnath C. Roy; IIT Madras, India

Heterojunction design is an effective strategy for separation of photogenerated charges and reduce recombination in a semiconductor. In the nanostructured form, such heterojunctions have the added advantage of higher specific surface area that serves as efficient catalyst, chemical sensors etc. CuO and Cu₂O, both *p* type materials with the band gap values of 1.6 and 2.1 eV respectively, form type II heterostructure, wherein electrons and holes are favorably separated and migrate in opposite directions. The heterojunctions between these materials have been studied in planar or thin film configuration. Here we present fabrication of Cu₂O nanowire- CuO nanoflake heterojunctions fabricated by a combination of electrochemical anodization followed by hydrothermal processing techniques. The Cu₂O nanowires formed by electrochemical anodization of Copper foil are treated in hydrothermal conditions at 150 °C to grow CuO nanoflakes in a perpendicular direction on the nanowire surface. Such nanoscale 3D morphologies result in a photocurrent an order of magnitude higher than bare Cu₂O nanowires. The heterojunction system is characterized by x-ray diffraction, scanning and transmission electron microscope, optical absorption spectroscopy and photoelectrochemical impedance spectroscopy. Our investigations indicate that, in addition to solar energy harvesting, the Cu₂O-CuO nanostructured heterojunctions can also be potentially effective in rechargeable batteries and supercapacitor applications.

SESSION NM05.11: Functional Nanoparticle Materials—Synthesis, Property and Applications XI
Session Chairs: Ou Chen and Yu Han
Tuesday Afternoon, April 20, 2021
NM05

2:15 PM *NM05.11.01

Assembling Magnetic Nanoparticles into Superparamagnetic Nanocomposites Dale L. Huber; Sandia National Laboratories, United States

Magnetic nanoparticles can exhibit a property known as superparamagnetism where they have extremely high susceptibility and a complete absence of magnetic hysteresis. This would represent an ideal inductor or transformer material if it could be maintained in a bulk material. To do this, magnetic nanoparticles must be densely packed without touching, as contact would lead to the formation of ferromagnetic domains and loss of superparamagnetism. The formation of bulk superparamagnetic materials can be discussed in terms of two

fundamental steps. The first is the large-scale synthesis of precisely size controlled magnetic nanoparticles, and the second is the densification of these particles into a highly magnetic material. The properties of magnetic nanoparticles vary dramatically with size, with an abrupt transition from superparamagnetic to ferromagnetic behavior. The highest magnetic susceptibility, however, is typically found just before this transition to ferromagnetism. Therefore, careful control of particle size and reproducibility of particle size are critical for real world application. The chosen approach here is high temperature decomposition reactions with precise control over reaction kinetics. The second required step is densification while maintaining a critical separation. As particles move closer together, they undergo an abrupt transition where they begin forming multi-particle ferromagnetic domains. An ideal nanocomposite would be close to this critical distance to maximize magnetic particle loading without showing deleterious interparticle magnetic interactions. Careful control of the particles' surface chemistry and appropriate chemical crosslinking can generate strong nanocomposites with excellent magnetic properties that extend to the MHz frequency regime with low losses and little to no decrease in susceptibility. We have designed and synthesized a number of these composites and are currently investigating their application in high frequency switching circuits for power electronics. SNL is managed and operated by NTESS under DOE NNSA contract DE-NA0003525.

2:40 PM NM05.11.02

Functional $\text{Sr}_{0.5}\text{Ba}_{0.5}\text{Sm}_{0.02}\text{Fe}_{11.98}\text{O}_4/x(\text{Ni}_{0.8}\text{Zn}_{0.2}\text{Fe}_2\text{O}_4)$ Hard-Soft Ferrite Nanocomposite Material—Structural, Magnetic and Microwave Analyses [Sadik Güner](#)¹, [Yassine Slimani](#)², [Munirah A. Almessiere](#)², [Alex V. Thrukhanov](#)³ and [Abdulhadi Baykal](#)⁴; ¹RWTH Aachen University, Germany; ²Imam Abdulrahman Bin Faisal University, Saudi Arabia; ³National University of Science and Technology MISiS, Russian Federation; ⁴Institute for Research and Medical Consultations (IRMC), Imam Abdulrahman Bin Faisal University, Saudi Arabia

The structural, magnetic and microwave characteristics of $\text{Sr}_{0.5}\text{Ba}_{0.5}\text{Sm}_{0.02}\text{Fe}_{11.98}\text{O}_4$ (SrBaSmFe) and $x(\text{Ni}_{0.8}\text{Zn}_{0.2}\text{Fe}_2\text{O}_4)$ (NiZnFe) 1:x ($0.0 \leq x \leq 3.0$) hard/soft ferrites nanocomposites (NCs) are presented in this study. SrBaSmFe/x(NiZnFe) hard/soft ferrite NCs were synthesized applying one-pot citrate combustion approach. The structural analyses of all NCs were performed via XRD, SEM, TEM and HR-TEM. Room temperature (RT) 300 K and 10 K magnetization curves were investigated by VSM measurements. Both RT and 10 K magnetization and coercivity data have maximum values for SrBaSmFe/1.0(NiZnFe) NCs (i.e. $x = 1.0$) and continuously reduce with the increasing weight fraction of NiZnFe soft ferrite. Some magnetic hysteresis loops are seen with a kink shape. Magnetic analyses revealed the ongoing hard ferrimagnetic nature of NCs at both temperatures. Squareness ratios (SQRs) were specified to be inferior to the theoretical limit value of 0.50, assigning the multi-magnetic domain nature for NCs. The plots of switching field distribution (SDF) showed the presence of two distinct peaks. This means that the exchange coupling was not accomplished in these NCs by one-pot approach. Frequency dependence of microwave characteristics were discussed utilizing co-axial method in frequency range 0.7-18 GHz. Non-linear dependences of the main microwave properties with varying composition rate might originate from the soft magnetic phase influence. Behavior of the microwave properties are correlated well with the composite theory.

2:55 PM NM05.11.03

Late News: Single Nanoparticle and Virion Mass Spectrometry in Air by Self-Focusing Nanomechanical Sensors [Selim Hanay](#)¹, [Ramazan Tufan Erdogan](#)¹, [Hadi Pisheh](#)¹, [Mohammed Alkhaled](#)¹, [Mehmet Kelleci](#)¹, [Hashim Alhmoud](#)¹, [Ilbey Karakurt](#)¹, [Batuhan E. Kaynak](#)¹, [Cenk Yanik](#)² and [Aykut Özkul](#)³; ¹Bilkent University, Turkey; ²Sabancı University, Turkey; ³Ankara University, Turkey

The COVID-19 pandemic highlighted the necessity to develop rapid *in situ* viral detection techniques to isolate infection breakouts. Current biochemical detection techniques, such as polymerase chain reaction (PCR), remain inadequate for initial response due to the delay associated with sequencing the viral genome and reagent development. Alternatively, physical properties of the virus such as mass and size can be quickly profiled and utilized for rapid detection using mass spectrometry (MS). The recent developments in Nanoelectromechanical Systems (NEMS) have made it possible to measure the mass of single particulates with high accuracy; however,

significant challenges still exist in adapting NEMS-MS for real-life samples. Sample delivery to the sensing element generally requires the use of delicate vacuum systems and the sensing element suffers from low capture efficiency due to its miniscule size. Here, we develop a NEMS-MS device with an integrated polymeric electrostatic lens to enhance the capture efficiency by several orders-of-magnitude compared to the state-of-the-art, while allowing for operation under atmospheric conditions. After benchmarking and validating device performance with polystyrene and gold nanoparticles, we successfully detected the mass of single inactivated SARS-CoV-2 virions from cell lysates with minimum sample preparation. The results establish NEMS technology as an effective approach for the label-free detection of nanoparticles and emerging viruses.

3:10 PM NM05.11.04

Liquid Porous Nanomaterials for Liquid-Liquid Extraction Justine Ben Ghazi-Bouvrande, Sandrine Dourdain and Stéphane Pellet-Rostaing; Institut de Chimie Séparative de Marcoule, CEA, CNRS, ENSCM, Univ.Montpellier, France

Nowadays, separation of chemical elements is an important stake for applications as broad as ore mining, metal recycling or pharmaceutical industry. Although liquid-liquid extraction represents the most applied method at industrial scale, it involves many economic and environmental constraints related to the use of large quantities of solvents. There is therefore a growing interest for alternatives as solid-liquid separation and flotation processes, which however, would require re-designing the actual industrial installations. These alternatives present moreover limited performances, in terms of extraction and selectivity capacities. This project proposes to evaluate a new approach by replacing the organic phases of liquid-liquid extraction processes, with a porous liquid. The Oak Ridge Corporation proposed in 2014 [1], a new class of porous liquid, based on hollow silica nanospheres (HS) obtained by a surfactant templated silica sol gel. To form the “liquid material”, the HS are grafted with an organosilane and a PEG. This ionic bond between the functions gives the interesting property to render the HS liquid and to provide solid empty cavities in a liquid state, without any solvent. In this work, we evaluate the application of such liquid empty cavities to extract metals from an aqueous phase. This extraction approach would be at the exact junction between the conventional liquid-liquid and solid-liquid extraction processes, taking the advantages of the two processes.

To form the porous liquid, HS were prepared thanks to the self-assembly of a surfactant in presence of oil and silica precursors. After the synthesis, the surfactant is removed by calcination and monodisperse HS are made. Various synthesis parameters were investigated to control and understand the morphology of the HS. Indeed, the size of the core, the shape and the homogeneity of the particles could be changed and controlled. TEM micrograph and SAXS data showed that we obtain highly monodisperse HS with a core radius of 6nm and silica shell of 7nm.

The HS are further grafted with an organosilane and a PEG interacting thanks to an ionic bond. This ionic corona has the property to turn the solid nanospheres into a liquid material.

For extraction application, it appears essential to characterize in details the structure and the permeability of these HS, not only to metallic species but in the first place, to aqueous solutions and gaz.

In order to optimize the synthesis route for enhanced permeability, adsorption of argon and nitrogen were carried out with the solid and the liquid to highlight the accessibility to gas of the porosity throughout all the steps of grafting. Gaz sorption reveals that the porosity is becoming less accessible after the grafting step, which means when the solid becomes liquid. This first result showed that the synthesis procedure has to be optimized to limit this loss of opened porosity (which may be due to a closure of the microporous network present in the silica shell of the HS).

An adsorption study was also conducted with liquid solutions by matching the contrast of various solvent and silica by SAXS and SANS to rely the permeability and the pores structure. The SANS signal of the non-grafted HS was completely extinguished with a H₂O/D₂O ratio matching the scattering length density of nanosphere's silica. It allowed us understanding the permeability of reference HS to solvent, specifically if and how the grafting influences the solvent permeability.

Finally, some preliminary extraction tests performed on the solid non-grafted HS, showed that significant amounts of metallic cations can be extracted.

This study confirm that all the synthesis process has to be optimized and understood to maintain the extraction

efficiency of the material when it is in the liquid state.

References

[1] J. Zhang, "Porous liquids: a promising class of media for gas separation" in *Angew. Chem.*, 127, pp 946-950 (2015).

3:25 PM NM05.11.05

Synthesis and the Magnetocaloric Behavior of $\text{La}_{0.7}\text{Sr}_{0.3}\text{MnO}_3/\text{SrFe}_{12}\text{O}_{19}$ Nanocomposites Surendra Dhungana, Sanjay R. Mishra and Dipesh Neupane; The University of Memphis, United States

Recently there has been a renewed interest in exploring novel materials with a large magnetocaloric effect (MCE), due to the fact that solid magnetic refrigeration potentially could replace gas refrigerants. The ferromagnetic perovskite manganites have drawn attention due to its outstanding physical properties as this system displays a rich phase diagram in the magnetotransport, structural properties, and magnetocaloric. The typical way to enhance the MCE is to introduce an insulating phase to the grain boundaries and at the surfaces of manganites as a second phase. Therefore, the composite of the high resistive second phase compound and manganite could be an effective route to improve the MCE properties. In this view, the study is being conducted to understand the impact of the second phase ($\text{SrFe}_{12}\text{O}_{19}$) on the magnetization and magnetocaloric effect of the $\text{La}_{0.7}\text{Sr}_{0.3}\text{MnO}_3$ manganites. With the possibility of the exchange interaction between soft LaSrMnO_3 and hard- $\text{SrFe}_{12}\text{O}_{19}$, a modulation in MCE in the composite is expected.

One-pot auto-combustion technique followed by calcination at 1100 C was used to prepare magnetically hard-soft $x\text{SrFe}_{12}\text{O}_{19-x}$ (100-x) wt % $\text{La}_{0.7}\text{Sr}_{0.3}\text{MnO}_3$ ($x=0, 10, 20, 30, 40, 100$) nanocomposites using nitrite salts. X-ray diffraction (XRD) and scanning electron microscopy (SEM) were used to characterize the structural properties of the samples. The XRD plots showed no trace of secondary phases in the composite. The hexagonal structure (spacegroup-P63) of $\text{SrFe}_{12}\text{O}_{19}$, as well as the perovskite cubic structure (spacegroup-Pm-3m) of $\text{La}_{0.7}\text{Sr}_{0.3}\text{MnO}_3$, were confirmed. Furthermore, magnetic and magnetocaloric properties were studied using SQUID analysis. An exchange coupling behavior was obtained between the soft LaSrMnO_3 and the hard $\text{SrFe}_{12}\text{O}_{19}$ phase. Magnetic isotherms are being collected using PPMS to study the magnetocaloric effect in the as-synthesized composites.

3:30 PM NM05.11.08

Single Molecular Magnet(SMM) Induced Strong Antiferromagnetic Exchange Coupling on a Magnetic Tunnel Junction Based Molecular Spintronics Device Pawan Tyagi, Edward Friebe and Christopher D'Angelo; University of the District of Columbia, United States

Monte Carlo simulations were performed to study the effect of magnetic molecule induced exchange coupling on the magnetic properties of the magnetic tunnel junction based molecular spintronics devices (MTJMSD). We considered all the possible permutations and combinations and nature of interactions between a paramagnetic molecule and the two ferromagnetic (FM) electrodes of an MTJMSD to understand the experimental results. Experimentally observed molecule induced strong antiferromagnetic coupling was only possible when a molecule, with a net spin state, established ferromagnetic coupling with one FM electrode and antiferromagnetic coupling with the other FM electrode. Our MC simulations effectively explain the origin of the experimental data obtained from SQUID magnetometer, ferromagnetic resonance, and MFM studies on MTJMSD. The experimentally estimated molecular coupling strength was in agreement with our results of MC simulations. Increasing MTJMSD size was found to weaken the molecular coupling effect. However, it is quite possible that we underestimated the impact of molecular coupling on the MTJMSD size. In this study, we mainly focused on the Heisenberg type magnetic interaction among nearest neighbors. In reality, molecules are expected to have other modes of couplings such as biquadratic coupling, dipolar coupling, and most importantly paramagnetic molecules are also capable of invoking spin fluctuation assisted coupling between two FM electrodes

3:35 PM NM05.11.09

Impact of Anisotropy of Ferromagnetic Electrodes on Magnetic Tunnel Junction Based Molecular

Spintronics Device (MTJMSD) Properties Bishnu R. Dahal, Marzieh Savadkoohi, Andrew Grizzle, Uzma Amir, Pius Suh, Christopher D'Angelo and Pawan Tyagi; University of the District of Columbia, United States

Covalently bonded Paramagnetic molecular bridges between two ferromagnets (FM) electrodes of a magnetic tunnel junction (MTJ) may enable highly efficient spin transport properties for futuristic computers. The MTJ based molecular spintronics device (MTJMSD) approach can solve the decades' long problems of fabricating robust and mass-producible molecular spintronics device[1]. MTJMSD provides opportunities to connect FM electrodes of a vast range of anisotropy properties to a variety of molecules of length scale. Our prior studies showed that the paramagnetic molecules can produce strong antiferromagnetic coupling with FM electrodes when the molecule establishes a ferromagnetic coupling with one FM electrode and antiferromagnetic coupling with another FM electrode of an MTJ[2]. The device properties of MTJMSD depends upon various factors such as the anisotropy of the FM electrodes, thermal energy (kT), ferromagnet-molecular coupling strengths, spin states of molecules, etc. In this paper, we report a theoretical Monte Carlo Simulation (MCS) study to explain the impact of anisotropy on the MTJMSD equilibrium properties and related experimental observations[3]. Our MCS also studied the impact of thermal energy (kT). The MTJMSD used in this study was represented by an 11x 50 x 50 Ising model, with 11 being the thickness of the MTJMSD and 5x10x50 being the size of each electrode. We ran Markov process for 200 to 500 Million iterations to reach the equilibrium state and record MTJMSD properties such as magnetization of each electrode and complete device. We also studied the energy variation of the MTJMSD system with time as a function of FM electrode anisotropy. We found that increasing anisotropy strength starts exhibiting diverse domain structures within an FM electrode. Increasing anisotropy was found to create stripe-shaped domains with opposite spins. These phases are impacting the overall magnetic properties of the FM electrode where anisotropy was varied. At $kT = 0.1$ we observed that for the high anisotropy magnitude the magnetic moment of the FM electrode settled close to zero. Our MCS study agreed with the experimentally observed stiped domain on MTJMSD and Magnetic force microscopy data[4]. MCS study showed that the anisotropy was the most influential parameter in defining the properties of MTJMSD. The effect of anisotropy enabled MTJMSDs to compete with the increasing thermal energy. High anisotropy enabled MTJMSD to conserve a high magnetization state close to Curie temperature. Anisotropy factor was instrumental even when all the coupling effects get nullified due to thermal energy induced disorders in the MTJMSD. These MCS studies are expected to inform the designing of the MTJMSD for the logic and memory operation.

This research is supported by National Science Foundation-CREST Award (Contract # HRD- 1914751), Department of Energy/ National Nuclear Security Agency (DE-FOA-0003945).

[1] P. Tyagi, Multilayer edge molecular electronics devices: a review, Journal of Materials Chemistry 21(13) (2011) 4733-4742.

[2] P. Tyagi, C. Baker, C. D'Angelo, Paramagnetic molecule induced strong antiferromagnetic exchange coupling on a magnetic tunnel junction based molecular spintronics device, Nanotechnology 26(30) (2015) 305602.

[3] M. Newman, G. Barkema, Monte carlo methods in statistical physics chapter 1-4, Oxford University Press: New York, USA1999.

[4] P. Tyagi, C. Riso, Magnetic force microscopy revealing long range molecule impact on magnetic tunnel junction based molecular spintronics devices, Organic Electronics 75 (2019) 105421.

3:50 PM NM05.11.10

Designing Magnetic Metal Oxide Colloidal Nanoparticles for Spatially Resolved Thermometry Adam Biacchi, Thinh Bui, Eduardo De Lima Correa, Cindi Dennis, Solomon Woods and Angela Hight Walker; National Institute of Standards and Technology, United States

Colloidal magnetic nanoparticles (MNPs) of metal oxides are becoming increasingly important for applications such as biomedical imaging, sensing, drug delivery, and hyperthermia. These exploit the very soft magnetism

found in nanoscale ferrimagnets, often ferrites, which yield a strong collective response to applied alternating (AC) magnetic fields while simultaneously remaining dispersed in media. Their synthesis relies on reproducible, scalable, colloidal solution chemistry routes. Further, the size, shape, structure, and composition are tunable, which serve as levers to design and manipulate the magnetic behavior of these functional nanoparticle materials.

Remote 3D magnetic thermometry is an emerging application of MNPs. The technique employs colloidal nanoparticles to measure and image temperature remotely with high spatial resolution throughout a three-dimensional volume. This metrology is based on the temperature-dependent nature of the particles' magnetization, their dispersibility throughout a liquid or solid of interest, and the ability of applied AC magnetic fields to penetrate through many materials. Although progress has been made in the development of magnetic nanothermometry, commercially available MNPs often lack several properties necessary for widespread application, including particle-to-particle consistency, thermosensitivity response, and a non-exothermic response to applied AC magnetic fields.

Here, we report colloidal MNPs specifically designed for remote 3D thermometry. A series of shape- and size-controlled colloidal MNPs based on ferrites were synthesized *via* the thermal decomposition of organometallic precursors. Further, we exploited compositional doping of transition metal elements and exchange coupling between core-shell magnetic heterostructures as means of generating improved temperature-dependent magnetization (200-400 K at <0.001 T applied AC field) from designed spin interaction within the nanoparticles. Extensive structural characterization was performed to better understand the underlying factors influencing the magnetic response. Results collected from X-ray photoelectron spectroscopy, Raman spectroscopy, and high-resolution electron microscopies, including spatially resolved electron energy loss and energy-dispersive X-ray spectroscopies, revealed correlations between the nanoscale atomic structure of these particles with their magnetic performance. Finally, we used a home-built AC magnetic particle spectrometer to determine the magnetization-dependence of these nanothermometers as a function of temperature, frequency, and field amplitude. These studies allow us to interrogate the fundamental response dynamics of dispersed and deposited magnetic nanoparticles under AC driving fields. Collectively, we show that carefully designed complex metal oxide MNPs display tunable thermosensitivity and AC field signal response, which represents a potential pathway to the implementation of a practical 3D thermal imaging platform based on magnetometry.

SESSION NM05.12: Functional Nanoparticle Materials—Synthesis, Property and Applications XII
Session Chairs: Mei Cai and Ou Chen
Tuesday Afternoon, April 20, 2021
NM05

9:00 PM NM05.12.01

Impact of Heisenberg Exchange Coupling Strength of Ferromagnetic Electrodes on Magnetic Tunnel Junction Based Molecular Spintronics Devices (MTJMSD) Eva Mutunga¹, Bishnu R. Dahal¹, Marzieh Savadkoochi¹, Andrew Grizzle¹, Christopher D'Angelo¹, Vincent Lamberti² and Pawan Tyagi¹; ¹University of the District of Columbia, United States; ²Y-12 National Security Complex, United States

Molecules are highly tunable nanostructures because synthetic chemistry can customize their optical, electrical, and magnetic properties. Thus, molecules used as active device elements open a new pathway towards the miniaturization of advanced logic and memory devices, as well as a new class of metamaterials altogether [1]. The anticipation is that molecular electronic devices will function at significantly low power and reach the ultimate device size limits [2]. Prior research [3] shows that when molecules are bridged between two ferromagnetic electrodes they can serve as novel molecular spintronics-based magnetoresistance devices. Moreover, when the molecule itself possesses a net magnetic spin and interacts with the electrodes' spin state,

more dramatic results are observed. With the magnetic tunnel junction based molecular spintronics device (MTJMSD) we observed paramagnetic molecules produced strong exchange coupling between ferromagnetic electrodes. MTJMSD is fabricated by chemically bonding the molecular channels to the ferromagnetic electrodes of a prefabricated magnetic tunnel junction [4]. We observed that molecule impact was dependent on the type of MTJMSD's ferromagnetic electrodes [5]. However, it is challenging to experimentally study the effect of a wide range of ferromagnetic electrodes on MTJMSD properties. This paper discusses our Monte Carlo simulation study focusing on understanding the effect of ferromagnetic electrodes on magnetic and physical properties of MTJMSD. This paper utilized the 3D Ising model to realistically simulate the experimentally studied MTJMSD design. We varied the Heisenberg exchange coupling parameter for the MTJMSD's two ferromagnetic electrodes. This variation simulated the ferromagnetic electrodes with low to high Curie temperature. We recorded the evolution of MTJMSD magnetization with time and observed the impact of ferromagnet type on the nature of evolution of equilibrium state. We varied thermal energy to understand the role of ferromagnetic electrode type on MTJMSD. We also studied the effect of molecular coupling strength in conjunction with the ferromagnetic electrode's Heisenberg exchange coupling. We have recorded spatial distribution of the magnetic moment of the ferromagnetic electrodes to elucidate the impact range of molecules as a function of ferromagnetic electrode type.

This work is supported by National Science Foundation-CREST Award (Contract # HRD- 1914751), Department of Energy/ National Nuclear Security Agency (DE-FOA-0003945).

References

1. Bogani, L. and W. Wernsdorfer, *Molecular spintronics using single-molecule magnets*. Nature Materials, 2008. **7**(3): p. 179-186.
2. Tyagi, P., C. Riso, and E. Friebe, *Magnetic Tunnel Junction Based Molecular Spintronics Devices Exhibiting Current Suppression At Room Temperature*. Organic Electronics, 2019. **64**: p. 188-194.
3. Rocha, A.R., et al., *Towards molecular spintronics*. Nature Materials, 2005. **4**(4): p. 335-339.
4. Tyagi, P., *Multilayer edge molecular electronics devices: a review*. Journal of Materials Chemistry, 2011. **21**(13): p. 4733-4742.
5. Tyagi, P., C. Baker, and C. D'Angelo, *Paramagnetic molecule induced strong antiferromagnetic exchange coupling on a magnetic tunnel junction based molecular spintronics device*. Nanotechnology, 2015. **26**(30): p. 305602.

9:15 PM NM05.12.02

Multicomponent CoCrFeMnNi Nanoalloy Particle Formation in Hydrogel Nanofibers Yuen Yee Li Sip, David Fox and Lei Zhai; University of Central Florida, United States

Multicomponent and high entropy alloys (HEAs) are a novel class of metallic material systems in the field of materials science and engineering. Such alloys are comprised multiple principal elements with various multicomponent compositions. HEAs are typically formed at elevated temperatures and require high-energy systems to promote high entropy of mixing and ensure equimolar concentration and distribution. However, our study investigated the idea of distributing metal ions inside a hydrogel nanofiber (NF) at ambient temperatures, with random probability and high entropy via absorption and strong interactions in the NF. The subsequent reduction of the metal ions and the formation of nanoparticles (NPs) in the NF will be influenced by this distribution, leading to the potential for kinetic control of HEA NPs. In this study, we have produced the quinary CoCrFeMnNi nanoalloy particles in stable flexible electrospun hydrogel fibers composed of poly(acrylic acid) (PAA) and poly(allylamine hydrochloride) (PAH). The metal ions were loaded into the NFs by immersion into a solution mix containing the required metal salts, followed by chemical reduction to form the metal NPs. The composition of the metal in the alloy could be tuned by varying the metal salt ratio. The proposed method resulted in random capturing by the carboxyl groups of PAA where the metal ions were kinetically trapped and in minimizing the coalescence of the reduced metals. The hydrogel fiber matrix also allowed for aqueous absorption and provided a viscous environment to promote particle formation in the small diameter range. The fabrication process is beneficial in terms of controllability, simplicity and versatility. The

HEA NP loaded fiber composite was characterized for alloy morphology and distribution, electronic states and overall composition. The structural and functional capabilities of the multicomponent nanoalloys create high-performance materials applicable in the aerospace, catalysis and energy industries. Catalysis is one field of interest to incorporate multicomponent nanoalloy composite because the various constituting metals enable an enhanced and more selective catalytic property when compared to monometallic NPs.

9:30 PM NM05.12.03

Late News: Fog Sensor Cameras Using Upconverting Nanoparticles Udit Kumar¹, Scott Hoos², Tamil Selvan Sakthivel¹, Christina Drake² and Sudipta Seal^{1,1}; ¹University of Central Florida, United States; ²Kismet Technologies, United States

Fog formation is often unforeseen and rather hard to predict due to the thermodynamics and kinetics of fog formation overland type and surrounding air conditions. Reduced visibility is one of the substantial causes of vehicular crashes. Despite having multiple meteorological equipment types for measuring and studying fog characteristics, many are suitable only for marine environments and ports. The current state-of-the-art real-time scattering of the light-based roadside fog detection system is riddled with false-negative and false-positive identifications. Considering this situation, we report a novel Upconverting nanoparticles (UCNPs) cameras-based fog sensor concept that is easy and cost-effective for roadside deployment. For the upconverting application, we have fabricated NaYF₄ (Yb, Er) nanoparticles using a facile hydrothermal based route. It has a primarily β - NaYF₄ (hexagonal) phase with an average particle size of around 15 nm and 5 nm and fluorescence spectroscopy showing multiple emission in blue-green-red spectrum with an excitation from NIR light (980 nm).

To eliminate false negatives/positives results, our sensor methodology utilizes two fog detection methods. First, based on Koschmieder's law, it involves estimating visibility conditions and scattering light due to fog, and the second one based on contrast change of an engineered object in the field of view of a traffic camera. NIR light within a black background with UCNPs (in front of the camera utilized in a thin film outside of the front of the camera lens) acts as both a scattering source and an object for contrast measurement. UCNPs also take care of the automatic NIR light filters, common in roadside cameras during daytime use. We have observed fog detection at levels 1-6 (Thick fog to light haze) of the International visibility code at both day and nighttime conditions using the synergic complementary scattering-contrast measurement approach.

9:35 PM NM05.12.04

Late News: Diamine Functionalized Mg₂(dobpdc) Micro-Beads with Hydrophobicity for CO₂ Capture Jong Hyeak Choe, Yun Seok Chae, Dae Won Kim, Doo San Choi, Hyojin Kim, Minjung Kang and Chang Seop Hong; Korea University, Korea (the Republic of)

Metal-organic frameworks (MOFs) is a new type of adsorbents for removing CO₂. In particular, Mg₂(dobpdc) shows high performance in CO₂ capture. Shaping of Mg₂(dobpdc) is important for practical applications. Here, we present a scalable synthesis method for Mg₂(dobpdc) MOF and its shaped beads, which are obtained by using a spray dry method after mixing Mg₂(dobpdc) powders with alumina sol. The synthesized Mg₂(dobpdc)/Al beads have micron-sized diameters. In addition, *N*-ethylethylenediamine (een) functionalization and coating with long alkyl chain silanes results in **een-MOF/Al-Si**, which shows high CO₂ uptake and hydrophobicity. The **een-MOF/Al-Si** microbeads maintain their crystallinity and enhanced CO₂ uptake upon exposure to humid conditions for three days at a high temperature. More details can be found on the poster.

9:40 PM NM05.12.06

Bimetal-Organic Framework as a Wearable Electrochemical Glucose Sensors for Real-Time Sweat Analysis Maowen Xie, Guang Yao and Yuan Lin; University of Electronic Science and Technology of China, China

Flexible wearable sensor are widely reported as emerging tools for target diagnosis and healthcare management,

mainly for detect biomarkers in various body fluids.[1] Place the sensing element on the skin and engineering a detector that can sense glucose without piercing the skin in real time. The rational design of sensing element is the key for the sensing performance of wearable electrochemical sensors.[2] Carbon materials (graphene, carbon nanotubes, carbon nanofibers, etc.), macromolecule polymers, metallic materials, and biological enzyme-based materials are used as highly efficient functional materials for biosensor with high sensitivity and low detection limit, but poor stability, inferior electrical conductivity, limited flexibility still hinder their practical application. [3-5]

Metal-organic frameworks (MOFs) have attracted considerable attention because their uniform-structured cavities and open channels pave the way for entering and escaping molecules. In particular, MOFs and transition metal-MOFs have been used as various sensors, such as gas sensors, DNA sensors, and glucose sensors.[6] In recent years, Co and Fe are an interesting transition metal that has catalytic activity for glucose oxidation due to the excellent catalytic performance and electronic properties.[7,8] Herein, we describe the development of cobalt-foil MOF nanowire array on ultrathin copper foam (Co-Fe MOF/CF) via hydrothermal method possesses high catalytic activity towards glucose electro-oxidation. Benefits from synergies between bimetals, this electrode shows a short response time of less than 3 s, a wide linear range of 0.04–7 mM, a low detection limit of 0.1 μM ($S/N = 3$), and a higher sensitivity of $4424.9 \mu\text{A mM}^{-1} \text{cm}^{-2}$, as well as satisfactory reproducibility, stability and selectivity. In general, our work provided an effective and stable flexible biosensor for the detection of small biological molecules which overcomes the disadvantages of traditional enzyme-based materials. This non-invasive electrochemical biosensor is expected to have considerable applications in personal health monitoring applications, sport and military applications.

References:

- [1] Anneng Y., Feng Y. Flexible electrochemical biosensors for health monitoring. *ACS Appl. Electron. Mater.*, (2020) DOI:10.1021/acsaelm.0c00534.
- [2] Huanfen Y. et al. A contact lens with embedded sensor for monitoring tear glucose level. *Biosens. Bioelectron.*, **26**, (2011) 3290–3296 .
- [3] Songyue L. et al. A flexible and highly sensitive nonenzymatic glucose sensor based on DVD laser scribed graphene substrate. *Biosens. Bioelectron.*, **110**, (2018) 89–96 .
- [4] Su-Kyoung K. et al. Hyaluronate–Gold Nanoparticle/Glucose Oxidase Complex for Highly Sensitive Wireless Noninvasive Glucose Sensors. *ACS Appl. Mater. Interfaces*, **11**, (2019) 37347–37356 .
- [5] Yagmur K. et al. Highly sensitive glucose sensor based on monodisperse palladium nickel/activated carbon nanocomposites. *Anal. Chim. Acta.*, (2018) **1010**, 37–43.
- [6] Furukawa H., et al. The Chemistry and Applications of Metal-Organic Frameworks. *Science*, **341**, (2013) 1230444.
- [7] Yan W., et al. Preparation and characterization of reduced graphene oxide/Fe₃O₄ nanocomposite by a facile in-situ deposition method for glucose biosensor applications. *Mater. Res. Bull.*, **101**, (2018) 340–346.
- [8] Pengcheng Q., et al. A hierarchical cobalt/carbon nanotube hybrid nanocomplex-based ratiometric fluorescent nanosensor for ultrasensitive detection of hydrogen peroxide and glucose in human serum. *Anal. Bioanal. Chem.*, **411**, (2019) 1517–1524.

9:55 PM NM05.12.07

A Soft Mechanotransducer Based on Ionic Polymer-Metal Composite for High-Performance Haptic Feedback Hanbin Choi¹, Youngchan Kim², Joo Sung Kim¹, Changhyeon Cho², Hyukmin Kweon¹, Seonho Kim³, U Hyeok Choi³, Hojin Lee^{2,2} and Do Hwan Kim¹; ¹Hanyang University, Korea (the Republic of); ²Soongsil University, Korea (the Republic of); ³Inha University, Korea (the Republic of)

With the development of soft electronics, an ionic electroactive polymer (i-EAP) actuator has dominated research in various fields because, they provide a lot of advantages such as lightweight, flexibility, simple process, and low operating power. However, many i-EAP studies have demonstrated some drawbacks including low blocking force, displacement and so on, in the utilization of various applications. In order to apply these i-EAP actuators to various fields, it is important to provide the optimum characteristics of the i-EAP actuator suitable for the target application. Among the various applications, for soft haptic feedback, it is required to

achieve high blocking force as well as wide bandwidth. Thus, in order to enhance the blocking force of the i-EAP actuator, highly-performance actuators take advantage of inorganic materials having a high mechanical modulus. Although the inorganic material embedded EAP actuator possesses high blocking force, it's application in soft haptic feedback is questionable due to the narrow bandwidth.

In this work, we described an ionic polymer-metal composite based mechanotransducer (IPMCM), with high blocking force and wide bandwidth consisting of ionic conducting polymer electrodes and a IPMCM material. The composite material based on hydrogen bond increases the actuation performance of blocking force and wide bandwidth through the high modulus of inorganic materials. Also, our actuator could control an interface between ionic polymer and electrodes using conducting polymer (PEDOT:PSS) with ionic liquids and DMSO as additives. As a result, the developed IPMCM with ionic conducting polymer was operated with a wide bandwidth of up to 100 Hz as well as a high blocking force of 1.0 mN. In addition, our ionic polymer-metal composite exhibited the different ion transport mechanism containing inorganic particles with similar activation energy of ionic polymers. We believe that our proposed actuator can serve as an ideal guide to human-machine soft haptic interface.

SESSION NM05.13: On-demand
Wednesday Morning, April 14, 2021
NM05

8:00 AM NM05.07.04

Late News: A Biophilic Composite Multi-Functionalized on the Nanoscale [Alexandra Rempe](#)¹, Joseph Plumitallo¹, Jin Ho Kim¹, Haelin Jang² and Jimmy Xu^{1,1,2}; ¹Brown University, United States; ²Harvard University, United States

This work is a continuation of a growing interest and effort to incorporate into nanocomposites functionalities beyond load-bearing. We report on the concepts and findings of engineering nanocomposites to acquire surface self-disinfection, self-enhanced cell adhesion and growth, on top of internal self-transport of nutrient and growth factors, self-healing and self-lubrication.

Biocomposites have been engineered to repair or replace human mechanics, damaged due to age or injury or deceases, and are of increasing clinical importance. In particular, many surgical procedures require implanting bone-like biomaterials to perform necessary operations. Oftentimes these operations lead to dangerous surgical site infections, as foreign surfaces are an attractive site for bacterial adherence, thus, biocompatibility studies on implantable device require a series of in-depth experiments analyzing both in vitro and in vivo applications.¹ Bone implant biomaterials are generally made of calcium phosphate ceramics, of which hydroxyapatite (HAp) and Whitlockite (WH) have shown notable biocompatibility and bioactivity. Previous research on HAp and WH biomaterials, has created novel advancements seen in dental work, bone implants, and biocoatings.

In an effort to advance such composites beyond the load-bearing function, we have succeeded in engineering a 3D network of nanochannels inside the composite that enables nutrient absorption and transport along with growth factors and enabled self-sustained bone cell growth for selfhealing². With such a built-in network and its Laplace (capillary) force within, lubricants and coolants could also be delivered to the interface of a joint^{3,4}. We show a further advance of this effort – surface engineering to enable on-command self-infection and enhanced celladhesion/growth, via incorporation of TaN and/or TiO₂ nanocomposites and photocatalytic and heterointerface field-induce reactions as representative approaches.

We plan to leverage the visible-light photocatalytic activity and electrical conductivity of copper oxide nanoparticles (CUO NPs) to further contribute to self-disinfection, self-enhanced cell adherence and growth material. Likely because of the electrical conductivity, CuO-Hap nanobiocomposites present high cell viability⁵,

thus, we expect this to further the functionality of the TiO₂-Hap composite, creating a strong application for the future of biocomposites. We hope by the end of this process we will have pioneered a technique that will help minimize the invasive and inflammatory effects of implant debris and microphage reactivity, setting a new ground for the future and reduction of osteogenesis infections.

Referneces:

1. Biocompatibility. (n.d.). Retrieved February 02, 2021, from <https://www.sciencedirect.com/topics/materials-science/biocompatibility>
2. Jang, H. L., Lee, K., Kang, C. S., Lee, H. K., Ahn, H.-Y., Jeong, H.-Y., Park, S., Kim, S. C., Jin, K., Park, J., Yang, T.-Y., Kim, J. H., Shin, S. A., Han, H. N., Oh, K. H., Lee, H.-Y., Lim, J., Hong, K. S., Snead, M. L., ... Nam, K. T. (2015). Biofunctionalized Ceramic with Self-Assembled Networks of Nanochannels. *ACS Nano*, 9(4), 4447–4457
3. C. Wu, J-H Kim, Jimmy Xu System and methods for nanostructure protected delivery of treatment agent and selective release thereof, US Patent 14600188
4. J-H Kim, K-T Nam, Jimmy Xu, “Bioceramics with Self-Powered Fluidic Delivery and Lubrication”, 15th Conference and Exhibition of the European Ceramic Society, (ECerS 2017), Budapest, Hungary, July 9-13, 2017
5. Sahmani, S., Shahali, M., Ghadiri Nejad, M. et al. Effect of copper oxide nanoparticles on electrical conductivity and cell viability of calcium phosphate scaffolds with improved mechanical strength for bone tissue engineering. *Eur. Phys. J. Plus* 134, 7 (2019). <https://doi.org/10.1140/epjp/i2019-12375-x>

SYMPOSIUM NM06

Manipulation and Detection of Physical Properties of Two-Dimensional Quantum Materials
April 14 - April 20, 2021

Symposium Organizers

Jian-Hao Chen, Peking University
Divine Kumah, North Carolina State Univ
Tania Roy, University of Central Florida
Srinivasa Rao Singamaneni, The University of Texas at El Paso

Symposium Support

Platinum
National Science Foundation

* Invited Paper

Tutorial NM06: Manipulation and Detection of Physical Properties of Two Dimensional Quantum Materials
Session Chairs: Sergey Budko, Judy Cha, Archana Raja and Srinivasa Rao Singamaneni
Saturday Afternoon, April 17, 2021
NM06

5:00 PM *

Optical Spectroscopy—2D Materials Archana Raja; Lawrence Berkeley National Laboratory, United States

Optical spectroscopy is a powerful tool to study nanoscale materials, and in particular atomically thin 2D materials that exhibit extraordinarily strong light-matter coupling in 2D materials. In this tutorial I will introduce the optical spectroscopy of 2D transition metal dichalcogenides that are layered semiconductors, and the concept of excitonic Rydberg states to non-invasively understand electronic processes in these materials. In particular I will discuss how excitonic states can be a probe of local strain, doping, dielectric screening and interfacial magnetic exchange. Technical aspects of micro-spectroscopy will be covered along with an overview of advanced capabilities available at national labs that can enable unique insights through correlated, multimodal measurements.

6:00 PM BREAK

6:15 PM *

Quantum Materials—Under Pressure Sergey Budko; Ames Laboratory of US DOE, United States

Pressure is known to control the physical properties of quantum materials. This tutorial will focus on the hydrostatic and uniaxial pressure spanning from general principles to pressure cell design. This includes hydrostaticity, pressure media, experimental techniques under pressure/strain. In particular, this tutorial covers the properties of quantum materials such as superconductors, fragile magnets, novel semimetals under pressure.

7:15 PM BREAK

7:30 PM *

Electrochemical Properties—*In Situ* Characterization Judy Cha; Yale University, United States

Many layered materials have been explored as electrocatalysts for various energy-relevant reactions, most notably for hydrogen evolution reaction (HER). This tutorial will provide basic information on electrochemically driven HER, such as the reaction pathways, mechanisms, and standard experimental set-ups, and present our current understanding of the active sites of layered materials, mostly focusing on transition metal dichalcogenides. The tutorial will discuss the effects of hydrogen adsorption energy, density of catalytically active sites, and catalyst-support interface on the overall activity of HER. Moreover, the tutorial will highlight *in situ* characterization techniques and HER studies based on nanoscale devices, which can provide detailed information on the effects of microstructure and transport properties on HER during reaction.

SESSION NM06.01: Topological/Graphene/Thin Film Magnetism/Anisotropy

Session Chairs: Judy Cha and Srinivasa Rao Singamaneni

Sunday Morning, April 18, 2021

NM06

8:00 AM NM06.01.01

Tuning Fermi Levels in Intrinsic Antiferromagnetic Topological Insulators MnBi_2Te_4 and MnBi_4Te_7 by Defect Engineering and Chemical Doping Mao-hua Du, Jiaqiang Yan, Valentino R. Cooper and Markus Eisenbach; Oak Ridge National Laboratory, United States

MnBi_2Te_4 and MnBi_4Te_7 are intrinsic antiferromagnetic topological insulators, offering a promising materials

platform for realizing exotic topological quantum states. However, high densities of intrinsic defects in these materials not only cause bulk metallic conductivity, preventing the measurement of quantum transport in surface states, but may also affect magnetism and topological properties. In this paper, systematic density functional theory calculations reveal specific material chemistry and growth conditions that determine the defect formation and dopant incorporation in MnBi_2Te_4 and MnBi_4Te_7 . The large strain induced by the internal heterostructure promotes the formation of large-size-mismatched antisite defects and substitutional dopants. Our results show that the abundance of antisite defects is responsible for the observed n-type metallic conductivity. We predict that a Te-rich growth condition should reduce the bulk free electron density, which is confirmed by experimental synthesis and transport measurements in MnBi_2Te_4 . Furthermore, Na doping is proposed to be an effective acceptor dopant to pin the Fermi level within the bulk band gap to enable the observation of surface quantum transport.

M. -H. Du, J. -Q. Yan, V. R. Cooper, M. Eisenbach, *Adv. Func. Mater.* DOI: 10.1002/adfm.202006516.

8:15 AM *NM06.01.02

Visualization of Topological States of Matter Using Microwave Impedance Microscopy Monica Allen; University of California, San Diego, United States

A main thrust of condensed matter physics concerns the discovery of new electronic states in emerging quantum materials. One example is the rapidly expanding class of topological materials, which are posited to enable realization of non-abelian particles and topological quantum computing. In this talk, I will discuss how exotic electronic phenomena can arise from the interplay of topology and magnetism in epitaxially-grown topological insulator thin films. Our experiments employ low-temperature microwave impedance microscopy (MIM), which characterizes the local complex conductivity of a material, to directly image chiral edge modes and phase transitions in a magnetic topological insulator. Finally, I will outline how MIM could be used in the future to visualize and manipulate Majorana modes, an emerging platform for topological quantum information processing.

8:40 AM *NM06.01.03

Spectro-Microscopy of 30° Twisted Bilayer Graphene Jerzy Sadowski; Brookhaven National Laboratory, United States

A discovery of unconventional superconductivity in a twisted bilayer graphene (tBLG) system has spurred intensive discussions about the importance of interlayer coupling in the tBLG. Even though the electronic valence band structure of this system has been thoroughly studied, much of its macroscale properties, such as conducting electron behavior and light-matter interactions remain uncertain. A 30° twisted bilayer graphene (30° -tBLG) is another material system of interest that was recently enabled experimentally. Here, I present the results of the investigations of the interlayer coupling effects in the twisted 30° bilayer graphene system using surface sensitive low energy electron microscopy (LEEM), micro-spot low energy electron diffraction (μ LEED), x-ray photoemission electron microscopy (XPEEM), Raman scattering spectroscopy and scattering-type scanning near-field optical microscopy (sSNOM). Two types of samples were studied in detail – as-grown graphene structures on a copper foil and the graphene transferred to a $\text{TiO}_x/\text{SiO}_2/\text{Si}$ substrate. Strong interlayer coupling between two individual graphene sheets rotated by 30° was revealed by a sharp 12-fold symmetrical LEED pattern acquired in the LEEM microscope. Distinct electron reflectivity contrasts in the LEEM experiment observed between 30° -tBLG and AB-stacked bilayer graphene yielded differences in the conduction band electronic structure between these two systems. Enhancement of interlayer light scattering was observed by the Raman scattering spectroscopy. Most surprisingly, the plasmonic interaction was observed to be sharply quenched on 30° -tBLG, in contrast to enhanced plasmonic interaction observed on chemically similar, AB-stacked bilayer graphene. The plasmonic interactions and sharp contrast in the 30° -tBLG on $\text{TiO}_x/\text{SiO}_2/\text{Si}$ was directly captured in real-space in the sSNOM measurements. We conclude that the 30° -tBLG interface features a unique interlayer resonant interaction in which the interlayer scattering is greatly enhanced. This enhanced interlayer scattering promotes nearly energy-free charge carrier exchange in between two twisted atomic planes.

This research used resources of the Center for Functional Nanomaterials and National Synchrotron Light Source II, which are U.S. DOE Office of Science Facilities, at Brookhaven National Laboratory under Contract No. DE-SC0012704.

9:05 AM NM06.01.04

Probing Magnetic Anisotropy and Interfacial Exchange Interactions at Complex Oxide Interfaces Sanaz Koohfar, Yasemin Ozbek, Hayden Bland and Divine Kumah; North Carolina State University, United States

The control of magnetic ordering and magnetic anisotropy in ultrathin complex oxide films plays a critical role in advancing the development of novel spin-based sensors, storage devices and magnetic tunnel junctions. Perovskite complex oxide interfaces provide an ideal platform for manipulating magnetic ground states due to the strong coupling of spin, electronic, orbital and structural degrees of freedom at these interfaces. Using a combination temperature-dependent magnetometry and element-specific X-ray magnetic circular dichroism, we investigate the competition between epitaxial strain in interfacial magnetic exchange interactions on the magnetic anisotropy in ferromagnetic LaSrCrO₃(LSCO)/LaSrMnO₃(LSMO) heterostructures grown by molecular beam epitaxy. Here, we observe an in-plane easy axis for 2 unit cell LSCO/2 unit cell LSMO heterostructures independent of the substrate-induced epitaxial strain and an antiferromagnetic Mn-Cr exchange across the LSMO/LSCO interface. These results highlight the critical role of interfacial magnetic exchange interactions in tuning magnetic anisotropy at complex oxide interfaces.

*This work was supported by the US National Science Foundation under Grant No. NSF DMR1751455

9:20 AM NM06.01.05

Room-Temperature Ferromagnetism, Perpendicular Anisotropy, and Reverse Magnetostriction in 2-D MnGaN Yingqiao Ma¹, Diego Hunt², Kengyuan Meng³, Tyler Erickson¹, Fengyuan Yang³, Maria Andrea Barral², Valeria Ferrari² and Arthur R. Smith¹; ¹Ohio University, United States; ²Departamento de Física de la Materia Condensada, GIYA, CAC, Comisión Nacional de Energía Atómica, Argentina; ³The Ohio State University, United States

Two-dimensional (2-D) magnetic materials are of great interest for fundamental science and advanced applications while dilute magnetic semiconductors (DMS) have captured worldwide interest in the hope of combining magnetism with electronic properties. At the intersection of these fields, MnGaN-2D is discovered as an ultimately-thin, 2D-DMS material, consisting of a densely concentrated, hexagonal-like arrangement of Mn, Ga, and N, but with a crystal structure unique from its wurtzite GaN substrate. MnGaN-2D shows room-temperature ferromagnetism as demonstrated using spin-polarized scanning tunneling microscopy and as a function of applied magnetic field. This is also predicted by first-principles theoretical calculations which reveal the origins of the ferromagnetism through its highly spin-split and spin-polarized manganese states.[1]

The SP-STM results have been furthermore confirmed by SQUID magnetometry which reveals a high spin-polarization of ~79% at room temperature and perpendicular magnetic anisotropy.[2] New results for this novel system also suggest the possibility of switching the magnetic anisotropy using strain. Theoretical calculations reveal sensitivity of the filled states magnetic Mn peak to compressive versus tensile strain. Spin-orbit coupling is included in the calculations, which indicate either *out-of-plane* or *in-plane* anisotropy, dependent on the type of strain.

Clear evidence for both compressive and tensile local lattice strains is found by detailed analysis of atomic resolution STM images which reveal a wide, non-Gaussian range of lattice spacings (-18% to +18% variations), unlike normal materials. Furthermore, scanning tunneling spectroscopy measurements, showing the clear spin-polarized, filled states manganese peak, find fluctuations in the electronic position of this peak. The filled-states Mn peak energy is also found to fluctuate depending on lattice strain in the theoretical calculations, thus indicating a connection between electronic states and magnetic anisotropy in this RT ferromagnetic 2D

layer.

[1] Yingqiao Ma, Abhijit V. Chinchore, Arthur R. Smith, María Andrea Barral, and Valeria Ferrari, A Two-Dimensional Manganese Gallium Nitride Surface Structure Showing Ferromagnetism at Room Temperature, *Nano Letters*, Vol. 18, p. 158 (2018)

[2] Yingqiao Ma, Diego Hunt, Kengyuan Meng, Tyler Erickson, Fengyuan Yang, María Andrea Barral, Valeria Ferrari, and Arthur R. Smith, Local strain-dependent electronic structure and perpendicular magnetic anisotropy of a MnGaN 2D magnetic monolayer, *Physical Review Materials*, Vol. 4, p. 064006 (2020)

9:35 AM *NM06.01.06

2D Magnetic Materials Alberto Morpurgo; University of Geneva, Switzerland

In this presentation I will review our work on different 2D magnetic materials. I will mainly focus on tunnelling magnetoresistance measurements, in which thin layers of different semiconducting 2D magnetic materials are used as tunnel barrier, whose magnetoresistance exhibit new and interesting effects. I will concentrate on three different systems and of the evolution of their magnetic properties with thickness. The first is CrI₃, a ferromagnet in bulk form that exhibit layered antiferromagnetism when exfoliated in thin multilayer form. When used as tunnel barriers, these multilayers exhibit a 10'000% magnetoresistance that originates from a spin-valvbe effect in the transmission probability of the barrier. The second is CrCl₃, also a layered antiferromagnet in multilayer form, that contrary to CrI₃ (which is an easy axis material), has an easy plane with only weak anisotropy. I will discuss in detail how the evolution of the tunneling magnetoresistance as a function of magnetic field, number of layers and temperature allows the full magnetic phase diagram of these atomically thin crystals to be determined experimentally, and reproduced theoretically in terms of a simple "linear antiferromagnetic chain" model. Finally, I will address the case of MnPS₃, which contrary to the other two materials exhibit antiferromagnetic ordering within the individual layers of the the material. I will show that the tunneling magnetoresistance of sufficiently thick multilayers (i.e., 6-layer) allows the bulk magnetic phase boundaries to be traced. As the thickness is reduced to mono or bilayer, a large magnetoresistance persists, indicating the persistence of magnetism, event though its functional dependence differs from that observed in thicker multilayers. Overall, these examples show how tunneling magnetoresistance is a powerful technique to extract information about the magnetic state of 2D magnetic materials, which would not be easy to obtain otherwise.

SESSION NM06.02: 2D Semiconductors/Structure

Session Chairs: Monica Allen and Divine Kumah

Sunday Morning, April 18, 2021

NM06

10:30 AM NM06.02.01

Dynamic Control of Localized Exciton Emission and Plasmon-Exciton Coupling in Monolayer WSe₂ using a Novel Nanobubble-Nano Gap Architecture Thomas P. Darlington; Columbia University, United States

Applied strain has proven to be one of the most powerful tools in the study of semiconductors, enabling control of fundamental material properties such as the bandgap and electron-phonon coupling. In the context of the 2D semiconductors such as WSe₂, inhomogeneous strain in particular has received significant scientific attention with the discovery of localized excitons (LXs) associated with structural features such as nanobubbles, wrinkles, and nanotents. Such LX states have been shown to become single photon sources at cryogenic temperatures, potentially allowing for deterministic placement of single photon sources in-plane by depositing

single 2D layers over designer structures, e.g. nano-pillars, nano-pits, and nano-antennas. While deposition over fabricated structures allows for high spatial precision in LX location, important parameters such as the strain distribution and resulting emitter emission energy are fixed, and can only approximately controlled during deposition of the 2D layer.

In this presentation, I will show a novel approach that allows for the dynamic tuning of the LX emission energy and coupling to a plasmonic cavity. Using a metallized nano-optical probe as an indenter and, we show that nanobubbles in monolayer WSe₂ can be controllably deformed, tuning the local strain profile, and leading to controllable redshift in the emission energy. High resolution nano-Raman spectroscopy shows that high strains of order 1 - 2 % can be induced, consistent with naturally formed wrinkles that have been shown to host strongly LXs. Finally dramatic line splitting of the LX luminescence is seen, indicating possible strong-coupling with the gap mode plasmon formed between the metallized nano-optical probe and the gold substrate. Our results show the power of the combined plasmonic cavity-nanobubble approach to control the optical coupling and emission localized excitons in WSe₂, and provide greater insight for developing excitonic light sources in 2D materials.

10:45 AM NM06.02.02

WSe₂ as a 2D Quantum Material Integrated into non-Pb Based Bulk Perovskite for Critical Optoelectronics Tunability in an Effort to Enhance Signal-to-Noise Ratio for Non-Invasive Biomedical Device Sensing Saquib Ahmed¹, Sankha Banerjee² and Diedra Hodges³; ¹Buffalo State College, United States; ²California State University, Fresno, United States; ³The University of Texas at El Paso, United States

Integration of 3D bulk materials with 2D quantum materials for physical coupling and applications has been a relatively new area of research. Interfacing of these materials, excitingly, leads to drastic modulations in optoelectronic properties beyond those of the individual materials, thereby leading to an entire genre of innovation and technologies. In this research, DFT studies of 2D WSe₂ coupled with Cs₂AgBiBr₆, a non-Pb based perovskite structure, provide a suite of exciting modulations in electronic properties including higher density of states, and conversion of bandgap from indirect to direct type. Additionally, the charge contribution to the HOMO level of the coupled heterostructure is shown to be predominantly by the p orbital of Br atoms, whereas the LUMO level is seen to receive electrons from the d orbital of W, showcasing the critical transition of the excited electron from the bulk Cs₂AgBiBr₆ to WSe₂ monolayer upon irradiation. Moreover, the energy levels of the surface states are located just above the top of the valence bands in the bulk AgBiBr₂, indicating that the energy loss through charge transfer via surface states is expected to be considerably small. Lastly no mid-gap surface states are seen from density of states plots, indicating that electron-hole recombination hardly occurs even at the surfaces, and thus, long lifetimes of the photoexcited carriers can be realized. Optical properties show enhanced absorption and reflectivity of the 2D-3D heterostructure over each system by itself, together with critically modulated refractive index, dielectric constant (both real and imaginary) and loss term, and extinction index. Thermal and transport properties show similar modulations in the Seebeck coefficient and thermal conductivity. These results provide motivation for the application of such a 2D-3D heterostructure for a novel non-invasive glucose monitoring device. Such a device depends on a highly accurate detection of a signal (from an LED light source) that has undergone a change in intensity after passing through the sugar solution. The enhanced electronic, optical, thermal and transport modulations that the 2D-3D heterostructure showcases upon irradiation across a range of frequencies offers multiple modalities for amplifying and detecting such a signal. Importantly, these modalities can be utilized to detect not only changes in blood sugar level, but other markers in the blood (all non-invasively) that indicate changing health conditions.

11:00 AM NM06.02.04

Fast Bayesian Force Fields from Active Learning—Study of Inter-Dimensional Transformation of Stanene Yu Xie¹, Jonathan Vandermause¹, Lixin Sun¹, Andrea Cepellotti¹ and Boris Kozinsky^{1,2}; ¹Harvard University, United States; ²Robert Bosch LLC, Research and Technology Center, United States

Machine learning force field has attracted more and more attentions because those powerful function-fitting schemes are capable to reach first principle accuracy and simulate large scale systems that are prohibited for

quantum molecular dynamics (QMD). Gaussian process (GP) regression is one promising technique among them, whose remarkable competitive advantage over empirical interatomic force fields is the built-in uncertainty quantification based on Bayesian posterior inference, which can be used to monitor the quality of GP predictions. A current limitation of existing GP force fields is that accurate predictions are only enabled by large training data set. However, the prediction cost grows linearly with the size of the training data set, making accurate GP predictions slow and defying the competitive advantage over more accurate ab-initio techniques.

In this work, we present a way to dramatically accelerate Gaussian process models for interatomic force fields based on many-body kernels by mapping both forces and uncertainties onto functions of low-dimensional features. This allows for automated active learning of models combining near-quantum accuracy, built-in uncertainty, and constant cost of evaluation that is comparable to classical analytical models, capable of simulating millions of atoms.

Using this approach, we train force fields and perform large scale molecular dynamics simulations of stanene monolayer. The monolayer dynamics reveals an unusual phase transformation mechanism of 2D stanene, where ripples lead to nucleation of bilayer defects, densification into a disordered multilayer structure, followed by formation of bulk liquid at high temperature or nucleation and growth of the 3D bcc crystal at low temperature.

The presented method opens possibilities for rapid development of fast accurate uncertainty-aware models for simulating long-time large-scale dynamics of complex materials.

11:15 AM *NM06.02.05

The Synthesis and Engineering of Two-Dimensional Janus Quantum Layers Sefaattin Tongay; Arizona State University, United States

Named after the two faced Roman God Janus, 2D Janus layers contain two different atomic types on its top and bottom faces. Previous theoretical studies have shown that broken mirror symmetry together with large charge transfer across the top and bottom face opens up completely new quantum properties including Rashba effect, colossal Janus field, dipolar excitons, and Skyrmion formation. Despite the theoretical advances in the field, experimental results are still limited due to limitations in high quality 2D Janus layer synthesis. In this talk, I will introduce recent discoveries made at Arizona State University towards different types of Janus layers. The growth process relies on Plasma enhanced low pressure chemical vapor deposition (PE-LPCVD). With this all room temperature technique, our team can synthesize different Janus layers as well as their vertical / lateral heterojunctions, and Janus nanoscrolls. Further studies from our team will introduce on-demand fabrication of 2D Janus layers with unique in-situ growth capabilities that allows us to collect spectroscopy data during the course of Janus material growth. Results are presented along with microscopy, spectroscopy, high -pressure studies, and electronic transport datasets for complete understanding of these systems.

11:40 AM *NM06.10.06

Intertwined Topological and Magnetic Orders in Atomically Thin Chern Insulator MnBi_2Te_4 Xiaodong Xu; University of Washington, United States

The interplay between topology and broken time reversal symmetry in a solid-state system can create a Chern insulator. The non-trivial property of its band structure enables quantized Hall transport with dissipation-free chiral edge states. The recently-discovered topological magnet, MnBi_2Te_4 , provides a desirable platform to study tunable Chern insulator phase. In this talk, I will describe our recent progress in understanding this new material system by the combination of transport, magneto-optical Kerr effect, and microwave impedance microscopy measurement. These probes reveal the formation of the Chern insulator gap, image the associated chiral edge states, and visualize the band-crossing in atomically thin MnBi_2Te_4 devices. Our results offer insights into the topological character of the band structure in this new Chern insulator.

SESSION NM06.03: Calcogenides/van der waals
Session Chairs: Divine Kumah and Srinivasa Rao Singamaneni
Sunday Afternoon, April 18, 2021
NM06

1:00 PM NM06.03.02

Structure of Twisted Transition Metal Dichalcogenide Bilayers Madeleine Phillips and C. Stephen Hellberg; U.S. Naval Research Laboratory, United States

We present density functional theory (DFT) calculations of the reconstruction in MoSe₂/WSe₂ hetero-bilayers twisted a small angle away from 180-degree stacking. The bilayer reconstructs to increase the area of the domains with the lowest energy stacking. The overall twist is concentrated in the domain walls and vertices, where the energetic cost of twisting away from 180 degrees is reduced. We consider the local stacking, order parameter, and strain in the relaxed twisted bilayer.

1:15 PM *NM06.03.03

Magnetic Order and Spin Excitations in Two-Dimensional Honeycomb Lattice van der Waals Ferromagnets Pengcheng Dai; Rice University, United States

We use neutron scattering to study magnetic order and spin excitations in honeycomb lattice van der Waals ferromagnet CrI₃ and CrGeTe₃. In the case of CrI₃, we show that ferromagnetic phase transition is first order in nature, and controlled by spin-orbit coupling (SOC) induced magnetic anisotropy, instead of magnetic exchange coupling as in a conventional ferromagnet. We discuss the role of the next-nearest-neighbor Dzyaloshinskii-Moriya interaction and Kitaev's interaction plays on the spin-wave spectra of CrI₃. For CrGeTe₃, we show evidence of a novel spin-lattice coupling that induce a very large spin-wave broadening over a wide energy and momentum space. We discuss the possible presence of topological spin excitations in CrI₃ and CrGeTe₃.

1:40 PM *NM06.03.04

Spin-Phonon Dynamics in Layered van der Waals Magnets Arun Paramakanti; University of Toronto, Canada

Layered van der Waals magnets, such as CrI₃, show enormous potential for using light to drive phonons and to control magnetic exchange interactions. We present a numerical investigation of such coupled spin-phonon dynamics in model Hamiltonians which incorporate Heisenberg exchange as well as bond-anisotropic Kitaev couplings or Dzyaloshinskii-Moriya interactions. We discuss our results in the context of recent optical pump-probe experiments which observe an oscillatory time-resolved polarization rotation below T_c which may stem from coherent oscillations in the Kerr angle.

2:05 PM NM06.03.05

Flat Bands in Twisted Transition Metal Dichalcogenide Bilayers C. Stephen Hellberg and Madeleine Phillips; U.S. Naval Research Laboratory, United States

The electronic properties of transition metal dichalcogenide (TMD) bilayers vary according to the local atomic structure [1]. In minimally twisted bilayers, there is significant atomic reconstruction away from the rigid moiré pattern [2]. We present the results of density functional theory (DFT) calculations that model the electronic properties of MoSe₂/WSe₂ bilayers with a small twist away from commensurate 180-degree stacking. We present band structures and local densities of states that exhibit flat bands in the gap near the band edges.

[1] M. Phillips and C. S. Hellberg, arXiv:1909.02495

[2] S. Carr, et al, Phys. Rev. B 98, 224102

2:20 PM *NM06.03.06

Manipulation of Dimensionality, Edge State and Strain in Transition Metal Dichalcogenide Nanocrystals

Tomojit Chowdhury¹, Erick Sadler¹, Kiyoun Jo², Surendra B. Anantharaman², Todd Brintlinger³, Deep M. Jariwala² and Thomas J. Kempa^{1,1}; ¹Johns Hopkins University, United States; ²University of Pennsylvania, United States; ³U.S. Naval Research Laboratory, United States

Two-dimensional (2D) transition metal dichalcogenide (TMD) crystals exhibit electronic, magnetic, and optical properties which can be manipulated through control of crystal dimensionality, edge character, and strain state. We recently introduced a rational chemical synthesis strategy, based on gas-phase growth of TMD crystals on designer surfaces, that substantially improves control over the dimensions, morphology, and crystalline edges of 2D TMDs without top-down fabrication. TMD nanoribbons prepared in this manner exhibit atomically sharp edges, readily controllable dimensions, and anomalous photoluminescence features. This talk will focus on our recent efforts to better understand some of these optical anomalies. A mixed-dimensional architecture comprised of a 2D TMD crystal carefully interfaced with a Si nanowire enables the introduction of localized strain fields. Detailed structural and optical characterization of these architectures reveals unique edge- and strain-mediated photoluminescence that is localized and significantly red-shifted in energy. Our results highlight how rational design of low-dimensional materials can enable future optoelectronic and quantum device goals.

SESSION NM06.04 Ultrafast/Light/Photonics
Session Chairs: Divine Kumah and Harikrishnan Nair
Sunday Afternoon, April 18, 2021
NM06

4:00 PM *NM06.04.01

Late News: Controlled Spin Dynamics in Layered Antiferromagnet MnPS₃ via Sub-Gap Optical

Excitation of Orbitals and Lattice Mattias Matthiesen¹, Jorrit Hortensius¹, Dmytro Afanasiev¹, Andrea Caviglia¹, Eugenio Coronado², Peter Steeneken¹, Makars Šiškins¹, Martin Lee¹, Samuel Mañas-Valero² and Herre van der Zant¹; ¹Kavli Institute of Nanoscience, Netherlands; ²Universitat de Valencia, Spain

It has in recent years become clear that optical pumping of specific solid state modes using ultrashort pulses of light can provide highly targeted access to magnetic order. Resonant excitation of phonons or of electronic orbitals in magnetic ions has been shown to drive non-equilibrium magnetic dynamics, modify magnetic interactions and induce magnetic phase transitions. Such demonstrations have been mainly focused on three-dimensional crystals, and it is of interest to expand this approach to two-dimensional magnets where the magnetic order is intrinsically fragile and is expected to be more sensitive to perturbation. Here, using time-resolved optical second harmonic generation, we study picosecond dynamics of the antiferromagnetic order in the layered van der Waals antiferromagnet manganese thiosulfate (MnPS₃) in response to excitation of various sub-gap transitions. We demonstrate that resonant pumping of an orbital *d-d* transition within the Mn²⁺ electronic multiplet launches coherent antiferromagnetic spin precession, while excitation of high-energy phonons leads to quasithermal incoherent magnetic melting.

4:25 PM NM06.04.02

Ultrafast Optical Control of Magnetism in a Topological Insulator Hari Padmanabhan¹, Nathan Koocher², Vladimir Stoica¹, Peter Kim³, Maxwell Poore³, Danilo Puggioni², Seng Huat Lee¹, Richard Schaller², Zhiqiang Mao¹, Richard Averitt³, James Rondinelli² and Venkatraman Gopalan¹; ¹The Pennsylvania State University, United States; ²Northwestern University, United States; ³University of California, San Diego, United States

Magnetic order in topologically non-trivial materials gives rise to new, unconventional topological phases.

These phases exhibit unique properties such as quantized electronic transport and magnetoelectric coupling, which can result in potentially groundbreaking applications in error-tolerant quantum computing and spintronics. The key to harnessing these properties lies in being able to control magnetism in these materials. In this work, we demonstrate that ultrafast optical pulses can be used to coherently control magnetism in the topological insulator MnBi_2Te_4 , through coupling to optical phonons. First, we find using Raman spectroscopy that optical phonons strongly modulate the exchange interaction, resulting in large changes in phonon energies and linewidths across the magnetic transition in MnBi_2Te_4 . The spin-induced phonon renormalization observed here is the largest reported in any two-dimensional magnet to date. We exploit this strong spin-phonon coupling to optically engineer the spin Hamiltonian through ultrafast modulation of the exchange interaction through displacively excited coherent phonons. Using a time-resolved Kerr effect probe, we find that this results in a coherent modulation of the magnetization at femtosecond timescales. Our work thus unlocks a new mode of control of magnetism in topological materials.

4:40 PM *NM06.04.03

Using Ultrafast Electron Diffraction to Visualize Lattice Dynamics at Two-Dimensional van der Waals Interfaces Archana Raja; Lawrence Berkeley National Laboratory, United States

Two-dimensional (2D), van der Waals crystals allow the creation of arbitrary, atomically precise heterostructures simply by stacking disparate monolayers without the constraints of covalent bonding or epitaxy. Charge and energy transfer processes at these novel junctions is an area of burgeoning interest both from the fundamental and application points of view. At a type II heterojunction between two 2D semiconductors, ultrafast charge transfer has been previously determined to occur on the order of 10's of femtoseconds after photoexcitation. However, the coupling between the lattice degrees of freedom of the photoexcited monolayers remains less understood. We use ultrafast electron diffraction to directly visualize lattice dynamics in the individual monolayers of the van der Waals heterojunction. We are able to track the transfer of energy from one layer to another by following the change in intensity of the Bragg peaks after photoexcitation. With the aid of first principles calculations, we are able to shed light on the role of lattice dynamics during ultrafast electronic processes at 2D van der Waals heterojunctions.

5:05 PM NM06.04.04

Exploring Nonlinear Light-Matter Interaction and Electrostatic Doping in 2D Quantum Materials Xiaofeng Qian; Texas A&M University, United States

The ability to achieve noninvasive detection and efficient control of electric and magnetic orders in 2D quantum materials is of great importance to the development of ultrathin quantum electronics, optics, spintronics. Here we present our recent theoretical predictions of nonlinear response and sensing of 2D topological materials [1, 2, 3] and electrostatic doping induced switching of magnetic orders in 2D high Curie temperature ferromagnetic semiconductors CrSBr and CrSeBr [4]. First, we will show that time-reversal invariant few-layer WTe_2 holds out-of-plane polarization which can be switched via slight interlayer sliding under vertical electric field. Moreover, ferroicity-driven switching of nonreciprocal nonlinear photocurrent [5] such as ferroelectric nonlinear anomalous Hall effect can be achieved in few-layer WTe_2 by utilizing the intrinsic coupling among nonlinear susceptibility, crystalline symmetry, and quantum geometry of electronic states [1], paving theoretical foundation for nonlinear quantum memory such as Berry curvature memory. We will discuss the very recent experimental demonstration of ferroelectric nonlinear anomalous Hall effect in tri-layer WTe_2 [2]. We will also introduce our recent work on nonlinear photocurrent in PT-symmetry magnetic topological quantum materials [3], where magnetic shift photocurrent can be magnetically switched between two antiferromagnetic states in bilayer antiferromagnetic MnBi_2Te_4 . Moreover, external electric field can break PT-symmetry and enable normal shift photocurrent that are electrically switchable and tunable down to a few THz regime, suggesting bilayer antiferromagnetic MnBi_2Te_4 as a tunable platform with rich THz and magneto-optoelectronic applications. Finally, we will briefly present our recent theoretical prediction of long-range two-dimensional ferromagnetism in monolayer semiconductors CrSBr and CrSeBr with high Curie temperature of $\sim 150\text{K}$ [4] which was also experimentally demonstrated recently, offering potential alternatives to dilute magnetic

semiconductors. We show that electrostatic doping can switch magnetization easy axis, providing unprecedented opportunities for 2D spintronics such as spin valves and spin FETs [4].

References: [1] npj Computational Materials 5, 119 (2019). [2] Nature Physics 16, 1028-1034 (2020). [3] arXiv Preprint, arXiv:2006.13573 (2020). [4] Applied Physics Letters 117, 083102 (2020). [5] Science Advances 5, eaav9743 (2019).

5:20 PM NM06.04.05

Coupling Monolayer WS₂ with a Photonic Polymer Waveguide Through Mode-Center Placement

Angelina Frank, Justin Zhou Yong, James Grieve, Ivan Verzhbitskiy, Alexander Ling and Goki Eda; National University of Singapore, Singapore

The core requirement and challenge for integrated hybrid photonic platforms is effective coupling between the guided mode of a photon-routing structure and a photo-active material. In traditional (e.g. silicon nitride) platforms, the mode center is inaccessible which significantly limits the interaction between material and platform. Here, we overcome this limitation through integration of an atomically thin 2D material (WS₂) on hBN into the mode center of a novel elastomeric single-mode rib waveguide. This is achieved through transfer of the emitter onto a precured polymer layer and its subsequent bonding to the supporting polymer matrix by oxygen-plasma activation. We verify waveguide-emitter coupling by various means: observing polarization-dependent excitation of the integrated emitter when excited through the waveguide, collection of emission from the guide's output face, as well as polarization-dependent extinction in transmission measurements. Representative for room-temperature curing polymers, this work opens up new ways for the integration of (single-photon) emitters into polymer-based optical circuits.

5:35 PM *NM06.04.06

Optical Spectroscopy of Twisted Heterostructures of Transition Metal Dichalcogenides Hyeonsik Cheong; Sogang University, Korea (the Republic of)

Heterostructures of transition metal dichalcogenides (TMDs) have been extensively studied as the alignment of the bands in the constituent materials allow for manipulation of optoelectronic and transport properties. The band offset between the bands is usually the most important parameter in determining the physical properties of these structures. However, as evidenced in the so-called 'magic-angle graphene' [1], the twist angle between the crystallographic directions of the two layers is an important parameter that affect the physical properties. As the twist angle between two layers of a given set of materials is varied, the phonon spectrum as well as the electronic band structure and optoelectronic properties change systematically. Furthermore, at very small twist angles, atomic-scale lattice reconstruction [2] is observed and should be accounted for in describing the physical properties of heterostructures. In this talk, I will present some of the latest experimental data on the phonon spectra and the band structures from twisted heterostructures of TMDs.

References

- [1] Cao Y., *et al.*, *Nature* (2018); **556**, 43; *Ibid.* 80.
- [2] Yoo H., *et al.*, *Nature Materials* (2019), **18**, 448.

SESSION NM06.05: 2D Magnetism

Session Chairs: Pengcheng Dai, Divine Kumah and Srinivasa Rao Singamaneni

Sunday Afternoon, April 18, 2021

NM06

6:30 PM NM06.05.01

Ab Initio Spin-Phonon Relaxation in Graphene in Presence of External Electric Field and hBN Adela

Habib¹, Junqing Xu², Yuan Ping² and Ravishankar Sundararaman¹; ¹Rensselaer Polytechnic Institute, United States; ²University of California, Santa Cruz, United States

For the last two decades, graphene's impressive prospect as a material to revolutionize technologies from electronics to spintronics and quantum computing has prompted numerous studies of its spin dynamics. One of the puzzling phenomena in these studies has been a large discrepancy, at best by two orders of magnitude, between the observed and the predicted spin relaxation lifetimes. Several theoretical studies based on various models have proposed that external factors including but not limited to the substrate and externally applied electric field can influence relaxation reducing spin lifetimes from the predicted microseconds to nanoseconds in measurements. In particular, both these factors are expected to break space-inversion symmetry enhancing spin-orbit coupling strength significantly and consequently increasing spin relaxation rates in graphene. However, past theoretical models do not capture the effects of real substrates and hence do not explain the spin lifetime anisotropy at a graphene/hBN interface with an applied electric field. Consequently, a first-principles approach to explain these relaxation channels is necessary.

Here, we present our investigations of spin dynamics and in particular spin-phonon relaxation fully from first-principles in single layer graphene in the presence of an external electric field and/or hBN substrate. Using our *ab initio* computational method based on density matrices[1], we evolve electron(hole) spins for microseconds after an initial perturbation by a small magnetic field all the while fully accounting for their scattering against phonons. From our results, we predict that room-temperature spin lifetimes in graphene range from hundreds of picoseconds to a few nanoseconds in the presence of an external electric field or hBN. We find that the out-of-plane vs. in-plane spin lifetime anisotropy is greater than 0.5 in graphene on hBN, in a remarkable agreement with experimental observations but deviates from the general consensus in model-based theoretical studies. We report spin anisotropy of 0.5 only as a result of external applied electric field on free-standing graphene confirming its origin to the Bychkov-Rashba type spin-orbit field as widely accepted in theoretical studies. Our findings suggest that both substrate-induced spin-orbit fields and substrate phonons influence spin relaxation substantially and reduce lifetimes to the orders observed in experiments. [1] J. Xu et al, Nat. Commun. 11, 2780 (2020)

This work is funded by the National Science Foundation under grant number 1904547, and Adela Habib acknowledges support from the American Association of University Women(AAUW) fellowship program.

6:45 PM *NM06.05.02

Chiral and Helical Edge Transport in High Mobility 2D Materials Chun Ning (Jeanie) Lau; The Ohio State University, United States

Two-dimensional (2D) materials and heterostructures provide excellent platforms for exploring and understanding chiral and helical edge transport. Here we present our works on magnetotransport in high mobility 2D heterostructures. In few-layer black phosphorus devices, we use p-p'-p junctions to study the equilibration and transmission of edge states at the interfaces of regions with different charge densities. We observe both full equilibration, where all edge channels equilibrate and are equally partitioned at the interfaces, and partial equilibration, where only equilibration only takes place among modes of the same spin polarization. Furthermore, the inner p'-region with low-doping level in the junction can function as a filter for highly doped p-regions which demonstrates gate-tunable transmission of edge channels. In Bernal-stacked tetralayer graphene, we observe two topologically distinct phases supporting helical edge states at the charge neutrality point. As the magnetic field and out-of-plane displacement field D are varied, we observe a phase diagram consisting of an insulating phase and two metallic phases, with 0, 1 and 2 helical edge states, respectively. These phases are accounted for by a theoretical model that relates their conductance to spin-polarization plateaus. Transitions between them arise from a competition among inter-layer hopping, electrostatic and exchange interaction energies.

7:10 PM *NM06.05.03

Stacking Dependent 2D Magnetism Shiwei Wu; Fudan University, China

In van der Waals layered materials, the symmetries and functionalities could be controlled by modifying the stacking order through rotation and translation between the layers. Whereas most previous work has focused on the electronic and optical properties associated with the van der Waals stacking, the recent discovery of magnetism in 2D materials, achieved through both mechanical exfoliation and molecular beam epitaxy (MBE), provides an exciting opportunity to explore the effects of stacking order on a material's magnetic properties. In this talk, I will present two of our recent studies in this direction. 1) By discovering a giant nonreciprocal second harmonic generation from layered antiferromagnetism in mechanically exfoliated bilayer CrI₃, we revealed the underlying C_{2h} symmetry, and thus monoclinic stacking order in bilayer CrI₃, providing crucial structural information for the microscopic origin of layered antiferromagnetism. 2) By using the molecular beam epitaxy to grow monolayer and bilayer CrBr₃ and in situ characterization with a spin-polarized scanning tunneling microscopy and spectroscopy, we observed that while individual CrBr₃ monolayer is ferromagnetic, the interlayer coupling in bilayer depends strongly on the stacking structure and can be either ferromagnetic or antiferromagnetic. Thus, the direct correlation between stacking order and interlayer magnetism pave the way for manipulating 2D magnetism.

7:35 PM NM06.05.04

2D Correlations in the van der Waals Ferromagnet CrBr₃ Using High Frequency Electron Spin

Resonance Spectroscopy Christian Saiz¹, Jose A. Delgado¹, Johan van Tol², Fazel Fallah Tafti³ and Srinivasa Rao Singamaneni¹; ¹The University of Texas at El Paso, United States; ²Florida State University, United States; ³Boston College, United States

Broadening the knowledge and understanding on the magnetic correlations in van der Waals layered magnets is critical in realizing their potential next-generation applications. In this study, we employ high frequency (240 GHz) electron spin resonance (ESR) spectroscopy on plate-like CrBr₃ to gain insight into the magnetic interactions as a function of temperature (200 – 4 K) and the angle of rotation θ . We find that the temperature dependence of ESR linewidth is well described by the Ginzberg-Landau critical model as well as Berezinskii-Kosterlitz-Thouless (BKT) transition model, indicative of the presence of two-dimensional (2D) correlations. Furthermore, our findings show that the resonance field follows a $(3\cos^2\theta - 1)$ -like angular dependence, while the linewidth follows a $(3\cos^2\theta - 1)^2$ -like angular dependence. This observed angular dependence of the resonance field and linewidth further confirm an unanticipated 2D magnetic behavior in CrBr₃. This behavior is likely due to the interaction of the external magnetic field applied during the ESR experiment that allows for the mediation of long-range vortex-like correlations between the spin clusters that possibly formed due to magnetic phase separation. This study demonstrates the significance of employing spin sensitive techniques such as ESR to better understand the magnetic correlations in similar van der Waals magnets and suggests the need to study the magnetic correlations in CrBr₃ more closely.

7:50 PM NM06.05.05

Creating Half-Metallicity in Two-Dimensional Magnetoelectric Materials Cheng Gong¹, Shi-Jing Gong², Geunsik Lee³, Andrew Rappe⁴ and Xiang Zhang⁵; ¹University of Maryland, United States; ²East China Normal University, China; ³Ulsan National Institute of Science and Technology, Korea (the Republic of); ⁴University of Pennsylvania, United States; ⁵University of California, Berkeley, United States

Magnetic two-dimensional (2D) materials [1, 2] opened up unprecedented opportunities for nanoscale spintronic devices in the miniaturized form factor. With the aggressive pursuit for dimensional downscaling is the other paramount endeavor for high energy efficiency [3]. Under the umbrella of the pursuit for the low energy consumption, the realization of high spin polarization via minimal amount of electrical input is a critical prerequisite. In this talk, I will introduce two schemes [4, 5] to create half-metallicity in 2D layered material systems. In scheme I [4], electric field will be applied across the bilayer A-type antiferromagnetic 2D materials. In scheme II [5], a multiferroic superlattice consisting of alternative ferroelectrics and A-type antiferromagnets is constructed for the ferroelectric control of half-metallicity. Both schemes are experimentally relevant, and

will provide valuable contributions to the developments of miniaturized high-efficiency spintronic devices.

- [1] C. Gong *et al.*, Discovery of intrinsic ferromagnetism in two-dimensional van der Waals crystals, *Nature* 546, 265–269 (2017).
- [2] C. Gong, X. Zhang, Two-dimensional magnetic crystals and emergent heterostructure devices, *Science* 363, eaav4450 (2019).
- [3] C. Gong *et al.*, Multiferroicity in atomic van der Waals heterostructures, *Nat. Commun.* 10, 2657 (2019).
- [4] S.-J. Gong, *et al.*, Electrically induced 2D half-metallic antiferromagnets and spin field effect transistors, *Proc. Natl. Acad. Sci.* 115, 8511–8516 (2018).
- [5] E.-W. Du, *et al.*, Ferroelectric switching of pure spin polarization in two-dimensional electron gas, *Nano Lett.* 20, 7230–7236 (2020).

8:05 PM *NM06.05.06

Gigantic Current Control of Coercive Field and Intrinsic Spin-Orbit-Torque in Topological van-der-Waals Ferromagnetic Metal Fe₃GeTe₂ Kaixuan Zhang; Seoul National University, Korea (the Republic of)

Controlling magnetic states by a small current is essential for the next-generation of energy-efficient spintronic devices. The emerging spin-orbit-torque-Magnetic-Random-Access-Memory (SOT-MRAM) is the most promising commercial magnetic-RAM in the near future[1]. Unfortunately, the switching current density and power dissipation are still too high for conventional magnet/heavy-metal based SOT-MRAM[1], prompting the development of new large-SOT systems. On the other hand, very recently, van-der-Waals (vdW) magnetic materials have rapidly emerged as key members of the field of two-dimensional materials and device physics [2-7]. Among all the magnetic vdW materials, Fe₃GeTe₂ received special attention because it is the only topological ferromagnetic vdW metal[8].

Here we report that surprisingly an in-plane current can tune the magnetic state of nm-thin vdW ferromagnet Fe₃GeTe₂ from a hard magnetic state to a soft magnetic state, through substantial reduction of the coercive field. This surprising finding is possible because the in-plane current produces a highly unusual type of gigantic spin-orbit torque for Fe₃GeTe₂, which is directly related to the large Berry curvature and so its band topology. And we further demonstrate a working model of a new nonvolatile magnetic memory based on the principle of our discovery in Fe₃GeTe₂, controlled by a tiny current. Our findings open up a new window of exciting opportunities for magnetic vdW materials with potentially huge impacts on the future development of spintronic.

- [1] M. Cubukcu, O. Boulle, M. Drouard, K. Garello, C. O. Avci, I. M. Miron, J. Langer, B. Ocker, P. Gambardella, G. Gaudin, *Appl. Phys. Lett.* 2014, 104, 042406.
- [2] J. G. Park, *J. Phys. Condens. Matter* 2016, 28, 301001.
- [3] J. U. Lee, S. Lee, J. H. Ryoo, S. Kang, T. Y. Kim, P. Kim, C. H. Park, J. G. Park, H. Cheong, *Nano Lett.* 2016, 16, 7433.
- [4] B. Huang, G. Clark, E. Navarro-Moratalla, D. R. Klein, R. Cheng, K. L. Seyler, D. Zhong, E. Schmidgall, M. A. McGuire, D. H. Cobden, W. Yao, D. Xiao, P. Jarillo-Herrero, X. Xu, *Nature* 2017, 546, 270.
- [5] C. Gong, L. Li, Z. Li, H. Ji, A. Stern, Y. Xia, T. Cao, W. Bao, C. Wang, Y. Wang, Z. Q. Qiu, R. J. Cava, S. G. Louie, J. Xia, X. Zhang, *Nature* 2017, 546, 265.
- [6] K. S. Burch, D. Mandrus, J. G. Park, *Nature* 2018, 563, 47.
- [7] S. Kang, K. Kim, B. H. Kim, J. Kim, K. I. Sim, J.-U. Lee, S. Lee, K. Park, S. Yun, T. Kim, A. Nag, A. Walters, M. Garcia-Fernandez, J. Li, L. Chapon, K.-J. Zhou, Y.-W. Son, J. H. Kim, H. Cheong, J.-G. Park, *Nature* 2020, 583, 785.
- [8] K. Kim, J. Seo, E. Lee, K. T. Ko, B. S. Kim, B. G. Jang, J. M. Ok, J. Lee, Y. J. Jo, W. Kang, J. H. Shim, C. Kim, H. W. Yeom, B. Il Min, B. J. Yang, J. S. Kim, *Nat. Mater.* 2018, 17, 794.

8:00 AM *NM06.06.01

Giant c-axis Nonlinear Anomalous Hall Effect in T_d -MoTe₂ Adam W. Tsen¹, Archana Tiwari¹, Fangchu Chen¹, Shazhou Zhong¹, Elizabeth Druke², Jahyun Koo³, Austin Kaczmarek², Cong Xiao⁴, Jingjing Gao⁵, Xuan Luo⁵, Qian Niu⁴, Yuping Sun⁵, Binghai Yan³ and Liuyan Zhao²; ¹University of Waterloo, Canada; ²University of Michigan–Ann Arbor, United States; ³Weizmann Institute of Science, Israel; ⁴The University of Texas at Austin, United States; ⁵Chinese Academy of Sciences, China

We report the observation of a giant c-axis nonlinear anomalous Hall effect in the non-centrosymmetric T_d phase of MoTe₂, where application of an in-plane current generates a Hall field perpendicular to the layers. By measuring samples across different thicknesses and temperatures, we find that the nonlinear susceptibility obeys a universal scaling with sample conductivity. Application of higher bias yields an extremely large anomalous Hall ratio and conductivity.

8:25 AM NM06.06.02

Spin-Dependent Transport Through Colloidal Quantum Dots—The Role of the Exchange Interaction John P. Philbin¹, Amikam Levy², Prineha Narang¹ and Wenjie Dou³; ¹Harvard University, United States; ²Bar-Ilan University, Israel; ³University of California, Berkeley, United States

The study of spin transport through semiconductor quantum dots is experiencing a renaissance due to recent advances in nano-fabrication and the realization of quantum dots as candidates for quantum computing. In this work, we combine atomistic electronic structure calculations with quantum master equation methods to study the transport of electrons and holes through quantum dots coupled to two leads with a voltage bias. We find that a competition between the energy spacing between the two lowest quasiparticle energy levels and the strength of the exchange interaction determines if a spin singlet or triplet is the lowest energy two quasiparticle state. Specifically, the low density of electron states results in a spin singlet being the lowest energy two electron state whereas, in contrast, a spin triplet is the lowest energy two hole state due to the high density of states and significant exchange interaction. The exchange interaction is also responsible for spin blockades that our transport calculations suggest persist up to temperatures as high as 77 K for colloidal quantum dots with small core diameters. Lastly, we relate the findings of this study to both optical experiments and the preparation and manipulation of singlet and triplet spin states in quantum dots using voltage biases.

This work is partially supported by the Army Research Office MURI (Ab-Initio Solid-State Quantum Materials) under Grant No. W911NF-18-1-0431. JP is a Ziff Fellow at the Harvard University Center for the Environment.

8:40 AM NM06.06.03

Observing Quantum-Confinement Effects on the In-Plane Translational Motion of Excitons in CdSe Nanoplatelets Laurens Siebbeles; Delft University of Technology, Netherlands

Colloidal CdSe nanoplatelets (NPLs) can be made with a thickness of atomic precision in the range of about one to a few nanometers only. The lateral sizes are of the order of several to tens of nanometers. The thickness is less than the bulk exciton bohr radius and consequently leads to strong effects of spatial confinement on the internal energy of an exciton. Variation of the thickness of a NPL thus allows one to tune the photoluminescence (PL) and optical absorption spectra.

Interestingly, however, the experimental shape of PL and absorption spectra also depends on the lateral sizes of a NPL. To date, the latter has not received much attention, with the exception of a few (mainly theoretical) studies and the origin of this effect has been inconclusive.

We measured the PL and absorption spectra for a series of NPLs with different lateral sizes and find that the dependence of the optical spectra on the lateral size is fully explained by taking into account the quantum-confinement effects on the translational motion of excitons in the plane of the NPLs. The spectra of all samples considered can be reproduced very accurately by a theoretical description of exciton energies and oscillator strengths based on the quantum mechanical particle-in-a-box model and the known size-distribution of the NPLs.

8:55 AM *NM06.06.05

Magnetic van der Waals Materials Under Pressure Sergey Budko; Ames Laboratory, Iowa State University, United States

Magnetic van der Waals (vdW) materials are considered as promising candidates for low-dimensional magnetism since their vdW nature suggests the possibility of exfoliation down to the monolayer level and their low crystalline symmetry implies an intrinsic magnetic anisotropy. An understanding of the details of their bulk magnetic structure and the tunability of their properties is an important step towards potential applications. In this talk, a brief overview of the effects of hydrostatic pressure magnetic vdW materials will be presented with a particular emphasis on the recent magnetization and heat capacity results under pressure for VI_3 and CrPS_4 , where a complex interplay between different phases is observed at moderate pressure values.

Work at the Ames Laboratory was supported by the US Department of Energy, Office of Science, Basic Energy Sciences, Materials Sciences and Engineering Division. Ames Laboratory is operated for the US Department of Energy by Iowa State University under Contract No. DE-AC02-07CH11358.

9:20 AM *NM06.06.06

Long and Short-Range Ordered Magnetism in Honeycomb $\text{Na}_2\text{Ni}_2\text{TeO}_6$ Nathan Episcopo¹, Po-Hao Chang¹, Thomas W. Heitmann², Kinley Wangmo¹, James M. Guthrie², Magdalena Fitta³, Ryan Klein⁴, Narayan Poudel⁵, Krzysztof Gofryk⁵, Rajendra R. Zope¹, Craig Brown⁶ and Harikrishnan S. Nair¹; ¹The University of Texas at El Paso, United States; ²University of Missouri–Columbia, United States; ³Polish Academy of Sciences, Poland; ⁴National Renewable Energy Laboratory, United States; ⁵Idaho National Laboratory, United States; ⁶National Institute of Standards and Technology (NIST), United States

Low dimensional magnetic lattices are being studied recently owing to the possibility of realizing flatbands in the magnon spectrum which can then lead to dissipation-less spin transport and associated magnon Hall effect. One could expect to find a magnon insulator, similar to a topological insulator. In the present work we present a rather less-studied honeycomb material $\text{Na}_2\text{Ni}_2\text{TeO}_6$. Our samples of $\text{Na}_2\text{Ni}_2\text{TeO}_6$ conform to hexagonal $P6_3/mcm$ space group with refined lattice parameters, $a = 5.2023(1)$ Å and $c = 11.1552(8)$ Å. The physical properties of the present sample are characterized using magnetic susceptibility and specific heat, both of which confirm a phase transition at 28 K. Application of 8 T magnetic field only slightly polarizes the moment at the transition. We obtain a Curie-Weiss temperature of $-9.7(2)$ K and effective paramagnetic moment of $2.24(4)$ μ_B/Ni . This matches well with the spin-only moment of Ni^{2+} . Neutron diffraction experiments are used to determine the static magnetic structure and inelastic neutron scattering reveals a rather flat spin wave excitation at 5 meV. Combining neutron diffraction with density functional theory computations, we obtain a handle on the magnetism of honeycomb layers of Ni in $\text{Na}_2\text{Ni}_2\text{TeO}_6$.

SESSION NM06.07: Poster Session: Manipulation and Detection of Physical Properties of Two-Dimensional Quantum Materials

Session Chairs: Divine Kumah, Srinivasa Rao Singamaneni and Srinivasa Rao Singamaneni

Monday Morning, April 19, 2021

10:30 AM - 11:15 AM

NM06

NM06.07.02

***In Situ* Electron Spin Resonance Studies of MoS₂ During the Hydrogen Evolution** Jose A. Delgado¹, Yulu Ge¹, Dawn Blazer¹, Chinnathambi Karthik², Russell Chianelli¹, Dino Villagran¹ and Srinivasa Rao Singamaneni¹; ¹The University of Texas at El Paso, United States; ²Boise State University, United States

Finding energy efficient, earth-abundant catalysts to aid in the production of hydrogen has been the subject of intense research for several decades. Characterizing new catalysts is an important step in replacing rare-earth Pt-based catalysts for the hydrogen evolution reaction (HER). To the best of our knowledge, the earth-abundant catalyst MoS₂ has not been studied under HER reaction conditions using spin sensitive techniques. Therefore, our objective is to study the relationship between crystal defects and reactivity on the surface and edge sites of hydrothermally grown nanocrystalline MoS₂ using *in situ* Electron Spin Resonance (ESR). For this purpose, we have developed an *in situ* ESR cell to characterize MoS₂ during HER. This technique is useful for tracing the dynamics of conduction electrons and ferromagnetic/paramagnetic species, which can be used to understand reaction mechanisms and charge transfer processes. The charge transfer mechanisms and defect – reactivity relationships in MoS₂ during HER will be discussed in terms of this highly sensitive *in situ* technique.

NM06.07.03

Proton Fluence-Dependent Magnetic Properties of Irradiated van der Waals CrSiTe₃ Hector Iturriaga¹, Rubyann Olmos¹, Dawn Blazer¹, Luis M. Martinez¹, Kinjal Gandha², Cajetan I. Nlebedim², Yu Liu³, Cedomir Petrovic³, Lin Shao⁴, Qiang Wang⁵, Ju Chen⁶, Martin L. Kirk⁶ and Srinivasa Rao Singamaneni¹; ¹The University of Texas at El Paso, United States; ²Ames Laboratory, United States; ³Brookhaven National Laboratory, United States; ⁴Texas A&M University, United States; ⁵West Virginia University, United States; ⁶The University of New Mexico, United States

The emergence of novel properties in layered van der Waals magnets subject to external stimuli, such as exfoliation or doping, creates opportunities to favorably adjust their characteristics for the production of functional devices [Nat Rev Phys **1**, 646–661 (2019)]. In particular, Mn₃Si₂Te₆, a vdW ferrimagnet, has shown enhanced magnetization after irradiation [Appl. Phys. Lett. **116**, 172404 (2020)]. Therefore, we present the effects of proton irradiation on the magnetic properties of CrSiTe₃ (CST), a similar compound that has garnered attention for its potential use in atomically thin devices. Bulk CST is a layered van der Waals semiconducting ferromagnet with a previously reported Curie temperature (T_C) of 32 K [Phys. Rev. Materials **3**, 014001]. In this study, bulk CST crystals were irradiated at several fluences ranging from 10¹⁵ – 10¹⁸ protons/cm². Low-temperature SQUID magnetometry measurements reveal changes in the reported behavior of the magnetic phases of CST; for example, we find a T_C of up to 37 K in the sample irradiated with 10¹⁸ protons/cm². The evolution of the temperature and magnetic field dependence of the magnetization provides further insight into the differences between pristine and irradiated CST. Furthermore, the magnetic properties of CST will be described by our experimental findings on saturation magnetization, coercivity, T_C, and magnetocrystalline anisotropy.

NM06.07.04

Stability, Electronic States and Magnetization of WTe₂ Edges with Cu Adsorbates Zexi Lu, Micah P. Prange and Peter V. Sushko; Pacific Northwest National Laboratory, United States

Understanding the intrinsic stability, electronic and magnetic properties of functional materials, and their response to external chemical environments is crucial for their application in devices. Two-dimensional (2D) transition metal dichalcogenides (TMDCs) draw great attention due to their unusual electronic properties promising for applications in quantum information sciences (QIS). In particular, edges in some TMDCs exhibit non-trivial topological states that enable spin-momentum locking critical for realization of topological qubits. Utilization of these states in practical devices depends on our ability to control the details of their properties upon integrating them into larger materials systems. It is therefore critical to understand how the structure,

stability, and electronic properties of these edges are affected by their interfaces with other materials and by intrinsic and extrinsic defects.

In this study, we use first-principles simulations to quantify the stability of several types of edges in pristine and functionalized 1T'-phase WTe_2 and describe their electronic properties. We consider one-dimensional (1D) edges along $\{010\}$, $\{100\}$, $\{110\}$ and $\{310\}$ lattice directions and investigate the effects of the interactions with Cu atoms and clusters depending on the distribution and concentration of the adsorbed Cu species. We find that Cu atoms prefer to either cluster or form a quasi-1D chain along (010) edge, depending on the details of its atomic termination. Our simulations also predict that Cu clusters introduce magnetization and break the non-trivial topological order of WTe_2 protected by time-reversal symmetry. In contrast, the quasi-1D chain of the Cu atoms introduces a deformation that shifts the energy levels of the edge states, most of which remain intrinsic to WTe_2 and support quantum spin Hall effect. Our study suggests avenues for a controlled modification of the critical properties of WTe_2 through the control of its external chemical environments, which can be potentially generalized to a broader class of TMDCs and provide guidance for the design of new devices and manufacturing process.

NM06.07.05

Fluence -Dependent Magnetic Properties of Proton Irradiated Antiferromagnets MPS_3 (M= Mn, Fe, and Ni) Samir A. Muniz¹, Hector Iturriaga¹, Luis M. Martinez¹, Lin Shao², Suhan Son³, Je-Geun Park³ and Srinivasa Rao Singamaneni¹; ¹The University of Texas at El Paso, United States; ²Texas A&M University, United States; ³Institute for Basic Science, Korea (the Republic of)

Magnetic ordering in the two-dimensional (2D) limit has been one of the most important research topics in condensed matter physics for the past couple of years. Layered quasi 2D materials such as MnPS_3 , FePS_3 and NiPS_3 form a unique class of compounds. All three compounds are isostructural with the magnetic lattice being the two-dimensional honeycomb, the spin dimensionalities for the three compounds are different. While MnPS_3 is best described by the isotropic Heisenberg Hamiltonian, FePS_3 is most effectively described by the Ising model and NiPS_3 by the anisotropic Heisenberg Hamiltonian. The materials order antiferromagnetically at low temperatures, the Neel temperatures being 78,123 and 155K, respectively. Our main objective of this study is to investigate the magnetic properties of the above compounds upon proton irradiation, which is the versatile strategy in tuning the magnetic properties¹. These crystals were subjected to proton irradiation at fluences ranging from unirradiated, 1×10^{15} , 5×10^{15} , 1×10^{16} and 5×10^{16} protons/cm². We performed Raman, electron spin resonance, and magnetization measurements on all the proton irradiated samples, including the pristine crystals. We will present and discuss the comprehensive experimental findings, and offer the possible explanation for the observed trends.

NM06.07.06

Magnetic Properties of Bulk CrBr_3 Crystals Under Hydrostatic Pressure Rubyann Olmos¹, Shamsul Alam¹, Hector Iturriaga¹, Kinjal Gandha², Ikenna Nlebedim², Fazel Fallah Tafti³, Rajendra R. Zope¹ and Srinivasa Rao Singamaneni¹; ¹The University of Texas at El Paso, United States; ²Ames Laboratory, United States; ³Boston College, United States

The van der Waals class of materials offer a new approach for two-dimensional magnetism allowing spin fluctuations to be tuned upon exfoliation of layers. Moreover, it has recently been shown that spin lattice coupling and long-range magnetic order can be modified with pressure in van der Waals materials. In this study we look to understand the magnetic structure and properties of CrBr_3 , a member of the highly anisotropic MX_3 (M = Cr, V; X = Cl, Br, I) compounds. As research on pressure induced magnetic properties of CrX_3 is at its nascent stage, we seek to gain further insight into whether pressure increases or decreases the long-range magnetic ordering on bulk CrBr_3 crystals. The application of pressure (0 - 0.8 GPa) shows a decrease in saturation magnetization with small decrease in the Curie temperature from 32.8 K to 29.2 K at 0.8 GPa. Density functional theory calculations with pressure from 0 - 1 GPa show a reduction in volume and interplanar distance as pressure increases. To further understand magnetic properties with applied pressure we calculate the

magnetocrystalline anisotropy energy (MAE) and exchange coupling parameter (J). There is minimal decrease in MAE and the first nearest neighbor interaction (J_1) with a Hubbard U parameter, $U = 0$ eV, shows a reduction in J_1 with respect to pressure. Overall, CrBr₃ displays ferromagnetic interlayer coupling and the calculated parameters match well with experiment. We also explore the magnetocaloric effect as a function of pressure for this compound and in the future, further insight will be collected on the local electronic and magnetic structure of this material by employing x-ray magnetic circular dichroism (XMCD) (Cr L_{2,3} edge) measurements at high pressure (0-10 GPa).

NM06.07.07

Probing the Stability of Shastry Sutherland Lattice in Er₂Pd₂Sn and Er₂Pd₂In Gicela G. Saucedo Salas¹, Baidyanath Sahu², C. M. Naveen Kumar³, Andre Strydom², Stuart Calder⁴, Qiang Zhang⁴ and Harikrishnan S. Nair¹; ¹The University of Texas at El Paso, United States; ²University of Johannesburg, South Africa; ³Institut für Festkörperphysik, Austria; ⁴Oak Ridge National Laboratory, United States

The Shastry-Sutherland lattice-based compounds have perennial interest in the condensed matter physics community owing to the quantum phases that it realizes due to frustration. The R_2T_2X intermetallic compounds (R = rare earth, T = transition metal, X = main group), have been reinvestigated recently owing to the spin liquid state in the underlying Shastry-Sutherland lattice (SSL) formed by the *rare earth* [1, 2]. These compounds crystallizing in the Mo₂FeB₂ structure type display an interplay of frustration and quantum criticality. For the current study, we have selected the less-investigated Er₂Pd₂In and Er₂Pd₂Sn. X-ray powder diffraction and subsequent Rietveld refinements confirmed that the compounds were phase-pure and crystallize with tetragonal Mo₂FeB₂ structure. Both the compounds obeyed Curie-Weiss law in the paramagnetic regime, as judged from magnetic susceptibility data, which indicated anti-ferromagnetism. Specific heat data on both the compounds revealed a double peak indicating complex magnetic structure and phase transitions close to 6 K. We will present a detailed analysis of the magnetization and specific heat on both Er₂Pd₂(Sn/In) and the microscopic magnetic structure determined from neutron powder diffraction which indicates an incommensurate wave vector, k (0.09 0.09 0.5).

[1] Shastry B. S. and Sutherland B., Physica B 108B, 1069, 1981

[2] Kim M. S., Aronson M. C., Phys. Rev. Lett. 110, 017201, 2013

SESSION NM06.08: Emergent Magnetic Phenomena

Session Chairs: Divine Kumah, Arun Paramakanti and Srinivasa Rao Singamaneni

Monday Afternoon, April 19, 2021

NM06

1:00 PM NM06.08.01

Late News: Controlling the Anisotropy of a van der Waals Antiferromagnet with Light Dmytro Afanasiev^{1,2}, Jorrit Hortensius¹, Matthias Matthiesen¹, Samuel Mañas-Valero³, Makars Šiškins¹, Martin Lee¹, Edouard Lesne¹, Herre van der Zant¹, Peter Steeneken¹, Boris A. Ivanov⁴, Eugenio Coronado³ and Andrea Cavaglia¹; ¹Delft University of Technology, Netherlands; ²Universität Regensburg, Germany; ³Universitat de València, Spain; ⁴National Academy of Sciences and Ministry of Education and Science, Ukraine

Magnetic van der Waals materials provide an ideal playground for exploring the fundamentals of low-dimensional magnetism and open new opportunities for ultrathin spin-processing devices. The Mermin-Wagner theorem dictates that as in reduced dimensions isotropic spin interactions cannot retain long-range correlations; the order is stabilized by magnetic anisotropy. Here, using ultrashort pulses of light, we demonstrate all-optical control of magnetic anisotropy in the two-dimensional van der Waals antiferromagnet NiPS₃. Tuning the photon energy in resonance with an orbital transition between crystal-field split levels of the nickel ions, we

demonstrate the selective activation of a sub-THz magnon mode with markedly two-dimensional behaviour. The pump polarization control of the magnon amplitude confirms that the activation is governed by the instantaneous magnetic anisotropy axis emergent in response to photoexcitation of electronic orbitals with a lowered symmetry. Our results establish pumping of orbital resonances as a universal route for manipulating magnetic order in low-dimensional (anti)ferromagnets.

1:15 PM *NM06.08.02

Nanoscale Quantum Sensing of Two-Dimensional Spin Systems Patrick Maletinsky; University of Basel, Switzerland

The recent discovery of long-range magnetic order in atomically thin ``van der Waals'' (vdW) crystals [1] has attracted significant attention due to their fundamental and technological interest, including predictions of exotic magnetic phases and unique opportunities to control magnetism at the atomic scale.

I will present recent experiments, where we employ single-spin-based quantum sensors for quantitative, nanoscale probing of atomically thin vdW magnets [2]. Specifically, I will describe experiments, where we employ this technology to address magnetism in the prototypical vdW magnet CrI₃ [3], down to the level of atomic monolayers. Our approach enabled nanoscale imaging of magnetic domains, quantitative determination of CrI₃'s layer-dependent magnetization, and revealed a delicate interplay between magnetic and crystalline order in CrI₃.

Further, I will present recent results where we employ our quantum sensors to study two-dimensional systems of uncompensated magnetic moments that arise on surfaces of specific antiferromagnets [4]. On the use-case of a single-crystal of the prototypical, magnetoelectric antiferromagnet of Cr₂O₃, we establish how these spin systems can act as reports for the underlying antiferromagnetic order parameter and use this principle to gain new insight into the behavior of domain-walls in this antiferromagnet. Our results show remarkably pristine domain wall behavior in this material, and offer new routes to engineered domain-wall behavior and its application in the field of antiferromagnetic spintronics [5].

I will conclude with an outlook of future engineering challenges [6][7] for nanoscale quantum sensors and our ongoing developments of single spin magnetometers for extreme conditions, such as high magnetic fields, millikelvin temperatures or for high-frequency sensors to probe the dynamics of nanomagnetic systems.

B. Huang et al., Nature 546, 270; C. Gong et al, ibid 265 (2017)

L. Thiel et al., Science 364, 973 (2019)

M. Gibertini et al., Nature Nanotechnology 14, 408 (2019)

P. Appel et al., Nano Letters **19**, 1682 (2019)

N. Hedrich et al., arXiv: 2009.08986 (2020)

P. Appel et al., Review of Scientific Instruments **87**, 063703 (2016)

N. Hedrich et al. arXiv:2003.01733 (2020)

1:40 PM *NM06.08.03

Spontaneous Valley Polarization of Interacting Carriers in a Monolayer Semiconductor Scott Crooker; Los Alamos National Laboratory, United States

This talk will discuss recent magneto-absorption optical spectroscopy studies of dual-gated WSe₂ monolayers in high magnetic fields up to 60 T. When doped with a 2D Fermi sea of mobile holes, well-resolved sequences of optical transitions are observed in both left- and right- circular polarization, which unambiguously and separately indicate the number of filled Landau levels (LLs) in both K and K' valleys. This reveals the interaction-enhanced valley Zeeman energy, which is found to be highly tunable with hole density. We exploit this tunability to align the LLs in K and K', and find that the 2D hole gas becomes unstable against small changes in LL filling and can spontaneously valley polarize [1]. These results cannot be understood within a

single-particle picture, highlighting the importance of exchange interactions in determining the ground state of 2D carriers in monolayer semiconductors. [1] Jing Li, Mateusz Goryca, Nathan Wilson, Andreas Stier, Xiaodong Xu, & Scott A. Crooker, Phys. Rev. Lett. 125, 147602 (2020).

2:05 PM NM06.08.04

Late News: Towards Scalable High-Resolution Characterization of 2D van der Waals Heterostructures Hesham El-Sherif¹, Natalie Briggs², Joshua Robinson² and Nabil Bassim¹; ¹McMaster University, Canada; ²The Pennsylvania State University, United States

Scalable synthesis of heterostructures is recently realized through the *confinement heteroepitaxy* (CHet) technique. In this technique, atoms intercalate the epitaxial graphene (EG) interface and silicon carbide (SiC) substrates, which facilitates large-area environmentally stable 2D Nitrides, 2D Oxides, and 2D metals. One of the recently advanced 2D metals is gallium (2D Ga or Gallene), which is characterized as a half-van der Waal 2D metal heterostructure due to the bonding variation across the interface. Interestingly, 2D Ga exhibits exotic optical and electronic properties, such as enormous non-linear optical response, superconductivity, and near-zero index. In prior work, the spectroscopic ellipsometry technique reports that 2D Ga is mainly grown with bilayer thickness. However, the heterostructure's thickness, uniformity, and area coverage are not quantitatively understood with high spatial resolution techniques.

Here, we unlock the contrast from scanning electron microscope (SEM) images as a function of the 2D Ga position and the EG thicknesses. The SEM contrast is directly related to the local surface potential. We applied multiple correlative electron microscopy techniques, including the SEM and surface chemical maps in plan view for understanding the secondary electron (SE) emission contrast in SEM images. We also verified the 2D Ga location and the number of layers by correlating SEM with Scanning-Transmission electron microscopy (STEM) imaging and spectroscopy obtained from multiple site-specific cross-sections. Furthermore, we stitched hundreds of atomic-resolution STEM images over 7 μm FIB lamella to confirm that the 2D Ga grows with uniform bilayer Ga covered by EG with thicknesses that vary from 2-layers and up.

Besides, locating the uniform 2D Ga heterostructure positions enables us to segment SEM images that cover few millimeters in area. This segmentation process can be done manually from the image histogram or unsupervised by machine learning techniques. We form a montage view of $\sim 2 \text{ mm} \times 1.5 \text{ mm}$ area by stitching low-magnification and pixel-dense SEM images. This panorama retains lateral resolution controlled by the SEM resolution (few nm) but preserves atomic-resolution as resolved by correlative microscopy of the heterostructure's thicknesses.

Unlike spectroscopic techniques (ellipsometry or XPS), the *spectroscopic imaging* in SEM allows high-spatial-resolution for tracking intercalants, identify relative surface potentials, or determining the number of 2D layers. This could be further employed to characterize wafers' scalability and uniformity of 2D materials and 2D Van der Waals heterostructures.

2:20 PM *NM06.08.05

MXenes—2D Plasmonic Materials with Metallic Conductivity Yury Gogotsi; Drexel University, United States

MXenes (carbides and/or nitrides of early transition metals) are a very large family of 2D materials. They have a chemical formula of $\text{M}_{n+1}\text{X}_n\text{T}_x$, where M represents a transition metal (Ti, Mo, Nb, V, Cr, etc.), X is either carbon and/or nitrogen ($n=1, 2, 3$ or 4), and T_x represents surface terminations. The diversity in compositions (>30 stoichiometric MXenes have already been reported, >100 predicted), availability of solid solutions on M and X sites, and control of surface terminations, such as O, OH, F, Cl, S, etc., offers a plethora of structures and chemistries to investigate.¹

Combining the plasmonic properties with ease in processing, high electronic conductivity (up to 20 S/cm) and mechanical properties exceeding other solution-processable 2D materials, MXenes have the characteristics

necessary to develop as optical and electronic materials. Optical, electronic and transport properties of MXenes can be manipulated by tuning of their chemical composition. This presentation will provide insight into control of the optoelectronic properties (plasmon resonance frequency, electrical conductivity, carrier concentration, mobility and work function) and describe potential applications of MXenes as well as spectroscopic information, which can be applied to designing photonic and optoelectronic devices, such as electron transport layers for solar cells, optical sensors, electrochromic devices, metamaterials, EMI shields, antennas, etc.

2:45 PM NM06.08.06

Low Dimensional $\text{Bi}_2\text{Te}_3\text{-Sb}_2\text{Te}_3$ In-Plane Heterostructures—A Tunable Plasmonic Platform Beyond Noble Metals Parivash Moradifar¹, Austin G. Nixon², Tiva Sharifi^{3,4}, Pulickel Ajayan³, David Masiello² and Nasim Alem¹; ¹The Pennsylvania State University, United States; ²University of Washington, United States; ³Rice University, United States; ⁴Umea University, Sweden

Surface plasmons enable routing and manipulating of light on sub-diffraction limit length scales. Surface plasmons are commonly excited by coupling to an electromagnetic field leading to confined local field enhancements effect that be used for strengthening the sub-diffraction light-matter interaction and potentially offer a transformative solution for a wide range of high impact applications such as ultra-efficient nanostructured solar cells, high speed nano-devices, and photothermal biomedical therapeutic applications. Various conventional noble metals (gold and silver) based nanostructures have been extensively studied for their well-known plasmonic responses in the visible spectral range due to their long relaxation time. However, there are strong motivations in exploring alternative plasmonic structures that exhibit lower resistive losses at optical frequencies and more functionally diverse properties. Novel plasmonic building blocks such as topological insulators are considered to be a promising path for exploring low-loss plasmonic alternatives with exotic physical properties at optical frequencies in compare to conventional noble metals-based nanostructures.

Recently, two dimensional materials and group V-VI chalcogenides, known for their excellent thermoelectric and topological insulator (TI) properties, attracted a lot of attention for their exotic plasmonic phenomena. From the group of V-VI chalcogenides, this study will focus on low-dimensional $\text{Bi}_2\text{Te}_3\text{-Sb}_2\text{Te}_3$ in-plane heterostructures as low-band gap semiconductors and topological insulators providing gapless metallic surface states. $\text{Bi}_2\text{Te}_3\text{-Sb}_2\text{Te}_3$ in-plane heterostructure flakes contain a heterointerface between Bi_2Te_3 and Sb_2Te_3 that is formed under multi-step solvothermal synthesis process Bi_2Te_3 and Sb_2Te_3 have a rhombohedral crystal structure with space group of Rm. The bulk structure consists of alternating hexagonal monatomic crystal planes of Bi and Te arranging in ABC order along c-axis.

Monochromated electron energy loss spectroscopy (Mono-EELS) in conjunction with aberration corrected scanning transmission electron microscopy (STEM), in-situ transmission electron microscopy (TEM) and x-ray energy dispersive (XEDS) combined with singular value decomposition (SVD) analysis was used to identify and spatially resolve various surface plasmon excitation modes in these nanostructures. Furthermore, the effect of edge, heterointerface and defects (intrinsic and extrinsic) as potential paths to tailor the plasmonic response in low-dimensional $\text{Bi}_2\text{Te}_3\text{-Sb}_2\text{Te}_3$ in-plane heterostructures was explored. This work is also combined e-DDA calculations to further elaborate the experimental EELS measurements. These findings open a new path to design tunable plasmonic nanostructures with unique functionalities beyond noble metals.

SESSION NM06.09: Doping and Electric Field Effects in Low Dimensional Systems
Session Chairs: Divine Kumah, Harikrishnan Nair and Srinivasa Rao Singamaneni
Monday Afternoon, April 19, 2021
NM06

4:00 PM *NM06.09.01

A 2D Crystalline Acceptor for Modulation Doping in van der Waals Heterostructures Erik Henriksen,
Washington University in St. Louis, United States

a-RuCl₃ is a layered antiferromagnetic Mott insulator exhibiting phenomena related to the Kitaev quantum spin liquid. It can be readily exfoliated down to monolayer thicknesses and incorporated into van der Waals heterostructures along with graphene and myriad other atomically thin materials. In such devices, proximity of a-RuCl₃ to graphene leads to a significant charge transfer between the two that, surprisingly, persists even when a thin insulating layer is inserted between them, a phenomenon analogous to modulation doping in epitaxially-grown semiconductors. The effect can be observed in other materials including WSe₂, bilayer graphene, and EuS. This enables a new method of control over the charge distribution in van der Waals stacks, for instance by patterning RuCl to create local charge variations. As but one application, we describe the potential to create sharp pn junctions in graphene.

4:25 PM NM06.09.02

Late News: Highly Effective Gating of Graphene on GaN—Bias-Switchable Raman G Band Splitting

Jakub A. Kierdaszuk¹, Ewelina Rozbiegala^{2,3}, Karolina Pietak^{2,3}, Sebastian Zlotnik^{2,4}, Aleksandra Przewłoka^{2,5,4}, Wawrzyniec Kaszub², Andrzej Wyszomolek¹, Johannes Binder¹ and Aneta Drabinska¹; ¹University of Warsaw, Poland; ²Lukasiewicz Research Network - Institute of Microelectronics and Photonics, Centre for Electronic Materials Technology, Poland; ³Warsaw University of Technology, Poland; ⁴Military University of Technology, Poland; ⁵Center for Terahertz Research and Applications (CENTERA), Poland

In this communication we present results of highly effective gating of multilayer graphene in structure containing GaN epilayer with undoped GaN spacer. Bias switchable G band splitting showed great perspectives in characterization of devices based on graphene/GaN heterostructures and gives new opportunities in construction of nanosensors.

A 100 nm thick layer of undoped GaN preceded by a 1.3 μm thick layer of highly conductive GaN (n-doped) was grown on a sapphire substrate by MOCVD technique. Four-layer graphene (4-LGr) was used as a top contact to the GaN structures and was prepared in three steps. Firstly, a graphene monolayer grown on a copper substrate was transferred onto another graphene monolayer on a copper substrate by high-speed electrochemical delamination method. Then, a third graphene monolayer was transferred on the two layers of graphene obtained in the previous step. Finally, a fourth graphene monolayer was transferred on the graphene trilayer obtained in the previous step. 4-LGr was transferred on GaN heterostructure by polymer frame method [1]. So fabricated multi-layer graphene has an inhomogeneous and uncontrolled layer stacking.

A detailed analysis of Raman spectra showed three different types of spectra with G-band splitting into one, two or three subbands. No splitting of 2D band was identified. The presence of G band splitting is related to the turbostratic order and suggest different carrier concentrations of subsequent graphene layers in the 4-LGr structure. Therefore, high potential gradient near graphene/GaN junction is present even without bias. Additionally a strong shift of the G bands as a function of gate bias was observed. G band energy shift trends suggest n-doping of graphene. Interestingly, the most significant G band energy shift up to 8.5 cm⁻¹ occurs for the lowest bias, in the range between 1 V and -1 V. Further G band energy shift up to 1.4 cm⁻¹ in the range between -1 V and -5 V was observed. Raman micromapping showed that strong gating effect as well as band splitting is present over large surface area. Electroreflectance as well as band alignment analysis showed that undoped GaN spacer at reverse bias behaves like capacitor. Current-voltage characteristics exhibit Schottky-like behaviour. Graphene Fermi level shift calculated from current-voltage characteristic and electroreflectance measurements agree with Raman results. Fermi level shifts from 88 meV at 0 V to 200 meV at -5 V. For forward bias, a rapid decrease of electron concentration in graphene occurs (by 9x10¹² cm⁻²), the carrier concentration in across subsequent layers becomes more uniform so band splitting is less significant.

A substantial Raman position shifts occurs in our Schottky diode structures at one order of magnitude smaller voltages than for graphene deposited on SiO₂ substrates in capacitor type devices [2]. Obtained gating

efficiency is comparable to the results for solution-gated graphene. This strongly suggest that the diode junction is located directly near the graphene layers [3]. Thus, graphene gating is effective at very low voltages which is highly promising for further electron-phonon studies. Moreover, bias switchable G band splitting in turbostratic graphene enable to construct sensors based not on precise fitting of G band position shift but on tracing more significant band splitting.

REFERENCES

- I. Pasternak, et al., AIP Advances 4, 9, 097133 (2014).
J. Yan, et al., PRL 101, 136804 (2008).
J. Binder, et al., Nanotechnology 27, 045704 (2016).

4:40 PM NM06.09.03

Light-Induced Electron Spin Resonance Properties of van der Waals CrX_3 ($X = \text{Cl, I}$) Crystals Srinivasa Rao Singamaneni¹, Luis M. Martinez¹, Jens Niklas², Oleg Poluektov², Ravi Yadav^{3,4}, Michele Pizzochero^{3,4}, Oleg Yazyev^{3,4} and Michael McGuire⁵; ¹The University of Texas at El Paso, United States; ²Argonne National Laboratory, United States; ³Ecole Polytechnique Federale de Lausanne, Switzerland; ⁴Ecole PolyTechnique Federale de Lausanne, Switzerland; ⁵Oak Ridge National Laboratory, United States

The research on layered van der Waals (vdW) magnets is rapidly progressing owing to exciting fundamental science and potential applications. In bulk crystal form, CrCl_3 is a vdW antiferromagnet with in-plane ferromagnetic ordering below 17 K, and CrI_3 is a vdW ferromagnet below 61 K. Here, we report on the electron spin resonance (ESR) properties of CrCl_3 and CrI_3 single crystals upon photo-excitation in the visible range. We noticed remarkable changes in the ESR spectra upon illumination. In the case of CrCl_3 , at 10 K, the ESR signal is shifted from $g = 1.492$ (dark) to 1.661 (light), line width increased from 376 to 506 Oe, and the signal intensity is reduced by 1.5 times. Most interestingly, the observed change in the signal intensity is reversible when the light is cycled on/off. We observed almost no change in the ESR spectral parameters in the paramagnetic phase (>20 K) upon illumination. Upon photo-excitation of CrI_3 , the ESR signal intensity is reduced by 1.9 times; the g -value increased from 1.956 to 1.990; the linewidth increased from 1170 to 1260 Oe at 60 K. These findings are discussed by taking into account the skin depth, the slow relaxation mechanism and the appearance of low-symmetry fields at the photo-generated Cr^{2+} Jahn-Teller centers. Such an increase in the g -value as a result of photo-generated Cr^{2+} ions is further supported by our many-body wavefunction calculations. This work has the potential to extend to monolayer vdWs magnets by combining ESR spectroscopy with optical excitation and detection.

4:55 PM NM06.09.04

Local Magnetic Measurements of a Few-Layer van der Waals Superconductor Alexander Jarjour, Brian Schaefer, George M. Ferguson, Menyoun Lee, Debanjan Chowdhury and Katja C. Nowack; Cornell University, United States

Measurements of thermodynamic properties of few-layer van der Waals superconductors are scarce due to the inherently small volume of mechanically exfoliated samples. Here we measure the magnetic susceptibility of a van der Waals superconductor by using local magnetic measurements enabled by scanning SQUID microscopy. Specifically, we study transition metal dichalcogenide MoS_2 which exhibits a superconducting dome with a maximum critical temperature of nearly 10 K in ionic-gated few-layer devices. We combine the magnetic measurements with simultaneous electrical transport and map out changes in superfluid stiffness as a function of temperature and carrier density across the dome. We observe magnetic signatures consistent with a Kosterlitz-Thouless transition, and report our progress towards extracting absolute values of the superfluid stiffness and density from these measurements.

5:10 PM NM06.09.06

Determination of the In-Plane Exciton Radius in Two-Dimensional, Colloidal Semiconductor Nanoplatelets via Magneto-Optical Spectroscopy Alexandra Brumberg¹, Samantha Harvey¹, John Philbin², Benjamin Diroll³, Scott Crooker⁴, Eran Rabani² and Richard Schaller^{1,3}; ¹Northwestern University, United

States; ²University of California, Berkeley, United States; ³Argonne National Laboratory, United States; ⁴Los Alamos National Laboratory, United States

Nanoplatelets (NPLs), the colloidal analogues of more conventional two-dimensional materials such as transition metal dichalcogenide (TMD) layers and graphene, likewise exhibit modified electronic structure that arises from quantum confinement in only one dimension. It is often assumed that the lack of quantum confinement in the lateral plane yields a spatially extended exciton; however, studies in monolayer TMDs have shown that this is not the case. For colloidal NPLs, smaller exciton binding energies potentially challenge this picture, and reduced dielectric screening at the nanoparticle surface imposed by organic ligands provides additional considerations.

In this work, we implement absorption spectroscopy of CdSe NPLs in pulsed magnetic fields up to 60 T at the National High Magnetic Field Laboratory. The shift of the exciton energy as a function of magnetic field is probed for three different thicknesses and three different lateral areas of CdSe NPLs. Application of magnetic fields up to 60 T allows for the determination of the diamagnetic shift, the (small) second-order modification of the exciton energy. The diamagnetic shift provides insight into exciton lateral extent, as larger spatially extended excitons experience greater perturbations in a magnetic field. We calculate exciton lateral extents based on diamagnetic shift coefficients and find that exciton lateral extent is comparable to NPL thickness, indicating that the quantum confinement and reduced dielectric screening concomitant with few-monolayer thickness strongly reduces the exciton lateral extent. Atomistic electronic structure calculations of the exciton size for varying lengths, widths, and thicknesses support the substantially smaller in-plane exciton extent. This work follows similar studies of exciton spatial extent in monolayer TMDs and provides clear insight into the spatial extent of excitons in these promising, highly processable and scalable, two-dimensional materials.

5:25 PM NM06.09.07

Anisotropic Critical Behavior in $\text{Fe}_{2.7}\text{GeTe}_2$ Jose A. Delgado, Rubyann Olmos and Srinivasa Rao Singamaneni; The University of Texas at El Paso, United States

The presence of magnetocrystalline anisotropy in $\text{Fe}_{2.7}\text{GeTe}_2$ has previously been predicted by DFT calculations and confirmed through bulk magnetization measurements. This feature of $\text{Fe}_{2.7}\text{GeTe}_2$ makes it potentially useful for magnetic storage applications. For this material to be utilized in next-generation spintronic applications, the critical behavior, dimensionality of interaction, and magnetic exchange distance of $\text{Fe}_{2.7}\text{GeTe}_2$ must be fully understood. Here the hard-axis critical behavior was studied using a modified asymptotic analysis from bulk magnetization measurements for the first time. While much work has been previously done to study the critical behavior of $\text{Fe}_{2.7}\text{GeTe}_2$, we have found that the critical exponents and exchange distance vary between $H//ab$ and $H//c$. We have characterized the orientation-dependent critical phenomena of $\text{Fe}_{2.7}\text{GeTe}_2$, thus establishing a basis for the magnetocrystalline anisotropy from the perspective of competing universality classes.

5:40 PM NM06.07.09

Late News: Using Optical Pulses to Characterize Epitaxial Semiconductor Wafers Sam Mil'shtein and Brandon Keating; University of Massachusetts Lowell, United States

Abstract. In any commercial production of semiconductor wafers the required final step is characterization, producing the information about density of carriers (density of doping), and electron /holes mobilities. These characterization parameters are vital for design of any type of semiconductor electronics. The common, widely used characterization method consists of conductivity measurements combined with Hall effect testing. This common characterization technology requires to produce repeatedly the Van-der-Paw pattern with 6 contacts at testing pattern. The hetero-structured devices and thus hetero-structured wafers are common nowadays in mass production. Some of these layers are intentionally two-dimensional. For these wafers, the photolithography of Van-der-Paw pattern repeated for each epitaxial layer grown one above the other is complicated and costly by itself. Additional equipment, i.e., DC magnet positioned below the tested wafer is needed to finish Hall effect measurements. We developed a new characterization method to be used for testing of one after the other layers,

or selected test of only given layer by optical pulses of controlled wavelength. The optical pulses of selected wavelengths (colors) are produced by wide spectrum source of light and controlled by monochromator. Two ohmic probes are positioned on tested epilayer with distance of few millimeters between them. Focused light spot generates optical pulses with controllable amplitude and frequency near one contact. The second ohmic contact collects pulses of the photocurrent. At the end of this photocurrent stripe the amplitude and shape of moving pulses of carriers are analyzed by oscilloscope. The high amplitude of box-like pulse is registered at first contact. As the pulse proceeds, its amplitude decays and the pulse widens. Changes of pulse width, recorded by the scope, help to calculate diffusivity coefficient of generated photo carriers (D_n or D_p). Voltage bias at probes and direction of current defines the type (electrons or holes) of carriers. Einstein ratio ($D/\mu=kT/q$) is used to calculate the mobility of photo carriers. Simple measurement of current and voltage drop between two ohmic contacts, when the light is switched off, generates information about density of free carriers (density of doping). We discuss experimental setup of the new wafer characterization method [1] and how selection of light wavelengths defines selection of the tested layer.

1. S. Mil'shtein, B. Keating, "Novel Characterization Method for Semiconductor Wafers" Patent Application, December, 2021

SESSION NM06.10: Topological/Spin Ordering
Session Chairs: Divine Kumah and Srinivasa Rao Singamaneni
Tuesday Morning, April 20, 2021
NM06

8:00 AM *NM06.10.02

Interfacial Magnetic Anisotropy in $Y_3Fe_5O_{12}$ Induced by Low Crystalline Symmetry of Transition Metal Dichalcogenide WTe_2 Guanzhong Wu¹, Dongying Wang¹, Nish Verma¹, Yang Cheng¹, Side Guo¹, Guixin Cao¹, Kenji Watanabe², Takashi Taniguchi², Chun Ning (Jenie) Lau¹, Fengyuan Yang¹, Mohit Randeria¹, Marc Bockrath¹ and P. Chris Hammel¹; ¹The Ohio State University, United States; ²National Institute for Materials Science (NIMS), Japan

The breaking of inversion symmetry at the surface of a magnet significantly alters its properties and can induce a uniaxial anisotropy with its symmetry axis along the surface normal. In a complex oxide, such as ferrimagnetic garnet, this surface anisotropy is easy-plane in nature and can be enhanced by deposition of a non-magnetic material such as a heavy metal or a topological insulator, a phenomenon attributed to the enhanced Rashba spin orbit coupling. In striking contrast, we show here that if low symmetry, semi-metallic WTe_2 is placed in contact with $Y_3Fe_5O_{12}$ (YIG), an additional interfacial perpendicular magnetic anisotropy (iPMA) results. We probe the magnetism of the micron-sized YIG/ WTe_2 /hBN heterostructure using a high sensitivity ferromagnetic resonance force microscope, that can measure local ferromagnetic resonance with spatial resolution of 100nm and spectral resolution of 1 Oe. The magnitude of iPMA remains constant down to monolayer WTe_2 , indicating its interfacial origin. In addition, we probe the spin pumping effect from YIG to WTe_2 and find no WTe_2 thickness dependence, suggesting that interfacial spin relaxation plays the dominant role or that the spin diffusion length along the WTe_2 c axis is extremely short. This demonstrates the power of this approach in enabling studies of non-traditional heterostructures such as stacks of two-dimensional materials on epitaxially grown thin films. Our result further suggests that interfacial magnetic anisotropy in complex oxide ferro- or ferrimagnetic insulators is highly tunable by choice of non-magnetic overlayers, and could play an essential role in the development of next generation magnetic solid state devices.

8:25 AM NM06.10.03

Late News: Substrate Vicinality Effect on the Electronic Properties of Epitaxial Graphene Maya Narayanan Nair^{1,2}, Arlensiu Celis^{2,3}, Francois Nicolas², Stefan Kubsky², Amina Taleb-Ibrahimi² and Antonio Tejada^{3,2}; ¹Advanced Science Research Center (ASRC) at the Graduate Center at City University of New York,

United States; ²Synchrotron Soleil, France; ³Université Paris-Saclay, CNRS, Laboratoire de Physique des Solides, France

Many efforts to control the electronic properties of atomically thin two-dimensional materials (2D), either by twisted stacks or by deposition on a patterned substrate, are an intense line of research nowadays. Tuning the electronic properties of graphene by periodic potentials has resulted in many interesting properties such as Fermi velocity renormalization, extra Dirac points and tunable bandgap. However, it is still challenging to couple graphene to a lithographic structure with a periodicity of few nanometers. A very promising option consists of growing graphene on an appropriate periodical substrate, a natural route to induce periodic potentials in graphene [1]. However, the interaction of graphene with the substrate is still challenging [2,3]. Graphene on Ir(111) and Pt(111) substrates are particularly interesting because it exhibits a very weak graphene-substrate interaction, so the effect on the band structure as a function of the periodicity could exhibit a transition from mild coupling towards no coupling at all. In our recent work, we have investigated the influence of the one-dimensional periodic nanostructured substrate on graphene electronic properties. We have shown that graphene is extremely sensitive to periodic arrays, as demonstrated on two different nanostructured substrates, namely Ir (332) and Pt (111)[4,5]. The observed minigaps in graphene band structure by angle-resolved photoemission spectroscopy (ARPES) is related to the spatial periodicity. In this talk, I will present, the successful preparation of graphene on periodically nanostructured Pt (111) substrate and discuss how it is possible to control the superperiodicity and thus the bandgap by tuning the vicinity of the substrate, a simple way to engineer the electronic properties of graphene and other 2D materials.

1. I. Palacio et al., Nano Lett. 15,182 (2015)
2. M.S.Nevius et al., Phy. Rev. Lett.115,136802 (2015)
3. M. N. Nair et al., Nano Lett. 17, 2681 (2017)
4. A.Celis et al., Phy. Rev. B 97,195410 (2018)
5. A. Celis et al., Nanotechnology 31, 285601 (2020)

8:40 AM NM06.10.04

Late News: Nonradiative Recombination Free Monolayer Semiconductors Shiekh Zia Z. Uddin and Ali Javey; University of California, Berkeley, United States

Photoluminescence (PL) quantum yield (QY) is a key metric of optoelectronic performance that directly dictates the maximum optoelectronic device efficiency. In conventional semiconductors, defects act as a trapping center for nonradiative Shockley-Read-Hall or Auger recombination mechanism and drastically reduces PL QY at all generation rates. Two-dimensional transition-metal dichalcogenides (TMDCs), such as monolayer MoS₂, often exhibit low PL QY for as-processed samples, which has typically been attributed to a large native defect density. However, we show that the PLQY of as-processed MoS₂ and WS₂ monolayers reaches near-unity when they are made intrinsic through either by electrostatic or chemical doping. In the presence of background charge carriers, photogenerated excitons create positive or negative trions, which mostly recombine nonradiatively, leading to a low PL QY. This could be a result of a defect-assisted decay and/or a geminate Auger-like process in which the electron provides the third particle required for momentum conservation. On the other hand, if the semiconductor is intrinsic, the photogenerated exciton stays neutral and near unity PL QY is observed. Surprisingly, neutral exciton recombination is entirely radiative even in the presence of a high native defect density. This finding enables TMDC monolayers for optoelectronic device applications as the stringent requirement of low defect density is eased. Furthermore, the observed PL QY as a function of doping and generation rate in all four major TMDC monolayers (WS₂, WSe₂, MoS₂, MoSe₂) can be understood by considering the interaction of neutral excitons, charged trions, and free charge carriers and their subsequent recombination channels. This raises the intriguing possibility that the principle that excitonic systems show maximum PL QY when they are intrinsic is general enough to be applied to other material systems without the need for material-specific passivation techniques.

8:55 AM *NM06.10.05

Kitaev Interaction and Possible Quantum Spin Liquid State in 2D Materials with $S=3/2$ Changsong Xu;
University of Arkansas, Fayetteville, United States

Quantum spin liquids (QSLs) form an extremely unusual magnetic state in which the spins are highly correlated and fluctuate coherently down to the lowest temperatures, but without symmetry breaking and without the formation of any static long-range-ordered magnetism. Such intriguing phenomena are not only of great fundamental relevance in themselves, but also hold promise for quantum computing and quantum information. Among different types of QSLs, the exactly solvable Kitaev model is attracting much attention, with most proposed candidate materials, e.g., RuCl₃ and Na₂IrO₃, having an effective $S=1/2$ spin value with 4d/5d heavy transition metal. Here in this talk, I will first report the prediction of nonnegligible Kitaev interaction in 3d Cr-based 2D materials, e.g. CrI₃ and CrGeTe₃, from first-principles; then, via extensive first-principles-based simulations, I will further report the investigation of the Kitaev physics and possible Kitaev QSL state in epitaxially strained Cr-based monolayers, such as CrSiTe₃, that rather possess a $S=3/2$ spin value. Our study thus extends the playground of Kitaev physics and QSLs to 3d transition metal compounds.

9:20 AM *NM06.02.06

Temperature- and Intercalation-Induced Phase Transitions of MoTe₂ and MoS₂ Nanoflakes and Heterostructures Judy Cha; Yale University, United States

Owing to the small energy differences between the polymorphs, tellurium-based transition metal dichalcogenides, such as MoTe₂ and WTe₂, can access a full spectrum of electronic states, from the 2H semiconducting state to the 1T' semimetallic state, and from the T_d topological semimetallic state to the superconducting state in the 1T' and T_d phase at low temperature. Thus, it is a model system for phase transformation studies and applications as well as for studies of quantum phenomena such as the quantum spin Hall effect and potential topological superconductivity.

In this talk, I will first discuss our synthesis strategy to obtain cm²-scale thin films of 2H and 1T' MoTe₂ with layer control and large grains, which was achieved by tellurizing MoO_x thin films deposited by atomic layer deposition. Despite the van der Waals epitaxy, we show that the precursor-substrate interface critically determines the uniformity in thickness and grain size of the resulting MoTe₂ films: MoTe₂ grown on sapphire show uniform films while MoTe₂ grown on amorphous SiO₂ substrates form islands.

Phase transition from the 1T' phase to the T_d phase of MoTe₂ is explored using *in situ* cryogenic transmission electron microscopy, in which flakes of MoTe₂ are cooled from room temperature to liquid nitrogen temperature. Distinct changes in the electron diffraction patterns as a function of temperature demonstrate the phase change. Thus, *in situ* cryo-TEM enables studies of phase transitions as a function of thickness and morphology of 2D flakes in real space, providing important information to study the nucleation and growth of the new phase during phase transition. Finally, I will discuss the effects of heterointerface and mechanical strain on lithium-induced phase transition of MoS₂ and 2D heterostructures during lithium intercalation, which was investigated by combining field-effect transistor platforms with *in situ* probes during electrochemically controlled intercalation of lithium.

SESSION NM06.11: On-demand
Wednesday Morning, April 14, 2021
NM06

8:00 AM NM06.06.04

Multi-Level Manipulation of MXenes Electronic and Transport Properties Kanit Hantanasirisakul^{1,2}, Steven J. May¹ and Yury Gogotsi^{1,2}; ¹Drexel University, United States; ²A.J. Drexel Nanomaterials Institute,

United States

Two-dimensional (2D) transition metal carbides and nitrides, known as MXenes, have shown great promise in applications such as electromagnetic interference shielding, electrode and current collector in energy storage devices, transparent conductive electrodes, and optoelectronics. These applications are enabled by MXenes' high electronic conductivity, specifically $Ti_3C_2T_x$ (where T_x stands for surface termination such as O, F, and Cl) with metallic conductivity reaching 20,000 S/cm. Benefiting from a large variety of transition metals, C and/or N in the X layers, and versatile surface terminations, MXenes provide for multi-level tuning of electronic and transport properties. In this talk, we show that electronic and transport properties of MXenes can be manipulated by careful tuning of their chemical compositions. For instance, having a mix of C and N in the X layer of Ti_3CNT_x leads to a lower electrical conductivity, carrier concentration, and mobility compared to $Ti_3C_2T_x$. Moreover, the work function of $Ti_3C_2T_x$ thin films can be continuously tuned from ~4 to ~5 eV upon desorption of surface terminations *via* thermal annealing in vacuum. In addition, we also show that the intercalants, governing MXene interlayer spacing, play a crucial role in electronic transport properties in MXene free-standing films. This multi-level control of electronic properties is a unique advantage of MXenes compared to other 2D materials. This work is supported by the U.S. Department of Energy (DOE), Office of Science, Office of Basic Energy Sciences, grant #DESC0018618.

SYMPOSIUM NM07

Beyond Graphene 2D Materials—Synthesis, Properties and Device Applications
April 14 - April 20, 2021

Symposium Organizers

Zakaria Al Balushi, University of California, Berkeley
Ying Fang, National Center for Nanoscience and Technology
Deep Jariwala, University of Pennsylvania
Thomas Kempa, Johns Hopkins University

Symposium Support

Bronze
MilliporeSigma

* Invited Paper

SESSION NM07.01: Controlled Synthesis and Chemical Functionalization of 2D Materials I
Session Chairs: Surendra Anantharaman and Thomas Kempa
Sunday Morning, April 18, 2021
NM07

8:00 AM OPENING REMARKS

8:10 AM *NM07.01.01

Wafer-Scale Epitaxial Growth of Unidirectional TMD Monolayers Haoyue Zhu, Tanushree Choudhury, Benjamin Huet, Anushka Bansal, Thomas McKnight, Nicholas Trainor and Joan M. Redwing; The Pennsylvania State University, United States

Wafer-scale synthesis of semiconducting transition metal dichalcogenide (TMDs) monolayers is of significant interest for device applications to circumvent size limitations associated with the use of exfoliated flakes. Promising results have been demonstrated for epitaxial films deposited by vapor phase techniques such as CVD and MOCVD. However, the three-fold symmetry of TMDs such as MoS₂ and WSe₂, results in two energetically equivalent domain alignments, often referred to as 0° and 60° domains, when grown on substrates such as c-plane sapphire and graphene. The oppositely oriented domains give rise to inversion domain boundaries (IDBs) upon coalescence which exhibit a metallic character and are generally undesirable. In this study, we demonstrate the epitaxial growth of unidirectional TMD monolayers on 2" diameter c-plane sapphire substrates with a significantly reduced density of inversion domains. Steps on the sapphire surface are shown to play a key role in domain alignment by altering the energy landscape for nucleation and adatom diffusion.

Metalorganic chemical vapor deposition (MOCVD) was used for the epitaxial growth of WSe₂ and WS₂ monolayers on c-plane sapphire in a cold-wall horizontal quartz-tube reactor. The as-received sapphire substrates, which are miscut ~0.3° toward <110>, consist of steps with sub-1 nm step height separated by 50-70 nm wide terraces. A three-step nucleation-ripening-lateral growth process, carried out at temperatures ranging from 850°C to 1000°C, was used to achieve epitaxial films using W(CO)₆, H₂Se and H₂S as precursors in a H₂ carrier gas. Nucleation was observed to occur at the terrace edge and the growing domains align epitaxially with the underlying (0001) sapphire lattice. As a result of the nucleation process, the domains grow with a zig-zag edge facing the terrace edge which imparts a preferential direction to the domains. The percentage of domains with a preferred direction ranges from 75%-86% depending on MOCVD growth conditions. Continued lateral growth for times ranging from 10-30 minutes results in fully coalesced TMD monolayers that are epitaxially oriented on the sapphire, as assessed by in-plane x-ray diffraction, with a reduced density of inversion domain boundaries. The results demonstrate the important role of surface structure in nucleation and epitaxial growth of TMD monolayers.

8:35 AM *NM07.01.02

In-Plane Heterostructures of Graphene and Hexagonal Boron Nitride Hyeon Suk Shin; Ulsan National Institute of Science and Technology, Korea (the Republic of)

Two-dimensional (2D) heterostructures combining several individual 2D materials provide unique platforms to create unprecedented physical properties, thereby exploring new applications. In particular, heterostructures of hexagonal boron nitride (h-BN) and graphene have attracted a great deal of attention for potential applications. Although several methods have been developed to produce in-plane heterostructures of graphene and h-BN through the partial substitution reaction of graphene, the reverse reaction has not been reported. Though the endothermic nature of this reaction might account for the difficulty and previous absence of such a process, we demonstrated a new chemical route in which the Pt substrate plays a catalytic role. We also proposed that this reaction proceeds through h-BN hydrogenation; subsequent graphene growth quickly replaces the initially etched region. Importantly, this conversion reaction enabled the controlled formation of patterned in-plane graphene/h-BN heterostructures, without needing the commonly employed protecting mask, simply by using a patterned Pt substrate [1]. It means that we could fabricate spatially controlled in-plane heterostructures of h-BN and graphene.

We expanded the spatially controlled conversion of h-BN to graphene on an array of Pt nanoparticles (NPs) to realize an array of uniform GQDs embedded in an h-BN sheet. A uniform Pt NP array was formed on a SiO₂/Si substrate with the aid of self-patterning diblock copolymer micelles, and the h-BN sheet was transferred on the Pt NPs array, followed by the conversion of h-BN on Pt to GQDs. The size of the obtained GQDs corresponded with the sizes of the Pt NPs, because of the selective conversion of h-BN on top of Pt NPs. Uniform and precisely controlled size of the GQDs ranging from 7 to 13 nm was achieved. Finally, we demonstrated electron transport by the size-controlled GQDs isolated by insulating h-BN like a Coulomb blockade, indicating that the splitting energy of the GQD is 70–140 meV, compatible with its dimension [2].

In addition, a new photoluminescence peak in the GQD/h-BN heterostructures was observed at 410 nm. This blue-emitting photoluminescence occurs at 1D heterojunctions of h-BN and graphene, which is originated from

the localized energy states at the disordered boundaries of h-BN and graphene [3].

[1] G. Kim, et al., Nano Letters 15, 4769 (2015)

[2] G. Kim, et al., Nature Communications 10, 230 (2019)

[3] G. Kim, et al., Nature Communications 11, 5359 (2020)

9:00 AM NM07.01.03

Vertically-Oriented MoS₂ and WS₂ for Nonlinear Nanophotonics—From Nanosheets to Heterostructures

Maarten Bolhuis¹, Javier Hernández¹, Sabrya E. van Heijst¹, Miguel Tinoco Rivas^{1,2}, Kobus Kuipers¹ and Sonia Conesa-Boj¹; ¹Delft University of Technology, Netherlands; ²Universidad Complutense, Spain

Transition Metal Dichalcogenide (TMDC) materials such as molybdenum disulfide (MoS₂) and tungsten disulfide (WS₂) exhibit unique optoelectronic properties. This makes TMDCs particularly promising candidates for building blocks of ultra-thin nanophotonic devices. For such applications, the vertically-oriented configuration of TMDCs could be advantageous as compared to the conventional horizontal configuration, because the inherent broken symmetry of the vertically orientated MoS₂ and WS₂ would favor an enhanced nonlinear response. Further, these attractive optoelectronic properties of vertically-oriented MoS₂ and WS₂ can be augmented by fabricating heterostructures based on their combination. Up to now, most of these heterostructures have been fabricated by utilizing transfer techniques or by performing separate chemical vapor deposition (CVD) steps for each material.

As a starting point, we show that the direct sulfurization of predeposited Mo metal results in vertically orientated MoS₂ (v-MoS₂) nanosheets. A systematic study on these v-MoS₂ nanosheets shows that the sulfurization rate is strongly dependent on the reaction temperature and reaction time. By systematically varying the reaction time and temperature we were able to determine both the activation energy and the diffusion constant for the sulfurization process. We verify an enhanced nonlinear response in the resulting v-MoS₂ nanostructures as compared to their horizontal counterparts.

Building upon these results, we demonstrate the feasibility of creating vertically-oriented TMDC heterostructures via a one-step CVD process without relying on transfer techniques, utilizing the direct sulfurization of molybdenum (Mo) and tungsten (W) heterostructures and multilayers. By depositing different configurations of Mo and W metal and carefully controlling the sulfurization depth we can design different TMDC heterostructures and multilayers. Utilizing FIB tomography and 3D reconstructions, we determine that the grain boundaries at the interface between the Mo and W metals are continuous and that, after sulfurization, these continuous metal grains facilitate the synthesis of in-plane vertical heterostructures. HR-TEM analysis confirms that these in-plane heterostructures are continuous and uniformly distributed along the interface.

This versatile method of fabricating in-plane and vertically aligned MoS₂ and WS₂ heterostructures can be further extended to different arrangements of TMDC heterostructures and multilayers, thus represents a steppingstone towards the fabrication of low-dimensional TMD-based nanostructures for versatile nonlinear nanophotonic devices.

9:15 AM NM07.01.04

Impact of Oxygen on CVD Grown Boron Nitride Layers **Mohammad W. Malik¹, Bin Wang^{1,2}, Sahar Jaddi¹, Yiyi Yan¹, Victor Reis¹, Yun Zeng², Thomas Pardoen¹, Benoît Hackens¹ and Jean-Pierre Raskin¹; ¹UCLouvain, Belgium; ²Hunan University, China**

h-BN is an eminent member of the 2D materials family with exceptional and peculiar properties such as atomically smooth surface, ultra-high flexibility, and transparency. h-BN is an attractive candidate for application in flexible electronics, optoelectronics, and electro-mechanics devices. Moreover, h-BN encapsulated 2D materials ^[1] demonstrate elevated throughput and enhanced physical properties.

h-BN is a binary element material produced in various shapes via the CVD process ^[2]. The coalescence of the

different shape and orientation domains generate a range of grain boundaries (GBs) that can be composed of N-N, B-B, and N-B (5, 7) defects^[3]. Indeed, defective GBs lead to high leakage current and low mechanical strength, making it unsuitable for electro/mechanical devices and other applications. Therefore, the synthesis of large-area and defect-free h-BN is pivotal. Attempts have been made to grow large-area h-BN relying on pre-treatment of the substrate^[4], the alloyed substrate^[5], water vapors^[2], and monocrystalline substrate^[6]. These processes have shown promising results, but the impact of oxygen to reduce the nucleation density has not been widely scrutinized in the literature.

In this work, we investigated the impact of oxygen on the growth of large-area h-BN. CVD growth of h-BN was carried out on polycrystalline copper (Cu) foils using ammonia borane as a precursor. Our investigation suggests that pre-oxidation of Cu foils by a few hundred ppm of oxygen leads to an increase of the h-BN domains size by at least a factor of 5 when compared to the h-BN domains synthesized by sole hydrogen annealing of Cu foils^[4,6]. Typical samples contain the various shapes of domains with a maximum lateral size of hundreds of microns ($> 100 \mu\text{m}$), which have not been reported so far.

The quality of h-BN is confirmed by Raman, XPS, ToF-SIMS, and UV-Vis spectroscopies. An intense peak is observed in the frequency range of $1360\text{-}1370 \text{ cm}^{-1}$ that is the typical E_{2g} mode of h-BN reported in the literature. The binding energy of boron and nitrogen is about 190 eV and 398 eV, respectively. We also confirm the stoichiometry of h-BN, i.e., the N: B ratio is close to 1 in good agreement with high-quality h-BN growth. UV-Vis spectroscopy shows strong absorption around 202 nm that corresponds to the 6.13 eV optical bandgap. The combined results of Raman spectra with UV-Vis spectroscopy confirm the formation of h-BN and reject the possibilities of other crystallographic BN structures such as r-BN, c-BN, and w-BN. The tunneling current was measured for hundreds of metal/h-BN/metal structures with an overlap area of $25 \mu\text{m}^2$. For a typical device, the thickness of h-BN is 2.6 nm, as confirmed by AFM. The normalized current density was found to be $1.79 \text{ nA}/\mu\text{m}^2$ at a DC bias of 1 V, proving the good insulator potential of the synthesized h-BN.

The achieved large areas of grown h-BN are attributed to an optimum concentration of intrinsic carbon and organic species present in the Cu foil. These species presumably play a critical role in determining the size of the h-BN domains. An excessive degree of oxidation deteriorates surface quality during the process, leading to voids on the substrate and gives rise to defective growth, whilst an inadequate degree of oxidation results in smaller domains ($< 5\text{-}10 \mu\text{m}$). There is a tradeoff between the residual impurities and the h-BN grain size that can be tuned by the degree of oxidation of Cu foils, as demonstrated in this work.

References

- 1- J. Holler *et al.*, 2D Mater. 7, 015012, (2019).
- 2- L. Wang *et al.*, Mater. Chem. Front. 1, 1836-1840, (2017).
- 3- J. Strand *et al.*, J. Phys.: Condens Matt., 32, 055706, (2019).
- 4- R. Y. Tay *et al.*, Nano Lett., 14, 839-846, (2014).
- 5- G. Lu *et al.*, Nat. Comm., 6, 6160, (2015).
- 6- L. Wang *et al.*, Nat., 570, 91-95, (2019).

9:30 AM NM07.01.05

Versatile Roles of Monolayered Inorganic Nanosheets in Multifunctional Nanohybrids Seong-Ju Hwang; Yonsei University, Korea (the Republic of)

The monolayered 2D nanosheets of layered inorganic solids (layered metal oxides, layered double hydroxides, layered metal chalcogenides, and graphene) attract intense research interest because of their versatile roles in multifunctional nanohybrids applicable for energy and environmental technologies. The monolayered 2D nanosheets of inorganic solids can be synthesized by soft-chemical exfoliation reaction of the pristine layered materials. A great diversity in the chemical compositions and crystal structures of inorganic nanosheets

provides this class of materials with a wide spectrum of physical properties and functionalities. The inorganic nanosheets can be used as powerful building blocks for exploring high performance hybrid photocatalysts and electrocatalysts. These materials can play a role as catalytically active components as well as conductive additives for improving the catalyst performance of hybridized species. In this talk, several practical examples of 2D monolayered nanosheet-based photocatalysts and electrocatalysts active for solar fuel production will be presented together with the discussion about the relationship between catalyst performance and chemical bonding nature.

9:45 AM NM07.01.06

Synthesis and Properties of Supertwisted Spirals of 2D Materials Enabled by Non-Euclidean Surfaces

Yuzhou Zhao, Chenyu Zhang, Daniel Kohler, Jason Scheeler, John Wright, Paul M. Voyles and Song Jin; University of Wisconsin–Madison, United States

Euclidean geometry is the fundamental mathematical framework of classical crystallography. Traditionally, layered materials are grown on flat substrates, but growing Euclidean crystals on non-Euclidean surfaces has rarely been studied. Here, we present a general model describing the growth of layered materials with screw-dislocation spirals on non-Euclidean surfaces and show that it leads to continuously twisted multilayer superstructures. This model is experimentally demonstrated by growing supertwisted spirals of tungsten disulfide (WS_2) and tungsten diselenide (WSe_2) draped over nanoparticles near the centers of spirals. Microscopic structural analysis shows that the crystal lattice twist is consistent with the geometric twist of the layers, leading to moiré superlattices between the atomic layers, which further influence the electronic structures of the material. The preliminary studies on the physical properties of such multilayer twisting 2D materials will be discussed. Our results introduce new concepts in the growth of exotic nanomaterials and a rational strategy for potentially controlling the twist angle in layered materials from direct synthesis, which opens up new opportunities for the study of twisted moiré superlattices and chirality-related properties.

SESSION NM07.02: Controlled Synthesis and Chemical Functionalization of 2D Materials II

Session Chairs: Surendra Anantharaman and Thomas Kempa

Sunday Morning, April 18, 2021

NM07

10:30 AM *NM07.02.01

Ledge-Directed Epitaxy of Single-Crystalline Nanoribbons of Transition Metal Dichalcogenides

Areej A. Aljarb¹, Jui-Han Fu¹, Thomas Anthopoulos¹, Jeehwan Kim², Lain-Jong Li¹ and Vincent Tung¹; ¹King Abdullah University of Science and Technology, Saudi Arabia; ²Massachusetts Institute of Technology, United States

Two-dimensional (2D) transition metal dichalcogenides (TMDs) monolayers are considered promising for future extreme device downscaling. For wafer scale manufacturing of advanced logic and memory devices, dense arrays of single-crystal, globally aligned TMD monolayer nanoribbons that can be controllably grown, are highly desired. Demonstrated top-down approaches to form such nanoribbons require large-area, single-crystal TMDs and damage-free etching processes, which are not available currently. Bottom-up growth methodologies for TMD nanoribbons have been reported to individually achieve control of layer number, single-crystallinity, local alignment, and dimensionalities. However, controlled nanoribbon growth with all aforementioned properties synergistically remains a major challenge. In this talk, we will demonstrate a ledge-directed epitaxy (LDE) of dense arrays of continuous, self-aligned, monolayer and predominantly single-crystalline MoS_2 nanoribbons on β -gallium (III) oxide (β - Ga_2O_3) (100) substrates. Experimental observation and density function theory (DFT) simulation indicate that the presence of intrinsic ledges on β - Ga_2O_3 (100) leads to the reduction in binding energy. The two previously indistinguishable and nearly degenerate configurations are now remarkably uncoupled from each other by ~ 2 eV, overcoming the atomic registry—the

van der Waals (vdW) epitaxy constraint and thus ensuring the mono-orientated nucleation. Meanwhile, potential energy surface (PES) mapping sheds light on a surface diffusion limited pathway along the ledge, hence driving the energetically preferred and directionally modulated growth of aligned MoS₂ domains into single-crystalline nanoribbons. The stitching of unidirectional seeds into continuous, single-crystal and -orientated MoS₂ nanoribbons was confirmed by second harmonic generation (SHG) and dark field-scanning transmission electron microscopy (DF-STEM). The MoS₂ nanoribbons can be readily transferred to arbitrary substrates while the underlying β -Ga₂O₃ can be re-used after mechanical exfoliation. Prototype MoS₂ nanoribbon-based field-effect transistors exhibit high on/off ratios of 10⁸ and an averaged room temperature electron mobility of 65 cm²V⁻¹s⁻¹, both on par with values reported for mechanically exfoliated MoS₂ devices. We further demonstrate, for the first time, the LDE growth as a general strategy for single-crystal p-type WSe₂ nanoribbons and lateral n-p-n heterostructures made of p-WSe₂ and n-MoS₂ nanoribbons. Our findings pave the way to direct the growth of single-crystalline TMDs and their heterostructures for futuristic electronics applications.

10:55 AM NM07.02.02

Illuminating the Electronic Properties of WS₂ Polytypism with Electron Microscopy Sabrya E. van Heijst¹, Masaki Mukai², Eiji Okunishi², Hiroki Hashiguchi², Laurien I. Roest¹, Louis Maduro¹, Juan Rojo^{3,4} and Sonia Conesa-Boj¹; ¹Delft University of Technology, Netherlands; ²EMBU JEOL Ltd, Japan; ³Nikhef Theory Group, Netherlands; ⁴Vrije Universiteit Amsterdam, Netherlands

Tailoring the specific stacking sequences (polytypes) of layered materials represents a powerful strategy to identify and design novel physical properties. While nanostructures built upon transition-metal dichalcogenides (TMDs) with either the 2H or 3R crystalline phases have been routinely studied, our knowledge of those based on mixed 2H/3R polytypes is far more limited. Here we report on the characterization of mixed 2H/3R free-standing WS₂ nanostructures displaying a flower-like configuration by means of advanced transmission electron microscopy. We correlate their rich variety of shape-morphology combinations with relevant local electronic properties such as their edge, surface, and bulk plasmons. Electron energy-loss spectroscopy combined with machine learning reveals that the 2H/3R polytype displays an indirect band gap with $E_{BG} = 1.6$ eV. Further, we identify the presence of energy-gain peaks in the EEL spectra characterized by a gain-to-loss ratio $I_G / I_L > 1$. Such property could be exploited to develop novel cooling strategies for atomically thin TMD nanostructures and devices built upon them. Our results represent a stepping stone towards an improved understanding of TMDs nanostructures based on mixed crystalline phases.

11:10 AM NM07.02.03

Frank–van der Merwe Growth of Two-Dimensional Transition Metal Dichalcogenide by Strain-Engineering Yi Wan and Vincent Tung; King Abdullah University of Science and Technology, Saudi Arabia

Two-dimensional transition metal dichalcogenides (TMDCs) have attracted widespread attention due to their prospective for the next-generation non-silicon electronics and optoelectronics. Among these two-dimensional TMDCs research, the most highlight has been given to single-layer TMDCs because of its intriguing electrical and optical properties. However, the fabrication demands and the physics of TMDCs suggest that few-layer TMDCs may be more attractive than single layer TMDCs for the industrial manufacturers because few-layer TMDCs equit more density of states for application in electronics, better light absorption and wider spectral response in optical application. To realize full potential of few-layer TMDCs, there is still much effort in the scalable and layer-controllable growth of highly crystalline TMDCs need to be achieved. In this work, WSe₂ is treated as a representative of common TMDCs growth, and we report an experimental observation that strain presenting in the first WSe₂ layers plays a critical role in the determination of growth manners for the following layers. Frank–van der Merwe Growth mode can be realized through inducing built-in tensile strain in first WSe₂ layers during the CVD process. Moreover, we demonstrate the stacking angle between the successive layers and the first layers by second harmonic generation (SHG) measurement. The foundational understanding of growth mechanism is assessed by a comprehensive density functional theory (DFT) simulation. This work provides a crucial hint to realize uniform layer control over the large scale, which is an important step for TMDCs towards

real applications.

11:25 AM NM07.02.05

Stabilization of NbTe₃, VTe₃, and TiTe₃ via Nanotube Encapsulation Scott Stonemeyer^{1,2,3}, Jeffrey D. Cain^{1,2,3}, Sehoon Oh^{1,3}, Amin Azizi^{1,2}, Peter Ercius³, Marvin L. Cohen^{1,3} and Alex Zettl^{1,2,3}; ¹University of California, Berkeley, United States; ²Kavli Energy NanoScience Institute, Berkeley, United States; ³Lawrence Berkeley National Laboratory, United States

One of the primary objectives of nanoscience is the precise control over the processing-structure-property relationship intrinsic to traditional materials science. Recently, the concept of dimensionality, and the engineering of materials' structure and properties *via* changes in dimensionality, has emerged as an additional degree of freedom within this paradigm. To this end, the isolation of single atomic-planes (*e.g.* graphene and the transition metal dichalcogenides) and chains (*e.g.* transition metal trichalcogenides, TMTs) from quasi-low-dimensional materials has been extremely fruitful. The archetypal quasi-1D materials family is the TMTs, commonly referred to as MX₃ compounds, with M a transition metal and X a chalcogen. Typically for these materials, 1D MX₃ chains are weakly coupled by interchain vdW interactions to form coherent, but highly anisotropic, three-dimensional crystals. The bulk synthesis and properties of the TMTs has been well explored and they are canonical examples of superconductors and charge density wave materials. This structural motif is common across a range of M and X atoms (*e.g.* NbSe₃, HfTe₃, TaS₃), but not all M and X combinations are stable. Here, we demonstrate the successful synthesis of three previously unreported MX₃ TMT compounds: NbTe₃, VTe₃, and TiTe₃. This is accomplished through nano-confined growth within the cavity of multi-walled carbon nanotubes (MWCNTs). Depending upon the inner diameter of the encapsulating MWCNTs, specimens ranging from many chains, to few chains (2-3), and even single chain, can be isolated and studied. The MWCNT sheath stabilizes the chainlike morphology, enabling synthesis and characterization with transmission electron microscopy (TEM) and aberration-corrected scanning transmission electron microscopy (STEM). It is found that few-chain specimens of the new TMTs can exhibit a coordinated interchain spiraling, while the single-chain limit exhibits a trigonal anti-prismatic (TAP) rocking distortion, which we experimentally resolve for the first time here. First principles calculations give insight into the integral role that the encapsulating CNT plays in stabilization and provide information regarding the electronic structure of the new materials.

11:40 AM NM07.02.06

Deterministic Fabrication of Arbitrary Vertical Heterostructures of 2D Ruddlesden-Popper Halide Perovskites Dongxu Pan, Yongping Fu, Natalia Spitha, Yuzhou Zhao, Christopher Roy, Darien Morrow, Daniel Kohler, John Wright and Song Jin; University of Wisconsin–Madison, United States

Ruddlesden-Popper (RP) phase lead halide perovskites have emerged as a new class of 2D semiconductors that exhibit tunable electronic and optical properties, potentially offering unlimited heterostructure configurations for exploration. However, the promise of such heterostructures has not been fulfilled, because halide perovskites' highly mobile and fragile crystal lattices make controllable direct synthesis or van der Waals integration extremely difficult. Here, we report the direct growth of large-area free-standing nanosheets of diverse phase-pure RP perovskites with thickness down to a monolayer at the solution-air interface and a gentle and reliable approach for transferring and stacking these nanosheets. These advances enabled the deterministic fabrication of arbitrary vertical heterostructures and multi-heterostructures of different RP perovskites with unprecedented structural degrees of freedom that define the electronic structures of the heterojunctions. Such rationally designed heterostructures exhibit interesting interlayer properties such as interlayer carrier transfer and reduction of photoluminescence linewidth, and would enable the exploration of exciton physics and optoelectronic applications.

11:55 AM NM07.02.08

Late News: Ionic 2D Covalent Organic Frameworks for the Innovative Remediation of Toxic Chromium and Arsenic Oxyanions in Water Ping Li, Santa Jansone-Popova, Josh Damron, Vyacheslav Bryantsev and Bruce A. Moyer; Oak Ridge National Laboratory, United States

Accumulation of highly toxic oxyanions such as chromate and arsenate in ground and surface waters from the geological processes and/or man-made pollution has led to a wide range of health and environmental problems. Thus, the development of innovative materials that can selectively remove target toxic oxyanions has attracted enormous research interest in academia and industry. Ionic 2D covalent organic frameworks (iCOFs) offer a unique means to effectively incorporate well-defined anion binding motifs into chemically robust, highly periodic, low-density polymeric materials. Structural modifications can be easily implemented to fine-tune the local environments of anion binding sites inside iCOFs providing insights into the selectivity and efficiency of the ion exchange process. A series of guanidinium-based 2D iCOFs have been developed to systematically examine the impacts of steric, electrostatic, and H-bond groups on the anion exchange process of chromate and arsenate anions. Interesting conclusions include: 1) well-position H-bonds seem to play a crucial role in determining the weak binding of arsenate anions, 2) electrostatic tuning significantly impacts the nature and incorporation of guanidinium sites in iCOFs, 3) moderate steric alteration imposes little influences on chromate and arsenate selectivity. Results and knowledge from this study are expected to aid the development of new guanidinium-based polymeric and composite anion exchange materials for toxic oxyanion remediation and other extraction applications.

SESSION NM07.03: Controlled Synthesis and Chemical Functionalization of 2D Materials III
Session Chairs: Surendra Anantharaman and Thomas Kempa
Sunday Afternoon, April 18, 2021
NM07

1:00 PM *NM07.03.01

Chemically Tailoring Interfaces in Two-Dimensional Heterostructures Mark C. Hersam; Northwestern University, United States

As a result of their unique electronic, optical, and physical properties, two-dimensional (2D) materials are actively being explored for applications in optoelectronics [1], neuromorphic computing [2], quantum information science [3], and energy technologies [4]. With exceptionally high surface-to-volume ratios, 2D materials are highly sensitive to their environment, resulting in a strong dependence of their properties on substrate effects, extrinsic adsorbates, and interfacial defects. Furthermore, the integration of 2D materials into heterostructure devices introduces further demands for controlling interfaces with atomic precision. With this motivation, this talk will explore emerging efforts to understand and utilize interfacial chemical functionalization to influence the properties of 2D heterostructures. For example, organic adlayers can tailor chemical reactivity to enable conformal atomic layer deposition of pinhole-free encapsulation layers that mitigate the deleterious effects of ambient exposure, particularly for ambient-unstable 2D materials such as black phosphorus and monochalcogenides [5]. The integration of organic self-assembled monolayers with 2D semiconductors also allows for tailoring of electronic and optical properties such as photoinduced charge separation in fullerene/InSe heterojunctions [6] and mixed-dimensional excitonic states in phthalocyanine/MoS₂ heterojunctions [7]. By exploiting spatially inhomogeneous surface chemistry, seamless lateral 2D heterointerfaces can also be realized including perylene/borophene [8], graphene/borophene [9], and concentric borophene superlattices [10], each of which show atomically sharp electronic interfaces as confirmed by ultrahigh vacuum scanning tunneling microscopy and spectroscopy. Overall, by providing precise tailoring of interfaces, chemical functionalization presents opportunities for improved functionality in 2D heterostructure devices.

[1] M. E. Beck and M. C. Hersam, *ACS Nano*, **14**, 6498 (2020).

[2] V. K. Sangwan and M. C. Hersam, *Nature Nanotechnology*, **15**, 517 (2020).

[3] X. Liu and M. C. Hersam, *Nature Reviews Materials*, **4**, 669 (2019).

- [4] S. Padgaonkar, *et al.*, *Accounts of Chemical Research*, **53**, 763 (2020).
[5] S. A. Wells, *et al.*, *Nano Letters*, **18**, 7876 (2018).
[6] S. Li, *et al.*, *ACS Nano*, **14**, 3509 (2020).
[7] S. H. Amsterdam, *et al.*, *ACS Nano*, **13**, 4183 (2019).
[8] X. Liu, *et al.*, *Science Advances*, **3**, e1602356 (2017).
[9] X. Liu, *et al.*, *Science Advances*, **5**, eaax6444 (2019).
[10] L. Liu, *et al.*, *Nano Letters*, **20**, 1315 (2020).

1:25 PM NM07.03.02

Ledge-Directed Epitaxy of Continuously Self-Aligned Single-Crystalline Nanoribbons of Transition Metals Dichalcogenides Areej A. Aljarb^{1,2}, Jui-Han Fu¹, Lain-Jong Li^{1,3} and Vincent Tung¹; ¹King Abdullah University of Science and Technology, Saudi Arabia; ²King Abdulaziz University, Saudi Arabia; ³Taiwan semiconductor Manufacturing Company, Taiwan

Two-dimensional (2D) transition metal dichalcogenides (TMDs) monolayers have been considered promising for future device scaling. For wafer-scale manufacturing, dense arrays of single-crystal, globally aligned TMD monolayer nanoribbons are desired for advanced logic and memory devices. The top-down approach to form such nanoribbons requires large-area, single-crystal TMD, and deliberate lithography/etching processes, which are not available currently. The bottom-up growth approaches toward TMD nanoribbons have been reported to individually achieve the control of layer number, single-crystallinity, local alignment, and dimensionalities. However, the nanoribbon growth with all the above-mentioned properties synergistically remains a major challenge. Here, we demonstrate a ledge-directed epitaxy (LDE) of dense arrays of centimeter-long, self-aligned, monolayer, and predominantly single-crystalline MoS₂ nanoribbons on β -gallium(III) oxide (β -Ga₂O₃) (100) substrates. Experimental observations and density functional theory (DFT) simulation suggest that nucleation and growth of the nanoribbons follow the β -Ga₂O₃ ledges. The stitching of unidirectional seeds into continuous, single-crystal, and -orientation MoS₂ nanoribbons was confirmed by second harmonic generation (SHG) and dark field-scanning transmission electron microscopy (DF-STEM). The MoS₂ nanoribbons can be readily transferred to arbitrary substrates while the underlying β -Ga₂O₃ can be re-used after mechanical exfoliation. Our prototype MoS₂ nanoribbon-based field-effect transistor exhibits an on-off ratio of 10⁸ and room temperature carrier mobility of 65 cm²V⁻¹s⁻¹ comparable to those mechanically exfoliated benchmarks. We further demonstrate the LDE growth of p-type WSe₂ nanoribbons and lateral heterostructures made of p-n WSe₂-MoS₂ nanoribbons. Our findings pave the way to miniaturization of single-crystalline TMDs and their heterostructures with potential applications not available by other means.

1:40 PM DISCUSSION

2:10 PM NM07.03.05

Electron Wind Force Annealing of MXene Films John Sherbondy¹, Abu Rassel¹, Brian Wyatt Jr.², Babak Anasori² and Aman Haque¹; ¹The Pennsylvania State University, United States; ²Indiana University–Purdue University Indianapolis, United States

MXenes are a family of two-dimensional (2D) transitional metal carbides and nitrides, obtained by selective etching of the A element from the parent MAX phases, where M is an early transition metal, A is an element of the A group, mostly group 13 or 14 of the periodic table (in particular, Al, Si, and Ga), and X stands for carbon and/or nitrogen. Their atomic-scale nature, scalable processing, and attractive electrical properties (up to 20,000 S/cm conductivity) make them strong candidates for a diverse range of applications such next generation energy storage systems, electromagnetic interference (EMI) shielding, antibacterial agents, and water purification. However, MXenes are solution-based 2D materials with abundant surface functional groups and intra-flake separations, which decrease the overall electrical conductivity in film form. This renders film annealing a critical post processing step.

While annealing of MXene films is typically performed in the 700-1500 °C range, we present a novel, athermal

process to achieve similar results. We explore annealing with the electron wind force (EWF) at near-room temperature conditions in contrast to traditional heating methods. EWF is an atomic scale mechanical force that acts only in the defective regions, which is proposed to provide very high defect mobility. The process is demonstrated on nominally 5 microns thick, freestanding $Ti_3C_2T_x$ films. We report 30-50% decrease in resistance after applying only 20 amp/mm² current density. The specimen temperature remains below 100 °C during the process. The resistance change was permanent and did not increase back when the current was removed. We acquired Raman spectroscopy on as-received and EWF-annealed specimens to observe remarkable decrease of intensity in the T_x , M- T_x and the Carbon regions. In the T_x (230–470 cm⁻¹) largest intensity drop occurred at wave shift of 286 cm⁻¹. This range represents the in-plane vibrations of surface groups attached to titanium atoms. Therefore, our remarkable intensity drop suggests elimination of the surface terminated bonds, which are helpful for the electrical conductivity. Further, the C region (580 – 730 cm⁻¹) represents carbon vibrations, where we observed remarkable intensity drops in the 600 and 720 cm⁻¹ peaks. We also observed remarkable decrease in the 123 cm⁻¹ peak, which represents the surface plasmon resonance. The most remarkable feature of this annealing process is that no increase in disordered carbon peaks (typically seen in high temperature annealing) were observed. Rather, the decreased peak intensity in the C region indicates loss of carbon atoms. The Raman results were verified by Energy-dispersive Spectroscopy performed in a SEM. We also prepared cross-sectional specimens to highlight the decrease of the intra-layer defects (mostly micron scale voids).

To summarize, we have demonstrated a low temperature (<100 °C) process to anneal MXene thick films to decrease their resistivity up to 50%. Raman and EDS analyses suggest that such improvement in electrical conductivity comes from the removal of the surface terminated bonds. The advantages of this new process are (a) low temperature will allow temperature sensitive substrates, such as polymers and (b) absence of high temperature induced formation of TiO_2 or disordered carbon.

2:25 PM NM07.03.06

New Methods and Observations in Contact Scaling for 2D FETs Zhihui Cheng^{1,2,3}, Huairuo Zhang¹, Hattan Abuzaid³, Jonathan Backman⁴, Yifei Yu⁵, Shreya Singh³, Albert Davydov¹, Mathieu Luisier⁴, Linyou Cao⁵, Curt Richter¹ and Aaron Franklin^{3,3}; ¹National Institute of Standards and Technology, United States; ²Purdue University, United States; ³Duke University, United States; ⁴ETH Zürich, Switzerland; ⁵North Carolina State University, United States

Atomically thin two-dimensional (2D) crystals are promising channel materials for extremely scaled field-effect transistors (FETs) for the 2030 era [1]. In the quest of ultra-scaled transistors, both channel length (distance from source to drain contacts) and contact length (distance that the contacts overlap the 2D channel) must be scaled. However, contacting 2D materials at scaled contact lengths ($L_c < 30$ nm) has rarely been pursued or studied in-depth. In this work, we experimentally scaled contact length for Ni-contacted MoS_2 FETs and use asymmetrical contact measurements (ACM) as a new approach for characterizing the devices. We found that, contrary to most previous reports, top contacts can be scaled down to ~30 nm without noticeable degradation in contact resistance. Surprisingly, we also observed significant self-heating in scaled contacts in the saturation regime. While the first observation is promising for extremely scaled FET technologies, the second illustrates that current crowding in metal-2D contacts is a challenge toward the development for future scaled devices. [1] IEEE International Roadmap for Devices and Systems. <https://irds.ieee.org/> (2020).

2:40 PM NM07.03.07

Fabrication and Structural Characterisation of MoS_2 Nanowires Louis Maduro, Maarten Bolhuis and Sonia Conesa-Boj; Delft University of Technology, Netherlands

Molybdenum disulfide (MoS_2) and MoS_2 -based nanowire arrays have garnered significant attention recently due to several potential applications, including being used as interconnects for nanoelectronic devices, for efficient electron emission, their structural stability, and in connection promoting hydrogen evolution reaction. In particular, MoS_2 nanowires display decreasing resistivity with decreasing nanowire diameter. For this reason,

relatively large electric currents can be sustained for nanowires with diameters in the tens of nanometer range, even though the resistivity of such nanosized MoS₂ nanowires increases to values larger than bulk MoS₂. This property makes MoS₂ nanowires promising candidates to be deployed as interconnects for nanodevices.

Furthermore, arranging MoS₂ nanowires into bundles whose axis is perpendicular to the substrate surface is a promising strategy for creating efficient electron emitters, where a lower voltage is required for electron extraction when decreasing the diameter of these nanowires. In order to create an ideal electron emitter device, the density of MoS₂ nanowires has to be such that the field enhancement effect of single nanowires is preserved while having a large density of MoS₂ nanowires to achieve a high electron current density.

Previous work in the fabrication of MoS₂ nanowires mostly focuses on bottom-up approaches based on hydrothermal synthesis, self-assembly, and chemical vapour deposition. However, these bottom-up methods lack precise control of the nanowire shape, nanowire-to-nanowire distance, and nanowire orientation. We propose a top-down approach for the fabrication of MoS₂ nanostructures which has not been widely explored. Here demonstrate the feasibility of a top-down approach to fabricate ordered arrays of MoS₂ nanowires where the shape, diameter, pitch, and length of these nanowires can be controlled in detail by means of the combination of sputter-deposition, electron beam lithography, and reactive ion etching.

SESSION NM07.04: Controlled Synthesis and Chemical Functionalization of 2D Materials IV and Imaging, Spectroscopy, and Quantitative Analysis of 2 Materials I
Session Chairs: Surendra Anantharam and Thomas Kempa
Sunday Afternoon, April 18, 2021
NM07

4:00 PM *NM07.04.01

Controlled and Scalable Synthesis of Two-Dimensional Carbides (MXenes) Yury Gogotsi; Drexel University, United States

Two-dimensional metal carbides and nitrides, known as MXenes, are the largest and yet quickly expanding family of 2D materials. Their diverse electronic, optical, and electrochemical properties have already distinguished them from other 2D materials. MXenes are produced by selective etching processes in which A layer atoms (i.e., Al, Si, Ga, etc.) are chemically removed from layered ceramics known as MAX phases or related layered carbides. MXenes have a general formula of M_{n+1}X_nT_x where M is a transition metal (i.e., Ti, V, Nb, Mo, etc.), X is carbon and nitrogen, n can be from 1 to 4, and T_x indicates to presence of mixed surface terminations (O, OH, Cl, F, etc.) on the surface of outer transition metal layers of MXenes. MXenes can also contain two or more transition metals in the M sites in a random solid solution (such as (Ti,V)₂CT_x) or ordered (in-plane or out-of-plane, such as Mo₂TiC₂T_x) structure, which further expands their range of compositions and therefore, properties. The surface functional groups of MXenes provide them with chemical stability and control their electronic properties. Titanium carbide MXene, Ti₃C₂T_x, has metallic conductivity reaching over 15,000 S cm⁻¹, while some other MXenes showed 2-3 orders of magnitude lower values. The tunable electronic properties of MXenes along with their high mechanical stiffness (Young's modulus reaching ~0.4 TPa for Nb₄C₃T_x MXene) and high bending rigidity as well as rapid ion-transport properties, redox-active surfaces, tunable electrochemical and optical properties have rendered these materials as promising candidates for various high-tech applications such as transparent conductive electrodes (TCE) for organic light-emitting diodes, smart and conductive textiles for sensing and energy-storing wearable devices, thin-film transistors, biomedical and biosensing, photovoltaics, and high energy and power density supercapacitors. Herein, we aim to discuss synthesis of MXenes, as well as effect of synthesis process parameters on surface chemistry and properties. Scalability of MXene synthesis and its processing from aqueous solutions by a variety of techniques will be addressed in detail.

4:25 PM NM07.04.02

AFM Additive Nanopatterning on Ionic Liquid Monolayer-Decorated Surfaces by Combined Mechanical and Electrical Stimuli Zixuan Li¹, Filippo Mangolini¹, Jerzy Sadowski², Raluca I. Gearba¹, Karalee Jarvis¹, Oscar Morales-Collazo¹, Andrei Dolocan¹ and Joan F. Brennecke¹; ¹The University of Texas at Austin, United States; ²Brookhaven National Laboratory, United States

The development of direct-write nanopatterning approaches enabling the accurate and reliable production of nanoscale architecture is critical for exploiting the unique functionalities of materials at reduced length scales. In the last few decades, several atomic force microscopy (AFM) lithography techniques, which use a sharp probe to write on a solid surface, have been developed as cost-effective methods for patterning with nanoscale resolution. Common AFM lithography techniques usually exploit the meniscus formed around the tip-substrate contact to dissolve and transfer the reactants for surface patterning. This mechanism can be problematic in large scale production due to the restricted ink capacity, as well as the inconsistency in the transfer process by varying experimental and environmental factors. Here we highlight a new AFM patterning method with which an adsorbed ionic liquid (IL) monolayer on the substrate will be used as the ink material. The unique interfacial properties of ILs combined with electrical and mechanical stimuli can realize nanoscale patterning without the reliance of the meniscus for ink transfer. The chemical nature and physical properties of the deposited material will be evaluated.

4:40 PM NM07.04.03

Rational Synthesis and Assembly of Transition Metal Dichalcogenide Nanocrystals with Tunable Optical Properties Tomojit Chowdhury¹, Erick Sadler¹, Kiyoun Jo², Todd Brintlinger³, Deep M. Jariwala² and Thomas J. Kempa¹; ¹Johns Hopkins University, United States; ²University of Pennsylvania, United States; ³U.S. Naval Research Laboratory, United States

Reducing the dimensionality of semiconducting transition metal dichalcogenides (TMDs) substantially alters their physical properties. Two-dimensional (2D) TMD crystals also exhibit electronic, magnetic, and optical properties which are sensitive to any manipulation of edge and strain states. We have introduced a rational chemical synthesis strategy that drastically improves control over the dimensions, morphology, and crystalline edges of 2D TMDs without the need for lithography and etching. TMD nanoribbons prepared through gas-phase growth on our designer surfaces exhibit atomically sharp edges and have enabled the exploration of anomalous exciton emission features. Moreover, we show that judicious assembly of mixed-dimensional architectures containing 2D TMD crystals and Si nanowires enables the introduction of nanoscale strain fields. Detailed nanoscale structural and optical characterization of these systems reveals unique edge and strain states that manifest localized photoluminescence with anomalous shifts in energy. Our results open a path toward the rational design of inorganic low-dimensional architectures with clear relevance for enabling future photonic and optoelectronic device studies.

4:55 PM OPENING REMARKS

5:00 PM *NM07.04.04

Toward 2D Heat and Light in 2D Crystals Jiwoong Park; The University of Chicago, United States

2D crystals and superlattices possess extremely anisotropic structures originating from different in-plane intralayer and out-of-plane interlayer bondings. This extreme structural anisotropy leads to anisotropic transport of electrons, phonons and photons. Indeed, 2D materials have recently shown several exciting 2D electronic transport phenomena. However, its impacts on the transport of heat and light in different directions have not been fully explored. In this talk, I will discuss two recent results related to this topic. First, we will discuss extremely anisotropic thermal conduction in stacked multilayers of transition metal dichalcogenides, where interlayer rotations lead to air-like thermal insulation along the through-plane direction. This leads to a giant thermal conductivity anisotropy ratio ~ 900 , which is much larger than that of graphite. Second, we will discuss

the long-range (~cm) guiding and non-linear switching of 2D photonic waves using a "delta-waveguide" built based on wafer-scale MoS₂. We show that this becomes an optical analog of quantum mechanical delta potential trap with a single trapped wavefunction. If time allows, we will also discuss how to realize these novel anisotropic properties by synthesizing and integrating other, molecule-based 2D materials.

5:25 PM NM07.04.05

Atomic-Step-Induced Screw-Dislocation-Driven Spiral Growth of PVD SnS Yih-Ren Chang¹, Chien-Ju Lee², Tomonori Nishimura¹, Wen-Hao Chang² and Kosuke Nagashio¹; ¹The University of Tokyo, Japan; ²National Chiao Tung University, Taiwan

The in-plane piezoelectricity or ferroelectricity of two-dimensional (2D) materials can vanish due to the appearance of inversion symmetry with increasing flake thickness, which drastically limits the development of their energy-harvesting application. On the other hand, although screw dislocation has long been regarded as an undesired line defect in three dimensional materials, screw dislocation driven growth in 2D materials could result in non-centrosymmetric structure even in bulk materials. The non-centrosymmetric structure in 2D materials can bring about plenty of intriguing properties such as vertical conductivity through the screw dislocation core and nonlinear optical generation, piezoelectricity and ferroelectricity and these properties might be further used in various applications like memory devices or piezoelectric generators. [1-3] However, despite the fact that the inversion symmetry breaking characteristic in spiral structure may solve the above-mentioned problem in 2D materials, the control of spiral growth remains immature owing to random occurrence of screw dislocation which limits the development of applications based on spiral 2D materials by poor nucleation site control and low percentage of spiral flakes.

In this research, a novel mechanism to achieve high percentage of spiral SnS flakes with superior control of nucleation position is demonstrated. By introducing atomic steps on substrates, the screw dislocation can be easily formed when SnS partially grows across these steps and leads to over 90% of spiral SnS flakes grown by physical vapor deposition (PVD). Furthermore, the preference for SnS to nucleate at steps can introduce remarkable nucleation site control of spiral growth even on substrates with artificially transferred graphene atomic steps. Through second harmonic generation (SHG) spectroscopy and cross sectional STEM analysis, it turns out that the spiral SnS structure exhibits inversion symmetry characteristic. Contrary to common understanding that spiral 2D material with single screw dislocation and Burgers vector equaling single layer thickness would show non-centrosymmetric structure, single-spiral SnS flakes with Burgers vector equaling the thickness of single layer SnS exhibits centrosymmetric structure. One possible reason that lead to centrosymmetric structure in spiral SnS could be ascribed to its ferroelectricity, [4] indicating that the orientation switching of SnS layer and the formation of AB stacking structure could be induced by strain.

This is the first work to control the formation position of spiral 2D materials and point out 2D materials with single spiral morphology and Burgers vector equaling single layer thickness do not guarantee non-centrosymmetric structure. High spiral flake percentage and precise control of nucleation sites in this study will facilitate future development of spiral 2D materials.

Reference:

- [1] T. H. Ly, *et al.*, *Advanced Materials* 2016, 28, 7723.
- [2] L. M. Zhang, *et al.*, *Nano Letters* 2014, 14, 6418.
- [3] W. Z. Wu, *et al.*, *Nature* 2014, 514, 470.
- [4] M. H. Wu, *et al.*, *Nano Letters* 2016, 16, 3236.

5:40 PM NM07.04.06

Late News: WS₂ Films Obtained with a Low Thermal Budget Sulfurization Process Dheryck S. Cabeda, Bruno C. Ferreira, Guilherme K. Rolim, Gabriel V. Soares and Claudio Radtke; UFRGS, Brazil

Transition metal dichalcogenides (TMDs) with lamellar structures similar to that of graphite have received

significant attention because some of them are semiconductors with sizable bandgaps and are naturally abundant. This offers opportunities for fundamental and technological research in a variety of fields including catalysis, energy storage, sensing, and electronic devices. Among them, bulk WS₂ exhibits an indirect band gap of 1.2 eV, while single-layer WS₂ exhibits a direct band gap of 1.8 eV. In order to fully exploit this versatility, obtaining layers of this material over large areas with the desired properties (in particular the number of monolayers composing the stack) is mandatory. Despite recent advances in the growth techniques of such a material, further investigation is needed especially in the basic mechanisms involved in the growth of WS₂ layers aiming at expanding their applicability. In view of this scenario, we sulfurized sputtered WO₃ films on SiO₂/Si substrates, varying the processing parameters. The objective was i) to identify the role of hydrogen added to the carrier gas in the sulfurization process and ii) to determine sulfurization parameters that result in fully sulfurized WO₃ films. For that, WO₃/SiO₂/Si stacks were introduced in a quartz tube where they were heated for variable times and temperatures. Pure Ar and a Ar:H₂ gas mixture were used as carrier gases. Sulfur powder was independently heated. X-ray Photoemission Spectroscopy (XPS), Rutherford Backscattering Spectrometry (RBS), and Raman Spectroscopy were used to characterize the products of the sulfurization process and also to infer about W loss from the sample during sulfurization. Results evidence that H₂ promotes an efficient sulfurization of the WO₃ film. Using pure Ar as the carrier gas, higher temperatures must be employed aiming at a complete sulfurization. Moreover, W loss takes place during sulfurization, if S is not supplied in a specific moment of the sample's heating ramp. This latter effect can be strongly suppressed by the use of H₂, which also significantly lowers the temperature needed for sulfurization. These results evidence a synthesis of WS₂ layers with a low thermal budget as well as details of the sulfurization process of WO₃ films. Such knowledge is fundamental for further improvements of WS₂ films' properties and to new applications of this material.

5:55 PM NM07.04.07

The Phonon Dispersion Relation as a Unique Identifier of Ordered BC₃ “Flower” Units in Graphene-Like Materials Devin McGlamery¹, Alexander A. Baker², Yi-Sheng Liu³, Martin A. Mosquera¹ and Nicholas Stadie¹; ¹Montana State University, United States; ²Lawrence Livermore National Laboratory, United States; ³Lawrence Berkeley National Laboratory, United States

Boron doped graphene and related materials, especially crystalline BC₃, have long been sought as promising materials for applications such as hydrogen and lithium-ion storage. Among the materials presented by experimentalists so far, boron presents as a notoriously difficult structural/chemical environment to unambiguously probe in the presence of carbon, frustrating the report of a successful synthesis of single-layer BC₃. Herein we report that the hexagonally symmetric C₆B₆ flower-like units that make up the structure of BC₃ exhibit a characteristic “breathing mode” detectable by Raman spectroscopy in the place of the usual D peak associated with graphene. This mode has a distinctly different dispersion relation, which is easily measured using a typical benchtop Raman spectrometer. Boron-substituted graphitic materials were synthesized by the direct route in the temperature range of 750 °C to 1100 °C across a range of compositions and levels of structural order, as characterized by a complement of techniques: Raman spectroscopy, X-ray diffraction, X-ray absorption spectroscopy, energy dispersive X-ray spectroscopy, and Auger electron spectroscopy. The dispersion relation was shown to be directly correlated with the structure and composition of the resulting materials, culminating in the detection of extended BC₃ units in samples of composition ~BC₅ prepared at 800 °C.

SESSION NM07.05: Imaging, Spectroscopy, and Quantitative Analysis of 2D Materials II

Session Chairs: Ying Fang and Thomas Kempa

Sunday Afternoon, April 18, 2021

NM07

6:30 PM *NM07.05.01

Manipulation of Magnetic Properties of van der Waals Crystals by Protons and Photons Srinivasa Rao Singamaneni; The University of Texas at El Paso, United States

van der Waals (vdW) engineering of magnetism is a topic of increasing research interest in the community at present. In the first part of my talk, I will present and discuss our recent efforts¹ in manipulating the magnetic properties of quasi-two-dimensional layered vdW $\text{Mn}_3\text{Si}_2\text{Te}_6$ (MST) crystals upon proton irradiation as a function of fluence 1×10^{15} , 5×10^{15} , 1×10^{16} , and 1×10^{18} H^+/cm^2 . We find that the magnetization is significantly enhanced by 53% and 37% in the ferrimagnetic phase (at 50 K) when the MST was irradiated with the proton fluence of 5×10^{15} , both in *ab* and *c* plane, respectively. The ferrimagnetic ordering temperature and magnetic anisotropy retained even after proton irradiation.

In the second part of my talk, I will discuss on the electron spin resonance (ESR) properties² of CrCl_3 and CrI_3 single crystals upon photo-excitation in the visible range. We noticed remarkable changes in the ESR spectra upon illumination. In the case of CrCl_3 , at 10 K, the ESR signal is shifted from $g = 1.492$ (dark) to 1.661 (light), line width increased from 376 to 506 Oe, and the signal intensity is reduced by 1.5 times. Most interestingly, the observed change in the signal intensity is reversible when the light is cycled on/off. We observed almost no change in the ESR spectral parameters in the paramagnetic phase (>20 K) upon illumination. Upon photo-excitation of CrI_3 , the ESR signal intensity is reduced by 1.9 times; the g -value increased from 1.956 to 1.990; the linewidth increased from 1170 to 1260 Oe at 60 K. These findings are discussed by taking into account the skin depth, the slow relaxation mechanism and the appearance of low-symmetry fields at the photo-generated Cr^{2+} Jahn-Teller centers. Such an increase in the g -value as a result of photo-generated Cr^{2+} ions is further supported by our many-body wavefunction calculations. This work has the potential to extend to monolayer vdWs magnets by combining ESR spectroscopy with optical excitation and detection. Our work shows that it is possible to employ proton and photon excitation in tuning the magnetic properties of vdW crystals, and provide many opportunities to design desired magnetic phases.

¹L. M. Martinez, H. Iturriaga, R. Olmos, L. Shao, Y. Liu, Thuc T. Mai, C. Petrovic, Angela R. Hight Walker, and **S. R. Singamaneni**, Enhanced magnetization in proton irradiated, $\text{Mn}_3\text{Si}_2\text{Te}_6$ van der Waals crystals, Appl. Phys. Lett. **116**, 172404 (2020); doi: 10.1063/5.0002168

²**S. R. Singamaneni**, L. M. Martinez, J. Niklas, O. G. Poluektov, R. Yadav, M. Pizzochero, O. V. Yazyev, and M. A. McGuire, Light Induced Electron Spin Resonance Properties of van der Waals CrX_3 ($X = \text{Cl}, \text{I}$) Crystals, Applied Physics Letters **117**, 082406 (2020); doi: 10.1063/5.0010888.

6:55 PM NM07.05.02

2D Confinement Heteroepitaxy Metals—Atomistic Insights of Interface Structure and Layer Intermixing Hesham El-Sheri¹, Natalie Briggs², Joshua Robinson² and Nabil Bassim¹; ¹McMaster University, Canada; ²The Pennsylvania State University, United States

Confinement heteroepitaxy (CHet) is a fabrication technique for 2D heterostructure in which atoms are intercalated between defective epitaxial graphene and substrates of silicon carbide in a CVD process typically at 800 °C. The confined layers can be designed with the merit of intercalation in several combinations, including metals, refractory, nitrides, and oxides. With all of these combinations, the CHet layers attract interest for many next-generation 2D devices in the field of photonics, plasmonic, hot-electron transistors, and optical polarization substrates.

Using a double-corrected aberration electron microscope and many FIB cross-section samples, we noted that the CHet layers' structure is not a superficial metallic layer on a perfect 6H-SiC stacking. We found that the SiC terminations vary from terrace-to-terrace, including a significant 3C-SiC termination on the topmost layer. Accordingly, this termination variation is found to affect the CHet layers structure and physical properties. For example, the 2D metals – called half-Van der Waals metals – exhibit a non-centrosymmetric structure with a lateral direction variance of the stacking order, structure, and the number of layers, which adds to the vertical direction bonding variance; from covalent (SiC) to metallic (Ga or In) to Van der Waal (Graphene). This makes

the 2D CHet surfaces a candidate for generating non-linear optical response and implemented as Surface-enhanced Raman Scattering substrates.

Besides, we observed a picometer-to-angstrom lattice spacing variation at the Si-metal interface. We also investigated epitaxial graphene samples, just before the intercalation process, to understand the Si-graphene and Si-carbon buffer layer interface. Here, we could provide the first direct microscopic evidence that the SiC termination induces Si sublimation from the topmost layer through controlled electron beam damage experiments. Our TEM observations were also consentient with many previous theoretical expectations that explained epitaxial graphene growth due to a pico-scale corrugation in the Si-face atoms due to a $(\sqrt{3} \times \sqrt{3})R30^\circ$ reconstruction on hexagonal (0001) 6H-SiC.

With these observations, we could explain anomalous but repeatable STEM-HAADF images of 2D Gallium and indium interfaces. These images show a significant EELS signal of Ga and In co-located with the topmost SiC layer in addition to Si and C signal within the 2D Ga and In layer. This interface mixing is observed to be limited to the topmost SiC layer but could be propagated into few layers in severe cases. The Si-metal interface instabilities are essential to be fully understood to optimize the growth conditions to avoid them. However, the presence of few doped Si and C atoms within 2D Ga and In could also be exciting if it induces extra orbital hybridization that may generate local and confined magnetism from the metallic layer, which we are currently investigating.

7:10 PM NM07.05.03

Ambipolar Thermoelectric Measurements of Multilayer WSe₂ Victoria Chen, Hye Ryoung Lee, Cagil Koroglu, Connor McClellan, Alwin Daus and Eric Pop; Stanford University, United States

Layered, two-dimensional (2D) semiconducting materials are promising candidates for thermoelectrics [1,2]. Among them, WSe₂ has one of the lowest thermal conductivities [3], in part due to its heavier atoms, which is an important consideration. In addition, WSe₂ is one of the few 2D materials that has been demonstrated as both *n*- and *p*-type (i.e. ambipolar) [4], thus satisfying the need of a thermoelectric generator with one material. Despite these promising material characteristics, only a few experimental studies on the thermoelectric properties of 2D WSe₂ have been performed [5,6], and their dependence on thickness and temperature is still unknown to date.

In this work, we conduct thickness- and temperature- dependent in-plane thermoelectric measurements of WSe₂ films. In order to tune the Fermi level and modulate the carrier density in the channel, we use an ionic-liquid, 1-Ethyl-3-methylimidazolium bis(trifluoromethylsulfonyl)imide (EMIM-TFSI), for electrolyte gating. WSe₂ flakes are exfoliated onto a glass substrate and contacted from the top with 50 nm of evaporated Pd. By using ionic-liquid gating, we are able to sweep across a large range of carrier densities with relatively low applied gate bias. Furthermore, the low thermal conductivity of both the ionic-liquid and substrate contribute to a larger lateral temperature gradient along the WSe₂, which is important for an accurate measurement of the Seebeck voltage. The thermoelectric measurements are conducted in vacuum, with on-chip Pd metal lines serving as resistive heaters and thermometers.

We sweep the gate voltage and measure the in-plane Seebeck coefficient ($S_{n,p}$) and electrical conductance of WSe₂ flakes with thicknesses from ~10 to 90 nm between 296 to 400 K. At room temperature, we measure S_p up to 700 $\mu\text{V}/\text{K}$ for holes and S_n down to -400 $\mu\text{V}/\text{K}$ for electrons in the same device, which are some of the largest reported for sub-100 nm WSe₂ [5,6]. In addition, we measure power factor values up to 50 $\mu\text{W}/\text{K}^2/\text{cm}$, which are comparable to bulk Bi₂Te₃, a common commercially used thermoelectric material, at room temperature [7]. We examine the trends of thermoelectric performance vs. electron and hole density as well as temperature and observe an increasing power factor with decreasing flake thickness. Overall, our results demonstrate the potential for WSe₂ to eventually compete with bulk materials for use in thermoelectric energy harvesters and we contribute to further understanding the fundamental properties of WSe₂.

- [1] M. Dresselhaus et al., *Adv. Mat.*, **19**, 1043 (2007)
- [2] J. Wu et al., *Adv. Elec. Mat.*, **4**, 1800248 (2018)
- [3] A. Mavrokefalos et al., *Appl. Phys. Lett.*, **91**, 171912 (2007)
- [4] S. Das et al., *Appl. Phys. Lett.*, **103**, 103501 (2013)
- [5] J. Pu et al., *Phys. Rev. B*, **94**, 014312 (2016)
- [6] M. Yoshida et al., *Nano Lett.*, **16**, 2061 (2016)
- [7] I Witting et al., *Adv. Elec. Mat.*, **5**, 1800904 (2019)

7:25 PM NM07.05.05

Pyrene-tethered Poly(4-vinylpyridine) for Liquid Phase Exfoliation of Hexagonal Boron Nitride

Allotropes and Their Thermal Conductive Nanocomposite Hyeokjung Lee, Seung Won Lee, Chanho Park, Kyuho Lee and Cheolmin Park; Yonsei University, Korea (the Republic of)

Owing to its favorable solution processability, the development of a stable dispersion of two-dimensional (2D) boron nitride (BN) has received significant attention for cutting-edge optic/electronic applications. Herein, we report an efficient method to disperse BN nanosheets (BNNSs) in polar solvents via dual noncovalent interactions using pyrene-tethered poly(4-vinylpyridine) (P4VP-Py). As a dispersion agent, P4VP-Py enables dual-functionalization with BNNS through π - π and Lewis acid-base interactions arising from the pyrene and pyridine moiety, respectively, resulting in highly stable BNNS dispersions in different solvents. The blend of P4VP-Py-functionalized BNNS with the pristine P4VP matrix resulted in increased thermal conductivity and dielectric constant combined with superior thermal stability by forming a compatible interface between the P4VP-Py matrix and the BNNS adjacent to the P4VP-Py. We demonstrated that dual noncovalent functionalization of BNNSs based on molecular design presents a strategy to achieve high dispersion of 2D materials into various media, ranging from polar solvents to solid matrices, for the expansion of advanced optic/electronic applications using BNNSs.

7:28 PM NM07.05.06

ALD Growth of Wafer-Scale WS₂ Film and Device Applications with Non-Toxic and Less Corrosive

Precursors Hanjie Yang¹, Yang Wang¹, Tao Chen¹, Rongxu Bai¹, Zecheng Wu¹, Zhongya Pang², Xingli Zou², Hao Zhu¹, Lin Chen¹, Qingqing Sun¹ and Li Ji¹; ¹Fudan University, China; ²Shanghai University, China

Tungsten disulfide (WS₂), as a member of two-dimensional transition metal dichalcogenides family, has attracted great attention due to its tunable band structure, excellent electrical transportation, unique optical properties and good air-stability. Despite the fact that WS₂ is a potential candidate for next-generation channel materials, preparing wafer-scale WS₂ film (8 inch or larger) with good uniformity and film quality remains challenging. Moreover, the bandgap of WS₂ with different layer numbers was tunable, which implied the necessity to precisely control the thickness. Chemical vapor deposition (CVD) is a common method to achieve high quality WS₂ films [1]. However, it is difficult to synthesize 2-inch or larger size WS₂ films with precisely controllable thickness. Atomic layer deposition (ALD) is an effective method to achieve wafer-scale WS₂ film. The self-limiting growth mode enabled the thickness of WS₂ film to be accurately controlled through changing the cycle numbers. The S sources of most ALD WS₂ research works were H₂S, which was highly toxic and dangerous. In addition, F-based precursor were used in many studies[2-5], resulting in an accelerated degradation of deposition system due to the highly corrosive nature of F-based precursors. In this work, low-toxic and less-corrosive tungsten hexachloride and hexamethyldisilathiane ((CH₃)₃SiSSi(CH₃)₃, HMDST) were used as W and S precursors, respectively, to achieve wafer-scale and thickness-controllable WS₂ films. The annealing process was carried out to improve the crystallinity of WS₂ film at 800°C for 2h. The XPS spectra, Raman spectra and plane-view and cross-sectional TEM indicated the good quality and controllable thickness of WS₂ film. Moreover, arrays of field-effect transistors based on WS₂ channel were further fabricated showing homogeneous electrical properties. The on/off ratio of WS₂ FET was nearly 10⁵ and the average electron mobility of WS₂ FET was 3.5 cm²V⁻¹s⁻¹. Our results paved a new path to synthesize wafer-scale and thickness-controllable WS₂ film in use of low-toxic and less-harmful precursors through ALD process, while the electrical properties demonstrated the attractive and promising potentials for WS₂ films in future nano-electronic device

integrations and applications.

References

- [1] C.Y. Lan, Z.Y. Zhou, Z.F. Zhou, et al. "Wafer-scale synthesis of monolayer WS₂ for high-performance flexible photodetectors by enhanced chemical vapor deposition", *Nano Res.*, 2018, 11, (6), pp. 3371-3384.
- [2] A. Delabie, M. Caymax, B. Groven, et al. "Low temperature deposition of 2D WS₂ layers from WF₆ and H₂S precursors: impact of reducing agents", *Chem. Commun.*, 2015, 51, (86), pp. 15692-15695.
- [3] B. Groven, M. Heyne, A. Nalin Mehta, et al. "Plasma-Enhanced Atomic Layer Deposition of Two-Dimensional WS₂ from WF₆, H₂ Plasma, and H₂S", *Chem. Mat.*, 2017, 29, (7), pp. 2927-2938.
- [4] B. Groven, A.N. Mehta, H. Bender, et al. "Two-Dimensional Crystal Grain Size Tuning in WS₂ Atomic Layer Deposition: An Insight in the Nucleation Mechanism", *Chem. Mat.*, 2018, 30, (21), pp. 7648-7663.
- [5] B. Groven, A.N. Mehta, H. Bender, et al. "Nucleation mechanism during WS₂ plasma enhanced atomic layer deposition on amorphous Al₂O₃ and sapphire substrates", *J. Vac. Sci. Technol. A*, 2018, 36, (1), pp. 11.

7:31 PM NM07.05.07

An Effective Lattice Engineering Way of the Defect and Stacking Structure of Inorganic Nanosheets for Optimizing Their Electrode and Electrocatalyst Performances Tae-Ha Gu¹ and Seong-Ju Hwang²; ¹Ewha Womans University, Korea (the Republic of); ²Yonsei University, Korea (the Republic of)

An effective chemical way to optimize the electrochemical functionalities of layered inorganic solids is developed by controlled restacking of exfoliated 2D nanosheet (NS). The fine-control of the stacking number and oxygen defect of restacked inorganic NSs can be achieved by employing diverse intercalants having various ionic sizes and charge densities. In contrast to conventional expectation, the supercapacitor electrode and electrocatalyst performances of inorganic NSs are well-correlated with their stacking numbers and oxygen defects, rather than with their basal spacings. The application of appropriate intercalant ion is quite effective in enhancing the electrode/electrocatalyst performances of restacked NSs via the creation of oxygen defect and the decrease of stacking number, resulting in improvement of catalysis kinetics and charge transfer property, and electrochemical surface area (ECSA). The present study highlights that the controlled restacking of exfoliated inorganic NSs can provide an effective way to optimize its electrochemical functionalities.

7:34 PM NM07.05.08

Exfoliated g-C₃N₄ Nanosheet as an Emerging Cationic Building Block for 2D Superlattice Bifunctional Catalyst Nam Hee Kwon and Seong-Ju Hwang; Yonsei University, Korea (the Republic of)

The interstratified superlattices of graphitic carbon nitride (g-C₃N₄)-molybdenum disulfide (MoS₂) monolayers with improved bifunctional catalytic performance are synthesized by an electrostatically-driven self-assembly between oppositely-charged exfoliated nanosheets (NSs). In contrast to other exfoliated inorganic NSs, the cationic form of g-C₃N₄ NS can be obtained via the tuning of suspension pH, which is applicable as a new type of cationic building block for superlattice nanohybrids. The resulting superlattice nanohybrids display strong interfacial interaction between restacked g-C₃N₄ and MoS₂ NSs, leading to creation of nitrogen vacancy, stabilization of 1T'-MoS₂ phase, and efficient interfacial electronic transition between the interstratified NSs. The superlattice g-C₃N₄-MoS₂ nanohybrids display remarkably enhanced bifunctionality as electrocatalysts for hydrogen evolution reaction and photocatalysts for visible light-induced N₂ fixation with high selectivity. The beneficial effect of hybridization on catalyst performances is attributable to the promoted adsorption of H⁺/N₂, the provision of many active sites, and the enhancement of charge transfer kinetics, the charge separation, and the visible light absorptivity. The present study highlights that the application of g-C₃N₄ NS as a cationic building block provides valuable opportunity to widen the library of multifunctional NS-based superlattice nanohybrids.

7:37 PM NM07.05.10

Synthesis and Structural Characterization of Graphene and Boron Nitride Angela Luis Matos¹, Vladimir Makarov^{2,1}, Brad Weiner¹ and Gerardo Morell¹; ¹University of Puerto Rico at Río Piedras, United States; ²University of Puerto Rico, United States

Graphene and Boron nitride are 2D materials that has been widely investigated due to their excellent features and potential applications in optoelectronic devices because of their high absorbance and transmittance properties. Graphene has been grown by several methods such as chemical vapor deposition (CVD), chemical or plasma exfoliation from natural graphite, mechanical cleavage (exfoliation) from natural graphite, microwave synthesis, etc.

CVD has demonstrated to be the most remarkable process for large-scale graphene fabrication. When the thermal CVD process is carried out in a resistive heating furnace, it is known as thermal CVD, and when the process consists of plasma assisted growth, it is called plasma enhanced CVD or PECVD. In this work it is presented graphene growth by hot filament CVD. Here methane gas it is used as a carbon source which is decomposed with a filament at high temperature. In this technique it is possible to obtain a single to few layers graphene by adjusting the growth parameters. To characterize graphene one of the main techniques used is Raman spectroscopy. A nondestructive tool for investigating atomic vibrational properties. Using the important features such as the D, G and 2D band of graphene, can be distinguish the number of layers, the presence of defects, edge orientation and to monitor the temperature. In this work will be presented how the Raman spectra change depending on the substrate where graphene has been grown or transferred, as well as the dependence on the temperature of the G band in bilayer graphene. Also, hexagonal-boron nitride (h-BN) has been known as the best substrate dielectric for studying 2D physics of graphene and for the high-performance of graphene electronics, due to its atomically smooth surface, lattice constant similar to that of graphene, large optical phonon modes, and a large electrical band gap. H-BN have been used to encapsulate graphene to avoid the impurities and as well to tailor the electronic properties of graphene. In this work, it will be presented the synthesis of h-BN and its structural characterization.

7:40 PM NM07.05.12

Alkalide-Assisted Direct Electron Injection for the Non-Invasive N-Type Doping of Graphene Sanghwan Park and Chang Young Lee; Ulsan National Institute of Science and Technology, Korea (the Republic of)

Although the doping of graphene grown by chemical vapor deposition is crucial in graphene-based electronics, non-invasive methods of n-type doping have not been widely investigated in comparison with p-type doping methods. We developed a convenient and robust method for the non-invasive n-type doping of graphene, wherein electrons are directly injected from sodium anions into the graphene. This method involves immersing the graphene in solutions of $[K(15\text{-crown-5})_2]Na$ prepared by dissolving NaK alloy in 15-crown-5 solution. The n-type doping of the graphene was confirmed by down-shifted G and 2D bands in Raman spectra and by the Dirac point shifting to a negative voltage. The electron-injected graphene showed no sign of structural damage, exhibited higher carrier mobilities than that of pristine graphene, and remained n-doped for over a month of storage in air. In addition, we demonstrated that electron injection enhances noncovalent interactions between graphene and metallomacrocyclic molecules without requiring a linker, as used in previous studies, suggesting several potential applications of the method in modifying graphene with various functionalities.

7:43 PM NM07.05.13

Salt-Assisted Growth of 2D Transition Metal Dichalcogenides Shisheng Li; National Institute for Materials Science, Japan

Abstracts

Chemical vapor deposition (CVD) of 2D transition metal dichalcogenides (TMDCs) always involves the conversion of vapor precursors to solid products in a vapor-solid-solid (VSS) growth mode (e.g., $WO_3 + S \rightarrow WS_2 + SO_2$). This often requires very high temperatures to sublime metal oxide precursors (e.g., WO_3). Our pioneering work on salt-assisted CVD (**Salt 1.0 technique**) enables the growth of 2D WS_2 and WSe_2 monolayers in a mild condition (lower temperature and atmospheric pressure) [1,2]. In the last five years, the use of alkali (alkaline earth) metal halides (AH, A = Li, Na, K, Ba, Ca; H = F, Cl, Br, I) in CVD has demonstrated great success in growing tens of atomically thin metal chalcogenides, graphene & h-BN

monolayers [3,4]. This is due to the formation of volatile MO_nCl_v and non-volatile NaM_yO_z when alkali (alkaline earth) metal halides react with metal oxides. They are highly efficient precursors for growing 2D TMDC monolayers.

The recent discovery and use of non-volatile molten salts in CVD (**Salt 2.0 technique**) trigger the vapor-liquid-solid (VLS) growth of 1D/2D TMDC monolayers [5]. The Salt 2.0 technique shows great improvements in the high-efficient and reproducible growth of large-area, uniform, and high-quality 2D TMDC monolayers. The Salt 2.0 technique also demonstrates great potentials in growing 2D TMDC materials in the following aspects: wafer-scale single crystals, patterns, heterostructure, and alloys [6]. It represents a new trend in the CVD growth of 2D TMDC materials.

References

- [1] S. Li, S. Wang, D.-M. Tang, W. Zhao, H. Xu, L. Chu, Y. Bando, D. Golberg and G. Eda, *Appl. Mater. Today* **1** 60-66 (2015).
- [2] D. Bradley, *Mater. Today* **18** 533 (2015).
- [3] J. Zhou, J. Lin, X. Huang, Y. Zhou, Y. Chen, J. Xia, H. Wang, Y. Xie, H. Yu, J. Lei, D. Wu, F. Liu, Q. Fu, Q. Zeng, C.-H. Hsu, C. Yang, L. Lu, T. Yu, Z. Shen, H. Lin, B. I. Yakobson, Q. Liu, K. Suenaga, G. Liu and Z. Liu, *Nature* **556** 355 (2018).
- [4] C. Liu, X. Xu, L. Qiu, M. Wu, R. Qiao, L. Wang, J. Wang, J. Niu, J. Liang, X. Zhou, Z. Zhang, M. Peng, P. Gao, W. Wang, X. Bai, D. Ma, Y. Jiang, X. Wu, D. Yu, E. Wang, J. Xiong, F. Ding and K. Liu *Nat. Chem.* **11**, 730 (2019).
- [5] S. Li, Y.-C. Lin, W. Zhao, J. Wu, Z. Wang, Z. Hu, Y. Shen, D.-M. Tang, J. Wang, Q. Zhang, H. Zhu, L. Chu, W. Zhao, C. Liu, Z. Sun, T. Taniguchi, M. Osada, W. Chen, Q. Xu, A. T. S. Wee, K. Suenaga, F. Ding and G. Eda, *Nat. Mater.* **17** 535 (2018).
- [6] S. Li, Y.-C. Lin, X.-Y. Liu, Z. Hu, J. Wu, H. Nakajima, S. Liu, T. Okazaki, W. Chen, T. Minari, Y. Sakuma, K. Tsukagoshi, K. Suenaga, T. Taniguchi and M. Osada, *Nanoscale* **11** 16122 (2019).

7:46 PM NM07.05.14

Layer-Controlled Nb Doped MoS_2 Thin Film with Wafer-Scaled Uniformity Jae-Hwan Jung¹, Ahrum Sohn¹, Changhyun Kim², Kyung-Eun Byun², Yeonchoo Cho², Hyeon Jin Shin² and Sang-Woo Kim¹;
¹Sungkyunkwan University, Korea (the Republic of); ²Samsung Advanced Institute of Technology, Korea (the Republic of)

Recently, due to the physical limitations of silicon-based transistors, studies using 2-dimensional (2D) materials as next-generation transistors have become more active. Graphene, widely known as a representative next-generation 2D material, has attracted a great deal of attention due to its high electrical conductivity, thermal conductivity and stiffness coefficient. However, since it does not have a zero-bandgap, it is limited to use as a semiconductor. Molybdenum disulfide (MoS_2), one of the TMD materials consisting of chalcogenide elements on both sides of the transition metal, has been reported to have n-type property, a direct band gap of 1.9 eV in a single layer and high absorptivity. Synthesis of MoS_2 films with a different carrier type is a very desirable technology because it can overcome the scaling issues in the further CMOS technology. However, most doping techniques of MoS_2 are difficult to satisfy well-controlled the number of layers, and large-scaled uniformity at the same time. Herein, we propose that an outstanding method with two steps enables us to obtain 2-inch wafer sized MoS_2 thin film with controlled the number of layers and even metal-doped MoS_2 with different carrier type in significantly short time. Various experiments have verified the quality of grown MoS_2 including thickness-dependent electrical behavior, and especially an innovative TEM analysis has confirmed an existence of dopants regardless of an atomic size.

7:49 PM NM07.05.15

Controlling Two-Dimensional Growth Through Interfacial Interactions and Dynamics Maria Sushko, Jinhui Tao, Biao Jin, Praveen Thallapally, James J. De Yoreo and Jun Liu; Pacific Northwest National Laboratory, United States

Solution synthesis may prove to be one of the most scalable synthesis methods of 2D materials providing that the thermodynamic and kinetic drivers that determine the phase, nucleation, and growth kinetics, and the degree of perfection, can be understood and controlled. A combination of in situ characterization and simulations of crystallization pathways demonstrated the dependence of specific pathways on local chemical environments. Using well-defined model systems these studies identified the factors for particle morphology control during homogeneous nucleation and growth and highlighted the importance of interfacial precursor kinetics and surface stress in inducing asymmetric growth. In particular, fast ion deposition kinetics at twin planes was shown to promote the growth of nanoplates in pure precursor solution. In ligand assisted homogeneous and heterogeneous growth ion- and ligand-induced interfacial strain relief was found to control the growth of asymmetric nanoparticles and single-layer metal organic framework films, respectively. The detailed analysis of the dependence of crystallization pathways on synthesis parameters (pH, precursor and ligand concentrations, temperature) and the systematic approaches to control synthesis of 2D materials using homogeneous and heterogeneous solution-based synthesis will be discussed.

SESSION NM07.06: Imaging, Spectroscopy, and Quantitative Analysis of 2D Materials III
Session Chairs: Ying Fang and Thomas Kempa
Sunday Afternoon, April 18, 2021
NM07

9:00 PM NM07.06.02

Late News: Imaging Strain Fields in Moiré Heterostructures Daniel K. Bediako; University of California, Berkeley, United States

Strain plays a key role in defining both the electronic and chemical behavior of materials. The properties of two-dimensional (2D) materials are particularly susceptible to strain and the controllable creation and analysis of strain in such systems is critically important to understand their behavior. In recent years, moiré superlattices that are formed by a small lattice mismatch or the azimuthal misorientation (interlayer twist) of two 2D layers have emerged as some of the most fascinating platforms to probe a host of emergent phenomena. Twisted bilayer graphene, with one sheet twisted relative to another, results in a moiré superlattice with a wavelength that is inversely proportional to the twist angle. Because of the variation in stacking of AA vs AB/BA sites in the two graphene layers, the individual sheets strain from the graphene hexagonal lattice in order to minimize free energy. This talk will discuss our work to precisely map this atomic reconstruction and measure the resultant strain in twisted bilayer graphene using a new methodology called Bragg interferometry based on 4-dimensional scanning transmission electron microscopy (4D-STEM). Intralayer strain and reconstruction mechanics are determined from mapping the displacement vectors between the graphene lattices by acquiring diffraction patterns at each position of the scanning electron probe. By quantitatively mapping strain tensor fields we uncover two distinct regimes of structural relaxation—in contrast to previous models depicting a single continuous process—and we disentangle the electronic contributions of the rotation modes that comprise this relaxation. Further, we find that applied heterostrain accumulates anisotropically in saddle point regions to generate distinctive striped shear strain phases. Our results thus establish the reconstruction mechanics underpinning the twist angle dependent electronic behaviour of twisted bilayer graphene, and provide a new framework for directly visualizing structural relaxation, disorder, and strain in any moiré material.

9:15 PM NM07.06.03

Enhanced Electronic Quality of Monolayer WS₂ via Re-Doping Leyi Loh, Michel Bosman and Goki Eda; National University of Singapore, Singapore

It is known that the electronic quality of monolayer transition metal dichalcogenides (TMDs) is strongly compromised by the presence of chalcogen vacancy defects. These defects are commonly present in densities

of $> 10^{13} \text{ cm}^{-2}$ and result in unintentional n-type doping and sub-gap optical emission features. In this study, we report suppression of sulfur vacancy formation during chemical vapor deposition of monolayer WS_2 by means of intentional in-situ Re-doping. Using aberration-corrected scanning transmission electron microscopy (STEM), we reveal that the sulfur vacancy density consistently decreases by up to 52% with increasing Re content. Interestingly, despite the possible electron-doping behavior of substitutional Re, we find the Re-doped WS_2 to be less n-type, indicating the suppression of unintentional doping effects of sulfur vacancies and high activation energy of Re impurities. We further show that substrate-induced exciton line broadening and sub-gap emission features are strongly suppressed in Re-doped samples, demonstrating their high electronic quality.

9:30 PM NM07.06.04

Strategies to Induce Selectivity in 2D Material Chemical Sensors Through Integration with Covalent Organic Frameworks Lucas K. Beagle^{1,2}, Ly D. Tran^{1,2}, Rahul Rao¹, Luke A. Baldwin¹ and Nicholas Glavin¹;
¹Air Force Research Laboratory, United States; ²UES, Inc., United States

Chemical and biological sensing using 2-D nanomaterials has been an area of intense investigation including inorganic materials that exhibit high sensitivity, however it has been limited as a field due to the lack of selectivity among analytes. While 2D inorganic materials can readily decipher between donor/acceptor groups, strategies to incorporate selectivity in these devices is crucial. Organic 2D materials known as covalent organic frameworks are large porous and repeated organic frameworks which have been shown to act as selectivity agents due to functionalization and porosity. This research focuses on the association of COFs with 2-D nanomaterials using top-down microwave-assisted activation of TMDs and deposition of COF particles. Several known COF species have been examined in order to understand the fundamental surface interactions between 2-D nanomaterials and COFs. Kinetics and mechanistic studies were used to determine the manner of association of the inorganic and organic substrates.

9:45 PM NM07.06.06

Metal Atoms on WTe_2 —Surface Diffusion, Interactions with Defects and Clustering Peter V. Sushko, Zexi Lu, Micah P. Prange, Yang Wang and Zdenek Dohnalek; Pacific Northwest National Laboratory, United States

Electronic properties of 2-dimensional (2D) van der Waals materials can be modified by adsorbing and intercalating metal atoms. Controlled aggregation of isolated atoms into clusters and other low-dimensional features can be used to generate new functional properties with potential applications in electronic devices and energy storage and conversion. Our ability to utilize these possibilities are predicated on the development of new synthesis strategies that, in turn, require detailed understanding of diffusion and aggregation pathways of adsorbed species on surfaces of these materials.

Here we report on binding, diffusion, and aggregation of transition metal atoms (Pd, Cu, Fe) adsorbed on a prototype 2D transition metal dichalcogenide (TMD) WTe_2 investigated using ab initio (density functional theory) simulations. While we find four distinct surface binding sites, the diffusion activation barriers between them differ dramatically, creating an asymmetry in surface migration. Metal dimers are only marginally more stable ($\sim 0.1 \text{ eV}$) than isolated adsorbed atoms; however, clusters of three atoms are stabilized by as much as $\sim 0.4 \text{ eV}$. Further increase of the cluster size up to 11 atoms is not significantly favored on the non-defective surface, which suggests that such clusters can decompose under mild thermal treatment. In contrast, adsorption of metal atoms at the Te vacancy sites is strongly favored. This is particularly evident in the case of Pd, which is slightly more electronegative than Te. As the size of the vacancy bound Pd cluster increases, the amount of the electron charge transferred to the cluster from the surface Te increases as well. This charge redistribution is accompanied by Pd atoms displacing Te atoms from their lattice sites leading to significant lattice damage. Finally, we investigated pathways for Te substitution with the adsorbed metal species on pristine surfaces. Our results suggest that formation of transient Pd dimers and trimers can trigger Te-to-Pd charge transfer sufficient to destabilize surface Te atoms and induce Pd for Te substitution. These results are consistent with the formation of two types of small Pd clusters on WTe_2 observed using scanning tunneling microscopy and their responses to thermal treatment. We discuss the similarities and the differences in behavior of the adsorbed metal species and their effect on the electronic properties of WTe_2 as well as implications for functionalization of

other TMDs.

10:00 PM NM07.06.08

Evidence of Large Absorption in the UV-Vis Region from Chemically Exfoliated MoS₂ Nanoparticles

Wafa Alnaqbi¹, Juveiriah M. Ashraf¹, Ayman Rezk¹, Aisha Alhammadi¹, Sabina Abdul Hadi² and Ammar Nayfeh¹; ¹Khalifa University of Science and Technology, United Arab Emirates; ²University of Dubai, United Arab Emirates

Molybdenum disulphide (MoS₂) is a transition metal dichalcogenide (TMD) semiconductor that has unique optical and electronic properties making it attractive for future electronic and photonic devices [1]. Due to the quantum confinement effect in 2D MoS₂, it has a tuneable band gap which increases as the size decreases. Bulk MoS₂ has an indirect band gap of ~1.2eV, while 2D MoS₂ has a direct band gap of ~1.8eV. In this work, we present MoS₂ nanoparticles (NPs) synthesized using a chemical exfoliation method and investigate the optical properties. First, we disperse 0.5 grams of MoS₂ powder in 50 mL of N-Methyl-2-pyrrolidone (NMP). Next, sonication using a probe set at 50% amplitude, and 10/2 seconds duty cycle for 6 hours in an ice bath maintained at 0 °C. The dispersion is then centrifuged at 1500 rpm for 60 min to remove unexfoliated particles, then at higher speed (7500 rpm) for 30 min to remove soluble impurities from the dispersion. The NMP is then removed, and the MoS₂ nanoparticles are filtered and re-dispersed in 25 mL of IPA. In order to first characterize the chemically exfoliated MoS₂ (ce-MoS₂) nanoparticles, we first deposit them on 3 cm x 3 cm pieces of fused silica by spin coating. Three coats of 100 µL were deposited with a total of 300 µL. The samples were left to dry for 1 hour between each coat at room temperature. The spin coating was conducted at 150 rpm for 40s. Optical microscopy of the samples under ultra-violet (UV) illumination showed a homogenous distribution of the MoS₂ NPs, exhibiting a red photoluminescence (PL) which is correlated to the quantum-confinement effect in MoS₂ at the nanoscale where direct band gap transitions can occur with a stable tunable PL depending on the NPs size. The films showed a smooth layer at low particle densities with cluster sizes below the resolution of the microscope (< 300 nm). At higher particle densities, larger clusters begin to form, with an approximate size of 1 µm and above, with a majority of clusters in the range of 2-5 µm in diameter. Both reflection and transmission spectra are measured after each coat using a UV-VIS spectrophotometer (Lambda 850, PerkinElmer) to investigate the behaviour of MoS₂ NPs, and the effect of the number of coats applied on the reflectance of the substrate. The corresponding reflection spectra were captured as a function of the incident wavelength, ranging from 250 nm to 1500 nm. Coated samples show a severe reduction in transmission to almost ~0% at UV-Vis (250 to 850 nm) and ~ 10% at NIR (850 to 1500 nm) after three coats. However, reflectance was around ~20% for UV-Vis and increased to ~50% at NIR. Which got absorption to increase from ~0% to ~80% at UV-Vis and ~40% at NIR after the third coat. We also deposited the MoS₂ on low temperature PECVD Ge films grown on (100) P doped (n-type) Si described in detail in our previous work [2]. A large drop in reflectance below 800 nm is seen which can be attributed to absorption in the MoS₂ nanoparticles. Above 800 nm, reflectance increases. This asymmetrical behaviour, which will be investigated further, can be explained by increased scattering in the non-absorption region. To summarize, in this work, we investigate the optical properties of chemically exfoliated MoS₂ NPs on fused silica and PECVD Ge films. The results show a large reduction in reflectance due to absorption in the MoS₂ in the UV-Vis region. Moreover, these results show that MoS₂ can have potential applications in photonics and PV-based devices.

[1] Singh, E., Singh, P., Kim, K. S., Yeom, G. Y., & Nalwa, H. S. (2019). Flexible Molybdenum Disulfide (MoS₂) Atomic Layers for Wearable Electronics and Optoelectronics. *ACS Applied Materials & Interfaces*, 11(12), 11061-11105.

[2] Ghada H. Dushaq, Mahmoud S. Rasras, Ammar M. Nayfeh, "Low temperature deposition of germanium on silicon using Radio Frequency Plasma Enhanced Chemical Vapor Deposition," *Thin Solid Films*, page 585-592, 2017

8:00 AM OPENING REMARKS

8:05 AM *NM07.07.01

Electrical and Chemical Control of Magnetism in van der Waals Ferromagnetic Materials Goki Eda^{1,1,2};

¹National University of Singapore, Singapore; ²Centre for Advanced 2D Materials, Singapore

Recent discoveries of gate-tunable magnetism in ferromagnetic two-dimensional (2D) materials such as CrI₃ and Fe₃GeTe₂ highlight the unique potential of this class of materials for novel spintronic devices. Understanding the interplay between magnetic order, free electron density, and electric field in the 2D limit is essential for uncovering the full potential of these materials. In this talk, we will first discuss electrical control of magnetism in Cr₂Ge₂Te₆ (CGT), a van der Waals ferromagnetic semiconductor, in an electric double-layer transistor (EDLT) geometry. We show that degenerately electron-doped CGT exhibits enhanced Curie temperature of up to 200 K, and rotation of its easy axis from out-of-plane to in-plane orientation. We demonstrate that similar changes in Curie temperature and easy axis can be induced by Na intercalation, which is accompanied by heavy electron doping of the host. We will further discuss our exploration of magnetism in other van der Waals materials such as NbFeTe₂ and magnetically doped transition metal dichalcogenides.

8:30 AM NM07.07.02

Thickness-Dependent Ambient Effects on the Curie Temperatures and Magnetic Domains of Metallic Two-Dimensional Magnets Ti Xie¹, Yeonghun Lee², Jinling Zhou^{1,3}, Alemayehu S. Admasu⁴, Nagarajan Valanoor³, John Cumings¹, Sang-Wook Cheong⁴, Ichiro Takeuchi¹, Kyeongjae Cho² and Cheng Gong¹;

¹University of Maryland, United States; ²The University of Texas at Dallas, United States; ³University of New South Wales, Australia; ⁴Rutgers, The State University of New Jersey, United States

The emergent magnetic two-dimensional (2D) materials provide ideal solid-state platforms for a broad range of applications including miniaturized spintronics and magnetoelectric sensors. Owing to the general environmental sensitivity of 2D magnets, the understanding of ambient effects on 2D magnetism is critical. Apparently, the nature of itinerant ferromagnetism potentially makes metallic 2D magnets insensitive to environmental disturbance. Nevertheless, our systematic study showed that the Curie temperature of metallic 2D Fe₃GeTe₂ decreases dramatically in the air but thick Fe₃GeTe₂ exhibits self-protection. Remarkably, we found the air exposure effectively promotes the formation of multiple magnetic domains in 2D Fe₃GeTe₂, but not in bulk Fe₃GeTe₂. Our first-principles calculations support the scenario that substrate-induced roughness and tellurium vacancies boost the interaction of 2D Fe₃GeTe₂ with the air. Our elucidation of the thickness-dependent air-catalyzed evolution of Curie temperatures and magnetic domains in 2D magnets provides critical insights for chemically decorating and manipulating 2D magnets.

8:45 AM NM07.07.03

Atomic-Scale Understanding of Defect Dynamics in Phosphorene Under Ion Bombardment Saransh

Gupta¹, Prakash Periasamy² and Badri Narayanan¹; ¹University of Louisville, United States; ²LAM Research Corporation, United States

The unique opto-electronic properties of two-dimensional monolayer of phosphorus (namely phosphorene) makes them lucrative for a variety of applications in nano-scale electronic devices, including field-effect transistors, photovoltaic junctions and thin-film solar cells. In particular, the lure of phosphorene arises from its semiconducting nature, thickness-dependent electronic band gap (1.5 eV in monolayer to 0.3 eV in bulk), high hole mobility ($\sim 10^5$ cm²/V/s), and large drain current modulation. The properties of phosphorene can be further

engineered by precise introduction of defects via ion bombardment or electron-irradiation. For instance, isolated mono-vacancies can induce hole doping as well as local magnetic moments; which can be leveraged to achieve specific functionality in opto-electronic devices. Despite this promise, precise defect engineering of phosphorene via ion/electron beams has remained challenging due to lack of fundamental understanding of the atomic-scale mechanisms underlying production, accumulation, and subsequent annealing of defects during irradiation. Indeed, previous first-principles modeling and electron microscopy studies provide insights into the atomic structure of defects, their thermodynamic stability, and threshold ion energy required to produce them. However, the effect of dose on defect accumulation, atomistic details of temporal evolution of defects, and defect dynamics under irradiation as well as subsequent annealing are largely unclear. Here, we employed reactive molecular dynamics (MD) simulations to unravel the dynamical atomic-scale processes underlying formation, accumulation, and re-organization/annealing of defects during Ar-ion bombardment of phosphorene. We found that radiation dosage strongly influences the type of defects that form, as well as their subsequent annealing. At low doses (10^{13} Ar⁺ions/cm² at 25 keV), the predominant defects that form are isolated mono-vacancies or Stone-Wales type defects that largely retain the planarity of the sheet. Interestingly, even small voids (1-2 nm) that form at these low doses can be healed by subsequent annealing; such healing proceeds via local re-arrangement of rings. Beyond a critical dosage (10^{14} Ar⁺ ions/cm² at 25 keV), large nanopores form whose edges are stabilized by formation of 3D structures consisting of P₄ tetrahedra. During subsequent annealing, these 3D structures facilitate the coalescence of nanopores, which further degrades the structure. These results will be discussed in the context of designing novel routes to precisely tune opto-electronic properties of phosphorene-based devices using ion beams.

8:50 AM NM07.07.08

Spatial Defects Nanoengineering for Bipolar Conductivity in MoS₂ Annalisa Calo^{1,2}; ¹University of Barcelona, Spain; ²Institute for Bioengineering of Catalonia, Spain

Two-dimensional transition metal dichalcogenides show great potential as a new class of atomically thin semiconductors for electronics and optoelectronics. Understanding the atomistic origin of defects in these materials and their impact on the electronic properties, as well as finding viable ways to dope them is matter of intense scientific and technological interest. In particular, controlling defects could be envisioned as a strategy for the design of ad-hoc electronic and optoelectronic properties. Here, we demonstrate a new integration of thermochemical scanning probe lithography (tc-SPL) with a flow-through reactive gas cell to achieve a nanoscale control of the local thermal activation of defects in monolayer MoS₂. The tc-SPL activated nanopatterns can present either p- or n-type doping on demand, depending on the used gasses, allowing the realization of field effect transistors, and p-n junctions with precise sub-mm spatial control and a rectification ratio over 10⁴. Doping and defects formation mechanisms are elucidated at the molecular level by means of X-Ray photoelectron spectroscopy, scanning transmission electron microscopy, and density functional theory. The p-type doping of locally heated MoS₂ in HCl/H₂O atmosphere is found to be related to the rearrangement of sulfur atoms and the formation of new protruding covalent S-S bonds on the surface, which produce a band structure with p-character. Alternatively, local heating MoS₂ in N₂ produces n-character.

SESSION NM07.08: Fundamental Properties of 2D Materials and Heterostructures II

Session Chairs: Zakaria Al Balushi and Surendra Anantharaman

Monday Morning, April 19, 2021

NM07

10:30 AM *NM07.08.01

TMD Alloys—Phase Diagrams, Synthesis, Optical and Electrical Properties Albert Davydov; National Institute of Standards and Technology, United States

Pending

10:55 AM NM07.08.02

Strong and Flaw-Insensitive Two-Dimensional Covalent Organic Frameworks Qiyi Fang¹, Chao Sui¹, Chao Wang¹, Tianshu Zhai¹, Jing Zhang¹, Jia Liang¹, Hua Guo¹, Emil Sandoz-Rosado² and Jun Lou¹; ¹Rice University, United States; ²U.S. Army Research Laboratory, United States

Recently, two-dimensional covalent-organic-frameworks (COFs), an structural analogue of graphene, have attracted great interests because of their tailorable structures lacking in other 2D materials. The topological design principles of monomers enable researchers to control the pore size and the unit cell geometry of 2D COFs allowing for highly tunable functionalities and properties. The unique structural features make 2D COFs possess exciting multifunctional properties with broad applications in liquid/gas separation, water filtration, energy storage/conversion, catalysis and ionic conduction, etc. However, the understanding of its mechanical properties and fracture mechanisms remains elusive. Here we report a quantitative in-situ tensile study of ultrathin COFs films. The fracture strength was measured to be 0.75 ± 0.34 GPa, and the tensile modulus was measured to be 10.38 ± 3.42 GPa, with a nominal density of 0.393 g/cc, thus having specific strength equivalent to Kevlar (2 GPa cc/g), and specific modulus comparable to titanium alloys (23 GPa cc/g). Additionally, the fracture toughness was measured to be 0.55 ± 0.09 MPa \sqrt{m} , and it was found that the crack propagation could be insensitive to the pre-crack when the size of pre-crack is below a critical value, leading to intriguing flaw insensitivity in such ultrathin nanomaterials. This work provides in-depth insights into the fracture properties of 2D COF films and lays a foundation for their future applications.

11:10 AM NM07.08.03

Recycling of Two-Dimensional Materials for van der Waals and Remote Epitaxy Dongheun Kim, Yeonhoo Kim, Eric Auchter, Enkeleda Dervishi-Whetham and Jinkyong Yoo; Los Alamos National Laboratory, United States

The absence of surface dangling bonds on two-dimensional (2D) materials mitigates materials compatibility issues of heterostructuring. Conventional materials synthesis on 2D materials have been prepared by van der Waals (vdW) and remote epitaxy techniques. In principle conventional or other 2D materials epitaxially grown on a 2D materials can be feasibly delaminated from the 2D layer as a substrate via applying mechanical force. Previous reports have shown that semiconductor nanomaterials and thin films for device applications can be prepared on 2D materials, especially graphene. Then the grown materials were detached from the host substrate, and applied for flexible devices. However the 2D layer in between the grown materials and the host substrate has not been thoroughly investigated. The 2D layer as a substrate or interlayer for vdW and remote epitaxy techniques has been considered as damaged. Thus there was no systematic characterizations of 2D layer after the epitaxy procedures and no attempt to recycling the 2D layer multiple times.

In the presentation recycling graphene and transition metal dichalcogenides layers for vdW and remote epitaxy will be demonstrated and discussed. Surface morphology and optical characteristics of the recycled 2D layers along repetition of the vdW and remote epitaxy were studied. Moreover the electrical/optical characterizations of semiconductors/2D heterostructures were performed to obtain insights of 2D/conventional materials interfacial properties.

11:25 AM NM07.08.04

Optimizing the Schottky Barrier at Metal-MoS₂ Junctions Through Metal Selection and Annealing Meghan Bush, Timothy Ismael, Kazi Islam, Claire Luthy and Matthew Escarra; Tulane University, United States

Monolayer molybdenum disulfide (MoS₂) is an attractive semiconductor for nano-optoelectronic devices due to its direct bandgap, open-air stability, and potential for large-scale synthesis. To optimize the electrical performance of these devices for applications such as photovoltaics, the relationship between the semiconductor and metal contacts must be fully understood and optimized.

The Schottky barrier height, denoted as Φ_B , is a potential energy barrier that exists at the junction of a metal and a semiconductor due to the difference in work functions. This directly impacts device performance, as a higher barrier decreases minority carrier transport since electrons cannot easily flow back into the semiconductor. We report here the experimental measurements of Φ_B between monolayer MoS₂ and a number of metals with varying work functions and process conditions. Large-area monolayer MoS₂ is grown using chemical vapor deposition (CVD) and metal contacts are deposited using electron beam evaporation on patterns written by electron beam lithography.

Different metals have different electrical performances and Schottky barriers resulting from their interaction with a semiconductor. The metals used for contacts are Ti and Sc (low work functions) and Pt (high work function). Here, the barrier height is extracted using the thermionic emission model, which implies that the Schottky barrier is temperature dependent. With an applied source-drain bias of 1 V, a source-drain sweep is taken for the nanoscale transistors over the gate voltage range -30 V to 30 V. These sweeps are repeated at 25 K temperature increments over 100-400 K. This data is plotted on an Arrhenius plot, with logarithmic gate voltages on the y-axis and the inverse of temperature on the x-axis. The initial linear slopes are related to the barrier height using the thermionic emission model, which results in an approximate barrier vs gate voltage plot from which the actual Schottky barrier height is extracted.^{1,2} So far, we have experimentally determined the Schottky barrier height of titanium, $\Phi_{Ti} = 0.21$. We will be repeating this process with the other metal contacts listed above to fully document how our CVD grown 2D MoS₂ interacts with these metals.

Thermal treatments have been used for decades to improve electrical performance in traditional III-V solar cells and semiconductor devices. Building on this, we posit that there are optimal annealing parameters that can improve the desired transport properties in electron and hole-selective Schottky barriers between 2D materials and metals. This annealing is done using a Rapid Thermal Annealer (RTA) to expose the device to high temperatures for short periods of time. Since RTA is scalable, it directly translates to manufacturing for large area 2D PV. By comparing the Schottky barrier heights without annealing and after various annealing conditions, we will establish a better understanding of how this process impacts the metal-semiconductor junction. The ability to tune the barrier height allows devices to be further customized with improved performance.

Understanding the barrier of the MoS₂-metal junction will allow for more complex devices to be designed and fabricated, including but not limited to photovoltaics, photo-emitters, photodetectors, etc. Future work entails optimizing device preparation and treatment to result in Schottky barriers for different 2D electronic applications. These measured barrier heights are also being included in a computational device model to study various MoS₂-based optoelectronic devices.

¹ Das, S., Chen, H., Penumatcha, A. V., & Appenzeller, J. (2012). High Performance Multilayer MoS₂ Transistors with Scandium Contacts. *Nano Letters*, 13(13), 100-105

² Wang, W., Liu, Y., Tang, L., Jin, Y., Zhao, T., & Xiu, F. (2014). Controllable Schottky Barriers between MoS₂ and Permalloy. *Scientific Reports, Sci Rep* 4, 6928 (2014)

11:30 AM NM07.08.06

Collective Modes in Substitutionally Doped 2H-NbS₂ Amin Azizi¹, Mehmet Dogan^{1,2}, Jeffrey D. Cain^{1,2}, Kyunghoon Lee^{1,2}, Xuanze Yu¹, Marvin L. Cohen^{1,2} and Alex Zettl^{1,2}; ¹University of California, Berkeley, United States; ²Lawrence Berkeley National Laboratory, United States

Metallic transition-metal dichalcogenides (TMD) are rich material systems in which the interplay between strong electron-electron and electron-phonon interactions results in a variety of instabilities such as charge density waves (CDWs). While most metallic TMDs exhibit coexistence of superconductivity and CDWs, 2H-NbS₂, with a superconducting transition temperature (T_C) of ~6K, shows no CDW order. Most recently, the

existence of an incommensurate CDW pinned by atomic impurities (such as vacancies) has been reported in 2H-NbS₂. Substitutional dopants, depending on their atomic number and electronic state, can considerably affect electronic behavior in these systems.

Here, we substitutionally dope 2H-NbS₂ with heavy atoms via chemical vapor transport. Using aberration-corrected scanning transmission electron microscopy (STEM) imaging, we confirm the 2H phase of NbS₂ and determine the distribution and concentration of dopant atoms. Using a combination of low temperature transport measurements and density functional theory calculations, we demonstrate how heavy dopant atoms can modify the collective electronic states (such as superconductivity and CDW) in 2H-NbS₂.

11:45 AM NM07.08.07

Late News: Exfoliation and Optical Properties of Near-Infrared Fluorescent Silicate Nanosheets Gabriele Selvaggio^{1,2}, Milan Weitzel², Nazar Oleksiievets², Tabea A. Oswald², Robert Nißler^{1,2}, Ingo Mey², Volker Karius², Jörg Enderlein², Roman Tsukanov² and Sebastian Kruss^{1,2,3}; ¹Ruhr University Bochum, Germany; ²University of Göttingen, Germany; ³Fraunhofer Institute for Microelectronic Circuits and Systems, Germany

The near-infrared (NIR) region of the electromagnetic spectrum presents optimal characteristics for imaging of complex (biological) samples due to reduced light scattering, absorption, phototoxicity and autofluorescence. However, despite their clear potential over commonly employed visible fluorophores, only few NIR fluorescent materials are known so far, and even less are suitable for biomedical applications. For this reason, it is of great interest to identify novel NIR fluorophores and use them for biomedical applications.

Here, we exfoliated a class of layered silicates: Egyptian Blue (CaCuSi₄O₁₀, EB), Han Blue (BaCuSi₄O₁₀, HB) and Han Purple (BaCuSi₂O₆, HP). These pigments fluoresce in the NIR ($\lambda_{\text{emi}} \approx 920\text{-}950$ nm) with a long excited state lifetime ($\tau \approx 10\text{-}100$ μs). By milling, tip sonication and several centrifugation steps, small and monodisperse 2D nanosheets (NS) could be exfoliated. The morphology of such NS was then fully characterized by atomic force (AFM) and scanning electron microscopy (SEM). Most interestingly, the intense NIR fluorescence emission of the bulk counterparts is retained in these nanostructures. In comparison to state-of-the-art fluorophores, EB-NS show no bleaching while displaying outstanding fluorescence intensity. These qualities of EB-NS enabled us to inject them into systems of biological relevance such as developing *Drosophila* embryos, and perform *in vivo* single-particle tracking and microrheology measurements.

Furthermore, because of their high biocompatibility, it is possible to use them for NIR imaging in plants. [1] The above mentioned three silicate NS are very bright and can be imaged through several cm of tissue phantoms, which demonstrates the potential for (bio)photonics. Finally, we used the microsecond fluorescence lifetimes of EB-NS, HB-NS and HP-NS for micro- and macroscopic fluorescence lifetime imaging (FLIM). The results show that lifetime engineering of these silicate nanostructures is possible and can be used for lifetime-encoded imaging. [2]

In summary, we present a new exfoliation route that yields NIR fluorescent nanosheets with high potential for bioimaging and photonics.

Literature:

[1] G. Selvaggio *et al.*, Nat. Commun. 11, 1495 (2020)

[2] G. Selvaggio *et al.*, <https://doi.org/10.26434/chemrxiv.13350728.v1> (2021)

12:00 PM NM07.08.08

Late News: Strain Tuning of the Optoelectronic Properties of Two-Dimensional Crystals Elena Blundo¹, Marzia Cuccu¹, Pettinari Giorgio², Cinzia Di Giorgio³, Tanju Yildirim⁴, Paulo E. Faria Junior⁵, Marco Felici¹, Fabrizio Bobba³ and Antonio Polimeni¹; ¹Sapienza, University of Rome, Italy; ²National Research Council, Italy; ³University of Salerno, Italy; ⁴National Institute for Materials Science, Japan; ⁵Universität Regensburg, Germany

The variegated family of two-dimensional materials comprises crystals that have attracted great interest for diverse characteristics and peculiarities. Among them, semiconducting transition-metal dichalcogenides (TMDs) possess alluring optoelectronic and spin properties when reduced to the single layer. In particular,

TMD monolayers are characterised by a direct bandgap, resulting in an efficient light emission in the visible/infrared range, which renders them appealing for optoelectronic devices. Furthermore, a strong spin-orbit coupling makes them interesting candidates for valley- and spin-tronics. Indeed, the inherent plane-confined nature of these materials -coupled to their exceptional mechanical flexibility and robustness- makes them highly sensitive to external stimuli. Methods to tailor their unique properties on demand have been thus sought after, and protocols based on controllable external perturbations such as mechanical deformations have shown promise in this respect.

Here, we present a novel technique to induce controllable strain-fields in TMD monolayers and study their effect on the optical and spin properties. Localised strains are created via low-energy hydrogen-ion irradiation of bulk TMDs, leading to the production and accumulation of molecular hydrogen in the first interlayer region. The trapped gas coalesces, leading to a local blistering of the material, and thus to the formation of one-monolayer-thick micro/nano-bubbles, which stud the crystal surface and locally turn the dark bulk material into an efficient light emitter. [1] Electron-beam-lithography-based approaches allowed us to achieve control over the formation process of the bubbles, and to create them in ordered arrays and with the desired dimensions (from few tens of nm to few microns). [1-2] These bubbles are durable and incredibly robust [3] and host complex strain fields, evaluated numerically, that cause dramatic changes in the TMD optoelectronic properties. Photoluminescence steady-state and time-resolved studies enabled the characterisation of the strain-induced band-structure modifications and revealed intriguing phenomena, such as bandgap crossovers enabling the creation of exciton states with long lifetimes. [4] Magneto-optical experiments allowed us to achieve unprecedented information on the spin and valley properties of strained TMDs, and led to the observation of hybridisation mechanisms between different band states.

Recently, the interest for TMD monolayers has surged due to the possibility to stack them via weak van der Waals forces to create heterostructures. TMDs have also been coupled with other semiconducting two-dimensional materials, such as post-transition-metal chalcogenides. Novel excitonic states -referred to as interlayer excitons- have been observed in TMD-based heterostructures, in which the two oppositely charged carriers forming the exciton are localised in different monolayers. Here, we exploit the same approach used for the formation of single monolayer bubbles to strain-tune the electronic properties of novel van der Waals heterostructures, and show how strain can play a crucial role by changing the relative band alignment of the stacked materials.

Our results unveil unprecedented information on the strain effects on TMDs and their heterostructures, the understanding of which represents an essential step towards their integration into flexible electronic devices.

[1] D. Tedeschi, E. Blundo, et al., *Adv. Mater.* 31, 1903795 (2019).

[2] E. Blundo et al., *Adv. Mater. Interfaces* 7, 2000621 (2020).

[3] C. Di Giorgio et al., *Adv. Mater. Interfaces* 7, 2001024 (2020).

[4] E. Blundo et al., *Phys. Rev. Res.* 2, 012024 (2020).

SESSION NM07.09: Fundamental Properties of 2D Materials and Heterostructures III

Session Chairs: Zakaria Al Balushi and Surendra Anantharaman

Monday Afternoon, April 19, 2021

NM07

1:00 PM NM07.09.01

Late News: Zero-Dimensional Graphene and Its Behavior During Mechanochemical Activation of Nanoferrites [Monica Sorescu](#)¹, Alice Perrin² and Michael McHenry³; ¹Duquesne University, United States; ²MIT, United States; ³Carnegie Mellon University, United States

Nickel ferrite nanoparticles were subjected to mechanochemical activation for ball milling times ranging from 0 to 12 hours. The milling was performed with and without the addition of equimolar concentrations of graphene nanoparticles. Characterization of resulting nano-powders was undertaken by Mossbauer spectroscopy and magnetic measurements. The hyperfine magnetic field was studied as function of milling time for octahedral and tetrahedral sites. An additional quadrupole split doublet represented the occurrence of superparamagnetic particles in the as-obtained and milled specimens. A new phase was obtained in the graphene-milled set of samples, which could be assigned to carbon-rich particles. The degree of inversion and canting angle were derived from the Mossbauer measurements and studied as function of ball milling time. The degree of inversion was found to decrease with milling time, especially for the set without graphene and evidenced a transition from inverse to normal spinels. The canting angle decreased with time for the graphene milled nanoparticles. The recoilless fraction was determined as function of milling time and was consistent with the observation – for the first time in literature – of a distribution of recoilless fractions in the studied specimens. The saturation magnetization, remanence magnetization and coercive field were derived from the hysteresis loops, recorded at 5K and 5T. The zero-field-cooling-field-cooling measurements were obtained in a magnetic field of 200 Oe and the blocking temperature was determined. Our results show new features of the behavior of nickel ferrite nanoparticles under mechanochemical activation with and without graphene.

Cobalt ferrite nanoparticles were exposed to mechanochemical activation, with and without equimolar amounts of graphene nanoparticles, for time periods ranging from 0 to 12 hours. Their structural and magnetic properties were detailed from Mossbauer spectroscopy and magnetic measurements. The Mossbauer spectrum corresponding to the unmilled cobalt ferrite powder was analyzed using 2 sextets, corresponding to the tetrahedral and octahedral sites of ferrites. The rest of the spectra was deconvoluted using an additional quadrupole-split doublet, with an abundance close to 30% and was assigned to superparamagnetic particles. Moreover, the spectra corresponding to milling with graphene at the longest times needed a third sextet, which could be assigned to iron carbide. The degree of inversion was determined from the Mossbauer spectra and found to decrease with milling time, both for the set with and that without graphene. The canting angle was derived and studied as function of the ball milling time for both sets of samples. Hysteresis loops were recorded at 5 K in an applied magnetic field of 5 T and was found to exhibit a constricted shape. Magnetization was plotted as function of temperature in the range 5-300 K with an applied magnetic field of 200 Oe using zero-field-cooling-field-cooling (ZFC-FC) measurements. These made it possible to determine the blocking temperature of the samples. Our data exhibit new characteristics of the cobalt ferrite nanopowders milled with and without graphene nanoparticles.

1:15 PM NM07.09.02

Acoustic Transport of Room Temperature Excitons in Monolayer WSe₂ Kanak Datta¹, Zidong Li¹, Zhengyang Lyu¹, Takashi Taniguchi², Kenji Watanabe² and Parag Deotare¹; ¹University of Michigan–Ann Arbor, United States; ²National Institute for Materials Science, Japan

In recent years, monolayer transition metal dichalcogenides (TMD) have garnered widespread interest from the research community across the world due to their exciting optical properties and strong light-matter interaction. As the optical properties of these materials are extremely sensitive to external mechanical stimuli, controlled static strain has been successfully applied to tune the light-matter interaction in these materials [1]. However, the interaction of excitons with the travelling strain and piezoelectric field generated by surface acoustic wave remains widely unexplored. Here, we experimentally investigate exciton transport in monolayer WSe₂ under surface acoustic wave.

We generate high-frequency Rayleigh type surface acoustic wave (SAW) by patterning interdigitated electrodes (IDTs) on 128^o Y-cut piezoelectric lithium niobate (LiNbO₃) substrate using standard photolithography methods. The SAW resonators are designed for a resonance frequency of 600 MHz (SAW wavelength ~ 6 μm). We characterize the transport of excitons in hexagonal boron nitride (hBN) encapsulated WSe₂ monolayer using phase locked time correlated single photon counting (TCSPC). Upon RF excitation the travelling hydrostatic strain wave of the SAW modulates the conduction and valance band of the monolayer WSe₂ in opposite phase resulting in localized potential pockets, commonly referred as type – II bandgap modulation [2]. The resulting

potential pockets can capture and result in long-range transport of excitonic species.

We observed strong coupling of monolayer exciton species to the travelling strain field generated by the surface acoustic wave that resulted in remote recombination of the transported excitons. Using measured exciton lifetime of 1.27 ns, we estimate the exciton velocity under acoustic modulation to be $0.78 \times 10^3 \text{ ms}^{-1}$. Using experimentally reported value of strain mobility in monolayer WSe₂ [3], we estimate the hydrostatic strain on the monolayer to be 0.4%. Our observations show that the transport distance is mostly limited by the intrinsic exciton mobility and lifetime in monolayer WSe₂.

References:

- [1] C. Martella, C. Mennucci, A. Lamperti, E. Cappelluti, F. B. de Mongeot, and A. Molle, *Adv. Mater.* (2018).
- [2] J. Rudolph, R. Hey, and P. V. Santos, *Phys. Rev. Lett.* **99**, 1 (2007).
- [3] D. F. Cordovilla Leon, Z. Li, S. W. Jang, C. H. Cheng, and P. B. Deotare, *Appl. Phys. Lett.* (2018).

1:20 PM NM07.09.04

Late News: Structural and Spectroscopic Investigation of Layered Semiconductor-Iron Phosphorus

Trisulfide-FePS₃ Adam K. Budniak¹, Szymon J. Zelewski², Magdalena Birowska³, Tomasz Wozniak², Tatyana Bendikov⁴, Yaron Kauffmann¹, Yaron Amouyal¹, Robert Kudrawiec² and Efrat Lifshitz¹; ¹Technion - Israel Institute of Technology, Israel; ²Wroclaw University of Science and Technology, Poland; ³University of Warsaw, Poland; ⁴Weizmann Institute of Science, Israel

Binary layered semiconductors, especially transition metal dichalcogenides (TMDs), are among the most studied van der Waals (vdW) semiconductors. Recently ternary layered materials are drawing more attention due to their attractive properties.[1]

Amid ternary vdW semiconductors, iron phosphorus trisulfide - FePS₃ - is an interesting material. It belongs to a family of transition metal phosphorus trisulfides (TMTs) with general formula MPS₃. FePS₃ is magnetic semiconductor, absorbing in near IR, and it is also relatively stable in exfoliated form. Large FePS₃ crystals (almost centimeter size) have been obtained in big amounts (more than 70% chemical yield) via chemical vapor transport (CVT). Bulk material is investigated by X-Ray and ultraviolet photoelectron spectroscopy (XPS and UPS). Optical properties are carefully studied with temperature change. The results are further corroborated with DFT calculations. FePS₃ is both mechanically and liquid exfoliated and obtained products are compared by X-Ray diffraction (XRD) and then by conventional transmission electron microscopy (cTEM), carefully proceeded for chosen crystallographic directions with high-resolution analysis for both kinds of samples.[2] Here, a simple, one-step protocol for mechanical exfoliation directly onto transmission electron microscope grid is used as an efficient sample preparation method.[1,2,3] Finally, atomic resolution elemental maps are registered with high-resolution scanning transmission electron microscope (HR-STEM) and reveal directly the atom columns arrangement.[2]

At last, the large-scale project will be briefly described, where vdW materials are used for the first time for tunable X-Ray emission. The X-Ray radiation is produced from two combined mechanisms [called parametric coherent bremsstrahlung (PCB) collectively]: parametric X-ray radiation (PXR) and coherent bremsstrahlung (CBS). FePS₃ with other ternary vdW materials CrPS₄, MnPS₃, CoPS₃, NiPS₃, and also binary WSe₂, are mechanically exfoliated and transferred to electron microscopy grids. Next, they are irradiated by an electron beam inside a transmission electron microscope. The tunability of energy of emitted X-Ray is achieved both by adjusting electrons acceleration voltage or using different material as the emitter.[3]

References:

- [1] A.K. Budniak, N.A. Killilea, S.J. Zelewski, M. Sytnyk, Y. Kauffmann, Y. Amouyal, R. Kudrawiec, W. Heiss, E. Lifshitz, "Exfoliated CrPS₄ with promising photoconductivity", *Small*, **2020**, 16 (1), 1905924
- [2] A.K. Budniak, S.J. Zelewski, M. Birowska, T. Wozniak, T. Bendikov, Y. Kauffmann, Y. Amouyal, R. Kudrawiec, E. Lifshitz, "Spectroscopic and structural investigation of bulk and exfoliated iron phosphorus trisulfide - FePS₃", **manuscript in preparation**
- [3] M. Shentcis, A.K. Budniak, X. Shi, R. Dahan, Y. Kurman, M. Kalina, H. Herzig Sheinflux, M. Blei, M.

Kamper Svendsen, Y. Amouyal, S. Tongay, K. Sommer Thygesen, F.H.L. Koppens, E. Lifshitz, F. J. García de Abajo, L.J. Wong, I. Kaminer, “Tunable free-electron X-ray radiation from van der Waals materials”, *Nature Photonics*, **2020**, 14 (11), 686-692

1:35 PM NM07.09.05

Late News: Mobile Charges and Intertube Excitons in 1D van der Waals Coaxial Nano-Cables Maria Burdanova¹, Reza Kashtiban¹, Yongjia Zheng², Rong Xiang², Shohei Chiashi², Shigeo Maruyama² and James Lloyd-Hughes¹; ¹University of Warwick, United Kingdom; ²The University of Tokyo, Japan

Heterostructures built from atomically thin 2D crystals, and bound by the van der Waals force, are well known to exhibit attractive optoelectronic properties and exotic physics. For instance, the strong Coulomb interactions can create bound charges across an interface, creating interlayer excitons with longer lifetimes. However the quantum confinement of electrons in quasi-1D structures creates distinctly different possibilities than available in 2D, as can be seen by contrasting graphene (a semi-metal in 2D with no excitonic absorption) and carbon nanotubes (semiconducting for certain chiralities, and featuring strong excitonic absorption).

Here we report the structure, composition and optoelectronic properties of a 1D van der Waals heterostructure consisting of nano-scale coaxial cables [1,2]. Carbon nanotubes (CNTs) formed the “core” of the cable, and were wrapped by atomically-thin nanotubes of the insulator boron nitride, and then by molybdenum disulfide (MoS₂). The high quality of the composite was directly evident on the atomic scale from high-resolution transmission electron microscopy, and on the macroscopic scale by a study of its equilibrium and ultrafast optoelectronics [2].

We used THz spectroscopy to establish the good conductance of the CNT cores within the coaxial nano-cable, which can be therefore be regarded as a radial metal/insulator/semiconductor heterojunction. Via optical pump, THz probe spectroscopy we investigated the electron mobility of the MoS₂ nanotubes, finding that it was comparable to that of high-quality atomically-thin 2D crystals of MoS₂. The high mobility of the MoS₂ nanotubes highlights the huge potential of the coaxial “hetero-nanotube” growth platform for nanoscale optoelectronic devices [3].

Finally, we addressed the intriguing question: can the optical properties of such coaxial nano-cables be described by the average properties of each material in isolation, or do interactions between the materials lead to unique new properties? To investigate, we used multi-colour infrared pump, visible probe spectroscopy to selectively create excitons in the carbon nanotubes, while probing the response of the A and B excitons in the MoS₂ nanotube sheath. We observed a rapid and strong excitonic response of the MoS₂ to the presence of excitons in the carbon nanotube core. This observation is surprising as in the single-photon, single particle picture a photon from the infrared pump pulse (0.6eV) does not give an electron sufficient energy to cross the MoS₂ excitonic gap (1.9eV). Further, charge transfer processes are prohibited by the intermediate BN insulating layer. However, our experimental findings can be understood by considering the strong Coulomb correlations between the carbon nanotube core and the MoS₂ sheath, which created the intertube excitonic and biexcitonic absorption features observed in the transient spectra. This first observation of intertube excitons, analogous to the interlayer excitons of 2D heterostructures, further underscores the potential of 1D van der Waals materials for basic science and future applications.

[1] Xiang et al., *Science* (2020) 367, 537-542, DOI: 10.1126/science.aaz2570

[2] Burdanova et al., *Nano Letters* (2020) 20, 3560-3567, DOI: 10.1021/acs.nanolett.0c00504

[3] Xiang and Maruyama (2021), *Heteronanotubes: Challenges and Opportunities*. *Small Sci.* 2000039, DOI: 10.1002/smsc.202000039

1:50 PM *NM07.09.06

Van der Waals Heterostructure Magnetic Josephson Junction Philip Kim; Harvard University, United

States

When two superconductors are connected through a ferromagnet, spin configuration of the transferred Cooper pairs can be modulated due to the exchange interaction. The resulting supercurrent can reverse its sign across the Josephson junction, depending on the thickness of the ferromagnetic weak link. In this talk, we present Josephson phase engineering in van der Waals heterostructures of atomically thin magnetic insulator Cr₂Ge₂Te₆ sandwiched between NbSe₂ van der Waals superconductors. Employing a superconducting quantum interference device based on our magnetic insulator Josephson Junctions, we reveal a doubly degenerate nontrivial Josephson phase originating from the magnetic barrier. We find that these unusual magnetic Josephson junctions are formed by momentum conserving tunneling of Ising Cooper pairs of NbSe₂ across the magnetic domains of atomically thin Cr₂Ge₂Te₆. The doubly degenerate ground states in magnetic insulator Josephson junction provide a quantum two-level system which can be utilized as a new component for superconducting quantum devices

SESSION NM07.10: Fundamental Properties of 2D Materials and Heterostructures IV
Session Chairs: Surendra Anantharaman and Thomas Kempa
Monday Afternoon, April 19, 2021
NM07

4:00 PM *NM07.10.01

Orbital Magnetism in Graphene Heterostructures Andrea Young; University of California, Santa Barbara, United States

Ferromagnetism arises from the interplay of the Coulomb repulsion between electrons and their fermionic statistics. The vast majority of magnets consist of ordered arrangements of the electron spins stabilized by the spin orbit interaction. In my talk, I will describe a new class of magnets based on the spontaneous alignment of electron orbitals. Such orbital ferromagnetism may be a generic phenomena, but has, to date, found its fullest expression in graphene heterostructures in which the two dimensional orbits of electrons in distinct momentum space valleys provide the underlying degree of freedom for magnetic order. These magnetic degrees of freedom arise directly from the band wavefunctions, making orbital magnets exquisitely sensitive to both the design of the electronic wavefunctions as well as in situ control parameters. For example, in systems in which interlayer lattice mismatches lead to a moire superlattice potential, the resulting superlattice band structure may feature nontrivial topology, which in conjunction with orbital magnetism can give rise to precise quantization off the Hall effect at zero magnet field. Remarkably, the conduction electrons themselves can also directly influence the magnetic order, leading to field-effect switchable magnetic moments. Finally, I will conclude with our progress towards using orbital magnetism to engineer "topologically ordered" states at zero magnetic field, in which the electron splits into fractionally charged anyons.

4:25 PM NM07.10.02

Late News: Molybdenum Disulfide Nanoribbons—Scalable Fabrication, Structure-Properties Correlation, Precision Manipulation and Applications Yun Huang¹, Kang Yu^{1,2}, Huaizhi Li¹, Kai Xu³, Zexi Liang¹, Debora Walker⁴, Paulo Ferreira^{1,2,5}, Peer Fischer^{6,7} and Donglei (Emma) Fan^{1,1}; ¹The University of Texas at Austin, United States; ²International Iberian Nanotechnology Laboratory, Portugal; ³University of Illinois at Urbana-Champaign, United States; ⁴Harvard University, United States; ⁵University of Lisbon, Portugal; ⁶Max-Planck-Institute for Intelligent Systems, Germany; ⁷University of Stuttgart, Germany

In the family of two-dimensional (2D) transition metal dichalcogenide (TMD) materials, molybdenum disulfide (MoS₂) has received immense attention owing to its desirable electrical, chemical, and mechanical properties. Similar to single-crystalline MoS₂ nanostructures, polycrystalline MoS₂ structures also possess many desirable

properties for applications, such as outstanding catalytic properties. Recently we reported an innovative and scalable approach to synthesize MoS₂ nanoribbons with tunable dimensions and excellent dispersibility in suspension [1]. The obtained polycrystalline MoS₂ nanoribbons exhibit high chemical purity which endows them with much-enhanced surface reactivity compared to those of their single-crystal counterparts. They can be readily grafted with UV-triggered click-chemistry; they effectively react and remove mercury contaminants from water. They also possess an ultrafast optoelectronic response from 450 nm to 750 nm that is the same as the single-crystal forms. In this presentation, we highlight these properties and describe in detail our newly obtained unpublished result on the electronic properties of the MoS₂ nanostructures and how these determine their manipulation and electro-rotation behavior. We show that the nanoribbons can be manipulated efficiently in a high-frequency electric field. They propel along arbitrary paths on a 2D surface, assemble rapidly on prepatterned microelectrodes, and rotate clockwise and counter-clockwise. Their mechanical behaviors reflect their semiconductor electronic type, distinct from those of metals or insulators, which provides additional support to their optoelectronic characterizations. The fabrication, manipulation, assembly, and unique properties of the obtained MoS₂ is useful for device fabrication, and applications of the TMD family.

[1] Huang, Y., Yu, K., Li, H., Liang, Z., Walker, D., Ferreira, P., Fischer, P., Fan, D., "Scalable Fabrication of Molybdenum Disulfide Nanostructures and their Assembly", *Adv. Mater.*, 2003439, 2020.

4:40 PM NM07.10.03

Late News: Narrow Excitonic Lines and Large-Scale Homogeneity of Transition Metal Dichalcogenides

Grown by MBE on hBN Wojciech Pacuski¹, Magdalena Grzeszczyk¹, Karol Nogajewski¹, Aleksander Bogucki¹, Kacper Oreszczuk¹, Aleksander Rodek¹, Julia Kucharek¹, Karolina E. Polczynska¹, Bartłomiej Seredynski¹, Rafal Bozek¹, Slawomir Kret², Takashi Taniguchi³, Kenji Watanabe³, Janusz Sadowski^{1,2,4}, Tomasz Kazimierzczuk¹, Marek Potemski^{1,5} and Piotr Kossacki¹; ¹University of Warsaw, Poland; ²Institute of Physics of the Polish Academy of Sciences, Poland; ³National Institute for Materials Science, Japan; ⁴Linnaeus University, Sweden; ⁵Laboratoire National des Champs Magnétiques Intenses, France

Monolayer transition metal dichalcogenides (TMDs) are two-dimensional materials with exceptional optical properties such as high oscillator strength, valley related excitonic physics, efficient photoluminescence, and several narrow excitonic resonances. However, above effects have been so far explored only for structures produced by techniques involving mechanical exfoliation and for the best results, encapsulation in hBN, both procedures inevitably inducing considerable large-scale inhomogeneity. On the other hand, techniques which are essentially free from this disadvantage, such as molecular beam epitaxy (MBE), have to date yielded only structures characterized by considerable spectral broadening, which hinders most of interesting optical effects.

We report for the first time on the MBE-grown TMD exhibiting narrow and fully resolved spectral lines of neutral and charged exciton. Moreover, our MBE-grown TMD exhibits unprecedented high spatial homogeneity of optical properties, with variation of the exciton energy as small as 0.16 meV over a distance of tens of micrometers. Our recipe for MBE growth [1,2] is presented for MoSe₂ and includes extremely slow growth rate, the use of atomically flat hexagonal boron nitride (hBN) substrate and the annealing at very high temperature. Importantly, good optical properties are achieved for as-grown sample, without any post growth exfoliation and encapsulation in hBN. This novel recipe opens a possibility of MBE growth of TMD and their heterostructures with optical quality, dimensions and homogeneity required for optoelectronic applications.

[1] W. Pacuski, M. Grzeszczyk, K. Nogajewski, A. Bogucki, K. Oreszczuk, J. Kucharek, K.E. Polczynska, B. Seredynski, A. Rodek, R. Bozek, T. Taniguchi, K. Watanabe, S. Kret, J. Sadowski, T. Kazimierzczuk, M. Potemski, P. Kossacki; *Nano Letters* 20, (2020) pp. 3058-3066.

[2] Z. Ogorzalek, B. Seredynski, S. Kret, A. Kwiatkowski, K. P. Korona, M. Grzeszczyk, J. Mierzejewski, D. Wasik, W. Pacuski, J. Sadowski and M. Borysiewicz; *Nanoscale* 12 (2020) pp. 16535-16542.

4:55 PM NM07.10.04

Electrical Control of Strong-Light Matter Interactions in MoTe₂ Souvik Biswas¹, Zakaria Al Balushi^{1,2},

Eoin Caffrey¹, Sergiy Krylyuk³, Joeson Wong¹, Kenji Watanabe⁴, Takashi Taniguchi⁴, Albert Davydov³ and Harry A. Atwater¹; ¹California Institute of Technology, United States; ²University of California, Berkeley, United States; ³National Institute of Standards and Technology, United States; ⁴National Institute for Materials Science, Japan

Light matter interaction between excitonic resonances in atomically thin TMDCs, which are highly susceptible to electrostatic stimulus, and cavity polaritonic modes can enable novel electro-optic functionalities. In this work, we investigated electrical control of strong light-matter interactions in molybdenum ditelluride via opto-electronic modulation of an h-BN encapsulated monolayer MoTe₂ gated heterostructure designed also as a ‘Salisbury-screen’ photonic resonant absorber.

Using low temperature reflection contrast and photoluminescence measurements at different Fermi-level values, we observed strong modulation of the A 1s, 2s and B 1s exciton and trion peaks. Our results can be primarily understood from increased electronic doping which gives rise to enhanced elastic Coulomb scattering and screening – resulting in oscillator strength shifts from excitons to trions and also spectral broadening of the individual resonances. Moreover, many body effects leading to band-structure renormalization were seen from the changes in the binding energy of the different excitonic species with increased charge density. We performed transfer matrix calculations to obtain the complex dielectric function of MoTe₂ at each Fermi level position. Notably, we observed unity-order refractive index modulation at the A1s exciton. Additionally, we also studied the influence of optical pumping by performing laser fluence dependent emission measurements. Spectral broadening of the excitonic features was observed, indicating exciton-exciton interaction at higher pump powers. Our results shed light on the strongly correlated many-body interactions in MoTe₂ and suggest paths for integration into active devices such as near infrared electro-optical modulators.

5:10 PM NM07.10.05

Fracture Toughness and Fracture Strain of Single-Layer Freestanding Graphene Extracted by On-Chip Testing Sahar Jaddi¹, Bin Wang^{1,2}, Mohammad W. Malik¹, Yun Zeng², Jean-Pierre Raskin¹ and Thomas Pardoën¹; ¹UCLouvain, Belgium; ²Hunan University, China

Graphene has attracted the attention of the scientific community for the last two decades, thanks to an astounding set of properties such as high thermal conductivity (5000 W/mK), superior electron mobility (250,000 cm²/V-s), high modulus of elasticity (~1 T Pa), and ultra-high flexibility. Graphene’s C-C bonds are sp² hybridized providing superior mechanical stability in the basal plane directions. Graphene appears as the perfect material constituent for a wide range of application fields, like in flexible electronics, in electromechanical devices, and in reinforced lightweight composites that rely on both electrical and mechanical performances. It remains crucial to determine the latter properties under realistic and well-controlled conditions to guide the fail-safe design of graphene-based applications.

While the mechanical behavior of graphene has been very much investigated numerically for both perfect and defected lattice structures [1,2], most experimental works remain partly inconclusive regarding the fracture resistance. Nanoindentation of a suspended single layer (SLG) and of multilayer graphene (MLG) on top of holes [3,4], and uniaxial tensile test using the so-called push-to-pull device, are mostly used to deform graphene [8,9]. Testing graphene using a valid fracture mechanics approach is very complex due to the nature of the fabrication, the difficulty of pre-cracking, and the delicate data analysis. Two reports on the fracture toughness of SLG have been published [5,6], while other data are for MLG [7, 8]. The aforementioned works have provided insight into the fracture mechanisms of graphene, using a notch as a starter crack. This can potentially lead to an overestimation of the fracture toughness with a dependence on the notch root radius, which is difficult to deconvolute. Furthermore, the notch is produced by a focus ion beam, which may introduce damage. These tensile and fracture tests relied on external equipment either for loading or sensing, leading to cumbersome manipulation and allowing only a few specimens to be tested, preventing statistical analysis.

In the present work, we report two novel extensions of methods developed in our laboratory to study the mechanical and fracture properties of freestanding SLG. The method relies on the use of residual tensile-stress involved in a beam layer called the actuator beam. This beam is attached to the graphene specimen. Removing the sacrificial layer induces the release of internal stress in the actuator, pulling then on the graphene specimen. Hence, the use of external (electro-)mechanical actuation is avoided. In a first configuration, the actuator layer is pulling on a dog-bone shape or rectangular graphene specimen, from which the uniaxial stress-strain curve is extracted up to fracture [10]. In a second configuration, two actuator beams pull on a notched specimen but using a crack arrest method to determine the fracture toughness suppressing the problem of notch blunting effect at crack initiation [11]. Benefiting from the lithography process, numerous devices have been fabricated hence providing statistically representative data. Our investigation shows fracture strains larger than 10% and tensile strength larger than 100 GPa for specimens with an area larger than 160 mm². Brittle fracture behavior is observed with fracture toughness value equal to about 4 MPa m^{0.5} in agreement with literature.

References

1. F. Liu *et al.*, Phys. Rev. B 76, 2007
2. A. Shekhawat *et al.*, Nat. Commun. 7, 10546, 2016.
3. C. Lee *et al.*, Science 321, 2008.
4. H.I. Rasool *et al.*, Nature Commun. 4, 2013.
5. Y. Hwangbo *et al.*, Sci. Rep. 4, 2014.
6. P. Zhang *et al.*, Nature Commun. 5, 2014.
7. X. Wei *et al.*, Nano Lett. 15, 2015.
8. B. Jang *et al.*, Extrem. Mech. Lett. 14, 2017.
9. K. Cao *et al.*, Nat. Commun, 11, 92020.
10. M. Coulombier *et al.*, thin films. Scr. Mater. 62, 2010.
11. S. Jaddi *et al.*, JMPS, 123, 2019.

5:15 PM NM07.10.07

Nanoscale Anisotropic Strain Dynamics in MoS₂ Imaged with Ultrafast Electron Microscopy Yichao Zhang and David Flannigan; University of Minnesota Twin Cities, United States

The large anisotropy of the bonding states in layered transition metal dichalcogenides (TMDs) provides an additional dimension to modulate materials properties [1,2]. For example, relatively weak interlayer van der Waals forces lead to distinctly different electronic, mechanical, vibrational, and electrochemical properties along the *c*-axis of MoS₂ compared to the basal plane. Efforts have been focused on probing photoinduced structural dynamics in the basal plane, where strong covalent bonding dominates the response of the material [3,4]. Comparatively few ultrafast studies have shown the different nature of photoexcited structural dynamics along the *c*-axis as compared to the in-plane behaviors [5,6]. In addition, defects play an important role in the nucleation of coherent strain waves studied with the bright-field imaging modality of ultrafast electron microscopy (UEM) [7-9].

Here, we report the combined study of direct imaging of photoinduced localized *c*-axis acoustic-phonon dynamics of a free-standing, multilayer MoS₂ flake with UEM and finite element transient deformation analysis with COMSOL. With nanometer-picosecond spatiotemporal resolutions in bright-field imaging, we observe and quantify the emergence and oscillation of two spatially localized interlayer breathing modes separated by a 10-nm thick step edge, with the difference in frequency due to the different thicknesses in the two respective regions. The onset of coherent contrast dynamics in the thicker region of the terrace is delayed by 2 to 3 ps, indicating a more rapid structural response to photoexcitation in the thin region of the terrace. Time-dependent finite element analysis on a terrace of the same dimensions as the specimen shows excellent agreement with experimental results. Photoexcitation was modeled by applying a spatially varying strain profile along the *c*-axis calculated based on the absorption of multilayer MoS₂ and the thickness of the terrace, leading to a discontinuity of the *c*-axis strain profile at the step edge. Both experiment and simulation captured a gradual decrease of 1 to 2 GHz of the oscillation frequencies starting 50 to 100 nm away from the step edge on both

sides of the terrace, likely due to the additional force component along the c -axis opposed to wave propagation because of the distortion of the basal-plane covalent bonds. These results provide insights into the local, nanoscale nature of transient lattice deformations and the associated impacts on phonon dynamics in layered materials [10].

[1] A. P. Nayak, *et al.*, Nature **5**, (2014) 3731.

[2] S. Tongay, *et al.*, Nano Lett. **13**, (2013) 2831.

[3] E. M. Mannebach, *et al.*, Nano Lett. **15**, (2015) 6889.

[4] D. R. Cremons, *et al.*, Nat. Commun. **7**, (2016) 11230.

[5] A. J. McKenna, *et al.*, Nano Lett. **17**, (2017) 3952.

[6] E. M. Mannebach, *et al.*, Nano Lett. **17**, (2017) 7761.

[7] D. R. Cremons, *et al.*, Struct. Dyn. **4**, (2017) 044019.

[8] S. A. Reisbick, *et al.*, J. Phys. Chem. A **124**, (2019) 1877.

[9] Y. Zhang, *et al.*, Nano Lett. **19**, (2019) 8216.

[10] This material is based upon work supported by the National Science Foundation under Grant No. DMR-1654318. This work was partially supported by the National Science Foundation through the University of Minnesota MERSEC under Award Number DMR-2011401.

5:20 PM NM07.10.08

Unconventional Superconductivity Mediated by Spin Fluctuations in Single-Layer NbSe₂ Wen Wan, Paul Dreher, Rishav Harsh, Francisco Guinea and Miguel M. Ugeda; Donostia International Physics Center, Spain

Van der Waals materials provide an ideal platform to explore superconductivity in the presence of strong electronic correlations, which are detrimental of the conventional phonon-mediated Cooper pairing in the BCS-Eliashberg theory and, simultaneously, promote magnetic fluctuations. Despite recent progress in understanding superconductivity in layered materials, the glue pairing mechanism remains largely unexplored in the single-layer limit, where electron-electron interactions are dramatically enhanced. Here we report experimental evidence of unconventional Cooper pairing mediated by magnetic excitations in single-layer NbSe₂, a model strongly correlated 2D material. Our high-resolution spectroscopic measurements reveal a characteristic spin resonance excitation in the density of states that emerges from the quasiparticle coupling to a collective bosonic mode. This resonance, observed along with higher harmonics, gradually vanishes by increasing the temperature and upon applying a magnetic field up to the critical values (T_C and H_{C2}), which sets an unambiguous link to the superconducting state. Furthermore, we find clear anticorrelation between the energy of the spin resonance and its harmonics (Ω_n) and the local superconducting gap (Δ), which invokes a pairing of electronic origin associated with spin fluctuations. Our findings demonstrate the fundamental role that electronic correlations play in the development of superconductivity in 2D transition metal dichalcogenides, and open the tantalizing possibility to explore unconventional superconductivity in simple, scalable and transferable 2D superconductors.

5:23 PM NM07.10.14

Multiscale Phonon Green's Function for Silicene with and without Lattice Defects and Its Applications Vinod K. Tewary and Edward Garboczi; National Institute of Standards and Technology, United States

Since the advent of graphene, many new two-dimensional (2D) materials have been either fabricated or theoretically proposed. These new materials, the so called 2D materials beyond graphene, represent a revolutionary new development in the science and technology of materials. Silicene, a 2D allotrope of silicon, is one of these materials. Compared to the normal 3D solids, the electronic as well as phononic characteristics of these materials are quite unusual. It has a stronger spin-orbit coupling, which gives rise to quantum spin Hall effect. Further, it has an electrically tunable band gap, a property useful in the design of field effect transistors at room temperatures. Hence, there is a strong interest in silicene for solid state devices for diverse applications such as thermal management, thermoelectric energy conversion, quantum computing, and spintronic devices. A reliable and robust mathematical model is necessary for industrial development of new materials. It is needed

for development of their characterization and testing systems and for virtual experimentation for providing answers to “what if” type questions. The conventional modelling techniques based upon the continuum approximation of solids are not applicable to 2d materials. One obvious reason is that the solid has almost 0 thickness. This introduces a discontinuity in the derivatives of field quantities, in the direction of the thickness. Hence all components of the standard continuum parameters, like stress and strain tensors, are not rigorously defined for 2d materials. Modeling 2d materials is, therefore, a multiscale many body problem, which must be valid at the atomistic scales.

Further, it has been recognized that the performance and stability of quantum materials are sensitive to the presence of lattice defects. Lattice defects induce displacement field in the solid, which strongly affects thermal, optical and electronic parameters of the solid. The elastic displacement field due to a point defect in the plane of the solid has a logarithmic behavior, which introduces a size effect in the material parameters, which must be accounted for in modeling and interpretation of measurements. Hence a discrete atomistic scale model needs to be large in order to avoid spurious size effects.

Finally, the model should be able to simulate low frequency phonons and their interaction with the electrons, which make a significant contribution to the thermal and possibly even quantum response of the solid. All these requirements make modeling of silicene a highly challenging task for which special techniques are needed. A conventional molecular dynamics based model is computationally inefficient for modeling low frequency phonons in large crystallites because of rather poor mathematical convergence.

At NIST, we have developed a multiscale phonon Green’s function method, which is very efficient for modeling the phononic response of 2d quantum materials. Our method can simulate a million atoms over an extended time range on an ordinary desktop computer. The power of the Green’s function method arises from the fact that we retain up to second order terms in the expansion of the lattice Hamiltonian in terms of the atomic displacements. In contrast, only the first order terms are retained in standard molecular dynamics. The second order term is crucial for phonon applications because the phonon energies are determined by the second order term.

In this talk I will briefly describe our Green’s function method and its application to calculation of phonon related properties of 2d quantum materials with and without lattice defects, such as vacancy, lithium, phosphorous, and boron. Numerical results will be presented for silicene.

5:26 PM NM07.10.15

Theoretical Performance Limits of Graphene Hot Electron Emission Ragib Ahsan, Hyun Uk Chae and Rehan Kapadia; University of Southern California, United States

Electron emission devices with ultrahigh emission current density and ultrafast response are instrumental to applications including but not limited to electron microscopy, high power microwave generation, and free electron lasers. A key limitation to achieving the ultrahigh emission current density and ultrafast response lies in the 3D nature of electron emitters. In a 3D photoemitter, the photons are absorbed at a finite depth and the excited electrons need to transit to the emitting surface before they can be extracted. During this transit process, these high energy electrons lose their excess energy due to electron-phonon and electron-electron scattering. In a 2D material like graphene, the excited electrons are always at the emitting surface and therefore the transit length is effectively eliminated. In a recent experimental study, it has been demonstrated experimentally that a waveguide integrated graphene photoemitter can absorb nearly 100% of the photons traveling through the waveguide and the excited electrons can be extracted by applying a dc electric field with a quantum efficiency that exceeds 5 orders of magnitude compared to that of multiphoton and strong field photoemitters. In this work, we have performed a theoretical investigation of the performance limits of such a photoemitter by solving for the Monte Carlo Boltzmann Transport Equation (MCBTE) accounting for the scattering processes in graphene as well as the tunneling rates into the vacuum as a function of absorbed optical power density, photon energy and applied dc electric field. The rates of different scattering and tunneling processes were calculated by quantum mechanical theory using Fermi’s golden rule. We have shown that the theoretical model can reproduce the experimental results with good quantitative agreement. Our results predict two regimes of operation for graphene hot electron emitters: (a) single hot electron emission at lower power densities ($< 10^9$ W/m²) and (2) ensemble hot electron emission at higher power densities ($> 10^9$ W/m²) where the electronic temperature of

graphene increases beyond the lattice temperature. In the ensemble hot electron emission regime, it is possible to achieve a quantum efficiency that exceeds 100% with a response time below a picosecond. This theoretical study demonstrates an experimental roadmap towards realizing high efficiency electron emission with large emission current densities and ultrafast response times.

5:29 PM NM07.10.16

Atomistic Mechanism of Stress Modulated Phase Transition in Monolayer MoTe₂ Wei Gao; The University of Texas at San Antonio, United States

Monolayer MoTe₂, one of the 2D transition metal dichalcogenide (TMD) materials, exhibits two stable structural phases: semiconducting 2H phase and metallic 1T' phase. The dynamic control of the transition between these two phases on a single atomically thin sheet holds promise for a variety of revolutionary device applications. Particularly, stress could be utilized to dynamically modulate such phase transition. To date, the atomistic and kinetic mechanism of the phase transition under stress is not clear. In this study, the finite deformation nudged elastic band method and density functional theory are applied to determine the phase transition barriers and pathways of monolayer MoTe₂ as a function of applied stress. It is found that the stress can greatly influence the thermodynamics and kinetics of the phase nucleation and propagation. The results shed light on the phase engineering of 2D TMD materials with stress at the atomic level.

5:32 PM NM07.10.17

Mode-Dependent Thermal Conductivity and Size Effects in Planar SiC and h-BN Sheets Yuqing Huang, Anant Raj and Jacob Eapen; North Carolina State University, United States

Low-dimensional systems such as graphene and planar h-BN sheets exhibit anomalous size-dependent thermal transport. Non-equilibrium atomistic simulations using a constant heat current or a temperature gradient are ideal for analyzing this size dependency. Most analyses to date have employed the Fourier representation with complex normal mode coordinates to describe the phonon modes; while this representation is sufficient for computing the phonon dispersion relationships or spectral energy density, it lacks a precise capability to express the modal energy, and more importantly, a real modal heat current along a specified wave-vector. In this work, we adopt our recent non-equilibrium molecular dynamics approach [*J. Chem. Phys.*, **151**, 104110 (2019)], which employs a set of real asymmetric normal mode amplitudes that can unambiguously define the exact modal heat currents in a given direction, to extract the size-dependent modal thermal conductivity in planar SiC and h-BN sheets under a temperature gradient. We capture both the left-going and right-going modal heat current and phonon population independently, which is theoretically impossible with the traditional complex normal mode coordinates, and contrast their size-dependent behavior in planar SiC and h-BN sheets. While a modified Tersoff potential is used to describe the interatomic interactions in the planar SiC, the recently developed EXTEP potential is employed for h-BN. We anticipate that our approach would particularly be useful to characterize thermal transport in low-dimensional systems and molecular junctions where bulk or effective thermal properties are ill-defined or difficult to access.

SESSION NM07.11: Fundamental Properties of 2D Materials and Heterostructures V and Modeling and Machine Learning for 2D Materials Discovery I
Session Chairs: Surendra Anantharaman and Goki Eda
Monday Afternoon, April 19, 2021
NM07

7:45 PM NM07.11.03

Late News: Substitutional Doping of Fe on Magnetism in MoS₂ and WS₂ Monolayers Siwei Chen, Kyungham Kang, Shichen Fu and Eui-Hyeok Yang; Stevens Institute of Technology, United States

The doping of two-dimensional (2D) semiconductors has been intensively studied toward modulating their electrical, optical, and magnetic properties. While ferromagnetic 2D semiconductors hold promise for future spintronics and valleytronics, the origin of ferromagnetism in 2D materials remains unclear. Here, we present that substitutional Fe-doping into MoS₂ and WS₂ monolayers to induce magnetic properties. The Fe-doped monolayers were directly synthesized *via* chemical vapor deposition. A Fe₃O₄ powder was sandwiched between a bare SiO₂/Si substrate and the transition metal oxide-deposited substrate for the growth. After loading the substrates and precursors, Ar gas was supplied, and the furnace temperature was increased up to 900 °C. Fe substitutional doping was *successfully* achieved, as confirmed using scanning transmission electron microscopy. While both Fe:MoS₂ and Fe:WS₂ showed PL quenching and n-type doping, Fe dopants in WS₂ monolayers were found to assume deep-level trap states, in contrast to the case of Fe:MoS₂, where the states were found to be shallow. Unlike MoS₂ monolayers showing ferromagnetic behavior, WS₂ monolayers showed paramagnetic behavior upon Fe-doping. These contrasting magnetic behaviors caused by paired Fe atoms can be attributed to paired Fe atoms generating more accumulated electric charge in Fe:WS₂ by pulling the Fe atoms apart. These findings allow us to control the material's magnetic properties layer-by-layer and can be applied for spintronics.

7:50 PM NM07.11.04

Late News: Quasi-Fermi Level Splitting in Monolayer Transitional Metal Dichalcogenides and Its Manipulation Thereof. Mike Tebyetekerwa, Daniel Macdonald and Hieu Nguyen; Australian National University, Australia

Quasi-Fermi level splitting ($\Delta\mu$) of any material under illumination symbolizes the maximum possible open-circuit voltage (V_{oc}) that a photovoltaic device can reach if made out of that material in ideal conditions. We have experimentally quantified the $\Delta\mu$ (V_{oc}) values of various monolayer transitional metal dichalcogenides (TMDs). Briefly, we employed optical non-destructive techniques of micro-photoluminescence and micro-absorption spectroscopy with reference to the generalized Planck law of emission. We report that the photovoltaic devices made of monolayer WS₂, MoS₂, WSe₂, and MoSe₂ can possibly yield V_{oc} values of up to ~1.4, 1.12, 1.06, and 0.93 V at 1 Sun illumination, respectively. We further show some of the different possible ways to manipulate the reported V_{oc} performance using external voltage and chemical molecules of aggregation-induced emission in Type-I heterostructures.

7:55 PM NM07.11.05

Late News: Small-Nanostructure-Size-Limited Phonon Transport within Composite Films Made of Single-Wall Carbon Nanotubes and Reduced Graphene Oxides Qiyu Chen¹, Xiaolu Yan², Leyuan Wu², Yue Xiao¹, Sien Wang¹, Guoan Cheng², Ruiting Zheng² and Qing Hao¹; ¹University of Arizona, United States; ²Beijing Normal University, China

Nanocarbon materials have been widely used for nanoelectronics and other energy-related applications. In the kinetic relationship, the phonon (lattice) thermal conductivity is given as $k_L \sim C_p v_g A$, with C_p as the phonon specific heat, v_g as phonon group velocity, A as phonon mean free paths (MFPs). Within general composite films made of reduced graphene oxides (rGO) and carbon nanotubes (CNTs), the existence of many nanocontacts results in a k reduction but the loss in k can be overshadowed by the significant advantages of using bulk composites for large-scale applications. Detailed thermal analysis of composite films made of rGO and CNTs is still lacking, particularly for the individual in-plane k_{\parallel} contribution from each constituent material within the complicated 3D nanocarbons. In this work, composite films consisting of rGO nanosheets and varied weight percentage of single-wall CNTs (SWCNTs) are synthesized and studied for their in-plane thermal conductivities, in which increased SWCNTs percentage leads to a reduced k_{\parallel} . Different from pristine graphene and other composite nanocarbon films with decreased thermal conductivities above 300 K, the in-plane thermal conductivities of these composite films are found to follow the trend of the specific heat of graphene from 100 K to 400 K, i.e., monotonously increasing at elevated temperatures. For investigated samples, the extracted k_{\parallel} can be matched by a scaled curve for the product $C_p v_g$ summed up for all phonon modes that are computed for pristine graphene. This indicates that the rGO nanosheets contribute significantly to the k_{\parallel} but their MFPs are

largely restricted by the dense SWCNT-graphene junctions and additional graphene-graphene nanocontacts. Such a trend has seldom been observed for nanocarbon. This unique temperature dependence of thermal conductivities is attributed to the so-called small-nanostructure-size (SNS) limit, at which the phonon MFPs are simply restricted as the structure size. This SNS limit is often found at cryogenic temperatures where the majority bulk phonon MFPs are much longer than the sample size. But in this study, the intrinsically long phonon MFPs within the initial graphene sheets and the dense SWCNT-graphene/graphene-graphene nanocontacts result in $k \approx k_L$ following the SNS limit even up to 400 K. The highest in-plane thermal conductivity among samples with different synthesis conditions is 62.8 W/mK at 300 K which is significantly higher than amorphous materials with a similar temperature dependence of thermal conductivities. Such a high thermal conductivity, combined with its unique temperature dependency, can be ideal for applications such as flexible film-like thermal diodes based on the junction between two materials with a large contrast for their temperature dependence of the thermal conductivity.

8:00 PM NM07.11.06

Late News: Effect of Ti-Doping on Group-14 Elemental Two-Dimensional Materials as a Method for Improving the Quantum Capacitances Juven Rihm¹, Eun Seob Sim¹, Sung Beom Cho² and Yong-Chae Chung¹; ¹Hanyang University, Korea (the Republic of); ²Korea Institute of Ceramic Engineering and Technology, Korea (the Republic of)

Electric double-layer capacitors (EDLCs) are one of the most promising candidates for environmentally friendly and sustainable energy storage systems due to their balanced energy-power density compared to conventional batteries and capacitors. As key materials for EDLCs, group-14 elemental two-dimensional materials (ETDMs) possess extremely large surface area for doping and ion adsorption, which is advantageous for maximizing the charge storage. However, one of the bottlenecks that limits the performance as EDLCs is the ETDMs' lack of density of states (DOS) near the Fermi level (E_F) that can store the charge transferred from the ions. In this study, to provide additional DOS near the E_F , Ti-doping was introduced to the ETDMs. The density functional theory (DFT) calculation revealed that additional DOS was provided to ETDMs by the d band of doped Ti atom. Since the surface charge densities increased due to the newly formed DOS near the E_F , the quantum capacitances were also enhanced. In addition, among the Ti-doped ETDMs, Ti-doped silicene is found to have superior characteristics at the low voltage range. These findings may provide practical guidelines for improving the performance of EDLCs.

8:05 PM NM07.11.07

Late News: Enhanced Metallicity in Defected Zigzag Graphene Nano Ribbons—Role of Oxygen Doping Sonal Agrawal, Anurag Srivastava and Gaurav Kaushal; Atal Bihari Vajpayee Indian Institute of Information Technology and Management, India

The effect of Oxygen (O) doping in Zigzag Graphene Nano ribbons (GNR) has been investigated in terms of their stability and electronic properties, using density-functional theory-based ab-initio approach. The Zigzag GNR has been subjected to mono vacancy and decorated with three possible sites of oxygen impurities around the MonoVacancy (MV). The stability of the systems has been analysed in terms of cohesive energy, and the electronic properties in terms of band structure, and density of states profiles. The cohesive energy calculations suggest that formation of the pyridine-type defects with oxygen doping, have nearly the same stability in the case of monovacancy introduced system. The electronic bandstructure and density of state profile observed that the metallicity of the ZGNR enhances with O doping, validated through increase in density of states at the fermi level. This enhanced metallicity in ZGNR, defends its application as metallic electrodes as well as interconnects in electronic industry.

8:10 PM NM07.11.08

Large-Scale Lithium-Intercalated Multilayer Graphene Production Joseph Andrade¹, Mohamed Boukhicha², Jan Folkson¹, Amanda Carr¹ and Matthew Eisaman¹; ¹Stony Brook University, The State University of New York, United States; ²Brookhaven National Laboratory, United States

For more than 70 years, Graphite Intercalated Compounds (GICs) have been extensively studied, wherein LiC₆ was discovered as a lead material for high-capacity electrical energy storage. With the recent surge of compact electronic devices in commercial production, we present a novel fabrication technique for ultra-thin LiC₆ devices. Here we present a new transfer method, termed “bifacial float transfer”, which enables large-scale multilayer graphene transfer from both sides of a nickel growth catalyst [1]. Bifacial float transfer has the potential to reduce graphene production costs by transferring chemically vapor deposited (CVD) graphene films from both sides of their native nickel substrate, with one graphene film transferred to a polymer and the other graphene film transferred to another target substrate. In traditional transfer methods, the graphene on the “non-preferred” side, that is, the bottom of the substrate, is removed with oxygen plasma before removal of the metal catalyst in etchant solution. Although this treatment prevents undesired aggregation of the graphene films, it fails to utilize both sides of CVD-grown graphene. In this talk, we compare the quality of graphene transferred from both sides onto target glass and polymer substrates. The results of optical microscopy, confocal Raman spectroscopy, atomic force microscopy, and electronic transport measurements suggest that the quality of the multilayer graphene on the “non-preferred” side does not differ significantly from that of the “preferred” side. This method will allow more efficient and cost-effective use of graphene by doubling the usable graphene per area of growth substrate, and by eliminating the need for intermediate sacrificial transfer substrates such as poly(methyl methacrylate). By modifying the air-liquid interface, we also attempt similar polymer-free transfer of progressively thinner multilayer graphene films. The fabricated samples are then lithiated using the in-situ short-circuit direct contact method [2]. The ultra-thin LiC₆ exhibits metallic behaviour at room temperature with low sheet resistance and improved optical transparency in the visible spectrum [3]. We present preliminary results on the fabrication and characterization of these large-scale, stable LiC₆ films.

[1] Andrade J. A. et al., *Adv. Funct. Mater.*, 2005103 (2020)

[2] Shellikeri A. et al., *J. of Elec. Soc.*, 164, 14 (2017)

[3] Bao W. et al., *Nat. Communication*, 5, 4224 (2014)

8:15 PM NM07.11.09

High Efficiency Hot Electron Emission from Waveguide Integrated Graphene Ragib Ahsan, Fatemeh Rezaeifar, Hyun Uk Chae and Rehan Kapadia; University of Southern California, United States

Electron emission devices are important for applications in electron microscopy, free electron lasers, radio frequency (RF) amplifiers, and accelerators. Photoemission plays an important role in realizing high efficiency electron emission by exciting lower energy electrons above the workfunction barrier. There are three fundamental limitations to improving the efficiency of photoemission from cathodes: (1) low optical absorption (2) large absorption depth leading to a large transit length to the emitting surface for the excited electrons and (3) high workfunction barrier to extracting the electrons. As a result, most of the works on photoemitters have focused ultraviolet photons with energy that exceeds the workfunction barrier ($> \sim 5$ eV), multiphoton absorption, and strong field photoemission processes to realize electron emission. In this work, we have addressed these limitations by using a waveguide integrated graphene electron emitter excited by subworkfunction photons (3.06 eV). While monolayer graphene absorbs only 2.303% of the free space incident light, a waveguide integrated graphene can absorb nearly 100% of the light traveling through the waveguide. In addition, the monolayer thickness of graphene ensures that the excited electrons are always at the emitting surface which eliminates the transit length and reduces the energy loss in electrons due to electron-phonon scattering and electron-electron scattering. This waveguide integrated graphene electron emitter absorbs photons at 3.06 eV which is significantly smaller than the workfunction barrier in graphene (~ 4.5 eV) and a dc electric field then assists these electrons to tunnel out of graphene before they lose energy. This device experimentally demonstrates an efficiency exceeding the efficiency of multiphoton and strong field photoemitters available in literature by 5 orders of magnitude. Finally, we have modified the graphene surface by introducing a coating of LaB₆ nanoparticles which have a low workfunction (~ 2.7 eV). This coating of LaB₆ nanoparticles further reduces the workfunction of graphene to 3.5 eV resulting in a tenfold increase in the hot electron emission efficiency. Therefore, we have addressed all three fundamental limitations of a photoemitter by (a) using the waveguide integrated structure that allows $\sim 100\%$ optical absorption (b) using monolayer

graphene that eliminates transit length for excited electrons, and (3) reducing the workfunction barrier with a LaB₆ nanoparticle coating. The strategy to this work can be extended to optical resonators which allows higher optical power densities and other 2D materials including transition metal dichalcogenides which may allow a further increase the efficiency of hot electron emission.

8:20 PM BREAK

9:05 PM OPENING REMARKS

9:10 PM *NM07.11.10

New Directions in Topological 2D Materials without Translational Symmetry Sinéad Griffin; Lawrence Berkeley National Laboratory, United States

Topological order is intimately connected to the presence of translational symmetries - these result in symmetry-protected phases in quantum materials and the resulting classification of topological materials. However, recent experiments have hinted at the presence of topologically protected states even in the absence of translational symmetry. In this talk, I will discuss how theoretical calculations have uncovered topological phases in materials without translational symmetry -- namely in a quasicrystal material and in an amorphous material. I will first describe how a two-dimensional Ta-Te chalcogenide quasicrystal and approximant hosts a layer-tunable topologically nontrivial electronic bandstructure. Next, I will show how introducing disorder into the BiTeI layered family of Rashba materials can induce a trivial-to-nontrivial topological phase transition. Finally, I will discuss the amorphous limit of this case where theory and ARPES measurements suggest topologically protected surface states in amorphous Bi₂Se₃.

9:35 PM NM07.11.11

Electrically Tunable 2D Ferromagnetic Semiconductors CrSBr and CrSeBr with High Curie Temperature Xiaofeng Qian; Texas A&M University, United States

Identifying intrinsic low-dimensional ferromagnets with high transition temperature and electrically tunable magnetism is crucial for the development of miniaturized spintronics and magnetoelectrics. Recently, monolayer CrI₃ and Cr₂Ge₂Te₆ semiconductors were found to exhibit long-range two-dimensional ferromagnetism with relatively low Curie transition temperature. Here we present our theoretical study of van der Waals layered magnetic semiconductors CrSBr and CrSeBr. Using first-principles electronic structure theory and renormalized spin-wave theory, we predict that monolayer CrSBr and CrSeBr exhibit highly anisotropic electronic structure with bandgap of 1.66 eV and 0.78 eV. More importantly, monolayer CrSBr and CrSeBr possess high Curie temperature of ~150K which was recently verified by experiments, well beyond that of CrI₃ and Cr₂Ge₂Te₆. The origin of the high Curie temperature is attributed to strong anion-mediated superexchange interaction and sizable spin-wave excitation gap due to large exchange and single-ion anisotropy. Our results also show that it may be possible to switch magnetization easy axis via electrostatic doping can, suggesting the possibility of realizing spin field effect transistor controlled by electrostatic doping. Finally, we will also discuss linear and nonlinear optical properties of van der Waals layered CrSBr and CrSeBr. Monolayer CrSBr and CrSeBr semiconducting ferromagnets offer long-desired alternatives to dilute magnetic semiconductors and provide unprecedented opportunities for 2D spintronics such as spin valves and spin FETs.

9:50 PM NM07.11.14

Understanding Carrier Mobility in Two-Dimensional Semiconductors Chenmu Zhang, Long Cheng and Yuanyue Liu; The University of Texas at Austin, United States

Atomically thin (two-dimensional, 2D) semiconductors have shown great potential as the fundamental building blocks for next-generation electronics. However, all the 2D semiconductors that have been experimentally made so far have room-temperature electron mobility lower than that of bulk silicon, which is not understood. Here,

by using first-principles calculations and reformulating the transport equations to isolate and quantify contributions of different mobility-determining factors, we show that the universally low mobility of 2D semiconductors originates from the high “density of scatterings,” which is intrinsic to the 2D material with a parabolic electron band. The density of scatterings characterizes the density of phonons that can interact with the electrons and can be fully determined from the electron and phonon band structures without knowledge of electron-phonon coupling strength. Our work reveals the underlying physics limiting the electron mobility of 2D semiconductors and offers a descriptor to quickly assess the mobility. [1,2,3]

[1] L. Cheng, C. Zhang, Y. Liu, PRL 2020, DOI: 10.1103/PhysRevLett.125.177701 (Editor’s suggestion)

[2] L. Cheng, C. Zhang, Y. Liu, JACS, 2019, DOI: 10.1021/jacs.9b05923

[3] L. Cheng, Y. Liu, JACS, 2018, DOI: 10.1021/jacs.8b07871

10:05 PM NM07.11.15

Late News: Van der Waals Hetero-Structures of 1H-MoS₂ and N-Substituted Graphene for Catalysis of Hydrogen Evolution Reaction Lakshay Dheer; Jawaharlal Nehru Centre For Advanced Scientific Research, India

First-principles theoretical analysis of the catalytic activity of van der Waals hetero-structures of 1H-MoS₂ and graphene substituted with three chemical types of nitrogen species (i) Graphitic (G), (ii) Pyridinic (Pn), and (iii) Pyrrolic (Pr), for application in catalysis of hydrogen evolution reaction (HER) has been presented. Graphitic and pyrrolic N substituents result in n-type electronic structure, whereas substitution of pyridinic N imparts p-type electronic character to the hetero-structure. Work functions (ϕ) of the hetero-structures suggest that graphitic N-graphene:MoS₂ hetero-structure (ϕ) is expected to be effective in catalysing the reduction of H⁺ to evolve H₂. 1H-MoS₂ monolayer in the hetero-structure contributes by enabling increased H₂O adsorption and offsetting the band edge energies optimal for the catalytic activity. Near optimum Gibbs free energy of H-adsorption (ΔG_{H}) were obtained for graphitic (~ 0.29 eV) and pyrrolic (~ -0.2 eV) N-graphene:MoS₂ hetero-structures. Our work showcases how catalytic and electronic properties of the N-doped graphene:MoS₂ hetero-structure depends on the chemical identity of N-sites and uncovers a route to 2D hetero-structures with high catalytic activity.

SESSION NM07.12: Modeling and Machine Learning for 2D Materials Discovery II

Session Chairs: Surendra Anantharaman and Vincent Tung

Tuesday Morning, April 20, 2021

NM07

8:00 AM *NM07.12.01

Synthesizable Yet Unsynthesized Low Dimensional Materials Revealed by Data Science Gowoon Cheon, Evan Antoniuk and Evan J. Reed; Stanford University, United States

We have utilized data mining approaches to elucidate over 1000 2D materials and several hundred 3D materials consisting of van der Waals bonded 1D subcomponents, or molecular wires. We find that hundreds of these 2D materials have the potential to exhibit observable piezoelectric effects, representing a new class of piezoelectrics. A further class of layered materials consists of naturally occurring vertical hetero structures, i.e. . bulk crystals that consist of stacks of chemically dissimilar van der Waals bonded layers like a 2-D super lattice. We further combine this data set with physics-based machine learning to discover the chemical composition of an additional 1000 materials that are likely to exhibit layered and two-dimensional phases but have yet to be synthesized. This includes two materials our calculations indicate can exist in distinct structures with different band gaps, expanding the short list of two-dimensional phase change materials. We find our model performs five times better than practitioners in the field at identifying layered materials and is comparable or better than professional solid-state chemists. Finally, we find that semi-supervised learning can offer benefits for materials design where labels for some of the materials are unknown.

8:25 AM NM07.12.02

Late News: Theory-Based Strategy of Nitrogen Doping for Optimized Electronic Structure of Ti₂CO₂ Toward High Hydrogen Evolution Reaction Activity Hyunjun Nam¹, Eun Seob Sim¹, Minyeong Je², Heechae Choi² and Yong-Chae Chung¹; ¹Hanyang University, Korea (the Republic of); ²University of Cologne, Germany

Finding inexpensive and active catalyst is essential to produce renewable energy, hydrogen, in a sustainable method. MXenes have been reported as a potential hydrogen evolution reaction (HER) catalysts with the advantages of their unique surface properties and excellent electrical conductivity. Recent studies on MXenes, especially titanium carbide, have showed that nitrogen-doping improves the catalytic performances in HER. However, various nitrogen-containing by-products are formed on the surface of MXene during the doping processing, and the origins of catalytic performance variations or the theoretical optimal doping concentration have not been fully studied. In this study, to find the optimum nitrogen doping concentration of Ti₂CO₂, the adsorption energies of hydrogen and the conductivity, were investigated using the density functional theory (DFT) calculations. From the calculations of the doping formation energy, C-site of Ti₂CO₂ was found to be the most favored nitrogen substitution. To determine the optimum nitrogen concentration, the Gibbs free energy of hydrogen adsorption and the conductivity were calculated for various N doping concentration. As the doping concentration increased, both the Gibbs free energy of hydrogen adsorption and the conductivity were enhanced and reached an apex point at the specific doping concentration. As the doping concentration further increased, deterioration of the catalytic performance was expected as the values of the two properties decreased. Through these results, it can be inferred that the doping concentration of N at C site influences the catalytic properties of N-doped Ti₂CO₂ and that optimum catalytic performance can be achieved at the specific doping concentration. This study suggests a frame of systematic and theoretical predictions to optimize doping processing of MXene-based HER catalysts.

8:40 AM NM07.12.04

Late News: First-Principles Study of a MoS₂-PbS van der Waals Heterostructure Inspired by Naturally Occurring Merelaniite Gemechis D. Degagaa¹, Sumandeep Kaur², Ravindra Pandey² and John A. Jaszczak²; ¹Oak Ridge National Laboratory, United States; ²Michigan Technological University, United States

Vertically stacked, layered van der Waals (vdW) heterostructures offer the possibility to design materials, within a range of chemistries and structures, to possess tailored properties. Inspired by the naturally occurring mineral merelaniite, we investigate a vdW heterostructure composed of MoS₂ monolayer and PbS bilayer, using density functional theory. The results find such a heterostructure to be stable and possesses p-type semiconducting characteristics. Due to the heterostructure's weak interlayer bonding, its carrier mobility is essentially governed by the constituent layers; the hole mobility is governed by the PbS bilayer, whereas the electron mobility is governed by the MoS₂ monolayer. Furthermore, we estimate the hole mobility to be relatively high ($\sim 10^6$ cm²V⁻¹s⁻¹), which can be useful for ultra-fast devices at the nanoscale.

8:55 AM NM07.12.05

Flat Bands in Transition Metal Dichalcogenide with Strong Spin-Orbit Interaction Sudipta Kundu¹, Mit H. Naik², Indrajit Maity¹, Hulikal R. Krishnamurthy¹ and Manish Jain¹; ¹Indian Institute of Science, India; ²University of California, Berkeley, United States

Since the discovery of flat bands at magic angle in twisted bilayer graphene, the formation of flat bands has been predicted for several other materials, especially twisted transition metal dichalcogenides (TMD). WSe₂ possesses strong spin-orbit interaction which makes it different from other TMDs. Using a multiscale approach, based on classical force-fields for structural relaxation and density functional theory calculations for electronic structure, we study the effect of spin-orbit coupling on the formation of flat bands in relaxed twisted WSe₂. The spin-orbit interaction affects the flat bands with the twist angle close to 0° differently than those near 60°. The flat bands at valence and conduction band edge arise from K and Q points of the unit cell Brillouin zone

respectively. For twist angle near 60° , we find that the flattening of the bands arising from K point is a result of the atomic reconstruction in the individual layers and not due to interlayer coupling. On the other hand, for twist angle close to 0° , the interlayer interaction between the two layers becomes important. Additionally, we also find flat bands folded from the Γ point of the unit cell Brillouin zone. The wave function localization of the flat bands matches well with STM measurements from existing literature [1]. Furthermore, we find that the atomistic spin-orbit splitting in moiré remains unchanged from the monolayer. We extend our study to strain-induced moiré in homobilayer TMD. The mismatch in lattice constant gives rise to moiré pattern. Relaxation of the system distributes the strain unevenly in the moiré lattice with increased strain at the highest energy stacking. Several well separated flat bands emerge at both valence and conduction band edges and we observe a significant reduction in the band gap. Thus, both twist and strain engineered moiré generate pathway to manipulate holes and electrons in TMD.

Reference:

1. Z. Zhang et al. Nat. Phys. doi:10.1038/s41567-020-0958-x (2020).

SESSION NM07.13: Devices for Sensing, Energy Conversion, and QIS I
Session Chairs: Zakaria Al Balushi and Thomas Kempa
Tuesday Morning, April 20, 2021
NM07

11:45 AM *NM07.13.01

P-Type van der Waals Contacts on 2D Semiconductors Manish Chhowalla; University of Cambridge, United Kingdom

Ultra-clean van der Waals interfaces can be achieved between soft indium metal and monolayer 2D transition metal dichalcogenide semiconductors. Such interfaces lead to low contact resistance and n-type field effect transistors with high mobilities – in excess of $100 \text{ cm}^2\text{-V}^{-1}\text{-s}^{-1}$. It has been, however, challenging to make similarly clean interfaces between refractory metals with high work functions to achieve efficient hole injection. Here, I will present our efforts on realizing p-type contacts using high work function metals and their alloys. This method preserves the ultra-clean interface between the monolayer semiconductor and alloy while increasing the work function so that p-type devices can be realized. We also demonstrate clean interfaces using metals such as Pd and Pt via direct deposition. These interfaces reveal low contact resistance and also high performance p-type devices.

12:10 PM NM07.13.03

Deformed All-2D Electronics and Strain Engineering Enabled by 3D Deformation in 2D Monolayer Semiconductors Mohammad A. Hossain¹, Jaehyung Yu², Yue Zhang¹ and Arend van der Zande¹; ¹University of Illinois at Urbana-Champaign, United States; ²The University of Chicago, United States

Emerging technologies like stretchable electronics and straintronics require materials that are highly deformable yet electronically active. With high breaking strain, high electronic mobilities and diverse properties, two dimensional (2D) materials are ideal for such applications. Moreover, due to their low bending stiffness, 2D materials are excellent candidates for engineering three-dimensional (3D) nanostructures to relieve strain or engineer inhomogeneous strain under compression. In crumpled systems, highly deformed surfaces of 2D materials lead to applications in wearable electronics and multifunctional surfaces. Engineering inhomogeneous strain gradients into device architectures enables access and control of strain-dependent quantum states like single quantum emitters, exciton diffusion and asymmetric valley states.

To fully realize the potential of 2D materials for deformable electronics or straintronics, it is necessary to tailor the transfer of strain into the materials and resulting morphologies. Here we demonstrate tuning of the

interfacial interaction between 2D membrane and elastomer substrate resulting in either crumpling through buckle delamination or conformal wrinkling, corresponding with low and high transfer of strain into the 2D membrane respectively. We then explore systems leveraging these tuned interactions resulting in strain resilient electronics from crumpled 2D heterostructures, and inhomogeneous or mechanically reconfigurable strain engineering from wrinkled 2D materials.

First, we demonstrate phototransistors from crumpled 2D heterostructures formed from graphene contacts to a monolayer transition-metal dichalcogenide (MoS_2 , WSe_2) channel and quantify the membrane morphology and optoelectronic performance.[1] Under uniaxial compression, the heterostructure and constituent monolayers relieve the stress by creating nearly periodic delaminated folds whose spacing depends on the membrane type. The matched mechanical stiffness of the constituting layers allows the heterostructure to maintain a conformal interface through large deformations. Photoluminescence (PL) spectroscopy shows that the optical band gap of WSe_2 shifts by less than 2 meV under 15% biaxial crumpling, corresponding to a change in strain of less than 0.05%. Photocurrent revealed that the crumpled heterostructure behave as a phototransistor where photoresponsivity scaled as $P^{-0.38}$, with behavior similar to flat devices. Photocurrent maps reveal biaxial crumpling by 15% marginally increases the photoresponsivity, by only 20%. PL and photoresponse confirm that crumpling and delamination prevent the buildup of compressive strain leading to highly deformed materials and devices with similar performance to their flat analogs.

While crumpling leads to strain resilient structures, increased substrate interaction actually results in wrinkling and increased strain transfer. We demonstrate a method to tune the strain in 2D materials by wrinkling monolayer WSe_2 attached to a 15 nm thick Al_2O_3 support layer and compressing the heterostructure on a soft substrate.[2] The Al_2O_3 film stiffens the 2D material, enabling optically resolvable micron scale wrinkling rather than nanometer scale crumpling. Using PL spectroscopy, we show that the wrinkling introduces periodic modulation of the bandgap by 47 meV, corresponding with strain modulation from +0.67% tensile strain at the wrinkle crest to -0.31% compressive strain at the trough. Moreover, we show that cycling the substrate strain mechanically reconfigures the magnitude and direction of wrinkling and resulting band tuning.

Taken together, these results set a foundation for deformable all-2D heterostructure devices and circuitry for stretchable electronic applications, and articulate strategies for maximizing or minimizing strain transfer.

References:

- [1] Hossain, M. A., et al. *ACS Appl. Mater. Interfaces* 2020, 12 (43), 48910–48916.
- [2] Hossain, M. A., et al. *Proceedings of SPIE* 2020, 1146404, 1–7.

12:25 PM NM07.13.04

Mobile and Continuous Stress Monitoring Using Imperceptible Graphene E-Tattoos (GET) Robustly Connected to a Wristwatch Hongwoo Jang, Eunbin Kim, Siyi Liu, Xiangxing Yang, Kyoung-Ho Ha, Seungmin Kang, Rebecca Wang and Nanshu Lu; The University of Texas at Austin, United States

Mental stress negatively impacts more than 77% population in our modern societies. Continuous and objective assessment of stress level enables proactive management for depression, evasion, and suicidal tendency. Electrodermal activity (EDA), a.k.a. galvanic skin response (GSR), is an emotion-induced skin conductance change due to sweat gland activity. EDA has been widely used as a quantitative index of mental stress levels for decades. Palm has the highest density of eccrine sweat glands which are filled up under psychological stimuli, such as mental stress, primarily. However, state-of-the-art EDA monitors suffer from limitations such as obstructiveness, undesirable location, short-term wearability, motion artifacts, etc. Herein, we introduce a long-term wearable (e.g. 24 hours), high-fidelity palm EDA sensor using dry, sub-micron-thick graphene e-tattoos (GET). The filamentary-serpentine-shaped GET is so thin (only 150-nm-thick) and so soft that it is imperceptible optically, mechanically, and also physiologically. The GET can fully conform to the finest texture of human skin, resulting in an interface impedance even lower than wet Ag/AgCl gel electrodes as well as reduced susceptibility to motion artifacts. GET is laminated on the palm and extended to the wrist to connect to

a wristwatch which provides data acquisition, storage, and wireless transmission. The orders of magnitude mismatch of stiffness and thickness between the GET and the wristwatch poses an outstanding challenge for the connection in between. We propose a simple yet effective solution named “heterogenous serpentine ribbon (HSR).” Due to the ultimate conformability of GET, simply laminating serpentine GET ribbon on an ultrathin serpentine metal ribbon without any interfacial adhesive could yield a conductive and stretchable interface. Compared with contacts between straight GET and metal ribbons, HSR offers a ten-fold strain reduction. To achieve a mechanically robust and reversible electrical connection between the ultrathin metal ribbon and the wristwatch, a soft interlayer is added in between to serve as a mechanical insulator but electrical conductor. We have successfully applied such GET-watch-based wearable EDA sensor for long-term, continuous, and ambulatory EDA sensing during our daily activities as well as during sleep. We argue that our HSR plus soft interlayer structure is a generic solution to robustly connect any ultrathin and ultrasoft e-tattoos to smartwatches, which will significantly extend the sensing modalities of future smartwatches.

12:40 PM NM07.13.05

Structural Engineering of Two-Dimensional Nanomaterials for Electrocatalysis Zhiwei Fang and Guihua Yu; The University of Texas at Austin, United States

Research on beyond graphene two-dimensional (2D) nanomaterials is becoming critically important for wide-ranging technological applications. In parallel with the discovery of new candidate materials and exploration of their unique characteristics, there are significant interests to rationally control the properties of 2D nanomaterials to meet requirements for energy-related applications. Electrocatalysis powered by renewable energy is expected to play a pivotal role in achieving sustainable energy goals. Recent advances in structural engineering have demonstrated their ability to overcome intrinsic material limitations, showing great potential for promoting catalytic activity and stability to a new level. Here we will discuss several important strategies to provide insights into application-oriented tailoring of material properties, and focus on our recent progress in developing 2D nanomaterials with tunable pore sizes or multidimensional interconnection for catalyzing several key electrochemical reactions, such as oxygen evolution, hydrogen evolution, and nitrogen reduction. Constructing porous and/or hierarchical 2D nanosheets enables improved ionic/electronic transport to achieve high active surface area for reactant adsorption/desorption, and meanwhile maintains high structural stability. These works demonstrate valuable insights, regarding material selection, structural modification and electronic tuning, into developing earth-abundant 2D electrocatalysts as alternatives to noble metal catalysts for efficient and stable electrocatalysis.

12:55 PM NM07.13.06

Late News: Tailored Graphene Micropatterns by Wafer-Scale Direct Transfer for Flexible Chemical Sensor Platform Yeonhoo Kim¹, Taehoon Kim², Jinwoo Lee³, Yong Seok Choi², Joonhee Moon⁴, Seo Yun Park², Tae Hyung Lee², Hoon Kee Park², Sol A Lee², Min Sang Kwon², Hyung-Gi Byun⁵, Jong-Heun Lee⁶, Myoung-Gyu Lee², Byung Hee Hong² and Ho Won Jang²; ¹Los Alamos National Laboratory, United States; ²Seoul National University, Korea (the Republic of); ³Korea Institute of Materials Science, Korea (the Republic of); ⁴Korea Basic Science Institute, Korea (the Republic of); ⁵Kangwon National University, Korea (the Republic of); ⁶Korea University, Korea (the Republic of)

Emerging novel technologies, such as flexible, rollable, and wearable electronics, need to meet their special requirements such as ease of controlling electronic properties, flexibility, and transparency. To date, metal and semiconducting materials have been used for conventional electronics, but the materials are brittle and nontransparent. In contrast, two-dimensional (2D) materials such as graphene and transition dichalcogenides have demonstrated great potential for flexible electronics and transparent electrodes due to their unique mechanical and electronic properties. In order to fully utilize 2D materials for the next-generation of flexible electronics, geometric micropatterns of 2D materials on flexible substrates such as polymer substrates are essential to fulfill technological purposes. However, due to harsh conditions such as cleaning, developing, and etching processes in the existing lithography procedure, defining elaborate micropatterns of 2D materials using the conventional microelectromechanical systems on polymer substrates is difficult to achieve.

Here, we demonstrate a novel strategy to obtain micropatterned graphene on flexible substrates, which is an alternative to the conventional wet transfer method. Graphene microchannels, which are prepared by the conventional lithography process are transferred by direct polymer curing transfer. With this method, entirely flexible, transparent, self-activated graphene sensor arrays are fabricated on 4-inch wafer-scale polymer substrates. A sensor array with four sensors using micropatterned graphene channels with noble metal decoration provides different sensing information and discriminates chemical species. Finite element method simulations were employed to investigate the potential of this patterning technique. The calculation results demonstrate that the performance of the sensors can be highly enhanced when the active channels are suspended and nanoscaled. This study provides higher reliability compared to the present state-of-the-art flexible electronic fabrication techniques and also demonstrates future-oriented flexible chemical sensor platforms.

1:10 PM NM07.13.08

Late News: Atomically-Thin Tellurene Based Biosensor for Selective and Sensitive Electrochemical Detection of Dopamine Ruifang Zhang and Wenzhuo Wu; Purdue University, United States

The effective and accurate sensing of dopamine (DA) has important implications due to its essential roles in the neurobiological system. The release process of dopamine is closely linked with neurological diseases such as Parkinson's, drug addiction, and attention deficit hyperactivity disorder (ADHD). Here we report a novel electrochemical biosensor based on atomically-thin tellurene, a 2D *p*-type semiconductor, for selective and sensitive detection of dopamine with a sensitivity for 2.81 mA/mM*cm², which is more superior to glassy carbon electrodes. Our device exhibits good linearity of oxidation current at the concentration of DA over a range of 1-2.875 mM, which presents the largest range reported in the literature. Enabled by the specific binding between Te and nitrogen atoms on biomolecules (DA), tellurene based sensors show greater selectivity of DA in the presence of uric acid and ascorbic acid. In addition, well-dispersed Au nanoparticles (Au-NPs) on 2D tellurene can enable excellent catalytic activity and a hospitable environment for biomolecules. We further demonstrated the successful sensing operation of tellurene/Au-NP based hybrid biosensors for the quantification of dopamine concentrations in human blood samples with satisfactory recoveries.

SESSION NM07.14: Devices for Sensing, Energy Conversion, and QIS II

Session Chairs: Zakaria Al Balushi and Thomas Kempa

Tuesday Afternoon, April 20, 2021

NM07

2:15 PM *NM07.14.01

Logic-in-Memory Based on an Atomically Thin Semiconductor Andras Kis; EPFL, Switzerland

The growing importance of applications based on machine learning is driving the need to develop dedicated, energy-efficient electronic hardware. Compared with von-Neumann architectures, brain-inspired in-memory computing uses the same basic device structure for logic operations and data storage, thus promising to reduce the energy cost of data-centric computing significantly. Two-dimensional materials such as semiconducting MoS₂ could stand out as a promising candidate to face this obstacle thanks to their exceptional electrical and mechanical properties. Here, we show that wafer-scale grown MoS₂ can be used as an active channel material for developing logic-in-memory devices and circuits based on floating-gate field-effect transistors (FGFET). The conductance of our FGFETs can be precisely and continuously tuned, allowing us to use them as building blocks for reconfigurable logic circuits where logic operations can be directly performed using the memory elements. We show that this design can be simply extended to implement more complex programmable logic and functionally complete sets of functions. Our findings highlight the potential of atomically thin semiconductors for the development of next-generation low-power electronics.

2:40 PM NM07.14.02

Device Integration of Atomically Precise Graphene Nanoribbons (GNRs) Oliver Braun^{1,2}, Jan Overbeck¹, Mickael Perrin¹, Gabriela Borin Barin¹, Maria El Abbassi^{1,3}, Qiang Sun¹, Sara Sangtarash^{4,5}, Akimitsu Narita⁶, Klaus Müllen⁶, Edward Ditler¹, Kristjan Eimre¹, Colin Daniels⁷, Vincent Meunier⁷, Hatef Sadeghi^{4,5}, Carlo Pignedoli¹, Colin Lambert⁵, Oliver Gröning¹, Pascal Ruffieux¹, Roman Fasel¹ and Michel Calame^{1,2}; ¹Empa–Swiss Federal Laboratories for Materials Science and Technology, Switzerland; ²University of Basel, Switzerland; ³Kavli Institute of Nanoscience, Netherlands; ⁴University of Warwick, United Kingdom; ⁵Lancaster University, United Kingdom; ⁶Max Planck Institute for Polymer Research, Germany; ⁷Rensselaer Polytechnic Institute, United States

Graphene nanoribbons (GNRs) have attracted considerable interest due to their largely modifiable electronic properties, including width-dependent bandgaps for armchair GNRs and spin-polarized edge states for GNRs with zigzag edges.^{1,2,3,4} Manifestation of these properties requires atomically precise GNRs, which can be achieved through a bottom-up synthesis approach under ultrahigh vacuum conditions. We show that 5-atom wide armchair GNRs as well as pyrene-GNRs can be processed under ambient conditions and incorporated as the active material in a field effect transistor.^{5,6} At room temperature, a film like behavior is observed while at cryogenic temperatures coulomb blockade and single electron tunnelling can be seen. Our recent results may enable the realization of devices based on carbon nanomaterials with exotic quantum properties.

¹ Cai, J. *et al.*, *Nature* **466**, 470–473, (2010)

² Chen, Y.-C *et al.*, *ACS Nano* **7**, 7, 6123–6128, (2013)

³ Ruffieux, P. *et al.*, *Nature* **531**, 489–492, (2016)

⁴ Gröning, O. *et al.*, *Nature* **560**, 209–213, (2018)

⁵ El Abbassi, M. *et al.*, *ACS Nano* **14**, 5, 5754–5762 (2020)

⁶ Sun, Q. *et al.*, *Advanced Materials* **32**, 1906054 (2020)

2:55 PM *NM07.14.03

High Yield, Bottom-Up/Top-Down CVD Synthesis of 2D Layered Metal Selenides—A Promising Class of Materials for Applications in Electronics and Electrochemistry Gilbert D. Nessim; Bar Ilan University, Israel

Since the excitement about graphene, a monolayer of graphite, with its 2010 Nobel Prize, there has been extensive research in the synthesis of other non-carbon few/mono-layers exhibiting a variety of bandgaps and semiconducting properties (e.g., n or p type). The main approaches to deposit few/monolayers on a substrate are: (a) bottom-up synthesis from precursors using chemical vapor deposition (CVD) or (b) top-down exfoliation (liquid or mechanical) of bulk layered material. Using a Lego approach of superposing monolayers, we can envisage the fabrication of heterojunctions with original electronic behavior.

Here we show a combined bottom-up and top-down approach where (a) we synthesize in one step high yields of bulk layered materials by annealing a metal in the presence of a gas precursor (sublimated selenium from selenium powder) using chemical vapor deposition (CVD) and (b) we exfoliate and deposited (dropcast or Langmuir Blodgett) few/mono-layers on a substrate from a sonicated mixture of our material in a specific solvent. It is interesting to note that, besides the structure being 2D layered, the properties of the nanomaterials synthesized slightly differ from the materials with the same stoichiometry synthesized using conventional chemical methods (e.g., solvothermal).

In this talk, we will discuss the chemical synthesis, the very extensive characterizations, and the lessons we learned in making multiple metal selenides (Ag-Se, Cu-Se, W-Se, Mo-Se). We will see how we integrated these new materials into sensors and into electrochemical devices (see selected published papers below).

R. Konar, S. Das, E. Teblum, A. Modak, I. Perelshtein, J.J. Richter, A. Schechter*, and G.D. Nessim*
Facile and Scalable Ambient Pressure Chemical Vapor Deposition-Assisted Synthesis of Layered Silver Selenide (β -Ag₂Se) on Ag foil as an Oxygen Reduction Catalyst in Alkaline Medium

A. Moumen, R. Konar, D. Zappa, E. Teblum, I. Perelshtein, G.D. Nessim*, and E. Comini*

Exfoliated 2D few-layered tungsten di-selenide (2H-WSe₂) nanosheets for exceptionally sensitive and selective nitrogen dioxide (NO₂) detection at room temperature

ACS Applied Materials and Interfaces (in press)

R. Konar, Rosy, I. Perelshtein, E. Teblum, M. Telkhozhayeva, M. Tkachev, J.J. Richter, E. Cattaruzza, A. Pietropolli Charmet, P. Stoppa, M. Noked*, G.D. Nessim*

Scalable synthesis of few-layered 2D tungsten di-selenide (2H-WSe₂) nanosheets directly grown on tungsten (W) foil using ambient pressure chemical vapor deposition for reversible Li-ion storage

ACS Omega (inside cover) 5 (31), 19409-19421, July 2020

3:20 PM NM07.14.04

Late News: A Homoepitaxial Approach of Large Scale, High Quality Boron Nitride Growth by MOVPE

Aleksandra K. Dabrowska, Mateusz Tokarczyk, Grzegorz Kowalski, Johannes Binder, Rafal Bozek, Roman Stepniewski and Andrzej Wyszomolek; Faculty of Physics, University of Warsaw, Poland

The importance of hexagonal boron nitride (BN) in the world of two-dimensional crystals (2D) is constantly increasing. This is due to the fact that it combines the properties of 2D materials, like a layered structure and possibility of exfoliation with those of classic nitrides – a wide bandgap and high chemical and physical resistance [1]. All of these aspects make it a perfect candidate for example for deep UV light source and detector, insulating barriers in van der Waals heterostructures or protecting layers for other, more sensitive materials [2]. Metal Organic Vapor Phase Epitaxy (MOVPE) is a very promising technique to obtain high quality boron nitride on the wafer-scale, which could facilitate the implementation of the before mentioned applications

The MOVPE growth of boron nitride requires careful selection of growth conditions – as this is a van der Waals material, effective synthesis is usually connected with a bad surface morphology and poor optical properties. Epitaxial material, oriented parallel to the sapphire substrate could be obtained basically with two different growth modes. The first mode is the Continuous Flow Growth (CFG) regime when the boron (TEB) and nitrogen (ammonia) precursors enter the reactor simultaneously, conducted at extremely high temperature (about 1300 °C) and with a large NH₃/TEB flow ratio resulting in thin, smooth BN layers [3]. The optical properties and surface morphology of such layers are satisfactory. Unfortunately the longer the growth, the more three-dimensional precipitates appear on the surface, thus the maximum thickness of a good quality layer, possible to obtain by this method is about 5 nm. The second growth regime is Flow-rate Modulated Epitaxy (FME) for which ammonia and TEB are delivered to the reactor in alternating pulses. This growth mode allows to obtain tens of nanometer thick BN but the supersaturation of boron in TEB pulses support the formation of structural defects, responsible for mid-gap luminescence [3].

The method we propose combines these two growth regimes by using CFG BN as a buffer layer for homoepitaxial growth of a FME layer on the top of it. This approach allows to obtain FME BN layers with much better optical and structural quality reaching a thickness of several tens of nanometers [4]. Moreover, this semi-homoepitaxial boron nitride exhibits high homogeneity on the entire two-inch surface. Further optimization of this method allows us to obtain better quality samples. The relationship between the growth parameters and the crystallographic structure, concentration of point defects and surface morphology of BN grown by this Combined Growth Mode (CGM) will be presented. Our results bring boron nitride significantly closer to large-scale applications.

[1] K.S. Novoselov, A. Mishchenko, A. Carvalho, A.H. Castro Neto “2D materials and van der Waals heterostructures”. Science 353.6298, aac9439 (2016)

[2] N. Izyumskaya, D.O. Demchenko, S. Das, Ü. Özgür, V. Avrutin, H. Morkoç. “Recent Development of

Boron Nitride towards Electronic Applications”, *Advanced Electronic Materials* 3, 5:1600485 (2017)

[3] K. Pakula, A. Dabrowska, M. Tokarczyk, R. Bozek, J. Binder, G. Kowalski, A. Wyszomolek, R. Stepniewski ”Fundamental mechanisms of hBN growth by MOVPE” arXiv: 1906.05319 (2019)

[4] A.K. Dabrowska, M. Tokarczyk, G. Kowalski, J. Binder, R. Bozek, J. Borysiuk, R. Stepniewski, A. Wyszomolek, ”Two stage epitaxial growth of wafer-size multilayer h-BN by metal-organic vapor phase epitaxy – a homoepitaxial approach”, *2D Mater.*, 8, 015017 (2021)

3:35 PM NM07.14.05

Mixed-Dimensional MXene-Hydrogel Heterostructures for Electronic Skin Sensors with Ultrabroad Working Range Yichen Cai and Vincent Tung; King Abdullah University of Science and Technology, Saudi Arabia

Skin-mountable microelectronic devices (i.e., electronic skin, e-skin) are garnering substantial interest for various promising applications including human–machine interfaces, bio-integrated devices, and personalized medicines¹⁻³. However, it remains a critical challenge to develop reliable, durable, and biocompatible e-skins to mimic the human somatosensory system in a full working range⁴. Herein, we present a multifunctional e-skin system with a heterostructured configuration that couples a vinyl hybrid silica nanoparticles (VSNP) modified polyacrylamide hydrogel (VSNP-PAM) with two-dimensional (2D) MXene. The VSNP-PAM hydrogel is engineered to achieve both high toughness and low hysteresis, serving as an elastic substrate for the e-skin that overcomes the toughness-hysteresis correlation. Then, a nano-bridging layer of 1D polypyrrole (Ppy) nanowires is applied to dynamically link the interfaces between the hydrogel substrate and the sensing layer of 2D MXene. These material configurations endow the e-skin with tunable sensing mechanisms, exhibiting an extraordinary stretchable working range (0–2,800%), ultrafast responsiveness (~90 ms) and outstanding resilience (~240 ms), good linearity (0–800%) and excellent reproducibility (>5,000 cycles). In parallel, this e-skin is capable of detecting, quantifying and remotely monitoring of stretching motions in multi-dimensions, pressure exertions (40 Pa-30 kPa), tactile and proximity sensing (from a distance of ~20 cm), temperature, and light variations, providing a promising platform for next-generation smart flexible electronics with a ultrabroad working range.

References:

1. Wang, S. et al., *Nature* **555**, 83 (2018)
2. Larson, C. et al., *Science* **351**, 1071-1074 (2016)
3. Gao, W. et al., *Nature* **529**, 509 (2016)
4. McEvoy, M. A. & Correll, N. et al., *Science* **347**, 1261689 (2015)

3:50 PM NM07.14.06

Experimental Demonstration of Room Temperature 2D TMD Excitonic Perfect Absorbers for High Efficiency Excitonic Solar Cells Joeson Wong, Tyler Colenbrander and Harry A. Atwater; California Institute of Technology, United States

We experimentally demonstrate near-unity absorption in monolayer WS₂ via a van der Waals heterostructure coupled to an optical cavity. To achieve this perfect absorption at the excitonic frequency, we match the WS₂ radiative and non-radiative excitonic decay rates, which impedance matches the exciton to free space. With the presence of an Ag back mirror, this impedance matching condition results in perfect absorption at the excitonic frequency. We show that this impedance matching condition can be readily achieved at cryogenic temperatures by lowering the non-radiative decay rate due to homogeneous broadening but can also be achieved at room temperature by increasing the radiative decay rate, via Purcell enhancement of the excitonic emitter. We further show theoretically that perfect absorption with multiple excitonic species (e.g. WS₂ and WSe₂) is possible, suggesting that solar cells comprised of multiple excitonic perfect absorbers can achieve detailed balance photovoltaic efficiencies surpassing the Shockley-Queisser Limit. We find that monolayer 2D perfect absorbers have potential for highly efficient van der Waals optoelectronic and photovoltaic devices.

4:05 PM NM07.14.08

Laser Photothermal Nano-assembly of Palladium Nanoparticles and 3D Porous Graphene for Wireless,

Flexible, High-Sensitive Hydrogen Detection Seung Min Lee¹, Minsu Kim², Byoung Gak Kim² and Pilgyu Kang¹; ¹George Mason University, United States; ²Korea Research Institute of Chemical Technology, Korea (the Republic of)

A simple and facile method to produce a hybrid nano-assembly of 3-dimensionally (3D) structured and palladium nanoparticles (PdNPs) embedded graphitic carbon with high-performance polymers would be highly desirable. All existing approaches to synthesize hybrid materials comprising graphene and metal NPs involve complicated processes; carbon nanomaterials are mostly fabricated based on chemical vapor deposition or reduction of graphene oxides methods and PdNPs are further integrated on carbon nanomaterials through thermal annealing or chemical processes. Recently, a scalable and fast laser photothermal method to generate laser-induced graphene (LIG) with high electrical conductivity and large specific surface area from commercial polyimide films has been demonstrated and triggered a significant research development in various applications, including energy storage, harvesting, and detection. The method has been further utilized to fabricate LIG based hybrids including heteroatoms-doped LIG, LIG-metal-sulfides nanocomposite materials, as well as LIG-metal-oxides nanocomposite materials for high-performance energy storage, detection, and generation. However, the application of the laser photothermal method in the fabrication of porous graphene-PdNPs nanocomposite material has yet been demonstrated especially for the hydrogen leakage system hence achieving the hybrid materials remains a challenge due to the processing requirements of high thermal/chemical energy, and the lengthy period of time consumption. Here, we report a one-step, fast laser photothermal nano-assembly method to synchronously Pd-NPs and porous graphene from polymer films of mixed Pd and carbon precursors. We used the polymers of intrinsic microporosity (PIM-1) as a precursor to obtaining porous graphene, which has polybenzodioxane structure with cyano groups, high solubility in a volatile solvent, and miscibility with inorganic materials enabling to fabricate homogeneous polymer films with evenly and highly dispersed Pd-ligands. We demonstrated a scalable laser photothermal method to form the nano-assembly of 3D porous graphene and PdNPs from the polymer film for wireless and flexible hydrogen detection systems with the limit of detection (LOD) of 1 ppm hydrogen gas concentration. With the combined advantages of high sensitivity/selectivity/surface of 3D porous graphene and rapid response/recovery speed of PdNPs, we could obtain high sensitivity with the fast response time at low H₂ concentration ranges (1-50 ppm). Moreover, the hybrids exhibit outstanding flexibility and durability under bending and twisting and the nano-assembly is further integrated with a wireless communication system via BLE protocol to transfer the monitored signal of conductance to the change of hydrogen concentrations to a mobile device. The innovative sensing technology based on laser nanomanufacturing of the nano-assembly for highly sensitive, flexible, wireless sensing systems has future potential for broad applications in various industries and military fields.

SESSION NM07.15: Devices for Sensing, Energy Conversion, and QIS III

Session Chairs: Daniel Bediako, Ying Fang and Thomas Kempa

Tuesday Afternoon, April 20, 2021

NM07

5:15 PM NM07.15.04

Late News: Broadband Photodetectors Based on Tellurene/CdS Quantum Dots Mixed-Dimension heterostructure Ruifang Zhang and Wenzhuo Wu; Purdue University, United States

Photodetectors capable of detecting light in a broad spectrum is central to diversified optoelectronic applications in spectroscopy, remote sensing, imaging, and optical communication. Two-dimensional (2D) materials, such as graphene, borophene, phosphorene, and transition metal dichalcogenides (TMDs), are good candidates due to their unique semiconductor and structural characteristics. Tellurene is an emerging 2D semiconductor boasting characteristics potentially relevant for photodetection.

However, the small bandgap of tellurene makes it more suitable to detect long-wavelength light. Here, we

demonstrate a highly sensitive, fast-response photodetector based on tellurene-CdS quantum dots mixed-dimension heterostructures, which enables the efficient separation of the photogenerated electron-hole pairs and inhibits the rate of undesirable recombination. The heterostructured device exhibits a low dark current (0.4 nA) and good quantum efficiency. A systematic characterization of the device performance indicates that such mixed-dimensional heterostructured photodetector exhibits superior photodetection performance with a broadened spectrum response, improved response speed, sensitivity and responsivity.

5:20 PM NM07.15.05

CVD-Grown 2D Material Schottky Photovoltaics with Interlocking Asymmetric Contacts Timothy Ismael, Kazi Islam, Meghan Bush, Claire Luthy and Matthew D. Escarra; Tulane University, United States

Two-dimensional (2D) transition metal dichalcogenides (TMDCs) have received increased attention in recent years for optoelectronics due to their strong light-matter interactions. This includes ultra-thin molybdenum disulfide (MoS_2), which is a suitable material for flexible, wearable, and high specific power photovoltaics (PV)¹. Obtaining high efficiency PV through doping of 2D materials has been a challenge; however, Schottky PV is an alternative route to overcoming this challenge. In this work, we present a Schottky-type photovoltaic device using 2D MoS_2 films and asymmetric contacts.

Chemical vapor deposition (CVD) is utilized to synthesize MoS_2 films on sapphire substrate, with MoO_3 and S as the precursors, carried by Ar. High-quality monolayer films with sparse bi-layer regions are obtained, and film uniformity, optical performance, and electronic quality are confirmed through transmittance and photoluminescence spatial mapping. Ti contact MoS_2 transistors and photodetectors were fabricated from which an external quantum efficiency (EQE) of 25% at 620 nm laser illumination and a carrier mobility of $3.3 \text{ cm}^2/\text{V}\cdot\text{s}$ was obtained, indicating high quality CVD grown MoS_2 .

For the Schottky PV device, Ti is selected as one of the asymmetric metal contacts due to its work-function of 4.33 eV, while Pt is selected as the second contact due to its relatively high work-function of 5.64 eV. These Schottky PV device contacts are fabricated on SiO_2/Si substrates as an asymmetric interlocking-finger type design onto which the MoS_2 films are transferred using a surface energy assisted transfer technique. The MoS_2 /metal configuration maximizes the PV active area by eliminating contact shading losses and utilizes lateral transport to minimize electrical shunts between contacts. A band offset of -0.9 eV arises between the Fermi levels of Ti and MoS_2 at their interface while an offset of 0.41 eV arise at the Pt- MoS_2 interface. The resulting selectivity of Ti to electrons and of Pt to holes in the Ti-Pt asymmetric contact device creates the condition for photo-generated carrier separation.

The $300 \mu\text{m} \times 400 \mu\text{m}$ active area Schottky PV shows a V_{OC} of 260 mV under 660 nm laser illumination with a $1.07 \mu\text{A}/\text{cm}^2$ J_{SC} , while 125 mV V_{OC} was obtained under 1 sun AM1.5G illumination using a solar simulator with J_{SC} of $0.17 \mu\text{A}/\text{cm}^2$. Device modeling using COMSOL Multiphysics (Semiconductor Module) shows that a V_{OC} of 900 mV and $41 \mu\text{A}/\text{cm}^2$ [EMD1] J_{SC} is attainable for a Pt-Ti asymmetric contact 2D PV device. The low photocurrent and poor J_{SC} obtained from the fabricated asymmetric contact device can partly be attributed to the small diffusion length of carriers in these CVD-grown films, especially for holes. Furthermore, relatively large sheet and contact resistance was identified in the device through transmission line measurement (TLM). However, the relatively high V_{OC} and absorption, the promising carrier mobility obtained from the symmetric contact devices, and the device modeling all indicate that efficient photovoltaic devices are attainable.

Current efforts towards improving PV device performance include contact engineering, film growth/thickness, and device architecture optimization guided through spatial mapping of device properties. Atomistic investigation of interfaces through density functional theory, PV device modeling, and contact selection supported through Schottky barrier height extraction and work function measurements will also support the realization of high efficiency 2D PV.

¹Bernardi, M., Palummo, M., & Grossman, J. C. (2013). Extraordinary sunlight absorption and one nanometer thick photovoltaics using two-dimensional monolayer materials. *Nano letters*, 13(8), 3664-3670.

5:25 PM NM07.15.07

Tuning the Electrical Properties of Monolayer TMDs via Chemical Doping and Interface Engineering

The fundamental properties of two-dimensional (2D) materials, as well as the quality of 2D films and device interfaces, give rise to inherent limitations in their device performance. The ultrathin nature and large surface area of two-dimensional (2D) materials make them quite sensitive to their surrounding environments, which enables their optical and electrical properties to be tuned through surface modification. Developing processes to controllably dope transition-metal dichalcogenides (TMDs) and their electrical contact interfaces are critical to achieving commercial viability for optical and electrical applications. Previously, we successfully expanded the application of electron-transfer doping using molecular reductants and oxidants to various TMDs, including monolayer MoS₂, MoSe₂, WS₂, and WSe₂. The chemical doping is introduced onto the 2D material by exposing it to solutions of molecular reductant (n-dopant) or oxidant (p-dopant). Both n- and p-type transport properties were achieved in all four monolayer-TMDs, and both non-degenerate and degenerate regimes are accessible.¹ The degree of doping can be finely controlled by choice of dopants, treatment time, and the concentration of doping solution. Detailed physical characterization was conducted to study the doping effect and to understand the underlying mechanisms. MoS₂ is known to show stubborn n-type behavior due to its intrinsic band structure and Fermi level pinning. Here, we investigate the combined effects of molecular doping and contact engineering on the transport and contact properties of the monolayer (ML) MoS₂ devices. Our study showed that p-type MoS₂ can only be achieved by combining molecular doping with high-work function Pd contacts.² Molecular doped p-FETs show effective hole mobilities of 2.3 cm² V⁻¹ S⁻¹, an on/off ratio exceeding 10⁶, and improved contact resistance of ≈482 kΩ μm. Devices with low work function Ti metal contacts only showed ambipolar behavior. It was shown that the contact resistance and Schottky barrier heights can be effectively modulated through doping of the channel materials and by changing the contact metal. A relatively low hole injection barrier of ≈156 meV was obtained for p-doped MoS₂ with Pd contacts. A MoS₂ inverter based on pristine (n-type) and p-doped monolayer MoS₂ was fabricated, demonstrating the potential application of 2D-based complementary electronic devices. In summary, we have demonstrated a solution-based charge transfer doping on several 2D semiconductors. This technique provides a simple yet effective route to tailor the band structure of the 2D materials and control the resulting electrical and optical properties.

References

1. S. Zhang, H. M. Hill, K. Moudgil, C. A. Richter, A. R. Hight Walker, S. Barlow, S. R. Marder, C. A. Hacker and S. J. Pookpanratana, *Adv. Mater.*, 2018, 30, 1802991.
2. S. Zhang, S. T. Le, C. A. Richter and C. A. Hacker, *Appl. Phys. Lett.*, 2019, 115, 073106.

5:30 PM NM07.15.10

Graphene Oxide as a Catalytic Agent in Polymer Electrolyte Membrane Fuel Cell Shristi Silwal, Abdelrahman Elkhatib, Olabode Ajayi, Jayson Treml, Puteri M. Hamari and Bhushan V. Dharmadhikari; Minnesota State University, United States

Platinum (Pt) is commonly used as a catalyst in fuel cell production. Platinum being an expensive metal, makes commercialization of fuel cells uneconomical. Many research groups are working on finding the alternative catalytic material. Graphene and carbon based nanomaterials have potential to replace Pt as catalyst in polymer electrolyte membrane fuel cell (PEMFC) due to their properties such as broad electrochemically active surface area, fast carrier mobility, high conductivity, and ability to stabilize and increase the durability of fuel cells. Proton conducting Polymer Electrolyte Membranes (PEMs) are used in PEMFCs to allow protons (H⁺) to pass through the electrodes. An effective PEM should be able to facilitate ion transfer in fuel cells. Nafion is one of the most widely used electrolytes in PEMs due to its high ionic conductivity and highly resistance to chemical reactions such as corrosion. However, water retention in Nafion membrane give rise to fouling effect, which reduces the ion transfer and performance of PEMFC. The amount of water retained also causes the polymer to swell, therefore, decreasing the efficiency of fuel cells. To overcome this drawback, hydrophobic Polycaprolactone (PCL) is being considered a potential electrolyte in this study. The objective of our research is to use Graphene Oxide as catalyst in electrodes of PEMFC and find alternative for Nafion membrane by using electrospun PCL nanofibers instead. The use of carbon based nanomaterials has delivered commendable performance making commercialization of fuel cell products possible in near future.

5:35 PM NM07.15.12

Strong Interfacial Interaction of Prussian Blue and Inorganic Nanosheet with Improved Supercapacitor Performance Xiaoyan Jin and Seong-Ju Hwang; Yonsei University, Korea (the Republic of)

An efficient interfacial interaction between Prussian blue (PB) nanocrystals and exfoliated inorganic nanosheets (NSs) enables to synthesize strongly-coupled composite materials with remarkably improved electrode functionality for supercapacitor. The highly porous nanohybrids of PB-inorganic NS are synthesized by crystal growth of PB nanocrystals on the inorganic NSs. The coordinative bonding between cyanide ligand of PB and inorganic NS induces significant interfacial charge transfer and the increase of the metal oxidation state of PB. The obtained nanocomposites possess expanded surface area than does the pristine PB material, indicating the enhancement of porosity by the hybridization. Of prime importance is that the present nanocomposites show larger specific capacitances with better cyclability and better stability than does the MnO₂ free-PB material, underscoring the beneficial effect of incorporated inorganic NS on the electrode functionality of PB. The present study clearly demonstrates that the composite formation of PB nanocrystals with inorganic NSs can provide an effective way to explore high performance electrode for supercapacitor.

5:40 PM NM07.15.15

Flexible Piezotronic Transport Behavior and Transistors from 2D Zinc-Oxide Nanosheets Corey Carlos, Kevin J. Berg, Yizhan Wang and Xudong Wang; University of Wisconsin–Madison, United States

Since graphene, the growing family of 2-dimensional (2D) materials spanning transition-metal dichalcogenides (TMDs), metal-organic frameworks (MOFs), oxides, and organics, has led to the broader development of nanomaterials and creative use of nanotechnology. Often, it is this reduced dimensionality that enables enhanced structure-property relationships necessary for advancing the field. Wearable flexible electronics is one research area that has seen tremendous growth in recent decades and has benefited by advances in 2D nanomaterials. Considered a fundamental building block, transistors are ubiquitous in modern technology. We demonstrate a novel approach for utilizing the piezoelectric and semiconducting properties of 2D zinc-oxide (ZnO) nanosheets (NS), synthesized via Ionic Layer Epitaxy (ILE), as strain-gated flexible transistors. We examine the effects of strain and immobile piezoelectric surface charge on the semiconducting properties of ZnO-NSs. Given the polar structure of ZnO, we show that the accumulation of piezoelectric charge can change depending on the crystallographic orientation with the respect to the gated contacts of the flexible transistor. As a consequence, the Schottky barriers at the metal-semiconductor interface can be asymmetrically modulated through the application of strain.

5:45 PM NM07.15.16

Low-Voltage Operating 2D MoS₂ Channel Based Electron Devices Using Lead-Free High-k/Ferroelectric Ba_xSr_{1-x}TiO₃ Yeonsu Jeong, Hye-Jin Jin, Ji Hoon Park and Seongil Im; Yonsei University, Korea (the Republic of)

Combining lead-free high-k materials and two dimensional (2D) semiconductor has been attracted many attentions owing to need for environmental-friendly and low-voltage operating devices. Especially, low voltage switching ferroelectric memory devices are rare in report. Here, we have successfully fabricated low-voltage operating field effect transistor (FET) and ferroelectric switching memory transistor using 2D MoS₂ channel and high-k/ferroelectric dielectric Ba_xSr_{1-x}TiO₃ (BST). Ferroelectricity of BST can be controlled by changing composition ratio of Ba and Sr in the BST film. In this study, Ba_{0.5}Sr_{0.5}TiO₃ (50BST, x=0.5) and Ba_{0.8}Sr_{0.2}TiO₃ (80BST, x=0.8) have been used as dielectric materials for low-voltage operating FET and nonvolatile ferroelectric memory transistor, respectively. Mechanically exfoliated MoS₂ flakes were transferred on PMMA brush-treated 50BST and 80BST oxide. The 5 nm-thin PMMA brush was used for reduction of the surface roughness of BST. As a result, we have successfully demonstrated extremely low voltage operating MoS₂ FET, which uses only 0.5 V gate voltage for ON/OFF switching due to high-k 50BST. And using 80BST, MoS₂ based ferroelectric memory transistor has been well operated in a nonvolatile manner under ±3 V pulses. Since

employed high-k dielectric and ferroelectric oxides are lead-free in particular, the approaches applying high-k BST gate oxide for 2D MoS₂ FET are not only novel but also practical towards future low voltage nanoelectronics and green technology.

SESSION NM07.16: Devices for Sensing, Energy Conversion, and QIS IV
Session Chairs: Ying Fang and Thomas Kempa
Tuesday Afternoon, April 20, 2021
NM07

9:00 PM *NM07.16.01

2D Transistors—Promises, Pitfalls and Prospects Xiangfeng Duan; University of California, Los Angeles, United States

Two-dimensional (2D) semiconductors have attracted tremendous interest as an atomically thin channel for the continued transistor scaling. However, despite many proof-of-concept demonstrations, the full potential of 2D transistors remains elusive. To this end, the fundamental merits and technological limits of 2D transistors need a critical assessment, reality check and objective projection. In this talk, I will briefly review the promises and the current status of 2D transistors, and highlight the widely used device parameters (e.g., carrier mobility, contact resistance) could be frequently misestimated or misinterpreted, and may not be the most reliable performance metrics for benchmarking 2D transistors. We suggest the saturation or on-state current density, especially in the short channel limit, could provide a more reliable measure for assessing the potential of diverse 2D semiconductors, and should be applied for cross-checking different studies, especially when milestone performance metrics are claimed. We next summarize the key technical challenges in optimizing the channel, contacts, dielectric and substrate interfaces and outline the potential pathways to push the limit of 2D transistors; and lastly conclude with a prospect on the critical technical targets, the key technological hurdles to enable the lab-to-fab transition, and the potential opportunities arising in these atomically thin semiconductors.

9:25 PM *NM07.16.02

Ultrathin Electronic Tattoos Based on PtSe₂ and PtTe₂ Dmitry Kireev^{1,1}, Emmanuel Okogbue^{2,2}, Jayanth RT¹, Tae-Jun Ko², YeonWoong Jung^{2,2,2} and Deji Akinwande^{1,1}; ¹The University of Texas at Austin, United States; ²University of Central Florida, United States

In this work, we present the unique ultrathin platinum-based two-dimensional dichalcogenide (Pt-TMDs) based electronic tattoos. These ultrathin electronic tattoos are fabricated utilizing large-scale CVD-grown platinum diselenide (PtSe₂) and platinum ditelluride (PtTe₂). The growth is performed at moderate temperatures, at about 400°C, allowing for direct coating onto temperature-sensitive polymers, such as Kapton. Confirming the quality of TMD materials, we show a thorough characterization of PtSe₂ and PtTe₂'s electrical and electrochemical properties along with advanced healthcare-related applications. First of all, both PtSe₂ and PtTe₂ tattoos were found to have lower sheet resistance and electrode-skin impedance compared to graphene-based tattoos. Among themselves, PtTe₂ tattoos were found to be the most attractive, with sheet resistance as low as 13 Ohm/sq and electrode-to-skin impedance averaging at 4.94±1.61 kΩ (@10 kHz), clearly outperforming the state-of-the-art gold tattoos and even medical-grade Ag/AgCl gel electrodes. We used these ultrathin tattoos for a plurality of human physiological vital signs monitoring, such as the heart and the brain's electrical activity, muscle contractions, eye movements, and temperature. Moreover, to showcase an advanced application of the Pt-TMDs for human-machine interfacing, we built a multi-tattoo system that can easily distinguish eye movement and identify sight direction.

9:50 PM NM07.16.04

Late News: Controlled and Scalable Fabrication of Non-Stoichiometric 2D Bi₂S₃ and Its Intriguing

Optoelectronic Properties Jagadeesh Suriyaprakash and Lijun Wu; School of Information and Optoelectronic Science and Engineering, China

Two-dimensional (2D) materials are considered as ground-breaking foundations for novel optoelectronic devices owing to their tunable optoelectronic features, which rely on band/strain/defect engineering. However, early studies have limitations of precise tuning of new chemical composition correlated with electronic and crystal structure, which provides the space for developing a new strategy. In this context, we fabricated the novel non-stoichiometric $\text{Bi}_x\text{-Bi}_{2-x}\text{S}_{3-y}$ 2D-layered materials by simple e-beam lithography. Furthermore, an *in-situ* HRTEM study reveals that newly formed Bi metallic nanocrystals on the edge of $\text{Bi}_{2-x}\text{S}_{3-y}$ 2D layer show structural dynamics behavior followed by surface and structural transformation. We observed the nucleation, coagulation and Ostwald ripening process in the metallic nanocrystals with respect to the irradiation time. This functional material shows unique electronic structures, which can be manipulated by the non-stoichiometric ratio (Fermi level changes: p-type \rightarrow n-type \rightarrow quasi metallic). X-ray photoelectron spectroscopy studies supported the results of *in-situ* TEM analysis. Also, complete optoelectronic characteristics of newly synthesized materials were studied. We propose the possible mechanism involving the Auger decay of sulfur and local bond-breaking phenomenon in Bi_2S_3 material by considering the specimen heating effect and radiolysis process. This *in-situ* study opens the new corridor to the materials researchers to design the novel 2D transition metal chalcogenides materials by the one-step route and tune their physicochemical properties precisely.

10:05 PM NM07.16.05

Conductor-Free Anode of Transition Metal Dichalcogenide Nanosheets Self-Assembled with Graft Polymer Binder Chanho Park, Hyeokjung Lee, Seung Won Lee, Kyuho Lee and Cheolmin Park; Yonsei University, Korea (the Republic of)

The development of anodes for lithium-ion batteries (LIBs) has garnered considerable interest. In particular, anodes based on liquid-phase-exfoliated two-dimensional transition metal dichalcogenide (TMD) nanosheets are studied extensively because their intrinsic capacity is higher than graphite. As most semiconducting TMDs possess low electrical conductivity and lithium-ion diffusivity, costly processes are needed—such as the addition of conductive fillers, chemically converted metallic phase transformation, and topological nanofabrication—to decrease the ion diffusion length and increase the surface area. Here, we introduce a novel conductor-free TMD nanosheet anode with graft-polymer ionic channels that ensures high stability and rate capability of the LIB. The fluorinated polymer binder grafted with ionomers allows not only the efficient exfoliation of TMD nanosheets in the liquid phase to guarantee stable sheet-to-sheet separation but also provides self-assembled ionic channels through which lithium ions in the electrolyte readily arrive close to the surface of the nanosheets. Efficient electrochemical reduction of lithium ions occurs on the surface of our simple binary anode of MoS_2 nanosheets, self-assembled with graft binder ionic channels, resulting in a high-performance LIB with stability (90% retention rate after 1,000 cycles), rate capability (50% at 5 A/g), and high cell capacity (933.1 mAh/g at 0.1 A/g). Our TMD anodes that do not require additional processes for enhancing electric as well as ionic conductivity offer a novel strategy for developing high performance large-scale TMD-based LIBs.

10:20 PM NM07.16.06

QD Hybridized 2D Material Based Nanoscroll—A New Paradigm for Efficient Light-Harvesting and Polarized Emission Rapti Ghosh¹, Ya-Ping Hsieh¹ and Yang-Fang Chen²; ¹Academia Sinica, Taiwan; ²National Taiwan University, Taiwan

The light-matter interaction in the 2D materials can greatly be enhanced by exploiting their flexural strength. These materials either be twisted^[1] or wrinkled^[2] in order to decrease the substrate interaction. This generates enhanced carrier mobility in the suspended material and strong light confinement due to multiple internal reflections. Spirally rolling of 2D material (eg. MoS_2 , WS_2) strictly restricts the electronic motion in a uniaxial direction. This encapsulated structure after getting hybridized with high yield QDs form type-II band alignment

at the heterostructure interface. The photo-generated excitons after getting dissociated at the QD/2D interfaces transferred to the conductive 2D channel. The subsequent presence of QDs as a strong photoabsorptive material and multiple reflections at the inner wall of the nanocavity increase the photoconductivity in the nanoscale regime. Nanoscroll (NS) stimulates coherent lasing action with an unprecedentedly low lasing threshold and enhances the photosensitivity almost 3000 fold^[1] compared to the nanosheet counterpart. This spirally rolled helical structure predominately generates polarized photosensitivity due to preferential excitons localization along the circumference of the scroll. Our approach of QD hybridized NS formation thus enables feasible ways to discover exotic physical phenomena and to develop novel high-performance flexible devices toward realistic applications.

References:

[1] R. Ghosh *et al.*, *Small*, 2003944. DOI: 10.1002/sml.202003944.

[2] R. Ghosh *et al.*, *ACS Appl. Mater. Interfaces* 2019, 11, 26518. DOI: 10.1021/acsami.9b08294.

10:35 PM CLOSING REMARKS

SESSION NM07.17: On-demand
Wednesday Morning, April 14, 2021
NM07

8:00 AM NM07.10.09

Mitigating the Substrate Effect on Two-Dimensional Molybdenum Disulfide Kory Burns; University of Florida, United States

Valley excitons has proven to play a significant role in the photoconductivity and light emission processes of two-dimensional (2D) Molybdenum Disulfide (MoS₂). Exploring ways to manipulate energy levels of excitons opens the possibility to tune quantum degrees of freedom such as electron spin, layer pseudospin, and valley pseudospin. In this contribution, we first introduce a new method to produce single-layer sheets of MoS₂ using miscible organic solvents to minimize the exfoliation energy in the fabrication process. The atomically thin membranes were suspended on four different epitaxial substrates and analyzed using Raman spectroscopy, Photoluminescence (PL), Atomic Force Microscopy (AFM) and X-ray photoelectron spectroscopy (XPS). We report on the strain induced from the lattice mismatch between the substrate and the material, correlate the effect this has on the binding energy of MoS₂, and lastly explore the impact substrates have on the optical properties of MoS₂ by measuring the exciton binding energy, spin-orbit coupling, and optical and electronic band gap. This work serves as a foundational piece to assist researchers with choosing a formidable substrate to build field effect transistors.

SYMPOSIUM NM08

Nanoscale Heat Transport—Fundamentals
April 14 - April 20, 2021

Symposium Organizers

Kedar Hippalgaonkar, Nanyang Technological University
Sangyeop Lee, University of Pittsburgh

* Invited Paper

SESSION NM08.01: Surface Phonon Polaritons / Phonon Hydrodynamics / Polymers
Session Chairs: Keivan Esfarjani and Martin Maldovan
Sunday Morning, April 18, 2021
NM08

8:00 AM NM08.01.01

Late News: Experimental Observation of Quasi-Ballistic Thermal Transport of Surface Phonon-Polaritons Over Hundreds of Micrometers Yunhui Wu, Jose Ordonez-Miranda, Laurent Jalabert, Saeko Tachikawa, Roman Anufriev, Sebastian Volz and Masahiro Nomura; The University of Tokyo, Japan

At the nanoscale, enhancing the propagation distance of heat carriers in solids attracts intensive attention for improving the thermal performance in micro- and nanoelectronics. However, the major heat carriers, phonons, propagate ballistically over the distances shorter than one micrometer above room temperature. To compensate this limited propagation range, we propose a novel heat carrier, surface phonon polariton (SPhP), which is generated from the hybridization of the optical phonon and the photon and propagate in the range of a few hundred micrometers. In this study, we conduct a 3ω measurement of SiN suspended submicron films to investigate the thermal transport by SPhP in hundreds of micrometers range.

As a result, we report the thermal conductivity (TC) measurements in silicon nitride (SiN) films with different thicknesses ($h = 30, 50, 100, \text{ and } 200 \text{ nm}$) measured in the 300 - 400 K temperature range. We detect the higher TC with the sensor further from the heater ($d = 200 \mu\text{m}$) in thin films ($h = 30, 50 \text{ nm}$). This phenomenon suggests that the heat propagation due to SPhPs remains quasi-ballistic in the hundreds of micrometers range, which is consistent with our previous study [1]. When the 30-nm-thick film heats up to 400 K, we detect approximately 13% enhancement of the TC compared to 300 K. Meanwhile, for 100- and 200-nm-thick membranes, the TC is nearly independent of both temperature and the distance. The results presented here have potential applications in the fields of heat transfer, thermal management, near-field radiation, and polaritonics.

[1] Y. Wu et al. "Enhanced thermal conduction by surface phonon-polaritons", Science Advances 6, eabb4461 (2020)

8:15 AM NM08.01.02

Late News: Thickness Dependence of Surface Phonon-Polariton Propagation Length in SiO₂/Si/SiO₂ Structures Saeko Tachikawa¹, Jose Ordonez-Miranda², Yunhui Wu¹, Laurent Jalabert², Roman Anufriev¹, Sebastian Volz² and Masahiro Nomura^{1,2}; ¹IIS, the University of Tokyo, Japan; ²The University of Tokyo, Japan

Surface phonon-polaritons (SPhPs) are surface waves generated by the coupling of electromagnetic waves and optical phonons at the interface of polar materials. In suspended nanofilms, SPhPs propagate over typical distances of a few hundreds of micrometers along their interfaces [1], which positions them as powerful energy carriers to transport energy along the plane of nanomaterials. However, such nanometric films are mechanically unstable and hence their practical application is limited. In this work, we study the SPhP propagation along a three-layer structure made up of a Si film, acting as a mechanical support, sandwiched by two nanofilms of SiO₂, which is the SPhP active material. This is done by determining the SPhP propagation length as a function of the spectral frequency and thicknesses of the Si and SiO₂ films. Longer propagation lengths are obtained for

thinner SiO₂ films, due to the reduction of energy absorption [2]. By contrast, as the Si film thickness reduces, the propagation length increases (decreases) for thicknesses smaller (greater) than the SPhP wavelength. This behavior is generated by the tradeoff between the energy absorption and coupling of SPhPs propagating along the top and bottom SiO₂ layers. It is shown that the resulting SPhP contribution to the in-plane thermal conductivity of the considered structure exhibits a minimum value for a given Si film thickness. The obtained results thus shed light on the physical understanding of the propagation of SPhPs and the modulation of their thermal transport inside a layered and mechanically stable structure.

[1] Chen D.Z.A., *et al.*, Phys. Rev. B 72, 155435 (2005)

[2] Tachikawa S., *et al.*, Nanomaterials 10, 1383 (2020)

8:30 AM NM08.01.04

Late News: Near-Field Radiative Heat Transfer Mediated by Graphene Plasmons Behrad Zeinali Tajani and Sheila Edalatpour; University of Maine, United States

Radiative heat transfer is said to be in the near-field regime when the separation distance between the heat exchanging media is smaller than or comparable to the dominant thermal wavelength ($\lambda_{\max} \approx 10$ mm at room temperature). Near-field radiative heat transfer can be quasi-monochromatic and exceed the blackbody far-field limit by several orders of magnitude. The enhancement beyond the blackbody limit is due to the extraneous contribution to radiative heat transfer by evanescent waves that are confined to a distance of about the thermal wavelength from the surface of the thermal emitter. Near-field radiative heat transfer can be quasi-monochromatic when the heat exchanging media support surface phonon and plasmon polaritons. These unique properties of near-field regime of radiative heat transfer are highly promising for many advanced and state-of-the-art technologies such as waste heat recovery, nanoscale-resolution imaging, nanomanufacturing, thermal management of electronic devices, and thermal rectification through a vacuum gap. The quasi-monochromatic behavior of near-field radiative heat transfer plays a central role in these technologies. Development of the near-field applications requires materials with plasmonic or phononic resonances in the mid-infrared where these modes can be thermally excited.

The number of materials with plasmonic/phononic resonances in the mid-infrared is very limited, and the spectral location (wavelength) of these resonances does not often match the ones required by practical applications. Graphene supports surface plasmons in the mid-infrared and terahertz ranges. It is thermally very stable, and due to the two-dimensional nature of graphene, free electrons or holes can effectively be induced into this material using chemical doping or electrical gating rendering dramatically tunable optical properties. Due to these advantages, graphene has recently gained significant attention for increasing or modulating thermal radiation in the near-field regime. In this presentation, the possibility of tuning the spectrum of near-field radiative heat transfer using graphene-based materials is discussed. Radiative heat transfer between graphene sheets of various chemical potentials, temperatures, and separation distances is analyzed. The dispersion relation of graphene plasmons is derived, and the conditions under which graphene plasmons can result in quasi-monochromatic near-field conductance is discussed.

8:45 AM NM08.01.05

Late News: Phonon Hydrodynamics for Resistive Dominated Materials F. Xavier Alvarez, Albert Beardo Ricol, Lluç Sendra Molin, Juan Camacho and Javier Bafaluy; Universitat Autònoma de Barcelona, Spain

Phonon hydrodynamics is the framework to understand thermal transport in materials where momentum conservation is important. This is the case of 2D materials like graphene or transition metal dichalcogenides but also 3D materials like graphite and diamond. In these materials, momentum conservation is granted by the dominance of the normal phonon-phonon collision.

In the last decades, phonon hydrodynamics has been shown to offer also an explanation for the anomalous thermal behaviour of semiconductors like silicon or germanium, where normal scattering is not dominant. Despite also based in the momentum conservation, the appearance of hydrodynamics in materials like silicon is related to surface and interface physics. In this case, a boundary layer is created that is the responsible to transfer momentum between the surfaces and the inner regions of the materials. In that layer, conservation rules

are also crucial and modify the heat equations. The final result is that a hydrodynamic equation like Guyer and Krumhansl is also valid to describe these materials.

We present a multiscale analysis going from the microscopic fundamentals for the appearance of a hydrodynamic behaviour in silicon to the experimental evidences in favour of using the Guyer and Krumhansl equation to describe this kind of materials. We will also demonstrate that in the samples where this happens, traditional approaches based on an effective Fourier equation are completely ruled out.

Moreover, the proposed framework allows to understand why using a Fourier approach, a size dependent thermal boundary resistance at nanoscale contacts between metals and substrates is required. It will be shown that this size dependence understood through the hydrodynamic behaviour of the substrate near the metal line.

9:00 AM NM08.01.06

Late News: Observation of a Hydrodynamic Relaxation Time Scale Governing the Thermal Evolution of Nanoscale Heat Sources in Silicon Substrate Albert Beardo Ricol¹, Lluc Sendra Molin¹, Joshua Knobloch², Brendan McBennett², Travis D. Frazer², Javier Bafaluy¹, Jorge Nicolas Hernandez Charpak², Begoña Abad Mayor², Henry Kapteyn², Margaret Murnane², F. Xavier Alvarez¹ and Juan Camacho¹; ¹Universitat Autònoma de Barcelona, Spain; ²University of Colorado Boulder, United States

Recent experiments revealed non-Fourier thermal conduction in general semiconductors like Silicon [1-3]. The use of a hydrodynamic heat transport equation has shown to capture thermal transport beyond Fourier's law through new phenomena like phonon vorticity and viscosity [4-6].

We focus on the process of energy release from a nanoscale heat source towards a Silicon substrate. By monitoring the heater thermal relaxation through EUV-scatterometry techniques [2], we demonstrate that the heater temperature follows a double exponential decay [7]. This system response cannot be explained if using Fourier's law with effective parameters to model the substrate conduction, which provides a single exponential thermal decay followed by a power law. In contrast, the hydrodynamic model with geometry independent parameters naturally predicts the two exponential decay and provides analytic expressions for each characteristic time scale. The shorter time scale (~100ps) is dominated by the interfacial resistance and the second one (~1ns) is dominated by hydrodynamic effects in the substrate. The geometry dependencies of the second characteristic time accurately predict the observed slower relaxation of the heater by reducing its size. Furthermore, the model provides a simple analogy based in an electrical circuit to illustrate the heater thermal evolution.

References:

- [1] A. Ziabari et.al., Nat. Comm. 9, 255 (2018).
- [2] K. M. Hoogeboom-Pot et. al., PNAS 112 16 4851 (2015)
- [3] R.B. Wilson, D. Cahill, Nat Comm. 5, 5075 (2014)
- [4] S. Alajlouni, A. Beardo et al. Nano Research 14 945–952 (2020)
- [5] P. Torres et al. Phys Rev. Materials 2, 076001 (2018)
- [6] A. Beardo et al. Phys Rev. B 101, 075303 (2020)
- [7] A. Beardo, J. Knobloch, et al. submitted

9:15 AM NM08.01.07

Late News: New Formalism to Derive a Hydrodynamic Heat Transport Equation for General Semiconductors from the Phonon Boltzmann Equation Lluc Sendra Molin, Albert Beardo Ricol, Javier Bafaluy, F. Xavier Alvarez and Juan Camacho; Universitat Autònoma de Barcelona, Spain

We present a new formalism that solves the Boltzmann Transport Equation (BTE) and derives a hydrodynamic heat transport equation (Guyer-Krumhansl equation) [1] similar to Navier-Stokes, which generalizes the Fourier's law [2]. This generalization applies from systems dominated by momentum-preserving collisions to kinetic materials dominated by resistive collisions. Therefore, it can be applied to general semiconductors like Silicon, in contrast to the common belief [1]; and arbitrary complex geometries by using Finite elements

methods at a low computational cost.

This contrasts with other approaches, where efforts have been made to use Fourier's law with effective coefficients depending on the physical situation [3,4] or through alternative solutions of the phonon BTE [5,6], whose complexity only allows to face simple geometries.

Our model allows the understanding of the experimentally observed Fourier's law breakdown at small length and time scales by using geometry independent parameters calculated from ab initio, resulting in a predictive model [7-9].

Furthermore, it supplies a connection between microscopic variables (phonon properties) and mesoscopic ones (temperature, heat flux, ...), providing an explicit solution for the nonequilibrium phonon distribution function. Furthermore, this approach allows to derive consistent boundary conditions for arbitrary complex surfaces and interfaces between different materials.

References:

- [1] R. A. Guyer and J. A. Krumhansl, *Physical Review* **148**, 766 (1966).
- [2] L. Sendra et al., submitted to PRB.
- [3] K. M. Hoogeboom-Pot et al., *Proceedings of the National Academy of Sciences* **112**, 4846 (2015).
- [4] K. T. Regner et al., *Nat. Comm.* **4**, 1640 (2013).
- [5] A. Cepellotti and N. Marzari, *Phys. Rev. X* **6**, 041013 (2016).
- [6] C. Hua et al., *Phys. Rev. B* **100**, 085203 (2019).
- [7] A. Beardo et al., *Phys. Rev. Applied* **11**, 034003 (2019).
- [8] S. Alajlouni et al., *Nano Res.* (2020), 10.1007/s12274-020- 3129-6.
- [9] A. Beardo et al., *Phys. Rev. B* **101**, 075303 (2020).

9:30 AM NM08.01.08

Late News: Mechanical Tuning of the Thermal Conductance of Molecular Junctions Mohammadhasan Dinpajoo and Abraham Nitzan; University of Pennsylvania, United States

Understanding the thermal conductance in molecular junctions offers important insights in designing future thermoelectric devices. One of the most interesting features in molecular junctions is the possibility to exert external control through mechanical forces. We use non-equilibrium molecular dynamics simulations to study the steady state thermal conductance of different molecular junctions consisting of finite macromolecules at various end-to-end distances/electrode displacements. We find that the nature of the thermal conductance along such polymer chains strongly depends on mechanical tuning, leading to significantly different heat conductions and temperature profiles along the chain in the compressed-chain and stretched-chain limits. This transition between modes of behaviors appears to be a threshold phenomenon: at relatively small end-to-end distances/electrode displacements, the thermal conductance remains almost constant as one stretches the polymer chain. At given critical end-to-end distances/electrode displacements, thermal conductances start to increase, reaching the fully extended chain values. In addition, we find that the thermal conductances of molecular junctions sandwiched between metal leads significantly depend on the nature of metal leads and are much smaller than the corresponding intrinsic thermal conductances, i.e. in the absence of metal leads. We then address how the thermal conductance is correlated with the vibrational density of states and study the metal-molecule coupling and anharmonic effects upon stretching. We also conduct similar studies for disordered polymer chains and bundles of several polymer chains, which show remnants of the same behaviors of the aforementioned systems.

10:30 AM *NM08.02.01

Geometry-Modulated Metamaterials for Enhanced Thermoelectric Effects and Decreased Thermal Conduction Xanthippi Zianni; National and Kapodistrian University of Athens, Greece

Geometry-modulated nanostructures consist a class of metamaterials promising for efficient thermoelectric applications and nanoscale heat management. In these metamaterials, it is possible to achieve enhanced thermoelectric effects and decreased thermal conductivity by designing the geometry-modulation in the nanometric scale. We indicated this possibility in 2010 when we proposed diameter-modulated nanowires for enhanced thermoelectric efficiency [1]. We showed that coupling between propagating waves and resonances of the modulation units modifies the carriers transmission coefficients and results in enhanced thermoelectric power factor and decreased electron and phonon thermal conduction [2,3,4]. Electron and phonon scattering can be controlled by designing the shape of the geometry-modulation [5,6]. Ballistic or diffusive transport effects may dominate depending on characteristic dimensions of the geometry modulation [7,8]. We will discuss physics aspects of electron and phonon transport in geometry-modulated metamaterials based on our work and the evolution of the research in this field that is currently gaining increased interest for advanced applications.

- [1] X.Zianni, Applied Physics Letters **97**, 233106 (2010)
- [2] X.Zianni, Nanoscale Research Letters **6**, 286 (2011)
- [3] X.Zianni, Journal of Solid State Chemistry **193** 53 (2012)
- [4] X.Zianni, Microelectronic Engineering **112**, 235 (2013)
- [5] X.Zianni and P.Chantrenne, Journal of Electronic Materials, DOI: 10.1007/s11664-012-2304-2 (2012)
- [6] X.Zianni, V. Jean, K. Termentzidis and D. Lacroix, Nanotechnology **25**, 465402 (2014)
- [7] X.Zianni, K.Termentzidis and D.Lacroix, Journal of Physics: Conf. Series **785**, 012011 (2017)
- [8] X.Zianni, J. Phys. D: Appl. Phys. **51** 114003 (2018)

10:55 AM NM08.02.03

Late News: Ba_{1/3}CoO₂, a Promising Candidate for Oxide Thermoelectric Material Yuqiao Zhang¹, Yugo Takashima¹, Liao Wu¹, Jiake Wei^{2,3}, Bin Feng³, Yuichi Ikuhara^{2,3}, Hai Jun Cho¹ and Hiromichi Ohta¹; ¹Hokkaido University, Japan; ²Kyoto University, Japan; ³The University of Tokyo, Japan

Layered cobalt oxide such as Na_{0.75}CoO₂ and Ca₃Co₄O₉ are known as good candidates for oxide thermoelectric material. Although layered cobalt oxides have several advantages such as environmental compatibility and thermal-chemical stabilities compared to heavy metal-based chalcogenides like Bi₂Te₃ and PbTe, their *ZT* is low as compared to that of heavy metal-based chalcogenides, mainly due to rather high thermal conductivity. In order to overcome the difficulty, we hypothesized that the thermal conductivity of layered cobalt oxide can be reduced by heavier ion substitution^[1]. Firstly, we fabricated Na_{0.75}CoO₂ epitaxial films on sapphire or YSZ substrate by the R-SPE method^[2]. Then, the Na ions were exchanged with Ba ions by the ion exchange treatment. The resultant film was Ba_{1/3}CoO₂, which was clarified from the XRD patterns and HAADF-STEM images. Although Na_{0.75}CoO₂ is unstable at high temperature in air, the resultant Ba_{1/3}CoO₂ epitaxial films show excellent thermal stability at high temperature (700 °C) in air. The room temperature thermal conductivity of Ba_{1/3}CoO₂ epitaxial films along the layered structure was ~3 W m⁻¹ K⁻¹, which is approximately half of that of Na_{0.75}CoO₂ (~5.5 W m⁻¹ K⁻¹), indicating that our hypothesis is true. Since the power factor was almost unchanged, the *ZT* was greatly improved (*ZT* = 0.11^[3] at room temperature and 0.2 at 200 °C). These *ZT* values are the highest among oxides ever reported as a “reliable value”. The present result clearly indicates that Ba_{1/3}CoO₂ shows rather large *ZT* at high temperatures in air, exerting a potential high temperature application prospect.

References

- [1] H.J. Cho*, *Adv. Mater. Interfaces* **7**, 1901816 (2019).

[2] H. Ohta *et al.*, *Cryst. Growth Des.* **5**, 25 (2005).

[3] Y. Takashima, Y. Zhang* *et al.*, *J. Mater. Chem. A* **9**, 274 (2020).

11:10 AM NM08.02.04

Origin of Unexpectedly Low Thermal Conductivity In AMg_2X_2 ($A = Mg, Ca, Yb, X = Sb, Bi$) Jingxuan Ding¹, Tyson Lanigan-Atkins¹, Mario R. Calderon Cueva², Alexandra Zevalkink² and Olivier Delaire^{1,1}; ¹Duke University, United States; ²Michigan State University, United States

Thermoelectric materials enable direct conversion of waste heat into electrical energy. The conversion efficiency is inversely proportional to the thermal conductivity, which is generally dominated by phonons in semiconductors. Zintl compounds AMg_2X_2 constitute a class of new thermoelectric compounds with excellent thermoelectric performance in n-type $Mg_3(Sb,Bi)_2$ alloys, with zT values up to 1.6 reported so far. Mg_3Sb_2 exhibits very low lattice thermal conductivity ($\sim 1-1.5$ W/m/K at 300K), comparable with PbTe and Bi_2Te_3 , despite a much lighter average ionic mass. We report on neutron scattering and first-principles studies of the lattice dynamics of AMg_2X_2 . Inelastic neutron scattering measurements provided the temperature dependence of the phonon density of states (DOS). Extra peaks and overall softer phonons were found at low frequency in Mg_3Sb_2 and Mg_3Bi_2 compared to $CaMg_2X_2$ or $YbMg_2X_2$. Combined with simulations, we highlight the importance of a specific soft Mg-X chemical bond that suppresses phonon group velocities and drastically enlarges the scattering phase-space, enabling the threefold suppression in thermal conductivity.

11:25 AM NM08.02.05

Nanokelvin-Resolution Band-Edge Thermometry at Room Temperature Amin Reihani, Edgar Meyhofer and Pramod Sangi Reddy; University of Michigan, United States

High-resolution thermometry is essential in calorimetry and bolometry with broad applications in studies of dissipation in electronics and quantum systems [1, 2], metabolism in biological systems [3], and millimeter-wave sensing for astronomy [4]. Achieving high-resolution thermometry combined with small device size, at room temperature, is highly desirable. In this presentation, we will describe a novel thermometer capable of <100 nK resolution in a 0.1 Hz measurement bandwidth. Our thermometer is composed of a microfabricated suspended GaAs device with lateral sensing dimensions of <200 μm and employs an optical readout scheme. The temperature sensing mechanism is based on the Fabry-Pérot resonance at the Urbach edge of direct band-gap semiconductors, where the optical properties of the medium, namely the absorption coefficient and refractive index, change abruptly by variation of incident photon energy relative to the band gap [5]. We show that the temperature dependence of band gap provides a highly temperature-sensitive reflection or transmission signal at the Fabry-Pérot resonance peaks. The device we describe here represents a first demonstration of a micro-thermometer for all-optical, nano-Kelvin thermometry at and above room temperatures.

[1] K. Kim, W. Jeong, W. Lee, and P. Reddy, *Acs Nano* **6**, 4248 (2012).

[2] D. Halbertal *et al.*, *Nature* **539**, 407 (2016).

[3] S. Hur, R. Mittapally, S. Yadlapalli, P. Reddy, and E. Meyhofer, *Nature Communications* **11**, 1 (2020).

[4] R. Kokkoniemi *et al.*, *Communications Physics* **2**, 1 (2019).

[5] S. Johnson and T. Tiedje, *Journal of Applied Physics* **78**, 5609 (1995)

11:40 AM NM08.02.06

Cathodoluminescence Nanothermometry for Thermal Transport Measurements Kelly W. Mauser¹, Magdalena Solà-García¹, Matthias Liebrau¹, Benjamin Damilano², Pierre-Marie Coulon³, Stéphane Vézian², Philip Shields³, Sophie Meuret⁴ and Albert Polman¹; ¹AMOLF, Netherlands; ²Université Côte d'Azur, France; ³University of Bath, United Kingdom; ⁴CEMES/CNRS, France

As structures in nanodevices approach the size of the phonon mean-free-path of materials, studying thermal transport properties becomes increasingly difficult due to the need for nanoscale thermal probes. Many different techniques exist to study these nanoscale effects, however, measurement speed and/or the diffraction limit of

light is often a limiting factor. Here, we present new methods for measuring temperature and thermal conductivity of semiconductor nanostructures rapidly with nanometer resolution using cathodoluminescence spectroscopy in a scanning electron microscope (SEM).

First, we demonstrate the first measurements, to our knowledge, of cathodoluminescence (CL) nanothermometry in semiconductors. In semiconductor CL, a 5-30 keV electron beam from a scanning electron microscope excites electrical carriers, that recombine and emit radiation at energies near their bandgap, which is then collected and analyzed [1]. We perform CL imaging of 7-micron-long, 200-nm-diameter GaN nanowires, made by a top-down approach based on sublimation under vacuum, which are suspended across a 6.5 micron hole in a TEM membrane. The wires are thermally clamped on both sides using focused ion beam deposition of Pt and we record the bandgap emission near 3.4 eV at every position in the SEM image. By precisely measuring shifts in the bandgap, we map the temperature as the electron beam is scanned over the wire by using the Varshni relation fit to calibration data. We find a 6 K temperature resolution with our samples, limited primarily by small doping variations in the wires which can be corrected for by mapping the doping profile with a low-current electron beam with nm-resolution[2]. Using low-current electron beams which deposit less than 1 μ W of power into the wire, we can measure temperature in a non-perturbative way. Using large currents of 70 nA which can deposit 100's of μ W of power, we can heat the wires by over 400 K.

Next, we will discuss three techniques for measuring thermal conductivity using this novel method of CL nanothermometry. The first two use a continuous electron beam current scanned over the wires with the beam acting as both a delta-function-like heat source and local temperature probe with resolution of the electron cascade. We fit the temperature rise as a function of position, correcting for doping variations in the wire. The final method uses an electrostatic beam blanker[3], with which we measure the frequency dependence of the thermal response of the GaN nanowires to electron beam heating in the range of 100 Hz to 5 MHz in a matter of minutes. We develop a theoretical model to fit the data and find a cut-off frequency of \sim 500 kHz from which we derive a thermal conductivity of 54 ± 13.2 W/m \cdot K, which agrees within error with the other techniques we discuss. We will discuss the advantages and limitations of each technique and future directions. With minor modifications, the underlying principles of methods like time-domain thermo-reflectance are applicable to CL nanothermometry experiments, especially with the rise of electron microscopy with fs-photoexcited field-emission guns[4]. Because of the nanoscale nature of these measurements, CL nanothermometry methods could prove useful for probing thermal transport and phonon properties at small dimensions, including ballistic thermal transport, near-field heat transfer, or in studies of thermal contact resistance.

[1] Edwards P. R. and Martin R. W., *Semicond. Sci. Technol.* **26** 064005 (2011)

[2] Chen, H.-L. *et al. Nano Lett.* **17**, 6667–6675 (2017)

[3] S. Meuret, *et al., Ultramicroscopy* **197**, 28 (2019)

[4] M. Solà Garcia, *et al., ACS Photon.* **7**, 232 (2019)

11:55 AM NM08.02.07

Direct Electrocaloric Measurements via ThermoReflectance Layla Farhat^{1,2}, Mathieu Bardoux¹, Stéphane Longuemart¹, Ziad Herro² and Abdelhak Hadj Sahraoui¹; ¹Université du Littoral Côte d'Opale, France; ²Université Libanaise, Lebanon

Electrocaloric (EC) effect refers to the isothermal entropy or adiabatic temperature changes of a dielectric material induced by an external electric field. This phenomenon has been largely ignored for application because only small EC effects (2.6K) have been detected in bulk materials such as $\text{Pb}_{0.99}\text{Nb}_{0.02}(\text{Zr}_{0.75}\text{Sn}_{0.20}\text{Ti}_{0.05})_{0.98}\text{O}_3$. The discovery of a giant electrocaloric effect by Mischenko *et al.* in thin films (up to 12°C with $E=480\text{kV}\cdot\text{cm}^{-1}$) renewed interest in electrocaloric materials and related cooling technologies. It is indeed the development of thin structures that has made it possible to obtain high dielectric rigidity and significant electrocaloric effects.

Several methods have been developed to characterize EC effect. “Direct methods” measure the EC temperature

change or released heat in the material on application or withdrawal of the electric field. “Indirect method” employs Maxwell equations to calculate the EC effect from the change of polarization with temperature.

In fact, ferroelectric thin films exhibit significant dielectric losses ($\tan\delta > 0.1$). Furthermore, EC thin layer being deposited on a solid substrate, the thermal capacity of the assembly is very high compared to that of the thin layer alone. Thus, even if the change in specific entropy following the application of an electric field is very large, the change in total entropy is almost undetectable because of the very low volume of the thin films. The temperature variation will also be hardly detectable because of the rapid dissipation of the heat in the substrate that is behaving as a heat sink. Due to these limitations, till now it has been difficult to present experimental values of electrocaloric properties in thin films from direct measurements, only estimates by indirect characterization are accessible. It is therefore imperative to study these materials using instruments offering high resolution.

To overcome these difficulties, we propose a novel characterization method based on thermorefectance for measuring directly the electrocaloric effect. This method allows the study of systems such as thin films, multilayers, and nanoparticle. It is a non-contact and non-destructive measurement method with a very large temporal dynamic, which allows the study of extremely rapid phenomena. It exploits the temperature-dependent reflectivity of a surface which is probed using the intensity variation of a reflected laser beam. We report laser-based direct measurements of ECE in various solid ferroelectric materials in the form of multilayered capacitor and thin films as a function of the applied electric field. Using appropriate model, the signal can be used to retrieve Electrocaloric properties of embedded or stacked electrocaloric layers.

Acknowledgment: We are grateful to Université du Littoral Côte d’Opale and the National Council for Scientific Research in Lebanon for the support of this work

SESSION NM08.03: Magnetic and Piezoelectric Materials / Methods
Session Chairs: Sangyeop Lee and Pramod Sangi Reddy
Sunday Afternoon, April 18, 2021
NM08

1:00 PM NM08.03.01

Thermal Switching via the Thermal Chiral Anomaly in the Magnetic-Field Induced Ideal Weyl Phase of $\text{Bi}_{1-x}\text{Sb}_x$ Topological Insulators Dung D. Vu and Joseph Heremans; The Ohio State University, United States

The chiral anomaly in Weyl semimetals has a thermal analog [1]. In electrical measurements, an electric field applied parallel to a magnetic field and parallel to the direction of separation of the Weyl points produces a charge transfer between the Weyl points that results in an anomalous charge current and a negative magnetoresistance; this is the chiral anomaly. In thermal measurements, there is no charge transfer between the Weyl points, but an energy transfer, which produces an anomalous heat current and an increase in thermal conductivity in magnetic field. We unambiguously demonstrate this experimentally in the topological insulator bismuth-antimony alloys ($\text{Bi}_{89}\text{Sb}_{11}$ and $\text{Bi}_{85}\text{Sb}_{15}$) driven into an ideal Weyl semimetal state by a Zeeman field, with the chemical potential pinned at the Weyl points, and in which the Fermi surface has no trivial pockets. The experimental signature is a 300% enhancement of the electronic thermal conductivity in a 9T applied magnetic field parallel to the thermal gradient that follows the Wiedemann-Franz law above 60 K. The same material shows an equally strong decrease in thermal conductivity in a magnetic field applied perpendicularly to the direction of Weyl point separation. The talk will emphasize how the material is potentially useful in heat switches in applications, such as adiabatic demagnetization refrigeration, where an external magnetic field is already being used to induce ordering in a paramagnetic salt.

[1] Vu et al., arXiv:1906.02248 (2019).

Funding: Center for Emergent Materials, NSF-DMR-2011876.

1:15 PM NM08.03.02

Ultrafast Spin Seebeck Measurements on Rare-Earth Iron Garnets Victor Ortiz, Michael Gomez, Yawen Liu, Mohammed Aldosary, Jing Shi and Richard B. Wilson; University of California, Riverside, United States

Understanding the thermal generation of spin currents in magnetic materials is an important goal for the field of spin caloritronics. Among magnetic materials, rare earth iron garnets (REIG) display intriguing magnetic transport properties as result of strong antiferromagnetic exchange interactions and low magnetic damping. We report on ultrafast longitudinal spin Seebeck effect (LSSE) experiments on thin film REIG / heavy metal (HM) heterostructures (RE: Y, Tm, Eu, Tb; HM: Au). We use time-resolved magneto optic Kerr effect measurements to directly observe the transfer of magnetization from the REIG into the HM on femto-second timescales, allowing us to selectively probe the interfacial SSE. We observe a factor of 4 difference in the magnitude of the LSSE among the different REIG samples. Our results provide insight regarding the different contributions to the spin current from the different REIGs and the relevance of the interface between the REIG and the HM layers. This work was supported by the U.S. Army Research Laboratory and the U.S. Army Research Office under contract/grant number W911NF-18-1-0364; and SHINES, an Energy Frontier Research Center funded by the U.S. Department of Energy, Office of Science, Basic Energy Sciences under Award SC0012670.

References

[1] J. Kimling, G. M. Choi, J. T. Brangham, T. Matalla-Wagner, T. Huebner, T. Kuschel, F. Y. Yang and D. G. Cahill, "Picosecond Spin Seebeck Effect," *Phys. Rev. Lett.*, vol. 118, no. 5, 2017.

1:30 PM NM08.03.03

Thermal Conductivity Study of Piezoelectric PZT Stack Brandi Wooten and Joseph Heremans; The Ohio State University, United States

We present new data on the polarization-dependent thermal conductivity of ferroelectric materials, and a new hypothesis on its possible physical origin. Hopkins and colleagues [1] report that piezoelectric materials have a thermal conductivity that is a function of the external electric field. Further, they assert that the decrease as the field is applied is due to an increase in ferroelectric domain wall density, which increases the phonon scattering. While their experiment is conducted on a thin film, we investigate the field and temperature dependency of thermal conductivity on a PZT stack with interwoven electrodes. We present data that are consistent with [1], but with a sensitivity to the applied field that is an order of magnitude larger. The thermal conductivity changes are hysteretic and follow the polarization of the material, but the signal is too large to be explained by volume or sound velocity changes. Our data hint at an alternate hypothesis, in which local thermal fluctuations of the polarization in the material may carry heat, by analogy to magnons carrying heat in ferromagnets [2].

[1] *Nano Lett.* **15**, 1791-1795 (2015); [2] *Phys. Rev. B* **91** 226401 (2015)

Funding: NSF DMR 2011876

1:45 PM NM08.03.04

PHONONICA—An Object-Oriented Code for Probing Phonon Modes and Interactions Jacob Eapen and Anant Raj; North Carolina State University, United States

The traditional normal mode analysis, which employs complex normal mode coordinates, cannot distinguish the normal (N) phonon interactions from the Umklapp (U) interactions. In our recent work [*Sci. Rep.* **9**, 7982 (2019)], we have demonstrated that both N and U processes can be resolved from atomistic simulations by adopting a set of real asymmetric normal mode amplitudes. In the current work, we have developed an object-oriented code – Phononica, which when dynamically paired with the popular molecular dynamics (MD)

simulator – LAMMPS, transforms the atomistic trajectories, on the fly, to real normal mode amplitudes that can be used for analyzing phonon interactions, and phonon modes in non-equilibrium thermal transport. Additionally, Phononica can read-in the dynamical trajectories from *ab initio* MD codes such as VASP or Quantum Espresso for phonon analysis; using the recently developed ZTR-2 method [*Comp. Phys. Comm.* **238**, 124 (2019)], both crystalline and disordered materials can be analyzed even when the mean displacements are not defined or known. Phononica is particularly suited for (i) computing phonon dispersion curves, (ii) analyzing elementary phonon-phonon interactions, (iii) computing phonon modal conductivities from equilibrium and non-equilibrium simulations using our approach outlined in *J. Chem. Phys.*, **151**, 104110 (2019), (iv) analyzing defect-phonon interactions, and (v) modeling phonon transport across low dimensional molecular junctions and interfaces. In this talk, we summarize the capability of Phononica by elucidating the phonon and heat current modes in representative bulk and low-dimensional materials in both equilibrium and non-equilibrium conditions.

2:00 PM NM08.03.05

Atomistic Simulation of Phonon Behavior in Crystalline Cellulose I β Zhiyu Liu, Gaurav Kumar and Peter Chung; University of Maryland, College Park, United States

Cellulose is an inexhaustible naturally occurring plant-based polymer. Because of its sustainability and renewable properties, it has drawn significant research interest recently including simulation-based studies of thermal [1] and mechanical properties [2]. However, the phonon behavior in Crystalline Cellulose I β , especially the anharmonicity, is less studied. In this work, we investigate the intrinsic anharmonicity of Cellulose I β by calculating both harmonic and anharmonic phonon behaviors using molecular dynamics simulation using a reactive molecular forcefield (ReaxFF). To improve the performance of geometry optimization and get better energy conservation, a modified version of ReaxFF [3] is used in our study. The contributions of different phonon modes towards thermal conductivity and the mediating effects of anharmonicity are shown using both diffusive and ballistic models. Comparisons of the results using different models reveal the unconventional way heat is transported by phonons in Cellulose I β and help to understand nanoscale thermal transport mechanisms in this highly complex crystal. Moreover, similar to other organic molecular crystals, such as α -RDX [4], we show the unusual role of certain phonon-phonon scattering processes. Unlike ordered crystal, our study will demonstrate the diffusive behaviors of phonon in complex organic crystals. These results indicate complex materials like Cellulose I β can diverge strongly from accepted multiscale and multiphysical notions of phonon contributions to the macroscale thermal transport behavior.

References

- [1] R.-Y. Dong, Y. Dong, Q. Li and C. Wan, Ballistic-diffusive phonon transport in cellulose nanocrystals by ReaxFF molecular dynamics simulations, *International Journal of Heat and Mass Transfer* 148, 119155 (2020).
- [2] X. Wu, R. J. Moon and A. Martini, Tensile strength of I β crystalline cellulose predicted by molecular dynamics simulation, *Cellulose* 21, 2233-2245 (2014).
- [3] D. Furman and D. J. Wales, Transforming the Accuracy and Numerical Stability of ReaxFF Reactive Force Fields, *The Journal of Physical Chemistry Letters* 10(22), 7215-7223 (2019).
- [4] G. Kumar, F. G. VanGessel and P. W. Chung, Bond Strain and Rotation Behaviors of Anharmonic Thermal Carriers in α -RDX, *Propellants, Explosives, Pyrotechnics* 44, 1-9 (2019).

2:15 PM NM08.03.06

Late News: Causal Phonon Green's Function for Simulation of Thermal Transport in Nanomaterials Vinod K. Tewary and Edward Garboczi; National Institute of Standards and Technology, United States

The development of nanomaterials has revolutionized the materials industry. In order to exploit the full industrial potential of these materials, it is necessary to have a reliable mathematical model to simulate the physical processes that are relevant for specific applications. Such a model is needed, for example, for their characterization and testing and for virtual experimentation, useful for designing new devices.

Thermal transport in nanomaterials is a subject of strong topical interest because of its wide-ranging practical

applications. Examples are thermoelectric energy conversion as well as heat management systems. Almost all solid-state electronic devices are sensitive to heat and require efficient heat dissipation mechanisms. The conventional modeling techniques based upon the continuum approximation of solids are not applicable to nanomaterials. This is because phonons play a major role in the thermal transport and their mean free path is comparable to the interatomic spacing and the device dimensions.

Another modeling challenge is that the thermal transport characteristics of solids, specifically their thermal conductivities, are sensitive to the low frequency (GHz - MHz) phonons. These quasiparticles require modeling of a many particle system over extended times. The iterative numerical techniques, based upon the use of conventional molecular dynamics (MD), suffer from poor temporal convergence. They are, therefore, limited to small times and are more suitable for simulating high frequency phonons. For example, the basic MD formulation is limited to a few picoseconds, whereas simulation of GHz -MHz phonons need the simulations to extend to nano-micro seconds.

At NIST, we have developed a causal phonon Green's function (CGF) method, which is very efficient for modeling the phononic response of nanomaterials at the atomistic length scales and large temporal scales. In the conventional MD, a typical function $Z(r,t)$ in the Hamiltonian is expanded to first order in the space variable 'r', as well as the time variable 't'. The differentials are approximated by finite differences. In our CGF method, we first make the problem mathematically more complicated by expanding the $Z(r,t)$ to quadratic powers in 'r' but not in t. Then we exploit the fact that the CGF for Hamiltonian with quadratic dependence on r can be calculated analytically. This enables us to construct the CGF to obtain an exact solution in 't'. It breaks the limitation of the small time steps in temporal integration.

We still need to iterate because of the need to include the anharmonic (cubic and higher) terms in $Z(r,t)$. This introduces some constraints on the iteration steps but they are much less severe than those in the conventional MD. For some idealized cases, we had shown that our CGF technique can model the temporal processes over an unprecedented wide range from femto to microseconds.

One problem was that the calculation of CGF needs diagonalization of an $N \times N$ matrix, where N is the number of atoms in the model. This can be done for symmetric lattices but becomes computationally expensive for lattices with defects and disorders. We have now developed an ICGF (Iterative CGF) scheme for calculating the CGF for realistic nanomaterials without invoking any symmetry. We have tested the validity of the ICGF by applying it to a model problem, for which exact results are available for comparison.

The CGF is useful for a variety of modeling problems in nanomaterials. For example, it gives pair correlation functions and is useful for solving problems on scattering of quasi particles. The poles of the CGF give phonon frequencies and the imaginary part of its diagonal elements give the frequency spectrum. In this talk I will briefly describe our CGF and ICGF techniques and discuss their efficacy and validity by giving a numerical example.

2:30 PM NM08.03.07

Late News: Linearized Peierls Boltzmann Transport Solution of Heat Accumulation at Interfaces

Abhishek Pathak¹, Avinash Pawnday², Aditya P. Roy², Amjad Aref¹, Gary Dargush¹ and Dipanshu Bansal²;

¹University at Buffalo, The State University of New York, United States; ²Indian Institute of Technology Bombay, India

Interfaces impede phonon transmission and cause heat accumulation. This heat accumulation degrades the performance of nanoscale transistors and microprocessor chips used in our everyday life. Hence effective thermal management strategies are desirable to control the heat carriers both at an atomic scale and at the device level. Several phenomenological elastic phonon transmission models, such as the acoustic mismatch model, diffuse mismatch model, atomistic Green's function, are proposed to spectrally resolve the phonon conductance across the interface¹. More recently, the conductance is shown to have a significant (~50%) contribution from inelastic phonon transmission assisted by interfacial modes². Moreover, within both elastic and inelastic phonon transmission, phonons can retain or lose their coherency³. Simulation of these elastic and inelastic models at the device level is necessary to design effective thermal management strategies.

To this end, we have developed a variance-reduced Monte Carlo solver for linearized Peierls Boltzmann transport equation in three-dimensions⁴. Using phonon dispersions and lifetime from inelastic scattering

experiments, ab-initio simulations, or empirical models, we simulate domains ranging from a few nanometers to hundreds of microns. Simulations are performed on both periodic and non-periodic geometries. Since phonons scatter differently from physical domain boundaries, interface, impurity, and other phonons, we simulate boundary scattering, three-phonon processes, two-phonon processes, and impurity scattering independently. A frequency-dependent transmission probability and interface roughness (specularity) capture the size-effects and device-level conditions. Grain-boundary scattering models and interface transmission models are incorporated separately. Our interface modeling strategy is not limited to elastic energy transport and allows us to include inelastic transport across the interface by energy exchange between high- and low-frequency modes. We compare our interface conductance results in quasi-ballistic and diffusive regimes measured using near-IR pump EUV/X-ray probe experiments^{5,6,7}. The spectrally-resolved contribution to temperature and flux at the interface provides critical insights into the heat accumulation. We are presently simulating interfacial conductance in layered materials to compare with available near-IR pump and X-ray probe experiments⁸. We anticipate our code will further find applications in evaluating the nano-structuring and nano-patterning efficiency to thermal conduction properties of mesoscale devices.

References:

1. Monachon, C., Weber, L., & Dames, C. (2016), *Annual Review of Materials Research*, 46, 433–463.
2. Feng, T., Zhong, Y., Shi, J., & Ruan, X. (2019). *Physical Review B*, 99(4), 045301.
3. Ravichandran, N. K., & Minnich, A. J. (2014). *Physical Review B*, 89(20), 205432.
4. MCBTE-v0.1. Nov. 2020. <https://github.com/abhipath90/MCBTE>
5. Siemens, M. E., Li, Q., Yang, R., Nelson, K. A., Anderson, E. H., Murnane, M. M., & Kapteyn, H. C. (2010). *Nature Materials*, 9(1), 26–30.
6. Hoogeboom-Pot, K. M., Hernandez-Charpak, J. N., Gu, X., Frazer, T. D., Anderson, E. H., Chao, W., Falcone, R. W., Yang, R., Murnane, M. M., Kapteyn, H. C., & Nardi, D. (2015). *Proceedings of the National Academy of Sciences of the United States of America*, 112(16), 4846–4851.
7. Frazer, T. D., D., Knobloch, J. L., Hoogeboom-Pot, K. M., Nardi, D., Chao, W., Falcone, R. W., Murnane, M. M., Kapteyn, H. C., & Hernandez-Charpak, J. N. (2019). *Physical Review Applied*, 11(2), 1.
8. Nyby, C., Sood, A., Zalden, P., Gabourie, A.J., Muscher, P., Rhodes, D., Mannebach, E., Corbett, J., Mehta, A., Pop, E. and Heinz, T.F., (2020). *Advanced Functional Materials*, 30(34), p.2002282.

2:45 PM NM08.03.08

Late News: Ultrafast Thermo-Optical Dynamics for Thermal Boundary Resistance Measurements on Single Nano-Objects Michele Diego¹, Romain Rouxel¹, Fabio Medeghini¹, Aurélien Crut¹, Francesco Rossella^{2,3}, Paolo Maioli¹, Fabrice Vallée¹, Francesco Banfi¹ and Natalia Del Fatti¹; ¹FemtoNanoOptics Group, Université de Lyon, CNRS, University Claude Bernard Lyon 1, Institut Lumière Matière, France; ²NEST, Scuola Normale Superiore, Italy; ³Istituto Nanoscienze-CNR, Italy

Michele Diego, Romain Rouxel, Fabio Medeghini, Aurélien Crut, Francesco Rossella, Paolo Maioli, Fabrice Vallée, Francesco Banfi and Natalia Del Fatti

Single-particle optical spectroscopy methods have enabled quantitative investigations of the optical [1], electronic [2], and vibrational [3,4] responses of nano-objects in the recent years. In this work, we exploit single-particle pump-probe optical spectroscopy to investigate the cooling dynamics of individual gold nanodisks supported on a sapphire substrate. Although this topic has already been theoretically investigated in the past [5,6], quantitative measurements have so far proved very challenging. We here show time-resolved signals encompassing the temporal evolution of the single nanodisk temperature following its impulsive excitation [7]. By comparing the experimental signals (measured on individual nanodisks with different sizes) to the results of analytical [4] and finite-element simulations, we are able to retrieve the thermal boundary resistance at the single gold nanodisk-sapphire interface, which limits the nanodisk cooling rate. The present findings pave the way for quantitatively characterizing the temperature-dependent optical response of a single nano-object by investigating the probe-wavelength dependence of time-resolved signals, and for correlating the nano-object thermal properties to its specific morphology and composition. Moreover, it bears great relevance

for post-processing inspection of nanopatterned metal nano-objects [8].

- [1] A. Crut, P. Maioli, N. Del Fatti, and F. Vallee; *Chem. Soc. Rev.* **43**, 3921 (2014)
- [2] H. Baida, D. Mongin, D. Christofilos, G. Bachelier, A. Crut, P. Maioli, N. Del Fatti, and F. Vallee; *Phys. Rev. Lett.* **107**, 057402 (2011)
- [3] P. V. Ruijgrok, P. Zijlstra, A. L. Tchebotareva, and M. Orrit; *Nano Lett.* **12**, 1063 (2012)
- [4] A. Crut, P. Maioli, N. Del Fatti, and F. Vallee; *Phys. Rep.* **549**, 1 (2015)
- [5] F. Banfi, F. Pressacco, B. Revaz, C. Giannetti, D. Nardi, G. Ferrini, and F. Parmigiani; *Phys. Rev. B* **81**, 155426 (2010)
- [6] M. Gandolfi, A. Crut, F. Medeghini, T. Stoll, P. Maioli, F. Vallee, F. Banfi, and N. Del Fatti; *J. Phys. Chem. C* **122**, 8655 (2018)
- [7] R. Rouxel, M. Diego, F. Medeghini, P. Maioli, F. Rossella, F. Vallee, F. Banfi, A. Crut, and N. Del Fatti; *J. Phys. Chem. C* **124**, 15625 (2020)
- [8] S. Peli, A. Ronchi, G. Bianchetti, F. Rossella, C. Giannetti, M. Chiari, P. Pingue, F. Banfi, and G. Ferrini; *Scientific Reports* **10**, 16230 (2020)

SESSION NM08.04: Phase Change Materials
Session Chairs: Keivan Esfarjani and Sangyeop Lee
Sunday Afternoon, April 18, 2021
NM08

4:00 PM *NM08.04.01

Lattice Thermal Conductivity Enhancement at the Ferroelectric Phase Transition in GeTe Ivana Savic¹ and Djordje Dangic^{2,1}; ¹Tyndall National Institute, Ireland; ²University College Cork, Ireland

Materials near structural phase transitions usually have large phonon anharmonicity and low lattice thermal conductivity. The proximity to structural phase transitions in IV-VI materials is one of the main reasons for their low thermal conductivity and high thermoelectric figure of merit [1,2]. However, experiments indicate that the lattice thermal conductivity of germanium telluride (GeTe) actually increases near the ferroelectric phase transition around 600-700 K. In this work, we elucidate this unexpected effect using first principles calculations [3].

We first compute the lattice thermal conductivity of GeTe for a range of temperatures using the temperature dependent effective potential method [4] and the standard Boltzmann transport equation. We find that, although anharmonicity increases near the phase transition in the low symmetry phase (below the Curie temperature), the phonon group velocities increase as well, leading to a rise in the lattice thermal conductivity. Furthermore, anharmonicity decreases in the high symmetry cubic phase, further enhancing the phonon lifetimes and thermal conductivity.

Strong anharmonicity near the phase transition induces non-Lorentzian shapes of the phonon power spectra, which exhibit large softening of the peaks for soft phonon modes near the phase transition. To account for these effects, we implement a novel method of calculating lattice thermal conductivity based on the Green-Kubo approach [3]. Using this approach, we find that the Boltzmann transport equation underestimates the lattice thermal conductivity of GeTe near the phase transition. Our findings elucidate the influence of structural phase transitions on lattice thermal conductivity and provide guidance for design of better thermoelectric materials.

This work is done in collaboration with Djordje Dangic, Olle Helman and Stephen Fahy. The work is supported by Science Foundation Ireland PI Award 15/IA/3160.

[1] T. Shiga et al., Phys. Rev. B 85, 155203 (2011).

[2] R. M. Murphy, E. D. Murray, S. Fahy, and I. Savic, Phys. Rev. B 93, 104304 (2016).

[3] D. Dangic, O. Hellman, S. Fahy, and I. Savic, in preparation.

[4] O. Hellman and I. A. Abrikosov, Phys. Rev. B 88, 144301 (2013).

4:25 PM NM08.04.02

High Asymmetric Heat Transport in Multilayer Phase Change Materials Timm Swoboda¹, Katja Klinar², Andrej Kitanovski² and Miguel Muñoz Rojo¹; ¹University of Twente, Netherlands; ²University of Ljubljana, Slovenia

In this work, we determine how a multilayer structure made of different types of nanoscale phase change materials results in a highly non-linear and asymmetric heat flow depending on thermal bias directionality. This will set the basis of solid-state thermal diodes that can be scaled up for integration in energy management, conversion or storage applications. Thermal diodes (TD) or rectifiers are capable to manage heat in a similar manner as how electronic diodes control electricity, propagating heat preferably in one direction.^[1] The rectification ratio is defined as, $RR = (Q_{fwd} - Q_{rev}) / Q_{rev}$, where Q_{fwd} and Q_{rev} correspond to the heat flux in the forward and reverse direction, respectively. Unfortunately, current solid-state thermal diodes typically present moderate RR s, complex fabrication designs, and/or lack of operating temperature tuneability.^[1]

Phase change materials (PCM) have become popular for the development of TDs due to their thermal conductivity (k) change during the phase transition at a critical temperature (T_{crit}), e.g. VO₂ ($k_{low} = 1.5$ W/(m×K) to $k_{high} = 3.5$ W/(m×K) at $T_{crit} \sim 340$ K).^[1,2] These materials are often combined with phase invariant materials (PIM) to develop TDs.^[1] As an example, in a PIM/PCM structure based on VO₂, when the heat source is at temperatures $T > T_{crit}$ and close to the PCM side, both PIM and PCM conduct the heat well (Q_{fwd}). The situation is reversed when the heat source is applied to the PIM (Q_{rev}). This typically leads to RR larger than those found for individual PCMs.^[1]

Here, we used finite element modeling (COMSOL®) to develop a versatile TD based on a novel multilayer PCM/PIM structure. Our design includes an alternating combination of two PCM layers with two PIM layers. The total length of the multilayer structure was set to 1 μm, while the thickness of the individual layers was varied at the nanoscale. We selected carefully different types of PCM and PIM materials, whose experimental thermal properties were extracted from literature, to find the optimum PCM/PIM configuration that led to the highest RR . Then, we applied a temperature difference across the two ends of this structure. RR s larger than 100% were observed when we used Si and SiO₂ as PIMs and Ag₂Te and Ag₂S_{0.6}Se_{0.4} as PCMs with transition temperatures at 420 K and 360 K, respectively.^[3] Compared to the state of the art^[1] of PCM/PIM diodes, this configuration represents one of the highest RR s at room temperature as well as offers new possibilities for advanced thermal control. Additionally, from the point of view of applicability, this thermal diode offers numerous advantages over previously reported TDs, including simple design, scalability and operating temperature tunability.

To determine the potential of this thermal device for solid state refrigeration, we analyzed the effect of integrating this TD into a magnetocaloric (MC) device. For that purpose, we used a one-dimensional MC device consisting of gadolinium as MC material with two TDs at their ends, sandwiched between the heat sink and the heat source. The presence of TDs avoids the heat to flow back to the heat source improving the efficiency of the MC device.^[4] We selected a PIM/PCM structure that worked optimally for the MC system operating temperature and we considered quasi-steady-state operation in an alternating magnetic field with 1 T change. We observed that the integration of this TD enables higher operating frequencies compared to the conventional active magnetic regeneration process, increasing the cooling power density. Beyond MC refrigeration, this

versatile and unique TD can be used in other solid state refrigeration, heat pump and energy harvesting technologies to improve their performances or efficiencies.^[1,4]

References

- [1] Swoboda *et al.*, *Adv. Electron. Mater.*, **2020** (Accepted Review) DOI: 10.1002/aelm.202000625
- [2] Oh *et al.*, *Appl. Phys. Lett.*, **96**, **2010**
- [3] Hirata *et al.*, *J. Electron. Mater.*, **49**, **2020**
- [4] Kitanovski, *Adv. Energy Mater.*, **10**, **2020**

4:40 PM NM08.04.03

Phonon Softening Near Topological Phase Transitions Shengying Yue and Bolin Liao; University of California, Santa Barbara, United States

Topological phase transitions occur when the electronic bands change their topological properties, typically featuring the closing of the bandgap. While the influence of topological phase transitions on electronic and optical properties has been extensively studied, its implication on phononic properties and thermal transport remains unexplored. In this work, we use first-principles simulations to show that certain phonon modes are significantly softened near topological phase transitions, leading to increased phonon-phonon scattering and reduced lattice thermal conductivity. We demonstrate this effect using two model systems: pressure-induced topological phase transition in ZrTe₅ and chemical composition induced topological phase transition in Hg_{1-x}Cd_xTe. We attribute the phonon softening to emergent Kohn anomalies associated with the closing of the bandgap. Our study reveals the strong connection between electronic band structures and lattice instabilities and opens up a potential direction towards controlling heat conduction in solids. This work is based on research supported by DOE under the award number DE-SC0019244 and the UC Santa Barbara NSF Quantum Foundry funded via the Q-AMASE-i program under award DMR-1906325.

SESSION NM08.05: Coherent Phonons / Phase Change / Posters

Session Chairs: Sangyeop Lee and Martin Maldovan

Sunday Afternoon, April 18, 2021

NM08

6:30 PM NM08.05.01

Role of Coherent Phonons on Thermal Transport in Lead Sulfide Nanocrystal Superlattice Cheng Shao and Junichiro Shiomi; The University of Tokyo, Japan

Colloidal nanocrystal superlattices that are made of uniform-sized quantum dots (QD) connected by organic ligands have shown promising applications for photon detectors, solar cells, and thermoelectrics, among many others. Due to the secondary periodicity, the nanocrystal superlattice is also an ideal platform for phonon engineering, and the existence of coherent superlattice phonon mode is confirmed through the inelastic neutron scattering measurement recently. [1] However, it is also found that such coherent phonons are sensitive to the rotational motions of the building block [2], [3], and the surface morphology. [4] In this work, based on molecular dynamics simulation techniques, we explored the preconditions that are required to sustain the coherent phonons in the lead sulfide nanocrystal superlattice and the possible margins to engineering the thermal conductivity by manipulating such coherent phonons. We found that the mean free paths of the low-frequency coherent modes are tens of nanometers. However, those coherent modes, of which the frequency is less than 0.2 THz, carrier negligible amount of heat due to their small weights in the overall vibrational spectrum. We have shown that phonon in the frequency range of 0–5 THz dominates the thermal transport. In this frequency range, the interatomic vibrations of QDs have the maximum overlapping with the translation and bending modes in the ligands. We also identified the ligand coverage ratio as the key parameter that will affect

the morphology of the nanocrystal superlattice and thus dictate the thermal transport.

- [1] N. Yazdani *et al.*, “Nanocrystal superlattices as phonon-engineered solids and acoustic metamaterials,” *Nat Commun*, vol. 10, no. 1, pp. 1–6, Sep. 2019, doi: 10.1038/s41467-019-12305-3.
- [2] W.-L. Ong *et al.*, “Orientational order controls crystalline and amorphous thermal transport in superatomic crystals,” *Nature Materials*, vol. 16, no. 1, p. 83, Jan. 2017, doi: 10.1038/nmat4739.
- [3] S. Kumar, C. Shao, S. Lu, and A. J. H. McGaughey, “Contributions of different degrees of freedom to thermal transport in the C60 molecular crystal,” *Phys. Rev. B*, vol. 97, no. 10, p. 104303, Mar. 2018, doi: 10.1103/PhysRevB.97.104303.
- [4] K. J. Schnitzenbaumer and G. Dukovic, “Comparison of Phonon Damping Behavior in Quantum Dots Capped with Organic and Inorganic Ligands,” *Nano Lett.*, vol. 18, no. 6, pp. 3667–3674, Jun. 2018, doi: 10.1021/acs.nanolett.8b00800.

6:45 PM NM08.05.02

Late News: Anisotropic Heat Conduction of Coherent Phonons in Defect-Free Superlattices Hai Jun Cho and Hiromichi Ohta; Hokkaido University, Japan

Heat conduction due to phonons is usually dominated by diffuse scattering processes from crystal defects and anharmonicity. As such, doping and grain boundary engineering have been the primary approach for controlling the heat conduction in solids. While the contributions from coherently scattered low frequency phonons are not significant, they are challenging to control since they are not sensitive to crystal defects and therefore, remain as a major challenge for mastering the conduction of heat in solid. As such, understanding the propagation of coherent phonons is of fundamental interest in thermal management technologies. Superlattices in this regard provide an excellent platform since its heat conduction is attributed to coherent phonons. Experimental studies are typically performed on artificial superlattices, but they exhibit dislocations at interfaces, which increases anharmonicity and affect coherent scattering processes. For this reason, there has been some discrepancies between experimental and theoretical research efforts. In this study, we investigated the heat conduction in defect-free $\text{InGaO}_3(\text{ZnO})_m$ superlattice films to experimentally demonstrate several important concepts in phonon engineering, including the discrepancy between coherence length and mean free path, scattering mechanism changes according to the coherence length, specular phonon propagation along the in-plane direction, and the suppression of Umklapp processes.

7:00 PM NM08.05.03

Enhanced Environmental Scanning Electron Microscopy for Analyzing Material Dynamics in High-Pressure Gaseous Environments Lenan Zhang¹, Jinlong Zhu², Ryuichi Iwata¹, Lin Zhao¹, Kyle Wilke¹, Xiangyu Li¹, Zhengmao Lu¹, Yang Zhong¹ and Evelyn Wang¹; ¹Massachusetts Institute of Technology, United States; ²University of Illinois at Urbana-Champaign, United States

Environmental scanning electron microscopy (ESEM) is an important micro-to-nanoscale inspection tool to image diverse wet or insulating samples, such as liquid, polymer, and biomaterials in a gaseous environment. However, the presence of gas induces intensive electron-gas collisions, which leads to significant degradation of imaging quality. For this reason, the operating pressure of ESEM is typically below 1000 Pa. In this work, we enhanced the performance of ESEM by referring to the phase and scattering force of electron. Much higher contrast of ESEM images was obtained from the phase and scattering force reconstruction without any hardware changes. The limit of operating pressure was also extended up to 2500 Pa. More importantly, a close connection between the sample morphology and scattering force distribution was observed, which promises to advance the quantitative analysis using ESEM. To demonstrate the effectiveness of this enhanced ESEM technique, we studied the nucleation site distribution during droplet condensation, which cannot be precisely probed in previous studies due to the micro/nanoscale nature of nucleation. We show that the population of nucleation sites is governed by the Poisson distribution while the nearest neighbor distance follows the Rayleigh distribution, instead of the commonly used Poisson distribution. Our work provides a simple approach to enhance the performance of ESEM and can be widely used to study a variety of material dynamic processes in

gaseous environments.

7:15 PM NM08.05.04

Late News: Maximum Evaporating Flux of Molecular Fluids from a Planar Liquid Surface [Zhi Liang](#) and Eric Bird; California State University, Fresno, United States

Fast evaporation of liquids is a process of great importance to many industrial applications such as evaporative cooling of gas turbines, efficient combustion in engines, and superfine inkjet printing. Accurate prediction of the maximum evaporation flux from a condensed phase is one of the basic problems in the study of fast evaporation processes. The maximum evaporation flux occurs during the evaporation into a vacuum. In spite of the extensive work on the process of evaporation into a vacuum in the past decades, most of modeling studies only focused on the evaporation of monatomic substances. Whether these modeling results on monatomic fluids can be applied to predict the maximum evaporation flux of more complex fluids such as water and polymers is questionable. To address this question, one must have a fundamental and quantitative understanding of how the internal motions including rotations and vibrations of polyatomic fluid molecules affect the evaporation process and the maximum evaporation flux.

In this work, we use the kinetic theory of gases (KTG) to develop a theoretical model to understand the role of internal motions of molecules on the maximum evaporation flux from a planar liquid surface. The kinetic theory is applied to study the evaporation of molecular fluids into a vacuum and predict the dimensionless maximum evaporation flux ($J_{R,max}$, i.e. the ratio of the maximum evaporation flux to the molar flux emitted from a liquid surface). The key assumptions regarding the velocity distribution function (VDF) of polyatomic molecules in the highly non-equilibrium vapor near the evaporating surface are validated by the VDF obtained directly from molecular dynamics (MD) simulations. Our KTG-based analysis show that $J_{R,max}$ is affected by the specific heat ($c_{v,int}$) associated with internal degrees of freedom of fluid molecules. When the maximum evaporation flux is reached, the isotropic evaporating vapor far from the liquid surface moves at its speed of sound regardless of whether it is a monatomic vapor or polyatomic vapor. To fundamentally understand the evaporation of a molecular fluid into a vacuum, we solve the Boltzmann transport equation (BTE) to obtain the temperature, density, and flow speed distributions in the highly non-equilibrium evaporating vapor flow. Our BTE solutions indicate that there are several universal features of the evaporating vapor when the maximum evaporation flux occurs. In particular, we find that the evaporating vapor flow speed reaches the maximum value of $\sqrt{1.5}$ times the most probable thermal speed in the vapor flow direction at the vacuum boundary, and this maximum value is independent of fluid properties. All theoretical predictions in this work are verified by the MD simulation results of the evaporation of the model liquid Ar and the model liquid n-dodecane into a vacuum, and existing experimental data.

7:30 PM NM08.05.06

Interfacial Thermal Transport in Spin Caloritronic Material Systems [Frank Angeles](#) and Richard B. Wilson; University of California, Riverside, United States

Interfaces often govern the thermal performance of nanoscale devices and nanostructured materials. As a result, accurate knowledge of thermal interface conductance is necessary to model the temperature response of nanoscale devices or nanostructured materials to external heating. We report the thermal boundary conductance between metals and insulators that are commonly used in spin-caloritronic experiments. We use time-domain thermoreflectance to measure the interface conductance between metals such as Au, Pt, Ta, Cu, and Al with garnet and oxide substrates, e.g. NiO, YIG, EuIG, Cr₂O₃, and sapphire. We find that, at room temperature, the interface conductance in these types of material systems range from 50 and 300 MW m⁻² K⁻¹. We also measure the interface conductance between Pt/YIG at temperatures between 80 and 350 K.

7:35 PM NM08.05.07

Late News: Influence of the Crystallization on the Thermal Resistance of the GST-Based Structures [Kazimierz J. Plucinski](#); Military University of Technology, Poland

Correct estimation of the thermal resistance of the PCM memory structure is crucial due to the optimization of its parameters. The thermal resistance of PCM memory consists of thermal boundary interface resistances and GST bulk resistance. After entering the reset state, the crystallization of bulk GST begins and as a result a composite of GST crystallites distributed in an amorphous GST matrix is formed and thermal conductivity of such composite depends on the stage of the crystallization. Influence of the time-spatial distribution of the function defining the volume of the transformed fraction of the GST on the thermal resistance of the GST-based PCM structure is presented.

7:40 PM NM08.05.08

Control of Periodic Structure in a Homologous Series of Titanium Oxide Bulk Crystals in Atomic Scale
Shunta Harada^{1,2}, Shunya Sugimoto¹, Miho Tagawa¹ and Toru Ujihara¹; ¹Nagoya University, Japan; ²Japan Science and Technology Agency, Japan

Control of heat conduction through the manipulation of phonons as coherent waves have been attracted great interest for the advanced thermal management. Although smooth interfaces were reported to be obtained in artificial superlattices, preparation of coherent interfaces for terahertz phonons having nanoscale periodicity with atomic-scale perfection are still challenging since MOCVD and MBE were nonequilibrium growth process. Therefore, we focus on natural superlattice titanium oxides, in which periodic structures are obtained as thermodynamically stable phases. A homologous series of the titanium oxides is so-called crystallographic shear (CS) structure, in which planar faults are periodically introduced in the mother rutile structure with their spacing depending on the oxygen. Recently we have revealed that the titanium oxide with CS structure possesses the periodicity and the interface with high perfection and the coherent interface for almost all phonons are formed. In the present study, we demonstrated the control of the period of the CS structure in titanium oxides by the addition of chromium oxides to form oxygen deficiency.

The polycrystalline crystals of the titanium oxides with the addition was fabricated by the following process: firstly mixture of titanium and chromium oxides were sintered and obtained ceramics were melted by arc melting in an argon atmosphere and subsequently annealed in air for homogenization and oxidization of the crystals. The structure of the crystals were investigated by x-ray diffraction (XRD) as well as scanning transmission electron microscopy (STEM) with atomic-scale observation.

Judging from the XRD measurement, it seemed that the obtained crystals were of single phases and the structure was systematically changing according to the chromium content. Atomic-scale STEM observation revealed that the interval of the interfaces in the crystals were decreasing with increasing chromium content and we obtained the titanium oxides with the different interval of the interfaces ranging from 1.2 to 2.0 nm. From the STEM observation, not only the interval but also the atomic structure of the interfaces were changing depending on the chromium content. We have successfully control the periodic structure in a homologous series of titanium oxide bulk crystals. The current results indicates that the tuning of phonon band gap formation at higher frequency is possible in titanium oxide natural superlattices.

7:45 PM NM08.05.09

Late News: Generalized Law of Heat Conduction Including the Intrinsic Coherence of Thermal Phonons
Zhongwei Zhang¹, Yangyu Guo¹, Masahiro Nomura¹, Jie Chen² and Sebastian Volz¹; ¹The University of Tokyo, Japan; ²Tongji University, China

While coherent effects in solid heat conduction have recently been exemplified in superlattices and disordered structures [1-3], those evidences have remained essentially qualitative because the understanding of the intrinsic coherence of thermal phonons remains unclear. We propose a formalism supported by theoretical arguments and direct atomic simulations, which takes into account both the conventional phonon gas model and the internal wave nature of thermal phonons. By naturally introducing wavepackets in the heat flux from fundamental concepts, we derive an original thermal conductivity formula including coherence times and lifetimes. We then estimate the deviation between the predictions of the conventional model and ours by using atomic simulations to highlight significant effects in graphene. This contribution establishes a new frame for

understanding and quantifying the intrinsic coherence of phononic heat carriers, which has a general impact on the estimation of the thermal properties in nanostructures as well as in bulk materials.

References

- [1] Luckyanova, M. N., *et al.*, *Science* (2012) **338** (6109), 936
- [2] Isaeva, L., *et al.*, *Nat. Commun.* (2019) **10** (1), 3853
- [3] Simoncelli, M., *et al.*, *Nat. Phys.* (2019) **15** (8), 809

7:50 PM NM08.05.10

Anchor-Shaped Surfactants Enhance Evaporation on a Flat Liquid-Vapor Interface Xiaoman Wang¹, Jiong Chen², Jonathan Malen¹ and Alan McGaughey¹; ¹Carnegie Mellon University, United States; ²Zhejiang University-University of Illinois at Urbana-Champaign Institute, China

Surfactants are amphiphilic molecules that can be used to control the evaporation rate on a liquid-vapor interface. Previous experimental work has shown that molecular monolayers can reduce the evaporation rate on a flat liquid-vapor interface, while surfactant-modified sessile droplets show an increased evaporation rate due to changes in their wetting properties. A surfactant-induced increase in evaporation rate on a flat interface has yet to be demonstrated.

We applied molecular dynamics (MD) simulations to study the evaporation of a Lennard-Jones liquid with a variety of surfactants. A non-equilibrium MD (NEMD) simulation with a temperature difference was designed to directly extract the evaporation mass flux. Surfactants are added to the liquid-vapor interface. We found that an anchor-shaped surfactant with a flat hydrophobic top and hydrophilic chains enhances the evaporation rate by a factor of around 1.4 compared to the pure liquid.

To determine the origin of the evaporation rate enhancement, additional equilibrium MD simulations of the pure liquid and liquid-surfactant systems were performed to calculate thermal conductivities, diffusion coefficients, latent heats, vapor pressures, and mass accommodation coefficients. The results cumulatively point towards the evaporation enhancement being a result of liquid structuring around the surfactant, which lowers the thermal resistance to evaporation. Different surfactant sizes and structures are currently being investigated to further elucidate the origin and limits of the enhanced evaporation rate.

7:55 PM NM08.05.12

The Effect of Electrochemical Lithium Insertion on Thermal Transport of Titanate-Based Thin Films Azat Abdullaev, Bakhtiyar Soltabayev, Berik Uzakbaiuly, Almagul Mentbayeva, Zhumabay Bakenov and Zhandos Utegulov; Nazarbayev University, Kazakhstan

Understanding the heat transport in intercalated layered materials has attracted significant interest in Li-ion battery (LIB)-based electrochemical energy storage devices because they act as electrode materials. Heat dissipation affects a battery lifetime. Moreover, thermal runaway is one of the main faults of modern LIBs [1]. Therefore, tuning thermal conductivity in these devices becomes a key challenge. Chemical intercalation has proved to be an effective approach to control thermal transport in this application [2,3].

In our recent work, we have demonstrated thermal conductivity variation across amorphous Si thin films during Li intercalation [4]. In the present work, we further extend this research on titanium oxide and lithium titanate electrode materials, which were proved to be good alternatives for high power applications due to high cycling stability and long lifetime [5]. To study the effects of Li intercalation on their subsurface thermal conductivity, a picosecond time-domain thermoreflectance (TDTR) [4,6] was employed. Corresponding thin films were deposited by RF magnetron sputtering system and galvanostatic cycling was used between 0.5 and 3 V for Li insertion. Raman microscopy measurements were exploited to study chemical evolution during Li insertion into lithium titanate samples.

Thermal conductivity measurements revealed an average 50% increase in as-deposited TiO₂ thin films upon lithiation. Raman spectra indicated the formation of Li_xTiO₂ phase formation. Also, samples with different annealing temperatures have been prepared to study the effect of crystallinity on thermal conduction during Li

intercalation.

Reference

- [1] Q. Wang, P. Ping, X. Zhao, G. Chu, J. Sun and C. Chen, *Journal of Power Sources* 208 (2012): 210-224.
- [2] J. Cho, M. D. Losego, H. G. Zhang, H. Kim, J. Zuo, I. Petrov, D. Cahill and P. V. Braun, *Nature Communications* 5 (2014): 1–6.
- [3] Y. Xiong, N. C. Lai, Y. C. Lu and D. Xu, *International Journal of Heat and Mass Transfer* 159 (2020): 120077.
- [4] A. Abdullaev, A. Mukanova, T. Yakupov, A. Mentbayeva, Z. Bakenov and Z. N. Utegulov, *Materials Today: Proceedings* 25 (2020): 88-92.
- [5] M. V. Reddy, G. V. Subba Rao and B. V. R Chowdari, *Chemical reviews*, 113(7) (2013): 5364-5457.
- [6] D.G. Cahill, *Review of Scientific Instruments* 75 (2004): 5119–5122.

8:00 PM NM08.05.13

Nano- and Micro-Scale Thermal Conduction in AlN and Si₃N₄ Ceramics Irradiated by Swift Heavy Ions

Ainur Koshkinbayeva¹, Azat Abdullaev¹, Vinay Chauhan², Mostafa Valadkhani³, Ruslan Rymzhanov⁴, S. Mehdi Vaez Allaei³, Marat Khafizov⁵, Vladimir Skuratov⁴ and Zhandos Utegulov¹; ¹Nazarbayev University, Kazakhstan; ²Intel Corporation, United States; ³University of Tehran, Iran (the Islamic Republic of); ⁴Joint Institute for Nuclear Research, Russian Federation; ⁵The Ohio State University, United States

Displaying unique thermal, mechanical, electrical and magnetic properties [1], nitride ceramics have been widely used in nuclear engineering [2] and microelectronics applications [3]. In particular, the effect of swift heavy ion (SHI) irradiation on thermal transport of radiolysis-resistant nitride ceramics is a matter of interest [4]. However, there has been no prior study of the impact of SHI irradiation on the thermal conductivity of these materials on the subsurface scale.

AlN and Si₃N₄ polycrystalline ceramics were irradiated at the U-400 FLNR JINR cyclotron facility in Dubna, Russia by 167 MeV Xe and 700 MeV Bi ions at fluences between 1×10^{11} and 1×10^{14} cm⁻². The projected ion ranges were 13.6 (Si₃N₄) and 13.2 (AlN) μ m as calculated using SRIM 2013 in full cascade mode. Structural analysis with corresponding molecular dynamics (MD) simulations revealed formation of ion induced tracks in Si₃N₄, while no tracks were observed in AlN.

We report the results of cross-plane heat transport measurements of SHI irradiated aluminum nitride and silicon nitride ceramics as a function of ion dose by femtosecond laser pulse-based time-domain thermo-reflectance (TDTR) and continuous laser wave-based modulated thermoreflectance (MTR) techniques on nano- and micrometer subsurface scales, respectively. TDTR technique revealed thermally probed region extending down to hundreds of nanometers, where the electronic stopping / ionization processes dominate over nuclear stopping, while MTR approach has revealed thermal wave penetration depths down to microns. Thermal transport in these sub-surface domains irradiated by Xe and Bi ions for the given fluences has degraded by the factor of ~ 3 compared to non-irradiated as-received sample for both nitrides.

Using theoretical modeling based on Debye approximation and Klemens analytical thermal transport model [5], we analyzed defects concentrations extracted from experimentally measured thermal property data fitted to thermal diffusion model. In addition MD simulations were employed to model phonon scattering at ion tracks in Si₃N₄ ceramics. Given TDTR probed sub-surface region overlapped with ionization depth determined by SRIM calculation, whereas MTR probed region spanned nuclear displacive domain.

References

- [1] G. A. Slack, R. A. Tanzilli, R. O. Pohl, and J. W. Vandersande, "The intrinsic thermal conductivity of AlN," *J. Phys. Chem. Solids*, vol. 48, no. 7, pp. 641–647, 1987, doi: 10.1016/0022-3697(87)90153-3.
- [2] A. Janse Van Vuuren, V. Skuratov, A. Ibrayeva, and M. Zdorovets, "Microstructural Effects of Al Doping

on Si₃N₄ Irradiated with Swift Heavy Ions,” vol. 136, 2019, doi: 10.12693/APhysPolA.136.241.

[3] A. J. Griffin, F. R. Brotzen, and P. J. Loos, “The effective transverse thermal conductivity of amorphous Si₃N₄ thin films,” *J. Appl. Phys.*, vol. 76, no. 7, pp. 4007–4011, Oct. 1994, doi: 10.1063/1.357347.

[4] S. J. Zinkle, V. A. Skuratov, and D. T. Hoelzer, “On the conflicting roles of ionizing radiation in ceramics,” *Nucl. Instruments Methods Phys. Res. Sect. B Beam Interact. with Mater. Atoms*, vol. 191, no. 1–4, pp. 758–766, May 2002, doi: 10.1016/S0168-583X(02)00648-1.

[5] A. Koshkinbayeva, A. Abdullaev, Z. Nurekeyev, V. A. Skuratov, Y. Wang, M. Khafizov, Z. N. Utegulov “Thermal transport and optical spectroscopy of swift heavy ion irradiated LiF Crystals”, *Nuclear Instruments and Methods in Physics Research Section B: Beam Interactions with Materials and Atoms*, 475, 14-19 (2020).

8:05 PM NM08.05.14

Thermal Transport Properties of Dried Colloidal Silicon Nanoparticle Films by Micro-Raman

Spectroscopy Bayan A. Kurbanova¹, Gauhar Mussabek², Victor Timoshenko³ and Zhandos Utegulov¹;

¹Nazarbayev University, Kazakhstan; ²Al-Farabi Kazakh National University, Kazakhstan; ³Lomonosov Moscow State University, Russian Federation

We report on the heat conduction properties of smooth layers prepared from dried colloidal pure crystalline silicon (Si) nanoparticle (NP), which were probed by weak continuum wave (cw) laser light-induced heating with simultaneous Raman scattering detection under atmospheric conditions. The same approach of heating measurement was applied for the bulk silicon at high laser powers [1, 2]. Low thermally conductive Si NP films are envisioned as heat insulators for thermal management of optoelectronic devices. Laser heating causes softening of the first-order Raman Si-Si transverse optical phonon mode and a decrease in the corresponding phonon lifetimes [3]. The temperatures of laser-heated Si NP films were assessed from measured ratio of Stokes-to-Anti-Stokes integrated peak intensities of the Raman probed phonon mode and were compared with the external heater-heated temperature and temperature evaluation for cw-laser heated bulk crystalline Si [4]. It was revealed that the evaporation rate of the colloidal Si NP droplets and heating of deposited thin layers of variable thickness were heavily influenced by the thermal conductivities of the substrates, on which the films were deposited. It is suggested that the heat conduction of nanostructured layers is governed by the ballistic transfer of phonons across the boundaries of nanoparticles and varied with an increase in the layer thickness [5]. Our experimental results are in good agreement with theoretical molecular dynamics calculations [6] and Raman measurements in meso-porous nanocrystalline Si layer [7]. Micro-Raman-based thermal conduction measurements in our Si NP films are discussed in the light of variation of deposited colloidal NP film thickness, NP size, heating laser beam diameter and the substrate type.

References:

1. M. Balkanski, R.F. Wallis, and E. Haro, “Anharmonic effects in light scattering due to optical phonons in silicon”, *Phys. Rev. B*, 28 (4), 1928-1934 (1983).
2. M. Yamada, K. Nambu, Y. Itoh and K. Yamamoto, “Raman microprobe study on temperature distribution during CW laser heating of silicon on sapphire”, *J. Appl. Phys.*, 59(4), 1350-1354(1986).
3. P. Mishra and K. P. Jain, “Temperature-dependent Raman scattering studies in nanocrystalline silicon and finite-size effects”, *Phys. Rev. B*, 62 (22), 790-795 (2000)
4. J. Ready “Effects of High-Power Laser Radiation”, Academic Press (London), 1971.
5. Z. Wang, J. E. Alaniz, W. Jang, J. E. Garay and C. Dames. “Thermal Conductivity of Nanocrystalline Silicon: Importance of Grain Size and Frequency-Dependent Mean Free Paths”, *Nano Lett.*, 11, 2206–2213 (2000).
6. S. Ju and X. Lianga, “Thermal conductivity of nanocrystalline silicon by direct molecular dynamics simulation”, *J. Appl. Phys.*, 112, 064305 (2012).
7. V. Lysenko, S. Perichon, B. Remaki, D. Barbier, B. Champagnon, “Thermal conductivity of thick meso-

porous silicon layers by micro-Raman scattering”, J. Appl. Phys, 86 (12), 6841-6846 (1999).

SESSION NM08.06: Challenges and Opportunities/Boron Arsenide
Session Chairs: Martin Maldovan and Konstantinos Termentzidis
Monday Morning, April 19, 2021
NM08

8:00 AM *NM08.06.01

Phonon Heat Conduction Regime Map Gang Chen; Massachusetts Institute of Technology, United States

Beyond the Fourier diffusion theory on heat conduction, the classical size effects---the Casimir regime---caused by phonon boundary scattering is well known and extensively studied. However, over the last three decades, new regimes beyond the Fourier and the Casimir pictures of heat conduction have been demonstrated. In this talk, I will discuss different phonon heat conduction regimes, including the Knudsen regime, the hydrodynamic regime, the quantization regime, the coherence and localization regimes, and the divergence regime. The Knudsen regime expands Casimir’s picture to many other quasi-ballistic transport geometries, and is being exploited to develop phonon mean free path spectroscopy techniques. Phonon hydrodynamic transport happens when the normal scattering dominates over the resistive scattering, which is a condition difficult to satisfy and only observed at a narrow temperature range less than 20K. However, recent experiments have observed second sound---a consequence of phonon hydrodynamic transport---at much higher temperatures, while simulations point to possibility of observing hydrodynamic heat conduction even at room temperature. Quantized phonon transport was observed at very low temperatures. Signatures of coherent heat conduction, including localization, will be discussed, together with experimental evidences. Divergent thermal conductivity, implying thermal superconductors, is predicted to be possible in low-dimensional materials, although no experiments have provided conclusive evidence. These different phonon heat conduction regimes will be summarized in a regime map, demonstrating the rich phonon transport physics rivaling that of electrons.

8:25 AM NM08.06.02

Ray Phononics for Advanced Heat Flux Manipulations in Ballistic Regime Roman Anufriev and Masahiro Nomura; The University of Tokyo, Japan

Manipulation of thermal fluxes is essential in modern science and technology. Modern thermal phononics tries to achieve coherent control of heat conduction based on the wave interference of phonons that occurs in periodic nanostructures, called phononic crystals. However, the past decade of the research demonstrated that such a coherent control of heat is truly efficient either at sub-kelvin temperatures or in nanostructures with features at atomic scale.

In this work, we propose an alternative concept of heat manipulation based on the particle picture of phonons and their ballistic transport. We call this concept ray phononics as a thermal analogy of ray optics. Our simulations demonstrate the formation of directional thermal fluxes in phononic crystals due to the stochastic phonon motion in phononic crystals. We illustrate possible application of such directional fluxes for emitting directional heat rays, filtering the phonon spectrum, and even protecting a specific region from a thermal gradient.

Finally, we show that the proposed concept is not bound to only low temperatures, and ray-phononic nanostructures can control heat fluxes even at room temperature using modern materials like boron arsenide. Moreover, ray phononics is free from limitations of the traditional thermal phononics and enables creating and guiding thermal fluxes in realistic nanostructures regardless of their surface roughness. This makes us believe that advances in material synthesis may soon enable creation of devices capable of thermal guiding, emitting, filtering, and shielding using the proposed ray-phononics principles at room temperature.

Reference:

Anufriev and Nomura, "Ray phononics: thermal guides, emitters, filters, and shields powered by ballistic phonon transport", *Materials Today Physics* 15, 100272 (2020)

8:40 AM *NM08.06.04

Phonon-Phonon Interactions: Selection Rules and Higher-Order Processes David Broido¹ and Navaneetha Krishnan Ravichandran²; ¹Boston College, United States; ²Indian Institute of Science, India

Applying a first-principles theory that includes both the lowest-order three-phonon and the higher-order four-phonon processes to zinc blende semiconductors, we find that the lowest-order theory of phonon-phonon interactions drastically overestimates the measured thermal conductivities, k , for many of these materials, while inclusion of four-phonon scattering gives significantly improved agreement with measurements [1]. We identify new selection rules on the phase space of three-phonon processes that help explain many of these failures in terms of anomalously weak anharmonic phonon decay rates predicted by the lowest-order theory competing with four-phonon processes. We also show that zinc blende compounds containing boron (B), carbon (C), or nitrogen (N) atoms have exceptionally weak four-phonon scattering, much weaker than in compounds that do not contain B, C, or N atoms. This new understanding helps explain the ultrahigh k in several technologically important materials like cubic boron arsenide, boron phosphide, and silicon carbide. At the same time, it not only makes the possibility of achieving high k in materials without B, C, or N atoms unlikely, but it also suggests that it may be necessary to include four-phonon processes in many future studies. Finally, we show that the hidden influence of selection rules on three-phonon scattering can be exposed through anomalous signatures in the pressure (P) and temperature (T) dependence of the k of certain compounds [2]. In particular, boron phosphide reveals such underlying behavior through an exceptionally sharp initial rise in k with increasing P , which may be the steepest of any material, and also a peak and decrease in k at high P . These features are in stark contrast to the measured behavior for many solids, and occur at experimentally accessible conditions.

This work was supported by the Office of Naval Research under MURI Grant No. N00014-16-1-2436. N.K.R. acknowledges a start-up fund from the Indian Institute of Science, Bangalore, that supported a part of this work.

[1] Navaneetha K. Ravichandran and David Broido, *Phys. Rev. X* 10, 021063 (2020).

[2] Navaneetha K. Ravichandran and David Broido, <https://arxiv.org/abs/2009.01464>

9:05 AM *NM08.06.05

First Principles Predictions of Four-Phonon Scattering and Related Thermal Conductivity and Radiative Properties Xiulin Ruan; Purdue University, United States

For decades, the three-phonon scattering process had been considered to govern thermal transport in solids, while the role of higher-order four-phonon scattering had been persistently unclear and so ignored. However, recent quantitative calculations of three-phonon scattering had often overestimated thermal conductivity as compared to experimental data. We developed a rigorous perturbation method to predict four-phonon scattering rates and investigated its significant impact on thermal conductivity and infrared thermal radiative properties. We show that four-phonon scattering is generally important in solids. For silicon and diamond, the predicted thermal conductivity is reduced by 30% at 1000 K after including four-phonon scattering, bringing predictions in excellent agreement with measurements in the entire temperature range. For the projected ultrahigh-thermal conductivity material, BAs, a competitor of diamond as a heat sink material, four-phonon scattering is found to be strikingly strong as three-phonon processes have an extremely limited phase space for scattering. The four-phonon scattering reduces the predicted thermal conductivity from 2200 to 1400 W/m K at room temperature. The reduction at 1000 K is 60%. Our prediction on BAs has been confirmed by three independent experimental breakthroughs. Four-phonon scattering also significantly reduces the thermal conductivity of ZA phonons in graphene due to the fact the reflection symmetry does not restrict four-phonon scattering. Moreover, we find that four-phonon scattering universally plays a significant or even dominant role on the zone-center optical

phonon linewidth over three phonon scattering, for a wide range of materials including diamond, Si, Ge, GaAs, boron arsenide (BAs), cubic silicon carbide (3C-SiC), and α -quartz. This is enabled by the large four-phonon scattering phase space of zone-center optical phonons. Raman measurements on BAs were conducted, and their linewidth verifies our predictions. The predicted infrared optical properties through the Lorentz oscillator model, after including four-phonon scattering, show much better agreement with experimental measurements than those three-phonon-based predictions.

SESSION NM08.07: Machine Learning / Amorphous Materials
Session Chairs: Martin Maldovan and Konstantinos Termentzidis
Monday Morning, April 19, 2021
NM08

10:30 AM *NM08.07.01

Enhanced Controllability of Coherent Phonon Heat Conduction by Non-Random Aperiodic Nanostructures Junichiro Shiomi; The University of Tokyo, Japan

How and how much we can control transport of thermal phonons by nanostructures utilizing their wave nature is a central issue in science and engineering of nanoscale heat conduction. Phonon-particle scattering can impede heat conduction but, for that, large disorder needs to be introduced, which makes it inherently difficult to balance the impact with those on other quasi particles like electron and magnons. Furthermore, in the best scenario, the wave interference should be superior to particle scattering in impeding phonon transport as the former allows localization. The general difficulty in realizing interference by artificial nanostructure particularly for phonon transport is that the coherent lengths of phonons are typically quite short at room temperature, but thanks to the efforts of the researchers in the field, the control of phonon coherent heat conduction can be realized in heterostructures with nanometers lengths and clear interfaces like the semiconductor superlattices. Over the last few years we Thermal Energy Engineering Lab (TEEL) at the University of Tokyo, together with the collaborators, have been pushing the limit of controllability of coherent phonon heat conduction by exploring the effect of “non-random aperiodicity” in the superlattice. Since the design of aperiodic superlattice involves vast degrees of freedom, one of the key tools has been the machine learning, where we are now capable of efficiently handling extremely large search space using various machine learning schemes [1, 2] and hardware such as quantum annealer [3]. We performed a thorough demonstration from designing the structure by coupling coherent phonon transport calculation and machine learning to experimental fabrication and characterization for the GaAl/GaAs superlattice [4]. We further found a large controllability by the non-random aperiodicity in graphene/MoS₂ heterostructure [5]. An interesting finding here is that non-random aperiodic structure performs better than random aperiodic structure. Each part of the aperiodic structure selectively imposes interference of specific phonon band, allowing the overall structure to act on the entire thermal phonon spectrum. Here, competition with Anderson localization, which works best with full randomness, becomes important and we find that non-random structure is superior when the sample length/thickness is at nanoscale.

[1] S. Ju, et al, Physical Review X, 7, 021024 (2017)

[2] T. Dieb, et al, Science and Technology of Advanced Materials, 18, 498 (2017).

[3] K. Kitai, et al, Physical Review Research, 2, 013319 (2020).

[4] R. Hu, et al, Physical Review X, 10 (2), 021050 (2020).

[5] S. Hu, et al, (submitted).

10:55 AM NM08.07.02

Fast Simulations of Thermal Transport in Complex Materials using Machine Learning and Bayesian Force Fields Anders Johansson, Jonathan Vandermause, Andrea Cepellotti and Boris Kozinsky; Harvard University, United States

Controlling thermal conductivities of materials is important for a wide range of applications, from thermoelectrics for clean energy generation to electronic devices and thermal barrier coatings. The thermal conductivity is commonly estimated using molecular dynamics simulations within the Green-Kubo formulation. This requires a force field that is both 1) an accurate estimate of the interatomic interactions and 2) fast enough to allow simulations with sufficiently large length and time scales. Traditionally, only empirical force fields have fulfilled both of these requirements, which severely limits the applicability of the method.

In this work, we employ the Gaussian Process-based FLARE force field, which automatically learns the interactions of more complex materials than empirical force fields. The resulting model can then be mapped to a low-dimensional, computationally efficient model. Through GPU-acceleration with LAMMPS and the Kokkos library, we achieve excellent performance and obtain well-converged estimates for the thermal conductivity. Furthermore, we investigate state-of-the-art sampling and spectral denoising methods for further acceleration of the simulations.

11:10 AM NM08.07.03

Machine Learning Interatomic Potentials from Small Dataset for Grain Boundaries—A Case Study for Graphene Ruiqiang Guo, Sangyeop Lee and [Amirreza Hashemi](#); University of Pittsburgh, United States

Grain boundaries (GBs) often control a variety of properties of polycrystalline materials, which are widely used for practical applications. Atomistic simulations are helpful for understanding the relationship between GBs and materials properties. However such a simulation is largely limited by the lack of accurate and computationally efficient interatomic potentials. Machine learning has recently demonstrated its ability to develop interatomic potentials at first-principles level accuracy while costs a few orders of magnitude cheaper computational expense. However, for disordered structures like GBs, developing a high-fidelity machine learning interatomic potential (MLIP) usually requires a large training dataset to cover most of atomistic configurational space. Building the training dataset typically from first-principles calculations is very time-consuming. Here, we propose an efficient scheme for developing MLIPs for GBs from small dataset, while covering the entire atomistic configurational space. Using graphene GBs as an example, we show that the trained MLIP can achieve first-principles accuracy in the prediction of a broad range of structures and properties, including grain boundary energies, elastic constants, phonon spectra, etc. Our MLIP shows the almost same level of accuracy even for GBs not included in the training dataset, demonstrating an excellent transferability. We expect the proposed scheme will facilitate the efficient and rationale development of MLIPs of general GBs, enabling large-scale simulations of GB systems with high accuracy and low computational cost.

11:25 AM *NM08.07.04

Low, High and Switchable Thermal Conductivity in Soft Materials [David Cahill](#); University of Illinois at Urbana-Champaign, United States

A century of experiment and theory have produced a thorough understanding of heat conduction by phonons in simple inorganic crystals. By contrast, basic understanding of heat conduction by molecular vibrations in soft materials (amorphous and crystalline polymers, small molecule solids, and biological materials) is much less mature. Complex, non-periodic structures spanning multiple length scales are difficult to characterize and model. Low thermal conductivity, fiber morphologies, poor control of defects, and anisotropy created by molecular order create daunting challenges for experiment. I will discuss our past work on the thermal conductivity and elastic constants of a wide variety of polymeric materials in the form of thin films and fibers that span a factor of 300 range in thermal conductivity, 0.06 to 20 W/m-K. Time-domain thermoreflectance (TDTR) provides a common experimental platform for these studies; varying the thickness and modulation frequency changes the relative sensitivities of the TDTR measurement to thermal conductivity and heat capacity. Our recent work has employed light-activated changes in the morphology azo-polymers to switch the thermal conductivity by a factor of 3 between a low conductivity amorphous state and higher thermal conductivity crystalline state. We are developing frequency-domain probe beam deflection and optical-fiber

based TDTR measurements to provide new capabilities for measurements of the thermal effusivity and thermal diffusivity of small volumes of soft materials.

11:50 AM NM08.07.05

Strong Localization of Diffusons in Low-Coordinated Amorphous Networks Kiumars Aryana¹, Derek Stewart², John Gaskins¹, Joyeeta Nag², John Read², David Olson¹, Ashutosh Giri³, Michael Grobis² and Patrick Hopkins^{1,1,1}; ¹University of Virginia, United States; ²Western Digital Corporation, United States; ³University of Rhode Island, United States

Amorphous chalcogenide alloys are key materials for optical/electronic data storage and thermoelectric applications due to their threshold switching and low lattice thermal conductivity. Here, we report on a mechanism to suppress the thermal transport in a representative system, silicon telluride (SiTe), nearly by an order of magnitude via systematically engineering the cross-linking network between the atoms. As such, we experimentally demonstrate that in fully dense amorphous silicon telluride the thermal conductivity can be reduced to as low as 0.1 ± 0.01 W/m/K for high tellurium content with a density nearly twice that of amorphous silicon. With no fitting parameter, our estimation for thermal conductivity using ab-initio simulations integrated with lattice dynamics shows excellent agreement with the empirical measurements. We attribute the ultralow thermal conductivity of SiTe to suppressed contribution of propagons and a large shift in the mobility edge - a factor of five- towards lower frequency modes, leading to strong localization of extended modes of vibration, namely diffusons. This localization is the result of large atomic mismatch and a transition from over-constrained amorphous network to under-constrained atomic structure.

12:05 PM NM08.07.06

Effects of Medium Range Order on Propagon Thermal Conductivity in Amorphous Silicon Amirreza Hashemi¹ and Sangyeop Lee^{2,2}; ¹University of Pittsburgh, United States; ²University of Pittsburgh, United States

Several recent experimental and computational studies show that the thermal conductivity of amorphous silicon varies with sample size.¹⁻⁴ This suggests that phonon-like propagating vibrational modes (propagons) carry a significant amount of heat in amorphous silicon. The previous computational studies used the continuous random network (CRN) atomistic structure that represents an ideal random structure without medium- and long-range orders. However, recent spectroscopy results reveal that the actual atomistic structure of amorphous silicon contains medium-range order (MRO) that the CRN structure does not.⁵ In this work, we show the dependence of the propagon thermal conductivity on the MRO which has not been discussed in the previous studies. We compare the extent of MRO and the propagon thermal conductivity in several model amorphous silicon structures using simulated fluctuation electron microscopy, dihedral angle distribution, and molecular dynamics simulation. The results indicate that the structures with MRO show significantly larger propagon thermal conductivity (over 50 %) than the structures without MRO. As the extent of MRO depends on the material preparation methods, our study suggests that the thermal conductivity of amorphous Si also should depend on the material preparation method.⁶

References

- ¹ H.-S. Yang, D.G. Cahill, X. Liu, J.L. Feldman, R.S. Crandall, B.A. Sperling, and J.R. Abelson, *Phys. Rev. B* **81**, 104203 (2010).
- ² S. Kwon, J. Zheng, M.C. Wingert, S. Cui, and R. Chen, *ACS Nano* **11**, 2470 (2017).
- ³ J.L. Braun, C.H. Baker, A. Giri, M. Elahi, K. Artyushkova, T.E. Beechem, P.M. Norris, Z.C. Leseman, J.T. Gaskins, and P.E. Hopkins, *Phys. Rev. B* **93**, 1 (2016).
- ⁴ K.T. Regner, D.P. Sellan, Z. Su, C.H. Amon, A.J.H. McGaughey, and J.A. Malen, *Nat. Commun.* **4**, 1640 (2013).
- ⁵ M.M.J. Treacy and K.B. Borisenko, *Science* **335**, 950 (2012).
- ⁶ A. Hashemi, H. Babaei, and S. Lee, *J. Appl. Phys.* **127**, 45109 (2020).

12:20 PM NM08.07.07

Late News: Understanding Thermal Transport in Nanostructured Polymers Yu Guo and Yanfei Xu;
University of Massachusetts Amherst, United States

A continuous increase in power density and miniaturizing electronics makes heat dissipation one of the most important and complex technological challenges [1]. A major issue is that vast amounts of waste heat generated during device operation leads to overheating problems [2, 3]. A need for new materials to manage overheating arises. Polymers have been used for electronics packaging, thanks to their unparalleled properties: light weight, electrical insulation, chemical resistance and easy processability [4]. However, common polymers are generally regarded as thermal insulators with low thermal conductivity and are undesirable for efficient heat dissipation [5]. Understanding thermal transport in polymers and turning polymer insulators into heat conductors are needed for better thermal management [5, 6]. In this poster, we will present the recent work on improving thermal conductivity of polymers and understanding the relationships between thermal conductivity and polymer structures [5, 6]. We have developed polyethylene films with a high thermal conductivity of $\sim 62 \text{ W m}^{-1} \text{ K}^{-1}$, which is two orders of magnitude greater than that of traditional polymers ($\sim 0.1 \text{ W m}^{-1} \text{ K}^{-1}$) and is higher than that of many metals (e.g. 304-stainless steel $\sim 15 \text{ W m}^{-1} \text{ K}^{-1}$) and ceramics (e.g. aluminum oxide $\sim 30 \text{ W m}^{-1} \text{ K}^{-1}$). Unlike conventional approaches focusing on crystalline phase in polymers that can only marginally increase the thermal conductivity, we have engineered the non-crystalline chains through disentanglement and alignment and achieved a remarkably high thermal conductivity of $\sim 16 \text{ W m}^{-1} \text{ K}^{-1}$ [5]. We will also discuss our current work on investigating the relationships between thermal conductivity and polymer structures such as chain morphology and radius of gyration [6].

Reference:

1. Goyal, V. and A.A. Balandin, Thermal properties of the hybrid graphene-metal nano-micro-composites: Applications in thermal interface materials. *Applied Physics Letters*, 2012. **100**(7): p. 073113.
2. Ball, P., Computer engineering: Feeling the heat. *Nature*, 2012. **492**(7428): p. 174-6.
3. Waldrop, M.M., The chips are down for Moore's law. *Nature*, 2016. **530**(7589): p. 144-7.
4. Peplow, M., The plastics revolution: how chemists are pushing polymers to new limits. *Nature*, 2016. **536**(7616): p. 266-8.
5. Y. Xu, D. Kraemer, B. Song, Z. Jiang, J. Zhou, J. Loomis, J. Wang, M. Li, H. Ghasemi, X. Huang, X. Li & G. Chen, Nanostructured polymer films with metal-like thermal conductivity. *Nature Communications*, 2019. **10**(1): p. 1771.
6. Y. Xu, X. Wang, and Q. Hao, A mini review on thermally conductive polymers and polymer-based composites. *Composites Communications*, 2021. **24**: p. 100617.

SESSION NM08.08: 2D Materials / Machine Learning
Session Chairs: David Broido and Konstantinos Termentzidis
Monday Afternoon, April 19, 2021
NM08

1:00 PM *NM08.08.01

Thermal Transport in 2D Materials—Few-Layer Membranes and Heterostructures Clivia Sotomayor-Torres^{1,2} and Marianna Sledzinska¹; ¹Catalan Institute of Nanoscience and Nanotechnology, Spain; ²ICREA, Spain

Two-dimensional materials offer a wide range of options to study thermal transport in the nanoscale. The current understanding of thermal transport by phonons will be reviewed considering a few exemplary cases. We will discuss the case of free-standing polycrystalline membranes of MoS₂ where the grain size, their orientation and its distribution all play important roles to control the thermal conductivity, for which we have carried out

experiments and simulations. We explore the case of single crystal membranes containing few monolayers in which the sample preparation is crucial to eliminate effects of imperfections and contamination focusing on the thickness dependence of the thermal conductance. The role of the surface and interfaces will be discussed using the example of MoS₂/hBN heterostructures. Recent laser Raman thermometry data obtained from MoS₂ crystalline membranes supported on patterned substrates, with patterns covering the crossover range of phonon confinement to ballistic transport and from supported single-layer membranes of PtSe will be reported. In the former the focus is on the impact of phonon hybridization between the membrane and the patterned substrate, which has been observed and discussed in free-standing Si membranes on a phononic crystal, on the thermal transport. In the latter material, new challenges emerge and these will be discussed. On the methodological part, the sources of errors in the determination of thermal properties and outstanding questions concerning phonon transport in TMDCs will be discussed with view to find reliable figures of merits for a future benchmarking. Work in collaboration with M. Sledzinska, E. Chavez Angel, A. El-Sachat, X. Peng, M-J Esplandiu, R. Quey, B. Mortazavi, B. Graczykowski, M. Placidi, D. Saleta Reig, F. Alzina, L. Colombo, S. Roche, F. Bonell and M. Jamet.

1:25 PM NM08.08.02

Thermal Characterization of MoS₂ Mono/Few Layers Using Scanning Thermal Microscopy C. Mateo Frausto Avila^{1,2}, Victor Manuel Arellano Arreola¹, J. Martin Yañez Limon¹, Andres De Luna-Bugallo¹, Severine Gomes² and Pierre-Olivier Chapuis²; ¹Cinvestav Queretaro, Mexico; ²CNRS-CETHIL, France

Molybdenum disulfide (MoS₂) is a promising material for optoelectronics that belongs to the Transition Metal Dichalcogenide (TMDC) family and that can be grown in monolayers. Studies of such materials have led to a broad range of values for thermal conductivity and thermal contact conductance, both on simulation [1] and experimental [2] sides, probably due to the variety of configurations considered. Scanning Thermal Microscopy (SThM) is an Atomic Force Microscopy-based technique dedicated to the thermal investigation of micro and nanometric structures such as membranes, grains, films, etc, especially useful for cross-plane transport studies [2]. In this work, we apply the technique to characterize MoS₂ monolayers grown by Chemical Vapor Deposition (CVD) on Silicon Dioxide SiO₂_300nm/Si substrates. Our technique employs a self-heated resistive probe that is brought into contact with the surface of the sample to be characterized. Scanning the sample surface provides simultaneously the topography and thermal contrast images of sample. Using either the Wollaston microprobe or the Palladium nanoprobe in ambient environment, we find that SThM images show a clear thermal contrast between the substrate and MoS₂. Based on a calibration of the SThM probe using reference bulk materials and an original set of {oxide films on silicon substrate} samples of varying thickness, we are able to trace back to the effect of the MoS₂ layers. We find that the boundary dominates heat conduction on supported samples, and provide estimates of associated thermal contact resistance. Simulations reproducing the full {SThM probe + MoS₂ sample} experiment allows to clarify heat conduction in such systems.

[1] D.D. Fan et al., Applied Physics Letters, 103(13), 133113 (2014); A.N. Gandi et al., EuroPhysics Letters, 113(3), 36002 (2016); W. Li et al., Applied Physics Letters, 103(25), 253103 (2013)

[2] R. Yan et al., ACS nano 8.1 (2014): 986-993 (2104); X. Zhang et al., ACS applied materials & interfaces, 7(46), 25923-25929 (2015); A. Taube et al., ACS applied materials & interfaces, 7(9), 5061-5065; S. Vaziri et al., Sci Adv. 5(8): eaax1325 (2019)

[3] S. Gomès, A. Assy, P.O. Chapuis, Physica status solidi (a), 212(3), 477-494.(2015).

1:40 PM NM08.08.03

Tracking Energy Transport Across Atomic Junctions Using Femtosecond Diffraction Aditya Sood¹, Jonah Haber², Johan Carlstrom³, Elizabeth Peterson², Elyse Barre¹, Alexander Reid⁴, Xiaozhe Shen⁴, Marc Zajac¹, Suji Park⁴, Michael Kozina⁴, Emma Regan², Feng Wang², Xijie Wang⁴, Jeffrey B. Neaton³, Tony Heinz¹, Felipe H. Jornada¹, Aaron Lindenberg¹ and Archana Raja³; ¹Stanford University, United States; ²University of California, Berkeley, United States; ³Lawrence Berkeley National Laboratory, United States; ⁴SLAC, United States

Understanding and controlling interfacial heat transport is crucial for several applications in nanoelectronics, photonics, and energy conversion. Over the past few years, ultrafast optical techniques have enabled high-accuracy measurements of the thermal boundary conductance. Typically, these measurements are performed on systems that are thick compared to atomic lengthscales (at least several nm), and lack the ability to distinguish materials on both sides of the interface. The emergence of two-dimensional (2D) materials and heterostructures has revealed the need for techniques that can provide *angstrom-scale, material-selective* characterization of heat flow on picosecond timescales. Here, using mega-electron-volt ultrafast electron diffraction (MeV-UED), we present time-resolved measurements of thermal transport across type-II heterojunctions of monolayer 2D materials. Such heterostructures are of significant interest due to ultrafast (<100 fs) charge separation that is known to occur following photoexcitation. However, it has remained unclear how these electronic processes dissipate energy to the lattice. In this work, we prepare electron-transparent samples of 2D heterostructures, and selectively excite layer(s) within the stack using a tunable wavelength source. Layer-specific heating is subsequently monitored through the time-dependent dimming of Bragg peak intensities, thereby enabling picosecond tracking of energy flow across angstrom-scale junctions. Using *ab initio* calculations, we uncover the fundamental coupling between the electronic and lattice degrees of freedom in van der Waals 2D heterostructures.

1:55 PM NM08.08.04

Van der Waals Binding Effect Mediated Optimal Heat Transfer Through 2D Heterostructures Yang Zhong¹, Lenan Zhang¹, Xin Qian¹, Qichen Song¹, Jiawei Zhou¹, Long Li², Liang Guo², Gang Chen¹ and Evelyn Wang¹; ¹Massachusetts Institute of Technology, United States; ²Southern University of Science and Technology, China

Two-dimensional (2D) materials and their heterogeneous integration promise to advance the applications in electronics and photonics. However, the high thermal resistance at the interfaces bonded by weak van der Waals (vdW) interaction largely limits the energy dissipation, which may induce significant temperature rise and large thermal mismatch, and therefore degrades the device performance. Considering the practical tunability of vdW binding for 2D heterostructures reported by experimental studies, we investigated the thermal transport through an MoS₂-amorphous silica (a-SiO₂) heterostructure using molecular dynamics (MD) simulation, where the effects of vdW binding on both the in-plane and the cross-plane heat transfer are considered. We model the vdW interaction between MoS₂ and a-SiO₂ using the Lennard-Jones (LJ) potentials and scale the binding energy of the LJ force field. The in-plane thermal conductivity of the MoS₂ monolayer was calculated using the Green-Kubo formalism from the equilibrium MD simulation. The cross-plane thermal conductance between the MoS₂ monolayer and the a-SiO₂ substrate was calculated by the thermal circuit model using the approach-to-equilibrium MD. We show that the increase of vdW binding energy leads to a decrease of in-plane thermal conductivity and increased cross-plane thermal conductance. In particular, we observed saturation of the cross-plane thermal conductance at high vdW binding energy, which is attributed to the substrate-induced localized phonon modes in the MoS₂ with high phonon relaxation times and low participation ratios. The insights gained at the atomistic level lead to a device level optimization strategy of heat dissipation in the solid-state 2D nanodevice thermal management. Through the finite element analysis based on MD-calculated thermal properties, we show that three length scales, i.e., the hotspot size, the size of the 2D film, and characteristic length of the lateral heat spread, determine the device level thermal transport and the optimal vdW binding energy that maximizes heat dissipation. We identified two distinct heat transfer regimes that are characterized by the coupling of in-plane and cross-plane heat transfer and the cross-plane heat transfer, because of the interplay among the three length scales. At each regime, the optimal heat transfer for device operation was analyzed. Our study elucidates how the vdW binding affects the thermal transport through the 2D heterostructure from the atomistic level to the device level, which provides a general guideline to optimize the heat dissipation of high-performance 2D nanoscale devices.

2:10 PM OPEN SLOT

2:25 PM NM08.08.08

Mapping Nanoscale Thermal Transport Properties with Deep Learning Algorithms Sanghamitra Neogi, Artem Pimachev and Morgan Henderson; University of Colorado Boulder, United States

Confining heat carriers at the nanoscale significantly affects thermal transport in materials, even resulting in the breakdown of Fourier's law. For example, the thermal conductivities (TC) of one- and two-dimensional (1D and 2D) materials exhibit anomalous size dependencies and anisotropies. Confinement and surface roughness due to oxidation, amorphization, and nanostructuring have similar effects and have been investigated extensively as means for TC reduction, especially for thermoelectric applications. The end of conventional transistor scaling inspired extensive research on alternative integrated chip (IC) architectures to meet these increasing computing demands. Samsung announced limited manufacturing of a 3nm node IC featuring a new nanosheet architecture (Multi-Bridge-Channel FET). The greatest challenge in practically implementing such devices is the emergence of thermal bottlenecks that arise due to nanoscale structuring and material interfaces associated with tightly packed transistors, greatly reducing device performance. Although the nanoscale heat transport processes in semiconductors could be drastically different, as highlighted above, thermal modeling of these ICs is mostly done at the continuum level. New designs with controlled thermal environments guided by microscopic phonon physics models will directly impact the performance of nanostructured devices. To gain control over thermal transport processes in nanostructures, it is essential to fully map the vibrational properties of the materials. However, sampling of a high-dimensional parameter space is unavoidable to design nanostructured materials with controlled phonon transport properties due to the large variability of their geometric features, broad spectra of vibrational modes, and thermal transport properties; making analysis via first-principles models highly expensive. On the other hand, the rich dynamics of data in these spaces makes the problem of establishing a phonon-control design strategy ideal for the application of data-driven techniques. To understand thermal buildup in the active structures within modern field-effect transistor (FET) devices, we combine atomistic modeling techniques and first-principles calculations for constituent components with novel machine learning (ML) approaches to predict the thermal properties of the structures themselves. We generate temperature profiles for material components of several FET structures and identify phonon modes that contribute strongly to thermal transport in them using atomistic lattice dynamics calculations. We then establish a relationship between component features, temperature profiles, and corresponding phonon dynamics using a machine learning (ML) algorithm. Once the algorithm has been trained, the relationship is used to predict the full phonon dynamics of the FET structures. We acknowledge funding from the National Science Foundation [Award No.: HDR-DIRSE-1940153].

SESSION NM08.09: Structure and Interfaces I / BAs
Session Chairs: David Broido and Alan McGaughey
Monday Afternoon, April 19, 2021
NM08

4:00 PM *NM08.09.01

Nanoscale Thermal Transport in Hybrid Materials and Across Interfaces Zhiting Tian; Cornell University, United States

Understanding nanoscale thermal transport processes is essential to design nano-materials and devices with desired thermal transport properties for thermal energy conversion and management. Despite the significant progress in thermal transport of inorganic crystals, thermal transport in more complicated materials and across material interfaces remains largely unexplored. In this talk, I will present my research group's efforts to understand nanoscale thermal transport in hybrid organic-inorganic materials and across interfaces, using atomic modeling and experimental characterization. I will start with our study on phonon dynamics in hybrid

perovskites using inelastic x-ray scattering. It provides useful insights into their ultralow thermal conductivity. I will then share our recent development on anharmonic atomistic Green's function, which allows us to capture the importance of inelastic scattering at the interfaces. Lastly, I will share our latest work on phonon Anderson localization and quantum thermal rectification.

4:25 PM NM08.09.02

Optimizing Top-Side Device Cooling via Metal/Nanocrystalline Diamond Interfaces Henry Aller¹, Nicholas Golio¹, Karl Hobart², Tatyana Feygelson², Alan McGaughey¹, Andrew Gellman¹ and Jonathan Malen¹; ¹Carnegie Mellon University, United States; ²U.S. Naval Research Laboratory, United States

Top-side device cooling methods, e.g., diamond heat sinks on top of the metal contacts, facilitate heat removal from hot spots near the gate, directly lowering local and global temperature rises. Because the top-side surface of modern devices is often complex and rarely flat, conformal nanocrystalline diamond (NCD) growth techniques are critical to maximize the contact area between the device and the heat sink. Weak adhesion at this interface will cripple thermal transport, acting as a large thermal resistance. As a result, thin adhesive metal layers are often deposited between the device and the heat sink. The effectiveness of heat sinks is directly dependent on the thermal boundary conductance of the metal/NCD interface. In this study, we seek to optimize thermal transport across Au/Cr/Pd/NCD stacks. Cr was chosen for its thermal merits. Excellent adhesive properties and high maximum phonon frequencies has enabled Cr to produce some of the largest thermal boundary conductance interfaces for materials like Diamond, Al₂O₃, and AlN. Despite this, Cr is predicted to react with NCD to form enthalpically favorable carbides, which will lower the thermal boundary conductance. We hypothesize that a thin non-reactive Pd layer can eliminate these reactions and preserve the metal/NCD thermal boundary conductance in heated conditions. Pd and then Cr layers are deposited as perpendicular wedges with thickness of 0 to 20 nm on a single NCD sample, allowing us to test all thickness combinations of Pd and Cr. The thermal boundary conductance is measured using a non-destructive pump-probe optical technique, frequency domain thermorefectance (FDTR). By scanning the FDTR across the sample surface, a 2D map of thermal boundary conductance is created for all Pd/Cr thickness combinations. A local maximum in thermal boundary conductance is observed for a specific Cr/Pd thickness combination, providing evidence that our hypothesis is correct. Using Tunneling Electron Microscopy (TEM), we inspect a lift-out sample taken from our original NCD results, at the location of the TBC local maximum. Using image filtering, we identify the structure of this metal interface and determine the thickness of each metallic and reacted-carbide layers. The sample was then annealed and remeasured multiple times. Changes in the 2D thermal boundary conductance map following each heating cycle is used to quantify the ability for thin Pd layers to improve the thermal stability of metal contacts like Cr. Since large temperature rises will alloy and chemically react metal films and interfaces, it is crucial that we evaluate the thermal performance of metal stacks throughout the entire device's lifetime, not just when it's first made.

4:40 PM NM08.09.03

Interplay of Interfacial Scattering and Internal Phonon Scattering for Thermal Interfacial Transport in a Si/Ge Interface Xun Li and Sangyeop Lee; University of Pittsburgh, United States

Interfacial resistance between solids has drawn great interest due to its importance for various applications such as thermal management in electronic devices and energy conversion. The simple Landauer formula, which had been widely used, fails in describing interfacial resistance because it neglects internal phonon scattering. Past studies have shown that the modified Landauer formula proposed by S. Simons could give a much smaller interfacial resistance by considering internal phonon scattering [S. Simons, Journal of Physics C: Solid State Physics, 1974]. However, it assumes that phonons near the interface follow the distribution of bulk phase (i.e., distribution in an infinitely large sample with homogeneous temperature gradient), neglecting the non-equilibrium phonon distribution due to the interface and the complex interplay between the interface scattering and internal phonon scattering. We study the phonon transport across an interface between silicon and germanium by solving the Peierls-Boltzmann transport equation with inputs from first-principles. The phonon distribution is solved in both real and reciprocal spaces, and the local effects can be well captured. The results

show that both the Landauer formula and its modified version fail for interfacial phonon transport due to their assumptions neglecting highly non-equilibrium phonon distribution near an interface. The highly non-equilibrium phonon distribution decays with a distance from the interface and finally recovers to the phonon distribution of bulk phase at the distance which we define as an effective interfacial region. We find that the internal phonon scattering within the interfacial region provides an important contribution to overall interfacial resistance. Our study can help to understand the large discrepancy between experimentally measured interfacial resistance and that from the Landauer formula that is often found in literature, providing a useful way to interpret experimental data.

4:55 PM NM08.09.04

Theoretical Analysis of Factors Affecting the Thermal Boundary Conductance Variability between a 2-Dimensional Layered Material and Its Substrate Zhun-Yong Ong, Gang Zhang and Yong-Wei Zhang; Institute of High Performance Computing, Singapore

Effective heat dissipation from a two-dimensional semiconducting transition metal dichalcogenide (TMD), such as MoS₂ or WS₂, to its substrate is constrained by the thermal boundary conductance (TBC) of their planar interface which can exhibit significant variability with: (1) the charge carrier density, (2) surface roughness, (3) substrate elastic property, and (4) TMD thickness. Hence, insights into the factors affecting the TBC variability can lead to superior thermally aware design and more effective thermal management of TMD-based nanoelectronic devices through the optimal use of materials. We probe the physical origins of the TBC variability by modeling the underlying electronic and phononic processes in the TBC.

We quantify the temperature-dependent electronic TBC G_{el} between a single-layer TMD (MoS₂ or WS₂) and different dielectric insulating substrates (SiO₂, HfO₂ or Al₂O₃) and find that it varies significantly with the dielectric material and electron density, indicating that G_{el} is strongly tunable with a metal gate especially with Al₂O₃ [1]. To account for the effect of surface roughness on the phononic TBC G_{ph} , we introduce a phenomenological theory for diffuse phonon scattering between the TMD and its substrate [2]. The G_{ph} from diffuse scattering is compared to and found to be substantially higher than the G_{ph} from coherent scattering as well as comparable to experimentally measured TBC values for the MoS₂-SiO₂ interface, suggesting that the TMD-SiO₂ interface is highly disordered. To understand the effects of anisotropic elasticity in the substrate, we formulate an elasticity theory-based model of stacked thin plates to model the phononic TBC between a TMD and h-BN, a layered substrate [3]. Good agreement between the model and experimental TBC data is obtained for the MoS₂-BN interface. Our results reveal that h-BN is substantially more effective for heat dissipation than SiO₂, especially when the number of layers in the MoS₂ is large, because of the effective coupling of flexural modes across the MoS₂-BN interface.

References

1. Z.-Y. Ong, G. Zhang, Y.-W. Zhang, and L.Y. Cao, "Gate-tunable cross-plane heat dissipation in single-layer transition metal dichalcogenides," *Phys. Rev. Research* 2(3), 033470 (2020).
2. Z.-Y. Ong, Y. Cai, G. Zhang and Y.-W. Zhang, "Theoretical analysis of thermal boundary conductance of MoS₂-SiO₂ and WS₂-SiO₂ interface," Submitted.
3. Z.-Y. Ong, G. Zhang and Y.-W. Zhang, "Theory of phononic heat dissipation to a hexagonal boron nitride substrate," Submitted.

5:10 PM BREAK

5:20 PM NM08.09.05

Nanoscale Thermal Transport at Bi₂Te₃ Interfaces Aoife K. Lucid¹, Javier Fernandez-Troncoso², Jorge Kohanoff², Stephen B. Fahy¹ and Ivana Savic¹; ¹Tyndall National Institute, Ireland; ²Queen's University Belfast, United Kingdom

Nanostructured thermoelectric materials are generally highly polycrystalline, meaning that defects such as interfaces are prevalent. Advancing beyond the current state-of-the-art nanostructured thermoelectric materials requires a detailed understanding of the impact of interfaces on their thermal properties. In addition to the

importance of nanoscale engineering, it is highly desirable to achieve high thermoelectric performance at room temperature for Internet of Things, energy harvesting, and active cooling applications. Bismuth telluride (Bi_2Te_3) is the best performing thermoelectric material at room temperature. One route to achieving highly efficient thermoelectrics at room temperature is to understand the impact of interfaces in materials such as Bi_2Te_3 on thermal transport at an atomistic level.

In this work, we utilise reverse non-equilibrium molecular dynamics (rNEMD) simulations, with a recently developed empirical interatomic potential [1], to elucidate the impact of specific twin boundary structures on thermal transport in Bi_2Te_3 . Three basal plane twin boundaries terminated at different layers in Bi_2Te_3 and the 60° twin boundary [2] are investigated. The interfacial thermal resistance (Kapitza resistance) is calculated, along with an analysis of the structural changes observed at interfaces. We find that interfacial thermal resistance increases with decreasing stability of the interface, suggesting that the most effective interfaces may require more effort to fabricate. Despite large structural differences between the basal twin boundaries and the 60° twin boundary, we do not see significant variance in interfacial thermal resistance when comparing these interfaces. A comparison of the properties of these four twin boundaries is carried out, enabling us to identify those that may be the most impactful in terms of suppressing lattice thermal conductivity at room temperature.

[1] B. Huang et al., J. Phys. D Appl. Phys. 52, 425303 (2019)

[2] K. Kim et al., Nat. Commun. 7, 1-6 (2016)

This work is supported by a research grant from Science Foundation Ireland (SFI) and the Department for the Economy Northern Ireland under the SFI-DfE Investigators Programme Partnership, Grant No. 15/IA/3160. This work is also supported by SFI Grant No. 13/RC/2077.

5:35 PM *NM08.09.06

Peak Thermal Conductivity Measurements of Bulk Boron Arsenide Crystals and Individual Carbon Nanotubes Yuanyuan Zhou¹, Qianru Jia¹, Chunhua Li², Geethal Amila Gamage³, Zhifeng Ren³, David Broido² and Li Shi¹; ¹The University of Texas at Austin, United States; ²Boston College, United States; ³University of Houston, United States

The ultrahigh lattice thermal conductivities reported near the room temperature for boron arsenide (BAs) and carbon nanotubes (CNTs) make them useful for both thermal management applications and fundamental studies of phonon transport. The peak thermal conductivity of a single crystal usually appears at a low temperature and provides insight into the competition between extrinsic phonon-defect scattering with intrinsic phonon-phonon processes. However, existing measurements have yet to obtain the peak thermal conductivity of BAs and reported a much higher peak temperature for CNTs than for high-quality graphite. Here we report highly sensitive electro-thermal bridge measurements of the peak thermal conductivities of both bulk BAs crystals and individual CNTs. Theoretical calculations are used to correlate the thermal transport measurement results with the structure and chemical composition characterization data.

SESSION NM08.10: Thermoelectricity / Electron-Phonon / Thermionics

Session Chairs: Yee Kan Koh and Sangyeop Lee

Monday Afternoon, April 19, 2021

NM08

7:45 PM *NM08.10.01

Transport Properties of Chalcogenide Systems—The Effects of Atomic Re-Arrangement and Doping Lilia Woods; University of South Florida, United States

Multinary chalcogenides are diverse systems, which can be derived from simpler binary compositions by cation substitution and preserving the octet rule. One can achieve different classes of materials with more complicated compositions, which share some common features and yet have distinct properties. By using first principles simulations we study the electronic and vibrational properties of quaternary chalcogenides from the I₂-II-IV-VI₄, I-II₂-III-VI₄, and I-IV-V-VI₃ families. These systems have inherently low thermal conductivity, which is directly related to the lattice structures and underlying anharmonic phonon scattering mechanisms. Our first principles simulations help us understand from a microscopic perspective the phonon conduction processes in these classes of materials. We also find that there are various possibilities for different atomic arrangements which can lead to distinct structural phases. Also, various types of doping are possible, which can further be used for electronic property optimization. The inherently low thermal conductivity and the available earth-abundant chemical compositions make these materials attractive for applications in thermoelectricity and solar cells among others.

Support from the US National Science Foundation under Grant No. DMR-1748188 is acknowledged.

8:10 PM NM08.10.02

Improvement of Thermoelectric Efficiency of Si-Based Clathrate Masato Ohnishi¹, Koji Fujimura², Takahiro Yamamoto², Hiroshi Shimizu², Kiyoshi Yamamoto² and Junichiro Shiomi¹; ¹The University of Tokyo, Japan; ²Furukawa Electric, Japan

Clathrate compounds are promising candidates for thermoelectric materials in terms of the “electron-crystal phonon-glass” concept. Clathrate compounds are composed of guest atoms encapsulated in cagelike structures. It is expected that electrons can smoothly transport in the frame work while phonons are scattered by guest atoms. Particularly, in type-I clathrate compounds, guest atoms vibrate in a strong anharmonic potential because they are composed of a Weaire-Phelan structure, which divides a space with the maximum volume with the same cross-sectional area. While off-center clathrates such as type-I Ba₈Ga₁₆Sn₃₀, in which guest atoms vibrate in a double-well anharmonic potential, have low thermal conductivity, silicon-based clathrates are preferable for actual use in terms of the material cost.

In this study, we show that aluminum substitutions can enhance thermoelectric performance of silicon-based clathrates, type-I Ba₈Ga₁₆Si₃₀. Comparing calculated thermoelectric figure of merits (ZT) with those obtained in experiment, we concluded that (a) aluminum additive enhances ZT with lowering doping level and (b) further suppression of doping level can enhance ZT significantly. To investigate thermoelectric properties, we obtained possible structures at finite temperature with using a cluster expansion and Monte Carlo method [M. Ångqvist, P. Erhart et al., Chem. Mater. 29, 7554 (2017) and 28, 6877 (2016)] and thermoelectric properties were averaged for different possible structures. Phonon properties of the clathrates were calculated with using a self-consistent phonon (SCP) theory based on first-principles calculations [Tadano *et al.* Phys. Rev. Lett 120, 105901 (2018)]. Our state-of-the-art analysis method shows a good agreement with experimental data.

8:25 PM BREAK

8:50 PM *NM08.10.04

Nonequilibrium Energy Dynamics in Nanoscale Metal Multilayers After Femtosecond Heating Richard B. Wilson^{1,2}, Ramya Mohan², Kexin Liu¹, Xinping Shi¹ and Michael Gomez²; ¹University of California, Riverside, United States; ²University of California, RIverside, United States

Understanding the ultrafast energy dynamics in a metal after laser heating is critical for many engineering applications, including nanoscale thermal engineering, photocatalysis, and spintronics. Despite the topic’s importance, and decades of study, fundamental questions about the topic remain unanswered. In this talk, I discuss my group’s experimental work to answer two such questions. (i) Do photoexcited electrons transport energy ballistically, super-diffusively, or diffusively before thermalizing with phonons? (ii) Can we control the energy dynamics in metal alloys by using the effect of alloy composition on electronic band structure to control the strength of quasi-particle interactions? To answer the first question, we combine wavelength-dependent time-domain thermoreflectance experiments and time-resolved magneto-optic Kerr effect experiments to study

nanoscale heat-transfer in Au/Co multilayers. We perform measurements on a series of samples with varied Au thickness. Our experiments show that, while the energy dynamics in Au after photoexcitation are nonthermal, heat is still transported diffusively. To answer the second question, we perform pump/probe experiments on $Au_{1-x}Al_x$ and $Co_{1-x}Fe_x$ alloys. We find the ultrafast energy dynamics in these alloys depends strongly on composition. In $Au_{1-x}Al_x$ alloys, we credit the observed relationship between alloy composition and electron-phonon energy relaxation time to changes in the strength of electron-phonon interactions. In $Co_{1-x}Fe_x$ alloys, we credit the observed composition dependence of the electron-magnon energy relaxation time to changes in the strength of electron-magnon interactions. I conclude my talk by discussing the implications of our findings to the plasmonics and spintronics communities.

9:15 PM NM08.10.05

Long-Lived Modulation of Plasmonic Absorption by Ballistic Thermal Injection John A. Tomko¹, Evan Runnerstrom², Yi-siang Wang³, Weibin Chu³, Joshua R. Nolen⁴, David Olson¹, Kyle Kelley⁵, Angela Cleri⁶, Josh Nordlander⁶, Oleg Prezhdo³, Jon-Paul Maria⁶ and Patrick Hopkins¹; ¹University of Virginia, United States; ²CCDC US Army Research Laboratory, United States; ³University of Southern California, United States; ⁴Vanderbilt University, United States; ⁵Oak Ridge National Laboratory, United States; ⁶The Pennsylvania State University, United States

Light-matter interactions that induce charge and energy transfer across interfaces form the foundation for photocatalysis, energy harvesting and photodetection, among other technologies. One of the most common mechanisms associated with these processes relies on carrier injection. However, the exact role of the energy transport associated with this hot-electron injection remains unclear. Plasmon-assisted photocatalytic efficiencies can improve when intermediate insulation layers are used to inhibit the charge transfer or when off-resonance excitation is used, which suggests that additional energy transport and thermal effects could play an explicit role even if the charge transfer is inhibited. This provides an additional interfacial mechanism for the catalytic and plasmonic enhancement at interfaces that moves beyond the traditionally assumed physical charge injection. In this work, we report on a series of ultrafast plasmonic measurements that provide a direct measure of electronic distributions, both spatially and temporally, after the optical excitation of a metal/semiconductor heterostructure. We explicitly demonstrate that in cases of strong non-equilibrium, a novel energy transduction mechanism arises at the metal/semiconductor interface. We found that hot electrons in the metal contact transfer their energy to pre-existing free electrons in the semiconductor, without an equivalent spatiotemporal transfer of charge. Further, we demonstrate that this ballistic thermal injection mechanism can be utilized as a unique means to modulate plasmonic interactions. These experimental results are well-supported by both rigorous multilayer optical modelling and first-principle ab initio calculations.

9:30 PM NM08.10.06

Dependence of Electron-Phonon Energy Relaxation Times on Electron-Electron and Electron-Phonon Interactions Strengths Xinping Shi, Kexin Liu and Richard B. Wilson; University of California, Riverside, United States

Photoexcitation of a metal results in hot electrons that cool on femto to picosecond time-scales because of electron-phonon interactions. The energy relaxation times of hot electrons can vary a lot depending on the metal. For example, the electron-phonon energy relaxation time in Pt is less than 200 fs^[1]. Alternatively, in Au experiments suggest the energy relaxation is between 1 and 3 ps^[2-5]. In this work, we experimentally study how energy relaxation times in metals are determined by the interplay of electron-electron (e-e) interaction and electron-phonon (e-p) interaction strengths. We report on pump/probe measurements of picosecond acoustic signals in Au, Al, and their alloys. We perform these measurements on wedge samples with varied thicknesses. These metals have a wide range of e-e and e-p interaction strengths, and therefore provide a rigorous test on existing theories for hot electron dynamics. The picosecond acoustic signals we measure are caused by the rapid change in lattice temperature as a function of depth that occurs following laser excitation. Therefore, our experimental signals are a sensitive probe of electron-phonon energy relaxation times. Our results provide insight into how quasi-particle interactions govern nanoscale heat transfer in metal systems, which is important

to many disciplines, including nanophotonics, plasmonics, and ultrafast magnetism.

Reference

1. Hyejin Jang, Johannes Kimling, and David G. Cahill. Nonequilibrium heat transport in Pt and Ru probed by an ultrathin Co thermometer. *Phys. Rev. B* 101, 064304
2. Mueller, B. & Rethfeld, B. Relaxation dynamics in laser-excited metals under nonequilibrium conditions. *Physical Review B* 87, 035139 (2013).
3. Groeneveld, R. H. M., Sprik, R. & Lagendijk, A. Femtosecond spectroscopy of electron-electron and electron-phonon energy relaxation in Ag and Au. *PRB* 51, 11433-11445, doi:10.1103/PhysRevB.51.11433 (1995).
4. Del Fatti, N., Voisin, C., Achermann, M., Tzortzakis, S., Christofilos, D. & Vallée, F. Nonequilibrium electron dynamics in noble metals. *PRB* 61, 16956-16966, doi:10.1103/PhysRevB.61.16956 (2000).
5. Gusev, V. E. & Wright, O. B. Ultrafast nonequilibrium dynamics of electrons in metals. *PRB* 57, 2878-2888, doi:10.1103/PhysRevB.57.2878 (1998).

9:45 PM NM08.10.07

Microscopic Insulating Spacers for Thermionic Energy Conversion Mohsen Azadi¹, Zhipeng Lu¹, Matthew F. Campbell¹, Wujoon Cha¹, Josue Leon¹, Kyana Van Houten², Felix Schmitt², Jared W. Schwede² and Igor Bargatin¹; ¹University of Pennsylvania, United States; ²Spark Thermionics, United States

We introduce thermally insulating corrugated spacers that establish micron-scale electrode gaps without electrical shorting in thermionic energy converters, allowing temperature differences of hundreds of kelvins to be achieved with only a few watts of conductive heat transfer per square centimeter. These films' microscale corrugation serves both structural and thermodynamic functions, namely, to increase their robustness^{1,2} and to increase their overall thermal resistivity to limit heat transfer between the electrodes^{3,4}. Our thermomechanical testing reveals that these films have thermal resistance values high enough to reduce parasitic conduction to levels below that of thermionic heat transfer even at moderate (~1300 K) emitter temperatures, resulting in great enhancements in output current density and thermionic conversion efficiency while minimizing heat loss. These results represent a significant step toward high power density, mass producible, commercially viable direct heat-to-electricity energy conversion.

Thermionic energy converters are solid-state heat engines in which electrons are produced by a hot cathode, cross a vacuum gap, and impinge on a cold anode, delivering electric current. Maximizing efficiency and power density in these devices requires minimizing their vacuum gap thicknesses to roughly 2 μm . Establishing gaps of this scale by intricate external positioning mechanisms is impractical for mass-produced devices, thereby necessitating intra-gap spacers to internally maintain spacings. Previous methods of establishing these gaps have had limited success for reasons related to their high conductive losses or other manufacturing difficulties^{5,6}.

Therefore, we have developed spacers made through alumina atomic layer deposition with micron-scale thicknesses and square centimeter-scale areas that can be mass-produced using standard microfabrication techniques and subsequently transferred to thermionic energy converter electrodes. These films include hexagonal apertures to allow high electron currents (several A/cm^2), can tolerate compressive pressures of several atmospheres to ensure electrode parallelism, and have high thermal resistances (hundreds of $\text{cm}^2\text{K}/\text{mW}$) to minimize conductive losses. Our films' low conductance values stem from the high contact resistance they exhibit where they touch the electrodes³ and their carefully architected nanoscale corrugation, which reduces the area through which conduction can occur⁴.

We fabricate our spacer films by (1) constructing a silicon mold *via* sequential cycles of photolithography and deep reactive ion etching, (2) conformally coating the mold with insulating materials such as alumina using atomic layer deposition, (3) cutting hexagonal apertures in the insulating layer using inductively coupled plasma etching, and (4) releasing the film using XeF_2 etching. In addition, we have developed an ultra-high vacuum testing apparatus to probe the interactions between the mechanical and thermal properties of our films and in addition are conducting extensive electrical testing of these spacers in thermionic devices.

- 1) Davami *Nat. Commun.* 6(2015)10019
- 2) Jiao *Extreme Mech. Lett.* 34(2020)100599
- 3) Nicaise *Microsyst. Nanoeng.* 5(2019)31
- 4) Campbell *J. Microelectromech. Syst.* 29(2020)637
- 5) Littau *Phys. Chem. Chem. Phys.* 15(2013)14442
- 6) Belbachir *J. Micromech. Microeng.* 24(2014)085009

10:00 PM NM08.10.08

Comprehensive Modeling of Thermionic Energy Conversion with Micro/Nanoscale Vacuum Gaps with Constant Heat Flux Input Moh'd-Eslam Dahdolan and Mohammad Ghashami; University of Nebraska–Lincoln, United States

Thermionic energy conversion is the direct conversion of heat into electricity by the spontaneous emission of high-energy electrons from a surface. Although the physical mechanism of thermionic emission has been suggested to be used for energy conversion applications for over century now, thermionic energy converters (TEC) have not been widely implemented due to low conversion efficiency even at high temperatures. Recently, it has been suggested that by reducing the inter-electrode gap distance in a thermionic converter, electron emission can increase remarkably mainly due to the mitigation of excessive potential barriers (i.e., negative space charge). However, by shrinking the inter-electrode dimensions, other physical phenomena now need to be considered including near-field thermal radiation and image-charge effects. Therefore, significant knowledge gaps remain in the comprehensive modeling and analysis of thermionically induced electron and photon emission, particularly across nanometer distances. In this study, we present a comprehensive model describing the performance of a tungsten-based TEC by developing an energy balance with various heat flux inputs to the emitter and considering the effects of negative space charge, image charge, and near-field thermal radiation between the two electrodes. The steady-state temperatures of the emitter and collector are found to satisfy the energy balance of the TEC and the effects of inter-electrode gap distance, operating voltage, and work functions of the electrodes on the operating performance are further investigated for different heat input scenarios. The dependence of work output and efficiency on gap distance is highlighted to show the maximum efficiency and maximum power points, which are helpful in selecting gap distance for optimum performance. By clear illustration of the trade-off between the aforementioned physical phenomena at the nanoscale regime using this comprehensive model, our results prove that the power output and the conversion efficiency of a nanoscale TEC system can surpass those of conventional TECs and other competitive solid-state converters.

SESSION NM08.11: Nanostructures

Session Chairs: Martin Maldovan and Konstantinos Termentzidis

Tuesday Morning, April 20, 2021

NM08

8:00 AM *NM08.11.01

Phonon Transport Physics in Well-Controlled Various Nanomaterials Yoshiaki Nakamura and Takafumi Ishibe; Osaka University, Japan

With miniaturizing electronic devices, thermal management has attracted great interest for overcoming various heat issues in nanoscale world: dissipating heat, energy harvesting from the wasted heat, and so on. Therefore, much effort has been made to reveal the phonon transport physics in nanoscale leading to tailoring heat conduction. Nowadays, some studies experimentally demonstrated the interesting coherence property of phonon using superlattice structures [1, 2]. On the other hand, in the thermoelectric research field, phonon transport in nanostructured materials has also drawn much attention because of the thermal conductivity reduction. However, in general, the materials including nanostructures have unintentional defective structures:

uncontrolled crystal orientation, composition deviation, strains and crystal defects. It needs the atomically-controlled nanostructured materials to elucidate the phonon transport physics in the material system containing nanostructures.

We have developed various kinds of unique well-controlled nanostructures: IV group element-based nanodot structures, etc [3-6]. This talk will discuss the phonon transport physics in the unique nanomaterial films containing atomically-controlled nanocrystals where the thermal conductivity is drastically reduced. One example of our nanostructures is Si-based films including ultrasmall Ge nanodots with sharp interfaces and without strain unlike the conventional Stranski Krastanov nanodots. When Ge nanodots get smaller than 10 nm, the thermal resistance of Ge nanodot layers in Si films decreases, while that of Ge nanodot layers in SiGe films does not depend on Ge nanodot size. The tendency can be explained by phonon scattering theory. In this talk, we will introduce phonon transport in some kinds of well-controlled nanostructured materials. These findings will give a new insight for thermal management.

This work was supported by Grant-in-Aid for Scientific Research A (19H00853), Exploratory Research (19K22110). This work was also supported by JST CREST.

References

- [1] M. N. Luckyanova, et al., *Science* 338, 936 (2012).
- [2] J. Ravichandran, et al., *Nat. Mater.* 13, 168 (2014).
- [3] S. Yamasaka, et al., *Sci. Rep.* 5, 14490 (2015).
- [4] Y. Nakamura, et al., *Nano Energy* 12, 845 (2015).
- [5] Y. Nakamura, et al., *Sci. Technol. Adv. Mater.* 18, 31 (2018).
- [6] T. Taniguchi, et al., *ACS Appl. Mater. Interfaces* 12, 25428 (2020).

8:25 AM NM08.11.02

Phonon Mean Free Path Spectroscopy in Semiconductor Membranes Roman Anufriev¹, Jose Ordonez-Miranda² and Masahiro Nomura¹; ¹The University of Tokyo, Japan; ²Institute Pprime, France

Distributions of the phonon mean free path (MFP) in materials and nanostructures are important for understanding and engineering their thermal properties. In the past years, the phonon MFP in bulk semiconductors has been extensively studied both theoretically and experimentally. However, modern MEMS devices often rely on thin membranes rather than bulk material, yet the MFP spectra in thin membranes have not been measured experimentally.

In this work, we demonstrate an experimental method to probe the phonon MFP spectra in suspended semiconductor membranes. The method consists in measuring the thermal conductivity of membranes with arrays of slits and extracting the accumulated thermal conductivity as a function of the MFP through a fully analytical approach based on the semi-analytical procedure proposed by Hao et al. [1]. In silicon, we find that the phonon MFP in 145-nm-thick membranes is much shorter than that in bulk due to the scattering at the membrane boundaries [2]. At room temperature, the phonon MFP spans from 10 nm up to only 400 nm. Yet, at 4 K, the MFP becomes longer, and most phonons can travel ballistically for more than 100 nm. These results thus shed light on the long-lasting question of the range of ballistic and coherent phonon transport at different temperatures in nanostructures based on semiconductor membranes.

References:

- [1] Hao et al, *Materials Today Physics* 10, 10012 (2019)
- [2] Anufriev et al, *Physical Review B*, 101, 115301 (2020)

8:40 AM NM08.11.03

Artefacts in Scanning Thermal Microscopy—Nanometre-Scale Roughness and Oxide Films Down to Native Thickness Eloise Guen¹, Pierre-Olivier Chapuis¹, NJ Kaur², Petr Klapetek², Ravish Rajkumar³, Gordon Mills³, Philipp S. Dobson⁴, Jonathan M. Weaver⁴ and Severine Gomes¹; ¹CNRS-CETHIL, France; ²CMI, Czechia; ³Kelvin NanoTechnology, United Kingdom; ⁴University of Glasgow, United Kingdom

Scanning Thermal Microscopy (S_TH_M) allows the thermal characterization of materials with a sub-micrometric spatial resolution [1]. While obtaining qualitative trends, e.g. by means of images, is straightforward, determining reliable quantitative thermal data from the experiments is challenging because the probe-sample heat exchange depends strongly on parameters such as the size, geometry and surface states of probe and sample. In this work, we study first the impact of sample roughness on the thermal conductance at the probe/sample contact and then the impact of thin films of oxide on the surface.

Rough samples consisting of several sets of silicon surfaces with out-of-plane S_q roughness parameters of ~ 0 , 0.5, 4, 7 and 12 nm were prepared by anodic oxidation [2] and measured with three types of probe (Wollaston, palladium and doped Si probes) in vacuum conditions. Sample roughness is clearly shown to reduce the thermal conductance very significantly compared to a flat Si sample, up to 40-95% depending on the probe. S_TH_M sensitivity is low for highly conductive materials, so erroneous thermal conductivity can be deduced from a calibration curve performed for flat samples [3].

In a second step, we analyze the impact of thin oxide films on the determined thermal conductivity. It was shown that heat conduction in the cross-plane direction is strongly affected by native oxide in nanometre-thin suspended silicon membranes [4]. Here we extend the study to supported films of thickness varying between few nanometres and one micrometre. We find a logarithmic dependence on thickness for the apparent thermal conductivity and show that arbitrarily-small thicknesses may be detected. Nanoprobes are found to be less sensitive to the oxide thickness, as they probe only at the very surface [5]. We discuss the impact of thermal boundary resistances and ballistic dissipation in the samples.

All these results allow to envisage precise calibration of nanometre-scale thermal studies.

[1] S. Gomes, A. Assy, P.O. Chapuis, *Physical status solidi (a)* 3, 447 52015)

[2] J. Zemek, K. Olejnik, P. Klapetek, *Surface Science*, 602, 7, 1440-1446 (2008)

[3] E. Guen, P.O. Chapuis, N.J. Kaur, P. Klapetek, S. Gomes, submitted (2020)

[4] A.M. Massoud, J.-M. Bluet, V. Lacatena, M. Haras, J.-F. Robillard, P.-O. Chapuis, *Applied Physics Letters* 111, 063106 (2017)

[5] E. Guen, P.O. Chapuis, R. Rajkumar, P. S. Dobson, G. Mills, J. M. R. Weaver, S. Gomes, submitted (2020)

We acknowledge support from EU project QuantiHeat.

8:55 AM NM08.11.04

Heat Trapping and Thermal Conductivity Reduction Due to Specular Scattering in Nanoporous Si Laura de Sousa Oliveira¹, Seyed Aria Hosseini², Alex Greaney² and Neophytos Neophytou³; ¹University of Wyoming, United States; ²University of California, Riverside, United States; ³University of Warwick, United Kingdom

Nanostructuring has been successfully used to improve thermal transport performance across a wide range of materials, whether a high or low thermal conductivity is desired. This includes applications ranging from latent heat storage to thermoelectrics and phononic crystals. Nanoscale porosity has been shown to substantially decrease the thermal conductivity of semiconducting materials — thereby improving their thermoelectric efficiency — and, in some cases, even enhance transport. In this work [1], we identify an unusual anticorrelated specular phonon scattering effect which yields an additional $\sim 80\%$ decrease (at maximum efficiency) in the thermal conductivity of specific nanoporous geometries and which lends itself to a high degree of control by manipulating pore size and distribution.

Large-scale equilibrium molecular dynamics (MD) simulations show the presence of negatively correlated (or anticorrelated) heat flux for specific nanoporous geometries. Wave-packet MD simulations show how the heat becomes trapped between large pores with narrow necks due to specular scattering. We further reproduce the behavior observed in the MD simulations and demonstrate how specular scattering can give rise to negatively correlated heat flux using a heuristic ray-tracing analytical model. While specular scattering does not necessarily indicate the presence of coherence effects it is a necessary requirement for coherent interference, and our simulations support the notion that coherence effects could in principle be present at room temperature. We show with MD how the pore size/neck ratio and pore periodicity can be manipulated to control the strength

and duration of the correlated reflections and thus the reduction in thermal conductivity. In addition to thermoelectrics, we believe this work could have a broader application in phononics.

[1] de Sousa Oliveira, L., Hosseini, S. A., Greaney, A., & Neophytou, N. Heat current anticorrelation effects leading to thermal conductivity reduction in nanoporous Si. Phys. Rev. B. Accepted October 2020.

9:10 AM NM08.11.05

Thermal Rectification in Asymmetric Core/Shell Nanowires Paul Desmarchelier^{1,2}, Konstantinos Termentzidis¹ and Anne Tanguy^{2,3}; ¹CETHIL-INSA de Lyon, France; ²LaMCoS, France; ³ONERA, France

Thermal rectification is one of the next steps for a better thermal management. In this study, this effect has been assessed, in an original nanostructuring, thanks to non equilibrium molecular dynamics and wave packets propagation simulations. The direction dependent thermal conductivity results from the use of asymmetric crystalline-core/amorphous-conical-shell nanowires that induces variable axial and radial phonon propagation/confinement. This effect is linked to the combination of a crystalline/amorphous interfaces parallel to the heat flux, and with the variable amount of amorphous coating due to the conical shell of the nanowire. Rectification is analyzed terms of mean free path of phonons, axial and radial energy transfer, energy diffusivity, and vibrational density of states restricted to different constitutive elements of the nanowire.

9:25 AM NM08.11.06

Interplay Between Thermal Boundary Resistance and Ballistic Transport in In-Plane Phonon Heat Conduction Ali Alkurdi and Pierre-Olivier Chapuis; CNRS-CETHIL, France

When the characteristic size becomes comparable to the mean free path of phonons, the quasi-ballistic heat conduction regime arises while interactions with boundaries become significant. Both thermal boundary resistance and ballistic transport flatten the temperature profile and induce temperature jumps in comparison to macroscopic heat conduction: it is therefore difficult to disentangle the two effects by simply observing a temperature profile. We solve the phonon Boltzmann Transport Equation using the Discrete Ordinate Method, which accounts for the directional and non-local aspects of the energy flux, in order to analyze independently the effects and observe their interplay in a system of two contacted thin films. In particular, we find that the effective thermal conductivity for in-plane heat conduction is a function on the nondimensional figure Kn_T/τ , where Kn_T is the mean Knudsen number (ratio of average mean free path to sum of the thicknesses of the two films) and τ the mean transmissivity at their interface. The impact of the specularity of the film boundaries and interface is also evidenced, especially on the angular distribution of phonons. These results shed light on the relation between local energy non-equilibrium and transport properties.

The support of project EU project EFINEED is acknowledged. We thank E. Nefzaoui (ESIEE), D. Lemmonier (Pprime), and C. Abs Da Cruz.

9:40 AM NM08.11.07

Coherent Phonon Transport in Ultra-Low Thermal Conductivity Two-Dimensional Ruddlesden-Popper Phase Perovskites Alexander D. Christodoulides¹, Peijun Guo², Lingyun Dai¹, Justin M. Hoffman³, Xiaotong Li³, Xiaobing Zuo⁴, Daniel Rosenmann⁴, Alexandra Brumberg³, Mercouri G. Kanatzidis³, Richard Schaller⁴ and Jonathan Malen¹; ¹Carnegie Mellon University, United States; ²Yale University, United States; ³Northwestern University, United States; ⁴Argonne National Laboratory, United States

An emerging class of methylammonium lead iodide (MAPbI₃) based Ruddlesden-Popper (RP) phase perovskites, BA₂MA_{n-1}Pb_nI_{3n+1} ($n = 1 - 7$), exhibit enhanced stability to environmental conditions relative to MAPbI₃, yet still degrade at elevated temperatures. We use Frequency-Domain Thermoreflectance (FDTR) to experimentally determine the thermal conductivities of these layered RP phases for $n = 1 - 4$ thin films and $n = 3 - 6$ single crystals. We find that the initially decreasing trend of thermal conductivity in similarly oriented perovskites with increasing n results from the transport properties of coherent phonons, emergent from the

superstructure, that do not scatter at the interfaces of organic butylammonium (BA) chains and perovskite octahedra. With the exception of $n = 1$, the perovskites' thermal conductivities are lower than the range of 0.34 – 0.50 W/m/K reported for single crystal MAPbI₃. Reduced-order lattice dynamics modeling suggests that reduced group velocity of coherent phonons in $n = 3 - 6$, a consequence of band flattening in the phonon dispersion, is primarily responsible for their ultralow thermal conductivities. Similar effects on thermal conductivity have been experimentally demonstrated in deposited superlattices, but never in naturally defined materials like RP phases. GIWAXS measurements reveal that higher n RP phase thin films are less orientationally controlled, and therefore possess apparently elevated thermal conductivities relative to single crystals of the same n .

9:55 AM NM08.11.08

Late News: Modeling the Quasiballistic Phonon Thermal Resistance During Electron Beam Heating of Thin Films Geoffrey Wehmeyer; Rice University, United States

Electron beams with sub-10 nm diameters can be used as nanoscale heaters or thermometers, enabling new techniques to probe heat transfer in nanostructures. However, since the electron beam diameter is often smaller than the energy carrier mean free path, using Fourier's law will underpredict the (quasi-)temperature rise due to electron-beam induced heating. Here, we solve the Boltzmann transport equation (BTE) under the relaxation time approximation to quantify electron-beam induced heating in thin dielectric samples. In both thin and thick samples, the full BTE solution is in agreement with a simple "resistors in series model" that sums the ballistic resistance and the typical Fourier conduction resistance (considering the thin-film classical size effect). For nanoscale thermometry applications, the temperature rise under typical imaging conditions is predicted to remain negligibly small (<1 K), even when considering the dominant ballistic thermal resistance. Therefore, this BTE modeling indicates that nanoscale thermometry methods are not expected to display notable electron beam heating artifacts, even though the ballistic resistance is the dominant contributor to the total thermal resistance in experiments using nanoscale heat sources.

Ref: Wehmeyer, J. of Appl. Phys. 126, 124306 (2019).

*Support from the Welch Foundation (Grant No. C-2023).

SESSION NM08.12: Thermal Conductivity

Session Chairs: Martin Maldovan and Konstantinos Termentzidis

Tuesday Morning, April 20, 2021

NM08

11:45 AM *NM08.12.01

Thermal Transport and Fullerene Dynamics in Superatomic Crystals Alan McGaughey¹, Qi Liang^{1,2}, Wee Liat Ong^{1,3,4}, Matthew Bartnof¹, Ya-Ling He², Xavier Roy⁴ and Jonathan Malen¹; ¹Carnegie Mellon University, United States; ²Xi'an Jiaotong University, China; ³Zhejiang University, China; ⁴Columbia University, United States

Superatoms are atomically-precise and chemically-stable clusters that can emulate atoms, but at the nanometer scale. Ordered arrangements of superatoms are called superatomic crystals (SACs), which have potential use as electronic, thermoelectric, and phononic materials. In this talk, I will describe experiments and molecular dynamics (MD) simulations performed on SACs built from C₆₀ fullerene, Co₆Se₈(PET₃)₆, and Co₆Te₈(PET₃)₆ superatoms to characterize their thermal transport properties.

Thermal conductivity measurements on the [C₆₀] and [Co₆Se₈(PET₃)₆][C₆₀]₂ SACs show a decreasing thermal conductivity with increasing temperature, as it typical for a crystal. The thermal conductivity of the

[Co₆Te₈(PEt₃)₆][C₆₀]₂ SAC, on the other hand, is lower and temperature-independent, as is typical for an amorphous solid. X-ray diffraction measurements suggest that the temperature dependencies result from the C₆₀s being either locked-in-place (crystalline behavior) or freely-rotating (amorphous behavior).

The MD-predicted thermal conductivities agree with the experimental trends and offer additional insight into the underlying mechanisms. The C₆₀ rotational dynamics and orientation are quantified using the root mean square displacements of the carbon atoms and the relative orientations of the C₆₀s. At low temperatures, the C₆₀s exhibit small rotations around equilibrium positions (i.e., librations). When the librating C₆₀s are orientationally-ordered, as in the [C₆₀] and [Co₆Se₈(PEt₃)₆][C₆₀]₂ SACs, thermal conductivity decreases with increasing temperature. When the librating C₆₀s are orientationally-disordered, however, as in the [Co₆Te₈(PEt₃)₆][C₆₀]₂ SAC, thermal conductivity is temperature independent. At higher temperatures, where the C₆₀s in all three SACs freely-rotate and are thus dynamically disordered, thermal conductivity is temperature independent. The abrupt changes driven by the C₆₀ dynamics suggest that fullerene-based SACs can be designed to be thermal conductivity switches based on a variety of external stimuli.

12:10 PM NM08.12.02

Impact of Dimensional Crossover on Phonon Transport in van der Waals Materials—A Case Study of Graphite and Graphene Patrick Strongman and Jesse Maassen; Dalhousie University, Canada

Low-dimensional materials are the focus of intense research due to their unusual and tailorable properties, including their thermal transport characteristics. Examples of distinctive features include flexural acoustic phonons with quadratic dispersions and, in the case of graphene, selection rules that prohibit certain 3-phonon scattering processes. Often the bulk counterparts to these 2D materials are layered van der Waals materials, with the only difference between bulk and monolayer originating from weak inter-layer coupling. Thus, 2D materials can be expected to retain much of the bulk character, and vice versa. In this talk, I will present our work investigating how phonon transport evolves in van der Waals materials when going from 3D to 2D, using graphite/graphene as a case study. Focus is placed on identifying the features impacting thermal conductivity that may be shared with other layered materials. Our calculations are carried out using density functional theory in combination with a self-consistent solution of the phonon Boltzmann transport equation.

Unlike previous studies that compare the thermal properties of mono- and few-layer to bulk, in this work the transition from 3D to 2D is investigated by gradually increasing the inter-layer distance in graphite to form graphene. This approach provides a different perspective on how the phonon and scattering characteristics continuously evolve from bulk to monolayer. We find that changes in the phonon dispersion play a significant role in the lower thermal conductivity of graphite, versus graphene. Specifically, as the graphene sheets are brought closer together, the acoustic flexural phonons form low-energy optical phonons with lower velocities, density-of-states, and phonon occupation, which reduce thermal conductivity. Interestingly, our findings on the 3-phonon scattering properties indicate that the selection rules are mostly upheld as the atomic layers are brought together to form graphite. While the selection rules only strictly apply to graphene, in practice similar scattering behavior is displayed due to the weak inter-layer coupling. Lastly, we attempt to identify key features in the 3D-to-2D transition, that impact thermal conductivity, which may be shared with a broader class of van der Waals materials.

12:25 PM NM08.12.03

Evolution of Microstructure and Thermal Conductivity of Multifunctional Environmental Barrier Coating Systems David Olson, Jeroen Deijkers, Kathleen Kate-Quiambao, John Gaskins, Bradley Richards, Elizabeth Opila, Patrick Hopkins and Haydn Wadley; University of Virginia, United States

Environmental barrier coating (EBC) systems are applied to the surface of silicon-based composites exposed to high temperature combustion gas flow paths in gas turbine engines. They reduce the rate of composite oxidation, its volatilization by reactions with water vapor, and the temperature of the composite as their thermal conductivity decreases. Current EBC systems consist of a silicon bond coat covered by an yttrium disilicate

($\text{Yb}_2\text{O}_3 \bullet 2\text{SiO}_2$: YbDS) permeation resistant and low silica activity barrier. When applied by atmospheric-plasma spray deposition, this outer layer contains 10–15% of a secondary ytterbium monosilicate ($\text{Yb}_2\text{O}_3 \bullet \text{SiO}_2$: YbMS) phase. YbDS has a coefficient of thermal expansion (CTE) of $4\text{--}5 \times 10^{-6} \text{ }^\circ\text{C}^{-1}$, similar to those of the silicon and the silicon-based composite, but a relatively high thermal conductivity of $5\text{--}7 \text{ W m}^{-1} \text{ K}^{-1}$. YbMS has a higher steam volatility resistance than YbDS, and it has a much lower thermal conductivity ($\sim 2\text{--}2.5 \text{ W m}^{-1} \text{ K}^{-1}$) at ambient temperature compared to YbDS, but its higher, highly anisotropic CTE ($3\text{--}11 \times 10^{-6} \text{ }^\circ\text{C}^{-1}$) results in channel cracking which reduces environmental protection. Here, we use a combination of scanning electron beam and laser-based thermoreflectance methods to spatially map the distribution of the silicate phases and thermal conductivity at ambient temperature in a Si-ytterbium disilicate EBC system exposed to thermal cycling in water vapor. We show that during thermal cycling, diffusion of silica from the thermally grown oxide on the Si bond coat surface to nearby YbMS regions transforms this phase to YbDS, thereby reducing the risk of thermomechanical coating failure but decreasing its effective thermal resistance. We also show that as silica is volatilized at the water vapor–ytterbium silicate interface, YbDS is transformed to YbMS, restoring some of the thermal protection of the coating system lost by its reduction in thickness and the YbMS to YbDS transformation near the bond coat.

12:40 PM NM08.12.04

Predicting Phonon Properties and Thermal Conductivity of Crystals with Rigid Molecules Using Rotational Lattice Dynamics Hyun-Young Kim and Alan McGaughey; Carnegie Mellon University, United States

Phonons are the primary heat carriers in semiconducting and insulating crystals. By calculating their harmonic (i.e., frequency) and anharmonic (i.e., lifetime) properties, it is possible to predict thermal conductivity. These calculations can be performed using a technique called lattice dynamics, which uses the force constants between individual atoms as inputs to solve the Boltzmann transport equation. Some crystals, however, include molecules with strong internal bonds. For such materials, the atomic degrees of freedom can be restricted in order to model the system as rigid molecules rather than as individual atoms. This choice allows for an examination of the effect of small rotations about equilibrium (i.e., librations) on the thermal properties, as well as the impact of removing the intra-molecular vibrations. For example, this approach was used in molecular dynamics simulations of the C60 molecular crystal to explain how its thermal conductivity varies with respect to temperature.

A formulation exists to perform harmonic lattice dynamics calculations in the presence of rigid molecules. Here, we extend this rigid molecule formulation to anharmonic lattice dynamics calculations, allowing us to examine the impact on full thermal transport properties. The ability to perform these calculations allows us to examine the phonon scattering caused by librations, as well as the effect of removing intra-molecular vibrations on the associated scattering phase space.

We used an in-house lattice dynamics code for our calculations and modeled a modified toy Lennard-Jones argon system. Bonds were placed between the basis atoms to form diatomic molecules. Green Kubo calculations were performed in molecular dynamics simulations to provide a thermal conductivity benchmark for the lattice dynamics results. The predicted thermal conductivities are in reasonable agreement, with values of 5.50 W/m-K and 4.33 W/m-K from lattice dynamics along the two non-isotropic directions at 5 K, compared against $5.45 \pm 0.52 \text{ W/m-K}$ and $4.55 \pm 0.68 \text{ W/m-K}$ from molecular dynamics. The phonon properties and scattering rates were then examined in order to identify the cause behind the decrease in thermal conductivity compared to a full degree of freedom system. With the success of the modified lattice dynamics code in calculating the thermal conductivity of this toy system, it can now be extended to real materials such as sodium superoxide and organic-inorganic perovskites.

12:55 PM NM08.12.05

Thermal Conductivity of Phonon-Engineered Hygroscopic Nanocellulose-Based Foams Varvara Apostolopoulou Kalkavoura, Pierre Munier and Lennart Bergström; Stockholm University, Sweden

Cellulose and cellulose nanomaterials (CNMs) can be used to produce light-weight foams and aerogels with

heat transport properties that can be phonon-engineered for thermal management and thermal insulation applications^[1].

Cellulose possesses an intrinsic anisotropy of the thermal conductivity, which has been utilized to produce foams made with aligned CNM particles that exhibit highly anisotropic thermal conductivities. Anisotropic foams based on cellulose nanofibrils (CNF) made by ice-templating exhibit very low radial – perpendicular to the fibrils – thermal conductivity^[2,3], which suggests that CNM-based foams could reduce both the carbon footprint and the energy consumption in buildings.

Cellulose is a hygroscopic material, and it is thus essential to understand how the heat transfer mechanisms are influenced by water uptake and the relative humidity in air. We have investigated how the thermal conductivity of anisotropic CNM-based foams depends on moisture uptake and temperature, together with the diameter and degree of alignment of the fibrils, and the density and nanoporosity of the foams. Combining molecular simulations, thermal conductivity measurements, and moisture uptake experiments we have identified the importance of swelling in reducing the radial thermal conductivity. Tuning the surface properties of cellulose nanomaterials or increasing their degree of crystallinity and temperature has a significant effect on the moisture uptake which plays important role in governing the heat transfer within CNM foams at humid conditions. Furthermore, here we show potential routes to achieve very low thermal conductivity by tuning the gaseous and solid conduction contributions. Apart from the degree of the alignment and the sizes of pores, the CNM entanglement and the plethora of solid/solid and solid/air interfaces are crucial parameters to consider. To this end, enhancing the diffuse phonon scattering by tuning the length and number of interfaces seems to be the most efficient way to reduce the thermal conductivity below the superinsulating level in highly porous (>95%) CNM foams.

References

- [1] V. Apostolopoulou-Kalkavoura, P. Munier, L. Bergström, *Adv. Mater.* **2020**, 2001839, 1.
- [2] B. Wicklein, A. Kocjan, G. Salazar-Alvarez, F. Carosio, G. Camino, M. Antonietti, L. Bergström, *Nat. Nanotechnol.* **2015**, 10, 277.
- [3] P. Munier, V. Apostolopoulou-Kalkavoura, M. Persson, L. Bergström, *Cellulose* **2019**, 1.

1:10 PM NM08.12.06

Dual Crystal- and Glass-Like Heat Transport in Silicon Thin-Films with Nanscale Surface Substructures Sanghamitra Neogi; University of Colorado Boulder, United States

Resonance hybridization (RH) can be described as the coupling between wavenumber-independent vibrons in a substructure and wavenumber-dependent modes (phonons) of the host medium. This mechanism showed remarkable consequences for thermoelectric applications such as the ~40-fold reduction of thermal conductivity (TC) of silicon (Si) membranes due to resonances induced by native oxide at membrane surfaces [1]. In particular, nanopillar resonators on silicon thin-films have been illustrated to exhibit unique subwavelength phonon properties at the nanoscale, resulting in strong TC reduction. Our recent study reported the first remarkable observation that the RH mechanism can enforce directional mode propagation, and therefore anisotropic TC at room temperature, in otherwise isotropic single-crystal thin films of materials with isotropic bond symmetries (e.g. cubic or hexagonal). In Si membranes with surface nanofins, TC is ~100% greater in the direction parallel to the fins than in the perpendicular direction [2]. Anisotropic in-plane TC has been observed or predicted in 2D and 3D materials due to direction-dependent bonding environments and anisotropic pore spacing, and in two to four monolayer thick silicene due to surface reconstruction, the effect decreasing with thickness. However, anisotropic in-plane TC in the Si membranes beneath nanofins is remarkable as it is the first time such an effect has been observed in isotropic semiconductors at room temperature. This method of inducing anisotropy is particularly valuable, since modern fabrication techniques allow for more precise control over the addition of surface resonators than embedding Bragg scattering mechanisms within the material. This study further suggested that hybridized modes within the base material of such structures, deemed nanophononic metamaterials (NPMs), may not retain their full crystalline character. In fact, RH potentially induces "glass-like" phonon transport, rendering the host membrane or film a disordered "phonon-glass" for low frequency modes. Heat conduction mechanisms in crystals and glasses are fundamentally different. The

structural periodicity of crystals allows propagating phonons (propagons) to become excited and carry heat. In glasses, a lack of periodicity breaks the quasi-particle nature of heat carriers so that heat is transported mainly by the coupling of vibrational modes (diffusons) as described by the Allen and Feldman (AF) model. In NPMs, some hybridized modes retain a propagating character while others become localized with ~ 0 group velocity and display glassy heat transport behavior. The presence of both types of modes within 'simple' crystalline materials has not been adequately probed, and therefore further research is essential to describe the phenomenon. In this work, we use a combination of classical molecular dynamics, harmonic and anharmonic lattice dynamics and the newly proposed lattice dynamics based quasi-harmonic Green-Kubo approach to provide a complete microscopic description of the transport processes of the hybridized modes. We aim to establish the extent to which established phonon physics models remain valid for these systems.

1. S. Neogi, et al., *ACS nano*, vol. 9, no. 4, pp. 3820–3828, (2015).

2. S. Neogi, S. and D. Donadio, *Physical Review Applied*, 14(2), p.024004 (2020).

1:25 PM NM08.12.07

Nanoscale Thermal Transport in PVDF-Al Nanocomposites Ramya Mohan¹, Dylan Kline^{2,1}, Victor Ortiz¹, Michael Zachariah^{2,1} and Richard B. Wilson^{1,1}; ¹University of California, Riverside, United States; ²University of Maryland, United States

Fluorine-rich polymers incorporated with aluminum particles are of interest to the energetics community due to their enhanced flame propagation characteristics. Recent investigations have shown that PVDF-Al demonstrates better ignition and sustained combustion when compared to similar fluoropolymer-metal composites such as Viton-Al and THV-Al [1]. Enhanced thermal conduction in PVDF-Al nanocomposites due to the Al nanoparticles is speculated to contribute to their superior energetic properties. My talk will focus on nanoscale thermal transport in PVDF-Al films and their influence on flame propagation. Using time-domain thermo-reflectance (TDTR), I present high resolution 2-dimensional thermal conductivity maps of thin PVDF-Al films. The PVDF-Al composite samples have varying volume fractions of Al. The TDTR maps provide spatially correlated thermal conductivity and heat capacity measurements across the polymer, metal particles, and heterogeneous metal-polymer interfaces. I also report the results of TDTR measurements as a function of heating frequency. Heating frequency dependent measurements allow us to study how homogeneous the transport properties of the composites are as a function of thermal penetration depth. My investigation provides important insights into the nanoscale thermal transport in Al/PVDF nanocomposite systems, which could be used to predict their flame propagation and combustion characteristics.

Ref:

[1] Wang, Haiyang, et al. "Comparison study of the ignition and combustion characteristics of directly-written Al/PVDF, Al/Viton and Al/THV composites." *Combustion and Flame* 201 (2019): 181-186.

SESSION NM08.13: Density Functional Theory / Phase Transformations
Session Chairs: Martin Maldovan, Konstantinos Termentzidis and Richard Wilson
Tuesday Afternoon, April 20, 2021
NM08

2:15 PM *NM08.13.01

High Temperature Formalism of Phonon Transport Keivan Esfarjani; University of Virginia, United States

In this talk we report on recent progress in modeling phonon transport in bulk and across interfaces at high temperatures beyond the harmonic approximation. In bulk crystalline materials the self-consistent phonon theory has been extended within a variational formalism to include thermal strain and phase transitions. The anharmonic hamiltonian parameters of the high-symmetry phase are first extracted from a set of total-energy

and force calculations (from first-principles DFT calculations) in a supercell. Then a variational free energy is constructed which when minimized, produces the equilibrium structure and its lattice dynamical properties at any temperature, beyond the quasi harmonic approximation.

As for the interfacial thermal conductance, within the Landauer formalism, an expression is derived for the non-equilibrium thermal current of the anharmonic system based on the Green's function formalism. This non-perturbative expression is made to satisfy the detailed balance and current conservation constraints. Examples illustrating both methodologies will be shown.

2:40 PM NM08.13.02

Effect of Four-Phonon Scattering on the Phonon Lineshapes in Weakly-Bonded Solids from First Principles Navaneetha Krishnan Ravichandran; Indian Institute of Science, India

Recently, it has been shown computationally and experimentally that the inclusion of higher-order scattering among four phonons is crucial to accurately represent the phonon thermal conductivities of several strongly-bonded materials like boron arsenide and indium phosphide [1-3], as well as weakly-bonded solids like sodium chloride (NaCl) [4]. Here we show, from rigorous first-principles calculations, that four phonon scattering also critically affects the phonon lineshapes of NaCl and other weakly-bonded solids typically observed in inelastic neutron/x-ray scattering and Raman scattering experiments. These calculations are performed by building on the unified first-principles framework [4], which already includes the effects of the lowest-order three-phonon and higher-order four-phonon scattering processes on the thermal conductivity of materials, a many-body self-consistent anharmonic phonon renormalization step to address the possible ill-defined nature of certain phonon quasiparticles in weakly-bonded solids, and the determination of the stable lattice constants at finite temperatures, by explicitly evaluating and minimizing the fourth-order accurate free energy of the crystal. By performing these calculations over a broad range of temperatures, we show that the four-phonon scattering processes significantly broaden the phonon lineshapes compared to their three-phonon counterparts - particularly at high temperatures, and their inclusion into the calculations are pivotal to explain the experimental data.

This work has been supported by a start-up fund from the Indian Institute of Science, Bangalore, India.

[1] Navaneetha K. Ravichandran and D. A. Broido, Phys. Rev. X 10, 021063 (2020).

[2] Navaneetha K. Ravichandran and D. A. Broido, Nature Comm. 10, 827 (2019).

[3] Fei Tian, Bai Song, Xi Chen, Navaneetha K. Ravichandran et al., Science 361, 6402 (2018).

[4] Navaneetha K. Ravichandran and D. A. Broido, Phys. Rev. B 98 (8), 085205 (2018).

2:55 PM NM08.13.03

Uncertainty Quantification in First-Principles Predictions of Phonon Properties and Lattice Thermal Conductivity Holden Parks, Hyun Kim, Venkatasubramanian Viswanathan and Alan McGaughey; Carnegie Mellon University, United States

Density functional theory (DFT) is an ab-initio method that has been successfully used to predict the phonon dispersion and thermal conductivity of a variety of insulating and semiconducting materials. DFT-based calculations are attractive because, unlike calculations based on empirical potentials, they are free from fitting parameters. A DFT calculation is made computationally tractable by describing the complicated exchange-correlation (XC) electron interactions with an effective potential, called an XC functional. There is no a priori method of choosing an XC functional for a given material, so that choosing any single XC functional introduces uncertainty in any quantity derived from that calculation.

We present a framework for quantifying the uncertainty that results from the choice of XC functional in predictions of phonon properties and thermal conductivity that use DFT to calculate the atomic force constants. The framework uses the energy ensemble capabilities of the BEEF-vdW XC functional to predict ensembles of interatomic force constants, which are then used as inputs to lattice dynamics calculations and a solution of the

Boltzmann transport equation. We apply the framework to isotopically-pure silicon and find that the ensembles bound property predictions (e.g., phonon dispersion, specific heat, thermal conductivity) from other XC functionals and experiments. We distinguish between properties in silicon that are correlated with the predicted thermal conductivity [e.g., the transverse acoustic branch sound speed (Pearson correlation coefficient, R_2 , of 0.89) and average Gruneisen parameter ($R_2 = 0.85$)] and those that are not [e.g., longitudinal acoustic branch soundspeed ($R_2 = 0.23$) and specific heat ($R_2 = 0.00$)]. We find that differences in ensemble predictions of thermal conductivity are correlated with the behavior of transverse acoustic phonons with mean free paths between 100 and 300 nm. This framework systematically accounts for XC uncertainty in phonon calculations and should be used whenever it is suspected that the choice of XC functional is influencing physical interpretations.

3:10 PM *NM08.13.04

Monte Carlo and DFT Calculations Coupling; Application to Heat Transfer in Nanostructures David Lacroix and Laurent Chaput; Université de Lorraine, France

Models and tools devoted to the theoretical modeling of heat transport in new materials and nanostructures are of very different natures. Strong interest for DFT based methods has raised to compute thermal properties of bulk material from scratch, just knowing the atom organization in a supercell. In this field, tools such as those provided by the Phonopy [1] environment developed by A. Togo have paved the way to the discovery of new compounds with optimal thermal properties. The main strength of such an approach is its intrinsic reliability that usually matches very well with the available experimental data [2]. Yet, such an approach also has drawbacks, the most prominent is related to computing resources needed to carry out calculations. In addition, this approach basically addresses bulk materials. Dealing directly with nanostructures is currently impossible with such methods, as they remain too large for the actual computing facilities and probably even for the next generation ones. Nevertheless, we can circumvent this limitation by the coupling of ab-initio outputs with mesoscale modelling tools such as Monte Carlo solution of the Boltzmann transport equation (BTE) for phonons. For the latter technique, MC simulation of BTE is often limited by the knowledge of phonon dispersion properties and lifetimes of any kind of material.

However, what is a weakness for one method is a force for the other. Thus, coupling both techniques make sense and should allow to overcome intrinsic limitations of DFT and MC approaches. Within the group, but also in collaboration with the “Centre de Nanosciences et Nanotechnologies” (Université Paris-Saclay), we work on this coupling. As a first challenge, we investigate how to combine full band modelling approach in K-space, given by DFT calculations. Furthermore, for MC model the scattering term of the BTE was treated in the frame of the relaxation time approximation, considering the Matthiessen rule and statistics on phonon populations to define relevant lifetimes. Considering DFT coupling, a direct access to the mode lifetime with respect to the K-grid discretization is now possible.

On this basis, we have modified our existing MC tool for phonon transport in order to take into account full band phonon properties and lifetimes given by the DFT calculations. Among the main improvements of this new ab-initio/MC model, there is the resolution of BTE along characteristic lines. With this method there is a rigorous balance between energy and momentum as we follow each phonon bundle sampled on the K-grid. This new technique is much more rigorous as this is no longer necessary to compute scattering probability of phonon to restore equilibrium. Results concerning those calculations have been recently published in Applied Physics Letters [3], demonstrating the ability of the method to handle phonon lifetimes extracted from DFT calculations. In addition, for the first time, we extend the methodology to the coupling of phonon-phonon and electron-phonon interactions in doped Si, Ge and C compounds using DFT simulations that provide the relevant lifetimes. Application to such coupling are numerous, especially for materials where electron transport can hindered/increase heat transfer.

1 - <https://atztogo.github.io/phonopy/>

2 - A. Seko et al., *Prediction of Low-Thermal-Conductivity Compounds with First-Principles Anharmonic Lattice-Dynamics Calculations and Bayesian Optimization*, Phys. Rev. Lett. 115, 205901 (2015)

3 - L. Chaput et al., *Ab initio based calculation of the thermal conductivity at the micron scale*, Applied Physics Letters, vol. 112, (3), 033104 (2018)

3:35 PM *NM08.13.05

Phonons and Thermal Transport Near Lattice Instabilities—From Soft-Mode Transitions to Phonon Breakdown in Superionics Olivier Delaire; Duke University, United States

Using detailed measurements of inelastic scattering of neutrons and x-rays, complemented with first-principles simulations of atomic dynamics, we investigate strongly anharmonic effects on phonons near or across phase transitions, and their impact on thermal transport. This presentation will focus on transitions ranging from soft-mode condensation to sublattice melting in the case of superionic compounds. In particular, we will highlight systems undergoing ferroelectric transitions or related Jahn-Teller distortions (e.g. SnS and SnSe across their high-temperature structural transition [1]), which strongly renormalize group velocities and scattering phase-space, as well as “phonon-liquid electron-crystal” systems, in which selective phonon modes collapse to relaxational dynamics, as in Cu or Ag-based superionics [2,3].

[1] T. Lanigan-Atkins*, S. Yang*, J. L. Niedziela, D. Bansal, A. F. May, A. A. Puretzky, J.Y.Y. Lin, D. Pajerowski, T. Hong, S. Chi, G. Ehlers, and O. Delaire, Nature Communications 11 (1), 1-9 (2020).

[2] J. Ding, J. L. Niedziela, D. Bansal, J. Wang, X. He, A. F. May, G. Ehlers, D. L. Abernathy, A. Said, A. Alatas, Y. Ren, G. Arya, and O. Delaire, PNAS 117 (8) 3930-3937 (2020).

[3] J. L. Niedziela, D. Bansal, A. F. May, J. Ding, T. Lanigan-Atkins, G. Ehlers, D. L. Abernathy, A. Said, and O. Delaire, Nature Physics, 15, 73–78 (2019).

4:00 PM NM08.13.06

Local Study of the Evaporation Mass Flux in a Thin Liquid Film Using Thermoreflectance Experiments and Numerical Methods Xiaoman Wang, S. Arman Ghaffarizadeh, Alan McGaughey and Jonathan Malen; Carnegie Mellon University, United States

Thin film evaporation is important in the design of heat pipes, desalination, lubrication, air conditioning, and medical devices. Existing theories suggest that with smaller film thickness, the local evaporation mass flux will increase due in part to an increased interfacial temperature that results from lower conduction resistance in the liquid. However, this mass flux will sharply decrease to zero as the film gets even thinner due to the increased interface forces that inhibit the escape of interfacial vapor molecules.

In this project, we present the first experimental effort to locally measure the evaporation mass flux in a liquid meniscus. The microscale lateral extent of the meniscus and sub-Kelvin liquid-vapor temperature differences (superheats) challenge conventional thermometry. Here, Frequency domain thermoreflectance (FDTR), a non-contact laser-based method with a lateral resolution of micrometers, is used. A non-monotonic experimental signal change is observed as a function of position in the thin film portion of the meniscus, where a high evaporation heat flux is expected. This experimental technique has been hitherto widely employed with micron-scale lateral resolution in thin solid films, but not when evaporation is present. To extract the evaporation heat transfer coefficient in the meniscus region from the obtained signal, we modify the analytical solution to the heat diffusion equation to account for the phase change. This modification provides a new paradigm for investigating heat flux discontinuity in thermal models. Furthermore, to account for the thickness variation in the meniscus we also analyze the data using a finite element simulation performed with ANSYS. The ANSYS simulations are first validated against the modified FDTR equation for uniform liquid thicknesses. The ANSYS model is also able to capture account for the variation in evaporative heat transfer coefficient that occurs within the region interrogated by the 3 μm laser spot. A machine learning framework that uses neural networks is then used to find the optimal combination of meniscus thickness and evaporative heat transfer coefficient distribution to match the ANSYS model to the experimental data.

SESSION NM08.14: Thermal Radiation
Session Chairs: Martin Maldovan and Richard Wilson
Tuesday Afternoon, April 20, 2021
NM08

5:15 PM NM08.14.02

Near-Field Thermophotovoltaic Conversion with High Electrical Power Density and Efficiency Above 14% Christophe Lucchesi¹, Dilek Cakiroglu², Jean-Philippe Perez², Thierry Taliercio², Eric Tournié², Pierre-Olivier Chapuis¹ and Rodolphe Vaillon²; ¹CNRS-CETHIL, France; ²IES Montpellier, France

A thermophotovoltaic (TPV) device converts infrared radiation from hot sources into electrical power via a specifically designed photovoltaic cell. In order to increase the generated electrical power, the cell can be coupled with an infrared emitter brought in its near field ($< 4 \mu\text{m}$ at 700 K), where the emitter-cell radiative heat exchange can be enhanced by several orders of magnitude. This enhancement is well described theoretically but near-field TPV devices have been demonstrated experimentally only recently [1-3], unfortunately with very low electrical output power densities ($< 10 \text{ W}\cdot\text{m}^{-2}$) and conversion efficiencies ($< 1 \%$).

In this work, we first characterize experimentally fully-functional InSb TPV cells [4] that operate below room temperature (77 K). Indium antimonide (InSb) is an attractive material for TPV cells since its very low energy band gap ($\sim 5 \mu\text{m}$ at 77 K) matches well the blackbody spectrum of infrared emitters. We then demonstrate strong electrical power photogeneration by placing a graphite spherical emitter in the near field of the InSb TPV cells. In order to maximize the electrical power, large temperature differences are investigated: the emitter can be heated up to temperatures higher than 1000 °C. Impacts of emitter material and cell design on the near-field radiative heat transfer and near-field TPV conversion are investigated as a function of emitter-cell distance down to a few tens of nanometers. We measure a 7-fold enhancement of the generated electrical power when bringing the emitter in the near field, leading to an electrical power as high as $7500 \text{ W}\cdot\text{m}^{-2}$, three orders of magnitude higher than previous works [1-3], and near-field conversion efficiency larger than 14 % [5].

[1] A. Fiorino et al., Nature Nanotechnology (2018). [2] T. Inoue et al., Nano Letters (2019). G. Bhatt et al., Nature Com. (2020). [4] D. Cakiroglu et al. Solar Energy Materials and Solar Cells (2019). [5] C. Lucchesi, et al., arXiv:1912.09394 (2019)

Financial support by the French National Research Agency (ANR) under grant No. ANR-16-CE05-0013 and partial funding by the French "Investment for the Future" program (EquipEx EXTRA ANR-11-EQPX-0016 and IDEXLYON ANR-16-IDEX-0005) and by the Occitanie region are acknowledged.

5:30 PM NM08.14.03

Late News: Thermal Transport Across Nanoscale Gaps and Across Single-Molecule Junctions Merabia Samy¹, Ali Alkurdi², Christophe Adessi¹, Fatemeh Tabatabaei¹, Manuel Cobian³, Konstantinos Termentzidis², Pierre-Olivier Chapuis² and Thomas Niehaus¹; ¹Universite de Lyon, CNRS, UCBL, ILM, UMR5306, France; ²Institut National des Sciences Appliquées, France; ³Ecole Centrale de Lyon, France

Heat transfer in the extreme near field has shown recently an increased interest driven by the development of scanning probe techniques allowing to measure thermal transport across a nanoscale gap and across single molecule junctions. On the one hand, recent experimental studies reported giant heat flux transfer between gold surfaces separated by nanometer distances [1]. These results showed discrepancies with the conventional theory which are attributed to phonon tunneling neglected in the standard picture. On the other hand, the thermal conductance of single molecule junctions has been recently determined experimentally [2,3] opening the door to confirm the high thermoelectric efficiency displayed by these junctions. All these experiments call for models capable of describing accurately phonon tunneling and phonon thermal transport across molecules.

In this contribution, we model heat transfer across nanometer gaps and across single-molecule junctions using a combination of molecular dynamics and ab-initio simulations. First; we demonstrate, using a combination of ab-

initio lattice dynamics [4] and molecular dynamics simulations, that phonons dominate heat transport at nanometer distances, even in the presence of molecules in the gap [5]. This conclusion is shown to hold for nanogaps separating different types of materials. The computed thermal conductance turn out to be several orders of magnitude higher than the predictions of acoustic continuous models. We show that these discrepancies originate from the contribution of intermediate phonon frequencies which are not accurately described by acoustic models. Moreover, we highlight the leading role played by phonon scattering as compared with electron tunneling and electron/phonon processes at interfaces [6].

The second issue to be discussed concerns thermal transfer across molecular junctions [7]. We consider junctions made of OPE3 derivatives, as these molecules are commonly synthesized by experimentalists and already extensively studied for electronic transport.

The phonon thermal conductance of the corresponding gold-molecule-gold junctions are computed here using a combination of molecular dynamics and ab-initio calculations. In particular, we parametrize the interaction between the gold surface and the OPE3 derivative using an ab-initio adiabatic connection scheme [8]. For Au-OPE3-Au junctions, the computed thermal conductance obtained is in good agreement with the experimental value [3]. Next, we characterize the phonon thermal conductance of cross-linked molecules junctions, as a function of their length and the nature of the cross-linker. In particular, we show that constrained cross-linked molecules display relatively low thermal conductance, which makes them promising for thermoelectric applications. These low conductance levels are interpreted based on phonon transmission calculations.

References:

- [1] K. Kloppstech et al., *Nat. Comm.* 8 (2017) 144505
- [2] Cui et al., *Nature* 572 (2019) 628
- [3] Nico Mosso et al., *Nano Letters*, 19 (2019) 7614–7622.
- [4] A. Alkurdi, S. Pailhès and S. Merabia, *Appl. Phys. Lett.* 111 (2017) 093101
- [5] A. Alkurdi, C. Adessi, F. Tabatabaei, S. Li, K. Termentzidis and S. Merabia, *Int. Jour. Heat Mass Transf.* 158 (2020) 119963
- [6] J. Lombard, F. Detcheverry and S. Merabia, *J. Phys. Cond. Mat.* 27, 015007 (2015)
- [7] F. Tabatabaei, T. Niehaus and S. Merabia, in preparation
- [8] Zou, W., Kalescky, R., Kraka, E., & Cremer, D. *The Journal of chemical physics*, 137 (2012), 084114.

Acknowledgment: This work has been financially supported by the iMUST Labex project ATTSSEM and by the EU project EFINE (Project No. 76685).

5:45 PM *NM08.14.04

Energy Transfer and Conversion in Nanoscale Gaps Pramod Sangi Reddy; University of Michigan–Ann Arbor, United States

Understanding radiative heat transfer in nanoscale gaps and devices is of considerable interest for creating novel energy conversion devices. In this talk, I will first describe ongoing efforts in our group to experimentally elucidate nanoscale radiative heat transfer. Specifically, I will present our recent experimental work where we have addressed the following questions: Can existing theories accurately describe radiative heat transfer in single nanometer sized gaps? Can radiative thermal conductances that are orders of magnitude larger than those between blackbodies be achieved? In order to address these questions we have developed a variety of instrumentation including novel nanopositioning platforms and microdevices, which will also be described. Further, I will discuss possible applications of near-field thermal radiation for energy conversion and photonic cooling. Finally, I will briefly outline how these technical advances can be leveraged for future investigations of nanoscale heat transport and near-field thermophotovoltaic energy conversion.

6:10 PM NM08.14.05

Experimental Techniques for Exploring Near-Field Thermophotovoltaic Energy Conversion at High Temperatures Rohith Mittapally¹, Linxiao Zhu², Anthony Fiorino¹, Dakotah Thompson³, Ju Won Lim¹, Pramod Sangi Reddy¹ and Edgar Meyhofer¹; ¹University of Michigan–Ann Arbor, United States; ²The

Pennsylvania State University, United States; ³University of Wisconsin–Madison, United States

Thermophotovoltaic (TPV) systems are based on solid-state energy conversion technique and involve a hot emitter to radiate photons that excite electron hole pairs in a photovoltaic (PV) cell. Recent TPV studies in the far-field demonstrated impressively high efficiencies, but at low power densities. Several theoretical proposals have shown that dramatic enhancement in power density can be achieved by reducing the gap to tens of nanometers. However, such demonstrations have been elusive due to the challenge of maintaining such nano-separations between a hot emitter (~1000 K) and a cold cell (~300 K). Here, we will describe how high resolution calorimetry and a custom-built nano-positioning platform have made possible the first demonstration of ~40-fold increase in the power output, compared to far field, when the gap between the PV cell and thermal emitter at 650 K is reduced from ~10 μm to 60 nm. Further, we will discuss our recent work aimed at achieving larger power densities and efficiencies by developing thermal emitters that can operate at high temperatures (~1300 K) that may lead to power densities exceeding 1 W/cm².

6:25 PM NM08.14.06

Late News: Near-Filed Heat Transfer in High-Tc Superconductors. Bulk and Thin Films Raul Esquivel-Sirvent, Giuseppe Pirruccio, Shunashi Castillo-López and Carlos Villarreal; Universidad Nacional Autonoma de Mexico, Mexico

We investigate the near field radiative heat transfer between two slabs made of high temperature superconductors, namely, YBCO. We find a three orders of magnitude decrease in the total heat flux when the temperature of at least one of the slabs is below the critical temperature. We interpret this suppression as a consequence of the detailed balance of the charge carrier density: the increased density of the condensed electron pairs is accompanied by the simultaneous decrease of the density of the unpaired electrons. This effectively increases the conductivity of the superconductor by suddenly suppressing the electron damping mechanisms. Consequently, we observe a reduction of the contribution of the p-polarized waves compared to the s-polarized ones to the spectral heat flux.

The difference between using free-standing films and bulk media is also discussed. Thin-films allow for more modes that modify the radiative heat transfer making it larger than the case of bulk-materials.

SESSION NM08.15: Interfaces II

Session Chairs: Yee Kan Koh and Zhiting Tian

Tuesday Afternoon, April 20, 2021

NM08

9:00 PM *NM08.15.01

Atomistic to Continuum Modeling of Two-Phase Cooling Processes Anirban Chandra¹, Assad Oberai², Zhi Liang³ and Pawel Keblinski¹; ¹Rensselaer Polytechnic Institute, United States; ²University of Southern California, United States; ³California State University, Fresno, United States

Two-phase cooling is one of the most powerful approaches for removal of large amounts of thermal energy, which is required in a number of applications ranging from high power electronics to nuclear reactor safety. The analysis of the two-phase cooling processes is typically based on continuum modeling of heat and mass transport equations. While the constitutive laws for these transport processes in the bulk are well established, the quantitative, physics-based description of the transport processes at the liquid-vapor interface is still a challenge. A typical assumption here is that the interface is in a local thermal equilibrium. While such assumption might be appropriate for modeling systems with large feature sizes, it might lead to inaccurate predictions for micro/nanoscale systems, particularly for highly driven systems.

In our presentation I will describe an approach that enables high fidelity, predictive modeling of the two-phase flow systems based a continuum modeling framework informed via physics-based and molecular dynamics simulations verified “interfacial constitutive laws”. These interfacial laws provide quantitatively the rate of phase change in terms of local thermodynamic variables, such as temperature and pressure, and allow for non-equilibrium vapor pressure and temperature discontinuity at the interface. We demonstrated the fidelity of this approach in the case of planar heat pipe geometry, even in the limit of nanoscale systems and highly transient heating processes. We will discuss avenues and challenges for the development of this approach for more complex systems and processes.

9:25 PM *NM08.15.02

Heat Transfer Across van-der-Waals Interfaces and Au/thiol Heterojunctions Through Remote Coupling of Charge Carriers and Polar Vibration Modes Yee Kan Koh; National University of Singapore, Singapore

Most previous studies of interfacial heat transport focus on transmission of vibration modes across the interfaces. It is generally believed that heat is predominantly carried by vibration modes, even for metal/dielectric interfaces in which electrons in metals could be coupled remotely to the polar vibration modes in dielectrics due to the long-range nature of Coulomb force. In this talk, we will discuss our recent attempts to experimentally measure the interfacial heat transfer due to this remote coupling. In the first work, we measured the heat transport across van-der-Waals graphene interfaces, due to remote coupling of induced charge carriers in graphene and polar phonons in oxide substrate, by a newly developed technique called voltage-modulated thermoreflectance (VMTR). We find that the thermal conductance of SiO₂/graphene/SiO₂ interfaces increases by up to $\approx 1.5 \text{ MW m}^{-2} \text{ K}^{-1}$ under electrostatic fields of $< 0.2 \text{ V nm}^{-1}$, and hence establish an upper limit for direct heat transfer from graphene to SiO₂ substrates via remote interfacial phonon (RIP) scattering. In the second work, we integrate two pump-probe techniques, the picosecond transient absorption and time-resolved Raman spectroscopy, to concurrently monitor heating and cooling of gold nanorods and bonds in the conjugated ligands, with a sub-picosecond time resolution and an atomic spatial resolution. We find that bonds in the conjugated ligands are heated almost instantaneously and reach a peak temperature within $\sim 1 \text{ ps}$ after the nanorods were heated by the laser pulse. We attribute this fast heating to direct heating of bond by the non-equilibrium electrons in gold nanorods, due to the remote coupling across the Au-thiol heterojunction. Our analysis suggests that the remote coupling could contribute substantially to heat transport across Au-thiol heterojunctions. Our work could provide a new pathway to enhance and control heat transport across interfaces and heterojunctions, through remote coupling of charge carriers and polar vibration modes.

9:50 PM NM08.15.04

Thermal Conductance of Nitride/Diamond Interfaces Samreen Khan and Richard B. Wilson; University of California, Riverside, United States

The interface conductance between two strongly bonded materials is determined by the vibrational stiffness of the constituent materials. In theory, because diamond is very vibrationally stiff, interfaces between diamond and other materials should have a high interface conductance. In practice however, the interface conductance values observed in diamond systems are small. Observed conductance values in diamond systems range from 30-60 MW/m²-K for Pb and Au on diamond to $\approx 150 \text{ MW/m}^2\text{-K}$ for Al or Pt on diamond [1]. Low thermal boundary conductance in diamond systems is an obstacle to efforts to improve thermal performance in nitride electronic devices by using diamond substrates. In this work, we report time-domain thermoreflectance (TDTR) measurements of the interface conductance between nitride metals and diamond. Nitride metals are amongst the most acoustically stiff metals and are therefore good candidates for investigating the upper limits to the conductance of metal/diamond interfaces. We find TiN/diamond has a large interface conductance of $\approx 400 \text{ MW/m}^2\text{-K}$, much larger than typical in diamond systems.

[1] Hohensee, G., Wilson, R. & Cahill, D. Thermal conductance of metal–diamond interfaces at high pressure. Nat Communications 6, 6578 (2015).

10:05 PM NM08.15.05

Modeling of Phonon Transport Across Defected and Atomically Precise Interfaces Zexi Lu, Anne Chaka, Nathaniel P. Smith and Raymond Bunker; Pacific Northwest National Laboratory, United States

Phonons play important roles in quantum information science (QIS) devices through heat dissipation and transduction of signals. To better engineer such devices, it is critical to understand the phonon transport mechanism, especially how they interact with the interfaces. While defects, including vacancies, impurities, oxidations etc., naturally appear in all materials and their interfaces, recent developments in techniques such as molecular beam epitaxy also make possible the formation of atomically perfect interfaces between metals and semiconductors. Therefore, considering interfaces from both perspectives is necessary towards a deeper understanding of phonon transport in realistic devices. However, so far the detailed phonon scattering mechanism at such interfaces is not well understood.

In this study, we applied two complementary classical molecular dynamics (MD) techniques to elucidate an understanding of interfacial phonon transport mechanisms: 1) non-equilibrium MD to identify the overall transport mechanism of the entire phonon spectrum, and 2) wave packet formalism to reveal the individual scattering behavior of a single phonon at an interface. With NEMD we identified the effects of atomic vacancies at a Cu(100)/Si(100) interface, finding that interfacial phonon conductance can be increased by up to 76% with just a 3% concentration of vacancies. Further analysis based on phonon normal modes and density of states showed that the increase is primarily due to high-frequency phonons through enhanced inelastic scattering. On the other end, we revealed how individual phonons interact with atomically perfect Si(111)/Al(111) interfaces using wave packet simulations, considering 1×1 , $\sqrt{3} \times \sqrt{3}$ and 7×7 Si surface reconstructions. It was found that interfacial scatterings differ depending on the interfacial bonding, phonon mode and frequency. Our study provides insights on manipulating interfacial phonon transport through defect and atomically precise engineering, and interpreting measurements involving phonon signals in QIS.

10:20 PM NM08.15.06

Anisotropic Transient Disordering of Colloidal, Two-Dimensional CdSe Nanoplatelets Following High-Fluence Photoexcitation Alexandra Brumberg¹, Matthew Kirschner¹, Benjamin Diroll², Xiaoyi Zhang² and Richard Schaller^{2,1}; ¹Northwestern University, United States; ²Argonne National Laboratory, United States

Colloidal, two-dimensional nanocrystals (NCs) known as nanoplatelets (NPLs) exhibit many advantages over more traditional spherical NCs while maintaining the benefits of colloidal processability and bandgap tunability. Namely, the lack of size dispersion in the single quantum-confined dimension bestows NPLs with exceptionally narrow emission linewidths that bolster their use in optoelectronic applications such as light-emitting diodes and lasers. However, these applications operate under high-fluence conditions that raise a fundamental concern regarding NC stability and the effect of such excitation conditions on desired properties such as optical bandgap. NPLs in particular may exhibit reduced thermodynamic stability even beyond that of other NCs, owing to the presence of high surface energy corners and edges. While some movement toward understanding impacts of heat on electronic properties of NCs is underway, the influence of NC morphology, and especially dimensionality, to the material stability remain largely unexplored.

To this end, here we employ time-resolved x-ray diffraction at the Advanced Photon Source to study the effect of heating on anisotropic NCs. NPLs are excited using a picosecond pulsed laser and then probed using synchrotron x-rays, which reveals both thermal expansion and transient disordering following photoexcitation. Photoexcitation induces greater out-of-plane than in-plane disordering, with thicker NPLs producing more anisotropic responses. Recovery dynamics suggest that out-of-plane cooling slightly outpaces in-plane cooling, with recrystallization occurring on indistinguishable time scales. This response to high-fluence excitation differs significantly from the response of spherical NCs, which both respond and recover isotropically to photoexcitation and recover on faster timescales. These findings offer significant implications for optoelectronic devices, where the ability to operate at high excitation densities without loss of efficiency is advantageous. Our results suggest that both the composition and structure of the NC must be taken into account when considering

crystal lattice stability and optical performance, and that NPLs are likely to exhibit superior performance over traditional, zero-dimensional nanocrystals.

SESSION NM08.16: On-demand
Wednesday Morning, April 14, 2021
NM08

8:00 AM NM08.15.03

Late News: Grain-Boundary Thermal Resistance—An Important Factor in Thermal Conductivity Reduction Observed in Micro-Grained Bismuth Telluride Sien Wang¹, Xiaowei Lu², Ankit Negi³, Jixiong He³, Kyunghoon Kim³, Hezhu Shao⁴, Peng Jiang², Jun Liu³ and Qing Hao¹; ¹University of Arizona, United States; ²Dalian Institute of Chemical Physics, Chinese Academy of Sciences, China; ³North Carolina State University, United States; ⁴Wenzhou University, China

As the dominant thermoelectric material around the room temperature, Bi₂Te₃-based alloys have been intensively studied for its applications in power generation and refrigeration. Nanograined bulk Bi₂Te₃ can be synthesized by grinding down bulk Bi₂Te₃ or mixed element ingot into nanopowder and then hot pressing the nanopowder into a bulk disc. The obtained nanostructured bulk material has even better thermoelectric performance due to the largely suppressed lattice thermal conductivity by high-density grain boundaries (GBs) inside the material. In kinetic theory, lattice thermal conductivity reduction is attributed to the effective phonon mean free path (MFP) reduced from the bulk value due to the restriction of grain sizes. In this aspect, atomistic simulations suggest bulk phonon MFPs in Bi₂Te₃ are below 100 nm along major axis directions. Therefore, a reduced effective phonon MFP cannot explain the lattice thermal conductivity reduction observed in micro-grained Bi₂Te₃. To better understand thermal transportation in crystalline Bi₂Te₃, high-quality single crystals for accurate thermal measurements and modeling is needed.

In this work, high-quality Bi₂Te₃ nanoflakes are synthesized using chemical vapor deposition on a SiO₂/Si substrate. Thickness-dependent thermal conductivity has been measured along the cross-plane direction using the time-domain thermoreflectance (TDTR) method at room temperature. The film thickness ranges from 20 nm to 300 nm, as confirmed using the atomic force microscopy.

To explain the experimental data, first-principles calculations are carried out to extract both in-plane and cross-plane phonon MFP distributions for bulk Bi₂Te₃. Calculations based on the computed cross-plane phonon MFPs and measurement data agree well with each other.

These validated bulk phonon MFPs are then used to explain the reported lattice thermal conductivities of various polycrystalline Bi₂Te₃ and its alloys. It is found that the observed lattice thermal conductivity reduction is mainly attributed to the GB thermal resistance that results from the GB reflection and transmission of phonons. Particularly, optical phonons are largely filtered out by GBs to explain the data for micro-grained samples. This result could provide important guidance for thermal studies of general polycrystalline materials.

SYMPOSIUM NM09

Nanogenerators and Piezotronics
April 17 - April 20, 2021

Symposium Organizers
Philippe Basset, ESIEE Paris

Sang-Woo Kim, Sungkyunkwan University
Sihong Wang, University of Chicago
Yunlong Zi, Chinese University of Hong Kong

Symposium Support
Bronze
MilliporeSigma

* Invited Paper

Tutorial NM09: Nanogenerators and Piezotronics—Fundamentals and Applications I
Session Chairs: Philippe Basset, Caofeng Pan, Zhong Lin Wang, Yan Zhang and Yunlong Zi
Saturday Morning, April 17, 2021
NM09

8:00 AM *

Nanogenerators and Piezotronics—History and Fundamental Principles Zhong Lin Wang; Georgia Institute of Technology, United States

Prof. Wang will first introduce the fundamental science, engineering approach and technological applications of nanogenerator as a sustainable, self-sufficient power source for micro-/nanosystems by harvesting energy from our body and living environment. Prof. Wang will then introduce the fundamentals of piezotronics and piezophotonics and to give an updated progress about their applications in energy science, electronics and sensors.

9:00 AM BREAK

9:15 AM *

Piezotronics and Piezo-Phototronics—From Fundamental Science to Applications Caofeng Pan; Chinese Academy of Sciences, China

Piezotronics concerns the devices fabricated using the piezopotential as a “gate” voltage to tune/control charge carrier transport at a contact or junction. The piezo-phototronic effect is to use the piezopotential to control the carrier generation, separation, transport, and/or recombination for improving the performance of optoelectronic devices, such as photon detector, solar cell, and LED. In this tutorial, Prof. Pan will first give an in-depth introduction of the mechanisms and applications of nanowire-based piezotronics and piezo-phototronics

10:15 AM BREAK

10:30 AM *

Theory of Piezotronics Yan Zhang; University of Electronic Science and Technology of China, China

Prof. Zhang will introduce fundamental piezotronic theory established, piezotronic p-n junction and metal-semiconductor contact models. The class of materials includes wurtzite and two-dimensional piezoelectric semiconductors, such as ZnO, GaN, InN, CdS and monolayer MoS₂.

11:30 AM BREAK

11:45 AM *

Modeling and Conditioning Triboelectric Nanogenerators Philippe Basset; ESIEE Paris, France

For TENG, a power management circuit is needed to generate a low DC voltage for the load, while implementing a high voltage interface at the transducer's side, so to maximize the converted power. Prof. Basset will present an overview of the main architectures for power management systems proposed to date for triboelectric nanogenerators, and the various circuits will be compared based on electrical simulations.

Tutorial NM09: Nanogenerators and Piezotronics—Fundamentals and Applications II

Session Chairs: Sang-Woo Kim, Yong Qin, Sihong Wang and Yunlong Zi

Saturday Afternoon, April 17, 2021

NM09

5:00 PM *

Human-Compatible Designs of Nanogenerators for Harvesting Energy from Human Bodies Sihong Wang; University of Chicago, United States

Prof. Sihong Wang will first introduce the overall needs and technological challenges for harvesting mechanical energy from human bodies, towards realizing sustainable power sources for human-integrated electronics. Then Prof. Wang will introduce the major approaches in material and device designs for achieving both high power output and multi-aspect biocompatibility, based on the requirements from different body locations.

6:00 PM BREAK

6:15 PM *

Standardized Evaluation of Nanogenerators Yunlong Zi; Chinese University of Hong Kong, Hong Kong

Prof. Zi will systematically introduce the evaluation standards and standardized evaluation methods for nanogenerators. Starting from cycles of maximized energy output, the figures-of-merit will be proposed. And then, considering the breakdown effect, the maximized energy output should be modified by reducing the breakdown areas. Finally the experimental characterization methods will be introduced and the output energy density will be introduced and compared between different nanogenerators.

7:15 PM BREAK

7:30 PM *

Triboelectric Nanogenerator as a New Platform for Energy Harvesting and Wireless Energy Transfer Technologies Sang-Woo Kim; Sungkyunkwan University, Korea (the Republic of)

As main topics, Prof. Kim will introduce recent global achievements regarding highly robust and efficient TENGs with multifunctional materials, which provides new insights to an innovative energy solution for various wearable electronics, IoT sensors, bio/healthcare applications. In addition, he will share with audiences about a new wireless energy transfer technology based on ultrasound-driven TENG in a body.

8:30 PM BREAK

8:45 PM *

Flexotronics in Centrosymmetric Semiconductors Yong Qin; Lanzhou University, China

Prof. Yong Qin will first elaborate on the fundamental science of flexotronic effect in centrosymmetric semiconductors, which serve as the basis for understanding and utilizing the interfacial polarization engineering in the new area of flexotronics. Then he will provide an overview of the development of flexotronics, and

discuss the relationship between the piezotronics and the flexotronics. Finally, he gave a perspective about their further development and potential applications in emerging fields of enhanced solar technology, active electronics/optoelectronics, hybrid-spintronics etc.

SESSION NM09.01: Nanogenerator I
Session Chairs: Zuankai Wang and Yunlong Zi
Sunday Morning, April 18, 2021
NM09

8:00 AM *NM09.01.01

The Physics of Contact-Electrification and the Theory of Triboelectric Nanogenerators Zhong Lin Wang^{1,2} and Aurelia Chi Wang²; ¹Beijing Institute of Nanoenergy and Nanosystems, Chinese Academy of Sciences, China; ²Georgia Institute of Technology, United States

Contact electrification (CE) (or usually called “triboelectrification”) effect, the most fundamental effect for electricity, has been known for over 2600 years since ancient Greek time, but its scientific mechanism remains unclear. The study of triboelectrification is recently revived due to the invention of the triboelectric nanogenerators (TENGs) by using the coupling of triboelectrification and electrostatic induction effects. In this talk, we first present the physics mechanism of triboelectrification for general materials. Our model is extended to liquid-solid contact electrification, reviving the classical understanding about the formation of electric double layers. Secondly, the fundamental theory of the TENGs is explored based on a group of reformulated Maxwell equations. In the Maxwell’s displacement current proposed in 1861, the term $d\mathbf{E}/dt$ gives the birth of electromagnetic wave, which is the foundation of wireless communication, radar and later the information technology. Our study indicates that, owing to the presence of surface polarization charges present on the surfaces of the dielectric media in TENG, an additional term $d\mathbf{P}_s/dt$ that is due to non-electric field induced polarization should be added in the Maxwell’s displacement current, which is the output electric current of the TENG. Therefore, our TENGs are the applications of Maxwell’s displacement current in energy and sensors.

[1] Z.L. Wang and A.C. Wang “On the origin of contact electrification“ (Review), *Materials Today*, 30 (2019) 34-51; <https://doi.org/10.1016/j.mattod.2019.05.016>

[2] S. Lin, L. Xu, A.C. Wang, and Z.L. Wang* “Quantifying electron-transfer and ion-transfer in liquid-solid contact electrification and the formation mechanism of electric double-layer”, *Nature Communication*, 11 (2020) 399; <https://doi.org/10.1038/s41467-019-14278-9>.

[2] Z.L. Wang, “On the first principle theory of nanaogenerators from Maxwell’s equations“, *Nano Energy*, *Nano Energy*, 68 (2020) 104272; <https://doi.org/10.1016/j.nanoen.2019.104272>

8:20 AM *NM09.01.02

Self-Powered Flexible Electronics Beyond Thermal Limits Keon Jae Lee; Korea Advanced Institute of Science and Technology, Korea (the Republic of)

This seminar introduces three recent progresses of self-powered flexible electronic systems beyond thermal limits. The first part will introduce self-powered systems for IoT sensors and flexible energy source. Flexible nanogenerator converts external bio-mechanical movement into electrical energy for self-powered IoT and biomedical devices such as pacemaker and transportation. In addition, flexible piezoelectric materials detects the minute vibration of membrane or human skin that expands the application of self-powered acoustic sensor and healthcare monitor. The second part will introduce laser material interaction for flexible applications. Laser technology of ultra-short pulse duration becomes important for future flexible electronics since high temperature process can be adopted on plastic substrates, which is essential for high performance electronics. Exciting results of flexible laser material interaction will be explored from both material and device

perspectives including nanomaterial synthesis, inorganic laser liftoff and plasmonic material reaction. The third part will discuss flexible large scale integration (f-LSI) for flexible CPU and high density memory. Flexible LSI is an essential part of future electronics for data processing, storage, and radio frequency (RF) communication. To fabricate f-LSI, we integrated 0.18 CMOS process of single crystal silicon nano-transistors with flexible electronics. Simultaneous roll transfer and interconnection of flexible NAND Flash memory was achieved using anisotropic conductive film (ACF). Finally, we introduce the highly efficient and long-term stable flexible vertical micro LED (f-VLED) for full color displays, wearable and biomedical applications. Using optogenetic mouse models, f-VLED stimulated motor neurons deep below layer III from the brain surface and induced mouse behavior changes. These f-VLED can be also used as tools of skin research and phototherapy.

References of Keon's corresponding authors since 2014

- [1] Nature Comm. 7, 13562, 2016 [2] Adv. Mater. 32, 1904020, 2020
- [3] Adv. Mater. 30, 1800649, 2018 [4] Adv. Mater. 29, 1702308, 2017
- [5] Adv. Mater. 30, 1870094, 2018 [6] Adv. Mater. 27, 3982, 2015
- [7] Adv. Mater. 27, 2866, 2015 [8] Adv. Mater. 26, 7480, 2014
- [9] Adv. Mater. 28, 8371, 2016 [10] Adv. Mater. 26, 2514, 2014.
- [11] Adv. Mater., 29, 1603473, 2017 [12] Adv. Mater. 29, 1606586, 2017
- [13] Adv. Mater. 27, 1701138, 2017 [14] Adv. Mater. 29, 1700595, 2017
- [15] Adv. Mater. 26, 4880, 2014 [16] Energy Environ. Sci. 8, 2677, 2015
- [17] Energy Environ. Sci., 7, 4035, 2014 [18] Adv. Energy Mater. 6, 1600237, 2016
- [19] Adv. Energy Mater. 5, 1500051, 2015 [20] ACS Nano 9, 4120, 2015
- [21] ACS Nano, 10, 3435, 2016 [22] ACS Nano 8, 9492, 2014
- [23] ACS Nano 8, 7671, 2014 [24] ACS Nano, 9, 6587, 2015
- [25] ACS Nano, 10, 10851, 2016 [26] ACS Nano, 10, 9478, 2016
- [27] ACS Nano, 12, 9587, 2018 [28] Adv. Func. Mater. 24, 6914, 2014
- [29] Adv. Func. Mater. 26, 6170, 2016 [30] Adv. Func. Mater. 27, 1700341, 2017
- [31] Adv. Func. Mater. 28, 1801690, 2018 [32] Adv. Func. Mater. 24, 2620, 2014
- [33] Adv. Funct. Mater. 29, 1808075, 2019 [34] Nano Energy, 14, 111, 2015
- [35] Nano Energy, 44, 447, 2018 [36] Nano Energy 53, 198, 2018
- [37] Nano Energy, 53, 658, 2018 [38] Nano Energy, 35, 415, 2017
- [39] Nano Letters 14, 7031, 2014 [40] Adv. Sci., 1801146, 2018

8:40 AM *NM09.01.03

Sustainable Output Power Generation Based on Triboelectric Nanogenerator Jeong Min Baik;
Sungkyunkwan University, Korea (the Republic of)

Contact electrification (CE) is a well-known phenomenon in physics, in which opposite charges are created at surfaces due to continuous contact and separation processes occurring between two materials, followed by the generation of electric potentials between them. To date, CE has been exploited in a vast range of ways to affect our lives and industry, it has been used in fields such as photocopying, laser printing, and electrostatic separation. Recently, during the COVID-19 pandemic, many kinds of face masks have included filters with electrostatic charges that were created using the CE, these masks have been employed as public and personal health measures against the spread of coronavirus. Here, we will present the strategies for the sustainable output power generation of the triboelectric nanogenerator (TENG) based on the CE in terms of materials aspect by synthesizing a new dielectric, a C₆₀-containing block polyimide (PI-*b*-C₆₀). Two non-contact mode applications, a keyless electronic door lock system and a speed sensor with a tone wheel for a car, will be demonstrated. A new facile approach to increasing the output voltage of a thermoelectric generator that does not involve material modification will be also reported.

9:00 AM *NM09.01.04

Strategies for Maximizing Output Charge Density of Triboelectric Nanogenerator Chenguo Hu;

Chongqing University, China

Triboelectric nanogenerator (TENG) is one of the most important technology to solve the problem of distributed energy supply of wireless sensor networks. However, the low charge density constrains TENG output performance and application field. Poor contact with the tribo-material interface, air breakdown effect and insufficient charge generation capability are the main factors affecting TENG charge density. In this talk, I will introduce the strategies for maximizing output charge density of triboelectric nanogenerator in our group, including the material modification, structure design and energy management, specifically, establishing criteria to quantitatively evaluate the contact status and inhibition of the interface air breakdown effect for contact/separation TENG, and the enhancement of charge generation capacity by shielding layer and device structural design of the sliding TENG.

References

1. Yike Liu, Wenlin Liu, Zhao Wang, Wencong He, Qian Tang, Yi Xi, Xue Wang, Hengyu Guo and Chenguo Hu, Quantifying contact status and air breakdown model of charge excitation TENG for maximum charge density, *Nature Communications*, 2020, 11:1599
2. Wencong He, Wenlin Liu, Jie Chen, Zhao Wang, Yike Liu, Xianjie Pu, Qian tang, Hengyu Guo, Chenguo Hu, Boosting output performance of sliding mode triboelectric nanogenerator by screening layer enabled charge space accumulation effect, *Nature Communications*, 2020 11:4277
3. Wenlin Liu, Zhao Wang, Gao Wang, Qixuan Zeng, Wencong He, Liyu Liu, Xue Wang, Yi Xi, Hengyu Guo, Chenguo Hu and Zhong Lin Wang, Switched-capacitor-convertors based on fractal designed configurations for double-function output power management of triboelectric nanogenerator, *Nature Communications*, (2020) 11:1883
4. Wenlin Liu, Zhao Wang, Gao Wang, Guanlin Liu, Jie Chen, Xianjie Pu, Yi Xi, Xue Wang, Hengyu Guo, Chenguo Hu, Zhong Lin Wang, Integrated charge excitation triboelectric nanogenerator, *Nature Communications*, 2019, 10:1426

9:20 AM NM09.01.05

Achieving Ultrahigh Output Energy Density of Triboelectric Nanogenerator in High-Pressure Gas Environment Jingjing Fu; The Chinese University of Hong Kong, Hong Kong

Through years of development, the triboelectric nanogenerator (TENG) has been demonstrated as a burgeoning efficient energy harvester. Plenty of efforts have been devoted to further improving the electric output performance through material/surface optimization, ion implantation or the external electric circuit. However, all these methods cannot break through the fundamental limitation brought by the inevitable electrical breakdown effect, and thus the output energy density is restricted. Here we proposed a method for enhancing the threshold output energy density of TENGs by suppressing the breakdown effects in the high-pressure gas environment. With that, the output energy density of the contact-separation mode TENG can be increased by over 25 times in 10 atm than that in the atmosphere, and that of the freestanding sliding TENG can also achieve over 5 times increase in 6 atm. Our research demonstrated the excellent suppression effect of the electric breakdown brought by the high-pressure gas environment, which may provide a practical and effective technological route to promote the output performance of TENGs.

SESSION NM09.02: Nanogenerator II

Session Chairs: Canan Dagdeviren and Sihong Wang

Sunday Morning, April 18, 2021

NM09

10:30 AM *NM09.02.01

Piezoelectric Nanotransducers—What's Next? Christian Falconi; University of Rome Tor Vergata, Italy

Nanoscale piezoelectric transducers can outperform conventional piezoelectric devices for energy harvesting (nanogenerators), sensing (e.g. piezotronics), implantable systems, wireless piezoelectric nanotransducers, and more. In fact, the properties of transducers greatly depend on dimensions due to both classic scaling laws and, at nanoscale, quantum effects. Consistently, a systematic analysis allowed to identify up to 16 possibly significant advantage of nanoscale piezoelectricity [1]. For instance, nanoscale materials can withstand larger deformations (which translate into higher piezopotentials, more robust and flexible devices and extended measurement ranges), have higher piezoelectric coefficients, offer superior mechanical force-to-displacement sensitivities and operate at higher speed. Moreover, several materials which are not piezoelectric in their bulk form due to the opposite orientations of adjacent atomic layers, are piezoelectric as single layer [1,2]. Besides, some working mechanisms are only possible at nanoscale [1,2]. Additionally, nanoscale results in more degrees of freedom for structures [3], types of mechanical input, positions of contacts, dimensionalities, and shapes [3,4]. Downscaling also uniquely offers the opportunity to fabricate piezoelectric transducers which can be used *in vivo* for a variety of tasks [5,6].

Despite such an impressive potential, practical applications can be complicated by many difficulties, with special reference to synthesis, characterization, modeling and device implementation. In this talk, also taking advantage of our last results, I will discuss some of the most important open challenges and possible strategies to address them, namely rational design of synthesis procedures [7], real time monitoring [8], dynamic synthesis procedures [8], 3D geometrical characterizations of quasi-1D single crystal nanostructures from conventional SEM images [9] and recent results for both modeling and synthesis.

References

- [1] C. Falconi, Piezoelectric nanotransducers, *Nano Energy*. 59 (2019) 730–744. <https://doi.org/10.1016/j.nanoen.2019.03.027>.
- [2] R. Hinchet, U. Khan, C. Falconi, S.W. Kim, Piezoelectric properties in two-dimensional materials: Simulations and experiments, *Mater. Today*. 21 (2018) 611–630. <https://doi.org/10.1016/j.mattod.2018.01.031>.
- [3] C. Falconi, G. Mantini, A. D’Amico, Z.L. Wang, Studying piezoelectric nanowires and nanowalls for energy harvesting, *Sensors Actuators, B Chem*. 139 (2009) 511–519. <https://doi.org/10.1016/j.snb.2009.02.071>.
- [4] R. Araneo, G. Lovat, P. Burghignoli, C. Falconi, Piezo-semiconductive quasi-1D nanodevices with or without anti-symmetry., *Adv. Mater*. 24 (2012) 4719–24. <https://doi.org/10.1002/adma.201104588>.
- [5] C. Falconi, A. D’Amico, Z.L. Wang, Wireless nanosensors and nanoactuators for in-vivo biomedical applications, in: *Eurosensors*, Göteborg, 2006.
- [6] C. Falconi, A. D’Amico, Z.L. Wang, Wireless Joule nanoheaters, *Sensors Actuators, B Chem*. 127 (2007) 54–62. <https://doi.org/10.1016/j.snb.2007.07.002>.
- [7] G. Arrabito, V. Errico, Z. Zhang, W. Han, C. Falconi, Nanotransducers on printed circuit boards by rational design of high-density, long, thin and untapered ZnO nanowires, *Nano Energy*. 46 (2018) 54–62. <https://doi.org/10.1016/j.nanoen.2018.01.029>.
- [8] A. Orsini, C. Falconi, Real-time monitoring of the solution growth of ZnO nanorods arrays by quartz microbalances and in-situ temperature sensors, *Sci. Rep.* 4 (2014) 1–7. <https://doi.org/10.1038/srep06285>.
- [9] A. Mencattini, A. Orsini, C. Falconi, 3D Reconstruction of Quasi-1D Single-Crystal Nanostructures, *Adv. Mater*. 27 (2015) 6271–6276. <https://doi.org/10.1002/adma.201503522>.

10:50 AM NM09.02.03

High-resolution 3D Printing of Piezoelectric Structures Using Micro-CLIP Process Siying Liu, Luyang Liu, Wenbo Wang and Xiangfan Chen; Arizona State University, United States

Piezoelectric materials and composites enable a wide range of energy harvesting and sensing applications owing to their intrinsic capability of converting mechanical energy to electrical energy and vice versa. Additive manufacturing (AM), also known as 3D printing, is thriving as a category of effective and robust techniques in manufacturing three-dimensionally (3D) architected piezoelectric composites comprising of inorganic/organic piezoelectric materials, and these architected structures possess the potential of delivering

anisotropic piezoelectric responses upon specific structural designs. Nonetheless, the serial nature of the additive building processes results in the inherent speed-accuracy trade-off, which seriously limits the scalability and efficiency of manufacturing functional devices that require precise control of fine features. As a result, the reported progress in this field either limit themselves to macroscale devices due to relatively low printing resolution, e.g, fused deposition modeling (FDM), or require extensive amount of fabrication time, e.g., projection micro- stereolithography (PμSL). On the contrary, micro continuous liquid interface production (μCLIP), a recently developed 3D printing technology, has been shown to create 3D geometries at very high speeds, with good surface finish, and uniform mechanical properties.

Herein, we report rapid 3D printing of architected barium titanate (BTO) composite structures with high resolution by using mCLIP. The BTO nanoparticles were surface functionalized prior to mixing to enable stable dispersion in poly(ethylene glycol) diacrylate (PEGDA). Resins with up to 25 wt% of functionalized-BTO (f-BTO) nanoparticles were prepared and printed continuously to yield a variety of architected structures with unprecedented longitudinal printing speeds of up to ~ 25 μm/s. The architected structures were tested with a customized piezoelectric characterization setup and demonstrate effective piezoelectric constant d_{33} of 37.9 pC/N, and piezoelectric voltage constant g_{33} of 0.92 Vm N⁻¹, which is comparable to other reported work. This work not only enables the rapid 3D printing of architected piezoelectric structures with tailorable properties via compositional and structural modifications, but also intrinsically enlightens its potential capability for eco-friendly and biocompatible applications.

11:00 AM NM09.02.04

High-Performance Polyvinylidene Difluoride/Dopamine Core/Shell Piezoelectric Nanofiber and Its Application for Biomedical Sensors Tong Li, Long Gu, Corey Carlos and Xudong Wang; University of Wisconsin-Madison, United States

Soft piezoelectric materials are an important group of functional material for state-of-the-art energy harvesting, energy conversion and sensing technologies. Driven by the rapid evolution of internet of things and biomedical engineering, current energy and sensor technologies, particularly those interfacing with human beings, are placing tremendous emphasizes on the flexibility, processability, conformality and biocompatibility to the piezoelectric components, in addition to their high performance. While polyvinylidene difluoride (PVDF) has been a well-known and broadly used piezoelectric polymer material over years, their mechanical property, piezoelectric performance and processability still cannot meet the high requirements of wearable devices. Recent years see a surge of research efforts on PVDF-based nanostructures to interface with biological systems for energy or sensing applications. However, unlike ceramic-based piezoelectric materials, to reach desired high piezoelectric property and long-term stability in biological environment still stand as a big challenge in PVDF soft nanomaterial development.

In this work, we report a one-step strategy for fabricating core/shell polyvinylidene difluoride (PVDF)/dopamine (DA) nanofibers (NFs) with a very high β-phase content and self-aligned polarization. The self-assembled core/shell structure is believed essential for the formation and alignment of β-phase PVDF, where strong intermolecular interaction between the -NH₂ groups on DA and -CF₂ groups on PVDF is responsible for aligning the PVDF chains and promoting β-phase nucleation. As-received PVDF/DA NFs exhibit significantly enhanced piezoelectric performance and excellent stability and biocompatibility. An all-fiber-based soft sensor is fabricated and tested on human skin and in vivo in mice. The devices show a high sensitivity and accuracy for detecting weak physiological mechanical stimulation from diaphragm motions and blood pulsation. This sensing capability offers great diagnostic potential for the early assessment and prevention of cardiovascular diseases and respiratory disorders.

11:10 AM *NM09.02.05

Closed-Loop Electrostimulation Enabled by Nanogenerator Technology Xudong Wang; University of Wisconsin-Madison, United States

Electrostimulation (ES) has long been utilized as a versatile therapeutic strategy for treating human diseases. The nanogenerator technology stands at a unique position for connecting biological ES to body motions by

converting biomechanical energy to electric pulses. This process forms a closed-loop ES in both energy flow and function feedback. This talk will first elaborate how the closed-loop ES operates as a close analogue to how the body controls its own functions. The most recent progresses of flexible and complex piezoelectric material innovations in our group will be viewed for implantable nanogenerator development, including 3D printing techniques and degradable piezoelectric biomaterials. These materials exhibited tissue-matching mechanical property as well as excellent electromechanical coupling properties, ideal for in situ electrostimulation generation. In our recent research, we also successfully implemented the closed-loop electrostimulation concept for skin wound healing, hair growth, bone healing and vagus nerve stimulation for obesity control with superb performance. An electrical stimulation bandage was developed that could accelerate skin wounds recovery to within 3 days as compared to 12 days of usual contraction-based healing processes in rodents. Via a similar design, the electrical pulses were applied to stimulate hair growth. In another work, an implanted vagus nerve stimulation system was developed in responsive to the peristalsis of stomach. The electric signals generated by this device stimulates the vagal afferent fibers to reduce food intake and achieve weight control. With the advanced electromechanical material and device design and engineering, the closed-loop electrostimulation concept will quickly grow into a very impactful application direction of nanogenerator technology for human wellbeing.

11:30 AM NM09.02.06

Quantifying and Understanding the Triboelectric Series of Inorganic Non-Metallic Materials Haiyang Zou and Zhong Lin Wang; Georgia Institute of Technology, United States

Contact-electrification is a universal effect for all existing materials, but it still lacks a quantitative materials database to systematically understand its scientific mechanisms. Using an established measurement method, this study quantifies the triboelectric charge densities of nearly 30 inorganic nonmetallic materials. From the matrix of their triboelectric charge densities and band structures, it is found that the triboelectric output is strongly related to the work functions of the materials. Our study verifies that contact-electrification is an electronic quantum transition effect under ambient conditions. The basic driving force for contact-electrification is that electrons seek to fill the lowest available states once two materials are forced to reach atomically close distance so that electron transitions are possible through strongly overlapping electron wave functions. We hope that the quantified series could serve as a textbook standard and a fundamental database for scientific research, practical manufacturing, and engineering.

11:40 AM *NM09.02.07

Conformable Facial Code Extrapolation Sensor (cFaCES) for Non-Verbal Communication Canan Dagdeviren; Massachusetts Institute of Technology, United States

Devices that facilitate nonverbal communication typically require high computational loads or have rigid and bulky form factors unsuitable for use on the face or on other curvilinear body surfaces. Here, we report the design and pilot testing of an integrated system for the decoding of facial strains and for predicting facial kinematics. The system consists of mass-manufacturable, conformable piezoelectric thin films for strain mapping, multiphysics modelling for the analysis of the nonlinear mechanical interactions between the conformable device and the epidermis, and three-dimensional digital image correlation for the reconstruction of soft-tissue surfaces under dynamic deformations and for informing device design and placement. In healthy subjects and in subjects with amyotrophic lateral sclerosis, we show that the piezoelectric thin films, coupled with algorithms for the real-time detection and classification of distinct skin-deformation signatures, enable the reliable decoding of facial movements. The integrated system could be adapted for use in clinical settings as a nonverbal communication technology or for use in the monitoring of neuromuscular conditions.

1:00 PM *NM09.03.01

Turn the Triboelectric Charges on the Body into Energy and Signals Renyun Zhang; Mid Sweden University, Sweden

The triboelectric charges on the human body are generated by the contact electrification of the human skin and other surfaces. The mechanism behind this is that the human skin has a very positive charge affinity due to its surface biological composition. Such a high positive charge affinity leads to electron transfer between the skin and other materials when the physical contact-separation process is happening.

Utilizing such unique properties of the human skin, we have constructed different types of triboelectric nanogenerators (TENGs) including human body based TENGs (H-TENGs) for harvesting energy from body motions with maximum output power density above 30 W/m². Moreover, due to the unique charge generating process of the body, we have developed new types of body motion sensors that can sense the movements of the human body. Such sensors have great applications in healthcare and security areas. Beyond these, one can also create human-machine interactions based on the charges generated on the human body.

Our studies have discovered the fundamentals of the triboelectricity of the human body, as well as future applications in different areas. New types of human-machine interaction prototype are expecting to be developed in the future.

References:

- (1) Zhang, R.; Hummelgård, M.; Örtégren, J.; Yang, Y.; Andersson, H.; Balliu, E.; Blomquist, N.; Engholm, M.; Olsen, M.; Wang, Z. L.; Olin, H. Sensing Body Motions Based on Charges Generated on the Body. *Nano Energy* **2019**, *63*, 103842. <https://doi.org/10.1016/j.nanoen.2019.06.038>.
- (2) Zhang, R.; Hummelgård, M.; Örtégren, J.; Olsen, M.; Andersson, H.; Olin, H. Interaction of the Human Body with Triboelectric Nanogenerators. *Nano Energy* **2019**, *57* (October 2018), 279–292. <https://doi.org/10.1016/j.nanoen.2018.12.059>.
- (3) Zhang, R.; Hummelgård, M.; Örtégren, J.; Olsen, M.; Andersson, H.; Yang, Y.; Olin, H. Human Body Constituted Triboelectric Nanogenerators as Energy Harvesters, Code Transmitters, and Motion Sensors. *ACS Appl. Energy Mater.* **2018**, *1* (6), 2955–2960. <https://doi.org/10.1021/acs.aem.8b00667>.
- (4) Zhang, R.; Örtégren, J.; Hummelgård, M.; Olsen, M.; Andersson, H.; Olin, H. Harvesting Triboelectricity from the Human Body Using Non-Electrode Triboelectric Nanogenerators. *Nano Energy* **2018**, *45*, 298–303. <https://doi.org/10.1016/j.nanoen.2017.12.053>.

1:20 PM DISCUSSION

1:40 PM *NM09.03.03

Zinc Oxide Nanowires Based Nanogenerator: Design, Manufacture, Modelling and Characterization Guylaine Poulin-Vittrant^{1,2}, Taoufik Slimani Tlemcani¹, Kevin Nadaud¹, Emmanuel Dumons², Louis P. Tran-Huu-Hue² and Daniel Alquier¹; ¹CNRS, Université de Tours, France; ²CNRS, INSA-CVL, Université de Tours, France

Piezoelectric composites based on PZT ceramic rods or fibers have emerged long time ago for ultrasonic applications [1]. With the progress in nanotechnologies, similar composites incorporating piezoelectric nanowires have been manufactured for mechanical energy harvesting, generally called nanogenerators [2]. These devices have attracted increasing research interest, as possible micro-power supplies for wireless and mobile electronics, with the growing importance of the Internet of Things (IoT) [2,3].

Here, we will present an original design as well as a modelling strategy of nanogenerator devices. The flexible nanogenerator is manufactured on a polydimethylsiloxane (PDMS) substrate. It consists in a multilayer device with a Ti/Au bottom electrode, a nucleation layer, a zinc oxide (ZnO)/parlylene C composite layer, a Ti/Al top electrode, and a final PDMS encapsulation [4]. ZnO nanowires are synthesized using a low temperature Chemical Bath Deposition (CBD) process (85°C), compatible with various substrates and transferable to industrial processes.

Some of the key properties of the nanogenerator constitutive elements have been studied and optimized: the flexible substrate [4], the bottom electrode layer and the nucleation layer – which may be the same layer and, indeed, the ZnO crystalline quality. The ZnO nanowires properties have been adjusted through the CBD growth conditions (temperature, duration, reactants) [5,6] and the nucleation layer type and thickness (Au, ZnO or Al-doped ZnO) [7,8].

A dedicated test bench has been designed in order to measure the electrical power or energy delivered to an external circuit. Average electrical power and RMS voltage are measured thanks to a double buffer amplifier [9]. The nanogenerator produces a $0.4 \mu\text{W}/\text{cm}^2$ average power (or $2 \mu\text{W}/\text{cm}^2$ peak power) for a 6N force applied at 5Hz [10]. The force sensitivity of the device is 2 V/N at 5Hz. In order to determine the doping properties of the ZnO nanowires, single nanowire – Field Effect Transistors (FETs) were manufactured and characterized [5]. A 10^{18}cm^{-3} doping level is estimated for pristine nanowires, decreasing by two orders of magnitude thanks to thermal annealing of the nanowires in air. This intrinsic doping, resulting from native defects, is increasing with HMTA (hexamethylenetetramine) concentration used for CBD growth. The ZnO doping values estimated thanks to single nanowire FETs have been correlated to photoluminescence spectroscopy results [6].

In terms of modelling, an analytical model and a Finite Element (FE) model have been developed depending on the simulation purpose. In particular, the analytical model takes into account the possible wide frequency band of the mechanical excitation and allows the prediction of the harvested power for a mechanical force with an arbitrary time-domain form [11]. The FE model of a single cell – with appropriate symmetry conditions – containing a piezoelectric and semiconducting material embedded into a dielectric polymer matrix, on a given rigid or flexible substrate, provides a better understanding of the electromechanical behavior of the transducer. Based on this model, energetic considerations are discussed, like conversion rate or electromechanical coupling factor.

References

- [1] R.E. Newnham et al., *Mat. Res. Bull.* 13 (1978) 525-536
- [2] L. Jin et al., *Nano Energy* 66 (2019) 104086
- [3] A.S. Dahiya et al., *Journal of The Electrochemical Society* 167 (2020) 037516
- [4] A. S. Dahiya et al., *Advanced Materials Technologies* (2017) 1700249
- [5] S. Boubenia et al., *Scientific Reports* 7 (2017) 15187
- [6] A. S. Dahiya et al., *Nanoscale Research Letters* (2018) 13:249, 9 pp.
- [7] T. Slimani Tlemcani et al., *Chemosensors* 7, 7 (2019)
- [8] C. Justeau et al., *Materials* 12 (2019) 2511
- [9] K. Nadaud et al., *Appl. Phys. Lett.* 112 (2018) 063901
- [10] S. Boubenia, PhD thesis, Université de Tours, 4th July 2019
- [11] K. Nadaud et al., *Mechanical Systems and Signal Processing* 133 (2019) 106278

2:00 PM NM09.03.04

Photoinduced Strain in Ferroelectric-Based Cantilevers Stéphane Gable, Komalika Rani, Thomas Maroutian, Guillaume Agnus, Philippe Lecoeur and Sylvia Matzen; Université Paris-Saclay, France

Due to their large number of properties, such as switchable polarization, piezoelectricity or optical absorption, ferroelectrics are particularly promising in order to develop the next generation of electronic microdevices. Among these ferroelectrics, lead zirconium titanate (PZT) has been widely investigated for its high electromechanical properties and more recently for its light-induced deformation¹, commonly named photostriction, combining simultaneously bulk photovoltaic and converse piezoelectric effects². Although this

phenomenon was discovered in multiple ferroelectrics materials these last decades³, the photostriction is not fully understood and thus requires further studies in order to promote the future electronic microdevices. In this work, the interplay between the electric polarization and the photoinduced strain is investigated in PZT epitaxial-based cantilevers. For this purpose, the resonance frequencies of the cantilevers and their deflection were studied under UV illumination, through electrical measurements and optical profilometry respectively. The recent results have shown that the sign of both the photoinduced shift of resonance frequency and photoinduced deflection strongly depend on the polarization state in the ferroelectric thin film.

¹ S. Matzen *et al.*, « Tuning Ultrafast Photoinduced Strain in Ferroelectric-Based Devices », *Adv. Electron. Mater.*, p. 1800709, mai 2019, doi: 10.1002/aelm.201800709.

² C. Paillard, B. Xu, B. Dkhil, G. Geneste, et L. Bellaiche, « Photostriction in Ferroelectrics from Density Functional Theory », *Physical Review Letters*, vol. 116, n° 24, juin 2016, doi: 10.1103/PhysRevLett.116.247401.

³ B. Kundys, « Photostrictive materials », *Applied Physics Reviews*, vol. 2, n° 1, p. 011301, mars 2015, doi: 10.1063/1.4905505.

2:10 PM *NM09.03.05

Revealing Fundamental Multi-Scale, Multi-Physics Interaction in Contact Electrification Jun Liu;
University at Buffalo, The State University of New York, United States

Understanding the fundamental mechanism of contact electrification has been the Holy Grail for physicists for centuries. The direct-current generation in semiconductor-based dynamic contacts is a newly discovered triboelectric phenomenon, where multi-scale interaction and multi-physics coupling of contact interfaces under non-equilibrium condition are involved. At microscopic level, mechanical modulation is exerted at local single asperities due to surface roughness. Lattice distortion of a dynamic contact could be extremely large considering a high local pressure at GPa level at the single asperity. As a result, one would expect an ultrahigh ‘local’ temperature as high as 1000 K given rise by the rigorously perturbed surface atoms. In an effort to elucidate the physical picture of the energy conversion process, we investigate the long-existing problem from different scales and different angles: At microscopic level, the contribution of flexoelectric effect due to strain gradient on the interfacial electric field; At atomic level, the contribution of surface dipole formation due to perturbation of surface to the interfacial electric field; At quantum level, the contribution of non-adiabatic electron-phonon interaction on the electronic excitation. It is proposed that those factors should be considered comprehensively, in addition to the simple charge transfer theory based on thermodynamic fermi-level alignment, in order to understand the fundamental mechanism of contact electrification.

SESSION NM09.04: Nanogenerator IV
Session Chairs: Giuseppina Pace and Wenzhuo Wu
Sunday Afternoon, April 18, 2021
NM09

4:00 PM NM09.04.01

Holistic Engineering of Biocompatible and Biodegradable Polymers as Wearable Triboelectric Devices for Self-Powered Cardiovascular Monitoring Ruoxing Wang and Wenzhuo Wu; Purdue University, United States

Personalized real-time health monitoring in non-clinical environments can significantly improve the life quality by regularly evaluating health status, immediate warning of abnormality, and remote diagnosis. The continuous detection of various vital signals such as respiration, perspiration, and temperature have been realized by wearable sensors. Heart rate is another critical parameter which is closely related to cardiovascular health.

Cardiovascular disease is one of the leading causes of death globally, which costs more than \$219 billion each year in healthcare service, medicine, and loss of productivity. The precise continuous monitoring of pulse waveform is critical for assessing overall cardiovascular health and the state of the autonomic nervous system (ANS) responsible for regulating cardiac activity.

The emerging frontiers in real-time cardiovascular health monitoring demand that the corresponding sensors be biocompatible, wearable, and self-sustainable. The capability of sensor systems to efficiently scavenge the stray, weak environmental energies through sustainable pathways would enable self-powered bioelectronic systems. Triboelectric nanogenerators (TENG) can effectively transform the otherwise wasted environmental, mechanical energy into electrical power. Recent advances in TENGs witness a significant boost in the output performance. However, obstacles hindering the development of efficient triboelectric devices based on biocompatible materials continue to prevail. Being naturally degradable, biocompatible, low-cost, and lacking in cytotoxicity, chitosan and polyvinyl alcohol (PVA) are two materials with great potential being functional constituents in biomedical devices.

Here, we present for the first time the holistic engineering of chitosan and PVA with tunable mechanical properties, biodegradable rates, and electrical outputs for wearable TENGs, through revealing and understanding the interactions between the constituent materials and the structure-property-performance relations.^[1, 2] The feasibility of laser processing of biopolymers was explored for the first time to improve the TENG performances. Leveraging the high mechanical deformability and biocompatibility of the constituent materials, the optimized triboelectric devices built with PVA composite films and chitosan composite films exhibit stable and robust triboelectricity outputs. Such wearable devices are capable of detecting the imperceptible degree of skin deformation induced by human pulse and capture the cardiovascular information encoded in the pulse signals with high fidelity for self-powered cardiovascular health monitoring. The gained fundamental understanding and demonstrated capabilities are expected to enable the rational design and holistic engineering of novel materials for more capable biocompatible triboelectric devices that can continuously monitor vital physiological signals for self-powered health diagnostic and therapeutic systems.

[1] R. Wang, S. Gao, Z. Yang, Y. Li, W. Chen, B. Wu and W. Wu, *Adv. Mater.* **2018**, 30, 1706267.

[2] R. Wang, L. Mu, Y. Bao, H. Lin, T. Ji, Y. Shi, J. Zhu and W. Wu, *Adv. Mater.* **2020**, 32, 2002878.

4:10 PM NM09.04.02

Plasma Nanoengineering for the Development of Hybrid Piezo and Tribonanogenerators Xabier García-Casas¹, Nicolas Filippin¹, Javier Castillo-Seoane², Francisco J. Aparicio¹, Ali Ghafarnejad¹, Jorge Budagoski¹, Carmen Lopez-Santos², Angel Barranco¹, Juan R. Sanchez-Valencia² and Ana Borrás¹; ¹Spanish National Research Council (CSIC), Spain; ²Universidad de Sevilla, Spain

In this communication, we show an innovative approach to the production of piezoelectric nanogenerators by combining polycrystalline and texturized ZnO layers fabricated at room temperature by plasma enhanced chemical vapor deposition with flexible small-molecule organic nanowires (ONWs) acting as 1D and 3D soft-template. We address the one-wire / one-device concept by developing a core-multishell piezoelectric nanogenerator including gold and silver shells acting as inner nanoscopic electrodes.^[1] Besides, this nanoarchitecture is integrated in high density in a contact-separation mode triboelectric nanogenerator. We aim to demonstrate the advantages of the application of plasma assisted deposition and plasma nanoengineering to optimize the output power of the hybrid nanogenerator at two levels, namely, the nanoengineering of the piezoelectric nanowires and the plasma treatment and functionalization of the triboelectric surfaces. On the one hand, we discuss the role of the piezoelectric shell microstructure, texture, and hierarchical formation of nanotrees. On the other hand, the plasma assisted fluorinated functionalization of PDMS is evaluated as a sustainable approach to increase the electronegativity and hydrophobicity of the negative friction layer. For the optimized vertical separation-contact TENG on ITO/PET, the measured output on manual pressing stimulation reached values higher than 75 V of open-circuit voltage and 0.5 μ A of short-circuit current. A setup for the generation of reproducible mechanical stimuli either in frequency or amplitude was developed and applied, which allowed us to obtain a characteristic frequency for the maximal output of the device. Finally, the wetting properties of TENGs surfaces have been tuned by controlling the surface micro and nanoroughness and superhydrophobic hierarchical structures ranging from Petal to Lotus mechanisms. The liquid-solid

electrification and its application for fabricating a single electrode TENG have been exploited to harvest energy from microdroplets' impacts and sliding.

4:20 PM NM09.04.04

Towards Flexible and Scaled-up Schottky Direct Current Generator Ruizhe Yang, Matthew Benner and Jun Liu; University at Buffalo, The State University of New York, United States

High-current density dynamic Schottky junctions hold great promise for ambient energy harvesting, which overcome the transient and limited current output as faced by traditional piezoelectric/triboelectric nanogenerators. However, self-powered applications for wearable/implantable electronics call for excellent flexibility for the device, whereas the materials of dynamic Schottky junction being used hitherto are inorganic bulk materials with poor flexibility. In addition, the low open-circuit voltage and high-cost scaling up have hampered its further implement for practical applications in self-powered electronic devices. Here, we design and optimize the scalable DC generators with high power output as well as excellent flexibility. The flexible DC power generator exhibits a robust mechanical stability and durability under ambient temperature. The design of flexibility in such DC energy generator is inherited from the long chain polymer concept. The Schottky DC power generation nature provides such flexible generator with high current density performance without rectification. The demonstration of scalable and flexible of high current density DC energy generator opens up energy conversion applications with remarkable power output performance (approaching mA level of short-circuit current, and 1 volt open-circuit voltage for single unit) enabled by low frequency movement, high flexibility, and excellent durability performances.

4:30 PM *NM09.04.05

Nylon-11 Nanowires for Triboelectric Energy Harvesting Yeon Sik Choi¹ and Sohini Kar-Narayan²; ¹Northwestern University, United States; ²University of Cambridge, United Kingdom

Triboelectric energy harvesting from ambient mechanical sources relies on motion-generated surface charge transfer between materials with different electron affinities. In order to achieve highly efficient energy harvesting performance, choosing materials with a high surface charge density is crucial, and odd-numbered polyamides (Nylons), such as Nylon-11, are particularly promising due to their strong electron-donating characteristics and the possibility to achieve dipolar alignment leading to high surface potential. The use of Nylon-11 as a material for triboelectric energy harvesting has been rather limited due to the extreme processing conditions required for film fabrication, and the high-voltage poling process required for dipole alignment. However, several methods to achieve “self-poled” Nylon-11 nanowires via facile nanoconfinement techniques have been demonstrated recently, leading to highly efficient Nylon-11 nanowire-based triboelectric nanogenerators. In this talk, I will discuss the most recent advances in the fabrication of Nylon-11 nanowires, with a focus on how nanoconfinement-based fabrication methods can be used to control phase and crystallinity. These growth methods lead to self-poled nanowires without the requirement for subsequent electrical poling, facilitating their integration into triboelectric energy harvesting devices. Strategies to fabricate Nylon-11 nanowires for applications in triboelectric devices can be extended to other polymeric families as well, giving rise to improvements in energy harvesting performance.

[1] "Unprecedented dipole alignment in α -phase nylon-11 nanowires for high-performance energy-harvesting applications" Y. S. Choi, S. K. Kim, M. Smith, F. Williams, M. E. Vickers, J. A. Elliott and S. Kar-Narayan*, Science Advances 6, eaay5065 (2020), DOI: 10.1126/sciadv.aay5065

4:50 PM NM09.04.07

Two-Stage Conditioning System for Triboelectric Nanogenerators Using a High-Voltage MEMS Plasma Switch Hemin Zhang^{1,2}, Frédéric Marty¹, Dimitri Galayko³, Naida Hodzic¹ and Philippe Basset¹; ¹ESYCOM, Univ Gustave Eiffel, CNRS, CNAM, ESIEE Paris, France; ²University of Cambridge, Cambridge, United Kingdom; ³Sorbonne Université, France

Adding a switch at the output of a TENG or in its conditioning circuit largely promotes the energy harvesting efficiency. However, the switch has to be self-activated with a minimum consumption, so electronic switches are not suitable. We propose to apply MEMS technologies to develop a self-sustained, high-voltage and well-controlled narrow-hysteresis switch for high-efficiency energy transfer.

Our plasma switch is made of bulk silicon. It is part of a 2-stage conditioning system with a first stage including a $\sim 35\text{cm}^2$ flexible TENG and a Bennet doubler circuit, plus a second stage including the MEMS switch and a buck converter. The switch includes a movable anode connected to the Bennet output, a fixed cathode connected to the buck input, and a ground reference. At start, the switch is OFF and the voltage progressively increases across the rectifier capacitance C_{buf} , while an electrostatic force pulls the anode close to the cathode. According to Paschen's Law, if the plasma breakdown voltage is higher than the physical-contact voltage, a contact occurs between the electrodes and a full-hysteresis ON-OFF loop appears because the contact current is high enough to release all the energy from C_{buf} . If the breakdown voltage is lower than the physical-contact voltage, micro-plasma occurs before contact, leading to a narrow-hysteresis ON-OFF loop because the low plasma current cannot fully release the energy stored in C_{buf} due to the end of the plasma.

We used a 2-stage circuits with a Bennet doubler and a MEMS switch having an initial gap of $6\mu\text{m}$ and $9\mu\text{m}$ to charge a larger capacitor C_{store} , or using only a full-wave rectifier. Defining the charging efficiency as the energy per cycle in C_{store} at 4.5V (the regulator's operation voltage) divided by the charging time to this voltage, we can conclude that using the 2-stage conditioning circuit with a $6\mu\text{m}$ -gap MEMS switch improves the energy transfer efficiency by 145 times compared to only a full-wave rectifier. With the $6\mu\text{m}$ -switch, contact occurs with a full hysteresis, while with the $9\mu\text{m}$ -switch a μ -plasma is obtained with a very narrow hysteresis. Despite its full-hysteresis, the $6\mu\text{m}$ switch has a better energy conversion per mechanical cycle without any load because of its much higher ON voltage. However, in a practical implementation with a commercial regulator and a 660kW load, the circuit with the $6\mu\text{m}$ -switch has many glitches at the regulated output, on the contrary to the one with the $9\mu\text{m}$ -switch. This is explained by the longer time for recharging C_{buf} induced by the full-hysteresis that drastically decreases the mean value of the voltage across C_{buf} . Therefore, the switch can be further improved by designing a $6\mu\text{m}$ -switch with plasma discharge and no contact.

5:00 PM NM09.04.08

Slide Electrification to Supply Power for Smart Contact Lenses Erfan Pourshaban, Aishwaryadev Banerjee, Mohit Karkhanis, Chayanjit Ghosh, Adwait Deshpande, Hanseup Kim and Carlos Mastrangelo; The University of Utah, United States

One of the essential components for practical realization of the smart wearables, is an efficient and standalone power scavenging system. Photovoltaics and wireless power transfer are widely used for such purposes. However, these techniques depend on the presence of an external energy source which poses certain limitations on their practical deployment. Alternatively, conversion of mechanical motion to electrical energy can be considered as a practical and standalone method to generate power for wearable electronics systems such as smart contact lenses. Due to its high output power density, triboelectric power generators are an attractive choice for such purposes. Here, we have investigated a slide triboelectric power generation of liquid-solid movements with respect to each other. Our results confirm the feasibility of supplying power for biomedical electronics just by natural human muscle motions. In this talk we present a triboelectric generator driven by eye blinks suitable for powering up smart contact lenses. A human's average eye blinking speed is approximately 200 mm/s [1]. Furthermore, an adult blinks about 12 times per minute[2].

One of the main shortcomings of the common solid-solid triboelectric power generators is the materials' surface properties. Micro and nanoscale surface roughness, together with surface destruction by the friction effect, deteriorate the performance of the solid-solid triboelectric devices. However, in the present study, we have used the liquid as one side of our slide electrification system. Having liquid as one side of the mechanical to electrical power generators, not only benefits from touching all possible surface area of the solid's surface but also offers a higher lifetime to the triboelectric power generation devices. The solid plate of our device is made up of a grating aluminum (Al) with a surface area and spacing of $1\times 5\text{ mm}^2$ and 5 mm , respectively. 300 nm of silicon dioxide (SiO_2) was sputtered, followed by coating 800 nm of polytetrafluoroethylene (PTFE). SiO_2 prevents any leakage current from the slide electrification process. In addition, thin layer of PTFE is used to

make the solid's surface hydrophobic and prevent the wetting of the surface by the motion of the liquid. The liquid side is composed of a simple Al electrode and different types of liquids. Results confirm that the motion of the liquid with respect to the solid plate generates an alternative voltage which is due to the capacitor behavior. Furthermore, the liquid's ion concentration and the movement speed determine the output generated voltage of the liquid-solid triboelectric system.

A noise-free, battery operated digital oscilloscope (Yeapock ADS1013D) with the input impedance of 1 M Ω was used for the output voltage measurements. In addition, an operational amplifier (ST Microelectronics LM358D) was configured as a unity-gain voltage follower which buffered our device to detect the open-circuit voltage of the triboelectric power generators, properly. We have used different NaCl concentrations (0, 0.01, 0.1, and 1M) as the liquid part of our triboelectric power generator. Higher NaCl concentration results in higher output voltage. At the movement speed of 30 mm/s, deionized (DI) water without NaCl shows no output voltage

while the same value is outstandingly rising to 3.7 V by adding 1 M NaCl to the DI water. Using the commercially available moisturizing eye drop as the liquid part of the slide electrification device at the movement speed of 30 mm/s results in an output voltage of 3.7 V and 4.7V at of 200 mm/s. The calculated effective power density was $\sim 0.4 \text{ Wm}^{-2}$.

References

- [1] K.-A. Kwon et al., "High-speed camera characterization of voluntary eye blinking kinematics," J. R. Soc. Interface, vol. 10, no. 85, p. 20130227, Aug. 2013, doi: 10.1098/rsif.2013.0227.
- [2] Physiology of the Eye. Elsevier, 1992.

5:10 PM *NM09.04.09

Smart Textiles for Personalized Health Care Jun Chen; University of California, Los Angeles, United States

There is nothing more personal than healthcare. Health care must move from its current reactive and disease-centric system to a personalized, predictive, preventative and participatory model with a focus on disease prevention and health promotion. As the world marches into the era of Internet of Things (IoT) and 5G wireless, technology renovation enables industry to offer a more individually tailored approach to healthcare with more successful health outcomes, higher quality and lower costs. However, empowering the utility of IoT enabled technology in personalized health care is still significantly challenged by the shortage of cost-effective and wearable biomedical devices to continuously provide real-time, patient-generated health data. Textiles have been concomitant and playing a vital role in the long history of human civilization. In this talk, I will introduce our current research on smart textiles for biomedical monitoring and personalized diagnosis, textile for therapy, and textile power generation as an energy solution for the future wearable medical devices.

SESSION NM09.05: Nanogenerator V
Session Chairs: Hengyu Guo and Xudong Wang
Sunday Afternoon, April 18, 2021
NM09

6:30 PM NM09.05.01

A Flexible Piezoelectret Actuator/Sensor for Mechanical Human-Machine Interfaces Junwen Zhong;
University of Macau, China

Flexible and wearable devices with the capabilities of both detecting and generating mechanical stimulations are critical for applications in human-machine interfaces, such as augmented reality (AR) and virtual reality (VR). Herein, a flexible patch based on a sandwiched piezoelectret structure is demonstrated to have a high equivalent piezoelectric coefficient of d_{33} to selectively perform either the actuating or sensing function. As an actuator, mechanical vibrations with peak output force of more than hundreds of mN have been produced, similar to

those from the vibration mode of a modern cell phone and can be easily sensed by human skin. As a sensor, both high sensitivity of 1.84 Pa for sensing resolution and excellent stability of less than 1% variations in thousands of cycles have been achieved. The design principle together with the sensing and driving characteristics can be further developed and extended to other soft matters and flexible devices.

6:40 PM NM09.05.02

Polymer-Based Multifunctional Self-Powered Systems for Energy Harvesting and Active Sensing Ruiyuan Liu; Soochow University, China

Functional polymers provide unique advantages in flexible electronics to improve their electrical performance, flexibility and functions. An integration of flexible energy harvesting and storage components enables a self-powered system that can simultaneously harvest solar/mechanical energy and store electricity for soft robotics, the internet of things and portable electronics. The introduction of functional polymers into a self-powered system pave a new direction for the multifunctional applications in energy harvesting, storage and mechanosensing.

1. R. Liu; M Takakuwa, A Li, et al. An efficient ultra-flexible photo-charging system integrating organic photovoltaics and supercapacitors. *Adv. Energy Mater.* 2020, 10, 2000523
2. R. Liu, X. Kuang, J. Deng, et al. Shape memory polymers for body motion energy harvesting and self powered mechanosensing. *Adv. Mater.* 2018, 30, 1705195.
3. R. Liu, J. Wang, T. Sun, et al. Silicon nanowire/polymer hybrid solar cell-supercapacitor: a self-charging power unit with a total efficiency of 10.5%. *Nano Lett.* 2017, 17, 4240.
4. R. Liu, Y. Liu, H. Zou, et al. Integrated solar capacitors for energy conversion and storage. *Nano Res.* 2017, 10, 1545.

6:50 PM NM09.05.04

A Constant Direct-Current Triboelectric Nanogenerator Arising from Electrostatic Breakdown Jie Wang; Beijing Institute of Nanoenergy and Nanosystems, Chinese Academy of Sciences, China

In-situ converting mechanical energy to electricity is a feasible solution to satisfy the increasing power demand of wearable electronics and Internet of Things (IoTs). Triboelectric nanogenerator (TENG) is considered as a potential solution via building self-powered systems. With its pulsed alternating-current (AC) output characteristics, a conventional TENG, based on triboelectrification effect and electrostatic induction, always needs rectification and energy storage units to obtain a constant direct-current (DC) output to drive electronic devices. Here we report a next-generation TENG, which realizes constant current (crest factor ~ 1) output for the first time by coupling triboelectrification effect and electrostatic breakdown, which has similar essence of lightning. Meanwhile, its output charge density can be improved by nanostructure design, working temperature and atmosphere control. Until now, its charge density is reach $\sim 5.4 \text{ mC m}^{-2}$, which is over 2-fold the state-of-art of TENGs. The novel direct-current triboelectric nanogenerator (DC-TENG) is demonstrated to power electronics directly without any rectifier or energy storage units. Our findings not only promote the miniaturization trend of the self-powered system used in wearable electronics and IoTs, but also provide a paradigm shifting technique to harvest mechanical energy efficiently.

7:00 PM *NM09.05.05

Tribotronics for Active Mechanosensation and Self-Powered Microsystems Chi Zhang and Tianzhao Bu; Beijing Institute of Nanoenergy and Nanosystems, Chinese Academy of Sciences, China

Tribotronics has attracted great attentions as a new research field about the control and tuning of semiconductor transport by triboelectricity. Here, the tribotronics is firstly reviewed for active mechanosensation and human-machine interfacing. As the fundamental component, contact electrification field-effect transistor is analyzed, in which the triboelectric potential could be used to control the electrical transport in semiconductors. On the basis, several tribotronic functional devices have been developed including tribotronic smart skin, tactile

sensing array and tuning diode, which has demonstrated triboelectricity-controlled electronics and established the active mechanosensation for external environment. In addition, the triboelectric power management strategy is also reviewed, in which the triboelectricity can be managed by electronics in reverse action. With the implantation of triboelectric power management module, the harvested triboelectricity by various kinds of human kinetic and environmental mechanical energy could be effectively managed as a power source for self-powered microsystems. By the research prospects for interactions between triboelectricity and semiconductor, tribotronics is expected for significant impacts and potential applications in MEMS/NEMS, flexible electronics, robotics, wireless sensor network, and Internet of Things.

7:20 PM *NM09.05.06

Stand-Alone Printed Flexible DC TENGs with Ion-Gel Supercapacitor Ju Hyun Lee, Sungjune Jung and Unyong Jeong; Pohang University of Science and Technology, Korea (the Republic of)

The voltage output of TENG without a rectifier and a capacitor intrinsically displays in sharp AC spikes of several hundred volts. However, numerous functional devices demand continuous DC voltage from the triboelectric power source. Two components are needed for TENG generating a DC voltage (DC-TENG): a rectifier, and a capacitor. Many researches on TENG have employed the conventional silicon diodes to obtain unipolar peaks. Utilizing typical silicon diodes and commercially available aluminum oxide capacitors has been a common way of converting AC voltage to constant voltage, but the integrated triboelectric system based on the hard materials restricts flexibility and patterning. Direct application of the energy harvester as wearable device necessitates a standalone DC-TENG system with flexibility as well as printability. This talk presents the conversion of the spike voltage to continuous DC voltage with the integrated triboelectric system by printing all components of TENG, rectifier, and capacitor on the flexible substrate. And also it demonstrates the self-powered electrochromic display on a single flexible substrate and show the change in color due to the charge accumulation in the ion gel capacitor unit. It holds potential to realize completely wireless and wearable self-power in the future.

7:40 PM NM09.05.09

Dynamic Mechanical Stimuli Communication via Switchable Ionic Polarization Dong-Min Lee, Hong-Joon Yoon and Sang-Woo Kim; Sungkyunkwan University, Korea (the Republic of)

Awareness of diverse tactile experiences has been a challenge toward greater human-machine interaction, which requires its full comprehension for both static and dynamic stimuli. Recent advances in triboelectricity-based touch sensors take great advantages in regard of cost, simplicity of design, and use of a wider range of materials. Due to their reliance on the level of contact electrification at the interface of materials, they encounter major difficulties to measure the extent of deformation of materials under a given mechanical force. Here, we describe an ion-doped gelatin hydrogel-based touch sensor, identifying not only contact with an object but also deformation under a certain level of force. Switchable ionic polarization plays an essential role to allow different sensing mechanisms when the touch sensor is contacted and deformed. We successfully demonstrate that this sensor provides dynamic deformation-responsive signals that can be used to control the motion of a miniature car, thereby broadening the potential applications in a human-machine communication system.

SESSION NM09.06: Nanogenerator VI
Session Chairs: Jianhua Hao and Chengkuo Lee
Sunday Afternoon, April 18, 2021
NM09

9:00 PM *NM09.06.01

Piezoelectric Response of In_2Se_3 Layered Nanosheet Based Heterostructures for Diverse Devices Jianhua

Hao; The Hong Kong Polytechnic University, Hong Kong

Currently, technological progress has pushed increasingly miniaturized devices and systems, stimulating a search for nanoscale piezoelectric materials. Taking the mechanical property with large elastic strain limits, excellent flexibility and the observed piezoelectricity into account, it is expected to develop diverse devices based on the 2D layered nanosheets and their heterostructures, giving rise to ultrathin device technologies towards piezoelectric nanogenerators, actuators, piezo-phototronics, active human-machine smart sensors and self-powered stretchable/wearable devices. Noted that the out-of-plane and in-plane piezoelectricity found in mono- and multilayered α -In₂Se₃ nanosheets offers an opportunity to enable a variety of piezoelectric devices. In my group, we design several kinds of In₂Se₃ layered nanosheet based heterostructures. We have demonstrated the high tunability of In₂Se₃ Raman spectra and PL characteristics under compressive biaxial strain induced by the piezoelectric substrate. The controllable biaxial strain is experimentally imposed on α -In₂Se₃ nanosheets by an electromechanical device. By precisely *in situ* modulating bias voltage on the substrate, the biaxial strain can be generated and delivered to In₂Se₃ nanosheets, resulting in the prominent shift in Raman and PL spectra. The vibrational behavior of In₂Se₃ is examined based on the Grüneisen parameter. On the other hand, we have demonstrated superior out-of-plane piezoelectric coefficient d_{33} for In₂Se₃/MoS₂ vdW heterostructure. By combining the experimental studies and density functional theory calculations, the enhanced piezoelectric properties of In₂Se₃/MoS₂ are ascribed to a larger interfacial dipole moment result from the type II band alignment. The high-precision piezoelectric actuators in 2D atomic scale are conceived based on the out-of-plane piezoelectricity of In₂Se₃ based heterostructure. Lastly, we present enhanced performance in the photodetectors based on In₂Se₃ van der Waals heterostructure according to the piezo-phototronic effect. Consequently, our design and strategies enable us not only to achieve enhanced piezoelectric response in the In₂Se₃ nanosheets, but also to offer the possibility for realizing various high-performance devices. The works are supported by the grants from RGC GRF (PolyU153025/19P), CRF (C7036-17W) and NSFC (No. 51972279).

9:20 PM NM09.06.04

Self-Powered Microbial Disinfection System Using the Nanowire-Enhanced Localized Electric Field

Young Jun Kim, Zheng-Yang Huo and Sang-Woo Kim; Sungkyunkwan University(SKKU), Korea (the Republic of)

Air-transfer pathogens can cause severe epidemics (e.g., COVID-19), which shows a substantial public health threat. Inactivation of the pathogenic microbes in the air is an essential process, whereas the feasibility of existing air disinfection technologies has encountered obstacles including only achieving physical separation but no inactivation, noticeable pressure drops, and energy intensiveness. Here we report a rapid disinfection method for inactivating air-transfer bacteria and viruses using the nanowire-enhanced localized electric field to damage microbes' outer structures. This air disinfection system is driven by a triboelectric nanogenerator that effectively converts mechanical vibration to electricity and achieves self-powered. Assisted by a rational design for accelerated microbes' accelerated charging and trapping, this self-powered air disinfection system promotes microbial transport. It achieves high performance: >99.99% microbial inactivation within 0.025s in a fast airflow (2 m/s) while only causing low pressure drops (<24 Pa). This rapid, self-powered air disinfection method may fill the urgent need for the air-transmitted microbial inactivation to protect public health.

9:30 PM NM09.06.05

Fully Biodegradable Triboelectric Nanogenerator Based on Nature-Derived Polysaccharide with Tunable Lifetime and Tunable Output Performance Minki Kang, Muhammad Syafiq Bin Mohammed Khusrin and Sang-Woo Kim; Sungkyunkwan University, Korea (the Republic of)

Development of biocompatible, biodegradable polymer with tunable properties is essential for multifunctioning implantable electronic devices (IEDs). To address this issue, we propose nature-derived polysaccharide, Kappa Carrageenan-Agar composite (kC-Agar composite) based fully biodegradable triboelectric nanogenerator (TENG). We found that triboelectric property of kC-Agar composite can be largely enhanced because of

electron-donating oxygen-rich functional groups and abundant presence of Ca^{2+} cations via ionic crosslinking. Through the evaluation of surface potential and triboelectric output, we demonstrate 80 wt% kC-Agar composite is the most highly triboelectric positive as well as surface potential is largely increased by at most 58 % compared to kC and Agar. In addition, to reveal the potential of kC-Agar composite for fully biodegradable triboelectric and encapsulation materials, we demonstrate tunable output performance and lifetime of fully biodegradable triboelectric nanogenerator (BDTENG) based on kC-Agar composite by simply varying the concentration. We believe that our findings would provide multiple options for researchers and engineers in the field of IEDs and biodegradable materials.

9:40 PM NM09.06.06

Long-Lifetime Triboelectric Nanogenerator Operated in Conjunction Modes and Low Crest Factor
Xinyuan Li, Jie Wang and Zhong Lin Wang; Beijing Institute of Nanoenergy and Nanosystems, Chinese Academy of Sciences, China

The high-output triboelectric nanogenerator (TENG) is indispensable for its practical applications toward industrial products. However, the electricity loss in simple parallel connection among all units and the typically high crest factor output seriously hamper the practical applications of TENG. Here, a rectified TENG is reported in parallel structure to solve the problem of electricity loss in simple parallel connection. The rotational contact-separation structure with phase difference between rectified TENGs addresses high crest factor output and extends service life of rotational TENG simultaneously. The current crest factor is dramatically decreased to 1.31 in multiple rectifier multiple TENG in parallel (MRM-TENG), while that of TENG in simple parallel is higher than 6. A theory based on simulation results was also proposed to reduce the high crest factor and avoid energy loss of traditional TENG in parallel, and its feasibility was confirmed by the experiment. Meanwhile, the current output can retain up to ~93% of its initial performance after 7 200 000 rotations under 2.00 r s^{-1} of 1000 h. Furthermore, the equivalent current can be in linear growth with low crest factor by making MRM-TENG in parallel for distributed energy supply without electricity loss. This work may provide a new strategy for TENG in parallel to achieve a low crest factor output and long-term cycling stability power generation in distributed energy harvesting for large-scale power application.

9:50 PM *NM09.06.07

Microscopic Models of Contact Electrification Morten Willatzen^{1,2} and Zhong Lin Wang^{1,3}; ¹Beijing Institute of Nanoenergy and Nanosystems, Chinese Academy of Sciences, China; ²Technical University of Denmark, Denmark; ³Georgia Institute of Technology, United States

Quantum-mechanical models for contact electrification are presented by virtue of tunneling and light-assisted electron transfer between dissimilar solids. Firstly, a description of electronic states in solids (either metal/semiconductor/dielectric) is presented using the one-band effective-mass approach. Then, based on continuity of the wavefunction and its derivative (multiplied by the inverse effective mass), computation of the transmission probability through a barrier potential of vacuum (air) is carried out and weighted by the Fermi functions of the solids to the left and right of the vacuum barrier and the electron density of states. The model captures details of the Fermi levels of the two solids in contact, their temperatures, and the vacuum (air) layer thickness. We investigate the strength of the electron transfer as a function of the effective mass, Fermi levels, temperatures, and the vacuum barrier thickness using the Landauer-Boettiker equation in a one-dimensional formulation. Secondly, we take into account the Coulomb repulsion effect that is gradually established as electrons transfer from one material to the other. This is done by solving for the electric field as a function of the temporal build up of surface charges (positive on the material from which electrons are emitted and equally negative on the other material). The resulting electric potential is a linear function of distance in the vacuum region and the envelope of the electron wavefunction becomes a linear combination of Airy functions. Due to the linearly increasing barrier potential, the electron transfer rate is increasingly reduced as the surface charge build up takes place. This leads to a saturation effect such that the Fermi levels do not become equal as time goes. On the other hand, if the electron transfer is small at all times, the two Fermi levels eventually become equal. In the second part of the talk, light-assisted electron transfer models (spontaneous emission, stimulated

emission or absorption) are described using Einstein rate equations and the Fermi Golden Rule. This is first done for a system of coupled atoms separated by a barrier potential and later generalized to arbitrary solids described by Fermi levels.

References

- [1] M. Willatzen and Z. L. Wang, "Theory of contact electrification: Optical transitions in two-level systems", *Nano Energy* 52, 517 (2018).
- [2] M. Willatzen and Z. L. Wang, "Quantum-mechanical model for optical transitions between solids," *Nano Energy* 61, 311 (2019).

10:10 PM *NM09.06.08

Stretchable Nanogenerators for Wearables and Human-Machine Interface Pooi See Lee; Nanyang Technological University, Singapore

Development of mechanical energy harvesting devices that are compliant to curvilinear surfaces or mountable onto human body or skin are attractive for human-machine interface and wearable applications. Fabric based or textile based wearable triboelectric nanogenerators (TENGs) have attracted attention since it is conformable and feasible for users to generate electricity from simple biomechanical motions. We develop a conformable textile nanogenerator utilizing black phosphorus as charge trapping layer. The conformable textile nanogenerator was found to deliver considerably high output with a small force (~ 5 N) and low frequency (~ 4 Hz), which can be used to power small electronic gadgets. Fabric based TENGs with self-cleaning and antifouling properties are important attributes. Through the preparation of hydrophobic cellulose oleoyl ester nanoparticles, a low-cost and nontoxic coating material can be realized to harvest mechanical energy from water flow. The all-fabric-based dual-mode device harvests both the electrostatic energy and mechanical energy of water, achieving the maximum instantaneous output power density of 0.30 W m^{-2} . Recently, with the aim of attaining stretchability, breathability and waterproofness simultaneously for wearable applications, we fabricated mechanical interlocked stretchable nanofibers using electrospinning and electrospraying, delivering breathable TENG for tactile interactive sensing and energy harvesting. Designing thermoplastic elastomer that can be 3D printable attains the function of stretchable triboelectric active layer and simultaneously a stretchable current collector. In addition, we have synthesized self-healable elastomers based on porous supramolecular polyurethane which exhibited gas-solid interacted triboelectric behaviour, with high stretchability and adhesion properties.

SESSION NM09.07: Nanogenerator and Piezotronics I
Session Chairs: Unyong Jeong and Qing Yang
Monday Morning, April 19, 2021
NM09

8:00 AM *NM09.07.01

Innovations at Interfaces for Water Energy Harvesting Zuankai Wang; City University of Hong Kong, Hong Kong

Water covers about 70% of the earth's surface and contains tremendous renewable and clean energy. Despite success in the harvesting hydrodynamic energy based on heavy-weight and bulky electromagnetic generators, a great deal of water energies stored in the low-frequency flow of water, such as in the form of raindrop, river/ocean wave, tide, remain largely untapped. In recent years, numerous promising techniques that allow for the efficient harvesting of water/liquid energy have emerged [1-3].

In this talk, I will discuss our recent progress in taking advantage of the fusion of slippery surfaces and transistor-inspired architecture on efficient water energy [4]. On the research line of liquid/liquid-interface based energy harvesting, we developed a novel slippery lubricant-impregnated porous surface (SLIPS) based

TENG, termed as SLIPS-TENG, that exhibits distinctive advantages including optical transparency, self-cleaning, impact tolerance, flexibility, and enhanced power generation stability even under harsh environments [5]. On the research line of solid/liquid-interface based energy harvesting, we report an original droplet-based energy generator (DEG) with field-effect transistor (FET)-like architecture that fundamentally overcomes the physical limitation inherent in the traditional approaches which are imposed by the undesirable interfacial effect and achieves the highest energy conversion efficiency [6]. Such a unique design allows for the reversible and efficient transfer of charges between the source and drain, resulting in the enhancement of power density by several orders of magnitude over its counterparts.

References:

1. Scruggs, J. & Jacob, P. Harvesting ocean wave energy. **Science**, 323, 1176-1178 (2009)
2. Logan, B. E. & Elimelech, M. Membrane-based processes for sustainable power generation using water. **Nature**, 488, 313-319 (2012).
3. Lin, Z.-H., Cheng, G., Lee, S., Pradel, K. C. & Wang, Z. L. Harvesting water drop energy by a sequential contact-electrification and electrostatic-induction process. **Adv. Mater.** 26, 4690-4696 (2014).
4. Wanghui Xu, Zuankai Wang. Fusion of slippery interfaces and transistor-inspired architecture for water kinetic energy harvesting. *Joule*, <https://www.sciencedirect.com/science/article/abs/pii/S2542435120304438>
5. Xu, W., Zhou, X., Hao, C., Zheng, H., Yan, X., Liu, Y., Yang, Z., Leung, M., Zeng, X.C., Xu, R., Wang, Z. SLIPS-TENG: Robust triboelectric nanogenerator with optical and charge transparency using slippery interface. **Nat. Sci. Review**, 6, 540 (2019).
6. Xu, W., Zheng, H., Liu, Y., Zhou, X., Zhang, C., Song, Y., Deng, X., Leung, M., Yang, Z., Xu, R., Wang, Z., Zeng, X.C., Wang, Z. A droplet-based electricity generator with high instantaneous power density. **Nature**, 578, 392(2020).

8:20 AM NM09.07.02

Self-Polarized PVDF Based Thin-Film Nanogenerator—An Approach Towards Developing Self-Powered Devices Vaibhav Khurana and Dipti Gupta; Indian Institute of Technology Bombay, India

Over the years, self-powered devices (SPDs) have been investigated to reduce the dependency of various electronic components on externally connected power sources. These components not only range from biomedical sensors but also basic building blocks of modern electronics—thin film transistors. SPDs are capable of not only powering and storing the energy but also provide the required driving potential to the sensors, which run at minimal input energy. In general, mechanically powered SPDs work on the principle of piezoelectricity; as human motion-powered devices can be considered as the mechanical power source of energy, these self-powered devices can be produced using the same principle. With this motivation, we have fabricated a piezoelectric nanogenerator (PNG) using poly-vinylidene fluoride (PVDF) as an active material spin-coated on a polyethylene terephthalate (PET) coated aluminum substrate. The adopted approach takes care of the device flexibility along with the extrication of mechanical energy via several degrees of motion owing to the involvement of polymeric components. Piezoelectricity in PVDF matrix is due to an electroactive all-trans β phase (re-orientation of H-F dipoles across C-C chain along one direction). To create a self-polarized PVDF film, we have made use of the quenching process, which has not been much explored in fabricating PNGs. The quenching based polarization solely depends on nucleation and growth concept, specifically nucleation of β crystallites under lower temperature. The employed organic solvents during the fabrication process contributed to the appearance of the β phase, which is confirmed by X-ray diffraction and Fourier transform infrared spectroscopy. These films were then incorporated into a PNG device that had a single active layer providing a thin device that is self-polarized and paves the way towards a small area, robust energy harvester. A two-step approach fabrication of the PVDF device showed exceptional performance, resulting in an open-circuit peak-to-peak voltage of 19.2 V upon human hand pressing and short-circuit current $>0.7 \mu\text{A}$. The average d_{33} value for the quenched PVDF film is observed to be $-15.16 \pm 5.81 \text{ pm/V}$. Further, charging of a capacitor and powering the liquid crystal displays (LCDs) are realized through the nanogenerator, thus validating mechanical energy conversion, storage, and powering applications.

8:30 AM NM09.07.03

Poly(vinyl alcohol)/Polyethyleneimine Composite for Energy Harvesting and Self-Powered Sensing Applications Lingyun Wang^{1,2}, Yunlong Zi² and Walid A. Daoud¹; ¹City University of Hong Kong, China; ²The Chinese University of Hong Kong, China

The advances of wearable electronics and the Internet of things has triggered tremendous demands for wearable power sources as well as sensors, with multifunctionalities, such as transparency and flexibility/stretchability. Since 2012, triboelectric nanogenerators (TENG) have demonstrated themselves as promising power sources as well as self-powered sensors for various applications. Scientists are devoted to enhancing the output performance of TENG through materials exploration, structural design, and circuit management. From a material point of view, developing tribo-materials with a strong affinity to gain/lose electrons, good mechanical, dielectric, surface properties, and other functionalities is one of the key factors to maximize the output power of TENG.

Herein, we explore a poly(vinyl alcohol)/polyethyleneimine composite, featuring high transparency, ionic conductivity, flexibility, good mechanical property, and plenty of functional groups. These features enable the polymer composite capable of serving as both a tribo-material and a current collector for TENG applications. Through embedding conductive nanofillers with surface capping ligands, the dielectric constant of the composite can be fine-tuned, where the higher power output of the resultant TENG can be achieved. In addition, the ionic conductivity of the composite can be enhanced by tuning the weight ratio of polyethyleneimine in the composite, facilitating its charge collection as a current collector. In this regard, a metal-electrode-free transparent wearable power source and a fully integrated self-powered triboelectric sensor array for self-powered tactile sensing are developed. Furthermore, the interfacial interactions between the functional groups of the composite and the carbon dots enable the composite with enhanced transmittance, resulting in a dual-functional layer for both solar energy and raindrop energy harvesting.

References:

1. L. Wang, W. A. Daoud. Highly flexible and transparent polyionic-skin triboelectric nanogenerator for biomechanical motion harvesting. *Advanced Energy Materials*, 2019, 9, 1803183.
2. L. Wang, X. Yang, W. A. Daoud. High power-output mechanical energy harvester based on flexible and transparent Au nanoparticle-embedded polymer matrix. *Nano Energy*, 2019, 55, 433-440.
3. L. Wang, Y. Liu, Q. Liu, Y. Zhu, H. Wang, Z. Xie, X. Yu, Y. Zi. A metal-electrode-free, fully-integrated, soft triboelectric sensor array for self-powered tactile sensing. *Microsystems & Nanoengineering*, 2020, 6, 1-9.
4. L. Wang, Y. Wang, H. Wang, G. Xu, A. Doring, W. A. Daoud, J. Xu, A. L. Rogach, Y. Xi, Y. Zi. Carbon dot-based composite films for simultaneously harvesting raindrop energy and boosting solar energy conversion efficiency in hybrid cells. *ACS Nano*, 2020, 14, 10359-10369.

8:40 AM DISCUSSION

8:50 AM NM09.07.06

Triboelectrification Behaviors and Photoinduced Enhancement of All-Inorganic Perovskite Triboelectric Nanogenerators Yudi Wang, Xiya Yang, Jialong Duan and Qunwei Tang; Institute of New Energy Technology, College of Information Science and Technology, Jinan University, China

The in-depth understanding on the electrification behavior of dielectric materials is a prerequisite to improve the surface triboelectric charge density for triboelectric nanogenerators (TENGs). Dielectric property is favorable for triboelectric materials due to its high charge sustaining capability and dielectrics are commonly utilized for TENG devices. However, the inherent large impedance of dielectric materials undoubtedly causes limited current and power density outputs, alternatively, semiconductors with higher charge mobility can facilitate the charge transfer thus enhancing the electrical output performances.

Halide perovskites, as one of the most promising semiconductors, have gained tremendous attentions in the past decade given its fascinating optical and electronic properties in solar cells, light emitting diodes and

electrochemical sensors. Herein, triboelectric charging affinities and polarities of all-inorganic cesium lead tri-bromine (CsPbBr_3) and ions doped (alkaline earth / alkali metal ions) perovskites are systematically investigated by assembling into vertical contact-separation TENGs. An enriched triboelectric series supplemented with inorganic perovskites and quantified triboelectric charging polarities is delivered through analyzing their dielectric properties, electrical output performances, figure-of-merits (FOM), work function, bond energy and electron binding energy. Moreover, the photoinduced charges play significant role in enhancing the triboelectrification charges and altering charging polarity of perovskite based TENGs under illumination. This work not only supplements inorganic perovskites to triboelectric series and also provides new insights of inorganic perovskite in the foundation of tribo-photovoltaic theory and hybrid devices.

9:00 AM DISCUSSION

9:10 AM NM09.07.10

Micro Triboelectric Ultrasonic Device for Acoustic Energy Transfer and Signal Communication Chen Chen, Xuhui Sun and Zhen Wen; Soochow University, China

As a promising energy converter, the requirements for miniaturization and high-accuracy of triboelectric nanogenerator (TENG) always keep urgent. In this presentation, a micro triboelectric ultrasonic device will be introduced by integrating TENG and micro-electro-mechanical systems (MEMS) technology. To date, it sets a world record of smallest TENG with a 50 μm -sized diaphragm, and enables to bring the working frequency to Mega Hertz. This dramatically improves the miniaturization and chip integration of triboelectric nanogenerator. With 63 kPa@1 MHz ultrasound input, the micro triboelectric ultrasonic device can generate the voltage signal of 16.8 mV and 12.7 mV through oil and sound-attenuation medium, respectively. It also achieved the signal-to-ratio of 20.54 dB and exhibited the practical potential for signal communication by modulating the incident ultrasound. Finally, the detailed optimization approaches have also been proposed to further improve the output power of the micro triboelectric ultrasonic device.

Reference:

C. Chen, Z. Wen, J. Shi, X. Jian, P. Li, J.T.W. Yeow, X. Sun, Micro triboelectric ultrasonic device for acoustic energy transfer and signal communication, *Nature Communications*, 11(2020) 4143.

SESSION NM09.08: Nanogenerator VII
Session Chairs: Jun Chen and Haiyang Zou
Monday Morning, April 19, 2021
NM09

10:30 AM NM09.08.01

Implanted Battery-Free Direct-Current Micro-Power Supply from *In Vivo* Breath Energy Harvesting Jun Li and Xudong Wang; University of Wisconsin–Madison, United States

Majority of current IMDs are powered by conventional primary or secondary batteries that contribute up to 90% weight and volume of the entire device. [1,2] While replacement of or recharging the batteries requires substantial surgical or technical efforts, introducing additional suffering and complexity to the patients, other batteries potential issues such as overheat and leakage of toxic electrolyte further prohibit the advancement and miniaturization of IMDs. Therefore, increasing efforts are now being focused on the innovation of designated IMD power sources. Implantable nanogenerators (i-NGs) have been designed to convert biomechanical energy into electricity. [3,4] In spite of their numerous merits, the outputs of state-of-the-art i-NGs are always in a form of largely discrete pulses. Although their theoretical output power could be sufficient for IMDs, battery component is still needed in the i-NG design to produce a steady and useable direct current (DC) output.

Moreover, most i-NGs are non-stretchable with incompatible mechanical properties compared to soft biological tissues, which further challenges their practical applications.

In this work, we reported an ultra-soft stretchable i-NG system that could function as a battery-free DC micro-power supply. The i-NG consisted of ultrafine micro-scale interdigital electrodes (IDEs) and multi tribo-active layers with a small working area (approximately 2 cm²), packaged with biocompatible silicone elastomer. While the micro IDEs support the output of high frequency electricity (1 μ A at 70 Hz) driven by slow mechanical stimulation, the silicone elastomer and an embedded cavity design enable i-NGs with extremely low Young's Modulus (46 kPa), exactly matching the mechanical property range of most soft biological tissues. By implanted inside the abdominal cavity of Sprague Dawley (SD) adult rats, the i-NG could convert slow diaphragm movement during normal breath into stable high-frequency electrical spikes, which were readily transmitted into a continuous \sim 2.2 V DC output on a LED load after being integrated with a basic electrical circuit (rectifier and capacitor) for a relatively long period of time.

This electric output could continuously power the LED without any observable power decay, successfully demonstrating a constant operation of small electronics DC power free of the battery component. This solely biomechanical-energy driven DC micro power supply offers a very promising solution for the development of self-powered IMDs in the near future.

References:

- [1] A. B. Amar, A. B. Kouki and H. Cao, *Sensors*, 2015, 15, 28889-28914.
- [2] D. C. Bock, A. C. Marschilok, K. J. Takeuchi and E. S. Takeuchi, *Electrochimica Acta*, 2012, 84, 155-164.
- [3] J. Li and X. Wang, *APL Materials*, 2017, 5, 073801.
- [4] M. Parvez Mahmud, N. Huda, S.H. Farjana, M. Asadnia, C. Lang, *Advanced Energy Materials*, 2018, 8, 1701210.

10:40 AM NM09.08.02

Self-Activated Omnidirectional Electrostimulator for Effective Hair Regeneration Guang Yao, Xiaoyi Mo, Jingyi Yan, Qian Wang, Chenhui Yin and Yuan Lin; University of Electronic Science and Technology of China, China

Hair loss is classified as a dermatological disorder due to growth factors deficiency and/or hair cycle disorder, which is a common disease for both men and women throughout the world and the number of hair loss cases in 2011 has exceeded 30% of the global population.[1,2] Major current treatments for hair loss including topical treatments, oral medicine and hair transplant to re-establish healthy hair growth cycles, where topical treatments are the most common choice by patients due to the non-invasive nature and high absorbability. Minoxidil (MNX) and oral finasteride are the two FDA-approved drugs to treat hair loss, but they may still induce severe side effects. Hair transplant is invasive and associated with high cost, discomfortness and time commitment.[3] Recent study showed electric stimulation can induce a non-invasive biological effect named electrotrichogenesis (ETG), which could enhance the influx of calcium ions into the dermal papilla cells via voltage-gated transmembrane ion channels, facilitate ATP synthesis in mitochondria, activate protein kinases, and stimulate protein synthesis and cell division.[4,5] As a result, the ETG effect is believed to be able to regulate secretion of multiple hair growth factors, promote hair follicles (HFs) proliferation, prolong the anagen stage, and ultimately promote hair regeneration. However, the electrical stimulation is typically complicated for implementation and not quite suitable for everyday treatment.

Here, a universal motion-activated and wearable electric stimulation device (*m*-ESD) that can effectively promote hair regeneration via random body motions was designed.[6] Significantly facilitated hair regeneration results were obtained from Sprague-Dawley (SD) rats and nude mice. On shaved SD rats, compared to the other conventional pharmacological MNX and vitamin D₃ treatments, the hair growth rate in *m*-ESD region is 0.73 mm per day, and the final hair shaft length under *m*-ESD was 1.8 times and 2.2 times longer than those treated by MNS and vitamin D₃, respectively. Meanwhile, the HF density from *m*-ESD stimulating was 141% of the MNX and vitamin D₃ regions. We also showed that *m*-ESD can promote HFs proliferation and improve the secretion of vascular endothelial growth factor and keratinocyte growth factor, and thereby alleviate hair keratin disorder, increase the number of HFs and promote hair regeneration on genetically defective nude mice. In general, our work provided an effective hair regeneration strategy in the context of non-pharmacological self-

powered wearable electronic device, and possessed a great value in reshape modern pharmacological physical approaches in biomedical treatments. It is expected to be able to quickly evolve into a practical and facile solution to address the hair loss problem suffered by billions of people over the world.

References:

- [1] Lei, M., Chuong, C. M. Aging, alopecia, and stem cells. *Science* **351** (2016) 559.
- [2] Matsumura, H., Mohri, Y., Binh, N. T., Morinaga, H., Fukuda, M., Ito, M., Kurata, S., Hoeijmakers, J., Nishimura, E. K. Hair follicle aging is driven by transepidermal elimination of stem cells *via* COL17A1 proteolysis. *Science* **351** (2016) aad4395.
- [3] Shapiro, J. Hair Loss in Women. *Engl. J. Med.* **357** (2007) 1620-1630.
- [4] Benjamin, B., Ziginskis, D., Harman, J., Meakin, T. Pulsed electrostatic fields (ETG) to reduce hair loss in women undergoing chemotherapy for breast carcinoma: a pilot study. *Psychooncology* **11** (2010) 244-248.
- [5] Yao, G., Kang, L., Li, J., Long, Y., Wei, H., Ferreira, CA., et al., Effective weight control via an implanted self-powered vagus nerve stimulation device, *Nat Commun* **9** (2018) 5349.
- [6] Yao, G., Jiang, D., Li, J., Kang, L., Chen, S., Long, Y., et al, Self-activated electrical stimulation for effective hair regeneration via a wearable omnidirectional pulse generator, *ACS Nano* **13** (2019) 12345-56.

10:50 AM NM09.08.03

Flexible Symbiotic Non-Pharmacological Biomedical Therapy Systems Guang Yao, Xiaoyi Mo, Jingyi Yan, Maowen Xie, Tianyao Zhang and Yuan Lin; University of Electronic Science and Technology of China, China

Flexible bioelectronics, integrated into a variety of accessories, seamlessly fitting to the skin, or even implanted in the living body, have been extensively researched and have made great progress in biomedical fields such as electronic skin, intelligent monitoring and human-machine interface.[1,2] In particular, a significant interest of flexible bioelectronics lies in monitoring physiological signals, revealing timely information on the state of our body and further providing actionable feedback for disease treatment to sustain a healthy lifestyle.[3,4] In addition, non-pharmacological neuromodulation can manipulate influencing neurophysiological signals or body functions by stimulating through the neural networks to achieve therapeutic purpose, which is a non-destructive and reversible therapeutic strategy.[5,6] However, the device power source still faces the limitation of large size, rigidity and short working life.[7] If wearable electronic devices can be attached to a living body to collect energy generated by low-frequency motion and directly drive a flexible smart biomedical device, the nonnegligible problem of the size, rigidity and working life can be solved.

Here, we present a novel symbiotic non-pharmacological therapy system through low-invasive electrical intervention methods, including a wearable hair regeneration device, an implantable weight loss device and a biodegradable tissue repair device, emphasizing their role in biomedical applications *in vivo* and problems in practical applications. The work of weight loss provides an efficient and low-invasive strategy, and the weight of the device-implanted rat group was reduced by ~40% compared with the control group. A closed-loop feedback regulation system through food intake, gastric motion, electrical neuromodulation and brain control was established. Meanwhile, in the experiments of hair regeneration and tissue repair, the non-pharmacological electrical stimulation can regulate secretion of multiple growth factors, promote cell proliferation, and ultimately achieve the efficient repair effect. In general, due to the non-pharmacological and low-invasive nature, the widespread application of symbiotic bioelectronics will effectively treat more diseases or symptoms.

References:

- [1] J. Y. Sun, C. Keplinger, G.M. Whitesides, Z. Suo, Ionic skin, *Adv Mater*, 26 (2014), 7608-7614.
- [2] T. Someya, Z. Bao, G.G. Malliaras, The rise of plastic bioelectronics, *Nature*, 540 (2016) 379.
- [3] P.J. Soh, G.A.E. Vandenbosch, M. Mercuri, D.M.M. Schreurs, Wearable wireless health monitoring: current developments, challenges, and future trends, *IEEE Microw Mag*, 16 (2015) 55-70.
- [4] M.M. Rodgers, V.M. Pai, R.S. Conroy, Recent advances in wearable sensors for health monitoring, *IEEE Sens J*, 15 (2015) 3119-3126

- [5] Y. Long, H. Wei, J. Li, G. Yao, B. Yu, D. Ni et.al., Effective wound healing enabled by discrete alternative electric fields from wearable nanogenerators, *ACS Nano*, 12 (2018) 12533-12540.
- [6] Yao, G., Jiang, D., Li, J., Kang, L., Chen, S., Long, Y., et al, Self-activated electrical stimulation for effective hair regeneration via a wearable omnidirectional pulse generator, *ACS Nano* **13** (2019) 12345-56.
- [7] T.R. Ray, J. Choi, A.J. Bandonkar, S. Krishnan, P. Gutruf, L. Tian, R. Ghaffari, J.A. Rogers, Bio-Integrated Wearable Systems: A Comprehensive Review, *Chem Rev*, 119 (2019) 5461-5533.

11:00 AM *NM09.08.04

Energy Harvesting and Ultra-Low Power Electronics for Implantable Biosensors and Sustainable Iot

Tharun R. Kandukuri¹, Pelumi Oluwasanya¹, Ioannis Prattis¹, Vincenzo Pecunia² and Luigi G. Occhipinti¹;

¹University of Cambridge, United Kingdom; ²Soochow University, China

Energy-autonomous smart sensor systems have been the subject of intense research and innovation activities for applications in multiple and diverse sectors, from wearable wireless sensor patches in sport, wellness and healthcare to battery-assisted distributed sensor nodes for the Internet of Things [1]. Selecting and combining energy harvesting from multiple sources, including from mechanical displacements, thermal gradients and electromagnetic radiations, from radiofrequencies to visible and infrared light, provides a unique opportunity to extend the battery life throughout the entire lifetime of the device [2]. This is particularly important in applications where physical access to the system once in operation is not convenient, such as in distributed environmental sensors for air quality monitoring in metropolitan or rural areas, and indoor [3], as well as in implantable medical devices, such as those operating low voltage (<1V) biosensors in contact with organs and tissues in order to avoid water electrolysis and faradaic reactions [4].

Both fields are critically affected by the appropriate choice of materials in terms of environmental sustainability at the end of life, such as the battery component materials. In recent work we have demonstrated the possibility to operate the front-end and digital electronics via printable thin-film transistors with a carbon nanotube-based channel and hybrid nanodielectrics operating in the deep-subthreshold ambipolar regime, achieving ultralow voltage (<0.5V) and record-low power consumption of 10^{-15} - 10^{-12} W/ μ m per gate [5].

Hence our research focuses on combining smart sensor technologies with energy harvesting and ultra-low power electronics to achieve long-lifetime and battery-less biosensor systems and sustainable IoT nodes for “place and forget” applications.

Different types and forms of piezoelectric materials such as thin films, bulk or nanowires have been subject of intense research as a route towards mechanical energy harvesting and triboelectric nanogenerators with both environmental sustainability and biocompatibility. Piezoelectricity has been theoretically predicted first [6] and then reported in low dimensional materials, such as hexagonal boron nitride (hBN), transition metal dichalcogenides (TMDs), including MoS₂, MoSe₂, WS₂, WSe₂, MoTe₂ WTe₂, and graphene engineered by atom adsorption (with e.g. Li, K, F, H) or by incorporating non-centrosymmetric in-plane defects [7], with coefficients of piezoelectric strain (d_{11}) and piezoelectric stress (e_{11}) of the 2H-TMD monolayers comparable to, sometimes even better than, those of the conventional bulk piezoelectric materials, such as AlN and GaN.

Additionally, it has been discovered that ultrathin MoS₂ with odd-layers could produce oscillating piezoelectric voltage and current outputs with highest values of the piezoelectric coefficient recorded in the case of a monolayer of MoS₂, whereas no piezoelectric output was observed for the MoS₂ with even-layers [8]. More recent works have reported enhanced values of the piezoelectric effect induced in butterfly-shaped monolayers of MoS₂ with grain boundaries (GB-MoS₂) achieving current densities 50% higher than those measured in MoS₂ monolayers without grain boundaries [9] paving the way towards practical energy harvesting applications for self-powered printed electronic devices.

11:20 AM NM09.08.05

Comparison Between a Selection of Stable and Unstable Charge-Pumps for TENG Conditioning Ahmad

Delbani¹, Naida Hodzic¹, Armine Karami¹, Dimitri Galyko² and Philippe Basset¹; ¹ESYCOM, Université Gustave Eiffel, France; ²LIP6, Sorbonne Université, France

Triboelectric energy generators (TENGs) are characterized by their high electric field and relatively high output

power. They usually generate high AC open-circuit voltage around hundreds of volts peak-to-peak, with relatively low short-circuit current around tens of micro ampere (μA) peak-to-peak. However, most applications require DC voltages around a few volts, with DC current of at least a few hundreds of μA , and a conditioning circuit for the TENG is needed to rectify the high AC voltage. Moreover, for a better kinetic-to-electrical energy conversion, TENGs need to maximize their bias voltage, which can be improved with dedicated conditioning circuits (CC). CC can be separated in two categories: Stable Charge Pumps (SCP) and Unstable Charge Pumps (UCP). SCPs reach constant saturation voltage after a few mechanical cycles, whereas the UCPs can generate an exponential increase of the output voltage until the components' limitation, even with a basic TENG.

Although the unstable charge pumps can show biasing advantages over the stable charge pumps, UCP must have a minimum TENG's capacitance variation for an adequate operation, characterized by the max-to-min ratio η . This constraint may differ from one UCP architecture to another.

In this presentation, we will compare several stable charge pumps (half/full-wave bridge rectifiers and Cockroft Walton multipliers) with different architectures of unstable charge pumps such as Bennet's doubler and its variations from Lefeuvre and Karami. A series of simulations are conducted for all the conditioning circuits under the same parameters for the TENG and the same simulation conditions. The transducer used in simulations has a surface area $S=9\text{ cm}^2$, and a surface charge density $\sigma = -50\mu\text{C}/\text{m}^2$.

It is not simple to make a valid comparison between the UCPs and SCPs. SCPs reach a saturation voltage so the optimal power and the energy conversion is achieved during a specific mechanical cycle. On the other hand, UCPs' rectified voltage is always increasing thus the energy, and there is no specific optimal power. Due to such discrepancy between the two, the comparison will be done by choosing a certain mechanical cycle at a given maximal voltage and calculating its QV-cycle area. We show that there is a tradeoff between the time needed to reach the high energy conversion state and the amount of the converted energy. SCPs are more convenient if we need to reach a significant energy conversion rate very quickly. On the contrary, if we want much higher energy conversion, UCPs need to be chosen, but it requires more time, thus average power cannot be that good, unless a 2-stage power management system is used.

11:30 AM NM09.08.06

Study of the Bennet Doubler Conditioning a TENG with a Double Anti-Phase Variable Capacitance

Naida Hodzic¹, Ahmad Delbani¹, Minki Kang², Armine Karami¹, Sang-Woo Kim², Dimitri Galayko³ and Philippe Basset¹; ¹ESYCOM, Université Gustave Eiffel, CNRS, CNAM, France; ²Sungkyunkwan University (SKKU), Korea (the Republic of); ³Sorbonne Université, LIP6, France

Kinetic energy harvesters (KEHs) are typically not considered as stand-alone devices having very high voltage and low current at the output. Given that the direct converted energy cannot be sufficient for powering a system, and at minimum need to be rectified, conditioning circuits are necessary. Traditionally, stable charge pumps such as half- full-wave rectifier, or unstable charge pumps such as Bennet's doubler are used. It has been previously shown that unstable charge pumps can be significantly more efficient due to no limitations or saturation points in charge multiplication. Keeping the high energy conversion in mind, Bennet's charge doubler has been studied in detail and applied to different architectures and types of electrostatic KEHs, such as triboelectret nanogenerators (TENGs). Several variations of this circuit have also shown the expected exponential increase with various optimum for specific TENG configurations.

By adding a third electrode to a classical 2-electrode TENG, we can obtain a device with three terminals and two variable capacitors having a 180° phase-shift. Converted energy of such device is higher than of a similar TENG with one variable capacitor, but specific conditioning is needed. In this work, we demonstrate that replacing the fixed capacitor in Bennet's charge doubler by the 2nd variable capacitor of the 3-electrode TENG leads to higher converted energy. While this new combination gives promising results, its behavior and details about each phase that occurs during one conversion cycle have not been fully analyzed yet.

To obtain the most information about the circuit's behavior during the energy conversion process, the best is to observe the change of voltage and charge over the two TENG's variable capacitors. Taking each of them and examining their behavior through variation of the two mentioned parameters gives the converted energy in each mechanical cycle. This study discussed critical points occurring during one conversion cycle that are a combination of mechanical and electrical variations occurring at the same time. Constraints are set for the

TENG, particularly the physical parameters defining $\eta = C_{max}/C_{min}$ ratio conditioning the start of the circuit. Furthermore, we broke down and analytically expressed each significant moment within one mechanical cycle of double variable TENG. Each crucial point is defined by relevant parameters such as local capacitance, voltage and charge over the capacitor, leading to the full definition of such a system.

The analytical study of double variable TENGs is corroborated with simulation models with Bennet's charge doubler circuit operating in steady state, or in other words, when exponential output is guaranteed. Theoretical study and simulation results have been completed by experimental test through practical implementation of a gap-closing double variable TENG and the charge doubler circuit, leading to the conclusion that, indeed, realistic systems convert expected higher amounts of energy.

Even though this study has been conducted on double variable gap-closing TENG, it can be universally applied to any three-terminal KEH with a phase shift of 180° between its output signals, ensuring steady exponential output.

11:40 AM NM09.08.07

Late News: Combined Design of Wind Tunnel and Triboelectric Structure for Optimized Power Conversion Elias Kharbouche, Cyril Calmes, Marc Ramuz, Roger Delattre and Sylvain Blayac; Mines Saint-Etienne, France

The last decade highlighted Triboelectric Nanogenerators (TENGs) as a very promising technology for the conversion of mechanical energy into reliable electrical power sources. This technique takes advantage of the triboelectrification effect. Nowadays, lithium batteries supply the biggest part of Internet of Things (IoT) nodes since their energy storage density is significant. However, considering the limits in terms of maintenance cost, resources consumption and environmental dissemination, it is highly desirable to develop alternative self-powering solutions. In the context of the fourth industry era, the wind energy extraction from ventilation systems or areas with permanent airflows can supply enough power for the operation of numerous sensors deployed in the facilities. Ambient energy harvesting is then to be considered as an attractive solution to provide sustainable power sources.

Our initial investigation of an Insulator-Metal-Insulator (IMI) composite thin-film reported an attractive way to obtain compact devices with high power density. The presented work highlighted the great potential of this multilayer structure in a high-performance Wind Actuated Triboelectric Nanogenerator (WATENG). For this study, the collecting wind tunnel is improved. This solution converts wind power to lateral oscillations in a symmetric triboelectric structure using mobile flexible electrodes. This innovative architecture optimizes the triboelectric charges accumulation into metal islands to boost the output power of the WATENG. Different customized stacks and materials are investigated to overcome the localized charge density saturation into the triboelectric harvesting layers.

This study demonstrates the great potential of an IMI structure coupled to a pioneering WATENG architecture in the same device, to greatly enhance the potential airflow-powered connected objects.

SESSION NM09.09: Nanogenerator VIII

Session Chairs: Aurelia Chi Wang and Renyun Zhang

Monday Afternoon, April 19, 2021

NM09

1:00 PM NM09.09.02

Late News: Ultraflexible and High-Durable Ferroelectric Transducers and Organic Circuits for Energy-Efficient Wireless Health Patches Andreas Petritz^{1,2}, Esther Karner-Petritz^{1,2}, Takafumi Uemura², Philipp Schöffner¹, Teppei Araki², Barbara Stadlober¹ and Tsuyoshi Sekitani²; ¹Joanneum Research

Health is a very precious commodity, as we experience every day and especially in these times shaken by a pandemic. Continuous recording of health status through diagnostic techniques that combine high wearing comfort with high reliability, accuracy and cost-effectiveness is therefore very desirable. In this context, we present an ultraflexible solution for the power supply of wireless medical patches for monitoring of heart rate and blood pressure. The ultraflexibility is due to the very low overall thickness (only 2.5 μm in total) of the ferroelectric polymer transducers, organic rectifiers and capacitor components manufactured on a substrate only 1 μm thick, and it guarantees high sensitivity (15 nC N^{-1}), superior component reliability (over 6000 cyclic loading) and a very high peak power density (1 mW cm^{-3} at 2 Hz excitation). Our health patch solution not only includes this radically reduced layer thickness, but also new material combinations (ferroelectric polymers on parylene), novel device concepts (organic thin-film transistor-based diodes) and new integration principles (multi-stack transducers on 3D curved surfaces).¹

¹Petritz et al. submitted; preprint DOI: 10.21203/rs.3.rs-86704/v1;

1:10 PM NM09.09.03

Late News: Fully Spray Coated Flexible Triboelectric Devices for Self-Powered Wearable and Ubiquitous Sensors Shujia Xu^{1,2} and Wenzhuo Wu^{1,2,3}; ¹Purdue University, United States; ²Flex Laboratory, United States; ³Birck Nanotechnology Center, United States

Triboelectric nanogenerator (TENG) has been widely used as self-powered wearable sensor, and progresses on novel material for high output TENG have attracted tremendous attention. However, simultaneous consideration on materials system design and manufacture process receives limited attention. Manufacture and encapsulation techniques feasible for large scale fabrication compile with functional materials systems need to be developed. Spray coating is an attractive method due to its potential for large scale deposition of ink-based materials. Here, we demonstrate fully sprayed TENG using ink-based functional materials. Several functional inks compatible with spray coating are formulated to fabricate flexible TENG for human pulse monitoring and human-machine interaction. All functional materials are solution processable and can be sprayed layer-by-layer to form the triboelectric sensor. Such flexible sensors could also be sprayed and integrated on arbitrary surfaces for ubiquitous electronics and sensors.

1:20 PM *NM09.09.04

Bio-Derived Materials Based Wearable Triboelectric Sensors for Human-Integrated Technologies
Wenzhuo Wu; Purdue University, United States

The capability of sensor systems to efficiently scavenge their operational power from stray, weak environmental energies through sustainable pathways could enable viable schemes for self-powered health diagnostics and therapeutics. Triboelectric nanogenerators (TENG) can effectively transform the otherwise wasted environmental, mechanical energy into electrical power. However, obstacles hindering the development of efficient triboelectric devices based on biocompatible materials continue to prevail. I will discuss our recent progress in the design and engineering of bio-derived materials for biocompatible, wearable triboelectric devices.

Such wearable devices are conformable to human skins and can sustainably perform non-invasive functions, e.g., gesture recognition, by harvesting the operation power from the human body. These devices can also detect the imperceptible skin deformation induced by the human pulse and capture the cardiovascular information encoded in the pulse signals with high fidelity. The gained fundamental understanding and demonstrated capabilities enable the rational design and holistic engineering of novel materials for more capable biocompatible triboelectric devices that can continuously monitor vital physiological signals for self-powered health diagnostics and therapeutics.

1:40 PM NM09.09.05

High-Performance Tactile Graphene-Based TENG Devices Based on Simple Laser-Assisted Fabrication Method

Method Kapil K. Bhorkar^{1,2}, Nikolaos Samartzis^{1,3} and Spyros N. Yannopoulos¹; ¹FORTH, Greece; ²Univ Rennes, France; ³University of Patras, Greece

Strong research efforts have been dedicated towards the miniaturization of energy conversion devices to support the development of self-powered sensors and relevant devices. The harvesting of ambient energy, predominantly vibrational motion, has been demonstrated to convert into the electrical energy by employing various mechanisms, such as electrostatic, electromagnetic, and piezoelectric. These devices face a number of unachievable targets related to the proper output power demanding by specific applications, durability to withstand long life time and flexibility to conform to requirements of wearable electronics. Triboelectric nanogenerators have emerged as an alternative technology to confront with the above challenges. The first TENG devices have been envisaged and fabricated by Wang and co-workers [1]. The working principle is based upon the coupling between electrostatic induction and triboelectric effect. In the current work, we apply a novel method which entails the simultaneous growth and deposition of graphene on any substrate with the use of laser-assisted decomposition of organic compounds. The method allows the deposition of hybrid nanomaterials with a single laser processing step. Employing this method, a single-electrode TENG device architecture was implemented by the direct laser-assisted forward transfer of graphene and graphene/SiO_x hybrids on PDMS substrate acting as one of the tribo-materials. A fairly low sheet resistance of the graphene film and its ability to withstand several cycles of operation are key factors towards replacing the precious metals deposited on the back side of the contact material. The electrical features and the output power of the flexible single-electrode TENG devices were evaluated against various external loads. A remarkable finding of this work is that the current external resistance value providing maximum output of the TENG, is much lower than values reported in the literature. Given the high impedance of other TENGs, this is a significant advantage of the current device, considering that the reduction of the internal impedance is highly desirable in a number of applications requiring low impedance loads for many practical applications.

[1] Fan, F. R., Tian, Z. Q. & Wang, Z. L. Flexible triboelectric generator. *Nano Energy* 1, 328–334 (2012).

1:50 PM NM09.09.06

Understanding the Fundamental Role Played by Electrodes Design for Increasing Triboelectric

Nanogenerators Power Output Giuseppina Pace¹, Michele Serri², Alberto Ansaldo², Antonio Esau Del Rio Castillo³ and Francesco Bonaccorso³; ¹Consiglio Nazionale delle Ricerche, Italy; ²Istituto Italiano di Tecnologia, Italy; ³BeDimensional S.p.A., Italy

The operation of wearable and portable electronics requires only few tens of microwatts of power supply. These new low power devices, such as the one largely developed for the internet of Things technologies (IoT), have fostered the development of low power energy sources which harvest the environmental green energy. In particular, the fast-growing demand for new sustainable energy, and the ubiquitous and abundant environmental mechanical energy, has raised the interest in energy harvesters able to convert such energy into electrical power. Triboelectric nanogenerators (TENGs) can provide such green power supply. Recent developments in TENGs technology show that they can be used in different applications ranging from wearable self-powered sensors to wind and sea wave energy harvesting (blue energy). Despite the wide number of TENGs developed so far, an in depth understanding of their working mechanism operating at the sub-microscale is still missing. In this work, we highlight the fundamental role played by the interface between the triboelectric material and the electrode collector in contributing to the TENG's power generation. In particular, we will show the fundamental role played by the electrodes work function and capacitance in boosting triboelectric nanogenerators power outputs. We will describe the guidelines for the combination of electrode and triboelectric materials to optimize the mechanical energy conversion efficiency in TENGs. The outcomes of our studies provide essential insights for the proper design of new TENGs to the aim of further enhancing their performances.

2:00 PM NM09.09.07

Strain-Induced Piezoelectric Polarization of Zinc-Oxide Nanosheets Studied via Piezo Force Microscopy

Corey Carlos, Kevin J. Berg and Xudong Wang; University of Wisconsin–Madison, United States

Flexible, wearable, and human-compatible electronics are helping shape a future of integrated nanotechnologies. As such, piezoelectric and semiconducting materials have drawn intense interest by many research groups for the excellent potential to advance the field of wearable devices. Moreover, two-dimensional (2D) nanomaterials, valued for their enhanced mechanical, electronic, and structural properties, have moved to the forefront of compliant electronic devices. Therefore, a thorough understanding of the interfacial charge distribution is required when utilizing flexible piezoelectric semiconductors, such as zinc-oxide (ZnO). We present a method for monitoring the piezoelectric response of nanometer-thick 2D ZNO nanosheets (NS) grown via Ionic Layer Epitaxy (ILE). The direct piezoelectric effect, and the coupling of electronic dipole polarization to lattice strain within ZnO-NSs, is monitored *in situ* via piezo force microscopy (PFM). Using PFM, we illustrate the effects of modulating strain in piezoelectric nanomaterials and its role in the polarization charge distribution across the surface of the 2D ZnO-NS. Our results illustrate the critical need for understanding the interdependent roles of static piezoelectric charges, semiconducting properties, and strain, for future flexible devices.

SESSION NM09.10: Poster Session: Nanogenerators and Piezotronics I

Session Chairs: Wenbo Ding and Sang-Woo Kim

Monday Afternoon, April 19, 2021

9:15 PM - 10:10 PM

NM09

NM09.10.01

Self-Powered Electronic Paper with Energy Supplies and Information Inputs Solely from Mechanical Motions

Tingting Hou^{1,2}, Bo-ru Yang³, Xiong Pu^{1,2} and Zhong Lin Wang^{1,2}; ¹Beijing Institute of Nanoenergy and Nanosystems, Chinese Academy of Sciences, China; ²University of Chinese Academy of Sciences, China; ³Sun Yat-sen University, China

The electronic paper (E-paper) display features flexibility, sunlight visibility and low power consumption, which makes it ideal for Internet of Things (IoT) applications where maintenance of bulky power modules is better to be eliminated. In electrophoretic E-papers, the most successfully commercialized E-paper technology, there are generally different color particles, and these particles are usually surface-modified and charged by charge control agents (CCAs) for good stability in nonpolar solvent. The color of a pixel is updated by changing the distribution of charged pigment particles of different colors between two electrodes with an external electric field. With the specific driving waveforms, different distributions of pigment particles are formed to provide various colors according to Grassmann's laws, which indicates the possibility of full-color E-paper.

Currently, smart sensor networks of the emerging Internet of Things (IoT) have to be self-powered by the energy *in-situ* harvested from the working environment, so as to avoid the impossible maintenance of numerous smart devices. This trend bring E-papers new opportunities, especially if a low-power E-paper can be integrated with an energy-generating device for self-powered displays.

Therefore, we report a unique self-powered E-paper (SPEP), where information inputs and energy supplies are all converted from mechanical motions by a sliding-mode triboelectric nanogenerator (TENG). The operation of an electrophoretic E-paper is firstly investigated, identifying the current density as a determinative parameter for driving pigment particles motion and color change. Electrical and optical responses of the E-paper driven by a sliding-mode TENG are then found to be consistent with that under a current source mode. All-in-one monochromatic and chromatic SPEPs integrated with a flexible transparent TENG are finally demonstrated. The sliding-driven mechanism of SPEP allows potential handwriting function, is free of extra power supply and promises certainly a wide range of future applications.

NM09.10.02

Acoustic Sensor Based on Two-Dimensional Piezoelectric MoS₂ Hyoung Taek Kim, Ahrum Sohn, Jae-Hwan Jung and Sang-Woo Kim; Sungkyunkwan University, Korea (the Republic of)

Experimental studies on the physical properties of two-dimensional (2D) materials have grown exponentially since 2D materials offer unique advantages for use in such next-generation devices. Various semiconducting 2D materials have been studied, including transition metal dichalcogenides (TMDs) such as molybdenum disulfide (MoS₂), molybdenum diselenide (MoSe₂), tungsten diselenide (WSe₂), which are likely to bring breakthroughs in future electronic and optoelectronic devices. The physical properties of 2D MoS₂ nanosheets have been actively explored particularly as a result of their possible integration in both nano/microelectromechanical devices and energy harvesting devices. Monolayer MoS₂ has a direct band gap and high mobility and has been used to successfully fabricate field-effect transistors so it has emerged as an interesting complement to graphene in various semiconducting applications. In addition, it is expected that piezoelectric properties of 2D layered materials are very useful to realize highly sensitive, high impact resistive, self-powered sensor. However, studies on the suspended model of 2D MoS₂ have been done mainly on studies on the measurement method or photosensitivity, and studies using the piezoelectric characteristics of suspended MoS₂ have not been actively done. Here we demonstrate a new way to use 2D MoS₂ for highly sensitive 2D piezoelectric acoustic sensor. The acoustic sensor fabricated by using suspended structure of MoS₂ that generate piezoelectric output potential due to vibration transmitted by sound. We have achieved high sensitivity and high impact resistance by using single layer or several layers of MoS₂, and by using piezoelectric properties of MoS₂, we have produced an acoustic sensor that does not require standby power. This study demonstrates a new way of studying 2D MoS₂ research and acoustic sensors by developing a high-sensitivity and high-durability acoustic sensor using suspended MoS₂.

NM09.10.05

Anisotropic Structural Index for Ferroelectric Properties of Strained KNbO₃ Perovskite Polymorphs Woohyun Hwang, Seungjae Yoon, Jihwan Lee and Aloysius Soon; Yonsei University, Korea (the Republic of)

Despite many attempts to harness a strain-driven control of ferroelectric properties in thin films, there remains a technical hurdle to understand the delicate relationship between crystal structure, spontaneous polarization (P_s), and the electronic band gap (ϵ_{gap}) modulation under the anisotropic strain. To further our understanding of how these complex anisotropic structure-property relationships may be rationalized by their local atomic arrangements in ferroelectric materials, we perform first-principles density-functional (perturbation) theory calculations to understand how applied epitaxial strain may influence their structural, thermodynamic, electronic, and (anisotropic) polarization properties in polar KNbO₃ polymorphs – a potential contender for Pb-free piezoelectric applications. Specifically, we examine the displacement of the center metal cation (niobium, Nb) as a key descriptor for its polar behavior and find that it exhibits an anisotropic nonlinear relationship between ϵ_{gap} and the commonly-used isotropic scalar quadratic elongation ($\langle\lambda\rangle$). To overcome the inadequacy of the simple $\langle\lambda\rangle$, we propound a revised definition of this key structural descriptor – the new bond elongation index (λ_i), that contains vectorial structural information. Using λ_i , we successfully rationalize the linear dependency of direction-dependent P_s on λ_i for strained KNbO₃ polymorphs with a R^2 value of 0.998. We further demonstrate and verify that this newfound linear relationship can be used to predict direction-dependent P_s in BaTiO₃ polymorphs without further expensive calculations under strain, and thus allows for the fast and consistent determination of direction-dependent P_s in strained perovskite polymorphs in the course of high-throughput polar materials design.

NM09.10.07

Auxetic Structure Enabling the Bending Energy Harvesting Mode of Piezoelectric Nanogenerator Xinran Zhou^{1,2}, Shlomo Magdassi^{3,2} and Pooi See Lee^{1,2}; ¹Nanyang Technological University, Singapore; ²Campus for Research Excellence and Technological Enterprise (CREATE), Singapore; ³The Hebrew University of Jerusalem, Israel

Piezoelectric nanogenerator (PENG) is a kind of mechanical energy harvester, which utilizes the dipole moment in piezoelectric material to convert mechanical energy to electrical energy. Among all piezoelectric materials, PVDF-based piezoelectric polymer is one of the best materials for PENG due to its high piezoelectricity, light weight, simple fabrication, and high toughness and flexibility comparing with the ceramics. However, since the elasticity of PVDF-based polymers is low, the piezoelectricity in the 31 and 32 directions are underutilized. In this work, auxetic structure is 3D printed onto the drop casted piezoelectric film, of which the synclastic effect enables the bending mode energy harvesting of piezoelectric films by slightly stretching the film in 1 and 2 directions during bending, activating the 31 and 32 direction piezoelectric effect, at the same time the tensile strain of the film can be controlled to avoid over-stretching the device. The structure design and strain distribution are evaluated by finite element analysis. The piezoelectric composites made of P(VDF-TrFE) copolymer and surface modified barium titanate nanoparticles effectively improves the piezoelectricity. With the auxetic structure, the PENG can generate voltage over six times of that without the auxetic structure. Under slight bending, it generates 350 nW/cm² power density. The PENG is also demonstrated as a sensor to detect the motion at various positions on human body.

NM09.10.08

Self-Powered Flexible Fiber-Based Triboelectric Sensors Toward Traffic Monitoring System Guangqing Liu, Xiya Yang, Jialong Duan and Qunwei Tang; Institute of New Energy Technology, College of Information Science and Technology, Jinan University, China

With the rapid development of 5G network and internet of things (IoT), there are incredibly increasing sensors and corresponding applications emerging to benefit our daily lives. However, the power supplies for the countless sensors become an issue to suppress the IoT further expansion. In this work, we present a strategy which applies triboelectric nanogenerator (TEG) as self-powered sensor in traffic control system. Flexible and reliable polyvinylidene fluoride (PVDF) embedded with multi-wall carbon nanotubes (MWCNTs) fiber-based composite membrane is synthesized by electrospinning to act as triboelectric layers. Vertical contact-separation mode is adopted to design the fiber-based triboelectric sensor toward detecting the incoming vehicles signals on roads. Through systematically investigating the impacts of MWCNT concentration and controlling the electrospinning parameters, the electrical output performances of the fiber-based triboelectric sensors are optimized and an ultra-sensitivity can be achieved for detecting the vehicles signals. Based on the sensors' electrical charges outputs and the advanced cloud IoT services, a traffic control system including traffic flow management, offending vehicle such as overlapping and overspeed capture, and plate number recognition is developed to facilitate the potential application scenarios of the fiber-based triboelectric sensors. This engineered self-powered triboelectric sensors not only open a new potential area for TENG in traffic monitoring, but also significantly popularized the application of TENG in IoT industry.

NM09.10.09

Honeycomb Structured Triboelectric Nanogenerator for High-Efficiency Particulate Matter Filtration Toward Vehicle Exhaust Scavenging Dahao Chen^{1,2}, Xiya Yang¹, Chuanyong Xu^{1,2}, Xiaozhen Du² and Qunwei Tang¹; ¹Institute of New Energy Technology, College of Information Science and Technology, Jinan University, China; ²College of Mechanical and Electronic Engineering, Shandong University of Science and Technology, China

Air pollution has become a major environmental concern due to the large amount of air pollutants emitted from human activities such as traffic, industry, and power plants. Particulate matter (PM) serious impacts the living environment in terms of air quality, visibility, climate effects and ecosystems. Haze is mainly formed by PM_{2.5} (PM with diameter of 2.5μm or less), which results in serious health issues such as cardiovascular and respiratory diseases and even lung cancer, increasing the morbidity and mortality. Based on the coupling of the triboelectric effect and electrostatic induction effect, the typical characteristic of triboelectric nanogenerator (TEG) is its high voltage output of hundreds to thousand volts, which is promising for capturing the PMs using electrostatic effect without external power supply. Herein, a honeycomb ceramic based triboelectric PM

vehicle exhaust filter (HTPMF) filled with fluorinated ethylene propylene (FEP) particles is introduced to efficiently capture the PMs from vehicle exhaust. Finite element analysis software (COMSOL) is applied to simulate the dynamic behaviors of the triboelectrification process of the PMs in the HTPMF. An open-circuit voltage of 63V can be achieved in one single hole of the HTPMF. Through well controlling the number of FEP particles, the achieved filtration efficiency for PM1.0, PM2.5, PM4.0, PM10 are all over 90% with the highest filtration efficiency of 93.49% for PM2.5. This honeycomb triboelectric PM filter presents promising potential in the application for industrial dust emission and vehicle emission removal.

SESSION NM09.11: Nanogenerator and Pieztronics II
Session Chairs: Yong Qin and Zhen Wen
Tuesday Morning, April 20, 2021
NM09

8:00 AM NM09.11.01

Fusion of Slippery Interfaces and Transistor-Inspired Architecture for Water Kinetic Energy Harvesting Wanghuai Xu and Zuankai Wang; City University of Hong Kong, Hong Kong

Water and energy, as two fundamental components of our 21st-century life, cannot be considered separately. Solving this water-energy nexus becomes a promising strategy to relieve the global energy and water crisis facing humanity today. In this regard, the diversiform water-related energies, such as tidal energy, wave kinetic energy, and thermal differential energy, are being explored to generate electricity. Recently, interfacial energy harvesting, relying on the interfacial charges and relative motion between two different materials, is drawing significant attention, as it provides new pathways for collecting the low-frequency water energy. In spite of the extensive progress, the state of the art low-frequency water energy harvesting devices are generally limited by low energy density, poor durability, and hence it remains challenging for multiscale practical implementations. In this talk, I will focus on high-performance water kinetic energy harvesting by designing novel slippery materials and novel electrode architecture. First, I will report an original droplet-based energy generator (DEG) with transistor-inspired architecture that fundamentally overcomes the physical limitation inherent in the traditional approaches, which are imposed by the undesirable interfacial effect, and achieves the highest energy conversion efficiency and power density. Second, inspired by hierarchical structures on the peristome of the Nepenthes pitcher, we will also report a novel slippery lubricant-impregnated porous surface (SLIPS)-based TENG, termed as SLIPS-TENG, that exhibits distinctive advantages including optical transparency, self-cleaning, impact tolerance, flexibility, and enhanced power generation stability even under harsh environments. In the future, we envision fusing the advantages inherent in slippery interfaces and transistor-inspired architecture will provide a paradigm shift in the design of efficient energy harvesting devices, and trigger a new wave in the research of the water energy harvesting, including basic fundamental understanding, material design, as well as the multiscale practical applications.

8:10 AM NM09.11.05

A Highly Efficient Triboelectric Negative Air Ion Generator Hengyu Guo; Chongqing University, China

Negative air ions (NAIs) have been widely harnessed in recent technologies for air pollutant removal and their beneficial effects on human health, including allergy relief and neurotransmitter modulation. Herein, we report a corona-type, mechanically stimulated triboelectric NAI generator. Using the high output voltage from a triboelectric nanogenerator, air molecules can be locally ionized from carbon fibre electrodes through various movements, with the electron-ion transformation efficiency reaching up to 97%. Using a palm-sized device, 1×10^{13} NAIs (theoretically 1×10^5 ions cm^{-3} in 100 m^3 space) are produced in one sliding motion, and particulate matter (PM 2.5) can be rapidly reduced from 999 to 0 $\mu\text{g m}^{-3}$ in 80 s (in a 5,086 cm^3 glass chamber) under an operation frequency of 0.25 Hz. This triboelectric NAI generator is simple, safe and

effective, providing an appealing alternative, sustainable avenue to improving health and contributing to a cleaner environment.

8:20 AM NM09.11.06

Effect of Surface Modification on the Electromechanical Properties of Lead-Free (Na,K)(Nb,Sb)O₃-BaZrO₃-(Bi,K)ZrO₃ Nanoparticle-Embedded Piezoelectric Composite Nanofiber for Flexible Nanogenerators Seung-Rok Kim, Ju-Hyun Yoo, Ji Ho Kim, Yong Soo Cho and Jin-Woo Park; Yonsei University, Korea (the Republic of)

Emerging deformable energy harvesting systems gain a significant interest as power sources for wearable and implantable electronics because they acquire and convert readily available mechanical, ambient light, biochemical, and thermal energies from the human body and surroundings into electrical energy. Among deformable energy harvesting systems, piezoelectric nanogenerators (PNGs) are the most promising because they harvest the mechanical energy provided by the evermoving and deforming human body to empower wearable electronics. Although PZT is one of the most extensively exploited ceramic piezoelectric materials because of their high piezoelectric coefficient, high Curie temperature, and low cost, the inherent toxicity and rigidity of Pb-based PZT restrict its application to wearable electronics. Hence, tremendous efforts have been made to develop Pb-free perovskite-structured ceramic alternatives to solve the safety issues of PZTs, while the hybrid composite of Pb-free perovskite-structured ceramics with organic polymers ensures the deformability of f-PNGs as the power sources of wearable electronics. However, the excellent mechanical energy harvesting performance of flexible PNGs made of perovskite ceramic nanoparticles (PCNPs) embedded in piezoelectric polymer NFs is challenging to achieve because of the poor adhesion between the ceramic and polymer materials. Because of the weak interaction of the ceramics and polymers together with the very high surface-to-volume ratio of the nanoparticles, the PCNPs easily form agglomerates within the polymer NFs. In this work, we investigated the mechanical and piezoelectric properties of Pb-free NKNS-BZ-BKZ PCNPs uniformly embedded in c-NFs for f-PNGs. A significant reduction in the agglomerate size of the PCNPs and their enhanced interfacial adhesion with the P(VDF-TrFE) matrix were achieved through a tetradecylphosphonic acid (TDPA) surface treatment of the PCNPs. The surfaces of the NKNS-BZ-BKZ PCNPs were modified with TDPA to enhance the interfacial interaction of the PCNPs with the P(VDF-TrFE) matrices. We used the electrospinning method for fabricating the c-NFs of NKNS-BZ-BKZ PCNPs and P(VDF-TrFE) piezoelectric polymers. Particle size distribution analysis, transmission electron microscopy (TEM), and in situ tensile testing in a scanning electron microscope chamber were used to evaluate the effect of the TDPA surface treatment of the PCNPs on the mechanical properties of the c-NFs. The piezoelectric properties of the c-NFs were characterized through Kelvin probe force microscopy (KPFM) and PNG cell performance evaluation. The uniform distribution of the embedded PCNPs made the web of c-NFs highly negative relative surface potential and a high effective modulus of approximately 170 MPa. Consequently, the f-PNG with the TDPA surface-treated PCNPs maintained an open-circuit voltage, a high maximum generated power, and an output voltage of approximately 12.2 V, 33.2 nW, and 1.25 V, respectively, despite being bent for 10,000 cycles at a bending radius (r) of 15 mm.

8:30 AM NM09.11.07

Tactile Electronic Skin to Simultaneously Detect and Distinguish Between Temperature and Pressure Based on a Triboelectric Nanogenerator Fang Yi; Sun Yat-sen University, China

Tactile electronic skin (e-skin) aims to mimic the functions of skin, which could have profound implications for areas including medical care, prosthetics and robotics. However, it faces a great challenge to simultaneously detect and distinguish between multiple stimuli by a single device. Here, a tactile e-skin that can simultaneously detect and distinguish between temperature and pressure in real time is developed, based on a single-electrode-mode triboelectric nanogenerator (TEENG) with a specially prepared thermoresistive electrode combining BiTO and rGO. The TEENG based tactile e-skin outputs voltage in response to pressure and its electrode resistance changes in response to temperature (thermal sensitivity $\beta_{25/100}$: 1024 K, temperature coefficient of resistance: -1.15 %/K at 25 °C, range: 25~100 °C). The pressure sensing performance maintains stable with varying

temperatures and the temperature sensing performance is undisturbed under pressure. The tactile e-skin also demonstrates excellent sensing reproducibility and durability. When the e-skin is mounted on the human body, it can monitor and distinguish between temperature and pressure with the two signals imposing no interference on each other. This work provides new routes for wearable sensing and sheds new light on the development of electronic skin.

8:40 AM DISCUSSION

8:50 AM NM09.11.10

Fabrication of Piezoelectric Biomaterials for Energy Applications Rusen Yang; Xidian University, China

Multifunctional materials have received increasing attention in recent years. Owing to their inherent biological nature as well as piezoelectric properties, piezoelectric biomaterials are considered as promising candidates for application in fields ranging from electrochemical energy storage to biological systems. Rational material design is important to enhance their piezoelectric and biological activity. Herein, recent advancements to piezoelectric biomaterials like peptide-based micro/nanostructures are provided. Synthetic methods, morphological features, and piezoelectric performance of piezoelectric biomaterials are presented. The effect of growth direction, phase and structure of piezoelectric biomaterials on their piezoelectric activity are discussed. The applications of piezoelectric biomaterials in the field of nanogenerators are provided at the end.

9:00 AM NM09.11.12

Electrostatic Interaction Assembled Transparent Piezoelectret Zisheng Xu, Jun Zhou and Bin Hu; Huazhong University of Science & Technology, China

Piezoelectric polymers hold physical properties, such as high mechanical flexibility and smaller acoustical impedance, that ceramics do not. Nevertheless, owing to the lack of dipoles, most non-crystalline polymers are hard to generate a high piezoelectric response. Here, we developed a class of hybrid electret films with high piezoelectric performance via electrostatic self-assembly. Their piezoelectric effect stems from an out-plane electric-dipole structure in the inner dielectric polymer constructed by two electret films. The piezoelectret exhibits direct and converse piezoelectric effect (d_{33} of 77 pC/N, g_{33} of 4 V m/N), pyroelectric effect, and high mechanical flexibility. Additionally, we also developed different hybrid piezoelectric films and applied them to wearable electronics, such as ultrathin strain sensors and acoustic transducers, based on the ultrathin characteristic ($\sim 25 \mu\text{m}$ thickness), providing a different class of polymer piezoelectric film.

SESSION NM09.12: Poster Session: Nanogenerators and Piezotronics II

Session Chairs: Philippe Basset and Guylaine Poulin-Vittrant

Tuesday Morning, April 20, 2021

11:45 AM - 12:05 PM

NM09

NM09.12.01

Late News: *In Vivo* Self-Powered Wireless Transmission Using Biocompatible Flexible Energy Harvester Min SeongWook and Dong Hyun Kim; KAIST, United States

The practical use of biomechanical energy is demonstrated with flexible single crystal PMN-PZT energy harvesters. A flexible PMN-PZT piezoelectric energy harvester is used to demonstrate powered, wireless data transmission activated by biomechanical energy in vivo derived from the movement of the heart in a large animal model. In the contraction and relaxation of the pig's heart, the single crystal flexible energy harvester produced an open circuit voltage of 17.8V and short circuit currents 1.74 μA , 4.45 and 17.4 times higher. To

demonstrate the biocompatibility of the piezoelectric energy harvesting PMN-PZT flexible energy harvester, various cell viability tests and histological methods were conducted, but no signs of biological damage and inflammatory reactions were shown. Finally, an automated driving system was used to collect the pig's heart energy and transmit communication data wirelessly. It is also visually proven to repeat the light bulb on and off at a distance of about 5 meters without using another power source. This successful automated driving data transfer demonstrates potential applications in implantable biomedical devices that use direct biomechanical energy.

NM09.12.02

Late News: Decentralized Triboelectric Electronic Health Monitoring Flexible Microdevice Ulises G. Vidaurri Romero; University of Texas Rio Grande Valley, United States

In recent years, triboelectric nanogenerators (TENGs) have been the center of attention for research due to its wide range of applications as a microsystem component. This environmentally friendly energy framework can be implemented in advanced healthcare monitoring as a wearable electronic for sensory applications. Unfortunately, the production cost of TENGs are high and lead to loss of accessibility and production. Our research focuses on a triboelectric universal health monitoring device (TUHMD) that is biocompatible, highly sensible, self powered and economically advantageous simple structured, multifunctional, and wearable. The fabrication of the device shows the combination of cellulose paper and polydimethylsiloxane (PDMS) / polytetrafluoroethylene (PTFE) copolymer electrodes. The addition of this gadget into a wearable hardware provides real-time data of physiological movements and vibrations. The TUHMD shows promise as it can potentially be used for personalized medicine, rehabilitation, and remote monitoring of patients. The TUHMD reported a response as a triboelectric nanogenerator with a range of 12 V with negligible charge accumulation, along with a maximum capacitive performance of 11 F. The smart device demonstrated the capability of maintaining full health care monitoring applications.

Keywords

Nanogenerator, Triboelectric nanogenerator, Wearable electronics, Motion Sensor, Health care Monitoring, Remote monitoring

NM09.12.03

Late News: Spray Printed Triboelectric Tactile Sensors Powered by Artificial Intelligence Shengjie Gao and Wenzhuo Wu; Purdue University, United States

The seamless and adaptive interactions between functional devices and their environment are critical for advancing emerging technologies. The state-of-the-art technologies, however, require a complex integration of heterogeneous components to interface the environmental mechanical stimulus, which is ubiquitous and abundant in the above applications. Here we report a convenient layer-by-layer spray printing method to fabricate Triboelectric Nanogenerator (TENG) sensing unit for tactile sensing. In addition to the general optimization of fabrication process, we also carry out learning-based quantitative study between TENG signals and external factors to extract more in-depth relationship. This research is expected to help construct a smarter sensing system with potential application in biomedical monitoring, consumer electronics, and intelligent robotics.

NM09.12.04

Remote Plasma Assisted Vacuum Deposition of Functional Organic and Polymeric Layers for the Development of thin Film Piezoelectric Nanogenerators and UV Piezotronic Detectors Xabier García-Casas¹, Francisco J. Aparicio¹, Jose M. Obrero¹, Jorge Budagoski¹, Angel Barranco¹, Juan R. Sanchez-Valencia² and Ana Borrás¹; ¹Spanish National Research Council (CSIC), Spain; ²Universidad de Sevilla, Spain

In this communication, we present the advantages of the application of the remote plasma assisted vacuum

deposition method for the development of nanocomposite layers of organic functional molecules as adamantane and Spiro-OMETAD and polymers as PVDF. The synthesis is carried out at room temperature and under a low power plasma activation in an ERC-MW reactor to avoid energetic species or UV radiation of the plasma to reach the substrate surface. This methodology has been previously applied for the fabrication of photonics films based on organic dyes and small functional molecules working as optical sensors, optical filters, tunable photoluminescence emitters and lasing gain media. We present for the first time the exploitation of this approach to develop PENGs and UV photodetectors in combination with texturized ZnO thin films fabricated by plasma enhanced chemical vapour deposition.

SESSION NM09.13: Nanogenerator IX
Session Chairs: Tianzhao Bu and Xiong Pu
Tuesday Afternoon, April 20, 2021
NM09

9:00 PM *NM09.13.01

Triboelectric Human Machine Interfaces Chengkuo Lee; National University of Singapore, Singapore

Triboelectric nanogenerator (TENG), since its first invention in 2012, has been proved as a promising energy harvesting technology and widely adopted in energy generation, self-powered sensing, actuation, and self-sustained systems, etc. In recent decades, advances in the Human Machine Interface (HMI) have improved from tactile sensors, such as touchpads and joysticks, to now include the accurate detection of dexterous body movements in more diversified and sophisticated devices. In this talk, we discuss a few triboelectric based human-machine interfaces with unique design of electrode patterns aiming for the gaming control. In addition, artificial intelligence (AI) as an effective data analytics tool has been integrated with various triboelectric sensors to achieve intelligent monitoring and recognition system. The AI-enabled triboelectric glove-based HMIs are investigated for gaming and VR/AR applications. On the other hand, the AI-enabled soft robotic manipulator is demonstrated with object recognition capability. Lastly, a smart floor monitoring system is reported with the merits of low cost, high scalability, and self-powered sensing capability, based on the integration of triboelectric sensors and deep learning-based data analytics.

9:20 PM *NM09.13.02

Integrated High Resolution Imaging Based on Micro-/Nanomaterials Qing Yang^{1,2,3}; ¹Zhejiang University, Joint International Research Laboratory of Photonics, China; ²Zhejiang Lab, Res Ctr Smart Sensing, China; ³Shanxi University, China

High resolution imaging is a key technology for physics, biology, medicine and material development. Most high resolution imaging relies on cost, large volume and complex equipment. It is desired to have integrated high resolution imaging for invasive internal diagnosis and low cost drug discovery. Here we report our recent results on integrated high resolution imaging based on micro-/nanomaterials: chip-based super-resolution imaging [1-4] and multimode fiber based high resolution endoscope [5,6].

A majority of developed super-resolution techniques rely on nonlinear response to achieve nanoscale resolutions, while their low throughput could limit their practical applications. To achieve fast imaging with a large field-of-view (FOV), linear super-resolution microscopy via synthesis aperture approach is an alternative way that can be used. However, current linear super-resolution imaging is limited in resolution because a missing spatial-frequency band occurs when trying to use a shift magnitude surpassing the cutoff frequency of the detection system beyond a factor of two. In the presentation, we will show our recent results in wide-field far-field super-resolution imaging based on tunable frequency shifting. The missing of spatial-frequency can be effectively solved by developing a spatial-frequency-shift actively tuning approach through wave vector

manipulation and operation of optical modes propagating along multiple azimuthal directions on a waveguide chip to interfere.

Multimode fiber, as a potential minimally invasive endoscope, possesses larger mode capacity, higher efficiency of light collection, and much lower cost than fiber bundle. The main challenge in multimode fiber imaging is the complex light propagation process inside multimode fibers: light suffers from modal scrambling caused by environmental fluctuation, meaning that an image injected from one end of a fiber will become scrambled as very little fluctuation of environments. In this presentation, we propose some potential methods to increase the contrast-to-noise ratio (CNR) and stability of multimode fiber imaging. Wavelength modulation is introduced to suppress the background without increasing the number of controllable modes. Bending effect was investigated carefully and used to improve the imaging stability. We combine exhaustive bending and Convolutional Neural Networks to find the bending status precisely and compensate it fast. The results will improve the flexibility of multimode fiber imaging system, paving the way for deep and volumetric tissue endoscope imaging based on multimode fiber.

Acknowledgement

The authors are grateful to the supports from the National Natural Science Foundation of China (No. 51672245, 61822510, 61735017, 62020106002), the Zhejiang Provincial Natural Science of China (No. R17F050003), the Zhejiang University Education Foundation Global Partnership Fund.

9:40 PM NM09.13.03

Wireless Passive Pressure Sensor for Wound Repair by Electrical Stimulation Qian Wang, Guang Yao and Yuan Lin; University of Electronic Science and Technology of China, China

Flexible intelligent sensor-stimulation integrated devices can dynamically capture the physiological signals of human tissues and organs, sensing real-time health information, and provide timely and accurate stimulation or treatment for injuries and diseases, which plays a key role in the next generation of intelligent healthcare systems.[1] However, almost all of the wearable electronic devices rely on some form of power supply and battery, and still face the problems of large volume and short working life. If the wearable electronic devices can be attached to the organism to collect the energy generated by low-frequency motion and directly applied to the flexible intelligent sensor-excitation device, it can get rid of the traditional battery and realize the infinite power supply of symbiosis in a sense.[2-4] Piezoelectric materials are the core part of piezoelectric electronic devices and the decisive component to realize the conversion of mechanical energy to electrical energy. Therefore, the research and development of high energy density piezoelectric materials is of great significance for the practical application of miniaturization and high sensing excitation performance flexible electronic devices. However, under the condition of large deformation and extensibility, rigid piezoelectric components are seriously limited due to the relaxation of human-machine interface coupling, low electromechanical coupling conversion/ wearing comfort and brittleness, resulting in short working life. It is not appropriate to directly use hard materials as functional components of wearable devices.

Here, a flexible wireless passive piezoelectric polymer polyvinylidene fluoride (PVDF) film stimulation device is designed for effective wound healing and repair. Firstly, compared with the traditional inorganic piezoelectric materials, organic piezoelectric polymer PVDF has the advantages of excellent stability, flexibility and low density.[5] Secondly, we designed the flexible PVDF film into grids, at the same time, the pyramid microstructure is introduced. The introduction of the microstructure plays an important role in improving the comprehensive performance of the flexible pressure sensor. Compared with the flexible device that is not combined with the pyramid structure, the piezoelectric output of this device has been increased from the original (3.43 V) to the current (4.61 V), and it can continue to work stably for at least 60 minutes. This provides the possibility for effective wound treatment. In summary, flexible piezoelectric film devices can not only prepare flexible wearable devices for disease treatment, but also the passive devices can get rid of the traditional batteries, which makes the devices further develop towards lightweight, miniaturization and integration. Therefore, the application of piezoelectric passive devices in wound treatment is an important research direction in the field of wearable devices.

References:

[1] Gao, Y., Yu, L., Yeo, J., Lim, C. Flexible Hybrid Sensors for Health Monitoring: Materials and Mechanisms

to Render Wearability. *Adv. Mater.* **32** (2019) 1902133.

[2] Chu, B., Burnett, W., Chung, J., Bao, Z. Bring on the body NET, *Nature*, **549** (2017) 328.

[3] Wang, X., Dong, L., Zhang, H., Yu, R., Pan, C., Wang, Z. Recent Progress in Electronic Skin, *Advanced Science*. **2** (2015) 1500169.

[4] Yao, G., Kang, L., Li, J., Long, Y., Wei, H., Ferreira, C., Jeffery, J., Lin, Y., Cai, W., Wang, X. Effective weight control via an implanted self-powered vagus nerve stimulation device. *Nat Commun.* **9** (2018) 5349.

[5] Sang, M., Wang, S., Liu, S., Liu, M., Bai L., Jiang, W., Xuan, S., Gong, X. A Hydrophobic, Self-Powered, Electromagnetic Shielding PVDF-Based Wearable Device for Human Body Monitoring and Protection. *ACS Appl. Mater. Interfaces.* **11** (2019) 47340.

9:50 PM NM09.13.04

Multifunctional Self-Powered Switch toward Delay-Characteristic Sensors Haoyu Wang and Yunlong Zi;
The Chinese University of Hong Kong, China

With the development of smart city which has been considered as a new lifestyle in the future, the Internet of Things (IoT) technology becomes more and more mature and important. According to a recent report there will be 20 billion devices connected by 2020. Nowadays, with a great progress in communication and embedded technology, emerging technologies such as the big data transfer and microprocessor distributed computing are being rapidly developed. Therefore, research on sensors requires sensing systems to be accurate, stable and small. However, in traditional sensing systems, the power supply circuits are usually complex and may cause environmental issues. In this case, self-powered devices which could work without external power source provide a more sustainable solution to meet the power requirement of such a big sensor network. Triboelectric nanogenerators (TENGs) which work based on the triboelectric effect and electrostatic induction have a list of great advantages, such as high sensitivity to detect motions, significant output voltage, flexibility, light weight, low cost, environmentally friendliness. With that, TENG plays an important role in detecting movement, direction, force, speed, and acceleration signal. However, the extremely-high-voltage output from TENG makes it difficult to directly power most electronics. By using the output electrical signals from TENGs to trigger the traditional electronic control devices, the extremely-high-voltage output from TENGs could break down these electronic devices. Furthermore, the TENG's output current is too low to meet the power requirement of some switches. Alternatively, TENG's output signal could be transferred to other kinds of signals which are easily detected and processed, such as transferring to optical signal to realize free-space optical communication. The switching devices which can directly transfer the high-voltage TENG output signal to other types of signals that can be easily processed are highly preferred. On the other hand, the delay characteristic plays an important role in fields of control and signal transmission. It brings convenience and energy-saving features to daily life, for example the delay light control system and the delay air conditioner control system. It can maintain safe operation of systems, such as the alternating current (AC) motor control and the time-limit current quick-break protection. It is also used in controlling the time delay of signals to improve the system's bandwidth, a.k.a. delay line. A wide kinds of delay characteristic switches have been designed with different mechanical structures or electrical circuits. However, current devices are usually complex and need external power source. It is demanded to achieve delay characteristic switching function in a simple but self-powered way, enabling smart systems. With the principle of dielectric polarization and electrostatic force, an electrostatic force based self-powered switch (EFS) which can work as an electrostatic force optical switch (EFOS) or a controlled electrostatic force electrical switch (CEFES) has been developed. It could be used to detect slight motions through TENG, or work as a high-threshold-voltage (over 1000 V) switch with a high sensitivity and delay characteristic. Upon applying a voltage on the EFOS, the nitrile butadiene rubber (NBR) film in EFOS will be attracted by the electrostatic force to block the light beam with a certain delay time, converting high-voltage electrical signal to optical signal. CEFES could conduct a controlled circuit when the control voltage reaches the threshold value with the delay characteristic. The self-powered EFS is achieved by using a freestanding sliding mode TENG (FS-TENG) as the power and controlling unit to realize the function of delay-characteristic self-powered sensing, which can be applied in various fields such as coding communication, human-machine interface, architecture auto-monitor, etc.

10:00 PM NM09.13.05

Water-Based Electricity Generator and Applications Hao Wu^{1,2}; ¹City University of Hong Kong, Hong Kong; ²The Chinese University of Hong Kong, Hong Kong

Water is ubiquitously existing on the earth. Natural water sources including rainfall, river water, and ocean waves always contain a certain amount of mechanical energy. When water contacts a specific solid surface, it will either generate a static surface tribo-charge or lead to electrostatic induction. In some circumstances, these both occur. By properly using the static charges generated by water/solid contact and the electrostatic induction process, the mechanical energy contained in the water movements can be converted into electrical energy. In this presentation, I will first introduce the mechanism of electricity generated from water/solid contact and then demonstrate some related application cases.

10:10 PM NM09.13.06

Deformable, Green, and Self-Healable Triboelectric Nanogenerators and Their Applications in Flexible Electronics and Self-Powered Sensing Uses Ying-Chih Lai; National Chung Hsing University, Taiwan

Deformable and wearable soft devices have attracted great interest because they cannot only extend the scope of smart systems but also provide compliant user experience. Operating those devices inevitably need power sources. However, traditional batteries suffer from heavy weight, bulky volume, and limited capacity and lifetime, hindering the progress and practical uses of those emerging devices. Toward the soft future, it is necessary to explore new energy technology. In this talk, deformable, mechanically-durable, green, and even self-healable energy-collecting triboelectric nanogenerators will be demonstrated for not only serving as new energy providers but also self-powered sensing uses. First, super-stretchable triboelectric nanogenerators will be presented for generating electricity by contacting with other materials regardless of various extreme deformation required from uses, such as extreme stretching, multiple twists and folds. Particularly, even experiencing severe tearing damages, the device can retain its functionality to act as a power source for other components. Such technology can also be introduced into fabric materials for wearable energy and fabric-based self-powered sensing uses. Then, we will discuss the use in self-powered and deformable electronic skins that can actively sense proximity, contact, and pressure to external stimuli via self-generating electricity. Further, the perfect integration of the tribo-skins and soft actuators enables soft robots to perform various actively sensing and interactive tasks including actively perceiving their muscle motions and working states, checking baby diaper conditions, and even detecting subtle human physiological signals. The self-generating signals can even drive optoelectronic devices for visual communication and be processed for diverse sophisticated uses. Then, a self-healing, highly-transparent, and super-stretchable triboelectric nanogenerator with energy-extracting and activity-sensing abilities will be demonstrated in the use of self-powered electronic skin, human-interactive interfaces, and so forth. Last, a triboelectric nanogenerator based on recycled coffee waste is presented for future low-cost and green energy devices. These works may open the crucial doors for the tremendous potentials of wearable/stretchable/deformable electronics, and energy devices.

[Ref]

1. Advanced Functional Materials, 2019, 190426.
2. Nano Energy, 2020, 105405
3. Advanced Science, 2019, 1801883.
4. Advanced Materials, 2018, 30,1801114.
5. Advanced Materials, 2018, 30, 1705918.
6. Advanced Materials, 2016, 28, 10024-10032

10:20 PM NM09.13.07

Modulus Controllable HEMA-Based Hydrogel for Ultrasound-Driven Implantable Triboelectric Nanogenerator Bosung Kim, Hong-Joon Yoon and Sang-Woo Kim; Sungkyunkwan University, Korea (the Republic of)

Recently, the demand for implantable medical devices has steadily increased as the number of the adult patients is on the rise with westernized diet and aging population. Implantable medical devices normally use batteries, which have a limitation in the lifetime and a need for replacement surgery at the end of life. To overcome these limitations of the batteries, various studies have been conducted and a paper using triboelectric nanogenerator which is capable of transmitting vibration energy using ultrasonic waves from the outside of the body, has been published. The implantable energy harvesting devices for medical devices need to be packaged with titanium plate when they are implanted in the body to avoid unintended immune response or inflammatory reaction from toxic material. However, there is a major disadvantage that large amount of energy is reflected and lost from the titanium surface because titanium has large acoustic impedance compared to the human body tissues. Therefore, we produced an ultrasound implantable triboelectric nanogenerator with bio-implantable and modulus controllable HEMA-based hydrogel which does not require titanium packaging. The voltage and current generated in-vivo by ultrasonic energy transmission reached 3.42 volts and 130 microamps under rat's tissue which can charge the 100 μ F capacitor at the rate of 23.9 μ C/s. This HEMA-based US TENG shows higher output than the titanium packaged US TENG device and it generates sufficient energy level to charge the batteries of implantable medical devices.

10:30 PM NM09.13.08

Continuous, Low-Level Pressure Sensor Enabled by a Convolution of Electrostatic Induction in Triboelectric Nanogenerator Soyeon Lee and Jin-Woo Park; Yonsei University, Korea (the Republic of)

A pressure sensor is one of the essential electronic devices for human-machine interfaces that enables monitoring from low-level pressure such as vibration and acoustic signals to moderate-level pressure such as physical body signals, including heart rate and blood pressure. Capacitive, resistive, piezoelectric, and triboelectric pressure sensors are commonly used as an electrical signal modifier or transducer responding to mechanical stimuli. Among those sensors, piezoelectric and triboelectric based pressure sensors have been established as self-powered active sensor as they do not consume electrical energy during sensing. Recently, triboelectric-based active sensors are exponentially used, having many advantages such as abundant materials candidate, fast response, and broad dynamic sensing range with linearity. Furthermore, many studies employed hierarchical nano/microstructure in the friction surface of the triboelectric pressure sensor since the micropattern structure improves deformability and contact area variation and enhances the friction surface and charge density. However, the effect of deformation and contact area variation is not significant in a small pressure range (<1kPa), which results in incorrect information in the low-level pressure signal. Herein, a highly sensitive and amplified electrical signal upon low-level pressure input can be achieved by using the convolution of electrostatic induction in a micropatterned triboelectric nanogenerator. By defining electrostatic induction in individual micro-ridge of the microstructure, distance variation between the two separate films can be continuously encoded. The microstructure was fabricated by mold casting of PVDF-TrFE using a commercial 3D printer (Formlabs), and electrodes were prepared by spray coating of AgNW. Face centered cubic (FCC) structure induced-hemisphere micro-ridge patterns were fabricated with diameter varied from 100 to 1000 micro-meter—of which scale pattern cannot be achieved in etched Si mold, and FCC interlocked structure of two separate films enabled spacer-free paired triboelectric system. To identify the electrostatic induction in microstructure, electrodes were embedded at a different distance from the friction surface, and PVDF-TrFE/AgNW/PVDF-TrFE layered structures were formed. Here, spray coating of AgNW on the micro-structured PVDF-TrFE films enabled the conformal distribution of electrode along every micro-ridge morphology, which was confirmed by FE-SEM images and EDS mapping of the respective film layers. As the electrode distance from the friction surface decreased, the open-circuit voltage and short circuit current are exponentially increased. Here, to exclude the capacitance increase effect due to the thinner dielectric layer in a closer distance electrode system, flat samples are also prepared alike the micropattern PVDF-TrFE/AgNW/PVDF-TrFE layered structure. Compared to the linear increase of electrical output when varying the distance between friction surface and electrode in the flat samples, an exponential increase of output signal in micropatterned samples with varying electrode distance can be explained by the convolution of electrostatic induction term from every near micro-ridge. The electric field applied on every surface of the micro-ridge can

participate in the triboelectric charge generation and, finally, sensitively respond to every distance variation from individual micro-ridge patterns. This enhancement is typically helpful for detecting pressure levels under 1kPa.

10:40 PM NM09.13.09

Stretchable and Mechanically-Durable Triboelectric Nanogenerator Based on Recycled Coffee Waste as Flexible Power Sources and Self-Powered Smart Sensors Ying-Chih Lai; National Chung Hsing University, Taiwan

Maximizing resource recycling and finding renewable energy sources are important for a sustainable environment considering the development and consumption of electronic products with the advancement of the internet of things and artificial intelligence technologies. Herein, an economic and environment-friendly triboelectric nanogenerator derived from the discarded coffee ground waste (CG-TENG) is developed to serve as a light-weight and shape-adaptive energy source and self-powered sensitive sensor (CG-TENG sensor). The coffee ground, embedded into the silicone rubber elastomer, is first used as the metal-free electrode feedstock to minimize waste generation. Based on the triboelectrification and electrostatic induction, the shape-adaptive CG-TENG, as wearable power, is capable of harvesting surrounding energy from human motions and extreme deformations, exhibiting excellent stretchability and mechanical durability. The generated electricity can be stored in the conductive coffee ground-derived capacitors to drive portable electronics, which is beneficial for building completely green power systems using coffee waste. Furthermore, the self-powered CG-TENG sensor with optimized structure endows its ultra-high sensitivity for sensing human physiological signals, monitoring motions, emulating gestures, as well as for developing smart tactile epidermal controller and intelligent vending coaster, paving the way for building large-scale energy-efficient artificial sensors and eco-environmental wearable electronics towards humanoid robotics and human-machine interfaces.

10:50 PM NM09.13.10

Triboelectric Nanogenerator as Highly Sensitive Sensors for Human Machine Interface Xianjie Pu; Chongqing University, China

Human-machine interface (HMI) has become an indispensable part of our lives. From the original keyboards to the virtual reality today, the goal of HMI is to make life more convenient and fascinating. In certain scenarios, for example, when a user's two hands are fully occupied, or the disabled expect to achieve necessary self-care, a hands-free operation via eye movement or voice is most definitely the approach of choice for human-machine interfacing. Based on the unique advantages of high sensitivity, low cost, light weight, applicability of structure design, prominent stability, robustness, etc. of triboelectric nanogenerator (TENG), we design a mechnosensational TENG (msTENG) and a triboelectric auditory sensor (TAS) for controlling the equipment via eye-blink and interacting with the robotic via voice, respectively. While in the scenarios of manufacturing industry, deep-sea exploration, telesurgery and disaster salvation etc., gesture control can help bringing about an intuitive interface instead of operation based on amount of learning and training. From this point, we design a joint motion triboelectric quantization sensor (jmTQS) for constructing a robotic hand synchronous control system. Then, keeping on investigating into intuitive interface and coming down to the universal experience in daily life, some traditional interactive modes such as mouse and keyboards, still have a strong vitality and practical value. Thus, we develop a 3D triboelectric touch pad (3D-TTP) for an effective and efficient touch-screen graphical user interface. These studies cover the control modes of eye-movement, voice, gesture, and touch of HMI nowadays. While in the feedback phase of HMI, TENG as a highly sensitive sensor transform mechanic movements into electric signals can also do benefits as in visual, auditory, and tactile modes. Take the TAS study above for example, this resonant frequency-tunable auditory sensor is also a hearing aid for people with impaired hearing in the feedback stage between robotics and them. Further, the 3D-TTP can be another kind of electronic skin of the robotics. With above successful attempts, we may foresee more potentials of TENG-based sensors in the control-feedback loop of HMIs.

SYMPOSIUM SM01

Materials Modulating Stem Cells and Immune Response
April 18 - April 18, 2021

Symposium Organizers

Jianping Fu, University of Michigan
Shaoyi Jiang, Cornell University
Nan Ma, Helmholtz-Zentrum Geesthacht
Henry Yu, National University of Singapore

* Invited Paper

SESSION SM01.01: Mechanosensing and Cell
Session Chairs: Nan Ma and Henry Yu
Sunday Morning, April 18, 2021
SM01

8:00 AM *SM01.01.01

Mechanobiology of Epithelial Folding and Migration in Intestinal Organoids Xavier Trepats; Institute For Bioengineering Of Catalonia, Spain

Intestinal organoids capture essential features of the intestinal epithelium such as folding of the crypt, spatial compartmentalization of different cell types, and cellular movements from crypt to villus-like domains. Each of these processes and their coordination in time and space requires patterned physical forces that are currently unknown. In this study, we map the three-dimensional cell-ECM and cell-cell forces in mouse intestinal organoids grown on soft hydrogels. We show that these organoids exhibit a non-monotonic stress distribution that defines mechanical and functional compartments. The stem cell compartment pushes the ECM and folds through apical constriction, whereas the transit amplifying zone pulls the ECM and elongates through basal constriction. Tension measurements establish that the transit amplifying zone isolates mechanically the stem cell compartment and the villus-like domain. A 3D vertex model shows that the shape and force distribution of the crypt can be largely explained by cell surface tensions following the measured apical and basal actomyosin density. Finally, we show that cells are pulled out of the crypt along a gradient of increasing tension, rather than pushed by a compressive stress downstream of mitotic pressure as previously assumed. Our study unveils how patterned forces enable folding and collective migration in the intestinal crypt.

8:25 AM *SM01.01.02

Force-FAK Signaling Coupling at Individual Focal Adhesions Coordinates Mechanosensing and Microtissue Repair Andrés J. García; Georgia Institute of Technology, United States

How adhesive forces are transduced and integrated into biochemical signals at focal adhesions (FAs) is poorly understood. Using cells adhering to deformable micropillar arrays, we demonstrate that traction force and FAK localization and traction force and Y397-FAK phosphorylation are linearly coupled at individual FAs on stiff, but not soft, substrates. Similarly, FAK phosphorylation increases linearly with external forces applied to FAs using magnetic beads. This mechanosignaling coupling requires actomyosin contractility, talin-FAK binding, and full-length vinculin that binds talin and actin. Using an in vitro 3D biomimetic wound healing model, we show that force-FAK coupling coordinates cell migration and tissue-scale forces to promote microtissue repair.

A simple kinetic binding model of talin-FAK binding interactions under force can recapitulate the experimental observations. This study provides insights on how talin and vinculin convert forces into FAK signaling events regulating cell migration and tissue repair.

8:50 AM SM01.01.04

The Response of Human Induced Pluripotent Stem Cells to Cyclic Cold Shock Yan Nie^{1,2}, Weiwei Wang^{1,3}, Xun Xu^{1,3}, Nan Ma^{1,3} and Andreas Lendlein^{1,2,3}; ¹Institute of Biomaterial Research and Berlin-Brandenburg Center for Regenerative Therapies, Helmholtz-Zentrum Geesthacht, Germany; ²Institute of Biochemistry and Biology, University of Potsdam, Germany; ³Helmholtz Virtual Institute – Multifunctional Biomaterials for Medicine, Germany

Human induced pluripotent stem cells (hiPSCs) attract interest to develop patient-specific therapeutic tools for their clinical applications [1]. The *in vitro* culture of hiPSCs with high quality is dependent on the signals from their extracellular environments [2, 3]. In this study, we explore the effect of cyclic cold shock on hiPSCs behavior. A computer-controlled thermo-chamber was employed to exert cyclic cold stress on hiPSCs, in which temperature was alternately varied between 10 °C and 37 °C, whereby each temperature was kept for 30 min. The expression of pluripotent markers was evaluated 24 h after culture either under constant temperature at 37 °C or under cyclic temperature changes (ΔT). An atomic force microscope (AFM) was used to detect changes in cellular mechanics and the decellularized extracellular matrix (ECM). Immunofluorescence analysis showed that the expression of pluripotent markers, NANOG and SOX2, was maintained within 24 h of culture. A slight change in Young's modulus of hiPSCs cultured under different conditions was observed. This observation might be a result of an alteration in the arrangement of the actin cytoskeleton revealed by the immunofluorescence analysis. Notably, the topography of decellularized ECM showed an increase in surface roughness in the ΔT group. The average surface roughness (Ra) and roughness mean square (Rms) of decellularized surfaces under the ΔT condition were 31.56 ± 2.82 nm and 38.07 ± 3.58 nm, while under the constant temperature were 39.52 ± 2.83 nm and 49.14 ± 4.23 nm. This result suggested that the component and/or the arrangement of ECM protein was altered by the cold stress. This was supported by the enzyme-linked immunosorbent assay (ELISA), which showed the cyclic cold shock promoted the secretion of laminin. The presented findings provide an insight into the interactions between hiPSCs and factors of their microenvironment, which would contribute to a better understanding of the interactions between hiPSCs and their local microenvironment.

Reference

1. Rowe, R.G. and G.Q. Daley, *Induced pluripotent stem cells in disease modelling and drug discovery*. Nature Reviews Genetics, 2019. **20**(7): p. 377-388.
2. Garreta, E., et al., *Fine tuning the extracellular environment accelerates the derivation of kidney organoids from human pluripotent stem cells*. Nature materials, 2019. **18**(4): p. 397-405.
3. Han, U., et al., *Construction of nano-scale cellular environments by coating a multilayer nanofilm on the surface of human induced pluripotent stem cells*. Nanoscale, 2019. **11**(28): p. 13541-13551.
1. Rowe, R.G. and G.Q. Daley, *Induced pluripotent stem cells in disease modelling and drug discovery*. Nature Reviews Genetics, 2019. **20**(7): p. 377-388.

9:05 AM *SM01.01.05

The Spatial Self-Organization within Pluripotent Stem Cell Colonies is Continued in Detaching Aggregates Mohamed H. Elsafi Mabrouk^{1,1}, Roman Goetzke^{1,1}, Giulio Abagnale², Burcu Yesilyurt¹, Lucia Salz^{1,1}, Kira Zeevaert^{1,1}, Zhiyao Ma¹, Marcello A. Toledo³, Ronghui Li¹, Ivan G. Costa¹, Vivek Pachauri³, Uwe Schnakenberg³, Martin Zenke^{1,1} and Wolfgang Wagner¹; ¹RWTH Aachen University Medical School, Germany; ²St. Anna Children's Cancer Research Institute (CCRI), Austria; ³RWTH Aachen University, Germany

Colonies of induced pluripotent stem cells (iPSCs) reveal aspects of self-organization even under culture conditions that maintain pluripotency. To investigate the dynamics of this process under spatial confinement, we used either polydimethylsiloxane (PDMS) pillars or micro-contact printing of vitronectin. There was a

progressive upregulation of OCT4, E-cadherin, and NANOG within 70 μm from the outer rim of iPSC colonies. Single-cell RNA-sequencing demonstrated that *OCT4*^{high} subsets have pronounced up-regulation of the TGF- β pathway, particularly of NODAL and its inhibitor LEFTY, at the rim of the colonies. Furthermore, calcium-dependent cell-cell interactions were found to be relevant for the self-organization. Interestingly, after 5 to 7 days, the iPSC colonies detached spontaneously from micro-contact printed substrates to form 3D aggregates. This new method allowed generation of embryoid bodies (EBs) of controlled size, without any enzymatic or mechanical treatment. Within the early 3D aggregates, the radial organization and differential gene expression continued in analogy to the changes observed during self-organization of iPSC colonies. Our results provide further insight into the gradual self-organization within iPSC colonies and at their transition into EBs.

SESSION SM01.02: Deciphering Cell and Materials Interaction
Session Chairs: Jianping Fu, Nan Ma, Weiwei Wang and Xun Xu
Sunday Morning, April 18, 2021
SM01

10:30 AM

Panel Discussion: Xavier Trepát; Andreas Garcia; and Mohamed H. Elsafi Mabrouk Moderators: Nan Ma and Jianping Fu [Nan Ma](#)¹, [Jianping Fu](#)², [Fiona Watt](#)³, [Xavier Trepát](#)⁴ and [Wolfgang Wagner](#)⁵; ¹Helmholtz-Zentrum Geesthacht, Germany; ²University of Michigan, United States; ³King's College London, United Kingdom; ⁴Institute for Bioengineering of Catalonia, Spain; ⁵RWTH Aachen University, Germany

Panel discussion

11:40 AM *SM01.02.01

Enzymatically Crosslinked Hydrogels for the Encapsulation of Living Cells and Enzymes [Changzhu Wu](#); University of Southern Denmark, Denmark

Hydrogels are the ubiquitous three-dimensional networks that can store a great amount of water in their porous scaffolds, holding great potential for bio-related applications.[1] In particular, their biophysical similarity to living tissues and extracellular matrix has made them valuable for tissue engineering, drug/gene delivery, biocatalysis, and regenerative medicine. However, the preparation of robust hydrogels in a mild fashion remains a technical challenge. Typically, hydrogels are prepared by physical interactions or chemical reactions. However, physically crosslinked hydrogels are generally limited by the instability due to their weak interactions, while chemical approaches are often associated with the problems of involving toxic reagents and harsh reaction conditions. Therefore, there has been a quest to establish a reliable and efficient methodology to construct stable hydrogels under physiological conditions.

Here, we demonstrate an enzymatic approach to creating hydrogels to encapsulate living cells and biocatalytically active enzymes for regenerative therapy, catalysis, and antibacterial study, respectively.[2-4] In the first study, the hydrogels were prepared using horseradish peroxidase (HRP) to enzymatically crosslink phenolic derivatized dendritic polyglycerol polymer into hydrogels in a buffer.[2] Our results showed that the resultant gels were not only biocompatible to fibroblast murine cells but also allowed for their encapsulation with high viability over 48 hours. This successful demonstration suggests the potential of our hydrogels for future use in regenerative medicine. Furthermore, we used the same enzymatic crosslinking method and materials to prepare nanogels for the encapsulation of HRP and *Candida antarctica* lipase B, respectively.[3] The advantage of this method is the mild condition that maintains the good enzyme activity, and more importantly, the process doesn't require any quench steps, thus substantially simplifying purifications. Therefore, this study proves a new concept of "enzymatic nanogelations" for biocatalysis. Lastly, the enzymatically crosslinked hydrogels were explored for antibacterial applications.[4] Similar to the previous,

hydrogels were crosslinked on glass slides by HRP, but differently, a second enzyme, glucose oxidase (GOD), was co-encapsulated. The existence of GOD could generate toxic H₂O₂ when supplying glucose, and kill *Pseudomonas putida* (Gram-negative) by 100% and *Staphylococcus aureus* (Gram-positive) by $\geq 40\%$, respectively.

Overall, we show a facile method to prepare hydrogels using enzymatic crosslinking for diverse applications. The success of this method suggests its great potential in future biomedicine and biotechnology.

Reference.

1. Seliktar, D., Designing cell-compatible hydrogels for biomedical applications. *Science* 2012, 336 (6085), 1124-1128.
2. Wu, C.; Strehmel, C.; Achazi, K.; Chiappisi, L.; Dervede, J.; Lensen, M. C.; Gradzielski, M.; Ansorge-Schumacher, M. B.; Haag, R., Enzymatically crosslinked hyperbranched polyglycerol hydrogels as scaffolds for living cells. *Biomacromolecules* 2014, 15 (11), 3881-3890.
3. Wu, C.; Böttcher, C.; Haag, R., Enzymatically crosslinked dendritic polyglycerol nanogels for encapsulation of catalytically active proteins. *Soft Matter* 2015, 11 (5), 972-980.
4. Wu, C.; Schwibbert, K.; Achazi, K.; Landsberger, P.; Gorbushina, A.; Haag, R., Active antibacterial and antifouling surface coating via a facile one-step enzymatic cross-linking. *Biomacromolecules* 2017, 18 (1), 210-216.

SESSION SM01.03: Engineering Approach for the Biointerface
Session Chairs: Jianping Fu, Shaoyi Jiang, Nan Ma and Weiwei Wang
Sunday Afternoon, April 18, 2021
SM01

1:00 PM *SM01.03.01

Engineering Liquid Interfaces with Viscoelastic 2D Protein Networks—Microdroplet Design for Stem Cell Technologies Julien Gautrot, Dexu Kong, Lihui Peng and Minerva Bosch; Queen Mary, University of London, United Kingdom

Adherent cell production is hindered by the use of solid substrates or hydrogels for culture and expansion. Such materials and platforms are difficult to scale up and parallelise. In contrast, liquid-liquid technologies and microdroplet platforms have been applied very successfully in the field of Chemical Engineering for the scale up of synthesis and purification of fine chemicals, therapeutics, polymers and nanomaterials. Yet, their use in the field of biotechnologies is restricted to the high throughput screening of single planktonic cells. However, we recently reported that the culture of adherent cells at the surface of liquids [1, 2], previously observed with fibroblasts, was mediated by the self-assembly of protein nanosheets forming mechanically strong interfaces [3, 4]. This enabled the adhesion of stem cells such as keratinocytes and mesenchymal stem cells and the regulation of their spreading via the classic integrin and acto-myosin machinery, allowing the retention of stem cell phenotypes despite the extreme compliance of liquid substrates [5]. We now examine the chemical design of protein nanosheets systematically and identify groups of pro-surfactant molecules effectively supporting stem cell expansion at liquid interfaces. Surprisingly, the shear moduli of associated interfaces does not correlate with cell expansion. Instead, we observe that the viscoelastic behaviour of protein nanosheets correlates with stem cell proliferation. We identify that particularly stiff nanosheets that display poor elasticity do not support stem cell expansion and that this phenomenon is associated with the formation of brittle domains that can relax and dissipate energy in response to cell mediated forces. Hence the multi-scale viscoelasticity of liquid-liquid interfaces, rather than shear moduli, is the primary physical determinant of stem cell proliferation. Based on neutron reflectometry, TEM and polarised optical microscopy, we report that this behaviour is controlled by the nanoscale organisation of prosurfactant-mediated rigid domains. To demonstrate the capacity to expand stem

cells at liquid interfaces whilst retaining their phenotype, and the relevance of these systems for stem cell manufacturing, we characterised the expansion of mesenchymal stem cells over multiple passages, their retention of stem cell markers and ability to differentiate into multiple lineages. Cells cultured on nanosheet-stabilised emulsions displayed comparable phenotype in long-term expansion compared to stem cells cultured on 2D plastic and solid microcarriers. Overall, our results pave the way to the use of microdroplet technologies and liquid-liquid interfaces in the field of tissue engineering and for stem cell technologies.

1. Keese et al. Proc. Natl. Acad. Sci., 1983. **80**, 5622. 2. Keese et al. Science, 1983. **219**, 1448. 3. Kong, D., et al. Nano Lett., 2018. **18**, 1946. 4. Kong, D., et al. Faraday Discuss., 2017. **204**, 367. 5. Kong, D., et al. ACS Nano, 2018. **12**, 9206.

1:25 PM SM01.03.02

An Innovative Approach to Study Cell Mechanics—A Skin-Over-Liquid Platform with Compliant Microbumps Actuated by pyro-EHD Pressure Martina Mugnano¹, Romina Rega¹, Emilia Oleandro^{1,2}, Vito Pagliarulo¹, Pietro Ferraro¹ and Simonetta Grilli¹; ¹Institute of Applied Sciences and Intelligent Systems of the National Research Council (CNR-ISASI), Italy; ²Department of Mathematics and Physics, University of Campania “L. Vanvitelli”, Italy

Investigating the mechanical crosstalk between cells and their surrounding environment is fundamental to understand the influence of forces on cell functions and responses. In attempt to better elucidate the material – cell interaction *in-vitro* during adhesion process, here we report a new concept for a reliable and dynamic skin-over-liquid system for studying mechanobiology. It is made of a periodic array of highly compliant microbumps actuated through electrode-free electrohydrodynamic (EHD) pressure. These structures are highly repeatable and capable of swelling and deflating easily under a simple thermal stimulation driven by the pyroelectric effect, thus providing an innovative and easy tool that can be actively controlled at the microscale. To confirm the formation of the cytoskeleton structures after the stimulation, a fluorescence imaging system was used as a control to visualize actin filaments. The strategy here proposed portends broad applicability to investigate the correlation between the mechanical stress applied to cells by swelling these microbumps and their cytoskeleton assembly process. Moreover, the preliminary results are promising and permit us to consider skin-over-liquid platform as an easy assay for cell nanomechanic investigations in the future.

References

- [1] Gennari, O., Rega, R., Mugnano, M., Oleandro, E., Mecozzi, L., Pagliarulo, V., Mazzon, E., Bramanti, A., Vettoliere, A., Granata, C. and Ferraro, P., 2019. A skin-over-liquid platform with compliant microbumps actuated by pyro-EHD pressure. *NPG Asia Materials*, *11*(1), pp.1-8.
- [2] Fusco, S., Memmolo, P., Miccio, L., Merola, F., Mugnano, M., Paciello, A., Ferraro, P. and Netti, P.A., 2016. Nanomechanics of a fibroblast suspended using point-like anchors reveal cytoskeleton formation. *RSC advances*, *6*(29), pp.24245-24249.
- [3] Marchesano, V., Gennari, O., Mecozzi, L., Grilli, S., & Ferraro, P. (2015). Effects of lithium niobate polarization on cell adhesion and morphology. *ACS applied materials & interfaces*, *7*(32), 18113-18119.
- [4] Rega, R., Gennari, O., Mecozzi, L., Grilli, S., Pagliarulo, V., & Ferraro, P. (2016). Bipolar patterning of polymer membranes by pyroelectrification. *Advanced Materials*, *28*(3), 454-459.

1:40 PM SM01.03.03

Late News: Intranasal Vaccination with Polycation/HA/CpG Nanoparticles Confers Cross-Protection Against Influenza Viruses Chunhong Dong and Baozhong Wang; Georgia State University, United States

Influenza remains one of the most severe threats to public health. Influenza mucosal immunity could confer broad cross-protection against influenza viruses. Intranasal (*i.n.*) vaccination with recombinant protein/peptide vaccines is a safe and promising strategy in the prevention of influenza virus infection due to the capability of generating both systemic immunity and local mucosal immunity. However, the intranasally administered protein/peptide vaccines are poorly immunogenic due to the harsh and tolerogenic mucosal environment.

Adjuvants could program the dimension and magnitude of antigen-specific immune responses and are helpful boosters to promote rapid and strong immune responses with a dose sparing effect. Nevertheless, few mucosal adjuvants are currently licensed for human use.

Nanoparticles are a special and promising class of vaccine adjuvants as it could not only serve as effective delivery carriers for antigen and/or molecular adjuvants but also synergistically work with molecular adjuvants like TLR agonists in a whole system. Polyethyleneimine (PEI) is a kind of organic polycations that could form nanoscale complexes with viral glycoprotein antigens. In our study, we prepared PEI-hemagglutinin (HA) nanocomplexes with or without CpG ODN molecules, and comprehensively studied the humoral and cellular immune responses after *i.n.* vaccination with the nanocomplexes. Our results showed that the PEI-HA nanocomplexes induced significantly enhanced mucosal and systematic antibody responses than soluble HA antigens. The combination of PEI and CpG in PEI-HA/CpG further boosted the responses. Furthermore, we would investigate the induced cellular responses and study the cross-protection efficacy of these nanocomplexes against different influenza strains in mice. The role of PEI, CpG and the nanoparticulate feature in regulating the immune responses would be further discussed. Our study will provide perspectives to guide the development of effective mucosal adjuvants for influenza vaccines.

1:45 PM SM01.03.04

Late News: One-Step Synthesis of Water-Soluble Fullerene Derivative with Myogenic Activity and Pronounced Antiviral Properties Olga A. Kraevaya¹, Alexander Shestakov^{1,2}, Dominique Schols³, Svetlana Kostyuk⁴ and Pavel Troshin¹; ¹ICPC RAS, Russian Federation; ²Department of Physical and Chemical Engineering, Lomonosov Moscow State University, Russian Federation; ³Rega Institute for Medical Research, Belgium; ⁴Research Centre for Medical Genetics RAMS, Russian Federation

We will discuss a straightforward method for the synthesis of a water-soluble C₆₀ fullerene derivative (F1) with five attached residues of phosphonic acid. Self-assembly of the synthesized compound in an aqueous solution leads to the formation of various nanostructures, as observed by AFM and DLS methods.

Antiviral screening of the synthesized compound *in vitro* demonstrated its activity against ten different viruses such as Feline coronavirus, Influenza A virus (H3N2 and H1N1), Influenza B virus, Varicella zoster virus, Cytomegalovirus, Herpes simplex virus (HSV-1, HSV-2), Cowpox virus, Feline herpes virus, and Human immunodeficiency virus (HIV-1, HIV-2).

The most unexpected effect of the water-soluble fullerene derivative F1 was its ability to promote myogenic differentiation of human mesenchymal stem cells (MSCs). In the absence of the fullerene derivative, stem cells from adipose tissue partially differentiate into adipocytes in the non-differentiating culture medium. During prolonged cultivation of MSCs in the presence of F1, the morphology of the cells changes spectacularly: fragments of stem cells with an ordered structure, which express markers of myogenic differentiation, appear. This kind of activity is unknown for all other reported water-soluble fullerene derivatives.

The obtained results open new horizons for the development of fullerene-based drugs for the regeneration of damaged muscle tissue and the treatment of severe muscle atrophy.

This work was supported by the Russian Science Foundation (project 19-13-00411).

1:50 PM SM01.03.05

Late News: *In Vitro* Assessment of Polymer Thrombogenicity—The Effect of Endothelial Culture Conditions on Platelet Responses Skadi Lau¹, Anna Maier¹, Steffen Braune¹, Manfred Gossen¹, Andreas Lendlein^{1,2} and Yue Liu¹; ¹Institute of Active Polymers and Berlin-Brandenburg Center for Regenerative Therapies, Helmholtz-Zentrum Geesthacht, Germany; ²Institute of Chemistry, University of Potsdam, Germany

The establishment of near-physiological *in vitro* thrombogenicity test systems for the evaluation of blood-contacting biomaterials requires co-cultivation of endothelialized materials and platelets (PLT) under blood flow-like conditions. Commercial perfusion systems for this purpose are equipped with gas plasma-treated cyclic olefin copolymer (COC)-based standard slides for endothelialization. Here, COC was characterized for physicochemical properties prior to co-culture studies. Moreover, endothelial culture conditions were systematically analyzed regarding PLT responses considering their sensitivity to external influences, both of

their handling and their environment, and their central role in hemostasis and innate immunity. A basic chemical characterization of COC and of its physical surface properties was performed. Human platelet rich plasma (PRP) was mixed with EGM-2 basal medium (BM) or with BM separately containing each of nine supplements or with BM containing all supplements together. PLT adherence analysis was carried out on COC and poly(tetrafluoro ethylene) (PTFE) as a control. PLT activation and aggregation were analyzed using light transmission aggregometry and flow cytometry (CD62P). COC endothelialized with human umbilical vein endothelial cells was co-cultivated with 150.000 PLT/ μL for 1 h under static conditions and laminar flow (10 dyn/cm²).

The physical and chemical characteristics as determined were in line with COC's cell adhesive properties. Medium supplements had no effect on PLT activation and aggregation. Regarding PLT adherence, supplements differentially affected PLT number, size and PLT covered area on COC and PTFE. EC count was significantly higher under laminar flow than under static conditions. PLT count and PLT covered area increased under static culture conditions compared to flow both on endothelialized and non-endothelialized surfaces.

Gas plasma-treated COC is suitable for the establishment of an in vitro thrombogenicity test system. Systematical medium analysis showed that according to the readouts employed here, the use of standard endothelial growth medium maintains functionality of PLT under EC compatible conditions without masking the differences of PLT adherence on different polymeric substrates. Moreover, improved EC attachment and reduced PLT adhesion under flow underlines the importance of blood flow-like conditions. These findings are important prerequisites for the assessment of polymer-based cardiovascular implant materials in contact with EC, PLT and, in the future, possibly also with further immune cells to grasp the complex role of blood homeostasis in contributing to thrombogenic events.

2:05 PM SM01.03.06

Covalent Cell Surface Conjugation of Nanoparticles by a Combination of Metabolic Labeling and Click Chemistry Alexander Lamoot, Annemiek Uvyn and Bruno G. De Geest; Ghent University, Belgium

Modification of the cell surface with nanoparticles (NP) can be of interest for a wide variety of biomedical applications. An attractive therapeutic strategy involving conjugation of NP to living cells is to exploit the tissue homing properties of specific cell types for targeted delivery of drugs loaded into NP (e.g. *ex vivo* engineering of tumor infiltrating T lymphocytes and CAR T cells). Cell surface conjugation requires either a covalent or non-covalent reaction. Non-covalent conjugation with ligand decorated NP is challenging and involve a dynamic equilibrium between the bound and unbound state. By contrast, covalent NP conjugation where reactive groups on the NP surface react with a complementary reaction partners in the cellular glycocalyx, results in a permanently bound state of NP. Current routes for cell surface conjugation predominantly make use of natural occurring lysines and cysteines on the cell surface and respectively activated esters and maleimides on the surface of NP. However also these routes tend to be challenging due to slow reaction kinetics, random conjugation to proteins in the glycocalyx etc. Therefore, there is strong need for new strategies that allow for efficient covalent cell surface conjugation. In particular, bio-orthogonal click reactions are an attractive alternative and in this context, introducing azides on the cells surface through metabolic labelling with azido sugars is attractive to introduce unnatural functional groups on the cell surface that can be addressed further on using biorthogonal strain promoted azide-alkyne cycloaddition (SPAAC) click chemistry. To explore this strategy, we used dibenzyl cyclooctyne (DBCO) functionalized lipid nanoparticles (LNP) formed by electrostatic complexation of an ionizable lipid and a double stranded RNA synthetic analogue, polyinosinic: polycytidylic acid (polyIC). Interestingly, we found that, whereas the reaction between small molecule dye-labeled DBCO and azido-labeled cells is extremely fast and efficient, reaction between DBCO-LNP and azide-labelled cells is rather inefficient, leading to a low degree of functionalization and high unspecific background adsorption of LNP to cells when attempting at optimizing conjugation conditions. We attribute this to a combination of sterical hindrance and the low concentration and slow Brownian motion of the reaction partners. This issue could be circumvented by designing LNP that contain a diisopropylamino-functionalized lipid that has a pKa below physiological pH. A short co-incubation time at pH 7.4 shows almost no association between DBCO-LNP and azido-labelled cells, but at pH 5, where the diisopropylamino moieties bear a cationic charge, strong LNP adsorption takes place due to electrostatic interaction. Due to the close contact between DBCO-

LNP and azide-labelled cells, SPAAC takes place and LNP remain permanently bound to the cell surface. However, this route leads to an extremely high non-specific background adsorption of control non-SPAAC-reactive LNP and on control cells, despite multiple washing steps with neutral buffer. To tackle the issue of low reactivity and high non-specific binding, we explored the ultra-fast bio-orthogonal inverse electron demand Diels–Alder (IEDDA) reaction between tetrazines (Tz) and trans-cyclooctene (TCO). We developed a 2-step conjugation sequence in which metabolically azide labelled cells first react with sulfo-6-methyl-*tetrazine-DBCO* (Tz-DBCO), followed by co-incubation with TCO-LNP. Eventually, this strategy gives a highly specific cell surface conjugation of LNP, with very low non-specific background fluorescence for controls cells and for control LNP lacking TCO, as evidenced by flow cytometry and confocal microscopy. Hence, we believe that this last strategy holds a general applicability for cell surface modification in view of adoptive cell transfer therapy with NP-backpacked cells.

2:20 PM *SM01.03.07

Multifunctional Biomaterials for Directing and Orchestrating Behavior and Functions of Stem Cells via Mechanical Cues Weiwei Wang¹, Zijun Deng^{1,2}, Xun Xu¹, Nan Ma^{1,2} and Andreas Lendlein^{1,2,3}; ¹Helmholtz-Zentrum Geesthacht, Germany; ²Free University of Berlin, Germany; ³University of Potsdam, Germany

Stem cells are highly relevant in tissue regeneration due to their self-renewal capacity and differentiation potential. Given the capacity of stem cells to sense the environmental cues and to convert the perceived information to intracellular signaling cascades, the use of external stimulation through biomaterials to regulate stem cells has become a safe and effective approach to guide them towards a desired function and lineage commitment. We designed and fabricated polymer based cell culture substrates with well-defined geometric micro-wells (size, shape) to exhibit static mechanical cues or thermally controlled artificial muscles as dynamic substrates. We investigated how the stem cells respond to these mechanical stimuli provided by the biomaterial and elucidated the underlying mechanism.

The micro-topography of the differently structured substrates exerted highly distinct effects on the major cellular process of mesenchymal stem cells (MSCs), including cell morphology, cytoskeleton organization, focal adhesion distribution, migration, gene expression, proliferation, and differentiation. Taking advantage of an AB copolymer network with a thermally controlled shape-memory actuation capability, we studied MSC response to the thermal (environmental temperature change) and mechanical (substrate shape change) stimuli. The combinational and synergetic effect of the dual stimuli as well as the activated signaling cascades were explored. The Ca²⁺ dynamics was shown to regulate the intercellular connection of mechano- and thermosensing components, promoting the osteogenic differentiation of MSCs.

These results provide a fundamental principle for design and application of advanced multifunctional biomaterials in regenerative medicine.

2:45 PM SM01.03.08

Late News: Gradient Granular Microgels for Spatial Differentiation of Mesenchymal Stem Cells Thomas G. Molley, Gagan Jalandhra, Tzong-tyng Hung and Kristopher Kilian; University of New South Wales, Australia

During tissue development, progenitor stem cells form functional tissue with high cellular diversity and intricate micro and macro architecture. Current approaches have attempted to replicate this process with materials cues or through spontaneous cell self-organization. However, it has become increasingly clear that cell-directed and material-directed organization are both required to achieve native structure and function. Here, I will present a biomanufacturing method to deposit stem cells in freeform within a granular matrix while spatially guiding their differentiation. The directed combination of varied microgels establish a 3D bioprinting support medium with gradients of mechanical stiffness and growth factor release. The packed suspension of gelatin methacrylate microgels crosslink together under near UV light, locking the cells and gradients in place. And controlled deposition of mesenchymal stem cells across these gradients within the gel enables guided differentiation to osteogenic, adipogenic, or chondrogenic phenotypes. As a demonstration of this method, we combine a gradient of stiffness and growth factor release with a gradient of hyaluronic acid to create a model meniscus. We

anticipate this material platform will open new avenues for regenerative medicine and fundamental studies on the role matrix cues play in stem cell differentiation.

SESSION SM01.04: Biomimetic ECM and Cell Modulation
Session Chairs: Xuesi Chen, Nan Ma, Xun Xu and Harry Yu
Sunday Afternoon, April 18, 2021
SM01

4:00 PM *SM01.04.01

Metabonegenic Citrate-Based Biomaterials for Orthopedic Applications Jian Yang; The Pennsylvania State University, United States

Citrate-based biodegradable polymer has recently joined in a handful of biodegradable synthetic polymers used in Food and Drug Administration (FDA) approved implantable medical devices such as orthopedic fixation devices. Citrate, historically known as an intermediate in the Krebs cycle, is a multifunctional, nontoxic, readily available, and inexpensive cornerstone monomer used in the design of citrate-based biomaterials. We have recently identified citrate as an osteo-promotive factor and revealed a key link between citrate metabolism and its downstream effects on osteogenic differentiation of human mesenchymal stem cells (hMSCs), named metabonegenic regulation. Our studies show that extracellular citrate uptake through solute carrier family 13, member 5 (SLC13a5) supported osteogenic differentiation via regulation of energy-producing metabolic pathways, which led to elevated cell energy status to fuel osteo-differentiation of hMSCs with high metabolic demands. We have also identified other factors such as phosphoserine (PSer) that can synergize with citrate to exhibit concerted action not only in metabonegenic potential for orthopedic regeneration, but also in functionalizing materials with imaging capability for materials tracking and monitoring. This unique citrate metabonegenic regulation has allowed us to design new citrate-based platform biomaterials to meet the dynamic biological, biochemical, and biophysical needs in tissue regeneration. The recent regulatory success of citrate-based biomaterials makes them promising candidate materials for technology translation and commercialization. In this presentation, a methodology for the design of citrate-based biomaterials in various regenerative engineering applications with a focus on orthopedic applications will be discussed.

4:25 PM SM01.04.02

Integrating Transferrable Chemically Modified Graphene with Materials and Biological Substrates Keith E. Whitener¹, Dhanya Haridas¹, Woo-Kyung Lee¹, Saron Yoseph² and Christopher So¹; ¹U.S. Naval Research Laboratory, United States; ²Howard University, United States

Developing interfaces between active materials and biological structures is becoming increasingly important for manipulating and interrogating living systems for use in advanced biological engineering. We have developed techniques for transferring graphene-based thin film materials from one substrate to another without needing to use harsh chemicals to detach the films from their initial substrates. This allows us to interface a number of materials directly with biological substrates including live stem cells without sacrificing viability. We found that partially reduced graphene oxide can be used as a transferrable surface for printing a number of materials, including metallic structures, fluorescent cell dyes, and phase-separated block copolymers. The mild transfer techniques we have developed allow us to easily probe biological systems at the scale of individual cells, and we can also use our transferrable block copolymer technology to lithographically pattern novel hierarchical structures on arbitrary substrates. These capabilities offer a cheap and easy way to exert spatiotemporal control over single cells and cell-cell interactions.

4:40 PM SM01.04.03

Mechanical Characterization of Collagen Hydrogels by Quasi-Static Uniaxial Tension Jieung Kim¹,

Sangmin Lee¹, Taek-soo Kim¹, Hyunjoon Kong² and Dongchan Jang¹; ¹Korea Advanced Institute of Science and Technology, Korea (the Republic of); ²University of Illinois at Urbana-Champaign, United States

Collagen is one of the most abundant extracellular matrix of animal tissues and also serves as the main structural material by providing mechanical environments for cells. Especially, collagen hydrogels are widely used as scaffold materials in vitro since the chemo-mechanical environments they give the cells are almost identical to those in vivo. Thus, providing physical reliability of the collagen hydrogel presents significant challenges for tissue engineering applications, and it is essential to understand its mechanical behavior and deformation mechanisms. In this study, we aim to investigate the mechanical behavior of collagen hydrogels under quasi-static uniaxial tensile strain to present the complex tempo-mechanical response of biomaterials apart from the rheometric response. A combination of tensile testing in a hydrogel-friendly hydrated environment and microstructure analysis including structural parameters and strain evolution demonstrates the mechanism of tensile properties, complementarily. When the tensile strain is applied, the stress-strain relationship of collagen hydrogels shows a non-linear response with strain-stiffening. This non-linearity of the physical properties of collagen hydrogel comes from the shift of deformation mechanism and the unfolding dominated deformation of the collagen fiber network is completed as the very first stage, the mechanical response gradually turns to the stretching dominated deformation of the collagen fibers by aligning their microstructure. These results illustrate that collagen hydrogels respond to tensile strain with two main different deformation mechanisms, unfolding and stretching of collagen fibers, which shows the non-linear stress-strain relationship, and the topology of collagen hydrogels can control the mechanical response. Furthermore, it is a new approach to physical behavior for soft and hydrated materials that can be applied throughout the bioengineering field.

4:55 PM SM01.04.04

Late News: Mesenchymal Stem Cells Derived Exosomes Promote the Expansion of Bregs and Alleviate the Collagen-Induced Arthritis Qiugang Zhu, Ke Rui, Shengjun Wang and Jie Tian; Jiangsu University, China

Olfactory ecto-mesenchymal stem cells (OE-MSCs) exert protective effects in some autoimmune diseases, partly through the regulation of activation, proliferation and differentiation of lymphocytes. Extracellular vesicles (EVs), including exosomes, released by MSCs contain bioactive factors, such as microRNAs, proteins, lipids, and some studies have confirmed that the immunoregulatory function of MSCs was mediated by exosomes. However, it is unclear whether OE-MSC-derived exosomes (OE-MSC-Exos) influence regulatory B cells in collagen-induced arthritis (CIA). In this study, we found that OE-MSC-Exos could promote the expansion of interleukin-10-producing B cells (B10 cells) with regulatory function in an Epstein-Barr virus-induced gene 3 (EBI3)-dependent pathway. In vivo, intravenous injection of OE-MSC-Exos into CIA mice significantly inhibited the disease progression and reduced the severity of both clinical score and joint damage. Taken together, our findings identified that OE-MSC-Exos might become a new cell-free therapy for the treatment of RA and other inflammatory diseases.

5:00 PM SM01.04.09

Thermomechanical Modulation of Toll-Like Receptor Internalization and Expression Profile in Mesenchymal Stromal Cells Xun Xu¹, Weiwei Wang¹, Yan Nie^{1,2}, Nan Ma^{1,3} and Andreas Lendlein^{1,2,3}; ¹Institute of Biomaterial Science and Berlin-Brandenburg Center for Regenerative Therapies, Helmholtz-Zentrum Geesthacht, Germany; ²Institute of Biochemistry and Biology, University of Potsdam, Germany; ³Institute of Chemistry and Biochemistry, Freie Universität Berlin, Germany

During the current SARS-CoV-2 pandemic, intravenous infusion of mesenchymal stromal cells (MSCs) is emerging as one of the promising therapeutic tools for treating the severe respiratory syndrome in COVID-19, which mainly relies on the regenerative capacity and superior immunomodulatory function of MSCs [1, 2]. The transplanted MSCs were found to be recruited at the interface of alveoli and surrounding capillaries, where respiratory airway structures are exposed to periodic heat exchange and mechanical stresses with respiratory

cycles [2, 3]. Toll-like receptor (TLR) triggers innate immune response against virus including SARS-CoV-2 [4, 5]. TLR also plays a key role in regulation of differentiation and immune polarization of MSCs, which highly associated with the MSC therapeutic efficacy. However, TLR expression profiles and distributions are varying in MSCs not only depending on the cell sources but also the culture conditions [6]. To date, little is known about the influence of the thermomechanical cues on regulating the TLRs in MSCs. Here, thermally-controlled polymer sheets with programmable actuation capacity (cPCLBA) were created to autonomously synchronize and transfer the thermomechanical signal to MSCs. With the periodic temperature change between 10 °C and 37 °C, $14 \pm 1\%$ elongation of programmed sheets can be achieved at both macro- and micro-scales. As a result, in response to thermomechanical stimuli, the proportion of cells expressing SARS-CoV-2 responsive TLRs (TLR4+TLR7+) were significantly increased from $69 \pm 5\%$ to $81 \pm 3\%$, while the TLR3+TLR9+ cells that sensing double-stranded RNA and unmethylated DNA virus was decreased from $41 \pm 5\%$ to $26 \pm 4\%$. Moreover, the internalization of cell surface expressed TLR4 was promoted and the intracellular TLR4 was co-localized with TLR7, and retained closely to the endoplasmic reticula where viral entry, replication and assembly takes place [7]. In summary, the programmed cPCLBA sheet provided a simple, cost effective and efficient respiratory cycle model, which synchronized and transduced the thermomechanical stimuli into MSCs. Such stimuli were able to accumulate TLR4 and TLR7 at endoplasmic reticula and selectively amplified the TLR4+TLR7+ MSCs, which can specifically react to single-stranded RNA virus including SARS-CoV-2. These results highlight the potential application of boosting the anti-viral immunity via preconditioning of MSCs with thermomechanical cues prior to cell infusion.

References:

1. Chowdhury, M.A., et al., Immune response in COVID-19: A review. *J Infect Public Health*, 2020.
2. Leng, Z., et al., Transplantation of ACE2(-) Mesenchymal Stem Cells Improves the Outcome of Patients with COVID-19 Pneumonia. *Aging Dis*, 2020. 11(2): p. 216-228.
3. Garcia, C.S., et al., Understanding the mechanisms of lung mechanical stress. *Braz J Med Biol Res*, 2006. 39(6): p. 697-706.
4. Patra, R., N. Chandra Das, and S. Mukherjee, Targeting human TLRs to combat COVID-19: A solution? *J Med Virol*, 2020.
5. Heil, F., et al., Species-specific recognition of single-stranded RNA via toll-like receptor 7 and 8. *Science*, 2004. 303(5663): p. 1526-9.
6. Seo, Y., T.H. Shin, and H.S. Kim, Current Strategies to Enhance Adipose Stem Cell Function: An Update. *Int J Mol Sci*, 2019. 20(15).
7. Inoue, T. and B. Tsai, How viruses use the endoplasmic reticulum for entry, replication, and assembly. *Cold Spring Harb Perspect Biol*, 2013. 5(1): p. a013250.

5:15 PM *SM01.04.10

The Mechanical Responses of Tension-Transmission Supramolecular Linkages Jie Yan; National University of Singapore, Singapore

The task of mechanosensing of cells involves dynamic assembly of various tension-transmission supramolecular linkages, which enable the cells to properly sense and respond to the level of tension in the linkages. A tension-transmission linkage typically consists of a few non-covalently linked proteins, in which the domains and protein-protein interfaces are subject to dynamic fluctuation of intracellular tensions. This leads to highly complex tension-dependent connectivity of the supramolecular linkages, conformational changes of the domains and the resulting tension-dependent interactions of binding sites in the linkage with signalling proteins. Increasing evidence has suggested that protein-protein interfaces and protein domains in various mechanosensing tension-transmission supramolecular linkages have been evolved with special structural and topological features that impart them with special mechanical properties. In this talk, I will introduce our recent single-molecule and theoretical investigations of the effects of the structural-topological features shared by many tension bearing protein-protein interfaces and protein domains on the mechanical stability and

mechanosensing function of tension-transmission supramolecular linkages.

SESSION SM01.05: Immunological Modulation and Biomaterial

Session Chairs: Nan Ma and Jie Yan

Sunday Afternoon, April 18, 2021

SM01

6:30 PM SM01.05.03

Poly(I:C) Delivery Strategies to Selectively Activate TLR3 and MDA-5 Pathways for Immunotherapy

Apoorv Shanker¹, Imane Bouzit¹, Sandeep Koshy², Janelle Velez², Stephanie Schwartz² and Paula Hammond^{1,1};

¹Massachusetts Institute of Technology, United States; ²Novartis Institutes for BioMedical Research, United States

Agonists of toll-like receptors (TLRs) form an important class of adjuvants employed in cancer immunotherapies and prophylactic vaccines. Among the various TLR agonists, polyriboinosinic acid:polyribocytidylic acid (poly(I:C)), a synthetic mimic of viral dsRNA, has been shown to activate and boost antigen cross-presentation by dendritic cell (DCs), promote NK cell cytotoxicity as well as effect direct tumor-killing to generate tumor-associated antigens for DC presentation. Poly(I:C) is recognized by the endosomal receptor TLR3 as well as cytosolic receptors such as RIG-I and MDA-5. Poly(I:C) binding to its receptor initiates a cascade of signaling pathways resulting in the activation of NF- κ B and production of pro-inflammatory cytokines (TLR3), or IRF and production of type-I interferons (MDA-5). Despite its potent immunogenic properties, safety concerns including inadvertent immune over-stimulation, induction of autoimmune diseases, and short half-life *in vivo* have limited the scope of poly(I:C). Several strategies including liposomal and polymeric encapsulation, polycationic complexes or polyplexes, and surface-assembly on nanoparticles (NPs) or microparticles (MPs) have been explored to overcome these issues.

Here, we present a comparative study of poly(I:C) polyplexes and layer-by-layer (LbL)-assembled NPs/MPs carrying poly(I:C) to selectively activate the TLR3 and MDA-5 receptors. Poly(I:C) delivery platforms were fabricated using three classes of polycations: polypeptides, polysaccharides, and synthetic polymers. Dynamic light scattering, zeta potential measurements, gel electrophoresis, fluorophore exclusion titration assay, circular dichroism, and isothermal titration calorimetry were utilized to characterize the polyplexes and assess the structural integrity of poly(I:C) complexed with different polycations. LbL particles were built on a negatively-charged core using the polycations to electrostatically assemble poly(I:C) on the particle surface. HEK-Blue mTLR3 reporter cell line was used to assess the ability of polyplexes and LbL particles to activate the endosomal TLR3 receptors. For the polyplexes with varying poly(I:C):polycation ratios, TLR3 activation was found to be roughly inversely correlated with the poly(I:C) binding strength of the polycations. While poly(I:C)-loaded LbL particles were as effective as free poly(I:C) in activating TLR3 when in direct contact with the cells, significant loss of bioactivity was observed when the cells and the particles were separated using a trans-well. This was likely due to enhanced cellular uptake of the LbL particles or degradation of poly(I:C) released from the LbL particles in the latter case. The selectivity of polyplexes and LbL particles toward TLR3 and MDA-5 receptors was assessed in A549 dual NF- κ B-SEAP and IRF-luciferase reporter cell line. Activation of the two pathways was further correlated with cellular uptake and trafficking of the polyplexes and LbL particles. We elucidate the role of the delivery mechanism and polycationic carriers in stabilizing poly(I:C) against serum nucleases, reducing cellular toxicity and selectivity toward endosomal or cytosolic receptors. The presented biophysical studies provide critical insight into the design of poly(I:C) delivery platforms toward more potent adjuvants.

6:45 PM *SM01.05.05

Immunomodulating Nano-Adaptors Potentiate Antibody-Based Cancer Immunotherapy Cheng-Tao

Jiang¹, Kai-Ge Chen¹, Song Shen^{1,2} and Jun Wang^{1,2,2}; ¹South China University of Technology, Guangzhou International Campus, China; ²South China University of Technology, China

Modulating effector immune cells via monoclonal antibodies (mAbs) and facilitating co-engagement of T cells and tumor cells via CAR T cells or bispecific T cell-engaging antibodies are two typical cancer immunotherapy approaches¹⁻³. We speculated that immobilizing two types of mAbs against effector cells and tumor cells onto single nanoparticle could integrate the functions of these two approaches, as the engineered formulation (immunomodulating nano-adaptor, imNA) could potentially associate with both cells and bridge them together like an 'adaptor' while maintaining the immunomodulatory properties of parental mAbs. However, existing mAbs immobilization strategies mainly rely on chemical reaction, a process that is rough and difficult to control. Here, we built up a versatile antibody immobilization platform by conjugating anti-IgG (Fc specific) antibody (α Fc) onto nanoparticle surface (α Fc-NP), and confirmed that α Fc-NP could conveniently and efficiently immobilize two types of mAbs through Fc-specific noncovalent interactions to form imNAs. The superiority of imNAs over the mixture of parental mAbs were validated in T cell-, natural killer cell- and macrophage-mediated antitumor immune responses in multiple murine tumor models.

1. Velasquez, M.P., Bonifant, C.L. & Gottschalk, S. Redirecting T cells to hematological malignancies with bispecific antibodies. *Blood* 131, 30-38 (2018).
2. Slaney, C.Y., Wang, P., Darcy, P.K. & Kershaw, M.H. CARs versus BiTEs: a comparison between T cell-redirected strategies for cancer treatment. *Cancer Discov.* 8, 1-11 (2018).
3. Sadelain, M., Riviere, I. & Riddell, S. Therapeutic T cell engineering. *Nature* 545, 423-431 (2017).

SYMPOSIUM SM02

Next-Generation Antimicrobial Materials—Combating Multidrug Resistance and Biofilm Formation
April 14 - April 19, 2021

Symposium Organizers

Karen Lienkamp, Universität des Saarlandes
Haitao Liu, University of Pittsburgh
Edmund Palermo, Rensselaer Polytechnic Institute
Lihua Yang, University of Science and Technology of China

* Invited Paper

SESSION SM02.01: Materials Against AMR
Session Chairs: Haitao Liu and Edmund Palermo
Monday Morning, April 19, 2021
SM02

8:00 AM *SM02.01.01

Antibacterial Cationic Molecular Umbrellas Edmund F. Palermo and Ao Chen; Rensselaer Polytechnic Institute, United States

We synthesized "cationic molecular umbrellas", which are dendrons of multivalent cationic charge attached to a

hydrophobic alkyl chain. The generation number and alkyl chain length are key determinants of activity against bacteria and red blood cells. In the best case, we identified a very promising composition that exerts potent, broad-spectrum antibacterial activity (MIC = 4–8 $\mu\text{g}/\text{mL}$) while remaining non-hemolytic ($\text{HC}_{50} \sim 5000 \mu\text{g}/\text{mL}$) even at concentrations 1000x higher than the effective antibacterial dose. Although these compounds do self-assemble into stable micelles in aqueous solutions, the antibacterial activity is observed at concentrations far lower than the CMC, suggesting that the active species is the individually solvated dendron. Mechanistic studies strongly point to a mechanism involving membrane disruption.

8:15 AM *SM02.01.02

Development of Nanoantibiotics to Fight Drug-Resistant Bacterial Infections Hongjun Liang; Texas Tech University Health Sciences Center, United States

Antibacterial nanomaterials, or nanoantibiotics, are emerging contenders to fend off drug-resistant bacteria when conventional antibiotics fail. Nanostructure itself is widely and sometimes blithely speculated to instigate added benefits in killing bacteria, but whether it plays any role on defining the encounter between nanoantibiotics with bacteria that seals the dour fate of the microbes is not clear. In order for nanoantibiotics to stay relevant in the clinical battlegrounds against bacterial infections, it is imperative to dissect the antibacterial role of nanostructures from the inherent and external chemical moieties associated with the nanoantibiotics that are detrimental to both bacteria and mammalian cells. In this talk, I will discuss our effort to elucidate the antibiotic role of nanostructures using model spherical and rod-like polymer molecular brushes (PMBs) that mimic the two basic structural motifs of bacteriophages. While the individual linear-chain polymer branch that makes up the PMBs is hydrophilic and a weak antimicrobial, amphiphilicity is not a required antibiotic trait once nanostructures come into play. The phage-mimicking PMBs induce an unusual topological transition of bacterial but not mammalian membranes to form pores. The sizes and shapes of the nanostructured PMBs further help define their antibiotic activity and selectivity against different families of bacteria. This nanostructure-induced transformation of antibacterial activities further suggests that nanoantibiotics have the potential to serve as a generic platform for the design of “smart” antibiotics with in-demand activity and selectivity in response to external stimuli by assembly or disassembly of their nanostructures. To exploit this concept for the design of environmentally benign antibiotics that remain fully active in clinical services but become deactivated rapidly once released into the environment, I will discuss an example of antibiotic PMB design that epitomizes the concept of carrying a built-in “OFF” switch responsive to natural stimuli. In their nanostructured forms in services, these PMBs are potent killers for both Gram-positive and Gram-negative bacteria, including clinical multidrug-resistant strains; after services and being discharged into the environment, they are shredded into antimicrobially inactive pieces by bioorthogonal chemistry that does not exist in human body but occurs abundantly in natural habitats.

8:40 AM DISCUSSION

9:05 AM SM02.01.04

Broad-Spectrum Polyimidazolium Against Pan-Resistant Bacteria Wenbin Zhong and Mary Chan-Park; Nanyang Technological University, Singapore

Antimicrobial resistance (AMR) has become a global severe problem and is aggravated by the slow pace of antibiotic development. Antimicrobial peptides and its mimics have emerged as alternative therapeutic agents but most failed in clinical trials due to varied reasons like limited antimicrobial spectrum, reduced activity in physiological condition, toxicity issue etc. Here we applied one-pot multicomponent polymerization and prepared a series of main-chain cationic polyimidazoliums (PIMs). The lead compound, PIM1, demonstrated good biocompatibility and potent broad-spectrum antimicrobial efficacy against both multi-drug resistant Gram-positive and Gram-negative bacteria even including colistin-resistant *burkholderia*, and it's an anti-mycobacterial agent. Unlike classic antimicrobial peptides, PIM1 does not permeabilize bacterial cell membrane but accumulates into cells with assistance of membrane potential, and ultimately leads to cell death. PIM1 does not develop resistance in Gram-negative *P. aeruginosa* cells while has menaquinone mutation in

Gram-positive *S. aureus*. In murine wound model, PIM1 demonstrated good potency in preventing topical skin infection, but systemic toxicity in mice was found via intraperitoneal injection of PIM1. We further developed PIM1 derivative, PIM1D, which has amide bond and become less hydrophobic. Experiments showed that PIM1D does not cause systemic toxicity to mice even with 7-days repetitive dosing but maintained good antimicrobial potency and demonstrated the ability to rescue mice suffering sepsis infection. Overall, we successfully showed a potential drug candidate in fighting against pan-resistant bacterial infections.

9:20 AM SM02.01.05

Cost-Effective Hybrid Membranes with Antimicrobial Efficacy for Burn Treatments Kausik

Mukhopadhyay, Suvash Ghimire, Kasey Rigby and Kaitlyn E. Crawford; University of Central Florida, United States

There are about 1.1 million burn injuries that receive medical attention every year in the United States, of which majority are related to first- and second-degree burns. Burns are among the most painful and debilitating wounds and often turn deadly when infection sets in. Approximately 50,000 of these require hospitalization; around 20,000 suffer from major third degree burns, and an estimated 4,500 die from burn wounds. Patients who are admitted to the hospital after sustaining a large burn injury are at high risk for developing hospital-associated infections. If patients survive the initial three days after a burn injury, infections are the most common cause of death. The risk of infections caused by multidrug-resistant bacteria increases as the patients stays longer time in the hospitals. While susceptible gram-positive organisms predominate in the initial days, the more resistant gram-negative organisms are found later. These findings affect the choice of empiric antibiotics in critically ill burn patients.

To combat such infections only a handful of FDA-approved products are available in the market to treat second and third degree burns, and hardly a handful treat scars associated with such burns. Topical agents in treating wounds such as chlorhexidine, proflavine, iodine, hydrogen peroxide, silver etc. have been used to combat wound infections. However, the relentless emergence of antibiotic resistant strains of pathogens, often with multiple antibiotic resistances, together with the discovery of novel antibiotics has led to the need to find alternative treatments.

We have developed a series of hybrid membranes engineered using material modification through intercalation and exfoliation of silicate-based materials and metal ions to prevent infections from ESKAPE pathogens sans the expensive or environmentally toxic ions or nanoparticles while promoting rapid wound and scar healing. Further, we will also display a metal-less hybrid organic-inorganic system that shows huge promise in antimicrobial efficacy against gram-negative and gram-positive bacteria. Complete characterization including physico-chemical, spectroscopic and mechanical analyses corroborates our hypothesis for the structures, properties, mechanisms, mechanical durability and microbial activity of such membranes. The membranes also exhibit optimal water vapor transport through the pores and skin - an important feature that helps with the healing and quick recovery. Cost-effective, near-zero toxicity, biodegradable and durability features, together with easy application on the wound areas, make these hybrid membranes unique for burn treatments.

9:35 AM SM02.01.06

What Nanozymes Preferentially Kill Bacteria Over Mammalian Cells and Bio-Compatibly Inhibit

Biofilm Formation (Those Generating Surface-Bound Reactive Oxygen Species) Feng Gao, Tianyi Shao, Yunpeng Yu, Yujie Xiong and Lihua Yang; University of Science and Technology of China, China

Nanozymes kill bacteria with reactive oxygen species (ROS) they produce *in situ*. Because ROS can simultaneously oxidize diverse substances crucial for proper cell functions, nanozymes are recognized as a class of novel antimicrobial agents that are promising for tackling antimicrobial resistance. However, the intrinsic inability of ROS to distinguish bacteria from mammalian cells deprives nanozymes of the selectivity necessary for an ideal antimicrobial. Note that mammalian cells, but not bacteria, actively internalize nanoparticles via endocytosis and that reactive ROS have extremely short lifetimes. We hypothesize that nanozymes that generate

surface-bound ROS may selectively kill bacteria over mammalian cells, thereby offering disinfection and biofilm inhibition in a biocompatible manner. To prove this hypothesis, we identified AgPd, a silver-palladium bimetallic alloy nanoparticle, to be an oxidase-like nanozyme that generates surface-bound ROS and, using AgPd as a model for surface-bound ROS-generating nanozymes, carried out antibacterial assays and mammalian cell cytotoxicity tests both in vitro and in animal models. We further excluded the possibility that our hypothesis applies only to AgPd, by examining the performances of another two nanozymes that are distinct in materials from AgPd but generate surface-stabilized ROS in oxidase-like way as well. To examine whether or not the surface-bound nature of ROS on AgPd impacts its potential in eliminating antibiotic-resistant bacteria or delaying the onset of bacterial resistance emergence, we performed serial antibacterial assays in vitro. Moreover, to evaluate the potential of AgPd as antibacterial additive for surface coating, we coated AgPd onto an inert substrate and tested the potency of the resulting surface in thwarting biofilm formation both in vitro and in mouse models. Results from above in vitro assays and animal experiments will be reported.

SESSION SM02.02: Anti-Viral Materials
Session Chairs: Karen Lienkamp, Haitao Liu and Lihua Yang
Monday Morning, April 19, 2021
SM02

10:30 AM *SM02.02.04

Engineering Antimicrobial Biomaterials—The Fight Against Bacteria, Fungi and Viruses Jayanta Haldar; Jawaharlal Nehru Centre for Advanced Scientific Research (JNCASR), India

Emergence of antimicrobial resistance (AMR) caused by superbugs, has threatened the global public health thereby constituting a major share of the annual mortality, worldwide. On top of that, COVID-19 pandemic in the recent times has further worsened the prevailing scenario. In this context, the global community has been realizing the significant role of surfaces in infection transmission and necessity for the development of effective preventive measures and therapeutics. Towards this goal of mitigating the spread of pathogens through fomites, our group has engineered numerous polymeric antimicrobial paints.¹⁻² Recently, we have developed a one-step curable, covalent antimicrobial coating, which can be applied to various surfaces such as cotton, plastic, polyurethane, surgical mask, apron, gloves.³ The coating displays excellent activity against drug resistant bacteria, and pathogenic fungi. Remarkably, this coating shows complete killing of human influenza viruses and is also being investigated for ability to inactivate SARS-CoV-2. Our interest into biomaterial researched has also led to antimicrobial hydrogels and injectable antimicrobial sealant with superior adhesive strength and haemostatic ability and potent therapeutic effect against corneal infections.⁴⁻⁶ Alongside, we have contributed significantly in the development of synthetic peptidomimetic antimicrobial polymers.⁷⁻⁹ These membrane-active macromolecules demonstrate excellent activity against multidrug resistant pathogenic bacteria and fungi in *in-vitro* as well as *in-vivo*, without any detectable resistance development. Overall, the aforementioned inventions hold promise leading to be developed as smart technologies in future to combat microbial infections and antimicrobial resistance.

Reference:

(1) Hoque, J. *et al. ACS Biomater. Sci. Eng.* **2019**, 5, 81. (2) Hoque, J. *et al. ACS Appl. Mater. Interfaces*, **2019**, 11, 39150. (3) Ghosh, S. *et al. ACS Appl. Mater. Interfaces* **2020**, 12, 27853. (4) Hoque, J. *et al. ACS Appl. Mater. Interfaces* **2017**, 9, 15975. (5) Hoque, J. *et al. Biomacromolecules* **2017**, 19, 267. (6) Hoque, J. *et al. Mol. Pharmaceutics* **2017**, 14, 1218. (7) Barman *et al, ACS Appl. Bio Mater.* **2019**, 2, 5404-5414; (8) Barman, S. *et al. ACS Appl. Mater. Interfaces* **2019**, 11, 33559. (9) Mukherjee, S. *et al. Front. Bioeng. Biotechnol.* **2020**, 8, 55.

10:55 AM SM02.02.02

On-Mask Chemical Modulation of Respiratory Droplets Haiyue Huang, Hun Park, Yihan Liu and Jiaxing Huang; Northwestern University, United States

Mask-wearing has become a new normal in many parts of the world in the COVID-19 pandemic. There has been much interest in enhanced masks that can better protect the wearers. However, a mask or face covering is much more effective in protecting others, because it can block and reroute a large portion of the virus-laden respiratory droplets from symptomatic or asymptomatic infected wearers during coughing and sneezing. Here we report an on-mask chemical modulation strategy, where droplets escaping a masking layer are chemically contaminated with antipathogen molecules (*e.g.*, mineral acids or copper salts) pre-loaded on polyaniline-coated fabrics. Colorimetric method based on the color change of polyaniline and fluorometric method utilizing fluorescence quenching microscopy are developed for visualizing the degree of modification of the escaped droplets by H^+ and Cu^{2+} , respectively. It is found that even fabrics with low fiber packing densities (*e.g.*, 19%) can readily modify 49% of the escaped droplets by number, which accounts for about 82% by volume. The chemical modulation strategy could offer additional public health benefits to the use of face covering to make the sources less infectious, helping to strengthen the response to the current pandemic or future outbreaks of infectious respiratory diseases.

11:10 AM SM02.02.03

A FAST Platform to Counter Antimicrobial Resistance and Pandemics Anushree Chatterjee^{1,2}; ¹University of Colorado Boulder, United States; ²Sachi Bioworks Inc, United States

The rapid rise of multidrug-resistant (MDR) superbugs and the declining antibiotic pipeline are serious challenges to global health. Rational design and synthesis of therapeutics can accelerate development of effective therapies against MDR bacteria. In this talk, I will describe multi-pronged systems, synthetic biology, and nano-biotechnology based approaches being devised in our lab to rationally engineer therapeutics that can overcome antimicrobial resistance. We have developed a synthetic biology and materials-engineering based platform called Facile Accelerated Specific Therapeutic (FAST) for developing accelerated therapeutics in less than a week. This approach relies on designing, building and testing engineered antisense therapeutics that can block translation or increase transcription of any desired gene in a species-specific manner. We have used this approach to uncover and target novel genes to re-sensitize MDR clinical isolates of bacteria to antibiotics, develop new classes of antibiotics, as well as develop therapeutics effective against SARS-CoV2 in very short periods of time. I will also present a nano-biotechnology based approach involving development of a unique semiconductor material-based quantum dot-antibiotic (QD ABx) which, when activated by stimuli, release reactive oxygen species to eliminate a broad range of MDR bacterial clinical isolates. This approach has been shown to eliminate MDR clinical isolates under both planktonic and biofilm conditions. Pre-clinical animal studies evaluating the FAST and QD Abx platform demonstrate low toxicity and high efficacy, and thus promise for further translation. The FAST and QD Abx platforms and inter-disciplinary approaches presented in this talk offer novel methods for rationally engineering new therapeutics to combat disease challenges.

11:35 AM *SM02.02.01

Viral Inhibition with DNA Star Strategy Xing Wang; University of Illinois at Urbana-Champaign, United States

Many infectious diseases including viruses, bacteria, and toxins, present unique spatial patterns of antigens on their surfaces [1-3]. These specific patterns facilitate multivalent binding to host cells, resulting in enhanced pathogenic infectivity. Based on this naturally occurring multivalent binding mechanism, synthetic multivalent entry blockers were previously introduced by linking epitopes-binding ligands to a scaffold to improve multivalent binding avidity [4-7]. Recently, the anti-influenza assays by Kwon *et al.* has suggested that matching ligand spacing with the distance of viral epitopes is a critical factor in inhibiting viral infection, while higher ligand densities have resulted in null or much weaker inhibition of influenza infection [8]. However, existing scaffolds, which include polymers, dendrimers, nanofibers, inorganic nanoparticles and lipid nanoemulsions, have shown toxicity [9,10]. Furthermore, the complex geometric patterns of viral epitopes

cannot be matched by existing scaffolds because they are not as precise in ligand spacing or provide limited control over the scaffold shape and ligand valency.

A customizable molecular scaffold strategy capable of incorporating pathogen-specific ligands and patterns may address these issues on both therapeutic and diagnostic fronts. DNA, when folded into nanostructures with a specific shape, is capable of spacing and arranging binding sites into a complex geometric pattern with nanometer-precision. Here we demonstrate designer DNA nanostructures (DDNs) that can act as templates to display multiple binding motifs with precise spatial pattern-recognition properties, and that this approach has been shown to confer exceptional potent viral inhibitory capabilities against dengue virus (DENV) and SARS-CoV-2.

As a proof-of-concept, we designed and synthesized a star-shaped DNA architecture to display 10 DENV envelope domain III (ED3)-targeting aptamers into a two-dimensional pattern precisely matching the spatial arrangement of ED3 clusters on the viral surface [11]. DENV was chosen as a representative target because its epitopes represent the most complex spatial pattern among all known viruses. The binding strength of monovalent ligand to proteins on a viral or cell surface is often relatively weak [8,11]. However, the “DNA star” allows for polyvalent and spatial pattern-matching interactions, affording dramatic improvement in DENV-binding avidity and providing highly potent DENV inhibitor in human blood with an EC₅₀ of 2 nM (~7,500-fold more effective than the monovalent aptamer). Live confocal imaging confirmed that dengue virions lost their cell internalization ability after binding by the DNA stars in blood. Our molecular-platform design strategy could be adapted to combat other disease-causing pathogens by generating the requisite ligand patterns on customized DNA nanoarchitectures. The design and characterization of our SARS-CoV-2 inhibitors will be also discussed.

References:

1. *Science* 2010, **329** (5995), 1026-1027.
2. *Science* 2005, **309** (5735), 777-781.
3. *J Am Chem Soc* 2017, **139** (45), 16389-16397.
4. *Nat Biotechnol* 2001, **19** (10), 958-961.
5. *Nat Biotechnol* 2006, **24** (5), 582-586.
6. *Nat Nanotechnol* 2008, **3** (1), 41-45.
7. *Nature* 2000, **403** (6770), 669-672.
8. *Nat Nanotechnol* 2017, **12** (1), 48-54.
9. *Rev Environ Health* 1989, **8** (1-4), 3-16.
10. *J Control Release* 2000, **65** (1-2), 133-148.
11. *Nat Chem* 2020, **12** (1), 26-35.

SESSION SM02.03: Anti-Biofilm Materials I

Session Chair: Haitao Liu

Monday Afternoon, April 19, 2021

SM02

1:00 PM *SM02.03.01

Nanogenerator-Enabled Electrical Strategy for Suppressing Biofouling Xudong Wang and Yin Long;
University of Wisconsin-Madison, United States

The attachment and accumulation of organic substances and subsequent microbe attaching on submerged solid surfaces can cause substantial energy waste and severe damage. In addition to conventional antifouling coatings, alternating strong electric fields have also been investigated as a promising anti-biofouling strategy via

the effects of killing microbes by irreversible electroporation of cell membranes or to repel microbes via the dielectrophoresis effect. We recently investigated nanogenerator technology as an effective approach to generate alternative electric fields by harvesting mechanical energy from ambient environment. With appropriate design, the electric potential generated directly from water agitation can be utilized as a self-sustainable energy source to effectively prevent microbe adhesion by changing surface charge distribution on microbes. We demonstrated an efficient and eco-friendly anti-biofouling system using an alternating low-intensity and discrete electric field generated by a water-driven nanogenerator. The anti-biofouling mechanism was attributed to the electric field-induced disturbance to the double layer, which impairs the stable adsorption of organic substances and the subsequent microbe attachments. The anti-biofouling efficacy was directly related to the strength of the electric field but less dependent to the alternating frequency. A long-time on-site demonstration in lake demonstrated superior performance compared to copper based surfaces and commercial coatings. This development brings a novel, effective and eco-friendly solution for protecting a broad range of surfaces against biofouling, including underwater surface and maybe even for implanted medical devices.

1:25 PM *SM02.03.03

Entrapment of Commensal Skin Bacteria in Polymer Materials: An Approach to Treat Skin Disorders due to Pathogens? Karine Glinel, Wanlin Xu, Sophie Demoustier-Champagne and Alain M. Jonas; Université Catholique de Louvain, Belgium

Usual approaches to treat skin infections are based on the use of antimicrobial products such as disinfectants or antibiotics. However, these compounds are rarely fully selective so that they act not only on pathogens responsible for the skin infection but also against commensal bacteria living on the human skin and which are now recognized as a part of the host defense system. Indeed, some bacteria involved in the skin microbiota play a major role against proliferation of pathogens by secreting active substances such as antimicrobial peptides, quorum sensing molecules, etc. These microorganisms produce also substances which stimulate the wound repair and limit the inflammation related to the infection.

As a consequence, treatments impacting this community can give rise to serious skin disorders leading to pathologies even more serious than the initial infection to be treated. Therefore, it is now well-admitted that skin treatments need to be targeted to preserve the bacterial community composing the skin microbiota. In this context, recent approaches explored the use of commensal bacteria known for their beneficial activity against pathogens to treat skin diseases. However, applying directly such bacteria on the patient's skin is not without risk considering their tremendous ability to mute or to become pathogenic in certain conditions. Therefore, an approach allowing to manipulate such bacteria to treat skin disorders while avoiding their uncontrolled proliferation could be a promising approach for topical applications.

In this presentation, we present different approaches to entrap *Staphylococcus epidermidis*, a predominant commensal skin bacterium known for its active role in the host defense system but also reputed to be an opportunistic agent being a major source of hospital-acquired infections, mostly associated with the use of invasive medical devices. The objective is to develop polymer envelopes which preserve the viability and the activity of bacteria and allow the diffusion of secreted molecules but also avoid the release of cells to prevent their uncontrolled growth on human skin. Different strategies based on encapsulation of individual cells in a polymer shell, entrapment of cells in mats of polymer nanotubes, in polymer microtubes and in pores of polymer membranes will be presented. The advantages and the limitations of these different approaches towards the final application, i.e., the development of new therapeutic strategies to treat skin disorders, will be discussed.

1:50 PM SM02.03.04

DNA-Based Nanofabrication for Antifouling Applications Liwei Hui and Haitao Liu; University of Pittsburgh, United States

This talk will present our recent work on the fabrication of antifouling surface using DNA-based nanofabrication. We used DNA triangle nanostructures as templates to produce triangular-shaped trenches *ca.* 100 nm in size on a SiO₂ surface. Using *B.subtilis* as a bacterial model, we found that such nanopatterned

surface showed a 75% reduction in bacterial adhesion and 74% reduction in biofilm density at only 35% surface coverage of the nanoscale triangle trenches. Our work demonstrates the potential of DNA-based nanofabrication in antifouling and other surface engineering applications.

2:05 PM SM02.03.05

Antimicrobially Active Polymer Materials for Interfaces and Applications [Karen Lienkamp](#)^{1,2}; ¹Albert-Ludwigs-Universität Freiburg, Germany; ²University of Saarland, Germany

Bacterial infections of patients often initiate at the surface of medical devices. In consequence, biofilms form, often with life-threatening consequences. It is estimated that by 2050, up to 10 million people will die every year due to bacterial infections if the current trends cannot be reverted. Thus, antimicrobial polymers are currently experiencing a renaissance both as drugs and materials. Polycationic materials have long been known for their antimicrobial activity; however, they fail once they are fully covered by bacterial debris. To overcome this problem, we followed different strategies. First, we designed micro- and nanostructured polymer surfaces from a protein-repellent and an antimicrobial poly(oxanorbornene) by colloidal lithography and microcontact printing. By varying the polymer patch sizes, we obtained structure-property relationships for the interaction of these patterned polymer surfaces with proteins, bacteria, and human cells, and found that they were simultaneously protein-repellent, antimicrobial, and cell-compatible at a spacing of 1-2 μm , a size matching bacterial dimensions. We also serendipitously found a stimulus-responsive poly(oxanorbornenes) that was protein-repellent and cell adhesive, yet antimicrobial when in contact with bacteria, and thus makes ideal material for implant coatings. Finally, we investigated interfaces that can shed their functional skin when contaminated, like a reptile, and thereby regenerate their original surface functionality.

SESSION SM02.04: Hybrids Against Bacteria
Session Chairs: Karen Lienkamp and Haitao Liu
Monday Afternoon, April 19, 2021
SM02

4:00 PM SM02.04.01

Late News: Synergistic Antimicrobial Activity of Nanopillars Combined with an Inherently Antimicrobial Hydrogel [Sara Heedy](#)¹, Michaela Marshall², Juvarelli Pineda², Eric Pearlman² and Albert Yee¹;
¹University of California, Irvine, United States; ²University of California Irvine, United States

Microbial keratitis has ~1 million new cases annually worldwide and is the principal cause of blindness in Asia. The most frequent cases occur in Nepal and South India, which have an incidence rate of 799 and 113 per 100,000 individuals, respectively. One study in India found up to 44% of these infections were caused by fungi. These fungal infections are usually caused by injuries contaminated by soil, allowing invasive molds into the wound area. In humid regions across the world, keratitis is often caused by the invasive mold *Fusarium oxysporum*, while in the United States, keratitis is often caused by the opportunistic bacteria *Pseudomonas aeruginosa*.

The current method to prevent microbial infection is overused chemical solutions that lead to antimicrobial resistance. This leads to the development of antimicrobial surfaces which aim to limit the spread of microbes in the first place. The two main methods of antimicrobial surfaces are inherently antimicrobial materials, and physical nanopattern topography. Inherently antimicrobial materials include cationic polymers and chemical tethering of antimicrobial agents. These are simple, effective, but may suffer from leaching. Natural, nanotextured surfaces such as those on cicada wings cause bacterial and fungal cell rupture and death. These textures are promising as a long term solution, but many times the fabrication steps use harsh chemicals. This leads to our work that harnesses the synergistic antimicrobial activity of the inherently antimicrobial biopolymer

chitosan and a nanopillar coating. We examined the growth of pathogenic fungi and bacteria on these hydrogel surfaces. After 24 hours, we found fewer viable fungi on all of the hydrogel films compared to a control. While dense biofilm was observed on the control surface, the surface without nanopillars inhibited biofilm development due to the antimicrobial activity of the chitosan material. The addition of nanopillars onto the chitosan surfaces appear to stunt the germination and germ tube development even further compared to the film without nanotextures. Additionally, there was a decrease in viable bacteria on the hydrogel surfaces compared to a control. We conclude that the nanopillars act synergistically with the inherently antimicrobial chitosan material to inhibit disease causing microbial growth. This study may inspire the design of future antimicrobial systems that harness multiple antimicrobial effects.

4:15 PM SM02.04.02

Late News: Development of Antibiofilm Surfaces' Coating -Pickering Emulsion Based Mor Maayan^{1,2}, Karthik Ananth^{1,2}, Michal Natan³, Ehud Banin³ and Guy Mechrez²; ¹The Hebrew University of Jerusalem, Israel; ²Volcani Institute, ARO, Israel; ³Bar-Ilan University, Israel

This research presents bio-friendly and cost-effective antibiofilm coating formulations based on Pickering emulsion templating. The coating does not contain any active material, where its antibiofilm function is based on passive mechanisms, laying solely on the superhydrophobic nature of the coating, and thus highly suitable for food and medical applications.

The coating formulation is based on water in toluene or xylene emulsions that are stabilized by commercial hydrophobic silica, with Polydimethylsiloxane (PDMS) that is dissolved in the organic phase. The stability of the emulsions and their structure were studied by microscopy methods. The most stable emulsions were applied on polypropylene surfaces and dried in an oven to form PDMS/silica rough coatings. The surface morphology of the coatings shows a honeycomb-like structure that exhibits a combination of micron-scale and nano-scale roughness resulting in a Superhydrophobic property.

The superhydrophobicity of the resulting coatings has been tuned to meet the demands of highly efficient antibiofilm passive activity. The obtained coatings have shown a decrease of one order of magnitude in the *E. coli* accumulation on the surface, that is a significant value for coating with a passive based antibiofilm coating.

4:30 PM SM02.04.03

Late News: Encapsulation of Bacteria in Membrane-Based Patches with Antibacterial Surface Wanlin Xu, Karine Glinel, Sophie Demoustier-Champagne and Alain M. Jonas; University Catholique Louvain, Belgium

Bacteria communities are essential components of the skin ecosystem, whose disbalance can be related to several skin disorders, such as acne, eczema or psoriasis. Therefore, exogenously supplying skin-beneficial bacteria to dysbiotic skin is increasingly considered as a way to restore immune response, inhibit infection and treat skin inflammation. This requires encapsulation to control the dispersion and proliferation of bacteria while keeping their benefits. Encapsulation of bacteria was previously studied in spherical particles, microcapsules, gels and electrospun fibers; here, we investigate the encapsulation and growth of bacteria in the micropores of track-etched membranes, aiming at checking the role of channel confinement on bacteria proliferation and at producing soft patches for direct topical application.

Well-defined cylindrical micropores of polycarbonate (PC) membranes were modified by a biocompatible coating based on chitosan and alginate. *Staphylococcus epidermidis* (*S. epidermidis*), a Gram-positive commensal skin bacterium that is known to have potential benefits to human hosts, was then introduced in the modified micropores. The metabolic activity of *S. epidermidis* was then tested, showing the proliferation of encapsulated bacteria in the microchannels. However, the release of *S. epidermidis* from the microchannels is not desirable for practical skincare applications, since *S. epidermidis* proves to be a dangerous pathogen when it passes the skin barrier. Therefore, to prevent the free growth of *S. epidermidis* and maintain its metabolic activity, the modified PC membrane was coated with a layer of agarose gel, followed by coating of this gel with layer-by-layer assembled multilayers, either based on alginate/chitosan, or on polyethylenimine/poly(styrenesulfonate) (PEI/PSS). These barrier layers were demonstrated to efficiently delay the leaking of bacteria from the membrane-in-gel patch, with the lag time depending on bilayer number (coating

thickness). In this respect, PEI/PSS is more efficient than alginate/chitosan multilayer in controlling the release of bacteria, with only four bilayers sufficient to effectively prevent bacterial escape over long times. The polyelectrolyte multilayers coatings act as barriers preventing bacteria from escaping, while the agarose gel protects them from direct contact with this antibacterial coating and keeps them alive. The resulting soft patches are thus ideally suited to topical applications of *S. epidermidis*.

4:45 PM SM02.04.04

Late News: Synthesis and Characterization of Silver Chloride Nanocolloids in Aqueous Medium for Antimicrobial Application Syed I. Hossain^{1,2}, Maria C. Sportelli¹, Rosaria Anna Picca^{1,2}, Nicoletta Ditaranto^{1,2} and Nicola Cioffi^{1,2}; ¹Dipartimento di Chimica, Università degli Studi di Bari “Aldo Moro”, Italy; ²CSGI (Center for Colloid and Surface Science) Bari Unit, Università degli Studi di Bari “Aldo Moro”, Italy

Synthesis and characterization of silver halides (AgX) have drawn much attention due to its specific properties and promising application [1,2]. Particularly, AgX have the potential to be nanoantimicrobials (NAMs) by providing a constant concentration of biocidal Ag⁺ ions in aqueous medium and tailoring control release of Ag⁺ ions into the surrounding environment. Nonetheless, it is known that AgX salts in pure crystalline form are unstable [3], whereas AgX salts in a dispersed state are considered stable [4]. Therefore, it is worth pursuing to study the convenient ways to prepare a stable dispersion of AgX with intrinsic antimicrobial activity. In the present study, nano colloidal dispersion of silver chloride (AgCl) in aqueous medium is prepared by using AgNO₃ as precursor and quaternary ammonium chlorides (QAC) as both source of chloride, and stabilizer. Tetra-octyl-ammonium chloride (TOAC) and Benzyl-hexadecyl-dimethyl-ammonium chloride (BAC) were chosen as model QAC systems, holding a symmetric or asymmetric molecular structure. The synthetic approach resulted to be scalable and green. Morphology and stability of AgCl nanocolloids were investigated as a function of different molar fractions of the reagents. Size distribution and kinetics of the particle growth were monitored by dynamic light scattering, which predicted the formation of QAC bilayered structures associated with the AgCl nanoparticles (NPs). Nanocolloids were further characterized by transmission electron microscopy, X-ray photoelectron and infrared spectroscopies. Zeta potential measurements revealed a highly positive potential value at every stage of synthesis. Experimental evidences support the morphological stability of the nanocolloids, along with their antimicrobial property. Application of the antimicrobial NPs is being investigated as slow-releasing active phases in the Food Packaging industry, mainly aiming at bacteriostatic, long term effects.

References

- [1] Physica E 33, (2006), 308–314
- [2] Mater. Sci. Eng. C 29, (2009), 1216–1219
- [3] Spectrochim. Acta, Part A 77, (2010), 1108–1114
- [4] J. Phys. Chem. B 103, (1999), 5917–5919

Acknowledgements

Financial support is acknowledged from European Union’s 2020 research and innovation program under the Marie Skłodowska-Curie Grant Agreement No. 813439.

5:00 PM SM02.04.05

Late News: Electrosynthesized ZnO Nanoantimicrobials for Cultural Heritage Applications Margherita IZZI¹, Maria C. Sportelli¹, Roberto Gristina², Rosaria Anna Picca¹ and Nicola Cioffi¹; ¹University of Bari Aldo Moro, Italy; ²Institute of Nanotechnology, National Research Council of Italy (CNR-NANOTEC), c/o Department of Chemistry, Italy

The employment of bioactive nanomaterials is one of the most strategical approach to fight antimicrobial resistance and biofilm formation. In particular, metal and metal oxide nanoparticles with controlled ion release can show a noteworthy antimicrobial activity [1]. The use of zinc oxide (ZnO) nanostructures for these purposes is continuously expanding, due to its biocompatibility and low toxicity. In our research group we are exploring

electrochemical strategies for the preparation of ZnO nanostructures based on the use of a sacrificial Zn anode in an aqueous electrolytic bath [2] as alternative approach to conventional methods. By tuning the synthesis parameters and selecting the proper stabilizer, spheroidal and flower-like ZnO nanostructures are synthesized. Particularly, poly-sodium-4-styrenesulfonate (PSS), cetyltrimethylammonium bromide (CTAB), benzyl-hexadecyl-dimethylammonium chloride (BAC) and poly-diallyl-(dimethylammonium) chloride (PDDA) have been tested as capping agents [3–5]. Novel hybrid coatings were developed by dispersing the as-synthesized ZnO into commercially-available consolidating agents. The nanostructured coatings were deposited on stone monuments as multifunctional films, providing antimicrobial and consolidating properties [6,7]. More recently, flower-like nanostructures have been successfully tested against *Bacillus subtilis* as a Gram-positive model microorganism [5]. Morphological analyses carried out on the ZnO-based nanomaterials will be presented. The combination of UV–Vis, FTIR and XPS spectroscopies afforded for the univocal assessment of the material composition as a function of different processing and deposition conditions. A critical comparison of the different materials will be presented, outlining the effects of the stabilizer.

1. Sportelli, M.C.; Picca, R.A.; Cioffi, N. Nano-Antimicrobials Based on Metals. In *Novel Antimicrobial Agents and Strategies*; Wiley-Blackwell, 2014; pp. 181–218 ISBN 978-3-527-67613-2.
2. Izzi, M.; Sportelli, M.C.; Ditaranto, N.; Picca, R.A.; Innocenti, M.; Sabbatini, L.; Cioffi, N. Pros and Cons of Sacrificial Anode Electrolysis for the Preparation of Transition Metal Colloids: A Review. *ChemElectroChem* **2020**, *7*, 386–394, doi:10.1002/celec.201901837.
3. Picca, R.A.; Sportelli, M.C.; Hötger, D.; Manoli, K.; Kranz, C.; Mizaikoff, B.; Torsi, L.; Cioffi, N. Electrosynthesis and Characterization of ZnO Nanoparticles as Inorganic Component in Organic Thin-Film Transistor Active Layers. *Electrochimica Acta* **2015**, *178*, 45–54, doi:10.1016/j.electacta.2015.07.122.
4. Picca, R.A.; Sportelli, M.C.; Lopetuso, R.; Cioffi, N. Electrosynthesis of ZnO Nanomaterials in Aqueous Medium with CTAB Cationic Stabilizer. *J. Sol-Gel Sci. Technol.* **2017**, *81*, 338–345, doi:10.1007/s10971-016-4268-9.
5. Sportelli, M.C.; Picca, R.A.; Izzi, M.; Palazzo, G.; Gristina, R.; Innocenti, M.; Torsi, L.; Cioffi, N. ZnO Nanostructures with Antibacterial Properties Prepared by a Green Electrochemical-Thermal Approach. *Nanomaterials* **2020**, *10*, 473, doi:10.3390/nano10030473.
6. Ditaranto, N.; Werf, I.D. van der; Picca, R.A.; Sportelli, M.C.; Giannossa, L.C.; Bonerba, E.; Tantillo, G.; Sabbatini, L. Characterization and Behaviour of ZnO-Based Nanocomposites Designed for the Control of Biodeterioration of Patrimonial Stoneworks. *New J. Chem.* **2015**, *39*, 6836–6843, doi:10.1039/C5NJ00527B.
7. van der Werf, I.D.; Ditaranto, N.; Picca, R.A.; Sportelli, M.C.; Sabbatini, L. Development of a Novel Conservation Treatment of Stone Monuments with Bioactive Nanocomposites. *Herit. Sci.* **2015**, *3*, 29, doi:10.1186/s40494-015-0060-3.

5:15 PM SM02.04.06

Late News: Cu-Based Hybrid Nanoantimicrobials (Nams)—Electrochemical Synthesis And

Characterization Ekaterina Kukushkina, Maria C. Sportelli, Rosaria Anna Picca, Nicoletta Ditaranto and Nicola Cioffi; University of Bari, Italy

Copper is one of the most promising agents to fight antimicrobial resistance (AMR) and growth of biofilms: it is commonly incorporated as part of the novel composite systems with synergistic effects [1]. In this study, organic/inorganic Cu-based nanohybrids were prepared by Sacrificial Anode Electrolysis (SAE) technique in organic medium. Several quaternary ammonium compounds (QAC) were used as cationic stabilizers and supplementary organic components with intrinsic antimicrobial properties [2]. These organic species, carrying positive charge, are well-known for their ability to bind to a negatively-charged outer surface of majority of pathogens. In particular, Benzyl-hexadecyl-dimethyl-ammonium chloride (BAC) and Tetra-butyl-ammonium perchlorate (TBAP) were used as a “shell” for comprising a hybrid composite: these organic compounds are widely used as disinfectants with ability to prevent formation of biofilms [3].

Morphological and spectroscopic characterization of these nanocomposites was performed: UV-vis spectroscopy, transmission electron microscopy (TEM), X-ray photoelectron spectroscopy (XPS), and Fourier Transform infrared spectroscopy (FTIR) were used. Stability and kinetics were studied at different conditions: organic to inorganic component ratio, time and applied potential to the working electrode among other

parameters. Stability of the colloids and surface potential were studied by dynamic light scattering (DLS) and Zeta potential measurements. These hybrid nanoantimicrobials (NAMs) are subjects for further microbiological and toxicological tests as potential materials for controlling and inhibiting biofilm and pathogen growth. Inclusion of the NAMs in biodegradable polymers and their use as active coatings for Food Packaging applications are being investigated, as well.

[1] *Nanomaterials* 2020, 10, 2491

[2] *ACS Infect. Dis.* 2015, 1, 7, 288–303

[3] *Molecules* 2020, 25, 49

Acknowledgements

Financial support is acknowledged from European Union's 2020 research and innovation program under the Marie Skłodowska-Curie Grant Agreement No. 813439.

SESSION SM02.05: Poster Session: Next-Generation Antimicrobial Materials—Combating Multidrug Resistance and Biofilm Formation
Session Chairs: Edmund Palermo and Lihua Yang
Monday Afternoon, April 19, 2021
7:45 PM - 8:15 PM
SM02

SM02.05.01

Computational Modeling of Antimicrobial Materials using Zinc Oxide Nanoparticles Roxanne Esparza and Sungwook Hong; California State University, Bakersfield, United States

The use of zinc oxide nanoparticles (ZnO NPs), biologically safe and compatible, has gained a great amount of attention in a wide range of biotechnological applications due to their ability to act as antimicrobial materials. That is, ZnO NPs could interact with a small cluster of bacteria like *Escherichia coli* (*E. coli*) preventing a growth of *E. coli* molecules. While many studies showed the antimicrobial behavior of the ZnO NPs, bioactivities of the ZnO NPs with *E. Coli* have not been clearly understood at a molecular level. Here, we perform reactive molecular dynamics (RMD) simulations based on ReaxFF to investigate effects of the addition of ZnO NPs on the growth of *E. coli* molecules. We found that the addition of ZnO NPs could successfully delay the growth of *E. coli* clusters. We also identified key reaction pathways for the antibacterial behaviors of ZnO NPs. As such, our work will help guide experimental design of Antimicrobial materials using ZnO NPs for a wide range of medical solutions like lotions and ointments.

R.E. and S.H. acknowledge new tenure-track faculty start-up funds from School of Natural Science, Mathematics and Engineering at California State University, Bakersfield (CSUB).

SM02.05.02

A Study of the Interaction Between BSA Conjugated Silver Nanoparticles and Hyaluronic Acid-PEG Based Hydrogel for the Design of an Antimicrobial Hydrogel Nanocomposite Olufolasade F. Atoyebi¹, Berhanu Zewde¹, Ayele Gugsa¹, Karen Gaskell² and Dharmaraj Raghavan¹; ¹Howard University, United States; ²University of Maryland, United States

Significant interest has been directed to synthesizing topical gel formulations capable of encapsulating silver nanoparticles where the nanoparticles released can be effective against antibiotic resistant bacterial strains. The release of nanoparticles from the hydrogel nanocomposite is dictated by the interaction between nanoparticles

and the crosslinked hydrogel. The objective of this study is to develop an understanding of the interactions that exist within the nanocomposite hydrogel between the bovine serum albumin stabilized silver nanoparticles (Ag/BSA) and the hydrogel (hyaluronic acid-PEG based hydrogel) using XPS and FTIR, as well as AAS to quantify the release of Ag/BSA nanoparticles from the hydrogel nanocomposite. Characteristic IR peaks in the nanocomposite were found to have broadened and/or red shifted compared to the neat hydrogel; suggesting possible hydrogen bonding or weak interactions between the nanoparticles and the hydrogel in the nanocomposite. A striking difference in the C1s XPS spectrum of the neat hydrogel and the nanocomposite suggested structural rearrangement of the hydrogel in the presence of the BSA coated nanoparticles. Specifically, a large increase in C-O bonding at the surface relative to hydrocarbon bonds in the composite was observed and is indicative of the hydrogel molecule rearranging such that PEG is pointing towards the surface while the ends of the hyaluronic acid are interacting with the BSA of nanoparticles. Additionally, only 50% and 20% of nanoparticles were desorbed from the lightly and highly crosslinked nanocomposite matrix, respectively, after a 14 day of desorption study. This suggests that the role of the nanostructure and the importance of nanoparticle-hydrogel interaction is in controlling the release of nanoparticles from the hydrogel matrix. Antimicrobial studies of the neat hydrogel against *E. coli 107*, *L. monocytogenes*, and *S. sonnei* showed poor antibacterial activity. All the while the nanocomposite showed excellent bactericidal activity against the three kinds of bacteria; indicating that the observed antimicrobial properties are a direct result of the nanoparticles released from the hydrogel. Future studies will explore the potential wound healing properties of the hydrogel nanocomposite when dosed with antibiotic resistant bacterial strains.

SM02.05.03

Impact of ZnO Microcrystal Morphology and Surface Chemistry on Growth Inhibition of *s. aureus* Bacteria

John Reeks, Iman Ali, Jacob Tzoka, Dustin Johnson, Daniel Lopez, Shauna McGillivray and Yuri Strzhemechny; Texas Christian University, United States

Microscale ZnO particles are known to inhibit the growth of bacteria. The fundamental mechanisms driving this process, however, are not completely understood. While there are many contributing factors to consider, we hypothesize that the antimicrobial action is most fundamentally derived from the ZnO surface and its interaction with growth media and the bacteria's extracellular material. In this work, we implement minimum inhibition concentration and novel comparative assays to evaluate the antibacterial activity of ZnO microcrystals produced by us using a hydrothermal chemical growth method. The samples were synthesized in the range of sizes from 1 μ m to 5 μ m with varying abundances of surfaces with different polarities. This approach prevents the ZnO particles from being internalized by the bacterial cells with diameters ca. 500 nm, thus allowing one to study correlations between overall surface polarity and antibacterial action. These experiments were performed in conjunction with optoelectronic studies of ZnO crystals (photoluminescence, surface photovoltage) to characterize electronic structure and dominant charge transport mechanisms as fundamental phenomena, which could potentially govern the processes leading to an antibacterial behavior in our samples. We report on the results of these comparative studies relating antibacterial properties with surface morphology and electronic behavior.

SM02.05.05

Late News: Nanostructured Antibacterial Aluminum Foil Produced by Hot Water Treatment Against *E. coli* in Meat

Quinshell Smith^{1,1}, Nawzat Saadi¹, Khulud Alotaibi¹, Khalidah Al-Mayalee¹, Atikur Rahman¹, Nawab Ali¹, Ashraf Khan² and Tansel Karabacak¹; ¹University of Arkansas–Little Rock, United States; ²National Center for Toxicological Research,, United States

Antibiotic resistance has been on the rise due to the overuse of antibiotics in the livestock and fishing industry. This has led to an increase in foodborne illnesses and a need for alternative modes of action to help mitigate bacterial growth. This study broaches the potential applications of hot water treated (HWT) aluminum foil for use in the food packaging industry. Through HWT, a layer of aluminum oxide nanostructures is formed on the surface of the foil, which conveys antibacterial properties. In this study, we analyze the efficacy of HWT aluminum foil in preventing bacterial growth of *Escherichia coli* on red meat. Aluminum foil samples were

treated in hot water at different temperatures including 75°C, 85°C, and 95°C. It was found that HWT foils were on average 80% more effective than untreated foil samples at preventing bacterial colony growth. This research shows promising alternative modes of action against foodborne illnesses by offering a green and cost-effective means of curbing bacterial growth.

SM02.05.06

Late News: The Antibacterial Efficacy of Aluminum Oxide Nanostructures for HVAC Systems Quinshell Smith, Kenneth Burnnett, Ashley Esparza, John Bush and Tansel Karabacak; University of Arkansas–Little Rock, United States

Air quality is the most important factor in heating, ventilating, and air conditioning (HVAC) systems. This is even more important in an environment where the population is composed of an already immunocompromised segment. Nowhere is this more apparent than in hospitals and health facilities. A review of the current literature suggest that these HVAC systems increase the risk of nosocomial infections if not properly maintained and frequently scrutinized via quality checks. Bacteria, viruses, and fungi find entry into health facilities via equipment, people, and air flow. It is the latter which this research has as its focus. This airflow, once inside the health care center, recirculates throughout the facility, carrying with it the microorganisms it has within it. We utilized a novel hot water treatment (HWT) to produce aluminum oxide nanostructures on the surface of aluminum sheets which are used as ductwork for heating, ventilating, and air conditioning (HVAC) systems. We hypothesized that our HWT duct would greatly reduce the bacterial activity in the air circulating through the HVAC system as well as on the surface of the HWT duct. Air and surface analysis were done with an untreated ventilation system and compared to a ventilation system which had received the hot water treatment to produce Aluminum oxide nanostructures. This research was carried out at temperatures of 20–22 °C. Our results show the extreme effectiveness of using this novel, inexpensive, chemical-free method of producing aluminum oxide nanostructures to decrease bacteria growth in HVAC systems, and in turn significantly improving the air quality.

SESSION SM02.06: Anti-Biofilm Materials II

Session Chairs: Haitao Liu and Lihua Yang

Monday Afternoon, April 19, 2021

SM02

9:15 PM SM02.06.01

High-Performance 3D Printing and Coatings with Graphene Oxide Anti-Pathogenic Properties Rigoberto C. Advincula^{1,2,3}; ¹The University of Tennessee, Knoxville, United States; ²Oak Ridge National Laboratory, United States; ³Case Western Reserve University, United States

Optimized polymer and nanocomposite materials for additive manufacturing (3D printing) and smart coatings play an important role in improving thermo-mechanical properties, preventing corrosion, influencing the wetting properties of surfaces. And improving any process industry. Graphene nanomaterials and their unique processing methods have been reported and be optimum with a minimum percolation threshold and optimum performance peak. They have been demonstrated to have anti-microbial, anti-fungal, and anti-viral properties, including preventing biofilm formation. Nanostructuring of these materials is important to understand its efficacy. In this talk, we will describe nanostructured graphene composite materials' use to demonstrate and distinguish this anti-pathogenic effect in 3D printed materials and coatings and applications even with high-temperature environments. The use and characterization of these nanocomposite materials coatings are described. Graphene oxide (GO) additives also enhance their surface chemistry ability, having acid, hydroxy, and other oxidized species sufficient for interaction with silanes. The interest is in utilizing the capabilities of GO to form a hierarchical structure capable of anti-microbial properties, non-cytotoxicity, and preventing

biofilm formation. Important surface analytical and characterization methods will also be described.

9:30 PM SM02.06.02

Hydrogen Sulfide Slow Releasing Peptide as an Antimicrobial in Burn Wounds Nicole Levi¹, Afnan Altamimi¹, Yun Qian², Shaina A. Yates Alston¹, Mingjun Zhou², Santu Sarkar¹ and John Matson²; ¹Wake Forest School of Medicine, United States; ²Virginia Tech, United States

Burn wounds are a devastating form of injury that leads to substantial morbidity, mortality, and costs. One of the critical complications of burn wounds is infections, especially with *Staphylococcus aureus*. Rising antimicrobial resistance is contributing to the complexity of wound management. Topical antimicrobial therapy, early wound debridement and grafting, and advances in trauma care and intensive management have all contributed to the decline in burn injury mortality. Management for these burns is challenging and is dependent on many factors including but not limited to patient age, total body surface area (TBSA) involved, the cause of the burn and other aspects that shape the treatment plan. *Staphylococcus aureus* and *Pseudomonas aeruginosa* are the most common pathogens isolated from wound infections including burn wounds. These microorganisms commonly attach to any surface and start producing extracellular polysaccharides, creating a film like a matrix. Biofilms are a serious problem for public health because of the protective effect of this matrix to the microorganisms they house, shielding them from antibiotics or immune cells, and set the path for development of chronic wounds, and failure of skin grafts. Hydrogen Sulfide (H₂S) is a novel gasotransmitter that has many physiological functions and acts as a signaling molecule, with pro-inflammatory effects. It also acts as a vasodilator allowing for more blood perfusion to the burn wound, We hypothesized that the a slow releasing H₂S peptide, based on the S-arylothiooxime (SATO) functional group (S-FE), that self-assembles into nanofibers that form into a gel, could provide benefits in an infected burn wound model. Dipeptide gels were examined *in vitro* to evaluate the antimicrobial effects on *S. aureus*. Assays showed bactericidal and bacteriostatic properties of both S-FE and control (non-H₂S releasing) hydrogels. We next evaluated the H₂S dipeptides in an *ex vivo* burn model using porcine skin and established *S. aureus* biofilm. These results aligned with the *in vitro* results showing a decrease in bacterial burden with both S-FE and control gels compared to the bacteria only group. Building on the behavior of bacterial populations after S-FE and control treatments *in vitro* and *ex vivo* experiments the dipeptides were further *in vivo* on a well-established infected porcine burn model. The S-FE dipeptide hydrogels resulted in reduced bacterial burden, improved blood perfusion to the burn area and better wound healing compared to the control hydrogels.

9:45 PM SM02.06.03

Tailoring Surface Physicochemical Properties of SU-8 to Modulate Bacterial Motility, Adhesion and Biofilm Formation of *Xylella fastidiosa*. Silambarasan Anbumani¹, Aldeliane M. da Silva¹, Mariana de Souza de S. Silva², Hernandes F. Carvalho¹, Alessandra A. de Souza² and Monica A. Cotta¹; ¹University of Campinas, Brazil; ²Agronomic Institute of Campinas, Brazil

SU-8 is an epoxy-based photo resist which has been used as a novel platform for biomedical applications due to its chemically tunable and biocompatible surface in addition to its relatively high stiffness, chemical resistance, optical transparency and ease of processing properties. Such properties can have a deep impact on the adhesion of single prokaryote cells and subsequent biofilm formation. In this work, we tailor SU-8 surface properties to investigate single cell motility and adhesion of the bacteria *Xylella fastidiosa*.

Different SU-8 samples have been prepared using UV illumination, thermal processing and oxygen plasma treatment. In addition, flat InP substrates were used for reference control since adhesion on InP surfaces has been well studied in our group. Atomic Force Microscopy and X-Ray Photoelectron Spectroscopy were used to determine nanoscale surface properties; *ex-vivo* studies at the level from single cell to biofilm formation were carried out with Confocal Laser Scanning Microscopy (CLSM) for different bacterial growth times. The mean velocity and displacement of single cells have been extracted from CLSM tracking information data and the size and quantity of biofilms are compared for different samples. We observed a significant difference in bacterial cell motility, adhesion and biofilm architecture on SU-8 as nanoscale surface property changes. Larger density

of carboxyl groups in treated SU-8 surfaces provide enhanced cell motility, while denser biofilms are found in pristine SU-8. Our results can improve understanding of the role of nanoscale properties on bacteria-surface interaction and thereby create strategies to prevent microbial adhesion and consequently, biofilm development of pathogenic species.

10:00 PM SM02.06.04

Investigation of Organic Polymer Nanoparticle Photothermal Ablation and Combination Antibiotic Treatment Against *S. aureus* Biofilms Shaina A. Yates Alston^{1,2}, Santu Sarkar², Matthew Cochran², Scott Northrup² and Nicole Levi^{2,1}; ¹Wake Forest School of Medicine, United States; ²Wake Forest Baptist Medical Center, United States

Biofilm infections are suggested to be associated with over 99,000 deaths annually and are thought to be responsible for over 80% of bacterial infections. It has been reported that over 90% of chronic wounds become colonized by biofilm, like that caused by *Staphylococcus aureus*. These ubiquitous biofilms are also a well-known cause of medical device implant infections and are thought to be responsible for 80% of limb amputations. These biofilms consist of an extracellular matrix (ECM) of extracellular polymeric substances (EPS), composed of polysaccharides, various proteins and glycoproteins, extracellular DNA (eDNA), and other host-derived factors and substances. These aspects of the biofilm help to confer resistance to the host immune response and antimicrobial resistance, as well as tolerance to other stressors like heat. Research demonstrates that antibiotic efficacy can be increased against biofilms after exposure to both mildly hyperthermic ($T < 45^{\circ}\text{C}$) and ablative ($T > 45^{\circ}\text{C}$) temperatures. Studies indicate that hyperthermia alone can alter biofilm structural integrity and viability, but the lack of localization of hyperthermia upon the biofilm matrix creates a challenge for clinical application. This study investigates the impact of near-infrared photothermal ablation (NIR-PTA), via polymer nanoparticles and combined antibiotic treatment, on *S. aureus* biofilms.

We have synthesized biocompatible polymer dynamic organic theranostic spheres (PolyDOTS) composed of two polymers: Poly[4,4-bis(2-ethylhexyl)-cyclopenta[2,1-b;3,4-b']dithiophene-2,6-diyl-alt-2,1,3-benzoselenadiazole-4,7-diyl] (PCPDTBSe) for heat generation and Poly(3-hexylthiophene-2,5-diyl) (P3HT) for fluorescence. PolyDOTS are capable of repeated photothermal generation under NIR irradiation and exhibit no photobleaching. They absorb in the NIR range, peaking at 760 nm. Thermocouple measurements determined the photothermal generating capacity of PolyDOTS at different concentrations, under 5 W, 60 secs 800 nm irradiation. They exhibited increasing heat generation at increasing concentrations, with an approximate plateau of 80°C .

Biofilms were challenged with a one-log (90%) effective minimal bacterial eradication concentration (MBEC-90) of clindamycin and a similarly effective dose (100 $\mu\text{g}/\text{mL}$) of PolyDOTS NIR-PTA. Clindamycin was administered either simultaneously with, 24-hours before or immediately after PolyDOTS NIR-PTA. Results showed that simultaneous administration was the most effective, up to a clinically significant three-log (99.9%) reduction in biofilm viability, compared to controls. The least efficacy occurred when clindamycin was added after NIR-PTA, suggesting that the observed ECM changes can inhibit antibiotic efficacy. Confocal microscopy using LIVE/DEAD stain surprisingly showed no confirmation of viability reduction, which is suggestive of a hyperthermia-induced loss of the biofilm layers. Biofilm biomass and structural changes were analyzed via an ECM confocal stain, scanning electron microscopy, and crystal violet assay. *S. aureus* biofilms showed increasingly pronounced aggregation on SEM and uncharacteristic coalescence, suggestive of compaction of the ECM. The crystal violet assay and spectrophotometry seemed to support the suspected ECM compaction of the PolyDOTS NIR-PTA-treated *S. aureus* biofilms. The results of this study provide evidence that PolyDOTS NIR-PTA alone, and in combination with an antibiotic, can significantly mitigate biofilm viability. While further investigation into the ECM structural changes resulting from localized biofilm hyperthermia would be merited, this study suggests that the combination treatment may improve existing biofilm infection therapy by enhancing antimicrobial efficacy.

8:00 AM SM02.03.02

The Pyro-Electrification of Polymer Sheets as a New Platform for the Evaluation of Biofilm Formation

Emilia Oleandro^{1,2}, Romina Rega¹, Martina Mugnano¹, Vito Pagliarulo¹, Filomena Nazzaro³, Pietro Ferraro¹ and Simonetta Grilli¹; ¹Institute of Applied Sciences and Intelligent Systems of the National Research Council (CNR-ISASI), Italy; ²Department of Mathematics and Physics, University of Campania "L. Vanvitelli", Italy; ³Institute of Food Sciences, National Research Council of Italy (CNR-ISA), Italy

The availability of surface-charged polymer-based materials opens up new perspectives for many industrial applications. In recent years, we developed a new technique for achieving such kind of surfaces through a chemical-free procedure that what we call pyro-electrification (PE). It exploits the electrostatic fields spontaneously generated on the surface of pyroelectric lithium niobate (LN) crystals. We present here how this technique can be used in various applications ranging from live cell patterning to biofilm formation for bacteria. In fact, the bacteria intrinsically become more resistant to environmental stresses under biofilm configuration, and may be a serious problem in different industrial sectors. Therefore, the possibility of monitoring the adhesion and the biofilm formation of bacteria is a very important issue, and has numerous advantages, since a fast detection of the presence of bacteria can significantly reduce the risk of contamination. In particular, we show the characterization of biofilm formation through qualitative and quantitative procedures in order to demonstrate the reliability of technique even for different bacterial strains.

References

- 1) Rega, R., Gennari, O., Mecozzi, L., Grilli, S., Pagliarulo, V., & Ferraro, P. (2016). Bipolar patterning of polymer membranes by pyroelectrification. *Advanced Materials*, 28(3), 454-459.
- 2) Mandracchia, B., Palpacuer, J., Nazzaro, F., Bianco, V., Rega, R., Ferraro, P., & Grilli, S. (2018). Biospeckle decorrelation quantifies the performance of alginate-encapsulated probiotic bacteria. *IEEE Journal of Selected Topics in Quantum Electronics*, 25(1), 1-6.
- 3) Gennari, O., Marchesano, V., Rega, R., Mecozzi, L., Nazzaro, F., Fratianni, F., ... & Ferraro, P. (2018). Pyroelectric effect enables simple and rapid evaluation of biofilm formation. *ACS applied materials & interfaces*, 10(18), 15467-15476.
- 4) Rega, R., Gennari, O., Mecozzi, L., Pagliarulo, V., Mugnano, M., Oleandro, E., ... & Grilli, S. (2019). Pyro-electrification of freestanding polymer sheets: a new tool for cation-free manipulation of cell adhesion in vitro. *Frontiers in chemistry*, 7, 429.

SYMPOSIUM SM03

Advanced Neural Materials and Devices
April 14 - April 20, 2021

Symposium Organizers

Mohammad Reza Abidian, University of Houston
Dion Khodagholy, Columbia University
Daniel Simon, Linköping University
Flavia Vitale, University of Pennsylvania

* Invited Paper

SESSION SM03.01: Advanced Neural Materials and Devices I
Session Chairs: Mohammad Reza Abidian and Daniel Simon
Tuesday Morning, April 20, 2021
SM03

8:00 AM *SM03.01.01

PEDOT:PSS-Based Neural Devices George Malliaras; University of Cambridge, United Kingdom

Neural devices are important for understanding how the brain works and for treating neurological disorders. The commercially available conducting polymer PEDOT:PSS has emerged as a state-of-the-art material for neural devices due to its mixed conductivity, biocompatibility, and convenient deposition. I will present examples of implantable and cutaneous neural devices for bidirectional neural interfaces, explaining the advantages of this material over commonly used metal electrodes. I will discuss the relationship between materials properties and device performance, elaborate on device fabrication techniques, and discuss lessons learned in the design of competitive materials.

8:20 AM *SM03.01.02

Soft Electronic and Ionic Materials and Devices for Neural Interfaces Klas Tybrandt; Linköping University, Sweden

Two-way communication between electronics and neural tissue is key for advancing diagnosis and therapies for neurological diseases and disorders in both the central and peripheral nervous systems. Establishing such neural interfaces is a major challenge, as the tissue response to implants can have a detrimental effect on the signal quality and functionality of the implant. Also, electrical stimulation is inherently limited in its stimulation of neural tissue, in comparison to the sophisticated chemical signaling processes within biological tissue. Here, I present our efforts in addressing two critical material and device aspects for the creation of versatile neural interfaces: the matching of mechanical properties of tissues and electronics, and the development of fast and low-leakage chemical interfaces. Soft electronic biomedical implants have a demanding set of requirements, including biocompatibility, desirable mechanical and electromechanical properties, long-term stability and good electrode performance. To meet these requirements, we have developed a high-performance, long-term stable soft and stretchable conducting nanowire composite. Several fabrication strategies have been developed around this composite to enable the fabrication of soft neural electrodes of different dimensions and geometries. Based on this technology, we have developed devices for both the central and peripheral nervous systems. Next, I will outline our strategy for creating high-speed low-leakage chemical neural interfaces by first discussing the relationship between delivery delay and leakage, and then present an iontronic approach to achieve low leakage and small delivery delay simultaneously.

<http://www.liu.se/soft-electronics>

8:40 AM SM03.01.03

Late News: Diamond-Based Multielectrode Sensors for *In Vitro* Detection of Excitable Cells Activity
Veronica Varzi¹, Pietro Aprà¹, Giulia Tomagra¹, Andrea Marcantoni¹, Alberto Pasquarelli², Paolo Olivero¹, Valentina Carabelli¹ and Federico Picollo¹; ¹University of Torino, Italy; ²Ulm University, Germany

To better understand neuronal signalling behind brain activity, a proper detection of both electrical and chemical signals is essential. Indeed, action potentials (APs) generation and synaptic quantal release of neurotransmitters play a fundamental role in the cellular mechanisms underlying brain functions, being at the basis of information transmission and signal communication in neuronal microcircuits.

In the present work, we present the employment of diamond-based micro-patterned graphitic biosensors to extracellularly record the activity of excitable cells, to resolve APs waveforms and neurotransmitter release [1-2]. The multi-electrode-array sensors were fabricated using a three-dimensional patterning process by means of MeV He ion-beam-based lithography on an artificial-type-IIa single-crystal monocrystalline diamond sample ($4.5 \times 4.5 \times 0.5 \text{ mm}^3$), thus creating 16 independent graphitic electrodes embedded in its matrix. Being electrically conductive, the micro-channels of the sensors were used to investigate the in-vitro neuron activity both in terms of electrical signals generation (APs firing) and neurotransmitter secretion (quantal exocytic events). The diamond biocompatibility allowed neuronal cells to be plated directly over the diamond device. Potentiometric measurements of APs generation were recorded from cultured hippocampal neurons, while quantal secretory events were amperometrically recorded from plated mouse dopaminergic neurons [3]. The electrical activity of an intact mouse sinoatrial node directly placed on the sensor was also recorded. These results demonstrated the usability of diamond-based biosensors as promising devices for the simultaneous multi-parametric in-vitro detection of both electrical and chemical signals, representing in perspective a further step for a better understanding of brain functioning.

[1] Picollo, F. et al. *Anal. Chem.* 88, 7493–7499 (2016).

[2] Tomagra, G. et al. *Front. Neurosci.* 13, 288 (2019).

[3] Tomagra, G. et al. *Carbon* 152, 424-433 (2019).

8:55 AM SM03.01.04

Flexible ITO-Based Electrolyte Gated FETs for Bioelectronic Applications Mary J. Donahue, Ludovico Migliaccio, Mehmet Say, Gaurav Pathak and Eric Glowacki; Linköping University, Sweden

Electrochemical and electrolyte-gated transistor architectures have emerged as powerful components for bioelectronic sensors and biopotential recording devices. For amplification of weak electrophysiological signals, maximum transconductance, high cutoff frequencies, and large on/off ratios are key desired parameters. Organic conducting polymer devices have recently dominated the field, especially where flexible and conformable *in vivo* electronics are necessary. Herein we report ultrathin, flexible indium tin oxide (ITO) electrolyte-gated field-effect transistors (EGFETs). These accumulation-mode devices combine high transconductance ($g_m > 30 \text{ mS}$), excellent on/off ratio (10^5), and fast modulation with excellent stability and the possibility of optically transparent layouts. While oxides are normally considered brittle, we obtain mechanically flexible and robust ITO layers by room temperature deposition of ultrathin (30 nm) amorphous layers onto parylene substrates. This approach results in low strain and the devices survive bending and deformation tests over hundreds of cycles. In addition to favorable material properties, these transistors offer low power consumption, as a result of the normally off state and low off currents. Furthermore, a wide variety of biosensor applications can be envisioned since the material is an oxide with active oxygen surface chemistry (hydroxyl groups) and facile chemical functionalization approaches may be employed. Based on the demonstrated stability and performance, as well as the future possibilities using these transistors, indium tin oxide EGFETs represent a promising avenue for bioelectronic devices.

9:10 AM SM03.01.05

High Performance Conducting Polymer Nanofiber Actuators Operate in Liquid and Gel-Polymer Electrolytes Mohammadjavad Eslamian, Fereshtehsadat Mirab, Vijay Krishna Raghunathan, Sheereen Majid and Mohammad Reza Abidian; University of Houston, United States

Electrochemical actuators that transform electrical energy to mechanical energy through electrochemical reactions have numerous applications for biomedical devices, soft robotics, and bioelectronics. However, the design of high performance and durable electrochemical actuators that efficiently operate in biological environment remains a challenge yet. To address this challenge, here we developed and characterized a flexible organic electronic actuator based on poly(pyrrole) nanofibers (PPy NFs) that reversibly operates in liquid and gel polymer electrolytes under electrical stimulation. PPy is a versatile biocompatible CP which has been widely employed for bioactuators due to its low weight, fracture tolerance, and relatively large actuation strain.

To fabricate the PPy NFs actuator, we electrodeposited an electroactive layer of PPy doped with polystyrene sulfonate (PSS) around template poly-L-lactide (PLLA) nanofibers that were previously electrospun onto a thin layer of gold coated poly(propylene) (PP) film (20 mm × 1 mm × 30 μm). The average diameter of template nanofibers and the resultant PPy NFs were 140 ± 4 nm and 626 ± 16 nm, respectively. The PPy NFs were subjected to cyclic voltammetry (CV) in an aqueous solution and 0.2 wt.% agarose hydrogel both containing 0.1 M poly(sodium 4-styrenesulfonate) (NaPSS) at various scan rates of 10, 50, 100, and 200 mV/s with the potential window of -0.8 V to +0.4 V. We demonstrated that the actuator kinematics (i.e. displacement and speed) can be tuned by adjusting the CV parameters (voltage and scan rate). Remarkably, the PPy NFs actuator demonstrated excellent properties, including low power consumption/strain (as low as 1 mW/cm²/%), relatively high actuation strain (up to 1.85%) a controlled cycling response, and excellent cycling stability (>96.5 % bending stability over 15000 actuations equivalent to 25 hr continuous operation). Overall, this study presents a new strategy for development of flexible, mechanically durable and dynamically tunable organic electronic actuators for variety of applications ranging from soft robotics to biomedical devices.

9:13 AM SM03.01.06

Late News: Patterning PEDOT:PSS Microgel Based Electrodes to Interface Cell Culture Models

Sebastian Buchmann, Liangqi Ouyang, Mahiar Hamedi and Anna Herland; KTH Royal Institute of Technology, Sweden

Conjugated polymers such as PEDOT:PSS provide soft interfaces with cells and tissue. Their large surface area and innate ability to transport ions make them attractive, high-performance materials that work in ion-rich, wet conditions.¹

We have developed a method of patterning PEDOT:PSS microgels into functional devices with heterogeneous structures. Using an out-of-shelf wax printer, we patterned filtrations membranes and have PEDOT:PSS microgels filtered through the membrane. PEDOT:PSS was retained on the hydrophilic region that was not covered by wax. We reached a resolution of ~100 μm both at the patterned thickness and the gap distances between materials. Utilizing its microgel nature, we show that the patterns can be healed by water treatment. In its hydrated state, it can also be stretched by over 30% to 70%, depending on the stretching directions and the geometry of PEDOT.

By transferring PEDOT:PSS patterns onto adhesive substrates, followed by consecutive transferring of other colloidal materials, such as carbon nanotube (CNT), we demonstrate functional PEDOT:PSS electrodes and electrochemical transistors. We also developed methods to tune the water stability of the devices. This allowed us to perform ON/OFF switching cycles on the transistors in water for over 500 cycles.

Finally, we demonstrated biocompatibility of the materials by cultivating human tumor-derived U87 glioma cells as well as Lund Human Mesencephalic (LUHMES) neuronal cells on patterned PEDOT:PSS microgels electrodes, thus showing the possibility to use this method in both tumor-biology studies and more demanding neural models.

(1) Zeglio, Erica, et al. "Conjugated Polymers for Assessing and Controlling Biological Functions." *Advanced Materials* 31.22 (2019): 1806712.

9:16 AM *SM03.01.07

CMOS Microelectronic Systems to Characterize Neurons and Networks at Subcellular Resolution

Andreas Hierlemann; ETH Zürich, Switzerland

Microelectrode arrays (MEAs) have been widely used in recent years for in-vitro investigation of neuronal cells and neural networks, as they enable long-term bi-directional interfacing with networks of living cells [1, 2]. Modern CMOS-based active MEA devices, especially high-density MEAs, provide the capability to

simultaneously perform electrophysiological recordings from thousands of electrodes at cellular/subcellular spatial resolution [3-6]. The high spatio-temporal resolution enables better separation and assignment of neural activities for closely spaced neurons as well as localized and specific stimulation of single individual neurons [7].

An exemplary CMOS high-density microelectrode system includes a large sensing area of $4.48 \times 2.43 \text{ mm}^2$ comprising 59'760 (332×180) electrodes of $3 \times 7.5 \text{ }\mu\text{m}^2$ size at a pitch of $13.5 \text{ }\mu\text{m}$ [6]. The system incorporates several types of sensing units with the aim of extracting a wide spectrum of information from the same neuronal culture or brain slice: 16 dual-mode stimulation buffers, 2048 action-potential recording channels, 32 local-field-potential recording channels, 32 current recording units, 32 impedance measurement units and 28 neurotransmitter detection units [6].

By using such a system it was possible to record subcellular-resolution data in various preparations, ranging from organotypic and acute slices to cultures of dissociated neurons and stem-cell derived neurons. It was also possible to detect low-amplitude signals of action potentials traveling along thin axons ($\sim 100 \text{ nm}$ diameter). Moreover, the stimulation features of CMOS microtransducer arrays and integrated microsystems offer the capability to bi-directionally interact, also in closed loop and real time, with potentially every single neuron in a given neuronal network. Applications include research in neural diseases and pharmacology.

Acknowledgements

The work was supported by the European Community through the ERC Advanced Grant “neuroXscales” under contract number AdG 694829.

References

1. M. E. J. Obien, K. Deligkaris, T. Bullmann, D. J. Bakkum, and U. Frey, *Front. Neurosci.*, Vol. 9, pp. 423 ff, 2015.
2. A. Hierlemann, U. Frey, S. Hafizovic, F. Heer, *Proc. IEEE*, vol. 99, no. 2, pp. 252-284, 2011.
3. L. Berdondini, K. Imfeld, A. Maccione, M. Tedesco, S. Neukom, M. Koudelka-Hep, and S. Martinoia, *Lab Chip*, vol. 9, no. 18, pp. 2644–2651, 2009.
4. B. Eversmann, A. Lambacher, T. Gerling, A. Kunze, P. Fromherz, and R. Thewes, *Eur. Solid-State Circuits Conf.*, pp. 211–214, 2011.
5. M. Ballini, J. Müller, P. Livi, et al., *IEEE J. Solid-State Circuits*, Vol. 49, no. 11, pp. 2705–2719, 2014.
6. J. Dragas, V. Viswam, A. Shadmani, Y. Chen, R. Bounik, A. Stettler, M. Radivojevic, S. Geissler, M. Obien, J. Müller, A. Hierlemann, *IEEE J. Solid-State Circuits*, Vol. 52, no. 6, pp. 1576-1590, 2017.
7. M. Radivojevic, D. Jäckel, M. Altermatt, J. Müller, V. Viswam, A. Hierlemann, D. Bakkum, *Scientific Reports* 6, Art. 31332, 2016.

9:36 AM *SM03.01.08

Closing the Gap Between Organic Bioelectronics and Neuronal Systems Magnus Berggren; Linköping University, Sweden

Organic Bioelectronics operating in the electrochemical mode has been widely explored to record and stimulate signaling of neuronal systems. To make this technology successful in therapy and prosthesis applications as a future med-tech platform, included devices and materials should possess minimal invasiveness and must operate at a proximity, addressability and signal specificity to capture as much as possible of the signaling spectrum of the nervous system. Here, recent progress of the development of Organic Bioelectronics is presented that address these challenges, specifically targeting the development of devices integrated into capillaries and also self-organized neuro-bioelectronics.

2:15 PM *SM03.02.01

3D Multifunctional Mesoscale Frameworks as Neural Interfaces to Cortical Spheroids John A. Rogers; Northwestern University, United States

Three-dimensional (3D), sub-millimeter-scale constructs of neural cells, known as cortical spheroids, are of rapidly growing importance in biological research because these systems reproduce complex features of brain architecture and organization in vitro, at levels qualitatively more sophisticated than those found in traditional two-dimensional (2D) cell cultures. Despite their great potential for studies of neurodevelopment, neurological disease modeling and evolution, detailed investigations of these miniature, 3D living objects cannot be accomplished easily using conventional approaches to neuromodulation, sensing and manipulation. This talk describes classes of microfabricated 3D frameworks as mechanically compliant, multifunctional neural interfaces to individual spheroids and to engineered, interconnected collections of them, known as assembloids. Electrical, optical, chemical and thermal interfaces to cortical spheroids derived from human induced pluripotent stem cells demonstrate some of the capabilities. Complex architectures and high-resolution features, in isolated or arrayed configurations, and in layouts that enable full surface coverage highlight the design versatility. Detailed studies of the spreading of coordinated bursting events across the 3D surface of an isolated cortical spheroid and of the cascade of processes associated with formation and regrowth of bridging tissues across a pair of such spheroids represent two of the many opportunities in basic neuroscience research and regenerative medicine uniquely enabled by these platforms.

2:35 PM *SM03.02.02

Materials and Bioactive Strategies Towards Better Neural Electronics-Tissue Interface Xinyan T. Cui; University of Pittsburgh, United States

Microelectronic devices placed in the nervous system present tremendous potentials for mapping neural circuits and treating neurological disorders. Currently, the performance of these devices is sub-optimum due to electrode material limitations and undesired host tissue responses. Quantitative histology and 2-photon imaging have revealed neuronal damage and degeneration, inflammatory gliosis, blood brain barrier leakage and oxidative stress at the site of implants which may compromise the intended recording/stimulation/neurochemical sensing function. We use several biomaterial strategies to minimize these responses in order to achieve seamless and stable device-tissue interface. Conducting polymer based nanocomposites have been investigated as electrode coatings and facilitate the signal transduction/charge transfer between the ionically conductive tissue and the electrical device. Nanostructuring is employed to improve the adhesion, stability and charge injection and drug delivery capability of the conducting polymers to meet the material challenges at the neural interface. As we continue to improve our understanding of the implant induced tissue response, bioactive approaches are being developed to modulate the cellular responses for seamless integration. Surface modification with bioactive molecules or anti-fouling materials have been found to significantly improve neuronal health and inhibit the inflammatory tissue response around the implants. Alternatively, therapeutics that control inflammation, neurodegeneration and oxidative stress can be delivered systemically or locally. These bioactive approaches demonstrated significant benefit in neural recording quality and longevity. The ultimate solution to a seamless device/tissue interface may be a combinatorial approach that takes advantage of multiple biomaterial strategies discussed above and beyond.

2:55 PM *SM03.02.03

NIH/NINDS Funding Opportunities for Technology Development and Translation Eric Hudak, Kari Ashmont, Brooks Gross and Nick Langhals; National Institutes of Health, United States

The mission of the NINDS Division of Translational Research (DTR) is to accelerate basic research findings

towards patient use for neurological disorders and stroke by providing funding, expertise, and resources to the research community. DTR provides funding and resources through grants, cooperative agreements, and contracts to academic and industry researchers to advance early-stage neurological technologies, devices, and therapeutic programs to industry adoption (i.e. investor funding and corporate partnerships). We have created a variety of programs that support the design, implementation, and management of research activities critical to translational challenges in the treatment of neurological disease. In addition, DTR plays an active role in the NIH BRAIN Initiative, the Blueprint for Neuroscience Research, the HEAL Initiative, and the SPARC Program. DTR is actively managing programs that support small molecule, biologic, and neural device therapeutics, biomarkers, and training through grants, contracts, and consultants. These programs cover all stages of translational research from early assay/biomaterial/device development and optimization to preclinical development and early clinical development. Funding opportunities and resources are actively supporting translational research in preclinical discovery and development of new therapeutic interventions for neurological disorders and stroke, as well as neuropsychiatric disorders and neurotraumatic injuries (BRAIN Initiative). An overview of NIH/NINDS translational programs and resources will be presented.

3:15 PM *SM03.02.04

Local Cytostatic Hypothermia to Control Glioblastoma Syed Faaiz Enam, Cem Y. Kilic, Jianxi Huang, Brian J. Kang, Reed Chen, Connor S. Tribble, Martha I. Betancur, Ekaterina Ilich, Stephanie J. Blocker, Steven Owen, Johnathan G. Lyon and Ravi Bellamkonda; Duke University, United States

As a cancer therapy, hypothermia has been used at sub-zero temperatures to cryosurgically ablate tumors. However, these temperatures indiscriminately damage both tumorous and healthy cells. Additionally, therapies targeting single molecules or pathways are highly susceptible to evolutionary escape. To address these limitations, we studied the use of hypothermia as a broad cytostatic tool against cancer and deployed it in rodent models of glioblastoma (GBM). To identify the minimal dosage of 'cytostatic hypothermia', we cultured at least 4 GBM lines at 4 continuous or intermittent degrees of hypothermia and evaluated their growth rates through a custom imaging-based assay. This revealed cell-specific sensitivities to hypothermia. Subsequently, we examined the effects of cytostatic hypothermia on these cells by a study of their cell-cycle, energy metabolism, and protein synthesis. To assess the efficacy of cytostatic hypothermia *in vivo*, we report the design of an implantable device to focally administer cytostatic hypothermia in rats bearing F98 and U87-MG GBMs. Hypothermia at supra-cytostatic temperatures significantly doubled the median survival of rats bearing F98. Cytostatic hypothermia delivered in rats bearing U87-MG resulted in no deaths during the study period. An absence of gross behavioral alterations was also observed and in concurrence with literature suggesting the brain is naturally resilient to focal hypothermia. We also investigated the use of cytostatic hypothermia as an adjuvant to chemotherapy and CAR T immunotherapy. Our studies demonstrated that cytostatic hypothermia did not interfere with Temozolomide *in vitro* and may have been synergistic against at least 1 GBM line. Interestingly, we also demonstrated that CAR T immunotherapy can function under cytostatic hypothermia. Based on these findings, we anticipate that focally administered cytostatic hypothermia alone has the potential to delay tumor recurrence or increase progression-free survival in patients. Additionally, it could also provide more time to evaluate concomitant, curative cytotoxic treatments.

3:35 PM *SM03.02.06

Cholesterol-Functionalized Poly(3,4-ethylenedioxythiophene) (PEDOT-cholesterol) Samadhan Nagane, Shirang Chhatre, Yuhang Wu, Vivek Subramanian, Peter Sitarik, Quintin Baugh, Junghyun Lee and David C. Martin; The University of Delaware, United States

We continue to investigate the design, synthesis, and characterization of functionalized variants of poly(3,4-ethylenedioxythiophene) (PEDOT). PEDOT and its derivatives have proven to be of considerable interest for a variety of applications, particularly bioelectronic neural interfaces. Substituted variants of the 3,4-ethylenedioxythiophene (EDOT) monomer, including EDOT-carboxylic acid (EDOT-acid) and EDOT-maleimide (EDOT-MA) make it possible for us to create a variety of functionalized PEDOT copolymers. This allows us to optimize electronic and ionic transport, adhesion to surfaces and biological tissue, and mechanical

properties. Here, we will present results from our recent studies of PEDOT functionalized with cholesterol side groups, attached either via the EDOT-acid (PEDOT-cholesterol) or EDOT-MA (PEDOT-MA-cholesterol) chemistries. Cholesterol is the most abundant steroid in the animal kingdom, and provides flexibility and resilience to cell membranes. It is also known to promote the formation of chiral liquid crystalline mesophases. We will discuss the structure and properties of PEDOT-cholesterol using a variety of characterization techniques, and compare these results with previous studies of PEDOT and PEDOT copolymers.

SESSION SM03.03: Advanced Neural Materials and Devices III
Session Chairs: Mohammad Reza Abidian and Dion Khodagholy
Tuesday Afternoon, April 20, 2021
SM03

9:00 PM *SM03.03.01

Neural Interface via Iontronics and Synaptic Interface Taek Dong Chung, Min-Ah Oh, Seok Hee Han, Joohee Jeon, Sung Il Kim, Wonkyung Cho, Sun-heui Yoon, Ji Young Kim and Chang Il Shin; Seoul National University, Korea (the Republic of)

Ongoing interest in the interface between the manmade device and live neural system is at the heart of many researchers that develop new materials to facilitate the neural interface. The ultimate goal in the neural materials is to seamlessly integrate the neural system with the device so as to monitor and modulate signals from neurons. In this regard, there are two major technical hurdles in connecting electronic devices and neural systems. First, the neural signal transmits across synaptic cleft through elaborate secretion and recognition of neurotransmitters, which are tricky to mimic using artificial gadgets. Second, it is difficult to secure stable and intimate contact between the neural system and the electronic device because of dissimilar material properties such as flexibility and softness. In this talk, we suggest our two approaches to get over the challenges.

One is the gel-based iontronics to the neural interface. Iontronics is the field of ion-based information processing inspired by the neural system and various biological structures such as ion channels. Materials that allow an electric field to manage gradients of ions, such as polyelectrolyte gels (charged hydrogel), can be used as components of iontronics. Taking hints from it, we constructed microfluidic chips such as a bipolar ionic diode, transistor, and logic circuits through polyelectrolyte gels. Even a fully aqueous and ionic circuit can be created on a chip powered by reverse electrodialysis (RED), which is reminiscent of neurons that transduce signals just by the ion transport. PDMS, a transparent and flexible material, can be employed as a chip substrate to expand the libraries of materials available for iontronics. Recently, we invented a new form of iontronic tools, i.e. an ion current rectifying micropipette, to address the neural system for chemical stimulation with high spatial and temporal resolutions.

The other is a biologically spontaneous and steady conjugation between the neural systems and electrode through synaptic proteins. One of the key issues in functional neural materials is persistent stability to minimize inflammation and neuron cell loss. We materialized the neural interface harnessing the synaptic proteins, paying attention to the fact that neuron stably transmits signals through neurotransmitter secretion in the synapse.

Engineered the Neuroligin1 (Nlg1) as known to induce the presynaptic differentiation is immobilized onto the substrate to call for its counterpart protein, Neurexin (Nrx), in the live neuron that contact with the modified electrode. Heterogeneous association of the two proteins belonging to natural and artificial surfaces facing each other comes to form a unique junction that is mechanically as well as biologically stable enough to be persistent for several days.

9:20 PM SM03.03.03

Late News: Customizable and Rapidly Manufacturable 3D-Printed Neural Probes for Wireless Optogenetics Juhyun Lee¹, Kyle E. Parker^{2,3,4}, Chinatsu Kawakami⁵, Jenny R. Kim^{2,3,4}, Raza Qazi¹, Junwoo Yea⁶, Shun Zhang⁷, Choong Yeon Kim¹, John Bilbily^{2,3,4}, Jianliang Xiao⁷, Kyung-In Jang⁶, Jordan G.

McCall^{2,3,4} and Jae-Woong Jeong¹; ¹Korea Advanced Institute of Science and Technology, Korea (the Republic of); ²Washington University in St. Louis, United States; ³St. Louis College of Pharmacy, United States; ⁴St. Louis College of Pharmacy and Washington University School of Medicine, United States; ⁵Toyohashi University of Technology, Japan; ⁶Daegu Gyeongbuk Institute of Science and Technology, Korea (the Republic of); ⁷University of Colorado Boulder, United States

Optogenetics is a powerful neuromodulation technique that enables dissection of neural circuitry and treatment of neurodegenerative diseases based on its cell-type specificity and high temporal resolution in control. Implementing optogenetics traditionally relies on fiber optics or microfabricated optical probes. Although highly reliable and effective, however, these approaches do not support facile and rapid design adjustment to meet various needs for *in vivo* neuroscience. Specifically, optical fibers are hard to be transformed to 2D or 3D configurations to enable multisite neural interfacing. Microfabricated probes can address this limitation by providing design versatility. However, the fact that microfabrication requires special cleanroom facilities and complex processes makes this approach expensive and time-consuming, hampering easy optimization and rapid prototyping for targeted *in vivo* applications.

To address these issues, we have developed a 3D printing-based manufacturing technique for rapid and customizable fabrication of optogenetic probes. The 3D printed optogenetic probes (3D-POPs) consist of microscale inorganic light-emitting diodes, electrical interconnects made of silver paste, and thin 3D printed substrates (60 μm thick). The 3-D printed patterned substrate determines the overall framework of the probe and facilitates electrode formation using silver paste in its groove patterns. The design can be easily altered using a 3D computer-aided design (CAD) program, thus providing facile design customizability. This straightforward 3D printing scheme can not only enable low-cost (\$0.54 per 5 mm-long probe) and mass production of probes (fabrication of 50 probes (printing area of 1800 mm^2) in 3 minutes), but also significantly reduce the time and cost needed for developing new devices optimized for specific applications. Successful experiments with live mice show biocompatibility as well as wireless functionality of 3D-POPs, verifying their practicality for *in vivo* optogenetics. We foresee that this 3D printing strategy can be applied to cost-effective production of diverse bioelectronics beyond neural probes.

9:35 PM *SM03.03.04

Dimensional Stability of Conductive Hydrogel Electrode Coatings for Deep Brain Stimulation Laura Poole-Warren; University of New South Wales, Australia

Background: Low charge transfer, mechanical mismatch and host response to the implant, can ultimately compromise the long-term performance of deep brain stimulation (DBS) devices. Conductive hydrogel (CH) electrode coatings are hybrid systems that address these limitations by combining the high electroactivity of conductive polymers with the soft mechanical properties of hydrogels. Successful use of CHs on DBS electrode arrays relies on their ability to withstand mechanical stress during electrode placement. A key challenge in use of CH electrode coatings is dimensional change due to swelling of the hydrogel component. This work aimed to control CH swelling via modifying hydrogel chemistry, and assessing the effect of insertion on electrode coating stability *in vitro* and *in vivo*.

Methods: Two CH formulations based on poly(vinyl alcohol) were fabricated with low or high crosslinking densities (CD). DBS arrays modified for use in rats were dip-coated in polymer solution, polymerised, electrodeposited with poly(ethylenedioxythiophene) (PEDOT), and ethylene oxide (ETO) sterilised. Electrode coating stability was assessed *in vitro* via insertion in 0.6% agarose gels before and after ETO sterilisation. Stability was evaluated by impedance spectroscopy (EIS), charge storage capacity (CSC), and charge injection limit (CIL). The higher-crosslinked, lower swelling formulation was tested in a rat animal model and compared to Pt DBS arrays over 8-weeks implantation.

Results: CH coated DBS arrays maintained superior electrochemical performance when compared to Pt model electrodes *in vitro*. Following insertion in agarose gels, there was no significant impact on electrical properties of DBS coated arrays. ETO sterilisation significantly affected CSC and CIL as well as the coat adhesion on Pt electrode substrates. Nonetheless CH coated electrodes electrically outperformed Pt counterparts *in vivo* allowing for high fidelity neuronal recordings following chronic implantation.

Conclusions: CH coat dimensional stability can be improved by tailoring hydrogel crosslinking density without affecting electrical performance. Further research is required to understand the effect of sterilisation techniques on coating stability.

9:55 PM SM03.03.05

Carbon Nanotubes Embedded Silk Film Enables the Photoacoustic Neural Stimulation and the Control of Neurite Outgrowth Nan Zheng and Chen Yang; Boston University, United States

Neural regeneration is important for repairing nerve injuries and treating neurological disease. Despite with improved understanding of pathophysiology, a critical problem of slow nerve regeneration remains unsolved and often leads to a delayed and incomplete functionality recovery. Current stimulation technologies, such as electrical, ultrasound stimulation and optogenetics were found to improve nerve regeneration often due to an enhanced production of neurotrophic factors. However, electrical stimulation is invasive. Ultrasound lacks spatial specificity. Optogenetics, as a genetics-based technique, has limitation in translation from bench to patients.

Photoacoustic (PA) neural modulation is an emerging light-mediated technique allows temporally and spatially precise control of neural activity. The photoacoustic process is initiated by shining a pulsed laser on the absorber, and then broadband acoustic waves will be generated by the transient heating and thermal expansion. In this study, we developed a composite film of silk fibroin and carbon nanotubes (CNT) as a novel neural interface with the function of PA stimulation upon near infrared (NIR) second window excitation. PA signals can be controlled by varying the laser power and the concentration of CNT. To investigate the neural stimulation function, we examined the response of cultured cortical neurons to PA stimulation under different stimulation conditions. By time-resolved calcium imaging, we demonstrated this PA stimulation can robustly generate neural activations. Furthermore, as a key messenger in nerve system, we found that the calcium influx triggered by the PA stimulation can also modulate the neurite outgrowth of cultured rat dorsal root ganglion (DRG).

10:10 PM SM03.03.06

Late News: Nanostructured Biohybrid Material Composed of Metalloprotein/DNA/Gold Nanoparticle/Electrically Controllable Complex for Electrical Control of Neural Differentiation Joungpyo Lim, Jinho Yoon and Jeong-Woo Choi; Sogang Univ., Korea (the Republic of)

Accurate control of cell differentiation has received lots of attention because of due to its high applicability in personalized medicine. For this reason, numerous researches for control of cell differentiation have been reported such as introduction of functionalized nanoparticles or surface modified electrodes. However, these methods are difficult to apply directly to cell-based therapy because it is hard to simultaneously control the time and region in which cells are induced to differentiate into desired lineages. In this study, nanostructured biohybrid material composed of metalloprotein, DNA, gold nanoparticle (GNP), and electrically controllable complex was developed to control the neural differentiation electrically. The electrically controllable complex composed of 5,5-Bis(mercaptomethyl)-2,2-bipyridine, cucurbit [8] uril, and retinoic acid modified WGG tripeptide (RA-WGG). The result indicates that the neural differentiation was successfully conducted due to the release of the RA-WGG from electrically controllable complex by applied electrical stimulation. Furthermore, by adjusting the time and location of applying electrical stimulation to nanostructured biohybrid material, it was possible to increase the efficiency of neural differentiation over a long period of time and various regions on substrate. Proposed nanostructured biohybrid material should be used for differentiation of various stem cells as an innovative method in cell therapy. **Acknowledgments:** This research was supported by the National Research Foundation of Korea (NRF) grant funded by the Korea government (MSIT) (No. 2019R1A2C3002300) and by the Ministry of Education (No. 2016R1A6A1A03012845).

10:13 PM SM03.03.07

Stem Cell-Laden Gelatin-Based Microelectrode Arrays Applied for Nerve Tissue Engineering and Neuromodulation Shu-Han Li¹, Yue-Xian Lin², Hwei-Min Stu³ and Wei-Chen Huang⁴; ¹Undergraduate Honors

Program of Nano Science and Engineering, National Chiao Tung University, Taiwan; ²Department of Materials Science And Engineering, National Chiao Tung University, Taiwan; ³National Chiao Tung University, Taiwan; ⁴Department of Electrical and Computer Engineering, National Chiao Tung University, Taiwan

Implanted neural prosthetics are electrical interfaces enabling neural recording and stimulation for the treatment of multiple neurological diseases. The typical neural prosthetic devices are designed for neuromodulation, while they cannot permit neuroreplacement or neuroregeneration which is a critical goal for rehabilitation in nervous injury. Herein, we developed tissue-like microelectrode arrays (MEAs) composed of bioresorbable materials to show the functions including neural recording, neural stimulation, and stem cell therapy. The electrode, PDGA, was synthesized with copolymerized poly(3,4-ethylenedioxythiophene) (PEDOT) and gelatin methacrylate (GelMA) to exhibit both nerve tissue-mimicked properties and hydroresponsive conductivity. Based on the thermal-responsive and photo-responsive sol-gel transition properties, PDGA can be directly micropatterned into a circuit in a resolution down to 30 μm , followed which an adhesive hydrogel substrate synthesized by gelatin and Transglutaminase (mTG) can directly transfer print the PDGA micropatterns. Applied with PLGA as the insulation layer, the integrated final MEAs demonstrated tissue-like mechanical and structural properties, adipose tissue-derived stem cell (ADSC) -laden capability, and electrical monitoring/neuromodulation. With the examination of physical, chemical, and biological properties, this device was expected as a revolutionary platform to promote nerve regeneration.

10:16 PM *SM03.03.08

Wirelessly-Controlled Implantable Drug Delivery Devices for Brain Diseases Dae-Hyeong Kim; Seoul National University, Korea (the Republic of)

Treatment of brain tumours, particularly malignant one such as glioblastoma, is extremely challenging because the efficacy of the conventional chemotherapy is quite limited due to the blood-brain barrier. Meanwhile, the wireless integration of wearable devices with implantable drug delivery devices can present a new opportunity in the development of unconventional devices for the treatment of fatal seizures. In this talk, recent progresses in the wirelessly-controlled implantable drug delivery devices for brain diseases, such as brain tumour and fatal seizure, will be presented. In the first part, an implantable drug delivery device using a flexible, sticky, and bioresorbable drug reservoir integrated with the biodegradable wireless electronics for the treatment of glioblastoma will be presented. In the second part, a device that consists of a soft implantable drug delivery device integrated wirelessly with a wearable electrophysiology sensor for the treatment of status epilepticus will be presented. Such novel wirelessly-controlled drug delivery devices are expected to present new opportunities for the treatment of brain diseases.

SESSION SM03.04: On-demand
Wednesday Morning, April 14, 2021
SM03

8:00 AM SM03.04.02

Multimodal Neural Probe for Simultaneous Optogenetics, Neuropharmacology and Neurochemical Sampling Guangfu Wu and Yi Zhang; University of Connecticut, United States

The multimodal neural probe for simultaneous monitoring and manipulation of neuronal circuits in small animal models during behavioral tasks has advanced the understanding of complex brain functions. Although sophisticated and powerful in the manipulation and analysis of neural circuits, these multimodal neural probes are constrained by their inability to monitor changes in neurochemicals, which leaves many of the molecular mechanisms underlying neurological and psychological disorders unresolved. This limitation can be overcome by using systems that combine independently controlled neuromodulation with neurochemical sampling within

a single platform. Conventional *in vivo* extracellular fluid sampling approaches such as microdialysis technology rely on rigid probes and semipermeable membranes, and therefore suffer from poor spatial resolution ($\sim 1 \text{ mm}^2$), low temporal resolution (several minutes), and limited capacity to collect large molecules, such as neuropeptides and neuroproteins. Here, we demonstrate a battery-free, wireless, “all-in-one” neural probe for simultaneous optogenetics, neuropharmacology and neurochemical sampling in awake, freely moving animals. *In vitro* studies demonstrate the programmable operation for efficiently sampling various neurochemicals (K^+ , dopamine, and neuropeptide Y) with a small sampling area ($10 \times 10 \text{ }\mu\text{m}^2$) and fast dynamics ($< 1 \text{ min}$). Open field test reveals that the device implantation does not impact the movement and spatial preferences of mice. The probe is implanted in the brain of freely moving mice and could successfully sample the pharmacologically evoked release of the large molecule neuropeptide Y. The soft mechanics and lightweight construction allow for applications in freely moving small animal models to uncover the basis of brain disorders.

8:10 AM SM03.04.03

High Density, Individually Addressable Silicon-Based Nanowire Arrays Record Native Intracellular Activity from Primary Rodent Neurons without Electroporation Jihwan Lee¹, Ren Liu^{1,2}, Youngbin Tchoe¹, Andrew Bourhis¹, Sang Heon Lee¹, Deborah Pre³, Gaëlle Robin³, Mary Elizabeth Phipps⁴, Jennifer S. Martinez⁴, Anne Bang³ and Shadi Dayeh^{1,1,1}; ¹University of California, San Diego, United States; ²Harvard University, United States; ³Sanford Burnham Prebys Medical Discovery Institute, United States; ⁴Center for Integrated Nanotechnologies, United States

New technologies that can provide intracellular electrophysical access with high spatiotemporal resolution and minimal invasiveness could assist neurophysiological undertakings that aim to gain an in-depth understanding of how neurons regulate and orchestrate large network activity to coordinate cognition, disease, and function. Numerous nanoscale devices were invented in the last decade for probing intracellular potentials but such methods exhibit a compromise between stability and scalability. Of these, vertical nanowire arrays generally employ electroporation techniques which lead to a compromised stability of the nanowire-neuron interface and additionally suffer from low sensitivity. We address these challenges by innovating large scale vertical ultra-sharp nanowire arrays that are individually addressable and exhibit sub-10 nm tips. This silicon-based nanowire array interface system enables native recording of graded potentials proceeding high-amplitude intracellular action potentials without resorting to electroporation methods. Passive intracellular recording is performed stably with *in vitro* rat cortical neurons without attenuation of the amplitude for the duration of the experiment (several minutes). Systematic studies show chronically stable nanowire-neuron interfaces with somas naturally permeated by the nanowire, validated by FIB-SEM image of the cross-section at the nanowire-neuron interface. Pharmacological stimulation and inhibition of electrophysiological activities confirmed our results. By constructing a comprehensive small signal model used for modeling potential transients at nanowire-neuron interfaces, we demonstrate by simulation and experimental investigations the significant reduction of signal amplitude as we deliberately increased the number of nanowires per recording channel. Overall, our ultra-sharp nanowire array platform may pave the way to high-throughput and low-cost drug screening for neurological diseases and can enable future investigations of neuronal dynamics that coordinate function and of relevance to brain-machine interfaces.

8:20 AM SM03.04.04

Action Potential-Like Oscillations in Biomolecular Neuristors Sijie He¹, Ahmed S. Mohamed¹, Md Sakib Hasan² and Joseph S. Najem¹; ¹The Pennsylvania State University, United States; ²The University of Mississippi, United States

Biological neurons process signals and compute by integrating incoming stimuli and initiating action potentials to convey information within the nervous system without loss. The process from generation to propagation is regulated by membrane potential and voltage-activated sodium and potassium channels. These key features inspire the design of neuron-like materials and neuristors for applications in signal processing, computing, and lossless propagation of information. To date, despite success in emulating neural functionalities, the state-of-

the-art neuristors consisting of nanoscale memristors fall short in energy efficiency compared to biological neurons due to their electronic nature. Further, while suitable for neuromorphic computing applications, current neuristors lack biocompatibility and operate at non-biological timescales, which makes them incompatible with biological applications. In contrast, neuristors assembled from synthetic biomolecular elements are biocompatible, bear similarities in structure and dynamics to their biological counterpart, and can operate at biological timescales.

Here, we demonstrate a dynamic neuristor consisting of two biomolecular memristors in parallel operating according to the same principles as Hodgkin-Huxley. The biomolecular memristors consist of insulating biomembrane doped with voltage-driven, pore-forming peptide, *alamethicin*. To capture the switching dynamics of the sodium and potassium channels, we used DPhPC- and BTLE-based memristors, which can offer fast and slow-switching dynamics, respectively. The neuristor exhibits a firing behavior similar to a biological neuron as well as power efficiency that far exceeds metal oxide-based memristors. Further, we confirm that the addition of a lipid-based memcapacitor into the circuit embeds short-term synaptic plasticity dynamics within the neuristor—adding another layer of nonlinearity and complexity in signal processing. Our results demonstrate that the addition of a symmetrical memcapacitor resulted in a decreased firing rate (inhibition), while an asymmetrical memcapacitor resulted in an increased firing rate (facilitation). This novel neuristor composition can be implemented in an adaptive nonlinear control system, a brain-machine interface (BMI) device, as well as a wide range of applications in signal processing. Further, this neuristor can serve as a model to aid in fathoming the neuronal structure and functions.

8:30 AM SM03.04.05

Flexible Crossbar Arrays of Biomolecular Memristors for Brain-Inspired Computing Nicholas Armendarez and Joseph S. Najem; The Pennsylvania State University, United States

With the rise of Artificial Intelligence and the Internet of Things in biological domains, it is imperative to construct computing devices that are biocompatible, low-power, and preferably ionic. We believe an approach that takes inspiration from the brain can yield a computational system that mimics synaptic and neuronal functionalities with the scalability of semiconductor processors, all while maintaining the biocompatibility and mechanical flexibility of biological materials. To this end, we have recently demonstrated that lipid bilayer membranes formed between two lipid-encased water droplets in oil (i.e., droplet interface bilayers or DIBs) can exhibit memcapacitive and memristive properties. To leverage all the diverse functionalities exhibited by a single membrane, large networks of functional membrane-based elements need to be assembled to achieve vast interconnectivity and flexibility—similar to how individual synapses/neurons operate together to perform complex tasks and functions in the brain. However, previous efforts to incorporate such components at a scale that could be usefully comparable to modern solid-state processors have been blocked by the difficulty of organizing liquid state DIBs into a dense, digitally addressable material. To address these shortcomings, we propose a pressure-driven PDMS microfluidic device to form lipid-encased water droplets in the initially liquid oil phase, organize them into DIBs, and connect them to electrodes forming a crossbar array. Crossbar arrays have been used in solid-state computers as a method to densely pack two-terminal devices while maintaining individual addressability to each device. The microfluidic system operates on the principle of a shift register where droplets pumped into the device fill the first available empty register and subsequent droplets move past onto the next register. This allows for the exact positioning of droplets within a 2D geometry which, in this case, is an n -by- n arbitrary-sized array with equal spacing between each DIB. Electrodes run the length of the top and bottom of the device such that the top electrodes electrically connect each row of the array, and the bottom electrodes connect each column of the array. Each DIB inside the device can be addressed by one combination of a single top and bottom electrode pair. Once all DIBs have been sorted inside the device, the oil phase is solidified, locking all the droplets in place. The solidified oil phase inside the PDMS microfluidic makes for a durable, yet flexible material that is capable of energy-efficient computation.

8:40 AM SM03.04.06

Direct Laser Writing of Organic Electronics Omid Dadras, Milad Khorrami and Mohammad Reza Abidian;

University of Houston, United States

Development of soft and conductive microstructures has become a key research topic in organic electronics. Among various 3D printing techniques, Two-Photon Polymerization (TPP) based on direct laser writing technology stands out due to its unique capability to fabricate 3D complex architectures in sub-micron resolution. Herein, we have formulated a novel resin that can be fabricated into conductive microstructures via TPP lithography. We have also developed a strategy to fabricate multi-material (combination of conductive / non-conductive resin) microelectrodes with low impedance and high charge storage capacity.

Conductive resin consisted of poly(ethylene glycol) diacrylate (PEGDA), poly(3,4-ethylenedioxythiophene)-poly(styrenesulfonate) (PEDOT:PSS), dimethyl sulfoxide, and ethyl (2,4,6-trimethylbenzoyl) phenylphosphinate. Microstructures were constructed on a glass slide through 3D movement of XYZ stages and irradiation of 130 femtosecond pulses, which solidified the resin at the laser focal point. I-V measurements revealed that conductivity of microstructures fabricated by non-conductive resin (PEGDA) significantly improved from $3.4 \pm 0.8 \text{ S m}^{-1}$ to $24248 \pm 929.7 \text{ S m}^{-1}$ ($n=5$) by incorporation of PEDOT:PSS in the resin.

Michigan-style neural microelectrodes were fabricated in two steps via TPP: 1. Construction of conductive microstructures including cylindrical electrode sites with diameters of 1 μm (site 1), 5 μm (site 2), 10 μm (site 3), 20 μm (site 4), 40 μm (site 5), and 80 μm (site 6) with height of 7 μm , which were individually connected to cubical contact pads with dimensions of 20 μm (width) \times 20 μm (length) \times 7 μm (height) by wire connectors with height of 2 μm , using conductive resin (PEGDA/PEDOT:PSS), 2. Fabrication of electrode shank with height of 5 μm using non-conductive resin (PEGDA), which isolated the wiring and partially exposed the cylindrical sites and cubic pads. Electrochemical characterization of microelectrodes indicated that the impedance at 1 kHz was $63.13 \pm 4.56 \text{ k}\Omega$, $49.33 \pm 2.98 \text{ k}\Omega$, $42.82 \pm 2.95 \text{ k}\Omega$, $33.21 \pm 3.69 \text{ k}\Omega$, $26.66 \pm 2.07 \text{ k}\Omega$, and $19.28 \pm 3.08 \text{ k}\Omega$, and charge storage capacity was $2.38 \pm 0.18 \text{ nC } \mu\text{m}^{-2}$, $8.61 \pm 1.03 \text{ nC } \mu\text{m}^{-2}$, $16.36 \pm 1.67 \text{ nC } \mu\text{m}^{-2}$, $28.43 \pm 4.28 \text{ nC } \mu\text{m}^{-2}$, $61.07 \pm 5.96 \text{ nC } \mu\text{m}^{-2}$, and $89.73 \pm 15.14 \text{ nC } \mu\text{m}^{-2}$ for site 1, 2, 3, 4, 5, and 6, respectively ($n=3$). Development of these soft and electrically functional microelectrodes paves the way towards minimally invasive neural recording and stimulation.

8:50 AM SM03.04.07

Transparent Neuroelectronic Interfaces and Novel Modeling Paradigms to Elucidate the Dynamics of Neural Networks at Microscale Nicolette Driscoll¹, Richard Rosch¹, Brendan Murphy¹, Arian Ashourvan¹, Ramya Vishnubhotla¹, Olivia Dickens¹, A.T. Charlie Johnson¹, Kathryn A. Davis¹, Brian Litt¹, Danielle S. Bassett¹, Hajime Takano² and Flavia Vitale¹; ¹University of Pennsylvania, United States; ²Children's Hospital of Philadelphia, United States

Our current understanding of the spatiotemporal dynamics underlying neural function and disease is limited by (i) our inability to record brain dynamics at sufficient spatial and temporal resolutions and (ii) a lack of established frameworks for applying novel data analysis techniques to high-dimensional neuronal datasets. Light-based approaches to manipulate and monitor neuronal activity have established neuroimaging as the principle technique for mapping the brain at cell-specific resolution and at large scale ($>10^6$ cells). Optical imaging techniques, like calcium and voltage imaging, however, typically suffer from the slow kinetics, suboptimal intensity, and low photostability of the fluorescent reporter molecules, as well as from the limited speed of currently available imaging systems. Electrophysiological recordings with implantable microelectrode arrays can capture spikes from single neurons, but they can only resolve few tens of cells at a time. Combining electrophysiological and optical modalities presents a unique opportunity to harness the spatial resolution of optical imaging along with the temporal resolution of electrophysiology. However, such a combination requires imaging and recording simultaneously in the same location, which is not possible with conventional microelectrode arrays composed of opaque metallic materials, as these block optical access and suffer from photoelectric artifacts. Furthermore, there is no established framework to combine these multimodal datasets operating at different spatiotemporal scales to elucidate the dynamics of brain networks during normal function and disease.

Here, we show how to address this essential challenge by leveraging flexible, transparent graphene microelectrode arrays to map the dynamics of onset and evolution of epileptic seizures. Through the transparent arrays, we acquired simultaneous electrophysiology and calcium imaging *in vivo* in mouse models during the transition from baseline to chemically-induced epileptiform activity. To integrate data features from both modalities, we established an analytical framework based on non-negative matrix factorization to identify transitions in brain state that occur during an epileptic seizure. Our analysis demonstrates that it is possible to capture complementary and otherwise hidden aspects of ictal dynamics operating on different spatial and temporal scales by leveraging data features from multiple modalities. Furthermore, we show how microscale brain dynamics are linked to clinically measurable markers of seizure states.

9:00 AM SM03.04.08

Integrated Electrochemical and Electrophysiological *In Vivo* Micro Electrode Arrays with Zwitterionic Polymer Coating Bingchen Wu^{1,2}, Elisa Castagnola^{1,2} and Xinyan T. Cui^{1,1}; ¹University of Pittsburgh, United States; ²Center for Neural Basis of Cognition, United States

The number of people using Illicit drug aged 12 years and older reached 30 million in 2016, among which 2 million are cocaine users based on the national data. In order to fully understand the mechanism of action and develop effective therapy for addiction, a tool that can reliably and consistently measure *in vivo* cocaine concentration and neural activity with high spatial and temporal resolution is needed. Integrated biochemical sensing devices based upon microelectrode arrays (MEA) have emerged as a powerful tool for such purpose. The implanted MEA devices often face challenges in the *in vivo* environment where biological reactions could have detrimental effects on the sensing and recording capability of the device. To protect implanted MEAs from biofouling and harmful tissue reaction, zwitterionic polymer coatings have recently emerged as a promising candidate. In current work, cocaine electrochemical sensors made from synthetic DNA aptamers were functionalized on flexible MEAs and protected with antifouling zwitterionic poly (sulfobetaine methacrylate) (PSB) coating which prevents sensors from being degraded by host tissue. *In vitro* experiments showed that biofouling of plasma protein doesn't play a significant role in sensor performance decline, while exposure to DNase have detrimental effects on sensor performance, causing a 57.2% signal reduction. The PSB coating successfully protected sensors from DNase enzyme digestion over a 24hrs period. Also, the sensor is stable after 12hrs of continuously applied square waver voltammetry (SWV). This novel integrated cocaine sensor can serve as a valuable tool for study of cocaine addiction mechanism, while the sensing and coating technology can be generalized to detect many other biochemicals of interest.

9:10 AM SM03.04.09

Imaging the Stimulation Efficiency of Electrodes Coated with PEDOT/CNT and Iridium Oxide Xin Sally Zheng^{1,1}, Alberto Vasquez^{1,1,1} and Xinyan T. Cui^{1,2,1}; ¹University of Pittsburgh, United States; ²Center for Neural Basis of Cognition, United States

Intracortical microstimulation is not only a useful tool in neuroscience research for dissecting circuitry and modulating brain activity, it has also shown promise in restoring sensory functions in humans with neural deficits. Current electrode materials like platinum do not meet charge injection requirements for chronic microstimulation, which motivates the development of new stimulating electrode materials. One such material is the conducting polymer poly(3,4-ethylenedioxythiophene) (PEDOT) doped with acid functionalized multi-wall carbon nanotubes (CNT). Although promising, the *in vivo* stimulation performance of PEDOT/CNT(PC) remains to be fully characterized. Traditionally, characterizations of stimulation performance have been based on electrophysiological, behavioral or endpoint histology. Using advanced imaging technologies, we directly measured neuronal activity evoked by microstimulation in transgenic animals in real-time. Herein, we implanted microelectrode arrays coated with PEDOT/CNT (PC) and iridium oxide (IrOx) (a commonly used high charge injection stimulation material) in GCAMP6s mice and applied electrical stimulation while imaging neuronal calcium responses. We observed that PC coated electrodes produce more intense and broader GCaMP responses than IrOx. Using TPM we examined the effect of stimulation modality and pulse-width modulation on neuronal activation. We found that stimulating via PC coated electrodes activates significantly more

neuronal soma and neuropil than via IrOx electrodes in constant-voltage stimulation and significantly more neuronal soma in constant-current stimulation. Furthermore, for both materials and the same injected charge, stimulating with a shorter pulse activated neural elements that are more spatially confined than longer pulses, providing an accessible means to tune stimulation selectivity. Using finite element analysis, we observed that the non-directional and rough edges of PC surfaces result in a more non-uniform and dense electric field, which increases the likelihood of activating nearby neural elements. Our results show that PC coated electrodes provide essential improvements in electrical stimulation applications in terms of energy efficiency for activating local excitable tissue.

9:20 AM SM03.04.10

Late News: Efficient Gating of PEDOT:PSS Organic Electrochemical Transistors with In-Plane Gate Electrodes Dimitrios Koutsouras¹, Fabrizio Torricelli², Paschalis Gkoupidenis¹ and Paul Blom¹; ¹Max Planck Institute for Polymer Research, Germany; ²University of Brescia, Italy

Organic Electrochemical Transistors (OECTs) belong to a class of electrolyte-gated transistors with tremendous applications in bioelectronics due to their unique device architecture. The absence of an insulating layer between gate and channel and its replacement by an electrolyte creates an ideal environment for biological driven measurements as it allows for a direct integration of cell tissue on the device. For efficient gating, a non-polarizable Ag/AgCl electrode is used, which however limits the option for integrating more gates on a chip. Patterned polarizable Au gates on the other hand show strongly reduced gating due to a large voltage drop at the gate/electrolyte interface. Here, we demonstrate a novel method to induce efficient gating by patterned in-plane gate electrodes. For this, we make use of the fact that poly(3,4-ethylenedioxythiophene) polystyrene sulfonate (PEDOT:PSS) exhibits a volumetric capacitance in an electrolyte. As a result, the capacity of PEDOT:PSS based gates can be strongly enhanced by increasing their thickness, thereby reducing the voltage loss at the gate/electrolyte interface. By combining two different fabrication approaches (spin coating and electrodeposition), we create gate electrodes of different thicknesses on the same chip. These electrodes gate the same channel revealing the effect of the gate film thickness on the gating efficiency. The results are compared to the ones of the typically used Ag/AgCl gate electrode, showing that the gating performed by a PEDOT:PSS electrode can be tuned to be comparable to the one from a Ag/AgCl electrode. Using these in-plane gates we study the device physics of multi-gated Organic Electrochemical Transistors and disentangle the part that the gate capacitance plays in gating. Our findings offer an extra degree of freedom in the design of OECT-based biosensors. Most importantly, they pave the way for an elegant integration of in-plane gate electrodes into the latter, leading towards the realization of “organ-on-a-chip” platforms.

SYMPOSIUM SM04

Beyond Nano—Challenges and Opportunities in Drug Delivery
April 14 - April 21, 2021

Symposium Organizers

Yosi Shamay, Technion-Israel Institute of Technology
Youqing Shen, Zhejiang University
Patrick Stayton, University of Washington
Yoon Yeo, Purdue University

Symposium Support

Gold
National Institutes of Health

Bronze
MilliporeSigma

* Invited Paper

SESSION SM04.01/SM01.06: Joint Session: Immunoengineering/Nanotechnology
Session Chairs: Nan Ma, Xun Xu and Yoon Yeo
Tuesday Morning, April 20, 2021
SM04

8:00 AM *SM04.01/SM01.06.01

Multifunctional Nanocarriers for Efficient Cancer Immunotherapy Yunching Chen¹, Shu-Yi Lin² and Kuan-Wei Huang¹; ¹National Tsing Hua University, Taiwan; ²National Health Research Institutes, Taiwan

While immunotherapy holds great promise for combating cancer, the limited efficacy due to an immunosuppressive tumor microenvironment and systemic toxicity hinder the broader application of cancer immunotherapy. We engineered tumor-targeted lipid-dendrimer-calcium-phosphate (TT-LDCP) nanoparticles (NPs) with thymine-functionalized dendrimers that not only exhibited enhanced gene delivery capacity but also immune adjuvant properties by activating the stimulator of interferon genes (STING)-cGAS pathway. TT-LDCP NPs delivered siRNA against immune checkpoint ligand PD-L1 and immunostimulatory IL-2-encoding plasmid DNA to hepatocellular carcinoma (HCC), increased tumoral infiltration and activation of CD8⁺ T cells, augmented the efficacy of cancer vaccine immunotherapy, and suppressed HCC progression. Our work presents nanotechnology-enabled dual delivery of siRNA and plasmid DNA that selectively targets and reprograms the immunosuppressive tumor microenvironment to improve cancer immunotherapy.

8:25 AM *SM04.01/SM01.06.02

Immuno-Engineered Biomaterials Reduce Implant-Related Infections Bingyun Li and Shichao Zhang; West Virginia University School of Medicine, United States

Introduction: Although responsible for reducing infection, widespread antibiotic use has also created the latest grave challenge in wound care, i.e., antibiotic resistant bacteria. Antibiotic resistance has been making our drug choices for infection control increasingly limited and more expensive. According to the Centers for Disease Control and Prevention (CDC), in the U.S. alone, antibiotic resistant bacteria cause at least 2.8 million infections and 35,000 deaths a year and \$55-70 billion per year in economic impact. Meanwhile, it is known that trauma (e.g. open fractures) and major burns lead to decreased resistance to infection (“immunosuppression”) and thereby have high infection rates. Here, we present the engineering of biomaterials with interleukin 12p70 (IL-12) and other cytokines to tune the immune responses locally against open fracture associated infections.

Methods: IL-12 nanocoatings and microcapsules were prepared using electrostatic layer-by-layer (LbL) self-assembly. Polymers like poly(L-lysine) or PLL, poly(L-glutamic acid) or PLGA, and bovine serum albumin (BSA) were used to prepare the coatings, and the release properties and stabilities of the nanocoatings were examined. Next, an open femur fracture infection model was created using Sprague-Dawley rats. The rats’ femurs were fractured, inoculated with 100 mL 10² colony-forming unit (CFU/0.1mL) *Staphylococcus aureus*, left open for one hour, mimicking the “golden hour” of trauma patients, and then fixed with a stainless steel Kirschner wire (K-wire) with or without IL-12 nanocoatings. Animals were euthanized and samples of blood, bone, and K-wires were collected for analysis.

Results: IL-12 nanocoatings were prepared on orthopedic implant models (e.g., K-wires and stainless steel

sheets). The loading and release of IL-12 from polypeptide nanocoatings were tuned and a sustained release of IL-12 for approximately 10 days was achieved by controlling the LbL self-assembly process. Polypeptide microcapsules were also prepared and loaded with IL-12. Our *in vivo* studies showed that IL-12 nanocoatings and microcapsules reduced open fracture associated infection and were advantageous compared to systemic or percutaneous injections of IL-12.

Discussion and Conclusions: Trauma like open fractures have been reported to result in diminished production of IL-12, reduced type 1 helper T (Th1) responses, and decreased resistance to infection. IL-12 displays multiple biologic effects on immune cells; for instance, IL-12 stimulates natural killer (NK) cells to release interferon γ , induces Th1 cell and cytotoxic T lymphocyte proliferation, and promotes the progression of cell-mediated immunity. Local application of IL-12 may restore the capability of the host's inherent resistance to infection, and have led to decreased infection in open fractures.

Acknowledgements: This work is supported by the Office of the Assistant Secretary of Defense for Health Affairs under Award No. W81XWH-17-1-0603. We also acknowledge financial support from AO Foundation, Osteosynthesis & Trauma Care Foundation, WVU PSCoR, and WVCTSI.

8:50 AM SM04.01/SM01.06.03

Polydopamine Capped Gold Nanoparticles for Double NIR-Stimulated Photodynamic Therapy Miso Lee, Mao Wei, Ju Won Lee, Jae Keun Park, Vu O. Pham-Nguyen, Wan Ho Cho and Hyuk Sang Yoo; Kangwon National University, Korea (the Republic of)

Photodynamic therapy (PDT), a treatment method using reactive oxygen species (ROS), have recently been widely used in anticancer treatments. In this study, 130nm gold nanoparticles (AuNP) were stepwise coated with high biocompatible polydopamine(PDA) and photosensitizer chlorin-e-6 (Ce6). The PDA on AuNP surface allowed Ce6 to adhere on the particles through amide bond. Herein, we employed of 2 different NIR light wavelength (650nm and 808nm) to achieve PDT effect. Ce6@PDA@AuNP would absorb by 808nm laser light and generate heat by SPR effect, and Ce6 would absorb 650nm laser light and generate ROS, which can cause the death of target cells. To characterize the nanoparticle, DLS, zeta-potential and Raman spectroscopy of Ce6@PDA@AuNP particle were analyzed. There were an increase in hydrodynamic diameter of the AuNP in the order of AuNP (~130nm), PDA@AuNP (~210nm) and Ce6@PDA@AuNP (~240nm). Due to the anionic charge of PDA, the surface charge of the AuNP decreases after PDA coating, and Raman spectroscopy shows that Ce6@PDA@AuNP shows sharper peak at 1480cm^{-1} and 1580cm^{-1} than those of PDA@AuNP, and the 983cm^{-1} new peaks indicating that Ce6 is attached to the nanoparticle. Besides, Ce6 release behaviors under several pHs were recorded. The more Ce6 release was observed in the lower pH with laser irradiation. Moreover, when Ce6@PDA@AuNP were irradiated with lasers (650nm and 808nm), it was confirmed that the temperature would rise to 58°C and the PDA layer surrounding the AuNP was consequently peeled off after 20 minutes of the irradiation resulted in the release of Ce6 and enhanced ROS generation under the irradiation of 650nm laser. Likewise, since PDA affected by pH, more Ce6 was released from nanoparticles at lower pH, even during the same laser irradiation time resulting better cell apoptosis effect *in vitro*. These results suggested that Ce6@PDA@AuNP has antitumor effects under near-infrared (NIR) irradiation based on the PDT effect.

9:05 AM SM04.01/SM01.06.04

Less (Radiation) is More—Bi₂S₃ Nanoparticles as Efficient Radiosensitizers for Breast Cancer Cells Isabel Galain¹, Emilia Tejeria¹, María Elena Cardoso¹, Gustavo Mourglia¹, Paula Arbildi¹, Mariella Terán¹, Maria Perez Barthaburu² and Ivana Aguiar¹; ¹Facultad de Química - Universidad de la República, Uruguay; ²Centro Universitario Regional del Este - Universidad de la República, Uruguay

Cancer is one of the main threats to human health, due to the large number of cases and high mortality rates. These rates are only expected to increase in future years. Although radiotherapy is the main course of treatment, it is not specific for tumor cells, affecting also healthy cells. Radiosensitizers provide a novel and simple solution to this problem, since they increase the amount of radiation a cell can absorb. This allows for cancer treatments that use a lower dose of radiation, leading to less secondary effects for the patient. Our group synthesized bismuth sulfide (Bi₂S₃) nanoscale particles using a hot injection method followed by a ligand

exchange, for use as radiosensitizers. We synthesized Bi₂S₃ nanorods measuring in average 4.1 ± 1.2 nm in width and 20.2 ± 7.0 nm in length. These nanoparticles were successfully coated with polyvinylpyrrolidone (PVP) to improve their biocompatibility. According to IR and DSC results, we achieved a successful ligand exchange to PVP, with a defined binding with the nanoparticle. We studied the nanoparticles' stability in different biological media (water, culture medium, fetal bovine serum, and human plasma). The stability tests showed that the suspensions were more stable for media with higher protein components. This may aid in the ability of the nanoparticles to move through the bloodstream. We studied the nanoparticles' cytotoxicity in human breast cancer cells (MCF7), over 72 hours of incubation. The coated nanoparticles did not evidence cytotoxicity up to 2500 µg/mL. Also, we conducted radiosensitivity tests using a Co-60 source. We determined that the best condition for adequate radiosensitizing test is a dose of 2 Gy and a post-irradiation incubation time of 48 hours. MCF7 cells that were incubated with a nanoparticle concentration of 50 µg/mL and irradiated showed a 38% increase in cell death when compared to cells that were only irradiated, without nanoparticles. Our results confirm that PVP-coated Bi₂S₃ nanoparticles are stable in many biological media, and that they are not-cytotoxic in a wide range of concentrations. When combined with gamma radiation, the nanoparticles increase the efficiency of radiotherapy. This outstanding results certainly grant hope for this line of research, to develop cancer treatments that have less secondary effects and a better quality of life for patients.

9:20 AM SM04.01/SM01.06.05

Nucleic Acid Mediated Reversal of Charge—An Useful Methodology to Prevent the Immunostimulatory Activity of Positively Charged Lipid Nanocarrier Arindam Dey^{1,2}, Adrien Nougarede^{1,3}, Flora Clément^{1,2,4}, Carole Fournier^{1,2}, Evelyne J. Marche^{1,2}, Marie Escude^{1,3}, Dorothée Jary^{1,3}, Fabrice P. Navarro^{1,3} and Patrice N. Marche^{1,2}; ¹Université Grenoble Alpes, France; ²Research Center, CNRS, France; ³Microfluidic Systems and Bioengineering Lab, France; ⁴CEA, INSERM, IRIG-BIOMICS, France

Use of nanotechnology in gene therapy to deliver therapeutic nucleic acid such as siRNA could open up a new avenue to cure genetic disorders. Lipid nanoparticles currently in use for several biomedical applications integrate cationic lipids in order to form complexes with nucleic acid cargo and enable their uptake by target cells. However, larger surface area and highly charged nature of these nanocarriers increase their interaction with host cells which might induce toxicity. While gene mediated off-target effects have been extensively studied, it is crucial to consider the carrier toxicity and side effects including immunological parameters. In the immune system, phagocytes can engulf foreign materials, therefore they are appropriate to screen for immunotoxicity by monitoring their functions in unspecific and specific immune responses.

In our study, we evaluated the function of primary bone marrow derived macrophages (BMDMs) in response to cationic nanostructured lipid carriers (cNLCs), which are positively charged (+45.8 mV). The effect of cNLCs was investigated in non-activated and IL-4 or LPS-activated BMDMs. We assessed the secretion of proinflammatory molecules including, IL-6, TNF- α , MCP-1, Nitric Oxide (NO). We also addressed the effect of cNLCs on metabolism by evaluating glycolytic activity (glycolysis and glycolytic capacity) and oxidative phosphorylation (basal respiration, proton leak, ATP production, maximal respiratory capacity, spare respiratory capacity). Our results showed that cNLCs remarkably enhanced the secretion of several molecules (IL-6, TNF- α , MCP-1, NO) as well as the energy flux in non-activated or LPS- or IL-4-activated BMDMs. Furthermore, we combined cNLCs with negatively charged siRNA at different N/P ratios (the ratio of positively-charged amine groups of cNLCs (N = nitrogen) to negatively-charged phosphate (P) groups of nucleic acid) (N/P = 8/4/2/1). Our experiments showed that reversing the surface charge prevent the effect induced by positively charged cNLCs on IL-6, TNF- α , MCP-1, and NO productions as well as on cellular metabolism (glycolysis and oxidative phosphorylation) of BMDMs. Our results highlight that reversing the surface charge of cationic lipid nanocarriers with an oppositely charged biomaterial, for instance nucleic acid, could attenuate immunostimulatory activities of the cationic nanocarrier. This issue needs to be addressed during the use of cationic nanocarriers in different biomedical applications, such as nucleic acid delivery for therapies or vaccines.

Finally, we propose to tune the nucleic acid load, hence the surface charge of lipid nanocarriers is critical for their therapeutic use, to prevent the alteration of immune cell response to positive charge stimuli. We also recommend to measure the zeta potential of the nanocomplexes, keeping in mind that charged nanocomplexes

can alter the immune cell function which may lead to several side-effects.

This project has received funding from the European Union's Horizon 2020 research and innovation program H2020 "NEWDEAL" (grant agreement No. 720905).

9:35 AM SM04.01/SM01.06.06

Tagging the Cancer Cell Surface for Innate Immune Recognition and Destruction by Bifunctional Multivalent Antibody-Recruiting Polymers Annemiek Uvyn¹, Bas de Waal², Bert Meijer² and Bruno G. De Geest¹; ¹Ghent University, Belgium; ²Technische Universiteit Eindhoven, Netherlands

Binding antibodies onto a cell surface triggers antibody-mediated effector killing by innate immune cells through complement activation (CDC), antibody-dependent cellular cytotoxicity (ADCC) and antibody-dependent phagocytosis (ADCP), which is the mechanism of action of many monoclonal antibody (mAbs) therapeutics. As an alternative to mAbs, synthetic systems that can recruit endogenous antibodies, i.e. antibodies against small molecule haptens that are found in the blood of virtually every human being, from the blood stream to a cancer cell surface could be of great relevance. Herein, we explore antibody-recruiting polymers as a novel class of immunotherapy. These polymers are functionalized on their surface with multiple cell-binding and antibody-binding hapten motifs such as dinitrophenol and rhamnose. As cell surface binding motifs, we employ alkyl lipid and dibenzoylcyclooctyne motifs, for respectively hydrophobically-driven insertion into the phospholipid cell membrane or strain promoted alkyne-azide cycloaddition with azide motifs in the glycocalyx of cancer cells. *In vitro* on cancer cell cultures, we demonstrate that antibody-recruiting polymers allow for high avidity antibody binding and drive antibody recruitment to treated cells for several days and elicit robust innate immune effector killing.

9:50 AM PANEL DISCUSSION

SESSION SM04.02: Machine Learning for Drug Delivery Design

Session Chair: Yosi Shamay

Tuesday Morning, April 20, 2021

SM04

11:45 AM *SM04.02.01

Machine Learning-Enabled High-Throughput Virtual Screening for Novel Mitochondrial Membrane Dyes Kirill Shmilovich¹, Bernadette Mohr², Tristan Bereau² and Andrew Ferguson¹; ¹The University of Chicago, United States; ²University of Amsterdam, Netherlands

Mitochondria are energy-producing organelles that exist within eukaryotic cells contained within a double phospholipid membrane. The inner membrane is composed of about 20% cardiolipin (CL), an unusual dimeric phospholipid in which a pair of phosphatidic acids are linked by glycerol to yield a molecule with four acyl chains. CL is the hallmark of energy transducing membranes and is implicated in a number of critical pathways in mitochondrial metabolism, regulation, and apoptosis. Abnormalities in CL composition profiles are linked to several diseases, including Barth syndrome, Tangier disease, heart failure, and neurodegenerative disorders [1]. The acridine orange derivative, 10-N-nonyl acridine orange (NAO), is a high-affinity probe that is 30 times more specific for CL than for other cationic phospholipids and is used as a stain for fluorescent visualization and quantification of mitochondrial CL [2]. Enhancing probe uptake by CL enables the use of lower dye concentrations and lowers cellular toxicity, but efforts to rationally engineer NAO to increase staining efficiency have compromised its phospholipid selectivity [3]. In this work, we have combined coarse-grained molecular simulation, alchemical free energy calculations, deep representational learning, and Bayesian optimization to perform high-throughput virtual screening of candidate organic molecules as CL dyes with

superior uptake and selectivity than NAO. We consider as our search the $>10^{11}$ small organic molecules up to 400 Da molecular weight and use our computational platform to rationally traverse this space. Our analysis efficiently identifies novel high performing dye molecules and informs new understanding of the molecular properties responsible for good efficiency and selectivity. After just a few rounds of iterative molecular simulation and data-driven model building, we have identified three candidates predicted to have up to 4-fold superior uptake and 99 candidates with up to 34-fold superior selectivity relative to NAO. Future collaborative work is planned to synthesize and test the top compounds identified in the computational screen.

1. G. Paradies, V. Paradies, F.M. Ruggiero, and G. Petrosillo, *Cells* 8 (7) 728 (2019)
2. M.E. Rodriguez, K. Azizuddin, P. Zhang, S.-M. Chiu, M. Lam, M.E. Kenney, C. Burda, and N.L. Oleinick, *Mitochondrion* 8 (3) 237-246 (2008)
3. J. Zielonka, J. Joseph, A. Sikora, M. Hardy, O. Ouari, J. Vasquez-Vivar, G. Cheng, M. Lopez, and B. Kalyanaraman, *Chemical Reviews* 117 (15) 10043-10120 (2017)

12:10 PM *SM04.02.02

Development of Kinase Inhibitor Nanomedicines for Intracranial Tumor Delivery Daniel Heller^{1,2}, Daniel Tylawsky², Yosi Shamay³ and Kiroto Kiguchi⁴; ¹Memorial Sloan Kettering Cancer Center, United States; ²Weill Cornell Medicine, United States; ³Technion–Israel Institute of Technology, Israel; ⁴Children’s Hospital of Philadelphia, United States

Therapy based on personalized medicine has become a leading strategy to treat cancer. Small molecule drugs such as kinase inhibitors, which target key effectors of cancer signaling pathways, constitute a major component of this strategy. This class of drugs is diverse and each has different issues regarding pharmacokinetics, toxicity, and therapeutic index, especially in intracranial tumors due to the blood-brain barrier. Kinase inhibitors also inhabit a diverse chemical space, making it difficult to develop nanomedicines against the wide set of precision drug targets. We developed data science/machine learning-driven processes to predict and facilitate the encapsulation of diverse drug classes into nanoparticles based on the molecular structures of the drugs. These included quantitative structure-nanoparticle assembly prediction models for drug payload selection. We found molecular descriptors that are highly predictive indicators of nano-assembly and nanoparticle size. For the treatment of pediatric tumors with an intact blood-brain barrier, we developed a therapeutic nanoformulation capable of traversing the blood-brain barrier via transendothelial transport across tumor vasculature to improve kinase inhibitor therapeutic index.

12:35 PM SM04.02.03

Micro-Nozzle Integration for Controlled Drug Delivery via a Microfluidic Imaging Window Tristen Head^{1,2}, Natalya Tokranova¹ and Nathaniel Cady¹; ¹State University of New York Polytechnic Institute, United States; ²University at Albany, State University of New York, United States

Novel imaging and drug delivery methods are needed to understand the cellular and molecular events of cancer metastasis. We have developed a microfluidic imaging window (MFIW) platform that enables precise delivery of drugs, labeling agents, and cells during longitudinal intravital imaging of the tumor microenvironment. Intravital imaging with the MFIW platform enables *in vivo* evaluation of drug effects on tumors, and observation of cellular events, such as the intravasation of tumor cells into blood vessels. An important aspect of fluid delivery is to precisely control the fluid flow vector field and three-dimensional distribution of reagents in the target tissue. Using a dry film SU-8 photoresist we have implemented a novel photolithography process dubbed post-exposure lamination (PEL). Using PEL we have successfully integrated micro-nozzle structures with planar microfluidics, to significantly enhance three-dimensional control of fluid infusion. The PEL method enables control of the vertical and horizontal morphology of micro-nozzle structures, yielding nozzles that produce unique flow profiles. The micro-nozzle structure improves the convective transport of reagents into a projected delivery area that is 70% smaller than the projected delivery area of devices with a planar outlet. Confocal microscopy and computational fluid dynamic simulations are currently being used to assess the depth penetration and radial spreading of fluid in a tissue phantom, with initial results showing improved penetration

depth and radial profile when micro-nozzle outlets are employed. Ongoing work is focused on localized delivery of transfection reagents to cells in three-dimensional culture, to demonstrate the therapeutic potential of the platform.

12:50 PM SM04.02.04

Dialysate Regeneration by Efficient Urea Decomposition with TiO₂ Nanowire Photoelectrochemical Cell Guozheng Shao, Yushi Zang and Bruce Hinds; University of Washington, United States

More than 2 million End Stage Renal Disease (ESRD) patients receive dialysis to sustain life, with this number likely to represent less than 10% of the actual need. In the United States alone, over 460,000 people are on dialysis. Conventional hemodialysis removes urea and other metabolic wastes from the body by running ~120 L of dialysate over hollow fiber dialysis membranes each session, which is typically 3-4 hours per session and thrice a week. The intermittent character of hemodialysis results in large fluctuations in blood metabolite concentrations. Observations show that long term survival in dialysis patients treated by extended hemodialysis are improved compared to conventional hemodialysis. Thus a portable dialysis machine that is working continuously would bring in significant health, quality of life and economic benefits.

To enable portable kidney dialysis for ESRD, the regeneration of the dialysate in a closed loop system is a primary critical technical barrier. Currently the ~120 L (kg) of dialysate per session, far exceeds usable weights for a portable system. We have developed an efficient photooxidation system based on hydrothermally grown TiO₂ nanowires, UV LEDs, and catalytic gas diffusion barriers to decompose urea from the dialysate at rates sufficient to remove daily production of urea at 15 g/day.

A photoelectrical decomposition cell with SiO₂/FTO/TiO₂ nanowire anode, 10 mM urea/0.15 M NaCl electrolyte, and 4 mg/cm² Pt black loaded carbon paper cathode was characterized for urea decomposition efficiency. Under 4 mW/cm² illumination of the 365 nm LED with 40% quantum efficiency, the device yielded a photocurrent density of ~1 mA/cm² in a dialysate simulant of corresponding to 40% quantum efficiency in urea decomposition per incident photon. From performance parameters, a feasible portable device with ~0.23 m² active area and a current draw of 11 A is able to decompose a daily 15 g urea production sufficient to regenerate dialysate. Also high selectivity (80%) for urea decomposition over Cl₂ formation is shown. For comparison, prior reports in literature [J. Photochem. Photobiol. AChem, 2009, 205, 168] for urea fuel cells of agricultural waste, > 5000 A would be required. Improvements reported here are based on nanowire microstructure to efficiently separate electron holed pairs and efficiently adsorb incident UV irradiation.

1:05 PM SM04.02.05

Late News: Filamentous Self-Assembly Based on Lithocholic Acid-Polyethyleneimine Conjugate for Local Delivery of Drug and Gene Therapeutics Jianping Wang, Fanfei Meng and Yoon Yeo; Purdue University, United States

Introduction: Filamentous nanoparticle (FN) refers to a polymeric self-assembly with a high aspect ratio, nanometer scale in diameter and micrometer scale in length. FN has great potential in drug delivery because it shows a longer circulation time, low phagocytic cell uptake, and longer retention in tissues as compared to spherical counterparts. FN is produced with amphiphilic block-co-polymers, which interact with each other via directional and reversible noncovalent interactions. For biomedical applications, FN is usually prepared with a peptide-drug conjugate, in which a drug is part of the building block of the FN. We report a lithocholic acid-polyethyleneimine conjugate (lp) that can form FN in the presence of hydrophobic drugs, with no need of the drug being part of the polymer, and serve as their carrier for local drug delivery. We characterized the properties of FN, studied the conditions that enable FN formation, and tested the feasibility of using FN for local drug delivery.

Methods: FN was prepared by the membrane hydration method. Various small molecule drugs or model compounds were screened to test the ability to form FN with lp. Retrospective quantitative structure-property relationship (QSPR) analysis was performed by AlvaDesc software to identify common structure features of FN

formers. The formation of FN and FN hydrogel was studied varying the conditions such as aging time, temperature, lp/drug ratio, and drug concentration. Tissue retention of paclitaxel FN labeled with DiR was monitored by intratumoral injection of FN to CT26 colon tumors in Balb/c mice and whole-body fluorescence imaging.

Results: Out of 19 drugs screened, 6 drugs formed FN with lp, 4 formed short filaments, and 9 did not form FN. QSPR analysis revealed that FN formers had amido bond in common. The diameter of FN was measured to be 26.3 ± 4.3 nm, and the average length ranged from 1 to 2 μm depending on the type of drug and the weight ratio of lp to drug. The rate of FN formation increased with temperature. Paclitaxel-loaded FN formed a hydrogel at 37.8 mg/mL or higher, likely due to the physical entanglement of FN. FN injected at 4.46 mg/mL to subcutaneous CT26 tumors persisted for more than 8 days showing 80% of the initial FN signal in the tumor on day 8. In contrast, spherical counterparts diffused away with only 50% FN remaining after day 1 and all disappearing after 1 week. This result indicates the potential of FN to serve as a local drug delivery system.

Conclusion: Lithocholic acid-polyethyleneimine conjugate formed FN with a group of hydrophobic drugs. The drug-loaded FN can serve as a local depot of the drug in tumors. The lithocholic acid-polyethyleneimine conjugate can be combined with various hydrophobic drugs with amido bond structure to form FN and FN-based hydrogel for systemic and local drug delivery.

1:20 PM *SM04.02.07

Improving RNA Delivery by Testing Thousands of Nanoparticles *In Vivo* James Dahlman; Georgia Institute of Technology, United States

DNA and RNA can manipulate the expression of any gene, making these molecules promising drugs. However, whether the drug is comprised of DNA, siRNA, mRNA, lncRNA, or another nucleic acid, it is limited by one problem: drug delivery. Chemists design thousands of distinct nanoparticles to deliver DNA or RNA to the desired cell type. However, after nanoparticles are synthesized, their ability to deliver drugs is evaluated using *in vitro* systems devoid of a liver, kidney, spleen, immune system, pulsatile blood flow, and other selection pressures known to affect nanoparticle delivery *in vivo*.

We have designed a series of increasingly advanced DNA barcoding platforms to quantify how thousands of nanoparticles deliver nucleic acids *in vivo*. Our goal is to quantify how up to 300 nanoparticles deliver DNA, mRNA, ASOs, or siRNA into up to 30 cell types, all in a single animal. To analyze these large *in vivo* drug delivery datasets, we have also developed an open source bioinformatics pipeline to iteratively 'evolve' nanoparticles that target cells *in vivo*. Using this high throughput, iterative, *in vivo* approach, we have identified nanoparticles with tropism to many novel cell types, in many different tissues.

SESSION SM04.03: Biomaterials and Drug Delivery for Immunotherapy I

Session Chairs: John Wilson and Yoon Yeo

Tuesday Afternoon, April 20, 2021

SM04

2:15 PM *SM04.03.01

Engineering Innate Immune Activation with Amphiphilic Biomaterials Bruno G. De Geest; Ghent University, Belgium

Uncontrolled systemic inflammatory immune triggering hampers clinical translation of many classes of small molecule immunomodulators for vaccine design and cancer immunotherapy. Potent small molecule agonists of pathogen recognition receptors such as toll like receptors and agonists of STING have been discovered, but like many other small molecule drugs, they are prone to rapid distribution throughout the body, thereby losing sitespecific activity and causing unwanted systemic inflammation.

Noncovalent albumin binding has proven a powerful strategy for lymphoid delivery. By taking advantage of the

inherent serum protein binding property of lipid motifs and their tendency to accumulate in lymphoid tissue, we designed lipid amphiphile conjugates that show robust lymphatic translocation by hitch hiking onto albumin molecules in the interstitial flow from the injection site to draining lymphoid tissue. By conjugating a small molecule immunomodulator (exemplified in our work by an imidazoquinoline TLR7/8 agonist) to lipid amphiphiles through a degradable linker we obtain well water soluble prodrugs that, upon subcutaneous or intramuscular administration provoke potent lymph node immune activation but suppress systemic overstimulation of the immune system.

Lipid conjugation of potent small molecule immunomodulators has shown to reduce systemic toxicity but comes at a cost of a dramatic reduction in biological activity due to the formation of an insoluble depot. Our approach results in a well water soluble lipid amphiphile prodrug, showing high biological activity *in vitro* and *in vivo* in mouse models.

2:40 PM *SM04.03.02

Engineering Approaches to Modulate the Immune System James J. Moon; University of Michigan–Ann Arbor, United States

With profound advances in immune-oncology, cancer immunotherapy is now considered the fourth pillar of cancer therapy, joining the ranks of surgery, radiotherapy, and chemotherapy. For some cancers, including advanced non-small cell lung cancer, combination immunotherapy is FDA-approved as the frontline therapy, showing promise for applying immunotherapy to a wide range of advanced cancers. Currently, immune checkpoint blockade involves systemic administration of monoclonal antibodies, which can cause off-target side effects by inducing activation of self-antigen reactive T-cells. The combination of multiple immune checkpoint blockers generally improves the clinical responses; however, this can lead to severe immune-related adverse events that result in clinical manifestations of dermatitis, colitis and hepatitis. Thus, to fully realize the potential of cancer immunotherapy, approaches are needed to amplify anti-tumour T-cell immune responses, to convert cold tumours into hot tumours and to sensitize tumours to immunotherapies with minimal off-target toxicity and immune-related adverse events. Here, we highlight new opportunities for combination immunotherapy based on nanomedicines that are well poised tackle the challenges faced by the field of cancer immunotherapy. We present biomaterial-based strategies for amplifying anti-tumor immune responses and sensitizing tumors to immunotherapies in a safe and effective manner. Briefly, we show that lipid-based nanodiscs can efficiently co-deliver antigen and immunostimulatory molecules to draining lymph nodes and elicit potent CD8⁺ cytotoxic T lymphocyte responses directed against tumor antigens, leading to substantially enhanced anti-tumor efficacy in multiple murine tumor models, including colon carcinoma, melanoma, and glioblastoma multiforme. In a second research thrust, we have shown that this nano-platform can deliver chemotherapeutic agents in a synergistic manner with immune checkpoint blockers. In a third research thrust, we are developing new biomaterials for *in situ* modulation of the gut microbiome for regulation of local and systemic immune responses. We will share our latest results showing the therapeutic potential of our gut modulation approach in the context of combination cancer immunotherapy. Owing to the facile manufacturing process, robust therapeutic efficacy, and good safety profiles, our biomaterial-based approaches may offer powerful and convenient platforms for combination cancer immunotherapy.

3:05 PM SM04.03.03

Late News: Poly(ethylene glycol)-b-poly(D,L-lactide) Nanoparticles as Potential Carriers for Anticancer Drug Oxaliplatin Nikita Sedush¹, Yulia Kadina¹, Ekaterina Razuvaeva¹, Dmitry Streltsov¹, Alevtina Kulebyakina¹, Alexander Puchkov¹, Alexey Nazarov² and Sergei Chvalun^{1,3}; ¹National Research Center Kurchatov Institute, Russian Federation; ²Department of Chemistry, Lomonosov Moscow State University, Russian Federation; ³Enikolopov Institute of Synthetic Polymeric Materials Russian Academy of Sciences, Russian Federation

In the last decades, great attention has been paid to developing of nanoscale vehicles for drug delivery. Incorporation of drug molecules into nanocarriers allows to overcome poor water solubility of hydrophobic drugs as well as increase stability against hydrolytic degradation of hydrophilic ones. Moreover, nanoparticulate

drug formulations can act in a targeted and prolonged manner enhancing the efficacy of treatment, e.g. cancer treatment. Platinum-based complexes (cisplatin, carboplatin, oxaliplatin etc.) are widely used chemotherapeutics agents for the treatment of various types of cancer. Oxaliplatin ((trans-R,R-cyclohexane-1,2-diamine)oxalatoplatinum(II)) is the third-generation platinum complex that was designed to overcome cellular resistance to cisplatin and carboplatin. Oxaliplatin shows higher solubility and less toxicity than cisplatin. It is used as a standard treatment for colorectal cancer. Moreover, oxaliplatin can be active against refractory ovarian cancer, germ-cell cancers, non-small cell lung cancer etc. Nevertheless, its low water solubility, short half-life in the bloodstream and non-selective biodistribution reduces the effective dose of oxaliplatin in the targeted tissues and enhances the systemic toxicity. The design of new types of nanocarriers for delivery of oxaliplatin is of high interest. We believe that P(D,L)LA-b-PEG nanoparticles is a promising platform due to its flexibility and successful track record as a nanocarrier for development of targeted anticancer drug formulations.

Biodegradable drug-free and oxaliplatin-loaded mPEG₁₁₃-b-P(D,L)LA_n nanoparticles were prepared by a simple nanoprecipitation technique. The effect of hydrophobic block length on the structure, size, morphology and drug loading content of mPEG₁₁₃-b-P(D,L)LA_n nanoparticles was investigated. It was observed that in aqueous solution mPEG₁₁₃-b-P(D,L)LA_n copolymers, where n = 62 – 173 monomer units, form spherical nanoparticles with hydrodynamic diameters ranging from 32 to 56 nm. The “core-corona” structure of the block copolymer nanoparticles was confirmed by SAXS. Tailoring of P(D,L)LA block length results in variation both core-corona interface area and tethering density of hydrophilic PEG chains on the surface of P(D,L)LA core of the mPEG₁₁₃-b-P(D,L)LA_n nanoparticles, which affects oxaliplatin loading content. An increase in P(D,L)LA block length from 62 to 173 monomer units results in a decrease in core-corona interface area from 2.7×10^{20} to 1.5×10^{20} nm²/g and tethering density of PEG chains from 1.6 to 1.0 nm⁻² and a reduction in the oxaliplatin loading content from 3.8 to 1.5% wt./wt. Thus, we suppose that oxaliplatin is adsorbed on the core-corona interface of the mPEG₁₁₃-b-P(D,L)LA_n nanoparticles. SAXS measurements revealed that oxaliplatin loading does not affect the size and structure of the block copolymer nanoparticles.

The size and structure of polymeric nanoparticles are crucial characteristics that should be considered in the design of targeted nanoformulations of anticancer agents. The developed formulations of oxaliplatin can be considered as promising candidates for treatment of various types of cancer. In vitro tests were performed in order to compare its efficacy and toxicological profile with pure oxaliplatin.

This research was funded by the Russian Science Foundation, grant number 18-73-10079.

3:20 PM SM04.03.04

Donor-Acceptor Based Photothermal Nanoparticles for Augmenting Oxaliplatin Chemotherapy Against Colorectal Cancer Santu Sarkar and Nicole Levi; Wake Forest University School of Medicine, United States

Colorectal Cancer (CRC) is the fourth leading cause of cancer-related deaths with few available treatment options. Common treatment techniques are surgery and chemotherapy. Among the available chemotherapeutic drugs, oxaliplatin is a cornerstone for the treatment of CRC. As an adjuvant technique, hyperthermia i.e. an elevated temperature (39–42 °C), has been shown to increase chemotherapy treatment outcomes clinically. Hyperthermia increases the drug uptake by affecting cell membranes and produces drug-induced DNA damage leading to enhanced tumor cell death. It has been demonstrated that the synergistic effect of hyperthermia with oxaliplatin can treat CRC. One of the major disadvantages is, due to the intermittent exposures of oxaliplatin the cells become chemo-resistance complicating the treatment procedure. To improve the precision of the technique, instead of using a bulk carrier fluid along with a heat exchanger in the traditional hyperthermia delivery, photothermal nanoparticles can be used to deliver more specific and effective hyperthermia. In our laboratory, semiconducting polymer nanoparticles have been used as photothermal agents to ablate cancer cells. Recently, variable molecular weight nanoparticles (VMWNPs) produced from the oligomer and high MW segments of a single polymer poly[4,4-bis(2-ethylhexyl)-cyclopenta-[2,1-b:3,4-b'']-dithiophene-2,6-diyl-alt-2,1,3-benzoselenadiazole-4,7-diyl] (PCPDTBSe) were demonstrated as a promising photothermal agent for the ablation of breast cancer. VMWNPs generated heat upon 800 nm laser irradiation and produced fluorescence emission at 825 nm upon excitation at 550 nm. Therefore, VMWNPs can be used to detect CRC through near infra-red fluorescence imaging and hyperthermia delivery. Here we have explored the synergistic effect of oxaliplatin and hyperthermia generated through VMWNPs to augment chemotherapy treatment of

chemo-sensitive and chemo-resistant CRC cells.

The process of hyperthermia generation using VMWNPs was optimized, and it was found that a 25 µg/ml concentration of VMWNPs could produce hyperthermia (39–42 °C) effect upon 800 nm (3W) laser exposure for 20 seconds. Various concentrations of VMWNPs were incubated with mouse-derived CRC CT-26 cells for 24 hours and no cytotoxic effect was observed up to 100 µg/ml. Whereas upon incubation of oxaliplatin with increasing concentrations there was a 50% decrease in cell viability at 300 µM concentration was observed. To monitor the thermal dose, first, the chemo-sensitive and chemo-resistant CRC cells were incubated with varying concentrations of oxaliplatin and kept at 42 °C for two hours. An 80% and 75% decrease in cell viability was observed for chemo-sensitive cells and chemo-resistant cells respectively. To observe the effect of VMWNPs induced hyperthermia, CRC chemo-sensitive cells were incubated with oxaliplatin and VMWNPs followed by laser exposure (800 nm, 3W, 20 secs) in three cycles. A 63% reduction in cell viability was observed for VMWNPs generated hyperthermia. This result confirmed that VMWNPs could successfully deliver hyperthermia to augment chemotherapy. In the future, oxaliplatin, and hyperthermia using VMWNPs will be utilized to treat chemo-resistant CRC cells.

3:35 PM SM04.03.05

Late News: Polymersome Encapsulation of a Lipophilic Protein-Protein Interaction Inhibitor to Achieve Increased Solubility and Therapeutic Index Yu Tian, Mathew Schnorenberg, James LaBelle and Matthew Tirrell; The University of Chicago, United States

Protein-protein interactions (PPIs) dictate most biological processes, including those responsible for carcinogenesis. Targeted therapeutics acting on these oncogenic PPIs have naturally become the focus of novel drug discovery. Currently, one small molecule PPI inhibitor, Venetoclax (AbbVie) is FDA approved to treat a number of hematologic malignancies through its inhibition of an antiapoptotic protein, BCL-2. However, considering that there are ~650,000 human PPIs as potential targets, the development of other PPI inhibiting drugs has been lagging due to the off-target and delivery issues. For example, a PPI inhibitor, ABT-263, although possessing potent nanomolar binding affinity to BCL-2, can lead to severe thrombocytopenia when administered systemically, which is due to the off-target BCL-XL inhibition in platelets. This is limiting its therapeutic index. We have developed a nanocarrier system, targeted polymersome (PSOM) nanoparticle, made of biocompatible poly(ethylene glycol)-disulfide-poly(propylene sulfide) (PEG-SS-PPS) with surface conjugated anti-CD19 F(ab) antibody fragments (aCD19 Fabs) as targeting motif to B cell lymphoma. PSOMs are fabricated by flash nanoprecipitation (FNP) and extrusion resulting in uniform vesicular morphology and size distribution (~130 nm in diameter). Moreover, ABT-263 was successfully encapsulated by PSOM at an efficiency over 90%, which increases the solubility of the lipophilic ABT-263 to over 10mM in PBS. From *in vivo* platelet-counting experiment, the intravenous administration of PSOM encapsulated ABT-263, in contrast to orally administered non-encapsulated drug, led to the mitigated thrombocytopenia in mice. Importantly, flow cytometric analyses on a panel of human CD19 positive diffuse large B cell lymphoma cell lines demonstrated specific uptake of aCD19-PSOM nanoparticles. We believe the results indicate the great promise of *in vivo* targeted delivery of ABT-263 by PSOM to B cell lymphoma.

3:50 PM SM04.03.06

Late News: Activatable Perfluorocarbon Bubble Inflation and Drug Release Using Superheated Perfluorocarbon Nanodroplets Caroline de Gracia Lux, Jacques Lux and Robert F. Mattrey; University of Texas Southwestern Medical Center, United States

The field of acoustic droplet vaporization (ADV) was introduced nearly 20 years ago to embolize tissues non-invasively. ADV used 1-5 µm perfluorocarbon (PFC) droplets and converted them into large gas bodies in the feeding artery with ultrasound to embolize tissues downstream. Despite its potential clinical impact, the ADV field has not advanced. The manufacture of nanodroplets (ND) using PFC that boils near 0 °C to ease vaporization, was introduced 10 years later to rescue ADV, and to capitalize on the nanosize ND for tumor detection. Despite this advance, the field remains stagnant because of critical efficacy and safety challenges hindering its translation and widespread use. Some important challenges include the energetics required to

cavitate the PFC into gas, and the resultant rapid expansion that could injure tissues. We recently discovered that PFC nanobubbles (NBs) and microbubbles (MBs) inflate when exposed to superheated PFC NDs. While *in vitro* and *in vivo* preliminary data confirmed the proof of concept, the translational success of our novel approach will rely on our ability to control bubble inflation to safely improve tumor detection when NBs are used or occlude tumor microvascular when MBs are used. We showed that both rate and degree of expansion is affected by the type of PFC used, ND and NB/MB size and type of lipid emulsifier that affect both interfacial tension and the ability of bubbles to expand. We showed that MBs with a stiff polymeric shell made of denatured albumin when exposed to liquid PFC NDs expand more rapidly, but to only half the diameter of typical phospholipid-based MBs, encouraging us to optimize shell formulation to limit inflation.

As this non-invasive platform can be used to perform chemoembolization as is currently done to treat liver tumors but without the need for angiography or prior tumor visualization, one of our current goal is to load chemotherapeutics in NDs or MBs and promote drug release in only tissues expressing the receptor of interest, analogous to trans-arterial chemoembolization. However, since this approach is not image guided, tumors do not need to be visible pre-treatment. We believe that these accomplishments show promise and potential to translating our novel approach to the clinic while creating new paradigms for early detection and treatment of cancer. This talk will be focused on the impact of formulation on MB growth and translational opportunities.

4:05 PM PANEL DISCUSSION

SESSION SM04.04: Biomaterials and Drug Delivery for Immunotherapy II

Session Chairs: Ciana Lopez, Patrick Stayton and Yoon Yeo

Tuesday Afternoon, April 20, 2021

SM04

5:15 PM *SM04.04.02

Programming Immunity with Smart Materials John T. Wilson; Vanderbilt University, United States

Interventions that engage the power and specificity of the immune system have enormous potential to improve human health, yet the efficacy, safety, and utility of many promising immunomodulatory agents is limited by critical drug delivery barriers. This talk will describe current research in my laboratory focused on engineering nanomaterials for intracellular delivery of immunomodulatory proteins, nucleic acids, and small molecules. Specifically, I will discuss our recent efforts in developing environmentally-responsive “smart” materials that open access cytosolic immune surveillance pathways, including STING and RIG-I, and how we are leveraging these platforms to enhance responses in cancer immunotherapy and augment the efficacy of subunit vaccines against respiratory viral pathogens.

5:40 PM SM04.04.03

A Novel Upconversion Nano Platform for NIR Triggered Drug Release and PDT Therapy Lei Ma¹, Olivia Fernandez¹, Hao Zhang², Lu Li², Luis Echegoyen¹ and Xiujun J. Li¹; ¹The University of Texas at El Paso, United States; ²Shandong Normal University, China

The development of an efficient phototherapeutic system is highly desirable but still a big challenge, because of its significant limitations at tissue penetration. NIR photo upconversion can be an effective key to assist electromagnetic energy penetrating deep tissue into most tumor locations. Herein, a novel 808 nm triggered upconverting system was designed and applied for NIR triggered drug release and simultaneous photodynamic therapy. A core-shell NaYF₄:Nd/Yb@NaYF₄:Yb/Er nanocrystal was rationally synthesized, exhibiting photoluminescence emissions at the wavelength around 538 nm, under NIR laser radiation. The UCNPs were surface modified with silanization and amine terminals decoration. Subsequently, via a carbodiimide coupling

reaction, UCNPs were grafted with bifunctionalized C₆₀ derivative, as the photosensitizer. Then the C₆₀ coated UCNPs were further conjugated with chemotherapy model drug Doxorubicin (Dox), through a covalent oxalyl linkage. Notably, under NIR laser irradiation, singlet oxygen was effectively generated from an upconverting photodynamic combination of UCNPs and C₆₀. And Dox got a controlled release from cleavage of the peroxide sensitive oxalyl bridge. The drug release and therapeutic efficacy were investigated in vitro on breast cancer cell lines MCF-7 and MDA-MB-231 by various microscopic and biochemical studies under a significantly mild NIR irradiation and low dosage of the treatment. The combination of controlled release for localized chemotherapy with simultaneous photodynamic treatment has great potential for clinical photo cancer therapy.

5:55 PM SM04.04.04

Polymeric Microcapsules Designed for On-Demand Local Heating and Drug Release in Synergistic Chemo-Photothermal Therapy Ji-Won Kim, Sang Hoon Han and Shin-Hyun Kim; Korea Advanced Institute of Science and Technology (KAIST), Korea (the Republic of)

Photothermal therapy is promising for cancer treatment as it is noninvasive and localized. The way to treat tumors is elevating the temperature through conversion of radiation energy to heat under near-infrared (NIR) light. To further enhance the therapeutic effect of cancer treatment, anti-cancer drugs are released to the photothermally-heated tumors. The chemo-photothermal therapy can synergistically enhance the efficacy of tumor treatment. For the chemo-photothermal therapy, it is required to design drug carriers that provide photothermal heating and on-demand release of drugs. At the same time, the carriers should have high payload and high efficiency of encapsulation for the drugs. However, there have been few reports on such an advanced carrier for the synergistic chemo-photothermal therapy.

Herein, we report a pragmatic microfluidic approach to produce monodisperse microcapsules for chemo-photothermal therapy. The microcapsules contain highly concentrated polydopamine (PDA) nanoparticles and drugs in their aqueous lumens, enclosed by thermo-responsive membrane. The microcapsules are templated by water-in-oil-in-water (W/O/W) double-emulsion droplets. With a glass capillary microfluidic device, monodisperse double-emulsion droplets are produced to have the innermost water drops containing PDA nanoparticles and drug and the outer oil drops of photocurable monomer, phase-change materials (PCM), and molecular compatibilizer. As a continuous phase, an aqueous solution of high concentration of salt and surfactant is used to make a hypertonic condition. The double-emulsion drops shrink downstream as water in the innermost drops is pumped out through the oil shell by the osmotic-pressure difference, which concentrates the PDA nanoparticles and drugs during the flow. The resulting droplets are irradiated by ultraviolet (UV), which photopolymerizes the monomer in the oil shell. In the presence of a molecular compatibilizer between the monomer and PCM, the polymerization does not cause any macrophase separation, resulting in a composite membrane with continuous microscopic PCM domains. The polymer framework in the membrane provides mechanical stability, whereas PCM domains provide channels for transmembrane transport at the temperature above a melting point for molecules dissolvable in the molten PCM. To use the microcapsules for in-vivo drug release, tetradecanol with melting point of 38°C is chosen as a PCM so that the microcapsules retain drugs at body temperature while secreting them when temperature is elevated; many anti-cancer drugs are dissolvable in organic solvents as they are not highly polar.

The microcapsules show a rapid temperature increase under the irradiation of 808 nm laser as highly-concentrated PDA nanoparticles in the lumen provide a high photothermal conversion efficiency. Therefore, the PCM in the membrane is molten under the laser irradiation and the drugs in the lumen is gradually released out. As the heating is highly localized, the microcapsules are cooled down as the laser is off, holding up the release. Therefore, the release as well as local temperature can be controlled in a programmed manner by controlling the duration and interval of stepwise irradiation. With the microcapsules, we successfully treat breast cancers using animal models through chemo-photothermal therapy where palbociclib is used as an anti-cancer drug. The combination of drug and local heating shows higher efficacy of the treatment than the photothermal therapy or chemotherapy used only. We believe the resultant microcapsules with synergistic chemo-photothermal effect are highly attractive in use of advanced chemo-photothermal therapy.

6:10 PM *SM04.04.05

Cancer Immunotherapy Using Nanomaterial-Based Delivery Systems of Oncolytic Adenovirus Chae-Ok Yun; Hanyang University, Korea (the Republic of)

Intratumoral injection of adenovirus (Ad) into diseased tissues remains a conventional route for viral gene delivery. Nonetheless, locally administered virus often disseminates to the surrounding nontarget tissues from the injection site, leading to poor localization and retainment of the virus in tumor tissues. Rapid induction of antiviral immune response against Ad also contributes to poor longevity of virus at tumor site. To address these limitations, diverse array of nanomaterial-based delivery systems for oncolytic Ad have been investigated to improve intratumoral retainment and accumulation of virus at tumor tissues, while attenuating nonspecific sequestration into healthy organs. Importantly, nanomaterial coating on the surface of viral capsid can facily endow novel properties to the resulting nanohybrid complex, which cannot be achieved through genetic engineering of the virus genome. For instance, masking of viral capsid with nanomaterials can endow “stealth” ability to the virus, enabling it to evade the detection by host immune system and subsequently attenuate antiviral immune response against Ad, ultimately prolonging virus’ biological activity at tumor tissues. Importantly, optimization of nanohybrid system can ensure that oncolytic Ad’s ability to induce robust antitumor immune response can be preserved while selectively attenuating induction antiviral immune response, thus resulting in improved potency and safety profile. Another advantage of nanohybrid system is that diverse array of cancer targeting moieties, like antibodies and peptides, can be easily incorporated on the surface to redirect the virus tropism to wide range of tumors expressing complementary receptors. Sustained or controlled release of the virus at tumor sites can also be achieved by nanomaterial-based delivery system to improve and prolong virus retention at tumor sites. Collectively, nanomaterial-based delivery systems for oncolytic adenovirus is a promising strategy to overcome many of the clinical hurdles to achieving optimal virus delivery to tumor tissues.

6:35 PM *SM04.04.01

Modulating the Immune System with Nanostructured Biomaterials Tejal Desai; University of California, San Francisco, United States

Biomaterials can improve the safety and presentation of therapeutic agents for effective immunotherapy, and a high level of control over surface functionalization is essential for immune cell modulation. Here, I will discuss biocompatible immune cell engaging particles that use synthetic short DNA as scaffolds for efficient and tunable protein loading. The use of DNA scaffolds allows for ratiometric control and high-density biomolecular loading. Moreover, intratumorally injected immune cell engaging particles presenting a high density of priming antigens activated CAR-T cells drove local tumor clearance while sparing uninjected tumors in immunodeficient mice. The ratiometric control of costimulatory ligands and the surface presentation of a cytokine on immune cell engaging particles were shown to significantly impact human primary T cell activation phenotypes. I will also discuss ways to use nanostructured biomaterials to selectively capture endogenous cytokines in order to preferentially engage specific immune cells. These modular and versatile biomaterial platforms can provide new opportunities for immunotherapies.

7:00 PM PANEL DISCUSSION

SESSION SM04.05: Advances in Nanomedicine
Session Chairs: Wenguang Liu and Youqing Shen
Tuesday Afternoon, April 20, 2021
SM04

9:00 PM *SM04.05.01

Biomolecule-Based Nanostructures for Tumor Microenvironment Targeting and Regulation Guangjun

Nie; National Center for Nanoscience and Technology, China

It has witnessed that the rapid development on precision design and fabrication of intelligent next generation nanomedicines hold great potential to revolutionize the current landscape of drug development. It is also clear that tumor microenvironment plays critical roles on either promotion or restriction on primary tumor rapid growth and metastasis. Those achievements have made targeting and regulation of tumor microenvironment via responsive nanomedicines a feasible and fruitful strategy, to improve the therapeutic outcomes for cancer treatment. This presentation will feature our recent development on using biomolecule-based nanostructures as intelligent nanomedicines to regulate tumor microenvironment to block tumor microvessels or re-store the homeostasis of tumor stroma. Robotic molecular systems have great potential as intelligent vehicles to enable the delivery of various potent molecules, which otherwise never could be used as therapeutics due to numerous limitations. Yet, achieving in vivo, precise molecular-level, and on-demand targeting and delivery has proven extremely challenging. We developed nanorobotic systems for targeted cancer therapy, programmed to transport molecular payloads and cause on-site tumor infarction. Given the robust self-assembly behavior, exceptional designability, potent antitumor activity and minimal in vivo adversity, the development represents a promising strategy for precise drug design for cancer therapeutics.

References

- Yinlong Zhang, Xuexiang Han, Guangjun Nie*, Responsive and activable nanomedicines for remodeling the tumor microenvironment, *Nature Protocols*, in press
- Shaoli Liu, Qiao Jiang, Zhao X, Zhao R, Wang Y, Wang Y, Liu J, Shang Y, Zhao S, Wu T, Zhang Y, Guangjun Nie, Baoquan Ding*, A DNA nanodevice-based vaccine for cancer immunotherapy, *Nature Materials*. 2020 Sep 7. doi: 10.1038/s41563-020-0793-6.
- Suping Li, Yinlong Zhang, et al, Guangjun Nie, Combination of tumour-infarction therapy and chemotherapy via the co-delivery of doxorubicin and thrombin encapsulated in tumour-targeted nanoparticles. *Nature Biomedical Engineering*, 2020 Jun 22. doi: 10.1038/s41551-020-0573-2.
- Xin Zeng, Jie Sun, Suping Li, Jiyun Shi, Han Gao, Wei Sun Leong, Yiqi Wu, Minghui Li, Chengxin Liu, Ping Li, Jing Kong, Yi-Zhou Wu, Guangjun Nie, Yuming Fu & Gen Zhang, Blood-triggered generation of platinum nanoparticle functions as an anti-cancer agent, *Nature Communications*, 2020, 11, 567.
- Xuexiang Han, Yiye Li*, Xiao Zhao, Yinlong Zhang, Xiao Yang, Yongwei Wang, Ying Xu, Ruifang Zhao, Gregory J. Anderson, Yuliang Zhao*, Guangjun Nie*, Reversal of pancreatic desmoplasia by re-educating stellate cells with a tumour microenvironment-activated nanosystem, *Nature Communications*, 2018, 9, 3390.
- Suping Li, Qiao Jiang, Shaoli Liu, Yinlong Zhang, Yanhua Tian, Chen Song, Jing Wang, Yiguo Zou, Gregory J Anderson, Jing-Yan Han, Yung Chang, Yan Liu, Chen Zhang, Liang Chen, Guangbiao Zhou, Guangjun Nie*, Hao Yan*, Baoquan Ding*, Yuliang Zhao*, A DNA nanorobot functions as a cancer therapeutic in response to a molecular trigger in vivo, *Nature Biotechnology*, 2018, 36, 258-264.
- Suping Li, Yinlong Zhang, Jing Wang, Ying Zhao, Tianjiao Ji, Xiao Zhao, Yanping Ding, Xiaozheng Zhao, Ruifang Zhao, Feng Li, Xiao Yang, Shaoli Liu, Zhaoifei Liu, Jianhao Lai, Andrew K. Whittaker, Gregory J Anderson, Jingyan Wei, Guangjun Nie*, Nanoparticle-mediated local depletion of tumour associated platelets disrupts vascular barriers and augments drug accumulation in tumours, *Nature Biomedical Engineering*, 2017,1, 667–679.

9:25 PM *SM04.05.02

Engineering Nano-Based Neurotherapeutics for Pediatric Brain Disease Elizabeth Nance; University of Washington, United States

Of the clinically approved nanotechnologies in 2019, none are indicated for non-cancerous neurological disease, which represents 13% of the global disease burden. Therefore, our lab has worked to develop tools that inform how we can more effectively treat the diseased brain, using nanotechnology as both a probe and as a therapeutic delivery vehicle. When delivery limitations of a nanoparticle platform are better understood, an optimal formulation can be engineered and evaluated for therapeutic efficacy in clinically relevant animal models of brain disease. We focus on developing nanoparticle-based therapeutic approaches for improved neurological

outcomes in perinatal brain injury. We use therapeutic nanoparticle platforms that are polymer-based, incorporate materials that are FDA approved, and have been utilized extensively in adult populations but have not been used in children or newborns. We identify drugs that can affect multiple pathways and have a solubility and/or delivery problem - that is, the drug is either not soluble in aqueous solutions or it is not able to reach its target site in high enough concentrations to be effective. We use a range of *in vitro*, *ex vivo*, and *in vivo* models to screen and evaluate efficacy of nanotherapeutic platforms. Our *ex vivo* cultures include stimuli that replicate aspects of *in vivo* injury conditions, such as oxygen-glucose deprivation, glutamate toxicity, or exposure to lipopolysaccharide. *In vitro* and *ex vivo*, we test for toxicity and dose response; *ex vivo*, we evaluate regionally dependent cellular uptake and downstream mechanistic effects of the nanotherapeutic platform; *in vivo*, we quantify biodistribution and measure improvements in gross injury and neuropathology in response to treatment. We have shown curcumin-loaded polymer nanoparticles could reduce brain injury via gross injury analysis and neuropathology in neonatal rats with hypoxic-ischemic (HI) brain injury. We expanded on this work to show that superoxide dismutase can be an effective treatment against HI injury in cultured rat brain slices, and screened promising preclinical therapeutics in a ferret brain slice model of HI injury. Importantly, we've furthered our targeting capabilities by showing how the (1) disease severity alters nanoparticle-cellular interactions, (2) formulation conditions can impart pathology-specific toxicity, and (3) surfactant used to stabilize polymer formulations can direct site-specific cell-specific uptake in the neonatal brain. In this talk, we demonstrate the importance of using multiple platforms to evaluate nanotherapeutic behavior in the brain, and the impact formulation methods can have on polymeric nanoparticle effect and fate in the brain. Further, we show that we can engineer more effective nanotherapeutics for the treatment of neurological disease with a specific emphasis on the neonatal and pediatric populations, which are vastly underserved by technology development.

9:50 PM SM04.05.04

Polymeric Micelles for Delivery of Gasotransmitter Hydrogen Sulfide with Proangiogenic Activity Urara Hasegawa and Andre J. van der Vlies; The Pennsylvania State University, United States

Hydrogen sulfide (H₂S), a gaseous signal-transmitter molecule (gasotransmitter), has pivotal roles in the human body by regulating physiological and pathological processes such as angiogenesis, inflammation and neurotransmission. With the discovery of the biological significance of H₂S, the potential for H₂S-based therapies has attracted growing attention. However, the lack of H₂S delivery systems that enable controlled release of H₂S at the site of interest limits its biomedical applications. One common approach is to use H₂S donor compounds, such as anethole dithiolethione (ADT) derivatives, which generate H₂S under physiological conditions. However, the uncontrolled rate of H₂S release and toxic side effects of the donor compounds and/or their decomposition byproducts remain as the major problems associated with the use of small H₂S donor compounds. To address this issue, we developed polymeric micelles carrying H₂S-donating ADT groups (H₂S donor micelles), which release H₂S in a sustained manner under physiological conditions. Here, we report design, synthesis and characterization of polymeric H₂S donor micelles. The proangiogenic activities of these micelles were also evaluated in the *in vitro* cell culture assays as well as the *in ovo* chick chorioallantoic membrane (CAM) assay.

10:05 PM *SM04.05.05

Theragnosis Inspired by Real-Time Molecular Imaging Ick Chan Kwon; Harvard Medical School, United States

Molecular imaging is recognized as a key technology for theragnosis which is known as an emerging paradigm for future personalized medicine. Peptide which have been used as a useful carrier for drug delivery system could also be served as an excellent tool for molecular imaging. Approaches to combine these two important functionalities all together in a peptide conjugate are proposed in this presentation. Recent advances in biotechnology have contributed to the development of various peptide conjugates that enable targeted delivery of imaging agents as well as therapeutic agents for biomedical applications. Compared to small molecules (e.g., imaging agents and therapeutic agents), peptide conjugates possess unique characteristics such as high target-

specificity and multi-functionality. As a result, peptide conjugates hold great potential in the future biomedical field such as molecular imaging, diagnostics, and the drug delivery system. Moreover, combination of both imaging agents and therapeutic agents within a single peptide conjugates, often referred to as theragnostics, make it possible to provide useful information in drug developments. Theragnostic peptide conjugates allow in vivo real-time imaging of the diseased site, monitoring the biodistribution of drug and determining the optimal therapeutic efficacy following treatments. These features can allow clinicians to select optimal therapeutic options for personalized medicine. In recent studies, we developed epidermal growth factor receptor (EGFR) and CD 47 receptor-specific self-quenched imaging probes, which can emit fluorescence (activate) via de-quenching reaction in lysosome, resulting in showing target-specific fluorescence signal in vitro as well as in vivo condition. This presentation will highlight our recent advances that have been made in the development of multifunctional peptide conjugates and the applications into theragnosis.

10:30 PM PANEL DISCUSSION

SESSION SM04.06: Gene Delivery I
Session Chairs: Youqing Shen and Yoon Yeo
Wednesday Morning, April 21, 2021
SM04

8:00 AM *SM04.06.01

The Direction of Nucleic Acid Drug Delivery—From RNA Interference to Genome Editing Jun Wang^{1,2,2}; ¹South China University of Technology, Guangzhou International Campus, China; ²South China University of Technology, China

Nucleic acids have paved new avenues for the development of therapeutic interventions against a spectrum of diseases; however, their clinical translation is limited by successful delivery to the target cells. To solve this problem, we fabricated cationic lipid-assisted nanoparticle (CLAN) by double emulsion method. In our initial design, the CLAN system was constructed using PEG-*b*-PLA and BHEM-Chol, which achieved >95% encapsulation efficiency of siRNA. Using CLAN, we and collaborators delivered siRNA, CpG and other nucleic acids for cancer and HBV treatment. To further improve its therapeutic efficacy, we synthesized a tumor pH-labile linkage-bridged block copolymer of poly(ethylene glycol) with poly(lacide-*co*-glycolide) (PEG-*Dlink*_m-PLGA) to prepare DCLAN_{PLGA} for siRNA delivery. The PEG surface layer of DCLAN_{PLGA} can be detached in response to the tumor acidic microenvironment to facilitate cellular uptake, and the siRNA was rapidly released within tumor cells due to the hydrophobic PLGA layer. Thus, PEG-*Dlink*_m-PLGA-based CLANs exhibited an enhanced siRNA delivery efficacy. Most recently, to rationally design the delivery system of CRISPR-Cas9 genome editing tools, we constructed a library of CLANs with different properties (e.g. surface PEG density, zeta potentials, cationic lipid types) by adjusting the weight and types of the cationic lipid and incorporating the homopolymer PLGA. After systemic administration, the uptake of these CLANs by different immune cells was evaluated, and the optimal CLANs were screened. Using this strategy, we efficiently delivered CRISPR-Cas9 into macrophages, neutrophils, B cells and dendritic cells for treating inflammatory diseases, type II diabetes, autoimmune diseases *et al.*. In summary, our CLAN is an effective platform for developing the delivery systems of siRNA, CRISPR-Cas9 and other nucleic acids.

8:25 AM *SM04.06.02

Polyplexes for Local Delivery of siRNA. Tina Vermonden, Lies Fliervoet and Cristina Casadidio; Utrecht University, Netherlands

Purpose. Polymeric vectors have been extensively studied to function as gene delivery systems, but their widespread applications have been restricted by inefficient *in vivo* delivery of therapeutic nucleic acids. In our

studies, we investigate local and sustained delivery of nucleic acids making use of a polyplex-containing injectable hydrogel.

Methods. Complexes are formed between nucleic acids and cationic poly(2-dimethylaminoethyl methacrylate) (PDMAEMA)-based polymers (referred to as polyplexes), followed by the encapsulation of the polyplexes in a thermosensitive hydrogel. The designed triblock copolymer (PNIPAM-PEG-PDMAEMA, NPD) used for polyplex formation combines multiple functionalities, including cationic properties, needed for complexation with nucleic acids, and thermosensitive properties to anchor the polyplexes in the thermosensitive hydrogel. The physico-chemical properties of siRNA complexed to the multiresponsive polymer were evaluated and compared with polyplexes made with a non-thermosensitive polymer (PEG-PDMAEMA, PD) in 2D and 3D multicellular tumor spheroid models (MCTS).

Results. We found that stable polyplexes could be formed at physiological temperature by tuning the block lengths of the NPD polymers and the N/P ratio, reflecting the ratio between cationic nitrogen of the polymer and anionic phosphate groups in the nucleic acids, respectively. Upon encapsulation of siRNA polyplexes in the thermosensitive hydrogel, a sustained release profile was observed *in vitro* and thorough characterization of the released particles showed that they are stable, have the same size as before encapsulation and retain similar transfection activity. Penetration and diffusion of free siRNA polyplexes were monitored via live-cell imaging into MCTS, reaching the core of spheroids after 24 hours of incubation. A pilot *in vivo* study showed that fluorescently labeled polyplexes could be released locally for at least 7 days after injection intraperitoneally and subcutaneously.

Conclusions. Injectable hydrogels can enhance the local concentrations of delivered nanoparticles. We showed successful encapsulation of siRNA based polyplexes and sustained release from an injectable matrix both *in vitro* and *in vivo*. Moreover, *in situ* released polyplexes proved to easily penetrate hard tissue models. These formulations showed to extend the residence time of siRNA therapeutics and thereby have great potential for local therapeutic delivery.

Acknowledgment.

The Netherlands Organization for Scientific Research (NWO/VIDI 13457 and NWO/Aspasia 015.009.038) is acknowledged for funding.

8:50 AM SM04.06.03

Nucleic Acid Co-Delivery—How to Modulate Protein Co-Expression by Formulation of Payload Hanieh Moradian^{1,2,3}, Andreas Lendlein^{1,2,3} and Manfred Gossen^{1,2}; ¹Helmholtz-Zentrum Geesthacht, Germany; ²Berlin-Brandenburg Center for Regenerative Therapies (BCRT), Germany; ³University of Potsdam, Germany

Co-delivery of two genes into individual cells by means of polymeric or lipid nanocarriers is of utmost importance in many experimental settings, addressing either fundamental scientific questions or therapeutic applications. Examples are the expression of heterodimeric proteins such as antibodies or the co-introduction of an imaging marker. For widely used DNA-based gene transfer, multiple transcription units can be easily integrated on one molecule, e.g., plasmids. This strategy is not feasible for mRNA delivery. Here, co-delivery has to be achieved by mixing independent functional units or shifting the separation of functional entities to the level of proteins. In this study, we investigated multiple approaches to achieve simultaneous expression of two proteins at the same cells with a focus on formulation of nucleic acid (NA) payload, here mRNA as well as pDNA. The first strategy relies on the delivery of the genetic information via two independent “monocistronic” NAs, whereas in the second approach, this information is combined in a single NA molecule, referred here as “bicistronic”. The latter results in expression of two proteins from a single open reading frame and its co-translational separation by so called “2A” sequences. Two reporter proteins, enhanced green fluorescent protein (EGFP) and mCherry, as well as EGFP together with another non-fluorescent protein were utilized to evaluate these alternative methods, an advantageous feature of using NA as delivery entity. The data revealed that there was negligible differences between monocistronic and bicistronic delivery of genes of the same size, i.e. EGFP

and mCherry. However, a significant difference between cells transfected with two genes with different molecular size was observed, in terms of cell population expressing both proteins, i.e. double positive cells. More precisely quantified by flow cytometry, $36.76 \pm 2.03\%$ of cells were double positive for bicistronic method versus $90.43 \pm 1.27\%$ double positive cells, which was recorded for cells co-transfected with two monocistronic NAs. Our findings could be served as guideline for selecting the best-suited approach by choosing payload properties that can be complemented by adapting the formulation, e.g., polymer- or lipid-based, to the intended application.

9:05 AM SM04.06.04

Antibacterial Activities of Cationic Porphyrins and Gold Nanorod Encapsulated Porphyrins and Their Activities on Bacterial Cell Lines Nthabeleng Hlapisi; University of Zululand, South Africa

Bacterial infections form part of the major causes of mortality and mobility around the world more especially in developing and under-developed countries. This study is based on the synthesis of two cationic porphyrins, 5,10,15,20-tetra-kis(4-aminophenyl)porphyrin (TAP) and 5,10,15,20-tetra-kis(4-pyridyl)porphyrin (TPyP) that are evaluated against bacterial strains by the micro-well assay and the micro-dilution method. Gold nanorods were encapsulated with each of these porphyrins and dissolved in DMSO. At 50mg/ml, the porphyrin-AuNRs produced zones of inhibition of 10-12mm against *S. aurea* (ATCC 25925), *E. Faecalis* and *K. pneumonia* (ATCC 4352). The minimum inhibitory concentration (MIC) values that were obtained using the micro-dilution method were, 0.78, 1.5 and 2.6mg/ml for *S. aurea* (ATCC 25925), *E. Faecalis* and *K. pneumonia* (ATCC 4352) respectively for all bacterial strains using TPyP@AuNRs, and 1.8, 0.42 and 0.76 mg/ml for *S. aurea* (ATCC 25925), *E. Faecalis* and *K. pneumonia* (ATCC 4352) respectively using TAP@AuNRs. The results show the porphyrin-AuNR conjugates to have a potential as anti-bacterial agents.

9:20 AM *SM04.06.05

PNAGA-based Hydrogels for Diverse Biomedical Applications Chunyan Cui, Chuanchuan Fan and Wenguang Liu; Tianjin University, China

It has been fifty-four years since N-acryloyl glycinamide (NAGA) monomer and its polymer (PNAGA) were reported in 1964. It is characterized by two amides in its side chain. The concentrated aqueous solution of PNAGA has been shown to form supramolecular polymer (SP) hydrogels which are physically crosslinked by dual-amide hydrogen bonds, and the SP hydrogels' mechanical properties can be tuned by varying initial monomer concentration, substitution groups as well as feature monomer copolymerization. Recently, our group has reported on high strength and soft PNAGA SP hydrogels by modulating hydrogen bonding density, and these SP hydrogels are developed as 3D printing bioinks for regeneration of osteochondral defect, an autolytic high strength instant adhesive hydrogel for emergency self-rescue, and a Janus hydrogel wet adhesive for internal tissue repair and anti-postoperative adhesion. The Janus hydrogel wet adhesive with strikingly distinct adhesive/nonadhesive properties on its two sides is fabricated by gradient polyelectrolyte complexation via one-sided dipping of carboxyl-containing hydrogel in cationic oligosaccharide solution. This Janus hydrogel demonstrates an instantly robust adhesion to soft tissues under water, and is successfully used for repairing perforated stomach of rabbits, meanwhile preventing post-operative tissue adhesion in vivo.

9:45 AM PANEL DISCUSSION

SESSION SM04.07: Gene Delivery II

Session Chair: Yosi Shamay

Wednesday Morning, April 21, 2021

SM04

11:45 AM *SM04.07.01

RNA Therapeutics Using Targeted Lipid Nanoparticles—From Gene Silencing to Gene Editing Dan Peer;
Tel Aviv University, Israel

Accumulating work points out relevant genes and signaling pathways hampered in human disorders as potential candidates for therapeutics. Developing nucleic acid-based tools to manipulate gene expression, such as siRNAs, mRNA and genome editing strategies, open up opportunities for personalized medicine. Yet, although major progress was achieved in developing RNA targeted delivery carriers, mainly by utilizing monoclonal antibodies (mAbs) for targeting, their clinical translation has not occurred. In part because of massive development and production requirements and high batch-to-batch variability of current technologies, which relies on chemical conjugation. Here we present a self-assembled modular platform that enables to construct theoretically unlimited repertoire of RNA targeted carriers. The platform self-assembly is based on a membrane-anchored lipoprotein, incorporated into RNA-loaded lipid nanoparticles that interact with the antibody Fc domain. We show that a simple switch of 8 different mAbs, redirects specific uptake of siRNAs by diverse leukocyte subsets *in vivo*. The platform therapeutic potential is demonstrated in an inflammatory bowel disease model, by targeting colon macrophages to reduce inflammatory symptoms, and in Mantle Cell Lymphoma xenograft model, by targeting cancer cells to induce cell death and improve survival. In addition, I will discuss novel approach for delivering mRNA to specific cell types *in vivo* utilizing this platform. Finally, I will share new data showing high efficiency genome editing approaches in glioma and metastatic ovarian cancer. This modular delivery platform can serve as a milestone in turning precision medicine feasible.

12:10 PM *SM04.07.02

RNA Delivery Manfred Gossen; Helmholtz-Zentrum Geesthacht, Germany

The cellular uptake of engineered RNA, both as research tool or for (envisaged) therapeutic application came in the focus of nanomedicine by studies using short interfering RNAs (siRNA). While chemical modifications of the active ingredient siRNA proved important for efficacy of *in vitro* delivery, the major technological hurdles for *in vivo* delivery were targeting the RNA-containing nanoparticles to the right location and their *in vivo* delivery and survival. These bottlenecks have to be addressed by application-tailored formulations, mostly based on lipids or polymers. Part of the lessons learned can be applied for the more recent emergence of *in vitro* transcribed messenger RNAs (IVT-mRNA) for either vaccination or therapeutic gain-of-function approaches. Part of this spike in interest results from the safety profile (and record) of IVT-mRNA, due to its distinct chemical identity when compared to other “gene medicines”: mRNA only interferes transiently with the homeostasis of a cell’s transcriptome and does not effect the integrity of a cell’s genome composed of DNA, as has been shown for, e.g., viral delivery. Still, aside from the already mentioned hurdles in targeting and *in vivo* uptake, effective delivery of mRNAs requires further research in immune evasion strategies, as transfected mRNAs – among other reasons – are mistaken as viral invaders and tackled accordingly. I report on the proper use of chemically modified nucleotides as IVT-mRNA building blocks, and cell-based *in vitro* readout systems to monitor and ultimately modulate the innate immune response in the context of different formulations for delivery.

References:

Dammes N & Peer D (2020) Paving the Road for RNA Therapeutics, *Trends in Pharmacological Sciences*, 41:755

Moradian H, Roch T, Lendlein A & Gossen M (2020) mRNA Transfection-Induced Activation of Primary Human Monocytes and Macrophages: Dependence on Carrier System and Nucleotide Modification, *Scientific Reports* 10:4181

Moradian H, Lendlein A & Gossen M (2020) Strategies for Simultaneous and Successive Delivery of RNA,

12:35 PM SM04.07.03

Late News: Effect of Nucleotide Chemistry on Expression of *In Vitro* Transcribed mRNA Hanieh Moradian^{1,2,3}, Andreas Lendlein^{1,2,3} and Manfred Gossen^{1,2}; ¹Helmholtz-Zentrum Geesthacht, Institute of Active Polymers, Germany; ²Berlin-Brandenburg Center for Regenerative Therapies (BCRT), Germany; ³Institute of Biochemistry and Biology, University of Potsdam, Germany

Recent technological advances in the production of *in vitro* transcribed mRNA (IVT-mRNA) facilitate its clinical use as well as application in basic research. In this regards, numerous chemical modifications, which are not observed in nature, have been introduced and successfully implemented to increase its stability, biological performance, and in particular the resulting protein production levels. Despite pronounced differences in expression levels of chemically modified IVT-mRNA as observed between different modifications, it is unclear whether these differences are exclusively due to translation capacity of chemically modified mRNAs, or if it is also caused by, e.g. differences in complex formation efficiency of modified mRNAs or in different uptake rates of IVT-mRNA/carrier complexes. Here a co-transfection experiment was designed using IVT-mRNA coding either of the two different fluorescent protein markers, i.e. EGFP and mCherry, which were synthesized with 5-methoxy-uridine (5moU) or a combination of pseudouridine and 5-methyl-cytidine (Ψ /5meC) modifications, respectively – and vice versa. We found that 5moU modified IVT-mRNA resulted in a much higher transgene expression, when transfected in human macrophages. This analysis was completed by biochemical experiments clarifying the contribution of other steps identified as possible causes for the observed differences in apparent expression levels. We predict that our findings shed light on the applicability of different mRNA modifications, and benefit future research by helping to select the proper chemical composition to accomplish their experimental/scientific requirements.

12:50 PM SM04.07.04

Competitive Binding and Molecular Crowding Regulate the Cytoplasmic Interactome of Non-Viral Polymeric Gene Delivery Vectors Alex Raynold, Danyang Li, Fengjin Qu and Julien Gautrot; Queen Mary, University of London, United Kingdom

Although polycationic vectors display excellent performance *in vitro* with many cellular systems, their clinical use remains very restricted. To some level, this is due to the poor compatibility of such systems with biological fluids and tissues. In addition, in contrast to the processes controlling the complexation, targeting and uptake of polycationic gene delivery vectors, such as poly(ethylene imine) and poly(dimethylaminoethyl methacrylate), the detailed molecular mechanisms regulating their cytoplasmic dissociation remains poorly understood. Upon cytosolic entry, gene delivery vectors become exposed to a complex, concentrated mixture of molecules and biomacromolecules. To explore cytosolic release mechanisms, we characterised the cytoplasmic interactome associated with a polycationic vector based on poly(dimethylaminoethyl methacrylate) (PDMAEMA) brushes grafted from nanoparticles. Such cationic brushes were found to be particularly effective at trapping small RNAs, resulting in high knock down efficiencies¹⁻³. However, how such stable association is disrupted in the cytosol was not clear. To quantify the contribution of different classes of low molar mass molecules and biomacromolecules to RNA release, we used fluorescence microscopy and developed a kinetic model based on competitive binding. We propose that the molecular structure and architecture (in particular the high surface density) of cationic brush-decorated nanoparticles, together with the cytosolic molecular crowding, modulate competitive binding and, in turn, the long term release of RNA. Based on these observations, we chemically designed polymer brushes with improved RNA retention in the cytosol, avoiding burst release, and enabling to achieve long term (at least 10 days) knock down (>70%) with one single transfection. Understanding the mechanism regulating cytosolic dissociation will enable the improved design of cationic vectors for long term gene release and therapeutic efficacy.

ACKNOWLEDGEMENTS

Funding from the ERC (ProLiCell, 772462) is gratefully acknowledged.

REFERENCES

- (1) Li, D.; Sharili, A. S.; Connelly, J.; Gautrot, J. E. Highly stable RNA capture by dense cationic polymer brushes for the design of cytocompatible, serum-stable siRNA delivery vectors. *Biomacromolecules* **2018**, *19* (2), 606.
- (2) Li, D.; Wu, L.; Qu, F.; Ribadeneyra, M. C.; Tu, G.; Gautrot, J. Core-independent approach for polymer brush-functionalised nanomaterials with a fluorescent tag for RNA delivery. *Chemical Communications* **2019**, *55* (94), 14166.
- (3) Qu, F.; Li, D.; Ma, X.; Chen, F.; Gautrot, J. E. A kinetic model of oligonucleotide-brush interactions for the rational design of gene delivery vectors. *Biomacromolecules* **2019**, *20*, 2218.

1:05 PM SM04.07.05

Cell Nucleus Decoration with Oxidized Nano-Graphene—A New Opportunity in Drug Delivery Martina Mugnano¹, Giuseppe Cesare Lama², Rachele Castaldo², Francesco Merola¹, Gennaro Gentile², Veronica Ambrogi³, Piero Cerruti², Pasquale Memmolo¹, Vito Pagliarulo¹, Pietro Ferraro¹ and Simonetta Grilli¹;
¹Institute of Applied Science & Intelligent Systems ‘E. Caianiello’, National Council of Research of Italy (ISASI-CNR), Italy; ²Institute for Polymers, Composites and Biomaterials, National Council of Research of Italy (IPCB-CNR), Italy; ³University of Naples Federico II, Italy

The perspective of using graphene and its derivatives in bionanotechnology opens innovative and fascinating scenarios in the future of biomedicine for drug delivery, DNA sensing, protein assays, tissue engineering and cell imaging studies. For these purposes, there is an increasing interest in shedding light on the interaction mechanisms of graphene oxide (GO) live matter. In fact, the effects on human health of GO, and on cytotoxicity, are still largely unknown. Here we show that, by minimizing the oxidation degree of GO, its toxicity is significantly reduced in mouse fibroblasts. We discover a peculiar internalization of the oxidised nano graphene (nGO) leading to an intriguing nucleus decoration (ND) that could open the route to new opportunities in drug delivery. We demonstrate that it is possible to quantitatively assess the cell morphology during decoration process with nGO by a time-lapse monitoring in phase-contrast digital holography configuration. This study could open the route for further investigations on the use of label-free and quantitative imaging for characterizing the effect of graphene-based nanomaterials and their interactions with biological systems.

References

- [1] Mugnano, M., Lama, G.C., Castaldo, R., Marchesano, V., Merola, F., del Giudice, D., Calabuig, A., Gentile, G., Ambrogi, V., Cerruti, P. and Memmolo, P., 2019. Cellular Uptake of Mildly Oxidized Nanographene for Drug-Delivery Applications. *ACS Applied Nano Materials*, *3*(1), pp.428-439.
- [2] Castaldo, R.; Lama, G. C.; Aprea, P.; Gentile, G.; Lavorgna, M.; Ambrogi, V.; Cerruti, P. Effect of the Oxidation Degree on SelfAssembly, Adsorption and Barrier Properties of Nano-Graphene. *Microporous Mesoporous Mater.* 2018, *260*, 102–115.
- [3] Paturzo, M.; Pagliarulo, V.; Bianco, V.; Memmolo, P.; Miccio, L.; Merola, F.; Ferraro, P. Digital Holography, a Metrological Tool for Quantitative Analysis: Trends and Future Applications. *Optics and Lasers in Engineering* 2018, *104*, 32–47.
- [4] Calabuig, A.; Mugnano, M.; Miccio, L.; Grilli, S.; Ferraro, P. Investigating Fibroblast Cells Under “Safe” and “Injurious” Blue-Light Exposure by Holographic Microscopy. *Journal of biophotonics* 2017, *10*, 919–927.

1:20 PM PANEL DISCUSSION

SESSION SM04.08: Biomaterials and Bioinspired Materials I
Session Chairs: Kim Woodrow and Yoon Yeo
Wednesday Afternoon, April 21, 2021
SM04

2:15 PM *SM04.08.01

Developing Therapeutic Materials to Redirect Cellular Chatter Juliane Nguyen; University of North Carolina at Chapel Hill, United States

An increasing number of studies report that exosomes play critical roles in intercellular communication. While exosomes are essential to maintain physiological conditions, aberrant exosomal communication can lead to the development of cancer, diabetes, and many other diseases. Here we will describe new materials to redirect and modulate cellular communication mediated by exosomes for therapeutic applications. Specifically, we have identified RNA-based materials to modulate exosomal function by repackaging them with different types of cargoes. This presentation will discuss how beneficial exosomal communication can be enhanced for therapeutic purposes.

2:40 PM *SM04.08.02

Nanoscale Metal-Organic Frameworks for Chemoradiation and Radioluminescent Imaging Megan Neufeld¹, Allison DuRoss¹, Madeleine Landry¹ and Conroy Sun^{1,2}; ¹Oregon State University, United States; ²Oregon Health & Science University, United States

Metal-organic frameworks (MOFs) have emerged as promising functional biomaterials for a wide range of applications in drug delivery and biomedical imaging. In particular, nanoscale MOFs (nMOFs) have drawn significant attention as novel therapeutic agents in oncology both as drug carriers and as stimuli-responsive materials. Here we present our recent findings utilizing nMOFs as a multipronged radiosensitizer for chemoradiation in breast and colorectal cancer models. Through incorporation of high-Z elements, such as Hf, we demonstrated an enhanced physical radiation dose deposition observed through increased production of reactive oxygen species generation and subsequent DNA double strand breaks in X-ray irradiated cells. Coupled with delivery of DNA repair inhibitors, such as talazoparib (PARPi), we found improved control of tumor growth when employing nMOFs with radiation therapy (RT). We further investigated the integration of functional coatings, including fucoidan targeting P-selectin expression, to improve delivery of these nanomaterials during fractionated RT. In addition, we describe here the interaction of X-rays with lanthanide-based nMOFs to serve as energy mediators in deep tissue photodynamic therapy (PDT) or molecular probes in radioluminescence imaging. Detailed physiochemical characterization and in vivo toxicity data will be presented to promote discussion on clinical translation challenges of these novel materials.

3:05 PM SM04.08.03

Late News: 3D Printing of Spatiotemporally Controlled Drug Delivery Dental Device Valentine M. Berger, Zhi Luo and Jean-Christophe Leroux; ETH Zurich, Switzerland

Sustained and localized drug delivery in the oral cavity remains an important challenge in pharmaceutical sciences.¹ Currently, existing self-applied dosage forms such as gels, toothpaste or mouthrinses are rapidly washed away after administration, resulting in modest efficacy and thus require repeated applications. Therefore, oral devices that fit precisely patient's anatomy² with spatiotemporally controlled drug release profiles represent a promising approach to improve drug delivery in the oral cavity. Here, we demonstrate how the 3D printing of drug-polymer composite materials could be utilized to achieve this goal. Thanks to the possibility of printing complex 3D geometries with multiple materials³, the fused deposition modelling (FDM) technique was chosen to fabricate personalized mouthguards that allow local and prolonged elution of drugs. As a model drug compound, sodium fluoride (NaF), a salt commonly used to prevent tooth decay, was combined with a variety of polymer mixtures containing different ratios of poly(ϵ -caprolactone), poly(ethylene glycol) and poly(vinyl alcohol). Composite filaments with tunable hydrophobicity were then produced from the blends of thermoplastics with varying loads of NaF and fed into the FDM printer. The mechanical properties were assessed with standard tensile testing to confirm the suitable toughness and durability of the printed materials. *In vitro* dissolution studies further demonstrated the tunable release kinetics of the devices.

Finally, toothguard models that fit precisely the geometries of human teeth were designed after 3D scanning of the specimens and were then printed in high resolution. To evaluate the therapeutic effects of the devices, the toothguards were used *ex-vivo* on the decayed teeth for 7 days. The lesion was characterized by scanning electron microscopy and the fluoride incorporation was measured by energy-dispersive X-ray spectroscopy. A significant elevation of fluoride contents in the enamel was found in the specimen in contact with the fluoride-loaded devices compared with the one in contact with simple control solutions. In conclusion, the data show that a slow and local drug release of fluoride could improve the buccal delivery of therapeutic compounds.

3:20 PM SM04.08.05

Late News: Dissecting How Cells Internalize and Process Nano-Sized Drug Carriers for Nanomedicine Applications Anna Salvati; University of Groningen, Netherlands

Nano-sized materials have the unique capacity to distribute in organisms and enter cells easily using cellular pathways. This has opened up tremendous opportunity in nanomedicine for the use of nano-sized carriers to deliver drugs more efficiently to their site of action. However, the molecular details of the mechanisms of uptake and intracellular trafficking of nano-sized materials are in most cases still not clear. Such knowledge could allow us to further improve the design of truly targeted nanomedicines.

To this aim, we have combined the use of transport inhibitors and RNA interference with proteomic based methods to identify the cell surface receptor interacting with nano-sized materials and characterize the mechanisms by which they are internalized by cells.^{1,2} Additional efforts have been focused on developing *in vitro* endothelial cell barriers more closely resembling the barriers nanomedicines encounter *in vivo*.³ Uptake and distribution of nanoparticles have also been studied in precision cut tissue slices from the major organs in which nanoparticles distribute, such as the liver, lungs and kidneys, as an advanced *ex vivo* 3D model.^{4,5} Our results show that the same cells process nanoparticles in different ways when they are developed into an endothelial cell barrier rather than at different degrees of cell density, as commonly applied for *in vitro* studies.³ Furthermore we show that liver tissue slices allow to resemble *ex vivo* some of the major outcomes of *in vivo* distribution studies, i.e. the preferential accumulation of nanoparticles by Kupffer cells, the liver macrophages.⁴ Finally, we show that the corona molecules adsorbing on the nanoparticle surface once applied in serum or plasma can be recognized by specific cell receptors, and they can also affect the details of the following uptake mechanism by cells.⁶ Thus, in other words, the same nanoparticles enter cells via different pathways when different coronas are formed on their surface. Using liposomes of different composition, we also show how the composition of the corona forming in serum can be tuned, thus affecting uptake efficiency and uptake kinetics.⁷

References:

¹ Comparison of the uptake mechanisms of zwitterionic and negatively charged liposomes by HeLa cells, D Montizaan, et al, Nanomedicine NBM, 2020, 30, 102300

² Limits and challenges in using transport inhibitors to characterize how nano-sized drug carriers enter cells, V Francia, et al, Nanomedicine 2019, 14 (12), 1533-1549

³ Effect of the development of a cell barrier on nanoparticle uptake in endothelial cells
V Francia, et al, Nanoscale 2018 10 (35), 16645-16656

⁴ Time-Resolved Quantification of Nanoparticle Uptake, Distribution, and Impact in Precision-Cut Liver Slices, R Bartucci, et al, Small, 2020, 1906523

⁵ Comparative study of nanoparticle uptake and impact in murine lung, liver and kidney tissue slices
R Bartucci, et al, Nanotoxicology, 2020, 14 (6), 847-865

⁶ Corona Composition Can Affect the Mechanisms Cells Use to Internalize Nanoparticles
V Francia, et al, ACS nano 2019 13 (10), 11107-11121

⁷ Tuning Liposome Composition to Modulate the Corona Forming in Human Serum and Uptake by Cells, K Yang, et al, Acta Biomaterialia, 2020, 106, 314-327

3:35 PM SM04.08.06

Late News: Controlling Porosity and Protein Release Profile of Nanofibrillar Chitosan Scaffolds

Muhammad Haji Mansor^{1,2}, Jean-Michel Thomassin¹, Alain Colige¹, Emmanuel Garcion², Frank Boury² and Christine Jerome¹; ¹Univ de Liege, Belgium; ²Université d'Angers, France

Chitosan is an abundantly common, naturally occurring, polysaccharide biopolymer. Its biocompatible, biodegradable, and antimicrobial properties have led to significant research toward biological applications such as drug delivery, artificial tissue scaffolds for functional tissue engineering, and wound-healing dressings. For applications such as tissue scaffolding, formation of highly porous mats of nanometer-sized fibers, such as those fabricated via electrospinning demonstrated high potentials.

In this framework, we have as first objective to control better the scaffold porosity by decreasing the fiber density while keeping enough mechanical performances to be handled and implanted. By playing on the design of the collector used for electrospinning, we have developed structured fiber mats that meet both targeted high porosity and mechanical resistance properties.

In a second objective, strategies have been developed allowing proteins encapsulation within the chitosan scaffolds for locoregional release. The electrospinning process has been optimized in order to preserve the protein integrity and its biological activity. Various release profiles of the protein have been achieved from the structured electrospun scaffolds. A sustained release has been obtained by the use of proteins loaded poly(lactic-co-glycolic acid) (PLGA) nanoparticles [1].

The developed electrospinning process allowing both the precise control of the porosity and of the release profile of a protein will be useful for elaborating porosity and concentration gradients which are critical when developing biomimetic scaffolds aiming to control cell migration and trapping.

[1] Haji Mansor M, Najberg M, Contini A, Alvarez-Lorenzo C, Garcion E, Jérôme C & Boury F. Development of a non-toxic and non-denaturing formulation process for encapsulation of SDF-1 α into PLGA/PEG-PLGA nanoparticles to achieve sustained release. *European Journal of Pharmaceutics and Biopharmaceutics*. 2018; 125: 38-50

3:50 PM PANEL DISCUSSION

SESSION SM04.09: Biomaterials and Bioinspired Materials II
Session Chairs: Ciana Lopez and Patrick Stayton
Wednesday Afternoon, April 21, 2021
SM04

5:15 PM *SM04.09.01

Long-Acting Parenteral Products for Global Health—Challenges and Opportunities Dennis Lee^{1,2}; ¹Bill & Melinda Gates Foundation, United States; ²Global Health, United States

Daily drug regimen adherence is a widespread challenge for individuals living in all countries. For those in low and middle income countries (LMICs), there is an added layer of complexity due to a number of systemic factors, including poor access to medications in rural areas in combination with a shortage of healthcare workers and facilities, weak supply chains, and the challenge of “last mile” transportation. The lack of infrastructure in LMICs presents further challenges for product development. Cold chain is sporadic and often absent, and electricity often is not reliable or available. Hence, there is a need for products that provide long-term shelf stability at ambient temperatures. The Gates Foundation has built a broad portfolio of long-acting drug delivery technologies that address these several of these issues and have the potential to increase uptake of essential medicines. These investments span a spectrum of materials science approaches and support a diverse

array of use cases in HIV prevention and family planning contraception.

5:40 PM *SM04.09.02

***In Situ* 3D-Patterning of Electrospun Fibers Using Two-Layer Composite Materials** Kim Woodrow;
University of Washington, United States

Polymeric electrospun nanofibers have extensive applications in filtration, sensing, drug delivery, and tissue engineering that often require the fibers to be patterned or integrated with a larger device. Here, we describe a highly versatile *in situ* strategy for three-dimensional electrospun fiber patterning using collectors with an insulative surface layer and conductive recessed patterns. We show that two-layer collectors with pattern dimensions down to 100-micrometers are easily fabricated using available laboratory equipment. We use finite element method simulation and experimental validation to demonstrate that the fiber patterning strategy is effective for a variety of pattern dimensions and fiber materials. Finally, the potential for this strategy to enable new applications of electrospun fibers is demonstrated by incorporating electrospun fibers into dissolving microneedles for the first time. These studies provide a framework for the adaptation of this fiber patterning strategy to many different applications of electrospun fibers.

6:05 PM SM04.09.03

Malleable Hydrogel Containing Micellar Cargo-Expellers for Prompt Transdermal Patch Sung-Ho Shin^{1,2}, Youngho Eom³, Eun Seong Lee⁴, Sung Yeon Hwang^{1,5}, Dongyeop X. Oh^{1,5} and Jeyoung Park^{1,5}; ¹Korea Research Institute of Chemical Technology, Korea (the Republic of); ²Purdue University, United States; ³Pukyong National University, Korea (the Republic of); ⁴The Catholic University of Korea, Korea (the Republic of); ⁵University of Science and Technology, Korea (the Republic of)

Hydrogels, water-swollen cross-linked polymeric networks, resemble natural soft tissues (e.g. skins) more than any other types of materials including silicones. They are representative soft biomedical materials in terms of a high water content over 70%, good biocompatibility, low foreign body sensation, and favorable capacity of water-soluble molecules. In this regard, hydrogels are promising materials for drug delivery system as the form of patches, contact lens, and synthetic skins. As a platform for drug delivery, simultaneously accomplishing the fast delivery of a drug and shape conformity of a hydrogel can find its use of pharmaceutical or cosmetic patches. However, there exists the trade-off between the liquid and solid properties that the liquid medium like eye-drops rapidly releases a drug but cannot be used as a patch on human skins, whereas a solid-state hydrogel realizes the stable drug delivery platform but inevitably exhibits a slow release of the drugs.

Herein, a malleable and biocompatible hydrogel containing micellar cargo-expellers was prepared. The *in situ* polymerization of poly(hydroxyethyl methacrylate) (PHEMA) within the poly(vinyl alcohol) (PVA)-borax hydrogel matrix produces large compound micelle particles (micelles) that are not bound by the matrix. Notably, as the micelles do not form any chemical crosslinks with the matrix, they rapidly release outside of the hydrogel network in a wet condition. The micelles act as cargo-expellers through a concentration gradient, which delivers a 25-fold larger quantity of a model cargo than the control hydrogel. Also, the dynamic borate-diol bonds of the hydrogel matrix engender the hydrogel with self-healing properties, and mechanical shock-absorbing property of micelles enables the hydrogel to tightly contact highly curved skin. Moreover, biocompatibility of the hydrogel was confirmed by both *in vivo* cytotoxicity and *in vivo* skin irritation tests. Consequently, this malleable hydrogel will inspire novel prompt skin-patch systems for pharmaceutical and cosmetic purposes. [1]

[1] S.-H. Shin et al. Adv. Healthc. Mater. 2020, 9(19), 2000876.

6:20 PM SM04.09.04

Late News: A Platform for Macrophage-Mediated Delivery of Polymeric Prodrugs to Solid Tumors Ciana L. Lopez^{1,2}, Katherine J. Brempeles², James F. Matthaei², Kate S. Montgomery¹, Selvi Srinivasan¹, Debashish Roy¹, Shannon Kreuser², John Chiefari³, Courtney A. Crane² and Patrick S. Stayton¹; ¹University of Washington, United States; ²Seattle Children's Research Institute, United States; ³CSIRO Manufacturing,

Australia

Current approaches for drug delivery to solid tumors like glioblastoma are insufficient. Delivery of passive- and active-targeting nanomaterials is diffusion-limited, hindered by heterogenous tumor vasculature, and has resulted in few improvements to the standard of care for rapid and lethal disease. Macrophages readily survey solid tumors and are actively involved at all stages of tumor development. Here we introduce genetically engineered macrophages (GEMs) with a fully bioorthogonal, genetically encoded receptor capable of loading with polymeric prodrugs (referred to as ‘drugamers’) in a titratable manner. These RAFT-based polymers are multi-functional: affording biocompatibility, solubility, and sustained release of a small molecule drug cargo. Using the PI3K inhibitor, PI-103, as a model drug, we demonstrate how our polymeric formulation’s optimized release kinetics compliment the drug’s mechanism of action, leading to improved and sustained activity against cancer cells. Furthermore, our drugamer-loaded GEM platform introduces a new cell-mediated and kinetically regulated mechanism for delivery of small molecule drugs to tumors. We have previously demonstrated that GEMs home to and persist in tumors following both intratumoral and intravenous delivery, suggesting the potential of this cellular therapeutic to be administered intravenously to localize to single sites or even metastases.

6:35 PM *SM04.09.05

Boosting Intracellular Delivery of Messenger RNA Gaurav Sahay; Oregon State University, United States

Endosomal sequestration of lipid-based nanoparticles (LNPs) remains a formidable barrier to intracellular delivery of mRNA. Herein, structure-activity analysis of cholesterol analogues reveals that incorporation of C-24 alkyl phytosterols into LNPs (eLNPs) enhances gene transfection and the length of alkyl tail, flexibility of sterol ring and polarity due to -OH group is required to maintain high transfection. Cryo-TEM displays a polyhedral shape for eLNPs compared to spherical LNPs, while x-ray scattering shows little disparity in internal structure. eLNPs exhibit higher cellular uptake and retention, potentially leading to a steady release from the endosomes over time. 3D single-particle tracking shows enhanced intracellular diffusivity of eLNPs relative to LNPs, suggesting eLNP traffic to productive pathways for escape. Our findings show the importance of cholesterol in subcellular transport of LNPs carrying mRNA and emphasize the need for greater insights into surface composition and structural properties of nanoparticles, and their subcellular interactions which enable designs to boost intracellular delivery of mRNA. I will briefly discuss three applications of LNPs to deliver mRNA i.e. for the treatment of cystic fibrosis, retinal degeneration and COVID-19 therapeutics.

7:00 PM PANEL DISCUSSION

SESSION SM04.10: On-demand
Wednesday Morning, April 14, 2021
SM04

SYMPOSIUM SM05

Progress in Multimaterials and Multiphase-Based Multifunctional Materials
April 14 - April 23, 2021

Symposium Organizers

H. Jerry Qi, Georgia Institution of Technology
Richard Trask, University of Bristol
Tao Xie, Zhejiang University
Ruike Renee Zhao, The Ohio State University

* Invited Paper

SESSION SM05.01: Manufacturing of Functional Materials I
Session Chairs: Sung Kang and H. Jerry Qi
Wednesday Morning, April 21, 2021
SM05

8:00 AM SM05.01.04

Late News: Selective Laser Sintering Process of Tungsten Oxide (WO₃) Thin Films for Electrochromic Applications Jinhyeong Kwon¹, Hyunmin Cho², Jinki Min², Daeyeon Won² and Seung Hwan Ko²; ¹Korea Institute of Industrial Technology, Korea (the Republic of); ²Seoul National University, Korea (the Republic of)

A selective laser sintering (SLS) process has opened a novel patterning way for advanced electronic applications. The SLS process bases on the photothermal effect and features for high precision, fast processing, and room temperature accessibility without inert gas. Therefore, the effectiveness of the interaction between the nanomaterials and laser has examined the various conductive metal nanomaterials such as gold, silver, and copper. Although the laser sintering process has shown many achievements on metal nanomaterials, it has rarely studied for the interaction for the metal oxide nanomaterials. In this study, WO_x thin film layer employs the SLS process for post-processing which enables patterning and annealing simultaneously with inducing photochemical reaction as well as photothermal effect. The SLS-processed WO_x thin film has shown similar electrochemical performances for the electrochromic application to the thermal annealed WO_x thin film. We have established facile and fast fabrication for electrochromic devices with the SLS-processed WO_x thin film layer and demonstrated feasibility for the indoor temperature controllable feature.

8:05 AM SM05.01.05

Shape Controllable Building Blocks for 3D Collective Assembly via Residual Stress Design Woongbi Cho^{1,2}, Dong Gyun Kim³, Yong Seok Kim³ and Jeong Jae Wie^{1,2}; ¹Inha University, Korea (the Republic of); ²Inha University, Korea (the Republic of); ³Korea Research Institute of Chemical Technology, Korea (the Republic of)

In nature, the collective assembly is often observed which enrich the structural and functional diversities. For example, DNA for various creatures consist with double helix architecture via collective assembly of only 4 distinct types of building blocks (Adenine, Guanine, Cytosine, Tymine). The hierarchical structures via collective assembly can highly release the limitations on geometries and functionalities through a spatial arrangement of diversely designed 3D building blocks. In this presentation, geometrically tailorable 3D building blocks are introduced by controlling residual stress with rapid and reproducible fabrication without complicate and/or expensive equipment. Frontal photopolymerization (FPP) with variously designed photomask and different curing time are employed for spatiotemporal regulation of photopolymerization. The employed photocurable resin is composed of bio-compatible poly(ethylene glycol)diacrylate (PEGDA) matrix, photo-initiator and photo-absorber. The photo-absorber generates drastic gradient of light intensity during the photopolymerization, resulting in a residual stress via crosslinking density mismatch through the thickness. When the photopolymerization is terminated, a curvilinear 3D shape morphing occurs within 1 min as a result of shrinkage mismatch induced by immediate relaxation of the residual stress. The geometries of 3D building blocks are programmed by systematic change of spatiotemporal conditions of pre- and post-curing. The 3D

morphed structures are hierarchically assembled to achieve self-similar scaled-up structures inspired by designs of famous landmark (e.g. the great pyramid in Giza). The regularly stacked geometry allows 3D assembled structure to withstand 150 times of its own weight by homogeneous distribution of normal stress. Furthermore, the electrically conductive property is rendered to 3D assembled structural by applying conductive silver pastes on the 3D layered structures. Hence, our design strategy of tailorable 3D building blocks for collective assembly can be a promising candidate for prototyping several platforms of electronics, optics, and metamaterials.

8:10 AM SM05.01.06

Magnetic Collective Swimming of Bioinspired Ternary Nanocomposites Sukyong Won¹, Hee Eun Lee¹, Young Shik Cho², Jeong Eun Park¹, Seung Jae Jang¹ and Jeong Jae Wie¹; ¹Inha University, Korea (the Republic of); ²Seoul National University, Korea (the Republic of)

Stimuli-responsive unary materials and binary composites have employed for actuation of soft robots. However, collective motion of multiple soft robots is challenging when stimuli-responses are implemented without batteries and sensors. Herein, we present magnetic collective swimming of ternary polymeric nanocomposites capable of adaptably organizing. Core-shell design of nanoporous carbon nanotube yarn (CNTY) and magnetic particles is inspired by skeletal muscles surrounding spongy bone in musculoskeletal system. The magnetic particles are attached to the CNTY owing to sol-gel polymerized elastomers providing the function of connective tissue. The polymeric soft robots swim with multimodal motility of rectilinear translational motion and rotational motion under a rotating quadrupolar electromagnetic field. Multiple soft robots can be adaptably organized through magnetically interactive dynamic soft joints when varying the rotational frequency of the magnetic field. We will discuss collective swimming of modular soft robots that transport 850 microbeads above water and a semi-submerged milli-bead.

8:15 AM SM05.01.07

Late News: Cross-Reactive poly(ethylene oxide) and poly(ϵ -caprolactone) Stars Towards Covalent Adaptative Networks Exhibiting Water and Temperature Triggered Shape-Memory Properties Jérémie Caprasse, Jean-Michel Thomassin, Raphaël G. Riva and Christine Jerome; University of Liege, Belgium

Covalent networks of semi-crystalline poly(ϵ -caprolactone) (PCL) are highly performant shape-memory materials (SMM) i.e. high fixity of the temporary shape and high recovery of the thermally triggered permanent shape. Being in addition biocompatible and degradable, applications in the biomedical field are foreseen. Advantageously, inserting reversible bonds in the network, adaptative materials are obtained which allows reconfiguration of the permanent shape while preserving the shape memory properties at the body temperature [1].

As an answer to the increasingly demanding biomedical field, we aim at providing to such covalent adaptative networks, an additional shape transition triggered by the presence of water at constant temperature. For this purpose, poly(ethylene oxide) has been selected as a hydrophilic component introduced in the PCL networks.

In the present work, a covalent adaptative PEO/PCL hybrid network is formed by Diels-Alder reaction between PCL and PEO stars purposely end-capped by maleimide and furan, respectively. After melt-mixing of these cross-reacting stars and a post-curing, the resulting covalent adaptable hybrid networks shows high crosslinking density, as demonstrated by swelling experiments while preserving enough crystallinity to exhibit high thermal triggered shape-memory performances that remain as good as the ones of PCL covalent networks. Thanks to the insertion of furane-maleimide Diels-Alder adduct in the covalent networks, this material can be recycled by solvent-free hot-melt reprocessing and the permanent shape of this SMM can be reconfigured, e.g. by using mold of a complex shape. In addition, water triggered shape transition was evidenced allowing to achieve medical devices of complex shapes exhibiting in vivo self-deploying properties.

[1] Defize, T.; Riva, R.; Jérôme, C.; Alexandre, M., Multifunctional Poly(ϵ -caprolactone)-Forming Networks by Diels–Alder Cycloaddition: Effect of the Adduct on the Shape-Memory Properties. *Macromolecular Chemistry and Physics* **2012**, *213* (2), 187-197.

8:20 AM SM05.01.08

Late News: Silicon Nanowires Decorated with Gold Nanoparticles—Synthesis and Analytical

Characterization Margherita Izzi^{1,2}, Rosaria Anna Picca^{1,2}, Antonio A. Leonardi^{3,4}, Maria J. Lo Faro^{3,4}, Maria C. Sportelli¹, Alessia Irrera⁴ and Nicola Cioffi^{1,2}; ¹University of Bari Aldo Moro, Italy; ²CSGI (Center for Colloid and Surface Science) c/o Dept. Chemistry, University of Bari, Italy; ³University of Catania, Italy; ⁴IPCF-CNR, Italy

Hybrid nanomaterials combining semiconductor and metal nanostructures represent an efficient way to develop novel platforms for advanced applications, ranging from sensing to catalysis [1–3]. In particular, silicon nanowires (SiNWs) are a promising host matrix for the dispersion of metal nanoparticles (MeNPs). They exhibit excellent characteristics such as large surface area, relatively high mechanical stability and low cost [4]. SiNWs are prepared by a wet-etching technique, assisted by the deposition of an ultrathin metal film on (p-, n-doped or highly doped) Si single crystal. SiNWs with very high density and controllable aspect ratios can be obtained. In the last years, we have studied the decoration of the proposed SiNWs with different MeNPs, including gold, by pulsed laser deposition [2,3]. This technique allows for loading “naked” NPs on the NWs. As alternative approaches, wet-methods can be used to decorate the semiconductor nanostructures. In this communication, we report on the modification of SiNW platforms with chemically produced AuNPs by electrophoretic deposition (EPD). We exploit an innovative synthesis based on stainless steel as solid reductant for H₂AuCl₄ to prepare AuNPs [5,6]. This method is very easy, quick, cost-effective, and scalable, allowing the synthesis of highly stable NPs without additional capping agents [6]. Pros and cons of EPD of preformed NPs will be highlighted in comparison with direct reduction of gold precursor on SiNW surface. The role of silicon doping will be investigated in combination with the charge of AuNP surface to evaluate their influence on final material properties. To this aim, electrochemical, spectroscopic and morphological characterizations will be proposed.

1. D’Andrea, C.; Faro, M.J.L.; Bertino, G.; Ossi, P.M.; Neri, F.; Trusso, S.; Musumeci, P.; Galli, M.; Cioffi, N.; Irrera, A.; et al. Decoration of Silicon Nanowires with Silver Nanoparticles for Ultrasensitive Surface Enhanced Raman Scattering. *Nanotechnology* **2016**, *27*, 375603, doi:10.1088/0957-4484/27/37/375603.

2. Picca, R.A.; Calvano, C.D.; Faro, M.J.L.; Fazio, B.; Trusso, S.; Ossi, P.M.; Neri, F.; D’Andrea, C.; Irrera, A.; Cioffi, N. Functionalization of Silicon Nanowire Arrays by Silver Nanoparticles for the Laser Desorption Ionization Mass Spectrometry Analysis of Vegetable Oils. *J. Mass Spectrom.* **2016**, *51*, 849–856, doi:https://doi.org/10.1002/jms.3826.

3. Casiello, M.; Picca, R.A.; Fusco, C.; D’Accolti, L.; Leonardi, A.A.; Lo Faro, M.J.; Irrera, A.; Trusso, S.; Cotugno, P.; Sportelli, M.C.; et al. Catalytic Activity of Silicon Nanowires Decorated with Gold and Copper Nanoparticles Deposited by Pulsed Laser Ablation. *Nanomaterials* **2018**, *8*, 78, doi:10.3390/nano8020078.

4. Irrera, A.; Faro, M.J.L.; D’Andrea, C.; Leonardi, A.A.; Artoni, P.; Fazio, B.; Picca, R.A.; Cioffi, N.; Trusso, S.; Franzò, G.; et al. Light-Emitting Silicon Nanowires Obtained by Metal-Assisted Chemical Etching. *Semicond. Sci. Technol.* **2017**, *32*, 043004, doi:10.1088/1361-6641/aa60b8.

5. Izzi, M.; Sportelli, M.C.; Tursellino, L.; Palazzo, G.; Picca, R.A.; Cioffi, N.; López Lorente, Á.I. Gold Nanoparticles Synthesis Using Stainless Steel as Solid Reductant: A Critical Overview. *Nanomaterials* **2020**, *10*, 622, doi:10.3390/nano10040622.

6. López-Lorente, A.I.; Simonet, B.M.; Valcárcel, M.; Eppler, S.; Schindl, R.; Kranz, C.; Mizaiakoff, B. Characterization of Stainless Steel Assisted Bare Gold Nanoparticles and Their Analytical Potential. *Talanta* **2014**, *118*, 321–327, doi:10.1016/j.talanta.2013.10.028.

8:25 AM SM05.01.09

Inkjet Printed Nanodielectrics for High-Energy Microcapacitors Jinkai Yuan, Fernando Torres-Canas and Philippe Poulin; Centre de recherche Paul Pascal, France

Micro-energy storage devices are appealing, and highly demanded for diverse miniaturized electronic devices, ranging from microelectromechanical system, robotics, to sensing microsystems and wearable electronics.[1,2] However, making high-energy microcapacitors with currently available printing technologies remains

challenging. Herein, we show the possibility to use latex polyvinylidene fluoride (PVDF) as aqueous ink for making dielectric capacitors on the microscale. The dielectric properties of printed microcapacitors can be optimized based on a novel approach, i.e., mixing PVDF latex with polyvinyl alcohol (PVA) to realize dielectric organic nanocomposites. The PVA prevents the coalescence of PVDF nanoparticles and serves as a continuous matrix phase with high dielectric breakdown strength. While the well-dispersed PVDF nanoparticles serve as highly polarizable and isolated domains, providing large electric displacement under high fields. Consequently, a high discharged energy density of 12 Jcm^{-3} is achieved at 550 MVm^{-1} . [3] These printed microcapacitors demonstrate mechanical robustness and dielectric stability over time.

[1] Z. S. Wu, X. Feng, H. M. Cheng, *Natl. Sci. Rev.* 2014, 1, 277.

[2] M. Beidaghi, Y. Gogotsi, *Energy Environ. Sci.* 2014, 7, 867.

[3] F. Torres-Canas, J. Yuan, I. Ly, W. Neri, A. Colin, P. Poulin, *Adv. Funct. Mater.* 2019, 1901884.

8:40 AM SM05.01.10

Digital Microfluidic Activated by Physical Intelligence Sara Coppola, Veronica Vespini and Pietro Ferraro; Institute of Applied Sciences and Intelligent Systems “E. Caianiello”, Italy

Robots and intelligent systems will be the key factor of Industry 4.0 revolution for aiding at any stage engineering and manufacturing processes. One of the most challenging demanded issue is to make available appropriate tools for full control of liquids. In fact, the manipulation of the liquid matter is of strategic importance in many procedures and facilities involving many fields of applications i.e. biomedicine, biotechnologies, food, cosmetics, just to cite few. Liquids, polymers and more in general soft-matter requires even more accurate, precise and full controlled handling apparatuses. So far, several engineering methods have been proposed for furnishing intelligent responses to environmental changes in order to drive liquids by external magnetic, electric or optical fields. However, until now, very few and shy approaches for locomotion and remote control have been featured to manage liquid actuation. The design of innovative portable devices, working in non-contact mode, easy to use, totally safe for the medical staff and based on handling of small amount of reagent and liquid to be analysed, is certainly a strategic ambition for all the researchers, scientist and industries all over the world. Actually, most of the systems in use are made of rigid components, not friendly, unable to self-adapt to various configurations and most important require the manual intervention by the operators (i.e. classical manual pipetting) so exposed to cross-contamination problems. Here we introduce a new working principle for liquid manipulation and a complete exploration of the opportunities of a multipurpose platform guided by physical intelligence, enlarging the opportunity of liquid handling via pyro-electrohydrodynamics (EHD). The platform is able to handle liquid volumes by reacting to thermal external stimulus on a functionalized substrate (i.e. ferroelectric crystal). The innovation consists in creating a multiscale digital microfluidic system for handling small amount of liquids and multiphase samples with volumes in a wide range from microliter to milliliter, in air and in three-dimensions. In fact, the huge electric field generated via the pyroelectric effect allows to manage the on/off activation system of the pyro-Electro-Hydro-Dynamic driving force for commanding a fast response in a smart way and for easily moving units of liquid with different size and volumes. We prove remote locomotion of liquid volume as a sort of tweezers able to move liquids along desired paths. Beyond the guiding property, we proved also additional functionalities like merging, stretching, mixing and jumping of liquid volumes and millimeter objects using a working distance of millimeter, i.e. bigger than the conventional distances used for liquid handling in classical digital microfluidic.

1. Nasti, G., Coppola, S., Vespini, V., Grilli, S., Vettoliere, A., Granata, C., & Ferraro, P. (2020). Pyroelectric tweezers for handling liquid unit volumes. *Advanced Intelligent Systems*, <https://doi.org/10.1002/aisy.202000044>

8:55 AM *SM05.01.11

Rapid Synthesis of Elastomers and Thermosets with Tunable Multifunctional Properties Nancy R. Sottos, Leon Dean, Qiong Wu and Jeffrey Moore; University of Illinois at Urbana-Champaign, United States

Frontal polymerization (FP) has emerged as a promising technique for rapid, energy-efficient preparation of

bulk polymeric materials in ambient conditions without solvents. In FP, the monomer is converted to a polymer within a localized reaction zone that propagates spatially as a consequence of heat transfer from the exothermic polymerization to unreacted monomer. FP requires a minimal amount of energy to initiate the process, after which the polymerization front continues to propagate without further energy input. In this talk, we report the rapid, solvent-free synthesis of poly(1,4-butadiene) by FROMP of neat 1,5-cyclooctadiene (COD). Moreover, we find that FROMP of comonomer mixtures of COD and dicyclopentadiene (DCPD) produces mechanically robust cross-linked polymeric materials having a wide range of properties, from soft elastomers to rigid thermosets, which are tuned simply by varying the comonomer ratio. We use the ability to spatially control copolymer composition to rapidly fabricate materials with spatially varying properties capable of multistage shape memory actuation. By triggering instabilities in the front propagation, we can also create materials with complex gradients in materials properties.

SESSION SM05.02: Manufacturing of Functional Materials II

Session Chairs: H. Jerry Qi and Kenan Song

Wednesday Morning, April 21, 2021

SM05

11:45 AM SM05.02.01

Evolutionary Design of Cactus-Inspired Soft Robotics Based on 3D-Printed Multi-Material Construct

Anil K. Bastola¹, Marc Behl¹, Patricia Soffiatti², Nick P. Rowe³ and Andreas Lendlein^{1,4}; ¹Institute of Biomaterial Science, Helmholtz-Zentrum Geesthacht, Germany; ²Federal University of Parana State, Brazil; ³AMAP, Univ Montpellier, CIRAD, CNRS, INRAE, IRD, France; ⁴Berlin-Brandenburg Center for Regenerative Therapies, Helmholtz-Zentrum Geesthacht, Germany

Nature is a magnificent source of inspiration to develop new technologies. The evolutionary development of plants leads to functional traits that can anchor, twine, vine, or search. An interesting representative in this context is *Selenicereus setaceus*, a cactus found in the Atlantic forest of Brazil capable of climbing¹. Such biological functional system can serve as a source for bio-inspired robots with the potential ability to anchor, attach, and climb^{2,3}. We questioned how the process of development could be a shortcut to different forms. Our approach is the evolutionary design of a multi-material system inspired by the cactus. *Selenicereus setaceus* demonstrates a unique structural configuration along the different stages of the growth: the stem is circular at the base while the younger parts are star-like in shape at the apex. The cactus consists of soft tissues surrounded by a thin skin layer. The capability of transformation in shape not only optimizes its flexural rigidity but also provides flexibility to allow the cactus to search for light in the challenging environment of the seasonally dry Atlantic forest.

In our design concept for this evolutionary cactus-inspired artificial system, we selected the unique geometry, a star-like shape, of the cactus at the apex. Such a unique shape is 3D printed using a soft elastomeric polymer. Another soft material, a water-swollen polymer, hydrogel, is synthesized on the 3D printed structure. Herein, we demonstrated two developments directly inspired by the functional traits of the cactus. In the first, we demonstrated a controlled movement similar to the searcher component of the natural cactus, when the humidity is changed the hydrogel-elastomer system could bend toward low humidity through anisotropic swelling and de-swelling of the hydrogel. In the second, we demonstrated the change in geometry from star-like to circular shape, as the natural cactus does in nature as it grows, partly by means of isotropic swelling and de-swelling of the hydrogel. These evolutions show the possibility that we can directly learn from the behavior and structural configurations of plants to develop functional artificial systems. We hope that this study stimulates the design of novel plant-inspired ecological robotic systems.

References

1. P. Soffiatti and N.P. Rowe: Mechanical innovations of a climbing cactus: functional insights for a new

generation of growing robots. *Frontiers in Robotics and AI* **7** (2020).

2. B. Mazzolai, L. Beccai and V. Mattoli: Plants as model in biomimetics and biorobotics: new perspectives. *Frontiers in bioengineering and biotechnology* **2**, 2 (2014).

3. B. Mazzolai, F. Tramacere, I. Fiorello and L. Margheri: The bio-engineering approach for plant investigations and growing robots. A mini-review. *Frontiers in Robotics and AI* **7**, 130 (2020).

12:00 PM SM05.02.03

Fabrication and Characterization of Ferromagnetic Organic Semi-Crystalline Polymers Scott

Newacheck^{1,2} and George Youssef¹; ¹San Diego State University, United States; ²University of California, San Diego, United States

Multifunctional material systems are breaking the elusive boundaries between functions previously deemed independent, necessitating a composite approach but with inferior response. While research in multifunctional materials for magnetoelectric coupling is thriving, polymeric (or organic) multiferroics are lagging behind due to several processing, characterization, and performance challenges. Commonly trending organic multiferroics exhibit lower magnetoelectric properties than their composite oxide-based counterparts, but report a measureable coupling at room temperature, positioning them as a superior class of materials in comparison to intrinsic single phase multiferroic materials. The latter has a diminished response at room temperature, deeming them impractical for any translational applications. The magnetoelectric response of organic multiferroics, on the other hand, can be further enhanced through the addition of mechanical or photonic energies. However, organic multiferroics suffer from complex phasic structure consisting of multiscale crystalline phases surrounded by amorphous regions, which can be tuned based on fundamental understanding of the process-structure-property interrelations. Thus, the objective of this research is to characterize a blend organic framework with multiferroic properties to elucidate the interdependence of the properties on the processing approach. Here, regioregular poly(3-hexylthiophene) polymer (P3HT) is blended with organic compound phenyl-C₆₁-butyric acid methyl ester (PCBM) to synthesize an excitonic multiferroic polymer with tunable properties. The structure of P3HT consists of a crystalline phase surrounded by amorphous regions, while PCBM forms nanocrystalline aggregates. The interrelationship between primary processing parameters, including the concentration of P3HT and the ratio of P3HT to PCBM, are discussed as a function of triphasic structure. The ferromagnetic polymers were characterized for their photomagnetic, piezomagnetic, and mechanical properties using a modified vibrating sample magnetometer with illumination source matching the absorbance band of the blend polymer and a mechanical loading mechanism. Overall, this study reports the first process-structure-property map of the blend P3HT:PCBM organic framework for magnetoelectric coupling, which will accelerate translation applications in flexible and wearable electronics. Future research will focus on multiscale characterization of the interaction between the boundaries separating the amorphous and crystalline phases of P3HT and the interfaces between P3HT and PCBM.

12:15 PM SM05.02.04

Harnessing Instabilities During Frontal Polymerization for Patterning Justine E. Paul, Julian C. Cooper, Anisha Sharma, Jeffrey Moore and Nancy R. Sottos; University of Illinois at Urbana-Champaign, United States

We have developed a new approach to manufacturing thermoset materials with complex morphology and function using frontal ring-opening metathesis polymerization (FROMP). Propagation of uniform fronts enables rapid, efficient fabrication of neat polymers and composites. In this work, we explore the instabilities that arise during FROMP, which lead to non-uniform front propagation and complex patterns and property gradients within the material. We utilize the synthetic reaction-thermal diffusion system that arises from the FROMP of dicyclopentadiene (DCPD), 5-ethylidene-2-norbornene (ENB), and 1,5-cyclooctadiene (COD) to take advantage of the positive and negative feedback loops for patterning. Spontaneous pattern formation is achieved in an open mold geometry which causes non-uniform front propagation and gives rise to the competition between thermal transport and reaction rates. The effects of boundary conditions, co-monomers, chemical inhibitors, and energy inputs are investigated and monitored visually using an infrared camera. By tuning the reaction kinetics, ambient temperature, and thermal initiation conditions, we achieve a spin mode propagation,

causing wavelike surface patterns to develop across the entire length of the material. The wavelength of the surface patterns is systematically varied by adjusting the parameters of the experimental system. By layering comonomers based on density differences, we achieve materials with functionally graded properties. The thermophysical properties of these functional materials are tunable and highly reproducible.

12:30 PM SM05.02.05

Stimuli-Responsive 2D Metal-Organic Frameworks Prepared by Chemical Vapor Deposition F. James Claire¹, Marina Solomos¹, Jungkil Kim¹, Gaoqiang Wang^{2,3}, Maxime Siegler¹, Michael Crommie^{2,3} and Thomas J. Kempa^{1,1}; ¹Johns Hopkins University, United States; ²University of California, Berkeley, United States; ³Lawrence Berkeley National Laboratory, United States

The incorporation of metal organic frameworks into advanced devices remains a desirable goal, but progress is hindered by difficulties in preparing high quality, multifunctional metal-organic framework (MOF) films with suitable electronic performance. We demonstrate the direct growth of large-area, high quality, and phase pure single MOF crystals through chemical vapor deposition of a dimolybdenum paddlewheel precursor, Mo₂(INA)₄. These exceptionally uniform crystals cover areas up to 8600 μm² and can be grown down to thicknesses of 30 nm. Scanning tunneling microscopy indicates that the Mo₂(INA)₄ clusters assemble into a two-dimensional, single-layer framework. Devices fabricated from single vapor-phase grown crystals exhibit reversible nearly 10-fold changes in conductivity upon illumination at modest powers. Moreover, we identify vapor-induced single crystal transitions that are reversible and responsible for 30-fold changes in conductivity of the MOF as monitored by *in situ* device measurements. Gas-phase methods, including chemical vapor deposition, show broader promise for the preparation of multifunctional molecular frameworks, and may enable the integration of these materials into devices, including detectors and actuators.

12:45 PM SM05.02.06

Late News: Design and Fabrication of Hybrid 3D-Printed Conductive Wires on Epoxy Substrates for Self-Sensing Applications Haley Hilborn and H. Jerry Qi; Georgia Institute of Technology, United States

Additive manufacturing (AM) allows for rapid fabrication of complex structures with the advantage of multi-material composition and high structural complexity, or a unique combination of the two. Recently, there is an increasing interest in creating multi-material components which have optimal interfacial interactions between layers. However, the challenge lies with determining optimal compatibility between printed components, and how those influence bulk property of the multi-material structure. Previous investigation of direct-ink write (DIW) printed epoxy-silver composite structures did not produce conductive parts. Therefore, we study silver conductive ink material composition and compatibility with epoxy, including interfacial connections and layer-by-layer material adhesion. As a result, an optimal material for multi-functional composite parts was developed for a variety of thermal, mechanical and electrical applications. Electronics such as strain gauges and light sensors were DIW 3D printed. Additionally, we demonstrate a deicing unit for potential use on an aircraft, such as unmanned aerial vehicle (UAV) wings. Thus, utilizing material science, we solve material compatibility issues that frequently arise when 3D printing multi-material components, eliciting desired features within a printed part.

SESSION SM05.03: Novel Soft Composites I
Session Chairs: H. Jerry Qi and Ruike Renee Zhao
Wednesday Afternoon, April 21, 2021
SM05

2:15 PM SM05.03.01

Multi-Phase Multifunctional Materials that Sense Mechanical Loading and Adapt Sung H. Kang; Johns

Hopkins University, United States

Bone is a multi-phase multifunctional material that can sense the mechanical loading and adjust itself by adding more minerals to the region of high stress and reducing them to the low stress region so that it can increase the efficiency and lifespan of the material. However, it has been a challenge to synthesize load-bearing materials with such capabilities. Inspired by bone mineralization mechanisms, we have investigated a multi-phase material system that self-senses mechanical loading and proportionally triggers mineral formation from media with mineral ions so that the material can mitigate damages and increase lifespan. The mineralization rate within the material system is autonomously modulated in response to changing loading conditions, resulting in a 30-180% increase in the modulus of the material upon 1 to 5 N cyclic loadings. Moreover, the multifunctional material adds more minerals to the region of high stress and vice versa for that of low stress so that the material can mitigate the damage and enhance its lifetime. We envision that our findings can open new strategies for making synthetic multifunctional materials with self-adaptable mechanical properties.

Acknowledgements: This work was supported by the Air Force Office of Scientific Research Young Investigator Program Award (Award number: FA9550-18-1-0073, Program manager: Dr. Byung-Lip (Les) Lee), Johns Hopkins University Whiting School of Engineering start-up fund, and Temple University Maurice Kornberg School of Dentistry start-up fund.

Reference: S. Orrego, Z. Chen, U. Krekora, D. Hou, S.-Y Jeon, M. Pittman, C. Montoya, Y. Chen, S. H. Kang, *Advanced Materials*, 1906970 (2020).

2:30 PM SM05.03.02

Grayscale Digital Light Processing Enabled 3D/4D Printing for Multimaterial Multifunctional

Composites H. Jerry Qi, Xiao Kuang and Stuart M. Montgomery; Georgia Institute of Technology, United States

Digital light processing (DLP) based 3D printing is an additive manufacturing process which utilizes light patterns to photopolymerize a liquid resin into a solid. Due to the accuracy of modern digital micromirror devices (DMD) and a layer of thin resin being cured rapidly (1-5s), DLP has the advantage of high speed and high resolution. However, conventional DLP method is not suitable for multimaterial printing because it uses a single vat of resin. Recent advances in resin chemistry now make it possible to create functionally graded structures using different light intensity values, also known as grey-scale DLP (g-DLP). In this talk, we present some of our recent efforts in using g-DLP to 3D/4D print multimaterial multifunctional composites, including creating functionally graded materials with modulus spanning three orders of magnitude, creating inflatable structures. As a digitally graded light pattern can impose concentration gradients upon the different reacting chemical species, which in turn can cause diffusion of these components throughout both the liquid resin and the solidified regions. This effect can affect both spatial resolution as well as physical property resolution in g-DLP printing. In this talk, we will briefly present a reaction-diffusion model coupled with radiative transfer to analyse the effects of component diffusion and its impact upon the resulting mechanical property resolution on a sub-pixel and macro scale. Our aim is to accurately model the underlying physics along with the additive manufacturing process to quantify these phenomena and use the information gained to optimize printing parameters such as light exposure time, grey-scale distributions, and resin composition.

2:45 PM SM07.07.02

Structural and Electrical Properties of Self-Assembled Monolayers on Germanium as Passivating and

Insulating Layers Mohamed-Amine Guerboukha¹, Virginie Gadenne¹, Hela Mrezguia², Luca Giovanelli², Younal Ksari², Guillaume Monier³, Victorien Jeux⁴, Jean-Manuel Raimundo⁵ and Lionel Patrone¹; ¹Aix Marseille Univ., Université de Toulon, CNRS, IM2NP UMR 7334, Yncréa Méditerranée, ISEN-Toulon, France; ²Aix Marseille Univ., Université de Toulon, CNRS, IM2NP UMR 7334, Domaine de St Jérôme, Service 151, France; ³Univ Clermont Auvergne, CNRS, SIGMA Clermont, Inst Pascal, France; ⁴ESCOM Chimie, France; ⁵Aix Marseille Univ, CNRS, CINaM UMR 7325, France

Due to its high intrinsic mobility, germanium (Ge) is emerging as a likely alternative material to replace silicon in the next generation of high-mobility and high-frequency field effect transistors. However, unlike silicon dioxide, Ge oxide is neither stable nor of good quality. Thus, the preparation of an interfacial layer enabling to passivate and insulate Ge surface is still problematic. A promising approach consists in using self-assembled molecular monolayers (SAMs) [1] with high dielectric constant K. In this perspective, the aim of this work is to design new SAMs grafted on Ge exhibiting highly insulating and passivating properties as new high-K self-assembled nanodielectrics [2].

We have studied SAMs of model molecules such as alkylthiols and fluoro-alkylthiols, and of specially synthesized non-charged novel push-pull chromophores bearing electron donor and acceptor groups, separated by a pi-conjugated bithiophene bridge which promotes electron transfer and a subsequent dipole formation [3]. Indeed, due to the alignment of the oriented dipoles promoted by the SAM deposition strategy, such push-pull chromophores have been shown to form highly polarizable insulating films in the literature [2]. We have adapted and developed the original Ge deoxidation/grafting technique in hydro-alcoholic solution [4] and shown that, compared to the usual deoxidizing acid treatment, it gives smoother surfaces and well-organized SAMs, which is proven by ellipsometry, wettability measurements, and scanning probe microscopy analyses. The grafting of alkylthiols and fluoro-alkylthiols on Ge has been performed directly in a single step thanks to the affinity of sulfur with Ge, whereas for the push-pull chromophores designed with a carboxylic anchoring group, we have achieved a two-step grafting with amide bonding on pre-assembled amine-terminated sticking layers. Among the latter, we have demonstrated aminothiophenol SAMs exhibit a better arrangement than cysteamine, with a smooth monolayer film suitable for grafting ordered push-pull SAMs on top. UV-Visible absorption spectroscopy has been carried out to probe push-pull chromophores in solution to determine the concentration limit to avoid aggregation. X-ray photoelectron spectroscopy (XPS) and infrared spectroscopy (FTIR) analyses demonstrate the oxide removal from the Ge surface after the SAM formation process. Statistical electrical analyses of the various SAMs on Ge have been carried out by using eutectic GaIn contacts. With such push-pull SAMs, we have been able to decrease the current by a factor of 10^5 compared to Ge, and 10^4 compared to dodecane SAMs of similar thickness. Results have been analyzed by transition voltage spectroscopy [5], and successfully correlated with spectroscopic analyses of molecular levels, using inverse photoemission spectroscopy and XPS valence band determination for probing the unoccupied and occupied molecular orbitals respectively, as well as with DFT calculations, thus allowing to identify the highest occupied molecular orbital as the level involved in the electronic transport through the push-pull SAM. Dipole formation has also been evidenced in the SAM. Further work will address multilayers of aligned organic push-pull chromophores to increase the overall dipole of the films for enhanced dielectric properties.

1. A. Ulman, *An Introduction to Ultrathin Organic Films*, Academic Press (Ed.), Boston (1991)
2. A. Facchetti, M.H. Yoon, T.J. Marks., *Adv. Mater.* **17**, 1705 (2005) ; Y.G. Ha, A. Facchetti, T.J. Marks, *Chem. Mater.* **21**, 1173 (2009)
3. V. Malyskiy, V. Gadenne, Y. Ksari, L. Patrone, J.M. Raimundo, *Tetrahedron* **73**, 5738 (2017)
4. J.N. Hohman, M. Kim, H.R. Bednar, J.A. Lawrence, P.D. McClanahan, P.S. Weiss, *Chem. Sci.* **2**, 1334 (2011)
5. X. Lefevre, F. Moggia, O. Segut, Y.-P. Lin, Y. Ksari, G. Delafosse, K. Smaali, D. Guérin, V. Derycke, D. Vuillaume, S. Lenfant, L. Patrone, B. Jousselme, *J. Phys. Chem. C* **119**, 5703 (2015).

3:00 PM SM05.03.04

Magnetic Soft Composites with Multifunctional Shape Manipulations Ruike Renee Zhao; The Ohio State University, United States

Shape-programmable soft materials that exhibit integrated multifunctional shape manipulations, including reprogrammable, untethered, fast, and reversible shape transformation and locking, are highly desirable for a plethora of applications, including soft robotics, morphing structures, and biomedical devices. Despite recent progress, it remains challenging to achieve multiple shape manipulations in one material system. Here, a novel magnetic shape memory polymer

composite is reported to achieve this. The composite consists of two types of magnetic particles in an amorphous shape memory polymer matrix. The matrix softens via magnetic inductive heating of low-coercivity particles, and high-remanence particles with reprogrammable magnetization profiles drive the rapid and reversible shape change under actuation magnetic fields. Once cooled, the actuated shape can be locked. Additionally, varying the particle loadings for heating enables sequential actuation. The integrated multifunctional shape manipulations are further exploited for applications including soft magnetic grippers with large grabbing force, reconfigurable antennas, and sequential logic for computing.

3:15 PM *SM05.03.05

Layered Transition Metal Dichalcogenide Assemblies and Nanocomposites Ali Jawaaid, Jason Streit, Peter Stevenson, Robert Busch, W. Joshua Kennedy, Jonathan Vernon and Richard A. Vaia; Air Force Research Laboratory, United States

Layered Transition Metal Dichalcogenides (LTMD, MX_2) exhibit metallic, semi-metallic, semiconducting, insulating, or superconducting character depending on chemical composition and structure. Recent high-yield, exfoliation methods (i.e. Redox Exfoliation), which are sonication and surfactant-free, are providing oxidatively-resistant and colloiddally-stable dispersions of Group IV-VI TMDs (>14 compositions) at high volume fraction (>10% v/v) in a broad range of polar and anhydrous solvents (e.g. acetonitrile, acetone, alcohols). In addition to expanding the range of surface hybridization chemistries, these methods are transforming approaches to LTMD nanocomposite fabrication, ink formulation, and film processing. These opportunities will be highlighted by examples of multi-functional materials and hetero-structures with unique optical performance for optical filters, GRIN optics, and non-linear absorbers.

3:45 PM *SM05.03.06

Bio-enabled Nanocomposites with Novel Physical Properties Vladimir Tsukruk; Georgia Institute of Technology, United States

Bio-enabled nanocomposites represent a novel class of functional materials, which uses principles of bioinspiration to design hybrid materials and structures with co-assembled biological and synthetic components to bring best of two worlds: versatile functions with responses to mechanical, optical, chemical, and light stimuli and mechanical strength, flexibility, environmental robustness, and scalability (see general reviews [1, 2]). We discuss general principles of organization in most popular biological components frequently explored for bio-hybrid materials including proteins (silk fibroins), polysaccharides (nanocelluloses) and common synthetic components such as metal and semiconducting nanoparticles/nanowires and two-dimensional metal oxides, nanoclays and graphene derivatives. For specific illustrations, we select recent results from our research group on designing flexible and strong nanomaterials with electrical conductivity, actuation, bright emission, and controlled photonic properties. In particular, we demonstrated robust patterned metallized biographene papers from graphene oxide monolayers “glued” by silk fibroins with intriguing biosensing properties and corresponding Kirigami structures with large stretchability and ability to transform from planar to 3D structures. Among most recent results, we reported chiral emission in organized biopolymer photonic films with embedded carbon quantum dots mediated by polymer linkers [3], co-assembly of cellulose nanocrystals with amorphous polysaccharides resulted in the preservation of the original structural colors and intercalation into the interstitial defects of nematic monolayers [4], and stable and robust MXene-silk composites [5].

[1] R. Xiong, J. Luan, S. Kang, S. Singamaneni, V. V. Tsukruk, Natural Biopolymers for Organized Photonic Structures, *Chem. Soc. Review*, **2020**, *49*, 983.

[2] R. Xiong, A. M. Grant, R. Ma, S. Zhang, V. V. Tsukruk, Naturally-derived biopolymer nanocomposite: interfacial design, properties and emerging applications, *Mat. Sci. & Eng. Reports*, **2018**, *125*, 1.

[3] R. Xiong, X. Zhang, M. Kreckler, S. Kang, M. J. Smith, V. V. Tsukruk, Large and Emissive Crystals from Carbon Quantum Dots onto Interfacial Organized Templates, *Angew. Chem.*, **2020**, *59*, 2

[4] K. Adstedt, et al., Intercalation of amorphous polysaccharides into chiral cellulose nanocrystal organization

for controlled iridescence and enhanced mechanics, *Adv. Funct. Mater.*, **2020**, 202003597

[5] M. C. Kreckler, et al., Bio-encapsulated MXene Flakes for Enhanced Stability and Composite Precursors, *Adv. Funct. Mater.*, **2020**, 2004554

SESSION SM05.04: Novel Soft Composites II
Session Chairs: Michael Bartlett and Jacques Lux
Wednesday Afternoon, April 21, 2021
SM05

5:15 PM SM05.04.01

A New 3D Printing for Multiphase-Based Nanocomposites Dharneedar Ravichandran, Yuxiang Zhu, Weiheng Xu, Sayli Jambhulkar and Kenan Song; Arizona State University, United States

3D printing has been known as additive manufacturing, with advantages of flexible design and rapid prototyping over subtractive manufacturing. Current 3D printing on the market includes material extrusion, ink jetting, photopolymer curing, and powder fusion. However, these methods rely on simple blending or premixing to fabricate multiple materials or multiphase composites. As a result, the dispersion quality and interfacial interactions have been a bottleneck to overcome during the layer-by-layer manufacturing that leads to weak properties in 3D printed composites. Our study reports an in-house 3D printer based on multiphase printing that can selectively deposit polymers and nanoparticles within distinct phases. In this way, the particle dispersions and their interactions with neighbor polymer chains can be precisely manipulated. Therefore, the composites will demonstrate improved mechanical and functional properties. We will demonstrate the uses of polyvinyl alcohol (PVA) and polyacrylonitrile (PAN) in this unique multiphase 3D printing. Carbon nanotubes (CNTs) and carbon nanofibers (CNFs) with simple sonication will serve as printing inks. The composite structures (e.g., hierarchies, architectures), thermal transitions (e.g., glass transition or melting), and mechanical properties (e.g., strength and stiffness), as well as the performance of printed systems, will be the focus of our research.

5:30 PM SM05.04.02

Oxide-Mediated Mechanisms of Gallium Foam Formation During Ambient Shear Mixing Processes Wilson Kong¹, Najam U. Shah¹, Taylor V. Neumann², Man Hou Vong², Praveen Kotagama¹, Michael Dickey², Robert Y. Wang¹ and Konrad Rykaczewski¹; ¹Arizona State University, United States; ²North Carolina State University, United States

Liquid metals (LMs) based on gallium have been explored as prospective functional materials in soft electronics and wearable technology. LMs are useful in applications which require high electrical and thermal conductivity while remaining mechanically deformable. Their widespread use is hindered by its high surface tension, large density, high cost, and rapid surface oxidation in ambient conditions. Augmentation to its rheology through the addition of solid particles or air bubbles can enable LM to be patterned and dispensed onto different surfaces while reducing the overall LM used [1]. Previous studies have demonstrated the need for particle-induced stabilization of air bubbles for traditional metal foams while gallium foaming can occur through simple stirring in air [2-3]. Furthermore, the mechanism for gallium foam formation during shear mixing in air is currently not well understood. In this work, we elucidate the mechanisms for which this foaming process occurs for liquid gallium and the effects of air entrapment on its density, rheology, and thermal properties [4]. We systematically show the structure-property relationships of gallium foam during shear mixing in air and how the surface oxide contributes to the formation and stabilization of air bubbles. From this, it is revealed that a critical amount of surface oxide fragments is necessary to transition the gallium LM into a foam-like LM. These studies provide fundamental insights into the effects of LM-processing on its material properties and open a pathway for exploring other methods to engineer multifunctional LM soft composites.

References:

- [1] W. Kong et al., *Adv. Mater.*, 2019, 31, 1904309
- [2] X. Wang et al., *Adv. Funct. Mater.*, 2019, 1907063
- [3] J. Banhart, *Adv. Eng. Mater.*, 2006, 8, 781–794
- [4] W. Kong and N. U. H. Shah et al., *Soft Matter*, 2019, 16, 5801-5805

5:45 PM SM05.04.03

Field-Assisted 3D-Printing of Functional Composites Tyler Ray¹, Drew Melchert², Matthew Begley² and Daniel Gianola²; ¹University of Hawaii at Manoa, United States; ²University of California, Santa Barbara, United States

Acoustic forces are an attractive pathway to achieve directed assembly for multi-phase materials *via* additive processes. Programmatic integration of microstructure and structural features during deposition offers opportunities for optimizing printed component performance. Here, we demonstrate that acoustic fields can effectively assemble conductive particles into networks within polymer matrices, whose configuration is modulated prior to curing, to produce 2-D conductive, 1-D conductive, or insulating materials on-demand, all using the same precursor ink. Furthermore, patterning efficient percolated networks in this manner increases conductivity an order of magnitude over conventional dispersed-fiber composites with an order of magnitude lower particle loading, improving printability and allowing versatile orthogonal control of other properties. Although the focus is on electrical conductivity, the approach described is extensible to other transport phenomena. As a relatively material agnostic technique for microstructural control, acoustic-focusing-assisted additive manufacturing offers an expanded library of printable multiphase inks. This technology demonstrates a novel approach to modulating material properties via microstructure control to pave the way for 3D printing components with embedded electrical circuits or other spatially modulated properties.

6:00 PM SM05.04.04

Microcapsule-Based Self-Healing Chemistry for Glass Fiber-Reinforced Thermoplastic Composites Dhawal Thakare^{1,2}, Ian L. Flueck^{1,2} and Nancy R. Sottos^{1,2}; ¹University of Illinois at Urbana-Champaign, United States; ²Beckman Institute for Advanced Science and Technology, United States

Fiber-reinforced thermoplastic composites are increasingly being used for industrial applications as they reduce the weight versus traditional materials such as metals and thermosets without compromising structural strength while also allowing better stiffness, recyclability and short processing times. Traditional methods of healing thermoplastics by heating or inducing local heat through embedding heat sources requires external intervention and energy. This strategy may not be suitable for many large-scale industrial applications. Microcapsule-based strategies present an attractive alternative as they are autonomous, scalable and can be incorporated into traditional composite systems. Capsule-based self-healing has been widely shown in bulk polymers, and to some extent in thermoset composites, but autonomous healing in fiber-reinforced thermoplastic composites remains a challenge. The healing strategy proposed in this work utilizes a robust dual microcapsule system containing monomeric healing compositions which will undergo complete polymerization upon release from ruptured microcapsules within a damage zone. Multi-shell walled microcapsules coated with polydopamine are used to encapsulate a methacrylate-alkylborane based chemistry. One part of the microcapsule system contains a trialkyl borane-amine complex and the other microcapsule contains an acrylic monomer with an anhydride-based decomplexer. The microcapsule size has been tuned to the order of a few microns to avoid agglomeration and aid survival during composite manufacturing. The core content of the microcapsules is confirmed and quantified using ¹H NMR and elemental analysis techniques. Thermogravimetric analysis of the microcapsule system reveals enhanced thermal stability at temperatures up to 200 °C, which is required to survive stringent composite manufacturing conditions. Subsequently, the microcapsules are incorporated into a model glass fiber-reinforced polyethylene composite to assess its ability to heal delamination and quantify its healing performance. In addition to autonomous healing, this healing strategy offers other advantages such applicability of the healing chemistry to a wide variety of inert low surface energy thermoplastics and healing at room temperature.

6:15 PM SM05.04.05

Soft Organic Multiferroic Polymer Composites Scott Newacheck and George Youssef; San Diego State University, United States

The prominence of interactions between multiphysical domains give rise to the need for multifunctional materials that satisfy the broad requirements for the emerging fields of soft robotics and biomedical devices. These fields require efficient coupling of electrical and magnetic energies for sensing, actuation, and communication, preferably done with the same components to reduce system complexity. Composite multiferroic materials offer tunable extrinsic magnetoelectric coupling by engineering the piezomagnetic and piezoelectric materials in different proportions, geometries, and configurations. A major limitation for nearly all multiferroic composites stems from their composition of brittle and stiff ceramic and metallic materials, highlighting a greater property mismatch between the constituents. Such mismatch is detrimental in straintronics, where the main mediator between electricity and magnetism is mechanical strain. On the other hand, organic multiferroic materials are attracting scientific and technological interest due to their tunable properties while reducing the mismatch challenges since the entire framework is made of compliant polymers. However, a shortcoming of organic multiferroics is the basis that the donor-acceptor paradigm is an inferior magnetoelectric coupling mechanism due to the limited excitonic interactions. Presented herein is a novel approach to enhance the magnetoelectric performance of organic multiferroics through the addition of lattice deformation and charge injection mechanisms. The novel organic ferromagnetic polymer blend, P3HT-PCBM is interfaced with a well-established electroactive polymer, PVDF-TrFE, for its piezoelectric properties. The application of an electric field across the PVDF-TrFE surfaces result in a mechanical strain that can transfer to the adjacent P3HT:PCBM framework, enhancing the spin-lattice interaction. The polarization of PVDF-TrFE is also dependent on the electric field resulting in an accumulation of charges on the surface, hence improving the spin-electron interactions of the blend polymer. Therefore, the addition of PVDF-TrFE strategically and dynamically tunes the magnetoelectric properties of the blend polymer on demand. Furthermore, monochromatic illumination of the newly created composite has shown to manipulate the magnetic behavior through photon-exciton-spin coupling. Future research will focus on gaining an insight into magnetoelastic and magnetocrystalline anisotropies of this novel class of material which is forecasted to be fundamentally different from traditional magnetic materials.

6:30 PM SM05.04.06

TEM Image Processing Analysis of BTO-polymer Nanocomposites to Construct a Finite Element Model for Extracting the Particle Dielectric Constant of BTO Dithi Ganjam¹, Giovanni Ferro², Maia Gibson¹, Katherine Partington¹, Akshay Trikha¹, Albert Dato¹ and Todd Monson³; ¹Harvey Mudd College, United States; ²Pomona College, United States; ³Sandia National Laboratories, United States

Barium titanate (BTO) is a ferroelectric perovskite material that is currently used in energy storage applications because of its high dielectric constant. Wada et al. reported that the size of BTO strongly affects its dielectric constant [2]. In the study, BTO powders with diameters larger than 300 nm were found to have a dielectric constant of 4000, while BTO nanoparticles with a diameter of 70 nm exhibited a dielectric constant of over 15,000. These results are highly contested, but their implications to energy storage have motivated us to investigate the dielectric constants of BTO nanoparticles of various sizes. Here we present the relationship between BTO diameter and BTO dielectric constant, which was obtained through (1) capacitance measurements of polymer-matrix nanocomposites containing BTO nanoparticles, (2) a novel method of processing transmission electron microscope (TEM) images of highly agglomerated nanocomposites, and (3) more accurate COMSOL models of the nanocomposites using data obtained from our image processing method. The positions, agglomeration, shapes, and diameters of BTO nanoparticles in a polymer matrix were determined through our image processing method that extracts this information directly from TEM images of nanocomposites. We then developed a COMSOL Multiphysics model that simulates BTO nanoparticles embedded in a polymer matrix. The COMSOL model takes the results of our image processing technique as inputs and computes the dielectric constants of nanocomposites. By comparing experimental composite

dielectric constants to those obtained through COMSOL modeling, we explored the relationship between BTO nanoparticle diameter and dielectric constant.

Sandia National Laboratories is a multimission laboratory managed and operated by National Technology and Engineering Solutions of Sandia, LLC., a wholly owned subsidiary of Honeywell International, Inc., for the U.S. Department of Energy's National Nuclear Security Administration under contract DE-NA0003525.

6:45 PM SM05.04.07

Late News: Self-Healing Vitrimer Coating for Robust Hydrophobicity Jingcheng Ma, Laura E. Porath, Christopher Evans and Nenad Miljkovic; University of Illinois at Urbana-Champaign, United States

Durable hydrophobic coatings have seen considerable interest in the last decade. Currently, the most popular strategy to achieve mechanical robustness is by combining perfluoro-compounds (PFCs) with 'armor' structures for coating protection. These protective structures are usually large (>10 μm in thickness). However, in many cases thin (<100 nm) hydrophobic coatings are desired. For example, in dropwise condensation, atmospheric water harvesting, anti-icing, and water desalination, the heat and mass transfer rate can be significantly enhanced using hydrophobic surfaces that are less than 100 nm in thickness. Here, we achieve stable hydrophobicity with high mechanical robustness using polydimethylsiloxane-based self-healing thin films that are 1-10 nm thick. We designed and synthesized the vitrimer with polydimethylsiloxane network strands and dynamic boronic ester crosslinks (dyn-PDMS) to take advantage of the inherent hydrophobic nature of silicones. The dynamic bonds provide a mechanism for self-healing and damage resistance. We show that even for films having nanoscale thickness (<10 nm), the transparent coating maintains exceptional hydrophobicity after scratching, cutting, indenting, and steam condensation. The dynamic coating can also be easily deposited through scalable techniques like dip-coating on a variety of substrates including silicon wafer, aluminum, copper, and glass. The developed dynamic polymer chemistry is fluorine-free for better environmental sustainability compared to commonly used PFC-based materials. The presented work develops a paradigm shift in achieving long-term durable hydrophobicity enabling the implementation of self-cleaning, anti-icing, heat transfer, and microfluidic applications.

7:00 PM SM05.04.08

Late News: Encapsulation of Phase Change Materials in Fibers for Renewable Thermal Energy Storage Ping Lu, Wanying Wei, Ryan Hart, Dev Patel and Harmann Singh; Rowan University, United States

A natural phase change material, lauric acid (LA), was encapsulated in polystyrene (PS) hollow fibers through three green approaches: 1) co-fabrication of the mixture solutions, 2) thermally triggered nanocapillary transportation and encapsulation, and 3) solvent-assisted nanochannel encapsulation. By simply tuning the encapsulation parameters such as the LA/PS weight ratio, temperature and concentration, the obtained LAPS composite fibers achieved an unprecedented thermal energy storage capacity up to 82.0% (147.8 J/g) of pristine LA (180.2 J/g) owing to the high LA loading and the lightweight and porous nature of the PS matrix. Simultaneous TGA-DSC, ATR, Raman, and SEM measurements confirmed the homogeneous distribution of LA inside the fibers across the whole membranes. Further, the LAPS composite fibers showed a long-lasting stability during cycling without storage capacity deterioration, as well as an exceptional structural stability without LA leaking and fiber rupture during 100 heating-cooling cycles. The energy-dense and form-stable LAPS composite fibers have a great potential for various thermal energy storage applications including solar energy storage, "temperature-smart" buildings, thermal regulating textiles, and thermal therapy devices.

8:15 PM SM05.05.01

Late News: Microbubbles Cloaked with Hydrogels as pH-Activatable Ultrasound Contrast Agents Mary W. Burns, Robert F. Mattrey and Jacques Lux; UT Southwestern, United States

While microbubbles (MBs) are currently mainly used as cardiac and perfusion imaging agents in the clinic, engineering MBs with bioresponsive properties would expand their use to detect pathophysiologic changes. This can be achieved by stiffening the MBs shell with a bioresponsive “cloak” to decrease their oscillations and silence their signal, and rescuing the MB elasticity when they are exposed to a biomarker of interest. This strategy would allow the switching between a stiff 'OFF' state and an elastic 'ON' state that would allow MBs to become detectable only when exposed to biomarkers of interest (*e.g.*, pH, reactive oxygen species, hypoxia, or enzymes).

To validate our hypothesis, we used conjugated MBs with hyaluronic acid (HA) and crosslinked the resulting polymeric shell with pH-sensitive crosslinkers to obtain activatable pH-sensitive MBs (pH-MBs). We first validated the successful conjugation of HA to MBs and targeting of pH-MBs to CD44-positive cells. Using ultrasound imaging, we confirmed the harmonic signal loss that is associated with the stiffening of pH-MBs. We used a clinical ultrasound scanner equipped with Cadence contrast pulse sequencing to image pH-MBs before and after acidification and observed a fivefold increase in harmonic signal. Because the crosslinker cleavage is reversible, we were able to silence harmonic signal again by neutralizing the acidic suspension was neutralized, confirming that harmonic signal is dependent on the cross-linked HA. Interestingly, the rate of rise and the magnitude of harmonic signal increase could be manipulated by varying the phospholipid composition and the number of crosslinkers, indicating that the platform can be tuned to the desired response needed.

8:30 PM SM05.05.02

Late News: Highly Recyclable and Tough Polyurethane Elastomeric Thermosets for Soft Electronic via Well-Defined Network Design Jiancheng Luo¹, Sheng Zhao² and Pengfei Cao¹; ¹Oak Ridge National Laboratory, United States; ²The University of Tennessee, Knoxville, United States

Jiancheng Luo, Sheng Zhao, and Pengfei Cao*

Chemical Sciences Division, Oak Ridge National Laboratory, Oak Ridge, TN 37830, USA

Thermoset elastomers with multifunctionality such as self-healable and recyclable capability, stretchability, and stimuli-responsive shape, are attractive to numerous applications. In this work, polyurethane (PU) vitrimers with well-defined network topology are design by connecting tetra-armed crosslinkers with PDMS chains bearing disulfide bonds. Compared with the random network, the well-defined network endows elastomeric vitrimers significant improvement on their mechanical performance. Through tuning PDMS chain length, the elastomers exhibit outstanding mechanical properties with ultimate tensile stress ranging from 1.5 MPa to 11.2 MPa, and elongation at break ranging from 290% to 884%. The elastomers also exhibit good solvent resistance and self-healability, and meanwhile show no obvious loss on mechanical performance after 5 reprocessing cycles. By embedding carbon nanotubes (CNT) into polymer network, the as-prepared conductive elastomers can be used to fabricate various soft electronics, *i.e.*, strain and electrocardiogram sensors. The network design principle here provides a feasible approach to achieve recyclable thermoset elastomers with excellent mechanical performance.

8:45 PM SM05.05.03

Late News: Multifunctional Origami Patch for Minimally Invasive Tissue Sealing Sarah Wu, Hyunwoo Yuk, Jingjing Wu and Xuanhe Zhao; Massachusetts Institute of Technology, United States

For decades, bioadhesive materials have garnered great attention due to their potential to replace sutures and staples for sealing and repairing tissues during minimally invasive surgical procedures. However, the complexities of delivering bioadhesives through narrow spaces and achieving strong adhesion in fluid-rich

physiological environments continue to present substantial limitations to the surgical translation of existing glues and sealants. We introduce a new strategy for minimally invasive tissue sealing and repair based on a multilayer bioadhesive patch, which is designed to repel body fluids, form fast, pressure-triggered adhesion with wet tissue surfaces, and resist biofouling and inflammation. The multifunctional patch is realized by a synergistic combination of three distinct functional layers: (i) a micro-textured bioadhesive layer, (ii) a dynamic, blood-repellent hydrophobic fluid layer, and (iii) an antifouling zwitterionic non-adhesive layer. The bioadhesive patch is capable of forming fast and robust adhesion to tissue surfaces in the presence of blood, and exhibits superior resistance to bacterial adhesion, fibrinogen adsorption, and *in vivo* fibrous capsule formation. By adopting origami-based fabrication strategies, we demonstrate that the multilayer bioadhesive patch can be readily integrated with a variety of minimally invasive end effectors to provide facile and effective tissue sealing in ex vivo porcine models, offering new opportunities for minimally invasive tissue sealing and repair in diverse clinical scenarios.

9:00 PM SM05.05.04

Late News: Photo Patterning of Dynamic Covalent Polymer Hydrogels Towards Sustainable and Flexible Micromanufacturing Di Chen, Qian Zhao and Tao Xie; Zhejiang university, China

Dynamic covalent polymer networks will go through topological rearrangements under stimulations to relax internal stress and switch the features of materials. Via continuously exploring new internal force programming approaches, the structure of dynamic materials can be manipulated in a more and more controllable fashion. Here, besides the generally deformed by macroscopic stretching, bending or twisting, we present a microscopical way which is freezing, to impose internal force toward a dynamic hydrogel and establish a flexible micromanufacturing method. Specifically, the hydrogel is crosslinked by disulfide bonds and owns capability of photo-induced network rearrangements. During freezing, microphase separation occurs, forming two phases: ice crystals and a squeezed polymer phase. After spatial UV exposure, polymer chains are relaxed due to the disulfide bond exchange and entropy of the network is increasing as well. Subsequent ice melting will lead to porous patterns with the feature size of 20 μm , and the obtained porous hydrogels can be directly utilized to spatially store functional inks for transfer printing. Additionally, the present ice-templating photo patterning method requires no solvent washing step, and uses mostly water (98%) with the remaining organic component easily recyclable, thus generating zero organic waste. Therefore, it can open up an avenue for sustainable and flexible micromanufacturing.

9:15 PM SM05.05.05

A One-Pot Immunosensor Composed of Metal-Enhanced Fluorescence Probes and a Photocatalytic Film Kihyeun Kim and Min-Gon Kim; Gwangju Institute of Science and Technology (GIST), Korea (the Republic of)

To overcome a limitation of typical immunoassays like an enzyme-linked immunosorbent assay (ELISA) in terms of multi-step procedure, one-pot immunoassays are in high demand for point-of-care (POC) testing that can be used by individuals at any time and anywhere.

In this study, we suggest a one-pot immunosensor composed of Cy5/capture antibody/gold nanorod conjugates and an Au/TiO₂ photocatalytic film. After injection of solution for an immunoassay, delayed production of H₂O₂ from the photocatalyst by ultraviolet illumination enabled a one-pot assay by quenching of Cy5 due to 4-chloro-1-naphthol precipitates that produced by the enzymes bound to the conjugates via interleukin 8 (IL-8) antigens. As a result, our one-pot immunosensors could detect IL-8 within the range of 1 pg mL⁻¹ – 1,000 pg mL⁻¹, which was as sensitive as the purchased ELISA kit for IL-8 detection. Therefore, this sensor platform could pave the way for highly sensitive, portable, easy-to-use POC biosensors for individuals.

9:30 PM SM05.05.06

Late News: Light-Coded Digital Heterogeneity Toward Multifunctional Shape Shifting of Shape Memory Polymers Wenjun Peng and Tao Xie; Zhejiang University, China

Homogeneous single synthetic materials typically have limited functions as multifunction is always related to multimaterial systems. By mimicking the nature of biological species to introduce spatially heterogeneous distribution of active components in synthetic materials, the design space for advanced multifunction is widened. Here, we introduce the heterogeneity at the programming process after material synthesis/fabrication step by a digital photothermal effect. Our first work allows spatio-selective programming of crystallinity in a shape memory polymer (SMP). Consequently, a pre-stretched 2D film with spatial heterogeneity in shape recovery ratio can morph into designable 3D permanent shapes, achieving the 4D transformation. Following the first work, we design a supramolecular SMP with intrinsic time-temperature dependency. Spatial controlling of deformation temperature and time brings heterogeneity in shape recovery rate, thus leading to highly non-monotonic shape-shifting pathways and tunable evolution lifetime. The benefits of these unique features are demonstrated by multi-shape transformation, an “invisible” color based clock and a time-temperature indicator (TTI). Heterogeneous material in our work, as a novel kind of multimaterials, provides a versatile idea for manufacturing multifunctional devices.

SESSION SM05.06: Novel Soft Composites IV
Session Chairs: Di Chen and Yujie Wei
Thursday Morning, April 22, 2021
SM05

8:00 AM SM05.06.02

Spatially Patterned Magnetic Hydrogels—Towards Controllable Structures and Responses Jacek Wychowaniec¹, Patricia Monks^{1,2}, Eoin P. Mckiernan¹, Krutika Singh¹, Danielle Winning¹, Katie McGarry¹, Esther R. Aluri¹, Shane Clerkin¹, Niall Treacy¹, Andreas Heise², John Crean¹, Emmanuel Reynaud¹, Brian Rodriguez^{1,1} and Dermot Brougham¹; ¹University College Dublin, Ireland; ²Royal College of Surgeons in Ireland, Ireland

Multifunctional nanocomposites which exhibit well-defined physical properties and encode spatio-temporally controlled responses (including changes of shape, microscopic morphology, mechanical strength and permeability) are emerging as components for advanced responsive systems. For instance in the case of biomedical applications magnetic nanocomposite materials have attracted significant attention due to their ability to respond to spatially and temporally varying magnetic fields changing their intrinsic structure, undergoing time-dependent deformations, or releasing cargo on demand.¹⁻³

The combination of MNPs and established 3D printable polymeric hydrogel formulations can provide multifunctional and stimuli-sensitive systems with spatial-, temporal- and dosage-controlled release properties. Here, our work towards bio-applications of magnetic hydrogels is described in two fabrication cases, (i) conventional manufacturing, where magnetic materials are utilized in conventional manufacturing processes during solidification/gelation, as well as (ii), magnetic structuring, where the presence of magnetic fields or 3D printing was used to spatially pattern materials with encoded magnetic responsiveness.

A combination of in-house built multi-head and commercial 3D printers was used to extrude selection of magnetic composite hydrogels. Magnetic nanoparticles were synthesised, stabilized and dispersed homogeneously through the gels to optimise their hyperthermic responses. Oscillatory and rotational rheology measurements confirmed the viscoelastic properties providing ideal materials for 3D printing well-defined architectures with high fidelity for both magnetic and non-magnetic components of integrated multi-component builds. The hybrid inks showed complete shear- and temperature-recoverability/reversibility to their initial state, confirming that at particle concentrations that enable magnetic responses the necessary printability is not lost. Multiple complex structures were printed with high resolution (~150 μm) with independent magnetic and non-magnetic patterned components and these were shown to be reproducible and robust. Post-printing chemical

crosslinking was used to retain long-term fidelity of the printed structures, whilst retaining magnetically responsive hyperthermic responses at low particle concentrations. Thermoresponsive contractile elements were also embedded from selection of polymers based on poly(N-isopropylmethacrylamide) with chemically programmed volume temperature transitions at physiologically relevant range of 32 to 45°C.

For AC-magnetic field responsiveness, high resolution IR thermography confirmed that incorporated magnetic nanoparticles retain sufficient magnetic response to provide spatial temperature gradients for cell stimulus and for stimulus-responsive timed delivery of biomolecules. The advantages of spatial patterning of thermally active components will be described in the context of kidney and cerebral organoids, as well as for stem cell differentiation. Applications of DC-magnetic fields to physical stimulation of patterned magnetic gels will also be presented.

1. Zhang, X. *et al.*, The Pathway to Intelligence: Using Stimuli-Responsive Materials as Building Blocks for Constructing Smart and Functional Systems. *Advanced Materials* **2019**, *0* (0), 1804540.
2. Lyons, S.; Mc Kiernan, E. P.; Dee, G.; Brougham, D. F.; Morrin, A., Electrostatically modulated magnetophoretic transport of functionalised iron-oxide nanoparticles through hydrated networks. *Nanoscale* **2020**, *12* (19), 10550-
3. Stolarczyk, J. K. *et al.*, Nanoparticle Clusters: Assembly and Control Over Internal Order, Current Capabilities, and Future Potential. *Advanced Materials* **2016**, *28* (27), 5400-5424.

ACKNOWLEDGMENTS

The authors acknowledge support from Science Foundation Ireland (16/IA/4584 and 13/IA/1840).

8:15 AM SM05.06.03

Artificial Tendrils Mimicking Plant Movements by Mismatching Modulus and Length in Multimaterial Polymeric Systems Muhammad Farhan¹, Andraz Resetic², Anil K. Bastola¹, Marc Behl¹ and Andreas Lendlein¹; ¹Helmholtz-Zentrum Geesthacht, Germany; ²Jozef Stefan Institute, Slovenia

Plants structures and their motions are a result of long-term interplay between evolution, failure, and adaptation to their local environments. Motions of plants are driven by their growth. Typical examples of the plant kingdom where the motion is relevant are searchers of liana or the tendrils of climbing plants. In both examples, the capability of coordinated actuation such as coiling upon response to specific external stimuli can be observed. To enable biomimetic innovations, special attention has been paid to understand the coiling of plant structures. [1, 2] A promising approach to mimic this behavior are multifunctional multimaterial systems, in which orchestrated interplay of functions could provide this coiling behavior. Here we report on development of a multimaterial fiber as an artificial tendril. The multimaterial fiber is composed of shape-memory polymer fiber core and an elastic outer matrix. As fiber core we selected a poly[ethylene-co-(vinyl acetate)] (PEVA) fiber ($d \approx 400 \mu\text{m}$), whereas a silicone based soft elastomer was chosen as a matrix. The core fiber provides a temperature dependent actuation (expansion/contraction) that propagates coiling of the tendril due to the mismatch in the modulus of outer matrix and inner core. Therefore, we considered the mismatch in elastic modulus as a control parameter. The modulus of the matrix (E_{matrix}) was varied between 0.1 and 0.5 MPa to achieve various coiling behaviors of such multimaterial tendrils. The maximum number of coiling per unit centimeter ($N = 0.35$) was observed for the tendril with an intermediate $E_{\text{matrix}} = 0.29$ MPa. Our study stimulates the design for plant inspired multimaterial tendrils with tunable coiling and reversible motion responses.

References

Gerbode, S.J., et al., *How the Cucumber Tendril Coils and Overwinds*. *Science*, 2012. 337(6098): p. 1087-1091.
Xiao, Y.Y., et al., *Biomimetic Locomotion of Electrically Powered "Janus" Soft Robots Using a Liquid Crystal Polymer*. *Advanced Materials*, 2019. 31(36).

8:30 AM SM05.06.04

Control of Direct Crystallization by a Running Magnetic Field Sergey M. Karabanov, Dmitry V. Suvorov,

Dmitriy Y. Tarabrin, Evgeny V. Slivkin and Andrey S. Karabanov; Ryazan State Radio Engineering University, Russian Federation

Direct crystallization is widely used in the production of multicrystalline silicon for solar energy and electronics. In the process of direct crystallization, the melt flow is controlled by the heat convection force resulting from a temperature gradient. This leads to the appearance of convective disturbances and melt turbulence. These effects have a negative impact on the quality of the obtained material.

The efficient way to control the melt mixing is to use both continuous and variable magnetic fields. Continuous magnetic fields smooth effectively convection flows in the melt, and variable magnetic fields influence substantively on the melt mixing.

This paper presents the results of mathematical modeling of electromagnetic stirring of silicon melt under various conditions. Mathematical modeling was carried out using COMSOL Multiphysics software. In the course of modeling, the distributions of the magnetic field induction, the densities of the Lorentz force, and the melt stirring rates were obtained. The distribution of the surface rate of melt movement was determined. Experimental studies were carried out on a direct crystallization unit with the crucible size of 860x860x450 mm and the ingot weight of up to 500 kg. To create a running magnetic field, a current pulse generator was made. The current amplitude of an inductor was regulated in the range from 10 A to 700 A, the frequency of current pulses was from 20 Hz to 200 Hz, and the phase shift was from zero to 180 degrees.

The research results are as follows:

- a physical and mathematical model of electromagnetic stirring of silicon melt was developed, modeling of electromagnetic stirring was carried out;
 - on the basis of the developed model, the configuration of the pilot unit was selected;
 - a pilot unit was created and experimental studies on the influence of the magnetic field parameters on the melt surface rate were carried out;
 - the optimal conditions for obtaining a stable, repeatable process of silicon melt stirring were established.
- The obtained results were used for multicrystalline silicon production. Studies on the effect of the current shape in inductors were conducted.

8:35 AM SM05.06.05

Stepwise Magnetic Self-Organization of Micropillar Arrays Jeong Eun Park¹, Augustine Urbas², Zahyun Ku² and Jeong Jae Wie¹; ¹Inha University, Korea (the Republic of); ²Air Force Research Laboratory, United States

Long-range ordering of magnetic particles has been reported by generating magnetic dipole moments and dynamic swarming motion in aqueous medium under external magnetic field. However, the self-organization is not reversible and reliable because the position of magnetic particles is not stationary. Alternatively, we suggest periodic polymeric micropillar arrays with inclusion of magnetic particles for reversible and programmable magnetic self-organization in a stepwise manner. When magnetic field is applied, individual micropillars are magnetized and operate as micromagnets. The vicinal pair of pillar tops magnetically attract each other for magnetic self-organization while the pillar base is still fixed to the substrates. As the magnetic flux density increases, the paired micropillars undergo quad-body organization, and then the long-range connectivity of pillar tops is accomplished. We will discuss the influence of spacing and anisotropic cross-sections of the micropillars on the stepwise magnetic self-organization by investigating the geometry form factors such as rectangular, square and circular cross-section.

8:40 AM SM05.06.06

Thermo-Responsive Microcapsules with Tunable Cut-Off Threshold of Molecular Permeation for Temperature-Controlled Encapsulation and Release Yehun Choi¹, Seog-Jin Jeon² and Shin-Hyun Kim¹; ¹Korea Advanced Institute of Science and Technology, Korea (the Republic of); ²Kumoh National Institute of Technology, Korea (the Republic of)

Microcapsules with a liquid core and solid shell have been used for storage and release of materials in various

purposes. The shells that have regular size of continuous pores or microchannels provide molecular-size-selective permeation so that they allow transmembrane transport for smaller molecules than the pores while excluding or retaining larger molecules. The size-selective permeation is of great importance for protection of delicate large encapsulants while allowing transmembrane transport of small molecules, in particular for encapsulation of catalysts or enzymes and nanoparticle-based sensors. The shells with tunable cut-off threshold of size-selective permeation are promising for reversible encapsulation and release of encapsulants in a highly controlled and programmed manner. The molecules smaller than the cut-off threshold can be inserted into the core of the microcapsules by diffusion, which is encapsulated by lowering the cut-off below the size of the molecules. The encapsulants will be released into surrounding by increasing the cut-off, which can be done in single step or multiple steps.

Hydrogels are one of the promising shell materials to achieve the tunable cut-off threshold. Hydrogels have three-dimensional network of hydrophilic polymers. When the network is swollen by water, large free volume is formed in the mesh, through which small molecules can diffuse. More importantly, the use of stimuli-responsive polymers to form the mesh enables to control the degree of swelling. However, the precursors for hydrogels are usually hydrophilic and soluble in water, which makes it challenging to produce microcapsules with water core and hydrogel shell using conventional templates of water-in-oil-in-water (W/O/W) or oil-in-water-in-oil (O/W/O) double-emulsion drops.

In this work, we use a novel thermoresponsive hydrogel precursor to produce the semipermeable microcapsules with tunable cut-off threshold of permeation with a template of W/O/W double-emulsion drops. The precursor is poly(N, N-diethylacrylamide) (PDEAM) functionalized with benzophenone (BP). BP self-initiates the reaction under the irradiation of ultraviolet (UV) in the absence of photoinitiator, crosslinking PDEAM to form a mesh. PDEAM has the lower critical solution temperature (LCST) around 34°C with water. Due to the hydrophobic BP moiety, PDEAM-BP is highly soluble in organic solvent and weakly soluble in water even at room temperature. Using the solution of PDEAM-BP in chloroform as an oil phase, we produce W/O/W double-emulsion drops with ultra-thin oil shell with a glass capillary microfluidic device. The innermost water drops and continuous phase contain a high concentration of salt, which exerts an osmotic pressure and helps prevent the formation of tiny water droplets in the oil shell. The double-emulsion drops are incubated at 50°C for removal of chloroform, which makes the PDEAM-BP more hydrophobic and further suppresses the formation of water droplets in the oil shell. After complete consolidation, PDEAM-BP is crosslinked by UV irradiation and the resulting microcapsules are washed with distilled water at room temperature. The microcapsules show temperature-dependent changes of diameter and shell thickness. The cut-off threshold is estimated to be below 4kDa in size at 50°C, whereas that is between 4kDa and 10kDa at 25°C and 4°C. The temperature-dependent change of the cut-off threshold is highly reversible, which enables us to load and release molecules in a programmed manner. In addition, the release can be done in multiple steps by repeating heating and cooling. Moreover, the cut-off threshold of the microcapsules can be further controlled through the controlled irradiation of near infrared light by encapsulating photothermal agent of polydopamine (PDA) nanoparticles in the core. We believe our microcapsules with tunable cut-off threshold will provide new opportunities for microreactors and microsensors as well as drug carriers.

8:45 AM SM05.06.07

Multi-Functional Curvilinear Shape-Morphing with Patterned Adhesive Tapes via Localized Photothermal Effects Jae Gyeong Lee, Sukeyoung Won, Jeong Eun Park and Jeong Jae Wie; Inha university, Korea (the Republic of)

Construction of a 3D structure from 2D flat geometry has received great attention in the materials community. Although various methods are reported to achieve 2D to 3D shape-morphing, photothermal actuation has been emerged as a promising method for contactless shape-reconfiguration. The photothermal heating method often use black inks on the shape memory polymers to localize photothermal heating. However, this method could cause further undesirable actuation as the ink patterns remain even after creating the desirable 3D structures. In this study, adhesive tape patterns were employed instead of the ink patterns in order to achieve transparent 3D structures as well as prevent undesirable actuations. When black adhesive tapes were irradiated with NIR light, the patterned areas absorb photons and generate photothermal heating. When the temperature exceeds the

polymer glass transition temperature, shrinkage of polymer occurs by recovery of random coil conformation from biaxially pre-strained coils. We discuss the effects of various radial and chiral tape patterns on curvature control for complex 3D structures. Furthermore, we will demonstrate sequential folding by temporal regulation of the NIR irradiation. We will also discuss shape-reconfiguration of heterogeneous materials with the addition of compliant papers and introduction of conductive functions on 3D morphed polymers.

8:50 AM SM05.06.09

Late News: Gallium-Based Transformative Electronic System Integrated with Graphene and Flexible Thermoelectric Device for Rapid Bi-Directional Stiffness Tuning Sang-Hyuk Byun¹, Choong Sun Kim¹, Karen-Christian Agno¹, Simok Lee¹, Zhuo Li², Byung Jin Cho¹ and Jae-Woong Jeong¹; ¹Korea Advanced Institute of Science and Technology, Korea (the Republic of); ²Fudan University, China

While the predetermined mechanical properties of both conventional rigid electronics and emerging soft electronics allow them to perform target-specific functions, their fixed rigidity limits their extensive applications. Rigid electronics such as smartphones and laptops are easy to handle and can endure external stress owing to their robust structures. However, their high stiffness makes them incompatible with soft biological tissue, thus they are not suitable for use in wearables and implantable devices. While the compliant interface of soft electronics allows conformal contact with the curvilinear body, it does not provide sufficient load-bearing capability when operated in an off-body application. Stiffness tuning is one of the promising solutions in order to leverage the key features of both rigid and soft electronics. Recently, transformative electronic systems (TES) with reconfigurable shape and stiffness have been developed by using gallium as a thermally-tunable mechanical platform. However, the gallium platform experiences supercooling phenomenon during its liquid-to-solid phase transition which prevents soft-rigid TES mode conversion at its freezing temperature (29.76 °C) and makes the fast bi-directional soft-rigid conversion of TES a challenging task. Here, we present an advanced architecture for gallium-based TES, which integrates graphene and a flexible thermoelectric device (f-TED) to enable a rapid bi-directional soft-rigid transformation mode. Graphene facilitates the mitigation of the degree of supercooling as a catalyst to accelerate the nucleation of gallium during the liquid-to-solid phase transition, while the f-TED offers active temperature control to accelerate the overall phase transition of the gallium platform. During the solidification process, the f-TED lowers the temperature which assists in overcoming the supercooling of gallium that leads to a reduction in the liquid-to-solid transition time. In a similar way, the f-TED can shorten the time required for the solid-to-liquid transition of gallium by actively heating the TES platform. By integrating the graphene-gallium interface platform and f-TED, we could significantly reduce the time for the melting and freezing, by 91% (from 255 to 23 s) and 55% (from 175 to 79 s), respectively, as compared to TES design built with pure gallium. Based on this design strategy, we could successfully demonstrate a TES that can facilitate rapid conversion between a rigid handheld display and a flexible wearable pulsimeter/display. The proof-of-principle demonstration of TES capable of rapid bi-directional transformation suggests broad utility of the proposed design, which may open new opportunities for electronics, robotics, and biomedical devices.

9:05 AM *SM05.06.10

Micro- and Nano-Structured Dynamic Soft Matter Material Design by Light Christopher Barner-Kowollik; Queensland University of Technology, Australia

The tuning of both covalent bond formation as well as dissociation remains a grand challenge in the design of photodynamic systems. The light-responsive adaptation of polymer materials requires different wavelengths to induce reversible covalent bond formation and dissociation. Our efforts have been devoted to pioneer a toolbox of photocycloadditions that can be triggered by lower energy visible light, while their cycloreversion should function at the least energetic wavelength, too. The lecture will showcase the latest applications of reversible photochemistry for the generation of light adaptive micro-structured materials via 3D laser lithography.¹

Further, the lecture will explore visible light-triggered reversible triazolinedione (TAD) chemistry and its application in materials science. We have recently pioneered the photo-chemically driven reaction of TADs

with naphthalene as a dynamic covalent cross-linking platform that enables green light-induced network formation (525 nm), while network degradation is triggered by merely switching off the light, thus introducing the new class of Light Stabilized Dynamic Materials (LSDMs).² These materials can undergo a repeatable change in morphology from a covalently cross-linked material into a liquid polymer formulation by switching the visible light source on-and-off without the need for any additional triggers. Furthermore, TADs exhibit a strong purple colour which fades upon reaction with suitable substrates, thus facilitating online monitoring of the material's property transformation with the naked eye.

We subsequently expanded TAD photochemistry in the field of light-fuelled covalent non-equilibrium chemistry. Under green light, naphthalene-containing polymers can be folded into single chain nanoparticles (SCNPs) driven by [2+4] cycloadditions with a bivalent TAD crosslinker, whereas the SCNPs unfold into their linear parent polymers in the absence of light.³ Such photonic fuel driven dynamic SCNPs constitute the first example of a reversible light triggered folding of single polymer chains, mimicking their naturally observed spontaneous folding of proteins.

Moreover, we have established a new method for the photoinitiated, additive-free precipitation-driven synthesis of particles by crosslinking pre-synthesized low molecular weight polymers. Microspheres were produced by employing the nitrile-imine mediated tetrazole-ene cycloaddition reaction upon UV irradiation ($\lambda = 300$ nm), therefore forming intrinsically fluorescent particles.⁴ The reaction wavelength was subsequently red-shifted to 415 nm by exploiting *o*-quinodimethanes that undergo [2+4] cycloadditions with suitable dienophiles or [4+4] via self-dimerization.⁵ Critically, a variety of crosslinking molecules and dienophiles were investigated, imparting unique properties to the particles such as chemical degradability, chemiluminescence and acid triggered fluorescence switch-on. Finally, we combined our visible light driven particle design platform technology with the visible light-driven reversible [2+4] cycloaddition of TADs with naphthalene prepolymers, creating degradable microparticles that do not require any external degradation trigger other than darkness.⁶

¹ Gernhardt, M.; Frisch, H.; Welle, A.; Jones, R.; Wegener, M.; Blasco, E.; Barner-Kowollik, C. *J. Mater. Chem. C* **2020**, 8, 10993-11000.

² Houck, H. A.; Blasco, E.; Du Prez, F. E.; Barner-Kowollik, C. *J. Am. Chem. Soc.* **2019**, 141, 12329-12337

³ Kodura, D.; Houck, H. A.; Bloesser, F. R.; Goldmann, A. S.; Du Prez, F. E.; Frisch, H.; Barner-Kowollik, C. **2020**, submitted.

⁴ Hooker, J.; Delafresnaye, L.; Barner, L.; Barner-Kowollik, C. *Mater. Horiz.* **2019**, 6, 356-363.

⁵ Hooker, J.; Feist, F.; Delafresnaye, L.; Barner, L.; Barner-Kowollik, C. *Adv. Funct. Mater.* **2020**, 30, 1905399

⁶ Schmitt, C. W.; Walden, S. L.; Delafresnaye, L.; Houck, H. A.; Barner, L.; Barner-Kowollik, C. **2020**, submitted

SESSION SM05.07: Novel Soft Composites V
Session Chairs: Jianliang Xiao and Ruike Renee Zhao
Thursday Morning, April 22, 2021
SM05

10:30 AM SM05.07.01

Programmable Liquid Metal Microstructures for Multifunctional Soft Thermal Composites Michael D. Bartlett, A B M Tahidul Haque and Ravi Tutika; Virginia Tech, United States

Soft, elastically deformable composites can enable new generations of multifunctional materials for flexible devices and reconfigurable structures. An emerging material architecture is to create solid-liquid composites with liquid metal (LM) inclusions dispersed in elastomer matrices. These materials have shown exceptional combinations of soft mechanical response, tunable electrical properties, and high thermal conductivity. Such

properties are strongly dependent on the material composition and microstructure. However, approaches to control the liquid metal microdroplet morphology to program mechanical and functional properties are lacking. Here, we overcome this limitation by thermo–mechanically shaping LM droplets in soft composites to create programmable microstructures. This enables LM loadings up to 70% by volume with prescribed particle aspect ratios and orientation, enabling control of microstructure throughout the bulk of the material in stress–free conditions. The influence of microstructure on the mechanical and functional response is theoretically and experimentally determined and a general framework is developed to design soft composites with desired functional characteristics. Through this microstructural control in soft composites, we simultaneously achieve a thermal conductivity as high as 13 W/mK (> 70 x increase over polymer matrix) with low elastic modulus (< 1.0 MPa) and high stretchability ($> 750\%$ strain), representing one of the highest thermal conductivities for soft, deformable materials. The exceptional thermo–mechanical properties of LM programmed composites enables thermal control in rigid and highly deformable systems. We demonstrate this capability with electronics integrated into 3D printed materials, soft heat sinks, and thermal shielding in artificial muscles for a prosthetic hand. We envision that the ability to program microstructure in solid–liquid composites will enable further advances in flexible electronics and robotics, medical devices, and shape morphing structures.

10:45 AM SM05.07.02

Control of ROMP Polymer Architecture and Chemistry for High Temperature Stability and

Recyclability Douglas Ivanoff¹, Julian C. Cooper¹, Peyton Shieh², Jeremiah A. Johnson², Jeffrey Moore¹ and Nancy R. Sottos¹; ¹University of Illinois at Urbana-Champaign, United States; ²Massachusetts Institute of Technology, United States

High temperature thermosets display exceptional thermomechanical behavior due to densely crosslinked networks and chemically resistant bonds. Traditionally, increases in polymer crosslink density present greater challenges for recyclability. Here we show incorporation of a selectively cleavable moiety at the crosslink junction allows for significant increases in crosslink density and glass transition temperature while maintaining a pathway for recyclability. Co-polymerization of multi-functional cyclic olefins featuring silyl ether moieties with dicyclopentadiene (DCPD) produces degradable poly(DCPD)-based thermosets with high glass transition temperatures (T_g). Crosslinking density and glass transition temperature are controlled by tuning structure and molar concentration of the degradable co-monomers. These robust thermosets are degraded via exposure to a triggering fluoride stimulus, and the resulting soluble products can be incorporated into new polymers networks. The effects of these multifunctional cyclic olefins on crosslink density, glass transition temperature, and the rate of structural degradation are studied, and the properties of the recycled materials are characterized. Incorporation of silyl ether crosslinking units leads to thermosetting materials with high T_g (> 180 °C) and that are readily recyclable.

11:00 AM SM05.07.03

Lightweight, Liquid Metal Elastomer Composite Ethan Krings and Eric Markvicka; University of Nebraska–Lincoln, United States

Soft, elastically deformable materials with high thermal conductivity are critical for numerous industries including healthcare, aerospace, automotive, and flexible electronics, where combinations of high mechanical compliance and high thermal conductivity are required. An emerging material architecture are elastomer composites that are composed of liquid-metal (LM) microdroplets embedded in hyperelastic polymers. These all soft-matter systems exhibit exceptional thermal properties, are electrical insulating even at high volume loadings, and remain soft and stretchable even at extremely low temperatures (-80 °C). Although these materials exhibit a unique combination of properties, the high density and high volume loading of the LM filler significantly increases the density of the composite, which is problematic for large-area thermal management and weight sensitive applications such as wearable electronics, aerospace thermal control, and clothing. Here, we introduce a new lightweight, LM inclusion that has a unique combination of properties including high thermal conductivity, low mass density, and high deformability when embedded into an elastomer matrix. Furthermore, the composition of the lightweight, LM inclusion can be tailored, enabling a large range in density

with negligible changes to the thermal conductivity of the inclusion as the thermal conductivity is dominated by electrons. Experimental thermal conductivity results measured using the transient hot-wire method agree well with the Bruggeman and Cheng-Vachon models of effective medium theory. As with previously reported LM embedded elastomer composites, this composite shows increased thermal conductivity under strain and is able to achieve maximum strain above 400%. This work presents a new material architecture to enable independent control of the thermal conductivity and density of LM elastomer composites, offering new opportunities to tune functional properties of systems where weight is critical.

11:15 AM SM05.07.04

Inverted Shape Memory Elastomeric Composite (i-SMEC) with Matrix-Enabled Fixing and Fiber-Driven Recovery Caitlin D'Ambrosio¹, Melodie I. Lawton², Kelly Tillman³, Devon Shipp³ and Patrick T. Mather¹; ¹Bucknell University, United States; ²University of Rochester, United States; ³Clarkson University, United States

The demand for shape memory polymer (SMP) development has risen due to their multifunctional abilities and numerous applications in a variety of industries. This project explores a new approach to reconfigurable shape memory elastomeric composites (Re-SMEC) by altering the roles of the individual phases to create an inverted shape memory elastomeric composite (i-SMEC). In our previous work, we confirmed the feasibility of reconfiguration attributed to a dynamic covalent exchange between neighboring anhydride groups occurred, enabling the customization of the target geometry during shape memory activation. In the present work, we exploit these properties in the form of a new type of shape memory elastomeric composite that features a fibrous thermoplastic elastomer web combined with a reconfigurable elastomeric polyanhydride (PAH) matrix in a novel geometry controlled and manipulated thermomechanically. Contrary to traditional fiber-reinforced composites, where the fibrous phase temporarily fixes the geometry, this shape memory system utilizes the reconfigurable matrix for shape-fixing and elastic fibers as the memory retaining phase. We report the morphology, quantification of the mechanical properties, and the effect of fiber diameter on the shape memory abilities. Further, we introduce a new shape memory testing methodology of particular use for SMPs with fixing via matrix reconfiguration.

11:30 AM *SM05.07.05

Soft Multifunctional Composites Using Liquid Metals Michael Dickey; North Carolina State University, United States

This talk will discuss new work in our group (and with collaborators) on soft composites that utilize liquid metals. Liquid metals composed of gallium are compelling materials for multifunctional materials because they can be incorporated, patterned, or mixed readily into elastomer. The addition of the metal alters the electrical and thermal properties, but without significantly stiffening the composite relative to the pure elastomer. In addition to imparting metallic thermal or electrical properties (the latter of which is useful for creating wires, antennas, and electrodes), it can also tune the effective dielectric properties of the material and also go through phase transitions to produce enormous changes in modulus. I will discuss several aspects and implementations of these multifunctional properties. First, characterizing the dielectric and electrical properties of such soft composites for pressure sensor applications. Second, utilizing such materials for conductors and electrodes that can undergo enormous changes in mechanical properties. Third, describing composites with electrical conductivity that increases with deformation, which is highly unusual. Fourth, printing of such composites by modifying the rheology to enable 3D printing. This work has implications for stretchable electronics, responsive materials, and soft robotics.

11:55 AM *SM05.07.06

Sharpening and Amplifying the Actuation of Liquid Crystalline Elastomers Timothy White; University of Colorado Boulder, United States

Liquid crystalline materials are pervasive in our homes, purses, and pockets. It has been long-known that liquid

crystallinity in polymers enables exceptional characteristics in high performance applications such as transparent armor or bulletproof vests. This talk will generally focus on a class of polymeric liquid crystalline materials: liquid crystalline elastomers. These materials were predicted by de Gennes to have exceptional promise as artificial muscles, owing to the unique assimilation of anisotropy and elasticity. Subsequent experimental studies have confirmed the salient features of these materials, with respect to other forms of stimuli-responsive soft matter, are large stroke actuation up to 400% as well “soft elasticity” (stretch at minimal stress).

This presentation will survey our efforts in directing the self-assembly of these materials to realize distinctive functional behavior with implications to soft robotics, flexible electronics, and biology. Most notably, enabled by the chemistries and processing methods developed in my laboratories, we have prepared liquid crystal elastomers with distinctive actuation and mechanical properties realizing nearly 40 J/kg work capacities in homogenous material compositions.

SESSION SM05.08: Novel Functionalities of Multiphase Materials I
Session Chairs: H. Jerry Qi and Ruike Renee Zhao
Thursday Afternoon, April 22, 2021
SM05

1:00 PM *SM05.08.01

Functional Materials in Soft, Skin-Interfaced Haptic Systems for Virtual/Augmented Reality John A. Rogers; Northwestern University, United States

Advanced, immersive systems for virtual and augmented reality (VR/AR) will transform the way that we interact with computer-generated environments and, by extension, with one another. Although audio-visual aspects of VR/AR hardware are increasingly well developed, a frontier, underexplored opportunity for engineering science is in the development of interfaces that add spatio-temporally controlled physical sensations to the VR/AR experience, with the skin as the input interface. This talk summarizes a collection of foundational ideas in materials science and electrical engineering that enable a unique class of technology for this purpose – thin, soft, lightweight sheets that embed wirelessly powered and programmed arrays of high-speed, millimeter-scale mechanical actuators, capable of gently laminating onto the skin at nearly any location on the body, including but not limited to the fingertips. These systems qualitatively expand the VR/AR interface through complex patterns of physical sensory inputs across substantial areas of the body, time-coordinated with visual and auditory cues. Three example applications – one in social media interactions, a second in feedback for the control of robotic prosthetics, and a third in video gaming – illustrate the operational possibilities.

1:30 PM SM05.08.02

Magnetic Multimaterials with Multiphysics Controls for Widely Tunable Physical Properties Shuai Wu; The Ohio State University, United States

Metamaterials are architected materials that possess unique properties not observed in nature, which makes them promising candidates for a broad range of applications. After fabrication, existing metamaterial systems can only tune their properties to a limited extent. The coupled multimaterial system and multiphysics control provide a new strategy to achieve active metamaterials with widely tunable physical properties. Fabricated by recently developed magnetic shape memory polymer, demonstrated metamaterials can soften upon heating, and the embedded high-remanence magnetic particles drive the rapid and reversible shape change under the application of magnetic field. Once cooled, the stiffness of the composite can increase by three orders of magnitude to lock the deformed shape. Furthermore, the coupled magneto-mechanical actuation at high temperature realizes various deformation modes, which lead to widely tunable physical properties including

stiffness, Poisson's ratio and elastic wave bandgaps. Additionally, the combination of magnetic shape memory polymers with magnetic soft materials, together with the cooperative stimuli of magnetic field, mechanical loading and temperature, enable dexterous manipulations of material systems with tunable physical properties and shiftable mechanical behaviors.

1:45 PM SM05.08.03

Wearable Thermoelectric Generator with Self-healing, Recycling and Lego-Like Reconfiguring Capabilities Jianliang Xiao; University of Colorado Boulder, United States

Thermoelectric generators (TEGs) can directly convert low-grade heat to electricity, and thus are very promising energy sources for wearable electronics and 'Internet of Things'. However, conventional TEGs are rigid and brittle, and thus are not adaptable to the complex geometrical and compliant material properties of human body. Recently, developing flexible TEG systems has attracted a lot of attention, including using thermoelectric (TE) films, TE bulks, printable TE inks, TE fibers and organic TE materials. However, very few studies reported TEGs with good stretchability, which is critical to ensure conformal contact with complex geometries of human body for optimal thermoelectric performance. Inspired by the self-healing capability of human skin, self-healable electronics has also shown promising potential in wearable electronics for improved reliability and durability. However, this capability has not been achieved in TEG systems yet.

In this work, a high-performance wearable thermoelectric generator with superior stretching, self-healing, recycling, and Lego-like reconfiguration capabilities is reported. To achieve these properties, high-performance modular thermoelectric chips, dynamic covalent thermoset polyimine as substrate and encapsulation, and flowable liquid metal as electrical wiring are integrated through a novel mechanical architecture design of "soft motherboard-rigid plugin modules". This TEG can self-heal when it's damaged by mechanical cut. When not needed, this TEG can be fully recycled, and the recycled polymer solution, thermoelectric chips and liquid metal can all be used to fabricate a new generation of TEG device. The lego-like reconfiguration capability allows reconfiguring multiple TEGs into a single TEG with increased power output. This TEG can produce a record high open-circuit voltage density of 1 V/cm² at temperature difference 95 K, which is promising for harvesting low-grade heat to power 'Internet of Things' and wearable electronics. These features enable TEGs to be adaptable to the rapidly changing mechanical and thermal conditions, and user requirements. The reported TEG demonstrate superior mechanical compliance and deformability. It can be bent and stretched without sacrificing the thermoelectric performance. Cyclic bending test of the TEG for 1000 times led to no obvious degradation. When subjected to a tensile strain of 120%, the TEG still functioned well. Furthermore, a wavelength-selective metamaterial film is integrated at the cold side of the TEG to simultaneously maximize the radiative cooling and minimize the absorption of solar irradiation. Therefore the thermoelectric performance can be greatly enhanced under solar irradiation, which is critically important for wearable energy harvesting during outdoor activities. The design concepts, approaches and properties of the TEG system reported in this work can pave the way for delivering the next-generation high-performance, adaptable, customizable, durable, economical and eco-friendly energy harvesting devices with wide applications.

2:00 PM SM05.08.05

Local Stiffness Control and Anti-Bacterial Properties by a Metal Redox Reaction in Double Network Hydrogels Sooik Im, Ethan Frey, Jinwoo Ma, Jan Genzer, Michael Dickey and Vi Khanh Truong; North Carolina State University, United States

Hydrogels are hydrophilic polymer networks, which contain water and electrolytes. Double network hydrogels have enhanced mechanical properties relative to single networks [1]. The presence of a secondary network that consists of a bioderived material, alginate, can dissipate energy through sacrificial bonds that break during elongation, while the first polymer network remains intact. The double network hydrogel can be toughened further by ionic crosslinking between carboxylic groups in alginate and di- or trivalent metal ions. With this interaction, hydrogel stiffness can be tuned locally. Previously, ionoprinting with Cu²⁺ was employed to increase stiffness locally to actuate and modify the stiffness of hydrogels [2]. However, this method can increase stiffness only at the surface of the gel. Here, we used metal redox reactions between Bi particles and

Ag⁺ to tune hydrogel stiffness locally. By controlling particle distribution and reaction time, we control the properties of the gel. The gel is multifunctional since it has both tunable mechanical and anti-bacterial properties arising from the ions.

We fabricated polyacrylamide/alginate double network hydrogels embedded with Bi particles. The hydrogels were dipped into AgNO₃ solution to initiate a reaction between Bi and Ag⁺. Bi particles are ionized into Bi³⁺, which crosslinks with carboxylic groups (COO⁻) of the alginate. The crosslinking bonds stiffen the hydrogels, leading to an increase of the dynamic modulus by two-fold. The local strain level within the hydrogel was mapped using digital image correlation (DIC). By correlating the particle distribution with the local strain level, we confirmed Bi³⁺ produced on the Bi particle surfaces caused a heterogeneous local strain level in the gel. Tuning the dipping time in AgNO₃ solution leads to the gradient of modulus in the hydrogels. We mapped dynamic gradient modulus by cutting the hydrogels into different parts, which were measured separately. Modulus gradient hydrogels from the reactions can act as a bridge between soft and hard materials. This modulus gradient was similar to that of cartilage. With Bi particles settling in the pre-gel solution, the hydrogel was found to bend toward the side with high particle density due to the difference in modulus within the hydrogels. As an application, we confirmed Ag particles generated by the redox reaction could be used as antibacterial agents. Bacterial inhibition zone increased with increasing concentration of AgNO₃.

References

- [1] Jeong-Yun Sun, Xuanhe Zhao, Widusha R. K. Illeperuma, Ovijit Chaudhuri, Kyu Hwan Oh, David J. Mooney, Joost J. Vlassak, and Zhigang Suo (2012). Highly Stretchable and Tough Hydrogels. *Nature*, 489: 133–136.
- [2] Etienne Palleau, Daniel Morales, Michael D. Dickey, and Orlin D. Velev (2013). Reversible Patterning and Actuation of Hydrogels by Electrically Assisted Ionoprinting. *Nat. Commun.*, 4: 2257.

2:15 PM *SM05.08.06

Biomimetic Complexity and Graph Theory (GT) of Chiral Nanostructures Nicholas A. Kotov; University of Michigan–Ann Arbor, United States

The structural complexity and multifunctionality of composite biomaterials and biomineralized particles arises from the hierarchical ordering of inorganic building blocks over multiple scales. While empirical observations of complex nanoassemblies are abundant, physicochemical mechanisms leading to their geometrical complexity are still puzzling, especially for non-uniformly sized components. Here we report the assembly of hierarchically organized particles (HOPs) with twisted spikes and other morphologies from polydisperse Au-Cys nanoplatelets [1]. The complexity of Au-Cys HOPs is higher than biological counterparts or other complex particles as enumerated by graph theory (GT). Complexity Index (*CI*) and other GT parameters can be applied to a variety of different nanoscale materials to assess their structural organization. As the result of this analysis, we determined that intricate organization of HOPs emerges from competing chirality-dependent assembly restrictions that render assembly pathways primarily dependent on nanoparticle symmetry rather than size. These findings and HOPs phase diagrams open a pathway to a large family of colloids with complex architectures and unusual chiroptical and chemical properties. Developed GT methods and new index-property relations were also applied to design complex biomimetic composites for energy and robotics applications [2].

References

- [1] W. Jiang, Z.-B. Qu, P. Kumar, D. Vecchio, Y. Wang, Y. Ma, J. H. Bahng, K. Bernardino, W. R. Gomes, F. M. Colombari, A. Lozada-Blanco, M. Veksler, E. Marino, A. Simon, C. Murray, S. Ricardo Muniz, A. F. de Moura, N. A. Kotov, Emergence of Complexity in Hierarchically Organized Chiral Particles, *Science*, **2020**, 368, 6491, 642-648.
- [2] Wang, M.; Vecchio, D.; Wang, C.; Emre, A.; Xiao, X.; Jiang, Z.; Bogdan, P.; Huang, Y.; Kotov, N. A. Biomimetic Structural Batteries for Robotics. *Sci. Robot.* **2020**, 5 (45), eaba1912. <https://doi.org/10.1126/scirobotics.aba1912>.

SESSION SM05.09: Novel Functionalities of Multiphase Materials II
Session Chairs: Shuai Wu and Ruike Renee Zhao
Thursday Afternoon, April 22, 2021
SM05

4:00 PM SM05.09.01

Energy-Efficient Adaptive Multimodal Thermal Management for Personal Health—The Nexus of Light, Heat and Smart Materials Po-Chun Hsu; Duke University, United States

As warm-blooded mammals, the human body is constantly maintaining its core temperature against ambient fluctuation. For extreme temperatures or suboptimal physiological conditions, it may result in serious health issues. For example, at low ambient temperature, blood pressure and viscosity may increase, which are strongly correlated with cardiovascular diseases. This is the reason why cardiovascular diseases often have seasonal dependence. On the other hand, at high ambient temperature, excessive sweating can cause electrolyte imbalance or even heat stroke. Commercial body heating/cooling devices, such as Joule heating or Peltier cooling, are prohibitively energy-intensive or bulky for continuous use. In this talk, I will demonstrate our recent research progress in energy-efficient adaptive textiles that can adjust the heat balance via controlling the heat transfer coefficients rather than actively supplying power. First, I will introduce the wearable varied emittance (WeaVE) device that modulates the human body radiative heat transfer to accomplish thermoregulation with ultralow energy consumption. The electrochemically-operated WeaVE can switch the mid-IR emissivity by more than 40% within less than one minute. Kirigami design enables superior stretchability and conformality when applying to the human body. By communicating with ambient temperature and humidity sensors, the WeaVE can autonomously stabilize the body heat loss to accomplish thermal comfort in a natural and continuous manner. Second, I will demonstrate the multimodal moisture-responsive wearable device that modulates both radiative and convective heat transfer to accomplish large tunability. In both projects, I will explain how the judicious choice of materials and design, based on fundamental physical principles, can directly result in high performances in multiple aspects.

4:15 PM SM05.09.02

Soft and Stretchable Energy Harvesting Using Liquid Metals Veenasri Vallem, Erin Roosa, Tyler Ledinh and Michael Dickey; North Carolina State University, United States

With a fast-growing interest in flexible and stretchable soft electronic devices (e.g. electronic skin, soft robotics, implantable devices, tactile sensors, wearable electronics, smart textiles, etc.), there has been an increasing demand for similar sustainable power sources. Commonly used power sources such as batteries are rigid and require frequent recharging. Rigidity inhibits the stretchability/wearability, limiting the usage of the device, and frequent recharging limits the operating range of the device. Moreover, implantable devices that utilize batteries exhibit a limited life-time and require additional surgeries to replace the battery thereby presenting a huge risk to the users. To address these limitations, efforts have been made to develop soft energy harvesters that can convert human motion/ambient mechanical energy to electrical energy. Energy harvesting can eliminate the need for frequent recharging, which allows the device to operate in a tether-free manner. Furthermore, users can generate mechanical energy at their will, which enables the harvesters to power the devices in remote settings. Triboelectric and piezoelectric generators are prominently used harvesters for converting mechanical energy to electrical energy. Triboelectric harvesters have gained great popularity due to their relatively straightforward fabrication. They induce electrical current based on contact electrification (rubbing two surfaces) and electrostatic induction (oscillating the distance between charged surfaces). Triboelectric harvesters generate high voltages and low currents. They require moisture-free environments and rubbing components to enable contact electrification. Piezoelectric generators, in contrast, generate electricity due to inherent polarization

when subjected to mechanical deformation. However, they require extensive fabrication techniques and suffer loss in energy conversion when converted to flexible/stretchable devices, as their fundamental materials are intrinsically hard and brittle. We report a new approach to energy harvesting that utilizes liquid metals. These devices generate about 0.2 mW m^{-2} by harnessing energy from mechanical motion. We have characterized the behavior of these devices as a function of a variety of parameters including material properties (chemical composition), design parameters (organization and volume of each component), and physical deformation (amplitude and frequency of the mechanical energy input). We have developed a physics-based model to predict device performance. The devices behave as expected and the response of the devices to deformation matches the model. The liquid metal-based soft device is stretchable and can generate an electrical signal when deformed, which may be useful for energy harvesting as well as wearable self-powered sensors. These devices can be used to monitor human activities thereby find many applications in wearable electronics, dynamic tactile surfaces, healthcare systems like rehabilitation and prosthetics.

4:30 PM SM05.09.03

Harnessing a Molecular Switch in an Energy-Efficient Thermal Actuating Bilayer Michael Leveille, Wenxin Fu, Jacqueline Bustamante, Sayantani Ghosh and Jennifer Lu; University of California, Merced, United States

Stimuli-responsive materials have proliferated in recent years due to their potential for a broad range of applications including switching, actuating, sensing, energy harvesting, and soft biorobotics and wearable devices. Herein we describe a bilayer system that can generate programmable deformation reversibly in response to photothermal stimuli (e.g. low-energy near infrared-induced photothermal heating) or heating a few degrees above room temperature.

The bilayer film consists of a polyarylamide layer containing a small amount of crosslinking dibenzocycloocta-1,5-diene (DBCOD) and is covalently bonded to a sheet of aligned carbon nanotubes (CNTs). Our design takes advantage of self-assembly of DBCOD units along the CNT longitudinal direction to generate directional thermal contraction upon the DBCOD conformational change. The coefficient of thermal expansion of CNTs is near zero while the polymer layer exhibits a large negative thermal expansion. This mismatch results in substantial thermal stress and thus large deflection of the bilayer with small changes in temperature. We have demonstrated a deflection of 6.5 mm per cm by heating from 20 to 60 °C. This deformation can be pre-programmed with the selection of CNT/cut pattern. Additionally, the bilayer inherits excellent cycle stability, moving as a single unit without separation due to the covalent bonds between polymer and CNT layers. This actuator offers thermal to mechanical energy conversion at an efficiency at least on par with state of the art of mechanoresponsive polymer systems. Finally, we have also demonstrated that electricity can be generated by photo- or thermal fluctuations by coupling the actuation to piezoelectric effects in a trilayer device.

Such a low-energy stimulus induced high-efficiency system paves pathways to develop remotely controlled actuators, low-energy driven artificial fingers as well as thermal-to-electric energy harvesting.

4:45 PM SM05.09.04

Late News: Amplification and Modulation of Compliant Mechanisms by Shape Memory Polymers Johan Dag Valentin Baeckemo^{1,2}, Yue Liu^{1,2} and Andreas Lendlein^{1,2}; ¹Institute of Active Polymers, Helmholtz-Zentrum Geesthacht, Germany; ²Institute of Chemistry, University of Potsdam, Germany

Compliant mechanisms have attracted tremendous interest for application in fields such as consumer products, soft robotics, and even animatronics. The fundamental design principle is the non-linear bending behavior of beams, which for non-trivial geometry and large deformations cannot be solved for analytically by using classical Euler-Bernoulli and Timoshenko-based equations. Therefore models are demanded that can predict said behavior through numerical solvers, or even analytically. The improvement of computing performance and more sophisticated software enabled such models which have incidentally become an integral part in the design process.

Examples are the Pseudo-Rigid-Body (PRB)(1) model and the Beam Constraint Model (BCM)(2). Here the Chained Beam Constraint Model (CBCM)(3), a development on the BCM, was applied, which to a high degree of accuracy can predict the complex bending behaviour of thin beams. This model is applied to a selection of beam shapes and were further developed as 3D-structures. These were manufactured using a shape-memory polymer (SMP) which when programmed through a counter-mold could add additional functionalities such as the switching of bi-stability of a given design or the amplification of deformation. We explored a design and fabrication scheme from conception of compliant mechanisms through the application of the CBCM, the design of molds to create demonstrators out of SMP and later the evaluation of functionalities through mechanical testing.

The modelling was realized through Python programming and implementing its non-linear solvers from the SciPy package to solve the governing equations of the CBCM. 3D-printed master molds were created to cast the polydimethylsiloxane (PDMS) molds. Consequently, demonstrators were created by casting poly[ethylene-co(vinyl acetate)] (PEVA) as a SMP in the PDMS molds.

This study demonstrates how one can conceptualize design and forecast complex bending behaviours using computational tools, and in turn apply SMPs such as PEVA to further amplify or modulate functionalities. This study could be seen as a step to create novel manufacturing schemes for the use in growing fields such as soft robotics.

1. H. Larry L., in *21st Century Kinematics*, J. M. McCarthy, Ed. (Springer, 2013), chap. Chapter 7 - Compliant Mechanisms.
2. S. Awtar, S. Sen, A generalized constraint model for two-dimensional beam flexures: nonlinear load-displacement formulation. *Journal of Mechanical Design* **132**, (2010).
3. G. Chen, F. Ma, G. Hao, W. Zhu, Modeling Large Deflections of Initially Curved Beams in Compliant Mechanisms Using Chained Beam Constraint Model. *Journal of Mechanisms and Robotics* **11**, (2019).

5:00 PM SM05.09.05

Late News: Dynamic, Remote-Controllable Electroactive Hydrogel Waveguide Architectures Oscar Alejandro Herrera Cortes and Kalaichelvi Saravanamuttu; McMaster University, Canada

We generated electroactive hydrogel light-guiding structures and demonstrated that their orientation, motion and - thereby the direction of their light output - can be precisely and remotely controlled through external electrical fields. This was achieved with a range of architectures including planar slab waveguides, individual and small arrays of cylindrical waveguides as well as long-range waveguide lattices ($> 10\,000\text{ cm}^2$).

Waveguides were induced in electroactive photopolymerizable hydrogels by self-trapped visible beams from light-emitting diodes (LEDs). These nonlinear waves are elicited when photo-induced refractive index changes counter the natural divergence of light beams launched into the hydrogels. Because the refractive index changes are irreversible, self-trapped beams permanently inscribe cylindrical waveguides along their paths. Such structures would be impossible to fabricate through conventional photolithographic methods. Because they are electroactive, we could apply and vary external electric fields to dynamically control the bending, angular orientation, and rotation (up to 360°) of these pliant light-guiding structures.

5:15 PM SM05.09.06

Late News: A Practical Hydrogenated Graphene Gas Sensor for CO₂ Monitoring Samuel Escobar, Solimar Collazo Hernandez, Marcel Grau, Ernesto Espada, Brad Weiner and Gerardo Morell; University of Puerto Rico, Río Piedras, Puerto Rico

The development of a practical gas sensor is of great interest for monitoring toxic and non-toxic gases that might endanger our safety and wellbeing in different settings. Hereby we present a practical gas sensor based on hydrogenated graphene for CO₂ monitoring. Hydrogenated graphene was synthesized by a

single-step method directly onto an Au-pattern insulating substrate. Hydrogenated graphene was then characterized using RAMAN spectroscopy, X-ray photoelectron spectroscopy (XPS), and X-ray Diffraction (XRD). The materials interaction with CO₂ was systematically study at different PPM to determine our sensor's detection limits. Some preliminary research reveals that the hydrogenated graphene-based sensor is capable of sensing CO₂ at the mid-ppm-level.

5:30 PM SM05.09.07

Late News: Single-Step Synthesis of Highly Ferromagnetic Hydrogenated Graphene Samuel Escobar¹, Marcel Grau¹, Solimar Collazo Hernandez¹, Ernesto Espada², Brad Weiner¹ and Gerardo Morell¹; ¹University of Puerto Rico, Río Piedras, Puerto Rico; ²University of Puerto Rico at Río Piedras, Puerto Rico

Hydrogenated graphene has been of great interest for the scientific community due to properties like ferromagnetism that are not usually present in graphene; requiring subsequent functionalization after synthesis to obtain them. Hereby, we present a novel method for synthesizing hydrogenated graphene via a single-step process. Hydrogenated graphene was characterized primarily by Raman spectroscopy, X-ray Photoelectron Spectroscopy (XPS), X-ray Diffraction spectroscopy (XRD) and Physical Properties measurement system (PPMS). Our Raman spectra confirms the presence of the 2930 cm⁻¹ peak associated with hydrogen functionalization, while the PPMS reveals the strongest ferromagnetism at room-temperature of a carbon-based material with a curie temperature higher than 350 K. These results are strong evidence of hydrogenated graphene's capabilities for its implementation to spintronics & memory applications.

5:45 PM SM05.09.08

Late News: Waveguide Encoded Lattices (WELs)—Slim Polymer Films with Enhanced Fields of View Inspired by Arthropodal Compound Eyes Kathryn Benincasa, Hao Lin, Cécile Fradin and Kalaichelvi Saravanamuttu; McMaster University, Canada

We have generated slim (2 mm to 3 mm thick), soft polymer films inscribed with Waveguide Encoded Lattices which - like arthropodal compound eyes - have enhanced panoramic field of view (FOV) and multiple optical functionalities. [1-3] These include an exceptionally high density of light harvesting waveguide units (>15,000 cm⁻²), excellent imaging resolution, infinite depth of field and operability at all visible wavelengths including broad incandescent spectra (like sunlight) and discrete spectral ranges of lasers and LEDs. WELs transmit, focus and invert images without need for bulky optics and conversely, control the shape and trajectory of light beams. Different from the curved architectures of compound eyes, WELs are plane-faced, optically flat, slim films, which due to their translational symmetry could be extended over large areas (e.g. through roll-to-roll manufacturing) and due to their flexibility, integrated with ease into technologies such as LCDs, solar cells, cameras and smart phones.

1. Hosein, I. D.; Lin, H.; Ponte, M. R.; Basker, D. K.; Brook, M. A.; Saravanamuttu, K. *Adv. Funct. Mater.* **2017**, *27*, 1–11.
2. Lin, H.; Hosein, I. D.; Benincasa, K. A.; Saravanamuttu, K. *Adv. Opt. Mater.* **2019**, *7*, 1801091 (1-9).
3. Lin, H., Benincasa, K., Fradin, C., Saravanamuttu, K. *Adv. Opt. Mater.* **2019**, *7*, 1801487 (1-9).

SESSION SM05.10: Novel Functionalities of Multiphase Materials III

Session Chairs: H. Jerry Qi and Shuai Wu

Thursday Afternoon, April 22, 2021

SM05

8:15 PM SM05.10.01

Enabling Near-Hysteresis-Free Tactile Sensitive Electronic Skin Haicheng Yao, Weidong Yang, Wen

Cheng and Benjamin Tee; National University of Singapore, Singapore

The development of polymeric electronic skins (e-skins) enables applications such as telehealthcare, human-machine interfaces, prosthesis, and robotic perceptions.^{1,2} The reliable sensing and monitoring require e-skin sensors to respond to mechanical stimuli sensitively and accurately with minimal data variation between contact cycles. However, hysteresis is always a trade-off with sensitivity in polymer-based sensors to limit their reliability. We propose a soft indentation process to generate annular metallic cracks on three-dimensional (3D) micro-elastomers.³ The cracking mechanism is explored via theoretical analysis and numerical simulations. Good control of crack morphology on elastomers enables a piezoresistive e-skin sensor (TRACE) with high tactile sensitivity yet a large reduction of hysteresis ($2.99 \pm 1.37\%$). The assembled TRACE sensors array achieves precise monitoring of pulse waveforms and continuous track of pulse wave velocity (PWV). It also enables robotic perceptions on surface textures with improved reliability compared to large-hysteresis e-skin sensors.

References:

1. Ray, T. R. *et al.* Bio-integrated wearable systems: A comprehensive review. *Chem. Rev.* **119**, 5461–5533 (2019).
2. Yang, W., Hon, M., Yao, H. & Tee, B. C. K. *An Atlas for Large-Area Electronic Skins*. **3840**, (Cambridge University Press, 2020).
3. Yao, H. *et al.* Near-hysteresis-free soft tactile electronic skins for wearables and reliable machine learning. *Proc. Natl. Acad. Sci.* **117**, 25352–25359 (2020).

8:30 PM SM05.10.02

Nanopillar-Guided Nuclear Deformation for Cancer Grading Yongpeng Zeng, Yinyin Zhuang, Aninda Mitra, Weibo Gao and Wenting Zhao; Nanyang Technological University, Singapore

Nuclear shape irregularities, especially subnuclear features like invagination and folds on the nuclear envelope, are commonly found in metastatic cancer cells. Assessment of nuclear irregularities, i.e. nuclear grading, has long been used to diagnose and grade cancer in clinical practice. However, the current evaluation of cancer nuclear morphology is mainly through human-based inspection of microscopy images, and largely relies on the experience and judgment of individual pathologist. Inevitably, it suffers from low consistency and reproducibility. Though the reproducibility and precision can be enhanced with the aid of artificial intelligence, the most available algorithm for automatic assessment only uses the whole-nucleus morphological parameters for grading. The subnuclear and nanoscale features are often overlooked due to the randomness of their distribution and thus difficult to locate and segment for quantitative analysis. In this work, we introduced vertically aligned nanopillar arrays with defined geometry and pattern to enable effective guidance on subnuclear abnormal features in cancer cells. Taking breast cancer cells as a model, we found that the low malignant MCF7 cells generated isotropic subnuclear deformation feature on nanopillars, while the high malignant MDA-MB-231 cells exhibited anisotropic patterns with the subnuclear features aligned with nanopillar arrays. By quantitative assessment of the isotropy of subnuclear features guided on nanopillars, differentiation of cancer cells in high and low malignancies was successfully achieved. We further demonstrated that the heterogeneity in a population of cancer cells can be quantitatively mapped. In addition, the therapeutic potential of drugs specifically targeting metastatic cells was also evaluated effectively using nanopillar arrays. We envision that the nanopillar-based nuclear grading will provide a new tool to improve both cancer diagnosis and anti-cancer drug screening.

8:45 PM SM05.10.03

Late News: Reconfigurable Soft Magnetic Actuators with Reprogrammable Magnetization Pattern Hyeonseong Song¹, Hajun Lee¹, Jaebyeong Lee¹, Jun Kyu Choi¹, Suwoo Lee¹, Jee Yoon Yi¹, Sunghoon Park¹, Jung-Woo Yoo¹, Min Sang Kwon² and Jiyun Kim¹; ¹Ulsan National Institute of Science and Technology, Korea

(the Republic of); ²Seoul National University, Korea (the Republic of)

Soft magnetic materials have shown promise in diverse applications due to their fast response, remote actuation, and large penetration range for various conditions. Those are usually composed of hard magnetic particles or discrete magnets incorporated in a base material, and the actuation of these materials arises from spatiotemporal interactions between the applied magnetic field, environment, and programmed magnetization. However, a limitation arises because actuation is constrained by the programmed magnetization profile because magnetic fillers are usually physically confined in the soft matrix after fabrication is completed. Here, we propose a new soft material composite, the ferromagnetic domain pattern of which can be reprogrammed without changing intrinsic magnetic properties of embedded magnetic particles or the molecular properties of the base material.

Our reprogrammable magnetic composite is composed of spatially separated magnetic microspheres embedded in the elastomeric matrix (Ecoflex 00-30). Each magnetic microsphere consists of neodymium-iron-boron (NdFeB) microparticles, with an average size of 5 μm , encapsulated in oligomeric polyethylene glycol (PEG). The magnetization profile of our composite can be easily reprogrammed using the phase transition of oligomeric polyethylene glycol which is encapsulating the magnetic microparticles.

If the encapsulating polymer changes from solid to liquid, the magnetic particles can freely move or rotate in the microspheres along the external magnetic field. As the material cools, the encapsulating polymer solidifies and it fixes the reprogrammed magnetic particle alignment. To verify the re-programmability of the magnetic composite, we measure the magnetic moment density in samples at various angles relative to the external magnetic field applied by the vibrating sample magnetometer.

As an illustrative example to demonstrate the ability to reprogram the magnetization pattern of our composite, we demonstrate several reconfigurable soft magnetic actuators. The actuators can be classified into three types; (1) complex transformations of a continuous magnetic membrane are realized as a fully functional origami. (2) various transformations of a magnetic origami sheet with discrete magnetic layers on a flexible substrate layer are demonstrated by utilizing our magnetic composite as a functional layer. (3) *in situ* reprogramming scenario is proposed by adding a conductive heating layer to the reprogrammable magnetic layer.

We expect that this soft magnetic composite with a reprogrammable magnetization pattern could be used to make reconfigurable soft material systems for a wide range of applications including biomedical engineering, flexible electronics, and soft robotics.

9:00 PM SM05.10.04

Modified Structures with Crack based Sensors for Physiology Detection Byeonghak Park and Tae-il Kim; Sungkyunkwan University, Korea (the Republic of)

From so-called “smartwatches” to implantable pacemakers, wearable/implantable mechanosensors have been regarded as essentials and promising potentials for biomedical applications and even for raising the quality of daily life. Crack based mechanosensors have risen promising potentials for communicating with the human, so that they have been developed in the aspect of sensitivity, stretchability, durability, visualizing, and multi-functionality for few years. While valuable mechanical physiology is composed of complex stimuli such as strain, pressure, and torsion, however, due to the geometrical and mechanical properties of the cracks, the sensitivity of the crack based sensors is limited to the strain stimulus. Here, we describe the modified inner structures for transforming pressure to the plane strain, enabling the highly sensitive ability to the pressure. As a given pressure, the strain can be amplified over 3 times, which is a big advantage for the strain-sensitive mechanosensors. Attributed to the structure, the crack based sensor can detect the pressure up to 10 MPa with a $3 \times 10^6/\text{Pa}$ sensitivity, which is more than 100 times sensitive than the normal crack based sensors. We found the advantages of the biomedical application which has complex strain and pressure, and especially, the jaw rehabilitation devices for the neck and head cancer patients. Despite the 3D printed supporters of the device, the sensor array can successfully discriminate each position and each pressure of the rehabilitating bite trials. The

structures can be huge potentials for the biomedical physiology detection for the electronics.

9:15 PM *SM05.10.05

Scaling of Internal Dissipation of Polycrystalline Solids on Grain-Size and Frequency Chuangchuang Duan^{1,2} and Yujie Wei^{1,2}; ¹Chinese Academy of Sciences, China; ²University of Chinese Academy of Sciences, China

Internal friction is essential for nearly all solids to dissipate kinetic energy through internal mechanisms. The pioneering analyses by Zener (Phys. Rev. 60 (1941) 906-908) and Kê (Phys. Rev. 71 (1947) 533-546) demonstrated the existence of a single friction peak in the loss modulus spectrum of polycrystalline solids, which is attributed to viscous sliding in grain boundaries. In this study, we establish a continuum model coupled elastic deformation, viscous creep and diffusion in grain boundaries and reveal the existence of a second loss modulus peak resulted from viscous deformation within grain boundaries [1]. The corresponding two frequencies, when internal dissipation reaches its local maximum, depend on grain size d : the lower frequency one is proportional to d^{-3} , and the higher frequency one is proportional to d^{-1} . The underlying deformation mechanisms accounting for the two peaks and the scaling laws are identified. The inherent scaling laws are related to the combination and architecture of the dissipative soft grain boundary layers and hard grains in polycrystalline solids. The effects of local elasticity and diffusion in grain boundaries on the loss modulus spectrum are examined. The findings can be applied to granular and porous materials, and complex rheology in geosciences, where internal dissipation is momentous for waves and seismic activities. The unifying picture revealed based on the combination of hard grains and soft grain boundary layers could be employed to many heterogeneous systems for their design for high damping performance.

Reference

[1] C Duan, Y Wei, Acta Materialia, 201(2020), 350-363. <https://doi.org/10.1016/j.actamat.2020.10.004>.

SESSION SM05.11: Novel Functionalities of Multiphase Materials IV

Session Chairs: H. Jerry Qi and Shuai Wu

Friday Afternoon, April 23, 2021

SM05

2:15 PM SM05.11.01

Late News: Benchmarking of Molecular Dynamics Force Fields for Solid-Liquid and Solid-Solid Phase Transitions in Alkanes Stephen Burrows and Stoyan K. Smoukov; Queen Mary University of London, United Kingdom

Accurate prediction of alkane phase transitions involving solids are needed to prevent catastrophic pipeline blockages, improve lubrication formulations, smart insulation and energy storage, and bring fundamental understanding to processes such as artificial morphogenesis. Solid-solid phase transitions are rarely modeled due to difficulties in long timescales for nucleation and dynamics, as well as lack of order descriptors. We report on the applicability, accuracy and computational performance of seven representative molecular dynamics models (TraPPE, PYS, CHARMM36, L-OPLS, COMPASS, Williams, and the newly optimized Williams 7B).

2:30 PM SM05.11.03

Late News: Microfluidic-Assisted Phase Separation and Phase Transition of Liquid Proteinaceous Materials Yufan Xu¹, Yi Shen^{1,2} and Tuomas P. Knowles^{1,1}; ¹University of Cambridge, United Kingdom; ²The University of Sydney, Australia

Liquid-liquid phase separation (LLPS) of proteinaceous materials and crowding agents is emerging as a significant model facilitating the understanding of protein functions and malfunctions, which can find healthcare-related applications in the understanding, diagnosis, and treatment of diseases. In this presentation, we will report the construction, characterisation, and application of multiphase-based all-aqueous materials generated from the concept and mechanism of LLPS of extracellular proteins and crowding agents using microfluidic devices. Smart multiphase-based protein microgels, dynamic phase-separated protein microgels, and spatially inhomogeneous one-phase protein microgels will be demonstrated. The demixed states of proteins in crowding agents highlight the LLPS of the all-aqueous material systems. We will report the LLPS findings and explanations in micron-scaled compartments containing multiphase-based materials, and the LLPS of extracellular proteins and their surrounding environments at a larger scale. As a control study, spatially inhomogeneous one-phase protein microgels will be displayed. The possible mechanisms, fabrication techniques, applications, as well as the opportunities and challenges of the multiphase-based material systems will be presented. Microfluidic platforms can open up new routes for the advanced processing and precise controlling of biocompatible and bioactive materials at the microscale, in a fashion where conventional manufacturing was thought to be impossible. The microgels are promising models for temperature sensing, soft robots, as well as cell-culture scaffolds, which can promote the development of bioengineering and biophysics.

References:

Xu Y, et al. doi.org/10.1101/2020.12.08.416867, 2020. Submitted.

Xu Y, et al. arXiv preprint arXiv:2009.13413, 2020. Submitted.

Xu Y, et al. Small 16 (32), 2000432, 2020.

2:45 PM SM05.11.04

Late News: Active Polymeric Sheets for Plant Protection Based on Pickering Emulsion Templating

Karthik Ananth Mani¹, Meche Tefang Aureole Berenice¹ and Guy Mechrez²; ¹The Hebrew University of Jerusalem, Israel; ²Agricultural Research Organization, Israel

In the past few years, there has been a tremendous amount of scientific activity in the field of controlled release of volatile antimicrobial agents such as Thymol and Carvacrol, which have shown high antimicrobial activity and suitability for food and agriculture applications from the regulatory point of view. However, the ability to develop efficient and cost-effective controlled release formulations for essential oils is still highly challenging. This research presents the development of an active polymeric sheet for plant protection. Thymol is a natural monoterpenoid phenol, which is isomeric with Carvacrol found in thyme oil and has beneficial properties. Thymol will be dissolved and encapsulated in the minor phase of toluene-in-water Pickering emulsion or in the major phase of an inverse emulsion. Polycaprolactone or polydimethylsiloxane will be dissolved in the toluene phase. The studied emulsions with the encapsulated Thymol will be impregnated in a non-woven polypropylene sheet. After evaporation of the water and toluene, polymeric structures with Thymol in their matrix will be formed inside the non-woven sheet. The activity of the resulting sheets along with their release properties will be compressively investigated for protecting these plants; rosemary, mint, and thyme through bioassay infectivity analysis. The system, which will be developed in this proposed research, is expected to exhibit high tunability in terms of the release rates and clear ability to encapsulate known amounts of Thymol in the resulting capsule. In addition, this Pickering emulsion-based formulation has shown clear feasibility to be impregnated in polypropylene non-woven sheet, which results in the formation of active silica/polyacrylate microspheres on the filaments of the sheet.

3:00 PM SM05.11.05

Late News: The Role of End Groups in the Structure and Microscopic Dynamics of Unentangled Poly(ethylene glycol) Silica Nanocomposite Melts—Simulation and Theory Emmanuel Skountzos^{1,2},

Katerina S. Karadima^{1,2} and Vlas Mavrantzas^{1,2,3}; ¹University of Patras, Greece; ²FORTH-ICE/HT, Greece; ³ETH Zürich, Switzerland

Molecular dynamics simulations are employed to study an unentangled poly(ethylene glycol) (PEG) - silica

nanocomposite melt with emphasis on the structure of the adsorbed layer around the nanoparticle and the dynamics of adsorbed and free chains in the melt. The simulations reveal significant differences depending on the type of PEG terminal group assumed (hydroxyl versus methoxy) arising from the different ways that polymer chains adsorb on the silica surface in the two cases: hydroxyl-terminated PEG chains are adsorbed by their ends giving rise to a brush-like structure, whereas methoxy-terminated ones are adsorbed equally probably along their entire contour which results in better local packing of adsorbed segments. In both cases, the dominant mechanism for the strong adsorption of PEG chains onto silica is the development of hydrogen bonds. Hydroxyl-terminated chains, in particular, prefer to develop hydrogen bonds through their terminal OH groups implying the development of graft-like conformations. Additional information about the structure of the adsorbed layer on silica is provided through a detailed analysis of adsorbed chain conformations in terms of trains, loops and tails, revealing appreciable differences in the statistical properties (population per adsorbed chain and length) between the two nanocomposites examined. How the dense interfacial layer that develops in both cases affects the dynamic behavior of free chains, especially in the nanocomposite where PEG chains are terminated with hydroxyl groups, is also discussed. MD simulation results for the relative population of tails, trains and loops are used to parameterize a theoretical model based on the Rouse model¹ on the assumption of a set of mixing (additive) rules. Overall, the proposed analytical model seems to provide a very satisfactory description (qualitative and quantitative) of the simulation findings, which in turn are found to practically match experimentally measured data for the dynamic structure factor already reported in the literature^{2,3} for the two types of nanocomposites addressed in our work under exactly the same conditions.

References

- 1) Rouse, P. Jr, *J. Chem. Phys* 21, 1272, **1953**.
- 2) Glomann, T.; Hamm, A.; Allgaier, J.; Hübner, E. G.; Radulescu, A.; Farago, B.; Schneider, G. J., *Soft Matter* 9, 10559, **2013**.
- 3) Glomann, T.; Schneider, G. J.; Allgaier, J.; Radulescu, A.; Lohstroh, W.; Farago, B.; Richter, D., *Phys. Rev. Lett.* 110, 178001, **2013**.

3:15 PM SM05.11.06

Late News: Single Cell Encapsulation via Pickering Emulsion Stabilized by TiO₂ Nanoparticles Providing Biopesticides Resistance Against UV Radiation Reut Amar Feldbaum^{1,2}, Noga Yaakov¹, Karthik Ananth^{1,3}, Dana Ment¹ and Guy Mechrez¹; ¹Agricultural Research Organization - the Volcani Center, Israel; ²Bar-Ilan University, Israel; ³The Hebrew University of Jerusalem, Israel

This study presents highly stable oil-in-water Pickering emulsions with tunable droplet size, suitable for individual encapsulation of fungal spores. The emulsions were stabilized by amine-functionalized TiO₂ (titania) nanoparticles (NPs). These emulsions were utilized for the development of a novel formulation for biological pest control with significant UV protection capability. The droplet size, stability, and structure of the emulsions were investigated at different titania contents and oil/water phase ratios. Most of the emulsions remained stable for 6 months. The Pickering emulsions' structural properties have been characterized by confocal microscopy and high-resolution cryogenic scanning electron microscopy (cryo-HRSEM). The presence of the titania particles at the interface was confirmed by both confocal microscopy and cryo-HRSEM. *Metarhizium brunneum* Ma7 conidia were incorporated into the emulsions. The successful encapsulation of individual conidia in the oil droplets was confirmed by confocal microscopy. The individual encapsulation of the conidia in the emulsions was significantly improved by dispersing the conidia in a 0.02% Triton X-100 solution prior to emulsification. Individually encapsulated conidia in a titania-based o/w Pickering emulsion have exhibited high UV protection levels, demonstrating the feasibility of the developed formulation to exhibit significant protection against UV for biopesticides.

3:30 PM *SM05.11.07

Autonomous Material Robotics—From Self-Sensing and Movement to Molecular Dynamics Simulations Stoyan K. Smoukov; Queen Mary University of London, United Kingdom

Our combinatorial multi-functional materials have demonstrated self-sensing, movement, and programmability. Recent advances have allowed us to grow shapes from the bottom up. Now we are advancing to the ability to start growing autonomous material robots bottom-up from single molecules. In this invited talk reporting results of large collaborations, we highlight tools we have developed, including molecular dynamics simulations, to predict liquid-solid and solid-solid phase transitions. These enable the growth of functional swimming robots that are powered by environmental fluctuations and manufacturing processes by artificial morphogenesis.

SESSION SM05.12: Novel Functionalities of Multiphase Materials V
Session Chairs: H. Jerry Qi and Shuai Wu
Friday Afternoon, April 23, 2021
SM05

5:15 PM SM05.12.01

Effects of Surfactants on the Microencapsulation of Off-the-Shelf Phase Change Thermochromic Materials for Thermal Storage Applications Abdullatif A. Hakami¹, Sesa Srinivasan², Keon Sahebkar¹, Mingyang Huang¹ and Elias Stefanakos¹; ¹University of South Florida, United States; ²Florida Polytechnic University, United States

We have investigated the effects of different surfactants and their concentrations in the microencapsulation of TiO₂ of phase change thermochromic materials procured commercially. These off-the-shelf phase change materials involve Leuco dye particles that has demonstrated color change (black to white) behavior at the low transition temperatures of about 36 °C. The role of TiO₂ encapsulation is to protect these thermochromic particles from the degradation due to solar radiation. Various surfactants such as CTAB, SDBS, Hexadecanol and Tetradecanol at different concentrations have been used to synthesize the TiO₂ microencapsulated phase change thermochromic particles. A number of physico-chemical characterizations such as XRD, SEM, EDS, FTIR and TGA/DSC have been carried out to understand the surface morphology, composition and thermal behavior of TiO₂ microencapsulated phase change thermochromic materials for thermal storage applications.

5:30 PM SM05.12.02

Late News: Efficient and Accurate Modeling of Thermoset Systems Using a Synergistic Combination of First-Principles Quantum Chemistry and Molecular Dynamics Atif Afzal, Thomas Mustard, Andrea R. Browning and Mathew Halls; Schrodinger Inc., United States

Fiber-reinforced composites containing epoxy-matrix are one of the key structural materials used in designing high-performance aircraft, automobiles, and athletic equipment. Several properties, including the deformation characteristics, thermal stability, fluid sensitivity, and interfacial properties, of these composite materials are dependent on the polymer matrix. Thus, understanding the matrix chemistry would allow us to improve their performance by tailoring the chemical structure. For example, using multifunctional epoxides has shown to augment the thermophysical and mechanical properties of such composite materials. Using computational techniques, we can enumerate large combinations of epoxides and amines and evaluate their properties. To efficiently model such polymer systems, we have built robust workflows using both quantum mechanics (QM) and molecular dynamics (MD). The workflows employ automated QM tools to identify key reaction steps and their kinetics involved in polymer synthesis and matrix-crosslinking. In this work, we have screened the key reaction barriers of amine/epoxy/accelerant combinations yielding 252 reactive barriers. The kinetics information for a subset of these epoxy-amine systems was then cast into our crosslinking workflows to obtain realistic in-silico systems. Subsequently, we computed the structural, thermophysical, mechanical, and water uptake properties of these systems. We demonstrate that by combining our QM tools with our accurate forcefield and GPU accelerated MD code, we can generate physically meaningful morphologies and efficiently

study the properties of crosslinked polymer systems.

5:45 PM SM05.12.03

Alternating Polymer/Nanoparticle Layers for Enhanced Composite Performance Dharnedar

Ravichandran, Yuxiang Zhu, Weiheng Xu, Sayli Jambhulkar and Kenan Song; Arizona State University, United States

Alternating layers originated from natural systems can display high-performance mechanical, thermal, electrical, optical, and other functional properties. We have developed new manufacturing that can blend polymers and nanoparticles from different channels and selectively place them in alternating layers. These layers contain nanoparticles confined within a phase and bond each of these phases via polymer phases. This structure is similar to the brick-and-mortar structure in nacre, namely, the stiff and rigid calcium carbonate and soft polymer materials. The interface formation is critical in forming superior properties. We studied the fabricated filaments, thin films, and laminates, thus confirming the layered structures' scalability. Our results also validated the high reinforcement efficiency of carbon nanotubes and nanofibers. We will also study how the particle loading, particle morphology, and interfacial interactions influence their electrical and other properties.

5:50 PM SM05.12.04

Kinetics of Crack Healing and Self-Repair Behaviors in a Sealant Glass for SOFC Application

Padmanapan Rao and Raj N. Singh; Oklahoma State University, United States

A sealant is required for the Solid Oxide Fuel Cell (SOFC) to maintain hermeticity at high operating temperatures, keep fuel and oxidant from mixing, and avoid shorting of the cell stack. Glass and Glass-Ceramic materials are widely used as a sealant since their properties can be tailored to meet the stringent requirements of SOFC stack. This study used a self-repairable glass for crack healing kinetics and independent measurement of glass viscosity. The cracks on the glass surface are created using a Vickers's indenter to achieve a well-defined crack geometry, and then the glass is exposed to elevated temperatures for different length of time to study the crack-healing kinetics. The crack-healing kinetics is compared with the predictions of our theoretical model and found to be in good agreement. In addition, glass viscosity is extracted from the healing kinetics and compared with the independent measurement of viscosity from dilatometric and sintering data to further validate the crack-healing theoretical model. These results will be presented and discussed.

5:55 PM SM05.12.05

Late News: Integration of Aptamer-Based 3D Structures and Biological Reporters for Design of

Multiplexed Biosensor Platform Irina Drachuk^{1,2}, Amy M. Ehrenworth Breedon^{1,2}, Yaroslav Chushak^{3,2} and Jorge L. Chavez²; ¹UES, Inc., United States; ²711 HPW, Airman Systems Directorate, WPAFB, United States; ³Henry M. Jackson Foundation/ WPAFB, United States

Development of biological sensors that track basal and during-duty changes in biomarker levels can provide vital information for monitoring personnel workload and implementing remediation strategies. While biological systems (i.e. bacteria or yeast) have been proven to be robust systems for engineering sensing pathways to produce modular, tunable, and dynamic responses, the discovery or engineering of novel biorecognition elements (BREs) is a time consuming and tedious challenge. Aptamers, on the other hand, provide necessary selectivity and sensitivity. However, they do not provide easy means to capture a measurable signal. Therefore, we introduce a platform that combines *Biomarker-Responsive 3D Aptamer-based Structures* with *Biological Cell-based Reporters* to develop multiplexed sensing platform for rapid tracking of multiple stress- and fatigue-related biomarkers. The platform's design combines DNA-based microcapsules with a well-established cell-based biological reporter, *S. cerevisiae*. The activation of the biosensor platform is based on a step-wise mechanism involving release of encapsulated chemical cargo upon ligand binding to an aptamer-based structure, followed by the activation of a yeast-based biosensor by released cargo. The large dynamic range exhibited by both sensing units makes them ideal for use in pseudo two-component systems, where diverse

DNA aptamers can be reliably linked to a common whole-cell biosensor output without need for additional reengineering of the sensor with each novel analyte and/or reporter. Moreover, this design can include the activation of different genetic pathways to provide different type of readout outputs, including optical or electrochemical sensing. Alternatively, the genetic output can be linked to synthesizing active compounds for remediation purposes. Hence, by combining the best features of the biological systems and DNA structures, we aim to create a suitable multiplexed platform for monitoring of different analytes of interest and mitigation of performance degrading effects.

6:00 PM SM05.12.06

Late News: Improvement of Sensor Selectivity to Butanone by Modification of ZnO Hollow with NiS

Tarcísio M. Perfecto, Cecilia A. Zito and Diogo P. Volanti; Unesp - São Paulo State University, Brazil

With the exponential advance of industries in the world comes the great concern with the possible contaminants generated in industrial processes and the health of the population. Clean and contaminant-free air is essential for the well-being of the population and environmental preservation. In this sense, the need to detect toxic and harmful volatile organic compounds (VOCs) generated in industrial processes and environments is essential, requiring a system or a device for this task, with precision and low detection limits [1–4].

In addition to the harmful problems on human health caused by toxic VOCs, recent analyses of exhaled air have demonstrated the association of diseases and VOCs [5–9]. Some compounds have proven to be efficient disease biomarkers, such as diabetes [10] and lung cancer [11].

Developing a device or material to detect volatile organic compounds (VOC) is no longer a challenge, despite its great interest. The difficulty is linked to developing a material that does not suffer from interferences, such as from humidity, other gases, or volatiles present in the analyzes. In this sense, we present a new way to modify zinc oxide (ZnO) hollow spheres with nickel (II) sulfide (NiS) nanosheets, a barely studied material in the literature, to increase the butanone selectivity and to reduce the negative effect of humidity in the final response of the sensor.

Under dry conditions, pure ZnO hollow sphere presents the best sensing response of 705.3 to 100 ppm of butanone followed by the 5%-NiS-ZnO heterostructure with a response of 123.8. However, the selectivity of 5%-NiS-ZnO improves and reaches a value of 12.92, which is more than four times higher than the selectivity of pure ZnO (3.12). Furthermore, the performance under humidity atmospheres shows that NiS heterostructures suffer less effect of the humidity. The responses to 100 ppm of butanone under 55% of relative humidity were 40.2 and 23.7 for 5%-NiS-ZnO and pure ZnO, respectively. Therefore, the developed butanone sensor demonstrated excellent response, selectivity, and a promising possibility for its practical use in sensing devices under real conditions of humidity.

Acknowledgments

This research was funded by São Paulo Research Foundation (FAPESP; grants 2018/00033-0, 2016/25267-8, 2017/01267-1).

[1] United States Environmental Protection Agency, (2016).

[2] A. Manzoli, C. Steffens, R.T. Paschoalin, A.A. Correa, W.F. Alves, F.L. Leite, P.S.P. Herrmann, *Sensors* 11 (2011) 6425–6434.

[3] V. V. Deo, D.M. Patil, L.A. Patil, M.P. Kaushik, *Sensors Actuators, B Chem.* 196 (2014) 489–494.

[4] F. Tsow, E. Forzani, a. Rai, R.W.R. Wang, R. Tsui, S. Mastroianni, C. Knobbe, A.J. Gandolfi, N.J. Tao, *IEEE Sens. J.* 9 (2009) 1734–1740.

[5] B.M. Ross, *BMC Res. Notes* 1 (2008) 41.

[6] Z.Q. Xu, Y.Y. Broza, R. Ionsecu, U. Tisch, L. Ding, H. Liu, Q. Song, Y.Y. Pan, F.X. Xiong, K.S. Gu, G.P. Sun, Z.D. Chen, M. Leja, H. Haick, *Br. J. Cancer* 108 (2013) 941–950.

[7] S. van den Velde, M. Quirynen, P. Van hee, D. van Steenberghe, *J. Chromatogr. B Anal. Technol. Biomed. Life Sci.* 853 (2007) 54–61.

[8] J. Pereira, P. Porto-Figueira, C. Cavaco, K. Taunk, S. Rapole, R. Dhakne, H. Nagarajaram, J.S. Câmara, *Metabolites* 5 (2015) 3–55.

[9] W. Li, Y. Liu, Y. Liu, S. Cheng, Y. Duan, RSC Adv. 7 (2017) 17480–17488.

[10] Y. Qiao, Z. Gao, Y. Liu, Y. Cheng, M. Yu, L. Zhao, Y. Duan, Y. Liu, Biomed Res. Int. 2014 (2014) 1–5.

[11] R.J. Knipp, M. Li, M. Bousamra, X.-A. Fu, M.H. Nantz, Cancer Med. 3 (2013) 174–181.

6:05 PM SM05.12.07

Late News: Revealing Surface Chemistry of Archaeological and Ethnographic Glass Beads Using X-Ray Photoelectron Spectroscopy Tamil Selvan Sakthivel¹, Joseph Lehner^{2,1}, Scott Branting¹ and Sudipta Seal¹;

¹University of Central Florida, United States; ²The University of Sydney, Australia

The scientific analysis of 2600-year-old archaeological and ethnographic materials has led to new perspectives on societies of past and present. Tangible cultural heritage objects are quite unlike materials prepared in known laboratory conditions because they were produced using traditional technologies in highly variable conditions. Particularly, In the Mediterranean region and Western Asia, the earliest man-made glasses in the Iron age were made from melting mixtures of natron (soda) and sand containing shell fragments (silica and lime), or ash derived from halophytic plants (soda and lime) and calcium-free sand or crushed quartzite (silica). Often knowledge about the source materials and technologies are lost, and they can only be reconstructed with careful scientific and forensic analyses. The present study focuses on two black glass beads decorated with either yellow or blue trails from 8th to 7th century BCE Sardis, glass beads that are exceptionally uncommon for this period, and on this site. A surface chemical analysis of the glass beads was made using high-resolution Imaging X-ray photoelectron spectroscopy (XPS) to understand the spatial relationships and historical evolution of chemical states inherent. We identified that the yellow glass is produced using lead stannate in which Tin in the glass is an opacifier. In the case of blue glass, copper and cobalt were the colorants. Exact chemical species identification of minerals and surface oxidation states of colorant metallic materials helps discriminate among source materials and thermodynamic processes, thereby permitting the reconstruction of technologies, provenance determination, and ancient trade routes. Funding is acknowledged NSF MRI: ECCS:1726636.

SESSION SM05.13: On-demand
Wednesday Morning, April 14, 2021
SM05

8:00 AM SM05.11.02

Late News: Silica Based Pickering Emulsions for Food and Agriculture Avital B. Benhaim and Guy Mechrez; Volcani Center, ARO, Israel, Israel

A simple and effective way to prepare multi walled carbon nanotubes (MWNT)/silica hybrid colloidosomes is presented. The colloidosomes have been generated by emulsion templating in a biphasic oil-in-water (o/w) system. Two trialkoxysilanes of complementary polarity, (3-aminopropyl)triethoxysilane and dodecyltriethoxysilane, were used to chemically immobilize the silica nanoparticles at the o/w interface and stabilize the as-generated PICKERING emulsions. The effects of varying the o/w ratio and the concentration of the added solids on the type of emulsion formed, the oil droplet size, as well as the emulsion stability have been investigated. The emulsion phase fraction was dependent on the silica content while the droplet size increased with increasing oil volume percentage. A solid shell emerged around the oil droplets from copolymerization between silane monomers. The thickness of the resulting shells was several hundreds of nm. Although MWNTs and silica nanoparticles both were co-assembled at the o/w interface, silica has shown to be the sole stabilizer, with APTES being crucial for the formation of the shell structure. Drop-casting of the emulsion and air-drying led to hierarchical open porous MWNT-silica nanocomposites. These new structures are promising as electrically conductive thin films for variety of applications, such as electro-optics, encapsulation, or chemical sensing. To the best of our knowledge, this is the first time that a CNT/silica colloidosome is prepared¹.
Reference

Grzegorzewski, F., Benhaim, A., Itzhaik Alkotzer, Y., Zelinger, E. and Mechrez, G., (2019). In situ fabrication of MWNT/silica hybrid colloidosomes by Pickering emulsion templating using trialkoxysilanes of opposite polarity, *Polymers*, 11(9): 1480.

8:15 AM SM05.02.02

Fibers Deposition Control by Innovative Pyro-Electrospinning Romina Rega, Vito Pagliarulo, Sara Coppola, Veronica Vespini, Pietro Ferraro and Simonetta Grilli; National Research Council, Italy

The electrospinning (ES) technique is able to produce polymer fibres at micro- and nano-metric scale that find application in various technological and biomedical sectors. Although the technique is well established, it still has several limitations, such as the restricted variety of printable inks (due to nozzle clogging problems) and the low control of fiber deposition (due to bending phenomena). Indeed, for some applications, the orderly arrangement, and in general the control of the deposition of these fibers, is highly desirable and people try to achieve it typically by structuring the external electrodes or using very expensive masks. Here we propose an innovative approach, which turns out to be easy to apply and economical which we have called “pyro-electrospinning” (p-ES). This technology is able to print high viscosity inks by regulating the deposition of the fibers with true regularity at the microscale. The p-ES system is based on the pyroelectric effect of polar dielectric crystals such as lithium niobate (LN). The electric field generated by the pyroelectric effect acts electro-hydrodynamically on the liquid sample, allowing the ordered deposition of the fibers. Therefore, the use of syringes, electrodes, and nozzles generally used in standard technologies is avoided. The reliability of the technique has been demonstrated both in the production of ordered periodic array fibers mats of D, L-poly (lactic acid) (PDLLA) and in spiral-shaped polymethyl methacrylate (PMMA) fibers (up to 300 nm thick) directly on a support with a true regularity at the microscale. The technique proves valid also for the deposition of fibers of highly dense materials such as poly(lactic-co-glycolic acid) (PLGA) avoiding the limitations mentioned above. The results show that these structures are useful for cell patterning applications.

References

- [1] Sun, D., Chang, C., Li, S., & Lin, L. 2006. Near-field electrospinning. *Nano letters*, 6(4), 839-842.
- [2] Xue, J., Wu, T., Dai, Y., & Xia, Y. 2019. Electrospinning and electrospun nanofibers: methods, materials, and applications. *Chemical reviews*, 119(8), 5298-5415.
- [3] Hohman, M. M., Shin, M., Rutledge, G., & Brenner, M. P. (2001). Electrospinning and electrically forced jets. I. Stability theory. *Physics of fluids*, 13(8), 2201-2220.
- [4] Rega, R., Gennari, O., Mecozzi, L., Pagliarulo, V., Bramanti, A., Ferraro, P., Grilli, S. 2019. Maskless arrayed nanofiber mats by bipolar pyroelectrospinning. *ACS applied materials & interfaces*, 11(3), 3382-3387.
- [5] Mecozzi, L., Gennari, O., Rega, R., Grilli, S., Bhowmick, S., Gioffrè, M. A., Grilli, S., Ferraro, P. 2016. Spiral formation at the microscale by μ -pyro-electrospinning. *Soft matter*, 12(25), 5542-5550.
- [6] Mecozzi, L., Gennari, O., Coppola, S., Olivieri, F., Rega, R., Mandracchia, B., Grilli, S. 2018. Easy Printing of High Viscous Microdots by Spontaneous Breakup of Thin Fibers. *ACS applied materials & interfaces*, 10(2), 2122-2129.

SYMPOSIUM SM06

Materials and Fabrication Schemes for Robotics
April 19 - April 20, 2021

Symposium Organizers

Donglei (Emma) Fan, The University of Texas at Austin
Peer Fischer, Max Planck Institute for Intelligent Systems

* Invited Paper

SESSION SM06.01: Micro/Nanorobotics
Session Chairs: Donglei (Emma) Fan, Peer Fischer and Bradley Nelson
Monday Morning, April 19, 2021
SM06

8:00 AM *SM06.01.01

Multifunctional Helical Nanobots: Roles of Material and Geometry Ambarish Ghosh; Indian Institute of Science, India

Helical nanobots driven by magnetic fields can provide mechanical information about their local surrounding with sub-micron spatial resolution, probe complex, heterogenous biological environments, such as the intracellular environment, as well as the extracellular matrix; and provide a rich and powerful platform towards futuristic drug delivery. The same system can be used for sub-micron colloidal cargo manipulation in microfluidic devices and on-chip assembly applications. Their fabrication is based on shadow evaporation allowing a wafer scale route towards integration of many different functionalities in a single nanostructure. Crucially, their properties and functionalities can be tuned with great control using intelligent design of material and geometry, and I will present few examples of the same.

8:30 AM *SM06.01.02

Driven Nanomachines—Symmetry, Controlled Propulsion and Complex Environments Alexander Leshansky; Technion–Israel Institute of Technology, Israel

Steering of nano-/microhelices by a rotating magnetic field is considered a promising technique for controlled navigation of tiny objects through viscous fluidic environments. It was recently demonstrated that simple geometrically achiral planar structures can also be steered quite efficiently [1]. Such planar propellers are interesting for practical reasons, as they can be mass-fabricated using standard photolithography techniques. Following the earlier development of a theory of driven rotation and propulsion of magnetized object of an *arbitrary shape* in an in-plane rotating magnetic field [2], we propose general symmetry arguments (involving parity and charge conjugation) establishing correspondence between propulsive solutions of simple planar V-shaped structures on orientation of the dipolar magnetic moment [3]. In particular, it can be shown that in-plane magnetization results in propulsion due to a spontaneous symmetry breaking, whereas the rotating motors swim either parallel or anti-parallel to the field rotation axis depending on their initial orientation. Particular off-plane magnetization yields *unidirectional* propulsion typically associated with chiral structures, such as helices. Since planar micro/nano-structures are prone to in-plane magnetization and their uniform off-plane magnetization is not an easy task, the interesting question is whether they can be steered in a controllable fashion? Here we demonstrate that actuation by a *conical* rotating magnetic field (i.e., superposition of an in-plane rotating field and constant field orthogonal to it) can yield efficient unidirectional propulsion of planar and in-plane magnetized structures [4]. In particular, we found that the symmetrical V-shape magnetized along its symmetry axis which exhibits no net propulsion in in-plane rotating field, shows unidirectional in-sync propulsion with a *constant* (frequency-independent) velocity when actuated by the conical field. When the constant field is imposed in plane of the rotating field, it results in the net propulsion accompanied by the *drift* orthogonal to the axis of the field rotation [5]. Such setup can potentially be used to achieve *spatial* control over motion of individual propellers and their swarms.

Until now most of the theories considered propulsion through purely viscous Newtonian fluids. However, most practical (e.g., biomedical) applications of micro-/nanopropellers involve complex heterogeneous non-Newtonian (viscoelastic) fluidic environments. Modeling of such complex media would typically require advanced numerical approaches. In this talk I shall present the hydrodynamic slender-body theory based on phenomenological “two-fluid model” first introduced by de Gennes to study entangled polymer solutions. The model describes coupled dynamics of two phases – the viscous solvent and the embedded elastic polymer network. We demonstrate that the type of the boundary condition employed for the polymer network at the surface of the particle (e.g., slip, stick or depletion layer) plays a crucial role in determining its hydrodynamic mobility.

Acknowledgement. This work was supported in part by the Israel Science Foundation (ISF) via the grant No. 1744/17.

References

- [1] U. K. Cheang et al., *Phys. Rev. E*, **2014**, 90, 033007.
- [2] K. I. Morozov et al., *Phys. Rev. Fluids*, **2017**, 2, 044202.
- [3] J. Sachs et al. *Phys Rev. E*, **2018**, 98, 063105
- [4] K.-J. Cohen et al., *Phys. Rev Appl.* **2019**, 12, 014025
- [5] K. I. Morozov and A. M. Leshansky, *Phys. Chem. Chem. Phys.* **2020**, 16407

9:00 AM SM06.01.03

Materials for Magnetically Actuated Micro and Nanorobots Vincent M. Kadiri^{1,2}, Hyunah Kwon¹ and Peer Fischer^{1,2}; ¹Max Planck Institute for Intelligent Systems, Germany; ²Universität Stuttgart, Germany

Magnetic micromotors and microrobotic systems benefit from hard magnetic and biocompatible materials, as well as schemes to avoid adhesion and overcome biological barriers.

While chemical targeting enables tissue-specific delivery, magnetically propelled microrobots can navigate through complex biological media through surface functionalization^[1-2] and can transport material towards individual cells. However, many commonly used magnetic materials or coatings are not biocompatible (Ni, Co) or possess weak magnetic moments (Fe, Fe₃O₄).

Here, we discuss both non-cytotoxic materials^[3] and medically approved coatings^[1-2] for magnetically actuated microrobots. Exciting applications range from targeted delivery through real tissues and to cells, as well as mobile contrast agents. In addition to passive coatings, it is also possible to consider chemically-active coatings where enzymes are immobilized^[2] or assembled onto selected proteinaceous templates^[4] which can facilitate the transport through complex biological fluids. Fully biocompatible magnetic microrobots combined with a suitable surface-chemistry are promising tools for biomedical applications.

1. Wu, Z.; Troll, J.; Jeong, H.-H.; Wei, Q.; Stang, M.; Ziemssen, F.; Wang, Z.; Dong, M.; Schnichels, S.; Qiu, T.; Fischer, P., A swarm of slippery micropropellers penetrates the vitreous body of the eye. *Science Advances* **2018**, 4 (11), eaat4388.
2. Walker, D.; Käs Dorf, B. T.; Jeong, H.-H.; Lieleg, O.; Fischer, P., Enzymatically active biomimetic micropropellers for the penetration of mucin gels. *Science Advances* **2015**, 1 (11), e1500501.
3. Kadiri, V.M., Bussi, C., Holle, A.W., Son, K., Kwon, H., Schütz, G., Gutierrez, M.G. and Fischer, P., Biocompatible magnetic micro and nanodevices: fabrication of FePt nanopropellers and cell transfection. *Advanced Materials* **2020**: 1-9.
4. Alarcon-Correa M, Guenther JP, Troll J, Kadiri VM, Bill J, Fischer P, Rothenstein D. Self-assembled phage-based colloids for high localized enzymatic activity, *ACS nano*, **2019**, 13(5):5810-5.

9:15 AM SM06.01.04

Substantially Accelerating Sensing Speed of Low-Concentration Molecules with Motorized Microsensors and the Working Mechanism Zexi Liang, Jianhe Guo and Donglei (Emma) Fan; The University of Texas at

Austin, United States

Vigorous research efforts have advanced the state-of-the-art nanosensors with ultrahigh sensitivity for bioanalysis. However, a dilemmatic challenge remains: it is extremely difficult to obtain nanosensors that are both sensitive and high-speed for the detection of low-concentration molecules in aqueous samples. In this work, we demonstrate substantially accelerated sensing speed of low-concentration DNA molecules in aqueous suspension with retained high sensitivity by rotationally motorizing microsensors. An improvement of at least 3 to 4 times has been obtained from a sensor rotating at 630-1200 rpm. Theoretical analysis and modeling concerning both the convective-diffusion and the diffusion-absorption processes unveil the underlying working mechanism and the application range and limitation. This work provides a device scheme that could be applied to alleviate the dilemmatic challenge in biochemical sensing. The understanding of the complex interactions of molecules and moving micro-objects may assist the design of desired microrobotic systems for the capture, translocation, sensing, and release of biocargo.

9:30 AM SM06.01.05

Late News: Synergistic Magnetism- and Light- Fields Manipulation Enables Omnidirectional Walking of Graphene Mini-Robots Bing Han¹, Zhuo-Chen Ma², Yong-Lai Zhang³, Guang-Zhong Yang² and Hong-Bo Sun¹; ¹Tsinghua University, China; ²Institute of Medical Robotics Shanghai Jiao Tong University, China; ³Jilin University, China

Miniaturized soft robots capable of omnidirectional walking through rough terrain are particularly promising for cutting-edge applications such as planetary exploration, military reconnaissance and disaster rescue. Especially, inspired by natural animals with sophisticated motion systems, great efforts have been devoted to developing walking robots based on different mechanisms. Nevertheless, most of the reported mini-robots are incapable of omnidirectional walking, which limits their controllability, active obstacle-avoidance ability, full space utilization and dead-corners elimination. The essential difficulty lies in that mini-robots with simplified components and reduced load-bearing are incapable of breaking motion symmetry in all directions through a highly controlled manner. In this study, we fabricated a small-scale crab robot (CraBot, overall dimension 2.5 cm) that enables omnidirectional walking via in-situ laser synergistic integration (LSI) of multiple graphene actuators at specified positions as joints. In this way, for the first time, we manipulated a mini-robot through coupled magnetism- and light- fields. The magnetic field regulates the center-of-mass of the CraBot, leading to an asymmetrical energy storage within the robot; meanwhile, the addressable light field selectively triggers the deformation of specific joints, releasing the accumulated energy into mechanical walk. In this way, the light field produces effective walking gait under the guidance of magnetic field synchronously. As a proof-of-concept walking to the left/right/front/back, as well as 45° off its lateral directions are presented as typical walking paths. Such dual-field-coupled manipulation strategy may serve as a versatile mechanism for future robot designs.

9:45 AM SM06.01.06

3D Metal-Organic Microrobots Fabian Landers, Carlos C. Alcantara, Bradley J. Nelson and Salvador Pané; Swiss Federal Institute of Technology (ETH) Zurich, Switzerland

The last two decades have seen significant efforts in developing micro and nanoscale machines with the ability to locomote through fluids and realizing tasks that require small-scale precision. One of the primary motivations of this research has been the realization of machines that could navigate the human body's vessels and ultimately perform medical missions, such as targeted drug delivery, microsurgery, localized diagnosis, or tissue regeneration. To this end, the use of magnetically driven small-scale robots is among the most investigated strategies, as magnetic fields are biocompatible in a wide range of conditions and they allow for a rich spectrum of locomotion mechanisms. While traditionally, research on small-scale magnetic robots has been done with rigid magnetic micro- and nanostructures made of metals or ceramics, recent efforts are dedicated to creating softer versions with the incorporation of organic materials such as polymers or hydrogels. Soft materials are usually more biocompatible, their mechanical properties resemble those of biological tissues, and

they can be easily processed in different sizes and shapes. Composites consisting of small magnetic particulates dispersed in organic matrices are typically used to render these materials magnetic. Another approach involves coating polymers with magnetic films. Yet, these strategies are usually not optimal for magnetic manipulation. Note that the force or torque exerted in a magnetic body is proportional to the magnetic material's volume. Composites comprise a reduced number of particulates that can be hosted in their matrices, while films are limited in thickness. Additionally, when polymers are coated, some of their potential functionalities such as cargo transportation, shape transformation, or degradation can be severely compromised or inhibited. To exploit the full capabilities of both stiff magnetic and soft organic materials, we present a process to manufacture interlocked metal-organic micromachines. The devices are fabricated by combining template-assisted metal electrodeposition and polymer microcasting in 3D printed molds obtained by two-photon polymerization (2PP). Sophisticated micrometric architectures such as cage-bar-ring metallic structures connected to multiple polymeric legs or metallic helices framed by a polymer casing can be successfully manufactured. We demonstrate the versatility of our approach by fabricating micromachines with iron as the magnetic component, and three prototypical polymers used for biomedical applications such as shape-memory polyurethane-based polymer (NOA-63), polydimethylsiloxane, and pure gelatin. Note that iron is the platable element with the highest saturation magnetization and displays optimal biocompatibility characteristics. Importantly, as our method involves mold-casting of polymers, the need for toxic cross-linkable moieties or photoinitiators can be avoided. In this talk, we will show the detailed manufacturing of these devices, the rich locomotion mechanisms of several complex interlocked microrobots, as well as strategies to tailor the buoyancy of the magnetic micromachines by means of the solvophobicity of the threaded polymeric structures. Finally, prospective applications such as control over the agglomeration of magnetic swarms will be discussed.

SESSION SM06.02: Soft Robotics I

Session Chairs: Donglei (Emma) Fan, Peer Fischer and Bradley Nelson

Monday Morning, April 19, 2021

SM06

10:30 AM *SM06.02.01

High-Performance Soft Actuators Based on Electrostatic Forces [Herbert R. Shea](#); Ecole Polytechnique Fédérale de Lausanne (EPFL), Switzerland

Directly electrically driving soft actuators offers clear system-level advantages over pneumatic actuation, but adds a number of challenges. For a wide range of soft robotic applications, such as haptics, and mobile robots, getting rid of the compressor, with its bulk, noise and low overall energy efficiency is a key step towards untethered and portable operation.

Due to its high energy density, we have focused on electrostatic actuation, using high electric fields to deform elastomers or textile structures. By using thin dielectrics, high permittivity and high electrical breakdown strength films, and low stiffness electrodes, we can both push up energy density and reduced drive voltage.

For a fully stretchable device, we reduced the drive voltage of Dielectric Elastomer Actuators (DEAs) from several kV to 400 V, a level at which we can use SMD components for compact control electronics (mass 350 mg). We report “feel-through” untethered cutaneous haptics, with DEA actuators only 18 μm thick[1], so thin the user does not feel them mounted on his or her fingertip when they are off. However, when the 3 mm diameter devices are turned on, the user feels localized pulsation that allows receiving rich haptic information.

Using zipping electrostatic actuation, such as electro-ribbon from prof. Rossiter's group and peano-HASELS from prof. Keplinger's group allows for higher energy density than DEAs because thin flexible materials such as polyimide have generally much better electrical properties than thin elastomers. We have developed arrays of

sub-mm thick flexible actuators that generate over 60% strain and operate at over 300 Hz [2]. A 6 mm diameter actuator generates 300 mN normal force and 500 μm displacement. This is achieved using fluidically coupled electrostatic zipping and a combination of flexible polymers with high breakdown field and central silicone elastomer region in which no electric field is applied. We have made 5x5 arrays, mounted them directly on the arm and on consumer products, and report on user feedback for notification, control and navigation.

Finally, I will present an additive manufacturing approach to such devices, using ink jet printing to freely deposit elastomer, electrode and sacrificial layers for fluidic channels[3]. I will close by going over the challenges of integrating these technologies in a glove or suit and the promise of this field of soft electrostatic actuators.

[1] X. Ji *et al.*, “Untethered Feel-Through Haptics Using 18- μm Thick Dielectric Elastomer Actuators,” *Advanced Functional Materials*, p. 2006639, 2020,

[2] E. Leroy, R. Hinchet, and H. Shea, “Multimode Hydraulically Amplified Electrostatic Actuators for Wearable Haptics,” *Advanced Materials Technologies*, 2020.

[3] S. Schlatter, G. Grasso, S. Rosset, and H. Shea, “Inkjet Printing of Complex Soft Machines with Densely Integrated Electrostatic Actuators,” *Advanced Intelligent Systems*, p. 2000136, 2020.

11:00 AM *SM06.02.02

Soft Micro-Sensors and Micro-Actuators Fabricated by Direct Laser Writing Larisa Florea¹, Colm B. Delaney¹, Alexa Ennis¹, Deanna Nicdao¹, Marc del Pozo² and Albert P. Schenning²; ¹School of Chemistry and AMBER, the SFI Research Centre for Advanced Materials and BioEngineering Research, Trinity College Dublin, Ireland; ²Department of Chemical Engineering, Eindhoven University of Technology, Netherlands

Reversible actuation through external stimuli is a critical component for the realization of smart devices in micro-mechanical, micro-optical and microfluidic systems. Significant advances in additive manufacturing has allowed for the creation of three-dimensional (3D) structures with sub-100 nm resolution(1). These advances in fabrication have allowed for considerable progress in the realization of micro-robots, such as micro-swimmers (2) or micro-grippers(3). Soft polymeric materials, such as responsive hydrogels, have the potential of augmenting the capabilities of hard micro-robotic units through the introduction of soft modules that mimic actuation of natural organisms. Hydrogels are hydrophilic, crosslinked polymer networks, that can absorb large quantities of water. Introduction of stimuli-responsive units in their structure, allows for their reversible transition from a hydrophilic (swollen) to a hydrophobic (contracted) state under external stimulation, in response to, for example, pH, temperature, light and magnetic fields. However, the main drawback of osmotically driven hydrogel actuators is their low actuation speed, where actuation force and response time are inextricably linked. This represents one of the major challenges for stimuli-responsive hydrogels which rely on the diffusion of analytes or bioanalytes. As response rate is dependent on the square of the hydrogel’s characteristic dimensions, reduction of hydrogel size to a micro regime could yield an accelerated and augmented response.

Herein we demonstrate the use of Direct Laser Writing (DLW) by multi-photon polymerization for the realization of 3D micro-actuators and sensors based on stimuli-responsive hydrogels and soft polymeric materials. We present the high resolution fabrication of a variety of structures, in a wide range of materials, including acrylated monomers, liquid crystal elastomers (4) and poly(ionic liquids)(5). These 3D structures can increase their size by over 300% through the absorption of water or solvent and can expel a large amount of the hydration media upon photo-, thermal or chemical stimulation (4D effect). Furthermore, domains of varying stiffness (e.g. hinges, joints) are integrated on demand by altering the laser exposure. Regions of low stiffness (reduced laser exposure) allow for increased swelling of the hydrogel material whilst high stiffness (e.g. obtained via increased laser exposure) act as hinges to control the direction of the fold. The single fabrication step and single resist formulation used to tailor the mechanical properties of soft polymer structures enables a simple processing method for the fabrication of complex 4D architectures via DLW.

3D micro-fabrication by DLW coupled with intrinsic (molecular) alignment is also demonstrated for the realization of dual-responsive soft polymer micro-structures. In this example, a supramolecular cholesteric liquid crystalline (CLC) elastomer is used for the fabrication of 4D structures, where the on-demand actuation is coupled with a color change. The CLC networks exhibit a self-organized helical photonic structure that can selectively reflect light, giving the 3D structures an initial color. Upon stimulation, via humidity (directly) and temperature (indirectly) changes, the network expands triggering a change in pitch of the CLC's helical structure, therefore resulting in a shift of the reflection band. The micro-actuator's expansion (up to 42 % in height at 75 %RH and at 19 °C) is accompanied by a color change. Such dual-response would be beneficial in microrobotics, enabling real-time interrogation of actuator status, through observation of the intrinsic color of the material.

1. M. Farsari, B. N. Chichkov, *Nature photonics* **3**, 450 (2009).
2. C. Alcântara *et al.*, *Small* **15**, 1805006 (2019).
3. M. Power *et al.*, *Small* **14**, 1703964 (2018).
4. M. Del Pozo *et al.*, *ACS Nano* **14**, 9832 (2020).
5. A. Tudor *et al.*, *Materials Today* **21**, 807 (2018).

11:25 AM SM06.02.03

Soft Robots with Reconfigurable and Deactivatable Skeleton Yueping Wang, Xiyue Zou, Aaron Mazzeo and Howon Lee; Rutgers, The State University of New Jersey, United States

Soft robots have been attracting great attention for their high flexibility and versatility. One of the most significant shortcomings of inflatable soft robots is the low bending stiffness due to the intrinsic soft nature of elastomers. As a result, it becomes challenging to maintain the shape of a soft robot against gravitational force when the aspect ratio of a soft robotic manipulator increases (e.g. long and slender). To address this inherent drawback, we present a soft robot with reconfigurable and deactivatable skeleton. It consists of a soft elastomeric body reinforced with a rigid shape memory polymer (SMP) skeleton. Exploiting viscoelasticity of the SMP, the stiffness of the SMP skeleton can be varied over two orders of magnitude from ~ 1.2 GPa to ~ 2.4 MPa by resistive heating through an embedded liquid metal channel. At room temperature, the rigid SMP skeleton provides structural stability, making it possible for a large-scale soft robot to maintain its shape against gravity as vertebrates do. When flexible soft robotic actuation is needed, resistive heating is applied to deactivate the SMP skeleton mechanically, thereby rendering the soft robot flexible and pneumatically actuable. Furthermore, the SMP allows the soft robot to be reconfigured into different shapes. This approach enables simple soft robotic gripping actuation with a large length scale of ~ 50 cm. We also demonstrate an amphibious locomotion of a soft robot which can reconfigure its four soft robotic limbs from straight flap for swimming in water, to curved legs for multi-pedal gaiting on rough terrains, to wheel-like geometry for driving on flat surfaces. The reconfigurable and deactivatable skeleton may expand the applications of soft robots to diverse practical and industrial uses.

11:40 AM SM06.02.04

Late News: Electrically Responsive Elastomers—From Synthesis to Applications Dorina M. Opris; Empa—Swiss Federal Laboratories for Materials Science and Technology, Switzerland

Often the doors to major technological innovations are opened by the discovery of novel functional materials. Dielectric elastomer transducers (DET) are an emerging technology, which gained importance over the last years. For this technology, the need for high dielectric permittivity polymers is higher than ever before. They hold great promise as active components in actuators, sensors, energy harvesting, artificial muscles, and soft robotics.

This presentation will give an overview of how we synthesized high dielectric permittivity elastomers. One approach to increase the dielectric permittivity consists of blending highly polarizable fillers in matrices with good elasticity. This approach failed because the materials are inhomogeneous at the molecular level and the mechanical and electromechanical properties are deteriorated. The second approach uses a chemical

modification of polymers with polar groups. This allows the formation of homogenous materials, but it has the downside that the glass transition temperature (T_g) increases too much and turns unattractive for practical applications.

Using a highly flexible polymer backbone, we have shown that it is possible to achieve polymers with increased dielectric permittivity and low T_g . Our strategy is to chemically modify polymers that have a very low T_g with polar groups. Despite the increase in T_g due to dipolar interactions, the T_g of the modified polymers is still attractively low. Using this approach, we were able to achieve the highest dielectric permittivity ever for a neat elastomer, which exhibit unprecedentedly high dielectric breakdown fields. Such elastomers respond to both low electric fields and low voltages.

11:55 AM *SM06.02.05

Soft BioRobotics—Rethinking Material Role for Life-Like Robot Behaviour Cecilia Laschi^{1,2}, Matteo Cianchetti², Leonardo Ricotti², Marcello Calisti² and Hilda Gómez Bernal²; ¹National University of Singapore, Singapore; ²Scuola Superiore Sant'Anna, Italy

BioRobotics is a successful approach for designing robots from and for living beings. Bioinspired robot design is based on principles observed and modelled on living beings. In a beneficial loop, bioinspired robots also contribute to gain insight in biology. Either bioinspired or not, biorobots are those applied in the biomedical field.

A lesson learnt from living beings is that the physical body has a more important role in shaping intelligence than we think. Behaviour is not only controlled by the computation happening in the nervous system but emerges from the interaction of the body with the environment. It then depends on the physical properties of the body itself, on its morphology, on the environment it is operating in. This concept of embodied intelligence brought to rethink bodyware in robotics. Compliance became key and either compliant joints or soft materials have been used.

In this scenario, recent advances in materials, smart materials and fabrication techniques are enabling the development of soft robots, with new technologies for actuation, sensing, control, energy supply. Among the many possible applications of soft robots are the biomedical ones, e.g. surgery, prosthetics, rehabilitation [1]. Soft robotics technologies can also be used for building biomimetic organs or physical models of human body parts. The EU HybridHeart project is developing a fully soft artificial heart. A physical model of vocal cords was developed for studying larynx physiology and pathologies.

Bioinspired soft robots find applications in explorations, in natural environments. They can access remote areas, confined spaces, complex or collapsed structures, both in land and at sea. Marine applications of soft robots give interesting challenges and opportunities for developing bioinspired swimming and locomotion. While current underwater robots operate in the water column, soft robots can afford the interaction with the seabed or underwater plants [2].

Soft robots open up unprecedented abilities. The classical robot abilities of manipulation and locomotion assume new forms and new abilities become possible, like morphing, growing, self-healing, biodegrading [3]. Soft robots enable a vision for life-like abilities and behaviour, thanks to the bioinspired principles they embed and to the materials they are built of. In this framework, bio-hybrid robots are another intriguing paradigm, pursuing the integration between artificial materials and living cells/tissues. The unique features of living cells, optimized by millions of years of natural evolution, can be actually exploited to enable specific robot abilities and to achieve robots scaling toward small dimensions [4].

Overall, soft biorobots support a vision for future robots where they have a full life cycle, in analogy to living beings [5]. They are born but grow in body and intelligence, they learn and adapt their bodies, find their energy, self-heal their bodies and biodegrade at the end of their life. The vision for life-like robot behaviour is still in its infancy but shows an enormous potential. It provides challenges and opportunities for revolutionizing robotics and for exploring new materials and fabrications schemes.

[1] M. Cianchetti, C. Laschi, "Pleasant to the touch", *IEEE Pulse Magazine*, 3, 34-37, 2016

[2] G. Picardi, M. Chellapurath, S. Iacoponi, S. Stefanni, C. Laschi, M. Calisti. "Bioinspired underwater legged robot for seabed exploration with low environmental disturbance", *Science Robotics* 5(42), 2020

- [3] C. Laschi, M. Cianchetti, B. Mazzolai, “Soft robotics: Technologies and systems pushing the boundaries of robot abilities”, *Science Robotics* 1(1), 2016
- [4] L. Ricotti, B. Trimmer, A.W. Feinberg, et al., “Biohybrid actuators for robotics: A review of devices actuated by living cells”, *Science Robotics* 2(12), 2017
- [5] B. Mazzolai, C. Laschi, “A vision for future bioinspired and biohybrid robots”, *Science Robotics* 5(1), 2020

SESSION SM06.03: Materials in Robotics
Session Chairs: Donglei (Emma) Fan and Peer Fischer
Monday Afternoon, April 19, 2021
SM06

1:00 PM *SM06.03.01

Pick-and-Place by Switchable Microstructures—A Sustainable Handling Paradigm Eduard Arzt^{1,2} and Marc Schöneich³; ¹INM–Leibniz Institute for New Materials, Germany; ²Universität des Saarlandes, Germany; ³INNOCISE GmbH, Germany

Reliable and sustainable automated manufacturing is predicted to play an even greater role in future industrial value creation than today. Automated handling processes are currently facing unprecedented challenges in terms of miniaturization, sustainability, and demanding production environments. Systems in worldwide use are mechanical grippers, electromagnetic actuators or vacuum suction devices. Requiring electrical energy and other valuable resources, these systems leave a large environmental footprint. They are dysfunctional with sensitive materials that suffer damage easily or with micro objects, causing low yields and high scrap rates. In this talk, it will be demonstrated that the new paradigm involving the tailoring of surface microstructures can offer innovative gripping solutions. Inspired by natural examples such as geckos and insects, micropatterning of polymeric surfaces allows the creation of various structure-related functionalities including the controlled adhesion and release of objects. These effects are based on van der Waals interactions and are largely independent of – sometimes environmentally harmful - materials chemistry; in particular, microfibrils can impart switchable stickiness to a material which is intrinsically non-adhesive. The sticking action is provided by a multitude of fine polymeric fibers (imitating a gecko foot); unsticking is provoked by actively switching the orientation of these hairs, resulting in accurate placement of an object. An elegant mechanical approach is to apply a compressive overload to the adhesive structures: the resulting elastic instability due to buckling of the fibrils leads to contact loss and creates a transition to a non-adhesive state. Such a load-controlled stimulus constitutes a reliable strategy and is straightforward to implement in industrial robotic systems. Subsequently, multistep switchable adhesives were developed, in which fibrils of varying length enable tuning of the adhesion strength. Other actuation mechanisms involve thermal stimuli, e.g. in combination with trained shape memory polymers or magnetic fields, which can trigger the bending of fibrils and induce a loss of contact.

The resulting Gecomer® technology has decisive advantages over conventional technologies: It is highly energy saving, resource sustainable, noise-free, compatible with sensitive surfaces, and applicable under extreme conditions where conventional solutions fail, e.g. in micro dimensions and in vacuum (as in space applications). To ensure reliable adhesion and controlled release, the pick-and-place process has been modelled by considering the interfacial stress distribution in the contact area. Governing parameters are the compressive preload, the size, shape and modulus of the fibril, the assumed defect statistics and the properties of the backing layer. An emerging challenge in microfabrication is the controlled release of small objects, where the weight of the objects to be handled is insufficient for easy detachment; for this, novel microstructure designs were developed that minimize the residual adhesion while ensuring high lateral precision during the placement step. Current developments included in-situ monitoring and machine learning to improve the reliability of the handling process. The new, precise and universal system solutions provided for automation, robotics and handling have already proven their practical suitability in demanding pilot applications. Examples of successful

implementation will be demonstrated.

1:30 PM *SM06.03.02

Liquid Metals for Soft Robotics Michael Dickey; North Carolina State University, United States

This talk will discuss recent progress in utilizing liquid metals as conductors for stretchable, soft, and reconfigurable components for soft robotics. Alloys of gallium are noted for their low viscosity, low toxicity, and near-zero vapor pressure. Despite the large surface tension of the metal, it can be patterned into non-spherical 2D and 3D shapes due to the presence of an ultra-thin oxide skin that forms on its surface. Because it is a liquid, the metal is extremely soft and flows in response to stress to retain electrical continuity under extreme deformation. By embedding the metal into elastomeric or gel substrates, it is possible to form soft, flexible, and conformal electrical components, stretchable antennas, and ultra-stretchable wires that maintain metallic conductivity up to ~800% strain. Thus, these materials are well-suited for soft robotics because they decouple electrical conductivity and mechanical properties. In addition to introducing the advantages of these materials for soft robotics, this talk will focus on recent work to utilize liquid metal for tactile sensors and energy harvesters. These advances have implications for soft machines and robots that have ultra-soft mechanical properties.

2:00 PM *SM06.03.03

Robotic Surfaces with Tunable Stiffness and Reversible Shape-Morphing Chiara Daraio; California Institute of Technology, United States

Robotic surfaces that can reshape and react to external stimuli offer opportunities to create soft, versatile machines that can multi-task, while interacting safely with their surroundings. Such systems are useful in applications that range from haptic interfaces, wearable exoskeletons and reconfigurable medical supports. Key properties of robotic surfaces include their ability to control their local stiffness, reprogram their target shape and have sufficient mechanical loadbearing ability, to support weights and manipulate objects. In this talk, I will describe recent solutions developed in our group, to create structured fabrics that have tunable bending stiffness and robotic surfaces that allow for large, reprogrammable, and pliable shape morphing into smooth 3D geometries. To develop these solutions, we design layered, architected materials, consisting of interlocking particles or networks of layered, polymeric ribbons. We employ different actuation methods, including vacuum pressure and Joule heating, to control the response of the surfaces. We demonstrate the ability to fabricate fabrics that become >25 times stiffer than their relaxed configuration, when a small external pressure (~93 kPa) is applied. We also show that robotic surfaces consisting of layers of heat responsive liquid crystal elastomers (LCEs) can be reprogrammed to assume arbitrary shapes.

2:30 PM SM06.03.04

Selective Curing of Carbon Fiber Reinforced Plastics to Fabricate Deployable Folding Structures Thomas Celenza, Matthew F. Campbell, George A. Popov, Luke Kasper, Wujoon Cha, Cynthia Sung, Mark Yim and Igor Bargatin; University of Pennsylvania, United States

We have developed a photolithography-inspired method of transferring predetermined fold patterns to carbon fiber veneers *via* selective ultraviolet epoxy curing, which allows us to create deployable structural components for microrobots and microflyers. Our technique uses photosensitive epoxies that require ultraviolet light for curing with a patterned mask to inhibit photopolymerization along fold lines but to allow light exposure and therefore hardening reactions to take place elsewhere. Using this technique, we constructed origami-inspired fold patterns on samples with thicknesses of 200 microns and areal densities of 20 mg/cm² from bi-woven carbon fiber fabrics without the need for cuts, living hinges, or buckling lines. This work represents, to our knowledge, the first use of ultraviolet epoxies to make folding composite materials.

Significant research has been devoted to improving aerial vehicles and robots by decreasing their sizes and reducing their masses. Toward the first strategy, small untethered microflyers with diameters of just 2 cm have

been demonstrated¹; however, these robots' small sizes were achieved by sacrificing aerodynamic components that provide maneuverability. To overcome this, deployable structures have been proposed as methods to increase microflyer control while maintaining compact dormant footprints². Toward the second strategy, new materials have been explored that provide enhanced strength with lower densities. A prime example is carbon fiber³, which has been widely used to fabricate micro aerial vehicles with dimensions >10 cm. Examples combining both of these performance enhancement strategies, *i.e.*, foldable composite sheets, are currently limited to large space assemblies and composite load bearing structures that have a single degree of freedom³⁻⁵. Employing these methods for small-scale vehicles has required specialized joint actuation and other design limitations^{6,7}.

There is thus a significant need for lightweight structural components that can be folded in multiple directions to allow arbitrary modular robot and microflyer designs. To bridge this gap, we have developed a method of transferring predetermined fold lines onto carbon fiber sheets using photosensitive epoxy resin and light-obstructing mask patterns. This method results in veneers with areas of high stiffness where ultraviolet light was exposed but thin foldable elastic areas where radiation was blocked. Importantly, our folds do not require cuts or fractures; rather, due to the absence of cured epoxy in the hinge areas, the carbon fibers can undergo microbuckling in a repeatable fashion⁸. Moreover, our technique allows fold patterns, such as those previously used in space applications⁹, to be quickly imparted to carbon fiber sheets in a reproducible and mass producible fashion at a smaller scale than previous work.

To fabricate our folding veneers, we impregnated a bi-woven carbon fiber fabric with photocurable epoxy, exposed it to ultraviolet light through a 2-mm-wide frame, additively manufactured mask, and cleaned the resulting veneer to remove excess uncured resin. We are currently subjecting our samples to mechanical testing to identify their bending stiffnesses and radii of curvature and are designing complex fold patterns to demonstrate these veneers' deployable functionality. Our results represent a significant step forward in modular design and assembly toward deployable and lightweight components for robots and microflyers at such a small scale.

- 1) Piccoli *ICRA* (2017)3328
- 2) Cha *J. Microelectromech. Syst.* 29(2020)1127
- 3) Shi *IOP Conf. Ser., Mater. Sci. Eng.* 531(2019)012067
- 4) Peterson *AIAA* (2013)1667
- 5) Leclerc *AIAA* (2019)1522
- 6) Dufour *IROS* (2016)1576
- 7) Jacob *AIAA* (2009)745
- 8) Jimenez *AIAA* (2009)2633
- 9) Miura *Int. J. Space Struct.* 8(1993)3

This material is based upon work supported by the Defense Advanced Research Projects Agency (DARPA) under Contract No. HR0011-19-C-0052. Approved for Public Release, Distribution Unlimited.

2:45 PM SM06.03.05

Multi-Assembly of Soft Electroactive Polymeric Yarn Actuators by Using Textile Processes Carin Backe¹, Jose G. Martinez², Li Guo¹, Edwin Jager² and Nils-Krister Persson¹; ¹University of Borås, Sweden; ²University of Linköping, Sweden

Textile assembly methods offer great possibilities to create complex, large-scale, multi-functional 2D materials (fabrics) by a continuous process of structuring yarns together, in an architected manner. By designing a specific pattern and using functionalized yarns the properties of such a fabric can enable a variety of roles for example actuation and mechanical stimuli. Moreover, actuation can be achieved in several directions as the textile assembly enables the construction of a network where yarns can be independently addressed in X and/or Y direction. These are advantages that can be utilized in the field of soft robotics in many ways. The

requirements for human-robotic interactions call for soft and compliant materials that are safe for such collaborative interactions and involve several types of functionalities. Textiles are easily conformed to the body, whether that is a robotic or a human one. Here we report on the integration of novel functional actuating yarns in the purpose of creating pliable textile actuators that also exhibit versatile morphing capabilities. The yarns consist of three layers; two of which are made of thin poly (3, 4-ethylenedioxythiophene): poly (styrene sulfonate) (PEDOT: PSS) coatings that cover opposite sides of the third layer, an ionogel. This stretchable gel supplies the system with ions for the actuation mechanism and therefore enables in-air actuation. The yarns are transformed into fabrics by using woven assembly techniques. This is an additive method that structures one set of yarns in a parallel sequence that is perpendicular to another second set of yarns. By structuring a number of yarns together in parallel the performance in terms of force output including blocking force is shown to increase. The textile assembly process allows for two approaches, collective and individual addressing for the actuating yarns. For the former, arranging the yarns into different pre-determined segments enable collective actuation of each segment to change the overall shape of the textile structure. In regards to the latter, by individual addressing we show that a specific and targeted actuation can be achieved. Furthermore, the arrangement in which the yarns are interlaced in the fabric enables switching the modality of the actuation. This means that we can alter a motion specific to the yarns into another by their arrangement in the textile structure. With our developed textile assembly method, we are approaching low-cost, large-scale production of actuating systems for human-robotic applications.

SESSION SM06.04: Poster Session: Materials and Fabrication Schemes for Robotics
Session Chairs: Donglei (Emma) Fan and Peer Fischer
Monday Afternoon, April 19, 2021
9:15 PM - 10:05 PM
SM06

SM06.04.01

Late News: Photoreversible Q-Silsesquioxane/Azo Network Sponges Joseph Furgal and Nai-hsuan Hu; Bowling Green State University, United States

The synthesis and mechanical properties of photoswitchable silsesquioxane/azobenzene hybrid 3D-polymers (“dynamic sponges”) are presented and discussed. The hybrid is capable of extensive macroscopic movement, and overcomes previously problematic crosslink locking issues. A hydride-functionalized Q-type silsesquioxane ($Q_8M_8^H$) was reacted with di-allyloxyazobenzene using hydrosilylation methods. The properties of the resulting materials are controlled via careful choice of starting material ratios and solvent, leading to gels or films. Both morphologies show pronounced photoresponsive behavior in and on the surfaces of different solvents. Photoactuation is tracked by microscopy, DMA and UV/Vis spectroscopy. The gel system has a porous structure similar to a sponge. It undergoes shrinkage in volume by 18.3% in toluene under UV irradiation, and shows excellent recovery to the swollen state after irradiation with visible light. These novel photodynamic materials offer reversible modulus switching from 160 kPa in the swollen state to 500 kPa in the “wrung-out” sponge. The sponges can engage in uptake and release of a range of substances (i.e., reversible hydrophobic sponging), with overall performance determined by substrate size and polarity. Such behavior gives these materials high potential for soft robotics applications and great promise as reusable environmental remediators.

SM06.04.03

Biomimicking the Property Modulation and Self-Healing Characteristics of Biological Tissues Through an Electrochemical Cell with Soluble Porous Anode Changquan Lai; Nanyang Technological University, Singapore

Current structural materials for robotics generally possess mechanical properties that are static and can operate only within a narrow range of environmental conditions. In an effort to imitate living biological tissues that can modulate their properties dynamically in response to an environmental stimulus, we developed an electrochemical cell with a soluble porous anode (ECSPA). This cell allows material to be added to or removed from the structural electrode according to the duration, polarity and magnitude of the applied potential difference, bringing about precise and reversible modulation in the material's modulus, strength and energy absorption characteristics over 3 orders of magnitude. In response to a complete fracture, the cell was shown to be able to self-heal, achieving ~ 50% of its original load-bearing capability with as little as 6 hours of treatment. A self-contained ECSPA setup was also demonstrated as a proof-of-concept for how the cell can possibly be integrated into a robotic assembly for real-world applications.

SM06.04.04

High Fracture Toughness and Self-Healable Elastomers for Soft Robotics [Matthew Tan](#) and Pooi See Lee; Nanyang Technological University, Singapore

Fracture toughness and self-healing capabilities in synthetic soft materials are attractive features to prolong the lifetime of soft robotics and enable their usability in extreme or harsh environment. To achieve these two attributes, soft materials such as elastomers are often endowed with dynamic supramolecular bonds such as hydrogen bonds. In this work, we describe two toughening modes that arise from tuning the polymeric chain mobilities of carboxyl functionalized polyurethane (CPU) using plasticizers. Without plasticizers, intrinsic toughening was found to dominate as a result of strong hydrogen bonds that resist crack propagation. Under such conditions, CPU achieves a fracture toughness of ($\sim 105 \text{ kJ m}^{-2}$) at which a sharp crack tends to propagate when stretched. In contrast, upon the addition of plasticizers, extrinsic toughening mechanism dominates with energy dissipation from the breakage of weaker hydrogen bond interactions. Furthermore, large blunted cracks propagate within plasticized CPU with larger stretchability. By tuning the content of plasticizers within CPU, both toughening mechanisms can be combined, enhancing the fracture toughness of CPU ($\sim 122 \text{ kJ m}^{-2}$). To prove this hypothesis, we perform in-situ studies where notched CPU was stretched at various temperatures to modulate the chain mobilities. Also, at higher plasticizer content, CPU was found to display higher self-healing capabilities, retaining greater mechanical toughness. Overall, this work provides a fundamental mechanical understanding to tune the fracture toughness and self-healing of elastomers, making them attractive for soft robotic applications.

SM06.04.05

Late News: 3D Printable Silicone Double Networks for Soft Robotics [Thomas J. Wallin](#); Facebook Reality Labs, United States

We report a framework for creating tough, 3D printable silicone double networks (SiIDNs) by combining thiol-ene and condensation cured polydimethylsiloxanes. These two chemical reactions are "orthogonal"—each proceeds without hindering the other. Thus, photocurable thiol-ene network forms the shape during 3D printing and entraps the precursors to our latent condensation network which dominates the final mechanical properties. Thus, we can break the endemic process-structure-property trade-off in 3D printed polymers and create a family of soft ($100 \text{ kPa} < E < 1 \text{ MPa}$), highly extensible ($\epsilon > 100\%$) elastomers. The slower condensation reaction can also form interfacial bonds with diverse materials including ceramics, metals, and other polymers. With this strategy, we can create mechanical gradients spanning almost seven orders of magnitude, a similar range found in natural systems. We demonstrate the utility of this system by building soft robotic devices cohesively affixed to electronic circuitry and commercial garments. Further, we use machine learning to generate mechanical metamaterial structures based on the assembled structures of 3D printed rigid bodies with SiIDNs. Lastly, we demonstrate a ternary chemistry where this framework can be extended to create multimaterial foamed elastomers.

SM06.04.07

Late News: Synergistic Integration of Smart Materials into 3D Printed Programmable Tensegrity [Hajun](#)

Lee, Yeonwoo Jang, Jun Kyu Choi, Suwoo Lee, Hyeonseong Song, Jin Pyo Lee, Nasreena Lone and Jiyun Kim; Ulsan National Institute of Science and Technology, Korea (the Republic of)

Successful designs of soft robots rely on both clever morphology and material properties. Many researchers have pursued the intelligent embodiment of smart materials into the soft systems, which results in the dynamic interaction of architecture, material, and environment. However, body designs of soft robots have lagged behind biological analogs because of the inherent complexities in both form and function in generating suitable environmental behaviors at desired scales.

Structural approaches are essential to increasing the systematic complexity and the functional diversity of soft material-based intelligent systems. Smart structures can represent unconventional but programmable mechanical properties, reacting to environmental changes in morphologically and functionally adaptive ways. These features distinguish smart structures from typical static structures with a primary purpose of providing load capacity. However, in most smart structures, most loads are focused on the flexible joints or hinges, and thus, combining multiple materials has limited synergistic effects in programming system-level mechanics to include both morphology and structural mechanics efficiently. Therefore, to increase programmable complexity and synergistic integration in 3D, more scalable and systematic approaches should be promoted because of combinatorial issues brought about by embedding multiple distinct materials in a seamless and synergistic way. We propose the adoption of tensegrity as a class of metamaterial strategy for smart material-based robotic systems. Tensegrity systems are composed of both isolated compressive “struts” and a network of elastic “tendons” with a specific configuration of nodes. The main advantages of tensegrity structures include high stiffness-to-mass ratio, controllability, reliability, structural flexibility, and large deployment. Furthermore, by preserving the self-equilibrium of normal forces applied to its elements, tensegrities are easily stabilized as the structure stands or is deformed. This harmonious balancing of forces enables distinctive material components to be formed in a network, instead of piling up simple cellular units, and thus provides ample design space of morphology and mechanical properties. Despite its advantages, smart materials are rarely used as mechanical elements for the construction of smart tensegrity structures because of a lack of proper manufacturing processes allowing generation of multi-material parts with intricate 3D shapes.

In this work, we adopted the tensegrity for the development of soft structures with programmable mechanical responses in 3D. We endowed tensegrity with additional functionality by using magnetic materials as tendon components and used a 3D printing technology combined with sacrificial molding to fabricate tensegrities at a diverse scale. This method makes the construction of tensegrity a lot easier because it eliminates any post-assembly process of beam elements.

As a result of printing tensegrity with coordinated soft and stiff elements, we could use design parameters (such as geometry, topology, density, coordination number, and complexity) to program structure-level mechanics in a soft structure. On the basis of the programmed mechanics of tensegrity structures, we developed diverse smart structures and demonstrated a tensegrity robot capable of walking in any direction. We demonstrated several tensegrity actuators (such as auxetic behavior, locomotion, and intaking) by leveraging smart tendons with magnetic functionality. This physical realization of complex 3D metamaterials with multiple mechanical components can pave the way toward more analytical and algorithmic designs of scalable geometry and contribute to complex morphing for 3D soft systems. Furthermore, this may provide new form factors for 3D flexible devices in the fields of flexible electronics, biomedicine, and soft robotics.

SM06.04.08

Rehealable and Highly Stretchable Strain Sensing System Enabled by Dynamic Covalent Thermoset

Jianliang Xiao; University of Colorado Boulder, United States

Soft and stretchable integrated electronic systems have gained wide popularity recently due to their superior mechanical compliance and conformability, which distinguishes them from conventional rigid electronic devices. Cutting-edge technologies of stretchable, skin-mountable, and wearable electronics are able to effectively accommodate large strain when integrated onto soft, elastic and curved surfaces. Ultralow modulus and high stretchability of electronic systems are achieved by designing new structural layouts and developing novel materials. However, stretchable conductors made of metallic materials often suffer from cycling induced

fatigue, which cannot be easily improved by new structural designs.

Recently, various wearable strain sensors with high stretchability have been developed for their broad applications in human motion detection, health care, human-machine interfaces. Strain sensors can be classified into two types: resistive-type and capacitive-type sensors. Resistive-type sensors are typically composed of composites combining electrically conductive sensing films with flexible substrates. When stretched, the microstructure of sensing films evolves, and the electrical resistance changes accordingly. On the other hand, a capacitive-type sensor consists of a highly compliant dielectric layer between a pair of stretchable electrodes. When stretched, two electrodes become closer, and the capacitance increases. Alternatively, stretchable and wearable strain sensors can also be classified according to their materials, into categories such as fiber, liquid metal (LM), and piezoelectricity based strain sensors. As a liquid-state conductor, the LM features excellent electrical conductivity, fatigue-free characteristics and extremely high deformability, thus is an ideal component for wearable strain sensors.

Moreover, materials that can heal/reheal like natural skins have also been developed in wearable electronics. Self-healing/rehealing can help wearable electronics to gain benefits of reliability, durability, cost and performance. While some self-healing mechanisms can automatically respond to damages without stimuli, most self-healing/rehealing materials still require moderate external stimulation—such as heat, light, water and chemicals—to trigger the healing process. Various strategies have also been investigated to achieve self-healability/rehealability, including metal-ligand supramolecular, microvascular agents, hydrogen bonds, semiconducting polymers, and dynamic covalent bonds. Among the many self-healing mechanisms, dynamic covalent bonding in polymer networks is usually stronger than supramolecular interactions, thus making such materials more robust and can operate under a wider range of conditions⁴⁴. More recently, a series of dynamic covalent thermoset polyimine that can self-heal/reheal under modest external stimuli have been developed. Here, we present a new type of flexible, highly stretchable, and rehealable strain sensing system enabled by eutectic LM alloy and dynamic covalent thermoset polyimine. As LM is a liquid, it doesn't add rigidity and provides excellent deformability to the strain sensing system. Moreover, unlike conventional metal conductors, LM conductors doesn't experience fatigue. Furthermore, a dynamic covalent thermoset polyimine matrix is not only highly stretchable, but also rehealable from damages. To provide prediction to the strain sensing system, we have also established an analytical model to describe the resistance change under applied strain, which shows good agreement with finite element simulations and experimental measurements.

SESSION SM06.05: Chemical Systems in Robotics I
Session Chairs: Donglei (Emma) Fan and Peer Fischer
Tuesday Morning, April 20, 2021
SM06

8:00 AM *SM06.05.01

Mechanics and Thermodynamics of Hygroresponsive Soft Machines and Engines Ho-Young Kim,
Beomjune Shin and Moonkyung Choi; Seoul National University, Korea (the Republic of)

Hygroresponsive soft materials can convert environmental humidity directly into mechanical motions, as can be mundanely observed in curling of wet paper, swelling of kitchen sponges, and opening of dry pine cones. Although the bending and coiling motions of such moisture-sensitive materials are recently explored for powering tiny robots, a lack of mechanistic and thermodynamic understanding of the soft actuation systems has hindered optimization of their mechanical designs and evaluation of energy conversion efficiency. Here, we construct a theoretical model to predict the temporal evolution of actuator shape and resulting force under environmental humidity change. We demonstrate how our mechanistic theory optimizes designs of various hygroresponsive machines developed in this work, including a crawler, a wheel, a seesaw, and a vehicle. Furthermore, we introduce a stress-volume diagram of soft power generators to calculate the thermodynamic efficiency of natural and artificial hygroresponsive engines.

8:25 AM *SM06.05.02

Biologically Inspired Polymerization Motor Gels for Building Soft Robots Controlled by Biomolecular Reactions Rebecca Schulman, Ruohong Shi, Joshua Fern and David H. Gracias; Johns Hopkins University, United States

Shape-changing hydrogels that can bend, twist, or actuate in response are critical elements of soft robots. Chemomechanical devices, which are controlled by chemical signals, have critical advantages for miniaturizing soft robots. The chemicals that control these devices can diffuse over large distances and into small or tortuous spaces, and the huge number of chemicals that can be synthesized offers unprecedented tunability and specificity. Chemomechanical devices require no batteries and can easily be miniaturized and integrated with other devices. We demonstrate hydrogels differentially responsive to different DNA signals. Specific DNA molecules can induce 100-fold volumetric expansion of hydrogels by successive extension of cross-links via the operation of polymerization motors. These structures can be photopatterned at size scales up to centimeters to create composite gels containing multiple domains. The resulting devices undergo different shape changes in response to different DNA sequences that selectively swell different domains. A simple design rule derived from experiments and material simulations suggests a means to control shape change. Methods of rational DNA design and control of DNA stoichiometry can, by altering polymerization motor operation, alter the amount and rate of swelling. Finally, multicomponent hydrogels using a variety of scaffold polymers, including polyethylene-glycol, acrylamide can be photopatterned into distinct shapes, have a broad range of mechanical properties, including tunable shear moduli across more than an order of magnitude, and enhanced biocompatibility. These materials offer a new possible means of building soft robots: because DNA molecules can be outputs and inputs to molecular sensors, amplifiers, and logic circuits, this strategy introduces the possibility of building soft devices autonomously controlled by chemical networks.

8:55 AM *SM06.05.03

Biohybrid Devices—Harnessing Biofunctional Materials in Micro-Devices Shoji Takeuchi^{1,2,1}; ¹The University of Tokyo, Japan; ²Kanagawa Institute of Industrial Science and Technology (KISTEC), Japan

Biohybrid devices can be categorized into 4 groups: (i) biohybrid-sensors that can detect target molecules at highly selective and sensitive manner, (ii) biohybrid-reactors that mimic biological reaction in our body, and thus are useful for drug testing or tissue transplant for cell therapy, (iii) biohybrid-actuators that shows highly energy efficient motion and (iv) biohybrid-processors that achieve low-energy and highly parallel computing like our brain. In this talk, I would like to talk about a couple of our recent results regarding biohybrid sensors and actuators.

9:25 AM SM06.05.04

Artificially Innervated Foams—Biomimetic Self-Healing Synthetic Piezo-Impedance Sensor Skins Hongchen Guo, Yu Jun Tan and Benjamin Tee; National University of Singapore, Singapore

The mechanoreceptors buried in human skin is known for enabling the skin to be tactile sensitive. Meanwhile, the innervations of the mechanoreceptors, which function via three-dimensionally distributed nerves extending from deep skin upwards, also enable the skin to detect complex tactile stimuli like normal and shear forces. Here, we design a biomimetic e-skin sensor by embedding three-dimensional metal wire electrodes as ‘nerves’ in a low-modulus yet elastic self-healing foam named Artificially Innervated Foam (AiFoam). The three-dimensional electrodes in the sensing material enable the sensor to detect both normal and shear forces, as opposed to the conventional sensors with two-dimensional planar electrodes which can only detect normal forces. We also develop a unique bimodal piezo-impedance pressure sensing foam material with both piezoresistive and piezocapacitive sensing capabilities. The near-percolation metal particle foam composite can be obtained through a new one-step self-foaming process. The elastic foam material has a low modulus of 600 kPa and self-heals through strong dipole-dipole interactions and hydrogen bonding. In addition to the detection of tactile signals, the AiFoam e-skin can also function beyond the human skin by perceiving proximity.[1]

1. Guo H., Tan Y. J., *et al.* Artificially Innervated Self-healing Foams as Synthetic Piezo-Impedance Sensor Skins. *Nat Commun.* (in press).

9:40 AM SM06.05.05

Autonomously Self-Healable, Super-Stretchable, Highly Transparent and Energy-Harvesting Self-Powered Triboelectric Skins Ying-Chih Lai; National Chung Hsing University, Taiwan

Soft devices (including sensors, electronics, and machines) have attracted huge interest because they cannot only extend the scope of smart systems but also provide compliant and safer user experience. Particularly, power and electronic components that are self-healable, deformable, transparent, and even self-powered are highly desired for future robotic applications. Here, we present the first triboelectric-based energy-harvesting and self-powered robotic skin that is entirely, intrinsically, and autonomously self-healable and simultaneously highly transparent and extraordinarily stretchable. Not only can this energy-harvesting robotic skin serve as an untethered and robust power source for personal electronics, but it can also be used as elegant robotic sensing skin that combine all desired attributes including self-healing, self-powered, highly transparent, and super-stretchable. This is the first time that not only the structure of an self-powered robotic skin is entirely and intrinsically self-healable at room conditions but also the device can be operated via self-generating electricity. Additionally, the self-powered robotic skin possesses a fast healing time (30 min, 100% efficiency at 900% strain), high transparency (88.6%), and extraordinary inherent stretchability (>900%). Even after 500 cutting-and-healing cycles or under extreme 900 %-strain, the energy-harvesting robotic skin can retain its functionality. The generated electricity from the robotic skin can be used directly or stored to power commercial electronics. Further, the robotic skin is designed for self-powered tactile-sensing matrix in diverse human-machine interfaces including smart glass, an epidermal controller, and cell phone panel. The unprecedented triboelectric-based robotic skin that is entirely and inherently ambient self-healable, highly transparent, and intrinsically stretchable, and possesses energy-harvesting and actively-sensing ability, can meet wide application needs ranging from deformable/portable/transparent electronics, smart interfaces, energy devices, artificial skins, to soft robotics.

[Ref]

[1] Paper cover: <https://onlinelibrary.wiley.com/doi/10.1002/adfm.201970273>

[2] Ying-Chih Lai,^{‡*} Hsing-Mei Wu,[‡] Heng-Chuan Lin, Chih-Li Chang, Ho-Hsiu Chou,^{*} Yung-Chi Hsiao, and Yen-Cheng Wu, Entirely, Intrinsically, and Autonomously Self-Healable, Highly Transparent, and Superstretchable Triboelectric Nanogenerator for Personal Power Sources and Self-Powered Electronic Skins, *Advanced Functional Materials*, 2019, 190426. (Cover of the journal. VIP paper. This article was also selected in: Hot Topic: Flexible Electronics)

[News]

<https://www.youtube.com/watch?v=Gzt4PKGItcY>

<https://www.youtube.com/watch?v=g1huAexxiY4>

[Demo video]

<https://www.youtube.com/watch?v=eYKW63GFheU>

SESSION SM06.06: Chemical Systems in Robotics II

Session Chairs: Donglei (Emma) Fan and Peer Fischer

Tuesday Morning, April 20, 2021

SM06

11:45 AM *SM06.06.01

Molecular and Supramolecular Design of Robotic Soft Matter Samuel I. Stupp; Northwestern University, United States

Molecular and supramolecular level engineering of soft matter that exhibits autonomous or externally guided locomotion and dynamic morphogenesis is a grand challenge for materials science. If this happens at macroscopic scales it would be a pathway to create robotic objects from soft materials; at the microscopic scales we could begin to emulate cell behaviors with chemical defined materials; and distantly organelles as we approach the nanoscale. In this lecture we report on bio-inspired systems synthesized in a chemistry and materials science laboratory to design bottom up macroscopic robots under water. These macroscopic robots have the capacity to respond synergistically to photons and magnetic fields and reveal locomotion under water at speeds that approach those of biological systems, namely one body length per second. We found that we could control speeds, trajectories, and gait on the fly by manipulating light intensity and magnetic fields, and most interestingly it is possible to predict theoretically the response of the robots to design their behaviors. The lecture will also present results on light responsive materials that exhibit origami-like morphogenesis using constructs with macromolecules in which it is possible to design their response to photons.

12:15 PM *SM06.06.02

Shape-Memory Actuator Blends by Stereocomplexation of PLA Karl Kratz¹, [Victor Izraylit](#)^{1,2}, Matthias Heuchel¹ and Andreas Lendlein^{1,2}; ¹Helmholtz-Zentrum Geesthacht, Germany; ²University of Potsdam, Germany

Current approaches to modify the material composition, and in this way the mechanical behavior, of physically cross-linked polymeric actuator materials are reliant on synthetic alteration of the polymer architecture.¹ Here, we introduce a reprocessable shape-memory polymer actuator consisting of a multiblock copolymer with poly(ϵ -caprolactone) and poly(L-lactide) (PLLA-PCL) segments, which is blended with a poly(D lactide) (PDLA) oligomeric additive. By careful molecular design, the incorporation of structural units capable of stereocomplexation enabled the formation of the stable physical network necessary for actuation. By varying the relative concentration of the two blend components, a material with tunable reversible bidirectional actuation performance and reprocessability was created.² Moreover, through the study of the strain recovery and stress relaxation the macroscopic deformation patterns of the investigated materials were attributed to the microscopic deformation mechanisms of PCL crystallites and PLA stereocomplexes. The strain and composition ranges could be defined, in which PLLA-PCL / PDLA blends having PLA stereocomplexes as physical netpoints maintain elastic behavior typically attributed to polymer networks. The polymer blend system is of potential relevance as thermally controlled artificial muscles in soft robotics.³

References:

- A. Lendlein, M. Balk, N. Tarazona, O.E.C. Gould, *Biomacromolecules*, 20(19), 3627-3640 (2019)
- V. Izraylit, O. E. C. Gould, T. Rudolph, K. Kratz, A. Lendlein, *Biomacromolecules*, 21(2), 338-348 (2020)
- V. Izraylit, M. Heuchel, O.E.C. Gould, A. Lendlein, *Polymer* 209, 122984 (2020)

12:45 PM *SM06.06.03

Can Active Gels of the Muscle Proteins Actin and Myosin be Used as Soft Robotic Actuators? [José Alvarado](#); The University of Texas at Austin, United States

The proteins actin and myosin are well known for their roles as biological actuators, not only in muscle tissue, but also in the cytoskeleton of various non-muscle cells. When purified in a cell-free environment, these two proteins form the basis of an active gel, a material that is capable of undergoing deformation and exerting force. So far researchers have studied these gels to better understand actin-myosin contraction in living cells. Could these active gels find their way someday in robotics applications as actuators? In this talk, I will review the mechanical, force-generating, and rupture properties of active gels of actin and myosin. I will then explore the pros and cons of these materials as robotic actuators.

1:15 PM SM06.06.04

Self-Healing Biological Materials for Soft Robotics [Abdon Pena-Francesch](#)^{1,2}, Melik Demirel³ and Metin

Sitti²; ¹University of Michigan, United States; ²Max Planck Institute for Intelligent Systems, Germany; ³The Pennsylvania State University, United States

Recent research efforts have focused on developing soft, flexible, compliant materials for robotics, biointerfacing, and biosensing applications. Because of their intrinsic softness, these materials are susceptible to cut, puncture, scratch, and/or tear damage that compromise their physical integrity, and therefore self-healing properties are indispensable for soft machines and devices operating in dynamic environments. However, current self-healing materials have shortcomings that limit their practical application, such as low healing strength (below MPa) and long healing times (hours).

Here, we introduce high-strength, biodegradable protein-based materials that self-heal micro- and macro-scale mechanical damage within a second via reversible physical cross-linking. These proteins are systematically optimized to improve their hydrogen-bonded nanostructure and network morphology, with healing properties (~25 MPa strength after 1 second of healing) surpassing those found in other natural and synthetic soft materials by several orders of magnitude. We demonstrate soft gripper and artificial muscle prototypes integrating such biological materials. Such healing performance opens new opportunities for bioinspired materials design, and addresses current limitations in self-healing materials for soft robotics and wearable technology.

SESSION SM06.07: Soft Robotics II

Session Chairs: Donglei (Emma) Fan, Peer Fischer and Bradley Nelson

Tuesday Afternoon, April 20, 2021

SM06

2:15 PM *SM06.07.02

Bioinspired Functional Soft Materials for Soft Robotics and Wearable Devices Ximin He; University of California, Los Angeles, United States

Soft robots, advantageous in their compliance and flexibility, have advanced smart soft materials towards multifunctionality with local sensing, control and powering capabilities that approach human dexterity. Mimicking biological neuromuscular systems' sensory motion requires the unification of sensing and actuation in a singular artificial-muscle material, which must not only actuate but also sense their own motions and even has built-in feedback loop for basic-level control functions. Stimuli-responsive hydrogels are a class of synthetic materials that can change their volume upon environmental cues (temperature, light, and chemicals) to act as soft actuators and chemical sensors. They can also provide flexible porous scaffolds to load conductive components for constructing soft strain sensors, supercapacitors and other soft electronics. Their biocompatibility, easy functionalization, solution-based processing, and 3D printability are their additional merits for soft robotics. These together may lead to all-soft robots with higher flexibility, autonomy, and performance. Towards this goal, we have developed a series of material systems based on hydrogels and conducting polymers, including (i) beetle-inspired ultrafast colorimetric sensing of chemical and biological species (*Adv. Mater.* 2018; *Adv. Opt. Mater.* 2019), (ii) muscle-inspired high contractile tough actuators (*Sci. Adv.* 2020, *ACS Appl. Mater. Inter.* 2020), (iii) plant-mimetic adaptive light tracking and harvesting (*Nat. Nanotech.* 2019), (iv) phototactic soft swimming robot (*Sci. Robotics* 2019; *Sci. Adv.* 2020), (v) high-performance soft strain sensors and supercapacitors (*Adv. Funct. Mater.* 2020, *Matter* 2020), and (vi) a soft somatosensitive actuating material utilizing an electrically-conductive and photothermally-responsive hydrogel, which combines the functions of piezoresistive strain/pressure sensing and photo/thermal actuation into a single material. Overall, these intelligent material systems represent a step towards next-generation soft robots with life-like adaptiveness and higher-level autonomy.

2:45 PM SM06.07.03

Late News: 3D Printed Sweating Robots Anand K. Mishra¹, Thomas J. Wallin^{1,2} and Robert Shepherd¹;

¹Cornell University, United States; ²Facebook Reality Labs, United States

Despite the promise of operation in extreme environments and the use of high energy density power sources, strategies for thermoregulation remain underdeveloped in soft robots. Here, we present autonomically perspiring fluidic actuators based on multimaterial 3D printing of smart gels. We developed two custom hydrogel photochemistries—one based on poly-N-isopropylacrylamide (PNIPAm) and the other based on polyacrylamide (PAAm)—with opposing thermo-mechanical responses. At elevated temperatures, PAAm expands, and NIPAm contracts. Our actuator designs contain a porous dorsal layer of PAAm micropores that cap the fluidic channel embedded in the PNIPAm body. As the temperature rises above $\sim 37^{\circ}\text{C}$, the PNIPAm body collapses to expel water through the dilated PAAm pores. This material response is reversible and occurs without any additional control from the robot to enable localized sweating. We then create the experimental protocols to measure the thermoregulatory performance of soft robots and further develop mathematical models using Newton's Law of Cooling to quantify this behavior and compare it to that of their non-sweating counterparts under a variety of conditions. Our sweating actuator exhibit a 600% enhancement in cooling rate with $>100 \text{ W}\cdot\text{kg}^{-1}$ of additional cooling capacity, comparable to the best animal systems. We further combine multiple actuators into a hand and demonstrate the ability to grasp and thermally manipulate objects in the environment.

(1) Mishra, A.K., Wallin, T.J., Pan, W., Xu, P., Wang, K., Giannelis, E.P., Mazzolai, B. and Shepherd, R.F., 2020. Autonomic perspiration in 3D-printed hydrogel actuators. *Science Robotics*, 5(38).

(2) Mishra, A.K, Pan, W., Giannelis, E.P. and Shepherd, R.F., Wallin, T.J., 2020. Making Bioinspired 3D Printed Autonomic Perspiring Hydrogel Actuators, *Nature Protocols*

3:00 PM SM06.07.04

Growing Material Robotics —A Novel Type of Active Matter Stoyan K. Smoukov; Queen Mary University of London, United Kingdom

We report on a novel kind of material robotics micro-swimmers, ones that could be assembled bottom-up. They are able to harvest energy from their environment to move, and recharge on demand. We quantify the movement and reveal their propulsion mechanism. The robots form a new type of active matter, that is sustainable, as they could be grown from single molecules and almost no energy or materials are wasted. In this invited talk I will report on the large collaborative effort that resulted in this discovery and directions in which new fields of study can develop.

3:15 PM SM06.07.05

Multifunctional High-Swelling DNA Gels for Building Soft Robots Ruohong Shi, Joshua Fern, Rebecca Schulman and David H. Gracias; Johns Hopkins University, United States

Hydrogels with the ability to change shape in response to biochemical stimuli are important for biosensing, smart medicine, drug delivery, and soft robotics. Here, we create a new family of multicomponent DNA polymerization motor gels with different polymer backbones, including acrylamide-co-bis-acrylamide (Am-BIS); poly(ethylene glycol) diacrylate (PEGDA); and gelatin-methacryloyl (GelMA) that swell extensively in response to specific DNA sequences. A common actuation mechanism, a polymerization motor that induces swelling is driven by a cascade of DNA hairpin insertions into hydrogel crosslinks. These multicomponent hydrogels can be photopatterned into distinct shapes and structures, have a broad range of mechanical properties, tunable moduli, and enhanced biocompatibility. Human cells adhere to the GelMA-DNA gels and remain viable during approximately 70% volumetric swelling of the gel scaffold induced by DNA sequences. The results demonstrate the generality of sequential DNA hairpin insertion as a mechanism for inducing shape change in multicomponent hydrogels, suggesting new ways of building soft robotic devices and widespread applicability in biomaterials science and engineering.

3:20 PM SM06.07.06

Physical Intelligence Drives Liquid Handling Sara Coppola, Giuseppe Nasti, Veronica Vespini and Pietro Ferraro; Institute of Applied Sciences and Intelligent Systems “E. Caianiello”, Italy

Nature continually provides a rich and valuable source of inspiration for many fields of research. Looking to the natural development of life, researchers have been consistently inspired designing new functional and adaptive materials. Programmed and self-assembled deformations are widespread in nature, providing elegant paradigms to design self-morphing materials, responsive materials or engineered robots. In fact, it would be very powerful in different fields of technology and, in particular for indwelling or external biomedical devices, to have elements capable of responding to external stimuli in a simple way. Within this context, there is a lot of interest in creating artificial structures that can walk, swim, move and perform various tasks answering to an external stimulus. Conventional robots are usually entirely composed of hard materials and require complex control systems to accomplish different tasks. Their fabrication process is long-lasting and complicated, inhibiting downscaling and constraining the device to a single predefined behavior. Recently, an emerging class of soft robotics with flexible actuation, intelligent sensibility, and biomimetic functionality are driving advances in academic researches and commercial applications through the development in soft matter engineering and flexible actuation systems. One of the most challenging issues in developing enhanced robotic technology is making appropriate tools also for the full control of liquids. Liquid robots still represent an interesting outcome for the technology from micro to nano scale. In fact, liquid-manipulating systems extend to many fields with important industrial applications such as biomedicine, biotechnologies, food, chemistry, industry and cosmetics, to cite a few. To build these systems, liquids, polymers, and soft matter require accurate, precise, and fully controllable methods to be handled and processed. So far, several engineering methods have been proposed to control and drive liquids in response to external magnetic, electric, or optical fields. However, until now, all the approaches proposed for locomotion and remote liquid control are complicated and very expensive. Here we introduce a new and simple working mechanism for actuation, liquid manipulation and a complete exploration of the opportunities of a multipurpose platform guided by physical intelligence. Physical intelligence is a new way of furnishing intelligent responses (outputs) as a function of environmental changes (inputs); in particular, this disruptive technology proposed is based on the use of a pyroelectric material (Lithium Niobate) that can provide an electric field (output) as a consequence of temperature changes (input). The electric field generated by the pyroelectric effect allows one to manage the on/off function of the system in order to command a fast response in a smart way, and to easily move units of liquid with different volumes. The pyroelectric platform allows to manage and displace liquid unit volumes from a starting position to the desired endpoint, controlling with good resolution any intermediate step until the final position. Beyond the guiding property, we prove additional functionalities like merging, stretching, mixing and jumping of liquid volumes and millimeter objects using a working distance of millimeter, bigger than the conventional distances used for liquid handling in classical digital microfluidic. Multiple volumes can be dragged over the surface, moved simultaneously and mixed in case of need. The proposed technology for locomotion and tweezing of liquids and particles could open a new route for soft robotics, biomedicine, material science, fluid dynamic and also for application in microgravity environment, where it is well known that the managing of liquid is difficult and has safety concerns.

Nasti, G., Coppola, S. et al. (2020). Pyroelectric tweezers for handling liquid unit volumes. *Advanced Intelligent Systems*, 2000044.

SYMPOSIUM SM07

Symposium Organizers

Qian Chen, University of Illinois at Urbana-Champaign
Hong-Gang Liao, Xiamen University
Youhong Tang, Flinders University
Xin Zhang, Pacific Northwest National Laboratory

* Invited Paper

Tutorial SM07: Probing Self-Assembly via Advanced Microscopic Techniques

Session Chairs: Ou Chen, Qian Chen, James De Yoreo, Hongyou Fan, Dongsheng Li, Jungwon Park, Xingchen Ye, Xin Zhang and Haimei Zheng
Saturday Afternoon, April 17, 2021
SM07

1:00 PM *

Dynamics of Interface-Driven Nucleation and Assembly James J. De Yoreo; Pacific Northwest National Laboratory, United States

Heterogeneous distributions of ions and water at interfaces have a strong impact on processes of nucleation and assembly. This talk will introduce how to investigate these phenomena and their relationship to interfacial structure for a number of mineral systems in aqueous electrolyte solutions via using a combination of in situ imaging techniques such as in situ liquid cell atomic force microscopy (AFM) and in situ liquid phase scanning/transmission electron microscopy (S/TEM) and computational methods.

1:45 PM BREAK

2:00 PM *

Real Time Imaging of Dynamic Behavior of Individual Nanocrystals During Superlattice Phase Transformations Using *In Situ* Liquid Phase Transmission Electron Microscopy Haimei Zheng; Lawrence Berkeley National Laboratory, United States

Nanocrystals have attracted considerable attention because of their potential applications in catalysis, energy storage, microelectronic devices, biomedicines, etc. Monodisperse nanocrystals could form superlattices with emergent collective properties. Although there have been intensive studies on nanocrystal superlattices, how individual nanocrystals change and how they interact with each other during superlattice transformations are unclear. Direct observation with high spatial and temporal resolution using transmission electron microscopy (TEM) provides the opportunity to address these questions. This talk will introduce the development of high-resolution carbon-film liquid cells, which allow to directly observe nanocrystal superlattice transitions using TEM.

2:45 PM BREAK

3:00 PM *

Quantum Dot Nanomaterials—Synthesis, Assembly and Applications Ou Chen; Brown University, United States

Nanocrystal materials are emerging as an important class of tools that are revolutionizing both fundamental science and technological applications due to their many unique properties. In particular, quantum dots

nanocrystals have demonstrated their great potential to be applied in a wide variety of applications as a unique emissive material. In my talk, I will describe our experimental efforts for the synthesis and characterization of high-quality quantum dot nanocrystals. These dots combine, in one material, great optical performance metrics desired in quantum dot nanomaterials. Then, I will show how we can use colloidal quantum dot nanocrystals as building blocks to generate higher-order architectures in assemblies. At last, several quantum dot based applications studied in my lab will be discussed.

3:45 PM BREAK

4:00 PM *

Pressure Induced Nanoparticle Aggregation Hongyou Fan; Sandia National Laboratories, United States

This talk will summarize recent progress on the studies of pressure induced nanoparticle aggregation behavior. This talk starts with a brief overview of high pressure characterization techniques, coupled with synchrotron X-ray scattering, Raman, fluorescence, and absorption. Then, the pressure induced nanoparticle aggregation behavior including size dependent aggregation and threshold pressures using several typical NP material systems as examples. Finally, outlooks with future directions are discussed.

4:45 PM BREAK

5:00 PM *

Self-Assembly in Colloidal Nanoparticle Systems—Thermodynamics, Interaction Softness and Kinetics Xingchen Ye; Indiana University, United States

Nanoparticle superstructures are versatile materials platforms for fundamental study of colloidal assembly and exploration of technologically relevant applications. In this talk, I will describe our recent progress on kinetically controlled assembly of multicomponent superstructures using spherical nanoparticles with tunable softness. Characterization of kinetically arrested intermediates reveals a multistep crystallization pathway defying the classical nucleation theory. Next, I will present our work on assemblies of shape-anisotropic nanoparticles with tunable softness. The interplay between particle shape and interaction softness leads to rich phase behaviors.

5:45 PM BREAK

6:00 PM *

Direct Observation of Oriented Attachment in Nanoparticle Growth Dongsheng Li; Pacific Northwest National Laboratory, United States

The oriented attachment of molecular clusters and nanoparticles in solution is now recognized as an important mechanism of crystal growth in many materials. This talk will introduce the background of oriented attachment and the application of high-resolution fluid cell transmission electron microscopy (TEM) to directly observe oriented attachment of several nanoparticle systems, including iron oxyhydroxides, Au, Ag, and Pt.

6:45 PM BREAK

7:00 PM *

***In Situ* and Liquid TEM for Investigating Nanoparticles** Jungwon Park^{1,2}; ¹Seoul National University, Korea (the Republic of); ²Institute for Basic Science, Korea (the Republic of)

Molecular or atomistic mechanistic understanding of nucleation, growth, and structural changes of nanoparticles have not achieved enough at the nanoscale or below. It is mainly because of a lack of appropriate analytical methods that can obtain in-situ structural information with a spatial resolution at such small length scale along

with sub-msec temporal resolution. The in situ, both in liquid phase and dry state, transmission electron microscopy (TEM) offers an opportunity to directly observe diverse classes of chemical reactions. Here we introduce technical developments for those techniques. Topics will cover fabrication processes for TEM liquid cells with thin film window materials such as graphene and silicon nitride, and data processing of large sized in situ TEM images. In addition, we also present application of in situ TEM to study chemistry of colloidal nanoparticles. We reveal that the early stage of nanoparticle formation is driven by reversible transition between disordered and ordered phases before crystalline phase is stable above a certain size. It is also frequently observed that different types of non-classical pathway, including two-step nucleation, amorphous-to-crystalline transition, and coalescence of clusters, are heavily involved in different conditions of nanoparticle formation. We also present a new development using liquid phase TEM to investigate 3D atomic structures of nanoparticles directly in the colloidal synthesis batch.

7:45 PM BREAK

SESSION SM07.01: Self-Assembly of Nanoparticles I
Session Chairs: Qian Chen and Hong-Gang Liao
Sunday Morning, April 18, 2021
SM07

8:00 AM *SM07.01.01

Nucleation and Growth of Nanocrystals—Insights Derived from Direct TEM Imaging Utkur Mirsaidov;
National University of Singapore, Singapore

Understanding how materials form at the nanoscale is fundamental for materials engineering and fabrication in many functional nanodevices. Nucleation, growth, and self-assembly are key “bottom-up” processes through which these materials form in solution. Despite the importance of these processes both from basic science principles and technological stand-point, many of the chemical and physical details of these dynamic processes remain unknown. This gap in knowledge stems mainly from a lack of proper experimental techniques that enables visualize these nanoscale solution-based processes in real-time. Here, using in situ liquid cell transmission electron microscopy (TEM), I will describe how direct observations can shed new light on nucleation and growth of both organic and inorganic crystals.

Specifically, I will show that organic crystals such as metal-organic frameworks nucleate via a nonclassical pathway, involving phase separation of the precursor solution into dense solute-rich and solute poor-regions, followed by condensation of the dense phase into crystals. I will also discuss the nucleation and crystallization of other organic materials such as perovskites and illustrate that visualizing these crystallization pathways can teach us a lot in terms of materials synthesis.

Our studies highlight the importance of direct visualization of nanoscale processes for the rational design of materials.

8:25 AM *SM07.01.02

Approaching the What, How, and Why of Crystallization with Self-Assembly Simulations Julia Dshemuchadse;
Cornell University, United States

Many materials properties are determined through their underlying crystal structure, and often the search for new materials with improved functionalities requires the targeting of particular structure types and crystal geometries. While the science of crystallography has helped us to largely decipher the structure of materials over the past century, the art of structure prediction has remained elusive: our ability to rationalize why a certain system crystallizes in any given structure is severely constrained, for example by being applicable to only specific materials classes or by being predictive of ground-state structures without allowing to draw conclusions

about the aspect of synthesizability.

We investigate the enigma of crystal structure formation by simulating the growth of different crystal phases from particles with exquisitely simple interactions. By modeling the self-assembly of long-range ordered structures with varying complexity and symmetry, we aim to formulate the general principles of the development of crystallinity from local interactions. We hope to elucidate how complexity can emerge from simple particles, how long-range order emerges from short-range forces, and how symmetries are broken locally in concert with the appearance of global, crystal symmetries.

By developing a fundamental understanding of the process of self-assembly in crystalline matter, we can move forward with efforts of structure prediction at a level that will enable materials design from basic principles in the future.

8:50 AM SM07.01.03

Colloidal Quasicrystals Engineered with DNA Wenjie Zhou^{1,2}, Haixin Lin^{1,2}, Yein Lim³, Sangmin Lee³, Yuanwei Li^{1,2}, Ziyin Huang^{1,2}, Jingshan S. Du^{1,2}, Shunzhi Wang^{1,2}, Luis M. Liz-Marzán⁴, Sharon Glotzer³ and Chad Mirkin^{1,2,2}; ¹International Institute for Nanotechnology, United States; ²Northwestern University, United States; ³University of Michigan–Ann Arbor, United States; ⁴Ikerbasque, Basque Foundation for Science, Spain

Quasicrystals are structures that are ordered but not periodic. While they lack translational symmetry, they possess a high degree of rotational symmetry. Their experimental identification in 1984 brought the concept of aperiodic structures from mathematical tilings to physical existence. Since then, the experimental pursuit of these elusive materials has extended from atomic systems to colloidal superlattices. To date, all experimentally reported quasicrystalline superlattices possess either multiple sizes or the asymmetric functionalization of building blocks. The question of whether it is possible to synthetically achieve quasicrystals using one uniformly functionalized constituent remains elusive. Utilizing five-fold symmetric nanocrystals and elastically directional, oligonucleotide-based ligands, we report the first single-component dodecagonal colloidal quasicrystal assembled from DNA-functionalized decahedral nanocrystals. This discovery enriches the scope of colloidal quasicrystals, and sheds light on the design-based, enthalpy-driven crystallization of polyhedral nanocrystals.

9:05 AM SM07.01.04

Multivariate Analysis of Peptide-Driven Nucleation and Growth Processes in Plasmonic Nanoparticles Kacper J. Lachowski and Lilo D. Pozzo; University of Washington, United States

The localized surface plasmon resonance of metallic nanoparticles continues to be studied for light harvesting applications such as photocatalysis and biosensing. Control over the light response depends on careful synthetic control of the particle structure, composition, and state of assembly. Whereas the current theoretical understanding of nanoparticle growth has been sufficient for enabling the synthesis of monodisperse spherical nanoparticles, shortcomings in current theories hinder the prediction of synthetic outcomes in more complex experimental systems (e.g. non-spherical morphologies, particle superstructures). An underlying challenge which we seek to address is the development of methodologies for connecting large experimental design spaces to the outcomes of nanoparticle syntheses that may also span over multiple length and time scales. Herein, we present a multivariate analysis of how amphiphilic solid binding peptides can mediate the nucleation, growth, morphogenesis, and self-assembly of gold nanoparticles over a broad range of conditions. High-throughput synthesis using programable liquid-handling robots is coupled with UV-Vis characterization to create state diagrams for visualizing the relationship between surface plasmon resonance or colloidal stability, and sample composition and peptide sequence. We then demonstrate the utility of unsupervised learning techniques to identify these relationships and for guiding selection of samples for lower-throughput characterization techniques. The structure of selected samples is investigated further using transmission electron microscopy (TEM) and small angle x-ray scattering (SAXS). Together, these results motivate targeted *in situ* experiments which reveal how peptide self-assembly and complexation with precursors lead to distinct modes of growth and

self-assembly. Finally, we discuss how these methodologies can also be extended to the study of other hybrid inorganic-organic systems that are driven by nucleation and growth phenomena.

9:20 AM *SM07.01.05

Chiral Nanostructures Nicholas A. Kotov; University of Michigan–Ann Arbor, United States

The early observation of strong circular dichroism for individual nanoparticles (NPs) and their assemblies have developed into a rapidly expanding field of chiral inorganic nanostructures. They encompass a large family of mirror-asymmetric constructs from metals, semiconductors, ceramics, and nanocarbons with multiple chiral geometries with characteristic scales from *Ångströms* to microns. Versatility in dimensions and polarizability of the inorganic materials enables their multiscale engineering to attain a broad range of optical and chemical properties. This talk will address (1) the origin of the uniquely high values of optical anisotropy; (2) mechanisms of chirality transfer in inorganic materials; and (3) emergence of complexity in self-organized chiral nanoassemblies. Special attention will be given to the emerging venues for practical realizations of chiral nanoassemblies related to (1) chiral catalysis and (2) circular polarization spectroscopy in terahertz spectral window.

References

W. Jiang, Z.-B. Qu, P. Kumar, D. Vecchio, Y. Wang, Y. Ma, J. H. Bahng, K. Bernardino, W. R. Gomes, F. M. Colombari, A. Lozada-Blanco, M. Veksler, E. Marino, A. Simon, C. Murray, S. Ricardo Muniz, A. F. de Moura, N. A. Kotov, Emergence of Complexity in Hierarchically Organized Chiral Particles, *Science*, **2020**, 368, 6491, 642-648.

Si Li, Juan Liu, Naomi S. Ramesar, Hendrik Heinz, Liguang Xu, Chuanlai Xu, Nicholas A. Kotov, Single- and Multi-Component Chiral Supraparticles As Modular Enantioselective Catalysts, *Nature Comm*, **2019**, 10, 4826.

W.J. Choi, G. Cheng, Z. Huang, S. Zhang, T. B. Norris, N. A. Kotov, Chiroptical Kirigami Modulators for Terahertz Circular Dichroism Spectroscopy of Biomaterials, *Nature Materials*, **2019**, 18, 820–826.

9:45 AM SM07.01.06

Investigating Interparticle Interactions Mediating Fuel Driven Dissipative Self-Assembly of Colloids
Thilini U. Dissanayake, Justin Hughes and Taylor Woehl; University of Maryland, United States

Previous studies have demonstrated chemical fuel driven dissipative self-assembly of colloids initiated by adding a chemical fuel that converts hydrophilic surface groups to hydrophobic groups. The hydrophobic colloids aggregate over several hours while a slow hydrolysis back reaction converts hydrophobic groups back to hydrophilic, causing the aggregates to disassemble after tens of hours. While the chemical reactions involved in dissipative self-assembly process have been studied in detail, the colloidal scale interparticle interactions underlying self-assembly are not well understood. Here we demonstrate that the dissipative self-assembly of carboxylic acid functionalized polystyrene occurs over narrow ranges of fuel and particle concentrations that are dictated by the strength of hydrophobic interparticle interactions and the ligand-fuel reaction kinetics. We utilized optical microscopy to image dissipative self-assembly of sub-micron to micron sized particles to probe assembly behavior as a function of particle and fuel concentration. Particles showed either no assembly, dissipative self-assembly, or irreversible aggregation. A scaling analysis revealed that no assembly occurred if the lifetime of the surface hydrophobic groups was less than the characteristic time for colloidal aggregation as determined by the Fuch's stability parameter. Dissipative assembly occurred for fuel concentrations where there was a secondary minimum in the pairwise interaction potential, which lead to weak hydrophobic interparticle bonds and residual interstitial water layers that facilitated hydrolysis back reactions. Irreversible assembly occurred when hydrophobic attractive forces dominated electrostatic repulsion and caused permanent aggregation with no residual interstitial water layer. These results shed light on the interplay between colloidal interactions and kinetics that underly dissipative self-assembly of colloids and will enable rational design of

transient and reconfigurable colloid assemblies.

SESSION SM07.02: Self-Assembly of Nanoparticles II

Session Chairs: Xingchen Ye and Xin Zhang

Sunday Morning, April 18, 2021

SM07

10:30 AM *SM07.02.01

Self-Organization of Colloidal Nanocrystals—From Intricate Structures to Functional Materials Igor Coropceanu, Eric Janke and Dmitri V. Talapin; The University of Chicago, United States

Nanocrystals of different functional materials can self-assemble from colloidal solutions into long-range ordered periodic and quasicrystalline structures (superlattices). Such assemblies offer a powerful platform for designing hierarchically organized macroscopic solids. Unlike atomic and molecular crystals where atoms, lattice geometry, and interatomic distances are fixed entities, arrays of nanocrystals represent solids made of “designer atoms” with potential for continuous tuning their physical and chemical properties. The self-assembly process is guided by an intricate interplay of entropy-driven crystallization and soft interparticle interactions. The surface ligands also play an important and sometimes counterintuitive role, supporting many-body interactions and stabilizing complex structures which can be explained by specific topological textures developed within surface ligands.

The properties of nanocrystal superlattices are determined by the nanocrystalline building blocks and by the electronic couplings between individual nanocrystals. Strong electronic coupling between nanocrystals within a superlattice is an important prerequisite for the emergence of non-additive physical properties. By using optimized surface chemistries, the electronic coupling can be significantly enhanced, approaching the metal-insulator transition. The formation of strongly-coupled nanocrystal assemblies represents an important step toward the bottom-up design of functional materials. We will demonstrate the power of “modular” materials fabrication for electronic and optoelectronic devices and the utility of engineered nanocrystal assemblies for real-world technologies.

10:55 AM *SM07.02.02

Growth of Metal Nanocubes, Nanowires, and Nanoplates Kristen A. Fichthorn; The Pennsylvania State University, United States

Metal nanocrystals have gained tremendous attention due to their superior performance in various applications, ranging from selective catalysis to electronic devices to plasmonic applications. For these and many other applications, the properties of the nanocrystals are highly sensitive to their shape. However, it remains a challenge to achieve high shape selectivity in solution-phase syntheses. I will discuss our efforts to understand the growth of Cu and Ag nanocubes, nanowires and nanoplates, which is facilitated by a synergy between halide ions (chloride, bromide, and iodide) and capping molecules in the synthesis protocol. We use ab initio thermodynamics based on quantum density-functional theory (DFT) to demonstrate how the combination of capping molecules and halides create thermodynamic driving forces for cubes, plates and wires, by selectively altering surface energies. Using a combination of DFT and the theory of absorbing Markov chains, we demonstrate how a synergy between capping molecules and halides affect deposition, surface diffusion, and interfacet transport to drive the growth of particular nanoshapes. Our results agree with experiment and indicate a promising way to exact control over nanocrystal synthesis.

11:20 AM SM07.02.03

Synthesis of Polymer-Patched Nanoparticles and Their Self-Assembly into Open Lattices Ahyoung Kim¹, Thi Vo², Chansong Kim¹, Lehan Yao¹, Shan Zhou¹, Hyosung An¹, Sharon C. Glotzer² and Qian Chen¹;

¹University of Illinois at Urbana-Champaign, United States; ²University of Michigan–Ann Arbor, United States

I will present our most recent experiment-computation collaboration on a new strategy of “atomic stencil” to site-specifically coat gold nanoparticles (NPs) with polymer patches. We experimentally demonstrate the general applicability of the strategy in patterning polymer patches of precise size and shapes on a variety of anisotropic gold NPs. We realize highly uniform patchy NPs, from tip to facet-patches, as well as from symmetric to broken-symmetry patch arrangements. The patch grafting simulation based on scaling theory reveals the vital roles of interpolymer attraction and local surface curvature of NPs in polymer portioning. Finally, we show that the as-prepared library of patchy NPs can assemble into various structures, including small clusters (dimers, trimers) via self-limited attraction, and large-scale open lattices, which are challenging to be achieved from NPs of uniform surface chemistry. We foresee the method can generate hybrid NPs with site-specifically programmable chemistries and interactions for the applications in catalytic, delivery, and their directed assembly into exotic functional structures, including a Kagome lattice.

11:35 AM *SM07.02.04

Enabling Kinetic Control in the Self-Assembly of Polymer-Grafted Nanocrystals Xingchen Ye; Indiana University Bloomington, United States

Polymer-inorganic nanocomposites based on polymer-grafted nanocrystals (PGNCs) are enabling technologically relevant applications owing to their unique physical and chemical properties. While diverse PGNC superstructures have been realized through evaporation-driven self-assembly, this approach presents multifaceted challenges in understanding and ultimately controlling the assembly kinetics. In this talk, I will introduce our recent progress on the facile assembly of multicomponent superstructures from a homogeneous disordered PGNC mixture. We demonstrate that controlling the nature of assembly environment allows for exquisite control of the rate of PGNC assembly. Characterization of kinetically arrested intermediates reveals that assembly follows a multistep crystallization pathway. Our work opens up new avenues for the predictive synthesis of multicomponent PGNC superstructures exhibiting multifunctionality and emergent properties.

12:00 PM SM07.02.05

Crack-Free Colloid Self-Assembly for High-Strength Metallic Nanolattice Fabrication Zhimin Jiang and James H. Pikul; University of Pennsylvania, United States

Natural cellular materials have inspired researchers to create lightweight high-strength porous metals with chemical or physical functionalities. Traditional fabrication methods, however, have limited porous metals' strength to well below their theoretical limits because of the difficulties in controlling the pore morphology and the constituent metal's microstructure. 3D printing is one manufacturing technique that has realized nanolattices with periodic pores and nanostructures that approach the theoretical strength of their constituent materials [1], but it has inherent trade-offs between resolution and printing time that severely limit the scalability. In addition to 3D printing, advancements in self-assembly have realized relatively low cost and fast fabrication of large-area metallic and ceramic nanolattices with nanometer-sized features, but the assembled templates are subject to dense cracks unavoidable during solvent drying [2]. Filling the template voids with a solid material can fill the cracks, but these inverted crack structures divide the sample into small nanolattice domains (typically <0.01 mm² in area), cause stress concentrations, block fluid/gas transport, and increase optical scattering. A fabrication approach that uses self-assembled templates to produce large-area metallic nanolattices without inverted cracks has yet to be demonstrated.

This work overcomes these limitations by developing a crack-free colloid self-assembly approach to fabricate cm-scale porous nickel nanolattices with 30 nm grain size, 100 nm feature sizes, and an ultrahigh 227 MPa tensile strength, 3 times stronger than what has been reported for porous metals with the same relative density at any scale. We fabricate our nickel nanolattices by first self-assembling 400-800 nm diameter polystyrene (PS) particles with positive surface charges into single-crystalline FCC packed films on an indium tin oxide (ITO) coated substrate. We then electrodeposit nickel through the template voids and etch the PS by toluene. We found that the key to eliminating cracks in the colloid self-assembly process while maintaining high-quality

crystal growth, which reduces defects and improves optical properties, is to keep the template wet with 0.06% glycerol. After self-assembly of a wet uncracked colloid template, we then overcame the challenge of electrodepositing nickel in a wet unsintered template by taking advantage of electroosmotic forces on synthesized positively charged polystyrene particles that push the template onto the conductive substrate. Compared to traditional self-assembly, the new approach overcomes the long-standing cracking issues in self-assembled colloid templates to fabricate nanolattices, which have over 2 cm² area without inverted cracks, 20,000X increase in crack-free area compared to conventional self-assembled metallic nanolattices, 1,000X more units cells in the loaded direction than 3D printed nanolattices for tensile testing, and, for the first time, enable macroscopic tensile testing of metallic nanolattices.

1. Bauer, J., et al., Nanolattices: An Emerging Class of Mechanical Metamaterials. *Advanced Materials*, 2017. 29(40): p. 1701850.

2. Jiang, Z., Z. Hsain, and J.H. Pikul, Thick Free-Standing Metallic Inverse Opals Enabled by New Insights into the Fracture of Drying Particle Films. *Langmuir*, 2020. 36(26): p. 7315-7324.

12:15 PM SM07.02.06

Late News: 2D Magnetic Thin Sheets via Self-Assembly of Magnetic Nanoparticles Jiwoo Yu, Yeu-Wei Harn, Shuang Liang, Gyutae Nam, Zewei Wang, Martin Mourigal and Zhiqun Lin; Georgia Institute of Technology, United States

Centimeter-scale hydrophilic two-dimensional (2D) magnetic sheets are created via rapid self-assembly of magnetic nanoparticles at liquid-liquid interface. Such large-scale 2D sheets open up new avenue to engineering 2D materials. Assembly of nanoparticles at liquid interfaces has attracted much attention for decades. Yet, developing their assemblies of mechanically intact structure is comparatively few as most of assemblies collapsed when the interface is removed. Moreover, only a limited number of studies on the ability to form thin sheets with magnetic properties have been reported. In this context, our 2D magnetic thin sheets are structurally intact that retain the millimeter-scale continuity even after three times of centrifugation and washing with pure water, without additional crosslinking or polymerization processes. The formation of such mechanically robust sheets can be attributed to ligand interactions, hydrogen bonding, and favorable dipole-dipole interaction of magnetic nanoparticles. Furthermore, mechanical and magnetic properties of the 2D membrane are investigated. Finally, self-assembly is also carried out using magnetic nanoparticles of larger size distribution, demonstrating the versatility of this strategy for crafting 2D sheets.

SESSION SM07.03: Self-Assembly Nanoparticles III

Session Chairs: Qian Chen and Xin Zhang

Sunday Afternoon, April 18, 2021

SM07

1:00 PM *SM07.03.01

Interfacial Structure, Interparticle Forces and Assembly Dynamics During Oriented Attachment James J. De Yoreo^{1,2}, Elias Nakouzi¹, Lili Liu¹, Guomin Zhu^{2,1}, Sebastien Kerisit¹, Maria Sushko¹, Jaehun Chun^{1,3}, Gregory Schenter¹ and Christopher Mundy^{1,2}; ¹Pacific Northwest National Laboratory, United States; ²University of Washington, United States; ³The City University of New York, United States

Growth of single crystals via oriented attachment of primary nanocrystals is widespread phenomenon in both synthetic and natural environments. This process exhibits a range of styles including face-specific oriented attachment (OA) in which the primary particles and final crystal are of the same phase, attachment of a nanoscopic phase to a bulk phase followed by transformation to form a crystal with crystallographically matched or twinned interfaces, and mis-oriented aggregation followed by coarsening through elimination of

dislocations to a single crystal. While descriptions of assembly in these systems must share a commonality with continuum-based DLVO-type theories for simple colloids, nanocrystals present additional complexities, including face-specificity of dielectric properties, surfaces that are periodically structured at the Å-scale structure, and consequent solvent-responses that are expected to be of a comparable length scale. To understand the relationship between nanocrystal and solution structure, interparticle forces and consequent motion leading to attachment, we are investigating oriented attachment in a number of crystal systems including ZnO, Fe₂O₃ and AlO(OH). We use in situ AFM to map the structure of both the crystal surface and the near surface solution, in situ TEM to observe assembly dynamics, force spectroscopy with custom-made single crystal tips to measure face-specific interparticle forces, and molecular-scale simulations to define the relationships between these features. AFM-based fast force mapping shows that the structure of the solution near the interface exhibits the symmetry of the underlying crystal with lateral variations in density on the same scale as the atomic lattice, but the extent of these variations away from the surface varies between crystal systems and with ionic strength. Moreover, measurements with different kinds of tips combined with molecular dynamic simulations show that the measured solvent structure is impacted by the probe chemistry, implying that, as particles approach, the structure of the solvent evolves in response to the changing interfacial chemical environment. In situ TEM demonstrates that direction-specific forces align randomly diffusing particles prior to contact and that attachment occurs on lattice matched faces via a sudden jump to contact followed by coarsening to produce compact single crystal structures. Direct measurements of the forces between crystal surfaces reveal orientation dependent attractive interactions that also exhibit the symmetry of the underlying lattice. Simulations show that orienting, attractive forces arise from a number of sources, including hydration, ion correlation and dispersion forces and barriers to attachment are caused by hydration layers, which vary with surface hydrophobicity. In at least one case — ZnO — electric dipole forces dominate the interparticle interactions and lead to coalignment long before contact occurs. The integration of these complimentary techniques and their application to multiple crystal systems is helping to provide a comprehensive physical picture of OA.

1:25 PM SM07.03.02

Role of the Solvent–Surfactant Duality of Ionic Liquids in Directing Two-Dimensional Particle Assembly

Lili Liu, Duo Song, Biao Jin, Michael Sinnwell, Jun Liu, James J. De Yoreo and Maria Sushko; Pacific Northwest National Laboratory, United States

Nanoparticle self-assembly plays a key role in the formation of superlattices, which exhibit remarkable physical and chemical properties. However, controlling the assembly remains a challenge partly due to a lack of understanding of the assembly dynamics and the difficulty in linking interfacial solution properties to interparticle forces. Using liquid-cell transmission electron microscopy, the self-assembly of gold nanoparticles (NPs) into superlattices in mixtures of water and ionic liquid (IL) was visualized, revealing a dual role of the IL in the assembly process. At intermediate concentrations, the IL acts as a surfactant stabilizing the particles at a well-defined equilibrium separation corresponding to the length of hydrogen-bonded IL cations adsorbed onto neighboring NPs. Analysis of the interparticle forces reveals attractive long-range interactions of a van der Waals nature. At separations of 1–3 nm, the interactions are dominated by attractive ion correlation and repulsive hydration forces giving rise to an energy minimum at 1.5 nm separation. The superlattice is further stabilized by hydrogen bonding, which shifts the equilibrium interparticle distance to 1.1 nm. In contrast, at higher concentrations, IL accumulates and forms a structured network in the gap between nanoparticles, where it acts as a solvent that eliminates the repulsive barrier and thus promotes particle coalescence. This solvent–surfactant duality of IL opens new opportunities for its use in directing particle assembly.

1:40 PM SM07.03.03

Liquid-Phase TEM Imaging of Oriented Attachment of Nanoparticle Superlattices Assisted by Machine Learning Chang Liu, Lehan Yao and Qian Chen; University of Illinois at Urbana-Champaign, United States

We utilize nanoparticle dispersion as a model system to study the fundamentals of order emergence and evolution at the nanoscale. Diverse superlattices are achieved under liquid-phase TEM which enables single-particle level imaging in real time and real space. To be specific, coalescence and oriented attachment of two

dimensional/three dimensional (2D/3D) superlattices are observed, where both attach–rotation and prealign–attach behaviors occur. Machine learning is used for the first time to extract the structural information in 3D superlattices, which further helps to identify single particle behaviors. Furthermore, the high spatiotemporal resolution enables us to identify single particles and to map out their trajectories sampling the energy landscape. The individual fast motion (e.g. surface and volume diffusion) along with collective motion (e.g. transient neck formation, translational and translational motion of the domains) drives the coarsening of the nanoparticle superlattice, which is attributed to the features of different interactions involved at the nanoscale. Our work proposes novel data acquisition protocol and offers new dynamic observations on the superlattice evolution with high spatial and temporal resolution, which can provide insight into material engineering at the nanoscale.

1:55 PM *SM07.03.04

Nature's 3D Printing: Self-Assembly of Coral Skeletons Pupa Gilbert^{1,2}; ¹University of Wisconsin–Madison, United States; ²Lawrence Berkeley National Laboratory, United States

Corals reef ecosystems are extremely diverse, beautiful, and threatened by climate change. Learning how corals form their skeletons may be useful to save them from global warming, and to develop new synthesis strategies. Coral skeletons, in fact, are Nature's 3D printing. Recent synchrotron spectromicroscopy data reveal that all reef-building coral build their skeletons by two concomitant mechanisms:

1. Particle attachment, with nanoparticles of amorphous precursors nucleated in the tissue
2. Ion attachment, at the surface of the growing skeleton, from the calcifying fluid.

A new model for coral skeleton formation shows both mechanisms. See Sun et al. PNAS 2020.

2:20 PM *SM07.03.05

Probing Particle Mediated Growth Pathways of Metal Oxides Kevin Rosso, Xin Zhang, Yining Wang, Jianbin Zhou, Sebastian Mergelsberg, Maria Sushko, Duo Song, Eric Bylaska and James J. De Yoreo; Pacific Northwest National Laboratory, United States

Understanding particle mediated growth is critical to geoscience, material synthesis, catalysis, energy storage, environmental conservation, biological medicine, etc. Using a combination of scanning/transmission electron microscopy (S/TEM), atomic force microscopy (AFM), small angle X-ray scattering (SAXS), and molecular computations, we are investigating these phenomena for several metal oxide systems and their relationship to interfacial structure in vacuum, water vapor, and solutions. Here we discuss two cases. In the first, we explore the aggregation behaviors of hematite nanocrystals with different exposed facets including {001}, {012}, {104} and {116} in aqueous solutions at room temperature or hydrothermal conditions (120-180 °C). SAXS was used to study the aggregation behavior at room temperature. Remarkably, only {104} nanoparticles are well mono-dispersed in aqueous solutions from 1 to 30 mg/ml at 10, 30, and 60 days. In contrast, at similar conditions {001} and {116} nanoparticles are highly aggregated. High resolution TEM and scanning TEM (STEM) on aggregates formed at hydrothermal conditions suggest hematite crystallization by nanoparticle aggregation occurs predominantly on [001] facets. We then compare the results to the predictions of coupled plane-wave and classical density functional theory simulations to relate the behavior to surface interactions. In the second case, we report measurement of anisotropic forces between rutile TiO₂ (001) nanocrystals as a function of their azimuthal orientation and surface hydration extent using a combined environmental TEM-atomic force microscopy (AFM) technique. At tens of nanometers of separation, the attractive forces are weak and show no dependence on azimuthal alignment nor surface hydration. At separations of approximately one hydration layer, attractive forces are strongly dependent on azimuthal alignment and systematically decrease as intervening water density increases. Measured forces closely agree with predictions from Lifshitz theory and show that dispersion forces are capable of generating a torque between particles to align them. Ongoing adaptation of these modeling techniques to explain the observed aggregation behavior in the hematite system are motivated by the need to ultimately uncover common underlying mechanisms driving particle-mediated crystallization phenomena such as oriented aggregation.

2:45 PM SM07.03.06

Self-organization of Iron Sulfide Nanoparticles into Multi-Compartment Supraparticles Emine S. Turali-Emre, Ahmet Emre and Nicholas A. Kotov; University of Michigan–Ann Arbor, United States

Compartments are essential for any life, cells, prokaryotes, and even viruses. Recreation of their formation has both technological and fundamental importance. This study shows that *L*-cysteine stabilized iron sulfide NPs can self-assemble into multi-compartment supraparticles (SPs). The transmission electron microscopy results showed that NPs initially produce ~55nm cup-like structures and then mature into ~75nm SPs with *ca.* 190 interconnected compartments. The color change of the solution from black to yellow suggests the SP formation and particle oxidation. The selected area electron diffraction and energy dispersive X-ray spectroscopy confirm that SPs are formed from FeS₂ and Fe₂O₃ NPs. Elemental mapping showed that Fe₂O₃ NPs are located on the SP's surface and protecting FeS₂ and compartments from the surroundings. These compartmentalized particles can be used for the successful encapsulation of the DNA fragments and gene delivery.

SESSION SM07.04: Aggregation Induced Emissions (AIE)
Session Chairs: Benzhong Tang and Yun Yan
Monday Morning, April 19, 2021
SM07

8:00 AM *SM07.04.01

Late News: Self-Assembly of AIEgens Benzhong Tang; Hong Kong University of Science and Technology, China

Self-assemblies have attracted great scientific interests in recent few decades due to their various potential applications. Scientists can obtain different elaborate assemblies with multiple on-demand functionalities using various noncovalent interactions, such as hydrophilic-hydrophobic interaction, hydrogen bonding, host-guest interaction, π - π interaction, metal coordination, *etc.* Although the formation or responsive process of these assemblies can be monitored by various methods, such as NMR, IR, MS and electron microscopy, *etc.*, a problem associated with these methods is that they are either invisible to our naked eye or rely on harsh preparation methods. Luminescence is a perfect choice as technique for the applications in self-assemblies, in the light of its rich advantages such as superior sensitivity, high selectivity, fast response, low background noise and simplicity. More importantly, it can provide high spatiotemporal resolution for precise visualization into complicated processes in a noninvasive and on-site way. Another thing that need to be considered is that most of the assemblies function in the condensed phase which show notoriously ACQ effect to result in compromised sensitivity. Diametrically opposed to conventional luminophores, AIEgens are nearly non-luminescent in the isolated state but luminesce strongly in the aggregate/clustered state. Based on different AIEgens, we have fabricated various functional self-assemblies, such as helical assemblies with circularly polarized luminescence signal, surfactant micelles and microemulsion droplets with visible transition processes, interfacial dynamic self-assembly with *in situ* imaging technology, supramolecular polymers formed from TPE-based luminescent monomer, *etc.*

8:25 AM *SM07.04.02

Molecular Self-Assembly in Solid Phase Leading to Large Scale Fabrication of Supramolecular Films
Yun Yan; Peking University, China

General strategies leading to scale-span molecular self-assembly are of crucial importance in creating bulk supramolecular materials. We report that under mechanical pressure, caking of the precipitated molecular self-assemblies may lead to bulk supramolecular films. Massive fabrication of supramolecular films becomes possible using a simple house-hold noodle machine. The film can be endowed diversified functions by depositing various functional ingredients via co-precipitation. We expect the current work opens up a new

paradigm leading to large-scale functional solid molecular self-assembled materials.

8:50 AM *SM07.04.03

Assembling Dyes with Polymers into Small and Bright Fluorescent Nanoparticles for Biosensing and Bioimaging Andrey Klymchenko; University of Strasbourg, France

Dye-loaded fluorescent polymeric nanoparticles (NPs) appear as an attractive alternative to inorganic NPs, such as quantum dots (QDots).^[1] However, preparation of polymeric NPs featuring small size and high fluorescence brightness remains a challenge. To address it, we introduced a concept of charge-controlled nanoprecipitation of hydrophobic polymers in aqueous media.^[2] We found that a single charge in polymers, such as poly(methyl methacrylate) (PMMA), poly(lactic-co-glycolic acid) (PLGA) and polycaprolactone (PCL) can drive self-assembly of polymers into NPs of 20-40 nm size. Further addition of charges into these polymers (up to 10 mol%) can decrease particle size down to 7 nm.^[3] On the other hand, to ensure high brightness of polymeric NPs, we proposed to encapsulate charged dyes with bulky hydrophobic counterions.^[4] The latter serve as spacers between dyes, thus preventing aggregation-cause quenching and, at the same time, favor the co-assembly of the dyes with the polymer into stable NPs without dye leakage.^[5] Based on these design concepts, we obtained NPs that are ~100-fold brighter than QDots of similar size.^[6] Their small size was found essential for their free diffusion in cytosol of live cells^[3] and for their intracellular delivery by electroporation. Their high brightness enabled unprecedented single-particle tracking in the mice brain and visualization of crossing blood-brain barrier.^[7] Assembling dyes inside small polymeric NPs revealed also a unique cooperative behavior of dyes through ultrafast dye-dye energy migration, which led to the collective switching of >100 dyes in a single particle.^[4, 6] This collective behavior of dyes enabled efficient Förster resonance energy transfer (FRET) from ~10000 encapsulated dyes to a single acceptor. This light-harvesting nanoantenna provided >1000-fold signal amplification (antenna effect), allowing first single-molecule detection in ambient light.^[8] Functionalization of these nanoantennas with nucleic acids yielded ultrabright FRET-based nanoprobe for amplified detection of oligonucleotides,^[9] opening possibilities for rapid detection of cancer markers using a RGB camera of a smartphone.^[10] Nanoantennas of 20 nm size enabled efficient FRET to a single acceptor at their surface and detection of RNA/DNA with a single-molecule sensitivity.^[11] The light-harvesting concept was also applied to amplify phosphorescence of porphyrins for ratiometric sensing of oxygen with minimal phototoxicity.^[12] The developed small dye-loaded polymeric NPs open the route to ultrabright tools for sensing and tracking biomolecules in biosensing, bioimaging and diagnostics applications.

This work was supported by ERC Consolidator grant BrightSens 648528.

References

- [1] A. Reisch, A. S. Klymchenko, *Small* **2016**, *12*, 1968.
- [2] A. Reisch, A. Runser, Y. Arntz, Y. Mely, A. S. Klymchenko, *ACS Nano* **2015**, *9*, 5104.
- [3] A. Reisch, D. Heimbürger, P. Ernst, A. Runser, P. Didier, D. Dujardin, A. S. Klymchenko, *Adv. Funct. Mater.* **2018**, *28*, 1805157.
- [4] A. Reisch, P. Didier, L. Richert, S. Oncul, Y. Arntz, Y. Mely, A. S. Klymchenko, *Nature Commun.* **2014**, *5*, 4089.
- [5] B. Andreiuk, A. Reisch, E. Bernhardt, A. S. Klymchenko, *Chem. Asian J.* **2019**, *14*, 836.
- [6] A. Reisch, K. Trofymchuk, A. Runser, G. Fleith, M. Rawiso, A. S. Klymchenko, *ACS Appl. Mater. Interfaces* **2017**, *9*, 43030.
- [7] I. Khalin, D. Heimbürger, N. Melnychuk, M. Collot, B. Groschup, F. Hellal, A. Reisch, N. Plesnila, A. S. Klymchenko, *ACS Nano* **2020**, *14*, 9755.
- [8] K. Trofymchuk, A. Reisch, P. Didier, F. Frasn, P. Gilliot, Y. Mely, A. S. Klymchenko, *Nature Photonics* **2017**, *11*, 657.
- [9] N. Melnychuk, A. S. Klymchenko, *J. Am. Chem. Soc.* **2018**, *140*, 10856.
- [10] C. Severi, N. Melnychuk, A. S. Klymchenko, *Biosens. Bioelectron.* **2020**, *168*.
- [11] N. Melnychuk, S. Egloff, A. Runser, A. Reisch, A. S. Klymchenko, *Angew. Chem. Int. Ed.* **2020**, *59*, 6811.
- [12] P. Ashokkumar, N. Adarsh, A. S. Klymchenko, *Small* **2020**, *16*, 2002494.

SESSION SM07.05: Self-Assembly of Polymers and Clusters I
Session Chairs: Shuai Zhang and Xin Zhang
Monday Morning, April 19, 2021
SM07

10:30 AM *SM07.05.01

Supramolecular Engineering Strategies to Enable Hierarchical Self-Assembly Alvaro Mata^{1,2}; ¹University of Nottingham, United Kingdom; ²The University of Nottingham, United Kingdom

Nature has evolved in a hierarchical manner to achieve outstanding material properties and complex organismal behaviours. While great progress has been made engineering precise nanostructures through the self-assembly of molecular building blocks, the capacity to organize them beyond the nanoscale and into functional macroscopic structures, remains a challenge. In the fields of tissue engineering and regenerative medicine, it is essential to design materials, structures, and processes with hierarchy as a central principle. This talk will present our laboratory's efforts to exploit biological organization principles to guide self-assembly of multiple types of building blocks across size scales and enable the design of functional biomaterials. Examples will include the use of supramolecular events found in nature based on multicomponent self-assembly, protein order-disorder synergies, diffusion-reaction processes, and/or organic-inorganic interactions to organize multiple types of biological (*e.g.* proteins, polysaccharides) and/or synthetic (*e.g.* peptides, surfactants, graphene oxide) building blocks hierarchically. The resulting materials exhibit properties such as hierarchical organization (1-4), the capacity to grow and heal (1,2), tuneable mechanical properties (1,4), and biomimicry (4,5).

References

1. Wu et al (2020). Nature Communications 11, 1182, 10.1038/s41467-020-14716-z.
2. Inostroza-Brito et al (2015). Nature Chemistry 7(11), 10.1038/nchem.2349.
3. Hedegaard et al (2018). Advanced Functional Materials 28(16), 10.1002/adfm.201703716.
4. Elsharkawy et al (2018). Nature Communications 9(2145), 10.1038/s41467-018-04319-0.
5. Hedegaard et al (2020). Science Advances 6(4), 10.1126/sciadv.abb3298.

10:55 AM SM07.05.02

Late News: Time-Domain Programming of Self-Assembly with Chemical Clocks Guido Panzarasa; ETH Zurich, Switzerland

Living systems can grow a huge variety of materials with the highest degree of sophistication, and an overall efficiency that remains largely unparalleled by artificial fabrication techniques. Moreover, living materials are adaptive *i.e.* they exist and perform autonomously under dissipative conditions. These features are made possible by the ability to control complex reactions networks, carefully organized in spatiotemporal sequences. Developing autonomous chemical systems that could imitate the properties of living matter is a challenge at the meeting point of materials science and systems chemistry. Chemical clocks thus become versatile tools to program in time the autonomous and transient self-assembly of organic as well as inorganic building blocks. The design of such *ad hoc* reaction networks is at the core of my current research efforts. I will show how to “clock” molecules, polymers and metal cations into different structures, from nanoparticles to gels, without the need for external control, and demonstrate how this approach paves the way to the development of (almost) living artificial materials.

11:10 AM SM07.05.03

Late News: Single-Step Annealing and Incorporation of a Metal Complex into Block Copolymer Matrix

Modern nanotechnology fabrication relies on two opposite approaches, namely the “top-down” and the “bottom-up”. The former typically employs lithography techniques with which one can obtain nanometer-sized (10-100 nm) structures. This conventional "top-down" approach meets ultimately the physical limits, thus the further progress of the lithographic methods is hindered. The alternative, "bottom-up" strategy, utilizes chemical compounds, which self-assemble into more complex structures. An example of such compounds are block copolymers (BCPs), consisting of at least two different homopolymer blocks joined together with a covalent bond.

Our aim is to explore principles governing each block location (degree of order) and control it, prior to subsequent metal/oxide functionalization of such organic template. A straightforward approach, which we call Solvent Evaporation Annealing (SEA), offers a sensible balance between simplicity and economic cost. Here, the ordering process occurs at the same time while the layer is deposited on the substrate in a time-extended spin-coating process. The key element is an introduction of a low volatile compound in the mixture with BCP along with normally present high volatile solvent. Lower solution viscosity combined with an elongated evaporation time delivers a large grain size (more specifically correlation length), which is on the order of single micrometers.

BCP ordered films are designed to serve as matrices for the templated synthesis of inorganic nanostructures. Conversion methods follow the general idea of the affinity of metal precursor molecules to a specific functional group present in a selected homopolymer block. Thus, the metal precursor renders a pattern marked by one domain. Wet techniques accomplish the idea by a solution-based chemical reaction with a polymer, sometimes acting destructively on the polymer morphology. In our research, we combined Solvent Evaporation Annealing with the addition of metal precursor salt to successfully obtain BCP-templated metal nanostructures. The technique requires only the use of the spin-coating device and a proper selection of cosolvent with dissolved metal precursor salt. We have tested several compounds with metals incorporated, which reproduce the pattern of preferential homopolymer block. We further characterized the morphology of the obtained samples. Our profound investigations about this convenient process may open the facile way for obtaining precisely tuned functional nanostructures with sizes not exceeding single nanometers, which potential area of application ranges from membranes through memory devices to optical coatings.

11:25 AM SM07.05.04

Late News: Solvent Evaporation Annealing—An Efficient Path of Block Copolymer Self-Assembly

Arkadiusz A. Leniart, Przemyslaw Pula and Pawel W. Majewski; University of Warsaw, Poland

Large scale block copolymer self-assembly is hindered by relatively low defect formation energy – leading to high defect density, and relatively slow ordering kinetics. There are many processing methods used to overcome these obstacles, all aiming at obtaining highly ordered morphologies in a time- and cost-efficient manner. Among them, the two most straightforward techniques have been extensively explored – thermal annealing and solvent vapor annealing (SVA).

Solvent evaporation annealing (SEA) is a method based on a concept similar to SVA – in both cases, the acceleration of block copolymers self-assembly is obtained by an increase of mobility of polymeric chains in a presence of solvent molecules. However, instead of swelling of dry polymer film, in SEA preferable ordering conditions are achieved by evaporation of the solvent during single-step casting. It is possible due to binary solvent mixtures, in which the dominant solvent is much more volatile than a second one. Unlike in conventional spin-coating, during the casting process, the non-volatile addition remains in a block copolymer film for a significantly longer time. This residual solvent in a polymer wet film prolongs the evaporation process. We monitor the block copolymer grain coarsening – the long-range ordering of polymer domains – by control of multiple parameters, such as residual solvent concentration, temperature, and pressure of the environment.

In this study, we present kinetic data of grain growth in cylindrical block copolymer with a molecular weight range from 58 kg/mol to 275 kg/mol, consisting of polystyrene and poly(vinyl pyridine) blocks, conditioned in

different solvents mixtures and varying environmental conditions. The evaporation rate was controlled in both isothermal and non-isothermal manner. We determined a critical concentration of solvent in block copolymer wet film, at which order-disorder transition occurs. Moreover, we conducted a series of experiments in which different pathways of evaporation were scrutinized, including rapid quenches at certain thicknesses and delay of evaporation. The image analysis results were corroborated by large-scale SEM images and GISAXS studies. The obtained results indicate, that there is a power-law scaling between grain coarsening and evaporation rate as well as the time of retention near ODT.

SEA is a convenient method for the fast and cost-effective production of large block copolymer grains. In contrast to many other self-assembly methods, this technique is relatively simple and can be utilized without any complex processing setup.

11:40 AM SM07.05.05

Knotted and Macromolecular Catenanes—Synthesis and Surface Directed Assemblies Rigoberto C. Advincula^{1,2,3}; ¹The University of Tennessee, Knoxville, United States; ²Oak Ridge National Laboratory, United States; ³Case Western Reserve University, United States

Nanostructured and hierarchical assemblies are important for demonstrating the ability to understand directed or self-directed forces in defining function for polymers. Knotted and catenated macromolecular architectures in polymers are a departure from typical linear polymers. The lack of chain-ends, the topologically exact order, size, and composition can influence properties and applications such as rheology modifiers, adhesion promoters, and compatibilizers. Herein we demonstrate a supramolecular assembly approach towards these topologically exact polymers and demonstrate their self-assembly properties at interfaces. First, we demonstrate their programmable synthesis—next, their complexation and assembly properties. The goal is to understand structure-composition-property correlation at the macromolecular assembly scale and compare it to other architectures such as stars, dendrimers, and brushes. The ability to self-assemble at the air-water interface is demonstrated with PLA-PCL copolymers and catenanes, and the role of metal complexation is highlighted. Different surface-sensitive analytical spectroscopic and microscopic properties are utilized and reported.

11:55 AM SM07.05.06

Monolayer Fluidic Water in Nanoscale Confinement Shuai Zhang^{1,2}, Qiang Li^{3,2}, Flemming Besenbacher² and Mingdong Dong²; ¹University of Washington, United States; ²Aarhus University, Denmark; ³Shandong University, China

With distinct intermolecular network and dynamics, interfacial water is essential to modulate the surface behaviors, like growth and dissolution, redistribution of surface charge, and dewetting/wetting surfaces. It plays a crucial role in nano-fluidics, tribology, doping of semiconductors, (geo)-mineralization, and bio-macromolecule and nanoparticle assembly. Hence, characterizing and understanding the structures and dynamics of interfacial water is essential in designing and creating advanced materials.

In the last decade, it has been found that few-layer water confined between solid surfaces in sub-nanoscale can convert into two-dimensional (2D) ice-like structure (i-water). Although its growth dynamics and transition to three-dimensional phases, water droplets, and vapor, in response to humidity, temperature, organic vapor, and hydrophobicity of confining solid surface have been studied, it is unclear if there are other 2D water phases in sub-nanoscale confined space thermodynamically stable, and how it responds to environmental stimuli. The phase diagram of the confined 2D water in sub-nanoscale is not complete.

Recently, using in-situ thermal atomic force microscopy, we have confirmed the existence of 2D monolayer fluidic water confined by few-layer graphene and muscovite mica. The new phase thickness is less than 0.2 nm, adapting one unique hydrogen-bond network different from bulk water and i-water. It is a thermodynamically stable phase that coexists with i-water. The discovery of this new 2D water phase fills one missing part of the phase diagram of the confined 2D water in sub-nanoscale. It provides another opportunity to understand the physics of fluidics in the nanoscale other than the classical carbon nanotubes and protein-based nanopores. It will also inspire the new theory and scheme in understanding how interfacial water response to confinement and how such modulation can adjust material assembly.

12:10 PM SM07.05.07

Competing Self-Assembly Pathways for Metal Nanomembranes Divya J. Prakash^{1,1}, Hassan Dibaji¹, Mengistie L. Debasu¹, Donald E. Savage², Max G. Lagally² and Francesca Cavallo^{1,1}; ¹The University of New Mexico, United States; ²University of Wisconsin–Madison, United States

Competing relaxation mechanisms have been extensively modeled for strained and single-crystalline semiconductor nanomembranes (NMs) upon release from their substrate surface. As a result, a variety of 3D structures can be obtained by self-assembly of semiconductor NMs with a high degree of predictive control on their geometry. These structures include wrinkles, helices, twists, and rolled-up tubes. Guided self-assembly of metal NMs into different 3D objects has also been demonstrated. However, the ability to determine the relaxation pathway of a free-hanging metal NM remains elusive. A significant challenge in achieving predictive control on the geometry of metal NMs upon release from their substrate surface relates to a varying stress distribution across the NM thickness for a given set of deposition parameters. Moreover, different stress vs. thickness distributions have been reported for metals with low and high adatom mobilities.

Here, we demonstrate predictive control on the relaxation of metal NMs upon release from their substrate surface. The work encompasses continuum mechanics modeling and synthesis of 3D microstructures via self-assembly of metal NMs.

We investigate NMs comprising Cr and Au, i.e., metals with low and high adatom mobility. We use a force balance model to determine the preferential geometry of a released Cr and Au-based NMs as a function of various parameters. These parameters include the Cr and Au layer thickness, the number of Cr and Au layers and their stacking order within the NM, the substrate surface, and the two metals' deposition rates. The focus is on metal NMs obtained by evaporation. We also establish how the NMs' lateral geometry on the substrate surface will affect its self-assembly pathway upon release.

Our theoretical study yields the conditions to obtain rolled-up and inverted rolled-up tubes, helices and twists with an unprecedented degree of control on their diameter and pitch in the microscale range.

We validate our predictions via a comparison with experimentally fabricated 3D structures via guided self-assembly of Cr and Au-based NMs. The NMs are deposited via e-beam evaporation on bulk Si substrates coated with a sacrificial layer. In our work, we use Ge, GeO_x, and SiO₂ sacrificial layers. Upon selective removal of the sacrificial layer, we observe the formation of rolled-up structures by either upward or downward bending of the NM based on the NM composition, sacrificial layer, and thickness of the Cr and Au layers. The fabricated structures include tubes, helices, and twists. The geometry of the fabricated structures is consistent with the prediction of our model.

In conclusion, we have provided the theoretical framework to fundamentally understand and determine competing relaxation pathways for metal NMs that have been released from their substrate surface. Our work is timely and relevant as self-assembled metal NMs are increasingly proposed for various device applications (e.g., integrated inductors and transformers, slow-wave structures, and unit cells of metamaterials).

ACKNOWLEDGEMENT. The work was funded by US AFOSR under award No. FA9550-19-1-0086. This work was performed, in part, at the Center for Integrated Nanotechnologies, an Office of Science User Facility operated for the US Department of Energy (DOE) Office of Science by Los Alamos National Laboratory (Contract 89233218CNA000001) and Sandia National Laboratories (Contract DE-NA-KE,0003525).

SESSION SM07.06: Self-Assembly of Polymers and Clusters II

Session Chairs: Shuai Zhang and Xin Zhang

Monday Afternoon, April 19, 2021

SM07

1:00 PM SM07.06.01

Late News: Spectroscopic and Structural Characterization of Silver Nanoclusters with DNA Monomers and Dimers Using Mass Spectrometry Soonwoo Hong, Ines C. Santos, Yu-An Kuo, Yuan-I Chen, Trung D. Nguyen, Jennifer S. Brodbelt and Tim Yeh; The University of Texas at Austin, United States

As a special class of nanomaterial fluorophores, DNA-templated silver nanoclusters (DNA/AgNCs) have become important in molecular sensing, creating new tools for detection of metabolites, neurotransmitter and metal ions. Despite of their unique capabilities in molecular sensing, the mechanisms that mediate both the formation of DNA/AgNCs and the resulting optical properties are largely unknown. Here we utilized an advanced mass spectrometry, including electron spray ionization (ESI-MS) and activated-electron photodetachment mass spectrometry (aEPD-MS), to probe the fluorescence and structural properties of DNA/AgNCs, including stoichiometries, compositions and binding sites of DNA/AgNCs templated in seven DNA 10-mers. Our mass spectrum data revealed the presence of complexes containing one (monomeric) or two (dimeric) DNA hosts and a variable number of silver atoms. Interestingly, while monomeric species incorporated a low number of silver atoms ($Ag_1 - Ag_4$), the dimeric complexes contained a higher number of silver atoms ($Ag_4 - Ag_{18}$). Using polyacrylamide gel electrophoresis (PAGE), we validated that the higher number of silver atoms are associated with dimers responsible for the red fluorescence emission, while the low number of silver atoms are monomers that tend to give green fluorescence emission. The formation of nanocluster cores and the resulting spectroscopic properties vary by the base composition of the DNA template. Given the enhanced abundance of specific dimeric DNA/AgNCs, we hypothesize that certain magic-number of Ag atoms (e.g., Ag_6 , Ag_{10} , and Ag_{11}) with dimerization of short DNA may be a clue for having fluorescence with the different emission wavelengths (490 – 680 nm) observed. This study suggests that fluorescence can be strategically controlled by the certain design (e.g., consecutive cytosines and GC contents ratio) of the DNA host to guide the formation of monomeric or dimeric species with magic-number of silver atoms.

References:

1. M.S. Blevins, D. Kim, C.M. Crittenden, S. Hong, H.-C. Yeh, J.T. Petty and J.S. Brodbelt, "Footprints of nanoscale DNA-silver cluster chromophores via activated-electron photodetachment mass spectrometry", *ACS Nano* 13, 14070-14079, 2019.
2. I.C. Santos, S. Hong, H.-C. Yeh and J.S. Brodbelt, "Electron photodetachment mass spectrometry to study interactions of silver nanoclusters with DNA monomers and dimers", *under review*.

1:15 PM SM07.06.02

Ionic Liquid Directed Self-Assembly of Block Copolymers in Epoxy Resins Deborah Liu and Daniel Krogstad; University of Illinois at Urbana-Champaign, United States

Epoxy/block copolymer (BCP) blends have shown great promise in a variety of applications. The BCPs can form nanostructures in the resins, which improve the toughness of the thermoset as well as provide a template for nanoparticles (NPs). However, the BCPs can either form the nanostructures through reaction induced microphase separation (RIMPS) or by self-assembly. For toughness applications, the mechanism is not as critical, but for NP templating, the self-assembly mechanism is preferred in order to help mitigate NP aggregation. In this work, we demonstrated that using an ionic liquid (IL) hardener, rather than a traditional diamine hardener, results in the formation of the nanostructures through self-assembly rather than RIMPS for poly(ethylene oxide-*b*-propylene oxide-*b*-ethylene oxide) (Pluronic) BCPs. Small angle x-ray scattering (SAXS) was used to develop a ternary phase diagram that shows a range of stable nanostructures including higher ordered cubic, hexagonal and lamellar structures, even in these highly polydisperse BCPs. Additionally, *in situ* small angle x-ray scattering (SAXS) was used to show that there are significant morphological transitions during epoxy curing. These data show that there are competing changes that are driven by the epoxy cross-linking reactions and the increased thermal mobility of the BCPs in the epoxy. These results demonstrate new methods to drive self-assembly in epoxy/BCP blends, which is critical for their development as multifunctional nanocomposites.

1:30 PM SM07.06.03

Late News: Modulating and Modeling Charge of Hybrid Lipid/Polymer Vesicles Walter Paxton, Keith L. Willes, Trent Johnson, Sydney Johnson and Daniel R. Hart; Brigham Young University, United States

Amphiphilic block copolymers combined with lipid-based amphiphiles are capable of self-assembling into hybrid bilayers with properties of both lipid and polymer that are not always predictable. We aim to understand and predict the properties of polymer and hybrid vesicle membranes to better exploit them for use in drug delivery and modulating surface properties in biosensing devices. One of those key properties is the surface charge of vesicles, which influences how a membrane will interact with other materials and biological tissues, as well as the biological fate of vesicle assemblies in vivo. To study the modulation of surface charge in hybrid lipid/polymer bilayers, we have used DLS and zeta potential analysis to investigate the effects of incorporating charged lipids and polymers into hybrid lipid-polymer vesicles. We have found that polymer amphiphiles containing polyethylene oxide headgroups have a surprisingly strong ability to screen charged lipids within the vesicle membrane, complicating the task of predicting the surface properties of hybrid vesicles. To explain these results and provide a straightforward way of predicting the surface properties of synthetic, multicomponent membranes, we have devised a model that allows us to predict the zeta potential of hybrid vesicles quantitatively. We anticipate that our approach will greatly facilitate modulating zeta potential and other surface properties of biomimetic membrane materials.

1:45 PM SM07.06.04

Influence of Organic Solvent in Peptide Self-Assembly on Two-Dimensional Materials Robert Ccorahua, Hironaga Noguchi, Kazunori Motai and Yuhei Hayamizu; Tokyo Institute of Technology, Japan

The controllable nanoscale self-assembly of biomolecules, such as peptides, on solid surfaces is an important issue in establishing functional bio/solid interfaces for biosensors. Two-dimensional (2D) nanomaterials such as graphene and MoS₂ are gaining a wide attention due to its unique electrical properties as a novel platform for biosensing. For this sake, we have established a method to control the self-assembly on these 2D materials by applying electrochemical bias¹ and designing new sequence of peptides². In this work, we studied basics of the assembly process of the self-assembling peptide Y(GA)₄Y: (Y4Y) on 2D materials by employing methanol (MeOH) and other organic solvents as mediators.

Flakes of graphite and MoS₂ were transferred on to silicon wafers by mechanical exfoliation method. A solution of Y4Y peptide (100 nM) dissolved in a mixture of water and methanol (MeOH) at different concentrations ranging from 0% to 50% were placed on both substrate graphite and MoS₂. After 1 hour of the incubation, the solution was removed by blowing with N₂ gas and the sample was dried overnight. Finally, Atomic Force Microscopy (AFM) characterization and analysis were carried out.

AFM analysis showed that, by using aqueous solution as a medium for the self-assembly of Y4Y, more than 85% of self-assembled peptide covered (coverage) the surface of graphite and MoS₂ forming a monolayer in the shape of nanowires with a hexagonal structure. When MeOH was employed as the mediator of Y4Y self-assembly, the coverage decreased drastically for both substrates at distinct threshold concentrations. While the coverage of peptides decreased to ~60% at more than 30% of MeOH concentration on graphite, the peptide coverage resulted in ~50% at more than 20% of MeOH for MoS₂. Higher concentrations of MeOH resulted in no self-assembled peptide for both substrates, thus evidencing the effect of MeOH in controlling the coverage of Y4Y structure over graphite and MoS₂. Additionally, we evaluated the influence of other water-miscible organic solvents (DMSO and acetone) in the self-assembly process of peptide on graphite and MoS₂. These AFM characterizations suggested that the organic-solvent mediated self-assembly process of peptide on 2D materials correlates with the relative polarity of the respective organic solvent. These results unveil promising properties of organic solvents as peptide self-assembly mediator on 2D materials.

(1) T. Seki, C. Page, D. Starkebaum, Y. Hayamizu, M. Sarikaya, *Langmuir*, 34, 1819 (2018).

(2) P. Li, K. Sakuma, S. Tsuchiya, L. Sun, Y. Hayamizu, *ACS Appl. Mater. Interfaces*, 11, 20670 (2019).

2:00 PM SM07.06.05

Layer-by-Layer Assembled Microparticle Vaccines for Combination Immunotherapy Apoorv Shanker¹, Imane Bouzit¹, Sandeep Koshy², Michael Nehil², Janelle Velez², Stephanie Schwartz² and Paula Hammond^{1,1}; ¹Massachusetts Institute of Technology, United States; ²Novartis Institutes for BioMedical Research, United States

Recent clinical successes of checkpoint inhibitors have led to a renaissance in the field of cancer immunotherapy. Combinatorial immunotherapy that targets multiple immune pathways offers a more potent strategy to improve patient outcomes. However, combination immunotherapies generally suffer from increased risk of immune-related adverse events that limit their utility. Optimal sequencing, timing, and duration of exposure of immune-modulators that resonate with the natural immune cycle can help rescue systemic toxicity and unleash the full potency of combination immunotherapies. Rational biomaterials- and nanotechnology-based drug delivery strategies that allow precise spatiotemporal control of the *in vivo* presentation of the immune-modulators can open the door to more effective immunotherapies.

One such strategy is the layer-by-layer (LbL) self-assembly technology which enables the fabrication of a modular drug delivery platform with multiple immune-modulating drugs stacked in a layered structure. The sequence of assembly of the bioactive agents and the choice of intervening non-bioactive “glue” layers provide precise control over the timing and duration of exposure of the assembled immune-modulators. Here, we present LbL-assembled structures on injectable microparticles as a tractable drug delivery system to achieve appropriately-timed delivery of poly(I:C), a TLR3 agonist, and interleukin-2 (IL-2), a pro-inflammatory cytokine. To fabricate the microparticle vaccines, the heparin-binding capability of IL-2 was leveraged and poly(I:C), a negatively-charged synthetic mimic of viral dsRNA, was employed as one of the polyelectrolytes in the LbL assembly. The chosen polycation functions as the “glue” layer to enable sequential assembly of the negatively-charged heparin/IL-2 complexes and poly(I:C), as well as to control their rate of release. Encapsulation efficiencies of 30-50% and 60-90% for poly(I:C) and IL-2, respectively, at a high formulation yield (> 80%). For a milligram of the microparticle core, a single layer of IL-2 and poly(I:C) can hold 3-4 μg and 5-10 μg , respectively. Differential release rates of IL-2 from the LbL- microparticles were achieved by the choice of polycations. While LbL-microparticles built with the hydrolytically-degradable poly(β -amino ester) (PBAE) as the polycation released ~90% IL-2 over three days, less than 15% was released from the formulation with the non- degradable poly(L-lysine) (PLK) over eight days. A 4:1 mixture of PBAE and PLK yielded an intermediate release profile with 45% of loaded IL-2 released over eight days. For LbL-microparticles loaded with both poly(I:C) and IL- 2, the release kinetics were adjusted to achieve faster release of poly(I:C) (~90% over 3 days) required to trigger the innate immune response followed by a slow, sustained presentation of IL-2 over multiple weeks to augment the developing adaptive immunity. The microparticle vaccines were further characterized in subcutaneous murine tumor models to evaluate the time-course effects of the LbL-delivered poly(I:C) and IL-2 on immune activity, toxicity, and therapeutic efficacy.

LbL microparticle vaccines, thus, present a new paradigm to evaluate drug sequencing in combination immunotherapies in higher throughput than currently possible with conventional dosing in pre-clinical *in vivo* experiments.

2:15 PM SM07.06.06

Tracing the Formation of De Novo Binary Protein Arrays on Cells and Synthetic Membranes Ariel J. Ben-Sasson^{1,1}, Joseph Watson², Alice Bittleston², Ioanna Mela², Greg Hura³, Clemens Kaminski², Emmanuel Derivery² and David Baker^{1,1,1}; ¹University of Washington, United States; ²University of Cambridge, United Kingdom; ³Lawrence Berkeley National Lab, United States

Co-assembling genetically encoded protein materials represent a paradigm shift in engineering of complex biomaterials.^{1,2} Compared to their single-component counterparts^{3,4} they offer facile components production and functionalization, as well as control over the temporal, spatial, and composition aspects of the formation process, that is only initiated by mixing two different building

blocks.1 Here we go beyond homogeneous protein materials formation, whether in a tube or inside a living cell, and demonstrate formation of biologically-active hybrid arrays on mammalian cell membranes and their synthetic counterparts to tunable dimensions, showcasing ordered receptor clustering and tunable endocytosis properties.

To this end we first selected a membrane receptor, genetically- or peptide-fused a compatible ligand to one of the arrays components, saturated the cell membrane receptors with said component, removed unbound components from the cell environment, and triggered arrays formation by introducing the second component into the system. While this seemed as a valid assembly pathway we found that the arrays' dihedral building blocks that need to first anchor to the membrane, were not suited for this task. We hypothesized this is likely because cell membranes can wrap around the dihedral components' identical two sides, each displaying an equal number of binding sites, thereby blocking assembly. We therefore devised cyclic pseudo-dihedral versions of the array components, which are partly dihedral to allow proper formation of a 2D array, but overall cyclic to allow directional anchoring.

To follow array formation we label the array components and the targeted receptor's intracellular domain and demonstrate a fast, uniform, and synchronised assembly process that is robust to derive useful information from, using quantitative microscopy.

Through a rigorous quantitative microscopy study on cell membranes combined with AFM characterization of arrays assembled on supported bilayers we show that arrays formed on cells are likely of an ordered single layer structure and thus that our material can impose order onto fundamentally disordered substrates like cell membranes receptors.

We envision the design approach and the system demonstrated here will enable deeper investigation into assembly processes both in-vivo and in-vitro, and will pave the way towards a new generation of multi-protein and hybrid biomaterials designed to modulate cell responses and reshape synthetic and living systems.

References:

- 1. Ben-Sasson, A. J. et al. Design of Biologically Active Binary Protein 2D Materials. bioRxiv 2020.09.19.304253 (2020) doi:10.1101/2020.09.19.304253.**
- 2. Vantomme, G. & Meijer, E. W. The construction of supramolecular systems. *Science* 363, 1396–1397 (2019).**
- 3. Chen, Z. et al. Self-Assembling 2D Arrays with de Novo Protein Building Blocks. *J. Am. Chem. Soc.* 141, 8891–8895 (2019).**
- 4. Sleytr, U. B., Schuster, B., Egelseer, E.-M. & Pum, D. S-layers: principles and applications. *FEMS Microbiol. Rev.* 38, 823–864 (2014).**

2:30 PM SM07.06.07

AI Guided Discovery of Self-Assembly Peptide Sequences Using Monte Carlo Tree Search and Coarse-Grained Simulations Rohit Batra, Troy D. Loeffler, Henry Chan, Srilok Srinivasan, Christopher Fry and Subramanian Sankaranarayanan; Argonne National Laboratory, United States

Peptide materials have a wide array of functions from tissue engineering, surface coatings, catalysis, and sensing. This class of biopolymer is composed of a sequence of 20 naturally occurring amino acids. As the peptide sequence increases, so does the searchable sequence space (trimer = 20^3 or 8,000 peptides and a pentamer = 20^5 or 3.2 M). Empirically, peptide design is guided by the use of structural propensity tables, hydrophobicity scales, or other desired properties and typically yields <10 peptides per study, barely scraping the surface of the search space. Here, we combine machine learning techniques, such as Monte Carlo tree search and random forest, with coarse-grained molecular dynamics (MD) simulations to efficiently search large spaces of trimer, pentamer and octamer peptide sequences with high self-assembly propensity. Subsequent experiments on identified sequences support our findings, and demonstrate the ability of this approach for peptide design.

2:45 PM SM07.06.08

Reconfiguration of Amorphous Complex Oxides as a Route to Self-Assembly of Inorganic

Nanomembranes Divya J. Prakash^{1,1}, Mengistie L. Debasu¹, Yajin Chen², Donald E. Savage², Chaiyapat Tangpatjaroen², Christoph F. Deneke³, Angelo M. Da Souza⁴, Adam D. Alfieri², Izabela Szlufarska², Paul G. Evans² and Francesca Cavallo^{1,1}; ¹The University of New Mexico, United States; ²University of Wisconsin–Madison, United States; ³Universidade Estadual de Campinas, Brazil; ⁴Universidade Federal de Minas Gerais, Brazil

We report and investigate a novel approach to self-assembly of complex oxide-based nanomembranes (NMs) in radial geometries, including radially stacked complex oxides and complex oxides/single-crystalline semiconductors superlattices. These structures will offer a tremendous opportunity for discovery-driven science and new functionalities. For example, the proximity of single-crystalline semiconductors and complex oxides will potentially result in superlattices with intriguing magnetic and electronic properties through modulating the oxides' intrinsic spin-lattice coupling and other coupling effects. Moreover, we expect that curvature will significantly affect the electronic band structure of the stack and produce unique electrical and thermal transport features.

Amorphous SrTiO₃/Si/Si_{1-x}Ge_x nanomembranes (NMs) roll up into micron-scale tubes upon release from the growth substrate due to the elastic relaxation of stress from two sources: (i) the epitaxial mismatch of SiGe and Si and (ii) stress resulting from the deposition of the amorphous SrTiO₃. Crucially, the NMs are in a metastable structural configuration after release because the SrTiO₃ layer remains in the amorphous state.

Heating transforms NMs scrolls into swiss roll structures that alternate single-crystalline semiconductors and amorphous complex oxides in a radial geometry. A detailed continuum mechanics study establishes that the relaxation of the hybrid NM during heating involves large irreversible compressive stress arising from structural changes in the oxide. Mechanical modeling also shows that this stress is responsible for NM assembly. X-ray reflectivity, x-ray diffraction, and transmission electron microscopy probe changes in the structure of the SrTiO₃ layer that are consistent with densification of the complex oxide.

Based on our experimental results and continuum mechanics modeling, we predict that a variety of complex oxides-based heterostructures can be obtained via reconfiguration-driven assembly of amorphous oxides, including SrTiO₃/Si and SrTiO₃/LaAlO₃.

ACKNOWLEDGEMENT. This research was supported by the U.S. Department of Energy (DOE), Office of Science, Basic Energy Sciences (BES), under Award # DE-SC0020186 (electron microscopy, data analysis, and mechanical modeling) and by the National Science Foundation (NSF) under Award # DMR-1720415 (synthesis of the samples). This work was performed, in part, at the Center for Integrated Nanotechnologies, an Office of Science User Facility operated for the U.S. Department of Energy (DOE) Office of Science by Los Alamos National Laboratory (Contract 89233218CNA000001) and Sandia National Laboratories (Contract DE-NA-KE,0003525). X-ray diffraction was performed at the XRD2 beamline within the Laboratorio Nacional de Luz Sincrotron.

SESSION SM07.07: Applications of Assemblies I
Session Chairs: Lili Liu and Xin Zhang
Monday Afternoon, April 19, 2021
SM07

4:00 PM SM07.07.01

Structure and Properties of Ice-Templated Cellulose Nanomaterial-Based Composite Foams for Thermal Insulation Pierre Munier, Varvara Apostolopoulou Kalkavoura and Lennart Bergström; Stockholm University, Sweden

Cellulose nanomaterials (CNM) have emerged in the last decades as a potential candidate for renewable thermally insulating foams and aerogels ^[1]. The intrinsic anisotropy of cellulose chains has been exploited in the design of anisotropic foams with aligned nanoparticles and lower-than-air thermal conductivities in a specific

direction [2]. It was recently shown [3] that the (nano)porosity, particle alignment and tailoring of heterogeneous interfaces can have a significant effect on the heat transfer properties within foams. Here, we will present work on the heat transfer and mechanical properties of ice-templated anisotropic foams based on TEMPO-oxidized cellulose nanofibrils (TCNF) and cellulose nanocrystals (CNC). Anisotropic CNM-based foams with a wide range of densities were prepared by freeze casting aqueous dispersions with different particle concentrations. We will discuss how the radial thermal conductivity (perpendicularly to the freezing direction) of the foams was related to the nanoporosity in the pore walls and the degree of particle alignment. It will also be shown that ice-templating of composite foams, by adding for instance montmorillonite clay nanoplatelets or colloidal silica [4], could mechanically strengthen the foams while specific co-assemblies could favor certain heat dissipation mechanisms and therefore preserve or even improve the thermal insulating performance.

References

- [1] N. Lavoine, L. Bergström, *J. Mater. Chem. A* **2017**, *5*, 16105.
[2] B. Wicklein, A. Kocjan, G. Salazar-Alvarez, F. Carosio, G. Camino, M. Antonietti, L. Bergström, *Nat. Nanotechnol.* **2015**, *10*, 277.
[3] V. Apostolopoulou-Kalkavoura, P. Munier, L. Bergström, *Adv. Mater.* **2020**, *2001839*, 1.
[4] P. Munier, V. Apostolopoulou-Kalkavoura, M. Persson, L. Bergström, *Cellulose* **2019**, 1.

4:15 PM SM07.07.03

3D Printed Pattern for Directing Nanoparticle Alignment for Device Applications Sayli Jambhulkar, Dharneedar Ravichandran, Weiheng Xu, Yuxiang Zhu and Kenan Song; Arizona State University, United States

Nanoparticle assembly can enable broad applications in electronics, optics, optoelectronics, resonators, and thermal dissipations or conductions. Current methods to tailor nanoparticle structures include electrical field, magnetism, mechanical stretching, surface functionalization, and template directing. Most substrates for template-based nanoparticle assembly have crimped surfaces from elastomer compression, transfer imprinting, and other methods with similar slow-manufacturing. Our study has demonstrated the use of different 3D printing, including stereolithography (SLA) and continuous liquid interface processing (CLIP), in making microscale surface patterns for nanoparticle assembly. Via the combination of 3D printing and layer-by-layer assembly (LbL), we demonstrated the capability of aligning nanoparticles between surface grooves. The density of the aligned particles will transport electrons or phonons with different efficiencies. As a result, these rapidly prototyped devices showed varied conductivity and sensitivity. We demonstrated the manufacturability and scalability of our manufacturing with different nanoparticles. The inclusion of these nanoparticles with different concentrations showed high sensitivity and selectivity to different gas analytes, making them ideal platforms for detecting toxic gases or monitoring human health.

4:30 PM SM07.07.04

Late News: Polymer and Surfactant Assisted Crystallization for Electronics and Ionics Applications Jihua Chen; Oak Ridge National Laboratory, United States

Crystallization is a process that can be affected by many internal and external factors, which can in turn correspond to varied crystal structures, polymorphism and stunning differences in functions. Numerous examples can be found in oxides, silicon carbide, organic electronics, pharmaceutical compounds, and energetic materials. Ways to navigate nucleation and crystallizations of molecular crystals are explored, including frontline boundary control, temperature, and most importantly modified microenvironment by polymer additive.[1-2] Low-dose energy filtered TEM was used in combination with impedance analysis and equivalent circuit modelling to study ion transport, while hole transport in organic thin film transistor was studied as a function of pi-pi interaction strength. Recently, a similar approach has been adapted to grow ionic crystals with a surfactant additive. Improved grain boundary structure and facet

distribution lead to enhanced capacitance performance. Explanation of these results are given in light of surface energy, growth kinetics, and nucleation.[3]

Reference:

1. Z. He, et al., *Sci. Rep.* **2020**, *10*, 4344

2. S. Bi, et al, *J. Polym Sci. B*, **2015**, *53*, 1450

3. Part of this research was conducted at the Center for Nanophase Materials Sciences, which is a DOE Office of Science User Facility.

(This manuscript has been authored in part by UT-Battelle, LLC, under contract DE-AC05-00OR22725 with the US Department of Energy (DOE). The US government retains and the publisher, by accepting the article for publication, acknowledges that the US government retains a nonexclusive, paid-up, irrevocable, worldwide license to publish or reproduce the published form of this manuscript, or allow others to do so, for US government purposes. DOE will provide public access to these results of federally sponsored research in accordance with the DOE Public Access Plan (<http://energy.gov/downloads/doe-public-access-plan>.)

4:45 PM SM07.07.05

Late News: Ultrahigh- Block Copolymer Materials with Versatile Etch Selectivity for Sub-10 nm Pattern Transfer Jian Sun¹, Koei Azuma², Changyeon Lee³, Youngwoo Choo⁴, Teruaki Hayakawa², Chinedum Osuji³ and Padma Gopalan¹; ¹University of Wisconsin-Madison, United States; ²Tokyo Institute of Technology, Japan; ³University of Pennsylvania, United States; ⁴Yale University, United States

Studies of block copolymer (BCP) materials and their phase separation in bulk and thin-film forms have exploded over the last decades, due to the wide range of accessible morphologies (e.g. spheres, cylinders, gyroid, and lamellae) and sizes (5-200 nm) of features. The phase separation of a BCP is governed by three factors which include the relative volume fraction (f) of the blocks A and B ($f_A = 1 - f_B$), the degree of polymerization (N), and the Flory-Huggins interaction parameter (χ). The basic BCP self-assembly principles have enabled the BCP community to control the morphology as well as to tune the domain size and have driven the community to target the smallest size possible by synthesizing BCPs with high interaction parameter. Accessing sub-5 nm feature size is no longer a challenge utilizing BCP self-assembly. However, transferring the self-assembled BCP features to a substrate over a large area with high fidelity presents additional challenges, especially at the 10 nm length scale. In this work, the highly polar, functional and hydrophilic poly(3-hydroxystyrene) (P3HS) is incorporated with the acid sensitive poly(dimethylsiloxane) (PDMS). A tetrahydroxydopyranoyloxy (THP) protecting group which requires mild deprotection condition is introduced to the system and hence PDMS block remains intact after deprotection. We explore both P3HS/PDMS-based diblocks and triblocks synthesized by sequential living anionic polymerization and atom transfer radical polymerization, respectively. P3HS-*b*-PDMS shows well-defined lamellae or hexagonally packed cylinders with characteristic dimensions ranging from 7.4 to 17.7 nm. Mean-field theory analysis of the temperature-dependent correlation-hole scattering derived from a disordered symmetric P3HS-*b*-PDMS gives $\chi_{(T)} = 33.491/T + 0.3126$, which is more than 4-fold increase over PS-*b*-PDMS. Triblocks P3HS-*b*-PDMS-*b*-P3HS also show well-ordered lamellae and cylinder structures in bulk with the successful access to sub-5 nm feature size. Additionally, the unique architecture of ABA triblock allows the thin film of P3HS-*b*-PDMS-*b*-P3HS to be aligned vertically to the substrate, making this material a promising candidate for pattern transfer. Etching study indicates that the etch contrast between P3HS and PDMS is 15:1 under oxygen plasma treatment. Due to the functionality from the hydroxy group, inorganic precursors such as trimethylaluminium can selectively penetrate into P3HS domain which can be further converted into alumina mask for pattern transfer. These new BCPs not only exhibit high interaction parameter to achieve sub-10 nm feature size, but also present high etch contrast and versatile etch selectivity to facilitate the pattern transfer.

5:00 PM SM07.07.06

Late News: Domain-Selective Thermal Decomposition within Supramolecular Nanoribbons Yukio Cho¹, Ty Christoff-Tempesta¹, Dae-Yoon Kim^{1,2} and Julia Ortony¹; ¹Massachusetts Institute of Technology, United States; ²Korea Institute of Science and Technology, Korea (the Republic of)

Self-assembly is a powerful way to organize small molecules with tunable molecular chemistries into nanostructures with high surface areas. However, in order to exploit molecular self-assembly, the molecules must be amphiphilic and must fulfill particular packing parameter guidelines. These constraints have limited the use of small molecule self-assembly to a narrow range of molecular species with specific chemical attributes. Here, we introduce a new approach to supramolecular nanoribbons composed of untraditional hydrophobic small molecules. We pre-program into the nanostructure thermal stability in hydrophobic domain, and we use thermal decomposition to selectively remove the hydrophilic labile groups. The selective decomposition of labile groups with maintained nanoribbon morphology was confirmed by the combination of thermogravimetric analysis with mass spectrometry, ¹H NMR, and infrared spectroscopy. This molecular design strategy represents a new pathway to non-amphiphilic small molecule nanostructures through domain-specific selective decomposition, and broadens the potential utility of this materials class for new targets, including superhydrophobic coatings and self-assembled molecular electronics.

SESSION SM07.08: Applications of Assemblies II and Poster Session
Session Chairs: Lili Liu and Xin Zhang
Monday Afternoon, April 19, 2021
SM07

7:45 PM SM07.08.01

Atomistic Simulation Studies of Synthetic Melanin Particles in Aqueous Solutions with Poly (ethylene glycol) and Chitin Utkarsh Kapoor and Arthi Jayaraman; University of Delaware, United States

Melanin, a natural pigment known for imparting color to human skin/hair, is mimicked in synthetic materials for use in a variety of applications with the desired optical, photonic, thermal, and electrical property. In the past decade, polydopamine has served as one such synthetic form dominating the fundamental and applied research on melanin-based materials. While past experimental studies have focused on the synthesis and characterization of these melanin synthetic mimics, much less is known about the preferential interactions of these materials with other polymers, biocompatible and/or bio-derived. In this work, we use atomistic molecular dynamics (MD) simulation to simulate synthetic melanin nanoparticles, self-assembled using oligomers (e.g., 2-mer, 4-mer, and 8-mer) of polydopamine in an explicit solvent with and without added polymers, poly (ethylene glycol), and chitin. Using these simulations, we understand the nature of the polydopamine nanoparticle surface and its interactions with these polymers. We quantify the hydrophobic vs. hydrophilic character of the surfaces of the different assembled polydopamine oligomers, behavior of water molecules near the surface in the presence and absence of biopolymers. The impact of the polydopamine nanoparticle surface on the polymer is quantified via pair-wise correlation functions, polymer-particle hydrogen bonds, chain conformations, and interaction with water in the presence/absence of the polydopamine particle.

8:00 PM SM07.08.02

The Effect of Crystal Morphology on Hydrophobicity and Electrical Charge Retention in Melt-Blown Isotactic Polypropylene Fibers Farshad Nazari^{1,2} and Mohammad Reza Rahimpour²; ¹Florida State University, United States; ²Shiraz University, Iran (the Islamic Republic of)

From extrusion, melt-blown Isotactic polypropylene (iPP) submicron fibers were produced to be used in air purification. Scanning Electron Microscopy images revealed the lower the iPP molecular weight (MW), the lower the resulting melt-blown fiber diameter. For iPP fibers with MW~50 kg/mol, the average diameter was

~0.7 μm . The base weight in the melt-blown mats was adjusted by tuning the collector speed. Filtration properties, namely air resistance (AR) and filtration efficiency (FE%), were measured for the melt-blown iPP mats with different base weight, 5-75 gsm. Filtration efficiency increased exponentially as air resistance increased almost linearly with base weight. However, the filtration quality factor ($Q_f = -\ln(1 - \text{FE}/100)/\text{AR}$) was the highest, ~0.04 Pa^{-1} , at 50 gsm. The effect of discharging, using saturated isopropyl alcohol (IPA) vapor, on filtration quality factor was also studied. The mats maintained ~50% of their filtration quality factor, reflecting the existence of residual electrostatic charges from the melt-blown process and their significant effect on filtration.

Charge retention is crucial in air filter media, in which the nonwoven fibers are electrically charged. Nano-roughness is known to improve hydrophobicity at the solid-liquid interphase. In this work, nano-roughness is introduced to melt-blown iPP fibers via the formation of shish-kebab crystallites.

The shish-kebab formation seems to occur only in the presence of high MW iPP chains. Hence, using microscopy and thermal analysis, crystalline structure in melt-blown iPP fibers with MW~50 kg/mol was studied; at the presence of different amounts (0.0-12.8 wt.%) of high MW~500 kg/mol iPP, blended via melt extrusion. In addition, electrical charge retention in the resulting nonwoven media was investigated through discharging, using saturated IPA vapor. Not only from microscopy and thermal analysis was it evident that the shish-kebab structure was most prevailing for the iPP fibers with 3.0 wt.% high MW component, but also charge retention was the highest for these fibers. Based on the increasing trend in fiber diameter and melt viscosity among fibers with 3.0-12.8 wt.% high MW component, the smaller presence of shish-kebab in the crystalline structure of these fibers is attributed to lower elongation in the melt-spinning process for these fibers. The shish-kebab structure adds nano-roughness to the surface of the melt-blown iPP fibers, causing the formation of IPA droplets to become more difficult. This seems to contribute to the resulting fibers' resistance to IPA-induced discharging.

8:15 PM SM07.08.03

Late News: A Fabrication Process Based on Block Copolymer Self-Assembly for Three-Dimensional and Hollow Composite Nanostructures with Noble Metal Nanoparticles Embedded in Carbon Matrices Gun Ho Lee and Yeon Sik Jung; Korea Advanced Institute of Science and Technology, Korea (the Republic of)

In the last decades, growing concerns in global warming and environmental issues have inspired developments of diverse green and sustainable energy technologies. In particular, proton exchange membrane fuel cells (PEMFCs), which produce electrical energy from hydrogen fuel, have gained significant interests as one of the leading candidates to replace conventional internal combustion engines that rely on hydrocarbon fuels. Despite their low greenhouse gas emissions, PEMFCs have been limited to niche applications due to the high cost and scarcity of platinum, which is an essential electrocatalyst material in the energy conversion system.

Consequently, most commercially available PEMFCs have adopted composite catalysts in forms of platinum nanoparticles randomly dispersed on zero- or one-dimensional carbon support materials to increase its catalytic efficiency and minimize the noble metal load. However, such platinum/carbon (Pt/C) electrocatalysts have yet to meet the cost, catalytic activity, and durability requirements to be commercially viable and demand further improvements in the electrocatalytic performance *via* morphological and compositional control.

Here, we present a fabrication method based on block copolymer self-assembly for highly controlled carbon-platinum composite electrocatalysts with superior catalytic performance. Self-assembled diblock copolymers were used as structure-directing frameworks, selectively incorporated with platinum precursor ions, and pyrolyzed to prepare carbon-metal composite nanostructures with well-defined, three-dimensional morphologies. The calcination process produced evenly distributed, size-controlled platinum nanoparticles embedded in the carbon matrices, which increased the carbon-metal interactions and enhanced the durability of the catalytic materials. We also discuss a novel self-assembly technique to develop hollow channels throughout the carbon support structures using the chemical differences between the two polymer blocks. The three-dimensional morphologies and hollow channels provided pathways for superior mass transport within the nanostructures and enhanced the catalytic activity of the noble metal nanoparticles. Electrochemical evaluations revealed that the fabricated composite nanostructures exhibited greater electrochemical surface area and durability compared to those of commercially available Pt/C catalysts, demonstrating the significant

enhancements in the catalytic properties made *via* morphological controls.

In addition, the fabrication process can be utilized to develop composite nanostructures with various noble metals other than platinum. We demonstrated three-dimensional composite nanostructures prepared with a number of noble metals nanoparticles, including ruthenium, rhodium, osmium, and iridium nanoparticles, embedded in carbon matrices. The block copolymer self-assembly technique was also employed here for flexible control of the nanostructures, including formation of the hollow channels. The versatility of the process can be utilized to fabricate composite nanostructures of carbon and noble metals arranged in diverse morphologies and compositions, optimized for respective applications.

8:30 PM SM07.08.04

Late News: Highly Dynamic BP-Based Nanocomposite Hydrogels for Biomedical Applications Weihao Yuan, Kunyu Zhang and Liming Bian; The Chinese University of Hong Kong, Hong Kong

Hydrogels are emerging biomaterials with desirable physicochemical characteristics. Doping of metal ions such as Ca^{2+} , Mg^{2+} , and Fe^{2+} provides the hydrogels with unique attributes, including bioactivity, conductivity, and tunability. Traditionally, this doping is achieved by the interaction between metal ions and corresponding ligands or the direct incorporation of as-prepared metal-based nanoparticles (NPs). However, these approaches rely on a complex and laborious preparation and are typically restricted to few selected ion species. Herein, by mixing aqueous solutions of ligands (bisphosphonates, BPs), polymer grafted with ligands, and metal ions, a series of self-assembled metallic-ion nanocomposite hydrogels that are stabilized by the in situ formed ligand-metal ion (BP-M) NPs are prepared. Owing to the universal coordination between BPs and multivalent metal ions, the strategy is highly versatile and can be generalized for a wide array of metal ions. Such hydrogels exhibit a wide spectrum of mechanical properties and remarkable dynamic properties, such as excellent injectability, rapid stress relaxation, efficient ion diffusion, and triggered disassembly for harvesting encapsulated cells. Meanwhile, the hydrogels can be conveniently coated or patterned onto the surface of metals via electrophoresis. This work presents a universal strategy to prepare designer nanocomposite materials with highly tunable and dynamic behaviors. Moreover, we demonstrated that the nanocomposite hydrogels doped with lanthanide ions exhibited a highly tunable fluorescent spectrum. We next applied the developed hydrogels to treat peripheral nerve injuries, which are of great clinical significance. We demonstrated that the nanocomposite hydrogels containing magnesium and bisphosphonates promoted peripheral nerve regeneration and achieved partial functional recovery in sciatic nerve injury rat model.

8:45 PM BREAK

9:15 PM SM07.08.05

Greener Synthesis of High Aspect Ratio Copper Oxide Nanowires for Potential Applications Gayani Chathurika Pathiraja and Hemali Rathnayake; University of North Carolina at Greensboro, United States

Controlled synthesis of one-dimensional nanostructures such as nanowires are most fascinating for wide range applications due to their superior performances based on quantum confinement effects. Here, we demonstrate a novel facile and greener synthesis method to fabricate high aspect ratio of one-dimensional CuO nanowires from directed self-assembly of $\text{Cu}(\text{OH})_2$ nanocrystals guided by the oriented attachment mechanism via post-annealing. This surfactant free, one-pot sol-gel route at low temperature allows us to make higher aspect ratio of CuO nanowires with controlled-dimensions over a large area. The respective Raman, XRD and XPS spectroscopies confirm the chemical composition of CuO nanowires and their purity. The synthesized CuO nanowires has average diameter of 26.5 ± 2.4 nm and aspect ratio of 280.9 ± 18.0 . Further, the analysis of electrochemical properties of synthesized CuO nanowires have shown the suitability for potential electrochemical applications of capacitors and energy storage devices.

9:20 PM SM07.08.06

Selective Nanoparticle Deposition in Polymers for Functional Composite Applications Sayli Jambhulkar, Dharnedar Ravichandran, Weiheng Xu, Yuxiang Zhu and Kenan Song; Arizona State University, United

States

Self-assembly can organize structures beyond the synthesis nanoscale and bridge to macroscale manufacturing, thus providing many device fabrications opportunities. For composite devices, the mixing of nanoparticles in polymers involves dispersion quality, interfacial interactions, and nanoparticle alignment. Among these parameters, the nanoparticle alignment is the most challenging. Our study has shown an efficient way to self-assemble nanoparticles based on surface topologies, roughness, and wetting conditions. In this research, we used photopolymers for the first layer deposition and surface topology control. Following the deposition of nanoparticles complies with this first layer and form cluster-based assembly with different densities. Our manipulation of the nanoparticle density via the secondary-bonding can tune the layered structure's mechanical and electrical properties, thus making them multifunctional devices. The same manufacturing is also applicable in general nanoparticles based on our observation of feasibility using 1D nanofibers and 2D nanoplatelets. The fabricated devices showed enormous potential in microelectronics, sensors, actuators, and smart materials in robotics.

9:25 PM SM07.08.09

High-Throughput Printing of Semiconducting Polymers by Meniscus Oscillated Self Assembly Jisoo Jeon^{1,1}, Alvin Tan², Jaeyong Lee³, Jin Kon Kim³, John Hart² and Jeong Jae Wie^{1,1}; ¹Inha University, Korea (the Republic of); ²Massachusetts Institute of Technology, United States; ³Pohang University of Science and Technology, Korea (the Republic of)

Controlled evaporative self-assembly of semiconducting polymers has mostly been limited to time-consuming solvent evaporation or non-continuous blade-casting techniques. In this study, we report a novel high-throughput continuous printing of poly (3-hexylthiophene 2,5-diyl) (P3HT) by a custom-made oscillatory roller. The roller oscillation generates a cycle of meniscus stick and slip motion per single rotation of the roller that induces a rapid self-assembly of P3HT lines. The printed P3HT lines demonstrate hierarchical structures: nanometer scale thickness, micron scale width, sub-millimeter pattern intervals, and millimeter to centimeter scale length with highly defined boundaries. Remarkably, the line width and the interval of P3HT patterns can be independently controlled by varying polymer concentrations, the rotation rates of the roller, and the stage speed. Furthermore, grazing incidence wide angle X-ray scattering (GIWAXS) revealed that the roller-blading technique dramatically enhances crystallinity of P3HT by shear-induced crystallization. This high-throughput printing process for hierarchical assembly will open new opportunities for printed electronics with wide ranges of engineering capability.

9:30 PM SM07.08.12

Phase Behavior of Colloidal Particles with Attractive Potentials Sanghyuk Park, Seung Yeol Lee and Shin-Hyun Kim; Korea Advanced Institute of Science and Technology, Korea (the Republic of)

The behavior of colloidal particles has been widely studied with interests in their dynamics and self-assembly. Specifically, since the phase behavior and lattice structures of colloids are similar to those of atoms, the main focus is on how to treat colloids as model atoms. In previous studies, colloids have been primarily considered as hard spheres on which only the infinite repulsion at contact distance is acting. This is to reflect a repulsion between atoms due to the overlap of electron clouds when they are getting close. Such hard-sphere systems have also been realized by matching refractive indices. The real atomic interactions, however, are different from that due to van der Waals (vdW) attraction. They are represented by well-known models such as Lennard-Jones, Mie, and Morse potential. Therefore, a colloidal system that takes attractive interactions into account should be developed for the modeling. Here, in that sense, the phase behavior of colloidal particles with attractive potentials is studied. Systems are designed to have both repulsive and attractive force among particles and analyzed using both DLVO theory and a non-DLVO interaction. To observe crystals with an optical microscope and UV-Vis spectrometer, dielectric colloids are chosen properly so that crystal lattices diffract a selected wavelength in the visible range resulting in structural colors. In experiments, polystyrene nanoparticles (PS NPs) synthesized via emulsion polymerization are used as building blocks. Then, PS NPs, sodium chloride, and

poly(Acrylamide-*co*-acrylic acid) (p(AM-*co*-AAc)) are mixed with different compositions in de-ionized water. The suspensions are confined in glass cells immediately and observed continuously until reaching an equilibrium state. There are three interactions among PS NPs. VdW attraction arises from the different dielectric constants between PS and water. Electric double-layer repulsion is derived by sulfate groups on the surface of PS NPs, which is reduced by charge screening due to a salt, sodium chloride. A depletion attractive force is given and modulated by depletants, p(AM-*co*-AAc). Within two days, colloidal systems have been clearly distinguished into 4 phases depending on the composition; each phase is labeled as “fluid”, “crystal/fluid”, “crystal/glass/fluid”, and “glass/fluid” phase based on whether crystals and aggregates are dominantly formed. At a low concentration of depletant and salt, none of the crystal or aggregate are observed at equilibrium, while only the aggregates are formed at high concentrations. In between, crystals with distinctive structural colors are detected. However, not all of the samples reach the equilibrium states in this short term. It was figured out that after a month, crystals are formed in the samples of which the compositions are at the boundary between the fluid and crystal/fluid phases, and their growth stops after 3 months. Interestingly, these crystals are dendritic-like and much larger over a few mm, while crystals formed in other conditions are polygon-shaped and smaller up to a few hundreds of μm . The interactions are then analyzed with pair-potentials derived from DLVO theory, Lifshitz’s continuum theory, and Asakura-Oosawa’s model. The osmotic contribution of depletants is adjusted theoretically because of its size-dependency. A total pair-potential is calculated by summing up three interaction potentials. From the developed potential curves, which are analogous to the atomic potentials, the information about equilibrium points as well as collision kinetics is obtained. By matching experimental results with pair-potentials, the energetic and kinetic range for the crystallization of spherical colloids have been demonstrated. The validity of analysis is verified using other types and sizes of colloids. In conclusion, the developed colloidal systems with attractive force will be a lot more reasonable to analyze the crystallization in terms of modeling the real atoms.

SYMPOSIUM SM08

Next-Generation Materials and Technologies for 3D Printing and Bioprinting
April 21 - April 22, 2021

Symposium Organizers

Shervanthi Homer-Vanniasinkam, University College London
Roger Narayan, North Carolina State University
Wai Yee Yeong, Nanyang Technological University
James Yoo, Wake Forest Baptist Health

Symposium Support

Bronze
MilliporeSigma

* Invited Paper

SESSION SM08.01: 3D Printing and Bioprinting I
Session Chairs: Roger Narayan, Franz Weber and Ian Wong
Wednesday Morning, April 21, 2021
SM08

8:00 AM INTRODUCTION

8:05 AM SM08.01.01

Expanding the Frontiers of Design and Additive Manufacturing for Biomaterials Joseph P. Crolla, Barnaby Hawthorn, Jackson C. Kirkman-Brown, Galane J. Luo, Rosemary J. Dyson and Lauren E. Thomas-Seale; University of Birmingham, United Kingdom

Design for Additive Manufacturing (AM) is widely acknowledged as a severe barrier to the progression of the technology. In terms of biomaterials, whilst AM provides unique opportunities for the design of geometries and material compositions, there remains a persistent problem in the trade-off between the desired mechanical properties and the material properties [1]. To overcome this challenge, a radically new interdisciplinary approach to the development of AM systems and design techniques for biomaterials is required. Rather than a bioinspired method towards designing a single product, this research outlines how the exploration of developmental biology can expand the frontiers of AM systems and design techniques [2].

The majority of AM techniques increase the part size through incremental fusion of the material. Considering the development of the human in-utero; life begins as a single cell, which eventually forms tissues and organs, growing and functioning in synergy. The essence of foetal development is a very sophisticated AM process; in-utero growth demonstrates intrinsically intertwined materials, design and manufacturing [2]. However, this synergy between materials, design and manufacturing is not reflected in AM.

The development of the foetus is fundamentally dependent on varying spatial and temporal stimuli through the pregnancy. Analogical reasoning between foetal development and AM highlights a complete lack of any tailored process parameters during manufacturing. Process parameters are currently predefined and remain constant. Yet the process parameters underpin the properties of the material. Temporal DfAM, the design of process parameters during an AM build, is proposed as a method of designing the properties of a material through a single part [3]. Whilst this approach has been demonstrated computationally, its application to biomaterials is novel.

Poly(vinyl alcohol) (PVA) cryogel is a biocompatible, synthetic hydrogel that can be physically cross-linked at sub-zero temperatures. The mechanical properties of PVA are tailored through concentration, molecular weight and the number and temperature profile of freezing and thawing cycles. This makes it a widely applicable biomaterial as a component of tissue constructs and diagnostic phantoms. A novel cryogenic 3D printer has been developed to facilitate the AM of PVA. In doing so, the geometric complexity of the meso and micro-structure of the material is vastly increased.

This presentation will demonstrate the application of the novel design technique TDfAM to a cryogenic 3D printing platform for PVA. Changing the fixed process parameters of cryogenic 3D printing leads to a change in the mechanical properties of the PVA. Thus, TDfAM, the variation of process parameters during an AM build, will be explored with respect to the local and global material heterogeneity and mechanical properties. This experimental work will be validated through computational simulations.

The limitations of the TDfAM technique and cryogenic 3D printing of PVA will be discussed with respect to the current barriers to their industrial and clinical translation. Finally, we will outline the next steps of this unique research trajectory, exploring new dimensions of developmental biology and how we can develop current research and extract more novel innovations in AM design and manufacturing systems.

[1] S. Miramini et al. (2020) *Journal of the Mechanical Behaviour of Biomedical Materials*, 103: 103544

[2] L.E.J. Thomas-Seale et al. (2019) *Cogent Engineering*, 6:1662631

[3] S. Saliba et al. (2020) *International Journal of Advanced Manufacturing Technology*, 106: 3849-3857

8:15 AM SM08.01.03

3D Printing of Active Devices for Drug Delivery and Sensing Roger Narayan; North Carolina State University, United States

Two photon polymerization is a 3D printing process that relies on the use of ultrashort laser pulses to selectively polymerize and solidify photosensitive materials. The quadratic character of the two photon absorption probability and the well-defined polymerization threshold of this process allow for the diffraction limit to be exceeded and structures with features below one micrometer to be prepared. Two photon polymerization has recently been used to fabricate many types of microstructured and nanostructured medical devices out of biocompatible inorganic-organic hybrid materials (such as zirconium oxide hybrid materials) and polymers for medical applications. The use of biocompatible photoinitiators, including a combination of riboflavin and triethanolamine, for two photon polymerization will be considered. Integration of electrochemical sensors with two photon polymerization-processed microneedles will be discussed. Assessment of the biocompatibility of two photon polymerization-processed materials using in vitro biological studies will be discussed. In addition, application-specific studies of two photon polymerization-processed medical devices for biosensing and drug delivery, including in vivo studies, will be described. Our results indicate that two photon polymerization provides many benefits for fabricating medical devices with small-scale features and unique drug delivery and biosensing functionalities.

8:25 AM *SM08.01.04

Maneuvering and Printing Liquids by Means of a Pyro-Electrohydrodynamics—How Overcome the Current Limits of Micro- and Nanoscale Bio-Printing Pietro Ferraro, Veronica Vespini, Romina Rega and Simonetta Grilli; Intelligent Systems CNR, Italy

Inkjet printing is a powerful enabling technology for formation of structures at micro and nanoscale for current most advanced fields of applications. As it is a direct fabrication approach, it has the undisputed advantage to avoid any masks, molds or lithography steps. Furthermore, in addition to this great flexibility, recently it has been demonstrated the capability of inkjet printing approaches to reach very high spatial resolution, down to nanoscale and over large area. Direct printing of micro and nano structures has been proofed with a variety of different inks and different types of materials. Different technologies exist, such as thermal jetting, piezo-based jetting, Electrohydrodynamic (EHD) jetting, syringe-based pumping or simply contact-dispensing printing. Each of the above-mentioned technologies is based on liquid media to be delivered in the jet printing process. Moreover, most of the existing methods include needles for liquid dispensing. Unfortunately, the use of needles has some severe limitations such as clogging and cross contamination. Here it will be presented some recent developments about a novel and special platform based on EHD jetting driven by a pyroelectric effect activated in a bulk ferroelectric crystal. What we named Pyro-EHD exhibits significant potentialities in allowing liquid dispensing and printing for a number of applications ranging from microelectronics to biotechnologies. One of the interesting features is that pyro-EHD can easily work in nozzle-less modality thus avoiding needles and consequently the related clogging drawbacks. The pyro-EHD printer approach usually dispenses liquids from a liquid reservoir that can be a sessile droplet or even the free surface of a liquid. The high potentials easily attainable through the ignition of the pyroelectric effect allow to maneuvering and dispense and print also high viscous polymers and liquids droplets. Description of the pyro-EHD will be provided. The results obtained will be shown and discussed. Several examples will be illustrated for direct printing of liquids under both single and multiphase forms that can find useful exploitation in a multiplicity of fields from microelectronics to biomedical applications.

[1] P. Ferraro, S. Coppola, S. Grilli, M. Paturzo, V. Vespini, *Nature nanotechnology*, (2010), 5, 429.

[2] Grilli, S., Coppola, S., Vespini, V., Merola, F., Finizio, A., & Ferraro, P. (2011). 3D lithography by rapid curing of the liquid instabilities at nanoscale. *Proceedings of the National Academy of Sciences*, 108(37), 15106-15111.

[3] Ferraro, P., Grilli, S., Miccio, L., & Vespini, V. (2008). Wettability patterning of lithium niobate substrate by modulating pyroelectric effect to form microarray of sessile droplets. *Applied Physics Letters*, 92(21), 213107.

[4] Coppola, S., Vespini, V., Nasti, G., Gennari, O., Grilli, S., Ventre, M., ... & Ferraro, P. (2014). Tethered

pyro-electrohydrodynamic spinning for patterning well-ordered structures at micro-and nanoscale. *Chemistry of Materials*, 26(11), 3357-3360.

[5] Nasti, G., Coppola, S., Vespini, V., Grilli, S., Vettoliere, A., Granata, C., & Ferraro, P. (2020). Pyroelectric tweezers for handling liquid unit volumes. *Advanced Intelligent Systems*, 2000044.

[6] Coppola, S., Nasti, G., Vespini, V., & Ferraro, P. (2020). Layered 3D printing by tethered pyro-electrospinning. *Advances in Polymer Technology*, 2020.

[7] Vecchione, R., Coppola, S., Esposito, E., Casale, C., Vespini, V., Grilli, S., ... & Netti, P. A. (2014). Electro drawn drug loaded biodegradable polymer microneedles as a viable route to hypodermic injection. *Advanced Functional Materials*, 24(23), 3515-3523.

8:50 AM *SM08.01.05

Osteoconduction and Bone Augmentation—When 3D-Printed Designs Meet Bone Biology Franz E. Weber; University Zurich, Switzerland

In the last decades, advances in bone tissue engineering mainly based on osteoinduction and on stem cell research. Only recently, new efforts by others and us focused on the micro- and nanoarchitecture needed to improve and accelerate bone regeneration. By the use of additive manufacturing, libraries of diverse microarchitectures were produced and tested to identify the ideal pore size or rod distance for osteoconduction to occur. Presently, we try to elucidate the dependency of osteoconduction on microporosity and expand our view on micro- and nanoarchitecture of bone substitutes for optimal bone augmentation.

For the production of scaffolds, we applied for titanium-based scaffolds selective laser melting and for ceramics the CeraFab 7500 from Lithoz, a lithography-based additive manufacturing machine. As in vivo test model, we used a calvarial defect and a bone augmentation model in rabbits. The histomorphometric analysis showed that bone formation was significantly increased with pores between 0.7-1.2 mm in diameter. Moreover, microporosity appeared to be a strong driver of osteoconduction and influenced osteoclastic degradation. Best microarchitecture for osteoconduction and bone augmentation are different.

In essence, additive manufacturing enabled us to generate libraries of microarchitectures to search for the most osteoconductive microarchitecture and the ideal microarchitecture for bone augmentation purposes. Moreover, additive manufacturing appears as a promising tool for the production of personalized bone tissue engineering scaffolds to be used in cranio-maxillofacial surgery, dentistry, and orthopedics.

9:15 AM *SM08.01.06

Light-Directed 3D Printing of Hydrogels and Elastomers for Microfluidic Devices Ian Y. Wong; Brown University, United States

Additive manufacturing of hydrogels or elastomers can be used to fabricate microfluidic channels with biomimetic functionality. For instance, atomically thin sheets of nanomaterials can augment organic polymers with enhanced mechanical and physical functionalities. These 3D printed structures can further exhibit stimuli-responsive behaviors such as actuation, self-adhesion, or degradation. Here, we present recent results on light-directed 3D printing of next generation materials using covalent and ionic crosslinking. First, we explore the use of versatile alginate hydrogels with graphene oxide to pattern collective cell migration, tune stimuli-responsive behaviors, and repel oil in seawater like conditions. Second, we demonstrate double network hydrogels that are stimuli-responsive and self-adhesive as a simple “do-it-yourself” construction set for soft machines and microfluidic devices. This approach enables “plug-and-play” hydrogel parts for ionic soft machines that emulate actuation, sensing, and fluid transport in living systems. Finally, we investigate the use of 3D printed elastomers for microfluidic devices to achieve perfusion of tissue fragments for preclinical testing of immunotherapies. Overall, 3D printing enables multiscale integration of nanomaterial and polymeric building blocks into bespoke larger scale structures for advanced materials and biomedicine.

SESSION SM08.02: 3D Printing and Bioprinting II

Session Chair: Fiorenzo Vetrone

Wednesday Morning, April 21, 2021

SM08

11:45 AM INTRODUCTION

11:50 AM *SM08.02.02

Using Bioprinting to Create Personalized In Vitro Tumor Models Joseph Kinsella, Jacqueline Kort-Mascort, Salvador Flores-Torres and Veena Sangwan; McGill University, Canada

The tumor microenvironment (TME) is a dynamic cellular and biochemical system, integrating multiple positive and negative biological feedback loops that influence cell physiology. Cell-extracellular matrix, secreted factor-cell signaling pathways, and cell-cell interactions are known factors in tumorigenicity and drivers of therapeutic resistance. There is, therefore, an urgent need to develop clinically relevant in vitro platforms comprising epithelial and stromal cells in an extracellular matrix mimicking microenvironment. Three-dimensional (3D) cell culture and co-culture of cancer cells have demonstrated that creating physiologically representative tumor microenvironment in vitro models enables patient-specific experiments to be performed. Typically, these are performed by casting cells within a droplet of Matrigel, or commercially available biocompatible hydrogels, promoting the self-assembly of multi-cellular organoids. While these systems provide a more relevant microenvironment than monolayers, the resulting organoids have limited user input over parameters such as the initial location of different cell types.

We have recently developed extracellular matrix mimicking hydrogel biomaterials capable of hosting cells, and subsequently, being extruded to form complex in vitro tumor models. Our lab has previously demonstrated that composite materials constituted of sodium alginate, a seaweed-derived polysaccharide, and gelatin, a bovine or porcine-derived denatured collagen, can be tuned to recapitulate the mechanical properties of soft tissues while keeping their biocompatibility and printability. Here, we report a bioink prepared by decellularizing tissue and incorporating sodium alginate and gelatin at controlled weight percentages as rheological modifiers to reinforce and positively impact the composite material's mechanical integrity. dECM contains structural proteins, glycosaminoglycans, and growth factors preserved from the tissue of origin. Gelatin provides mechanical stability during the printing process, and crosslinked-alginate chains maintain sample integrity in long-term cell culture conditions.

We have demonstrated this methodology to create breast and head and neck tumor models using immortalized cell lines and, more recently, lung, gastric, and breast models derived from patient tumor samples to create precision interventional schemes. Of particular interest is the ability to build complex 3D geometric structures using soft materials (bioinks) that recapitulate the mechanical properties such as the stiffness of solid tumors and their microenvironment. Bioprinting permits more complex geometric matrices to be printed with high cell density, control over cell location, and viability. Bioprinted models can be created directly with precise reproducibility from cell-hydrogel suspensions with high throughput and scalability directly on to well plate platforms. In collaboration with the Sangwan and Ferri labs at the Goodman Cancer Research Centre at McGill University, we have further explored using biobanked tissue samples to develop personalized tumor models.

12:15 PM SM08.02.03

3D Printing of Cellulose with Controllable Mechanical Properties Jungang Jiang, Yuan Chen, Jason Yu and Feng Jiang; The University of British Columbia, Canada

Three-dimensional hierarchical structures with controllable mechanical properties are expected to have wide range of applications. In general, material properties depend on the building block and it remains challenging to develop materials with dramatically different mechanical properties from the same type of material. In this

presentation, cellulose was demonstrated for 3D printing of two types of structure. In one case, a lightweight ($\sim 90 \text{ mg/cm}^3$) and super-strong (16.6 MPa compressive Young's modulus) honeycomb structure is constructed by 3D printing of cellulose ink dissolved in NaOH/urea solution. The 3D printed cellulose structure demonstrated switchable high elasticity (to withstand varied repetitive elastic deformation) at the wet state and high rigidity (to support over 15,800 of its own weight) at dry state. In another case, we demonstrated a compressible and superelastic 3D printed structure based on cellulose nanofibrils. The 3D structure showed superb elasticity (over 91% strain recovery after 500 cycles of compressive test) and compressibility (up to 90% compressive strain). In addition, with the incorporation of salt, the 3D printed CNF structure was demonstrated to serve as pressure sensor with high pressure sensitivity of 0.337 kPa^{-1} at 43% relative humidity. These results indicate that the mechanical properties of the 3D printed cellulose structure can be facilely controlled by the inter-fibril interactions, leading to either super-strong or super-elastic materials properties.

12:25 PM SM08.02.04

3D Printed Bioplastics with Shape-Memory Behavior Based on Bovine Serum Albumin Eva Sanchez^{1,2}, Patrick Smith¹, Alvaro Gomez-Lopez², Maxence Fernandez³, Aitziber Cortajarena³, Haritz Sardon² and Alshakim Nelson¹; ¹University of Washington, United States; ²University of the Basque Country, Spain; ³CIC biomaGUNE, Spain

Bio-sourced materials that can replace existing petroleum-based materials are an integral component of sustainability. Moreover, biomaterials with greater complexity and functionality will be required to meet the demands for the full spectrum of applications from aerospace to medicine. The unique features of proteins (such as the mechanical properties of spider silk) have inspired the development of protein-based plastics, but their application is limited by poor processability and limitations in mechanical performance.

Both 3D and 4D additive manufacturing (AM) processes that utilize vat photopolymerization have tremendous potential in industrial manufacturing for the future production of parts and supplies. Naturally occurring polymers often require modification with photocurable functionalities to become printable. Most notably, methacryl groups have been introduced onto the amines of biopolymers to afford polymerizable materials like gelatin methacrylamide (Gel-MA), silk fibroin methacrylate (Sil-MA), and methacrylated bovine serum albumin (MA-BSA). While 4D printed structures that undergo chemical or physical changes in response to their environment are often inspired by nature, there are relatively few examples that use bio-sourced and biodegradable materials.

Both structural and globular proteins are known as macromolecules that can introduce material plasticity or elasticity based on the unfolding or disassembly of the proteins. Proteins can be unravelled reversibly or irreversibly upon the application of a tensile force, thus, the secondary and tertiary structure of proteins have been utilized to achieve biomaterials with unique combinations of extensibility, strength, and resilience. More recently, BSA was incorporated into hydrogel networks to provide an energy dissipation mechanism via protein unfolding. However, there has not been a demonstration of a protein-based material that exhibits plasticity due to unfolding, with a corresponding shape recovery back to its original form.

We formulated a simple aqueous-based resin for laser-scanning SLA printing based on BSA in a photocurable resin. BSA is an abundant globular protein with excellent aqueous solubility and low viscosity at concentrations up to 30 wt%. Furthermore, we demonstrated that the native conformation of these globular proteins is largely retained in the 3D printed constructs, and that each protein molecule possesses a "stored length" that could be revealed during mechanical deformation (extension or compression) of the 3D bioplastic objects. Given the large molecular weight of BSA (66 kDa), the potential for unfolding individual protein chains can be significant, as exhibited by the plasticity observed in these thermoset materials. We expect this strategy – wherein globular proteins are utilized to afford 3D printed bioplastics with mechanical properties that utilize the stored length of these macromolecules – is broadly applicable to other forms of vat photopolymerization to create constructs that can create a closed loop life cycle with bioplastics. In short, we introduced a bio-sourced resin for additive manufacturing that can be used to fabricate in a rapid manner complex elements for a wide range of applications, with a very interesting stimuli response of the printed parts, due to the conformational changes of proteins at the molecular level.

12:35 PM *SM08.02.05

NIR Excited, UV Emitting Nanoparticles Fiorenzo Vetrono; Institut National de la Recherche Scientifique, Université du Québec, Canada

Luminescent lanthanide doped nanoparticles have received significant attention due to their fascinating optical properties. At the core of this interest is their ability to convert near-infrared (NIR) excitation light (typically 980 or 800 nm) to higher energies spanning the ultraviolet (UV), visible and higher energy NIR regions of the spectrum through a multiphoton process known as upconversion. Upconversion differs from conventional multiphoton excitation in other materials where no real intermediate states are present necessitating the use of ultrafast lasers (in the femtosecond regime) for simultaneous excitation to the upper emitting state. The lanthanide ions possess a multitude of $4f$ electronic energy states that have long lifetimes (micro- to millisecond) thus act as population reservoirs in the upconversion process. Hence, upconversion occurs through real, long-lived intermediate states through a sequential photon absorption process. This eliminates the need for ultrafast excitation and as a result, upconversion can be observed using inexpensive, continuous wave diode lasers. Upconversion luminescence can be exploited for a number of applications in nanomedicine, theranostics, photovoltaics, photocatalysis, as well as many others.

In this presentation, we will discuss the synthesis of these nanoparticles, establish how changing their nanoscale architecture can affect their luminescence properties and upconversion, as well as discuss their applications in nanomedicine, theranostics and potentially in 3D printing.

1:00 PM SM08.02.06

Feedstock Engineering and Rheology Scaling of Metal-Polymer Composites for the Filament Extrusion and Fused Deposition Modeling Amm G. Hasib and Bruno Azeredo; Arizona State University, United States

Fused Deposition Modeling (FDM) has been adapted to metals using filaments made of metal particle reinforced polymer matrix composites (PMC). However, there is still a fundamental gap in understanding how its melt suspension rheology affects the ability to extrude and print filaments continuously without jamming. In this correlative study, a framework for studying rheological scaling is presented as function of increasing metal content (i.e. gas atomized NiCu) in a thermoplastic binder (i.e. PLA), and it was shown that, even with high zero-shear viscosities (more than 1×10^5 Pa-s), high metal content composites showed a dramatic shear thinning behavior and hence were extrudable at a content of 54 vol% of metal. Extruded filaments were re-melted and submitted to flow sweep rheology test. The zero-shear viscosity scaling with metal content fits well with the existing theoretical model of Krieger and Daugherty, but it was not sufficient to predict the extrudability of the filament due to its complex shear thinning behavior. Additionally, the filaments displayed premature slippage onset at $<10 \text{ s}^{-1}$ which is typically below those observed inside of the die during extrusion indicating potential change in the flow regime during extrusion. The homogeneity of composite filaments was also analyzed in global scale (by doing thermogravimetric analysis of the 12 ft continuously extruded filaments along the length to find out the metal vol%) and local scale (by analyzing a small cross-section in X-ray micro-tomography). It was verified that the filament content was uniform up in filaments with a maximum metal content of 54%. This strategy of homogeneously packing gas atomized metal spheres at higher metal content, gave us the insights on how to scale and modulate the melt rheology to create consistently extrudable and uniform dense metal filaments easily without using any kind of additives.

1:10 PM SM08.02.07

Integrated Nonthermal Plasma Synthesis and Inkless Aerosol Jet Printing of Nanoparticles Alexander Ho and Rebecca Anthony; Michigan State University, United States

Nonthermal plasmas have proven to be an effective method for the synthesis of high-quality nanoparticles. The nonthermal plasma environment allows for crystallization despite the low temperature, suppression of particle agglomeration, and control over particle size through manipulation of the synthesis conditions. Typical nonthermal plasma reactors operating under vacuum are fairly large and costly. By operating at atmospheric

pressure and miniaturizing the reactor, costs of the system are reduced and the ability to scale the process is enhanced. Reactors often benefit from confinement to the microscale at atmospheric pressure, this reduction in size lends itself well to act as a deposition head for additive manufacturing processes. Here we present our work on the synthesis and deposition of nanoparticles into ordered patterns and structures. A 13.56 MHz RF power supply was used to generate a plasma in a glass capillary tube between two external ring electrodes at atmospheric pressure. Supplied to the reactor was a precursor gas of silane and a background gas of argon for the synthesis of silicon nanoparticles. The reactor was attached to a computer-controlled gantry and stage for the controlled deposition of the nanoparticles. The gas phase synthesis method inherently produces an aerosol of nanoparticles without the need of an atomizer as is required in typical aerosol jet printing processes (AJP). Typical AJP requires the use of an ink for atomization whose properties must be precisely to known to reduce losses during transportation and deposition. From TEM and XRD analysis we have been able to deposit crystalline silicon nanoparticles with tunable particle sizes approaching the Bohr-exciton radius of silicon that also exhibit a fairly narrow size distribution without the use of an ink. Further by varying synthesis conditions during deposition we have been able to print materials whose properties vary spatially along the deposition. Further the particles were deposited with linewidths as small as 100 microns and layer thicknesses of 1.5 microns.

SESSION SM08.03: 3D Printing and Bioprinting III
Session Chairs: Sankha Banerjee and Wenzhuo Wu
Wednesday Afternoon, April 21, 2021
SM08

2:15 PM SM08.03.01

Water Confinement and Swelling Kinetics of Photo-Crosslinked Hydrogels Using Micro-3D Printing Afra S. Alketbi, Hongxia Li, Aikifa Raza and TieJun Zhang; Khalifa University of Science and Technology, United Arab Emirates

Hydrogels are recognized as one of the most promising functional materials, as it is dynamic, tunable, biocompatible, biodegradable and able to encapsulate large water content. Owing to these unique characteristics, hydrogel based systems are revolutionizing many applications in solar energy water nexus, biomedical engineering, drug delivery and soft electronics. Hydrogel materials endow an intriguing activation phenomenon on water molecules confined in hydrogel meshes. By altering resin formulation and crosslinking density of photocrosslinked hydrogels, we are able to manipulate the water states within the hydrogel. The water states as well as the degree of photopolymerization are characterized by confocal Raman microscopy. Moreover, 3D microstructures of responsive hydrogels are fabricated using high resolution micro projection stereolithography. The transition from 3D hydrogel microstructures to 4D is studied during its response to external stimuli such as temperature and moisture, and its swelling dynamics is monitored through in situ condensation experiments using the environmental scanning electron microscopy. Finally, by fabricating functional hydrogel devices with tunable water states, we aim at developing high resolution 3D printing technologies for broad energy and sustainability applications.

2:25 PM SM08.03.02

Wear Resistance and Microstructure of 3D-Printed High Density Polyethylene/Ultra High Molecular Weight Polyethylene Reactor Blend Sahitya Movva, Hamid Garmestani and Karl Jacob; Georgia Institute of Technology, United States

Wear resistance and microstructure of potential prosthetic hip and joint bioimplant material system, a reactor blend of high density polyethylene (HDPE) and 10 wt% ultra high molecular weight polyethylene (UHMWPE), 3D printed using fused deposition modeling (FDM) with different printing speeds and printing orientations have

been studied using microscratch tester and wide angle X-ray diffraction respectively and compared with those of injection molded samples. The microstructure has been represented in terms of texture components using pole figures and orientation distribution functions (ODFs). This study investigates how 3D printing parameters affect texture and how global combination of the texture components prevalent in different plastic regimes engender material responses to wear resistance. The effect of abrasion and change in wear resistance of the bioimplant material (HDPE+10wt%UHMWPE) system have been explored by varying the loads applied, scratch directions, scratch speeds and the number of recurring scratches within the microscratch tests. This study of correlation between wear resistance and texture suggests that improved wear resistance in the (HDPE+10wt%UHMWPE) system can be achieved by texturing the bioimplant material in the loading direction.

Keywords: High density polyethylene; Ultra high molecular weight polyethylene; 3D printing; Fused Deposition Modeling (FDM); Wear resistance; Texture; Bioimplant material;

2:35 PM SM08.03.03

Additively Manufactured Magnetolectric Multifunctional Materials Steven Malley, Scott Newacheck and George Youssef; San Diego State University, United States

Magnetolectric materials are an important class of multifunctional materials with applications spanning from wearable electronics to space exploration. The current state-of-the-art in processing this exciting class of materials heavily rely on vacuum-based methods, increasing the complexity and hindering their translational potential. Magnetolectric materials couple, intrinsically or extrinsically, the magnetic and electric energies through several mediators, including strain, charge, and spin, making them imperative for straintronics, optoelectrics, and spintronics applications. The objective of this research is to report a novel processing method of polymer-based magnetolectric composite materials using additive manufacturing technique. The latter is parametrically different than the state-of-the-art, resulting in reducing cost, increasing yield, and streamlining processing of multifunctional materials. The approach is realized composites of electroactive polymer with large piezoelectric properties and magnetic particles using digital light processing technique (DLP), whereas the application of an electric field across the surface results in change in magnetization while a magnetic field changes the state of polarization, hence the magnetolectric coupling. Notably, previous research has shown that the suspension of nanoscale magnetic particles increased the dielectric properties of the electroactive phase without affecting its piezoelectric response. A photopolymer resin is used as the binder, which is activated by the light source in the printer within the ultraviolet spectrum. Additive manufacturing with DLP technique produces lightweight and nearly isotropic structures with high geometrical accuracy, in comparison with other methods such as material extrusion. Samples with different volume fractions of magnetic particles and electroactive polymers were fabricated and characterized. To establish the process-property-performance interrelationship, the mechanical, electrical, magnetic, and magnetolectric properties were exhaustively investigated of DLP processed sample. The mechanical properties were investigated using a standard load frame equipped with a ± 1 kN load cell and long travel extensometer. The response of the material to external load will describe the mechanical utility of the material. The electrical properties were characterized based on the hysteretic response collected using the Sawyer-Tower circuit while subjecting the sample to AC electric field. Finally, the magnetolectric (ME) coupling coefficient was measured using vibrating-sample magnetometer (VSM), inducing an AC magnetization in the sample while measuring the resulting change in voltage. The ME coefficient, defined as the ratio between the resulting electric field to applied magnetic field, is the main performance matrix of the efficacy of the magnetic to electric energy conversion. The results indicate the suitability of DLP additive manufacturing to efficiently produce magnetolectric composites. Future research will focus on enhancing the properties and further streamline the fabrication process.

2:45 PM *SM08.03.04

Hybrid Nanomanufacturing for Wearable Intelligence Wenzhuo Wu; Purdue University, United States

The seamless and adaptive interactions between functional devices and their environment (e.g., the human body) are critical for advancing emerging technologies, e.g., wearable devices, consumer electronics, and

human-machine interface. The state-of-the-art technologies, however, require a complex integration of heterogeneous components to interface the environmental mechanical stimulus, which is ubiquitous and abundant in the above applications. Moreover, all existing technologies require a power source, which complicates the system design and limits operation schemes.

I will discuss our recent progress in developing self-powered human-integrated nanodevices through the hybrid nanomanufacturing (e.g., 3D printing of self-assembled function materials) of heterostructured nanodevices with hierarchical architectures. This new class of wearable devices are conformable to human skins and can sustainably perform non-invasive functions, e.g., physiological monitoring and gesture recognition, by harvesting the operation power from the human body. This research is expected to have a positive impact and immediate relevance to many societally pervasive areas, e.g., biomedical monitoring, consumer electronics, and intelligent robotics.

3:10 PM SM08.03.05

Adaptive Multinozzle for Conformal Direct Ink Writing Sebastien Uzel^{1,2}, Robert Weeks¹, Michael Eriksson¹, Dimitri Kokkinis¹ and Jennifer Lewis^{1,2}; ¹Harvard University, United States; ²Wyss Institute, United States

Direct ink writing (DIW) is a versatile additive manufacturing technique for patterning a wide variety of materials in three dimensions and is particularly well suited for printing assemblies of multiple functional materials, with electrical, optical, structural or biological properties. Currently, DIW is hindered by a relatively low throughput, which limits the potential applications and suitability for larger-scale manufacturing. To increase the throughput of DIW while retaining its unique advantages, multinozzle DIW printheads have been developed in order to accommodate for the simultaneous deposition of up to 64 filaments. However, this process has been constrained to printing on flat substrates, thereby excluding its use for the functionalization of pre-existing surfaces. To circumvent this shortcoming, we designed an adaptive multinozzle printhead and combined it with non-contact surface profilometry for high throughput printing on non-planar surfaces. The printhead is comprised of 16 nozzles positioned in a linear array and individually actuatable by a set of stepper motors in order to conform its geometry to the underlying substrate topography. We demonstrate that this novel printhead can successfully and rapidly deposit viscoplastic inks onto surfaces with complex profiles. More importantly, we show that this adaptive multinozzle approach can be applied to restore the mechanical integrity of damaged solids via the conformal extrusion of structural elastomeric inks or cover wound regions of human limb models using biological inks.

3:20 PM DISCUSSION

3:45 PM SM08.03.07

Hydrogel 3D Fabrication to Introduce Vascular Networks Using Digital Light Processing Livia Kalossaka, Ali Mohammed and Connor Myant; Imperial College London, United Kingdom

Biomaterials that closely mimic the complex structural organization of natural tissues hold great promise for regeneration of tissues. Hydrogels have emerged as leading candidates to reproduce native extracellular matrix. In order to provide structures and functions similar to native tissues, controlled porosity and vascular networks are required. However, fabrication techniques to introduce these are still limited. In this study we propose a comparison on fabrication techniques to achieve 3D vascular networks using water based solvents only. Diagnostic methodologies to optimize printing parameters and mechanical characterization are performed on the formulated hydrogel compositions.

With the adequate choice of ingredients and fillers for photocurable formulations, structural and functional properties of the fabricates scaffold can be tailored, opening the path for advanced applications.

Exploring both natural and synthetic hydrogels formulations, fabrication of vascular networks using Digital Light Processing (DLP) is assessed. An analysis of the achieved vascularization morphologies is performed to yield a library of fabrication parameters and hydrogel formulations for future applications.

3:55 PM SM08.03.08

Printed Biofoams via Large Scale Additive Manufacturing: Microcellulose Fiber - PLA Foams Halil L. Tekinalp¹, Stefan Dopatka², Tyler Smith¹, Vipin Kumar¹, Katie Copenhaver¹, James Anderson³, Yousoo Han³, Douglas Gardner³, William Peter¹ and Soydan Ozcan¹; ¹Oak Ridge National Laboratory, United States; ²Oak Ridge Associated Universities, United States; ³University of Maine, United States

Polymer additive manufacturing (AM) is a rapidly growing technology and it is transitioning to become an advanced manufacturing technique with the introduction of fibrillar reinforcing materials and the recent developments in large scale AM. While carbon and glass fibers are mainly used as reinforcing phase in polymer composites, as a result of increasing environmental and long-term sustainability concerns, there is an increasing interest in using bio-derived cellulose fibers to reinforce polymers instead. The ability of freeform manufacturing of parts with complex geometries makes large scale AM attractive for various applications; however, different applications require different material properties. One of the interesting application areas for large scale AM is printing of lightweight materials via extrusion foaming. While density is a key property in light weighting, mechanical performance is also important for many lightweight applications. The purpose of this study is to understand the impact of microcellulose fibers (MCF) on foaming behavior and the mechanical properties of additively manufactured parts. MCF-PLA feedstock pellets at varying MCF content (5, 10, 15 and 20wt%) were prepared to understand the impact of cellulose fiber content on density and mechanical properties of the AM biocomposites. Also, the impact of foaming agent content as well as extrusion rate on the AM biocomposites are investigated. Although achieving printed parts with uniform foam structure with the presence of cellulose fibers was challenging, initial results are promising, reaching density values below 0.5g/cm³.

4:05 PM SM08.03.09

Ex-Situ Surface Modification of Biocompatible 3D Printed Polylactic Acid (PLA) using Plasma Micro Discharge: Towards the Enhancement of Cell-Selective Surfaces Jack Luong¹, Mai T. Yang¹, Mandeep Singh¹, Shervin Zoghi¹, Subhadip Sarkar¹, Edbertho Leal-Quiros², Saquib Ahmed³ and Sankha Banerjee¹; ¹California State University, Fresno, United States; ²University of California, Merced, United States; ³Buffalo State College, United States

Cell growth and cell adhesion on biocompatible polymers are affected by the surface energy and the interfacial properties. One of the major factors that affect adhesion is contamination by different microorganisms. This contamination and simultaneous growth of microorganisms can affect the quality and quantity of healthy cells that grow on the surface. Polylactic Acid (PLA) is a biodegradable polyester material produced from renewable resources like biomass. Additionally, its biocompatibility has permitted its use in the food packaging and the biomedical industry. Despite its benefits, PLA intrinsically lacks in strength, durability, and adhesiveness. This study focuses on mitigating these problems by incorporating surface modification techniques to increase the surface roughness of PLA. PLA samples were 3D printed and then treated with Corona discharge, a method widely used in a variety of industries because of its safety, low cost, and overall effectiveness. After treatment and surface modification, the material properties of the samples were characterized by using Impedance Spectroscopy, Raman spectroscopy analysis, and Optical Profilometry. The results of these studies showed a significant improvement in the surface properties that promote cell affinity and adhesion.

SESSION SM08.04: 3D Printing and Bioprinting IV
Session Chairs: Showan Nazhat and Swee Leong Sing
Wednesday Afternoon, April 21, 2021
SM08

5:15 PM *SM08.04.01

Injectable Hydrogel Micro-Scaffolds Encapsulating Conjunctival Stem Cells for Subconjunctival Ocular

Delivery Zheng Zhong, Wisarut Kiratitanaporn, Jacob Schimelman, Min Tang and Shaochen Chen; University of California, San Diego, United States

Ocular surface diseases including conjunctival disorders are multifactorial progressive conditions that can severely affect vision and quality of life. With more than ten million new diagnosis worldwide each year, patients suffering from these severe forms of ocular diseases will often need surgical intervention to regenerate the ocular surface, especially the conjunctiva, to restore vision. With the development of advanced regenerative medicine and stem cell technologies, growing attention over the past decade has turned towards the utilization of stem cell therapy for ocular surface diseases, and stem cell therapies based on conjunctival stem cells (CjSCs) have become a potential solution for treating ocular surface diseases. However, neither an efficient culture of CjSCs nor the development of a minimally invasive ocular surface CjSC transplantation therapy has been reported. The goal of this study was to develop a robust *in vitro* expansion method for primary rabbit-derived CjSCs and applied digital light processing (DLP)-based bioprinting to produce CjSC-loaded hydrogel micro-scaffolds for injectable delivery. Expansion medium containing small molecule cocktail that performed dual SMAD signaling inhibition (dSMADi) and ROCK signaling inhibition (ROCKi) generated fast dividing and highly homogenous CjSCs for more than 10 passages in feeder-free culture while maintaining the expression of stemness markers (ABCG2, KRT14, P63). With our customized DLP-bioprinting system, the elastic modulus of gelatin methacryloyl (GelMA) hydrogel micro-scaffolds was tuned to enable the 3D culture of CjSCs while supporting their viability, stem cell phenotypes, and the differentiation potential into conjunctival goblet cells. Our bioprinting system also enabled rapid fabrication of 18 cellularized hydrogel micro-scaffolds simultaneously with customizable geometries in less than a minute. These hydrogel micro-scaffolds were well-suited for scalable dynamic suspension culture of CjSCs. The bioprinted hydrogel micro-scaffolds in (100 μm diameter and 100 μm in height) were shear thinning and successfully delivered to the bulbar conjunctival epithelium via minimally invasive subconjunctival injection. This is the first report on the development of bioprinted injectable CjSC-loaded hydrogel micro-scaffolds and the establishment of protocols for robust *in vitro* expansion of CjSCs. Overall, this work serves as an important framework for understanding the conjunctival stem cell population, conjunctival epithelial biology, as well as the application of CjSCs as a clinically translatable strategy for minimally invasive treatments of severe ocular surface diseases.

5:40 PM *SM08.04.02

***In Situ* Alloying by Powder Bed Fusion as a Rapid Alloy Design Tool for Biomedical Applications** Swee Leong Sing; Nanyang Technological University, Singapore

The design of new alloys for metal additive manufacturing (AM), or 3D printing, is an essential research field to encourage higher adaption of AM in the industries. Currently, pre-alloyed powders are typically used in metal AM. Pre-alloyed powders are expensive and inflexible in terms of chemical composition. *In-situ* alloying, which makes use of powder blends, enables high-throughput experimental alloy design and screening. This production approach allows high flexibility in varying the chemical composition.

For bulk sample production, laser powder bed fusion of elemental powder blends was applied to build up titanium-tantalum alloy as proof of concept. Tantalum is an excellent choice for alloying with titanium for biomedical applications due to its' high biocompatibility, corrosion resistance and good mechanical properties. Furthermore, titanium-tantalum alloys are promising materials for such applications because of high strength to modulus ratio. Despite the promising characteristics, they are still not widely used due to the difficulty in alloying titanium with tantalum as a result of their difference in melting point and density. *In-situ* alloying has been shown to be an effective approach in creating these alloys. The material processed were characterised using optical microscopy, electron backscatter diffraction, scanning electron microscopy, energy-dispersive X-ray spectroscopy, X-ray diffraction, hardness and tensile testing.

6:05 PM SM08.04.04

Mechanical Properties of Aligned Graphene-Polymer Composites Fabricated Through Stereolithographic 3D Printing Changquan Lai; Nanyang Technological University, Singapore

The advent of additive manufacturing has enabled many complex, optimized structures to be realized efficiently and reliably, improving the performance of many applications where these architected materials are employed. Nevertheless, many of the materials that are currently compatible with 3D printing exhibit mechanical properties that are far from the desired levels, significantly curtailing the benefits that this technique can provide. To address this, we have developed a method of incorporating graphene nanoplatelets into a commercial PMMA-based photosensitive resin and successfully demonstrated the 3D printing of graphene-polymer composites. The static and dynamic (*i.e.* viscoelastic and high strain rate) mechanical responses of the printed structures were characterized and found to improve tremendously with as little as 0.02wt% of graphene addition. An important reason for this improvement was that the 3D printing process of graphene-polymer resins involved the Selection of Naturally Aligned Graphene (SNAG), which lined the graphene platelets along the printing axis, reinforcing the stiffness and strength of the material in this direction. The effect of various processing parameters, such as the use of post-print baking and addition of acetone to disperse the graphene nanoplatelets, will be presented in detail as well.

6:20 PM SM08.04.05

Voxel-scale Conversion Mapping in Stereolithographic Additive Manufacturing Tobin Brown, Callie Higgins and [Jason Killgore](#); National Institute of Standards and Technology, United States

Due to the parallelized nature of digital light processing (DLP), additive manufacturing based on this technique has the unique capability to deliver fine resolution over a large area with reasonable print times. This is advantageous in applications such as tissue bioprinting, where micron-scale complexity persists throughout a tissue which may be tens of centimeters in length. In practice, such high resolution is difficult to achieve due to diffusion of reactive species between light and dark regions of the printing plane. Partially crosslinked macromolecules diffuse away from initiating regions while oxygen and other inhibitors diffuse into them. The combined effect is overpolymerization in dark zones, undercuring in light regions, and a loss of print fidelity. Additionally, gradients within polymerized structures cause mechanical heterogeneity in the final part. Because these processes occur on the individual voxel scale, measurement techniques such as photorheology and infrared spectroscopy are unable to adequately measure them, and new measurement techniques are needed.

In this talk, I will describe an atomic force microscopy (AFM) technique to directly map the generation and diffusion of polymeric species during localized photopolymerization. We use an AFM cantilever with a nanocylinder extending from the tip, and when the cylindrical probe is inserted into a resin, the drag on the cylinder can be used to measure the local viscosity of the liquid, and in turn, the local extent of reaction. Vibrating the cantilever at one of its resonance frequencies (10^4 Hz - 10^7 Hz) affords high temporal resolution. Computational fluid dynamics modeling indicates that the fluid motion induced by the oscillating cantilever is localized within 1 μm of the probe. Employing a custom-built instrument, we can direct arbitrary light patterns to resin in the imaging plane of the AFM to achieve photopolymerization. By translating the tip and light pattern relative to one another, the full spatial evolution of the reaction profile can be measured.

We employed this technique to measure the reaction dynamics during DLP photopolymerization of a thiol-ene resin. The thiol-ene click reaction has some advantages over the photopolymerization of acrylate resins, including reduced shrinkage stress and insensitivity to oxygen inhibition. We find a non-reciprocal dependence of the reaction on light intensity; increasing the light intensity decreases the efficiency of the reaction, likely by increasing the bi-radical termination rate. Thus, at constant light dose, lower light intensities lead to increased conversion in the reaction volume, even accounting for increased time for diffusion. This disproves a common assumption in stereolithography, namely that gelation depends solely on the light dose, often referred to as the “critical dose.”

Mapping the spatial evolution of the polymer conversion profile also allows us to easily identify the diffusion length scales during the reaction, and we measure polymer accumulation 20 μm away from the illuminated region within one second of light exposure, identifying the relevant length scale of our process. We then created

an open ring test structure (inner diameter = 15 μm , outer diameter = 45 μm) based on this finding to determine the effect that diffusion plays on the resolution of a printed part. Consistent with our measurements of the reaction profile, we observe significant overpolymerization in the ring center, leading to gelation and loss of fidelity to the projected mask. This new technique provides adequate spatial (1 μm) and temporal (<1 ms) resolution for modern stereolithography applications, and it can be used to predict the ultimate printing resolution and rapidly determine the optimal exposure conditions for a given resin.

6:30 PM SM08.04.06

4D Printing of High-Performance Thermoset and Elastomer Materials Rigoberto C. Advincula^{1,2,3}; ¹The University of Tennessee, Knoxville, United States; ²Oak Ridge National Laboratory, United States; ³Case Western Reserve University, United States

3D printing can be used to create prototypes and devices from polymeric materials which have appended the design functionality for new materials including uses in biomedical devices enabling their rapid development. While 3D printed polymers can be further classified into thermoplastics, thermosets, and elastomers based on their thermo-mechanical properties – new opportunities for multi-materials and composites are possible. The processability and functionality of thermosets and elastomers make it a challenge to employ using most 3D printing methods for polymer additive manufacturing. The transition to a final phase or cross-linked structure results in new properties in combination with the processing method. However, 4D printing allows the design of new materials and applications based on integrating the chemistry of conversion with the printing mode and final stimuli-responsive property on the printed part. In this talk, we will demonstrate the 4D fabrication of multi-materials including thermosets and thermoset elastomers with concept objects and elastomeric properties unlock with stimuli-response. This is based on the use of extruded viscous solutions. The result is an extrudable precursor and nanocomposite elastomers which can be printed via viscous extrusion printing (VEP) or viscous solution printing (VSP) and then converted to an elastomeric actuating material with very high cyclic compressibility or a shape memory thermoset. Other works based on the use of SLA, SLS, FDM, towards high strength epoxy, silicones and nanocomposite materials will be discussed.

6:40 PM *SM08.04.07

Automated Biofabrication of Tailored Dense Collagen Tissue Building Blocks Gabriele Griffanti, Ehsan Rezaeigi, William Lepry and Showan Nazhat; McGill University, Canada

The convergence of three-dimensional (3D) printing of cell seeded bioinks and regenerative medicine offers promise in the biofabrication of tissue building blocks with tailored structural, biological and mechanical properties. However, current 3D bioprinting approaches are limited in their ability to print fibrous collagen bioinks at different length scales that replicate the complex hierarchical architecture of native tissues. Collagen-based hydrogel bioinks are restricted by their narrow printability range, where protein structure, seeded cell viability, and bioactivity of incorporated biomolecules all need to be maintained within physiological boundaries. Herein, a unique approach to biofabricate tissues has been developed to overcome these challenges. Automated gel aspiration-ejection (GAE) leverages the properties of dense collagen gels as tissue models and templates for regenerative medicine. Automated-GAE fabricates highly defined mini-tissue building blocks of various dimensions and shapes, *e.g.*, cylindrical, quadrangular and tubular as well as with tunable microstructural and mechanical properties that modulate seeded cellular responses.

Acellular and cell seeded cylindrical highly hydrated precursor gels were initially cast in different volumes. Automated-GAE was carried out using a uniquely configured instrument equipped with multiple syringe pumps connected to various densification needles to generate dense collagen gel bioinks of different sizes and microstructures. Through the creation of a pressure differential, GAE aspirates the precursor highly hydrated gels into the needles, expelling their unbound fluid and simultaneously inducing their compaction and meso-scale anisotropy. By subsequent reversal of the pressure, dense collagen gel bioinks can be controllably ejected that can be cylindrical, quadrangular or tubular in shape. The incorporation of bioactive materials can also facilitate the production of rapidly mineralizable tissue blocks.

A simple mathematical relationship defining the bioink compaction factor by relating changes between initial highly hydrated hydrogel precursor and final dense gel dimensions was found to be surprisingly highly effective in predicting the initial and temporal properties of the bioinks in culture. Bioink collagen fibrillar density and alignment, tissue building block mechanical properties, as well as seeded cell density, morphology, viability and proliferation were all quantitatively correlated with fabrication compaction factor. Furthermore, by controlling initial bioink parameters, seeded cellular function, in terms of differentiation and extent of matrix remodelling ability were modulated. To this end, automated-GAE will potentially also enable a fourth dimension to biofabrication, where cell-cell communications and cell-extracellular matrix interactions as a function of time in culture can be predicted and modelled.

Therefore, by initially using naturally derived reconstituted collagen hydrogels incorporating cells, and negating the need to directly extrude pre-polymerized collagen molecules, the automated-GAE fabricated mini tissue blocks can be tailored to mimic protein fibril density and alignment of target native tissues, as well as cell loading, density and orientation according to the intended use. Furthermore, the mini tissue blocks can be combined to generate more intricate structures resembling those found in native tissues. Thus, a pre-defined microenvironment can be designed and tuned along with controlling cellular function to meet specific structural requirements of both, mineralized and soft tissues. This breakthrough development will also potentially enable the rapid 3D printing of tissues with varying architectures based on a platform bioink system.

SESSION SM08.05: 3D Printing and Bioprinting V

Session Chair: Hongsoo Choi

Wednesday Afternoon, April 21, 2021

SM08

8:15 PM *SM08.05.01

Hydroxyapatite/Collagen Bone-Like Nanocomposite Paste for 3D Printing Masanori Kikuchi; National Institute for Materials Science, Japan

Hydroxyapatite/collagen nanocomposite (HAp/Col) is a material mimicking bone nanostructure and chemical composition and the world first material reported as completely incorporated into bone remodeling process and substituted with new bone. Porous HAp/Col has been already applied in Japan as a bone void filler and is also considered as a scaffold for bone tissue regenerative medicine. The HAp/Col contains collagen molecules; thus the porous body is prepared by freeze casting and pore structure is only controlled by ice crystals formation in its suspension. Since pore structure influences on cell behaviors including activation of various functions, control of pore structure is one topic for the HAp/Col functionalization. Extrusion type 3D printing is a good technique to fabricate designed pore structure for collagen containing materials. Alginate-based and silane coupling agent (SCA)-based HAp/Col pastes were prepared for 3D printing. The alginate-based HAp/Col paste was immediately hardened to viscoelastic body by extruding into Ca^{2+} containing solution and can be applied to fabricate cell-scaffold construct. The SCA-based HAp/Col paste maintains its shape even if it extrudes directly into water and hardened in 30 min.

The SCA-based HAp/Col pastes were directly injected into bone hole of SD-Rat and remained the injected site by hardened. They were started to remodeled in 7 days without any bad symptoms. The SCA-based HAp/Col paste injected directly into holes of porcine tibia completely substituted with new bone in 3 months without any bad symptoms. The HAp/Col pastes are good candidate for fabrication of cell-scaffold constructs in bone and maybe other tissues due to their bioresorbable and viscoelastic nature.

8:40 PM SM08.05.02

3D Printing of Personalized Medical Device—From Material Properties to Scale-Up Production Sze Yi Mak¹, Chun Hong Jasper Yeung¹, Ah Yiu Chong¹, Tsz Wai Boris Lee¹ and Ching Hang Bob Yung²; ¹The University of Hong Kong, Hong Kong; ²Koln 3D Technology (Medical) Limited, Hong Kong

Personalized medical device fabricated by additive manufacturing is a booming research field for it enables innovative solutions to cater for patients' specific needs. Seemingly, the predominant limitations to scale up in the medical industry arise from the suboptimal biomechanical properties and challenge in boosting the productivity. In this study, we introduce a hybrid laser sintering-heat treatment approach to address this problem. We first examine the microstructure of additive manufactured components under various sintering and heat treatment parameters, and thereby reveal the optimization in terms of material and biomechanical properties, efficacy of bio-functions, and efficiency in cost and time of manufacturing. In addition, the biocompatibility of the 3D printed alloy is validated via haemolysis assay, cytotoxicity and implantation tests. We further present a pathway from proof-of-concept to clinical application with our state-of-the-art examples. Our work will shed lights on the industrialization of additive manufacturing in medical device industry.

8:50 PM *SM08.05.03

Active Hydrogel Towards Miniaturized Robots Yong Feng Mei and Hong Zhu; Fudan University, China

Hydrogels are promising material candidates in diverse applications including drug delivery, tissue engineering and soft robotics, owing to their excellent properties of biocompatibility, wetness, softness, deformability and responsiveness [1]. However, the intrinsic activeness of hydrogels for autonomous locomotion is not achieved yet. The existing activeness of hydrogels are realized by capping active nanoparticles like MnO₂ and TiO₂, which undergo relative catalytic reactions to perform tasks for environmental applications [2,3]. Furthermore, we fabricated versatile printable active hydrogels which possesses the ability to move on water surface. Utilizing the surface tension, the homogeneous active hydrogels propel themselves and show well-controlled and intelligent locomotion on water surface. Incorporated with stimuli-responsive groups, the active hydrogels are able to change their geometries with time under relative stimulus, which adds the dimension of time (4th dimension) to the 3D-printable active hydrogels. The processing technique of these active hydrogels are fully compatible to existing photo-curing 3D-printing equipment. These active hydrogels provide new opportunities for 3D-printing technology to be applied in the field of miniaturized robots.

Reference:

- [1] Xinyi Lin, et al. *Research* 1-15 (2020).
- [2] Xinyi Lin, et al. *Adv. Mater. Technol.* **5** 1-10 (2020).
- [3] Jinrun Liu, et al. *Environ. Sci.: Nano*, **7** 656-664 (2020).

9:15 PM SM08.05.04

Soft Hydrogels as Anti-Adhesion Interfaces for Rapid Digital Light 3D Printing Jingjun Wu; Zhejiang University, China

3D printing is ideal for prototyping yet its low productivity prevents it from being further applied in large-scale manufacture. Some innovative techniques have been developed to break the limitation of printing speed, however, sophisticated facilities or costly consumables are required, which still substantially restricts the economic efficiency. Here we report that a most common stereolithographic 3D printing facility can achieve a very high printing speed (400 mm/h) using a green and inexpensive hydrogel as an anti-adhesion interface (release films). The anti-adhesion mechanism relies on large deformation of the soft hydrogel, which is distinct from that of other techniques. Adhesive force of the solid-solid interface during the layer-by-layer photo curing can be largely reduced according to such mechanism. The technique shows an excellent printing stability even for fabricating large continuous solid structures, which is challenging for other rapid 3D printing techniques.

9:25 PM SM08.05.05

High-Speed VEGF Recognition via Microbead-Based Fluorescence-Linked Immunosorbent Assay Using the 3D-Printed Micro Incubation Chamber in the Lab-on-a-Disk Dong Hee Kang, Na Kyong Kim and Hyun Wook Kang; Chonnam National University, Korea (the Republic of)

A commercialized fluorescence-linked immunosorbent assay (FLISA) is a quantitative technique for detecting bio-chemicals through antigen-antibody binding reaction using well-plate platform. As the manufacturing technology of microfluidic systems has improved, the FLISA is implemented onto the microfluidic disk platform which shows detection of trace bio-chemicals with high resolution. It is possible to reduce time from the reagent loading to the detection step within an hour, in addition to benefits of reducing the amount of reagents to 1/10. Since the high density antibodies on the surface of microbeads, the potential is increased for immobilization of bio-molecules. The incubation process requires not only the binding the antigen-antibody, but also the several steps for binding fluorogenic substrates to target protein. And the unbound reagents should be removed by a washing process. The FLISA protocol in the microfluidic platform, it is necessary to properly execute of liquid reagents movement in each process of FLISA in order to perform the binding reaction sufficiently. The precise control of reagent liquids is required such as fluidic isolation of the incubation chamber and repetitive angular rotation control of disk. We suggest a novel microfluidic disk including a 3D incubation chamber using multi-material to low cost which is fabricated to simple mechanical assembly. VEGF detection is performed sequentially one-step using a 3D microfluidic disk within an hour. On the 3D microfluidic disk, the microbead-based FLISA protocol is operated from the incubation process to the detection process in hand-free without additional components to liquid control. For the incubation process, the microbead movement is controlled through the centrifugal force by disk rotation and gravitational force by bead sedimentation on a slope of chamber.

9:35 PM *SM08.05.06

A Magnetically Actuated Microrobot by on Two-Photon Polymerization for Targeted Neural Cell Delivery and Active Connection Hongsoo Choi^{1,2,3}; ¹Daegu Gyeongbuk Institute of Science and Technology (DGIST), Korea (the Republic of); ²DGIST-ETH Microrobotics Research Center, Korea (the Republic of); ³DGIST, Korea (the Republic of)

Several *in vitro* neural network models have been developed to mimic the reconstruction and interconnection of neural networks and to study brain function and related diseases. Such *in vitro* neural networks require predefined neural connections at the target location and the measurement of neural activity using a multi-electrode array (MEA). The predefined neural connections sometimes limit the adaptation of the user to the change in the neural connection patterns. Here we report a three-dimensional (3D) magnetically actuated microrobot fabricated by 3D laser lithography based on two-photon polymerization for selective neurite alignment and neuronal connections. Using confocal immunofluorescence imaging, the aligned neurite outgrowth and synaptic connections in the neural network were measured. The microrobot, in which the rat's primary hippocampal cells were cultivated, was transmitted between two neural clusters by a magnetic field and then structurally and functionally connected to a neural network that can transmit neural activity signals. Neuronal activities were measured with a complementary metal-oxide-semiconductor-based MEA system to monitor the propagation of extracellular axonal signals from the neural clusters. The proposed microrobot shows the potential for *in vitro* neural experiments to understand how neurons communicate in the neural network by actively connecting neural clusters.

10:00 PM SM08.05.07

Late News: One-Step 3D Structuring of Protein-Based Microneedles Using Digital Light Processing Donghyeok Shin and Jinho Hyun; Seoul National University, Korea (the Republic of)

Microneedles are a transdermal drug delivery system with length dimensions of several hundred micrometers. To be considered in biomedical applications, the biocompatibility and safety of materials are critical factors. The use of protein-based biomaterials such as silk fibroin(SF) can clearly reduce immunological risks resulting from accidental breakage of microneedles during injection into the skin. In the experiment, one-step 3D structuring of SF-based microneedles is challenged using riboflavin as an enzymatic photoinitiator. Digital light processing (DLP) 3D printing is adopted because it is advantageous for direct 3D construction of molecules dissolved in aqueous solution at relatively low concentration through photocrosslinking. Oblique and sharp microneedles are printed using an anti-aliasing strategy and shrinkage of the hydrogel in a dehydration process.

The SF microneedle is strong and showed no severe damage to the structure upon application of ~300 mN of compressive stress. A flexible SF microneedle array pad is fabricated and subsequently utilized for delivery of fluorescence dye molecules into pig skin.

10:10 PM SM08.05.08

Late News: Reversible Morphing of 3D Printed Reinforced Multifunctional Composites Wing Chung Liu¹, Shanthini Puthanveetil¹, Katherine Riley², Andres Arrieta² and Hortense Le Ferrand¹; ¹Nanyang Technological University, Singapore; ²Purdue University, United States

4D printing gives 3D printed structures shape morphing properties when exposed to external stimuli. Many such materials have been reported using hydrogels, liquid crystals and shape memory polymers. However, these materials generally lack the mechanical strength and stiffness required for common applications in the robotics and aerospace industries. In this work, we employ direct-ink-writing to fabricate stiff fibre-reinforced epoxy composites which exhibit temperature controlled reversible morphing. The composite is printed flat initially and the morphing behaviour is activated by heating the material to a temperature above its glass transition temperature. The reversible morphing is enabled by the microstructuring of the printed material arising from the shear-induced fibre alignment during printing. This local alignment controls local anisotropy in the material properties that drives deformation upon heating.

The experimental results, along with finite elemental analysis reveal that by varying the layer print orientation and activation temperature of the prints, the resultant shape and curvature of the morphed material can be controlled precisely as desired. Using an appropriate print design, structures which exhibit high temperature bistability could be achieved, which allows reversible morphing into multiple stable shapes in stiff materials. Furthermore, the ink composition can be tuned to generate shape-dependent functional properties, such as electrical conductivity. Therefore, our method has the potential to fabricate functional composites with tailored made morphing behaviours for applications such as actuators and sensors.

SESSION SM08.06: 3D Printing and Bioprinting VI
Session Chairs: Hannes Schniepp and Min Wang
Thursday Morning, April 22, 2021
SM08

8:00 AM *SM08.06.01

Fabrication of Multi-Analyte Microbiosensors by Microcontact Printing of Enzymes Harold Monbouquette, Bo Wang, Bonhye Koo, I-wen Huang and Yan Cao; University of California, Los Angeles, United States

High performance microprobes for combined sensing of glucose and choline were fabricated using microcontact printing (μ CP) to transfer choline oxidase (ChOx) and glucose oxidase (GOx) onto targeted sites on implantable microelectrode arrays (MEAs). Many neuroscience studies require the monitoring of multiple species, including metabolites and neurotransmitters, with high spatiotemporal resolution *in vivo*. Choline is of interest as a surrogate for the neurotransmitter, acetylcholine, which is turned over rapidly by acetylcholinesterase in the brain. Most electroenzymatic sensing sites on MEAs for neuroscience applications have been created by manual enzyme deposition, however this approach becomes problematic when the array feature size is less than or equal to $\sim 100 \mu\text{m}$. The μ CP process used here relies on use of soft lithography to create features on a polydimethylsiloxane (PDMS) microstamp that correspond to the dimensions and array locations of targeted, microscale sites on a MEA. Precise alignment of the stamp with the MEA is also required to transfer enzyme only onto the specified microelectrode(s). The dual sensor fabrication process began with polyphenylenediamine (PPD) electrodeposition on all Pt microelectrodes to block common interferents (*e.g.*,

ascorbic acid and dopamine) found in brain extracellular fluid. Next, a chitosan film was electrodeposited to serve as an adhesive layer. The two enzymes, ChOx and GOx, were transferred onto different microelectrodes of 2×2 arrays using two different PDMS stamps and a microscope for stamp alignment. Using constant potential amperometry, the combined sensing microprobe was confirmed to have high sensitivity for both choline and glucose (286 and $117 \mu\text{A mM}^{-1} \text{cm}^{-2}$, respectively) accompanied by low detection limits (1 and $3 \mu\text{M}$, respectively) and rapid response times (≤ 2 s). The performance of the dual sensing microprobe was validated in the dorsal striatum of anesthetized rats. This work demonstrates the use of μCP for facile creation of multi-analyte sensing microprobes by targeted deposition of enzymes onto preselected sites of a microelectrode array. Such technology will enable neuroscientists to monitor multiple species at the same location in the brain and to integrate chemical sensing sites with microelectrodes for electrophysiological recordings so as to better correlate neurochemical signaling with neuronal activity.

8:25 AM *SM08.06.02

Diatom-Based 3D Printed Hierarchical Materials Aaron Stapel and Hannes C. Schniepp; William and Mary, United States

We synthesize 3D-printable inks containing live diatoms and diatom nutrients. The glass skeletons of the diatoms form the basis for structures of high complexity and with many levels of hierarchy reaching from the nanometer scale to the centimeter scale. The diatoms survive the printing process and keep reproducing in the printed structures. We have succeeded implementing this method for several types of diatoms featuring different morphologies and sizes. The printed structures can be converted into several types of material, such as composites with diatoms as the reinforcing agent, or into materials entirely consisting of glass. Due to their nano-structured morphology, the highly heat resistant all-glass materials exhibit significantly enhanced mechanical properties compared to bulk glass, while being much lighter. Based on home-grown biological feedstock, we consider this a promising approach for the scalable production of sustainable performance materials with a negative carbon footprint and widely tunable properties and functionality.

8:50 AM *SM08.06.03

5D Printing and Its Application in Tissue Engineering Min Wang; The University of Hong Kong, Hong Kong

Tissue engineering offers a promising approach to treat difficult problems in human body tissue repair. It involves using live cells to form implantable devices for body tissue regeneration. In scaffold-based tissue engineering, a porous scaffold provides a microenvironment for cells to adhere, proliferate and differentiate and a structural framework for new tissue formation. Most human body tissues are complex and their regeneration requires structurally complex scaffolds that resemble tissue structures and can provide biochemical cues such as growth factors (GFs). Incorporating GFs and even live cells in scaffolds can greatly facilitate tissue regeneration. 3D printing has many advantages in scaffold fabrication, such as control of pore shape, size, porosity, etc. Furthermore, 3D printing can make complex tissue engineering scaffolds, including multilayered scaffolds with different layer characteristics for regenerating body tissues that exhibit multilayered structures such as osteochondral tissue. Therefore, like in other industries, 3D printing has already made a high impact in the tissue engineering field, with numerous researchers around the world using 3D printing technologies to produce various tissue engineering products. 4D printing emerged in 2013 and immediately attracted world's attention. 4D printing uses 3D printing technologies to produce shape-morphing objects. Such objects can meet the demanding requirements in particular applications. The concept of 4D printing has been evolving and one current popular definition of 4D printing is that the shape, property and functionality of a 3D printed object can change with time in a predefined design. 4D printing relies on advances in 3D printing technologies, smart materials, and smart designs. It has become an actively pursued subject in both academia of different disciplines and industry, including tissue engineering. We have conceptualized 5D printing and are applying it in tissue engineering. 5D printing produces shape-morphing and information-embedded structures, and the information, which is the 5th dimension in 5D printed structures, is delivered *in situ* during applications of these structures. More importantly, with 5D printed structures, the delivered information affects the surrounding environment (or

5D printed structures) and guide changes in the environment (or 5D printed structures). For 5D printing in tissue engineering, the embedded information can be biomolecules such as GFs. Using 5D printing, shape-morphing, mesenchymal stem cell (MSC)-containing and GF-delivering multilayered complex scaffolds may be constructed for gastrointestinal (GI) tissue engineering. Under GFs' guidance, MSCs will differentiate into different types of cells in the cell-scaffold constructs for GI tissue regeneration. This talk will present our work in 3D/4D/5D printing of scaffolds for body tissue regeneration. It will focus on the design and construction of complex tissue engineering scaffolds.

9:15 AM SM08.06.04

3D Printed Nanofiber Reinforced Tissue Engineering Scaffolds with Controlled Release of Growth Factor Jiahui Lai and Min Wang; The University of Hong Kong, Hong Kong

3D printing has greatly improved our ability to create complex tissue engineering scaffolds with high precision. Biomaterials, growth factors or even living cells are accurately deposited layer-by-layer in 3D printing to construct the scaffolds. Hydrogels have been commonly used biomaterials in 3D printing of scaffolds owing to their various advantages. However, most hydrogels, particularly natural hydrogels, have poor mechanical properties, which severely limit their tissue engineering applications. It has been shown that adding polymer nanofibers into hydrogels can lead to improved mechanical properties that can be comparable to the body tissues. Growth factors (GFs) in the body can promote wound healing, cell growth, proliferation and differentiation. Incorporating GFs into scaffolds may accelerate tissue regeneration. Fibroblast growth factor (FGF) is generally used in the regeneration of tissues such as cornea and skin. In this study, nanofiber reinforced scaffolds with the controlled release of GF were investigated with 3D printing of PLGA nanofiber (PLGA_f) reinforced alginate hydrogel containing FGF. To control the FGF release, two strategies were adopted: (1) FGF was directly included in the biomaterial (PLGA_f and alginate hydrogel mixture) for 3D printing, (2) FGF was firstly encapsulated in PLGA nanofibers via emulsion electrospinning and the nanofibers were then dispersed in alginate hydrogel for 3D printing. Thus two types of inks were made for 3D printing: FGF/alginate/PLGA_f ink, and alginate/PLGA_f-FGF ink. They were used in an extrusion-based 3D bioprinter to fabricate reinforced scaffolds according to the CAD design. The experiments showed that the addition of PLGA_f into alginate hydrogel greatly improved its viscosity and mechanical strength. *In vitro* release studies were conducted for scaffolds 3D printed from the two type of inks. Release results showed that both types of scaffolds exhibited two-stage release profiles: an initial fast release period in the first 2 days, and the subsequent slower and sustained release period. In addition, alginate/PLGA_f-FGF scaffolds displayed a slower release than FGF/alginate/PLGA_f scaffolds, which was mainly due to the different incorporation site of FGF within the scaffolds. It can be concluded that the GF release behaviour from 3D printed scaffolds can be controlled through choosing the loading site in scaffolds for GFs, which enables designing personalized GF delivery specific for the targeted tissue engineering application.

SESSION SM08.07: 3D Printing and Bioprinting VII

Session Chairs: Shervanthi Homer-Vanniasinkam and Parisa Pour Shahid Saeed Abadi

Thursday Morning, April 22, 2021

SM08

10:30 AM *SM08.07.01

Synthesis, Rheology and 3D Printability of Novel Polyesters for Solvent- and Additive-Free Extrusion-Based 3D Printing Tanmay Jain, David Kaplan and Irada Isayeva; U.S. Food and Drug Administration, United States

Three-dimensional (3D) printing offers the unparalleled capability to create medical devices with complex architectures matched to the patient's anatomy. However, most of the currently used polymers require high

processing temperatures and pressures and/or a combination with leachable additives like initiators, crosslinkers, plasticizers, and solvents to enable extrusion-based direct-write 3D printing (EDP). Such conditions may raise safety concerns for the final medical product. Therefore, it is desirable to develop polymers that could be printed at ambient conditions and without additives. To develop such polymers, it is necessary to systematically understand the relationship between polymer molecular structure, rheology, and 3D printability. Herein, we present a library of novel polyesters with modular functionalities, which can be used to create customized 3D constructs using EDP. The polyesters with various pendant functional groups were synthesized and their physical properties, rheology, and 3D printability were analyzed.

Methods: The polyesters were synthesized at room temperature using carbodiimide-mediated polymerization of pendant functionalized diols and succinic acid, and characterized using $^1\text{H-NMR}$ and variable temperature-FTIR. Polymer viscosity as a function of shear rate was measured under steady state shear flow. Small amplitude oscillatory shear experiments were done to plot master curves of viscoelastic properties for each polyester over a wide frequency range using the time-temperature superposition (TTS) principle. The 3D printability of the polyesters was assessed based on parameters such as the ability to extrude polymer as continuous filaments through a narrow nozzle at a consistent flow rate, retain the printed shape, form bridge-spanning filaments without significant sagging or collapse, and form multilayer constructs.

Results: Data demonstrated that the synthesized polyesters exhibit properties that are desirable for the extrusion-based 3D printing. $^1\text{H-NMR}$ confirmed the presence of the appropriate functional groups for each synthesized polyester suggesting successful synthesis. All synthesized polyesters exhibit shear thinning behavior at EDP relevant shear rates and respective 3D printing temperatures, which is important for solvent-free printing. The tangent delta peak observed at temperatures higher than polymer T_g indicated the presence of a “secondary network” and supramolecular interactions. Variable temperature-FTIR supported the presence of supramolecular interactions, such as H-bonding. The presence of “secondary network” along with supramolecular interactions appear to facilitate the retention of printed shape and improve the overall quality of the 3D printed constructs. Based on observed correlations between 3D printability and the rheology of each polyester a “3D printability window” is proposed. The insights derived from this study can be used to inform the design of new biodegradable polymers for extrusion-based direct-write 3D printing for biomedical applications.

10:55 AM SM08.07.02

Late News: Sub-10 nm Resolution Patterning of Pockets for Enzyme Immobilization via tc-SPL Annalisa Calo^{1,2}; ¹University of Barcelona, Spain; ²Institute for Bioengineering of Catalonia, Spain

The ability to precisely control the localization of enzymes on a surface is critical for several applications including biosensing, nano-bioreactors and single molecule studies. Despite recent advances, fabrication of enzyme patterns with resolution at the single enzyme level is limited by the lack of lithography methods that combine high resolution, compatibility with soft, polymeric structures, ease of fabrication and high throughput. Here, a method to generate enzyme nanopatterns on a polymer surface is demonstrated using thermochemical scanning probe lithography (tc-SPL) and the enzyme Thermolysin as a model system. Electrostatic immobilization of negatively charged sulfonated enzymes occurs selectively at positively charged amine nanopatterns produced by thermal deprotection of amines along the side-chain of a methacrylate-based copolymer film via tc-SPL. This process occurs simultaneously with local thermal quasi-3D topographical patterning of the same polymer, offering lateral sub-10 nm resolution and vertical 1 nm resolution, as well as high throughput ($5.2 \times 10^4 \text{ mm}^2/\text{h}$). The obtained patterns with single enzyme resolution are characterized by atomic force microscopy (AFM) and fluorescent microscopy. The enzyme density, the surface passivation and the quasi 3D arbitrary geometry of these patterned pockets are directly controlled in a single step, without the need of markers or masks. Other unique features of this patterning approach include the combined single-enzyme resolution over mm^2 areas and the possibility of fabricating enzymes gradients at the nanoscale.

11:05 AM SM08.07.03

Late News: Vapor-Phase Organic Electronic Processes to Pattern Cells Jeffrey Horowitz, Xiaoyang Zhong, Samuel DePalma, Maria Ward Rashidi, Brendon Baker, Joerg Lahann and Stephen Forrest; University of

With the development of stem cells, *in vitro* tissue engineering has become a promising technology for research, clinical testing, and medical treatment. One consistent focus of research has been the high-precision patterning of cells, necessary because material surface properties, environment, and organization of cells in two- and three-dimensions all significantly impact the growth and development of tissue. While many different cell patterning techniques have been explored for cell patterning, the integration of organic electronic processes has been previously overlooked. In this presentation, we demonstrate a process whereby organic semiconductors are used to pattern cells and discuss the unique advantages of such a process. Using vacuum thermal evaporation (VTE) and organic vapor jet printing (OVJP), two organic electronic materials are precisely deposited in the vapor-phase as adhesion points on a biocompatible poly(p-xylylene) surface. The small molecular weight organics prevent the subsequent growth of anti-fouling polyethylene glycol methacrylate (PEGMA) polymer brushes, rendering the background areas of the substrate protein and cell resistant. Fibronectin then attaches to the deposited organic semiconductor regions, followed by the selective adhesion of fibroblasts. For VTE, the adhesion regions consist of hexagons with side-lengths of 25 μm , while OVJP is used to form patterns varying in width from several hundred micrometers to about 10 μm . At smaller widths, cells show considerable alignment to the OVJP-formed patterns, moving to random orientation at a threshold width of about 110 μm . The surface properties of the different organic semiconductor materials also prove important, demonstrating different patterning tendencies. The cell-patterning process presented here diverges from other techniques in i) the usage of organic small-molecule semiconductors as adhesion regions, ii) the formation of adhesion via vapor-phase deposition. Some of the many advantages include the vast number of evaporable organic semiconductor materials, the ability to deposit onto a fragile scaffold without contact, and the potential for high-throughput manufacturing. Therefore, this process is a useful development in cell patterning with many potential applications.

11:15 AM SM08.07.04

Late News: Roll-to-Roll Large-Scale Manufacturing of Polymer Biochips for Multiplexed DNA Testing

Pelin Toren¹, Martin Smolka¹, Anja Haase¹, Dieter Nees¹, Stephan Ruttloff¹, Markus Rumppler¹, Manuel W. Thesen², Max Sonnleitner³, Wilfried Weigel⁴, Barbara Stadlober¹ and Jan Hesse¹; ¹Joanneum Research Forschungsgesellschaft mbH, Austria; ²micro resist technology GmbH, Germany; ³GENSPEED Biotech GmbH, Austria; ⁴SCIENION AG, Germany

We successfully developed a complete process chain of production lines for foil-based bioanalytical lab-on-chip devices. The process is based on high-throughput structuring and lamination using roll-to-roll (R2R) UV micro or nano-imprinting on several hundred meters-long flexible, polymeric foils. Bio-functionalization of the imprinted structures is achieved via R2R microarray printing. In our pilot line, the polymer foil is roto-gravure coated using a photopolymer with tuneable properties, which is then structured via R2R UV nanoimprint lithography (NIL).^[1] The technology allows producing various kinds of fluidic structures; such as, capillary force-driven fluidic channels, reservoirs or pumps as well as production of optical structures with different geometries for effective guiding of light for *in-vitro* diagnostic (*IVD*) products. Following R2R UV NIL imprinting, bio-functionalization is achieved using a custom-made, semi-automated R2R microarray spotting unit. For specific bio-detections via *IVD* chips, various probe DNAs or proteins can be printed at different sections of biochips. With layout design flexibility and rapid prototyping possibilities, up to 7500 biochips per 100 meters are produced via our technology. The feasibility of the approach for massively parallel production of lab-on-a-foil products is demonstrated based on a model application of *in-vitro* multiplexed DNA testing for markers of a methicillin resistant pathogen.^[2] The manufactured foil chips show similar detection performance as commercial injection-moulded chips, thus demonstrating that our lab-on-a-foil technology is a potential replacement for the commercially available, disposable chips for *IVD* applications.

REFERENCES

[1] M. Leitgeb et al., *ACS Nano*, **10**, (2016) 4926-4941.

[2] P. Toren et al., *Lab on a Chip*, **20**, (2020) 4106-4117, featured as inner front cover.

ACKNOWLEDGEMENT

This research was supported by NextGenMicrofluidics project (www.nextgenmicrofluidics.eu) Horizon2020 European Union Research and Innovation Programme with grant agreement n° 862092.

11:25 AM SM08.07.07

Late News: Development of a Bionic Patient-Specific Temporomandibular Joint Prosthesis Stijn Huys¹, Nikolas De Meurechy², Annabel Braem¹, Maurice Mommaerts³ and Jos Vander Sloten¹; ¹KU Leuven, Belgium; ²VUB, Belgium; ³UZ Brussel, Belgium

With vital functions like talking, chewing, and swallowing, an optimized implant should replace a diseased temporomandibular joint (TMJ). Moreover, it is unique as the only bilateral joint in the human body acting as one unit, its movements are a combination of rotations and translations, and it is the most regularly used joint on a daily basis, suggesting a broad range of highly customized TMJ prostheses. In reality, the vast majority of available options contradict these prerequisites, because they are mainly focused on shape reconstruction, rather than functional reconstruction, e.g., no features are foreseen for laterotrusive movements (which are necessary for proper grinding of food) and the implants are not adapted to allow contralateral movements. This leads to partial improvement in functionality (an increase of maximum mouth opening of ± 1 cm), but there is room for optimization.

During this research, the entire concept was revised based on all prerequisites and new advances in technology and surgery. Based on experience and various simulations, a thorough analysis was conducted to determine the optimal building blocks for this concept; crosslinked ultrahigh molecular weight polyethylene has shown its excellence in various medical joints, while biocompatible Ti6Al4V (Grade 23, ELI) allows for high customization when using three-dimensional printing (Selective Laser Melting). Combining these raw materials with biofunctionalization (e.g., surface treatments and lattice structures) and a promising HadSat[®]-coating has led to excellent wear properties and long-term *in vivo* results (simulated in a sheep study).

The importance of function-reconstruction translated into specific design parameters; the bilateral nature of the TMJ's caused the prosthetic side to greatly influence the healthy side (and vice versa) and, with that, all mandibular movements (e.g., opening, closing, protrusive, and lateral movements). To consider these challenges during the patient-specific design of the implant, it was reverse-engineered. Starting from the desired mandibular movements for a specific patient, the topology of the custom-made implant was derived. These desired mandibular movements were based on the pre-diseased anatomy of the patient, using a statistical shape model. This methodology allowed the designers to incorporate important anatomical features (such as condylar path angulation and Bennet movements), and to achieve the optimized patient-specific design.

By incorporating several additional distinctive features, the “bionic” prosthesis was developed. Several lattice structures (scaffolds) were used in the design, to allow for bone ingrowth. This osseointegration served as a secondary fixation method and, together with a lateral movement-restricting lip, reduced the number of necessary screws and thus surgical time. Furthermore, by implementing a scaffold into the condylar neck, the pterygoideus lateralis muscle could be reattached, which helped the patient during lateral movements. This unique feature, together with the abovementioned materials and patient-specific design, next to the sheep experiments, resulted in extensive simulation using finite element analyses to ensure both patient safety and long-term results.

By incorporating all of the abovementioned features into a novel TMJ prosthesis concept, a major advance in function-reconstructive temporomandibular joint replacement was achieved. Early *in vivo* results (1 year after surgery) showed promising outcomes, involving both high increases in mandibular movements and decreases in pain scores.

11:35 AM SM08.07.08

Late News: Additive Manufacturing of Conductive and High-Strength Epoxy-Nanocaly-Carbon Nanotube Composites Masoud Kasraie and Parisa Pour Shahid Saeed Abadi; Michigan Technological

University, United States

Additive Manufacturing has increased our ability to fabricate complex shapes and multi-material structures. Epoxy is excellent as the base for structural composite materials. Furthermore, carbon nanotube (CNT) is an outstanding filler due to its unique properties and functionalities. Here, conductive epoxy-nanoclay-CNT nanocomposite structures were fabricated by direct-write 3D printing. In this process, 3D-printable composite inks were synthesized by incorporation of nanoclay and different concentrations of CNTs – 0.25, 0.5, and 1 vol%, 0.43, 0.86, and 1.7 wt% – in epoxy. CNTs were found to significantly improve the electrical and mechanical properties. Rheological characterization of the inks revealed a shear-thinning behavior for all the nanocomposite inks and an increase in the complex viscosity, storage, and loss moduli with the incorporation of CNTs. The CNT concentration of 0.5 vol% was found to be the optimum condition for enhancement of mechanical properties; an average increase of 61, 59, and 31% was measured for flexural strength, flexural modulus, and tensile strength, respectively, compared to the 3D printed epoxy-nanoclay nanocomposite structures. The electrical conductivity of 2.4×10^{-8} and 2.2×10^{-6} S/cm was measured for the nanocomposites containing 0.5 and 1 vol% CNTs, respectively. Multi-scale characterization of the morphology revealed partial alignment of CNTs in the direction of printing, CNT pull-out and breakage at the fracture surfaces, and nano-scale interactions of the constituents, all of which contribute to the superiority of the nanocomposite with CNTs. The findings show the promise of this ink material and printing method for various applications such as aerospace structures and electronics.

11:45 AM SM08.07.09

Late News: 3D Printing of MXene Composite Sensor and Capacitor via Binder Jetting Technique Terek L. Li; University of Toronto, Canada

This work presents a MXene polymer composite directly 3D printed via binder jet technique. We introduce a strategy to print poly(vinyl alcohol) (PVOH) composite with optimized MXene ink. By ejecting highly conductive MXene particles onto a PVOH matrix, the resulting sample is able to achieve semi-conducting behaviour with the potential for strain sensing and energy storage. The printed component can be used as a strain sensor capable of sensing tensile strains between 11 to 250%. The component could also be used as electrode material in a sandwich-structured pseudo-capacitor with an energy density of 36.4 mJcm^{-3} and a power density of 2.8 mWcm^{-3} . This study demonstrates that binder jet printing has the potential to directly fabricate polymer composite materials end different end applications.

In order to briefly explain why this submission will appeal to broad and interdisciplinary researchers in both 3D manufacturing and 2D materials, it should be noted that although binder jet printing is widely adopted in industrial setting to print ceramic and metallic components. However, it has only been proven very recently as a viable method to print polymer composite materials. The submitted manuscript not only offers a guideline toward ink optimization for binder jet printing with polymeric material, but also for the first time demonstrates different end applications of printed components. This work is believed to be highly capable of providing the readers in the field of 3D printing with a framework on the modification of particle morphology and ink composition in order to further explore the potential limit of binder jet printing of polymeric composite.

11:55 AM SM08.07.10

3D-Printed Organ Phantom for Simulation and Quantitative Evaluation of Medical Procedures Eunjin Choi^{1,2}, Moonkwang Jeong², Dandan Li¹, Rodrigo Suarez-Ibarrola³, Arkadiusz Miernik³, Frank Waldbillig⁴, Tian Qiu^{1,2} and Peer Fischer^{1,2}; ¹Max Planck Institute for Intelligent Systems, Germany; ²University of Stuttgart, Germany; ³University Medical Center Freiburg, Germany; ⁴University Medical Centre Mannheim, Germany

Organ phantoms have been recognized as a testing platform in medicine and have become more realistic as the 3D printing technology has advanced. Typical 3D printers can achieve resolutions of tens of microns and offer a number of printing materials [1]. This allows detailed anatomical features to be resolved by choosing different

materials [2,3]. While most printing materials do not have properties that reflect those of tissues, 3D printing with biocompatible hydrogels show tissue-like properties [4]. However, most of the work to date has focused on reproducing structural details resemblance, which is mainly of interest for visual comparison. Here, we present high-fidelity organ phantoms of the full urinary tract that can also be used to simulate and evaluate medical procedures, including surgery. We used 3D-printed molds to build the phantom. The 3D-printed molds were designed with computer-aided design (CAD) and are based on high-resolution X-Ray images. The casting method allows the use of materials that match the mechanical, optical, and imaging contrast properties of biological tissues.

Our phantom has been validated for the simulation and evaluation of many medical procedures, such as lithotripsy [5], cystoscopy [6], and the transurethral resection of the prostate [7]. A major advantage of the phantom is that the surgery can be quantitatively evaluated using multi-modality medical imaging to an extent that cannot be achieved in a real surgery. Both user-feedback as well as the physical parameters of time, accuracy, geometrical centricity, and surface smoothness of the surgical resection can be quantitatively evaluated. These phantom are expected to be important tools for medical training, surgical planning as well as the development of new medical instruments.

[1] V. Filippou et al., Recent advances on the development of phantoms using 3D printing for imaging with CT, MRI, PET, SPECT, and ultrasound, *Med Phys* 45, e740 - e760 (2018)

[2] F. Adams et al., Soft 3D-Printed Phantom of the Human Kidney with Collecting System. *Ann Biomed Eng* 45, 963–972 (2017)

[3] K. Qiu et al., 3D Printed Organ Models for Surgical Applications, *Annu Rev Anal Chem* 11, 287–306 (2018)

[4] J. Li et al., 3D printing of hydrogels: Rational design strategies and emerging biomedical applications, *Mater. Sci. Eng. R Rep*, 140, 100543 (2020)

[5] D. Li et al., Soft Phantom for the Training of Renal Calculi Diagnostics and Lithotripsy, 41th IEEE EMBC, 19109241 (2019)

[6] E. Choi et al., Soft Urinary Bladder Phantom for Endoscopic Training, submitted

[7] E. Choi et al., A High-Fidelity Phantom for the Simulation and Quantitative Evaluation of Transurethral Resection of the Prostate. *Ann Biomed Eng* 48, 437–446 (2020)

SESSION SM08.08: 3D Printing and Bioprinting VIII

Session Chair: Chrystelle Salameh

Thursday Afternoon, April 22, 2021

SM08

1:00 PM SM08.08.01

3D Printing of Ingestible Gastric Resident Electronics and Biomedical Devices Yong Lin Kong; The University of Utah, United States

The integration of electronics with the human body, such as wireless sensors and a drug delivery system can enable a personalized digital-based diagnosis and treatment strategies. Nevertheless, surgically placed medical implants are associated with eliciting foreign body immune responses and can serve as a nidus for infection. Recent advances in 3D printing have enabled the creation of novel 3D architecture and devices with an unprecedented level of complexity, properties, and functionalities. The development of a multi-scale, multi-material 3D printing approach can overcome the geometrical, mechanical and material dichotomies between conventional manufacturing technologies and a broad range of three-dimensional systems. Here, we discuss the creation of 3D printed gastric resident electronics (GRE) that can circumvent the potential complications associated with surgically placed medical implants by leveraging the significant space and immune-tolerant of the stomach. We propose biomedical applications with the further advancement of this system that can be

potentially realized with a multiscale 3D printing process that synergistically integrates functional nanomaterials.

1:10 PM SM08.08.02

Late News: Tissue Specific 3D Bioprinting Using Ready-to-Use TissueFab™ Bioinks Kevin T. Dicker, Juyi Li, David Settles, Hanying Luo, Nicolynn E. Davis and Gangadhar Panambur; MilliporeSigma, United States

3D bioprinting is an enabling tool for regenerative medicine and drug discovery. Despite promising advancements 3D bioprinting technology, a need remains for reproducible commercially available ready-to-use bioinks to replicate 3D tissue microenvironments. To address this, we have developed a platform of bioink formulations, *TissueFab™*, that are compatible with diverse cell types, bioprinting platforms and have high batch-to-batch consistency. *TissueFab™* is a family of general purpose and tissue specific ready-to-use bioinks based on natural proteins and polysaccharides and synthetic polymers. *These bioinks are designed for* optimal viscosity and mechanical properties for high resolution bioprinting and to maintain high cell viability (>80%) in a wide range of curing wavelengths. Printability of our bioinks are assessed on multiple microextrusion based commercial bioprinters thus demonstrating the printer agnostic characteristic of the bioinks. Bioink formulations were validated for high cell viability, proliferation and metabolic activity using C2C12 mouse myoblast cells, human mesenchymal stem cells (hMSCs) or human adult dermal fibroblasts (HDFa). For bone tissue engineering applications, we have shown that hMSCs bioprinted in *TissueFab™ - Bone bioinks* show an increase in osteogenic differentiation. Additionally, *TissueFab™ - Conductive bioinks* exhibit enhanced conductivity making them attractive for bioprinting electroactive tissues such as neural or muscular tissue. *TissueFab™* bioinks provide a robust tissue-mimetic platform for microextrusion-based bioprinting various cell types with both high printability and cell viability. *TissueFab™* bioinks enable on-demand tissue printing which is a tangible step forward for addressing drug testing and tissue engineering challenges.

1:20 PM SM08.08.03

Late News: Multimaterial 3D Printing of Functional Objects Using Polymerization-Induced-Phase-Separation Chantal Paquet¹, Bhavana Deore¹, Katie Sampson¹, Thomas Lacelle¹, Derek Aranguren van Egmond¹ and Hendrick W. de Haan²; ¹National Research Council of Canada, Canada; ²Ontario Tech University, Canada

Advances in materials and processes are required to transform 3D printing into a manufacturing platform capable of generating complex objects with integrated function. Despite its high dimensional accuracy and resolution, excellent surface finish, versatile modification of feedstock chemistry, and low cost printers, vat polymerization 3D printing lacks the versatility to generate multimaterial objects. In this presentation, we describe a strategy to generate functional multimaterial objects by vat polymerization 3D printing that relies on controlled phase separation. Using photoresins comprising of judiciously selected components, the diffusion of phase separating components are modulated via the kinetics of gelation, the density of the polymer network and the diffusivity of materials to control the material phases spatially. The insight gained in controlling the material phases allows a rationalized approach to formulating resins to access a wide range of material morphologies for specific applications. The approach was used to fabricate dipole antenna arrays that function at 2.4 GHz, trusses that response to compression and anti-bacterial surface. Due to the universality of this approach 3D PIPS represents a powerful method to create materials with controlled sub-phases and will accelerate the adoption of vat polymerization as a viable technique to generate functional 3D objects.

1:30 PM SM08.08.04

Late News: 3D Printed Porous Polymer-Derived Bioceramics for Bone Tissue Engineering Joelle El Hayek, Mikhael Bechelany, Philippe Miele and Chrystelle Salameh; European Institute of Membranes, France

The production of biomaterials for tissue and bone engineering is still a real challenge for repairing, implanting or filling damaged bone or connective tissue. Silicate-based bioceramics have excellent bioactivity and are

considered promising materials for bone regeneration; however, their synthesis and design in complex geometric forms using conventional techniques is still challenging. The design of scaffolds for tissue engineering with the mechanical and microstructural properties required to promoting cell attachment, growth and new tissue formation is one of the major challenges facing researchers in the field. Their main disadvantage is their low strength and high brittleness under applied loads.

The Polymer-Derived Ceramics (PDCs) route is one of the most advantageous approaches in the manufacture of bioceramics due to the ability to control both synthesis and shaping.

In this work, we investigated 3D printing of two preceramic polymers precursors of Ca_2SiO_4 using Stereolithography (SLA). We studied the effect of the precursor's composition and ceramic yield on the physico-chemical properties of the glass-ceramic. After pyrolysis, the scaffolds were functionalized with silver-reduced graphene oxide composites in order to assess their antibacterial activity.

The bioceramics, characterized with good mechanical strength, showed regular geometries and a high interconnected porosity (60%) with an average pore size between 200 and 400 μm . Cell viability and cytotoxicity tests showed that the scaffolds were biocompatible and nontoxic suggesting that such 3D bioceramics are suitable for tissue engineering.

1:40 PM SM08.08.05

Late News: Tailoring Slurry Formulation to Manufacture Fine-Scale Ceramic Structures via Material Extrusion Huseyin Utkucan Kayaci and Simge Cinar; Middle East Technical University, Turkey

Additive manufacturing is a highly advantageous manufacturing technique that enables the production of complex shapes which cannot be produced by any other technique, and it provides an opportunity for fast prototyping and personal based productions. Despite the advantages of additive ceramics manufacturing, obtaining superior mechanical properties using this technique is still a challenge because of the need to use inks with significant additive percentage. Among the other ceramic additive manufacturing techniques, extrusion-based robocasting technique offers a low-cost opportunity for the production of high-density and high strength bodies; yet, it requires strict control over the rheological behavior of the ceramic ink and the processing conditions. The increasing interest in the topic leads to significant improvements in the design of the printing parameters. However, the studies on the relation between the slurry properties, the rheological properties, the processing conditions, and the resulting properties of the green and sintered bodies are overlooked. In this study, the importance of the powder properties on the suspension rheology and the resulting properties of the extruded green and sintered bodies were investigated. Proper choice of particles, particle size and the processing additives enabled better controlled rheological properties of suspensions, smoother extrusion through narrow channels, and eliminated clogging during extrusion and crack formation in green bodies. Moreover, sintered ceramic bodies with even 200 – 300 μm size features could be produced. The sintered bodies exhibited densities above 97% of their theoretical density. In the present work, alumina was used as a model ceramic material, but the findings can certainly be extrapolated to other ceramic systems. Such findings are particularly critical for the biological, electronic and robotic applications where the mechanical requirements are demanding.

This work has been supported by Scientific Research Projects Coordination Unit of Middle East Technical University under grant number YOP-308-2018-2677.

1:50 PM *SM08.08.06

One-Shot Bioprinting with Ultrasound Zhichao Ma¹, Kai Melde¹ and Peer Fischer^{1,2}; ¹Max Planck Institute for Intelligent Systems, Germany; ²University of Stuttgart, Germany

Ultrasound is benign and can exert forces on particles and cells. A recent advance makes it possible to form high-resolution arbitrary shaped ultrasound pressure distributions [1]. By encoding the necessary phase information into the topography of a 3D-printed plate that is placed in front of a simple ultrasound transducer, it is now possible to generate sophisticated acoustic fields inside a fluid volume. We have shown that particles can be assembled into pre-defined shapes and that the particle-assemblies can be fixed to form permanent objects [2]. The advantage of directed-assembly via ultrasound fields is that the particles assemble at once to form the

object. This promises a general one-shot fabrication method. Of particular interest is to apply this method to the patterning of biological cells. We could show that the acoustic amplitude distribution of a complex image, defined by the hologram, exerts forces on biological cells and the biocompatible hydrogel they are suspended in. The resultant convection flow gently delivers the suspended cells to the image plane where they form the desired pattern [3]. The hydrogel can then crosslink to immobilize the cell pattern. The use of acoustic holography for the assembly of cells structures shows great potential to grow tissue-like structures. A spatial ultrasound modulator based on microbubble arrays [4] can replace the static 3D-printed hologram and opens the possibility to form dynamic, reconfigurable assemblies.

References

- [1] K. Melde, A. G. Mark, T. Qiu, P. Fischer. *Nature* 537, 518-522 (2016).
- [2] K. Melde, E. Choi, Z. Wu, S. Palagi, T. Qiu, P. Fischer. *Adv. Mater.* 30:1704507 (2018).
- [3] Z. Ma, A. Holle, K. Melde, T. Qiu, K. Pöppel, V. Kadiri, P. Fischer. *Adv. Mater.* 32:1904181 (2020).
- [4] Z. Ma, K. Melde, A.G. Athanassiadis, M. Schau, H. Richter, T. Qiu, P. Fischer. *Nat. Comm.* 11:4537 (2020).

2:15 PM SM08.08.07

Late News: Additive Manufacturing of Ceramic Components via UV-Assisted Direct Ink Writing Connor Wyckoff^{1,2}, Matthew Dickerson¹ and Lisa Rueschhoff¹; ¹Air Force Research Laboratory, United States; ²UES, Inc., United States

Ceramic additive manufacturing has the potential to be a disruptive technology enabling rapid prototyping and the production of complex geometries. A relatively new approach for ceramic part fabrication is additive manufacturing via UV-assisted direct ink writing (UV-DIW). UV photopolymerization during the print process modifies ink rheology to enable the fabrication of more complex geometries such as overhanging or spanning structures that are otherwise difficult to make with traditional DIW processes. We have developed a UV-DIW optimized ink that consists of a preceramic polymer-based system loaded with ceramic powder, containing all off the shelf components. This ink shows easy printability as well as limited shrinkage after pyrolysis, making it ideal for near net shape fabrication and rapid prototyping without the need for time consuming synthesis steps. The relationship between ink formulation, rheology, printability, as well as the structure of the final ceramic components will be presented

2:25 PM *SM08.06.05

Engineering The Cellular Niche Via CAD/CAM Laser Processing Douglas B. Chrisey¹, Jayant Saksena¹ and Yong Huang²; ¹Tulane University, United States; ²University of Florida, United States

We have developed a laser-biomaterial interaction-based prototyping platform capable of three fabrication modes: (1) laser direct write of cells, microbeads, and other biomaterials; (2) fabrication of cell encapsulating microspheres (microcapsules); and (3) laser micromachining of substrates. Using this system, we are able to precisely place biomaterials, such as cells, into substrates with spatial constraints from laser micromachining or wholly fabricate scaffolds that are cell laden. This enables fabrication of co-cultures in almost any geometry and controlled gradients of chemical factors. In addition, the process is parallelizable, thus allowing for numerous potential bioassay applications. One such assay is a differential system for quantifying multiple outcomes in response to multiple parallel biophysicochemical cues in competition. These novel assays are complex, reproducible, and disposable microenvironments. This presentation will summarize the control integration developed for Laser Direct Write, a 2D model of laser ablation, with a computational method demonstrating preliminary results. The biofabrication methods discussed are applied to an Organ-On-a-Chip model to develop a fully automated fabrication process.

SYMPOSIUM SM09

Peptide and Protein Design for Responsive Materials
April 23 - April 23, 2021

Symposium Organizers

Chris Kloxin, University of Delaware
Aline Miller, Manchester BIOGEL
Jacek Wychowanec, University College Dublin
Xuehai Yan, Institute of Process Engineering, Chinese Academy of Sciences

Symposium Support

Bronze

Royal Society of Chemistry Scientific Meetings Grant (S19-0365)
University of Delaware, Materials Science and Engineering

* Invited Paper

SESSION SM09.01: Assembly Rules of Responsive Peptide and Protein based Materials
Session Chairs: Aline Miller, Jacek Wychowanec and Xuehai Yan
Friday Morning, April 23, 2021
SM09

8:00 AM *SM09.01.01

Socially Distant at the Nanoscale—It's a (Soft) Matter of Heterochirality Silvia Marchesan; Università degli Studi di Trieste, Italy

Diphenylalanine (Phe-Phe) is a popular building block in nanotechnology and materials science. This motif derives from the sequence of Amyloid beta peptide that is prone to self-aggregation and it is associated to Alzheimer's disease. Phe-Phe is well-known to self-assemble into nanotubes with an inner water-channel, but their uncontrolled growth results into hierarchical assembly into toxic microtubes. In this work, we show that the hydrophobic inter-molecular (social) interactions are responsible for the association into microtubes, and their replacement with intra-molecular (asocial) contacts is key to avoid microtube formation and alleviate cytotoxicity in vitro.

Interestingly, substitution of one amino acid with its mirror-image to yield D-Phe-L-Phe is sufficient to hinder microtube formation. As a result, a homogenous population of 4-nm wide fibrils is obtained that form a network yielding a macroscopic hydrogel. Full-atom molecular dynamics simulations, single-crystal XRD data and spectroscopic analyses allowed us to unravel the fine (supra)molecular details of the process. Furthermore, halogenation of the building blocks is an additional variable proved to be effective to fine-tune self-organization.

The soft matter formed by self-assembly of short, heterochiral peptides is reversible and gel/sol transitions can be triggered by a variety of stimuli, including not only temperature and pH, but also light for instance. The talk will provide examples of the recent research avenues undertaken on using heterochirality as a design strategy to achieve supramolecular soft matter to serve different functions.

S.Kralj et al. ACS Nano 2020 doi:10.1021/acsnano.0c06041

8:25 AM SM09.01.02

Ultra-Short Ionic-Complementary Constrained Peptides (UICPs) as a Chemical Platform for the Development of Bioinspired Multifunctional Nanofibrous Materials Mohamed Elsayw¹, Joseph Hayes² and Jacek Wychowaniec³; ¹De Montfort University, United Kingdom; ²University of Central Lancashire, United Kingdom; ³University College Dublin, Ireland

Peptide non-covalent assembly has been classically studied as the main culprit implicated in a variety of 'protein aggregation' diseases, such as Alzheimer's, Parkinson's, Huntington's, Prion diseases, and others. In the last three decades, the process has attracted material designers as a bioinspired strategy for the development of peptide-based assembling functional nanomaterials; which showed great potential for a wide variety of biomedical and pharmaceutical applications (X. Zhao & S. Zhang. *Macromol Biosci.* 2007, 7, 13; R.V. Ulijn & A.M. Smith. *Chem. Soc. Rev.* 2008, 37, 664; A.L. Boyle & D.N. Woolfson. *Chem. Soc. Rev.* 2011, 40, 4295; A. Altunbas & D.J. Pochan. *Top Curr Chem.* 2012, 310, 135; Dasgupta et al. *RSC Advances* 2013, 3, 9117; C. Edwards-Gayle & I. Hamley. *Org. Biomol. Chem.* 2017, 15, 5867). The high versatility of material requirements for different applications makes it important to have a tuneable and multifunctional system by molecular design.

Recent endeavours in our group focus on the molecular engineering of Ultra-short Ionic-complementary Constrained Peptides (UICPs) as a chemical platform for the development of bioinspired cost-effective multifunctional materials. Using bottom-up rational design approach combined with computational modelling, we have developed the parent UICP tetrapeptide sequence Phg4, which is the shortest reported ionic-complementary peptide that self-assemble into thermodynamically stable β -sheet structures forming amphiphilic nanofibers capable of both gelation and emulsification (J. Wychowaniec *et al.* *Biomacromolecules* 2020, 21, 2670). Phg4 nanofibers demonstrated unique surface activity in the presence of immiscible oils and were superior to commercial emulsifiers in stabilizing emulsions and emulgels (EMGs) under a range of storage and stress conditions. These results imply the considerable potential of UICPs as biocompatible excipients in pharmaceutical, cosmetics, and food industries. In addition, interfacial self-assembly has led to the fabrication of nanofibrillar microspheres suitable for cell microencapsulation and scaffolding for supporting cells proliferation and differentiation processes. UICP microspheres were also manipulated for fine-tuning release kinetics of multiple drug cargos, both of hydrophobic and hydrophilic nature.

We are currently developing a range of next generation UICP sequences with a variety of aromatic residue designs and charged residues distributions, for further adjusting molecular assembly, gelation and interfacial properties to meet the intended application needs.

ACKNOWLEDGMENTS

The authors would like to thank International Newton Fund (Newton-Mosharafa Scheme) and the Engineering and Physical Sciences Research Council (EPSRC Grant no: EP/G03737X/1) for financial support of this work, and Diamond Light Source for the Beam Time Award (SM17102). Authors would like to thank Prof. Alberto Saiani from School of Materials, University of Manchester for scientific discussions of SAXS data analysis.

8:40 AM *SM09.01.03

Harnessing Biological Organization Principles to Engineer Active and Dynamic Materials Alvaro Mata; The University of Nottingham, United Kingdom

Living systems have evolved to grow and heal through self-assembling processes capable of organizing a wide variety of molecular building-blocks at multiple size scales. While advances in nanotechnology and biofabrication are enhancing our capacity to emulate features of some of these biological structures, it is increasingly evident that recreation of their complexity and adaptability will require new ways to build with molecules such as peptides and proteins. This talk will present our laboratory's efforts to combine

supramolecular events found in nature such as disorder-to-order transitions(1,2), diffusion-reaction processes(2,3), and organic-inorganic interactions(1) with engineering (e.g. biofabrication techniques)(4) or materials science (e.g. host-guest complexes)(5) approaches to organize peptides and proteins into hierarchical and functional materials with emergent properties.

References

1. Elsharkawy et al (2018). Nature Communications, 10.1038/s41467-018-04319-0.
2. Wu et al (2020). Nature Communications, 10.1038/s41467-020-14716-z.
3. Inostroza-Brito et al (2015). Nature Chemistry, 10.1038/nchem.2349.
4. Hedegaard and Mata (2020). Biofabrication, 10.1088/1758-5090/ab84cb
5. Redondo-Gomez et al (2020). Biomacromolecules, 10.1021/acs.biomac.9b00224.

9:05 AM SM09.01.04

Protein-Based Conductive Polymers—From Flexible and Stretchable Electronics to a Platform for Light-Stimuli-Responsive Material Nadav Amdursky; Technion–Israel Institute of Technology, Israel

We are inspired by nature for its utilization of proteins for a variety of function, and specifically to our work, the ability of proteins to form high-hierarchical structures and the ability of proteins to mediate charges (electrons, protons and ions) across specific pathways from the nm-scale up to the μm scale. and we use proteins for the formation of responsive materials. With this biological inspiration, we report here on a new family of conductive and free-standing biological materials, where we use different types of proteins as building blocks to form various types of materials. With this in mind, we focus only on proteins that can be produced in bulk quantities and in low cost from raw materials, in which most of our work to date has been focused on the bovine serum albumin protein. We show that using our (bio-)polymerization approach we can form highly elastic polymers in large scale, capable of stretching more than 5 times their length. Due to the relatively high water uptake of our protein-based polymers and the presence of many amino acids residues that can participate in hydrogen bonding, our new protein-based polymers showing good protonic and ionic conductivity. Following the formation of the biopolymer, we show that it can be further functionalized in different ways. For enhanced protonic conductivity we add oxo-acids to the polymer, resulting in measured ionic conduction of >10 mS/cm at room temperature. For enhanced electronic conductivity we can dope the formed polymer with natural electron mediating small molecules. For gaining new light-stimuli-responsive we attach to the protein-based polymer light-responsive molecules, resulting in the large light attenuation of its electrical properties. From blue skies research perspective, the protein-based nature of our materials enables us to explore the governing factors and mechanisms of long-range biological charge transport. Nonetheless, our new protein-based biopolymers have several attractive properties for their possible integration in various applications. Our materials are environmentally friendly, they possess inherent biodegradability and biocompatibility, they have attractive mechanical properties and their formation obeys to most principals of green chemistry. From a practical point of view, we introduce here a very easy polymerization method that requires no synthesis and it is energy efficient, and in addition, our chosen proteins are having low price tag, resulting in a materials cost of around $\$1/\text{cm}^2$. Currently, our main targeted application for our new family of materials is for biological interfaces, while other lines of applications include the use of our biopolymers for biomedical application (tissue engineering) and for energy applications such as membranes for fuel cells.

9:20 AM SM09.01.05

Late News: Artificial Protein Design Rules to Harness Protein Tertiary Structures for Polymeric Materials with Exotic Mechanical Behaviors Minkyu Kim; The University of Arizona, United States

Unprecedented physical, chemical, and biological properties of natural materials inspire next-generation polymeric materials for healthcare, defense, and industrial applications. For example, muscle tissues and red blood cells (RBC) largely alter their structures under mechanical stresses to dissipate energy and prevent tissue or cellular damage before recovering when environmental stresses decrease. Single molecule studies revealed that the macroscopic mechanical behaviors are strongly correlated to exotic nanomechanics from their protein

tertiary structures. Design rules are in place to guide the incorporation of intrinsically disordered proteins into polymeric materials, which have been established using synthetic polymers. However, design rules to harness protein tertiary structures into macroscopic polymeric materials are unclear because the strand flexibility with structured proteins is significantly dissimilar with nonstructured polymer-based strands.

Here, we designed artificial proteins, composed of rigid tertiary and flexible nonstructured protein modules in specific ratios and arrangements to identify design rules for incorporating protein tertiary structures in polymeric materials. The rigid module consists of RBC ankyrin repeats, known for its solenoidal shape and nanospring behavior under applied external forces. The flexible module comprises polyelectrolytic, nonstructured protein repeats. These protein modules were genetically inserted into a telechelic, associative construct with self-oligomerizing protein endblocks to form hydrogels in aqueous conditions. Using mechanical testing, we identified that an asymmetric flexible-rigid protein design with an optimal flexible length enhances the hydrogel rheological properties compared to hydrogels composed of only flexible or rigid protein modules. This indicates that controlling strand flexibility can improve the crosslinking effectiveness in polymeric materials, which can potentially enhance the macroscopic material performance. Furthermore, our current effort to identify specific and strong self-oligomerizing protein endblocks that will properly exhibit protein nanomechanics at the macroscopic material level will be discussed. This design discovery will culminate in an artificial protein platform that harnesses mechanical proteins with diverse tertiary structures into self-assembled materials for exotic mechanical behaviors, which we expect to advance a wide variety of healthcare applications, including but not limited to tissue engineering, drug delivery, and regenerative medicine.

9:35 AM SM09.01.07

A Protein-Based Free-Standing and Proton-Conducting Transparent Elastomer as a Sustainable Material for Large Scale Sensing Applications Ramesh Nandi; Technion–Israel Institute of Technology, Israel

A most important endeavor in modern materials research is shifting toward green environmental and sustainable materials. Natural resources are one of the attractive sustainable building-blocks for making environmentally-friendly materials. However, in most cases, the performance of nature-derived materials does not match the performance of carefully designed synthetic materials, particularly for conductive polymers, which is the topic here. Inspired by the natural role of proteins in mediating protons, we show here their utilization for making free-standing transparent polymer having highly-elastic nature and proton conductivity comparable to synthetic polymers. Importantly, the polymerization process is relying on the natural protein crosslinkers and is spontaneous and energy-efficient. The used protein, bovine serum albumin, is one of the most affordable proteins, resulting in the ability to form large-scale materials at low cost. Due to the inherent biodegradability and biocompatibility of the elastomer, it is promising for biomedical application, and here we show its immediate utilization as a solid-state electrode for sensing physiological signals.

9:39 AM SM09.01.08

Late News: Artificial Protein Design as an Effective Material Platform for Antimicrobial Peptides Fathima T. Doole¹, Lauren G. Melcher¹, Christopher P. Camp¹, Anne M. Wertheimer^{1,1}, Abhishek Singharoy², Michael F. Brown^{1,1} and Minkyu Kim^{1,1}; ¹University of Arizona, United States; ²Arizona State University, United States

Antimicrobial peptides (AMPs) are a promising solution to combat antibiotic-resistant superbugs. The major drawbacks of AMPs are their rapid *in vivo* degradation and renal filtration which have led to poor AMP efficacy. Anchoring AMPs with synthetic polymer tethers on biomaterial surfaces can overcome these obstacles by enhancing AMP stability and protecting AMPs from renal filtration. Further, modulating the physicochemical properties of synthetic polymer tethers can potentially maximize AMP efficacy. However, intricate material synthesis and inconsistent yields of tethering AMPs on material surfaces result in varying material performance.

Using artificial protein technology, we developed an “All-in-One” (AiO) protein-based antimicrobial material that contains three major components, similar to conventional AMP-incorporated materials: a material scaffold, biopolymer tether, and an AMP. An elastin-like protein (ELP) was designed as the material scaffold that when in aqueous solution under physiological temperature will make micelles or the ELP can be photo-crosslinked to make hydrogels. Next, a hydrophilic, flexible protein sequence was introduced to the material scaffold to act as a biopolymer tether. Finally, two of the most common AMPs, LL37 and Pexiganan, were chosen to demonstrate and evaluate AiO protein-based antimicrobial materials. To investigate the role of the biopolymer tether, AiO antimicrobial materials with and without tethers were biosynthesized. The AiO material with the tether reduced the growth of *Staphylococcus aureus*, gram-positive bacteria, by 50% more than the material with non-tethered AMP. This could be due to greater flexibility and degrees of freedom of tethered AMPs, which can effectively interact with the bacteria. To investigate this hypothesis, all-atom molecular dynamics simulations are being employed to understand the atomistic level details of the biopolymer tether on AMP activity and membrane interaction. Artificial AiO protein development provides consistent yields and materials performance, as well as the opportunity to engineer material components at a single amino acid level precision to improve the AMP efficacy. Therefore, we anticipate that the AiO protein will advance the use of diverse AMPs as an effective and wide-reaching therapeutic strategy to mitigate antimicrobial resistance

9:43 AM SM09.01.09

Role of Calcium Signaling on Regulated Cell Death Induced by Membrane-Interacting Peptide

Amphiphiles Damien Samways¹, Shantanu Sur¹, Samuel I. Stupp², Morgan Reynolds¹, Michael Sanborn¹ and Manal A. Binqabbus¹; ¹Clarkson University, United States; ²Northwestern University, United States

Peptide amphiphiles (PA) consist of short peptide chains linked to an alkyl tail that can undergo self-assembly into nanofibers. Previous studies have shown that exposure to many types of PA results in cell death, and the assumption has been that this is primarily due to disruption of cell plasma membrane integrity. However, preliminary data in our laboratory has indicated that the effects of certain weak beta-sheet forming cationic PAs on inducing cell death might involve specific stimulation of signal transduction pathways rather than coarse disruption of biological membranes. Our goal was to investigate the effect of PA exposure on intracellular Ca²⁺ homeostasis, which is known to be a major regulator of cell survival. Utilizing live cell Ca²⁺ imaging with the Ca²⁺ indicator Fluo-4, we found that exposure to PA stimulated slow sustained elevations in intracellular Ca²⁺ concentration ([Ca²⁺]_i). This PA-induced [Ca²⁺]_i persisted in the absence of added extracellular Ca²⁺ ruling out the possibility that it was due to Ca²⁺ leak across a disrupted plasma membrane. Rather, the elevation in [Ca²⁺]_i appears consistent with the mobilization of Ca²⁺ from the intracellular endoplasmic reticulum stores, in part through a phospholipase C (PLC)-dependent signal transduction pathway. We hypothesized that the PA-dependent elevation in [Ca²⁺]_i marked the first step in the observed PA-induced cell death. However, surprisingly the cytotoxicity of PA was not significantly reduced by either PLC inhibition or by suppressing Ca²⁺ elevations in the cervical cancer cells by pre-incubating them with the intracellularly active Ca²⁺ chelator, BAPTA-AM. While PA-induced changes in [Ca²⁺]_i do not appear to cause the subsequent PA-associated cell death, these data nevertheless support the hypothesis that PAs can influence vital intracellular signaling processes.

9:47 AM SM09.01.10

Identifying New Strategies to Promoted Adhesion to Non-Polar Substrates by Bacterial Surface Display

Mark T. Kozłowski, Joshua Orlicki, Randall A. Hughes, Thomas H. Segall-Shapiro, Randi M. Pullen and Jimmy Gollihar; U.S. Army Research Laboratory, United States

Polystyrene (PS) and polypropylene (PP) are ubiquitous plastics in our modern world. However, their highly non-polar characteristics can lead to difficulty forming a good adhesive bond. Current methods for PS and PP adhesion rely on high temperatures, solvent plasticization, or extensive pre-treatment and priming. Identifying new strategies to enable good adhesive bonding would provide opportunities for facile repair in the field, new designs for capacitors, and the creation of new types of composite materials.

Biology may point the way to these new strategies for chemically-based adhesion of non-polar substrates. For

example, the filamentous projections (hyphae) of fungi must breach an air-water interface when colonizing new environments and seeking nutrients, and do so by the secretion of a family of natural surfactants known as hydrophobins [1]. Hydrophobins have already been shown to adhere to highly non-polar surfaces, such as Teflon [2], and there is at least one previous report of a designed chimeric hydrophobin successfully adhering to polystyrene [3], meaning this is a promising class of materials deserving further exploration.

Screening the chemical compositional space afforded by peptides and the natural amino acids would be nearly impossible if undertaken in a serial fashion. Recently, the Army Research Laboratory developed a peptide surface display and high-throughput library screening system to find candidate peptides capable of adhering to polylactic acid [4], and to gold nanoparticles [5]. The on-cell peptide screening has the advantages of easy recoverability, the ability to propagate and sequence the genetic code of the adhesive peptides, and possible further improvements of the peptides by directed evolution. In the present work, we use these previously-developed surface display methodology, a peptide library, and a separate hydrophobin library, to screen for affinity and (hopefully) adhesion to non-polar plastics. We believe this work will encourage further exploration of biologically-inspired adhesive agents for non-polar plastics, and provide key insights for the chemical synthesis of new types of non-polar material adhesives.

References

- [1] P.W. Cox, P. Hooley, Hydrophobins: New prospects for biotechnology, *Fungal Biology Reviews* 23(1) (2009) 40-47.
- [2] M. Linder, G.R. Szilvay, T. Nakari-Setälä, H. Söderlund, M. Penttilä, Surface adhesion of fusion proteins containing the hydrophobins HFBI and HFBI from *Trichoderma reesei*, *Protein Sci* 11(9) (2002) 2257-2266.
- [3] I. Sorrentino, M. Gargano, A. Ricciardelli, E. Parrilli, C. Buonocore, D. de Pascale, P. Giardina, A. Piscitelli, Development of anti-bacterial surfaces using a hydrophobin chimeric protein, *International Journal of Biological Macromolecules* 164 (2020) 2293-2300.
- [4] S.D. Stellwagen, D.A. Sarkes, B.L. Adams, M.A. Hunt, R.L. Renberg, M.M. Hurley, D.N. Stratis-Cullum, The next generation of biopanning: next gen sequencing improves analysis of bacterial display libraries, *BMC Biotechnol.* 19(1) (2019) 12.
- [5] J.P. Jahnke, H. Dong, D.A. Sarkes, J.J. Sumner, D.N. Stratis-Cullum, M.M. Hurley, Peptide-mediated binding of gold nanoparticles to *E. coli* for enhanced microbial fuel cell power generation, *MRS Commun.* 9(3) (2019) 904-909.

Distribution Statement A: Approved for public release: distribution unlimited.

9:51 AM SM09.01.11

Late News: A Peptide Based Latent Crosslinker Activated by Thiol-Thioester Exchange Reaction

Makafui Y. Folikumah^{1,2}, Marc Behl¹ and Andreas Lendlein^{1,2}; ¹Institute of Active Polymers and Berlin-Brandenburg Centre for Regenerative Therapies, Helmholtz-Zentrum Geesthacht, Germany; ²University of Potsdam, Germany

Thiol-thioester exchange (TTE) reaction can occur smoothly in neutral aqueous media and is therefore worthwhile to be considered as potential dynamic covalent chemistry for physiological environments ^[1-2].

Typically, the thiol and the thioester functionalities reacting here are part of two separate molecules. Systems making use of a single molecule providing both functional groups employ hydrophobic aromatic moieties. In these cases, a catalyst might be required in order to control the direction of the equilibrium ^[3].

The hydrophobicity of these substrates and the liberation of foul-smelling aromatic thiols limit their use for biomedical application. Here we report on a thio-depsipeptide (TDP), Ac-Pro-Leu-Gly-SLeu-Leu-Gly-NEtSH synthesized by the modification of a standard collagenase activity peptide, Ac-Pro-Leu-Gly-SLeu-Leu-Gly-OEt. TDP was capable of a 'pseudo' intramolecular TTE reaction to yield α , ω -free thiol bearing peptide crosslinker without perceivable foul-smell. We could demonstrate in electrospray ionization mass spectrometry studies that the TDP, Ac-Pro-Leu-Gly-SLeu-Leu-Gly-NEtSH, self-generates a dithiol peptide crosslinker, HSLeu-Leu-Gly-NEtSH (BTDP) as a TTE product in aqueous medium in addition to Ac-Pro-Leu-Gly-SLeu-Leu-Gly-NEtS-Gly-

Leu-AcPro (TXP). When mixed with a panel of thiols, cysteine (pKa 10.8), glutathione (pKa 9.6), methylthioglycolate (pKa 7.8), 4-mercaptobenzoic (pKa 5.9), and *para*-nitrophenol (pKa 4.6) in equimolar concentrations, the fate of exchange products between TDP and the external thiols was found to be dependent on the relative pK_a of these thiols to the attacking TDP thiol. *L*-cysteine with similar thiol pK_a as the attacking TDP thiol yields an additional exchange product Ac-Pro-Leu-Gly-SCys-OH, with a corresponding increase in BTDP peak intensity than observed for TDP only. 4-mercaptobenzoic and *para*-nitrophenol with more acidic thiols relative to the attacking TDP thiol however resulted in a decrease of BTDP peak intensity caused by the lack of breakdown of their respective tetrahedral intermediates, which were clearly visible in the recorded spectra.

A concept for the design of water-soluble single TTE substrates without the need for incorporation of acidic aromatic thiols is presented. Since aromatic thiols are known for their toxicity and unpleasant smell after TTE reactions the newly developed TDP could potentially enable in situ bioconjugation and crosslinking applications.

References

- [1] M.G. Woll and Gellman, S. H., J. Am. Chem. Soc., **126** (36), 11172-11174, 2004
- [2] R. Larsson, Z. Pei, O. Ramström, Angew. Chem. Int. Ed., **43** (28), 3716-3718, 2004
- [3] C. Wang, S. Mavila, B. T. Worrell, W. Xi, T. M. Goldman, C. N. Bowman, ACS Macro Lett, **7** (11), 1312-1316, 2018

SESSION SM09.02: Peptide and Protein based Materials: From Assembly to Applications in Biological Context I

Session Chairs: Chris Kloxin, Aline Miller and Jacek Wychowaniec

Friday Morning, April 23, 2021

SM09

11:45 AM *SM09.02.01

β-Sheet Forming Peptide Hydrogels—From Self-Assembly to Functional Biomaterials [Alberto Saiani](#); The University of Manchester, United Kingdom

The use of non-covalent self-assembly to construct materials has become a prominent strategy in biomaterials science offering practical routes for the construction of increasingly functional materials for a variety of applications ranging from cell culture and tissue engineering to in-vivo cell and drug delivery.[1] A variety of molecular building blocks can be used for this purpose, one such block that has attracted considerable attention in the last 20 years is *de-novo* designed peptides.[2] The β-sheet motif is of particular interest as short peptides can be designed to form β-sheet rich fibres that entangle and consequently form very stable hydrogels. These hydrogels can be easily functionalised using specific biological signals and can also be made responsive through the use of enzymatic catalysis [3-4] and/or conjugation with responsive polymers [5]. Through the fundamental understanding of the self-assembly and gelation of these peptides across length scales [6-8] we have been able to design hydrogels with tailored properties for a range of applications including for the culture of a variety of cells[9-11], injectable and sprayable hydrogels for cell and drug delivery [12-13] as well as shear thinning hydrogel for 3D bio-printing [14-15]. The intrinsic biocompatibility [16] and low immunogenicity [17] of these materials makes them also ideal for TERM applications. Recently we have demonstrated their potential in a range of TERM applications including, oesophagus [18], nerve [19], intervertebral disk [20] and cardiac [21] regeneration.

References:

1. Zhang, S. G., *Nature Biotechnology* 2003, 21, 1171; 2. Zelzer, M. et al. *Chemical Society Reviews* 2010, 39, 3351; 3. Guilbaud J.B. et al. *Langmuir* 2010, 26, 11297; 4. Guilbaud J.B. et al. *Biomacromolecules* 2013, 14,

1403; **5.** Maslovskis A. et al. *Langmuir* 2014, 30, 10471; **6.** Elsayy, M. A. et al., *Langmuir* 2016, 32, 4917; **7.** Gao, J. et al., *Biomacromolecules* 2017, 18, 826; **8.** Wychowaniec, J. Et al. *Biomacromolecules* 2020, 21, 2285; **9.** Mujeeb, A. et al., *Acta Biomaterialia* 2013, 9, 4609-4617; **10.** Castillo Diaz, L. A. et al., *Journal of Tissue Engineering* 2014, 5, 2041731414539344; **11.** Castillo Diaz, L. A. et al. *Journal of Tissue Engineering* 2016, 7, 2041731416649789; **12.** Roberts, D. et al. *Langmuir* 2012, 28, 16196; **13.** Tang, C. et al., *International Journal of Pharmaceutics* 2014, 465, 427; **14.** Raphael, B. et al., *Materials Letters* 2017, 190, 103; **15.** Chiesa J. Et al. *Frontiers in Medical Technology* DOI:10.3389/fmedt.2020.571626 (2020); **16.** Morris O. et al. *Journal of Labelled Compounds and Radiopharmaceuticals* 2017, 60, 481; **17.** Markey A. et al. *Journal of Peptide Science* 2017, 23, 148; **18.** Kumar D. et al. *Advanced Functional Materials* 2017, 27, 1702424; **19.** Faroni et al. *Advanced Healthcare Materials*, 2019, 1900410; **20.** Corimo L. et al. *Acta Biomaterialia* 2019, 92, 92; **21.** Burgess K. et al. *Materials Science & Engineering C* 2020 in press.

12:10 PM SM09.02.02

Simulating Peptide Self-Assembly on Single Layer Materials via Asynchronous Markov Chain Algorithms Siddharth S. Rath, Michael Malone, Chandler King and Mehmet Sarikaya; University of Washington, United States

Predictively controlling the self-assembly of biomolecules at solid interfaces is crucial for the development of functional substrates at bio/nano soft interfaces. The self-assembly of peptides is largely impacted by environmental conditions such as temperature, pH, and concentration. However, the extent to which these environmental conditions dictate peptide self-assembly on atomically single-layer materials is largely unknown. Here we show a computational modeling approach that enables a greater understanding of how adjustments of environmental conditions affect peptide self-assembly. We modify asynchronous Markov chain algorithms to investigate the impact of environmental conditions on peptide self-assembly. The original purpose of the Markov model was to visualize programmable matter that can achieve complex self-organizing ensembles. This is carried out using particles with extremely limited computational power. We modify these algorithms to achieve a virtual self-organizing particle system representative of self-organizing solid binding peptides. The overall self-assembly process is simplified to include the most significant steps: 1. Peptide adsorption/desorption, 2. Diffusion across substrate, 3. Clustering of peptides, and 4. Break-up of clusters into linear formations based on favorable conformation-mediated intermolecular interactions. Our Markov model currently allows for variable adjustments in particle surface concentration, adsorption rate, strength of intermolecular interactions, and diffusion coefficients. Various combinations of these bias parameters yield unique self-organizing particle systems with distinct characteristics, similar to the differences in self-assembly characteristics between various solid binding peptides. We show, therefore, that Asynchronous Markov Models provide a simple modeling platform for biomolecular self-assembly on atomically flat solids along with avenues to tune binding energies, adsorption/desorption rates, temperature, effects of concentration, pH, and structure-mediated intermolecular interaction energies as well as lattice mismatch parameters. Such models allow one to fit simulated models with AFM images, including grain size, chiral angles, degree of ordering, and surface coverage, estimate several energetic parameters involved in the self-assembly process, towards better characterization and understanding of interfacial properties in soft bio/nano interfaces and their implementation into practical devices. The research is supported by NSF-DMREF program.

12:20 PM *SM09.02.03

Programming Sequence-Defined Peptoids for Bio-Inspired Synthesis of Functional Nanomaterials Chun-Long Chen; Pacific Northwest National Laboratory, United States

Proteins are the molecular machines that carry out the vast array of functions needed for the survival and propagation of all cellular organisms. Many proteins form this machinery by folding into functional building blocks that self-assemble into extended networks to deliver sequence-specific functions ranging from photosynthesis, to molecular separation, selective ion transport, and tissue mineralization. Inspired by nature, many sequence-defined molecules have been exploited for the preparation of nanostructured functional materials. Peptoids are one of the most advanced classes of sequence-defined synthetic foldamers. By bridging

the properties of proteins and polymers, they offer unique opportunities for the synthesis of biomimetic materials with controlled structures and tunable functions.

In this talk, I will discuss our recent efforts in designing amphiphilic peptoid sequences for bio-inspired synthesis of functional materials (e.g. membrane-mimetic 2D nanosheets, dynamic nanotubes, pore-forming networks, and flower-like fluorinated nanoparticles). For these self-assembly systems, peptoid-peptoid and peptoid-substrate interactions play critical roles in the peptoid assembly and can be tuned through the peptoid sidechain chemistry. By programming these peptoids with responsive functional groups and sidechains, we developed a variety of responsive hierarchical nanomaterials. Due to the high stability and programmability of these biomimetic materials, we further demonstrated the incorporation of various functional groups into these peptoid-based materials for specific applications. Our results indicate that self-assembly of amphiphilic peptoids into hierarchical structures can be used as a robust platform to develop biomimetic materials with tunable structures and controllable functions.

12:45 PM SM09.02.04

Designed Interfaces Between Proteins and Inorganic Crystals for Templated Assembly and Co-Assembly
Sakshi Yadav; Pacific Northwest National Laboratory, United States

Previously we have shown we could use Rosetta to design proteins that exhibited a lattice match to mineral surfaces. We discovered that we could exploit those interactions and designed protein-protein interfaces to generate a variety of ordered 2D phases (micrometer-long wires and extensive honeycomb arrays) that were strongly dependent on electrolyte type, electrolyte and protein concentration, and protein sequence. Even without designed protein-protein interfaces, rod shaped proteins with the protein-mineral interface assembled into 2D ordered phase with defined planes characteristic of smectic phases, which is surprising considering that 2D smectic phases have not been observed in colloidal nanorod systems nor are they predicted by Monte Carlo simulations of non-interacting rods. Thus, these assemblies must result from the competition between protein-protein interactions, protein-mineral interactions, and colloidal forces. Our knowledge of the protein-mineral interactions is informed by machine learning analysis that shows the orientation dependent energy landscape is complex and depends on electrolyte type and concentration, and theoretical analysis that shows a far-field reversal in the polarization response which may be the cause the distinct behavior seen with Na^+ vs K^+ . We are now exploring the co-assembly of different proteins at a solid-liquid interface to both investigate the role of complementarity and frustration in defining order and to generate higher-order assemblies. In addition, we are working to “lock” the protein assemblies formed in one set of conditions as a means of creating extensive, anisotropic 2D protein layers as scaffolds for subsequent mineralization and 2nd component assembly under disparate conditions.

12:55 PM SM09.02.05

Understanding the Impact of Sequence Length, Composition, and Dispersity on the Melting Transition and Assembly of Collagen-Like-Peptide (CLP) Triple Helices
Phillip Taylor, April Kloxin and Arthi Jayaraman; University of Delaware, United States

Recent advances in materials design, synthesis, and simulation have allowed the creation of biomimetic materials with responsive yet controllable physicochemical properties. Materials that self-assemble into desired morphologies such as fibrils and supramolecular networks are of particular interest, where their ability to self-assemble can be tuned by applying external stimuli such as heat, light, pH, and salt for a range of applications including in drug delivery and tissue engineering. In this talk, we will present our recent work involving coarse-grained (CG) simulation studies on the melting transitions, fibrillar assembly, and gelation of collagen-like peptides (CLPs). CLPs are thermoresponsive biopolymers in which each CLP chain is made up of repeat units of amino acid triplets, (X-Y-G), where X and Y are usually proline (P) and hydroxyproline (O), respectively. Like native collagen, CLPs have been shown to assemble to form triple helices, fibrils, and gels in aqueous solutions thus exhibiting self-assembly at multiple length scales. In this work, we extend our CG CLP model to simulate CLP heterotrimers in which the length of each of the three CLP strands forming the triple helix can be

different. Inspired by the heterotrimeric nature of natural collagens, we investigate CLP heterotrimers with sticky ends which self-assemble to form fibrils and fibrillar networks driven by interchain hydrogen bonding. We explore how various design parameters including the length and number of sticky ends in each CLP triple helix, CLP triple helix concentration, and temperature (above and below CLP melting transition) impact CLP assembly. Overall, our work highlights the predictive capabilities of MD simulations in guiding experiments, as these complex peptide systems with unique molecular insights can inform new system designs and streamline the discovery of new, biomimetic platforms.

1:05 PM *SM09.02.06

Stimuli Responsive Protein Vesicles for Biocatalysis and Drug Delivery Julie Champion; Georgia Institute of Technology, United States

Protein vesicles incorporating functional, globular proteins have potential in a number of bio-applications such as drug delivery, biocatalysis, and sensing. We have previously created protein vesicles from mCherry-zipper-ELP protein complexes where ELP is a thermo-responsive elastin-like polypeptide, zipper is a coiled-coil, and mCherry is a model folded protein. As we utilize these vesicles, we have replaced mCherry with more useful functional proteins and have engineered the vesicles to provide both stability and responsiveness. We implemented non-natural amino acid incorporation to enable photocrosslinking strategies to stabilize vesicles and control their swelling and release of cargo as a function of salt concentration. We have modified the ELP amino acid sequence to create vesicles that are pH sensitive and swell or disassemble at acidic pH. With this information, we have demonstrated assembly of biocatalytic vesicles with significant improvements in activity over soluble enzyme and produced vesicles for drug delivery capable of carrying and releasing therapeutic cargoes. The wide range of vesicle properties and functions exhibited in these examples, highlight the versatility of protein vesicles as functional and responsive protein materials.

1:30 PM SM09.02.07

Controlling Blood Coagulation in Supramolecular Vascular Access Grafts via a Feedback-Response Mechanism Boris Arts^{1,2} and Patricia Dankers^{1,2}; ¹Technische Universiteit Eindhoven, Netherlands; ²Institute for Complex Molecular Systems, Netherlands

Introduction

Currently 1 in 1000 people in Europe suffer from end-stage renal disease and require hemodialysis¹. Hemodialysis is a medical procedure to remove waste products from the blood where the blood circulation of the patient is directly connected to a dialysis machine, often, *via* a vascular access graft (VAG). The primary failure of VAGs are due to its low patency rate. Several studies showed that coating the inner lining of the graft, e.g. with heparin, improves the patency rate². However major concerns are expressed regarding the long-term efficacy of those coatings. Hereto the aim of this study is to improve the hemocompatibility of these grafts by controlling blood coagulation through a feedback-response mechanism.

Here we make use of bisurea (BU)-based supramolecular polymers. BU motifs can self-assemble *via* hydrogen bonding resulting in dynamic crosslinks embedded in a soft amorphous polymer phase. Bioactive molecules, e.g. peptides, can be functionalized with BU and mixed in through a modular approach to implement specific properties in the material³.

In our approach heparin is conjugated to the surface of our VAGs *via* a thrombin cleavable peptide (TCP). When in contact with whole blood the enzyme thrombin is designed to cleave the peptide causing heparin to be released (response). In turn heparin can form an inhibitory complex with anti-thrombin, naturally present in blood, thereby inhibiting thrombin activity and decreasing heparin release (feedback).

Experimental methods

TCPs were synthesized by solid phase peptide synthesis. Next, heparin (Hep) was functionalized with TCPs (Hep-TCP). To surface functionalize the graft material an inverse electron demand Diels Alder (iEDDA)

reaction was utilized between tetrazine (Tz) and bicyclooctyne (BCN). Hereto BU-Tz motifs were mixed in the material, while TCPs were functionalized with a BCN moiety.

Fibrous scaffolds were produced by electrospinning of the BU-polymer with or without BU-Tz. Scaffold morphology and fiber diameter were assessed by scanning electron microscopy (SEM). The iEDDA reaction was carried out by incubating the scaffold in reaction mixture containing Hep-TCP. Surface functionalization was investigated through x-ray photoelectron spectroscopy (XPS), water contact angle (WCA) measurements, and toluidine blue staining.

Results and discussion

TCPs were successfully synthesized. The grafting density of TCP on heparin was analysed by $^1\text{H-NMR}$ and UV/vis spectroscopy. A grafting density of 7 was obtained. Scaffolds were obtained by electrospinning with an average fiber diameter of $0.9 \pm 0.1 \mu\text{m}$ and $1.0 \pm 0.1 \mu\text{m}$ for pristine and BU-Tz containing scaffolds, respectively, as observed by SEM.

Activity of thrombin towards TCP and Hep-TCP was assessed in solution by fluorescence spectroscopy. Michaelis-Menten kinetics was used to determine the Michaelis-Menten constant (K_m) and maximum rate of cleavage (V_{max}). Both TCP and Hep-TCP showed similar values of K_m . However, V_{max} almost decreased by a factor 2. This difference might be attributed to inhibitory effects of heparin towards thrombin. Next, scaffolds were surface functionalized with Hep-TCP by incubation in reaction mixture. XPS, WCA and toluidine blue staining revealed the presence of heparin at the surface of the scaffold.

Conclusion

It was shown that heparin could be successfully functionalized at the surface of our supramolecular polymer scaffolds. Next, further investigation towards the cleavage of heparin from the surface of the scaffold should be carried out.

1. Kramer, A. *et al.* The European Renal Association – European Dialysis and Transplant Association (ERA-EDTA) Registry Annual Report 2015: A summary. *Clin. Kidney J.* **11**, 108–122 (2018).
2. Walpoth, B. H. *et al.* Improvement of patency rate in heparin-coated small synthetic vascular grafts. *Circulation* **98**, II319-23; discussion II324 (1998).
3. Koevoets, R. A. *et al.* Molecular recognition in a thermoplastic elastomer. *J. Am. Chem. Soc.* **127**, 2999–3003 (2005).

1:40 PM SM09.02.08

Late News: Binding Affinity of Oligomers Towards SARS CoV 2 S-Protein Through Machine Learning and Experimental Validation [Craig J. Neal](#)¹, Katalina Biondi¹, Elayaraja Kolanthai¹, Aida Tayebi¹, Niloofar Yousefi¹, Ganesh Balasubramanian², Ozlem Ozmen^{1,1}, Ivan Garibay¹ and Sudipta Seal^{1,1}; ¹University of Central Florida, United States; ²Lehigh University, United States

The COVID-19 pandemic has led to over 80 million people becoming infected and has claimed more than 1.7 million lives worldwide. As the pandemic progresses, it has become evident that long term solutions for what can be considered as “new normal” are needed. In this work, we ultimately aim to develop a multi-layer, functional coating architecture to *capture-and-kill* SARS-CoV-2, the virus responsible for COVID-19, which can be formed over personal protective equipment and high-touch surfaces requiring frequent sanitation such as in airports, airplanes, hospitals, public spaces, etc. To facilitate the initial *capture* of SARS-CoV-2, a high-specificity binding element must be determined. Given the immediate, dire need to block viral transmission: our approach aims to accelerate the discovery of such components. We use machine learning techniques such as transfer learning to leverage the vast amount of data that exists in drug discovery databases to overcome limitations of data sparsity for COVID-19-related protein/molecular interactions. First, graph convolutional neural network (GCNN) is pre-trained using a dataset curated from public databases such as DrugBank, ChemBL, and DUDE to build a binary classifier. This classifier is used for virtual screening of binding affinities between small molecules (ligands, aptamers) and relevant proteins (targets). Next, we fine-tune the

resulting GCNN on COVID-19-related data. This GCNN model automatically extracts features from defined “protein pockets” (i.e. binding regions; e.g. SARS-CoV2 S-protein receptor binding domain site) and molecular graph representations of ligands, and classifies them as inactive or active. We rank candidate ligands based on binding scores using molecular docking studies for test priority/potential efficacy. Umbrella sampling simulations using molecular dynamics are employed to determine the free energy of binding for the protein-ligand complex as well as to examine the hydrogen bonding, hydrophobic and non-bonded interaction energies to identify possible stimulus for enhancing the specificity of the binding element. Finally, higher priority candidates are further evaluated and experimentally validated using a commercial binding (S-protein/ACE2) inhibition based assay.

1:43 PM SM09.02.09

High Performance Computing and the Covid-19 Virus Bhushan V. Dharmadhikari¹, Sreejita Patra² and Prabir Patra^{3,4}; ¹Minnesota State University, Mankato, United States; ²Fairfield Warde High School, United States; ³University of Bridgeport, Bridgeport, United States; ⁴University of Bridgeport, United States

An effective way to predict the binding sites of SARS-COV-2 proteins, and enzymes in pulmonary surfactant, is by taking advantage of present-day High-Performance Computing (HPC) capabilities. These are able to identify the response of various pulmonary surfactant proteins, as well as enzymes on the Covid-19 spike proteins. The fundamental dynamics of COVID-19 and lung defender proteins; such as, but not limited to, pulmonary surfactant protein D (SP-D); need to be understood at the atomic level in order to develop new target-specific drugs that can fight against the infection. Amongst many computational and bioinformatics tools available today, the Molecular dynamics (MD) simulation is of great importance.

We performed an MD simulation on two pulmonary surfactant proteins: SP-A and SP-D, using NAMD and CHARMM27 force field parameters. Molecules were solvated using the TIP3P water model with 150 mM of sodium and chloride ions. All the parameters of the simulation were set according to the parameters described in Jeong et al., 2020. The goal of our simulation study is to help develop a carbon nanotube-based (CNT) protein sensor, which will detect the ultra-low quantity of pulmonary surfactant protein levels with a potential of lung disease implications. The MD results show higher readings of RMSD and SASA in the case of SP-D and CNT interactions. SP-D considers CNT to be a foreign body, and shows a higher level of protein structure change in comparison to SP-A. This may also be the case in the presence of COVID-19 pathogens, and could be a factor in the elevated levels of SP-D. Performing similar HPC simulations with COVID-19 can give us insight into how the proteins and lipid complex inside the pulmonary surfactant are affected by the deadly pathogen.

SESSION SM09.03: Peptide and Protein based Materials: From Assembly to Applications in Biological Context I

Session Chairs: Chris Kloxin and Jacek Wychowaniec

Friday Afternoon, April 23, 2021

SM09

2:15 PM *SM09.03.01

Modulating the Temperature Response and Performance of Elastin-Based Adhesives Julie C. Liu; Purdue University, United States

Our group has developed bioinspired protein-based adhesives that combine adhesion from DOPA residues found in mussel adhesive proteins with the mechanical properties of elastin, which can also coacervate in response to the environment. These proteins are cytocompatible, provide the strongest bonds of any rationally designed protein when used completely underwater, and can be easily applied underwater because they coacervate in physiological conditions. Recently, we demonstrated that incorporating short, charged peptide tags can be used to tune the coacervation temperature of these proteins. Furthermore, the recombinant protein

design allowed us to systematically probe the individual contributions and interactions of DOPA and thiol chemistries to adhesion.

2:40 PM DISCUSSION

3:05 PM SM09.03.03

Hierarchically Organized Structure of Electrospun Nanofibers from Computationally Designed Peptide Bundlomers Kyunghee Kim¹, Chris Kloxin¹, Jeffery Saven² and Darrin J. Pochan¹; ¹University of Delaware, United States; ²University of Pennsylvania, United States

Fiber materials from natural proteins or synthetic polymers are ubiquitous in technology due to many features including a high aspect ratio, large surface area, structural tunability, and excellent/tunable mechanical properties. In contrast to synthetic polymers, which involve a distribution of chain lengths/molecular weights and random coil structures, proteins and peptides can have defined sequences of amino acids with uniform lengths/molecular weights, allowing for precise control over molecules, supramolecular structures, and overall hierarchical assemblies. Herein, computationally designed peptides were used to assemble coiled-coil, or 'bundlerner' building blocks for the construction of higher-order fiber materials. The two different, designed bundlomers are coiled-coil bundles that, subsequent to coiled-coil formation, covalently interact with each other to produce rigid-rod, peptide-based polymers. The extreme rod-like morphology and resultant properties of the bundlerner polymers are confirmed by transmission microscopy (TEM) and rheology. Due to its molecular rigidity, the rod chains can exhibit lyotropic liquid crystalline behavior in concentrated solution. The resultant rod chains are subsequently employed to fabricate fiber materials via electrospinning, preserving their unique orientational behavior within the fibers. The rod chains are preferentially aligned along the fiber axis, which is confirmed by x-ray scattering, scanning microscopy, and polarized optical microscopy. Additionally, the mechanical properties of the final nanofibers will be presented.

3:15 PM *SM09.03.04

Programming Phase Separation of (Poly)Peptides for Controlled Nano- and Micro-Structured Materials Kristi Kiick; University of Delaware, United States

Significant attention has been paid to the sequence specificity of intrinsically disordered peptide and proteins owing to their importance in regulating spatiotemporal organization of membraneless organelles in cells and their demonstrated versatility in producing hydrogels, nanoparticles, and sensor platforms. In our laboratory, we have employed amino acid sequences inspired by structural proteins such as collagen, elastin, and resilin, and have tailored their stimuli-responsive behavior to enable finely tuned control over both microscale and nanoscale structures. Their conjugation via chemical methods affords biomaterials with diverse properties responsive to multiple triggers, and select modification of their sequences facilitates nuanced manipulation of their assembly and responsiveness. We have also investigated the controlled retention and release of cargo via biomimetic mechanisms, offering substantial improvement in activity for both small molecule and macromolecular cargo, with targeted applications in tissue repair.

3:40 PM *SM09.03.05

Adaptable Hydrogels for Organoid Culture Sarah C. Heilshorn; Stanford University, United States

The term "organoid" refers to an artificially grown collection of cells that resembles aspects of a native organ. While organoid culture has the potential to revolutionize our understanding of human biology, current protocols rely on the use of Matrigel, a complex, heterogeneous protein-based material with large batch-to-batch variations that hinder reproducibility. In response, several groups have begun designing synthetic hydrogel systems based on polyethylene glycol to enable the reproducible culture of organoids. As a fully biodegradable alternative, here we present the design of an engineered protein hydrogel system for reproducible organoid culture. Our family of double-network hydrogels undergo two stages of crosslinking: the first stage uses reversibly dynamic covalent chemistry bonds, while the second stage reinforces the hydrogel through thermal-

induced protein aggregation. Recently, the matrix stress relaxation rate (i.e. the ability of a hydrogel to remodel its network connectivity in response to an applied stress) has been demonstrated to have profound effects on encapsulated cells. To date, the role of matrix stress relaxation on organoid cultures has been underexplored. Our engineered double-network of physical interactions results in a gel with a broad dynamic range of tunable mechanical properties, where the gel stiffness is set by the number of crosslinks and the gel stress relaxation rate is independently set by the kinetics of the crosslink binding and unbinding. These novel, double-network hydrogels are being used to study the role of mechanotransduction in the culture of several different types of patient-derived, human organoids.

4:05 PM SM09.03.06

Designed 2D Binary Protein Materials Geared to Modulate Cells Behavior Ariel J. Ben-Sasson¹, Joseph Watson², Alice Bittleston², Logeshwaran Somasundaram¹, Justin Decarreau¹, Andrew Drabek³, Stephen Blacklow^{3,4}, Hannele Ruohola-Baker^{1,1}, Emmanuel Derivery² and David Baker^{1,1,1}; ¹University of Washington, United States; ²University of Cambridge, United Kingdom; ³Harvard Medical School, United States; ⁴Dana-Farber Cancer Institute, United States

Imposing order onto the fundamentally disordered 2D cell membrane matrix upon introduction of an external cue, enables to modulate and reshape the cell behavior. We recently designed a de novo binary 2D protein co-assembling system¹ which, unlike its natural single component counterparts such as S-layers,^{2,3} rapidly assemble into an ordered hexagonal array only upon mixing of its two distinct building blocks (protein components). In a binary architecture, individual components can be designed to remain soluble and amenable for facile functionalization in ambient conditions, and the assembly onset timing and location can be directed and determined by the experimental setup.⁴ We leverage these novel properties of the binary 2D material and repurpose the system to specifically interact with cell membrane proteins and modulate their surface distribution and downstream signaling.

To this end we first selected a membrane receptor, genetically- or peptide-fused a compatible ligand to one of the arrays components, saturated the cell membrane receptors with said component, removed unbound components from the cell environment, and triggered arrays formation by introducing the second component into the system. We found that the arrays' dihedral building blocks (each component monomer first forms a dihedral homooligomer and the mixture of these forms the arrays) that need to first anchor to the membrane, were not suited for this task. We hypothesized this is likely because cell membranes can wrap around the dihedral components' identical two sides, each displaying an equal number of binding sites, thereby blocking assembly. We therefore devised cyclic pseudo-dihedral versions of the array components, which are partly dihedral to allow proper formation of a 2D array, but overall cyclic to allow directional anchoring.

Because the components are individually stable in ambient conditions and peptide fusion provides a rapid and simple way to diversify the components' functionality prior to array formation (and thereby the system functionality post-array formation), we fused to either or both components optical labels as well as ligands to specifically interact with cell surface receptors. A partial list includes: sfGFP to GBP, a GFP binding peptide, F domain to Tie2, EGFR-binder⁵ to EGFR, etc. We exploit the system's multi-parameter controllability to demonstrate formation of biologically-active structures on mammalian cell membranes to tunable dimensions, showcasing ordered receptor clustering and tunable endocytosis properties.

The system's functional modularity, temporal controllability, and targeted location assembly demonstrated here will enable new methods for characterization of structural-functional relations in living systems. This work marries protein engineering and cell biology into a brand new field that would allow probing and elucidating fundamental biological questions.

1. Ben-Sasson, A. J. et al. Design of Biologically Active Binary Protein 2D Materials. bioRxiv 2020.09.19.304253 (2020) doi:10.1101/2020.09.19.304253.

2. Sleytr, U. B., Schuster, B., Egelseer, E.-M. & Pum, D. S-layers: principles and applications. FEMS Microbiol Rev 38, 823–864 (2014).

3. Baneyx, F. & Mattheaei, J. F. Self-assembled two-dimensional protein arrays in bionanotechnology: from S-layers to designed lattices. Current Opinion in Biotechnology 28, 39–45 (2014).

4. Vantomme, G. & Meijer, E. W. The construction of supramolecular systems. *Science* 363, 1396–1397 (2019).

5. Pedersen, M. W. et al. Sym004: A Novel Synergistic Anti–Epidermal Growth Factor Receptor Antibody Mixture with Superior Anticancer Efficacy. *Cancer Res* 70, 588–597 (2010).

SYMPOSIUM SM10

Progress in Green Chemistry Approaches for Sustainable Polymer Materials
April 19 - April 19, 2021

Symposium Organizers

Henri Cramail, Université de Bordeaux
Steven Howdle, The University of Nottingham
Christine Jerome, Univ de Liege
Kyoko Nozaki, The University of Tokyo

* Invited Paper

SESSION SM10.01: Progress In Green Chemistry Approaches for Sustainable Polymer Materials I
Session Chairs: Christophe Detrembleur, Masami Kamigaito and Kyoko Nozaki
Monday Morning, April 19, 2021
SM10

8:00 AM INTRODUCTION

8:05 AM *SM10.01.01

Terpenes as Feedstock for Polymers—Structural Diversity and Post-Synthetic Opportunities Arjan W. Kleij, Francesco Della Monica and Jeroen Rintjema; ICIQ & ICREA, Spain

Terpenes are naturally occurring unsaturated hydrocarbon compounds produced predominantly by plants. Their unsaturation in combination with their rich structural diversity make them interesting building block candidates for biosourced polymer development. While direct homopolymerization of terpenes is a well-known approach to more complex polyolefin analogues, formation of polyester or polycarbonate macrostructures that incorporate terpene monomers is still at its infancy. In this regard, development of novel catalysts that can address the copolymerization of terpene oxides with either cyclic anhydrides (to form polyesters) or CO₂ (to provide polycarbonates) is of high current interest. Our group has been interested in the use of renewable compounds for heterocyclic and polymer synthesis, and initially our focus was on the copolymerization of *D*-limonene and CO₂. The resultant polycarbonates demonstrated a versatile synthetic behavior allowing to fine-tune functionality, thermal behavior and application potential such as increasing the hydrophobicity. At a later stage, we developed polyesters from a range of terpene oxides (including those on limonene, menthene and carene) illustrating a further diversity of structurally useful polymer backbones that allowed to fine-tune the thermal properties over an extensive glass transition temperature range (50-235 deg). In a more recent embodiment of our work, we have used beta-elemene (a terpene with three distinct double bonds) as a precursor towards functional polymer structures by copolymerization with cyclic anhydrides. This has allowed us to devise polyesters with two built-in functional groups that can be addressed and transformed individually giving

impetus to materials with tunable mechanical and thermal features that are not easily feasible through conventional polymerization processes. Key to the development of all these poly-carbonates and poly-esters has been the enabling power of aluminium- and iron-based aminotriphenolate complexes that have privileged catalytic reactivity in the activation of sterically congested terpene oxide monomers. In this presentation, both the importance of catalyst design and the potential of the functional terpene-derived polymers will be discussed in detail.

8:30 AM SM10.01.03

Late News: Recyclable Epoxy Vitrimers Based on Imidazolium-Catalyzed Dynamic Ester Cross-Links Antoine Debuigne, Panagiotis Falireas and Jean-Michel Thomassin; University of Liege, Belgium

Thermosets, and epoxy resins in particular, constitute an important class of materials on the global polymer market that are valued in plethora of applications requiring superior mechanical properties as well as thermal and chemical stability. As downside, however, they can hardly be recycled and reprocessed due to their permanent cross-linked architecture. In response to this concern, adaptable covalent networks featuring dynamic cross-linking based on associative exchange reactions, also called vitrimers, emerged some years ago.[1-4] Above a certain temperature, the kinetic of the exchange reactions increases significantly, the topology of the network changes and the material can be reshaped or healed. In the case of epoxy-acid vitrimers, the relaxation of the network relies on transesterification exchanges promoted by catalysts such as zinc carboxylates, organotin compounds, triphenylphosphine, etc.[1-4] Despite the recognized activity of the latter, the search for alternative non-toxic catalysts with high efficiency, low leaching tendency as well as heat and air sensitivity is still relevant.

As will be discussed in the communication, driven by the attractive properties and catalytic activity of ionic liquids (ILs),[5-6] we designed epoxy-acid resins in the presence of ILs for the first time and produced unprecedented imidazolium-catalyzed epoxy vitrimers.[7] In addition to outstanding features such as chemical and thermal stability, low vapor pressure, high conductivity, imidazolium salts are known as very efficient homogeneous and heterogeneous catalysts especially in transesterification reactions.[5-6] In practice, a series of cross-linked epoxy-acid networks were synthesized from diepoxy and diacid compounds cured in the presence of imidazolium acetate catalysts obtained via a single-step and atom economical Radziszewski multicomponent reaction. The impact of the imidazolium on the course of the curing reaction, the structure of networks and the mechanical properties, will be discussed. The vitrimer-like properties of these IL-containing networks, and so the ability of the imidazolium additives to catalyze the transesterification exchange reactions, will also be demonstrated via stress relaxation experiments. The effect of the nature and concentration of the imidazolium derivatives on the network dynamics will also be discussed. Finally, it will be shown that such imidazolium-containing resins can be recycled several times while preserving their excellent mechanical properties. In addition to demonstrate the capacity of ILs to play the role of catalysts in the field of adaptable networks, this contribution also emphasizes that a low amount of imidazolium within ester networks is likely to induce some relaxation. Moreover, given the great variety of ILs and the large set of reactions they can catalyze, this approach should be applicable to adaptable networks governed by other types of crosslinking bonds and could contribute to the recycling of various polymer resins in the future.

[1] D. Montarnal, M. Capelot, F. Tournilhac, L. Leibler, *Science*, **2011**, 334, 965-968.

[2] M. Capelot, M.M. Unterlass, F. Tournilhac, L. Leibler, *ACS Macro Lett.*, **2012**, 1(7), 789-792.

[3] T. Liu, B. Zhao, J. Zhang, *Polymer*, **2020**, 194, 122392.

[4] M. Guerre, C. Taplan, J. M. Winne and F. Du Prez, *Chem. Sci.*, **2020**, 11, 4855-4870

[5] Z.I. Ishak, N.A. Sairi, Y. Alias, M.K.T. Aroua, R. Yusoff, *Catal. Rev*, **2017**, 59(1), 44-93.

[6] P. Stiernet, A. Aqil, X. Zhu, A. Debuigne, *ACS Macro Lett.*, **2020**, 9(1), 134-139.

[7] P. G. Falireas, J.-M. Thomassin, A. Debuigne, *Eur. Polym. J.*, **2020**, in press.

Funding: F.R.S.-FNRS, PDR, VITRIPILS project (ID 9236)

8:45 AM SM10.01.04

Late News: Predicting Polymer Degradation by Combining Monte Carlo Simulations and Analytical Models Falk Hoffmann¹, Rainhard Machatschek¹ and Andreas Lendlein^{1,2}; ¹Helmholtz-Zentrum Geesthacht, Germany; ²University of Potsdam, Germany

Degradability as a material function is characterized by its kinetics and the degradation time period depending on the specific system environment. (Co)Polyesters like PLGA (poly[*rac*-lactide-*co*-glycolide]) or PCL (poly(ϵ -caprolactone)) degrade in aqueous environments via a hydrolysis reaction, which can be catalyzed by enzymes. In case of these two polymers, water molecules diffuse into the polymer in order to reach the ester bonds in the bulk. The degradation depends on the crystallinity and starts in the amorphous region of the polymer. In these regions, polymers are degraded by chain cuts that are occurring either randomly between all repeating units of the polymer (random chain cut mechanism) or preferentially at the end of the polymer chains (chain end cut mechanism). If the generated fragments are small enough, they dissolve in water and diffuse away, which leads to polymer mass loss. We recently showed with a Monte Carlo simulation that the direction of the diffusion of water molecules or small fragments through a semi-crystalline polymer is not influenced by the internal morphology of its crystalline regions and can be described with a random walk behavior through the amorphous regions of the polymer. [1] Here, we present an equation for the degradation of polymer chains for the random chain cut and the end chain cut mechanism depending on the initial number of repeating units, the initial number of chain ends and the length of diffusive fragments. The degradation function of molecular mass consists of three regions, which are characterized by the current molecular weight of the polymer. It is further investigated, how the type of the chain cut mechanism changes the degradation behavior and additional modifications, e.g. the effect of increasing water sorption and/or autocatalysis, are discussed. Based on the analytical models, which are verified with a Monte Carlo model, we suggest new ways to present and evaluate experimental polymer degradation data that are more precise than the currently established first order assumptions. We demonstrate this by evaluating experimental data and discuss how the model helps to advance degradable material design.

[1] Hoffmann, F., Machatschek, R., & Lendlein, A. (2020). Understanding the impact of crystal lamellae organization on small molecule diffusion using a Monte Carlo approach. *MRS Advances*, 5(52-53), 2737-2749.

8:50 AM SM10.01.05

Late News: Supercritical CO₂ Foaming of PCL Covalent Networks—Taking Benefit From the Thermoreversible Diels–Alder Cycloaddition Maxime Houbben and Jérôme Christine; Center for Education and Research on Macromolecules (CERM), University of Liege (ULiege), Belgium

Foams are versatile materials encountered in our daily life for a wide variety of uses such as cushioning, thermal and acoustic insulation or medical applications. The combination of the mixed properties between a continuous matrix and gas cells and the diversity of pore structures represent a powerful tool for the design of new materials. Among the different polymer foam fabrication processes, the use of supercritical CO₂ has been one of the most investigated in the past decade. Nevertheless, the design of crosslinked polymer foams with high foaming ratio still remains a challenge. Various crosslinking processes mainly based on heating, irradiation with the addition of an external agent have been applied after foaming but remain difficult to perform due to mass transfer issues of the crosslinking agent. When crosslinking occurs before foaming, it dramatically limits the material expansion.

In order to overcome these drawbacks, the present work aims taking advantage of the thermoreversible Diels–Alder cycloaddition to elaborate foams of poly(ϵ -caprolactone) (PCL) covalent networks. Based on this reaction, we considered to induce cross-linking after the foam expansion by playing on the thermal equilibrium of the thermoreversible Diels–Alder cycloaddition. Therefore, low molar mass star-shape PCL end-capped by furan or maleimide were impregnated with CO₂ under supercritical conditions and then foamed under appropriate control of the pressure and temperature. The resulting foam possesses a much higher volume expansion than a pre-crosslinked sample foamed in the same conditions, thanks to the low crosslinking ratio during foaming. These foams exhibit also improved thermal stability thanks to its chemical crosslinking as

compared to non-crosslinked PCL foams. Interestingly, these foams possess shape memory properties due to the semi-crystallinity of the PCL. Thermal stability and shape memory properties were evaluated by dynamic mechanical analysis in both tensile and compression testing with controlled force mode, stress and temperature ramps. Since significant maleimide/furan adduct cyclereversion can be achieved at high temperature, system reversibility and recyclability have also been attested.

This foaming process proves itself very interesting by the formation of highly physically expanded and recyclable crosslinked foams from a non-initially foamable material. This contribution aims at reporting a new concept that can be used for the preparation of highly expanded and crosslinked polymers foams from any semi-crystalline polymers.

8:55 AM SM10.01.06

Late News: Decarbonization and Sustainability Assessment of the Aerospace Phenolic Resin Supply Chain Alicia Piscitelli and Ross Lee; Villanova University, United States

The establishment of fiber reinforced polymers (FRPs) as lightweight structural components is driven by the need for strong, stable materials in stressful environments. Mainly fashioned from glass or carbon reinforcing fibers impregnated with polymer matrices, these composites can significantly reduce fuel consumption in aircrafts, lowering carbon emissions. Nevertheless, they are currently derived from depletable, greenhouse gas (GHG) emitting fossil fuel sources. FRPs present an opportunity to aid the effort of mitigating climate change, a global phenomenon attributed to the accumulation of atmospheric GHGs and associated with negative, irreparable impacts on ecosystems and humanity. Polymer synthesis using alternative, renewable monomer feedstocks would allow for regenerative material origins while providing a pathway to GHG reductions associated with virgin supplies.

One of the most common polymer matrices in aerospace composites is phenolic resin, a material used in secondary structural components for its low flammability and high temperature resistance. Due to strict material specifications within the aerospace industry, the phenol and formaldehyde monomers used to synthesize phenolics must be identical to current supplies. Therefore, the foundational requirements in decarbonizing phenolic's supply chain are scaling up benchtop methods or leveraging currently industrialized processes that produce pure monomers which are also renewably sourced. Current efforts include thermochemical conversion of biomass and fermentation of sugars for phenol and oxidation of bio-methanol for formaldehyde. Another benefit of creating pure supplies is the opportunity to directly substitute feedstocks taking advantage of downstream infrastructure.

Establishing the sustainability of renewable polymer feedstocks requires a balance of whole system perspectives which include social, technical, economic, environmental, and political aspects. This work will assess material criticality and resiliency of feedstocks for organic materials through metrics such as the magnitude and location of material reserves, material substitutability, and corporate importance from a whole systems perspective.

9:10 AM *SM10.01.07

Development and Applications of Self-Immolative Polyglyoxylates Quinton E. Sirianni, Amir Rabiee Kenaree, Rebecca Yardley and Elizabeth Gillies; The University of Western Ontario, Canada

Many traditional applications of polymers have relied on their high long-term stability. For example, it is desired that plastic packaging retains its structure and properties for months or years, while the plastic used in joint replacements should survive for decades in the human body. However, there are growing concerns about the impact of plastic pollution on humans and the environment. It is predicted that almost 12,000 metric tons of plastic will have accumulated in landfills and the environment by 2050. Furthermore, for many applications of polymers in therapeutics and regenerative medicine, it is desired that polymers break down, rather than accumulate in the body. Therefore, interest in developing degradable polymers has been growing. Significant progress has been made in the preparation and application of polyesters and polysaccharides. However, these polymers degrade gradually in many different environments, sometimes more slowly or more rapidly than desired, which hinders their widespread application. To gain a new level of control over when and where

polymers degrade, we have been developing “self-immolative polymers” (SIPs). These polymers are designed to be stable during their use, but then to degrade (depolymerize) rapidly when triggered by a stimulus. Their mechanism of degradation involves a reaction cascade such that a single stimulus event is sufficient to degrade an entire polymer chain. In addition, the stimulus to which they respond can be easily changed by switching a single capping molecule at the end of the polymer. This presentation will describe our research on polyglyoxylates. Polyglyoxylates were synthesized by anionic-like polymerization mechanisms. A diverse library of end-caps was developed, allowing depolymerization to be triggered by stimuli including light, heat, pH changes, reducing agents, and reactive oxygen species. The properties of the polyglyoxylates were tuned by incorporating different pendent groups, either through polymerization of different glyoxylate monomers or through post-polymerization transesterification reactions. Furthermore, amidation reactions were used to convert readily accessible poly(ethyl glyoxylate) to various polyglyoxylamides, which exhibit very different properties than the polyglyoxylates. The function of these degradable polymers was demonstrated through formation of polymer particles, micelles, and vesicles that were capable of loading and releasing molecules on demand. In addition, polyglyoxylates were applied as coatings to release agricultural chemicals in response to stimuli. Overall, this work demonstrates the versatility and applicability of self-immolative polymers across a range of fields.

SESSION SM10.02: Progress In Green Chemistry Approaches for Sustainable Polymer Materials II
Session Chairs: Andrew Dove and Steven Howdle
Monday Morning, April 19, 2021
SM10

10:30 AM *SM10.02.01

From Natural Phenols to High Properties Sustainable Polymers—A Platform Approach Sylvain Caillol; Université de Montpellier, France

Recent years have witnessed an increasing demand on renewable resource-derived polymers owing to increasing environmental concern and restricted availability of petrochemical re-sources. Thus, a great deal of attention was paid to renewable resources-derived polymers and to thermosetting materials especially, since they are crosslinked polymers and thus cannot be recycled. Also, most of thermosetting materials contain aromatic monomers, able to confer high mechanical and thermal properties to the network. Therefore, the access to biobased, non-harmful, and available aromatic monomers is one of the main challenges of the years to come. Starting from phenols available in large volumes from renewable resources, our team designed platforms of chemicals usable for the synthesis of various polymers. Hence, we studied, tanins, lignin-derived vanillin, eugenol or cardanol. Various aromatic building blocks bearing polymerizable functions were synthesized: epoxy, amine, acid, carbonate, alcohol, (meth)acrylates... (Figure 1). These bio-based aromatic monomers can potentially lead to numerous polymers. The substitution of bisphenol A was studied in epoxy thermosets. Materials were prepared from the biobased epoxy monomers obtained from vanillin. Their thermo-mechanical properties were investigated and the effect of the monomer structure was discussed. High Tg phenol-free phenolic thermosets have been synthesized. Phenol and formaldehyde free phenolic thermosets were also prepared with high thermal stability. The properties of the materials prepared were found to be comparable to the current industrial references, indicating a potential replacement of fossil resources. The tunability of the final properties was achieved through the choice of monomer and through a well-controlled oligomerization reaction of these monomers.

10:55 AM SM10.02.02

Characterization of Fibril Hierarchical Self-Assembly of Sugar-Based Poly(D-glucose carbonate) Amphiphilic Block Copolymers in Solution Jee Young Lee¹, Yue Song², Michiel G. Wessels¹, Arthi Jayaraman^{1,1}, Karen L. Wooley² and Darrin J. Pochan¹; ¹University of Delaware, United States; ²Texas A&M

Motivated by the recent drive to replace petrochemical plastics for more renewable source-based materials, our efforts focus on designing and characterizing a next generation biomolecular-based polymer for solution assembly applications. Sugar-derived poly(D-glucose carbonate) (PGC) molecules are synthesized, and their solution chain dynamics and assembly behavior are analyzed in the production of nanoparticles. Unlike conventional vinyl-based polymers with flexible coil-like chains, the PGC system is characterized by its entire backbone composed of semiflexible, hydrophobic glucose monomers where its chain rigidity and local amphiphilicity created by the backbone compared to added side chains are expected to significantly impact both local and global solution chain behavior. First, with a PGC-containing amphiphilic diblock copolymer system, we explored kinetically controlled assembly pathways by variation of solvent composition that lead to the hierarchical assembly of ribbon-like fibers with features that do not follow the traditional BCP micellar-like packing. We show that while the stiffness of the PGC backbone impacts the local BCP chain conformation and chain packing within the assembled nanostructure, the backbone hydrophobicity drives the unidirectional hierarchical fibril growth by the formation of soft patchy precursor particles. Second, to understand how the chain behavior affects the final assembly morphology, the hydrophilic block equivalent homopolymers were studied using small-angle neutron scattering techniques to obtain polymer chain solution properties for a better understanding of the PGC block copolymer chains in similar solvent conditions. These results suggest polymers with unconventional backbone chemistries, frequently found in natural carbohydrate-based molecules, can shed light on the effects of polymer backbone rigidity and hydrophobicity on the assembly pathway and final assembled structures while also presenting opportunities to better understand other bio-inspired green chemistries-based molecules can organize and assemble in various environment conditions.

11:10 AM SM10.02.03

Late News: Multifunctionality by Core/Shell Design of PLLA/PDLA Nanofibres Axel T. Neffe¹, Quanchao Zhang¹, Paul J. Hommes-Schattmann¹, Weiwei Wang¹, Xun Xu¹, Bilal S. Ahmad², Gareth Williams² and Andreas Lendlein¹; ¹Helmholtz-Zentrum Geesthacht, Germany; ²University College London, United Kingdom

Polymeric materials modulating regenerative processes in vivo need to fulfill multiple requirements that include handling, macroscopic performance after implantation, guiding of cellular behavior, as well as degradation creating space for new tissue to form. Addressing the individual requirements by macromolecular chemistry is likely to lead to highly complex polymer systems. In addition, biomaterials with novel chemistry face substantial hurdles in the regulatory process. For translation, use of components already established in the clinic would be highly beneficial, but requires the realization of multifunctionality [1] by material design. Electrospun polymer meshes are of interest as they allow a multiscale design by adjustment of fiber diameter and fiber organization in the mesh (orientation, density) in addition to the macroscopic shape. Furthermore, the porous structure allows facilitates cell migration. Polylactide (PLA) is – due to the histocompatibility with different tissues and its hydrolytic degradability - commonly applied in biomedicine. The rate of crystallization of PLA is however quite slow, and as crystallinity of the polymer matrix is of importance for its mechanical behavior, control over the crystallization would be advantageous. Interestingly, mixtures of isotactic Poly(L-lactide) (PLLA) and Poly(D-lactide) (PDLA) form stereocrystallites [2] that are formed faster than PLA homocrystallites, and moreover have higher thermal, mechanical, and hydrolytic resistance. Furthermore, lactide is considered a green polymer.

Here, we hypothesized that by forming coaxial nanofibers of PLLA and PDLA, it is possible to initiate the formation of stereocrystallites at the interface of the two layers and therefore have a temporal and spatial control over the crystallization of the matrix. In fact, electrospinning of coaxial fibers consisting of a lower M_w ($= 47 \text{ kg mol}^{-1}$) PLLA core and a higher M_w ($= 147 \text{ kg mol}^{-1}$) PDLA shell resulted in amorphous fibers. Annealing of the fibers above the glass transition temperature T_g led to stereocrystallization as shown by Wide Angle X-Ray Scattering. DSC studies could be used to quantify crystallization, but does not represent the situation after spinning as crystallization also happened during the heating phase. The crystallization led to changes in the mechanical behavior as determined in tensile tests at room and temperature in the dry state and under physiological conditions. Interestingly, the stereocrystal containing materials had lower Young's moduli E (9 ± 1

MPa) compared to the as-spun materials (46 ± 8 MPa), and were also softer than PDLA or PLLA, which can be rationalized by localization of the crystals and relaxation effects. In a second step, gelatin was added to the PDLA phase in order to generate fibers that display adhesion sites for cells on the surface, which was shown by labelling of gelatin on the fiber surface. Gelatin did not negatively influence the (stereo)crystallization of PLA and led to a slight reduction of the T_g . The overall morphology can therefore be understood as semi-interpenetrating polymer network with physical netpoints (crystallites). Altogether, a material system with crystallization controlled by design as well as with cell adhesion sites could be formed in one step based on components established in the clinics.

1: A. Lendlein, R. Trask, *Multifunct. Mater.* **2018**, *1*, 010201.

2: V. Izraylit, P. Hommes-Schattmann, A.T. Neffe, O.E. Gould, A. Lendlein, *Eur. Polymer J.* **2020**, *137*, 109916.

11:25 AM SM10.02.04

Late News: A Semi-Continuous Flow Platform for the Direct Preparation of Novel Cyclic Phosphate Monomers from Bulk Chemicals and Their Further Polymerization Toward Functional

Polyphosphoesters Romain Morodo, Raphaël G. Riva, Christine Jerome and Jean-Christophe M. Monbaliu; University of Liège, Belgium

Polyphosphoesters have recently emerged as new materials for biomedical applications thanks to their biocompatibility and biodegradability properties that can be finely tuned by varying their functional side-chains linked to a pentavalent phosphorus. The preparation of polyphosphoesters frequently relies on the ring-opening polymerization of 5-membered cyclic phosphate monomers (CPMs), which are generally synthesized through a 3-step procedure. Starting from bulk chemicals the preparation of such monomers by a batch process is time-consuming, difficult to scale-up and involves safety concerns such as the uncontrolled generation of HCl by-product and the handling of sensitive and corrosive intermediates. To this end, we developed a semi-continuous flow platform allowing the direct preparation of CPMs starting from PCl_3 and a 1,2-diol derivative without isolation of the intermediates. The first step involved the preparation of cyclic chlorophosphite derivatives by reacting a neat diol with a highly concentrated organic solution of PCl_3 at room temperature with an associated residence time of 1 minute in a compact coil reactor. This procedure allowed to produce a wide range of novel cyclic chlorophosphites starting from various diols in moderate to high yields and with a daily productivity of up to ~ 500 g. The scope was also extended to thioalcohol, dithiol, aminoalcohol and diamine derivatives and the process was eventually adapted to a base-involving procedure allowing the conversion of more demanding substrates such as highly hindered pinacol-type diols. The next oxidation step toward cyclic chlorophosphates was directly concatenated with the upstream production of chlorophosphites in a single continuous flow system. A high pressure and an improved mixing capacity allowed to perform the oxidation using 4 equivalents of molecular oxygen in only 21 seconds of residence time at 65°C toward a quantitative conversion while batch procedures usually require tens of hours or days of reaction time. A final functionalization of chlorophosphates toward various CPMs was subsequently integrated in a semi-continuous flow platform where the effluent coming from the oxidation step is directly reacted in a batch reactor. The system allowed to produce the CPMs directly from PCl_3 in an extremely shortened time by a single process without purification and isolation of the sensitive intermediates while mitigating the hazards linked to the corrosive derivatives produced. Among the novel monomers prepared, a bifunctional derivative was successfully copolymerized by ring-opening polymerization allowing the introduction of a typical alkoxy pendant group linked to a pentavalent phosphorus and an additional convertible chloromethyl function directly linked to a main-chain carbon. The introduction of such functionalizations opens new opportunities for the preparation of novel materials with various properties which could be time-dependent through the quick (P-linked group) or slower (C-linked group) degradation of the polyphosphoester linkages.

11:40 AM SM10.02.05

Late News: Fabrication of Hemp Fiber Composites for Hydroponic Application via PVA-Assisted Crosslinking of Hemp Lignin Avinash Kumar Both, Mark A. Helle and Chin Li Cheung; University of Nebraska–Lincoln, United States

Lignin is an abundant, under-utilized, and cheaply available bioresource. It is a phenolic macromolecule which substantially differs depending on the plant species and the type of isolation process. In this presentation, we describe a green approach to make chemically reactive lignins and lignin-containing composite materials. These composite materials were shown to be applicable as growing media for hydroponics. Our reaction scheme was to couple lignin with a bifunctional linker molecule comprising of an aromatic amine group and a protected vinyl sulfone group. The chemical process begins with the conversion of the aniline-amine group of this linker to an electrophilic diazonium salt to react with the electron-rich naphthalene rings of the lignin. The other functional end of the linker was then deprotected under basic conditions to yield the vinyl sulfone for forming covalent bonds to the hydroxyl groups of substrates via the Michael reaction. The only byproducts are harmless inorganic salts. Unlike common composite fabrication processes that require organic solvent, the process is performed in water and thus is eco-friendly.

The increase in hemp farming in the U.S. in recent years has resulted in a large supply of hemp fibers. We demonstrated the application of our green approach to fabricate hemp fiber composites for hydroponics. The lignin inside hemp fibers was functionalized by employing a bifunctional linker to make chemically reactive hemp. The anchored vinyl sulfonate group of the linker was then used to cross-link hemp fibers with polyvinyl alcohol (PVA) to yield hemp fiber composites. These hemp composites were analyzed to have a Young's modulus of 5.4×10^{-3} GPa but were also found durable. Other properties of this composite such as water retention capacity values, C/N ratios, and salinity were evaluated to discern their suitability for hydroponic applications. The hemp fiber composites were applied as hydroponic growing media to grow model plant systems. Our results demonstrated that the hemp composites can be as effective growing media as other commercially available ones.

11:55 AM *SM10.02.06

Carbon Dioxide for Producing Non-Isocyanate Polyurethane Foams, Adhesives, Hydrogels and—Much More! Christophe Detrembleur, Fabiana Siragusa, Thomas Habets, Florent Monie, Maxime Bourguignon, Christine Jerome and Bruno Grignard; CERM, University of Liege, Belgium

The recycling of carbon dioxide (CO₂) by transforming this waste into value has become a major goal in contemporary science. Strategies are emerging to turn this renewable carbon feedstock into valuable engineering plastics while diversifying renewable resources for the sustainable production of consumer materials.¹ Novel routes to efficiently turn CO₂ into polymers are expected to accelerate and facilitate the transition from existing fossil-based to future generations of more sustainable materials while trying to meet the requirements of a circular economy for consumer plastics.

In the first part of this talk, we will discuss how CO₂ can be converted into monomers² that are then involved in step-growth copolymerizations with diamines to produce non-isocyanate polyurethanes (NIPUs)³, greener variants of conventional polyurethanes that are commonly prepared by the toxic isocyanate chemistry. These monomers can be easily and quantitatively produced at the multi-kg scale under solvent-free conditions in our lab. We will show how they can be exploited to design some representative high performance NIPUs materials. We will first discuss how adhesives and coatings can be produced under solvent-free conditions, with adhesion performances on various substrates (aluminum, wood, stainless steel, glass) that compete to those of commercial products, provided that appropriate curing is applied.⁴ We will then report on an innovative robust and solvent-free process for the construction of flexible or rigid self-blown NIPU foams that offers the first realistic alternative to the traditional isocyanate route.⁵ In this process, the CO₂-based monomer is not only exploited to construct the NIPU matrix but also for its self-blowing. If time permits, we will also show that NIPUs hydrogels can be produced in water at room temperature without any catalyst with impressive short gel times.⁶ These hydrogels can be easily reinforced by introducing natural polymers or clay in the formulations prior to curing. All these technologies can be easily scaled-up and are highly versatile, opening new opportunities in the design of more sustainable materials while valorizing CO₂ as a renewable carbon feedstock. In the second part of the talk, we will describe an innovative approach for the facile preparation of new regioregular functional NIPUs (e.g. poly(oxo-urethane)s and poly(oxazolidone)s) at room temperature by using a novel family of monomers prepared by the CO₂ chemistry.⁷ The special reactivity of these monomers will be

discussed, and if time permits, we will show how they can be exploited for the facile construction of other relevant polymers (e.g. polycarbonates, sulfur-containing polymers) under mild operating conditions.^{7,8}

References.

1. Detrembleur et al. *Chem. Soc. Rev.* **2019**, 48, 4466.
2. Detrembleur et al. *Catal. Sci. Technol.* **2017**, 7, 2651.
3. Cramail et al. *Chem. Rev.* **2015**, 115, 12407.
4. Detrembleur et al. *ACS Sustainable Chem. & Eng* **2018**, 6, 14936; *Polym. Chem.* **2018**, 9, 2650; *Polym. Chem.* **2017**, 8, 5897.
5. Detrembleur et al. *Angew. Chem. Int. Ed.* **2020**, 59, 17033 ; patent application EP3760664(A1)
6. Detrembleur et al. *ACS Sustainable Chem. & Eng* **2019**, 7, 12601; *Macromol. Rapid Commun.* **2020**, 2000482.
7. Detrembleur et al. *Angew. Chem., Int. Ed.* **2017**, 56, 10394; *Macromolecules* **2020**, 53, 6396
8. Detrembleur et al. *Angew. Chem. Int. Ed.* **2019**, 58, 11768; *J. Mater. Chem. A.* **2019**, 7, 9844; *ACS Appl. Polym. Mater.* **2020**, 2, 922.

SESSION SM10.03: Progress In Green Chemistry Approaches for Sustainable Polymer Materials III
Session Chairs: Sylvain Caillol and Henri Cramail
Monday Afternoon, April 19, 2021
SM10

1:00 PM *SM10.03.01

New Exo-Vinylencarbonates Based on CO₂ for the Synthesis of Polyurethanes and Polycarbonates
Thomas Schaub^{1,2}; ¹BASF SE, Germany; ²Catalysis Research Laboratory (CaRLa), Germany

Based on the bulk chemical 1,4-butanediol, readily available epoxides and carbon dioxide, a new series of unsubstituted exovinylene carbonates were synthesised. Chemoselective additions of diamines or diols to these cyclic carbonates allow the regiocontrolled synthesis of new functionalised polyurethanes and polycarbonates under mild conditions. This route to polyurethanes avoids the use of toxic isocyanates.

For the monomer synthesis, we also developed a straight-forward approach to separate the catalyst from the exo-vinylene carbonate (EVC) products of the carboxylative cyclisation of primary propargylic alcohols. The liquid-liquid phase synthesis utilises lipophilic silver(I) carboxylate salts and *N,N*-dioctyl modified phosphine (FatPhos) ligands to enhance catalyst solubility in non-polar solvents. Following simple liquid-liquid phase separation, EVCs relevant as monomers for poly(hydroxyurethane) and poly(carbonate) synthesis were isolated in the non-miscible polar phase in good yields and the catalyst was used in recycle experiments.

References:

- 1] Saumya Dabral, Ulrike Licht, Peter Rudolf, Gerard Bollmann, A. Stephen K. Hashmi, Thomas Schaub, *Green Chem.* **2020**, 22, 1553-1558.
- 2] Chloe Johnson, Saumya Dabral, Peter Rudolf, Ulrike Licht, A. Stephen K. Hashmi, Thomas Schaub, *ChemCatChem*, **2020**, DOI: 10.1002/cctc.202001551
- 3] Saumya Dabral, Bilguun Bayarmagnai, Marko Hermsen, Jasmin Schiessl, Verena Mormul, A. Stephen K. Hashmi, Thomas Schaub, *Org. Lett.* **2019**, 21, 1422-1425.

1:25 PM SM10.03.02

Late News: Biodegradable Aliphatic Polyphosphoester-Based Particles—Green Production by Batch and Flow Processes Philippe J. Lecomte, Christine Jerome, Jean-Christophe M. Monbaliu, Raphaël G. Riva, Jérémie Caprasse and Romain Morodo; University of Liège (ULiège), Belgium

Nano- and microparticles are used as carriers for the controlled delivery of an active ingredient with a high potential for applications for, among others, the health care and personal care industry. Particles made up of aliphatic polylactones, typically, polylactide, polyglycolide and polycaprolactone are very well-known since many years. Aliphatic polyphosphoesters less popular even though they this class of polymers has witnessed a renewed interest. This communication aims at comparing the potential of aliphatic polylactones and aliphatic polyphosphoesters with a special attention paid on particles, based on the recent developments carried out in the Center of Education and Research of Macromolecules of the University of Liège.

Ring-opening polymerization of 5-membered cyclic polyphosphoesters is very efficient for the synthesis of high molar mass aliphatic polyphosphoesters. As far as cyclic 5-membered phosphates are concerned, their extremely high sensitivity to hydrolysis remains a strong limitation at the time being. In this context, efficient processes allowing the synthesis of a wide range of aliphatic polyphosphoesters, functionalized or not, will be reported based on: (1) flow technologies, (2) organocatalysis and (3) chemical modification of the polymers. Advantages and drawbacks of aliphatic polyphosphoesters compared to polyesters will be detailed with a special attention on both the synthesis of these polymers and their properties, to assess their potential for future applications. Particles made up of biodegradable poly(phospho)esters will be shown to be prepared by the self-assembly of amphiphilic polymers or by nanoprecipitation in batch or in flow reactors. Depending on the preparation process and the chemical structure of the polyesters, the size and size-dispersity of particles as well as the loading content, loading efficiency and release rate of a model active ingredient will be discussed.

Acknowledgements: Philippe Lecomte is research associate by the Belgian FNRS. The authors thank all the partners of the IN-Flow project carried out under the Interreg V-A Euregio Meuse-Rhine Programme, with €2.1 million from the European Regional Development Fund (ERDF). By investing EU funds in Interreg projects, the European Union invests directly in economic development, innovation, territorial development, social inclusion, and education in the Euregio Meuse-Rhine.

1:40 PM SM10.03.03

3D Printing Sustainable High-Performance Nanocellulose and Chitosan Composites Rigoberto C. Advincula^{1,2,3}; ¹The University of Tennessee, Knoxville, United States; ²Oak Ridge National Laboratory, United States; ³Case Western Reserve University, United States

The ecosystem of 3D printing to fabricate objects from polymeric nanocomposite materials is important for wide use and rapid scale development towards high-performance materials. Other materials based on metallic, ceramic, hydrogels, and other non-metallic do not have as wide a range of properties leading to new structure-composition-property relationships. Nanomaterials together with sustainable biobased polymers can be used to enhance performance in thermoplastics, thermosets, and elastomers and their thermo-mechanical properties. In this talk, we emphasize the use of sustainable cellulosic and non-cellulosic additives to improve the performance of composite polymer materials. This has been demonstrated in the choices of 3D printing methodologies (FDM, SLA, SLS, VSP) which can make use of blended or formulated compositions of these sustainable filler materials. By incorporating nanomaterials such as nanocellulose, nanosilica, nanoclays with 3D printing new designs of toughened materials on commodity polymers, the value chain of biobased materials can be extended to higher values. 4D Printing will be demonstrated based on stimuli-responsive properties as reported.

1:55 PM SM10.03.04

Late News: Recyclable Porous Ionic Liquid Catalysts from One-Pot Emulsion Templating Multicomponent Polymerization Pierre Stiernet, Abdelhafid Aqil and Antoine Debuigne; Uliège, Belgium

Porous poly(ionic liquid)s (PILs) combine the intrinsic features of ionic liquids (ILs) with properties of polymers and porous structures notably enlarged surface area, high ionic density, spatial structuration, and the tunability of their properties via counterions exchange. Over the years, they have become essential materials for many applications, i.e., gas separation, CO₂ capture, energy storage, polymer electrolyte in Li-batteries, sensors and catalysis.^[1] Amongst them, porous poly(imidazolium)s (PIMs) are of great interest for cutting edge

applications, especially for heterogeneous catalysis. Their chemical composition catalyzes a wide range of reactions while their macrostructure allows easy recyclability without the need of advanced purification methods. However, structuring PIMs into porous materials is not trivial and requires multistep approaches based on the polymerization of preformed imidazolium monomers^[2] or by post-modification of porous organic networks. Therefore, the search for simpler and straightforward synthesis of porous PILs is highly relevant. In this respect, the emergence of multicomponent reactions (MCR), in which three or more compounds react and form a product containing essentially all atoms of the starting reagents, offers new opportunities.^[3] This communication aims at reporting a straightforward and atom economical approach for designing interconnected macroporous imidazolium-based networks. The latter combines for the first time the aqueous mediated Radziszewski MCR^[4] under high internal phase emulsion (HIPE) conditions. The catalytic activity and recyclability of these materials are illustrated for transesterification and decarboxylation reactions.^[5]

[1] S. Zhang, K. Dokko, M. Watanabe, *Chem. Sci.* **2015**, *6*, 3684–3691.

[2] K. Mathieu, C. Jérôme, A. Debuigne, *Polym. Chem.* **2018**, *9*, 428–437.

[3] R. Kakuchi, *Angew. Chem. Int. Ed.* **2013**, *53*, 46–48.

[4] S. Saxer, C. Marestin, R. Mercier, J. Dupuy, *Polym. Chem.* **2018**, *9*, 1927–1933.

[5] P. Stienet, A. Aqil, X. Zhu, A. Debuigne, *ACS Macro Lett.* **2020**, *9*, 134–139.

2:00 PM SM10.03.05

Late News: Full Circle Recycling of Silicones and Their Resins Joseph Furgal and Buddhima Rupasinghe; Bowling Green State University, United States

Siloxane based polymeric materials are widely used all over the world due to their chemical, mechanical, and thermal stability, and low-toxicity. Despite their usefulness, a critical issue has been the ability to recycle them effectively. The present methods used to recycle silicone-based materials, such as PDMS, involve high temperatures/pressures, and complicated setups. To address this issue, we have established an efficient room temperature technique for depolymerization of silicone-based polymers and resins in the presence of low catalytic amounts of fluoride in specific high swell organic solvents. The products primarily contain cyclic siloxane units (D4, D5, D6) as verified by GCMS and ²⁹Si NMR. Nearly any silicone resin can be depolymerized quite rapidly using our methods. Silicone rich systems result in the best conversions and the highest quantity of identifiable cyclics, while complex resins resulted in complicated products alongside discernable cyclics. We have also repolymerized the products from this process to reform silicones via acid, base and fluoride catalysis. Our discovery has the potential for large scale industrial processing due to the use of mild conditions and solvent recycling ability.

2:15 PM *SM10.03.06

Using Efficient Chemistries to Create Sustainable Materials Andrew P. Dove; University of Birmingham, United Kingdom

The global need to devise strategies that can provide applicable solutions to recycling plastics is clear and urgent. It is estimated that a total of 8300 million metric tonnes of plastics have been produced to date. Incredibly, more than 40 years after the launch of the recycling symbol, less than 10% of plastics that have been manufactured are recycled; the rest are either poured into landfill, burned to produce CO₂ and other harmful gases or, worst of all, discarded into the environment. There are several potential approaches to solving the plastic problem, all of which have merit and will address a part of the problem in a different way. To ensure success, all approaches need to be followed. One of the best known is the creation of a circular economy, in which used plastic is recycled chemically to yield virgin grade materials. Our work has focussed on new methods to catalytically recycle polymers as well as develop new materials with interesting properties that can be fully recycled by chemical means. Efficiency of the chemistry used is an important aspect to ensure that the energy requirements remain low and waste is limited. To this end, we have focussed on applying highly efficient click chemistries to create new materials, including those from sustainably sourced starting materials, that can be assembled and disassembled on demand. This presentation will cover some of the latest developments from our laboratory in these areas.

2:40 PM SM10.03.07

Late News: Degradation Kinetics of oligo(ϵ -caprolactone) Ultrathin Films—Influence of crystallinity
Shivam Saretia^{1,2}, Rainhard Machatschek¹ and Andreas Lendlein^{1,2}; ¹Helmholtz Zentrum-Geesthacht, Germany;
²University of Potsdam, Germany

Besides the hydrolysis rate of the ester bonds, the degradation behavior of polymers is also influenced by their crystallinity.¹ The tight assembly of polymer chains restricts the access of water/ions to cleavable chemical bonds. In bulk, it is often very difficult to quantify this effect. Degradation-induced crystallization can promote an increase in crystallinity during degradation, which cannot be distinguished from an increase in crystallinity simple because of faster degradation of amorphous segments. Polymers like oligo(ϵ -caprolactone) (OCL) exhibit hydrolytic degradation times even at acidic pH in the range of several days to months. During that time period other ageing phenomena can occur as well. In contrast, the degradation of OCL in ultrathin films takes only a few hours. Here, we hypothesize that we can determine the degradation rate of OCL segments in amorphous and crystalline domains via this approach, which can further be utilized to tailor the degradation of ultrathin OCL films in acidic environments.

We apply the Langmuir technique to generate ultrathin OCL films at the air-liquid interface with precisely adjusted semi-crystalline morphology, including crystal size, number density, thickness, and melting temperature.² Partially crystalline or highly crystalline films of hydroxy and methacrylate end capped linear oligomers are prepared by crystallization at different film areas and surface pressures. Both semi-crystalline films and amorphous films are hydrolytically degraded at pH \sim 1.5 both at room- and at elevated temperature, either at constant surface pressure at the air-water interface or as transferred films on silicon surfaces. By comparing the data for highly crystalline with amorphous films using appropriate quantitative models, we are able to extract the degradation rate constants of OCL segments in amorphous and crystalline domains. The comparison between the polymers with two different end-groups enables further insights whether the chain packing at the crystal surfaces affects free volume within crystalline regions, thereby increasing the permeation of proteolytic ions for faster hydrolytic degradation. Amorphous ultrathin films of OCL diol degraded completely at pH 1.2 within \sim 16 h. Yet, highly crystalline ultrathin films of OCL diol degraded only by \sim 10 % after 14 h at the same pH, even at an elevated temperature of 46 °C.

The present work demonstrates the option to control the hydrolytic degradation of OCL in ultrathin films via crystallization. Besides for determination of degradation rate constants, thin layers with controlled crystallinity can be further investigated as degradable coatings. These coatings are thermoswitchable and the difference in degradation behavior between crystalline/amorphous films suggest a thermally induced acceleration of degradation.

SESSION SM10.04: Progress In Green Chemistry Approaches for Sustainable Polymer Materials IV
Session Chairs: Elizabeth Gillies and Christine Jerome
Monday Afternoon, April 19, 2021
SM10

4:00 PM *SM10.04.01

Renewable Polymers via Precision Polymerization of Plant-Derived Vinyl Monomers Masami Kamigaito;
Nagoya University, Japan

Renewable polymer is now indispensable for sustainable developments of modern materials. Vinyl polymers constitute one of the largest families among various synthetic polymers and are generally prepared from

petroleum-derived vinyl monomers. Nature also produces a variety of vinyl compounds with unique structures, which are often observed in terpenoids and phenylpropanoids. We found that these natural vinyl compounds can be classified into several families such as non-polar olefins, styrenes, and acrylates in a similar way to petroleum-derived vinyl monomers depending on the substituents attached to the vinyl groups. This suggests that they can be polymerized by designing suitable catalysts and initiating systems for the monomers. In addition, their unique natural structures will give specific properties and functions to the resulting bio-based polymers, which cannot be easily attained by polymerization of common simple vinyl monomers derived from petroleum.

From this viewpoint, we have been investigating polymerization of various unique bio-based vinyl compounds, which can be directly obtained from plants or indirectly derived from natural compounds via simple transformation reactions. In particular, we have been focusing on the controlled polymerizations because the controlled polymer structures will further bestow special properties and functions to the bio-based polymers. In this talk, I will discuss our recent results on controlled radical and cationic polymerizations of bio-based vinyl monomers derived from terpenoids and phenylpropanoids for high-performance and functional sustainable polymeric materials.

4:25 PM SM10.04.02

Directional Evaporative Crystallization of Poly(Lactic Acid) in Presence of Polyphenols Yejin Park and Jongwhi Lee; Chung-Ang University, Korea (the Republic of)

The biodegradable polymer, poly(lactic acid) (PLA), has become a material of high industrial value. However, the low toughness and low heat distortion temperature of PLA still limits its industrial use. Since controlling crystallinity is a convenient strategy to improve the heat distortion temperature, many studies have been conducted on PLA crystal engineering. The use of crystallization additives could accelerate the nucleation and growth behavior of PLA, but they should have environmentally friendly properties. Herein, natural polyphenols were employed to improve the crystallinity of PLA, which have strong antioxidant properties. Natural polyphenols can be obtained from various fruits and plants, and they are environmentally friendly and harmless to humans. Polyphenols were used as nucleants for the heterogeneous nucleation of PLA chains by adding in solutions for film casting. Polyphenols were prepared with controlling their sizes in two ways, a top-down ball milling method and a bottom-up precipitation method. PLA was dissolved into a volatile solvent at room temperature, and the biopolymer films were made by a solvent-casting technique. The cast film of solution was partially contacted with a hot plate and experienced directional evaporation under one-way air flow. As a nucleation agent, the existence of polyphenols improved the crystallinity of the PLA films. The polyphenols prepared by the ball milling and precipitation methods have smaller particle sizes than the corresponding raw polyphenols. The degree of PLA crystallinity reflects the size of the polyphenol particles: The smaller the particle size, the larger the surface area, and more nuclei could result. The one-way airflow at a proper temperature produced controlled moving of crystallization front, and as a result, uniform PLA films having polyphenol nuclei were produced. It is expected that natural polyphenols, which have biocompatibility and biodegradability, could serve as crystallization seeds in making PLA films by controlling the crystallinity of PLA, and this novel way to control the crystallinity of PLA could offer new solutions for the future replacement of plastics.

4:30 PM SM10.04.04

Large Thermal Conductivity Anisotropy of Orientated Cellulose-Clay Composite for Fire Retardancy Guantong Wang¹, Jing Liu¹, Lilian Medina², Lengwan Li², Bin Xu¹, Lars Berglund² and Junichiro Shiomi¹; ¹The University of Tokyo, Japan; ²KTH Royal Institute of Technology, Sweden

Flame-retardant materials are widely used in various applications. Most of the flame-retardant materials contain Br and Cl that are reported to form toxins. Montmorillonite-clay/cellulose nanocomposite, a new green functional flame retardant material, shows excellent mechanical properties, gas barrier properties, biodegradability, and flame retardant properties. When the multilayered montmorillonite-clay/cellulose composites are subjected to fire, montmorillonite forms protective surface barriers of intaking oxygen and

volatiles, meanwhile, outside layers of dilative fire retardant composites form a char layer to protect further propagation and insulate the underlayer materials. Nano-cellulose is induced as for its high strength, and high crystalline stiffness to improve composites' mechanical properties, and it is considered as an excellent candidate in the use of thermal management with high thermal conductivity. This intrinsic high thermal conductivity of nano-fibrillated cellulose has brought a new concept for montmorillonite clay/cellulose flame retardant materials [1], reducing the highest temperature by modifying thermal degradation route with the help of high anisotropy ratio of thermal conductivity composites in in-plane direction to dissipate heat. However, the anisotropy of thermal conductivities of composites has not been fully investigated. In this work, we prepared CNF water suspension and clay suspension and mixed them for around five minutes. Next, clay-CNF co-suspension was filtered under vacuum conditions for several hours by using ultra-filtration membranes. The samples which obtained after filtration was finally dried in a dryer under 93 °C for 15 minutes[1]. we measured the anisotropy ratio of thermal conductivity as a function of montmorillonite-clay/cellulose content. We result shows that the cross-plane thermal conductivity depends on the clay content non-monotonically; as the clay content increases from 0% (pure cellulose), the thermal conductivity decreases until the content reaches 80% and then increases until 100%. The in-plane thermal conductivity also shows a non-monotonic dependence on the content; increasing until 50 % and then decreases. This gives rise to the largest anisotropy at clay content of 50 %, where in-plane thermal conductivity is 30 times larger than the cross-plane thermal conductivity. Furthermore, Raman spectroscopy was performed to investigate the orientation of cellulose nanofibrils in the composite, and the analysis reveals that the degree of alignment strongly depends on the clay content with the maximum achieved at 50 % content, revealing that the large anisotropy is originated from the alignment of the cellulose nanofibrils.

KEYWORDS: montmorillonite, nanocellulose, thermal conductivity, anisotropy ratio

[1] Medina L, Nishiyama Y, Daicho K, et al. Nanostructure and Properties of Nacre-Inspired Clay/Cellulose Nanocomposites—Synchrotron X-ray Scattering Analysis[J]. *Macromolecules*, 2019, 52(8): 3131-3140.

4:45 PM SM10.04.05

Catalysts for Polymer Synthesis and Degradation toward Utilization of Renewable Resources Kyoko Nozaki; The University of Tokyo, Japan

Two chemical transformation reactions for polymer synthesis and degradation will be presented aiming at efficient utilization of renewable resources.

1. Polymer synthesis using CO₂

Homopolymerization and copolymerization of 3-ethylidene-6-vinyltetrahydro-2H-pyran-2-one, made from butadiene and CO₂ will be presented.

2. C-C and C-O bond cleavage

Catalyst design for hydrogenative cleavage of C-C and C-O bonds and its use to degrade beta-O-4 structure often found in lignin will be discussed.

SYMPOSIUM SM11

Design and Analysis of Bioderived and Bioinspired Multifunctional Materials
April 20 - April 21, 2021

Symposium Organizers

Patricia Dankers, Technische Universiteit Eindhoven
Feng Jiang, University of British Columbia

* Invited Paper

SESSION SM11.01: Materials Inspired by or Derived From Plant Resources
Session Chairs: Runye Zha and Hongli Zhu
Tuesday Morning, April 20, 2021
SM11

8:00 AM *SM11.01.01

Lignin Fractionation and Valorization with Aqueous Renewable Solvents—Focusing on Higher-Value Applications Mark Thies¹, Amod A. Ogale¹ and Mojgan Nejad²; ¹Clemson University, United States; ²Michigan State University, United States

By exploiting the novel liquid–liquid equilibrium (LLE) that exists between lignin and hot, one-phase solutions of aqueous renewable solvents, crude bulk lignins can be simultaneously fractionated, cleaned, and solvated for conversion to higher-value, high-quality bioproducts. This unusual LLE phase behavior forms the basis for a fractionation process that we refer to as Aqueous Lignin Purification with Hot Agents, or ALPHA. With this recently patented technology, simultaneous control of both lignin purity and molecular weight becomes possible. Furthermore, ALPHA has also been developed for continuous operation, so it can be commercially scaled-up. Finally, the technology has the added advantage of using renewable solvents that are produced within the biorefinery itself, including acetic acid and ethanol.

Lignin is like any other polymer in that the molecular weight can have a dramatic impact on its suitability for a given application. In addition, polymer purity can also be an important requirement if the desired materials properties are to be achieved. Two large and growing markets have been identified for our “ALPHA” lignins: (1) high-performance carbon fibers for automotive applications and (2) rigid polyurethane foams for building spray insulation. In both cases, we are showing how lignin fractions isolated by ALPHA with preferred molecular weights, purities, and chemical functionalities yield decidedly superior performance vs. the starting bulk feed lignins, whether they be Kraft lignins or agriculturally based lignins derived from hybrid poplar or corn stover. In particular, ALPHA lignins exhibit superior spinnability and result in carbon fibers having improved strength and modulus. Alternatively, other ALPHA lignins tuned to have a completely different set of properties are being used to make polyurethane foams at polyol substitution rates of up to 60%, with most foam properties showing improvement over the polyol-based control.

8:25 AM SM11.01.02

Bioinspired Lignocellulose Matrices for Tunable Sorption and Release—From Sustainable Agriculture to Environment Remediation Tahira Pirzada, Jacob John, Charles H. Opperman and Saad A. Khan; North Carolina State University, United States

Being significant components of woody and non-woody plants, lignocellulosic have recently found enormous applications in various fields ranging from biofuels and filtration to battery materials. We present an innovative approach to fabricate bioinspired lignocellulosic materials with tunable sorption and release profiles. We have prepared lignin-cellulose hybrid nanofibers and particles via respective electrospinning and anti-solvent precipitation of mixtures containing biodegradable cellulose and alkali lignin. We find an interesting correlation between the precursor mixture composition and the fiber/particle physical properties. When the sorption and release profile of these matrices is investigated, the matrix composition seems to monitor its capacity and kinetics to sorb and release various types of molecules. In particular, we have examined the scope of these matrices as sorbents for industrial contaminants using model dyes, while efficacy of these matrices as sustained-

release media for agrochemicals is analyzed by using abamectin as the model pesticide. We have also determined the bioavailability of abamectin from various matrices using *in-vitro* bioassays. We believe that by manipulating the composition of the matrices, we can fine-tune their sorption and release profiles, while flexibility in fabricating the matrices in different physical forms further enhance the scope of our approach to be applied in diverse applications.

8:40 AM SM11.01.03

Plant-Inspired Phenyl Chemistry to Engineer Electroconductive Hydrogel Ink for 3D Printing Technique

Mikyung Shin¹, Subin Jin¹ and Jason Burdick²; ¹Sungkyunkwan University, Korea (the Republic of);

²University of Pennsylvania, United States

Electroconductive hydrogels are promising materials for mimicking electrophysiological environments of biological system towards cardiac/neural tissue engineering, therapeutic applications, and bioelectronics. Considering recent approaches of 3D printing technique to fabricate desirable objects for medical applications, injectability, biocompatibility and mechanical strength of those conductive hydrogels are necessarily required. However, current strategy of simple imbedding of conductive additives (e.g., carbon materials, metal nanoparticles, and conducting polymers) into the hydrogel network has challenges to achieve stable gelation, toughness, and high conductivity before and after 3D printing. Herein, we propose two types of plant-inspired phenyl chemistry, i) gallol oxidation and ii) biphenyl formation via Suzuki-miyaura coupling, for *in situ* fabrication of electroconductive hydrogel inks applicable to extrusion-based 3D printing. In the first topic, injectable and conductive microgels are developed for *in situ* deposition of silver nanoparticles on the surface of the hydrogels via redox activity of the gallol moieties - which is abundant polyphenol in plant kingdom, further applying to 3D printing and electrophysiological muscle tissue support. In the second topic, the phenylborate-triggered conductive hydrogels are formed by biphenyl coupling upon gold reduction, exhibiting high cytocompatibility and temporal injectability for printing of biotic-abiotic interfacing layers in bioelectronics. Our finding of the phenyl chemistry would provide an insight to a variety of applications where conductive materials are needed.

8:55 AM SM11.01.04

Design of Fluorescent and Encapsulating Particles from Biosourced Monomers— Shaping,

Characterization, Degradation and Controlled Release Chaohe Hu^{1,2} and Jacques Fattaccioli^{1,2}; ¹École

Normale Supérieure, France; ²Institut Pierre-Gilles de Gennes, France

Since its beginning, in the early 1920's, polymeric industry relies heavily on fossil fuel resources. Approximately 4%-8% oil, gas and their derivatives are nowadays transformed into polymeric materials. Most of them are non-recyclable and non-degradable, hence leading to serious environmental issues, detrimental to wildlife and humans. In this context, there is a need for the development of alternative polymeric products, which, starting from renewable commodities, will share the same level of complexity than current ones derived from oil industry.

Among the various biosourced raw products used to make polymeric materials, vegetable oils are promising for their low cost and intrinsic degradability, but also because their production is already optimized for the food industry. Acrylated epoxidized soybean oil (AESO) is one example of the vegetable oil derivatives that are used as e.g. plastifying additives for the formulation of PVC. Alone, AESO can be readily and rapidly polymerized to give a thermoset polymer. However, as a consequence of its high intrinsic viscosity, most of the research on AESO-based polymer so far is only focused on the bulk, coating or film properties of this material, leaving the possibility to fabricate high added value materials a blind spot.

Herein, we present the development of a simple, “one-pot” approach to manufacture monodispersed AESO microparticles, based on a microfluidic chip with a flow-focusing structure for emulsification and the serpentine zone for UV-induced reticulation. We show that the size and shape of particles can be tailored easily by precisely tuning the nature and concentration of a co-solvent, used to decrease the viscosity of the dispersed

phase, and monitoring the hydrodynamics of the flow. Exploiting the presence of triglycerides structures within the thermoset, we show that the particles are degradable in alkaline conditions. In addition, we show that AESO particles are good at encapsulating model amphiphilic or hydrophobic fluorescent molecules, and at releasing them on long timescales in the external, continuous phase.

Our work is a first step towards the development of a full range of functional microspheres from biosourced raw materials.

9:10 AM SM11.01.05

Deformation Processing of Palm Leaf Materials for Eco-Friendly Food Packaging Debapriya Pinaki

Mohanty¹, Anirudh Udupa¹, James B. Mann² and Srinivasan Chandrasekar¹; ¹Purdue University, United States; ²M4 Sciences Corporation, United States

The proliferation of single-use plastics (e.g., food packaging) has led to investigation of sustainable plant-based substitutes. We report on the immense potential of leaf-sheath from a palm tree—*Areca catechu*—for manufacturing of eco-friendly, single-use food ware, by direct single-step forming of the sheath material. Using microstructural analyses and different mechanical loading paths, we show that this sheath material can accommodate large forming strains of up to 200% prior to failure. The sheath's deformation response is highly sensitive to hydration, with up to 400% increase in forming strain, so that present manufacturing techniques, largely driven by empiricism and heuristics, are far from optimal. The embodied energy for the palm products is 4-5 orders of magnitude smaller than for equivalent plastic or paper products. Our results delineate product shapes that can be formed in a single step using this material, without intermediate pulping processes, thus demonstrating its versatility. The manufacturing approach demonstrated with the palm leaf has inherent advantages over other resource-intensive, multi-step processing methods commonly used with plant materials.

9:25 AM *SM11.01.06

Understanding Structure/Property Relationships of Lignocellulosic Biopolymer Assemblies Through Molecular Modeling and NMR Peter Ciesielski; National Renewable Energy Laboratory, United States

Plant cell walls are highly-evolved nanocomposite materials with impressive properties and useful functionality. The macromolecular assembly of cellulose, hemicellulose, and lignin, collectively termed lignocellulose, serves multiple functions to plants including structural support, transport of water and nutrients, and biological defense. This same material has also served humanity since the beginning of civilization in applications spanning construction materials, clothing, and fuel. Advances in our understanding of the molecular-level structure/property/function relationships of lignocellulose will enable us to use this natural, renewable material to meet the technological demands of modern society, and thereby displace incumbent materials and fuels derived from fossil carbon which are the cause of increasing environmental detriment. In this presentation, I will discuss modeling approaches to understand how molecular characteristics give rise the emergent properties that ultimately govern the bulk behavior of lignocellulosic composites. Specifically, I will present a study of how the molecular structure of xylan, a hemicellulose, impacts its binding affinity to cellulose nanofibrils. Our findings indicate that xylan of degree of polymerization (DP) less than 20 will detach from the surface of cellulose fibrils in an aqueous environment, while xylan polymers with DP greater than 20 remain strongly bound. Next, I will discuss the construction of simulations of a 3-component system including multiple cellulose nanofibrils, cellulose, and lignin. The starting configuration of the polymers is informed by NMR experiments. Simulations varying the monomeric composition of the lignin polymers show that monomers that contain more methoxy groups on the aromatic rings increase the mechanical integrity of the assembly. Finally, I will present recent progress towards development of a coarse-grained dynamics modeling framework that will enable investigations biopolymer assemblies several orders of magnitude larger than those accessible to molecular dynamics simulations.

11:45 AM *SM11.02.01

Thermal Enhancement of Bioinspired Catecholamine Coatings Kyueui Lee¹, Minok Park¹, Katerina Malollari¹, Peyman Delparastan¹, Costas Grigoropoulos¹ and Phillip B. Messersmith^{1,1,2}; ¹University of California, Berkeley, United States; ²Lawrence Berkeley National Laboratory, United States

In nature, catecholamines play important and diverse roles, including neurotransmission, wet adhesion, pigmentation and photoprotection. The special combination of catechols and amines is a subject of high interest, not only for understanding the biological roles of catecholamines, but also as building blocks for synthetic materials. In the proteins that enable adhesion of marine mussels to wet surfaces, the intimate association of catechols and amines is believed to be essential to interfacial adhesion. As a result, combinations of catechols and amines have featured prominently in the design of synthetic adhesive polymers and in multifunctional ‘polydopamine’ coatings. Polydopamine coatings derived from polymerization of catecholamines can be exploited for a variety of practical applications. In this talk we will describe our recent elucidation of the macromolecular nature of polydopamine and describe our attempts to improve the mechanical performance of these coatings. In particular, we recently showed that laser thermal annealing of pDA produced further polymerization of monomeric and oligomeric species leading to fundamental changes in molecular and bulk mechanical behavior, including vast improvement in scratch resistance. Laser-annealed pDA has better scratch resistance than titania and silica, while preserving the multifunctional properties of pDA that are attractive in a variety of contexts. The results of this work suggest new opportunities for the use of PDA in mechanically demanding applications.

12:10 PM SM11.02.03

Diatoms Microalgae as Living Platforms for Optoelectronics Gianluca M. Farinola¹, Stefania R. Cicco², Roberta Ragni¹, Danilo Vona¹, Gabriella Buscemi¹ and Gabriella Leone¹; ¹Università degli Studi di Bari Aldo Moro, Italy; ²CNR-ICCOM, Italy

Diatoms are single celled microalgae which couple photosynthetic activity with the biomineralization process of conversion of inorganic silicate into complex and nanostructured biosilica. Biosilica shells (frustules) exhibit high surface area, periodic porosity, transparency and mechanical resistance. All these features of their silica shells make diatoms appealing living sources of sustainable smart materials for applications in photonics, optoelectronics, sensing and biomedicine [1].

Recently, we demonstrated an *in vivo* protocol which enables frustules’ silica modification by simple introduction of functional molecules into the culture medium. Many functional molecules can be introduced into the biosilica by this approach, including organic [2] and organometallic emitters [3] and also compounds of pharmacological interest [4].

We recently demonstrated that a surface adherent diatom species, *Phaeodactylum tricornutum*, can self-populate and propagate on transparent conductive ITO electrodes, producing photocurrents. In addition, these diatoms can uptake luminescent and optoelectronically active organometallic complexes during their growth and adhesion process. The combination of these features enables to envision microalgae as a platform which can self-assemble in optoelectronically active layers, suitable for producing living micro-devices.

[1] R. Ragni, S. R. Cicco, D. Vona and G. M. Farinola, *Adv. Mater.*, 1704289, 1-23 (2017).

[2] R. Ragni, F. Scotognella, D. Vona, L. Moretti, E. Altamura, G. Ceccone, D. Mehn, S.-R. Cicco, F. Palumbo, G. Lanzani and G. M. Farinola, *Adv. Funct. Mater.*, 28 (24), 1706214-1706223 (2018).

[3] G. Della Rosa, D. Vona, A. Aloisi, R. Ragni, R. Di Corato, M. Lo Presti, S. R. Cicco, E. Altamura, A. Taurino, M. Catalano, G.-M. Farinola and R. Rinaldi, *ACS Sust. Chem. & Eng.*, 7(2), 2207-2215 (2018).

[4] S.R. Cicco, D. Vona, G. Leone, E. De Giglio, M.A. Bonifacio, S. Cometa, S. Fiore, F. Palumbo, R. Ragni, G.M. Farinola, *Mat. Sci and Eng.: C*, 104, (2019).

12:25 PM SM11.02.04

Late News: Robust Biocompatible Composites Inspired from Marine Shell Nacre Hemant K. Raut and Javier G. Fernandez; Singapore University of Technology and Design, Singapore

Addressing the global challenges of sustainability calls for the development of materials using bio-based constituents that can outperform conventional materials. An example of one such bio-based material is chitosan (that is derived from marine shells). However, the use of chitosan in load-bearing structural and industrial applications is limited due to its inferior mechanical properties in comparison to a variety of engineered materials such as ceramics and metals.

Interestingly, the shells of marine species – nacre, from which chitosan is extracted, is one of the strongest known natural materials. This is possible because in nacre the chitin (from which chitosan is derived) is embedded with mineral platelets of calcium carbonate, forming a brick-mortar architecture.

Based on this bio-inspiration, a nacre-mimetic composite comprising bio-based constituents (chitosan and silk) and calcium carbonate minerals is manufactured by a green bio-mineralization approach. The approach enables synthesis of mineralized (calcium carbonate) films with teeth-like patterned microstructures. The films comprising the patterned minerals are then stacked with the patterned sides facing each other and infused with silk fibroin. Subsequent drying consolidates the mineralized films into a nacre-mimetic composite where across successive layers, the films are laterally interlocked due to their patterned topography. The resultant composite exhibits nearly 85% higher tensile strength and elastic modulus at least 10 times higher than that of chitosan owing to the distinctive micro-level interlocking between the mineralized films.

Owing to its bio-based constitution, the nacre-mimetic composite also exhibits biocompatibility and mechanical properties similar to that of mammalian bone, making it potentially useful for hard-tissue regeneration applications.

12:40 PM SM11.02.05

Late News: Micro- and Nano-Structured Camouflage Surfaces Inspired by Cephalopods Yinuan Liu, Zhijing Feng, Chengyi Xu and Alon Gorodetsky; University of California, Irvine, United States

Wrinkled surfaces and materials are widespread throughout the natural world and underpin the functionality of a variety of emerging modern technologies. Indeed, the implementation of wrinkles can improve the performance of controllably-wettable surfaces, conductive electrodes, photovoltaics, and dielectric elastomer actuators. However, despite tremendous progress to date, the reversible post-fabrication tuning of wrinkle sizes across multiple length scales has remained quite challenging, and the development of comprehensive relationships between structure and function for optically-active wrinkled surfaces has often been fraught with difficulties. Herein, by drawing inspiration from natural micro- or nano-structured cephalopod skin components and leveraging methodologies established for artificial adaptive infrared-reflecting and infrared-transmitting soft actuators, we engineer camouflage surfaces with dynamically-reconfigurable morphologies and concomitant tunable visible-to-infrared spectroscopic properties, while also developing an enhanced understanding of the relationship between their local surface structures and global functionalities. When mechanically actuated, our systems can reconfigure their height frequency distributions by ≈ 180 -fold and root-mean-square roughnesses by ≈ 215 -fold; alter their visible to near-infrared total reflectances, transmittances, and absorptances by $\approx 10\%$, $\approx 20\%$, and $\approx 30\%$ and their mid- to long-wavelength infrared total reflectances, transmittances, and absorptances by $\approx 26\%$, $\approx 27\%$, and $\approx 36\%$; and modulate their specular-to-diffuse reflectance and transmittance ratios by ≈ 18 -fold and ≈ 60 -fold within the visible to near-infrared and by ≈ 5 -fold and ≈ 38 -fold within the mid- to long-wavelength infrared. When electrically actuated, our systems maintain their highly-desirable visible and thermal functionalities and feature competitive figures of merit, e.g., reasonable maximum areal strains of $\approx 60\%$, rapid response times of ≈ 0.7 s, and good stabilities upon repeated actuation. Overall, our findings constitute another step forward in the continued development of cephalopod-inspired light- and heat-manipulating architectures and appear well-positioned to facilitate new opportunities in

areas as varied as sensing, electronics, optics, soft robotics, and thermal management.

SESSION SM11.03: Cellulose-Based Materials I

Session Chairs: Feng Jiang and Hongli Zhu

Tuesday Afternoon, April 20, 2021

SM11

2:15 PM *SM11.03.01

New Photonic Materials from Cellulose Nanocrystals Mark Maclachlan; The University of British Columbia, Canada

In nature, structural organization of biopolymers at the nanoscale leads to iridescent coloration, as observed in beetle shells and bird feathers. These structural colors can be mimicked in synthetic materials derived from cellulose nanocrystals (CNCs) because CNCs organize into a helical structure (known as a chiral nematic liquid crystal). When a suspension of CNCs is dried, the resulting film has a chiral nematic structure and, if the pitch of the helical structure matches the wavelength of visible light, the film will appear iridescent.¹

Over the past decade, we have been developing new materials derived from CNCs, with a particular emphasis on creating new photonic materials. For example, we have exploited CNCs as a template to construct novel chiral nematic mesoporous materials with photonic properties.² We have succeeded in preparing silica,³ organosilica,⁴ and polymeric materials⁵ through self-assembly or templating methods.

In this presentation, I will discuss our recent progress using CNCs to create flexible photonic materials that respond to stimuli.^{6,7}

[1] Revol, J.-F.; Godbout, L.; Gray, D. G. *J. Pulp Pap. Sci.* **1998**, *24*, 146.

[2] Giese, M.; Blusch, L. K.; Khan, M. K.; MacLachlan, M. J. *Angew. Chem. Int. Ed.* **2015**, *54*, 2888.

[3] Shopsowitz, K. E.; Qi, H.; Hamad, W. Y.; MacLachlan, M.J. *Nature* **2010**, *468*, 422.

[4] Shopsowitz, K.E.; Hamad, W.Y.; MacLachlan, M.J. *J. Am. Chem. Soc.* **2012**, *134*, 867.

[5] Cao, Y.; Lewis, L.; Hamad, W.Y.; MacLachlan, M.J. *Adv. Mater.* **2019**, *31*, 1808186.

[6] Kose, O.; Tran, A.; Lewis, L.; Hamad, W.Y.; MacLachlan, M.J.; *Nature Commun.* **2019**, *10*, 510.

[7] Boott, C.E.; Tran, A.; Hamad, W.Y.; MacLachlan, M.J. *Angew. Chem. Int. Ed.* **2020**, *59*, 226-231.

2:40 PM *SM11.03.02

Wood Nanotechnologies Liangbing Hu; University of Maryland, United States

I will give an overview of our published work on nanotechnologies using cellulose nanomaterials, with a focus on assembly and functionalization strategies of **wood nanocellulose** aimed at specific properties, with an eye toward high impact applications including energy, electronics, building materials and water treatment, including nanomanufacturing and light management in transparent nanopaper for optoelectronics (as a replacement of plastics); mechanical properties of densely packed nanocellulose for lightweight structural materials (replacement of steel, **Nature** 2018); artificial tree for high-performance water desalination and solar steam generations; mesoporous, three-dimensional carbon derived from wood for advanced batteries (replacement of metal current collectors for beyond Li-ion batteries); nano-ionic thermoelectrics (**Nature Materials**, 2019); radiation cooling (**Science**, 2019).

3:05 PM *SM11.03.03

Renewable Nanoparticles in Superstructured Materials Rojas Orlando^{1,2}; ¹Aalto University, Finland; ²The

University of British Columbia, Canada

Superstructured colloidal materials are proposed to endow new functions to renewable nanoparticles, including chitin and cellulose which can be isolated as large axial aspect nanofibrils or shorter nanorods. Interparticle interactions and ensuing adhesive forces are used for building macroscale assemblies displaying networks with tailorable strength, cohesion, porosity and with opto-mechanical response. Here, we demonstrate that the topology of nanonetworks formed from the respective system enables robust superstructuring of diverse particles, including mineral and organic, representing a generic pathway for the fabrication of a new class of constructs. An intermixed network of fibrils with particles increases the toughness of the assemblies by up to three orders of magnitude compared, for instance, to sintering. Supramolecular cohesion is transferred from the fibrils to the constructs following a power law, with a constant decay factor. Our results are expected to expand the development of functional colloids from laboratory-scale towards their implementation in nanomanufacturing of bulk materials.

3:30 PM SM11.03.04

Super Thermal Insulating Cellulose Aerogel with Quasi-Closed Micropores via Emulsion Templating

Mingyao Song, Jungang Jiang and Feng Jiang; The University of British Columbia, Canada

Due to its lightweight and high porosity, aerogel has been considered a promising material with great potential in thermal insulation application. Although silica aerogel demonstrates ultralow thermal conductivity of less than 15 mW/(m K), its brittleness has limited its wide application. Therefore, flexible and durable aerogel with low thermal conductivity has been actively pursued, especially those derived from natural polymers. In this presentation, we report a cellulose nanofibrils (CNF)/Pickering emulsion composite aerogel with quasi-closed internal pores with extremely low thermal conductivity. The composite CNF/emulsion aerogel was fabricated by Pickering emulsion templating and solvent exchange methods. By removing the oil phase from the emulsion, quasi-closed pores could be generated inside the aerogel, which can reduce the thermal conductivity to 15.5 mW/(m K). The presence of quasi-closed pore from emulsion templating is verified from both confocal microscopy and scanning electron microscopy images. The composite aerogel showed very low density of 11.4 mg/cm³, high mesoporosity, high specific modulus of 18.2 kPa/(mg cm³), and specific yield strength of 1.6 kPa/(mg cm³). The CNF/emulsion composite aerogel also demonstrates superb flexibility and infrared shielding performance. It is expected such all-cellulose aerogel can be used in textile and clothing, as well as building and construction for thermal insulation and management.

3:45 PM SM11.03.05

Nanocellulose-Enhanced High Performance Ionic Conductive Organohydrogels—A Versatile and Adaptive Platform for Multi-Functional Sensors

Yuhang Ye, Yifan Zhang, Yuan Chen, Xiaoshuai Han and Feng Jiang; The University of British Columbia, Canada

To date, ionic conducting hydrogel has attracted tremendous focus as an alternative to the conventional rigid metallic conductors in fabricating flexible and soft electronics, owing to their intrinsic characteristics of high stretchability, transparency, tunable mechanical property, consistent conductive phase, and biocompatibility. However, the current ionic conductive hydrogels still suffer from two long-standing dilemmas, which is between the strength and toughness, as well as between the mechanical strength and ionic conductivity. In addition, ionic conductive (organo)hydrogel with freezing tolerance has not been widely reported, and the current anti-freezing ionic conductive (organo)hydrogel showed unsatisfactorily low ionic conductivity at subzero temperature. Therefore, simultaneous realization of high strength, stretchability, toughness, ionic conductivity, and freezing tolerance through a simple approach is still a challenge.

In this work, a novel polyvinyl alcohol (PVA)- cellulose nanofibrils (CNF) ionic conducting organohydrogel with integrated characteristics, including superb mechanical performance (stress up to 2.1MPa, strain up to 660%), high conductivity (3.2 S/m at room temperature), transparency (90%), freezing tolerance (-70 °C), and long-term solvent retention, was facilely fabricated through a simple sol-gel transition method. Owing to the

existence of DMSO/H₂O binary solvent system, the organohydrogel maintains flexible and conductive (1.1 S/m) even at -70 °C. This material design verifies the synergistic effect of CNF in enhancing both mechanical properties and ionic conductivity, providing a facile solution to address the long-standing dilemma among strength, toughness, and ionic conductivity for the ionic conducting hydrogel. In addition, the ionic conductive organohydrogel exhibits excellent sensing performance and can be rationally assembled into multi-functional sensors to detect full-range human body movement with high sensitivity, stability, and durability. Attributed to these characteristics, this PVA-CNF ionic conducting organohydrogel is believed to function as a versatile and adaptive platform for future manufacturing of multi-functional sensors in extensive applications such as health monitoring, electronic skin, and wearable electronics.

4:00 PM SM11.03.06

Nanocellulose Alignment and Its Application Zhangkang Li and Jinguang Hu; University of Calgary, Canada

Nanocellulose research has addressed increased attention in the bioprocessing community, especially the utility of these materials in different fields including biomedical and materials applications. However, the major concern in today's nanocellulose research is not about production but matters a lot to find a better application where its structural characteristics could be tailored by different methods. In this presentation, a scalable method for the assembly of oriented bacterial nanocellulose (BC) films is presented, based on using wrinkled thin silicone substrates of meter square size as templates during BC biotechnological synthesis. Control samples, including flat templated and template-free oriented bacterial cellulose, along with the oriented BC, are morphologically characterized using scanning electron microscopy (SEM). Multiple functional properties including wettability, birefringence, mechanical strength, crystallinity, water retention, thermal stability, etc., are being characterized for the BC samples, where the wrinkling induced in-situ BC alignment not only significantly improved material mechanical properties (both strength and toughness) but also endowed unique material surface characteristics such as wettability, crystallinity and thermal stability. Owing to the enhanced properties observed, potential applications of wrinkle templated BC in printing and cell culture is being demonstrated as a proof of concept. The excellent improved mechanical properties and respectable printability of wrinkle templated BC also opens the door for various cellulose-based wearable and printable electronic devices and sensors application.

SESSION SM11.04: Protein and Peptide-Based Materials I

Session Chairs: Feng Jiang and Runye Zha

Tuesday Afternoon, April 20, 2021

SM11

5:15 PM DISCUSSION

5:40 PM *SM11.04.02

Programming Self-Assembling Protein Engineered Biomaterials Michael Meleties, Priya Katyal, Kamia Punia, Yao Wang and Jin Montclare; NYU Tandon School of Engineering, United States

Inspired by nature's biopolymers, we engineer artificial protein materials on the genetic and chemical level leading to new properties and function. We employ synthetic and chemical biology to construct our materials and endow them with stimuli-responsiveness. In particular, we have fabricated protein-derived nanomaterials: coiled-coil fibers and helix-elastin block polymers. We investigate the fundamental self-assembly and molecular recognition capabilities of these systems. More importantly, we are able to harness these structure as well as others to interface with small molecule therapeutics and cells. Our studies lead to insights in how we can program self-assembling protein biomaterials to be sensed and respond to external stimuli.

6:05 PM SM11.04.03

Experimental Synthesis and Computational Modeling of Silk-Mimetic Polymers Amrita Sarkar, Tanner Fink, Yanming Zhang, Yunfeng Shi and Runye H. Zha; Rensselaer Polytechnic Institute, United States

Silk fibroins are naturally occurring proteins that can exhibit a combination of strength and toughness far exceeding those achieved by man-made polymers. For example, the dragline silk of the European garden spider has higher tensile strength and stiffness than nylon 6/6, with three times the toughness of Kevlar. The exemplary properties of silk fibroins arise from their chemical architecture, in which rigid hydrophobic and flexible hydrophilic peptide segments linearly alternate. Supramolecular assembly of silk fibroins yield a nanostructured material with crystalline beta-sheet domains, which provide strength and stiffness, dispersed in an amorphous matrix, which provides toughness. Interestingly, silk fibroins bear structural resemblance to synthetic segmented copolymers such as poly(ether-block-amide) (PEBA), yet man-made PEBA are vastly inferior in mechanical properties compared to many natural silk fibroins. Thus, mimicking silk fibroin architecture in synthetic polymers can unlock the path to synthesizing exceptionally strong and robust next-generation polymers. Unfortunately, rational design of silk-mimetic polymers is hindered by: 1) the challenges faced in rapid synthesis of well-defined segmented polymers bearing multiple aggregation-prone "blocks", and 2) the lack of knowledge in predicting how chemical structure and sequence dictates supramolecular structure and mechanical properties. This talk will present our recent work in developing a new route towards efficient synthesis of silk-mimetic polymers. In particular, we discuss a two-stage modular approach based on microwave-assisted chemistry that is capable of generating silk-mimetic polymers with well-defined beta-sheet forming peptide segments and improved molecular weights. This work is the first to demonstrate Cu(I)-mediated click chemistry as a new approach toward efficient step-growth polymerization of silk-mimetic polymers. Notably, this synthetic approach can reach molecular weights within 20 min that far surpass those obtained by traditional peptide coupling reagents, and the resulting polymers readily form silk-like supramolecular structures. The speed and modularity of this synthetic approach offers possibility for creating libraries of silk-mimetic polymers for systematic study of structure-property relationships. Furthermore, this talk will also briefly discuss a new computational model for predicting materials properties based on chemical structure in silk-mimetic polymers. This computational model can reveal fundamental mechanisms in the mechanical behavior of silk-mimetic polymers in relation to molecular and supramolecular structure. Thus, these experimental and computational tools are crucial steps towards enabling rational design and synthesis of silk-mimetic polymers.

6:20 PM SM11.04.04

Programming *Bombyx Mori* Silk's Water-Responsive Actuation Using Silica Nanoparticles Yejin Jung^{1,2}, Raymond S. Tu^{1,2} and Xi Chen^{1,2}; ¹The City College of New York, United States; ²Advanced Science Research Center at City University of New York, United States

Spider silk that mechanically swells and shrinks in response to changes in relative humidity or water gradient has shown capability to exert higher energy than conventional actuators and artificial muscles, and thus holds potential to be used as high-energy actuating components for various engineering applications, including robotics, shape morphing, and smart structures. However, spider silk's low availability largely limits these potential applications. We found that water-responsiveness of *Bombyx (B.) mori* silk, which possesses a similar supramolecular structure to that of spider silk, could be dramatically increased, and even surpasses that of spider silk, by simply adding silica nanoparticles. Mechanical and microstructural analyses using FTIR and AFM, together with our previous studies on water-responsiveness of regenerated silk with various β -sheet crystallinity, suggest that stiff silica nanoparticles could dramatically reduce energy dissipation within silk's supramolecular network, and increase energy conversion efficiency during silk's water-responsive actuation. We also demonstrate that a large-scale actuator of *B. mori* silk/silica nanoparticles composites that reversibly lift a weight powered by humidity changes, showing the possibility of using silk with lower-cost and wider availability as building blocks for high-energy water-responsive structures.

6:35 PM SM11.04.05

Photo-Crosslinking Silks Under Stretches for Boosting Strength Chang Liu and Bin Fei; The Hong Kong Polytechnic University, Hong Kong

Silk fibroin fibers (FFs), produced from natural silk by removing their sericin coating layer, have been used as a biomedical suture material for centuries. Both physical and chemical methods have been used to enhance the strength of silk fibroin. However, the current methods have limitations. For example, the physical methods lead to the brittle nature of silk fibroin due to the increasing of β -sheet content. The chemical crosslink methods show better nature, but they may be time-consuming or lead to cytotoxicity under certain conditions, limiting the fields, especially in biomedical. Therefore, a rapid and mild chemical crosslink method is necessary to develop.

In this study, silk fibroin fibers were crosslinked by employing photoredox catalysis. The chemical crosslink through dityrosine connection was confirmed, and further evaluated by the crosslink density. Further applying tension stretch to the fibers, the break stress and modulus of stretched photo-crosslinked FFs increased by nearly 70% and 50% than that of original FFs. This approach constitutes an easy and straightforward strategy for the strengthening of FFs, promotes the FF applications in broad engineering fields.

6:50 PM SM11.04.06

Dry Cell-Free Protein Synthesis Formulations are Compatible with Polymer Casting Techniques Marilyn Lee¹, Rebecca Raig^{2,3}, Danielle Kuhn¹, Matthew Lux¹ and Maneesh Gupta³; ¹U.S. Army CCDC Chemical Biological Center, United States; ²UES, Inc., United States; ³Air Force Research Laboratory, United States

Cell-free systems have growing importance as a way to use synthetic biology tools in resource-poor environments. Lysates may be dried for storage, delivering biochemical activity for sensing or producing molecules on-demand upon rehydration at the point of need. Up to now, cell-free protein synthesis (CFPS) reactions have been studied as aqueous solutions in test tubes or absorbed onto paper or cloth. Embedding biological functionality into broadly-used materials, such as plastic polymers, has long been an attractive goal. Unfortunately, this goal has for the most part remained out of reach, often due to the fragility of biological systems outside of aqueous environments. In this work, we describe and utilize a surprising and useful feature of lyophilized cell-free lysate systems: tolerance to casting methods involving exposure to organic solvents or heat up to 90°C. To explore this newly discovered feature, a variety of solvents were tested and CFPS reaction components were screened for protective properties. CFPS is compatible with several polymer types. Tolerance to polymer casting enables the delivery of dry cell-free reactions in the form of coatings or fibers, among other processing possibilities.

SESSION SM11.05: Cellulose-Based Materials II

Session Chairs: Runye Zha and Hongli Zhu

Wednesday Morning, April 21, 2021

SM11

8:25 AM *SM11.05.02

Structured Materials from Cellulose Nanofibrils Lars Wagberg, Tobias Bensefelt and Daniel Söderberg; KTH Royal Institute of Technology, Sweden

Biobased Cellulose NanoFibrils (CNFs) constitute a highly anisotropic nanomaterial with excellent mechanical properties with a well defined surface chemistry and outstanding durability in harsh environments. During the last two decades CNFs have been used in numerous applications ranging from antibacterial, composite, energy storage, display and fire proofing applications, to mention a few, where different aspects of their inherent

applications have been utilized. The Young's modulus of the fibrils is around 130 GPa and it should hence be possible to create outstanding materials of these materials provided that the nanostructure of the prepared materials could be controlled. Since materials from CNFs are almost exclusively formed from water it is essential to control their colloidal interactions in dispersion to create an ideal structure for a certain end-purpose. In the present contribution two different strategies will be handled in detail. In the first approach anionically modified CNFs were well dispersed at low concentrations together with small amounts of high molecular mass sodium alginate before dewatering of the dispersion to a solid gel before drying. The so prepared materials were then re-swollen in aqueous solutions containing different di-valent or tri-valent counterions resulting in wet films with excellent mechanical properties. A wet film of these materials with 50 % water was shown to have modulus, strength and stress at break comparable and even better than HD polyethylene. The reason to this extraordinary behaviour is that the fibrils form a volume spanning arrested state (VAS) as the concentration is increased during dewatering and this creates a lamellar structure in the concentrated wet film with an intertwined network of alginate polymers. As the dry films are re-swollen this network basically expands in one direction and by using multivalent ions the alginate molecules are able to lock the structure creating a type of interpenetrated network of CNF and alginate. In the second approach the CNFs are converted to end-less filaments using a flow-focusing methodology. In this approach the well dispersed fibrils are oriented in an elongational flow in a flow-focusing device and by using an acidic solution to create this flow the fibrils are locked in an oriented structure where their excellent mechanical properties can be fully utilized to create strong and thin filaments. This concept can also be developed by using coaxial arrangements where different types of interactive filaments can be prepared.

8:50 AM *SM11.05.03

Multifunctional Cellulose Biocomposites of High Strength and Optical Transmittance Lars Berglund; KTH Royal Institute of Technology, Sweden

Polymer matrix cellulose biocomposites are widely used in the form of molded components in industry exemplified by automotive applications. Improved control of the nanostructure makes it possible to significantly widen the range of properties and potential applications. Top-down approaches are particularly interesting, since the nanostructure can be controlled both in terms of spatial nanocellulose fibril distribution and its orientation. One can also prepare optically transparent materials by selection of an appropriate polymer matrix. By the addition of functional components in the form of nanoparticles or dyes, the photonics functionality can be extended further for applications such as smart windows, wood for solid state lasing and heat storage. Molecular and nanoscale understanding of processing for nanostructural control is essential, as well as the effect of nanostructure on physical properties. Materials design in terms of wood substrate modification, chemical treatment and polymer impregnation strategies will be discussed. This includes methods for nanostructural characterization, mechanisms for light transmission, reduction of moisture sensitivity and effects from refractive index matching between the polymer and the wood substrate. An important argument for cellulosic materials is their role in sustainable development, and this topic will be analyzed. There is a tendency to emphasize the renewable resource origin of cellulose, but this may not always be sufficient to justify the replacement of established materials.

9:15 AM SM11.05.04

Bacteria Cellulose Derived Functionalized Separator for Lithium Sulfur Batteries Wenyue Li and Zhaoyang Fan; Arizona State University, United States

Other than its superior mechanical strength and thermal stability, bacterial cellulose (BC)-derived thin sheet could also provide other crucial functions as an excellent separator candidate used in emerging battery technologies. Particularly, for lithium sulfur batteries (LSBs), polysulfide shuttling effect and lithium dendrites are two tough issues that cause numerous problems including low cell efficiencies, fast battery decay and safety concerns. To attack these two problems simultaneously, this study presents a functionalized BC separator by manipulating its oxygen-containing functional groups. With enhanced repulsive force between polysulfides and the carboxyl-altered BC film, the polysulfide shuttling can be effectively suppressed on the cathode side.

Correspondingly, the tendency of lithium ion absorption to the oxygen functional groups is capable of generating uniform lithium ion diffusion at the interface of the lithium anode and the BC separator, resulting in stable lithium stripping/plating processes by inhibiting lithium dendrite growth. As a result, the LSB cell with a BC separator, at a sulfur load of 4 mg cm^{-2} , delivers a specific capacity of 1450 mAh g^{-1} at 0.1C, or 1000 mAh g^{-1} at 0.3C over 100 cycles, suggesting the superior performance of BC separators in LSB.

9:30 AM SM11.05.05

Optimization of Spray-Drying Cellulose Nanofibrils for Biocomposites Xianhui Zhao¹, Lu Wang², Kai Li¹, Katie Copenhaver¹, Halil L. Tekinalp¹, Douglas Gardner² and Soydan Ozcan¹; ¹Oak Ridge National Laboratory, United States; ²University of Maine, United States

Growing interest in using cellulose nanofibrils (CNFs) to reinforce polymers is attributable to CNFs' unique properties such as high aspect ratio, high specific strength, light weight, low cost, and renewability. However, drying CNFs effectively with less agglomeration at low cost is a main challenge for enabling use of CNFs in biocomposites. In the present study, CNFs derived from bleached pulps were spray-dried at six different conditions: two temperatures ($\sim 125 \text{ }^\circ\text{C}$ and $\sim 110 \text{ }^\circ\text{C}$) and three feed concentrations (1.3%, 1.5%, and 1.8%). The spray-dried CNFs were compounded with polylactic acid (PLA) (at 5 wt% CNF level) to form CNF/PLA biocomposites. The biocomposites obtained were characterized using techniques including tensile testing, rheological analyses, dynamic mechanical analysis (DMA), differential scanning calorimetry (DSC), thermogravimetric analysis (TGA), and scanning electron microscopy (SEM). The tensile strengths of the CNF/PLA biocomposites varied largely from 32 to 54 MPa (69% change). When the CNFs were spray-dried at the higher temperature ($\sim 125 \text{ }^\circ\text{C}$) with a feed concentration of 1.3%, the CNF/PLA biocomposite had the highest tensile strength among all composites. This indicates that the CNF spray-drying condition has a significant effect on the mechanical properties of the CNF/PLA composites. Some physicochemical treatments on CNFs will be utilized in the future to further improve the properties of CNF/PLA composites.

SESSION SM11.06: Protein and Peptide Based Materials II

Session Chairs: Feng Jiang and Yuhang Ye

Wednesday Afternoon, April 21, 2021

SM11

2:15 PM SM11.06.01

Biomimetic Tooth Repair—Peptide-Guided Remineralization of Functional Dental Tissues Deniz T. Yucesoy^{1,2,2}, Hanson D. Fong^{2,2}, Jacob Rodriguez^{2,2}, John Hamann^{2,2}, Sami Dogan² and Mehmet Sarikaya^{2,2,2}; ¹Izmir Institute of Technology, Turkey; ²University of Washington, United States

Dental diseases are a global health problem affecting large populations despite the widespread use of fluoride and other preventive treatments. Primarily as result of demineralization, i.e., loss of mineral from teeth, these ailments are associated with incipient caries, gum recession, hypersensitivity, and gingivitis. Current dental therapies mostly rely on replacement defective or lost tissue with synthetic restorative dental materials with limited long-term success, often causing post-therapeutic problems, e.g., gingival inflammation, secondary caries, and even tooth loss. Incorporating a functional mineral layer that can be fully integrated into underlying molecular tooth structure in repairing the tissue has been a long-standing challenge. Following lessons from biology where proteins guide tissue formation, we develop a peptide-based biomimetic remineralization methodology to restore demineralized dental hard tissues in enamel, dentin and cementum using peptides derived from biomineralizing proteins, such as amelogenin, the key protein in enamel. Dubbed as amelogenin-derived peptides, ADPs are designed through a multipronged approach including biocombinatorial selection, bioinformatics, molecular simulations, and by iteratively testing via binding and mineralization assays. The ADPs are used in guiding remineralization *in vitro* on artificially demineralized teeth of extracted human, rat,

and porcine teeth as under simulated physiological conditions and in vivo rat model. In a variety of treatment modalities, the peptide treated test groups displayed structure and morphology with well-integrated interfaces exhibiting local mechanical properties mimicking the restored tissues, e.g., similar to dentin-enamel junction (DEJ) and dentin-cementum junction (DCJ). The highly potent materials and methods developed in this work pose to drastically alter the current dental health care by highly effective practical products and procedures in restorative and cosmetic dentistry as well as in preventive daily oral care.

2:30 PM SM11.06.02

Late News: Functionalization of Supramolecular Ureidopyrimidinone-Materials by Photo-Induced Oxygen-Tolerant Polymerization Muhabbat Komil¹, Bastiaan Ippel¹, Paul Bartels¹, Serge Söntjens², Maarten Pouderoijen² and Patricia Dankers¹; ¹Technische Universiteit Eindhoven, Netherlands; ²SyMo-Chem, Netherlands

An elegant way of biomaterial synthesis is through supramolecular chemistry, where functional moieties are held together via dynamic and reversible bonds. An example of such a supramolecular moiety is the ureidopyrimidinone (UPy), which dimerizes by four-fold hydrogen bonding and distinctly self-assembles into nanofibrous structures. Various polymers, functionalized with multiple UPy-motifs, can be processed into films and scaffolds, giving a wide choice of materials characteristics for numerous biomedical applications. Furthermore, because of the supramolecular nature, countless different additives modified with a UPy-motif are easily incorporated into the supramolecular materials to achieve the desired functionality for potential applications as biomedical materials.

Previously, we demonstrated the design of a UPy-functional alkyl halide initiator, including its incorporation into the UPy-functional polycaprolactone (UPy-PCL) films at different concentrations by solvent casting. Grafting of antifouling polymers by atom transfer radical polymerization (ATRP) in form of polyzwitterions in a fully aqueous medium at room temperature was described. Furthermore, we were able to successfully functionalize microporous supramolecular electrospun scaffolds prepared from telechelic UPy-PCL with polyzwitterions. Post-polymerization surface elemental composition measurements, revealed presence of two distinct signals that reflected the charged atoms of the polyzwitterions. The charges strongly affected the wettability of the grafted materials. Additionally, presence of the new polymer layer on the surfaces was characterized by differences in surface morphology and cellular adhesion pre- and post-polymerization. The amount of polymer was dependent on the concentrations of UPy-initiator incorporated into the supramolecular films, as well as polymerization times.

We have now further improved our approach by utilizing photo-induced ATRP to gain temporal control over the polymerization. Photo-induced ATRP allows us to pattern our supramolecular material surfaces with functional polymers. With recent developments in the field of radical polymerization, we now utilize enzymatically degassed ATRP, which is oxygen-tolerant and has alleviated the need for inert atmosphere. Thus, we can perform open-to-air polymerization and effortlessly upscale supramolecular material functionalization to multiple materials at a time. With catalytic amounts of glucose oxidase enzyme, we have observed excellent control over the polymerization in a fully aqueous medium at room temperature, by means of linear first-order kinetic behaviour and narrow molecular weight distributions. We have successfully synthesized hydrophilic oligo(ethylene glycol) (OEG) polymer brushes with varying brush lengths, which resulted in thermoresponsive materials. Additionally, functional OEG copolymer brushes were prepared with multiple pendant amine moieties, which were positively charged at physiological conditions. Amine moieties can act as anchors to conjugate various peptides, dyes and bioactive motifs, post-polymerization. Currently, we are continuing implementation of photo-induced oxygen-tolerant ATRP for the design of bioactive materials with carbohydrate moieties. Materials functionalized with carbohydrate moieties serve as excellent candidates for extracellular matrix mimics. We are excited to further investigate a plethora of possible applications of our functional supramolecular materials in the field of tissue engineering and regenerative medicine.

2:45 PM SM11.06.03

Biologically Engineered Living Bacterial Thin Film with Tunable Stiffness and Self-regeneration Capability Dong Li¹, Victor Mann¹, Marimikel Charrier², Caroline Ajo-Franklin³ and Paul Ashby¹; ¹Lawrence

Berkeley National Laboratory, United States; ²Colorado University, United States; ³Rice University, United States

Natural biological materials often demonstrate intriguing properties that are difficult to replicate in man-made materials, such as self-repairing/-regeneration, adaptable morphological and mechanical switch, sensing and responding. One promising strategy of incorporating these living aspects into creating new materials is to genetically program microbes and use them as the major building blocks. Here we report a new Engineered Living Material (ELM) that harnesses the active properties of bacterial cells to create an ultra-stiff, regenerable, and responsive film. The material is assembled from tightly packed cells whose solid surfaces are densely crosslinked. The surface layer (S-layer) protein of *C. crescentus* was engineered to display SpyTag over the entire cell body. These functionalized bacterial cells crosslink into tight assemblies with close cell-cell contact mediated by nanoparticles displaying SpyCatcher and the formation of SpyCatcher-SpyTag iso-peptide bonds. We found (1) A layer of densely packed Qdots can be displayed on living bacterial surface. (2) Stiffness of the crosslinked bacterial film increases over 30 times compared to non-crosslinked biofilms. Cleavage of a disulfide bond inserted between SpyCatcher and the nanoparticles melts the crosslinked film, confirming the specific covalent linkage is responsible for the enhanced mechanical properties. (3) The engineered ultra-stiff bacterial film can harvest nutrients to both continue to manufacture new material and regenerate damaged regions due to the continuous growth of *C. crescentus* cells and the expression of new S-layer proteins in the presence of crosslinking agent. (4) The crosslinked living bacterial film exhibits dynamic morphological and mechanical response to environmental osmotic stressing caused by a neutral polymer macromolecule polyethylene glycol 8000. With these materials we introduce a new design principle for creating high stiffness in liquid content materials.

3:00 PM SM11.06.04

Decellularized Extracellular Matrix Bioinks for Cancers-on-Chips Hee-Gyeong Yi; Chonnam National University, Korea (the Republic of)

Microphysiological cancer systems (Cancers-on-Chips) are emerging cancer models for better cancer research. Conventional cancer models have failed in capturing the underlying mechanisms of how cancer reacts to the current anti-cancer approaches due to the lack of similarities with the original cancer of patients. The challenge is modeling a complex and heterogeneous cancer environment where every element contributes to cancer hallmarks development. Recently, biofabrication technologies have been advanced to spatially control multiple types of cells and biomaterials to mimic the native physiology of human tissue and organs. In particular, 3D cell-printing has beauty in manipulating the 3D anatomical structure of cancerous tissue through a layer-by-layer process that stacks up cells and bioinks following a precisely designed sequence. The decellularized extracellular matrix bioinks that mimic the tissue-specific environment has recapitulated the pathology and aggressiveness of cancer. In addition, 3D cell-printing has shown the possibilities in modeling various types of cancers for future cancer research.

3:15 PM SM11.06.05

A Novel Supramolecular Cryopreservation Nanoagent Based on Self-Assembly of Peptide Hayeon Kim and Eunji Lee; Gwangju Institute of Science and Technology, Korea (the Republic of)

Cryopreservation is very important in biotechnological, pharmaceutical, biochemical or food industries as the purpose of storage of protein drugs, cells, tissues and food, and ice slurries for refrigeration systems. Antifreeze protein (AFP) have been received attention with their potential as a cryopreservation agent by their ability to prevent the organisms from freezing at the subzero environment through antifreeze activity such as ice recrystallization inhibition or thermal hysteresis effect. However, it is struggling to apply the natural AFP in practical industries as cryopreservation agent because of their irreversible denaturation and the difficulty in extraction from nature. These challenges have led to developing artificial cryopreservation agents like dimethyl sulfoxide and sodium phosphates but due to the cytotoxicity and less biocompatible of them, the recovery rate of the target matter is too low when they are added. Here, the natural AFP mimetic short peptides conjugated

with specific amino acids showing antifreeze activity and fibrous assembly with enhanced π - π stacking are prepared by supramolecular chemistry to increase both antifreeze activity and biocompatibility. This research might provide a useful strategy to fabricate the cryopreservation agent through the supramolecular nanomaterials and to figure out the mechanism of ice binding to antifreeze protein.

SESSION SM11.07: Bioinspired Devices
Session Chairs: Runye Zha and Hongli Zhu
Wednesday Afternoon, April 21, 2021
SM11

5:15 PM INTRODUCTION

5:20 PM SM11.07.03

Near-Field Electrospun Hybrid Biodegradable Polymer/M13-Bacteriophage Whispering Gallery Mode Biosensors Stephen T. Hsieh, Joseph E. Cheeney, Xi Ding, Nosang V. Myung and Elaine D. Haberer; University of California, Riverside, United States

Polymer/virus based biosensors are a compelling system for medical diagnostics, environmental monitoring, and food security. The hybrid system of a biocompatible polymer with a virus bio-recognition element, results in a bio-friendly device that is solution processable. Typically, antibodies or aptamers are used as the bio-recognition element, however they can be costly and time consuming to produce, lack stability under sensing or surface functionalization conditions, and be poorly oriented during functionalization rendering a fraction of receptor sites useless. In contrast, the M13 virus, a harmless and non-toxic filamentous bacteriophage, can be manufactured in large quantities through inexpensive infection of a bacterial host and can withstand a large range of temperatures and pHs. Moreover, this combinatorial phage display workhorse can be genetically modified to display thousands of well-ordered, densely packed affinity peptide fusions with controlled orientation along its less than one micron length.

Recent work has demonstrated that electrospun polymer fibers can be utilized as optical resonator whispering gallery mode (WGM) sensors. These WGM sensors have potential as highly sensitive, label-free sensors. The high quality (Q) cavities are of particular interest as they enable light to recirculate hundreds to millions of times or more, significantly increasing interaction with an analyte and improving device sensitivity. Light propagating at the periphery of these radially symmetric resonators is confined by total internal reflection such that its evanescent field serves as a probe for analyte binding events on the resonator surface. A promising biosensor device would combine the polymer/virus bio-recognition with the WGM sensing mechanism. An ideal method would be to electrospinning polymer/M13 fibers capable of supporting WGM while still maintaining the M13 bio-recognition properties

Here, we used near-field electrospinning, a direct write fabrication method utilizing a low strength electric field, to create polyvinyl alcohol (PVA) WGM fiber resonators with incorporated M13 biorecognition elements. A streptavidin-binding phage functioned as a model bioreceptor to demonstrate the utility of the sensing platform. The surface concentration of M13 was evaluated via streptavidin-conjugated gold nanoparticle binding and x-ray photoelectron spectroscopy (XPS). Rhodamine 6G (R6G) was then incorporated into the fiber as an emitter. Sharp peaks associated with WGMs decorated the broad dye fluorescence. The resonant modes were identified using Mie theory, and Q values and free spectral range were measured. Subsequently, the fibers were used to detect streptavidin and the sensitivity of these novel PVA/M13 biosensors was determined. These studies demonstrate the potential of electrospun WGM resonators with incorporated phage-based bioreceptors as a robust platform for highly sensitive biosensing.

5:35 PM SM11.07.04

Bioinspired Interphase Engineering for 1D and 2D Nanocarbon-Included Functional Composites

Weiheng Xu, Sayli Jambhulkar, Dharnedar Ravichandran, Yuxiang Zhu and Kenan Song; Arizona State University, United States

Layer-structured composites have broad applications in the biomedical device, tissue scaffolds, skin membranes, solar cell devices, battery and supercapacitor devices, sensors, and actuators. Here we report the biosystem-mimicking structure of layers along the thickness or radial directions. These polymer/nanoparticle composites display in different material forms, such as fibers, thin films, or laminates. The combination of the soft micromoles and hard nanoparticles have synergistic effects in mechanical robustness and functional versatility. We demonstrate via a few polymers of polyvinyl alcohol (PVA), polyacrylonitrile (PAN), and thermoplastic polyurethane (TPU). Different nanoparticles in one-dimension and two-dimension are incorporated in these polymers, for example, carbon nanotubes (CNTs), carbon nanofibers (CNFs), and graphene nanoplatelets (GNPs). The composites' compositions and structures in each layer can be tuned via manufacturing customization and material modification. We will demonstrate how uniquely designed structures benefit mechanical enhancement, electrical conductivity, and gas sensitivity.

5:50 PM SM11.07.05

Late News: Blends of Beeswax and Soy Wax as Encapsulating Materials for Soil-Biodegradable Electronics Madhur Atreya, Gabrielle Marinick, Karan Dikshit, Charlotte Bellerjeau, Yongkun Sui, Carson Bruns and Gregory Whiting; University of Colorado Boulder, United States

The growing field of printed biodegradable electronics provides the opportunity to monitor soils at a high spatial density without the risk of increased waste. A tunably degradable encapsulant is a critical component of soil-degradable electronics, as it acts to delay the ingress of water, microbes, and other agents responsible for degradation. Existing biodegradable polymers such as poly(lactic acid) tend to have limited utility due to their uptake of water which could in turn expose components underneath. Candelilla wax has been shown to be an effective encapsulating material in biomedical applications [1]. We have recently demonstrated that a blend of beeswax and soy wax is an effective encapsulant for printed biodegradable soil moisture sensors [2]. In this presentation, we elaborate on the thermal/mechanical properties of beeswax-soy wax blends to explore the conditions required for melt processing and coating substrates. In addition, we explore the tunability of degradation and introduce a novel wax-based soil degradation sensor, where time to sensor failure can be correlated to microbial or enzymatic activity.

[1] Won, S. M.; Koo, J.; Crawford, K. E.; Mickle, A. D.; Xue, Y.; Min, S.; McIlvried, L. A.; Yan, Y.; Kim, S. B.; Lee, S. M.; et al. Natural Wax for Transient Electronics. *Adv. Funct. Mater.* 2018, 28 (32), 1–10. <https://doi.org/10.1002/adfm.201801819>.

[2] Sui, Y.; Atreya, M.; Dahal, S.; Gopalakrishnan, A.; Khosla; Whiting, G. Controlled Biodegradation of an Additively Fabricated Capacitive Soil Moisture Sensor. *ACS Sustainable Chem. Eng.* in press.

6:05 PM SM11.07.06

Late News: Sub-Micron Topography Modulates Strain-Stiffening Behavior in Fibrous Hydrogels Sara Heedy, Juviarelli Pineda and Albert Yee; University of California, Irvine, United States

Nature provides soft materials, such as gels, capable of complex mechanical responses that vary with hydration level and other environmental factors such as pH and salinity. Such biological “soft” polymers often consist of nanofibers capable of aggregating further into microbundles. These biopolymers contain relatively rigid building blocks along the chain backbone, which is necessary to form hierarchical structures characteristic of fibers. The fiber forming hierarchical biopolymers exhibit a nonlinear stress-strain response – typically a ‘J-shape’ stress-strain curve that demonstrates strain-stiffening behavior. Being able to replicate this strain-stiffening behavior is critical for the success of future bio-electronic interfaces and medical devices. Systems designed to exhibit strain-stiffening responses demonstrate unfolding, deformation, and straightening of the network. Recent designs include wavy-textures induced by pre-straining, self-assembled elastomers, and kirigami-inspired systems. Yet, it remains a worthwhile goal to develop tunable strain-stiffening systems,

particularly from biocompatible polymers. Here, we demonstrate a new approach to modulating the strain-stiffening response of monolithic fibrous hydrogels through application of a physical surface topography.

We fabricated periodic pillar nanostructures on a fibrous chitosan hydrogel using solvent dropcast lithography. We produced a range of regularly spaced nanopillars with periodicities of approximately 200 nm, 300 nm, and 500 nm, which is comparable to the biopolymer radius of gyration (~ 250 nm). We performed tensile testing in the plane of the hydrated films with and without nanopatterns to determine the effect of surface nanostructures on film stiffness. We found, surprisingly, that the elastic moduli increased in the films with nanopillar topography, and that the amount of increase was correlated to the increasing feature size of the films. Furthermore, the nanopillar topography strongly modulated the strain-stiffening response.

To determine the origin of the processing-structure-mechanical property relation, we systematically investigated the nanoscale topography deformation utilizing atomic force microscopy, and observed significant alignment of the nanofibers at deformations above the nonlinear stress-strain transition point. In this presentation, we report on our study to examine the role of interactions and ionic linkages in the hydrogels and to determine if there is a limit to the tunable mechanical properties. The simple method to fabricate a monolithic strain-stiffening system from fibrous hydrogels could be translated towards other biopolymer-based devices and materials including electronically active biopolymers.

6:20 PM SM11.07.07

Muscle-Inspired Hydrogels of High Toughness and High Contractile Force Ximin He, Mutian Hua and Shuwang Wu; University of California, Los Angeles, United States

Hydrogels are a class of water-laid crosslinked polymers with tissue-like microstructure and unique stimuli-responsive deformability, with great potential for tissue engineering, humane-machine interface, and artificial muscle for soft robots and wearable electronics. However, due to the high porosity their intrinsic mechanical weakness and low deliverable actuation force limit their applications. We have recently made progresses on developing a new generic method to construct hydrogels of (1) ultra-toughness and (2) high deliverable force and power density during actuation. First, Natural load-bearing materials like tendons are strong and tough, owing to the hierarchically assembly of anisotropic structures across multi-length-scales. We have developed a strategy to produce polymers with tendon-like hierarchical architecture. Multiple mechanisms originating from these structures at different length-scales were integrated in the water-rich polymer (70-95% water) to feature both ultra-high ultimate stress (23.5 MPa) and strain (2900%), which yields giant toughness (210 MJ/m^3 , 170 kJ/m^2) and remarkable fatigue resistance, 10-time tougher than natural tendon, Kevlar and rubber. This research may make hydrogels capable of practical applications that requires long-term services with high-loads and abrupt-impacts, and extend to the optimization of various polymeric materials. Second, inspired by the energy conversion mechanism of many creatures during jumping, we designed an elastic-driven strong contractile hydrogel through storing and releasing elastic potential energy in polymer network. It can generate high contractile force (40 KPa) rapidly at ultra-high work density (15.3 KJ/m^3), outperforming current hydrogels ($\sim 0.01 \text{ KJ/m}^3$) and even biological muscles ($\sim 8 \text{ KJ/m}^3$). This demonstrated elastic-energy storing and releasing method endows hydrogels with elasticity-plasticity switchability, multi-stable deformability in fully reversible and programmable manners, and anisotropic or isotropic deformation. With the high power density and programmability via this customizable modular design, these hydrogels demonstrated potential for broad applications in artificial muscles, contractile wound dressing, and high-power actuators.

6:35 PM SM11.07.08

Plant-Inspired hydrogels for Phototropic Energy Harvesting and Flexible Storage Devices Ximin He and Yusen Zhao; University of California, Los Angeles, United States

Nature with the 3.8 billion years of research and development experiences can always provide us with out-of-the-box ideas for man-made materials from their superior design and functionality. Recent progresses by our group on energy harvesting (Nat. Nanotech. 2019) and energy storage (Adv. Funct. Mater. 2019; Matter 2020)

materials will be presented. First, plant can turn its head following the sun, known as phototropism, to maximize the photo(thermal) energy harvesting. Engineering such a self-adaptive actuation ability in synthetic materials would be highly advantageous for advancing intelligent energy-efficient systems and enhancing the performance of optical or optoelectronic devices, avoiding computer programming or electromechanical control and external power supply. We have an artificial phototropic system based on nanostructured stimuli-responsive polymers that can aim and align to the incident light direction in the three-dimensions over a broad temperature range. Such adaptive reconfiguration is realized through a built-in feedback loop rooted in the photothermal and mechanical properties of the material. This system is termed a sunflower-like biomimetic omnidirectional tracker (SunBOT). We show that an array of SunBOTs can, in principle, be used in solar vapour generation devices, as it achieves up to a 400% solar energy-harvesting enhancement over non-tropistic materials at oblique illumination angles. The principle behind our SunBOTs is universal and can be extended to many responsive materials and a broad range of stimuli. Second, wood in nature has well-defined vertical structure with low tortuosity to facilitate the mass transport. Inspired from the wood structure, we designed anisotropic hydrogels with alignment to increase the ionic conductivity of materials. The pore size can be rationalized and reduced even smaller than natural wood to increase the specific area, while maintaining the alignment. Conducting polymer, owing to its mesoporous structure and high electrical conductivity has been widely used for supercapacitors. By incorporating the conducting polymer in hydrogel-based matrix, the all-solid-state supercapacitor with high electrochemical performance can be fabricated. Such conducting polymer-hydrogel composites exhibit unprecedented ionic conductivity, areal supercapacitance, power density, energy density, capacitance retention and cyclic stability. Besides, the hydrogel matrix also provides excellent flexibility under cyclic bending, making it possible for flexible electronics.

SESSION SM11.08: Poster Session: Design and Analysis of Bioderived and Bioinspired Multifunctional Materials

Session Chairs: Feng Jiang and Runye Zha

Wednesday Afternoon, April 21, 2021

10:00 PM - 10:55 PM

SM11

SM11.08.02

BioInspired Fish Scales—A Kinematic and Numerical Approach for Flexible Armor Design Ailin Chen, Komal Thind, Kahraman Demir and Grace X. Gu; University of California, Berkeley, United States

Fish scales serve as a natural dermal armor with remarkable flexibility and puncture resistance. Through biomimetic scales, researchers are able to acquire these properties and tune them by adjusting their design parameters. Overlapping scales, as seen in elasmoid scales, can lead to complex interactions between each scale. These interactions are able to maintain stiffness while improving flexibility. Hence, it is important to understand these interactions in order to design biomimetic fish scales. As the scaled substrate deforms and the scales start to engage, modeling the flexibility requires accounting for nonlinear relations. Current studies focus on characterizing these kinematic linear and nonlinear regions but fall short in modeling the kinematic phase shift. Here we propose an approach that will predict when the transition from linear to nonlinear will occur, allowing for more control of the substrate's overall behavior. Using a kinematic analysis of the interacting scales, we can model the flexibility at the transition point where the scales start to engage in a nonlinear manner. The validity of these kinematic predictions will be investigated through finite element analysis. The results of this investigation could allow for an efficient optimization method for scale-like designs that can be applied to various applications.

SM11.08.03

Hierarchical Alginate Hydrogel Architectures and Multi-Layered Encapsulation Yoon Jeong and Joseph

Irudayaraj; University of Illinois at Urbana-Champaign, United States

Hierarchically ordered structures can be found in a variety of biological systems ranging from microscopic to the macroscopic scale in nature. Not surprisingly, inspiration from nature has provided cues to stimulate research in materials preparation to obtain functional hierarchy. For instance, hierarchical and ordered biological structures, in many tissues such as cartilage, and cornea, are well exemplified. Extensive efforts have been made to mimic the native biological structures of a tissue on cell layers and stratification. We attempt to develop hierarchical and layered hydrogel architectures with robust design necessary for cellular encapsulation.

Research on hierarchical structured hydrogels is still in its infancy. More recently, new hierarchical hydrogel architectures have been pioneered to create multi-layered chitosan hydrogels in a concentric fashion. Pioneering efforts to develop hierarchical architectures with hydrogel have provided fundamental insights at the molecular level. Yet the strategies might not be standardized because substantial different design considerations is required due to a wide range of biochemical processes involved. In some cases, cytotoxic processes and/or chemicals to form a gel structure are utilized which results in an inevitable cell damage. Furthermore, at small scales, the fabrication of micro-size architectures requires higher reaction rates than that of macroscopic objects, which causes agglomeration between gels in a reaction bath. Due to the agglomeration issue, there has been an absence of reliably scale-down models for mass production. Only a few methods have been introduced to produce a single multi-layered capsule with diameters between 4 and 20 mm. Even with predictive mechanisms in various hydrogels, challenges exist in both mass production and scaling-down of the size of hydrogel architectures, and multi-layered techniques for cell encapsulation studies are even sparse.

We propose the fabrication of multi-layered alginate capsules to resolve the technical bottlenecks through precise control of hydrogel modalities and shell thickness at micron scale enabling scaleup for mass production. The multi-layered capsules comprise of natural alginate polymer crosslinked with Ca^{2+} ions without auxiliary crosslinking agents. To the best of our knowledge, no theoretical or empirical formulation has been suggested to describe the process underlying our hierarchical alginate structures. In addition to the materials we also suggest a hypothetical mechanism to explain how different alginate hierarchical structures can be fabricated and demonstrate its encapsulant application for heterogenous microbial spatial distribution. We believe our proposed encapsulation methodology with alginate hydrogels will be an effective avenue to organize cells into sophisticated and stratified structures to study intra and multi-cellular communication.

SM11.08.04

***In Situ* Investigations of Biochar as a Tunable Platform for Aqueous Malathion Adsorption** John Kirtley, Daniel Goettlich, Abdul Hadi and Kelsi McEnaney; Montana Technological University, United States

Biochar, a highly porous carbonaceous product of biomass pyrolysis, offers a wide array of surface functional groups and structural modalities that depend on biomass properties and pyrolysis conditions. This tunable platform promises versatility in capturing aqueous organophosphates, including malathion, a hazardous pesticide and chemical warfare agent surrogate. While some studies have elucidated the general mechanisms associated with biomass pyrolysis, the relationship between material evolution and efficacy toward a variety of emerging applications is largely unknown. In this work, we use Raman spectroscopy and Diffuse Reflectance Infrared Fourier Transform Spectroscopy (DRIFTS) to probe *in situ* the molecular and structural changes of coir biochar at various temperatures up to 850 °C. Raman signatures from biochar reflect the complex structural changes of the amorphous carbon as it gradually transforms to larger aromatic structures, during a slow temperature ramp and subsequent 2-hr dwell. DRIFTS similarly indicates increasing aromatic character and fewer aliphatic groups as pyrolysis temperature increases, while some oxygen-containing functional groups (hydroxyl, carbonyl) are largely eliminated by 500 °C. These tunable chemical groups/carbon structures are expected to significantly impact the adsorption of aqueous malathion onto the meso and micro pore surfaces of biochar due to various non-covalent interactions. To test this hypothesis, we use high-performance liquid chromatography (HPLC) to record the concentrations of aqueous malathion containing biochar suspensions, over time. Initial work suggests that biochar is effective in adsorbing malathion, and continued studies elucidate

the nature of the biochar-malathion interactions. In particular, during the course of an adsorption experiment, biochar suspensions are removed and analyzed using attenuated-reflectance FTIR. Spectra from suspensions containing the highest concentrations of malathion near equilibrium suggest the highest density of surface-adsorbed malathion, and that the malathion carbonyl groups may be responsible for this interaction.

SM11.08.05

Polydopamine-Coated Silica Aerogels with Enhanced UV-Absorption Gabrielle S. Rey¹, Stephanie L. Vivod², Saranshu Singla¹, Theresa Benyo² and Ali Dhinojwala¹; ¹The University of Akron, United States; ²NASA Glenn Research Center, United States

Silica aerogels are lightweight, open-celled, porous structures that have advantageous properties such as low density and high surface area. Due to these characteristics, silica aerogels would be great candidates for aeronautical applications. Recently, there has been considerable interest in functionalizing substrates with polydopamine (PDA), a polymeric, bio-inspired synthetic analogue of melanin. Due to the catechol functionalities in PDA, PDA can easily adhere to a variety of substrates. While many studies coat two-dimensional substrates easily, very few studies exist that coat three-dimensional scaffolds with PDA while maintaining the scaffold's original properties. Here we demonstrate an in-situ coating method for depositing PDA on silica aerogel by utilizing the amine functionalities within the aerogel. The coated PDA-aerogel maintain high porosity (> 90%) and high surface areas (around 600 m²/g). It also exhibits strong absorption of UV-light in comparison to the uncoated aerogel monolith due to UV-absorption ability of PDA. PDA-coated aerogels have promising potential to serve as radiation-mitigating materials for space exploration.

SM11.08.08

Bioinspired Nano and Macro Composite Structures as Thermoelectric Devices Yuxiang Zhu, Weiheng Xu, Dharneedar Ravichandran, Sayli Jambhulkar and Kenan Song; Arizona State University, United States

Thermoelectric devices can collect heat and convert them as electricity; thus, fabrication of composites with programmable electrical conductivity, thermal conductivity, and Seebeck coefficient parameters can enable highly efficient energy generation and storage. Our research reported the processing of polymer and nanoparticles from a molecular scale via the in-situ polymerization method. The nanoscale polymer/nanoparticle hybrid mimicked biosystems such as blood vessels or cellular structures in plants. Via the interphase formation, the thermal and electrical conductivity of the macroscale composites showed optimized properties. As compared to the simple blending of the polymer and the nanoparticles, our in-situ polymerized composites exhibited much enhanced thermoelectrical performance and shed light on manufacturing that transfer the nanoscale properties to the macroscale device performance.

SM11.08.09

Late News: Direct Laser Written Microstructures Displaying Reversible Sugar-Induced Actuation Alexa Ennis, Deanna Nicdao, Colm B. Delaney and Larisa Florea; Trinity College Dublin and The University of Dublin, Ireland

The reversible binding of phenyl boronic acids (PBA) to 1,2 or 1,3 diols has been explored for over 20 years.¹ Solution based studies have used these molecules to generate measurable colorimetric, fluorescent, or electrochemical change in response to common saccharides, such as glucose and fructose. As the nature of their reversible bond formation remains relatively unspecific to the nature of the sugar present, their application has struggled to ever compete with the accuracy of enzymatic systems based on glucose oxidase. However, the potential to incorporate these materials, in a facile manner, into soft polymeric matrices can offer significant advantage in the generation of passive sampling and even self-regulating systems.

To this end, sensors and actuators based on the PBA-containing hydrogels have found application in optically, electrically, and even mechanically responsive materials. A large proportion of the research which generates binding-induced shape changes, relies on swelling or shrinkage of PBA materials, caused by modulating osmotic pressure upon bond formation with the sugar molecule, a phenomenon first exploited by Matsumoto et

al. in 2004.² Volume change of PBA in hydrogel structures can be hampered by slow response times as the speed of the response relies on the volume-dependent diffusion times of analytes to receptor sites. To date, such systems have primarily been implemented in macro-sized gels which have contributed to this effect. As the kinetics of hydration process are typically proportional to the square of the linear dimension³, a reduction in hydrogel size from mm to μm (as presented herein) reduces the response time by a factor of 1 million. We present a system compatible with two photon polymerization (2PP) which allows for the fabrication of structures on the micron and sub-micron scale. The advantage of having such small structures is that the traditionally slow responses times associated with PBA based hydrogels are overcome by the fast diffusion of the analyte throughout the structure.

To study the actuation of microstructures fabricated using our novel photoresist, arrays of pillars with 20 μm diameter and 30 μm height were fabricated. When exposed to a D-fructose solution, the pillars underwent a significant swelling response. Up to a 90 % increase in area of the pillars was observed within 30 seconds of the addition of 100 mM fructose solution. It was demonstrated that this response was reversible and reproducible over multiple cycles.

Interestingly, the degree of actuation can be tailored by adjusting the laser dosage used to fabricate the structures. As expected, structures fabricated using higher laser powers were more densely crosslinked and therefore exhibit a reduced swelling response when compared to structures fabricated at lower laser powers. For example, the area of structures fabricated at a 20 mW laser power increased by almost 90 %, while structures fabricated at a 40 mW laser power only underwent a 40 % increase in area.

This work enables the realization of soft complex 3D microstructures and actuators with programmable response and fast response-time.

1. Lorand, J. P.; Edwards, J. O., Polyol Complexes and Structure of the Benzenboronate Ion. *The Journal of Organic Chemistry* **1959**, 24 (6), 769-774.

2. Matsumoto, A.; Kurata, T.; Shiino, D.; Kataoka, K., Swelling and Shrinking Kinetics of Totally Synthetic, Glucose-Responsive Polymer Gel Bearing Phenylborate Derivative as a Glucose-Sensing Moiety. *Macromolecules* **2004**, 37 (4), 1502-1510.

3. Shibayama, M.; Tanaka, T., Volume phase transition and related phenomena of polymer gels. In *Responsive Gels: Volume Transitions I*, Springer Berlin Heidelberg: Berlin, Heidelberg, 1993; pp 1-62.

SM11.08.10

Late News: Teroligomers from Morpholine-2,5-Diones Providing a Large Variety of Repeating Unit Sequences Xiao Liang¹, Marc Behl¹ and Andreas Lendlein^{1,2}; ¹Institute of Active Polymers Helmholtz-Zentrum Geesthacht Centre for Materials and Coastal Research, Germany; ²University of Potsdam, Germany

The structural variation of functional side groups and sequence structures of repeating units in oligodepsipeptides (ODPs) allows the design of matrix materials exhibiting strong physical interactions with specific drug molecules^[1,2]. In this way high drug loading can be achieved. Here teroligomers are prepared by a ring-opening polymerization of three different morpholine-2,5-diones. Dibutyl tin(II) oxide were reacted with 2-hydroxyethyl disulfide forming the catalyst / initiator system for the library of teroligomers^[3]. It was designed to potentially introduce redox sensitivity to the ter-ODPs. The optimized synthetic route enabled the presence of dihydroxy terminal groups on the ter-ODPs, and minimized the formation of macrocycles as a potential side reaction. The systematical variation of repeating units composition in ter-ODPs samples was quantitatively calculated by ¹H-NMR according to the intensity variation of the methyl/methylene signals from the different repeating units, and it was in line with the variation of comonomer ratio of the feed composition for the ROP reactions. As the repeating units in ter-ODPs have different molecular weight, the composition variation in different ter-ODPs was also reflected by MALDI-TOF-MS results. The intensity of m/z^+ peaks assigned to telechelic ter-ODPs with high methyl-modified MD units (MMD_{units}) content increased accordingly as the composition of the MMD_{units} increased, and thus a shift of m/z^+ peaks of telechelic structures was observed. In addition, the intensity change of the $\delta_s(\text{CH}_3)$ band at 1375 cm^{-1} in the fingerprint area of the FT-IR spectra of different ter-ODPs samples, attributed to the iso-butyl modified MD units could be an additional hint for the composition variation of ter-ODPs. The good end group functionality of ter-ODPs was reflected by the further

linkage with isophorone diisocyanate (IPDI) via the coupling of hydroxy ends of ter-ODPs and one of the isocyanate group of IPDI. In future, these ter-ODPs could be used as interesting candidate matrix materials for drug releasing implants such as particulate dosage forms.

References

- [1] N. Brunacci, A.T. Neffe, C. Wischke, T. Naolou, U. Nöchel, A. Lendlein, Oligodepsipeptide (nano) carriers: Computational design and analysis of enhanced drug loading, *J. Controlled Release* 301 (2019) 146-156.
- [2] Y.K. Feng, J.A. Lu, M. Behl, A. Lendlein, Progress in Depsipeptide-Based Biomaterials, *Macromol. Biosci.* 10(9) (2010) 1008-1021.
- [3] Peng, X., Behl, M., Zhang, P., Mazurek-Budzynska, M., Feng, Y., & Lendlein, A, Synthesis of Well-Defined Dihydroxy Telechelics by (Co) polymerization of Morpholine-2,5-Diones Catalyzed by Sn (IV) Alkoxide. *Macromol. Biosci.*, 18(12) (2018) 1800257.

SM11.08.11

Late News: Microbe-Assisted Titanium Oxide Composite Development for Lithium-Ion Battery (LIB) Anodes with Super-Concentrated Aqueous Electrolytes Pei-en Weng¹, Alexander Gooyandeh¹, Avinash Godara², Tianyu Li³, Jocelyn Vanlenzuela¹, Steven Mancini¹, Samuel Ming Tuk Yeung¹, Katy Kao¹ and Dahyun Oh¹; ¹SJSU, United States; ²Texas A&M University, United States; ³North Carolina State University, United States

Unique structural and intermolecular properties found in nature for generations have inspired humanity to engineer more efficient products. Biomaterials-driven nanostructures have also shown remarkable performance improvements in electronics. The recent development of carbon-coated TiO₂ has been proved to improve the performance of TiO₂ as an anode material in Li-ion batteries (LIBs). Microbes, such as *E. coli*, contain a high amount of carbon, making them a promising precursor for the formation of carbon layers. In this presentation, we report a bioinspired synthesis method to fabricate a composite using microbes and anatase TiO₂ to improve the energy density and cycle life of aqueous LIBs with the water-in-salt electrolyte (WiSE), (aqueous electrolyte composed of 21m LiTFSI (lithium-bis(trifluoromethanesulfonyl)-imide)). Anatase TiO₂ synthesized by the sol-gel method can reach a high theoretical capacity (167 mAh/g) and increase batteries' energy density. The volumetric changes in its crystalline structure during the lithiation/delithiation is less than 4%, making the anatase TiO₂ a possible anode material for stable batteries. By using two different strains at different growth stages, we were able to control the microstructure of the microbe-assisted TiO₂ (m-TiO₂) composite based on the variability of the shape of the microbes. The synthesis process involved subsequent mixing and dehydration of the microbe and TiO₂ mixture, followed by an annealing process. The microbes acted as carbon precursors and formed a carbonaceous layer on the anatase TiO₂. These carbonaceous biofilms are expected to improve the composite's conductivity and prevent direct contact between the anode and water molecules in WiSE. With m-TiO₂ anodes, we achieved 37.2% higher specific capacity at the fortieth cycle at the C/5 rate and 49.2% higher at the C/2 rate compared to the performance of bare TiO₂ anodes.

SYMPOSIUM SM12

Bioinspired Macromolecular Assembly and Hybrid Materials—From Fundamental Science to Applications
April 14 - April 23, 2021

Symposium Organizers

Chun-Long Chen, Pacific Northwest National Laboratory
Fiona Meldrum, University of Leeds
Ki Tae Nam, Seoul National University
Tiffany Walsh, Deakin University

* Invited Paper

SESSION SM12.01: Bio-Inspired Hybrid Materials I
Session Chairs: Fiona Meldrum and Ki Tae Nam
Thursday Morning, April 22, 2021
SM12

8:00 AM *SM12.01.01

Assemblies of Ordered Nano-Hybrids Obtained by Biomineralization-Inspired Processes Takashi Kato;
The University of Tokyo, Japan

Biomineralization processes are controlled by organic templates such as peptides and polysaccharides. Acidic peptides and proteins exert effects on morphologies of biominerals, which are organic/inorganic hybrids [1-3]. Inspired by these processes, we have obtained a variety of synthetic organic/inorganic hybrids. Here we show recent developments of nanorod and nanodisk hybrid materials based on calcium carbonate [4] and hydroxyapatites (HAP) [5-8]. These hybrid materials are obtained in the presence of an acidic synthetic polymer, poly(acrylic acid). These nano-hybrids form colloidal liquid-crystalline states due to their anisotropic shapes. The dynamic and alignment behavior has been examined for these nano-hybrids by x-ray and neutron scattering [6,7]. Biofunctions of these materials have been studied for HAP nanomaterials [8].

References

- [1] M. Suzuki, T. Kato, and H. Nagasawa et al., *Science*, **325**, 1388-1390 (2009).
- [2] A. Sugawara, H. Nagasawa, T. Kato et al., *Angew. Chem. Int. Ed.*, **45**(18), 2876-2879 (2006).
- [3] T. Kato et al., *MRS Bulletin*, 35(2), 127-132 (2010).
- [4] M. Nakayama and T. Kato et al. *Chem. Sci.*, **6**(11), 6230-6234 (2015); *Nanoscale Adv.*, 2(6), 2326-2332 (2020).
- [5] M. Nakayama and T. Kato et al. *Nat. Commun.*, **9**, 568 (2018).
- [6] T. Hoshino, M. Nakayama and T. Kato et al., *Soft Matter*, **15**(16), 3315-3322 (2019).
- [7] S. Kajiyama, H. Seto, and T. Kato et al., *Nanoscale*, **12**, 11468-11479 (2020).
- [8] M. Nakayama, T. Kato and Y. Zhao et al. *ACS Appl. Mater. Interfaces*, **11**(19), 17759-17765 (2019).

8:25 AM *SM12.01.02

Diverse and Unique Colloidal Particles Assembled from Polydisperse Liquid Crystalline Oligomers Shu Yang;
University of Pennsylvania, United States

Polymeric colloidal particles play important roles in applications including coatings, adhesives, paintings, drug delivery, and personal cares. Often they are prepared from emulsion polymerization with well-controlled chemical compositions of surfactants and monomers. Polydispersity tends to impede self-assembly processes and the control of particle morphologies. In contrast, nature provided us diverse examples of microparticles that have unique surface textures from mixtures of polypeptides. Further, shape transformation from one state to another is not uncommon in biology.

Here, I will present two examples of self-assembled colloidal particles polymerized from nematic liquid crystal

oligomers (LCOs), where oligomerization and polydispersity of the chain lengths is a feature. In the first example, we synthesize microparticles using a microfluidic device, followed by solvent evaporation and photopolymerization, leading to with robust, tunable surface patterns. Phase separation of LCOs occurs at the interface of the oil-in-water droplet upon organic solvent evaporation, which is facilitated by the mechanical coupling of LCOs of different chain lengths at the droplet interface. In the second example, we show dramatic shape transition of nematic LCO drops to a rich variety of non-spherical morphologies with unique internal structures upon cooling from the isotropic state to the nematic state. Here, molecular heterogeneity *promotes* and stabilize the reversible transitions. These studies suggest that heterogeneity and anisotropy together with shape control will offer new exciting routes to create a wide variety of bioinspired materials.

8:50 AM SM12.01.03

The Dynamics of Chemical Interactions in a Fluid Medium as Revealed by Turing Patterns—A Model Study for Exoskeletal Patterns in Morphogenesis Renuka Rajasekaran; Luella High School, United States

Allen Turing suggested that a system of chemicals reacting with each other and diffusing across space, termed a reaction-diffusion system, could account for the chief phenomena producing exoskeletal patterns in morphogenesis. Turing Patterns remained dormant for some time due to Turing's untimely death and the dominance of the Second Law of Thermodynamics in the scientific world. Some alternatives to the reaction-diffusion theory have also been proposed now. For instance the mechanochemical theory of morphogenesis. However, there are several puzzles to be solved in Turing Patterns. Chief among such puzzles is: which chemicals are the most fundamental of biological patterns? Neither Turing, nor the latter researchers have addressed this question. The present work is an effort to seek answer to this question through a simplistic approach.

The study's focus started with melanin, which is the chief pigment of exoskeleton color and pattern prints. Evidence shows that in the complex genetic expression of melanin, casein is involved through an enzyme called casein kinase. Therefore, it was realized that exploration of caesin's Turing patterns in a physiological fluid model deserves a study. In the simplified model of the physiological fluid chosen for this study, certain key ingredients were incorporated into cow's milk; they are: sucrose, collagen, and sodium chloride. The rationale for the choice of these ingredients is given below.

Sucrose is involved in embryonic development as the energy source and it also serves as the signaling material for gene expression. Collagen is a fibrous protein and constitutes nearly 50% of body protein in mammals. Collagen also comes to the central stage from the osteogenesis (bone development) phase in embryonic development. Given that casein, collagen, and sucrose are macromolecules, they serve a major role as the basic building blocks of embryonic development. The importance of sodium chloride comes from the fact that it is the dominant physiological electrolyte.

Casein is a popular globular protein; as is well known, globular proteins have complex structures (conformation) and have a far greater variety of biological functions. They are thus very dynamic rather than static in their activities. Notably, casein is involved from the start in the embryonic development both in vertebrate and invertebrate animals as well as in plants.

In consideration of the relevance to morphogenesis, Turing patterns of the interaction between casein, sucrose, collagen, and sodium chloride in aqueous medium were investigated in the present study. The stains used are the dye/pigment components of common food coloring agents. The present investigation provides a strong support to casein being the most fundamental macromolecule, which initiates, controls, and guides pattern formation. Salt helps in the polarization of casein and loosens the micelles to different patterns depending on the degree of polarization determined by salt concentration. Sucrose cross links casein strands in unique ways to produce different patterns, guided by its concentration. As revealed by the Turing patterns, sucrose's effect is so magical and seemingly different unique conformational structures are created by casein-sucrose interaction. The Turing patterns also indicate that the effects of these substances are synergistic. Furthermore, some of the patterns revealed by casein and collagen are similar to that of the embryo in gastrulation and neurulation. The present investigation also leads to an understanding that stripes of alternative colors we see on the animal skins (such as zebras) do not seem to come from two different pigments; but they seem to be different tones of the same color. The tone is determined by the kinetics of the underlying physicochemical phenomena.

9:05 AM *SM12.01.04

Light-Responsive Shape-Shifting Nanoparticle Superstructures Nathaniel Rosi and Yicheng Zhou; University of Pittsburgh, United States

We have developed a peptide-based approach for designing and constructing structurally complex nanoparticle superstructures. In this approach, peptide conjugate molecules bind to inorganic nanoparticles and direct their assembly. This presentation will detail first generation ‘static’ superstructures, including 1-D assemblies such as gold nanoparticle helices and discrete 0-D assemblies such as hollow spherical superstructures. We will discuss the subtle differences between the peptide conjugates which direct the assembly of these morphologically distinct superstructures and suggest design criteria for conjugates that can be used to construct second generation ‘dynamic’ superstructures. As a proof of principle, we design a family of photoresponsive peptide conjugates to control the reversible assembly of gold nanoparticles. The conjugates have different responses to input of UV radiation. We demonstrate that the nanoparticle superstructures constructed from these conjugates can undergo morphological shifts from spheres to 1-D assemblies. These results point toward new methods for dynamically controlling nanoparticle assembly via photo stimulus and new families of structurally complex dynamic nanoparticle superstructures.

9:30 AM SM12.01.06

Doping Silicon, Using DNA Ruobing Bai and Haitao Liu; University of Pittsburgh, United States

This talk will present our recent effort towards achieving nanoscale site-specific doping of Si wafer using DNA as both the template and the dopant carrier. Upon thermal treatment, the phosphorous atoms in the DNA diffuse into Si wafer, resulting in doping within the defined region right below the DNA template. A doping depth of 30 nm is achieved for 10s of thermal treatment. We have fabricated prototype field effect transistors using the DNA-doped Si substrate. By using DNA nanostructures to pattern self-assembled monolayers, we are able to achieve both *n*-type and *p*-type site-specific doping of Si. This work shows that DNA nanostructure template is a dual-use template that can both pattern Si and deliver dopants.

SESSION SM12.02: Bio-Inspired Macromolecular Assembly
Session Chairs: Chun-Long Chen and Ki Tae Nam
Thursday Morning, April 22, 2021
SM12

10:30 AM *SM12.02.01

Designing Self-Assembling and Gradient Materials for Regenerative Medicine Molly Stevens; Imperial College London, United Kingdom

This talk will provide an overview of our recent developments in self-assembling and gradient materials for regenerative medicine. We are using remote fields to engineer complex 3D architectures that mimic anisotropic and multiscale tissue structures and produce spatially arranged bioinstructive biochemical cues. We have used acoustic stimulation to produce engineered muscle with bundles of aligned fibres [1], and magnetic fields and buoyancy to achieve biochemical gradients in osteochondral scaffolds [2]. These versatile technologies can be applied to wide range of tissue engineering and drug delivery. We also use light stimulation on our photocaging gRNA strategy for spatiotemporally resolved CRISPR-Cas gene editing [3]. Using this system, we have achieved *in vivo* spatiotemporally controlled gene editing in living zebra fish embryos upon brief exposure to UV light. Finally, we will discuss recent developments in our tunable nanoneedle arrays for multiplexed intracellular biosensing at sub-cellular resolution and modulation of biological processes [4].

[1] J. P. K. Armstrong, J. L. Puetzer, A. Serio, A. G. Guex, M. Kapnisi, A. Breant, Y. Zong, V. Assal, S. C.

Skaalure, O. King, T. Murty, C. Meinert, A. C. Franklin, P. G. Bassindale, M. K. Nichols, C. M. Terracciano, D. W. Huttmacher, B. W. Drinkwater, T. J. Klein, A. W. Perriman, M. M. Stevens. "Engineering anisotropic muscle tissue using acoustic cell patterning." *Advanced Materials*. 30(43): 1802649.

[2] C. Li, L. Ouyang, I. J. Pence, A. C. Moore, Y. Lin, C. W. Winter, J. P. K. Armstrong. "Buoyancy-driven gradients for biomaterial fabrication and tissue engineering." *Advanced Materials*. 31(17): 1900291.

[3] E. V. Moroz-Omori, D. Satyapertiwi, M.-C. Ramel, H. Hogset, I. K. Sunyovszki, Z. Liu, J. P. Wojciechowski, Y. Zhang, C. L. Grigsby, L. Brito, L. Bugeon, M. J. Dallman, M. M. Stevens. "Photoswitchable gRNAs for spatiotemporally controlled CRISPR-Cas-based genomic regulation." *ACS Central Science*. 2020. 6(5): 695-703.

[4] C. Chiappini, E. De Rosa, J. O. Martinez, X. W. Liu, J. Steele, M. M. Stevens, E. Tasciotti. "Biodegradable silicon nanoneedles delivering nucleic acids intracellularly induce localized in vivo neovascularization." *Nature Materials*. 2015. 14: 532-539.

10:55 AM *SM12.02.02

Self-Assembling Peptides for Regenerative Medicine Applications Fabrizio Gelain; IRCCS Casa Sollievo della Sofferenza, Italy

Peptidic biomaterials have been receiving great interest because of their easiness of scale-up production, absence of pathogen-transfer risk, biomimetic properties, nanostructured morphology and customization potential for the specific tissue engineering application. However, their proper usage requires the understanding of multiple phenomena taking place at different scale levels during self-assembling. In this presentation, focused on the nanotech advancements in the field of regenerative medicine, we will see some multi-disciplinary researches and advances toward the regeneration of nervous tissues and pancreatic islets transplantation. This will bring us from molecular dynamics to cross-linking and electro-spinning of self-assembling peptides, from high-density 3D cells cultures to in vivo testing.

11:20 AM SM12.02.03

Biomimetic Self-Templating Fibrillogenesis Seungwook Ji^{1,2}, JuHun Lee^{1,2} and Seung-Wuk Lee^{1,2};

¹University of California, Berkeley, United States; ²Lawrence Berkeley National Laboratory, United States

In nature, many filamentous macromolecules self-assemble into complex, hierarchically ordered fiber structures. The formation of fibers proceeds as cells secrete the macromolecules into a confined extracellular space. The filamentous macromolecules stabilize into diverse non-equilibrium structures that exhibit exquisite optical, mechanical and biological functions. To explain the mechanism of fiber formation in nature, biophysicists have constructed a variety of theoretical and experimental models. These models could not propose real-time processes of fiber formation and assume no interaction between macromolecules in general. Because it is not trivial to design an interaction-controllable system; this basic limitation and assumption, however, is highly simplified and does not represent the reality of nature. We demonstrate our recent efforts to design a biomimetic self-templating fiber formation process under the interaction-controllable system. M13 bacteriophage possesses a long filamentous shape with a helically-arranged protein surface, analogous to naturally existing basic building blocks. As a result of amplification through bacterial infection, M13 bacteriophage is identical, homogenous, and can be easily genetically engineered to make M13 bacteriophage a promising biomaterial in designing a biomimetic system. In this study, we genetically engineer M13 bacteriophage to install a functional peptide motif (VGVPGVG (V: Valine, P: Proline, G: Glycine)) at the end of the major capsid protein p8 to tune interactions between biomolecules during assembly. The introduced functional peptide motif possesses hydrophobic residue which can trigger hydrophobic interaction between phages. In addition, we applied depletion attraction force to manipulate interaction more precisely. We demonstrate that by controlling thermodynamic factors (e.g. concentration of phage and depletant, ionic strength and temperature, etc) we could investigate real-time evolution process of fibrous structure formation and understand how the molecular level interaction acts to the process. Engineered phages go through loosely assembled tactoids, densely packed domains, stacking of domains to fibrils formation and further hierarchical structures. Our approach provides the understanding how the formation of each ordered structure could be the

basis of the next hierarchical structure formation. To investigate the time dependent evolution process of fibrous hierarchical structures, we employed polarized optical microscopy (POM). Other microscopic and nanoscopic structure characterization were carried out by atomic force microscopy (AFM) and scanning electron microscopy (SEM).

11:35 AM SM12.02.04

Pyroelectricity of M13 Bacteriophages Han Kim¹, Seungwook Ji¹, Inseok Chae¹, Kento Okada^{1,1} and Seung-Wuk Lee^{1,1,2}; ¹University of California, Berkeley, United States; ²Lawrence Berkeley National Laboratory, United States

Pyroelectricity is a physical phenomenon of polarization change under temperature fluctuation in the environment. Biological building blocks such as amino acids, deoxyribonucleic acid (DNA), ribonucleic acid (RNA), proteins, and biomaterials such as soft and hard and tissues with hierarchical structures are composed of polar molecules and also known to induce pyroelectric property. However, the molecular mechanism of the pyroelectric effect in biological materials is still elusive. Here we report M13 bacteriophage (phage) as a programmable biomacromolecule building block to study the structure and function relationship of the pyroelectric biomaterials. M13 phage is a benign and non-harmful virus to infect only bacterial host cells. It has a filamentous shape with 880 nm in length and 6.6 nm in diameter. The M13 phage is assembled with 2700 copies of major pVIII coat protein hierarchically with spontaneous polarization. Through genetic modification, we can precisely control the chemical and physical structures of the phage proteins and investigate how the polarization changes under heat application. We can further easily amplify to produce identical copies of the phage on a large scale and self-assemble the phage into highly ordered arrangements. Here we developed a novel pyroelectric material and device using M13 phage. We first created a unidirectionally polarized monolayer phage film and characterized its pyroelectric characteristics. To determine how the heat can manifest polarization of the phage, we used piezoresponse force microscopy and Kelvin probe force microscopy and observed the polarization changes by visualizing the changes in the amplitude, phase, and surface potential under temperature changes. We then modified the polarization of the phage protein by inserting a variable number of negatively charged amino acids to demonstrate the origin of the pyroelectricity of the phage and to suggest the controllability of the pyroelectricity in biomaterials. We finally fabricated phage-based pyroelectric devices that can be used for thermosensor and energy harvester to show the feasibility of future applications. Our approach shows how the hierarchical assembled polar molecules contribute to the pyroelectricity in a biological system in a molecular level and how we can utilize the pyroelectric biological materials for future self-powered system and biomedical applications.

11:50 AM SM12.02.05

Self-Assembly of Aramid Amphiphiles into Ultra-Stable Nanoribbons and Aligned Nanoribbon Threads Ty Christoff-Tempesta and Julia Ortony; Massachusetts Institute of Technology, United States

Small molecule assemblies in biological systems, such as cell membranes, benefit from high-surface-areas, tunable surface decoration, and responsiveness for interaction with their environments. In these systems and the synthetic analogues inspired by them (e.g. those derived from peptides), molecular migration, molecular exchange, and other dynamic instabilities are pervasive. These dynamic processes can be beneficial in applying supramolecular assemblies in biological environments, but increasing nanostructure stability may provide a route to their use in non-biological contexts. Here, we introduce the design of the aramid amphiphile (AA) motif to form microns-long nanoribbons with a dense, percolated hydrogen bonding network. These nanoribbons exhibit suppressed molecular exchange dynamics, mechanical properties on par with silk, and morphological stability outside of water. We utilize this stability to, for the first time, produce dried macroscopic threads of small molecule amphiphiles and demonstrate tunability of their mechanical properties. Finally, we incorporate photoswitchable moieties into the amphiphile design and show their triggerable, reversible morphological transitions between nanoribbon and nanotube states. Both morphologies exhibit months-long stability, persistence in air, and convert fully upon triggering. The AA platform overcomes dynamic limitations of conventional supramolecular systems to provide a novel route to solid-state

nanostructured molecular materials.

12:05 PM *SM12.02.06

Bio-Inspired Photosynthetic and Bioactive Hydrogels Samuel I. Stupp; Northwestern University, United States

Our laboratory is focused on the design of synthetic functional systems that can emulate the most intelligent processes in supramolecular structures of plantae and animalia kingdoms. Two functional hallmarks of naturally occurring chemical systems are the photosynthetic machinery of green plants, which “safely” sustains life on the planet, and the amazing signaling pathways that rule the behavior of cells. Both use hydrogels as the “material” environment in which evolutionary events have optimized their respective functions. In this lecture we describe bio-inspired synthetic hydrogels inspired by green leaves that are based on light harvesting supramolecular polymers and enzymes. These systems synthesize molecules such as hydrogen peroxide, potentially useful as liquid fuels in sustainable energy systems. The lecture will also describe highly dynamic supramolecular polymer hydrogels that mimic extracellular matrices and effectively signal cells to promote regenerative signaling pathways. This particular work will highlight the use of hydrogels in promoting regeneration in the central nervous system, a goal that for many reasons has great societal impact to be explained in the lecture.

SESSION SM12.03: Peptoid-Based Nanomaterials
Session Chairs: Chun-Long Chen and Adrienne Rosales
Thursday Afternoon, April 22, 2021
SM12

1:00 PM *SM12.03.01

Metal-Binding Peptoids as a New Platform for the Development of Functional Bio-Inspired Materials and Supramolecular Peptoid Architectures Galia Maayan; Technion–Israel Institute of Technology, Israel

Peptoids, N-substituted glycine oligomers, are an important class of peptide mimics that are generated from primary amines rather than from amino acids. Their facile and efficient synthesis on solid phase support enables the incorporation of various functional groups at specified *N*-positions along their spine including metal-binding ligands and catalysts.¹ Peptoids can adopt polyproline type helices if the majority of their sequence consists of chiral bulky pendent groups.² Such side-chains are structure inducers but they have no functional value. In my talk I will present the inclusion of metal-binding ligands within peptoid sequences as a new platform for the development of functional bio-inspired materials and supramolecular peptoid architectures. Thus, I will describe: (i) Controlled aggregation of Ag(0) NPs at room temperature in water near neutral pH mediated by peptoids, where tuning the sequence or of the peptoid or changing the metal-binding ligand impact the morphology of the Ag(0) NPs assemblies.³ (ii) Cu(II) mediated self-assembly of short peptoids to form double-stranded peptoid helicates,⁴ and distinct copper-peptoid duplexes, where changing only one non-coordinating side-chain leads to different supramolecular structures including tightly packed helical rods or nano-channels, and to different the pore sizes of the nano-channels.⁵ The selective recognition abilities of the nano-channels towards biologically relevant small molecules and anions will be also demonstrated. (iii) The direct correlation between the structure of short metal-binding peptoids varied in their monomer sequence, and the photoluminescence of their Ru(II) complexes, where .helical peptoids do not affect the fluorescence of the embedded Ru(II) chromophore, while unstructured peptoids lead to its significant decay.⁶

References:

1. (a) T. Zabrodski, M. Baskin, P. Jeya Kaniraj, G. Maayan *Synlett* **2015**, A1. (b) P. Jeya Kaniraj, G. Maayan, *Chem. Commun.* **2015**, 11096. (c) M. Baskin, G. Maayan, *Chem. Sci.* **2016**, 7, 2809.

2. (a) K. Kirshenbaum *et al.*, *Proc. Natl. Acad. Sci., USA* **1998**, *95*, 4303. (b) B.C. Gorske, *et al. J. Am. Chem. Soc.*, 2007, **129**, 8928. (c) O. Royet, *et al.*, *J. Am. Chem. Soc.* **2017**, *139*, 13533
3. (a) H. Tigger-Zaborov, G. Maayan, *J. Coll. Inter. Sci.* **2017**, *508*, 56-64. (b) H. Tigger-Zaborov, G. Maayan *J. Coll. Inter. Sci.* **2019**, *533*, 598-603.
4. T. Ghosh, N. Fridman, M. Kosa, G. Maayan, *Angew. Chem. Int. Ed.* **2018**, *57*, 7703.
5. P. Ghosh, N. Fridman, G. Maayan, *Chem – A Eur. J.*, in press.
6. L. Zborovsky, H. Tigger-Zaborov, G. Maayan, *Chem. Eur. J.* **2019**, *25*, 9098 –9107.

1:25 PM *SM12.03.02

Expanding Hydrogel Functionality using Hierarchical Structure in Precision Polymers Adrienne M. Rosales; The University of Texas at Austin, United States

Tissue engineering offers great promise as a therapy for damaged tissues, a replacement for whole organs, or a platform for drug screening; however, many biomaterial scaffolds fall short on yielding reproducible and functional constructs. Hydrogels in particular have garnered intense interest as tissue engineering scaffolds due to their tailorable permeability, mechanics, and degradability. Synthetic materials are attractive due to their known chemical compositions and reproducibility, but the challenge with their use lies in the lack of complexity as compared to biological systems, especially with regard to sequence-specific bioactivity and hierarchical structure. Hence, our work aims to expand the toolbox for building complexity and functionality into synthetic hydrogel biomaterials by using precise polymer architectures, specifically those of polypeptoids. Using non-natural polypeptoid crosslinkers, we achieved control over the mechanics of poly(ethylene glycol) (PEG) hydrogel platforms by varying monomer sequence and chain structure. Unlike traditional crosslinking methods, our polypeptoid crosslinkers enabled control over hydrogel mechanics without altering network connectivity. Due to their biomimetic backbone, the polypeptoid crosslinkers also conferred stability to cellularly-secreted proteases, as compared to biological substrates. Furthermore, we examined the ability of non-natural peptoid monomers to tune proteolytic degradation rate using hybrid peptide-peptoid structures. Overall, our results suggest that sequence control of synthetic polymers may be a general strategy for expanding the functionality of biomaterial scaffolds for tissue engineering, particularly with respect to mechanics and degradation in complex biological environments.

1:50 PM SM12.03.03

Peptoid-Directed Assembly of CdSe Nanoparticles Madison Monahan¹, Bin Cai², Tengyue Jian², Shuai Zhang^{2,1}, Guomin Zhu^{2,1}, Chun-Long Chen^{2,1}, James J. De Yoreo^{1,2,1} and Brandi Cossairt¹; ¹University of Washington, United States; ²Pacific Northwest National Laboratory, United States

The high information content of proteins drives their hierarchical assembly and complex function, including the organization of inorganic nanomaterials. Peptoids offer an organic scaffold very similar to proteins, but with a wider solubility range and easily tunable side chains and functional groups to create a variety of self-assembling architectures with atomic precision. If we could harness this paradigm and understand the factors that govern how they direct nucleation and assembly of inorganic materials to design order within such materials, new dimensions of function and fundamental science would emerge. In this work, peptoid tubes and sheets were explored as platforms to assemble colloidal quantum dots (QDs) and clusters. We have successfully synthesized CdSe QDs with difunctionalized capping ligands containing both carboxylic acid and thiol groups and mixed them with maleimide containing peptoids, to create an assembly of the QDs on the peptoid surface via a covalent linkage. This conjugation was seen to be successful with peptoid tubes, sheets and CdSe QDs and clusters. Particle identity was confirmed on the peptoid surface using EDX and high-resolution TEM. The particles were seen to have a high preference for the peptoid surface but non-specific interactions with carboxylic acid groups on the peptoids limited control over QD density via the maleimide conjugation. Replacing the carboxylic acid groups with methoxy ethers allowed for control over QD density as a function of maleimide concentration. ¹H NMR analysis demonstrated that binding of QDs to peptoids involved a subset of surface ligands bound via the carboxylate functional group, allowing sulfur to bind via covalent linkage to the maleimide. Overall, we have shown the compatibility and control of CdSe-peptoid interactions via a covalent

linkage with varying peptoid structures and CdSe particles to create complex hybrid structures. Future work looks to expand the library of compatible nanoparticles to tune the properties of the hybrid materials and pattern complimentary nanoparticles onto a single peptoid surface and to investigate the assembly of peptoid nanostructures after conjugation with nanoparticles

2:05 PM *SM12.03.04

Protein-Mimetic Materials from Sequence-Defined Peptoid Polymers Ronald N. Zuckermann; Lawrence Berkeley National Laboratory, United States

A fundamental challenge in materials science is to create synthetic, organic nanostructures with the same architectural sophistication as proteins. One of the most exciting ways to do this is to mimic nature, and synthesize sequence-defined, non-natural polymer chains that spontaneously fold and assemble into precise three-dimensional structures. Peptoid polymers offer a unique platform to advance this general approach. We developed an automated synthesis method, the solid-phase submonomer method, which can efficiently synthesize high-purity, sequence-defined peptoid polymers up to 50 monomers in length. The method uses readily available primary amine synthons, allowing hundreds of chemically diverse sidechains to be cheaply introduced. We use this method, along with computational modeling, to design, synthesize, assemble and engineer a variety of protein-mimetic nanostructures, and to probe fundamental questions in self-assembly and polymer physics. Here, we show by NMR, direct imaging using cryo-TEM, X-ray scattering, and MD simulations, that all known crystalline peptoid assemblies share a fundamental secondary structure motif based on a backbone fold containing all *cis*-amide bonds. This unexpected universality of peptoid backbone folding offers a unique opportunity to rationally design and engineer these materials to create robust, atomically-defined nanomaterials capable of protein-like functions.

2:30 PM SM12.03.05

Designing and Building Hierarchical Heterostructures through Solid-Binding Proteins Functionalized Peptoid Nanosheets Jinrong Ma¹, Bin Cai², Shuai Zhang^{1,1}, Tengyue Jian², James J. De Yoreo², Chun-Long Chen² and Francois Baneyx^{1,1}; ¹University of Washington, United States; ²Pacific Northwest National Laboratory, United States

Despite their technological potential and decades of advances in synthetic and biological chemistry, the construction of hierarchical architectures that intimately integrate synthetic polymer, natural biomolecules and inorganic components remains difficult. Two promising building blocks to tackle this challenge are peptoids, a class of peptide mimics that can be designed for self-assembly into well-defined structures, and solid-binding peptides (SBPs), which offer a biological path to controlled inorganic assembly and mineralization. Here, we report on the synthesis of ~3.3 nm-thick, thiol-reactive peptoid nanosheets assembled from equimolar mixtures of unmodified and maleimide-derivatized version of the Nbpe₆Nce₆ oligomer, optimize the location of cysteine residues in silica-binding derivatives of superfolder green fluorescent protein (sfGFP) for maleimide conjugation, react the two components to form peptoid-protein hybrids that exhibit partial or uniform protein coverage on both of their surfaces, and use 10 nm silica nanoparticles to trigger the stacking of these 2D structures into a multi-layer material comprised of alternating peptoid, protein and inorganic layers. We also exploit the display of solid-binding proteins on peptoid nanosheets and nanotubes to template the organization and control the precipitation of various inorganic materials, establishing peptoid-protein hybrids as a promising platform for materials science.

2:45 PM SM12.03.06

Multi-Phase Assembly of Short-Sequence Peptoid on MoS₂ Shuai Zhang^{1,2}, Peng Mu², Chun-Long Chen^{2,1} and James J. De Yoreo^{2,1}; ¹University of Washington, United States; ²Pacific Northwest National Laboratory, United States

Inspired by Nature, numerous biomolecules with complementary binding affinity to inorganic surfaces have been designed. These biomimetic molecules, including peptides, proteins, and peptoids, have convincing

applications in molecular recognition, fabrication of bio-hybrid materials, (bio)mineralization, energy conversion, storage, and transportation of matter and information, etc.

Peptoid is a class of biomimetic polymer with compatible bio-functions to peptide but has better thermal and chemical stabilities. It offers unique advantages for creating hierarchical assemblies at solid-liquid interfaces, serving as templates with outstanding spatial order for further functionalization. In this talk, I will present the most recent achievements of assembling short peptoid oligomers on MoS₂. By adjusting the pH of the assembly solution and the size of peptoid hydrophobic side chains, we demonstrated that peptoid assembly on MoS₂ could have diversity phases, including the homogeneous film with high crystallinity, disk-like single-layer domains, and lamella patterns. We further found that these phases can co-exist with each other, and the homogeneous film is the template for the growths of the other two phases. After comparing the results to the simulations, it is clear that the peptoid-peptoid interaction and peptoid-MoS₂ interaction, mediated by pH, both play crucial roles in this multi-phase assembly. These results improve the knowledge of designing hierarchical architectures with biomolecules at solid-liquid interfaces. It also provides opportunities to optimize the performance of semiconductor devices in the future.

SESSION SM12.04: Bio-Inspired Hybrid Materials II
Session Chairs: Chun-Long Chen, Marc Knecht and Tiffany Walsh
Thursday Afternoon, April 22, 2021
SM12

4:00 PM *SM12.04.01

Bio-Inspired Approaches for Assembly—Insights for Graphene and *h*-BN Marc R. Knecht; University of Miami, United States

Controllable assembly of materials with regiospatial precision remains a grand challenge where complex arrangements are required to achieve emergent properties. Such structures are required for a wide range of applications, including metamaterials, optical limiting, catalysis, biosensing, etc. Bio-inspired approaches represent unique avenues to achieve such organized structures based upon the precision achieved through biorecognition. Such assembly capabilities are well known in biological systems; however, translation of these approaches to non-natural materials remains difficult to achieve due to the lack of fundamental information concerning the interactions between biomolecules and material surfaces, especially for material compositions not typically observed in nature. In this talk, initial steps to access bio-based approaches for the assembly of two dimensional nanosheets of graphene and hexagonal boron nitride (*h*-BN) in three dimensions will be discussed. Our research has demonstrated that peptides can be used to drive graphene exfoliation from bulk graphite where modification of the peptides with fatty acid domains can be exploited to minimize defect incorporation in the final materials. Through a combination of experimental analyses and computational modeling, we have identified key parameters to control both the binding at the nanosheet surface for both graphene and *h*-BN, as well as the selectivity between the two different materials. Interestingly, the length of fatty acid modifications to the peptide sequence plays an important role in controlling the final bound structure, including achieving highly viscoelastic biointerfaces. Such capabilities are key for the design of new biomolecules with multiple materials binding domains, which could eventually be exploited to drive nanosheet heterostructure formation.

4:25 PM SM12.04.02

Periodic Phosphorylation and Disordered Domain in Amyloid Nanoribbons Impact Nucleation and Growth of Amorphous Mineral Susrut Akkineni^{1,2}, Cheng Zhu³, Jiajun Chen⁴, Miao Song², Samuel Hoff³, Johan S. Bonde⁵, Jinhui Tao², Stefan Habelitz⁶, Hendrik Heinz³ and James J. De Yoreo^{2,1}; ¹University of Washington, United States; ²Pacific Northwest National Laboratory, United States; ³University of Colorado Boulder, United States; ⁴Lawrence Berkeley National Laboratory, United States; ⁵Lund University, Sweden; ⁶University of California, San Francisco, United States

Protein nanoribbons are believed to direct the organization of soft, amorphous mineral into tough, crystalline composites, however, how these ribbons scaffold an amorphous layer remains elusive. Inspired by tooth enamel, wherein amyloid-like amelogenin protein guides apatite mineralization, we investigated the impact of protein and peptide nanoribbon structure on thermodynamics and kinetics of heterogeneous calcium phosphate nucleation and growth. Using *in situ* atomic force microscopy, supported by X-ray diffraction and molecular dynamics simulations, the molecular self-assembly, structure and function of nanoribbons arrays on graphite were resolved. We find that the nanoribbons lowered the barrier for formation of an amorphous phase, likely due to the hydrophilic side groups that protrude into solution with periodicity. Modification of the periodic domain with phosphorylation enhanced nucleation rates, whereas addition of a hydrophilic, disordered domain at C terminus promoted growth rates. These relationships provide empirical evidence for mineralization scaffolded by amelogenin nanoribbons and fundamentals for synthesis of hierarchical hybrid composites controlled by functional domains in nanoribbons.

4:40 PM SM12.04.03

From Nanoscale Interfacial Control to Bioinspired, Macroscale Thermoelectric Devices in Polyaniline/Nanocarbon Composites Yuxiang Zhu, Weiheng Xu, Dharneedar Ravichandran, Sayli Jambhulkar and Kenan Song; Arizona State University, United States

A thermoelectric generator is a promising approach to recovering this low-grade energy and provides a circular economy method for energy sustainability. So far, only 70% of humanity's total energy dissipates as waste heat, further exacerbating the energy crisis and global warming. This study will demonstrate the scalability of coating polyaniline (PANI) on carbon nanotubes (CNTs) for efficient thermoelectrical energy conversions. We start from the in-situ polymerization of aniline with mixed CNTs, and found that the coating of PANi on CNTs showed distinct phases as compared to mixed PANi/CNTs blends. A further examination of their properties showed higher thermal stability and mechanical robustness. More importantly, with different CNT concentrations, the thermoelectric performance was optimized in bioinspired gill structures. We demonstrated the uses of this structure in current/voltage measurement and showed efficiency in powering in-house designed sensors. Our manufacturing is applicable in conjugating polymers for thermoelectric devices.

4:55 PM SM12.04.04

Symbiotic Binary Assembly of Peptide Nano-Mosaics at Graphite Interfaces Tyler D. Jorgenson, You-Hsin Chen, Hadi Zareie, Mehmet Sarikaya and Rene Overney; University of Washington, United States

Control over the self-assembled hierarchical structure of functional biomolecules at solid interfaces is essential for the fabrication of micron-scale bio-nanodevices. Promising candidates are solid-binding peptides selected for specific inorganic solids by directed evolution techniques. Many of these selected peptides exhibit spontaneously long-range ordering at two-dimensional atomically flat solid surfaces. Advanced bio-nanotechnologies, such as multi-enzymatic bioreactors, require multiple, independently tunable functionalization of two or more different peptides to tailor interfacial molecular structures and functions. However, the current understanding of miscibility and binary assembly of peptides at interfaces is lacking. Here we present our findings on binary peptide assemblies at cleaved graphite surfaces with extraordinarily well behaved immiscible long-range ordered structures. We show that nucleation rates of the binary assembled system exceed those of the constituent peptide systems and are tunable by blending ratio and total peptide concentration. Molecular dynamics simulations and nanoscale atomic force microscopy attribute peptide immiscibility to peptide specific substrate recognition and self-assembly directions. Collectively, these findings lead to model predictions of the binary assembly structures of immiscible peptides based on 2D nucleation parameters of the single peptide assemblies. Our findings facilitate the molecular scale engineering of structured bio-nano interfaces through a multi-species self-assembly process and advance the fabrication of high-density patterning of biomolecules for biomimetic technologies, e.g., in multienzyme bioreactors and multiplexed biosensors. The research was supported by NSF-DMREF program through the grant DMR-1629071, 1848911, and 1922020 as part of the Materials Genome Initiative.

5:10 PM *SM12.04.05

Balancing Interactions Over Multiple Length Scales to Direct Assembly of Engineered Proteins at Mineral Surfaces

James J. De Yoreo^{1,2}, Shuai Zhang^{2,1}, Robert Alberstein³, Harley Pyles², Jiajun Chen^{4,2,1}, Faik A. Tezcan³ and David Baker^{2,2,2}; ¹Pacific Northwest National Laboratory, United States; ²University of Washington, United States; ³University of California, San Diego, United States; ⁴Lawrence Berkeley National Laboratory, United States

Self-assembly of particles to form superlattices and other ordered structures is typically thought of in terms of colloidal forces and liquid crystal ordering. Considerations of shape and solvent entropy dominate the controls on organization while atomic-scale details are of lesser importance due to the fairly homogeneous nature of the building blocks. Proteins offer unique advantages over inorganic particles as nanoscale building blocks, including monodisperse structures and specific interactions that are both atomically precise in their location on the protein and tuneable in their strengths. For this reason, ordered assemblies of protein building blocks exhibit a wide range of structural motifs including 1D nanofibers and tubes, 2D lattices and 3D capsids and frameworks. Protein-based systems have the further advantage that they are readily assembled in interrogated in mild aqueous conditions, making them amenable to molecular resolution imaging techniques that provide a unique window into the assembly process. Here we report on two systems of engineered proteins. The first consists of a highly patchy 4-fold symmetric protein building block (L-rhamnulose-1-phosphate aldolase; RhuA), whose self-assembly is driven at the shortest length scale by disulphide bonds designed into four corners of the protein. By introducing a charged, atomically patterned substrate and varying charge states via solution ionic strength, we achieve simultaneous control of four different classes of interactions (covalent bonding, electrostatic surface templating, dipole-dipole interactions and desolvation-induced complexation) to yield four distinct, precisely patterned 2D crystals. The second system consists of a de novo designed rod-shaped helical repeat protein, DHR MicaN whose length can be set arbitrarily to N units of one repeat. These MicaN proteins are designed to interact in an epitaxial manner with the K⁺-sublattice of muscovite mica. Variation of the design created an end-to-end hydrophobic interactions that were either dimeric at both ends or trimeric interface at one end and dimeric at the other. As with RhuA, we show that the interplay of the specific intermolecular interactions, regional electrostatic interactions and global colloidal forces lead to a variety of distinct ordered phases that are not expected for uniform or non-interacting colloids. In all cases, in situ AFM reveals the development of order and its relationship to protein design and surface and solution interactions. The results provide a mechanistic picture of assembly by protein building blocks that links pathways and outcomes to the influence of interactions over many length scales.

5:35 PM *SM12.04.06

Biological Synthesis and Structural Developments in Ultrahard Teeth of Chiton

Taifeng Wang¹, Anna Pohl¹, Steven Herrera¹, Y. Narahara¹, M. Nemoto¹ and David Kisailus^{1,2}; ¹University of California, Riverside, United States; ²University of California, Irvine, United States

There is an increasing need for the development of multifunctional lightweight materials with high strength and toughness. Natural systems have evolved efficient strategies, exemplified in the biological tissues of numerous animal and plant species, to synthesize and construct composites from a limited selection of available starting materials that often exhibit exceptional mechanical properties that are similar, and frequently superior to, mechanical properties exhibited by many engineering materials. These biological systems have accomplished this feat by establishing controlled synthesis and hierarchical assembly of nano- to micro-scaled building blocks. This controlled synthesis and assembly require organic that is used to transport mineral precursors to organic scaffolds, which not only precisely guide the formation and phase development of minerals, but also significantly improve the mechanical performance of otherwise brittle materials.

Here, we investigate an organism that have taken advantage of hundreds of millions of years of evolutionary changes to derive structures, which are not only strong and tough, but also demonstrate abrasion resistance. All of this is controlled by the underlying organic-inorganic components. Specifically, we discuss the formation of heavily crystallized radular teeth the chitons, a group of elongated mollusks that graze on hard substrates for

algae.

Our investigation of the formation of a fully mature radular tooth from *Cryptochiton stelleri* found in the eastern Pacific, occurs over a series of more than 40 teeth. The initial stage of tooth formation begins with the synthesis of a three-dimensional fibrous α -chitin organic matrix, prior to the onset of crystallization. Microscope analysis of early stage teeth shows ferrihydrite mineral particles growing on α -chitin fibers. Synchrotron x-ray, combined with TEM analyses show that ferrihydrite exists as randomly oriented aggregates, but undergoes a phase transformation to magnetite within a few rows of teeth. We discuss potential mechanisms of nucleation of ferrihydrite, its transformation to magnetite as well as its subsequent mesoscale ordering, crystal growth and the resulting mechanical properties. From the investigation of synthesis-structure-property relationships in these unique organisms, we are now developing and fabricating multifunctional engineering materials for energy and water purification based applications.

SESSION SM12.05: Bio-Inspired Hybrid Materials III and Poster Session
Session Chairs: Chun-Long Chen and Ki Tae Nam
Thursday Afternoon, April 22, 2021
SM12

8:15 PM SM12.05.01

Particle Analogs of Electrons in Colloidal Crystals Martin Girard¹, Shunzhi Wang^{1,2}, Jingshan S. Du¹, Anindita Das¹, Chad Mirkin¹ and Monica Olvera de la Cruz¹; ¹Northwestern University, United States; ²University of Washington, United States

A versatile method for the design of colloidal crystals involves the use of DNA as a particle-directing ligand. With such systems, DNA-nanoparticle conjugates are considered programmable atom equivalents (PAEs), and design rules have been devised to engineer crystallization outcomes. This work shows that when reduced in size and DNA grafting density, PAEs behave as electron equivalents (EEs), roaming through and stabilizing the lattices defined by larger PAEs, as electrons do in metals in the classical picture. This discovery defines a new property of colloidal crystals—metallicity—that is characterized by the extent of EE delocalization and diffusion. As the number of strands increases or the temperature decreases, the EEs localize, which is structurally reminiscent of a metal-insulator transition. Colloidal crystal metallicity, therefore, provides new routes to metallic, intermetallic, and compound phases.

8:30 PM SM12.05.02

***In Situ* Generated Silver Nanodot FRET Pair Reveals Nanocage Size** Junhua Yu and Sungmoon Choi; Seoul National University, Korea (the Republic of)

Deciphering the structure and function of nanocages in macromolecules is essential to understand how the confined and finely tuned nanostructure assists and catalyzes reactions. Furthermore, we have been able to develop new strategies to employ unique functionalities of these nanocages unavailable by conventional methods. However, the identification and characterization of nanocages in macromolecules are always challenging; particularly, a fast and straightforward detection of the nanocage size is still missing. FRET can sense nanometer-scale dimensions while keeping the target intact. We have applied the silver nanodot FRET pair to the measurement of nanocages in reverse micelles successfully. Our results also clearly demonstrate that the water nanocage size of the Triton X-100/1-hexanol/cyclohexane-based reverse micelles expanded as more water was added into the system, clarifying long-term confusion regarding the size of the nonionic surfactant-based reverse micelles. The diameter of the nanocage obtained from the FRET of the nanodots was consistent with the size of the nanocage revealed by the cryo-TEM, suggesting that the FRET of silver nanodots to detect nanocage size is an easy and accurate tool. Our approach can be further applied to the measurement of

nanocages in proteins in the future.

References.

1. Jeon, S. M., et al., *J. Photochem. Photobiol. A* **2018**, 355, 479.
2. Yang, S.-A., et al., *Scientific Reports* **2018**, 8, 185.
3. Choi, S., et al., *Chem.-Eur. J.* **2016**, 22, 12660.
4. Choi, S., et al., *Chem. Commun.* **2013**, 49, 10908.
5. Choi, S., et al., *Chem. Soc. Rev.* **2012**, 41, 1867.
6. Zhao, Y. L., et al., *J. Phys. Chem. Lett.* **2020**, 11, 6867.

8:45 PM SM12.05.04

Electrostatically Driven Assembly of Gold Nanorods Using *De-Novo* Designed Protein Fiber Muammer Y. Yaman¹, Kathryn N. Guye¹, Hao Shen¹, Maxim Ziatdinov², Sergei Kalinin², David Baker¹ and David Ginger¹;
¹University of Washington, United States; ²Oak Ridge National Laboratory, United States

Hierarchical inorganic materials are highly desirable for the development new advanced technologies¹. Using programmable macromolecular building blocks such as protein², peptoid³ and polymers³ as templating agent is an effective approach to achieve the hierarchy of inorganic materials. Inducing the successful preparation of functional inorganic materials, these programmable building blocks allow us to control their optical and electronic properties. Due to their outstanding properties, these materials can be applied in a wide range of applications, such as plasmonics¹ and quantum optics¹. However, there still lack of a conclusive guiding rule for the successful synthesis of hierarchical inorganic materials with desired properties via designing macromolecular building blocks. Here, we studied the assembly behavior in a simple system, where *de-novo* designed protein nanofibers⁴ act as the building block, and Au nanoparticles as the inorganic units, towards a general rule for the effect of ionic strength on macromolecule templated assembly of inorganic materials. The protein fibers were designed to be negatively charged and the Au nanorods were synthesized to be positively charged; the electrostatic force were assumed to be the driving force of the hybrid assembly. After electrostatic assembly of Au nanorods along the protein fibers were achieved, we conducted a series of experiments to study the influence of external parameters, such as the aspect ratio of Au nanorods and salt concentration (ionic strength) on the assembly of Au nanoparticles on protein fibers. Moreover, we have developed an automated image analysis tool to help understand the as-obtained experimental data including scanning electron microscope images. With the new image analysis tool, we were able to calculate and analyze the attachment angle of Au nanorods with respect to protein fibers. Our results demonstrate that the average attachment angle varies depending on the ionic strength of the solution. This work is a promising step to the successful synthesis of functional inorganic materials and provides a guiding rule of ionic strength on the orientation of inorganic building blocks in electrostatically-driven hierarchical assembly.

- 1) Qian, Z., Ginger, D.S. Reversibly Reconfigurable Colloidal Plasmonic Nanomaterials *J. Am. Chem. Soc.* **139**, 15, 5266-5276 (2017)
- 2) Dou, J., Vorobieva, A.A., Sheffler, W. *et al.* De novo design of a fluorescence-activating β -barrel. *Nature* **561**, 485–491 (2018)
- 3) Yan, F., Liu, L., Walsh, T.R. *et al.* Controlled synthesis of highly-branched plasmonic gold nanoparticles through peptoid engineering. *Nat. Commun.* **9**, 2327 (2018)
- 4) Shen, Hao, Fallas, J.A., Lynch E., *et al.* De novo design of self-assembling helical protein filaments. *Science* **362** (6415)705-709 (2019)

9:00 PM BREAK

9:30 PM SM12.05.06

Biodegradable Poly-L-lactic acid/Glycine Core/Shell Nanofibers with High Piezoelectricity via Self-Assembly Technology Tong Li, Jun Li, Long Gu and Xudong Wang; University of Wisconsin-Madison, United States

Soft piezoelectric materials are an important group of functional material for state-of-the-art energy harvesting, energy conversion and sensing technologies. Since piezoelectric materials can couple mechanical energy and electric polarization, they can serve as appealing sensing materials, alternative to the described passive semiconductors and capacitive polymers, for self-powered force sensors. While polyvinylidene difluoride has been a well-known and broadly used soft piezoelectric polymer material over years, non-degradability raises a significant concern in terms of safety issues and often requires an invasive removal surgery, which can damage directly interfaced tissues/organs. Poly-L-lactic acid (PLLA), a biodegradable medical polymer, has been shown to exhibit piezoelectricity when appropriately processed, thereby offering an excellent platform to construct safer, biodegradable piezoelectric implants, which can avoid problematic removal surgeries. However, unlike ceramic-based piezoelectric materials, to reach desired high piezoelectric property and long-term stability in biological environment still stand as a big challenge in PLLA soft biodegradable nanomaterial development. In our work, we report a one-step strategy for fabricating core/shell PLLA/Glycine (Gly) NFs with a very high crystalline content and orientation of the polymer chains. The self-assembled core/shell structure is believed essential for the formation of crystalline phase and alignment of polymer chains, where strong intermolecular interaction between the $-NH_2$ groups on Gly and $-C=O$ groups on PLLA is responsible for aligning the PLLA chains and promoting crystalline nucleation. The orientation of polymer chains in the PLLA/Gly NFs along their axes is up to 0.88 observed at atomic scale through high resolution transmission electron microscopy, and the crystallinity ratio is found to be 0.73. The as-obtained PLLA/Gly NFs exhibit significantly enhanced piezoelectric performance and excellent stability and biocompatibility. We also verify that PLLA/Gly NFs functioned well in its predefined lifetime and eventually self-degraded. In addition, the successful formation of high crystallinity ratio with a well-oriented polymer chains offers a structural-assisted design strategy, as opposite to traditional stretching and thermal process, to fabricate high-performance soft biodegradable piezoelectric materials at molecular level.

9:35 PM SM12.05.07

Oriented Crystal Growth of Phenylalanine and Dipeptide by Solution Shearing Kazunori Motai and Yuhei Hayamizu; Tokyo Institute of Technology, Japan

Crystallization of biomolecule offers to form long-range ordered molecular structures in an energy efficient manner under aqueous conditions[1]. Peptide sequences can be designed to establish desired crystal structures. These structured biomaterials will give rise to new functional devices which can be used for various applications. However, the method to form aligned peptide crystalline structures on substrates with a controlled manner is still limited. In this research, we aimed at developing a solution process to align crystals on a substrate in a thin film form. Solution shearing is a promising method to fabricate aligned molecular thin films, which has been studied with synthetic organic molecules, especially for organic semiconductor [2]. In this process, the solution is sandwiched between a blade and substrate. Evaporation of solution occurs at the meniscus formed at the edge of a blade. As the solution evaporates, molecules form thin film with a certain molecular orientation on the substrate. To the best of our knowledge, there is no report applying this method for biomolecules to form their oriented films. Biomolecules have different features from organic semiconductors for the solution shearing process. (1) while synthetic semiconductor organics are dissolved in organic solvents, biomolecules are dissolved in water. Water has a relatively higher boiling temperature than usual organic solvents. (2) while semiconductor organics have planar conformation which is advantageous for the crystallization, peptides or amino-acids are relatively flexible and hard to form a crystal. Thus, optimization of the sweeping speed and temperature of the substrate in the solution shearing is important for the formation of uniform and large-area thin film.

In this study, we developed a fabrication technique of oriented biomolecular thin film based on the solution shearing method. To achieve this goal, we developed a hand-made system for the solution shearing with biomolecules in aqueous solutions, and optimized the sweeping speed and temperature in the process. We utilized amino acids and peptides to test the ability of our system, and we analyzed the structures of deposited thin films of amino acids and peptides by X-ray diffraction (XRD) and angle dependent polarized Raman spectroscopy [3]. As a result of the parameter optimization, we succeeded in fabricating 300 nm-thick oriented films with a size of more than 500 μm square. We have characterized thin films using polarized Raman

spectroscopy and X-ray diffraction (XRD) measurements. Raman spectra revealed that the solution shearing allows us to form crystalline amino acids and dipeptides on Si wafers. These experiments exhibited that the crystal orientations were along the direction of shearing. Furthermore, XRD spectra also revealed a formation of polymorph. It was found that we can suppress the polymorph formation by optimizing the condition of the solution shearing.

Reference

- [1] Yuan, Chengqian, et al. "Hierarchically oriented organization in supramolecular peptide crystals." *Nature Reviews Chemistry* 3.10 (2019): 567-588.
- [2] Giri, G. et al. Tuning charge transport in solution-sheared organic semiconductors using lattice strain. *Nature* 480, 504–508 (2011).
- [3] Motai, K. et al. Oriented crystal growth of phenylalanine and dipeptide by solution shearing. *J. Mater. Chem. C* (2020) doi:10.1039/D0TC01208D.

9:40 PM SM12.05.08

Influence of Surface Charge on Protein-Directed Electrostatic Assembly of Metal Nanoparticles Kathryn N. Guye, Hao Shen, Muammer Y. Yaman, Gerald Liao, David Baker and David Ginger; University of Washington, United States

Achieving controlled assembly of functional inorganic nanoparticles is a requirement for developing new applications in areas such as optoelectronics, sensing, and photocatalysis. Traditional methods, however, are often diffraction-limited or confined to small scale assemblies. Bioorganic templating of inorganic nanomaterials capitalizes on nature's evolutionary design to achieve highly ordered nanostructures, often otherwise inaccessible through conventional ligand-mediated or nanofabrication methods. To efficiently design biological scaffolds for the controlled ordering of nanoparticles, we must first identify and characterize the intersurface interactions governing the assembly process. Here, we study the protein-directed electrostatic assembly of spherical gold nanoparticles along high aspect ratio, *de novo*-designed protein nanofibers anchored to an ITO substrate. We achieve these structures via a layer-by-layer assembly process, in which alternating surface charges of each component drive the highly specific attachment of gold nanoparticles to the anchored protein nanofibers. We then characterize the composite structures by scanning electron microscopy. To probe the charge-dependent particle-substrate and particle-fiber intersurface interactions, we vary particle diameter and pH of the nanoparticle solution and measure particle density and specific binding efficiency to benchmark these interactions. We find an inverse correlation between nanoparticle diameter and particle density. We attribute this trend to more effective screening of the like-charge repulsion between the nanoparticle and substrate by the oppositely-charged protein nanofiber. We then explore how varying pH can tune the local interactions to adjust particle density and the specific binding efficiency. We observe the maximum attachment density at neutral pH at which the layers of the assembly have alternating charges. Furthermore, we note a significant decrease in particle density at low pH at which all surface moieties are protonated and prohibit electrostatic attachment. However, only a slight decrease at high pH is observed as the result of a monotonic decrease of specific binding efficiency with increasing pH due to the neutralization of the substrate surface charge. Finally, we predict optical properties of these composite structures by finite-difference time-domain simulations. These results demonstrate the importance of understanding intersurface interactions for electrostatic assemblies and will guide the design of future bio-templates for the ordering of inorganic nanoparticles.

9:45 PM SM12.05.09

De Novo Designed Protein Templates for Directing TiO₂ Mineralization Amy E. Stegmann^{1,2,3}, Brittney Hellner¹, Harley Pyles^{1,2,3}, Fatima Davila^{1,3,2}, Francois Baneyx^{1,3}, David Baker^{1,2,3} and James J. De Yoreo^{3,1,1}; ¹University of Washington, United States; ²Institute for Protein Design, United States; ³CSASS, United States

De novo designed proteins enable the precise placement of functional groups in three-dimensional space, which can be leveraged to guide the precise nucleation and growth of inorganic phases to form complex hierarchical nanostructures. Proteins have diverse functional groups which enable them to access an array of applications.

Utilizing a strict control of chemical moieties in building blocks and designing repetitive interfaces enables precisely arranged structures to bridge scales. This control is shown to direct nucleation of precursors in solution at room temperature. Investigating the effect that organic molecules can have on nucleation by confining nucleation sites to specific geometries can lead to the formation of hierarchical materials with controlled microstructure. Understanding the effects that spatial presentation of different amino acid moieties has on the nucleated crystal phase and structure will facilitate the intentional design of self-assembled inorganic materials. Herein we demonstrate the influence that sequence can have on the phase of nucleated titania as well as the spatial control over nucleation that we can leverage using homo oligomeric *de novo* protein assemblies. We show that point mutations of different positively charged amino acids can favor anatase or beta phase titania. The templates shown here include small protein oligomers that display a favorable surface for nucleation, and large assemblies of protein fiber with mineralization directing moieties presented in the confined interior.

9:50 PM SM12.05.12

Forced Assembly of Polymer and Nanoparticles for Sensing Applications Weiheng Xu, Sayli Jambhulkar, Dharnedar Ravichandran, Yuxiang Zhu and Kenan Song; Arizona State University, United States

In fabricating polymer and nanoparticle composite or hybrid materials, the soft macromolecules' selective arrangement and the rigid nanoparticles's orders have been a bottleneck to overcome. We will use the bioinspired design of the composite structure to demonstrate the interface and interphase effects in stress transfer, energy transport, stabilization of dispersant, degree of confinement or bonding, and, other new property generations. This poster will introduce the polymer and nanolayered structures in fiber forms. Different polymers and different nanoparticles will be spun via in-house designed fiber spinning techniques. These fibers possess different layer thickness, nanoparticle concentration, and particle morphologies. As a result, these composite fibers display controllable mechanics and conductivity. We leveraged these properties for versatile sensors that are responsive to mechanical strain and gaseous analytes. Our manufacturing of the fibers has not been reported anywhere else and sheds light on a new sensor fabrication for environmental or human health monitoring.

9:55 PM SM12.05.13

Late News: Large-Scale Simulations of Nanostructures Formed During the Selective Binding of a M13 Biological Template to a Nanoscale Architecture Lunna Li^{1,2}, Angela Belcher¹ and Desmond Loke²; ¹Massachusetts Institute of Technology, United States; ²Singapore University of Technology and Design, Singapore

Biological templates that can facilitate nanostructure assembly are widely used in next-generation remediation, electrochemical, photovoltaic, catalytic, sensing and electronic memory devices, but the fundamental features that control their dynamics have yet to be elucidated. By using large-scale molecular dynamics simulations, we reveal, in atomistic detail, the M13-biotemplating kinetics. We observe the assembly of gold nanoparticles on two experimentally-based M13 phage types using full M13-capsid structural models and with polarizable gold nanoparticles in explicit solvent. Moreover, mechanistic and structural insight into the selective binding affinity of the M13 phage to gold nanoparticles are obtained based on a previously unconsidered clamp-based binding-pocket-favored N-terminal-domain assembly and also on surface-peptide flexibility. Our results may open the route for the prospects of utilizing computational tools for genetically engineering a wide range of 3D electrodes for high density low-cost device technologies.

10:00 PM SM12.05.14

Late News: Associate Polymer Theory-Inspired Modelling of Intrinsically Disordered Protein-Mimicking Polymer-Oligopeptide Hybrids for the Formation of Artificial Membraneless Organelles Kalindu S. Fernando, Ghodshiehsadat Jahanmir, Ilona Christy Unarta, Jianhui Liu and Ying Chau; The Hong Kong University of Science and Technology, Hong Kong

Membraneless organelles (MOs) formation via liquid-liquid phase separation (LLPS) is a versatile spatiotemporal organizing mechanism in biological cells. They control biochemical reactions efficiently while being molecule enhancing hubs. Due to these diversified functionalities of MOs, there has been an increasing interest to develop novel bio-active materials and drug delivery systems to imitate MOs in recent years. Intrinsically disordered proteins (IDPs) are found to be one of the significant constituents in MOs and our lab has been inspired to synthesize a new class of polymer-peptide conjugate known as Intrinsically disordered protein mimicking Polymer-oligopeptide Hybrid (IPH) to mimic Fused in Sarcoma (FUS) protein. Liquid droplets reminiscent of MOs have been formed by IPHs under physiological conditions in-vitro.

We develop a computational method to describe the phase separation of IPHs. To describe IPH in a minimalist model, we consider an IPH of having a stickers-spacers architecture, leveraging on classical associative polymer theory. We employ molecular dynamics simulations to estimate the driving forces from the interactive oligopeptide segments (as stickers). The favorable enthalpy between oligopeptide segments provides the driving force for reversible binding between IPHs. We estimated the average binding energy between a pair of stickers as 96 kJ/mol using the Molecular Mechanics Poisson-Boltzmann Surface Area (MMPBSA) method.

Next, we adopt Monte Carlo simulations to describe the stochastic movement of IPHs under physiological conditions. IPHs are structured as strings of stickers and spacers and randomly placed in a three-dimensional simple cubic lattice ($200 \times 200 \times 200$) as a canonical ensemble. We perform 10^5 order of hypothetical Monte Carlo movements as self-avoiding walks on the lattice to obtain energy minimized configuration using the Metropolis-Hastings algorithm as movement acceptance/rejection criteria. Then the radial distribution function is used to identify the phase boundaries of the system. The results provide insights about the propensity of the IPHs to phase separate.

In summary, the research will provide a theoretical framework for understanding the material requirement on the molecular and macromolecular level for the IPHs to form MO-like structures. It provides a fast and economical means to guide the design of synthetic materials for mimicking intrinsically disordered proteins.

10:05 PM SM12.05.15

Late News: Excited-State Dynamics in DNA-Templated Molecular Dye Aggregates [Jonathan S. Huff](#), Daniel B. Turner, Olga A. Mass, Matthew S. Barclay, Bernard Yurke, William B. Knowlton, Paul Davis and Ryan D. Pensack; Boise State University, United States

Molecular assemblies of dye molecules, known as dye aggregates, are of great interest for applications in light harvesting, nanoscale computing, and energy conversion, to name a few. When dye molecules are situated in close (few nm) proximity, short-range interactions modify their electronic structure, which is observed via dramatic changes in their optical properties. Recently, researchers have used DNA as a scaffold to template dye aggregates, raising the prospect that DNA nanotechnology may facilitate the development of aggregates with tunable optical properties. While the electronic structure (i.e., optical properties) of a variety of DNA-templated aggregates has been investigated via steady-state spectroscopic methods, their excited state dynamics, which are critical to their application, remain largely unexplored. In this contribution, we present time-resolved measurements of the excited-state lifetimes of a series of DNA-templated dye aggregates containing a prototypical cyanine dye, Cy5. We demonstrate that for all of the aggregate structures studied, the excited-state lifetimes are considerably shortened relative to that of the Cy5 monomer, exhibiting up to 20-fold lifetime reductions. We attribute the reduced lifetimes to enhanced nonradiative decay. Additionally, we discuss possible mechanisms of the enhanced nonradiative decay and ways that the nonradiative decay process might either be enhanced further or suppressed in order to meet the demands of various applications.

10:10 PM SM12.05.16

Late News: Artificial Membraneless Organelle-Based Therapeutic System for Regulation of RNAzyme Directed Gene Therapy [Fariza Zhorabek](#) and Jianhui Liu; The Hong Kong University of Science and Technology, Hong Kong

Stability and efficiency remain as a critical hurdle limiting clinical application of gene therapeutics, where development of protective gene carrier system has a potential to solve existing problems. In cells, nucleic acid molecules together with intrinsically disordered proteins (IDP) are actively localized in specialized compartments known as membraneless organelles (MO), that serve to stabilize, protect, and regulate corresponding reactions of molecules inside. Inspired by following beneficial aspects of MOs, here we report a new method for encapsulation and enhancement of functional activity of RNA therapeutics using membraneless organelle biomimetic system, reconstructed from IDP-mimicking polymer-oligopeptide hybrid (IPH). IPH, designed to display weak molecular attractions and RNA-binding capability, forms membraneless droplets under physiological mimicking conditions and demonstrates range of biomimetic properties. A model gene therapeutic, hammerhead RNAzyme against TNF- α cytokine mRNA, was preferentially recruited into IPH-droplets, along with target mRNA, with up to 30-folds enrichment. Owing to the liquid-like nature of the droplet interior, both recruited nucleic acid molecules exhibited free diffusion within the droplet environment as indicated by FRAP. Notably, RNAzyme catalytic activity was enhanced in the presence of the artificial MOs, demonstrated by gel electrophoresis and confocal fluorescence microscopy, presumably owing to localized increase of RNAzyme concentration and distinct droplet interior. This result also seems to indicate that localization within the IPH-droplet supports RNA folding, essential for its reactivity. Furthermore, methods for delivering RNAzyme loaded IPH-droplets into a macrophage cell line will be explored, where upon successful delivery, biocompatibility, stability, and suppression level of TNF- α production will be investigated. Overall, IPH-based MO biomimetics investigated here offers a potential as a gene carrier and bioreactor module, which may be useful for a range of gene therapeutic strategies.

SESSION SM12.06: Bio-Inspired Macromolecular Self-Assembly
Session Chairs: Chun-Long Chen, Fiona Meldrum and Ki Tae Nam
Friday Morning, April 23, 2021
SM12

8:00 AM *SM12.06.01

Functional Bioinspired Polypeptoids Jing Sun; Qingdao University of Science and Technology, China

Bioinspired polymeric materials receive considerable attention due to significant advantages over their natural counterparts: the ability to tune their structures over a broad range of chemical and physical properties, increased stability and improved processability. In particular, polypeptoids, or poly N-substituted glycines, are a promising class of peptidomimetic polymers, which offer great unique properties for both fundamental research and applications in biotechnology. The polypeptoid possess identical backbones to the polypeptide, but the side chain is attached to the nitrogen instead of α -carbon. It thus eliminates the inter- and intrachain hydrogen bonding and the chirality in the main chain. The peptoid polymers with high molecular weights and large scale yields can be obtained by ring-opening polymerization technique. Many polypeptoid-based block copolymers have therefore been synthesized and studied. We synthesized a series of functional polypeptoids with stimuli responsive properties by a combination of ring-opening polymerization and thiol-yne click chemistry. The obtained polymers show either LCST-type or UCST-type behaviour depending on the side-chain functionalities. We further reported a facile approach to prepare functional nanostructures such as highly flexible 2D crystalline nanosheets and superbrushes. The obtained bioinspired nanostructures are potential candidates for applications in nanoscience and biomedicine.

8:25 AM SM12.06.02

"Functional Fouling" of Surfaces by Interfacial Silk Fibroin Self-Assembly Tanner Fink, Caleb Wigham, Jeongae Kim and Runye H. Zha; Rensselaer Polytechnic Institute, United States

Silk fibroins are a class of proteins produced by a variety of insects and arachnids that can surpass man-made materials in specific strength and toughness. From a macromolecular perspective, silk fibroins have a linear architecture predominantly consisting of regularly alternating beta-sheet forming peptide segments and flexible peptide segments, resulting in a supramolecular network structure with stiff crystalline domains reinforcing an amorphous matrix. In nature, silk fibroins undergo a complex self-assembly process during spinning, rapidly transitioning from a soluble protein to an insoluble, highly robust material. Our work leverages the self-assembly of silk fibroin and silk-like macromolecules as a bottom-up method to form functional biomedical coatings. In particular, we have observed that non-specific interactions of silk fibroin with surfaces during supramolecular self-assembly can lead to the formation of stable and adherent thin-film coatings. These coatings provide complete surface coverage and can grow to tens of nanometers thick, completely transforming the physicochemical properties of a surface without requiring covalent chemistry or substrate pre-activation. Our studies also demonstrate that silk fibroin coatings can be generated on a variety of substrates ranging from hydrophobic Teflon to hydrophilic TiO₂. Furthermore, these coatings can readily exhibit beneficial biomedical properties, such as decreasing bacterial attachment and increasing neurite extension. Our research moreover delves into the complex interplay of surface-protein and protein-protein interactions underlying coating formation to establish methods by which we can tune the coating process. Through these investigations, we reveal a novel mechanism of protein adsorption that enables continuous, indefinite growth of robust protein layers on a variety of surfaces, which forms the foundation of a new approach towards modifying biomedical surfaces.

8:40 AM SM12.06.03

Computational Reverse-Engineering Analysis for Scattering Experiments (CREASE) on the Self-Assembly of Amphiphilic Polymer-Peptide Conjugates Ziyu Ye and Arthi Jayaraman; University of Delaware, United States

Peptide-based amphiphilic biomaterials that self-assemble into nanostructures provide a path for designing materials such as hydrogels and drug delivery vehicles. The engineering of these materials hinges upon the precise characterization of the self-assembled structures such as those obtained through small angle scattering techniques. The interpretation of these scattering profiles typically relies on analytical models for conventional shapes that may not capture the system geometry at hand. This calls for a method that is able to tie scattering profile features directly to the molecular level details in complex nanostructures without needing off-the-shelf scattering models. To address this need, we present recent developments in extending Computational Reverse-Engineering Analysis for Scattering Experiments (CREASE) to a system of polymer-peptide conjugates that self-assemble into bilayer and vesicle structures. Taking in scattering intensity profiles and polymer chemistries as inputs, CREASE combines genetic algorithm and molecular reconstruction simulations to determine the peptide amphiphile bilayer composition and vesicle dimensions (e.g. core diameter, layer thicknesses) and molecular level packing within the nanostructure.

8:55 AM SM12.06.04

Development of a Coarse-Grained Model to Simulate Assembly within Solutions of Cellulose and Cellulose Derivatives Zijie Wu and Arthi Jayaraman; University of Delaware, United States

In this talk we present a new coarse-grained (CG) model for cellulose and cellulose derivatives (e.g., methylcellulose) that enables simulations of their assembly in experimentally relevant solution conditions. This model balances the incorporation of chemical details at the monomer level (e.g., β , 1-4 linkage, relevant placement of groups that can/cannot form hydrogen bonds, directional hydrogen bonding interactions) as well as the reduction in degrees of freedom needed to simulate experimentally relevant length scales and time scales associated with assembly of multiple cellulose or methylcellulose chains in solution at finite concentration. We will first validate this CG model by comparing the cellulose single chain structure observed with the CG molecular dynamics (MD) simulations to that seen in atomistic MD simulations. We also compare the hydrogen bonding pattern, interchain distance and interchain orientation seen in multi-chain CG MD simulations with those observed in experimental crystallographic studies. After validation of cellulose CG model, we extend the

CG model to study impact of 'silenced' hydrogen bonding sites in order to simulate cellulose derivatives synthesized by substituting some of the hydrogen bonding -OH groups in cellulose with other non-hydrogen bonding groups (e.g., -OMe in methyl cellulose). We expect this type of CG model to be useful in predicting morphology of cellulose and its derivatives under a wide range of solution conditions and chemical modifications to the chains.

9:10 AM SM12.06.06

Late News: Antibacterial Alumochitin Thin Films Grown by Molecular Layer Deposition Karina

Ashurbekova¹, Kristina Ashurbekova², Arbresha Muriqi³, Leire B. Larrea¹, Borja A. Lerma¹, Iva Šarić⁴, Evgenii Modin¹, Raul Perez-Jimenez^{1,5}, Mladen Petravić⁴, Michael Nolan³ and Mato Knez^{1,5}; ¹CIC nanoGUNE, Spain; ²Dagestan State University, Russian Federation; ³Tyndall National Institute, Ireland; ⁴University of Rijeka, Croatia; ⁵IKERBASQUE, Basque Foundation for Science, Spain

Natural chitin and chitinoid materials have outstanding physical and biological properties, which inspired us to develop a process for biomimetic chitinoid organic and hybrid organic-inorganic thin film growth by Molecular Layer Deposition (MLD).

Here, we present a new class of organic-inorganic hybrid polymers called "metallo-saccharides", based on sugar-type precursors. For a controlled MLD growth, the hexosamine monosaccharide N-Acetyl-D-mannosamine (ManNAc) was coupled with trimethylaluminum (TMA) repetitively in a cyclic manner for the growth of the hybrid organic-inorganic alumochitin thin films.

The self-limiting behavior of the surface reactions and the growth rate were determined by in-situ quartz crystal microbalance (QCM) and X-ray reflectivity (XRR) studies. The QCM measurements revealed a linear mass increase with the number of MLD cycles, and a film growth rate of ~ 20 ng/cm²/cycle at 115 °C. XRR studies showed a growth rate of ~ 1.3 Å/cycle and a constant film density of ~ 2.5 g/cm³. The chemical structures of the coatings were studied with *ex-situ* X-ray photoelectron spectroscopy (XPS) and attenuated total reflectance Fourier transform infrared spectroscopy (ATR-FTIR). Characterization of the film structure, morphology, and conformality were performed by High-resolution transmission electron microscopy (HR-TEM), showing uniform and conformal alumochitin films wrapping ZrO₂ nanoparticles (NPs).

The chemical interaction between ManNAc and TMA, and the possibility of hybrid alumochitin film formation were modeled by density functional theory (DFT). The computed interaction energies between TMA and ManNAc are negative, meaning that there's a strong interaction between these precursors. Theoretical modeling revealed that the proposed reaction mechanism for the ManNAc/TMA MLD process is energetically favorable. The evaluation of the antimicrobial activity of the alumochitin thin film against Gram-positive (*Staphylococcus aureus*) and Gram-negative (*Escherichia coli*) bacteria was assessed. Bacteria attachment and proliferation on glass substrates, covered with MLD film, were analyzed by confocal microscopy. Both types of bacteria grow and proliferate on positive control samples, while neither *Staphylococcus aureus* nor *E. coli* bacteria attached to the surface of the alumochitin film. These results show a great antimicrobial activity of alumochitin against gram-positive and gram-negative bacteria, as well as its enormous application potential as bioactive surfaces.

This project has received funding from the European Unions Horizon 2020 research and innovation programme under the Marie Skłodowska -Curie grant agreement No 765378.

9:25 AM SM12.06.07

Late News: Structure, Tunable Self-Assembly and Optical Properties of a Model Cephalopod Protein

Preeta Pratakshya¹, Gregor Ilc², Matic Kovačič², Atrouli Chatterjee¹, Janez Plavec² and Alon Gorodetsky¹; ¹University of California, Irvine, United States; ²Slovenian NMR Centre, Slovenia

The study of natural and designer protein-based materials has enabled the development of ubiquitous modern technologies for applications in optics, electronics, bioengineering and even medicine. Within this context, unique cephalopod structural proteins called reflectins have garnered attention due to their technological potential for the development of biophotonic and bioelectronic devices. However, the development of reflectin-based materials has been impeded by an incomplete understanding of their structures and properties. Here we

highlight the proteins' structure, assembly and multi-faceted material properties within the context of biophotonic platforms. Specifically, we present the molecular-level structure of a model cephalopod protein, its tunable self-assembly, and the correlation between its structural characteristics and optical properties. Our findings not only provide useful insights into the structure-function relationships of reflectins but also underscore their potential as functional biomaterials and hold relevance for the development of cephalopod-inspired optical technologies.

SESSION SM12.07/SM09.04: Joint Session: Bio-Inspired Macromolecular Assembly
Session Chairs: Chun-Long Chen and Chris Kloxin
Friday Afternoon, April 23, 2021
SM12

5:15 PM *SM12.07/SM09.04.01

Biomolecules for Non-Biological Things—Materials Construction Through Peptide ‘Bundlemers’ Design and Solution Assembly Darrin J. Pochan; University of Delaware, United States

Self-assembly of molecules is an attractive materials construction strategy due to its simplicity in application. By considering peptidic molecules in the bottom-up materials self-assembly design process, one can take advantage of inherently biomolecular attributes; intramolecular folding events, secondary structure, and electrostatic interactions; in addition to more traditional self-assembling molecular attributes such as amphiphilicity, to define hierarchical material structure and consequent properties. A new solution assembled system comprised of theoretically designed coiled coil bundle motifs, also known as ‘bundlemers’ will be introduced. The molecules and nanostructures are not natural sequences and provide opportunity for arbitrary nanostructure creation with peptides. With control of the display of all amino acid side chains (both natural and non-natural) throughout the peptide bundles, desired physical and covalent (through appropriate ‘click’ chemistry) interactions have been designed to produce one and two-dimensional nanostructures. One-dimensional nanostructures span exotically rigid rod molecules that produce a wide variety of liquid crystal phases to semi-flexible chains, the flexibility of which are controlled by the interbundle linking chemistry. The two dimensional nanostructure is formed by physical and covalent interactions and are also nanostructures not observed in nature. All of the assemblies are responsive to temperature since the individual bundle building blocks are physically stabilized coiled coil bundles that can be melted and reformed with temperature. Additional, novel nanostructures to be discussed include uniform nanotubes as well as the templated growth of metallic phases. Included in the discussion will be molecule design, hierarchical assembly pathway design and control, click chemistry reactions, and the characterization of nanostructure via electron microscopy, neutron and x-ray scattering, and rheological measurements, as well as inherent material properties (e.g. extreme stiffness, responsiveness to temperature and pH, stability in aqueous and organic solvents).

5:40 PM *SM12.07/SM09.04.02

De Novo Design of Protein-Based Materials and Machines David Baker; University of Washington, United States

We are exploring the de novo design of proteins that self-assemble into 1D (fiber), 2D (array), or 3D (crystal) architectures. We have designed, with near-atomic accuracy, 1D helical filaments with a wide range of diameters that assemble into precisely ordered micron-scale fibers, as well as 2D hexagonal arrays that assemble rapidly upon mixing the two designed protein components. The arrays span multiple microns and are robust to fusion of a wide range of functional groups enabling. We have also extended these approaches to the design of protein-inorganic hybrid materials. Finally, we are pursuing the computational design of new mechanical systems made of proteins. With this work, we seek to create custom devices that can perform useful work at the nanoscale.

6:05 PM *SM12.07/SM09.04.03

Dynamic and Adaptive Protein Assemblies by Chemical Design Faik A. Tezcan; University of California, San Diego, United States

Proteins represent the most versatile building blocks available to living organisms or the laboratory scientist for constructing functional materials and molecular devices. Underlying this versatility is an immense structural and chemical heterogeneity that renders the programmable self-assembly of proteins a challenging design task. To circumvent the challenge of designing extensive non-covalent interfaces for controlling protein self-assembly, we have endeavoured to use bonding strategies based on fundamental principles of inorganic, supramolecular and polymer chemistry. These strategies have resulted in 0, 1, 2, and 3D protein assemblies that display high structural order over many length scales and possess emergent chemical, physical, functional and dynamic properties. In this talk, I will present some of the recent protein-based assemblies and materials constructed in our laboratory.

6:30 PM SM12.07/SM09.04.04

Late News: Nucleic Acids Modulate Stiffness of Artificial Membraneless Organelles Jianhui Liu, Fariza Zhorabek and Ying Chau; The Hong Kong University of Science and Technology, Hong Kong

Driven by liquid-liquid phase separation (LLPS), an emerging universal intracellular organization mechanism, membraneless organelles (MOs) generally harbor intrinsically disordered proteins (IDPs) and RNAs. As a minimalist biomimetic synthetic pathway, we synthesized IDP-mimicking polymer-oligopeptide hybrid (IPH) by conjugating cysteine-terminated peptides to vinylsulfone-modified dextran *via* facile click chemistry pathway through Michael addition between thiol and vinylsulfone. Two peptide sequences, namely, cysteine-terminated low complexity domain-like peptide (CLCDP) and cysteine-terminated arginine-glycine-glycine-containing peptide (CRP), were designed to impart weak molecular attraction and RNA-binding capacity to IPH, respectively. Most intriguingly, IPH underwent LLPS under physiology-mimicking conditions *in vitro*, resulting in micron-sized compartmentalized droplets, which could recruit RNA to generate complexed coacervate, namely, artificial MOs (AMOs). Stoichiometry of RNA, represented by N/P ratio between IPH and RNA, could exert effect on viscoelastic properties (storage modulus, G' , as an indicator of stiffness) of AMOs in a dose-dependent fashion, as will be quantified by microrheology, whilst no appreciable change of sphericity of AMOs was observed even for long RNAs (up to *ca.* 2.78 kbs) with high incorporation (up to N/P=1/25). Moreover, mobility, indicated by diffusion coefficient (D) measured by fluorescence recovery after photobleaching (FRAP), was also significantly affected by incorporation of RNAs. As an intracellular structural analogue which has also been shown implication in MO formation, (single/double stranded) DNA-based AMOs were also constructed and investigated. In stark contrast to RNA-based MOs, DNA modulates stiffness of AMO much more drastically, as is indicated by significant decrease of sphericity even at low incorporation (as low as N/P=1/0.1, similar length as RNA counterpart), as well as with very short DNA (*ca.* 36 bp, N/P=1/10), which will be further quantified by microrheology. Additionally, FRAP will be leveraged to quantify D of DNA-based AMO, which is expected to be drastically different from RNA-based AMO owing to occurrence of irregular-shaped assemblies. We reason the disparity between effect of RNA and DNA (single/double stranded) originates from the difference of intrinsic rigidity, as well as their non-specific interactions with IPH, which will be further elucidated *via* a biophysical model.

SESSION SM12.08: Bio-Inspired Hybrid Materials IV

Session Chairs: Chun-Long Chen and Ki Tae Nam

Friday Afternoon, April 23, 2021

SM12

8:15 PM SM12.08.01

Late News: Developing Complex Structures—A Micron-Scale Tree Trunk with Its Annual Rings Arash Momeni¹, Christopher Walters¹, Yi-Tao Xu¹, Wadood Hamad² and Mark Maclachlan^{1,3,4}; ¹The University of British Columbia, Canada; ²FPIInnovations, Canada; ³Stewart Blusson Quantum Matter Institute, Canada; ⁴Kanazawa University, Japan

Hierarchical biological materials, such as osteons and plant cell walls, are highly complex structures that are difficult to mimic. Here, we demonstrate that liquid crystal systems combined with polymerization techniques could be applied in confined spaces to develop complex structures. We report development of a highly ordered concentric chiral nematic polymeric fibers based on cellulose nanocrystals (CNCs).

CNCs are nano-sized needle-shaped crystalline cellulose particles obtained by treatment of cellulosic biomass with acids. CNC aqueous suspensions spontaneously form chiral nematic liquid crystalline structures above a critical concentration in water. Organization of CNC particles could be manipulated through confinement. In our experiments, CNC suspensions were mixed with polymeric precursors and confined within a glass capillary tube. The tube was aged for several days for the liquid crystalline structure to form, followed by UV-initiated polymerization to lock the structure. The resulting CNC/polymeric fiber could then be removed from the tube and shows a highly ordered single domain liquid crystalline structure throughout its length.

Polarized optical microscopy, electron microscopy, confocal microscopy and 2D X-ray diffraction showed highly uniform concentric rings throughout the length of the fiber. The concentric rings are formed by CNC particles arranging in a chiral nematic liquid crystalline order where the CNC particles' director rotates along the fiber diameter. A good analogy to describe the fiber structure is a tree trunk with its annual rings. The distance between the concentric rings of the fiber is equal to half of the pitch of the chiral nematic CNC liquid crystal. We tracked the formation of this highly ordered structure over time and under different conditions in which we varied the tube orientation, CNC concentration, CNC type, and capillary tube size.

Tube orientation during liquid crystalline phase formation was important because gravity causes sedimentation of tactoids, a predecessor to the long-range ordered phase. Tactoids are liquid crystalline anisotropic droplets that spontaneously nucleate above a critical CNC concentration and are the intermediate state bridging the isotropic phase and the macroscopic liquid crystalline phase with longer range order. CNC concentration and type were shown to determine the distance between concentric rings of the fiber. The capillary tube inner diameter was also important, and a single-domain structure was only obtained inside small-diameter tubes, not large ones. Mechanical tests showed similar properties for the chiral nematic and a pseudo-nematic CNC/polymeric fiber, both of which had superior mechanical properties compared to a polymer-alone fiber.

The structure of the single-domain chiral nematic concentric CNC/polymeric fiber is very similar to biological hierarchical structures, such as twisted plywood architecture of collagen fibers in cortical bone or twisting cellulose microfibrils of wood cell units. Indeed, liquid crystal systems, confined spaces, and polymerization techniques could be combined to achieve complex structures. These highly ordered CNC/polymeric fibers could become a platform for many applications from photonics to developing complex hierarchical materials.

8:30 PM SM12.08.02

Late News: Lipophilic Modification of Silica Coated Gold Nanorods Generates Enhanced Photoacoustic Signal Nonlinear with Laser Fluence Evan Mueller¹, Maju Kuriakose¹, Ke Ma², Marco Inzunza¹, Jennifer Cha¹, Todd Murray¹ and Andrew Goodwin¹; ¹University of Colorado Boulder, United States; ²Purdue University, United States

In this paper, lipophilically modified silica coated gold nanorods were developed to enhance the photoacoustic response of contrast agents. Photoacoustic imaging become a popular technique in the diagnostic imaging because it can utilize light at larger penetration depths and better resolution than optical coherence tomography or fluorescence imaging. In addition, photoacoustic imaging can augment optical microscopy to image in high

scattering tissue. To boost signal, many exogenous contrast agents have been synthesized. However, these agents are still limited to a linear dependence of signal on laser fluence, which limits the benefits for imaging in scattering media. The ability of agents to induce cavitation events in response to laser irradiation would both increase signal and promote nonlinearity. In this work, silica coated gold nanorods with a longitudinal plasmon peak of 750-800 nm were lipophilically modified to facilitate the formation of cavitation nuclei on the rod's surface. It was found that the lipophilically modified silica coated gold nanorods were able to achieve nonlinearity at pulse radiant exposures greater than 8 mJ/cm². At radiant exposures of 21 mJ/cm², the photoacoustic response was 13-15 times higher than unfunctionalized gold nanorods. The concentration of the samples was also investigated, and it was found that the photoacoustic response was greater for samples with higher concentrations than ones that were lower. Finally, the lipophilically modified silica coated gold nanorods were more resistant to etching in aqueous media, showing stability for more than one month in PBS.

8:45 PM SM12.08.03

Late News: Statistical Studies of Meniscus Splitting Using an Aqueous Mixture of Polysaccharides for Preparation of Bioinspired Functional Materials Isamu Saito, Koji Ogura, Yuiming Wu, Yoshiya Tonomura and Kosuke Okeyoshi; Japan Advanced Institute of Science and Technology, Japan

Influx and efflux of water is important for polysaccharides in living organisms, *e.g.* directional control of water diffusion on vascular bundle and water retention on fruits. While, it is possible to artificially create spatial patterns through water evaporation under physicochemically controlled environments. In fact, based on fingering phenomena, we could successfully obtain spatio-temporal patterns by drying aqueous mixture of polysaccharides.¹ The pattern formation has been demonstrated using several kinds of viscous aqueous mixtures of polysaccharides. The spatial pattern is formed by meniscus splitting with ordered depositions of polysaccharide self-assembly, from one space into multiple spaces. Differing from previous dissipative structures transiently showing spatial patterns, we successfully immobilized the structure as polymer deposition with uniaxial orientation. In this study, to clarify the factors on specific deposition nucleation, the nucleus position is statistically analyzed by changing the initial polymer concentration and drying temperature. Furthermore, by introducing crosslinking points into the membrane, the swelling characteristics as an anisotropic hydrogel were investigated. Reference 1. *Sci. Rep.* **2017**, *7*, 5615; *Polymer J.* **2020**, *52* 1185.

9:00 PM SM12.08.04

Late News: Iridescent Cellulose Nanocrystal Films Modified with Hydroxypropyl Cellulose Christopher Walters¹, Charlotte Bootte¹, Thanh Nguyen¹, Wadood Hamad² and Mark Maclachlan¹; ¹University of British Columbia, Canada; ²FPIInnovations, Canada

Cellulose nanocrystals (CNCs) are an abundant biorenewable resource that spontaneously organize into chiral nematic liquid crystals with hierarchical structure. This chiral nematic organization is retained in dried films of CNCs, giving films with brilliant iridescent colors.¹ The introduction of polymers into a chiral nematic cellulose nanocrystal (CNC) matrix allows for the tuning of optical and mechanical properties, enabling the development of responsive photonic materials.² Previously, researchers have investigated CNCs added to hydroxypropyl cellulose (HPC), but not the effects of small amounts of HPC on CNC.^{3, 4} In this study,⁵ we explored the incorporation of HPC into a CNC film prepared by slow evaporation. In the composite CNC/HPC thin films, the CNCs adopt a chiral nematic structure, which can selectively reflect certain wavelengths of light to yield a colored film. The color could be tuned across the visible spectrum by changing concentration or molecular weight of the HPC. Importantly, the composite films were more flexible than pure CNC films with up to a ten-fold increase in elasticity and a decrease in stiffness and tensile strength of up to six-times and four-times, respectively. Surface modification of the films with methacrylate groups increased the hydrophobicity of the films and therefore the water stability of these materials was also improved.

References:

1. Revol, J.-F.; Godbout, L.; Gray, D., Solid self-assembled films of cellulose with chiral nematic order and optically variable properties. *J. Pulp Pap. Sci.* **1998**, *24*, 146-149.
2. Tran, A.; Boott, C. E.; MacLachlan, M. J., Understanding the Self-Assembly of Cellulose Nanocrystals—Toward Chiral Photonic Materials. *Adv. Mater.* **2019**, *32*, 1905876.
3. Ma, L.; Wang, L.; Wu, L.; Zhuo, D.; Weng, Z.; Ren, R., Cellulosic nanocomposite membranes from hydroxypropyl cellulose reinforced by cellulose nanocrystals. *Cellulose* **2014**, *21*, 4443-4454.
4. Fernandes, S. N.; Geng, Y.; Vignolini, S.; Glover, B. J.; Trindade, A. C.; Canejo, J. P.; Almeida, P. L.; Brogueira, P.; Godinho, M. H., Structural Color and Iridescence in Transparent Sheared Cellulosic Films. *Macromol Chem Phys* **2013**, *214*, 25-32.
5. Walters, C. M.; Boott, C. E.; Nguyen, T.-D.; Hamad, W. Y.; MacLachlan, M. J., Iridescent Cellulose Nanocrystal Films Modified with Hydroxypropyl Cellulose. *Biomacromolecules* **2020**, *21*, 1295–1302.

9:15 PM SM12.08.05

Recombinant Spidroins for Fibrous Materials Applications Jinlian Hu; City University of Hong Kong, Hong Kong

Spiders can produce up to seven different types of silk fibers with varying mechanical properties and functions to support their survival. Some of their most characteristic properties that do not exist in other natural fibers are flat-stress strain behavior (tubuliform silk), supercontraction (dragline), and water collection (capture silk). These interesting properties can serve the requirements for smart functionality of materials for various applications. However, unlike silkworm silk spiders cannot be farmed due to their cannibalistic nature. This limits utilization of spider silks in their natural form for real world applications. The understanding of molecular structure of silks has inspired research by utilizing the repeating modules of spider silks with different gene sequence motifs to develop biomimic, novel and high performance materials. There are so far a range of recombinant spider silk proteins, namely, spidroins, being genetically produced by a variety of host organisms. Although such produced spidroins have been shown to be versatile proteins with the capability to be processed into different morphologies, fibrous materials are still one of the most attractive incentives since its natural counterparts due to the above reasons. This talk will present several examples of biomimetic fibrous materials with different properties including shape memory/supercontraction, mechanical toughness and directional water collection by using spidroins made from different gene motifs expressed in *E. Coli*.

Tubuliform spidroin 1, from a black widow spider-Lactrodectus Mactans, was first genetically engineered by using the single repeat unit and abbreviated as eTuSp1 for flat-stress-strain mechanical properties. In this work, in good agreement with previous studies, spherical aggregates were considered as intermediates and could be induced into β -sheet-rich silk fibers by the shear and elongation. The underlying mechanism for the assembly of silk spheres and fibers were demonstrated by the micelle theory. To investigate mechanical properties, individual spheres were subjected to the AFM indentation and the corresponding compressive modulus was determined by using Hertz model. In the tensile test, the modulus of silk fibers could be flexibly regulated in accordance to different post-spin drawing ratios. We also prepared an engineered major ampullate spidroin 2 (eMaSp2) by using N & C terminal domains from spidroins MaSp1 of Euprosthenoops australis and MiSp1 (minor ampullate spidroin) of Araneus ventricosus respectively for shape and stress memory fibers. Revealed by CD spectrum, eMaSp2 formed a dimer in the solution and predominantly obtained a α -helix structure. Upon exposure to the elevated temperature from 25 oC to 70 oC, a permanent transition from α -helix to β -sheet was observed. Followed by a biomimetic wet-spinning approach, eMaSp2 fiber was prepared and later displayed β -sheet-rich structure similar to natural counterpart.

Moreover, to obtain fibers to perform as a spider capture silk in spider web to collect water for recovering the daytime-distorted shape during night through water-sensitive shape memory effect. Different from using synthetic materials, an all silk-protein fiber (ASPF) with periodic knots to endow extremely high volume-to-mass water collection capability. This fiber has a main body of *B. mori* degummed silk coated with recombinant eMaSp2 of spider dragline silk. It is 252 times lighter than synthetic polymer coated nylon fibers that once was reported to have the highest water collection performance. The ASPF collected a volume of 6.6 μ L of water and

has 100 times higher water collection efficiency compared to existing best water collection artificial fibers in terms of volume-to-mass index (VTMI) at the shortest length (0.8 mm) of three phase contact line (TCL). Since silkworm silks are available abundantly, effective use of recombinant spidroins tandemly shows great potential for scalability.

9:30 PM SM12.06.05

Adsorption of Soy Protein Globulins at the Water/Oil Interface: Viscoelastic Effects Farshad Nazari^{1,2} and Mohammad Reza Rahimpour²; ¹Florida State University, United States; ²Shiraz University, Iran (the Islamic Republic of)

Possessing an amphiphilic character, proteins are commonly used to stabilize the oil-water interface of the food-grade emulsions. Soybeans are a particularly good source of edible proteins because of their relative abundance, sustainable supply, and low cost. Soy proteins can be isolated from other components of the beans and converted into functional ingredients using commercially viable extraction and purification methods. The major fractions in soy protein are globulins, namely β -conglycinin (a 7S globulin) and glycinin (an 11S globulin). These protein globulins are one of the most commonly used plant proteins for the fabrication of food-grade particles as Pickering emulsion stabilizers. As the use of soy protein isolates in complex food systems such as emulsions and suspensions, gains more momentum, it is important to fully understand the amphiphilic properties of these protein globulins and study their adsorbance at the oil-water interface.

Diffusing away from the aqueous phase, soy protein (SPI) globulins adsorbed at the water/oil interface. For this film of adsorbed SPI, the viscoelastic effects were investigated using a rotational rheometer equipped with the double-wall ring geometry (DWR). Steady-shear time sweeps using DWR revealed an increase in the interfacial viscosity similar to the Kelvin-Voigt model. The relaxation time (as a measure of the initial adsorbance rate) scaled linearly with the SPI bulk concentration ($E/\eta \sim c^{1.0}$). It was concluded that perhaps, at the early stages of SPI adsorbance, the transport mechanism is driven by the concentration gradient between the layer adjacent to the interface and the interface itself ($c/2 \cdot R_h$, with R_h being the hydrodynamic radius of the SPI globulins). Moreover, frequency sweeps (at 0.01-100 rad/s) from the DWR indicated a highly entangled layer of SPI globulins at the interface. However, pressure-driven flow through a pipe at high shear rates (steady flow at ~ 10 -1000 1/s with zero interface) showed Newtonian flow behavior ($n \sim 1.0$). This was attributed to the difference in conformation for the SPI chain at the oil/water interface vs in the aqueous bulk, causing the SPI globulin to unfold in the former case.

SESSION SM12.09: Social Activity
Session Chair: Chun-Long Chen
Friday Afternoon, April 23, 2021
SM12

2:15 PM PLACEHOLDER

SESSION SM12.10: On-demand
Wednesday Morning, April 14, 2021
SM12

8:00 AM SM12.01.05

Cell-Type-Specific CRISPR/Cas9 Delivery by Biomimetic Metal-Organic Frameworks Mram Z. Alyami; King Abdullah University of Science and Technology, Saudi Arabia

Effective and cell-type-specific delivery of CRISPR/Cas9 gene-editing elements remains a challenging open problem. Here we report the development of biomimetic cancer cell coated zeolitic imidazolate frameworks (ZIFs) for targeted and cell-specific delivery of this genome editing machinery. Coating ZIF-8 that is encapsulating CRISPR/Cas9 (CC-ZIF) with a cancer cell membrane resulted in the uniformly covered C3-ZIF(cell membrane type). Incubation of C3-ZIFMCF with MCF-7, HeLa, HDFn, and aTC cell lines showed the highest uptake by MCF-7 cells and negligible uptake by the healthy cells (i.e., HDFn and aTC). As to genome editing, a 3-fold repression in the EGFP expression was observed when MCF-7 were transfected with C3-ZIFMCF compared to 1-fold repression in the EGFP expression when MCF-7 were transfected with C3-ZIFHELA. In vivo testing confirmed the selectivity of C3-ZIFMCF to accumulate in MCF-7 tumor cells. This supports the ability of this biomimetic approach to matching the needs of cell-specific targeting, which is unquestionably the most critical step in the future translation of genome editing technologies.

SYMPOSIUM SM13

Advances in Membrane and Water Treatment Materials for Sustainable Environmental Remediation
April 14 - April 23, 2021

Symposium Organizers

Frank Gu, University of Toronto
Suzanne Lackner, Technische Universität Darmstadt
Rob Simm, Stantec

* Invited Paper

SESSION SM13.05: On-demand
Wednesday Morning, April 14, 2021
SM13

8:00 AM SM13.01.09

Late News: 3D Graphene-Based Sponge for Superior Separation of Heavy Oil-in-Water Emulsions

Ahmed S. Khalil^{1,2}; ¹Faculty of Science, Fayoum University, Egypt; ²School of Innovative Design Engineering, Egypt-Japan University of Science and Technology (E-JUST), Egypt

Oily wastewater generated by industries such as crude oil production, oil refining, and metal manufacturing, can cause major environmental issues, and affect human health [1]. In oily wastewater, oils are classified into two types, a mixture of oil/water, and oil-in-water emulsion. The later has stable microdroplets smaller than 20 μm with complex wetting behavior [2]. The separation of oil-in-water emulsions has become an extremely important for both environmentally and industrial related applications. Various traditional methods have been used to separate oils [3,4,5]. Herein, a graphene-based sponge (rGO@MF) was developed and utilized for separating various heavy oil-in-water emulsions as well as oil/water mixtures [6]. The superhydrophobic sponge was engineered through facile surface-treatment and hydrothermal steps. The commercially available MF sponges were initially surface treated and subsequently coated with rGO sheets. The surface and structural properties of the rGO@MF sponge and the nanoemulsions were thoroughly characterized by advanced techniques. The high-resolution SEM and EDX mapping confirmed

the homogeneous distribution of rGO sheets surrounding the fibers. The developed rGO@MF sponge showed excellent chemical stability and durability. Five different oils and organic solvents with high concentration (up to 30 g/l) were tested. We aimed to formulate stable and different sized emulsions to explore and study in detail the correlation between the oil type, droplet size and concentration of oil/water mixtures and emulsions, and the rGO@MF adsorption capacity and removal efficiency. The developed superhydrophobic rGO@MF sponge showed water contact angle of $\sim 164^\circ$ and exhibited superior adsorption capacity and removal efficiency of up to 5647 mg/g and $95 \pm 3\%$ respectively, for crude oil-in-water emulsions of 30 g/l. In addition, the rGO@MF sponge maintained its high separation performance over ten consecutive adsorption cycles. The adsorption capacity of the rGO@MF sponge maintained up to 92% of its initial values after ten cycles. The calculated activated adsorption energy for crude oil-in-water emulsion on rGO@MF sponge was $16.59 \text{ kJ mol}^{-1}$ indicating a physical adsorption process. The adsorption kinetics and interactions were carefully explored and a general mechanism of separation for both oil-in-water nanoemulsions and oil/water mixtures was introduced.

References

- [1] B. Dubansky, A. Whitehead, T. Miller, C. D. Rice, F. Galvez, Multitissue Molecular, Genomic, and Developmental Effect of the Deep water Horizon Oil Spill on Resident Gulf Killifish (*Fundulus grandis*), *Environ. Sci. Technol.* (2013): 5074-5082.
- [2] A. Gupta, H. B. Eral, T. A. Hatton, P. S. Doyle, Nanoemulsions: Formation, properties and applications, *Soft Matter*. 12 (2016) 2826–2841.
- [3] J. Saththasivam, K. Loganathan, S. Sarp, An overview of oil-water separation using gas flotation systems, *Chemosphere*. 144 (2016) 671–680.
- [4] J. Huang, Z. Yan, Adsorption Mechanism of Oil by Resilient Graphene Aerogels from Oil-Water Emulsion, *Langmuir*. 34 (2018) 1890–1898.
- [5] S.V. Thakkar, A. Pinna, C.M. Carbonaro, L. Malfatti, P. Guardia, A. Cabot, M.F. Casula, Performance of oil sorbents based on reduced graphene oxide-silica composite aerogels, *J. Environ. Chem. Eng.* 8 (2020) 103632.
- [6] R. M. G. Ahmed, B. Anis, A. S. G. Khalil. "Facile surface treatment and decoration of graphene-based 3D polymeric sponges for high performance separation of heavy oil-in-water emulsions." *Journal of Environmental Chemical Engineering*: 9 (2021) 105087.

8:15 AM SM13.01.10

Late News: Efficient Separation of Heavy Oil-in-Water Emulsion Using Isotropic Polyethersulfone Membranes [Ahmed S. Khalil](#)^{1,2}; ¹Faculty of Science, Fayoum University, Egypt; ²School of Innovative Design Engineering, Egypt-Japan University of Science and Technology (E-JUST), Egypt

Recently, oil-contaminated wastewater treatment has become a research hotspot for both the scientific community and the industry due to the potential disastrous impact of oily wastewater on environment and human health. Huge volumes of stable oil/water emulsions are usually produced from a variety of industries such as oil and natural gas exploration and processing, metallurgical, petrochemical, pharmaceutical, and food industries [1]. Several previously reported techniques are widely used for separation of oil/water mixtures, which involve gravity separation, dissolved air flotation, solvent extraction, coagulation, biodegradation and adsorption [2]. However, these conventional methods have their own drawbacks, such as, high cost, using toxic compounds, large space for installation and generation of secondary pollutants [3]. Membrane separation technology, in particular, ultrafiltration (UF), has attracted attention as an effective approach for removing dispersed oil droplets smaller than $\sim 10 \mu\text{m}$ in emulsions. However, membrane fouling is regarded as the key challenge for membrane-based separation processes that results from deposition of oil droplets/aggregates on membrane surface or inside membrane pores causing a severe flux decline

Here, we present the separation performance of isotropic PES membrane that has been successfully developed via VIPS, for different high concentration oil-in-water nanoemulsions [4,5]. Detailed comparison with the well-developed anisotropic membrane was carried out. The as-prepared membranes were analyzed with respect to surface morphology, surface roughness, pore size, overall porosity, water uptake, underwater oil contact angle (UOCA) and surface wettability. The membrane separation performances were evaluated in terms of water

permeance, oil separation efficiency, antifouling performance, and cyclic reusability. Remarkably improved surface hydrophilicity for isotropic PES membrane (contact angle, CA=39°) compared to anisotropic PES membrane (CA=70°), resulting in superior pure water permeance, attaining 4721 L/h.m².bar at operating pressure of 0.5 bar. The isotropic PES membrane achieved superior crude oil-in-water nanoemulsion separation (permeance of 713 L/h.m².bar and 100 % rejection) at oil concentration of 1 g/L. At extremely high oil concentration of 50 g/L, the PES membrane was not completely fouled and showed permeance of 65 L/h.m².bar and 98.2% rejection. Moreover, the flux recovery of the fouled isotropic PES membrane exceeded 59.5% over three subsequent cycles of filtration and back-washing with water. Overall, this study might provide substantial guidance for large-scale manufacturing and application of isotropic PES membrane in treating oil-in-water nanoemulsion under harsh conditions.

Keywords: Isotropic PES membrane, oil-water emulsion separation, super permeance, fouling mitigation

References

- [1] T. Sirivedhin, L. Dallbauman, Organic matrix in produced water from the Osage-Skiatook Petroleum Environmental Research site, Osage county, Oklahoma, *Chemosphere* 57 (2004) 463–469.
- [2] S. Jamaly, A. Giwa, S.W. Hasan, Recent improvements in oily wastewater treatment: Progress, challenges, and future opportunities, *Int. J. Environ. Sci.* 37 (2015) 15–30.
- [3] G. Crini, E. Lichtfouse, Advantages and disadvantages of techniques used for wastewater treatment, *Environ. Chem. Lett.* 17 (2019) 145–155.
- [4] Abdel-Aty, A. A., Aziz, Y. S. A., Ahmed, R. M., ElSherbiny, I. M., Panglisch, S., Ulbricht, M., & Khalil, A. S. G. (2020). High performance isotropic polyethersulfone membranes for heavy oil-in-water emulsion separation. *Separation and Purification Technology*, 253, 117467.
- [5] Elrouby, A. A., Ali, A. S., Abdel-Aty, A. A., Abu-Elnaga, A. M., & Khalil, A. S. (2020, November). Low-Cost Production of 3D Printed Lab-on Chip (LOC) Device for Oil-in-Water Emulsion Separation. In 2020 27th IEEE International Conference on Electronics, Circuits and Systems (ICECS) (pp. 1-4).

SESSION SM13.01: Advances in Membrane and Water Treatment Materials for Sustainable Environmental Remediation I

Session Chairs: Frank Gu and Rob Simm

Friday Morning, April 23, 2021

SM13

8:00 AM SM13.01.01

Late News: Cross-Linking of Polyetherimide by Bi- and Tetrafunctional Nucleophiles in Ultrathin Layers
Rainhard Machatschek^{1,2}, Matthias Heuchel¹ and Andreas Lendlein^{1,2}; ¹Helmholtz Zentrum Geesthacht, Germany; ²University of Potsdam, Germany

Polyetherimide (PEI) is a membrane forming material with excellent chemical and mechanical stability. Nevertheless, further chemical modification might be demanded by the designated application. The hydrophobic nature of PEI could cause adsorption of solutes if the material is used in aqueous environments, whereas application in organic solvents may necessitate further stabilization via cross-linking [1]. In these cases PEI has the additional advantage that a ring-opening at the imide groups in the polymer backbone using suitable nucleophiles allows for chemical modification, a strategy that has been widely explored as a method for post-functionalization of PEI membranes and particles. The reaction with water soluble diamines can result in cross-linking via formation of amide or imine groups. An excess of diamine would drive the reaction towards a non-crosslinked state, while also hydrolysis could occur if the pH exceeds a certain value[2]. Also, the chain-length and stiffness of the diamine is likely to have an effect.

Here, we use ultrathin films (1-2 nm) at the air-water interface to investigate the chemical functionalization of

PEI surfaces. In contrast to thicker films or bulk materials, where the majority of molecules is not accessible for chemical reactions, nearly all imide groups can be converted in ultrathin films, making them especially sensitive tools to study the effects of post-functionalization.

By means of interfacial rheology, we determine the optimal conditions for cross-linking of PEI, together with surface potential measurements to detect the formation of a positively or negatively charged groups in consequence of either partial hydrolysis or protonation of free amine groups. We further evaluate the effects of catalytic strategies for amine bonding based on carbodiimides or Lewis acids, and investigate whether tetrafunctional amines result in a better cross-linking than bifunctional ones. The outcome of the chemical modifications is further investigated using IR and/or Raman spectroscopy. In addition, we evaluate the influence of the chemical treatments on the Young's modulus of the modified PEI and determine the molecular arrangement of the chains by atomic force and electron microscopy.

The ultrathin PEI films presented here are not only of interest as model systems for the surfaces of PEI membranes, but also as present stable thin films with can be functionalized and transferred onto almost any substrate.

References

- [1] K. Vanherck, A. Cano-Odena, G. Koeckelberghs, T. Dedroog and I. Vankelecom, *J. Membr. Sci.* **353** (1), 135-143 (2010).
- [2] S. Basu, M. Heuchel, T. Weigel, K. Kratz and A. Lendlein, *Polymers for Advanced Technologies* **26** (12), 1447-1455 (2015).

8:10 AM SM13.01.02

ZnO Molecular Foams for Micropollutant Removal Zachary Warren, Thais Tasso Guaraldo, Davide Mattia and Jannis Wenk; University of Bath, United Kingdom

The accumulation of micro-pollutants such as pesticides and pharmaceuticals in water supplies is of growing concern to public health, as these compounds can bioaccumulate, causing potential health issues as well as being resistant to the methods of wastewater treatment currently employed. Photocatalysis shows promise as a potential solution to this problem but is currently hindered in two main ways:.. Photocatalytic slurries require downstream separation or can pose a risk to health themselves, while supported photocatalysts suffer from low exposed surface areas and efficiencies as well as potential leaching, again potentially posing a health risk. In this work, we present a novel ZnO photocatalytic foam. Briefly, the synthesis is a modification to abased on sol gel synthesis of ZnO, incorporating direct aeration during gel formation followed by high temperature sintering (900 °C, 12 hrs) to form a highly porous yet mechanically stable ZnO structure in as macroscale foam monoliths (20 mm in height and diameter) without the use of foaming agents nor supercritical drying. These “monoliths or “molecular foams”” were then used in the photocatalytic degradation of carbamazepine as a target pollutant in both batch and recirculating systems. This novel work solves both issues traditionally associated with photocatalysts, as the highly porous nature of the monoliths allows for a high surface area of catalyst to be used, similar to a slurry, while the removal of a support and having a structure of ZnO only, means that there are no binding interactions between catalyst and support, removing the risk of leaching entirely.

These foamsmonoliths were characterised as pure wurtzite ZnO and highly crystalline in nature as well as showing high porosity (90 %), measured using an Archimedes method, and a hierarchical structure, which showed promise for the degradation of target pollutants. FE-SEM micrographs of the foams show a structure consisting of both large channels and smaller pores, allowing for both flow through the foamsmonoliths and a reactive surface for degradation to occur at. Initial photocatalytic tests in the batch system showed 55 % degradation after 4 hours and a kinetic constant of $3.3 \times 10^{-3} \text{ min}^{-1}$ using 0.5 g L^{-1} loading of foam catalyst. The batch kinetics of the foam system shows promise, as it they are is higher than literature values for immobilised catalysts, but still lower than those reported for slurry systems. and the next goal of the project is to demonstrate

kinetics that are comparable to slurries. Building upon this, further studies were conducted, applying foams in a recirculating batch system where an increase in photocatalytic activities, of both removal and kinetic constant, was observed. This is attributed, as when applied in this manner to a fuller use of the as flow of solution through the foam takes advantage of the highly porous and hierarchical structure of the foams, allowing for greater utilisation of the photocatalyst as well as greater mass transfer of the pollutant to the catalyst surface. These results show promise for the potential application of photocatalytic foam structures as a tertiary treatment step in addition to traditional wastewater treatment, for the removal of currently persistent micropollutants. The proposed 3D structure combines the advantages of slurries and immobilised catalysts while simultaneously addressing drawbacks.

8:20 AM SM13.01.03

Quick Formation of Polymeric Membranes at Water/Air Interface [Sara Coppola](#), Giuseppe Nasti, Veronica Vespini and Pietro Ferraro; Institute of Applied Sciences and Intelligent Systems “E. Caianiello”, Italy

Nowadays various methods and technological process are conventionally employed for water treatment and filtration, attempting to contrast the pollution of chemicals, particles and emerging contaminants (i.e. microplastics, industrial residue, oil, pharmaceutical components..). Generally all the processes proposed for water treatment require multistep protocols and the use of expensive device. Over the last decade, a wide range of functional materials have been investigated to separate multiphase liquids and immiscible mixtures, electrochemical catalysts, photocatalysts, reactive and nanomaterials have been recently successful tested for water treatment. Good results in terms of efficiency in separating oil/water mixtures have been obtained using polymeric functionalized membranes but big restrictions still remain unsolved. Different technological methods of microfabrication (two-photon polymerization, soft interference lithography, replica molding and self-folding polymers) have been used but, chemical-physical pre-treatments are often required to gain the desired final properties. To avoid this problem a number of methods have been developed for the fabrication of polymer films, such as solution casting method, interfacial methods, layer-by layer technique or solvent evaporation method. Unfortunately, all this techniques still require special equipment and have severe limitations with respect to the substrate size as well as film quality, stability and, moreover, until now the self-assembling of thin polymeric film into complex 3D structures remains problem. Actually there is a growing interest in competitive candidates methods for membrane technology with the following properties: large area coverage, high structural flexibility, low temperature processing, especially low cost, formation in situ and three-dimensional shaping. Here we describe a water-based bottom-up approach in which we let a biopolymer self-assemble with unprecedented degree of freedom over the water surface. Being a liquid, water can assume flexible shapes taking on the form of its container and, as a direct consequence, the polymer, dispensed over the water using the method described, could self-assemble into different geometries generating thin polymeric films following the existent water profile in a very direct and simple way. The membranes are formed *in-situ*, directly in the place of interest without the need of handling thin membranes and the subsequent risk of deforming and damaging them. The polymer film could be the external container of a liquid core or a free standing layer with personalized design. The membranes produced encasing water have been characterized in terms of physical properties and morphology. The quick liquid packaging approach could be used to lay a film over micropillars, organic and inorganic micro-objects and colloidal particles. With the same technology it is possible to create also millimetre membrane accommodating the area of interest. The packaging process is described in details reporting, for the first time, the real time characterization of the membrane formation in static and dynamic condition, while various application are proposed. We believe that the proposed technology could be further improved in the future also for selective adsorption of pollutants, filtering and liquid separation moreover, being the polymer used a biodegradable one we foresee application of biocompatibility.

1. Yulaev, A. Lipatov, A. X. Lu, A. Sinitskii, M. S. Leite, A. Kolmakov, Adv. Mater. Interfaces 4, 1600734 (2016).
2. Wickman, H. H. and Korley, J. N. Nature 393, 445–447 (1998).
3. Coppola S. et al. Science Advances 5, eaat5189 DOI: 10.1126/sciadv.aat5189 (2019)

8:30 AM SM13.01.04

Quantitative Holographic Thickness Mapping Reveals the Full-Field Drainage During Thin-Film Moving

Vincenzo Ferraro¹, Zhe Wang^{2,1}, Lisa Miccio² and Pier Luca Maffettone¹; ¹University of Naples Federico II, Italy; ²ISASI-CNR, Italy

Thin-film is one of the important components in material world. From semiconductor layer detection to water membrane measurement, quantitative thickness mapping for thin-film has been a widely studied issue in the past decade. However, with the development of imaging technology, single-point measurement of film thickness has been unable to meet the changing scientific requirements. Full-field visualizing and characterizing for thin-film evolution is taking place as a principal tool for related study, which can provide effective data support for membrane science, polymer chemistry, biomaterials, applied Chemistry, etc. In this paper, we show that digital holographic thickness mapping could be a powerful solution to reveal the full-field drainage of thin liquid film. Digital holography (DH) is an interference imaging technology, it has possibility to achieve requisite spatial and temporal resolution for evolution measurement of transparent and translucent materials. In our study, DH has been performed to reveal the thickness mapping of soap films when moving inside a cylindrical metal tube. Herein, customized tubes with different customized radius were used to generate and hold flat thin soap films. The thin-film is formed inside the tube by immersion. The drainage with different air pumping rates is analyzed. In the recording geometry, the tube is placed vertically, then the object beam of DH passes through the film when the film is moved from the middle of the tube to the top. The object beam will carry full-field thickness information and meet the reference beam on the screen of the camera. Finally, the hologram of related thickness distribution will be created by interference. The film will start to drainage and create multiple fingerings due to Marangoni flows around the edges of the film once it moves inside the tube. Thanks to DH, the full-field evolution process of film thickness will be continuously recorded, so we can quantitatively analyze all features of the film surface, by means of a-posteriori holographic numerical reconstruction. In this case, the relationship between film thickness features with motion speed and tube diameter was studied, this will allow revealing the Marangoni flow formation process in the flat film. In order to obtain highly continuous full-field thickness evolution data, we also proposed a 4D phase unwrapping algorithm based on time series in holographic numerical reconstruction. Comparing with the conventional phase unwrapping algorithm, the new approach utilizes the phase change of the same points in the field of view under a long-time sequence to achieve phase tracking, then the accurate phase unwrapping is achieved. Once supported by the large number of continuous experimental records, 4D phase unwrapping allow us to obtain no phase-jump full-field phase distribution, which is the key to perform quantitative holographic thickness mapping with nanometer precision. In this paper, thanks to the customized thin-film generator and 4D holographic thickness extraction algorithm, the drainage process of the flat film during pumping uplift is quantitatively revealed. A series of space-time drainage modes are made to show the thinning process of the soap films, based on holographic thickness mapping. The results show that DH is a reliable and powerful tool that can effectively reveal the full-field thickness variation of thin liquid film under different conditions.

8:40 AM SM13.01.06

Late News: The Design and Process Development of Electro-Thermal Membranes for Membrane Distillation Applications

Noora A. Almarzooqi; Khalifa University of Science and Technology, United Arab Emirates

Introduction

Electro-thermal (ET) membranes based on the joule heating concept were developed for evaporation and membrane distillation applications. This approach is novel since voltage is applied to a porous thin-film carbon nanotube (CNT)/polymer composite membrane, creating a localized heating effect within the bulk of the membrane, allowing vapour pressure difference to occur and flux of fresh water to permeate. We investigated the effect of joule heating in ionizable environments such as high-salinity brines through the use of a novel class of freestanding MWCNT/PVDF composites within an ET setup.

Methods

CNT/PVDF membranes were fabricated using a tape casting method, as illustrated in figure 1. This method

requires low energy and is scalable.

Figure 1 – Fabrication of freestanding CNT/PVDF membranes using tape casting method, different concentrations percentages of CNT were used to test their joule heating behaviour.

Evaporation experiments were performed to provide supplementary understandings for electrothermal powered MD, as illustrated in figure 2.

Figure 2 – Electrothermal evaporation setup incorporating different membrane compositions.

Results

The results show the high temperatures achievable in response to current passage through the in-lab developed CNT/PVDF composite sheets. Moreover, the thermoelectric effect only resulted in fresh water flux when A.C. voltage was applied.

Figure 3 – The temperature response for the CNT composite sheets under different applied voltages, and the performance of the thermoelectric sheets under different D.C. and A.C. voltages.

Discussion

A big challenge was given by the ionisable nature of the saline water, but was overcome by performing A.C. voltage experiments, which have likely prevented concentration polarization effects and limited both the side reactions and electrode degradation. The ET technology presents a great filtration ability to purify different types of feed streams such as high salinity water, brines and brackish water, and calls for the need for further developments.

8:50 AM SM13.01.08

Pore Size Tuning of Fouling-Resistant, Self-Assembled Zwitterionic Copolymer Nanofiltration

Membranes Through Click Chemistry Abhishek N. Mondal, Samuel J. Lounder, Luca Mazzaferro and Ayse Asatekin; Tufts University, United States

Membrane based water purification processes are of enormous importance in water and wastewater treatment due to their scalability, reliability, energy efficiency, and high effluent quality. Fouling, defined by performance loss due to the adsorption and accumulation of feed components on the membrane surface, is likely the most important obstacle to broader use of membranes in these applications. Zwitterions, moieties with equal numbers of positive & negative electrostatic charges, strongly resist the adsorption of biomacromolecules due to their high degree of hydration. This unique characteristic of zwitterions makes them a promising candidate to be incorporated into membranes to restrict fouling. Linear random copolymers of zwitterionic segments and non-zwitterionic (hydrophobic) segments have recently been shown to be extremely promising materials for membrane selective layers that combine exceptional fouling resistance, narrow pore size distribution, and high water permeability. These copolymers self-assemble to form a bicontinuous zwitterionic network with an approximate ~ 1.5 nm interconnected domains, held together by a hydrophobic phase. While this pore size is intriguing for a variety of wastewater treatment applications, there is a need for a novel, fast, scalable, and versatile approach to tune the effective pore size of these zwitterionic membranes while retaining their fouling resistance and water permeability. This approach needs to be fast and efficient enough to be integrated into roll-to-roll manufacturing techniques. In this current work, we introduce the first use of thiol-ene click chemistry to tune the effective pore size of self-assembled membranes, leading to the formation of robust membranes with high flux, divalent ion rejection, and fouling resistance. The use of click chemistry allows significant changes in effective pore size, measured through the rejection of both organic solutes and salts, in a matter of seconds, with 40 seconds of cross-linking leading to the doubling of riboflavin rejection. These highly cross-linked membranes also combine high divalent salt rejection (e.g. 80% Na_2SO_4 rejection) whereas the monovalent salt rejection was fairly low (e.g. 28% NaCl rejection). The pore size can be easily tuned by simply changing the crosslinking time, hence the selectivity of these membranes are easily tunable for various membrane selectivity. This unique crosslinking technique can be beneficial for tunable separation properties to address specific processes in bio-separations as well as water and wastewater treatment.

SESSION SM13.02: Advances in Membrane and Water Treatment Materials for Sustainable Environmental Remediation II
Session Chairs: Frank Gu and Rob Simm
Friday Morning, April 23, 2021
SM13

11:45 AM *SM13.02.01

Block-Polymer Membranes and Membrane-Like Capsules for Aqueous Separations Jay Werber^{1,2};

¹University of Minnesota, United States; ²University of Toronto, Canada

The self-assembly of block polymers into microphase-separated domains provides exciting opportunities for the design of high-performance membranes. In this talk, two block-polymer-based membrane systems will be discussed. In the first, we used a co-casting strategy to rapidly and scalably synthesize membranes that exploit the disordered morphology of block polymers. The polymer in our demonstration contained an etchable poly(lactide) block and a copolymer block comprising poly(methyl methacrylate-*stat*-styrene), with the polymer chemistry tuned to enable an accessible order-disorder transition temperature (T_{ODT}). Rapid thermal quenching from the disordered state kinetically trapped this bicontinuous morphology, with subsequent etching enabling continuous, tortuous pores without need for channel alignment. We employed a co-casting approach wherein a thin block polymer/solvent layer was coated atop a polysulfone/solvent layer. Rapid drying followed by immersion in non-solvent (water) created composite membranes with discrete layers. Competitive water permeances along with sharp molecular-weight cut-offs were achieved. In the second system, we explore the synthesis of polymeric microcapsules as a proof of concept for dispersible facilitated transport membranes, particularly serving as robust analogs of emulsion liquid membranes. The microcapsules were fabricated using a double-emulsion technique and comprised a commercial poly(styrene)-*block*-poly(butadiene)-*block*-poly(styrene) as a diffusive matrix for facilitated transport, in which a copper-selective small-molecule ligand was dissolved. The ligand allowed for selective uptake of copper ions, which were transported into inner acid-containing, aqueous compartments in exchange for protons. Furthermore, the microcapsule approach allows for simple packing into columns to enable simple cycling of extraction and stripping steps. The two systems are both promising demonstrations of block polymer membranes for practical aqueous separations.

12:05 PM SM13.02.04

Oil-Water Separations Using Nanostructured Coatings and 3D Printed Membranes Rigoberto C.

Advincula^{1,2,3}; ¹The University of Tennessee, Knoxville, United States; ²Oak Ridge National Laboratory, United States; ³Case Western Reserve University, United States

Oil and water separation and treatment are significant for the oil and gas industry, including clean-up. The preparation of filter formats or coatings has been used to improve the efficiency of the process. We will focus on using new high-performance thermoset and nanocomposite materials for both coatings and 3D printing format in this talk. Polybenzoxazine chemistry and polymerization have enjoyed tremendous growth due to its versatility in chemistry. Several advantages in properties for high-temperature applications compared to epoxy, PU, PF, resins. We report on the preparation of nanostructured polybenzoxazine (PBZ) nanocomposites prepared with nano clay, nano-silica, and graphene to obtain very robust and superhydrophobic coatings that have resulted in efficient anti-corrosion properties and oil-water separators, including anti-icing properties. The monomers are prepared by simpler chemistry enabling additives and other preparation protocols that lead to robust coatings. The addition of telechelic polybutadiene and polyaniline as part of the interpenetrating network (IPN) and semi-interpenetrating network (SIPN) composition results in robust and very conformal coating compositions. Excellent adhesion properties to substrates even at higher temperature (HT) operations may enable these materials to be applied in more demanding conditions. Nanostructured and nanocellulose materials have also been used to produce highly efficient oil-water separators based on the superhydrophobic and super oleophilic properties of coated filters. In another aspect of high-performance materials, we have demonstrated the use of 3D printing to create membranes and oil soaking objects that can be used for clean-up based on

elastomeric silicone materials. Lastly, we demonstrate the use of 3D printing of superhydrophobic structures to demonstrate controlled wetting behavior.

12:15 PM SM13.02.05

Eco-Friendly and Efficient Carbon-Based Adsorbents Produced from Organic Feedstocks for Removing Toxic Organic Pollutants from Groundwater Suraj Pochampally, Soroosh Mortazavian, Padmanabhan Krishnaswamy, Christina Obra, Ashtin Hofert, Erica Marti and Jaeyun Moon; University of Nevada, Las Vegas, United States

Contamination of groundwater by organic compounds, heavy metals, and chlorinated compounds is a current environmental issue. In-situ remediation techniques that use adsorptive materials have recently been developed for more sustainable treatment of contaminated aquifers. Biochars (BCs) are a biomass-derived black carbon with a highly ordered, interconnected networks of micropores, mesopores, and macropores, which is an economical substitute for conventional adsorbents. In this work, we studied the physical and chemical modification processes of the BCs on their surface area, adsorptive capacity, and surface functional groups. We focused on investigating BCs made from three different shell-type biomasses: walnut shells, pecan shells, and peanut shells. The BCs were produced through pyrolysis process at varied temperatures in the range between 500 °C and 900 °C in an inert gas environment. To tailor the physical and chemical properties of the BCs, the pre-pyrolysis processes and post-pyrolysis techniques (e.g., base treatment and acid activation) were employed. The different BCs were used and assessed for effective remediation of toxic pollutants (i.e., trichloroethylene (TCE), and perchloroethylene (PCE)) from water. The unmodified and modified BCs were compared in terms of microstructures and surface states as well as TCE and PCE adsorptive capacity in this study.

The materials were physically and chemically characterized using various tools. Scanning electron microscopy (SEM) characterization showed different porous surface morphologies of various BCs. The surface hydrophilicity of the different types of BCs were characterized by a sessile test, which was correlated with surface functional groups analyzed by Fourier transform infrared spectroscopy (FT-IR). The pyrolysis process of BCs has been fully understood with thermogravimetric analysis (TGA). The results of this work can advance the understanding of different modification effects on BCs' properties, aiming at the wide adoption of cost-effective and eco-friendly adsorbents.

12:25 PM SM13.02.06

Functionalized Cellulose-Chitosan Membranes for Adsorption of Amine Compounds Marshall Frye, Shangradhanva Eswara Vasisth and Juan Nino; University of Florida, United States

According to several recent reports from the United Nations, WHO, and UNICEF, water contamination is a prevalent issue around the world that needs to be addressed. The current water treatment methods, specifically the primary and secondary treatments, are very good at removing large scale waste but fail at removing some microcontaminants and emerging pharmaceutical water contaminants. Developing novel materials for adsorption to complement the filtration of granular materials in the tertiary treatment step of water processing is a promising way to resolve this issue. Nanocellulose is a strong candidate for a filtration material due to its high surface area, zeta potential, and capability for functionalization. It is an excellent adsorbent for dyes, metals, and other organic molecules. Here, we will demonstrate the high potential of cellulose-based materials as an adsorbent for conventional contaminants, as well as emerging microcontaminants, such as opioids. In the case of amine compounds, through adsorption testing we have recently shown that sulfonated cellulose membranes have high adsorption capacity (i.e. 68.56 mg/g). These membranes are fabricated via a two-step process, first sulfonated the cellulose and then crosslinked with chitosan for mechanical stability. We will also discuss the opportunities for using agricultural cellulose waste streams like rice husks and sugarcane bagasse for producing these filters. Scanning electron microscopy demonstrated degradation of the cellulose surfaces after sulfonation, and a reorganization of the cellulose layers when crosslinked with chitosan. Through Fourier transform infrared spectroscopy it was determined that there were chemical changes through the oxidation and sulfonation steps. The maximum concentration of sulfonate groups was determined to be 194.4 mmol/g using a conductometric titration method. The thermal stability of the cellulose membranes was demonstrated through TGA, showing an

extrapolated onset temperature of 281°C. The adsorptive capabilities of these membranes, tested through kinetic and isothermal models, will be presented. Finally, a performance comparison between activated carbon and these cellulose membranes will be performed.

12:35 PM SM13.02.07

Photocatalysts on Transparent Fibers Improve Light and Mass Transport for a "Chemical-Free" UV-AOP Daniel E. Willis, Ella C. Sheets and Kevin M. McPeak; Louisiana State University, United States

Water scarcity is a growing concern across the globe.^{1,2} It is imperative that communities develop and implement energy efficient technologies to treat water contaminated by industrial activity, human waste, or harmful microorganisms. Current best methods, such as advanced oxidative processes (AOPs), can be highly effective against targeted contaminants, but often require chemical additives (e.g. chlorine, peroxide, ozone) which increase costs and may lead to the formation of undesirable disinfection byproducts.^{3,4} The use of immobilized photocatalysts with strong light absorption, chemical stability, and high surface area could greatly reduce the need for oxidant feedstocks and improve the affordability of UV-AOPs.

Here, we report on the fabrication and characterization titania-based photocatalysts immobilized on quartz-fiber felt for UV-driven water treatment. Our supported titania is mesoporous which, combined with the macroporous ($\Phi > 0.95$) fiber, yields a high surface area beneficial for mass transport. By using quartz fibers, we maximize the optical path length of UV (250 – 400 nm) light through our system. Our titania may also be loaded with Au nanoparticles to increase the generation of reactive oxygen species (ROS) and provide alternative reaction pathways for degrading contaminants. We propose a cost/benefit breakdown for the addition of Au in our photocatalytic system.

We test the long-term (>24 hours) stability and efficacy of our fiber-supported photocatalysts to degrade model contaminants under illumination from both UV-A LEDs and germicidal UV-C lamps. Our immobilized photocatalysts produce >100 μM $\cdot\text{OH}$ in 20 seconds in a flow reactor and achieve an Electrical Energy per Order (EEo) of <0.6 for the degradation of Rhodamine B. We also examine the impact of water quality (pH, TOC, scavengers) and propose mechanisms for pollutant breakdown. Lastly, we will discuss the reactor design and relevant transport conditions for our supported photocatalysts, and the improvements necessary to scale our material for practical applications.

1. Liu, et al. Environ. Sci. Technol. 2016, 50, 17, 9736–9745.

2. Stefan, Mihaela I. (Ed.) Advanced Oxidation Processes for Water Treatment: Fundamentals and Applications. London: IWA Publishing, 2019.

3. Richardson, et al. Environ. Sci. Technol. 1996, 30, 3327-3334.

4. Mian, et al. Water Research. 2018, 147, 112-131.

12:45 PM SM13.02.08

Late News: Activated Agro-Industrial Waste Biochars for Heavy Metal Remediation and Nutrient Management Zoe Pollard and Jillian Goldfarb; Cornell University, United States

Sustainable water treatment materials can be derived from carbon-rich agro-industrial wastes through thermal treatment and physical activation, thus shifting away from traditional disposal – landfilling or composting. Cherry pits are an abundant carbon-rich waste biomass in the Great Lakes region and represent a viable feedstock for conversion to biochars and activated biochars for soil amendments and heavy metal adsorbents. These sustainable materials have the potential to remediate local water quality issues including the hazardous eutrophication of the Great Lakes and heavy metal contamination of the region's drinking water. In this work, slow pyrolysis was used to convert waste cherry pits to biochars (1 hour at peak temperatures of 450 and 600°C) and activated biochars (1 hour at peak temperatures of 800 and 900°C). Biochars produced have surface areas between 206 and 274 m^2/g and increased bioavailability of Fe, K, Mg, Mn, and P. The biochars can be implemented as soil amendments to reduce nutrient run-off and serve as a valuable carbon sink (biochars

contain 74-79% carbon), potentially mitigating harmful algal blooms in the Great Lakes. The CO₂-activated biochars exhibited selective metal adsorption of As, Cu, Pb, and Zn from simulated contaminated drinking water. Physical activation increased the metal adsorption capacity by 2.8 and 4.2 times for the biochars activated at 800 and 900°C, respectively. The increased capacity is attributed to high surface areas (up to 629 m²/g) and a hydrophilic surface (confirmed via FTIR functional group analysis). Through sustainable waste-to-byproduct valorization we convert this waste food biomass into biochar for use as a soil amendment and into activated biochars to remove metals from drinking water, thus alleviating economic issues associated with cherry pit waste handling and reducing the environmental impact of the cherry processing industry.

12:55 PM SM13.02.09

Late News: Facile Size-Selective Defect Sealing in Large-Area Atomically Thin Graphene Membranes for Sub-Nanometer Scale Separations Piran Ravichandran Kidambi; Vanderbilt University, United States

Atomically thin graphene with a high-density of precise subnanometer pores represents the ideal membrane for ionic and molecular separations. However, a single large-nanopore can severely compromise membrane performance and differential etching between pre-existing defects/grain boundaries in graphene and pristine regions presents fundamental limitations. Here, we show for the first time that size-selective interfacial polymerization after high-density nanopore formation in graphene not only seals larger defects (>0.5 nm) and macroscopic tears but also successfully preserves the smaller subnanometer pores. Low-temperature growth followed by mild UV/ozon oxidation allows for facile and scalable formation of high-density ($4-5.5 \times 10^{12} / \text{cm}^2$) useful subnanometer pores in the graphene lattice. We demonstrate scalable synthesis of fully functional centimeter-scale nanoporous atomically thin membranes (NATMs) with water (~0.28 nm) permeance $\sim 23\times$ higher than commercially available membranes and excellent rejection to salt ions (~0.66 nm, >97% rejection) as well as small organic molecules (~0.7–1.5 nm, ~100% rejection) under forward osmosis.

Cheng et al. Nano Lett. 2020

Cheng et al. Nanoscale. 2021

Kidambi et al. Adv. Mat. 2018

Kidambi et al. Adv. Mat. 2018

Kidambi et al. ACS App. Mat. Int. 2018

Kidambi et al. Adv. Mat. 2017

Kidambi et al. Adv. Mat. 2017

Kidambi et al. Nanoscale 2017

SESSION SM13.03: Advances in Membrane and Water Treatment Materials for Sustainable Environmental Remediation III

Session Chairs: Frank Gu and Rob Simm

Friday Afternoon, April 23, 2021

SM13

2:15 PM SM13.03.02

Late News: Zinc Oxide Nanostructures by Hot Water Treatment for Photocatalytic Water Treatment Ranjitha Hariharalakshmanan, Juan Martinez and Tansel Karabacak; University of Arkansas at Little Rock, United States

Over the recent years, zinc oxide (ZnO) nanostructures have gained remarkable attention in the field of semiconductor photocatalysis for water treatment applications. In our previous work, we demonstrated that ZnO nanostructures can be produced in a simple, cost-effective, and environmentally-friendly manner by the method of hot water treatment (HWT) and the nanostructures produced by this method can be used to degrade organic

pollutants via photocatalysis. In this work, we investigate how the photocatalytic degradation is affected by changing the amount of the HWT ZnO nanostructure photocatalyst and the concentration of the organic pollutant. The ZnO nanostructure suspension was made by the HWT of zinc plates in DI water at 75°C for 5 hours. Since the ZnO nanostructures are released into the water as a result of the HWT of the Zn plates, our ZnO nanostructures are in the form of a suspension in water. In order to change the amount of photocatalyst, we changed the volume of the ZnO nanostructure suspension being added. We used 10 ml, 25 ml, and 50 ml of the ZnO nanostructure suspension, added it to methylene blue (MB) at an initial concentration of 2.5 ppm and exposed the mixture to UV light for 4 hours. We observed that 25 ml of the ZnO nanostructure suspension gave the maximum degradation of MB (~65%). When we used 50 ml, the degradation percentage decreased to about 45%. This might be due to increase in turbidity of the mixture, which can lead to a decrease in the penetration of UV light. We then used 25 ml of the ZnO nanostructure suspension and conducted MB degradation tests at 4 different initial concentrations of MB. Maximum MB degradation was at 1 ppm (~84%) and minimum at 10 ppm (~18%). This decrease in MB degradation can be due to the decrease in UV light being absorbed by the photocatalyst as more and more MB molecules get adsorbed to the photocatalyst surface. As a preliminary study, we also did HWT of Zn plates in tap water instead of DI water. We were able to form ZnO suspension in tap water too, and we observed ~47% degradation of MB during photocatalytic degradation experiment. This is an encouraging result as the use of tap water instead of DI water can further bring down the cost and increase the scalability of nanostructure fabrication by HWT.

2:25 PM SM13.03.04

Catalytic Reduction of Graphene Oxide Membranes in Water-Alcohol Separations and Its Impact on Permeation Behavior Yushi Zang¹, Alex Peek¹, Yongsoon Shin², David Gotthold² and Bruce Hinds¹;

¹University of Washington, United States; ²Pacific Northwest National Laboratory, United States

Graphene oxide (GO) is considered to have great potential for chemical separation applications due to its unique properties of enhanced 2-D nanofluidic and the ability to control interlayers spacing for size-based chemical selectivity. A GO membrane with highly aligned GO grains was fabricated through a slip casting process and studied for alcohol-water separation application. We found the pressure-driven permeance of water, MeOH and IPA through 5 µm thick GO membranes to be 0.4, 0.12 and 0.8 LMH/Bar (L/m²-hr-Bar) respectively consistent with literature examples without defects that had given erroneously high flows. Interestingly, the permeance of alcohol-water mixture was found to be dramatically lower (~0.01 LMH/Bar) than any of its individual components. Such a mixture of solvents does not permanently affect the GO membrane, as the permeance of pure solvent was recovered to its original level upon removal of alcohol-water solvent mixture. The drop in transmembrane flux was also observed in osmotic tests when alcohol-water solvent mixture was in the feed solution side of the membrane. The osmotic tests showed the selectivity of water over alcohol through GO membrane and rejection of salt. The interlayer space of a dried GO membrane was found to be 8.52 Å which increased to 12.19 Å, 13.26 Å and 16.20 Å upon addition of water, MeOH and IPA. When water saturated GO membranes were exposed to MeOH, a 2 Å decrease in interlayer spacing of GO membrane was seen suggesting the removal of OH groups from GO. Such phenomenon was accompanied by a color change of the membrane at the same time. Permeation was recovered with exposure to oxidants (H₂O₂). These observations support a newly proposed mechanism of a partial reduction of GO through a catalytic reaction with alcohol-water mixtures.

2:35 PM SM13.03.05

Strategies for the Scale-up of the Photocatalysis Process for Disinfecting Large Quantities of Water Niraj Ashutosh Vidwans, Johnathan Bockenstedt, John Boswell, Terry Gentry and Sreeram Vaddiraju; Texas A&M University, United States

Titanium dioxide (TiO₂) is one of the well-studied materials for applications in photocatalysis. Various forms of TiO₂, such as commercially available Aeroxide® P25, nanowires, phase-pure Anatase crystals, and phase-pure Rutile crystals have been explored for photocatalysis. The capability of TiO₂ in generating reactive oxygen species (ROS) when exposed to ultraviolet (UV) light has been extensively utilized for both removing

contaminants (e.g. dyes) from water and disinfecting water. Here, the high specific surface area obtained when TiO₂ is made in nanocrystalline form (nanoparticles and nanowires) aids in engineering both the efficiencies and the kinetics of the water remediation processes. However, one of the major hurdles in the widespread use of photocatalysis for water remediation is the need to extensively pre-process and post-process the source water and the treated water, respectively for making the source water transparent to light and for the recovery of the TiO₂ photocatalyst. This makes it tedious to employ photocatalysis, unlike processes such as chlorination. In this work, we present a few strategies useful for overcoming the above-mentioned bottlenecks. Flow pattern changes, photocatalyst morphology alterations, and surface chemical compositional changes in a TiO₂ nanowire-based photocatalyst have been employed to make the photocatalysis process useful for treating any kind of water with minimal post-processing. These strategies will be discussed in detail in this talk. The steps involved in implementing these strategies in a bench-scale setup capable of continuously disinfecting 3 gallons of water per minute will also be discussed. The central ideal here is that making photocatalysis easy to implement and effective makes it employable at any stage in the train of technologies used for treating water.

2:45 PM SM13.03.07

Removal of Low Concentration Water Contaminants with Biochar using Novel Mixing Methods Richard M. LaDouceur, Dario Prieto and Alyssa Cook; Montana Technological University, United States

Biochar is a carbonaceous solid commonly referred to as charcoal which results from the pyrolysis of organic matter. These materials are important domestic and industrial adsorbents due to their rich surface chemistry, large micropore volume, and high specific surface area. Recent research indicates that biochar can remove both organic and inorganic contaminants from gas and liquid streams. Careful biomass pyrolysis can lead to structures with the right combination of surface morphology and chemistry to adsorb specific adsorbates. However, biochar morphology and function are both inextricably linked to the pyrolysis conditions and the biomass source. Adsorption methodology has a large effect on the adsorption behavior of high surface area materials which hinders reproducibility. Therefore, a design of experiments was created to attempt to determine ideal conditions for maximum contaminant uptake. Experimental designs for three biochar-contaminant mixing methods, the orbital shaker, rotational mixer, and resonant acoustic mixer (RAM), were formed, with three variable factors being taken into consideration for each: biochar mass, length of mixing time, and intensity of mixing. High, middle range, and low values for each factor were combined to create the matrix for each mixing method. Similar adsorption behavior is noted for the three methods with the time required for maximum adsorption being considerably different between the three methods.

2:55 PM SM13.03.08

Material and Structural Designs of Hydrogels for Solar-driven Desalination and Water Purification Xingyi Zhou and Guihua Yu; The University of Texas at Austin, United States

Solar-powered water evaporation provides a means for sustainable seawater desalination and water purification technologies. Advanced material and structural designs of the evaporative materials are essential for efficient freshwater production. Here we will present our representative works on rational design and molecular engineering of hydrogels and their applications in solar-powered water purification. We designed hybrid hydrogels composed of a hydrophilic polymer framework and solar absorption materials to harvest solar energy and remove contaminants. By tuning the micro/nanostructures and chemical/physical interactions between components, the hybrid gels exhibit attractive synergistic characteristics including high solar absorption, reduced energy consumption for water evaporation, fast water transport, effective thermal management and antifouling property. The highly hydratable polymer networks can be architected to tune the water state, activating water molecules and facilitating water evaporation. The hydrogel evaporator with topology-controlled hydration behavior is also designed to achieve water and heat management simultaneously. These works provide fundamental design principles regarding material selection, molecular engineering and structural modification of these emerging hydrogels for the development of next-generation solar evaporators for seawater desalination and water purification.

3:05 PM SM13.03.09

Late News: The Role of Additional Oxidation of Graphene Oxide on the Removal of Methylene Blue

Cecilia A. Zito¹, Tarcísio M. Perfecto¹, Talita Mazon² and Diogo P. Volanti¹; ¹São Paulo State University, Brazil; ²Center for Information Technology Renato Archer (CTI), Brazil

Graphene oxide (GO) has emerged as an efficient adsorbent for environmental remediation, playing an important role in water treatment. GO-based materials have been developed for the sorption and removal of contaminants from water, including dyes,¹ metallic ions,² radionuclides,³ aromatic organic compounds,⁴ and so on. In particular, dyes can cause damages to humans and aquatic biota for being toxic and carcinogenic.⁵ The chemical composition, degree of oxidation, and size strongly affect the adsorption properties of GO. Herein, we report the repeated oxidation of GO using milder conditions of a modified Hummers' method to obtain the modified graphene oxide (Ox-GO). The impact of the repeated oxidation was evaluated by studying the adsorption performance of the materials towards methylene blue (MB), one of the most used cationic dyes. The materials were characterized by X-ray powder diffraction, scanning electron microscopy, atomic force microscopy, X-ray photoelectron spectroscopy, total X-ray scattering, and pair distribution function analysis. Our results show that the additional oxidation step does not lead to an increased content of oxygenated groups but instead, it causes a small change in the amounts of each functionality, reduces the size and introduces holes in the sheets, facilitates the exfoliation. The adsorption experiments reveal that when using an initial MB concentration of 200 mg L⁻¹ at pH 6, Ox-GO shows a dye adsorption capacity of 695.36 mg g⁻¹, nearly 1.32-fold higher than that of GO (527.07 mg g⁻¹). Thus, more than 90% of MB can be removed by Ox-GO, while GO removes only 72.2%. When the pH is decreased to 2 at the same dye concentration, the difference in removal for both materials is more pronounced, where Ox-GO adsorbs 1.45 times more MB than GO, reaching an efficiency of around 79.5%. On the other hand, under alkaline conditions (pH 10), GO can adsorb almost 100% of the dye, but Ox-GO presents a catalytic behavior to converting MB into a different species, violet-colored. Therefore, the additional oxidation step of GO is an efficient method to enhance the MB adsorption performance, enabling the application in water treatment. Moreover, the material also shows catalytic properties that allow more potential applications.

Acknowledgments

This research was funded by São Paulo Research Foundation (FAPESP; grants 2018/08271-7, 2016/25267-8, 2018/00033-0, 2017/01267-1).

References

- 1 G. K. Ramesha, A. Vijaya Kumara, H. B. Muralidhara and S. Sampath, *J. Colloid Interface Sci.*, 2011, **361**, 270–277.
- 2 L. Chaabane, E. Beyou, A. El Ghali and M. H. V. Baouab, *J. Hazard. Mater.*, 2020, **389**, 121839.
- 3 A. S. Kuzenkova, A. Y. Romanchuk, A. L. Trigub, K. I. Maslakov, A. V. Egorov, L. Amidani, C. Kittrell, K. O. Kvashnina, J. M. Tour, A. V. Talyzin and S. N. Kalmykov, *Carbon N. Y.*, 2020, **158**, 291–302.
- 4 H. Yan, H. Wu, K. Li, Y. Wang, X. Tao, H. Yang, A. Li and R. Cheng, *ACS Appl. Mater. Interfaces*, 2015, **7**, 6690–6697.
- 5 Z. Cheng, J. Liao, B. He, F. Zhang, F. Zhang, X. Huang and L. Zhou, *ACS Sustain. Chem. Eng.*, 2015, **3**, 1677–1685.

3:15 PM SM13.03.10

Late News: Elucidating Ionization Anomalies Observed in Nanoporous Polyamide Membranes

Cody Ritt¹, Jay Werber¹, Mengyi Wang^{2,2}, Zhongyue Yang², Yumeng Zhao¹, Heather J. Kulik² and Menachem Elimelech¹; ¹Yale University, United States; ²Massachusetts Institute of Technology, United States

Escalating global water scarcity necessitates high-performance desalination membranes, for which fundamental understanding of structure–property–performance relationships is required. In this study, we comprehensively assess the ionization behavior of nanoporous polyamide selective layers in state-of-the-art nanofiltration (NF) membranes. In these films, residual carboxylic acids and amines influence permeability and selectivity by imparting hydrophilicity and ionizable moieties that can exclude coions. We utilize layered interfacial polymerization to prepare physically and chemically similar selective layers of controlled thickness. We then

demonstrate location-dependent ionization of carboxyl groups in NF polyamide films. Specifically, only surface carboxyl groups ionize under neutral pH, whereas interior carboxyl ionization requires $\text{pH} > 9$. Conversely, amine ionization behaves invariably across the film. First-principles simulations reveal that the low permittivity of nanoconfined water drives the anomalous carboxyl ionization behavior. Furthermore, we report that interior carboxyl ionization could improve the water-salt permselectivity of NF membranes over fourfold, suggesting that interior charge density could be an important tool to enhance the selectivity of polyamide membranes. Our findings highlight the influence of nanoconfinement on membrane transport properties and provide enhanced fundamental understanding of ionization that could enable novel membrane design.

SESSION SM13.04: Advances in Membrane and Water Treatment Materials for Sustainable Environmental Remediation IV

Session Chairs: Frank Gu and Rob Simm

Friday Afternoon, April 23, 2021

SM13

5:15 PM SM13.04.01

Photocatalytic Degradation of Organic Dyes in Presence of Titanium Dioxide Under UV Light María J. Paz Ruiz and Alondra A. Lugo Ruiz; University of Puerto Rico at Ponce, Puerto Rico

There has been a high discharge of non-biodegradable dyes into natural streams and water bodies, thus contaminating them. Many of these dyes are synthesized by carcinogens and can be water-soluble, therefore being more problematic to remove. One of the largest categories of colorants are the azo dyes, over 50% of all the dyes used are azoic dyes. The problem with azo dyes is that they can be reduced into aromatic amines, which are potentially hazardous. One effective way to remove these dyes from our water sources is by using semiconductor nanoparticles in a photocatalytic degradation process. Titanium dioxide is a semiconductor material with intrinsic optical and electronic properties that promote its use in several applications including catalytic processes and organic synthesis. The photocatalytic capacity of TiO_2 nanostructures is based on the generation of electron-hole pairs due to the UV excitation of TiO_2 . The generated pairs diffuse to the surface of the material and participate in the surface reaction leading to the decomposition of absorbed matter. The generation of reactive oxygen species by the electron-hole pairs is responsible for the degradation of organic contaminants like dyes. Based on the considerations above, the objective of this research was to study and evaluate the photocatalytic capacity of the Titanium Dioxide NPs on organic dyes. The results evidenced that the photocatalytic properties of TiO_2 degraded the dyes in its majority. The effect of catalysts concentration on the reaction rate constants will be discussed.

5:20 PM SM13.04.02

Effect of the Particle Size and pH on the Photocatalytic Performance of CeO_2 Nanoparticles Natalie M. Lopés Velasco and Sonia J. Bailón- Ruíz; University of Puerto Rico at Ponce, Puerto Rico

Cerium Oxide Nanoparticles (CeO_2 NPs) are recognized as important functional materials because of their exciting applications. These nanoparticles are used as catalytic converters for; internal combustion engines, polishing lenses, optical instruments, pigments, solar cells, and photocatalytic processes. Preliminary studies have reported that CeO_2 has the potential capacity to destroy organic dyes because of their capacity to generate reactive oxygen species (ROS) in aquatic environments as hydroxide radicals (OH). However, there is a concern about the potential adsorption of CeO_2 in aquatic organisms and later toxicity in these living systems. In this way, scarce studies about the nanotoxicity of CeO_2 in the aquatic organism have been reported. Based on the mentioned before, the objectives of this work were: 1) Characterize Cerium Oxide Nanoparticles, 2) Study the photocatalytic degradation of organic dyes with two different sizes of CeO_2 NPs, 3) Evaluate the CeO_2 nanoparticles ROS production capacity (as toxicity in marine organisms), and 4) Determine the effect of the pH

in the photocatalytic capacity of CeO₂ NPs. Nanoparticles of CeO₂ evidenced a high absorption peak in the ultraviolet range, which suggests the charge-transfer transition from O₂- (2p) to Ce⁴⁺ (4f) orbitals in CeO₂. It is known that Azo dyes are disposed of in aquatic environments without treatment. These dyes are used in printing, pharmaceuticals, laboratory research, and in the textile industry. These toxins can enter the body through the skin and cause; fast heart rate, lung tissue death, and vomiting. In this research, we focused on the azo dye, Tropaeolin O. The catalytic activity of two different Cerium Oxide size nanoparticles were evaluated in aqueous solutions of Tropaeolin O at 70 μM of concentration. These solutions were put in a UV light at 302 nm for intervals until it reached 160 minutes. The smallest Cerium Oxide NPs (<5.0 nm) degraded about 40%. The biggest Cerium Oxide NPs (<25.0 nm) degraded about 20%. This result shows that (<5.0 nm) CeO₂ NPs degraded more due to its greater surface area and its capacity to generate more reactive oxygen species (ROS). The capacity of CeO₂ NPs to generate ROS was examined and investigated with the intoxication experiment of shrimps. The toxicity was evaluated in marine crustaceans at different CeO₂ concentrations in the 0ppm to 1000ppm range. The results indicated that Cerium Oxide had a negative interaction in marine organisms with increased concentration and exposure time. At 24 hours of exposure, the smallest NPs had a high mortality rate at CeO₂ concentrations higher than 100ppm. However, when the exposure time was increased by 48 hours, nanoparticles were toxic at concentrations higher than 10ppm. In contrast, the biggest NP showed no high mortality rate after 48 hours of exposure and higher concentrations. This experiment explains that (<5.0 nm) Cerium Oxide nanoparticles are more toxic because of the greater surface area and the generation of ROS radicals. We are currently working with the optimization of both sizes of the CeO₂ NPs by changing their acidic pH to a basic pH. In theory, this would optimize and give a better photocatalytic effect and a more significant degradation percent of different azo dyes like Tropaeolin O.

5:25 PM SM13.04.04

Solar Evaporators Based on Water Pump of Thermosensitive Hydrogels Hoyeon Kim and Jongwhi Lee; Chung-Ang University, Korea (the Republic of)

Solar desalination system shows great potential as a solution to the issues of global water scarcity because of its eco-friendliness and sustainability. However, the heat loss of evaporation surface to water reservoir, fouling due to the formation of salt crystals on evaporation surfaces, and the difficulty of continuous brine supply without external power are the major obstacles to the practical use of the solar desalination. Herein, using thermosensitive hydrogel composites, a solar evaporator was which could work by diurnal temperature variation with antifouling properties and no heat loss during evaporation. An irreversible water flow was achieved by using composites of thermosensitive poly(N-isopropylacrylamide) (PNIPAm) hydrogel and hydrophobic polydimethylsiloxane (PDMS), which have fast deswelling kinetics. The composites were made by directional melt crystallization (DMC) of solvent. By the DMC method, a porous PNIPAm having aligned and continuous three-dimensional pores was prepared. The structure enables a combination of two different materials. It can be achieved by the infiltration of PDMS to the aligned pores of PNIPAm. Anisotropic composites have PNIPAm/PDMS phase at the bottom of the composites, which has a faster deswelling rate than pure PNIPAm phase. As temperature rises above the LCST of PNIPAm, water can be released from the top surface of the PNIPAm, and this water pumping could be repeated by the diurnal temperature variance. Between the pumping composite and the water reservoir, another porous PNIPAm was placed. During diurnal temperature variance, this bottom PNIPAm can vary its length. At a temperature above LCST, the length of the PNIPAm is shortened, a thermal isolation from the water reservoir results. At a temperature below LCST, PNIPAm is lengthened, and it can absorb brine from the water reservoir and diffuse brine into the entire phases of PNIPAm/PDMS composites. Water from the pumped brine evaporates on the surface of nickel/cellulose composite, which could float on water. Nickel nanoparticles were prepared on the surfaces of cellulose papers. When brine is released, the nickel/cellulose composites float, and salt accumulation is formed at the bottom of the composites. This can solve the decrease in the efficiency of the evaporation due to the fouling by salt crystallization. Our three-dimensional solar desalination system could be operated without artificial power without the fouling problems. Diurnal operating strategy makes the solar evaporator eco-friendly, and the antifouling properties increase the sustainability of solar desalination.

5:30 PM SM13.04.06

In Situ Synthesis of Carbon Dot at Cellulose Nanofiber for Durable and Selective-Removal Membrane via Mild Hydrothermal Carbonization Jungbin Ahn and Hyungsup Kim; Konkuk Univ., Korea (the Republic of)

Researches on water treatment technology has been steadily studied for innovative improvement of the performances, i.e., high yield and speed of purification process. Conventionally, water treatment membrane was fabricated from synthetic polymers, such as polysulfone and polyethersulfone, with the controlled pore structure. Non-solvent induced phase separation (NIPs) is the most common method to control the pore structure. In the process, polymer solution should be immersed in a coagulation bath containing non-solvent. The overuse of hazard solvents is inevitable during the fabrication. In order to protect the earth from those kinds of pollutions, a substantial candidate for the membrane is crucial. TEMPO-oxidized cellulose nanofiber (CNF) has high potential for the membrane application due to its high aspect ratio and high mechanical strength. Owing to its carboxylate groups, CNF can be easily dispersed in water which enables the membrane fabrication without the help of toxic solvents. Up to now, a number of studies have been reported for high performance membrane based on CNF. However, it is still challenging to increase pollutant removal performance without sacrificing its water flux.

In the study, high-performance water treatment membrane was fabricated using *in-situ* synthesized carbon dot (CD) at CNF. Via simple hydrothermal treatment, CD was homogeneously attached to the CNF surface by amide bonding. CD@CNF had a fibrous structure with rough and bumpy morphology, while the chemical structure of cellulose was not changed. The CD attached on the surface decreased the repulsive force between the CNFs and remarkably increased the thermal and dimensional stabilities of the CNF film. With the structural robustness, CD@CNF showed excellent performance as a dye-rejection membrane of high-water flux and high rejection rate. As well the CD@CNF showed superior selective removal results toward cationic dyes. This study suggests the novel synthesizing method of durable CNF membrane by envelopment of CD for effective water treatment.

5:40 PM SM13.04.08

Doped Graphitic Carbon Nitride Nanocomposites with Various Dimensions for the Effective Photodegradation of Pharmaceuticals Ruey-An Doong¹ and Thanh Binh Nguyen²; ¹National Tsing Hua University, Taiwan; ²National Kaohsiung University of Science and Technology, Taiwan

In recent years, the presence of pharmaceuticals such as diclofenac and sulfamethoxazole in the aquatic environment has been of growing interest as it poses a threat to aquatic organisms and human health. Graphitic carbon nitride (g-C₃N₄) is a promising green photocatalyst with the visible-light-responsive property. However, the high e⁻-h⁺ recombination rate decreases the photo-activity of g-C₃N₄. Therefore, the doping with other ions as well as the combination with other photocatalysts can not only extends the absorption to the visible light region but also reduces the recombination rate of electron-hole pairs. Herein, the doped C₃N₄ with various morphologies and dimensional was successfully synthesized by a facile hydrothermal-assisted thermal approach as an effective photocatalyst for photocatalytic degradation of pharmaceuticals under visible-light irradiation. The 1-D B, P-codoped g-C₃N₄ various P loadings was fabricated for highly recyclable photodegradation of diclofenac (DFC) under visible light irradiation. The as-prepared 1-D B, P-C₃N₄ exhibits high surface area, visible-light response and photoinduced charge separation to effectively photodegrade > 99% of 10 mg/L diclofenac within 90 min of irradiation. The 1D-BPCN-3 shows good reusability in the photodegradation of DFC for at least 5 consecutive cycles without considerable loss in photocatalytic activity. Moreover, the 3-D flower-like g-C₃N₄@TiO₂ was prepared by the thermal exfoliation of urea and hydrothermal method. The g-C₃N₄@TiO₂ exhibits an excellent photocatalytic performance toward diclofenac degradation under solar light irradiation. The impedimetric and photoluminescence spectra show that 5 wt% g-C₃N₄ can increase the conductivity as well as reduce the recombination rate of g-C₃N₄@TiO₂ nanocomposites, resulting in the enhancement of photodegradation efficiency and rate of diclofenac. The rate constant for diclofenac degradation by 3-D g-C₃N₄@TiO₂ is 0.075 min⁻¹, which is 3–10 times higher than the other g-C₃N₄@TiO₂. These results clearly demonstrate that the various dimensions of doped g-C₃N₄ are reliable visible-light-

responsive photocatalysts for the decomposition of antibiotics and other emerging pollutants in aqueous solutions.

SYMPOSIUM ST01

Mechanical Behavior at Micro/Nano-Scale
April 14 - April 20, 2021

Symposium Organizers

Wendy Gu, Stanford University
Matt Pharr, Texas A&M University
Jagannathan Rajagopalan, Arizona State University
Gi-Dong Sim, Korea Advanced Institute of Science and Technology

* Invited Paper

SESSION ST01.01: Novel Methods to Tailor the Microstructures of Micro- and Nanoscale Materials I
Session Chairs: Jagannathan Rajagopalan and Gi-Dong Sim
Sunday Morning, April 18, 2021
ST01

8:00 AM *ST01.01.01

Heterostructured Material—New Science Produces Superior Properties Yuntian T. Zhu^{1,2}; ¹City University of Hong Kong, China; ²Southeast University, China

Strong and tough materials are desired for light-weight applications such as electric cars and aerospace applications. Recently, heterostructures are found to produce unprecedented strength and ductility that are considered impossible from our textbook knowledge and materials history. Heterostructured materials consist of heterogeneous zones with dramatic (>100%) variations in mechanical and/or physical properties. The interaction in these hetero-zones produces a synergistic effect where the integrated property exceeds the prediction by the rule-of-mixtures. Importantly, HS materials can be produced by current industrial facilities at large scale and low cost. There are many scientific issues with such materials that challenge the communities of experimental materials science and computational material mechanics. Heterostructured materials is quickly becoming a hot research field in the post-nanomaterials era. In this talk I'll present the current advances as well as future challenges and issues in this emerging field.

8:25 AM ST01.01.02

Late News: Characterization of Gamma to Alpha Phase Transition in Uranium via XRD and DSC
Christian J. Reiter, Julia Mausz, Christian Schwarz, Bruno Baumeister, Winfried Petry and Peter Muller-Buschbaum; Technische Universität München, Germany

For safety of nuclear fuel, pure metallic uranium disqualifies due to its anisotropic thermal expansion and cycling behavior of its equilibrium alpha phase under operation conditions. In contrast, the body-centered cubic gamma-phase provides the desired irradiation stability, but as this phase is not stable at room temperature, it is necessary to alloy it with elements such as Nb, Ti or Mo. Still, the alloy needs to be quenched rapidly from the

high temperature gamma-phase regime down to room temperature in order to preserve the gamma phase. Uranium-molybdenum alloys, with 4.5 wt.% to 15 wt.% Mo, have been favored, however, the best compromise between fuel performance and uranium density must be made. In order to provide a safe usage, two conditions must be ensured during the entire operation cycle: On the one hand, the stability of phases must be given throughout the operation cycle and on the other hand, the interaction with other materials, especially with the cladding, must be minor or at least predictable.

Exposed to elevated temperatures, the meta-stable gamma-phase of uranium-molybdenum alloys decomposes into other thermal equilibrium phases, i.e. U_2Mo and alpha-uranium following isothermal phase transformation kinetics. Until now, the transformation enthalpy, which is the energy required to transform the decomposed phases back into pure gamma, has not been studied by accounting for the relative fraction of the phases during this re-transformation. The enthalpy change of the phase transformation can be studied by differential scanning calorimetry (DSC).

In the present study, an uranium-molybdenum alloy with 7.8 wt.% has been used, which was deposited onto a copper substrate using physical vapor deposition (PVD). In order to compare the phase composition, X-ray diffraction (XRD) measurements were conducted on fresh and tempered samples, respectively. After heat treatment, the phase proportion between alpha and gamma phase exists according to the corresponding time temperature transformation (TTT) diagram. During the measurement, the respective fraction of the volume undergoes a transformation back from alpha- to gamma-uranium, which can be measured using DSC. However, the phase transition enthalpy cannot directly be normalized by the weight or volume of the sample. Hence, an additional correction of pre-measured fractional phase composition must be carried out. Analysis of DSC data is presented.

8:40 AM ST01.01.03

Nanoporous Gold Thin-Film Dealloying—Process-Structure Correlation Stanislau Niauzorau, Aliaksandr Sharstniou, Natalya Kublik, Venkata Sampath and Bruno Azeredo; Arizona State University, United States

Nanoporous metals with bi-continuous porosity attracts considerable interest due to its high surface area which opens their potential for use in sensing [1], catalysis [2], and energy storage [3]. However, processing-structure (PS) relations for nanoporous gold (NPG) have been largely not understood. Recently, McCue et al. constructed and analyzed a large dataset of porous gold SEM images from various publications to establish correlations between structural parameters (i.e. ligament diameter, aspect ratio, solid area fraction (SAF)), and processing conditions (such as dealloying times and temperatures) [5]. However, the large scatter of this dataset also suggests issues with the reproducibility of NPG synthesis even with the reported fixed dealloying protocol (e.g. precursor alloy composition, etching solution, concentration, etc.). In this study, we experimentally examine the reproducibility of the synthesis of NPG thin films fabricated at constant conditions (i.e. 60 at.% Ag in precursor alloy, 7.85 M HNO_3 , 65 °C) and extract structural data to find PS relations. Moreover, we test the influence of processing conditions previously not reported such as the temperature equilibration time of the etchant solution, and sample aging effects such as stress release, grain growth and surface oxidation, all of which have been found to affect the uncertainty of NPG synthesis. This ground work may shed more light at future understanding of the kinetics of morphology evolution in chemical dealloying at a more quantitative level.

[1]

B.-K. Chao, H.-C. Ho, P. Yiu, Y.-C. Lai, C.-H. Shek and C.-H. Hseuh, "Gold-rich ligament nanostructure by dealloying Au-based metallic glass ribbon for surface enhanced Raman scattering," *Scientific Reports*, vol. 7, no. 7485, 2017.

[2]

V. Vij, S. Sultan, A. Harzandi, A. Meena, J. Tiwari, W. Lee, T. Yoon and K. Kim, "Nickel-based electrocatalysts for energy-related applications: oxygen reduction, oxygen evolution, and hydrogen evolution reactions," *ACS Catalysis*, vol. 7, no. 10, pp. 7196-7225, 2017.

[3]

J. Li, J. Pu, Z. Liu, J. Wang, W. Wu, H. Zhang and H. Ma, "Porous-nickel-scaffolded Tin-Antimony anodes with enhances electrochemical properties for Li/Na-ion batteries," *Applied Materials and Interfaces*, vol. 9, pp. 25250-25256, 2017.

[4]

A. Sharstniou, S. Niazorau, P. M. Ferreira and B. P. Azeredo, "Electrochemical nanoimprinting of silicon," *PNAS*, vol. 116, no. 21, pp. 10264-10269, 2019.

[5]

I. McCue, J. Stuckner, M. Murayama and M. J. Demkowicz, "Gaining new insights into nanoporous gold by mining and analysis of published images," *Scientific Reports*, vol. 8, no. 6761, 2018.

8:55 AM ST01.01.04

Investigation of Fundamental Creep Behavior in Thermally Stable Hierarchical and Nanocrystalline Ni-Y Alloys Shruti Sharma, Pedro D. Peralta and Kiran Solanki; Arizona State University, United States

There is a growing interest in developing strategies to increase the high temperature performance of metallic alloys used in extreme conditions, such as those found in many energy generations and propulsion systems, among others. Microstructure refinement has long been considered a potential route for improvement in this regard; however, nanocrystalline (NC) metals and alloys (with grain size less than 100 nm) exhibit significant microstructure instability at high temperatures and even at room temperatures under, e.g., cyclic loads. Thermodynamic (solute segregation to reduce grain boundary energy) and/or kinetic approaches (solute drag, Zener pinning, etc., to pin grain boundaries) can be used to suppress grain growth through the addition of alloying elements and second phases. Some NC alloys such as Cu-10%Ta fabricated using far from equilibrium processing techniques have displayed stability of their microstructures mostly through kinetic mechanisms at various thermo-mechanical loading conditions, leading to an enhanced creep behavior compared to its coarse-grained (CG) counterparts. However, the low melting point of Cu makes Cu alloys ill-suited for advanced applications compared to Ni and Ti. The fundamental creep mechanisms in these alloys also need to be studied in more detail.

This work seeks to study the microstructure stability as well as the fundamental creep mechanisms in hierarchical and NC Ni-Y alloys, where the hierarchical alloys were synthesized using the conventional arc-melting technique in an inert atmosphere and NC alloys by consolidating powders at high temperatures through equal channel angular extrusion (ECAE) processing to retain a fully dense NC microstructure. For the Ni-Y alloys, using a Ni-rich matrix can impart high ductility and formability while leading to high stiffness and a relatively high melting point, thereby delaying the onset of diffusional creep mechanisms. Small additions of Y to Ni would introduce second phase particles from Ni-Y (Ni_{17}Y_2), thus possibly improving the kinetic stability (Zener pinning of grain boundaries).

Current research is divided into three major tasks: a) evaluating microstructure and mechanical properties of hierarchical Ni-Y alloys over an appropriate range of compositions to establish a baseline to assess binary alloy behavior, b) high temperature uniaxial compression and creep-testing of both hierarchical and NC alloys, and c) advanced characterization techniques to understand the creep behavior of the alloys. The microstructure of hierarchical alloys studied using characterization techniques like optical microscopy, BSE imaging, EDX, and WDX analysis displayed three major length scales. The ultrafine eutectic length scale of ~ 300 nm led to the microhardness and yield strength of the alloys comparable to the existing Ni-superalloys. Furthermore, the matrix of the alloys defined by dendritic arm spacing of ~ 10 μm controlled the microstructural stability of alloys, ascertained by heat treatments and high temperature compression tests. Additionally, grain size (200 μm) in hierarchical alloys is expected to play a significant role in improving creep properties based on the observation of the creep rate possessed by the ultrafine-grained Ni-Y alloys being comparable to that of Ni-

based single crystal superalloys. Characterization has also been performed on as-deformed hierarchical Ni-Y samples using EBSD techniques before and after deformation to see a combination of RT and temperature deformation in the matrix and eutectic phases, understand the deformation behavior, e.g., slip behavior, and correlate crystallography with slip behavior. EBSD combined with higher resolution imaging has also been used to see the effect on the eutectic phase with deformation. Furthermore, SAXS measurements are also performed on the deformed samples to understand the average particle size, particle size distribution, particle surface area, etc. in hierarchical and NC alloys.

9:10 AM ST01.01.05

Microstructure and Mechanical Property Gradients in Stainless Steels Induced by Thermal Gradients in Spark Plasma Sintering Alexander D. Preston and Kaka Ma; Colorado State University, United States

Spark plasma sintering (SPS) is a unique powder metallurgy technique capable of rapid densification due to a combination of joule heating and pressure. The rapid heating rates in SPS and the tooling-sample contact resistances cause thermal gradients, which in turn lead to microstructural gradients. To elucidate the nature of the interaction between starting powder morphology, electric current pathways, and thermal gradients in SPS, the present work investigated the microstructure and mechanical properties of nominally austenitic stainless-steel samples fabricated via SPS of gas atomized and ball milled powders. Microhardness testing and nanoindentation were applied to investigate local mechanical properties at both a micro- and a nanoscopic level. Nanoscratch testing was incorporated to understand the effect of different particle-particle interfaces including the deformation behavior. It was found that a grain size gradient arising from the thermal gradients in SPS lead to changes in local microhardness ($\Delta H=100\text{MPa}\sim 150\text{MPa}$). Nanoindentation results revealed radial porosity gradients in the samples lead to a radial gradient in Young's modulus ($\Delta E=30\text{GPa}\sim 65\text{GPa}$).

9:25 AM *ST01.01.06

Tailoring the Configuration of Nanotwins in Sputter Deposited Alloys as a Route to Isolate Dislocation-Twin Interactions Francisco Andrade Chavez, Orcun Koray Celebi, Ahmed Sameer Khan Mohammed, Huseyin Sehitoglu and Jessica A. Krogstad; University of Illinois at Urbana-Champaign, United States

The remarkable strength of nanotwinned metals and metallic alloys has been attributed to a number of mechanisms, all involving frequent dislocation-twin interactions. Despite the high density of nanotwins that have been achieved through a variety of processing routes, the relative distribution of twins remain stochastic. For simple deformation modes, such a distribution of dislocation barriers can be accommodated by adapting traditional strengthening models. However, under cyclic loading conditions, the configuration and spacing between obstacles play a much more nuanced role. Modeling approaches have begun to tackle this problem, but without experimental validation in a controlled microstructure, the impact remains limited. We will emphasize the processing science necessary to develop well defined nanotwin microstructures, complemented by characterization of select twin-dislocation interactions enabled by these configurations. We will demonstrate the impact of deposition conditions and intrinsic properties on the nature and density of nanotwins using Ni-rich Ni-Ti alloys. Specifically, we have employed alloy chemistry, stacking fault energy and substrate constraint to engineer nanotwins that are inclined to the plane of the film. In such a configuration, simple tensile loading can activate complex dislocation-twin interactions, while still allowing for a systematic characterization of these interactions. When paired with computational tools and developing analytical model, these observations provide fundamental insight on the interfacial reactions relevant to fatigue damage accumulation.

SESSION ST01.02: Novel Methods to Tailor the Microstructures of Micro- and Nanoscale Materials II

Session Chairs: Matt Pharr and Jagannathan Rajagopalan

Sunday Morning, April 18, 2021

ST01

10:30 AM *ST01.02.01

Local Phase Transformations—A New Creep Strengthening Mechanism in Ni-Base Superalloys A. Egan^{1,1}, S. Mukhopadaya^{1,1}, T.M. Smith², Maryam Ghazisaeidi¹, S.R. Niezgodna¹, Y. Wang¹ and Michael J. Mills^{1,1}; ¹The Ohio State University, United States; ²NASA Glenn Research Center, United States

Polycrystalline Ni-based superalloys are vital materials for disks in the hot section of aerospace and land-based turbine engines due to their exceptional microstructural stability and strength at high temperatures. In the drive to increase operating temperatures and hold times in these engines, hence increasing engine efficiency and reduction of carbon emissions, creep properties of these alloys becomes increasingly important. At these higher temperatures, new deformation modes become active. Several alloy compositions and microstructure variants of commercial disk alloys are being explored, including g' strengthened alloys as well as compositions promoting g' and g'' co-precipitation. Microtwinning and stacking fault shearing are important operative mechanisms in the critical 600-800°C temperature range. Advanced characterization techniques using scanning transmission electron microscopy with diffraction contrast imaging, high resolution imaging, and energy dispersive spectroscopy have been used to gain new insights into these mechanisms and the rate-limiting processes during high temperature deformation. Atomic-scale chemical and structural changes associated with stacking fault and microtwin interfaces within g' precipitates have been identified and indicate that local phase transformations (LPT) occur commonly during creep of superalloys. Three distinct LPT scenarios have been identified. In the first, the stacking faults and twin interfaces adopt a composition similar to that of the solid solution g matrix and is associated with alloys having lower creep strength. In the second scenario, the superlattice extrinsic stacking fault structure transforms to the DO₂₄ η phase and is associated with alloys having improved creep resistance. In the third scenario, superlattice intrinsic stacking faults transform to a local X (DO₁₉) phase, and also appears to provide creep strengthening. Thus, these important deformation modes can be modulated by LPT formation. For instance, for alloys in which η phase formation is favorable, microtwinning is inhibited as a deformation mechanism. The thermodynamic driving force for LPT formation is being explored using DFT modeling, and the predicted segregation profiles are compared with experiment. Phase field dislocation dynamics modeling is being used to explore the interaction of dislocations with g' microstructures under the cooperative shearing and local compositional changes associated with the LPT mechanism. Finally, these time-dependent processes are being incorporated into a microstructure-based crystal plasticity model for creep.

10:55 AM DISCUSSION

11:10 AM ST01.02.03

Experimental Evidence of Auxeticity in Ion Implanted Single Crystalline Calcite Substrates Michael E. Liao¹, Chao Li², Nachiket Shah³, Gaurav Sant^{1,1} and Mark S. Goorsky¹; ¹University of California, Los Angeles, United States; ²Applied Materials, Inc., United States; ³University of Illinois at Urbana-Champaign, United States

Calcite, a polymorph of calcium carbonate with a trigonal crystal structure, has been predicted to exhibit auxetic behavior – materials with negative Poisson's ratios – but this has not been experimentally determined. Work by Aouni et al.,¹ for example, calculated the predicted crystallographic directions of maximum auxeticity in calcite. In this work, we report the first experimental evidence of auxeticity in calcite by ion implanting (10 $\bar{1}$ 0) oriented single crystalline calcite substrates with Ar ions. Calcite substrates were implanted at room temperature using an ion energy of 400 keV and a dose of 1.0×10^{14} cm⁻², resulting in a projected range of ~400 nm. Lattice compression normal to the substrate surface was observed, which is an atypical result when ion implanting materials. Usually lattice expansion normal to the substrate surface is expected when implanting substrates.²⁻⁴ This is due to the ions inducing lattice expansion during the implantation process. The bulk of the substrate beneath the ion projected range applies compressive biaxial stress to the expanding ion implanted region. Hence, materials with positive Poisson's ratios would expand normal to the surface, which can be measured as tensile strain with diffraction measurements. Triple-axis X-ray diffraction measurements were employed to

examine the strain state of the implanted calcite substrates. Reciprocal space maps for the symmetric $30\bar{3}0$ and asymmetric $14\bar{5}0$ reflections were measured and revealed that the implanted region was fully strained (pseudomorphic) to the bulk of the substrate beyond the projected range of the implant. A symmetric $\omega:2\theta$ line scan of the $(30\bar{3}0)$ reflection was also measured and X-ray dynamical diffraction simulations were used to model the strain profile to extract the variation of compressive strain as a function of depth normal to the substrate surface. SRIM calculations were also performed to obtain a displacement-per-atom profile. It was found that the strain profile generally follows the displacement-per-atom profile. This study demonstrated the use of ion implantation and X-ray diffraction methods to probe mechanical properties of materials and to test predictions such as the auxeticity on the scale of nanometers to microns depending on the ion energy used.

References

1. N. Aouni, et al., Phys. Stat. Sol. (b), 245(11), 2454 (2008).
2. C. Mićlaus, et al., J. Phys. D: Appl. Phys., 36, A177 (2003).
3. M.E. Liao, et al., ECS J. of Solid State Sci. and Technol., 8(11), P673 (2019).
4. Y. Wang, et al., Phys. Status Solidi B, 257, 1900705 (2020).

11:25 AM ST01.02.04

Mechanical Behavior of Bicrystalline Nickel Thin Films with High Strength and Ductility Rohit Berlia and Jagannathan Rajagopalan; Arizona State University, United States

Metallic thin films typically show high strength but low strain hardening capacity, which leads premature failure. For example, Ni films with a mean grain size less than 100 nm shows ultimate tensile strength of around 1.5 GPa but fail at strains below 3%. Here, we report the mechanical behavior of bicrystalline (111) textured Ni films with incoherent twin boundaries that exhibit high strength and significant ductility. Ni films of thickness varying from 200 nm to 2.5 μm were deposited on Si (111) substrates with a 25 nm Ag buffer layer at room temperature using magnetron sputtering. The microstructure of the films was characterized by TEM, EBSD and XRD, which revealed the presence of two grain variants with (111) out-of-plane texture with an incoherent twin boundary at their interface. Freestanding, dog-bone shaped samples of the films were co-fabricated with MEMS tensile testing stages using standard microfabrication techniques and their uniaxial tensile stress – strain response was measured at quasi – static strain rates. The experiments revealed flow stresses approaching 1 GPa as well as significant strain hardening capacity, which resulted in uniform elongation >10% in the thickest films. Possible mechanisms for this unusually high strength and ductility will be discussed.

SESSION ST01.03: Deformation Behavior of Low-Dimensional Materials I

Session Chairs: Matt Pharr and Gi-Dong Sim

Sunday Afternoon, April 18, 2021

ST01

1:00 PM *ST01.03.01

Contact Quality of 2D Materials—How Interfacial Atomic Structure Controls Nanoscale Contact, Friction and Adhesion Robert W. Carpick; University of Pennsylvania, United States

2D and layered materials are generating excitement due to their multitude of novel properties. Exciting applications include as high-performance solid lubricants due to their ability to achieve “superlubricity” (nearly zero friction), and as functional materials for flexible electronics due to their exceptional bendability, strength, and electronic behavior. Yet the limits of their durability, friction, and adhesion behavior are not understood.

To explore these limits, we study nanocontacts with 2D and layered materials including graphene, MoS₂, and other transition metal dichalcogenides (TMDs) with atomic force microscopy (AFM). We previously found that

friction is intrinsically low for these materials, but depends strongly on the number of layers underneath the AFM tip. A model attributing this to adhesion-induced “puckering” of the ultrathin 2D layers around the tip [1] was then enhanced by molecular dynamics (MD) simulations showing a strong role of the “quality” of the contact. In particular, energy barriers to sliding are affected by interfacial pinning and commensurability due to subtle deformations of the 2D material [2].

We then discovered another contact quality effect when probing nanoscale sliding against graphite while varying the relative humidity. Water acts as a lubricant only above a threshold humidity; below that, adsorbed water increases friction six-fold relative to dry sliding. Such a non-monotonic dependence of friction has been previously attributed to a humidity-dependent water meniscus. We reveal a new possibility, where the number and location of water molecules at the interface controls friction [3].

Finally, we have discovered another factor that strongly affects static friction, namely, the lattice constant. We compared the friction behavior for a nanoscale single asperity sliding on MoS₂, MoSe₂, and MoTe₂ in both bulk and monolayer form through a combination of AFM experiments and molecular dynamics (MD) simulations [4]. Under otherwise identical conditions, MoS₂ has the highest friction and MoTe₂ the lowest. Simulations and further analysis revealed that the friction contrast is attributable to their lattice constants. While the energy barriers to sliding are similar for all three materials, the larger lattice constants associated with larger chalcogen atoms permit the tip to slide more easily across correspondingly wider saddle points in the potential energy landscape. This emphasizes the critical role of the lattice constant, which can be the determining factor for nanoscale friction behavior.

[1] C. Lee *et al.* *Frictional Characteristics of Atomically-Thin Sheets*. **Science**, 328, 76 (2010).

[2] S. Li *et al.* *The Evolving Quality of Frictional Contact with Graphene*. **Nature** 539, 541 (2016).

[3] Hasz, K. *et al.* *Experiments and Simulations of the Humidity Dependence of Friction between Nanoasperities and Graphite: The Role of Interfacial Contact Quality*. **Phys. Rev. Mat.** 2, 126001 (2018).

[4] Vazirisereshk, M.R. *et al.*, *Nanoscale Friction Behavior of Transition-Metal Dichalcogenides: Role of the Chalcogenide*, **ACS Nano** (2020).

1:25 PM ST01.03.02

Late News: Mechanical Strains at Quasi van der Waals Interfaces Cyril Guedj¹, Stéphane Cadot¹, Rémy Gassilloud¹, Damien Caliste² and Pascal Pochet²; ¹Univ. Grenoble Alpes, CEA, LETI, France; ²IriG, Univ. Grenoble Alpes & CEA, France

The nanomechanical properties of materials critically depend on the nature of atomic bonds. In the conventional epitaxy, large lattice mismatches inevitably result in the formation of defects which are usually detrimental for the device performances. The weak bonds obtained at quasi van der Waals interfaces on 2D layers can relax this constraint [1], but the detailed mechanical relaxation processes are not fully understood yet, since charge transfers and defect creation might occur, up to the buckling-driven delamination of the 2D films. The strain engineering is critical for devices applications because it can tune the optical and electronic properties [2],[3],[4] at the interface. Hence, a precise insight into the mechanical properties at the atomic scale is needed to probe the links between the grown structures and their physical properties.

In this work, we investigate the strain relaxation mechanisms at quasi van der Waals interfaces using aberration-corrected HRSTEM-HAADF imaging [5] with a spatial resolution of 50 pm. High resolution maps of mechanical strains and bond rotations are derived from cross-analysis of atomistic modeling and microscopy image simulations. In particular, the influence of the possible crystallographic phases on the simulated HRSTEM images is provided to guide our analysis. We report the case of AlN layers grown on multi-layered MoS₂. Our analysis shows that the lattice mismatch is mostly accommodated by interfacial shear strains and

heterogeneous localized distortions. Plastic deformations are prevalently located in MoS₂. These results are compared to recent theoretical predictions about the possible reordering phenomena in 2D layers due to in-plane uniaxial stress [6]. A global overview of the elastic strain fields around the quasi van der Waals interface will be presented. These results provide a basis for future strain and interface engineering of similar systems.

- [1] D. Liang et al., *Nano Energy* 69, 104463 (2020)
- [2] J. He, et al. *Phys. Rev. B* 89, 1–11 (2014)
- [3] F. Li et al., *Phys. Chem. Chem. Phys.*, 20, 29131 (2018)
- [4] P. Gant et al., *Materials Today*, Vol. 27 (2019)
- [5] O.L. Krivanek et al., *Nature* 464, 571–574 (2010)
- [6] A. B. Alencar et al., *J. Phys.: Condens. Matter* 33, 125401 (2021)

Acknowledgments: Nicolas Bernier is acknowledged for measuring the HRSTEM images, Audrey Jannaud for preparing the samples at the nano-characterization platform of Minatec, and François Martin for his valuable expertise.

1:40 PM ST01.03.03

Late News: Anisotropic Properties and Electron Redistribution in 3C-SiC Hannah Wiswell and Zubaer M. Hossain; University of Delaware, United States

It is understood that anisotropy in material behavior plays a critical role in deformation, but it is important to also understand how anisotropy is related to the very cores of materials, atoms and their structures, and how a material's genome can be altered at the atomic level to increase strength and toughness. In this study, we apply some of the basic principles of quantum mechanics to explore how strength and toughness change in diamond cubic solids, by taking SiC as an example material. We attempt to understand how electron density changes due to stress and strain under different loading conditions. Two distinct conditions were investigated: the first condition involved hydrostatic deformation which preserves the lattice symmetry, and the second condition involved symmetry-breaking uniaxial deformation along the three principal high-symmetry directions, [100], [110], and [111]. Under hydrostatic deformation, it was found that the nearest-neighbor bonds in 3C-SiC deform equally, regardless of the deformation state of the lattice; thus, there is no relaxation within the lattice, and there is symmetric distortion in the electron density. In contrast, under uniaxial stress deformation, it was found that the elastic energy was highest for loading along the [100] direction, while it was the least for loading along the [111] direction. This is due to the nearest-neighbor bonds during [100] directional loading deforming uniformly, so all energy is equally distributed throughout the lattice, while for the [110] and [111] loading directions, bond lengths change non-uniformly, so parts of the lattice relax while the others do not, leading to quicker failure. After evaluation of the electronic structure basis of the maximum stress the lattice can sustain under uniaxial stress deformation, it was found that for the Carbon atoms, electron redistribution in the s and px orbitals was highest for loading along the [100] direction, with the [111] loading direction inciting the least change in electron occupation. For the Silicon atoms, the opposite results were observed, with the [111] loading direction experiencing the highest change in electron density for those orbitals. Further discussion of the methodology and conclusions from this study will occur during the presentation. In this presentation, it will be shown just how significant this study is; with the connection between solid mechanics and quantum mechanics understood, the future of tough, strong, and electrically conductive materials is brighter, and will allow applications of energy-efficient materials to grow in abundance.

1:55 PM ST01.03.04

Late News: Extreme Mechanical Resilience in Nanolabyrinthine Self-Assembled Metamaterials Carlos Portela¹, A Vidyasagar², Daryl Yee¹, Julia Greer², Dennis M. Kochmann³, Sebastian Kroedel³ and Tamara Weissenbach³; ¹Massachusetts Institute of Technology, United States; ²California Institute of Technology, United States; ³ETH Zürich, Switzerland

Lightweight materials with tailorable properties have attracted attention for decades, yet stiff materials that can

resiliently tolerate extreme forces and deformation, while being manufactured at large scales, have remained a rare find. Bio-inspired designs such as hierarchical foams and atomic-lattice-mimicking trusses have achieved optimal combinations of mechanical parameters but suffer from limited mechanical tunability, limited long-term stability, and low throughput volumes. Most mechanical metamaterials have relied on symmetry, periodicity, and lack of defects to achieve the desired mechanical response, resulting in sub-optimal mechanical response under the presence of inevitable defects. Shell-type designs, which can mitigate stress concentrations and flaws, have come with high densities and limited recoverability.

We exploit non-periodic nanoscale ceramic shell architectures of ultralow density (reaching 4 mg/cm^3) whose engineered curvature distribution achieves close-to-optimal stiffness scaling and, moreover, whose careful combination of topology, geometry and base material results in mechanical resilience superior to previous mechanical metamaterials. We present a method for scalable fabrication of these materials, guided by natural spinodal decomposition, which results in shell-based ceramic architectures with thicknesses down to $\sim 10 \text{ nm}$ and overall sample volumes of up to a few cubic centimeters. We show the capability of these architectures to maintain more than 50% of their original stiffness and strength after ten cycles of compression up to 30% while exhibiting no visible permanent deformation. Guided by simulations, we show how controlling the material morphology leads to the (an)isotropic material response whose directional stiffness distribution, impressively, remains constant over a wide range of shell thicknesses, as demonstrated experimentally. Our approach highlights pathways to harness self-assembly methods in the design and scalable fabrication of novel micro/nanoscale metamaterials with both tunable high stiffness and unsurpassed recoverability, simultaneously unachievable by previously reported mechanical metamaterials.

2:10 PM ST01.03.05

Late News: Effects of H₂O Interaction with Graphene Grain-Boundary Under Strain Julia T. Hatoum, Claire Andreasen and Zubaer M. Hossain; University of Delaware, United States

In recent years, graphene has captured wide attention among engineers and researchers for its unique electronic, thermal, chemical, and mechanical properties, which could revolutionize a number of application areas including electronics, nanotechnology, drug delivery, sensors, and catalysis. Since discovery, extensive research has been conducted theoretically, experimentally, and computationally to investigate the behavior of pristine graphene under no strain conditions. With the goal of applications in mind, it is critical to develop a fundamental understanding of the properties of defective graphene under deformed or strained conditions. While line-defects (such as grain boundary) within the graphene lattice are known to degrade its mechanical properties, they can serve as an important source for making the graphene layer function as a chemically reactive 2D material which may be unattainable otherwise. Under defect-free conditions, an ideal and infinite graphene lattice can be deemed non-polar, due to its symmetry preservation across the sheet, which can prevent any measurable interaction with external molecules that may come in contact with. In this work, using density functional theory simulations, we investigate the energetics of an isolated H₂O molecule at a grain-boundary formed between armchair and zigzag graphene sheets. By placing the molecule at different heights from the graphene lattice, we calculate the total groundstate energy of the system. Our findings suggest that if the initial placement of the molecule is parallel to the lattice within the van der Waals interaction distance, the molecule undergoes a reorientation, and the O atom faces the graphene lattice. On the other hand, if the initial position of the molecule is parallel but closer to the graphene lattice, the H atoms become more reactive and they face toward the graphene lattice. We considered six different sites on the hexagon and found similar behavior. An electronic structure analysis suggests that the electron redistribution at the grain boundary affects the behavior of the molecule. Also, due to a separation-distance dependent distinct chemical affinities between the C-O atom vs. C-H atom pairs, the groundstate interaction is strongly affected by the initial position of the molecule. The results are expected to have important implications to our understanding of strain-chemistry of defective graphene. This talk will present the analysis of the results from an electronic structure perspective.

2:25 PM ST01.03.06

Late News: Electron Redistribution Surrounding a Deformed Graphene Mono Vacancy Claire Andreasen,

Julia Hatoum and Zubaer M. Hossain; University of Delaware, United States

Vacancy defects are unavoidable in 2D materials due to the challenges involved in fabricating defect-free lattice from experimental methods. While defects are known to degrade the mechanical properties of a lattice, they offer unique opportunities to tailor the electronic and thermal properties by controlling the mean free path of electrons and phonons. It is therefore important to develop a fundamental understanding of the role of defects in modulating the local electronic character of a lattice. Nevertheless, the understanding of defect-induced alteration of electronic properties (the electronic states for example) remains less understood, particularly under finite deformation. Although researchers have investigated the mechanical and electronic properties of pristine graphene under stress, there is little research on the chirality effects on electron distribution at defective sites in 2D materials under applied stress. In this work, we use the density functional theory simulations and the Mulliken charge population analysis to investigate the electronic behavior of an isolated defect in graphene under the uniaxial loading condition for five different chiralities of the lattice. We analyze how chirality and intensity of loading affect the mechanical properties, bond length and bond angle change, charge distributions, the density of states, and the partial density of states surrounding the vacancy. Our results show that there is a uniform pattern for bond length redistribution as well as electron redistribution at all orientation angles and that such bond and electron redistributions are directly correlated. During all simulations, we observe a bond reconstruction at the defective site at higher deformation. In terms of the orientation angle, we demonstrate that increased orientation angle yields changes in the strength, toughness, stiffness, bond distributions, and electronics surrounding a mono vacancy. We find that differing orientation angles result in different failure processes and speeds. Additionally, the redistribution at the defective site is chirality-dependent, and there is a significant localization of electronic states at the defective site. The pattern of density of states is deformation-dependent. This talk will present a comprehensive view on the specific effects of electron redistribution on mechanical and electronic characteristics of the defective lattice.

SESSION ST01.04: Deformation Behavior of Low-Dimensional Materials II
Session Chairs: Wendy Gu and Matt Pharr
Sunday Afternoon, April 18, 2021
ST01

4:00 PM *ST01.04.01

Fracture of Two-Dimensional Materials Jun Lou; Rice University, United States

Two-dimensional (2D) materials, such as Graphene, hBN and MoS₂, are promising candidates in a number of advanced functional and structural applications, owing to their exceptional electrical, thermal and mechanical properties. Understanding mechanical properties of 2D materials is critically important for their reliable integration into future electronic, composite and energy storage applications. However, it has been a significant challenge to quantitatively measure mechanical responses of 2D materials, due to technical difficulties in the nanomechanical testing of atomically thin membranes. In this talk, we will report our recent effort to determine the engineering relevant fracture toughness of graphene with pre-existing defects, rather than the intrinsic strength that governs the uniform breaking of atomic bonds in perfect graphene. Our combined experiment and modeling verify the applicability of the classic Griffith theory of brittle fracture to graphene. Strategies on how to improve the fracture resistance in graphene, and the implications of the effects of defects on mechanical properties of other 2D atomic layers will be discussed. More interestingly, stable crack propagation in monolayer 2D *h*-BN is observed and the corresponding crack resistance curve is obtained for the first time in 2D crystals. Inspired by the asymmetric lattice structure of *h*-BN, an intrinsic toughening mechanism without loss of high strength is validated based on theoretical efforts. The crack deflection and branching occur repeatedly due to asymmetric edge elastic properties at the crack tip and edge swapping during crack propagation, which toughens *h*-BN tremendously and enables stable crack propagation not seen in graphene.

4:25 PM ST01.04.02

Anharmonicity and Universal Response of Linear Carbon Chain Mechanical Properties Under Hydrostatic Pressure Keshav Sharma; The University of Alabama, United States

Isolated linear carbon chains (LCCs) encapsulated by multiwalled carbon nanotubes are studied under hydrostatic pressure (P) via resonance Raman scattering. The LCCs' spectroscopic signature C band around 1850 cm^{-1} softens linearly with increasing P. A simple anharmonic force-constant model not only describes such softening but also shows that the LCCs' Young's modulus (E), Grüneisen parameter (γ), and strain (ϵ) follow universal P⁻¹ and P² laws, respectively. In particular, γ also presents a unified behavior for all LCCs. To the best of our knowledge, these are the first results reported on such isolated systems and the first work to explore universal P-dependent responses for LCCs' E, ϵ , and γ .

4:40 PM ST01.04.04

Mechanical Properties of 3D Freestanding DNA-Inorganic Nanostructure Hybrid Haitao Liu¹ and Feng Zhou²; ¹University of Pittsburgh, United States; ²New York University, United States

This talk will present our recent study on the mechanical properties of free-standing wire-frame 3D DNA tetrahedra in air. The structure was coated with a nanometer thick layer of uranyl acetate. The free-standing DNA tetrahedron structure, $93 \pm 2\text{ nm}$ high in air, withstands $42 \pm 22\text{ nN}$ of loading force. The effective hardness ($9.1 \pm 5.1\text{ MPa}$) and Young's modulus ($77 \pm 48\text{ MPa}$) of this low-density (70.7 kg/m^3) DNA nanostructure are comparable to other reported low-density high-strength materials. Our result suggests a new approach to fabricate low density materials.

4:55 PM ST01.04.05

Strain-Resilient Electrical Functionality Enabled by Two-Dimensional Interlayer Chullhee Cho¹, Pilgyu Kang², Amir Taqieddin¹, Yuhang Jing¹, Keong H. Yong¹, Jin Myung Kim¹, Md Farhadul Haque¹, Narayana R. Aluru¹ and SungWoo Nam^{1,1}; ¹University of Illinois at Urbana-Champaign, United States; ²George Mason University, United States

Flexible electrodes suffer unexpected, complete electrical disconnection after the onset of inevitable mechanical fracture across metal thin-films during their uses, severely reducing the functional lifespan of flexible/wearable electronics. Sudden, unperturbed straight in-plane mechanical fracture of metal thin-film was revealed to cause a catastrophic electrical failure of complete disconnection. Here, we report two-dimensional (2D)-interlayer approach that modulates in-plane fracture modes of metals and results in augmented strain-resilient electrical performance of metal thin-film electrodes under a high degree of multimodal deformation. Atomically thin 2D-interlayers, such as semi-metallic graphene, semiconducting MoS₂ and/or insulating hBN, induce continuous in-plane crack deflection (vs. straight) of metal thin-film electrodes and enable unique electrical characteristics which we term 'electrical ductility', where electrical resistance gradually (vs. abruptly) increases with strain allowing extended regions of stable resistance. 2D-interlayer electrodes maintain several orders-of-magnitude ($>10^4\sim 10^5$) lower electrical resistance with resistance locking beyond a strain where conventional metal electrodes would be completely disconnected. Our 2D-interlayer approach is not limited to a certain combination of metals and 2D materials. The electrical ductility enabled by 2D-interlayer offers strategies for early damage diagnosis for the next-generation flexible/wearable electronics preventing abrupt, complete device functional failures.

5:10 PM ST01.02.05

Late News: Crystallographic Anisotropy Dependence of Interfacial Sliding Phenomenon in Nanoindentation of Cu/Nb ARB (Accumulated Rolling Bonding) Nanolayers as Revealed by 4-Axis X-Ray Diffractometer Arief S. Budiman^{1,2}, Rahul Sahay² and Nagarajan Raghavan²; ¹BINUS University, Indonesia; ²Singapore University of Technology and Design, Singapore

Metallic FCC-BCC nanolayers, such as Cu/Nb, have received wide attention due to their extraordinary mechanical properties as well as the unique self-healing capacities due to the interface characteristics. Most recently, the materials have also been shown to exhibit significant and tunable interfacial sliding mechanisms (based on defect structures in the interface). The significant interfacial sliding is all along while maintaining full contact between the layers, and thus one could expect negligible resistance increase upon straining, which would be attractive for stretchable metallic conductor technology. The interfacial sliding has been modeled with some combination of diffusional and displacive mechanisms – the extreme extents of which are afforded by the nanoscale layering in the materials. The exact mechanisms continue to be fully investigated with some of the most cutting-edge materials experimental/characterization techniques as reported in the literature in the past 2-3 years. Nanoindentation has been used widely to investigate mechanical properties of small scale materials such as elastic modulus, hardness and work hardening. In this work, we report a study using nanoindentation with particular emphasis on depth profile (of the indented surface) and the pile-up height upon Berkovich nanoindentation of Cu/Nb nanolayers fabricated by Accumulated Rolling Bonding (ARB) method. The Cu/Nb ARB nanolayers have been reported to have strong anisotropy in mechanical properties in general, but specifically in this study, we show there is strong correlation between pile-up height and the extent of interfacial sliding. Cu/Nb ARB nanolayers (with 16nm individual layer thickness) has been used as a test material due to its crystallographic anisotropy owing to the presence of contrasting interfaces along rolling (RD) and transverse direction (TD). The Cu/Nb ARB nanolayers were first characterized with X-ray Diffraction with 4-axis diffractometer, resulting in complete 3D crystal orientation/texture of the nanolayers. Nanoindentation was then performed along TD as well as RD of ARB Cu/Nb nanolaminate and subsequently Scanning Probe Microscopy (SPM) data was collected to measure the pile-up along RD and TD in the Cu/Nb nanolaminate. The 16 nm Cu/Nb ARB nanolaminate along RD was found to exhibit significantly higher surface pile-up than TD which is attributed to the variation in the Cu/Nb interface-mediated plasticity (sliding, rotation, etc.) along RD and TD, as well as the crystallography and texture of the nanolayers which determine the availability of slip systems in both Cu and Nb crystals. Further, 2D axisymmetric FEA analysis was performed to compare and validate experimental indentation data. The simulated data was found to compare well with the experimentally generated load-displacement curves whereas qualitative agreement was obtained with the experimentally obtained pileup data. The authors believe that the characterization of surface pile-up is of significant importance for enabling the Cu/Nb ARB nanolayers as the novel stretchable metallic conductor technology (for emerging applications such as electronic skins, soft robotics, etc.).

SESSION ST01.05: Nanocomposites
Session Chairs: Wendy Gu and Matt Pharr
Sunday Afternoon, April 18, 2021
ST01

6:30 PM ST01.05.01

Room-Temperature Shear-Banding in CuAl₂-CuAl Intermetallic Composite Yuki Ikeda^{1,2}, Jose Mancias¹ and Robert Maass^{2,1}; ¹University of Illinois at Urbana-Champaign, United States; ²Federal Institute for Materials Research and Testing (BAM), Germany

Intermetallics are generally brittle by nature and exhibit little or no plasticity at ambient conditions. However, lamellar eutectics containing an intermetallic phase, such as CuAl₂-Al, may exhibit room-temperature plasticity due to confinement effects. In this study, we apply the same idea of plasticity confinement to a CuAl system by designing a CuAl₂ matrix containing a nano-scale CuAl-phase via the diffusion-couple approach. This nanocomposite is found to undergo room temperature shear deformation during nano-indentation. The indentation curves exhibit a continuously increasing pop-in size with increasing load, a feature typically not known for crystalline nano-indentation plasticity. High-Angle-Annular-Dark-Field Scanning Transmission Electron Microscopy (HAADF-STEM) observation of deformed regions underneath the indent locations provide

evidence for shear-banding in the otherwise brittle CuAl₂ phase. TEM observations of the microstructure underneath the indent revealed furthermore the existence of a phase with three-fold symmetry, of which we discuss the origin and structure.

6:45 PM ST01.05.02

Fracture Toughness and Nanowear Behavior of Alumina-Yttria Stabilized Zirconia Composites Yuchen Lin and Kaka Ma; Colorado State University, United States

Yttria stabilized zirconia (YSZ) has important applications in thermal barrier coatings, dental implants and ceramic blades. Fracture toughness and wear resistance are two critical mechanical properties that determine the performance of YSZ. Al₂O₃-YSZ composites have the potential to combine the high hardness of Al₂O₃ and the enhanced toughness of the tetragonal phase of zirconia. The present work aimed to investigate the effect of adding Al₂O₃, specifically, the particle size and distribution of Al₂O₃, on the mechanical behavior of YSZ at both micro- and nanoscale, via the combination of micro-indentation, nanoindentation and nanoscratch. Spark plasma sintering was utilized to fabricate the Al₂O₃-YSZ ceramic composites for its rapid densification rate to minimize grain growth. The results show that the as-sintered Al₂O₃-YSZ composites retain the tetragonal zirconia phase and the grain size of the YSZ matrix decreases with increasing amount of Al₂O₃ addition. Enhanced fracture toughness, as high as 11.32 MPa×m^{0.5}, is achieved by tailoring the distribution of the Al₂O₃. Homogeneous distribution of Al₂O₃ with reduced particle size alters the nanoscratch-induced plastic deformation mechanism and increases the wear resistance of the Al₂O₃-YSZ composites.

7:00 PM ST01.05.03

Molecular Dynamics Simulations on the Mechanical Behavior of Multilayer Polymer/Metal Nanostructures Under Impact Loading Nuwan Dewapriya and Ronald Miller; Carleton University, Canada

Even though numerous engineering applications of ultrathin multilayers have already been demonstrated, their mechanical behavior under dynamic loading remains poorly understood. Recent advances in experimental techniques have enabled the dynamic testing of nanoscale films. For example, microprojectile impact tests have revealed that ultrathin polymer films absorb approximately ten times more energy per unit mass during the penetration process than that of traditional bulk armor materials. At the same time, it has been well established that metallic nanostructures possess extraordinary mechanical properties when their characteristic dimension is few nanometers. Therefore, multilayer arrangements of nanoscale polymer and metal films could possess superior ballistic performance, and more importantly, their ballistic performance could even be engineered by altering the relative domain size and the spatial arrangement. We tested this hypothesis by conducting a comprehensive molecular dynamics (MD) study on the ballistic impact response of multilayer aluminum-polyurea nanostructures.

Macroscopic experiments have shown that placing a polymer layer on the back face of a metallic target is more effective in terms of impact energy absorption. In contrast, our MD simulations revealed that placing a nanoscopic polymer layer on the strike face is more effective when the individual layer thickness is in the order of a few nanometers. Furthermore, our dislocation analysis revealed that the polymer layer has a remarkable influence on the dislocation processes in the metallic layer. Moreover, the MD simulations demonstrated that the ballistic limit velocity (V_{50}) and the specific penetration energy of the nanoscale multilayers are significantly higher than the experimentally measured values for any nanomaterial. In order to gain further insights into the nanoscale energy dissipation mechanisms, we computed the V_{50} of the multilayers using two existing membrane models. The results of this study demonstrate a potential bottom-up design pathway for developing new structural barrier materials with superior dynamic properties.

Acknowledgement: This work was supported by the Natural Sciences and Engineering Research Council of Canada.

7:15 PM ST01.05.04

Effect of Co-Deformation of Ceramic Layer in Ag/Al-Doped ZnO Nanolayered Composites DongGyu

Kang, Hyeongyun Nam, Dae ho Kim and Seung Min Han; Korea Advanced Institute of Science and Technology, Korea (the Republic of)

Nanolayered composites composed of metal-ceramic layers have been studied to have high strength by effectively constraining the dislocation motion at the interfaces, but unfortunately, unstable deformation occurs due to the brittleness of the ceramic layer. In this study, In order to investigate the effects of the brittle-to ductile transition of the ceramic layer, we explore the deformation behavior of metal-ceramic nanolayered composites at varying ceramic layer thicknesses. Ag and Al-doped ZnO was chosen for metal-ceramic material system. The thickness of Al-doped ZnO was first fixed at 9 nm, which is theoretically expected to be ductile, and the metal thickness varies from 85 nm to 240 nm. For further comparison with thicker Al-doped ZnO that is expected to be brittle, 150 nm Ag/120 nm Al-doped ZnO was studied. In-situ SEM pillar compression showed stable deformation for 9 nm thick Al-doped ZnO samples, and TEM analysis of the deformed specimen was used to confirm the co-deformation of metal and ceramic. For the same 9 nm thick Al-doped ZnO samples, systematic increase in strength was observed with reduction in Ag thickness from 240 nm to 85 nm. For the 150 nm Ag/120 nm Al-doped ZnO, A brittle fracture of the Al-doped ZnO layer was observed to lead to a reduction in flow stress or strain softening after 30% deformation. Finite element analysis showed that the stress of the Ag and the Al-doped ZnO layer reached the stress required for the co-deformation of the two phases.

7:30 PM ST01.05.05

Effect of Cellulose Nanocrystal and Low Molecular Weight Molecules on the Mechanical Properties of Polyacrylonitrile/Cellulose Nanocrystal Fibers from *In Situ* Polymerization to Carbonization Hyejin Ju, Jung-Eun Lee, Min Jeong Kim and Han Gi Chae; Ulsan National Institute of Science and Technology, Korea (the Republic of)

Cellulose Nanocrystal(CNC) is a naturally abundant environmentally benign material. The large aspect ratio and many hydroxyl groups attached on the surface of CNCs greatly contribute to the orientation of polymer chains when produced as a polymer nanocomposite. In addition, CNC causes a strong interaction with polyacrylonitrile (PAN), a semi-crystalline polymer having nitrile groups used as a carbon fiber precursor, leading to an increase in physical and mechanical properties of polymer nanocomposite.

In the current study, PAN/CNC polymer fibers were prepared through in-situ polymerization by combining CNC to the PAN synthesis. We have conducted the thorough characterizations of CNC dispersion and polymers (molecular weight, molecular weight distribution, rheological properties, and the structure-property of the resulting precursor fibers). The orientation factor of the post-drawn PAN/CNC fiber increased about 2 times compared to the as-spun PAN/CNC fiber, and PAN/CNC fibers by in-situ polymerization had the highest mechanical properties at total draw ratio 18 than mechanical stirred PAN/CNC and control PAN fibers. . In other words, it was confirmed that the fiber with CNC can have high mechanical properties because crystallinity is clearly improved even if it is slightly stretched.

Also, in heat treatment for manufacturing carbon fiber, it is observed that the crystallinity improvement effect by CNC and the influence of low molecular weight molecules with a wide polydispersity index (PDI). These low molecular weight molecules play a role in increasing the intensity ratio of the D and G band (IG/ID) in Raman spectroscopy analysis in the heat treatment. And it confirmed that after carbonization in-situ polymerized PAN/CNC fibers acted as an element capable of having a tensile property value of 1.6 times or more compared to the carbonized control PAN fiber.

This experiment could suggest that the PAN/CNC nanocomposite fiber may be used as a precursor for high-performance carbon fiber.

7:45 PM ST01.05.06

Manufacturing of Bulk Al/rGO Nanolayered Composite by Accumulative Roll Bonding Sieun Choi and Seung Min Han; Korea Advanced Institute of Science and Technology, Korea (the Republic of)

Metal/graphene nanolayered composites are known to have ultra high strength due to the effectiveness of graphene in constraining the dislocation propagation during plastic deformation. Earlier study on

metal/graphene nanolayered composites involved repeated physical vapor deposition of metal and wet-transfer of graphene and the fabrication method, therefore, has limitations in terms of scalability. Powder metallurgy techniques through mixing graphene flakes into metallic powders has also been reported, but the achieved strengthening effect is not as pronounced as in nanolayered composite produced by alternated thin film deposition and graphene transfer layer-by-layer. In this study, we report a scalable fabrication method for Al/reduced graphene oxide (rGO) nanocomposite with interlayer spacing of ~200 nm in the bulk form using Accumulative Roll Bonding (ARB). rGO flakes are first sprayed on the surface of an aluminum sheet of thickness using air-spray gun, and the resulting rGO on Al sheet was used in ARB where the Al sheet was stacked, rolled, sectioned and stacked for subsequent rolling. A bulk Al/rGO nanolayered composite with ~200 nm interlayer spacing was successfully fabricated and the mechanical properties of the developed bulk nanocomposite was analyzed for mechanical properties using nanopillar compression testing to show the strengthening effect in comparison to the specimen prepared using layer-by-layer deposition. In order to study the effectiveness of the Al/rGO interfaces in hindering dislocation motion, deformed nanopillars were analyzed using TEM.

SESSION ST01.06: Fracture and Fatigue of Micro/Nano-Scale Materials

Session Chairs: Wendy Gu and Gi-Dong Sim

Sunday Afternoon, April 18, 2021

ST01

9:00 PM *ST01.06.01

Experimental Study on Fracture Nanomechanics Takayuki Kitamura and Takashi Sumigawa; Kyoto University, Japan

The strength of nanoscale materials is one of key properties in development of advanced devices such as semiconductors, small sensors, and micro- and nano-electromechanical-systems (MEMS and NEMS). It is inevitable to understand their fracture behavior in terms of the mechanics for keeping high reliability in manufacturing as well as in service. Especially, focus must be put on the point that the mechanics and mechanism for materials in nanoscale might be significantly different from that in macroscale counterpart. The internal nanostructures including dislocations, grain boundaries, and various defects strongly affect the mechanical properties coupling with the external structures (geometric factor), shape and size of components. Although there are many excellent papers published on the deformation behavior on the bases of nanoscale experiments, few research works have been conducted on the fracture characteristics. It is mainly due to the difficulty of fracture experiments in nanoscale. For describing the fracture laws of materials in macroscale, it is essential to understand the fracture characteristics under diverse fracture mechanism including toughness, fatigue, creep and so on. We have conducted various fracture experiments with *in situ* SEM/TEM observation. In this lecture, we present two topics on the experimental study in terms of the fracture nanomechanics. Smallest applicable limit of the conventional fracture mechanics [T.Sumigawa *et al*, ACS Nano, 11, p. 6271, 2017]

Fracture of bulk brittle materials such as silicon is characterized by cracking and the mechanics is well explained by the singular stress field formed near the crack tip according to the fracture mechanics (Griffith) theory. The applicability of these continuum-based theories is, however, uncertain and questionable in a nanoscale system due to its extremely small singular stress field of only a few nanometers. We directly conduct *in situ* fracture toughness testing for silicon specimens with a nanocrack using a transmission electron microscope and demonstrate that the Griffith theory can be applied to even 4 nm stress singularity despite their continuum-based concept. We show that the fracture toughness of clean silicon is independent of the dimension of materials and therefore inherent. Quantum mechanics/atomistic modeling explains and provides insight into these experimental results. It also shows that the limit is on around 2-3nm. This work therefore provides a fundamental understanding of fracture criterion and fracture properties in brittle nanomaterials.

Fatigue process of small metal [T.Sumigawa *et al*, Acta Materialia, 153, p.270, 2018]

We develop an *in situ* scanning electron microscope observation technique of micron-scale metal specimens under fully-reversed tension-compression cyclic loading and investigate the unique cracking process in low-cycle fatigue of single crystal copper in micron scale under a constant displacement amplitude. While crystallographic slips spread over the entire test section during the tensile first half-cycle, a locally concentrated slip band appears during the first reverse loading (compression). Crystallographic slip takes place only near the localized band in consecutive cycles, and strain localization due to slip bands leads to nanoscale extrusion/intrusion at the surface. This indicates that, unlike during the fatigue of a typical bulk pure metal, no characteristic dislocation substructure is formed during the extrusion/intrusion process. Moreover, the process required a much higher stress amplitude than in the case of bulk copper specimen. Thus, the fatigue cracking process for copper micro-scale specimen differs significantly from that for bulk copper specimen.

9:25 PM ST01.06.02

A Combined Atomistic-Continuum Model to Examine Interfacial Fracture in Multilayer Ceramics

Aniruddh Vashisth¹ and Mirmilad Mirsayar²; ¹University of Washington, United States; ²Florida Institute of Technology, United States

Ceramic composites have various applications ranging from medical to high-temperature aerospace structures. These multi-material composites usually have two brittle materials sharing a bonded interface. For example, ceramic composites with SiC/SiO₂ interface find applications as microelectronics in semiconductors. However, like other bonded components, performance challenges are inevitable due to the high density of defects existing at SiC/SiO₂ composite interface. A crack or defect can be initiated at the interface during fabrication or as a result of residual mechanical/thermal stresses between the two components. We developed a multi-scale model that simulates the mechanics of interfacial fracture at a strong interface by combining reactive molecular dynamics (ReaxFF) and continuum fracture theory.

Cracks existing in strong interfaces tend to propagate out of interface under mixed-mode (i.e., combined opening/sliding) loading conditions. As temperature varies, the material properties change, thereby affecting the interfacial crack propagation behavior. The mechanical response of both the constitutive materials, namely silicon carbide and amorphous silica, was simulated within a temperature range of 300–1200 K. Amorphous silica (SiO₂) shows a continuous decrease in modulus and strength with increasing temperatures. The modulus of silicon carbide (SiC) plateau between 700 and 900 K while its strength drops continuously as temperature increases. Next, using a multi-scale modeling approach, these temperature-dependent properties are used as inputs to a continuum-based model to investigate fracture behavior as a function of temperature; by employing maximum tangential stress (MTS) criterion.

We found that altering the ambient temperature influences the interfacial fracture toughness in all crack tip deformation modes (pure mode I, mixed-mode I/II, and pure mode II). Depending on the imperfection level, the limits depicted in the mixed-mode fracture toughness curves should vary. It is worth mentioning that the current research was a preliminary analysis, and other significant parameters such as specimen geometry require additional investigations. Depending on the specimen geometry and applied loading configuration, the coefficients of the higher-order terms in the crack tip stress field may also be important in the fracture criteria as well as the singular terms. Future investigations will look into combined environmental and geometric effects for various materials, not only for ceramic composites but also for advanced composites.

9:40 PM ST01.06.03

Enhancing the Fracture Toughness of Polymer-Infiltrated Nanoparticle Films via Polymer Bridging and Entanglement Yiwei Qiang, Daeyeon Lee and Kevin Turner; University of Pennsylvania, United States

The mechanical properties of disordered nanoparticle (NP) packings can be significantly improved through the infiltration of polymers to enhance the interactions between the NPs. Previous work has shown that capillary rise infiltration (CaRI) is a simple and highly effective route to stiffen, harden, and toughen NP packings. While results from previous nanoindentation-based fracture measurements suggest that polymer infiltration can improve the toughness of NP films, it is challenging to fully understand how the relative size of polymer and

nanoparticles and the extent of confinement affect the toughness using nanoindentation-based measurements of fracture toughness. In the present work, a thin-film fracture testing method based on the double cantilever beam (DCB) specimen is developed and used to investigate the fracture properties of polymer-infiltrated nanoparticle films. In the DCB specimen, a crack is propagated in NP films over distances of tens of millimeters, allowing for highly accurate measurements of toughness in a mode I (tensile opening) configuration. The fracture toughness of the polymer-infiltrated NP films is found to be strongly dependent on polymer molecular weight (MW) and NP size. Low MW, unentangled polymers, effectively toughen small NP packings; whereas high MW, entangled polymers, show enhanced toughening in large NP packings. Possible toughening mechanisms, including confinement-induced polymer bridging and polymer entanglement, will be discussed.

9:55 PM *ST01.06.06

Fracture and Plasticity of Nano-Sized Brittle Materials Dongchan Jang¹ and Dahye Shin^{1,2}; ¹Korea Advanced Institute of Science and Technology, Korea (the Republic of); ²Korea Research Institute of Standards and Science, Korea (the Republic of)

Most of the brittle materials are usually very vulnerable to the existence of the crack because a lack of the intrinsic toughening mechanism, such as tip blunting by the plastic deformation, renders it to propagate unimpededly once a critical condition is reached. Therefore, most of the efforts to mitigate the sudden failure of brittle ceramics have been focused on developing the extrinsic toughening mechanisms that hinder crack propagation behind the tip, such as the fiber bridging. In this work, we experimentally demonstrate that the intrinsic toughening arises even in the brittle monolithic ceramic material like diamond-like carbon (DLC) when its external dimension reduces down to sub-micron scales. This unique phenomenon owes its origin to the decrease of the crack driving force in the small samples, which in turn enables them to bear high enough stresses to activate the local atomic plasticity. Through nanomechanical tensile and bending experiments, electron energy loss spectroscopy analysis and finite element method for stress distribution calculation, we confirmed that the local atomic plasticity associated with sp^3 to sp^2 rehybridization is responsible for the intrinsic toughening.

SESSION ST01.07: Integration of Micro/Nano-Scale Materials into Applications and Devices I
Session Chairs: Jagannathan Rajagopalan and Gi-Dong Sim
Monday Morning, April 19, 2021
ST01

8:00 AM *ST01.07.01

Programmable Materials—A New Materials' Design Space? Franziska Wenz^{1,2}, Ingo Schmidt¹, Alexander Lechner³, Tobias Lichti³, Sascha Baumann⁴, Heiko Andrä³ and Christoph Eberl^{1,2}; ¹Fraunhofer IWM, Germany; ²Universität Freiburg, Germany; ³Fraunhofer ITWM, Germany; ⁴Fraunhofer ICT, Germany

Today's materials design space reaches from electronic structure to microstructure and metamaterials structured on a mesoscopic scale. Nevertheless, the aim is typically to implement novel properties or tune them to a specific task. Instead, Programmable Materials aim to design materials' behavior and let them interact and adapt to the environment. In this talk, an outline will be given how this new design space could be approached and structured. The approach is based on translating physical and mechanical mechanisms into classes similar to modern programming languages. Materials' specific molecular and mechanical mechanisms will be discussed which enable Programmable Materials to process information or specific user interactions. For a concerted behavior, the interaction between compartmentalized unit cells needs to be finely tuned. Based on simulations and optimization routines, local programming of mechanical metamaterials can be used to implement complex shape morphing into 3D-printed parts. Furthermore, possible routes for mass manufacturing Programmable Materials will be presented.

8:25 AM ST01.07.02

Vertical Graphene—*In Vivo* Biocompatible Strain Sensor Sunghun Lee¹, Seung-Hyun Chun¹, C-Yoon Kim² and Yong Ju Yun³; ¹Sejong University, Korea (the Republic of); ²Konkuk University, Korea (the Republic of); ³Korea University, Korea (the Republic of)

Resistive strain sensors (RSS) with ultrasensitivity has been investigated for widespread applications. However, due to physical/mechanical limits, the development of mechanosensors satisfying the prerequisite of stability, durability and controllability remains a challenge. Also, in-depth toxicology in *in vivo* system is imperative because of in direct contact with skin, even applied to organs, yet has not been reported for RSS. Here, we demonstrate that vertical graphene (VG) RSS can serve *in vivo* biocompatible sensors, and show remarkable sensitivity (gauge factor of 5,000) with revivable status even after broken current path. Three-dimensional tufted VG network structure allowed charge transport depending on crack geometry. We further showed that the signals from rat heartbeat depend on the direction of VG sensor directly attached to the heart, enabling to distinguish the cardiac contractility through its ventricle and atrium. Our finding provides new insight for controllable and permanent mechanosensing system, making VG promising option for *in vivo* biocompatible platform.

8:40 AM ST01.07.03

Measurement of Acoustic Emission Using Ti₃C₂-MXene Films Krzysztof Grabowski¹, Pavitra Belthangadi², Shreyas Srivatsa¹, Prosenjit Sen², Tadeusz Uhl¹, Saurabh Kumar² and Manjunath M. Nayak²; ¹AGH University of Science and Technology, Poland; ²Indian Institute of Science, India

Structural Health Monitoring (SHM) of engineering structures involves damage detection and monitoring during its life-cycle. One of the phenomena used to detect changes within the structure is Acoustic Emission (AE). Structure undergoing the damage mechanism releases the energy in the form of elastic waves. These elastic waves propagating in a structure when captured could be used to characterize and localize the damage. In this work, we demonstrate the measurement of AE waves using the capabilities of two-dimensional nanomaterials - Titanium Carbide MXene (Ti₃C₂-MXene) films. Ti₃C₂-MXenes, discovered in 2011, have good electromechanical properties, film-forming ability, piezoresistivity, and relatively good dynamic response behavior to impact loads. Utilizing these properties of Ti₃C₂-MXene, we subject the films to the Hsu-Nielsen source. The test is performed with the pencil lead in contact with the Ti₃C₂-MXene film sample and the breakage of the pencil lead (which generates the acoustic wave) is detected by the Ti₃C₂-MXene film. Sensors based on Ti₃C₂-MXene can be deposited on the surface of the structure as a coating or potentially as a thin film layer. Ti₃C₂-MXene with its dynamic response properties provide a wide range of opportunities for SHM applications and these are discussed with the experimental results.

8:55 AM ST01.07.04

Printable Magneto-resistive Sensors for On-Skin Interactive Electronics Eduardo Sergio Oliveros Mata¹, Gilbert Santiago Canon Bermudez¹, Minjeong Ha², Yevhen Zabala³, Jürgen Faßbender¹ and Denys Makarov¹; ¹Helmholtz-Zentrum Dresden-Rossendorf, Germany; ²Electronics and Telecommunications Research Institute, Korea (the Republic of); ³Polish Academy of Sciences, Poland

Ultra-portable, imperceptible^[1], and shapeable^[2] devices are expected to be widespread due to the emergence of flexible electronics as an industrial technology^[3,4]. Printing is an affordable and high throughput method to process electronics in soft substrates that is still to be optimized to deliver electrically and mechanically reliable electronic devices^[5].

In particular, printable magneto-resistive pastes have been developed as an alternative single-step fabrication method to obtain magnetic field sensors^[6]. These pastes usually consist of composites of magnetic particles embedded in a non-magnetic matrix^[7,8]. Particle-based pastes can achieve large magneto-resistance ratios at the expense of high resistivity and noise levels^[7-9]. Previously, Karnaushenko et al. reported magneto-resistive

pastes based on giant magnetoresistive (GMR) microflakes as an alternative to overcome the problems presented in particle-based pastes^[10,11]. Magnetoresistive flakes were produced after the delamination of thin-film stacks from a deposited sacrificial layer. With this technology, it was shown that flakes-based Co/Cu printed sensors exhibit low resistance and 37% GMR response at moderate magnetic fields (500 mT)^[11].

Despite the advances in printable magnetic sensors, there are no reports of systems that show good sensitivity at low magnetic fields relevant for safe integration into wearable electronics. Electronics with magnetic components have to perform below the WHO limit of continuous exposure to magnetic fields (<40mT) to comply with this health standard^[12]. Furthermore, for on-skin electronics that experience considerable strain, there are not examples of magnetic printed sensors that deliver steady sensing behaviour upon mechanical stretching.

Here, we will present low-noise printable magnetic field sensors sensitive down to sub-mT, which are mechanically stretchable after printing. We demonstrate the fabrication of printable sensors in ultrathin foils (3- μm -thick Mylar) based on magnetoresistive pastes that can undergo 100 % strain and 16 μm bending radius maintaining stable sensing and mechanical performance. The pastes are composites of poly(styrene-butadiene-styrene) copolymer (SBS) with embedded magnetoresistive microflakes. Using [Py/Cu]₃₀ and [Ta/Py] flakes, we obtained printed GMR and anisotropic magnetoresistive (AMR) sensors, respectively. We address the key role of SBS to enable an enhancement of two orders of magnitude improvement in bendability and sensitivity at low magnetic fields.

Due to the good performance at low fields, reduced noise levels and high compliance, we will show the direct lamination of the printed sensors as an on-skin interactive device for scrolling through documents or digital maps. We envision that the proposed magnetic sensors will enable printing on-demand utilities for physical activity tracking systems or human-machine interfaces that can improve and even expand our sensing capabilities.

- [1] M. Melzer et al., *Nat. Commun.* **6**, 6080 (2015)
- [2] D. Makarov et al., *Appl. Phys. Rev.* **3**, 011101 (2016)
- [3] S. Huang et al., *Adv. Funct. Mater.* **29**, 1805924 (2019)
- [4] W. Wu, *Sci. Technol. Adv. Mater.* **20**, 187 (2019)
- [5] Q. Huang et al., *Adv. Mater. Technol.* **4**, 1800546 (2019)
- [6] D. Makarov et al., *ChemPhysChem* **14**, 1771 (2013)
- [7] J. Meyer et al., *Smart Mater. Struct.* **22**, 025032 (2013)
- [8] J. L. Mietta et al., *Langmuir* **28**, 6985 (2012)
- [9] L. Ding et al. *ACS Appl. Mater. Interfaces* **12**, 20955 (2020)
- [10] D. Karnaushenko et al., *Adv. Mater.* **24**, 4518 (2012)
- [11] D. Karnaushenko et al., *Adv. Mater.* **27**, 880 (2015)
- [12] World Health Organization, Static fields (2006)

9:10 AM ST01.07.05

ZnO Nanostructures in SAW Sensing Aurelian Marcu¹, Razvan Mihalcea¹, Cosmin Samoil², Emil Slushanschi², Viorel Chihai³, Ionut Nicolae¹ and Cristian Viespe¹; ¹National Institute for Laser Plasma and Radiation Physics, Romania; ²University Politehnica of Bucharest, Romania; ³National Institute of Physical Chemistry "Ilie Murgulescu", Romania

Sensors are a key issue in the present technological development and Surface Acoustic Wave (SAW) sensing is just one of the development directions in fluids detection with application from security to industry and medicine. Depending of the fluid composition there are various sensor types and used materials but all of them are basing their functionality on the mechanical and structural properties changes of an 'active layer' material in the presence of the detected fluid. Nanostructure or nanostructured materials present a series of enhanced properties compared with the bulk materials, due to the high surface-to-volume ration but their specific

parameters are sometimes rather challenging to control for optimizing sensor performances. For SAW sensor fabrication we use ZnO material as a versatile bio-compatible wide band-gap semiconductor, with a good absorption of various gases including hydrogen isotopes. Through the 'Bottom-UP' approach, we use Pulsed Laser Deposition (PLD) - Vapour-Liquid-Solid (VLS) techniques to grow ZnO single crystal [0001] nanowires on sensor patterned active surface area. By controlling several experimental parameters and respectively VLS grow elementary processes we control nanowires morpho-structural properties. Some correlations between these parameters and sensor experimental response are presented. Results interpretation is presented together with few wave propagation theoretical modeling through the sensor active area and respectively simulations on ZnO nanowire absorption. Presented results are aimed for SAW applications in gas detection and pressure measurement and are exemplified for hydrogen isotopes detection.

9:25 AM ST01.06.05

Compliance Grading Motif in Nacre for Enhanced Structural Performance S Kumar; University of Glasgow, United Kingdom

Natural materials exhibit high specific toughness, strength, stiffness and impact resistance¹. The excellent properties of many such natural materials are attributed to hierarchical arrangement of their structure and spatial material gradients at different length scales². Nacre- an iridescent material, exhibits enhanced strength and toughness though it majorly (>95vol.%) comprises an extremely brittle phase (aragonite)³. Nacreous structures show extraordinary toughness due to sliding of the bricks (macroscopic work hardening) over neighboring bricks together with other energy dissipation processes such as crack deflection, micro cracking and crack bridging⁵. Failure in such nacreous materials usually initiates in structurally weak mortar near the corners of the bricks where steep stress gradients exist. In this study, we introduce compliant grading motif (CGM) observed in many natural materials such as spider fang, byssal thread and squid beak, in the mortar of nacreous structure utilizing multimaterial additive manufacturing (AM). We postulate that the CGMs in mortar could play a role in toughening and strengthening the nacreous system by diffusing the peak stresses and moving the stress concentration away from the potential failure zones. Mechanical performance assessment of the AM realized nacreous structures with CGMs in mortar show ~60% improvement in strength, ~ 70% in toughness, and ~30% in strain-to-break, while retaining the macroscopic stiffness. The nature inspired CGMs introduced here is easily realizable in a wide range of 3D printing techniques for developing high performance architected materials with unprecedented properties.

References

- (1) Gu, G. X.; Takaffoli, M.; Hsieh, A. J.; Buehler, M. J. Biomimetic Additive Manufactured Polymer Composites for Improved Impact Resistance. *Extreme Mechanics Letters* **2016**, *9*, 317-323.
- (2) Studart, A. R. Biological and Bioinspired Composites with Spatially Tunable Heterogeneous Architectures. *Adv. Funct. Mater.* **2013**, *23* (36), 4423-4436.
- (3) Munch, E.; Launey, M. E.; Alsem, D. H.; Saiz, E.; Tomsia, A. P.; Ritchie, R. O. Tough, Bio-Inspired Hybrid Materials. *Science* **2008**, *322* (5907), 1516-1520.
- (4) Rabiei, R.; Bekah, S.; Barthelat, F. Acta Biomaterialia Failure Mode Transition in Nacre and Bone-Like Materials. *Acta Biomaterialia* **2010**, *6*, 4081-4089.
- (5) Nalla, R.; Kinney, J.; Ritchie, R. Effect of Orientation on the in Vitro Fracture Toughness of Dentin: The Role of Toughening Mechanisms. *Biomaterials* **2003**, *24* (22), 3955-3968.

SESSION ST01.08: Integration of Micro/Nano-Scale Materials into Applications and Devices II
Session Chairs: Matt Pharr and Jagannathan Rajagopalan
Monday Morning, April 19, 2021
ST01

10:30 AM ST01.08.01

Carbon Fiber-Aluminum Sandwich Plates with Microscale Thickness for Microflyers and Miniature Robots Wujoon Cha, Luke Kasper, Matthew F. Campbell, Thomas Celenza, George A. Popov, Jeremy Wang, Cynthia Sung, Mark Yim and Igor Bargatin; University of Pennsylvania, United States

We have developed hollow carbon fiber-aluminum sandwich plates with high strength-to-weight ratios and microscale thicknesses that can serve as structural components in microflyers and miniature robots. These panels consist of perforated aluminum sheet cores fixed between face plates of carbon fiber-reinforced polymer using epoxy. This combination of aluminum and carbon fiber exhibits both high impact resistance and high specific stiffness and strength^{1,2} with areal densities of only 100-200 mg/cm² and normalized flexural rigidity values of up to ~7 N-m. Our work represents a simple and inexpensive platform for creating structural components of microflyers and small robots.

Emerging micro-aerial vehicles and small-scale robots require low-weight materials with sufficient structural rigidity to survive substantial collisions^{3,4}. This is difficult to achieve because thin light-weight elements suffer from low bending stiffness, which scales cubically with plate thickness. Because of this, sandwich composite plates with lightweight cores and rigid face sheets are widely used to achieve enhanced resistance to bending while maintaining low weight. Although there have been many efforts in creating sandwich plates with microscale thickness^{5,6}, many require costly and complicated microfabrication. For quick prototyping of mesoscale devices, such as microflyers and small robots, more straightforward methods of producing sandwich plate materials are required.

To fill this gap, we have developed sandwich plates whose faces are carbon-fiber reinforced polymer veneers and cores are aluminum sheets. This combination results in high strength with resistance to the brittle fracture failures that characterize single carbon fiber veneers. We fabricate these plates by using time-curing two-part epoxy to bond 300- μ m thick carbon fiber weaves to both sides of a 300- μ m thick aluminum sheet. To reduce the weight of our plates, we use waterjet cutting to remove material from the aluminum sheet, yielding a low-density honeycomb-patterned core spacer.

To test our specimens, we subject them to three-point bending experiments in which we monitor their mechanical properties as a function of the plates' micro- and macro-scale geometry and composition, and subsequently we compare our results with finite element simulations. Our results reveal that the flexural rigidity values of our sandwich plates are enhanced by 1 to 2 orders of magnitude relative to those theoretically expected from carbon fiber veneers alone. We are currently exploring more aggressive mass-reducing methods, such as decreasing the fill factor of the aluminum honeycomb core and reducing the volume fraction of epoxy in the composite. Although we are currently investigating aluminum cores, our method can be easily adapted for other lightweight cores, such as a laser-micromachined polyurethane layers.

- 1) Aslan *Pam. Univ. J. Eng. Sci.* 24(2018)1062
- 2) Tamilarasan *Mat. Res.* 18(2015)1029
- 3) Sareh *Sci. Robot.* 3(2018)EAAH5228
- 4) Mulgaonkar *IDETC-CIE* (2015)47864
- 5) Arias *J. Mat. Res.* 16(2011)597
- 6) Kolodziejska *APL Mat.* 3(2015)050701

This material is based upon work supported by the Defense Advanced Research Projects Agency (DARPA) under Contract No. HR0011-19-C-0052. Any opinions, findings and conclusions or recommendations expressed in this material are those of the author(s) and do not necessarily reflect the views of the DARPA. Approved for Public Release, Distribution Unlimited.

10:45 AM ST01.08.02

Mechanical Behavior of Kirigami-Inspired Three-Dimensional Polymer Structures Jungkyu Lee¹, Kian

Bashandeh² and Andreas Polycarpou²; ¹Bruker Nano Surfaces, United States; ²Texas A&M University, United States

By using kirigami-inspired structures, highly deformable microscale shape memory polymer structures can be realized. These have a variety of applications in the wearable electronics, biomedical, and aerospace industries. Since many types of structures can be made, a complex assortment of mechanical responses can be observed. Since it's desirable to measure and verify performance, a sensitive mechanical testing instrument is needed. To that end, we fabricated various three-dimensional shape memory polymer (SMP) structures composed of epoxy monomers and studied their mechanical behavior using a nanoindentation instrument. Several important mechanical responses, such as load bearing capacity, hysteresis, and the effect of pre-existing cracks were investigated in detail. Full load-displacement curves were determined for the various structures, both at room temperature and an elevated temperature of 72 °C using a heating stage. The experimental results were coupling with modeling, which was performed to examine the internal stress distributions of the structure under compression conditions, both at room temperature and elevated temperature. This study demonstrates with detail how the mechanical performance of kirigami structures is significantly altered by its design.

11:00 AM ST01.08.03

Strain Sensing and Electrically-Conductive Kevlar-Reinforced Composites Enabled by Atomic Layer Deposition Robin E. Rodríguez¹, Tae H. Lee¹, Yuxin Chen¹, Tae H. Cho¹, Claire Huang¹, Eric Kazyak¹, Andrea Poli¹, William S. LePage², Mihaela Banu¹, M. D. Thouless^{1,1} and Neil P. Dasgupta^{1,1}; ¹University of Michigan–Ann Arbor, United States; ²The University of Tulsa, United States

There is a growing motivation to impart electrical properties into polymer fibers and textile structures, in order to enable multi-functional composites¹. A common approach to manufacturing electrically-conductive fiber-reinforced polymer-matrix composites (PMCs) is to modify the matrix polymer with conductive additives. However, these particle additives can affect the bulk mechanical properties of the final product, which may not be desired. An alternative method to impart electrical conductivity without significantly affecting the bulk mechanical properties is to modify the surface of the fibers by adding a thin, conductive coating. Among the coating techniques that can be utilized, atomic layer deposition (ALD) is an attractive technology that provides unparalleled conformality and sub-nanometer resolution in film thickness and composition.

In this work we demonstrate the fabrication of electrically-conductive Kevlar-reinforced PMCs without measurably affecting the bulk material properties, by pre-coating Kevlar 49 fabrics with aluminum-doped zinc oxide (AZO) via ALD. The core-shell fabric morphology and structure were characterized by SEM, XPS, and XRD. Four-point probe cyclic voltammetry measurements were performed to measure the electrical resistance of the AZO-coated Kevlar. Measurements were taken at both the single-fiber and fabric scales, after varying the thickness of AZO from 40-120 nm. At 40 nm the Kevlar fabric exhibits a low electrical conductivity, which is attributed to the film morphology. As the film thickness increases, the sheet resistance decreases, reaching a value 55.1 Ω/sq at 120 nm. The thickness-dependence of conductivity is well described by an analytical model, which allows for predictive design. This is sufficiently conductive to serves as an electrode material in textile-based devices ranging from thin-film electronics to energy storage devices.

Additionally, we studied the electrical conductivity and strain-sensing capabilities of AZO-coated Kevlar fabrics in PMCs. We demonstrate the potential for these conductive composites in strain-sensing and damage-monitoring applications. The electrical resistance of the sample was continually monitored *in-situ* while loading the sample to failure in a tensile load frame. The average ultimate tensile strength and Young's modulus of the Kevlar-reinforced PMC was not affected by AZO interface coatings, illustrating the advantage of this approach over bulk conductive additives. Furthermore, significant changes in the electrical resistance $(R-R_0)/R_0$ as a function of the strain were observed. These results demonstrate the potential of AZO-coated Kevlar to monitor the strain and provide electrical feedback during the linear elastic regime of the composite, which could be used for structural health monitoring prior to failure.

References

1. Sabetzadeh, N.; Najar, S. S.; Bahrami, S. H. Electrical Conductivity of Vapor-Grown Carbon Nanofiber/Polyester Textile-Based Composites. *J. Appl. Polym. Sci.* 2013, 130 (4), 3009-30017. <https://doi.org/10.1002/app.39447>.

11:15 AM ST01.08.04

Late News: Soft Nanofiber Forests Embedded in Liquid Crystals—Sharing of Strain and Emergent Electrooptical Properties Sangchul Roh¹, John Kim², Divya Varadharajan³, Joerg Lahann^{2,3} and Nicholas L. Abbott¹; ¹Cornell University, United States; ²University of Michigan—Ann Arbor, United States; ³Karlsruhe Institute of Technology (KIT), Germany

We report the synthesis of surface-attached nanofibers by chemical vapor polymerization of 4-hydroxymethyl-[2,2]paracyclophane into films of nematic liquid crystals (LC) (4-(trans-4-pentylcyclohexyl) benzonitrile and 4-(trans-4-propylcyclohexyl) benzonitrile) supported on indium tin oxide (ITO)-coated glass. Dense arrays of end-attached polymeric nanofibers are observed to form with shapes programmed by the strain engineered into the confined LC film. Upon application of an electric field across the LC-nanofiber film, we observe reorganization of the LC to be coupled to the deformation of the soft nanofibers, generating an electrooptical response that reflects coupling of elastic strain in both the LC and nanofiber. We construct a microscopic electromechanical model that captures the transmission of torques between the LC and nanofibers. We also observe patterned orientations of LCs to lead to patterned arrays of nanofibers (e.g., defining mesoscale vortices) during synthesis, which generate complex electro-optical responses that arise from elastic energy stored in both the LC and nanofiber arrays. Overall, these results reveal that LC-templated nanofiber arrays offer a promising route to optical metamaterials with emergent properties generated by the sharing of strain between soft nanofibers and LCs.

11:30 AM *ST01.08.05

Linking Local and Global Strains—From Films to Lattices Mitra Taheri; Johns Hopkins University, United States

In the quest for improved materials, length scale effects are an option for tuning properties. Reduction in grain size can increase strength and manipulation of strut size and distribution in lattice structures can alter myriad properties. A key challenge in using length scale as a tuning parameter is understanding stresses and strains across scales to inform the design process. This talk reviews recent work that leverages a suite of spatially resolved, electron imaging, diffraction, and spectroscopy techniques to correlate global and local strains and stresses. Specifically, linking grain to subgrain scales is addressed. The work presented describes a platform for reliable, multiscale tuning in systems such as additively manufactured materials, high entropy alloys, and fine-grained metals.

11:55 AM ST01.05.07

Late News: Characterization of Wear Debris from Carbon-Carbon Composites in Braking Applications Matthew Noor^{1,2}, Peter Filip², Neil Murdie³, Yanmei Piao³, Angela Walker¹ and Jeffrey Fagan¹; ¹National Institute of Standards and Technology, United States; ²Southern Illinois University, United States; ³Honeywell International, United States

Carbon-carbon (C-C) composites are often used as friction and brake materials due to their high strength, low density, excellent frictional properties, high thermal conductivity and high heat capacity. When worn, C-C composites produce particulate wear debris. The fine wear debris particles then form a layer on the wear surface, known as a friction film layer, which has the potential to change the overall frictional performance of the system. The size, shape and chemistry of these wear debris particles and friction layers can give information about the mechanisms of wear in the composite and the effects of temperature, humidity, oxidation and other chemical modifications that can occur depending on the wear environment. However, this analysis is rather

difficult to perform due to the wide range of particle size, from small nanoscale primary particles to large microscale aggregates. The chemical and material similarities of the carbon fiber and matrix further complicates decoupling the effects of the different components of wear debris on performance. This research explores particle separation and characterization techniques to obtain information about the C-C wear process. The principle technique for particle separation is density gradient ultra-centrifugation (DGU) in which fibrous and matrix-rich particles are separated based on their density. Orthogonal analysis with Raman and UV-vis spectroscopy, optical and electron microscopy, and X-ray Photoelectron spectroscopy can then be made on separated aliquots. Understanding the properties of the wear particles and friction film gives information about the wear process and can help inform future design and material considerations.

SESSION ST01.09: Micro/Nano-Scale Characterization and Mechanics I

Session Chairs: Matt Pharr and Jagannathan Rajagopalan

Monday Afternoon, April 19, 2021

ST01

1:00 PM ST01.09.01

Late News: Studying the Surface and Residual Stress Effects in the Bending Response of Silicon Nanowires—Testing and Modeling [Sina Zarepakzad](#)¹, Mohammad Nasr Esfahani², Zuhail Tasdemir³, Nicole Wollschläger⁴, XueFei Li⁵, Taotao Li⁵, Mustafa Yilmaz¹, Yusuf Leblebici^{6,7} and B. Erdem Alaca^{1,1}; ¹Koc University, Turkey; ²University of York, United Kingdom; ³Paul Scherrer Institute, Switzerland; ⁴Bundesanstalt für Materialforschung und -prüfung, Germany; ⁵Nanjing University, China; ⁶Swiss Federal Institute of Technology – Lausanne (EPFL), Switzerland; ⁷Sabancı University, Turkey

Nanowires (NWs) are frequently employed as critical components in innovative devices including gate-all-around transistors and next-generation mass spectrometers. Despite all their promising aspects, the level of commercialization of such new technologies remains surprisingly low. There has been a vast effort towards the characterization of materials behavior at the nanoscale while a lot of improvement remains to be accomplished depending on the optimization or development of NW fabrication technologies, physical characterization tests, and integration techniques. Mechanical characterization of NWs considered as building blocks of nanoelectromechanical systems (NEMS) is mainly carried out through tensile or bending tests. The interpretation of test data obtained through such experimental measurements necessitates a comprehensive modeling effort to address the current challenge of understanding the size-dependent behavior of NWs. For instance, modeling of NW deformation at the atomistic level predicts size-dependent elastic properties for NWs only with cross-sectional dimensions less than ~10 nm. We undertake such a study by investigating the elastic modulus of Si NWs with a critical dimension of 28 nm via three-point bending test. Testing effort is accompanied by a comprehensive non-linear model of NW bending, including surface and intrinsic stress effects. The model considers all relevant effects including large deformations, intrinsic stresses, and surface effect with native oxide. The presence of intrinsic stresses is studied through micro-Raman spectroscopy with a precise evaluation of strain profile in the structure. Raman mapping was performed for analysis of the spectra as a line scan along the NW where residual stresses were quantified. In addition, we examine the surface effect by implementing the surface stress and surface elastic through atomistic simulations coupled with the continuum model by introducing the presence of native oxide layer covering the silicon NW. The native oxide structure is characterized through high-resolution transmission electron microscopy where inclusion of oxide layer effect into calculations verifies that the size effect is postulated to be primarily a result of differences in the NW surface and core elastic moduli. An in-depth understanding of the surface effect in NW mechanical properties is a critical step which requires an extensive mechanical analysis including all effective parameters in the deformation behavior of NWs. Overall, the study presents a comprehensive model for completely considering effects from axial extension, surface effect, and intrinsic stress to tackle the bending response of Si NWs.

1:15 PM ST01.09.02

Late News: Mechanical Behavior of ZrTa Metallic Glass Thin Films and Nanolayered Composites Ali Bagheri Behboud¹, Amir Motallebzadeh² and Sezer Ozerinc¹; ¹Middle East Technical University, Turkey; ²Koç University, Turkey

Metallic glasses are alloys that exhibit a disordered atomic structure. The lack of dislocations makes these materials stronger and harder than their crystalline counterparts. Furthermore, the lack of grain boundaries provides a desirable microstructure for corrosion resistance. Therefore, metallic glasses provide a promising design space for the development of wear-resistant and corrosion-resistant coatings.

Magnetron sputtering of thin films provides binary metallic glasses over wide compositional ranges due to the process's ultra-fast cooling rates. As a result, the sputtering approach enables systematic studies exploring the effect of composition on metallic glass thin films' mechanical behavior. Zr-Ta is one of the promising systems for coating applications, whose constituent elements possess desirable properties of high strength, biocompatibility, and corrosion resistance. However, there has been no study to date focusing on this binary system and its potential as a metallic glass coating. In this work, we explored the structure-property relationships of magnetron sputtered ZrTa metallic glasses.

A magnetron sputterer deposited 1 μm -thick films of ZrTa on oxidized silicon substrates. We employed combinatorial sputtering, which provided a wide range of compositions at a single deposition step. EDS measurements verified the composition, and X-ray diffraction characterized the microstructure. Transmission electron microscopy analyzed selected compositions in further detail. Nanoindentation with Berkovich and cube corner tips determined the elastic modulus, hardness, and fracture toughness of the specimens.

EDS measurements show that the Zr content varies between 21 and 70 at.%. For Zr contents below 30 at.%, the microstructure includes nanocrystalline and amorphous domains. For Zr in the range of 30 to 70 at.%, the microstructure becomes fully XRD-amorphous. Nanoindentation measurements exhibit a monotonic decrease of elastic modulus and hardness with increasing Zr content. For the amorphous films, hardness varies in the range of 5.5 – 9 GPa, and elastic modulus varies in the range of 105 – 130 GPa. Energy-based analysis of nanoindentation data provided the fracture toughness of the coatings. Fracture toughness decreases with increasing Zr content.

The second part of the study investigated nanolayered films composed of alternating layers of $\text{Zr}_{35}\text{Ta}_{65}$ and $\text{Zr}_{70}\text{Ta}_{30}$, for layer thicknesses in the range of 10 – 100 nm. The results show that the nanolayered films provide a desirable combination of high strength and fracture toughness. We attribute these results to the strong modulation of strength and elastic modulus at a length scale comparable to the size of the shear bands. The abrupt variations in the mechanical properties distort the stress state in the structure and hinder the rapid propagation of the shear bands.

In summary, we obtained ZrTa metallic glass thin films over a wide compositional range and determined the effect of composition on the mechanical behavior. The nanolayered form of the metallic glass thin film provided promising results that combine high hardness and fracture toughness. The findings can guide future studies towards the development of wear-resistant coatings that exhibit corrosion resistance and biocompatibility.

1:30 PM ST01.09.03

Understanding Hardness and Imprint Formation in Low-Load Nanoindentations of FCC, BCC and HCP Metals Jorge Alcalá¹, Javier Varillas^{2,3} and Jan Ocenasek²; ¹Universitat Politècnica de Catalunya, Spain; ²University of West Bohemia in Pilsen, Czechia; ³The Czech Academy of Sciences, Czechia

Nanocontact plasticity of metal surfaces involves sudden imprint formation processes along with the inception and evolution of entangled defect networks in the subsurface. Our investigation provides a fundamental

comprehension to nanoindentation experiments through massive molecular dynamics simulations of face-centered cubic Al, Cu and Ni; body-centered cubic Ta and Fe, and hexagonal closed-packed Mg performed across temperatures, tip penetration velocities, and nanoindenter tip sizes. We first investigate the critical contact resistance p_c rendering defect inception as a function of the incipient defect nucleation mechanisms and effective elastic modulus E of the crystal. Systematic analyses are performed on the subsequent pop-in events attained with increasing tip penetration, which lead to the onset of a steady-state nanoindentation regime characterized by constant hardness p_p . An insight is then gained into the specific nanoimprint formation mechanisms in cubic and hexagonal metals which comprise specific, collective dislocation emission and glide processes, individual nanotwin inception, and the development of unique nanostructured subgrain arrangements. A discussion is given on the role of these mechanisms upon the onset of higher values for the p_p/E ratio in BCC Ta and Fe and for the smaller p_p/E attained in FCC Cu, FCC Ni and HCP Mg. Finally, we investigate the correlation between the nanoimprint formation at the steady-state hardness p_p and the dislocation mobilization events triggered within the incepted defect networks at the uniaxial yield strength σ_{ys} . It is found that the p_p/σ_{ys} ratio approaches ≈ 7 and ≈ 10 in FCC and BCC metals, respectively.

1:45 PM ST01.09.04

Revealing the Lattice Scale in Microcompression of Nb Quentin Rizzardi¹, Cameron Elfresh², Douglas Stauffer³, Jaime Marian² and Robert Maass^{4,1}; ¹University of Illinois at Urbana-Champaign, United States; ²University of California, Los Angeles, United States; ³Bruker Nano Surfaces, United States; ⁴Federal Institute of Materials Research and Testing (BAM), Germany

Here we present temperature-dependent micro-compression data of Nb single crystals. We focus on the changes of the discrete plastic flow response between 370 and 170 K. Whilst the flow stress as a function of temperature is in excellent agreement with thermally-activated bulk plasticity models for bcc metals, a temperature insensitive component is revealed when tracing the change of displacement discontinuities with decreasing temperature. It is found that the scale of the displacement jumps changes from a scale-free like behavior at high temperatures to a scale-dependent behavior at the lowest temperature, where the length scale converges towards the scale of the lattice parameter. 3D discrete dislocation dynamics simulations are done to shed light onto the underlying dislocation behavior, revealing that the athermal plasticity component is governed by screw-dislocation activity. The temperature insensitivity of this screw-dominated plasticity can be shown to depend on high local stresses that significantly exceed the Peierls stress in the studied Nb microcrystals. This work is based on earlier efforts that aim at understanding stress-strain fluctuations in microcrystals (Phys. Rev. Mat. 2 (2018) 120601; Phys. Rev. Mat. 3 (2019) 080601).

2:00 PM *ST01.09.06

Fabrication and Mechanical Characterization of Ultra-Stiff and Ultra-Light Nano-Cardboard Structures Joost J. Vlassak and Jong-hyoung Kim; Harvard University, United States

Nano-cardboard structures are shell structures that consist of two face plates held together by hollow tubes that serve as ligaments [1]. These structures are fabricated entirely using thin films with thicknesses on the order of 100 nm or less. As a result of their geometry, nano-cardboard structures have a very low density and are ten times stiffer than aerogels or nanolattices of the same densities (5-20 kg/m³). Additionally, they exhibit recoverable deformation similar to nanolattices and have a low thermal conductivity similar to aerogels [2, 3]. Nano-cardboard structures are light enough to be levitated by photophoretic forces [4, 5], they can serve as substrates for sensors, and may be of interest in geoenvironmental applications [5]. Here, we describe a low-cost and fast process for fabricating scalable nano-cardboard structures. The fabrication process relies on inexpensive silicon wafers that are patterned by means of deep reactive ion etching to form sacrificial scaffolds. The sacrificial scaffolds are then uniformly coated with a thin ceramic layer using atomic layer deposition. In a final step, the silicon is etched away through small openings in the top face using XeF₂ gas, leaving a ceramic nano-cardboard with dimensions comparable to those of the original silicon wafer. Using this approach, nano-cardboard can be fabricated from many different ceramics and metals, with no limitation on the size of the nano-cardboard other than the wafer dimensions. We have analyzed the mechanical behavior of nano-cardboard

with various periodic ligament patterns including a hexagonal and basket-weave patterns using finite elements. The nano-cardboard stiffness, buckling load, and post-buckling behavior depend sensitively on both the ligament pattern and dimensions, allowing optimization of the structure for maximum specific stiffness and strength. Because of their macroscopic dimensions, nano-cardboard structures can be tested relatively easily using a range of different mechanical techniques. Here, we present results of bending experiments on nano-cardboard structures with various patterns performed using nanoindentation.

- [1] C Lin et al., Nanocardboard as a nanoscale analog of hollow sandwich plates, Nat. Commun., 2018
- [2] L Meza et al., Strong, lightweight, and recoverable three-dimensional ceramic nanolattices, Science, 2014
- [3] Zhang et al., Lightweight, flaw-tolerant, and ultrastrong nanoarchitected carbon, PNAS, 2019
- [4] J Cortes et al., Photophoretic Levitation of Macroscopic Nanocardboard Plates, Adv. Mater., 2020
- [5] D Keith, Photophoretic levitation of engineered aerosols for geoengineering, PNAS, 2010

SESSION ST01.10: Micro/Nano-Scale Characterization and Mechanics II
Session Chairs: Wendy Gu and Matt Pharr
Monday Afternoon, April 19, 2021
ST01

4:00 PM *ST01.10.01

High-Cycle Fatigue *In Situ* in the Transmission Electron Microscope Christopher M. Barr¹, Ta Duong², Daniel C. Bufford¹, Abhilash Molkeri², Nathan Heckman¹, David P. Adams¹, Ankit Srivastava², Michael Demkowicz², Brad L. Boyce¹ and Khalid Hattar¹; ¹Sandia National Laboratories, United States; ²Texas A&M University, United States

The exceptional properties that have been reported for nanostructured metals have made them appealing in both applications at decreasing dimensions and increasingly complex environments. The incorporation of nanoscale metals into thin-film solar cells, electrical sensors, and electronic textiles means that these materials will experience the day-to-day fatigue from thermal cycling through bodily motion. Fatigue is one of the most common causes of failure in metals, but to date is poorly explored in nanostructured metals. This presentation will highlight recent in-situ transmission electron microscope (TEM) investigations into the tension-tension fatigue behavior of nanocrystalline copper and platinum at frequencies from 1 Hz to 100s of Hz, enabling accumulations of up to 10^6 cycles within 1 h. Fatigue loading combined with the high spatial resolution of the TEM permits observations at crack growth rates of $\sim 10^{-12}$ m/cycle. As a result of this exceptional resolution, new insights into grain growth, twin elongation, and crack healing mechanisms that occur in the crack initiation regime of pure nanocrystalline metals can now be directly observed. When in-situ TEM fatigue experiments are coupled with automated crystal orientation mapping (ACOM), the interplay among grain orientation, grain boundary character, and fatigue crack propagation becomes apparent. This addition of ACOM also permits direct coupling to atomistic and mesoscale modeling, which can add or remove microstructural elements not possible experimentally to fully elucidate the active mechanisms. This new capability to directly observe with nanometer resolution grain growth, twin elongation, crack healing and potentially other active mechanisms has the potential to drastically change our understanding of the crack initiation portion of fatigue failure. Ongoing efforts to expand this in-situ TEM to approach and other materials systems and extreme environments will also be highlighted if time permits.

This work is supported partially by the Division of Materials Science and Engineering, Office of Basic Energy Sciences, U.S. Department of Energy. This work was performed, in part, at the Center for Integrated Nanotechnologies, an Office of Science User Facility operated for the U.S. Department of Energy (DOE) Office of Science. Sandia National Laboratories is a multimission laboratory managed and operated by National Technology & Engineering Solutions of Sandia, LLC, a wholly owned subsidiary of Honeywell International,

Inc., for the U.S. DOE's National Nuclear Security Administration under contract DE-NA-0003525. The views expressed in the article do not necessarily represent the views of the U.S. DOE or the United States Government.

4:25 PM ST01.10.02

Full Characterization of an Individual 5nm Film Within a Bilayer—Stiffness Degradation Due to Surfaces and Dopants in Low-k Dielectrics Travis D. Frazer¹, Joshua Knobloch¹, Jorge Nicolas Hernandez Charpak¹, Kathleen Hoogeboom-Pot¹, Damiano Nardi¹, Sadegh Yazdi¹, Weilun Chao², Erik Anderson², Marie Tripp³, Sean King³, Henry Kapteyn¹, Margaret Murnane¹ and Begoña Abad Mayor¹; ¹University of Colorado Boulder, United States; ²Lawrence Berkeley National Laboratory, United States; ³Intel Corporation, United States

Nanofabricated systems, from electronics, to spintronics, to quantum devices, rely on increasingly 3D stacks of ultrathin films. However, as feature sizes push below 10nm, there are both new and long-standing challenges to improving device performance. For example, an established problem in nanoelectronics is that doping interlayer dielectric films with hydrogen (hydrogenation) to improve electrical performance can degrade mechanical performance to the point of device failure [1]. However, a potential new challenge is the dominant influence of surfaces and interfaces for ultrathin nanoscale films, which can change the film's properties compared to bulk materials. Depending on the composition of the film, the influence of surfaces has been shown to either increase stiffness or increase compliance in ultrathin films [2,3]. Moreover, for sub-25 nm films at the leading edge of technology, traditional techniques struggle to measure the mechanical properties of films without overwhelming influence from the substrate. In this work, we use our ultrafast acoustic technique based on coherent extreme ultraviolet (EUV) light [4] to fully and nondestructively characterize the mechanical properties of films as thin as 5nm, even for an individual film in a bilayer. We study SiOC:H films and SiC:H bilayers to illuminate how surfaces affect the mechanical properties of these low-k ($k < 4.2$) dielectric materials being developed for next-generation nanoelectronics. Comparing the two materials, we distinguish between the stiffness degradation induced by dopants and that induced by the surface of the film. In particular, in very thin (5-nm) SiC:H films with low hydrogen doping, we find that surface effects induce a substantial reduction in stiffness—by almost an order of magnitude—compared with the same doping in thicker (46-nm) films [5]. However, for SiOC:H films with high hydrogenation, we observe no change in mechanical properties down to 11 nm. We attribute this difference in behaviors to the large loss of stiffness already induced by the hydrogen doping in SiOC:H, such that the surface has less of a relative effect. These findings have important implications for informed design of ultrathin films in a host of nano- and quantum technologies and most directly for improving the switching speed and efficiency of advanced nanoelectronics.

[1] D. Shamiryan, et al., Low-k dielectric materials, *Mater. Today* **7**, 34–39 (2004).

[2] C. Q. Sun, Size dependence of nanostructures: Impact of bond order deficiency, *Prog. Solid State Chem.* **35**, 1–159 (2007).

[3] R. J. Wang, et al., Effective geometric size and bond-loss effect in nanoelasticity of GaN nanowires, *Int. J. Mech. Sci.* **130**, 267–273 (2017).

[4] A. Rundquist, et al., Phase-Matched Generation of Coherent Soft X-rays, *Science* **280**, 1412–1415 (1998).

[5] T. D. Frazer, et al., Full characterization of ultrathin 5-nm low-k dielectric bilayers: Influence of dopants and surfaces on the mechanical properties, *Phys. Rev. Mater.* **4**, 073603 (2020).

4:40 PM ST01.10.03

Late News: Exploring Three-Dimensional Architectures of Crystalline III-V Thin Films by Compressive Buckling Jihun Lim, Dejiu Fan, Byungjun Lee and Stephen Forrest; University of Michigan–Ann Arbor, United States

Three-dimensional (3D) microstructures of thin film materials are emerging technologies with a growing range of applications. The formation of residual compressive stresses is a common method to transform in-plane microstructures to 3D architectures. Here, we present a 3D strain scheme for compressive buckling in free-

standing semiconductor thin films spanning between thin gold gridlines. The residual stresses are determined while transferring and bonding the films with the gridlines on their surfaces onto a substrate by cold pressure welding. Computational models are implemented using finite element analysis to predict the residual stresses and post-buckling morphologies in the free-standing films. Experimental results demonstrate a variety of scalable 3D architectures from nanometers to tens of microns, depending on the gridline spacings and bonding conditions. Additionally, the buckling microstructures elastically respond to external forces. We show the thickness dependent buckling mode transitions in the free-standing films. The film buckling phenomena offer an opportunity for achieving a diversity of 3D shapes such as nearly flat surface, upward buckling, telephone-cord buckling, and geometrical circle segmentation. Indeed, strain engineering of 3D thin metamaterial microstructures on inelastic platforms can lead to unprecedented material functions useful for energy harvesting and deployable microstructures.

4:55 PM ST01.10.04

Late News: High-Strain-Rate Behavior of Polyurea Under Microparticle Impact David Veyssset^{1,2}, Yuchen Sun¹, Steven E. Kooi¹ and Keith Nelson¹; ¹Massachusetts Institute of Technology, United States; ²Stanford University, United States

Hierarchical elastomers, such as polyureas or polyurethanes, have gained interest for their high energy absorption capabilities and impact protection performance, where deformation-induced glass transition has been suggested to play a determining role. Here, we investigate the dynamic response of polyurea under temperature-controlled micro-impact experiments. We impact micron-scale silica projectiles at subsonic velocities on a polyurea target using the laser-induced microparticle impact test platform. Using high-speed imaging, we measure impact and rebound velocities and determine the absorbed impact energy as a function of target temperature from 20°C to 160°C. We observe a local elevated energy absorption around 115°C, which we attribute to the dynamic glass-to-rubber transition. The soft-segmental α_2 -relaxation is extracted and fit with a Havriliak–Negami function from dielectric spectroscopy measurements. We find that the α_2 -relaxation at 115°C correlates well with the characteristic strain rate of the impact experiments. The results confirm that the deformation-induced glass transition leads to enhanced energy dissipation. This work further supports the importance of the dynamical T_g as an important factor in the design of impact-resistant materials.

5:10 PM ST01.10.05

Late News: Atomistic Processes of Surface-Diffusion-Induced Abnormal Softening in Nanoscale Metallic Crystals Sixue Zheng, Xiang Wang and Scott X. Mao; University of Pittsburgh, United States

Ultrahigh surface-to-volume ratio in nanoscale materials, could dramatically facilitate mass transport, leading to surface-mediated diffusion similar to Coble-type creep in polycrystalline materials. Unfortunately, the Coble creep is just a conceptual model, and the associated physical mechanisms of mass transport have never been revealed at atomic scale. Akin to the ambiguities in Coble creep, surface atomic diffusion in nanoscale crystals remains largely unclear, especially when mediating the process of yielding and plastic flow. Here, by using *in situ* nanomechanical testing under high-resolution transmission electron microscope, we found that the diffusion-assisted dislocation nucleation induced the transition from a normal to an inverse Hall-Petch relation of the strength-size dependence, and the surface diffusional creep led to an abnormal softening in flow stress with the reduction in the size of silver nanocrystals, contrary to the classical “alternating dislocation starvation” behavior in nanoscale platinum. This work provides novel insights into the atomic-scale mechanisms of diffusion-mediated deformation in nanoscale materials, and impact on the design for ultrasmall-sized nanomechanical devices.

5:25 PM *ST01.10.06

Nanomechanical Behavior of Hierarchical Metallic Microstructures Amit Misra; University of Michigan–Ann Arbor, United States

In metallic microstructures, hierarchical architectures of multiple phases with varying sizes and morphologies

shown to be effective in simultaneously enhancing yield strength, due to the strong glide dislocation interactions with their nanoscale features, and plastic deformability, due to increased strain hardening from microstructure hierarchy. In some hierarchical microstructures, impedance of crack growth via deflection along interfaces that have relatively low shear strength and bridging via relatively softer micro-scale composite domains can also lead to enhanced crack growth resistance. Examples will be presented from a variety of microstructures produced by magnetron co-sputtering (Cu-Mo, Cu-Ta), laser rapid solidification (Al-Si) and laser direct metal deposition (Cu-Fe). The challenges and opportunities in elucidating nanomechanical response of a microstructure comprised of multiple length scales, morphologies and chemical heterogeneities will be discussed.

SESSION ST01.11: Micro/Nano-Scale Characterization and Mechanics III and Poster Session
Session Chairs: Wendy Gu and Gi-Dong Sim
Monday Afternoon, April 19, 2021
ST01

7:45 PM ST01.11.03

Late News: Mechanical Behavior of Micro/Nanostructures Based on the Couple Stress Theory Jae-Hoon Choi, Hojang Kim, Byung-Chai Lee and Gi-Dong Sim; Korea Advanced Institute of Science and Technology, Korea (the Republic of)

Classical continuum theory is widely used as a tool to predict structural behavior. However, the behavior of micro/nanostructures cannot be appropriately predicted based on classical continuum mechanics. The structural stiffness predicted by classical continuum theory is much more flexible than that of the real structure. In the past decades, various higher-order deformation theories have been developed to simulate size effect within a continuum scale. In higher-order deformation theories, additional material properties are introduced besides the Lamé constants. Since the additional material properties have a unit of length, they are called length scale parameters. In the couple stress theory, which has only one length scale parameter, couple stress is introduced as additional resistance to deformation.

In this study, structural behavior at micro/nano-scale is analyzed based on the couple stress theory by using the finite element method. It is observed that the bending rigidity increases as the thickness of microcantilever beams decreases. When a tensile load is applied to a flat plate with a hole, the stress concentration factor decreases as the size decreases. The buckling load of the thin structure increases as the thickness decreases. In order to predict the structural behavior of micro/nanostructures based on the higher-order deformation theory, measurement of the length scale parameter must be preceded. We introduce two experiments to measure the length scale parameter. The first experiment is bending test. Microcantilevers can be fabricated via MEMS fabrication process and a line load is applied using a nanoindenter equipped with a wedge tip. The second experiment is buckling of membranes. After fabricating free-standing thin membranes, the temperature is gradually increased to measure the temperature at which buckling occurs. The material length scale parameter can be calculated inversely from the magnitude of the buckling loads. The experimental results are predicted from the finite element analysis based on the couple stress theory.

8:00 PM BREAK

8:35 PM ST01.11.05

Thermo-Mechanical Characterization of Graphitized and Activated Carbon Structures Formed from Polyacrylonitrile/Carbon Nanotube Composites Exhibiting Interphase Structural Control Conor Doyle, Kenneth Benson and Marilyn L. Minus; Northeastern University, United States

This research focuses on observations of polyacrylonitrile (PAN)/single wall carbon nanotube (SWNT)

composite films processed through pyrolyzation cycles for the production of ordered graphitic and activated carbon structures. The precursor composite films were processed using a solvent-based phase separation approach to promote the formation of extended-chain PAN interphase development at the SWNT surface as well as a hybrid through-thickness morphology. Previously reported work has outlined the advantages of this structural formation of crystalline PAN interphase regions within the precursor for the formation of ordered carbon at low temperatures between 900 °C to 1100 °C. In this work, PAN/SWNT precursor films underwent identical stabilization and carbonization cycles in air and argon gas, respectively. After low temperature turbostratic carbon formation, annealing cycles were then performed for various time and temperature combinations (up to 10 hours at 1700 °C) before activating the samples in carbon dioxide. These studies aim to correlate the stability of the low-temperature carbon forms to heal during annealing and subsequently survive activation toward forming graded porosity structures in these hybrid films. Dynamic mechanical analysis was used at each intermediary step of pyrolysis to evaluate the development of tensile strength (σ) and modulus (i.e., Storage (E') and Loss (E'') moduli). Overall material morphological composition was also evaluated using X-ray diffraction/scattering and electron microscopy both before and after activation. The results to be presented demonstrate the development and thermo-mechanical characterization of unique graded activated carbon architectures with potential applications such as filtration, electrochemical, and shielding.

8:40 PM ST01.11.06

Mechanical Behavior of Passivated Al Thin Films Hojang Kim, Sun Kun Choi and Gi-Dong Sim; Korea Advanced Institute of Science and Technology, Korea (the Republic of)

Metal thin films are widely used in various small-scale devices such as integrated circuits, gas sensors, micro-actuators, and micro-heaters. In most of the devices, it is hard to find freestanding thin films; instead, a number of layers of different materials are stacked in a complex way. In other words, metal films are generally surrounded by other materials. Dielectric materials commonly cover metal thin films in order to insulate electricity and heat conducted through the metal layer, and to prevent oxidation of the metal surface.

In this presentation, we will introduce two *in-situ* experimental techniques utilizing Si-based micromachining process to characterize the mechanical behavior of passivated metal thin films. Experiments were carried out on submicron thick aluminum thin films passivated with a few tens of nm thick SiN_x.

The first technique is performed through use of a custom-built in-situ scanning electron microscope (SEM) mechanical tester for measurement of the mechanical properties of Al thin films with and without a passivation layer. The apparatus has a stroke of 250 μ m with a displacement resolution of 10nm and a load resolution of 9.7 μ N. It utilizes pre-calibrated leaf spring, capacitive displacement gauge, and piezo actuator with a built-in displacement sensor. The second technique utilizes an in-situ SEM nanoindentation system equipped with a diamond wedge tip. Micro-scale bridge-shaped membranes and cantilever samples are fabricated via standard microfabrication process, and deflected by applying a line load. Stress-strain curves can be determined from load-displacement curves. Metallic thin films with a passivation layer exhibit enhanced strain hardening behavior because the passivation layer forms a strong interface, which acts as an obstacle to dislocation motion. Future plans for measurements at elevated temperatures will be introduced.

8:45 PM ST01.11.07

Mapping Elastic and Viscoelastic Contacts Across the Surfaces of High-Entropy Alloys Catherine B. Ott¹, Quentin Rizzardi¹ and Robert Maass^{2,1}; ¹University of Illinois at Urbana-Champaign, United States; ²BAM, Germany

Complex multi-principle element alloys, also referred to as high-entropy alloys (HEAs), have complex chemical and topological fluctuations at the atomic scale. This lead to a pronounced locality of the dislocation behavior and therefore the plastic response of such alloys. Here we focus on single-phase solid solution HEAs and trace the microplastic response of collective dislocation rearrangements (avalanches). A detailed analysis of the time-resolved response of crystallographic slip suggests that internal length scales much larger than the interatomic distance control the dislocation motion. To shed further light onto this observation, we use spatially resolved property mapping at the nano-scale with the aim of linking the length-scales derived from time-resolved slip

with correlation lengths determined from nano-mechanical fluctuations.

8:50 PM ST01.11.08

Structure Evolution and Corresponding Mechanical Behavior of Carbon Fibers Upon Post Heat-Treatment Jung-Eun Lee, Hyejin Ju and Han Gi Chae; UNIST, Korea (the Republic of)

Carbon fibers have been of great interest in many industrial applications due to their high specific mechanical properties as compared to steel or glass fibers. The polyacrylonitrile (PAN)-based commercial carbon fiber has as high as 7 GPa of tensile strength, and the highest tensile modulus is about 600 GPa although their theoretical properties are known to be 150 GPa and 1060 GPa, respectively. The property discrepancy, especially in tensile strength, is attributed to the defective structures such as bulk defects (voids, cracks, and cavities), surface defects (notches and punctures), and structural defects (disordered carbon and radial heterogeneity). Therefore, many researches regarding the correlation between microstructure and corresponding mechanical properties of carbon fibers upon carbonization have been conducted. Irrespective of carbon fiber's intrinsic properties, one has to keep in mind that it is mainly used in the form of carbon fiber-reinforced plastics (CFRP) or carbon-carbon composites rather than being used by itself. The carbon fibers are oftentimes subjected to very high temperature not only in the application but also during processing. In the due course, the structure and properties of carbon fibers are supposed to be varied. It would be beneficial that one has the information how their structure and the corresponding mechanical properties are changed upon application of such an extreme condition.

In the current study, the structure evolution and respective mechanical behavior of commercial PAN-based carbon fibers, H2550 and H3055 (Hyosung Co.), were analyzed upon post heat-treatment from 1600 to 2400 °C. With increasing heat-treatment temperature, the tensile modulus continuously increased due to the improvement of crystal size and orientation factor. However, the tensile strength exhibited abnormal behavior, which decreased in the temperature range of 1600-1800 °C, increased in the range of 2000-2200 °C, and decreased again at higher temperature than 2200 °C. This is correlated with the microstructure by considering above-mentioned various defects. The fibers heat-treated in the range of 2000-2200 °C showed the highest tensile strength value among them because of a high fraction of amorphous and disordered carbon, leading to effective energy dissipation. On the other hand, at 2400 °C, the strength was drastically diminished due to the graphitization and the generation of a rough surface. Radial heterogeneity and elongated void development were also observed at high temperatures, but it appeared that they don't have a significant effect on strength. It is noticeable that the Weibull modulus, which represented the fiber's uniformity and reliability in fracture, also showed unusual behavior depending on the temperature, and was highest at 2400 °C for both fibers (8.8 of H2550 and 6.4 for H3055). This suggests that post heat-treatment can also tailor the structural uniformity of fibers. The current study will provide the fundamental information of carbon fibers' structure-property relationship and can be used to predict the property variations of fibers in composites when used in high-temperature applications.

8:55 PM ST01.11.09

Late News: Atomistic Basis of Anisotropic Poisson's Ratio in 3C-SiC Zubaer M. Hossain and Henry Fidlow; University of Delaware, United States

Poisson's ratio (PR) of a material plays an important role in governing the lateral response of a solid subjected to symmetry-breaking deformation. Traditionally, PR is represented as a single material constant which, by construction, refers to the linear part of the stress-strain curve. The understanding of a possible coupling between crystallographic direction and PR remains more elusive. Here, we report the observation of anisotropic PR in defect-free 3C-SiC lattice, using quantum simulations based on the Density Functional Theory. We analyze the lateral response of 3C-SiC to an applied strain along the three high-symmetry crystallographic directions, [100], [110], and [111]. From our ab initio calculations, we use the linear and nonlinear regimes of mechanical deformation to determine Poisson's ratio as a function of applied strain for a given axial and transverse direction. Asymmetric deformation in the lattice of the [110] direction results in two Poisson functions dependent on the lateral orientation. One of these indicates a positive value, while the other a negative

value (regardless of the strain state of the lattice). This suggests simultaneous existence of both positive and negative PRs in the material. Conversely, uniaxial loading along either of the other two high-symmetry directions, the [100] and [111] directions, yields identical lateral behavior, allowing for a single Poisson function. From the four Poisson's functions, the maximum and minimum Poisson's ratios are reached in the two different lateral directions of the [110] direction. The first function reaches a maximum Poisson's ratio of 0.5, indicating incompressibility and maximum contraction of the lateral direction for applied tensile loads. The second function is auxetic, exhibiting purely negative Poisson's ratios throughout the true strain range. This translates to lateral expansion in tension and lateral contraction in compression. In both the [100] and [111] directions, all values of the Poisson's functions exist within the range of 0 to 0.3. Anisotropic behavior is similarly witnessed in the strength and toughness of 3C-SiC for the three high-symmetry directions. Here it can be noted that loading along the [100] direction exhibits optimal strength and toughness while loading in the [111] direction displays maximum stiffness. Analysis at the atomic scale reveals relationships between crystallographic structure and anisotropy of Poisson's ratio. Linear and angular bond deformation influences the lateral strain behavior based on lattice symmetry with respect to the axial direction. Additionally, further investigation of the electron redistribution properties of both silicon and carbon atoms was investigated to determine relationships between Poisson's ratio and electron density in the various orbitals. Coupled with improvements in grain manufacturing technologies, these observations can be utilized toward the optimization of mechanical properties of 3C-SiC and other diamond cubic structures in practical applications.

9:00 PM ST01.11.10

Mechanical Behavior of Micro-Scale NiTi Shape Memory Alloys Ji-Young Kim, Abdul Rehman and Gi-Dong Sim; Korea Advanced Institute of Science and Technology (KAIST), Korea (the Republic of)

Shape memory alloys (SMA) are a class of alloys which show unusual deformation depending on temperature or loading condition. Nickel-Titanium (NiTi) alloys is one of the most attractive SMAs due to its remarkable work output per unit volume, significantly higher strain recovery, and superior thermo-mechanical stability. However, majority of research on NiTi alloys have focused on the bulk-scale mechanical properties, and it is still challenging to apply NiTi SMAs in micron-scale applications such as electric and/or biomedical sensor. Few studies have reported that small-scale NiTi shows different shape memory behavior compared to its bulk counterpart, but our understanding on size effect is yet premature and a comprehensive study is required. In this study, we conducted in-situ tensile test of NiTi alloys, utilizing two experimental techniques for investigation of the small-scale mechanical behavior. In the first technique, tensile specimens are prepared by sputter deposition and Micro-electro-mechanical-system (MEMS) fabrication process. Tensile tests are conducted by using a customized in-situ scanning electron microscope (SEM) tensile tester. In the second experimental technique, micro-scale tensile bars are fabricated within a bulk-scale NiTi sheet by utilizing femtosecond laser and focused ion beam (FIB) milling. Femtosecond laser machining is used for fast, but rough, specimen mass production, and FIB milling is performed for fine cleaning. Micro-scale mechanical testing is conducted utilizing a nanoindenter equipped with a diamond gripper. By comparing the mechanical response between sputter deposited NiTi thin films and micro-scale tensile bars carved out from a bulk crystal, we aim to gain better understanding of microstructural effect on the superelastic behavior of micro-scale NiTi SMA alloys.

9:05 PM ST01.11.11

Late News: Investigating Grain Size, Grain Arrangement and Dislocation's Structure on Mechanical Behavior of Heterogeneous Materials Khaled Adam^{1,2}; ¹Kennesaw State University, United States; ²University of Benghazi, Libya

It is well known that the mechanical behavior of polycrystalline material changes largely with their mean grain diameter. In this work, we explore the grain size-dependent phenomenon in heterogeneous structure material using a continuum dislocation theory coupled with ViscoPlastic Fast Fourier Transform (VP-FFT) method. A dislocation-based strain gradient plasticity model was developed to predict the grain size effect over a wide range of length scales. The effect of the GNDs density was incorporated into the model for the mean free path

of dislocations.

9:10 PM ST01.11.12

Late News: Combinatorial and High-Throughput Experiments on Co-Based Alloy Thin Films Taeyeop Kim¹, Daegun You¹, Kooknoh Yoon², Eun Soo Park² and Dongwoo Lee¹; ¹Sungkyunkwan University, Korea (the Republic of); ²Seoul National University, Korea (the Republic of)

Superalloys are structural materials for high-temperature applications such as gas turbines and space vehicles. Co-based superalloys have been spotlighted as they can be utilized at a higher temperature than traditional Ni-based alloys. Investigations of composition-microstructure-property relationships are required to develop next generation superalloys. However, due to the enormous number of the possible combinations, it is challenging to acquire the property data that can illustrate the relationships. In this study, we carried out the combinatorial synthesis and high-throughput experiments to investigate the composition and microstructure dependent properties of Co-Cr-Ti alloy thin films library, which are known to produce the γ/γ' microstructures in bulk scale. Combination synthesis and high throughput experiments provide an effective pathway for obtaining large amounts of experimental property data. We used magnetron co-sputtering to produce hundreds of different Co-Cr-Ti thin-film alloys on a single wafer. We then characterized composition-dependent phase formation as well as electrical and mechanical properties by performing X-ray diffraction, 4-probe resistance mapping, and nanoindentation experiments. The correlation among the measured properties and their implication on bulk properties will be discussed.

9:15 PM ST01.11.13

Late News: Tribological Properties of Magnetic Nanoparticles Reinforced Polymer Nanocomposites Salman Ahmed Syed and Zainuddin Shaik; Tuskegee University, United States

In this study, Fe_3O_4 and Fe_2O_3 nanoparticles were used to improve the tribological performance of the Epoxy resins. The composites were prepared by adding the nanoparticles to the epoxy resin and techniques like sonification and thinky mixing were used to get good dispersion of the nanoparticles. The effects of Fe_3O_4 and Fe_2O_3 nanoparticles on the wear rate, friction coefficient and hardness of the composites were investigated using Bruker's UMT Tribolab. The results showed that the composite exhibited improved wear resistance, lower friction coefficient and better hardness values compared to neat epoxy resin. With the incorporation of 3% Fe_2O_3 , the hardness values of the composites enhanced to 9.3 HV (increased by 165%), 16.9 HV (increased by 160%) and 26.2 HV (increased by 159%) for 20 N, 40 N and 60 N, respectively. Similar increasing trend can be seen with incorporation of 3% Fe_3O_4 , with hardness values increased to 9.1 HV (increased by 160%), 17.1 HV (increased by 163%) and 27 HV (increased by 167%) for 20 N, 40 N and 60 N, respectively. From the scratch test results, we can see a decreasing trend in the COF values for the samples, with 5% samples showing the lowest COF values. The improved tribological performance of the composites can be ascribed to the improved mechanical and lubricating properties of the nanoparticles.

9:20 PM ST01.11.14

Late News: Property Degradation of Helium Ion Irradiated Tungsten Based Alloy Thin Films Haechan Jo, Sanghun Park, Daegun You and Dongwoo Lee; Sungkyunkwan University, Korea (the Republic of)

Tungsten (W) is one of the promising candidate materials for plasma-facing materials (PFMs) in fusion reactors due to its high melting point, high thermal conductivity, and low sputtering rate. PFMs are known to be irradiated by the by-products of fusion reaction, such as helium ions & neutron, which can lead to structural and mechanical degradation. It has been reported that the addition of rhenium (Re) and tantalum (Ta) can mitigate irradiated damages and hinders helium bubble formation. In this work, we performed helium irradiation experiments on combinatorially sputter deposited W-based alloy thin films to investigate the microstructure- and composition-dependent irradiation damages. XRD was used to analyze the structural damages, and nanoindentation and 4-point measurement were used to measure the mechanical and electrical property changes, respectively. The correlation between the microstructural changes and the materials' properties are discussed.

9:25 PM ST01.11.15

Late News: Mechanical and Thermal Properties of Multi-Walled Carbon Nanotube w/ PHBV Azizi Turner; Tuskegee University, United States

Biocomposites can be specifically tailored to improve their multifunctional properties for a wide variety of applications by the addition of carbon nanoparticles. In this study, thin films of Poly(3-hydroxybutyrate-co-3-hydroxyvalerate) (PHBV) nanocomposites were prepared by adding 0.1- 0.5 % Multi-Walled Carbon Nanotubes (MWCNTs). In the construction of the films, chloroform was used as the solvent for the PHBV nanocomposites and the MWCNTs. Sonication was used to enhance the dispersion of the MWCNT throughout the solvent, and a magnetic stirrer was used to help in mixing the solution with the polymer. When adding MWCNT into PHBV, there was an improvement during the following tests: tensile test, thermogravimetric analyses, and differential scanning calorimetry. In addition, the tested samples were analyzed using scanning electron microscopy and transmission electron microscopy to see how the effect of MWCNT's addition on the surface of PHBV.

9:30 PM ST01.11.16

Multiscale Mechanical Characterization of Additively Manufactured Inconel 718 Kwanghyeok Lim¹, Ken-Hee Ryou¹, Jeong-Hwan Lee², Gwang-Hyo Choi¹, Won-Seok Choi¹, Pyuck-Pa Choi¹ and Gi-Dong Sim¹; ¹Korea Advanced Institute of Science and Technology, Korea (the Republic of); ²Samsung Electronics, Korea (the Republic of)

Additive manufacturing is an emerging technology due to its superiority in complex and customized design. These advantages lead to applications such as turbofan engines, power plant turbines, and spacecraft engine parts. Inconel 718, which is widely applied to the above applications, has now become one of the main additive manufacturing research targets. However, it has the possibility of containing inclusions such as titanium nitride (TiN) due to being exposed to air during deposition despite the injection of shielding gas. The effect of such inclusions on the high-temperature mechanical properties of additively manufactured Inconel 718 is not yet well understood.

In this study, multi-scale (bulk-scale and meso-scale) uniaxial tensile tests are performed to investigate the effect of TiN inclusions on the mechanical properties of additively manufactured Inconel 718 at elevated temperatures. Inconel 718 is deposited on the substrate using the direct laser deposition (DLD) method. Wire electrical discharge machining (EDM) is applied to fabricate dog-bone shaped bulk-scale specimens with gauge lengths of 10mm, gauge widths of 2mm, and thickness of 0.3mm. Tensile tests are carried out at room temperature, 400°C, 600°C, 650°C, 700°C, 750°C, and 800°C at the strain rate of 10⁻⁴/s. According to the experimental results, additively manufactured Inconel 718 maintains a yield strength of 550MPa while increasing the temperature up to 650°C, and exhibits the highest value of 670MPa at 700°C. In addition, as temperature increases, uniform elongation decreases from 16.5% at room temperature to 1% at 700°C. Scanning electron microscope (SEM), energy-dispersive spectroscopy (EDS), and X-ray diffraction (XRD) analysis are conducted to examine the presence of TiN inclusions and the failure mechanisms of additively manufactured Inconel 718. EDS and XRD results show that TiN inclusions are contained numerously, and SEM images indicate that TiN inclusions show a trace of brittle fracture, while the matrix of the material is ductile. We will also introduce ongoing efforts trying to understand the effects of a single TiN inclusion on the high-temperature tensile properties via small scale experiments. Femtosecond laser machining is utilized to fabricate dog-bone shaped meso-scale specimens with gauge lengths of 2mm, gauge widths of 0.5mm, and thickness of 30. A meso-scale tensile tester, capable of testing at temperatures up to 1000°C has been custom-built. Future plans of meso-scale experiments at elevated temperatures will be discussed.

9:35 PM ST01.11.17

Late News: The Measurement of Modulus and Hardness of Different Cross-Linked SU-8 via Nanoindentation Prakash Sarkar, Prita Pant and Hemant Nanavati; Indian Institute of Technology Bombay, India

The effect of cross-linking on the modulus (E) and hardness (H) of an epoxy polymer was studied using nanoindentation. Experiments were carried out on SU-8, which is an epoxy-based thermoset polymer extensively used for fabricating micro-electrical mechanical system (MEMS) components. The extent of cross-linking was varied by modifying the curing steps (post-exposure baking, hard baking) of standard photolithography process. The amount of cross-linked segments was measured via in-situ Fourier-transform infrared spectroscopy. Nanoindentation experiments were carried out under constant strain rate conditions. Using the conventional Oliver-Pharr method yielded high E and H values for less cross-linked sample and less values for high cross-linked samples. A careful analysis showed that the main reasons for these inverse values are adhesion between the tip surface and sample surface, viscoelastic effect on unloading and errors in calculation of contact area. We propose a new methodology to correct for these potential sources of error. Thereafter, E values of 4.61 ± 0.13 GPa and 5.02 ± 0.18 GPa, and H values of 256.97 ± 1.42 MPa and 285.48 ± 1.17 MPa were obtained for less (~ 82 %) and high (~ 95 %) cross-linked samples, respectively.

Keywords: SU-8; Photolithography process; FTIR; Nanoindentation; SPM

9:40 PM ST01.11.18

Late News: Mechanical Properties of Sputter Deposited Aluminum-Carbon Alloy Thin Films Injong Oh¹, Hojang Kim¹, Hyunjoo Choi² and Gi-Dong Sim¹; ¹Korea Advanced Institute of Science and Technology, Korea (the Republic of); ²Kookmin University, Korea (the Republic of)

Aluminum is a widely used metal in transportation, aviation, and energy due to its advantages of low density. Aluminum and its alloys are also being used in MEMS (Micro-electromechanical system) devices due to properties such as low resistivity, high conductance, high reflectance, and low residual stress. However, as aluminum possesses low strength, it is crucial to increase strength by tailoring the microstructure via altering deposition conditions, heat treatment, and/or alloying. In previous works, nickel, molybdenum, and copper were alloyed with Al to increase the strength. One possible way to enhance the mechanical properties of aluminum is to reinforce it with strong materials (e.g., carbon nanotubes, graphene, etc.), producing aluminum-based composite. However, it is still challenging to uniformly disperse nano-carbon material in the aluminum matrix without forming carbides. Recently, a new way to increase strength of aluminum using super-saturated Al-C phases has been proposed. Carbon atoms from individually dispersed C60-fullerenes, are intercalated into the interstitials of aluminum matrix, producing supersaturated Al-C phases with artificially moderated lattice structures. However, the underlying strengthening mechanism of atomically adding carbon atoms to aluminum matrix has not been deeply understood.

In this presentation, we discuss the mechanical properties and microstructure of sputter deposited aluminum (Al)-carbon (C) alloy thin films. Aluminum-carbon alloy thin films with various compositions were produced by co-sputtering aluminum and carbon without substrate rotation. Through this method, Al-C coatings with compositional spread can be fabricated, and the effect of carbon on the deformation mechanism can be analyzed. Thin film specimens having micro-scale dimensions were fabricated utilizing MEMS processing techniques. The tensile characteristics of thin film specimens were evaluated utilizing a custom-built micro tensile tester. The sputter deposited Al-C alloy thin films exhibit higher yield stress (~ 420 MPa) compared to that of pure aluminum thin films without loss of ductility (~ 10%). The deformation mechanism of the aluminum-carbon alloy thin films was analyzed based on mechanical and microstructural analysis.

9:45 PM ST01.11.19

Late News: Misorientation Development Near Grain Boundaries and Twin Boundaries in Pure Copper and Copper-Aluminium Alloy Sandhya Verma, Prita Pant and M. P. Gururajan; Indian Institute of Technology Bombay, India

During deformation of bulk polycrystalline materials, boundaries impose constraints due to requirements of compatibility across boundaries. Pure bulk Copper and Copper-aluminium samples were subjected to interrupted tensile tests coupled with electron backscatter diffraction (EBSD) analysis, to study the evolution of misorientation at specific boundaries. Our results show that misorientation development (in terms of Kernel

Average Misorientation, KAM) near boundaries is a function of orientation of grains on each side, but it is also influenced by the presence of other boundaries nearby, and constraints such as triple points. We have noticed that KAM values near boundaries does not behave monotonically for both Cu and Cu8Al. For Cu, in one case it increases as well as decreases in values, while in other case it remains constant. Similarly, for Cu8Al it reduces in values for most of the cases and increases or remains constant with strain in few cases. So while developing models for deformation of polycrystals, detailed information regarding grain orientation and neighbouring grains should also be incorporated. We have analysed our results in terms of Schmid factors of the grains on either side of the boundaries. Results for copper are compared with Cu-Al alloy, which has significantly finer twins in the microstructure. Hence there are greater constraints.

Keywords: EBSD; Misorientation; Orientation gradient; Grain boundary; Schmid factor; KAM

9:50 PM ST01.07.06

Optimization of Micro/Nano-Scale Mechanical and Surface Properties of PMMA Thin Layer for Simple and Low Cost-Nanoimprinting Process Silambarasan Anbumani, Mariana Zavarize, Helio T. Obata, A.A.G. von Zuben and Monica A. Cotta; University of Campinas, Brazil

Surface micro/nano patterning is essential for diverse applications including next generation-solar cells, photonics and bio-interface devices. Nanoimprint lithography offers such patterning with high resolution and high throughput. However, since such technology usually requires sophisticated instruments and clean room facilities, it is cost-effective only if performed in high-volume mass production that limits its role in most research and development needs and various niche applications. To overcome such limitations of nanoimprinting process, we utilize a thermoplastic polymer with a thorough knowledge of the imprinting conditions at micron to nano scale such as filling behavior, pattern fidelity, and surface properties.

In the present study, we describe an optimized process for imprinting sub-micron to nano-structures to poly(methyl methacrylate) (PMMA), a thermoplastic polymer, using simple soft PDMS (Polydimethylsiloxane) templates. Initially, a range of imprinting depth of 200nm PMMA thin layer was explored with micron to nano scale features of a template for a low imprinting pressure (~3 bar). Sub-micron patterned features have complete depth of trenches as template compared to micron size patterns; in both cases, the obtained patterns depend on applied pressure and imprinting temperature. The imprinting at temperatures higher than that for PMMA glass transition leads to increased pattern trench depths; however the imprinted PMMA layer shows poor surface quality due to the high temperatures employed. We addressed this problem by using PMMA solvent mixed with acetone to improve the surface quality of PMMA layer. Therefore, relatively low surface roughness and good anti-sticking properties were obtained. The thermal behavior and etching rate of the polymer prepared with mixed solvent were studied. By tuning nanoscale mechanical and surface properties, we successfully imprinted features at submicron and nano scales and demonstrate pattern transfer to substrates after metallization and lift off process.

SESSION ST01.12: Micro/Nano-Scale Characterization and Mechanics IV

Session Chairs: Jagannathan Rajagopalan and Gi-Dong Sim

Tuesday Afternoon, April 20, 2021

ST01

2:15 PM *ST01.12.01

Measurement of Hardness and Elastic Modulus by Depth Sensing Indentation—Improvements to the Technique Based on Continuous Stiffness Measurement Warren C. Oliver¹, Phani Sudharshan² and George M. Pharr³; ¹KLA Corporation, United States; ²ARCI, India; ³Texas A&M University, United States

The method to measure hardness and elastic modulus of small volumes of material by instrumented indentation presented in the seminal works of Oliver and Pharr in 1992 and 2004, has revolutionized the field of small scale nanomechanical testing. Several recent advances in measurement electronics have enabled testing over a wider range of test conditions (speeds) using methodologies that were developed earlier, which requires a critical assessment. In the backdrop of the latest developments in instrumentation and test methodologies, an overview of the various factors affecting the precision and accuracy of the nanoindentation test results at different test conditions with specific focus on Continuous Stiffness Measurement (CSM) technique will be presented.

2:40 PM ST01.12.02

Late News: High-Pressure Studies of Nanostructured Ultra-Incompressible Superhard Materials [Shanlin Hu](#)¹, Jialin Lei², Richard Kaner¹ and Sarah Tolbert¹; ¹University of California, Los Angeles, United States; ²Washington State University, United States

Hardness is a complex physical property that includes both intrinsic and extrinsic effects. In the past, to design intrinsically hard materials, we have explored the use of late transition metal borides that possess intrinsically high incompressibility due to high valence electron density, and added covalency through the formation of metal borides as a way to increase resistance to shear. At the opposite end of the spectrum, we find extrinsic effects, including grain boundary processes, such as grain boundary sliding, diffusion and grain rotation. In nanocrystalline material, these extrinsic effects compete with intrinsic effects (grain interior dislocations) and lead to unique plastic deformation behavior. While the size effects have been explored in the ductile metal system, little is known about whether these same phenomena dominate in nanocrystals of much harder materials, such as transition metal boride nanocrystals, mostly due to a lack of materials with size tunable nanosized domains.

Here, we demonstrate the size dependency of plastic deformation mechanism in the nanosized superhard ReB₂ system. In order to understand the lattice specific mechanical failure that is related to bonding motifs, in-situ high-pressure radial X-ray diffraction was conducted. A large magnitude of uniaxial stress state was generated in the diamond-anvil cell (DAC), while X-ray diffraction is simultaneously collected, allowing us to probe the changes in bonds under compression and obtain the differential strain (t/G), which describes the material's ability to resist shear stress. In addition, texture analysis on the radial diffraction data provides quantitative information on slip planes within a material, revealing the extrinsic effects interacting with the grain interior dislocations. Different sizes of nano-ReB₂ (20 nm and 50 nm) were synthesized by molten-salt method and bulk-ReB₂ was synthesized by arc-melting method. In-situ radial X-ray diffraction was performed under high pressure up to ~60 GPa. The lattice specific differential strain was experimentally measured and the diffraction patterns were analyzed by Rietveld refinement. In the nano-ReB₂, extrinsic effects compete with grain interior dislocations and lead to plastic deformation behavior that is very different from bulk-ReB₂. A Hall-Petch size dependence was observed, as the grain size gets smaller, the increasing the grain boundary content impedes plastic deformation and results in enhanced resistance to dislocation glide. Texture analysis was performed on the nano-ReB₂ system, because the grains in the nano-samples are fine enough that the peak intensity variation with azimuth angle correlates to the slip systems and grain orientation. From the inverse pole figures, the texture has its maximum intensity along the (0001) direction in both nano-samples, suggesting that the deformation is primarily controlled by the basal slip system. Furthermore, the pole density is more concentrated at (0001) pole as the grain size gets smaller, suggesting closing of slip system as the grain boundary concentration increases.

2:55 PM *ST01.12.03

Low-Temperature Time-Dependent Ductility in Single Crystal Silicon at Micro Scale [Taher Saif](#), University of Illinois at Urbana-Champaign, United States

Materials at small scale behave differently from their bulk counterparts. This deviation originates from the abundance of interfaces at small scale. Quantifying the properties and revealing the underlying mechanisms requires experiments with small samples in situ in analytical chambers. However, small size poses the challenge

of sample handling, but offers the opportunity of in situ inspection of mechanism during testing in analytical chambers. In order to overcome the challenge and take advantage of the opportunity, we developed a MEMS based micro scale testing stage where the sample and the stage are co-fabricated. The stage suppresses any misalignment error in loading by five orders of magnitude. The stage allows in situ inspection of samples during testing in SEM and TEM. We employed the stage to explore the effect of size on brittle to ductile transition (BDT) temperature (540C) in single crystal silicon. Here, the sample is a micro scale single crystal silicon beam subjected to bending which limits the high stress region to a small volume of the sample, and minimizes the probability of premature failure from random flaws. We found that silicon indeed deforms plastically at small scale at temperatures much lower than 540C. Ductility is achieved through a competition between fracture stress and the stress needed to nucleate dislocations from the surface. Our combined SEM, TEM and AFM analysis reveals that as a threshold stress is approached, multiple dislocation nucleation sites appear simultaneously from the high stressed surface of the beam with a uniform spacing of about 200 nm between them. Dislocations then emanate from these sites with time, lowering the stress while bending the beam plastically. This process continues until the effective shear stress drops and dislocation activities stop. A simple mechanistic model is presented to relate dislocation nucleation with plasticity in silicon.

3:20 PM *ST01.12.04

Nanoscale Science for Geoscale Phenomena: Mechanisms of Rock Friction Revealed by Atomic Force Microscopy, Nanoindentation and Atomistic Simulations David L. Goldsby¹, John McClimon¹, Zhuohan Li², Izabela Szlufarska², Robert W. Carpick¹, James Batteas³, George M. Pharr³, Xin Zhang⁴ and Kevin Rosso⁴; ¹University of Pennsylvania, United States; ²University of Wisconsin–Madison, United States; ³Texas A&M University, United States; ⁴Pacific Northwest National Laboratory, United States

Earthquakes are frictional instabilities that initiate on faults in Earth's crust at slow, quasi-static slip rates of nm/s to $\mu\text{m/s}$. Unstable fault slip results from interactions between the mechanical properties of the rocks which load the fault and the frictional behavior of the fault itself. Like several engineering materials, the quasi-static frictional behavior of rocks is described by rate-variable and state-variable friction (RSF) “laws”, which are actually empirical relations based on data from laboratory experiments. These descriptions of friction agree with many (but not all) data from lab experiments, and reproduce a rich variety of earthquake behavior when employed in full-cycle earthquake rupture models. However, the physical and/or chemical mechanisms that yield the observed rock friction behavior are unknown, making extrapolations of RSF laws beyond the limited range of conditions of the experiments that form their basis fraught with uncertainty.

The most fundamental observation from experimental studies of rock friction is that friction increases with the log of the time of stationary (or nearly stationary) contact. This is typically studied in slide-hold-slide experiments, wherein restarting sliding after a “hold” period without sliding results in an increase in peak static friction. This increase in *state* of the frictional interface during the hold may occur with the time of stationary contact, or with the slow slip of shear-loaded contacts. Time- or slip-dependent aging manifests as a velocity dependence of friction, the sign of which determines whether unstable frictional sliding (an earthquake) is possible.

Because the frictional behavior of faults emerges from the collective behavior of myriad nanometers- to microns-sized contacting asperities, fundamental rock friction mechanisms can be studied at the single-asperity level by atomic force microscopy (AFM) and nanoindentation. The canonical view is that aging results from increases in contact area due to plasticity and creep of asperities in contact. Results of our recent AFM and nanoindentation experiments, coupled with first-principles simulations, however, point to chemical bonding across frictional interfaces as an important mechanism of friction. Extensive AFM studies with oxidized silicon tips and samples, and more recently with quartz tips on quartz samples, and coordinated simulations demonstrate that log-time aging results from chemical bonding across asperity contacts, in the absence of plastic deformation. Moreover, our AFM experiments reveal many of the phenomena observed in friction experiments on rocks - notably a critical slip (or memory) distance D_c , variations in the dependences of friction on sliding velocity, increases of friction with slow as well as no slip during holds, and stick-slip behavior. Our

nanindentation experiments show that the yield stress and creep behavior of quartz at room temperature are independent of relative humidity (RH) in the range ~0 to 50%, whereas macroscale friction tests on quartz reveal no aging at RH <5% due to a supposed lack of asperity yielding and creep. These observations thus preclude plastic deformation as the primary mechanism of frictional aging. Our studies collectively point to chemical bonding as an important mechanism of rock friction, and motivate our current models of rough rock surfaces in contact that incorporate both chemical bonding and asperity yielding and creep.

3:45 PM ST01.12.05

Late News: A New Machine Learning Framework for Accelerating Mechanical Characterization at Small Scales Christos E. Athanasiou, Xing Liu, Nitin Padture, Brian W. Sheldon and Huajian Gao; Brown University, United States

Investigating mechanical properties at small scales is a challenging endeavor. It requires sophisticated micro-/nano-scale experimental methods combined with laborious/time-intensive finite element computations. In this talk, a new framework for materials characterization at small scales using the latest developments in machine learning will be presented. This framework involves multi-fidelity deep learning and active learning methods limiting the need for finite element simulations. Its application for predicting the fracture toughness of microscale pentagonal cross-sectional ceramic cantilevers will be showcased, demonstrating that it can significantly accelerate fracture toughness characterizations at small scales.

4:00 PM ST01.12.06

Microparticle Impact at Very High Velocities Does Not Necessarily Improve Bonding Ahmed A. Tamiyu, Yuchen Sun, Keith Nelson and Christopher Schuh; Massachusetts Institute of Technology, United States

Impacts at very high velocities have been widely perceived to promote particle flattening and bonding during additive manufacturing processes such as cold spray. Using the laser-induced particle impact tester, we perform site-specific studies with well-known particle sizes and velocities, and show that particle impact at some very high velocities can counter-intuitively deteriorate coating quality. We identify a particle rim peeling mode that hinders extensive lateral particle flattening and also appear to cause debonding at the particle-substrate interface close to the particle periphery, even prior to the undesirable hydrodynamic particle penetration regime. To the extent that high velocities are required for permanent particle adhesion, this work points to the possibility of a more narrow velocity range within which high quality particle bonding may be achieved.

SESSION ST01.13: On-demand
Wednesday Morning, April 14, 2021
ST01

8:00 AM ST01.04.03

Inverse Layer Dependence of Friction on MoS₂ Achieved Through Intercalation of Dopants Ogulcan Acikgoz¹, Alper Yanilmaz², Omur E. Dagdeviren^{3,4}, Cem Çelebi² and Mehmet Z. Baykara¹; ¹University of California, United States; ²Izmir Institute of Technology, Turkey; ³McGill University, Canada; ⁴École de Technologie Supérieure, Canada

We present the results of atomic-force-microscopy-based friction measurements on Re-doped molybdenum disulfide (MoS₂). In stark contrast to the seemingly universal observation of decreasing friction with increasing number of layers on two-dimensional (2D) materials, friction on Re-doped MoS₂ exhibits an anomalous, i.e. inverse dependency on the number of layers. Raman spectroscopy measurements reveal signatures of Re intercalation, leading to a decoupling between neighboring MoS₂ layers and enhanced electron-phonon interactions, thus resulting in increasing friction with increasing number of layers – a new paradigm in the

mechanics of 2D materials.

8:15 AM ST01.07.07

Tuning Field-Effect Mobility of Ultrasensitive Hybrid Transistors with UV Light Che-Hsuan Cheng, Kanak Datta, Da Seul Yang, Jinsang Kim and Parag Deotare; University of Michigan–Ann Arbor, United States

Light-powered and chemically fueled artificial molecular applications have long been recognized as the key building blocks of the functional materials of the future. In this work we employ an azobenzene based molecules A3 that undergoes reversible structural change between *trans* and *cis* forms upon irradiations of UV and visible light respectively. Using this, we develop highly sensitive phototransistors with tunable and ultra-high field-effect carrier mobility based on tungsten diselenide (WSe₂) monolayer. By stretching and contracting the underlying A3 molecules using UV and visible light (from 9 Å to 5.5 Å), the hole mobility of the hybrid FET device can be tuned from 100 cm²/Vs to as high as 1025 cm²/Vs, which is over an order of magnitude higher than typical TMDs based transistors. The observed mobility is comparable to that of conventional semiconductors such as silicon and germanium. We investigated the enhancement mechanisms by electrically characterizing the hybrid device before and after UV exposure. Consequently, we conclude strain to be the primary mechanism for channel current enhancement.

Furthermore, we monitored the UV photoresponse of the hybrid transistor and found that the UV photocurrent extinction ratio to be 75% higher than that of the bare WSe₂ device, making it a promising candidate for UV detection application. Such hybrid platform can potentially be used for designing next generation devices as well as ultrasensitive UV photodetectors.

SYMPOSIUM ST02

In Situ Mechanical Testing of Materials at Small Length Scales, Modeling and Data Analysis
April 14 - April 23, 2021

Symposium Organizers

Gerhard Dehm, Max Planck Institute
Christoph Gammer, Austrian Academy of Sciences
Sang Ho Oh, Sungkyunkwan University
Kelvin Xie, Texas A&M University

Symposium Support

Silver
JEOL Ltd.

Bronze
Alemnis AG
Bruker

* Invited Paper

SESSION ST02.01: Plasticity at Small Length Scales—Metals and Alloys
Session Chairs: Christoph Gammer and Erdmann Spiecker
Thursday Morning, April 22, 2021
ST02

8:00 AM *ST02.01.01

***In Situ* Transmission Electron Microscopy Deformation Study on Dislocation Plasticity in FeCoCrMnNi High-Entropy Alloy** Subin Lee¹, Christian Liebscher¹, Sang Ho Oh², Karsten Albe³ and Gerhard Dehm¹; ¹Max Planck Institute for Iron Research, Germany; ²Sungkyunkwan University, Korea (the Republic of); ³Technische Universität Darmstadt, Germany

In the past decades, high-entropy alloys (HEAs) have been intensively investigated not only because of fundamental scientific interests, but also their outstanding mechanical properties, for example, high ductility and fracture toughness. Among hundreds of different combinations of principal elements, the equiatomic FeCrCoMnNi alloy, the so-called Cantor alloy, has been studied as a model system, which is a single-phase material with face-centered cubic (FCC) structure at room temperature and shows outstanding ductility and strain hardening especially at cryogenic temperatures.

However, dislocation-based deformation mechanisms of HEAs remain elusive and require a fundamental understanding to tailor their mechanical properties. Several models have been suggested possible strengthening mechanisms of HEAs, for instance, the high entropy effect and the lattice distortion effect. In the case of the Cantor alloy, the main strengthening mechanism was identified as deformation twinning with critical twinning stress of 720 MPa. At room temperature, dislocation slip by full dislocations is dominant, however, at strains exceeding 20 % and high flow stresses, deformation twinning was also observed. To reveal the strengthening mechanism in more detail, direct observation of dislocation plasticity and deformation dynamics is required.

Here, we present a study correlating the microstructure and dislocation plasticity of FeCrCoMnNi FCC phase HEA by employing an in-situ transmission electron microscope (TEM) compression and tensile deformation. The threshold shear stress for dislocation glide in a thin foil is measured from dislocation curvature as exceeding 400 MPa. Interestingly, dislocations are prevented from straightening upon unloading due to high frictional stresses. Moreover, an atomic-scale chemical analysis is conducted by aberration-corrected scanning TEM energy-dispersive X-ray spectroscopy (STEM-EDS) and atom probe tomography to investigate chemical inhomogeneity. Lastly, the origin of the jerky glide motion of dislocations observed during the in-situ TEM straining tests is further analyzed by using atomistic simulations.

8:30 AM *ST02.01.02

***In Situ* TEM Straining Experiments Cantor's HEA Alloy at Liquid Nitrogen and Room Temperature** Daniela Oliveros¹, Anna Fraczkiewicz², Antonin Dloughy³, Stefan Sandfeld⁴ and Marc Legros¹; ¹CEMES-CNRS, France; ²Ecole des Mines de Sainte Etienne, Cours Fauriel, France; ³Czech Academy of Sciences, Czechia; ⁴Forschungszentrum Jülich GmbH, Germany

Despite possessing similar glide systems as an fcc metal, the equiatomic CoCrFeMnNi high entropy alloy (HEA) (Cantor alloy) continues to intrigue metallurgists around the world. Many key questions such as the origin of its strength, the preferential activation of twinning at low temperature or the nature of obstacles to dislocation movement remain to be understood. In particular, the possibility of a friction stress that would arise from the distorted structure of the HEA instead of an extended core as in bcc metals or covalent materials is still debated. In this study, we have carried out tens of in situ straining tests in a TEM at room and liquid nitrogen temperature to assess these questions. Dislocations are used as probes, whose dynamic behavior under stress serve as local markers of the average of punctual obstacles strength they have to overcome. Quantitative stress measurements are made and confronted to those provided by bulk tests, including the size effects arising from thin foil testing.

9:00 AM ST02.01.03

Late News: *In Situ* Synchrotron Diffraction Study of Structural Evolution in a Ductile Bulk Metallic Glass Under Tension at Micro-Scale Sinan Liu¹, Jiacheng Ge¹, Xun-li Wang² and Si Lan¹; ¹Nanjing

University of Science and Technology, China; ²City University of Hong Kong, Hong Kong

The development and application of metallic glasses can benefit from the in-depth understanding of the structure-properties relationship during plastic deformation. The limited tensile plasticity of metallic glasses hindered the in-situ study of structural response under tension. Here, we report an in-situ synchrotron study of a metallic glass after canning compression under tension at a micro-scale. Our experimental results show that the canning-compressed metallic glass has much better tensile ductility and much higher ultimate strength than its initial state. The real-space analysis of synchrotron diffraction data indicates that the cluster connectivity and ordering at medium-range length scale play an essential role in plastic deformation. Our results may shed light on developing ductile metallic glasses and their devices at micro-scales.

9:15 AM ST02.01.05

Spatial Localization of Dislocation Avalanches During Microplasticity of a High-Entropy Alloy Quentin Rizzardi¹ and Robert Maass^{1,2}; ¹University of Illinois at Urbana-Champaign, United States; ²Bundesanstalt für Materialforschung und -prüfung (BAM), Germany

We attempt here an in-situ experiment to reconcile the recorded mechanical activity of dislocation avalanches during small-scale plasticity of a high-entropy alloy with the observed formation and evolution of slip line morphology on the sample. Correlating the intermittent microplastic events with their corresponding slip-line pattern allows us to define two main event types: events that lead to the formation of new slip lines, and those that involve reactivation of already existing slip lines. The formation of new slip lines reveals statistically larger and faster avalanches that lower the stress-integrated scaling exponent of the global distribution of all occurring events. The opposite tendency is seen for avalanches involving reactivation of already existing slip lines. The combination of both these types of events represents the highest degree of spatial avalanche delocalization, forming a group of events that determine the truncation length-scale of the truncated power-law scaling. These observations link stress-strain fluctuations in a typical small-scale deformation experiment to the spatial localization of dislocation avalanches, underlining their non-trivial scaling behavior.

SESSION ST02.02: MEMS, High-Strain Rate, High Temperature & Environmental Testing
Session Chairs: Christoph Gammer and Thomas Pekin
Thursday Morning, April 22, 2021
ST02

10:30 AM *ST02.02.01

High Strain Rate Testing from Micro-to-Meso Scale Rajaprakash Ramachandramoorthy^{1,2}, Szilvia Kalácska², Patrik Schuerch³, Manish Jain², Jakob Schwiedrzik², Wabe Koelmans³, Laetitia Philippe², Xavier Maeder² and Johann Michler²; ¹Max-Planck-Institut für Eisenforschung, Germany; ²Empa–Swiss Federal Laboratories for Materials Science and Technology, Switzerland; ³Exaddon AG, Switzerland

Dynamic properties of materials at high strain rates are vital to assess their suitability and reliability in applications ranging from common drops to demanding impact-protection applications. Macroscale mechanical testing at high strain rates, though challenging, is already a well-established field of research. But recently, given the push towards miniaturization, small scale mechanics has also been a topic of intense research over the last two decades. However, till date the micro and nanomechanical experiments have been largely limited to testing samples made using focused ion beam (FIB) milling at quasi-static speeds. Small scale sample preparation using FIB-based milling is a serial and time-consuming process that typically limits the number of samples tested in micromechanical studies, while allowing the fabrication of only simple geometries. On the other hand, the limitation in testing speed is primarily attributed to the lack of instrumentation capable of high speed actuation and simultaneous high speed capture of loads and displacements with micronewton and

nanometer resolution.

This presentation will introduce a newly developed piezo-based micromechanical tester capable of conducting high strain rate micromechanical testing at speeds up to 10mm/s. The relevant hardware requirements and protocols specific to high speed testing at the small scale will be elaborated. Further, a localized electrodeposition based metal additive micromanufacturing (μ AM) technique will be introduced as a viable method for fabricating full-metal microarchitectures. A large array of ideal copper micropillar test-beds built using this technique will be presented along with electron backscatter diffraction (EBSD) based microstructural characterization showing two distinct microstructures: microcrystalline and ultrafine grain (UFG). The mechanical properties of these copper micropillars, explored as a function of strain rate from 0.001/s to 500/s, will be shown as a function of initial pillar microstructure. Relevant, stress-strain signatures, thermal activation parameters and post-deformation microstructural analysis using EBSD and transmission kikuchi diffraction (TKD) for the copper micropillars will also be presented.

The last part of the presentation will highlight the capabilities of μ AM to fabricate complex full-metal 3D microarchitectures such as microlattices and microsprings. Copper microlattices with different geometries, chosen from an energy absorption perspective, including honeycomb, octet and kelvin foam will be presented along with their dynamic compressive properties upto a strain rate of \sim 150/s. Further, a detailed structural and microstructural characterization conducted using FIB-based 3D slice-and-view and EBSD/transmission electron microscopy (TEM) respectively will be compared between the undeformed and deformed lattices. Finally, a finite element methods (FEM) based simulation aimed at understanding the structural evolution of the metal lattices under high speed deformation will be presented. It will be explained that the FEM simulation model takes into account the defect structures determined using the reconstructed 3D slice-and-view lattices and the appropriate constitutive laws identified from the high strain rate compression of copper micropillars.

11:00 AM ST02.02.02

Beyond Strain Bursts in Intermittent Crystal Plasticity—Ultrafast Dislocation Avalanches and Mean Swept Distances Across Microsample Sizes in FCC and BCC Metals Jan Ocenasek¹, Jeffrey Wheeler², Javier Varillas^{1,3}, Jaafar El-Awady⁴ and Jorge Alcalá⁵; ¹University of West Bohemia in Pilsen, Czechia; ²Swiss Federal Institute of Technology in Zürich, Switzerland; ³The Czech Academy of Sciences, Czechia; ⁴The Johns Hopkins University, United States; ⁵Universitat Politècnica de Catalunya, Spain

Plastic deformation in crystalline materials consists of an ensemble of collective dislocation glide processes, which lead to strain burst emissions in micro-scale samples. Prior investigations of plastic intermittencies involved the large strain bursts triggered with dynamically-reactive testing systems. Under these driving conditions, the microcrystal is rapidly compressed as a function of the system's dynamic response, which ultimately governs the termination of the instability and its overall size. We argue that a dynamically-induced plastic instability or strain burst is comprised of many of the currently measured individual dislocation avalanche events, propagating over minuscule time scales, which are ubiquitous to crystal plasticity.

To investigate the onset of the ultrafast individual dislocation avalanches, we performed a comprehensive set of strict displacement-controlled micropillar compression experiments in conjunction with large-scale molecular dynamics and physics-based discrete dislocation dynamics simulations. It is shown that the size distributions of these dislocation events exhibit a gradual transition from an incipient power-law slip regime (spanning \approx 2.5 decades of slip sizes) to a large avalanche domain (spanning \approx 4 decades of emission probability) at a cut-off slip magnitude s_c . This cut-off slip provides a statistical measure to the characteristic mean dislocation swept distance, which allows for the scaling of the avalanche distributions *vis-à-vis* the archetypal dislocation mechanisms in face-centered cubic (FCC) and body-centered cubic (BCC) metals. Our statistical findings provide a new pathway to characterizing metal plasticity and towards comprehension of the sample size effects that limit the mechanical reliability in small-scale structures.

11:15 AM ST02.02.03

High Temperature *In Situ* Mechanics of Ni-Based Superalloys and Bond Coatings Sanjit Bhowmick;

Bruker, United States

High-strength structural materials such as Ni-based superalloys and diffusion bond coats are widely used in challenging environments and with exposure to mechanical fatigue, particle impact, and erosion at elevated temperatures. Diffusion platinum-aluminide bond coatings are an example of compositionally and microstructurally graded coatings with significant variation in engineered mechanical properties across the cross-section. In this study, an SEM nanomechanical instrument with an integrated high-temperature stage and an active tip heating was used to conduct pillar compression of aluminide bond coating and substrate at room temperature to 1000°C. With combined analysis of chemistry and microstructural changes, the results were used to understand local mechanical properties variation as a function of temperature.

11:30 AM ST02.02.04

Isothermal, Self-Actuated MEMS-Based High-Temperature Nanomechanical Test Platform Longchang Ni¹, Ryan Pocratsky² and Maarten De Boer¹; ¹Carnegie Mellon University, United States; ²Fischione Instruments, United States

Relatively little is known about freestanding thin film creep at elevated temperature. In MEMS, polycrystalline silicon (polysilicon) thermal actuators are frequently used as on chip actuators, but they typically operate at temperatures 300-500 °C higher than the substrate to generate useable displacement and force output. This is because polysilicon's coefficient of thermal expansion (CTE, 2.7 $\mu\epsilon/^\circ\text{C}$) is the same as the silicon substrate. When actuated by Joule heating, heat flows to the specimen, which can induce experimental artifacts. Instead of using polysilicon, we demonstrate refractory metal tantalum (Ta) thin films as a new structural material for MEMS nanomechanical test platforms. The CTE of Ta films is double that of polysilicon (5.9 $\mu\epsilon/^\circ\text{C}$). Therefore, self-actuation simply by raising the temperature is possible. A stress relaxation test can be performed under an isothermal condition, and strains up to 30 % are possible. We have fabricated Ta thermal actuators using conventional surface micromachining after resolving key fabrication issues. Self-actuation has been successfully demonstrated. Using a platinum specimen for demonstration, we have validated a process flow to co-fabricate the specimen with Ta thermal actuators. High-temperature, stress relaxation experiments on structural Pt films at temperatures up to 500 °C will be performed and presented. This work demonstrates for the first time a powerful drift-free in-situ stress relaxation test of structural thin films at elevated temperatures.<!--![endif]----><!--![endif]---->

11:45 AM ST02.02.05

Variable-Humidity Nanoindentation—Challenges and Opportunities Joseph Jakes; USDA Forest Service, Forest Products Laboratory, United States

A wide variety of materials, including thin film microelectronics and lignocellulosic materials, have moisture-dependent mechanical properties that can vary substantially depending on the ambient relative humidity (RH). Under high RH conditions, moisture sorption can weaken interfaces or plasticize materials. The effects of moisture can be especially challenging to study at interfaces and in composite materials with small micron- and nanoscale components. To overcome this challenge, protocols were developed to perform nanoindentation experiments over a wide range of humidity. Using an external RH generator, the environment inside of a Hysitron TriboIndenter enclosure was controlled and varied from dry air up to 95% RH. Analysis of calibration nanoindentations in the air and in fused silica supported that the nanoindenter functioned properly over the entire humidity range provided that enough time was given to equilibrate at the RH. However, some corrosion was observed in metal fasteners on the instrument, which suggests that keeping the nanoindenter under high RH conditions is not advisable over the long term. Nanoindentation results studying the moisture-dependent properties of porous organosilicate glass (SiCOH) thin films and wood will be presented. In SiCOH, elastic modulus was found to not depend on humidity, whereas the hardness and fracture behavior were intimately linked to the nature and concentration of the absorbed water. Wood cell walls are plasticized by the absorbed water and both the elastic modulus and hardness decrease with increasing RH. Additionally, using dynamic nanoindentation the mechanical damping of the wood cell walls was assessed over three decades of frequency

and a moisture-dependent glass transition of the amorphous polysaccharides in the wood cell wall could also be observed as a peak in mechanical damping.

12:00 PM ST02.02.06

Electro-Chemo-Mechanical Coupling—A Novel Approach to Micro Actuation Evgeniy Makagon¹, Ellen Wachtel¹, Lothar Houben¹, Sidney Cohen¹, Yuanyuan Li², Junying Li², Anatoly Frenkel² and Igor Lubomirsky¹; ¹Weizmann Institute of Science, Israel; ²Stony Brook University, United States

The chemo-mechanical effect in solids refers to dimensional change due to change in stoichiometry. Dimensional change due to electrochemically-induced compositional change has been termed the electro-chemo-mechanical (ECM) effect. The mechanical instability inherent in this effect is clearly deleterious for batteries or fuel cells, but, as recently suggested, has potential for use in actuation[1]. The structure of an actuator device that operates on the ECM principle comprises a micrometer thick solid electrolyte (SE) sandwiched between two ECM-active, working body (WB) layers. An electrochemical reaction must occur in these layers, causing them to alternately expand or contract. In order to facilitate the ECM response, the WB layers should have mixed ionic and electronic conductivity and a large chemical expansion coefficient. We have constructed a 2mm diameter thin film membrane ECM actuator device comprising 20mol% Gd doped CeO₂ (20GDC) as the SE and [TiO_{2-δ}20GDC] or [V₂O_{5-δ}20GDC] composites as the WBs[2]. Selected area electron diffraction measurements showed the composite to be nanocrystalline, a morphology that promotes interfacial oxygen ion diffusion. Synchrotron X-ray absorption (XAS) measurements detected a mixture of Ce³⁺/Ce⁴⁺ (~[0.4]/[0.6]) and Ti³⁺/Ti⁴⁺ (~[0.1]/[0.9]) oxidation states in the WB. XAS measurements under bias showed changes in the short-range order of Ti and V oxides supporting the presence of a redox reaction. The deformation of the ECM actuator was observed to be in the bending regime producing large vertical displacements (~3 μm) and ~4 MPa stress. The stress/voltage ratio yields a pseudo piezoelectric stress coefficient of $e_{31}=1.26 \text{ C/m}^2$, comparable to common lead-free piezoelectrics such as lithium niobate, lithium tantalate and alkali niobates.

[1] J. G. Swallow *et al.*, Nat. Mater. (2017) **16**, 749

[2] E. Makagon et al. Adv. Funct. Mater. (2020), 2006712.

SESSION ST02.03: In Situ Techniques—Strain Mapping
Session Chairs: Christoph Gammer and Wendy Gu
Thursday Afternoon, April 22, 2021
ST02

1:00 PM *ST02.03.01

Imaging Defects and Their Dynamics Using Scanning Electron Microscopy Approaches Daniel Gianola; University of California, Santa Barbara, United States

The past several years has witnessed a surging popularity of two techniques for defect characterization in crystalline materials: (i) scanning transmission electron microscopy (STEM) using diffraction contrast imaging, and (ii) electron back-scattered diffraction (EBSD) mapping. Advantages of diffraction-contrast STEM methods over conventional TEM include the suppression of dynamical effects and spurious contrast, as well as the ability to image relatively thick specimens. In parallel, the use of transmission modalities in the scanning electron microscope (SEM) has attracted recent attention. Here, we link these capabilities by employing an field emission SEM equipped with a transmission detector for defect characterization – termed transmission SEM (TSEM). Imaging modes that are similar to conventional CTEM bright field (BF) and dark field (DF) and STEM are explored, and some of the differences due to the varying accelerating voltages highlighted. As an alternative approach more amenable to bulk materials, EBSD has evolved to be a widespread and

powerful characterization technique for the mapping and analysis of phases in crystalline materials, providing key information about crystal orientation, morphologies, lattice strain, topology, and crystallographic texture. Whereas the advent of direct electron detection (DED) that circumvents inefficient conversion between electrons and photons has revolutionized the field of TEM, owing to single electron sensitivity for beam sensitive samples and ultrafast detection for time-resolved studies, the use of DED in the vastly more accessible SEM environment is in its infancy. Here, we demonstrate how the richness of information encoded in EBSD patterns is amplified by a new generation of direct electron detectors that enable high speed mapping and acquisition of high-fidelity patterns that can be used for statistically-meaningful defect analyses. We further show that these SEM-based approaches provide significant advantages for dynamic *in situ* characterization. We employ location-specific *in situ* tensile experiments to study the nature of dislocations dynamics in several structural alloys. By selecting specific crystallographic orientations relative to the tensile axis, we observe the underpinnings of several plasticity mechanisms including shear localization, cross-slip, and dislocation junction formation and evolution. To illustrate the power of these new methods for defect-contrast studies, we show examples on several emerging structural materials such as superalloys and refractory multi-principal element alloys.

1:30 PM *ST02.03.02

***In Situ* 4D-STEM** Andrew M. Minor^{1,2}; ¹University of California, Berkeley, United States; ²Lawrence Berkeley National Laboratory, United States

In situ transmission electron microscopy (TEM) experiments are typically recorded either in real space or diffraction space. However, it would be ideal to have both real and diffraction space for when transient events occur that cannot be repeated exactly (ie- defect generation or irreversible phase transformations). Real space imaging provides context for these transient events by spatially-resolving microstructural features to one another while diffraction space provides better structural clarity about phase identification and lattice parameters. Four-dimensional scanning transmission electron microscopy (4D-STEM), can come close to providing both simultaneous real-space imaging and diffraction analysis during *in situ* testing. With the advent of fast direct electron detectors it is possible to perform strain mapping via diffraction pattern analysis during in-situ deformation in a TEM with the precision of a few nanometers without stopping the experiment. Images of the same overall experiment can then be formed using virtual apertures applied to the accumulated diffraction patterns. This talk will highlight recent *in situ* 4DSTEM experiments that explore transient events where both information from diffraction space and real space are used. The diffraction patterns are used to identify different phases, orientations and relative strain, while the images formed by using virtual apertures provide microstructural context for the analysis. Example experiments include defect generation and interactions in metals, local strain evolution in bulk metallic glasses, and structural transformations in functional oxides under deformation.

2:00 PM ST02.03.03

Assessment of Template Matching (TeMA) and Geometric Phase Analysis (GPA) in Quantifying Large Deformation Strains/Displacements Around Defects Ahmed Sameer Khan Mohammed, Florian Brenne and Huseyin Sehitoglu; University of Illinois at Urbana-Champaign, United States

This study assesses the applicability of advanced atomic resolution displacement measurement techniques to characterize dislocation character in metallic materials using simulated images derived from anisotropic elasticity and actual measurements in high entropy alloys. We draw attention to two techniques: the real space method of template matching (TeMA) and the reciprocal space method of geometric phase analysis (GPA) and provide a critical assessment. These techniques have limitations for direct evaluation of full dislocations Burgers vector or when local displacements exceed certain value. This value depends on the displacement direction in relation to the crystal structure. A cut-off for reliable displacement measurement is proposed as the boundaries of the Wigner-Seitz cell drawn on the 2D HRTEM image of the crystal structure. This effect is illustrated with simulated arctangent displacement profiles reminiscent of dislocation cores. An approach for circumventing this limitation is suggested in the form of a nearest neighbor correction. Additionally, a

methodology for determination of the Burgers vector is introduced on the basis of a vectorial rendering of the displacement field upon consideration of two zone axis measurements and applied to TeMA and GPA. The experimental results conform to the Burgers vector of a full lattice dislocation in the FCC crystal structure of the High-Entropy Alloy (HEA). The comparison of simulated and experimental images proves the efficacy of the HR-TEM (High Resolution Transmission Electron Microscopy) displacement mapping techniques while pointing to the need for caution in case of large displacements.

2:15 PM ST02.03.04

Stress and Crystal Orientation Mapping in Thin Films with Micro Reflectance Anisotropy Spectroscopy

Joan Sendra, Nerea Abando, Henning Galinski and Ralph Spolenak; ETH Zürich, Switzerland

The mechanical characterization at small length scales is of fundamental importance to obtain insights of deformation mechanisms. In particular, stress mapping is of great interest since it allows the study of fracture mechanics, e.g. visualizing the stress distribution around a crack tip. Conventional lab scale stress mapping techniques are based on electron microscopy and Raman spectroscopy. Common drawbacks are the required high vacuum for electron microscopy and the need of polarizable materials for Raman spectroscopy, hindering the range of materials that can be analyzed. X-ray diffraction is also an established technique for mechanical studies, however its need for a large interaction volume poses problems for ultra thin film studies while still being limited in lateral resolution. Synchrotron X-ray diffraction bypasses these drawbacks and achieves high spatial resolution and strain sensitivity for thin crystalline materials but requires significant resource investment. In contrast, reflectance anisotropy spectroscopy (RAS) can be employed for a wide range of materials, environments and sample thicknesses to become an attractive technique for non-destructive mechanical studies. RAS is an ellipsometric technique that measures the difference in reflectance between linearly polarized light along two orthogonal directions of the sample. However, usual resolution of conventional RAS setups is in the order of millimeters. Here, we present an advanced reflectance anisotropy spectroscopy (RAS) microscope based on a super continuum laser source as a non-destructive stress mapping technique. Our microscope enables insight into the electronic band structure, phase and crystal orientation.

We sputter metallic thin films on flexible substrates and employ focused ion beam (FIB) milling to modify surface topology. We then demonstrate the capabilities of the technique by externally applying uniaxial strain on the fabricated FIB structures and mapping of the strain distribution on the surface of the sample. Furthermore, mechanical properties are highly influenced by microstructure. Since RAS signal is dependent on crystal orientation, we also prove grain mapping in polycrystalline copper and compare the RAS signal of different grains to outline the possibility of grain orientation indexing in a similar fashion to electron backscattered diffraction. The potential simultaneous stress and grain orientation mapping will enable future studies on the fracture mechanics of thin films and novel materials with different microstructure and environmental conditions.

2:30 PM ST02.03.05

Nanoscale Imaging of Strain and Defect by Bragg Coherent X-Ray Diffractive Imaging Wonsuk Cha;

Argonne National Laboratory, United States

In the past decades, Coherent X-ray Diffractive Imaging in Bragg geometry (BCDI) has become one of major nanoscale imaging techniques. Unique sensitivity to lattice [1] enables BCDI to image three-dimensional morphology as well as internal deformation field distribution of nano-scaled and/or micro-scaled materials including metal, metal oxide, minerals, and so on. Nowadays, in-situ and operando BCDI is a main driver to address scientific questions on materials.

In this talk, I will introduce current state-of-the-art of BCDI and the 34-ID-C beamline in the Advanced Photon Source where BCDI experiments can be performed. This talk will also cover recent experimental results on in-situ and operando BCDI, e.g. unique lattice distortion in ZSM-5 zeolites [2], annealing effect on gold grains on gold thin films [3], dislocation imaging under tensile loading [4], and current development on combining Laue diffraction to BCDI [5]. In addition, some estimates of BCDI in the future will be discussed.

- [1] M. A. Pfeifer, et al., Nature 442, 63 (2006).
[2] W. Cha, et al., Nat. Mater. 12, 729 (2013).
[3] A. Yau, et al., Science 356, 739 (2017).
[4] M. Cherukara, et al., Nature Communications 9, 3776 (2018).
[5] A. Pateras, et al., Journal of Synchrotron Radiation 27, 1430 (2020).

SESSION ST02.04: Plasticity at Small Length Scales I
Session Chairs: Mitra Taheri and Kelvin Xie
Thursday Afternoon, April 22, 2021
ST02

4:00 PM *ST02.04.01

Deformation in Sub-10 nm Nanocrystals and Nanoclusters Wendy Gu, Abhinav Parakh and Qi Li; Stanford University, United States

Sub-10 nm metals have fascinating physical, optical and chemical properties. By applying stress to these nanomaterials, it is possible to study atomistic motion near surfaces, as well as investigate structure-property relationships at the smallest length scales.

Here, we use diamond anvil cell techniques to compress nanocrystals and nanoclusters under hydrostatic and non-hydrostatic pressures. Synchrotron X-ray diffraction is used to detect structural changes within 4 and 6 nm Au nanocrystals. It is found that crystalline defects (e.g. stacking faults) form in the 4 nm nanocrystals under pressure, and remain in the nanocrystals after pressure is removed. In contrast, twins within 6 nm Au nanocrystals are removed during high-pressure compression, such that single crystalline nanocrystals are formed. These single crystalline nanocrystals were found to be metastable. The nanocrystals were recovered after compression, and placed in the TEM, where the nanocrystals reverted to the twinned state under the electron beam.

At even smaller length scales, fcc cuboctahedral and icosahedral nanoclusters such as Au₂₁, Au₂₅, and Ag₂₈Pt₁ were compressed while optical absorbance and photoluminescence spectroscopy were performed in-situ. In combination with density-functional theory, it was found that increased interaction between surface metal atoms and the surrounding organic ligands leads to the observed high pressure behavior.

4:30 PM *ST02.04.02

In Situ TEM Tensile Testing of Crystalline Metallic Nanowires Yong Zhu; North Carolina State University, United States

Metallic nanowires have been widely used in a variety of nanoengineering applications, including nanoelectromechanical systems, nanosensors, transparent electrodes, optoelectronics, and flexible and stretchable electronics. Mechanical behaviors of metallic NWs play a crucial role in reliability of the nanowire-based devices. Here I will present the recent work in my group on in-situ nanomechanics of crystalline metallic nanowires inside transmission electron microscope (TEM). First, we report competition of deformation mechanisms - twinning and slip - in single-crystalline metallic nanowires. We found that the competition depends on the cross-sectional shape of the nanowire, which affects the change of surface energy associated with each deformation mechanism. Second, we found unexpectedly, through careful cross-sectional TEM study, that most of the synthesized single-crystalline nanowires include a central twin boundary along the entire length of the nanowire, so we call them bi-twinned nanowires. Here we also found two competing deformation mechanisms - localized dislocation slip and delocalized plasticity via an anomalous tensile detwinning mechanism - depending on the volume ratio between the two twin variants and the cross-sectional aspect ratio.

The mechanism of the observed tensile detwinning was investigated. Furthermore, the twin boundary was found to cause interesting recoverable plasticity and Bauschinger effect, as well as strain hardening. Finally, we probe hydrogen embrittlement using metallic nanowires as a model system. We found increasing yield strength and brittle failure with the presence of hydrogen, which was attributed to the hydrogen-induced suppression of dislocation nucleation at the free surface of nanowires.

5:00 PM ST02.04.03

Molecular Crystal Compaction at the Microscale Daniel Bufford, Christopher M. Barr, Jeremy Lechman and Marcia Cooper; Sandia National Laboratories, United States

Molecular crystals consist of discrete molecules bonded together not by ionic, covalent, or metallic bonds, but by weaker cohesive forces. The almost endless variety of molecular shapes and bonding forces gives rise to a plethora of structures, and, accordingly, deformation and fracture processes that vary greatly among molecular crystals. Mechanical behavior in these materials generally remains less completely understood than in other materials. Small-scale and in-situ mechanical testing approaches have made great contributions to the understanding of deformation mechanisms in many other classes of materials; nanoindentation has already proven useful in examining molecular crystals, but to date in-situ methods have seen little application. This talk present results from single particle compression studies conducted in-situ inside of a scanning electron microscope. Individual micron-sized particles of hexanitrohexaazaisowurtzitane, an organic molecular crystal and energetic material, were compressed to the point of fracture. Challenges and successes in sample preparation, experiment execution, and interpretation of the resulting data will be discussed. The combination of microscopy and quantitative load-displacement data allowed for estimation of stresses and strains associated with yielding and fracture processes, and may suggest an extrinsic size-dependent strength phenomenon. The approach here is generalizable, and may contribute to the understanding of deformation and fracture in other molecular crystals.

This work was performed, in part, at the Center for Integrated Nanotechnologies, an Office of Science User Facility operated for the U.S. Department of Energy (DOE) Office of Science. Sandia National Laboratories is a multimission laboratory managed and operated by National Technology & Engineering Solutions of Sandia, LLC, a wholly owned subsidiary of Honeywell International, Inc., for the U.S. DOE's National Nuclear Security Administration under contract DE-NA-0003525. The views expressed in the article do not necessarily represent the views of the U.S. DOE or the United States Government.

5:15 PM ST02.04.04

Quantifying Size-Dependent Deformation Mechanisms in Metal Nanoparticles via In Situ TEM Mechanical Testing Soodabeh Azadehnanjbar¹, Ruikang Ding¹, Andrew Baker¹, Ingrid M. Padilla Espinosa², Ashlie Martini² and Tevis Jacobs¹; ¹University of Pittsburgh, United States; ²University of California, Merced, United States

While bulk material strength is determined by the size of microstructural features, such as the size and distribution of grains, precipitates, twin boundaries or dislocations, nanoscale deformation is strongly dependent on the size of the body being deformed. In the range of tens of nanometers of particle diameter, deformation is accommodated through a Coble-creep-like mechanism where the strength depends on strain rate and the size of the spherical particle. However, even this Coble-creep-like mechanism may break down for single-digit-diameter nanoparticles, when surface faceting becomes dominant.

In the present work, we used *in situ* compression tests of platinum nanoparticles to quantify the size-dependence of deformation mechanisms. Platinum nanoparticles were synthesized with sizes ranging from tens of nanometers down to single-digit nanometers. These particles were compressed inside of a transmission electron microscope (TEM), enabling the combination of high-resolution video with real-time measurement of force and deformation. The morphology and load response of the deforming nanoparticles were analyzed to demonstrate the dominant deformation mechanism in various size regimes. Finally, results were compared with matched atomistic simulations for atomic-scale insight into driving forces and particle behavior.

5:30 PM ST02.04.05

Late News: *In Situ* Observations of Phase Transitions During Berkovich Indentation of Silicon Thin Films Yvonne B. Gerbig and Chris Michaels; National Institute of Standards and Technology, United States

The indentation-induced phase transformation of crystalline silicon thin films was studied *in-situ* during the indentation with a Berkovich probe using Raman spectroscopy-enhanced instrumented indentation. The *in-situ* Raman spectroscopic analysis showed the formation of high-pressure phases during indentation loading, calling into question the common view that pressure release is a pre-condition for this transformation. The observations suggest strain and time as important but overlooked factors in nucleation and growth of high-pressure phases and provide new context to previous works on the pressure-induced phase transformations of silicon.

SESSION ST02.05: Nanoscale Deformation & Fracture

Session Chairs: Yuichi Ikuhara and Sang Ho Oh

Thursday Afternoon, April 22, 2021

ST02

8:15 PM ST02.05.03

Deformation Twinning in Au₃₀Ag₇₀ Alloy Nanowire Under Tensile Strain Wonsik Kim¹, Kkotchorong Park¹, Seung Jo Yoo^{1,2}, Byungil Hwang³, Bongsoo Kim¹ and Seung Min Han¹; ¹Korea Advanced Institute of Science and Technology, Korea (the Republic of); ²Electron Microscopy Research Center, Korea Basic Science Institute, Korea (the Republic of); ³Chung-Ang University, Korea (the Republic of)

Single element metallic nanowires have been deeply studied for their wide range of applications. Alloyed nanowires are known to have distinct characteristics and deformation behavior compared with single element nanowires that comes from difference in stacking fault energies. They are known to have potential to be used in various plasmonic devices for their chemical stability and broad applicable range of wave lengths. However, more detailed analysis mechanical properties is needed for comprehensive understanding of such material systems. In this study, defect-free single crystalline Au₃₀Ag₇₀ alloy nanowires are synthesized by topotaxial growth method and tested in tension using an in-situ pico-indenter. Deformation twinning followed by superplastic deformation of the alloy nanowires is experimentally observed and the critical dimension of Au₃₀Ag₇₀ alloy nanowires at which transition from ordinary plasticity to deformation twinning is determined to be ~333 nm, which is about 2 time larger than that of Au nanowires. Stacking fault energy, which is the key element determining the deformation mode, of Au₃₀Ag₇₀ alloy nanowires is calculated to be 21 mJ/m², which is smaller than that of Au nanowire with stacking fault energy of 31 mJ/m². The decrease in the stacking fault energy in the alloy nanowire resulted in stabilization of deformation twinning to a larger critical dimension before transitioning to ordinary plasticity.

8:30 PM ST02.05.04

Late News: The Study of Structure-Mechanical Relationship of SU-8 via *In Situ* Characterization Prakash Sarkar, Prita Pant and Hemant Nanavati; Indian Institute of Technology (IIT), Bombay, India

SU-8 is a cross-linked thermoset polymer which is extensively used for design micro-electrical mechanical system (MEMS) components. The effect of cross-linking amount on the mechanical properties i.e. modulus (E) and hardness (H) was studied using nanoindentation. Different cross-linked samples were fabricated by changing the curing steps (post-exposure baking, hard baking) of standard photolithography process. The accurate measurement of cross-linked segments is done via in-situ Fourier-transform infrared spectroscopy. Nanoindentation experiments were performed under constant strain rate loading conditions. Using the conventional method yielded high E and H values for less cross-linked sample and less values for high cross-

linked samples. A careful analysis showed that the main reasons for these inverse values are adhesion between the tip surface and sample surface, viscoelastic effect on unloading and errors in calculation of contact area. We propose a new methodology to correct for these potential sources of error. Thereafter, less E and H values for less cross-linked sample and high values for high cross-linked sample were obtained. The values are 4.61 ± 0.13 GPa and 5.02 ± 0.18 GPa of E, and 256.97 ± 1.42 MPa and 285.48 ± 1.17 MPa of H for less (~ 82 %) and high (~ 95 %) cross-linked samples, respectively.

Keywords: SU-8; Photolithography process; FTIR; Nanoindentation; SPM

8:45 PM *ST02.05.05

Nanoscale Dynamic Observations of Grain Boundary Fracture, Deformation, Migration and Twin

Formation in Ceramics Yuichi Ikuhara^{1,2,3}; ¹University of Tokyo, Japan; ²Japan Fine Ceramics Center, Japan; ³Tohoku University, Japan

Ceramics have been widely used for structural applications because of their superior mechanical properties. It has been known that the behavior of GB fracture, deformation and migration is strongly dependent on the GB characters such as misorientation angle between two adjacent crystals and GB plane, however, such effect has not been clarified yet. In this study, in order to clarify the atomistic mechanisms of GB fracture and deformation, bicrystal studies have been performed to find the relationship between the atomic structures and GB behavior of SrTiO₃ and Al₂O₃ ceramics. Several kinds of bicrystals including GBs with specific geometrical configuration were fabricated, and some of them were doped by rare-earth elements to enhance the GB segregation.

It has been reported that single crystal of SrTiO₃ can be plastically deformed even at R.T. by dislocation slip like metals. So far, many experimental investigations have been tried for understanding the dislocation-grain boundary interaction, but these experiments were mostly carried out statically, and the fundamental processes are still not well understood yet. In this study, the nanoindentation experiments were conducted for SrTiO₃ crystals their bicrystals inside TEM. The SrTiO₃ single crystals were indented with the sharp diamond tip and successfully observed the dislocation dynamics. In the case of the GBs, the interaction between the introduced lattice dislocations and the GBs were directly observed. The dislocation-GB interaction and its dependence on the GB characters will be discussed in detail.

GB fracture in Al₂O₃ is strongly dependent on the GB characters and the dopant segregated at GBs. In order to clarify the atomistic GB fracture mechanism and its dopant effect in Al₂O₃ ceramics, Al₂O₃ bicrystals including GBs with specific geometrical configuration were systematically fabricated, and some of them were doped by rare-earth elements. Then, the atomic structures and chemistry in thus fabricated GBs were characterized by atom-resolved STEM, and the dynamic behavior of GB fracture was observed by TEM nanoindentation experiment. The relationship between GB characters, segregated dopants and GB fracture behavior of Al₂O₃ will be discussed in detail.

It is known that Al₂O₃ shows twin formation at R.T. under high stress concentration. So far, many experimental investigations have been tried for understanding the twin formation mechanism, but these experiments were also carried out statically, and the fundamental atomistic processes are still not well understood yet. In this study, TEM *in situ* nanoindentation experiments were conducted also for Al₂O₃ single crystals and the bicrystals. Al₂O₃ single crystals were indented with the sharp diamond tip, and the twinning dynamics were successfully observed. In this case, the deformation twinning often occurs in the present experimental condition, and the mechanism can be explained by a shear process for each lattice layer, which is caused by twinning dislocations. It is suggested that the non-basal twinning systems, such as the rhombohedral twinning in Al₂O₃, can be completed by not only simple shear but also atomic shuffling. In this study, the dynamic behavior and atomic structures of the twinning dislocations were investigated for rhombohedral twinning in Al₂O₃, and the twin -GB interaction and its dependence on the GB characters will be discussed in detail.

References:

- 1) S. Kondo, N. Shibata, T. Mitsuma, E. Tochigi, Y. Ikuhara, *Appl. Phys.Lett.*, 100(18), 181906(2012)
- 2) S. Kondo, T. Mitsuma, N. Shibata, Y. Ikuhara, *Sci. A dv.*, 2[11], e1501926(2016).
- 3) J. Wei, B. Feng, R. Ishikawa, T. Yokoi, K. Matsunaga, N. Shibata, Y. Ikuhara, *Nature Materials*, DOI : 10.1038/s41563-020-00879-z (2021)

9:15 PM ST02.05.06

Late News: Analysis of Mechanical Behaviour of Ti/TiN Multilayer Using Micro-Cantilever Beam

Bending Ashwini K. Mishra¹, Hariprasad Gopalan², Marcus Hans³, Christoph Kirchlechner⁴, Jochen Schneider³, Gerhard Dehm² and Nagamani Jaya Balila¹; ¹Indian Institute of Technology Bombay, India; ²Max-Planck-Institut für Eisenforschung GmbH, Germany; ³RWTH Aachen University, Germany; ⁴Karlsruhe Institute of Technology, Germany

Nitride ceramics have wide application as a protective coating but suffer extreme brittleness. In this work, the mechanical behavior of physical vapor deposited Ti/TiN multilayer has been studied. Effect of varying layer thickness and volume fraction of elastic-plastic Ti in Ti-TiN multilayer is observed by testing micro-cantilever bending. FEM simulations were carried out for various multilayer thickness and volume fraction to establish the theory behind it. R-curve behavior of multilayer is also discussed using simulation results. Finer spacing in multilayer enhances the fracture toughness of multilayer. Fracture properties of multilayer in comparison to monolithic TiN layer will be reported.

9:30 PM ST02.05.07

Late News: Microscale Mechanical Studies in Barium Titanate—Deformation and Fracture

Nidhin G. Mathews¹, Ashish K. Saxena^{2,3}, Christoph Kirchlechner^{2,4}, N Venkataramani¹, Gerhard Dehm² and Balila N. Jaya¹; ¹Indian Institute of Technology Bombay, India; ²Max-Planck-Institut für Eisenforschung GmbH, Germany; ³Vellore Institute of Technology, India; ⁴Karlsruhe Institute of Technology—Institute for Applied Materials, Germany

Barium Titanate (BTO) is a widely used lead-free piezoelectric ceramic used at micron length scales as thin films in MEMS applications. Here we study the mechanical behaviour BTO single crystals and thin film systems using different micromechanical experiments and finite element modelling (FEM). Microscale mechanical behaviour of single crystalline BTO was studied by uniaxial *in situ* micropillar compression for different sizes. It was observed that pillars below 1µm diameter reached their theoretical strength whereas larger pillars yielded at lower stress values with multiple stress drops confirming slip activity. The strain accommodation mechanism at smaller length scales is by plastic flow, with a size exponent close to 1 and enhances the elastic strain limit of the material, which is an important consequence that can be exploited in sensors/actuators. Microcantilever fracture measurements revealed that, single crystal BTO showed a 45% higher K_{IC} than the bulk, while the polycrystalline thin film showed a 60% lower K_{IC} due to the weak inter-columnar boundaries. Different geometrical aspects and loading parameters on the stress intensity factor of single cantilevers are investigated using FEM to propose testing standards that can be used by future users. The variation of stress intensity factor and mode mixity (K_{II}/K_I) with respect to the relative position of the notch, beam cross-section, notch tip radius, notch geometry and arm length of the cantilever and loading direction are studied. Effect of bilayers and elastic modulus mismatch between the layers on the crack driving force are also discussed.

SESSION ST02.06: Plasticity at Small Length Scales II

Session Chairs: Gerhard Dehm and Ruth Schwaiger

Friday Morning, April 23, 2021

ST02

8:00 AM *ST02.06.01

On the Role of Surfaces and Interfaces in Dislocation Nucleation-Controlled Plasticity of Nano-Objects—Comparison of In-Situ Experiments with Atomistic Simulations Zhuocheng Xie¹, Aruna Prakash², Saba Khadivianazar³, Nadine Schrenker³, Daniel Gianola⁴, Erdmann Spiecker³ and Erik Bitzek³; ¹RWTH Aachen University, Germany; ²Technische Universität Bergakademie Freiberg, Germany; ³FAU-Erlangen-Nürnberg, Germany; ⁴University of California, Santa Barbara, United States

Nanoscale metallic objects like thin films, nanoparticles, nanowires, or nanoporous metals receive sustained attention due to their size-dependent mechanical properties, which can include changes in deformation mechanisms, pseudoelastic behavior and increased yield strength compared to the bulk material. Many of these nano-objects have well-defined morphologies and are initially dislocation-free, which make them ideal model systems to study, e.g. dislocation nucleation and dislocation – interface interactions. These properties of such nano-objects also predestinate them for direct comparisons between experiments and simulations.

Here we present recent results on in situ experiments on single crystalline, nanotwinned and five-fold twinned nanowires as well as on nanoporous gold and compare them with atomistic simulations. The latter allow for controlled variation of the size and morphology, surface quality and loading conditions. Such careful studies allowed to show that twin boundaries not only act as obstacles to dislocation motion leading to hardening, but also fundamentally change the deformation mechanisms and failure mode. The loading mode (tension, compression, bending) and boundary conditions, the location of the twin boundary and most importantly the intersection of the twin boundaries with other interfaces are shown to critically influence the deformation behavior. These observations demonstrate the fundamental differences between dislocation processes in nanotwinned polycrystals and in nanotwinned nano-objects. The simulations furthermore highlight the need for realistic sample sizes and morphologies to capture and understand essential, experimentally-observed, deformation mechanisms.

8:30 AM *ST02.06.02

In Situ Mechanical Testing of Elastic and Plastic Properties of Metal Nanowires Erdmann Spiecker¹, Lilian Vogl¹, Peter Schweizer¹, Nadine Schrenker¹, Xin Zhou¹, Marco Moninger¹, Felix Werner¹ and Gunther Richter²; ¹University of Erlangen-Nuremberg, Germany; ²Max Planck Institute for Intelligent Systems, Germany

In situ microscopy has been established itself as a key technique for studying the mechanical properties of materials at small length scales. In particular, the application of in situ microscopy to nanowires and nanowhiskers has been very successful, not only because such nanostructures can be produced with high quality but also because preparation artefacts like FIB damage can be avoided. As result the intrinsic mechanical properties of nanowires and nanowhiskers can be reliably studied down to very small dimensions. Such investigations consolidated the notion of ‘smaller is stronger’ which refers to an almost universal trend of increased strength with decreasing size of nanostructures subjected to mechanical loads. Reducing the size of nanostructures not only affect their plastic deformation behavior but also changes their elastic properties as result of the increased surface-to-volume ratio. However, the observations of size effects on elastic properties are less consistent and the underlying mechanisms are still controversially discussed.

In this contribution we present results of in situ microscopy studies on individual metal nanowires carried out over the past years at the Center for Nanoanalysis and Electron Microscopy (CENEM) in Erlangen. In the first part we focus on the elastic properties of gold nanowires and demonstrate a profound influence of both, shape and size of the nanowires. The elastic properties are determined using in situ mechanical testing in SEM and TEM by means of resonance excitation and uniaxial tension. The combination of bending and tensile load types, performed subsequently on the same wire, allows for an independent and correlative calculation of the Young’s modulus. For this, the cross-sectional area and resulting second moment of area are determined for each individual nanowire by performing high resolution TEM on FIB cross sections of undisturbed nanowire areas after mechanical testing. Based on a detailed comparison of nanowires with different size and shape we find both cases of softening as well as stiffening, depending critically on the interplay between size and shape of the

wires. Our results clearly demonstrate that not only size but also shape matters for the elastic properties at small scales. Different models from the literature are discussed which can in part explain the behavior.

In the second part we focus on the plastic deformation behavior and failure modes of five-fold twinned silver nanowires which are used as conduction lines in flexible transparent electrodes. Upon uniaxial straining of such electrodes some nanowires experience tensile loading and fracture while others are set under compressive stress resulting in buckling and kink formation, depending on the orientation of the nanowires with respect to the external load axis. We employ different in situ microscopy techniques in TEM, SEM and light microscopy to study the mechanisms of kink formation for both freestanding nanowires and nanowires on flexible substrates, respectively. We determine the critical strain for kink formation under these conditions and study the fundamental defect mechanisms associated with this deformation mode. Moreover, we demonstrate the potential of in situ light microscopy to study the deformation behavior of single nanowires on flexible substrates under ambient conditions. Finally, we report on first in situ microscopy studies under conditions of cyclic loading and discuss the role of kink formation and nanowire fracture on the overall failure behavior of flexible transparent nanowire electrodes.

9:00 AM ST02.06.03

Late News: Correlating Intrinsic and Extrinsic Damping Factors of Single Nanowire Resonators Using *In Situ* SEM and LM Lilian Vogl¹, Peter Schweizer¹, Peter Denninger¹, Gunther Richter² and Erdmann Spiecker¹; ¹Friedrich-Alexander-Universität Erlangen-Nürnberg, Germany; ²Max Planck Institute for Intelligent Systems, Germany

Microcantilevers are already successfully implemented in mass sensing devices, offering an improved sensitivity down in the range of few picogram. The performance of such nanomechanical devices is given by a high resonance frequency combined with a high quality factor. While for mass sensing applications the frequency shift is used, the quality factor additionally depends on the ambient medium and scales inversely with the pressure in the molecular flow regime. However, the measurable pressure range of commercial micro-sized cantilevers is restricted, which limits the application ability. To expand the pressure range, the size of the cantilevers has to be further reduced: A beam with a thickness in nm range, would shift and additionally broaden the measurable regime to higher pressure values. Therefore, a precise characterisation of the vibrational properties of nanowires is required, which is the fundament for further research of next-generation devices. We present a correlative electron and light microscopic approach to characterize the vibrational properties of single nanowires in dependence of the gas atmospheres and pressure level. The resonance properties of nanowires and the assigned quality factor depends on the pressure of the ambient medium. The high vacuum state of $10^{-6} - 10^{-7}$ mbar in SEM and TEM enables the characterization of the intrinsic vibrational properties, which is directly related to the microstructure and surface quality. To analyze the damping effect caused by the interaction of the gas molecules with the nanobeam, the *in situ* resonance measurements have to be performed within the molecular flow regime (~ 50 mbar -200 mbar). For this purpose, the single nanowire is mounted within a compact chamber for the light microscope, which allows to observe the changing resonant behavior in dependence of the applied gas atmosphere (He, N₂, Air, Ar) and pressure level. By using the resonance vibration, we demonstrate the pressure sensing capability of a single nanowire. Moreover, the damping effect is used to examine the molar mass of the surrounding atmosphere and therefore the nanowire can be seen as ultrathin nanoscale resonant gas sensor. The *in situ* measurements of the same nanowire in the electron and light microscope offers the opportunity to analyze the complex interplay of several damping factors and gives direct insights in the vibrational behavior. While the intrinsic damping factor can be tuned by the microstructure, the nanowire thickness determines the sensitive pressure regime. The extrinsic factors are given by the interaction of the vibrating nanobeam with the surrounding gas atmosphere and are used for sensing applications.

9:15 AM DISCUSSION

9:30 AM ST02.06.05

A Study of Mechanical Size Effects by Optical Means—Using Reflectance Anisotropy Spectroscopy to Test Metallic Thin Films at Smaller Scales Micha Calvo and Ralph Spolenak; ETH Zürich, Switzerland

Thin film technologies have enabled the life we know today. There is barely any product released in today's market that does not involve thin film technologies at any point during its fabrication. As less material usually means lower costs, these thin films have been downsized to the dimension that is just barely sufficient to fulfill their purpose. For applications like e.g. diffusion-barriers or reflective coatings these dimensions are reaching nowadays well below 20 nm.

It is of interest to study films of small dimensions, because the material exhibit different properties at small length scales, usually referred to as size effects. Mechanical size effects have been studied extensively during the last two decades. Amongst others, by the means of Nano-indentation, Synchrotron XRD, Wafer-curvature, micropillar-compression, bulge-testing, cantilever-bending, nanowire-tensile experiments, and lately also by Reflectance Anisotropy Spectroscopy (RAS).

When it comes to polycrystalline thin films however, all the above mentioned techniques (except RAS) are getting less reliable when it comes to ultra-thin films, with thicknesses below 50 nm. This is due to the nature that the probed interaction volume becomes too small and the signal-to-noise ratio decreases. In our setup, we use white light from a common Xe-lamp for excitation. For metals at these optical frequencies, the interaction volume is confined to a few tens of nanometers below the surface. This makes RAS an excellent candidate to investigate metallic ultra-thin films below 50 nm.

RAS is best described as phase-modulated near-normal incidence Ellipsometry. It probes the difference of reflectance in two orthogonal directions, which correspond to anisotropies in the dielectric function. The Piezo-optical tensor relates strain to the dielectric function, which makes this technique highly sensitive to anisotropic changes in lattice spacing (e.g. under uniaxial loading). The method is not limited to any material or materials class, as long as the films are continuous and the material has an electronic transition in our detection range (1.5 - 5.5 eV). Our metallic films are on a flexible substrate, which allows us to strain them considerably in uniaxial tension. By the subsequent unloading of the stress the polymeric substrate drives the metallic film into compression. This is required as the technique is blind to residual biaxial strains.

We will present a new *in-situ* mechanical size effect study on pure fcc metals (namely gold, copper, and silver) down to 20nm thin polycrystalline films on flexible substrates. Sample fabrication has been proven most critical, as the technique is highly sensitive to surface morphology (e.g. anisotropic pores, roughness) and texture. To reduce roughness of the metal surface that is probed a substrate transfer is performed after deposition, usually referred to as template stripping. This results in metallic thin films on polymeric substrates with the same roughness as a silicon wafer. We will clearly outlay the potential as well as the limitations of this technique.

9:45 AM ST02.06.06

Analyzing the Fracture Characteristics of Twisted Tri-layer Graphene using Molecular Dynamics Hassan Shoaib^{1,2,3}, Qing Peng¹ and Abduljabar Alsayoud^{1,2,3}; ¹King Fahd University of Petroleum and Minerals, Saudi Arabia; ²Saudi Aramco, Saudi Arabia; ³King Abdullah University of Science and Technology, Saudi Arabia

The field of Graphene Twistrionics has been gaining significant traction in recent times due to the excellent superconductive behavior of these materials and their potential use in various applications. However, while the electronic properties of twisted multi-layered graphene have been extensively studied in the literature, there is a lack of research concerning the mechanical properties of twisted tri-layer graphene (tTLG). Therefore, this paper aims to mechanically test tTLG under tensile loading and evaluate the mechanical properties by constructing an accurate model of the system using a twist angle of $\pm 1.53^\circ$ which is known to exhibit highly superconductive behavior. To develop our system and assess the fracture mechanism, we opted to use the AIREBO-M potential to precisely mimic the behavior of multi-layer graphene with varying sizes of cracks. The results indicate that TTLG possesses exceptional mechanical properties with pristine tTLG exhibiting a Young's modulus of 1.506 TPa and an ultimate strength of 146.36 GPa. Furthermore, the fracture characteristics are also excellent with a fracture toughness of $4.79 \pm 0.085 \text{ MPa M}^{1/2}$ and as expected, the critical stress reduces with increasing crack size a_0 . It is also interesting to note that critical strain equilibrates to approximately 0.072 after a crack length of 1.85 nm. Twisted Tri-layer graphene has been known to exhibit exceptional electrical properties and this study validates the excellent mechanical properties as well.

SESSION ST02.07: Modelling, Big Data and Machine Learning
Session Chairs: Erik Bitzek and Gerhard Dehm
Friday Morning, April 23, 2021
ST02

11:45 AM *ST02.07.01

New Insights into Plasticity by Combining Nanomechanics, High-Resolution Characterization and Simulation Ruth Schwaiger; Forschungszentrum Jülich GmbH, Germany

Mechanical behavior of crystalline materials strongly depends on the microstructure and its evolution at different length scales which is governed by, e.g., crystallography, the distribution of defects, grain morphology, or texture. Understanding and predicting macroscopic mechanical responses requires appropriate descriptions of the micro- and nanoscale response, i.e., the evolution of the underlying microstructure, or intra- and inter-granular stresses. Following the advancement of experimental techniques, it is becoming possible to link computational models with real-life observations of deformation and failure.

In this presentation, an overview of current approaches integrating advanced experimental methods with high-resolution characterization and modeling will be discussed in the context of dislocation plasticity. In situ microcompression experiments, electron backscatter diffraction, and high-resolution digital image correlation allow the determination of local strains and identification of activated slip bands. In combination with transmission electron microscopy and computational analysis, the formation of dislocation structures and the interaction of dislocations with grain boundaries is analyzed. Geometrically necessary dislocation densities can be quantified at the nanoscale by using electron diffraction methods and the Kröner-Nye dislocation density tensor, thereby giving insights into, e.g., the indentation size effect. With those methods, experiment and simulation move closer together facilitating an understanding of relevant mechanisms in plasticity and fracture.

12:15 PM *ST02.07.02

Micromechanics with A.I.—Towards Combining High Resolution with Statistical Observations Setareh Medghalchi¹, Carl Kusche¹, Talal Al-Samman¹, Ulrich Kerzel^{1,2} and Sandra Korte-Kerzel¹; ¹RWTH Aachen University, Germany; ²IUBH International University of Applied Sciences, Germany

High performance materials, from natural bone over ancient damascene steel to modern superalloys, typically possess a complex structure at the microscale. Their properties exceed those of the individual components and their knowledge-based improvement therefore requires understanding beyond that of the components' individual behaviour. Electron microscopy has been instrumental in unravelling the most important mechanisms of co-deformation and in-situ deformation experiments have emerged as a popular and accessible technique. However, a challenge remains: to achieve high spatial resolution and statistical relevance in combination. Here, we overcome this limitation by using panoramic imaging and machine learning to study damage in a dual phase steel. This high-throughput approach now gives us strain and microstructure dependent insights into the prevalent damage mechanisms and allows the separation of inclusions and deformation-induced damage across a large area of this heterogeneous material. Aiming for the first time at automated classification of the majority of damage sites rather than only the most distinct, the new method also encourages us to expand current research past interpretation of exemplary cases of distinct damage sites towards the less clear-cut reality. Often, the collection of ground truth data may be the limiting step, for this reason we will also address using data augmentation to achieve transferability, for example between different stress states like uniaxial, bending and biaxial loading.

12:45 PM ST02.07.03

Atomistic Simulations of the Facet-Dependent Deformation of sub-10-nm Platinum Nanoparticles Ingrid M. Padilla Espinosa¹, Ruikang Ding², Andrew Baker², Soodabeh Azadehranjbar², Tevis Jacobs² and Ashlie Martini¹; ¹University of California, Merced, United States; ²University of Pittsburgh, United States

Small metallic nanoparticles are promising in a variety of fields due to their chemical, optical and electronic properties. Understanding the deformation mechanisms and mechanical response of these small nanoparticles to compression is necessary to determine their stability and suitability for applications. Most prior descriptions of nanoparticle deformation, such as Cobble-creep-like deformation, are defined assuming spherical nanoparticles. However, at very small sizes (<10 nm), metallic nanoparticles tend to form different shapes (such as icosahedra, dodecahedra, and cubes). The shape/size dependency of nanoparticles is a result of the anisotropy of the surface energies of the different facets. These facets determine the mechanical deformation of the small nanoparticles because different facets facilitate or impede processes such as atomic diffusion and defect nucleation. Here, molecular dynamics simulations were performed to understand the relationship between faceting and the mechanical deformation of platinum nanoparticles. Simulated compression tests were performed, with matched conditions to *in situ* experimental testing inside of a transmission electron microscope. Dynamic facet rearrangement was observed during compression, and qualitatively linked as a result of crystal deformation, dislocation mobility, and residual mechanical strain. Taken together, the simulated and experimental results demonstrate the size- and facet-dependence of deformation in small platinum nanoparticles.

1:00 PM ST02.07.04

Evaluation of Uncertainty in Clustering of Nanoindentation Data Bernard Becker, Eric Hintsala, Benjamin Stadnick, Ude Hangen and Douglas Stauffer; Bruker Nano Surfaces, United States

High throughput nanoindentation is a powerful technique for evaluating highly localized mechanical properties in materials with complex microstructures. This allows for study of spatial and statistical variations in properties for materials with different phases or features of interest. Prominent examples include composite materials, multi-phase metallic alloys, gradient microstructures, or heat affected zones from processing. This makes it useful for speeding up development of new structural materials, especially since a lot more data can be generated versus traditional bulk mechanical testing for the same sample preparation time. This data can furthermore be easily correlated to the microstructure through use of complementary techniques, such as scanning electron microscopy and electron backscatter diffraction. In order to extract useful information from these techniques, automated analyses also need to be developed in tandem since such datasets are composed of many thousands of points, typically.

We have been exploring clustering as such an accompanying analysis technique. This encompasses several algorithms which are used to group similar data together. The primary current application is getting statistics from individual phases in the microstructure. This can also identify the size and position of these phases. In the future, more advanced analyses are expected to be developed as well. For now, determining the best clustering methods is still a relevant question. Many algorithms exist to choose from, along with choosing the correct number of clusters, how to do outlier removal, and the number of measurements needed to capture the property distributions. To that end, we have been developing an analytical framework based upon bootstrapping to compare the bias and uncertainty in different clustering techniques, as applied to nanoindentation. This will be demonstrated on complex structural materials, including Damascus steel, dual-phase iron high entropy alloys, and additively manufactured T91.

1:15 PM ST02.07.05

Density Functional Theory and Molecular Dynamics Simulations of Shock Wave Propagation Through Polymer/Ceramic Multilayers Nuwan Dewapriya and Ronald Miller; Carleton University, Canada

The thermodynamic equilibrium states of materials under shock loading (i.e. the shock Hugoniot) can be used to characterize their high strain-rate behaviors. The shock Hugoniot for a given material is generally obtained by conducting shock wave experiments. The current experimental techniques are, however, unable to elucidate all the complex atomistic mechanisms associated with the shock wave propagation, which can only be realized

through comprehensive atomistic simulations. For example, first-principle density functional theory (DFT) calculations can be used to compute the shock Hugoniot of materials with very high accuracy. However, the system size that can be simulated in DFT is quite small (a few hundred atoms) due to the extremely high computational cost associated with DFT, which could be problematic if the dynamic response of the systems is size-dependent. Moreover, the high computational cost of DFT only allows us to model the equilibrium thermodynamic state behind the shock front (i.e. the Hugoniot states), rather than the dynamic shock wave propagation itself. Alternatively, classical molecular dynamics (MD) simulations can be used to explicitly model the shock wave propagation in larger systems containing millions of atoms. In addition to providing the shock Hugoniot, the explicit modeling of the shock wave propagation provides more useful information like spatiotemporal evolution of temperature and pressure.

In this work, we first conducted both DFT-based-quantum and classical MD simulations to obtain the shock Hugoniot of polymers and compared them with the existing experimental data. This exercise revealed the upper limits of the shock wave speed that can be accurately modeled using classical MD. Thereafter, we employed classical MD to explicitly model the dynamic shock wave propagation and spallation of polymers as well as polymer/ceramic multilayers. We conducted DFT calculations to obtain accurate MD force field parameters to model the adhesive interactions between the polymer and the ceramic. In order to investigate the atomistic mechanisms associated with the penetration process, we conducted full-scale classical MD simulations of ballistic impact tests of the polymer/ceramic multilayers. Our study demonstrates that the atomistic simulations provide a great insight into the nanoscale mechanisms associated with the dynamic behavior of materials under extreme conditions.

Acknowledgement: This work was supported by the Natural Sciences and Engineering Research Council of Canada.

1:30 PM ST02.07.06

Late News: Slip and Deformation Twinning Mechanisms on First Order Pyramidal Plane of Magnesium—Molecular Dynamics Simulations and First Principal Studies Reza Namakian¹, George Voyiadjis¹ and Piotr Kwasniak²; ¹Louisiana State University, United States; ²Center of Digital Science and Technology, Cardinal Stefan Wyszyński University in Warsaw, Poland

Molecular dynamics (MD) simulations and first-principles calculations are carried out on first order pyramidal plane (FOPP) of magnesium (Mg) to study both compression twinning (CTW) and dislocation slip. To this end, a generalized stacking fault energy (GSFE) analysis is employed on dense and loose spaced planes of Mg FOPP. The crystal shearing resistance is extracted by using a minimum-energy path (MEP) finder called the nudged elastic band (NEB) method. The MEP regarding slip system on loose plane of FOPP shows that the unfaulted crystal structure is recovered in the middle of the path with non-straight and pronounced curved slip trajectories. Besides, it will be revealed that metastable configurations on the half of the MEP for the slip system are indeed related to a dissociated extended dislocation of loose pyramidal-I slip. Also, after extracting the dissociation mechanism related to this dislocation, it will be shown that loose pyramidal-I slip can involve shuffling. Moreover, the MEP for dense pyramidal-I slip shows transmutation of this slip into CTW in the middle of the path. This transmutation process will be further examined on CTW growth, and it will be demonstrated that this CTW mechanism is energetically more favorable compared to other twinning mechanisms.

SESSION ST02.08: Quantitative In Situ Deformation

Session Chair: Kelvin Xie

Friday Afternoon, April 23, 2021

ST02

2:15 PM *ST02.08.01

Novel *In Situ* TEM Analysis for Amorphous Materials Enabled by Fast, Sensitive Detectors Thomas C. Pekin¹, Christoph Gammer², Colin Ophus³, Robert O. Ritchie^{3,4} and Andrew M. Minor^{3,4}; ¹Humboldt-Universität zu Berlin, Germany; ²Erich Schmid Institute of Materials Science, Austrian Academy of Sciences, Austria; ³Lawrence Berkeley National Laboratory, United States; ⁴University of California, Berkeley, United States

Four dimensional scanning transmission electron microscopy (4DSTEM) is a versatile and powerful electron microscopy technique that has been used to measure strain, polarization and orientation, among other properties, at the scale of traditional TEM analysis. This technique, enabled by a new generation of electron detectors, is based on the computational analysis of thousands to hundreds of thousands of diffraction patterns rapidly acquired while the electron beam is scanned across a sample. It can further be combined with *in situ* TEM to provide novel insight into bulk metallic glasses (BMG). This talk will highlight how the evolution of strain and structural order in bulk metallic glasses prior to shear band formation can be spatially correlated during *in situ* deformation. The development of *in situ* heating and crystallization 4DSTEM techniques for BMGs will also be discussed. Additionally, if time allows, this talk will cover some of the more versatile aspects of 4DSTEM, such as *in situ* strain mapping in crystalline materials, orientation mapping nanoparticle grains, and the development of the software required to perform the analysis shown.

2:45 PM *ST02.08.02

Probing Deformation Mechanisms in Ultrafine Grained Al and Au Thin Films by Quantitative *In Situ* TEM Deformation Josh Kacher, Sandra Stangebye, Yin Zhang, Ting Zhu and Olivier Pierron; Georgia Institute of Technology, United States

Understanding dislocation generation mechanisms and interactions with obstacles such as grain boundaries and other dislocations is central to understanding the mechanical behavior of metals and alloys. This has motivated decades of research into the unit processes governing dislocation interactions by *in situ* transmission electron microscopy (TEM) mechanical testing, resulting in the establishment of basic rules that govern how these interactions occur. However, much of this research has focused on the deformation of coarse-grained polycrystals where the grain boundaries are largely isolated from each other and dislocation glide is primarily transgranular. In ultrafine grained and nanocrystalline materials, the high volume fraction of grain boundaries can lead to the activation of additional deformation mechanisms, such as grain growth, grain boundary sliding, and intergranular dislocation propagation. This paper presents results on quantitative *in situ* TEM experiments of deformation of ultrafine grained materials with a focus on deformation-induced grain boundary migration. A unique aspect of this study is the ability to measure the apparent and true activation volumes associated with the material deformation using a micro-electromechanical system (MEMS)-based deformation platform. This study also takes advantage of progress in electron detection technology, with simultaneous high and low resolution recording now possible via digital zoom.

In this paper, I will discuss our results from two different systems: nanocrystalline Al and ultrafine grained Au thin films. In both cases, grain growth accompanies the deformation, but the rates and migration behavior differ significantly. The reasons for these differences, including the activity of disconnections and the role of grain boundary character, will be discussed and explored using atomistic simulations. I will also discuss the effects of the electron beam on deformation mechanisms, which are significant even when operating well below the knock-on damage threshold. This influence can be seen in the deformed microstructure and quantified via activation volume measurements.

3:15 PM *ST02.08.03

Integration of Microscopy and Data Science to Access Multiscale Defect Distributions Mitra Taheri; Johns Hopkins University, United States

Grain boundary (GB) stability may be defined as the ability of a GB to continue to absorb point defects without becoming saturated and without changing its macroscopic degrees of freedom (misorientation, inclination), or degrees of freedom. Much debate revolves around local GB stresses and how they evolve with radiation. Through the use of quantitative in situ microscopy, atomic and mesoscale simulations, and machine learning, we explore how GBs evolve as a function of point defect absorption, and specifically, how local stresses evolve throughout the dynamic radiation process. The results have profound implications in developing thermally stable, bulk nanocrystalline materials, and damage tolerant materials.

3:45 PM ST02.08.04

Late News: Atomistic Processes of Grain Boundary Phase Transformation During Shear-Mediated Migration Zhengwu Fang and Scott X. Mao; University of Pittsburgh, United States

Stress-driven grain boundary (GB) migration can lead to grain growth and GB network evolution during the deformation of polycrystalline materials. The theoretical models with disconnection, dislocation, and shuffling mechanisms have been proposed to describe the GB migration. However, GB phase transformation during migration, the process of which cannot be described by these models, has never been explored experimentally at the atomic scale, especially for asymmetrical tilt GBs (ATGBs), one of the most common GBs in polycrystalline materials. Here, by performing in-situ high-resolution transmission electron microscopy, GB phase transformation was discovered at two faceted ATGBs in Au. Both of them were found to form $\Sigma 11(113)$ symmetrical tilt GBs, either via facet phase transformation or GB dissociation, during the shear-mediated migration process, which was further confirmed by molecular dynamics simulations. This work provides the first insights into the atomistic mechanisms of GB dynamic phase transformation during the migration of ATGBs and the impact of it on the microstructural control during the thermal-mechanical processing in polycrystalline materials.

4:00 PM ST02.08.05

Quantitative *In Situ* Study of Strength-Governed Interfacial Failure Between h-BN and Polymer-Derived Ceramic Boyu Zhang¹, Xing Liu², Hua Guo¹, Kaiqi Yang¹, Brian W. Sheldon², Huajian Gao^{3,2} and Jun Lou¹; ¹Rice University, United States; ²Brown University, United States; ³Nanyang Technological University, Singapore

Nanomaterials, such as carbon nanotubes, hexagonal boron nitride (h-BN) and graphene platelets, are promising candidates for reinforcing ceramic matrix composites. They are known for their high strength and have shown potential for improving the fracture toughness of monolithic ceramics. Much of the current understanding of these nano-reinforcements is based on extrapolation from the existing literature on much larger reinforcements such as microfibers. According to these studies on micro-reinforcements, the interaction between a crack and the interface is typically an energy governed process. However, in the case of nano-reinforcements, especially 2D reinforcements, this mechanism has yet to be fully explored due to the lack of systematic experimental studies on the interfacial properties of composites reinforced with nanomaterials.

In this work, the interfacial behaviors between multi-layer h-BN nanosheets and a polymer-derived ceramic (PDC) were investigated to promote the understanding of interfacial failure at small scales with *in-situ* pull-out experiments. By using nanoindentation-assisted micro-mechanical devices integrated with scanning electron microscopy (SEM), the detailed interfacial sliding and debonding behaviors between 2D materials and ceramic matrix were quantitatively measured for the first time. Interfacial mechanical properties, *i.e.*, interfacial modulus and strength, were measured to be $5.65 \pm 1 \text{ GPa} \cdot \mu\text{m}^{-1}$ and $66.4 \pm 16.8 \text{ MPa}$, respectively. Furthermore, based on the experimental observations, an analytical cohesive shear-lag model was established to understand the failure mode of the interface in h-BN/PDC composite. It is found that the strength of the interface, rather than interfacial fracture energy, governs the interfacial failure at nanoscales, which provides valuable insight that is expected to motivate future work on the mechanical properties of nanomaterial-reinforced composites.

SESSION ST02.09: Glasses and Polymers
Session Chairs: Josh Kacher and Kelvin Xie
Friday Afternoon, April 23, 2021
ST02

5:15 PM ST02.09.01

Predicting the Long-Time Creep Dynamics of Gels from Their Static Structure by Machine Learning

Han Liu and Mathieu Bauchy; University of California, Los Angeles, United States

Upon sustained loading, gels tend to feature delayed viscoplastic creep deformations. However, the relationship, if any, between the structure and creep dynamics of gels remains elusive. Here, based on accelerated molecular dynamics simulations and classification-based machine learning, we reveal that the propensity of a gel to exhibit long-time creep is encoded in its static, unloaded structure. By taking the example of a calcium–silicate–hydrate gel (the binding phase of concrete), we extract a local, non-intuitive structural descriptor (“softness”) that is strongly correlated with the dynamics of the particles—wherein the macroscopic creep rate exhibits an exponential dependence on the average softness. We find that creep results in a decrease in softness in the gel structure, which, in turn, explains the gradual decay of the creep rate over time.

5:30 PM ST02.09.02

Late News: *In Situ* Raman Spectroscopic Measurements of Silicate Glasses During Indentation Yvonne B. Gerbig and Chris Michaels; National Institute of Standards and Technology, United States

This talk describes the design and integration of a custom-built optical instrument for in-situ Raman microscopy suitable for collecting high-quality spectroscopic data during the indentation of glass materials. It will further show that the reported experimental setup and optimized experimental parameters enable meaningful in-situ spectroscopic observations during indentation of fused silica at forces in the millinewton range. In this context, the talk will also touch upon possible pitfalls in in-situ Raman measurements on indented glasses and describe the misinterpretations that may result.

5:45 PM DISCUSSION

6:00 PM ST02.09.04

Spectroscopic Explorations of Thermal Transitions of Polyurea Nha Uyen Huynh^{1,2} and George Youssef¹;
¹San Diego State University, United States; ²University of California, San Diego, United States

The quest for in-situ characterization has placed an emphasis on spectroscopic methods with penetrative, noninvasive, nondestructive attributes, thus bringing terahertz-based techniques to the forefront. Terahertz time-domain spectroscopy operating in the transmission mode is most suitable for investigation of polymers in-situ or ex-situ. Polymers are nearly transparent to terahertz waves, indicating inheritance of the molecular information by the propagating electromagnetic wave as it interacts with the polymer continuum, regardless of the sample form. The research leading to the presentation is focused on elucidating the thermal transition, e.g., glass transition, of polyurea. Polyurea is a thermoset elastomer prepared by mixing oligomeric diamine and diphenylmethane diisocyanate at a stoichiometric ratio of 96%, yielding a viscoelastic polymer with significant strain-rate sensitivity. Polyurea has been integrated in a plethora of applications due to its superior physical properties, the prime of which is the impact mitigation to guard structures and human from hypervelocity projectiles and biomechanical dynamic loading, respectively. However, prolonged exposure to environmental conditions was reported to deteriorate the material and adversely affect its mechanical properties. Therefore, this research strives to elucidate the structure-property interrelationship of polyurea using the noninvasive THz-TDS technique as a function of temperature spanning from -103°C to -3°C since the glass transition temperature of polyurea was previously reported to be -49°C. The approach is to control the temperature of the sample in a cold finger by isothermally soaking at each temperature step for 2 min, before collecting the terahertz signal

with the sample in the propagation path with a spectral bandwidth of 1.7 THz extending from 0.3 - 2.0 THz and peak width of 0.18 mm. The time-domain data was transformed to the frequency domain using discrete Fourier transform. The optical and dielectric properties were deduced from the spectral data of each sample, where a shift in the sensitivity to change of the optical properties with respect to temperature was noticed around the thermal transition of polyurea. The polyurea samples, with ~16 mm diameter, were extracted from a 1 mm sheet that was prepared using slab molding technique, where a subset of the samples were continually exposed to ultraviolet radiation of 15 weeks at an exposure level of 5122 mJ/cm²/hr and 8553 mJ/cm²/hr of UV-A and UV-B, respectively. This prolonged exposure resulted in discoloration, minor changes in the elastic, hyperelastic, and viscoelastic behavior, and materials degradation in the form of crazing and microcracks. However, the extent of degradation was found to be limited to 45 μm below the surface, which is thought to attribute to the insignificance of the property changes. Investigation with THz-TDS in cryogenic temperature was able to accurately identify the glass transition temperature and radiation-related changes, since changes in molecular vibrations associated with conformational changes are encoded in the terahertz signal as it propagates through the sample. Future research seeks to couple the experimental results with molecular dynamic simulations to accurately elucidate the type and source of conformational changes.

6:15 PM ST02.09.05

Late News: Rheological Yielding in Nanotube Reinforced Metallic Composites Kang Pyo So, Myles Stapelberg, Yu Ren Zhou, Mingda Li, Mike Short, Ju Li and Sidney Yip; Massachusetts Institute of Technology, United States

We propose and demonstrate a rheological yielding mechanism in metallic matrix nanotube composites, which may aid in improving the mechanical properties of such composites. Machine learning-based analysis of *in situ* transmission electron microscopy (TEM) tensile test videos is used to identify microstructural defects in an aluminum-carbon nanotube (CNT) nanocomposite and thereby uncover nanoscale yielding processes during mechanical deformation. Observed defects near CNTs include notch evolution, new surface creation, material sliding, dislocation glide/cross-slip, and localized shear strain at <100nm length scale. Non-shearable CNTs provide strong pinning points against dislocation glide or cross-slip, triggering high local shear strains, which result in deformation via shear transformation. CNTs parallel to the load axis bridge evolving notches, hindering further penetration and inducing substantial nanoscale load transfer, which may contribute to the exceptional strength observed in these Al-CNT composites.

SESSION ST02.10: On-demand
Wednesday Morning, April 14, 2021
ST02

8:00 AM ST02.09.03

Late News: Condensation Induced Blistering as a Measurement Technique for Adhesion Energy of Nanoscale Polymer Films Jingcheng Ma, David Cahill and Nenad Miljkovic; University of Illinois at Urbana-Champaign, United States

Polymeric coatings having nano-to-microscale thickness show immense promise for enhancing thermal transport, catalysis, energy conversion, and water collection. Characterizing the work of adhesion (G) between these coatings and their substrates is key to understanding transport physics as well as mechanical reliability. Due to the rapid development of nanoscale devices and coatings, there is an increasing need to develop methods to quantitatively measure the work of adhesion at ever smaller length scales, both in terms of lateral spatial resolution (< 100 μm) and film thickness (< 100 nm). Experimentally quantifying the work of adhesion of nanoscale films with high spatial resolution is difficult. The most common method for measuring work of adhesion involves characterizing the contact or 'pull-off' force between a probe coated with the thin film of

interest and the surface of interest using atomic force microscopy. However, surface force measurement is highly sensitive to adsorption of airborne hydrocarbons or water vapor on the test surface. To obtain accurate measurements of adhesion, it is necessary to separate the two surfaces of interest prior to interaction with the surrounding atmosphere. Conventional mechanical approaches for adhesion energy measurement, such as the peel test and four-point bending test delaminate the film from its substrate directly, thus preserving the interface. However, these methods are only appropriate at larger scales (> 1 mm lateral length for adhesion measurement) due to the difficulty of applying the delamination force without damaging the film via stress concentration. Here, we demonstrate that water vapor condensation blistering is capable of *in situ* measurement of work of adhesion at the interface of polymer thin films with micrometer spatial resolution. We use our method to characterize adhesion of interfaces with controlled chemistry such as fluorocarbon/fluorocarbon (CF_n/CF_m , $n, m = 0 \sim 3$), fluorocarbon/hydrocarbon (CF_n/CH_m), fluorocarbon/silica (CF_n/SiO_2) and hydrocarbon/silica (CH_n/SiO_2) interfaces showing excellent agreement with adhesion energy measured by the contact angle approach. We demonstrate the capability of our condensation blister test to achieve measurement spatial resolutions as low as $10 \mu\text{m}$ with uncertainties of $\sim 10\%$. The minimization of energy dissipation enables us to probe extremely weak adhesion, which can be as low as 10^{-6} J/m^2 at Sapphire/Teflon interface. The outcomes of this work establish a simple tool to study interfacial adhesion.

SYMPOSIUM ST03

Design, Synthesis and Characterization of Architected Materials for Structural Applications
April 20 - April 21, 2021

Symposium Organizers

Dongchan Jang, Korea Advanced Institute of Science and Technology
Woo Soo Kim, Simon Fraser University
Lucas Meza, University of Washington
Ruth Schwaiger, Forschungszentrum Juelich GmbH

* Invited Paper

SESSION ST03.01: Deformation and Fracture Analysis
Session Chairs: Vikram Deshpande and Ruth Schwaiger
Tuesday Morning, April 20, 2021
ST03

8:30 AM *ST03.01.01

Fracture of Micro-Architected Solids—Does a Toughness Exist? Angkur Shaikeea¹, Huachen Cui², Rayne Zheng³ and Vikram S. Deshpande¹; ¹University of Cambridge, United Kingdom; ²Virginia Tech, United States; ³University of California, Los Angeles, United States

Rapid progress in additive manufacturing methods has led to the creation of a new class of ultralight, stiff and strong 3D architected metamaterials comprised of a network of struts resembling a periodic truss structure. The performance of these micro-architected metamaterials is ultimately be limited by their tolerance to damage and defects, yet experimental investigations of their fracture toughness have remained elusive primarily due to manufacturing limitations. Using octet-truss metamaterial specimens comprising in excess of a million unit-

cells we show that not only is stress intensity factor, as used in conventional elastic fracture mechanics, is insufficient to characterise fracture in these metamaterials but also that conventional fracture test methods using two-dimensional specimens with through-thickness cracks are inappropriate. Via a combination of finite element (FE) calculations and asymptotic analyses we extend the application of the ideas of fracture mechanics to metamaterials with a view to developing a continuum theory and measurement protocol for the failure of such architected metamaterials.

8:55 AM ST03.01.02

Effects of Buckling Struts on the Fracture Toughness of Triangular Lattices Melle Gruppelaar, Eral Bele and PJ Tan; University College London, United Kingdom

Introduction and Aim

Microarchitected lattices have attracted significant interest as lightweight, resource-efficient structural materials. One of their notable advantages is the ability to attain high weight-specific mechanical properties by manipulating how material is distributed in space. Here, we will present numerical and experimental results to reveal how the buckling of struts, hitherto neglected, affects the crack tip field, the location of fracture initiation and propagation, and their concomitant effects on the fracture toughness of regular triangular lattices.

Hitherto, the fracture toughness of lattices had mainly been studied numerically, assuming idealized geometry and material properties, and specimen size that is free from the influence of edge effects. The above can all have a significant impact upon the deformation of stretch-dominated lattices with slender struts (low relative density) even in the absence of material nonlinearities, but few studies have examined how local geometric instability affects fracture initiation and the subsequent crack growth in 2D prismatic lattices.

Methods

The influence of strut buckling in elastic-brittle triangular lattices is assessed numerically, through a Boundary Layer Method (BLM) for infinite-sized specimens, and results compared to those from simulations of finite-sized, Single Edge Notched Tension (SENT) specimens. In the former, crack-tip displacements field from LEFM were imposed as periodic boundary condition to a Representative Volume Element, and the latter follows the standard procedure described in BS8571:2018. Eigenvalue analysis was performed and it will be shown that stress-bifurcation (buckling) in the struts can occur under certain conditions prior to fracture. The effects of mixed-mode loading are also evaluated using the BLM through a range of boundary conditions with varying Mode I and Mode II contributions. Interaction between buckling and intrinsic size-effects of finite-sized specimens is addressed for lattices with $16 < W/l_0 < 128$ cells across the width, and crack-sizes of $0.15 < a/W < 0.65$, where W is specimen-width, a is the crack-length and l_0 is the characteristic length of the unit cell. For validation, experimental results using SENT specimens, manufactured by laser-cutting of PMMA sheets, will also be presented.

Results

It is demonstrated that stress bifurcation in struts near the crack-tip occurs below a critical transition relative density. The latter is sensitive to the nonlinear strain of the strut material and shows good agreement with predictions by elastic buckling calculations. In infinite-sized lattices, the fracture initiation in pure Mode I loading is insensitive to buckling, however increased Mode II contribution leads to earlier onset of buckling and fracture at loads up to 70% lower than initially predicted. These phenomena are observed at practically relevant relative densities (up to $\rho=0.2$), e.g. a reduction of 68% at $\rho=0.1$. Finite-sized SENT specimens reveal fracture initiation in the post-buckling regime, with toughness values up to 60% below that predicted by standard scaling law. In deeply notched finite-sized specimens ($a/W > 0.48$), buckling and fracture are first observed at the remote edge from the crack. Experimental results confirm the occurrence of strut buckling before fracture in SENT specimens and validate the numerically obtained fracture toughness scaling law.

Conclusions

It is shown that elastic strut buckling is an active mechanism in the fracture initiation of lattice materials, and

can lead to material failure at smaller loads than predicted by current analyses. Finite deformation of individual struts is shown to significantly affect the bulk mechanical properties of the lattices.

9:10 AM ST03.01.03

Tailoring the Mechanical Properties of High-Strength Mechanical Metamaterials Chantal Kurpiers¹, Artur Böttcher¹, Stefan Hengsbach¹ and Ruth Schwaiger²; ¹Karlsruhe Institute of Technology, Germany; ²Forschungszentrum Jülich GmbH, Germany

Technological advances in additive manufacturing techniques have enabled the fabrication of novel three-dimensional nano- and micro-architected lattice materials, which facilitate the exploration of yet unreachable property combinations. Specifically designed lattice materials have great potential in particular in the field of lightweight materials, since high specific strength and stiffness combined with low densities and remarkable robustness can be achieved. For the fabrication of geometrically complex structures with small feature size, light-based additive manufacturing methods, such as 3D direct laser writing (3D-DLW), are the most promising ones. In combination with various post-processing steps, such as annealing, pyrolysis, and the application of coatings, the overall behaviors of the printed structures can be further adapted. However, the failure processes are not yet clear, in particular since the writing parameters themselves might affect the materials properties very locally affecting individual components of the architectures.

In this work, we fabricated tetrahedral microlattices via 3D-DLW using two different photoresists (IP-Dip, IP-S). The writing parameters were varied during the writing process of the microlattices to induce local changes of the material properties. The polymeric structures were then converted into glassy carbon through pyrolysis, which is accompanied by significant shrinkage of the lattices depending on the selection of temperatures. The mechanical behaviors of both the lattices and materials was investigated by compression tests using a nanoindenter. Raman Spectroscopy and X-ray Photoelectron Spectroscopy (XPS) were applied to further characterize the structural variations. A variation of the 3D-DLW parameters and the post-processing steps showed a significant influence on the materials structures and therefore the deformation and failure behavior of the microlattices. Understanding the relation between the chemical morphology and the mechanical behavior will contribute to our understanding and prediction of properties of architectures fabricated through 3D-DLW, which will further enhance the applicability of high-strength mechanical metamaterials.

9:25 AM ST03.01.04

Late News: Mechanical Properties of a Truncated-Hexagonal Lattice Milad Omid and Luc St-Pierre; Aalto University, Finland

Bending-dominated lattices offer superior energy absorption capacities and one of the most commonly used topologies is the hexagonal lattice. This architecture is frequently used as the core of sandwich panels, for example, because its simple geometry can be manufactured easily. The rapid development of additive manufacturing, however, allows us to produce much more complex architectures and this raises the question: could other bending-dominated topologies outperform the hexagonal lattice? This study reports the behaviour of a truncated-hexagonal lattice: a 2D prismatic bending-dominated topology with mechanical properties superior to those of the hexagonal lattice.

The truncated-hexagonal lattice is a semi-regular tessellation where each vertex is connected to two dodecagons and a triangle. It has a nodal connectivity of three (like the hexagonal lattice) and consequently, its behaviour is bending-dominated. We derived analytical expressions for the elastic modulus and strength of the truncated-hexagonal lattice when subjected to (i) uniaxial compression and (ii) shear. These analytical expressions were then validated using finite element simulations. Both analytical and numerical work assumed that the lattice is made from an elastic, perfectly plastic solid and that the bars are sufficiently slender to behave as Euler-Bernoulli beams.

The results showed that a truncated-hexagonal lattice is particularly stiff for a bending-dominated lattice. In fact, its Young's and shear moduli are both 85% stiffer than those of the hexagonal lattice. This result is independent of orientation since the truncated-hexagonal lattice has in-plane isotropic elastic properties. The truncated-hexagonal lattice fails by plastic collapse when it is loaded in compression or in shear. Its plastic

collapse strength is 11% higher than that of the hexagonal lattice.

In summary, we conclude that the stiffer and slightly stronger truncated-hexagonal lattice would be a good replacement to the hexagonal lattice in applications where energy absorption is critical. Experimental work is currently underway to corroborate the analytical and numerical results reported above.

SESSION ST03.02: Mechanical Behavior of Architected Materials I

Session Chair: Lucas Meza

Tuesday Morning, April 20, 2021

ST03

11:45 AM *ST03.02.01

Double Elasticity Transition in Multistable Architected Materials Agustin Iniguez-Rabago¹ and Johannes Overvelde^{1,2}; ¹AMOLF, Netherlands; ²TU/e, Netherlands

Advances in fabrication technologies are enabling the production of architected materials with unprecedented properties. While most of these materials are characterized by a fixed geometry, an intriguing avenue is to incorporate internal mechanisms capable of reconfiguring their spatial architecture, therefore enabling tunable functionality. Inspired by the structural diversity and foldability exposed in origami, researchers have started to create reconfigurable materials comprising assemblies of plates and hinges. Here our focus is on achieving architected materials with a finite range of encoded behaviors. We achieve this by harnessing nonlinear mechanical behavior that arises either through the underlying 3D geometry, or by direct assuming a nonlinear description for the folding behavior of the hinges, resulting in multistability. Guided by numerical analysis and physical prototypes, we systematically explore the mobility of the designed structures through the use of local actuation, in an effort to uncover and classify their potential behavior. By doing so, we find two transitions in the elastic behavior of these materials depending on the ratio between the stiffness of the plates and hinges. Given that the underlying principles are scale-independent, our strategy can be applied to design the next generation of reconfigurable structures and materials, ranging from transformable meter-scale architectures to nanoscale tunable photonic systems.

12:10 PM ST03.02.03

Controlled Chemical Evolution of a 3D Biogenic Structure for Tailored Mechanics Sunghwan Hwang, Raheleh Rahimi, Mohsen Damadam, Jiaqi Li, Alexander Strayer, Mahdi Dehestani, Grigorios Itskos, David Bahr and Ken Sandhage; Purdue University, United States

Diatoms are single-celled algae that produce, and live within, 3-D, microscopic, nanostructured, porous silica glass-based shells (called “frustules”). Diatom frustules have evolved over hundreds of millions of years to provide resistance to being crushed by predators. Indeed, micromechanical tests and simulations have indicated that *Fragilariopsis kerguelensis* frustules are capable of accommodating local compressive and tensile stresses in excess of 600 MPa and 500 MPa, respectively (C. E. Hamm, et al., *Nature*, 421, 841-843 (2003)). The robust nature of silica-based *F. kerguelensis* diatom frustules has led us to question how such microscale structures would behave if these structures were comprised of metallic or oxide/metal composite materials (i.e., materials that are ordinarily more resistant to fracture than bulk monolithic silica).

To address this question, SiO₂-based *F. kerguelensis* diatom frustules were reactively converted into 3-D replicas comprised of Ti and MgO/Ti composites. Live *F. kerguelensis* diatoms were graciously provided by Prof. Rebecca Robinson (University of Rhode Island). Diatom culturing was conducted in L1 medium at 4°C using 13 h light/11 h dark cycles. After harvesting and then washing of the diatom cells in water and ethanol, the cells were heated in air at 600°C for 4 h to remove organic material to yield SiO₂ frustules. A series of gas/solid reactions was then used to convert these SiO₂ frustules into MgO/Ti and Ti replicas. Reactive

conversion experiments were conducted on two types of specimens: i) a shallow bed of frustules (to allow for X-ray diffraction analysis at each stage of reactive conversion), and ii) isolated individual frustules on inert polished substrates (to allow for evaluation of the preservation of the overall frustule morphology and surface features at each stage of conversion via electron microscopy and to allow for *in-situ* mechanical tests). The latter specimens were oriented with the valve or the girdle band of the frustule or frustule replica facing upwards (to allow for compression tests with both orientations). Secondary electron microscopic images of individual frustules confirmed that the 3-D frustule morphology was preserved at each stage of reactive conversion. The micro/nanochemical evolution during such shape-preserving reactive conversion was evaluated using X-ray diffraction analysis, energy-dispersive X-ray analysis, and selective area electron diffraction analysis (via transmission electron microscopy).

In-situ mechanical tests were conducted with a Hysitron PI-88 system installed in a scanning electron microscope to allow for direct observation of the deformation behavior of SiO₂ *F. kerguelensis* frustules, and of Ti and MgO/Ti replicas of such frustules. Single and partial loading-unloading load functions were applied to these diatom frustules and frustule replicas. Load-displacement plots indicated that the SiO₂ frustules exhibited fully elastic and brittle behavior, whereas appreciable plasticity was detected for the Ti frustule replicas. While the SiO₂ frustules and Ti frustule replicas exhibited some similarities in apparent crack initiation locations and in crack propagation behavior, higher failure loads were accommodated by the Ti frustule replicas prior to catastrophic failure than for the SiO₂ frustules. The MgO/Ti frustule replicas exhibited higher stiffness, and sustained appreciably higher loads prior to catastrophic failure, than the Ti frustule replicas, while retaining notable plasticity. The use of such *in-situ* micromechanical tests and simulations to evaluate structural motifs responsible for such mechanical behavior will be discussed.

12:25 PM ST03.02.04

Multifunctional Metallic Nanolattices with Ultra-High Tensile Strength Enabled by cm-Scale Crack-Free Self-Assembly Zhimin Jiang and James H. Pikul; University of Pennsylvania, United States

Biology creates complex porous structures to realize materials that are mechanically strong and lightweight, and have added chemical or physical functionalities, like bone or wood. Inspired by these remarkable materials, engineers have been adding pores to metals to make strong and lightweight multifunctional structures. Porous metals fabricated by traditional methods, however, have mechanical strengths far below their theoretical limits [1]. High-resolution 3D printing is one manufacturing technique that has realized nanolattices that approach the theoretical strength of their constituent materials through topological design, structural optimization, and size effects in nanomaterials. 3D printing, however, has inherent trade-offs between resolution and printing time that severely limit the scale-up of 3D printed nanolattices, which has restricted almost all nanolattice mechanical property measurements to compression by micro/nanoindentation [2]. The tensile properties of nanolattices, therefore, have been mostly unexplored. To truly take advantage of the remarkable properties of nanolattices, it is essential to realize new methods for fabricating macroscopic nanolattices and to understand how their chemistry and physical properties affect their tensile properties.

In this work, we demonstrate a crack-free self-assembly approach to fabricate 2 cm long multifunctional metallic nanolattices with 100 nm periodic features and 30 nm grain size, which translates to 1,000X more unit cells in the loading direction than prior studies. Benefiting from the scalability of this fabrication approach, we grow the first large-area multifunctional nickel nanolattices and measure the tensile properties with macroscopic testing equipment. We show that they can achieve an ultra-high 227 MPa tensile strength at a density less than aluminum, which is 3 times stronger than what has been reported for porous metals with the same relative density at any scale. We also found that the key to enhancing the tensile strength is to combine a lattice geometry that reduces stress concentrations with control of the nanostructure and grain size which reduce the size of inherent defects, such as voids, and increase the metal strength. The resulting nickel nanolattices have excellent structural photonic coloration, approach the theoretical limit of their upper tensile strength, and realize a new combination of strength and relative density for porous metals and nanolattices. The combination of high strength and high specific strength makes these nickel nanolattices ideal for resisting bending loads: they can resist the same load with 50% smaller volume than porous titanium, 50% lower mass than porous iron, and,

importantly, 10X less volume than other nanolattices. The new ways developed in this work to fabricate metal nanolattices and characterize their performance will further the design and fabrication of lightweight high-strength multifunctional porous metals.

1. Zhao, B., et al., A review on metallic porous materials: pore formation, mechanical properties, and their applications. *The International Journal of Advanced Manufacturing Technology*, 2018. 95(5): p. 2641-2659.
2. Zhang, X., et al., Design, Fabrication, and Mechanics of 3D Micro-/Nanolattices. *Small*, 2020. 16(15): p. e1902842.

12:40 PM ST03.02.05

Electrically-Driven Soft Robots via 3D Printed Handed Shearing Auxetics Ryan L. Truby, Lillian Chin and Daniela Rus; Massachusetts Institute of Technology, United States

Electrically-mediated actuation schemes offer great promise beyond popular pneumatic and suction-based approaches in soft robotics, but they often rely on bespoke materials and manufacturing approaches that constrain design flexibility and widespread adoption. Following the recent introduction of a class of architected materials called handed shearing auxetics (HSAs), we present a 3D printing method for rapidly fabricating HSAs and HSA-based soft robots that can be directly driven by servo motors. To date, HSA fabrication has been limited to laser cutting of extruded Teflon (PTFE) tubes. Our work expands the HSA materials palette to include flexible and elastomeric polyurethanes. Herein, we investigate the influence of material composition and geometry on printed HSAs' mechanical behavior. In addition to individual HSA performance, we evaluate printed HSAs in two robotic platforms - four degree-of-freedom (DoF) platform and a soft gripper - to confirm that printed HSAs perform similarly to the original PTFE HSA designs. Finally, we demonstrate new soft robotic capabilities with 3D printed HSAs, including fully 3D printed HSA actuators, higher force generation in multi-DoF devices, and demonstrations of soft grippers with internal HSA endoskeletons. We anticipate our methods will expedite the design and integration of novel HSAs in electrically-driven soft robots and facilitate broader adoption of HSAs in the field.

12:55 PM ST03.02.06

Effect of Fibre Length and Distribution on the Structural Properties of Bamboo-Fibre Foams Hosna Malekzadeh and Eral Bele; University College London, United Kingdom

Introduction/Aims

Solid foams are structurally efficient materials, and as such, are particularly attractive in weight sensitive applications, e.g. in packaging and insulation. The typical base materials of commercial foams are metallic or petrochemical, both of which pose some disadvantages due to energy intensity of manufacturing, and reliance on non-renewable resources respectively. Natural fibres can be exploited to create and reinforce biodegradable cellular materials, e.g. to increase rigidity, strength and energy absorption.

In this work we consider the use of cellulose fibres extracted from bamboo culms, and used in two configurations: as reinforcement for close-celled cellulose-matrix foams, and as a structural open-celled fibre network. Topology optimisation is used to improve the reinforcement efficiency of such fibres, with the aim of obtaining comparable mechanical properties to commercial foams. We present results on the effect of fibre length and distribution on the macroscopic mechanical response and deformation mechanisms in compression and bending.

Methods

This study uses relatively simple manufacturing techniques to fabricate closed and open-celled foams. Cellulose fibres are extracted from bamboo culms and used as the primary source of raw material, to reinforce a pulp slurry that is subsequently drained and solidified, and to create a fibre network that bound at the joints through microfibril bridges created by partial surface hydrolysis.

The material properties of fibres, the fibre/matrix interfacial strength, and critical fibre length are obtained through microtensile tests. The mechanical response of the resultant foams is reported in uniaxial compression and 3-point bending. These tests are coupled with strain mapping through digital image correlation (DIC), and microstructural investigation of deformation mechanisms through scanning electron microscopy (SEM).

Results

In close-celled foams, the internal microstructure consisted of interpenetrating ellipsoidal voids, with an aspect ratio of 1.5, and the compressive response was typical of elastic-brittle foams. Fibre reinforcement was exploited by two mechanisms: the delay of fracture propagation during uniaxial compression, and shear transfer during bending. The former resulted in an increase in the energy absorption/density ratio with fibre volume fraction, and the latter in an increase in the flexural rigidity and strength. A critical fibre length is reported for effective reinforcement in both cases. Bending stiffness and strength were largely determined by this parameter, but the reinforcement efficiency in compression was more sensitive to preferential fibre distribution than length.

In fibrous networks, surface treatment through partial hydrolysis was used to control the number of inter-fibre bridges. The latter increase density but reduce stiffness, due to a low joint strength. The effect of fibre length was shown in a linear compressive stiffness/density relationship, indicating that the network response was dominated by fibre stretching.

Conclusions

The response of these first cellular materials created from bamboo fibres showed that the mechanical properties are within the range of current foams. The results showed that there is a critical fibre length and distribution for optimal reinforcement efficiency. These findings indicate a potential route towards the manufacturing of sustainable lightweight materials for structural applications.

SESSION ST03.03: Design of Architected Materials I
Session Chairs: Woo Soo Kim and Jordan Raney
Tuesday Afternoon, April 20, 2021
ST03

2:15 PM *ST03.03.01

Bayesian Optimization with Multi-Fidelity Sources for the Design of Non-Uniform Architected Lattices with Optimal Failure Properties Chengyang Mo, Paris Perdikaris and Jordan R. Raney; University of Pennsylvania, United States

Architected cellular solids and lattices (2D and 3D) have been widely studied and integrated into many applications in mechanics. Past research has mainly focused on uniform, periodic lattices. However, lattices can be architected to possess non-uniform struts and non-periodic arrangements with interesting mechanical properties. Previous work has explored variations of non-uniformity, including linearly-graded or harmonically-graded lattices that result in staged failure. Yet designing more general non-uniform structures that optimize desired mechanical properties is challenging due to the large number of parameters. Machine learning algorithms such as neural networks can help in the design process by generating all possible geometric patterns and finding candidates that match the desired properties. However, this approach is limiting, as it is only feasible for low dimensions and can only be experimentally validated for a few design candidates that have been identified. Here, we discuss the use of a framework based on Bayesian optimization that incorporates multi-fidelity data originating from both experimental and numerical results in the pursuit of optimized properties. In this approach, the Bayesian optimization is a closed-loop design process based on Gaussian process regression which guides the choice of design variables for each iteration of experiments. We implemented this approach for the design of both 3D (body-centered cubic lattice) and 2D structures (square

cellular solids), seeking to optimize for desirable combinations of mechanical properties (such as toughness, yield stress, etc.). As a “low-fidelity” data source we use numerical simulations in ABAQUS to simulate compression of architected lattices with non-uniform strut thicknesses. As a “high-fidelity” data source we perform experimental compression tests on structures that have been 3D printed using stereolithography (SLA). These data sources are fed into the multi-fidelity Bayesian optimization algorithm. The algorithm guides the choice of the next experiments/numerical simulations until sets of optimal parameters are found.

2:40 PM ST03.03.02

Architected Liquid Crystalline Elastomers with Strain Rate-Adaptive Extreme Energy Absorption Sung H. Kang; Johns Hopkins University, United States

An architected material allows new opportunities in material design and synthesis by enabling new properties that are not observed in natural materials or from a bulk material that the “material” is made of based on the interplay between material and geometry. We have investigated liquid crystalline elastomer-based architected materials that harness energy absorption mechanisms across multiple length scales for extreme energy absorption. Moreover, the architected material shows strain-adaptive energy absorption behaviors with power-law relation between energy absorption and strain rate whose exponent can be tuned via controlling microscale mesogen alignment by couple nonlinear geometric and nonlinear material properties. We will report our characterization results of energy absorption behaviors of architected liquid crystalline elastomers over 6 orders of magnitudes strain rate ranges and numerical modeling results to investigate its strain-rate adaptive energy absorption mechanisms based on viscoelastic property characterization data of liquid crystalline elastomers over 20 orders of magnitudes frequency ranges. The findings from our study can contribute to realizing extremely lightweight and high energy absorbing materials, which will be beneficial for various applications, including automotive, aerospace, and personal protection.

Acknowledgements: This research is supported by the Army Research Office (Grant Number W911NF-17-1-0165) and the Johns Hopkins University Whiting School of Engineering start-up fund.

2:55 PM ST03.03.03

Late News: Kirigami-Inspired Graphene with Programmable Thermo-Mechanical Properties Jun Cai and Hamid Akbarzadeh; McGill University, Canada

Tuning and programming the multiphysical properties of advanced materials is of critical importance for developing the next generation of adaptable multifunctional metamaterials. This study demonstrates the tunability of thermo-mechanical properties of graphene sheets by inspiring from kirigami mechanical metamaterials. The theoretical investigation, multiscale simulation, and experimentations show that the stress-strain response, the buckling-induced 3D patterns, as well as the thermal conductivity of nano-architected kirigami metamaterials can be tuned by altering geometrical parameters and cutting patterns. The thermal conductivity of kirigami-inspired graphene metamaterial can be further regulated and managed by an external mechanical strain. By analyzing and comparing the results from atomic simulation and continuum-based simulation, the effect of the length scale is discussed to explore the connection across the scales. Analytical models are also developed to predict the thermo-mechanical properties of heterogeneous kirigami and offer an explicit tool for the rapid engineering of graphene-based metamaterials to achieve desired stress-strain response and thermal conductivity. This work facilitates the applications of programmable kirigami-inspired nano-metamaterials in wearable nanoelectronics and nanoscale heat transport systems.

3:10 PM ST03.03.04

Spectral Selective Transparent Porphyrin Thin Films with PT- and PV- Dual Modality for Energy-Efficient Building Skin Jou Lin and Donglu Shi; University of Cincinnati, United States

In solar harvesting for energy sustainability, the porphyrin compounds have been found to exhibit both photovoltaic (PV) and photothermal (PT) effects due to their unique structures. Both chlorophyll and

chlorophyllin belong to the porphyrin compounds that are structurally characterized with a large ring molecule consisting of four pyrroles, denoted as the porphyrin ring. The optical properties of these compounds are typically characterized with strong absorptions near the UV and NIR regions, and high average visible transmittance. The porphyrin compounds are well-known for dye-sensitized solar cells (DSSC), bulk-heterojunction solar cells (BHJSC), and perovskite solar cells (PSC). Some of the porphyrin compounds have also been shown to exhibit strong photothermal effects. Upon sufficient solar harvesting, the photon energy can be converted to electricity or thermal energy by PV or PT through the same porphyrin thin film in an alternative fashion. Therefore, a PT- and PV- dual-modality can be designed and engineered for energy applications. In this study, the spectral-selective porphyrin thin films are applied on the window inner surface for thermal insulation in a single pane design. Upon solar irradiation, the window surface temperature can increase appreciably by the PT coating resulting in significantly reduced heat transfer, characterized by a low U-factor. Therefore, thermal insulation can be achieved optically without any interfering medium as conventionally required in the double- or triple- glazing. The building skin with a large surface area with the PT coating can also serve as an ideal substrate for PV panel for energy generation, with the dual modality that can be altered seasonably. We report the experimental results on the PT- and PV dual modality building skin based on porphyrin thin films for energy saving and generation. Also reported are the porphyrin compounds synthesis, thin film deposition, optical absorption characterization, and the photothermal/photovoltaic measurements.

3:15 PM ST03.03.06

Late News: Nano-Architected Carbon for Supersonic Impact Mitigation [Carlos Portela](#)¹, Bryce Edwards², David Veysset¹, Yuchen Sun¹, Keith Nelson¹, Dennis M. Kochmann³ and Julia Greer²; ¹Massachusetts Institute of Technology, United States; ²California Institute of Technology, United States; ³ETH Zurich, Switzerland

The use of architecture in materials has been reported to enable novel combinations of mechanical properties such as high stiffness- and strength-to-density ratios. Furthermore, interesting size effects can appear when architected nanometer-scale features are achieved such as in pyrolytic carbon struts, which have recently been shown to exhibit rubber-like response. While this size effect has been explored in the quasi-static response of 3D beam-based architected materials, no work has explored its implications under extreme conditions. Exploiting these size effects in the dynamic regime has potential to enable ultralightweight impact-resistant materials for applications such as ballistic impact, blast loading, and micrometeoroid shielding in space. We propose a method to fabricate and test nano-architected carbon lattice materials at supersonic ballistic impact speeds of up to ~ 1 km/s, allowing for in situ and post-mortem characterization. Using beam-based architectures as the periodic building-blocks, we fabricate these materials using a two-photon lithography process followed by pyrolysis, yielding a carbon-based nano-architected material. Using ~ 2 μm tetrakaidekahedral unit cells, with beam diameters ranging from 300-800 nm, we explore the effects of relative density (i.e., fill fraction) on the impact response. Employing 14 μm -diameter projectiles via the laser-induced particle impact test (LIPIT), we analyze the effects of varying impact velocities from 50 – 1,100 m/s, attaining nominal strain rates on the order of 10^6 s⁻¹ to 10^7 s⁻¹. We observe three distinct response regimes: (i) elastic impact, (ii) cratering and particle rejection, and (iii) cratering and particle capture, depending on the relative density of the lattice material as well as the impact energy. Our experiments demonstrate impact energy dissipation of up to 1.1 MJ/kg in these materials, outperforming traditional impact-resistant materials such as steel, aluminum, PMMA, and Kevlar. By analogy to planetary impact, we also introduce predictive tools for crater formation in these materials using dimensional analysis. These results uncover an extreme-condition regime over which nano-architecture can enable the design of new generations of ultra-lightweight, impact-resistant materials.

SESSION ST03.04: Applications of Architected Materials

Session Chairs: In-Suk Choi and Dongchan Jang

Tuesday Afternoon, April 20, 2021

ST03

5:45 PM *ST03.04.01

Design of Patterned Structures for Deformable Devices In-Suk Choi; Seoul National University, Korea (the Republic of)

How can we overcome the formability of materials beyond original materiality? To answer this question, we have adopted “**simple geometric patterned structures**” that significantly enhance flexibility and stretchability of brittle or stiff materials. Geometrical design such as *auxetics*, *origami* and *kirigami* provides us many examples of the formation of delicate and, detailed patterns leading to the effective distribution of stresses. Instead of process control and complex structure design, we employed the simple juxtaposition of unit design leading to simple, cheap and easily processed flexible, stretchable and deployable structures for deformable devices. In addition, newly developed computational approach expands our design dimension to the next level. We believe that geometrical modulation by controlled size, shape, and symmetry adds another dimension unleashing the limitation of conventional design space of structure materials

6:10 PM ST03.04.02

Mechanical and Structural Properties of Nanostructured Metalattices Probed by Coherent EUV Beams Begoña Abad Mayor^{1,2}, Joshua Knobloch¹, Travis D. Frazer¹, Jorge Nicolas Hernandez Charpak¹, Hiu Yan Cheng³, Alex Grede³, Noel Giebink³, Tom Mallouk³, Pratibha Mahale³, Nabila Nova³, Andrew Tomaschke¹, Virginia Ferguson¹, Vincent Crespi³, Venkatraman Gopalan³, Henry Kapteyn¹, John Badding³ and Margaret Murnane¹; ¹University of Colorado Boulder, United States; ²University of Basel, Switzerland; ³The Pennsylvania State University, United States

Phononic crystals represent a very promising route for tuning the properties of next-generation nanoelectronics, thermoelectrics, and ultralight materials. These consist of periodic arrays embedded in an elastic medium, arranged in a specific lattice symmetry [1,2,3]. Nanofabrication techniques can now produce nanoscale phononic crystals with dimensions $\ll 100$ nm (referred to as metalattices) which make it possible to engineer new elastic and transport properties [4,5]. To fabricate metalattices, nanospheres are first assembled into a colloidal crystal with face centered cubic order. This base structure can be tuned from monolayer to microns in thickness, with sphere sizes from the nanometer (nanoscale opals) to microns (opals) [1,6]. The interstitial space between the nanospheres of the colloidal crystal is then infiltrated with another material, forming a metalattice structure for periodicities in the sub-100nm. To understand the mechanical properties of metalattices, studies to date have focused only on one component of the metalattice—either the template or the etched-out structures, and always for periodicities >100 nm. In this work, we present a nondestructive method to accurately extract, for the first time, the mechanical and structural properties of metalattices with much smaller feature sizes. Specifically, we probe silicon metalattices fabricated from sphere diameters of 14 nm and 30 nm, with periodicities of 19 nm and 42 nm, respectively. These metalattices contain feature sizes that are an order of magnitude smaller than opals that have been characterized to date. We use an ultrafast laser pulse to heat a set of transducer gratings, which impulsively launch surface acoustic waves (SAW) in the metalattice. The wavelength of the SAW can be tuned by varying the transducer grating periodicity, which also changes the SAW penetration depth into the metalattice and the silicon substrate. We then monitor the SAW frequency from the time-dependent change in extreme ultraviolet (EUV) light diffracted off the grating. This method allows us to simultaneously extract the acoustic dispersion, as well as the Young's modulus, thickness and filling fraction of the metalattice. Interestingly, the extracted mechanical and structural properties agree well with macroscopic predictions, while the transport properties of the same metalattices do not agree with bulk models. Additionally, the measured metalattice thicknesses agree with scanning electron microscopy images and the extracted Young's moduli agree with nanoindentation measurements, while achieving higher accuracy. Finally, this technique represents the only approach to date to nondestructively validate the filling fraction of deep-nanoscale metalattices. It also has advantages over destructive electron imaging because it probes over large areas and does not suffer from material contrast issues. These results can enable precise fabrication, characterization and understanding of materials with tailored mechanical and transport properties.

- [1] Armstrong, E. & O'Dwyer, C. *J. Mater. Chem. C* **3**, 6109–6143 (2015).
[2] Barako, M. T. *et al. Nano Lett.* **16**, 2754–2761 (2016).
[3] Liontas, R. & Greer, J. R. *Acta Mater.* **133**, 393–407 (2017).
[4] Liu, Y. *et al. Nano Lett.* **18**, 546–552 (2018).
[5] Maldovan, M. *Nature* **503**, 209–217 (2013).
[6] Vogel, N., Retsch, M., Fustin, C.-A., del Campo, A. & Jonas, U. *Chem. Rev.* **115**, 6265–6311 (2015).

6:25 PM ST03.04.03

Optimizing Steel-Reinforcement in Concrete—Using Topology Optimization and Digital Fabrication to Develop Ductile Concrete for Specific Loading Conditions [Brian Salazar](#), Parham Aghdasi, Michael Herrmann, Sharjeel Laeeq, Levi Seidel, Claudia Ostertag and Hayden Taylor; University of California, Berkeley, United States

As concrete is a brittle material, it must generally be reinforced for use in building applications. Steel-reinforced concrete is a composite in which the majority of the compressive strength stems from the concrete and the steel reinforcement provides the tensile strength. Typically, the steel reinforcement often takes the form of a 1-D reinforcing bar or 2-D cage. However, the reinforcement geometry is not usually optimized for the particular loading scenario that the structure will experience. Additionally, the placement of the concrete itself may be optimized for particular applications, which may reduce the CO₂ emissions for concrete structures.

The minimum amount of steel reinforcement in a concrete structure is dictated by the loads it must withstand. Further, building codes specify a maximum amount of steel allowed within a structure; concrete structures typically do not have a steel reinforcing ratio greater than 6%. As our goal is to optimize the amount and placement of both the steel reinforcement and the concrete within the overall structure, this is a constrained, multi-material topology optimization problem. Our approach is innovative, as we use the specific loading structure to inform where the steel and concrete should be placed and use digital manufacturing techniques to create that optimal steel reinforcing structure.

We use the Topology Optimization (TopOpt) Grasshopper tool developed at the Technical University of Denmark to inform the optimal steel placement within the concrete structures. TopOpt's objective is to minimize the structure's compliance, with constraints on the material volume and the void shape. TopOpt assumes that the concrete has a compressive stiffness that is 10 times greater than its tensile stiffness. This material anisotropy serves to ensure the concrete and steel are placed properly within the geometry. The loading scenario considered here is a flexural beam undergoing four-point bending. When using these topology optimization results to inform the 3-D reinforcement geometry design, the result is a steel volume fraction of 6%.

Digital fabrication technologies are well-suited to creating these complex reinforcement structures. We used an Omax 2626 to waterjet cut these architected, steel reinforcement geometries, placed this optimized steel reinforcement geometry into a 3" x 3" x 11" mold, and casted concrete around it. In this first structure, the placement of steel is optimized, but the placement of concrete is not. We created a second concrete geometry, wherein both the placement of steel and the concrete is optimized. This geometry contained 30% less concrete than the first geometry. Finally, we created a non-optimized, straight, steel rebar geometry and used it to reinforce a 3" x 3" x 11" concrete beam (for comparison purposes).

In four-point bending tests, we found that the beam with optimized steel reinforcement reached a peak load that is 1.28 times greater than the peak load reached by the beam with straight rebar reinforcement, despite the two beams having the same steel reinforcing ratio. Additionally, the beam with optimized steel reinforcement reached a toughness that is 1.38 times greater than the toughness reached by the beam with straight rebar reinforcement. When we compared the beam with optimized steel reinforcement and the beam with both optimized steel reinforcement and optimized concrete placement, we saw that the peak load is reduced by 18%, and the toughness is reduced by 26%.

These results suggest that optimizing the placement of steel reinforcement within concrete structures can have a significant improvement on the overall mechanical properties. Additionally, optimizing the placement of the concrete—and reducing the amount of concrete used—allowed us to create a structure with a 30% weight reduction, which may be beneficial in seismic applications.

6:40 PM ST03.04.04

Architecting Lithium-Ion Battery Electrodes with Acoustic Focusing Emilee Armstrong¹, Keith Johnson², Drew S. Melchert², Matthew R. Begley^{2,2} and Corie L. Cobb¹; ¹University of Washington, United States; ²University of California, Santa Barbara, United States

Lithium-ion batteries (LIBs) with high energy and power density are crucial for energy storage applications such as vehicle electrification. Traditional LIBs have planar electrodes wherein their performance can be optimized for energy or power, but not both simultaneously. Three-dimensional (3D) electrodes have been shown to mitigate these trade-offs by using 3D architecture to enable fast ion transport in thick battery electrodes.¹ However, there is a need for more scalable, large-area fabrication methods for 3D electrodes. In this work, we expand a computational model² to analyze the feasibility of combining acoustic focusing with additive manufacturing to fabricate line-patterned battery electrodes. Acoustic focusing uses acoustic forces to control particle placement in a fluid, and its ability to align particles on a micron-scale make it a promising technique for 3D electrode fabrication. In our model, we solve for trajectories of particles in a fluid using analytical models of the focusing forces, which we compare to experimental results. We apply this model to battery-relevant materials to determine how focusing parameters such as viscosity, particle size, and volume fraction impact electrode geometry for optimizing battery energy and power performance. Our initial results suggest that lithium cobalt oxide (LiCoO₂) and lithium nickel manganese cobalt oxide (LiNi_{0.33}Mn_{0.33}Co_{0.33}O₂) are highly compatible with acoustic focusing.

1. C. L. Cobb and M. Blanco, *J. Power Sources*, **249**, 357-366 (2014).
2. R. R. Collino, T. R. Ray, L. M. Friedrich, J. D. Cornell, C. D. Meinhart and M. R. Begley, *Mater. Res. Lett.*, **6**, 191–198 (2018).

6:45 PM ST03.04.05

Design Considerations and Performance of Bi-Material Lattices Amanda Ruschel and Frank Zok; University of California, Santa Barbara, United States

Cellular materials, including stochastic foams and ordered lattices, have been used extensively for their weight efficient properties. The nearly-constant crushing stress of stochastic foams make them ideal for energy absorption applications. Notwithstanding, their strengths are low relative to those of ordered lattices. Although ordered lattices can attain higher strengths, they exhibit internal buckling and concurrent strain softening during compressive loading, making them undesirable for energy absorption applications. Although the performance of single-material foams and lattices has been studied extensively, recent advancements in additive manufacturing have opened new possibilities of *multi-material* lattice structures.

This talk will outline the design considerations for bi-material lattices that have potential for tuning the balance between high strength and high straining capability. To begin, a primitive structural motif that exhibits the desired behavior is identified and its compressive response is analyzed. A 2D multi-cell lattice based on the primitive motif is designed and several material variants are fabricated and tested. Analysis of test results addresses effects of finite node dimensions, constraints on member rotation at the nodes, free edges, and friction with the loading platens as well as limits dictated by rupture of tensile members or buckling of compressive members. The study culminates with guidelines on design of bi-material lattices with high strength and high straining capability.

7:00 PM ST03.04.06

***De Novo* Discovery of Disordered Mechanical Metamaterials by Machine Learning** Han Liu and Mathieu Bauchy; University of California, Los Angeles, United States

Topology-optimized architected materials can feature unique mechanical behaviors, including unusual density-stiffness scaling. However, such materials have then been largely limited to periodic lattices. Here, we use machine learning and molecular dynamics to explore the effect of disorder as a new degree of freedom. We develop a Bayesian optimization framework that prescribes targeted topologies, which are subsequently validated by molecular dynamics simulations, which, in turn, generate new data to refine our machine learning model. This iterative learning pipeline is used to accelerate the discovery of light yet stiff disordered phases. We show that, at constant average local topology, disordered phases behave differently than their crystalline counterparts. This establishes disorder as a promising degree of freedom to discover new exotic phases with unusual mechanical properties.

SESSION ST03.05: Synthesis and Fabrication of Architected Materials I
Session Chairs: Dongchan Jang and Seokwoo Jeon
Tuesday Afternoon, April 20, 2021
ST03

9:00 PM *ST03.05.01

Mechanical Behavior of Ordered Porous Ceramic Architecture Made by PnP Seokwoo Jeon; KAIST, Korea (the Republic of)

Numerous three dimensional (3D) nanofabrication methods have been proposed for novel applications in mechanical metamaterials. However, highly periodic 3D fabrication in large area and volume has limited success. Here I present our recent efforts to expand the limit in size of highly periodic 3D nanostructures through Proximity field nanoPatterning (PnP) which uses conformal phase masks with outstanding scalability and easiness of the large area patterning. After brief overview of 3D nanofabrication technique and potential application fields, mechanical behaviors of nanocomposites based on 3D nanostructures will be discussed. Current applications are stretchable light scatter, interphase boundary nanocomposites (ceramic-polymer, ceramic-metal). The change of optical and mechanical behavior by changing the constitute materials and the geometry and thickness of cellular materials will prove the importance of structural motif in submicron, ordered porous materials and composites.

9:25 PM ST03.05.03

Bulk Fabrication 3D Ultralight Nanocomposite with High Resilience and Recoverability Jongbeom Kim and Seung Min Han; Korea Advanced Institute of Science and Technology, Korea (the Republic of)

3D lightweight, architected cellular structures that are fabricated via additive manufacturing methods are currently receiving much interest due to the tunable properties that can be realized by simply tuning the architecture. In addition, the use of nanoscale materials that have excellent mechanical properties as building blocks to create a large scale bulk material via hierarchical structuring allows for realization of a bulk material that display the excellent properties of the constitutive nanoscale materials. In this study, a simple bulk fabrication based on directional freeze-drying method was developed for synthesis of fully recoverable ultralight 3D porous nanocomposite that is composed of Ag nanowire/cellulose nanofiber(CNF). Freeze-drying method is a one-step process via ice crystal formation followed by sublimation of ice crystal which leaves behind the Ag nanowire/CNF nanocomposite walls to form the 3D porous structure. Compression tests on vertically and horizontally aligned Ag nanowire/CNF nanocomposite walls showed highly anisotropic mechanical properties. An optimized concentration of Ag nanowires resulted in the compressive strength of 100 kPa at a relative density of 0.96%, which has 1.5 times higher strength when normalized by the material density

compared to that of metal microlattices fabricated by lithography methods. Horizontally aligned 3D porous structure showed perfect restoration while maintaining sufficient electrical conductivity that is suitable for flexible electronics and 3D strain sensors. Proposed freeze-drying methodology was also used to fabricate other 3D nanocomposite using polyvinylalcohol and Ag nanowire as a hard core that was then infiltrated with PDMS to create a hard core-soft matrix composite. The compression tests of the developed 3D bulk nanocomposite indicated excellent resilience and recoverability.

9:40 PM ST03.05.04

Late News: The Twisting of Dome-Like Metamaterial from Brittle to Ductile Lizzie Cheng; City University of Hong Kong, Hong Kong

Architected materials can exhibit mechanical properties that do not occur with ordinary solids. By integrating hierarchy and size effects, micro-architected metamaterials fabricated by two-photon lithography with metallic or ceramic coating can be ultra-strong but lightweight. However, the attainment of both strength and ductility is generally mutually exclusive. Inspired by the Pantheon dome in Rome, which can withstand high load while keeping low density, micro-architected domes with a gradient helix are designed and deposited in a hierarchical nanostructured aluminum film with ultrahigh strength and considerable plasticity. Despite a thick coating usually causes catastrophic collapse, the thick-walled metallic dome shows recoverability during compression. The compressive strength significantly increases compared to current ductile-like micro-lattices. Detailed experimental and computational works reveal the graceful (non-catastrophic) failure due to the helical twisting and plastic flow in the supra-nano material. It is a promising method of suppressing brittle failure via a combination of architectural and material design. It can be used to impart enhanced functionality, making programmable stiffness, and tailored energy absorption all possible.

9:45 PM ST03.05.05

Mechanical and Microstructural Characterization of Non-Polymeric Architected Materials Fabricated Using a Cost-Effective and Scalable Stereolithography 3D Printing Technique Changquan Lai; Nanyang Technological University, Singapore

Architected materials hold much promise in achieving unprecedented structural properties that can significantly benefit applications are required to be stiff, strong and energy absorbent, with minimal mass, such as those in the aerospace, automobile and sports industries. The recent advent of additive manufacturing has sped up the pace of research in this field considerably by allowing complex, optimized designs to be realized easily and reliably. Nevertheless, many non-polymeric materials remain incompatible with most 3D printing schemes, and the few that are, require specialized equipment and treatments that remain far too costly for many industries to adopt. Here, we attempt to address this innovation gap by developing materials that are compatible with commercial stereolithography 3D printers originally designed for photosensitive polymers. Such printers are cost-effective, scalable and can produce structures that are mechanically isotropic with a fine resolution. Two strategies were adopted. First, non-polymeric powders were mixed into photosensitive resin and subjected to SLA 3D printing. Second, 3D printed polymeric structures were dip-coated in a mixture of non-polymeric powder and resin. In both cases, subsequent de-binding and sintering steps were required to remove the polymers and coalesce the non-polymeric powders. Lattices with solid struts and hollow tubes, made out of metal, ceramic and composites were successfully demonstrated. The microstructures of these lattices were examined in detail through SEM and micro-CT scans and related to their mechanical properties using simple analytical relationships.

10:00 PM ST03.05.06

Late News: Omnidirectional, Broadband Light Absorber with Hierarchical Nanoturf Structures for Solar-Thermal Conversion Jong Uk Kim¹, Seung Ji Kang¹, Seok Joon Kwon² and Tae-il Kim¹;
¹Sungkyunkwan University, Korea (the Republic of); ²Korea Institute of Science and Technology (KIST), Korea (the Republic of)

Although much attention has been paid to the development of photothermal materials and designs that can convert solar irradiation into exploitable thermal energy, it remains some obstacles such as limited light absorbing band and narrow incident angle. This study proposes a black gold-coated hierarchical nanoturf (Au/h-nanoturf) membrane incorporated with randomly distributed high aspect ratio (AR) nanostructures and micro-through holes. Thanks to structural advantages, this large area membrane exhibited good absorption of the broadband solar light spectrum. The h-nanoturf is further combined with a microcone array to enhance solar absorption extended to the near-infrared range as well as the omnidirectional incident direction of the light. The fundamental mechanism of the strong omnidirectional broadband absorption performance of the h-nanoturf was thoroughly analyzed with computational electrodynamics simulations. Consequently, we employed the Au/3D h-nanoturf with microscale hole (μ -hole) membrane to fabricate an advanced solar-vapor generator.

SESSION ST03.06: Mechanical Behavior of Architected Materials II

Session Chair: Ruth Schwaiger

Wednesday Morning, April 21, 2021

ST03

8:00 AM *ST03.06.01

Recent Progress on 3D Chiral Mechanical Metamaterials [Martin Wegener](#); Karlsruhe Institute of Technology (KIT), Germany

In this review talk, we present our experimental and conceptual progress on three-dimensional (3D) microstructured chiral mechanical metamaterials, which we have introduced (T. Frenzel et al., *Science* 358, 1072 (2017)) and summarized (I. Fernandez-Corbaton et al., *Adv. Mater.* 31, 1807742 (2019)) previously. This includes recent results for the dynamic as well as for the (quasi-)static regime.

In the dynamic regime, we have previously discussed the possibility of chiral metamaterial phonons and acoustical activity, the elastic counterpart of optical activity (T. Frenzel et al., *Nature Commun.* 10, 3384 (2019)). In 3D metamaterials, the magnitude of the polarization rotatory power as well as the operation frequency can be tailored by rational design. However, acoustical activity has been highly anisotropic in these simple-cubic lattices and essentially restricted special propagation directions. More recently, we have designed architectures enabling nearly isotropic chiral phonons and nearly isotropic acoustical activity in 3D over a large bandwidth. This includes the possibility of 3D chiral quasi-crystalline mechanical metamaterials (Y. Chen et al., *Phys. Rev. Lett.* 124, 235502 (2020)) as well as of chiral triclinic (Y. Chen et al., submitted (2020)) and chiral simple-cubic truss lattices (Y. Chen et al., in preparation (2020)). The different underlying principles behind obtaining isotropic elastic behavior in 3D are discussed and compared.

In the (quasi-) static regime, 3D chiral mechanical metamaterials allow for further behaviors “forbidden” in classical Cauchy elasticity such as, e.g., conversion of strain to twist. These behaviors are intimately connected to a loss of scale invariance, i.e., the mechanical behavior depends on the number of unit cells in the metamaterial specimen. We build on our previous conceptual work on tailoring a characteristic chiral length scale. When divided by the lattice constant, the characteristic length scale turns into the characteristic number (P. Ziemke et al., *Extreme Mech. Lett.* 32, 100553 (2019)). We have designed more practical architectures that we have manufactured by multi-focus multi-photon 3D laser nanoprinting with as many as more than one hundred thousand unit cells total and more than three hundred billion voxels. Specifically, we can tailor the twist/strain to increase linearly up to a characteristic number of unit cells, beyond which the twist/strain asymptotically decays inversely with the number of unit cells. We achieve characteristic numbers as large as about ten experimentally. Conceptually, the characteristic number can probably be made arbitrarily large. This statement is backed up by numerical simulations on different levels of approximations as well as by a simple and intuitive analytical model (T. Frenzel et al., in review (2020)).

8:25 AM *ST03.06.02

Metamaterials as a Platform for Sustainable Power Generation Miso Kim^{1,2}; ¹Korea Research Institute of Standards and Science, Korea (the Republic of); ²Sungkyunkwan University (SKKU), Korea (the Republic of)

Mechanical energy harvesting (MEH) is the technology that utilizes ambient mechanical energy available in nature such as sound, vibrations, and all human-derived kinetic motions to convert into useful electricity. MEH is regarded as a great platform to provide sustainable power solution to operate wireless sensors, one of the key essentials for Smart City, particularly without the need to replace after a certain amount of time. Although attractive, insufficient power generation is still the issue to solve in MEH. Metamaterials, artificially engineered structures, have proved useful for input mechanical energy manipulation, thus providing a new paradigm of solution to enhancing power generation in MEH. Here, I will summarize a collection of advances that push the boundaries to achieve a new paradigm of energy harvesting systems using various metamaterial designs ranging from phononic crystals, elastic and acoustic gradient index (GRIN) metamaterials, locally-resonant acoustic materials, to elastic instability-based mechanical metamaterials. These metamaterials exhibit unconventional material properties such as negative mass density, negative bulk modulus, and programmable stiffness, thus enabling intriguing phenomenon including band gaps, negative refractions, and shape and pattern transformation capabilities. All these unusual and intriguing phenomena can contribute to tailoring and amplifying input mechanical energies, ultimately leading to drastic enhancement in overall power generation of MEH systems.

8:50 AM ST03.06.03

Electrochemistry for Fabricating Nanoarchitected Mechanical Metamaterials Chris Gunderson, Nadia Rohbeck, Maxime Tranchant, Janne-Petteri Niemelä, Ivo Utke, Jakob Schwiedrzik, Laetitia Philippe and Johann Michler; Empa–Swiss Federal Laboratories for Materials Science and Technology, Switzerland

Two-photon lithography is a well-established technique for the creation of 3D polymer structures with sub-micron architecture. Recent work in the past few years has focused on the combination or integration of two-photon lithography with other fabrication processes for creating 3D nanoarchitected structures from other materials such as ceramics and metals. Toward this goal, two fabrication schemes will be presented for creating 3D nanoarchitected mechanical metamaterials from metals using electroforming, also called template-assisted electrodeposition. In the first example, two-photon lithography is used to create a 3D photoresist structure that serves as a template for fabricating a 3D nanoarchitected metal matrix composite with a ceramic nanolattice reinforcement through electroforming and atomic layer deposition. Structural characterization and initial *in situ* micromechanical testing data will be shown, including studies at high temperatures. In the second example, the resolution of 3D electroforming is improved to below 200 nm by pyrolysis of two-photon lithography templates. We fabricate metal nanolattices with strut diameters down to 150 nm and test the resolution of the technique by creating free-standing single metal nanowires/pillars with diameters down to 60 nm. *In situ* micromechanical testing of these lattices will be presented.

9:05 AM ST03.06.04

Late News: Fabrication of 3D Architectures Using Near-Field Electrospinning Ahsana Sadaf, Monsur Islam, Dario Mager and Jan Gerrit Korvink; Institute of Microstructure Technology, Karlsruhe Institute of Technology, Germany

In this work, we present preliminary results towards fabrication of 3D architectures using near field electrospinning as a novel additive manufacturing technology. Electrospinning is a technique of drawing a nanofibril string from a charged polymer droplet under a high electric field. In far-field electrospinning, the distance between the spinneret and the collector is quite large (5-10 cm), which leads to bending instability along the nanofiber jet resulting in random distribution of the deposited fibers on the collector. Keeping the electric field constant, reducing the distance between spinneret and collector (typically ≤ 1 cm) results in a highly focused electric field which leads to a precise deposition of the fibers. Such low-distance electrospinning

is termed as near-field electrospinning (NFES). NFES has enabled the fabrication of several 2D geometries of various materials ranging from polymers to ceramics for a wide range of applications including piezoelectric nanogenerators, biomedical devices, wearable sensors, FETs, photodetector, and MEMS structures. Due to the ability of precise nanofiber deposition, several researchers have attempted to develop NFES as an additive nanomanufacturing tool. However, these studies lack fundamental analysis of the NFES and involve additional complex components. Here we focus on exploring the fundamentals of NFES towards developing it as a high-speed additive nanomanufacturing tool. Currently we are characterizing several process parameters, such as electric field, printing speed, viscosity, conductivity, and dielectric constant of the solution towards enabling the nanofibers to stack onto each other leading to the fabrication of 3D structure. The outcome of this work will enable NFES to fabricate high aspect ratio 3D structures of stacked nanofibers with various geometries at a high processing speed, compared to other additive nanomanufacturing technologies. Such structures can be useful for various applications such as electrodes for energy devices and scaffolds in tissue engineering.

We have used polyethylene oxide (PEO) as the polymer, and a rotating drum as the high-speed moving collector to make 3D walls of stacked nanofibers. We have studied the effect of different solvents and collector material on the 3D stacking of the nanofibers. The results show that collector conductivity and vapor pressure of the solvent play a crucial role on the stacking of the fibers. The experiments so far have resulted in a 3D stacked wall of PEO with a maximum height of $\sim 250 \mu\text{m}$ and diameter of $\sim 10 \mu\text{m}$, while using a chromium/gold substrate and dichloromethane as the solvent.

Our ongoing work is to optimize the processing parameters to narrow down the diameter of nanofiber and to achieve the straight wall of stacked fibers with high aspect ratio. We plan to use these NFES-driven 3D stacked walls of nanofibers as scaffolds for tissue engineering. Furthermore, we target to achieve 3D structures of various other materials such as carbon and metal oxides using this NFES-driven additive nanomanufacturing process.

9:20 AM ST03.06.05

Late News: Extensible 3D Hierarchical Woven Materials [Carlos Portela](#)¹, Widiyanto Moestopo², Arturo Mateos², Ritchie Fuller³ and Julia Greer²; ¹Massachusetts Institute of Technology, United States; ²California Institute of Technology, United States; ³Independent Artist, United States

Most architected materials to date have enabled properties such as extreme stiffness and strength, at levels unattainable independently by their constituent materials, with few works focusing on the compliant, extensible regime pertinent to applications such as flexible electronics and tissue engineering. While exceptional mechanical properties such as extreme resilience and high deformability have been realized in many three-dimensional (3D) architected materials using beam-and-junction-based architectures, stress concentrations and constraints induced by the junctions limit their mechanical performance. Compliant architected materials that overcome these limitations, in combination with conductive components or constituent materials, could open a new path for the applicability of architected materials.

We present a new hierarchical design concept for flexible 3D architected materials in which fibers are interwoven to construct effective beams, such as the ones in classical monolithic-beam lattice architectures. Via in situ tension and compression experiments of additively manufactured polymeric woven and monolithic lattices at the microscale, we demonstrate the superior ability of woven architectures to achieve high tensile and compressive strains ($>50\%$)—without failure events—via smooth reconfiguration of woven microfibers in the effective beams and junctions. Cyclic compression experiments reveal that woven lattices accrue less damage compared to lattices with monolithic beams. We employ numerical studies of woven beams with varying geometric parameters to present new design spaces for the development of architected materials with tailored compliance that is unachievable by similarly configured monolithic-beam architectures. This woven hierarchical design offers a pathway to make traditionally stiff and brittle materials more deformable by introducing a new building block for 3D architected materials, with complex nonlinear mechanics, applicable to flexible electronics applications.

9:35 AM ST03.06.06

Late News: Liquid-Induced Topological Transformations of Cellular Microstructures Shucong Li, Bolei Deng, Alison Grinthal, Alyssa Schneider-Yamamura, Jinliang Kang, Reese S. Martens, Cathy T. Zhang, Jian Li, Siqin Yu, Katia Bertoldi and Joanna Aizenberg; Harvard University, United States

The fundamental topology of cellular structures -- the location, number, and connectivity of nodes and compartments -- can profoundly impact their acoustic, electrical, chemical, mechanical, and optical properties, as well as heat, fluid and particle transport. Approaches harnessing swelling, electromagnetic actuation as well as mechanical instabilities in cellular materials have enabled a variety of interesting wall deformations and compartment shape alterations, but the resulting structures generally preserve the defining connectivity features of the initial topology. Achieving topological transformation presents a distinct challenge for existing strategies: it requires complex reorganization, repacking, and coordinated bending, stretching, and folding, particularly around each node where elastic resistance is highest due to connectivity. Here we introduce a two-tiered dynamic strategy to achieve systematic reversible transformations of the fundamental topology of cellular microstructures that can be applied to a wide range of materials and geometries. Our approach only requires exposing the structure to a liquid whose composition is selected to have the ability to first infiltrate and plasticize the material at the molecular scale, and then, upon evaporation, to form a network of localized capillary forces at the architectural scale that zip the edges of the softened lattice into a new topological structure, which subsequently re-stiffens and remains kinetically trapped. Reversibility is induced by applying a mixture of liquids separately acting at the molecular and architectural scales -- thus offering modular temporal control over the sequence of the softening-evaporation-stiffening actions -- restoring the original topology or providing access to intermediate modes. Guided by a generalized theoretical model connecting cellular geometries, material stiffness and capillary forces, we demonstrate programmed reversible topological transformations of various lattice geometries and responsive materials, undergoing fast global or localized deformations. We then harness dynamic topologies for developing active surfaces with information encryption, selective particle trapping and bubble release, and tunable mechanical, chemical and acoustic properties.

SESSION ST03.07: Synthesis and Fabrication of Architected Materials II

Session Chairs: Brad Boyce and Lucas Meza

Wednesday Morning, April 21, 2021

ST03

11:45 AM *ST03.07.01

Late News: Contacting but not Connected—Interpenetrating Lattices Benjamin White^{1,2}, Anthony P. Garland^{1,2}, Ryan Alberdi^{1,2} and Brad L. Boyce^{1,2}; ¹Sandia National Laboratories, United States; ²Center for Integrated Nanotechnologies, United States

Traditional lattice metamaterials have greatly expanded the range of achievable material properties; however, they are generally physically continuous throughout their volume, and thus cannot take advantage of contact interactions or multi-body behavior. Here we present the new concept of an interpenetrating lattice, where two or more lattices interlace through the same volume without any direct connection to each other. Interpenetrating lattices greatly expand design possibilities, allowing single material printers of all types to print composite metamaterials irrespective of material or length scale. While the geometry defining interpenetrating lattices has been studied since the days of Euclid, additive manufacturing allows us to turn these mathematical concepts into physical objects with remarkable properties including reduced transmission of thermal, electrical, shock and vibration loads, increased toughness, multi-stable/negative stiffness behavior, and unusual energy transduction. In this first study on interpenetrating lattices, we reveal remarkable mechanical properties including improved toughness, multi-stable/negative stiffness behavior, and electromechanical coupling.

12:15 PM ST03.07.02

Direct Ink Writing of Short Carbon Fiber-Reinforced Phenolic Resins for Production of C/C Composites
Caitlyn M. Clarkson, Matthew Dickerson and Hilmar Koerner; Air Force Research Laboratory, United States

Carbon-carbon (C/C) composites are utilized by the aerospace industry primarily as structural materials due to their high thermal stability, low density, and good mechanical properties. Because of the aerospace industry relevance and unique properties of these materials this work will explore opportunities to manufacture complex parts via AM. Direct ink writing (DIW), an AM technique, offers a unique advantage in that it is amenable to printing of chopped fiber reinforcements and continuous fiber reinforcement. In DIW, complex structures are formed from the deposition of shear-thinning inks (suspensions or pastes) extruded through a nozzle. An added benefit of this process is that alignment of the fiber reinforcement is achieved during processing, allowing access to conventional fiber composite configurations. Here we present a route for the production of C/C composites by DIW of phenolic-based carbon fiber composite inks. Molecular gelators were employed as rheological modifiers to facilitate DIW of an otherwise low-viscosity liquid phenolic resin and chopped carbon fiber with an acid catalyst to accelerate low temperature curing. The rationale for ink formulation and assessment of the subsequent rheological behavior will be discussed as they pertain to printability in addition to its effects on the conversion of these materials to C/C.

12:30 PM ST03.07.03

Late News: Multifunctional 3D Self-Supported Hybrid Aerogels Prepared from Sol-Gel Electrospun Nanofibers Vahid Rahmanian, Tahira Pirzada and Saad A. Khan; North Carolina State University, United States

Owing to their outstanding properties including ultralow density, high specific surface area, and low thermal conductivity, aerogels are being considered for several applications including separation, thermal insulation, tissue scaffold, electromagnetic and sound absorption, sensors, supercapacitors, and catalysis. Generally, conventional aerogels are synthesized from a gel (either hydrogel or organogel) including multiple solvent exchange steps followed by solvent removal *via* oven, freeze, or supercritical drying. The complexity of this process not only raises the cost of fabrication but also significantly increases the duration of the process. We present a sustainable approach to prepare aerogels from sol-gel electrospun hybrid organic-inorganic nanofibers of polyvinylpyrrolidone (PVP)-titania (TiO₂). This facile and robust methodology resulted in the fabrication of a 3D self-supported cellular structure with elasticity, low density (~10 mg.cm⁻³), and hierarchical porosity consisting of primary (1-5 μm) and secondary pores (10-60 μm). XPS analysis and SEM demonstrate that titania networks developed during sol-gel electrospinning and uniformly distributed inside the nanofibers. Moreover, FTIR analysis provides evidence that PVP and TiO₂ components chemically interact during the sol-gel processing through Ti-O-C linkage. The PVP-TiO₂ nanofibrous aerogel exhibit high mechanical flexibility, hierarchical porosity, and low density demonstrating their possible applications in diverse fields like filtration, CO₂ capture, and antimicrobial.

12:45 PM ST03.07.04

Multiscale Modeling of Nanoarchitected Materials Under Large Deformations Joshua Crone, Richard Becker and Jaroslaw Knap; U.S. Army Research Laboratory, United States

Recent advances in additive manufacturing have enabled the production of nanoarchitected material, consisting of truss structures with sub-micron geometric features. These materials have achieved unprecedented specific stiffness and strength as well as extraordinary energy absorption and recoverable compressibility. As additive manufacturing techniques continue to improve, scaling of nanoarchitected materials will reach the component level. Modeling of these parts will require a multiscale approach to span the range of length scales between the sub-micron features of the trusses and the component scale. While numerous homogenization schemes have been developed for multiscale modeling of architected materials, most are limited to capturing material and geometric effects in the linear and early yield regimes. While these methods may be sufficient for predicting the specific stiffness and strength, they are not useful in designing materials for energy absorption and large deformation applications.

In this work, we present a multiscale model for architected materials that captures material nonlinearities including yield, hardening, and failure as well as geometric nonlinearities including buckling, post-buckling softening, and densification. We employ an FE² approach where the component-scale deformation is modeled by finite element (FE) analysis and the microscale deformation is modeled by another FE simulation of the representative unit cell (RUC). A homogenization scheme is used to determine the stress-strain constitutive relation for the component-scale FE simulation through numerous evaluations of the RUC. The model is integrated into a computational framework for multiscale modeling that handles resource management and fault tolerance to allow many RUC evaluations to occur in parallel, enabling efficient use of high-performance computing resources.

1:00 PM ST03.07.05

A Mechanical Analysis of Planar and Corrugated Metamaterials as Relativistic Light Sails for Interstellar Travel Matthew F. Campbell¹, Mohsen Azadi¹, Pawan Kumar¹, George A. Popov¹, John B. Brewer², Aaswath Raman², Prashant K. Purohit¹, Deep M. Jariwala¹ and Igor Bargatin¹; ¹University of Pennsylvania, United States; ²University of California, Los Angeles, United States

We propose a composite light sail composed of nanometer-thick corrugated layers of alumina and molybdenum disulfide that can be used to accelerate a gram-scale probe to relativistic velocities for interstellar space travel. Our mechanical calculations suggest that this sail can sustain radiation pressures of tens of Pa, necessary to achieve a velocity of roughly a fifth the speed of light. In addition to our numerical analysis, we are demonstrating the manufacturability of this concept by producing prototype sections of the composite material using standard microfabrication techniques. Our results represent one of the first evaluations of sail robustness and fabricability of ultrathin light sails and highlight the need for additional research on the optical and mechanical properties of thin Al₂O₃ and MoS₂ films, particularly at elevated temperatures.

The Breakthrough Starshot Initiative aims to send an ultralight spacecraft to Proxima Centauri B within the next half century by accelerating it using a highly reflective light sail and an array of Earth-bound high-power lasers¹. A sail that will accomplish this must have a total mass of approximately 1 g and an area of 1-10 m² to minimize the size of the laser system, a high reflectivity over the entire doppler-shifted laser wavelength range to minimize the required laser power, a high emissivity at mid-infrared wavelengths for efficient radiative cooling, a shape that provides beam-riding stability over long distances, and mechanical robustness to maintain its form without tearing or fracturing. Several recent studies have examined the optics and dynamic stability of sails, proposing spherical designs², planar photonic heterostructures³, and textured photonic metasurfaces⁴. However, few studies have incorporated mechanical robustness and manufacturability assessments into their proposals.

Therefore, we propose a novel sail that addresses mechanical robustness, manufacturability, beam-riding stability, optical characteristic, and mass property considerations. Our design involves a ~2 m circular, spherically curved sheet comprised of several interlocking gores, each of which is composed of roughly 70 layers (~50 nm) of highly reflective (>50%) MoS₂ sandwiched between two 5-nm optically transparent Al₂O₃ films. We have incorporated a micron-scale hexagonally patterned corrugated rib structure into the sail that increases its bending stiffness⁵ by 10-100× and reduces its tensile stiffness⁶ by 2-3× relative to planar films, preventing it from clinging to itself and making it more robust against deformation and fracture. Our stress calculations, performed using a thin-walled pressure vessel model, confirm that the sail can tolerate the laser-induced acceleration forces with failure margins of 10-30%. Planned next steps include using finite element methods to validate our calculations and implementing an energy balance to quantify the temperature variation of the sail throughout its acceleration and the impact of thermal effects on its mechanical response.

Finally, to demonstrate this concept, we are fabricating small prototype sections of this sail. We use photolithography and deep reactive ion etching on a silicon wafer to create a hexagonal rib mold, use atomic layer deposition to conformally-coat the mold with a thin Al₂O₃ film, transfer a thin MoS₂ flake to the surface of

the film, deposit a second Al₂O₃ film, and release the result using XeF₂ etching. We intend to extend this process to larger areas using chemical vapor deposition to directly synthesize MoS₂ upon the Al₂O₃. Taken together, our modeling and fabrication results indicate the possibility of laser-driven relativistic interstellar travel.

- 1) *Atwater Nat. Mater.* 17(2018)861
- 2) *Manchester Astrophys J. Lett.* 837(2017)L20
- 3) *Ilic Nano Lett.* 18(2018)5583
- 4) *Salary Laser Photonics Rev.* 14(2020)1900311
- 5) *Davami Nat. Commun.* 6(2015)10019
- 6) *Jiao Extreme Mech. Lett.* 34(2020)100599

1:15 PM ST03.07.06

Tensegrity-Inspired Nanoarchitected Materials Lucas Meza, Caelan Wisont and Lucas Meza; University of Washington, United States

The field of architected materials has been invigorated by a revolution in additive fabrication methods with micro- and nanoscale precision, enabling the creation of architected materials that can exploit the enhanced properties of nanomaterials. Despite many developments in this area, the mechanical properties of these nanoarchitected materials are impaired by designs that i) have little mechanical tunability and ii) have a poor distribution of load carrying elements. This work investigates the fabrication and mechanical characterization of a new class of highly tunable, tensegrity-inspired nanoarchitected materials. These are created in a two-step process involving two-photon lithography (TPL) to create a polymeric framework followed by pyrolysis to convert the material to amorphous carbon. This procedure relies on the size-dependent shrinkage of beams during pyrolysis, which enables nanoarchitectures to be controllably prestressed by varying the size of different elements in the structure. We demonstrate that these amorphous carbon nano-tensegrities have highly tunable mechanical properties that can be varied independently of their relative density, allowing more optimal strength and stiffness per unit mass.

SESSION ST03.08: Design of Architected Materials II
Session Chairs: Jonathan Hopkins and Woo Soo Kim
Wednesday Afternoon, April 21, 2021
ST03

2:15 PM *ST03.08.01

Design of Architected Materials Using Freedom and Constraint Topologies (FACT) Jonathan Hopkins; University of California, Los Angeles, United States

Designing architected metamaterials is overwhelming for many computational approaches because of the large number and complexity of flexible elements that constitute their architecture—especially if such elements don't repeat in periodic patterns or collectively occupy irregular bulk shapes. In this work, we introduce the freedom and constraint topologies (FACT) methodology, which leverages simplified assumptions regarding the topology, geometry, and constituent properties of such materials to enable their design with ~6 orders of magnitude greater computational efficiency than other approaches (e.g., topology optimization).

FACT utilizes a comprehensive library of intuitive geometric shapes, which embody the mathematics of screw theory, constraint-based design, and projective geometry. One set of shapes, called freedom spaces, represent all the ways a compliant system can deform with high compliance. Another set of shapes, called constraint spaces,

represent the region of space within which flexible elements should be placed for exhibiting the compliant deformations of their complementary freedom spaces. By obeying simple systematic rules, designers (or an automated code) can rapidly search the full design space of compliant topology solutions, embodied by the complementary geometric shapes of the complete FACT library.

In this work, we will explain how FACT can be used specifically to design directionally compliant metamaterials, transmission-based architected materials such as materials that achieve desired Poisson's ratios, and materials with Poisson's ratio's that fluctuated spatially and temporally.

2:40 PM ST03.08.02

Metallic Films with Architected Bimodal Microstructures—Synthesis and Mechanical Properties Rohit Berlia and Jagannathan Rajagopalan; Arizona State University, United States

Materials with heterogeneous microstructures have been shown to exhibit a superior combination of strength, ductility and toughness compared to both homogeneous nanostructured and coarse-grained materials. However, only limited progress has been made in the synthesis of heterogenous microstructure materials with robust control of key microstructural parameters. Here we report a novel technique to synthesize metallic films with precisely defined bimodal microstructures using magnetron sputtering, wherein the size, volume fraction and connectivity of nanocrystalline (< 100 nm) and coarse domains (> 1000 nm) can be explicitly controlled. Using this technique, we synthesized pure iron films in which the nanocrystalline and coarse-grained domains were configured to be in different spatial arrangements like series and parallel. Along with the spatial arrangements, the volume fraction was also varied by changing the size of these domains. The microstructure of these films was characterized using EBSD and TEM, and tensile testing was performed using MEMS based testing stages. As anticipated, the spatial arrangement (series versus parallel) of the nanocrystalline and coarse domains markedly altered the stress-strain response, with the parallel arrangement leading to co-deformation and higher strength. In addition, films containing higher volume fraction of nanocrystalline domains showed higher strength. More interestingly, the orientation of the coarse domains with respect to the loading axis also had a significant influence on the mechanical behavior due to the constraints it imposed on dislocation motion. These results indicate that this synthesis method can be used to systematically tailor the mechanical behavior of metallic films in a repeatable manner.

2:55 PM ST03.08.03

Nanoarchitected Coatings with Extreme Thermal and Mechanical Resilience Nishita Anandan and Lucas Meza; University of Washington, United States

Premature failure of materials in extreme thermal and mechanical environments has been a challenge for decades. Extreme temperatures can enable enhanced efficiencies, e.g. in jet engines, or they may be required for normal operation, e.g. in hypersonic vehicles and spacecraft. The ceramic coating layer used for protection are prone to cracks and delamination due to inherent property mismatch between the layers. This talk describes the development of durable nanoarchitected alumina coatings with high impact and thermal shock resistance.

The coating was designed to have a gradient spinodal shell structure, its uniform stress distribution and minimize stress concentrations to prevent cracking and the stiffness of the spinodal shell was tailored by setting a preferential surface formation direction. A spinodal structure with gradient stiffness is chosen to ensure better mechanical interfacing with the metal substrate. The mechanical resilience of the material is achieved by using an architecture that exploits shell buckling as the dominant deformation mechanism. The thermal shock resistance was enhanced by maintaining the relative density below 0.04. The performance of the coating was investigated through numerical and experimental investigations. High strain rate and sequential thermo-mechanical simulations were performed to evaluate the stress and temperature distribution in an extreme environment. Nanoindentation and laser thermal shock experiments were performed to explore the failure mechanism. Through this work we demonstrate a new approach to create thermal protection coatings. Instead of searching for new advanced materials, we use the existing materials and use nanoarchitecture to make them

resilient to extreme thermal and mechanical loads.

3:10 PM ST03.08.04

Analyzing Microscale Toughening Mechanisms in Bioinspired Nanoarchitected Materials Zainab S. Patel and Lucas Meza; University of Washington, United States

Natural materials exhibit remarkable toughness and damage tolerance, properties that stem from their hierarchical architecture built up from the nano- and microscale. Many of the underlying mechanisms behind these novel mechanical properties are not well understood at microstructural length scales. Replicating the architectural complexity of natural materials is not only challenging in terms of fabrication but is also time-consuming and expensive. Therefore, it is important to systematically develop and study complex nano- and microarchitectures to understand their effect on mechanical properties and thereby develop effective material design strategies.

In this study, we analyze crack propagation and energy absorption in dense microscale nanoarchitected Bouligand beams inspired by the dactyl club of a mantis shrimp. We developed a fabrication process utilizing two-photon lithography to create polymeric beams with increasing architectural complexity, starting from a beam with unidirectional fibers and moving to a herringbone structured beam with out-of-plane wavy fibers. We extended these methods to include a secondary ceramic phase between the polymeric fibers to understand the effect of material modulus mismatch on crack propagation at the microscale, a feature commonly witnessed in tough natural materials. We present the results of in-situ nanomechanical testing of microscale three-point bend specimens with nanoarchitected beams.

The results of this study help to develop a fundamental understanding of the effect of architectural tortuosity on crack propagation, energy dissipation, and toughening mechanisms at the microscale. Moreover, it reveals the microscale fracture properties of nanoarchitected materials, importantly illustrating how fracture processes change when the sample size is comparable to the process zone size and how that can affect macroscale properties. This combined understanding of the effect of both architecture and specimen length scale on toughness is crucial and will pave the way to successfully engineer tougher materials with bioinspired strategies.

3:25 PM ST03.08.05

Magnetron Sputtered Micro-Lattice Structures Alina Garcia Taormina¹, Chantal Kurpiers², Ruth Schwaiger³ and Andrea Hodge¹; ¹University of Southern California, United States; ²Karlsruhe Institute of Technology, Germany; ³Forschungszentrum Jülich GmbH, Germany

A prevalent focus of materials research is the development of ultra-lightweight, multifunctional materials that exhibit unparalleled mechanical properties. Within the last decade, technological advances in additive manufacturing (AM) have enabled the fabrication of novel three-dimensional nano- and micro-architected lattice materials, allowing researchers to investigate previously unexplored phenomena and property spaces. Current printing techniques are mainly restricted to polymer-based systems, which narrow the functionalities and mechanical robustness of these architected lattice materials. While a handful of nano-architected ceramic and metallic systems have been realized by way of pyrolysis, namely SiOC, nanoporous Ni, and glassy carbon, new printable material systems are limited by the chemistry of the resin blend and require further research. Thus, alternative approaches such as the deposition of metallic and ceramic coatings on polymer-based lattice scaffolds offer a flexible and feasible route for expanding the mechanical and functionality space of these advanced materials.

Several novel nano- and micro-lattice materials have been developed through means of various light-based AM methods and coating deposition approaches, namely atomic layer deposition and plating techniques. However, such methods are limited to materials that undergo specific chemical reactions. Thus, magnetron sputtering, a technique that allows for the deposition of a nearly unlimited selection of metals, alloys, and ceramics can be utilized to further expand the synthesis space of these materials. Several recent publications have employed

planar magnetron sputtering configurations to deposit a wide range of materials on nano- and micro-lattice structures, from high entropy alloys to bulk metallic glasses. Nonetheless, sputtering is a momentum-driven line-of-sight process, and thus achieving uniform coatings on fine-featured lattice materials remains a prominent challenge. As such, our work is based on inverted cylindrical magnetron sputtering, a novel coating approach that allows for an unprecedented 360° line-of-sight. With enhanced line-of-sight, it is expected that higher ionization rates and bombarding energy can be achieved as compared to planar cathodes under the same sputtering conditions. Overall, inverted cylindrical magnetron sputtering can lead to a greater understanding of the effect of cathode geometry and deposition parameters on coating uniformity on complex 3-D topologies.

SYMPOSIUM ST04

High Entropy Materials—From Fundamentals to Potential Applications
April 23 - April 23, 2021

Symposium Organizers

Cecilia Cao, University of West Florida
Peter Liaw, The University of Tennessee, Knoxville
Eun Soo Park, Seoul National University
Cemal Cem Tasan, Massachusetts Institute of Technology

* Invited Paper

SESSION ST04.01: High Entropy Materials I
Session Chair: Peter Liaw
Friday Morning, April 23, 2021
ST04

8:00 AM *ST04.01.01

Tuning Phase Formation, Microstructure and Properties of High Entropy Alloys and Chemically Complex Composites [Jurgen H. Eckert](#)^{1,2}; ¹Erich Schmid Institute of Materials Science, Austrian Academy of Sciences, Austria; ²Montanuniversität Leoben, Austria

This talk explores the structural diversity that can be achieved in high entropy alloys and multiphase composites developed through a combination of concepts for designing chemically complex alloys and metallic glasses using rapid quenching and annealing or severe plastic deformation for tuning phase formation and microstructure development. The role of length-scale modulation and phase transformation upon heating or loading will be critically assessed with respect to structural stability and mechanical behavior. Examples for changes in deformation mechanism, e.g. from crack-controlled to dislocation-dominated deformation, twinning or cooperative deformation of shear bands and interfacial sliding, will be presented and discussed as ways to control strength, ductility and fracture toughness in a wide range. Besides, also examples for developing novel nanostructured and ultrafine-grained complex materials via composition and process control will be given, attempting to derive guidelines for how to tune the microstructure and properties of non-equiatomic chemically complex alloys with optimized properties.

8:25 AM ST04.01.02

Late News: Discontinuous Deformation of FCC High and Medium Entropy Alloys at Close to 0 K Aditya Srinivasan¹, Theresa Hanemann¹, Klaus-Peter Weiss¹, Jens Freudenberger², Martin Heilmaier¹ and Alexander Kauffmann¹; ¹Karlsruhe Institute of Technology, Germany; ²Leibniz Institute for Solid State and Materials Research, Germany

Discontinuous deformation or serrated plastic deformation, at temperatures close to 0 K, has formerly been reported in some metals and alloys. Based on the previous reports, concentrated substitutional FCC solid solutions are expected to show this phenomenon in an intense fashion. This would correspondingly provide the conditions to most effectively evaluate the phenomenon. To that end CoCrNi and CoCrFeMnNi were tested and observed to exhibit very intense serrated plastic behavior during deformation near 0 K [Tirunilai et al. *Acta Materialia* 200 (2020) 980-991]. CoCrFeMnNi, was especially interesting, as it showed low temperature serrations at a higher temperature than previously reported for any other metal or alloy. While previous reports have put forth theories on the cause for serrations, the reports fail to characterize serration trends and make evaluations with respect to active deformation mechanisms. Presently, in order to understand and characterize this serrated plastic deformation, (i) general deformation characteristics at temperatures near 0 K have to be understood, (ii) the influence of the deformation mechanisms seen at these temperatures (dislocation based deformation, deformation twinning and epsilon martensite formation) have to be evaluated and (iii) the serrated plastic deformation has to be evaluated based on the influence of temperature and deformation. This was done using the alloys CoNi, CoCrNi and CoCrFeMnNi.

(i) The initial microstructure of the alloys in question was evaluated using XRD and SEM. Subsequently, the specimens were subjected to macroscopic tensile tests at different temperatures in the range between 295 and 4.2 K. Using SEM and TEM, deformation twinning was identified in CoCrNi and CoCrFeMnNi. Additionally, martensite was indexed post deformation in CoCrNi, but not in CoCrFeMnNi, contrary to the expectation based on SFE – temperature relation [Huang et al. *Scripta Materialia* 108 (2015) 44-47]. However, it was clear that in both these alloys deformation twinning was the primary contributor to strengthening.

(ii) Deformation twinning and martensitic transformations are associated with instability in single crystals and are influential in high temperature serrated plastic deformation. However, tensile tests conducted on CoCrFeMnNi at different temperatures indicate that no new deformation mechanism can be attributed as the cause for serrations. Additional tests on martensite forming CoCrNi and non-twinning CoNi verify the lack of influence of both, deformation twinning as well as martensite formation.

(iii) Serration intensity trends, measured as serration stress amplitude, were evaluated at different temperatures as well as in the pre-deformed condition. Correspondingly, the current results are consistent with the basis proposed by Seeger [Seeger in Fisher et al., *Dislocations and Mechanical Properties of Crystals*, Wiley, New York (1956)], according to which the serrations were a result of ‘avalanche slip’ of dislocations piled up at Lomer-Cottrell (LC) locks. This theory proposes a basis for the phenomenon, but the current work establishes a qualitative model that validates both present results as well as those in former publications.

8:40 AM ST04.01.03

Thermal Stability of the Microstructure and the Hardness of Multi-Principal Element Alloys Processed by Severe Plastic Deformation Hung T. Pham¹, Megumi Kawasaki², Jae-Kyung Han², János L. Lábár^{1,3} and Jenő Gubicza¹; ¹Eötvös Loránd University, Hungary; ²Oregon State University, United States; ³Institute for Technical Physics and Materials Science, Centre for Energy Research, Hungarian Academy of Sciences, Hungary

Multi-principal element alloys (MPEAs) or Complex Concentrated Alloys (CCA), including high-entropy alloys (HEAs) are designed with multiple principal elements of equal or near equal molar ratios. The strength of MPEAs can be further enhanced by refining the microstructure into the nanocrystalline state using severe plastic deformation (SPD) techniques. In this study, the influence of thermal treatment on the microstructure and hardness of nanocrystalline MPEAs processed by SPD was investigated. The SPD process was carried out using high-pressure torsion (HPT) technique up to ten turns at room temperature. The effect of heat treatment was studied from room temperature up to 1000K using differential scanning calorimetry (DSC). It was found that a single phase HfNbTiZr MPEA transformed into multiple phases at elevated temperatures. On the other

hand, CoCrFeNi MPEA remained single phase solid solution throughout the annealing process. The microstructures and the chemical compositions of the different phases were examined by transmission electron microscopy (TEM) and energy-dispersive X-ray spectroscopy (EDS). In addition, X-ray diffraction line profile analysis (XLP) technique was used to monitor the evolution of the crystallite size and the dislocation density of CoCrFeNi, as well as to identify the different decomposed phases in the nanocrystalline HfNbTiZr MPEA. The average hardness of the annealed samples was also measured and correlated to the microstructure. This study demonstrated a comparative analysis of the results obtained in these alloys.

8:55 AM ST04.01.04

Late News: High Entropy Alloy Multilayers—A Processing and Deformation Study Khushbu Dash¹, Satyam Suwas² and Gandham Phanikumar¹; ¹Indian Institute of Technology Madras, India; ²Indian Institute of Science, India

High entropy alloys are next generation potential materials which have the calibre of performing as a structural material. High entropy alloys show improved properties due to several underlying effects such as: high configurational entropy, lattice distortion, sluggish diffusion and cocktail effect. They exhibit strength-ductility synergy which is an important aspect which is a paradox in conventional materials. Recent works on high entropy alloys span from thermomechanical processing of the same to severe plastic deformation in order to enhance their mechanical performance. The severe plastic deformation induces fine grain structure making the material possess delayed failure. Metallic sheets have wide range of applications starting from large body structures to acting as small components in aerospace and automobile sectors. Sheet forming along with a high performance ensures a high-quality product. The sheet possessing ultrafine grains as well as a gradient microstructure and texture will enable better mechanical behaviour. Multilayered sheets are a method to achieve the above attributes, hence we propose to design this by accumulative roll bonding.

This work presents the processing of hard cantor alloy into ultrafine grained multilayered sheet using hot accumulative roll bonding (ARB) to study its microstructural and texture evolution. The Cantor alloy FeCrCoMnNi was cast and cold rolled to obtain a sheet of thickness of 0.4 mm followed by annealing. The sheet was characterized and studied for its microstructure and annealing texture, along with its mechanical properties. This sheet was then accumulatively roll bonded with a sheet of same alloy at 450 C by imparting a reduction of 50% in each pass upto 3rd pass using a cladding process. The ARB processed multilayer sheet was investigated for microstructure, bulk texture and microtexture. The strain gradient induced during accumulative roll bonding is instrumental in creating a gradient microstructure and texture along the thickness of the multilayered sheet. Electron back scattered diffraction will be helpful in predicting the grain structure and the local strain in the deformed material.

9:10 AM ST04.01.05

Late News: Exceptionally High Spallation Strength for a High-Entropy Alloy Demonstrated by Experiments and Simulations Daniel Thürmer¹, Shiteng Zhao², Hye-Sook Park³, Camelia Stan⁴, Iyad A. Alhafez⁵, Orlando Deluigi⁶, Eduardo M. Bringa^{6,7}, Herbert Urbassek⁵, Marc Meyers⁸ and Nina Gunkelmann¹; ¹Clausthal University of Applied Technology, Germany; ²University of California, United States; ³Lawrence Livermore National Laboratory, United States; ⁴Lawrence Berkeley National Laboratory, United States; ⁵University Kaiserslautern, Germany; ⁶University of Mendoza, Argentina; ⁷Universidad Mayor, Chile; ⁸University of California, San Diego, United States

High entropy alloys (HEA) are materials with an increasing number of technological applications. Among them, the Cantor Alloy, FeMnCoCrNi, shows desirable mechanical properties at normal loading conditions. In this study we focus on the performance of the Cantor alloy at ultrahigh deformation rates of shock waves.

Intense shock waves may lead to spallation of the sample. In this study we perform molecular dynamics simulations of shock-induced spallation and compare our results with experiments using laser shocks and scanning transmission electron microscopy of the unloaded samples. Our molecular dynamics simulations were carried out with three different piston velocities, which allow us to gather more information and compare the data about the influence of the velocity on a

microscale. Both experiments and simulations show a high spall strength which would be beneficial for certain applications, with experiments giving 12 GPa at 10^7s^{-1} and MD 30 GPa at 10^9s^{-1} . Post-mortem analysis of the experimental samples show nanotwins near the spall plane, while MD simulations show a highly disordered region giving rise to void nucleation and spall.

9:15 AM DISCUSSION

9:30 AM ST04.01.07

Late News: High-Entropy Ceramics for Electrochemical Applications Ben Breitung¹, Qingsong Wang¹, Miriam Botros¹, Simon Schweidler¹, Abhishek Sarkar², Yanjiao Ma¹, Torsten Brezesinski¹ and Horst Hahn^{1,2}; ¹Karlsruhe Institute of Technology, Germany; ²KIT-TUD Joint Research Laboratory Nanomaterials Institute of Materials Science, Technische Universität Darmstadt, Germany

In recent years, the transition from high-entropy alloys to high-entropy ceramics^[1] (e.g. high-entropy oxides, oxyfluorides, fluorides, etc.) has paved the way for a completely new field of materials and applications. The strong structure/property relationships and the unique possibility to tailor the compositions of high-entropy materials make them ideal candidates when aiming to prepare novel materials with adjustable properties for a variety of different applications.

Here, the utilization of several different high-entropy ceramics in the electrochemical sector will be presented. Conversion battery anodes and cathodes could be prepared using high-entropy oxides and fluorides, offering unexpected properties and advantages compared to conventional materials, which make them interesting for further research.^[2] It could be shown that the high entropy plays a decisive role regarding the performance of the electrodes and serves as an “adjusting screw” when the material is tailored towards a desired property. High-entropy insertion and intercalation materials could also be synthesized by introducing high-entropy oxyfluorides and layered high-entropy structures, respectively.^[3,4] Moreover, high-entropy oxides and high-entropy metal organic frameworks were applied to design post-Li battery electrodes for Na insertion. These materials do stand out due to their high reversibility and high accessible C-rates over reversible de/sodiation. Finally, the utilization of high-entropy molybdates and fluorides as catalysts for oxygen evolution reactions will shortly be demonstrated.^[5]

[1] C. M. Rost, E. Sacht, T. Borman, A. Moballegh, E. C. Dickey, D. Hou, J. L. Jones, S. Curtarolo, J.-P. Maria, *Nat. Commun.* **2015**, *6*, 8485.

[2] A. Sarkar, L. Velasco, D. Wang, Q. Wang, G. Talasila, L. de Biasi, C. Kübel, T. Brezesinski, S. S. Bhattacharya, H. Hahn, B. Breitung, *Nat. Commun.* **2018**, *9*, 3400.

[3] Q. Wang, A. Sarkar, D. Wang, L. Velasco, R. Azmi, S. S. Bhattacharya, T. Bergfeldt, A. Düvel, P. Heitjans, T. Brezesinski, H. Hahn, B. Breitung, *Energy Environ. Sci.* **2019**, *12*, 2433.

[4] J. Wang, Y. Cui, Q. Wang, K. Wang, X. Huang, D. Stenzel, A. Sarkar, R. Azmi, T. Bergfeldt, S. S. Bhattacharya, R. Kruk, H. Hahn, S. Schweidler, T. Brezesinski, B. Breitung, *Sci. Rep.* **2020**, *10*, 18430.

[5] D. Stenzel, I. Issac, K. Wang, R. Azmi, R. Singh, J. Jeong, S. Najib, S. S. Bhattacharya, H. Hahn, T. Brezesinski, S. Schweidler, B. Breitung, *Inorg. Chem.* **2021**, *60*, 115.

9:45 AM ST04.01.08

Late News: High Entropy Oxides for Reversible Energy Storage Simon Schweidler¹, Qingsong Wang¹, Miriam Botros¹, Abhishek Sarkar¹, Torsten Brezesinski¹, Ben Breitung¹ and Horst Hahn^{1,2}; ¹Karlsruhe Institute of Technology (KIT), Germany; ²Technische Universität Darmstadt (TUD), Germany

In recent years, transition metal oxides (TMOs) have gained increasing interest in the field of rechargeable energy storage materials. One of the reasons is that often TMOs have a large theoretical specific capacity > 1000 mAh/g, which is attributed to the conversion reaction mechanism with its multi-electron redox processes during cycling.¹ This makes TMOs promising anode materials compared to graphite (theoretical capacity = 372 mAh/g). However, conventional TMOs suffer from rapid capacity degradation due to severe structural changes (large volume changes) during cycling.

Our recent studies show that transition metal-based high entropy oxide (TM-HEOs) $(\text{CoCuMgNiZn})_1\text{O}_1$ exhibit reversible long-term lithium storage properties. The cycling stability might be attributed to an entropy stabilizing effect, additionally, it turned out that the electrochemical behavior of the TM-HEO is strongly influenced by each of the metal cations present. This makes it possible to change the electrochemical properties by simply changing the elemental composition.^{2,3} Furthermore, using *operando* XRD and SAED, it was shown that, unlike conventional TMOs, the entropy-stabilized crystal structure serves as a kind of host matrix for the conversion reaction and that it is retained even in the fully lithiated state. The *operando* gassing study further showed that similar cycling performance and stability was obtained for cells with EC and FEC containing electrolytes. The gas analyses showed that H_2 and C_2H_4 were the main gas species during cycling. After the first cycle, especially the evolution rate of C_2H_4 decreased significantly, indicating the formation of a stable SEI layer on the HEO particles and emphasizing further the unique entropy-stabilized mechanism.⁴ In addition, further preliminary electrochemical studies show the successful use of TM-HEO as anode material in coin-type and pouch-type full cells. The cells were found to provide an initial specific discharge capacity of 446 mAh/g, which was maintained at 300 and 256 mAh/g after 50 and 100 cycles, respectively.⁵

- (1) Qian, Y.; Niehoff, P.; Zhou, D.; Adam, R.; Mikhailova, D.; Pyschik, M.; Börner, M.; Klöpsch, R.; Rafaja, D.; Schumacher, G.; Ehrenberg H.; Winter M.; Schappacher F. *J. Mater. Chem. A* **2017**, *5*, 6556–6568.
- (2) Sarkar, A.; Velasco, L.; Wang, D.; Wang, Q.; Talasila, G.; de Biasi, L.; Kübel, C.; Brezesinski, T.; Bhattacharya, S. S.; Hahn, H.; Breitung B. *Nat. Commun.* **2018**, *9*, 3400.
- (3) Sarkar, A.; Wang, Q.; Schiele, A.; Chellali, M. R.; Bhattacharya, S. S.; Wang, D.; Brezesinski, T.; Hahn, H.; Velasco, L.; Breitung, B. *Adv. Mater.* **2019**, *31*, 1806236.
- (4) Breitung, B.; Wang, Q.; Schiele, A.; Tripković, D.; Sarkar, A.; Velasco, L.; Wang, D.; Bhattacharya, S. S.; Hahn, H.; Brezesinski, T. *Batter. Supercaps* **2020**, *3*, 1–10.
- (5) Wang, Q.; Sarkar, A.; Li, Z.; Lu, Y.; Velasco, L.; Bhattacharya, S. S.; Brezesinski, T.; Hahn, H.; Breitung, B. *Electrochem. commun.* **2019**, *100*, 121–125.

SESSION ST04.02: High Entropy Materials II
Session Chairs: Robert Ritchie and Cemal Cem Tasan
Friday Morning, April 23, 2021
ST04

11:45 AM *ST04.02.01

Damage-Tolerance and the Effects of Local Order in High-Entropy Alloys Robert O. Ritchie^{1,2}, Andrew M. Minor^{1,2}, Mark Asta^{1,2}, Jun Ding², Sheng Yin², Flynn Walsh^{2,1}, Ruopeng Zhang^{2,1}, Shiteng Zhao^{2,1}, Qin Yu², Jon Ell^{1,2} and Yang Yang²; ¹University of California, Berkeley, United States; ²Lawrence Berkeley National Laboratory, United States

Face-centered cubic (*fcc*) high-entropy alloys (HEAs) can display exceptional combinations of strength, tensile ductility and fracture toughness, properties that can be further enhanced at cryogenic temperatures. Body-centered cubic (*bcc*) refractory HEAs, conversely, can display exceptional strength and compressive ductility at elevated temperatures, but are often compromised by poor lower-temperature behavior. We examine here the damage-tolerance of these two classes of multiple principal-element alloys, and show that whereas some of the *fcc* HEAs exhibit the highest fracture toughness on record, the *bcc* HEAs can display extremely low toughness (and ductility) when subject to tensile loading. We further examine the role of short-range order (SRO) in these two alloy classes, theoretically using DFT-based Monte-Carlo and Molecular Dynamics simulations and experimentally using energy-filtered TEM and 4D-STEM techniques. Whereas atomistic simulations predict the existence of SRO in *fcc* and *bcc* HEAs, together with its influence on plastic deformation behavior, *e.g.*, slip behavior, dislocation mobility, *etc.*, direct experimental evidence is difficult. We believe that we have unequivocal evidence for SRO in *fcc* HEAs, with an understanding of the role of magnetically-driven ordering

in CrCoNi-based systems; studies for the *bcc* systems, however, are still in process. Our emphasis now is on defining the mechanistic role and quantitative effect on mechanical properties, with respect to how SRO can affect the strength, strain-hardening, ductility and toughness.

12:10 PM ST04.02.02

Short-Range Order Strengthening in 3D Transition Metal-Based Complex Concentrated Alloys Hyunseok Oh¹, Michael Xu¹, Jein Lee², Koichi Tsuchiya², James M. LeBeau¹ and Cemal Cem Tasan¹; ¹Massachusetts Institute of Technology, United States; ²National Institute for Materials Science, Japan

Due to their multi-component nature, preferential chemical ordering, which is otherwise known as short-range order, has been proposed in various concentrated alloys. Short-range order can be caused by various origins such as magnetic frustration, strong electronic interaction, and the formation of complexes with interstitial elements. Here we present a first systematic study of the methods to control the degree of SROs and the resultant mechanical properties in 3d transition metal-based complex concentrated alloys (3d CCAs). Theory-based proposals for the effects of short-range order will be discussed via the in-situ deformation studies using various scanning electron microscopy techniques. Our findings call for revisiting the classical understanding of the deformation behavior of 3d CCAs taking into account chemically ordered configuration effects.

12:25 PM ST04.02.04

Design of Multi-Principal Element Alloys with a Modified Miedema Scheme John D. Cavin, Zhaohan Zhang, Arashdeep Thind and Rohan Mishra; Washington University in St. Louis, United States

Traditionally, alloying has involved the addition of relatively small concentrations of foreign elements to a base metal. In recent years, there has been a paradigmatic shift in alloying wherein three or more elements are mixed in near equal fraction to obtain multi-principal element (MPE) alloys. The inclusion of many elements increases the mixing entropy and results in the stabilization of solid solutions and has been shown to improve mechanical and electrochemical properties. This approach has also been extended beyond pure metallic alloys to solid solutions of oxides and carbides with multiple cations. While the combinatorics of cation choice result in large phase spaces of possible MPE alloys, entropic stabilization is limited by its ability to overcome positive mixing enthalpies, i.e., not all MPE alloys will have single phase solid solutions at reasonable synthesis temperatures. A computational model that can predict the stability of MPE alloys based on a limited set of first-principles calculations would be an invaluable tool for rapid screening of promising candidates for subsequent synthesis and characterization. Here, we present a method for calculating the equilibrium phase diagram of N -component MPE alloys. This method combines the mixing enthalpy of equimolar components calculated using density-functional theory with a modified Miedema scheme [1,2] to predict temperatures above which a single-phase solid solution can be stabilized. A functional form for the mixing enthalpy is determined by fitting a $(N-1)$ -dimensional polynomial to the equimolar mixing enthalpies of an N -component MPE alloy and the $(N-1)$ -, ..., 2-component alloys of the constituent compounds. By including a contribution from the configurational entropy, $(N-1)$ -dimensional Gibbs free energy surfaces are generated and used to construct phase diagrams. In addition to providing miscibility temperatures for solid solutions, our method can identify regions of metastability and can be used to predict the stability of near-equimolar alloys. Where applicable, stable ordered alloys are also included in our analysis. Results for MPE alloys of refractory metals, oxides, carbides, and transition metal dichalcogenides will be discussed.

Acknowledgments: This work was funded by NSF DMREF-1729787.

1. Boer FR, Perrifor DG, editors. Cohesion in metals. Amsterdam: Elsevier; 1988.
2. Bakker H. In: Enthalpies in alloys, materials science foundations, vol. 1. Netherlands: Trans Tech Publications; 1998. p. 1-78.

12:40 PM ST04.02.05

Modeling, Prediction and Analysis of the Temperature-Dependent Strength Properties of High-Entropy

Alloys, and Comparison with Nickel-Based Superalloys Baldur Steingrímsson^{1,2}, Xuesong Fan³, Michael Gao⁴ and Peter K. Liaw³; ¹Portland State University, United States; ²Imagars LLC, United States; ³The University of Tennessee, Knoxville, United States; ⁴U.S. Department of Energy National Energy Technology Laboratory, United States

We present a bilinear log model for modeling and predicting the temperature-dependent strength properties of high-entropy alloys (HEAs). We have applied the model to prediction of the ultimate strength of HEAs and evaluated its effectiveness for 21 compositions. We model the logarithm of the yield or ultimate strength vs. temperature in terms of two linear regimes, a low-temperature and a high-temperature regime with a break temperature, T_{break} , in between. We present a global optimization approach for simultaneously optimizing the parameters of the bilinear model over the low-temperature and high-temperature regimes and for accurately estimating T_{break} . We consider the break temperature an important parameter for the design of materials with attractive high-temperature properties, one warranting inclusion in alloy specifications. For reliable operation, the operating temperature for the corresponding alloys may need to stay below T_{break} . Previous models for the temperature dependence of the yield strength of alloys only accounted for a single exponential. Hence, there was no break temperature.

The bilinear log model is founded on physical interpretations provided in a 2019 *Acta Materialia* paper by Senkov, Gorsse and Miracle titled “High Temperature Strength of Refractory Complex Concentrated Alloys”. Here, the authors show that, once above T_{break} , materials lose strengths rapidly due to rapid diffusion leading to easy dislocation motion and dissolution of strengthening phases (if any). According to Senkov et al., the diffusion processes required to initiate phase transformations generally become noticeable at temperatures $T > 0.4 T_m$, where T_m represents the melting temperature, while at $T < 0.4 T_m$ the phase transformations are kinetically restricted. In case of the low-temperature regime, atoms cannot move out of the lattice, and no phase transformations can take place. This is the case for low-entropy alloys (LEAs), medium-entropy alloys (MEAs), and HEAs, and serves to explain the two exponentials. A solid-solution strengthening model by Rao et al. does not take into account diffusion effects and agrees well with the experimental data only at relatively low temperatures, where diffusion-controlling deformation mechanisms can be ignored. Then, as the temperature increases, the chemical bonds between the elements become softer. The diffusion-controlled regime generally occurs above $\sim 0.5 - 0.6 T_m$. It can be distinguished from the low-temperature regime by a more rapid drop in strength with increasing temperature, because dislocations are able to move more easily around obstacles. We then investigate the suitability of our bilinear regression model to commercial alloys, including Ni-based superalloys. Anomalous yield stress behavior is common among superalloys strengthened by L12 order intermetallics. We analyze suitability of our bilinear model for predicting the yield strength of commercial alloys, with or without evidence of the anomalous yield stress phenomenon. We compare and contrast our observations with the physical interpretations of Senkov et al., per the 2019 paper in *Acta Materialia*.

12:55 PM ST04.02.06

Predictive Models for Slip-Twin Interactions Explaining Strain-Hardening of HEAs Ahmed Sameer Khan Mohammed, Orcun Koray Celebi and Huseyin Sehitoglu; University of Illinois at Urbana-Champaign, United States

Much of the outstanding mechanical behavior of High Entropy Alloys (HEAs) in monotonic loading and in fatigue can be attributed to its propensity to strain-harden under large deformation. Such strain-hardening fundamentally arises from interactions between dislocations and twin boundaries. Recent work from our group has shown the role of such slip-twin (also twin-twin) interactions in increasing strain-hardening rates (*M. Bönisch, Y. Wu, H. Sehitoglu, Acta Materialia 153 (2018) 391-403*), decelerating fatigue-crack growth, their dependence on crystallographic orientation with respect to load (*R. Sidharth, W. Abuzaid, H. Sehitoglu, Intermetallics 126 (2020) 106919*), and a strong correlation with Burgers vector residuals of slip-twin (or twin-twin) interactions. Although such interactions have been a subject of intensive study via Molecular Dynamics and Dislocation-Dynamics methods, the methods employed are not truly predictive as they rely on some form of empiricism. Tapping the full potential of strain-hardening from High-Entropy Alloys requires an ab-initio understanding of these interactions, one that does not involve any empiricism, captures the orientation-

dependence and roots the critical stresses of these interactions in fundamental fault energy parameters such as those parametrizing the Stacking-Fault Energy (SFE) landscape (e.g. intrinsic SFE, unstable SFE). We develop such a predictive framework for Dislocation-Twin-Boundary (D-TB) interactions within Generalized Peierls-Nabarro theory, predicting the critical stress for several dislocation reactions on twin boundaries. From a scientific standpoint, there has been a longstanding knowledge-gap in understanding core-structures of sessile dislocations such as stair-rods on twin boundaries. This gap has been the primary obstacle to modeling such dislocation reactions. We propose a core-structure for such dislocations, illustrating their evolution during their reaction and linking the changing core-width to the observed interaction stresses. The proposed framework establishes the dependence of the critical stresses on fundamental energy barriers of the crystal structure namely the intrinsic SFE, the unstable SFE and the unstable twinning energy. The physical fidelity of the model is validated by comparing against recent experimental data on HEAs showing good agreement, particularly in explaining the orientation-dependent behavior. By applying the model on several FCC materials and preparing Ashby-like plots we explain the reason behind such unseen strain hardening behavior of HEAs to be their critical stresses of D-TB interaction, finding them to be considerably higher than conventional FCC metals and alloys. We forward this predictive framework as a useful tool in designing HEA compositions and polycrystalline textures tailored to push boundaries of strength and toughness.

SESSION ST04.03: High Entropy Materials III
Session Chairs: Cecilia Cao, Hyunseok Oh and Yonggang Yao
Friday Afternoon, April 23, 2021
ST04

2:15 PM *ST04.03.01

High Entropy Nanomaterials—Synthesis, Application and Accelerated Discovery Yonggang Yao¹ and Liangbing Hu²; ¹Huazhong University of Science & Technology, China; ²University of Maryland, United States

High entropy materials have shown superior mechanical performances owing to the unique random mixing structure with multielement solid solution strengthening and stabilization. When scale down to nanometers, high entropy nanomaterials are promising for functional applications such as catalysis due to the exposed reactive surfaces. Particularly, the multielement mixing enables continuously tunable surfaces and properties while the high entropy structure provides the critical stability for using in harsh reactive conditions. However, in considering the large multielement compositional space and complex structures, the general synthesis of uniform mixing structure and the rapid screening of high entropy nanomaterials are still extremely challenging. In this report, we introduce the enabling and controllable thermal shock synthesis of high entropy nanomaterials (including alloys, oxides, and others) and their specific formation guidelines. In addition, the promising of high entropy nanomaterials as highly active and stable catalysts were demonstrated for both thermochemical and electrochemical reactions. Finally, combined with computational guide and high throughput screening, we briefly layout a potential way for accelerated discovery in the rarely explored multidimensional space.

2:40 PM ST04.03.02

Late News: Microwave Plasma Synthesis of High Entropy Transition Metal Diborides Bria C. Storr and Shane A. Catledge; University of Alabama at Birmingham, United States

The study explores the boro-carbothermal reduction synthesis of high entropy transition metal diborides via microwave plasma. High entropy diborides are promising materials due to ultra-hardness and resistance to high-temperature oxidation. The use of microwave plasma is a novel approach for high entropy diboride formation that capitalizes on its ability to transfer thermal energy to chemical reactions produced via the low-temperature plasma. Aiming to produce a five-component equimolar diboride, the starting powders consist of metal oxides (HfO₂, TiO₂, ZrO₂, Ta₂O₅, MoO₃) with carbon black blended by high energy ball mill, then combined with

boron carbide. By annealing the sample using microwave plasma, both boro-carbothermal reduction and a single-phase high entropy diboride ($\text{Hf}_{0.2}, \text{Zr}_{0.2}, \text{Ti}_{0.2}, \text{Ta}_{0.2}, \text{Mo}_{0.2}$) B_2 were achieved in a single step.

2:55 PM ST04.03.03

Manipulate Ionic Transport Through Entropic Design—Case Studies on Disordered Rocksalt Oxides Bin Ouyang¹, Zhengyan Lun¹, Deok-Hwang Kwon², Linze Li³, Chongmin Wang³ and Gerbrand Ceder¹; ¹University of California, Berkeley, United States; ²Lawrence Berkeley National Laboratory, United States; ³Pacific Northwest National Laboratory, United States

Metal oxides are promising materials for energy storage applications. For instance, disordered rocksalt types of metal oxides are promising Li-ion battery cathodes. Such materials are always made as a solid solution, in which short-range order (SRO) usually occurs and plays a crucial role on the Li transport properties. In this work, we developed a modeling suite that combines first-principles calculations, cluster expansion Monte Carlo simulations, electron diffraction prediction and Li percolation analyses to understand the evolution of Li transport properties with the increasing entropy. The impact of entropy on transport properties is evaluated from two types of compositional design: 1) Adding more species (such as F) into the anion site while maintaining three or four species on the cation sites; and 2) adding more than seven species on the cation sites. It has been found that the engineering of entropy on an anion site (O site) will lead to diverse evolution of transport properties, which is determined by how cations are mixed. On the other hand, once more than seven species are introduced to the cation site, the SRO generally evolves to be more favorable for Li transport. As a result, our findings lead to two routes of improving Li transport properties. For both directions of compositional engineering, we validated our theoretical predictions with experiments, which also lead to the discovery of new Li cathode materials with much higher capacities and rate capability than other state-of-the-art cathode materials. With the understanding of entropic effect on ionic transport, we hope to provide broader insights into understanding and exploring novel high entropy ceramic materials with extraordinary properties.

3:10 PM ST04.03.04

Catalytic High Entropy Oxide Heterostructures Stabilized with Vacancy Contributed Configurational Entropy Chris D. Riley¹, Andrew De La Riva², Abhaya Datye² and Stanley S. Chou¹; ¹Sandia National Laboratories, United States; ²The University of New Mexico, United States

High entropy oxides (HEO) are single phase oxides that combine traditionally immiscible metal cations through the increase of configurational entropy, by incorporating five or more cations. In some ways, this mimics a material's natural tendency to stabilize surfaces by the introduction of point defects to increase configurational possibilities of atoms. Using this concept, we demonstrate that a HEO can be designed with vacancies as an integral component of its structure. In this manner, we design structures with atomic porosities to yield a significantly vacant final product. For this, we utilize conventional alumina as a base, and through solid-state diffusion, induce sub-stoichiometric formations and vacancies as cations are introduced on its surface. The final product, a heterostructure, demonstrates a defined interface and unique vacancies sites that do not exist in conventional alumina-based structures, whether perovskites or spinel, and affords us to design catalytic active sites for tailored reactions. As a demonstration of the utility of this approach, we use the CO oxidation reaction as exemplar. In this case, the designed atomic porosities/vacancies engender oxidation pathways through the Mars Van Krevelen mechanism, which conventionally do not exist in alumina supports. In this manner, we demonstrate the catalytic potential of a highly engineered HEO, yielding a catalyst with performance that rivals the best state-of-the art single atom ceria-based catalysts.

This work was performed, in part, at the Center for Integrated Nanotechnologies, an Office of Science User Facility operated for the U.S. Department of Energy (DOE) Office of Science. Sandia National Laboratories is a multimission laboratory managed and operated by National Technology & Engineering Solutions of Sandia, LLC, a wholly owned subsidiary of Honeywell International, Inc., for the U.S. DOE's National Nuclear Security Administration under contract DE-NA-0003525. The views expressed in the article do not necessarily represent the views of the U.S. DOE or the United States Government.

3:25 PM ST04.03.05

Oxygen Vacancies in High Entropy Perovskite Oxides for Thermochemical Hydrogen Generation Jiyun Park¹, Jie Pan², Jian Luo³, Xingbo Liu⁴ and Yue Qi¹; ¹Brown University, United States; ²Michigan State University, United States; ³University of California, San Diego, United States; ⁴West Virginia University, United States

High entropy perovskite oxides (HEPOs) with A-, B-, or both-site mixing are promising redox materials to enable solar thermochemical hydrogen (STCH) generations with the improved efficiency, stability, and kinetics. In the STCH process, hydrogen is generated through a two-step cycle, where oxygen vacancies are created at high temperature and filled at low temperature by splitting water and releasing hydrogen. The efficiency of hydrogen production via the STCH process is, therefore, controlled by the difference between oxygen vacancy concentrations (δ) at the two steps, $\Delta\delta$. We hypothesized the HEPOs can allow more oxygen vacancies (V_o) without a phase transition. Thus, a thorough study on the oxygen vacancy formation in the HEPOs is needed.

In this study, we combined density functional theory (DFT) calculations with statistical thermodynamics to investigate the oxygen vacancy formation and interactions in the randomly mixed systems $\{A\}\{B\}O_{3-\delta}$. This method enabled us to investigate the effects of multi-ions mixing in $\{A\}\{B\}O_{3-\delta}$ and to calculate the oxygen vacancy concentrations (δ) and the difference in δ at two stages ($\Delta\delta$). The δ and $\Delta\delta$ are governed by the chemical potential of oxygen which varies with experimental conditions such as dry, wet, or ideal conditions. We analyzed a set of A-site elements, {Ba, Sr, La, Y, Gd, Nd, Pr, Sm}, and that of B-site elements, {Al, Ga, Mn, Fe, Ni, Co}, in $\{A\}\{B\}O_{3-\delta}$. We further compared the predicted vacancy concentration δ and $\Delta\delta$ with experimental observations in different STCH cycles. The atomistic insight, such as the oxygen formation energy was more sensitive to the charge of the {A} site ion, can be used to guide the design of new HEPO compositions with the improved properties for the STCH production.

3:40 PM ST04.03.06

Magnetocaloric Study of Aluminum-Doped $Gd_3Fe_{5-x}Al_xO_{12}$ Ferrite Dipesh Neupane¹, Arjun K. Pathak², Surendra Dhungana¹ and Sanjay R. Mishra¹; ¹The University of Memphis, United States; ²SUNY Buffalo State University, United States

The solid-state magnetic refrigeration technique is the convincing alternative reversible technique to replace the conventional gas compression refrigeration method based on the Magnetocaloric effect (MCE). The MCE is the intrinsic property of the magnetic materials. Rare earth (RE) iron garnets are complex ceramic oxides, having the chemical formula $A_3B_2C_3O_{12}$, (where A = RE^{3+} ion, B and C = Fe^{3+} ions) is suitable for MCE for low temperature. The garnet structure contains three different crystallographic sites, namely, dodecahedral (c), octahedral (a), and tetrahedral (d) site. The magnetic properties in rare-earth garnets arise from the antiferromagnetic exchange interactions of these sites. In $Gd_3Fe_5O_{12}$, two sublattices of ferric ions couple antiferromagnetically via the superexchange interaction through oxygen anions. The formula unit consists of three Fe^{3+} cations on tetrahedral sites and two Fe^{3+} cations on octahedral sites. The Gd^{3+} ions are also antiferromagnetically coupled to the net moment of the Fe^{3+} ions. Since the Gd^{3+} ions are disordered at room temperature and ordered at low temperature, the moment of Fe^{3+} ions are governed at high temperature, and Gd^{3+} dominates at low temperature. In this temperature range, interactions between neighboring spins and magnetic frustration result in finite entropy. In the present study, Al is doped in $Gd_3Fe_{5-x}Al_xO_{12}$ to investigate crystal structure and magnetic properties, including the magnetocaloric effect. $Gd_3Fe_{5-x}Al_xO_{12}$; x = 0.0, 0.25, 0.50 and 1.0 samples were synthesized via autocombustion method and heat-treated in air at 1100°C for 12 h. The phase identification and lattice parameter of the powders performed using x-ray diffraction show the presence of high-crystalline single phases garnet (JCPDS-48-0077). With Al^{3+} doping, a gradual shift in the peaks to the left as compared to pure garnet is observed that showed a decrease in lattice parameters from 12.50Å to 12.44Å due to smaller ionic radii of Al^{3+} ion (0.535 Å) replacing Fe^{3+} ions (0.645 Å). Magnetic measurements were performed using SQUID magnetometer. Temperature dependence of the zero-field-cooled (ZFC) curve exhibits transition temperature at ~50 K that is associated with glass transitions. Noticeably, there

is a sharp decrease in the FC magnetization below ~ 120 K, which coincides with the magnetic ordering temperature of the Gd sub-lattice. Saturation magnetization increased gradually with x content and reached an optimum value 43 emu/g for $x=0.5$ from 18 emu/g for $x = 0.0$ and followed by a decrease with x content at 5K. Observed enhanced magnetization for $x = 0.5$ is due to the optimal distance between Fe^{+3} ions, thus enhancing pair exchange interaction. To evaluate the MCE of the samples, the magnetization isothermal curves were collected at different fixed temperatures ranging from 10 to 250 K and in the field range between 1-3T. The magnetic entropy change (ΔS_M) as a function of the temperature curve shows a broad peak for $x = 0.0$. The peak position is shifted towards lower temperatures as x increases. This trend is consistent with our observation that the maximum magnetic entropy change (ΔS_M^{Max}) of the $x=0.50$ sample at 40K increases abruptly with an applied magnetic field of 3T. The increase in ΔS_M is mainly due to superexchange interaction between Fe-Fe ions and particle size. Arrot plots showed the positive slope of the curve, indicating a second-order phase transition in Al-doped nanoparticles. Cooling efficiency can be calculated from the peak position of ΔS_M^{Max} called relative cooling power(RCP). RCP values of our nanoparticle samples lie between 5 and 90 Jkg^{-1} , with 90 Jkg^{-1} being the maximum for $x = 0.50$. These results make our compounds promising materials for magnetic refrigeration technology. Our study suggests that up to a certain level of non-magnetic atom doping, enhancement in MCE is possible. Thus, the proposed compound is cost-effective in terms of reducing the expensive rare-earth element.

3:45 PM ST04.03.07

Magnetocaloric Properties of RE Doped $\text{Gd}_{3-x}\text{RE}_x\text{Fe}_5\text{O}_{12}$ (RE=Sm, Dy and Nd) Garnets Dipesh Neupane¹, Arjun K. Pathak², Surendra Dhungana¹ and Sanjay R. Mishra¹; ¹The University of Memphis, United States; ²University at Buffalo, State University of New York, United States

Rare earth(RE) iron garnets are complex ceramic oxides, having interesting magnetocaloric properties. The garnet structure contains three different crystallographic sites that hold a wide variety of cations. The magnetic properties in rare-earth garnets arise from the antiferromagnetic exchange interactions. In $\text{Gd}_3\text{Fe}_5\text{O}_{12}$, two sublattices of ferric ions couple antiferromagnetically via the superexchange interaction through oxygen anions. The formula unit consists of three Fe^{3+} cations on tetrahedral sites and two Fe^{3+} cations on octahedral sites. The Gd^{3+} ions are also antiferromagnetically coupled to the net moment of the Fe^{3+} ions, but this coupling is weaker than that between Fe^{3+} ions. Since the Gd^{3+} ions are disordered at room temperature, the ferrimagnetic properties of the material at high temperatures are governed by the moments of the Fe^{3+} ions. At low temperature, however, the Gd^{3+} lattice becomes ordered and dominates the magnetic properties of the material due to the larger magnetic moment of Gd compared with that of Fe ions. In this temperature range, despite interactions between neighboring spins, magnetic frustration due to the geometric configuration results in a disordered cooperative paramagnetic state with finite entropy. Besides structure, MCE also depends on morphology and defects. The present study investigates MCE in rare-earth-doped $\text{Gd}_{3-x}\text{RE}_x\text{Fe}_5\text{O}_{12}$ where Gd ion is replaced by RE=Dy, Sm, and Nd. Doped $\text{Gd}_{3-x}\text{RE}_x\text{Fe}_5\text{O}_{12}$ samples were synthesized via autocombustion method and heat-treated in the air at 1100°C for 12 h. The influence of replacing Gd^{3+} ions by rare-earth ions (RE^{3+}) ions on the structural, morphology, magnetic, and magnetocaloric properties have been investigated using X-ray diffraction, scanning electron microscopy, and SQUID. The diffraction patterns showed the garnet structure (JCPDS-48-0077) of the cubic group $\text{Ia}\bar{3}\text{d}$ with the absence of any impurity phases. The lattice parameter of the powders calculated from the XRD pattern. The analysis of the XRD data confirmed that all compositions are single phase with garnet structure. The Dy doped garnet showed a decrease while Sm and Nd-doped garnet showed an increase in lattice volume. This systemic changes in the lattice volume are the result of the difference in ionic radii of RE ions. The temperature-dependent magnetization of the as-prepared pure phase RE doped samples was measured with field and zero-field cooling(FC and ZFC). Dy doped garnet had transition temperature at 90K, whereas Nd and Sm doped samples showed similar transition temperature with pure garnet. All RE^{3+} doped samples showed paramagnetic behavior at RT and antiferromagnetic behavior at 5K. The isothermal magnetic entropy changes (ΔS_M) calculated by using Maxwell equation from the isothermal magnetization curves that were collected at different fixed temperatures ranging from 10 to 250 K. $-\Delta S_M$ as a function of temperature curve shows a broad peak for $x = 0.00$. The peak position is independent with applied fields for the same material, whereas the peak shifted as RE^{3+} doped. ΔS_M increased with Dy^{3+} increases,

whereas Nd^{3+} showed decreases with x content. For Sm^{3+} , $x = 0.25$ has maximum ΔS_M . This trend is consistent with our observation that the maximum magnetic entropy change (ΔS_M^{Max}) of the Sm^{3+} ($x=0.25$) sample at 40K increases abruptly with the applied magnetic field of 3T. The variation in ΔS_M^{Max} is mainly due to super-exchange interaction between Fe – Fe ions. By doping Dy^{3+} , the distance between Fe^{3+} – Fe^{2+} ions decreases, so the exchange interactions and the super-exchange interaction become strong, resulting in the enhance of . Moreover, increased $\sim 23\%$ for Dy^{3+} $x=0.75$ sample and $\sim 73\%$ for Sm^{3+} $x = 0.25$ sample. These values are relatively high and comparable to some noticeable magnetocaloric material. Thus, based on these results, our samples are promising materials for magnetic refrigeration technology.

SESSION ST04.04: High Entropy Materials IV

Session Chair: Eun Soo Park

Friday Afternoon, April 23, 2021

ST04

5:15 PM *ST04.04.01

Unique High-Temperature Deformation Dominated by Grain Boundary Sliding in Heterogeneous Necklace Structure Formed by Dynamic Recrystallization in HfNbTaTiZr High Entropy Alloy Nobuhiro Tsuji¹, Rajeshwar R. Eleti¹, Atul Chokshi² and Akinobu Shibata³; ¹Kyoto University, Japan; ²Indian Institute of Science, India; ³NIMS, Japan

Microstructural evolution of dynamically recrystallized (DRX) grains and grain boundary sliding (GBS) in the heterogeneous necklace structure of HfNbTaTiZr refractory high entropy alloy (RHEA) was studied systematically during high temperature deformation. Uniaxial compression testing was carried out to different strains at 1000 °C and a strain rate 10^{-3} s^{-1} . Significant bulging of grain boundaries led initially to the formation of DRX grains. The fraction of DRX grains increased with strain, and typical necklace structures of fine ($d \leq 1.5 \mu\text{m}$) DRX grains formed at strain $\epsilon \geq 0.3$. The DRX grains showed limited grain growth, and heterogeneous microstructures composed of coarse unrecrystallized regions surrounded by the characteristic DRX necklace structure were formed at larger strains. Interrupted testing with marker grids revealed that DRX grains deformed by a GBS mechanism. The DRX necklace regions connected mesoscopically and also displayed diamond network morphologies, with unique “Y-shaped”, “T-shaped” and “X-shaped” junctions. The formation of different types of junctions were rationalized on the basis of GBS accommodated by local dislocation slip in unrecrystallized regions. The unrecrystallized regions showed preferred $\langle 001 \rangle / \langle 111 \rangle$ micro-textures, consistent with conventional dislocation slip in the BCC crystals. On the other hand, the newly formed DRX grains initially had similar orientations to those of the parent grains, but they displayed a random texture with increasing strain, as expected from GBS. The randomized texture of DRX grains and the stability of DRX grains size represented GBS in the DRX necklace regions.

5:40 PM ST04.04.02

Late News: Element Redistributions During Early Stages of Oxidation in a Ni₃₈Cr₂₂Fe₂₀Mn₁₀Co₁₀ Multi-Principal Element Alloy Elizabeth J. Kautz¹, Sten Lambeets¹, Daniel Perea¹, Angela Gerard², Junsoo Han², John Scully², James Saal³ and Daniel Schreiber¹; ¹Pacific Northwest National Laboratory, United States; ²University of Virginia, United States; ³Citrine Informatics, United States

Element redistributions after initial oxidation of a Ni₃₈Cr₂₂Fe₂₀Mn₁₀Co₁₀ (at.%) multi-principle element alloy at 120 °C and 300 °C is captured via *in situ* atom probe tomography. All cations contribute to the oxide in both conditions, consisting of a Cr-rich inner oxide and a Fe, Mn, Co and Ni-rich outer oxide. At lower temperature, Ni tends to be trapped at the outer/inner oxide interface, while Ni enriches at the oxide/metal interface at higher temperature in tandem with Cr metal depletion. These observations confirm oxidation of complex alloys involves the formation of metastable, multi-layered oxide films, with a distinct tendency for solute trapping.

5:55 PM ST04.04.03

Cyclic-Deformation Behavior in a Ductile Multicomponent B2 Precipitates-Strengthened High-Entropy Alloy Rui Feng^{1,2}, You Rao³, Chuhao Liu⁴, Xie Xie¹, Dunji Yu², Yan Chen², Maryam Ghazisaeidi³, Tamas Ungar⁵, Huamiao Wang⁴, Ke An² and Peter K. Liaw¹; ¹The University of Tennessee, Knoxville, United States; ²Oak Ridge National Laboratory, United States; ³The Ohio State University, United States; ⁴Shanghai Jiao Tong University, China; ⁵Eötvös University, Hungary

Fatigue failures in engineering structures can cause catastrophic accidents without obvious warning. Thus, a fundamental understanding of cyclic-deformation and fatigue-failure mechanisms is critical for developing fatigue-resistant structural materials. Here we report a ductile multicomponent B2 precipitates-strengthened high-entropy alloy (HEA), which exhibits the outperforming fatigue life, relative to traditional materials, at low strain amplitudes. Its real-time cyclic-deformation mechanisms are revealed by *in-situ* neutron diffraction, transmission-electron microscopy, crystal-plasticity modeling, and Monte-Carlo simulation. Multiple cyclic-deformation mechanisms, including dislocation slips, multicomponent-precipitation strengthening, deformation twinning, and reversible stress-induced martensitic transformation, are observed in the studied HEA. Its excellent fatigue performance is attributed to the outstanding fatigue-crack-initiation resistance, resulting from the high elasticity, plastic deformability, and martensitic transformation of the B2 phase that leads to the effective load redistribution and strain partitioning with the face-centered-cubic (FCC) matrix. Guided by this study, fatigue-resistant alloys strengthened by ductile multicomponent intermetallic phases can be developed.

6:10 PM ST04.04.04

Late News: Phase Diagram and Phase Transformations of Refractory High Entropy Superalloy Sang Jun Kim, Ji Young Kim, Hyunseok Oh and Eun Soo Park; Seoul National University, Korea (the Republic of)

Recently, various refractory high entropy superalloys, which have unique microstructure containing cuboidal nano-precipitates in BCC high entropy alloy (HEA), reported. They exhibited superior mechanical properties at both ambient and high temperature. However, there are many unsolved issues to attract even greater attention such as precipitation control of unwanted compounds, optimal phase selection between ordered and disordered BCC, and optimization of mechanical properties etc. In the present study, we studied the phase diagram and phase transformations of refractory high entropy superalloy through a bulk combinatorial approach in Ti-Zr-Nb-Ta-Al quaternary HEAs. Microstructural evolution for the non-equiatomic HEA compositions obtained by a bulk combinatorial approach were systematically investigated by considering phase transformation mechanism as well as phase equilibria. This result could provide an effective guideline for tailoring microstructure of HEAs with ordered and disordered BCC phases, and developing a promising high entropy superalloy with customized microstructure for ultra-high temperature structural application.

6:25 PM ST04.04.05

Lattice Distortion in Refractory High-Entropy Alloy Chanho Lee¹, Yi-Chia Chou², George Kim³, Michael Gao⁴, Ke An⁵, Jamieson Brechtl⁵, Chuan Zhang⁶, Wei Chen³, Jonathan D. Poplawsky⁵, Gian Song⁷, Yang Ren⁸, Yi-Chia Chou², Nan Li¹, Saryu J. Fensin¹ and Peter K. Liaw⁹; ¹Los Alamos National Laboratory, United States; ²National Chiao Tung University, Taiwan; ³Illinois Institute of Technology, United States; ⁴U.S. Department of Energy National Energy Technology Laboratory, United States; ⁵Oak Ridge National Laboratory, United States; ⁶Computherm LLC, United States; ⁷Kongju National University, Korea (the Republic of); ⁸Argonne National Laboratory, United States; ⁹The University of Tennessee, Knoxville, United States

The lattice distortion is the core effect of HEAs to enhance the strength at room as well as high temperatures. The number of constituent elements with various atomic sizes have the identical possibility to occupy at atom positions of a crystal lattice, which induces a severe distortion of the crystalline lattice. Several studies have attempted to quantitatively measure the lattice distortion with increasing the number of alloying elements, using x-ray diffraction (XRD) and neutron diffraction (ND). However, only limited alloy systems have succeeded to demonstrate the correlation between lattice distortion and mechanical properties. In this study, we have

systematically investigated the evolution of lattice distortions for Nb-Ta-Ti-V-Zr systems as function of number of additional elements and its effect on mechanical properties, using experimental [atom-probe-tomography (APT at CNMS), transmission-electron microscopy (TEM)] and modeling methods [density-functional-theory (DFT)]. It is found that lattice distortions have a critical role in improving yield strength.

6:40 PM ST04.04.06

Late News: Microstructural Evolution of TRIPLEX Refractory High Entropy Alloy Composites Fabricated by Spark Plasma Sintering Sang Jun Kim¹, Jin Yeon Kim¹, Da Hye Song², Jin-Kyu Lee² and Eun Soo Park¹; ¹Seoul National University, Korea (the Republic of); ²Kongju National University, Korea (the Republic of)

Recently, BCC high entropy alloys (HEAs) composed by Group-4 to Group-6 elements were reported to exhibit superior mechanical properties up to high temperature above 1273 K comparing conventional Ni-based superalloy. However, RHEAs is their industrial application is limited due to the high melting point and poor ductility in room temperature. In this study, TiVNbTaW RHEA powder with single BCC phase was prepared by high-energy ball milling and the fabricated powder were sintered using spark plasma sintering. Sintered TiVNbTaW high entropy alloy exhibited TRIPLEX nanostructure consisting of (Nb,Ta)-rich BCC, W-rich BCC and TiO FCC phase, which was formed during the sintering process by decomposition of single BCC phase in as-milled powder. Microstructural evolution of TRIPLEX nanostructure was analyzed in terms of metastable thermodynamic equilibrium related with segregation of solutes and diffusion kinetics in a complex multi-principle system. This result could provide an effective guideline for tailoring the nanostructure of RHEAs fabricated by powder metallurgy.

6:45 PM ST04.04.07

Late News: Bi-Continuous Refractory HEA/Cu Composite with Superior Thermal Conductivity at High Temperature Kooknoh Yoon, Il Hwan Kim and Eun Soo Park; Seoul National University, Korea (the Republic of)

Due to its high melting point, low deuterium/tritium retention, high thermal conductivity and so on, Refractory metals including tungsten(W) has been recognized as the most promising candidate of plasma facing materials (PFMs) for fusion reactors. Moreover, Refractor high entropy alloys (RHEA) is known to exhibit higher strength and thermal conductivity at elevated temperatures than W alloys due to solid solution strengthening as well as high resistivity against neutron irradiation damage.

Meanwhile, copper(Cu) based alloys have been proposed as the heat sink materials behind the plasma facing material due to its excellent thermo-mechanical properties. The joining of W to copper based heat-sink (CuCrZr) remain a main problem in the development of plasma facing component (PFC) due to the large difference in the coefficient of thermal expansion (CTE) between these two materials.

In this research, therefore, we fabricated composites of R-HEA and Cu by liquid metal dealloying (LMD) process. To utilize this technique, we prepared a precursor material which contains elements having positive and negative enthalpy of mixing with Cu simultaneously, and we immersed it into high-temperature liquid copper to form bi-continuous composite material. Finally, we analyze strength and thermal conductivity of the composite systematically. This work will give a guide line for designing PFMs with improved properties.

SESSION ST04.05: High Entropy Materials V
Session Chairs: Eun Soo Park and Kooknoh Yoon
Friday Afternoon, April 23, 2021
ST04

8:15 PM *ST04.05.01

Single-Crystal Mechanical Properties of Equiatomic and Non-Equiatomic High-Entropy Alloys of the Cr-Mn-Fe-Co-Ni System Haruyuki Inui; Kyoto University, Japan

The plastic deformation behavior of single crystals of the FCC equiatomic and non-equiatomic high-entropy alloys of the Cr-Mn-Fe-Co-Ni system has been investigated in a temperature range of 10-1273 K both in tension and compression. Deformation occurs via slip of the $\{111\}\langle 110\rangle$ system exclusively in the whole temperature range for all alloys investigated. The CRSS values increase with decreasing temperature, especially below room temperature, so that the concept of 'stress equivalence' is obeyed. This is a clear indication that the strength of these alloys should be described by a mechanism based on solid-solution hardening. The CRSS values at 10 K seems to be well scaled by the mean-square atomic displacement from the regular FCC lattice points (calculated based on density-functional theory). Deformation twinning occurs in later stages of deformation at low temperatures below room temperature in many of these alloys. The correlation between twinning stress and the stacking-fault energy will be discussed.

8:40 PM ST04.05.02

Late News: Solid Solution Strengthening of Local Atomic Clusters (LAC) in CrMnFeCoNi High Entropy Alloys Kooknoh Yoon¹, Hyunseok Oh², Batiste Gault³, Dierk Raabe³ and Eun Soo Park¹; ¹Seoul National University, Korea (the Republic of); ²Massachusetts Institute of Technology, United States; ³Max-Planck-Institut für Eisenforschung GmbH, Germany

Since high entropy alloy (HEA) is constituted with multi-principal elements, it can be understood in a very severe condition of solid solution strengthening (SSS). In particular, the local atomic clusters (LAC), sub-nano scale atomic structure, can be easily formed in HEAs by having preferential bonding among specific elements with thermodynamic stability. Understandably, the LACs can drive HEAs to extreme condition of SSS.

Moreover, some former researches have reported that this structure can also affect on the bulk properties of HEAs, such as stacking fault energy (SFE) and so on.

In the present study, we systematically evaluate the influence of LAC formation on the degree of SSS in various CrMnFeCoNi HEAs. The LAC formation was carefully controlled by solidification history intensive structural analysis including APT, EXAFS and so on. Finally, this work will establish a tuning recipe for SSS in HEAs, which uses the sub-nano scale structural information.

8:55 PM ST04.05.03

Late News: *In Situ* Neutron Scattering Study of Plastic Deformation Mechanism in a High-Entropy Alloy with Chemical Short-Range Ordering Si Lan¹, Huiqiang Yin¹ and Xun-li Wang²; ¹School of Materials Science and Engineering, Nanjing University of Science and Technology, China; ²City University of Hong Kong, China

Like elements choose to gather together and tend to form chemical short-range ordering in compositionally complex alloys, i.e., high-entropy alloys. The role of chemical short-range ordering in plastic deformation of a CoCrFeNiPd alloy has been studied using in-situ neutron diffraction and small-angle neutron scattering. The FCC single-phase CoCrFeNiPd alloys show much more substantial nanoscale heterogeneity than CoCrFeNiMn Cantor alloy, indicating the existence of pronounced chemical short-range order. Moreover, lattice strain analysis reveals that the stacking fault probability is much higher in CoCrFeNiPd alloy than that of Cantor alloy due to the increase of stacking fault energy by chemical short-range ordering. Analysis of diffraction and microscopy data confirms that dislocations interactions and propagations, rather than stacking faults or twinning, play an essential role at the early stage of plastic deformation in CoCrFeNiPd, leading to higher yield strength without compromising strain hardening and tensile ductility than those in Cantor alloy.

9:10 PM ST04.05.04

Late News: Correlation Between Medium-Range Order and Magnetic Structure in a High-Entropy Fe-Er-Ho-Tm-Y-Dy-Nb-B Metallic Glass Jiacheng Ge¹, Sinan Liu¹, Si Lan¹ and Xun-li Wang²; ¹Nanjing University of Science and Technology, China; ²City University of Hong Kong, China

In-situ synchrotron high-energy X-ray diffraction and small-angle neutron scattering have been employed to study the kinetics of static structure and magnetic structure evolution in a high-entropy Fe-Er-Ho-Tm-Y-Dy-Nb-B metallic glass with an anomalous exothermic phenomenon upon heating. Our experimental evidence reveals that the high-entropy glassy alloy of a calorimetric anomaly would undergo a liquid-liquid phase transition accompanied by structure changes on medium-range ordering in the supercooled liquid region. Moreover, there is an increase of magnetic correlation length with the enhanced connectivity of medium-range ordering, resulting in the higher saturation magnetization for the sample after the liquid-liquid phase transition. Our results may help build a correlation between the medium-range order and the magnetic structures in soft-magnetic high-entropy metallic glasses.

9:25 PM ST04.05.05

High-Throughput, Combinatorial Study of Mechanical Properties of NiCoCr Thin Film Semin Park and Seung Min Han; Korea Advanced Institute of Science and Technology, Korea (the Republic of)

High- and medium-entropy alloys are presumed to form a stable single phase of a random solid solution due to the high configurational entropy and are reported to have novel mechanical properties where they hold decent combinations of strength and toughness even under extreme conditions. One of the critical factors in designing HEA and MEA is to ensure stability of the solid solution, which typically is metastable unless the heat treatment temperature is sufficiently high to ignore the enthalpy term. Therefore, solid solution of HEA or MEA cannot be designed based on entropy alone, but the extent of enthalpy affecting solid solution stability should also be considered. In addition, atomic interactions affecting the short-range order and stacking fault energy can largely affect the expected mechanical properties. In this study, non-equiatomic NiCoCr HEA alloy is chosen to study the effect of composition on the mechanical properties using combinatorial high throughput method. Thin film composition library was fabricated via co-sputtering at different processing temperatures. Chemical mapping of the composition library indicated formation of NiCoCr with composition range of Ni varies from 18 to 51 at.%, Co from 19 to 59 at.%, Cr from 20 to 56 at.%, and x-ray diffraction was performed to analyze the phases. Measurement of Young's modulus and hardness was performed using nanoindentation methods, where thin film model was used to accurately determine the mechanical properties of the NiCoCr thin film by removing substrate effects. This study is first to report a high throughput method involving a thin film combinatorial method in studying the effect of composition of NiCoCr on the mechanical properties via nanoindentation.

9:40 PM BREAK

10:00 PM ST04.05.06

Late News: Comprehensive Composition-Microstructure Maps of High-Entropy Alloys from High-Throughput First-Principles Study Zhidong Leong and Teck Leong Tan; Institute of High Performance Computing, A*STAR, Singapore

While refractory high-entropy alloys (HEAs) exhibit exceptional mechanical properties, insights into the underlying microstructures are limited—experimental data appear scarce relative to the vast composition space. Here, we present a high-throughput first-principles study of Mo-V-Nb-Ti-Zr, a refractory HEA known for its high-temperature strength and biomechanical compatibility. Using cluster expansion and Monte-Carlo simulations, we compute the temperature dependence of the microstructures across the whole composition space. We demonstrate that as the high-temperature solid solution cools, Zr preferably segregates from Mo and V (rather than from Nb and Ti), leading to secondary phases that are enriched in Zr with randomly dispersed Nb and Ti. Across compositions, the segregation is more pronounced for a higher segregation T_c , which increases with higher Mo and V contents. We elucidate the origins of the phase separation and elemental distribution via tracing the short-range ordering tendency of the different elemental pairs. Not only do our results reproduce numerous sets of experimental observations within a consistent framework, they also provide predictions for much of the compositional space lacking experimental data. Finally, using the segregation T_c , we discuss the

phase stability of solid solutions and identify compositions for which solid solution formation is prohibited. Our work provides the much needed insights into the HEA's microstructures, guiding future experiments in the design of HEAs with superior mechanical properties.

10:15 PM ST04.05.07

Late News: Development of Classical and Machine Learning Based Force Fields for Robust High Entropy Alloys Structure-Property Predictions Bhumika Longakshi, Siddharth Krishnan and Raghavan Ranganathan; Indian Institute of Technology Gandhinagar, India

High Entropy Alloys (HEA) form a fascinating class of materials with various technological applications arising from their interesting properties. Due to the complex nature of these systems, a detailed and reliable exposition of nanoscale structure-property correlations via full atomistic simulations is a considerable challenge. In this work, we generate robust parametrized Embedded Atom Method (EAM) potentials and critically compare it with a generalized Machine Learning-based Moment Tensor potential for predictions of mechanical properties in the Fe-Ni-Co-Cr-Cu alloy system. These potentials are fit to results from detailed ab initio Molecular Dynamics (AIMD) simulations yielding energies, stresses and atomic positions under various conditions (varying temperature, strains and defects), with the advantage of using the same DFT training set for both the classical EAM potential, and the Machine Learning Interatomic Potential. Model structures in training include constituent unaries, equiatomic binaries and ternaries and a few non-equiatomic compositions of the quinary alloy. We show that although the EAM potential for the alloy is able to capture the static structural properties and near-equilibrium dynamic properties well, the MTP potential with active learning of the potential resulting from on-the-fly calculations of atomic trajectories, yields superior results even for far-from-equilibrium dynamic conditions such as high-strain rate tension and compression. This modeling protocol serves as a high-fidelity approach for large-scale atomistic simulations of structure-property correlations in HEAs.

10:20 PM ST04.05.08

Late News: First-Principles Calculation of Stacking Fault Energy of Multi Principle Component Alloys Using Bilayer-SQS Sufyan M. Shaikh¹, Budaraju Srinivasa Murty^{1,2} and Satyesh K. Yadav¹; ¹Indian Institute of Technology Madras, India; ²Indian Institute of Technology Hyderabad, India

Deformability of high entropy alloys (HEAs) has been shown to strongly depend on their stacking fault energy (SFE). Reducing the SFE of HEAs can lead to enhanced twin susceptibility, which can ultimately lead to improved deformability of the alloys. CoCrFeMnNi shows good deformability at room temperature, which is attributed to low SFE. We observe that SFE of CoCrFeMnNi is lower than SFE of each of its constituent elements. This hints towards a way of lowering the SFE of BCC metals (which are less deformable than FCC alloys), by alloying them to form multi principal component alloys. To predict effect of alloying elements reliably, first-principle density functional theory (DFT) technique is used.

Special quasi-random structure (SQS) supercells are widely used to calculate the SFE of HEAs. Such SQS attempt to mimic random occupancy of each lattice site by constituent elements in the bulk, we call this approach as “bulk-SQS” method. This approach does not guarantee same stoichiometry in each plane as in the bulk, which results in large variation in calculated SFE depending on type and number of atoms in the two planes being sheared.

Here we propose a new “bilayer-SQS (bSQS)” methodology to reliably calculate the SFE of HEAs. Instead of considering the correlation in the entire volume of the supercell, in bSQS method, the correlations are considered only in the two neighboring planes. First, a bilayer, i.e. SQS with 2 planes (in which SFE need to be calculated) is generated with the same chemical composition as the alloy. This bSQS is then repeated 5 times to get 10 slip planes in the supercell. A minimum of 10Å of vacuum is added to prevent the effect of neighboring faults due to the periodic boundary condition.

The bSQS methodology gives the same SFE value irrespective of which slip plane is sheared. We also optimize the minimum number of slip planes and the minimum number of atoms per plane required to reliably calculate the SFE of HEAs. The SFE values are said to be converged when the values from two consecutive atoms per plane supercells are within 1meV/atom (which is typical DFT error). This gives us the minimum number of atoms required in the supercell to get a reliable SFE value. In present work, the bSQS methodology is used to calculate the SFE of $\{110\}\langle 111\rangle$, of Ti, Zr, Hf, Nb, Ta, and their equiatomic binaries, ternaries and quaternaries.

SYMPOSIUM ST05

Mechanics of Energy Storage Materials
April 14 - April 22, 2021

Symposium Organizers

Jang Wook Choi, Seoul National University
Dongping Lu, Pacific Northwest National Laboratory
Jodie Lutkenhaus, Texas A&M University
Yuan Yang, Columbia University

* Invited Paper

SESSION ST05.00: On-demand
Wednesday Morning, April 14, 2021
ST05

8:00 AM ST05.00.01

Insights of Capacitance Increase Over Repetitive Charge/Discharge for Lignin Carbon Nanofiber-Based Supercapacitors Azega Rajendra Babu K. Arasi, Qi Li, Mazharul Haque, Per Lundgren and Peter Enoksson; Chalmers University of Technology, Sweden

The production of free-standing carbonized electrospun lignin carbon fibers (ELCF) is similar to that used in large scale paper making. This makes ELCF highly prospective for commercially viable supercapacitor electrodes, being a low-cost and bio-renewable starting material. However, untreated ELCF -based electrodes for supercapacitors face several challenges due to their poor mechanical performance and limited conductivity. Thermal treatments applied for carbonization and activation vastly improve both electrochemical performances and mechanical properties by giving rise to fiber crystallization. Yet as supercapacitor electrodes, their microporous structure faces the issue of electrolyte ion accessibility. The charge transfer impedance is known to increase due to the inaccessibility of electrolyte ions to the porous structures, resulting in decreased charge storage ability [1]. Understanding the correlation between the electrode physiochemical properties and the charge storage is key to guide the production and commercialization of ELCF materials for supercapacitor applications. In this work, ELCF were fabricated by electrospinning and carbonized at 1000 °C. The ELCF performance was evaluated in a coin cell configuration with two symmetric electrodes in 6M KOH electrolyte over 5k, 10k, 20k, and 50k cycles. There was a constant increase in performance up to 2-fold from 3.8 mF/g to 7.7 mF/g after 50k cycles. The capacitance increase is accompanied by an interfacial resistance decrease that is caused by the interaction between the bulk electrolyte and the electrode's interface as inferred from the Nyquist

plots. This improvement behaviour with cycling is attributed to the better accessibility of the alkaline KOH electrolyte ions to outer pores over repeated cycling. Another contribution to the increased capacitance could be related to lignin being a complex natural biopolymer incorporated with various functional groups [2]; more reactive functional groups could be made available during the consecutive cycling for the charge transfer to take place [3]. The K^+ electrolyte ions are adsorbed on the exposed reactive sites in the larger lignin chains over their repeated intercalation and deintercalation during redox reactions resulting in slower and steady growth in capacitances with highly stable cycling behaviour. This can also be explained by the common behaviour during electrochemical analysis that the unreactive constituents remain inactive to capacitive behaviour initially and begin electroactivity additionally after the reaction. To further corroborate these explanations, the specific surface area, pore size, and functional groups of the ELCF before and after cycling will be investigated by using Brunauer-Emmett-Teller (BET) and X-ray Photoelectron Spectroscopy (XPS) characterization analysis. Additionally, a thorough electrochemical investigation will be carried out regarding the improved capacitive performance with cycling, alongside with the quantification of electrostatic (pore) and pseudocapacitive (functional group) charge storage of ELCF material.

Keywords: lignin, supercapacitors, cycling, pseudocapacitance, pore accessibility

[1] Inchan Yang, Sang-Gil Kim, Soon Hyung Kwon, Myung-Soo Kim, Ji Chul Jung, “Relationships between pore size and charge transfer resistance of carbon aerogels for organic electric double-layer capacitor electrodes”, *Electrochimica Acta*, 2017

[2] José Luis Espinoza-Acostaa , Patricia I. Torres-Chávez , Jorge L. Olmedo-Martínez , Alejandro Vega-Rios , Sergio Flores-Gallardo, E. Armando Zaragoza-Contreras , “ Lignin in storage and renewable energy applications: A review”, *Journal of Energy Chemistry* 27 (2018) 1422-1438

[3] Manohar D. Mehare, Abhay D. Deshmukh , S. J. Dhoble , “Preparation of porous agro-waste-derived carbon from onion peel for supercapacitor application”, *Journal of Materials Science* 55 (2020) pages 4213–4224

8:10 AM ST05.00.02

Late News: Mechanical Degradation in 3D Metal Scaffold Structured Silicon Anodes Soheil Daryadel, Benjamin Zahiri, Nathan J. Fritz, Paul Braun and Jessica A. Krogstad; The University of Illinois at Urbana-Champaign, United States

3D structuring significantly enhances the cycle life performance of silicon anodes by accommodating large volume changes during de/lithiation and enables fast charging. The accumulation of mechanical stress induced by large volume changes and understanding its impact on cell performance is key toward optimizing the cycle life of these structured anodes. In this presentation, we report on the contribution of mechanical degradation to capacity fading in Si-coated 3D Ni scaffolds. We propose a novel approach to investigate the mechanical properties of the electrode materials decoupling the geometry evolution. The mechanical resilience of the anodes, including the active material and metallic support, the SEI, and the associated interfaces, are probed throughout cycling using nanoindentation. Additionally, the microstructural evolution and structural disintegration of Si and the metallic scaffold were investigated at different stages of cycling. Results revealed a reduction of strength and connectivity in the Ni scaffold during cycling and provided critical insight into the design optimization of durable high energy density anodes. A fundamental understanding of the coupling between mechanics and electrochemistry in lithium-ion battery electrodes can be advantageous in developing reliable next-generation energy storage technologies.

8:20 AM ST05.00.03

Non-Classical Electrostrictive Phenomena in Hydrated Acceptor Doped BaZrO₃— Proton Trapping and Dopant Size Effect Evgeniy Makagon¹, Maximilian Hoedl², Rotraut Merkle², Eugene Kotomin^{2,3}, Joachim Maier² and Igor Lubomirsky¹; ¹Weizmann Institute of Science, Israel; ²Max Plank Institute for Solid State Research, Germany; ³University of Riga, Latvia

Acceptor-doped BaZrO₃ is a promising electrolyte for protonic ceramic fuel cells as it combines high bulk proton conductivity with good chemical stability. The protonic conductivity is achieved by dissociative water incorporation into oxygen vacancies formed by acceptors on Zr⁴⁺ sites. We have investigated the influence of

dopants, oxygen vacancies, and protons on the macroscopic elastic and electromechanical properties of acceptor-doped BaZrO₃ ceramics.

Ceramics of BaZr_{1-x}X_xO_{3-x/2+δ}H_{2δ} with X = Ga, Sc, In, Y, Eu and 0.05 ≤ x ≤ 0.2 were prepared by solid state reactive sintering and hydration. Ultrasonic pulsed echo time of flight measurements were used to infer the Young's and the shear moduli. Both moduli decrease by up to ~20% due to the presence of dopants and oxygen vacancies that cause local lattice distortions [1,2]. Water incorporation into the vacancies decreases the moduli even further. An unexpectedly large electrostriction coefficient ($M_{33} \sim 10^{-15} \text{ m}^2/\text{V}^2$) was detected with a capacitive proximity sensor for all dopants introducing a new class of non-classical electrostrictors. M_{33} of the hydrated ceramics exhibits a Debye-type relaxation with the relaxation frequency exponentially increasing with the ionic radius closely matching dielectric relaxation measured by impedance spectroscopy. This implies that the protons are associated with the dopants, and the binding strength decreases from Ga to Y.

[1] M. F. Hoedl, E. Makagon, I. Lubomirsky, R. Merkle, E. A. Kotomin, J. Maier, *Acta Mater.* (2018) **160**, 247

[2] E. Makagon, R. Merkle, J. Maier, I. Lubomirsky, *Solid State Ionics* (2020) **344**, 115130

8:30 AM ST05.00.04

Strain Induced Enhancement of Hydrogenation Capacity in rGO/Pd/rGO Nanolaminates Dae ho Kim¹, Jinseok Koh¹, ShinYoung Kang², Eun Seon Cho¹ and Seung Min Han¹; ¹Korea Advanced Institute of Science and Technology, Korea (the Republic of); ²Lawrence Livermore National Laboratory, United States

In this work, rGO/Pd/rGO nanolaminates for metal-hydride hydrogen storage material was studied for the first time that indicated an enhancement in the hydrogen storage capacity due to the mechanical strain imposed on the Pd nanoparticles. Pd nanoparticles were encapsulated by the graphene layers to fabricate rGO/Pd/rGO nanolaminates and reduced graphene oxide (rGO) wrapping induced strain on Pd nanoparticles were then analyzed using high resolution transmission electron microscope (HRTEM). The average strain induced on the Pd nanoparticles in the as synthesized rGO/Pd/rGO nanolaminates was 3.30% in tension, and this value of strain increased to 5.44% upon hydrogenation. The strain increase to 4.94% in Pd and 7.12% in PdH_x nanoparticle if the contracted lattice parameter by nanosize effect was considered. Atomistic simulations were performed to provide further analysis on the effect of surface tension on the reference lattice parameter of Pd nanoparticles to refine the calculated strain from the HRTEM analysis. Hydrogen storage performance indicates a significant improvement, where both kinetics and the hydrogen storage capacity are significantly improved without sacrificing nano-size effects, and this enhancement is due to the tensile strain on the Pd nanoparticles causing a reduction in the activation energy of hydride formation.

8:40 AM ST05.00.05

The Role of Surface Energy in Propagation of Stress-Induced Cracks in Li-Intercalated Hollow-Sphere Silicon Anodes—A Comprehensive Analytical Model Tejveer S. Anand, Jayant Choudhary, Akash Sonkar, Henam S. Devi and Madhusudan Singh; Indian Institute of Technology Delhi, India

Owing to their high theoretical capacity to incorporate substantial amounts of lithium, silicon anodes in lithium-ion batteries undergo significant volumetric changes during charge-discharge cycles, leading to battery failure due to pulverization and fracture of the anode material. We have constructed an analytical model based on concentration-driven diffusion and linear elasticity. This comprehensive model incorporates diffusion-induced stress (DIS), electrochemical (forward) reaction induced stress (RIS), and surface effects associated with a hollow silicon spherical electrode under potentiostatic operation. Also included are various forms of stress - radial, hoop and hydrostatic, coupled with various functional parameters to study variations in stress profiles for low lithium concentrations. Two surface effects are accounted for: a) surface energy, which is the Laplace pressure arising from lithium concentration difference at the silicon interface, and surface elastic modulus. To illustrate the importance of surface effects in this model, we carried out numerical solutions of the coupled problem in its natural geometry - spherical polar coordinates, to study a hollow silicon sphere with inner radius of 200 nm and outer radius of 500 nm. When aforementioned surface effects are ignored, the maximum value of radial stress is found to be 5.3 MPa (tensile) at 318 nm (close to the center of the hollow sphere). When surface

energy and surface modulus are included in the solution, the maximum value of radial stress reduces dramatically by nearly 59% and the location of the maximal stress moves inwards to ~285 nm. This consequently leads to the stress at the outer surface becoming compressive in nature. Further, with a systematic increase in surface energy parameters, radial as well as hoop stress at the outer interface becomes more compressive. Physically, in a manner somewhat analogous to hydrophobic liquids, this shift can be understood as the effect of enhanced surface energy countering the tendency of the system to expand and relieve its increased surface stress by propagating cracks. Unsurprisingly, as the surface to volume ratio increases for smaller hollow silicon spheres, the effect becomes even more discernible for low surface lithium-concentrations ($[Li] \sim 1 \text{ mol} / \text{m}^3$). This suggests that it may be advantageous to use slightly larger electrodes (at the cost of lower capacity), or to employ lower working lithium concentrations. We are currently studying the effect of suitable barrier layers for rational design of anodes with engineered stress profiles, while maintaining high capacity.

SESSION ST05.01: Alloy and Metal Anodes
Session Chairs: Dongping Lu and Yuan Yang
Wednesday Morning, April 21, 2021
ST05

11:45 AM *ST05.01.01

Creep-Enabled 3D Solid-State Lithium-Metal Battery Ju Li; Massachusetts Institute of Technology, United States

Existing all-solid-state Li-metal batteries suffer attacks by the chemically aggressive and mechanically stressful Li metal. Li metal is a soft crystal and may exhibit either displacive or diffusive deformation. Here, we describe a class of all-solid-state Li-metal batteries enabled by 3D porous Li-metal hosts made of electrochemically stable mixed Li-ion and electronic conductor (MIEC) and electronic and Li-ion insulators (ELI). Within 3D open porous MIEC/ELI structure, Li metal advances and retracts via interfacial diffusional creep as an "incompressible working fluid" with fast stress relaxation and minimal contact with a solid electrolyte (SE), thereby significantly improving the electrochemomechanical stability. In situ transmission electron microscopy corroborated with thermodynamic analyses offers design principles in materials, sizes, and interfaces of the 3D porous MIEC/ELI structures, which are applicable to other alkali-metal batteries. The successful construction of a creep-enabled battery engine opens a new avenue toward high-density, electrochemically and mechanically robust all-solid-state Li-metal batteries. [Nature 578 (2020) 251]

12:10 PM ST05.01.02

Structural Evolution and Failure Modes in High-Performance Silicon-Oxide Based Anode Driven by Electrochemistry and Mechanics Guoyu Qian; Peking University Shenzhen Graduate School, China

High-energy-density silicon oxide-based/ graphite composite anodes are promising to become the next-generation anode material in the lithium-ion battery industry. However, as the vital raw material of the newly designed anodes, micron-sized silicon oxide-based particles exhibit poor cycling stability, which limits its industrialization promotion. Due to the complex amorphous microstructure inside the silicon oxide-based particles, its evolution and failure mechanism during the electrochemical cycling process remains poorly understood.

Accurate sample preparation for the silicon oxide-based particles will be performed by FIB-SEM dual-beam system, so that the chemical compositions and structure in the internal space of silicon oxide-based particles would be characterized. Combining with the different results during the whole electrochemical cycling process,

we would obtain the formation and evolution principles of the internal microstructure for the silicon oxide-based particles.

Moreover, the dramatic volume change, the damage of ion pathway and conductive network inside the particles, the continuous growth and reconstruction of SEI, and the Si-ion loss to the silicon oxide-based particles during hundreds of electrochemical cycles would be comprehensively investigated, in order to summarize the negative factors of the particle failure and capacity loss.

Benefited from the results in this report, more effective strategies would be designed, which could be generalized for the preparation of other silicon oxide-based anode materials. Therefore, the next-generation anodes of Li-ion batteries with excellent cycling stability, high reversible capacity and superior rate performance would be obtained.

12:25 PM *ST05.01.03

Chemo-Mechanics of Battery Transformations Investigated with *In Situ* Imaging Methods Matthew T. McDowell; Georgia Institute of Technology, United States

Pathways to batteries with higher energy density necessarily involve the use of electrode materials that undergo substantial chemo-mechanical transformations in both liquid and solid-state electrolyte environments. Here, I discuss my group's efforts to use *in situ* and *operando* characterization to investigate the interplay between chemistry and mechanics during reactions of high-capacity battery electrode materials. First, our work on using *in situ* transmission electron microscopy (TEM) to investigate reversible void nucleation and growth during delithiation of antimony (Sb) alloy nanocrystals is presented. Sufficiently small Sb alloy nanocrystals were found to form single voids during dealloying rather than undergoing shrinkage, as in larger particles. This voiding behavior during dealloying was a result of the impact of stiff native oxide surface layers that retained their shape. This effect was found to be size dependent, and an analytical model was developed to show that small nanocrystals do not exhibit enough total strain energy during shrinkage of the Li-Sb phase to drive mechanical buckling of the shell. These observations translated to improved electrochemical behavior in battery cells, where the small nanocrystals were observed to exhibit the highest average Coulombic efficiency compared to larger particles. Next, a study on chemo-mechanical degradation of FeS₂ electrode materials reacting with different ions (lithium, sodium, and potassium) is presented. Despite larger volume changes during reaction with Na⁺ and K⁺, only reaction with Li⁺ was observed to cause fracture. Modeling showed that this surprising result was found to be due to the shape of the reaction front as it evolves during reaction, with sharp corners during lithiation resulting in stress concentration and fracture. Finally, our efforts on understanding interphase formation and mechanical contact at solid-state interfaces in all-solid-state batteries is discussed. The reaction of L_{1+x}Al_xGe_{2-x}(PO₄)₃ (LAGP) solid-state electrolyte with lithium is found to involve amorphization and volume expansion of ~130%. *In situ* X-ray tomography experiments of operating LAGP-based cells reveal that the growth of the interphase causes fracture, which is the underlying cause of impedance increase within the cell. Together, these studies highlight the controlling influence of chemo-mechanics in high-capacity battery electrolyte materials when used in both liquid and solid-state battery systems.

12:50 PM ST05.01.04

Real-time Control of Dendrites in Rechargeable Batteries Using Smart Feedback Asghar Aryanfar^{1,2}, Yara Ghamlouche¹ and William A Goddard III²; ¹American University of Beirut, Lebanon; ²California Institute of Technology, United States

The non-uniform growth of the microstructures in dendritic form inside the battery during prolonged charge-discharge cycles causes short-circuit as well as the capacity fade. We develop a feed-back control framework for the real-time minimization of such microstructures. Due to accelerating nature of the branched evolution, we focus on the early stages of growth, identify the critical ramified peaks and compute the effective time for the dissipation of ions from vicinity of those branching fingers. The control parameter is a function of the maximum interface curvature (i.e. minimum radius) where the rate of run-away is the highest. The minimization of total charging time is performed for generating the most packed microstructures which correlate closely with those of considerably higher charging periods, consisting of constant and uniform square waves. The developed

framework could be utilized as a smart charging protocol for the safe and sustainable operation the rechargeable batteries, where the branching of the microstructures could be correlated to the sudden variation in the current/voltage.

1:05 PM *ST05.01.05

Fundamental Understanding of the Coupled Mechanical and Chemical Degradation of Lithium Metal Electrodes Xingcheng Xiao; General Motors, United States

Low cycle efficiency and dendrite growth are two critical barriers for rechargeable batteries using Li metal as negative electrodes, mainly due to the coupled mechanical/chemical degradation of the SEI layer formed on Li metal surface. We have developed a comprehensive set of in situ diagnostic techniques combined with atomic/continuum modeling schemes to investigate and understand the coupled mechanical/chemical degradation of the SEI layer/Li system including fundamentally understanding the surface and interface phenomena. We have found that the mechanical incompatibility between SEI and soft Li leads to the complicated mechanical behaviors of the lithium metal electrode during the plating and stripping process. We systematically investigated the relationship between surface morphology and current density distribution which results in an inhomogeneous Li plating/stripping process. We also investigated the mechanical properties of Li metal electrode at different cycle period, including the stress evolution and deformation mechanism which have been significantly impacted by SEI formation. Based on the fundamental understanding from the integrated in-situ diagnostics, atomic simulation, and continuum framework, we have developed a new coating design strategy to achieve high cycle efficiency/dendrite free and extend the cycle life of lithium rechargeable batteries.

1:30 PM ST05.01.06

Sodium Metal Mechanics—Temperature and Grain-Rotation Effects on Plasticity and Creep William LePage^{1,2}, Yuxin Chen², Kuan-Hung Chen², Andrea Poli² and Neil P. Dasgupta²; ¹University of Tulsa, United States; ²University of Michigan, United States

Na-ion and Na-metal batteries are attractive alternatives to Li-ion, as they have the potential to reduce cost and add supply chain stability for energy storage portfolios. The raw materials for Na-based batteries are more readily sourced: Na is much more earth-abundant than Li, Na batteries can utilize aluminum for both current collectors (instead of copper), and they can also readily use cobalt-free cathodes. In order to advance the state-of-the-art for Na-ion and Na-metal batteries, reliable mechanical property data for Na is needed. However, few reports have characterized the mechanical properties of Na, especially in terms of its viscoplastic and creep properties [1]–[3].

In this study, we report the first temperature-dependent measurements of power-law creep of Na. While prior works on the viscoplastic and creep deformation of Na have reported values at room temperature, this work measured the tensile response of Na in inert environments between 273 and 348 K. Furthermore, this work revealed insights about sodium deformation in general that have implications for Na batteries. For example, tests at room temperature utilizing digital image correlation (DIC) were performed inside of an argon glovebox [4] to map the local deformation of Na tensile samples. Local strain and rotation maps from DIC revealed millimeter-scale inhomogeneity that was attributed to plastic grain rotation, due to the large (~1 mm) grain size in the Na. The full calibration of power-law creep behavior from this work is valuable for modeling efforts to understand the fundamental research of Na-based batteries.

[1] P. M. Sargent and M. F. Ashby, “Deformation mechanism maps for alkali metals,” *Scr. Metall.*, vol. 18, pp. 145–150, 1984, doi: 10.1016/0036-9748(84)90494-0.

[2] C. D. Fincher, D. Ojeda, Y. Zhang, G. M. Pharr, and M. Pharr, “Mechanical properties of metallic lithium: from nano to bulk scales,” *Acta Mater.*, vol. 186, pp. 215–222, 2020, doi: 10.1016/j.actamat.2019.12.036.

[3] M. J. Wang, J. Chang, J. B. Wolfenstine, and J. Sakamoto, “Analysis of Elastic, Plastic, and Creep Properties of Sodium Metal and Implications for Solid-State Batteries,” *Materialia*, p. 100792, 2020, doi: 10.1016/j.mtla.2020.100792.

[4] W. S. LePage *et al.*, “Lithium Mechanics: Roles of Strain Rate and Temperature and Implications for Lithium Metal Batteries,” *J. Electrochem. Soc.*, vol. 166, no. 2, pp. A89–A97, 2019, doi: 10.1149/2.0221902jes.

SESSION ST05.02: Intercalation Chemistry
Session Chairs: Yijin Liu and Yuan Yang
Wednesday Afternoon, April 21, 2021
ST05

2:15 PM *ST05.02.01

Gliding and Microcracking in a Single Crystalline Ni-Rich Cathode Jie Xiao; Pacific Northwest National Laboratory, United States

High energy Ni-rich cathode will play a key role in advanced Li-ion batteries, but it suffers from moisture sensitivity, side reactions and gas generation. Single crystalline Ni-rich cathode has a great potential to address the challenges present in its polycrystalline counterpart by reducing phase boundaries and materials surfaces. However, synthesis of high-performance single crystalline Ni-rich cathode is very challenging, not mentioning a fundamental linkage between over potential, microstructure and electrochemical behaviors in single crystalline Ni-rich cathodes. This talk will discuss the planar gliding and microcracking along the (003) plane in a single crystalline Ni-rich cathode by using in situ AFM and TEM. The formation of microstructure defects is correlated with the localized stresses induced by a concentration gradient of Li atoms in the lattice, providing clues to mitigate particle fracture from synthesis modifications.

2:40 PM *ST05.02.03

Cationic and Anionic Redox Heterogeneity in Layered Battery Cathode Yijin Liu; SLAC National Accelerator Laboratory, United States

Multiscale electro-chemo-mechanical interplay governs the local structural and chemical evolution and is fundamental to the global electrochemical behavior of batteries. Prolonged battery operation under realistic conditions induces state-of-charge (SoC) heterogeneity, builds up mechanical stress, and provokes morphological breakdown. These processes prevail in most battery electrodes and ultimately determine the device-level battery performance. In lithium-rich nickel-manganese-cobalt (LirNMC) layered material, a promising cathode for lithium-ion batteries with superior energy density however suffers from capacity and voltage fade, the coexisting cationic and anionic redox activities further complicate the redox heterogeneity, urging for a comprehensive investigation of at the nano- to meso- scales. In this talk, we will present a systematic study on the mesoscale degradation of the layered battery cathode material. We look into the intertwined lattice, redox, and micro-morphology properties as the cathode is cycled under different conditions. Our results suggest that the cathode particle engineering could be a viable approach for further improving the structural and chemical robustness of the Li-ion battery.

3:05 PM DISCUSSION

3:20 PM ST05.02.05

Unraveling the Role of Primary Particle Size and Morphology During Calcination of Layered NMC Cathodes for Li-Ion Batteries Mark Wolfman¹, Xiaoping Wang¹, Peter Eng², Joanne Stubbs², Vincent De Andrade¹, Pallab Barai¹, Juan C. Garcia¹, Hakim Iddir¹, Venkat Srinivasan¹ and Tim Fister¹; ¹Argonne National Laboratory, United States; ²The University of Chicago, United States

In modern layered cathodes for lithium-ion batteries, the sizes and morphologies of the primary particles play a key role in governing the electrochemical dynamics during cycling, since the desired charge-transfer reactions

and any competing solid-electrolyte interphases rely on the exposed particle surfaces. Synthesis of layered cathodes is a two-step process. The secondary structure is determined largely by the conditions used in the initial preparation of the transition metal precursor material. The subsequent high-temperature calcination transforms the precursor to the final lithiated cathode while largely preserving the structure of secondary particle agglomerates. Recent research has characterized the crystal structure during this transformation, but has been largely silent on the accompanying morphological changes in the primary particles. Through a combination of in-situ X-ray diffraction and X-ray tomography, the morphology and structure of layered NMC primary particles were tracked during calcination. Comparison with first principles calculations and continuum modeling provided additional insights into the changes in both phase and morphology. These results provide a foundation for a more deliberate design of cathode materials with the necessary performance characteristics to help meet the growing demand for electrochemical energy storage.

3:35 PM *ST05.02.06

Role of Mechanical Deformation on Rate Capability of Electrosorption and Insertion-Type Charge Storage Veronica Augustyn; North Carolina State University, United States

Extremely fast charging and discharging, along with long cyclability, require energy storage materials that respond with minimum mechanical deformation while at the same time storing significant amounts of charge. The coupling of mechanics with electrosorption and insertion leads to fundamental limits in the power capability of materials. During this presentation, I will discuss our use of operando atomic force microscopy to probe the real-time deformation of ion insertion materials at fast (minute and second) timescales. The nanoscale dimensions of the AFM tip allow us to probe not only the deformation but also the heterogeneity of the insertion process. Furthermore, I will share our insights into how understanding mechanical deformation can lead to the design of high power energy storage materials such as tungsten oxides with confined interlayer water.

SESSION ST05.03: Mechanics in Battery Materials

Session Chairs: Yuan Yang and Kejie Zhao

Wednesday Afternoon, April 21, 2021

ST05

8:15 PM ST05.03.01

Effect of Li Concentration-Dependent Material Properties on Diffusion Induced Stresses of a Sn Anode Hyeongyun Nam, Chung Su Hong and Seung Min Han; Korea Advanced Institute of Science and Technology, Korea (the Republic of)

Sn is one of promising anode materials with high theoretical capacity for Li ion batteries and has attractive mechanical properties for effective stress relaxation during lithiation. Soft, ductile nature as well as creep at room temperature allow for Sn to effectively relax the generated stress due to the volumetric strain as a result of lithiation. In this study, finite element simulation was used to study the evolution of diffusion induced stresses in Sn micropillar anode with the focus on the effect of concentration-dependent material properties in the diffusion induced stresses. Simulation results using concentration-dependent material properties indicated a different failure mode in comparison to that from simulations results using concentration-independent material properties. When modeled using constant material properties that are independent of Li composition, compressive hoop stress is developed at surface of pillar. If we assume elastic deformation, max hoop stress at the surface is 1000 MPa, but this reduced down to 150 MPa and 40 MPa in compression when plasticity and creep, respectively, is incorporated in simulation model. On the other hand, when concentration-dependent material properties were incorporated in the model, concentration profile of Li in Sn becomes homogeneous as lithiation is proceeded and compressive hoop stress at surface is transformed into tensile hoop stress in the early

stage of lithiation. This hoop stress transition at surface is found to be originated from the increase of diffusivity of Li in the lithiated phases; outer region near the surface that has already transformed to Li rich phases is pushed out as the core of the pillar undergoes lithiation reaction to result in tensile hoop stress at the surface of the micropillar. Development of tensile hoop stress at surface can then trigger the crack formation at the surface of Sn micropillar. In order to experimentally determine the critical dimension for Sn micropillar as a result of lithiation, Sn micropillars of varying sizes were studied which was determined to be 5.3 μm when charged at rate of C/10.

8:30 PM *ST05.03.02

Heterogeneous Damage in Li-Ion Batteries—Experimental Analysis and Theoretical Modeling Kejie Zhao; Purdue University, United States

We assess the heterogeneous electrochemistry and mechanics in a composite electrode of commercial batteries using synchrotron X-ray tomography analysis and microstructure-resolved computational modeling. Morphological defects are visualized at multi-scales ranging from the macroscopic composite, particle ensembles, to individual single particles. Particle fracture and interfacial debonding are identified in a large set of tomographic data of active particles. Mechanical failure in the regime near the separator is more severe than toward the current collector. The active particles close to the separator experience deeper charge and discharge over cycles and thus are more mechanically loaded. The difference in the Li activity originates from the polarization of the electrolyte potential and the non-uniform distribution of the activation energy for the charge transfer reaction. We model the kinetics of intergranular fracture and interfacial degradation to confirm that the various Li activities are the major cause of the heterogeneous damage. The interfacial failure may reconstruct the conductive network and redistribute the electrochemical activities that render a dynamic nature of electrochemistry and mechanics evolving over time in the composite electrodes. We further quantify the influence of the mechanical damage on the metrics of battery performance. We simulate the electrochemical impedance profile to build a relationship between the interfacial debonding and the impedance of electron transport and surface charge transfer. The mechanical failure disrupts the conduction path of electrons and results in significant polarization and capacity loss in batteries.

8:55 PM ST05.03.03

Structural Lithium-Ion Battery Electrodes Based on Branched Aramid Nanofibers Paraskevi Flouda, Suyash Oka, Dimitris Loufakis, Dimitris Lagoudas and Jodie Lutkenhaus; Texas A&M University, United States

Structural energy storage devices combine energy storage and structural functionalities in a single unit, leading to lighter and more efficient electric vehicles. However, conventional electrodes for batteries and supercapacitors are optimized for high energy but suffer from poor mechanical properties. Here, we use Kevlar® nanofibers to fabricate mechanically strong Li-ion battery anodes and cathodes. Specifically, we report on free-standing electrodes consisting of lithium iron phosphate (LFP, cathode) or silicon (Si, anode) particles, reduced graphene oxide (rGO), and branched aramid nanofibers (BANFs). LFP and Si have high theoretical capacity values. rGO has high electrical conductivity, high surface area, high capacitance, and excellent mechanical properties. Recently developed branched aramid nanofibers, nanoscale Kevlar® fibers, are of great interest due to their exceptional mechanical properties, such as ultimate strength and stiffness. rGO and BANFs interact with each other through hydrogen bonding and π - π stacking interactions allowing for load transfer within the electrodes. The composite electrodes were fabricated *via* vacuum-assisted filtration to achieve highly layered structures. Electrical, mechanical, and electrochemical properties for all composite electrodes were evaluated as a function of composition. Overall, we obtained up to two orders of magnitude improvements in Young's modulus and tensile strength compared to commercial battery electrodes while maintaining energy storage capability. The role of BANFs was further investigated using scanning electron microscopy (SEM), x-ray photoelectron microscopy (XPS), and electrochemical impedance spectroscopy (EIS) before and after electrochemical cycling. This work demonstrates an efficient route for designing structural Li-ion battery cathodes and anodes with enhanced mechanical properties. This work is supported by AFOSR under Grant No.

FA9550-19-1- 0170.

9:10 PM ST05.03.04

High-Density Hydrogen Storage on Zeolite-Templated Carbon Monoliths Seth Putnam¹, Dalton Compton¹, Atsushi Gabe², Hirotomo Nishihara² and Nicholas Stadie¹; ¹Montana State University, United States; ²Tohoku University, Japan

Volumetric hydrogen storage was investigated on compacted monoliths of zeolite-templated carbon, a material with unique mechanical properties allowing for extreme densification. Pellets were prepared by a hot-pressing method between 433-573 K and 50-345 MPa, with densities of up to ~1 g/mL. Hydrogen adsorption measurements were carried out on the so-obtained monolithic samples between 40-298 K and 0.0003-10 MPa, with a focus on volumetric storage and delivery metrics at 77 and 298 K. Under optimal pelletization conditions, a sample was prepared which demonstrates near-ideal stored and delivered quantities of hydrogen when compared to that of ZTC powder compacted to “crystalline” (periodic model) density. The improvement in hydrogen delivery is notable at room temperature, exhibiting a 10% advantage over compression alone. Higher capacities and deliveries could not be achieved with activated carbons owing to mechanical properties prohibitive to the preparation of pellets without the use of excessive binder, highlighting the unique advantage of ZTC as a soft, sponge-like material for high density energy storage applications.

9:15 PM ST05.03.05

Computational Electro-Chemo-Mechanics of Two-Dimensional Energy Materials Dibakar Datta; New Jersey Institute of Technology, United States

Two-dimensional materials (2DM) such as graphene, transition metal dichalcogenides (TMD), MXenes, and their heterostructures are among the most promising energy materials for radically advanced batteries. In this presentation, two important computational aspects of 2DM-based batteries are addressed – (i) 2DM and its heterostructures as anode materials, and (ii) 2DM as van der Waals (vdW) slippery interface. The conventional anode materials have several problems, such as low gravimetric capacity (e.g., graphite – 372 mAh/g) and high volume expansion (e.g., silicon – 300%). Our computational modeling shows that topologically modified 2DM can be utilized as high-capacity anode materials for ion batteries with capacity as high as 1000 mAh/g. However, despite enormous opportunities in 2DM anode, several challenges need to be addressed, such as trapping of adatoms at the defect sites, the effect of defects on the diffusivity of adatoms, mechanical degradation at defect sites during charging/discharging, etc. The second part of the presentation discusses the interface of anode and current-collector (e.g., silicon anode and copper current-collector in Li-ion battery). To combat the issue of high-stress development at the anode-current collector interface during charging/discharging, we propose the usage of the graphene layer over the current collector as a vdW slippery interface that reduces the interfacial stress and enhances the cycle life of batteries. Our computational results are in excellent agreement with the experimental findings.

SESSION ST05.04: Flexible Batteries
Session Chairs: Yuan Yang and Zijian Zheng
Wednesday Afternoon, April 21, 2021
ST05

10:00 PM *ST05.04.01

Fiber-Based Wearable Energy Storage Devices Zijian Zheng; The Hong Kong Polytechnic University, Hong Kong

Wearable energy storage devices are indispensable cornerstones for future wearable electronics. Current energy

storage technologies are based on materials and devices that are rigid, bulky, and heavy, making them difficult to wear. On the other hand, fibers are flexible and lightweight materials that can be assembled into different textiles and have been worn by human beings thousands of years. Different from conventional two-dimensional thin films and foils, the three-dimensional fiber and textile structures not only provide superior wearing ability but also much larger surface areas. This talk will introduce how our research group makes use of the attributes of fibers for high-performance wearable energy storage devices. We will demonstrate the strategies and discuss the perspectives to modify fibers and textiles for making wearable capacitors and batteries with excellent mechanical durability, electrochemical stability, and high energy/power density.

10:25 PM ST05.04.03

Self-Assembly of Polypyrrole Micro-Foam/Carbon Nanotube Composite Electrodes for Stretchable Self-Sensing Supercapacitor Devices HaoTian H. Shi and Hani E. Naguib; University of Toronto, Canada

Polypyrrole (PPy)-based electrochemical energy storage electrodes have been widely investigated due to its desired pseudocapacitive charge storage capabilities. However, with the inflexible nature of the conducting polymer, its utilization in fully flexible and stretchable supercapacitor electrodes has been hindered. Herein, a surface-modified thermoplastic polyurethane (TPU) was utilized as the flexible substrate, coated with a thin surface layer of carbon nanotubes (CNT) to provide the desired electrical conductivity and allowed better adhesion of the PPy micro-foam (PPyMF) structures. The fabrication process involved density difference induced alignment of surface CNTs for an even surface coating of the conducting carbon layer suitable for PPy polymerization. With the formation of high specific surface area PPyMF, the flexibility of the sandwiched structure was retained, while providing a highly conducting network with extremely porous active PPyMF for charge storage. The as-fabricated TPU/CNT/PPyMF electrodes were shown to produce a high 345 F/g gravimetric capacitance at a scanning rate of 5 mV/s, an exceptional electrical conductivity of 713 S/m, and a retained capacity of 71% after 3000 charge/discharge cycles, which was better than previously reported polypyrrole based electrode systems. The retained flexibility and charge storage capability during bending was tested to show that 78% of capacity was retained at a bending angle of 90 degrees. At the same time, the supercapacitor electrode was also designed to be self-sensing with an ability to sense strain based on resistance changes, allowing further monitoring of supercapacitor stretching and flexing during usage.

SESSION ST05.05: Solid State Batteries I

Session Chair: Dongping Lu

Thursday Morning, April 22, 2021

ST05

10:30 AM ST05.05.01

Interphase Influence on the Elastic Moduli of Functionalized Reduced Graphene Oxide and Aramid Nanofiber Nanocomposite Supercapacitor Electrodes Tianyang Zhou, James Boyd, Jodie Lutkenhaus and Dimitris Lagoudas; Texas A&M University, United States

Energy storage materials that also provide structural integrity are in need for the weight reduction of electrical automobiles. Structural supercapacitor electrodes consisting of aramid nanofiber (ANFs) and reduced graphene oxide (rGO) nanosheets have shown promising experimental combinations of mechanical properties and capacitance. Further, electrodes including chemically functionalized rGO nanosheets (frGO) has demonstrated even higher experimental moduli than that of the rGO/ANF nanocomposite. The purpose of the present work is to develop a micromechanics model for elastic moduli to analyze the influence of different functional groups and support the development of multifunctional composite electrodes. A three-step micromechanics model was developed to capture the influence of the functional groups on the overall elastic modulus of frGO/ANF composite electrode, as well as the waviness (or curvature) of the respective nanomaterials. The functional

groups on rGO were modeled as a separate phase surrounding the rGO. The interphase was introduced in the nano scale representative volume element (RVE) to form the effective frGO phase. In the microscale RVE, waviness and random orientation was introduced to both ANFs and the frGO. Then, the effective ANF and frGO phases were combined in the mesoscale RVE. Parametric studies on the interphase were carried out. The influence of the interphase thickness and interphase modulus was considered. The in-plane moduli increase significantly with initial interphase modulus increase. However, the increase of in-plane moduli of the composite films will reach a plateau after 30 GPa. Functionalized rGO/ANF composites have lower waviness and a wider waviness distribution per film compared to rGO/ANF composites according to scanning electron microscopy images, which was also captured by the model. Based on the modeling results, the sensitivity of elastic moduli to waviness is higher at lower waviness because of the nonlinear relationship between elastic moduli and waviness which led to the higher standard error of the elastic moduli observed in the experimental results.

10:45 AM *ST05.05.02

Structural Batteries for Mass-Less Energy Storage Leif E. Asp; Chalmers University of Technology, Sweden

Engineering materials that can store electric energy in structural load paths can revolutionise lightweight design across transport modes. Contemporary electric vehicles and aircraft use traditional lithium ion batteries for electrical energy storage. The battery is only providing an electrical energy storage function - adding weight to the system but does not contribute to its structural performance. This paper will present research aimed at the development and demonstration of a multifunctional material that can simultaneously store electrical energy and carry mechanical loads. We have coined this material as the *structural battery composite*. Structural battery composite materials will allow radical weight savings for any electrically powered structural systems, from laptops to cars and aircraft. We foresee that access to structural batteries would allow that practically all the weight of the current monofunctional battery is removed in satellites and significantly reduced in electric cars. Use of structural batteries will provide more energy efficient transport solutions and hence increase competitiveness and save money. As an example, for satellites, a 250 kg weight reduction corresponds to a cost reduction for launch of at least \$3.8M.

Over the last decade, Chalmers and KTH have performed research to realise structural battery composites. By this work, the Swedish team has established a position as leaders in the field [1]. Current structural battery composites have demonstrated an energy density of 24 Wh/kg at a Young's modulus of 25 GPa. We are currently in the process of developing and demonstrating the second-generation structural battery composite with an anticipated energy density of at least 50 Wh/kg and a modulus of 70 GPa. This is slightly lower than traditional composites and Li-ion batteries but combined into a multifunctional material providing significant mass savings.

Structural battery composites are made from carbon fibres in a structural battery electrolyte (SBE) matrix material. Neat carbon fibres are used as a structural negative electrode, exploiting their high mechanical properties, excellent lithium insertion capacity and high electrical conductivity. Lithium iron phosphate coated carbon fibres are used as the structural positive electrode. Here, the lithium iron phosphate is the electrochemically active substance and the fibres carry mechanical loads and conduct electrons. The surrounding SBE is lithium ion conductive and transfers mechanical loads between fibres. With these constituents, structural battery cells are realised.

The presented research relates to recent activities funded by EU's Clean Sky II and USAF. It further comprises ongoing research activities to realise the second-generation laminated structural battery composite full cells. The work comprises Multiphysics models for design and analysis of structural battery devices; separators to allow increased charge/discharge rates; highly multifunctional carbon fibre-reinforced positive electrodes; and design and characterisation of multifunctional electrodes/SBE and separator/SBE interfaces.

1. Our paper Fredi G, et al. *Multifunctional Materials*, 1, 2018, 015003 was appointed among the top-ten breakthroughs in physics in 2018 by the *Physics World* magazine.

11:10 AM *ST05.05.03

Modelling Challenges for Structural Supercapacitors E.S. Greenhalgh, S.N. Nguyen, M. Valkova, C. Lee, M.S.P. Shaffer, A. Kucernak and A. Panesar; Imperial College London, United Kingdom

Structural power composites is an important emerging technology which has the potential to address challenges associated with both lightweighting and electrical energy storage for a range of platforms, but particularly transportation. The focus of the work reported here are structural supercapacitors. Although these devices do not offer the high energy densities associated with batteries, they provide a research vehicle to understand the generic development and implementation hurdles associated with structural power. Structural supercapacitors consist of two electrodes (woven carbon fibre plies impregnated with carbon aerogel) which sandwich an electrically insulating (but ionically conducting) separator (spread tow woven glass fibre). This assembly is immersed in a structural electrolyte, which is a biphasic interconnecting network of a structural phase (typically epoxy) and an ionically conducting phase (typically ionic liquid).

Predictive modelling is discipline which could potentially accelerate the progress, but there is a dearth of work into such studies for structural power. This paper describes the modelling efforts which have been undertaken at Imperial College London, focusing on studies at three different lengthscales: *micro*, *meso* and *macro*.

Firstly, at the *micro* lengthscale, topology optimization (TO) methods are being adopted to identify the optimum microstructure of the structural electrolyte and hence maximize the multifunctional performance of the resulting structural power devices. The structural electrolyte needs to provide a balance between mechanical load-bearing and ionic transport functions. TO has been used to find solutions for the ideal microstructures under different loading cases (tension and shear) whilst maximizing ionic conductivity. This has led to the optimum microstructures for given volume fractions of each phase, over a range of weightings (ranging from dominated by mechanical loading requirements to dominated by ionic transport) having been identified. These predictions have been validated against 3D printed unit cells, the mechanical and electrochemical performance of which has been characterized.

At the *meso* lengthscale, a multiphysics numerical model has been developed, using a commercially available finite element code (ABAQUS), to predict both the mechanical and electrochemical response of our devices. Key to this is predicting the consolidation of the device during manufacture, since this will dictate the spacing between the electrodes (hence the electrochemical performance), but also the reinforcement volume fraction (hence the mechanical performance). The consolidated device geometries have been then been modelled to predict their mechanical response but also, using a modified user element, their electrochemical response. The future aspiration is to permit coupling in these models, such that the influence of mechanical cycling or damage on the electrochemical performance can be predicted. Ultimately this model will provide a means to support the certification of structural power components for transport applications.

Finally, at the *macro* lengthscale, is the challenge of multifunctional design: identifying how best to design with and adopt structural power composites. Methodologies have been developed to provide a clear comparison between conventional compartmentalized systems (such as load-bearing structure and conventional batteries) and structural power components. Hence, the energy and power densities need to be achieved in such multifunctional materials to offer a weight saving over existing systems have been determined. Such studies have considered a range of platforms, and provided an insight into target applications for future structural power materials.

It is anticipated that development of predictive models at these different lengthscales will underpin and accelerate the maturation of this emerging technology, and hasten its adoption by end-users.

11:35 AM ST05.05.04

Rational Interfaces Design for Structural Batteries with High Energy Densities and Electrochemical Performance Tianwei Jin and Yuan Yang; Columbia University, United States

In the past decades, lots of efforts are made by researchers to promote the development of structural lithium ion

batteries, which endow energy storage ability to structural parts for vehicle lightweighting. However, the two strategies people normally use nowadays still have major challenges. One method is introducing thick or heavy packaging and mechanically supporting parts to or inside cells, which intrinsically decreases the energy densities of these energy storage devices. The other one is replacing conventional cell parts like electrodes and electrolytes with materials which have strong mechanical properties but poor electrochemical cycling stability, which sacrifice cycling performance of batteries.

By finite element analysis, we find that the reason of unsatisfying flexural behavior of conventional lithium ion batteries is the sliding of separator and electrode layers relative to each other, and it will greatly increase if we can suppress this sliding. The reason is that if layers are bonded together, all components will participate in the resistance of bending rather than slide relatively, which inspires us with a new idea to improve the mechanical behavior of batteries.

Here we propose a straightforward and rational interfacial design to make cell parts of lithium ion batteries robust by applying suitable and strong “binders” to each interface inside. With a thin coating layer of porous PVDF-HFP, which is previously shown without detriment to cycling performance, electrodes can be bonded with PVDF-coated separators tightly by hot pressing. With these techniques, all components in cells can contribute to the overall mechanical strength, which allows the battery with greatly enhanced flexural strength than conventional batteries. On the other side, on account of the chemical simplicity of this strategy, the structural battery in this work can deliver a comparable specific capacity with conventional cells. This work comes up with a new and simple way to design structural batteries, with both mechanical performance and energy density satisfied, and the method can be easily transferred to large-scale production in industry. Thanks to the wide electrochemical stability of PVDF-HFP, nonflammable and fire-retardant electrolytes can also be utilized, once they are compatible with electrodes, to improve the safety of batteries for their practical application as structural parts in vehicles.

In addition, we apply finite element analysis to conduct simulations to compare the contribution of materials' intrinsic mechanical properties and interfacial adhesion strength in flexural behaviors of batteries, which provides a valuable insight into feasible structural batteries with balanced mechanical and electrochemical properties.

11:50 AM ST05.05.05

Reduced Graphene Oxide / Kevlar Aramid Nanofiber Electrodes as a Structural Supercapacitor

Platform Jodie Lutkenhaus¹, Dimitris Lagoudas¹, James Boyd¹, Micah Green¹ and Haleh Ardebili²; ¹Texas A&M University, United States; ²University of Houston, United States

Structural energy and power devices combine the mechanical properties of structural composites with the energy storage properties of capacitors or batteries. These multifunctional devices promise to reduce the mass and volume of electric vehicles, aircraft, and spacecraft. Carbon fiber mats have been proposed as platforms due to their high stiffness, but it is a challenge to achieve high specific energy and power because the carbon fiber occupies a large volume/mass and is not as electrochemically active due to its low surface area. In response to this challenge, we have explored composite electrodes containing reduced graphene oxide (rGO) nanosheets and Kevlar aramid nanofibers (ANFs). The rGO nanosheets are conductive, mechanically stiff, and have a high surface area; the ANFs are mechanically stiff and provided bridging among the rGO nanosheets via noncovalent interactions.

This talk will provide an overview of the rGO/ANF structural supercapacitor platform, experimentally emphasizing the role of non-covalent interfacial interactions and computationally emphasizing electrode architecture and interphase effects. We compare nacre-like and open-cell electrode morphologies, in which rGO/ANFs electrodes are made via vacuum filtration and hydrothermal synthesis, respectively. Experiments and COMSOL multi-physics modeling demonstrate tradeoffs among ion transport. Generally, the open cell structure results in poorer mechanical properties but satisfactory capacitance. We also compare different functional groups on chemically functionalized rGO, including dopamine, tannic acid, amine, carboxylic acid, and chelating ions. It is found that the mechanical stiffness increases with increasing non-covalent interaction strength, but this results in denser electrodes and poor ion transport. Further, micromechanical modeling shows

modulus and conductivity variations depending on electrode arrangement and waviness (i.e., curviness) of the rGO nanosheets and ANFs. The interphase, as described by modeling as a proxy for the non-covalent interacting layer, affects modulus and conductivity, as well. Together, these results indicate that rGO/ANF electrodes with good combinations of mechanical stiffness and capacitance should have a layered structure with flattened nanomaterials (not wavy, wrinkled, or curvy) with strong and numerous noncovalent interactions, but these electrodes should also have sufficient porosity to allow for ion access to the electrode's surfaces. Lastly, in comparison to the carbon fiber platform, the rGO/ANF capacitors have higher capacitance, but lower stiffness.

Looking to the future, structural energy and power devices bear tradeoffs among mechanical properties and energy storage performance that still need to be addressed with new materials and platforms. The effect of electrochemomechanical coupling is needed to understand failure modes and long term stability.

This work is supported by AFOSR under Grants No. FA9550-16-1-0230 and FA9550-19-1- 0170.

12:05 PM *ST05.05.06

Mechanical Modeling of Li-Ion Batteries—From Physics-Based to Data-Driven Juner Zhu, Wei Li, Martin Z. Bazant and Tomasz Wierzbicki; Massachusetts Institute of Technology, United States

Lithium-ion batteries (LIBs) are ubiquitous in modern society with a wide spectrum of applications from consumer electronics to electric vehicles and the future electric aircraft. The basic structure of a commercial LIB cell consists of alternating porous layers (electrodes and separator) and metal foils (current collectors). These solid materials are saturated with a liquid electrolyte. The first part of this talk will cover a comprehensive physics-based modeling program of the LIB structure, based on several key publications of our team. We will then show that conventional computational tools such as finite element simulations gradually lose their effectiveness as the dimensionality of the system increases. We will use the second part of the talk to demonstrate the applicability of physics-guided neural network approaches, both PDE-based and energy-based, in the mechanical modeling of LIBs in a few real-world scenarios.

SESSION ST05.06: Solid State Batteries II

Session Chairs: Jodie Lutkenhaus and Yuan Yang

Thursday Afternoon, April 22, 2021

ST05

1:00 PM *ST05.06.01

The Electrochemo-Mechanics of Interfaces in All-Solid-State Li-Ion Batteries Yue Qi^{1,2}, Hong-Kang Tian², Aritra Chakraborty², A. Talin³ and Philip Eisenlohr²; ¹Brown University, United States; ²Michigan State University, United States; ³Sandia National Laboratories, United States

Maintaining the physical contact at the electrolyte/electrode interface and preventing mechanical failure are critical to the performance of all-solid-state batteries (ASSB). The ceramics based solid electrolyte and electrode interface tends to have imperfect contact, which can be worsened due to cycling and improved due to cell stack pressure. The solid electrolyte is also subject to electrochemical decomposition at the interface, causing volume change, in addition to the well-known volume change in the electrodes during lithiation-and-delithiation. These chemical strains generate mechanical stress, which leads to fracture in the highly compliant all-solid-state batteries, especially in 3D ASSBs. In this presentation, new continuum models were developed to capture the highly coupled electrochemical-mechanical phenomena. First, we will present a 1D Newman battery model for a film-type Li|LiPON|LiCoO₂ ASSB that incorporated the effect of imperfect contact area with

battery performance by assuming the current and Li concentration will be localized at the contacted area. To establish the relationship between the applied pressure and the contact area, we applied Persson's contact mechanics theory as it uses self-affined surfaces to simplify the multi-length scale contacts in ASSLBs. The model is then used to suggest how much pressures should be applied to recover the capacity drop due to contact area loss. Furthermore, we will introduce a 3D Newman battery model for the experimentally-made 3D Si|LiPON|LiCoO₂ ASSB to incorporate the chemo-mechanical strains due to interfacial decomposition of LiPON and the lithium concentration gradient while cycling. This electrochemo-mechanical model could be used for predicting whether and where the fractures would be produced in order to guide the architecture design of 3D ASSB with balanced energy density and mechanical integrity.

1:25 PM ST05.06.02

Enabling Highly Conductive and Flexible Solid-State Electrolyte Film for All-Solid-State Li-Ion Battery Zhaoxin Yu, Kiseuk Ahn, Jie Xiao, Jun Liu and Dongping Lu; Pacific Northwest National Laboratory, United States

All-solid-state lithium batteries (ASSLBs) are pursued intensively as a promising next-generation energy storage technology due to their high potentials to achieve superior safety and high energy/power densities.¹ Sulfide solid-state electrolytes (SSEs) are arguably more viable for bulk-type ASSLBs than oxide and polymer-based SSEs, thanks to their higher ionic conductivities at room temperature and lower elastic modulus, which allows fast Li⁺ transportation and intimate contact with active materials.² However, deployment of sulfide solid-state electrolytes in practical bulk type ASSLBs are hindered by the processing of highly conductive and ultra-thin solid electrolyte films. Most ASSLBs are evaluated using thick sulfide SSE pellets (>300 microns) for appropriate mechanical strength. This method is not realistic since thick SSE pellet causes a serious penalty to energy density at the cell level.³ Therefore, it is urgent to develop highly conductive and ultra-thin sulfide SSE film with good mechanical properties for the deployment of ASSLBs.

Here, we report an up-scalable method for the preparation of highly conductive sulfide SSE films with a lean amount of polymeric binder. A new polymeric binder/solvent combination, which is compatible with sulfide SSEs, was identified to prepare the ultra-thin SSE film. Under processing, the polymeric binder is well-controlled into filament-shape and builds a 3D-matrix, providing superior confinement for SSE particles with decent flexibility. Effects of the polymeric binder on SSE film have been investigated in terms of film mechanical property, ionic conductivity, and electrochemical properties of Li/SSE/Li symmetric cells. As a result, ultra-thin SSE film with a thickness of 75-100 um was prepared with 2 wt. % of the polymeric binder and demonstrates an overall conductivity of about 1 mS/mcm at room temperature. More details of this research will be discussed at the symposium.

1. Randau, S. *et al.* Benchmarking the performance of all-solid-state lithium batteries. *Nat. Energy* **5**, 259–270 (2020).
2. Wang, Y. *et al.* Superionic conduction and interfacial properties of the low temperature phase Li₇P₂S₈Br_{0.5}I_{0.5}. *Energy Storage Mater.* (2019).
3. Lee, Y. G. *et al.* High-energy long-cycling all-solid-state lithium metal batteries enabled by silver-carbon composite anodes. *Nat. Energy* (2020).

1:40 PM *ST05.06.03

Mechanical Constriction Design of Stabilities for High Performance Solid-State Batteries Xin Li; Harvard University, United States

Mechanical constriction induced various stabilities greatly widen the operational voltage window of solid-state batteries. Bulk and interface stabilities can be modulated to operate at extreme voltages of high voltage cathodes

and Li metal anode. Ab-initio simulations and experimental characterizations are used to unveil chemical, electrochemical and microstructural details to support the unique physical picture of mechanical constriction modulated electrochemical behavior. Based on the design principle, up to 10 mA/cm² current density on lithium metal anode and up to 10 V voltage stability of sulfide electrolytes are demonstrated. The potential impact of this effect on the design of high voltage solid state batteries beyond the commercial level will also be discussed.

2:05 PM DISCUSSION

2:20 PM *ST05.06.05

Mechanical Properties of Metal Anodes of Rechargeable Batteries Matt Pharr; Texas A&M University, United States

Metallic anodes have the potential to enable batteries with enormous capacities. Indeed, lithium metal has the highest theoretical capacity, lowest density, and most negative electrochemical potential of known anode materials for rechargeable batteries. However, dendrites of Li can form during cycling, which lead to significant safety issues that have precluded their practical deployment. Sodium metal anodes have similar safety concerns but have recently received increased attention due to their natural abundance, relatively low cost, and potential for grid-scale energy storage. Potassium metal anodes are still very much in a developmental phase but have promise stemming from their potential for simple cell design with cheap fabrication, earth abundance, and relatively low cost. Magnesium metal anodes have enormous volumetric capacities but readily form passivating layers during recharging, and recent studies suggest dendrite formation can occur under certain conditions. While the electrochemistry of these systems has received extensive study, at the heart of many practical issues in these systems lies a mechanics of materials problem. Specifically, as atoms are deposited and stripped during electrochemical cycling, the material deforms, generating stresses under constraint. These stresses can result in fracture, delamination, detachment, and/or unstable deformation (e.g., the formation of dendritic structures) of the electrodes, diminishing their capacity or leading to severe safety issues. Likewise, the stresses in turn may affect the electrode kinetics, the growth morphology under cycling, and/or the integrity of the contact at the anode/solid-state-electrolyte interface. Studies that provide deeper understanding of mechanics in these systems may thus play a key role in mitigating or even preventing many of these issues. For instance, modelling studies have suggested that the mechanical properties of the anode materials (relative to the separators or solid-state electrolytes with which they are in contact) are key in guiding the suppression of dendritic growth during electrochemical operation. Experimental studies have shown that the morphology of Li during electrochemical deposition depends on external pressures applied to battery stacks, as does the propensity for maintaining interfacial contact in all-solid-state batteries. As such, prior to real applications, a comprehensive understanding of the mechanical properties of these materials is vital. To this end, through nanoindentation, microhardness, and bulk testing, this talk will present experimental studies of the mechanical properties of metallic Li, Na, K, and Mg anodes, including how these properties vary with loading rate, representative size scale, and temperature. These properties will be connected to implications in terms of potential battery performance, e.g., in preventing dendritic structures, detachment between solid-state electrolytes and metallic anodes, etc. Overall, this talk will provide insight into guiding the design of battery materials, architectures, and electrochemical (e.g., charging) conditions that mitigate unstable growth of metal anodes during electrochemical cycling.

2:45 PM ST05.06.06

Bioinspired Structural Ion Conductive Membranes for Energy Storage Applications Ahmet Emre, Jinchun Fan, Mingqiang Wang, Volkan Cecen and Nicholas A. Kotov; University of Michigan–Ann Arbor, United States

Bioinspired ion conductive membranes have been widely investigated for beyond lithium-ion battery

applications. The high theoretical specific energy density (2600Wh/kg) and high specific capacity (1675mA/g) along with the natural abundance and low toxicity of sulfur have been attracting significant attention for the development of an alternative battery system to replace traditional lithium-ion batteries which suffer from safety and capacity/energy density limitations in various applications. However, challenges such as polysulfide dissolution and shuttling prevent mass commercialization of metal sulfur batteries. Inspired from biological ion transport mechanisms, we show a practical yet comprehensive approach for the development of high-performance metal sulfur batteries. Aramid nanofiber (ANF) based composite ion conductive membranes not only prevent dendrite formation but also confine polysulfides on the cathode side. ANF composite battery separators provide diverse and opposing properties including high mechanical properties, high ionic conductivity, and high thermal/chemical stability. Moreover, the highly selective ion sieving properties of these strong biomimetic separators provide safe and high-performance structural batteries. Fabrication of such biocompatible, affordable, flexible, and high energy density structural battery is quite crucial in powering next-generation electric vehicles, robotics and electronics including but not limited to portable, wearable, and implantable biomedical devices.

SYMPOSIUM X

Frontiers of Materials Research
April 17 - April 23, 2021

* Invited Paper

SESSION X.01
Wednesday Morning, April 21, 2021
X

10:15 AM *X.01.01

Tropical Rain-Forest Plants—A Source of Bio-Inspired New Materials, New Technologies and New Concepts Nick P. Rowe; Centre National de la Recherche Scientifique (CNRS), France

Tropical rain forests represent some of the most complex and diverse living structures. Plants make up the three-dimensional complexity of these ecosystems not only as trees, but also as creepers, vines, lianas, and epiphytes. This diversity of growth forms has evolved and is adapted for a wide range of physical and mechanical constraints. Big trees are well designed to be mechanically stable under self-loading but are also compliant when the wind blows. Vines and lianas exploit the stature of big trees by attaching and climbing on them towards the light. They show highly specialized properties to reach and attach to supports and then climb by economically, narrow stems which are amazingly flexible and highly resistant to mechanical failure. In this talk we will go on a walkabout of tropical rain forests and visit highly adapted growth forms, their remarkable mechanical properties and also their capacity for movement. In fact, plants, especially climbing plants, do move. Not only rather slowly by growth but also by internally controlled circling, spiraling, waving and oscillating movements - movements by solid materials without muscles. So, our tour will not only be a story about the different materials and structures that exist in these environments—what we might call a static view, it will also be a story with a dynamic view, how plants grow and move adaptively using smart additive processes

(AKA growth), how they can move and position themselves, and how they can explore their environment and mechanically attach to supports.

Nick Rowe is a biologist and Director of Research in the CNRS, at the AMAP research Laboratory in Montpellier, France. He grew up in the southeast of England and was educated in Rochester, Kent. He obtained both his B.Sc. degree in honours botany and Ph.D. degree from the University of Bristol, England. Being British and having worked and lived in France, Germany and Great Britain, his personal outlook and his research interests and collaborations in science remain highly international and multidisciplinary. Originally trained as an evolutionary biologist focusing on the origin and evolution of plants, he became increasingly interested in plant functional biology and biomechanics—how different plant species have evolved and adapted diverse functional and biophysical properties for surviving in a complex world. In recent years, he established a biomechanics laboratory in France, forming a home-base for research into the biomechanics and diversity of plants from the tropical forests of South America, west Africa and southeast Asia. Most recently, his research has focused on the structures and properties we see in today's plant diversity and how this offers a source of inspiration for developing new materials, new technologies and new concepts. His latest projects are exploring the functional, ecological, evolutionary and developmental potential of plants as sources for new innovative technologies including research on climbing plant innovations for soft robotics.

SESSION X.02

Thursday Afternoon, April 22, 2021

X

6:15 PM *X.02.01

Nanotechnology for Sustainability Yi Cui; Stanford University, United States

One of the most challenging problems human beings are facing during the 21st century is the sustainability due to climate change and environment pollution. Nanotechnology provides new opportunities to address the sustainability issues, including energy and environment. In this talk, I will provide examples of nanotechnology for sustainability, including: 1) Nanomaterials design for reinventing batteries to achieve high energy density, long life, good safety and low cost to be used in the applications of transportation and grids. 2) Reinventing textiles with nanotechnology to control human body infrared radiation for the warming and cooling purpose, which could potentially save building energy consumption by 30%. 3) Air, water and soil nanotechnology for effective removing pollutants and disinfecting biopathogen. I will also discuss how to take these technologies from labs to markets in order to have a sustainability impact to the real world.

Biography

At Stanford University, Yi Cui is Director of the Precourt Institute for Energy, co-director of the StorageX Initiative, and professor of materials science and engineering and of photon science at SLAC National Accelerator Laboratory. A cleantech pioneer and entrepreneur, Cui earned his B.S. degree in chemistry in 1998 from the University of Science & Technology of China and his Ph.D. degree in chemistry from Harvard University in 2002. He was a Miller Postdoctoral Fellow at the University of California, Berkeley, from 2002 to 2005 before joining the Stanford faculty. Cui manages a large Stanford research group, from which alumni have succeeded in academia and businesses. He has founded five companies to commercialize the energy and environment technologies from his lab: Amprius Inc., 4C Air Inc., EEnotech Inc., EnerVenue Inc. and LifeLab Design Inc.

A preeminent researcher of nanotechnologies for better batteries and other sustainability technologies, Cui has published more than 500 studies and is one of the world's most cited scientists. He is an elected fellow of the American Association for the Advancement of Science, the Materials Research Society, and the Royal Society

of Chemistry. He is an executive editor of *Nano Letters* and co-director of the Battery 500 Consortium.

In 2021, U.S. Department of Energy awarded Cui an Ernest Orlando Lawrence Award which honors mid-career scientists and engineers in eight research fields. Other awards include: Materials Research Society Medal (2020), Electro Chemical Society Battery Technology Award (2019), Nano Today Award (2019), Blavatnik National Laureate (2017), and the Sloan Research Fellowship (2010).

SESSION X.03

Friday Morning, April 23, 2021

X

10:15 AM *X.03.01

How New and old Materials Research and Know-How Extend the Increase in Computation Power Iuliana Radu; imec, Belgium

For the past 20 years, doomsayers have been talking about the end of performance increase in compute because transistor scaling was supposed to end. We all know this was far from true and continue physical and performance scaling of the transistors has enabled continues increase in computing power. Maintaining physical or performance scaling of the switches themselves is becoming more difficult but other options exist and the field of very exciting research. Old concepts with new materials and new concepts with old materials are in the spotlight and materials research is paramount to enabling new growth in computing power and of the society in general.

In this talk, we will cover an old concept but with new materials: transistors with 2D semiconducting channels as these materials are expected to enable further scaling of transistor area and performance. At the other side of the spectrum, we will cover how better-understood materials such as Al, Nb, TiN contribute to better qubit for quantum computing. Uniting the two topics are not only the application of computing, but also the mindset and fundamental need for extreme control of materials and processes involved in fabricating these devices.

Transistors with 2D materials hold the promise for extreme gate length scaling compared to Si as they can be deposited with monolayer precision, and mobility is expected to be almost independent of material thickness. In this presentation, we will discuss imec's work on 2D materials emphasizing channel and dielectrics deposition and how process steps could change device performance. We will cover how device and circuit modelling guides choices in integration schemes and ultimately defines specifications for the materials involved. We will describe how variability analysis can help differentiate between one-off observations and consistent process control and understanding.

Quantum computing is fundamentally different that classical computing but many of the technology challenges are similar to those for building classical systems. In this talk, we will outline how learning and practices from standard semiconductor development can be used to enable quantum computing. We will discuss how materials and process development can improve device performance.

In both topics, we will outline what we believe main materials research directions to be investigated and where fundamental discovery and innovation is key.

Biography

Iuliana P. Radu is Director of Quantum and Exploratory Computing at imec. Her activities include work on beyond CMOS device concepts such as spintronic majority gates and switches with novel channel materials and their possible applications in the semiconductor industry. Quantum computing includes work on qubit devices and the periphery circuits meant to control them. Prior to establishing the Beyond CMOS program at imec in 2013, she was a Marie Curie and FWO fellow at KU Leuven and imec. Iuliana received a Ph.D. degree in physics from Massachusetts Institute of Technology in 2009 where she searched for Majorana fermions in the quest to build very reliable qubits for quantum computing. She has authored over 190 papers in leading peer-reviewed journals and conferences. She has given more than 40 invited talks at international conferences and seminars where she is a frequent speaker on quantum computing and exploratory devices for classical computing. She currently serves as program committee member for ESSDERC and SNW and is an associate editor for IEEE *TNANO*.